













TS  
200  
15



# THE JOURNAL OF THE INSTITUTE OF METALS

VOLUME LXXX  
1951-52

EDITOR

N. B. VAUGHAN, M.Sc.

*The Right of Publication and of Translation is Reserved.  
The Institute of Metals is not responsible for the statements  
made or for the opinions expressed in the following pages.*



LONDON

PUBLISHED BY THE INSTITUTE OF METALS  
4 GROSVENOR GARDENS, S.W.1

1952

Copyright]

[Entered at Stationers' Hall



## PAST-PRESIDENTS

Sir WILLIAM HENRY WHITE, K.C.B., LL.D., D.Eng., Sc.D., F.Inst.Met., F.R.S., 1908–1910 (*deceased*).

Sir GERARD ALBERT MUNTZ, Bart., 1910–1912 (*deceased*).

Professor WILLIAM GOWLAND, A.R.S.M., F.R.S., 1912–1913 (*deceased*).

Professor ALFRED KIRBY HUNTINGTON, A.R.S.M., 1913–1914 (*deceased*).

Engineer Vice-Admiral Sir HENRY JOHN ORAM, K.C.B., F.Inst.Met., F.R.S., 1914–1916 (*deceased*).

Sir GEORGE THOMAS BEILBY, LL.D., D.Sc., F.R.S., 1916–1918 (*deceased*).

Professor Sir HENRY CORT HAROLD CARPENTER, M.A., Ph.D., D.Sc., D.Met., A.R.S.M., F.Inst.Met., F.R.S., 1918–1920 (*deceased*).

Engineer Vice-Admiral Sir GEORGE GOODWIN GOODWIN, K.C.B., LL.D., F.Inst.Met., 1920–1922 (*deceased*).

LEONARD SUMNER, O.B.E., M.Sc., J.P., F.Inst.Met., 1922–1924 (*deceased*).

Professor-Emeritus THOMAS TURNER, M.Sc., A.R.S.M., F.Inst.Met., 1924–1926 (*deceased*).

Sir JOHN DEWRANCE, G.B.E., F.Inst.Met., 1926–1928 (*deceased*).

WALTER ROSENHAIN, D.Sc., B.C.E., F.Inst.Met., F.R.S., 1928–1930 (*deceased*).

RICHARD SELIGMAN, Ph.nat.D., F.Inst.Met., 1930–1932.

Sir HENRY FOWLER, K.B.E., LL.D., D.Sc., 1932–1934 (*deceased*).

HAROLD MOORE, C.B.E., D.Sc., Ph.D., F.Inst.Met., 1934–1936.

WILLIAM ROBB BARCLAY, O.B.E., F.Inst.Met., 1936–1938 (*deceased*).

CECIL HENRY DESCH, D.Sc., LL.D., Ph.D., F.Inst.Met., F.R.S., 1938–1940.

The Hon. RICHARD MARTIN PETER PRESTON, D.S.O., 1940–1942.

Lieut.-Colonel Sir JOHN HENRY MAITLAND GREENLY, K.C.M.G., C.B.E., M.A., F.Inst.Met., 1942–1944 (*deceased*).

Sir WILLIAM THOMAS GRIFFITHS, D.Sc., 1944–1946 (*deceased*).

Colonel Sir PAUL GOTTLIEB JULIUS GUETERBOCK, K.C.B., D.S.O., M.C., T.D., D.L., J.P., M.A., A.D.C.,  
F.Inst.Met., 1946–1948.

Sir ARTHUR JOHN GRIFFITHS SMOUT, J.P., 1948–1950.

HUBERT SANDERSON TASKER, B.A., 1950–1951.

Professor ALFRED JOHN MURPHY, M.Sc., 1951–1952.



# COUNCIL AND OFFICERS

FOR THE YEAR 1952-53

## PRESIDENT

C. J. SMITHELLS, M.C., D.Sc.

## PAST-PRESIDENTS

Professor A. J. MURPHY, M.Sc.

Sir ARTHUR SMOUT, J.P.

H. S. TASKER, B.A.

## VICE-PRESIDENTS

G. L. BAILEY, C.B.E., M.Sc.  
S. F. DOREY, C.B.E., D.Sc.,  
F.R.S.

A. B. GRAHAM  
P. V. HUNTER, C.B.E.

Professor H. O'NEILL, D.Sc., M.Met.  
Professor F. C. THOMPSON,  
D.Met., M.Sc.

## HON. TREASURER

E. H. JONES

## ORDINARY MEMBERS OF COUNCIL

ALFRED BAER, B.A.  
E. A. BOLTON, M.Sc.  
N. I. BOND-WILLIAMS, B.Sc.  
K. W. CLARKE  
C. H. DAVY  
N. P. INGLIS, Ph.D., M.Eng.

IVOR JENKINS, D.Sc.  
L. B. PFEIL, O.B.E., D.Sc.,  
A.R.S.M., F.R.S.  
Professor A. G. QUARRELL, D.Sc.,  
Ph.D., A.R.C.S.  
A. G. RAMSAY, Ph.D., B.Sc.

Professor G. V. RAYNOR, M.A.  
D.Phil., D.Sc.  
CHRISTOPHER SMITH  
H. SUTTON, C.B.E., D.Sc.  
Major P. L. TEED, A.R.S.M.  
W. J. THOMAS

## EX-OFFICIO MEMBERS OF COUNCIL

E. A. FOWLER, B.Sc., A.R.T.C.  
(*Scottish Local Section*)  
C. E. RANSLEY, Ph.D., M.Sc.  
(*London Local Section*)

H. M. FINNISTON, B.Sc., Ph.D.,  
A.R.T.C.  
(*Oxford Local Section*)  
K. M. SPRING  
(*South Wales Local Section*)

M. M. HALLETT, M.Sc.  
(*Sheffield Local Section*)  
H. H. SYMONDS  
(*Birmingham Local Section*)

## REPRESENTATIVES OF OTHER BODIES

The following, in accordance with Article 32, represent Government Departments and allied societies at Council meetings, for purposes of liaison

ADMIRALTY . . . . .	Capt. (E.) H. J. B. GRYLLS, R.N.
WAR OFFICE . . . . .	Major-General S. W. JOSLIN, C.B.E., M.A.
IRON AND STEEL INSTITUTE . . . . .	Capt. H. LEIGHTON DAVIES, C.B.E., J.P.
INSTITUTION OF METALLURGISTS . . . . .	MAURICE COOK, D.Sc., Ph.D.; E. G. WEST, B.Sc., Ph.D.

## SECRETARY

Lieut.-Colonel S. C. GUILLAN, T.D.

## ASSISTANT SECRETARY

Major R. E. MOORE

## EDITOR OF PUBLICATIONS

N. B. VAUGHAN, M.Sc.



# CHAIRMEN AND HONORARY SECRETARIES OF THE LOCAL SECTIONS

at 30 September 1952

## Birmingham

*Chairman* : H. H. SYMONDS, 77 Antrobus Road, Sutton Coldfield, Warwickshire.

*Hon. Secretary* : A. W. MATTHEWS, 124 Hay Green Lane, Birmingham 29.

*Hon. Treasurer* : R. CHADWICK, M.A., 5 Fairmead Rise, King's Norton, Birmingham 30.

## London

*Chairman* : C. E. RANSLEY, Ph.D., M.Sc., Research Laboratories, The British Aluminium Company, Ltd., Chalfont Park, Gerrards Cross, Bucks.

*Hon. Secretary* : E. C. RHODES, Ph.D., B.Sc., The Mond Nickel Company, Ltd., Development and Research Department, Bashley Road, London, N.W.10.

*Hon. Treasurer* : J. D. GROGAN, B.A., Metallurgy Division, National Physical Laboratory, Teddington, Middlesex.

## Oxford

*Chairman* : H. M. FINNISTON, B.Sc., Ph.D., A.R.T.C., Atomic Energy Research Establishment, Harwell, Berks.

*Hon. Secretary* : B. R. T. FROST, B.Sc., Ph.D., Atomic Energy Research Establishment, Harwell, Berks.

*Hon. Treasurer* : J. C. ARROWSMITH, M.Met., Pressed Steel Company of Great Britain, Ltd., Oxford.

## Scottish

*Chairman* : E. A. FOWLER, B.Sc., A.R.T.C., Scotts' Shipbuilding and Engineering Company, Ltd., Greenock, Renfrewshire.

*Hon. Secretary* : MATTHEW HAY, A. Cohen and Co., Ltd., Craigton Industrial Estate, Barfillan Drive, Cardonald, Glasgow, S.W.2.

*Hon. Treasurer* : N. J. MACLEOD, Steven and Struthers, Ltd., 86 Eastvale Place, Kelvinhaugh, Glasgow, C.3.

## Sheffield

*Chairman* : M. M. HALLETT, M.Sc., Sheepbridge Engineering, Ltd., Chesterfield.

*Hon. Secretary and Treasurer* : A. J. MACDOUGALL, M.Met., Department of Applied Science, The University, St. George's Square, Sheffield 1.

## South Wales

*Chairman* : K. M. SPRING, 36 Beechwood Road, Uplands, Swansea.

*Hon. Secretary* : W. H. GRENFELL, "The Woods", Bryn Terrace, Mumbles, Swansea.

*Hon. Treasurer* : R. G. L. MATTHEWS, Imperial Chemical Industries, Ltd., Metals Division, Landore, Swansea.



# CORRESPONDING MEMBERS TO THE COUNCIL

at 30 September 1952

## Australia

Professor H. K. WÖRNER, D.Sc.,  
Professor of Metallurgy, University of Melbourne, Carlton, N.3, Melbourne, Victoria.

## Belgium

H. P. A. FÉRON,  
Administrateur-Directeur, Visseries et Tréfileries Réunies, 2 Avenue Général Leman, Haren, Bruxelles.

## Canada

Professor BRUCE CHALMERS, Ph.D., D.Sc.,  
Department of Metallurgical Engineering, University of Toronto 5, Ontario.  
Professor G. LETENDRE, B.A., Ph.D.,  
Professor of Metallurgy and Director, Department of Mining and Metallurgical Engineering, Faculty of Sciences,  
Laval University, Boulevard de l'Entente, Quebec City, P.Q.

## France

Professor P. A. J. CHEVENARD,  
Administrateur et Conseiller Scientifique, Société Anonyme de Commentry-Fourchambault et Decazeville, 84 rue de Lille, Paris 7e.  
JEAN MATTER,  
Vice-Président et Directeur-Général, Société Centrale des Alliages Légers, Issoire, Puy-de-Dôme.

## India

N. P. GANDHI, M.A., B.Sc., A.R.S.M., D.I.C.,  
Kennaway House, Proctor Road, Girgaon, Bombay 4.

## Italy

LENO MATTEOLI, Dott.chim.,  
Vice-Director, Istituto Scientifico Tecnico Ernesto Breda, Sesto S. Giovanni, Milano.

## Netherlands

M. HAMBURGER,  
Director, N.V. Royal Nederlandsche Lood- en Zinkpletterijen voorheen A.D. Hamburger, Leidschekade 30, Utrecht.

## South Africa

G. H. STANLEY, D.Sc., A.R.S.M.  
24 Duncombe Road, Forest Town, Johannesburg, Transvaal.  
Professor L. TAVERNER, A.R.S.M., D.I.C.,  
Professor of Metallurgy and Assaying, University of the Witwatersrand, Johannesburg, Transvaal.

## Spain

Professor J. ORLAND, M.Sc., M.A., Ph.D., D.D.,  
Head of the Department of Metallography and Strength of Materials, Instituto Católico de Artes e Industrias,  
Alberto Aguilera 23, Madrid.

## Sweden

Professor CARL BENEDICKS, Fil.Dr., Dr.-Ing.e.h., Dr.Techn.h.c.,  
Drottningatan 95 B., Stockholm.  
Professor AXEL HULTGREN,  
Professor of Metallography, Kungl. Tekniska Högskolan, Stockholm.

## Switzerland

Professor A. VON ZEELEDER, Dr.-Ing.,  
Director, Research Laboratories, Société Anonyme pour l'Industrie de l'Aluminium Chippis, Rosenbergstrasse 25,  
Neuhausen a./Rheinfall.

## United States of America

Professor R. F. MEHL, Ph.D., Eng.D., Sc.D.,  
Director, Metals Research Laboratory, Carnegie Institute of Technology, Pittsburgh, Pa.  
Professor C. S. SMITH, Sc.D.,  
Professor of Metallurgy and Director of the Institute for the Study of Metals, University of Chicago, Chicago 37, Ill.  
Dr. R. A. WILKINS,  
Vice-President, Revere Copper and Brass, Inc., Rome, N.Y.





Digitized by the Internet Archive  
in 2024









C. J. SMITHELLS, M.C., D.Sc.  
(President, 1952-53)

# CONTENTS

## MINUTES OF PROCEEDINGS

	PAGE
General Meeting, 17 October 1951 . . . . .	xi
General Meeting, 3 January 1952 . . . . .	xi
Annual General Meeting, London, 24-27 March 1952 . . . . .	xi
Annual Autumn Meeting, Oxford, 15-19 September 1952 . . . . .	xiii
General Meeting, 19 November 1952 . . . . .	xvi

## PAPERS AND DISCUSSIONS

	PAGE	
	<i>Paper.</i>	<i>Discn.</i>
1319. The Grain Refinement of Aluminium Alloy Castings by Additions of Titanium and Boron. By A. Cibula, M.A., A.I.M. . . . .	1	685
1320. Some Observations on the Occurrence of Stretcher-Strain Markings in an Aluminium-Magnesium Alloy. By R. Chadwick, M.A., F.R.I.C., F.I.M., and W. H. L. Hooper, B.Sc., A.I.M. . . . .	17	689
1321. The Effect of Phosphorus on the Corrosion-Resistance of Magnesium and Some of Its Alloys. By E. F. Emley, B.Sc., Ph.D., A.I.M., F.R.I.C., A. C. Jessup, M.C., A.Inst.P., F.I.M., and W. F. Higgins, M.Sc., Ph.D., A.R.I.C. . . . .	23	
1322. Creep and Stress Rupture as Rate Processes. By Italo S. Servi, Dott., S.M., Sc.D., and N. J. Grant, B.S., Sc.D.	33	
1323. A Simple Method of X-Ray Microscopy and Its Application to the Study of Deformed Metals. By R. W. K. Honeycombe, M.Sc., Ph.D. . . . .	39	
1324. Inhomogeneities in the Plastic Deformation of Metal Crystals—I. II. I.—Occurrence of X-Ray Asterisms. II.—X-Ray and Optical Micrography of Aluminium. By R. W. K. Honeycombe, M.Sc., Ph.D. . . . .	45	690
1325. The Flow of Liquid Metals on Solid Metal Surfaces and Its Relation to Soldering, Brazing, and Hot-Dip Coating. By G. L. J. Bailey, Ph.D., A.R.C.S., D.I.C., F.Inst.P., and H. C. Watkins, L.I.M. . . . .	57	692
1326. The Spectrochemical Determination of Zinc, Lead, and Iron in Copper and Copper Alloys. By Frederick V. Schatz, M.A. . . . .	77	
1327. The Equilibrium Diagram of the System Nickel-Manganese. By B. R. Coles, B.Sc., and W. Hume-Rothery, M.A., D.Sc., F.R.S. . . . .	85	694
1328. The Nucleation of Cast Metals at the Mould Face. By J. A. Reynolds, B.Sc., and C. R. Tottle, M.Met., A.I.M.	93	
1329. Electrochemistry and the Science of Metals. Twenty-Second Autumn Lecture. By Professor Roberto Piontelli . . . . .	99	
1330. High-Temperature Thermal Analysis Using the Tungsten/Molybdenum Thermocouple. By H. T. Greenaway, B.Met.E., S. T. M. Johnstone, B.Met.E., and Marion K. McQuillan, M.A. . . . .	109	
1331. Slip Bands and Hardening Processes in Aluminium. By A. F. Brown, M.A., Ph.D. . . . .	115	690
1332. Experiments on the Reaction of Aluminium-Magnesium Alloys with Steam. By A. J. Swain, M.A. . . . .	125	598
1333. The Creep and Softening Properties of Copper for Alternator Rotor Windings. By N. D. Benson, M.Eng., J. McKeown, D.Sc., and D. N. Mends, B.Sc. . . . .	131	682
1334. The Alloys of Molybdenum and Tantalum. By G. A. Geach, M.Sc., Ph.D., F.I.M., and D. Summers-Smith, B.Sc., A.R.T.C. . . . .	143	528
1335. An Investigation of the Structural Changes Accompanying Creep in a Tin-Antimony Alloy. By W. Betteridge, Ph.D., F.Inst.P., and A. W. Franklin, M.Sc., A.I.M. . . . .	147	587
1336. Thermoelastic Analysis of Transformations in Copper Alloys. By R. Cabarat, P. Gence, Professor L. Guillet, and R. Le Roux . . . . .	151	700
1337. The Structure and Some Properties of Titanium-Oxygen Alloys Containing 0-5 At.-% Oxygen. By A. E. Jenkins, M.Eng.Sc., and H. W. Worner, M.Sc. . . . .	157	702
1338. Some Observations on the Deformation of Polycrystalline Zinc. By J. A. Ramsey, M.Sc. . . . .	167	706
1339. The Sigma Phase in Binary Alloys of the Transition Elements. By A. H. Sully, M.Sc., Ph.D., F.Inst.P., F.I.M. . . . .	173	694
1340. Some Metallographic Observations on the Fatigue of Metals. By P. J. E. Forsyth, A.I.M. . . . .	181	
1341. A Mechanism of Stress-Corrosion in Aluminium-Magnesium Alloys. By C. Edeleanu, M.A., Ph.D. . . . .	187	707
1342. The Production and Properties of Oxide-Reduced Copper Powder. By E. C. Ellwood, Ph.D., A.I.M., and W. A. Weddle, B.Sc. . . . .	193	711
1343. Unrelated Simultaneous Interdiffusion and Sintering in Copper-Nickel Compacts. By J. M. Butler, M.A., Ph.D., and T. P. Hoar, M.A., Ph.D., F.I.M. . . . .	207	711
1344. Heat-Treatment of Titanium-Rich Titanium-Iron Alloys. By H. W. Worner, M.Sc. . . . .	213	702
1345. The Solid Solutions of Zinc in Aluminium. By E. C. Ellwood, Ph.D., A.I.M. . . . .	217	713



		PAGE	
		Paper.	Discn.
1346. Metal Economics. I.—Primary Resources of Ferrous and Non-Ferrous Metals :			
Introduction. By Professor A. J. Murphy, M.Sc. . . . .	225		
The World Supply of Non-Ferrous Metals, Including the Light Metals. By R. Lewis Stubbs . . . .	226		
Metals as Natural Resources. By Professor S. Zuckerman, C.B., F.R.S. . . . .	233		
World Demand and Resources of Iron Ore. By T. P. Colclough, C.B.E., D.Sc. . . . .	234		
Joint Discussion . . . . .			237
Metal Economics. II.—Scrap Reclamation, Secondary Metals, and Substitute Metals :			
The Scope for Conservation of Metals, Ferrous and Non-Ferrous. By C. A. Bristow, B.Sc., A.R.S.M., A. J. Sidery, Assoc.Met., and H. Sutton, D.Sc. . . . .	240		
Economy by Standardization of Alloys and of the Method of Reclamation of Scrap Metals. By C. Dinsdale, M.Sc. . . . .	241		
The Influence of Specifications on Productivity and the Economic Utilization of Ferrous and Non-Ferrous Metals. By F. Hudson . . . . .	244		
Secondary Heavy Metals. By E. H. Jones . . . . .	245		
Secondary Aluminium and Magnesium. By Colonel W. C. Devereux, C.B.E. . . . .	248		
Joint Discussion . . . . .			252
SYMPOSIUM ON EQUIPMENT FOR THE THERMAL TREATMENT OF NON-FERROUS METALS AND ALLOYS			
1347. Electric Furnaces for the Thermal Treatment of Non-Ferrous Metals and Alloys. By C. J. Evans, A.M.I.E.E., P. F. Hancock, B.A., F.I.M., F. W. Haywood, Ph.D., B.Sc., F.R.I.C., F.I.M., and J. McMullen, A.I.M. . . . .	255		
1348. Gas Equipment for the Thermal Treatment of Non-Ferrous Metals and Alloys. By J. F. Waight, B.Sc.(Eng.), M.Inst.Gas E. . . . .	269		
1349. Batch and Continuous Annealing of Copper and Copper Alloys. By Edwin Davis, M.Sc., F.I.M., and S. G. Temple, M.Sc., A.I.M. . . . .	287		
1350. Bright Annealing of Nickel and Its Alloys. By H. J. Hartley, M.Sc., F.I.M., and E. J. Bradbury, M.Eng., A.M.I.Mech.E., A.I.M. . . . .	297		
1351. Batch Thermal Treatment of Light Alloys. By C. P. Paton, B.Eng. . . . .	311		
1352. Flash Annealing of Light Alloys. By R. T. Staples . . . . .	323		
1353. Continuous Heat-Treatment of Aluminium Alloys of the Duralumin Type. By Marcel Lamourdedieu . . . .	335		
Joint Discussion . . . . .			667
Report of Council for the Year Ended 31 December 1951 . . . . .	341		
Report of the Honorary Treasurer for the Financial Year Ended 30 June 1951 . . . . .	349		
1354. The Sintering of Copper-Zinc Powder Compacts. By D. D. Howat, B.Sc., Ph.D., F.R.I.C., R. L. Craik, B.Sc., A.R.T.C., and J. P. Cranston, B.Sc., Ph.D., A.R.T.C. . . . .	353		711
1355. The Effect of the Elements of the First Long Period on the $\alpha \rightleftharpoons \beta$ Transformation in Titanium. By A. D. McQuillan, Ph.D., B.Sc. . . . .	363		702
1356. Determination of Elastic Constants and Stress/Strain Relationship to Fracture of Sintered Tungsten Carbide- Cobalt Alloys. By E. Lardner, B.Sc., A.I.M., and N. B. McGregor . . . . .	369		
1357. The Constitution of the Copper-Rich Copper-Zinc-Germanium Alloys. By P. Greenfield, Ph.D., B.Sc., and Professor G. V. Raynor, M.A., D.Sc. . . . .	375		700
1358. Micrographic Aspects of the Diffusion of Zinc and Aluminium in Copper. By H. Bückle, Dr.-Ing., and J. Blin R. C. Hall, and R. F. Hehemann . . . . .	385		714
1359. Note on Sub-Crystal Structure in Cold-Rolled Aluminium. By A. E. L. Tate, A.I.M., and D. McLean, B.Sc. Appendix by O. Kubaschewski, Dr.phil.nat.habil. . . . .	390		
1360. Fundamental Reactions in the Vacuum-Fusion Method and Its Application to the Determination of O <sub>2</sub> , N <sub>2</sub> , and H <sub>2</sub> in Mo, Th, Ti, U, V, and Zr. By H. A. Sloman, M.A., F.R.I.C., F.I.M., and C. A. Harvey. With an Appendix by O. Kubaschewski, Dr.phil.nat.habil. . . . .	391		
1361. The Opaque-Stop Microscope as a Means of Studying Surface Relief. By W. M. Lomer, M.Sc., B.A., and P. L. Pratt, B.Sc. . . . .	409		715
1362. A Modified Dew-Point Method for Vapour-Pressure Measurements of Lead-Mercury Alloys. By B. R. Burgan, R. C. Hall, and R. F. Hehemann . . . . .	413		
1363. The Effect of Grain-Size on the Structural Changes Produced in Aluminium by Slow Deformation. By W. A. Rachinger, M.Sc. . . . .	415		
1364. Observations on the Structure and Properties of Wrought Copper-Aluminium-Nickel-Iron Alloys. By Maurice Cook, D.Sc., Ph.D., F.I.M., W. P. Fentiman, B.Sc., A.I.M., and Edwin Davis, M.Sc., F.I.M. . . . .	419		716
1365. The Solid Solubilities of Cadmium, Indium, and Tin in Aluminium. By H. K. Hardy, Ph.D., M.Sc., A.R.S.M., A.I.M. . . . .	431		

		PAGE	
		Paper.	Discn.
1366. The Constitution of the Aluminium-Chromium-Zinc Alloys at Low Chromium Contents.	By A. R. Harding, B.Sc., Ph.D., and Professor G. V. Raynor, M.A., D.Sc.	435	
1367. The Aluminium-Rich Alloys of the System Aluminium-Chromium-Iron.	By J. N. Pratt, B.Sc., Ph.D., and Professor G. V. Raynor, M.A., D.Sc.	449	
1368. The Equilibrium Diagram of the System Copper-Gallium in the Region 30-100 At.-% Gallium.	By J. O. Betterton, Jr., D.Phil., B.S., and William Hume-Rothery, O.B.E., F.R.S.	459	700
1369. Presidential Address.	By C. J. Smithells, M.C., D.Sc., F.I.M.	469	
1370. A Study of Some Factors Influencing the Young's Modulus of Solid Solutions.	By A. D. N. Smith, B.A.	477	
1371. The Ageing Characteristics of Ternary Aluminium-Copper Alloys with Cadmium, Indium, or Tin.	By H. K. Hardy, Ph.D., M.Sc., A.R.S.M., A.I.M.	483	
1372. Residual Stresses in Chill-Cast and Continuously Cast Aluminium Alloy Billets.	By R. A. Dodd, M.Sc., Ph.D., A.I.M., A.R.I.C.	493	
1373. Stress-Recovery in Aluminium.	By W. A. Wood, D.Sc., and J. W. Suiter, B.Sc.	501	
1374. Creep Processes in Coarse-Grained Aluminium.	By D. McLean, B.Sc.	507	
1375. Electron-Microscopic Studies of Slip in Aluminium During Creep.	By J. Trotter	521	
1376. Allotropic Transformation in Titanium-Zirconium Alloys.	By Professor Pol Duwez, D.Sc.	525	694
1377. The Place of Plastics in the Order of Matter. Forty-Second May Lecture.	By J. J. P. Staudinger, Dr.-Ing.	529	
1378. Boundary Slip in Bicrystals of Tin.	By K. E. Puttick, B.Sc., and Ronald King, B.Sc.	537	
1379. X-Ray Diffraction Studies in Relation to Creep.	By G. B. Greenough, Ph.D., (Mrs.) Catherine M. Bateman, B.Sc., and (Mrs.) Edna M. Smith, B.A.	545	
1380. The Formation of the Ni <sub>3</sub> Al Phase in Nickel-Aluminium Alloys.	By R. W. Floyd, B.Sc., A.I.M.	551	694
1381. The Effect of Metal/Mould Reaction on 85 : 5 : 5 : 5 Lead Gun-Metal Sand Castings.	By N. B. Rutherford, B.Sc., A.I.M.	555	718
1382. Segregation of Iron and Phosphorus at the Grain Boundaries in 70 : 30 Brass During Grain Growth.	By H. M. Miekkoja, Sc.D.	569	
1383. The Constitution of Nickel-Rich Alloys of the Nickel-Chromium-Titanium System.	By A. Taylor, Ph.D., F.I.M., F.Inst.P., and R. W. Floyd, B.Sc., A.I.M.	577	694
1384. The Constitutional Diagram of the Chromium-Tungsten System.	By H. T. Greenaway, B.Met.E.	589	694
1385. The Effect of Zirconium on the Properties and Structure of Superalumin, with Particular Reference to Forgings.	By M. Tournaire and M. Renouard	593	
1386. Lattice-Spacing Relationships in Aluminium-Rich Solid Solutions of the Aluminium-Magnesium and Aluminium-Magnesium-Copper Systems.	By D. M. Poole, B.Sc., and H. J. Axon, D.Phil.	599	
1387. Factors Affecting Equilibrium in Certain Aluminium Alloys.	By E. C. Ellwood, Ph.D., F.I.M.	605	
1388. The Factors Affecting the Formation of 21/13 Electron Compounds in Alloys of Copper and of Silver.	By W. Hume-Rothery, O.B.E., F.R.S., J. O. Betterton, Jr., D.Phil., B.S., and J. Reynolds, B.A.	609	700
1389. The Lattice Spacings and Densities of Gold-Nickel Alloys at 25° C.	By E. C. Ellwood, Ph.D., F.I.M., and K. Q. Bagley, Ph.D.	617	
1390. The Metallography of Uranium.	By B. W. Mott, M.A., and H. R. Haines	621	720
1391. The Application of Polarized Light to the Examination of Various Anisotropic Metals and Intermetallic Phases.	By B. W. Mott, M.A., and H. R. Haines	629	720
1392. The Equilibrium Diagram of the System Copper-Indium in the Region 25-35 At.-% Indium.	By J. Reynolds, B.A., W. A. Wiseman, and W. Hume-Rothery, O.B.E., F.R.S.	637	700
1393. The Constitution and Structure of Nickel-Vanadium Alloys in the Region 0-60 At.-% Vanadium.	By W. B. Pearson, D.F.C., M.A., and W. Hume-Rothery, O.B.E., F.R.S.	641	694
1394. Twin Accommodation in Zinc.	By P. L. Pratt, B.Sc., Ph.D., and S. F. Pugh, M.A., A.I.M.	653	723
1395. The Cubic-Tetragonal Transformation in Manganese-Copper Alloys.	By Z. S. Basinski, B.A., and J. W. Christian, M.A., D.Phil.	659	694

1396-1408. Papers Nos. 1396 to 1408, inclusive, are published in a separate volume "Properties of Metallic Surfaces" (*Monograph and Report Series*, No. 13).



# LIST OF PLATES

C. J. Smithells, M.C., D.Sc., President 1952-53 . . . . .	frontispiece
I-II. Paper by Mr. A. Cibula . . . . .	between pp. 8 and 9
III-VI. Paper by Mr. R. Chadwick and Mr. W. H. L. Hooper . . . . .	between pp. 20 and 21
VII. Paper by Dr. E. F. Emley, Mr. A. C. Jessup, and Dr. W. F. Higgins . . . . .	facing p. 24
VIII-IX. Paper by Dr. R. W. K. Honeycombe . . . . .	between pp. 40 and 41
X-XIII. Paper by Dr. R. W. K. Honeycombe . . . . .	between pp. 52 and 53
XIV-XIX. Paper by Dr. G. L. J. Bailey and Mr. H. C. Watkins . . . . .	between pp. 68 and 69
XX. Paper by Mr. F. V. Schatz . . . . .	facing p. 84
XXI. Paper by Mr. B. R. Coles and Dr. W. Hume-Rothery . . . . .	facing p. 92
XXII-XXIII. Paper by Mr. J. A. Reynolds and Mr. C. R. Tottle . . . . .	between pp. 96 and 97
XXIV. Paper by Mr. A. F. Brown . . . . .	facing p. 122
XXV. Paper by Mr. N. D. Benson, Dr. J. McKeown, and Mr. D. N. Mends . . . . .	facing p. 140
XXVI. Paper by Dr. G. A. Geach and Mr. D. Summers-Smith . . . . .	facing p. 146
XXVII-XXVIII. Paper by Dr. W. Betteridge and Mr. A. W. Franklin . . . . .	between pp. 150 and 151
XXIX. Paper by Mr. A. E. Jenkins and Mr. H. W. Worner . . . . .	facing p. 158
XXX-XXXI. Paper by Mr. J. A. Ramsey . . . . .	between pp. 168 and 169
XXXII-XXXIII. Paper by Mr. P. J. E. Forsyth . . . . .	between pp. 182 and 183
XXXIV-XXXV. Paper by Dr. C. Edeleanu . . . . .	between pp. 188 and 189
XXXVI-XXXVII. Paper by Dr. J. M. Butler and Dr. T. P. Hoar . . . . .	between pp. 208 and 209
XXXVIII-XXXIX. Paper by Mr. H. W. Worner . . . . .	between pp. 216 and 217
XL-XLV. Paper by Mr. C. J. Evans, Mr. P. F. Hancock, Dr. F. W. Haywood, and Mr. J. McMullen . . . . .	between pp. 262 and 263
XLVI-XLVII. Paper by Mr. J. F. Waight . . . . .	between pp. 278 and 279
XLVIII-XLIX. Paper by Mr. E. Davis and Mr. S. G. Temple . . . . .	between pp. 294 and 295
L. Paper by Mr. H. J. Hartley and Mr. E. J. Bradbury . . . . .	facing p. 302
LI-LII. Paper by Mr. C. P. Paton . . . . .	between pp. 318 and 319
LIII. Paper by Mr. R. T. Staples . . . . .	facing p. 326
LIV-LV. Paper by Dr. A. D. McQuillan . . . . .	between pp. 364 and 365
LVI. Paper by Mr. E. Lardner and Mr. N. B. McGregor . . . . .	facing p. 372
LVII. Paper by Dr. P. Greenfield and Professor G. V. Raynor . . . . .	facing p. 384
LVIII. Paper by Dr. H. Bückle and Mr. J. Blin . . . . .	facing p. 386
LIX. Paper by Mr. A. E. L. Tate and Mr. D. McLean . . . . .	facing p. 390
LX. Paper by Mr. W. M. Lomer and Mr. P. L. Pratt . . . . .	facing p. 410
LXI-LXII. Paper by Mr. W. A. Rachinger . . . . .	between pp. 430 and 431
LXIII-LXVI. Paper by Dr. M. Cook, Mr. W. P. Fentiman, and Mr. E. Davis . . . . .	between pp. 430 and 431
LXVII-LXVIII. Paper by Dr. H. K. Hardy . . . . .	between pp. 430 and 431
LXIX. Paper by Dr. J. N. Pratt and Professor G. V. Raynor . . . . .	between pp. 430 and 431
LXX. Paper by Dr. J. O. Betterton, Jr., and Dr. W. Hume-Rothery . . . . .	between pp. 430 and 431
LXXI-LXXII. Paper by Dr. W. A. Wood and Mr. J. W. Suiter . . . . .	between pp. 508 and 509
LXXIII-LXXX. Paper by Mr. D. McLean . . . . .	between pp. 508 and 509
LXXXI-LXXXIV. Paper by Mr. J. Trotter . . . . .	between pp. 508 and 509
LXXXV-LXXXVI. Lecture by Dr. J. J. P. Staudinger . . . . .	between pp. 544 and 545
LXXXVII-LXXXVIII. Paper by Mr. K. E. Puttick and Mr. R. King . . . . .	between pp. 544 and 545
LXXXIX-XC. Paper by Dr. G. B. Greenough, Mrs. C. M. Bateman, and Mrs. E. M. Smith . . . . .	between pp. 544 and 545
XCI. Paper by Mr. R. W. Floyd . . . . .	between pp. 544 and 545
XCII. Paper by Mr. N. B. Rutherford . . . . .	between pp. 544 and 545
XCIII-XCIV. Paper by Dr. A. Taylor and Mr. R. W. Floyd . . . . .	between pp. 592 and 593
XCV. Discussion on paper by Dr. W. Betteridge and Mr. A. W. Franklin . . . . .	between pp. 592 and 593
XCVI. Paper by Mr. H. T. Greenaway . . . . .	between pp. 592 and 593
XCVII-XCVIII. Paper by M. M. Tournaire and M. M. Renouard . . . . .	between pp. 592 and 593
XCIX-CIII. Papers by Mr. B. W. Mott and Mr. H. R. Haines . . . . .	between pp. 636 and 637
CIV. Paper by Mr. J. Reynolds, Mr. W. A. Wiseman, and Dr. W. Hume-Rothery . . . . .	between pp. 636 and 637
CV-CVI. Paper by Mr. W. B. Pearson and Dr. W. Hume-Rothery . . . . .	between pp. 636 and 637
CVII-CVIII. Paper by Dr. P. L. Pratt and Mr. S. F. Pugh . . . . .	between pp. 636 and 637
CIX. Paper by Mr. Z. S. Basinski and Dr. J. W. Christian . . . . .	between pp. 636 and 637
CX-CXIII. Discussion of various papers . . . . .	between pp. 700 and 701

# THE INSTITUTE OF METALS

## MINUTES OF PROCEEDINGS

### GENERAL MEETING

17 October 1951

A GENERAL MEETING of the Institute of Metals was held at the Park Lane Hotel, Piccadilly, London, W.1, on Wednesday, 17 October 1951, the President, Professor A. J. MURPHY, M.Sc., occupying the Chair.

#### DISCUSSION ON "METAL ECONOMICS"

A General Discussion took place, based on the papers listed below, at two sessions:

#### SESSION I (10 a.m.).—*Primary Resources of Ferrous and Non-ferrous Metals*

"Introduction", by Professor A. J. Murphy, M.Sc.

"The World Supply of Non-Ferrous Metals, Including the Light Metals", by R. Lewis Stubbs.

"Metals as Natural Resources", by Professor S. Zuckerman, C.B., F.R.S.

"World Demand and Resources of Iron Ore", by T. P. Colclough, C.B.E., D.Sc.

#### SESSION II (2.30 p.m.).—*Scrap Reclamation, Secondary Metals, and Substitute Metals*

"The Scope for Conservation of Metals, Ferrous and Non-Ferrous", by C. A. Bristow, B.Sc., A.R.S.M., A. J. Sidery, Assoc.Met., and H. Sutton, D.Sc.

"Economy by Standardization of Alloys and of the Method of Reclamation of Scrap Metals", by C. Dinsdale, M.Sc.

"The Influence of Specifications on Productivity and the Economic Utilization of Ferrous and Non-Ferrous Metals", by F. Hudson,

"Secondary Heavy Metals", by E. H. Jones.

"Secondary Aluminium and Magnesium", by Colonel W. C. Devereux, C.B.E.

(An abridged report of the papers and discussion is published in this volume of the *Journal*, pp. 225–254.)

At the conclusion of the meeting, a hearty vote of thanks to the authors was proposed by the Chairman and carried with acclamation.

### GENERAL MEETING

3 January 1952

A GENERAL MEETING of the Institute of Metals was held in the University, Edgbaston, Birmingham, at 2.30 p.m. on Thursday, 3 January 1952. The Chair was taken by Mr. CHRISTOPHER SMITH, Chairman of the Metallurgical Engineering Committee.

Before the meeting, members had paid a visit to the Aitchison Laboratories, by invitation of Professor A. J. MURPHY, M.Sc.

#### INFORMAL DISCUSSION ON "TOOL AND DIE MATERIALS FOR THE EXTRUSION OF NON-FERROUS METALS AND ALLOYS"

An informal discussion on the subject of "Tool and Die Materials for the Extrusion of Non-Ferrous Metals and Alloys" was opened by Mr. S. S. SMITH and Mr. E. W. COLBECK. About eighty contributions were made to the discussion, a very brief report of which is published in the *Bulletin*, 1951–52, vol. 1, p. 52.

At the conclusion of the meeting, votes of thanks were passed to the University authorities for permission to use the Chemistry Lecture Theatre for the meeting, and to Professor Murphy for his invitation to visit the Aitchison Laboratories.

### ANNUAL GENERAL MEETING

THE FORTY-FOURTH ANNUAL GENERAL MEETING of the Institute of Metals was held in London from Monday to Thursday, 24–27 March 1952.

Monday, 24 March

#### MAY LECTURE

The Forty-Second May Lecture was delivered by Dr. J. J. P. STAUDINGER on "The Place of Plastics in the Order of Matter", in the Lecture Theatre of the Royal Institution, Albemarle Street, W.1, at 6.0 p.m. The President, Professor A. J. MURPHY, M.Sc., occupied the Chair.

At the conclusion, Mr. H. W. G. HIGNETT, B.Sc., Member of Council, proposed a hearty vote of thanks to Dr. Staudinger for his lecture, which is printed on pp. 529–536 of this volume of the *Journal*.

In the evening, the Council entertained Dr. Staudinger to dinner at the Army and Navy Club, Pall Mall, S.W.1.

Tuesday, 25 March

The meeting was resumed at the Park Lane Hotel, Piccadilly, W.1, at 10.30 a.m. The retiring President, Professor A. J. MURPHY, M.Sc., occupied the Chair at the opening of the meeting.

The Chairman welcomed members and visitors attending the meeting from overseas.

The minutes of the previous General Meeting of the Institute, held in Birmingham on 3 January 1952, were taken as read and signed by the Chairman.

#### ELECTIONS OF ORDINARY MEMBERS, JUNIOR MEMBERS, AND STUDENT MEMBERS

The SECRETARY (Lieut.-Colonel S. C. GUILLAN, T.D.) announced that since the Annual Autumn Meeting, held in Italy in September 1951, 279 Ordinary Members, Junior Members, and Student Members had been elected on 18 October, 20 November, 17 December, and 31 December 1951, and 11 February, 20 February, 10 March and 24 March 1952, the lists of whose names are printed in the *Bulletin*, 1951–52, vol. 1, pp. 22, 30, 39, 40, 52, 65, and 73.

#### REPORT OF COUNCIL FOR THE YEAR ENDED 31 DECEMBER 1951

The CHAIRMAN moved, Dr. IVOR JENKINS seconded, and there was carried without dissent, a motion for the adoption of the Report of Council for the Year Ended 31 December 1951, which is printed on pp. 341–348 of this volume of the *Journal*.

#### REPORT OF THE HONORARY TREASURER FOR THE FINANCIAL YEAR ENDED 30 JUNE 1951

The HONORARY TREASURER (Mr. W. A. C. NEWMAN, O.B.E.) presented his Report and moved the adoption of the Institute's accounts for the financial year ended 30 June 1951, which is printed on pp. 349–352 of this volume of the *Journal*.



Major C. J. P. BALL, D.S.O., M.C. (Chairman, Finance and General Purposes Committee) seconded the motion, which was then put to the meeting and carried without dissent.

#### RE-ELECTION OF AUDITORS

It was proposed, seconded, and carried unanimously that Messrs. Poppleton and Appleby be re-elected auditors to the Institute for the ensuing year.

#### ELECTION OF OFFICERS FOR 1952-53

The SECRETARY announced that the following officers had been elected to fill vacancies on the Council for the year 1952-53:

##### President:

C. J. SMITHELLS, M.C., D.Sc.

##### Vice-Presidents:

G. L. BAILEY, C.B.E., M.Sc.  
S. F. DOREY, C.B.E., D.Sc., F.R.S.

##### Honorary Treasurer:

E. H. JONES.

##### Ordinary Members of Council:

ALFRED BAER, B.A.  
N. I. BOND-WILLIAMS, B.Sc.  
N. P. INGLIS, Ph.D., M.Eng.  
IVOR JENKINS, D.Sc.  
A. G. RAMSAY, Ph.D., B.Sc.  
H. SUTTON, C.B.E., D.Sc.  
Major P. LITHERLAND TEED, A.R.S.M.  
W. J. THOMAS.

#### SENIOR VICE-PRESIDENT FOR 1952-53

The SECRETARY announced that the Council had elected Professor F. C. THOMPSON, D.Met., M.Sc., to be Senior Vice-President for 1952-53, and that he would be its next nominee for the Presidency.

#### INSTITUTE OF METALS (PLATINUM) MEDAL

The CHAIRMAN announced that the Institute of Metals (Platinum) Medal for 1952 had been awarded to Mr. WILLIAM SYDNEY ROBINSON, until recently President of the Consolidated Zinc Corporation, Ltd., in recognition of his outstanding services to the non-ferrous metal industries in developing the Australian zinc-lead industry and the British zinc industry.

#### W. H. A. ROBERTSON MEDAL

The CHAIRMAN announced that the W. H. A. Robertson Medal had been awarded to Mr. C. E. DAVIES for his paper on "The Cold-Rolling of Non-Ferrous Metals in Sheet and Strip Form" (*Journal*, 1950-51, vol. 78, pp. 501-536).

#### ROSENHAIN MEDAL

The CHAIRMAN announced that the Rosenhain Medal for 1952 had been awarded to Professor ANDRÉ GUINIER, Professor of Physics at the Sorbonne, Paris, in recognition of his outstanding contributions in the field of physical metallurgy, particularly in connection with precipitation phenomena.

#### VOTE OF THANKS TO RETIRING OFFICERS

Professor F. C. THOMPSON, D.Met., M.Sc. (Senior Vice-President) proposed, Mr. E. A. BOLTON, M.Sc. (Member of Council) seconded, and there was carried with acclamation, a hearty vote of thanks to the following retiring officers for their services on the Council: Colonel Sir Paul Gueterbock, K.C.B., D.S.O., M.C., T.D., D.L., J.P., M.A., A.D.C., Past-President; Major C. J. P. Ball, D.S.O., M.C., Vice-President and Chairman of the Finance and General Purposes Committee; Mr. W. A. C. Newman, O.B.E., B.Sc., A.R.S.M., A.R.C.S., Honorary Treasurer; and Mr. D. F. Campbell, M.A., A.R.S.M. (first Chairman of the Metallurgical Engineering Committee), Mr. T. M. Herbert, M.A., Mr. H. W. G. Hignett, B.Sc. (Chairman of the Local Sections Committee), and Mr. A. R. Powell, Ordinary Members of Council.

Colonel Sir PAUL GUETERBOCK, on behalf of the retiring officers, briefly acknowledged the vote of thanks.

#### INDUCTION OF THE NEW PRESIDENT

The CHAIRMAN (Professor A. J. Murphy, M.Sc.) then introduced the new President, Dr. C. J. SMITHELLS, M.C., and inducted him into the Chair.

#### VOTE OF THANKS TO THE RETIRING PRESIDENT

Mr. CHRISTOPHER SMITH (Member of Council), in proposing a vote of thanks to Professor A. J. Murphy for his services as President for the year 1951-52, said that the members could congratulate their retiring President and themselves on a very full and interesting year's work. Twelve months ago they had listened to a Presidential Address full of wit and charm, and one which had about it a certain statesmanlike quality as well. He thought that the year's work had borne out the promise of that Address. The Institute's affairs had prospered and its field of activities had widened materially.

Mr. G. L. BAILEY, C.B.E., M.Sc. (Vice-President), in seconding the motion, said that he had had the pleasure of knowing Professor Murphy for many years, and of seeing the work that he had done for the Institute in various capacities. The duties of the President were more arduous than many members might realize. When, to his formal duties, the President added an enthusiastic interest in the Institute, they could become a severe task. The members were particularly grateful that Professor Murphy had been willing to sacrifice himself in that way; he had shown that enthusiasm and that real interest in the Institute's work which had made his year of office such a success.

The motion was put to the meeting, and carried with acclamation.

The retiring President briefly responded.

#### PRESIDENTIAL ADDRESS

The President, Dr. C. J. SMITHELLS, M.C., then delivered his Presidential Address, which is printed on pp. 469-475 of this volume of the *Journal*.

A vote of thanks to the President for his Address was proposed by Dr. L. B. PFEIL, F.R.S. (Member of Council), seconded by Mr. J. S. WALTON (Member), and carried with acclamation.

#### LUNCHEON

A Luncheon was held at the Park Lane Hotel, Piccadilly, W.1, at which Dr. C. J. SMITHELLS, M.C., President, presided.

At the conclusion of the Luncheon, the President presented the W. H. A. Robertson Medal to Mr. C. E. Davies and the Rosenhain Medal to Professor André Guinier.

#### DISCUSSION OF PAPERS

The Meeting was resumed at the Park Lane Hotel, when the President, Dr. C. J. SMITHELLS, M.C., occupied the Chair.

The following papers, which had previously been printed in the *Journal*, were discussed. In each case a vote of thanks to the authors was proposed by the Chairman and carried with acclamation.

"The Production and Properties of Oxide-Reduced Copper Powder", by E. C. Ellwood, Ph.D., A.I.M., and W. A. Weddle, B.Sc.

"Unrelated Simultaneous Interdiffusion and Sintering in Copper-Nickel Compacts", by J. W. Butler, M.A., Ph.D., and T. P. Hoar, M.A., Ph.D., F.I.M.

"The Sintering of Copper-Zinc Powder Compacts", by D. D. Howat, B.Sc., Ph.D., F.R.I.C., R. L. Craik, B.Sc., A.R.T.C., and J. P. Cranston, B.Sc., Ph.D., A.R.T.C.

"The Creep and Softening Properties of Copper for Alternator Rotor Windings", by N. D. Benson, M.Eng., J. McKeown, D.Sc., and D. N. Mends, B.Sc.

#### ANNUAL DINNER

In the evening a dinner and dance was held at the Park Lane Hotel.

## Wednesday, 26 March

At the resumed meeting, at 10.30 a.m., at the Park Lane Hotel, Piccadilly, W.1, two concurrent scientific sessions were held: (i) an all-day Symposium on "Equipment for the Thermal Treatment of Non-Ferrous Metals and Alloys", and (ii) a discussion of other scientific papers which had previously been printed in the *Journal*.

## SYMPOSIUM ON "EQUIPMENT FOR THE THERMAL TREATMENT OF NON-FERROUS METALS AND ALLOYS"

At the morning session, the Chair was taken by the President, Dr. C. J. SMITHELLS, M.C.

Mr. W. A. BAKER, B.Sc. (Member), as rapporteur, introduced the following 7 papers (see this volume, pp. 255-339) which had been contributed to the Symposium.

In the afternoon, the Chair was taken by Mr. CHRISTOPHER SMITH, Chairman of the Metallurgical Engineering Committee.

There was an all-day discussion, based on the papers contributed to the Symposium, a report of which is printed on pp. 667-681 of this volume of the *Journal*.

"Electric Furnaces for the Thermal Treatment of Non-Ferrous Metals and Alloys", by C. J. EVANS, A.M.I.E.E., P. F. HANCOCK, B.A., F.I.M., F. W. HAYWOOD, Ph.D., B.Sc., F.R.I.C., F.I.M., and J. McMULLEN, A.I.M.

"Gas Equipment for the Thermal Treatment of Non-Ferrous Metals and Alloys", by J. F. WRIGHT, B.Sc. (Eng.), M.Inst.Gas.E.

"Batch and Continuous Annealing of Copper and Copper Alloys", by EDWIN DAVIS, M.Sc., F.I.M., and S. G. TEMPLE, M.Sc., A.I.M.

"Bright Annealing of Nickel and Its Alloys", by H. J. HARTLEY, M.Sc., F.I.M., and E. J. BRADBURY, M.Eng., A.M.I.Mech.E., A.I.M.

"Batch Thermal Treatment of Light Alloys", by C. P. PATON, B.Eng.

"Flash Annealing of Light Alloys", by R. T. STAPLES.

"Continuous Heat-Treatment of Aluminium Alloys of the Duralumin Type", by MARCEL LAMOURDEDIEU.

At the conclusion of the Symposium, a vote of thanks to the authors was proposed by the Chairman and carried with acclamation.

## DISCUSSION OF OTHER SCIENTIFIC PAPERS

The Chair was taken by Professor F. C. THOMPSON, D.Met., M.Sc., Senior Vice-President.

At the morning session the following papers, which had previously been published in the *Journal*, were discussed:

"The Hardness and Strength of Metals", by D. TABOR, Ph.D.

"Some Observations on the  $\alpha$ - $\beta$  Transformation in Titanium", by A. D. McQUILLAN, Ph.D., B.Sc.

"The Application of Hydrogen Equilibrium-Pressure Measurements to the Investigation of Titanium Alloy Systems", by A. D. McQUILLAN, Ph.D., B.Sc.

"The Constitution of Titanium-Rich Alloys of Iron and Titanium", by H. W. WORNER, M.Sc.

"The Titanium-Hydrogen System for Magnesium-Reduced Titanium", by A. D. McQUILLAN, Ph.D., B.Sc.

"A Provisional Constitutional Diagram of the Chromium-Titanium System", by (Mrs.) M. K. McQUILLAN, M.A.

"An X-Ray Study of the Phases in the Copper-Titanium System", by NILS KARLSSON.

"The Structure and Some Properties of Titanium-Oxygen Alloys Containing 0-5 At.-% Oxygen", by A. E. JENKINS, M.Eng.Sc., and H. W. WORNER, M.Sc.

"Heat-Treatment of Titanium-Rich Titanium-Iron Alloys", by H. W. WORNER, M.Sc.

"The Effect of the Elements of the First Long Period on the  $\alpha \rightleftharpoons \beta$  Transformation in Titanium", by A. D. McQUILLAN, Ph.D., B.Sc.

In the afternoon, a discussion took place on the following papers, which had previously been published in the *Journal*:

"Mechanism of Precipitation in Aluminium-Magnesium Alloys", by E. C. W. PERRYMAN, M.A., A.I.M., and G. B. BROOK, B.Met.

"Experiments on the Reaction of Aluminium-Magnesium Alloys with Steam", by A. J. SWAIN, M.A.

"A Mechanism of Stress-Corrosion in Aluminium-Magnesium Alloys", by C. EDELEANU, M.A., Ph.D.

"The Ageing Characteristics of Binary Aluminium-Copper Alloys", by H. K. HARDY, Ph.D., M.Sc., A.R.S.M., A.I.M.

In each case a vote of thanks to the authors was proposed by the Chairman, and carried with acclamation.

## CONVERSAZIONE

In the evening, a conversazione and exhibition was held at the Institute's headquarters, 4 Grosvenor Gardens, London, S.W.1.

## Thursday, 27 March

## DISCUSSION OF SCIENTIFIC PAPERS

The meeting was resumed at 10.0 a.m. at the Park Lane Hotel, Piccadilly, London, W.1, when the Chair was taken by Professor A. G. QUARRELL, D.Sc., Ph.D., A.R.C.S., D.I.C., F.Inst.P., F.I.M., Chairman of the Metal Physics Committee.

Dr. F. C. FRANK, as rapporteur, presented the following papers, previously printed in the *Journal*, after which there was a discussion on fatigue:

"Some New Observations on the Mechanism of Fatigue in Metals", by W. A. WOOD, D.Sc., and A. K. HEAD, B.A., B.Sc.

"Some Metallographic Observations on the Fatigue of Metals", by P. J. E. FORSYTH, A.I.M.

Mr. F. R. N. NABARRO, M.B.E., M.A., B.Sc., as rapporteur, presented the following papers, previously printed in the *Journal*, after which there was a discussion on plastic deformation:

"Slip and Polygonization in Aluminium", by R. W. CAHN, B.A., Ph.D.

"Inhomogeneities in the Plastic Deformation of Metal Crystals", by R. W. K. HONEYCOMBE, M.Sc., Ph.D.

"Slip Bands and Hardening Processes in Aluminium", by A. F. BROWN, M.A., Ph.D.

## VISITS TO WORKS AND LABORATORIES

Visits were paid to the following works and laboratories: British Iron and Steel Research Association, Physics Department, Battersea.

Ford Motor Co., Ltd., Dagenham.

The General Electric Co., Ltd., Research Laboratories, Wembley.

The Mond Nickel Co., Ltd., Precious Metal Refinery, Acton.

J. Stone and Co. (Charlton), Ltd., Charlton.

The meeting then concluded.

## ANNUAL AUTUMN MEETING

THE FORTY-FOURTH ANNUAL AUTUMN MEETING of the Institute of Metals was held in Oxford from Monday to Friday, 15-19 September 1952.

## Monday, 15 September

A General Meeting was held in the Sheldonian Theatre, Oxford, at 8.30 p.m., the Chair being taken by the President, Dr. C. J. SMITHELLS, M.C.

The Chairman welcomed members, ladies, and delegates attending the meeting from overseas.

The minutes of the previous General Meeting, held in London from 24 to 27 March 1952, were taken as read and signed by the Chairman.



ELECTIONS OF ORDINARY MEMBERS, JUNIOR MEMBERS,  
AND STUDENT MEMBERS

The SECRETARY (Lieut.-Colonel S. C. GUILLAN, T.D.) announced that since the last General Meeting a total of 167 Ordinary Members, Junior Members, and Student Members had been elected on 15 April, 7 May, 2 June, 25 July, 12 August, and 4 September 1952, the lists of whose names are printed in the *Bulletin*, 1951-52, vol. 1, pp. 82, 94, 101, 111, and 117.

## ELECTION OF OFFICERS FOR 1953-54

The SECRETARY announced that the following members would retire from the Council at the 1953 Annual General Meeting, as required by the Articles of Association:

*President:*

C. J. SMITHELLS, M.C., D.Sc.

*Past-President:*

Sir ARTHUR SMOUT, J.P.

*Vice-Presidents:*

Professor H. O'NEILL, D.Sc., M.Met.  
Professor F. C. THOMPSON, D.Met., M.Sc.

*Ordinary Members of Council:*

E. A. BOLTON, M.Sc.  
C. H. DAVY  
Professor A. G. QUARRELL, D.Sc., Ph.D.  
Professor G. V. RAYNOR, M.A., D.Phil., D.Sc.

He stated that, in accordance with Article 19, Dr. C. J. SMITHELLS, M.C., would fill the vacancy as Past-President, and that, in accordance with Article 22, the Council had nominated the following members to fill the other vacancies:

*As President:*

Professor F. C. THOMPSON, D.Met., M.Sc.

*As Vice-Presidents:*

Major C. J. P. BALL, D.S.O., M.C.  
Professor G. V. RAYNOR, M.A., D.Phil., D.Sc.

*As Ordinary Members of Council:*

W. A. BAKER, B.Sc.  
J. C. COLQUHOUN, M.B.E.  
E. R. GADD  
The Hon. JOHN GRIMSTON, M.P.

He reminded the members of their rights, under Article 22, to make other nominations, if desired, before the conclusion of the meeting.

## SENIOR VICE-PRESIDENT FOR 1953-54

The SECRETARY announced that, in accordance with Article 42, the Council had elected Dr. S. F. DOREY, C.B.E., F.R.S., as Senior Vice-President for 1953-54, and that he would be their nominee for the Presidency in the year 1954-55.

## AUTUMN LECTURE

The Chairman introduced Professor H. W. SWIFT, M.A., D.Sc., who delivered the Twenty-Third Autumn Lecture entitled "On the Foot-Hills of the Plastic Range". At the conclusion of the lecture, a hearty vote of thanks to Professor Swift was proposed by Professor F. C. THOMPSON, D.Met., M.Sc. (Senior Vice-President) and carried with acclamation. The lecture is printed in the *Journal*, 1952-53, vol. 81, pp. 109-120.

## Tuesday, 16 September

## OFFICIAL WELCOME TO OXFORD

The meeting was resumed at 9.30 a.m. in the Lecture Theatre of the Clarendon Laboratory, when the Chair was taken by Dr. H. M. FINNISTON, Chairman of the Reception Committee.

The Right Worshipful the Mayor of Oxford (Alderman W. C. WALKER, O.B.E.) and the Vice-Chancellor of Oxford University (Sir MAURICE BOWRA, M.A., D.Litt.) welcomed the members to Oxford on behalf of the City and the University. The President, Dr. C. J. SMITHELLS, M.C., replied.

The meeting was then briefly adjourned and was resumed at 9.50 a.m., when two concurrent scientific sessions were held in the Lecture Theatres of the Clarendon Laboratory and the Electrical Laboratory, respectively.

## DISCUSSION OF PAPERS

Session A was held in the Lecture Theatre of the Clarendon Laboratory, the President, Dr. C. J. SMITHELLS, M.C., occupying the Chair. The following papers were presented and discussed. In each case a vote of thanks to the authors was proposed by the Chairman and carried with acclamation.

"Observations on the Structure and Properties of Wrought Copper-Aluminium-Nickel-Iron Alloys", by Maurice Cook, D.Sc., Ph.D., F.I.M., W. P. Fentiman, B.Sc., A.I.M., and Edwin Davis, M.Sc., F.I.M.

"The Flow of Liquid Metals on Solid Metal Surfaces and its Relation to Soldering, Brazing and Hot-Dip Coating", by G. L. J. Bailey, Ph.D., A.R.C.S., D.I.C., F.Inst.P., and H. C. Watkins, L.I.M.

Session B was held in the Electrical Laboratory, the Senior Vice-President, Professor F. C. THOMPSON, D.Met., M.Sc., occupying the Chair. The following papers were presented and discussed. In each case a vote of thanks to the authors was proposed by the Chairman and carried with acclamation.

"The Application of Polarized Light to the Examination of Various Anisotropic Metals and Intermetallic Phases", by B. W. Mott, M.A., and H. R. Haines.

"The Metallography of Uranium", by B. W. Mott, M.A., and H. R. Haines.

"Some Observations on the Deformation of Polycrystalline Zinc", by J. A. Ramsey, M.Sc.

"The Opaque-Stop Microscope as a Means of Studying Surface Relief", by W. M. Lomer, M.Sc., B.A., and P. L. Pratt, B.Sc., Ph.D.

"Twin Accommodation in Zinc", by P. L. Pratt, B.Sc., Ph.D., and S. F. Pugh, M.A., A.I.M.

## VISITS

In the afternoon, visits were paid by members to the Atomic Energy Research Establishment, Harwell; the Locomotive and Carriage and Waggon Works of British Railways, Swindon; the works of the M.G. Car Co., Ltd., and Riley Motors, Ltd., Abingdon-on-Thames; the works of the Northern Aluminium Co., Ltd., and Aluminium Laboratories, Banbury; and the works of the Pressed Steel Co., Ltd., Cowley. Other members and ladies paid visits to Chastleton House, Moreton-in-the-Marsh; the Colleges in Oxford; and Colonel Sir Ralph Glyn's Farm near Ardington.

## DINNER

In the evening members and their ladies were the guests of the Chairman and Committee of the Oxford Local Section at a Dinner in the Hall of Magdalen College. The Chair was taken by Dr. H. M. FINNISTON (Chairman of the Oxford Local Section), and the principal guests were The Right Worshipful the Mayor of Oxford (Alderman W. C. WALKER, O.B.E.) and the Mayoress of Oxford.

## Wednesday, 17 September

At the resumed meeting, two concurrent scientific sessions were again held:

## DISCUSSION OF PAPERS

Session A was resumed at 9.30 a.m. in the Lecture Theatre of the Clarendon Laboratory, when the President, Dr. C. J.

SMITHELLS, M.C., took the Chair. The following papers were presented and discussed :

"The Grain Refinement of Aluminium Alloy Castings by Additions of Titanium and Boron", by A. Cibula, M.A., A.I.M.

"The Nucleation of Cast Metals at the Mould Face", by J. A. Reynolds, B.Sc., and C. R. Tottle, M.Met., A.I.M.

The President then vacated the Chair, which was taken by Mr. A. B. GRAHAM, Vice-President. The following papers were then presented and discussed :

"The Effect of Mould Material and Alloying Elements on Metal/Mould Reaction in Copper-Base Alloys", by N. B. Rutherford, B.Sc., A.I.M.

"The Effect of Metal/Mould Reaction on 85:5:5:5 Lead Gun-Metal Castings", by N. B. Rutherford, B.Sc., A.I.M.

In each case a vote of thanks to the authors was proposed by the Chairman and carried with acclamation.

Session B was resumed at 9.30 a.m., in the Lecture Theatre of the Electrical Laboratory, when Professor G. V. RAYNOR, M.A., D.Sc., Member of Council, took the Chair. Discussions took place, based on two groups of papers :

(a) *Equilibrium Diagrams and the Theory of Copper Alloys*

"Thermoelastic Analysis of Transformations in Copper Alloys", by R. Cabarat, P. Gence, Professor L. Guillet, and R. Le Roux.

"The Constitution of the Copper-Rich Copper-Zinc-Germanium Alloys", by P. Greenfield, Ph.D., B.Sc., and Professor G. V. Raynor, M.A., D.Sc.

"The Equilibrium Diagram of the System Copper-Gallium in the Region 30-100 At.-% Gallium", by J. O. Betterton, Jr., D.Phil., B.S., and William Hume-Rothery, O.B.E., F.R.S.

"The Factors Affecting the Formation of 21/13 Electron Compounds in Alloys of Copper and of Silver", by W. Hume-Rothery, O.B.E., F.R.S., J. O. Betterton, Jr., D.Phil., B.S., and J. Reynolds, B.A.

"The Equilibrium Diagram of the System Copper-Indium in the Region 25-35 At.-% Indium", by J. Reynolds, B.A., W. A. Wiseman, and W. Hume-Rothery, O.B.E., F.R.S.

(b) *Equilibrium Diagrams and the Theory of Alloys of the Transition Metals*

"The Equilibrium Diagram of the System Nickel-Manganese", by B. R. Coles, B.Sc., and W. Hume-Rothery, M.A., D.Sc., F.R.S.

"The Alloys of Molybdenum and Tantalum", by G. A. Geach, M.Sc., Ph.D., F.I.M., and D. Summers-Smith, B.Sc., A.R.T.C.

"The Sigma Phase in Binary Alloys of the Transition Elements", by A. H. Sully, M.Sc., Ph.D., F.Inst.P., F.I.M.

"Allotropic Transformation in Titanium-Zirconium Alloys", by Professor Pol Duwez, D.Sc.

"The Formation of the Ni<sub>3</sub>Al Phase in Nickel-Aluminium Alloys", by R. W. Floyd, B.Sc., A.I.M.

"The Constitution of Nickel-Rich Alloys of the Nickel-Chromium-Titanium System", by A. Taylor, Ph.D., F.I.M., F.Inst.P., and R. W. Floyd, B.Sc., A.I.M.

"The Constitutional Diagram of the Chromium-Tungsten System", by H. T. Greenaway, B.Met.E.

"The Constitution and Structure of Nickel-Vanadium Alloys in the Region 0-60 At.-% Vanadium", by W. B. Pearson, D.F.C., M.A., and W. Hume-Rothery, O.B.E., F.R.S.

"The Cubic-Tetragonal Transformation in Manganese-Copper Alloys", by Z. S. Basinski, B.A., and J. W. Christian, M.A., D.Phil.

In each case, a vote of thanks to the authors was proposed by the Chairman and carried with acclamation.

## VISITS

In the afternoon, members paid visits to the Associated Electrical Industries, Ltd., Research Laboratory, Aldermaston; the Locomotive and Carriage and Waggon Works of British Railways, Swindon; the Atomic Energy Research Establishment, Harwell; the works of the M.G. Car Co., Ltd., and Riley Motors, Ltd., Abingdon-on-Thames; the works of Morris Motors, Ltd., Cowley; the works of the Northern Aluminium Co., Ltd., and Aluminium Laboratories, Ltd., Banbury; and the Clarendon Laboratory, Oxford. Other members and ladies visited the blanket factory of Charles Early and Co., Ltd., Witney, and the Colleges in Oxford.

## RECEPTION BY THE MAYOR OF OXFORD

In the evening members and their ladies were the guests of the Mayor and Mayoress of Oxford at a Reception, with dancing, at the Town Hall.

## Thursday, 18 September

### INFORMAL DISCUSSION ON "GRAIN BOUNDARIES"

The meeting was resumed at 9.30 a.m., in the Lecture Theatre of the Clarendon Laboratory, when the Chair was taken by Professor A. G. QUARRELL, D.Sc., Ph.D., A.R.C.S., Chairman of the Metal Physics Committee. An informal discussion took place on "Grain Boundaries", which concluded at 12.10 p.m.

### VOTES OF THANKS

At 12.15 p.m., the Chair was taken by the President, Dr. C. J. SMITHELLS, M.C.

Mr. A. B. GRAHAM, Vice-President, moved :

"That the best thanks of the Institute of Metals be, and are hereby, extended to :

(i) The Chairman, Committee, and Members of the Oxford Local Section, and the Patrons of the meeting, for their invitation to hold this meeting in Oxford, and for their generous hospitality.

(ii) Mrs. Hume-Rothery and the Ladies' Committee for the arrangements made for the ladies.

(iii) The Right Worshipful the Mayor of Oxford (Alderman W. C. Walker, O.B.E.) for his welcome to the City and for his hospitality.

(iv) The Vice-Chancellor of Oxford University (Sir Maurice Bowra, M.A., D.Litt.) for his welcome on behalf of the University.

(v) The companies and individuals who so generously subscribed to the hospitality fund in connection with this meeting.

(vi) Colonel Sir Ralph and Lady Glyn, for their hospitality.

(vii) The Directors of Aluminium Laboratories, Ltd., Banbury; Associated Electrical Industries, Ltd., Research Laboratory, Aldermaston; the Atomic Energy Research Establishment, Harwell; Charles Early and Co., Ltd., Witney; the M.G. Car Co., Ltd., and Riley Motors, Ltd., Abingdon-on-Thames; Morris Motors, Ltd., Cowley; Northern Aluminium Co., Ltd., Banbury; and Pressed Steel Co., Ltd., Cowley; and the Mechanical and Electrical Engineer, British Railways, Western Region Workshops, Swindon; and the Printer to the University, for their kind invitations to visit their works and laboratories, and for their hospitality.

(viii) The President and Bursar of Magdalen College for the facilities granted to members and guests in the College.

(ix) The Director, The Clarendon Laboratory, for granting permission for the scientific sessions of the meeting to be held in the Lecture Theatres, and for members to visit the Laboratory.

(x) The Curators of the Sheldonian Theatre for granting permission for the Autumn Lecture to be delivered in the Theatre.



(xi) All others who have contributed in any way to the success of this meeting."

Dr. J. C. CHASTON, Member, seconded the motion, which was put to the meeting by the President and carried with acclamation.

Dr. H. M. FINNISTON, Chairman of the Reception Committee, briefly replied.

The business meeting then terminated.

#### VISITS

In the afternoon visits were paid by members to the Associated Electrical Industries, Ltd., Research Laboratory, Aldermaston; the Atomic Energy Research Establishment, Harwell; the works of Morris Motors, Ltd., Cowley; the works of the Pressed Steel Co., Ltd., Cowley; and the Clarendon Laboratory, Oxford. Other members and ladies visited Blenheim Palace, Woodstock; the Colleges in Oxford; and the University Press.

#### DINNER

In the evening, members and their ladies were the guests of the Chairman and Committee of the Oxford Local Section at a Dinner in the Hall of Magdalen College. The Chair was taken by Dr. H. M. FINNISTON (Chairman of the Oxford Local Section), and the principal guest was the Vice-Chancellor of Oxford University (Sir MAURICE BOWRA, M.A., D.Litt.).

#### Friday, 19 September

##### TOUR OF THE COTSWOLDS

A party of members and ladies took part in an all-day tour of the Cotswolds.

The meeting then concluded.

#### PATRONS OF THE OXFORD MEETING

The Right Worshipful the Mayor of Oxford  
The Vice-Chancellor of Oxford University

Viscount Nuffield, G.B.E., F.R.S.

Lord Cherwell, P.C., F.R.S.

Dr. T. E. Allibone, F.R.S.

Fraser W. Bruce, Esq.

Sir John Cockcroft, C.B.E., F.R.S.

Colonel Sir Ralph Glyn, M.C., D.L., M.P.

Kenneth Hall, Esq.

Professor Sir Cyril Hinshelwood, F.R.S.

Major Albert Pam, O.B.E.

Professor F. E. Simon, C.B.E., F.R.S.

R. Lewis Stubbs, Esq., O.B.E.

The President of the Oxford Chamber of Trade.

#### RECEPTION COMMITTEE

H. M. Finniston, Ph.D., B.Sc., A.R.T.C. (*Chairman.*)  
W. Hume-Rothery, O.B.E., M.A., D.Sc., Ph.D., F.R.S.  
(*Vice-Chairman.*)

R. T. Parker, Ph.D., B.Sc., A.R.S.M. (*Vice-Chairman.*)

B. R. T. Frost, Ph.D., B.Sc. (*Honorary Secretary.*)

J. C. Arrowsmith, M.Met. (*Honorary Treasurer.*)

P. Buckman H. D. Mallon, B.Sc., A.R.T.C.

H. Chadwick, M.Sc. G. Murray, M.Sc.

G. Forrest, B.Sc. J. Reynolds, B.A.

R. H. Goddard D. W. Summers-Smith, B.Sc.

J. Thewlis, D.Sc.

#### LADIES' COMMITTEE

Mrs. W. Hume-Rothery (*Chairman.*)

Mrs. J. C. Arrowsmith

Mrs. G. Forrest

Mrs. J. G. Ball

Mrs. G. Murray

Mrs. H. Chadwick

Mrs. R. T. Parker

Mrs. J. Christian

Mrs. J. Stephenson

Mrs. H. M. Finniston

Mrs. J. D. Summers-Smith

## GENERAL MEETING

19 November, 1952

A GENERAL MEETING of the Institute of Metals was held at the Royal Institution, Albemarle Street, London, W.1, on Wednesday, 19 November 1952, from 9.45 a.m. to 5.0 p.m.

At the opening of the meeting, the Chair was taken by the President (Dr. C. J. SMITHELLS, M.C.) who welcomed members of allied societies, who were attending by special invitation, and particularly many who were present from overseas.

The minutes of the previous General Meeting, held in Oxford from 15-19 September 1952, were taken as read and signed by the Chairman.

The President outlined the Council's objects in arranging the meeting, and then vacated the Chair.

#### SYMPOSIUM ON "PROPERTIES OF METALLIC SURFACES"

##### Morning Session

At the morning session, the Chair was taken by Professor A. G. Quarrell, D.Sc., Ph.D., Chairman of the Metal Physics Committee.

Professor A. H. COTTRELL, B.Sc., Ph.D., as rapporteur, introduced the following papers, after which there was a general discussion:

"Specialized Microscopical Techniques in Metallurgy", by Professor S. Tolansky, D.Sc., F.R.S.

"Radioisotopes in the Study of Metal Surface Reactions in Solutions", by M. T. Simnad, Ph.D.

"The Crystalline Character of Abraded Surfaces", by P. Gay, M.A., Ph.D., and P. B. Hirsch, M.A., Ph.D.

"Diffusion Coatings", by D. M. Dovey, M.A., A.R.I.C., A.I.M., I. Jenkins, D.Sc., F.I.M., and K. C. Randall, B.Sc.

"The Nature and Properties of the Anodic Film on Aluminium and its Alloys", by H. W. L. Phillips, M.A., F.R.I.C., F.Inst.P., F.I.M.

"Chemical Behaviour as Influenced by Surface Condition", by U. R. Evans, Sc.D., M.A., F.R.S.

"The Effect of Method of Preparation on the High-Frequency Surface Resistance of Metals", by R. G. Chambers, M.A., Ph.D., and A. B. Pippard, M.A., Ph.D.

##### Afternoon Session

At the afternoon session, the Chair was taken by Dr. D. G. SORWITH, Director of the Mechanical Engineering Research Organization (D.S.I.R.), Thornton-hall, near Glasgow.

Mr. D. A. OLIVER, M.Sc., F.Inst.P., F.I.M., as rapporteur, introduced the following papers, after which there was a general discussion:

"The Influence of Machining and Grinding Methods on the Mechanical and Physical Condition of Metal Surfaces", by Peter Spear, B.Eng., Ian R. Robinson, B.Sc., and K. J. B. Wolfe, M.Sc.

"The Effect of Lubrication and Nature of Superficial Layer after Prolonged Periods of Running", by F. T. Barwell, Ph.D., D.I.C., B.Sc.(Eng.), Wh.Sch., M.I.Mech.E., A.I.M.M.E.

"The Effect of Surface Conditions on the Mechanical Properties of Metals, Mainly Single Crystals", by Professor E. N. da C. Andrade, F.R.S.

"The Effect of Surface Condition on the Strength of Brittle Materials", by Professor C. Gurney, M.A., D.Sc., F.Inst.P.

"The Influence of Surface Condition on the Fatigue Strength of Steel", by R. J. Love, Wh.Sch., A.M.I.Mech.E.

"The Influence of Surface Films on the Friction and Deformation of Surfaces", by F. P. Bowden, Sc.D., F.R.S., and D. Tabor, Ph.D.

At the conclusion of the meeting, a vote of thanks to the authors of the papers was moved by the Chairman and carried with acclamation.

The papers (Serial Nos. 1396-1408) will be published, together with a report of the discussion, as *Monograph and Report Series* No. 13.

# THE GRAIN REFINEMENT OF ALUMINIUM ALLOY CASTINGS BY ADDITIONS OF TITANIUM AND BORON\*

1319

By A. CIBULA,† M.A., A.I.M., MEMBER

(Communication from the British Non-Ferrous Metals Research Association.)

## SYNOPSIS

Previous work showed that the grain refinement produced by the addition of titanium or boron to aluminium casting alloys is primarily caused by nucleating particles in the melts; the nuclei in titanium-containing alloys were found to be titanium carbide crystals, though only a small proportion of the added titanium was present in this form. The main objects of the present work were to identify the nuclei in other fine-grained aluminium alloys and to find ways of increasing the proportion of the refining elements present as nucleating compounds.

By centrifuging the particles from molten alloys containing boron but no titanium and observing the change in grain-size produced, evidence was obtained that the nuclei in these alloys are aluminium boride crystals. The minimum boron addition for adequate refinement of these alloys therefore depends mainly on the solubility of aluminium boride in molten aluminium.

Attempts to increase the concentration of titanium carbide in alloys containing titanium achieved no useful results, owing to difficulties in forming or dispersing the carbide as fine particles. The addition of boron instead of carbon was more effective in producing refinement, nucleating particles of titanium boride being formed at very low concentrations of titanium and boron; moreover, boron was more easily added than carbon, as aluminium-boron master alloys could be used. The boride formed was isomorphous with pure  $TiB_2$ , but had slightly different lattice dimensions and a range of composition ( $a_0 = 3.010-3.016 \text{ \AA.}$ ,  $c_0 = 3.235-3.240 \text{ \AA.}$ ).

The grain refinement of some commercial casting alloys by simultaneous additions of titanium and boron was studied in detail; grain coarsening due to high casting temperatures, repeated remelting, or gravity segregation during solidification was less than in alloys containing much larger percentages of titanium alone. Alternative methods of adding titanium and boron and the refinement produced by borides of transition metals other than titanium were investigated.

As the boron additions required when titanium was present were small, the mould reaction previously encountered in alloys of high boron content was largely avoided.

## I.—INTRODUCTION

It has been shown in previous work<sup>1</sup> that the small grain-size produced by the addition of a grain-refining element to aluminium casting alloys is mainly caused by fine particles of a specific compound of this element, which are either introduced in the added hardener or formed by reaction with a constituent of the melt. This compound has certain properties which enable the particles to act as nuclei when the casting starts to solidify, and thus to produce a large number of grains.

The resulting refinement of the macrostructure greatly improves the properties of cast solid-solution-type alloys,<sup>2, 4, 5, 6, 7</sup> and one of the objects of the present work was to produce even finer grain-sizes, particularly when high casting temperatures have to be used. The refining element is used most effectively—and economically—when as much of it as possible is present as small particles of the nucleating compound, and the aim of most of the experiments described below was therefore to find ways of achieving this.

In some of these experiments it was first necessary to identify the nuclei. The earlier work<sup>1</sup> on grain refinement by the addition of boron, for example, did not establish the identity of the nuclei, although it was suggested that they were crystals of aluminium boride ( $AlB_2$ ); further experiments, described in Section III, have therefore been made to confirm this suggestion.

The nuclei in alloys refined by the addition of titanium and tantalum were found<sup>1</sup> to be interstitial carbides of these elements, and indirect evidence indicated that the nuclei in alloys containing other transition metals were the similar carbides formed by these elements; attempts have therefore been made to increase the carbon content of some titanium hardener alloys and to make direct additions of titanium carbide to molten aluminium alloys. The results are summarized in Section IV.

The work described in Section III confirmed that crystals of aluminium boride could act as solidification nuclei. This suggested that the isomorphous borides formed by several of the transition metals might also

\* Manuscript received 3 February 1951. The work described in this paper was made available to members of the B.N.F.M.R.A. in a confidential research report issued in

December 1950.

† Research Investigator, British Non-Ferrous Metals Research Association, London.



be suitable, particularly as these borides are similar to the interstitial carbides; it had already been reported to the Association\* that simultaneous additions of titanium and boron, which might be expected to form titanium boride in the melt, refined the grain-size of aluminium alloys more effectively than the addition of either element alone. The grain-refining effects of additions of titanium and boron together were therefore studied in some detail, including the identification of nuclei and the examination of the effects of remelting, increase in casting temperature, and gravity segregation during solidification. The grain-refining effects of additions of boron together with several other transition elements were examined briefly. The results are given in Section V.

## II.—EXPERIMENTAL TECHNIQUE

### 1. MATERIALS

The compositions of the two grades of aluminium, the commercial casting alloys, and the hardener alloys, and the methods of preparation of the hardener alloys, are described in Table I.

Super-purity aluminium was used as the basis metal in all the experiments in which it was important to avoid the presence of impurities, including the preparation of the hardener alloys which were required. Most of the experiments on the refinement of alloys of commercial composition and purity were carried out with aluminium-4.8 or 4.9% copper alloy (B.S. 1490, LM 11), made from commercial-purity aluminium and the hardener alloys described in Table I. A few other experiments were made with the commercial casting alloys noted in the table.

The fluxes used in the experiments described in Section IV, 3, were made from chemicals of Analar grade.

### 2. MELTING AND CASTING

The high-purity materials were melted in Salamander crucibles which were coated with pure alumina cement and, except in the preparation of hardeners, were heated in an electric furnace to minimize gas pick-up. These melts were stirred with pure alumina ( $\Delta R$ ) rods and were cast without being degassed. Bars of  $\frac{3}{4}$  in. dia. for grain-size measurement were cast in green Mansfield sand, and 1-in.-dia. bars, from which specimens to be centrifuged were machined, were made in cast-iron moulds.

The melts of commercial-grade alloys, usually 3 kg. in weight, were heated in uncoated crucibles in a gas-fired furnace. They were degassed with chlorine as soon as the temperature reached 660°–720° C., the flow of gas being gradually increased to raise the temperature of the melt up to, but not above, the selected casting temperature, making use of the heat generated by the strongly exothermic reaction be-

tween the chlorine and the melt. A constant time of degassing was used in each series of alloys poured at a constant temperature for comparison of grain-sizes. The reduced-pressure gas-test was used to check that the melts were substantially gas-free. With the exceptions noted below, the commercial-purity alloys were cast into inclined D.T.D. bar moulds in green synthetic sand and were poured in 8–12 sec. per bar.

Melt temperatures were measured to  $\pm 5^\circ$  C. with a Chromel/Alumel thermocouple.

### 3. EXAMINATION OF CASTINGS

Sections for grain-size determination were taken from the junction of the D.T.D. bars and the feeder-heads (before heat-treatment) and from the middle of the  $\frac{3}{4}$ -in.-dia. bars. The average grain diameters were measured with a rule, at a convenient magnification.

As previous work<sup>4</sup> had shown that boron promotes mould reaction in the aluminium-4.9% copper alloy, the distribution of porosity in the polished sections of the test-bars was noted and the overall percentage of voids in each bar calculated from its density, measured before heat-treatment. The density of the void-free alloy containing 4.90% copper was taken as 2.800 g./c.c. in the as-cast condition.

Some of the D.T.D. bars in the aluminium-copper alloy were solution-treated at 525°–535° C. for 16 hr. and aged at 140° C. for 16 hr. in a forced-air-circulation furnace, and the ultimate tensile strength and elongation were determined on 0.564-in.-dia. test-pieces machined from the bars.

### 4. CENTRIFUGING EXPERIMENTS

The use of the centrifuge developed by Baker for the identification of constituent particles in molten metals has been described previously.<sup>1,3,8</sup>

Cylindrical 12-g. specimens were melted in a closed graphite crucible which lay on its side in a horizontal tube-furnace mounted on the arm of the centrifuge. The melt was then rotated about a vertical axis with a centrifugal acceleration of 140 g. and was finally allowed to solidify with the centrifuge either rotating or stationary, as desired. The temperature of the metal could be measured to  $\pm 10^\circ$  C. or better by means of a thermocouple passing into the lid of the crucible with the weld close to the surface of the specimen.

## III.—THE IDENTIFICATION OF NUCLEI IN ALLOYS REFINED BY THE ADDITION OF BORON

### 1. PREVIOUS WORK

In earlier work<sup>1</sup> on the addition of boron to pure aluminium, it was observed that 0.01% boron was just sufficient to diminish undercooling before solidification and slightly to reduce the diameter of the

\* This information was originally given in 1948 by Dr. Strauss of Messrs. Foundry Services, Ltd., and has since

been confirmed by other members of the British Non-Ferrous Metals Research Association.

TABLE I.—Composition and Preparation of Alloys Used.

Alloy	Mark	Alloy Content, %	Impurities, %	Method of Preparation	Section of Report Describing Experiments in Which the Alloy is Used
Aluminium Metal					
S.p. Al	...	<0.01 total	0.001 Ti	...	III; IV, 3; V, 2.
C.p. Al	...	<0.3 „	0.11 Si; 0.16 Fe; 0.002 Ti	...	IV, 2 and 4; V, 3 and 4.
Hardener Alloys					
Al-Cu	NOU 501	50 Cu	...	Cathode Cu (99.99%) dissolved in molten s.p. Al.	III; IV; V.
Al-Ti	NKY 25	1.56 Ti	0.21 Si; 0.01 Fe; traces Mg, Mn, Cu, Zn.	Potassium titanofluoride stirred into molten s.p. Al in graphite crucible at 1100° C.	III; V, 3.
	NKY 21	1.81 Ti	...	As NKY 25, but prepared at 1300°-1400° C.	IV, 2.
	NKY 22	1.20 Ti	...	As NKY 25, but prepared at 1600° C. (approx.).	
	OJF 1	2.66 Ti	...	Commercial hardener, as received.	
	OJF 2	2.22 Ti	...	Commercial hardener (OJF 1) remelted to 1100° C. under cover of KF + graphite.	
Al-B	NLC 7	0.32 B	0.08 Si; 0.01 Fe; <0.002 Ti.	Potassium borofluoride stirred into molten s.p. Al at 1100° C.	III.
	NLC 10	0.50 B	0.16 Si; <0.01 Fe; <0.01 Ti; traces Mg, Cu, Zn.	in graphite crucible.	V, 2 and 4.
	NKY 27	1.3 Ti; 0.7-1.5 B	...	C.p. Al and commercial Al-2.7% Ti hardener melted to 1100° C. and commercial Al-25% B alloy added through cryolite flux. Cast at c. 1400° C.	V, 2.
Al-Ti-B	NKY 28	0.26 Ti; 0.16 B	...	As NKY 27 but commercial Al-10% Ti hardener added after boron at c. 1500° C., and alloy poured immediately at c. 1100° C.	
Al-V	OGQ 1	4.9 V	0.7 Fe; 0.23 Si; 0.06 Cu; 0.01 Ti; traces Mg, Mn, Ni, Zn.	Commercial Al-50% V alloy dissolved in molten Al under cryolite at 1100° C.	V, 4.
Al-Zr	NSK 10	1.75 Zr	...	Commercial Al-24% Zr alloy dissolved in molten Al at 1100° C.	
Al-Nb	NLA 6	0.21 Nb	...	Commercial Al-17% Nb + Ta alloy dissolved in molten Al at 1150° C.	
Al-Cr	NSH 3	6.95 Cr	...	Electrolytic Cr dissolved in molten Al at 1000° C.	
Commercial Casting Alloys					
B.S. 1490, LM 11	...	4.8 Cu; 0.13 Ti	...	...	V, 3.
B.S. 1490, LM 10	...	10.6 Mg	0.001 Ti	...	
B.S. 1490, LM 4	...	3.8 Cu; 4.0 Si; 0.6 Fe; 0.6 Mn; 0.08 Ti	...	...	

C.p. Al: commercial-purity aluminium; S.p. Al: super-purity aluminium.

columnar grains of the cast alloys, indicating that a very small number of nuclei were present at this boron content; larger additions produced more marked refinement and prevented any detectable undercooling. These effects approximately coincided with the appearance of aluminium boride ( $\text{AlB}_2$ ) crystals which were observed in alloys containing 0.02% or more boron, in agreement with recent data on the aluminium–boron system.<sup>9</sup>

The aluminium atoms in the boride lie on a simple hexagonal lattice,<sup>10</sup> in the close-packed planes of which the interatomic distance (3.00 Å.) is similar to the corresponding distance in solid aluminium

(2.86 Å.). This similarity and the above observations suggested that aluminium boride crystals were responsible for the observed grain refinement, nucleation of the aluminium-rich solid solution being accomplished by the deposition of the close-packed planes of aluminium atoms on to corresponding planes in the boride lattice.

It was also observed<sup>1,4</sup> that little or no grain coarsening occurred in alloys containing boron when the melts were superheated to temperatures up to 960° C. before casting, whereas alloys containing titanium showed considerable grain coarsening after superheating. This observation also agreed with the



suggestion that aluminium boride crystals function as nuclei. In the alloys containing titanium, the nuclei are particles of titanium carbide, both elements of which are minor constituents of the alloy; when the melt is superheated, the nuclei dissolve, but they do not easily re-precipitate on cooling, presumably because both the carbon and the titanium are greatly diluted and the nucleation of titanium carbide crystals is therefore difficult. The aluminium boride crystals must also dissolve when the melt is heated to the aluminium-boron liquidus temperature, but, as aluminium is the major constituent of the alloy, the formation of aluminium boride crystals should be less liable to suppression on cooling,\* and they should therefore re-precipitate when the casting cools and thereafter nucleate the aluminium-rich dendrites; the loss of refinement after superheating should therefore be less than in alloys containing titanium. (Nevertheless, some supersaturation occurs even with aluminium boride, as described in the Appendix.)

The absence of grain coarsening in alloys containing boron would be a useful property in commercial casting alloys, but, unfortunately, the addition of 0.03–0.05% boron required for grain refinement was also found to increase gas pick-up on melting and to produce mould reaction in sand castings of aluminium-copper<sup>4</sup> and aluminium-magnesium-beryllium alloys.<sup>11</sup> The following experiments were therefore made to confirm the identity of the nuclei in alloys containing boron, so that it could be decided whether the amount of boron required for refinement might be reduced and the undesirable effects of boron additions thus minimized.

## 2. PRIMARY PARTICLES IN AN ALUMINIUM-BORON ALLOY

In order to identify particles other than aluminium boride crystals, which might form the nuclei in alloys containing boron, attempts were made to concentrate the primary particles in a molten aluminium-boron alloy by centrifuging, and to identify the segregate by X-ray examination; a similar technique had been used successfully with alloys containing titanium.<sup>1</sup>

A specimen of high-purity aluminium–0.04% boron alloy was centrifuged at 680° C. for 15 min.; a section through the surface containing the segregated particles is shown in Fig. 1 (Plate I). All the lines in the diffraction pattern obtained by examination of the segregate with glancing-angle X-rays were identified as those of aluminium or aluminium boride ( $\text{AlB}_2$ ). Numerous crystals of this compound, often hexagonal in shape, could be seen in the section through the segregate, but the only other constituent which could be distinguished was occasional plates very similar to

those identified as aluminium carbide in other specimens. The latter compound has been observed in several boron-free alloys prepared from hardeners made under an active flux in graphite crucibles, and is unlikely to have any significant connection with the grain-refining effects of boron.

The above observations are consistent with the view that the solidification nuclei in the specimen were the crystals of aluminium boride; however, the possibility cannot be excluded that the nuclei were crystals of another compound which were very similar to the boride in appearance and too few to be detected by X-ray examination. The relation between grain-size and the presence of aluminium boride particles was studied further in the experiments described next.

The grain-refining effects of boron in aluminium are most marked when another element such as copper is present which produces concentration gradients during solidification and, by hindering crystal growth, allows the maximum number of nuclei to become effective in forming new crystallites. The experiments described in the remainder of this section were therefore carried out with alloys containing large percentages of copper to obtain the maximum range of grain-sizes; in the above experiments with binary aluminium-boron alloys, the detection of constituents was facilitated by the absence of  $\text{CuAl}_2$ , but the increase in grain-size caused by centrifuging was small.

## 3. THE REMOVAL OF ALUMINIUM BORIDE CRYSTALS FROM ALUMINIUM-COPPER-BORON ALLOYS BY CENTRIFUGING

### (a) *The Influence of Temperature*

The removal of the nuclei from a molten alloy by centrifuging should result in a coarse grain-size after solidification. If the nuclei are aluminium boride crystals, it should be possible to produce grain coarsening only by centrifuging at a temperature well below the aluminium boride liquidus temperature, for otherwise most or all of the boride would be in solution and could not be segregated at the bottom of the crucible. On the other hand, if the nuclei are not aluminium boride but are some other compound, grain coarsening would result from centrifuging even above the aluminium boride liquidus temperature if the other compound were not in solution at that temperature. Experiments were therefore made to determine whether the removal of aluminium boride crystals by centrifuging an aluminium–5% copper–0.04% boron alloy at a low temperature resulted in grain coarsening and whether grain coarsening was

\* The chance of a molecule of  $\text{AlB}_2$  forming in the melt is proportional to the square of the concentration of boron atoms (the concentration of aluminium atoms being practically unity); similarly, the chance of a molecule of  $\text{TiC}$  forming is proportional to the product of the concentrations of titanium and carbon atoms. The latter product is much smaller than

the former at the usual concentrations of these elements and the compound  $\text{TiC}$  is therefore probably more likely to supersaturate. This simple comparison of the tendency of the two compounds to supersaturate is only very approximate as the formation of the smallest stable crystal nuclei is dependent on several other factors (which cannot be calculated at present).

produced even at higher temperatures at which no segregation of aluminium boride occurred.

Two specimens of this alloy were centrifuged for 15 min., at 655° C. (only 10° C. above the aluminium-5% copper liquidus temperature) or 760° C., and were allowed to solidify with the machine stationary; two other specimens were merely heated in the stationary centrifuge for 15 min., one at each temperature, to obtain the grain-sizes of the non-centrifuged alloy for comparison.

As anticipated, a segregate of aluminium boride crystals (shown in Fig. 9, Plate II) was obtained only in the specimen centrifuged at the lower temperature; in the other centrifuged specimen the crystals were observed over the entire cross-section where they had re-precipitated only after centrifuging had stopped. Corresponding effects were observed in the macrostructures of the specimens: an increase in grain-size occurred after centrifuging at 655° C. (as may be seen by comparison of Figs. 5 and 6, Plate I), whereas the two specimens treated at 760° C. had identical grain-sizes (slightly larger than that shown in Fig. 6, Plate I).

The largest grain-sizes that could be obtained in specimens cooled from each of these two temperatures, if it were possible completely to remove the boron-containing nuclei in each case, should be the same as the grain-sizes of boron-free aluminium-5% copper specimens melted under the same conditions. The macrostructures of two specimens of the boron-free alloy, heated at 655° and 760° C., respectively, are shown in Figs. 7 and 8 (Plates I and II). Comparison of Figs. 7 and 5 (Plate I) shows that the grain coarsening which occurred in the specimen centrifuged at 655° C. was almost the maximum that could be produced, in contrast with the great difference in grain-size between the boron-free specimen heated at 760° C. (Fig. 8, Plate II), and the boron-containing alloy centrifuged at the same temperature.

These results confirm that grain coarsening occurs after centrifuging an aluminium-copper-boron alloy only if most of the aluminium boride crystals are thus removed from the molten alloy.

#### (b) *The Influence of Alloy Composition*

The densities of the aluminium boride crystals and the primary dendrites of solid solution in the aluminium-5% copper-0.04% boron alloy (3.2 and 2.56 g./c.c., respectively), are greater than that of the liquid metal (approximately 2.48 g./c.c.) during the first stages of solidification. When a specimen of this alloy is melted and is then allowed to solidify under centrifugal force, the boride crystals segregate to the base of the crucible (i.e. away from the axis of rotation) as the temperature falls and dendrites of solid solution then start to grow into the liquid metal from the same surface. Only the first dendrites are formed close to  $AlB_2$  crystals, and, whether these act as nuclei or not, the resulting macrostructure should be coarse grained. This is confirmed by the specimen shown in Fig. 10 (Plate II).

If the copper content is increased to 20%, however, the density of the primary solid-solution dendrites (2.62 g./c.c.) becomes lower than that of the copper-rich liquid (2.8-3.2 g./c.c.) throughout solidification, whereas the aluminium boride crystals are still denser than the liquid metal. If this alloy had solidified under centrifugal force, the first dendrites of solid solution formed at the face containing the segregated aluminium boride crystals would move towards the opposite face of the specimen (i.e. towards the axis of rotation), and this should be repeated with successive dendrites, all of which could thus be formed in the presence of aluminium boride crystals; consequently, if the latter function as nuclei the resulting grain-size should be much finer than in a boron-free alloy of the same copper content, in spite of the initial segregation of the boride and in contrast with the 5% copper alloy.

To confirm this conclusion, a specimen of aluminium-20% copper-0.04% boron alloy was centrifuged for 12 min. at 620° C. and solidified under centrifugal force; a boron-free alloy was similarly treated.

The macro-section of the boron-free specimen consisted mainly of large columnar dendrites, as shown in Fig. 11 (Plate II) (from the centre of the specimen) and Fig. 12 (Plate II) (from the base). The latter shows a dense band of dendrite-free eutectic at the base of the specimen.

The boron-containing alloy, however, consisted almost entirely of small equiaxial dendrites, as shown in Fig. 13 (Plate II) (from the centre of the specimen); the only large dendrites grew from the sides of the specimen near the base (they are visible at the right of Fig. 14, Plate II). A thin, discontinuous layer of segregated aluminium boride crystals was observed at the base of the specimen, but other crystals were scattered over the remainder of the specimen in the primary dendrites. Small dendrites, which had become trapped in the band of solid eutectic, were observed growing from the patches of boride crystals, Fig. 14 (Plate II), but none were observed at the corresponding face of the boron-free alloy, suggesting that the formation of primary dendrites was facilitated by the boride crystals and proceeded to a later stage of solidification.

#### 4. FURTHER DISCUSSION

The results obtained above are all in agreement with the suggestion that aluminium boride crystals are the nuclei in alloys containing boron. The only other explanation is that the nuclei are another compound of boron with a constituent of high-purity aluminium, which dissolve in molten aluminium over approximately the same range of temperature as aluminium boride and re-precipitate on cooling, but no evidence of the existence of such a compound has been obtained by visual or X-ray examination. For this reason and others which were discussed above, the second explanation is unlikely, and it seems



reasonable to conclude that the nucleating particles in aluminium-boron alloys are aluminium boride crystals.

The maximum proportion of the added boron that can be present as aluminium boride is determined by the aluminium-boron equilibrium diagram; it is, therefore, not possible to prevent undesirable mould reaction effects by reducing the amount of boron unless a third element can be found which, when present in small amounts, forms a similar boride at lower boron contents. This possibility is discussed further in Section V.

#### IV.—THE EFFICACY OF GRAIN REFINEMENT BY ADDITIONS OF TITANIUM

##### 1. PREVIOUS WORK

The results of previous experiments showed that the nuclei in fine-grained alloys containing titanium are particles of titanium carbide.<sup>1</sup> The amount of titanium present as titanium carbide was estimated to be only 0.001–0.01%, i.e. only 1–10% of the added titanium, in an alloy containing 0.1% titanium; it has also been estimated that of the remaining 0.09% titanium only about 0.003% is required in solution in the molten aluminium and in equilibrium with undissolved carbide, if excess carbon is present. This suggests that, if it were possible to prepare titanium hardener alloys containing greater proportions of carbon, smaller additions of titanium, down to 0.01% or less, might be sufficient to produce maximum grain refinement, provided that the alloy contained amounts of other alloying elements sufficient to produce the necessary concentration gradients round growing crystals of the aluminium-rich solid solution.

Micro-examination of the alloys described above showed that some of the titanium carbide crystals were as large as  $5\mu$  and had dendritic structures; this indicated that a larger carbon content in a titanium hardener alloy might increase the average size of the carbide particles rather than increase their number, and the amount of titanium required for refinement might therefore not be much reduced. Nevertheless, attempts were made to prepare titanium alloys of high carbon contents, and experiments on the direct addition of titanium carbide to aluminium alloy melts were also carried out.

In other work,<sup>4</sup> it was found that castings prepared from commercial alloy ingot already containing titanium had much larger grain-sizes than castings made from melts of the same composition which had been prepared from a laboratory titanium hardener. A possible reason for the smaller number of nuclei in the commercial alloy was that the titanium hardener used in its preparation had a lower carbon content than the laboratory hardener, which had deliberately been made under conditions which facilitated carbon pick-up. An alternative explanation was that the coarse grain-sizes of the commercial alloy were the result of remelting, flux treatments, flushing with an inert gas, or holding the molten alloy for long periods

at a low temperature during manufacture, all of which have been shown<sup>1, 4, 13</sup> to produce a reduction in the number of nuclei. To determine which was the correct explanation, the effectiveness of a commercial aluminium-titanium hardener alloy was compared with that of the laboratory hardener previously used, with the result described below.

#### 2. THE ADDITION OF CARBON TO TITANIUM HARDENER ALLOYS

##### (a) Commercial Titanium Hardener

A commercial titanium hardener containing 2.66% titanium was treated with graphite under a cryolite flux at approximately 1100°C. The effectiveness of

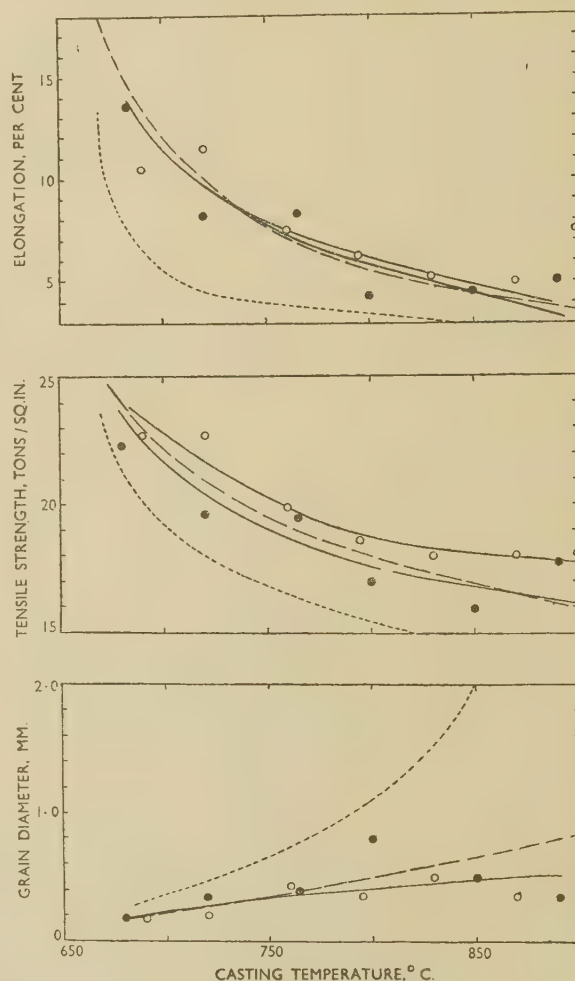


Fig. 15.—Comparison of Grain-Sizes and Tensile Properties of Test-Bars in Al-4.8% Cu-0.12% Ti Alloy, prepared from (●—●) as-received and (○—○) carbon-treated commercial titanium hardeners, (— — —) a laboratory titanium hardener, and (· · · · ·) commercial B.S. 1490, LM 11 alloy ingot.

the treated and as-received alloys was compared with that of the laboratory hardener previously used<sup>4</sup> by measuring the grain-sizes of test-bars in an aluminium-4.8% copper-0.12% titanium alloy prepared from each hardener and cast at a series of

temperatures between 680° and 900° C. The increase in grain-size with pouring temperature, caused by solution of the nuclei, should be least in castings containing the greatest proportion of titanium in the form of carbide, i.e. in the alloys made from the most effective titanium hardener alloy.

The results of grain-size, ultimate tensile strength, and elongation measurements are shown in Fig. 15; the results previously obtained with the laboratory titanium hardener and those obtained with commercial ingot already containing titanium have been included for comparison.

The results obtained from the carbon-treated and the as-received commercial hardener and the laboratory-made hardener were much the same, but the castings made with each of the three hardeners had considerably finer grain-sizes, with correspondingly higher tensile properties, than castings made from the commercial B.S. 1490, LM 11 alloy ingot. The scatter in the results obtained with the as-received commercial hardener was large; this was probably caused by segregation in the hardener which resulted in a variation in titanium content in the castings.

The commercial hardener was therefore as effective as the laboratory-made hardener and, assuming the former to be typical of commercial hardeners, the coarse grain-sizes of commercial aluminium-4.5% copper ingot already containing titanium are not caused by the use of an ineffective hardener in its preparation; the loss of refinement is probably, therefore, the result of the manufacturing process of the ingot.

The latter conclusion is supported by the even larger grain-sizes of castings made from some batches of secondary alloys; for example, test-bars made from a batch of B.S. 1490, LM 4 alloy containing 0.08% titanium had a grain-size of 2.5 mm. when poured at 700° C., compared with approximately 0.25 mm. which can be obtained by adding the same amount of titanium in a hardener alloy.

(b) *Aluminium-Titanium Hardener Alloys Prepared at High Temperatures*

The solution of the nuclei caused by superheating aluminium-titanium alloys indicates that the solubility of carbon in these alloys increases with tempera-

ture. Titanium hardener alloys were therefore prepared at higher temperatures than are normally used, in an attempt to saturate the alloys with carbon at these temperatures and obtain higher carbide contents.

The hardeners were made from potassium titanofluoride at approximately 1350° and 1600° C., respectively, graphite being added to the flux. To prevent the formation of larger titanium carbide crystals, the alloy prepared at the highest temperature was granulated in water instead of being cast into ingot moulds. The flux cover was very fluid at 1100° C., vigorously attacking the crucible and pieces of graphite, but at 1600° C. it formed a solid crust which apparently merely coated the graphite, and the advantage of the high temperature of preparation was thus partly lost.

These hardeners were compared with one made at 1100° C. by casting series of test-bars as described above. The results obtained with the hardener made at 1350° C. showed no improvement; considerably inferior results were obtained with the hardener prepared at 1600° C.

It is possible that the use of more stable fluxes which remain fluid at high temperatures might facilitate the introduction of carbon and yield more successful results, but the prospect was not sufficiently promising to warrant further work along these lines.

### 3. DIRECT ADDITIONS OF TITANIUM CARBIDE

Titanium carbide powder of particle size 1  $\mu$  (the finest available commercially) was mixed with 120-mesh aluminium powder and pressed into pellets containing 10% by weight of carbide. The pellets were then stirred into 600-g. melts of high-purity aluminium-5% copper alloy, from which bars for grain-size measurements were cast. A high casting temperature of 850° C. was used to produce a wide range of grain-sizes for ease of comparison.

No addition could be made without a flux, as the carbide merely oxidized and mixed with dross. Thin flux covers, of the compositions noted in Table II, were used in subsequent experiments, the results of which are included in the table.

The analysis shows that only 10% or less of the added titanium actually entered the melt and, although these small amounts were sufficient to

TABLE II.—*Additions of Titanium Carbide to Aluminium-5% Copper Alloy Cast at 850° C.*

Mark	Method of Addition	Flux	Titanium Addition		Grain Dia., mm.
			Nominal, %	By Analysis, %	
[Previous work (1-in.-dia. bars)]	Al-Ti hardeners	None	0.12	0.12	0.5-0.7
	Commercial ingot	None	...	0.12	1.9
NOU 150A	Titanium carbide pellets	None	None	...	3.5
B, D		{ 46% KF, 54% AlF <sub>3</sub> } (m.p. 570° C.)	None	...	1.5; 2.5
C, E			0.12	<0.01; 0.015	1.0; 0.9
F			0.20	0.010	0.75
G			0.30	0.025	0.5
H			None	...	1.5
J		{ 52% NaF, 48% KF } (m.p. 700° C.)	0.12	0.01	1.2
K			0.30	0.025	0.7



produce a marked reduction in grain-size, equal to that obtained by adding 0.12% titanium as a hardener alloy, the efficiency in the use of the added titanium was less than when a hardener is used.

In other experiments, attempts were made to reduce the amount of flux required and thus the proportion of carbide trapped in the flux. The carbide powder was stirred into small pellets of molten flux which, when solid, were plunged into molten aluminium-copper alloy. The results showed no significant improvement.

#### 4. FURTHER DISCUSSION

Although the results obtained above with titanium carbide additions confirmed that it is possible to produce grain refinement with much smaller titanium additions than are normally used, no method of practical value was found. The results showed that the obstacles in increasing the carbon content of aluminium-titanium alloys are largely caused by the difficulty of achieving intimate contact and wetting between carbon or titanium carbide and molten aluminium, either due to interference by oxide films or to inherently unsuitable angles of wetting. It has been suggested that one way of avoiding the difficulty would be by pre-wetting titanium carbide powder by sintering with nickel or cobalt powder, but the high melting point of these metals would be inconvenient with aluminium alloys and bridging between carbide particles might prevent their complete dispersion.

The introduction of carbon into molten aluminium-titanium alloys is also limited by the low solubility of carbon in the melt, for any excess of carbide would tend to remain where it was formed, in contact with the source of carbon, instead of dispersing in the melt, unless the carbide could be precipitated in the liquid metal.

In the work described in the next section on the use of titanium boride instead of titanium carbide, the difficulties described above were overcome by using separate aluminium-titanium and aluminium-boron hardener alloys; by this means it was possible to precipitate the boride particles in the melt and control the excess of either constituent. This could not be done with titanium carbide additions because carbon cannot be added already alloyed with aluminium.

### V.—GRAIN REFINEMENT BY SIMULTANEOUS ADDITIONS OF TITANIUM AND BORON

#### 1. THE TRANSITION-METAL BORIDES

Several transition metals form diborides which are isomorphous with aluminium boride ( $\text{AlB}_2$ ) and have very similar lattice dimensions<sup>14, 15, 16</sup> as shown in

Table III. These compounds have strongly metallic properties and a typical interstitial structure,\* and are similar to the interstitial compounds formed by carbon, nitrogen, and hydrogen with certain of the transition metals.

TABLE III.—*Lattice Parameters of Some Diborides with  $\text{AlB}_2$ -Type Hexagonal Structures.*<sup>14, 15, 16</sup>

Compound	$a_0$ , Å.	$c_0$ , Å.	$c/a$
$\text{AlB}_2$ . . .	3.00	3.25	1.08(3)
$\text{TiB}_2$ . . .	3.028	3.228	1.064
$\text{ZrB}_2$ . . .	3.170	3.533	1.114
$\text{NbB}_2$ . . .	3.086	3.306	1.071
$\text{TaB}_2$ . . .	3.088	3.318	1.074
$\text{VB}_2$ . . .	2.998	3.057	1.020
$\text{CrB}_2$ . . .	2.969	3.066	1.03

The similarity of the diborides to aluminium boride and to the interstitial carbides, all of which probably form nuclei in aluminium alloy melts, suggests that the diborides might function in the same way. This would be of practical value, however, only if the concentrations of boron required to precipitate the transition metal diborides in molten aluminium were less than the concentration necessary to form aluminium boride, for otherwise the latter would form in preference to the former. Unfortunately, no data have been published on the aluminium-transition metal-boron ternary systems or on the free energies or heats of formation of the borides, which would enable a comparison of the respective concentrations to be made. However, the information that the addition of boron and titanium together produced greater refinement than either element alone, suggested that crystals of titanium diboride did, in fact, form in the melt and act as nuclei during solidification.

If this were so, the addition of boron to alloys containing titanium would increase the proportion of titanium present in an effective form (either carbide or boride) and make it possible to reduce the amount of the metal required for refinement. The effects would thus be similar to those aimed at in the experiments on the addition of carbon described in the previous section, but the addition of boron is easier to carry out, by using, for example, an aluminium-boron hardener alloy. The objectionable effects of boron additions—the increase in the gas pick-up during melting and the promotion of mould reaction after casting—would also be reduced by the presence of titanium if smaller boron additions were required; this point is examined in more detail below.

It has been assumed that if the formation of a transition metal boride can occur in molten alu-

\* The borides differ, however, from the true interstitial compounds, in which the non-metallic atoms are isolated from each other in the interstices of a lattice of metal atoms, in that the boron atoms themselves form a network with fairly strong bonds.<sup>16</sup> For this reason the metal atoms in several of the diborides are more widely spaced than in the pure metals, and several transition metals can thus form interstitial

diborides even though the interstices in the metal lattices are not quite large enough to accommodate the isolated boron atom; the formation of an interstitial carbide, on the other hand, is closely limited by the relative sizes of the carbon atom and the transition metal atom, in accordance with Hägg's rule.

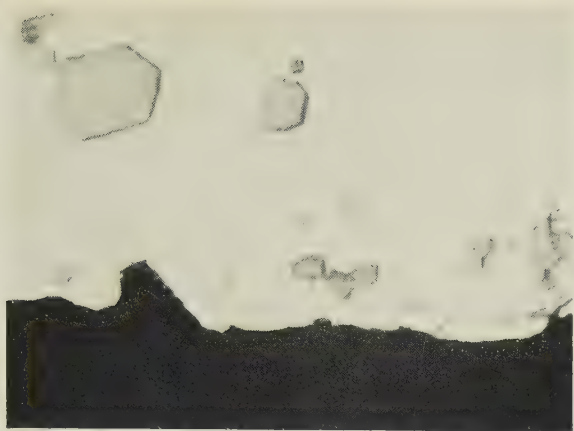


FIG. 1.—Segregated  $\text{AlB}_2$  Crystals in Centrifuged Al-0.04% B Alloy.  $\times 1000$ .

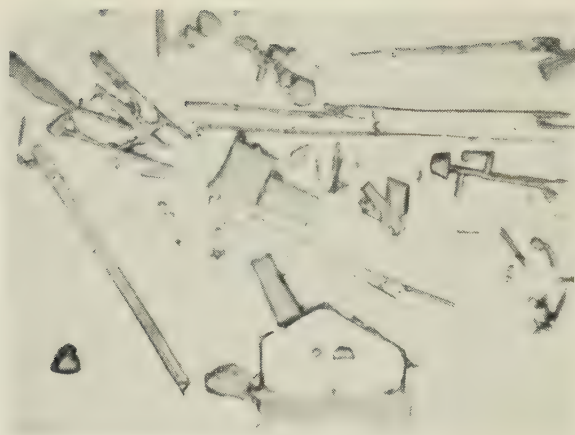


FIG. 2.—Segregated Primary Crystals in Centrifuged Al-0.04% B-0.12% Ti Alloy.  $\times 2000$ .



FIG. 3.—Precipitated Constituent in Interior of Centrifuged Al-0.04% B Alloy, after Ageing for 12 months at Room Temperature.  $\times 150$ .

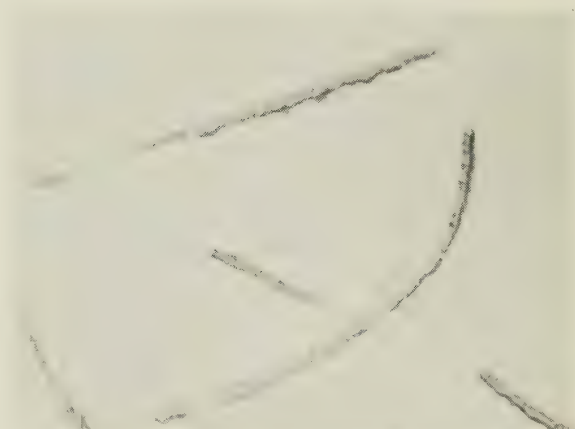


FIG. 4.—Same as Fig. 3.  $\times 1000$ .

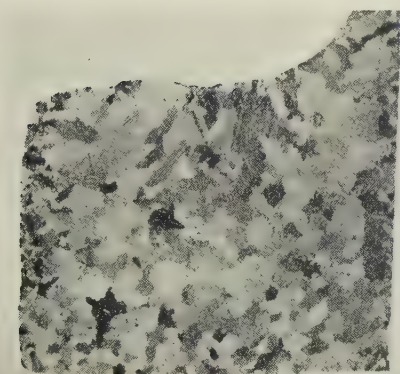


FIG. 5.—Al-5% Cu-0.04% B Alloy, Centrifuged for 15 min. at  $655^\circ\text{C}$ .  $\times 3$ .

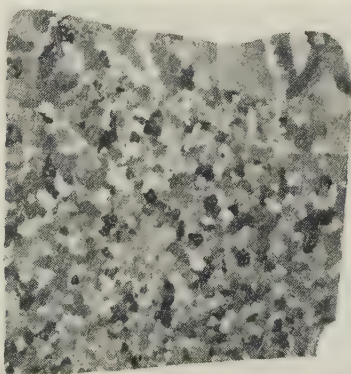


FIG. 6.—Al-5% Cu-0.04% B Alloy, Heated for 15 min. at  $655^\circ\text{C}$  in Stationary Centrifuge.  $\times 3$ .

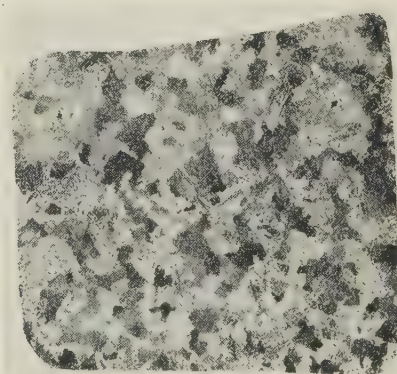


FIG. 7.—Al-5% Cu Alloy (boron-free), Heated for 15 min. at  $655^\circ\text{C}$  in Stationary Centrifuge.  $\times 3$ .

[To face p. 8.]



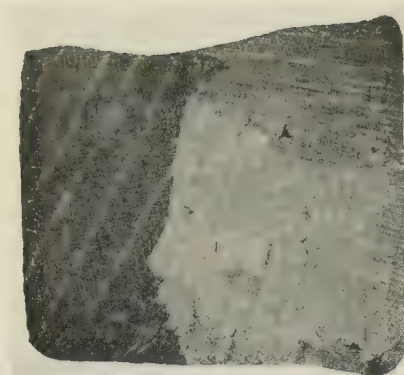


FIG. 8.—Al-5% Cu Alloy (boron-free), Heated for 15 min. at 760° C. in Stationary Centrifuge.  $\times 3$ .

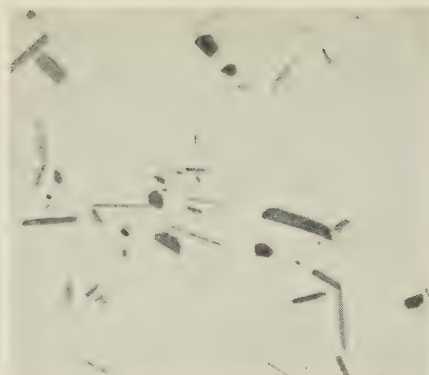


FIG. 9.—Segregate of  $\text{AlB}_2$  Crystals at Right-Hand Edge of Specimen shown in Fig. 5.  $\times 1000$ .

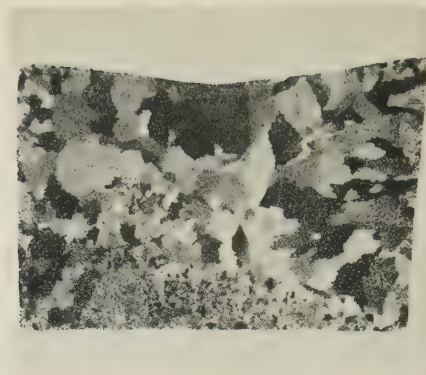


FIG. 10.—Al-5% Cu-0.04% B Alloy, Heated for 12 min. at 660° C. and Solidified under Centrifugal Force.  $\times 3$ .

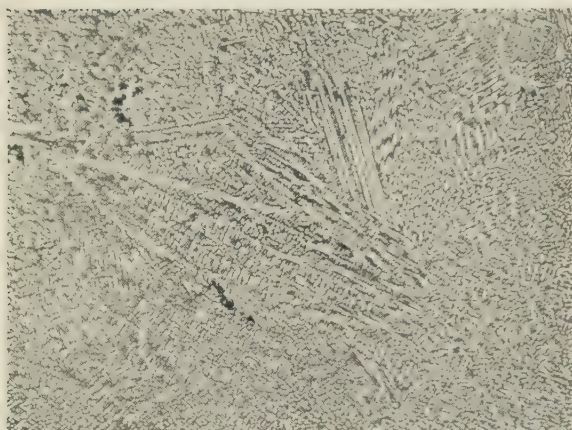


FIG. 11.—Large Dendrites in Interior of Al-20% Cu Alloy (boron-free), Solidified under Centrifugal Force. Etched in 0.5% HF.  $\times 15$ .



FIG. 12.—Large Dendrites near Base of Specimen Shown in Fig. 11. Etched in 0.5% HF.  $\times 15$ .

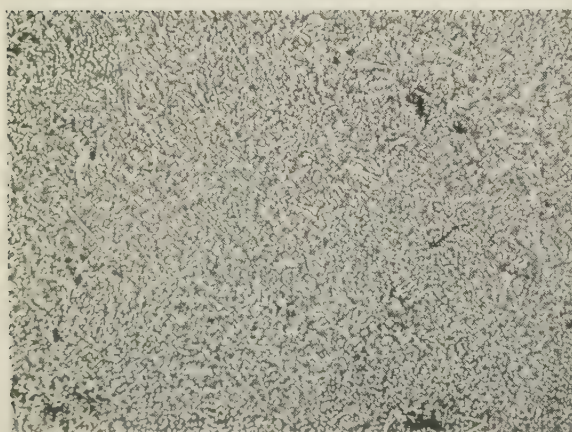


FIG. 13.—Small Dendrites in Interior of Al-20% Cu-0.04% B Alloy, Solidified under Centrifugal Force. Etched in 0.5% HF.  $\times 15$ .

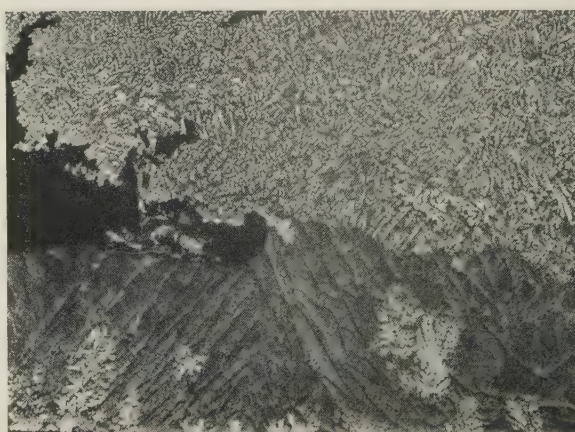


FIG. 14.—Small Dendrites Forming at Base of Specimen Shown in Fig. 13, from Segregated  $\text{AlB}_2$  Crystals. Etched in 0.5% HF.  $\times 15$ .



minium, the diborides described in Table III will be precipitated. Some of the transition metals, however, form other borides more complex than those described in the table, and the possibility that one of these complex borides may be formed, perhaps only over certain concentration ranges, must be remembered.

## 2. NUCLEI IN ALUMINIUM-TITANIUM-BORON ALLOYS

### (a) Addition of Boron to Coarse-Grained Aluminium-0.14% Titanium Alloy

In order to study the grain-refining effects of additions of boron to an aluminium-titanium alloy, nuclei of titanium carbide which were already present were first removed by bubbling nitrogen through the molten alloy under a cover of magnesium chloride/potassium chloride flux, as described previously.<sup>1</sup> A 4-kg. batch of coarse-grained aluminium-0.14% titanium alloy was thus prepared.

Melts of 300 g. of this alloy were then heated to 760°–770° C., at which temperature additions of the aluminium-0.5% boron hardener were made, and the grain-size bar was immediately cast at 760° C. Super-purity aluminium was substituted for the aluminium-titanium alloy in one melt to confirm the absence of refinement by 0.01% boron (the largest addition used) when only 0.001% titanium was present; 0.2% copper was also added to this melt to provide small concentration gradients during solidification similar to those caused by the presence of titanium in the other alloys.

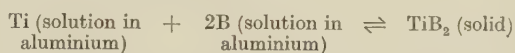
It was also desirable to confirm that the additions of the boron hardener did not re-introduce significant quantities of carbon into the titanium alloy. Unfortunately the carbon content of the hardener was not known, but an indication of the importance of this factor was obtained by making an addition of commercial-purity aluminium equal in weight to the largest addition of boron hardener alloy.

TABLE IV.—Effect of Boron Additions on Grain-Size of Aluminium-Titanium Alloys Cast at 760° C.

Mark, NKZ	Titanium Content of Melt, %	Additions, %	Grain Dia., mm.
136	0.14	None	Columnar grains
137		0.0001 B	0.8
135		0.001 B	0.23
131		0.01 B	0.23
132		2 c.p. Al	1.5 + columnar grains
133	approx. 0.001	0.01 B, 0.2 Cu	1 + columnar grains

The grain-sizes of the test-bars given in Table IV show clearly the marked effect of very small additions of boron, and confirm that the concentration of boron required to precipitate titanium boride particles is less than is required to form aluminium boride (0.0001% compared with approximately 0.01%).

The precise concentration of boron required probably varies with the titanium content, according to a reaction such as the following :



in which the presence of excess titanium reduces the concentration of boron in solution in equilibrium with titanium boride.

The boron addition required for maximum refinement (approximately 0.0001–0.001%) is of the same order as the estimated carbon content of a fine-grained aluminium-0.1% titanium alloy.<sup>1</sup>

### (b) Primary Particles in an Aluminium-0.12% Titanium-0.04% Boron Alloy

An aluminium-0.12% titanium-0.04% boron alloy was centrifuged at 680° C. for 15 min. to concentrate the primary particles. The surface at which the particles had segregated was then examined with glancing-angle X-rays and sectioned for micro-examination; scrapings from the surface were examined in an X-ray powder-camera for the determination of lattice parameters.

The diffraction pattern obtained was of an  $\text{AlB}_2$ -type structure, but the lattice parameters deduced from the pattern were not those of  $\text{TiB}_2$  or  $\text{AlB}_2$  but were of intermediate dimensions. Furthermore, the lines in the diffraction pattern were diffuse, whereas those produced by aluminium boride crystals in the aluminium-0.04% boron alloy described above were very sharp. As the size of the crystals was not small enough to account for this difference, it apparently indicated a range of composition with a corresponding range in lattice dimensions. The lattice parameters obtained in these experiments are given in Table V,

TABLE V.—Lattice Dimensions of the Hexagonal  $\text{AlB}_2$ -Type Structures Identified in Aluminium-Titanium-Boron and Aluminium-Boron Alloys.

Lattice Dimensions, Å.	$\text{AlB}_2$	$\text{TiB}_2$	Crystals in Al-0.04% B Alloy	Crystals in Al-0.04% B-0.12% Ti Alloy
$a_0$	3.00	3.028	3.000	3.010–3.016 approx.
$c_0$	3.25	3.228	3.243	3.235–3.240 „
$c/a$	1.08(3)	1.066	1.081	1.074

together with the parameters of the two pure borides. The results suggest that the boride which is formed in the aluminium-titanium-boron alloy is titanium boride with either excess titanium or considerable proportions of aluminium boride in solution; the latter explanation would not be altogether unexpected, in view of the close similarity of lattice structures and dimensions of the two borides and the fact that the crystals are formed in the presence of a great excess of aluminium.

The range of composition of the boride crystals indicates that they did not attain equilibrium



with the melt. This may have been caused by coring produced during the growth of the crystals, or by a coating of titanium boride formed on the original crystals of aluminium boride introduced in the hardener alloy; the hollow, shell-like structures seen in the micro-section through the segregated particles (Fig. 2, Plate I) may be evidence of such a coating.

### 3. GRAIN REFINEMENT OF SOME COMMERCIAL CASTING ALLOYS

#### (a) Grain-Sizes

To obtain information on the practical value of the above results, a number of test-bars were cast in commercial alloys refined with titanium and boron which were added as the hardener alloys in Table I.

Three series of castings were made in aluminium-4.9% copper alloy containing 0, 0.01, and 0.05% boron respectively; the titanium content in each series varied from approximately 0.002% (the inherent content of the commercial-purity aluminium) to 0.2%. Two melts of each composition were prepared, one being cast at 680° and the other at 800° C.

The grain-sizes of the test-bars are shown in Fig. 16. The bars cast at 800° C. show the differences in grain-size most clearly and indicate the effectiveness of the boron additions in reducing grain coarsening caused by the use of this high casting temperature. Although an addition of 0.01% boron was inadequate to produce refinement when the titanium content was only 0.002%, in the presence of 0.01% or more titanium this small boron addition was just as effective as much larger amounts. The addition of 0.02% titanium and 0.01% boron together had a refining effect somewhat greater than that of 0.05% boron or of 0.20% titanium added singly.

The bars cast at 680° C. had a much smaller range of grain-sizes, though the slight differences observed were in the same order as in the bars cast at 800° C. Measurements<sup>17</sup> of the temperatures of the metal entering the test-bar moulds during casting showed that, even at the beginning of pouring, the temperature of the metal was at the liquidus temperature of the alloy; the particles of solid metal formed in the pouring stream as it cooled would subsequently act as nuclei and thus account for the small maximum grain-size in the castings poured at a low temperature. The loss of heat and the amount of solid formed during pouring would vary with the melting and casting conditions, and would be greatest with small melts such as were used in the present work.

Two combinations of titanium and boron contents were selected from the above results—0.03% titanium + 0.01% boron, and 0.01% titanium + 0.003% boron—and the increase in grain-size with casting temperature of aluminium-4.9% copper alloys refined with these additions was investigated more fully by casting test-bars at various temperatures between 680° and 900° C.

The results (shown in Fig. 17) confirm that the increase in grain-size with casting temperature is considerably less than in alloys refined with the much larger titanium additions normally made<sup>4</sup> (shown by the dotted line in Fig. 17). For castings made from melts which need not be heated above 720° C. the smaller titanium and boron additions should be adequate.

The grain-sizes of bars cast from three melts in aluminium-10% magnesium-0.02% beryllium alloy

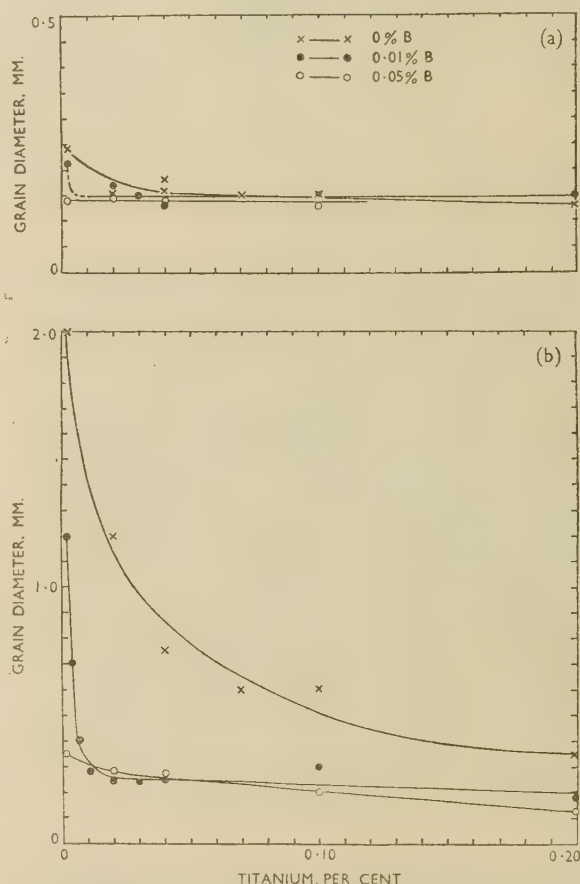


FIG. 16.—Variation of Grain-Size with Ti Content of Test-Bars in Al-4.9% Cu Alloy Containing 0, 0.01, or 0.05% B, poured at (a) 680° C. or (b) 800° C.

refined by the addition of 0.03% titanium + 0.01% boron are given in Table VI; the grain-sizes are similar to those obtained with aluminium-copper alloys.

The addition of 0.01% boron to a secondary alloy (B.S. 1490, LM 4) already containing 0.08% titanium also produced a marked reduction in grain-size in test-bars poured at 700° C., from 2.5 mm. in the boron-free alloy to 0.25 mm. Many commercial casting alloys, although containing 0.1% or more titanium, are nevertheless coarse grained, because of the absence of nucleating particles, and the addition of small quantities of boron alone to these alloys should produce satisfactory grain refinement.

The above results show that the addition of 0.01% titanium and 0.003% boron should adequately refine

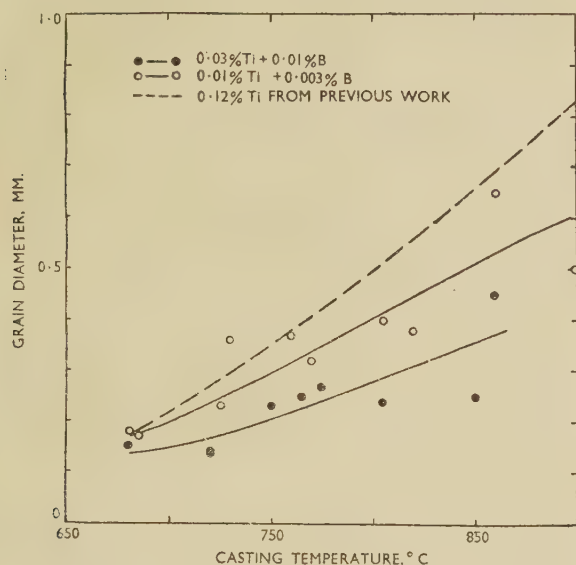


FIG. 17.—Variation of Grain-Size with Casting Temperature of Al-4.9% Cu Test-Bars Containing Ti and B.

the grain-size of aluminium alloy castings poured at temperatures below 720°C., but larger additions—up to 0.03% titanium and 0.01% boron—are required when higher casting temperatures are used. In attempts to prepare a hardener alloy containing both titanium and boron (described below, p. 13), severe gravity-segregation of titanium boride crystals occurred in the melt, suggesting that excessive additions

TABLE VI.—Grain-Sizes of Test-Bars in Aluminium-10% Magnesium-0.02% Beryllium Alloy Refined with 0.03% Titanium and 0.01% Boron.

Casting Temp., ° C.	Grain Dia., mm.
700	0.30
750	0.33
800	0.37

of titanium and boron would cause similar segregation in melts of commercial aluminium casting alloys. A member of the Association has encountered segregation of titanium boride in melts held at 700°C., and containing only 0.005% of each element. It is clear, therefore, that additions of titanium and boron must be made with caution, especially where the melt is liable to stand undisturbed for long periods.

#### (b) Gas Pick-Up and Mould Reaction

The increase in gas pick-up during melting and the promotion of mould reaction after casting, which were caused by large boron additions in previous work,<sup>4</sup> were confirmed in these experiments. The melts containing 0.05% boron required the longest periods of de-

gassing with chlorine before the reduced-pressure test indicated freedom from dissolved gas, and the percentages of voids in the test-bars poured from these melts were high when the titanium content was below 0.1%. These effects were most marked in the alloys cast at the highest temperatures, as shown in Fig. 18.

Fig. 19 illustrates the sub-surface pinhole formation typical of mould reaction caused by 0.05% boron, in an aluminium-copper alloy of low titanium content cast at 680°C. The pinholes in an alloy cast at 800°C. were less regular, and much more porosity occurred in the interior of the test-bars, as would be expected. The high boron content produced other noticeable surface effects—an increase in dross formation, and a green tinge on the top surface of the feeder heads in alloys cast at the lower temperature—which are no doubt connected with the effects described above.

There were no significant differences in the percentages of voids in test-bars containing 0.01% or less boron cast at 680°C., but when the pouring temperature was above 750°C. even 0.01% boron produced a significant, though small, increase in porosity in alloys of low titanium content, as shown in Fig. 18.

When the titanium content was 0.1% or greater, no mould-reaction effects were seen even with the highest boron additions, the percentages of voids in the test-bars being the same as in the boron-free bars. This was probably the result of the reduction in the concentration of boron in solution in equilibrium with excess titanium, as suggested in Section V, 2 (a), for it is unlikely that boron present as titanium boride crystals, instead of in solution, would promote reaction of the melt with moisture.

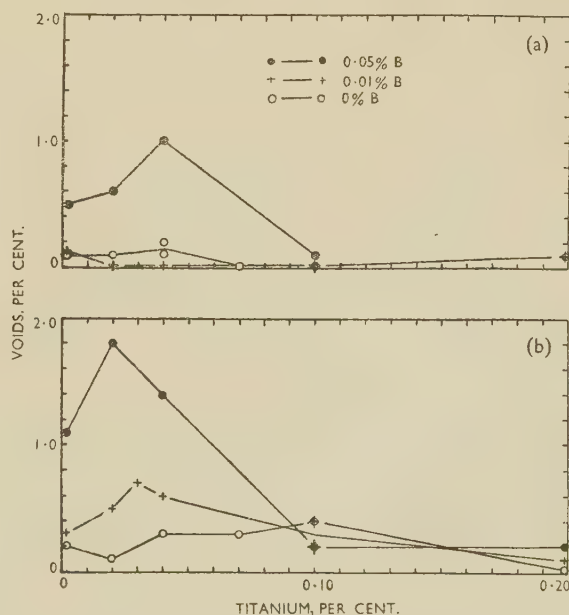


FIG. 18.—Variation of Percentage of Voids with Ti Content of Test Bars in Al-4.9% Cu Alloy Containing 0, 0.01, or 0.05% B, poured at (a) 680°C. or (b) 800°C.





FIG. 19.—Sub-Surface Pinholes Caused by Mould Reaction in Test-Bar of Al-4.9% Cu-0.05% B Alloy Cast at 680° C.  $\times 2.5$ .

### (c) Persistence of Refinement on Remelting

An increase in grain-size in aluminium casting alloys may result not only from the melt being superheated but also from repeated melting,<sup>13</sup> the effect being greater the higher the melt temperatures. The reason for the grain coarsening is probably the increasing solubility of the nucleus compound in the melt as the temperature rises above the melting point; the smallest nuclei would tend to dissolve completely and, when the melt is cooled again, they would probably re-precipitate on to existing, undissolved nuclei, thus progressively reducing the total number of nuclei.

As this effect is of practical importance, and experiments were made to compare the increases in grain-size of alloys refined with either 0.2% titanium alone or with 0.03% titanium + 0.01% boron. These additions were selected because the grain-sizes of castings from the initial melts were similar. A test-bar was cast at 780°–790° C. from each of the original 12-kg. melts, after degassing, and the remainder of the metal was ingotted and remelted; this procedure was repeated four times with each alloy, the melts thus being composed completely of “scrap”.

The results (the full lines in Fig. 20) show that the increases in grain-size of the two alloys were, within the limits of experimental error, the same. The results obtained by Sicha and Boehm<sup>13</sup> (the broken lines in Fig. 20), using somewhat different experimental conditions, suggest that remelting has more adverse effects in alloys containing only about 0.1% titanium.

It is concluded, therefore, that grain coarsening after remelting is no greater in alloys refined with titanium and boron additions than in alloys of the same initial grain-size refined with titanium alone. The grain coarsening after an addition of 0.03% titanium + 0.01% boron is less than in alloys containing the normal titanium additions of 0.10–0.15%.

### (d) Gravity Segregation During Solidification

It has been observed, in previous work by the Association and in industrial practice, that the upper parts of many aluminium alloy castings contain regions of large grain-size. The effect is more marked the greater the section-thickness and the higher the casting temperature, and although the coarse grains often occur only very close to the top surface, in large castings they sometimes form a wide zone of columnar grains. This type of grain coarsening is particularly objectionable because it occurs in castings which are otherwise adequately refined, though it can sometimes be confined to the feeders.

The explanation of this structure which has been put forward<sup>1,18</sup> is that the primary solid-solution crystals, being denser than the melt in most aluminium casting alloys, sink as they are formed and thus remove most of the effective nuclei from the upper parts of the castings. This grain coarsening cannot be entirely prevented, as it is primarily caused by the differences in the density of the constituents of the pasty alloy. However, it can be minimized by increasing the number of nuclei available so that new grains can form as the original crystals are removed by sedimentation; furthermore, the grains are finer and therefore sink through the melt more slowly.

Grain coarsening caused by sedimentation in alloys containing titanium should be reduced by additions of boron, for this should increase the number of

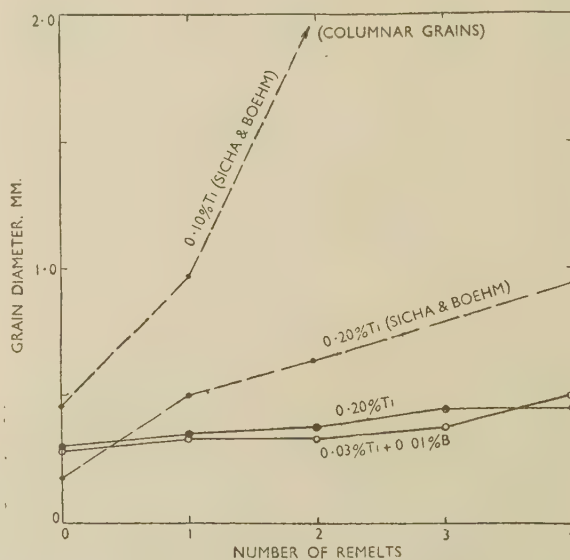


FIG. 20.—Increase of Grain-Size after Remelting in Al-4.9% Cu Alloy Test-Bars Refined with 0.20% Ti or 0.03% Ti + 0.01% B, Cast at 780°–790° C.

nuclei. To illustrate this effect of boron additions, horizontal cylinders of 5 in. dia. and 7 in. long were cast in aluminium-4.8% copper alloy containing (1) 0.13% titanium already present in the ingots of B.S. 1490, LM 11 alloy; (2) 0.13% titanium added as a hardener alloy; or (3) 0.03% titanium + 0.01%

boron added as hardener alloys. Each melt was poured at 725° C. after degassing.

Measurements of the grain-sizes in vertical sections through the castings, given in Table VII, show that

TABLE VII.—*Grain Coarsening Due to Gravity Segregation in 5-in.-dia. Castings of Aluminium-4.8% Copper Alloys.*

Pouring Temperature 725° C.

Grain-Refining Additions	Depth of Columnar Zone, mm.	Width of Columnar Grains, mm.	Dia. of Equi-axial Grains, mm.
0.13% Ti already present in comm. B.S. 1490, LM 11 ingot	18	3	0.7
0.13% Ti added as hardener alloy	17	3	0.4
0.03% Ti + 0.01% B added as hardeners	9	1	0.25

the zone of columnar grains was smallest and the equiaxial grains were finest in the alloy containing both titanium and boron. These results confirm that the additions of titanium and boron together, in the above amounts (3), reduce but do not eliminate grain coarsening caused by gravity segregation during solidification.

#### 4. ALTERNATIVE METHODS OF ADDING TITANIUM AND BORON

##### (a) *Aluminium-Titanium-Boron Hardeners*

As it would be of some advantage if the additions of titanium and boron could be made in a single hardener alloy, two attempts were made to prepare an alloy containing 1.5% titanium and 0.5% boron.

In the first experiment, an aluminium-1.5% titanium alloy was heated to 1600° C. and the required amount of aluminium-25% boron alloy was stirred into the melt through a flux of cryolite. The final alloy contained only 0.1% boron which was heavily segregated in the last-poured ingots, the titanium content being the same in all ingots.

Test-bars containing 0.03% titanium, made from this hardener and cast at temperatures up to 870° C., had grain-sizes only slightly coarser than are obtained by adding 0.12% titanium as a normal titanium hardener alloy. The addition of boron had therefore increased the effectiveness of the 1.5% titanium alloy as a grain-refiner, but the grain-sizes produced with this hardener were not as fine as can be obtained using separate additions of a boron hardener alloy.

The second titanium-boron hardener alloy was made by rapidly stirring an aluminium-10% titanium alloy into an aluminium-0.5% boron melt at 1600° C. and casting immediately. The first-poured ingot had titanium and boron contents of only 0.26 and 0.16%,

respectively, the boride crystals having segregated into the final ingot.

These results confirm that the solubility of titanium boride in molten aluminium is very low, and it is doubtful whether it would be practicable to prepare a single hardener alloy containing large percentages of both titanium and boron without marked segregation.

##### (b) *Reduction of Salts of Titanium and Boron*

Titanium and boron may also be introduced into aluminium alloy melts by the reduction of salts such as potassium titanofluoride ( $K_2TiF_6$ ) and potassium borofluoride ( $KBF_4$ ), and by using mixtures of these salts the additions may be made simultaneously. A proprietary mixture of two similar salts is available.

Several experiments were carried out in which quantities of the proprietary material were plunged into 3-kg. melts of aluminium-4.9% copper alloy at 750° C. After the dross had been removed, the temperature of the metal was raised to 800° C. by bubbling chlorine through the melt and grain-size bars were cast; the resulting grain-sizes were compared with those obtained using hardener alloys. One melt of aluminium-10% magnesium alloy was similarly treated. The results are given in the first three parts of Table VIII.

The grain-sizes obtained, though fine, were not as small as those obtainable by using hardener alloys, even when excess of the salt was added. The reason for this difference may have been that the boride crystals produced by the addition of mixed salts were larger than those formed from hardener alloys, for analyses showed that the transfer of titanium and boron was generally efficient by both methods. Only with the 10% magnesium alloy was the reduction of salts inefficient, which is in agreement with earlier work.<sup>3</sup> The best result was obtained with the commercial 4.8% copper alloy already containing 0.13% titanium.

Other results (in the last part of the table) obtained with a simple mixture of potassium titanofluoride and potassium borofluoride showed that the temperature of addition affected the resulting grain-size; the mixture melted completely only at 750°–770° C. and when this occurred the resulting grain-size was as fine as that obtained by using hardener alloys, but at lower temperatures the addition of the mixture of salts was less effective, apparently because of loss of boron. The results obtained with the proprietary mixture would possibly have been better if a higher temperature had been used, but it would usually not be desirable to exceed 750° C. in commercial melting practice because of the increase in gas pick-up. The size of the melt may also affect the results obtained with the proprietary mixture.

#### 5. THE EFFECT OF OTHER BORIDES

Zirconium, vanadium, niobium, and chromium form diborides similar to titanium boride, as described



TABLE VIII.—Addition of Titanium and Boron to Aluminium Alloy Melts by Reduction of Salts.

Mark, NOU	Alloy	Addition of Titanium and Boron						Grain- Size, mm.
		Source	Temperature of Addition, ° C.	Ti Content, %		B Content, %		
				Nominal	Analysis	Nominal	Analysis	
287 289 300	} Al-4.9% Cu-0.001% Ti Al-4.9% Cu-0.001% Ti	Commercial preparation of Ti and B salts.	750 {  With charge	0.03	0.03	0.005	0.01	0.5
		Hardener alloys.		0.12	0.08	0.02	0.02	0.5
				0.03	0.03	0.01	0.01	0.25
288	Al-10% Mg	Commercial preparation of salts.	750	0.03	<0.01	0.005	<0.005	1.0
307A 307B	} Al-4.8% Cu-0.13% { Ti (comm. ingot) {	No addition.	...	...	...	...	...	1.1
		Commercial preparation.	750	0.06	...	0.01	0.005	0.4
311 312	} Al-4.9% Cu-0.001% Ti	Potassium titanofluoride + potas-	710-730	0.03	0.03	0.01	<0.005	0.45
		sium borofluoride mixture.	750-770	0.03	0.04	0.01	0.005	0.27

in Table III. Series of aluminium-4.9% copper alloys were therefore made to which were added 0.01% boron and varying amounts of each of the above elements, to compare the effects of these additions with that produced by using titanium. All the additions were made as hardener alloys, and the melts were cast at 800° C.

The results of the grain-size measurements are plotted in Fig. 21, together with those obtained from bars containing titanium with 0.01% boron. None of the four alternative transition metals was more effective than titanium in reducing the grain-size at low concentration, if the additions are compared on the basis of either weight per cent. or atomic per cent. Both vanadium and niobium produced marked grain refinement, but none occurred with zirconium or chromium additions, presumably because the con-

centrations of the latter elements were too low to precipitate their respective diborides, or because other (unsuitable) borides were formed.

## VI.—SUMMARY AND CONCLUSIONS

(1) Substantial evidence has been obtained which shows that the grain refinement of aluminium alloys by the addition of boron is caused by nucleation by aluminium boride crystals in the melt. This conclusion was supported by other results obtained by using the isomorphous borides of certain transition metals. The metal atoms in these borides lie on simple hexagonal lattices, in the close-packed planes of which the interatomic distances are similar to the corresponding interatomic distance in solid aluminium.

(2) When boron is added to aluminium alloy melts containing titanium, marked grain refinement is produced which is thought to be caused by the formation of a boride with lattice dimensions similar to those of aluminium boride, which is probably titanium boride containing aluminium boride in solid solution. When the titanium content is over about 0.005%, this mixed boride is precipitated at very much smaller boron concentrations than are required to form pure aluminium boride in titanium-free alloys, and the boron addition necessary for maximum grain refinement is correspondingly less. For example, grain refinement of an aluminium-0.14% titanium alloy was produced by as little as 0.0001-0.001% boron—a quantity very similar to the estimated amount of carbon required to refine an alloy of similar titanium content.

(3) Two combinations of titanium and boron contents have been selected from these results for practical use—0.01% titanium + 0.003% boron for alloys cast at low temperatures, and 0.03% titanium + 0.01% boron for alloys which have to be heated above 720° C. before casting. Even the highest

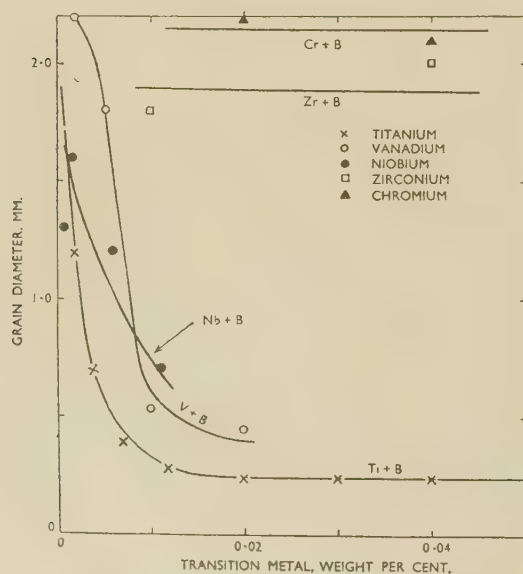


FIG. 21.—Grain-Sizes of Test-Bars in Al-4.9% Cu Alloy Containing 0.01% B and Small Quantities of a Transition Metal, Cast at 800° C.

additions represent a considerable saving in the use of titanium, and the grain refinement obtained is little affected by overheating the melt. Mould reaction and the loss of refinement caused by remelting in alloys containing the above additions are slight and not likely to be of any practical importance, and grain coarsening due to gravity segregation during solidification is reduced.

(4) Excessive additions of titanium and boron cause segregation of titanium boride crystals in the melt. As the loss of refinement on remelting is small, it should be unnecessary to make additions of titanium and boron to remelted scrap metal already containing these elements. Even with this precaution, however, segregation of titanium boride may still be encountered in quiescent melts unless the metal is stirred vigorously just before casting.

(5) Titanium and boron have also been added to aluminium alloy melts by the simultaneous reduction of molten salts of these elements, but the grain-sizes produced by this method are affected by the temperature of addition and the composition of the melt, and the method may be completely successful in practice only if the magnesium content is small and the temperature of addition high.

(6) Experiments on the addition of boron with transition metals other than titanium indicate that low concentrations of vanadium and niobium also produce marked refinement in the presence of boron.

(7) Very little success was obtained in attempts to increase the carbon content of alloys containing titanium; the addition of carbon presented much greater experimental difficulties than the addition of boron, and is unlikely to prove as successful as the latter.

#### ACKNOWLEDGEMENTS

The author is indebted to the Director and Council of the British Non-Ferrous Metals Research Association for permission to publish this paper. He also wishes to acknowledge information given to the Association by Messrs. Foundry Services, Ltd., and The British Aluminium Company, Ltd., and assistance received from Mr. E. Owden, Mr. J. Fox (who made the X-ray examinations), Mr. J. Day, and members of the Association's chemical laboratory.

#### APPENDIX

##### THE SUPERSATURATION OF ALUMINIUM BORIDE IN ALUMINIUM

When the centrifuged aluminium-0.04% boron specimen, which was discussed in Section III, 2, was examined again after twelve months, a new constituent was observed over the whole cross-section,

which was quite different in shape from the segregated aluminium boride crystals. The distribution of the new constituent suggested that it had precipitated from the solid metal on crystallographic planes and at the boundaries of dendrite arms as indicated in Fig. 3 (Plate I).<sup>\*</sup> At a high magnification, the precipitate was similar in appearance to aluminium boride ( $AlB_2$ ), but was quite different in shape, as shown in Fig. 4 (Plate I). It was largely situated in bands around what seemed to be sections of dendrite arms (as can be seen, for example, at the right of Fig. 3 (Plate I), so that the dendrites were revealed in a similar way to that usually produced by coring.

These observations can be interpreted in the following manner. The formation of primary aluminium boride crystals may be partly suppressed at high rates of cooling ( $40^\circ C./min.$ ) and the dissolved boron concentrates in the residual liquid as the super-saturated melt solidifies, producing coring. Some of the aluminium boride may form at the boundaries of dendrite arms, where its concentration is highest, at the moment when they solidify, but most of the compound precipitates from the solid metal on ageing.

This interpretation explains several observations which have been made in earlier work. For example, castings in high-purity aluminium-boron alloys, with a few exceptions, have columnar macrostructures, which can be explained by the absence of concentration gradients large enough to prevent the growth of the columnar grains in the solidifying alloys; some castings, however, have been observed with central zones, varying in size from casting to casting, of very fine equiaxial grains at the boundaries of which was a discontinuous constituent.<sup>1</sup> This phase now appears to have been aluminium boride which was formed in the way described above, and it is therefore possible that the concentration gradients which led to its formation caused the restriction of the growth of the dendrites which resulted in the fine equiaxial structures. The grain-boundary precipitate was observed in greatest amounts in castings made from melts which had been heated above  $860^\circ C.$ , but the reason for the variation from casting to casting cannot be given.

The lamellar pattern of the precipitate between the arms of dendrites in the centrifuged specimen is apparently identical with the eutectic-like structures which have been observed in previous work.<sup>3</sup> The observation may also explain the wide diversity of equilibrium diagrams which have been proposed for the binary aluminium-boron system,<sup>12</sup> one of which showed a eutectic point at more than 15% boron and  $565^\circ C.$ , and another a eutectic at less than 0.05% boron and  $658^\circ C.$ , with primary aluminium boride forming only at higher boron contents in both cases.

<sup>\*</sup> During the period of twelve months the metallographic specimen had been mounted twice, the temperature being raised to approximately  $130^\circ C.$  each time.



## REFERENCES

1. A. Cibula, *J. Inst. Metals*, 1949-50, **76**, 321.
2. W. A. Baker, *B.N.F.M.R.A. Research Rep.*, **A.550**, 1940.
3. M. D. Eborall, *J. Inst. Metals*, 1949-50, **76**, 295.
4. A. Cibula and R. W. Ruddle, *J. Inst. Metals*, 1949-50, **76**, 361.
5. D. C. G. Lees, *J. Inst. Metals*, 1946, **72**, 343.
6. A. L. Mincher, *Metal Ind.*, 1950, **76**, 435.
7. A. L. Mincher, *B.N.F.M.R.A. Research Rep.* **A.860**, 1949.
8. W. A. Baker and M. D. Smith, *B.N.F.M.R.A. Research Rep.* **A.694**, 1945.
9. W. L. Fink and L. A. Willey, "Metals Handbook", p. 1155. Cleveland, O.: **1948** (American Society for Metals).
10. W. Hofmann and W. Jäniche, *Z. Metallkunde*, 1936, **28**, 1.
11. N. B. Rutherford, B.N.F.M.R.A. unpublished work.
12. L. Mondolfo, "Metallography of Aluminium Alloys". New York: **1943** (John Wiley and Sons).
13. W. E. Sicha and R. C. Boehm, *Trans. Amer. Found. Soc.*, 1948, **56**, 398.
14. R. Kiessling, *Acta Chem. Scand.*, 1949, **3**, 90.
15. R. Kiessling, *Acta Chem. Scand.*, 1949, **3**, 595.
16. J. T. Norton, H. Blumenthal, and S. J. Sindeband, *Trans. Amer. Inst. Min. Met. Eng.*, 1950, **188**, 1060.
17. R. A. Skinner, B.N.F.M.R.A. unpublished work.
18. R. W. Ruddle, *J. Inst. Metals*, 1950, **77**, 1.

# SOME OBSERVATIONS ON THE OCCURRENCE OF STRETCHER-STRAIN MARKINGS IN AN ALUMINIUM-MAGNESIUM ALLOY\*

1320

By R. CHADWICK,† M.A., F.R.I.C., F.I.M., MEMBER, and  
W. H. L. HOOPER,‡ B.Sc., A.I.M., MEMBER

## SYNOPSIS

Detailed observations have been made of the appearance of and dimensional distortion associated with surface markings developed by the progressive stretching of aluminium-3% magnesium alloy sheet in different conditions of cold working and annealing. In material of 0.025 mm. grain-size, markings develop with a very small strain and are at first normal to the tension axis but subsequently become random in direction, reaching maximum intensity at about 1%, and decaying within a 2% extension. These random markings consist of a series of kinks, and there is no thinning of the sheet. Parallel, intersecting bands or shallow grooves at a definite angle to the direction of stretching first appear at about 2% extension and increase progressively in intensity up to the point of fracture. Parallel bands, which are caused by local thinning or necking, are of much less intensity than the random markings, which are the main cause of defects in pressing operations.

When the grain-size exceeds 0.05 mm., random markings do not occur in stretching, nor are they obtained in partially annealed or temper-rolled sheet irrespective of grain-size. Parallel bands are found in all these materials. When the grain-size is increased substantially, the well-known "orange-peel" effect develops on stretching and completely masks any other effect which might be present, the degree of roughening from this cause in sheet of 1.0 mm. grain-size being comparable with that produced by random markings in fine-grained sheet.

## I.—PREVIOUS WORK

STRETCHER-STRAIN markings are of particular significance in the manipulation of soft mild-steel sheet, and both practical and theoretical aspects of their occurrence have been the subject of numerous investigations. The physical appearance of strain markings and the conditions under which they occur have been discussed in some detail by Jevons,<sup>1</sup> who states that the uneven surface associated with stretcher-strains develops within an elongation of about 4%, beyond which the surface again becomes smooth and even. The standard method of preventing the occurrence of stretcher-strains in steel is by a light rolling reduction or passage through roller levellers, although the condition of immunity to strain marking is retained for only a short time.

Strain markings have been reported on several other metals, such as 70 : 30 brass, Duralumin,<sup>2</sup> and commercial aluminium,<sup>3</sup> but Jevons points out that in non-ferrous metals the effect is quite different from that experienced in steel, and occurs with much greater deformation. The intensity is also less, and all these metals are regularly used for deep and shallow pressings without any seriously detrimental stretcher-strain defects. Knight and Murray,<sup>4</sup> in a study of an aluminium-magnesium alloy, have shown that strain markings occurring with light stretching

have some resemblance to those observed on mild steel. The markings were found to be particularly intense in fine-grained sheet, and in this connection it is of interest to observe that in an investigation by one of the present authors,<sup>5</sup> covering a number of alloys of zinc, strain lines were obtained only in a zinc-magnesium alloy, which has the characteristic of recrystallizing with a very fine grain-size.

In recent scientific studies of stretcher-strain phenomena, particular attention has been paid to the associated discontinuities in stress/strain curves, rather than to the strain markings themselves. McReynolds<sup>3</sup> has reviewed work in this field, and has also carried out a detailed investigation of the behaviour in straining of commercial-purity aluminium sheet, but it is clear that the relationship between the steps or discontinuities and strain markings is by no means clearly defined. For example, it has been reported that both mild steel<sup>6,7</sup> and 70 : 30 brass<sup>8</sup> show stepped curves only at elevated temperatures, although pronounced markings develop in each case on stretching at room temperature. The extent to which discontinuities in the stress/strain curves are detected depends to some extent upon the elastic recovery in the straining mechanism, and studies of this type cannot be expected to provide information on the nature or range of occurrence of the strain markings themselves.

\* Manuscript received 12 April 1951.

† Assistant Research Manager, Imperial Chemical Industries, Ltd., Metals Division, Witton, Birmingham.

‡ Research Technical Officer, Imperial Chemical Industries, Ltd., Metals Division, Witton, Birmingham.



## II.—PRESENT INVESTIGATION

### 1. SCOPE

The experiments described were concerned with the appearance, magnitude, and conditions of occurrence of strain markings in an aluminium-3% magnesium alloy, which, from published literature and a preliminary survey made by the authors, was indicated as being probably the type of aluminium alloy most liable to such effects.

Various possible methods of measuring irregularities on a sheet surface were considered. For example, strained specimens were sectioned with the object of examining the surface under the microscope. However, even when tapered sections were cut at a narrow angle to the surface, and the precaution was taken of copper plating, in order to retain the sharpness of the surface, before mounting in methyl methacrylate, the magnitude of the effect was for the most part too small for an accurate assessment to be made by ordinary microscopical means. Mechanical methods proved more suitable and the experiments described were carried out with the Talysurf instrument, in which the displacement of a stylus traversing the specimen surface is magnified electronically and recorded on a paper chart.

The observation of Knight and Murray<sup>4</sup> that strain markings are most intense on annealed fine-grained material, was confirmed, and the stretching of fine-grained sheet up to the point of fracture was investigated in some detail. Additional observations were concerned with the study of markings in annealed sheet of different grain-sizes, and in temper-rolled and partially annealed sheet.

### 2. PREPARATION OF MATERIAL

All the sheet material required was rolled from a single ingot of 5 in. thickness, the composition of which, as determined by chemical analysis on the 0.25-in.-thick, hot-rolled stock, was: magnesium 3.03, manganese 0.46, iron 0.23, silicon 0.14, copper 0.03, titanium 0.01%, remainder aluminium. An earlier investigation<sup>9</sup> had shown that the final grain-size of this type of alloy depends mainly on the ultimate cold-rolling reduction and, to a smaller extent, on the rate of heating during subsequent annealing. Consequently, in order to obtain the largest possible range of grain-sizes in the present experiments, the sequence of cold-rolling and intermediate annealing operations was so arranged that final rolling reductions ranged from 5 to 80%, intermediate annealing being carried out at 400° C.

The cold-rolled samples were annealed by three alternative procedures, decided by reference to the curves reproduced in Fig. 1, which were plotted from hardness tests on samples reduced 10, 25, and 80% in thickness by cold rolling, and annealed for 2 hr. at suitable temperature intervals.

After final rolling, rectangular specimens 8 × 2 in. were cut from the flattened sheet and the following

treatment applied: (1) a rapid anneal in a salt bath at 500° C., designed to give the finest series of grain-sizes; (2) an anneal at 400° C. with slow heating in an air furnace, providing a series of coarser grain-sizes; or (3) an anneal at 325° C. in an air furnace in order to obtain the partially softened non-recrystallized condition on some of the specimens, and to increase still further the range of grain-sizes available.

A series of temper-rolled specimens was prepared from annealed 18-gauge sheet of fine grain-size, obtained by annealing at 400° C. after a final reduction of 80% in thickness, and therefore in its soft condition susceptible to stretcher-strain markings. Temper rolling was carried out in the same direction as previous cold rolling, and reduction in thickness ranged from 1 to 10%, control being effected by measurement of elongation on a length of 4 ft.

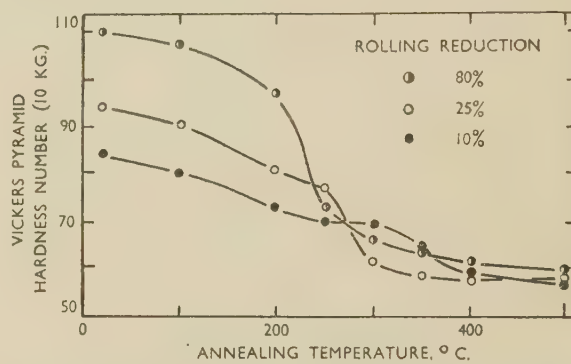


Fig. 1.—Annealing Curves of Aluminium-Magnesium Alloy Sheet.

Immediately before submitting them to stretching tests, all the 8 × 2-in. samples, whether annealed or temper-rolled, were polished by hand on both surfaces with metal polish, and then brightened by electrolytic treatment in a mixture of phosphoric acid and alcohol. The bright surface gave an almost level trace on the Talysurf apparatus and enabled markings to be seen or photographed with equal facility.

Surfaces were etched for grain-size measurement by immersing small areas at the ends of strips in the phosphoric acid mixture, and applying a lower voltage than that at which polishing takes place, for a period of some 10–20 sec. Grain-sizes were estimated by comparison, at a magnification of ×100, with a standard series of photomicrographs covering a range of mean grain diameters of 0.017–0.12 mm. For larger grain-sizes, the ×100 image was measured directly.

All strips annealed in a salt bath recrystallized. On the other hand, with specimens annealed in an air furnace at 400° or 325° C., recrystallization occurred only after rolling reductions greater than 5 and 10%, respectively. The grain-size of recrystallized material varied from 0.025 to 1.0 mm., the values obtained being included in Table III.

In the non-recrystallized specimens grain-sizes were apparently unchanged by the final rolling and annealing procedures. The X-ray diffraction patterns were,

however, characteristic of what is now regarded as the recovered condition, in which the individual grains seen under the microscope are apparently agglomerates of smaller crystals, differing in orientation by only a few minutes of a degree.

### 3. STRETCHING EXPERIMENTS

The  $8 \times 2$ -in. specimens were stretched in a hydraulic tensile-testing machine, the operation being interrupted at progressively increasing extensions for Talysurf traces to be made on the rolled surfaces. Extensions of up to 1% were measured with a Lamb extensometer of the mirror-and-scale type, and those between 1 and 2% with a direct-reading dial instrument, the gauge-length being 2 in. in both cases. Extensions greater than 2% were measured with spring-loaded dividers.

#### (a) *Fine-Grained Specimens*

The whole range of surface effects broadly termed stretcher-strain markings can be most readily described by reference to the stretching of a sample prepared by annealing after a cold reduction of 80%, when at 400° C. the grain-size developed is 0.025 mm. Two distinct types of strain markings were observed. The first of these, which has been termed "random markings", reaches a maximum intensity with about a 1% extension, thereafter diminishing rapidly in intensity with further stretching. The strain lines are often slightly curved and vary considerably in direction and in closeness of spacing, and the pattern appears to be identical on the two surfaces of the sheet. At an extension of about 2%, when random markings have virtually disappeared, the second type of marking begins to appear and consists of a cross-hatching of closely spaced parallel bands inclined at about 57° on either side of the line of stretching. These bands increase progressively in intensity, until necking and fracture eventually occur on one of them. The random markings at about 1% extension are by far the most significant and prominent of the two types of strain effect.

The nature of random markings, the progressive development of which is illustrated in Figs. 5, 6, and 7 (Plate IV), can best be understood by describing experiments carried out on a typical area of a stretched specimen, such as that illustrated in Fig. 2 (Plate III). The traces made by the Talysurf stylus on the two opposite faces of the sheet along the line *XX* are shown in Fig. 3 (Plate III), and in Figs. 2 and 3, the letters *A1*, *B1* to *A5*, *B5* refer to the successive areas over which the stylus passes. It will be noted that there is a sharp break or change in direction corresponding to the boundary line between light and dark areas. In effect, the surface can be regarded as consisting of planes inclined at variable small angles, which calculation shows to be generally smaller than 1°, to the general level of undistorted surface. Since, moreover, the traces are closely similar on the two sides of the specimen, it would seem that in effect the strip is concertina-ed, the two faces being parallel

with no perceptible thinning at any point. A further series of surface traces along parallel lines 1-9 is recorded in Fig. 4 (Plate III). It will be noted that where the tongue-shaped marking is narrow the inclination is steeper than where the marking is wide, and it is clear, therefore, that there is a slight degree of curvature of the individual segments. The form of the surface can be more clearly understood by reference to Fig. 12 (Plate VI), which shows a model of a strained specimen with markings similar to those illustrated in Fig. 2. The surface contour is on the same magnification as Figs. 3 and 4, but thickness is reduced relative to the other dimensions.

The first random markings were detected at very small extensions. A typical specimen in which the overall plastic strain is 0.015% is illustrated in Fig. 5 (Plate IV). The surface within the gauge-length itself is free from markings, and the points over which markings occur may therefore be assumed to have suffered an extension exceeding 0.015%. This is confirmed by continuing the stretching, for with the first intrusion of strain markings into the gauge-length (Fig. 6, Plate IV), the extension has increased to 0.03%, and calculations from measurements of surfaces partially affected by strain markings indicates that the development of random markings is accompanied by an extension of at least 0.5%. The spread of strain marking over the whole specimen is illustrated in Fig. 7 (Plate IV), in which the measured plastic strain over the gauge length is 1%. Smooth and uniform stretching of a specimen up to 1% extension is difficult to achieve, because of the sudden stress-relief that accompanies the formation of new areas of random strain markings, but with careful control it is possible to watch the movement of the strain lines or tongue-like formations, which can proceed either by a smooth and regular movement or by more rapid shooting and darting. When stretching first begins the lines are almost normal to the direction of strain, but as extension proceeds they tend to curve at the ends, and also to fork and branch, so that by the time they approach maximum intensity at about 1% extension, they take a great variety of forms, and their direction appears to be quite random. There is, however, some reason to believe that if uniform straining in one direction could be achieved, the lines would remain normal to that direction, the forking and branching being probably associated with lack of homogeneity in the material due to slight variations in gauge and temper.

The degree of roughening or magnitude of the strain-marking effect on each individual specimen was taken as the maximum vertical distance between any pair of adjacent inflections in the Talysurf trace; for example, in Fig. 5 the distance measured is *PQ*. Mean values of such measurement obtained at intervals in the progressive stretching of a number of fine-grained specimens are plotted in Fig. 13 (Plate VI), curve *A* (the broken line) representing strains over which the surface was only partly affected by markings. The strain markings are probably of maximum



intensity as soon as they appear, when their depth is about 0.003 in., although an exact evaluation is difficult when the surface is only partially affected. As stretching continues the bands multiply and groups of markings merge; accordingly, striations become less clearly defined, the measured roughness values diminishing rapidly so that at 2% elongation random marking has almost disappeared (Fig. 8, Plate IV) and surface irregularities are of the order of 0.0001 in. The sharp fall in roughness values between 1 and 2% extension will be observed in Fig. 13. Parallel bands, traversing specimens at an angle of about 57° to the direction of stretching, are just apparent at 2% extension, and roughness at this stage results partly from these bands and partly from residual random markings. As stretching is continued, parallel bands increase in depth and Fig. 9 (Plate V) illustrates the surface appearance of a specimen with a permanent extension of 5%, where the bands are closely spaced and quite conspicuous.

Features of parallel bands are their straightness, and manner of propagation, groups moving in a series of short jumps, seldom sweeping a distance greater than about 1 in. At 2% strain the magnitude of roughness associated with the bands is probably much less than 0.0001 in., but as stretching continues, the magnitude increases progressively, as indicated in Fig. 13, the maximum depth at an extension of 10% being 0.0003 in., when the operations were discontinued. Surface-contour records taken at this stage, Fig. 10 (Plate V), show that every depression in the system of parallel bands has an associated depression of similar magnitude in the opposite surface, causing in effect, a series of necks, in one of which, when stretching is continued, fracture eventually occurs.

#### (b) Specimens of Differing Grain-Size

Similar though less-detailed observations were made on the full range of annealed specimens, the appearance of which, after stretching to 1, 5, and 10% permanent extension, is recorded in Table I. Plots of the severity of strain marking, using the basis of measurement already described in connection with the sheets of fine-grained specimens, are shown in Fig. 13, for a representative series of grain-size values.

Behaviour in stretching was related entirely to grain-size. Specimens prepared by different rolling and annealing schedules, but with equal grain-size values, developed the same types and intensities of strain marking.

Random markings occurred with maximum intensity at about 1% extension in specimens with grain-sizes of from 0.025 to 0.042 mm. and were similar in appearance and of the same order of intensity over this range, as was also the decay of marking as the extension was increased from 1 to 2%. A specimen with the next largest grain-size of 0.05 mm., when stretched up to an extension of 1%, was, however, entirely free from random markings.

Clearly marked parallel bands developed in all specimens within the grain-size range of 0.025–0.06 mm., and the intensity of marking for any given degree of deformation appeared to be, within the limits of experimental error, independent of grain-size, as can be seen from the three curves relating to specimens within this range of grain-sizes plotted in Fig. 13. With grain-sizes of 0.05 mm. and over,

TABLE I.—*Stretching Characteristics of Annealed Sheet.*

Rolling Reduction, %	Grain-Size, mm.	Type of Marking				
		1% Extension	5% Extension	10% Extension		
<i>Annealed 30 min. in a salt bath at 500° C.</i>						
5	1.0	Severe orange-peel effect.	Severe orange-peel effect.	Severe orange-peel effect.		
10	0.15	Slight orange-peel effect.	Orange-peel effect and parallel bands.	Orange-peel effect and parallel bands.		
20	0.060	} No markings. } Severe random markings.	} Parallel bands.	} Parallel bands.		
25	0.057					
30	0.042					
40	0.040					
80	0.025					
<i>Annealed 2 hr. in an air furnace at 400° C.</i>						
5	0.025 *	Slight parallel bands.	Parallel bands.	Parallel bands.		
10	0.25	Slight orange-peel effect.	Orange-peel effect.	Orange-peel effect.		
20	0.08	} No markings. } Severe random markings.	} Parallel bands.	} Parallel bands.		
25	0.054					
30	0.042					
40	0.038					
80	0.025					
<i>Annealed 6 hr. in an air furnace at 325° C.</i>						
5	0.025 *	} Slight parallel bands.	} Parallel bands.	} Parallel bands.		
10	0.025 *					
20	0.057 †	} No markings. } Severe random markings.				
25	0.057					
30	0.05					
40	0.042					
80	0.026					

\* Not recrystallized.

† Partially recrystallized.

parallel bands were not masked by random markings, and in some instances were detected visually at 1% strain, but they were too shallow at this stage—less than 0.0001 in.—to measure with the Talysurf instrument. With increasing strain, parallel bands became progressively deeper, the merging of bands being the mechanism by which this occurred up to the point at which necking began at an extension of about 20%.

The upper grain-size limit for the appearance of parallel bands is governed by the occurrence of the well-known “orange-peel” effect, which results from non-homogeneous deformation within individual grains in material of large grain-size. In stretching sheet of 0.25 mm. grain-size the orange-peel effect is superimposed on parallel bands, but the roughness value at between 1 and 10% extension is only slightly higher than in fine-grained material. With further increase in grain-size the orange-peel markings are of much greater significance, and with a 1-mm. grain-size roughening is severe and completely masks parallel bands at all extensions (see Fig. 11, Plate V).

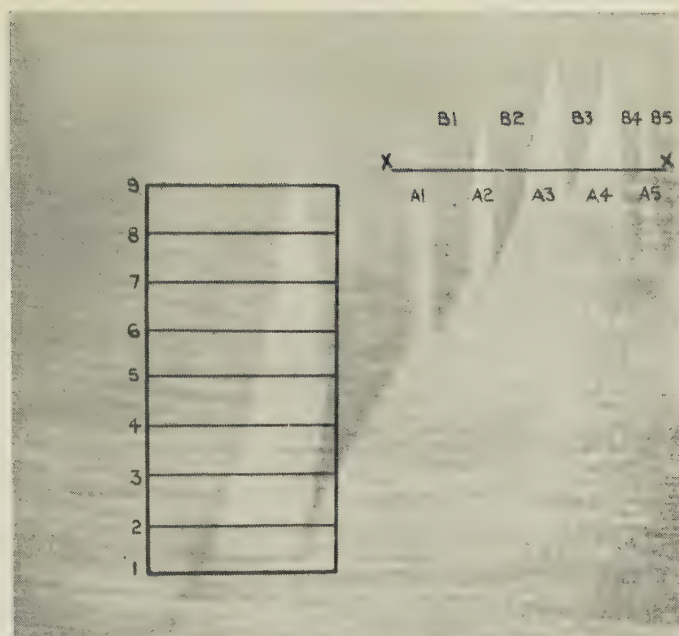


FIG. 2.—Typical Random Markings in Sheet of 0.025 mm. Grain-Size.  $\times 2$ .

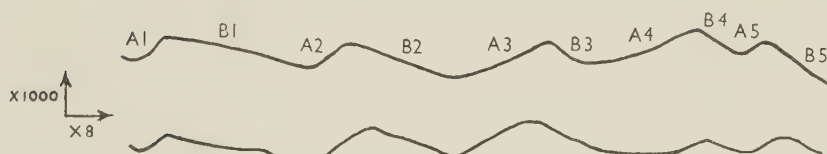


FIG. 3.—Talysurf Traces on Top and Bottom Surfaces Along Line XX in Fig. 2.

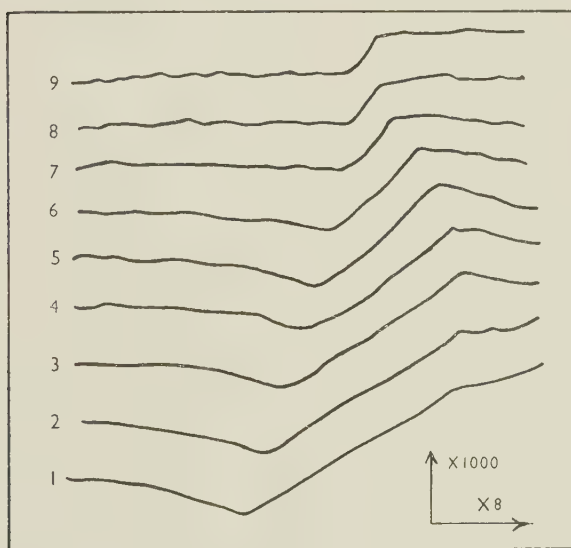


FIG. 4.—Talysurf Traces Along Lines 1 to 9 in Fig. 2.



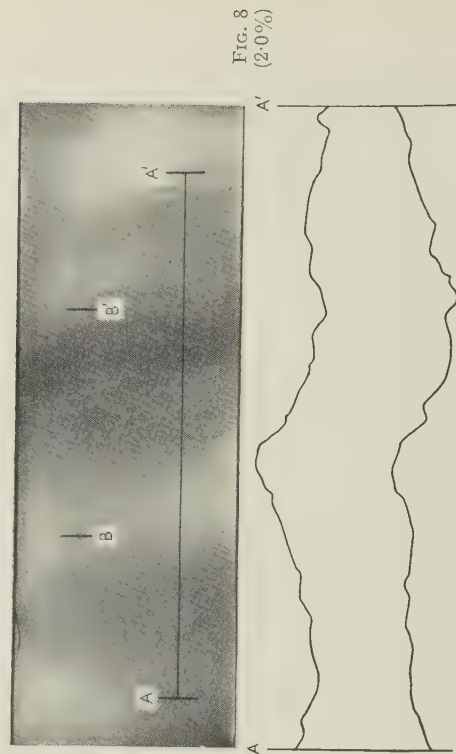
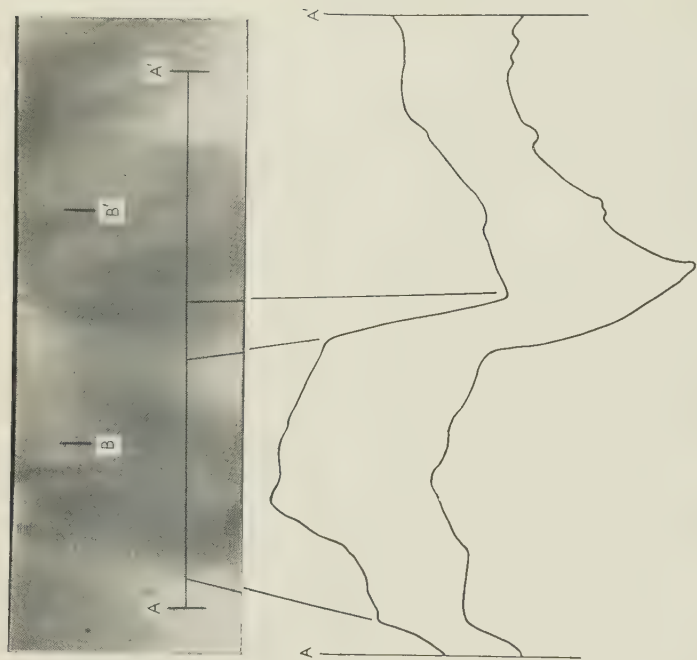
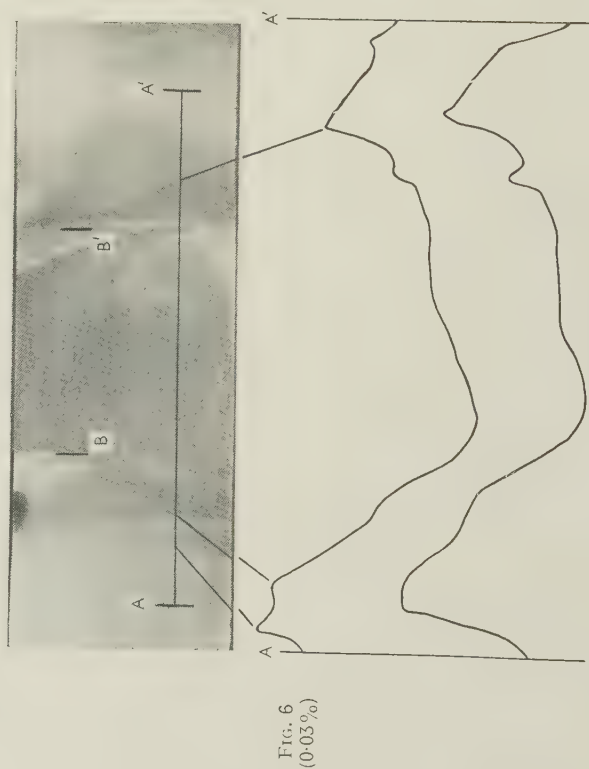
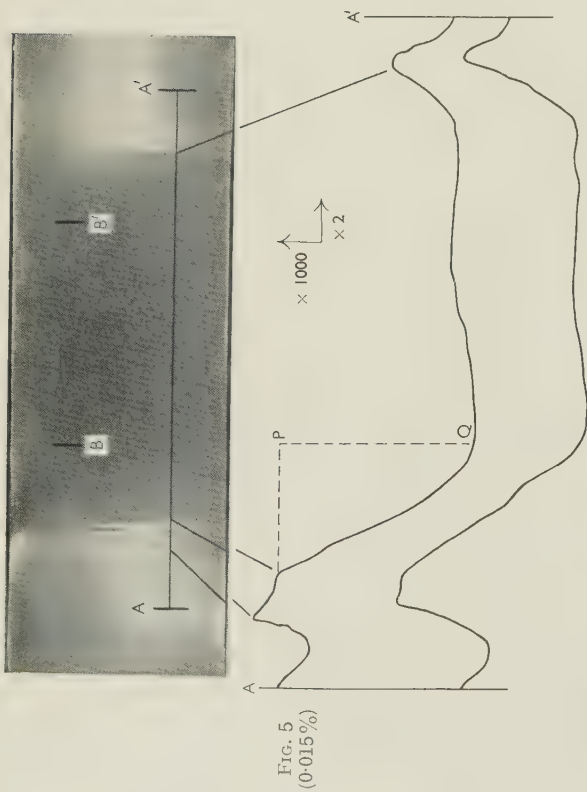




FIG. 9  
(5.0%)

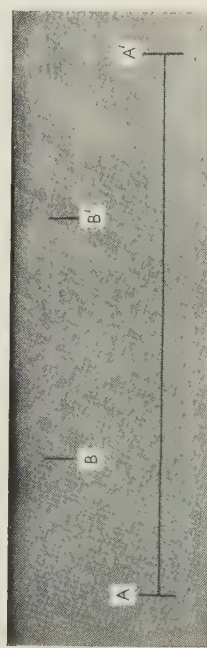
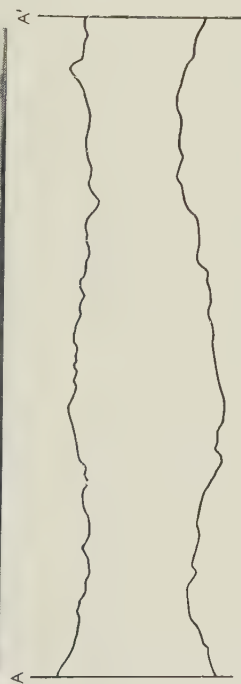


FIG. 10  
(10%)



FIGS. 5-10.—Strain Markings Obtained by the Progressive Stretching of an Aluminium-Magnesium Alloy Sheet of 0.025 mm. Grain-Size, with Talsurf Traces of Upper and Lower Surfaces from *A* to *A'*.  
FIG. 11.—Markings on Aluminium-Magnesium Alloy Sheet of 1.0 mm. Grain-Size.

Permanent extensions over the 2-in. gauge length *BB'* are as indicated in parentheses.

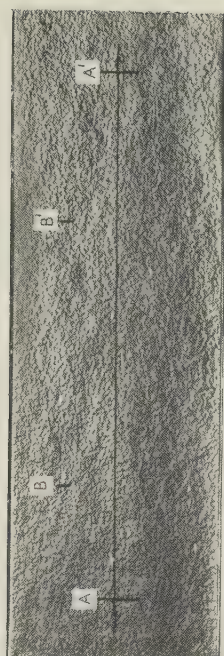
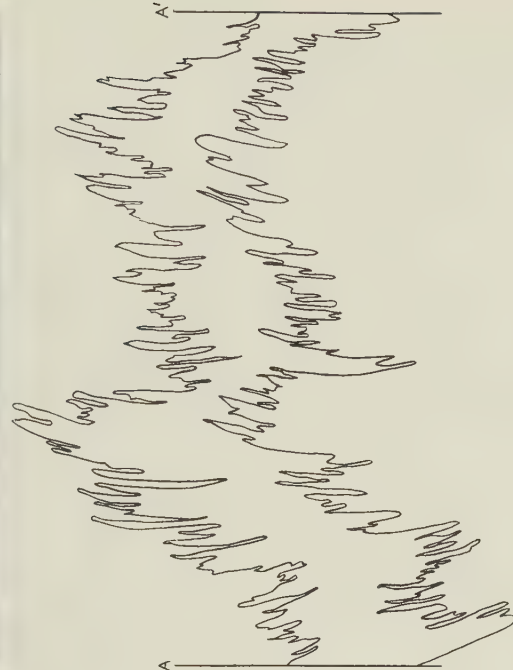


FIG. 11  
(10%)





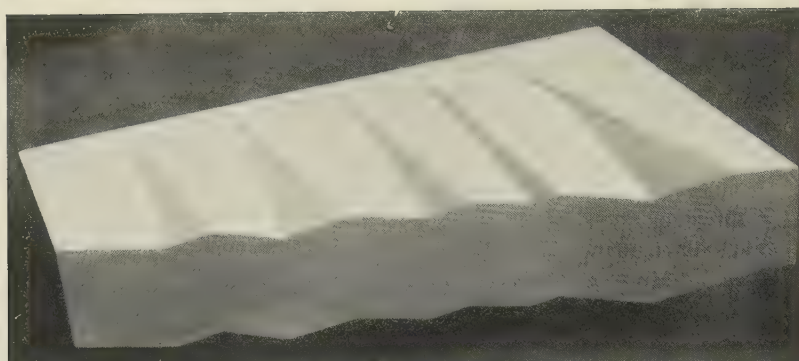


FIG. 12.—Solid Model of a Group of Random Markings.

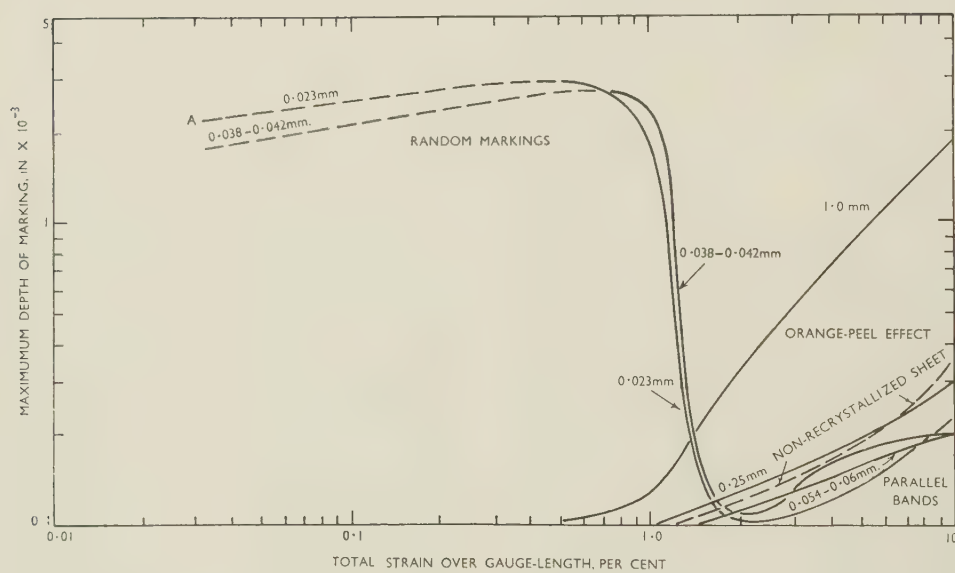


FIG. 13.—Effect of Strain on the Depth and Type of Markings on Annealed Sheets of Mean Grain-Size Ranging from 0.023 to 1.0 mm.

TABLE II.—*Stretching Characteristics of Temper-Rolled Sheet of Grain-Size, Before Rolling, 0.025 mm.*

Rolling Reduction, %	0.5% Extension		1% Extension		2% Extension		4% Extension	
	Maximum Talysurf Deviation, 10 <sup>-3</sup> in.	Type of Marking	Maximum Talysurf Deviation 10 <sup>-3</sup> in.	Type of Marking	Maximum Talysurf Deviation, 10 <sup>-3</sup> in.	Type of Marking	Maximum Talysurf Deviation, 10 <sup>-3</sup> in.	Type of Marking
1	0.1	Parallel bands	0.1	Parallel bands	0.15	Parallel bands	0.18	Parallel bands
2	0.1		0.1		0.15		0.18	
4	0.15		0.15		0.2		0.22	
10	0.18		0.2		0.22		0.3	

The degree of roughening resulting from orange-peel effect with a 1-mm. grain-size at 10% stretching is indicated in Fig. 1 (Plate VI), and it will be noted that the measured irregularities are of about the same order as those associated with random markings in fine-grained sheet with 1% stretching. Orange-peel effects, like parallel bands, are of relatively slight significance when the amount of stretching is small.

The non-recrystallized specimens, all three of which had about the same apparent grain-size of 0.025 mm., were entirely free from the random strain markings which are obtained in the fully recrystallized metal of similar grain-size. Parallel bands, however, began to appear at about 1% strain and deepened progressively with further stretching in precisely the same manner as in recrystallized sheet, a typical surface-roughness curve being shown as a broken line in Fig. 13.

#### (c) Temper-Rolled Specimens

As already stated, sheet for temper-rolling experiments was annealed at 400° C. after a final rolling reduction of 80%, and, having a grain-size of about 0.025 mm., was intensely susceptible to random markings.

Detailed observations were made and results are recorded in Table II on specimens subjected to rolling reductions of 1, 2, 4, and 10% in thickness; and in order to ascertain whether the behaviour in stretching is affected by strain-ageing effects, as it is in mild steel, the first series of experiments, carried out within 1 hr. of rolling (and in one or two instances within a few minutes of rolling) were repeated after an interval of three months.

None of the temper-rolled specimens showed any signs of random markings with light straining, as indeed might be expected by analogy with steel. Parallel bands, however, could be observed in every instance with only 0.5% strain and were, in all but the most lightly rolled specimens, of measurable depth with this extension, so that these bands were clearly of greater significance than in annealed sheet. The surface appearance and the maximum degree of irregularity of the various temper-rolled specimens with applied strains of 0.5, 1.0, 2.0, and 4.0% are recorded in Table II. It will be noted that the depth of the bands increases progressively with stretching, as in annealed sheet, while for a constant deformation, depth also increases slightly with temper-rolling

reduction; but even with a 10% temper rolling, the depth of parallel bands for any given extension is only about twice that obtaining in annealed sheet, and the total surface irregularity associated with parallel bands is small compared with that of random markings.

#### 4. MECHANICAL PROPERTIES OF SHEET

In annealed recrystallized sheet, hardness, proof stress, ultimate tensile strength, and elongation all increase by small progressive amounts with diminishing grain-size (Table III). For example, in alloys with a 0.05–0.06-mm. grain-size, and therefore free from random marking effects, the proof stress is about 1 ton lower than in sheet of 0.025-mm. grain-size, which is susceptible to random markings; in

TABLE III.—*Mechanical Properties of Annealed Sheet.*

Rolling Reduction, %	Grain-Size, mm.	Vickers D.P. Hardness Number (10 kg. load)	0.1% Proof Stress, tons/in. <sup>2</sup>	Ultimate Tensile Strength, tons/in. <sup>2</sup>	Elongation on 2 in., %
<i>Annealed 30 min. in a salt bath at 500° C.</i>					
5	1.0	55	4.8	13.6	24
10	0.15	57	4.9	14.0	24
20	0.060	57	5.6	14.2	23
25	0.057	58	5.6	13.8	23
30	0.042	58	5.6	13.9	26
40	0.040	59	6.0	14.0	26
80	0.025	60	6.6	14.2	26
<i>Annealed 2 hr. in an air furnace at 400° C.</i>					
5	0.025 *	64	7.4	14.7	20
10	0.25	52	5.1	13.9	21
20	0.08	52	6.0	14.1	22
25	0.054	53	5.7	14.0	23
30	0.042	53	6.0	14.0	23
40	0.038	55	6.4	14.3	23
80	0.025	55	6.9	14.4	24
<i>Annealed 6 hr. in an air furnace at 325° C.</i>					
5	0.025 *	66	7.5	14.4	20
10	0.025 *	67	7.6	14.4	19
20	0.057 †	61	7.1	14.2	23
25	0.057	58	6.2	14.2	22
30	0.05	59	6.2	14.0	21
40	0.042	59	6.5	14.2	23
80	0.026	61	7.1	14.4	25

\* Not recrystallized.

† Partially recrystallized.



other properties the proportionate differences are smaller. Again, sheet annealed at a low temperature so as to give a non-recrystallized or recovered structure is slightly higher in proof and tensile strength than fully annealed material. Temper-rolled sheet shows a wider range of mechanical properties (Table IV),

TABLE IV.—*Mechanical Properties of Temper-Rolled Sheet.*

Rolling Reduction, %	Vickers D.P. Hardness Number (10 kg. load)	0.1% Proof Stress, tons/in. <sup>2</sup>	Ultimate Tensile Strength, tons/in. <sup>2</sup>	Elongation on 2 in., %
Annealed	54.9	6.9	14.4	24
1	70	8.3	14.6	20
2	73	9.4	14.8	19½
4	82	11.4	15.3	15
10	84	12.2	16.2	9

strength increasing progressively with rolling reduction, but where this does not exceed 2%, ductility is not seriously impaired.

### III.—SIGNIFICANCE OF THE RESULTS

The experiments show that strain markings in annealed recrystallized sheet can be divided into two distinct types. Random markings are associated entirely with deformations of less than 2% and reach maximum intensity with about 1% stretching. They are found only in material with a grain-size below a sharply defined limit of about 0.05 mm. Parallel bands occur in all material irrespective of grain-size, but where this exceeds 1.0 mm. they are completely masked by the orange-peel effect. In annealed material parallel bands reach a measurable intensity at an extension of 2%, thereafter increasing progressively in magnitude up to the point of fracture. On the other hand, in sheet softened by a non-recrystallizing anneal or temper-rolled after a full anneal, parallel bands are of measurable depth at 1% strain, but in neither of these conditions is the surface affected by random markings.

The depth of random markings is about 0.003 in. at 1% extension, while parallel bands do not exceed a depth of 0.0003 in. with extensions of up to 10%, so that random markings are the only ones seriously detrimental in pressing. They can be avoided by subjecting sheet to one of the following procedures:

(1) By adjusting rolling and annealing schedules to give sheet with a final grain-size of 0.05–0.08 mm.

(2) By the application of a small final rolling reduction followed by a low-temperature non-recrystallizing anneal.

(3) By the application of a final temper-rolling reduction to fine-grained annealed sheet.

The third procedure, unlike temper rolling in mild steel, provides material which, over long periods of storage, is immune from any tendency to develop the more conspicuous, or random, type of strain effect on stretching.

It seems likely that the parallel markings, observed on every sample examined in the present investigation irrespective of its physical condition, are of more general occurrence than random markings, and indeed from careful reading of published work it appears probable that parallel banding is the type of marking reported in brass, Duralumin, aluminium, and a variety of other metals in sheet form. Random markings seem to be closely analogous to stretcher-strain effects in soft mild steel although according to Jevons the markings of steel are characterized by depressions on the two opposite faces of the sheet, giving rise to a local necking effect, and not to the kinking observed in the present investigation on aluminium-magnesium alloy sheet.

It is of interest to note that few metals or alloys can readily be obtained with the fine grain-size which the present experiments indicate to be essential to the development of random markings in aluminium-magnesium alloy, and this may well be one reason for the relatively rare occurrence of this phenomenon.

### ACKNOWLEDGEMENTS

The authors' thanks are due to Dr. Maurice Cook, for his helpful advice and encouragement, and to various colleagues who have assisted in the experimental work.

### REFERENCES

1. J. D. Jevons, "The Metallurgy of Deep Drawing and Pressing". 2nd edn. London: 1942 (Chapman and Hall, Ltd.).
2. E. W. Fell, *Carnegie Schol. Mem., Iron Steel Inst.*, 1936, **26**, 123.
3. A. W. McReynolds, *Trans. Amer. Inst. Min. Met. Eng.*, 1949, **185**, 32.
4. G. A. Knight and G. Murray, *Sheet Metal Ind.*, 1946, **23**, 1741.
5. R. Chadwick, *J. Inst. Metals*, 1933, **51**, 120.
6. A. Le Chatelier, *Rev. Mét.*, 1909, **6**, 914.
7. F. Körber and A. Pomp, *Mitt. K.W.-Inst. Eisenforsch.*, 1927, **9**, 346.
8. T. Sutoki, *Sci. Rep. Tôhoku Imp. Univ.*, 1941, [i], **29**, 673.
9. R. Chadwick and W. H. L. Hooper, *J. Inst. Metals*, 1948–49, **75**, 609.

# THE EFFECT OF PHOSPHORUS ON THE CORROSION-RESISTANCE OF MAGNESIUM AND SOME OF ITS ALLOYS \*

1321

By E. F. EMLEY,† B.Sc., Ph.D., A.I.M., F.R.I.C., MEMBER,  
A. C. JESSUP,‡ M.C., A.Inst.P., F.I.M., MEMBER, and  
W. F. HIGGINS,† M.Sc., Ph.D., A.R.I.C.

## SYNOPSIS

Corrosion tests have been carried out, by total immersion in salt solution, on samples of magnesium alloys containing various amounts of phosphorus and other impurities. It is concluded that the corrosion-resistance of pure magnesium is reduced by the presence of phosphorus in amounts over about 0.002%, but that this effect can be suppressed by addition of manganese. With a normal iron content, the adverse effect of phosphorus is not suppressed by manganese. Phosphorus also exerts a marked adverse effect on the corrosion-resistance of high-purity Elektron A8 (aluminium 8, zinc 0.4, manganese 0.25%, remainder magnesium).

The amount of phosphorus that can be introduced into magnesium is much greater in the presence of iron. Phosphorus increases iron pick-up in remelting A8 alloy.

Phosphorus is precipitated from magnesium by zirconium, and the corrosion-resistance of alloys containing zirconium is unaffected by phosphorus present in the metal used for their preparation.

## I.—INTRODUCTION

AN important study of factors affecting the corrosion-resistance of magnesium and its alloys has been made by Hanawalt, Nelson, and Peloubet.<sup>1</sup> This showed the general nature of the adverse effects of iron and nickel on corrosion-resistance, the existence of tolerance limits, and the manner in which the positions of these limits can be modified by the presence of aluminium, zinc, and manganese.

From the work of these authors it might be thought that, in order to prepare magnesium and its alloys in the state of highest corrosion-resistance, it would suffice to reduce the iron and nickel contents to below about 0.002% and 0.0005%, respectively, and to add sufficient manganese. This is by no means the case, however. Hanawalt, Nelson, and Peloubet were mainly concerned with the *total* quantities of impurities present, and the conditions of preparation of their samples, namely, slow cooling of the metal in a body of molten flux, were such as to favour settling out of insoluble particles. Since commercial alloys contain varying amounts of insoluble particles and may exhibit microporosity, a knowledge of the extent to which the presence of such defects can reduce corrosion-resistance is a matter of practical importance, and one which it is hoped to discuss in a later paper.

Except where otherwise stated, the present paper

refers to metal free from appreciable microporosity or abnormal numbers of particles. Even with such metal considerable variations in corrosion-resistance can occur; for instance, two samples of high-purity § Elektron A8 alloy, with iron and nickel contents below the limits mentioned above and containing 0.25% manganese, can differ in corrosion rate || by a factor of 100.

In considering the reasons for such large differences in corrosion-resistance, the possibility naturally arises that there may be other elements besides iron and nickel that can exert adverse effects. Comparative analyses for metallic impurities of samples of high-purity A8 of widely differing behaviour yielded no indications that any of the impurities detected might be harmful. Some circumstantial evidence suggested, however, that phosphorus might be a factor in determining corrosion-resistance. In particular, it was observed that the lowest corrosion rates obtained with A8 alloy prepared from electrolytic magnesium containing 0.015–0.025% phosphorus were appreciably higher than the lowest rates for the same alloy made from either ferro-silicon magnesium or electrolytic magnesium of very low phosphorus content; there was, however, little difference in average corrosion rate between the alloys made from these two grades of magnesium, at any rate on a production scale. It was accordingly decided to investigate the effect of phosphorus on corrosion-resistance, and an account

\* Manuscript received 13 November 1950.

† Metallurgist, Magnesium Elektron, Ltd., Clifton Junction, nr. Manchester.

‡ Chief Metallurgist, Magnesium Elektron, Ltd.

§ It is convenient to use this term to designate Elektron A8

of low iron and nickel contents.

|| Statements concerning corrosion-resistance and corrosion-rate figures in the present paper refer to weight loss (mg./cm.<sup>2</sup>/day) during 28 days' complete immersion in 3% NaCl solution saturated with Mg(OH)<sub>2</sub>.



of the work done and results obtained is given below.

## II.—INTRODUCTION AND REMOVAL OF PHOSPHORUS

In endeavouring to prepare corrosion specimens which would show unequivocally the effect of phosphorus, it was necessary to find a method of introducing the phosphorus without appreciable iron pick-up. Direct use of red phosphorus, even in conjunction with graphite crucibles and melting tools, proved unsatisfactory, and finally the phosphorus was introduced by plunging into the metal a mixture of A.R. calcium phosphate with sufficient Melrasal Z flux to control burning. This process had to be carried out in graphite crucibles using graphite plunging tools, as otherwise iron pick-up was excessive even at low temperatures, and it appeared that the presence of phosphorus in magnesium appreciably increased iron pick-up from mild-steel crucibles.

### 1. SOLUBILITY OF PHOSPHORUS IN MAGNESIUM

Using graphite crucibles and tools, the maximum amount of phosphorus that can be introduced into pure magnesium at normal operating temperatures is about 0.09%. If, however, iron crucibles are used,

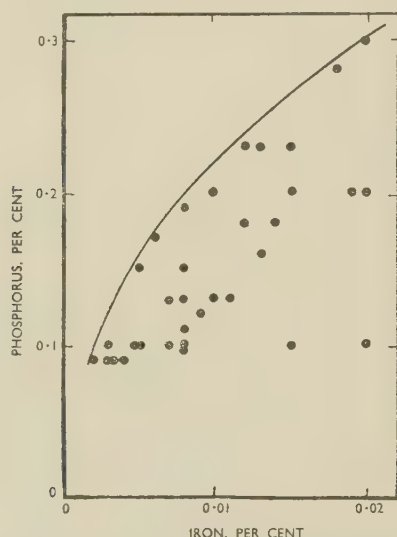


FIG. 1.—Relation Between Phosphorus and Iron Content for Melts Containing More Than 0.08% Phosphorus.

phosphorus contents up to about 0.4% can be achieved, introduction of the extra phosphorus being accompanied by iron pick-up. For each phosphorus content above about 0.09%, a *minimum* iron content is found (see Fig. 1), indicating some association of iron and phosphorus in the molten alloy. This is further confirmed by the observation that, in the presence of much phosphorus, removal of iron from A8 by addition of manganese and settling is incomplete.

With phosphorus contents above about 0.03%, small cavities are present in the solidified alloys (Figs. 2-5, Plate VII), and, from the number and size of these, the phosphorus content can be roughly estimated. The cavities are mentioned by Vosskühler,<sup>2</sup> but not by Bulian and Fahrenhorst,<sup>3</sup> who found in alloys containing phosphorus a constituent resembling  $Mg_2Si$  in habit which they attributed to the compound  $Mg_3P_2$ . In addition to these small cavities, metal saturated with phosphorus may develop considerable piping on solidification (Figs. 6 and 7, Plate VII), inflammable vapour, apparently phosphorus, being evolved. From the uniform distribution of cavities in metal containing phosphorus, it appears that the latter is largely in solution in the molten magnesium; and with less than 0.09% phosphorus and in the absence of more than about 0.002% iron, little analytical evidence of segregation has been obtained. With high phosphorus and iron contents, some segregation of phosphorus can occur in the molten alloy, especially if the melt is settled with the top kept hotter than the bottom to minimize convection; irregular phosphorus segregation in the solid metal is frequent. Repeated fluxing of magnesium with a high phosphorus content was found to reduce the phosphorus to about 0.1%. Treatment with a fully chlorinated hydrocarbon, such as hexachlorethane, does not remove phosphorus.

From the foregoing observations it appears probable that phosphorus can be present in molten magnesium, both in the dissolved state and as an insoluble complex with iron.

### 2. REMOVAL OF PHOSPHORUS BY PRECIPITATION AND SETTLING

The introduction into magnesium of zirconium and certain other of the less-common elements causes precipitation of any phosphorus present. With zirconium the phosphorus is precipitated in the form of insoluble zirconium-phosphorus particles. If the full zirconium content is not added, or if it is added and the metal is subsequently remelted, the precipitated phosphorus settles out to give a final content of not more than 0.002%. The phosphorus content of zirconium-containing alloys when the full zirconium content is added in one stage may be somewhat higher, e.g. 0.004%, presumably because settling of the precipitated phosphorus is less complete in the more viscous alloy.

When it is desired to remove phosphorus without leaving residual zirconium dissolved in the metal, the dephosphorization may be performed by adding a few per cent. of a zirconium-aluminium master alloy. This is itself insoluble in magnesium and forms insoluble particles on which the phosphorus precipitates and which are easily removed by settling. Dephosphorization without leaving residual precipitant in the final metal can also be effected by additions of rare-earth metals, the excess being removed by fluxing.

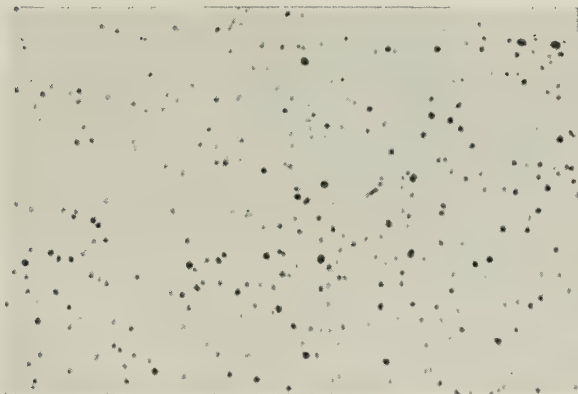


FIG. 2.—Polished Section of Magnesium Containing 0.2% P, 0.02% Fe, Showing Numerous Cavities. Unetched.  $\times 50$ .

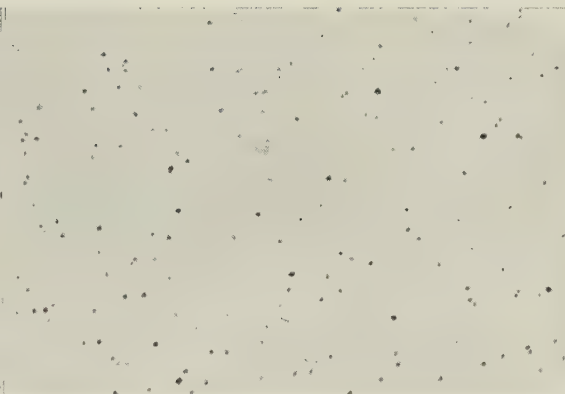


FIG. 3.—Section of Same Metal after Remelting and Repeated Fluxing. P = 0.1%. Unetched.  $\times 50$ .



FIG. 4.—Same Metal Polished Electrolytically.  $\times 1000$ .



FIG. 5.—Cavity Showing a Triangular Facet.  $\times 1000$ .



FIG. 6.—Ingot Poured at 750° C. from a Melt of Magnesium Saturated with Phosphorus, Showing Extensive Areas of Oxidation and General "Gassy" Appearance.  $\times \frac{1}{2}$ .

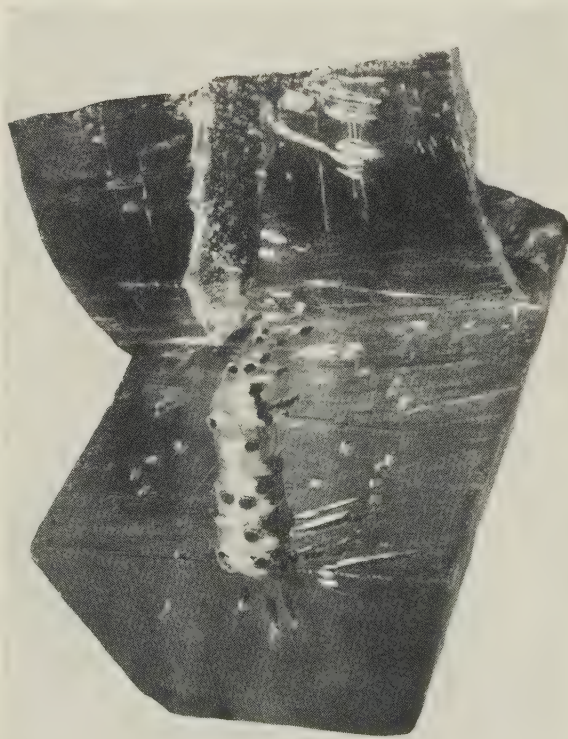


FIG. 7.—Horizontal Section Through the Same Ingot Showing Extensive Piping.  $\times 1$ .





## III.—CORROSION TEST METHODS

## 1. MATERIALS

The magnesium used in preparing the corrosion test specimens was made by the ferro-silicon process and its chemical composition was as follows :

Fe, %	P, %	Ni, %	Al, %	Ca, %	Cu, %	Mn, %	Na, %	Pb, %	Si, %	Zn, %
<0.002*	Up to 0.0004	0.005	0.005	0.002	0.002	0.003	0.01	0.001	0.002	<0.01
	0.005									

\* For most of the work magnesium containing less than 0.002% iron was selected. When difficulty was found in preparing samples rich in phosphorus with iron contents below 0.003%, subsequent "blank" and low-phosphorus melts were made from ferro-silicon magnesium with an initial iron content exceeding 0.002%. This appeared to be essential in order to avoid possible confusion of the effects of iron and phosphorus on the corrosion rates.

The aluminium and zinc used were of 99.99% purity. Manganese was added as  $\text{MnCl}_2$  (iron content 0.2%) or, where small amounts were required, as a magnesium-manganese hardener alloy made from  $\text{MnCl}_2$ . Phosphorus was added either directly as A.R. quality  $\text{Ca}_3(\text{PO}_4)_2$  mixed with Melrasal Z flux or as a hardener alloy with magnesium. Dephosphorization, where required, was carried out by means of a zirconium-aluminium master alloy or, in a few cases, with rare-earth metals.

## 2. MELTS

The following series of virgin melts with varying phosphorus contents were prepared in graphite crucibles on a 10-lb. scale, the phosphorus being added either directly as  $\text{Ca}_3(\text{PO}_4)_2$  or as a hardener alloy made in graphite crucibles :

Series A : Magnesium with low iron and varying manganese content.

Series B : Magnesium with at least 0.01% iron † and 0.2% manganese.

Series C : High-purity Elektron A8.

In addition, a further series was made as follows :

Series D : Remelts of high-purity A8 (prepared on a 250-lb. scale in steel crucibles) with phosphorus added as a hardener alloy made in steel crucibles.

## 3. SPECIMENS

Melts were cast into horizontal chill bar moulds of "keyhole" section to ensure maximum soundness and uniformity of composition of the three specimens into which each bar was machined. The analyses quoted relate to metal immediately adjacent to that from which the test specimens were taken. The analytical methods used are described elsewhere.<sup>7</sup>

Cylindrical specimens, approximately 0.7 in. dia.  $\times$  1½ in. long, were turned from the bar and cleaned with

moist pumice powder before immersion in the corrosion bath. This consisted of 3% NaCl solution saturated with  $\text{Mg}(\text{OH})_2$ . Cleaning of specimens after removal from the bath was effected by thorough washing with water and immersion in boiling chromic acid saturated with  $\text{Ag}_2\text{CrO}_4$ . By this means it was possible to remove practically all the corrosion product without dissolving any metal.

The immersion period was 28 days in all cases, and wherever possible all the specimens in one series were corroded at the same time in one bath. Where more than one bath was employed, the specimens in each were representative of the whole composition range of the series. To check that comparable corrosion rates were obtained irrespective of the bath used, separate tests were made on specimens all cut from the same piece of Elektron ZW3 sheet, and also on specimens cut from cast ZW3 slab made by the direct-chill process and known, from previous work, to have uniform corrosion rates. The average results on six pieces of sheet in each bath obtained in three separate and successive tests, and on four pieces of the slab in

TABLE I.—Variations in Corrosion Rate of ZW3 Alloy Due to Bath Used, and Range of Corrosion Rates among Similar Specimens.

Bath No.	Sheet			Direct-Chill-Cast Slab		
	No. of Specimens	Corrosion Rate, mg./cm. <sup>2</sup> /day		No. of Specimens	Corrosion Rate, mg./cm. <sup>2</sup> /day	
		Average	Max. and Min.		Average	Max. and Min.
1	6	0.335	0.431-0.276	4	0.167	0.249-0.135
2	6	0.408	0.472-0.314	4	0.197	0.262-0.124
3	6	0.264	0.313-0.204	4	0.170	0.190-0.142
4	6	0.263	0.294-0.224	4	0.145	0.156-0.129

a test made many months earlier, are given in Table I. The table also gives the maximum and minimum values for the specimens in each bath, showing the degree of variation commonly found between nominally identical specimens.

## IV.—DISCUSSION OF CORROSION TESTS

The results of the corrosion tests are given in Tables II–V and Figs. 8–10. Although the results on individual melts exhibit wide scatter, plots of corrosion rate against phosphorus content for each series disclose, in all cases except that of magnesium containing over 0.2% manganese, tendencies for the corrosion rate to increase with phosphorus content. These trends, shown on a single diagram in Fig. 10, are also evident from inspection of the mean results for each of the groups into which the tables have for convenience been divided (see also Fig. 9).

† Electrolytic magnesium contains at least 0.01% iron. Remelting of pure ferro-silicon magnesium once or twice in the usual steel crucibles increases the iron content to a similar

figure. The solubility of iron in magnesium appears to be about 0.025% at 650° C.<sup>4-6</sup>



TABLE II.—Effect of Phosphorus on the Corrosion Rate of Magnesium with Varying Manganese Content (Series A).

Virgin melts in 10-lb. graphite crucibles.

Range of Manganese Content, %	Range of Phosphorus Content, %	Melt No.	Chemical Analysis			Corrosion Rate, mg./cm. <sup>2</sup> /day	
			Fe, %	Mn, %	P, %	Mean of 3 Specimens	Range
0-0.05	<0.002	A1	0.004	0.004	0.001 *	0.117	0.096-0.155
		A2	0.005	0.027	<0.001	0.226	0.146-0.314
		A3	0.003	0.005	0.001	0.128	0.117-0.135
		A4	0.003	0.004	0.001 *	0.199	0.154-0.234
		A5	0.006	0.006	0.001	0.396	0.348-0.423
		A6	0.006	0.004	0.001	0.082	0.062-0.103
		Mean	0.0045	0.008	0.001	0.19	
	0.002-0.01	A7	0.003	0.005	0.002 *	4.790	4.48-5.15
		A8	0.005	0.032	0.002 *	0.388	0.276-0.501
		A9	0.002	0.040	0.003 *	1.997	1.845-2.221
		A10	0.002	0.004	0.008 *	5.100	4.67-5.52
		A11	0.005	0.028	0.007	0.590	0.572-0.612
		Mean	0.0034	0.022	0.0044	2.57	
	>0.01	A12	0.002	0.050	0.014	1.547	1.355-1.793
		A13	0.003	0.005	0.045	0.316	0.298-0.343
		A14	0.004	0.029	0.031	5.480	5.03-5.92
		A15	0.004	0.005	0.040	0.700	0.503-0.812
		A16	0.004	0.004	0.090	0.371	0.327-0.454
		Mean	0.0034	0.019	0.044	1.67	
0.051-0.2	<0.002	A17	0.004	0.084	<0.001	0.119	0.103-0.137
		A18	0.002	0.160	<0.001	0.083	0.080-0.086
		A19	0.002	0.150	<0.001 *	0.054	0.051-0.058
		Mean	0.0027	0.131	<0.001	0.085	
	0.002-0.01	A20	0.003	0.080	0.003 *	1.442	1.315-1.561
		A21	0.002	0.140	0.002	0.082	0.068-0.090
		A22	0.004	0.170	0.003 *	0.771	0.716-0.853
		Mean	0.003	0.130	0.0026	0.77	
	>0.01	A23	0.003	0.070	0.012	0.326	0.275-0.372
		A24	0.003	0.100	0.015	2.270	1.969-2.572
		A25	0.004	0.085	0.020	0.178	0.158-0.205
		A26	0.003	0.090	0.099	0.318	0.268-0.343
		A27	0.003	0.070	0.091	0.198	0.194-0.201
		A28	0.003	0.090	0.052	0.300	0.211-0.429
		A29	0.005	0.085	0.066	1.135	0.954-1.429
		A30	0.003	0.140	0.016	3.660	1.99-6.08
		A31	0.003	0.140	0.061	0.168	0.167-0.171
		Mean	0.0033	0.097	0.043	0.95	
>0.2	<0.002	A32	0.006	0.300	<0.001 *	0.385	0.348-0.432
		A33	0.004	0.650	<0.001 *	0.170	0.153-0.181
		A34	0.004	0.310	0.001	0.084	0.060-0.098
		Mean	0.0047	0.420	<0.001	0.21	
	0.002-0.01	A35	0.002	0.410	0.002 *	0.142	0.106-0.197
		A36	0.003	0.850	0.002 *	0.075	0.041-0.101
		A37	0.004	0.660	0.002	0.153	0.140-0.172
		A38	0.004	0.330	0.004 *	0.355	0.318-0.393
		A39	0.004	0.610	0.004 *	0.210	0.197-0.230
		Mean	0.0034	0.572	0.0028	0.19	
	>0.01	A40	0.004	0.220	0.016	0.614	0.402-0.900
		A41	0.004	0.300	0.015	0.079	0.062-0.089
		A42	0.006	0.650	0.033	0.083	0.057-0.107
		A43	0.003	0.290	0.065	0.213	0.162-0.273
		A44	0.006	0.660	0.068	0.061	0.031-0.080
		Mean	0.0046	0.424	0.039	0.21	

\* Prepared from ferro-silicon metal after dephosphorization with zirconium-aluminum alloy.

## 1. MAGNESIUM AND MAGNESIUM-MANGANESE ALLOY (SERIES A AND B)

From the results for Series A melts (Table II and Figs. 9 (a)-(c)) the following tentative conclusions can be drawn:

(i) Phosphorus has an adverse effect on the corrosion-resistance of pure magnesium.

(ii) The "tolerance limit" for phosphorus is about 0.002% (Fig. 8).

(iii) Addition of manganese suppresses the effect of phosphorus.

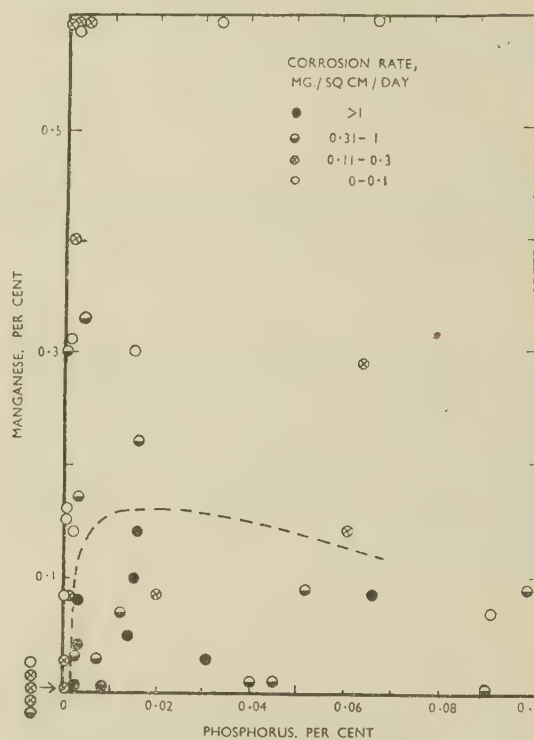


Fig. 8.—Effect of Phosphorus and Manganese on the Corrosion-Resistance of Magnesium.

The point nearest the origin represents the five melts indicated in the margin, which could not be plotted separately in the available space.

All melts with a corrosion rate exceeding 1 mg./cm.<sup>2</sup>/day lie within the marked area.

TABLE III.—Effect of Phosphorus on the Corrosion-Resistance of Magnesium Containing at Least 0.01% Iron and 0.2% Manganese (Series B).

Virgin melts in 10-lb. mild-steel crucibles.

Range of Phosphorus Content, %	Melt No.	Chemical Analysis			Corrosion Rate, mg./cm. <sup>2</sup> /day	
		Fe, %	Mn, %	P, %	Mean of 3 Specimens	Range
<0.005	B1	0.06	0.29	<0.002	0.601	0.551-0.673
	B2	0.06	0.29	<0.002	1.185	1.042-1.258
	B3	0.01	0.41	0.003	0.230	0.178-0.330
	Mean	0.043	0.33	0.002	0.67	
0.01-0.025	B4	0.015	0.36	0.012	1.43	0.610-2.32
	B5	0.024	0.33	0.023	1.68	1.46-2.03
	B6	0.015	0.25	0.023	1.79	1.500-1.975
	B7	0.024	0.33	0.023	2.45	1.951-3.405
	Mean	0.020	0.32	0.02	1.84	
>0.025	B8	0.015	0.21	0.033	5.07	2.162-9.250
	B9	0.02	0.28	0.06	7.45	1.85-10.89
	B10	0.02	0.28	0.06	12.20	10.67-13.78
	B11	0.018	0.23	0.08	2.19	1.73-2.46
	B12	0.018	0.24	0.17	2.13	1.68-2.60
	B13	0.018	0.20	0.19	11.10	8.42-13.15
	Mean	0.018	0.24	0.098	6.67	

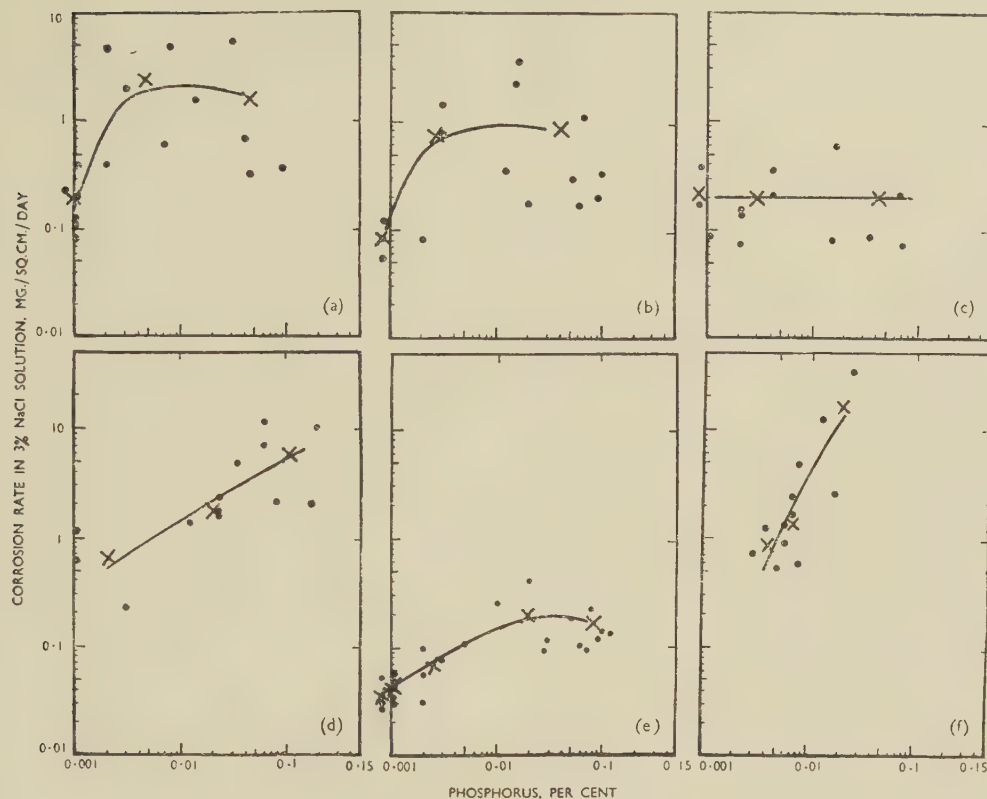


Fig. 9.—Effect of Phosphorus Content on Corrosion-Resistance.

- (a)–(c) Series A: Magnesium containing (a)  $<0.05\%$  Mn; (b)  $0.05$ – $0.2\%$  Mn; (c)  $>0.2\%$  Mn.  
 (d) Series B: Magnesium containing at least  $0.01\%$  Fe and  $0.2\%$  Mn.  
 (e) Series C: High-purity A8 (phosphorus added as pure  $\text{Ca}_3(\text{PO}_4)_2$ ).  
 (f) Series D: High-purity A8 (phosphorus added as hardener made in steel crucible).

● Individual melts.

× Grouped mean results.

The Series B results (Table III and Fig. 9 (d)) further indicate:

(iv) That when the iron content is “normal”, phosphorus exerts an adverse effect even with  $\frac{1}{4}\%$  manganese present.\*

It will be seen that, despite the use of graphite crucibles and tools, some iron pick-up occurred during preparation of the series A melts, five melts in particular containing as much as  $0.006\%$  iron. None of these shows a high corrosion rate, and it is evident that iron pick-up does not invalidate the results by itself contributing to the observed deterioration in corrosion-resistance which accompanies the introduction of phosphorus. This is in accordance with the high tolerance limit of pure magnesium for iron ( $0.017\%$ ) found by Hanawalt, Nelson, and Peloubet,<sup>1</sup> and the observation by Fox, Bushrod, and Mayer<sup>8</sup> that the corrosion-resistance of Elektron AM503 alloy (magnesium– $1.5\%$  manganese) is independent of the iron content.

The mean figure of  $0.19 \text{ mg./cm.}^2/\text{day}$  found for

magnesium of low iron, manganese, and phosphorus contents accords well with Hanawalt's figure of  $0.15 \text{ mg./cm.}^2/\text{day}$  for pure magnesium, obtained by intermittent as opposed to total immersion in salt solution. In general, however, the two forms of test are not dissimilar in effect,<sup>9</sup> and the values are found to be comparable, probably because of the short time of immersion in Hanawalt's test, which is too short to permit much draining, still less drying, of the specimen.

In view of the variable phosphorus content of the ferro-silicon magnesium available for the tests (up to  $0.005\%$ ), some of the melts were prepared from magnesium dephosphorized with zirconium–aluminum alloy, to assist in the control of phosphorus content in the lower ranges. These melts are indicated in Table II. The evidence available indicates that the dephosphorization process is without appreciable effect on the corrosion rate for a given phosphorus content. This has been verified on a large scale, a rate of  $0.16 \text{ mg./cm.}^2/\text{day}$ † being obtained for magnesium so dephosphorized, in agreement with the figure of about  $0.2 \text{ mg./cm.}^2/\text{day}$  found for the un-

\* Addition of several per cent. of manganese might, of course, suppress the effect of phosphorus in this case also.

† Mean of eight results ranging from  $0.12$  to  $0.18 \text{ mg./cm.}^2/\text{day}$ .



TABLE IV.—Effect of Phosphorus on the Corrosion-Resistance of High-Purity A8 (Series C).

Phosphorus added as pure  $\text{Ca}_3(\text{PO}_4)_2$  to 10-lb. virgin melts of A8 in graphite crucibles.

Range of Phosphorus Content, %	Melt No.	Chemical Analysis						Corrosion Rate, mg./cm. <sup>2</sup> /day	
		Al, %	Zn, %	Mn, %	Fe, %	Ni, %	P, %	Mean of 3 Specimens	Range
<0.001	C1	7.4	0.52	0.31	0.004	0.0002	<0.001 †	0.028	0.025–0.031
	C2	7.7	0.49	0.29	0.005	0.0003	<0.001 ‡	0.031	0.024–0.036
	C3	7.5	0.41	0.30	0.003	N.D.	<0.001 †	0.035	0.026–0.047
	C4	7.7	0.49	0.37	0.005	N.D.	<0.001 ‡	0.054	0.039–0.067
	Mean	...	...	...	0.004	0.0003	<0.001	0.037	
0.001	C5	7.9	0.62	0.40	0.0035	0.0004	0.001 †	0.031	0.024–0.039
	C6	7.4	0.59	0.33	0.0035	0.0004	0.001 ‡	0.032	0.026–0.039
	C7	8.2	0.49	0.38	0.005	0.0004	0.001 †	0.048	0.038–0.057
	C8	7.4	0.54	0.32	0.004	0.0004	0.001	0.045	0.035–0.061
	C9	7.6	0.55	0.45	0.0035	0.0004	0.001	0.056	0.040–0.075
	Mean	...	...	...	0.004	0.0004	0.001	0.042	
0.002–0.003	C10	7.4	0.51	0.36	0.0035	0.0004	0.002	0.031	0.031–0.032
	C11	7.5	0.45	0.36	0.0035	0.0004	0.002	0.056	0.045–0.077
	C12	7.2	0.41	0.40	0.005	N.D.	0.002 ‡	0.100	0.068–0.118
	C13	7.0	0.44	0.22	0.003	N.D.	0.003 †	0.078	0.065–0.105
	Mean	...	...	...	0.004	0.0004	0.0025	0.066	
0.005–0.03	C14	7.5	0.49	0.25	0.002	N.D.	0.005 †	0.111	0.067–0.162
	C15	7.7	0.51	0.22	0.004	N.D.	0.010	0.254	0.197–0.329
	C16	7.5	0.52	0.22	0.004	N.D.	0.02	0.409	0.187–0.531
	C17	7.5	0.48	0.28	0.005	0.0004	0.03	0.092	0.082–0.103
	C18	8.0	0.57	0.33	0.0045	0.0004	0.03	0.115	0.089–0.156
	Mean	...	...	...	0.004	0.0004	0.019	0.20	
>0.03	C19	7.7	0.70	0.35	0.005	0.0004	0.05	0.186	0.090–0.322
	C20	9.0	0.57	0.40	0.005	0.0004	0.06	0.103	0.046–0.202
	C21	8.8	0.72	0.48	0.005	N.D.	0.07	0.095	0.060–0.114
	C22	7.0	0.52	0.36	0.005	N.D.	0.08	0.224	0.198–0.263
	C23	7.2	0.32	0.31	0.005 *	0.0002	0.08	2.75	2.48–3.03
	C24	7.8	0.55	0.39	0.005	N.D.	0.09	0.118	0.097–0.148
	C25	4.3	0.31	0.47	0.005	N.D.	0.10	0.139	0.126–0.154
	C26	7.8	0.50	0.25	0.004	N.D.	0.12	0.131	0.090–0.162
	Mean	...	...	...	0.005	0.0004	0.081	0.14 §	

N.D. = Not determined.

\* Confirmed by analyses on the test specimen after corrosion.

† Melts dephosphorized with zirconium–aluminium alloy.

‡ Melts dephosphorized with Mischmetall (rare-earth metals of the cerium group).

§ Excluding Melt C23, the corrosion rate of which appeared to be anomalous.

treated pure magnesium. Table IV suggests that this dephosphorization process is without appreciable effect in the case of high-purity A8 also.

The fact that when the iron content is high the presence of  $\frac{1}{4}\%$  manganese does not suppress the adverse effect of phosphorus, appears to confirm earlier indications of the possible existence in magnesium of some iron–phosphorus complex.

## 2. ELEKTRON A8 (SERIES C AND D)

Results from series C (Table IV and Fig. 9 (e)) show a broad correlation of corrosion rate with phosphorus content, but none with that of any of the other constituents over the composition range covered. Neither of the processes employed for removing phosphorus appears to have affected the corrosion-resistance appreciably. (One melt with an ano-

malously high corrosion rate (2.75 mg./cm.<sup>2</sup>/day) has been excluded in calculating the mean rate for the appropriate group and also in drawing Fig. 9 (e); this is discussed later.)

The corrosion rates for the low-phosphorus high-purity A8 average less than one-fifth that of pure magnesium and are therefore very low indeed. Since the iron contents of these specimens extend to 0.005%, it must be assumed that the tolerance limit for iron in magnesium containing 8% aluminium is considerably higher than the figure of 0.002% given by Hanawalt, Nelson, and Peloubet,<sup>1</sup> at least in the presence of a few tenths per cent. of zinc. They reported that 0.5% zinc was without effect on the position of the iron tolerance limit but that 3% zinc raised it to 0.003%.

Corrosion rates from series D (Table V and Fig. 9 (f)) also show a broad correlation with phosphorus

TABLE V.—Effect of Phosphorus on the Corrosion-Resistance of High-Purity A8 (Series D).

Phosphorus added as a magnesium-phosphorus hardener alloy made in steel crucibles to 10-lb. melts in graphite crucibles of A8\* ingot made on a 250-lb. scale in steel crucibles and dephosphorized with zirconium.

Range of Phosphorus Content, %	Melt No.	Chemical Analysis			Corrosion Rate, mg./cm. <sup>2</sup> /day		
		Fe, %	Ni, %	P, %	No. of Specimens	Mean	Range
0-0.005	D1	0.004	0.0002	0.003	3	0.745	0.675-0.705
	D2	0.004	0.0002	0.004	2	1.298	0.655-1.94
	D3	0.003	0.0002	0.005	3	0.544	0.410-0.718
	Mean	0.004	0.0002	0.004		0.86	
0.006-0.01	D4	0.004	0.0002	0.006	2	0.90	0.726-1.09
	D5	0.003	0.0002	0.006	4	1.40	1.18-1.67
	D6	0.004	0.0002	0.007	5	1.69	1.25-1.98
	D7	0.004	0.0002	0.007	2	2.55	1.71-3.38
	D8	0.003	0.0003	0.008	4	0.59	0.151-1.30
	Mean	0.004	0.0002	0.007		1.43	
>0.01	D9	0.004	0.0002	0.013	5	13.10	11.9-11.4
	D10	0.004	0.0003	0.018	5	2.67	2.14-3.60
	D11	0.004	0.0003	0.026	5	37.20	36.2-38.6
	Mean	0.004	0.0003	0.019		17.7	

\* Composition of parent material: Al 7.6, Zn not determined (nominal 0.4), manganese 0.08%, magnesium remainder.

TABLE VI.—Comparative Corrosion Rates of High-Purity A8 Prepared on a Medium Scale in Mild-Steel and Graphite-Lined Carborundum Crucibles.

Crucible		Melt No.	Chemical Analysis			Corrosion Rate, mg./cm. <sup>2</sup> /day †
Material	Scale, lb.		Fe, %	Ni, %	P, %	
Mild steel	250	251B2	0.002	0.0005	<0.001	0.78
		420B	<0.002	0.0009	<0.002	0.98
		434B	0.001	0.0005	0.001	1.16
		469B	0.001	0.0006	<0.001	0.30
		470B	0.001	0.0003	<0.001	0.37
		505B	<0.001	0.0008	<0.001	0.22
		579B	<0.001	0.0007	<0.001	0.17
"Tercod" (graphite-lined carborundum)	100	554B	0.001	0.0004	0.002	0.049
		498B	0.0015	0.0003	0.002*	0.078

\* Melt dephosphorized with zirconium-aluminum alloy.

† Mean of 4 specimens.

content, but are much higher than those of series C for the same composition. One reason for these higher results might at first sight be taken to be the lower manganese content (0.08%) of the parent material, removal of some manganese having accompanied the dephosphorization process. On the other hand, Hanawalt, Nelson, and Peloubet<sup>1</sup> state that "a few hundredths per cent." of manganese is sufficient to raise the very low iron tolerance limit observed in the presence of aluminium to 0.002% for any aluminium content; and in the present work very low corrosion rates have been obtained with remelted dephosphorized high-purity A8 containing only 0.09% manganese.\* Moreover, the corrosion rates for the

low-phosphorus alloys of Table V are normal for high purity A8 of full manganese and negligible phosphorus contents made in 250-lb. steel crucibles (Table VI). It appears, therefore, that the higher corrosion rates of series D must be attributed at least partly to some factor associated with the scale of working or crucible material employed. Intensification of the adverse effect of phosphorus may result from addition of phosphorus as a hardener made in a mild-steel crucible and therefore probably existing as a phosphorus-iron complex. At the same time the low manganese content may have accentuated the adverse effect of the phosphorus.

Analysis and microscopic examination of the corroded test specimen of the anomalous melt C23 (Table IV) failed to show any reason for the high rate. The latter is intermediate between those of series C and D for the same phosphorus content, and the simplest explanation appears to be that part of the phosphorus was for some reason present in the same state as in the series D melts, i.e. probably as a complex with iron.† Although this melt has been excluded from the group mean, its implications are considered important, and further work on the matter is in progress.

It is interesting to note that the corrosion rates from series C (with phosphorus added in graphite crucibles) and series D melts (with phosphorus added in mild-steel crucibles) lie, in general, respectively below and above the figure of 0.2 mg./cm.<sup>2</sup>/day representing pure magnesium. A similar difference is found between the corrosion rates of high-purity A8 made in graphite and steel crucibles when a medium scale is employed (Table VI).

### 3. ALLOYS CONTAINING ZIRCONIUM

As already indicated, zirconium is a precipitant for phosphorus, and in commercial alloys containing zirconium the phosphorus content is below 0.005%. No indications have been obtained of any effect of phosphorus on the corrosion-resistance of alloys containing zirconium. This is to be expected, since the phosphorus is present in combination with zirconium in the form of insoluble particles and is thus analogous to iron, which in zirconium alloys is present as zirconium-rich particles and does not appreciably affect corrosion-resistance.

### V.—EFFECT OF PHOSPHORUS ON IRON PICK-UP IN THE REMELTING OF A8 IN MILD-STEEL CRUCIBLES

In view of the existence of a tolerance limit for iron in high-purity A8 alloy, the question of iron pick-up on remelting the alloy in the usual mild-steel crucibles is one of considerable practical importance.

\* Corrosion rate 0.055 mg./cm.<sup>2</sup>/day (mean of four results ranging from 0.018 to 0.097 mg./cm.<sup>2</sup>/day).

† The abnormally high degree of scatter in corrosion rate shown by melts (as distinct from individual test specimens) in

the present investigation, and, in particular, the tendency for scatter to increase with increasing phosphorus content, may also be attributable to variations in the state of the phosphorus.



The subject has been studied by Fox, Bushrod, and Mayer,<sup>8</sup> who called attention to the existence of a "seasoning" effect, as a result of which iron pick-up decreases on successive remeltings in the same crucible until, after two or three melts have been made, a roughly constant low iron pick-up occurs. This seasoning of the surface of the crucible is accompanied by decarburization and pick-up of aluminium and magnesium in the surface layers.\* Further work has shown that the seasoned surface deteriorates if the crucible is allowed to stand empty for a day or two, probably owing to the absorption of moisture by residual flux adhering to the crucible walls. Washing the crucibles also destroys the "seasoning". Even with seasoned crucibles, occasional melts high in iron are obtained at temperatures around 800° C. and above. This is no doubt due to local flaking off of the seasoned surface, leaving an area of unseasoned steel exposed to the magnesium.

In view of the probable existence of phosphorus as a complex with iron and the difficulty found in preparing high-phosphorus alloys with low iron content, experiments were made on the effect of phosphorus on iron pick-up in well-seasoned mild-steel crucibles. The results (Table VII) show that the effect is indeed pronounced.

TABLE VII.—Effect of Phosphorus on Iron Pick-Up in Remelting A8 in Seasoned Mild-Steel Crucibles.

(10-lb. Scale)

Phosphorus, %	Melting Cycle	Useful Life of Seasoned Surface *	Average Iron Pick-Up per Remelt, %
<0.001	Held for 30 min. at 800° C.	>12	0.0003
0.02	" " "	2	0.001
0.09	" " "	Nil	0.008

\* That is, number of consecutive melts with iron pick-up <0.002%.

TABLE VIII.—Effect of Remelting on Iron Content of A8.

Melt No.	Crucible		Chemical Analysis			Iron Pick-Up, %
	Material	Scale, lb.	P, % Initial	Fe, %		
				Initial	Final	
B358	Mild steel	10	0.001	0.003	0.003	0
B362			0.001	0.004	0.0025	-0.0015
B363			0.001	0.004	0.0025	-0.0015
B1000			N.D.	0.0015	<0.001	-0.001
B361	Cr-Mn-Al steel	20	0.002	0.003	0.002	-0.001
B366			0.001	0.004	0.001	-0.003
B231			<0.001	0.003	0.003	0
B236			<0.001	0.003	0.003	0
B237			<0.001	0.003	0.005	+0.002
B134	Mild steel	250	0.0015	0.0015	0.0015	0

N.D. = not determined.

\* This led to the subsequent suggestion of C. J. Bushrod to add aluminium to high-chrome-manganese steel for use in melting magnesium, and subsequent work by J. K. Davies

Further work on remelting the low-phosphorus high-purity alloy has shown that if, instead of holding the melt at fairly high temperatures for a period, the melt is merely raised to 750° C., stirred for 1 min., and poured after standing for, say, 5 min., the iron content may, in fact, fall. Table VIII illustrates this.

## VI.—FINAL CONSIDERATIONS

The work described has shown that in addition to iron and nickel a third element, phosphorus, can exert a pronounced adverse effect on the corrosion-resistance of magnesium when present in trace amounts.

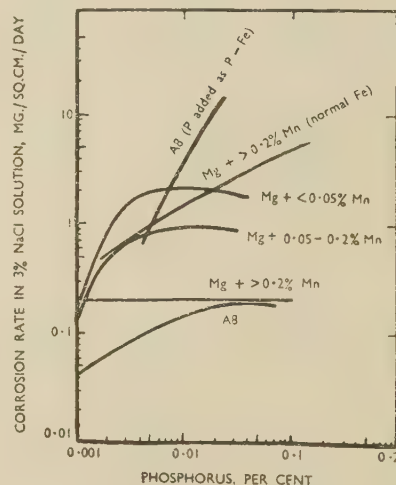


FIG. 10.—Effect of Phosphorus Content on Corrosion-Resistance.

From examination of the individual results, as well as the trends displayed in Fig. 10, it appears that corrosion discontinuities are less marked than with iron and nickel, the phenomena of sharp tolerance limits being not in general evident. The adverse effect of phosphorus shows, however, some analogies with that of nickel:

- (1) The most pronounced corrosion discontinuity occurs with magnesium alone.
- (2) The adverse effect is suppressed by manganese.
- (3) The adverse effect is not suppressed by manganese when aluminium is present.

The precise significance to be attached to the mutual effects of iron and phosphorus in promoting their entry into magnesium (Fig. 1 and Table VII) is not yet clear. It is possible that the solubility of iron in magnesium is increased in the presence of phosphorus and vice versa. On the other hand, some settling out of phosphorus and iron has been observed in the molten alloys, irrespective of whether the

and J. H. T. Petch has shown that such crucibles behave as if they were permanently in a "seasoned" condition.

phosphorus or the iron was introduced first into the magnesium; and this suggests the existence of some insoluble compound present in the molten alloy. The curve of Fig. 1 does not, however, represent a constant iron:phosphorus ratio, and the phosphorus increments, being between five and ten times the iron increments on an atomic basis, do not appear to correspond with likely compounds. Even higher phosphorus:iron ratios have been inferred from comparison of analyses taken from the top and bottom of settled melts. Unfortunately, it has not proved a simple matter to decide from metallographic evidence whether or not phosphorus and iron form a compound insoluble in the molten alloy. The cavities may be gas voids or, as suggested by Vosskühler,<sup>2</sup> they may be formed by the removal of soft particles during the polishing process. With mechanical polishing it is difficult to avoid partially filling cavities with polishing compound, and, with electrolytic polishing, cavities could arise through reaction of phosphide particles with the electrolyte. Very few of the particles described by Bulian and Fahrenheitst<sup>3</sup> and attributed to  $Mg_3P_2$  have been seen in any of the alloys examined.

On the question of the difference in corrosion rates shown by the two series of A8 melts for a given phosphorus content, it has been suggested that this may be largely attributable to the presence of phosphorus in series *D* melts in the form of a complex with iron. If this complex is unstable, or if a supersaturated solution is involved, decomposition might occur on solidification with liberation of iron on subsequent remelting, the liberated iron then settling out under the combined action of aluminium and manganese in the ordinary way. A process of this type would explain the frequent drop in iron content on remelting A8 when the phosphorus content is low. As a consequence it would be expected that the corrosion rate would improve. This has, in fact, been verified and in certain circumstances the remelting of high-purity A8 in steel crucibles has been found to reduce the corrosion rate by a factor of up to one hundred. Such work, however, lies beyond the intended scope of the present paper, the main object of which is to call attention to the adverse effects which phosphorus can exert on the corrosion-resistance of magnesium and its alloys.

#### ACKNOWLEDGEMENTS

The authors' thanks are due to Mr. W. Unsworth for carrying out most of the melting work, to Mr. W. R. Braithwaite for making some of the corrosion tests, to Messrs. J. B. Wilson and D. R. Knowles for helpful discussions on statistical aspects of the results and for making the majority of the calculations involved, and to the Directors of Magnesium Elektron, Ltd., for permission to publish the paper.

## APPENDIX

### NOTE ON STATISTICAL ASPECTS OF THE CORROSION TEST RESULTS

#### *Table II (Series A: Effect of Phosphorus on Magnesium of Varying Manganese Content)*

The results do not show a significant\* product-moment correlation coefficient ( $r$ ) between phosphorus content and corrosion rate, nor a significant partial correlation coefficient when the effect of manganese is eliminated. On the other hand, if the true curve of corrosion rate against phosphorus should be sigmoid with a sharp tolerance limit, a significant correlation coefficient would not necessarily be expected. In such a case, however, there should be a significant difference between the test results from samples with phosphorus contents above and below the tolerance limit when tested by the "Student"  $t$  test for comparison of means.

If the first occurrence of corrosion rates above 1 mg./cm.<sup>2</sup>/day is taken as evidence that a tolerance limit has been exceeded (as appears reasonable from a study of the diagram in Hanawalt's<sup>1</sup> paper), then the tolerance limit for phosphorus in pure magnesium will lie between 0.001 and 0.002% (Fig. 8). Applying this tolerance limit to all the melts containing less than 0.2% manganese (Figs. 9 (a) and (b)), the corrosion test results on melts with higher and lower phosphorus contents are found to differ significantly ( $p = 0.02$ ). The same applies to the melts containing less than 0.05% manganese (Fig. 9 (a)), the lower degree of significance ( $p = 0.05$ ) being due to the smaller number of melts falling below the tolerance limit.

Treated separately, the melts with intermediate manganese content (Fig. 9 (b)) indicate a slightly higher phosphorus tolerance limit between 0.002 and 0.003%, and division of the group here yields a significant difference ( $p = < 0.001$ ). Hanawalt, Nelson, and Peloubet<sup>1</sup> found that the nickel tolerance limit was raised by manganese, and, in view of the general resemblance in behaviour between nickel and phosphorus already noted, the same might apply to the phosphorus tolerance limit.

With manganese content greater than 0.2% (Fig. 9 (c)), corrosion rates above 1 mg./cm.<sup>2</sup>/day were not obtained, and at no point is it possible to divide the melts into two groups so as to yield a significant  $t$  test. (With a division at 0.0015% phosphorus  $p = 0.9$ .)

#### *Table III. (Series B: Effect of Phosphorus on Magnesium Containing at Least 0.01% Iron and 0.2% Manganese)*

The correlation coefficient between phosphorus and corrosion rate is not significant ( $p = 0.1$ ). If the results are grouped into those with phosphorus content above and below 0.025%, so as to obtain as nearly as possible groups of equal size, application of

\* The level of significance adopted is a chance probability  $p$  of 0.05, i.e. a 1 in 20 possibility that the observed distribution is due to chance.



the  $t$  test shows a significant difference in the means ( $p = < 0.01$ ).

Table IV. (Series C: Effect of Phosphorus on A8)

If, for the reasons discussed on p. 29, melt C23 is excluded, the partial correlation coefficient between phosphorus content and corrosion rate with the effect of manganese eliminated is just significant ( $p = 0.05$ ).

Table V. (Series D: Effect of "Phosphorus-Iron" on A8)

The correlation coefficient between phosphorus content and corrosion rate is significant ( $p = < 0.01$ ). In this case the analytical values obtained for iron and nickel are sufficiently constant to make the derivation of the second-order partial correlation coefficient appear unnecessary.

#### REFERENCES

1. J. D. Hanawalt, C. E. Nelson, and J. A. Peloubet, *Trans. Amer. Inst. Min. Met. Eng.*, 1942, **147**, 273.
2. H. Vosskühler, see "Technology of Magnesium and Its Alloys" (A. Beck), p. 45. London: 1940 (F. A. Hughes and Co., Ltd.).
3. W. Bulian and E. Fahrenhorst, "Metallography of Magnesium and Its Alloys", p. 31. London: 1944 (F. A. Hughes and Co., Ltd.).
4. E. Fahrenhorst and W. Bulian, *Z. Metallkunde*, 1941, **33**, 31.
5. G. Siebel, *Z. Metallkunde*, 1948, **39**, 22.
6. D. W. Mitchell, *Trans. Amer. Inst. Min. Met. Eng.*, 1948, **175**, 570.
7. "Methods of Analysis of Magnesium and Its Alloys". London: 1946 (F. A. Hughes and Co., Ltd.).
8. F. A. Fox, C. J. Bushrod, and S. E. Mayer, *J. Inst. Metals*, 1947, **73**, 55.
9. L. F. Le Brocq, *J. Inst. Metals*, 1944, **70**, 594 (discussion).

# CREEP AND STRESS RUPTURE AS RATE PROCESSES \*

1322

By ITALO S. SERVI,† Dott., S.M., ScD., and N. J. GRANT,‡ B.S., ScD.

## SYNOPSIS

Creep data for an iron-cobalt-chromium-nickel alloy reported by Grant and Bucklin (*Trans. Amer. Soc. Metals*, 1950, **42**, 720) are analysed according to the rate-process theory of plastic flow. The data indicate that the theory can be applied over only a limited range of creep rates.

An empirical equation, which relates the applied stress and the temperature to the minimum creep rate, is suggested for the analysis of creep data. This equation is valid only in the absence of structural instabilities.

## I.—INTRODUCTION

THE phenomenon of creep in metals has long been of great scientific and practical interest. The literature shows that much effort has been expended in analysing each curve and in relating families of curves to establish fundamental relationships between the variables involved in creep. The primary scientific aim has been to obtain a better understanding of the mechanism of creep, whereas the aim of the engineer has been the prediction of strain, strain rate, and life as a function of temperature, stress, and history of the material.

One of the recent important basic studies has considered the flow of metals to be a deformation process which takes place when a "unit of flow" is excited to an activated state. Such units of flow consist of groups of atoms which pass over one another by a shear process. The size of each unit of flow is a characteristic of the material and depends also on the temperature of testing.

The "theory of activated complex" or "rate-process theory" was first proposed by Eyring<sup>1</sup> and was applied to chemical reactions only. It was later applied to studies of viscosity, plasticity, and diffusion,<sup>2</sup> and subsequently by Kauzmann<sup>3</sup> and Dushman, Dunbar, and Huthsteiner<sup>4</sup> to the flow of solid metals. According to this theory, the rate of shear is proportional to the rate at which the unit of flow crosses a free-energy barrier, which is a function of the applied shear stress. By introducing several simplifying assumptions, the following ultimate equation is obtained:

$$r = Me^{-\Delta F/RT} \sinh(Ns) \quad (1)$$

where

$r$  = minimum creep rate.

$s$  = applied tensile stress.

$T$  = absolute temperature.

$\Delta F$  = free energy of activation.

$R$  = gas constant per mole.

$M, N$  are constants, at constant temperature.

Since

$$\sinh(Ns) \cong \frac{e^{Ns}}{2}$$

when  $Ns$  is sufficiently large, equation (1) can be written:

$$\log r = \log r_0 + Ps \quad (2)$$

where  $r_0$  and  $P$  are constants at constant temperature.

A further contribution to the study of flow of metals was made by Nowick and Machlin,<sup>5</sup> who derived a new equation for the steady-state rate of creep through the use of the rate-process theory and of the dislocation theory.

In an effort to find a practical application of the rate-process theory, Machlin and Nowick<sup>6</sup> developed an equation from stress-rupture tests which relates the rupture life to the stress and the temperature. This equation is based upon the assumption that the rupture life is inversely proportional to the rate at which the unit of flow crosses the energy barrier. Their suggested analysis of the data was intended to permit both extrapolation and interpolation to longer test times and higher test temperatures.

One of the more important observations common to all these applications of the rate-process theory is that, according to equation (2), a straight line should be obtained when the applied tensile stress is plotted against the logarithm of the minimum creep rate or against the logarithm of the rupture life for each constant temperature of testing. Further speculation, including the calculation of the "size of unit flow" and the calculation of the "free energy" and "entropy of activation", was based upon the applicability of the creep law as expressed by equation (2).

It is interesting to note that the rate-process theory is consistent with the empirical law suggested by Ludwick.<sup>7</sup> Such semi-log relationships are not in agreement with the observed straight-line relationships between stress and minimum creep rate when the data are plotted on a log/log basis. Since considerable experimental evidence has accumulated over

\* Manuscript received 19 January 1951.

† Research Assistant, Massachusetts Institute of Technology, Cambridge, Mass., U.S.A.

‡ Associate Professor, Massachusetts Institute of Technology, Cambridge, Mass., U.S.A.



a long period of time that such straight-line log/log plots are real, it is difficult to reconcile theory and test data.

The purpose of the present paper is to demonstrate that the creep law expressed by equation (2) cannot be applied when the creep-rate data are extended over a considerably wider range of creep rates than has previously been examined. The creep-rate data recently published by Grant and Bucklin<sup>8</sup> for the S 590 \* alloy will be used for this purpose, since these data are much more extensive than any other appearing in the literature.

Before presenting a detailed analysis of these data, a few general considerations should be discussed. Most creep data are reported in the literature in a graphical form. Calculations based on these plots can be greatly affected by the type of co-ordinates employed. It is suggested that the "range of accuracy" be plotted around each experimental point before deciding the position of the "best" experimental curve, especially when a large number of test points are not available. This is of the greatest importance when logarithmic co-ordinates are employed. It can be demonstrated that if a variable  $x$  is plotted on a logarithmic scale, a range of accuracy  $\pm ax$  plots on that scale as  $\pm \log(1 + a)$ . Although the range of accuracy is proportional to the variable, the graphical representation of this range is independent of the value of the variable. On the other hand, the graphical indication of constant uncertainties depends on the value of the variable.

The graphical analysis of creep data according to the rate-process theory may lead to rather uncertain results when the data present a considerable scatter. If the graphical method suggested by Dushman *et al.*<sup>4</sup> is used, the location of the straight line drawn in the semi-log plot of stress against creep rate has a great effect in the determination of the extrapolated intercept at zero stress. By re-examination of the data for high-purity aluminium presented by Dushman *et al.*<sup>4</sup> in graphical form, it was possible to calculate an activation energy  $Q_1$  whose values lay between 5000 and 20,000 cal., according to the way in which the best lines were plotted through the limited data on the semi-log basis.

Furthermore, for best results, the analysis of creep data must be restricted to data from samples which show, as far as can be determined metallographically and otherwise, a stable structure and a similar type of deformation. With this in mind, the analysis of the creep data for S-590 alloy will be restricted to that range in which the type of deformation is determined to be high-temperature behaviour,<sup>8</sup> and in which oxidation and other possible sources of instability have no marked effect. It is worth bearing in mind that oxidation was minimized through the addition of 20% chromium, and that the effect of other structural instabilities was greatly reduced by solution-treating and pre-ageing the test-bars for stability.

## II.—ANALYSIS OF THE CREEP DATA FOR S-590 ALLOY

The original data (Grant and Bucklin,<sup>8</sup> Table II), from which only the high-temperature-behaviour points were taken, were converted into C.G.S. units, and the logarithm of the minimum creep rate was plotted against the stress. It was observed that straight lines could not be drawn through the experimental points. The trend of the points follows a family of smooth curves, whose slope decreases as the strain rates increase (see Fig. 5). Within a given range of strain rates, the slope of the curves decreases as the temperature decreases.

It was first thought that, although straight lines could not be drawn on a semi-log plot, the experimental data might still be consistent with the rate-process theory, if they fitted the hyperbolic sine equation (1). In order to resolve this uncertainty, a hyperbolic sine curve was drawn near the experimental curve at 922° K. (1200° F.). Fig. 1 shows that the deviation of the theoretical hyperbolic sine curve from a straight line starts at a much lower stress than the deviation of the experimental curve. The same procedure was applied to other curves, with similar results.

Although the experimental data indicated that a semi-log relationship between stress and minimum creep rate cannot be applied to the behaviour of the

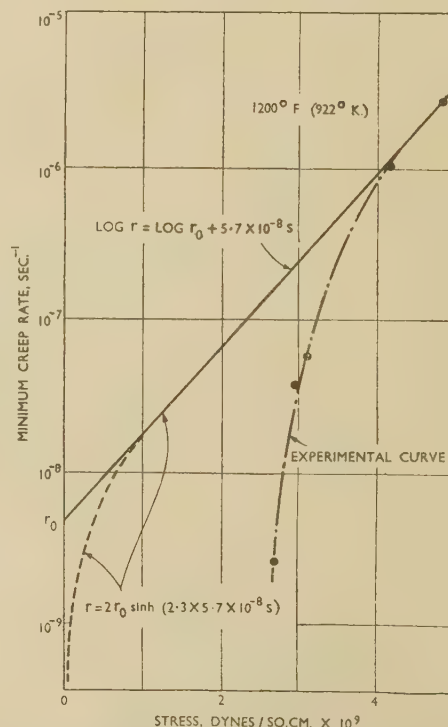


FIG. 1.—Plot of Logarithm of Minimum Creep Rate ( $r$ ) against Stress ( $s$ ) at 1200° F. (922° K.), Comparing the Experimental Curve and the Theoretical Hyperbolic Sine Curve.

\* 20% Co, 20% Cr, 20% Ni, 4% W, 4% Mo, 4% Nb, 0.5% C, balance Fe.

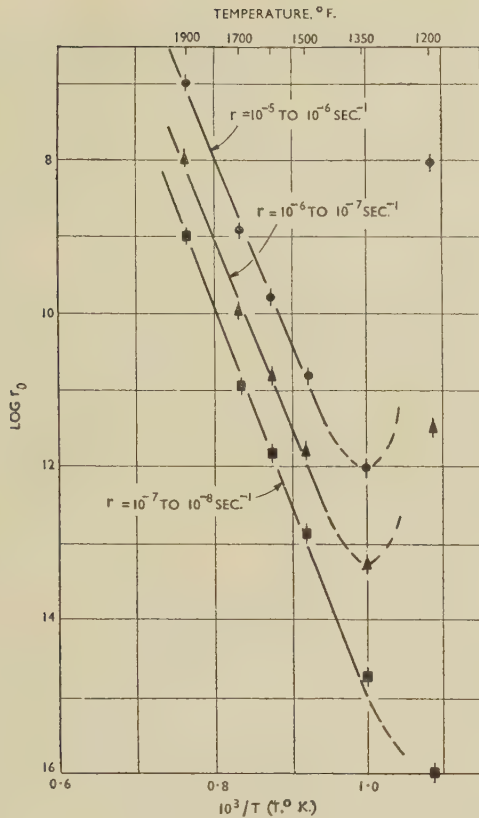


FIG. 2.—Plot of  $\log r_0$  against  $1/T$  for Three Ranges of Creep Rates ( $r$ ).

S-590 alloy, the rate-process theory was applied to the data by deliberately limiting the range of creep rates, the graphical method suggested by Dushman *et al.*<sup>4</sup> being used. The intercepts  $\log r_0$  at zero stress were determined for each curve after drawing the best average straight line in the limited range of creep rates. Three ranges, shown below, were selected at the lower creep rate end, where the approach to a straight-line semi-log relationship comes closest:

- (a)  $10^{-5}$ – $10^{-6}$  sec.<sup>-1</sup>
- (b)  $10^{-6}$ – $10^{-7}$  sec.<sup>-1</sup>
- (c)  $10^{-7}$ – $10^{-8}$  sec.<sup>-1</sup>

The values of  $\log r_0$  are plotted against the reciprocal of the absolute temperature in Fig. 2.

The uncertainty of the points plotted in Fig. 2 is great, and therefore any conclusion or calculation of the activation energy or the activation entropy is open to doubt. Nevertheless, it appears that a straight line may be obtained when the values of  $\log r_0$  are plotted against the reciprocal of the absolute temperature, except where the material approaches the transition from high-temperature to low-temperature behaviour. The trend of the points plotted in Fig. 2 indicates that an activation energy of the order of magnitude of 120,000 cal./g.-atom can be approximately estimated from these data; this value can vary between rather wide limits, according to the

way in which  $r_0$  is determined from the semi-log plot of stress against minimum creep rate.

In order to find a more general relationship between stress, minimum creep rate, and temperature, the data for S-590 alloy were replotted, using double logarithmic co-ordinates. The data included in the high-temperature range, in the absence of major sources of instability such as oxidation, show a definite linear trend when the logarithm of the minimum creep rate is plotted against the logarithm of the stress (Fig. 3). It was also observed that these straight lines drawn as shown converge at a single extrapolated point situated at a stress of  $10^{10.6}$  dynes/cm.<sup>2</sup> and at a creep rate of  $10^7$  sec.<sup>-1</sup>. When the slope of the isothermal lines is plotted against the reciprocal of the absolute temperature, a linear relationship is found (Fig. 4). Therefore, all the data included within the limits mentioned above may be expressed by a simple equation of the type:

$$\log r = a + (b/T - c)(\log s - d) \quad (3)$$

where:

$r$  = minimum creep rate,

$s$  = applied tensile stress,

$T$  = absolute temperature,

$a, b, c, d$  = constants depending on the material and structure.

For the S-590 alloy the constants are:  $a = 7$ ,  $b = 20,000$ ,  $c = 8.8$ ,  $d = 1.6$ , if the minimum creep rate is expressed in sec.<sup>-1</sup> and the stress in  $10^9$  dynes/cm.<sup>2</sup>.

Data calculated from equation (3) were recorded on a semi-log plot (solid lines in Fig. 5) together with

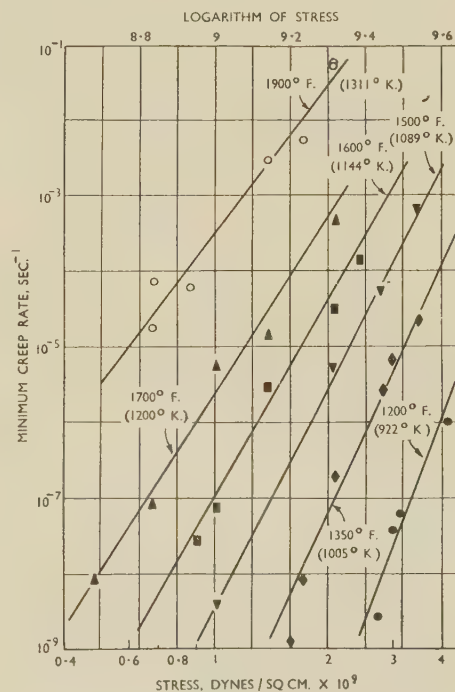


FIG. 3.—Log/Log Plot of Minimum Creep Rate against Stress for S-590 Alloy (in C.G.S. Units) at Different Temperatures.



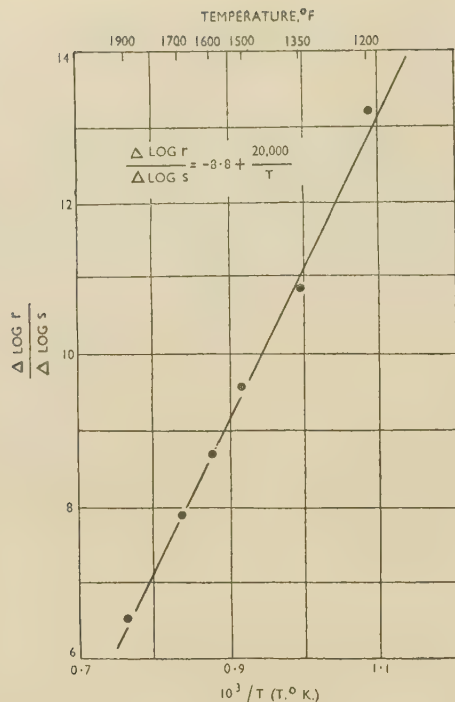


Fig. 4.—Plot of the Slopes of the Straight Lines from Fig. 3 against  $1/T$ .

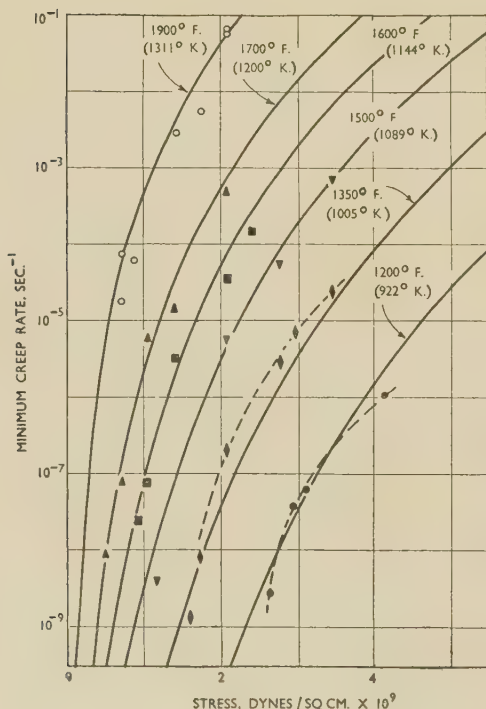


Fig. 5.—Semi-Log Plot of Minimum Creep Rate against Stress for S-590 Alloy.

— Replotted from curves of Fig. 3.  
 --- Curves through experimental points.

the experimental points. The best smooth curves to fit the experimental points (broken lines in Fig. 5) were also drawn for the two lower temperatures, where the deviation is more marked than at other temperatures. Fig. 5 shows that the experimental points follow the trend of the calculated curves, thus demonstrating that the linear trend observed on the log/log plot is not an artificial effect due to the type of co-ordinates used.

Equation (3) is not to be regarded as an equation of state, nor is it suggested as a basis for the extrapolation of creep data. It is simply reported as an empirical relationship between creep rate, stress, and temperature, and it can be used for interpolation with sufficient accuracy only if based on considerable experimental data. The position of the common point at which all the isothermal straight lines meet on the log/log plot cannot be determined within reasonable limits of accuracy, even with extensive experimental data. It is not possible to decide whether this point has physical significance or whether it is only an empirical reference point on which a mathematical analysis is based.

It may be suggested, at least as a first approximation, that at a certain very high strain rate, the strength of the grain boundaries would be constant, regardless of the temperature. This would be true if the mechanism of deformation and fracture common to high-temperature behaviour prevailed at that very high strain rate. Actually, it was proved experimentally that at a much lower strain rate a different mechanism of deformation and fracture becomes the controlling factor. This change is indicated on a log/log plot of minimum creep rate against stress by a change in slope of the experimental curves.

Although the physical significance of the reference point discussed above is doubtful, it is worth mentioning that a common point for all the curves plotted on double logarithmic co-ordinates was found to exist for other alloys, provided major instabilities were not operative. The data by White, Clark, and Wilson<sup>9</sup> for a Cr-Mo-Si steel, show this very clearly. The same evidence is found for the behaviour of 18:8 molybdenum stainless steel,<sup>10</sup> and for 3S-H12 aluminium alloy.<sup>11</sup> Even stress-rupture data have a similar trend, as can be shown using the data reported by Grant<sup>12</sup> for the cobalt-chromium "J" alloy.

It is obvious that at constant stress, equation (3) becomes of the same form as Boltzmann's equation:

$$\text{rate} = Ae^{-Q/RT}.$$

Moreover, it can be shown that the successful application of the rate-process theory to a limited range of creep rates, as demonstrated in Fig. 2, can be extended to any range of creep rates in a quite general way. In fact, equation (2), which is consistent with the rate-process theory, can be written:

$$\log r_1 = \log r_0 + \frac{d \log r}{ds} \cdot s \quad (4)$$

for each constant temperature. Differentiating equa-

tion (3) with respect to stress, at constant temperature, the following equation is obtained :

$$\frac{d \log r}{ds} = \frac{(b/T - c)}{s}$$

Substituting in (4) :

$$\log r_1 = \log r_0 + b/T - c$$

or

$$\log r_0 = -b/T + c + \log r_1. \quad (5)$$

Over a limited range of creep rates,  $\log r_1$  may be regarded as a constant, and therefore the logarithm of the intercept  $r_0$  of the best average curve at zero stress is a linear function of the reciprocal of the absolute temperature. The activation energy is proportional to  $b$ , and therefore constant in any range of creep rates. The activation entropy is proportional to  $(c + \log r_1)$ , and therefore it increases as the creep rate increases.

### III.—CONCLUSIONS

Creep data for the S-590 alloy reported by Grant and Bucklin<sup>8</sup> clearly show that a linear relationship is not obtained when the logarithm of the minimum creep rate is plotted against the stress over a fairly large range of creep rates. This experimental evidence is in disagreement with the fundamentals of the statistical theory of the rate process. The rate-process theory may be successfully applied only to a limited range of creep rates. If the experimental curves are compared with corresponding curves predicted by the rate-process theory, it may be concluded either that the theory cannot be applied or that the size of the unit of flow decreases (instead of remaining constant) as the strain rate increases at constant temperature.

Extrapolation of creep data based on the results of the rate-process theory cannot be safely carried out.

Interpolation leads to good accuracy only if restricted to the same range of creep rates.

A general approximate equation is suggested for interpolation of creep data in a wider range of creep rates. This empirical equation is based upon the experimental evidence of a linear relationship between the logarithm of the minimum creep rate and the logarithm of the stress. It is in good agreement with the results of the rate-process theory only over a limited range of creep rates, and it is found to be valid only in the absence of major instabilities and therefore cannot be safely used for extrapolation of data unless the absence of instabilities can be assured.

### ACKNOWLEDGEMENT

The authors wish to express their thanks to the U.S. Bureau of Ships, under whose sponsorship this research was carried out.

### REFERENCES

1. H. Eyring, *J. Chem. Physics*, 1935, **3**, 107.
2. H. Eyring, *J. Chem. Physics*, 1936, **4**, 283.
3. W. Kauzmann, *Trans. Amer. Inst. Min. Met. Eng.*, 1941, **143**, 57.
4. S. Dushman, L. W. Dunbar, and H. Huthsteiner, *J. Appl. Physics*, 1944, **15**, 108.
5. A. S. Nowick and E. S. Machlin, *J. Appl. Physics*, 1947, **18**, 79.
6. E. S. Machlin and A. S. Nowick, *Trans. Amer. Inst. Min. Met. Eng.*, 1947, **172**, 386.
7. P. Ludwick, "Elemente der Technologischen Mechanik". Berlin : 1908.
8. N. J. Grant and A. G. Bucklin, *Trans. Amer. Soc. Metals*, 1950, **42**, 720.
9. A. E. White, C. L. Clark, and R. L. Wilson, *Trans. Amer. Soc. Metals*, 1938, **26**, 60.
10. "Steels for Elevated-Temperature Service". 1949. (United States Steel Corp.).
11. J. E. Dorn and T. E. Tietz, *Proc. Amer. Soc. Test. Mat.*, 1949, **49**, 815.
12. N. J. Grant, *Trans. Amer. Soc. Metals*, 1948, **40**, 585.



## NOTICE TO AUTHORS OF PAPERS FOR THE "JOURNAL" AND CONTRIBUTORS TO DISCUSSIONS

1. **Papers will be considered for publication from non-members as well as members of the Institute.** They are accepted for publication in the *Journal* and not necessarily for presentation at any meeting of the Institute. MSS. should be addressed to The Editor of Publications, The Institute of Metals, 4 Grosvenor Gardens, London, S.W.1.

2. **Papers suitable for publication** may be classified as:

(a) Papers recording the results of original research.  
(b) First-class reviews of, or accounts of progress in, a particular field.

(c) Papers descriptive of works methods, or recent developments in metallurgical plant and practice.

(d) Papers in classes (a), (b), and (c) above, previously published in languages other than English, French, German, or Italian, if of sufficient merit.

3. **Manuscripts and illustrations** should be submitted in duplicate. MSS. must be typewritten (*double-line spacing*) on one side of the paper only, and authors are requested to sign a declaration that neither the paper nor a substantial part thereof has been published elsewhere. Exceptions may be made in certain cases where a paper has been published in a language other than English, French, German, or Italian (see 2(d) above). MSS. not accepted are normally returned within 6 months of receipt.

In the interests of economy, all papers must be written as concisely as possible; in general, internal research reports are not in suitable form for publication as papers in the *Journal*. All but the simplest mathematical expressions should be written by hand, with capital and small letters clearly distinguished. Superscript and subscript letters should also be plainly indicated. Greek letters and special signs should be identified in the margin. For style, spelling, and abbreviations used, any recent issue of the *Journal* may be consulted.

4. **Synopsis.** Every paper must have a synopsis (not exceeding 250 words in length) which, in the case of a paper reporting original research, should state its objects, the ground covered, and the nature of the results. The synopsis will appear at the beginning of the paper, and should be in a form suitable for use by abstracting organizations. Extracts from a "Guide for the Preparation of Synopses" drawn up by the Abstracting Services Consultative Committee are reproduced below.

5. **References** must be collected at the end of the paper and must be numbered in the order in which they occur in the MS. Initials of authors must be given, and the Institute's official abbreviations for periodical titles (as used in *Metallurgical Abstracts*) should be employed, where known. References to papers should be set out in the style:

A. L. Dighton and H. A. Miley, *Trans. Electrochem. Soc.*, 1942, 81, 321 (i.e. year, volume, page).

References to books should be in the following style:

C. Zener, "Elasticity and Anelasticity of Metals". Chicago: 1948 (University of Chicago Press).

6. **Illustrations.** Each illustration must have a number and description; only one set of numbers must be used in one paper, and it is desirable to number the half-tone illustrations consecutively, rather than to inter-spacer them with the line figures. The captions should be typed on a separate sheet.

The set of **line figures** sent for reproduction must be drawn (about twice the size to appear in the *Journal*) in Indian ink on smooth white Bristol board, good-quality drawing paper, co-ordinate paper, or tracing cloth, which are preferred in the order given. Co-ordinate paper, if used, must be blue-lined, with the co-ordinates to be reproduced finely drawn in Indian ink. Curves should be drawn boldly (i.e. at least twice the thickness of the frame). Experimental points should be indicated by open or closed circles, triangles, squares, &c. (preferably not crosses). Curves should be broken on each side of such symbols and plenty of allowance should be made for closing up in blockmaking. All lettering and numerals, &c., should preferably be in *pencil*, so that the Institute's standard lettering may be affixed, and ample margins must be left outside the framework of the figures to enable this to be done. The second set of line illustrations may be photostat copies.

**Photographs** must be restricted in number, owing to the expense of reproduction, and photomicrographs should be trimmed to the smallest possible of the following sizes consistent with adequate representation of the subject: 4 in. deep by 3 in. wide: 2 in. deep by 3 in. wide: 2 in. square. Magnifications of photomicrographs must be given in each case. Photographs for reproduction should be loose, not pasted down (and not fastened together with a clip, which damages them), and the figure number and author's name should be written on the back of each. Captions should be given to the photomicrographs, but these should be kept as brief as possible.

Because of the present high cost of printing and paper it is imperative that authors restrict illustrations (particularly photographs) to the absolute minimum deemed necessary to support their argument. Only in exceptional cases will illustrations be reproduced if already printed and readily available elsewhere.

7. **Tables or Diagrams.** Results of experiments, &c., may be given in the form of tables or figures, *but* (unless there are exceptional reasons) *not both*. Tables should bear Roman numbers, and each should have a heading that will make the data intelligible without reference to the text.

8. **Corrections.** A certain number of corrections in proof are inevitable, but any modification of the original text is to be avoided. Since corrections are very expensive, the Institute reserves the right to require authors to contribute towards their cost if the Editor deems them to be excessive. The Institute also reserves the right to require a contribution to the cost of remaking any block where this is necessitated by an error on the author's part.

9. **Reprints.** Individual authors are presented with a maximum of 25, and two or more authors with a maximum of 50 reprints from the *Journal*, without covers. Limited numbers of additional reprints can be supplied at the author's expense, if ordered before proofs are passed for press. (Orders should preferably be placed when submitting MSS.)

10. **Discussion.** Except in the case of special symposia, shorthand records of discussions are not taken at meetings. Written discussion may be submitted on any paper, preferably typewritten (*double-line spacing*). References should be given in the form of footnotes. Paragraphs 6 and 7 above are also applicable to such contributions. Reprints of discussion cannot be supplied to contributors.

## GUIDE FOR THE PREPARATION OF SYNOPSSES

(As recommended by the Abstracting Services Consultative Committee)

1. **Purpose.** The synopsis is not part of the paper; it is intended to convey briefly the content of the paper, to draw attention to all new information, and to the main conclusions. It should be factual.

2. **Style of writing.** The synopsis should be written concisely and in normal rather than abbreviated English. It is preferable to use the third person. Where possible use standard rather than proprietary terms, and avoid unnecessary contracting.

It should be presumed that the reader has some knowledge of the subject, but has not read the paper. The synopsis should therefore be intelligible in itself without reference to the paper; for example, it should not cite sections or illustrations by their numerical references in the text.

3. **Content.** The title of the paper is usually read as part of the synopsis. The opening sentence should be framed accordingly and repetition of the title avoided. If the title is insufficiently comprehensive, the opening should indicate the subjects covered. Usually the beginning of a synopsis should state the objective of the investigation.

It is sometimes valuable to indicate the treatment of the subject by such words as: brief, exhaustive, theoretical, &c.

The synopsis should indicate newly observed facts, conclusions of an

experiment or argument and, if possible, the essential parts of any new theory, treatment, apparatus, technique, &c.

It should contain the names of any new compound, mineral species, &c., and any new numerical data, such as physical constants; if this is not possible, it should draw attention to them. It is important to refer to new items and observations, even though some are incidental to the main purpose of the paper; such information may otherwise be hidden, though it is often very useful.

When giving experimental results the synopsis should indicate the methods used; for new methods the basic principle, range of operation, and degree of accuracy should be given.

4. **References.** If it is necessary to refer to earlier work in the summary, the reference should always be given in full and not by number. Otherwise references should be left out.

When a synopsis is completed, the author is urged to revise it carefully, removing redundant words, clarifying obscurities, and rectifying errors in copying from the paper. Particular attention should be paid by him to scientific and proper names, numerical data, and chemical and mathematical formulae.

# A SIMPLE METHOD OF X-RAY MICROSCOPY AND ITS APPLICATION TO THE STUDY OF DEFORMED METALS \*

1323

By R. W. K. HONEYCOMBE,† M.Sc., Ph.D., MEMBER

## SYNOPSIS

A method of obtaining images from metal crystals, using a line source of characteristic X-rays, is described. The images can be enlarged to at least 50 diameters to reveal significant microscopic phenomena, in particular distortions arising from slight plastic deformation which are not readily observed by optical micrography. However, optical micrography is of great assistance in the initial interpretation of the X-ray images, and the two techniques should be regarded as complementary. The scope of the method in the study of plastic deformation is illustrated by a series of X-ray and optical micrographs obtained from metal crystals deformed under varying conditions.

## I.—INTRODUCTION

It has been realized for many years that X-rays can be used to obtain images of crystal surfaces, but few attempts have been made to apply such methods to the study of deformed crystals. Berg<sup>1, 2</sup> has described two ways by which X-ray images could be obtained. Firstly he suggested the use of a point source of polychromatic X-rays, a method which has recently been used by Guinier and Tennevin<sup>3</sup> to obtain sharp images of crystals. The second method, which Berg adopted for his experiments, employed characteristic radiation from a line source; he showed that if the crystal was set at a suitable Bragg angle, a point-for-point image of the crystal surface was obtained. In this way Berg examined crystals of natural rock salt and detected striations in the image which he attributed to plastic deformation by slip along (110) planes in a [100] direction.

The matter was not investigated further until 1945, when Barrett<sup>4</sup> showed that a similar technique could be applied to the study of many metallurgical problems. Barrett found that a surprising degree of resolution could be obtained by using an ordinary line source of the type frequently available in X-ray tubes. With high-resolution photographic plates, he was able to obtain significant detail in the X-ray images at magnifications of 50 or more. This work was necessarily exploratory in character, but it sufficed to show that X-ray microscopy of this type would be a valuable new way of studying the deformation of metals, as well as other phenomena such as recrystallization and grain growth.

In the present work, the author has used a method based on the same principle and has applied it primarily to a study of the deformation of metal crystals. In conjunction with the classical methods of optical micrography it has proved very useful in

studying the inhomogeneities that develop during plastic deformation in both single-crystal and polycrystalline specimens. This work is the subject of a separate paper.<sup>5</sup> In the present paper it is proposed to describe and discuss the technique of X-ray microscopy and to show how some of the results can be interpreted.

## II.—DESCRIPTION OF TECHNIQUE

The principle of the method is shown schematically in Fig. 1. The crystal is rotated until a Bragg reflection occurs, and then, if the crystal is perfect, the X-rays reflected are defined by a series of cones

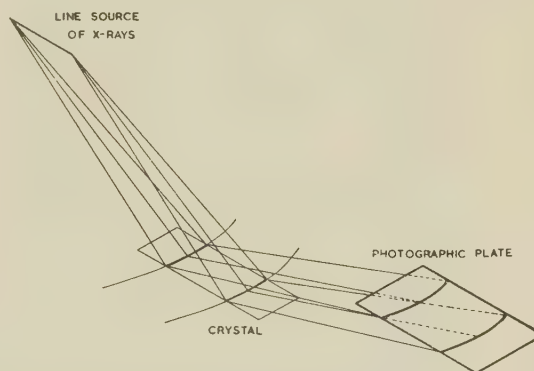


FIG. 1.—Schematic Diagram Showing Principle of X-Ray Technique.

with apexes on the line source. The rays forming these cones will give on reflection a point-for-point image of part of the crystal surface on a suitably placed photographic plate. Clearly, the image will be unique because each point on the crystal surface will reflect only one incident ray, namely, that which makes the correct Bragg angle with the set of reflect-

\* Manuscript received 6 February 1951.

† Armourers and Brasiers' Company Research Fellow, Cavendish Laboratory, Cambridge.



ing planes. As the crystal is rotated, other planes will, of course, reflect at different Bragg angles and result in similar images of the crystal. If the orientation of the crystal is not uniform, certain regions will not be in a position to reflect when the rest of the crystal is reflecting; this results in white areas in the X-ray image. The simplest case is that of a small included grain, which is revealed as a sharply bounded white area even if the orientation difference is quite small (see, for example, Fig. 5 (a), Plate VIII). The method has, however, been applied to the study of much smaller disorientations which occur as a result of plastic deformation. Here the interpretation is not quite so simple and will be dealt with in detail in a later section.

In practice, the apparatus is extremely simple. A demountable X-ray tube was employed for the present work, because the filament could be frequently replaced and the focal line on the target adjusted; normally the source was about 10 mm. long and 1 mm. wide. The target metal was chosen to give a radiation of relatively long wave-length, so that only a thin surface layer contributed to the reflection. Copper ( $\lambda_{K\alpha} = 1.59 \text{ \AA.}$ ) was frequently used, but equally satisfactory results were obtained with cobalt ( $\lambda_{K\alpha} = 1.74 \text{ \AA.}$ ) and manganese ( $\lambda_{K\alpha} = 2.10 \text{ \AA.}$ ) radiation. Fig. 4 (Plate VIII) is a photograph of the experimental arrangement. The window *W* of the X-ray tube was covered by a pair of adjustable slits, whose sole purpose was to limit the size of the beam. The crystal *C* to be examined was mounted on the spindle of a Unicam X-ray camera, and could be rotated about its vertical axis, or raised or lowered to bring different parts of the crystal into the beam. The camera was mounted on an adjustable bench which could be raised or lowered by means of the cantilever *L* or rotated about a pivot *P* directly beneath the window of the X-ray tube. The bench was sufficiently long for the camera to be moved up to 55 cm. from the target.

As the distance of the crystal from the focal line was increased, the better the resolution became and the smaller the disorientation that could be detected. The reverse was true, however, for the distance between the specimen and the photographic plate on which the reflected image was recorded. The plate or fluorescent screen holder was mounted on a rod *R* attached to the body of the camera, and could be easily adjusted to the required height. The holder could be moved horizontally so that the photographic plate was brought very close to the surface of the crystal, the usual working distance being between 2 and 5 mm. The holder was adjustable in three directions at right angles and therefore could make any desired angle with the crystal surface.

As the X-ray beam was very broad, it was necessary to reduce scattered radiation by means of a lead tube *T*, and to absorb the direct beam by a movable lead screen *S* which was guided along the camera table in brass slots.

To obtain an X-ray micrograph, the specimen,

usually a large single crystal or coarse-grained polycrystal, was mounted in the X-ray camera, as shown in Fig. 4 (Plate VIII), and a fluorescent screen was placed in the holder about 2 cm. from the specimen and parallel to the incident beam. After the eyes had become accustomed to complete darkness, it was possible to see the individual reflections on the screen as the crystal was slowly rotated. A suitable reflection was selected and the plate-holder brought as close to the crystal as feasible, the plate being still parallel to the incident beam. In these circumstances the photographic plate was adequately protected from the direct beam by the thin metal flange of the holder. Even without going to extreme lengths to improve the sharpness of the line source, the resolution of the method proved so satisfactory that the images obtained revealed significant detail when enlarged 50–100 diameters. This necessitated the use of fine-grained photographic emulsions. Kodak Maximum Resolution plates capable of resolving 1000 lines/mm. proved to be extremely satisfactory; the exposure time was usually between 2 and 6 hr. For work requiring magnifications of only 20 times or less, Kodak B.10 plates were adequate, the exposure time varying between 1 and 30 min., depending on the intensity of the reflection. Kodak D.8 developer was used.

### III.—SELECTION OF A SUITABLE REFLECTION

During rotation of the crystal, a large number of reflections were usually observed, but all were not suitable for detailed examination. The most obvious cause for rejection was the interference on the plate of two or more reflections. This frequently occurred, particularly with deformed crystals, as each reflection

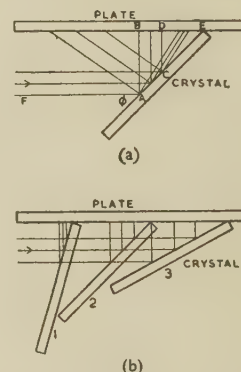


FIG. 2.—Effect of (a) Variation of Bragg Angle and (b) Variation of Angle between Specimen and Incident Beam.

then took place over an extended angular range. The likelihood of interference was also greater because the reflections were frequently larger than  $1 \text{ cm.}^2$  in area. Some reflections were excessively distorted as a result of striking the screen at a very oblique angle. Fig. 2 (a) shows the effect when the Bragg angle is altered by choosing a different set of reflecting planes (or by



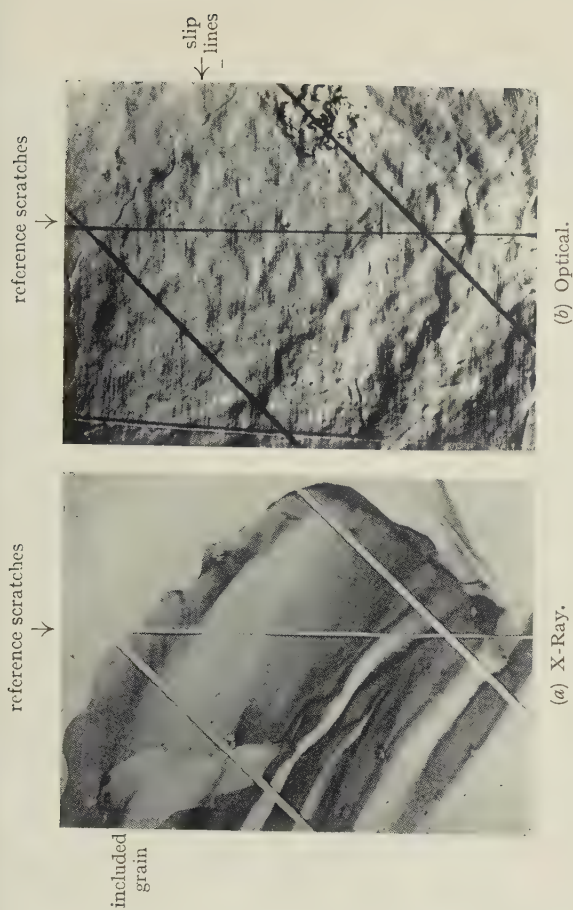


FIG. 5.—A Grain in Al Polycrystal (99.99% pure) After 0.6% Elongation in Tension at Room Temperature.  $\times 6$ .

FIG. 4.—Experimental Arrangement for X-Ray Microscopy.

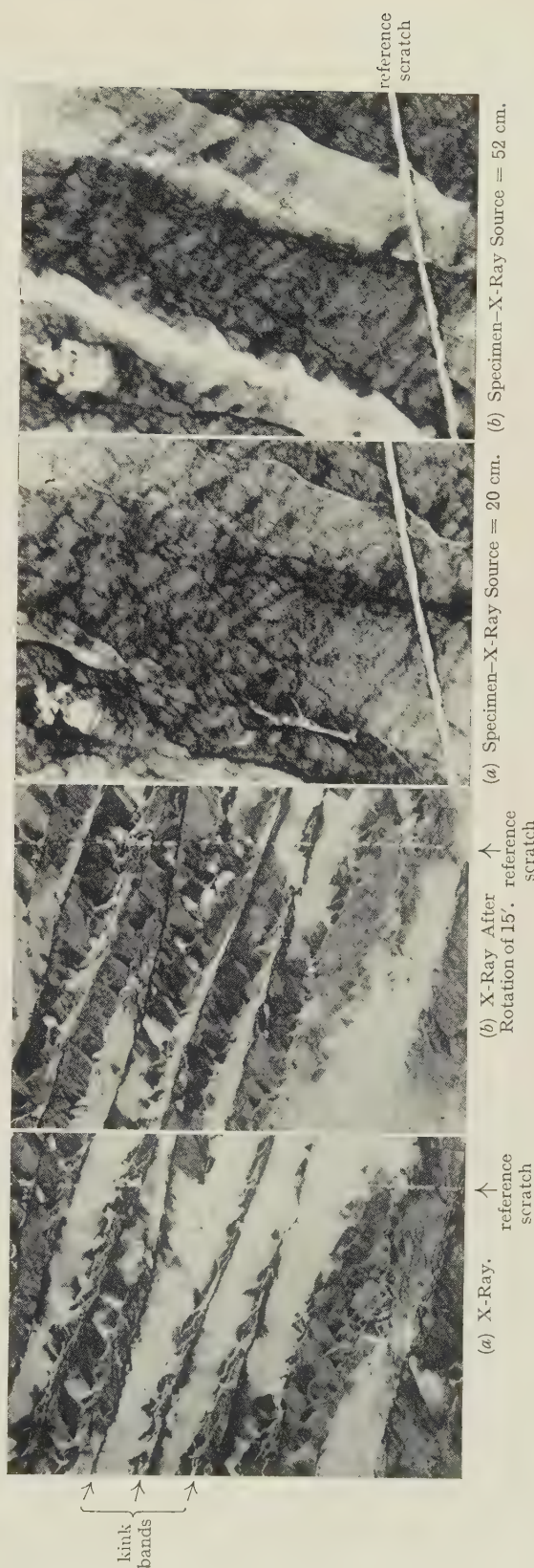
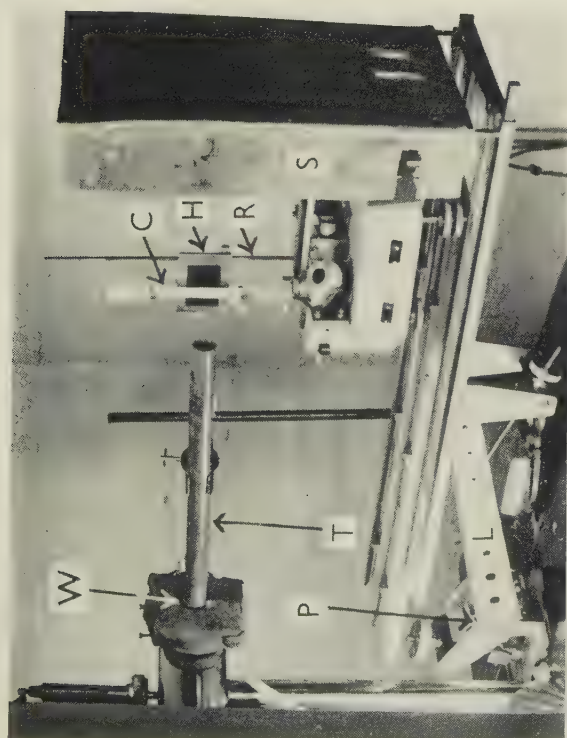
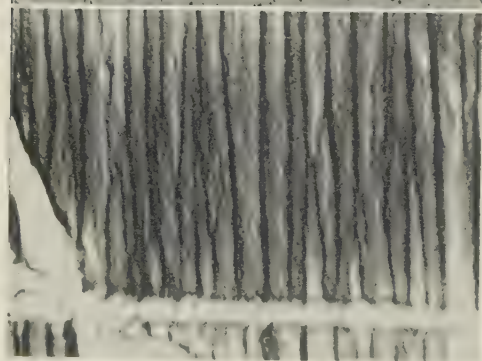


FIG. 6.—A Grain in Al Polycrystal (99.99% pure) After 3% Elongation During 4 Days' Slow Deformation at 300° C.  $\times 10$ .  
All except Fig. 4 reduced by  $\frac{1}{2}$  linear in reproduction.



reference scratches  
slip lines



(a) X-Ray,  $\times 25$ .



(b) Optical,  $\times 50$ .



FIG. 9.—X-Ray. Al Crystal (99.99% pure) After 4% Elongation at Room Temperature.  $\times 50$ .

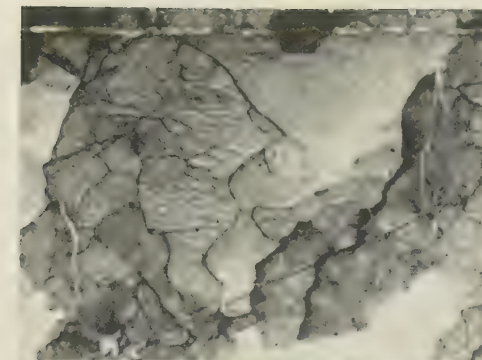
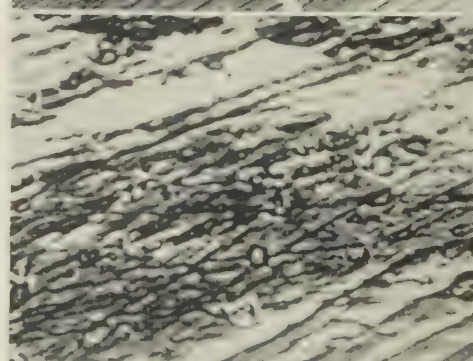
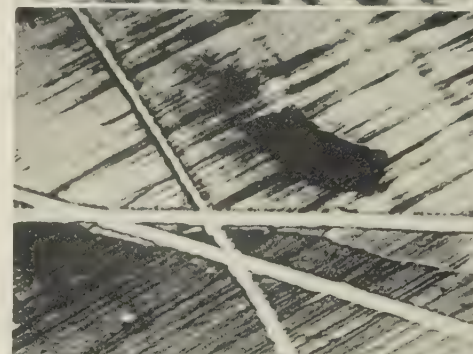


FIG. 10.—X-Ray. Al Crystal (99.99% pure) After 7% Elongation During 13 Days' Slow Extension at 300° C.  $\times 20$ .

kink  
bands



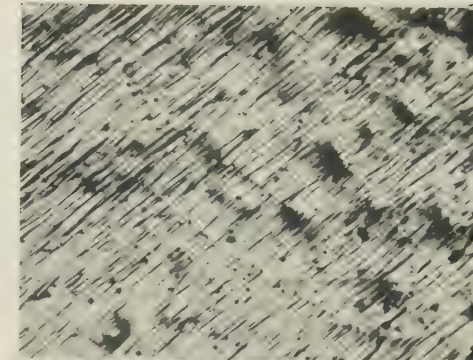
(a) X-Ray. After 2.9% elongation.



(b) X-Ray. As (a) after prolonged electrolytic polishing.



(a) X-Ray. After 4.6% elongation.  $\times 25$ .



(b) Optical. After 10% elongation.  $\times 50$ .

FIG. 11.—Cu Crystal, Originally Ground and then Electrolytically Polished.  $\times 25$ .

FIG. 12.—Al Crystal (99.5% pure) After Extension at Room Temperature.

All figures reduced by  $\frac{1}{4}$  linear in reproduction.

using a different wave-length), while the angle between the specimen and the photographic plate remains constant (in this case  $45^\circ$ ). It is clear that the image is the same size as the area irradiated when the triangle  $ABE$  is isosceles, in which case the Bragg angle is approximately  $56^\circ$ . As the Bragg angle increases beyond  $56^\circ$ , the image becomes larger, while if the angle is below  $56^\circ$  the image is correspondingly smaller. In practice, the best results are obtained when the reflection is not distorted greatly one way or the other.

Other factors remaining constant, the reflection comes from a larger area of the specimen if it is almost parallel to the incident beam than if it is almost normal to it. This is shown in Fig. 2 (*b*), where a Bragg angle of  $45^\circ$  is used for simplicity. When the photographic plate and the crystal are at a very acute angle, images are frequently obtained from the complete width of the surface presented to the incident beam. There is another reason for putting the plate at a very acute angle to the specimen. In practice, it is found that the resolution of the image is greater, the closer the plate is to the specimen, but some parts of the specimen are inevitably more distant from the photographic plate than others (Fig. 2). This difference is obviously minimized by making the angle between the plate and crystal as small as possible.

#### IV.—THE APPEARANCE AND INTERPRETATION OF X-RAY IMAGES FROM DEFORMED CRYSTALS

The image from an undeformed crystal is uniform, and no detail can be seen after considerable enlargement. Marked changes in orientation such as those occurring at grain boundaries and twin planes are clearly revealed by sharp breaks in the continuity of the reflection. However, when a metal crystal is deformed, local disorientations usually occur, the presence of which is shown indirectly by asterisms in X-ray Laue photographs. While the detailed nature of these inhomogeneities will be considered elsewhere, it is relevant now to consider how the X-ray images can be modified by them.

The most straightforward change in the image arises when the local rotation of the crystal is so great that this region is not able to reflect any of the incident X-rays. Thus the distorted region will behave exactly like an included grain of different orientation and a white area will appear in the X-ray image. Fig. 5 (*a*) (Plate VIII) illustrates this modification of the image in the case of a reflection from one grain of a coarsely crystalline aluminium specimen, which was deformed by 0.6% elongation in tension at room temperature. The white bands represent lamellar disorientations.

There are also white areas in Fig. 6 (Plate VIII) which correspond with regions of the crystal that, as a result of plastic deformation, have become disoriented so that they no longer contribute to the reflection. In these circumstances, it is reasonable to expect that a slight rotation of the specimen may

bring some of the non-reflecting regions into a reflecting position, while at the same time other regions may cease to reflect. In practice, a lightly deformed aluminium crystal will give a reflection over an angular range of  $1^\circ$ – $2^\circ$ , the angular spread increasing with the deformation; but at each particular setting of the crystal within this range a slightly different image will be obtained because of local variations in orientation. For example, Figs. 6 (*a*) and (*b*) (Plate VIII) represent the same reflection from a deformed aluminium crystal which has been rotated  $15'$  between the two photographs. The same general features are evident in both photographs, namely the lamellar disorientations, but some areas of the crystal which have not reflected in Fig. 6 (*a*) are reflecting in Fig. 6 (*b*) and vice versa.

If a disorientation in the crystal is sufficiently small, then the region concerned may be in a position to select rays which make the requisite Bragg angle from another point on the line source. Fig. 3 shows diagrammatically that this will result in a local displacement of the image which will cause interference on

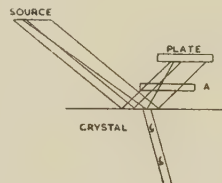


FIG. 3.—Effect of Local Rotation on the Image.

the photographic plate. It will be more pronounced the greater the distance of the plate from the specimen, and this is an additional reason for placing the photographic plate as near as possible to the crystal. If, on the other hand, the distance between the X-ray source and the crystal is increased, then the image will become more sensitive to orientation differences in the crystal. This follows directly from the fact that the angle subtended by the source to any point on the crystal will be smaller the greater the distance between them. The effect of changing this distance on the sensitivity of the technique is illustrated in Figs. 7 (*a*) and (*b*) (Plate VIII), which represent an X-ray reflection from an aluminium crystal after 1.7% elongation by slow straining at  $300^\circ\text{C}$ . Fig. 7 (*a*) was taken with the crystal 20 cm. from the X-ray source, and shows no large white regions representing disorientations. However, in Fig. 7 (*b*), which was taken with the crystal 52 cm. from the source, large disoriented regions are revealed.

There is obviously a practical limit to disorientations that can be detected with the technique as it stands; this is imposed by the dimensions of the X-ray source and by the workable distance of the specimen from the source. If the line source is assumed to be 10 mm. long and it is foreshortened to 1 mm. by using the X-ray tube in the usual way, then for a crystal 50 cm. away orientation differences of  $6'$  should be detected. In practice, the disorientations



which can be observed are rather smaller than this, but no quantitative estimate has been made. In this respect the method is not as sensitive as one devised by Guinier and Tennevin<sup>3</sup> for investigating the perfection of crystals. Their method employs a point source of polychromatic X-rays and by using the focusing condition it has been possible to detect disorientations as small as  $10''$ . However, this method does not reveal the *distribution* of inhomogeneities in the crystal, and thus does not fall into the category of X-ray microscopy. It should be mentioned that the technique described here is more than adequate for the study of lightly deformed crystals, because after about 1% elongation in tension the resulting disorientations are usually sufficiently large for detection by X-ray microscopy. In fact, after about 10% elongation in tension, the disorientations frequently become so great that the method is then too sensitive. This difficulty can be partly overcome by reducing the distance of the specimen from the X-ray source to a minimum.

It soon became evident that the above considerations were not the only ones defining the nature of the X-ray image. Within a totally reflecting area, it was found that the intensity of the image was not uniform. Some of the variations resulted from a lack of uniformity in the source, while others could be attributed to the displacement of incident radiation by disoriented regions so that they overlapped other parts of the image. When these causes had been eliminated, however, there remained narrow lines of high intensity in many of the X-ray images. By comparison with optical micrographs it was found that distorted regions of the crystal were responsible for the areas of high intensity. For example, one type of inhomogeneity resulting from deformation consists of narrow bands in which the crystal is sharply bent—*kink bands*. The lamellae between these narrow curved regions become disoriented as the deformation proceeds, and a lamellar type of disorientation results (see, for example, Fig. 6, Plate VIII). However, the bands themselves frequently show in the X-ray images as dark lines more intense than the adjacent regions of the crystal. This effect is best observed when the disorientations have been insufficient to produce the white non-reflecting lamellae in the images. Fig. 8 (a) (Plate IX) is an X-ray image from an aluminium crystal deformed by 2.9% elongation at 450°C. The dark bands correspond with narrow kink bands on (110) planes. In other circumstances, kink bands can also be revealed by the absence of a reflection when the rotations within them have been relatively great. These two effects of kink bands on the X-ray image are illustrated in Fig. 7 (a) (Plate VIII), in which both black and white lines can be seen. It should be mentioned that if a crystal containing kink bands is annealed at a high temperature, so that the curvatures are eliminated by polygonization, the intensity of the reflections from the bands diminishes markedly and more bands appear as white lines in the image.

The reason for these intense reflections may be the focusing by the bent lattice, but it seems more likely that it is an extinction phenomenon resulting from the distortions, which are in effect concentrations of dislocations. Some support for the latter view is found in the fact that other phenomena in deformed crystals which are associated with concentration of dislocations produce similar effects in the X-ray images. For example there is the slip process, which, although it occurs on a scale rather too fine for complete investigation by the X-ray technique at its present stage of development, nevertheless can be detected and studied under favourable conditions. Here also, the slip bands are revealed in the X-ray images as narrow bands of high intensity (Fig. 9, Plate IX).

Polygonization,<sup>6</sup> although it removes lattice curvatures by diffusion of dislocations and thus causes changes in the intensity of reflections from kink bands, does form narrow walls of dislocations separating regions differing slightly in orientation. These walls are often revealed in X-ray images as dark lines. Fig. 10 (Plate IX) is such an X-ray image taken from an aluminium crystal after 7% elongation in 13 days at 300°C., in which a complicated network of polygon boundaries is visible. In this case the disorientations between the polygons are so small that the majority are reflecting the incident X-rays, and they would not have been detected but for the stronger reflections from their boundaries.

Once it is appreciated that the X-ray image may be modified in the ways mentioned above, it is possible with some experience to interpret the images fairly accurately. Interpretation is greatly aided by using the X-ray method side by side with optical microscopy, although frequently the features which are observed in X-ray micrographs after small deformations, are not detected optically till after much heavier deformation. In the next section, a more detailed comparison of the results obtained by the two methods will be given.

## V.—A COMPARISON OF X-RAY AND OPTICAL MICROGRAPHY OF DEFORMED CRYSTALS

It should be emphasized first that the features of deformed crystals revealed by X-ray microscopy differ from those normally observed by optical microscopy. The optical examination of metals depends to a large extent on the observation of differences in surface level, e.g. grain boundaries and slip bands, and of differences in appearance produced by etching. X-ray microscopy on the other hand is not particularly sensitive to small changes in surface level; this can be seen by comparison of Figs. 5 (a) and (b) (Plate VIII), which represent X-ray and optical micrographs taken from one grain of a coarsely crystalline aluminium specimen after 0.6% elongation in tension at room temperature. Optical examination in oblique illumination has revealed slip bands and a number of irregular surface blemishes (Fig. 5 (b)), all

of which are absent in the X-ray macrograph (Fig. 5 (a)). The great advantage of X-ray micrography in the study of deformed crystals is in the detection of small local changes in orientation not revealed by optical microscopy. The X-ray reflection gives a map of the orientation changes which produce optically observable effects only at much heavier deformation. For example, Fig. 5 (a) contains several white bands representing disorientations in the crystal; on the other hand optically it is only just possible to detect some of the bands in oblique illumination (Fig. 5 (b)) because of slight changes in surface level. Furthermore, there is no indication in Fig. 5 (b) of the smaller included grain which is clearly delineated as a white area in Fig. 5 (a).

Scratches inscribed on specimens show up clearly in X-ray images (Figs. 5 (a), and 7, Plate VIII, and Fig. 8 (a), Plate IX) because the severe deformation in the scratch causes local disorientations. For this reason it is essential to eliminate mechanical polishing as a means of preparing the crystal surfaces. This need is further illustrated in Figs. 11 (a) and 11 (b) (Plate IX). A copper crystal was filed to produce a flat surface, ground, then electrolytically polished to remove all scratches. It was then deformed by 2.9% elongation, but the results of this deliberate deformation were entirely masked in the X-ray image by the effects of filing and grinding (Fig. 11 (a)). The crystal was then further electrolytically polished to remove 2 mm. of metal, approximately 25% of its original thickness. The X-ray micrograph taken at this stage revealed the more uniform effects of the tensile deformation and the coarse growth mosaic typical of cast single crystals (Fig. 11 (b)). X-ray micrography is thus a simple and sensitive way of studying the extent of deformation of metal crystals by various surface treatments.

The X-ray technique has proved very useful in a study of the plastic deformation of single crystals, the detailed results of which are to be discussed in a later paper.<sup>5</sup> While the method is applicable to an individual grain in polycrystalline aggregates, the use of single crystals is preferable so that simpler stresses can be applied to the specimen during deformation. X-ray micrographic examination of single crystals deformed in tension has revealed the presence of local disorientations or inhomogeneities long before they could be detected optically. For example, Fig. 12 (a) (Plate IX) shows an X-ray micrograph of an aluminium single crystal after 4.6% elongation in tension at room temperature, in which lamellar disorientations are evident. The cause of these disorientations proved to be narrow kink bands or regions of curvature which could not be detected optically until after much greater deformation. Fig. 12 (b) (Plate IX) is an optical micrograph taken on the same crystal after 10% elongation, in which the narrow kink bands can just be seen; however, there is no indication of the marked disorientations which have resulted in the

crystal. In Fig. 8 (a) (Plate IX), which is an X-ray micrograph from an aluminium crystal deformed by 2.9% elongation in tension at 450° C., the disorientations have not been sufficient to show up as white regions in the image, but the distorted regions appear as intense black bands. The corresponding optical micrograph reveals no sign of the kink bands, the only feature being the rather ill-defined high-temperature slip bands (Fig. 8 (b)).

It is not obvious at first sight that the bands of Figs. 8 (a) and 12 (a) (Plate IX), are identical, but a careful comparison of X-ray and optical micrographs at various stages of the deformation confirms this view. The most convincing evidence is obtained from the orientation of the bands within the crystals. The determination of the orientation of the bands is a simple matter in optical micrography if the orientation of the crystal itself is known; but with X-ray micrographs some distortion of angular relationships existing in the crystal usually results in the X-ray image. This follows because the reflected image may strike the photographic plate at any angle in space. A correction factor can be obtained by inscribing on the specimen two fine scratches making different angles with the axis. These will appear in the X-ray image (e.g. Fig. 11 (b), Plate IX), and the angles can again be measured.

Now it can be shown that:

$$\tan \alpha = A \tan \beta + B$$

where  $\alpha$  = angle on X-ray image,  $\beta$  = actual angle on specimen surface, and  $A$  and  $B$  are constants for a given reflection. With two pairs of angles, two simple equations are obtained from which the factors  $A$  and  $B$  can be determined.\* Thus the angles made by bands on surfaces of the crystal can be found when the bands are visible only in X-ray images. The orientation of the bands is then obtained by plotting the angles obtained from two faces of the crystal on a stereographic projection containing the crystal orientation. By this method it was found that the bands in Figs. 8 (a) and 12 (a) (Plate IX) occurred on (110) planes in the early stages of the deformation. In all the crystals examined these bands possessed the same crystallographic habit independent of temperature and speed of deformation.

X-ray micrography has revealed a second lamellar type of disorientation, but in most of the crystals examined the bands were initially almost parallel to the active slip plane, namely (111) in aluminium and copper. Fig. 11 (b) (Plate IX) is an X-ray image of a copper crystal deformed to 2.9% elongation by tension in which these lamellar disorientations are visible. Because of their crystallography they could easily be confused with slip bands, but optical examination at much greater deformations confirmed that such bands were present in the crystal and showed that they were regions in which a second slip system had operated, causing local disorientations.

\*  $B$  is usually quite small and can often be neglected.



Thus optical examination revealed how the bands were formed, while X-ray microscopy proved to be a much more sensitive means of detecting them.

The slow deformation of crystals at elevated temperatures usually results in the formation of similar inhomogeneities. For example, Figs. 6 (a) and (b) (Plate VIII) are X-ray micrographs taken from an aluminium crystal after four days' slow deformation at 300° C. (3% elongation). The large-scale lamellar form of the image is due to disorientations resulting from the formation of kink bands, which under these conditions cause almost macroscopic disorientations in aluminium of high purity. However, slow deformation at high temperatures is a rather different problem from that of deformation at low temperatures, because polygonization can occur simultaneously with the deformation. The work of Wood and his collaborators<sup>7, 8</sup> has shown the important part played by this phenomenon in the creep of aluminium polycrystals at elevated temperatures. By X-ray powder methods and optical micrography, they have found that strain-free fragments are formed within the individual crystals at an early stage of the deformation. But these methods do not reveal the origin of the fragments, nor do they show their exact mode of distribution within the grain and how it changes as the deformation proceeds further. X-ray microscopy is proving of value in this field, as it is capable of showing the mode of occurrence of the polygons at an early stage of the deformation, and the behaviour of individual fragments of a crystal can be followed. It has been mentioned already that the polygons are first revealed in X-ray micrographs by the intense reflections from their boundaries (Fig. 10, Plate IX); in this way the fragments can be detected in the early stages of the deformation when the orientation differences are too small to be revealed by absence of reflections. As the deformation proceeds the disorientations between the polygons become greater and they no longer all reflect simultaneously. This stage is shown in Figs. 6 (a) and (b) (Plate VIII) in which the long lamellæ are no longer reflecting uni-

formly—there are white areas within dark lamellæ which represent large individual polygons.

In conclusion, it is not suggested that the X-ray method described here is incapable of improvement. Certain alterations such as the provision of a much smaller source and a reduction of the divergence of the X-ray beam will certainly increase the sensitivity of the technique. However, the aim of this paper has been to show that the method as it stands provides a simple and effective way of studying the deformation of metal crystals, which yields information not normally obtained by optical micrography or more standard X-ray methods. The interpretation of the X-ray images can be a source of difficulty, particularly if the deformation is severe, but if the experiments are restricted to lightly deformed specimens and include optical micrography, then significant results can be obtained.

#### ACKNOWLEDGEMENTS

The author is indebted to Dr. E. Orowan, F.R.S., who first interested him in this problem, and to Professor Sir Lawrence Bragg, F.R.S., for laboratory facilities. The author wishes to thank his colleagues in the Cavendish Laboratory, in particular Mr. W. M. Lomer, for helpful discussions and also Mr. S. D. Charter for enthusiastic assistance. Finally, he is very grateful to the Armourers and Brasiers' Company for their Fellowship.

#### REFERENCES

1. W. Berg, *Naturwiss.*, 1931, **19**, 391.
2. W. Berg, *Z. Krist.*, 1934, **89**, 286.
3. A. Guinier and J. Tennevin, *Compt. rend.*, 1948, **226**, 1530.
4. C. S. Barrett, *Trans. Amer. Inst. Min. Met. Eng.*, 1945, **161**, 15.
5. R. W. K. Honeycombe, *J. Inst. Metals*, 1951-52, **80** (in the press).
6. R. W. Cahn, *J. Inst. Metals*, 1949-50, **76**, 121.
7. G. R. Wilms and W. A. Wood, *J. Inst. Metals*, 1948-49, **75**, 693.
8. W. A. Wood and W. A. Rachinger, *J. Inst. Metals*, 1949-50, **76**, 237.

# INHOMOGENEITIES IN THE PLASTIC DEFORMATION 1324 OF METAL CRYSTALS—I.—II.\*

## I.—Occurrence of X-Ray Asterisms

By R. W. K. HONEYCOMBE,† M.Sc., Ph.D., MEMBER

### SYNOPSIS

A study has been made of the occurrence of X-ray asterisms from deformed single crystals of a typical hexagonal metal (cadmium) and a typical cubic metal (aluminium). Cadmium can be extended by more than 100% elongation in tension without the appearance of asterisms in X-ray Laue photographs; asterisms occur only when the crystals are macroscopically bent or kinked. On the other hand, they are present in photographs from aluminium crystals after less than 4% elongation in tension. These asterisms contain intensity maxima which are shown to be a direct consequence of the deformation and not of a secondary phenomenon such as polygonization.

On annealing, extended cadmium crystals give sharp Laue spots, and the bent crystals polygonize very uniformly at 300° C. The appearance of asterisms from lightly extended aluminium crystals is unaltered by annealing at 250° C., at which temperature partial recovery of the yield stress occurs; but when the temperature is raised to 475° C. the asterisms become further fragmented as a result of polygonization.

These experiments suggest that tensile deformation causes aluminium, but not cadmium, crystals to break down into a series of slightly disoriented blocks connected by regions of distortion or lattice curvature.

### I.—INTRODUCTION

It has been realized for a long time that plastic deformation of metal crystals does not consist merely of simple translations along crystallographically defined slip planes. This is clearly shown in the shape of the stress/strain curves, which indicate that strain-hardening occurs to a greater or lesser degree. There is also metallographic evidence that even in deformed single crystals, deformation does not result in uniform shearing along glide lamellæ. The simple conception of plastic deformation is further belied by the occurrence of certain X-ray phenomena, such as asterisms in Laue photographs and line broadening in Debye-Scherrer photographs. X-ray asterisms show that local disorientations occur in deformed crystals, but these are related to the original orientation and do not amount to a random fragmentation of the crystal. In this and the second part of the paper, investigations of the nature of the phenomena in the deformed crystals giving rise to some of the above deviations from pure deformation by slip are described. These phenomena will be called inhomogeneities until at a later stage they can be referred to in more specific terms. A good starting point for the investigation is provided by a study of the origin and occurrence of X-ray asterisms.

### II.—THE ORIGIN OF X-RAY ASTERISMS

During the last twenty years there have been three main theories advanced to explain X-ray asterisms. Their origin has been variously attributed (1) to

local curvatures on the slip planes, (2) to macroscopic curvatures of the crystal, and (3) to fragmentation.

(1) Yamaguchi<sup>1</sup> considered that asterisms arose from the presence on the slip planes of local curvatures formed when glide processes became anchored in the lattice. This hypothesis was later supported by Taylor<sup>2</sup> and by J. M. Burgers,<sup>3</sup> who assumed that local curvatures occurred when dislocations of opposite sign approached each other. W. G. Burgers and Lebbink<sup>4</sup> did not consider macroscopic curvatures to be the basic cause of asterism, because they found that X-ray photographs of aluminium crystals showed asterisms even when the crystals were sheared along the slip plane in the slip direction by a special apparatus.

(2) Other workers hold the view that asterisms are caused by macroscopically bent regions of the crystals, and there are in fact cases where asterism clearly arises from this cause, e.g. the elastic bending of mica or thin metal sheet where asterism disappears on return to the unbent condition; this also occurs with some plastically bent crystals when they are re-straightened. Komar and Mochalov<sup>5</sup> have shown that with deformed magnesium crystals, the lengths of the Laue striæ diminish as the thickness of the crystals is reduced by etching, a result which suggests that the asterisms are due to macroscopic curvatures. Orowan and Pascoe<sup>6</sup> obtained further evidence for this view by the examination of X-ray rotation photographs from slightly deformed cadmium crystals. They found that certain reflections were very sharp, whereas other reflections from the same planes were

\* Manuscript received 24 January 1951.

† Formerly Armourers and Brasiers' Company Research

Fellow, Cavendish Laboratory, Cambridge; now at Metallurgy Department, University of Sheffield.



blurred, a result they explained by assuming a macroscopic curvature of the plane, the sharp reflection coming from the concave side, the blurred one from the convex. Kochendörfer<sup>7</sup> found that asterisms were absent in X-ray photographs from naphthalene crystals which had been sheared along the glide plane and in the glide direction, while tensile and compressive tests imposing similar strains resulted in strong asterisms. He concluded that the asterism was not due to local curvatures, as its occurrence depended clearly on the nature of the deformation process.

(3) A third explanation attributes X-ray asterism to the formation of lattice fragments with very small differences in orientation between neighbouring fragments, which if sufficiently small would make the asterism continuous. Manteuffel<sup>8</sup> and Komar<sup>9</sup> supported this view because they observed discontinuities in the asterisms from deformed metals. Wood,<sup>10</sup> on the basis of extensive experiments on X-ray line broadening, also considers that fragmentation occurs as a direct result of deformation. There is, in fact, much evidence that under certain conditions, e.g. deformation at high temperatures, X-ray asterisms contain a fine structure. This has been studied in recent years by Cahn<sup>11</sup> and by Guinier and Tennevin,<sup>12</sup> and from their experiments it seems clear that the breaking up of the asterisms results from the recovery of a bent lattice to a series of closely oriented, unbent blocks. This takes place by diffusion of dislocations to form the walls between the "fragments". It appears that this process, which Orowan has called polygonization, is a secondary one which removes lattice distortions caused by plastic deformation.

Apart from X-ray phenomena, there is direct metallographic evidence that inhomogeneities occur when metals deform. Band-like structures have been observed within deformed grains in many different metals in a variety of circumstances. In 1939 Barrett and Levenson<sup>13</sup> published an account of a detailed investigation into the occurrence of what they called *deformation bands* in iron and aluminium, using both polycrystalline and single-crystal specimens. In the early stages of deformation the bands occurred on planes of low indices, and the lattice within each band rotated away from the parent orientation to a gradually increasing degree. After heavy deformations the crystallographic features were obscured and the bands became curved and distorted. Barrett suggested that in view of the fact that the ranges of orientation in the bands correspond approximately with those determined from X-ray asterisms, the bands are a major source of these asterisms. These experiments demonstrated the important role of such inhomogeneities in the deformation of metals, but many points remain to be elucidated.

It is difficult to decide the real causes of asterism on the available evidence, because the experiments have been carried out on a variety of metals—and even non-metals such as mica, naphthalene, and rock salt—under widely differing conditions of deformation. It is perhaps unwise to expect non-metals to behave

similarly to metals, or indeed for metals as a class to behave uniformly. There is, in fact, ample evidence that metal crystals of cubic crystal structure, when plastically deformed, behave very differently from metals of hexagonal structure; e.g. the resolved shear stress/strain curves fall into two distinct groups,<sup>4</sup> the hexagonal metal crystals showing only a small degree of strain-hardening. It therefore seemed necessary to compare the behaviour of a typical hexagonal metal with that of a typical cubic metal. Experiments to this end on cadmium and aluminium are described below, in which the occurrence of asterisms is investigated together with the behaviour of the deformed crystals on annealing.

### III.—STUDY OF ASTERISMS FROM DEFORMED CRYSTALS

#### 1. CADMIUM

The single crystals used in these experiments were in the form of 1-mm.-dia. wires produced from the melt by the Andrade method. These were made from both spectroscopically pure (99.99%) and 99.9% pure metal. Crystals were selected in which the angle between the glide plane and the wire axis was 40°–60° (soft orientations), so that a large extension could be expected before twinning occurred. Specimens with gauge-lengths between 2 and 5 cm. long were carefully extended on a glass plate using small tweezers; in this way handling of the extremely fragile crystals was reduced to a minimum, and accidental distortion eliminated. Crystals were extended by this method to 100, 200, and even 300% elongation. Short lengths were then cut from the resulting flat ribbons by means of a sharp razor blade, and X-ray Laue photographs were taken using gold radiation. It was found that crystals extended by 100% produced practically no asterism in the Laue photographs and only a slight fine structure could be detected in the reflections (Fig. 4, Plate X). Prolonged annealing of the extended crystals in no case resulted in recrystallization and X-ray photographs revealed that the Laue spots were again extremely sharp and typical of an undeformed crystal.

Specimens from the extended crystals were then bent by controlled amounts around cylindrical mandrels (with radii of curvature from 5 to 1 mm.), the basal plane being almost parallel to the axis of bending. X-ray Laue photographs showed marked asterisms which were homogeneous, i.e. there were no pronounced intensity maxima (Fig. 5, Plate X). On annealing the bent crystals at 290° C. for 24 hr., a striking uniform fragmentation of the asterisms occurred, indicating that the bent lattice had polygonized (Fig. 6, Plate X). Prolonged annealing resulted in a coarsening of the polygonized structure, the range of orientation remaining constant. Recrystallization only occurred in the most severely bent crystals (radius of curvature 1.75 mm.), in which the new grain grew at the expense of a polygonized matrix (Fig. 7, Plate X).

Certain crystals were chosen with their basal plane parallel to the wire axis, so that on compression kinking took place. The structure of a kinked crystal, as given by Orowan<sup>15</sup> is shown in Fig. 1. This configuration occurs when the crystal suddenly collapses under load; there are two kink planes,  $k$  and  $k'$ , separated by a region in which the crystal is bent severely. X-ray photographs of kinked crystals did, in fact, show marked asterism in this region, but not elsewhere in the crystal. That kinking had led to a macroscopic bending of the crystal planes was shown directly by polishing flat faces on crystals such that the displacement would occur parallel to the face. The crystals were then kinked and examined microscopically. Fig. 8 (Plate X) shows a typical micrograph of a portion of a kink; the sharp change in direction of the slip lines at the kink plane is shown, and the slip lines in the region between the kink planes are macroscopically bent.

The bending caused by kinking was so severe that spectroscopically pure cadmium crystals after kinking either polygonized or recrystallized at room tempera-

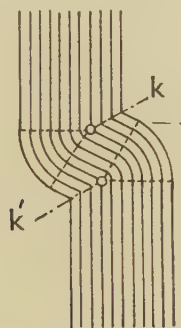


Fig. 1.—Schematic Diagram of a Kinked Crystal (Orowan<sup>15</sup>).

ture if left for several weeks. These changes were restricted to the bent regions of the crystal. If the kinked crystals were annealed at high temperatures (300° C.), the kinked region was almost invariably replaced by two new grains, each of which occupied one curved region of the kinked crystal, their boundaries with the old crystal being in the vicinity of the two kink planes.

## 2. ALUMINIUM

The aluminium crystals were prepared in a similar way to the cadmium crystals. They were in the form of wires 0.5 mm. in dia. and were of spectroscopic purity (99.99%). Specimens 1 in. long were cut from the crystals, and small copper U's were soldered to the ends so that the specimens could be suspended and deformed in a single-crystal extensometer.

Preliminary experiments showed that asterisms appeared in X-ray Laue photographs when the crystals had been elongated in tension by only small amounts. After 1% extension the Laue reflections were blurred and after 4–5% marked asterisms had developed. In all the cases examined the asterisms possessed a

pronounced fine structure which became apparent in the very early stages of the deformation (Fig. 9, Plate X). It was considered that a more valid comparison could be made with the experiments on cadmium if the aluminium crystals were deformed at elevated temperatures. However, asterisms were still obtained from crystals deformed at 400° C., and even after deformation at 600° C. Fig. 10 (Plate X) shows asterisms from a crystal deformed 20% at 600° C. Under such circumstances the asterisms were always built up of small discrete spots, indicating that fragmentation had occurred during deformation despite the fact that the deformed crystal was at 600° C. for only about 2 min. Microscopic examination confirmed that discrete crystallites with straight boundaries had been formed, in other words that the crystal had polygonized.

The fine structure in asterisms from crystals deformed at room temperature might be attributed to the partial occurrence of polygonization, which is pronounced in crystals deformed at much higher temperatures. However, such a recovery process would hardly be expected in aluminium crystals only slightly deformed at room temperature. For example, Guinier and Tennevin,<sup>12</sup> using a very sensitive X-ray focusing method, were unable to detect polygonization in aluminium at temperatures less than 300° C. and in most cases a considerably higher temperature was required. If polygonization does occur in aluminium crystals deformed slightly at room temperature, then changes in the mechanical properties, e.g. the yield point, might be expected to take place. To determine whether this was so, crystals were strained by small amounts in a single-crystal extensometer and the stress/strain curve obtained. The yield stress was subsequently measured after various periods at room temperature. Deformed crystals were also held at elevated temperatures (250°–450° C.) and changes in the yield stress were plotted against time to give recovery curves. The crystals thus investigated were mounted in small jigs that enabled them to be removed from the extensometer without distortion and to be fixed to the spindle of an X-ray camera. X-ray back-reflection Laue photographs were taken at various stages of the treatment and correlated with the changes in yield stress.

Several crystals were deformed small amounts (between 2 and 6% elongation) and allowed to remain at room temperature. It was found that the X-ray patterns showed intensity maxima when the exposure was made immediately after deformation. The pattern did not alter after two days at room temperature, and in the same time no change in the yield stress of the deformed crystals could be detected.

Certain of the deformed crystals were subsequently annealed at 250°–300° C., and the yield stress measured at intervals during the process. For example, Fig. 2 shows both the stress/strain curve and the recovery curve for crystal E Al 5; marked recovery has taken place on annealing at 250° C. X-ray Laue photographs taken with a fine collimator (0.3 mm.) revealed no change from those taken immediately after deforma-



tion. If a crystal annealed at 300° C. was subsequently annealed for 30 min. at 450° C. then the X-ray asterisms broke down further, giving the spots characteristic of polygonization. These new spots occurred in the originally diffuse portions of the

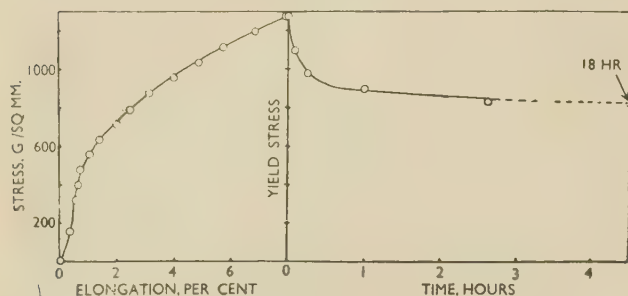


FIG. 2.—Stress/Strain and Recovery Curves for Aluminium Crystal E Al 5.

asterisms, while the original intensity maxima remained (Fig. 11, Plate X).

Other crystals after similar deformations were annealed immediately at 475° C. The yield stress fell markedly in the first 5 min. of the anneal (Fig. 3), during which time no perceptible change could be seen in the X-ray Laue patterns. However, at a later stage, when the recovery curve was almost horizontal, marked changes characteristic of poly-

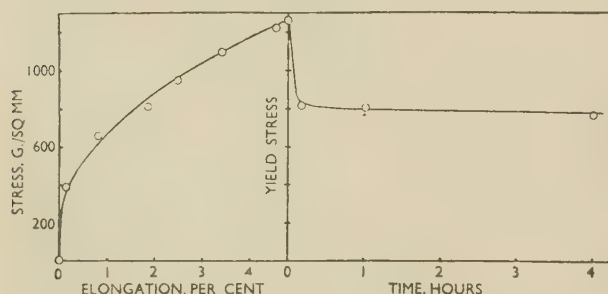


FIG. 3.—Stress/Strain and Recovery Curves for Aluminium Crystal E Al 1.

gonization were observed. It is interesting to note that after 5 minutes' annealing, the yield stress dropped almost to its final value. Further prolonged annealing did not result in a closer approach to the yield stress of the original crystal. It seems that changes resulting in the major part of the recovery are beyond the resolution of the X-ray method, which reveals only the final stage of polygonization when growth is taking place with little influence on the mechanical properties.

#### IV.—DISCUSSION AND CONCLUSIONS

The experiments with cadmium deformed in tension show that X-ray asterisms are not necessarily associated with the plastic deformation of this metal. That asterisms are obtained from cadmium crystals deformed inhomogeneously by bending or by kinking

is entirely in accord with the view that they result from macroscopic curvatures of the crystal, the occurrence of which in turn depends on the mode of deformation. On the other hand, asterisms appear in the photographs of aluminium crystals even after small elongations in tension, when marked macroscopic curvatures would not be expected. These asterisms differ from those obtained from bent cadmium crystals in so far as they contain marked intensity maxima after small deformations. It seems unlikely that these maxima are a result of polygonization, because they occur concurrently with the deformation at relatively low temperatures. They do not appear to result from spontaneous recovery at room temperature, because the Laue streaks show no further breakdown after several days at room temperature; furthermore, no change in yield stress occurs during this time. In fact, the asterisms remain unaltered even after annealing at 300° C., at which stage there is a definite fall in the yield stress which indicates that recovery is taking place. If the temperature is then raised to 450° C. for a short time, the Laue streaks alter, the diffuse arc breaking up into sharper spots typical of polygonization; however, the original intensity maxima remain.

The X-ray evidence suggests that in the case of aluminium deformed at room temperature, a fragmentation of the crystals has occurred. This view has been frequently put forward in the past to explain similar observations. However, the author believes that the "fragments" are responsible only for the intensity maxima in the asterisms, the diffuse background originating from distorted regions which join the fragments and allow the crystal to remain continuous although locally disoriented. In support of this hypothesis there is the observation referred to earlier that polygonization occurs primarily in the diffuse regions of the asterism, as would be expected if these regions were more severely bent than the rest of the crystal. It is clear that the tensile deformation of cubic metal crystals results not only in a greater degree of strain-hardening than is the case in hexagonal metals, but that the deformation is accompanied by much more distortion of the crystal. The obvious deduction is that the increased strain-hardening is a result of the greater amount of distortion in the crystals of cubic metals. Before this hypothesis can be further explored, the exact nature of the distortions should be known. This is dealt with in Part II.

A comparison of the behaviour of deformed crystals of cadmium and aluminium on annealing is significant. On the one hand cadmium, after extensions of 200–300% in tension, would not recrystallize or polygonize even on prolonged annealing at temperatures close to the melting point. The Laue spots originally only slightly affected by the severe deformation became extremely sharp after annealing. It thus appears that complete recovery occurred in these cases. In fact, measurements of the change in yield point of deformed zinc crystals made by Haase and Schmid<sup>16</sup> showed that even after 100% elongation complete

recovery to the original yield stress occurred, and Davies<sup>17</sup> has recently confirmed this behaviour for cadmium. On the other hand aluminium crystals deformed in tension do not recover to their original yield stress when annealed at high temperatures after relatively small deformation. Moreover, the X-ray reflections remain complex. It seems clear that once disorientations occur within a crystal they are not removed by recovery; nucleation and grain growth are the only way in which a uniform orientation can be re-created.

The experiments do not show conclusively whether polygonization is the sole mechanism by which recovery

occurs, for the resolution obtained in the X-ray Laue technique is insufficient to decide this. It is, however, significant that extended cadmium crystals are capable of complete recovery without the occurrence of polygonization. In this case it could be assumed that dislocations in the slip planes migrate through to the surface of the crystal, whereas if the crystal is bent this freedom of movement is restricted and the excess dislocations of one sign form polygon boundaries, leading to the observed X-ray effects. On the other hand, with aluminium crystals the movement of dislocations is hindered by the regions of distortion, which give rise to the X-ray asterisms.

## REFERENCES TO PART I.

1. K. Yamaguchi, *Sci. Papers Inst. Phys. Chem. Research (Tokyo)*, 1929, **11**, 151.
2. G. I. Taylor, *Proc. Roy. Soc.*, 1934, [A], **145**, 362.
3. J. M. Burgers, *Proc. Phys. Soc.*, 1940, **52**, 23.
4. W. G. Burgers and F. J. Lebbink, *Rec. Trav. Chim.*, 1945, **64**, 321.
5. A. P. Komar and M. D. Mochalov, *Physikal. Z. Sowjetunion*, 1936, **9**, 613.
6. E. Orowan and H. J. Pascoe, *Nature*, 1941, **148**, 467.
7. A. Kochendörfer, "Plastische Eigenschaften von Kristallen und metallischen Werkstoffen." Berlin: 1941 (Julius Springer).
8. I. Manteuffel, *Z. Physik*, 1931, **70**, 109.
9. A. P. Komar, *Physikal. Z. Sowjetunion*, 1936, **9**, 413.
10. W. A. Wood, *Proc. Phys. Soc.*, 1940, **52**, 110, &c.
11. R. W. Cahn, *J. Inst. Metals*, 1949-50, **76**, 121.
12. A. Guinier and J. Tennevin, *Compt. rend.*, 1948, **226**, 1530.
13. C. S. Barrett and L. H. Levenson, *Trans. Amer. Inst. Min. Met. Eng.*, 1939, **135**, 327; 1940, **137**, 112.
14. E. Schmid and W. Boas, "Plasticity of Crystals with Special Reference to Metals", p. 125. London: 1950 (F. A. Hughes and Co.).
15. E. Orowan, *Nature*, 1942, **149**, 643.
16. O. Haase and E. Schmid, *Z. Physik*, 1925, **33**, 413.
17. P. T. Davies, private communication.

## II.—X-Ray and Optical Micrography of Aluminium

### SYNOPSIS

A technique of X-ray microscopy is used in conjunction with optical micrography to investigate the structure of large aluminium crystals deformed by small amounts in tension. Two types of microscopic inhomogeneity which cause local variations in orientation are described. First, there are narrow regions of curvature or *kink bands* separating slightly disoriented lamellæ of the crystal; these bands occur initially on (110) planes, the normal to which coincides with the active slip direction. The second type of inhomogeneity comprises *bands of secondary slip*, which are regions nearly devoid of primary slip traces, in which slip on another system occurs preferentially. These bands are almost parallel to the primary slip planes in the early stages of deformation.

The effects of crystal orientation, temperature and speed of deformation, and purity of metal on the occurrence of kink bands are investigated, and it is found that these are usually present after deformation, except when this occurs from the beginning by conjugate slip. Bands of secondary slip also generally occur, and in crystals deforming by conjugate slip, they are often of macroscopic size.

The inhomogeneities play an important role in the deformation of aluminium and account for many of the differences between this metal and cadmium, such as the occurrence of X-ray asterisms, the marked differences in strain-hardening, and the extent to which recovery can occur on annealing.

### I.—INTRODUCTION

MUCH work has been done on the occurrence of so-called *deformation bands* in deformed metals, in particular by Barrett and Levenson,<sup>1</sup> which indicates that these bands may be the seat of the distortions in the crystals. However, the wealth of information relating to the bands is rather confusing and their exact nature is far from clear. If inquiry is restricted to aluminium single crystals deformed in tension, it is found that there is some evidence for the existence of regions of distortion on a microscopic scale. As

long ago as 1929, Yamaguchi<sup>2</sup> found microscopic regions in which the slip lines were bent, and Collins and Mathewson<sup>3</sup> observed narrow bands of crystallographic habit which they considered to be deformation bands. More recently Crussard<sup>4</sup> found regions in deformed aluminium crystals which he likened to the kinking that occurs in hexagonal metal crystals. Finally, Cahn,<sup>5</sup> during the course of the present work, has investigated by microscopic means bands of local flexural glide in deformed aluminium crystals of special orientation. There seems little doubt that all these observed phenomena are related and that they



are in need of further systematic study. Bearing in mind the limitations of optical micrography for detecting small local changes in orientation within crystals, a method of X-ray microscopy similar to that described by Berg<sup>6</sup> and Barrett,<sup>7</sup> which is suitable for the examination of lightly deformed crystals, has been developed. The main results obtained with deformed aluminium crystals are described below, but for convenience, the method employed and the detailed interpretation of the X-ray micrographs have been discussed in a separate paper.<sup>8</sup>

## II.—EXPERIMENTAL WORK

### 1. PREPARATION AND EXAMINATION OF CRYSTALS

The small crystals used in the previous experiments (reported in Part I) were unsuitable for micrographic examination, so large flat crystals 20 cm. long, 12.5 mm. wide, and 1.5–3 mm. thick, with a gauge-length of 7 cm., were produced by the Carpenter–Elam critical-strain method. Two grades of aluminium were used one 99.5% pure and the other 99.99% pure. Before deformation the crystals were electropolished, without previous mechanical polishing.

The crystals were deformed by various amounts between 0.5 and 20% elongation in a simple straining jig which, if necessary, could be heated in a furnace. The deformed crystals were examined in the optical microscope, often in oblique illumination, and by X-ray microscopy. Whereas the optical microscope revealed very small displacements in the crystal surface, e.g. slip lines, X-ray micrography showed local distortions and changes in orientation. As these disorientations did not occur on the slip planes, the latter were not usually an important feature of the X-ray photographs.

### 2. SUMMARY OF RESULTS

In aluminium crystals deformed between 0.5% and 20% elongation, two distinct types of inhomogeneity which had caused local disorientations were observed. First, narrow bent regions were found which separated relatively unbent regions of the crystals. These, which will be referred to as *kink bands*, were detected at a very early stage of the deformation on (110) planes. The essential feature of this type of inhomogeneity is the bending which can give rise to X-ray asterisms.

The other type of inhomogeneity comprised bands which were initially deficient in primary slip traces, i.e. traces of the slip system which would normally be expected to operate (applying the criterion of maximum resolved shear stress). In the very early stages of the deformation these bands were roughly parallel to the active slip planes. As the deformation proceeded, the bands became the preferential sites for secondary slip on planes not predicted by the criterion of maximum shear stress. For clarity, this type of inhomogeneity will be referred to as *bands of secondary slip*. These bands also lead to disorientations in the crystal, but are primarily free from severe curvatures.

## 3. KINK BANDS

### (a) Detection by X-Ray Micrography

X-ray micrographs of aluminium crystals of 99.5% purity after 4% elongation in tension were shown to possess a fine structure absent from images of undeformed crystals. When the X-ray images recorded on Kodak Maximum Resolution plates were enlarged to 50 diameters, two sets of dark bands were revealed (Fig. 12, Plate XI). One set, which predominated, had a spacing of about 0.05 mm.; furthermore, most of the bands ran completely across the crystal face. The fact that the reflections from the deformed crystal comprised alternate dark and light bands indicated that more or less regular disorientations had occurred. The crystal had broken up into long thin blocks, many of which were not in a position to reflect the incident X-rays. Optical examination at this stage of the deformation did not reveal the bands, but confirmed that they could not be due to the slip traces (Fig. 14, Plate XI). However, at heavier deformations (over 10% elongation) bands became visible and proved to be narrow regions within which the crystal was bent (Fig. 15, Plate XI). Optical examination at higher magnification showed clearly that the bands possessed a double curvature similar to that observed in kinked cadmium crystals. However, the planes bounding the bent regions were not as well defined as those in cadmium. Occasionally the presence of a small included grain caused the bands in its vicinity to widen and become more pronounced (Fig. 16, Plate XI).

The X-ray reflections from the slightly deformed crystals occurred over a greater angular range than those from the annealed crystals. It was not possible to relate directly the angular range of reflection to a given part of the crystal, because, as the crystal was rotated, the area contributing to the reflection changed gradually. However, by taking a series of photographs 6' apart, and by comparing the same region of the specimen represented in each, it was possible to determine the angular displacement over which a particular region contributed to the reflection. After 4% elongation, the angle was usually between 1° and 2° and increased with increasing deformation. While a small area, say 1 mm.<sup>2</sup>, might contribute to the reflection for 1° of rotation, it was obvious that different microscopic parts within the area contributed to the reflection at different stages of this rotation.

At certain settings of the crystal it was possible to obtain reflections from the slip planes rather than from the kink bands. Fig. 13 (Plate XI) shows the change which occurred in the image of Fig. 12 (Plate XI) after a rotation of only 20'. The dark bands representing the kink bands have been entirely replaced by a series of fine dark striations which are broken by horizontal white bands of similar orientation to the dark bands of Fig. 12. The kink bands are no longer in a reflecting position. In general, it was found that the kink bands caused striations which predominated in the image over most of the angular range

of reflection, whereas the reflections from the slip planes usually appeared over a much more restricted range (between  $10'$  and  $20'$ ). This predominance of the kink-band reflections is a consequence of the range of orientation created by these bent regions of the crystal, while the high intensity of the reflection is probably a result of the distortion in the bands.<sup>8</sup>

### (b) Crystallography of the Kink Bands

A number of crystals of different orientations were examined by X-ray micrography to determine whether the occurrence of the kink bands was dependent on orientation. The tension axes of 11 crystals which were systematically investigated are represented in the stereographic triangle of Fig. 26. Kink bands were detected in the crystals represented by the open circles, while the black circles represent crystals in which kink bands were not observed. In these two cases, conjugate slip on two or more systems occurred from the beginning of plastic deformation. While the

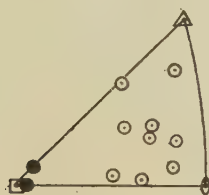


FIG. 26.—Stereographic Projection of Crystal Tension Axes.

○ Kink band present.      ● Kink band absent.

kink bands occurred to the same extent in crystals whose orientations lay near the centre of the stereographic triangle, they were much finer and more difficult to detect in crystals whose orientations were approaching the (111) pole. In these crystals the bands were not visible optically even after relatively heavy deformations. It is possible that the bands would be absent in orientations very close to (111), but crystals of this orientation have not yet been examined. Fig. 26 shows that several crystals have very similar orientations; these were chosen so that the investigation of such variables as speed and temperature of deformation could be made independent of orientation.

In all crystals which developed kink bands, the X-ray micrographs showed clearly that the bands possessed a marked crystallographic habit, so in every case the plane of the bands was determined in the manner described in a previous paper.<sup>8</sup> In addition to the plane of the kink bands, the active slip plane, as determined by measurement of angles of slip traces on two surfaces of the crystal, was plotted. The operative slip direction was obtained by selecting the [110] direction in the slip plane which gave the maximum resolved shear stress. In all cases it was found that in the early stages of plastic deformation,

the kink bands were on (110) planes, the normal to which coincided with the active slip direction.

### (c) The Formation of the Bands

It was found that the kink bands could occur after less than 1% elongation in tension. Fig. 21 (Plate XIII) is an X-ray micrograph of an aluminium crystal after 0.75% elongation. At this stage the local differences in orientation were very small and most of the crystal was contributing to the X-ray reflection; however, two sets of bands were visible because of differences in intensity within the reflection. On further deformation, one set of bands became much more pronounced in the X-ray images, and analysis showed that they were kink bands on (110) planes. The other set of bands originated from the second type of inhomogeneity, i.e. bands of secondary slip, which will be discussed later. In other crystals deformed by similar amounts the kink bands were not visible and appeared only after 1–2% elongation, but bands of secondary slip were always observed.

Optical examination revealed that many of the slip traces stopped in the kink bands (Figs. 15 and 16, Plate XI). This could mean that kink bands originated from barriers initially present in the crystal, but microscopic examination of crystals at different stages during deformation showed that the arrested slip lines were those which formed in the later stages. Initially all the slip lines were continuous, apart from occasional breaks due to cross-slip; moreover, no bending could be detected. The behaviour of the slip lines that appeared later was shown by a crystal deformed to 17.5% elongation, electropolished to remove all slip traces, and then re-strained slightly. All the new slip lines stopped abruptly in the kink bands (Fig. 17, Plate XII), which were also clearly shown to be regions of curvature.

Fig. 17 also shows that after moderate deformation, slip on a different set of planes occurs in the kink band. This suggests that rotation within the bands is more pronounced than in the bulk of the crystal. The amount of rotation necessary before secondary slip occurs is obviously dependent on the initial orientation of the crystal and on the direction of rotation. This occurrence of secondary slip may cause confusion between the kink bands and bands of secondary slip, particularly if the specimen is examined after heavy deformations. However, in the early stages of deformation, the difference can be easily seen and confirmed by determination of the crystallographic habit.

### (d) Purity of the Aluminium

Kink bands also occurred in deformed high-purity aluminium crystals (99.99%), but although they approximated to the same crystallographic habit as those in the less pure crystals, the bands were less regular and much further apart. Fig. 19 (Plate XII) is an X-ray micrograph of such a crystal after 2.8% elongation, which should be compared with Fig. 12 (Plate XI). There was also a more gradual development of the bands, the earlier ones being



between 0.2 and 1 mm. apart, but as the deformation became more severe, new bands appeared between them. This resulted in a more complex breakdown of the crystal, as shown in Fig. 20 (Plate XII) which represents the same area as Fig. 19 after 6% elongation. While the density of the bands was much less than in the less pure crystals, the rotations which occurred in the initial bands were greater. This usually resulted in a rumpling of the surface which was visible to the naked eye after small extensions (4%). Examination of such surfaces with a "Talysurf" profilometer revealed directly the tilting of the lamellæ between the kink bands. Optical examination at heavier deformation showed that these disoriented regions between the kink bands had frequently rotated to positions where duplex slip had begun (Fig. 18, Plate XII).

#### (e) *Temperature of Deformation*

Kink bands occurred in crystals deformed at widely differing temperatures. For example, crystals deformed rapidly at 500° C. developed kink bands to just as marked a degree as crystals deformed at room temperature. To investigate more precisely the effect of temperature, two crystals (99.5% pure) of similar orientation were compared; one was deformed rapidly at room temperature to an elongation of 4%, while the other was strained rapidly at 450° C. and immediately air-cooled. X-ray examination of the latter crystal showed that a widely spaced set of bands had formed.\* This should be compared with a typical result obtained at room temperature, as shown in Fig. 12 (Plate XI), from which it is clear there has been a two- or three-fold increase in spacing of the bands for an increase of 430° in the temperature of deformation. Analysis of the bands obtained in the crystals deformed at high temperatures showed that they had the same crystallographic habit as those formed at room temperature.

A crystal deformed at 450° C. was subsequently annealed at 630°–640° C., and X-ray micrographs were taken at various stages. It was found that the banded structure produced as a result of plastic deformation was still visible even after 89 hours' annealing, but the dark lines representing the kink bands were no longer intense and in many cases the incident X-rays were not reflected. This would be expected because of the tendency of the most severely bent regions, i.e. the kink bands, to polygonize during the long anneal and so eliminate the curvatures. However, as the kink bands are very narrow, this local polygonization is only a secondary source of disorientation, the primary source being the larger lamellæ formed between the kink bands during deformation.

Several high-purity crystals were deformed at the temperature of liquid nitrogen and again kink bands were detected in X-ray micrographs. These were much more closely spaced (0.05 mm. after 4.5% elongation) than those formed at room temperature

(Fig. 19, Plate XII) and could not be observed optically.

#### (f) *The Speed of Deformation*

The speed of deformation appeared to have little effect on the formation and habit of the kink bands. As in the investigation of the effect of temperature, crystals of similar orientation were compared after small deformations at widely differing rates of strain. A crystal of 99.5% aluminium deformed to 3.3% elongation at room temperature at a rate of 0.018% per hr. developed kink bands to much the same degree as a crystal deformed the same amount in several seconds. Again the bands occurred on (110) planes with the usual relation to the slip direction. Another crystal (99.5% purity) deformed at the same slow rate at 300° C., likewise developed kink bands. On the other hand the results obtained with high-purity (99.99%) crystals deformed slowly at 300° C. were very different from those at room temperature. Again, widely spaced, pronounced kink bands could be detected by X-ray microscopy. However, while the primary disorientations in the crystal were a result of the kink bands, the long lamellæ between the bands became the sites of smaller secondary disorientations.† This phenomenon is of great importance in the study of creep at elevated temperatures, but as discussion at this stage may obscure the simpler case of crystals deformed rapidly at relatively low temperatures, the matter will be discussed in detail elsewhere.

#### (g) *Crystals with Conjugate Slip*

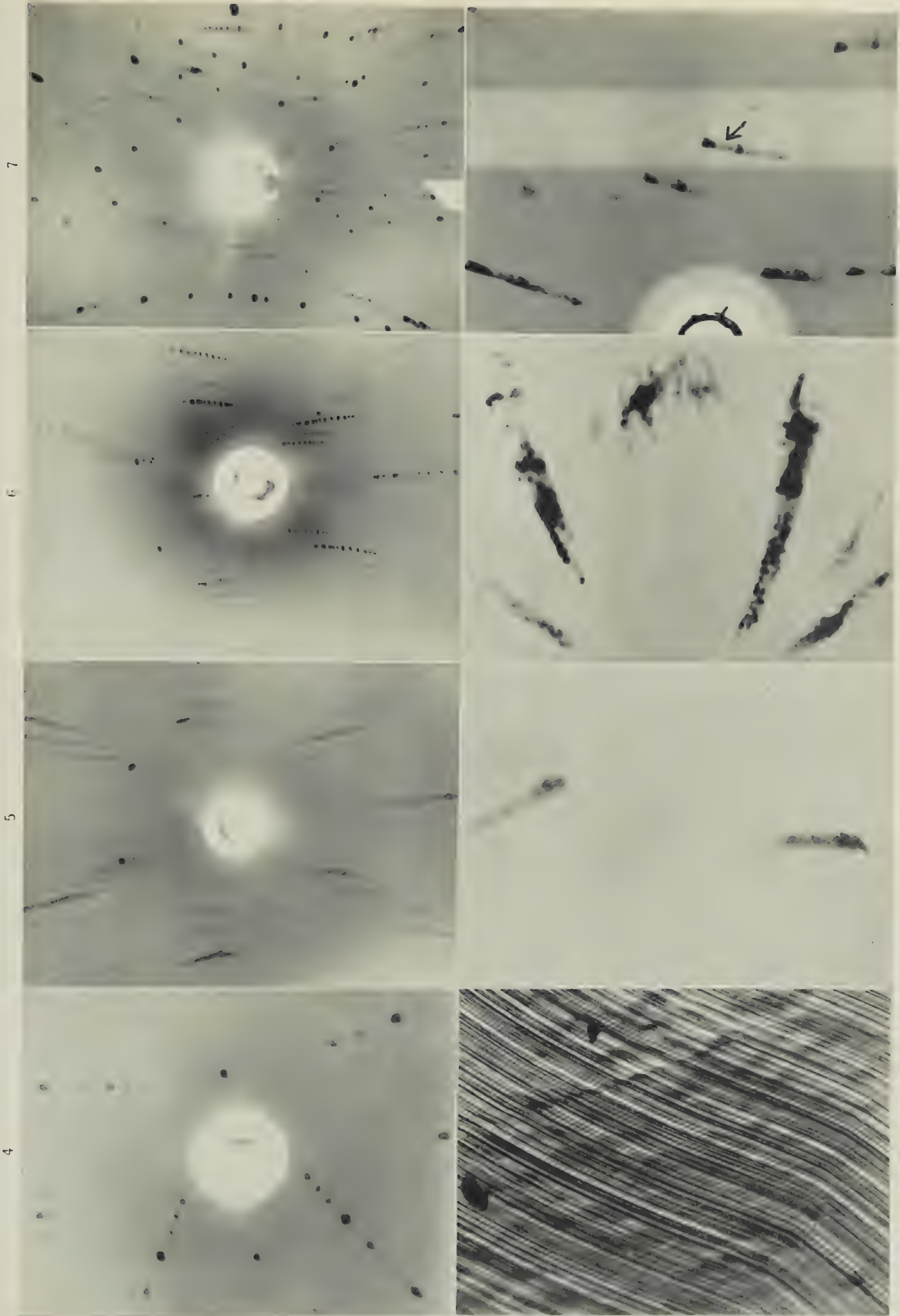
During the investigation several crystals were obtained, the orientations of which showed that conjugate or double slip could be expected at a very early stage of the deformation. The orientations of two crystals which were investigated in detail are represented in Fig. 26 as black circles. These crystals were of high-purity aluminium and were deformed at room temperature. They were examined at stages during the deformation both by X-ray and optical microscopy and in neither method were kink bands detected. A third crystal started to deform by conjugate slip after only a small amount of deformation, but in this case fine kink bands had already occurred in the early stages of the deformation. The bands, however, did not develop to the same degree as those found in crystals deforming on one primary set of slip planes.

### 4. BANDS OF SECONDARY SLIP

In X-ray micrographs of lightly deformed aluminium crystals two sets of bands were usually observed (Fig. 21, Plate XIII), particularly at small extensions (about 1% elongation). At a later stage the kink bands predominated in the X-ray micrographs, but optical examination showed that the other bands were still present. Microscopic examination revealed that in the early stages of deformation this second type of

\* See Fig. 8(a) (Plate IX), *J. Inst. Metals*, this vol.

† See Fig. 6(a) and (b), Plate VIII, *J. Inst. Metals*, this vol.



4

5

6

7

8

9

10

11

FIGS. 4-7.—X-Ray Laue Photographs of Cadmium Crystal After 100% Elongation. Au Radiation (Back Reflection).  
FIG. 8.—Micrograph of Kink Region of Cd. FIG. 9—4.6% Elongation at Room Temp. FIG. 10.—20% Elongation at 600° C. FIG. 11.—5.4% Elongation followed by Annealing for 4 Hr. at 300° C. + 30 Min. at 450° C.

FIG. 4.—As Extended.  
FIG. 5.—Bent to 3.5 mm. Radius.  
FIG. 6.—Bent to 3.5 mm. Radius and Annealed 24 Hr. at 290° C.

FIG. 8.—Micrograph of Kink Region of Cd. FIG. 9—4.6% Elongation at Room Temp. FIG. 10.—20% Elongation at 600° C. FIG. 11.—5.4% Elongation followed by Annealing for 4 Hr. at 300° C. + 30 Min. at 450° C.

FIG. 8.—Micrograph of Kink Region of Cd. FIG. 9—4.6% Elongation at Room Temp. FIG. 10.—20% Elongation at 600° C. FIG. 11.—5.4% Elongation followed by Annealing for 4 Hr. at 300° C. + 30 Min. at 450° C.



MICROGRAPHS OF 99.5% ALUMINIUM CRYSTAL AFTER 4% ELONGATION.  $\times 50$ .

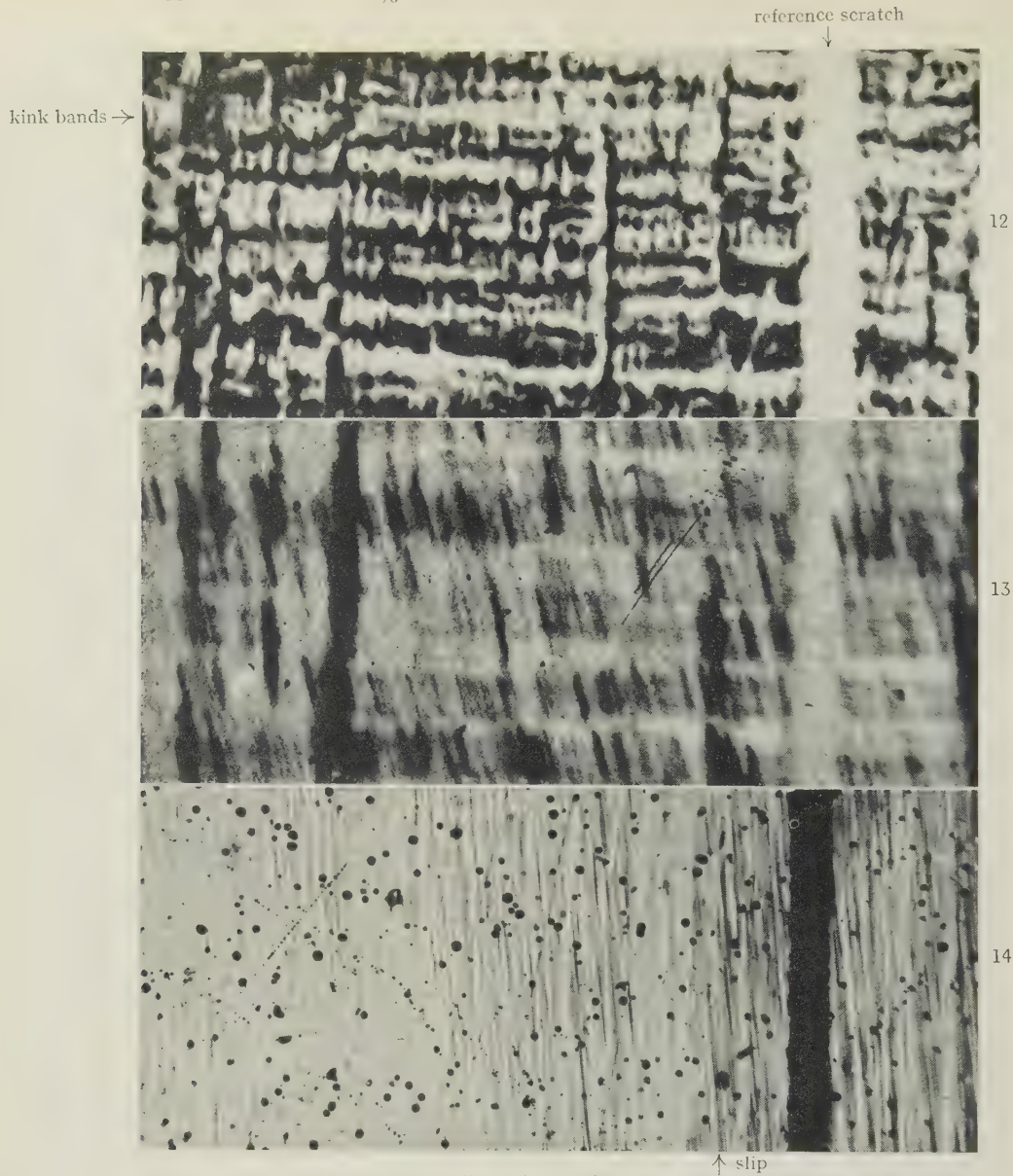


FIG. 12.—X-Ray Micrograph.

FIG. 13.—Same as Fig. 12 After Rotation of 20°.

FIG. 14.—Optical Micrograph.

OPTICAL MICROGRAPHS OF 99.5% ALUMINIUM CRYSTAL AFTER 20% ELONGATION.

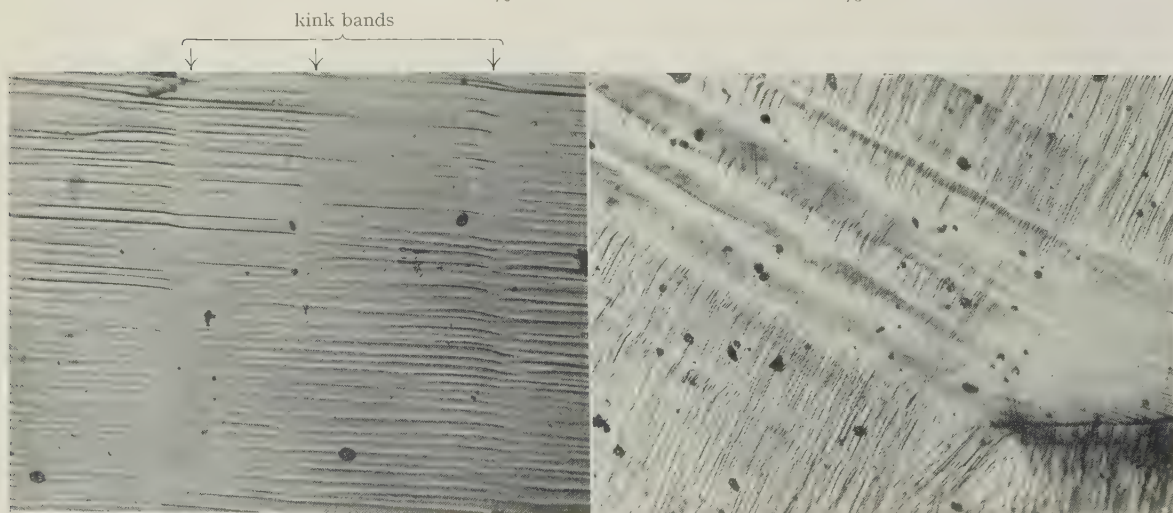


FIG. 15.—Kink Bands in Crystal.  $\times 500$ .

FIG. 16. Area Near Small Included Grain.  $\times 120$ .

OPTICAL MICROGRAPHS OF 99.99% ALUMINIUM CRYSTAL.

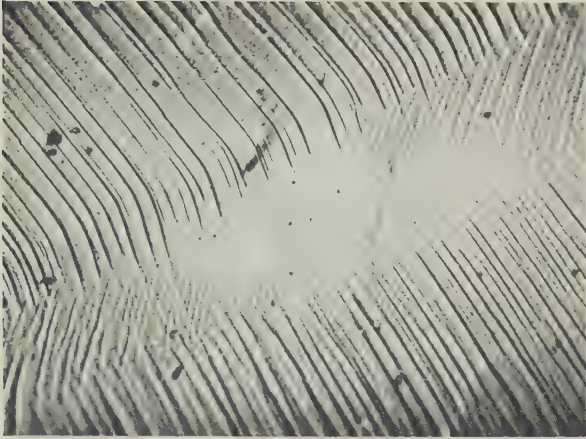


FIG. 17.—After 17.5% Elongation, Repolished, and Slightly Re-strained.  $\times 250$ .

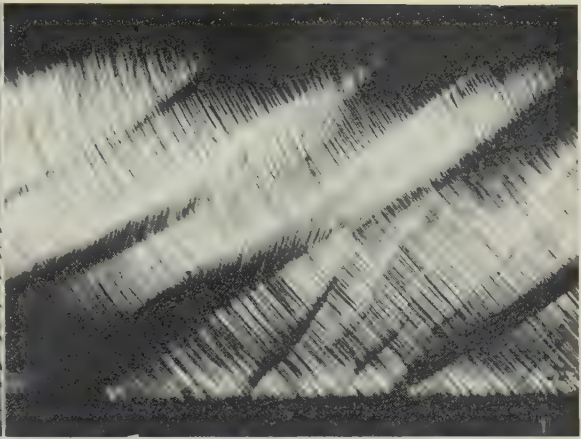


FIG. 18.—After 17.5% Elongation.  $\times 100$ .

X-RAY MICROGRAPHS OF 99.99% ALUMINIUM CRYSTAL.  $\times 20$ .

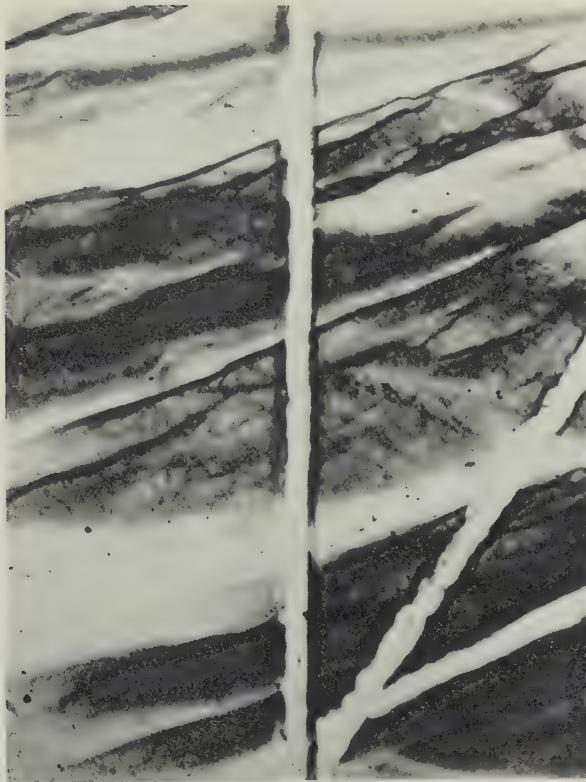


FIG. 19.—After 2.8% Elongation.

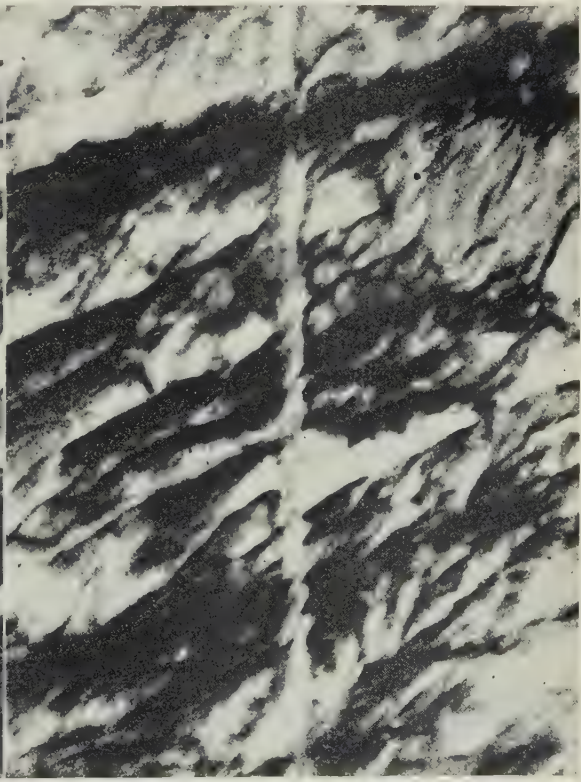


FIG. 20.—After 6% Elongation. Same area as Fig. 19.



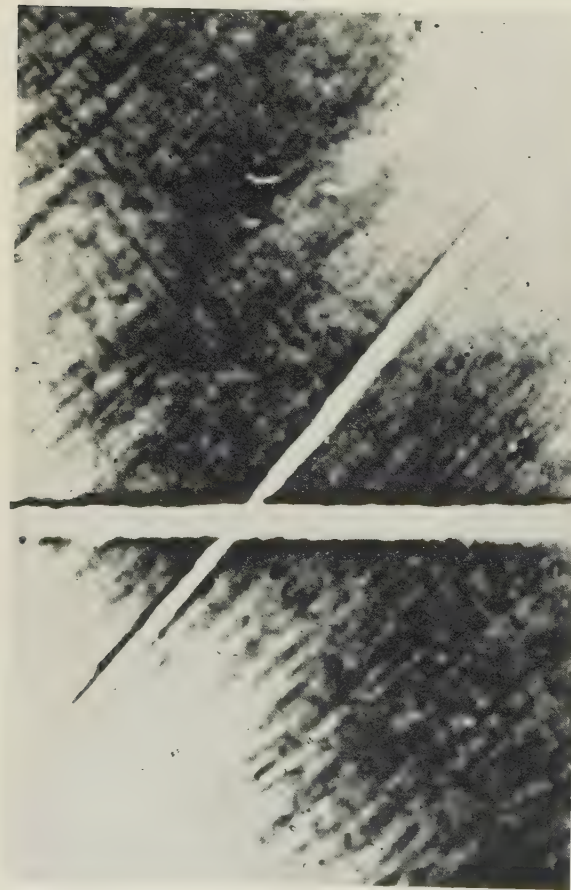


FIG. 21.—X-Ray Micrograph of 99.5% Aluminum Crystal After 0.75% Elongation.  $\times 25$ .  
OPTICAL MICROGRAPHS OF A BAND OF SECONDARY SLIP IN ALUMINUM CRYSTALS.

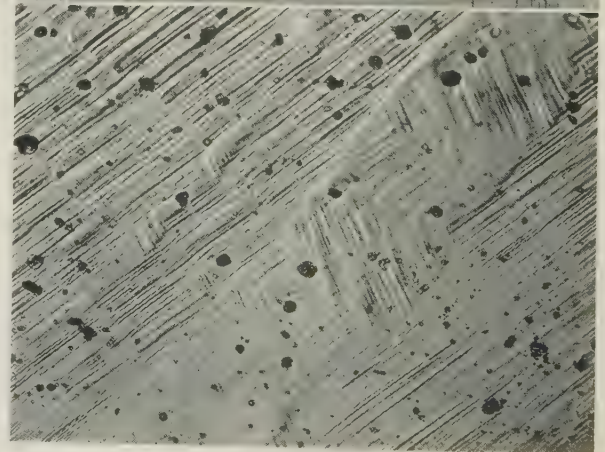


FIG. 23.—99.5% Al After 10% Elongation.  $\times 150$ .

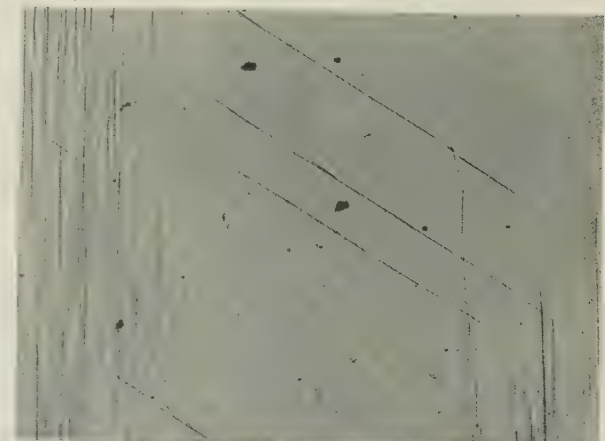


FIG. 24.—99.99% Al After 5.6% Elongation.  $\times 100$ .

kink bands

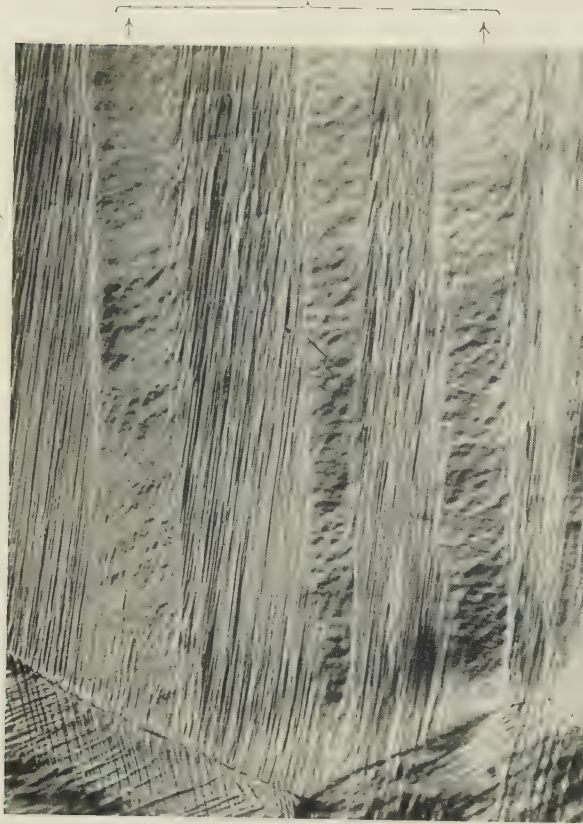


FIG. 22.—Optical Micrograph of Bands of Secondary Slip in a Grain of Coarse-Grained 99.9% Aluminum After 17% Elongation.  $\times 100$ .

coarse bands of secondary slip

primary system



FIG. 25.—Optical Macrograph of 99.99% Aluminum Crystal of Symmetrical Orientation After 5.6% Elongation.  $\times 5$ .



inhomogeneity occurred almost parallel to the octahedral slip planes, and comprised regions in which the primary slip traces were very weak or even absent. As the deformation became more severe, these bands were the preferential sites for slip on a system of planes different from those operating in adjacent parts of the crystal. For this reason the term "band of secondary slip" has been used to describe this type of inhomogeneity. A good example in an aluminium crystal (99.5% pure) after 10% elongation is shown in Fig. 23 (Plate XIII); in this case the secondary slip has developed to a considerable extent.

In many crystals the bands did not show sharp slip lines, but a rumpled appearance which at low magnifications revealed little crystallographic regularity. However, examination at higher magnifications

TABLE I.—*Primary and Secondary Slip in Crystal PA12 (99.99% Aluminium).*

Angles	Slip Planes		
	Primary	Secondary	
	1	2	3
$\lambda$ -angle between axis and slip direction . . . . .	42°	41°	42°
$\phi$ -angle between axis and slip plane normal . . . . .	55°	55°	59°
$\cos \lambda \cdot \cos \phi$ . . . . .	0.42	0.43	0.39

After slight tensile deformation, slip plane 1 operated, but there were large regions in which no primary slip lines were visible. After 5.6% elongation slip on at least one of the alternative systems occurred in these bands (Fig. 24, Plate XIII), in many cases to the complete exclusion of the primary system. Fig. 25 (Plate XIII) is a photomicrograph taken at this stage of the deformation, in which the bands of secondary slip show up as dark areas. When the specimen was deformed further to 16.3% extension, the bands became more pronounced as they rotated in a different direction from adjacent parts of the crystal, thus resulting in macroscopic disorientations within the crystal. By this stage the other parts of the crystal were deforming by conjugate slip on the primary plane and the first of the secondary planes. The smaller, more regularly spaced bands of Fig. 25 are approximately parallel to the primary slip plane and correspond to the bands observed in the many other aluminium crystals examined. The larger bands comprising about five large inhomogeneities were more or less regularly spaced along the crystal, and although they are similar in origin to the smaller bands, their unusual size and orientation must be attributed to the special orientation of the crystal.

## 5. POLYCRYSTALLINE HIGH-PURITY ALUMINIUM

While the majority of the experiments have been done with single crystals, some observations have also been made on polycrystalline high-purity aluminium deformed in tension. For convenience in observation the grain-size chosen was very large—between 2 and 10 mm.-dia. Under these conditions the deformation is much less homogeneous than in the case of single crystals, the effect of the crystal boundaries being to cause different parts of the one grain to deform to different extents (Boas and Hargreaves<sup>11</sup>). However, neglecting the variations in the vicinity of the boundaries, it can be said that the same inhomogeneities develop as in the single crystals. In fact, the two types of band are quite pronounced and can often be distinguished by macroscopic examination if the grain-size is large enough. Fig. 22 (Plate XIII) illustrates an example of bands of secondary slip typical of coarse-grained, high-purity aluminium; fine kink bands can also be seen. The grains which showed the most pronounced kink bands were those

showed that the rumpling was caused by the slip continually changing from the primary to the secondary slip system and back, thus following an irregular zig-zag path. The individual components of each slip line, as described by Heidenreich and Shockley<sup>9</sup> and Brown,<sup>10</sup> crossed over to the new glide plane at different points, thus somewhat obscuring crystallographic features. Fig. 22 (Plate XIII) shows some bands of secondary slip in which this has occurred; the photograph includes the major part of one grain of a coarse-grained aggregate which had been extended by 17% in tension after electrolytic polishing.

Crystals in which more than one slip system operated from the beginning of deformation allowed a detailed study of this type of inhomogeneity, for in these circumstances bands of macroscopic size were often obtained. Fig. 27 shows the stereographic projection of the orientation of one of these crystals, and it is clear that no less than four slip systems could take part in the deformation at an early stage. The data obtained by measurement on the crystal and its projection are tabulated in Table I.

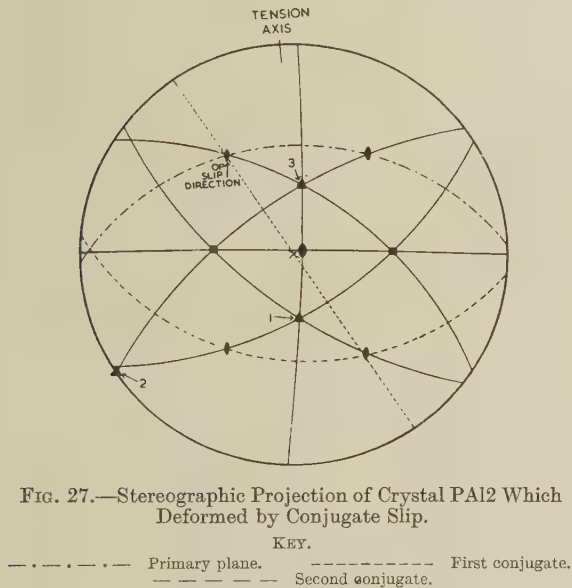


FIG. 27.—Stereographic Projection of Crystal PA12 Which Deformed by Conjugate Slip.

KEY.

— — — — — Primary plane.      - - - - - First conjugate.  
 . . . . . Second conjugate.



in which slip had predominantly occurred on one system; these grains also usually developed bands of secondary slip. Grains in which conjugate slip occurred at a very early stage of the deformation did not usually contain kink bands but the bands of secondary slip were quite pronounced. Again in some grains conjugate slip occurred as an almost uniform network.

#### 6. SOME OBSERVATIONS ON SINGLE CRYSTALS OF CADMIUM

Large cadmium crystals ( $10 \times 0.5 \times 0.3$  cm.) were prepared by solidification from the melt in a graphite-coated steel boat, the resultant undersurface of the crystal after electropolishing being tolerably flat for X-ray and optical micrography. The crystals were deformed in tension, and it was found that after 6% elongation X-ray micrographs showed no fine structure at all, whereas optical micrography revealed many straight slip lines. After 20% elongation some X-ray images showed some fine lines corresponding with optically observed slip bands; however, in no case were markings seen which could be attributed to kink bands or bands of secondary slip.

### III.—DISCUSSION AND CONCLUSIONS

In Part I it was stated that the structure of X-ray asterisms obtained from slightly deformed aluminium crystals could be interpreted in terms of microscopic disorientations within the crystals, the disoriented blocks being connected by bent regions. The results of X-ray and optical micrographic examinations in the present part have provided experimental evidence for this view, namely the occurrence of narrow kink bands separating disoriented lamellae of the crystal. It is suggested that the bands give rise to the diffuse background of the asterism, while the lamellae are responsible for the observed intensity maxima. The bands of secondary slip which are also present in aluminium crystals will result too in fragmentation of the asterisms, but because they are not primarily regions of curvature, would not be expected to contribute to the continuous background. Thus asterisms from slightly deformed aluminium crystals can be explained without recourse to the "local curvature" hypothesis of Burgers, which envisaged curvatures more on an atomic scale.

Burgers and Ploos van Amstel<sup>12</sup> have shown that the angular range of asterisms from deformed aluminium crystals is less for a given strain when the crystals deform from the start on two slip systems, than when slip occurs on a single system of planes. They contended that the asterism was less in the former case because the local curvatures were spread over twice as many glide planes. However, the above experiments indicate that the decrease in asterisms in crystals deforming by conjugate slip from the beginning of deformation is really due to the absence of kink bands. This view of the origin of asterisms is further supported by the experiments with cadmium crystals which showed no asterism after 100–200% elongation

in tension; X-ray micrographic examination of cadmium crystals did not reveal kink bands or other inhomogeneities after considerable plastic extension.

The axes of bending corresponding to the observed asterisms have been determined by numerous workers for various metal crystals. For example, Burgers and Louwerse<sup>13</sup> have shown that in aluminium crystals the curvatures are about an axis which lies in the glide plane perpendicular to the glide direction. Andrade and Tsien<sup>14</sup> have shown that a similar type of distortion occurs also in body-centred cubic metals such as sodium. Now kink bands occur on (110) planes, the normal to which coincides with the slip direction, so that the axis of rotation determined by Burgers and Louwerse is clearly compatible with the type of rotation occurring in the kink bands. It is not immediately evident that the axis of bending lies in the slip plane, but if the identity of kinks in cadmium crystals and kink bands in aluminium is complete (see later), then this will be so. However, while kink bands may be responsible for much of the asterism in the early stages of the deformation, after heavier deformation more general and less regular bending of the crystal may occur. For example, Barrett<sup>15</sup> has shown that the directions of the Laue striæ frequently cannot be explained in terms of the axis of curvature referred to above, and he has attributed these irregularities to the formation of deformation bands.

The question thus arises: what is a deformation band and what is its relation to the two types of inhomogeneity described above? In most of the earlier work on deformation bands, macroscopic etching methods were used to reveal the bands because they differed in orientation from the adjacent regions of the crystal. In fact, Barrett and Levenson<sup>1</sup> defined a deformation band as a region in which the orientation progressively rotated away from that in the neighbouring parts of the crystal, so it is likely that their deformation bands included the two types of inhomogeneity described in the present paper. Barrett and Levenson state in one of their papers: "we believe that the [deformation] bands form as a result of the operation of different sets of slip systems in different band-shaped regions". This would account for the bands of secondary slip, but not for the kink bands which appear to play an equally important part in the deformation. As the two types of inhomogeneity occur together in deformed crystals and as they possess different crystallographic habits, it is perhaps not surprising that the crystallographic features of deformation bands observed by earlier workers were rather variable. Furthermore, as the deformation proceeds, the bands rotate, and at heavy deformations there is no reason why they should occur any longer on planes of lower Miller indices.

The term *deformation band* has been used in the past to cover all disorientations encountered in deformed metals, and its continued use without qualification may lead to considerable confusion. In this paper the terms *kink band* and *band of secondary slip* have been deliberately used instead of the term

*deformation band*, because the two types of inhomogeneity arise through different initial mechanisms whatever their final result may be.

There is a close relationship between the kinking in compressed cadmium crystals described by Orowan<sup>16</sup> and the narrow kink bands found in aluminium crystals. It is clear from optical examination that both processes result in the formation of sharply bounded regions of the crystal within which the orientation is continuously changing because of lattice curvature. The kinks which occur when certain cadmium crystals are compressed are a more severe form of distortion than that in kink bands of aluminium crystals, but this is due to the different stress conditions. The characteristic kinking of cadmium crystals occurs suddenly on compression in a soft machine as a result of the inherent instability, but if a hard machine is employed the kinking can be stopped at an intermediate stage. This has been done by Hess and Barrett,<sup>17</sup> who used a compression machine in which a stiff action was produced by insertion of steel rods between the compression plates. They showed that the region bounded by the two kink planes became gradually disoriented from the rest of the crystal.

The similarity of the kinks in cadmium crystals and the kink bands observed in deformed aluminium crystals is further confirmed by a comparison of their crystallography. In all of a number of aluminium crystals having different orientations, the kink bands formed on (110) planes, the normal of the plane coinciding with the active slip direction. If we compare this behaviour with the geometry of a kink, the same conditions are found to apply; namely, the normal to the plane of kinking is identical with the original slip direction.

Kink bands are not observed in cadmium crystals elongated considerable amounts in tension; however, flexural glide, i.e. slip associated with macroscopic bending of the crystal, is found near the grips. This arises directly from the fact that although the crystal is being pulled in tension, it is attempting to deform by shear along slip planes. To do this the grips should be able to rotate relative to each other, but as is usual, they remain rigid and hinder rotation of the crystal, a circumstance which leads to macroscopic bending in their vicinity. It seems that in aluminium, the restraint of the grips is accommodated by the formation of kink bands which allow small units of the crystal to undergo rotation relative to neighbouring parts. It is significant that kink bands do not occur in crystals which deform from the beginning by conjugate slip on two or more slip planes. If another slip plane is available on which the resolved shear stress is similar to that on the primary plane, then the formation of kink bands is unnecessary, because the stresses set up as a result of the restraints imposed on the crystal, are reduced by slip on the alternative system.

The view that kink bands arise as a result of the mode of deformation is fully borne out by the recently published experiments of Röhm and Kochendörfer,<sup>18</sup>

who deformed long aluminium crystals in a special shear apparatus. Unlike results of earlier experiments carried out with the Bausch shear apparatus, they found that by arranging for the shear to take place along a (111) plane in the slip direction, they could obtain "pure gliding". This pure gliding was characterized by an absence of asterism in X-ray photographs, a very low value for the critical shear stress, and only a small degree of strain-hardening; in other words, aluminium crystals behaved rather like cadmium crystals in simple tension. It seems very likely that in these experiments kink bands were absent and that the grips had little influence on the deformation in the middle of the crystal.

The bands of secondary slip are in the first instance not regions in which the crystal is bent, but as the deformation becomes more severe, considerable distortions may arise within them. Evidence for this is provided by Barrett and Levenson,<sup>1</sup> who observed that deformation bands (into which general category bands of secondary slip certainly fall) become curved and distorted at high deformations. The present author has confirmed this observation in aluminium single crystals deformed in compression. This type of inhomogeneity may be related to the phenomenon of unpredicted cross-slip as described by Maddin, Mathewson, and Hibbard<sup>19</sup> in  $\alpha$ -brass crystals and Cahn<sup>5</sup> in aluminium crystals. However, this phenomenon in its various manifestations is usually very localized in character and the authors mentioned have not described the somewhat coarser band structures observed in the present work. The bands appear to be initially free from slip, but the presence of unpredicted cross-slip at the beginning of deformation could be the reason why primary slip traces are almost absent from the bands. It is well known that in deformed single crystals the latent slip systems are hardened by the primary slip, so that they do not operate until well past the position at which the resolved shear stresses on the two slip systems are the same. Thus the occurrence of cross-slip in a region before the primary slip would tend to inhibit slip on the primary system. The work of Maddin, Mathewson, and Hibbard<sup>19</sup> has established that cross-slip frequently occurs before primary slip. They explain it as an alternative to flexural glide: "[stress] relief could take place by action of the conjugate slip planes just prior to slip on the primary glide plane carrying the highest conventionally resolved shear stress".

The secondary slip observed in the bands was frequently straight, but if the bands were observed on a different face of the same specimen they then appeared to contain a zig-zag type of slip as a result of repeated alternate slip on two different planes. Recent work by Cahn<sup>5</sup> has shown that this is a general characteristic of slip processes in aluminium, which when observed in a plane containing the slip direction are straight but which frequently exhibit cross-slip when viewed in other planes. The apparent rumpling in the bands of secondary slip can be satisfactorily explained on this basis.



The occurrence of inhomogeneities in the tensile deformation of aluminium, which are absent in cadmium crystals deformed in a similar manner, may help to account for the great difference in strain-hardening in the two metals. The experiments with aluminium crystals indicate that the two types of inhomogeneity act as inhibitors of slip. On the one hand slip processes, particularly those occurring after the early stages of deformation, are halted at kink bands. Similarly the bands of secondary slip resist the penetration of primary slip traces and if examined at a late stage of the deformation, they clearly interrupt the progress of slip processes which have begun elsewhere (Fig. 22, Plate XIII). Thus, if we define the softness of a crystal as the ease with which a dislocation can proceed through it, then it is evident that both types of inhomogeneity are inhibitors of moving dislocations and hence should cause strain-hardening. Perhaps the most convincing support for this view is found in the experiments of Röhm and Kochendörfer already referred to. They found that the hardening was directly proportional to the amount of glide that occurred during deformation, i.e. the strain-hardening curve was linear and corresponded closely with those determined many years ago for hexagonal metals.<sup>20</sup> It therefore appears that inhomogeneities are responsible for a large part of the strain-hardening in aluminium crystals. The residual hardening as found in both cadmium and aluminium is considered by Kochendörfer to be due to the interaction of dislocations at their formation.

In Part I it has been shown that aluminium crystals deformed in tension do not recover completely and that the range of orientation produced in the crystals remains unaltered. However, Röhm and Kochendörfer<sup>18</sup> found that their sheared crystals recovered almost completely on annealing for 1 hr. at 350°C. after strains of 30–40%, i.e. they behaved like the cadmium crystals deformed in tension. On the other hand, they found that aluminium crystals deformed similar amounts in tension recovered by only 20–30% after the same annealing treatment. Thus the inhomogeneities which lead to X-ray asterisms and increase strain-hardening also influence the course of recovery. It is, in fact, difficult to see how disorientations of the type described above can be removed except by nucleation and grain growth.

In conclusion, it has been shown that in the tensile deformation of aluminium single crystals, inhomogeneities develop at an early stage and play an important part in determining the behaviour of the deformed crystal. In the first place, the microscopic inhomogeneities that have been described are the cause of the disorientations occurring in the crystal and are thus responsible for the asterisms in X-ray diffraction patterns. Further, it seems likely that the occurrence of inhomogeneities increases strain-hardening, and thus alters the shape of the stress/strain curve during deformation. Lastly, the inhomogeneities influence to a large degree the behaviour of a crystal during recovery. It appears that the inhomogeneities develop as a result of restrictions imposed by the mode of deformation, although the exact mechanisms involved are not yet understood. Quasi-homogeneous deformation, i.e. deformation by slip without the formation of kink bands, &c., can be achieved in special circumstances, and it has been shown that this condition is more readily attained in hexagonal metals, such as cadmium, than in aluminium. At the other extreme, the deformation of polycrystalline metals provides ample opportunity for the general development of the two types of inhomogeneity described in this paper, and which must undoubtedly be taken into account when the detailed plastic behaviour of metal aggregates is studied.

#### ACKNOWLEDGEMENTS

The author wishes to thank Professor Sir Lawrence Bragg, F.R.S., and Dr. E. Orowan, F.R.S., for their interest in this work. He is indebted to his colleagues at the Cavendish Laboratory for helpful discussions and also to Mr. S. D. Charter for his assistance in the preparation of single crystals and the construction of apparatus. Finally, the author gratefully acknowledges an I.C.I. Fellowship, during the tenure of which the work was begun, and the Research Fellowship of the Armourers and Brasiers' Company, which made possible its continuation.

#### REFERENCES TO PART II.

1. C. S. Barrett and L. H. Levenson, *Trans. Amer. Inst. Min. Met. Eng.*, 1939, **135**, 327; 1940, **137**, 112.
2. K. Yamaguchi, *Sci. Papers Inst. Phys. Chem. Research (Tokyo)*, 1929, **11**, 151.
3. J. A. Collins and C. H. Mathewson, *Trans. Amer. Inst. Min. Met. Eng.*, 1940, **137**, 150.
4. C. Crussard, *Bull. Soc. Franç. Minéral.*, 1945, **68**, 174.
5. R. W. Cahn, *Dissertation, Univ. Cambridge*, 1949.
6. W. F. Berg, *Naturwiss.*, 1931, **19**, 391; *Z. Krist.*, 1934, **89**, 286.
7. C. S. Barrett, *Trans. Amer. Inst. Min. Met. Eng.*, 1945, **161**, 15.
8. R. W. K. Honeycombe, *J. Inst. Metals*, 1951–52, **80**, 39.
9. R. D. Heidenreich and W. Shockley, *Phys. Soc.: Rep. Conf. on Strength of Solids*, 1948, 57.
10. A. F. Brown, *Metallurgical Applications of the Electron Microscope (Inst. Metals Monograph and Rep. Series No. 8)*, 1950, 103.
11. W. Boas and M. E. Hargreaves, *Proc. Roy. Soc.*, 1948, [A], **193**, 89.
12. W. G. Burgers and J. J. A. Ploos van Amstel, *Z. Physik*, 1933, **81**, 43.
13. W. G. Burgers and P. C. Louwerse, *Z. Physik*, 1931, **67**, 605.
14. E. N. da C. Andrade and L. C. Tsien, *Proc. Roy. Soc.*, 1937, [A], **163**, 1.
15. C. S. Barrett, *Trans. Amer. Inst. Min. Met. Eng.*, 1939, **135**, 296.
16. E. Orowan, *Nature*, 1942, **149**, 643.
17. J. B. Hess and C. S. Barrett, *Trans. Amer. Inst. Min. Met. Eng.*, 1949, **185**, 599.
18. F. Röhm and A. Kochendörfer, *Z. Metallkunde*, 1950, **41**, 265.
19. R. Maddin, C. H. Mathewson, and W. R. Hibbard, Jr., *Trans. Amer. Inst. Min. Met. Eng.*, 1948, **175**, 86; 1950, **185**, 527.
20. E. Schmid and W. Boas, "Plasticity of Crystals with Special Reference to Metals." London: 1950 (F. A. Hughes and Co.).

# THE FLOW OF LIQUID METALS ON SOLID METAL SURFACES AND ITS RELATION TO SOLDERING, BRAZING, AND HOT-DIP COATING \*

By G. L. J. BAILEY,† Ph.D., A.R.C.S., D.I.C., F.Inst.P., MEMBER,  
and H. C. WATKINS,‡ L.I.M., MEMBER

(Communication from The British Non-Ferrous Metals Research Association.)

## SYNOPSIS

Earlier investigations of soldering performance are reviewed and, after a theoretical discussion of factors expected to control the flow of liquids on solid surfaces, experimental investigations of the behaviour of several liquid metals and alloys in contact with various solid metals, are described. Most of the work was carried out using hydrogen as flux, but a few experiments with liquid fluxes are also described.

It is found that the contact angle between solid and liquid surfaces of the metals examined is not, in general, zero. Its true value in given circumstances is obscured by the effects of roughness of the solid surface, which cannot be allowed for. Roughness effects could also account for the fact that the contact angle against a surface over which liquid has receded is generally lower than that against a surface over which liquid has advanced. The development of the particularly low contact angles which are formed against copper by tin-lead alloys with compositions in the range preferred for practical soldering, appears to be preceded by the formation of an alloy layer in the surface of the copper over which the liquid metal spreads. The alloy layer may be formed relatively slowly by diffusion through the surface layers of the copper from the bulk of the liquid metal, or it may be formed relatively quickly as a result of transfer of metal ions through suitable liquid fluxes. The production of particularly low contact angles between lead and iron or copper and between tin and copper, through very small additions to the lead or tin, is described.

## I.—INTRODUCTION

THE use of soft soldering has for many centuries afforded a ready means of joining common metals such as steel, brass, and copper, without the use of equipment other than means of heating the joint to a comparatively low temperature. The essential characteristic of soldering is the ease and rapidity of making joints which are adequate for their purpose, and the most natural ways of assessing a soldering operation are in terms of ease of application of the solder and suitability for service of the resulting product.

The mechanical properties of joints can be measured, and the effects of variations of joint design, of method of soldering, and of materials used thereby usefully compared. In making joints, however, the liquid metal is required to flow, to an extent depending on the design of the joint, and it is found that, whatever methods of soldering are used, some combinations of solder, flux, and solid metal surfaces have better flow properties than others.

Although readily recognized in practice, the flowing power or "solderability" of a solder/flux/stock

system cannot be measured quantitatively. The causes of differences in "solderability" are not known, for the basic factors controlling flow are not well understood.

The British Non-Ferrous Metals Research Association first began to examine the properties of solders and soldered joints in 1922, and, since that time, has completed many investigations in this field. The most important conclusions of these researches are summarized in a monograph first issued in 1932 and subsequently, in a revised form, in 1942.<sup>1</sup> The imperative need for tin economy in the 1939-45 war stimulated much further work on low-tin or tin-free soft solders of which a description was recently published in another monograph.<sup>2</sup>

Much of the experimental data contained in these monographs is in the form of measurements of the mechanical properties of joints. In the earlier work, solders to British Standard No. 219 having tin contents in the range 30-65% were used. The war-time research was concerned largely with solders based on lead and containing small percentages of tin, antimony, and silver, either alone or in combination. Throughout, the effects on mechanical properties of

\* Manuscript received 8 February 1951. The work described in this paper was made available to members of the British Non-Ferrous Metals Research Association in a series of reports issued in June 1948 and January 1951.

† Deputy Research Manager, British Non-Ferrous Metals Research Association, London.

‡ Formerly Research Assistant, British Non-Ferrous Metals Research Association; now with Messrs. H. J. Enthoven and Sons, Ltd.



such variables as soldering temperature and time and joint design were of primary interest. In the work with conventional solders, sound joints were readily produced and the need for an investigation of the reasons for poor performance was therefore not felt, but war-time experience in the use of lead-rich solders containing less than 20% tin brought sharply into prominence the fact, already referred to, that marked variations existed between differing molten solder compositions in their readiness to flow when applied to solid metal surfaces, even when due allowance was made for differences in liquidus temperature. Difficulties were particularly evident in bit-soldering work and, since the reasons were not apparent, it was hard to foresee means of improving the performance.

At the end of the war, a study was started, on fundamental lines, of the factors of importance in making sound soldered and brazed joints. The initial stages of this research are described in the present paper.

As soon as the difficulties of using solders consisting substantially of lead became apparent, efforts were made to devise tests in which the power of a solder to fill a joint could be measured and its likely performance in practice readily assessed. Three such tests are described in the recent monograph,<sup>2</sup> in which, however, the significance of the results obtained is not discussed in detail. These tests are briefly described in the next section to illustrate the difficulties of explaining the results and assessing their practical value.

## II.—TESTS OF SOLDERING POWER

### 1. BIT-SOLDERING TESTS

Simple lap joints, 6 in. long, were made between strips cut from sheet material and clamped in contact. A gas-heated soldering bit, held at any desired temperature, was drawn at controlled rates along the lap which had been fluxed with zinc-ammonium chloride solution. These tests were intended to yield quantitative data on the penetration of solder into the lap joint, but "reproducibility was not generally adequate for this purpose, and the results had to be assessed on a purely qualitative basis". Special note was therefore taken of the external appearance of the joint, the penetration of the solder into and the soundness of the joint, and the ease with which the soldering bit could be tinned and maintained in a well-tinned condition.

Tests were made with joint members of blackplate and high-conductivity tough-pitch, and arsenical coppers, using a wide range of conventional and "tin-economy" solders. It was found that, even when allowance was made for the higher liquidus temperatures of the lead-rich solders by the use of higher bit temperatures, they did not adhere well to the bit and failed to form sound joints. Essentially, solders containing more than 30% tin gave good performance and those with less behaved poorly in application and gave badly filled joints.

### 2. AREA-OF-SPREAD TESTS

The markedly poorer flow characteristics of the lead-rich solders stimulated a series of experiments in which the area to which a pellet of solder spread when melted under flux on a heated copper or steel plate was measured. It was felt that, while the factors promoting spreading were not understood, the direct measurement of area of spread produced under standardized conditions approximating to bit soldering might form a rapid and simple means of classifying solders accord-

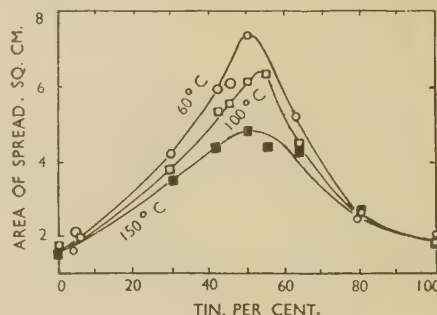


Fig. 1.—Spreading of Tin-Lead Solders on Copper With Zinc/Ammonium Chloride Flux at Various Degrees of Superheat.

ing to their expected performance in practical bit-soldering applications. In carrying out these tests, small square plates of copper or steel were fluxed and carried in the centre a pellet of solder in the form of a disc 8 mm. in dia. and 0.1 ml. in volume. They were placed on a hot plate held at a controlled temperature. The solder began to melt in about 10 sec. and spreading had ceased within a further 50 sec. After not longer than 1½ min., the plate was removed and cooled. No attempt was made to determine differences in the rate of spreading.

The results obtained on bright, electropolished copper surfaces, with zinc/ammonium chloride flux, may be summarized as follows. The area of spread for tin-lead solders varied with composition as shown in Fig. 1, in which the curves correspond to different superheats. Silver additions up to 3% of the tin content did not influence the amount of spread obtained. Antimony additions up to 6% of the tin content gave a marked reduction in area of spread, proportional to the antimony content and amounting to about 50% in the 50% tin solder containing 3% antimony. This effect of antimony was reduced somewhat by the presence of silver.

When a 20% solution of resin in industrial spirit was used as flux in place of zinc/ammonium chloride, the areas of spread remained in the same relative order, but the larger areas of spread were very much reduced.

When, instead of clean electropolished copper, oxidized specimens were used, the spreads obtained using zinc/ammonium chloride were rather greater than on clean surfaces; with the resin flux, very small areas of spread were obtained.

Similar experiments on mild-steel sheet, with zinc/ammonium chloride flux, showed that tin-lead

solders having tin contents of 20–50%, melted with 60° C. superheat, all spread to the same extent initially, the area of spread being about 3 cm.<sup>2</sup>. With solders containing 20% and 30% tin it was noted that spreading occurred in two stages. In the first stage, spreading took place rapidly once the solder became fully molten and then appeared to cease altogether. Subsequently, after a period depending on the temperature of the test, spreading began again, but only where molten flux remained upon the surface. This spreading was slower and generally very irregular, but amounted in some cases to an increase of 100% in area.

As with copper, silver additions to the solder were without effect, whereas antimony additions reduced the spread considerably. Both with copper and, especially, with steel, the addition of up to 5% tin to a lead–silver solder containing 1.5% silver, gave notably large areas of spread; the 5% alloy on steel spreading to an area of 6 cm.<sup>2</sup> at 360° C.

The applicability of the area-of-spread test to practice is not clear. Broadly, it may be stated that the solders most used industrially all show areas of spread greater than 3 cm.<sup>2</sup> in tests made as described by McKeown, and that those preferred for critical bit-soldering applications show areas of spread, on copper, of more than twice this area under suitable conditions of superheat. The differentiation shown between fluxes is in agreement with practical experience.

### 3. CAPILLARY-PENETRATION TESTS

Observation of the performance of solders in practice suggests that the impression of ease of flow which they give may be connected with the rate at which

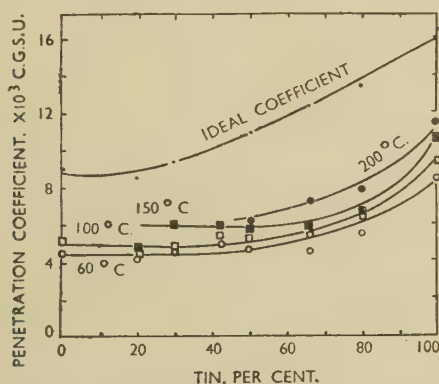


FIG. 2.—Penetration of Tin-Lead Solders in Copper Joints at Various Degrees of Superheat.

they penetrate into joints. From measurements of the time taken for solder to traverse a horizontal capillary space  $4\frac{1}{2}$  in. long  $\times$  1 in. wide and with a depth of either 0.0035 in. or 0.006 in., Latin<sup>2,3</sup> was able to calculate an “effective penetration coefficient”, characteristic of the solder/stock/flux combination at a chosen temperature. He compared this with the “ideal penetration coefficient” which he thought

would be obtained if the solder wetted the solid metal perfectly.

Latin's tests were made using joint members of copper and tinplate, with zinc–ammonium chloride and resin fluxes and with a wide range of solders. He found that, between copper surfaces, the highest effective penetration coefficient was obtained when the liquid metal was pure tin and that its value for any solder composition was always approximately half that of the corresponding ideal penetration coefficient. The effective penetration coefficient increased with increasing superheat, remaining at about half the ideal value, but was insensitive to the presence in the solder of additions of antimony, silver, and copper, and was the same whether zinc–ammonium chloride or resin flux was used. These results are shown in Fig. 2.

With tinplate surfaces, the penetration coefficient reached the ideal value when solders with tin contents in the range of 40–60% tin were used, but it fell to half the ideal value with solders containing less tin. No experiments on tinplate were reported with solders containing more than 63% tin.

The results of these tests are at variance with practical experience, which is that solder containing about 50% tin have the most useful flow characteristics, and that flow depends markedly on the flux used.

### III.—FACTORS CONTROLLING THE FLOW OF LIQUIDS UPON SOLID SURFACES

#### 1. SURFACE TENSION AND CONTACT ANGLE

In attempting to reconcile the results of the area and penetration tests with each other and with the results obtained in practice, it is necessary to consider the factors which control the flow of liquids in contact with solid surfaces. A liquid will flow under the action of forces to which it is subjected in an attempt to reach a position of equilibrium; the forces of particular importance in soldering, brazing, and hot-dip coating are those due to gravity and to surface tension. The surface-tension forces acting on the liquid metal are characterized by the value of the surface tension of the liquid metal and by the angle of contact between the liquid and solid surfaces at the line in which they meet.

The general features of the rate of flow and the equilibrium conditions under the combined influence of gravitational and surface-tension forces are most easily appreciated by considering that both the surface tension of a liquid and its contact angle against a solid surface remain constant. In these circumstances it is possible to examine flow and equilibrium theoretically in a number of examples of interest. The results of such examination are set out briefly in Appendix I. It will be noted that not every example can be given a completely satisfactory treatment. For instance, the relationship between the area of a drop of liquid on a solid surface, the surface tension of the liquid, and the contact angle is not simple unless the drop is small



enough for gravitational distortion to be negligible. When gravity can be neglected, however, the drop has the shape of a spherical cap; the area of spread is independent of the surface tension of the liquid, except in so far as this is one factor in determining the contact angle, and is connected in a relatively simple way with the value of the contact angle. Again, neither the rate at which a drop spreads or retracts to gain its equilibrium state, nor the rate at which a meniscus is formed when a solid surface is dipped into a liquid are at present calculable. For capillary spaces, however, both the equilibrium state and, with a good approximation, the rate of penetration, are calculable in all circumstances.

## 2. SIGNIFICANCE OF THE CONTACT ANGLE

Even the most casual observation of the flow of a liquid metal on a solid metal surface suggests that the contact angle is not constant and characteristic of the system. A discussion of the factors which determine its value is given in Appendices II and III. Briefly, Appendix II shows that if the solid surface is perfectly smooth, the contact angle which will be observed depends upon the value of the surface tension of the liquid ( $\gamma_{23}$ ) and on the values of two other surface tensions, attributable respectively to the solid surface where it is not covered by the liquid metal, ( $\gamma_{13}$ ), and to the solid metal/liquid metal interface ( $\gamma_{12}$ ).

In studies in fields other than those concerned with liquid metals,<sup>4</sup> it is almost always found that the contact angle of a liquid which has spread outwards over a smooth solid surface exceeds the contact angle observed after the liquid has retracted from the surface. This difference between the values of "advancing" and "receding" contact angles is generally attributed to the adsorption of molecules of liquid upon the solid surface and is known as "hysteresis of the contact angle". To distinguish such absorption hysteresis from hysteresis due to surface roughness, which is discussed below, it is proposed to employ the term "molecular hysteresis".

Unless the solid surface is perfectly smooth, the contact angle which is observed differs from the "true" contact angle, discussed in Appendix II, in a way which depends upon the surface roughness. The influence of roughness is discussed in Appendix III, in which it is shown that the contact angle observed after a liquid has spread outwards over a rough surface can exceed the angle observed after the liquid has receded over the surface. This effect may be described as "capillary hysteresis" to indicate the essential difference in its origin from "molecular hysteresis".

## 3. EFFECTS OF DIFFUSION BETWEEN SOLID AND LIQUID METALS

The discussion of the previous section indicates that, in a given system comprising liquid metal, flux, and solid metal, provided the three surface tensions referred to and the roughness of the solid

surface remain constant, values of the advancing and receding contact angle observed immediately the liquid has come to rest will be characteristic of the system and of the roughness of the solid surface. In fluxed metallic systems no such characteristic contact angles will necessarily be obtained, however, since intermetallic diffusion normally occurs, and in consequence both the roughness and the composition of the solid surface changes. Chemical and electrochemical action of the flux, and its evaporation and decomposition may also contribute to these changes.

## 4. REVIEW OF EARLIER EXPERIMENTAL WORK

This discussion throws some light on the results of several published accounts of experimental work. One important indication from the results of the spreading-drop experiments described by McKeown is that the contact angle, in the conditions of the tests, always exceeds zero. In fact, although no values were measured, it appears that the contact angle for compositions either very poor or very rich in tin must have been fairly large, say  $60^\circ$ . According to Latin, the contact angle accompanying penetration in his capillary joints was approximately  $60^\circ$  irrespective of solder or flux compositions. It may readily be shown that, in Latin's experiments, the lowest penetration velocity always exceeded 1 cm./sec. In the spreading-drop experiments, on the other hand, the mean rate of solder movement must obviously have been very much lower. It is possible, therefore, that in Latin's experiment the rate of movement was always so high that no time was available for the completion of reactions tending to bring about reduction of the contact angle to less than  $60^\circ$  such as may have taken place, in the spreading-drop experiments, with solders containing 30–70% tin. In narrower capillaries than those employed by Latin, penetration speeds would be lower and reduction of the contact angle might then occur.

Daniels and Macnaughtan<sup>5</sup> have reviewed the wetting of metals by metals, with particular reference to tinning and soldering. They state that a flux will assist the spreading of a drop of molten metal if it causes a reduction in the surface tension of the drop, and quote work by Coffman and Parr<sup>6</sup> and by Latin<sup>7</sup> in which the extent to which the surface tension of solders is reduced in various liquid fluxes was measured (comparison is made with values obtained in hydrogen or *in vacuo*). Daniels and Macnaughtan later point out that, with a given contact angle, joint penetration is greater, the higher the surface tension of the liquid, and they find some difficulty in reconciling the facts that an effective flux promotes both spreading and joint penetration. However, the area of spread of a drop is determined by the contact angle alone, i.e. indirectly by the values of three surface tensions, whereas joint penetration is determined by the product  $\gamma_{23} \cos \theta$ . Since  $\gamma_{23} \cos \theta = \gamma_{13} - \gamma_{12}$ , it is evident that joint penetration is determined directly by the difference in surface tension of two solid surfaces.

Chalmers and Wadie,<sup>8</sup> in investigating the dewetting

of tin and some tin alloys from hot-dipped O.F.H.C. copper, used the receding contact angle as a measure of the tendency to dewet and discussed the influence of the surface tension of the liquid and their experimental variables upon the measured receding contact angles. They derived Wenzel's expression for the effect of surface roughness upon contact angle (see Appendix III), but were unable to take roughness into quantitative account. In consequence, while they showed that the contact angle cannot depend only upon the value of the liquid surface tension, they were unable to decide whether the other factors causing contact angle variation were either roughness variations or variations in the two solid surface tensions, or a combination of these three variables. They added that the use of a flux which reduces the liquid surface tension will reduce the contact angle, but this involves the assumption that the other two surface tensions remain unaltered.

Daniels and Macnaughtan,<sup>5</sup> also discussing the dewetting of tin from oxygen-bearing copper, state that small additions of copper, nickel, or cobalt to the tin prevent collapse of the tin coatings. They account for this effect by supposing the viscosity of the coating to be increased by the small additions. It is improbable that any important change of viscosity is here involved, and it seems more likely that changes in roughness or true contact angle may provide an explanation.

In the course of his experiments designed to examine whether fluxes, besides acting as cleaning agents, also considerably lower the surface tension of the molten solder, Latin<sup>7</sup> noted that, around tin and solder drops heated in contact with copper in zinc-ammonium chloride flux, blue-coloured areas were obtained. He concluded that this blue coloration was due to tin which had been deposited from the flux and had subsequently alloyed with the copper. This action, he considered, might account for the greater spreading observed in zinc-ammonium chloride flux in comparison with that in resin flux. From a comparison of areas of spread of tin and eutectic tin-lead solder in either flux he deduced that the greater spreading of the eutectic solder was probably a consequence of its lower surface tension. If this were the only reason for greater spreading of the eutectic composition, it might be expected from measurements of surface tension in resin made by Chalmers and Wadie,<sup>8</sup> that the best spreading of all would be obtained with pure lead. Latin gives no evidence that this is so, and the spreading-drop results quoted by McKeown indicate that in fact lead does not spread as well as solders containing about 50% tin. The formation of "haloes" around drops of solder when a chloride flux is used, as observed by Latin, was also noted by Fine and Dowdell,<sup>9</sup> who suggested the addition of stannous chloride or lead chloride to zinc chloride fluxes used in the tinning and soldering of steel.

Daniels and Macnaughtan<sup>5</sup> point out that the rate of spreading of drops of solder upon solid surfaces has not been studied. However, Tammann and Arntz<sup>10</sup>

and Alty and Clark<sup>11</sup> measured the rate of spreading of mercury on a number of solid metals at room temperature, in air and under several liquids. In similar experiments using mercury, copper, and stannic bromide solution at temperatures above atmospheric, Daniels and Macnaughtan<sup>5</sup> found the rate of spreading suddenly to increase greatly above a critical temperature. They refer to the discovery by Latin of such a critical temperature for eutectic tin-lead solder on copper under molten zinc-ammonium chloride. It must be that at the "critical temperature" some reaction occurs which rapidly changes one or more of the factors determining the value of the contact angle.

Even when no liquid flux phase was present, and electrochemical reaction was therefore impossible, Tammann and Arntz<sup>10</sup> and Alty and Clark<sup>11</sup> noted the appearance of a band surrounding the drop of mercury in the surface of the solid metal. This band could be formed only as a result of the diffusion of liquid metal in the surface layers of the solid.

Daniels and Macnaughtan comment that it is unknown whether the formation of a "halo" (which it seems clear may take place by diffusion from the liquid metal or by deposition from some liquid fluxes) always accompanies the spreading of a drop of molten metal on a solid metal, or if it is an indispensable preliminary to the spreading of the main drop.

It will be clear that there is room for further experimental study of contact angles in soldering systems and of the factors which influence them. Such information may well have a bearing on the assessment of "solderability" in practice, even though the significance of this property cannot yet be appreciated.

#### IV.—EXPERIMENTAL INVESTIGATIONS ON THE TIN-LEAD/COPPER SYSTEM

##### 1. OBSERVATIONS OF THE SPREADING OF DROPS OF LIQUID METAL

The possibility of changes of contact angle taking place as a consequence of intermetallic diffusion<sup>10, 11</sup> has been pointed out. When a liquid flux is used, there is the further possibility of changes due to chemical and electrochemical reactions. Flux effects of this kind can be eliminated by studying the behaviour of liquid metals in contact with solid metal surfaces freed from oxide in a reducing atmosphere. It was considered that spreading-drop experiments, carried out using hydrogen as a flux, should be made to ascertain if changes in contact angle occurring only as a result of diffusion can in fact occur in the tin-lead/copper system and if so, in what circumstances.

In view of their exploratory nature, the precision of measurement aimed at in these tests was not high; instead, a procedure was adopted which would allow a large number of observations to be made quickly.

##### (a) Apparatus

The furnace used is shown in Fig. 3. Specimens of copper sheet rested on the furnace baseplate.



Just above the baseplate was a loose-fitting silica rod, with a spoon-shaped cavity ground at its end to hold a bead of liquid metal which could be gently dropped on to the copper specimen by rotating the rod. Spreading was observed through a silica window having a water-cooled wax seal, which was broken for insertion and removal of specimens. To aid in the estimation of drop diameters at any instant, a square of wire gauze was usually attached to the silica spoon in such a way that it could be rotated to lie over the drop. The drop diameter was estimated by counting the meshes of the gauze. The furnace was levelled by means of adjustable feet. In the experiments to be described, the furnace atmosphere was cylinder hydrogen which had been purified by passage over

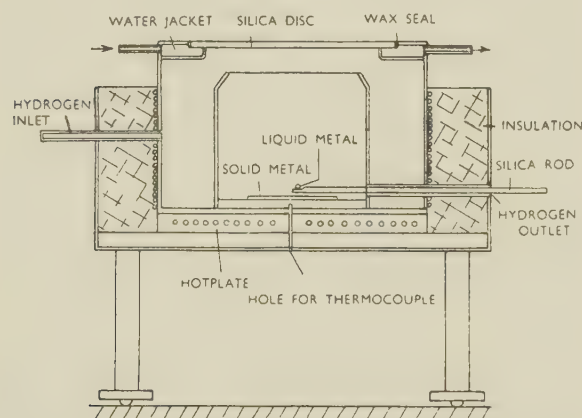


FIG. 3.—Sectional Diagram of Furnace for Spreading-Drop Experiments.

heated platinized asbestos and through a series of drying tubes.

### (b) Materials and Procedure

The copper used was oxygen-free, high-conductivity strip, 0.015 in. thick. Specimens  $1\frac{1}{2}$  in. square, were cathodically degreased, annealed in hydrogen for 1 hr. at  $600^{\circ}\text{C}$ ., flattened, and again degreased before insertion in the furnace. Pellets of high-purity tin and lead and of a range of alloys made up from them were cut and weighed to have a volume of 0.05 ml. A pellet of the required composition was loaded into the spoon. After the furnace had been sealed, hydrogen was passed for 15 min. to sweep out air and the temperature raised to  $600^{\circ}\text{C}$ . for a further 15 min. to complete the cleaning of the materials. The temperature was then adjusted to the required value and the drop of molten metal applied to the copper surface. Estimates of the area of spread were made at intervals over a period of 30 min.

### (c) Results

It was found that, with all the liquid alloys examined, a well-defined drop was formed immediately the liquid came into contact with the copper. In every case, the diameter of the drop was in the range 10–12 mm. With alloys of tin content less than 30% or

exceeding 70%, the shape of the drop did not change at all, or changed only slightly, during the 30 min. after its formation at any temperature between the liquidus of the alloy and  $500^{\circ}\text{C}$ . Within the composi-

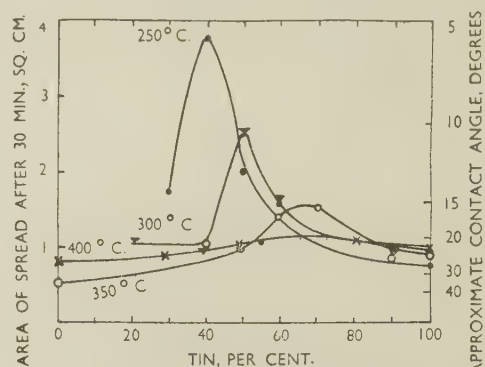


FIG. 4.—Effect of Tin Concentration on Spreading of Tin-Lead Alloys on Copper in Hydrogen Atmosphere at Different Temperatures.

tion range 30–70% tin, however, an appreciable and, in some cases, considerable increase of drop diameter occurred during this time. The extent of this secondary spreading was found to depend strongly on the composition of the alloy and on the temperature of the test.

The results are shown in Figs. 4 and 5. From Fig. 4 it is seen that a drop of 40% tin alloy spread in

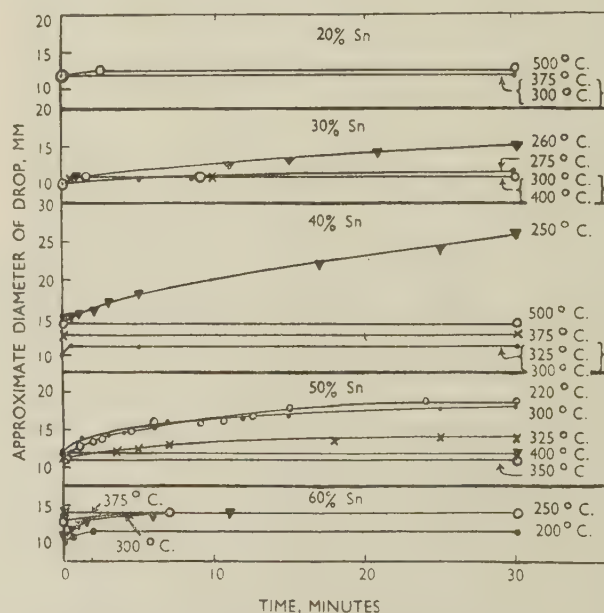


FIG. 5.—Effect of Temperature on Rate of Spreading of Tin-Lead Alloys on Copper in Hydrogen Atmosphere.

30 min. to an area of about  $4\text{ cm}^2$  when the temperature was  $250^{\circ}\text{C}$ . The initial area of all drops at all temperatures was roughly  $1\text{ cm}^2$ . Fig. 5 shows that a drop of 40% tin solder, at  $250^{\circ}\text{C}$ ., was still increasing in diameter at an approximately constant rate after

30 min., the average rate of movement of the liquid being 0.2 mm./min. At higher temperatures, a lower maximum was reached in 30 min. with alloys containing a greater percentage of tin, as shown in Fig. 4. The 30% tin alloy was still spreading at a comparatively low rate, after 30 min. at 260° C. (Fig. 5), but in the other cases a steady state had

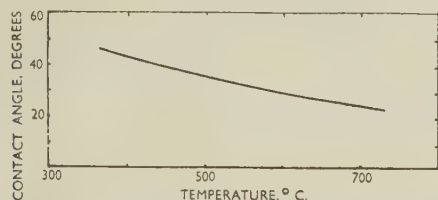


FIG. 6.—Change of Contact Angle with Temperature in the Lead/Copper System.

apparently been reached. Fig. 5 also illustrates the generally observed fact that when no marked secondary spreading took place, the area of drops was slightly greater at higher temperatures. This effect was examined over the temperature range 350°–950° C. for the lead/copper system. The contact angle of a drop of lead was found to decrease as the temperature was raised and to increase again as it was lowered, approximately as shown in Fig. 6, in which the contact angle is plotted against temperature. The fuller investigation of this effect in which the surface tension of the solid surface and that of the solid/liquid interface were measured is described elsewhere.<sup>12</sup>

According to the composition of the liquid alloy and the temperature of experiment, it was possible

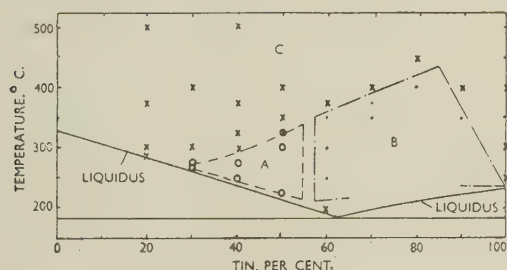


FIG. 7.—Spreading of Tin-Lead Alloys on Copper in Hydrogen Atmosphere.

to classify the spreading characteristics into three different categories :

(A) Marked secondary spreading, to areas greater than are obtained with the same composition at higher temperatures.

(B) Slight secondary spreading, to areas less than or equal to those obtained with the same composition at higher temperatures.

(C) No secondary spreading.

The temperature/composition fields corresponding to these three classifications are drawn in Fig. 7. It will be noted that the region of marked secondary

spreading includes a large part of the composition range within which the solders preferred in practice are found.

Two further observations of interest were made during the experiments. It was noted that when a drop of, for example, 40% tin alloy, applied at a temperature above 300° C. and therefore about 10 mm. in dia., was cooled slowly, it began to spread rapidly at the lower temperatures. A further feature frequently noted, particularly with alloys containing 30% tin or more, was the formation of a bright band in the copper surface immediately surrounding a drop. With compositions and at temperatures where slow spreading occurred, this band did not appear until the spreading became slower. Some observations on the character of these bands are made later in the paper (Section VI, 1 and 2).

## 2. AREA OF SPREAD AND CONTACT ANGLE

As is pointed out in Appendix I, only if a drop is sufficiently small in volume is the area of spread related

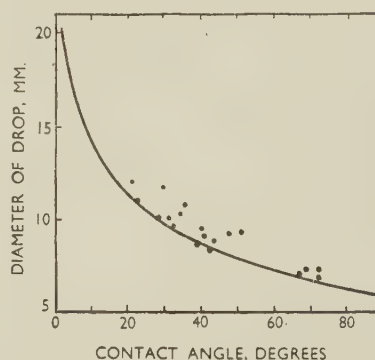


FIG. 8.—Relation of Drop Diameter and Contact Angle.

in a comparatively simple way to the contact angle. When the drop is so small in volume that gravitational effects are negligible it has the form of a spherical cap. The full curve of Fig. 8 shows the relationship between the diameter of the drop and the contact angle for a spherical cap of the volume used in these experiments. The points plotted in this figure show the measured diameter and contact angle of a number of drops of this volume. Contact angles were measured by an optical arrangement similar to that described by Chalmers and Wadie.<sup>8</sup> Various liquid and solid metals were used in obtaining these results, but the details are not of importance for the present purpose. It will be seen that the plotted points lie fairly close to the full curve of Fig. 8, and it is permissible therefore to derive an approximate value of the contact angle from the drop diameter or area of spread. Accordingly a scale for contact angle has been added to Fig. 4. It should be added that the measured height of the drops was in general appreciably less than it would have been if they were in fact spherical caps.

It will be noted from Fig. 4 that the secondary spreading undergone by certain of the alloys at appro-



appropriate temperatures corresponds to a reduction of the contact angle from the range  $20^{\circ}$ – $30^{\circ}$  down to  $10^{\circ}$  or less.

### 3. CONCLUSIONS FROM SPREADING-DROP EXPERIMENTS

The following conclusions may be drawn from the results of the simple experiments described above:

(i) The contact angle of tin, lead, and tin-lead alloys against a hydrogen-cleaned copper surface is not zero over the temperature range explored.

(ii) The enhanced spreading and consequent changes of contact angle obtained with certain compositions and temperatures are similar in extent to those found in spreading-drop tests using zinc-ammonium chloride flux, as comparison of Figs. 1 and 4 shows. In both sets of experiments, enhanced spreading is less marked at the higher temperatures. It may be noted that when, in the earlier tests, resin was used as flux, the same tendency to enhanced spreading was observed, though in this case its extent was slight. It thus seems probable that the potentialities for enhanced spreading reside in the metals themselves independently of the flux used and that they are most marked for a given composition at a particular temperature.

(iii) Although similar in other respects, there is a marked difference in the rate at which this secondary spreading occurs, depending on the nature of the flux phase.

### 4. POSSIBLE REASONS FOR SLOW SPREADING

The viscosity of the solder should not limit the spreading of a small drop to the rate observed during enhanced spreading in hydrogen unless the liquid became loaded with solid particles of intermetallic compounds. No evidence was found (e.g. by the exposure of particles in drops which had spread to large areas and become very thin) that this occurred, and it was concluded that such spreading is therefore due to a change in the conditions determining the contact angle, the rate of change controlling the rate of spreading. As has been pointed out earlier, a change of roughness or of composition, or a combination of these effects, may be expected to affect the contact angle. Whatever the detailed reason for the change of contact angle, it must certainly be associated with the occurrence of intermetallic diffusion between the liquid and solid metals.

If the surfaces are not perfectly clean in these experiments, the effect of diffusion may be merely to disperse contamination from the solid surface, allowing the drop to spread. If this is the only reason, it is difficult to see why pure tin should spread less well than some of the tin-lead alloys.

If, however, oxide films and gas-absorption effects are absent in the experiments in hydrogen, it can be concluded that, in the experiments using zinc-ammonium chloride flux, apart from any action in

removing oxide film and absorbed gas from the solid surface, the flux must also have some other action which leads to rapid secondary spreading. It has been suggested by Latin<sup>7</sup> that tin ions from the solder are taken into solution and re-deposited electrolytically on to the copper surface. The significance which may now be attached to this observation is that the slow diffusion from the edge of the drop is thereby replaced by a faster process, the occurrence of which is an essential preliminary to further spreading. The conditions in which such electrolytic deposition of tin occurs were examined experimentally in the following way.

### 5. ELECTROCHEMICAL EFFECTS IN FLUXES

Experiments were carried out with the object of determining at what stage of heating zinc-ammonium chloride flux the deposition of metallic ions could occur as a result of chemical or electrolytic reaction. The flux was contained in a small crucible furnace. At the bottom of the crucible was a thin layer of tin, lead, or tin-lead alloy into which dipped the exposed tip of an insulated connection. The procedure adopted was to insert a strip of copper into the flux at a chosen temperature, taking care to avoid contact with the metal at the bottom of the crucible. The copper strip was then connected externally directly to this metal layer and withdrawn without breaking contact after 10 sec. A fresh strip of copper was used for each immersion. The copper was cathodically degreased and pickled in a mixture of acids before use.

A plain zinc chloride flux, consisting of zinc chloride 50 g. and water 50 ml., was slowly heated to  $400^{\circ}$  C. over a period of 2 hr., a copper electrode being inserted as described above at regular temperature intervals. Under these conditions, no change in appearance of the copper was observed until boiling began at  $110^{\circ}$  C., when it became coated with a thin grey film. In the temperature range  $250^{\circ}$ – $300^{\circ}$  C. the coating was thin and irregular. Over this temperature interval the flux was either solid or very viscous. Coatings obtained above  $300^{\circ}$  C. were found to be much whiter than those obtained at lower temperatures, and spectrographic examination showed the presence of tin. These coatings appeared to be brittle, and it was thought probable that the tin was alloyed with the copper. A similar result was obtained when an addition of 5 g. ammonium chloride was made to this flux, and it was noted that the flux retained its fluidity throughout the experiment. When the tin was replaced by a 50% tin-lead alloy similar deposition was observed. Deposition was observed only when the external circuit between the copper and the liquid metal was completed. These experiments provide evidence that tin from a solder may be deposited on to a copper surface by electrolysis when a zinc or zinc-ammonium chloride flux is employed. Such deposition might well account for the far higher rate of spreading which must occur when such a flux is used in comparison with the rate in hydrogen.

## 6. FLOODING EXPERIMENTS

Although no detailed explanation of the way in which diffusion controls the rate of spreading of a drop in a hydrogen atmosphere is yet possible, the fact that it does so makes it important to obtain further information on diffusion characteristics. Useful results in this connection were obtained in experiments in which copper surfaces, cleaned in hydrogen, were covered with tin, lead, and tin-lead alloys for different lengths of time and then drained for a short period and observed. The apparatus used is shown in Fig. 9.

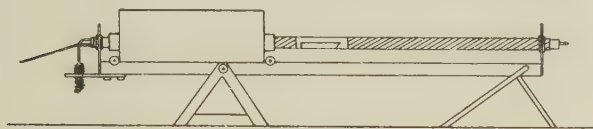


Fig. 9.—Apparatus for Flooding Tests.

It consisted essentially of a horizontal tube furnace which could be tilted through about  $15^\circ$ , and which was so arranged that the specimen could be examined visually during an experiment. A silica tube with a short central transparent insert was mounted concentrically within a horizontal tube furnace capable of operation at temperatures up to  $1000^\circ\text{C}$ . The furnace was carried on rails so that it could be withdrawn from the transparent section of the central tube, within which the specimen could thus be observed at will. The specimen was a narrow strip of metal foil, pressed on to the bottom of a silica boat which contained, in addition, a small piece of the more fusible metal, placed at one end, out of contact with the foil. When making an experiment, the furnace was tilted so that when the metal of lower melting point became liquid it remained out of contact with the solid foil. The specimen materials were cleaned by heating to  $600^\circ\text{C}$ . in purified hydrogen for 15 min. After cleaning, the furnace temperature was adjusted to the required value, and the specimen was then flooded by tilting the furnace into a horizontal position. After the specimen had been immersed for a chosen time, the furnace was again tilted to allow the liquid to drain, and draining could be observed by displacing the furnace from the window of the central tube. This was normally done 15 sec. after the beginning of draining. The draining angle was small, and the specimen cooled rapidly after removal of the furnace, and, in consequence, the apparatus was not operated in such a way as to provide a severe test of coating stability, the need for which was not appreciated at that time.

The solid surface was classified by observation after draining as follows:

- (a) Wetted surface: covered by a smooth, continuous liquid coating.
- (b) Dewetted surface: drops of liquid, formed by collapse of coating, adhering to the surface.
- (c) Unwetted surface: no liquid adhering as a film or as drops to the solid surface.

It was found that copper was unwetted by lead after immersion for 2 min. at  $400^\circ\text{C}$ . and also after 24 hr., at the same temperature. Experiments with tin-lead alloys containing tin in the range 2–50% were made at temperatures of  $380^\circ\text{C}$ . and  $450^\circ\text{C}$ . (below and above the decomposition temperature of the copper-tin  $\eta$ -phase,  $\text{Cu}_6\text{Sn}_5$ ). It was found that, whilst a coating was in all cases obtained after flooding for the shortest practicable time (about 10 sec.), it was unstable and broke up rapidly on draining, exposing a matt alloy layer on the surface of the copper foil. The stability of the coating was not improved by increasing the flooding time at  $450^\circ\text{C}$ ., but, at  $380^\circ\text{C}$ ., stability, within the limitations of the apparatus as mentioned above, was obtained by sufficiently prolonged immersion. The results of an assessment of the time required to develop a stable coating are shown in Table I.

TABLE I.—Time Required to Produce Stable Coating on Copper at  $380^\circ\text{C}$ .

Tin Concentration, wt.-%	Time Required, min.
2	60
5	20
10	6
20	5
50	<0.3

The stability of coatings produced in this way was found to be completely destroyed by a short treatment of the flooded specimen at  $450^\circ\text{C}$ ., but could be re-established by repeating the treatment at  $380^\circ\text{C}$ .

The marked dependence on tin concentration of the time required for the establishment of a relatively stable coating is noteworthy, and it may be suggested that, in the spreading tests in hydrogen, the rate of diffusion outwards from the drop might be extremely slow with solders containing less than 30% tin and thus not be observed in the 30 min. period allowed. Correspondingly, in the spreading tests using zinc-ammonium chloride flux, the deposition of tin might well fail to occur when low-tin solders are used. It may be suggested that if tin ions could be incorporated in the flux and be deposited electrolytically, enhanced spreading should be obtained even with low-tin or tin-free solders.

## 7. IMMERSION AND DRAINING EXPERIMENTS

Use of the tilting furnace just described did not conveniently allow the examination of effects produced during immersion periods of less than about 10 sec. In addition, the method failed to give as much information as was required on the approximate values of contact angle. An alternative method was therefore followed.

The object of these experiments was to observe:

- (a) The shape of the liquid meniscus formed against a vertically dipped, smooth, bright copper surface during slow immersion and while



held immersed in a fixed position for a few seconds.

(b) The shape of the meniscus during withdrawal from the liquid and the permanence of any liquid coating adhering to the withdrawn surface over a period of 30 sec., during which it was held vertically and maintained at the immersion temperature.

Tests were made with tin, lead, and a range of tin-lead alloys at temperatures up to 500° C., in hydrogen at atmospheric pressure, using the furnace shown in Fig. 3, in which a silica crucible was stood upon the furnace baseplate and a suitably bent strip of copper foil was attached to the rotatable silica rod.

It was found that the meniscus shape could be characterized by four contact angles as follows:

(i)  $\phi_I$ : the immersion contact angle, accompanying slow immersion of the solid surface.

(ii)  $\phi_A$ : the advancing contact angle, lower than  $\phi_I$ , assumed while the specimen was held immersed at a fixed depth.

(iii)  $\phi_W$ : the withdrawal contact angle, usually lower than  $\phi_A$ , accompanying slow withdrawal of the surface.

In most cases, the withdrawal contact angle was zero, i.e. a coating was withdrawn. This coating usually broke up into drops, and observations were made of a fourth angle.

(iv)  $\phi_R$ : the receding contact angle, less than  $\phi_A$ , typical of the "dewetted" drops formed on the collapse of a uniform coating.

It will be noted that two of the angles,  $\phi_A$  and  $\phi_R$  are "equilibrium" angles, whereas the other two,  $\phi_I$  and  $\phi_W$ , are unstable and change either when the immersion rate becomes zero or after the surface is withdrawn completely.

The magnitude of the angles was estimated by eye. To supplement these observations, the withdrawn surface could be described, at any stage after withdrawal, as wetted, dewetted, or unwetted. It was found that, with all liquid compositions and at all temperatures, the immersion angle,  $\phi_I$ , was approximately 90° and that this angle fell, very rapidly at the higher temperature and tin contents, to an advancing angle,  $\phi_A$ , of 40°–60°, as soon as the movement of the specimen stopped.

With tin and the tin-rich alloys the end of the fall from  $\phi_I$  to  $\phi_A$  was accompanied by the appearance of a band in the copper surface immediately above the meniscus, indicative of diffusion of the tin through the surface layers of the copper. With pure lead as liquid, the withdrawal angle  $\phi_W$  was estimated at 30° and no coating was formed. The copper surface remained smooth during immersion. When liquids containing 20% tin or more were used, the withdrawal angle was invariably zero, i.e. a coating was obtained, but the permanence of the coating depended on the composition of the liquid alloy and on the temperature. Thus,

coatings formed at 250° C., using a 45% tin alloy were classified as stable. A coating formed at 250° C. using a 60% tin alloy broke up slowly into separate drops. Coatings formed with a 45% tin alloy at 350° and 500° C., with a 60% tin alloy at 350° C., and with a 70% tin alloy or pure tin at temperatures in the range 250°–500° C. collapsed within two or three seconds of their withdrawal from the melt. The receding contact angle,  $\phi_R$ , was always in the range 5°–10°. With liquid alloys containing 20 and 30% tin a more stable coating could be obtained by repeated immersion. With alloys of high tin content, however, the copper sheet was completely dissolved if this was attempted. The solid surface exposed by the collapse of coatings was observed to be roughened, presumably by the formation of copper-tin intermetallic compounds.

## 8. CONCLUSIONS FROM COATING EXPERIMENTS

The changes occurring in these coating experiments are evidently of great complexity, and it is difficult to describe them with precision on the basis of the simple observations which were made. These observations do, however, enable the following suggestions to be put forward:

(a) Unless the receding contact angle,  $\phi_R$ , is less than about 20°, no coating can be withdrawn. When the receding contact angle is less than 20° a coating can be obtained, but such coatings exhibit varying degrees of stability. The degree of stability is indicated by the time which elapses after withdrawal before the coating is seen to break from a continuous film and coalesce into separate drops. It is also indicated by the area of uncoated surface relative to that covered by drops after coalescence. The lower the value of the receding contact angle, the higher is the stability of the coating.

(b) Coating stability increases with time of immersion only when some tin is present. This is clear for alloys containing tin in the range 1–50%. With more than 50% tin present in the lead, it may be presumed that the time required to develop the lowest value of receding contact angle is too short to be measurable. These observations indicate that formation of an alloy layer is required to enable the lowest value of receding contact angle to be developed. The reversible "wetting-dewetting," produced by heating at 380° and 450° C. supports this view and furthermore, indicates that the solid surface with which the lowest receding contact angles are associated must be the  $\eta$  phase,  $\text{Cu}_6\text{Sn}_5$ , rather than the  $\epsilon$  phase  $\text{Cu}_3\text{Sn}$ .

(c) It appears that coatings having the highest stability of any are obtained only with those solder compositions and in those temperature ranges for which marked secondary spreading is found in the spreading-drop experiments. It is possible that similar highly stable coatings may

be produced with solders of lower tin content than about 30% if sufficient time of immersion is allowed.

(d) There is evidence of marked contact-angle hysteresis. Except for lead, the receding contact angle, after a sufficient immersion time, is never more than about  $10^\circ$ , even with the least stable coatings. On the other hand, the advancing contact angle, determined in spreading-drop experiments, is not less than  $30^\circ$ , except in the cases of marked secondary spreading, for which the receding contact angle must be close to zero.

(e) The observation that the contact angle accompanying immersion,  $\phi_I$ , exceeds the advancing contact angle,  $\phi_A$ , to which  $\phi_I$  falls when the specimen becomes stationary, is in agreement with the supposition that the occurrence of diffusion reduces the contact angle.

## 9. SUMMARY OF MAIN CONCLUSIONS ON CONTACT ANGLES IN THE COPPER/TIN-LEAD/HYDROGEN SYSTEM

The main conclusions to be drawn as a result of the qualitative survey of contact angles in the copper/tin-lead/hydrogen system are as follows:

(a) There is no single value of contact angle characteristic of the liquid metal composition and temperature.

(b) The contact angle which is observed depends on the extent to which diffusion has occurred. This is evident in different ways according to whether the advancing or receding angle is examined.

(c) The experiments provide no evidence on the relative contributions of change of roughness and change of surface structure to the changes of contact angle consequent upon diffusion.

(d) Very low values of both advancing and receding contact angles may be obtained with certain liquid alloy compositions within limited temperature ranges.

## V.—EXPERIMENTAL OBSERVATIONS ON OTHER METAL SYSTEMS

It was of interest to compare the observations made upon the tin-lead/copper system with similar observations on other combinations of liquid and solid metals. Qualitative experiments, on the lines already described, are briefly reported below for several other combinations of solid and liquid metals.

### 1. FLOODING EXPERIMENTS

Flooding experiments, as described in Section IV, 6, were carried out with 38 pairs of pure metals selected from the following:

Liquid metal: Ag, Sb, Te, Zn, Pb, Cd, Bi, Sn, Al.

Solid metal: Fe, Ni, Cu, Au, Ag.

In 25 of the 38 pairs, it was expected that, at the temperature of the test, an intermetallic compound

TABLE II.—Summarized Results of Flooding Tests.

System	Temp., ° C.	Result
(a) Compounds Formed Between the Two Metals.		
Fe-Al	700	Wetting
Fe-Sb	700	Wetting
Ni-Sb	700	Wetting
Cu-Sb	600	Wetting †
Ag-Sb	550	Wetting †
Fe-Te	500	Wetting
Ni-Te	500	Wetting
Cu-Te	400	Wetting †
Ag-Te	500	Wetting
Fe-Zn	500	Wetting
Ni-Zn	500	Wetting
Cu-Zn	500	Wetting
Au-Zn	450	Wetting
Ag-Zn	500	Wetting
Ag-Pb	400	Wetting
Ni-Cd	400	Wetting
Cu-Cd	350	Wetting
Au-Cd	350	Wetting
Ag-Cd	400	Wetting
Ni-Bi	400	Wetting
Fe-Sn	400	Wetting
Ni-Sn	400	Wetting
Cu-Sn	400	Wetting
Au-Sn	275	Wetting
Ag-Sn	300	Wetting
(b) No Compounds Formed: the Solid Metal Can Take the Other into Solution.		
Ni-Ag	1000	Wetting
Cu-Ag	850	Wetting †
Au-Ag	1000	Wetting
Ni-Pb	(Fig. 10)	Wetting *
Ag-Pb	400	Wetting
Au-Bi	300	Wetting *
Ag-Bi	360	Wetting
(c) No Compounds or Solid Solutions Formed.		
Fe-Ag	1000	Dewetting
Fe-Pb	400	Non-wetting
Cu-Pb	400	Dewetting
Fe-Cd	400	Non-wetting
Fe-Bi	400	Non-wetting
Cu-Bi	400	Dewetting

\* A time factor was detected.

† Using eutectic liquid.

would be formed at the interface between solid and liquid metal and in all these cases wetting was observed. Of the remaining pairs, seven were examples

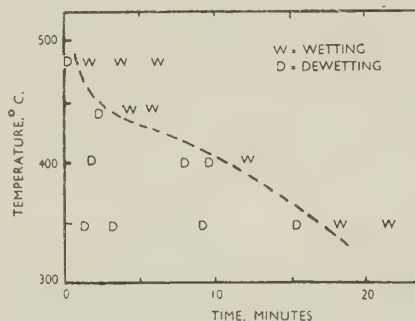


FIG. 10.—Effect of Time and Temperature of Immersion on Wetting of Nickel by Lead.

in which the solid could take the liquid metal into solution. Here again, the result was in all cases classified as "wetting." In the six remaining pairs,



no intermetallic compounds or solid solutions were expected to form at the temperature of experiments, and the result was either "dewetting" or "non-wetting." The results are set out briefly in Table II.

The combinations nickel/lead and gold/bismuth, both in the solid-solution-forming group, were of particular interest in that the development of a stable coating required a considerable time interval. An estimate of the time required to produce a stable lead coating on nickel is given in Fig. 10.

It was noted that although lead failed to wet copper and iron, the adhesion was strong when it was allowed to solidify in contact with either.

## 2. IMMERSION AND DRAINING EXPERIMENTS

Immersion and draining experiments were made with the following metal pairs:

- (a) Ag-Sn; Ni-Sn; Fe-Sn.
- (b) Ag-Pb; Ni-Pb.
- (c) Cu-Bi; Fe-Pb.

The pairs (a) above form intermetallic compounds at the solid liquid interface, pairs (b) are solid-solution types, and pairs (c) do not form solid solutions.

It was found that the liquid metals in group (a) formed coatings which dewetted rapidly, while those of group (b) gave comparatively stable coatings. In the nickel/lead system, immersion of at least 1 min. was needed at 500° C. to produce coating stability. The pairs of group (c) did not give a coating.

The nickel/lead pair was of interest in that the immersion contact angle exceeded 90° and did not change during the immersion period. The withdrawal angle was nevertheless zero.

It is clear from the results of these flooding and immersion experiments that there is a general correlation between the occurrence of alloy formation at the immersed solid surface and the occurrence of wetting. Coatings on "solid-solution" surfaces appear to be more stable than those on "intermetallic compound" surfaces. Coatings are not obtained on surfaces on which no alloy formation occurs, even though the solid metal may go into solution in the liquid. Both wetting and alloy formation normally take place very rapidly. Only with nickel/lead and gold/bismuth is the development of wetting observably slow, and nickel/lead shows in an extreme form the hysteresis of the contact angle which is present in all the other systems examined for the effect.

## 3. SPREADING-DROP EXPERIMENTS

In addition to the experiments with tin-lead alloys on copper already described (Section IV, 1, 2, and 3), similar observations were made with tin, lead, tin-lead alloys, and bismuth on iron, nickel, and silver.

### (a) *Spreading on Iron (Cold-Reduced, White-to-Edge Blackplate)*

Both lead and bismuth showed contact angles exceeding 90° against iron at temperatures up to 1000° C., but it was noted that the angle decreased with increase in temperature, especially near 1000° C., when it was probably just less than 90°. The contact angle of tin-lead solders on iron at 500° C. was 60°-70° irrespective of the solder composition. No slow secondary spreading was observed at this temperature, and no experiments were made at any other temperature.

### (b) *Spreading on Nickel*

The contact angle of bismuth on nickel was about 40° at 400° and 500° C., and no secondary spreading was observed. Using tin-lead alloys at 500° C., contact angles of about 30° were observed. Secondary spreading to a very low contact angle occurred fairly rapidly with a 1% tin alloy, but was not obtained with lead, tin, or tin-lead alloys containing 20% tin or more.

### (c) *Spreading on Silver*

Marked secondary spreading was observed when drops of tin, lead, and tin-lead alloys, and of bismuth, were applied to silver at temperatures above 400° C. Bismuth and lead behaved almost identically in this respect.

## 4. PRODUCTION OF STABLE LEAD COATINGS ON COPPER AND IRON

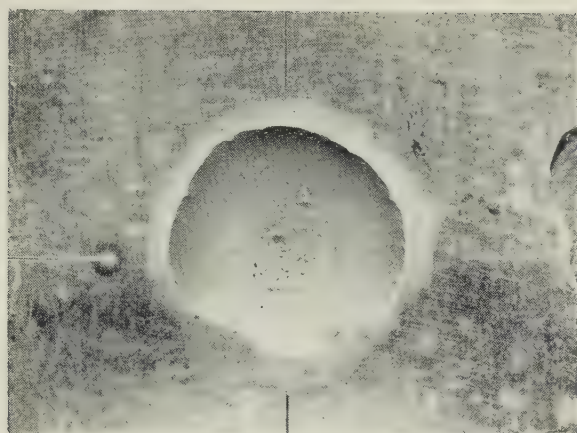
As has been pointed out, the failure of lead to form a hot-dipped coating on copper or iron is a consequence of the relatively high receding contact angles which characterize these systems. The immersion experiments just described show that comparatively stable lead coatings are readily produced upon silver and nickel surfaces. It was considered that the addition to lead of a small proportion of nickel should enable coatings of substantially pure lead to be formed on copper or iron surfaces, since the nickel by reason of its solubility in the solid metal, would tend to become adsorbed from the liquid solution at the solid/liquid surface. Dipping tests were carried out in hydrogen, using lead containing 0.1% nickel, on strips of copper and iron either as-rolled or after light etching. After immersion for 1 min. at 400° C., a coating was obtained on copper which showed little tendency to dewet. A similar coating was obtained on steel after immersion for 5 min., at 500° C. It was evident that the addition of a small proportion of nickel exerted a strongly marked effect in reducing the receding contact angle of lead against copper and iron.\*

## 5. PRODUCTION OF STABLE TIN COATINGS ON COPPER

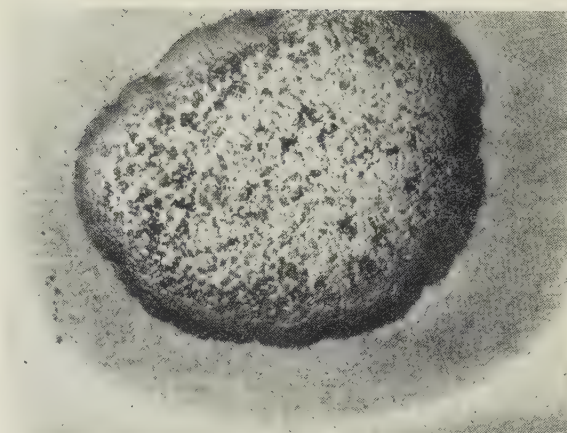
The fact that hot-dipped coatings of tin upon surfaces of O.F.H.C. copper and iron appear to be inherently unstable has been noted earlier. As a matter

\* Patent protection is being sought, in the interests of members of the Association, for processes for the production of lead coatings based upon these observations.



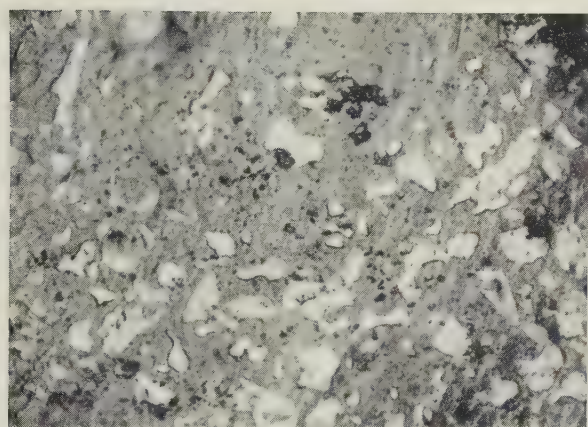


(a) 400° C.

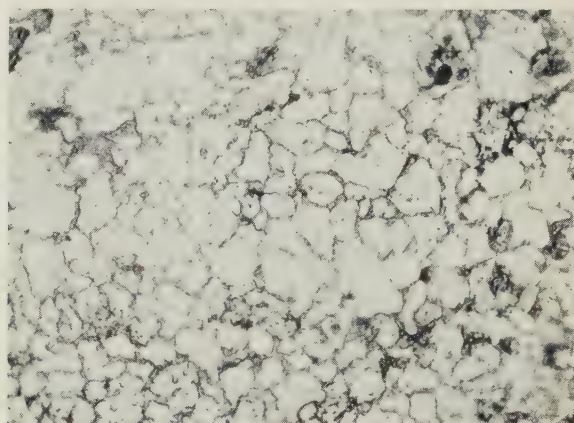


(b) 500° C.

FIG. 11.—Diffusion Bands Formed Around Drops of Lead Spreading upon Silver.  $\times 3$ .

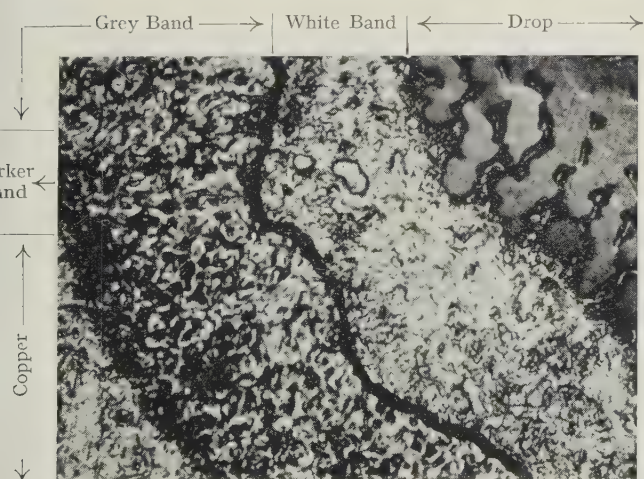


(a) Inner zone. Diffusion from grain boundaries into grains is evident.

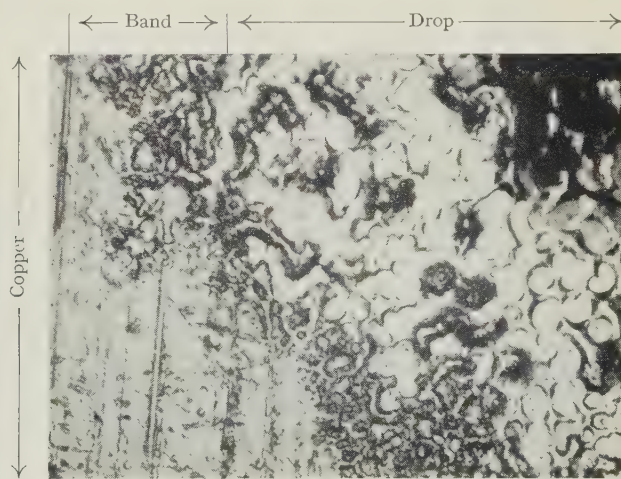


(b) Outer zone. Grain-boundary penetration is evident.

FIG. 12.—Diffusion Band Formed at 500° C. Around a Drop of Lead Spreading on Silver.  $\times 750$ .



(a) 250° C.



(b) 300° C.

FIG. 13.—Diffusion Bands Formed Around Spreading Drops of 40% Tin Solder on a Copper Surface.  $\times 300$ .



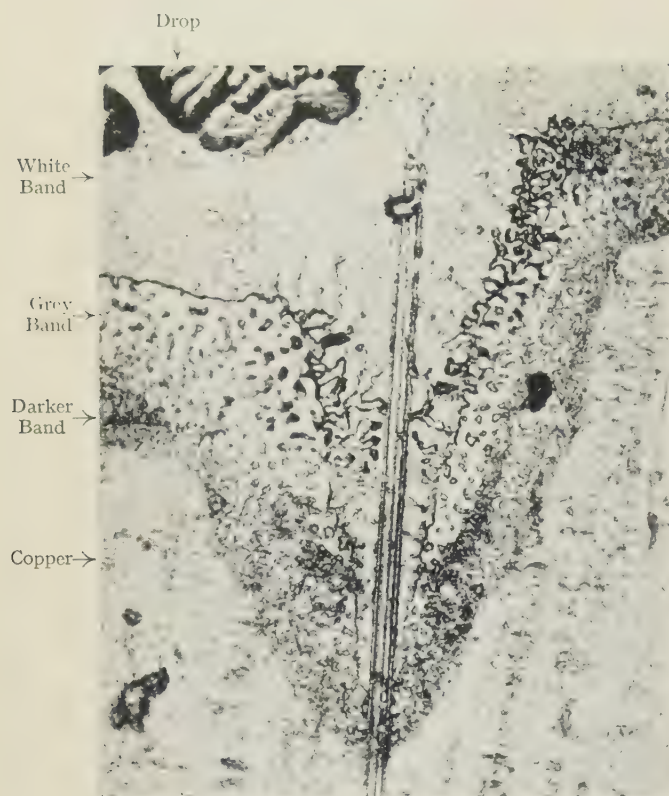


FIG. 14.—45% Tin Solder Spreading at 240° C. Along a Scratch in a Copper Surface.  $\times 150$ .



FIG. 16.—Dewetted Copper Surface Showing Attack at Grain Boundaries. Copper immersed in lead at 600° C. for 2 hr.  $\times 400$ .



(a)



(b)

FIG. 15.—Diffusion Band Formed Around Spreading Drop of 45% Tin Solder on Copper at 240° C. (a) Radiograph (the light areas correspond to strong X-ray absorption). (b) Micrograph of same field.  $\times 40$ .

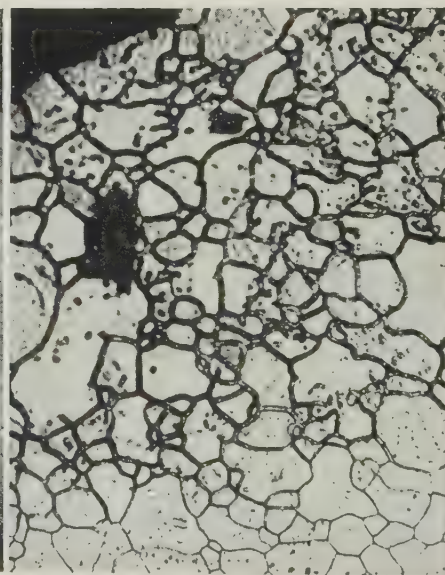


FIG. 17.—Dewetted Copper Surface Showing Lead Retained in Grain Boundaries. Copper immersed in lead at 600° C. for 2 min.  $\times 150$ .





FIG. 18.—Appearance of Copper Grain Face after Immersion in Lead Saturated with Copper and Very Slow Cooling to Precipitate Primary Copper. Showing development of preferred planes and “liquid” retained in grooves of structure.  $\times 400$ .

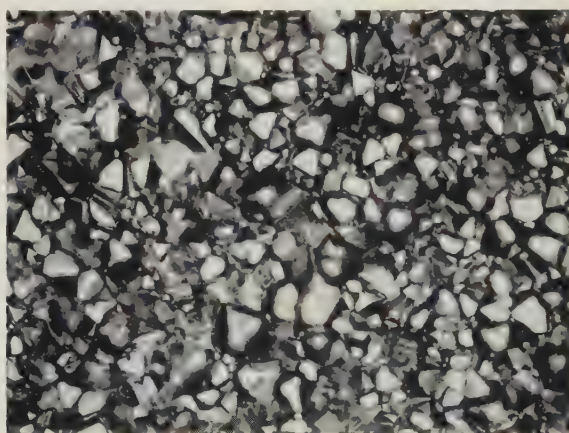
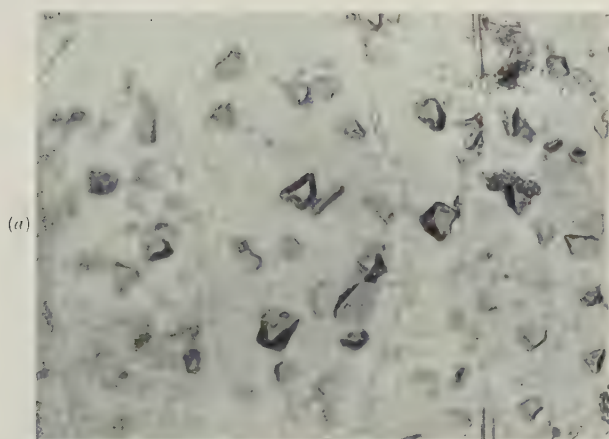


FIG. 19.—Copper Foil, Having Initially Smooth Surface, Flooded with 98 : 2 Lead-Tin Alloy for 60 min. and Drained at 450° C. Same area of surface photographed: (a) As dewetted, (b) after etching for 1 min. in 3 : 1 by volume glacial acetic acid and 20 vol. hydrogen peroxide.  $\times 500$ .



FIG. 20.—Copper Surface Immersed for 10 sec. at 400° C. in Lead Containing 0.05% Tin, Showing Cubic Etch-pits on the Least Attacked Grains.  $\times 750$ .

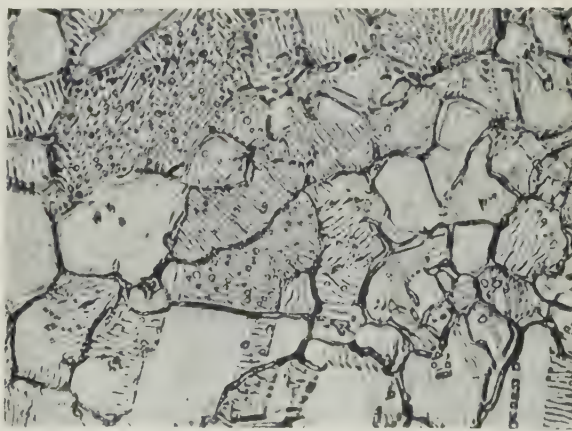


FIG. 21.—Copper Surface Immersed for 15 min. at 500° C. in Lead Containing 2.5% Silver, Showing Form of Etching.  $\times 500$ .



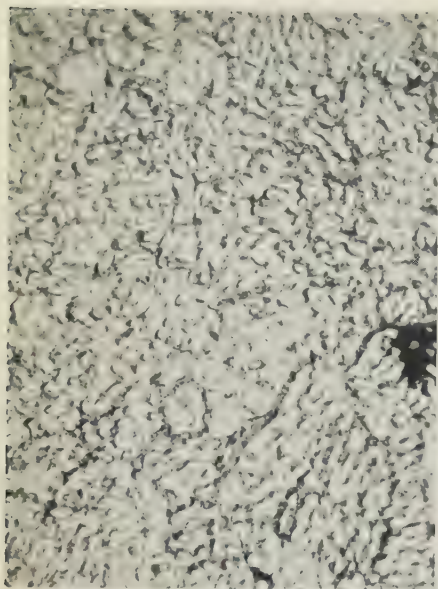


FIG. 22 (a).—Copper Surface after Immersion in Lead Containing 0.1% Nickel for 15 sec. at 400° C.  $\times 750$ .



FIG. 22 (b).—Copper Surface (larger grain-size produced by annealing 1 hr. at 1050° C.) after Immersion as in (a) Showing Enhanced Attack on Twin which has an Adherent Drop of Liquid.  $\times 400$ .

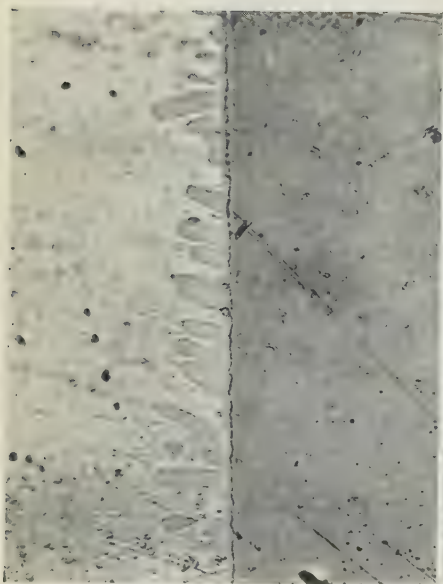


FIG. 23 (a).—Section of Copper Immersed for 2 min. at 300° C. in Pure Tin.  $\times 500$ .

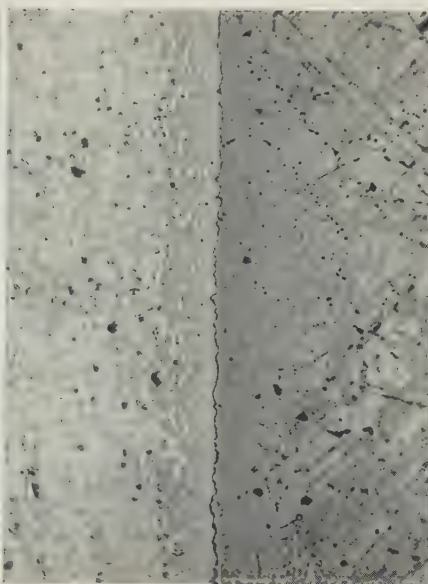


FIG. 23 (b).—As (a), but Immersed in Tin Containing 0.1% Nickel.  $\times 500$ .

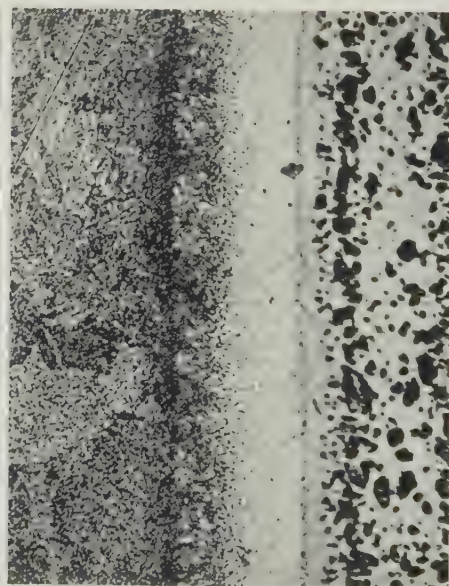
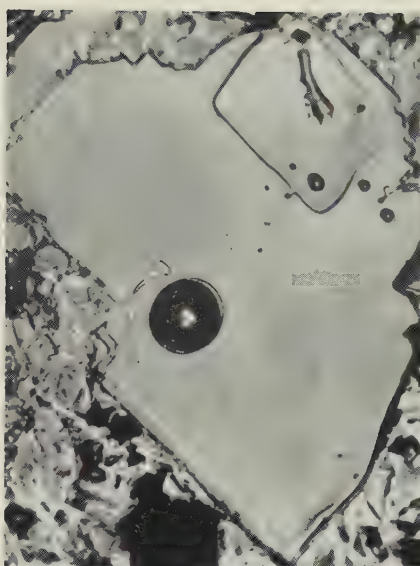


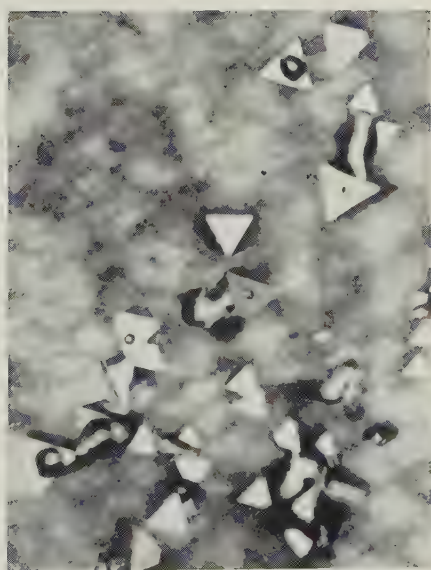
FIG. 24.—Oblique Section of 50% Tin Solder Coating Formed on Copper at 350° C.  $\times 500$ .



(a) Cu-Sn.



(b) Ag-Sn.



(c) Cu-Bi



(d) Cu-Pb

FIG. 25 (a)-(d).—Extracted Primary Crystals, Showing Adhesion of Drops of the Liquid.  $\times 200$ .



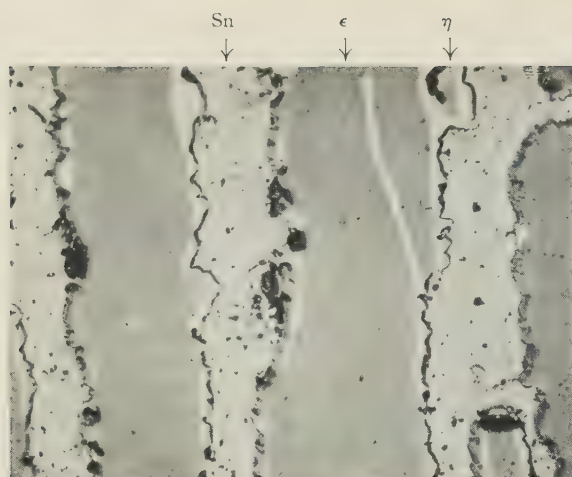


FIG. 26 (a).—Copper-Tin Alloy. As cast.  $\times 150$ .

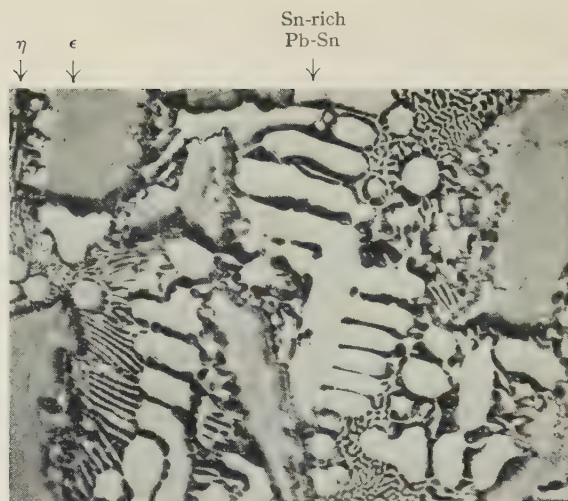


FIG. 26 (b).—Copper-Tin-Lead Alloy. As cast.  $\times 150$ .

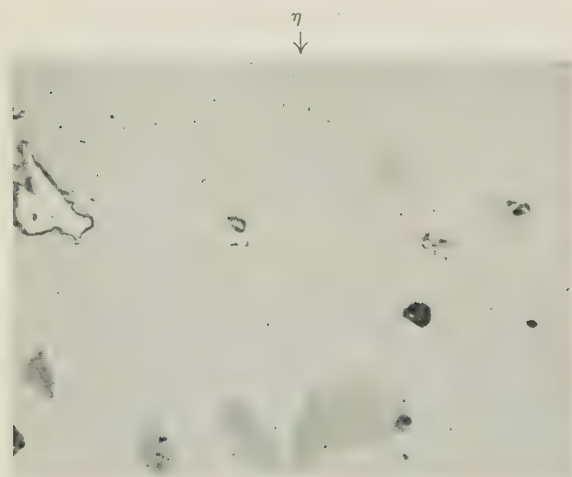


FIG. 27 (a).—Copper-Tin Alloy. Annealed 7 days at 400° C.  $\times 150$ .

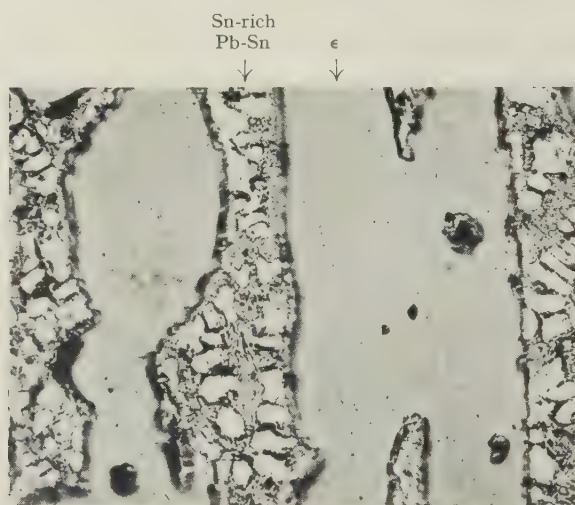


FIG. 27 (b).—Copper-Tin-Lead Alloy. Annealed 7 days at 400° C.  $\times 150$ .

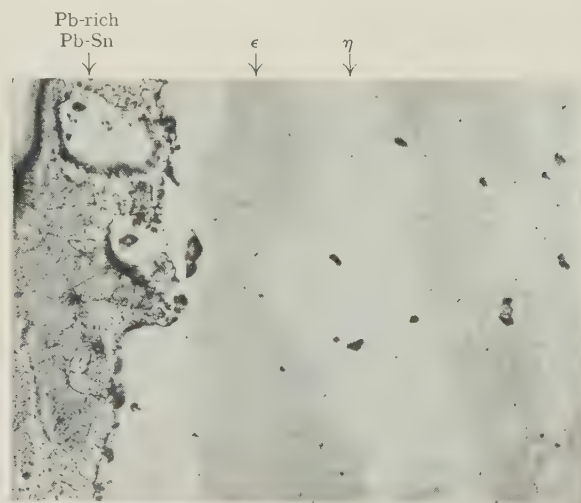


FIG. 28.—Copper-Tin-Lead Alloy. Annealed 21 days at 300° C.  $\times 150$ .

of interest arising from the improvement obtained by the addition of nickel to lead for coating copper and iron, similar experiments were made to observe the stability of a coating of tin, to which 0.1% of nickel had been added, upon these two metals. Strips of copper or iron were dipped simultaneously, at 300° C. for 2 min., one into pure tin and the other into tin containing 0.1% nickel. On withdrawal, both coatings on the iron specimens dewetted, but the nickel-bearing tin coating on the copper surfaces appeared to be very much more stable than that of pure tin.

#### 6. COATINGS OF LEAD-SILVER ALLOY ON COPPER

In similar experiments with a lead-silver alloy containing 2.5% silver upon copper surfaces with periods of immersion up to 15 min. at temperatures up to 500° C., it was found that, unlike lead, a coating could be obtained, but that this coating was comparatively unstable and dewetted fairly rapidly.

#### 7. ELECTROCHEMICAL DEPOSITION FROM FLUXES

The deposition of tin on to a copper surface by electrochemical action in a short-circuited cell consisting of tin/zinc-ammonium chloride/copper has been described (Section IV, 5), and its possible importance in promoting rapid spreading of solders in practice referred to. It was of interest to examine in a preliminary way the possibility of similar deposition on copper and iron from other metallic chlorides which might be incorporated into fluxes. Since the majority of the chlorides which were considered have high melting points, they were mixed with other chlorides with which eutectic systems are formed. The following compositions were examined:

- (a) Stannous chloride 80 g., potassium chloride 20 g.
- (b) Lead chloride 80 g., potassium chloride 20 g.
- (c) Cadmium chloride 60 g., potassium chloride 40 g.

In each case, a layer of the flux was heated in a silica crucible above a little of the appropriate metal (tin, lead, or cadmium) until both were molten and strips of copper and iron were dipped through the flux to make contact with the molten metal. After a few seconds' immersion, the specimen was removed and the part which had been in contact with the flux was examined. It was found that a coating had been deposited from the flux in every case except with steel immersed in the lead chloride flux. The coating of lead on the copper specimen had dewetted.

To repeat and extend the investigation, including other chlorides of interest, a standard flux base was adopted in which they could be incorporated. This consisted of equal parts of lithium, potassium, and ammonium chlorides, 10 g. of each being dissolved in 100 ml. of water. To this basic solution was added 10 g. of one of the following: nickel chloride, manganese chloride, cobalt chloride, stannous chloride, cadmium chloride.

These fluxes were tested by comparing their effectiveness in the hot-dip coating of copper and iron with lead at 400° C., zinc-ammonium chloride flux being used as a standard.

Before fluxing, the specimens were cathodically degreased, the copper was lightly etched in a chromate pickle and the steel in dilute nitric acid. The results showed that, while wetting of copper by lead could be produced with all the fluxes, only the stannous chloride, cadmium chloride, and zinc chloride fluxes were effective with iron. It was found that dewetting of copper was much less likely to occur with the flux containing nickel than with the standard flux.

Open-circuit voltage measurements at room temperature with lead as one electrode and copper or iron as the other, using the aqueous fluxes as electrolytes, gave the results shown in Table III.

TABLE III.—*E.M.F. Measurements.*

Flux	Open-Circuit Voltage at Room Temperature, V.	
	Steel	Copper
NiCl <sub>2</sub> . . . .	0.008 *	0.315
CoCl <sub>2</sub> . . . .	0.010 *	0.300
MnCl <sub>2</sub> . . . .	—0.015 *	0.252
SnCl <sub>2</sub> . . . .	0.095	0.215
CdCl <sub>2</sub> . . . .	0.100	0.235

\* No coating of lead obtained.

It will be seen that coatings were obtained only where an open-circuit voltage exceeding about +0.1V. existed between the electrodes. The polarity of the cells was in all but one case such as would result in the deposition of metallic ions on to the copper or steel.

#### VI.—METALLOGRAPHIC OBSERVATIONS

Throughout the experimental work described, metallographic studies were made of features of special interest. An account is given below of some of these observations.

##### 1. DIFFUSION BANDS IN SOLID SURFACES

The formation of bands in the exposed solid surfaces adjacent to the advancing edge of the liquid metal has been mentioned. These bands were most evident where secondary spreading occurred and were due to diffusion of the liquid in the surface layers of the solid metal. The appearance, after solidification, of drops of lead on a silver surface is shown in Figs. 11 (a) and (b) (Plate XIV). In both cases, the time of contact at temperature was 30 min., but the drop in Fig. 11 (a) was applied at 400° C. and showed no secondary spreading, whereas that of Fig. 11 (b) was applied at 500° C. and showed marked secondary spreading. In both cases a diffusion band is evident in the solid surface surrounding the drop. Closer examination of this band showed that in its outer zone grain-boundary penetration had occurred



(Fig. 12 (b) Plate XIV) while, nearer to the liquid, diffusion from the grain boundaries into the grains was evident (Fig. 12 (a) Plate XIV).

## 2. DIFFUSION BANDS IN THE COPPER/TIN-LEAD SYSTEM

The width and appearance of the diffusion bands formed in a copper surface at the periphery of a drop of molten tin-lead alloy was observed to depend on the tin content of the alloy, on the temperature, and on the duration of the experiment. Detailed examination could be made only after cooling, which may have been accompanied by an increase of contact angle, leading, with differential contraction, to shrinkage of the drop before solidification.

With pure tin, the diffusion band was always narrow, though wider at higher temperatures. In the range 250°–400° C. it consisted of two well-defined zones, a narrow, bright inner band, presumably of  $\eta$  phase ( $\text{Cu}_6\text{Sn}_5$ ) and a broader outer band, dark in colour, presumably of  $\epsilon$  phase ( $\text{Cu}_3\text{Sn}$ ). The diffusion zone round drops of tin applied at 500° C. showed only one band, presumably of  $\epsilon$  phase, since the  $\eta$  phase is unstable at that temperature.

No diffusion bands were observed surrounding drops of lead. With tin-lead alloys, the bands were broad only with compositions in the range 30–50% tin, and within limited ranges of temperature, i.e. in the circumstances in which secondary spreading was observed.

Reference to Fig. 4 shows that marked secondary spreading occurs with an alloy containing 40% tin applied at 250° C., the effect being entirely absent at 300° C. The corresponding diffusion zones formed at the periphery of the drop are compared in Figs. 13 (a) and (b) (Plate XIV). A similar difference was also obtained using a 50% tin alloy at 300° and 350° C. respectively. The width of the bands is sensitive to the texture of the surface. The effect of a scratch is shown in Fig. 14 (Plate XV).

An attempt was made, using the technique of micro-radiography, to obtain information on the materials composing the bands shown in Fig 13 (a) (Plate XIV). A drop of 45% tin alloy was allowed to spread at 240° C. on a copper foil 0.0006 in. thick and a radiograph was made of part of its periphery using cobalt radiation. The result is shown in Fig. 15 (a) (Plate XV). Fig. 15 (b) (Plate XV) is a normal micrograph of the same field. A marked difference in the X-ray absorption of the two principal diffusion bands is evident, suggesting that if, as is likely, the outer band is no thicker than the inner, it is lead-rich in comparison with the inner band. That this is very probably the case was confirmed by attacking the specimen with an etchant selective for lead. A micro-radiograph, taken after etching in acid ferric chloride solution, showed that the dense material was being removed. Removal by this etchant of the supposed lead-rich material exposed a light-coloured substrate similar to that seen in the inner band, Fig. 15 (a). Prolonged etching removed the light consti-

tuent from both inner and outer bands, exposing a darker surface. It must be remembered, however, that the X-ray examination could be made only on solidified drops and any interpretation of the result must take this fact into account.

## 3. ROUGHENING OF SURFACES ON IMMERSION

The examination of the solid/liquid interface of a coated surface is not easy, though some information is, of course, obtainable from sections. Dewetted surfaces may, however, be readily examined, and the changes which occur as a result of immersion are of interest. Thus, Fig. 16 (Plate XV) shows the dewetted surface of an initially polished copper specimen which has been covered by a small volume of lead for 2 hr. at 600° C. The resultant etching of the grain boundaries is clear. Fig. 17 (Plate XV) shows a similar specimen which has been immersed for 2 min. in a larger volume of lead at 600° C. The retention of lead in the grain boundaries near the lead drop at top left of the micrograph is evident, as is also the fact that the grain faces themselves are attacked. This attack results in the development of etch pits. The effect on a copper surface of slowly cooling a copper-saturated melt of lead in which it is immersed is shown in Fig. 18 (Plate XVI), in which the presence of residual "liquid" in the grooves of the surface is of interest.

Such retention of liquid from a coating drained off a roughened surface is clearly shown in Figs. 19 (a) and (b) (Plate XVI). A specimen of copper foil, having initially a smooth surface, was immersed for 60 min. in lead containing 2% tin, at 450° C. On withdrawal, the coating immediately dewetted, and the dewetted surface appeared as in Fig. 19 (a). This surface was treated in a lead-selective etch consisting of 3:1 by volume glacial acetic acid and 20 vol. hydrogen peroxide. Fig. 19 (b) shows the same field as Fig. 19 (a) after etching for 1 min. and the exposure of crystals, probably of  $\epsilon$ -copper-tin,  $\text{Cu}_3\text{Sn}$ , as "liquid" is removed is evident.

The marked effect in roughening a copper surface of the presence of as little as 0.05% tin in lead is shown in Fig. 20 (Plate XVI) which shows a polished copper surface after immersion for only 10 sec. at 400° C. It may be noted that those grains having a cubic plane in the surface appear to be least attacked, showing only a few cubic etch-pits. Similar selective roughening is shown when a copper surface is immersed in lead containing 2.5% silver, as is clear from Fig. 21 (Plate XVI), and when it is immersed in lead containing 0.1% nickel (Fig. 22, Plate XVII). The selective wetting of a twin is of interest in this last example, Fig. 22 (b). When intermetallic compounds are formed on immersion the solid surface is grossly roughened by the growth of crystals of the intermediate phase, as is clear from the sections shown in Fig. 23 (Plate XVII). The mode of growth of crystals of copper-tin compound appears to be greatly modified by the addition to the tin of 0.1% nickel, as shown by Fig. 23 (b), which should be compared with Fig. 23 (a).

The appearance of a section through a coating of 50% tin solder applied to copper at 350° C. shown in Fig. 24 (Plate XVII) resembles that of the tin-nickel alloy of Fig. 23 (b), and the solder coating had a similarly high stability.

#### 4. EXTRACTION OF PRIMARY CRYSTALS FROM MOLTEN ALLOYS

Some indication of the magnitude of the contact angle which is formed on comparatively smooth surfaces was obtained by the examination, after solidification, of the liquid phase adhering to the surface of primary crystals thrown out when saturated alloys were slowly cooled. These primary crystals were removed from the molten alloy on a copper or steel spatula, and allowed to cool in the furnace atmosphere of purified hydrogen. They were seen, by microscopic observation, in general to have comparatively smooth surfaces, to which there often adhered solidified drops of the liquid alloy. It was noted that the contact angle exhibited by these drops appeared to be comparatively high. Fig. 25 (a) (Plate XVIII) shows drops of tin-rich liquid adhering to the smooth face of a needle of  $\eta$  phase ( $\text{Cu}_6\text{Sn}_5$ ), extracted from a copper-tin liquid alloy at 250° C., Fig. 25 (d) (Plate XVIII) shows drops of lead-rich liquid on primary copper crystals extracted at 475° C., and Figs. 25 (b) and (c) (Plate XVIII) illustrate respectively the systems silver-tin and copper-bismuth. Similar behaviour was observed with molten copper-tin-lead alloys. Thus, with crystals extracted at 325° C. from a liquid containing 20% tin, drops with high contact angle were observed on the large primary crystals, blue-grey in colour, which had been formed by cooling the melt. Similarly, crystals extracted at 250° C. from a liquid containing 60% tin, showed adherent drops and were similar in appearance to those of Fig. 25 (a). However, crystals extracted at 300° C. from a 45% tin alloy appeared in general to be coated with liquid; where the coating had dewetted the contact angles were much lower than in the examples in which only adherent drops were observed.

#### 5. COMPARATIVE STRUCTURES OF TIN-COPPER AND TIN-COPPER-LEAD ALLOYS

The spreading and coating experiments with tin-lead alloys on copper surfaces in a hydrogen atmosphere show that the lowest contact angles are obtained upon an alloy layer, and that lower contact angles are observed when the layer is of the  $\eta$  phase ( $\text{Cu}_6\text{Sn}_5$ ) than when it is of the  $\epsilon$  phase ( $\text{Cu}_3\text{Sn}$ ). A possible reason for the failure of alloys containing less than about 30% tin to exhibit slow secondary spreading is that the rate of diffusion outwards from the drop is very slow because the reactivity of tin towards copper decreases as its dilution by lead increases. Relatively stable hot-dipped coatings are formed with alloys of lower tin content than 30% if sufficient time of immersion is allowed.

A micrographic study of alloy layers with the object of obtaining supporting evidence for these conclusions

might prove to be difficult, since undetectably thin alloy layers could influence the contact angle. An effort was therefore made to obtain information of the kind required by comparing the structures of cast and heat-treated tin-copper and tin-copper-lead alloys.

Small ingots were cast to the following compositions :

		Sn, wt.-%	Cu, wt.-%	Pb, wt.-%
Alloy A	:	59.0	41.0	...
Alloy B	:	53.1	36.9	10

In both alloys, the proportion of copper to tin was that of the  $\eta$  phase ( $\text{Cu}_6\text{Sn}_5$ ).

The as-cast structures of the two alloys are compared in Figs. 26 (a) and (b) (Plate XIX). It will be seen that these are similar in consisting of an open banded structure of  $\text{Cu}_3\text{Sn}$  (grey) fringed with  $\text{Cu}_6\text{Sn}_5$  (white), the intervening areas showing either tin (alloy A) or tin-lead eutectic with tin-rich primaries (alloy B). Figs. 27 (a) and (b) (Plate XIX) show the two alloys after annealing for 7 days at 400° C. It will be noted that while, in alloy A, the reaction  $\epsilon + \text{Sn} \rightarrow \eta$  has proceeded almost to completion, alloy B is apparently little changed. Annealing alloy B for a further period of 11 days at the lower temperature of 350° C. results in the appearance of substantial quantities of the white  $\eta$  phase and the depletion of the residual liquid approximately to the tin-lead eutectic composition, while annealing for 21 days at 300° C. gives a structure containing more of the white  $\eta$  phase and a lead-rich liquid phase Fig. 28 (Plate XIX).

Qualitatively, it appears that the lead present competes with the copper for the tin required to transform the  $\epsilon$  phase to the  $\eta$  phase, and that it competes more successfully at the higher than at the lower temperatures. At a temperature of 400° C., therefore,  $\text{Cu}_6\text{Sn}_5$  might be comparatively slow to form as an interfacial layer even in a tin-rich solder, and secondary spreading would accordingly not be marked with any solder composition at this temperature. At 350° C. there is a better chance of  $\text{Cu}_6\text{Sn}_5$  forming with solders containing less tin, while at 300° C. even less tin is necessary for the ready formation of  $\text{Cu}_6\text{Sn}_5$ . The rising liquidus temperature of lead-rich solders sets a limit to the range of solder compositions with which ready formation of  $\text{Cu}_6\text{Sn}_5$  is possible at appropriate temperatures. This tentative deduction from the examination of alloys A and B may in part explain the fact, shown in Fig. 4, that the greatest spreading occurs at lower tin contents as the temperature is decreased, and also the curious features shown in Figs. 13 (Plate XIV), 14, and 15 (Plate XV). It is evident, however, that a more extensive investigation would be needed to strengthen these views.

#### VII.—GENERAL CONCLUSION

The object of the investigation reported in this paper is to contribute to an understanding of the factors controlling the flow of liquid metals on solid metal surfaces, with particular reference to soldering,



brazing, and hot-dip coating. The experimental work described is of a preliminary kind, and is in several directions incomplete. It would be fruitless to attempt to summarize here the many experimental observations which have been made: conclusions are drawn at appropriate points in the paper. A more useful purpose is served by surveying briefly the main indications arising from the work.

Starting from the probable assumption that the forces controlling the flow of liquid are those due to surface tension aided or opposed by gravity, it is pointed out that the surface-tension forces depend on the value both of the surface tension of the liquid and of the contact angle. In capillary penetration both the rate and ultimate extent of penetration depend on the product of liquid surface tension and the cosine of the contact angle, whereas in spreading on a plane surface, particularly of small drops, the area covered depends solely on the value of the contact angle. This dependence is no longer as the cosine of the contact angle, but is more nearly inversely as the value of the contact angle itself.

It is not necessarily surprising, therefore, that solders are placed in differing orders of merit by spreading-drop and capillary-penetration tests, which, as hitherto employed, measure different surface-tension properties. The apparent discrepancies between the results of the two types of test may be explicable solely on these grounds. However, these discrepancies suggest alternatively, that with all tin-lead solder compositions the contact angle first formed against a solid surface is high (c. 60°), but that, if the solder moves sufficiently slowly over the surface, the contact angle of solders containing about 50% of tin falls to a low value. The experimental work on spreading over a copper surface in a hydrogen atmosphere shows that such slow spreading can occur. How quickly it occurs in the presence of liquid fluxes has not yet been determined. It evidently takes place to a greater extent under zinc-ammonium chloride flux than under plain resin flux. It appears that electrolytic deposition of metal from the flux on to the solid surface ahead of the spreading solder produces a modified solid surface against which the liquid develops a lower contact angle and as a result both the rate and the extent of the spreading are increased.

Theory anticipates and experiment readily shows that substantial hysteresis of the contact angle is usual. It is possible that the discrepancies between the results of spreading-drop experiments and practical assessments of solder performance may be explained by taking hysteresis into account. In spreading-drop experiments an advancing contact angle is established, whereas in most soldering practice, a coating of solder is formed, e.g. by tinning, dipping, or working with the bit and, if the contact angle is to be considered, the receding value should be more appropriate. It remains to be explained, however, why an area measurement should even approximately represent practical solder performance, in which the ability to penetrate joints appears to be the main requirement.

At present, theory does not allow the prediction of true contact angles, nor can they in general be measured directly because of the effects of surface roughness, which cannot be given quantitative expression. The nature of roughness effects can be foreseen to some extent, however. In particular, the promotion of spreading by previously roughening the solid surface by interlacing scratches is substantiated by theory.

Although true contact angles may be neither calculated nor measured, an indication of their value is obtainable by experiment, and some use may be made of such observations. For example, the observation that the receding contact angle of lead upon nickel is very low led to the successful attempt to produce lead coatings upon copper and iron by the addition of a small proportion of nickel to the lead.

#### ACKNOWLEDGEMENT

The authors are indebted to the Director and Council of the British Non-Ferrous Metals Research Association for permission to publish this paper.

#### APPENDIX I

##### SPREADING AND PENETRATION ON SMOOTH SURFACES: CONSTANT SURFACE TENSION AND CONTACT ANGLE

The purpose of this appendix is to state briefly and in simple form a number of expressions which are almost all derived in classical surface-tension theory<sup>4</sup> and relate to cases of particular interest in jointing and hot-dip coating.

##### (a) Shape of a Drop of Liquid on a Horizontal Plane Surface (Fig. 29)

The fundamental equation for the shape of the surface of a drop resting on a horizontal plane may be written:

$$\gamma \left( \frac{1}{r} + \frac{\sin \psi}{x} \right) = \frac{2\gamma}{b} + g\rho y \quad (1)$$

where  $\gamma$  = surface tension of liquid

$\rho$  = density of liquid

$g$  = acceleration due to gravity

$x, y$  = the co-ordinates of any point,  $P$ , on the surface (Fig. 29 (a))

$\psi$  = angle between the tangent to the drop at  $P$  and the  $x$ -axis

$r$  = that radius of curvature,  $PQ$ , at  $P$  which lies in the plane of the figure

$b = OM$ , the radius of curvature at the apex of the drop

The terms  $\sin \psi$ ,  $r$ , and  $b$  in equation (1) may be written as differential functions of  $x$  and  $y$ , so that equation (1) is in fact a differential equation in  $x, y$ , and the constants  $\gamma, \rho$ , and  $g$ . No general solution of this differential equation is possible, however. For a drop which is so large that its upper surface is flat,

and with contact angles exceeding  $90^\circ$  (Fig. 29 (b)), it is found by approximation that :

$$\gamma = \frac{g\rho h^2}{2} \quad (2)$$

$$\cos \theta = 1 - \frac{H^2}{h^2} \quad (3)$$

When the drop is so small that the gravitational term in equation (1) can be neglected, its surface forms part of a sphere. In these circumstances, the area of contact between the drop and the plane is independent of its surface tension and depends only on the volume of liquid composing the drop and the contact angle. This relationship may be written, Fig. 29 (c) :

$$V = \frac{\pi h}{6} (3R^2 + h^2) \quad (4)$$

$$\text{or} \quad V = \frac{\pi R^3}{3} \tan^2 \frac{\theta}{2} \left( 3 \operatorname{cosec} \theta - \tan \frac{\theta}{2} \right) \quad (5)$$

where  $V$  is the volume of the drop.

No useful solution of equation (1) is available when the drop is so large that the gravitational term cannot

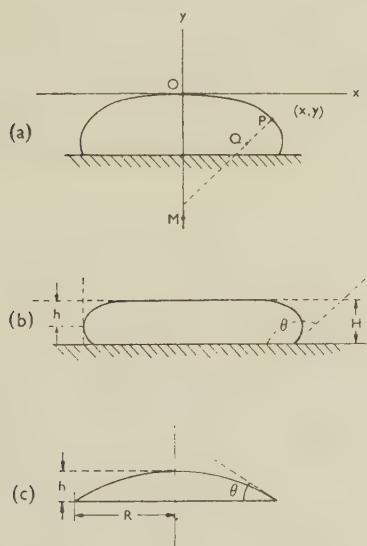


FIG. 29.—Shape of Liquid Drop on Horizontal Plane Surface.

be neglected and, at the same time, the contact angle is less than  $90^\circ$ .

#### (b) Rate at which a Drop of Liquid Attains its Equilibrium Shape

Because the fundamental equation for equilibrium drop shape, equation (1), is incapable of general solution, it is not possible to deduce either the rate at which a spherical drop applied to the surface will expand or the rate at which a given volume of liquid applied as a film of specified uniform thickness will contract to take up the equilibrium drop shape.

#### (c) Downward Pull Exerted by a Meniscus

When a plane surface is dipped vertically into a liquid which exhibits against it a contact angle  $\theta$ , the liquid surface assumes a shape shown in section in Fig. 30. The curve  $ABC$  is the "capillary curve"

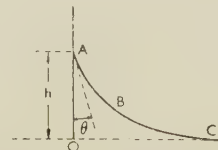


FIG. 30.—Shape of Liquid Surface at Vertical Plane Surface.

and its equation may be derived. Of greater interest, however, are the height ( $OA$ , Fig. 30) of the top of the liquid meniscus and the downward pull,  $W$ , exerted by the meniscus on the solid surface.

(i) The height of the meniscus is found from :

$$h = \sqrt{\frac{2\gamma}{g\rho} (1 - \sin \theta)} \quad (6)$$

(ii) The downward pull,  $W$ , is simply, per unit length of meniscus,

$$W = \gamma \cos \theta \quad (7)$$

#### (d) Rate of Formation of a Meniscus

The rate at which a meniscus achieves the equilibrium shape has not hitherto been calculated.

#### (e) Draining of Dipped Coatings

Jeffreys<sup>13</sup> derived a relationship for the thickness  $x$  of the liquid coating at a distance  $y$  below its top edge at any time  $t$  after withdrawal from immersion. This expression is :

$$x = \sqrt{\frac{\eta y}{gt}} \quad (8)$$

in which  $\eta$  is the kinematic viscosity of the liquid. It was derived under the assumption that the draining surface is vertical and that the contact angle is zero. No treatment has hitherto been given of the case when the contact angle is greater than zero, or of the collapse of coatings to form separate drops.

#### (f) Penetration of Capillary Spaces : Equilibrium Penetration Height

The height,  $H$ , to which a liquid rises in a vertical tube of circular cross-section is given by the expression :

$$H = \frac{2\gamma \cos \theta}{g\rho r} \quad (9)$$

where  $r$  is the radius of the tube. An identical expression in which  $r$  is now the separation of the surfaces, may be obtained for penetration between parallel plates. These expressions are also true for penetration in capillaries inclined to the vertical,  $H$  being the vertical component of the penetration distance; in the limiting case of a horizontal capillary it is clear



that equilibrium can never be reached in a tube of finite length.

(g) *Penetration of Capillary Spaces: Rate of Penetration*

The rate of flow into a capillary at any moment depends on its cross-section and on the length of the column of liquid already drawn up. In a vertical capillary, the velocity,  $V$ , at any height,  $h$ , is given by :

$$V = \frac{r^2 \rho g}{8\eta h} (H - h) \quad (10)$$

In this expression,  $\eta$  is the coefficient of viscosity of the liquid and  $H$  the equilibrium height. From equation (10), the time,  $t$ , to reach height  $h$  is found to be :

$$t = \frac{8\eta}{r^2 \rho g} \left( H \log_e \frac{H}{H - h} - h \right) \quad (11)$$

In a horizontal capillary, the corresponding expressions may be written :

$$V = \frac{r^2 \rho g H}{8\eta h} \quad (12)$$

$$t = \frac{4\eta h^2}{r^2 \rho g H} \quad (13)$$

These expressions form useful approximations for the early stages of penetration into a capillary space of any inclination. They may conveniently be re-written

$$V = \frac{r}{4\eta h} \cdot \gamma \cos \theta \quad (14)$$

$$t = \frac{2\eta h^2}{r} \cdot \frac{1}{\gamma \cos \theta} \quad (15)$$

## APPENDIX II

### FACTORS DETERMINING THE VALUE OF THE LIQUID SURFACE TENSION AND OF THE CONTACT ANGLE ON SMOOTH SURFACES

#### (a) *Surface Tension and Contact Angle*

For a general discussion of surface tension and contact angle reference should be made, for example, to Adam.<sup>4</sup> Here it is stated only that every surface separating different kinds of matter possesses, by virtue of its existence, surface energy, which resides in a surface layer only an atom or two thick, the value of which is determined by the nature and arrangement of the atoms in this layer. When a surface is mobile, as with a liquid, it will tend to adjust its shape until a condition of minimum free energy is achieved locally. The possession by a surface of a specific free energy per unit area may be regarded as equivalent to the presence of a numerically equal tension force per unit length, the surface tension, acting in the surface.

When a liquid is in contact with a smooth solid

surface, under equilibrium conditions, their surfaces meet at a characteristic angle, the contact angle, the value of which is determined by the surface tensions of three surfaces, as shown in Fig. 31, according to the expression : \*

$$\gamma_{13} = \gamma_{12} + \gamma_{23} \cos \theta \quad (16)$$

Of these three surface tensions, only that of the liquid,  $\gamma_{23}$ , is normally measurable. Clearly if  $\gamma_{13}$  equals or

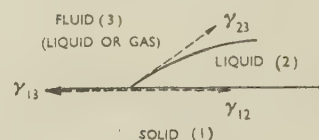


FIG. 31.—Determination of Contact Angle by Surface Tension of Three Surfaces.

exceeds the sum  $\gamma_{12} + \gamma_{23}$  the contact angle is zero and the liquid spreads indefinitely over the solid surface.

It is known that adsorption may occur from both the liquid and vapour phases on to a solid surface. The form of adsorption may well differ in the two cases, and thus the surface tension of a smooth solid surface may differ according as the liquid advances or recedes upon it. The contact angles accompanying advance and recession must thus also differ correspondingly, the receding angle being the lower. The possibility that such "molecular hysteresis" may occur indicates that two contact angles must be measured to specify a given system.

#### (b) *Direct Measurement or Estimation of Contact Angle*

The contact angle obtained in an experiment may frequently be measured directly by optical means. It may also be estimated by a method which does not involve any knowledge or assumption of the value of the surface tension of the liquid, from measurement of the area covered by small drops. By any other method of estimation, the contact angle is derived in terms of the liquid surface tension, the value of which in the circumstances in which the contact angle is investigated, may not be known. On smooth solid surfaces, it might be expected, in view of the possibility of molecular hysteresis, that different advancing and receding angles would be obtained, but these should be characteristic of the system. In Appendix III it is shown that, in general, when the surface is rough, it is impracticable to correct the observations for the effects of roughness and so derive these characteristic values. It is, however, the characteristic values which are of fundamental importance for spreading, capillary penetration, and coating stability. Since they cannot readily be measured directly, it is desirable to discuss individually the three surface tensions which determine them,

\* Surface tension at the surface between the solid (1) and liquid (2) is indicated by  $\gamma_{12}$ . Similarly the surface tension at

solid (1)/fluid (3) interface is  $\gamma_{13}$ , and at liquid (2)/fluid (3) interface  $\gamma_{23}$ .

(c) *Direct Determination of Surface Tensions*

While it is clear that the surface tension of a surface is determined by its atomic arrangement, the value cannot at present be calculated with accuracy for given arrangements of atoms. In any case, in view of the possible concentration at surfaces of impurities which are below detectable limits when a bulk sample is taken, such an approach would have little practical value. The surface tension of the liquid surface in contact with a fluid phase, either liquid or gaseous, may be measured directly, but those of the liquid metal/solid metal surface and of the solid metal/flux surface are not normally measurable.

(d) *Surface Tension of Liquid Metal/Flux Phase*

Direct measurement of the surface tension of a liquid metal in contact with a flux phase is possible by several methods which are independent of the contact angle. Bircumshaw<sup>14</sup> gives values for a number of tin-lead solders in contact with hydrogen, Chalmers and Wadie<sup>8</sup> obtained similar data employing a resin flux and Latin<sup>7</sup> determined the surface tension of tin and tin-lead solder of eutectic composition in contact with resin, zinc-ammonium chloride, and stannous chloride fluxes. Some of these results may be compared in Table IV.

TABLE IV.—*Surface Tensions of Tin, Lead, and Tin-Lead Eutectic (dynes/cm.) at Temperatures Just Above the Liquidus.*

Metal	Flux				
	Hydrogen <sup>14</sup>	Resin <sup>8</sup>	Resin <sup>7</sup>	Zinc/Ammonium Chloride <sup>7</sup>	Stannous Chloride <sup>7</sup>
Tin . . . . .	550	420	456	422	342
Tin-lead eutectic . .	490	380	390	331	...
Lead . . . . .	440	316	...	...	...

The complete series of results from which the first two columns of Table IV are selected show that, in both hydrogen and resin, surface tension decreases continuously with tin content. These results do not therefore at once suggest an explanation for the marked spreading of alloys in the centre of the composition range. If the two other surface tensions which determine the contact angle do not change, the largest spreads would be expected with the lead-rich solder compositions. It is, however, possible that the surface tension of the liquid metal may be influenced by the presence of the solid metal which is in contact with both solder and flux in soldering. This possibility has not hitherto been investigated, though the investigation might be attempted. One method would be to measure the downward pull exerted by a meniscus upon a vertical surface of the solid metal and at the same time to observe the contact angle directly.

(e) *Surface Tensions of Solid Surfaces*

No general methods are available for measurement of the surface tension of solid surfaces. An experi-

mental estimate for solid copper just below its melting point by Udin, Shaler, and Wulff<sup>15</sup> gives a value of 1370 dynes/cm., and another by Bailey and Watkins<sup>12</sup> gives a figure of 1800 dynes/cm. at temperatures of 800°–900° C. Bailey and Watkins were also able to measure the solid metal/liquid metal surface tension for the copper/lead/hydrogen system and obtained a value of 340 dynes/cm. at 800°–900° C. These values indicate that lead should spread completely on a copper surface at these temperatures. In fact, however, the contact angle is finite, though low. This is accounted for by supposing the surface tension of copper to be reduced as a result of adsorption of lead from the vapour phase. The surface tension of copper with an adsorbed lead layer was estimated to be 780 dynes/cm., less than half the "clean" value. A high value of the solid metal/flux phase surface tension, in the absence of adsorption, is not always to be expected, however. Shuttleworth<sup>16</sup> has calculated the surface tensions of some ionic crystals and found them to be of a lower order than those of metallic crystals. It might thus be expected that the surface tension of intermetallic compounds would in general be lower than that of metallic solid solutions.

C. S. Smith<sup>17</sup> considers that the solid metal/liquid metal surface tension is normally much lower than that of the solid metal surface in contact with its own vapour. He also describes experiments from which it is clear that the solid metal/liquid metal surface tension of lead-bismuth alloys in contact with copper varies considerably with the composition of the liquid alloy.

## APPENDIX III

## INFLUENCE OF SURFACE ROUGHNESS ON THE VALUE OF THE CONTACT ANGLE

## (a) "True" and "Observed" Contact Angles

The influence of roughness of the solid surface on the contact angle obtained in practice was first

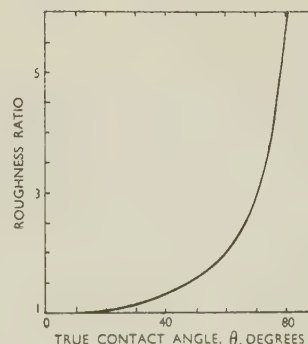


FIG. 32.—Relations Between True Contact Angle and Roughness Ratio.

discussed by Wenzel.<sup>18</sup> He considered that, if the true area of a rough surface is  $r$  times greater than its nominal area,  $r$  being called the "roughness ratio," the contact angle observed,  $\phi$ , is related to the true



contact angle,  $\theta$ , which is the angle observed on a smooth surface, by the expression:

$$\cos \phi = r \cos \theta. \quad (17)$$

Thus, when  $\theta$  is less than  $90^\circ$ , the observed contact angle is smaller than the true angle. The relationship between true contact angle and roughness ratio which gives an observed angle just equal to zero is plotted in Fig. 32 from which it will be seen, for example, that the observed angle is zero when  $r > 2$  and  $\theta < 60^\circ$ .

#### (b) *Influence of the Form of the Surface Roughness*

That Wenzel's solution of the problem is incomplete can be seen qualitatively from a consideration of Fig. 33. This represents an idealized rough surface in

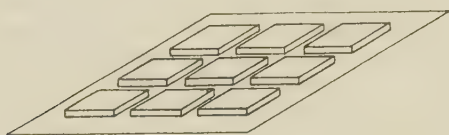


FIG. 33.—Idealized Rough Surface.

which the roughening has the form of a network of interlacing grooves. The spreading of a liquid on such a surface will be enhanced by the capillary effect of the grooves. Now consider a surface which is the "negative" of that of Fig. 33. This evidently consists of an array of pits. The roughness ratio of the "positive" and "negative" surfaces is the same, but spreading of a liquid on the negative will not be enhanced, as on the positive, by a network of capillary channels.

Using a similar model, Shuttleworth and Bailey<sup>19</sup> showed that Wenzel's expression, equation (17), is valid only when the roughness has the character of interlacing grooves. When this is not so the contact angle which is observed depends on whether the liquid has come to rest after spreading outwards over the surface or after receding over a surface which it has previously covered. The difference between advancing and receding values of the observed contact angle arising from this cause may be described as "capillary hysteresis" of the contact angle.

When this type of hysteresis occurs, it is impracticable to derive a quantitative relationship between observed and true contact angles. Whether or not it occurs in practice may be determined, not solely by a difference between advancing and receding contact angles which might be due only to "molecular hysteresis" but by the fact that, when an immersed surface is drained, pools of liquid remain trapped in the pits upon the surface.

By combining equation (16) (Appendix II) with equation (17) it is found that:

$$r\gamma_{13} = r\gamma_{12} + \gamma_{23} \cos \phi \quad (18)$$

This expression has the same form as equation (16), (Appendix II) and shows that, if Wenzel's equation is obeyed, the effect of the roughness is to increase the effective value of the surface tensions  $\gamma_{13}$  and  $\gamma_{12}$  by the roughness ratio,  $r$ .

The suggestion may be added that, with any real rough surface on which hysteresis is observed, the lower the true contact angle the more nearly does the surface behave as if it consisted of interlacing grooves. This suggestion arises from the view that a real surface consists of interlacing grooves of varying width and depth. When the true contact angle is high, grooves adjacent to the edge of a liquid drop will be incompletely filled, so that the variations in their depth will prevent capillary penetration. If the true contact angle is lower, this limitation on capillary penetration is less severe and the more nearly is an ideal system of interlacing grooves approached.

#### REFERENCES

1. S. J. Nightingale and O. F. Hudson, "Tin Solders: A Modern Study of the Properties of Tin Solders and Soldered Joints", (*Brit. N.-F. Metals Research Assoc. Research Monograph No. 1*), 1942.
2. J. McKeown, "The Properties of Soft Solders and Soldered Joints", (*Brit. N.-F. Metals Research Assoc. Research Monograph No. 5*), 1948.
3. A. Latin, *J. Inst. Metals*, 1946, **72**, 265.
4. N. K. Adam, "The Physics and Chemistry of Surfaces", 3rd Edition. London: 1941 (Oxford University Press).
5. E. J. Daniels and D. J. Macnaughtan, *Tech. Publ. Internat. Tin Research Develop. Council, Series B*, 1937, (6).
6. A. W. Coffmann and S. W. Parr, *Indust. and Eng. Chem.*, 1927, **19**, 1308.
7. A. Latin, *Trans. Faraday Soc.*, 1938, **34**, 1384.
8. B. Chalmers and R. H. Wadie, *J. Inst. Metals*, 1940, **66**, 241.
9. M. E. Fine and R. L. Dowdell, *Trans. Amer. Soc. Metals*, 1946, **37**, 245.
10. G. Tammann and F. Arntz, *Z. anorg. Chem.*, 1930, **192**, 45.
11. T. Alty and A. R. Clark, *Trans. Faraday Soc.*, 1935, **31**, 648.
12. G. L. J. Bailey and H. C. Watkins, *Proc. Phys. Soc.*, 1950, [B], **63**, 350.
13. H. Jeffreys, *Proc. Camb. Phil. Soc.*, 1930, **26**, 204.
14. L. L. Bircumshaw, *Phil. Mag.*, 1934, [vii], **17**, 181.
15. H. Udin, A. J. Shaler, and J. Wulff, *Trans. Amer. Inst. Min. Met. Eng.*, 1949, **185**, 186.
16. R. Shuttleworth, *Proc. Phys. Soc.*, 1949, [A], **62**, 167.
17. C. S. Smith, *Trans. Amer. Inst. Min. Met. Eng.*, 1948, **175**, 15.
18. R. N. Wenzel, *Indust. and Eng. Chem.*, 1936, **28**, 988.
19. R. Shuttleworth and G. L. J. Bailey, *Discussions Faraday Soc.*, 1948, (3), 16.

# THE SPECTROCHEMICAL DETERMINATION OF ZINC, LEAD, AND IRON IN COPPER AND COPPER ALLOYS\*

1326

By FREDERICK V. SCHATZ,† M.A.

## SYNOPSIS

A spectrochemical method suitable for the routine works control of copper and copper alloys has been developed. The procedure outlined is applicable to high-speed analysis, has a precision capable of determining zinc in brass with an error (expressed as a standard deviation) of 1.18% of the content or less, and has a sensitivity capable of detecting common impurities in copper alloys down to 0.005% or less. The determination of zinc, lead, and iron in brasses and leaded brasses is considered in detail. Factors important to the accuracy of the analysis are also considered; these include discharge characteristics, sample polarities, effects due to the nature of the lead dispersion, and curve shifts due to varying quantity of the matrix element.

## I.—INTRODUCTION

THE analysis of copper and copper alloys was among the earliest applications of the spectrograph in the field of practical analysis, and a great many papers have been published which describe spectrochemical methods designed to solve the special problems of individual investigators. Papers outlining procedures for practical works' control in the copper and brass industry, however, have been conspicuously small in number, and the development of suitable process control for copper alloys by means of the spectrograph has tended to lag behind the parallel development in the steel and aluminium works. This lag is not surprising when it is realized that a proper spectrographic procedure for the analysis of a simple high-purity brass should combine the extremes in spectrographic analysis, namely high-precision analysis of a constituent ranging from 5 to 40%, with a sensitive analysis of impurities ranging down to 0.005% or less. Only in recent years have the invention of high-precision sources, the development of photographic emulsions of great uniformity, and the progress in direct-reading equipment enabled the analyst to achieve control compatible with the specification limits of brasses.

The author has been engaged for several years in studying equipment and developing spectrochemical methods suitable for the complete analytical control of high-quality copper and brass alloys. This effort has been attended with considerable success, since at the present time up to 90% of all analyses at the Divisional Laboratories of Revere Copper and Brass Inc. are carried out on the spectrograph. The work described is concerned in detail only with the determination of zinc, lead, and iron in copper and the brasses. These elements are the most important encountered in

routine quality control, and analyses for them represent the greatest majority of those performed. Moreover, the procedures outlined are capable of extension to other elements. Work is in progress at the moment on a detailed consideration of the more complex copper alloys.

## II.—SOURCE CONSIDERATIONS

When the determination of high zinc contents in brass first engaged the author's attention, a new source, known as the Multisource, was being described in the literature.<sup>1,2</sup> Since a high-voltage Feussner interrupted spark had been used for high-zinc determinations with only fair results, a Multisource was obtained for detailed investigation.

The principle underlying the operation of the Multisource is very simple (Fig. 1). A half-wave rectifier charges a condenser to 940 V. during one half cycle. In the succeeding half cycle, the analytical gap is ionized by a low-power, high-tension spark discharge. This ionization allows the energy stored in the condenser to discharge across the gap through a selected inductance and resistance. Since the input rectifier and suitable filters isolate the discharge from all parts of the circuit except the analytical gap and a selected condenser, inductance, and resistance, the type of discharge and the energy associated with it can be very precisely controlled and maintained. Settings are combinations of 20, 20, 10, 5, 2, 2, and 1  $\mu$ F.; 200, 100, 50, 25, 10, 5, 5, 2, 2, and 1 ohm, and 200, 100, 50, and 25  $\mu$ H. There is also a distributed inductance of 25  $\mu$ H. and 0.4 ohm distributed resistance associated with the source, plus the distributed inductance, capacitance, and resistance of the leads used to connect the source and analytical gap.

The inventors of the Multisource claim that close to

\* Manuscript received 16 December 1950.

† Research Department, Revere Copper and Brass Inc., Rome, N.Y., U.S.A.



300,000 separate sources are possible. Of this multiplicity of sources, three have been found to be useful in the analysis of brasses. The three discharges are all unidirectional and pulse-like in nature. Os-

for most work, the Type 3 or Type 2 discharge has been used.

Examination of the oscilloscope pattern of the Type 3 discharge indicates that electrically it is slightly oscillatory. The contribution of the lower pip to the gap discharge, however, is so small that the pulse is unidirectional and has characteristics associated with high peak current and short duration.

If the Type 1 discharge is compared with Type 2, it is obvious that precision is associated with a short pulse and a low average current, while sensitivity is associated with a long pulse and a high average current. Consequently, there is a fundamental incompatibility between precision and sensitivity. Fortunately, the Type 3 discharge, which combines a pulse of short duration with a very high peak current, offers a compromise that enables the analyst to combine precision and sensitivity within reasonable limits.

Though the author has had no experience with the B.N.F.M.R.A. general-purpose source unit, descriptions<sup>3,4</sup> in the literature indicate that it is basically similar to the Multisource. The outstanding difference is that the triggered discharge voltage is 310 instead of 940 V. Consequently, equivalent settings on both units can be determined by the use of the relation:

$$R_c = 2\sqrt{L/C}$$

where  $R_c$  = critical damping resistance,  $L$  the inductance, and  $C$  the capacitance.

Distributed circuit constants may complicate the picture, especially in arriving at a proper resistance equivalent to the Type 3 discharge. This resistance is quite critical if a spectrum with optimum line-to-background intensity is desired. Walsh<sup>4</sup> in carrying out

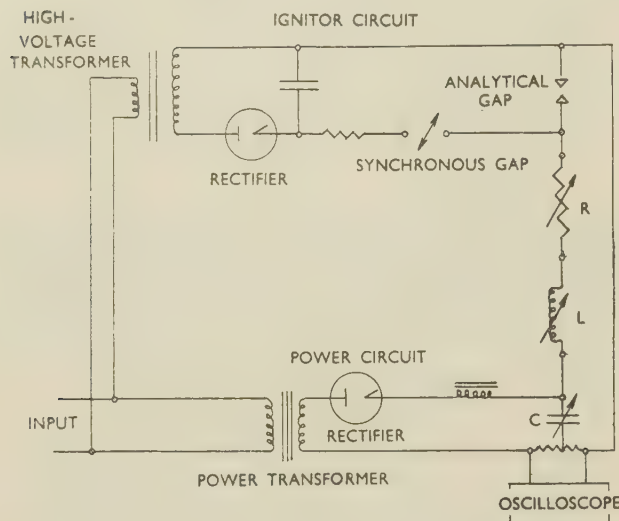


FIG. 1.—Schematic Diagram of Basic Multisource Circuit.

cillatory discharges from this type of circuit were found to be unsatisfactory owing not only to polarity considerations, but also to the nature of the copper spectrum, which in general was composed of broad, diffuse lines against a high background.

The discharges used are summarized in Table I.

TABLE I.—Types of Discharge.

Type	Sample Polarity	Precision	Sensitivity	Typical Setting
1. Slightly over-damped	+	< 2.0% Error	Poor	10 $\mu$ F., 200 $\mu$ H.,* 10 $\Omega$
2. Heavily over-damped	—	< 10% „	Excellent	60 $\mu$ F., 400 $\mu$ H.,* 20 $\Omega$
3. Slightly under-damped	+	< 2.0% „	Good	10 $\mu$ F., 200 $\mu$ H.,* 5 $\Omega$

\* Settings include 25  $\mu$ H. distributed inductance.

Oscilloscope patterns of each type of discharge are shown in Fig. 2 and form a convenient way of correlating settings between different source models. The Type 1 discharge, as applied to copper alloys, was first investigated by Hasler and Kemp,<sup>2</sup> who used it for aluminium bronze. They claimed a precision of better than 2% and a reduction in the effects of the specimen's metallurgical history. However, the Type 1 discharge is of only limited value in its applications to high-purity brasses, since its use makes necessary the application of either Type 2 or Type 3 discharges for the determination of impurities. The use of two discharges and the doubling of the analysis time may be unimportant in some laboratories, but not in a production laboratory where every minute counts. Consequently,

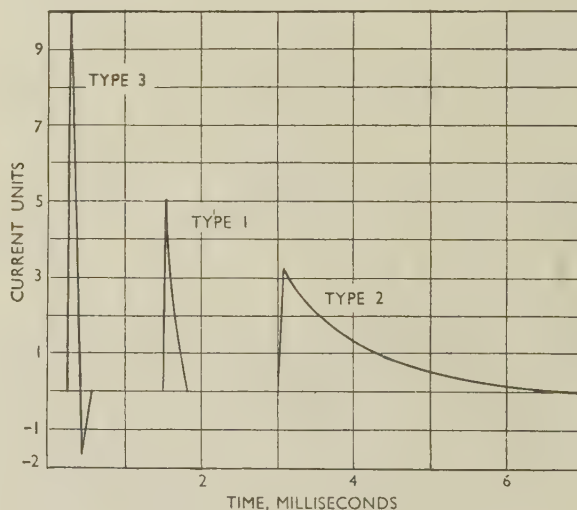


FIG. 2.—Discharge-Pulse Shapes.

the analysis of uranium with a B.N.F.M.R.A. general-purpose source unit, discovered a setting comparable in sensitivity to the over-damped arc-like discharge at resistance values between 0 and 1 when inductance

and capacitance settings were equal to 500  $\mu$ H. and 240  $\mu$ F. respectively. Calculation shows that if  $R = 0.97$  ohm Walsh setting is equivalent to the Type 3 discharge.

To summarize, the following working rules can be applied in deciding which discharge is most suitable for a specific copper alloy:

(1) Use Type 1 discharge on complex copper alloys where the metallurgical history is important and maximum impurity content is not too low, e.g. nickel silver, aluminium brass, and copper-silicon-manganese alloys.

(2) Use Type 2 discharge on materials where a very low maximum impurity content is important, e.g. copper, phosphor bronzes, and high-purity red brasses.

(3) Use Type 3 discharge where precision as well as low impurity content is important, e.g. copper, high-purity yellow brasses, leaded brasses, tin brasses, &c.

### III.—POLARITY CONSIDERATIONS

The sparking technique employed for these analyses is the point-to-plane spark, using a specimen with a machined flat opposed by a pointed graphite counter-electrode. Since the discharge is operating between dissimilar electrodes, polarity effects are important. For short-duration pulses of high peak current, positive polarity of the sample has been found to produce more desirable analysis conditions than negative polarity: the line-to-background ratios for impurity lines are greater, the curve for zinc has a greater slope, and random curve shifts are substantially less. A study of the zinc curve over a period of two years, under a variety of conditions, showed very little shift for positive sample polarity. At the same time curves for negative sample polarity showed shifts as high as 3% for 30% zinc.

For arc-like pulses of long duration, different conditions exist. For this type of discharge, sensitivity is the important factor. Investigation revealed that for the analysis of copper and brasses a five-fold increase in sensitivity resulted when the sample was negative instead of positive. Since a Type 2 discharge is over-damped as much as possible and the pulse maintained within the confines of one half cycle, it borders on a D.C. arc and as such is subject to some of the conditions controlling the D.C. copper arc.

Milbourn,<sup>5, 6</sup> in an investigation of the physical nature of the D.C. copper arc, demonstrated conclusively that in the presence of oxygen copper at the cathode is readily attacked and volatilizes as CuO. He also demonstrated that when no melting occurs at the anode, very little of the copper volatilizes from the positive pole. If the above conditions are observed, a copper arc of great uniformity results, having excellent analytical properties.

Early in 1946, the author had the opportunity to discuss personally with Mr. Milbourn the application of his D.C. copper-arc theories to a unidirectional pulse-like discharge, and there was agreement on the idea

that this type of discharge would give good precision and high sensitivity if the sample were negative instead of positive. As investigation proved, the over-damped discharge displayed these properties to a marked degree. In addition, the precision of the Type 2 discharge, though not as good as that of Types 1 and 3, is greatly superior to that of the D.C. arc.

### IV.—APPARATUS

Samples for analysis are in the form of small castings: discs  $2\frac{1}{2}$  in. in dia. and  $\frac{1}{2}$  in. thick; rectangular blocks  $2\frac{1}{2} \times 2\frac{1}{2} \times 1$  in. thick; or small squares  $1 \times 1 \times 1$  in. (see Fig. 4, Plate XX). Suitable flats for sparking are machined in a lathe or milling machine. In most cases, the analysis curves developed were independent of the shape or origin of the casting.

The spectrograph used is a large Bausch and Lomb prism spectrograph with quartz and glass optics, having a reciprocal dispersion of  $4\text{\AA}/\text{mm.}$  in the 2900 $\text{\AA.}$  wave-length region. A cylindrical quartz lens of 150 mm. focal length is placed directly in front of the slit. Its curvature is in the vertical plane and serves to focus the discharge vertically on the collimator opening. The distance between the discharge and the slit (23 cm.) keeps the wandering spark image within the horizontal aperture of the collimator. The discharge gap used (2.5 mm. or 0.1 in.) serves to keep the image of the electrodes just outside the vertical opening of the collimator. The slit width is 0.04 mm. With the above adjustments, the spectrum produced consists of easily measured lines against a satisfactory background.

The plates used are Eastman Kodak SA No. 1, which are developed at 70° F. (21° C.) in Kodak developer D19 for 5 min. The plates have high contrast, fine grain, and low background.

A Hilger non-recording microphotometer is used to read line densities. The scanning slit setting is  $0.10 \times 10$  mm., equivalent to a scanning area of 10,000 square microns at the plate. All line densities are read in terms of the percentage transmission on a scale 50 cm. long. Readings are recorded to within 0.5 mm. or 0.1% transmission. The percentage transmission readings are converted to arbitrary intensities by means of an emulsion characteristic curve.

The spectrum of a D.C. iron arc, photographed with a rotating stepped sector in front of the slit, is used to set up the emulsion characteristic curve. The spectrum consists of eight steps with an intensity relationship of the form  $\log \frac{I_1}{I_2} = 0.2$  between adjacent steps. The percentage transmissions of a sequence of steps of a number of iron lines are plotted against the corresponding intensity intervals on logarithmic co-ordinate paper. Since the curves obtained by this method are not sufficient to give the whole density range desired for an emulsion characteristic curve, the



various partial curves are shifted parallel to the intensity axis until they all overlap. Satisfactory overlapping is a good indication of self-consistency for all lines in the wave-length region used. Since logarithmic intensity ratios are used exclusively, there is no need to resort to absolute intensity determinations. Consequently, the emulsion characteristic curve may be very conveniently used with a negative logarithmic percentage transmission scale as the ordinate and a sliding logarithmic intensity scale as the abscissa.

Fundamental formulæ are :

$$D = \gamma \log E$$

$$\text{and} \quad D = \log 100/T$$

$\therefore$  for lines  $L_1$  and  $L_2$

$$D_1 - D_2 = \gamma \log \frac{E_1}{E_2} = \gamma \log \frac{I_1}{I_2}$$

$$\text{or} \quad -\log \frac{T_1}{T_2} = \gamma \log \frac{I_1}{I_2}$$

where  $D$  = film density,  $E$  = exposure,  $I$  = intensity,  $T$  = percentage transmission, and  $\gamma$  = development factor or film gamma.

Since the highest sensitivity as well as precision is required, background considerations are relevant, and in many cases background corrections are made. If the line intensity read is considered to be the sum of actual line intensity plus background intensity, the following derivation applies :

$$I(\text{line}) = I(\text{read}) - I(\text{background})$$

$$\therefore \quad \frac{I_L'}{I_L''} = \frac{I_R' - I_B'}{I_R'' - I_B''} \quad \text{or}$$

$$\frac{I_L'}{I_L''} = \frac{I_R'/I_B' - 1}{I_R''/I_B'' - 1} \times \frac{I_B'}{I_B''}$$

Thus the relative intensity of any two lines can be determined by manipulating two sliding logarithmic intensity scales which function as the scale of abscissæ for the emulsion characteristic curve.

## V.—DETERMINATION OF ZINC

As mentioned earlier, the Type 3 discharge has proved to be the most useful for the brasses, and the paper is confined to a detailed consideration of its application to the determination of zinc, lead, and iron.

The curve for the estimation of zinc in the range 20.0–40.0% appears in Fig. 3. Examination of curve *A* (relative intensity Zn 3018/Cu 3022 against zinc concentration, corrected for background) shows that its slope is greater than  $45^\circ$ . The slope of curve *B* (relative intensity Zn 3018/Cu 3022 against Zn/Cu relative concentration, corrected for background) is also greater than  $45^\circ$ . Therefore, the intensities of the zinc and copper lines are not linear functions of their respective concentrations. The increased slope of the zinc curve is probably due to the reduction in the

boiling point of the alloy with higher zinc content and a resulting enhancement of the intensity of the zinc line. (For the determination of nickel in cupronickel, the curves are quite flat probably owing to the opposite effect). This steep slope greatly contributes to the accuracy of the zinc determination by reducing the relative effect of emulsion and microphotometer errors.

For the determination of the precision of the spectrographic estimation of zinc in 70 : 30 brass, the author is indebted to the methods used by Vincent and Sawyer<sup>7-9</sup>. The total error associated with spectrochemical analysis can be considered as composed of errors due to : (1) sample inhomogeneity, (2) source, (3) microphotometer, and (4) emulsion. Inhomogeneity

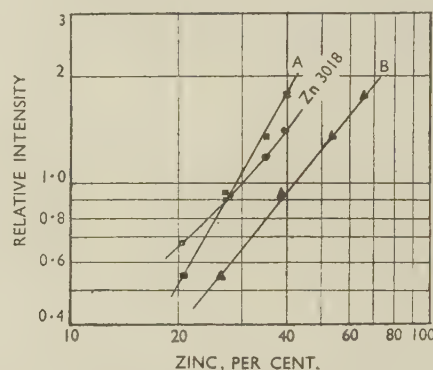


Fig. 3.—Curves for Determination of Zinc in Brass, with Type 3 Discharge, Using Cu 3022 as Reference.

Curve A : Relative intensity corrected for background vs. zinc concentration.

Curve B : Relative intensity corrected for background vs. relative zinc concentration.

geneity error was ignored, since copper and zinc form a homogeneous solid solution at 30% zinc. Emulsion and microphotometer error, though incidental to the analysis, were computed in order to arrive at a proper evaluation of error associated with the Type 3 discharge.

To arrive at a total error, three samples, poured from the same heat, were each sparked 32 times, making a total of 96 analyses. Six plates were used, 16 analyses per plate, and the samples were paired on the plates in the following manner :

Plate 1	Sample 1—eight analyses
	Sample 2— " "
Plate 2	Sample 3— " "
	Sample 1— " "
Plate 3	Sample 2— " "
	Sample 3— " " &c.

The plates were sparked over a period of a week in order to include variables associated with the passage of time, such as random curve shift, variation in plate-development conditions, optical misalignment, &c.

The standard deviation,  $\sigma_1$ , from an overall average was computed and found to be  $\pm 1.18\%$  of content or  $30\% \text{ Zn} \pm 0.355\%$ . In order to break this figure

down into a standard deviation per plate, the sixteen results on each plate were averaged and the difference between the individual results and the plate average was determined. The standard deviation,  $\sigma_2$ , of these differences was computed for the 96 analyses and found to be  $\pm 0.87\%$  of content or  $30\% \text{ Zn} \pm 0.261\%$ .

Microphotometer error,  $\sigma_m$ , was computed by taking three readings of percentage transmission  $R_1$ ,  $R_2$ , and  $R_3$  on 40 lines. Differences  $D_1$ ,  $D_2$ , and  $D_3$  for successive lines  $R'$  and  $R''$  were determined as  $D_1 = |R_1' - R_1''|$ ,  $D_2 = |R_2' - R_2''|$ , and  $D_3 = |R_3' - R_3''|$ . Deviations were computed as follows  $d_1 = |D_1 - D_2|$ ,  $d_2 = |D_1 - D_3|$ , and  $d_3 = |D_2 - D_3|$ . The standard deviation per pair of lines, computed from these deviations, was  $\pm 0.004$  intensity units.

Examination of the Zn 3018/Cu 3022 curve shows that a change of 0.01 in intensity unit at 30% zinc is equivalent to a change of 0.222% zinc or 0.74% of the content. Consequently, the microphotometer error is equivalent to  $\pm 0.30$  of the content or  $30\% \text{ Zn} \pm 0.09\%$ . This result is comparable with that of Grossman, Sawyer, and Vincent,<sup>9</sup> who obtained  $\pm 0.40\%$  of the content, and Vincent and Sawyer,<sup>8</sup> who obtained  $\pm 0.18\%$  of the content under the most favourable conditions.

Emulsion error  $\sigma_e$ , was determined by reading the relative intensity of Zn 3018/Cu 3022 at each end of the line pair. The paired readings, after adjustment for a slight constant difference due to the optics of the system, were subtracted to obtain the deviation due to emulsion error plus microphotometer error. The standard deviation per line pair for 47 deviations was computed and was found to be  $\pm 0.0086$  intensity unit. To compute  $\sigma_e$ , the following relation is used:

$$\begin{aligned}\sigma_e &= \pm \sqrt{0.0086^2 - \sigma_m^2} \\ &= \pm \sqrt{0.0086^2 - 0.004^2} \\ &= \pm 0.0076 \text{ intensity unit.}\end{aligned}$$

This result is equivalent to an error of  $\pm 0.57\%$  of content or  $30\% \text{ Zn} \pm 0.17\%$ .

To compute the source error due to the Type 3 discharge, the following relation is used:

$$\begin{aligned}\sigma_s &= \pm \sqrt{\sigma_2^2 - \sigma_m^2 - \sigma_e^2} \\ &= \pm \sqrt{0.886^2 - 0.30^2 - 0.57^2} \\ &= \pm 0.61\%\end{aligned}$$

Consequently, the source error is equivalent to  $\pm 0.61\%$  of the content, or  $30\% \text{ zinc} \pm 0.18\%$ . Owing to the indirect nature of its computation, the source error can be properly viewed with some scepticism. However, a check on this figure was furnished by Mr. M. F. Hasler who, at the request of the author, performed the analysis on the Quantometer, a direct-reading instrument. He reported a result of  $30\% \text{ zinc} \pm 0.18\%$ , using Type 3 excitation.

#### Note Added in Proof

For two under-damped discharges to be completely equivalent, both damping factor and period should be

equal. For a Type 3 discharge, the period of pulse length is closely approximated by:

$$\text{Period} = 2\pi\sqrt{LC} \times 10^{-3} \text{ millisecon.}$$

Thus  $L$  and  $C$  are uniquely defined by  $LC$  and  $L/C$ .

The author has recently been testing Type 3 discharges with pulse lengths ranging from 0.1 to 0.8 millisecon., the maximum obtainable on the Multi-source. As was to be expected, there is a deterioration in precision with increase in pulse length. For a discharge with constants  $40\mu\text{F}$ .,  $400\mu\text{H}$ ., and 2 ohms, and of 0.8 millisecon. duration, the standard deviation in the zinc determination computed from 2 plates and 32 analyses is  $\pm 1.55\%$  of content or  $30\% \pm 0.47\%$  zinc. Source error is  $1.39\%$  of content or  $30\% \pm 0.42\%$  zinc. Consequently source error, though still low, has more than doubled over that of the discharge ordinarily used, which has a pulse duration of approximately 0.3 millisecon. Any discharge of 1.0 millisecon. and over will probably have a precision equivalent to the over-damped case.

#### VI.—DETERMINATION OF LEAD IN LEADED BRASSES

Repeat determinations of 3% lead in selected leaded brass standards gave essentially the same accuracy as that associated with zinc. This accuracy is valid, only for samples with a uniform, very fine dispersion of the lead particles such as that shown in Figs. 5 (a) and (b) (Plate XX). In general, this very desirable fine particle dispersion can be obtained by pouring small samples into iron or steel moulds and causing a quick chill. Unfortunately, a structure where large agglomerates exist renders the spectrochemical determination of lead subject to large errors, and this structure sometimes occurs in the analysis sample in routine works' sampling procedures.

An investigation of the effect of lead dispersion on the lead curves shows a correlation between spectrographic relative intensities and the type of dispersion. In general, for samples of the same lead concentration, relative intensities for selected lead/copper lines increase with increased size of the lead particles. Moreover, this increase is complicated by greater scatter in individual results. Consequently, if lead dispersion is not controlled, it is impossible to obtain either a standardized curve or lead results with the required precision.

The photomicrographs of the six samples in Figs. 5 (a-f) (Plate XX) illustrate the forms of lead dispersion encountered in spectrographic samples of 3-4% leaded brass cast by routine procedures in the works. The relative intensities of the line pair Pb 2823/Cu 3022 were plotted against pre-spark time for the above six samples (Fig. 6). Samples 16 and 18, in which the lead is uniformly dispersed and has fine particle size, show the same decrease in relative intensities until 60 sec. is reached, when the relative intensities level off. The samples with large particle



size all show much higher initial relative intensities and steeper curves before the relative intensities level off. Border-line cases, such as sample 81, will event-

curves for the determination of lead in Fig. 7 are all based on samples that have been examined under the microscope and found to have a suitable fine particle dispersion.

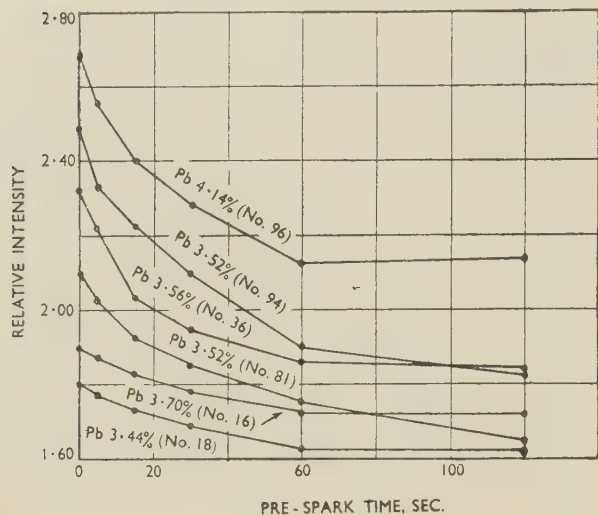


FIG. 6.—Relative Intensity of Pb 2823 to Cu 3022 Plotted Against Pre-Spark Time for Leaded Brass, Using Type 3 Discharge.

ually fall into line if the pre-sparking time is long enough. However, in most cases, relative intensities will level off at values much higher than those compatible with the curve. For routine procedures the author has found a 30-sec. pre-spark period adequate to align most samples with a normal range in lead dispersion. However, even with the greatest care, curve shifts due to differences in lead dispersion are all too common and contribute greatly to the analysis error. Changing the source excitation from Type 3 to Type 1 offers no improvement in a condition which originates in casting practice.

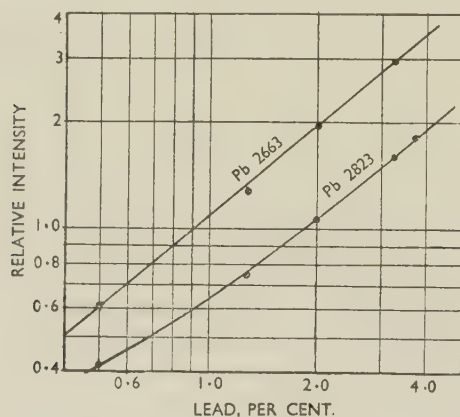


FIG. 7.—Curves for Determination of Lead in Leaded Brasses, with Type 3 Discharge, Using Cu 3022 as Reference.

Control of lead dispersion is a factor that enters into the analysis in the range 1–2% lead and becomes increasingly critical as lead content increases. The

## VII.—DETERMINATION OF IMPURITY ELEMENTS IN BRASS

Lead and iron in the range 0.01–0.2% are the two impurities most commonly encountered in high-purity brasses. Figs. 8 and 9 show the curves for these two impurities at various copper concentrations, using Type 3 discharge. Since background densities are an appreciable part of the measured densities, the curves are corrected for background in order to determine the curve shifts due to a variable matrix element.

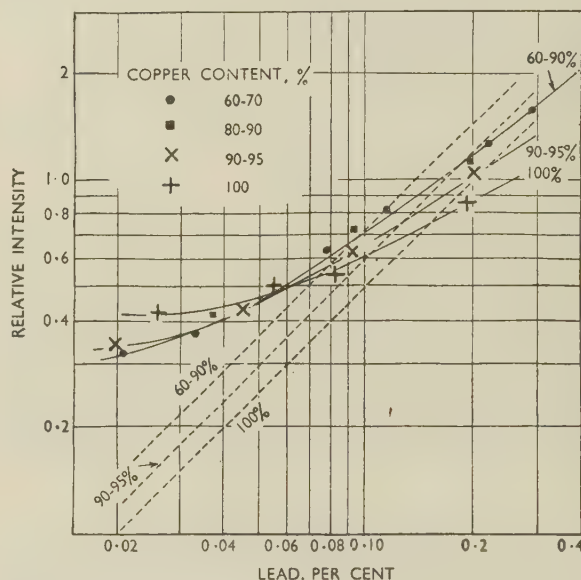


FIG. 8.—Relative Intensity of Pb 2833 to Cu 3022 Plotted Against Lead Concentration, Using Type 3 Discharge. Broken curves corrected for background.

With the exception of the curve for the determination of iron in copper, all curves, corrected for background, have slopes of  $45^\circ$ . Therefore, at a given copper concentration, the relative intensities of these lines of iron and lead are directly proportional to their respective concentrations, and no self-reversal is present. In the case of iron in copper, if the iron concentration is plotted against arbitrary intensity units for the iron line instead of relative intensities, to eliminate the effect of variation in the intensity of the copper line, the slope of this line also is  $45^\circ$ . Therefore, the relatively shallow slope of the line for the determination of iron in copper is due to the progressive enhancement of the copper spectrum by increasing amounts of iron. This enhancement extends to the lead line as well, since the curve for lead in copper maintains its  $45^\circ$  slope irrespective of the amount of iron present.

A single curve is adequate for lead in all brasses in the range 60–90% copper. Between 90 and 100% copper, however, close tolerances should be main-

tained on the copper content in order to preserve accuracy in the lead determination. With iron the situation is slightly different. Close tolerances should be maintained in the ranges 70–80% and 95–100% copper to preserve accuracy in the iron determination.

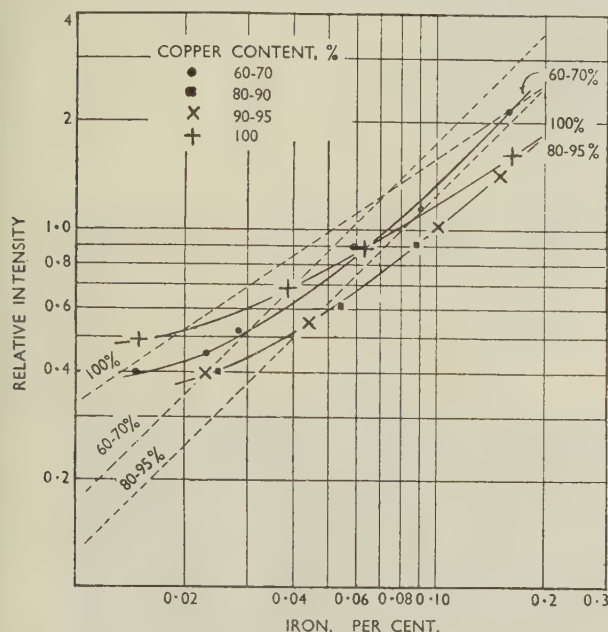


FIG. 9.—Relative Intensity of Fe 2739.6 to Cu 3022 Plotted Against Iron Concentration, Using Type 3 Discharge.  
Broken curves corrected for background.

#### ACKNOWLEDGEMENTS

\* The author wishes to express his appreciation to Dr. R. A. Wilkins for permission to publish the results obtained in this work, and to thank Messrs. F. F. Poland and L. H. Decker, whose co-operation enabled him to devote extensive time to this investigation. Thanks are also due to Mr. Robert Hahn for his many chemical analyses and to Mr. Donald Destito for his careful preparation of the photomicrographs.

#### REFERENCES

1. M. F. Hasler and H. W. Dietert, *J. Opt. Soc. Amer.*, 1943, **33**, 218.
2. M. F. Hasler and J. W. Kemp, *J. Opt. Soc. Amer.*, 1944, **34**, 31.
3. A. Walsh, *Bull. B.N.F.M.R.A.*, 1946, (201), 60.
4. A. Walsh, *Spectrochim. Acta*, 1950, **4**, 47.
5. M. Milbourn, *J. Inst. Metals*, 1943, **69**, 441.
6. M. Milbourn, *Proc. Phys. Soc.*, 1947, **59**, 273.
7. H. B. Vincent and R. A. Sawyer, *J. Opt. Soc. Amer.*, 1941, **31**, 639.
8. H. B. Vincent and R. A. Sawyer, *J. Opt. Soc. Amer.*, 1943, **32**, 686.
9. H. H. Grossman, R. A. Sawyer, and H. B. Vincent, *J. Opt. Soc. Amer.* 1943, **33**, 185.



## APPENDIX

## SUMMARY OF PROCEDURE

*Type 1 Setting, Slightly Over-Damped*

1. Source : Multisource  
10  $\mu$ F., 200  $\mu$ H., 10  $\Omega$ .  
 $R_c = 2\sqrt{\frac{200}{10}} = 8.95 \Omega$ .
2. Cast sample with machined flat.
3. Sample polarity : positive.
4. Counter-electrode :  $\frac{1}{4}$  in. graphite rod with 120° point.
5. Exposure : sufficient to yield Cu 2997 = 30% transmission.
6. Pre-spark : 5 sec.
7. Analysis line : Zn 3072 (20%–40% Zn).
8. Reference line : Cu 2997.
9. No background correction required.
10. Accuracy : <2.0% error.

*Type 2 Setting, Heavily Over-Damped*

1. Source : Multisource  
60  $\mu$ F., 400  $\mu$ H., 20  $\Omega$ .  
 $R_c = 2\sqrt{\frac{400}{60}} = 5.2 \Omega$ .
2. Cast sample with machined flat.
3. Sample polarity : negative.
4. Counter-electrode :  $\frac{1}{4}$  in. graphite rod with 120° point.
5. Exposure : sufficient to bring out Cu 2858.2 (background will vary according to amount of zinc present).
6. Pre-spark : 5 sec.
7. Analysis lines :  
Pb 2833 (0.005%–0.05%).  
Fe 2739.6 (0.005%–0.05%).  
P 2535.7 (0.02%–0.2%) (phosphor bronze).  
Te 2385.7 (0.05%–0.3%) (90 : 10 tellurium brass).  
As 2349.8 (0.02–0.1%).

8. Reference line : Cu 2858.2.
9. Background correction required for low impurity concentration in high-copper alloys.
10. Accuracy : <10% error.

*Type 3 Setting, Slightly Under-Damped*

1. Source : Multisource  
10  $\mu$ F., 200  $\mu$ H., 3  $\Omega$ .  
 $R_c = 2\sqrt{\frac{200}{10}} = 8.95 \Omega$ .
2. Cast sample with machined flat.
3. Sample polarity : positive.
4. Counter-electrode :  $\frac{1}{4}$  in. graphite rod with 120° point.
5. Exposure : sufficient to yield Cu 3022 = 30% transmission.
6. Pre-spark : 5 sec. (lead brass, 30 sec.).
7. Analysis lines :  
Zn 3345 (0.05–1.0%).  
Zn 3076 (5–10%).  
Zn 3072 (7–20%).  
Zn 3018 (20–40%).  
Pb 2823 (1.0–3.0%).  
Pb 2663 (0.5–2.0%).  
Pb 2833 (0.02–0.2%).  
Fe 2739.6 (0.02–0.2%).  
Sn 2840 (0.02–0.2%).  
Sn 2661 (0.2–1.0%).  
Ni 3050.6 (0.02–0.2%).  
Al 3092 (0.005–0.05%).  
Si 2881 (0.005–0.1%).  
Ag 3382.9 (0.003–0.05%).
8. Reference line : Cu 3022.
9. No background correction required except to maintain accuracy in very low concentration ranges.
10. Accuracy : <2.0% error.

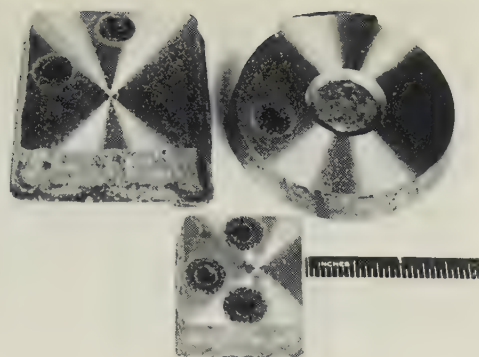
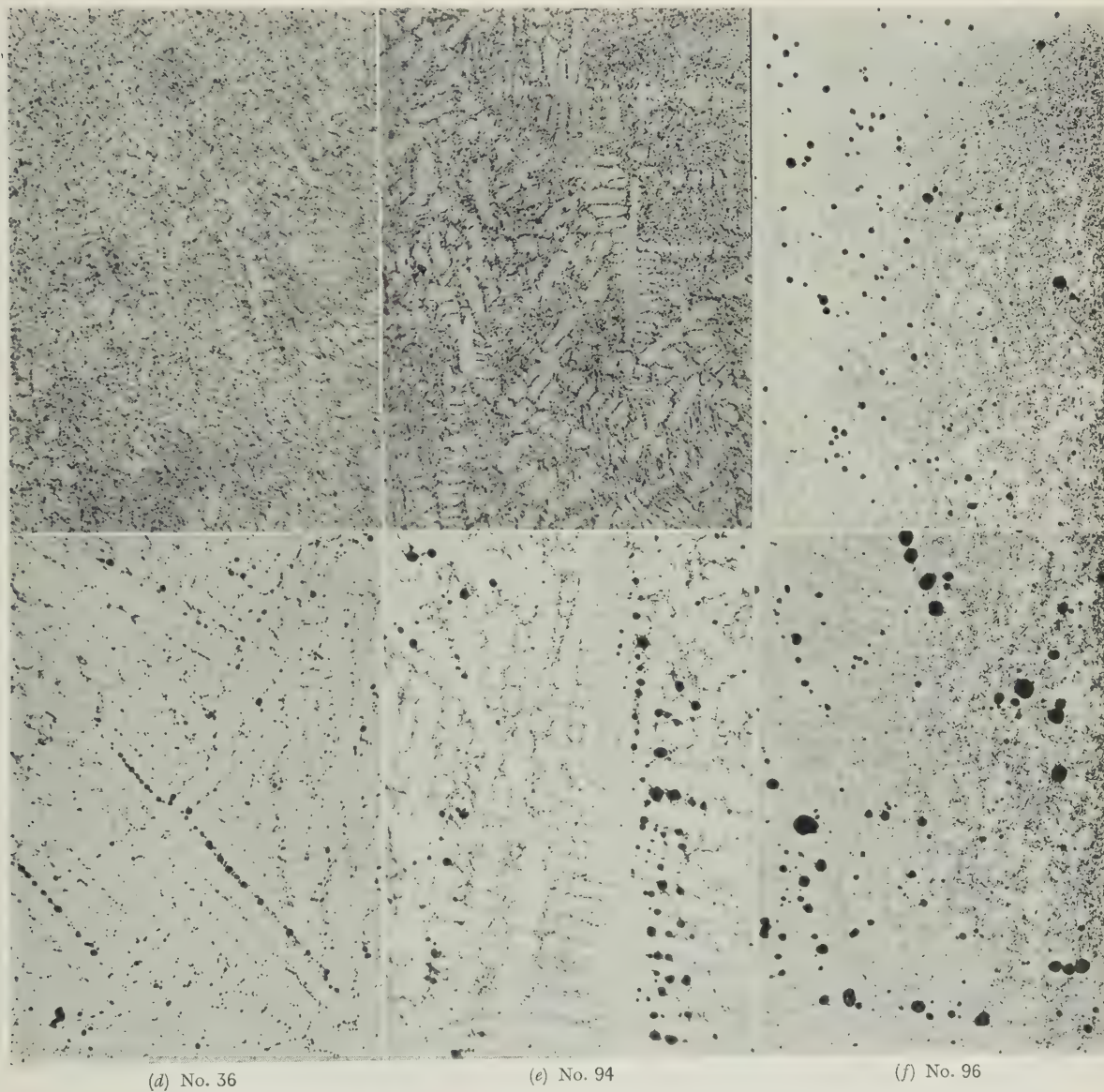


FIG. 4.--Sample Castings for Spectrographic Analysis, Showing Machined Surface and Discharge Spots.

(a) No. 16

(b) No. 18

(c) No. 81



(d) No. 36

(e) No. 94

(f) No. 96

FIG. 5 (a)-(f).—Photomicrographs Showing Range of Lead Particle Size Encountered in Leaded Brass Samples for Spectrographic Analysis.  $\times 100$ .

[To face p. 84.





# THE EQUILIBRIUM DIAGRAM OF THE SYSTEM NICKEL-MANGANESE \*

1327

By B. R. COLES,† B.Sc., JUNIOR MEMBER, and  
W. HUME-ROTHERY,‡ M.A., D.Sc., F.R.S., MEMBER

## SYNOPSIS

The equilibrium diagram of the nickel-manganese system above 800° C. has been determined by a combination of thermal, microscopical, and X-ray methods; some information about the diagram at lower temperatures was also obtained. The liquidus and solidus pass through a smooth minimum at 62 at.-% manganese and 1018° C. Nickel is freely soluble in  $\gamma$ -manganese and increases the axial ratio of the face-centred tetragonal structure until it becomes cubic and unites with the solid solution of manganese in nickel. Immediately below the solidus there is thus a complete range of solid solution extending across the diagram. At lower temperatures (c. 910° C.) this solid solution in the equi-atomic region is transformed into a  $\beta$  phase with a body-centred cubic structure which cannot be retained by quenching. At a still lower temperature the  $\beta$  phase is transformed into a phase with a face-centred tetragonal superlattice of the CuAu type. The temperature of the  $\delta \rightleftharpoons \gamma$  transformation of manganese is raised by the addition of nickel, whilst those of the  $\gamma \rightleftharpoons \beta$  and  $\beta \rightleftharpoons \alpha$  transformations of manganese are lowered. The diagram in some respects resembles that of the system nickel-zinc, and this suggests that manganese acts as a divalent element in some of the alloys.

## I.—INTRODUCTION AND PREVIOUS WORK

THE present investigation is concerned mainly with the equilibrium diagram of the system manganese-nickel at temperatures above 800° C., although some information has also been gained of the structures at lower temperatures. In describing the previous work it is not therefore proposed to discuss the earlier investigations of nickel-rich alloys at the relatively low temperatures where interesting magnetic properties are associated with ordered structures. When the present work was started the only general investigation of the system was that of Douridine,<sup>1,2</sup> who used impure alumino-thermic manganese. Shortly after the present work was begun, the results of a complete investigation of the system were published by Köster and Rauscher,<sup>3</sup> who used electrolytic manganese for alloys containing more than 75% of this metal, and less pure manganese for the remaining alloys. Their diagram is reproduced in Fig. 1 and is of interest in many ways. It shows a minimum in the liquidus at 62 at.-% manganese (61 wt.-% manganese). For convenience all alloys will be referred to by their atomic percentages of manganese. The minimum in the liquidus is smooth, and at high temperatures a continuous solid solution extends across the diagram from nickel to  $\gamma$ -manganese, the axial ratio of which is increased by the addition of nickel until, between 25 and 30 at.-% manganese, it becomes equal to 1.00, and the resulting face-centred cubic phase is continuous with the face-centred cubic solid solution in nickel. This solid solution is, however, broken into by a

phase denoted  $\delta$  in the equi-atomic region which, according to Köster and Rauscher, rises almost, but not quite, to the solidus curve, in contrast with the results of Douridine, which suggested that a peritectic reaction was involved. There is general agreement that at low temperatures the MnNi phase has a face-centred tetragonal structure. According to the thermal analysis of Köster and Rauscher MnNi transforms between 600° and 700° C. to an ordered face-centred cubic structure, but this has not been confirmed by the present work, which shows that at high temperatures the structure is that of a body-centred cube. The work of Douridine (*loc. cit.*) had suggested phases based on the compositions  $\text{Mn}_3\text{Ni}_2$  and  $\text{Mn}_3\text{Ni}_4$ , and Kaya and Kussmann<sup>4</sup> claimed to have discovered a face-centred cubic phase corresponding to the latter, although this was not confirmed by Valentiner and Becker,<sup>5</sup> and Köster and Rauscher (*loc. cit.*) considered that the only intermediate phases were those based on MnNi and  $\text{MnNi}_3$ , the latter being a superlattice structure. The work of Köster and Rauscher was not very thorough in the equi-atomic region, and their reliance on the results of X-ray examination of quenched specimens did not appear justified. For the manganese-rich alloys their results suggested that the temperature of the  $\alpha \rightleftharpoons \beta$  transformation was lowered markedly by the addition of nickel, which produced a similar but less-marked effect on the  $\beta \rightleftharpoons \gamma$  transformation, for which a broad ( $\beta + \gamma$ ) region was shown. The lines for the  $\gamma \rightleftharpoons \delta$  transformation in Fig. 1 were inserted on the basis of the microscopical

\* Manuscript received 29 January 1951.

† Lecturer, Imperial College of Science and Technology,

London. Formerly Inorganic Chemistry Laboratory, Oxford.

‡ Royal Society Warren Research Fellow, Oxford.



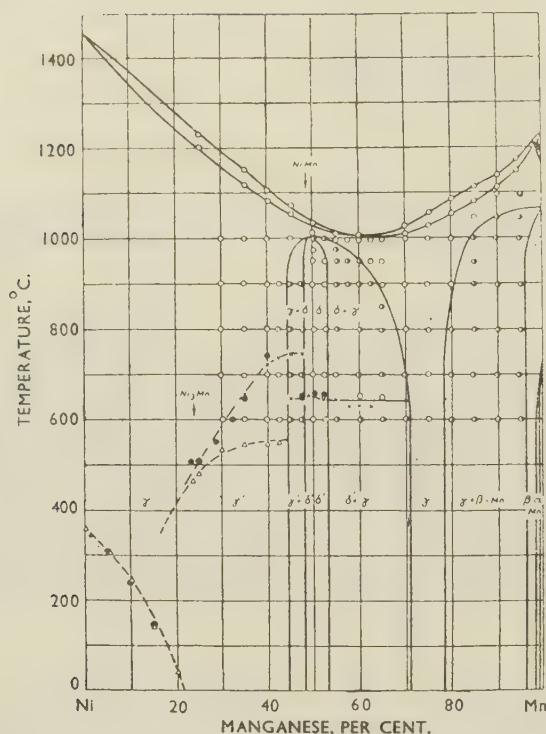


Fig. 1.—Equilibrium Diagram of the System Nickel-Manganese (according to Köster and Rauscher<sup>3</sup>).

examination of cooled alloys and were not detected by thermal analysis. In these circumstances complete re-investigation of the system has been made at the higher temperatures.

## II.—EXPERIMENTAL PROCEDURE

### 1. MATERIALS USED

The nickel used in the present work was specially selected Mond carbonyl nickel in the form of medium-sized shot. After the shot had been cleaned with ether to remove surface grease and dirt, the analysis obtained was 99.95% nickel, 0.02% carbon, and 0.02% iron. We have to thank The Mond Nickel Co., Ltd., for kindly presenting this metal. The manganese used was electrolytic metal of 99.98% purity, containing traces of iron and chromium. This was treated in purified hydrogen at 800° C., in order to remove superficial oxidation.

### 2. PREPARATION OF ALLOYS

The alloys, both for thermal analysis and for annealing, or X-ray experiments, were prepared in a valve-operated induction furnace without the use of a heater sleeve. The first alloys were melted in ΔRR alumina crucibles (Morgan Crucible Company), using an atmosphere of purified hydrogen, but these contained large gas holes owing to the great difference between the solubilities of hydrogen in the solid and liquid alloys. Later alloys were therefore prepared

under an atmosphere of purified argon and sound ingots were obtained. The vacuum system, furnace arrangements, and methods for the purification of hydrogen and argon have been described by Carlile, Christian, and Hume-Rothery<sup>6</sup> in their work on chromium-manganese alloys. The lower temperatures and reactivities involved in the present work reduced the risk of contamination by nitrogen, and as will be seen from what follows a satisfactory standard of purity was obtained. The loss of manganese by volatilization was also much smaller than in the work on chromium-manganese alloys, and even in manganese-rich alloys the loss rarely exceeded 1–2 g. in a 50-g. ingot.

### 3. THERMAL ANALYSIS OF THE ALLOYS

Thermal analysis was carried out by thermocouple methods, using the platinum-wound furnace shown in Fig. 1 of the paper by Carlile, Christian, and Hume-Rothery (*loc. cit.*). For this purpose the alloys were previously melted in the induction furnace, and were then remelted in the platinum furnace using a crucible with a re-entrant thermocouple sheath; to accommodate this the ingots were cut in half and grooved in order to allow the sheath to be inserted when the crucible was packed. The brittle manganese-rich alloys were broken up and packed into the crucible. The thermal analysis was carried out in an atmosphere of purified argon, and owing to the volatility of the manganese, whose vapour penetrates alumina thermocouple sheaths, it was necessary to calibrate the thermocouple during the actual experiment by the immersion-couple technique of Carlile, Christian, and Hume-Rothery. In this method a cooling curve is taken, the temperatures being read by means of the re-entrant thermocouple which may become contaminated during the process. As soon as the arrest is established the wires of a second or immersion thermocouple are pushed down a sheath which has also been in the melt and serves as a stirrer. Alternate readings are then taken on the two thermocouples until their temperature/time curves are parallel, after which the wires of the immersion thermocouple are withdrawn into a cold part of the sheath. In this way the re-entrant thermocouple is calibrated immediately after the arrest point against the immersion thermocouple which is exposed to high temperatures only for short periods. The immersion thermocouple itself was frequently recalibrated, and for high-temperature calibration it was found convenient to calibrate against the freezing point of pure nickel (1453° C.); the results obtained in this way agreed well with those obtained by the wire method for the gold and palladium points.

A complete experiment was usually carried out in the following way. After packing the crucible with material previously melted in the induction furnace, the apparatus was assembled and evacuated and the temperature raised to about 700° C. until the whole assembly was thoroughly outgassed. Argon was introduced and a heating curve was taken in which the

solidus was approached at a rate of about 5° C./min. The beginning and the end of the arrests on the heating curve gave a rough indication of the solidus and liquidus points, and the latter was then determined accurately by a cooling curve taken, with stirring, at a rate of 1°–3° C./min. When the alloy was completely solid, it was maintained at about 30° C. below the solidus for about half an hour, after which a slow heating curve was taken in order to determine the solidus point, and a second slow cooling curve to confirm that no appreciable change in composition had occurred. In general, the two liquidus determinations were in very good agreement, and if any slight difference occurred the second value was preferred because the composition was determined by the analysis of the complete ingot after the experiment. In some of the later experiments it was possible to prepare the initial ingots in the induction furnace in crucibles of the same size as those used for the subsequent thermal analysis. Under these conditions a close fit between the thermocouple sheath and alloy could be ensured, and after a preliminary anneal 30° C. below the solidus it was thought justifiable to take a single slow heating curve to determine the solidus, followed by a slow cooling curve for the liquidus. Experiments showed that it was essential to give a homogenizing treatment just below the solidus if the heating-curve points were to be relied upon; in work where this precaution was omitted the apparent solidus point might be as much as 20°–30° C. too low owing to coring of the ingot.

In general, the experiments for the determination of the liquidus and solidus were run by themselves, but in some cases cooling curves were followed to low temperatures, and the arrests due to low-temperature transformations were observed, and are discussed later.

The analysis of the cooling-curve ingots was carried out by Messrs. Johnson, Matthey & Co., Ltd., and the authors must express their thanks to Mr. A. R. Powell for his interest in the work. Both nickel and manganese were determined, and for the ingots included in Table I the analytical totals for the two metals lie between 99.92 and 100.06.

### III.—EXPERIMENTAL RESULTS

#### 1. THE LIQUIDUS

The results obtained from the cooling curves are shown in Table I. From the freezing point of nickel the liquidus falls smoothly to a flat minimum at 1018.3° C. and 62 at.-% manganese. The liquidus curve in this region is so flat that the exact composition of the minimum point could not be determined, although the curvature of the line through the adjacent points shows that it cannot be far from 62 at.-% manganese. In the experiment with alloy 62.5, the cooling curve was taken successfully, but an accident then occurred as a result of which the specimen was oxidized and could not be analysed. The composition

of this alloy was therefore estimated from the weights of metal used, and in view of the close agreement between the intended and analysed compositions in this region, the value is not likely to be in error by more than a few tenths per cent. The temperature of the minimum is appreciably higher than that obtained by previous workers, probably owing to the greater

TABLE I.—*Liquidus and Solidus Temperatures of Nickel-Manganese Alloys.*

Alloy	Mn, wt.-%	Mn, at.-%	Liquidus, °C.	Solidus, °C.
5	94.86	95.19	1198.2	1172.1
7.5	92.59	93.04	1181.0	1156.4
10	89.63	90.21	1161.6	1135.8
17	83.17	84.07	1124.0	1092.7
20 *	78.91	79.99	1094.8	1048.0
25	72.15	73.46	1057.6	1038.7
30	68.85	70.22	1038.7	1023.4
35	63.58	65.07	1018.1	
39 †	61	62.5	1018.5	
40	58.74	60.32	1018.3	1018.3
45	54.96	56.59	1027.4	1020.7
48.5	51.28	52.93	1039.3	1031.8
50	48.44	50.09	1053.0	1036.0
55	44.91	46.55	1072.8	1051.3
60	39.69	41.29	1110.3	1084.0
65	34.97	36.49	1145.5	1117.0
70	29.78	31.19	1188.2	1155.2
75	24.90	26.16	1228.6	1197.4
80	21.03	22.11	1265.4	1233.4
85	15.78	16.68	1315.9	1288.3
90	10.59	11.20	1363.2	1340.0
95	6.21	6.59	1407.8	1386.5

\* Showed effect of insufficient homogenization.

† Oxidized after liquidus arrest and not analysed.

purity of the metals used. This temperature was checked not only by the calibration methods described above, but also by a calibration against the freezing point of high-purity copper. In view of the previous suggestions of a peritectic horizontal connected with the formation of the NiMn phase, and of a eutectic in place of a smooth minimum, the cooling curves in the region 45–65 at.-% manganese were taken with great care and were examined in detail, but no sign of a second arrest could be detected. Microscopical examination of the cooling-curve ingots in the region of minimum freezing point gave no indication of a eutectic structure, and the evidence is therefore that the liquidus passes through a smooth minimum. With increasing manganese content the liquidus rises to 1162° C., where a change in direction occurs owing to the peritectic reaction:  $\gamma \rightleftharpoons \delta + \text{liquid}$ .

#### 2. THE SOLIDUS

The results of the solidus points taken from the final heating curves are shown in Column 5 of Table I. As in the case of the liquidus, a special search was made for the existence of a peritectic or eutectic horizontal in the middle of the diagram, but no evidence for this could be found and the conclusion is again that the liquidus and solidus fall to a smooth minimum at 62 at.-% manganese, and that a contin-



uous solid solution exists at the higher temperatures. The results of the heating and cooling curves are shown in Fig. 2. In the course of the work some annealing and quenching experiments were carried out which extended into the semi-liquid region, and the results of these are included in Fig. 2 and confirm the results obtained by the heating-curve method. The details of this work are described in later sections, and unless

points refer to alloys whose compositions were inferred from the analysis of another portion of the same ingot.

### 3. THE CONTINUITY OF THE $\text{Ni} \rightarrow \gamma \text{Mn}$ SOLID SOLUTION AT HIGH TEMPERATURES

Microscopical examination showed that all specimens in the range 0–49 at.-% manganese, when annealed

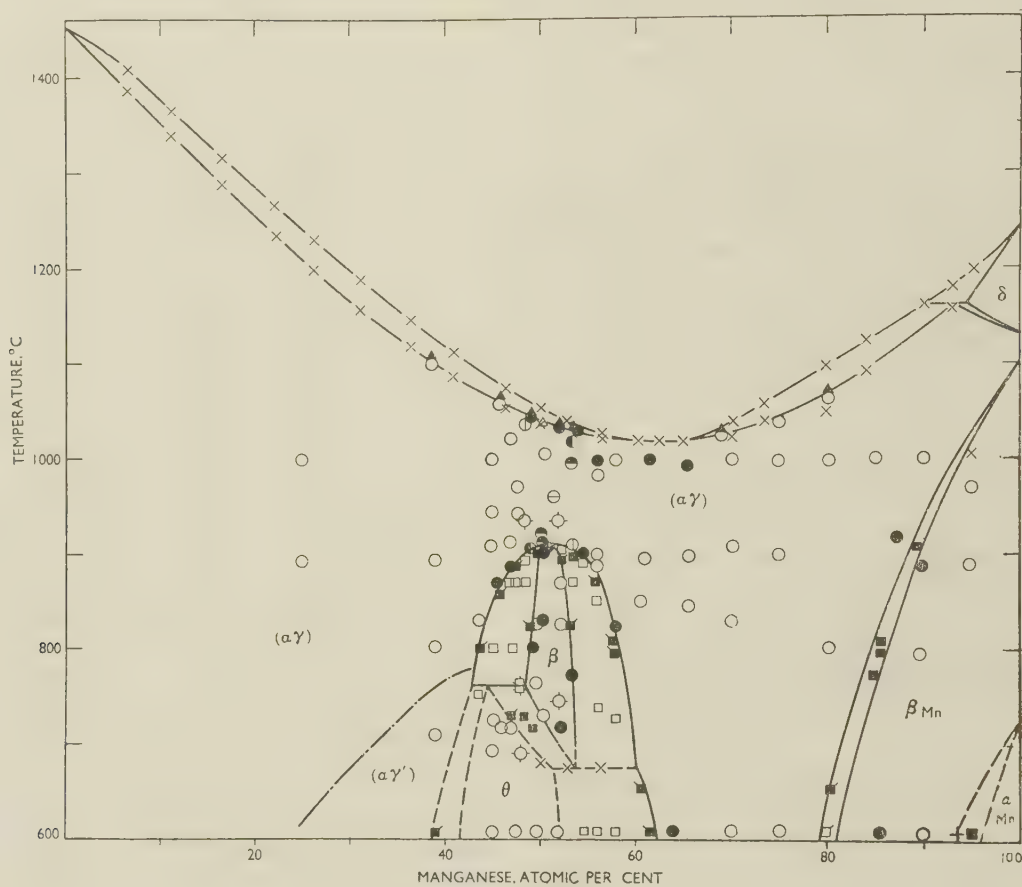


FIG. 2.—The Nickel-Manganese System.

#### KEY.

- |  |  |
|--|--|
| ○ ● Single-phase alloy.                        | ▲ Solid + liquid alloy.                |
| ⊖ ⊕ Single-phase alloys completely decomposed. | ⊕ High-temperature X-ray single-phase. |
| ⊕ ⊖ Single-phase alloys partly decomposed.     | ⊕ High-temperature X-ray two-phase.    |
| ■ Trace of second phase.                       | × Thermal arrests.                     |
| □ Two-phase alloy.                             | + X-ray boundary.                      |

The full or half-full symbols refer to alloys analysed after the heat-treatment shown. Open symbols refer to alloys whose compositions are based on the analysis of another portion of the same ingot, and sometimes to the synthetic compositions.

otherwise stated the microscopical points for the solidus in Fig. 2 were obtained by annealing previously homogenized specimens for at least 30 min. at the temperatures concerned; the temperature was kept constant to within  $\pm \frac{1}{2}^{\circ} \text{C.}$  by hand control of a Variac transformer. In this figure and in Fig. 3 the full points refer to alloys whose compositions were determined by the chemical analysis of the actual specimen examined microscopically, whereas the open

and quenched from temperatures above  $910^{\circ} \text{C.}$ , gave single-phase undecomposed structures, and single-phase structures were also obtained in alloys containing more than 54 at.-% manganese until the  $(\gamma\text{-Mn} + \beta\text{-Mn})$  region was reached. In the range 49–54 at.-% manganese, alloys quenched from above  $910^{\circ} \text{C.}$  showed decomposed microstructures; in some of these the whole section was of uniformly decomposed appearance, whilst in others structures

were obtained which simulated those of two-phase alloys, although careful examination suggested that these effects were really due to incomplete decomposition of the specimen. Thus Figs. 4 and 5 (Plate XXI) illustrate the structures of alloys 49.1 and 53.5 after quenching from 1035° and 995° C., respectively. They show smooth, light-etching areas in a background of decomposed material. The boundaries between the two are irregular and different in shape from those to be expected from an alloy consisting of two phases in equilibrium at the quenching temperature, and as these structures were not reproducible it was concluded that in Figs. 4 and 5 the light areas were portions which had not undergone decomposition during quenching. These regions were further examined by high-temperature Debye-Scherrer X-ray photography, using the camera of Hume-Rothery and Reynolds.<sup>7</sup> The filings were contained in evacuated silica capillaries, and chemical analyses were carried out on the actual specimens after the X-ray exposure. The first specimen examined contained 48.1 at.-% manganese and was prepared from a lump of alloy previously homogenized at 920° C. and quenched. The X-ray specimen was heated to 935° C. and kept at this temperature for 20 min., after which an exposure of  $1\frac{1}{2}$  hr. was made with unfiltered iron radiation. The film showed the diffraction lines of a face-centred cubic structure with  $a = 3.73$  kX, but an accidental fogging of one end of the film prevented an accurate determination of the lattice spacing. This result confirms the microscopical evidence. A similar experiment with an alloy containing 52.3 at.-% manganese also showed only the lines of a face-centred cubic structure with  $a = 3.741(0)$  kX. This experiment indicates that the intermediate MnNi phase which, as described below, has a body-centred cubic structure, does not exist at the higher temperature, but is replaced by a face-centred cubic solid solution. The conclusion of Köster and Rauscher is thus confirmed, although the temperature of the transformation is clearly much lower than was previously imagined. For convenience we shall denote this phase by the symbol  $\alpha\gamma$ .

#### 4. THE INTERMEDIATE PHASE IN THE EQUI-ATOMIC REGION

The work of previous investigators had shown that the low-temperature modification of the phase in the equi-atomic region possesses a face-centred tetragonal structure. This has been confirmed in the present work and a superlattice of the CuAu type has been identified; this phase will be denoted by  $\theta$ . In the region 670°–760° C. this phase is transformed into another which may be denoted  $\beta$ . Experiments with filings quenched from above the transformation temperature gave sharp lines of a face-centred cubic structure with no indication of the decomposition suggested by the microstructures of the quenched alloys. These X-ray films agree with those of Köster and Rauscher, but work with the high-temperature

camera has shown conclusively that the high-temperature phase has a body-centred cubic structure. The following two experiments are of interest:

(1) Alloy 52.3 when photographed at 745° C. showed only the lines of a body-centred cubic structure of  $a = 2.968(3)$  kX.

(2) Alloy 48.1 was carried through the sequence of treatments indicated in Table II in the high-temperature camera with the results given.

TABLE II.—Effect of Heat-Treatment on Structure of Alloy Containing 48.1 at.-% Manganese.

Heat-Treatment	Structure
Exposure at 763° C. . . .	b.c.c. + f.c.c.
Cooled to room temp. . . .	f.c. tetragonal.
Exposure at 783° C. . . .	b.c.c. + f.c.c.
Cooled to room temp. . . .	f.c. tetragonal.
Exposure at 700° C. . . .	f.c. tetragonal.
Cooled to room temp. and then exposed at 713° C. . . .	mixture of blurred lines.
Cooled from 713° to 687° C. and then exposed . . . .	f.c. tetragonal.
Heated from 687° to 800° C. . . .	b.c.c. + f.c.c.
Cooled to room temp. . . .	f.c. tetragonal.

The specimen was analysed after the above series of exposures, and the total of the percentages of nickel and manganese was 99.2. Mr. A. R. Powell gave it as his opinion that this low total was probably due to the extreme smallness of the sample and not to contamination. Another specimen made from the same batch of filings showed a face-centred tetragonal structure at room temperature, and a mixture of body-centred cubic and face-centred tetragonal structures at 759° C. These results show that the peritectoid decomposition of the  $\theta$  phase takes place at  $761^\circ \pm 2^\circ$  C. The way in which filings quenched from the homogeneous  $\beta$  region gave sharp lines of a face-centred cubic solid solution is very interesting, and emphasizes the desirability of combining X-ray and microscopical methods, because no suggestion of decomposition would have been obtained from the X-ray films.

#### 5. THE $(\alpha\gamma + \beta)$ , $(\theta + \beta)$ , AND $(\beta + \alpha\gamma)$ REGIONS

The boundaries of the phase fields in the region 40–60 at.-% manganese were determined by microscopical methods. For this purpose the furnace-cooled ingots were first homogenized by heating for 3 days at a temperature about 50° C. below the solidus of the alloys concerned. This treatment was carried out in a platinum furnace which was outgassed and filled with argon. For subsequent anneals in the range 800°–950° C. each specimen was placed in a sealed, evacuated silica capsule. Analysis of the specimens showed that no contamination by silicon occurred in this temperature range, although for the higher temperatures near to the solidus it was desirable to place the specimens in alumina collars inside the



silica capsules. The capsules were then heated in furnaces controlled by Foster temperature regulators, the accuracy of the control being of the order  $\pm 2^\circ \text{C}$ .

After quenching into iced water, the specimens were examined microscopically. When quenched from  $950^\circ \text{C}$ . all alloys except those in the range 45–55 at.-% manganese could be cut with a saw, but with specimens annealed at lower temperatures most of the alloys in the range 40–60 at.-% manganese were too hard for this and were therefore sectioned with a high-speed bonded carborundum disc, using a very light pressure and a continuous stream of cold water to prevent overheating. After the usual grinding on emery paper, the alloys were polished on a rotary wheel, using magnesia powder.

For alloys in the range 0–60 at.-% manganese the most suitable etching reagents were Merica's reagent,\* and the acidified alcoholic solution of ferric chloride recommended by Carapella.† The latter reagent does not remove much of the deformed layer produced by grinding and polishing, and it was therefore only used after a preliminary etch with Merica's reagent.

In the nickel-rich alloys the face-centred cubic  $\alpha$  phase is etched light by the above reagents, which also reveal the grain boundaries. On approaching the equi-atomic region decomposition readily takes place on quenching. Thus alloy 53.5 quenched from  $1017^\circ \text{C}$ . gave the structure shown in Fig. 6 (Plate XXI), with decomposition in the grain boundaries of the  $\alpha\gamma$  solid solution. Alloy 52.3, quenched from  $1036^\circ \text{C}$ ., gave the structure of Fig. 7 (Plate XXI), showing a little chilled liquid between crystals of the  $\alpha\gamma$  phase which has decomposed to an acicular structure resembling that illustrated in Figs. 4 and 5 (Plate XXI).

Alloys in the  $(\alpha\gamma + \beta)$  region etched so that the  $\alpha$  phase appeared light, while the  $\beta$  phase always decomposed. The pure  $\beta$  phase decomposed on quenching to give the characteristic martensitic structure shown in Fig. 8 (Plate XXI), which is a photomicrograph of the alloy 50.5 quenched from  $830^\circ \text{C}$ . In the  $(\beta + \gamma)$  region the  $\gamma$  phase appeared as light crystals in contrast to the decomposed  $\beta$  structure.

The present paper is concerned mainly with the diagram above  $800^\circ \text{C}$ ., but some quenching experiments were made at slightly lower temperatures, which showed that in an  $(\alpha + \theta)$  alloy, using Carapella's reagent, the  $\theta$  phase etched as the darker of the two phases. In the  $(\theta + \beta)$  alloys the  $\theta$  phase appeared light against the characteristic structure of decomposed  $\beta$ . In the  $(\theta + \gamma)$  region fine structures were obtained of the discontinuous precipitation type, and the  $\gamma$  phase was stained dark in comparison with the  $\theta$  phase. Single-phase  $\theta$  alloys at  $608^\circ \text{C}$ . were identified by X-ray powder photographs, because the microstructures were not easily distinguished from those of the  $\alpha$  phase.

## 6. THE $\alpha\gamma/(\alpha\gamma + \beta)$ , $(\alpha\gamma + \beta)/\beta$ , $\beta/(\beta + \alpha\gamma)$ , AND $(\beta + \alpha\gamma)/\alpha\gamma$ BOUNDARIES

The results of the annealing experiments for these phase boundaries are shown in Fig. 2 and in greater detail in Fig. 3. Annealing periods of from 1 week at the higher to 3 weeks at the lower temperatures were used in this part of the diagram, and further anneals up to 5 weeks at all these temperatures confirmed that equilibrium had been obtained.

The results show that the  $\beta$  phase field includes the equi-atomic composition. The phase field rises to a

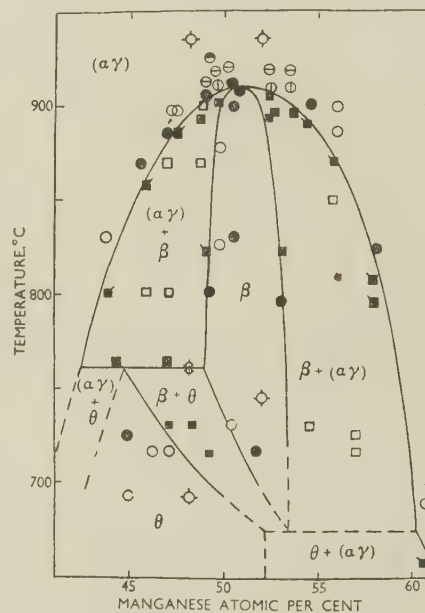
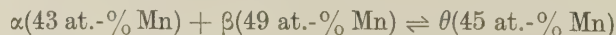


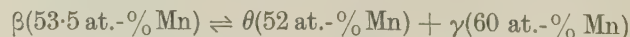
FIG. 3.—Constitution of Nickel-Manganese Alloys Below  $1000^\circ \text{C}$ . in the Range 40–60 At.-% Manganese.

maximum which is drawn at 50.3 at.-% manganese, but it is doubtful whether this can really be distinguished from the exact equi-atomic composition. The temperature of this maximum was determined as  $910^\circ \text{C}$ . by microscopical methods.

On the nickel-rich side the  $(\alpha\gamma + \beta)/\beta$  phase boundary with falling temperature slopes slightly in the direction of lower manganese content until  $761^\circ \text{C}$ ., at which temperature the  $\theta$  phase is formed by a peritectoid reaction which may be represented:



Below this temperature the nickel-rich boundary of the  $\beta$  phase moves in the direction of higher manganese content until at about  $675^\circ \text{C}$ . it undergoes a eutectoid decomposition which may be represented:



\* 1 part conc. nitric acid, 1 part glacial acetic acid, and 2 parts acetone by volume.

† 5 g. ferric chloride, 2 c.c. conc. hydrochloric acid, and 100 c.c. ethyl alcohol.

It is to be noted that the composition of the eutectoid is distinctly to the manganese-rich side of the equi-atomic value.

It is thought that the phase boundaries shown in Fig. 2 have been established accurately above 800° C. The low-temperature portion of the diagram is to be made the subject of a separate study, and the dotted lines shown in Figs. 2 and 3 are to be regarded as preliminary only.

## 7. THE SOLID SOLUTIONS IN MANGANESE

In pure manganese the  $\delta \rightleftharpoons \gamma$  transformation occurs at 1133° C., and in the present work the thermal analysis of alloy 95.2 showed arrests due to the transformation on both heating and cooling curves. The liquidus curve shows a slight change in direction at 1162° C., and in view of these facts the  $\delta$  field has been included in Fig. 2. The maximum solubility of nickel in  $\delta$ -manganese is about 6 at.-%.

In pure manganese the  $\gamma$  modification is stable between 1133° and 1100° C., below which the  $\beta$ -manganese allotrope is the stable phase. The temperature of the  $\beta \rightleftharpoons \gamma$  transformation is lowered by the addition of nickel. On cooling curves of manganese-rich alloys, arrests due to this transformation were detected, but they always showed some undercooling and were not at the equilibrium values. The phase boundaries indicated in Fig. 2 were determined by microscopical methods, using specimens which had first been homogenized in the  $\gamma$ -manganese region. Anneals varying from 4 days at 1000° C., to 7 weeks at 600° C. were used in this part of the diagram, though it is probable that these changes are fairly rapid and equilibrium is soon established. The alloys were etched in 1½% alcoholic nitric acid, which darkens the  $\beta_{\text{Mn}}$  phase. When present in small amounts the  $\beta_{\text{Mn}}$  phase appears olive after light etching, and brownish-blue after further etching. Fig. 9 (Plate XXI) illustrates the structure of alloy 85.5, quenched from 796° C., in which the  $\beta_{\text{Mn}}$  phase appears dark.

TABLE III. Lattice Spacing of  $\beta_{\text{Mn}}$  Phase with Varying Manganese Content.

Mn, at.-%	Lattice Spacing of $\beta_{\text{Mn}}$ Phase, kX
100	6.3030 *
94.63	6.3242
89.76	6.3434
85.36	6.3581

\* This value was obtained by Dr. J. W. Christian.

The lattice spacings of some alloys in the  $\beta_{\text{Mn}}$  field were measured with the results shown in Table III. For this purpose lumps of the alloys were first homogenized in the  $\beta_{\text{Mn}}$  region and quenched. The brittle

material was then ground to powder in an agate mortar, and was so fragile that sharp diffraction lines were obtained without further annealing.\* The chemical analyses were carried out on the actual powder after the above treatment, and the totals of the analytical percentages of nickel and manganese lay between 99.94 and 99.97.

## V.—DISCUSSION

The present work confirms the conclusion of Köster and Rauscher that at high temperatures the  $\alpha$  solid solution in nickel is continuous with the solid solution in  $\gamma$ -manganese, the axial ratio of the latter being increased by the solution of nickel. The present work suggests that the extent of the  $\gamma$ -manganese phase is much greater than had previously been imagined, and that the equi-atomic region has a quite different form. There is an interesting resemblance between the present equilibrium diagram and that of the system nickel-zinc, which also shows a typical body-centred cubic  $\beta$  phase in the equi-atomic region. It is of course well known that the divalent  $\text{Mn}^{++}$  salts are very stable owing to the presence of five 3d electrons which exactly half-fill the (3d)<sup>10</sup> sub-group. The resemblance between zinc and manganese can thus be understood, and if the  $\beta$  phases in the nickel-manganese and nickel-zinc systems were simple 3/2 electron compounds it would suggest that nickel was acting as a univalent element. On the other hand, the ferromagnetic properties of solid solutions of both zinc and manganese in nickel suggest that the holes in the 3d band of nickel have been filled by about 30 at.-% zinc or manganese. In the  $\beta$  phase of the nickel-zinc system, the proportion of zinc atoms is greater than in the  $\alpha$  (nickel-rich) solid solution, and there should be a greater tendency to fill up the holes in the d shell, so that the co-existence of univalent nickel and divalent zinc would seem improbable. The work of Schramm,<sup>8</sup> however, shows that the low-temperature  $\beta'$  modification of the nickel-zinc phase is paramagnetic and may involve holes in the d shell, so that the true state of affairs in this system is not yet understood. The resemblance between the systems nickel-zinc and nickel-manganese undoubtedly suggests that the manganese is acting as a divalent element in the equi-atomic region of the system manganese-nickel, but more extensive knowledge of nickel alloys is desirable before these phases can be understood.

Reference to Fig. 3 will show the very symmetrical nature of the ( $\alpha\gamma + \beta$ ) phase boundary about the composition 51 at.-% manganese. It is found that, except for a short length of the order of 1 at.-% at the extreme peak, this curve can be represented by the equation:

$$T = 2C^2,$$

where  $T$  is the temperature in °C. measured down-

\* Experiments by Dr. J. W. Christian have shown that in other solid solutions in  $\beta$ -manganese, no change in lattice

spacing is found if the "as-ground" powder is re-annealed and quenched from the  $\beta$ -region.



wards from 910° C., and  $C$  is the change in composition in either direction measured from the peak at 51 at.-% manganese.

## ACKNOWLEDGEMENTS

The authors must express their gratitude to Professor Sir Cyril Hinshelwood, F.R.S., for laboratory accommodation, and to Dr. F. M. Brewer for facilities and encouragement in their research work. Acknowledgement is also made to the Royal Society for grants towards the cost of apparatus used in the present work.

## REFERENCES

1. A. Dourdine, *Zhur. Russ. Met. Obshch.*, 1912, **1**, 341 (see *Rev. Mét.*, 1915, **12**, (Extraits), 125).
2. A. Dourdine, *Rev. Mét.*, 1932, **29**, 507 and 565.
3. W. Köster and W. Rauscher, *Z. Metallkunde*, 1948, **39**, 178.
4. S. Kaya and A. Kussmann, *Z. Physik*, 1931, **72**, 293.
5. S. Valentiner and G. Becker, *Z. Physik*, 1935, **93**, 795.
6. S. J. Carlile, J. W. Christian, and W. Hume-Rothery, *J. Inst. Metals*, 1949-50, **76**, 169.
7. W. Hume-Rothery and P. W. Reynolds, *Proc. Roy. Soc.*, 1938, [A], **167**, 25.
8. J. Schramm, *Z. Metallkunde*, 1938, **30**, 122, 131, and 327.

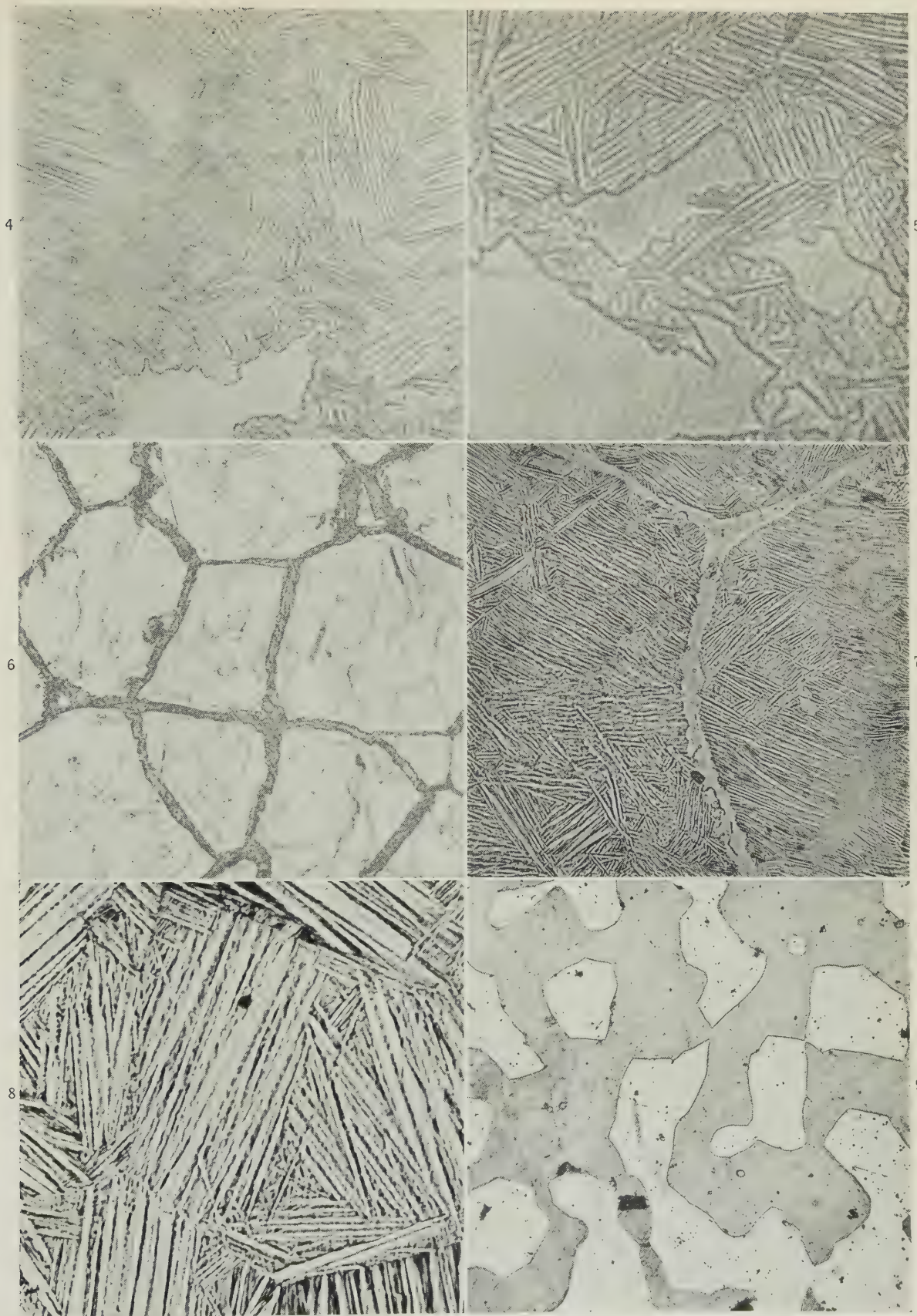


FIG. 4.—49.1 at.-% Mn Q. 1035° C. × 700.  
 FIG. 6.—53.5 at.-% Mn Q. 1017° C. × 420.  
 FIG. 8.—50.5 at.-% Mn Q. 830° C. × 200.

FIG. 5.—53.5 at.-% Mn Q. 995° C. × 900.  
 FIG. 7.—52.3 at.-% Mn Q. 1036° C. × 420.  
 FIG. 9.—85.5 at.-% Mn Q. 796° C. × 130.





# THE NUCLEATION OF CAST METALS AT THE MOULD FACE\*

1328

By J. A. REYNOLDS,† B.Sc., STUDENT MEMBER, and  
C. R. TOTTLE,‡ M.Met., A.I.M., MEMBER

## SYNOPSIS

The nucleation of some cast metals and alloys effected by applying metal powders to the face of a standard mould, has been investigated by comparing the grain-size of ingot surfaces produced with and without the coating.

In general, powdered metals having the same crystallographic form as the metal being cast are effective as nucleating agents, provided that the degree of lattice "misfit" does not exceed 5%, or in some cases 10%. This simple mechanism is found to apply to the solidification of tin, lead, zinc, antimony, aluminium, magnesium, and copper. Where the cast metal readily formed an oxide film, reduction of this film to the metal was found to occur when some coatings were applied, giving rise to simple homogeneous nucleation by the particles produced.

Homogeneous and heterogeneous nucleation of alloys can take place under the same conditions as with pure metals, the crystal structure of the solid first formed from the melt being the ruling factor. Reduction of oxide films also occurred, and in the case of an 18 : 8 austenitic steel resulted in isomorphous nucleation of the  $\delta$  solid solution by chromium particles reduced from the film.

## I.—INTRODUCTION

### 1. GENERAL

THE mechanism of solidification of cast metals has received considerable attention in recent years, chiefly from the thermal standpoint, in terms of rates of heat extraction and crystal growth. Contributions to the subject include a study of the thermal properties of some commercial moulding materials<sup>1</sup> and a bibliography<sup>2</sup> of experimental investigations. Two papers on the grain-refinement of aluminium alloys<sup>3,4</sup> have dealt with the formation of nuclei in the body of the melt, and Tammann's<sup>5</sup> experiments with organic and aqueous solutions have been extended to aluminium alloys.

In America, Turnbull<sup>6</sup> has investigated the mechanism of nucleation by supercooling droplets of liquid metals (mercury, gallium, and tin). His results support the "critical-size" concept of homogeneous nucleation, and have enabled the interfacial free energies between liquid metal and solid nuclei to be calculated. The thermodynamical aspects of nucleation have been discussed in a recent symposium.<sup>7,8</sup>

The nucleation of crystals at a mould face is mentioned in almost every text-book on founding, and in many on metallography, but little experimental evidence has been brought forward in support. Turnbull<sup>9</sup> states that "for liquid-solid transformations in relatively large volumes of liquid the evidence seems decisive that at least the first few nuclei that appear originate by a heterogeneous mechanism at the surfaces of the containing vessel or of colloidal inclusions in the system."

The work described below was undertaken with a view to establishing the connection between the physical and/or chemical properties of the mould face and the solidification of metals in contact with that face.

### 2. PRESENT INVESTIGATION

From the "critical-size" concept of nucleation,<sup>6</sup> it would appear that any particle acting as a nucleating agent must be of a specific size before growth can occur upon it. The addition of atoms to, or their subtraction from, a particle of critical size, results in a decrease of free energy; hence particles of diameter less than the critical size tend to vanish, while those of greater diameter tend to grow. The provision of nucleating particles would therefore demand a size greater than this critical value.

The requisite conditions are met by powders passing a 300-mesh sieve, as according to Turnbull the critical size is less than  $10^{-3}$  mm. radius.

The use of powdered metal to nucleate the same metal in the liquid state (homogeneous nucleation) can be extended to powders of dissimilar metals. These must have the same crystal structure, though the lattice spacing may differ to a certain extent (heterogeneous nucleation). No evidence was available on the permissible difference in lattice spacing between the nucleating particle and the metal to be cast, but in the experiments to be described it was assumed that a favourable spacing-factor might be essential.

In order to assess the lattice "misfit" involved in various combinations of powder and liquid metal, it was necessary to know the lattice constants at the operative temperatures. Initially, the values were

\* Manuscript received 21 November 1950.

† British Steel Founders' Research Association Research Student, Department of Metallurgy, King's College, Newcastle-upon-Tyne.

‡ Ministry of Supply, Division of Atomic Energy (Production); formerly Lecturer in Metallurgy, King's College, Newcastle-upon-Tyne.



calculated up to the freezing point of the cast metal but experiment showed that the powder on the mould face did not reach such a high temperature. The maximum temperature of the mould face was frequently of the order of 70% of the freezing point of the cast metal, and this was reached only some time after solidification had begun. It appeared that no great error was introduced by comparing the unit cell of the cast metal at its freezing point with that of the nucleating agent at room temperature. The crystal structure and lattice constants of the metals investigated are shown in Table I.

TABLE I.—*Crystal Structure and Lattice Constants of Possible Mould Coatings.*

Metal	Structure	$a_0$ , Å.*	$c_0$ , Å.*	Axial Ratio or Angle
Sroutium .	Face-centred cubic	6.075	...	...
Calcium .		5.56	...	...
Cerium .		5.143	...	...
Thorium .		5.077	...	...
Lead .		4.939	...	...
Silver .		4.532	...	...
Gold .		4.0701	...	...
Aluminium .		4.0414	...	...
Copper .		3.608	...	...
$\gamma$ -Iron .		3.564	...	...
Nickel .		(910° C.) 3.5167	...	...
Tungsten .	Body-centred cubic	3.1585	...	...
Molybdenum .		3.1409	...	...
Vanadium .		3.0338	...	...
$\delta$ -Iron .		2.93	...	...
Chromium .		(1425° C.) 2.8786	...	...
$\alpha$ -Iron .		2.8600	...	...
Magnesium .	Close-packed hexagonal	3.2022	...	...
Titanium .		2.953	...	...
Cobalt .		2.507	...	...
Beryllium .		2.268	...	...
Graphite .	Hexagonal	2.456	6.691	2.72
Zinc .		2.6595	4.9368	1.86
Cadmium .		2.927	5.607	1.84
Tellurium .		4.4469	5.9149	1.33
Antimony .	Rhombohedral	4.4974	...	57° 6.5'
Bismuth .		4.7361	...	57° 14.2'
Manganese .	Complex cubic	6.83	...	...
Silicon .	Diamond cubic	5.417	...	...
Tin .	Body-centred tetragonal	5.819	3.175	...

\* Room-temperature values unless otherwise stated.

## II.—EXPERIMENTAL METHODS

The principal difficulties in casting metals under specified conditions are to eliminate complicating variables and to provide rigid controls to simplify comparison. In the experiments described the mould coating was originally applied to one side only of a square-section pattern, thus allowing comparison to be made with three untreated surfaces. With the initial casts made in sand moulds, the mould cavity was duplicated, a common runner to both sections being employed. This proved an unnecessary precaution, and subsequently two coated faces were compared with two untreated ones, prepared in either single or double moulds. Casting temperatures were measured by means of immersion thermocouples, and dried moulds were used throughout, whatever the mould material.

### 1. MOULDS

#### (a) Sand

Northallerton naturally bonded sand was milled dry for 10 min., adjusted to a 5% moisture content, and milled for a further 5 min. The patterns were hand-rammed in this sand, the ingate of the runner being so disposed as to avoid sand wash or erosion of the powder-coated mould surface. The general arrangement is illustrated in Fig. 1. This shows a double mould, which produced an ingot 13 cm. high  $\times$  4 cm. square at the top, and 3 cm. square at the

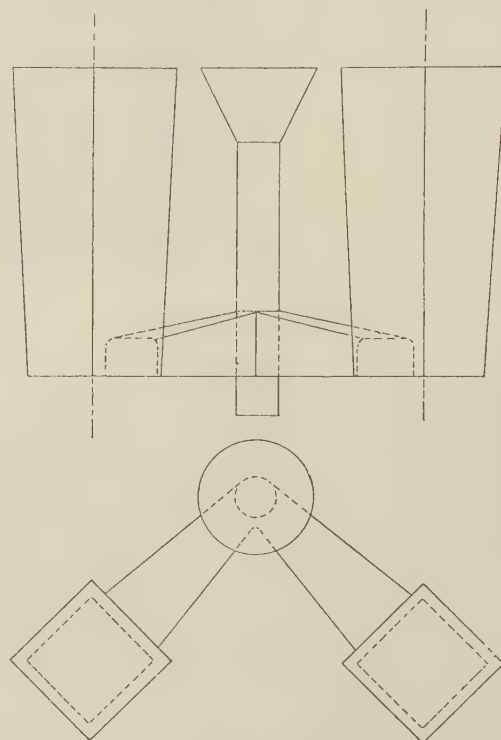


FIG. 1.—Mould Arrangement.

base. After moulding, the box was dried in an air-circulation oven at  $150^\circ \pm 10^\circ$  C. and allowed to cool to room temperature immediately before casting. The surface finish of ingots cast in sand moulds was rough in most cases, and this caused difficulty in assessing the degree of grain refinement.

#### (b) Synthetic

For synthetic moulds the Osborn-Shaw precision-casting process<sup>10</sup> was used, on the same patterns as for sand. The moulds are prepared by pouring over the pattern an unstable slurry of finely divided sillimanite in a suspension of ethyl silicates, which are undergoing a controlled hydrolysis to silica gel and ethyl alcohol. After setting, the pattern is withdrawn, the alcohol ignited, and the mould is heated to  $600^\circ$ – $700^\circ$  C. for a few minutes to remove residual alcohol. The final product is a mould of high refractoriness and resistance to thermal shock, with approximately 45% porosity.

To simplify moulding, and to permit examination of

both mould surface and casting after solidification, single moulds were employed; these were split along a diagonal, and were top poured. Owing to the porosity of the synthetic mould, cooling was very slow, and hence the grain-size of the cast metal when nucleation did not occur was large, which simplified comparison with the treated faces.

### (c) Metal

A rectangular "finger" mould of cast iron or steel, with a cavity measuring  $3 \times 1 \times \frac{3}{4}$  in., was used to investigate the effect of rapid chilling.

## 2. APPLICATION OF COATINGS

Metal powder passing a 300-mesh sieve was not always available, but it was found that coarse particles resulted in a poor surface finish on the ingots and rendered examination difficult. The purity of the powder employed was in general not less than 99.5%, and in some cases it was higher. The metals constituting the main impurities in any one powder were in the majority of cases themselves employed as powdered coatings during the investigation, which helped in determining the responsible nucleating agent. The magnitude of the effects produced in most cases suggested that impurities played only a minor role.

Where compounds of the metals were used, these were of analytical-reagent quality. The chief difficulty with the metal powders was to avoid oxidation during their preparation, handling, and application to the mould face. Strontium and calcium powders oxidized to such a degree that they were of little value, but it was possible to produce cerium powder by mechanical means without excessive oxidation.

For use with sand or chill moulds, a standard weight of powder (just sufficient to cover the mould face completely) was suspended in a weak solution of cellulose acetate in acetone, the viscosity of the solution being adjusted to allow uniform spreading of the final suspension. Application was by camel-hair brush, the acetone being allowed to evaporate in a warm atmosphere just before casting. As a periodic check, the cellulose solution alone was coated on to one face of the mould, but this was never found to influence the ingot grain-size.

The synthetic moulds were swabbed with ethyl silicate, the surplus solution allowed to evaporate, and the face to be treated dusted with the powder, any excess of which was removed by shaking or light tapping. A very thin coating, of the order of one particle thickness, was obtained by this means, and adhered well to the mould face. Iron and nickel powders agglomerated rapidly, and orientated themselves in the earth's magnetic field, thus preventing perfect removal of any excess powder.

## 3. MELTING PRACTICE

Commercial-purity metals were melted under flux according to normal practice in each case, and degassed where necessary. Gas-fired or electric-resistor

crucible furnaces were employed for all metals other than steel, for which an indirect-arc furnace was used. Since untreated faces of each individual ingot were compared with treated faces of the same ingot, any peculiarities due to melting conditions applied equally to both. In the case of magnesium castings made in sand moulds, sulphur was added to the moulding material, but this proved unnecessary with synthetic moulds. The sand moulds were bottom-poured, the remainder top-poured, turbulence being minimized in the latter case by careful pouring.

## 4. EXAMINATION OF INGOTS

Immediately after casting and cooling to room temperature, the ingots and mould faces were examined for any sign of change in appearance of the coating. The castings were then lightly pickled in appropriate reagents, details of which are given in Table II, without preparation. Sand castings, and

TABLE II.—*Pickling Reagents Used to Reveal Grain-Size.*

Cast Metal	On Ingot	On Transverse Slice
Aluminium and its alloys	5% HCl, HNO <sub>3</sub> , H <sub>2</sub> SO <sub>4</sub> in water	...
Antimony	10% HCl, HNO <sub>3</sub> in water (hot)	...
Copper and its alloys	10% HNO <sub>3</sub> (hot)	N/20 Iodine solution
Lead and its alloys	...	10% Nitromolybdic acid
Magnesium	...	60% Acetic acid + 10% ammonium acetate
Tin and its alloys	15% HCl	...
Zinc and its alloys	10% HCl (hot)	2% Chromic acid + sodium sulphate
18:8 Austenitic steel	Aqua regia (hot)	...
Mild steel	5% HCl	...

certain others with a poor surface finish, were often unsuitable for examination in the pickled state and from these a transverse slice was taken at a height two-thirds of the distance from the base of the ingot, lightly ground, and pickled as for the whole ingot.

After pickling, the grain-size was assessed by counting, with the naked eye or a binocular microscope, on all four faces of an ingot, and the four edges of a transverse slice. The number of grains per unit area (or unit length) was then calculated, and the nucleation effect expressed as the ratio of grains per unit on treated faces to the average number on untreated faces. In all cases where refinement had occurred, this was immediately obvious. Early casts, employing one treated to seven untreated faces (double mould) showed that 2-5% difference in ingot grain-size could be expected on the normal mould faces, whereas 50% or more reduction in grain-size was common for a treated face when nucleation had occurred.

## III.—DISCUSSION OF RESULTS

### 1. DIRECT NUCLEATION

The results obtained by using as coatings those metals whose crystal structure might be expected to influence nucleation are recorded in Table III. Those coatings which did not promote nucleation are also



included in the table. The term "homogeneous" nucleation is used where a powdered metal has refined the grain-size of the same metal cast against it, and "heterogeneous" nucleation where the two metals are different. In the latter case, the percentage difference in lattice spacing is given in the last column.

These results show that the general principle of homogeneous nucleation can be applied to cast zinc,

In the case of copper cast against iron powder, no effect was observed with a casting temperature below 1200° C, and it is presumed that the  $\gamma$  state is not reached by the iron coating under those conditions.

Fig. 2 (Plate XXII) illustrates refinement by a homogeneous coating and Fig. 3 (Plate XXII) demonstrates the absence of refinement where the lattice spacings differ by more than 10%.

TABLE III.—Nucleation by Isomorphous Coatings.

No. of Casts	Cast Metal	Casting Temp., °C.	Mould Material	Coating	Grain-Size Refinement Ratio *	Type of Nucleation	Lattice-Spacing Difference, %
4	Zinc	550-580	Sand	Zinc	2 : 1	Homogeneous	...
2		580	Synthetic	"	1.5 : 1	"	...
1		550	Steel	"	2 : 1	"	...
2		550	Sand	Graphite	1.5 : 1	Heterogeneous	8
2		560	"	Cadmium	1.2 : 1	"	9
2		560	"	Tellurium	1	Nil	>10
5	Aluminium	760	Sand	Aluminium	4 : 1 to 9 : 1	Homogeneous	...
3		760	Synthetic	"	10 : 1 to 15 : 1	"	...
1		750	Cast iron	"	10 : 1	"	...
1		730	Sand	Coarse aluminium	5 : 1	"	...
2		750	"	Lead	1	Nil	>10
2		750	"	Thorium	1	"	>10
2		750	"	Nickel	1	"	>10
2	Magnesium	730	Sand	Magnesium	2 : 1	Homogeneous	...
2		750	Synthetic	"	1.5 : 1	"	...
3		750	"	Titanium	1.2 : 1	Heterogeneous	8.5
1		750	Sand	Cobalt	1	Nil	>10
2		750	"	Beryllium	1	"	>10
2	Tin	400	Steel	Tin	20 : 1	Homogeneous	...
2	Lead	450-500	Steel	Lead	4 : 1 to 6 : 1	Homogeneous	...
3		500	"	Thorium	10 : 1	Heterogeneous	2.8
2		450	"	Cerium	2 : 1	"	4
2		450	Sand	Aluminium	1	Nil	>10
2		450	"	Copper	1	"	>10
2	Copper	1180	Synthetic	Copper	10 : 1	Homogeneous	...
2		1320	Steel	"	5 : 1	"	...
2		1220	Synthetic	Nickel	50 : 1	Heterogeneous	2.6
2		1220	Sand	"	25 : 1	"	2.6
2		1200	Synthetic	Aluminium	1.2 : 1	"	11
2		1200	Sand	$\gamma$ -Iron	1.2 : 1	"	1
2		1150	"	$\alpha$ -Iron	1	Nil	...
2		1200	"	Lead	1	"	>10
2	Antimony	770	Steel	Antimony	5 : 1	Homogeneous	...
2		750	"	Bismuth	2 : 1	Heterogeneous	5.4

\* Expressed as number of grains per unit area on treated face to average number on untreated faces.

aluminium, magnesium, tin, lead, copper, and antimony. As regards heterogeneous nucleation, the most marked effects arose with the combinations lead/thorium, lead/cerium, copper/nickel, and antimony/bismuth (the cast metal being placed first); positive results were also obtained with zinc/graphite, zinc/cadmium, magnesium/titanium, copper/aluminium, and copper/iron, though the results were not so perfectly reproducible. It appears that where the difference in lattice spacing between the coating and the cast metal is less than 5% simple heterogeneous nucleation will take place; with between 5 and 10% difference in spacing the results were variable, and beyond 11% no positive results were obtained.

## 2. NUCLEATION INVOLVING CHEMICAL REACTION

During the stripping of ingots cast against certain coatings (not specified in Table III), several instances occurred in which the coating had changed in colour and general appearance. The metal powders involved did not satisfy the principle of isomorphous nucleation, but the grain refinement was reproducible at will under a wide variety of conditions, and was in general greater in magnitude than the examples quoted in Table III.

Chemical and spectrographic analysis of residues scraped from the mould face showed that the oxide(s) of the metal originally applied as powder pre-



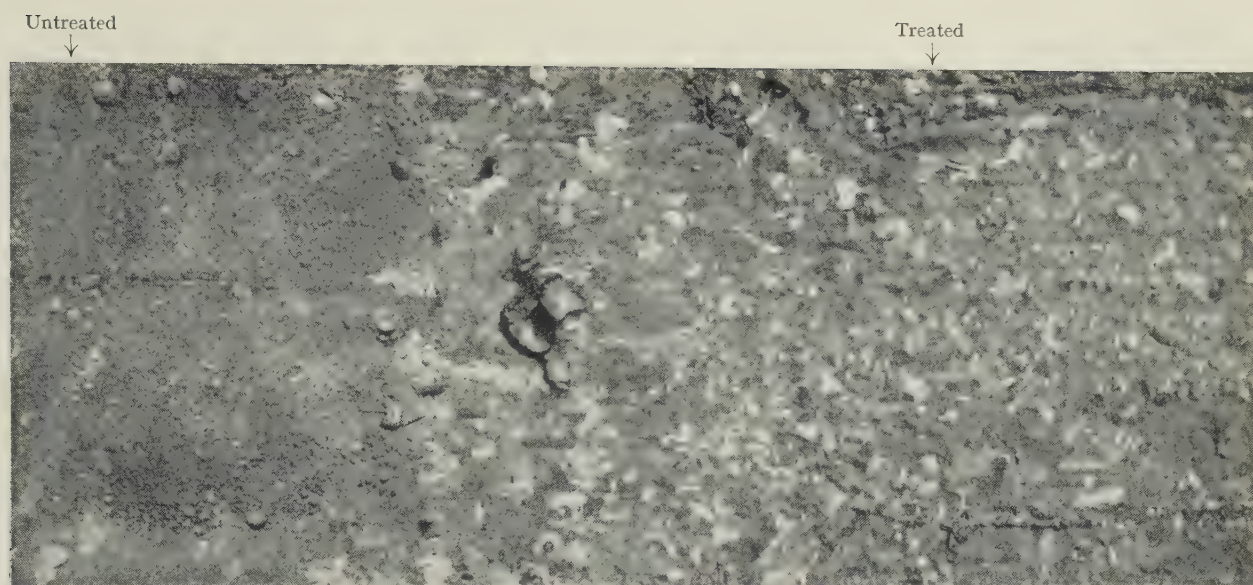


FIG. 2.—Lead Cast in Steel Mould Half Coated with Lead Powder.

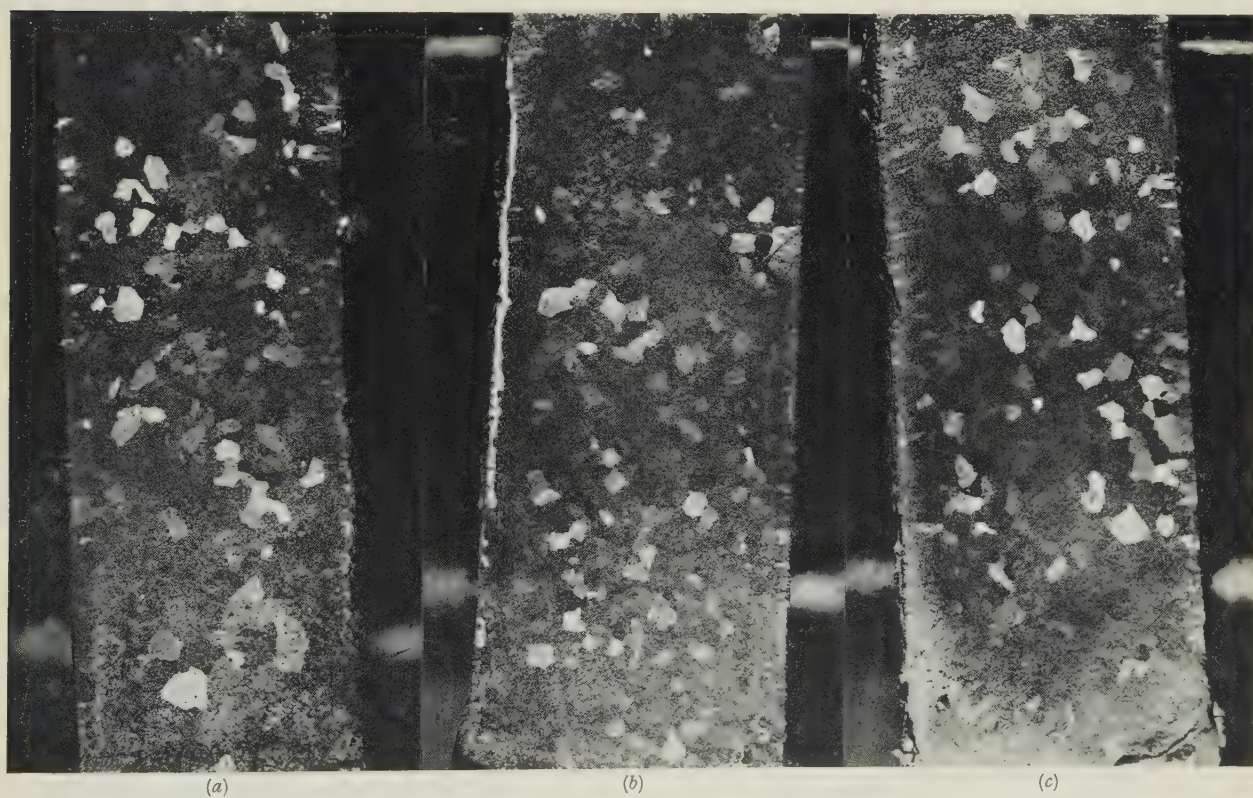


FIG. 3.—Lead Cast Against (a) Untreated Face; (b) Face Coated with Aluminium; (c) Face Coated with Copper.



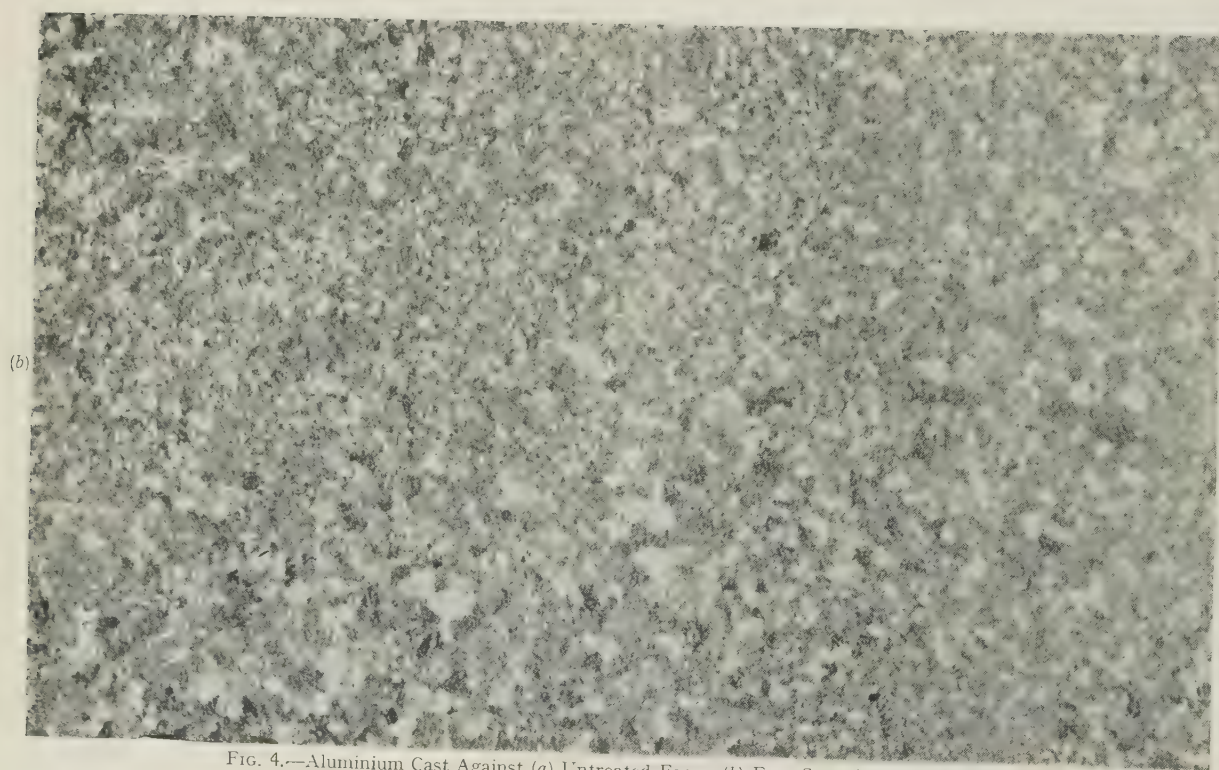
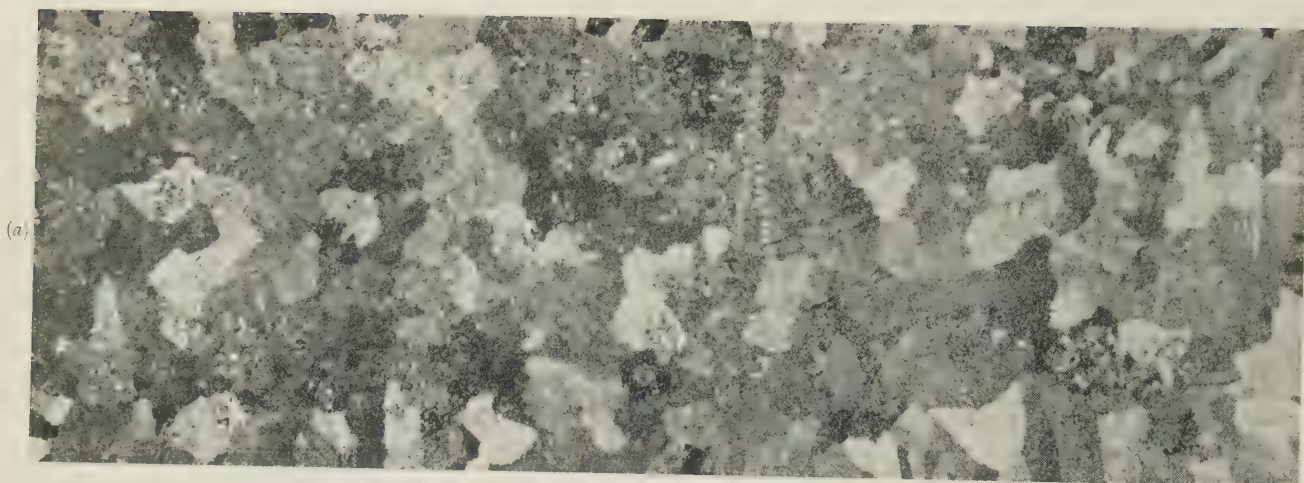


FIG. 4.—Aluminium Cast Against (a) Untreated Face; (b) Face Coated with Titanium.

dominated. It was therefore concluded that in such cases the powder had reduced the oxide film on the metal being cast, thus precipitating fine particles of

TABLE IV.—Free Energy of Formation ( $-\Delta G$ ) of Metallic Oxides at Room Temperature.<sup>11-14</sup>

Metal	Oxide	$-\Delta G$ , kg.cal./g.mol. oxygen (at 17° C.)	Accuracy ± kg.cal.
Calcium . . .	CaO	289	7
Thorium . . .	ThO <sub>2</sub>	281	25
Beryllium . . .	BeO	281	6
Magnesium . . .	MgO	273	1.5
Calcium silicide (Ca <sub>2</sub> Si)	2CaO + SiO <sub>2</sub>	260	?
Titanium . . .	TiO	257	8
Aluminium . . .	Al <sub>2</sub> O <sub>3</sub>	244	10
Titanium . . .	Ti <sub>2</sub> O <sub>3</sub>	236	15
" . . .	TiO <sub>2</sub>	206	6
Vanadium . . .	VO	199	8
Silicon . . .	SiO <sub>2</sub>	196	7
Vanadium . . .	V <sub>2</sub> O <sub>3</sub>	186	7
Manganese . . .	MnO	174	3
Chromium . . .	Cr <sub>2</sub> O <sub>3</sub>	167	4
Vanadium . . .	VO <sub>2</sub>	163	7
Zinc . . .	ZnO	153	4
Vanadium . . .	V <sub>2</sub> O <sub>5</sub>	141	5
Tin . . .	SnO	128	?
Iron . . .	FeO	115	3
Nickel . . .	NiO	103	2
Antimony . . .	Sb <sub>2</sub> O <sub>3</sub>	101	?
Lead . . .	PbO	91	4
Bismuth . . .	Bi <sub>2</sub> O <sub>3</sub>	84	?
Copper . . .	Cu <sub>2</sub> O	71	1

the cast metal, which then acted as homogeneous nuclei.

In determining which metals should be capable of reducing the oxide film on the cast metal, the values

of free energy of oxide formation given in recent publications were used.<sup>11-14</sup>

The rate of such reactions is governed by the activation energy ( $E$ ), and the free energy of formation ( $-\Delta G$ ) is only a guide to the possibility of deoxidation occurring. However, the results obtained do correspond to the expected behaviour based on the values of  $-\Delta G$  given in Table IV. Table V records the effects observed with grain-refined castings where oxidation of the coating took place and others where no refinement occurred. Fig. 4 (Plate XXIII) shows a typical example of nucleation involving oxide reaction.

It will be seen that aluminium provides the best example of a cast metal in which oxidation of the coating occurred. This is to be expected from the tenacious oxide film normally present on pouring the liquid metal. Magnesium behaves similarly, but the number of metals with a higher value of  $-\Delta G$  is limited, and of these, beryllium powder was not available at the time, and calcium powder was found difficult to produce without oxidation of the particles. Calcium silicide was used as a possible source of calcium, and has been included in Table IV. The compound Ca<sub>2</sub>Si was considered as a single component, and the free energy of oxide formation was made additive on a basis of the molecular ratios of the two constituents. Although this may not be justified, the calculated value is less than that of aluminium (see Table IV) and, as shown in Table V, calcium oxide is formed when aluminium reacts with the coating, and nucleation results to a limited degree.

The films remaining on titanium-coated mould faces after casting may contain TiO and Ti<sub>2</sub>O<sub>3</sub>, since both

TABLE V.—Nucleation Involving Deoxidation of the Cast Metal.

No. of Casts	Cast Metal	Casting Temp., °C.	Mould Material	Coating	Grain-size Refine- ment Ratio.*	Appearance of Coating After Casting
2	Aluminium	760	Sand	Magnesium	50 : 1	White; MgO confirmed
2		750	"	Titanium	50 : 1	Intense blue
2		750	"	Vanadium	2 : 1	Yellowish white
2		750	Cast iron	Titanium	50 : 1	Intense blue
2		750	"	Magnesium	10 : 1	White; MgO confirmed
4		720	Synthetic	Titanium	20 : 1	Intense blue
2		780	"	Calcium silicide	1.5 : 1	White; CaO confirmed
2		800	"	Vanadium	1.5 : 1	Yellow
2		740	"	Thorium	2 : 1	White
2		750	Sand	Iron	1	Metallic
2		750	"	Zinc	1	"
2		750	"	Antimony	1	"
2		750	Synthetic	Chromium	1	"
2		750	"	Silicon	1	"
2		750	Sand	TiO <sub>2</sub>	1	White
2		750	"	MgO	1	"
2		750	"	Al <sub>2</sub> O <sub>3</sub>	1	"
2	Magnesium	760	Synthetic	Thorium	2 : 1	White
2		760	"	Aluminium	1	Metallic
2		760	"	Silicon	1	"
2		770	Sand	Bismuth	1	"
2	Copper	1200	Synthetic	Aluminium	1.2 : 1	Some white specks
2		1180	"	Titanium	1.2 : 1	Slight blue film
2		1220	Sand	Antimony	1	Metallic
2		1220	Synthetic	Iron	1	"

\* Expressed as number of grains per unit area on treated face to average number on untreated faces.



these are blue in colour.<sup>15</sup> From Table V, it will be seen that the oxides of titanium and magnesium produce no grain refinement. Moulds heated to 200° C. after application of the coatings were also found to give negative results owing to oxidation of the powder at the surface.

Some attempt has been made to obtain X-ray back-reflection photographs of the treated surfaces of the castings, particularly where oxidation of the coating had occurred at the mould face. No traces of diffraction rings due to any metal other than the cast one were ever obtained. Reaction at the mould face, promoting turbulence, was also taken to be insignificant, after experimental casts had been made in which portions only of the mould face were coated. In these examples, the grain-refined areas showed sharp lines of demarcation, following exactly the pattern of the original coating.

### 3. NUCLEATION OF ALLOYS

In the nucleation of alloys the metal forming the basic constituent seems to exert the greatest influence, but where oxide films are involved, the composition of these films may prove the most important factor.

When the crystal structure of the first crystals to form from the alloy is identical with that of the principal constituent, isomorphous nucleation follows, as in the case of a pure metal. This was confirmed for some aluminium-, copper-, zinc-, lead-, and tin-base alloys. When the crystal structure of the first solid differs from that of the pure metal forming the basis of the alloy, then the 5% lattice-distortion rule appears to apply (see Section III, 1). Few results were obtained for such conditions, and they are not recorded here.

The most interesting example of alloy nucleation was provided by 18:8 austenitic steel. Here, the oxide film has been stated<sup>16</sup> to contain 90% chromium sesquioxide, 10% iron oxide, and a trace of nickel oxide. If a mould coating that will reduce chromium oxide is used, then the chromium particles formed may act as heterogeneous nuclei for the  $\delta$  solid solution which solidifies first from the melt, the lattice distortion being of the order of 2%. From the values of  $-\Delta G$  given in Table IV it appeared that thorium, magnesium, calcium silicide (as discussed above), aluminium, titanium, silicon, and possibly vanadium, should deoxidize the film on 18:8 austenitic steel at 1750° C, assuming this to consist mainly of chromic oxide. Table VI shows that these metals do, in fact, nucleate the steel.

As a practical test, a precision casting in this steel, containing sections tapering from  $\frac{1}{16}$  in. to a knife edge (necessitating high casting temperatures) was made, with and without coatings of aluminium powder. The pouring temperature of 1750° C. led to solidification in the thin section of one single grain, occupying the whole of the cross-section, when no powder was coated on to the synthetic mould. Using aluminium powder, the grain-size was refined at the surface, and solidification of the interior so modified as to produce from 5 to 100 grains across the narrow tapering section.

TABLE VI.—Nucleation of 18:8 Austenitic Steel.

No. of Casts	Casting Temp., °C.	Mould Material	Coating	Grain-Size Refinement Ratio *	Oxide-Film Coating After Casting
4	1720	} Synthetic {	Titanium	100:1	Blue
3	1700		Silicon	2:1	White SiO <sub>2</sub>
4	1720		Aluminium	50:1	White Al <sub>2</sub> O <sub>3</sub>
3	1700		Calcium silicide	20:1	White CaO
2	1750		Thorium	5:1	White
4	1750		Magnesium	4:1	White MgO
2	1720		Vanadium	1.5:1	Yellow

\* Expressed as number of grains per unit area on treated face to average number on untreated faces.

Note: Some ingots of 18:8 austenitic steel were cast using vanadium coatings in which refinement was negligible. No refinement was ever observed with iron, nickel, or zinc powder.

The improvement in mechanical properties was no doubt considerable, but the size of the casting prevented any direct measurement of these. No attempt was made to draw any conclusions from the experimental ingots as to the grain-size of the centre sections when nucleation at the surface had occurred, but it was observed that considerable influence was exerted on the crystals growing from the surface layer, often reaching to the centre of the ingot.

Further work is necessary to confirm the mechanism of nucleation in alloys.

### ACKNOWLEDGEMENTS

The authors wish to acknowledge the provision of materials, facilities, and advice on the Osborn-Shaw precision-casting process by Mr. Noel Shaw; and discussion of this work with their colleagues in the University.

### REFERENCES

1. R. W. Ruddle and A. L. Mincher, *J. Inst. Metals*, 1949–50, **76**, 43.
2. R. W. Ruddle, "The Solidification of Castings", *Inst. Metals Monograph and Rep. Series No. 7*, 1950.
3. M. D. Eborall, *J. Inst. Metals*, 1949–50, **76**, 295.
4. A. Cibula, *J. Inst. Metals*, 1949–50, **76**, 321.
5. G. Tammann, "A Textbook of Metallography". New York: 1925 (Chemical Catalog Co., Inc.).
6. D. Turnbull, *J. Appl. Physics*, 1949, **20**, 817; 1950, **21**, 1022. *Trans. Amer. Inst. Min. Met. Eng. (in J. Metals)*, 1950, **188**, 1144.
7. D. Turnbull, *Thermodynamics in Physical Metallurgy (Amer. Soc. Metals)*, 1950, 282.
8. J. H. Hollomon, *ibid.*, 161.
9. D. Turnbull, *J. Chem. Physics*, 1950, **18**, 198.
10. J. J. Marais, *Found. Trade J.*, 1949, **86**, 501.
11. M. de Kay Thompson, "The Total and Free Energies of Formation of the Oxides of Thirty-Two Metals". New York: 1943 (Electrochemical Society).
12. H. J. T. Ellingham, *J. Soc. Chem. Ind.*, 1944, **63**, 125.
13. F. D. Richardson and J. H. E. Jeffes, *J. Iron Steel Inst.*, 1948, **160**, 261; 1949, **163**, 397.
14. O. Kubaschewski and E. Ll. Evans, "Metallurgical Thermochemistry". London: 1951 (Butterworth-Springer).
15. J. W. Mellor, "Treatise on Inorganic and Theoretical Chemistry", Vol. VII, p. 28. London: 1927 (Longmans, Green and Co., Ltd.).
16. W. H. J. Vernon, F. Wormwell, and T. J. Nurse, *J. Iron Steel Inst.*, 1944, **150**, 81p.

ELECTROCHEMISTRY AND THE  
SCIENCE OF METALS \*

1329

By PROFESSOR ROBERTO PIONTELLI †

## SYNOPSIS

After giving an historical account of the origin and growth of electrochemistry, the author surveys the present state of knowledge on various aspects of electrochemistry that are closely related to metals. Particular attention is given to the question of the seat of electromotive force.

## I.—INTRODUCTION

FIRST, I should like to express my appreciation of the honour of having been invited to deliver this Autumn Lecture to the Institute of Metals. My choice of subject has been made on the one hand because electrochemistry is one of the few topics which I feel capable of treating at length; and on the other because it affords me an opportunity of directing the attention of an audience thoroughly versed in the science of metals to the problems of the electrochemist.

Every technologist will readily admit the important, in some respects unique, part played by electrochemistry in the field of metallurgy. The chemical action of electricity covers a wide range of free energies of reaction, and thereby exercises a predominating influence in certain directions, as, for instance, in the production of the less noble metals. The speed of such action and also its selectivity may be easily regulated, thus making possible a very high standard of purity of electrometallurgical products. The value of electrical instruments in control operations and in recording essential data does not need to be stressed. The measurement of electromotive forces at various temperatures affords a means of direct determination of free-energy and entropy changes in chemical processes, thereby supplying valuable data unobtainable by any other means.

Electrochemical methods are, moreover, finding wider and wider application in research on such subjects as the structure, reactivity, and catalytic power of metal surfaces; the mechanism of nucleation, growth, and breakdown of metal crystals; the genesis and significance of "secondary" structures; the existence and conditions of formation of unstable intermetallic phases; metal-gas systems, &c. Even so brief a summary indicates the importance of electrochemistry in extraction, refining, protection, finishing, analysis, research, and many other fields. The

sciences of metals, metallurgy, and electrochemistry are natural allies and the bonds between them are certainly not destined to relax.

For the future progress of both theoretical and applied electrochemistry it is in fact essential that the bonds should be drawn ever closer, and that the mechanism of their electrochemical behaviour should become as much a part of the study of metals as that of their mechanical and physical properties.

What I have to say will therefore constitute primarily an appeal, recalling that made by Sir Robert Boyle in the middle of the seventeenth century to the physical and corpuscular philosophers, urging on them a close and mutually profitable collaboration, inasmuch as it had been fully demonstrated how "*experimenta chymica per corpuscularium doctrinam feliciter explicari; ita vicissim huic ex illis vel lucem vel confirmationem non raro conciliari posse*".<sup>1</sup>

To demonstrate more clearly the essential features of present-day problems, I should like to draw on historical sources to trace their origin and development.

The lack of collaboration so greatly deplored by Boyle did not by any means denote, either in that or the preceding epoch, inactivity on the part of the philosophers of either of the two groups, in that very field of metals that we, too, have so closely at heart. It was the feverish activity of the alchemists that stored up the rich but confused fund of knowledge which made possible the development of modern chemistry; while the imaginative spirit of the "corpusculares" was also in ceaseless turmoil, endeavouring to establish in "formulations of everlasting philosophy" the protean nature of metals. To both groups the electrochemical problems of metals presented themselves in a particularly complicated form, in so far as behaviour towards atmospheric and chemical agents was concerned. It had long been known that iron coming into contact with waste water from copper mines was

\* Delivered at the Annual Autumn Meeting, Venice, 17 September 1951.

† Laboratori di Elettrochimica, di Chimica Fisica e Metallurgica e di Metallurgia del Politecnico, Milan.



transformed into copper. Such observations had led in distant times to the drawing up of the scale of "metallic perfection" headed by gold, and had been the source of endless illusions and misconceptions to those who, in good or in bad faith, saw in displacement reactions proof of the transmutability of metals—a road minutely explored with the object of appeasing the eternal lust for gold.

## II.—HISTORICAL SURVEY

I should like to survey briefly a few theories of the nature of metals from the wealth of historical material that I have accumulated.

First, there is the astrological conception—probably the most ancient—which attributed the behaviour of every metal to the more or less direct influence of a planet with which it was in affinity. Such affinity, for instance, was attributed by one school of thought to an infinite number of small corpuscles emerging from the planet and the metal, and possessing a form suitably adapted to the porosity of the planet and metal in question, but to no others. Let us not, however, too readily jeer at and condemn this apparently fantastic idea, lest the physics of cosmic rays should sooner or later disclose some phenomenon of a similar nature.

For centuries the most widely accepted explanation of the metallic state was based upon the blending of "constituent principles" (of Aristotelian inspiration): mercury, sulphur, and subsequently, salt. The purity of these materials, their relative proportions, the degree of their blending (accomplished in the depths of the earth but under the constant influence of the planets) determined the perfection of the various metals and the degree of their respective sympathies and antipathies.

The spread of clearly defined corpuscular theories during the second half of the seventeenth century—just at the time of Boyle's appeal—is worthy of note. The behaviour of individual metals was attributed to the form and compactness of the constituent corpuscles, which affected the size and shape of the pores accessible to reactive particles of the chemical agents. Behaviour therefore depended not only upon the penetrative properties of the agent, but also upon the internal and external structure of the metal.

\* "I have also observed that the alloys utilized for the welding of the copper plates on the sliding roof of the Florence Observatory have rapidly deteriorated, and transformed themselves into white oxide at all points of contact—welded joints—with the copper plates."<sup>2</sup>

† "Je n'ai jamais attribué aux métaux exclusivement la faculté d'inciter le fluide électrique par leur contact mutuel, lorsqu'ils sont de différentes espèces; ayant reconnu, et prouvé par un grand nombre d'expériences directes, que cette faculté appartenait, sans exception, à tous les conducteurs; et que si elle était en général plus marquée entre les métaux, elle ne laissait pas de se manifester dans le contact d'un métal . . . avec un de la seconde, ou conducteur humide. . . ."

"L'action électrique qui se déploie par le contact de plusieurs solutions salines avec les métaux—principalement de certains acides avec certains métaux, et des alkalis concentrés avec

The development of the phlogiston theory, however, represented a retrogression, inasmuch as the behaviour of metals was then attributed to the qualities of the phlogiston each possessed. Towards the end of the eighteenth century chemical doctrine was being radically revised. Bitter but fruitful disputation between Galvani and Volta and the ensuing clash between electricity and physiology definitely marked the advent of electrochemistry. Studies of the behaviour of metals by Fabbioni\* (1792), Ritter,<sup>3</sup> and others disclosed further and vaster fields open to electrochemistry. The discovery of the electric pile (1800) saw the problem of the day—the origin of galvanic fluid—extended to the working mechanism of the new apparatus. Volta had to oppose not only the supporters of "animal electricity", but also those of the "chemical theories"; moreover, he had to refute † the extreme opinions attributed to him—opinions which are still quite generally attributed to Volta to-day.

In a galvanic circuit Volta himself perceived a state of "electric tension" set up as a result of the formation of various heterogeneous contacts. The absolute or relative importance of the contributions of such contacts to the tension, and also the mechanism of these contributions, formed the crux of Volta's problem.

The supporters of the chemical theories refused to acknowledge any source other than the chemical effects at the metal/solution contacts. Volta was opposed to such an interpretation, being profoundly convinced of the importance of intermetallic contacts, and also because of the possibility of such chemical effects manifesting themselves independently of the galvanic phenomena, or even as a result of the circulation of the current.‡

The embittered nature of the controversy, together with the keen interest aroused by the phenomena involved—such as that of the decomposition of water (Nicholson and Carlisle<sup>5</sup>; 1800)—resulted in the advent of electrometallurgy (Cruikshank and Brugnatelli; 1800) passing almost unnoticed.

In his "History of Electricity"<sup>6</sup> Priestley attributes to G. B. Beccaria, the Turin physicist, the first experiments (about 1756) on the reduction of metallic compounds by friction machines. Although those experiments,<sup>7</sup> in which the thermal action of the

presque tous les métaux—est souvent plus forte et plus marquée que celle qui se déploie par le contact mutuel de deux métaux peu différents entre eux."<sup>4</sup>

‡ "L'oxidation est en partie indépendante de l'action galvanique, ou pour mieux dire électrique; car elle est l'effet chimique ordinaire de tel ou tel fluide sur tel ou tel métal; elle en dépend en partie, en tant que le courant électrique modifie singulièrement cette oxidation; en l'augmentant beaucoup dans le métal d'où le courant sort pour passer dans l'eau ou tout autre liquide oxydant, et en la diminuant ou supprimant tout à fait dans le métal où le courant électrique entre, et où le gaz hydrogène se développe. Ainsi donc le courant électrique exerce une action oxydante, et une désoxydante, suivant qu'il passe d'un métal dans un liquide, ou du liquide dans le métal; mais cette action n'est nullement la cause du courant, elle n'en est que l'effet."<sup>4</sup>

current certainly played a decisive part, contain in some respects the first germs of electrometallurgy, they remained undeveloped, and the true path to metallurgical applications was disclosed only with the discovery of the electric pile. In London Cruickshank, employing the Voltaic apparatus with the object of obtaining oxygen free from hydrogen, decided to eliminate the latter by utilizing it to reduce dissolved metallic compounds. Using lead acetate, he observed the formation on an electrode of tiny needles of lead and later of dendritic crystals; using copper sulphate, he observed the separation of copper.<sup>8</sup> Brugnatelli, who had the good fortune to work at Pavia, in close collaboration with Volta, and who concentrated on obtaining practical results rather than on establishing general laws, recorded the phenomena of the cathodic separation of silver, mercury, zinc, and copper.<sup>9</sup> At the time when Davy was entering upon his series of researches, which proved so valuable not only for the results obtained but also for the perfection of their technique, and the clarity of their interpretation, Brugnatelli<sup>10</sup> began work on galvanotechnical problems. This led to the discovery of his galvanic "gilding" process (1803), to the metallizing of carbon with gold, silver, and copper (1816), and to the successful electrodeposition of alloys of copper with gold, silver, and tin (1818).

In Faraday, the physical and chemical schools of thought, which had been becoming more and more divergent, met and temporarily achieved an harmonious union. "What is the source of power in a Voltaic pile?" he wrote. "This question is at present of the utmost importance in the theory and to the development of electrical science." And again: "All the facts show us that power, commonly called chemical affinity, can be communicated to a distance through the metals . . . that, in other words, the forces termed chemical activity and electricity are one and the same."<sup>11</sup> Faraday's contribution was indeed fundamental, and served to clothe with a true theory the ideas (bearing in part the highly original imprint of Davy) of the supporters of the chemical theory, whose numbers had in the meantime been augmented by such scientists as Oersted, De la Rive, Becquerel, Pouillet, Schönbein, and others. Divergencies of opinion nevertheless continued with increasing acrimony.

The activities of the physicists were, however, directed more and more towards new and promising fields of research in electrodynamics and electromagnetism; and, despite the fact that the results of Cruickshank and Brugnatelli were almost overlooked, applications of the electrochemistry of metals proceeded to increase and multiply.

The names of De la Rive, Jordan, Spencer, Elkington, Ruolz, Jacobi, Smee, Murray, and numerous others are still fresh in our memories, and it may be of interest to note that in his early days (about 1830) Sir Henry Bessemer did some valuable pioneer work in this field. Nobili<sup>12</sup> and Marianini<sup>13</sup> published important theoretical and applied studies of the subject; and

mention should be made of the name of Zantedeschi,<sup>14</sup> who was active in Venice and foremost among the pioneers in the art of galvanoplastics.

In the field of classical research the study of the Voltaic apparatus continued to provide a never-ending subject of discussion. The theoretical and experimental research work of Helmholtz, Joule, Clausius, Lord Kelvin, and others, provided a perfect working test-bench for the new doctrines of thermodynamics. From the science of energy as laid down by Ostwald,<sup>15</sup> a severe criticism emerged of the views of Volta and his followers in regard to the importance of intermetallic contacts. However, other authors, in particular Helmholtz, by virtue of the electromolecular-forces hypothesis and the electrical double-layer theory of contacts, had confirmed the importance of Volta's views, in a form which has continued to arouse interest down to the present day.

More recently, new chemical and physical concepts—in particular Arrhenius' theory of electrolytic dissociation and van't Hoff's osmotic theory of solutions—seem likely to shed important new light on the problem. Nernst's "osmotic theory of the pile" is confined substantially to contacts involving liquids (the contribution of the intermetallic contact being supposed to be represented by thermoelectric effects). While avoiding a crude conception of ionic-exchange processes, Nernst's theory attempts to explain, in terms of the solution pressure on the one hand and of the osmotic pressure on the other, the opposing chemical tendencies which the difference in electric potential is called upon to counterbalance.

The development of the new electron theories, and in particular their application to the phenomena of electronic emission from hot bodies (Richardson<sup>16</sup>), leads, however, to the conclusion that, in view of the different "affinities" of the various metals for electrons, the exchanges of electrons between metals must represent a definite amount of chemical energy. The origin of the electrical work accomplished by a Voltaic battery is essentially chemical (as thermodynamics requires), but henceforth all the particles constituting the electric fluid increasingly assume the aspect of a chemical species, thereby fully justifying the hypothesis of electromolecular forces which are also active at the intermetallic contact.

### III.—THE SEAT OF ELECTROMOTIVE FORCE

Chemical processes in a galvanic circuit can no longer be considered as exclusively confined to the contacts between metals and solutions, for the exchange of electrons at contacts between dissimilar metals forms an integral part of the overall chemical process in the battery, in the same way as does the exchange of ions between metals and solutions. If therefore Volta's substantial reasons for opposing chemical doctrines are demolished, the bases of the refutation of the ideas of Volta and his followers on the contribution of intermetallic contacts are likewise



destroyed. The curve of the progress of human knowledge is by no means a smooth one, but has many ups and downs. On the basis of experimental values of the work of extracting electrons some (so-called "neo-Voltian") physicists, are again seeking in the intermetallic contact the main or sole source of electromotive force.

The methodical revision of ideas, which is universally adopted in physics, when applied to electrochemical problems, leads to certain conclusions, which at first sight may appear discouraging, although they have already been clearly dealt with by Gibbs.<sup>17</sup> "The consideration of the electric potential in an electrolyte, and especially the consideration of the difference of potential in electrolyte and electrode, involves the consideration of quantities of which we have no apparent means of physical measurement, while the difference of potential in pieces of metal of the same kind attached to the electrode is exactly one of the things which we can and do measure."

And so we now come to the present position, which in certain respects may seem paradoxical: for while

periment furnishes us, by well-known direct methods, with the electric potential difference,  $E_M$ , between the terminals of the galvanic cell.

The series of equilibrium values  $E_M^\circ$ , determined for cells corresponding to the so-called "standard" conditions, constitutes the well-known "electrochemical series" or "scale of nobilities".

How is  $E_M$  made up of the contributions from the various contacts? Apart from the lack of an experimental method of determination, this problem is complicated by the absence of agreement on what constitutes such a "contribution". Any solution is of an essentially speculative character, but considering the extent and nature of past efforts in this direction, it seems unfair to ignore the problem altogether.

Let me therefore reaffirm an opinion that I have already discussed in detail elsewhere.<sup>19, 20</sup> When considering any one of the components of the circuit, isolated and electrically neutral, we find ourselves confronted with the problem (well defined both from the physico-structural and thermodynamic points of view) of the work needed to deprive it of its various constituent particles. As far as electrically charged particles (ions and electrons) are concerned, the forces—to the existence of which such work corresponds—may be supposed to be partly of an electrical and partly of a chemical nature.

This division is essentially arbitrary in character, inasmuch as according to the scale of atomic and subatomic dimensions at least one part of the forces we normally consider as being chemical appears to be of an electrical nature.<sup>19</sup> It is not my intention to enter deeply into such a difficult matter, and I shall confine myself to the view accepted by many writers, according to which a prudent application of mathematical electricity of the macroscopic type (Maxwell) is admissible, even internally, to a material.<sup>19-22</sup> The contour surface will be assumed to be uniform.

The average value of the internal potential of the phase is then essentially determined by the electric double layers existing on its surface. Such double layers may be present both for intrinsic structural reasons (for example, owing to the unsymmetrical configuration of the electronic atmospheres of the peripheral atoms), and as a result of a chemical alteration of the surface (adsorption of gas, oxidation, tarnishing, &c.), which may lead to the formation of new phases.

Let us now consider what happens when two different phases—initially isolated and electrically neutral—come in contact with each other without mixing. Owing to the different "affinities" (in the thermodynamic sense of the term) in respect of the various kinds of particles, we may suppose, generally, work to be available in the system that is liable to lead to an exchange of particles between the two phases. Such a mechanism (and in particular that of rearrangement of the interphase region and of the distribution of charges on the free surface of individual phases) will continue to operate until the available work is used up. The masses involved in these exchange

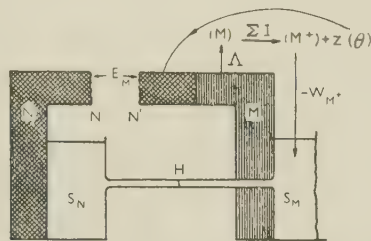


FIG. 1.—Cell for the Study of the Electrochemical Behaviour of a Metal.

$$E_M^\circ \simeq \Omega_M + K.$$

$$\Omega = \frac{1}{z} (\Delta + \Sigma I - W_{M^+}) = \frac{1}{z} (z\phi_0^{(M)} + \phi_{M^+}^{(M)} - W_{M^+})$$

$$= \frac{1}{z} (U^{(M)} - W_{M^+})$$

some physicists maintain that the problem of the seat of electromotive force is quite real, and one which may in some cases be regarded as solved, or as amenable to solution either experimentally (by various electrocapillary and electrokinetic methods) or theoretically (on the basis of our knowledge of the structure of the phases); others hold that the problem is devoid of any concrete physical significance.<sup>18</sup>

In order to get a clearer picture of the situation, let us endeavour to follow a course that cannot, from the very outset, be condemned on purely logical grounds.

Consider a system such as that shown in Fig. 1, which we will suppose to be isothermal, and in which the metal ( $M$ ), which it is proposed to study, is immersed in a solution ( $S_M$ ) of one of its salts. The solution is, in turn, connected (by means of an "interliquid contact") with a reference electrode ( $N/S_N$ ). As a precautionary measure, we shall choose physically identical materials for the two terminals of the circuit. Ordinary temperatures are considered.

Under these conditions it is possible to give the problem a fairly general significance. In fact, ex-

processes being extremely small, the internal chemical properties of the phases and the double layers on their free surfaces, will remain practically unaltered after the contact. The establishment of equilibrium is, however, essentially the result of these changes in the distribution of electrical charges.

The final distribution of these charges proves to be complicated, but it is always such as to satisfy the requirements necessary under equilibrium conditions to attain uniformity in the average electric potential in each of the phases in contact, and to neutralize the work available for the process of exchange of the particles between the phases.

At a given point in the interior of the phase, the electric potential is now determined by: (a) the double layers on the free surface of the phase which already existed before contact; (b) the free charges that have been superimposed on such layers as a result of the contact; and (c) the distribution of charges originating in the interphase region.

Turning from consideration of an internal point of a phase to an external one, though always one immediately adjacent to the surface (normally distances of the order of  $10^{-4}$  cm. are considered, namely those just out of the practical radius action of the so-called "image forces"), the variation of the electric potential is due exclusively to the double layers, either in the initial state or after the contact. Between two external points, immediately adjacent respectively to the two phases, the potential difference before the contact is zero, while after the contact an electric-potential difference exists, directly measurable by experiment, commonly called the "Voltaic potential difference". This Voltaic potential difference is very simply related to the work of extraction of the particles exchanged, and it expresses also the variation of the potential difference between internal points of the phases, with respect to the condition before the contact. This quantity, which thus represents the electrical consequences of the establishment of contact equilibrium, and the work initially available for which it must compensate, can therefore be reasonably supposed to be a measure of the "contribution" made to the overall electromotive force of the circuit by the contact itself, an assumption corresponding closely to Volta's original ideas.

Let us briefly examine the principal implications of this assumption. It is well known that  $E_M$  is the sum total of the Volta potential differences corresponding to the various contacts. The fact that a significant contribution to the electromotive force of a Daniell cell may derive from an intermetallic contact which is not a site of chemical changes, does not present any difficulty, inasmuch as the exchange of electrons between the phases, which is concentrated at the contact itself, is also a chemical process, and is governed by affinity.

The fact that the individual Volta potential differences depend on atmospheric action at the surfaces of the phases, whereas such action does not enter into the electromotive force of the circuit (at

identical terminals), also presents no difficulty, when we consider that each phase takes part in at least two contacts (one of them possibly with the atmosphere), the net contribution of which is independent of the influence of the double layers on the free surfaces. Such a contribution consisting of two contacts involving the same phase, also eliminates the indeterminateness inherent in the arbitrary value of the internal potential of the individual phases.

It thus seems to be proved that the problem of the seat of electromotive force is a definite one, and one which leads to-day to a somewhat Salomonic solution, inasmuch as it attributes importance to intermetallic contacts as well as to contacts between metals and liquids, and takes account also of the part played by the chemical changes at the surface due to the atmosphere, not as being the source of power, but as the cause of existence of or of variation in the surface double layers.

However, the indeterminateness inherent in the "absolute" electric potential differences, and in determining the part played in the above contributions by the internal properties or by the surface ones, still persists.

As may be gathered from the above outline, such a problem not only presupposes a definition (an arbitrary one, of course), but it admits only of theoretical solutions which could be based solely upon an adequate knowledge of internal structure and surface properties of the various phases, and in particular of the metallic ones.

Such knowledge, therefore, is one of the possible objectives that the collaboration between electrochemistry and the science of metals might seek to reach; it is a speculative aim and a somewhat distant one at that; but the road which leads to it would certainly reveal new horizons in the classical problems of thermionic and photoelectric emission, adsorption, catalysis, heterogeneous reactions, and so on.

#### IV.—ELECTROCHEMICAL PROPERTIES OF METALS

Let us now pass to the fundamental problem of the electrochemical behaviour of the various metals in relation to their other chemical and physical characteristics. We are not yet able to predict this behaviour on the basis solely of the electronic structure of the free atoms, but we may characterize the behaviour by means of properties more closely related to the atomic structure.

If we compare different galvanic cells, which vary only because of the nature of the metal  $M$  (and hence of the salt dissolved in  $S_M$ ), the differences in the values of  $E_M$  are essentially to be attributed to the contacts  $M/N$  and  $M/S_M$ , as the contribution of the liquid/liquid contact may be considered practically constant (and in any case very small). The problem of the relative values of  $E_M^\circ$  and of their relation to the properties of the various metals, thus leads back to the total contribution of the two above-mentioned



contacts. In consequence of the processes that take place at them (exchanges of electrons at the inter-metallic contact and of ions at the other contact), the phase  $M$  loses or gains atoms.

We may arrive indirectly at the same result (for the anodic direction of the reaction), if we assume the evaporation of the atoms  $M$ , their transformation into ions and electrons, and the passage of the former into  $S_M$  and of the latter into  $N$ . To a rough approximation (neglecting in particular some entropy changes)

free atoms, and  $W_{M^+}$  the chemical energy developed in the solvation of the gaseous ion;  $\phi_\theta^{[M]}$  and  $\phi_{M^+}^{[M]}$  are the "works of extraction" from the metal, of electrons and ions, respectively; while  $U^{[M]}$  represents the energy necessary for dissociating the crystal lattice into ions and electrons.

The values (in volts) of the ratios of some of these quantities to  $z^*$  for numerous metals, are shown in Fig. 2. It should be noted that: (1)  $\Lambda$  expresses the affinity of the lattice for the atoms  $M$ ; (2)  $\Sigma I$

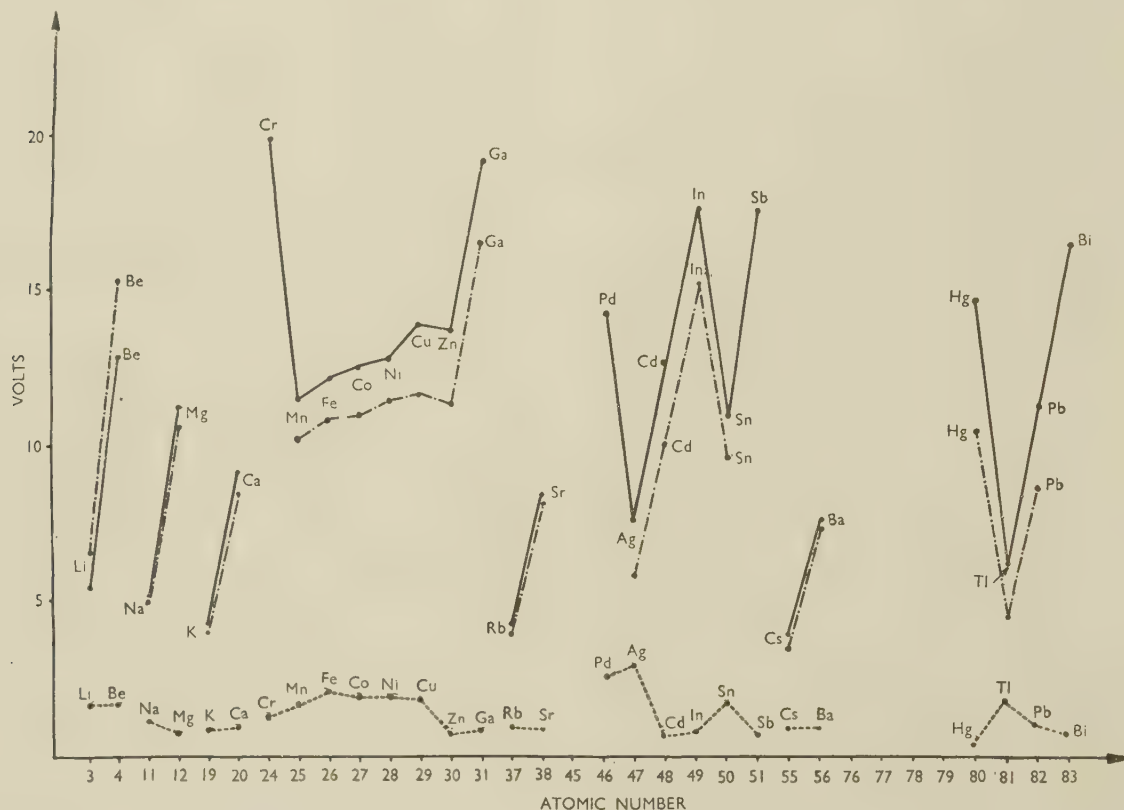


FIG. 2.—Values of  $\Lambda/z$  (---),  $\Sigma I/z$  (—), and  $W_{M^+}/z$  (- · -) as Functions of the Atomic Number. The abscissa is not uniform.

which nevertheless is sufficiently close for our present purpose, the part involving total chemical affinity of transformation, and therefore also the part of  $E_M^o$  which depends upon  $M$ , may be considered to be measured by the quantity  $\Omega_M$  (the so-called "nobility index" of the metal  $M$ ), which may be expressed in one of the equivalent forms:<sup>19, 20</sup>

$$\begin{aligned}\Omega_M &= \frac{1}{z}(\Lambda + \Sigma I - W_{M^+}) = \frac{1}{z}(z\phi_\theta^{[M]} + \phi_{M^+}^{[M]} - W_{M^+}) \\ &= \frac{1}{z}(U^{[M]} - W_{M^+})\end{aligned}$$

where  $z$  is the valency of the "normal" ionic form of  $M$ ;  $\Lambda$  is the energy required for the sublimation of  $M$ ;  $\Sigma I$  is the sum of the ionization potentials of the

measures the affinity of the individual atom for the valence electrons; and (3)  $W_{M^+}$  expresses the chemical affinity of the solution  $S_M$  for the ions  $M^+$ . Only the relative values of  $W_{M^+}$  can be indirectly determined by experiment, but for our present purposes, which are purely comparative, this does not matter.

The two largest terms ( $\Sigma I$  and  $W_{M^+}$ ) often counteract one another (in a certain sense the process of solvation tends to restore the electronic configuration of the atom); for this reason  $\Lambda$  is often of decisive importance. The works of extraction  $\phi_\theta^{[M]}$  and  $\phi_{M^+}^{[M]}$ , taken separately, cannot generally be considered as "purely chemical" work, for they comprise a chemical part and an electrical part (we here encounter once more the indeterminateness which obliged us

\* Taken from various sources<sup>23</sup> and in part original.

to abandon the problem of the absolute potential differences).

Taking the sum  $U^{[M]}$ , which corresponds to the loss from the metallic phase of equal charges of opposite sign, and which expresses the resistance of the lattice to dissociation into ions and electrons, we eliminate the electrical terms and thus obtain a quantity expressing the part of the active chemical affinity of the circuit, that depends solely upon  $M$ . This quantity, together with  $W_{M^+}$  (which also depends on the solution), determines the relative degree of nobility of  $M$ .

This fundamental property is thus correlated with others of more obvious significance. Fig. 3 shows the

plain solvation, it may be necessary to replace  $W_{M^+}$  by the heat of the reaction of formation, starting from the gaseous ion, of certain aggregates.

This holds good in the formation of complex ions in solution; and also in the formation of solid oxides, starting from the metal and gaseous oxygen. In the latter case, however, experiment shows (see Fig. 3) that the inverse variation of the heat of oxidation and the degree of nobility is well preserved, indicating that  $W_{M^+}$  runs parallel with the thermal output of the reaction between the ion  $M^+$  and the oxygen ion in the gaseous state.

Allow me to draw an analogy, which is perhaps rather far-fetched. A metallic phase is like a com-

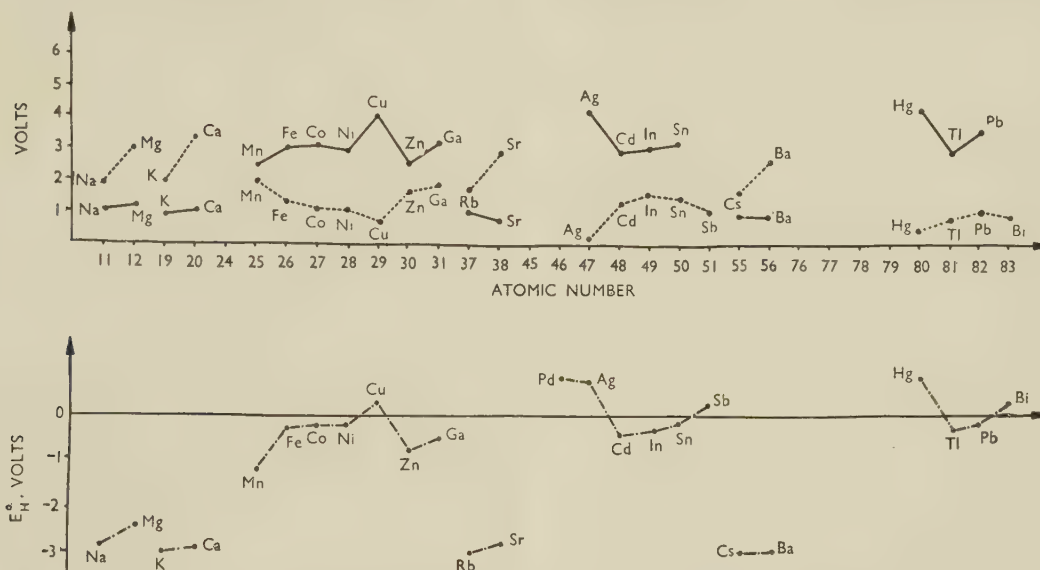


FIG. 3.—Values of  $\Omega_M$ ,  $-\Delta H_{ox}/z$ , and  $E_H^0$  as Functions of the Atomic Number. The abscissa is not uniform.

$$\text{—} = \frac{1}{z} (\Lambda + \Sigma I - W_{M^+}).$$

$$\text{---} = -\Delta H_{ox}/z.$$

good agreement existing between the values of  $\Omega_M$  and of  $E_H^0$ \*. In this figure are recorded together the values (both as divided by  $z$  and in volts) of the heats of formation (at 25° C.) of the oxides of  $M$  assuming the usual valency  $z$  ( $-\frac{\Delta H_{ox}}{z}$ ). These values vary inversely with those of  $\Omega_M$ . It is easy to see that the nobility index of the various metals also expresses, from a thermodynamic point of view (and in a relative way), their tendency to resist chemical attack from various sources and thus the predisposition of the metal not to return, as soon as a chance presents itself, to the "natural" forms of chemical bond from which the efforts of the metallurgist have torn it.

These reactions may be considered as the sum of two partial reactions, in which the metallic phase cedes ions and electrons, respectively, and in particular the thermodynamic affinity of reaction which depends on  $M$  can be measured, in a relative way, by  $\Omega_M$ . When, however, the final state of the ion is not that of

munity which may be considered to be composed of individuals of two species (electrons and ions) and of the families (atoms) formed by these individuals. When the phase is engaged in an electrochemical process, it is fighting, so to speak, on two fronts, against the attractions exercised by its surroundings. The ability of the aggregate to resist, upon which its degree of nobility depends, is determined by (a) solidarity between families ( $\Lambda$ ); (b) the resistance of a family when alone ( $\Sigma I$ ); and (c) by the disposition of the individuals, when free, not to become too easy a prey to their surroundings ( $-W_{M^+}$ ). We have noticed the important part played by solidarity in deciding the fate of the aggregate.

## V.—KINETIC ASPECTS OF ELECTRO-CHEMICAL BEHAVIOUR

Up to now we have considered exclusively the thermodynamic aspects of the electrochemical behaviour of metals. From a practical point of view, and in my opinion also from the theoretical standpoint,

\* Values of  $E_H^0$  referred to the "normal hydrogen electrode" at 25° C.



the kinetic aspect is of still more lively and real interest.

In all physicochemical problems, thermodynamic affinity, referred to the internal properties of homogeneous phases, taken in large masses, supplies adequate, but not overwhelming conditions for equilibrium. It is a measure of the availability of work, which is indispensable for producing a transformation but which may not be sufficient to initiate it; while the speed of transformation depends also on the other kinetic factor, the "resistance to reaction".

In electrochemistry, these resistances are closely bound up with the structural properties of the phases, and of the interphases. The true electrochemical behaviour of a metal, in processes which involve deposition as well as dissolution, does not depend only on its degree of nobility, but also, and sometimes in a decisive way, on the phenomena of cathodic and anodic overvoltages; and on processes that do not involve the ions of the metal, but, for example, hydrogen ions. As we know, even in deciding the true oxidizability, kinetic and structural factors of the metal and of its surface and of the oxide that it forms, play a part.

The electrochemical kinetics of metals can be studied experimentally by various means. One method, which, however, does not yet seem to have lived up to its initial promise, is that based on the use of radioactive tracers. Another method, of obvious interest in its application, is that based on the study of displacement reactions and concentration cells. The method, however, most frequently applied and most fruitful in results, is still that which depends on the direct determination of the anodic and cathodic polarization curves of metals under various conditions.

It should here be pointed out that the uncertainties which exist with regard to the absolute potential differences of contacts (intermetallic and metal/liquid) no longer figure in the case of polarization voltages. Everything leads us to believe that intermetallic contacts are unpolarizable, for which reason "overvoltages" can with certainty be attributed to metal/liquid contacts, and (under suitable conditions) they supply a measure of the "chemical resistance" which hinders the processes of ionic exchange.

It thus becomes possible to apply to metals the method so often used in chemistry to obtain evidence of the orientation of bonds; namely, that of examining the degree of ease with which they break down to give place to new configurations. In metals, the energy of cohesion and the work of extraction, although of rather indeterminate significance, are the result of a number of factors. Also the kinetics of the exchange processes of ions makes their bond conditions important, both in the lattice and in the solution; in addition, the surface condition of the metal, and, in general, the structure and properties of the interphase, are important.

The information regarding chemical resistance in the process of ionic exchange that can be obtained

from the study of overvoltages, is therefore still difficult to interpret, quite apart from the present difficulties of experimental technique. However, it is possible to say that this direction of research is full of promise.

In spite of the serious lack of experimental data at our disposal at present, concordant results yielded by the various methods of investigation mentioned above, show that the chemical resistances in the ionic-exchange processes are: (1) negligible in the case especially of mercury, lead, tin, cadmium, thallium (the so-called metals of normal behaviour); (2) important, or very large, for the transition metals that have been studied adequately up to the present time: iron, cobalt, nickel, metals of the platinum group (metals electrochemically inert); and (3) intermediate for the groups: silver, copper, gold, and bismuth, antimony, arsenic, in each of which the first-named metals (silver and bismuth) are practically normal while the chemical resistance (anodic and cathodic) increases in the order given.

It is interesting to note that in each of the categories, there occur elements of quite different nobilities. Contrary, therefore, to current opinion, the kinetic ease of ionic exchange does not depend on nobility.

It is also interesting to observe the tendency to symmetry in the effects of anodic and cathodic overvoltages. It seems legitimate to speak of an inherent disposition to processes of ionic exchange, a reasonable estimate of which may perhaps be based on the rate of these exchanges in both directions in the absence of any external current. At ordinary temperatures and concentrations of the dissolved ions, the exchange rates so far determined extend from values of the order of  $10^{-1}$  amp./cm.<sup>2</sup> for some normal metals, to very uncertain values, often lower than  $10^{-10}$  amp./cm.<sup>2</sup> for the inert ones.

The properties of the metallic phase which are relevant to the kinetics of the ionic-exchange processes seem to be: (1) the possible existence of *d* sub-shells which are incomplete in the free atom (or the purely metalloid character of the bonds, as is the case of arsenic); and (2) the minimum value of the interatomic distances in the lattices. The first property seems essential for the appearance of electrochemical inertia, which increases, in each group, with decrease of the interatomic distances. Both for the metals of intermediate behaviour and for the normal ones, the minimum interatomic distance seems to afford again a characteristic indication of the degree of normality.

The existence of an electrochemical inertia which is essentially determined by the nature of the bonds in the phases (crystal lattice and solution) also seems to be of importance in explaining the phenomena of passivity of metals; not so much in the sense of identifying inertia with passivity, as in finding in inertia the ideal basis for establishing states of passivity, which always seem liable to lead back to the surface condition, as Faraday foretold and U. R. Evans and others have clearly demonstrated.<sup>24</sup>

A serious gap in the study of the electrochemical kinetics of metals is the fact that up till now experiments have been concerned almost entirely with polycrystalline electrodes, and the existing data represent mean values, whose interpretation is by no means simple, of those corresponding to the various orientations of the lattice planes. The new and fairly simple methods for preparing single crystals are now opening up a very interesting field of investigation.

Another field which has been very little explored, owing to its inherent difficulty, though well deserving of study, is that of the part played, both in anodic and cathodic processes, by the so-called "secondary structures."

The possibilities of investigation into the electrochemical behaviour of alloys are still practically unlimited, ranging from the more classic examples to those "crypto-alloys" which all the commercial metals are in reality owing to the presence of impurities.

## VI.—CONCLUSION

In this lecture, which though lengthy is nevertheless in many respects incomplete, I have tried to describe those aspects of the development of the electrochemistry of metals which are most closely related to the science of metals. Let me remind you of a striking passage by Bacon<sup>25</sup>: "Qui tractaverunt scientias, aut empirici aut dogmatici fuerunt. Empirici, formicae more, congerunt tantum et utuntur; rationales, araneorum more, telas ex se conficiunt. Apis vero ratio media est, quae materiam ex floribus horti et agri elicit, sed tamen eam, propria facultate, vertit ad digerit."

The role of the bee is well suited to the electrochemistry of metals because of its character of an intermediate science. To extend the metaphor, the means of stimulating this increasingly fruitful collaboration between electrochemistry and the science of metals which I have predicted to-day, would perhaps be the opening to the electrochemical bees of the hothouses in which the beautiful flowers of the science of metals are grown.

## REFERENCES

1. R. Boyle, "Tentamina quaedam Physiologica", p. 178. Amsterdam: 1667.
2. G. Fabbroni, Communication to *Atti Accad. Georgofili*, Firenze, 1792; published in *J. Phys.*, 1799, **49**, 348.
3. W. Ritter, "Beweis, dass ein beständiger Galvanismus. . . ." Weimar: 1798; "Das Elektrische System der Körper." Leipzig: 1805.
4. A. Volta, Lettre aux Rédacteurs de la Bibliothèque Britannique (18 Mars, 1802); cited by G. Polvani, "Alessandro Volta". Pisa: 1942.
5. W. Nicholson and A. Carlisle, *Nicholson J.*, 1800, **4**, 179.
6. J. Priestley, "The History and Present State of Electricity, with Original Experiment". London: 1767.
7. G. B. Beccaria, "Elettricismo atmosferico", 2nd edn., p. 282. Bologna: 1758; "Elettricismo artificiale", p. 309. Torino: 1772.
8. W. Cruickshank, *Nicholson J.*, 1800, **4**, 187.
9. L. Brugnatelli, *Ann. Chim. Storia Naturale (Pavia)*, 1800, **18**, 136.
10. L. Brugnatelli, *Ann. Chim. Storia Naturale (Pavia)*, 1802, **20**, 148; 1803, **22**, 22; *J. Chim. Van Mons (Bruxelles)*, 1803, 257; *Giorn. Fis. Chim. (Pavia)*, 1808, **1**, 75; 1816, **9**, 145; 1818, **11**, 130.
11. M. Faraday, "Experimental Researches on Electricity", Vol. II, p. 18. London: 1844.
12. C. L. Nobili, "Memorie", Vol. I, pp. 18, 25, 57, 163. Firenze: 1834.
13. S. Marianini, *Giorn. Lett. Sci. Modenese*, 1840, **2**, 387; 1844, **7**, 90, 97.
14. F. Zantadeschi, "Della Elettropia". Venezia: 1841.
15. W. Ostwald, "Elektrochemie, ihre Geschichte und Lehre". Leipzig: 1896.
16. O. Richardson, *Proc. Camb. Phil. Soc.*, 1901, **11**, 286; *Phil. Trans. Roy. Soc.*, 1903, [A], **201**, 197.
17. J. W. Gibbs, "Collected Works", Vol. I, p. 429 (a letter of May 1899). New York: 1901.
18. E. A. Guggenheim, "Modern Thermodynamics with the Methods of J. W. Gibbs". London: 1933; "Thermodynamics", p. 330. Amsterdam: 1949.
- A. Sommerfeld and H. Bethe, "Handbuch der Physik", Vol. 24, Part 2, pp. 333, 444. 2nd edn. Berlin: 1933.
- J. A. Chalmers, *Phil. Mag.*, 1942, [vii], **33**, 399, 416, 496, 506, 594, 599, 608.
19. R. Piontelli, *Compt. rend. 2me Réunion Comité Internat. Thermodynamique Cinétique Electrochim.*, 1950, pp. 79, 185, 369. Milan: 1951; *Z. Elektrochem.*, 1951, **55**, 128.
20. R. Piontelli, *Compt. rend. 3me Réunion Comité Internat. Thermodynamique Cinétique Electrochim.*, 1951. Berne (in the press).
21. P. Duhem, "Leçons sur l'Electricité et le Magnétisme", Vol. I, p. 387. Paris: 1891.
22. E. Lange, "Handbuch der Experimentalphysik", Vol. XII, Part 2, p. 265. Leipzig: 1933.
23. F. R. Bichowsky and F. D. Rossini, "Thermochemistry of the Chemical Substances". New York: 1936.
- H. J. T. Ellingham, *J. Electrodepositors' Tech. Soc.*, 1940, **16**, 1.
- J. D. Bernal and R. H. Fowler, *J. Chem. Physics*, 1933, **1**, 515.
- J. A. V. Butler, "Electrocapillarity". London: 1940.
24. M. Faraday, "Experimental Researches on Electricity" Vol. II, p. 239. London: 1844.
- U. R. Evans, "Metallic Corrosion, Passivity, and Protection". 2nd edn. London: 1946.
25. F. Bacon, "Novum Organum Scientiarum", Vol. I, XCIV.





# HIGH-TEMPERATURE THERMAL ANALYSIS USING THE TUNGSTEN/MOLYBDENUM THERMOCOUPLE \*

1330

By H. T. GREENAWAY,† B.Met.E., S. T. M. JOHNSTONE,†  
B.Met.E., JUNIOR MEMBER, and MARION K. McQUILLAN,‡  
M.A., MEMBER

## SYNOPSIS

A technique which enables thermal analysis to be carried out at temperatures up to 2000° C. has been developed. High-frequency induction heating is used, and the temperature is measured by means of a tungsten/molybdenum thermocouple, for which a calibration curve is given. The method has been applied to the determination of the freezing point of pure chromium, which is shown to be  $1845^{\circ} \pm 10^{\circ}$  C., and the liquidus curve for the solid solution of manganese in chromium.

## I.—INTRODUCTION

DURING an investigation of the properties of several chromium-base alloys it became necessary to determine the freezing point of chromium and the liquidus curves of the systems under examination. It was decided that the induction heating method would be a satisfactory means of attaining the high temperatures involved and that a thermocouple would be the best means of measuring the temperature. The use of an optical pyrometer was dismissed because of vapour effects and of the personal factor in taking readings.

The work reported in the present paper includes the calibration of the tungsten/molybdenum thermocouple and examples of its use in determining the freezing point of chromium and the liquidus curve of the chromium-manganese system. The results are of special interest because of their recent determination by Carlile *et al.*,<sup>1</sup> using an optical pyrometer.

Some notes on the preparation of pure chromium have been included because of the importance of impurities in the determination of the freezing point and liquidus curves.

## II.—THE TUNGSTEN/MOLYBDENUM THERMOCOUPLE

The use of tungsten/molybdenum thermocouples is not new, but there has been considerable disagreement between the temperature/thermo-e.m.f. curves given for them by the various previous users, and they have had the reputation of being unreliable. The early workers<sup>2-6</sup> have shown, however, that the thermoelectric power of the thermocouples is sufficiently great, above 1250° C., to allow reasonably accurate temperature measurement. It has been

found that, with the better materials now available, a reproducible calibration curve can be established, and that after annealing the couples are quite stable. Although the tungsten and molybdenum wires are brittle after annealing, and require careful handling, their fragility is not a severe disadvantage to a careful worker.

The tungsten and molybdenum wires used were 0.05 in. in dia. and were obtained from commercial sources. Spectrographic examination indicated the presence of a trace of molybdenum in the tungsten and faint traces of magnesium and iron in the molybdenum, but the purity of both wires was of a high order. The wires were annealed in an atmosphere of hydrogen before use by passing a current of 65 amp. through them for 15 min. Thermocouples were made by welding in a tungsten arc. No protective atmosphere was used, but the operation was so rapid that very little oxidation took place, and good clean welds were obtained.

The thermocouples were calibrated over the temperature range 800°–2200° C. in two stages. From 800° to 1700° C. the temperature/e.m.f. relationship was established by direct comparison with a platinum/platinum-rhodium thermocouple; above 1700° C. the temperatures were measured by an optical pyrometer of the disappearing-filament type.

### 1. CALIBRATION FROM 800° TO 1700° C.

When using tungsten/molybdenum thermocouples, a protective atmosphere is necessary to prevent oxidation of the couple elements. Since the couples were required principally for use in hydrogen, the calibration was carried out under the same conditions. Although hydrogen is a more suitable medium than either air or vacuum in which to use platinum/

\* Manuscript received 25 January 1951.

† Research Officer, Aeronautical Research Laboratories, Melbourne, Australia.

‡ Formerly Research Officer, Aeronautical Research Laboratories, Melbourne, Australia.



platinum-rhodium thermocouples at high temperatures,<sup>7</sup> it involves the danger of contamination of the thermocouple if it is used in conjunction with silicon-bearing refractories in an apparatus in which carbon and sulphur are likely to be present.<sup>8</sup> In calibrating the tungsten/molybdenum thermocouple against a

each couple and using the means of all the readings taken. The thermo-e.m.f. readings given by the platinum/platinum-rhodium thermocouple were converted to temperatures, and plotted against the corresponding thermo-e.m.f. reading given by the tungsten/molybdenum thermocouple. A smooth and reproducible curve was obtained from 800° to 1700° C.

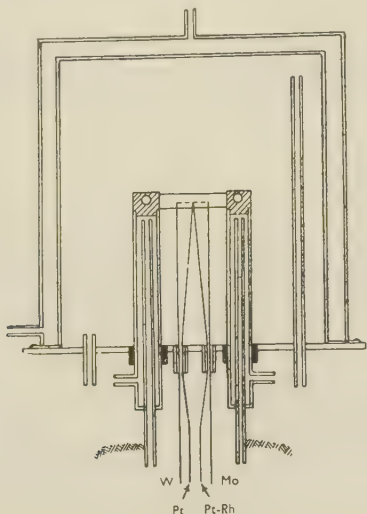


Fig. 1.—Molybdenum Strip Heating Apparatus for Calibration of Thermocouple from 800° to 1700° C.

platinum / platinum - rhodium thermocouple, this danger was avoided by the use of a heating apparatus in which no refractory materials were present.

A diagram of the apparatus is shown in Fig. 1. The heater consisted of two molybdenum strips 0.008 in. thick and about  $\frac{3}{8}$  in. wide, arranged in parallel in the form of a bow between two water-cooled electrodes spaced about  $2\frac{1}{2}$  in. apart. The strips, which were heated directly by resistance, acted as radiation shields as well as heaters, and very high temperatures were quickly and easily attained in the small space between them. In this space the hot junctions of the thermocouples were arranged. In order to ensure that the junctions of the two couples being compared were at the same temperature, the four wires were welded together to form a single bead. The electrodes were mounted in a base-plate, on to which was sealed a water-cooled copper bell which covered the heater assembly. The cold junctions of the thermocouples were allowed to remain at room temperature, which, during the course of the experiments, differed very little from 21° C. Any alternating currents picked up by the thermocouples were filtered out by means of a network of condensers and inductances.

The heating current was supplied by a transformer giving an output ranging from 0 to 15 V. At any transformer setting, thermo-e.m.f. readings were taken for the two couples alternately. The readings were sometimes found to vary slightly owing to fluctuations in the mains voltage, but these effects were overcome by taking a number of readings for

## 2. CALIBRATION FROM 1700° TO 2200° C.

Since there was no alternative to optical or radiation pyrometry for measuring temperatures above the range of the platinum/platinum-rhodium thermocouple, the disappearing-filament type of optical pyrometer was chosen as the most reliable and convenient means. The uniform temperature enclosure in which the thermocouple junction was heated was formed by three molybdenum blocks about  $\frac{3}{4}$  in. square and  $\frac{3}{8}$  in. thick, arranged as shown in Fig. 2. The thermocouple elements were not welded together, but were bent to a right angle at a distance of about  $\frac{3}{16}$  in. from one end, and were dropped through holes in the lower molybdenum block so that the short bent ends lay along a groove in the surface of the block running between the two holes, the remainder of the wires emerging downwards. Since the wires were not in contact with any part of the block other than the groove, the temperature of the hot junction could be safely assumed to be that of the grooved part of the block. The other blocks were placed on top of the grooved one and the three held together with a wrapping of molybdenum sheet. Holes drilled in the centres of the upper blocks formed a cavity which radiated effectively as a black body.

The blocks were mounted in a sealed silica tube. A totally reflecting prism above a window in the upper cover-plate of the tube was arranged so that the optical pyrometer might be conveniently sighted on the black-body cavity. The effect of the window and

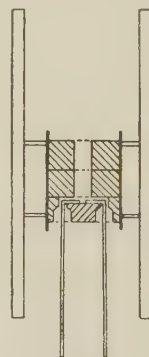


Fig. 2.—Molybdenum-Block Heater Assembly for Calibration from 1700° to 2200° C., Showing Arrangement of Thermocouple Elements.

prism on the optical-pyrometer readings was measured by means of a series of temperature determinations made on a calibrated tungsten-strip lamp with and without the window and mirror in the optical system, at temperatures from 1000° to 2000° C. A correction curve was thus established which enabled the optical-

pyrometer readings to be simply converted to true temperatures.

The molybdenum-block assembly was heated directly by high-frequency induction, any high-frequency currents picked up by the thermocouple being filtered out. Purified hydrogen was passed slowly through the apparatus during the experiment. The cold junctions of the thermocouple were again allowed to remain at room temperature. Using a pyrometer newly calibrated against a tungsten-strip lamp, it was found that the temperature/thermo-e.m.f. relationship obtained in this way agreed well with that obtained by comparison with a platinum thermocouple from 1000° to 1700° C. The calibration was then continued to 2200° C.

### 3. THE TEMPERATURE/THERMO-E.M.F. CURVE

The calibration curve obtained for the tungsten/molybdenum thermocouple is shown in Fig. 3. At

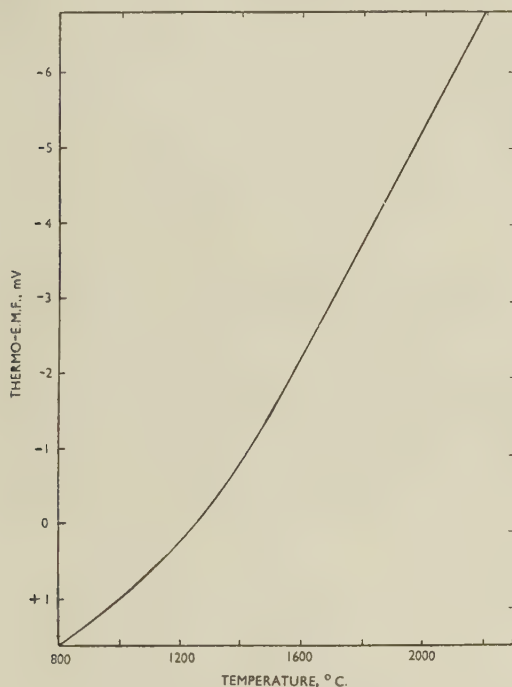


Fig. 3.—Calibration Curve for Tungsten/Molybdenum Thermocouple.

lower temperatures the curve is parabolic in form, but above 1500° C. it becomes linear. Below 1250° C. the thermo-e.m.f. generated is positive, decreasing to zero at 1250° C. and thereafter becoming increasingly negative. The reproducibility of the curve is about  $\pm 3^\circ$  C. below 1700° C. and  $\pm 5^\circ$  C. above this temperature. Its accuracy has been checked at the platinum point (1774° C.) by carrying out a cooling curve on a melt of pure platinum. The thermocouple gave a reading of 1776° C. at the freezing point, and its errors, therefore, lie within the limits of accuracy of the calibration of the optical pyrometer at this temperature.

It has been found that couples made from the same batch of material give reproducible calibration curves, and it is not necessary to calibrate each couple individually once the standard curve has been established. Furthermore, results obtained on a new batch of material indicate that there is no significant difference between its calibration and that of the earlier batch. Repeated heating to temperatures of about 2000° C. does not affect the couple once it has been annealed.

### 4. CONTAMINATION OF THE THERMOCOUPLE

Contamination of tungsten/molybdenum thermocouples is observed if they are heated in contact with beryllia, metallographic examination showing that severe intergranular penetration occurs. When the use of beryllia is unavoidable, it has been the practice to calibrate the couples before and after each significant experiment. Alumina has been found to cause no contamination of the thermocouple, but its low melting point (2050° C.) limits its usefulness. Experiments have recently been carried out on the use of magnesia. After heating to about 1900° C. in contact with magnesia, the thermocouple bead shows slight intergranular contamination near the surface, but this seems to have no marked effect on the calibration of the thermocouple. The contamination is very much less than that caused by beryllia under similar circumstances.

## III.—METHOD OF THERMAL ANALYSIS

The heating unit was a 20-kW. high-frequency generator manufactured by Amalgamated Wireless (Australasia), Ltd. The operating frequency is in the range 300-500 kc./s., depending on the characteristics of the work being heated. The power input to the work coil can be varied from about 20 to 100% of the power available for a given set of electrical conditions by a controlled positive voltage applied in opposition to a permanent negative bias on the grids of the oscillator valves.

The furnace arrangement is shown in Fig. 4. The alloy under investigation was placed in the crucible, *A*, which was supported at the mid-section of a cylindrical molybdenum heater, *B*, by means of an upturned crucible resting on a molybdenum wire grid, *C*. The heater was 8 in. long and 1.2 in. in dia., and was fabricated from 0.008-in.-thick molybdenum sheet by longitudinal spot welding with a tantalum strip interlayer. The heater was supported in turn on a section of molybdenum strip, *D*, resting on a fired alumina insulating piece, *E*. The whole of this assembly was contained in a silica tube, *F*, 30 in. long by 2 in. inner dia. The heater was located centrally in this tube by means of four molybdenum wire spacers, *G*, and was energized by induction from the work-coil, *H*, of the generator. The tube, *F*, was closed with water-cooled brass end-plates, *K*.

The thermocouple bead was protected by a sheath, *N*, which was held centrally in the crucible by a



molybdenum wire spacer, *P*. This spacer also served to locate the crucible centrally in the heater. The thermocouple wires were led out through a twin-bore silica insulator, *R*, to a pair of shielded extension leads, *S*, and thence through a radio-frequency filter, *T*, to a Negretti and Zambra quick-reading potentiometer. The filter consisted of an array of radio-frequency chokes and condensers which was necessary to eliminate stray e.m.f. induced

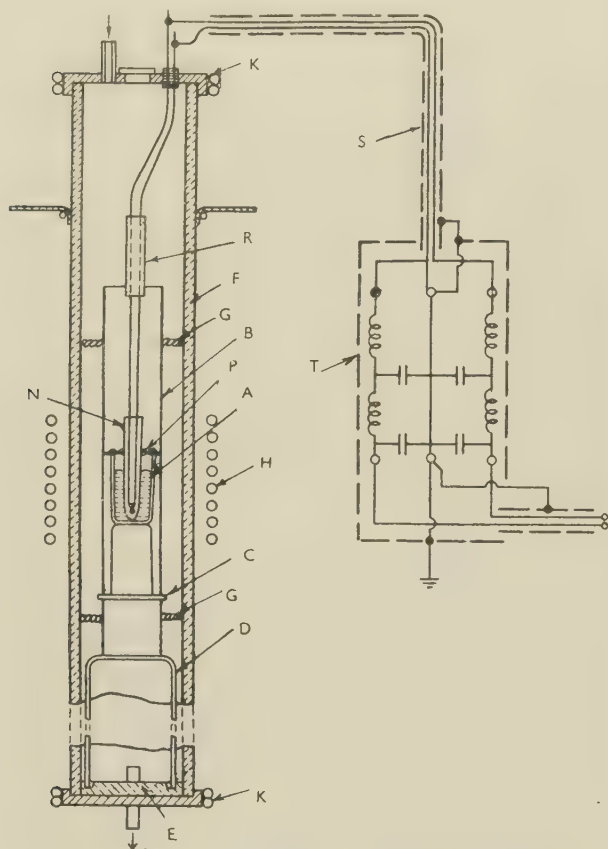


FIG. 4.—Furnace Arrangement for Thermal Analysis.

in the thermocouple by the H.F. current. Extension of the cylindrical heater well beyond the limits of the work-coil helped considerably to reduce these e.m.f.'s and also had the advantage of enabling the grid, *C*, and wire spacers, *G*, to be located outside the central hot zone. Failures of the heater at these points were frequent during earlier work when heating tubes 2.5 and 4 in. long were used. As a final precaution against inductive effects, one side of the thermocouple circuit was earthed, and the thermocouple wires were kept close together over the whole of their length, thus eliminating inductive "loops" in the vicinity of the work coil. The possibility of interfering e.m.f. could always be checked by momentarily shutting off the power supply and observing whether or not there was a corresponding jump in the potentiometer reading. With the arrangement shown in

Fig. 4, it was usual to find no interference of any kind. An atmosphere of purified hydrogen was maintained throughout a determination, the gas passing through at a slow constant rate.

For experiments in which the maximum thermocouple reading did not exceed about 1750° C., the crucible and thermocouple sheath were made of alumina. For maximum temperatures up to 1900° C., a beryllia crucible was used, and above this temperature both crucible and sheath were of beryllia or magnesia. When a combination of alumina and beryllia was used, care was taken to prevent contact between them in the hot zone, thus avoiding the formation of a low-melting mixture. Whenever a beryllia sheath was used it was necessary to recalibrate the thermocouple immediately after the experiment, as noted before (Section II, 4).

To determine a cooling curve after the melting of an alloy, the power input to the work-coil was quickly reduced to a predetermined setting—which would lead to a drop of temperature of 100°–200° C.—and the melt allowed to cool naturally to the lower temperature. During cooling the temperature was read on the potentiometer at 10-sec. intervals. This procedure was repeated with a series of overlapping temperature ranges, and on each occasion when an arrest or change of slope occurred, the determination was repeated at least once as a check.

#### IV.—THE DETERMINATION OF THE FREEZING POINT OF CHROMIUM

Previously published values for the freezing point of chromium vary from 1500° to 1920° C., the variation undoubtedly being due to contamination (particularly gaseous) of the melt and to faulty optical-pyrometer readings. The recent value of 1860° C. (after extrapolation to zero gas content) obtained by Carlile *et al.*,<sup>1</sup> using optical means, appears to be the most satisfactory published figure to date.

TABLE I.—Freezing Point of Chromium with Varying Gas Content.

Sample	Gas Content, wt.-%		Freezing Point, °C.	
	O <sub>2</sub>	N <sub>2</sub>	1st run	2nd run
1	0.02	0.014	1839	1841
2	0.02	0.033	1835	...
3	0.02	0.076	1834	1832
4	0.12	0.029	1831	...
Carlile <i>et al.</i> <sup>1</sup>	0.14	0.011	1845	

Using the apparatus and method described in the Appendix with melts of approximately 35 g. weight, a beryllia crucible, and an alumina sheath, the freezing points shown in Table I were determined. For comparative purposes the recent value obtained by Carlile *et al.*<sup>1</sup> is also given.

Extrapolations of these four results to zero gas

contents have given the freezing point of pure chromium as 1845°C. Taking into account the experimental errors, this value is estimated to be true to  $\pm 10^\circ\text{C}$ .

The determination of nitrogen was made by a modification of the Allen distillation method. Oxygen was determined by the chemical method described in the Appendix, a correction being made for the insoluble nitrogen content.

## V.—THE LIQUIDUS CURVE OF SOME CHROMIUM-MANGANESE ALLOYS

The method of thermal analysis described in Section III has also been used for the study of the liquidus curve of chromium-manganese alloys containing up to about 60 at.-% manganese. Electrolytic chromium and manganese were used, the chromium being prepared as described in the Appendix.

The alloys were prepared by melting together weighed quantities of the two metals in the thermal-analysis apparatus itself. The melts were very fluid, and sufficiently vigorous stirring occurred to produce uniformity. Each melt weighed about 30 g. Alumina crucibles and thermocouple sheaths were used.

A smooth liquidus curve, which fitted well with the determined value for the melting point of pure chromium, was obtained (Fig. 5). The melts were analysed for manganese and nitrogen. Some idea of relative oxygen contents was obtained from examination of the microstructures of the melts, and an indication of the results of such an examination has been given in Table II, which shows the manganese and nitrogen contents of a series of alloys. The relative amount of oxide present has been established in terms

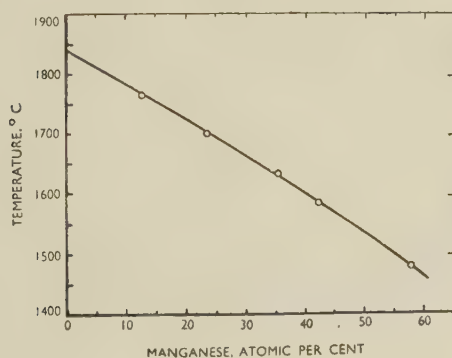


FIG. 5.—Liquidus Curve for the Solid Solution of Manganese in Chromium.

of the average amount present in the unalloyed chromium.

As a matter of interest, the approximate difference between the present results and those recently presented by Carlile *et al.*<sup>1</sup> for the same alloys have been included. An explanation of the observed differences was sought,

TABLE II.—Liquidus Temperature and Nitrogen and Relative Oxide Content of Chromium-Manganese Alloys.

Mn Content, at.-%	N <sub>2</sub> Content, at.-%	Relative Amount of Oxide Present as Compared with Amount in Unalloyed Cr	Difference Between Authors' Determination of Liquidus Temp. and that of Carlile <i>et al.</i> , <sup>1</sup> °C.
57.8	0.027	Less	22 lower
42.0	0.014	Slightly less	35 "
41.5	0.038	" "	35 "
35.3	0.018	Very much less	30 "
23.4	0.052	The same amount	35 "
12.5	0.037	" " "	20 "

unsuccessfully, in the gas contents of the alloys. No correlation was found between the gas contents of the alloys and the differences between the two sets of results. It may be seen in Table II that two alloys of closely similar manganese content show the same value for the liquidus temperature, even though the nitrogen content of one is more than twice that of the other. Furthermore, a specimen which shows one of the greatest differences between the present results and those of the earlier workers, has appreciably less oxide in its microstructure than any other specimen. The explanation is probably to be found in the different methods of temperature measurement used, the arrest points obtained by the authors having been obtained by thermocouple measurements, whereas Carlile *et al.* used an optical pyrometer.

## ACKNOWLEDGEMENTS

The work described above was carried out as part of the high-temperature materials programme of the Aeronautical Research Laboratories, Department of Supply, Melbourne. The authors wish to thank the Chief Scientist of the Department for permission to publish.

All the chemical analyses were done by Mr. E. J. T. Lumley of these laboratories, to whom acknowledgment is made. The authors are indebted to Dr. N. P. Allen of the National Physical Laboratory for the vacuum-fusion analyses of the chromium.

## APPENDIX

### THE PREPARATION OF PURE CHROMIUM

As high-purity chromium was not readily available, it was necessary to investigate means of producing the metal in the quantities required for the high-temperature materials programme of the Aeronautical Research Laboratories. Two methods were considered: (i) the electrolysis of chromic acid and (ii) the reduction of chromic oxide. The former was chosen, since it will produce, using suitable apparatus, metal containing only non-metallic impurities. The reduction of chromic oxide has one serious disadvantage—the probability of contamination of the product by the reducing element.



*Electrolytic Production of Low-Oxygen Chromium*

The apparatus employed was of the type used in normal electroplating, except for the following features:

(a) The acid bath and anode were made from pure lead, since antimonial lead was found to contaminate the electrodeposit with approximately 0.2% antimony.

(b) Polyvinyl chloride tubing was used for stopping off the cathode—a  $\frac{3}{8}$ -in.-dia. copper tube—since the commercial waxes available were unsuitable for the plating temperatures employed.

The bath contained 250 g./l. commercial chromic acid and 2.5 g./l. sulphate ion. Its composition was controlled chemically and additions made as required. The solution level was maintained constant, and the temperature thermostatically controlled to  $\pm 1^\circ\text{C}$ .

Spectrographic examination of chromium produced in this bath detected no metallic impurities. Gaseous impurities were hydrogen and oxygen; the latter was believed to be present in the form of hydrous chromic oxide. The hydrogen was readily evolved on heating to  $600^\circ\text{C}$ ., leaving oxygen as the remaining impurity. Brenner *et al.*<sup>9</sup> have shown that the oxide content of electrolytic chromium varies with plating conditions; temperature and current were therefore varied to determine the conditions which would yield the lowest oxygen content in the "as-deposited" condition. The results are given in Table III.

TABLE III.—*Variation of Oxygen Content with Temperature and Current Density.*

Current Density, amp./ft. <sup>2</sup>	Temperature, $^\circ\text{C}$ .	Oxygen, wt.-%
1100	68	0.23
1100	73	0.16
1100	75	0.13
1100	80	0.06
1100	83	0.08
850	80	0.07
960	80	0.07
1100	80	0.06
1250	80	0.06

From these results it is evident that the oxygen content varied only slightly with current density, but fell rapidly with increase in temperature. On this basis the conditions chosen for the production of all the chromium used in the programme were a

temperature of  $80^\circ\text{C}$ . and a current density of 1100 amp./ft.<sup>2</sup>.

Oxygen was determined by chemical means, which consisted essentially of dissolving a 1-g. sample in 10% hydrochloric acid, then determining the amount of chromium in the residues and converting to oxygen. This first necessitated a vacuum treatment at  $850^\circ\text{C}$ . to convert the soluble oxygen content of electrodeposited chromium into insoluble chromic oxide ( $\text{Cr}_2\text{O}_3$ ). The results of vacuum-fusion determinations as compared with the results of chemical analyses are given in Table IV. The low figures

TABLE IV.—*Comparison of Oxygen Content Determined by Vacuum-Fusion Method and Chemical Analysis.*

Sample	Condition	Oxygen, wt.-%	
		Vacuum Fusion	Chemical Analysis
A. Low- $\text{O}_2$ , bath temp. $80^\circ\text{C}$ .	As deposited.	0.06	0.02
B. "	Sample A, vacuum treated 1 hr. at $850^\circ\text{C}$ .	0.05	0.05
C. High- $\text{O}_2$ , bath temp. $68^\circ\text{C}$ .	As deposited.	...	0.04
D. "	Sample C, vacuum treated 1 hr. at $850^\circ\text{C}$ .	0.23	0.22

obtained by chemical analyses of samples A and C in this table indicate the need for vacuum treatment before analysis.

The nitrogen content of the chromium was less than 0.001%, as determined by vacuum fusion.

## REFERENCES

1. S. J. Carlile, J. W. Christian, and W. Hume-Rothery, *J. Inst. Metals*, 1949, **76**, 169.
2. S. Morugina, *Z. techn. Physik*, 1926, **7**, 486.
3. D. Binnie, *Roy. Tech. Coll. (Glasgow) Met. Club J.*, 1927-28, **6**, 35.
4. J. A. M. van Liempt, *Rec. Trav. Chim.*, 1929, **48**, 585.
5. J. H. Andrew and D. Binnie, *J. Iron Steel Inst.*, 1929, **119**, 309.
6. B. Osann and E. Schröder, *Arch. Eisenhüttenwesen*, 1933, **7**, 89.
7. M. K. McQuillan, *J. Sci. Instruments*, 1949, **26**, 329.
8. J. C. Chaston, R. A. Edwards, and F. M. Lever, *J. Iron Steel Inst.*, 1947, **155**, 229.
9. A. Brenner, P. Burkhead, and C. W. Jennings, *J. Research Nat. Bur. Stand.*, 1948, **40**, 31.

# SLIP BANDS AND HARDENING PROCESSES IN ALUMINIUM\*

1331

By A. F. BROWN,† M.A., Ph.D.

## SYNOPSIS

Slip bands on aluminium increase in number during plastic deformation and, at the same time, further slip occurs within each band. At higher temperatures and lower rates of deformation, as well as with increasing strain under all conditions, the latter process becomes increasingly predominant. This is interpreted on the basis of the fine structure of slip bands which has been resolved by the electron microscope. The differences in density and inner structure of slip bands formed under different conditions are compared with the differences between stress/strain curves, and it is shown that slip which forms a new band involves much more macroscopic hardening than slip within an existing band. A consequence of this conclusion is that a mechanical equation of state can exist only at very small strains.

## I.—INTRODUCTION

WHEN a metal crystal is deformed, the deformation is at first elastic and obeys Hooke's law: stress is proportional to strain. If the stress is progressively increased, the elastic limit is reached, after which the metal does not return to its original shape when the stress is released and increase of stress does not lead to a proportional increase of strain. The metal is then said to deform plastically.

In the elastic range, deformation is homogeneous, all atomic planes being strained alike, but in the plastic range all the deformation is concentrated on a few atomic planes; the crystal acquires a stepped appearance and the steps are visible on the surface as slip bands. However, in spite of the change in the character of the deformation, the elastic limit is not in general marked by an abrupt change in the slope of the stress/strain curve, and the stress needed to produce further plastic shear continues to rise with increasing strain. The metal is said to be work-hardening.

A satisfactory explanation of the origin of plastic work-hardening and of the shape of the stress/strain curve must take account of the observed inhomogeneity of plastic strain. In this paper it is shown that a very close correlation exists between the shape of the stress/strain curves and the differences in appearance of the slip bands formed under different conditions of temperature and strain rate.

In Section II of the paper experiments on aluminium are described which relate the amount of work-hardening to the number of slip bands and to the amount of slip within each. Plastic strain may arise either as a result of slip which produces new slip bands or as a result of slip producing extra shear on existing bands.

In Section III the experimental results are all summed up in the form of a simple picture of the

variation of stress in the space between slip bands. The sites where slip is observed most frequently to take place are indicated as places where the internal stresses are small. From this picture the result is obtained that slip on existing bands contributes little to the macroscopic stress. It is shown in Section IV that the form of the stress/strain curve under different conditions of temperature and strain rate can be accounted for in terms of this picture; a quantitative expression for the curve is obtained and gives good agreement with the evidence available for aluminium. Finally, in Section V, it is shown that a mechanical equation of state cannot exist under conditions which permit the strain within a slip band to increase after the formation of the band.

In a later paper it will be shown that similar conclusions are valid for several metals other than aluminium.

## II.—EXPERIMENTS ON THE FORM AND DISTRIBUTION OF SLIP BANDS

### 1. YAMAGUCHI'S EXPERIMENT

The classic experiment to show how the distribution of slip bands in aluminium is related to the amount of work-hardening was made by Yamaguchi in 1928.<sup>1</sup> The method was to polish single crystals of the purest aluminium then obtainable and extend them in a tensile testing machine. The experiment was stopped at intervals, the stress and strain recorded, and a count made of the number of slip bands per unit length in the direction normal to the slip planes. Slipping on one system only was allowed and if, with increasing strain, the specimen reached an orientation such that a second slip system became active, the experiment was stopped. With some specimens shear strains of 70% were reached.

Yamaguchi found that the number of slip bands per unit length was not proportional to strain, as would

\* Manuscript received 15 February 1951.

† I.C.I. Fellow, Cavendish Laboratory, Cambridge.



be the case if each band contributed a fixed amount of slip to the strain. However, the number of bands was related to the shear stress by an equation of the form:

$$\tau - \tau_0 = kN$$

where  $N$  is the number of bands per mm. counted as described above,  $\tau$  is the corresponding yield stress, and  $k$  is a constant of magnitude about  $5 \times 10^{-3}$  kg./mm.<sup>2</sup>.  $\tau_0$ , the yield stress corresponding to the elastic limit, is here defined as the stress which produces the first slip band. A curve of  $\tau$  against  $N$  plotted from a few of Yamaguchi's measurements is shown in Fig. 1 (a).

has been calculated from Yamaguchi's results and plotted as a function of the macroscopic shear strain. The resulting curve shows immediately that fresh slip occurs on existing bands at the same time as new bands are being formed.

It has been objected that Yamaguchi's procedure of counting slip bands could not give significant results, since the slip bands did not run right across the crystal but stopped or even ran into each other; however, it can be shown from Yamaguchi's photographs that the number of slip bands counted crossing a mark parallel to the axis of the specimen is independent of the position of the mark, provided that the

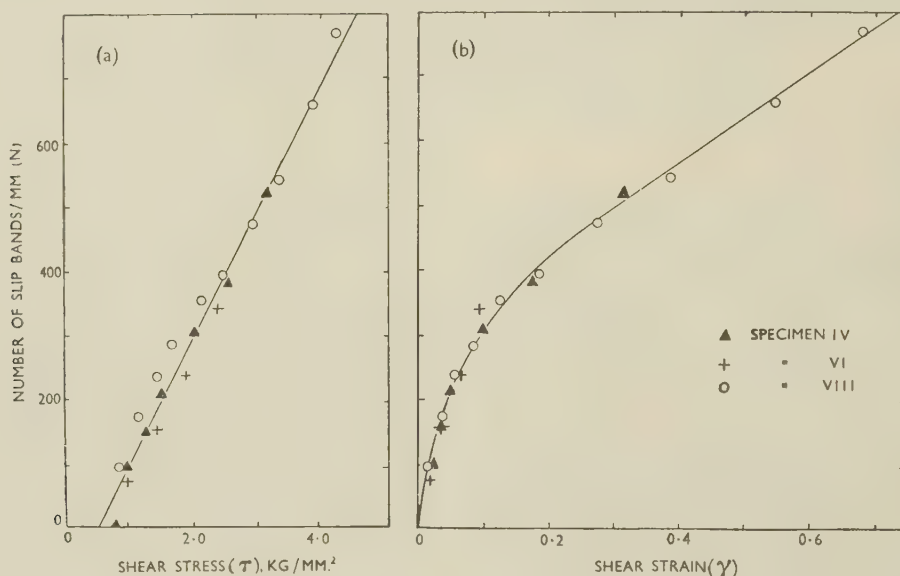


FIG. 1.—Curves from Results Obtained by Yamaguchi,<sup>1</sup> Relating the Density of the Slip Bands to (a) Stress and (b) Strain.

Yamaguchi's results are given in great detail in his paper, and it is possible to obtain additional information from them. Thus the relationship between  $N$  and the shear strain ( $\gamma$ ) has been extracted and is shown in Fig. 1 (b); this curve has the shape of the stress/strain curve. In Fig. 2, the amount of slip per band

number of bands is sufficiently great. Moreover, it is now possible to measure directly the amount of slip per band and to show that the values thus obtained agree well with those calculated from Yamaguchi's figures on the assumption that all bands make the same contribution to the macroscopic strain, at a given stress.

A recent attempt<sup>2</sup> to repeat Yamaguchi's experiments using aluminium of the highest modern purity gave the result that, up to 2% strain, both stress and strain are almost linear functions of the number of bands. (The authors of the paper are, however, concerned with the deviations from linearity.)

## 2. FINE STRUCTURE OF THE SLIP BANDS

The resolution of the light microscope is not sufficient to give definite information about the profiles of slip bands, i.e. the amount of slip occurring, or the number of crystallographic planes active in each. Recently, however, Heidenreich and Shockley<sup>3</sup> have shown by means of the electron microscope that the slip bands on aluminium can be resolved into bundles of finer lines as shown in Fig. 4. (Plate XXIV). These are interpreted as being the traces of slip lamellae such

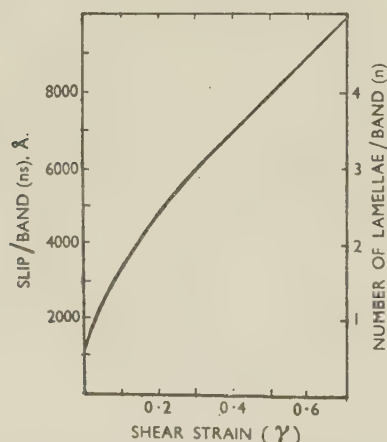


FIG. 2.—Curve from Results Obtained by Yamaguchi,<sup>1</sup> Relating Amount of Slip Per Band to Shear Strain.

as are shown schematically in Fig. 3. The slip distance per lamella, measured in the slip plane and slip direction is about 2000 Å., while the width of the lamellæ, i.e. the distance between active slip planes, is of the order of 200 Å.

Extended observations have now been made with the electron microscope on the variation with strain of the separation and fine structure of slip bands

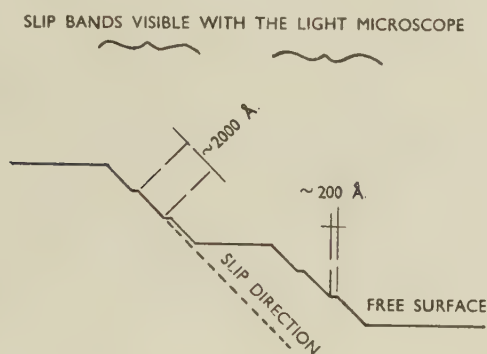


Fig. 3.—Schematic Representation of Fine Structure of Slip Bands.

in aluminium deformed at different temperatures. The methods employed and the results obtained have been described elsewhere.<sup>4</sup> The results for room-temperature deformation agree with those given by Heidenreich and Shockley, and no evidence was found of a finer structure. If such a structure exists, it must have dimensions of the order of a few atoms.

Within the limits of accuracy with which electron micrographs from metal replicas can be measured,<sup>4</sup> each lamella slips over its neighbours by approximately the same distance; in aluminium of the highest purity, measured distances range from 1600 to 2200 Å. There is no evidence either for uncompleted slip processes or for multiple slip processes on the same plane. Thus it may be concluded that slip takes place, under normal conditions, in avalanches and that the distance moved as a result of one avalanche is about 2000 Å.

Experiments on aluminium of lower purity<sup>5</sup> have given values of the slip distance between 1000 and 1200 Å. Thus, while the slip distance per lamella is rather less than in the pure metal, the range of values is still small. There is again no evidence that slipping of the lamellæ relative to each other can be otherwise than by avalanches.

At increasing values of the strain, the electron microscope shows that there are more lamellæ in each slip band, but that the amount of slip corresponding to the formation of each lamella is unchanged (within the limits specified above) from the smallest strains up to strains of the order of 90%. Thus the additional slip which Fig. 2 shows to occur within existing slip zones takes place by avalanches of length always about 2000 Å. on planes spaced some 200 Å. apart and leading to the formation of new lamellæ.

The numbers on the right-hand axis of Fig. 2

represent the number of lamellæ in each band, and are obtained from the figures on the left-hand axis by assuming that each lamella contributes just 2000 Å. of slip and that all bands in a uniformly sheared single crystal have the same number of lamellæ. The latter assumption is justified by experiment; the number of lamellæ in bands on a specimen deformed 40% will be normally about four, the observed range being 3–5. Thus bands formed late in the deformation rapidly catch up in total slip with those formed in the early stages. Experiment gives reasonable confirmation of the number of lamellæ calculated in the above manner.

At magnifications sufficient to resolve the lamellæ, the field of view of the electron microscope is not large enough to take in more than one or two slip bands. Thus, it is not possible to show in one photograph how the distribution of bands and, at the same time, their internal structure vary with strain. However, the evidence obtained from a number of electron micrographs of individual bands is shown diagrammatically in Fig. 6 where the lamellar spacing has been exaggerated some ten times relative to the band spacing. The diagram indicates that, at small strains, the bands are widely spaced and contain only one avalanche each. As the strain increases, more bands

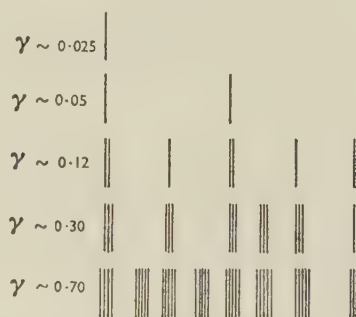


Fig. 6.—Development of a Field of Slip Bands at Room Temperature.

are formed in positions approximately midway between existing bands, and at the same time, fresh avalanches occur in the bands, giving rise to lamellæ.

### 3. EFFECT OF TEMPERATURE ON THE SLIP BANDS

The light microscope reveals differences between the slip bands on specimens which have been deformed at different temperatures. Bands formed in deformation at the temperature of liquid air appear as closely spaced, fine lines. As the temperature of deformation is raised, the spacing for a given strain increases until at high temperatures the bands are widely spaced and broad. Thus, with increasing temperature the same strain is concentrated into fewer and fewer bands.

The electron microscope<sup>4</sup> also enables this observation to be interpreted on the basis of formation of lamellæ. At low temperatures there are many bands, each containing few lamellæ, while as the temperature



of deformation is raised fewer bands are observed, with a corresponding increase of the number of lamellæ in each. The distance slipped in the formation of each lamella, i.e. the avalanche distance, does not alter appreciably with temperature. Values for this distance obtained by averaging observed values for many specimens are given in Table I.

TABLE I.—Distance Slipped [Avalanche Distance] in Formation of Each Lamella.

Deformation Temperature, °C.	Avalanche Distance, Å.	
	Mean	Limits Observed
—180	1500	1200–1800
20	2000	1600–2200
250	2200	1700–2500

Column 2 in this table gives the mean value obtained from 20 to 30 specimens for each temperature. Column 3 gives the limiting values measured; the spread is due in great part to the difficulty of measuring poorly contrasted lines on micrographs. The significance of the difference between the mean slip distances at 20° and 250° C. is doubtful, particularly since mean values higher than 2200 Å. are not found in experiments at temperatures above 250° C. However, experiments at the temperature of liquid helium<sup>5</sup> confirm that there is a real shortening of the avalanche distance as the temperature of deformation is reduced towards absolute zero.

The variation with temperature of the slip distance per lamella is thus small, and the main effect of temperature on the lamellæ is to alter their grouping, i.e. the number within each band. If all bands in a given specimen are assumed to be alike, the macroscopic shear strain,  $\gamma$ , is given by:

$$\gamma = ns/D \quad (1)$$

where  $n$  is the number of lamellæ per band,  $s$  is the avalanche distance, i.e. slip distance per lamellar slip, and  $D$  is the spacing of the slip bands measured, as usual, in a direction normal to the slip planes.

If, now, the small variations between the values of the avalanche distance,  $s$ , at temperatures between —180° and 250° C. are neglected:

$$n/D = \text{a constant for any given strain.}$$

How far this relationship is realized in practice is shown in Table II, where observed values of the number of lamellæ per band ( $n$ ) and the slip-band spacing are tabulated for various temperatures of deformation. The figures are for aluminium specimens which have undergone a shear strain of about 40%.<sup>4</sup> Greater accuracy of agreement than that shown in Table II cannot be expected owing to the difficulty of obtaining truly representative fields of slip bands with the small field of view of the electron microscope.

Thus the experimental evidence is that the geometry

TABLE II.—Variation of Number of Lamellæ per Band and the Slip-Band Spacing with Deformation Temperature.

Temperature of Deformation, °C.	Approx. Distance between Neighbouring Bands, $\mu$	No. of Avalanches per Band ( $n$ )
—180	$\frac{1}{2}$ –1	1–2
20	2	3–4
250	4	5–6
500	10	About 12

of plastic deformation varies at different temperatures. First, at small values of the strain, the slip bands consist, at all temperatures, of only one slip avalanche. As the strain increases, the predominating tendency is to form new bands at low temperatures and new lamellæ on existing bands at higher temperatures. The effect of this on the surface appearance of the bands is shown schematically in Fig. 7.

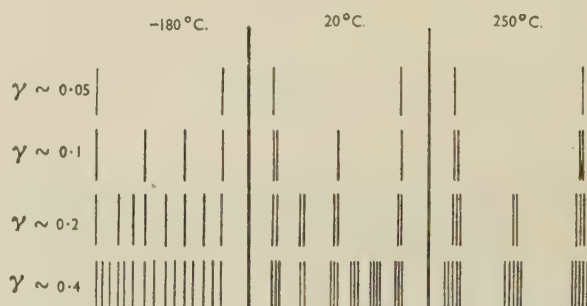


FIG. 7.—Comparison of Development of Slip Bands at Different Temperatures of Deformation.

#### 4. THE EFFECT OF VARYING THE RATE OF DEFORMATION ON THE SLIP BANDS

When the rate of deformation is reduced, the slip bands are found to be further apart so that, for a given total strain, there is more slip in each band. An extreme case is illustrated in Figs. 5 (a) and (b) (Plate XXIV): here a single crystal of aluminium has been extended at 450° C. at a constant strain rate of 1% per day. Fig. 5 (a) is a low-magnification photograph of the gross slip bands, some of which were found by differential focusing to be 10  $\mu$  in vertical height. Fig. 5 (b) shows part of the lamellar structure of one of these bands. In such conditions of high temperature and slow strain the lamellæ are no longer parallel, but the amount of slip corresponding to each is the same and is about 2000 Å. Although several days have elapsed between the formation of some of the lamellæ shown, and in spite of the high temperature, there is no evidence that more than one slip process has anywhere occurred on one slip plane.

### III.—THE RELATIONSHIP OF SLIP BANDS TO WORK-HARDENING

After plastic deformation has begun and slip bands have appeared, further increase in the strain is by means of slip processes that take place, either

on planes approximately midway between, or on planes situated very close to, the existing slip bands. Slip on other planes is unlikely, especially on those planes which have already slipped. These experimental observations are summarized in Fig. 8, which indicates what must be concluded to be the variation of hardness between two slip bands. The distance between the bands is plotted horizontally, while the vertical co-ordinate represents hardness, defined as the stress needed to force a slip process across the plane in question. The places of lowest hardness are the positions where slip has been found to be most likely to take place; the hardness there corresponds to the macroscopic hardness, since slip will occur on the softest available plane. The height of the hardness minimum corresponding to the position of fresh lamellar slip on an existing band must be comparable with that midway between the bands, since slip occurs in both positions with comparable frequency. The distance between adjacent slip bands is of the order of a hundred times the distance from a slip

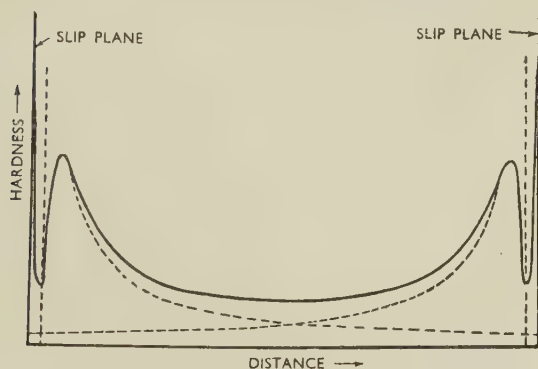


FIG. 8.—The Variation of Hardness Between Two Slip Bands.

band to the nearest plane of lamellar slip, so it is necessary, in the figure, to exaggerate the latter distance. Fig. 8 also shows the positions where slip is never observed to occur; these are the slip planes themselves and the hardness maximum on the other side of the lamellar trough. The full-line curve can be regarded as the sum of the separate hardening contributions of each of the two bounding slip zones. These latter curves are shown by dotted lines and represent the manner in which the hardening falls off with distance from the slip band. There are similar curves for the hardening on each side of every slip band.

### 1. THE REASON FOR PLANES OF EASY SLIP

The passage of a slip avalanche leaves the slip plane so disordered that slip never takes place on it again. At the same time internal stresses are set up throughout the metal which, as a result becomes harder throughout; higher stress is now required to force another slip avalanche through it. The stress required falls off with distance from the original slip plane in a manner such as is shown in Fig. 9. This

curve is of the same form as the dotted curves of Fig. 8, but without the minimum close to the slip plane. Fig. 9 is not to be regarded as a curve giving the

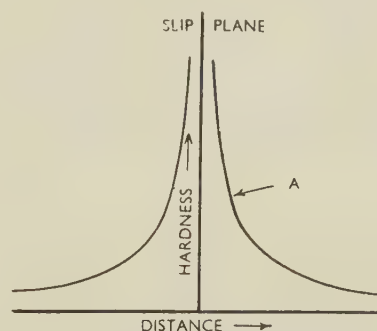


FIG. 9.—The Hardening Due to a Slip Process.

diminution of internal stress with distance from a single disordered plane, since the internal stresses that produce hardening cannot be all of one sign. On the contrary, Fig. 9 shows the diminution with distance of the hardening effect of internal stresses of rapidly varying sign produced by dislocations created during the slip avalanche but not on the apparent slip plane. It could perhaps be regarded as the envelope of the local stress peaks. The analytical shape of the curve will be discussed later.

Now experiment shows that there are planes of easy slip in positions where, as a result of the slip process, there should be the very high hardening stresses indicated in Fig. 9. By some process, therefore, the hardest parts must be softened. The means by which this occurs may be self-annealing, as discussed by Paterson and Orowan<sup>6</sup>; as soon as the internal stresses reach a critical magnitude, depending on the temperature, self-annealing would lead to softening. If this critical value corresponds to the point A (Fig. 9), then self-annealing would be expected to result in a hardness curve of the form shown in Fig. 10, in which the former slip plane has now become a

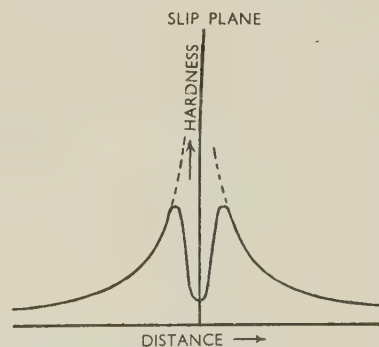


FIG. 10.—The Effect of Self-Annealing on Hardness Curve.

plane of relatively easy slip. However, experiment shows that the slip plane itself does not become a plane of easy slip, and the result of the softening



process is represented by the curve of Fig. 11. The hardness corresponding to the two troughs in this curve is comparable with the hardness midway between the bands. The amount of hardness remaining on the slip plane is not indicated; no more is known about it than that it is enough to prevent any further slip there. A curve of the form shown in Fig. 11 represents, then, the hardening effect of each separate slip band. The combined hardening

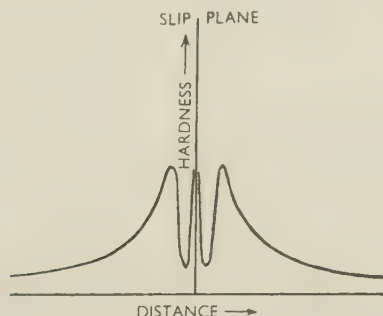


FIG. 11.—The Effect of Self-Annealing on Hardness Curve When the Slip Plane Remains Hard.

effect of two adjacent slip bands is thus obtained by summing the ordinates of two such curves, with their origins spaced apart by the inter-band distance. The result is the full curve shown in Fig. 8.

If each new slip process causes a hardening effect such as is represented by the curve of Fig. 11, then a new slip process occurring in the central trough of Fig. 8 will produce the result shown in Fig. 12. The addition of the new hardening results in a rise of the inter-band trough, and it becomes unlikely that a further new band can be formed until all the soft spots, close to the slip bands, are used up. A slip process, which occurs on one of these soft spots, has the same hardening effect on its own slip plane as a slip process which forms a new band. Its effect on the macroscopic hardness is different, however, since the metal on each side of it has reached limiting hardness and cannot be hardened further. The result is that the trough in which the slip occurred is wiped out, and there is no effect outside this trough. Thus the macroscopic hardness is unaltered, except by the circumstance that the elimination of one soft spot reduces the probability that further slip can find a spot of comparable hardness. The trough may, of course, be re-formed by further self-annealing.

The critical stress for self-annealing depends on temperature. At high temperatures the hardening due to a slip process readily reaches the critical value and then slip within existing bands is frequent. At the temperature of liquid air, however, self-annealing must be almost negligible. This is in agreement with the observation that at this temperature slip rarely takes place in existing bands until plastic shear strains of the order of 40% are reached.

As the strain increases each new slip process adds to the general hardening of the metal. Thus, at higher strains, it is more likely that the stresses produced by

a slip process, added to the higher general stresses, will be sufficient for self-annealing. Slip within existing bands, therefore, becomes more frequent as the strain becomes greater.

The contribution of a slip process to the macroscopic hardening will not vary greatly with the temperature of deformation. For slip takes place by avalanches occurring on the slip plane in a very brief space of time; the slip distance is limited by disordering which stops the avalanche. Since, as was shown above, the slip distance does not vary greatly with temperature, the hardening cannot vary greatly with temperature. That is, the curve in Fig. 9 is similar at all temperatures. At sufficiently high temperatures the hardening represented by this curve is modified, in the vicinity of the slip plane, by the self-annealing processes discussed above. In the region midway between slip bands, however, the hardness will be unaffected by self-annealing, since the stresses there are far below the critical value. It is the hardness in this region which determines the macroscopic hardness, for it must be assumed that slip will always take place on the softest plane.

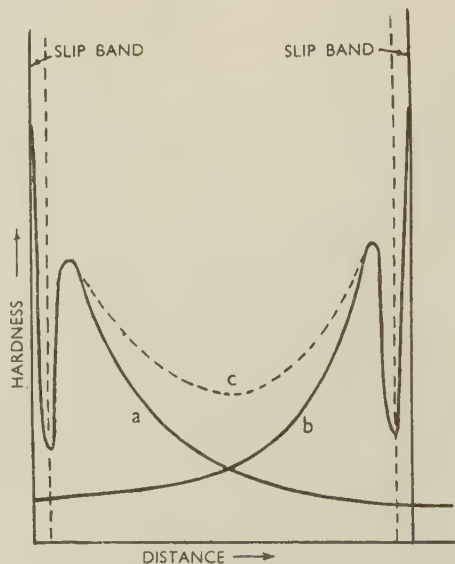


FIG. 12.—The Hardening Effect of a New Slip Band.

Curve (a): Hardness produced by slip band on left.  
Curve (b): Hardness produced by slip band on right.  
Curve (c): Combined effect of (a) and (b).

Similarly, since the slip distance is independent of strain, the effect of a slip process on the macroscopic hardness is also independent of strain.

## 2. THE RELATIONSHIP BETWEEN THE APPEARANCE OF THE SLIP BANDS AND THE SHAPE OF THE STRESS/STRAIN CURVE

The stress/strain curve is the macroscopic expression of the effect of the microscopic slip processes on the mechanical properties of the metal. Thus, if it is correct that the hardening effect of a slip process which forms a new slip band is much greater than that

of a similar slip process occurring within an already existing band, then there ought to be a close correlation between the density of slip bands and the amount of hardening. Moreover, since the hardening effect of a slip process does not vary greatly with the temperature of deformation, it may be expected that the differences observed between stress/strain curves corresponding to different temperatures must be related to the observed differences in the way these slip processes are grouped into bands.

The initial parts of the plastic stress/strain curve follow on without change of slope from the elastic region, and so are found to be <sup>7</sup> of similar gradient at all temperatures (cf. Fig. 14). Correspondingly, the slip bands resulting from small strains are similar at all temperatures, and consist of a single slip process (Fig. 7). As the strain is increased, differences appear between stress/strain curves measured at different temperatures. At the same time, the corresponding distributions of slip bands begin to differ; slip on existing bands is more common at high temperatures than at low. The differences in disposition of slip processes at various temperatures are shown for various values of the strain in Fig. 7; at the strain corresponding to the lowest line, for example, (about 40%) the specimen deformed at  $-180^{\circ}\text{C}$ . has developed more slip bands than that deformed at room temperature and many more than that deformed at  $250^{\circ}\text{C}$ . Reference to published families of stress/strain curves <sup>7</sup> (cf. Fig. 14) shows that the hardening is greatest for the specimen deformed at  $-180^{\circ}\text{C}$ . and least for the one deformed at  $250^{\circ}\text{C}$ .

Thus there is a qualitative correlation between the density of slip bands and the amount of work-hardening. Closely spaced bands, with little total slip in each, are associated with great hardening, while widely spaced bands with many slip processes in each correspond to little hardening. A quantitative correlation between hardening and the density of slip bands is provided by the relation already quoted which Yamaguchi <sup>1</sup> obtained for aluminium deformed at room temperature :

$$\tau - \tau_0 = kN$$

The simplest interpretation of Yamaguchi's equation is that work-hardening is a property solely of the density of slip bands, not of the amount of slip in each. Thus the contribution to the macroscopic hardness is made by the first slip process in a band. Subsequent slip processes, occurring on planes within the band which have recovered, do not contribute at all. Thus when slip occurs within an existing band, the strain increases without any corresponding increase in stress.

This circumstance provides a qualitative explanation of the curvature of the plastic stress/strain curve; at all strains a given stress increase produces the same number of new slip bands, but as the strain increases the amount of slip on existing bands increases relative to the amount of slip forming new bands. Hence the strain produced by a given increase of stress increases progressively with strain. The curvature of the stress/

strain curve is greater in proportion as the strain is produced by slip within existing bands rather than by formation of new bands. As shown above, this tendency increases as the temperature of deformation is increased, and consequently the curvature of the stress/strain curve becomes more pronounced with increasing temperature. In the next section it is shown how, on the basis of this interpretation of Yamaguchi's relation, an equation can be found for the stress/strain curve.

### 3. ANALYTICAL FORM OF THE STRESS DISTRIBUTION AROUND A SLIP BAND

If the hardness of a metal increases by the mechanism illustrated in Fig. 12, it is possible to obtain an equation for the empirical curves in the figure valid at places not too close to slip bands. Yamaguchi's result, that a doubling of the number of bands results in a doubling of the hardness, requires that the hardening due to a slip process falls off approximately reciprocally with distance from the slip plane. The hardening effect must be appreciable at distances of the order of the band spacing, i.e. several microns.

### IV.—AN EQUATION FOR THE STRESS/STRAIN CURVE

Consider a metal crystal of height 1 mm. measured normal to the slip planes and apply to it a steadily increasing shear stress until the first slip band appears. The stress required is the critical shear stress,  $\tau_0$ . The resulting strain is made up, partly of a strain,  $\gamma_0$ , corresponding to the first slip process in the band and partly of the strain corresponding to subsequent slip processes within the band. If the latter contribution to the strain is denoted by  $\gamma_0 f_0$  then :

$$\gamma = \gamma_0 + \gamma_0 f_0$$

At low temperatures  $f_0 = 0$ .

At this point in the deformation, the stress ( $\tau_1$ ) to produce a second slip band is given by Yamaguchi's relation :

$$\tau_1 - \tau_0 = k$$

The strain increase is again made up of two components :  $\gamma_0$ , corresponding to the slip process forming the second slip band, and  $\gamma_0 f_1$ , corresponding to subsequent slip processes which occur on the two slip bands at stress  $\tau_1$ . Proceeding thus, by increasing the stress at each stage just sufficiently to produce one more slip band and observing the resulting strain at each stage, after  $N$  slip bands have been formed the stress is :

$$\tau_N - \tau_0 = Nk \quad . \quad . \quad . \quad (2)$$

while the strain is :

$$\gamma_N = \gamma_0 \left( N + \sum_{r=0}^N f_r \right) \quad . \quad . \quad . \quad (3)$$

Equations (2) and (3) are the equations of the stress/strain curve.  $k$  is found by experiment and  $\gamma_0$  is the



shear strain corresponding to one slip process of distance  $s$  per mm. That is, if  $s$  is measured in Angstrom units:

$$\gamma_0 = s \times 10^{-7} \quad (4)$$

and with  $s = 2000 \text{ \AA.}$ :

$$\gamma_0 = 2 \times 10^{-4}$$

The first term in equation (3) gives the contribution of the bands, while the  $\Sigma$  term gives the contribution of the second and subsequent slip processes in each band. The function  $f$  is a measure of the relative importance of the two slip mechanisms.

With sufficient accuracy, the sum in equation (3) can be replaced by an integral, which gives the following strain equation:

$$\gamma_N = \gamma_0 \left( N + \int_0^N f(x) dx \right) \quad (5)$$

In the absence of theory,  $f$  is available to fit Yamaguchi's results to the equations; if  $f(x)$  is taken to be  $\beta x^m$ , where  $\beta$  and  $m$  are constants at a given temperature, equation (4) is integrable, giving (substituting for  $\gamma_0$ ):

$$\gamma_N = s \times 10^{-7} (N + \alpha N^{m+1}) \quad (6)$$

In Fig. 13 this curve is plotted with  $s = 2000 \text{ \AA.}$ ,  $\alpha = 1.6 \times 10^{-6}$ , and  $m = 2.25$ . Superposed on the

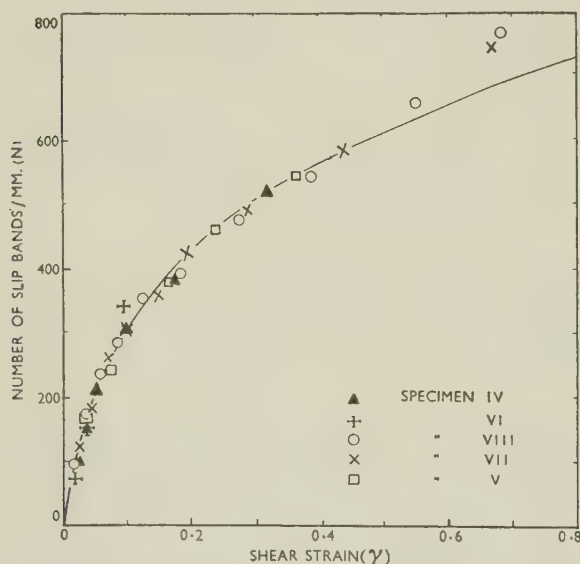


FIG. 13.—Comparison Between Yamaguchi's Results and Equation (6).

curve are the values measured by Yamaguchi for five specimens: his results for the specimens he numbered iv, vi, and viii are plotted directly and fit equation (6) well. In the case of specimens v and vii his results do not fit the equation with  $s = 2000 \text{ \AA.}$ , but fit it well if  $s$  is taken to be  $850 \text{ \AA.}$  for specimen v and  $1500 \text{ \AA.}$  for specimen vii. In order to show all five specimens fitting the same curve, Yamaguchi's

measurements of strain for specimens v and vii have been multiplied by  $2000/850$  and  $2000/1500$  respectively, and the values thus obtained plotted in Fig. 13. Values of  $s$  used in fitting Fig. 13 are given in Table III; the range of  $s$  required is comparable with the limits found for the avalanche distance in aluminium of different purities. For comparison Table III also gives values of  $k$  recalculated from Yamaguchi's results.

TABLE III.—Comparison of Avalanche Distance ( $s$ ) and the Rate of Hardening ( $k$ ).

Specimen No.	$s$ , $\text{\AA.}$	$k$ , $\text{kg./mm.}^2$
iv, vi, viii	2000	$5.0 \times 10^{-3}$
vii	1500	$4.8 \times 10^{-3}$
v	850	$4.0 \times 10^{-3}$

If the assumption that the differences between Yamaguchi's specimens lie in differences of unit slip distance is correct, then the table shows that the rate of hardening ( $k$ ) as a function of  $N$  is not very dependent on the slip distance, but that shorter slip distances are apparently associated with slightly less hardening. If slip occurs by means of avalanches, this result implies that, as the avalanche passes over the slip plane it produces work-hardening; the avalanche is stopped, not when it has produced a definite amount of slip but when it has produced a fairly definite amount of hardening.

#### 1. STRESS/STRAIN CURVES AT DIFFERENT TEMPERATURES

Fig. 14 illustrates graphically the mechanism just discussed. The steeply sloping parts of the curve marked "20° C." show the hardening effect of the formation of successive slip bands, while the parts drawn horizontally show the effects of the addition of subsequent slip processes to these bands. Since the relative probability of slip within a band as opposed to the formation of new bands increases with strain, the horizontal portions become longer as the strain becomes greater. The result of this construction is the stepped curve indicated, which in the limit of small steps becomes the observed stress/strain curve shown dotted.<sup>7</sup>

Now it is known<sup>4</sup> that, for a given strain, there are more lamellae in fewer zones at higher temperatures of deformation. Therefore, the horizontal portions of the curves corresponding to deformation at  $250^\circ$  and  $-180^\circ \text{ C.}$  are to be drawn longer and shorter respectively than the corresponding lines for room-temperature deformation. The results are, again in the limit, the steeply rising curve of liquid-air deformation ( $-180^\circ \text{ C.}$ ) and the curve, at first steeply rising but rapidly becoming almost horizontal, of deformation at high temperatures ( $250^\circ \text{ C.}$ ).<sup>7</sup>

Since, as was shown in Section III, the work-hardening in the absence of recovery is not very different at different temperatures, the sloping parts

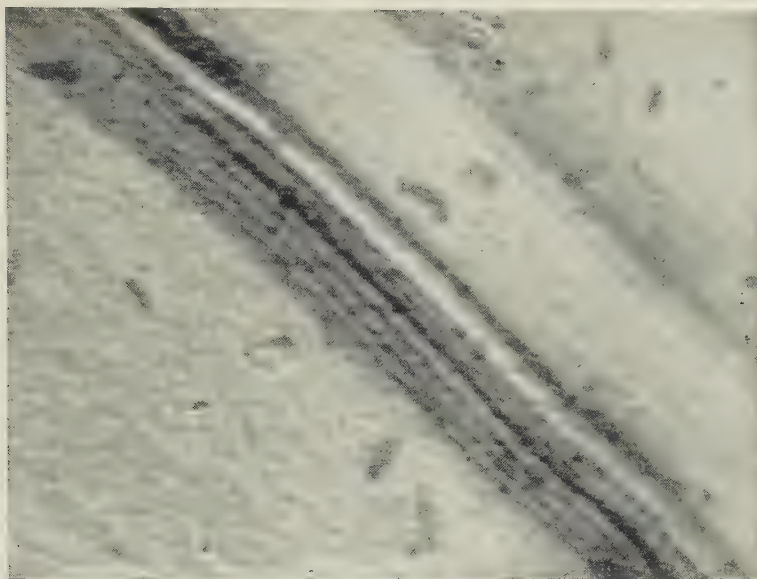


FIG. 4.—Slip Band on (100) Face of a Pure Aluminium Crystal. Approx. 70% shear strain. Aluminium oxide replica shadowed with gold-palladium.  $\times 25,000$ .

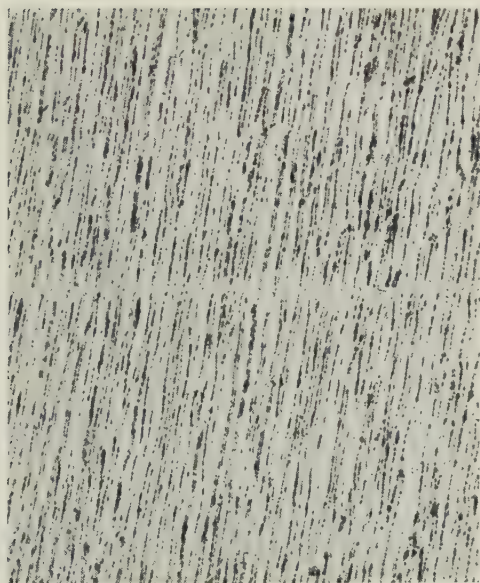


FIG. 5 (a).—Coarse Slip Bands on an Aluminium Single Crystal Extended at  $450^{\circ}\text{C}$ . at a Constant Strain Rate of 1% per Day. Total strain about 15%.  $\times 6$ .



FIG. 5 (b).—Part of the Lamellar Structure of One of the Slip Bands Shown in Fig. 5 (a). Aluminium oxide replica shadowed with gold-palladium.  $\times 25,000$ .





of the curves at all temperatures have been drawn of equal gradient; this implies that the differences between measured stress/strain curves at different

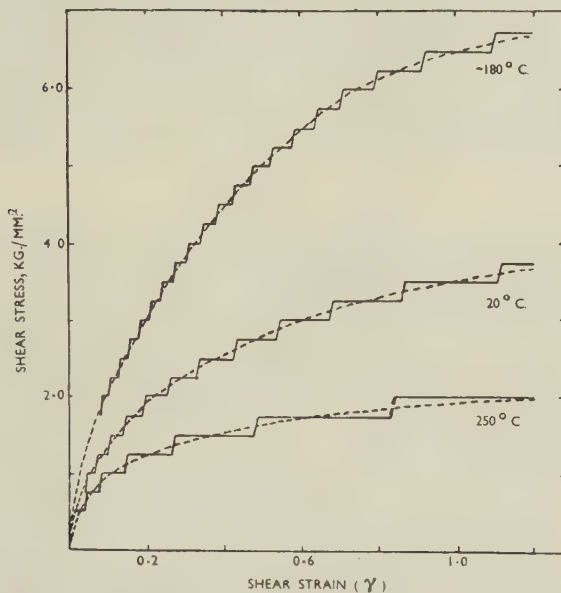


FIG. 14.—Stress/Strain Curves for Aluminium at Different Temperatures. Broken-line curves from Boas and Schmid.<sup>7</sup>

temperatures are almost entirely due to the mechanism of self-annealing discussed above.

## 2. DERIVATION OF THE FUNCTION $f$ FROM ORDINARY STRESS/STRAIN CURVES

By constructing stepped stress/strain curves to fit measured curves, it is possible to obtain information about the form of the function  $f$  without counting slip bands. Thus in the stepped stress/strain curve, the form of which is given by equation (3), the sloping parts are described by the first term on the right and the horizontal parts by the second. As drawn in Fig. 14, each sloping part represents the formation, not of one new slip band, as was the case in the analysis above, but of some 50 bands. The analysis is unchanged, but  $\gamma_0$  now represents the strain corresponding to that number of bands per mm. The length  $l(r)$  of the  $r$ -th horizontal part is, from equation (3):

$$l(r) = f(r) \gamma_0 \quad (7)$$

and if  $f(r)$  is taken to be of the form  $\beta r^m$  as before, this equation can be written, taking logarithms:

$$\log l(r) = m \log r + \log (\beta \gamma_0) \quad (8)$$

Hence the slope of a plot of  $\log r$  against  $\log l(r)$  gives  $m$ .

This method has been applied to the dotted curves of Fig. 14, which are stress/strain curves for aluminium obtained by Boas and Schmid.<sup>7</sup> The results obtained are shown in Table IV.

The agreement at 20° C. is rather lucky, since the curves obtained by Boas and Schmid are mean

TABLE IV.—Determinations of  $m$  by Equation (8) and by Yamaguchi.

Temp., °C.	$m$ (from equation (8))	$m$ (from Yamaguchi)
-180	1.3	...
20	2.3	2.25
250	3.7	...

values (though with only small scatter) from some ten specimens. Moreover, there is no evidence that their specimens were of purity comparable with Yamaguchi's.

## VI.—THE EQUATION OF STATE FOR PLASTIC DEFORMATION

The existence of a mechanical equation of state implies that work-hardening is a unique function of the strain ( $\gamma$ ), the strain rate ( $\dot{\gamma}$ ), and the temperature ( $T$ ), i.e.

$$\tau - \tau_0 = f(\gamma, \dot{\gamma}, T)$$

Thus, a metal deformed along the room-temperature curve of Fig. 15 (a) to the point  $A$  and then cooled to liquid-air temperature would continue to deform from  $B$  along the liquid-air-temperature curve and vice versa. Similarly, if an equation of state exists, it should be possible to pass from a high-speed test to a slow-speed test and vice versa by a path such as  $AB$  (Fig. 15 (b)).

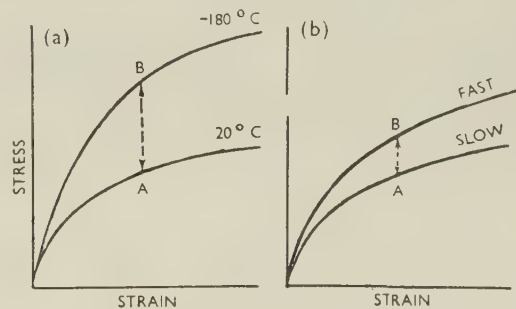


FIG. 15.—Transitions Between Stress/Strain Curves (a) at Different Temperatures, and (b) at Different Strain Rates, with Equation of State.

To see what, in fact, happens, consider two specimens both strained by the same amount, one at liquid-air temperature and the other at 20° C. The former has many more slip bands than the latter. If it is warmed up to 20° C., the stresses on the slip bands will be sufficient for self-annealing, giving rise to many more planes of easy slip than are available to the specimen deformed at 20° C. At the same time the stress to restart deformation will fall, say to the point  $B$  (Fig. 16 (b)). Then the metal, having a greater number of soft planes than correspond to its strain and temperature, deforms along an almost horizontal, i.e. non-hardening, curve until the surplus soft planes are used up. Thereafter its deformation follows the 20° C. curve.



Again, if the specimen deformed at 20° C. is cooled to liquid-air temperature, the stress to restart deformation is raised, say to the point *B* (Fig. 16 (a)). The metal has then many less slip bands than correspond to its strain and temperature. There will be available a few soft planes resulting from the last stages of

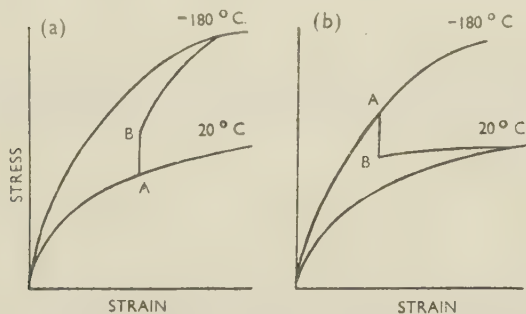


FIG. 16.—Transitions Between Stress/Strain Curves at Different Temperatures, with no Equation of State.

- (a) Transition from 20° C. curve to -180° C. curve.  
(b) Transition from -180° C. curve to 20° C. curve.

deformation at 20° C., but when these are used up they will not be replaced. Since the slip bands are far apart, the easiest sites for slip are then the planes midway between bands, and it is on these that new slip processes will occur predominantly. The result of this extra rapid formation of new bands is the steeply rising stress/strain curve shown in Fig. 16 (a). This curve will be followed until it intersects the curve of deformation at liquid-air temperature.

Transitions between stress/strain curves at different temperatures have been studied experimentally by Łoś.<sup>8</sup> The curves he obtained were of the form described above. Since the rate of band formation is also a function of strain rate, transitions between

stress/strain curves corresponding to different rates of strain are of similar form. Thus, when a substantial proportion of plastic strain takes place by slip on existing bands, i.e. by slip on planes which have softened during deformation of the specimen, a true equation of state cannot exist. On the other hand, at strains so small that the bands consist of only a single slip process at all temperatures, direct transitions like those shown in Fig. 15 may take place between stress/strain curves.

#### ACKNOWLEDGEMENTS

The author wishes to thank Professor Sir Lawrence Bragg, F.R.S., Dr. E. Orowan, F.R.S., and Dr. V. E. Cosslett for helpful discussions. It is also a pleasure to acknowledge the co-operation of Mr. R. W. Horne, assistant in research in electron microscopy at the Cavendish Laboratory. The work was carried out while the author was D.S.I.R. Senior Student and latterly I.C.I. Fellow.

#### REFERENCES

1. K. Yamaguchi, *Sci. Papers Inst. Phys. Chem. Research (Tokyo)*, 1928, **8**, 289.
2. F. D. Rosi and C. H. Mathewson, *Trans. Amer. Inst. Min. Met. Eng.*, 1950, **188**, 1159.
3. R. D. Heidenreich and W. Shockley, *J. Appl. Physics*, 1947, **18**, 1029.
4. A. F. Brown, *Metallurgical Applications of the Electron Microscope (Inst. Metals Monograph No. 8)*, 1950, 103; also *Nature*, 1949, **163**, 961.
5. A. F. Brown, *Compt. rend. 1<sup>er</sup> Congr. Internat. Microscopie Electronique, Paris*, 1950.
6. M. S. Paterson and E. Orowan, *Nature*, 1948, **162**, 991.
7. W. Boas and E. Schmid, *Z. Physik*, 1931, **71**, 703.
8. J. Łoś, *Abs. Dissert. Univ. Cambridge*, 1947-48, 124; see also E. Orowan, *J. West Scotland Iron Steel Inst.*, 1946-47, **54**, 45.

# EXPERIMENTS ON THE REACTION OF ALUMINIUM-MAGNESIUM ALLOYS WITH STEAM\*

1332

By A. J. SWAIN,† M.A., JUNIOR MEMBER

(Communication from the British Non-Ferrous Metals Research Association.)

## SYNOPSIS

The reaction of aluminium-magnesium alloys containing up to 25% magnesium with pure steam has been investigated over a range of temperatures from 450° to 700° C. A maximum reactivity, dependent on the composition, was found at temperatures between 550° and 625° C. The significance of these results in relation to metal/mould reaction in the aluminium-10% magnesium alloy is discussed briefly.

## I.—INTRODUCTION

CALCULATIONS indicate that when a metal is cast into a green-sand mould the water in the sand is almost immediately volatilized in sufficient quantity to sweep out practically all the air from the pores in the mould near the metal surface, so that the casting in effect solidifies in an atmosphere of practically 100% steam. The time for which the metal remains above the solidus temperature is likely to be of the order of 10 min. for a casting about 2 in. thick in an aluminium alloy of wide freezing range, and correspondingly longer for a larger casting.<sup>1</sup> When the metal contains a readily oxidized element, the latter may react with the steam during solidification to form oxide and hydrogen. This reaction, commonly known as metal/mould reaction, is prevalent in sand castings of aluminium-10% magnesium alloy, and the work described in the present paper is part of an investigation on metal/mould reaction in this alloy.

It is convenient to distinguish between "internal" hydrogen, which is absorbed by the metal and may give rise to porosity or disruption, and "external" hydrogen, which is released to the atmosphere. For an aluminium-7% magnesium<sup>2</sup> alloy reacting with water vapour at 16 mm. pressure at approximately 600° C., between the solidus and liquidus temperatures, the external hydrogen was much the greater, representing about 98% of the total hydrogen formed in the reaction. Thus the external hydrogen, although not so important in some respects as the internal hydrogen, is a convenient approximate measure of the total extent of the reaction. In these experiments, therefore, various alloys have been allowed to react with pure steam at temperatures between 450° and 700° C., and the external hydrogen collected and measured during the first 15 min.

Alloys with 1-25% magnesium have been studied. Although alloys containing more than 10% magnesium are not normally used in casting, they have been

included to investigate the effect of magnesium enrichment of the liquid phase in partially molten alloys. The use of small additions of beryllium to inhibit metal/mould reaction has been suggested, and preliminary experiments on such alloys have been carried out.

## II.—EXPERIMENTAL WORK

### 1. METHOD

The apparatus used is shown diagrammatically in Fig. 1. For some experiments with the alloys of higher magnesium content, a subsidiary, uncooled, collecting system of 900 c.c. capacity was used. Specimens used in the solid or partially molten state were cylinders 1 cm. dia. and 1 cm. long, with an axial hole of 1.5 mm. dia. drilled for half the length, so that the hot junction of a thermocouple could be placed at their centres. They were machined dry to size and degreased in acetone. Specimens used in the molten state were shaped to fit the boat by filing and were arranged so that the hot junction of the thermocouple was immersed when the specimen melted. The boats used with completely molten specimens were normally of such a size that the exposed surface area was approximately equal to that of the partially molten specimens. For alloys containing more than 20% magnesium the oxidized nickel boat, shown in Fig. 1, was replaced by one of fused alumina.

To ensure rapid response to temperature changes in the specimen, the hot junction of the thermocouple (28-gauge Chromel/Alumel) was insulated only by a thin coat of an aluminous cement. In operation, the apparatus was set up with the specimen *in situ*, and the reaction tube was swept out with purified argon, which was not collected. The temperature was then raised and when it was steady at the desired value the argon flow was stopped and steam substituted by closing clip 1 and opening clip 2 (Fig. 1). Approximately 20 sec. after admitting steam the collection

\* Manuscript received 8 February 1951. The work described in this paper was made available to members of the British Non-Ferrous Metals Research Association in a confidential research report issued in June 1949.

† Technical Liaison Section, Aluminium Wire and Cable Co., Ltd., Swansea; formerly Investigator, British Non-Ferrous Metals Research Association, London.



of gas in the burette was started, and readings taken at 1-min. intervals up to 15 min. The principal difficulty was in the control of temperature, since much heat is evolved in the reaction. By hand regulation of the furnace current, the temperature of the specimen was maintained constant to  $\pm 8^\circ \text{C}$ . for alloys with

to the hydrogen collected generally accounted for about 90% of the weight change.

The time lag between the evolution of hydrogen and its appearance in the burette was presumably less than 15 sec., since this time was sufficient to displace completely the argon initially present.

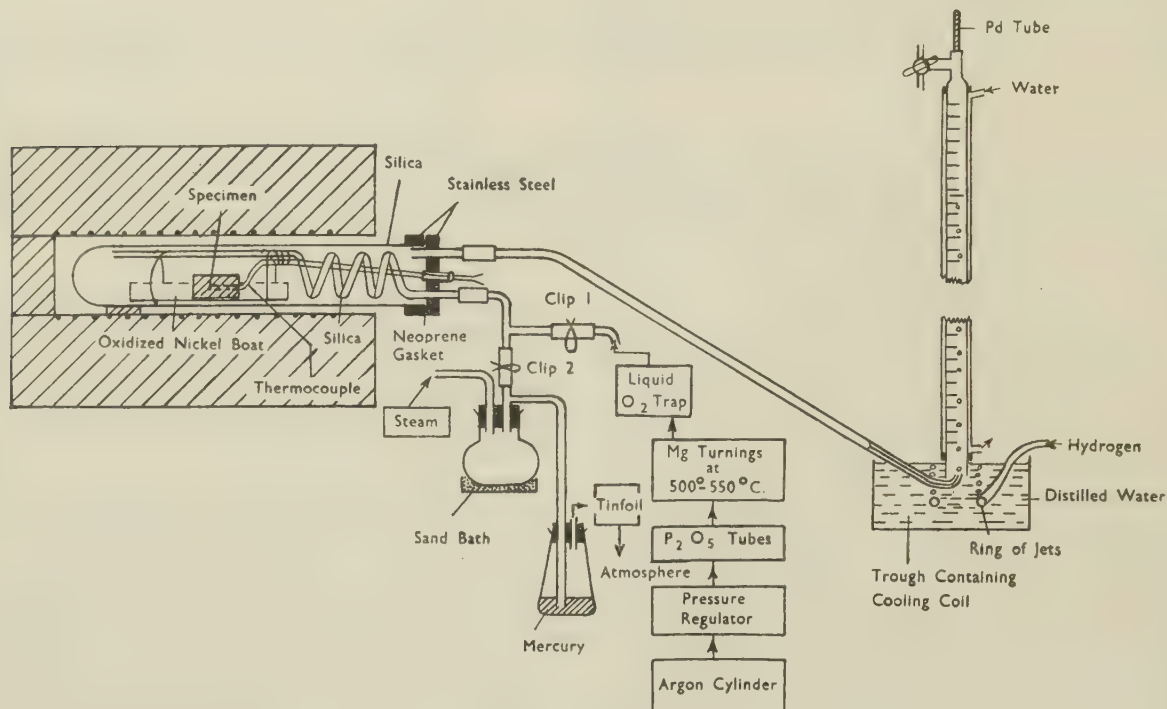


FIG. 1.—Diagram of Apparatus. A stainless steel flange is attached to the reaction tube, and various tubes are led through the end-plate, by compression joints with Neoprene washers.

less than 15% magnesium, and to  $\pm 15^\circ \text{C}$ . for alloys of higher magnesium content.

Preliminary experiments indicated that:

(a) Little or no oxidation of the specimen occurred during the heating up.

(b) No significant quantity of argon was collected in the burette.

(c) The blank, probably owing to the evolution of dissolved gases in the water in the collecting system, was substantially constant at 0.6(7) c.c. at  $15^\circ \text{C}$ . in 15 min. and was proportional to the time.

The palladium tube on the burette enabled a check to be made on the identity of the evolved gas. The percentage of gases other than hydrogen varied from about 2% for the largest quantities of hydrogen recorded in Table I to something approaching 10% for the smallest. It seems likely that this gas originated in the water in the burette. In the figures given in the table these gases have been included in the hydrogen figure. The total hydrogen collected during the time at temperature and subsequent cooling was, in many experiments, checked against increase in weight of the specimen, and the oxidation equivalent

## 2. MATERIALS

The alloys were made from aluminium and magnesium both of 99.99% purity. The melts were made in salamander crucibles and degassed with chlorine before casting. The alloys containing up to 18.25% magnesium were sand cast (2% boric acid in sand) in the form of D.T.D. bars (6 in. long and 1 in. dia. with a feeder head  $2\frac{1}{4}$  in. long by  $2\frac{1}{2}$  in. dia.); those of higher magnesium content were cast in a 1-in.-dia. iron chill mould. The bars were cut into four sections longitudinally, and the specimens were machined or filed from these sections.

The compositions given in Table I were obtained by chemical analysis.

## III.—RESULTS AND DISCUSSION

Figs. 2, 3, and 4 show the progress of the reaction for a number of the experiments. No allowance has been made for the blank.

Table I gives the quantities of hydrogen collected in 15 min., with due allowance for the blank, expressed as c.c. at N.T.P./100 g., and also as c.c. at N.T.P./unit surface area. The latter values have been calculated on the original surface area. In certain heavily

oxidized specimens considerable exudation had occurred.

The table also gives, where it is relevant, the

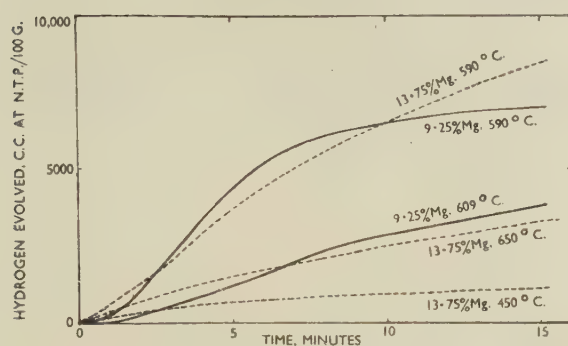


FIG. 2.—Progress of the Reaction for 9.25% and 13.75% Magnesium Alloys.

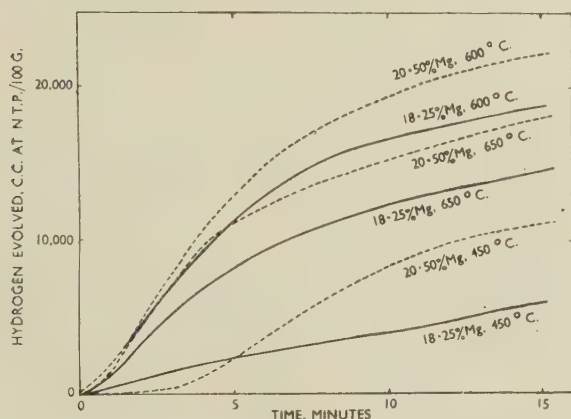


FIG. 3.—Progress of the Reaction for 18.25% and 20.50% Magnesium Alloys.

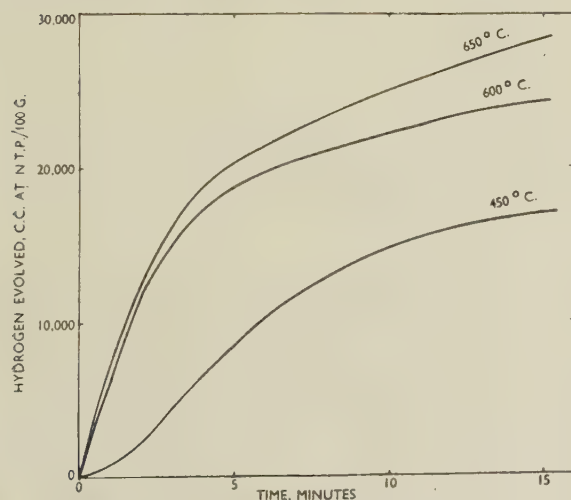


FIG. 4.—Progress of the Reaction for 24.75% Magnesium Alloy.

figure obtained by dividing the volume at N.T.P./unit area by the fraction of the alloy molten. This gives some basis for comparison between different alloy compositions at the same temperature. The maxi-

TABLE I.—Summary of Experimental Results.

Compn., % Mg	Temp., °C.	Fraction of Alloy Molten, %	Compn. of Liquid, % Mg	Hydrogen Collected in 15 min.			Max. Re- action Rate, c.c. at N.T.P./ g./min.
				c.c. at N.T.P./ 100 g.	c.c. at N.T.P./ cm. <sup>2</sup>	c.c. at N.T.P./ cm. <sup>2</sup> ÷ fraction molten	
0.75	652	50	2.0	93	0.3	0.6	...
	675	100	...	77	0.3	0.6	...
4.80	675	100	...	12	0.2	...	...
	550	0	...	0	0	...	...
	570	0	...	143	0.5	...	...
	590	0	...	1,150	3.2	...	1.5
	590	0	...	910	2.4	...	1.1
	609	12	11.2	830	3.2	26.6	0.8 (6)
	609	12	11.2	870	3.4	28.3	0.8 (6)
	613	18	10.5	620	2.4	13.3	0.7 (0)
	613	18	10.5	410	1.6	8.9	0.6 (0)
	628	46	7.5	70	0.3	0.65	...
	628	46	7.5	40	0.2	0.45	...
	650	100	...	5	0.1	...	...
	650	100	...	9	0.1	...	...
	675	100	...	21	0.3	...	...
	675	100	...	28	0.4	...	...
9.25	450	0	...	65	0.25	...	...
	450	0	...	128	0.37	...	...
	500	0	...	179	0.7	...	...
	500	0	...	153	0.6	...	...
	560	16	20	1,100	4.5	28.0	2.5
	560	16	20	1,300	4.7	29.4	2.9
	590	42.5	15.0	7,020	23.8	56.0	11.1
	590	42.5	15.0	6,430	22.8	53.3	9.0
	609	73	11.2	3,840	13.2	18.1	3.6
	609	73	11.2	4,000	15.8	21.6	3.1
	625	100	...	530	7.2	...	0.4 (6)
	625	100	...	460	5.6	...	0.4 (6)
13.75	650	100	...	180	2.5	...	...
	650	100	...	172	2.7	...	...
	675	100	...	60	1.0	...	...
	675	100	...	40	0.7	...	...
	700	100	...	27	0.05	...	...
	700	100	...	22	0.3	...	...
	450	0	...	810	3.07	...	0.8
	450	0	...	1,105	4.07	...	1.4
	500	11.5	28.8	2,410	8.68	75.3	3.7
	500	11.5	28.8	2,425	8.13	70.8	2.6
	545 †	38.0	22.2	11,800	41.2	108.5	23.4
	545 †	38.0	22.2	9,100	26.3	72.8	21.8
18.25	590	90	15.0	8,370	65.6	105.0	7.3
	590	90	15.0	9,520	94.7	...	8.7
	625	100	...	6,390	63.3	...	6.2
	625	100	...	6,790	73.2	...	6.8
	650 †	100	...	3,400	60.0	...	...
	650 †	100	...	3,230	32.0	...	4.4
	675 †	100	...	1,200	19.0	...	...
	675 †	100	...	770	7.8	...	0.5
	700	100	...	224	2.20	...	0.36
	700	100	...	231	2.20	...	0.37
	450	14.0	35.0	4,820	16.9	121.0	3.1
	450	14.0	35.0	5,840	18.2	130.0	5.5
20.50	500	37.5	28.8	11,400	33.5	89.2	17.6
	500	37.5	28.8	10,100	29.4	78.2	14.6
	560	86.5	20	17,600	219.0	242.0	17.6
	560	86.5	20	17,400	220.0	243.0	21.3
	600	100	...	17,890	136.2	...	26.5
	600	100	...	18,750	152.0	...	23.4
	625 †	100	...	15,750	76.5	...	25.2
	625 †	100	...	16,150	141.0	...	22.7
	650	100	...	14,450	170.0	...	21.7
	650	100	...	15,250	170.5	...	...
	675	100	...	9,790	101.0	...	11.8
	675	100	...	10,250	177.5	...	13.3
24.75	700	100	...	4,500	53.2	...	4.7
	700	100	...	4,210	61.8	...	4.8
	450	26.5	35.0	9,880	31.2	117.5	8.0
	450	26.5	35.0	10,950	30.0	113.0	13.7
	500	52.0	28.8	13,820	43.2	82.3	25.2
	500	52.0	28.8	14,780	47.5	91.4	34.3
	550 †	93.0	21.4	18,500	119.6	128.0	33.0
	550 †	93.0	21.4	19,550	219.0	235.0	22.5
	600	100	...	22,050	162.5	...	30.5
	600	100	...	21,000	162.0	...	38.5
	625	100	...	20,400	119.0	...	45.0
	625	100	...	20,000	111.5	...	52.5
24.75	650	100	...	17,200	91.5	...	20.7
	650	100	...	17,800	75.5	...	40.0
	675	100	...	13,850	76.7	...	23.5
	675	100	...	13,450	58.7	...	21.8
	700	100	...	7,730	75.7	...	11.4
	700	100	...	6,790	30.5	...	10.8

Continued.



TABLE I.—*continued.*

Compn., % Mg	Temp., °C.	Fraction of Alloy Molten,* %	Compn. of Liquid, % Mg	Hydrogen Collected in 15 min.			Max. Re- action Rate, c.c. at N.T.P./ g./min.
				c.c. at N.T.P./ 100 g.	c.c. at N.T.P./ cm. <sup>2</sup>	c.c. at N.T.P./ cm. <sup>2</sup> ÷ fraction molten	
24.75	450	48.0	35.0	16,250	43.6	90.9	16.0
				16,950	41.5	86.3	21.8
		76.0	28.8	20,100	34.8	133.0	50.0
				20,250	28.3	98.2	68.6
	500	100	...	22,350	171.5	...	51.8
				27,000	133.5	...	64.5
	550	100	...	27,300	121.0	...	70.3
				24,100	100.5	...	61.0
	600	100	...	26,450	150.0	...	80.0
				25,850	144.0	...	84.0
	625	100	...	28,250	182.5	...	72.0
				27,950	133.0	...	60.7
	650	100	...	27,000	175.5	...	44.5
				24,850	163.0	...	50.0
	675	100	...	25,700	129.0	...	48.6
				21,200	119.5	...	37.0

\* Calculated from Raynor's diagram.<sup>2</sup>

† The specimens used at this temperature had different volumes per unit surface area.

imum reaction rate obtained from the slope of the hydrogen-collection curves, expressed as c.c. at N.T.P./g./min., is also given.

The appearance of the specimens after reaction varied according to the extent of oxidation. Lightly oxidized specimens of low magnesium content retained their metallic appearance; others had a grey powdery surface layer of varying thickness, in some cases comprising the whole specimen. The grey powder was found by X-ray diffraction to consist of magnesium oxide and practically pure aluminium.

The weight per unit surface area for specimens which were heavily oxidized in the liquid state was deliberately varied, and good reproducibility was obtained for the figures for hydrogen collected expressed as c.c. at N.T.P./100 g., but not for the volume of hydrogen per unit surface area. This suggests that for vigorous reactions in the liquid state the oxidation penetrates rapidly into the specimen, so that the reaction is proceeding simultaneously at a number of centres, and consequently the reaction rate is independent of the original surface area with specimens of the sizes used. In fact, it has been observed that, a short time after the start of the reaction, the hydrogen boils off from the interior of the melt. The surface is thus disrupted and a new surface is constantly formed. Presumably this process results in the formation of channels throughout the metal by which further oxidation can proceed.

In some experiments the quantity of hydrogen collected exceeded that expected from complete oxidation of the magnesium present. This discrepancy can be explained by considering the hydrogen resulting from the surface oxidation of the particles of aluminium in the oxidation product, if it is assumed that they are fine and dispersed. For example, in one experiment with the 24.75% magnesium alloy, 28,250 c.c. hydrogen at N.T.P./100 g. were collected, whereas complete oxidation of the magnesium in this alloy would give 22,800 c.c. The excess hydrogen

obtained is equivalent to the formation of an alumina film 100 Å. thick on particles of aluminium approximately 2 microns in dia., assuming that the whole of the aluminium exists in this form.

Fig. 5 shows graphically the variation with temperature of the hydrogen collected in 15 min. (expressed as c.c. at N.T.P./100 g.) for each alloy. It will be seen that for each composition there is a temperature at

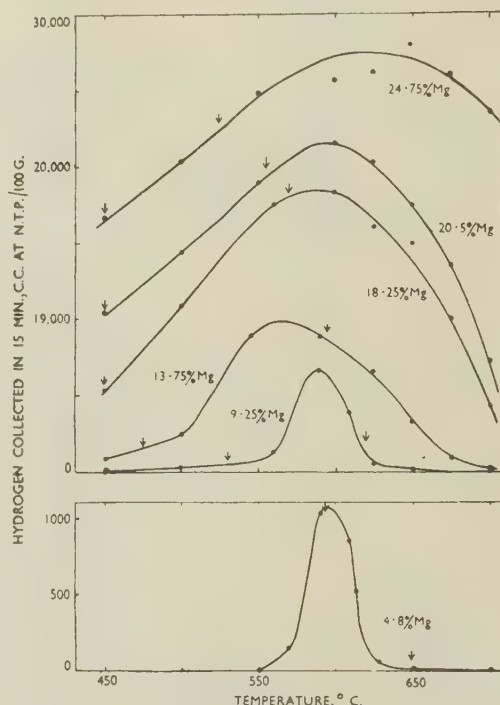


Fig. 5.—Variation of Hydrogen Collected in 15 Min. with Temperature. The arrows indicate the solidus (or eutectic) and liquidus temperatures.

which the quantity of hydrogen collected has a maximum value. For the 9.25% and 13.75% magnesium alloys this maximum lies between the solidus and liquidus temperatures, while for the higher magnesium alloys it occurs at temperatures above the liquidus.

Fig. 6 shows the variation of the maximum reaction rate with temperature for each alloy. For the 9.25% magnesium alloy there is a single maximum at 590° C. in the solidus/liquidus temperature range. With the 13.75% magnesium alloy the maximum, also in the solidus/liquidus temperature range, occurs at a lower temperature. The 18.25% magnesium alloy has a maximum at a temperature just above the liquidus. For the 20.50% and 24.75% magnesium alloys two maxima occur in each case, one within the solidus/liquidus temperature range and the second at approximately 625° C.

The solidus and liquidus temperatures indicated in Figs. 5 and 6 are the equilibrium values. In these experiments, however, the alloys may not have been

in equilibrium, and consequently the solidus temperatures quoted do not necessarily apply.

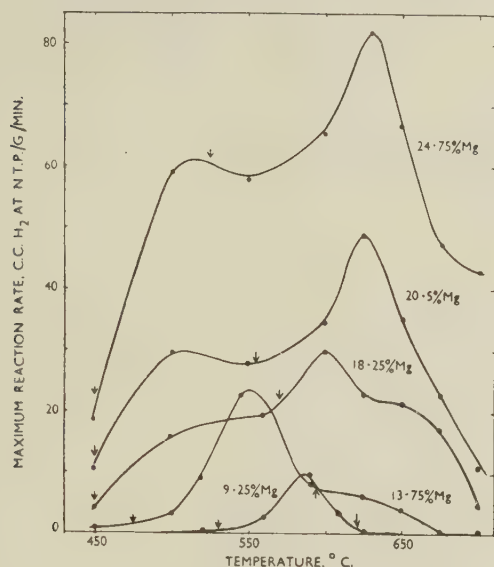


FIG. 6.—Variation of Maximum Reaction Rate with Temperature. The arrows indicate the solidus (or eutectic) and liquidus temperatures.

The maxima in the solidus/liquidus temperature range might be due to a combination of the effects of variations with temperature of the magnesium content of the liquid phase and the quantity of the latter present. For instance, it might be that for any

TABLE II.—Variation of Max. Reaction Rate/Fraction Molten with Temperature and Composition.

Temp., °C.	Composition of Alloy, % Mg	Fraction of Alloy Molten, %	Max. Reaction Rate (c.c. at N.T.P./g./min.) ÷ Fraction Molten
525	24.75	100.0	60.5
	20.50	71.5	40.6
	18.25	55.5	49.0
	13.75	25.5	32.5
555	20.50	100.0	28.0
	18.25	80.0	23.4
	13.75	47.0	48.9
	9.25	12.5	16.2
570	18.25	100.0	21.5
	13.75	62.5	28.0
	9.25	24.0	23.0
595	13.75	100.0	7.5
	9.25	48.5	15.4
620	9.25	100.0	1.0
	4.8	26.5	1.1

particular liquid composition the initial reaction rate is equal to the rate for a completely liquid specimen multiplied by the fraction of the surface which is molten, and that this fraction is equal to the volume fraction of molten metal. Table II shows, for a

number of temperatures, the maximum reaction rate divided by the fraction molten for alloys which are partially liquid at that temperature and have the same magnesium content in the liquid phase (assuming equilibrium between solid and liquid phases). The figures for each temperature vary considerably, and the assumptions made are, therefore, not correct except to a very rough approximation; the lack of agreement is probably due to the true reaction surface at the time of maximum reaction rate being different from the initial surface of the molten metal. However, it is clear from the figures for 100% liquid that the reactivity of the liquid phase in equilibrium with the solid at the temperature of test, does in fact increase as the temperature falls, owing to its increased magnesium content, in agreement with the general explanation of the maximum advanced above.

The occurrence of maxima in the curves of Fig. 6 at temperatures above the liquidus is very surprising, and no simple explanation can be advanced other than a change in the nature of the (rate-controlling) oxide films formed at these temperatures.

It has been found<sup>4</sup> that porosity caused by metal/mould reaction in the 10% magnesium alloy is confined to areas near the reacting surface. From the present results it can be seen that a large proportion of the hydrogen entering a casting of this alloy as a result of metal/mould reaction will do so at a comparatively late stage in the solidification process, namely, while the casting is partially solid, and thus would not be expected to diffuse far into the metal before being rejected from solution.

A few preliminary experiments have been carried out with a 10% magnesium alloy containing 0.025% beryllium, at temperatures between the solidus and liquidus. This alloy was made up from a 5% aluminium-beryllium hardener prepared from super-purity aluminium and commercially pure beryllium.

In all cases the quantity of hydrogen collected was of the same order as the blank value. The specimens after oxidation had a thin oxide film, which showed a bluish-green interference colour, similar to that found on inhibited castings of this alloy. Beryllium additions of 0.025% with the same hardener had been found to inhibit effectively metal/mould reaction in a 2-in.-dia. block casting of 10% magnesium alloy, so that in this instance there is agreement between the reaction rate and foundry experiments.

#### IV.—CONCLUSIONS

The reaction between aluminium-magnesium alloys and steam, as measured by the external hydrogen formed under the conditions of these experiments, reaches a maximum rate at a temperature dependent on the composition of the alloy, but within the range 550°–625° C. For the 10% magnesium alloy, which is widely used as a casting alloy, this maximum reaction rate occurs at a temperature within the solidus/liquidus range. This probably accounts for the fact that gas porosity caused by metal/mould reaction in



sand castings of this alloy occurs mainly in the surface layers of the castings.

No satisfactory explanation of these effects can be advanced at present.

#### ACKNOWLEDGEMENT

The author is indebted to the Director and Council of the British Non-Ferrous Metals Research Association for permission to publish this paper.

---

#### REFERENCES

1. R. W. Ruddle, *J. Inst. Metals*, 1950, **77**, 1.
2. R. Eborall and C. E. Ransley, *J. Inst. Metals*, 1945, **71**, 525.
3. G. V. Raynor, *Inst. Metals: Annotated Equilib. Diagr.* Series No. 5, 1945.
4. B. W. Peck, B.N.F.M.R.A., unpublished work.

# THE CREEP AND SOFTENING PROPERTIES OF COPPER FOR ALTERNATOR ROTOR WINDINGS\*

1333

By N. D. BENSON,† M.Eng., MEMBER, J. McKEOWN,‡ D.Sc.,  
MEMBER, and D. N. MENDS,§ B.Sc.

(Communication from the British Non-Ferrous Metals Research Association.)

## SYNOPSIS

The rotor windings of some large turbo-alternators are subject to longitudinal compressive stresses because of the higher coefficient of expansion of the copper relative to the steel rotor. These stresses may give rise to creep deformation and the resistance to creep of a number of high-conductivity coppers has been investigated in the temperature range 130°–225° C.

In cold-worked coppers resistance to creep may be reduced by softening occurring at the operating temperature. In consequence, the softening characteristics of high-conductivity coppers have been determined over the same temperature range.

The creep-resistance and the resistance to softening have been shown to be very much greater for silver-bearing (0.1% silver) than for silver-free, tough-pitch copper. The effect of the silver addition is such that the creep-resistance of the silver-bearing material at 225° C. is equal to that of the silver-free material at 130° C. The creep-resistance and the resistance to softening of O.F.H.C. copper are greater than those of tough-pitch copper when both are silver-free. Silver-bearing (0.1%) O.F.H.C. and tough-pitch coppers have very similar resistances to creep and softening.

In silver-bearing tough-pitch copper the resistance to creep increases with increase in the degree of cold work up to 10%. Beyond this amount there is no further increase in creep-resistance, and it is clear that maximum resistance to creep coupled with maximum resistance to softening is obtained with cold work of this degree.

## I.—INTRODUCTION

THE deformation, referred to as copper shortening, occurring in the rotor windings of some large turbo-alternators became a serious problem a few years before the Second World War. Since then, the problem has become more serious owing to the heavy power demands of war-time and post-war production and has been further aggravated by the shift working of alternators.

The generally accepted explanation of copper shortening in alternator rotor windings is given very briefly below. The subject has been discussed very thoroughly by a number of English and American authors.<sup>1-5</sup>

According to usual practice, an alternator is started up with the windings cold, and the excitation current is applied when the machine is running at speed. The effect of the centrifugal force on the windings in the rotor slot is to press them outwards against the retaining wedge and hence increase considerably, by reason of the frictional forces, the resistance to lengthwise movement. The temperature rise in the copper winding produced by the field-excitation current is

greater than that in the surrounding parts of the steel rotor, which are heated by the copper. For this reason, and also because the coefficient of expansion of copper is approximately 50% greater than that of steel, the copper will tend to expand lengthwise relative to the steel. This relative expansion is resisted by the frictional forces and as a consequence, the copper is subjected to compressive forces in the direction of its length. If the compressive stress in the copper due to these forces exceeds a certain value, plastic deformation and creep in compression will occur. This creep will be in the nature of relaxation, since, as it occurs, it will relieve the compressive stress and will progressively decrease as the stress is reduced.

The average temperature of the copper under normal running conditions would not exceed 130° C., in accordance with British Standard Specification No. 225, although some parts might approach 160° C., and under exceptional circumstances might even reach 190° C.<sup>6</sup>

The steel of the rotor may, according to Juhlin,<sup>2</sup> be as much as 50° C. lower in temperature. Assuming the copper at a temperature of 130° C., an analysis, based on elastic deformation only, shows that a stress

\* Manuscript received 29 March 1951.

† Formerly Investigator, B.N.F.M.R.A. Now Technical Officer, Imperial Chemical Industries Ltd., Metals Division, Birmingham.

‡ Head of Mechanical Testing Section, British Non-Ferrous Metals Research Association, London.

§ Formerly Investigator, British Non-Ferrous Metals Research Association, London.



as high as 17,500 lb./in.<sup>2</sup> may be induced in the copper. More recently, Horsley and Coates<sup>5</sup> have expressed the view that temperature differences between the conductors constitute the major factor determining the stresses built up in the copper, but have shown that stresses of the order quoted above may still be approached as the copper progressively work-hardens with each cycle of operation.

When the alternator is stopped, the exciting current, being switched off, will no longer heat the copper on the rotor, and contraction occurs, now with considerably reduced frictional restraint in the absence of centrifugal forces. Thermal contraction of the copper will be greater than that of the steel, and also the copper will have been shortened by any creep which occurred during operation. If on the one hand the ends of the windings are not held rigidly against this contraction, the end coils are pulled towards the rotor, leading in extreme cases to earthing faults after a number of repetitions of heating and cooling cycles. On the other hand, if the end coils are rigidly held against this contraction, tensile stresses will be set up in the copper.

Two different ways of solving this problem have been tried:

(1) By not running the alternator up to speed—and hence not bringing the centrifugal forces into full operation—until the copper windings have been raised to the operating temperature.

(2) By the use of rigid fixing of end coils against contraction. As already mentioned, this leads to tensile stresses in the copper when the rotor cools down, which has the effect of reducing the value of the compressive stress in the copper under full alternator load. This method has been combined with the use of copper having a high resistance to softening at the operating temperature.

The first method is only a palliative and not a complete solution; the second aims at ultimately limiting the compressive stresses to values at which plastic deformation and creep do not occur.

The failure of some earlier attempts to use hard-drawn coppers has been attributed to reduction in mechanical properties brought about by softening at the operating temperatures. It is known that the addition of silver to copper increases its resistance to softening, and hence it appears that the use of silver-bearing copper will reduce, if not eliminate, copper shortening. Clearly, if the copper were capable of withstanding, without plastic deformation, the compressive stresses imposed at the operating temperatures, no shortening would occur and the necessity for rigid end-coil fixing or preheating would not arise.

In view of the possible use of silver-bearing copper, data on the mechanical properties, particularly creep properties, of this material were required for comparison with those of ordinary tough-pitch copper. A programme of investigation was undertaken to determine the effect of elevated temperatures not exceeding 225° C. on these properties in high-conduc-

tivity tough-pitch copper, both with and without 0.1% silver. It is considered that, according to the copper-silver equilibrium diagram,<sup>7</sup> this amount of silver was virtually all in solid solution at the test-temperatures. Additionally, these properties were determined for silver-free and silver-bearing O.F.H.C. copper, since some recent American work<sup>8</sup> had suggested that these coppers have higher resistance to creep and to softening than the tough-pitch coppers.

Much of the present work is devoted to stress-free softening tests and creep testing in tension, and it is therefore appropriate at this point to explain the basic reasons underlying the decision to investigate, in particular, these physical properties. As already mentioned, the compressive stresses built up in the alternator rotor windings arise from the specific strain imposed on the copper by thermal expansion. Such stresses may be relieved by creep in compression, the copper increasing its cross-section. It might be thought, therefore, that a compression relaxation test would be the most suitable guide to probable service behaviour. If the copper shortening is to be entirely prevented, relaxation—and hence creep—must not occur. Creep tests in compression are difficult to carry out, and since very short specimens must be used, a high degree of sensitivity of strain measurement cannot be attained. The assumption is generally made that in most materials the mechanical properties in compression are similar to those in tension. This consideration, coupled with the fact that tensile creep-testing equipment was available, led to the use of tensile creep tests as a basis of comparison of the various coppers which have been used or are proposed for use in turbo-alternator windings.

The time to softening of cold-worked copper is known to depend on the degree of cold work and the temperature, and it was clearly important to establish how these variables are inter-related in the coppers used in turbo-alternators. Softening tests were therefore included in the investigation. The absence of softening in such tests does not necessarily mean that the materials will not soften under the same conditions of heat-treatment when simultaneously subjected to stress. Materials which soften in the absence of stress will also do so when stressed, and as the softening test is simple and does not require elaborate apparatus, it affords an easy method of sorting out those materials which will certainly be unsatisfactory under stress. Cook and Richards<sup>9</sup> have recently shown that the softening of cold-worked coppers at relatively low temperatures can be predicted with fair quantitative agreement on the basis of short-time tests at higher temperatures. Hence the softening test afforded a rapid method of assessing the behaviour of the materials as affected by low-temperature heat-treatment.

Although considerable importance is attached to the results of the softening tests, it is realized that the final assessment of suitability of materials must be in terms of creep behaviour, and creep testing therefore constituted the major part of the work.

TABLE I.—Analyses of Tough-Pitch and O.F.H.C. Coppers.

Type of Copper	O <sub>2</sub> , %	Ag, %	Fe, %	Pb, %	Ni, %	Sb, %	S, %	Remarks
Tough-pitch	0.03 *	0.002	0.0002	n.d.	0.0003	n.d.	0.002 *	Zn not detected.
Tough-pitch + silver	0.02 *	0.086 *	0.0002	n.d.	0.0001	n.d.	0.001 *	
O.F.H.C.	0.0002 †	0.001	0.0002	0.0003	0.0003	0.0008	0.002 *	As, Bi, Co, P, Si, Mn, Zn, Te, and Sn not detected.
O.F.H.C. + silver	0.0002– 0.0003 †	0.072 *	0.0002	0.0003	0.0003	0.0008	0.002 *	

\* Chemical analysis.

† Oxygen content measured by the method described by Baker.<sup>10</sup> Superficial oxidation of the sample between cleaning and insertion in the apparatus may account for about 0.0001% oxygen.

n.d. = not detected. Limits of detection are as follows: Zn, 0.001%; As, 0.002%; Bi, 0.0001%; Co, 0.0001%; P, 0.01%; Si, 0.005%; Mn, 0.001%; Te, 0.004%; Sn, 0.0005%; Sb, 0.0002%; Pb, 0.0003%.

## II.—MATERIALS

Primarily, two materials were selected for investigation: silver-free and silver-bearing (nominal 0.1% silver) tough-pitch, high-conductivity coppers. These were prepared by a member firm of the Association from O.R.C.-brand, vertically cast ingots. At a later stage silver-free and silver-bearing O.F.H.C. coppers were also obtained.

The materials were obtained in straight lengths in the form of strip  $1\frac{1}{4} \times 0.1$  in. cross-section, in the annealed condition and also with 10, 25, and 50% cold reduction of area.

All test materials were produced by a combination of hot rolling, annealing, and drawing, the final cold reduction of area being effected by drawing, except in the case of the coppers with 50% reduction. This final temper was produced by drawing (32% reduction) followed by rolling. In the production of copper strip to a given degree of cold work, the same programme was applied to all the coppers.

### 1. COMPOSITION

All materials were analysed spectrographically for minor constituents and chemically for main constituents. Results of these analyses are reported in Table I.

### 2. UNIFORMITY OF COLD WORKING OF THE COPPERS

The hardness was virtually constant across the width of the strip in the 50% cold-worked materials. In those with 25% cold work the variation from edge to centre was about 5%. The 10% cold-worked materials showed the greatest variation in hardness. Thus, in the tough-pitch coppers, the Vickers hardness ranged from 80 at the centre of a transverse section to 98 on the surface near the edge. In the O.F.H.C. coppers, corresponding figures were 91 to 97 in the silver-free and 81 to 94 in the silver-bearing strips. However, in all the materials the variation in hardness over the centre  $\frac{1}{2}$ -in. width, which formed the test width of a creep specimen, was negligible.

Hardness tests along the length of the strips

L 2

indicated that uniformity of cold working in this direction was good in all the materials.

### 3. COMPARISON OF HARDNESS AND GRAIN-SIZE

From Table II, it will be seen that the grain diameter of the O.F.H.C. copper is of the same order as that of the tough-pitch and that the tough-pitch is slightly

TABLE II.—Vickers Pyramid Hardness and Grain-Size of O.F.H.C. and Tough-Pitch Coppers.

Cold Work, %	V.P.N. (Mean of Five Impressions, 20 kg. Load)			
	Tough-Pitch	O.F.H.C.	Tough-Pitch + Silver	O.F.H.C. + Silver
0	48.0	36.8	44.9	37.8
10	94.1	91.0	96.1	93.4
25	105.0	101.3	105.0	102.0
50	114.5	111.0	116.0	115.0

Cold Work, %	Grain-Dia., mm.			
	Tough-Pitch	O.F.H.C.	Tough-Pitch + Silver	O.F.H.C. + Silver
0	0.030	0.040	0.030	0.040
10	0.035	0.040	0.030	0.040
25	0.030	0.035	0.035	0.035
50	...	...	...	...

harder than the O.F.H.C., especially in the annealed condition. In the materials with 50% cold work it was not possible to determine the grain diameter because of the elongated shape of the grains.

### 4. ROOM-TEMPERATURE TENSILE PROPERTIES

Results of tensile tests on all the coppers used are shown in Table III. It will be seen that there is little difference between the various coppers at any given degree of cold working.

### 5. ELECTRICAL CONDUCTIVITIES AT ROOM AND ELEVATED TEMPERATURES

In any changeover from high-conductivity copper to a material having improved properties, the alternator designer requires to know the extent to which



TABLE III.—Comparative Room-Temperature Tensile Properties of Silver-Free and Silver-Bearing O.F.H.C. and Tough-Pitch Coppers.

Each figure is the mean of two tests.

Cold Work, %	Property	Tough-Pitch	O.F.H.C.	Tough-Pitch + Silver	O.F.H.C. + Silver
0	0.1% P.S., tons/in. <sup>2</sup>	2.3	3.0	3.0	2.8
	U.T.S., tons/in. <sup>2</sup>	13.8	14.4	14.5	14.1
	Elongation, %	68	72	65	72
10	0.1% P.S., tons/in. <sup>2</sup>	13.3	13.5	13.7	13.5
	U.T.S., tons/in. <sup>2</sup>	16.3	15.7	16.0	15.6
	Elongation, %	41	44	46	52
25	0.1% P.S., tons/in. <sup>2</sup>	17.3	17.4	17.5	16.8
	U.T.S., tons/in. <sup>2</sup>	20.2	19.7	20.1	20.0
	Elongation, %	19	23	19	15
50	0.1% P.S., tons/in. <sup>2</sup>	20.5	21.2	21.3	21.1
	U.T.S., tons/in. <sup>2</sup>	23.4	23.8	23.8	23.3
	Elongation, %	14	12	13	12

conductivity must be sacrificed. It will be appreciated that any decrease in conductivity in the rotor copper, by virtue of the greater heat generation and higher temperature produced, would increase the tendency to copper shortening. The conductivity at the operating temperature is clearly the true criterion in the comparison, and therefore conductivity measurements have been made on the materials under investigation at 130° and 170° C., as well as at room temperature. The values obtained are listed in Table IV. No figures are quoted for cold-worked, silver-free, tough-pitch coppers at 170° C., as softening of these materials occurs in relatively short periods at this temperature.

TABLE IV.—Mass Conductivities of Silver-Bearing and Silver-Free O.F.H.C. and Tough-Pitch Coppers.

Type of Copper	Cold Work, %	Conductivity *		
		20°C.	130°C.	170°C.
Tough-pitch	0	102.3	70.6	63.7
	10	100.8	69.8	...
	25	100.3	69.2	...
	50	99.7	69.4	...
Tough-pitch + Silver	0	101.9	70.5	63.5
	10	100.5	69.8	63.3
	25	100.4	69.8	63.1
	50	99.5	69.6	62.9
O.F.H.C.	0	102.3	70.9	63.9
	10	101.5	70.4	63.2
	25	100.1	71.1	64.5
	50	100.5	70.1	63.1
O.F.H.C. + Silver	0	102.0	71.0	63.9
	10	101.6	70.7	63.6
	25	101.1	70.3	63.2
	50	97.8	69.0	62.4

\* International Annealed Copper Standard Units.

### III.—STRESS-FREE SOFTENING TESTS

It was initially intended to study the effect of long-term heat-treatments at temperatures of 130°, 175°, 200°, and 225° C. As testing proceeded, however, it

became clear that appreciable softening would occur in reasonable times only in the silver-free tough-pitch coppers and, in consequence, the initial tests were supplemented by tests at 250°, 275°, 300°, and 350° C. on the other coppers.

Heat-treatments of 8 hr. or less were carried out in a salt bath controlled to  $\pm 2^\circ$  C.; longer treatments were carried out in electric muffles, also controlled to  $\pm 2^\circ$  C. The surface hardness was measured by taking the average of five Vickers diamond impressions (20 kg. load) equally spaced across the full width of the strip, the two outer impressions being located  $\frac{3}{16}$  in. from the edges. Hardness measurements were taken initially and after periods of heat-treatment arranged

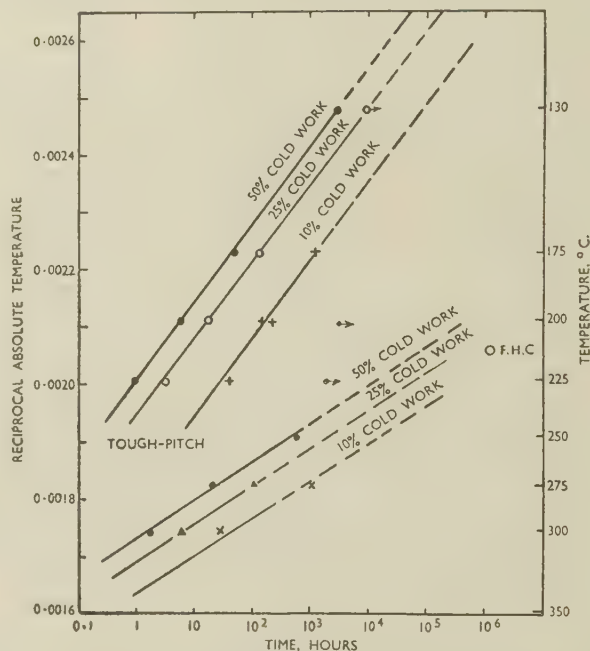


FIG. 1.—Relationship Between Time and Reciprocal Absolute Annealing Temperature to Produce 50% Softening of Cold-Worked Silver-Free O.F.H.C. and Tough-Pitch Coppers.

in geometrical progression. From the softening curves obtained the times to half-softening were determined, and the logarithms of these times were plotted against the reciprocal of the absolute temperatures at which the tests were made. This method of plotting has been shown by Cook and Richards<sup>9</sup> to give a linear relationship, a finding which is substantiated in the present tests.

The results obtained for the tough-pitch coppers are shown in Figs. 1 and 2 (a), from which it is seen that the resistance to softening of tough-pitch copper is considerably increased at all three degrees of cold work by the addition of 0.1% silver. Thus, in the materials with 50% cold work, half-softening is reached in the silver-free copper in 10–15 hr. at 190° C., whereas in the silver-bearing copper the corresponding time would be greater than 10<sup>6</sup> hr.

Figs. 1 and 2 (b) show the results to date of softening tests made on the O.F.H.C. coppers. In Fig. 1 it is

seen that the resistance to softening of silver-free O.F.H.C. copper is considerably greater than that of silver-free tough-pitch copper, probably because any impurities in the O.F.H.C. copper are in solution, whereas any in the tough-pitch copper exist as oxides. There is not such a great difference between the silver-free and the silver-bearing O.F.H.C. coppers as that which characterized the tough-pitch coppers. Comparing Figs. 2 (a) and 2 (b), it is seen that there is no appreciable difference in the resistance to softening, over the temperature range investigated, of the silver-bearing tough-pitch and O.F.H.C. coppers.

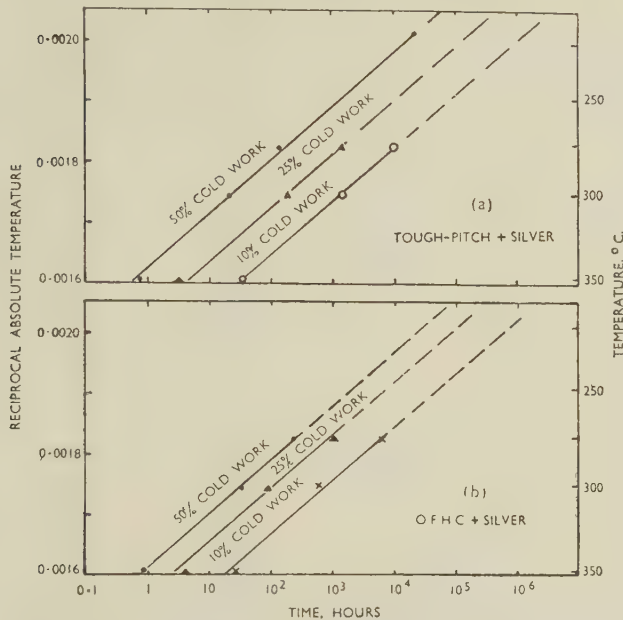


FIG. 2.—Relationship Between Time and Reciprocal Absolute Annealing Temperature to Produce 50% Softening of Cold-Worked Silver-Bearing O.F.H.C. and Tough-Pitch Coppers.

Thus it is clear that unless the presence of stress considerably modifies the softening characteristics—and the creep tests described later failed to show any evidence of this—softening of cold-worked copper used for alternator windings at temperatures up to 225° C. can be completely avoided by the use of silver-bearing copper.

#### IV.—CREEP TESTS

The specimens, to the dimensions shown in Fig. 3, were milled from the copper strips without surface machining. The effective gauge-length was 5 in. The extensometer was fixed rigidly to the enlarged ends of the specimen and the extension measured by two micrometers reading to  $1 \times 10^{-4}$  in., giving a strain sensitivity of  $1.7 \times 10^{-5}$ . The temperature of the specimen was maintained constant to  $\pm 1^\circ$  C., while uniformity of temperature along the parallel length was better than  $\pm 1^\circ$  C. The equipment used is described elsewhere.<sup>11</sup> In starting a test a period of 4–6 hr. was used to bring the specimen to within 2% of the test temperature, this being followed by a further soaking period of  $20 \pm 4$  hr. for close tempera-

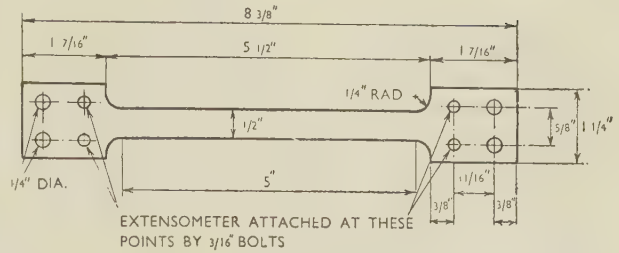


FIG. 3.—Creep-Test Specimen.

ture adjustment before loading. The load was applied in increments, and the Young's modulus of the specimen at the test temperature was determined. This enabled the elastic component of the total strain to be calculated and hence the plastic strain determined. Plastic creep strain is used in the tables and graphs where comparison of creep properties is made. Three test-temperatures were used, viz. 130°, 175°, and 225° C.

Creep tests up to 500 hr. in duration were carried out in triplicate at 130° C. on silver-free tough-pitch copper and at 225° C. on silver-bearing tough-pitch copper, and reproducibility of the results was found to be good.

The programme of tests was most complete for the tough-pitch coppers, the O.F.H.C. coppers being tested only at 130° and 225° C. and at a limited number of stresses. Some of the tests on the tough-pitch coppers were carried on to 10,000 hr. or even longer, but it became clear that comparisons made on a test duration of 5000 hr. or longer were equally valid at a duration of 1000 hr. In some of the longer tests at the lower stresses on the silver-bearing coppers, it was seen that the creep rate was still diminishing.

#### 1. COMPARISON OF SILVER-FREE AND SILVER-BEARING COPPERS

Some tests were made on the annealed tough-pitch coppers, and the results are shown in Fig. 4. It will

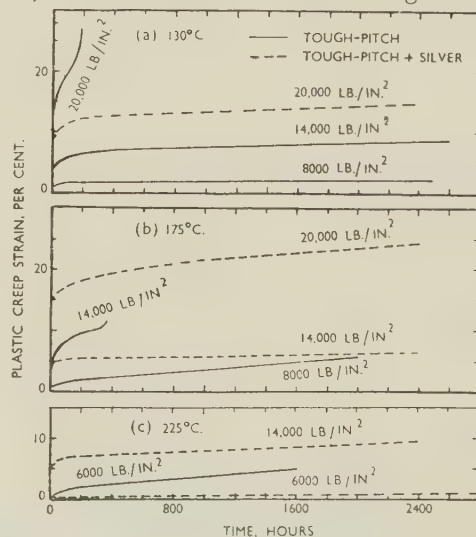


FIG. 4.—Creep Tests on Annealed Tough-Pitch Coppers Showing the Effect of Addition of 0.1% Silver.



be noted that the initial plastic strain is large, the transient creep is quite noticeable, and the secondary creep has a reasonably low rate. At each temperature the transient creep and the secondary creep rates were both greater for the silver-free than for the silver-bearing copper, at the same stress. As indicated in

Table II, the materials had the same grain-size. It is clear that the silver addition, which is probably in solid solution at the test temperatures, has increased the resistance to creep.

The results of the tests on the cold-worked materials are given in Table V. The first point to which

TABLE V.—Results of Creep Tests on Cold-Worked Silver-Free and Silver-Bearing Tough-Pitch and O.F.H.C. Coppers.

Test Temp., °C.	Cold Work, %	Type of Copper	Stress, lb./in. <sup>2</sup>	Plastic Creep Strain, %, at		Duration of Test, hr.	Plastic Creep Strain at End of Test, %
				1000 hr.	5000 hr.		
130 ( $E = 16.0 \times 10^6$ lb./in. <sup>2</sup> )	10	Tough-pitch	8,000	0.06	0.10	8,250	0.13
		" " + silver	8,000	0.02	0.03 *	4,750	0.03
		" " "	14,000	0.16	0.36	8,600	0.51
		" " + silver	14,000	0.04	0.06	9,800	0.08
		" " "	20,000	0.64	...	1,750B	2.40
		" " + silver	20,000	0.12	0.15	7,200	0.17
		O.F.H.C. + silver	20,000	0.09 *	...	750	0.09
	25	Tough-pitch	8,000	0.08	0.13	7,200	0.16
		" " + silver	8,000	0.02	0.02 *	4,750	0.02
		" " "	14,000	0.18	0.40	8,600	0.82
		" " + silver	14,000	0.05	0.07	10,200	0.07
		O.F.H.C. "	14,000	0.07	...	1,550	0.08
		" " + silver	14,000	0.06	...	1,550	0.06
		Tough-pitch	20,000	0.46	...	4,680B	3.30
		" " + silver	20,000	0.09	0.11	7,200	0.12
		O.F.H.C. "	20,000	0.15	...	1,550	0.17
		" " + silver	20,000	0.09	...	1,050	0.09
	50	Tough-pitch	8,000	0.07	0.42	8,250	1.36
		" " + silver	8,000	0.03	0.03 *	4,550	0.03
		" " "	14,000	0.13	1.51	8,700	6.44
		" " + silver	14,000	0.06	0.08	11,400	0.09
		" " "	20,000	0.29	...	4,030B	11.0
		" " + silver	20,000	0.10	0.13	7,250	0.13
		O.F.H.C. + silver	20,000	0.09 *	...	750	0.09
		O.F.H.C. + silver	20,000	0.09 *	...	750	0.09
175 ( $E = 15.5 \times 10^6$ lb./in. <sup>2</sup> )	10	Tough-pitch	8,000	0.16	0.62	6,850	0.96
		" " + silver	8,000	0.04	0.06 *	4,850	0.06
		" " "	14,000	1.12	...	1,100B	2.1
		" " + silver	14,000	0.09	0.12	12,900	0.16
		" " "	20,000	0.24	0.38 *	4,900	0.38
	25	Tough-pitch	8,000	2.93	...	1,050	2.96
		" " + silver	8,000	0.04	0.05 *	4,900	0.05
		" " "	14,000	0.08	0.10	12,900	0.13
		" " "	20,000	0.14	0.21	10,300	0.26
	50	Tough-pitch + silver	8,000	0.04	0.06	6,900	0.07
		" " "	14,000	0.09	0.14	12,900	0.16
		" " "	20,000	0.17	...	3,700	0.22
225 ( $E = 15.0 \times 10^6$ lb./in. <sup>2</sup> )	10	Tough-pitch + silver	8,000	0.09	0.15	8,900	0.18
		" " "	14,000	0.20	0.39	12,900	0.68
		O.F.H.C. + silver	14,000	0.16	...	1,050	0.16
	25	Tough-pitch + silver	8,000	0.07	0.11	8,900	0.13
		O.F.H.C. "	8,000	0.17	...	2,300	0.22
		" " + silver	8,000	0.08	...	3,150	0.11
		Tough-pitch + silver	14,000	0.16	0.27	11,500	0.47
		O.F.H.C. "	14,000	0.65	...	2,750	1.49
		" " + silver	14,000	0.21	...	3,100	0.31
		Tough-pitch + silver	20,000	0.35	0.76	9,870B	1.5
		O.F.H.C. "	20,000	...	...	275B	2.4
		" " + silver	20,000	0.61	2.43	5,000	2.43
		O.F.H.C. + silver	20,000	0.61	2.43	5,000	2.43
	50	Tough-pitch + silver	8,000	0.09	0.14	8,900	0.18
		" " "	14,000	0.20	0.34	12,900	0.62
		O.F.H.C. + silver	14,000	0.14	...	3,250	0.19
		Tough-pitch + silver	20,000	0.42	...	3,000	1.00

\* Extrapolated result.

B = broken.

$E$  = Young's Modulus.

attention should be drawn is that, provided it was retained at the test temperature, cold work materially increased the creep-resistance. Furthermore, the increase in creep-resistance was not essentially different for the three degrees of cold work used. Where the test temperature was such that softening of a cold-worked material occurred either during the preliminary heating period before application of the stress or at an early stage in the test, the subsequent creep-resistance became similar to that of the annealed material. Thus, the silver-free tough-pitch copper, with each degree of cold work, softened during the preliminary heating period when the test temperature was 225° C. Creep-strain values are not given in Table V, but they were similar to those shown for the annealed material in Fig. 4 (c). Only the 25% cold-

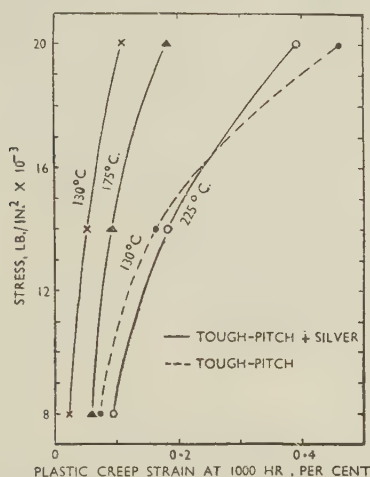


FIG. 5.—Creep Tests on Cold-Worked Tough-Pitch Coppers Showing the Effect of Addition of 0.1% Silver. Mean results for 10, 25, and 50% cold-worked materials.

Young's Modulus at Test Temperatures.

130° C.	16.0 × 10 <sup>6</sup> lb./in. <sup>2</sup> .
175° C.	15.5 × 10 <sup>6</sup> lb./in. <sup>2</sup> .
225° C.	15.0 × 10 <sup>6</sup> lb./in. <sup>2</sup> .

worked silver-free O.F.H.C. copper was tested at 225° C., and this gave no indications that softening was occurring during the creep tests lasting over 2000 hr.

In the tests at 130° C., at each degree of cold work and at each value of stress used, the silver-bearing tough-pitch copper was noticeably more resistant to creep than the silver-free, tough-pitch copper. At this temperature there was little, if any, difference between the two silver-bearing coppers, tough-pitch and O.F.H.C. The silver-free O.F.H.C. had greater creep-resistance than the silver-free tough-pitch, but the resistance was not as high as that of the silver-bearing coppers.

At 175° C. comparison was made only between the two tough-pitch coppers, and the creep-resistance of the silver-bearing copper was much greater than that of the silver-free.

At 225° C. there was again little difference between the creep-resistances of the silver-bearing coppers,

tough-pitch and O.F.H.C., while both were noticeably more resistant than the silver-free O.F.H.C. copper.

A more readily appreciated comparison of the creep properties of the silver-free and silver-bearing tough-pitch coppers is shown in Fig. 5. In this, the mean value of the plastic creep strain at 1000 hr. for the three degrees of cold working is plotted against the stress. It is seen that the silver-bearing copper has about the same creep-resistance at 225° C. as the silver-free copper at 130° C.

## 2. FRACTURES IN SILVER-FREE AND SILVER-BEARING COPPERS

Some fractures have been obtained in all materials under creep conditions and details are given in Table VI.

At 130° and 175° C. fractures have been obtained only of the silver-free tough-pitch coppers, while in the case of silver-free O.F.H.C. and silver-bearing tough-pitch and O.F.H.C. coppers, fractures have been obtained only at 225° C., because at the lower temperatures the stresses used in the creep tests were not high enough to cause fracture in the testing time. In all cases the fractures were intercrystalline, and intercrystalline cracking was observed in micro-specimens taken at different places along the parallel gauge-length of the creep specimens.

TABLE VI.—Details of Creep Fractures of Coppers.

Type of Copper	Cold Work, %	Test Temp., °C.	Stress, lb./in. <sup>2</sup>	Life, hr.	Total Elongation at Fracture, % on 5 in.
Tough-Pitch	Annealed	130	20,000	170	29.8
	10			1750	2.4
	25			4680	3.4
	50			4030	11.0 *
	10	175	14,000	1100	2.0
	25			365	14.6 *
	50			336	31.4 *
Tough-pitch + silver	25	225	25,000	800	6.0
	25		20,000	9870	1.5
	25		20,000	275	2.4
	10		20,000	1368	2.5
	25		25,000	520	2.8
O.F.H.C. + silver	25		25,000		

\* These specimens recrystallized during test.

The specimen of the 25% cold-worked, silver-bearing, tough-pitch copper stressed at 20,000 lb./in.<sup>2</sup> broke while still in the second stage of creep (minimum creep-rate stage), and gave no warning of its impending fracture by a turning-up of the creep curve. Plastic creep strain at fracture was 1.5%. The fracture was intercrystalline, and there was much intercrystalline cracking throughout the parallel length. Photographs showing cracking at and away from the fracture are given in Figs. 6 and 7 (Plate XXV).

A creep test has also been carried out at 25,000 lb./in.<sup>2</sup> and 225° C. on this material. This specimen fractured in 800 hr. with 2% extension, the fracture being intercrystalline, with some intercrystalline cracking along the parallel gauge-length. In this case the fracture took place in the final, or tertiary, stage of creep. Creep fractures obtained in the silver-free



and silver-bearing O.F.H.C. coppers were intercrystalline and similar to those obtained in the tough-pitch coppers.

The test results indicate that in the silver-free tough-pitch copper at 130° C. and stresses of 20,000 lb./in.<sup>2</sup> or less, or at 175° C. and stresses of 14,000 lb./in.<sup>2</sup> or less, any creep failures would be intercrystalline, since at a given temperature the probability that ultimate fracture will be intercrystalline increases with decrease in the rate of creep strain, i.e. with decrease in applied stress.

In the silver-bearing tough-pitch copper and silver-free and silver-bearing O.F.H.C. coppers, the only creep fractures obtained have been at 225° C. and 20,000 and 25,000 lb./in.<sup>2</sup>. For similar reasons to those given above, creep fractures in these materials at 225° C. and stresses of 20,000 lb./in.<sup>2</sup> or less would also be intercrystalline.

### 3. COMPARISON OF ROLLED AND DRAWN SILVER-BEARING TOUGH-PITCH COPPER AND THE EFFECT OF THICKNESS

Tests of 2000 and 3000 hr. duration were carried out at 175° C. and a stress of 14,000 lb./in.<sup>2</sup> on materials prepared by rolling and by drawing and at two different thicknesses, 0.1 and 0.2 in. The results obtained showed that there was no difference between the creep-resistance of material produced by these two methods, nor was there any significant effect of thickness of material.

### 4. EFFECT OF COLD WORK AND OF GRAIN-SIZE IN SILVER-BEARING TOUGH-PITCH COPPER

A comparison of the creep curves for the silver-bearing tough-pitch coppers under the same test conditions, but with different amounts of cold work

from 10 to 50% showed that there was no marked effect of degree of cold work within this range. This interesting result suggests the choice of a low temper for alternator windings, so that benefit may be derived from its greater resistance to softening. It was felt, however, that further information on this was required, and a number of tests was carried out to determine the influence on the creep-resistance of a range of cold work. At the same time the effect of grain-size was investigated.

Lengths of the silver-bearing tough-pitch coppers, originally with 10 and 50% cold work, were bright-annealed for 2 hr. at 570° C., giving annealed materials with two different grain sizes—0.023 and 0.043 mm. dia. Lengths of material of each grain-size were strained in tension at room temperature to give reductions in area of 5, 10, 15, and 20%. Creep specimens machined from these cold-worked materials were tested in creep at 14,000 lb./in.<sup>2</sup> at 175° C.

The creep curves obtained are shown in Fig. 8, while data derived from these curves and from the earlier work are shown in Fig. 9. It is seen that 5% cold work markedly reduced the amount of creep at 2000 hr., i.e. from 6.4 to 0.75 or 0.35% according to grain-size, while 10% cold work reduced these figures further to 0.15 or 0.08%.

It is seen from Fig. 9 that cold work in excess of 10% does not produce, in this material, any increase in creep-resistance at 175° C. Any further increase in cold work in fact decreases the time to the beginning of softening which brings about a decrease in creep-resistance.

The effect of grain-size on the creep-resistance is also shown by Figs. 8 and 9; at each degree of cold work the creep strain at 2000 hr. of the coarse-grained specimen was approximately one-half that of the fine-grained specimen.

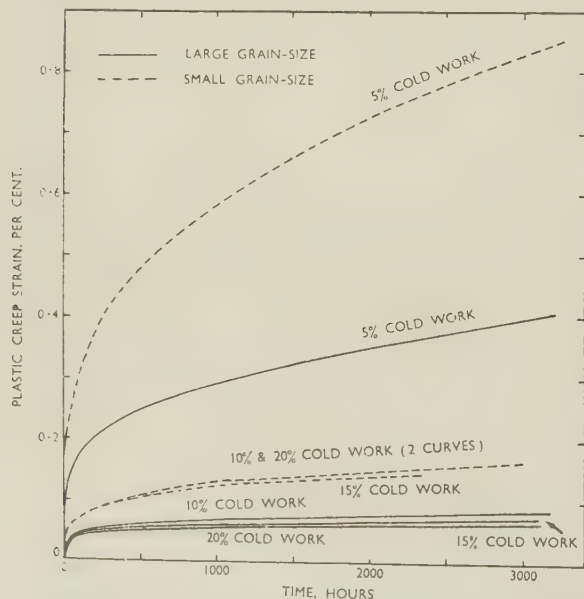


Fig. 8.—Effect of Cold Work and Grain-Size on the Creep of Silver-Bearing Tough-Pitch Coppers Stressed at 14,000 lb./in.<sup>2</sup> at 175° C.

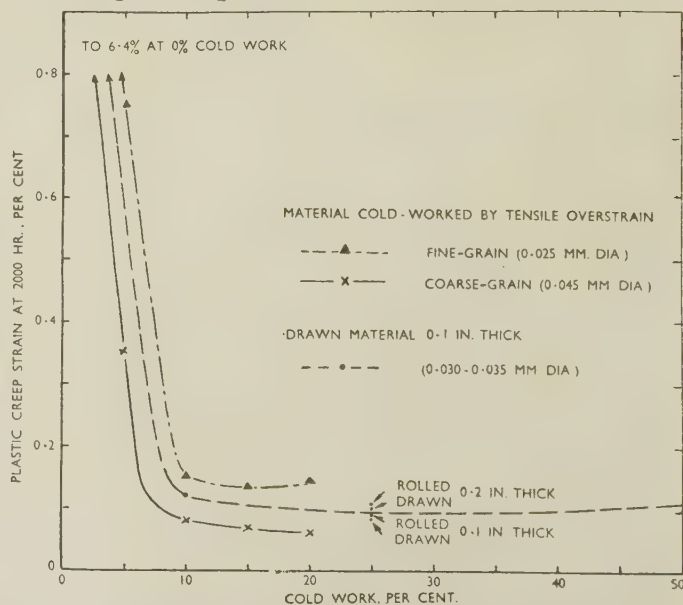


Fig. 9.—Effect of Cold-Work on the Creep of Silver-Bearing Tough-Pitch Coppers Stressed at 14,000 lb./in.<sup>2</sup> at 175° C.

### 5. THE EFFECT OF TENSILE AND OF COMPRESSIVE WORKING ON CREEP BEHAVIOUR

While the cold working of the copper conductors for alternator windings is generally carried out by drawing and hence is of the nature of tensile overstrain, the copper in service in the alternator is subjected to compressive stresses, under the action of which relaxation creep occurs. It is well known that if a specimen of any material is overstrained in tension and then tested in compression, there is a decrease in the stress below which a linear relationship exists between stress and strain. It was considered of interest in the general problem of copper shortening to observe the effect of previous tensile and compressive overstrains on the subsequent creep behaviour under tensile stress. Some 1-in.-dia. bar of 0.1% silver-bearing tough-pitch copper was annealed and part of the bar was overstrained in tension and part in compression, to produce in each case a change of 10% in the cross-sectional area. Specimens machined from each part were tested in creep at 175° C. and a tensile stress of 14,000 lb./in.<sup>2</sup>. The results of the

creep curve, the rate of plastic flow being high immediately the load is removed and decreasing with time. The curve appears to become asymptotic to some value of strain. In creep-recovery tests on coppers continued for 100 hr., two thirds of the total recovery occurred in the first 20 hr.

#### 1. PREVIOUS WORK

Tapsell<sup>12</sup> carried out creep-recovery tests on a nickel-chromium-molybdenum steel and on a 0.13% carbon steel at 450° C., on a 3% nickel steel at 400° C., and on lead at 60° C. The following conclusions were reported:

(a) Recovery over a given period after removal of stress was proportional to the original applied stress.

(b) The estimated final amount of creep recovery increased with the duration of the preceding creep test.

(c) The rate of recovery increased considerably with increase in temperature.

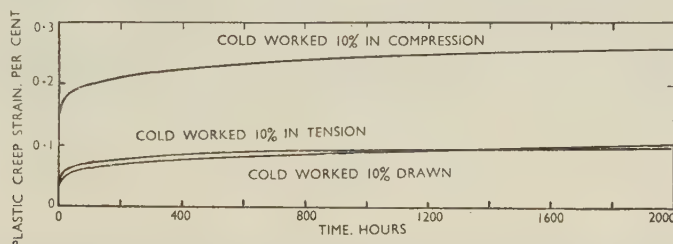


FIG. 10.—Creep Tests at 175° C. and 14,000 lb./in.<sup>2</sup> on Silver-Bearing Tough-Pitch Coppers Showing the Effect of the Direction of Working on Tensile Creep Behaviour.

tests are given in Fig. 10, where a comparison has also been made with the results of the creep test on the drawn silver-bearing strip cold worked 10% and used in the main programme. It will be seen that while the specimen overstrained in tension gave a similar creep curve to that of the drawn material, the specimen overstrained in compression gave a higher initial strain but subsequently the same rate of creep.

These results indicate that drawn material tested in creep under compressive stress will give a greater initial strain and a greater plastic strain at any subsequent time than when tested in creep under tensile stress. It is reasonable to suppose, however, that the greater resistance to plastic deformation of the silver-bearing compared with the silver-free copper shown in the tensile creep tests would also be shown in compressive creep tests.

### V.—CREEP RECOVERY

When a tensile creep specimen is unloaded at the test temperature, the strain in the specimen is reduced, first by an immediate contraction corresponding to the elastic recovery and hence related directly to the stress in the creep test, and then, gradually with time, by a further contraction resulting from plastic flow. The contraction/time curve is similar in shape to a normal

(d) A close approximation to a linear relationship existed in nearly all cases between the logarithm of the sum of the rapid elastic contraction and the creep recovery and the logarithm of the time.

Two theories have been put forward to account for creep recovery. The first supposes that in the material under test the grains, according to their orientation, will have varying resistance to deformation in the direction of stress. After a period of creep testing, some grains will be more heavily stressed than others and hence, on unloading, while there will be an immediate elastic recovery, additional recovery will occur with time as negative creep is produced by the action of the uneven stress distribution. Under some conditions, particularly at high temperatures, a large part of the creep recovery has been attributed to viscous flow in grain-boundary regions under the influence of elastic stresses in adjoining grains.

The second theory suggests that creep recovery may be due to an extra-elastic effect, i.e. a change in lattice strain with time in the direction of the applied stress during the creep test, and a change in the reverse direction during recovery. As creep recovery has not been observed in single-crystal specimens, the first theory is thought to be the more likely.



## 2. PRESENT EXPERIMENTAL WORK

In an attempt to obtain some information on the relative creep recovery of silver-bearing and silver-free coppers the following tests were made.

(a) *Effect of Creep Stress on Creep Recovery*

Four specimens of 25% cold-worked, silver-bearing, tough-pitch copper stressed at 8000, 14,000, 20,000, and 25,000 lb./in.<sup>2</sup> at 225° C. were unloaded when the plastic creep strain in each case reached approximately 0.15%. The creep recovery was followed at 225° C. and the results obtained are given in Table VII (a).

Only the specimen tested at 8000 lb./in.<sup>2</sup> was in the apparent minimum creep-rate stage before unloading; all the others were still in the primary stage of creep.

and 6000 lb./in.<sup>2</sup> were unloaded at approximately the same test times and creep strains, and the creep recovery followed at 225° C. Results are given in Table VII (c) and show that there is no effect of cold work from 10 to 50% on creep recovery. This result would be expected from the creep tests, which show no marked effect of this variation in cold work on the resistance to creep.

(d) *Cumulative Effect of Intermittent Creep and Creep Recovery*

In practice, some large turbo-alternators, forming part of stand-by equipment of power-stations, are run only at times of peak load. In consequence, the rotor windings of such machines are subjected to

TABLE VII.—*Factors Affecting Creep Recovery in Copper.*

Effect Investigated	Type of Copper	Test Temp., °C.	Cold Work, %	Creep Stress before Unloading, lb./in. <sup>2</sup>	Creep-Test Time before Unloading, hr.	Creep-Strain before Unloading, %	Creep Recovery at 100 hr., %
(a) Effect of creep stress at constant creep strain (0.15%)	Tough-pitch + silver	225	25	8,000 14,000 20,000 25,000	8856 265 29 1.3	0.130 0.148 0.138 0.148	0.020 0.041 0.043 0.031
(b) Effect of varying creep strain at constant creep stress (25,000 lb./in. <sup>2</sup> )	Tough-pitch	130	25	25,000	648 296 72	1.064 0.515 0.329	0.099 0.079 0.102
	Tough-pitch + silver	225	25	25,000	504 192 25 1.3	1.102 0.501 0.302 0.148	0.076 0.072 0.053 0.031
(c) Effect of varying amounts of cold work	O.F.H.C.	225	{ 10 25 50 }	{ 6,000 }	{ 1128 1104 1248 }	{ 0.071 0.097 0.090 }	{ 0.018* 0.018 0.016 }

\* In 48 hr. (thermostat failure).

The results do not indicate any simple relationship between creep recovery and creep-test stress.

(b) *Effect of Creep Strain at Constant Stress*

Specimens stressed at 25,000 lb./in.<sup>2</sup> were unloaded at plastic creep strains of approximately 0.3, 0.5, and 1.0%, and creep recovery allowed to occur at the creep-test temperature.

The tests were made on 25% cold-worked, silver-bearing, tough-pitch copper at 225° C., and on 25% cold-worked, silver-free, tough-pitch copper at 130° C. The results of these tests are given in Table VII (b). The results for the silver-bearing specimen unloaded at 0.148% strain, described in (a) above, is also included.

In the silver-bearing materials at 225° C., the greater the creep strain, the greater was the creep recovery; but in the silver-free material at 130° C. there was no systematic relationship between creep strain and creep recovery.

(c) *Effect of Cold Work on Creep Recovery*

Three creep specimens of silver-free O.F.H.C. copper with 10, 25, and 50% cold work tested at 225° C.

alternate stressing and unstressing, resulting in creep and creep recovery. It is usual for the running times at full load of such equipment to be short, say of a few hours' duration only, and for the creep recovery to occur under conditions of slow cooling of the windings. Such conditions cannot be reproduced conveniently in creep testing, where the requirements of temperature constancy impose certain limitations. It was considered however, that the approach described below gave information on the effect of creep recovery in conditions not too widely different from those met with in the actual windings of an alternator.

Two specimens of 50% cold-worked, silver-bearing, tough-pitch copper were tested in tensile creep at 175° C. and 20,000 lb./in.<sup>2</sup>. One specimen was stressed continuously. The other specimen was stressed first for 624 hr., and thereafter it was unloaded for 168 hr. (one week) and reloaded for 168 hr.; this cycle of loading and unloading being repeated up to a total time of 3000 hr. The total deformation (including elastic strain) with time in these tests is plotted in Fig. 11, and it is seen that a steady state of increase in total strain in each cycle has been reached.

CREEP FAILURE IN SILVER-BEARING TOUGH-PITCH COPPER, 25% COLD-  
WORKED.

Temperature : 225° C.  
Life : 9870 hr.

Stress : 20,000 lb./in.<sup>2</sup>  
Elongation : 1.5%

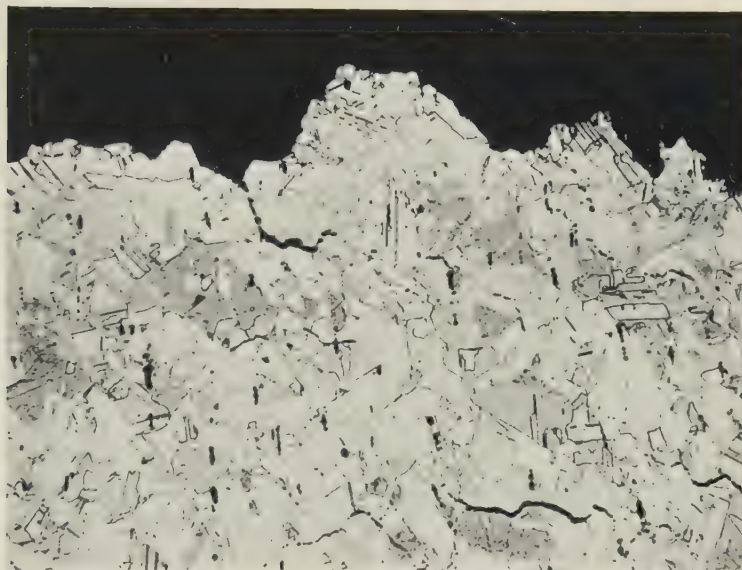


FIG. 6.—Intercrystalline Cracking in Vicinity of Fracture. Longitudinal section parallel to surface.  $\times 125$ .

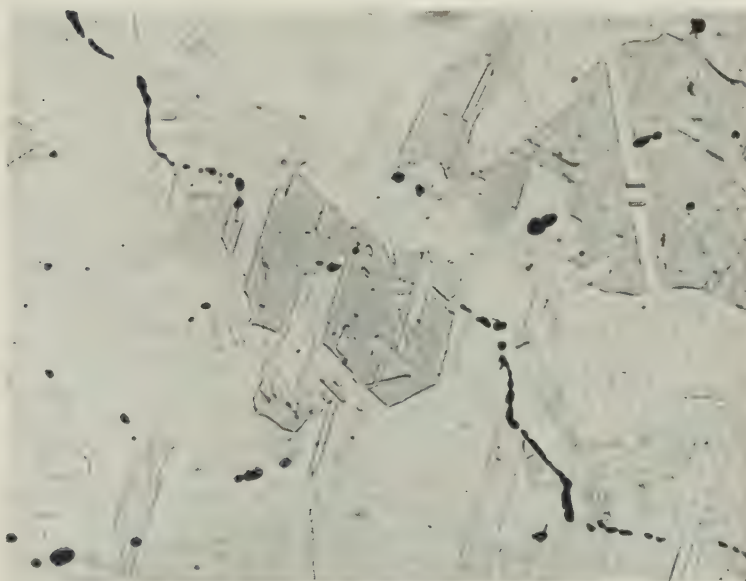


FIG. 7.—Intercrystalline Cracking 3 in. Away from Fracture. Longitudinal section parallel to surface.  $\times 500$ .





This comparison of the intermittently loaded specimen with the continuously loaded one is interesting, since the effective creep rate of the former approximates closely to half the steady creep rate of the latter, while the time under load in these two tests is in the same ratio as the creep rates. It is clear that the plastic strain recovered during negative

## VI.—CONCLUSIONS

The conclusions reached as a result of the investigations described above may be summarized briefly as follows:

(1) Creep tests at 130°–225° C. and of durations up to 10,000 hr. have shown that the addition of silver to cold-worked tough-pitch copper greatly increases its resistance to creep.

(2) The creep-resistance of all the coppers examined increased greatly with cold work up to 10% reduction and thereafter was little affected. In silver-bearing tough-pitch copper, 10% cold work is sufficient to produce the optimum combination of creep-resistance and resistance to softening over the temperature range 130°–225° C.

(3) Cold-worked O.F.H.C. copper containing silver has softening and creep characteristics closely similar to those of cold-worked tough-pitch copper containing silver.

(4) If both are free from silver, and in the absence of stress, the resistance to softening of cold-worked O.F.H.C. copper is much greater than that of cold-worked tough-pitch copper. If silver (0.08%) is added to each of these two coppers, their resistance to softening becomes equal and higher than that of either of the silver-free materials.

(5) In comparative creep tests at 130°–225° C. on cold-worked silver-free materials the creep-resistance of O.F.H.C. copper was much greater than that of tough-pitch copper. Presumably this is due in part to the increased resistance to softening of the O.F.H.C. copper and in part to its inherently greater resistance to creep deformation.

(6) Creep tests on rolled and drawn silver-bearing tough-pitch copper showed no effect of the method of production or of the thickness of the material.

(7) When recrystallization did not occur during a creep test, the fractures obtained were markedly intercrystalline, with intercrystalline cracking throughout the parallel length. Such fractures occurred at small extensions of the order of 2–3%. When recrystallization did occur during a test, considerably larger extensions were obtained, and in such cases, although the ultimate fracture was partially intercrystalline, relatively few intercrystalline cracks were observed in the regions of the specimen away from the fracture.

(8) An investigation of creep recovery in cold-worked silver-free and silver-bearing tough-pitch coppers at temperatures of 130° and 225° C. has shown that creep recovery is greater in the silver-free than in the silver-bearing copper, as would be expected from the greater creep-resistance of the latter.

(9) On reloading a specimen in which creep recovery has occurred, creep is more rapid until the strain reaches about the value before unloading. Thereafter it creeps at the same rate as before unloading. It follows that any creep recovery occurring in a turbo-alternator rotor winding during the shut-down period does not materially reduce copper shortening.

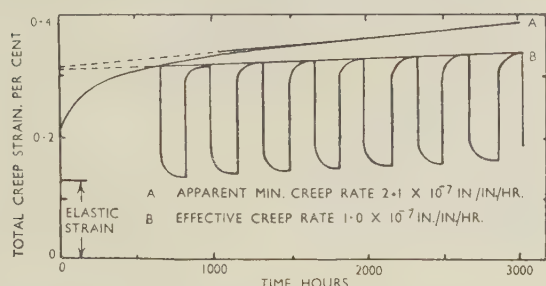


FIG. 11.—Comparisons of Creep Tests using Continuous and Intermittent Stress on 50% Cold-Worked Silver-Bearing Tough-Pitch Coppers at 175° C. and 20,000 lb./in.<sup>2</sup>.

creep is lost during the next loading cycle. Hence any differences in the creep-recovery characteristics of two materials are of no consequence, whereas differences in creep-resistance are important.

## 3. DISCUSSION OF RESULTS

In dealing with the subject of creep recovery in relation to the problem of copper shortening, the following considerations are relevant:

(a) The fullest extent of creep recovery is obtained only when the material is maintained after unloading at the same temperature as that at which creep had occurred. This condition is not normal in the rotor windings of a turbo-alternator, since when the machine is stopped the exciting current is switched off. Even when the creep-recovery temperature is the same as the creep-test temperature, the amount of recovery is small, 10–30% of the creep strain before unloading. When the recovery temperature is lower than the creep-test temperature, the amount of recovery will be still smaller, and hence is likely to be of negligible importance in turbo-alternator rotor windings.

(b) On re-stressing, creep occurs at first more rapidly than if recovery had not taken place, so that the recovery is to a large extent cancelled.

(c) Since creep recovery is a negative form of creep, the more resistant a material is to creep, the less creep recovery would be expected from it. Thus, since silver-bearing copper is more resistant to creep than silver-free copper, it must be expected to give less creep recovery, when unloaded from the same stress at the same temperature. It has been noted earlier that the creep-resistance of the silver-bearing tough-pitch copper at 225° C. is similar to that of the silver-free tough-pitch copper at 130° C. The test results given in Table VII (b) show that there is a corresponding similarity in the amount of creep recovery in the silver-bearing copper at 225° C. and the silver-free copper at 130° C.



## ACKNOWLEDGEMENTS

The authors wish to thank the Director and Council of the British Non-Ferrous Metals Research Association for permission to publish this paper. They also wish to record their thanks to Mr. R. D. S. Lushey, who carried out the many creep tests.

## REFERENCES

1. C. M. Laffoon and B. A. Rose, *Elect. J.*, 1936, **33**, 262.
2. G. A. Juhlin, *J. Inst. Elect. Eng.*, 1939, **85**, 544.
3. J. G. Noest, *Trans. Amer. Inst. Elect. Eng.*, 1944, **63**, 514.
4. R. H. Coates and B. C. Pyle, *J. Inst. Elect. Eng.*, 1946, **93**, 192.
5. W. D. Horsley and R. H. Coates, *Conf. Internat. Grands Réseaux Elect.*, Rep. No. **115**, 1946, 41 pp.
6. W. D. Horsley, private communication.
7. E. A. Owen and J. Rogers, *J. Inst. Metals*, 1935, **57**, 257.
8. A. D. Schwoppe, K. F. Smith, and L. R. Jackson, *Trans. Amer. Inst. Min. Met. Eng.*, 1949, **185**, 409.
9. M. Cook and T. Ll. Richards, *J. Inst. Metals*, 1946-47, **73**, 1.
10. W. A. Baker, *Metallurgia*, 1949, **40**, 188.
11. J. McKeown, *Metallurgia*, 1950, **42**, 189.
12. H. J. Tapsell, *Internat. Assoc. Test. Mat. London Congr. [Proc.]*, 1937, 1.

# THE ALLOYS OF MOLYBDENUM AND TANTALUM\*

1334

By G. A. GEACH,† M.Sc., Ph.D., F.I.M., MEMBER, and  
D. SUMMERS-SMITH,‡ B.Sc., A.R.T.C., MEMBER

## SYNOPSIS

An investigation of the binary system molybdenum-tantalum has shown that these metals form a continuous series of solid solutions. This is to be expected on theoretical grounds, as both metals crystallize with a body-centred cubic structure and the atoms are very similar in size. No superlattice was detected and no anomalies occur between the true and X-ray densities. Approximate melting points of the alloys have also been determined. The alloys of the transition metals of Groups IVA, VA, and VIA with each other are discussed briefly.

## I.—INTRODUCTION

THE binary alloy system molybdenum-tantalum has not been investigated in detail by previous workers. Von Bolten<sup>1</sup> in 1905 stated that molybdenum and tantalum alloyed in all proportions, but gave no further details. More recently Bückle<sup>2</sup> investigated the lattice parameter and hardness of three alloys and from them was able to postulate a continuous series of solid solutions. Myers<sup>3</sup> found that alloys containing up to 20 wt.-% molybdenum were single phase.

The two metals crystallize in the same structure, body-centred cubic, have similar electrochemical properties, and their atoms differ in size by less than 5%; thus it is to be expected that they will form extensive solid solutions with each other.

## II.—EXPERIMENTAL METHODS

### 1. MATERIALS USED

Alloys were prepared both from the metal powders and from the lump material. The metal powders were supplied by Murex, Ltd., who specify a purity of 99.8% for the molybdenum and 99.5% for the tantalum. The lump materials used were in the form of H.S. Spectrographic Standard rods supplied by Johnson, Matthey and Co., Ltd. The manufacturers claim a purity higher than 99.95% for the molybdenum and higher than 99.98% for the tantalum. Spectroscopic analysis indicated traces of copper, magnesium, and calcium in the molybdenum and of niobium, nickel, tungsten, silicon, iron, calcium, and copper in the tantalum.

### 2. PREPARATION OF THE ALLOYS

An initial attempt was made to prepare the alloys by powder-metallurgical methods. One-g. samples

of the powders in the desired proportions were mixed in a small ball mill, described elsewhere,<sup>4</sup> for 24 hr. The mixed powder was then compacted at 40 tons/in.<sup>2</sup> and the pellets sintered at 1500° C. for 24 hr. in a vacuum of 10<sup>-4</sup> mm. Hg or better. Even under these conditions some atmospheric contamination occurred, and equilibrium was not attained in the tantalum-rich alloys. It was not possible to attain equilibrium in these alloys in a reasonable time even when a sintering temperature of 1850° C. was used.

To overcome these difficulties further alloys were made by melting. When the metal powders were used, these were first mixed in the required proportions, pressed at 40 tons/in.<sup>2</sup> to form pellets about 1 cm. × 1 cm. dia. and weighing about 5 g. The pellets were sintered at 1500° C. for 2 hr. in a vacuum of 10<sup>-5</sup> mm. Hg to remove gases, and were then melted in a purified argon atmosphere in an arc furnace which is described in detail elsewhere.<sup>5</sup> With the spectroscopically pure metal rods no preliminary sintering was carried out, the alloys, weighing about 5 g., being made up directly by melting in the arc furnace. In this furnace the specimen forms the positive pole of a D.C. arc, the negative pole of which is a tungsten rod. The specimen rests on a water-cooled copper hearth and is melted in an atmosphere of argon at about 20 cm. pressure. The argon atmosphere in the sealed furnace vessel is first purified by melting a piece of zirconium, which effectively removes any residual gases. Spectroscopic analyses have shown that there is no pick-up of copper or tungsten during the melting, and other experiments with the furnace have shown that gaseous contamination is also negligible.

Both Myers,<sup>3</sup> with tantalum-rich alloys prepared by sintering *in vacuo* at 2600° C., and Schumb, Radtke, and Bever,<sup>6</sup> with alloys prepared by arc melting, found that there was a loss of molybdenum during

\* Manuscript received 12 April 1951.

† Physical Metallurgy Section Leader, Associated Electrical Industries Research Laboratory, Aldermaston, Berkshire.

‡ Research Metallurgist, Associated Electrical Industries Research Laboratory, Aldermaston, Berkshire.



heating due to evaporation. No such loss was found in the present case, as can be seen from Table I. The analyses in the table were carried out by Johnson, Matthey and Co., Ltd. The greatest deviation from the nominal composition is less than 1.5%, and is not significantly greater for the alloys prepared from the metal powders.

TABLE I.—*Compositions of Alloys Studied.*

Intended Composition, Ta, wt.-%	Analysed Composition		Tantalum, at.-%	Materials Used
	Mo, wt.-%	Ta, wt.-%		
0	100	...	0	Murex metal powders
20	80.66	19.28	11.2	
40	61.21	38.78	25.2	
60	40.28	59.76	44.1	
70	31.24	68.72	53.8	
80	20.32	79.64	67.5	
90	11.20	88.83	80.8	
100	...	100	100	H.S. Spec-pure metals
0	100	...	0	
10	90.24	9.70	5.4	
30	70.97	28.98	17.8	
50	49.90	50.12	34.8	
95	5.75	94.19	89.6	
100	...	100	100	

### III.—EXPERIMENTAL RESULTS

#### 1. X-RAY ANALYSIS

Powder photographs were taken in a 9-cm. "Unicam" camera, using copper radiation. This radiation is very suitable for the accurate determination of the lattice parameters of molybdenum and tantalum. For the former, the 400 reflection occurs at 78° and for the latter the 330 reflection at 82°. Nelson and Riley's <sup>7</sup> function was used to obtain the extrapolated values of the parameters at 90°.

The alloys of intermediate composition were brittle and could be powdered readily to pass a 200-mesh sieve; for the other alloys filings of less than 200 mesh were used. The powder samples were annealed at 1200°–1500° C. for 5 hr. in molybdenum boats in evacuated silica tubes. This annealing treatment was required to obtain sharp diffraction photographs with resolved high-angle doublets. All the alloys were single phase with a body-centred cubic structure. The lattice parameters, given in Table II, have been corrected to 20° C., assuming the thermal coefficients of expansion of the alloys to vary linearly between those of the two pure metals. The coefficients of expansion of molybdenum and tantalum are very similar,  $4.9 \times 10^{-6}$  and  $6.5 \times 10^{-6}$  respectively, and with the small temperature corrections that are involved this appears to be justified.

The parameters of the alloys prepared by sintering for 1 hr. at 1850° C. are also included in Table II for comparison. They show that equilibrium had not been obtained; this was most marked in the tantalum-rich alloys, which X-ray photographs showed to consist of two body-centred cubic phases.

TABLE II.—*Lattice Spacings of Molybdenum-Tantalum Alloys.*

Tantalum, at.-%	Lattice Spacing at 20° C., kX	
	Arc-Melted Alloys	Sintered Alloys
0	3.1406	3.1404
0	3.1404	...
11.2	3.1541	3.1478
25.2	3.1747	3.1690
34.8	3.1858	3.1795
44.1	3.2007	3.1923
53.8	3.2150	3.2140
67.5	3.2372	...
80.8	3.2627	...
100	3.2973	...
100	3.2974	...

To determine whether a superlattice was formed, powdered samples of alloys containing 44.1, 53.8, and 67.5% tantalum were annealed at 1500° C. for 5 hr. and then at 400° C. for 100 hr. No superlattice lines were detected in the X-ray powder photographs.

A lattice parameter/composition curve is plotted in Fig. 1. There is a slight negative deviation from

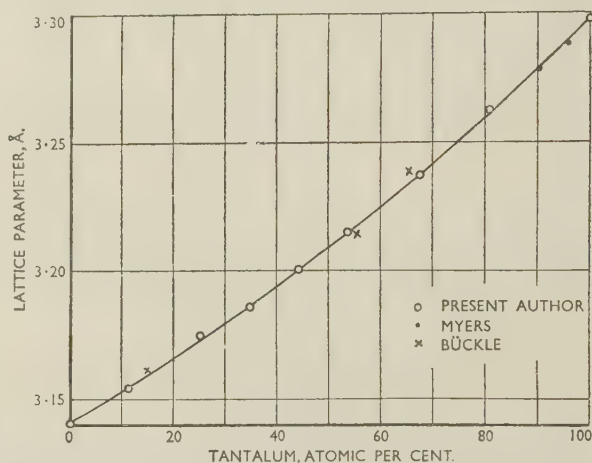


Fig. 1.—Lattice Parameters of Molybdenum-Tantalum Alloys.

Vegard's law, which reaches a maximum at 62.5% tantalum. Data from Bückle<sup>2</sup> and Myers<sup>3</sup> are also included in Fig. 1. The data from the former are for alloys sintered at 2100°–2600° C. and those from the latter for tantalum-rich alloys sintered at 2600° C. The values, particularly those of Myers, lie close to the curve.

#### 2. DENSITY MEASUREMENTS

Before density measurements were made, the alloys were sectioned or broken into lumps to determine whether there was any porosity. No blowholes were found, and the densities of the lump alloys were measured by means of a density bottle. The values are given in Table III, which also includes the densities calculated from the lattice parameters using the formula  $\rho = KnM/V^1$ , where  $n$  = the number of atoms per unit cell,  $M$  = the averaged

atomic weight,  $V^1$  = the volume of the unit cell in  $kX^3$  using the Siegbahn X-ray wave-lengths, and  $K$  a numerical constant = 1.6502, which takes account of Avogadro's number and the conversion of  $kX$  units to centimetres.

TABLE III.—*Densities of Molybdenum-Tantalum Alloys.*

Tantalum, at.-%	Density, g./c.c.	
	Measured at 20°C.	Calculated
0	10.17	10.22
5.4	10.65	10.64
17.8	11.65	11.68
34.8	12.87	12.80
44.1	13.50	13.43
53.8	14.13	14.06
67.5	14.95	14.91
80.8	15.70	15.63
100	16.61	16.65

The calculated densities agree with the experimentally determined values to within 0.5%, which is within the experimental error of the density measurements.

### 3. MELTING POINTS

The approximate melting points of some of the alloys were determined in the arc furnace, using an optical pyrometer. The alloys were loaded into the furnace with samples of pure molybdenum and tantalum, and were melted in turn without altering the conditions in the furnace. The technique used was to maintain a small molten pool of the alloy on the surface of the sample and to measure the temperature of the junction of the molten and solid metal with a disappearing-filament pyrometer. There was considerable adsorption of radiation in the argon atmosphere and the silica window, but from the observed melting points of the pure metals a correction factor can be obtained. To check that the adsorption conditions did not alter, the melting points of the standards were determined both before and after melting the alloys. For the degree of accuracy that can be realized by this method, which measures a

TABLE IV.—*Melting Point of Molybdenum-Tantalum Alloys.*

Tantalum, at.-%	Observed Melting Points, °C.		Corrected Melting Point, °C.
	Expt. No. 1	Expt. No. 2	
0	2240	2200	2620*
11.2	...	2200	2630
25.2	...	2260	2700
44.1	...	2300	2760
53.8	2390	...	2810
67.5	2420	...	2850
80.8	2450	...	2880
100	2560	2520	3000*

\* Assumed values.

temperature between the liquidus and solidus, a linear correction factor is justified; this varies from 400° C. at the melting point of molybdenum to 460° C. at that of tantalum. The observed and corrected melting points given in Table IV are possibly correct to about  $\pm 50^\circ$  C. Values of 2620° and 3000° C. are assumed for molybdenum and tantalum respectively.

The melting points lie on a smooth curve, without a maximum or minimum, which is very slightly curved towards the composition axis.

### 4. METALLOGRAPHY

Specimens for microscopical examination were prepared by grinding to 0000 grade emery paper and polishing with diamond dust ( $0-2\mu$ ), using white spirit as a lubricant. With these hard alloys this produced a surface substantially free from scratches and suitable for micro-examination.

The alloys as prepared in the arc furnace are virtually in the chill-cast condition and have a heavily cored solid-solution structure. This is best shown by a differential etch: 10 sec. in a 3% HF solution in concentrated  $HNO_3$ , followed by 10 sec. in 10%  $K_3Fe(CN)_6$ , 10% KOH in water. The first etchant brings up the grain boundaries and the second the cored structure of the grains. This structure is shown in Fig. 2 (a) (Plate XXVI), for the 34.8% tantalum alloy as melted in the furnace. Subsequent annealing for 12 days at 1200° C. did not remove the coring (Fig. 2 (b)), but by annealing for 30 min. in the arc furnace just below the melting point, homogeneous grains of the solid solution could be obtained (Fig. 2 (c)). After this arc-annealing treatment all the alloys had a homogeneous equi-axed grain structure. Hardness measurements were made on all alloys in the annealed and slowly cooled condition. The hardness values lie on a smooth curve reaching a flat maximum at about 500 V.P.N. between 50 and 60% tantalum.

### IV.—DISCUSSION

The experimental evidence shows that molybdenum and tantalum form a continuous series of body-centred cubic solid solutions with each other. No intermediate phases or superlattices forming at lower temperatures have been detected.

The alloys of the transition elements of Groups IVA, VA, and VIA with each other present an interesting series. All these elements crystallize in the  $A2$  (body-centred cubic) structure; in cases where there is more than one allotropic modification this is the high-temperature form. Hafnium is a possible exception; it is not definitely known whether it transforms to a cubic structure at high temperatures, though this is probably the case.

It is to be expected that a number of alloys of these metals would have continuous solid-solubility ranges, and this has proved to be the case for the binary system molybdenum-tantalum. Some information about other binary alloys that have been studied is



given in Table V. Only four ternary systems have been reported on, namely Nb-Ta-Mo, Nb-Ta-W, Nb-Mo-W, and Mo-Ta-W, all of which form continuous solid solutions.<sup>2</sup>

It can be seen from Table V that where the atomic

TABLE V.—Binary Alloy Systems Between Transition Elements of Groups IVA, VA, and VIA.

System	Remarks	Size Difference, %*	Deviation from Vegard's Law	Ref. No.
Ti-Cr	Continuous solubility below solidus. Cr <sub>3</sub> Ti <sub>2</sub> forms from this solid solution.	14.5	Not known	8
Ti-Zr	Continuous solubility in b.c.c. phase.	9	" "	9
Ti-Nb	"	0	" "	10
Ti-Mo	"	5	" "	10
Ti-Hf	"	...	" "	10
Ti-Ta	"	0	" "	10
Ti-W	"	4	" "	10
Cr-Zr	Compound Cr <sub>2</sub> Zr formed.	25	...	13
Cr-Nb	Compound Cr <sub>2</sub> Nb <sub>2</sub> formed.	14.5	...	15
Cr-Mo	Continuous solid solubility.	9	Positive	11
Cr-Ta	Compound Cr <sub>2</sub> Ta <sub>2</sub> formed.	14.5	...	15
Cr-W	Continuous solid solubility.	10	Positive	11
Zr-Mo	Compound ZrMo <sub>3</sub> formed.	14.5	...	13
Zr-Hf	Continuous solid solubility probable.	...	...	16
Zr-W	Compound ZrW <sub>2</sub> formed.	14	...	14
Nb-Mo	Continuous solid solubility.	5	Negative	7
Nb-Ta	" " "	0	" "	7
Nb-W	" " "	4	" "	7
Mo-Ta	" " "	5	" "	...
Mo-W	" " "	0	" "	12
Ta-W	" " "	4	" "	7

\* Values for interatomic spacing of  $\beta$ -Ti and  $\beta$ -Zr at room temperature taken as 2.85 and 3.10 Å., respectively.

radii differ by 14% or more, continuous solid-solubility ranges are not found, but intermediate phases occur. The system titanium-chromium presents a borderline case, for the size difference is about 14.5% and a continuous series of solid solutions occurs over a very restricted temperature range immediately below the

solidus. At lower temperatures an intermediate phase Cr<sub>3</sub>Ti<sub>2</sub> is formed. In all the other systems continuous solid solubility exists; with small size differences the deviations of the lattice parameters from the additivity rule (Vegard's law) are negative; for larger size differences they are positive. Superlattices have not been detected in any of the systems.

It may be predicted that continuous solid solutions will be formed in alloys of vanadium and titanium, chromium, niobium, molybdenum, tantalum, or tungsten, and in the systems zirconium-niobium and zirconium-tantalum. In the system vanadium-zirconium an intermetallic compound may be expected.

#### ACKNOWLEDGEMENT

The authors wish to express their appreciation to Dr. T. E. Allibone, F.R.S., for permission to publish this paper.

#### REFERENCES

1. W. von Bolten, *Z. Elektrochem.*, 1905, **11**, 51.
2. H. Bückle, *Metallforschung*, 1946, **1**, 53.
3. R. H. Myers, *Metallurgia*, 1950, **42**, 3.
4. D. Summers-Smith, *Metallurgia*, 1949, **39**, 309.
5. G. A. Geach and D. Summers-Smith, *Metallurgia*, 1950, **42**, 153.
6. W. C. Schumb, S. F. Radtke, and M. B. Bever, *Indust. and Eng. Chem.*, 1950, **42**, 826.
7. J. B. Nelson and D. P. Riley, *Proc. Phys. Soc.*, 1945, **57**, 160.
8. M. K. McQuillan, *J. Inst. Metals*, 1951, **79**, 379.
9. J. D. Fast, *Rec. Trav. Chim.*, 1939, **58**, 972.
10. B. W. Gonser, *Indust. and Eng. Chem.*, 1950, **42**, 222.
11. O. Kubaschewski and A. Schneider, *Z. Elektrochem.*, 1942, **48**, 671.
12. F. A. Fahrenwald, *Trans. Amer. Inst. Min. Eng.*, 1917, **56**, 612.
13. H. J. Wallbaum, *Naturwiss.*, 1942, **30**, 149.
14. A. Claassen and W. G. Burgers, *Z. Krist.*, 1933, **86**, 100.
15. O. Kubaschewski, A. Schneider, and M. Flad, *F.I.A.T. Rev. German Sci.*, 1939-1946. *General Metallurgy*, 1948, 75.
16. J. H. de Boer and J. D. Fast, *Z. anorg. Chem.*, 1930, **187**, 193.

PHOTOMICROGRAPHS OF 65.2 AT.-% MOLYBDENUM-34.8  
AT.-% TANTALUM ALLOYS.

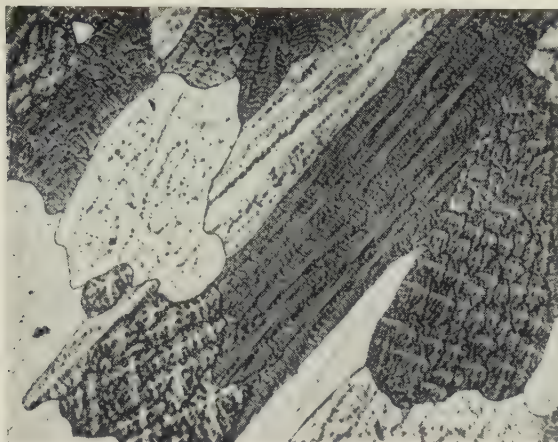


FIG. 2 (a).—As Melted.  $\times 30$ .



FIG. 2 (b).—Annealed 12 Days at  $1200^{\circ}\text{C}$ .  $\times 75$ .

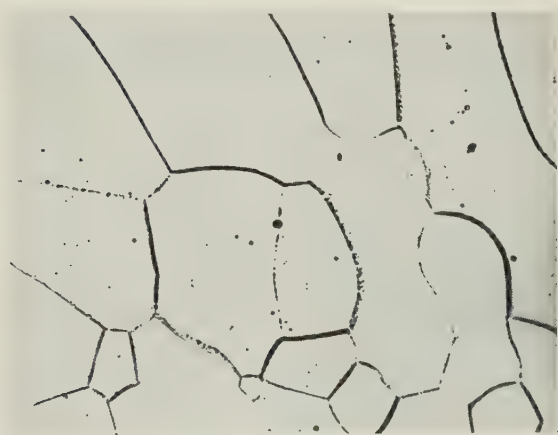


FIG. 2 (c).—Arc-Annealed 30 Min.  $\times 90$ .





# AN INVESTIGATION OF THE STRUCTURAL CHANGES ACCOMPANYING CREEP IN A TIN-ANTIMONY ALLOY \*

1335

By W. BETTERIDGE,† Ph.D., F.Inst.P., and A. W. FRANKLIN,†  
M.Sc., A.I.M., MEMBER

## SYNOPSIS

A tin-5% antimony alloy has been used for a microscopical study of the phenomena occurring during creep at room temperature. In addition to general slip within the grains and flow at the grain boundaries, it is shown that localized strain within the grains occurs in directions associated with the boundaries between adjacent grains. This latter plastic flow will be important in any consideration of the quasi-viscous flow of grain boundaries, since it will influence the effective shearing force acting on the flowing boundary. It is also suggested from this work, and from an examination of a pure aluminium sample strained in creep at 250° C., that the "cell structure" observed by X-ray examination is a consequence of the break-up of the grains by the slip bands and by the local strains.

## I.—INTRODUCTION

A NUMBER of recent papers have dealt with the mechanism of creep in metals as determined by X-ray and microscopic observation of samples strained at different rates and at different temperatures. These have generally supported the view that, while at lower temperatures and faster rates of straining the creep is largely due to crystallographic slip, at higher temperatures and slower straining rates the deformation is associated with the formation of a sub-structure within the grains. Sub-structures have been observed before, but their importance to the phenomenon of creep has been appreciated only in consequence of the recent X-ray investigations. The sub-structure so revealed has been referred to by Wood and his collaborators<sup>1,2,3</sup> as a "cell structure." The relationship between this cell structure and the sub-structure produced by straining and subsequent annealing which is described by the term "polygonization" has been discussed recently.<sup>4,5</sup>

The much earlier work of Hanson and Wheeler<sup>6</sup> has also shown that at fast strain rates the deformation is largely a consequence of slip-band formation within the grains, but that at slower rates grain-boundary flow is an important feature, although, of necessity, it is accompanied by distortion of the individual grains which occurs without the formation of well-marked slip bands. While grain-boundary flow has clearly occurred to a marked extent in the high-temperature, slow-strain tests of the recent investigators, attention has mainly been focused by them on the mechanism of deformation of the grains, without which appreciable grain-boundary flow cannot take place. Such an outlook is a consequence of the use of X-ray

methods which are not sensitive to grain-boundary flow. It is suggested that a better appreciation of the mechanism of creep deformation can be obtained if grain distortion and grain-boundary flow are considered together, although a detailed analysis of the separate processes is, of course, necessary in a complete theory.

Most of the work of earlier investigators has been carried out on pure aluminium. It was thought, however, that a microscopic study of the creep process in a tin-5% antimony alloy might furnish unique evidence which would be of value to a fuller understanding of the mechanism of the deformation process, since this alloy has been shown by Carpenter and Elam<sup>7</sup> to reveal grain-boundary movements on annealing without recourse to repeated etching.

## II.—EXPERIMENTAL PROCEDURE

The tin-antimony alloy for this work was prepared by melting under charcoal commercially pure tin and the required amount of antimony to give a 5% antimony alloy. No melting loss was allowed for, and it was assumed that the cast ingot was of satisfactory composition. The metal was cast into a slab 12 × 9 × 1 in. thick, which was machined all over and then cold rolled to approximately  $\frac{1}{4}$  in. thick. At this stage, some preliminary experiments were carried out which confirmed that grain-boundary migration could be seen when intermittent annealing of a microsection was carried out.

Flat creep specimens,  $\frac{3}{8} \times \frac{3}{16}$  in. with a 2-in. gauge-length, were machined from the rolled strip, rough polished by hand on one flat side, and then annealed for 16 hr. at 190° C. It was established by pre-

\* Manuscript received 11 January 1951.

† The Mond Nickel Co., Ltd., Birmingham.



liminary experiment that this annealing treatment would give a satisfactory grain-size. Specimens were finally prepared by alternate polishing and etching with concentrated ammonium sulphide solution. A simple dead-weight loading system was used for the creep tests, which were carried out at a room temperature of between 20° and 25° C.

### III.—EXPERIMENTAL RESULTS

The creep curves obtained by testing at stresses between 712 and 1420 lb./in.<sup>2</sup> are shown in Fig. 1.

Fig. 1) are shown in Figs. 4 and 5 (Plate XXVII) respectively, after both had been strained to approximately 0.2% extension, the first in 6 hr. and the second in 1000 hr. It is evident that similar changes have occurred in both specimens, even though there was a 200-fold difference in the rate of extension. The first of these two specimens was further strained to 1.4% in 71 hr. in order to develop the structure, typical examples of which are shown at low and high magnifications in Figs. 6 and 7 (Plate XXVII), respectively, and illustrate the salient characteristics

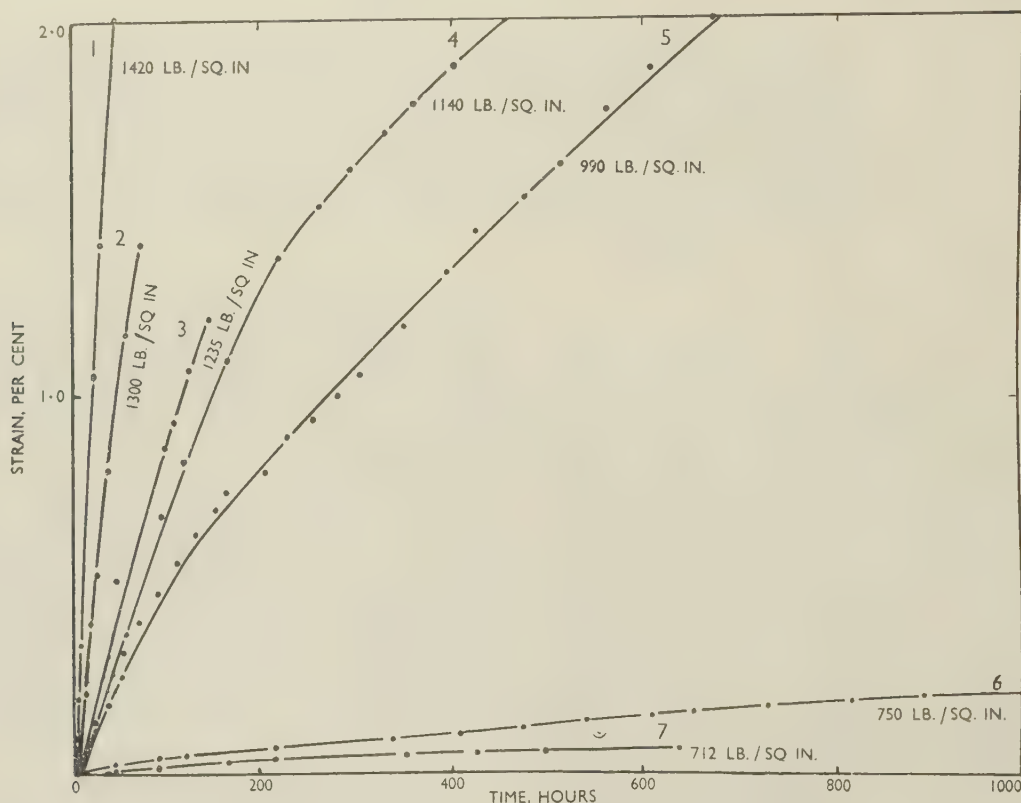


FIG. 1.—Experimental Creep Curves for Tin-5% Antimony Alloy.

The first specimen was etched before the test and strained 3.07% in 66 hr. A typical area after test is illustrated in Fig. 2 (Plate XXVII). Unfortunately, the method of protecting the specimen from dust was not adequate and the detailed structure is obscured, but locally concentrated strain marks and the displacement of scratches at or near grain boundaries could clearly be recognized. A typical example of scratch displacement is shown in Fig. 3 (Plate XXVII).

Further tests were carried out without initial etching of the specimens, it being postulated that if grain-boundary movements occurred then the grains should be revealed without etching.

Although eight specimens in all were tested, particular interest lay in specimens strained at high and low rates. Typical fields of specimens tested at 1300 and 750 lb./in.<sup>2</sup> (curves (2) and (6) in

which appeared to greater or less degrees in all specimens. These were:

(i) Rumpling of the surface of grains, varying from relatively sharp parallel lines characteristic of normal slip bands, to irregular markings with only an indication of a general direction. This effect tended to occur most markedly in the smallest grains of a specimen.

(ii) Severely localized strain marks within the grains, usually, but not invariably, running from points of intersection of grain boundaries. (A and B, Fig. 7, Plate XXVII).

(iii) Thickening of grain boundaries (C, Fig. 7).

(iv) Displacement of scratches at grain boundaries (E, Fig. 7).

(v) Subsidence of part of a grain (D, Fig. 7).

Examination of the first of these features at higher magnifications afforded no further information, as the slopes of the surface were too slight to give adequate contrast, but interesting observations were made on features (ii), (iii), and (iv). The thickening of the grain boundaries and the displacement of scratches were clearly due to grain-boundary flow, the former effect being caused by the component of motion perpendicular to the surface of the specimen and the latter to the component in the plane of the surface. The example shown in Fig. 8 (Plate XXVII) illustrates the apparent widening of grain boundaries by the step formed between the two grains. The escarpments were generally quite steep and, on examination under dark-field illumination, appeared light, as shown in Fig. 9 (Plate XXVII). Under these conditions of illumination the rumples within the grains did not show at all, proving that the slope of these rumples was much less steep than that of the grain-boundary steps.

All specimens were found to show grain-boundary movement to varying degrees, as determined by the amount of displacement of scratches, and the extent of movement differed considerably from boundary to boundary in any particular specimen. It must be remembered that only movements in the plane of the specimen are shown by these scratch displacements. An attempt was made to correlate the amount of boundary movement with the direction of the grain boundaries, as it was expected that the greatest amount of movement would occur on those boundaries lying in the direction of maximum shear stress, but although an indication of a linear relationship between the resolved shear stress and the displacement was obtained, the results were extremely scattered.

Such grain-boundary movements as are demonstrated by the above observations must produce corresponding modifications of the stress in the adjacent grains. Starr<sup>8</sup> has examined the case of a plane crack in an isotropic elastic medium and has shown that, if a uniform shear stress is applied in the plane of the crack, high shear-stress concentrations are produced in the direction of prolongation of the crack. If grain boundaries are regarded as cracks filled with viscous material, then the same considerations will apply to the equilibrium condition when grain-boundary flow has ceased owing to the elastic restraint of the surrounding matrix. If now the matrix is not perfectly elastic and the shear-stress concentrations reach a high enough level, grain slip will occur. When the grain boundary lies in a plane of maximum applied shear stress, the slip in the neighbouring grain will be exactly in the direction of prolongation of the boundary, but even if the boundary lies at an angle to the plane of maximum applied shear stress, the direction of slip in the neighbouring grain will deviate only slightly from the direction of the boundary. These conditions are illustrated diagrammatically in Fig. 15. The initial condition of three grains is shown in (a); after flow has occurred between grains *A* and *B* in the direction

indicated in (b), stress concentration leading to shear along the dotted line in grain *C* would occur. Such shear would, however, not be expected to be observed microscopically except by the displacement of scratches, since there would be no difference in level between the parts of grain *C* on either side of the line of shear. In Fig. 15 (c), however, grains *A* and *B* are supposed to move relatively to one another in a direction perpendicular to the diagram, so that *A* is higher than *B*; corresponding displacements of the two parts of grain *C* will occur, so that a visible step will be produced as a prolongation of the boundary

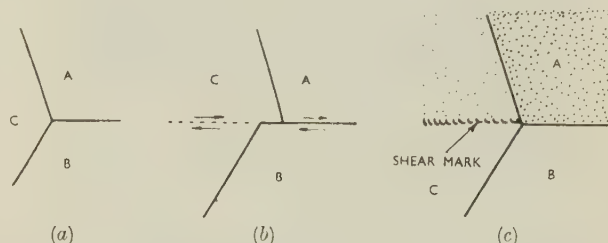


FIG. 15.—Diagrammatic Representation of How Grain-Boundary Movement Between Grains *A* and *B* is Accommodated by Shear in Grain *C*.

- (a) Before strain.
- (b) After strain. Grain boundary between *A* and *B* sheared to produce shear in grain *C*.
- (c) After strain. Same boundary sheared as in (b), but in direction normal to figure. Shaded part of *C* rises to produce a shear mark as a prolongation of the grain boundary.

between the grains *A* and *B*. This is put forward as an explanation of the many markings of type (ii) which were observed in all specimens. Specimens were closely examined in a search for such a mark which could be shown unambiguously to be due to the mechanism described, and Fig. 10 (a) (Plate XXVIII) provides the clearest example. The scratches crossing boundary *Y* are not displaced, those crossing *X* are only slightly displaced, while those crossing *Z* show a very large displacement, and the mark *A* is essentially a prolongation of this boundary. The mark would not, however, be visible, except for the displacement of scratches as at *B*, if the movement were only in the plane of the surface; but it is clear from the difference in focus on either side of the grain boundary *Z* and of the mark *A*, revealed in the high-magnification photograph Fig. 10 (b) (Plate XXVIII), that movement has also occurred perpendicular to the surface.

A careful search of all specimens was made for markings within the grains similar to those described as the cell structure by Wilms and Wood (Fig. 2 of their paper<sup>1</sup>). A few areas were found in which such markings were present, and Fig. 11 (Plate XXVIII) illustrates one of these under oblique illumination. In no case, however, was any displacement of scratches observed at the boundaries of such a network, and in view of the more obvious indications of strain of the grains by the presence of the irregular slip bands and the localized shear marks, it was felt that the



former markings must play a much less significant part.

In view of these observations on the tin-antimony alloy, it was thought desirable to examine a sample of pure aluminium in order to determine whether the microscopically observable cell structure was more readily developed in that material and whether any relationship between such a structure and other strain markings could be detected. A creep test-bar,  $\frac{1}{2}$  in. in dia. of wrought and annealed 99.99% aluminium was prepared with two diametrically opposite flats to facilitate microscopic examination. This bar was electrolytically polished in a standard perchloric acid-acetic anhydride bath,<sup>9</sup> using a potentiometric circuit, and was microscopically examined. A hazy network pattern was observed over the whole surface of the specimen when the polishing was carried out at the lower end of the range of current densities specified by Jacquet, and this network became more pronounced with reduction of the current density. It could be shown up most clearly by obliquely incident illumination, and is illustrated in Fig. 12 (Plate XXVIII). The structure appears very similar to that shown by Wilms and Wood as a typical example of the cell structure produced after slow straining.

The aluminium test-bar was then loaded in a creep-testing machine to a stress of 1000 lb./in.<sup>2</sup> at a temperature of 250°C., and after 25 hr. it had stretched 9.42%. A further microscopic examination of the surface showed that the structure referred to above was still clearly visible, under oblique illumination (Fig. 13, Plate XXVIII), but only faintly under normal illumination (Fig. 14, Plate XXVIII), when the additional markings due to the creep strain were exactly similar to those in the tin-antimony alloy, viz. rather irregular slip bands within the grains, displaced and thickened grain boundaries, and strain marks within the grains extending from adjacent boundaries. On this aluminium sample it was confirmed by back-reflection X-ray photographs that the initially perfect grains had each broken up into a number of small "cells."

#### IV.—DISCUSSION

The use of the tin-5% antimony alloy as the experimental material has not resulted in the observation of any unique phenomena, but three different microscopically detectable mechanisms appear to take part in the creep process, viz :

- (i) Viscous flow at the grain boundaries.
- (ii) General slip within the grains characterized by the formation of slip bands varying from fine straight bands to very irregular coarser bands.
- (iii) Localized strain within the grains, often associated with the grain boundaries between neighbouring grains which have flowed viscously.

The first two of these processes are well known and have been described by Hanson and Wheeler,<sup>6</sup> but

the importance of the last one does not appear to have been pointed out before. The elastic and plastic properties of the grains which are deforming in this manner will clearly be of importance in controlling the rate of viscous flow of the boundaries. A separate theoretical study of this problem is being made.

The microscopical examination of the unstrained pure aluminium shows that critical etching conditions can develop a structure very similar in appearance to that described as the cell structure by Wilms and Wood,<sup>1</sup> and Lacombe and Beaujard<sup>10</sup> have also shown that such structures can be formed in unstrained metals. True cell formation is convincingly proved by the X-ray examinations of Wilms and Wood, and since Wood and Rachinger<sup>2</sup> have shown that the number of cells into which a grain divides during creep increases with increasing rate of strain and also with decrease in temperature, while at the same time the number of slip bands increases, it is difficult not to associate the division of a grain into cells with its division by the intersecting slip bands, as in fact was suggested by Wood and Rachinger for the lower-temperature tests. Although, if the slip were perfectly regular, no relative rotation of the different portions into which a grain is divided would result, the irregularity in direction of the slip bands, particularly when the creep-rate becomes slower, suggests that some relative rotation must take place. In the creep tests at the slowest rates, after which according to Wood and Scrutton<sup>3</sup> no evidence of crystallographic slip is visible, subdivision of the grains would still occur by the third process mentioned above, viz. strain along the directions of extension of the boundaries between neighbouring grains. This phenomenon is clearly shown in the work of Wood and Scrutton<sup>3</sup> and of Wilms and Wood<sup>1</sup> for samples in which cell formation is claimed without the generation of slip bands.

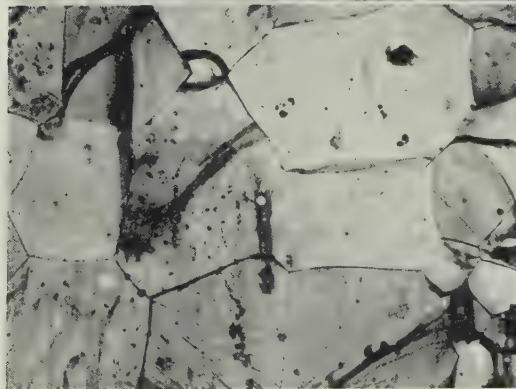
#### ACKNOWLEDGEMENTS

The authors wish to thank The Mond Nickel Co., Ltd., for permission to publish this paper. Their thanks are also due to Dr. L. B. Pfeil, O.B.E., F.R.S., for suggesting the investigation.

#### REFERENCES

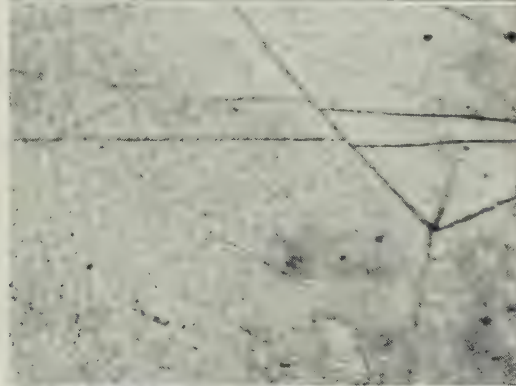
1. G. R. Wilms and W. A. Wood, *J. Inst. Metals*, 1948-49, **75**, 693.
2. W. A. Wood and W. A. Rachinger, *J. Inst. Metals*, 1949-50, **76**, 237.
3. W. A. Wood and R. F. Scrutton, *J. Inst. Metals*, 1950, **77**, 423.
4. R. Eborall, *J. Inst. Metals*, 1948-49, **75**, 1124 (discussion).
5. G. B. Greenough and E. M. Smith, *J. Inst. Metals*, 1950, **77**, 435.
6. D. Hanson and M. A. Wheeler, *J. Inst. Metals*, 1931, **45**, 229.
7. H. C. H. Carpenter and C. F. Elam, *J. Inst. Metals*, 1920, **24**, 83.
8. A. T. Starr, *Proc. Camb. Phil. Soc.*, 1928, **24**, 489.
9. P. Jacquet, *Métallurgie, Corrosion, Usure*, 1943, **18**, 198.
10. P. Lacombe and L. Beaujard, *J. Inst. Metals*, 1947-48, **74**, 1.

TIN-5% ANTIMONY ALLOY.



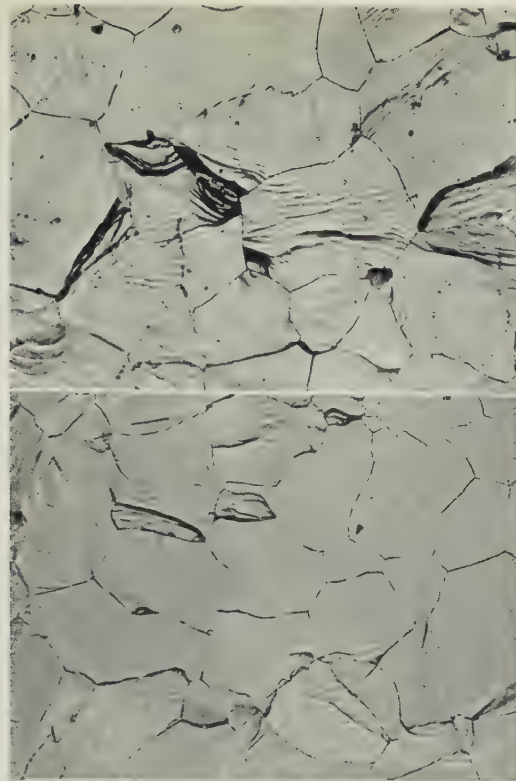
Typical Fields of Specimen Strained 3.07% in 66 Hr. at 1420 lb./in.².

FIG. 2.—Etched in Ammonium Sulphide Solution.  $\times 100$ .



Typical Fields of Specimens Strained Approximately 0.2%.  $\times 50$ .

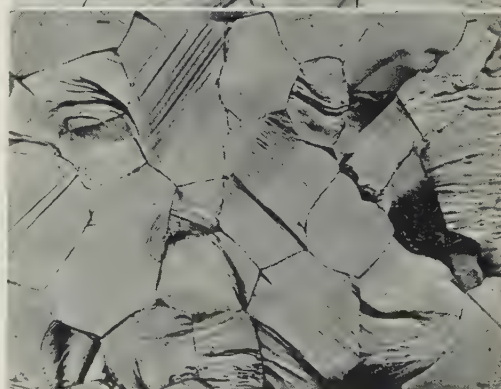
FIG. 3.—Showing Displacement of Scratches at Grain Boundary.  $\times 1000$ .



Typical Fields of Specimens Strained Approximately 0.2%.  $\times 50$ .

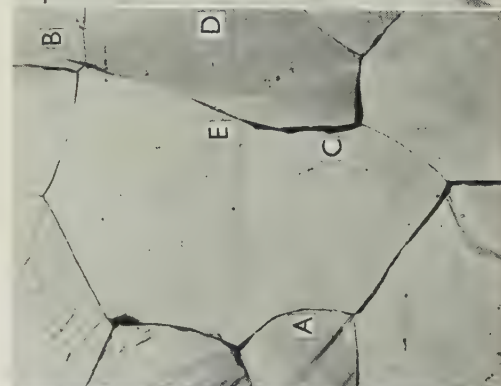
FIG. 4.—In 6 Hr. at 1300 lb./in.².

FIG. 5.—In 1000 Hr. at 750 lb./in.².



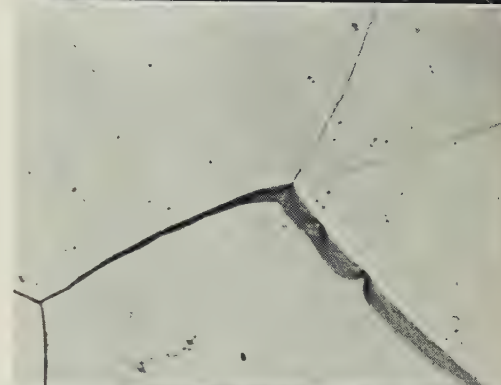
Specimen in Fig. 4 Further Strained to 1.4% in 71 Hr. at 1300 lb./in.².

FIG. 6.— $\times 75$ .



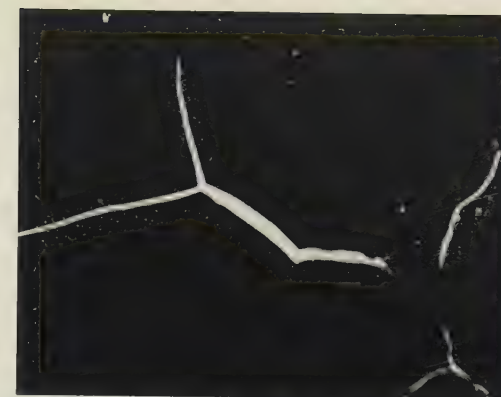
Specimen in Fig. 4 Further Strained to 1.4% in 71 Hr. at 1300 lb./in.².

FIG. 7.— $\times 500$ .



Specimen in Fig. 4 Further Strained to 1.4% in 71 Hr. at 1300 lb./in.².

FIG. 8.—Normal Illumination.  $\times 500$ .



Specimen in Fig. 4 Further Strained to 1.4% in 71 Hr. at 1300 lb./in.².

FIG. 9.—Dark-Field Illumination.  $\times 300$ .

All photomicrographs reduced by  $\frac{1}{10}$ th linear in reproduction.





FIG. 10.—Grain-Boundary Movements at Intersection of Three Grain Boundaries at C in Tin-5% Antimony Alloy.

(a) Shear at A arising from movement in grain boundary Z.  $\times 1500$ .

(b) Showing that movement perpendicular to the surface has occurred.  $\times 5000$ .

FIG. 11.

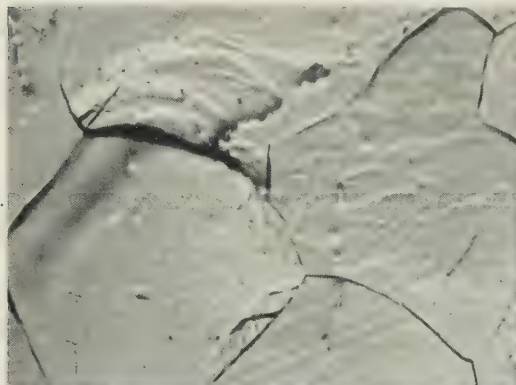


FIG. 12.

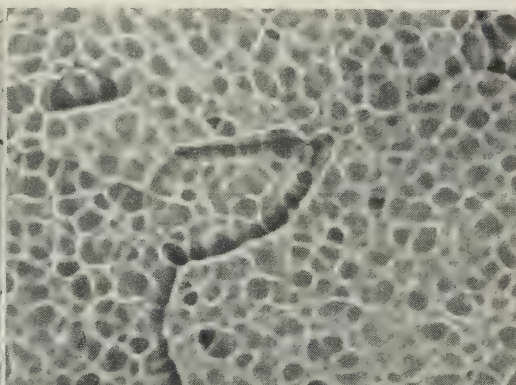


FIG. 13.

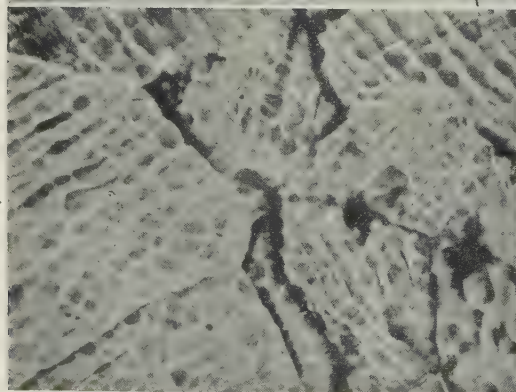


FIG. 14.

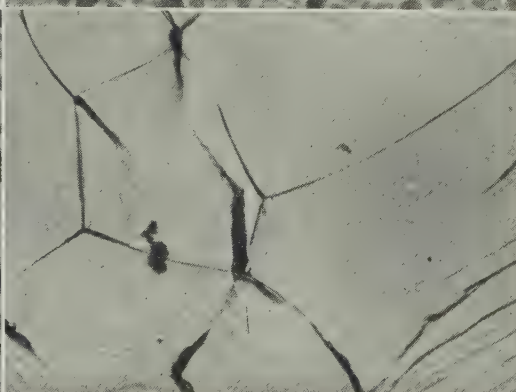


FIG. 11.—Examples of "Cells" in Tin-5% Antimony Alloy Strained 0.42% in 2051 hr. Similar to Those Described by Wilms and Wood in Aluminium. Oblique illumination.  $\times 300$ .

FIGS. 12-14.—Structure of Electropolished Pure Aluminium (99.99%) Before and After Straining 9.42% at 250° C. in 25 Hr. at 1000 lb./in.<sup>2</sup>.  $\times 200$ .

FIG. 12.—Before Creep Test. Oblique illumination.

FIG. 13.—After Creep Test. Oblique illumination.

FIG. 14.—After Creep Test. Normal illumination.

All photomicrographs reduced by  $\frac{1}{16}$ th linear in reproduction.

# THERMOELASTIC ANALYSIS OF TRANSFORMATIONS 1336 IN COPPER ALLOYS \*

By R. CABARAT,† P. GENCE,‡ PROFESSOR L. GUILLET,§  
and R. LE ROUX ||

## SYNOPSIS

The purpose of the investigation was to demonstrate the effect of allotropic transformations on the elastic modulus and logarithmic decrement of copper alloys. To determine these two properties a specimen was subjected to forced longitudinal vibrations of small amplitude and high frequency under reduced pressure. The formation of body-centred cubic phases on heating eutectoid copper-aluminium and copper-tin alloys results in a marked decrease in the elastic modulus, while the logarithmic decrement assumes large values before and during the transformation. The results are discussed in the light of present knowledge of the structure of alloys.

## I.—INTRODUCTION

THERMOELASTIC analysis is one of the physico-thermal methods that are often used to reveal transformations in alloys through the changes taking place in physical properties with temperature. Sudden changes in these properties occur at certain temperatures, corresponding to changes in lattice structure, the appearance or disappearance of a phase, &c. Physico-thermal methods have the advantage that their sensitivity is independent of the rate of heating and cooling.

Among the properties most frequently studied in this way are the coefficient of thermal expansion, electrical resistivity, thermoelectric power, specific heat, &c. The modulus of elasticity has been used to reveal anomalies in ferro-nickels,<sup>1</sup> cobalt,<sup>2</sup> and Monel metal,<sup>3</sup> allotropic transformations in steels<sup>4, 5</sup> and non-ferrous alloys,<sup>6, 7</sup> order-disorder transformations in gold-copper and copper-platinum alloys,<sup>7, 8</sup> as well as recrystallization phenomena in cold-worked metals.<sup>9, 10</sup> Variations in logarithmic decrement have also been determined in the case of order-disorder transformations in gold-copper and copper-platinum alloys and allotropic transformations in silver-zinc and silver-cadmium alloys.<sup>7</sup>

In order to measure the elastic properties accurately at high temperatures, viscous relaxation phenomena must be eliminated as far as possible, and dynamic methods are therefore particularly suitable. The present authors have already described<sup>11</sup> a new apparatus in which the specimen is subjected to forced longitudinal vibrations by means of an electrostatic field. This apparatus has since been improved so that it may be used at high temperatures, and the purpose of the present paper is to demonstrate its

suitability for revealing transformations in alloys. Copper-tin and copper-aluminium alloys were chosen for the work because their equilibrium diagrams are now well established; in addition, the transformation temperatures are not very high, so that there are no experimental difficulties. A slow rate of heating (1° C./min.) is necessary, to afford time to make the temperature measurements with the desired precision.

## II.—EXPERIMENTAL METHOD

The Cabarat elasticimeter depends on exciting longitudinal vibrations in a specimen electrostatically. The specimen, about 150–250 mm. long and 8–12 mm. in dia., is held in position by three hardened steel needles, between two adjustable electrodes *A* and *B* (Fig. 1).

A voltage amplified from a low-frequency oscillator is applied to electrode *A* and exerts a periodic electrostatic attraction on the specimen, thereby exciting longitudinal vibrations in it. Electrode *B* acts as an electrostatic microphone; the voltages produced in it by movements of the specimen are recorded after amplification on a cathode-ray oscilloscope, and can be measured by means of a valve voltmeter. The specimen is at earth potential. The amplitude of vibration is observable only if the frequency of the electrical vibrations coincides with the natural frequency of the specimen. Resonance is obtained by varying the frequency of the voltage between the electrode and earth by means of a variable condenser at the oscillator; the amplitude of the vibrations recorded on the oscillograph then passes through a very sharp maximum. The frequency read from the dial of the low-frequency oscillator (previously calibrated) is equal to the natural frequency ( $F_0$ ) of the specimen.

\* Manuscript received 15 March 1951. The investigation was sponsored by the Centre National de la Recherche Scientifique.

† Chef du Service d'Acoustique au Laboratoire d'Essais du Conservatoire National des Arts et Métiers, Paris.

‡ Ingénieur des Arts et Manufactures, Paris.

§ Professeur à l'Ecole Centrale et Chef de Travaux au Conservatoire National des Arts et Métiers, Paris.

|| Ingénieur du Conservatoire National des Arts et Métiers, Paris.



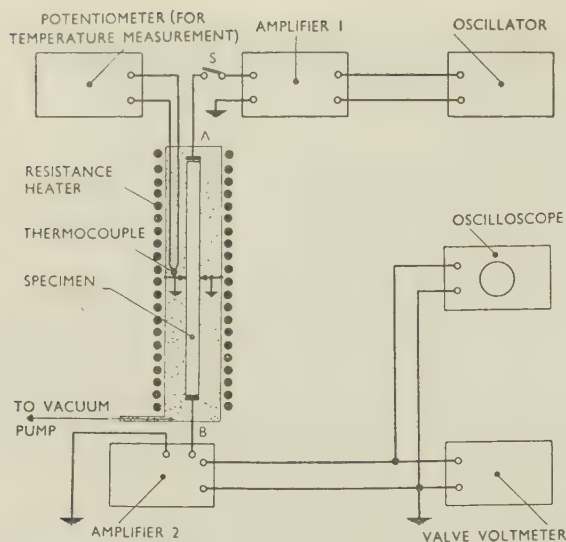


FIG. 1.—Schematic Diagram of the Apparatus.

If the density of the specimen is  $d$  and its length  $L$ , the elastic modulus ( $E$ ) is given by :

$$E = (2F_0L)^2d \quad (1)$$

The internal friction, represented by the logarithmic decrement ( $\delta$ ) of the vibrations, can be obtained from the resonance curve by the formula :

$$\delta = \pi \Delta F / F_0 \quad (2)$$

$\Delta F$  being the frequency interval separating two points on the resonance curve at which the amplitude is reduced to  $A_0/\sqrt{2}$  ( $A_0$  = peak amplitude).\*

The curve showing the exponential decay of the amplitude of vibration with time can also be recorded. The excitation of the specimen is cut off by the switch  $S$ , while leaving the microphone in action. To avoid errors due to the detection being no longer uniform at low microphone voltages, an amplifier having a logarithmic response is used. A straight line is thus obtained from which the value of the decrement can be calculated (Fig. 2). If  $t_s$  is the time in which the

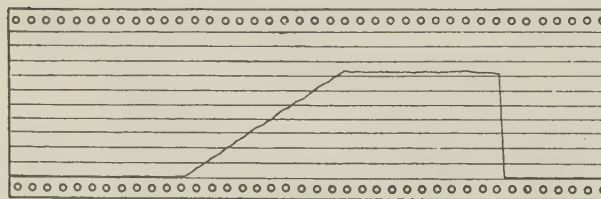


FIG. 2.—Oscillograph Record of Decay of Vibrations.

initial amplitude ( $A_0$ ) of vibration of the specimen is reduced to  $A_0/1000$ , then :

$$\delta = \frac{\log_e 1000}{F_0 \times t_s} = \frac{6.9}{F_0 \times t_s} \quad (3)$$

These two methods complement one another perfectly. For a material of high internal friction the resonance curve can conveniently be used; for a material with a very small damping capacity, however, the resonance curve is very sharp and the maximum amplitude is difficult to determine. In consequence  $\Delta F$  cannot be obtained accurately.

Acoustic radiation from the ends of the specimen can prove a serious source of error in measurements of internal friction, and for this reason the equipment for supporting the specimen and the electrodes is placed in a sealed tube in which the pressure is of the order of 0.1 mm. Hg. A systematic study of the damping of a steel specimen (250 mm. long  $\times$  10 mm. dia.) as a function of the degree of vacuum showed that the logarithmic decrement of the vibrations became constant at pressures below 1 mm. Hg (Fig. 3). The damping times corresponding to a reduction of the initial amplitude  $A_0$  to a value  $A_0/1000$  are reproducible to within about 5%.

This method has the advantage of being convenient for the study of the changes of elastic modulus and internal friction with temperature ( $\theta$ ); all that is necessary is to place the apparatus previously

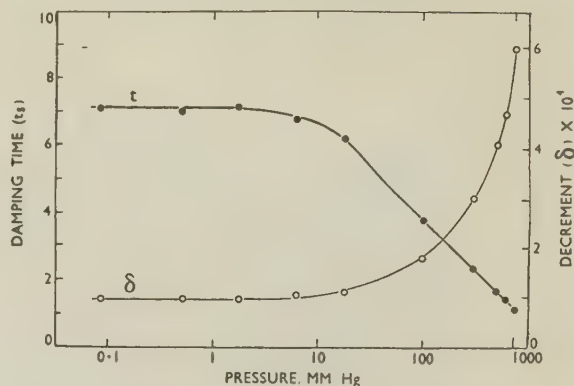


FIG. 3.—Time of Decay of Vibrations and Logarithmic Decrement of Steel Specimen as a Function of Pressure.

described in an electric furnace. To allow for the alteration in density and length of the specimen caused by the rise in temperature, a correction must be applied to the value of the modulus given by equation (1). If the density and length are measured at 20° C. and if  $\alpha$  is the mean coefficient of expansion of the metal between 20° C. and  $\theta$ , then

$$E_{\text{corr.}} = \frac{E_{\text{obs.}}}{1 + \alpha(\theta - 20)} \quad (4)$$

Chevenard's apparatus is used to obtain  $\alpha$ .

Fig. 4 shows the Cabarat elasticimeter, which is in the form of a desk. In the centre is the furnace  $D$  in which is situated the device for holding the specimen and the electrodes. Above the desk, on the left, is the cathode-ray oscilloscope  $C$  by means of which the electrodes are controlled, and the resonance of the specimen is observed when the condenser of the low-

\* See *J. Inst. Metals*, 1948-49, 75, 395 (Fig. 2).

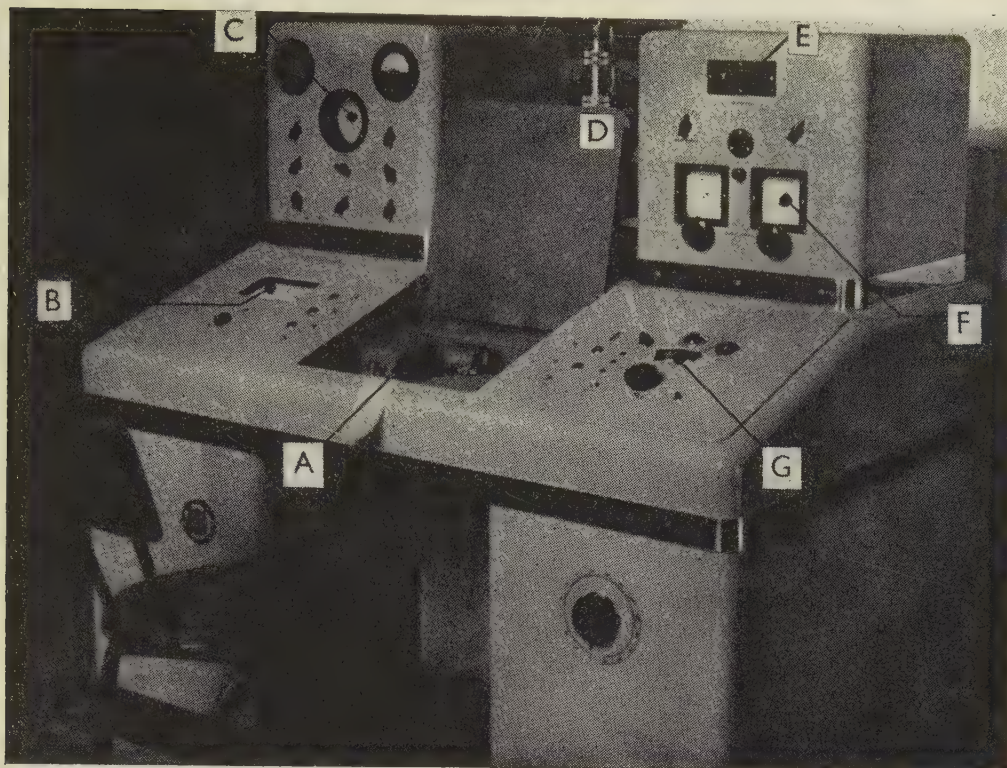


FIG. 4.—General View of the Apparatus.

frequency oscillator *F* on the right of the furnace is varied. On the desk itself, from left to right, are mounted the valve voltmeter *B*, the logarithmic recorder *A*, and the potentiometer *G* for measuring the temperature inside the furnace. *E* is the vacuum gauge.

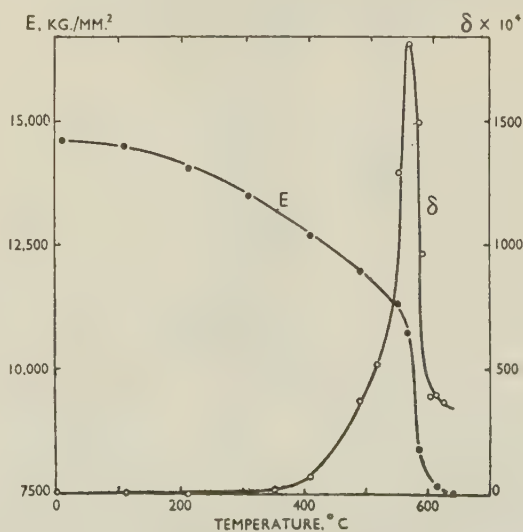
With this apparatus the frequency can be measured to  $\pm 1$  cycle in the range 5000–15,000 cycles/sec. To obtain this accuracy the low-frequency oscillator is calibrated against a tuning-fork having a frequency of 1000 cycles/sec. Particular care is taken to filter the supply current to the amplifiers, and the circuits are carefully shielded to avoid parasitic currents. Variations in the supply current have practically no effect on either the amplified microphone voltage or the frequency of the oscillator, as all the electrical equipment is fed through a voltage regulator.

The details of the furnace and of the specimen support are shown in Fig. 6. The furnace consists essentially of a steatite tube enclosing the well-lagged winding. Inside the furnace is a heat-resisting steel tube which can be evacuated at the lower end. A special tap cuts off the tube from the pump. The support for the specimen and the electrodes can easily be withdrawn from the tube, which is sealed by means of bolts and rubber joints. Finally, cooling fins reduce the heating of the upper part of the support, which comprises the rubber-sealed joints, soldered parts, and the milled knobs for controlling the electrodes.

### III.—EXPERIMENTAL RESULTS

#### 1. COPPER-ALUMINIUM ALLOYS

The alloy investigated was made from electrolytic copper and commercially pure aluminium (99.96%) and contained 11.95 wt.-% aluminium, which corresponds closely to the eutectoid composition (11.8%). It had been found that if a high-purity

FIG. 5.—Variation with Temperature of *E* and  $\delta$  for Annealed Copper-11.95% Aluminium Alloy.



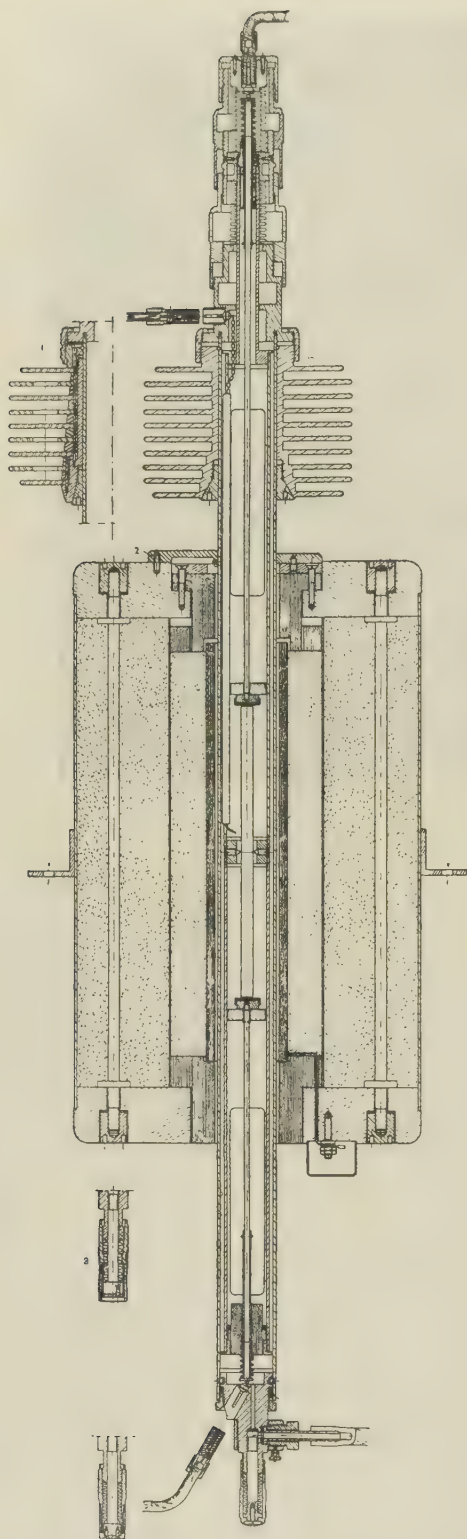
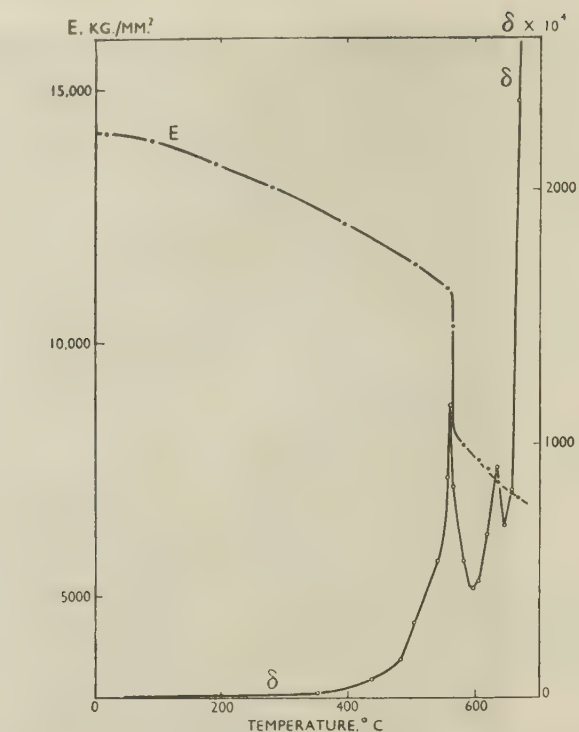
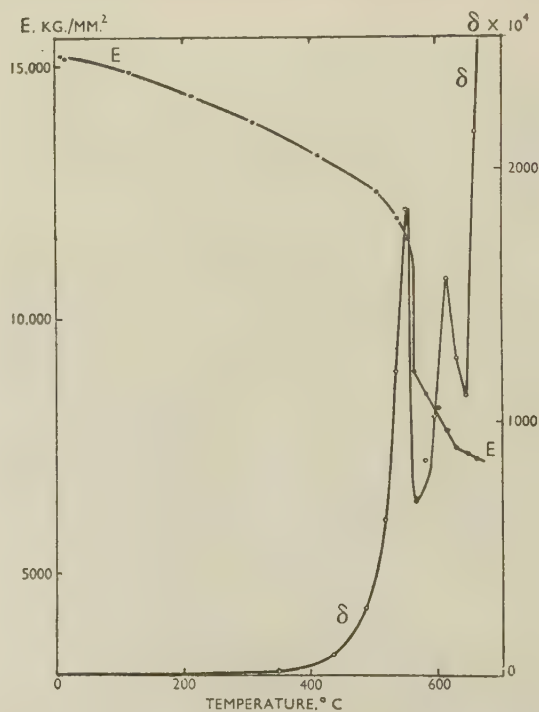


FIG. 6.—Sectional Diagram of the Furnace, Specimen, &amp;c.

aluminium was used a coarse structure always resulted in the alloy, whereas a fairly fine structure is desirable if adequate pseudo-isotropy is to be obtained. Ingots, 8 mm. in dia. and 150 mm. long, with a grain-size of 1150 grains/cm<sup>2</sup>, were made by casting into a

FIG. 7.—Variation with Temperature of  $E$  and  $\delta$  for Annealed Copper-11.40% Aluminium Alloy.FIG. 8.—Variation with Temperature of  $E$  and  $\delta$  for Annealed Copper-12.37% Aluminium Alloy.

graphite mould. The ingots were subsequently annealed for 100 hr. at 750°C.

Below 565°C., this alloy, when in equilibrium, consists of a mixture of  $\alpha$  (face-centred cubic, containing 9.4% aluminium) and  $\gamma$  (cubic with 52 atoms

per unit cell, containing 15.6% aluminium). This condition is obtained only if the rate of cooling is less than  $\frac{1}{2}^{\circ}\text{C./min.}$  If an alloy annealed as described is heated, it undergoes at  $565^{\circ}\text{C.}$  the transformation  $\alpha + \gamma \rightarrow \beta$ , accompanied by a very marked reduction in the elastic modulus  $E$  (see Fig. 5), owing to the disappearance of the  $\gamma$  phase, whose modulus is  $20,400\text{ kg./mm.}^2$  at  $20^{\circ}\text{C.}$ <sup>11</sup> The modulus of the body-centred cubic  $\beta$  phase obeys the law of mixtures at  $600^{\circ}\text{C.}$ , so that it can be calculated to within 5% from the moduli of copper and aluminium at that temperature. The logarithmic decrement  $\delta$  increases continuously as the temperature is raised and attains a considerable value *before* and during the transformation in spite of the fact that the latter is isothermal (see Fig. 5). The decrement is as small in the  $\beta$  condition as it is in the  $\alpha + \gamma$  state, but it reaches a value four times greater during the transformation.<sup>12</sup>

A hypo-eutectoid alloy and a hyper-eutectoid alloy, containing 11.40 and 12.37% aluminium respectively, were also studied. They undergo the  $\alpha + \gamma \rightarrow \beta$  transformation at  $565^{\circ}\text{C.}$ , but above this temperature the  $\alpha$  phase in the first case and the  $\gamma$  phase in the second have still not entirely disappeared, and the  $\beta$  phase field is reached at  $632^{\circ}$  and  $638^{\circ}\text{C.}$ , respectively.

The elastic-modulus/temperature and decrement/temperature curves therefore show two anomalies. The total disappearance of the  $\alpha$  and  $\gamma$  phases is preceded by a marked increase in internal friction, which reaches a maximum during the transformation; this is also revealed by a break in the modulus curve (see Figs. 7 and 8).

## 2. COPPER-TIN ALLOYS

The alloy investigated contained 24.9 wt.-% tin, whereas the eutectoid composition corresponds to 27 wt.-%. It was made from electrolytic copper and Union Minière du Haut Katanga tin and cast similarly to the copper-aluminium alloy; the ingots were subsequently annealed for 100 hr. at  $750^{\circ}\text{C.}$

Below  $520^{\circ}\text{C.}$ , the alloy when cooled at a rate of  $1^{\circ}\text{C./min.}$  consists of two phases:  $\alpha$ , which has a face-centred cubic lattice and contains 15% tin at  $500^{\circ}\text{C.}$ , and  $\delta$ , which has a cubic lattice of the  $\gamma$ -brass type and contains 32% tin.\* On heating, it undergoes a transformation similar to that in the aluminium bronzes, and above  $520^{\circ}\text{C.}$  it forms a body-centred cubic phase.

The disappearance of the  $\delta$  phase, with an elastic modulus of  $14,000\text{ kg./mm.}^2$  at  $20^{\circ}\text{C.}$ ,<sup>13</sup> results in a marked decrease in the modulus of the alloy. The decrement attains considerable values before the transformation and the decrement/temperature curve shows a relative maximum during the transformation (see Fig. 9).

Another hypo-eutectoid alloy containing only 20.2 wt.-% tin was also studied. In the annealed condi-

tion it contains the same phases as the previous alloy, but at  $20^{\circ}\text{C.}$   $\alpha$  is in excess.† The anomalies in the properties in the region of the transformation temperature are less marked, however, since above  $520^{\circ}\text{C.}$  this alloy still contains a considerable amount of  $\alpha$

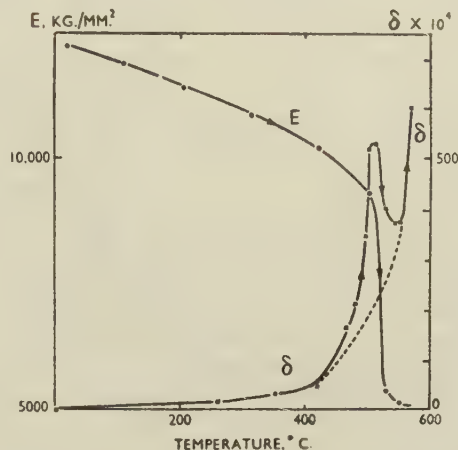


FIG. 9.—Variation with Temperature of  $E$  and  $\delta$  for Annealed Copper-24.9% Tin Alloy.

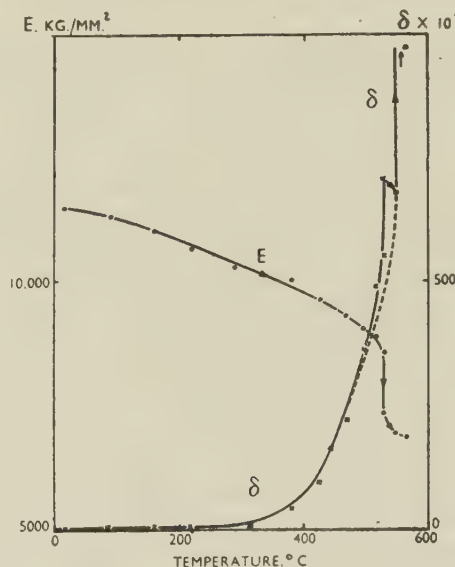


FIG. 10.—Variation with Temperature of  $E$  and  $\delta$  for Annealed Copper-20.2% Tin Alloy.

(see Fig. 10). At  $700^{\circ}\text{C.}$ , according to Raynor's diagram,<sup>14</sup> the body-centred cubic phase contains 23% tin and accounts for only 62% of the total mass.

The above examples have demonstrated the effect of a eutectoid-type transformation on the elastic modulus and decrement. Fig. 11, relating to an alloy containing 32.5 wt.-% tin (which corresponds exactly to the  $\delta$  phase or  $\text{Cu}_3\text{Sn}_8$ ) and having a grain-size of  $2300\text{ grains/cm.}^2$ , shows the effect of a transition

\* The  $\delta$  phase is not stable below  $350^{\circ}\text{C.}$ , but the rate of decomposition is very slow, and the present authors have not determined it.

† The modulus of elasticity of this alloy at  $20^{\circ}\text{C.}$  was less

than would be predicted from the curve already published<sup>13</sup>; this was due to the presence of some micro-blowholes in the specimen, but does not alter the form of the curves in Fig. 10.



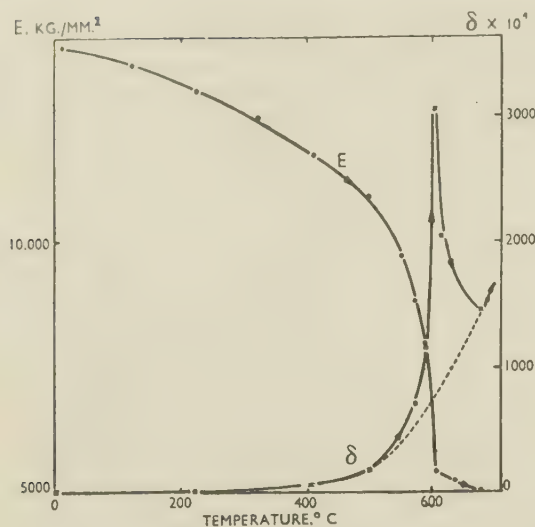


FIG. 11.—Variation with Temperature of  $E$  and  $\delta$  for Annealed Copper-32.5% Tin Alloy.

point. The  $\delta$  phase decomposes on heating to  $590^{\circ}\text{C.}$  into  $\zeta$  and  $\beta^*$ ,  $\zeta$  having an hexagonal lattice with 26 atoms per unit cell and  $\beta$  a body-centred cubic lattice. In the course of this transformation, the modulus and the decrement vary in a manner similar to the previous examples, but the decline in the modulus is steady and progressive over a certain range of temperature.

#### IV.—GENERAL CONCLUSIONS

The results described above show that transformations in the solid state in the copper alloys investigated are accompanied by important changes in their elastic modulus and logarithmic decrement.

The change in elastic modulus can be attributed quite simply to the disappearance of the  $\gamma$ -type phase and its replacement at high temperatures by the  $\beta$ -type phase whose modulus obeys the law of mixtures; it has been possible to confirm this explanation in the case of the copper-aluminium alloys, though the comparison cannot be made for copper-tin alloys owing to the low melting point of tin. It may, however, be said that at  $600^{\circ}\text{C.}$  the modulus of the body-centred cubic phase in the copper-tin system lies on the straight line joining the modulus of copper and that of the  $\epsilon$  phase (corresponding closely to  $\text{Cu}_3\text{Sn}$ ) at this temperature. At  $20^{\circ}\text{C.}$ , the modulus of  $\epsilon$  obeys the law of mixtures.<sup>11</sup>

As regards the hypo-eutectoid alloy containing 20.2% tin, if the change in the modulus on passing through the transformation point is less marked, this is because the alloy contains an excess of  $\alpha$  which does not take part in the transformation. Above the transformation temperature the modulus remains higher than that of the alloy containing 24.9% tin, since the  $\alpha$  phase in it, being less rich in tin, has a greater modulus. It is known that the decrease in the elastic modulus of copper alloys is roughly

proportional to the content of added element in the region of the face- and body-centred cubic phases.<sup>11</sup>

The results for the logarithmic decrement are particularly interesting. From the high values obtained and the frequencies employed, it appears that the internal friction is here due for the most part to irreversible phenomena initiated by the vibrations. The dislocations set up in the crystals may be caused by the transformation or by the process of preparation for it; they may also be in existence before the transformation begins at all. The case of the copper-aluminium alloy, in which the transformation is considered to be isothermal and the constitution of which undergoes no change before reaching  $565^{\circ}\text{C.}$ , is especially significant, for if the logarithmic decrement attains considerable values before reaching this temperature, it means that the isothermal transformation is preceded by a period of preparation, a phenomenon that appears to be revealed only by so sensitive a property as the internal friction. The same applies to the alloy containing 32.5% tin, consisting solely of  $\delta$ . It is during the isothermal transformation itself that the decrement passes through a maximum, and this indicates that the instability of the lattice structure is the cause of an energy loss which ceases when the transformation is complete because the state is then more stable.

#### ACKNOWLEDGEMENTS

The authors wish to acknowledge their indebtedness to M. Bellier, Directeur du Laboratoire d'Essais du Conservatoire National des Arts et Métiers, for providing facilities that made the work possible. They also wish to thank Messrs. A. Portevin and P. Chevenard, Membres de l'Académie des Sciences, for their valuable advice, and the company Le Bronze Industriel for preparing the alloys used.

#### REFERENCES

1. P. Chevenard, "Recherches experimentales sur les alliages de fer, de nickel et de chrome". Paris: 1927.
2. O. Engler, *Ann. Physik*, 1937, [v], 31, 145.
3. K. Nakamura, *Sci. Rep. Tôhoku Imp. Univ.*, 1936, [i], 25, 415.
4. E. Scheil and W. Thiele, *Arch. Eisenhüttenwesen*, 1937, 10, 477.
5. O. Vidal and P. Lescop, *Compt. rend.*, 1950, 230, 206.
6. F. Förster and W. Köster, *Z. Metallkunde*, 1937, 29, 116.
7. W. Köster, *Z. Metallkunde*, 1940, 32, 151.
8. G. E. Bennett and R. M. Davis, *J. Inst. Metals*, 1948-49, 75, 759.
9. P. Chevenard and A. Portevin, *Chim. et Ind.*, 1926, (Numéro spécial), 434.
10. J. T. Norton, *Trans. Amer. Inst. Min. Met. Eng.*, 1940, 137, 49.
11. R. Cabarat, L. Guillet, and R. Le Roux, *Compt. rend.*, 1948, 226, 1374.
12. R. Cabarat, L. Guillet, R. Le Roux, and A. Portevin, *Compt. rend.*, 1950, 231, 1373.
13. R. Cabarat, L. Guillet, and R. Le Roux, *J. Inst. Metals*, 1948-49, 75, 391.
14. G. V. Raynor, *Inst. Metals Annotated Equilib. Diagr. Series*, No. 2, 1949.

\* In Raynor's diagram<sup>14</sup> the body-centred cubic phase is designated  $\gamma$ , but the present authors prefer to use  $\beta$  for phases having this structure.

# THE STRUCTURE AND SOME PROPERTIES OF TITANIUM-OXYGEN ALLOYS CONTAINING 0-5 AT.-% OXYGEN \*

1337

By A. E. JENKINS,† M.Eng.Sc., JUNIOR MEMBER, and  
H. W. WORNER,‡ M.Sc., MEMBER

## SYNOPSIS

By means of measurements of thermoelectric power at various temperatures and by quenching experiments on alloys made with refined titanium, the limits of the ( $\alpha + \beta$ ) region up to 5 at.-% oxygen have been established. Alloys based on commercially pure titanium have also been studied, and it has been demonstrated that the impurities present in the commercial grade of metal cause a marked broadening of the  $\alpha \rightleftharpoons \beta$  transformation range.

The mechanical working and annealing of commercially pure alloys have been examined, and it has proved possible to develop techniques for forging and swaging alloys containing as much as 3.5 at.-% oxygen. Alloys containing more than 1.5 at.-% oxygen may be hot worked, but they are more or less brittle at normal temperatures. Special attention has been given to some of the main factors affecting the cold drawing and annealing of alloy wires. The proof stress, nominal ultimate stress, plastic elongation, and hardness of annealed alloys have been determined, chiefly with a view to providing some quantitative concept of the variation of these mechanical properties with oxygen content.

## I.—INTRODUCTION

UNTIL recently, many metallurgists have regarded oxygen as an undesirable impurity in titanium, particularly in relation to its mechanical and working properties. However, recent investigations have shown that concentrations of oxygen in the region of 1.5 at.-% (0.5 wt.-%) do not seriously impair the working characteristics of the metal. Such small concentrations of oxygen do in fact cause a marked increase in the proof stress and the ultimate tensile stress of titanium, and in this connection, oxygen can now be regarded as an alloying element which may be very desirable for many practical purposes. The investigation to be described in this paper was undertaken with this idea in mind.

The early work of de Boer, Burgers, and Fast <sup>1</sup> on the electrical resistance of titanium indicated that oxygen can be held in solid solution in titanium and that the  $\alpha \rightleftharpoons \beta$  transformation temperature is elevated by the introduction of oxygen. Subsequently, Ehrlich's <sup>2</sup> X-ray-diffraction investigations revealed that the maximum solid solubility of oxygen in  $\alpha$ -titanium is approximately 30 at.-%. Recently Clark <sup>3</sup> has reported more precise values of the lattice parameters of  $\alpha$ -titanium-oxygen solid solutions in the range up to 1.5 at.-%. Jaffee and Campbell <sup>4</sup> have investigated the effects of oxygen (up to 1 at.-%) on the electrical resistivity, microstructure, and cold-working characteristics of titanium, while Finlay and

Snyder <sup>5</sup> have studied in some detail the mechanical properties of titanium containing oxygen up to 0.75 at.-%. Since the completion of the present work, Jaffee, Ogden, and Maykuth <sup>6</sup> have published an account of their determination of part of the titanium-oxygen phase diagram. These workers have also reported some mechanical properties of alloys containing up to about 3 at.-% oxygen.

In the present investigation the range of oxygen contents studied was 0-5 at.-%. The first part of the work was aimed at establishing the  $\alpha \rightleftharpoons \beta$  transformation range up to 5 at.-% oxygen. A knowledge of this portion of the titanium-oxygen phase diagram proved useful in connection with high-temperature annealing experiments. The second part of the investigation covered the working and mechanical properties of the alloys, including the effects of cold working and the determination of annealing ranges.

## II.—EFFECT OF OXYGEN ON THE $\alpha \rightleftharpoons \beta$ TRANSFORMATION IN TITANIUM

### 1. MATERIALS EMPLOYED AND PREPARATION OF ALLOYS

Titanium refined by the iodide process in the Philips Laboratories, Eindhoven, was used as the basis metal, the impurities present being: nitrogen, 0.03; oxygen, 0.02; iron, 0.02 at.-%; tin, strong

\* Manuscript received 14 February 1951.

† Formerly Bage Memorial Research Scholar, University of Melbourne; now Research Officer, Physical Metallurgy Section, Commonwealth Scientific and Industrial Research Organization,

Baillieu Laboratory, University of Melbourne, Australia.

‡ Senior Research Officer, Physical Metallurgy Section, Commonwealth Scientific and Industrial Research Organization, Baillieu Laboratory, University of Melbourne, Australia.



trace; antimony, strong trace; and faint traces of copper, silicon, vanadium, magnesium, and manganese. The nitrogen and oxygen content were those reported by the Philips Laboratories.

The metal and the titanium-oxygen alloys were required in the form of wire or ribbon because it was decided to determine the ( $\alpha + \beta$ ) range by measuring the thermoelectric power/temperature relationship for each composition. The bar of refined titanium was therefore rolled down to ribbon 0.08 mm. thick, during which process two intermediate annealing treatments of  $\frac{1}{2}$  min. each at about 550° C. were required. This heating was done in the air, and the resulting thin oxide film was removed by abrasion with waterproof carborundum paper.

The alloys were made by introducing oxygen into the titanium ribbon in the following way. A convenient length, usually about 8 cm., of the ribbon was degreased with carbon tetrachloride. After drying and weighing, the ribbon was heated uniformly in air to a temperature in the range 500°–750° C. for several minutes, the actual temperature and heating period depending on the amount of oxidation required. Then the oxide-coated specimen was heated *in vacuo* to 850°–950° C. for about 30 hr. to enable interdiffusion between the oxide coating and the underlying metal to take place. To minimize the risk of the specimen becoming contaminated with carbon from oil vapours back-streaming from the diffusion pump or with silicon from the walls of the silica vacuum envelope, the ribbon was held within a long, hollow cylinder of titanium during the prolonged heating. The titanium receptacle was provided with a loosely-fitting titanium stopper, so that gases and vapours could not enter the inner chamber without having passed through the fine space between the stopper and the mouth of the cylinder. In this way, a gettered atmosphere was maintained around the specimen. It was considered that this precaution, together with the maintenance of a pressure in the range  $10^{-4}$ – $10^{-5}$  mm. Hg within the vacuum envelope, provided adequate protection for the specimen. At the end of the prolonged heating, the specimen was cooled and re-weighed, and the increase in weight was taken as the amount of oxygen introduced into the specimen. Careful chemical analyses revealed scarcely any detectable entry of nitrogen into the titanium, despite the fact that the metal was heated in air to produce the oxide coating. This was in agreement with the results of Carpenter and Reavell,<sup>7</sup> who have reported that the reaction between titanium and nitrogen is slow as compared with that between titanium and oxygen at temperatures up to 1000° C.

In most cases the amount of oxygen absorbed was too small to be determined accurately by chemical analysis. However, a specimen containing 4.9 at.-% oxygen (nominal composition) was analysed by the differential gravimetric method involving conversion of a weighed sample to  $\text{TiO}_2$  and determination of the increase in mass caused by the conversion:  $\text{TiO}_x \rightarrow \text{TiO}_2$ . The analytical result was  $4.7 \pm 0.1$

at.-% oxygen. In view of the small difference between the two figures, the nominal compositions were accepted in all cases.

In the early stages of the work, it was necessary to ascertain what period of heating at 850°–950° C. would be necessary to produce a practically uniform concentration of oxygen within the ribbon. Some exploratory work had indicated very approximately the location of the boundary between the  $\alpha$  and ( $\alpha + \beta$ ) fields, and it had been shown that alloys quenched from the ( $\alpha + \beta$ ) field exhibited a mixture of well-defined dark and light regions on etching in an aqueous solution of 3% HF and 2%  $\text{H}_2\text{O}_2$ . It became evident that the dark-etching regions had consisted of  $\beta$  solid solution at the quenching temperature, but that the  $\beta$  phase had very rapidly changed (presumably to  $\alpha$ ) during quenching. Now it will be evident that a specimen of uniform oxygen content would exhibit an even distribution of the light- and dark-etching areas after quenching from the ( $\alpha + \beta$ ) range. Hence, to determine whether or not a uniform concentration of oxygen had been produced in any given prolonged period of heating, it was simply necessary to examine a polished and etched cross-section of the ribbon after quenching from any temperature in the ( $\alpha + \beta$ ) range. In this way, it was found that 25–30 hr. heating at 850°–950° C. produced a close approach to equilibrium conditions in specimens containing up to 4.9 at.-% oxygen. It was realized that if the prolonged heating was carried out at temperatures in the ( $\alpha + \beta$ ) region, then there was the risk of the specimen finally consisting of an outer rim of  $\alpha$  encasing a core of  $\beta$ , each phase having its own equilibrium oxygen concentration at the temperature concerned. While such a specimen would be in an equilibrium state at the treatment temperature, it would not, of course, possess a uniform distribution of oxygen. Therefore, during the last 10–12 hr. of the homogenizing treatment, the temperature was kept in the range 850°–880° C., so that the specimen had an opportunity to approach a uniform concentration over the wholly  $\alpha$  field.

In view of the decision to employ a thermoelectric property in determining the ( $\alpha + \beta$ ) range, another aspect of specimen preparation had to be kept in mind, namely, the possibility of there being a preferred orientation in the samples. The specimens were made from rolled titanium ribbon, which in its original state exhibited a preferred orientation, the (0001) planes tending to lie parallel to the plane of rolling. However, one of the authors (H. W. W.) had previously found<sup>8</sup> that the preferred orientation in refined metal could be practically eliminated by heating just above the ( $\alpha + \beta$ ) range (883°–887° C.). Therefore it was decided to begin the homogenizing treatment by heating rapidly up to 900°–950° C., in an endeavour to eliminate the preferred orientation before the onset of the interdiffusion between the oxide layer and the underlying metal. This measure appeared to be successful in all cases except that of the 4.9 at.-% alloy. The results pertaining to this alloy will be discussed in Section II, 2.

COMMERCIALLY PURE TITANIUM.

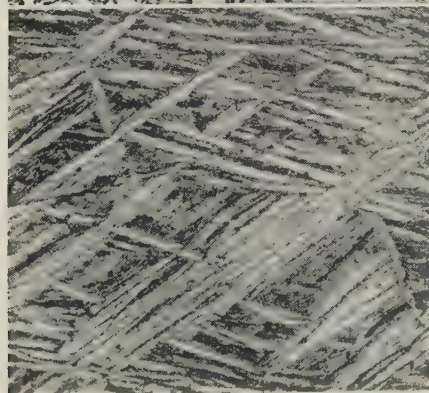


FIG. 7.—As Arc-Melted.  $\times 400$ .



FIG. 8.—As Forged in Range 600°-850° C.  $\times 400$ .

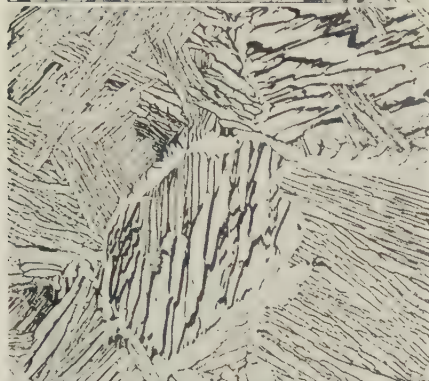


FIG. 9.—As Forged and Swaged at 600°-850° C., Heated at 900° C. for 4 Hr., and Cooled at 5° C./min. Single phase,  $\alpha$ -titanium; dark-etching areas formerly  $\beta$ .  $\times 100$ .



FIG. 10.—As Forged and Swaged at 900°-1000° C., Heated at 1000° C. for 4 Hr., and Cooled at 5° C./min. Single phase,  $\alpha$ -titanium; dark-etching areas formerly  $\beta$ .  $\times 100$ .

TITANIUM-OXYGEN ALLOYS.



FIG. 11.—3 at.-% Oxygen Alloy Swaged at 900°-1000° C., Heated at 1000° C. for 5 Hr., and Cooled at 5° C./min.  $\times 100$ .

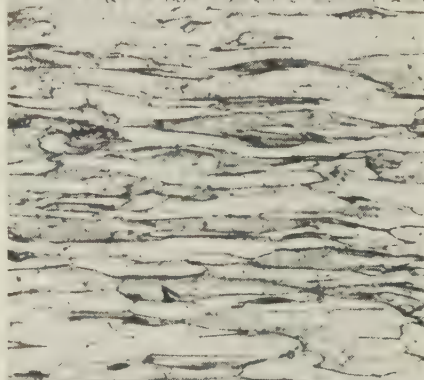


FIG. 12.—1 at.-% Oxygen Alloy Cold Drawn to 75% Reduction in Area.  $\times 200$ .

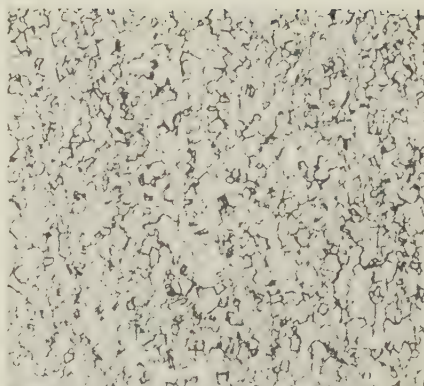


FIG. 13.—1 at.-% Oxygen Alloy Annealed for 3 Min. at 700° C.  $\times 100$ .

All specimens were etched in an aqueous solution of 3% hydrofluoric acid and 2% hydrogen peroxide.





## 2. DETERMINATION OF ( $\alpha + \beta$ ) RANGE BY THERMOELECTRIC-POWER MEASUREMENTS

In an earlier investigation, one of the authors (H. W. W.) had found that the  $\alpha \rightleftharpoons \beta$  transformation in refined titanium was accompanied by an abrupt change in thermoelectric properties.<sup>8</sup> The curve relating the thermoelectric power of a titanium/platinum couple with temperature exhibited two marked discontinuities which corresponded with the extremities of the ( $\alpha + \beta$ ) range in the refined titanium. It was therefore considered that the limits of the ( $\alpha + \beta$ ) region in an alloy could be determined by observing the temperatures at which the discontinuities occurred in the thermoelectric power/temperature curve for that alloy.

The equipment and experimental technique employed in the thermoelectric measurements were essentially identical with those used in earlier work on pure titanium.<sup>8</sup> It was expected that the  $\alpha \rightleftharpoons \beta$  transformation would be much slower in the alloys than in the pure metal because of the necessity for a considerable amount of diffusion to occur in them. The criterion for the establishment of equilibrium, or of a close approach to it, at a given temperature was the attainment of a steady value of the thermoelectric power. This required 20-30 min. at any temperature within the ( $\alpha + \beta$ ) region in the case of

correspondence between results obtained on heating and cooling is of value in revealing the extent to which equilibrium conditions had been achieved during the experiments. In this connection, the results for the 0.9, 2.7, and 3.6 at.-% oxygen alloys were satisfactory,

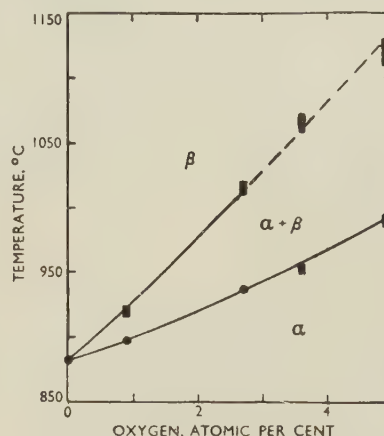


FIG. 2.—Phase Boundaries Deduced from Data in Fig. 1.

there being no definite signs of any hysteresis effects. In the case of the 4.9% oxygen alloy, the results pertaining to the first heating (curve *A'* in Fig. 1) did not coincide with those obtained in subsequent cooling and heating experiments. However, the upward turn in curve *A'* indicating the beginning of the  $\alpha \rightarrow \beta$  transformation occurred at the same temperature (990°C.) as that shown during subsequent cooling and heating. The same phenomenon had previously been noted in experiments on refined titanium which, in its initial state, had been annealed below the ( $\alpha + \beta$ ) range and which possessed residual preferred orientation until heated above the ( $\alpha + \beta$ ) region (cf. Worner<sup>8</sup>). In other words, the curve marked *A'* in Fig. 1 almost certainly pertains to an alloy which still possessed some degree of preferred orientation, whereas curve *A* represents the 4.9% alloy free from preferred orientation.

The ( $\alpha + \beta$ ) ranges deduced from the curves in Fig. 1 are presented in Fig. 2. The extremities of the ( $\alpha + \beta$ ) region cannot be accurately determined from the curves for 3.6 and 4.9 at.-% alloys in Fig. 1, since the changes in gradient,  $dP/dT$ , on passing from the  $\alpha$  or  $\beta$  field into the ( $\alpha + \beta$ ) region are not very sharply defined. This is especially true of the upper limit of the ( $\alpha + \beta$ ) range in each case. It is considered that this lack of sharpness is attributable to slight superficial contamination of the specimens during the experiments. Here it might be noted that exactly the same type of effect had been observed in earlier experiments on refined titanium which had suffered superficial contamination (cf. Worner<sup>8</sup>). In view of these observations, there is some uncertainty concerning the points denoting the high-oxygen portion of the  $\beta/(\alpha + \beta)$  boundary; hence the latter is shown as a dotted line in Fig. 2.

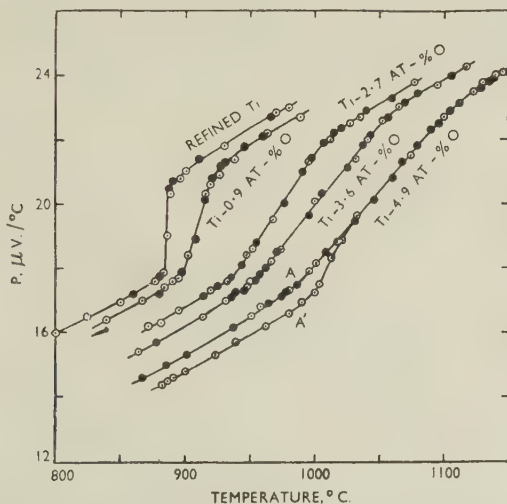


FIG. 1.—Temperature Dependence of the Thermoelectric Power (*P*) of Couples Comprising Pure Platinum and Titanium with 0-4.9 At.-% Oxygen.

### KEY.

*A'* represents first heating experiment with the Pt/Ti-4.9% O couple.  
*A* represents subsequent cooling and heating experiments with the Pt/Ti-4.9% O couple.  
 ○ Heating Curve. ● Cooling Curve.

the 4.9 at.-% oxygen alloy, which was the most sluggish of the alloys studied.

The thermoelectric-power determinations are set out in Fig. 1, in which points determined during both heating and cooling are included. The degree of



### 3. SOME METALLOGRAPHIC AND X-RAY-DIFFRACTION OBSERVATIONS ON QUENCHED ALLOYS

When quenched from the  $\beta$  region and etched in an aqueous solution of 3% HF and 2% H<sub>2</sub>O<sub>2</sub>, refined titanium exhibited a Widmanstätten pattern. Such a structure was not produced by quenching from any temperature in the  $\alpha$  region. These observations, together with X-ray-diffraction evidence that the  $\beta$  form of

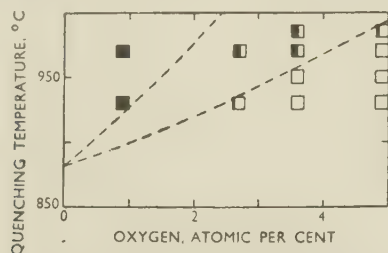


Fig. 3.—Results of Quenching Experiments on Refined Titanium-Oxygen Alloys. The broken-line boundaries are taken from Fig. 2.

#### KEY.

- =  $\beta$  at quenching temperature indicated by the structure resembling fine Widmanstätten pattern (cf. Fig. 7, Plate XXIX).
- =  $\alpha$  at quenching temperature.
- ◐ = ( $\alpha + \beta$ ) at quenching temperature.

titanium could not be retained by quenching, indicated that the Widmanstätten pattern was a manifestation of a rapid  $\beta \rightarrow \alpha$  change having occurred during quenching. Similar, but more marked Widmanstätten structures, rather like that illustrated in Fig. 7 (Plate XXIX), were found in oxygen-bearing titanium quenched from the  $\beta$  field shown in Fig. 2. As in the case of refined titanium, X-ray-diffraction tests revealed no evidence of retained  $\beta$  phase in oxygen alloys quenched from the  $\beta$  field. Hence the presence of a Widmanstätten structure in an etched as-quenched alloy could be taken as evidence of the  $\beta$  phase having been present at the quenching temperature, and of rapid transformation of the  $\beta$  phase during quenching.

The results of some quenching experiments are presented graphically in Fig. 3, which also contains the boundaries deduced from the thermoelectric-power experiments. In general, the results of the quenching tests are in concordance with those shown in Fig. 2. The quenching experiments on the 4.9 at.-% oxygen alloy would suggest that at this oxygen concentration the  $\alpha/(\alpha + \beta)$  boundary lies a little below that estimated from the thermoelectric-power results. This may mean that the thermoelectric power/temperature relationship does not reveal the very first appearance of  $\beta$  phase on passing from the  $\alpha$  into the ( $\alpha + \beta$ ) region. However, at lower oxygen concentrations, there is no marked discrepancy between the quenching-test results and those derived from the thermoelectric-power experiments.

### 4. EFFECT OF OXYGEN IN COMMERCIAL PURE TITANIUM

All of the results presented above pertain to titanium-oxygen alloys made with refined titanium. However, it was the authors' intention to study the

working and mechanical properties of alloys based on commercially pure titanium, i.e. metal made by the reduction of titanium tetrachloride with magnesium. Hence it was necessary to ascertain the transformation range in the alloys of commercial grade. Special interest was centred on the  $\alpha/(\alpha + \beta)$  boundary. It was hoped that most of the hot-working and annealing treatments could be carried out wholly in the  $\alpha$  field so that complications due to phase changes would not enter. For this purpose it was obviously necessary to determine the upper limit of the  $\alpha$  phase field.

In an earlier investigation, one of the authors (H. W. W.<sup>8</sup>) had found from thermoelectric power/temperature studies that the  $\alpha \rightleftharpoons \beta$  transformation in the commercial metal occurs over a broad temperature range. The transformation range could not be precisely ascertained, but it proved to be approximately 865°–970° C. Quenching experiments, similar to those outlined in the previous section, indicated that the range was from 860° C. up to some temperature between 965° and 980° C.

The  $\alpha/(\alpha + \beta)$  boundary in the system based on commercially pure titanium was determined by quenching experiments. The alloys were prepared by arc melting mixtures of titanium and titanium dioxide. Some details concerning the preparation and purity of the commercial alloys are given in Section III, 1 of the paper. Fig. 4 presents the results of the quenching tests. The results for the basis titanium are shown at 0.5 at.-% oxygen, this being the oxygen content of the commercial metal. For purposes of comparison, the phase boundaries pertaining to "pure" alloys are included as dotted lines.

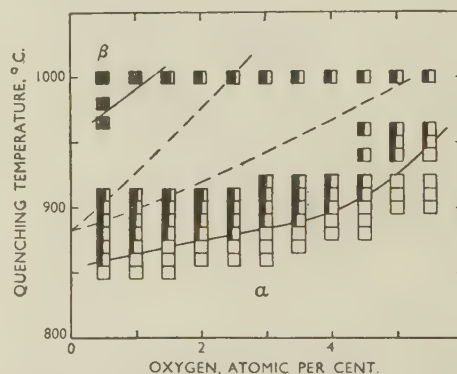


Fig. 4.—Results of Quenching Experiments on Commercially Pure Titanium-Oxygen Alloys. The broken-line boundaries refer to pure titanium alloys.

#### KEY.

- =  $\beta$  at quenching temperature.
- =  $\alpha$  at quenching temperature.
- ◐ = ( $\alpha + \beta$ ) at quenching temperature.

It is evident that the impurities in the commercial grade of metal exert a marked influence on the transformation range of the alloys. The  $\alpha/(\alpha + \beta)$  boundary for alloys of commercial purity lies well below the  $\alpha/(\alpha + \beta)$  boundary of Fig. 2. It seems that the  $\beta/(\alpha + \beta)$  boundary tends to rise rapidly to temperatures well above 1000° C., even at low oxygen

concentrations. The authors were not particularly concerned with the  $\beta$  region in this system; hence the investigation was not extended beyond 1000° C.

It will be noted that reference has been made to the  $(\alpha + \beta)$  region in alloys of commercial purity, though it is not known for certain that it is in fact a simple  $(\alpha + \beta)$  range. The commercial alloys contain several components, and it is possible that other phases may appear in the so-called  $(\alpha + \beta)$  zone. However, for the sake of brevity,  $(\alpha + \beta)$  has been used to denote the region between the  $\alpha$  and  $\beta$  solid-solution fields.

## 5. DISCUSSION ON THE TITANIUM-OXYGEN SOLID SOLUTIONS

Ehrlich<sup>2</sup> has shown that the titanium-oxygen  $\alpha$  solid solutions are of the interstitial type, there being an increase in density and lattice parameters on passing from 0 to approximately 30 at.-% oxygen. The oxygen is almost certainly accommodated in the octahedral interstices in the  $\alpha$ -titanium lattice, the bonding between the titanium and oxygen being essentially of the metallic-covalent type. If one adopts a "metallic" radius for oxygen, such as the value 0.80 Å. for co-ordination number 6 as deduced by Pauling,<sup>9</sup> then on the basis of the generally accepted rules pertaining to the lattice geometry of interstitial metallic phases, the extensive solubility of oxygen in  $\alpha$ -titanium can readily be understood (cf. Wörner<sup>10</sup>). On the other hand, considerations of lattice geometry suggest that serious distortion would occur if oxygen, having a "metallic" radius of approximately 0.80 Å., were introduced into the interstices of the body-centred cubic lattice of  $\beta$ -titanium. Hence it would be expected that the solubility of oxygen in  $\beta$ -titanium would be comparatively low. This idea is in agreement with the results obtained in the present investigation. In other words, considerations of lattice geometry explain in qualitative fashion why the addition of oxygen raises the  $\alpha \rightleftharpoons \beta$  transformation range.

As a matter of general interest, it was decided to ascertain thermodynamically where the  $\beta/(\alpha + \beta)$  boundary would lie using the following as bases for the calculation: (a) the  $\alpha/(\alpha + \beta)$  boundary shown in Fig. 2, and (b) the value 678 cal./g.-atom as the latent heat of the  $Ti_\alpha \rightleftharpoons Ti_\beta$  transformation in the neighbourhood of the transformation temperature. This figure was determined by McQuillan<sup>11</sup> in an investigation of the titanium-hydrogen system.

The relationship employed was:

$$\left( \frac{d \ln x_\alpha/x_\beta}{dT} \right)_{\text{const. pressure}} = - \frac{\Delta_i H}{RT^2}$$

where  $x_\alpha$  and  $x_\beta$  represent the atomic fractions of titanium in the  $\alpha$  and  $\beta$  phases respectively,  $T$  is in °K.,  $R$  is the gas constant, and  $-\Delta_i H$  the latent heat of  $\alpha \rightleftharpoons \beta$  transformation in pure titanium. It was assumed that the latent heat of transformation could be taken as constant in the range of temperature concerned.

Of course a boundary calculated in this way will be of interest only in the composition range in which the alloys can be described as dilute in the sense that the solvent (in this case titanium) obeys Raoult's law while the solute obeys Henry's law. There is some doubt as to the extent of the concentration range in which the titanium-oxygen solutions may, for practical purposes, be regarded as dilute in the above sense. In any case, the calculations have been restricted to the range 0-2 at.-% oxygen in the  $\alpha$  phase. To facilitate comparison, the  $\beta/(\alpha + \beta)$  boundary calculated as outlined above is included with the experimentally determined boundaries in Fig. 5. The calculated boundary

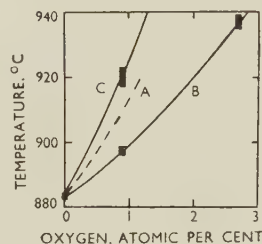


Fig. 5.—Comparison of the Calculated and Experimental  $\beta/(\alpha + \beta)$  Boundaries. Curve A is a portion of the  $\beta/(\alpha + \beta)$  boundary determined thermodynamically from the  $\alpha/(\alpha + \beta)$  boundary (curve B) assuming that both  $\alpha$  and  $\beta$  solid solutions obey the simple laws of dilute solutions. Curve C is the experimentally determined boundary.

lies well below the experimentally determined curve. In view of the fact that oxygen cannot be accommodated very readily as an interstitial solute in  $\beta$ -titanium, it is not unlikely that the  $\beta$  solid solutions will deviate from the laws pertaining to dilute solutions even at concentrations of the order of 0.5-1 at.-%. This factor is probably an important one contributing to the discrepancy in Fig. 5.

The  $\alpha/(\alpha + \beta)$  boundary shown in Fig. 2 agrees reasonably well with that deduced from quenching experiments by Jaffee, Ogden, and Maykuth.<sup>6</sup> These authors have placed the  $\beta/(\alpha + \beta)$  boundary somewhat higher than that obtained from thermoelectric power/temperature measurements in the present investigation. However, the discrepancy cannot be regarded as serious, especially when allowance is made for the experimental difficulties inherent in the determination of high-temperature phase boundaries in systems based on reactive metals such as titanium.

## III.—THE WORKING AND MECHANICAL PROPERTIES OF COMMERCIAL PURE TITANIUM-OXYGEN ALLOYS

### 1. PREPARATION OF THE ALLOYS

The alloys used in this part of the investigation were prepared by melting mixtures of chemically pure titanium dioxide powder and commercially pure titanium powder made by reducing titanium tetrachloride with magnesium. Impurities present in the basis titanium are listed in Table I. The value of



oxygen concentration was determined by vacuum-fusion analysis at the National Physical Laboratory, Teddington.

TABLE I.—Impurities Present in Commercially Pure Titanium After Melting in an Argon-Arc Furnace.

Impurity	Concentration	
	Wt.-%	At.-% (approx.)
Oxygen . . . .	0.17	0.5
Nitrogen . . . .	0.04	0.15
Carbon . . . .	0.10	0.40
Iron . . . .	0.20	0.18
Silicon . . . .	0.04	0.07
Manganese . . . .	0.04	0.04
Cobalt . . . .	0.015	0.01

Melting of the mixtures was effected by means of an argon-arc furnace of the type developed by Kroll.<sup>12</sup> Melting conditions were controlled to minimize spitting and fuming, so that there would be little risk of the final composition being significantly different from the nominal composition. When the main part of the investigation was in progress, no facilities were available for having the alloys analysed. However, one alloy, a 2 at.-% oxygen alloy (nominal composition) was analysed by the chlorination method, the result obtained being 1.95 at.-%. Mr. J. A. Corbett carried out the analysis, the method being briefly as follows. A weighed sample was subjected to the action of a stream of pure, dry chlorine at 400° C. so that practically all the metal was converted to titanium tetrachloride, while the oxygen remained as titanium dioxide in the residue. The latter was weighed and analysed, and from this result, the oxygen content of the original sample was calculated. In a more recent investigation, some titanium-oxygen alloys prepared as outlined above were analysed, and it was found that the nominal compositions agreed with the analytical results within  $\pm 5\%$ . The use of nominal compositions therefore seems justified. The following list indicates the nominal oxygen contents of all the commercially pure alloys used in the present investigation:

At.-%	Wt.-%	At.-%	Wt.-%
0.5 *	0.17 *	3.5	1.20
1.0	0.33	4.0	1.37
1.5	0.51	4.5	1.55
2.0	0.67	5.0	1.73
2.5	0.85	5.5	1.91
3.0	1.02		

\* Basis titanium.

The button-shaped specimens produced in the arc furnace were coarse grained, and on etching they exhibited a very marked Widmanstätten pattern, as shown in Fig. 7 (Plate XXIX). This structural feature was probably due to segregation during freezing of the alloys, and to the  $\beta \rightarrow \alpha$  transformation during cooling through the range 1000°–850° C. Early in the investigation it became apparent that alloys exhibiting structures like that shown in Fig. 7 were much less amenable to deformation than

specimens possessing a normal fine polygonal grain structure. The coarse Widmanstätten structures could be eliminated and the usual polygonal grain texture produced only by subjecting the alloys to very considerable amounts of hot working followed by long heating. Section III, 3 deals with an investigation of the homogenization of the alloys, i.e. with the elimination of the cast structure.

## 2. WORKING AND MACHINING QUALITIES

During the forging and swaging of the button-shaped as-melted specimens into useful shapes such as rod and wire, numerous observations of working qualities were made. The essential features of these observations are summarized graphically in Fig. 6. At normal temperatures, alloys containing more than 2.5 at.-% oxygen were brittle, no matter what the

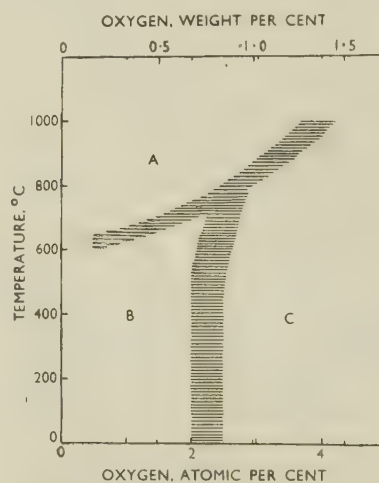


Fig. 6.—Working Qualities of Titanium-Oxygen Alloys at Various Temperatures.

### KEY.

- Region A: Alloys may be hot worked without intermediate annealing.  
 Region B: Alloys may be worked to a limited extent and require intermediate annealing at temperatures in the A region.  
 Region C: Alloys are, for all practical purposes, brittle in this region.

previous mechanical and thermal history of the specimens. In order to prevent the formation of cracks during forging or swaging of alloys containing more than 2.5 or 3 at.-% oxygen, working temperatures approaching 1000° C. had to be adopted. Even at 1000° C. alloys with 4% or more oxygen exhibited a marked tendency to crack during forging. Once a crack formed during hot forging, there was little chance of its healing during subsequent hot working, because of the rapidity of oxidation along the fissure. The transition from the hot-working temperature region (A in Fig. 6) to the range of brittleness (C) occurred over a comparatively small temperature interval, and this added to the difficulty of producing sound specimens of alloys containing more than 2.5 at.-% oxygen.

The production of alloy wires by drawing at room temperatures was investigated, and the results of this work are reported in Section III, 4.

The preparation of tensile-test specimens enabled the authors to compare the machining qualities of the alloys. High-speed steel tools were used, the rake and clearance angles being similar to those used in machining high-strength alloy steels. It proved advantageous to employ cutting fluids of the type used in machining steels. Table II summarizes the

TABLE II.—*Machining Properties of Annealed Titanium-Oxygen Alloys.*

Oxygen Content (nominal), at.-%	Comments
0.5 1.0 1.5 2.0	} Machined easily, there being no difficulty in drilling or screw cutting.
2.5 3.0	
3.5 4.0 4.5 5.0	
2.5 3.0	} Could be turned satisfactorily, but inclined to flake on screw cutting. Hard to drill.
3.5 4.0 4.5 5.0	
3.5 4.0 4.5 5.0	} Difficult to machine, screw-cutting and drilling being very unsatisfactory and practically impossible on 4.5% and 5.0% alloys.

observations made during turning, screw-cutting, and drilling operations. In general, it can be stated that machining alloys containing more than 2 at.-% oxygen proved difficult. In the range 0.5–2 at.-% oxygen, the machining qualities of the alloys were similar to those of high-strength structural alloy steels.

### 3. HOMOGENIZING TREATMENTS

In the early stages of the investigation some difficulty was experienced in producing alloy specimens with uniform polygonal grain structures. There was a marked tendency for the as-cast structure (Fig. 7, Plate XXIX) or a distorted form of it (Fig. 8, Plate XXIX) to persist despite the application of hot working and subsequent prolonged heat-treatments. It was therefore decided to make a systematic study of some of the main factors concerned in the elimination of the cast structure, viz. (a) the hot-working temperature, and (b) the subsequent heating conditions, i.e. temperature, duration of heating, and final cooling rate.

The amount of distortion effected during hot working was more or less constant, because all the buttons from the arc furnace had to be converted to specimens of rod form about  $\frac{3}{16}$ – $\frac{1}{4}$  in. in dia. Hence the total amount of hot working before the homogenizing heat-treatment did not enter as a variable factor. It should be noted that the buttons were shaped into rod by working in region A of Fig. 6, this being done largely to lighten the load on the working machinery. But the hot working alone did not suffice to eliminate completely the cast structure, even when temperatures as high as 900°–1000° C. were tried. The hot-working ranges could be broadly classified into: (a) within the  $\alpha$  range (approximately 600°–850° C.) and (b) within the  $(\alpha + \beta)$  range (900°–1000° C.).

Two ranges of homogenizing heat-treatment temperatures were tried: (a) within the  $\alpha$  range (800°–850° C.), followed by cooling at about 100° C./min. and (b) within the  $(\alpha + \beta)$  range (900°–1000° C.), followed by fairly slow cooling (about 1°–5° C./min.).

The heating periods ranged from 1 to 30 hr. In all cases the prolonged heat-treatments were carried out *in vacuo*, the pressure being kept below  $10^{-4}$  mm. Hg. As an extra precaution against contamination, the specimens were held within a loosely stoppered hollow titanium cylinder during the heat-treatments.

Most of the study of homogenization was concerned with alloys containing 0.5–2 at.-% oxygen, because it was in this range that greatest difficulty was experienced in producing uniform polygonal grain structures. Table III summarizes the observations.

A rather surprising feature of the results was that the most desirable structure was obtained by carrying out both the final hot working and subsequent homogenizing heat-treatment at comparatively low temperatures in the  $\alpha$  range.

It will be noted that coarse Widmanstätten structures persisted after slow cooling from the  $(\alpha + \beta)$  range. This is considered to be largely due to the broadness of the  $(\alpha + \beta)$  region in alloys of commercial purity (cf. Fig. 4). In other words, there is such a wide difference between the compositions of the  $\alpha$  and  $\beta$  phases at any temperature in the  $(\alpha + \beta)$  region,

TABLE III.—*Results of Investigation into Homogenization of Alloys Containing 0.5–2.0 At.-% Oxygen.*

Hot-Swaging Temp. Range		Homogenizing Temp. (periods up to 30 hr.)		Cooling Rate, °C./min.	Final Microstructure
Region	°C.	Region	°C.		
$\alpha$	600–850 (depending on oxygen content)	$\alpha$	800–850	100	Clean recrystallized $\alpha$ structure. Similar to Fig. 13 (Plate XXIX), but coarser. If worked consistently close to $(\alpha + \beta)$ region, tendency to leave unchanged the original broken-up cast structure (Fig. 8, Plate XXIX).
		$(\alpha + \beta)$	900–1000	1–5	Very coarse grain structure, $\alpha$ formed in Widmanstätten pattern (Fig. 9, Plate XXIX).
$(\alpha + \beta)$	900–1000 (depending on oxygen content)	$\alpha$	800–850	100	Similar to Fig. 8 (Plate XXIX) but coarser. No change from swaged structure.
		$(\alpha + \beta)$	900–1000	1–5	Very coarse grain structure (Fig. 10, Plate XXIX).

that diffusion during cooling at 1°–5° C./min. is unable to yield a uniform  $\alpha$  structure.

From a full consideration of the results presented in Table III, the following forging and swaging procedure was developed for alloys in the range 0.5–2.0 at.-% oxygen. The button-shaped ingots from the arc furnace were forged down to 0.5-in.-dia. bar, which was then swaged in four consecutive steps to about 0.3 in. in dia. All these operations were performed with the alloy at 900°–1000° C. Subsequently, the bars were reduced to 0.2 in. in dia. in two steps, in the



range 600°–850° C. After pickling in an aqueous solution containing 10% hydrofluoric acid and 50% nitric acid, the bars were heated *in vacuo* to 800°–850° C. for 4 hr. in order to complete the homogenizing process. The above sequence of hot working and heating operations produced a clean, polygonal grain structure, somewhat coarser than that shown in Fig. 13 (Plate XXIX).

Homogenization of alloys containing 3–5 at.-% oxygen did not prove as difficult as with the more dilute alloys. It was simply necessary to hot forge and swage the high-oxygen alloys at 1000° C., heat *in vacuo* to 1000° C. for about 5 hr., and finally cool at 1°–5° C./min. After this treatment, some of the oxygen-rich alloys exhibited an interesting “block” type of microstructure, as shown in Fig. 11 (Plate XXIX).

Whenever close temperature control during hot working was desired, the specimens were heated to the temperature by immersion in a charcoal-covered tin bath. This method of heating minimized the superficial oxidation of the specimens, and the tin itself caused no serious contamination. In many cases, heating in air was satisfactory when close temperature control was not required. The oxide layers were removed by acid solutions after hot working, as described above.

#### 4. DRAWING AND ANNEALING ALLOY WIRES

In this part of the investigation the composition range covered was 0.5–2.5 at.-% oxygen. The homogenized bars were hot swaged from 0.2 in. dia. down to 0.1 in. Table IV presents an outline of the essential features of working and annealing conditions, as well as the grain-size and hardness of the 0.1-in. wire stock.

TABLE IV.—*Preparation and Some Properties of Wire-Drawing Stock.*

	Oxygen Content (nominal), at.-%				
	0.5	1.0	1.5	2.0	2.5
Swaging temp., °C.	700	725	750	750	750
Stages at which annealed,* bar dia., in.	0.10	0.10	0.10	0.13 and 0.10	0.15 and 0.10
Approximate grain-size after final anneal, grains/mm. <sup>2</sup>	1000	1000	750	750	500
Vickers hardness number after final anneal	220	265	310	350	385

\* 15 min. at 800° C. *in vacuo*.

Before beginning to draw the wires through tungsten carbide dies, they were anodized in 5% aqueous acetic acid solution, the potential difference across the cell being about 50V. The anodized wires

were warmed and coated with a heavy gear-box oil to ensure smooth motion during wire drawing, which was done at room temperature. The wires were pointed by dipping into the nitric-hydrofluoric acid pickling mixture mentioned above.

TABLE V.—*Summary of First Part of Wire-Drawing Investigation.*

	Oxygen Content (nominal), at.-%				
	0.5	1.0	1.5	2.0	2.5
Dia. after final draw, in.	0.020	0.020	0.050	0.090	No reduction possible on account of brittleness at room temperature.
Reduction in area, %	96	96	75	20	
Vickers hardness after final draw	320	405	415	360	
Vickers hardness of initial annealed 0.1-in. stock (cf. Table IV)	220	265	310	350	
Comments	No sign of brittleness at finish.	No sign of brittleness at finish.	Fractured after 75% reduction.	Fractured after 20% reduction.	

Table V presents a summary of the first part of the wire-drawing investigation.

In order to produce wires of fine gauge from the basis titanium and the 1.0 and 1.5 at.-% oxygen alloy specimens, intermediate annealing treatments had to be given. It was also necessary to limit the amount of reduction in cross-sectional area by cold drawing before these annealing treatments, the aim being to prevent over-working of the alloys. For this purpose reductions approximating to 75% of the values shown in Table V were considered to be safe.

With a view to gaining a general understanding of the annealing characteristics of the 1.0 and 1.5 alloys as well as of the basis titanium, some short-term annealing experiments were conducted. In each case, the previous reductions were in accordance with the limits mentioned in the previous paragraph, and the actual values were:

	Redn. of Area, %
Basis titanium . . . .	approx. 73
1.0 at.-% oxygen . . . .	approx. 73
1.5 at.-% oxygen . . . .	approx. 55

Two methods of annealing were employed, the object being to compare a simple 3-min. heating in air with a 15 min. anneal *in vacuo* (pressure approximately 10<sup>-4</sup> mm. Hg). The anneal in air simply involved placing the specimen and a thermocouple in a small silica sheath which was dipped into a molten tin bath. A period of 3 min. was allowed after the attainment of a steady temperature, which generally took place within 30 sec. of immersion. The specimens annealed

*in vacuo* were heated for 15 min. at temperature and allowed to cool at a rate of about 75° C./min. Annealed specimens were set in Bakelite and a longi-

process, but the effect was not as marked as in the other two instances. Here it might be added that the first signs of recrystallization in the 1.5% alloy were noted after annealing at 600° C.

It will be evident that the 3-min. annealing treatments were almost as effective as the 15-min. treatments. Both sets of curves exhibited the same general features.

Completely recrystallized structures were observed in the basis titanium and the 1% alloy after heating to 600° C. for either 3 or 15 min. A slightly higher temperature (650° C.) was required for the 1.5% alloy. In general, it may be said that for all three compositions the most uniform fine-grained structures were produced by heating for either 3 or 15 min. at 700° C. A typical structure produced during a 3-min. anneal at 700° C. is shown in Fig. 13 (Plate XXIX). This is a 1 at.-% oxygen alloy which, in the cold-drawn condition (73% reduction of area), exhibited the structure shown in Fig. 12 (Plate XXIX).

## 5. SOME MECHANICAL PROPERTIES OF ANNEALED ALLOYS

All alloys examined in this part of the investigation had been annealed to produce fully recrystallized structures with a grain-size of the order of 1000 grains/mm.<sup>2</sup>. This was done so that variations in grain-size would not be a significant factor in the consideration of the results. The annealing temperatures used were in the range 700°-850° C., and the period of heating was usually 2-4 hr.

The modulus of elasticity of a 2 at.-% alloy was compared with that of the basis titanium. Specimens having a 0.2-in. dia. over a length of 4 in. were employed, and the elastic strain over a 2-in. gauge-length was determined by means of a Tuckerman

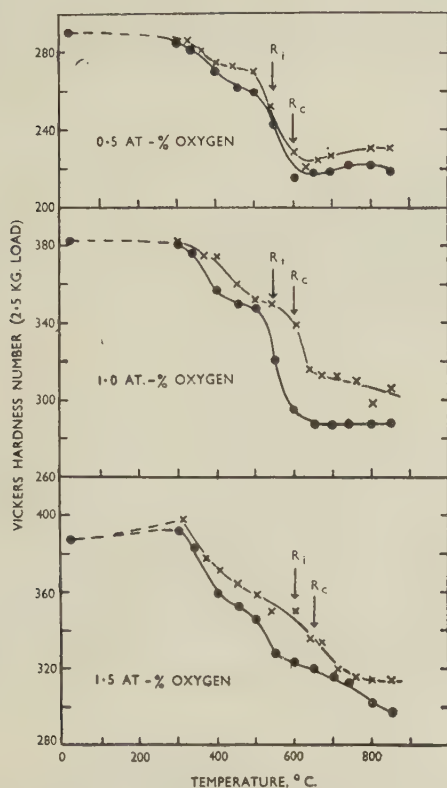


FIG. 14.—Results of Annealing Experiments on Cold-Drawn Wires. Amount of previous reduction :

Oxygen Content, %	Redn. of Area, %
0.5 (Basis Titanium)	73
1.0	73
1.5	55

### KEY.

- × 3 min. heating in air.
- 15 min. heating *in vacuo*.
- $R_i$  Beginning of recrystallization.
- $R_c$  End of recrystallization.

tudinal diametral section prepared for hardness testing and observation of the microstructure.

The results of the annealing investigation are presented graphically in Fig. 14., the hardness results being obtained from indentations made along the centre of the wire. In all cases the first signs of softening occurred on heating in the range 300°-400° C., even when the heating period was only 3 min. The hardness/temperature curves for the basis titanium and the 1.0% alloy suggest that there are two main stages in the softening process, one in the range 300°-450° C., the other from 500°-600° C. The first signs of recrystallization, as revealed by observation under the microscope, appeared in both the basis titanium and the 1% alloy after heating to 550° C. This suggests that recovery alone was occurring during heating at temperatures up to about 500° C., and that recrystallization became an important factor above 500° C. In the case of the 1.5% alloy, there was a suggestion of two stages in the annealing

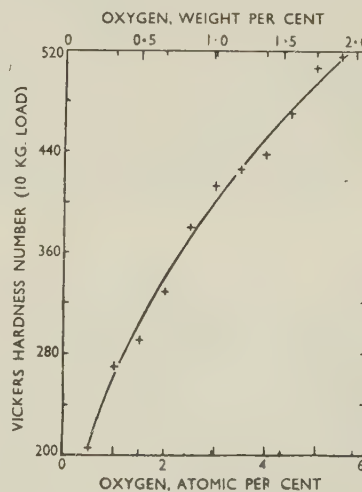


FIG. 15.—Hardness/Oxygen Concentration Relationship for Annealed Titanium-Oxygen Alloys.

optical strain-gauge with a sensitivity of  $\pm 5 \times 10^{-6}$  in./in. Within the limits of measurement, the value of Young's modulus for the 2% alloy equalled that



for the basis titanium, the actual result being  $(1.66 \pm 0.01) \times 10^7$  lb./in.<sup>2</sup>.

From the results of numerous Vickers hardness tests, it was possible to establish with reasonable certainty the hardness/concentration relationship for annealed alloys containing up to 5.5 at.-% oxygen. In Fig. 15, each point represents the mean of about 10 determinations made on 3 or 4 specimens. The scatter in the case of each alloy was of the order of

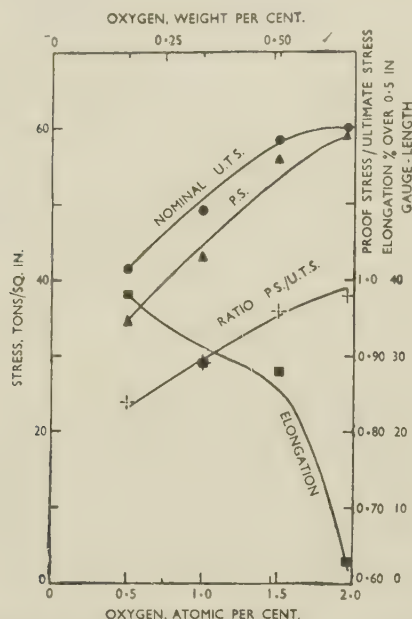


FIG. 16.—Mechanical Properties of Annealed Titanium-Oxygen Alloys. Proof stress is for approximately 0.2% permanent set.

$\pm 5$  Vickers units. It will be noted that the rise in hardness with increasing oxygen content is quite rapid.

Some values of the proof stress (approximately 0.2% permanent set), nominal ultimate tensile stress, and plastic elongation were ascertained in tensile tests on A.S.T.M. standard  $\frac{1}{8}$ -in.-dia. test specimens. Fig. 16 shows the tensile test results, each point representing the mean of two tests. A particular feature of the results was that the plastic range dropped markedly from about 28% elongation in the

case of the 1.5 at.-% oxygen alloy to just under 3% for the 2 at.-% oxygen alloy. Also, there was a marked rise in the ratio proof stress/nominal ultimate stress in the composition range studied. Extrapolation of the curves in Fig. 16 would suggest that alloys containing more than approximately 2.5 at.-% oxygen would be brittle at normal temperatures. Some very simple experiments on the 3 at.-% alloy confirmed this observation.

During the "necking down" stage in tensile tests, the basis titanium exhibited a non-uniformity of deformation near the point of fracture, resulting in the development of longitudinal ridges. This phenomenon was not observed in the alloys. The difference in behaviour between the basis metal and the alloys could not be attributed to grain-size, as all the specimens were similar in this respect.

## 6. CONCLUSION

The room-temperature properties of alloys containing up to 1.5 at.-% oxygen are such as to suggest that these alloys may be of value in certain engineering applications. A particular feature of the alloys is that they possess a comparatively high proof stress.

Finally, it is worth noting that the mechanical properties of the alloys could not be varied by quenching them from the  $\beta$  solid-solution field. It is thought that this was due to the great rapidity of the  $\beta \rightarrow \alpha$  transformation on cooling through the ( $\alpha + \beta$ ) range.

## ACKNOWLEDGEMENTS

Most of the investigation described in this paper was conducted as part of the programme of the Physical Metallurgy Section, Commonwealth Scientific and Industrial Research Organization, Australia. This Section forms part of the Baillieu Laboratory, University of Melbourne.

The authors gratefully acknowledge the assistance afforded by Professor J. Neill Greenwood. Thanks are also due to Mr. J. A. Corbett who carried out the necessary analytical work. The United States Bureau of Mines kindly provided the commercially pure titanium used in part of the investigation.

## REFERENCES

1. J. H. de Boer, W. G. Burgers, and J. D. Fast, *Proc. K. Akad. Wetensch. Amsterdam*, 1936, **39**, 515.
2. P. Ehrlich, *Z. anorg. Chem.*, 1941, **247**, 53.
3. H. T. Clark, *Trans. Amer. Inst. Min. Met. Eng.*, 1949, **185**, 588.
4. R. I. Jaffee and I. E. Campbell, *Trans. Amer. Inst. Min. Met. Eng.*, 1949, **185**, 646.
5. W. L. Finlay and J. A. Snyder, *Trans. Amer. Inst. Min. Met. Eng.*, 1950, **188**, 277.
6. R. I. Jaffee, H. R. Ogden, and D. J. Maykuth, *Trans. Amer. Inst. Min. Met. Eng.*, 1950, **188**, 1261.
7. L. G. Carpenter and F. R. Reavell, *Metallurgia*, 1948, **39**, 63.
8. H. W. Worner, *Australian J. Sci. Research*, 1951, [A], **4**, (1), 62.
9. L. Pauling, *J. Amer. Chem. Soc.*, 1947, **69**, 542.
10. H. W. Worner, *Australasian Eng.*, 1950, (Nov.), 52.
11. A. D. McQuillan, *Proc. Roy. Soc.*, 1950, [A], **204**, 309.
12. W. J. Kroll, *Trans. Electrochem. Soc.*, 1940, **78**, 35.

# SOME OBSERVATIONS ON THE DEFORMATION OF POLYCRYSTALLINE ZINC\*

1338

By J. A. RAMSEY,† M.Sc.

## SYNOPSIS

It is shown that polycrystalline zinc, when deformed, behaves in a similar way to aluminium in that, both at elevated temperature and at slow strain rates, it tends to form a sub-grain or cell structure within the grains. Evidence is presented in support of the view that the cell structure is produced directly by the deformation and cannot be adequately explained by the same mechanism as that suggested for polygonization.

## I.—INTRODUCTION

A NUMBER of papers<sup>1,2</sup> have appeared recently on the deformation of aluminium by creep at elevated temperatures, and it has been demonstrated that the grains break down into distinct elements or "cells". Similar observations having been made by the present author<sup>3</sup> on the rapid deformation of aluminium at an elevated temperature, it was thought desirable to seek confirmation with another metal, and zinc was chosen for the purpose because it belongs to a different crystal system and was readily available in a very pure form.

## II.—EXPERIMENTAL TECHNIQUE

Flat tensile specimens were prepared from strips of zinc produced by hot rolling cast ingots of purity 99.999%. Great difficulty was experienced in developing a uniform grain-size both within one specimen and from specimen to specimen after the same treatment. The method finally adopted was either to anneal the specimens at 270° C. after cutting from the rolled strip, or to anneal them at the same temperature after an elongation of 10%. Since the as-rolled strip was self-annealing, the former method depended upon grain growth and the latter upon recrystallization. The strain-anneal method was employed when a number of specimens of the same average grain-size were required, although it had the disadvantage of rumpling the surface in a manner which persisted even after electropolishing and made microscopic observation more difficult.

Electrolytic polishing was carried out by the method recommended by Rodda,<sup>4</sup> viz. by the use of a solution of 20 g. chromium trioxide in 1000 ml. of water. Satisfactory surfaces were obtained after 45 sec. with a current density of 16 amp./in.<sup>2</sup>. This electropolishing usually etched the grain boundaries adequately, but, if deeper etching was required, a reagent consisting of 15 g. sodium sulphate and 20 g. chromium trioxide in 1000 ml. of water was employed.

X-ray observations were made by the standard back-reflection technique, using cobalt radiation and reflections from the (105) and (114) planes.

Deformation was applied by stretching in a hand-operated tensile machine which could be encased in a furnace for work at elevated temperatures. Since it was necessary to cool the specimens before microscopic examination, it was not certain whether some of the features observed were a direct result of the deformation or whether they occurred during furnace-cooling. In order to overcome this objection, the changes in the microstructure of some specimens, such as those referred to in Section V, were followed while the specimen was being deformed at an elevated temperature. For this purpose, use was made of a small tensile machine which could be mounted on the stage of a Bausch and Lomb metallographic microscope and in which the specimen was surrounded by a small heating coil. In this way a given group of grains could be kept continuously under observation during the initial heating, whilst the specimen was being extended, and during cooling.

Specimens were generally extended at the rate used in normal tensile testing. Some specimens, however, were extended in a special machine at a low rate of approximately 0.15% elongation per hr. in order to examine the effect of the strain rate. For convenience the former will be referred to as rapid, and the latter, as slow straining.

## III.—RAPID DEFORMATION AT VARIOUS TEMPERATURES

Microscopic examination of specimens stretched at room temperature revealed slip and twinning. Fig. 1 (Plate XXX) illustrates a typical area on a specimen extended 5%, in which slip was confined to one set of planes. However, in a large number of grains, a set of faint, more or less parallel bands was present, which were at an angle to the slip lines. This phenomenon is clearly shown in Fig. 2 (Plate XXX) in the

\* Manuscript received 21 February 1951.

† Research Officer, Aeronautical Research Laboratories, Department of Supply, Melbourne, Australia.



direction indicated by the arrow, and appears very like a large number of small twins. Similar markings were noted recently by Jillson<sup>5</sup> and were attributed by him to "kinking". Another feature of the deformation was the existence of narrow bands running across the slip, the slip lines being deviated across them. These bands apparently provide a limit to the formation of twins, as shown in Fig. 2.

X-ray diffraction revealed that the arcs from individual grains consisted of a number of spots on a continuous background (Fig. 21, Plate XXXI), suggesting that the grains had broken down into a mixture of coarse fragments and very small fragments, the former being responsible for the spots and the latter for the continuous background. This type of fine structure has been correlated with kinking by Jillson, but, at least in the present case, the scale of the two phenomena appears to be quite different. From the microscopic appearance the only other evidence of discrete elements in the grains was the existence of the narrow deformation bands which could be considered to be the boundaries of areas in the grains of different degrees of tilting. However, though these were generally of about the right order of size, they were not observed in a very large number of grains. Whatever the cause of the fine structure, subsequent heat-treatment had the effect of sharpening the spots and reducing the continuous background, thus producing arcs consisting of a number of sharp spots. This suggests that the cause of the fine structure after recovery was present in the deformed state and was only made more easily observable by the heat-treatment. In comparing these structures with those resulting from deformation at elevated temperature, it should be noted that the grain boundaries in Fig. 1 (Plate XXX) are fairly sharp.

On raising the temperature of deformation, the most striking feature observed was a very definite sub-grain or "cell" structure in a large number of grains. This is illustrated in a very spectacular manner by Fig. 3 (Plate XXX), which shows the structure of a specimen extended 3.1% at 200° C. Fig. 4 (Plate XXX), which shows the same main grain shifted to the right and photographed with very slightly oblique illumination, clearly demonstrates that the surface of the grains was inclined differently from cell to cell. This was later confirmed by observations on the surface, using Tolansky<sup>6</sup> fringes. It will be noted that the cell boundaries are very regular and well marked, in contrast to those in aluminium, which are very irregular and difficult to observe.

Comparison between Figs. 5 and 6 (Plate XXX) which illustrate the condition after a 5% elongation at 100° and 200° C., respectively, shows that the cell structure is more clearly marked and is present in many more grains at the higher temperature. There was no significant difference in the cell sizes at the two temperatures. Recrystallization occurred during the process of elongation to 5% at 250° C.

At all temperatures, slip took place in the vast

majority of grains, and there was no change in spacing or thickness of the slip lines. This type of behaviour contrasts markedly with that of aluminium, in which both the spacing and "width" of the slip lines increased with the temperature and, at the highest temperatures, no slip at all was observed. However, in some grains of zinc, no slip was observed; this was always the case in those grains manifesting the most clearly developed cell structure.

Generally, the slip lines in the grains containing both cells and slip were continuous across the cell boundaries, and were either straight or slightly deviated. The slight directional changes appeared consistent with the tilting of the grain surface from cell to cell after the occurrence of slip. In a few cases very marked directional changes in the slip were found. This was so in grains in which the cell boundaries were more or less at right angles to the slip direction and is illustrated by Fig. 7 (Plate XXX), in which it appears to be similar to the effect obtained at room temperature (Fig. 2).

In large grains especially, the cell size was observed to vary within the grains, being finer along one of the boundaries and increasing in size towards the centre of the grain. Long narrow cells were often found lying parallel to the grain boundaries, as illustrated in Fig. 3 (lower right grain), giving the appearance of traces of a migrating boundary. That migration is not the explanation will be demonstrated later.

The increasing facility of twinning with increasing temperature of deformation in zinc, reported by Davidenkov, Kolesnikov, and Fedorov,<sup>7</sup> was not borne out by the present work. It was found that twinning was absent in fine-grained specimens and much diminished in coarse-grained ones, after deformation at elevated temperatures.

On electropolishing and re-etching the specimens, both the old boundaries and the cell boundaries reappeared, proving that the network of boundaries within the grains was not purely a surface effect and that recrystallization to a fine grain-size was not responsible (cf. the complete grain shown in Figs. 3 and 8, Plate XXX). The effect referred to earlier, viz. the presence of long narrow cells parallel to the grain boundaries, is shown also in Fig. 8 (Plate XXX) after repolishing and re-etching (lower right grain). The fact that the original boundary and the cell boundaries reappeared refutes the idea that the phenomenon was due to boundary migration since, if the latter were the case, only one line would reappear on the site of the final position of the boundary.

In order to study the relative orientation of the cells, a specimen that exhibited a cell structure was extended at room temperature after repolishing and re-etching. It was found that grains containing a very well-developed cell structure, such as the grain in Fig. 3 (Plate XXX), showed less tendency to slip than others, a greater overall extension being necessary before they manifested any slip. This may be interpreted in two ways; either the existence of

MICROSTRUCTURES OF POLYCRYSTALLINE ZINC AFTER DEFORMATION.

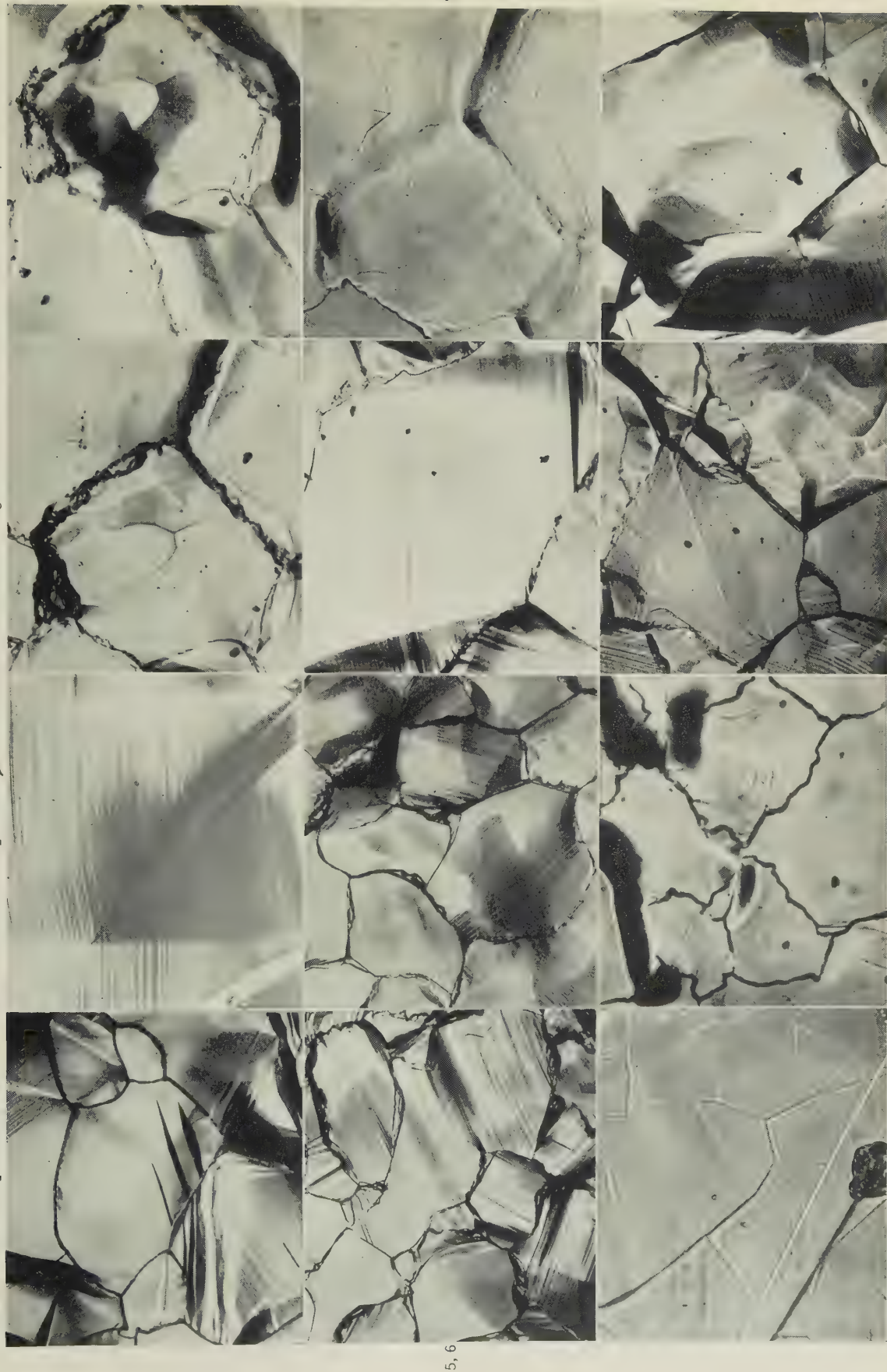
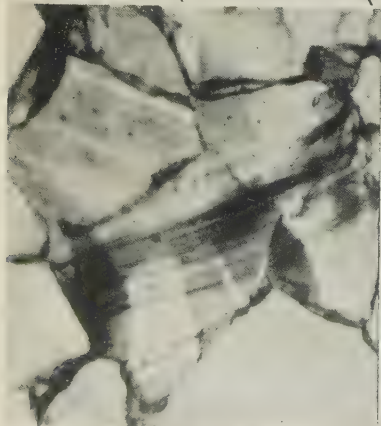


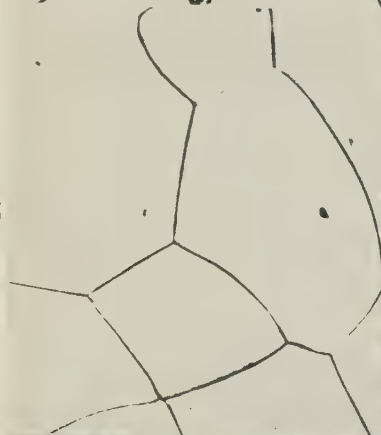
FIG. 1.—5% Extension at 21° C.  $\times 100$ .  
 FIG. 2.—5% Extension at 21° C. Coarser grain-size than in Fig. 1.  $\times 100$ .  
 FIG. 3.—3.1% Extension at 200° C. Vertical illumination.  $\times 100$ .  
 FIG. 4.—3.1% Extension at 200° C. Oblique illumination.  $\times 100$ .  
 FIG. 5.—5% Extension at 100° C.  $\times 100$ .  
 FIG. 6.—5% Extension at 200° C.  $\times 100$ .  
 FIG. 7.—3.1% Extension at 200° C.  $\times 100$ .  
 FIG. 8.—Fig. 3 After Repolishing and Re-Etching.  $\times 100$ .  
 FIG. 9.—Centre of Grain on Left in Fig. 8, after 3% Extension at Room Temperature, Showing Slip Lines and Twin Crossing Cell Boundaries.  $\times 250$ .  
 FIG. 10.—5% Extension at 200° C., Repolished and Re-Etched.  $\times 100$ .  
 FIG. 11.—10% Extension by Creep at 21° C.  $\times 100$ .  
 FIG. 12.—12% Extension by Creep at 100° C.  $\times 100$ .



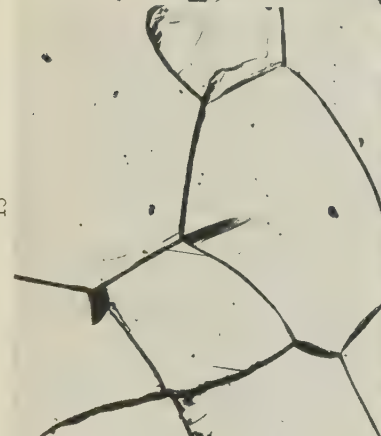
13



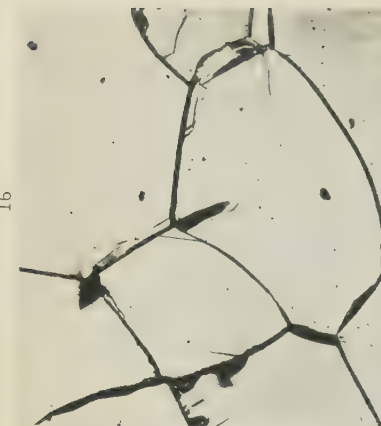
14



15



16



17



18



19



20



FIG. 13.—20% Extension by Creep at 21° C. Very fine grain-size.  $\times 500$ .  
FIG. 14.—Annealed Condition.  $\times 100$ .  
FIG. 15.—Fig. 14 After 2.5% Extension at 220° C.  $\times 100$ .  
FIG. 16.—Fig. 14 After 5% Extension at 220° C.  $\times 100$ .

FIG. 17.—Fig. 14 After 10% Extension at 220° C.  $\times 100$ .  
FIG. 18.—Fig. 14 After 15% Extension at 220° C.  $\times 100$ .  
FIG. 19.—Grain Boundary in Fig. 17 Marked by Arrow.  $\times 500$ .  
FIG. 20.—Same Boundary as in Fig. 18.  $\times 500$ .

X-RAY DIFFRACTION PATTERNS.



FIG. 21.—After 3.1% Extension at 21° C.

FIG. 22.—After 3.1% Extension at 200° C.

cells inhibited slipping or these grains were of such an orientation that slipping was difficult and thus they had found it easier to deform by cell formation and movement originally at the elevated temperature.

Fig. 9 (Plate XXX) illustrates the condition of the grain shown in Figs. 3, 4, and 8 after a 3% extension at room temperature. A number of points should be noted in this photograph. The general direction of the slip across the grain is the same, a fact which opposes the view that the sub-grain structure is due to recrystallization to a fine grain-size. However, there are some slight changes of direction from cell to cell and discontinuities in the slip lines across the cell boundaries. The former observation is consistent with the idea that slight relative rotations of the cells occurred during the deformation at elevated temperature. The observation of discontinuities in the slip is rather more difficult to understand. It can only be explained by relative movement along the cell boundaries if it be assumed that only certain groups of planes across a cell were capable of slipping and, in two neighbouring cells, had moved so that these planes were out of line across the boundary. A more reasonable explanation is that probably there is a difference of level between neighbouring cells at the boundary.

Another striking feature of deformation at an elevated temperature was the "broadening" of the grain boundaries. Such broadening was probably caused partly by boundary migration and, partly, by the relative movement of contiguous grains which resulted in deep shadows. The boundary-migration type of broadening is most clearly shown in Figs. 19 and 20 (Plate XXXI), in which it will be noted that the broad "boundary" consisted of a number of very fine, wavy lines, suggesting that the tendency to migrate was not uniform along the length of the boundary. Repolishing and etching revealed that the broad boundaries showed up as a single line, but that the new boundary was very "ragged". The cell structure appeared to be related to bumps in the grain boundary. This is illustrated by Fig. 10 (Plate XXX) which shows the same specimen as that in Fig. 6 after repolishing and re-etching, though the area photographed was different.

This observation strongly suggests that a boundary migrating into a grain with a well-developed cell structure does so by absorbing individual cells, the probability of a particular cell being absorbed depending on its orientation relative to the growing grain. Burgers<sup>8</sup> has drawn attention to a similar effect in a recrystallized grain growing into a polycrystalline matrix. The existence of cells parallel to the grain boundaries may be responsible for the jumps often noted during grain growth.<sup>9</sup> The whole question of boundary migration in grains with a cell structure is the subject of further investigation.

X-ray examination showed that the back-reflection arcs from individual grains consisted of a number of separate spots, and there can be no doubt that the

cells are responsible for the spots. The overall difference in orientation of the cells in a particular grain was estimated at 2° or 3°. Fig. 22 (Plate XXXI) shows a typical diffraction pattern.

#### IV.—THE EFFECT OF SLOW STRAINING

Since it was considered that decreasing the rate of straining would have a similar effect to raising the temperature, a few experiments were carried out at a low rate of strain. The slow straining was carried out at two temperatures, 21° and 100° C., at the rate of 0.15% extension per hr. At both temperatures the specimens manifested a cell structure similar to that discussed in Section III. It was more marked at the higher temperature (cf. Figs. 11 and 12, Plate XXX). Cottrell and Aytakin<sup>10</sup> have also recently made the same observation with polycrystalline zinc at elevated temperature under creep conditions.

In both cases the X-ray diagrams showed a Debye ring upon which a number of spots were superimposed. The spots tended to be rather diffuse in both cases, quite unlike the reflections from new recrystallized grains, and microscopic examination did not reveal any trace of recrystallization. The grain boundaries were "broad" at both temperatures, though more so at the higher temperature.

Twinning was present in the specimens strained at room temperature, though to a much lesser degree than after rapid extension. It was absent at the higher temperature. Repolishing and re-etching confirmed again that the cell structure was not a surface effect and also that the boundaries had become very ragged.

A specimen having a grain-size about the same as the cell size observed in the preceding experiments was slowly strained at the same rate at 21° C. It was thought that the grains might act as cells and that the deformation would occur by relative movement of small grains, but this did not prove to be so. Slip was present but, in contrast to the coarser-grained specimens, it was confined to broad bands and was not uniformly spread over the grains. This is similar to the effect of raising the deformation temperature or lowering the rate of deformation in the case of aluminium. Many grains manifested a cell structure. Twinning was absent, thus confirming the observation made in Section III that it occurs more readily the larger the grain-size, other things being equal. Fig. 13 (Plate XXXI) illustrates the condition after 20% elongation. It will be noted that the direction of slip changes across the cell boundaries in the grain at the centre of the photograph. The same grain at 10% elongation showed straight slip and no cells, so that during the extension from 10 to 20% the grain must have "buckled" along the cell boundaries, thus giving rise to the deviations of the slip shown in Fig. 13 (Plate XXXI). A similar effect was probably responsible for the changes in slip direction shown in Fig. 7 (Plate XXX).

It may be concluded that in zinc, as in aluminium



cell formation is facilitated by decreasing the rate of strain, and that zinc resembles aluminium more closely the smaller the grain-size.

### V.—THE PROCESS OF CELL-STRUCTURE FORMATION

In order to study the formation of a cell structure, a specimen was kept under observation continuously during the deformation at an elevated temperature. During the period of heating to the desired temperature before deformation, some grains showed evidence of slip which was possibly due to the anisotropy of thermal expansion.<sup>11</sup> In a few grains, too, a faint cell structure was observed which may be reasonably attributed to the same cause.

Fig. 14 (Plate XXXI) is a photograph of a typical area of a specimen taken at 220° C. before deformation. During the initial stages of deformation at 220° C. slip occurred in the majority of grains under observation. However, in the very early stages of deformation, some grains developed a cell structure before slip was observed. An example of such a grain is shown on the extreme right of Figs. 15–18 (Plate XXXI). The grains which exhibited slip in the early stages did not begin to show cells very clearly until the extension had reached about 5% (Fig. 16, Plate XXXI).

It will be noted that, accompanying the increasing deformation, the surface of the grains became tilted at different angles from cell to cell, and slight movements of the cells and changes in shape occurred. This latter is most strikingly shown near a grain boundary at high magnification in Figs. 19 and 20 (Plate XXXI), corresponding to 10 and 15% elongation respectively. In many instances cell structures apparently began as slight "puckering" near the grain boundary, possibly because of the greater degree of deformation along the grain boundaries.

The most important observation made during the deformation was that the initiation and subsequent developments in the cell structure occurred continuously with increasing extension, as though the formation and movement of the cell structure were a direct result of the deformation and not caused by a two-stage process of deformation followed by recovery.

An example of the broadening of a grain boundary by migration is shown in Figs. 19 and 20 (Plate XXXI), and illustrates quite clearly the raggedness of the migrating "front".

### VI.—DISCUSSION

The evidence adduced in the present paper shows clearly that, on deformation at elevated temperature or, if the strain rate is slow enough, at room temperature, the grains of polycrystalline zinc break down into a number of distinct elements or "cells", indicating that zinc behaves in a comparable way to that of aluminium deformed under similar conditions. However, zinc differs from aluminium in that the slip-line spacing and "thickness" was found to be

invariant over the ranges of strain rate and temperature considered in those experiments, and the cells show up in a much more striking way directly on deformation. The X-ray diagrams were similar to those obtained from aluminium.

The question has been raised in discussion of the work of Wood and his colleagues<sup>12, 13</sup> as to whether or not the cell structure obtained on deformation at elevated temperature is due to polygonization. Before embarking on a discussion of this matter, it is well to be clear as to the nature of the experimental evidence in both cases.

Considering in the first place the X-ray diffraction data, Cahn observed spotty asterisms in severely bent single crystals on annealing at a temperature very close to the melting point. Similar effects have been obtained by a number of other workers under conditions of deformation at room temperature and subsequent heating at an elevated temperature. Turning now to the question of cell formation, Wood and his co-workers, as well as a number of others, have found that discontinuous Debye arcs or asterisms can be obtained directly upon deformation at elevated temperatures, or as in the present work, at room temperature, if the deformation rate is low enough. Moreover, in the experience of the author, the spots on the X-ray diagrams indicate that the size and degree of perfection of the elements within the grains are greater when they are produced directly by deformation at elevated temperatures. Thus the X-ray evidence indicates some similarity between the final product in both cases.

On the other hand, the microscopic appearance is very different. Cahn<sup>14</sup> has shown that recovery after cold deformation produces long narrow elements, the boundaries of which run perpendicular to the slip planes, but the cells shown in the present paper have quite a different shape, and their boundaries bear no particular relation to the slip.

These, then, are the two major experimental facts upon which the concepts of "polygonization" and "cell formation" are based; one set of data shows a similarity between them and another a very striking difference. It is contended that the only experimental evidence for saying that cell formation is due to polygonization is the similarity of the X-ray diagrams.

Apart from this, a number of observations recorded in the previous section cast some doubt on the interpretation of cell formation as resulting from the same mechanism as polygonization, as interpreted by Cahn. In the first place, cells formed in a number of grains as soon as deformation began and developed strongly, though no slip was observed in the grains. If no slipping occurred, then the explanation of cell formation in terms of Cahn's theory of polygonization is improbable. Of course it may be argued that slip occurred, but not to an observable extent. If this were so, it is difficult to understand why polygonization did not occur in those grains showing much more marked slip. This can only mean that either there is a critical deformation at which "poly-

gonization" occurs most readily, or the orientation of the grains was such that their active slip plane lay parallel, or nearly parallel, to the specimen surface.

If the former were so in the present case, it would be expected that those grains which showed evidence of deformation by slip initially would not form a cell structure after a much greater degree of deformation, but in fact such a sequence was observed. If, on the other hand, it is suggested that slip was not visible in certain grains because the slip plane was parallel to the specimen surface, it is difficult to understand why slip appeared when the specimen was repolished and re-etched and then strained at room temperature.

These facts strongly suggest that slip is not a necessary prerequisite to the formation of cells, and therefore that the mechanism of their formation cannot be explained along the lines of Cahn's theory of polygonization.

An alternative view, which does not encounter these difficulties, is that at elevated temperatures some of the grains break down directly, on deformation, into a number of fragments identical with those shown in the photomicrographs, and these are responsible for the spottiness of the X-ray diagrams. It is suggested that such a direct breakdown occurs because at elevated temperature some grains find it easier to deform by the formation and relative movement of cells than by slip. In the grains which showed slip initially, it must be assumed that after a certain amount of deformation further changes in shape could not be provided by slipping and so cell formation and movement occurred. Of course, the problem

remains as to why cell formation is easier than slipping at elevated temperature.

The basic difference between the two points of view can be most clearly seen from a consideration of the atomic movements involved in each theory. The theory put forward in the present paper suggests that deformation at elevated temperatures causes the movement of atoms from their equilibrium lattice positions, but that the thermal energy available is sufficient to enable them to find new equilibrium positions continuously and spontaneously during the deformation; whereas the explanation of cell formation based on Cahn's theory of polygonization assumes a wholesale disordering of a large number of atoms, followed by a wholesale reordering. The latter theory therefore in effect presupposes that deformation at elevated temperatures involves the simple arithmetical addition of the effect of temperature and the effect of deformation, which is very different from the idea that, on deforming at elevated temperatures, the two factors combine to produce a different mode of deformation.

#### ACKNOWLEDGEMENTS

The author wishes to express his thanks to Professor J. N. Greenwood and Dr. W. A. Wood, of the Baillieu Laboratory, University of Melbourne, to Mr. J. B. Dance of the Aeronautical Research Laboratory, Department of Supply, and to his colleagues at both laboratories for helpful discussions and suggestions.

#### REFERENCES

1. G. R. Wilms and W. A. Wood, *J. Inst. Metals*, 1948-49, **75**, 693.
2. W. A. Wood and W. A. Rachinger, *J. Inst. Metals*, 1949-50, **76**, 237.
3. J. A. Ramsey, unpublished research.
4. J. L. Rodda, *Min. and Met.*, 1943, **43**, 323.
5. D. C. Jillson, *Trans. Amer. Inst. Min. Met. Eng.*, 1950, **188**, 1009.
6. S. Tolansky, "Multiple-Beam Interferometry of Surfaces and Films". Oxford: 1948 (Clarendon Press).
7. N. N. Davidenkov, A. F. Kolesnikov, and K. N. Fedorov, *Zhur. Eksper. Teoret. Fiziki*, 1933, **3**, 350.
8. W. G. Burgers, *Proc. K. Ned. Akad. Wetensch.*, 1947, **50**, 719.
9. W. Boas, *J. Inst. Metals*, 1947-48, **74**, 622 (discussion).
10. A. H. Cottrell and V. Aytakin, *J. Inst. Metals*, 1950, **77**, 389.
11. W. Boas and R. W. K. Honeycombe, *Proc. Roy. Soc.*, 1946, [A], **186**, 57.
12. Discussion on G. R. Wilms and W. A. Wood's paper, *J. Inst. Metals*, 1948-49, **75**, 1120.
13. Discussion on W. A. Wood and W. A. Rachinger's paper, *J. Inst. Metals*, 1949-50, **76**, 730.
14. R. W. Cahn, *J. Inst. Metals*, 1949-50, **76**, 121.





# THE SIGMA PHASE IN BINARY ALLOYS OF THE TRANSITION ELEMENTS\*

1339

By A. H. SULLY, M.Sc., Ph.D., F.Inst.P., F.I.M., MEMBER

## SYNOPSIS

The appearance of the sigma phase in alloys of elements of the First Long Period can be satisfactorily accounted for if it is assumed that the incidence of this phase is determined by a critical excess of electrons in bond orbitals over vacancies in the  $3d$  atomic orbitals. In the alloys of cobalt and iron with chromium; iron, nickel, and cobalt with vanadium; and chromium and vanadium with manganese, predictions of the boundary of the homogeneous sigma-phase region can be made on the basis of this hypothesis which accord well with experimental data where these are available. The fact that the sigma field does not include the equiatomic composition in certain alloy systems is also explained. It is probable that sigma phases occur in alloys between transition elements of the other long periods.

## I.—INTRODUCTION

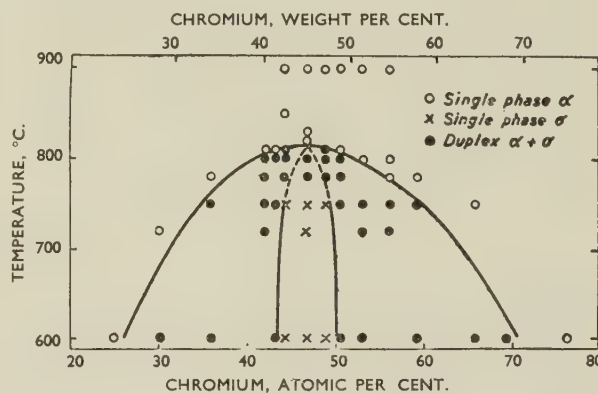
It was first shown by Bain and Griffiths<sup>1</sup> that a hard, brittle, and non-magnetic phase was formed in iron-chromium alloys of composition close to an equiatomic ratio, when the alloys were slowly cooled or annealed for long periods of time at temperatures below  $950^{\circ}\text{C}$ . The existence of this "sigma" phase was denied by other workers, notably by Adcock,<sup>2</sup> but its presence has since been adequately confirmed by Wever and Jellinghaus,<sup>3</sup> by Eriksson,<sup>4</sup> and by Bradley and Goldschmidt.<sup>5</sup> The extent of the sigma-phase region in equilibrium conditions in high-purity iron-chromium alloys had been determined by Cook and Jones,<sup>6</sup> whose diagram is reproduced in Fig. 1. The extension of the sigma-phase field into various ternary alloys containing iron and chromium has been investigated by many workers, and much study has also been devoted to the important effects which the formation of this phase has on the properties of industrial alloys, particularly of the austenitic stainless steels.

Until recently it was assumed that this phase was confined to alloys that contained both iron and chromium. In 1948, however, Sully and Heal<sup>7</sup> showed that a phase isomorphous with the sigma phase existed in the cobalt-chromium system. The most recently determined equilibrium diagram of this system, due to Elsea, Westerman, and Manning,<sup>8</sup> is shown in Fig. 2. The phase isomorphous with sigma is the gamma phase, the range of homogeneity of which is indicated to be from 53.5 to 58 wt.-% (56.6–61.0 at.-%) chromium.

Andrews<sup>9</sup> has shown that another isomorphous phase exists in the iron-vanadium system, the original investigation of which was made by Wever and Jellinghaus<sup>10</sup> (Fig. 3).

Goldschmidt<sup>11</sup> found that the phase based on  $\text{FeMo}$  in the iron-molybdenum system also has the sigma structure. In this system, however, the phase is

stable only at temperatures above  $1180^{\circ}\text{C}$ . and decomposes to  $\alpha$ -molybdenum and the  $\epsilon\text{-Fe}_3\text{Mo}_2$  phase at lower temperatures. This behaviour is markedly different from that in the iron-chromium, cobalt-chromium, and iron-vanadium systems, in which sigma is stable at relatively low temperatures and transforms below the melting point of the alloys in which it occurs.



[Courtesy Iron and Steel Institute.

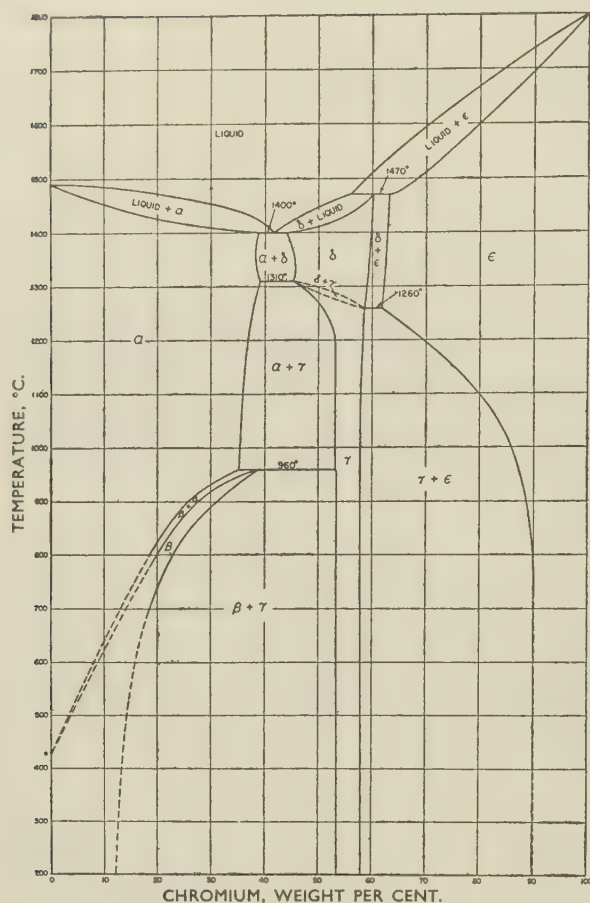
FIG. 1.—Sigma Phase in Iron-Chromium Alloys. (Cook and Jones.<sup>6</sup>)

Recently, the sigma phase has been encountered in four additional alloy systems. It has been found in nickel-vanadium and in cobalt-vanadium alloys by Pietrokowsky and Duwez<sup>12</sup> and by Pearson, Christian, and Hume-Rothery,<sup>13</sup> and by the latter investigators in chromium-manganese and vanadium-manganese. None of these systems has yet been examined in detail, but Pearson, Christian, and Hume-Rothery give the range of homogeneity of the sigma phase as 55 to more than 65 at.-% vanadium in the nickel-vanadium system, and from approximately 72 to 83 at.-% manganese in the chromium-manganese system.

\* Manuscript received 10 February 1951.

† Principal Physicist, Fulmer Research Institute, Stoke Poges, Bucks.





[Courtesy American Institute of Mining and Metallurgical Engineers.]

FIG. 2.—Equilibrium Diagram for Cobalt-Chromium Alloys.  
(Elsea, Westerman, and Manning.<sup>8</sup>)

In the cobalt-vanadium system the homogeneous sigma-phase region includes the 50:50 atomic composition, but in the vanadium-manganese system the 50:50 alloy has a body-centred cubic structure, although an alloy with 24.3 at.-% vanadium is in the homogeneous sigma-phase field.

## II.—ELECTRON COMPOUNDS

The existence of isomorphous phases of characteristic structure in different alloy systems at compositions which differ from one system to another has been satisfactorily explained by Hume-Rothery and his co-workers<sup>14</sup> on the basis that the phase appears at a critical ratio of valency electrons to atoms. Thus, the body-centred cubic  $\beta$  phase of the alloys of copper, silver, and gold with *B* sub-group and certain other elements occurs at a critical electron: atom ratio of 3:2. Similarly, it has been shown in the same alloys that  $\gamma$ -brass structures occur at electron: atom ratios of 21:13 and close-packed hexagonal structures at a ratio of 7:4. Such phases have come to be known as "electron compounds".

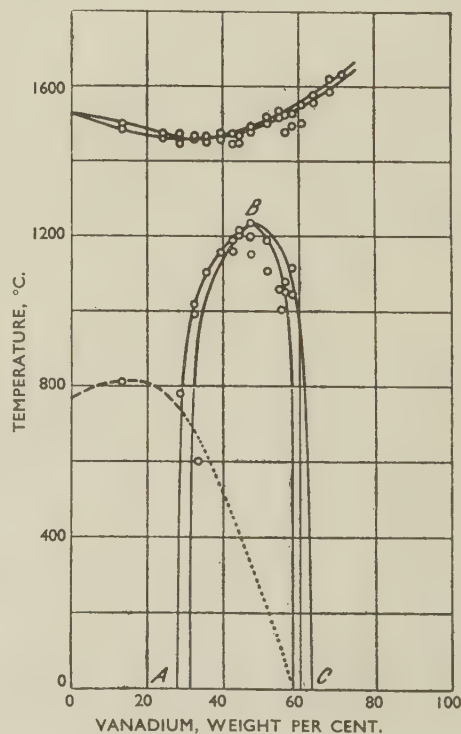
When the sigma phase was known only in the iron-chromium system, in which its range of homogeneity

includes the equiatomic composition, there was no reason to suppose that similar considerations applied to the formation of this phase. Indeed, Andrews<sup>9</sup> has suggested that its formation depends upon the onset of an ordered structure. However, it is now clear that in the systems cobalt-chromium, nickel-vanadium, chromium-manganese, and chromium-vanadium the range of homogeneity of the sigma phase does not include the equiatomic composition, and it is worth re-examining the suggestion, first made by Sully and Heal,<sup>7</sup> that the sigma phase is an electron compound.

## III.—ELECTRONIC STRUCTURE OF TRANSITION METALS

The chemical behaviour of transition metals is satisfactorily explained by the quantum theory, on the basis that the outermost quantum shell is filled to a constant level, while the next inner shell is incompletely full and is filled progressively as the atomic number increases within the transition group of elements. Thus, the electronic structure of the free atoms of the elements from potassium to copper is as set out in Table I.

Although the behaviour of free atoms is satisfactorily accounted for in this way, there are certain properties of the transition elements that are not explicable on this basis, notably the high bonding energy, high resistivity and specific heat, and the appearance of ferromagnetism in iron, cobalt, and nickel.



[Courtesy K. W. Institut für Eisenforschung.]

FIG. 3.—Sigma Phase in Iron-Vanadium Alloys. (Wever and Jellinghaus.<sup>10</sup>)

It was first proposed by Mott and Jones<sup>15</sup> that the numbers of electrons in the 3*d* and 4*s* bands of the transitional First Long Period elements were statistically non-integral, the average electron density being such that there were vacancies in the 3*d* band; the

On Pauling's theory, vanadium is regarded as having 5 and titanium 4 electrons available for bond formation, i.e. they have no electrons in atomic orbitals.

#### IV.—ALLOYING BEHAVIOUR OF TRANSITION METALS

In most of their alloys with non-transition metals, the transition metals chromium to nickel behave as if they have either zero or negative valency. For example, Ekman<sup>17</sup> showed that in the iron-zinc and nickel-zinc systems  $\gamma$ -brass structures occur at Fe<sub>5</sub>Zn<sub>21</sub> and Ni<sub>5</sub>Zn<sub>21</sub>, respectively. This conforms to the 21:13 electron:atom ratio, if iron and nickel behave as zero-valent, while zinc has its normal metallic valency of 2.

On the other hand, in some other systems these elements behave as if they have a negative valency, i.e. they accept electrons from the structure as a whole and contribute none themselves. Raynor<sup>18,19</sup> and his co-workers, in studying the alloys of aluminium with the transition metals iron, cobalt, and nickel, have shown that, if it is assumed that the transition-metal atoms absorb electrons to the full extent permitted by the vacancies in the 3*d* atomic orbitals, the appearance of compounds of the type X<sub>2</sub>Al<sub>9</sub>, where X represents one or more transition metals, is characterized by an excess electron:atom ratio of 2.06–2.28. It is apparently assumed that the transition elements themselves contribute no electrons to the structure, i.e. that the electrons in Pauling's bond orbitals play no part in determining the structure.

#### V.—ALLOYS OF THE TRANSITION METALS WITH EACH OTHER

##### 1. MODE OF BONDING

In the alloys of the transition metals with one another existing theory permits of no close definition of the detailed mode of cohesive bonding. If it is assumed that all the electrons in Pauling's bond orbitals are available as bond electrons, then the ratio of bond electrons to atoms remains constant at a value of 5.78 for all the alloys of chromium, manganese, iron, cobalt, and nickel with each other. If it is also assumed that vanadium contributes five electrons to the structure, then in the alloys of the transition metals with vanadium the electron:atom ratio can vary only between limits of 5.0 and 5.78. Obviously, on this basis it is not possible to explain the formation of the sigma phase by a critical electron:atom ratio. Another possibility which may be considered, however, is that under certain conditions an exchange of electrons can occur between bond and atomic orbitals, so that the latter are filled to the fullest permitted extent of 4.88 electrons per atom. Since the number of vacancies varies from one transition metal to the next, the ratio of atoms to electrons in excess of those required to fill the 3*d* vacancies can then vary considerably with composition.

TABLE I.—*Electronic Structure of Free Atoms of Transition Metals*

Element	Atomic Number	Number of Electrons for Indicated Quantum Number and Sub-Group						
		1	2 <i>s</i>	2 <i>p</i>	3 <i>s</i>	3 <i>p</i>	3 <i>d</i>	4 <i>s</i>
K . . .	19	2	2	6	2	6	...	1
Ca . . .	20	2	2	6	2	6	...	2
Sc . . .	21	2	2	6	2	6	1	2
Ti . . .	22	2	2	6	2	6	2	2
V . . .	23	2	2	6	2	6	3	2
Cr . . .	24	2	2	6	2	6	5	1
Mn . . .	25	2	2	6	2	6	5	2
Fe . . .	26	2	2	6	2	6	6	2
Co . . .	27	2	2	6	2	6	7	2
Ni . . .	28	2	2	6	2	6	8	2

number of unoccupied states was equal to the saturation intensity of magnetization in Bohr magnetons per atom, these values being 2.2 for iron, 1.7 for cobalt, and 0.6 for nickel.

This theory has been extended by Pauling,<sup>16</sup> who considers that bonding in the transition metals from chromium to nickel inclusive is due to both 4*s* and 3*d* electrons, but that the 3*d* electron states fall into two distinct groups. Of these 2.44 electron states or orbitals do not participate in bonding. Pauling calls these atomic orbitals. Two electrons, with opposite spins, can be accommodated in each orbital, so that 4.88 electrons can be accommodated in Pauling's atomic orbitals. The remaining 5.12 electrons, which make up the permitted maximum number of 10 in the 3*d* band, are accommodated in 2.66 "bond" orbitals, and electrons in these orbitals together with the 4*s*

TABLE II.—*Electronic Structure Based on Pauling's Theory*

Element	No. of Electrons in Bonding Orbitals		No. of Electrons in 3 <i>d</i> Atomic Orbitals			Vacancies in Atomic Orbitals
	3 <i>d</i>	4 <i>s</i>	Paired	Unpaired	Total	
Cr . . .	5.12	0.66	0	0.22	0.22	4.66
Mn . . .	5.12	0.66	0	1.22	1.22	3.66
Fe . . .	5.12	0.66	0	2.22	2.22	2.66
Co . . .	5.12	0.66	1.56	1.66	3.22	1.66
Ni . . .	5.12	0.66	3.56	0.66	4.22	0.66

electrons are available for bonding. The electrons in the 3*d* atomic orbitals will remain unpaired as long as possible, and the saturation magnetic moment may be equated with the number of unpaired electrons in the 3*d* atomic orbitals.

The electronic structures predicted by Pauling for the elements from chromium to nickel are given in Table II.



In considering the alloys of vanadium with the other transition metals, the simplest assumption is that it contributes 5 bonding electrons to the structure as a whole, but an additional assumption has been made that, like the following elements

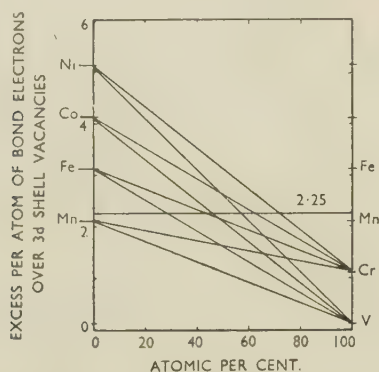


FIG. 4.—Excess Electron: Atom Ratios for Alloys of Elements from Vanadium to Nickel, Assuming Participation of 4s Electrons in Elements Chromium to Nickel.

chromium to nickel, it also has 2.44 atomic orbitals accommodating 4.88 electrons, which are normally empty.

With these assumptions and with the further assumption that in the sigma-phase structure electrons are absorbed to the full extent permitted by the vacancies in the 3d atomic orbitals, the ratio to atoms of the excess of bond electrons over 3d vacancies is found to vary considerably from system to system.

In considering the number of bonding electrons available, the simplest assumption is that both 3d and 4s electrons contribute to the structure, so that

TABLE III.—Sigma-Phase Boundary in Transition-Metal Alloys

System	Observed Boundary, At.-%	Range of Homogeneity, At.-%	Predicted Boundary, At.-%		
			4s Electrons Contributing (Ratio 2.25)	4s Electrons Not Contributing (Ratio 1.7)	4s Electrons Contributing (Ratio 1.7)
Fe-Cr	43.5 Cr	43.5-50.0 Cr	43 Cr	38 Cr	...
Co-Cr	56.6 Cr	56.6-61 Cr	62 Cr	59 Cr	...
Ni-Cr	Not observed	...	72 Cr	69 Cr	...
Fe-V	30 * V	30-60 * V	29 V	32 V	...
Co-V	40-45 V	40-45->54 V	47 V	52 V	...
Ni-V	55-60 V	55->65 V	57 V	63 V	...
Mn-Cr	17 Cr	17-28 Cr	...	...	24 Cr
Mn-V	?	Includes 24.3 V	...	...	20 V

\* Values not precisely defined. See discussion below.

there are 5.12 3d electrons and 0.66 4s electrons, or 5.78 electrons in all, available per atom of transition metal. Fig. 4 has been constructed on this model and shows the variation with composition of the ratio to atoms of electrons, in excess of those required to fill 3d atomic orbitals, for alloys of nickel, cobalt, and iron with manganese, chromium, and vanadium. It is

found that an excess electron:atom ratio of 2.25 accounts for the occurrence of sigma phase in the alloys with chromium and vanadium and also predicts fairly successfully the compositions at which the sigma phase appears in these systems.<sup>20</sup> The compositions are tabulated in the fourth column of Table III. The agreement with the experimentally determined boundary is in most cases quite satisfactory, and moreover the theory successfully accounts for the observed fact that the range of homogeneity of the phase does not include the equiatomic ratio in the systems cobalt-chromium and nickel-vanadium.

Although at first sight an excess electron:atom ratio of 2.25 appears to account satisfactorily for the appearance of the sigma phase in the systems shown in Table III, recent information indicates that the model chosen is not correct in detail. The Debye-Scherrer X-ray pattern of the sigma phase is characterized by a group of strong lines close together at low Bragg angles, and lends itself fairly readily to an approximate determination of the volume of the first

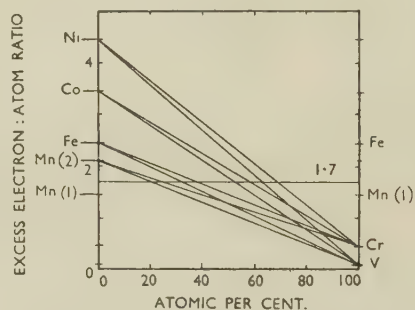


FIG. 5.—Excess Electron: Atom Ratios for Alloys of Elements from Vanadium to Nickel, Assuming no Participation of 4s Electrons in Elements Chromium to Nickel except for Manganese (2).

Brillouin zone. This enables an assessment to be made of the number of electrons that can be accommodated in the zone and consequently of the electron:atom ratio for the structure. In this way Douglas<sup>21</sup> has derived an approximate value of 1.72 for the sigma phase in cobalt-chromium alloys, while the author's colleagues Heal and Silcock<sup>22</sup> confirm this value and obtain an approximate value of 1.7 for the sigma phase in nickel-vanadium alloys at a composition of 62.5 at.-% vanadium.

These results show that the proposed electron:atom ratio of 2.25 cannot be correct and that, if the structure is an electron compound, one of the assumptions made must also be incorrect. A consideration of the results suggests that the incorrect assumption may be that the 0.66 4s electrons per atom play a part in the bonding process. If, instead, it is assumed that only the 3d electrons are involved, it is found that an excess electron:atom ratio of about 1.7 is appropriate to the sigma-phase composition ranges. Fig. 5 has been compiled by ignoring the 0.66 4s electrons per atom for the elements chromium to nickel and considering only the excess of 3d bond electrons

(5.12 per atom) over  $3d$  vacancies. The same assumptions as before are made about vanadium (5 electrons per atom and 4.88  $3d$  vacancies). The predicted composition of the sigma-phase boundary for an excess electron : atom ratio of 1.7 is given for the various systems in the fifth column of Table III. A detailed discussion of the degree of agreement in the various systems is given below.

## 2. ALLOYS WITH CHROMIUM

### (a) Iron-Chromium

According to Cook and Jones<sup>6</sup> (Fig. 1) the lower-chromium boundary of the sigma-phase region at 600° C. is at 43–44 at.-% chromium. The predicted value for an electron : atom ratio of 1.7, ignoring the  $4s$  electrons, is 38%. In view of the difficulty of achieving equilibrium conditions in alloys of this type, the agreement may be regarded as satisfactory. The homogeneous single-phase region extends to 50 at.-% chromium which corresponds to an excess electron : atom ratio of 1.46. Further investigation of these alloys, and those of the systems discussed below, is required in order to determine whether the structure can tolerate this degree of electron deficit or whether the electron : atom ratio is maintained at a higher level by the existence of a lattice deficient in chromium atoms as the chromium content increases across the range of homogeneity of the phase. An example of a lattice of this type, in which the electron : atom ratio is maintained approximately constant, is the  $Mn_3SiAl_3$  structure referred to by Robinson.<sup>23</sup>

### (b) Cobalt-Chromium

The lower-chromium boundary of the sigma region, according to Elsea, Westerman, and Manning<sup>8</sup> (Fig. 2) is at 56.6 at.-% chromium. The predicted boundary is 59 at.-% chromium, which agrees quite well and lies within the observed range of 56.6–61.0 at.-% chromium.

### (c) Nickel-Chromium

The theory predicts the appearance of the sigma phase in the nickel-chromium system at about 70 at.-% chromium. In fact, the sigma phase has never been observed in this system, which has been the subject of several investigations. Beck and Manly<sup>24</sup> have, however, noted that in the cobalt-chromium-nickel alloys the sigma phase persists for a considerable way towards the nickel-chromium boundary, and they infer that a tendency may exist to form a sigma phase in the nickel-chromium alloys. A possible reason for the non-appearance of the phase may be that its upper temperature limit of stability, which varies from system to system, is below about 600° C., so that transformations in these alloys do not take place within experimentally reasonable periods of time. It may be noted, although it may be fortuitous, that there is some correlation in the alloys with chromium, between the Curie temperature of the ferromagnetic component of the system and the

upper temperature limit of stability of the sigma phase. In the iron-chromium alloys, the upper temperature limit, according to Cook and Jones,<sup>6</sup> is at 800°–820° C., the Curie point of iron being 770° C.; while in cobalt-chromium alloys the sigma phase persists to 1250° C., the Curie point of cobalt being 1150° C. If this apparent correlation has any real significance, the upper temperature limit of stability of sigma may be related to the Curie point of nickel, which is only 360° C. In the alloys with vanadium, referred to below, no such considerations apply, however, the sigma phase being formed in nickel-vanadium alloys quite readily at the appropriate compositions at temperatures of the order of 700°–800° C.

## 3. ALLOYS WITH VANADIUM

### (a) Iron-Vanadium

The predicted boundary of the sigma region at the lower-vanadium end is 32 at.-% vanadium. Unfortunately, the range of homogeneity of the phase in this system is not reliably established. The diagram published by Wever and Jellinghaus<sup>10</sup> (Fig. 3) suggests a lower limit of just over 30% vanadium and a wide range of homogeneity up to about 58% by weight (60 at.-%). This at first sight indicates good agreement with the predicted value, but a closer examination of the data presented by Wever and Jellinghaus suggests that the range of homogeneity of the sigma phase may be narrower than that given by the diagram. The main evidence in favour of a wide range of homogeneity is provided by lattice-spacing measurements of the sigma phase which are reproduced in Table IV.

TABLE IV.—*Lattice Spacings for Two Lines of X-ray Spectrum of Sigma Phase in Fe-V Alloys (from Wever and Jellinghaus<sup>10</sup>).*

Vanadium Content		Lattice Spacing, Å.	
Wt.-%	At.-%	$d_1$	$d_2$
38.4	40.5	1.980	1.898
46.4	48.5	1.980	1.907
47.7	50.0	1.993	1.909
52.2	54.6	1.995	1.913
63.6	65.7	2.013	1.926

In a two-phase region the compositions of the separating phases, and consequently the lattice spacings, should be constant for a particular temperature of equilibrium. The increase of spacing over the above range of composition is interpreted by Wever and Jellinghaus as indicating that the sigma phase is homogeneous over most of the range. This conclusion may, however, be invalidated by the fact that the alloys on which these measurements were conducted were slowly cooled from 1400° C. and were not brought into equilibrium at a particular temperature by long isothermal heat-treatments. It would probably be unwise to draw any conclusion from Wever



and Jellinghaus's work, other than that it indicates a fairly wide range of homogeneity for the sigma phase, the precise limits of which must await further investigation. The predicted value for the low-vanadium boundary of 32 at.-% may, therefore, be too low in vanadium, but the extent of the disagreement cannot be assessed until the diagram is clarified. If it is assumed that the other boundary of the sigma-phase region is at 60 at.-% vanadium, then the sigma structure in these alloys can tolerate a much wider range of electron deficit than can the chromium alloys.

#### (b) Cobalt-Vanadium

The predicted boundary in this system is at 52 at.-% vanadium. There is no published work which enables the limits of the sigma-phase region to be precisely defined. Duwez and Baen<sup>25</sup> have shown that an alloy of the equiatomic composition lies in the homogeneous sigma field, and this is confirmed by Pearson, Christian, and Hume-Rothery.<sup>13</sup> The author's colleague, Miss J. M. Silcock, has carried out an X-ray investigation of some binary cobalt-vanadium alloys which were heated for long periods at 600° C. and at 700° C. The range of alloys examined was not sufficiently wide to enable the full extent of the homogeneous sigma-phase field to be determined, but the lower limit was found to be at an approximate value of 40-45 at.-% vanadium. The upper limit was greater than 54 at.-% vanadium. The predicted value thus lies to the vanadium-rich side of the correct boundary, but within the homogeneous sigma field.

#### (c) Nickel-Vanadium

The predicted boundary in this system is at 63 at.-% vanadium. Pearson, Christian, and Hume-Rothery<sup>13</sup> give the sigma range as 55 to more than 65 at.-% vanadium, and Duwez and Baen<sup>25</sup> note that the equiatomic composition lies in a two-phase region. The author's colleague, Miss J. M. Silcock, has confirmed that the lower limit is in the range 55-60 at.-% vanadium. The predicted value is not seriously in error and accords with the fact that the sigma region lies wholly to the vanadium-rich side of the stoichiometric composition NiV.

### 4. ALLOYS OF MANGANESE

If manganese shows the same behaviour as is suggested for the other metals in the same group, from chromium to nickel, the excess electron:atom ratio for the element would be  $5.12 - 3.66 = 1.46$ . If this were so, it would be expected that alloys at the manganese-rich end of the binary systems with iron, cobalt, and nickel, would tend to a sigma structure. As far as is known, however, this is not the case, although Bradley and Goldschmidt<sup>6</sup> have stated that similarities exist between the X-ray pattern of the sigma phase and that of  $\alpha$ -manganese. Instead, the sigma phase appears in the manganese-chromium and manganese-vanadium systems in which the excess

electron:atom ratio computed in the manner described above is appreciably less than 1.7. These facts suggest that manganese can behave in a way dissimilar from the other metals of the same group. Anomalous behaviour by manganese has been noted in other alloy systems. For example, in copper-aluminium ternary alloys the transition metals except manganese all behave as if they have a valency  $\leq 1$ , but Hume-Rothery<sup>26</sup> has shown that at concentrations less than 25% manganese behaves as a divalent element. A possible reason for this is that in manganese the 4s electrons participate in bonding, so that this element can have an excess electron:atom ratio of  $5.12 + 0.66 - 3.66 = 2.12$ . In this case, as will be seen from Fig. 5, sigma-phase formation at an electron:atom ratio of 1.7 is predictable in the systems manganese-chromium and manganese-vanadium.

In manganese-chromium alloys the range of homogeneity of the phase is given by Pearson, Christian, and Hume-Rothery<sup>13</sup> as 83-72 at.-% manganese (17-28 at.-% chromium). The predicted value at an electron:atom ratio of 1.7, assigning an excess electron:atom ratio of 2.12 to manganese, is 24 at.-% chromium, which lies within the observed range although on the chromium-rich side of the observed boundary.

In manganese-vanadium alloys the only information available at the present time is that an alloy with 24.3 at.-% vanadium is a sigma phase.<sup>13</sup> The boundary predicted on the above basis is at 20 at.-% vanadium, which is consistent with this observation.

## VI.—DISCUSSION OF RESULTS

The above approach to the problem of sigma-phase formation in the transition-metal alloys is somewhat speculative. It has, however, been shown on the basis of Pauling's theory of the electronic structure of the transition metals, that a number of predictions which conform to observed experimental facts can be made, if the factor that determines the appearance of the sigma phase is a critical excess of bond electrons over valencies in 3d atomic orbitals. Predictions can be made almost equally successfully with an excess electron:atom ratio of 2.25 and on the assumption that 4s electrons in the elements chromium to nickel contribute to bonding, or with an excess electron:atom ratio of 1.7 assuming no contribution from the 4s electrons, except in the case of manganese. Determinations of the volume of the first Brillouin zone in cobalt-chromium and nickel-vanadium alloys appear to favour the second model.

On this basis it is possible to explain the non-appearance of sigma phase in alloys of iron, nickel, and cobalt with each other. It is also possible to account for its appearance at approximately the correct composition in the systems iron-chromium, cobalt-chromium, iron-vanadium, cobalt-vanadium, nickel-vanadium, manganese-chromium, and manganese-vanadium. In particular, this hypothesis successfully explains the observed facts that the

homogeneous sigma-phase field does not include the equiatomic composition in the systems cobalt-chromium, nickel-vanadium, manganese-chromium, and manganese-vanadium. Such consistent agreement with experiment is hardly likely to be fortuitous and strongly suggests that the sigma phase is a type of electron compound.

Little is known about the detailed electronic structure of the  $d$  and  $s$  states in the transition elements of the other long periods. For this reason no attempt is made to account for Goldschmidt's<sup>11</sup> observation that a sigma phase is formed in alloys of iron and molybdenum, and the observation of Kasper, Decker, and Belanger<sup>27</sup> that it occurs in manganese-

molybdenum alloys. Obviously, however, similar considerations could apply to these alloys, and there is thus a strong possibility that similar phases may be formed in alloys between transitional metals of long periods other than the first. It is to be noted that, according to a recent publication,<sup>28</sup> the structure of  $\beta$ -uranium is also isomorphous with the sigma phase.

## ACKNOWLEDGEMENT

The author's thanks are due to his colleagues, Mr. T. J. Heal, B.Sc., A.Inst.P., and Miss J. M. Silcock, B.Sc., for helpful discussion on the subject matter of this paper and for the experimental evidence bearing on the subject which they have obtained.

## REFERENCES

1. E. C. Bain and W. E. Griffiths, *Trans. Amer. Inst. Min. Met. Eng.*, 1927, **75**, 166.
2. F. Adcock, *J. Iron Steel Inst.*, 1931, **124**, 147.
3. F. Wever and W. Jellinghaus, *Mitt. K.W. Inst. Eisenforsch.*, 1931, **13**, 93, 143.
4. S. Eriksson, *Jernkontorets Ann.*, 1934, **118**, 530.
5. A. J. Bradley and H. J. Goldschmidt, *J. Iron Steel Inst.*, 1941, **144**, 273p.
6. A. J. Cook and F. W. Jones, *J. Iron Steel Inst.*, 1943, **148**, 217p.
7. A. H. Sully and T. J. Heal, *Research*, 1948, **1**, 288.
8. A. R. Elsea, A. B. Westerman, and G. K. Manning, *Trans. Amer. Inst. Min. Met. Eng.*, 1949, **180**, 579.
9. K. W. Andrews, *Research*, 1948, **1**, 478.
10. F. Wever and W. Jellinghaus, *Mitt. K.W. Inst. Eisenforsch.*, 1930, **12**, 317.
11. H. J. Goldschmidt, *Research*, 1949, **2**, 343.
12. P. Pietrowsky and P. Duwez, *Trans. Amer. Inst. Min. Met. Eng.*, 1950, **188**, 1283.
13. W. B. Pearson, J. W. Christian, and W. Hume-Rothery, *Nature*, 1951, **167**, 110.
14. W. Hume-Rothery, G. W. Mabbott, and K. M. Channel-Evans, *Phil. Trans. Roy. Soc.*, 1934, [A], **233**, 11, 44, 87.
15. N. F. Mott and H. Jones, "The Theory of the Properties of Metals and Alloys". London: 1936 (Oxford University Press).
16. L. Pauling, *Phys. Rev.*, 1938, [ii], **54**, 899.
17. W. Ekman, *Z. physikal. Chem.*, 1931, [B], **12**, 57.
18. G. V. Raynor and P. C. L. Pfeil, *J. Inst. Metals*, 1947, **73**, 397, 609.
19. G. V. Raynor and M. B. Waldron, *Proc. Roy. Soc.*, 1948, [A], **194**, 362.
20. A. H. Sully, *Nature*, 1951, **167**, 365.
21. A. M. B. Douglas, Discussion at Conference of X-Ray Analysis Group of Institute of Physics, Leamington Spa, April 1951 (for summarized version see *Brit. J. Appl. Physics*, 1951, **2**, 305).
22. T. J. Heal and J. M. Silcock, *ibid.*
23. K. Robinson, *ibid.*
24. P. A. Beck and W. D. Manly, *J. Metals*, 1949, **1**, 354.
25. P. Duwez and S. A. Baen, *A.S.T.M. Symposium on the Nature, Occurrence, and Effects of Sigma Phase*, 1950, 48.
26. W. Hume-Rothery, *Phil. Mag.*, 1948, [vii], **39**, 89.
27. J. S. Kasper, B. F. Decker, and J. R. Belanger, *J. Appl. Physics*, 1951, **22**, 361.
28. C. W. Tucker, Jr., *Science*, 1950, **112**, 448, and private communication.  
Reported by G. J. Dickins, A. M. B. Douglas, and W. H. Taylor, *J. Iron Steel Inst.*, 1951, **167**, 27.





# SOME METALLOGRAPHIC OBSERVATIONS ON THE FATIGUE OF METALS \*

1340

By P. J. E. FORSYTH,† A.I.M., MEMBER

## SYNOPSIS

A metallographic investigation of the effects of cyclic stresses on the microstructure of an aluminium- $\frac{1}{2}$ % silver alloy has shown that factors other than simple slip are involved in the mechanism of fatigue at room temperature.

There is evidence of a recovery process associated with the formation of deformation bands and crystallites during fatiguing of the metal, and it is suggested that the observed anomalies in the effect of stress concentration on crack progress are the result of crystallite formation at the roots of the cracks.

## I.—INTRODUCTION

EWING and Humfrey<sup>1</sup> were among the first to make a study of the microstructural changes brought about by cyclic stressing. Their observations led them to suggest an "attrition" theory of fatigue in which the repeated applications of an unsafe stress produced repeated slip, resulting in attrition of the slip planes; this attrition eventually led to cracking and ultimate failure of the metal. Gough<sup>2</sup> examined metallographically several different metals, mainly in the form of single crystals, and concluded that the process of fatigue is one of strain-hardening by slip on the operative glide planes of the crystals until cracking occurs on these planes. From this he concluded that the strain-hardening process is identical with that of a crystal subjected to a static stress. He resolved the problem of fatigue cracking into one of cohesion between the metal atoms which will only be solved when a satisfactory theory of static rupture strength has been evolved. Gough also suggested that slip is accompanied by fragmentation of the original metal crystal into small crystallites in the region of the planes where slip has occurred, and that these crystallites suffer a slight rotation or re-orientation from the original crystal direction.

Theories that have so far been advanced to explain the phenomenon of fatigue in metals assume that during cyclic stressing a process of work-hardening takes place on the crystallographic slip planes. If the stress in the strain-hardened region eventually exceeds the rupture strength of the material, then cracking occurs.<sup>3</sup> No distinction has in the past been drawn between fatigue at high and at low stresses, since it has been assumed that the deformation is associated with slip alone; the degree of stressing would then control only the rate of work-hardening and the fatigue life of the metal. The characteristic shape of the fatigue curve for a metal might suggest that two mechanisms were in operation, but the

complex nature of the strain-hardening process has provided an alternative explanation.

The subject of deformation under static stress has been investigated more thoroughly than that of deformation under cyclic stresses. The classical idea of plastic deformation by glide on the operative crystallographic planes has long been known. Tammann<sup>4</sup> considered that the only possible means of deformation was by slip or twinning, but more recent work has shown that other forms of deformation may occur. Elam<sup>5</sup> has shown that deformation in

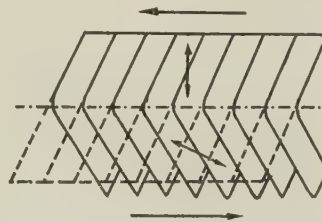


FIG. 1.—A Schematic Representation of a Lattice where Kinking has Occurred. The dotted lines represent the original lattice position and the continuous lines the new "kinked" or re-orientated material. (After Orowan.<sup>3</sup>)

$\beta$ -brass does not take place by slip on any definite crystal plane, but is brought about by movements of a complicated nature. These movements produce bands in the crystal, some of which have an orientation different from that of the original crystal and others which are thought to be layers of more highly strained material. A mechanism of deformation termed "kinking" has been described by Orowan,<sup>6</sup> who considers that there are many indications that deformation bands in metals, hitherto considered to be glide or twin bands, may be in reality "kink" bands. The mechanism of kinking is illustrated diagrammatically in Fig. 1. Honeycombe<sup>7</sup> has shown that kinking can produce deformation bands

\* Manuscript received 11 April 1951.

† Metallurgist, Royal Aircraft Establishment, Farnborough, Hants.



in single crystals of aluminium with as little as 1% extension. These bands are described as layers of varying orientation which are joined by narrow bent regions.

Flexural glide, either with or without accompanying relaxation in the form of polygonization, can also be considered as a possible form of deformation. The result of either form of deformation is a local variation in orientation, whereas pure glide causes no such change. These variations may be very small, and hence difficult to detect. Polygonization need not necessarily result in equiaxial crystallites. The term is used to describe the recovery of any form of lattice curvature. If the curvature is in one direction only, as in the case of kink bands, the resulting boundaries will be straight.

In undertaking the work described in the present paper, it was considered that developments in metallographic technique over recent years might bring to light features associated with the deformation of metals during cyclic stressing which have possibly escaped observation in the work previously reported. It is felt that the observations which have been recorded are of sufficient importance to justify a reconsideration of the present theories of fatigue by those working in the field of metal physics.

## II.—EXPERIMENTAL TECHNIQUE

### 1. METHOD OF STRESSING

The fatigue specimen of polycrystalline metal in the form of a cantilever with dimensions  $64 \times 8 \times 2$  mm., was vibrated in the apparatus described previously.<sup>8</sup> The specimen, while undergoing the fatigue test, was examined under the microscope, using stroboscopic illumination. No attempt was made to measure the stress accurately, since the investigation was concerned with the behaviour of the individual grains, for which the stress system would be complex. In the present paper the expression "high stress" is used where the maximum stress of the cycle is above the stress level of the "knee" of the  $S/N$  curve, and "low stress" is used where the maximum stress of the cycle is below the stress level of the "knee" of the curve.

### 2. MATERIALS EXAMINED

Most of the tests have been made on a high-purity aluminium- $\frac{1}{2}$ % silver alloy, although a few were made later on a commercially pure copper and an Armco iron. The aluminium-silver alloy was chosen because the solute causes negligible hardening as a result of the similarity in size of the aluminium and silver atoms, and because the solid-solubility range of silver in aluminium is sufficiently extensive to permit the study of the fatigue behaviour of single-phase and duplex structures. Unless otherwise stated, the observations and illustrations refer to the aluminium- $\frac{1}{2}$ % silver alloy.

### 3. PREPARATION OF SPECIMENS

(i) *Aluminium- $\frac{1}{2}$ % Silver Alloy*: This was cold rolled to 2 mm. from  $\frac{1}{2}$ -in. dia. extruded bar, machined, and then heat-treated for  $1\frac{1}{2}$  hr. at  $465^\circ\text{C}$ ., followed by cold water quenching. This treatment produced a grain-size of about 0.2 mm. dia.

(ii) *Commercial copper*: This was cold rolled to 2 mm. from  $\frac{1}{2}$ -in. dia. rolled bar, machined, and then heat-treated for 2 hr. at  $800^\circ\text{C}$ . in a nitrogen atmosphere and cooled in the furnace. This treatment produced a grain-size comparable with that of the aluminium-silver alloy specimens.

(iii) *Armco Iron*: This was cold rolled to 2 mm. thickness from  $\frac{1}{4}$ -in. plate, machined, and then annealed for 2 hr. at  $900^\circ\text{C}$ . in a nitrogen atmosphere and cooled in the furnace.

After heat-treatment the specimens were electro-polished without subsequent grinding, so as to ensure that no work-hardened surface layer existed.

The conditions of electrolytic polishing were as follows: Electrolyte, 50% orthophosphoric acid in water (specific gravity of the solution 1.35); temperature,  $30^\circ\text{--}40^\circ\text{C}$ .; current density, 15 amp./dm.<sup>2</sup>. The specimen was rotated within a cylindrical aluminium cathode.

The etching reagents found most suitable were:

(a) Aluminium- $\frac{1}{2}$ % silver alloy: 50% HF in water, followed by a dip in conc.  $\text{HNO}_3$ .

(b) Commercial copper:  $\text{FeCl}_3 + \text{HCl}$  in alcohol.

(c) Armco iron: 2% nital.

## III.—EFFECT OF STRESS ON THE STRUCTURE

The stresses imposed on the specimen were not measured accurately, owing to the complexity of

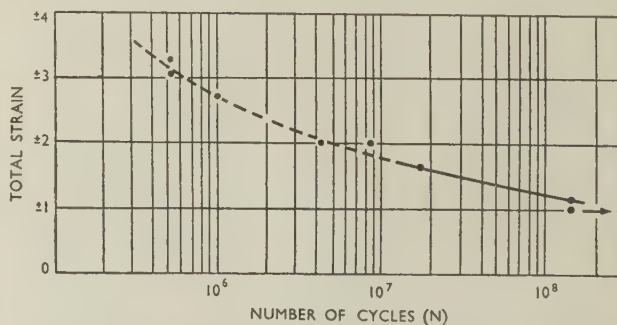
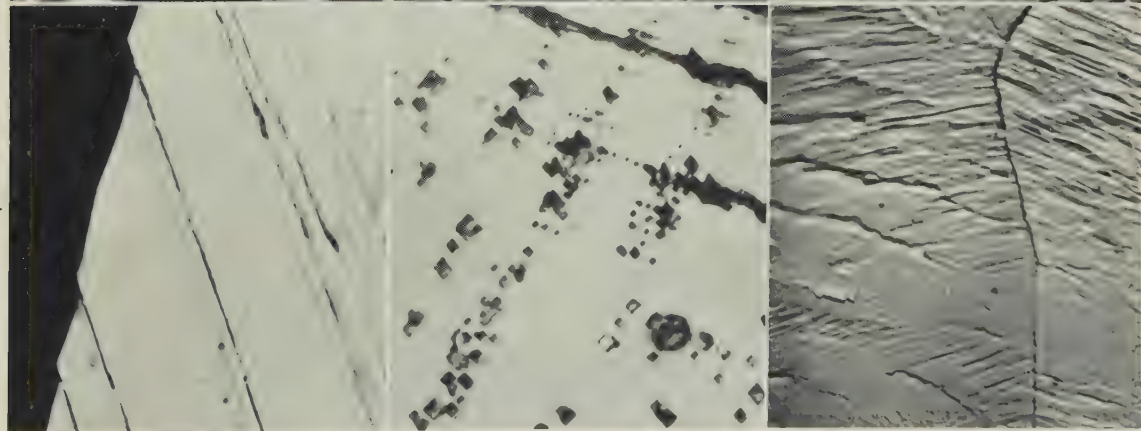


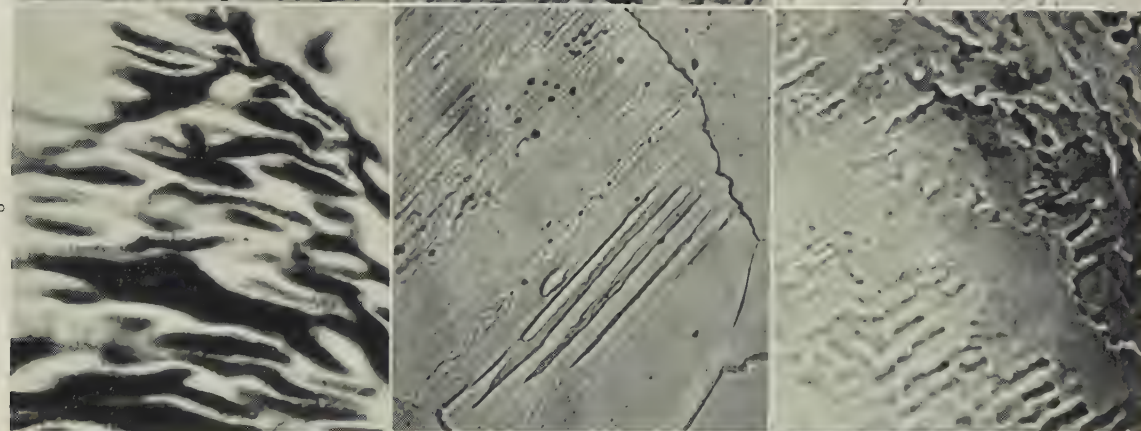
FIG. 2.—Strain/Log  $N$  Curve for Aluminium- $\frac{1}{2}$ % Silver Alloy. The strain is measured in arbitrary units.  
 - - - Widespread deformation with marked crystallite formation.  
 — Deformation bands with faintly defined crystallites.

stress distribution introduced by the notch that was provided to localize failure to the field of view, and because the materials were being stressed above their elastic limit. The form of curve obtained on the aluminium-silver alloy by operating under conditions

ALUMINUM- $\frac{1}{2}$ % SILVER ALLOY.



11, 12



15

16

17

18

FIG. 7.—Slip Displacement Produced by Static Stress. 1500.  
 FIG. 8.—Surface Corrugations Produced by High Fatigue Stress. 200.  
 FIG. 9.—Deformation Bands Produced by Cyclic Stresses. 1500.  
 FIG. 10.—Deformation Bands Produced by Static Stresses. 1500.  
 FIG. 11.—Deformation Bands Revealed by Etch-Pits. 100.  
 FIG. 12.—Deformation Bands Parallel to Slip Planes in Heavy Slip Regions. 500.  
 FIG. 13.—Relatively Large Displacements Produced by Slip Indicated by the Change of the Operative Slip Planes During Test. 500.

FIG. 14.—Grain-Boundary Irregularities Produced by Deformation. 1500.

FIG. 15.—Polygonized Kink Bands with Sharply Defined Boundaries. 1000.

FIG. 16.—Crystallites Produced by Interaction of Slip and "Kink"-Type Deformation Bands (Phase-contrast illumination). 700.

FIG. 17.—Polygonization Near an Original Grain-Boundary. 500.

FIG. 18.—Relatively Large Differences in Orientation Between Neighbouring Crystallites Indicated by Etch-Pits. 500.



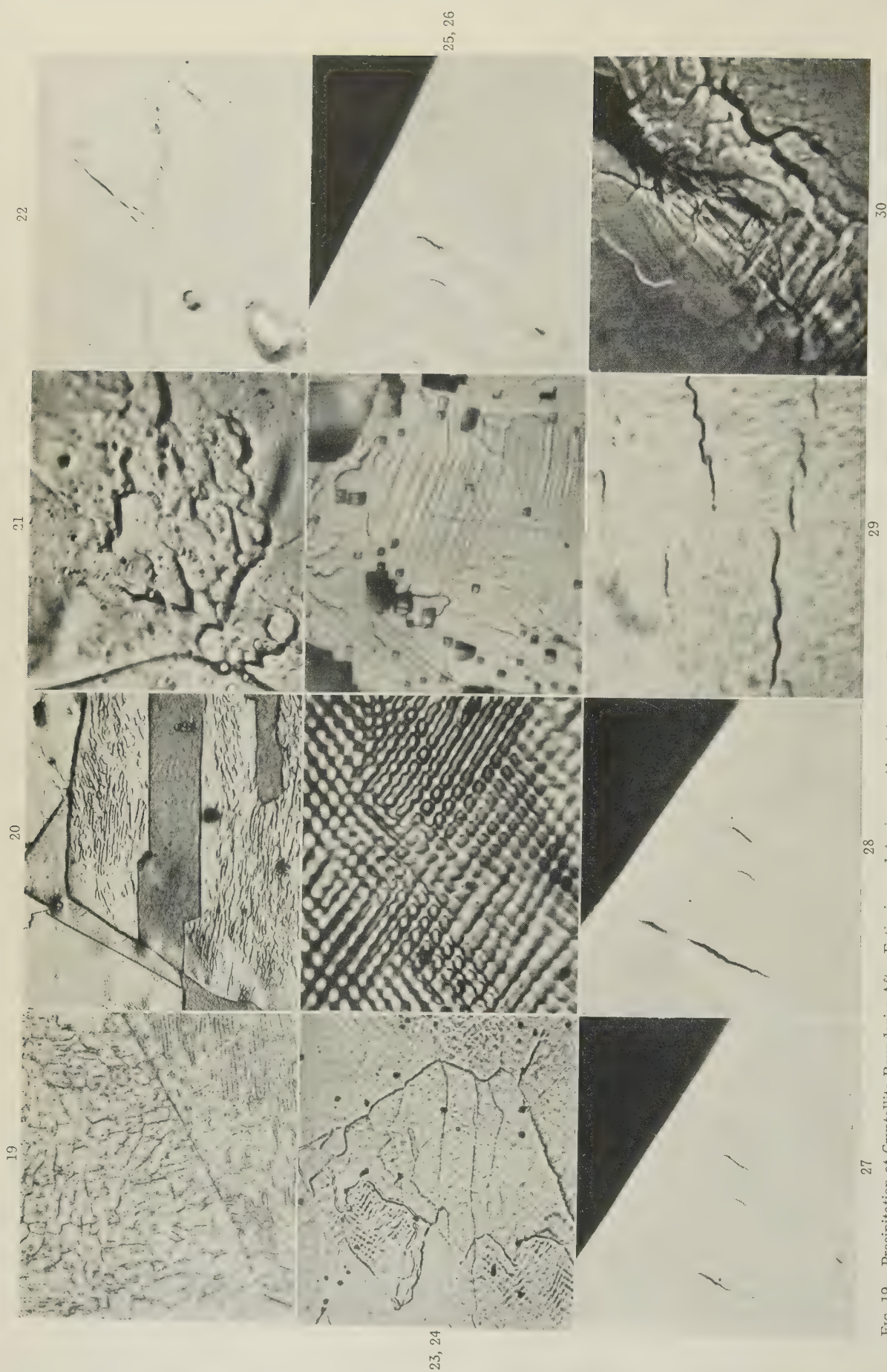


FIG. 19.—Precipitation at Crystallite Boundaries After Fatiguing and Ageing an Aluminium-4% Silver Alloy.  $\times 500$ .  
FIG. 20.—Crystallites in a Fatigued Copper.  $\times 1000$ .

FIG. 23.—Cellular Network Regions Produced by Fatigue Stresses (Etched).  $\times 500$ .  
FIG. 24.—Cellular Network Pattern Produced by Fatigue Stresses (Unetched).  $\times 1500$ .  
FIG. 25.—Changes in Direction of Slip Bands in an Aggregate of Crystallites.  $\times 500$ .  
FIG. 26.—Appearance of Specimen Surface after  $10^7$  Cycles.  $\times 500$ .

ALUMINIUM- $\frac{1}{2}$ % SILVER ALLOY.

FIG. 27.—As Fig. 26, after a Further 60,000 Cycles.  $\times 500$ .  
FIG. 28.—As Fig. 27, after a Further 60,000 Cycles.  $\times 500$ .  
FIG. 29.—Initial Fatigue Cracks.  $\times 2000$ .  
FIG. 30.—Region of Crystallites at Root of Fatigue Crack.  $\times 1500$ .



of constant strain for each specimen tested is shown in Fig. 2. The strain is plotted in arbitrary units derived from the deflection of the specimen.

During the course of the work it was found that the surface film formed on the aluminium-silver alloy during electrolytic polishing impeded the appearance of slip bands during deformation, although the formation of fine slip bands could readily be observed if the surface was etched to remove the film before stressing. This feature has been described in a recent paper by Wilms.<sup>9</sup> The practice was therefore adopted of etching the specimens before testing them. Fig. 7 (Plate XXXII) shows the displacement produced on slip bands by a static stress.

### 1. OBSERVATIONS AT HIGH CYCLIC STRESS

The high degree of deformation which may occur under high fatigue stresses can be seen from the rippled surface in Fig. 8 (Plate XXXII). Removal of the surface by electrolytic polishing of a specimen, which had been tested at a stress level above the knee of the fatigue curve but not at sufficiently high a level to produce the marked ripples to be seen in Fig. 8, followed by etching, revealed deformation bands of the type illustrated by Fig. 9 (Plate XXXII). It will be observed that these bands are not associated with any particular set of planes in the lattice, and are similar to kink bands which have been produced by static stress, as shown in Fig. 10 (Plate XXXII). In Fig. 11 (Plate XXXII), the deformation bands have been revealed by etch pits and by the slip bands.

Another type of band was formed parallel to the (111) slip planes in regions of heavy slip, although they were not usually as complete as those illustrated in Fig. 12 (Plate XXXII). The less-complete bands appeared to be elongated regions of high local curvature which were not removed by subsequent repolishing. The clarity with which the bands were defined depended on whether or not the regions of high local curvature had polygonized. The process of polygonization which occurs at elevated temperatures has been described by Cahn.<sup>10</sup> In the present tests, polygonization has taken place at room temperature, presumably because of the more severe lattice curvature.

The way in which these bands are formed by lattice curvature is depicted diagrammatically in Fig. 3, from which it will be seen that if the two halves of the stress cycle slip in opposite directions on groups of parallel planes (a) and (b), the general shape of the grain will remain unaltered. This is illustrated in Fig. 13 (Plate XXXII), where the extent of deformation is rendered clearly visible by slip on a second set of planes. The photographed area may not quite have reached the stage of polygonizing, but it is evident that when polygonization does occur in the regions of lattice curvature produced by the slip a new orientation will be derived, and it is suggested that this is the mechanism by which bands are formed. Another consequence of this form of slip is the movement that

occurs at the grain boundaries (see Fig. 14, Plate XXXII). This movement will be favoured by a condition in which there is little difference in orientation between two adjacent grains, i.e. where the restraint due to the neighbouring grains is small.

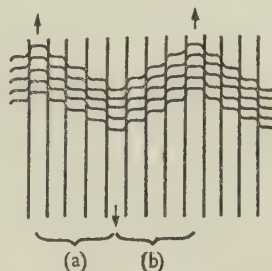


FIG. 3.—A Schematic Diagram Showing the Displacement Produced in a Crystal by Cyclic Stress. The bands marked (a) and (b) are deformed alternately as the stress direction changes.

It has been observed that the presence of deformation bands, produced either by kinking or polygonization of the curved lattice in regions of heavy slip, impedes the slip process. Since the appearance of such bands becomes more marked with increasing stress, it may well be that slip is not the predominant process of deformation at high stresses. This is illustrated by Fig. 15 (Plate XXXII), which shows a specimen that had been tested and then repolished and etched to reveal the deformation bands. These had sharply defined boundaries, indicating that polygonization had occurred. The specimen was then tested further to produce slip bands on the surface, and it will be seen from the photomicrograph that these bands are very incomplete and often confined to particular deformation bands.

As the result of further slip within the crystal, deformation bands formed in the initial stages of cyclic stressing are frequently broken down into crystallites. A photomicrograph taken with phase-contrast illumination reveals this effect in Fig. 16 (Plate XXXII). The formation of crystallites near grain boundaries, where the interaction of slip in neighbouring crystals may cause lattice bending with subsequent polygonization, is shown in Fig. 17 (Plate XXXII). In this particular photograph it will be seen that the boundaries of polygonized crystallites form contours. The etching of a specimen which contains these crystallites reveals that the boundary steps following the curvature are of the same sign; this is shown diagrammatically in Figs. 4 and 5.

Fig. 4 shows the original surface after fatigue (a), shows how repolishing tends to flatten the surface (b), and indicates the "stepped" surface (c), which will be observed after etching with a reagent that attacks the grains preferentially. The variation in orientation between adjacent crystallites may be appreciable, as is apparent from the etch-pits shown in Fig. 18 (Plate XXXII) where the crystallite boundaries are



clearly visible, the whole field being within one original grain. Etch figures have indicated that this difference may be as great as  $30^\circ$ , although the more usual variation is of the order of  $10^\circ$ . The use of X-ray technique has confirmed that a mean variation of  $10^\circ$  existed in the orientation of crystallites within one original crystal. Unfortunately this technique could not be used to determine the difference between two adjacent grains. The mean value of the crystallite size was  $10\ \mu$ , the smallest crystallites encountered being about  $1\ \mu$ . The observation does not exclude the possibility of the existence of a substructure within the crystallite boundaries, which could not be revealed by etching methods owing to the small difference in orientation between the component "blocks" of such a substructure. In fact, an aluminium-4% silver alloy which had been tested in the solution-heat-treated condition (i.e. as a single-phase

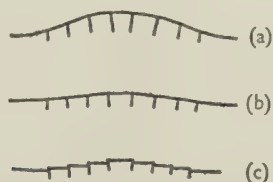


FIG. 4.—A Schematic Representation of Polygonization in a Region of Curvature (a) After Deformation, (b) After Re-polishing, and (c) After Repolishing and Etching.



FIG. 5.—A Three-Dimensional Representation of the Boundary Contours Produced by Etching a Curved Region as Shown in Fig. 17 (Plate XXXII).

alloy) to form crystallites, and then aged at  $300^\circ\text{C}$ . to effect precipitation of the  $\gamma$  phase on the crystallite boundaries, suggested evidence of a substructure within the crystallites, as will be seen in Fig. 19 (Plate XXXIII).

It is of interest to know whether crystallites are formed at room temperature during the fatigue testing of metals which have higher recrystallization temperatures than the aluminium-silver alloy has. For this purpose specimens in commercially pure copper and Armco iron were subjected to cyclic stress in a similar manner to the aluminium-silver alloy. The results are shown in Figs. 20 and 21 (Plate XXXIII), from which it is evident that the formation of crystallites does occur in copper and iron. It was also observed that, as in the aluminium-silver alloy, local boundary movement took place during the testing of these metals (see Fig. 22, Plate XXXIII).

A cellular network pattern was often observed on the polished surface of the aluminium-silver alloy specimens after fatiguing and is illustrated by Figs.

23 and 24 (Plate XXXIII). The specimen shown in Fig. 23 had been fatigued, re-polished, and etched to reveal crystallites, and then further tested to produce the cellular structure. It will be seen that the cellular structure appears in areas where crystallites have been formed, and that some of the crystallites, presumably with a favourable orientation for slip, show this structure very clearly. The repolishing and the etching treatment to which this specimen was subjected removed all evidence of the cellular pattern, but after further testing it re-appeared in certain crystallites, indicating that more deformation had taken place. Fig. 24 shows that these differences in orientation are observable in the unetched condition.

## 2. OBSERVATIONS AT LOW CYCLIC STRESSES

The essential difference observed to occur in specimens subjected to high and to low cyclic stresses was the absence of the kink-type deformation band in the latter. Slip was initially the predominant process at low stresses, but this eventually led to the formation of the type of deformation band associated with slip bands as the result of polygonization. Such an example is shown in Fig. 12 (Plate XXXII), in which the specimen had been tested for  $150 \times 10^6$  cycles when the photomicrograph was taken.

## 3. EFFECTS OF CRYSTALLITES ON DEFORMATION

An important effect of the presence of crystallites within a crystal would seem to be the increased resistance to slip offered by such an aggregate, as compared with the original crystal. Thus the slip bands in Fig. 25 (Plate XXXIII) change direction at the boundaries of the crystallites with a consequent decrease in the mean free path of slip. It will be observed that the slip bands are straight within any particular crystallite. Bragg<sup>11</sup> has advanced the theory that the specific shear energy required to initiate slip in a single crystal is an inverse function of the square of the crystal size, and Wood and Rachinger<sup>12</sup> have developed a theory of the strength of metals which depends on a limiting crystallite size for a particular metal. It is clearly important that the properties of such an aggregate be investigated.

## 4. THE FORMATION AND PROPAGATION OF CRACKS

The experiments described above have been concerned with a study of the structural changes which take place in a metal subjected to cyclic stressing before rupture of the crystal lattice. In this stage of the fatigue test it has been shown that the deformation which occurs is the result of a combination of crystallographic slip and the formation of deformation bands and crystallites. It might be expected that ultimate rupture of the lattice would be associated in some way with the structures so formed, and an attempt has been made to obtain evidence of this. However, the development of a

suitable technique to reveal the nature of a crack when it first appears has presented a difficulty. Thus, in attempting to determine whether or not the crack forms at the boundaries of the crystallites or deformation bands, an etched specimen in which such a structure had previously been developed by cyclic stressing was kept under observation during a further period of fatigue until a crack was formed. However, slip within the crystallites and the formation of the cellular structure prevented an accurate observation of the way in which a crack formed in the structure. If, after the formation of a crack, the specimen was electrolytically polished and etched to remove evidence of slip and of the cellular structure for better observation of the crystallite boundaries, detailed observation of the original form of the crack was prevented by rounding of the edges of the crack during the polishing.

Figs. 26–28 (Plate XXXIII) show the formation and growth of a crack as observed in a polished specimen. It will be noted that the crack first forms below that edge of the specimen which lies in the plane of maximum stress. Another feature of interest which has

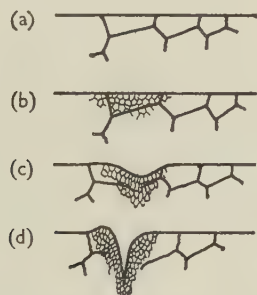


FIG. 6.—A Schematic Representation of the Formation of a Fatigue Crack in Aluminium- $\frac{1}{2}\%$  Silver Alloy at High Stress.

been observed is that it is not necessarily the first crack formed which propagates through the specimen to cause ultimate failure; it should be appreciated that observations have been limited to the surfaces of the specimen and that no attempt has yet been made to explore the path of the crack into the interior of the specimen.

Fig. 29 (Plate XXXIII) reveals, at a higher magnification, the corrugated nature of the cracks. It was found that the corrugations were of the same order of magnitude as the crystallites, which suggests a possible correlation between the two.

As the result of the examination of cracks in a large number of specimens, the impression has been formed that the cracks sometimes follow the crystallite boundaries and at other times are transcrystallite in character. However, it has not been possible to produce clear evidence of this in any of the individual photomicrographs that have been taken at room temperature, although the cracks which formed in a specimen fatigued at  $150^{\circ}\text{C}$ . definitely followed the crystallite boundaries.

A schematic description of the way in which a

crack is believed to form in an aluminium- $\frac{1}{2}\%$  silver alloy at high fatigue stresses is given by Fig. 6. Thus, the original grains of the annealed structure (a) are broken locally into small, faintly defined crystallites (b), and as fatiguing continues the crystallites become more sharply defined with evidence of surface flow (c); the crystallite formation then becomes more widespread and the surface corrugations become more severe, resulting in the formation of a deep groove (d), which eventually initiates a crack. The crack then progresses through the specimen, during which stage a region of crystallites precedes the root of the crack. Fig. 30 (Plate XXXIII) shows the condition of the structure in the region of the root of an advancing fatigue crack.

Reference has already been made to the fact that the first crack to form is not necessarily the one which propagates through the metal to produce failure. This would be difficult to appreciate if the region at the root of a fine crack were considered to be one of strain-hardened material subjected to a high stress concentration; however, the formation of crystallites ahead of the advancing crack may offer an explanation. Thus the relaxation which is associated with the formation of crystallites will result in a lower rate of strain-hardening than would occur in the absence of crystallites; in addition, the effectiveness of the crack as a stress-raiser will be reduced by the presence of branch cracks associated with the boundaries or cleavage planes of the crystallites.

#### IV.—CONCLUSIONS

Evidence obtained from a metallographic study of the structural changes that occur when an aluminium- $\frac{1}{2}\%$  silver alloy is subjected to cyclic stressing at room temperature has indicated that the process of fatigue is associated with the following phenomena:

(a) Slip occurs at all stresses which lie on the endurance curve.

(b) At a high stress level, i.e. above the "knee" of the  $S/N$  curve, deformation bands of the "kink" type occur in the early stage of fatigue, and deformation bands form along slip planes as the result of polygonization in regions of high lattice curvature.

(c) At a low stress level, i.e. below the "knee" of the  $S/N$  curve, deformation bands only of the second type described in (b) are formed.

(d) Crystallites are formed as the result of deformation bands being broken down by subsequent slip, or of the polygonization of regions of high lattice curvature, particularly near grain boundaries.

(e) The mean value of the crystallite size is about  $10\mu$ , the smallest value being about  $1\mu$ .

(f) The difference in orientation between neighbouring crystallites is up to about  $10^{\circ}$ .

(g) Final rupture of the lattice takes place in a region of crystallites, although it has not been definitely established whether the resulting crack forms at the crystallite boundary or within the crystallite; such



evidence as has been obtained, however, suggests that cracks originate at the crystallite boundaries.

(h) A region of crystallites is formed ahead of an advancing crack, which probably reduces the rate of strain-hardening in the lattice, whilst the development of branch cracks along crystallite boundaries reduces the effectiveness of the crack as a stress-raiser.

## ACKNOWLEDGEMENTS

Acknowledgement is made to the Chief Scientist, Ministry of Supply, and the Controller of H.M. Stationery Office for permission to publish this paper. The author also wishes to express his thanks to Mr. J. Harper for his interest in this subject and the many helpful discussions during the course of the work.

## REFERENCES

1. J. A. Ewing and J. W. C. Humfrey, *Phil. Trans. Roy. Soc.*, 1903, [A], **200**, 241.
2. H. J. Gough, *Proc. Amer. Soc. Test. Mat.*, 1933, **33**, [II], 3.
3. E. Orowan, *Proc. Roy. Soc.*, 1939, [A], **171**, 79.
4. G. Tammann, "Lehrbuch der Metallographie", Leipzig: **1923** (Leopold Voss).
5. C. F. Elam, *Proc. Roy. Soc.*, 1936, [A], **153**, 273.
6. E. Orowan, *Nature*, 1942, **149**, 643.
7. R. W. K. Honeycombe, *Proc. Phys. Soc.*, 1950, [A], **63**, 672.
8. P. J. E. Forsyth, *J. Sci. Instruments*, 1949, **26**, 160.
9. G. R. Wilms, *J. Inst. Metals*, 1949-50, **76**, 629.
10. R. W. Cahn, *J. Inst. Metals*, 1949-50, **76**, 121.
11. W. L. Bragg, *Nature*, 1942, **149**, 511.
12. W. A. Wood and W. A. Rachinger, *J. Inst. Metals*, 1948-49, **75**, 571.

# A MECHANISM OF STRESS-CORROSION IN ALUMINIUM-MAGNESIUM ALLOYS \*

1341

By C. EDELEANU,† M.A., Ph.D., MEMBER

## SYNOPSIS

The attack on aluminium and aluminium-rich alloys, immersed in neutral chloride solutions, tends to become restricted to a limited area owing to the autocatalytic nature of the anodic reaction. On homogeneous alloys, corrosion causes scattered pits which can increase either in depth or in area; but in the case of alloys possessing a path of easy corrosion, the attack takes the form of trenching and is confined to the tips of the cracks so formed. This latter type of corrosion leads to great mechanical weakening, even though the actual rate of attack per unit area may not be very different in the two instances.

The nature of the path of easy corrosion is unknown, but there is evidence that it is sub-microscopic in width. No indication has been found that, in the case of aluminium-magnesium alloys, it consists of the equilibrium second phase,  $\beta$ .

From experiments carried out on aluminium-7% magnesium alloy, it is concluded that stress exerts no influence during the first stages of the process (the greater part of the life), but that corrosion plays a vital role during the final rapid cracking.

## I.—INTRODUCTION

STRESS-CORROSION is known to involve a highly localized type of attack.<sup>1-4</sup> The mechanism of localized corrosion has been treated in a paper published elsewhere,<sup>5</sup> but it is desirable to summarize here the conclusions arrived at therein. This is done in Section II. Experiments carried out on aluminium-7% magnesium alloy and described in later Sections, were designed to establish:

- (1) The amount and rate of corrosion taking place before failure.
- (2) The effect of stress on the corrosion reaction.
- (3) The effect of corrosion on the progress of cracks.
- (4) The nature of the easily corrodible material found at the grain boundary.

Certain aspects of the mechanism of stress-corrosion are discussed in the light of these experiments and of the mechanism of localized attack outlined below.

## II.—LOCALIZED CORROSION OF ALUMINIUM

The slow rate of corrosion of aluminium and its alloys is due to the protective film of oxide which normally covers the metal, so that corrosion can take place only when either metal ions or some anion penetrate the film. (The two processes can be regarded as similar for the present purpose.) Aluminium ions arriving at the outer surface of the film can either leave the metal by becoming solvated or remain on the surface and form a solid product. If all the ions arriving at the outer surface are solvated, the film cannot thicken, and the continuous removal of

ions from beneath it will undermine the film. Eventually, therefore, the surface should become practically film-free. If, on the other hand, most of the ions arriving at the surface form, for example, an oxide, the film will thicken and the reaction must diminish rapidly with time.

In the case of a pure aluminium anode immersed in a neutral chloride solution, the proportion of ions that can become solvated is found to increase with time and with rise in current density,<sup>5</sup> and the film therefore tends to become thinnest, or weakest, at the place where the reaction is most rapid. In other words, the anodic reaction on aluminium is autocatalytic. This explains why corrosion, having started at one point, continues there in preference to any other points.

There is, however, an upper limit beyond which the rate of the anodic reaction cannot readily increase. This is believed to be due to the fact that aluminium anodes generally corrode faster than would be expected from Faraday's law, owing to a local reaction between aluminium and water by which a solid product and hydrogen<sup>5,6</sup> are formed. The anodic reaction is thus autocatalytic only up to a given point, beyond which thickening of the film due to the local reaction balances undermining due to the current flowing to distant cathodes. It is probable, therefore, that current densities lower or higher than that corresponding to minimum filming will be unstable. That is to say, for a given total corrosion rate the active anode area tends to become constant, and the rate of linear penetration down into the metal at the anodic points also tends to be constant.

The anodic behaviour of alloys is more complicated, but, qualitatively, aluminium-magnesium alloys

\* Manuscript received 12 December 1950.

† Brown-Firth Research Laboratories, Sheffield; formerly Metallurgy Department, University of Cambridge.



should behave in much the same way as pure aluminium. It is likely that, at a given *pH*, the proportion of soluble corrosion product resulting from attack on an alloy containing magnesium will increase with the magnesium content. Any relatively magnesium-rich paths should therefore corrode preferentially. It is still true, however, that for any alloy composition there is a rate of reaction for which filming is a minimum, and that faster or slower rates of corrosion are unstable. This minimum rate is not likely to alter by a large factor with small changes in composition.

### III.—AMOUNT AND RATE OF CORROSION

Unless otherwise stated, the alloy used in the experiments now described had the following composition: magnesium 7.3, copper 0.01, manganese 0.07, iron 0.045, silicon 0.009%, remainder aluminium. It was rolled to 18 S.W.G. sheet and given a solution-treatment before ageing.

Specimens were aged for 2 days at 200° C., and some were then bent beyond the yield point into U

cracking can occur after only a few micro-equivalents of metal have corroded and that there is no obvious difference between stressed and unstressed specimens.

### IV.—EFFECT OF STRESS ON CORROSION

The stress-corrosion life of specimens stressed throughout the entire duration of a test was compared with that of specimens which had first undergone a period of corrosion without stress, in order to establish whether the stress affected the corrosion reaction throughout the course of the experiment. Some of the results are given in Table II, from which it can be seen that the total life is not much affected if stress is absent during the greater part of the life of the specimen. It therefore appears probable that during this period corrosion is taking place at numerous grain boundaries and not only at those that will finally cause failure. Only a small proportion of the aluminium found in the solution during the experiments described in Section III therefore comes from the actual crack. The area of the fracture surface (which was intercrystalline) was probably of the

TABLE I.—*Effect of Stress on Corrosion Rate.*

Based on amount of aluminium found in solution after the corrosion of stressed and unstressed specimens.

Specimen No.	Nature of Solution	<i>pH</i> of Solution		Amount of Solution Used, c.c.	Duration of Experiment, min.	Exposed Area, cm. <sup>2</sup>	Stressed or Unstressed	Aluminium Found in Solution, × 10 <sup>-6</sup> g.
		Original	Final					
1	} 3% NaCl {	~4	...	25	10	0.5	S	4.8
2		~4	...	25	10	0.5	U	4.8
3	} 3% KCl {	2.45	2.46	35	15	1.0	S	12
4		2.45	2.49	35	15	1.0	U	12
5		2.45	2.49	35	15	1.0	S	26
6		2.45	2.52	35	15	1.0	U	36
7	} 3% KCl {	3.5	...	5	7	0.5	S	4
8		3.5	...	5	7	0.5	U	4

loops. These were forced into rectangular glass vessels, thus subjecting them to an elastic stress arising from the pressure against the walls of the vessel. Slightly acidified chloride solutions were added.

When the stressed specimens failed they were removed, together with the appropriate unstressed controls. The aluminium content of the solution was then estimated using Aluminon.<sup>7</sup> Results are given in Table I, from which it will be seen that specimens can fail when only a few microgrammes of aluminium have corroded and that no significant difference exists between the rate of corrosion of stressed and unstressed specimens.

The corrosion rate was also studied by following the changes in *pH* occurring in an almost neutral solution. This method has the advantage of being practically independent of the amount of diffusion of corrosion product out of the small cracks and of being highly sensitive. The experiments confirmed that

order of 1 cm.<sup>2</sup>, and from the quantity of aluminium found, the width of the corroded path may be estimated at less than 100 Å.

The effect of stress on corrosion during the last stages of the process was studied with the aid of a microscope fitted with a water-immersion lens. Stress was applied by means of the apparatus shown in Fig. 1 (Plate XXXIV), which is operated by metal bellows inside the cylindrical tube. It was noticed that a few hydrogen bubbles sometimes formed soon after immersion, but that large quantities appeared only a few minutes before failure, emerging from cracks which were already developing. These experiments prove that there is an increase in corrosion rate in the cracks during the final stages, but that the increase is not sufficiently great to be detected by the method described in Section III. It is impossible to tell how much of the increased corrosion is taking place at the tip of the crack and is connected with the cracking, and how much is taking place on the newly formed

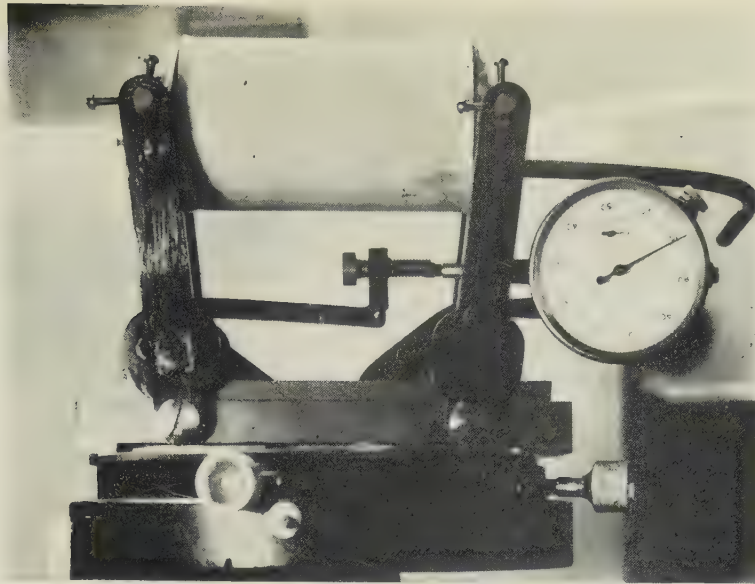


FIG. 1.—Apparatus Used for Stressing Specimens while under Microscopic Examination.

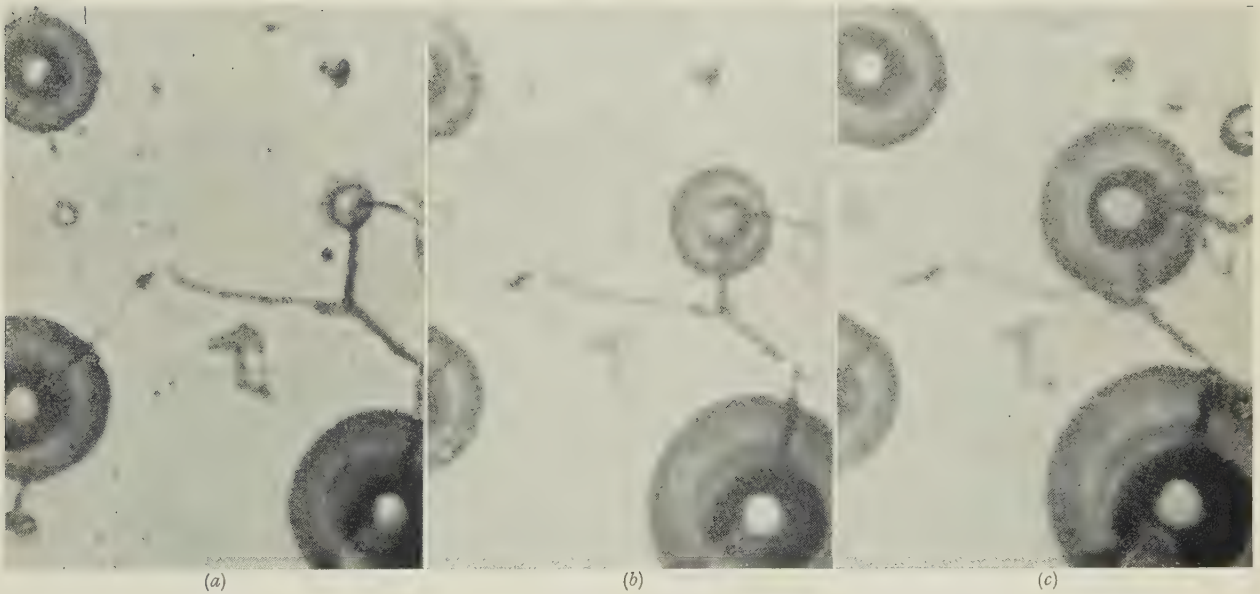


FIG. 2.—Evolution of Hydrogen Bubbles from a Specimen of Aluminium-7% Magnesium Alloy Cracking by Stress-Corrosion. (a), (b), and (c) were taken at intervals of approx. 1 sec.  $\times 1000$  approx.

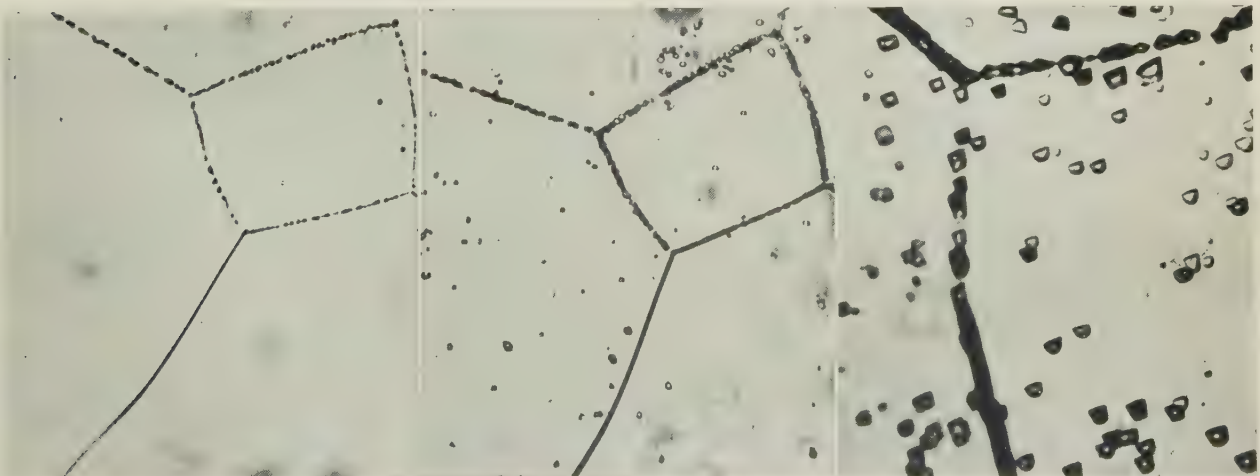


FIG. 6.—Grain-Boundary in Al-7% Mg Alloy Aged for 6 Hr. at  $200^{\circ}\text{C}$ . Etched for 10 sec. in Keller's Reagent.  $\times 1500$ .

FIG. 7.—Same Field as Fig. 6, after Etching for 2 Min.  $\times 1500$ .

FIG. 8.—Grain-Boundary in Al-7% Mg Alloy Aged for 2 Hr. at  $200^{\circ}\text{C}$ . Etched in Lacombe's Reagent.  $\times 1500$ .



ALUMINIUM-7% MAGNESIUM ALLOY.



FIG. 9.—Electron Micrograph of Grain-Boundary in Corrosion-Susceptible Alloy. Oxide replica (*Nutting*).  $\times 15,000$  reduced by  $\frac{1}{4}$  linear in reproduction.

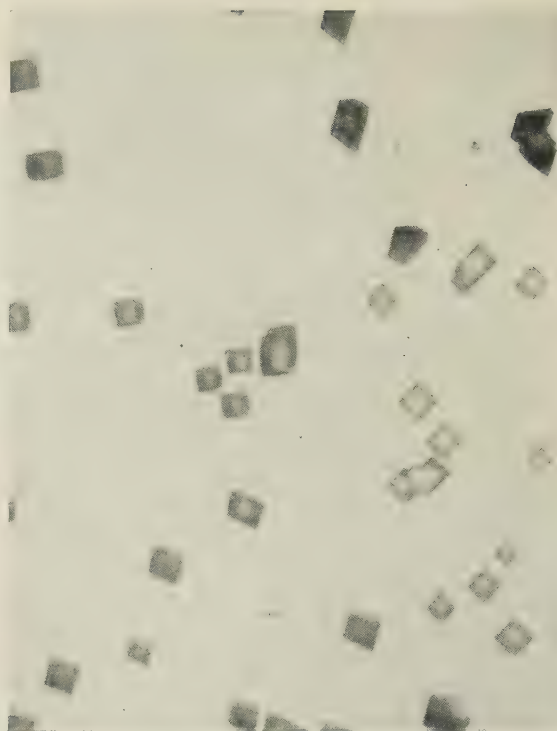
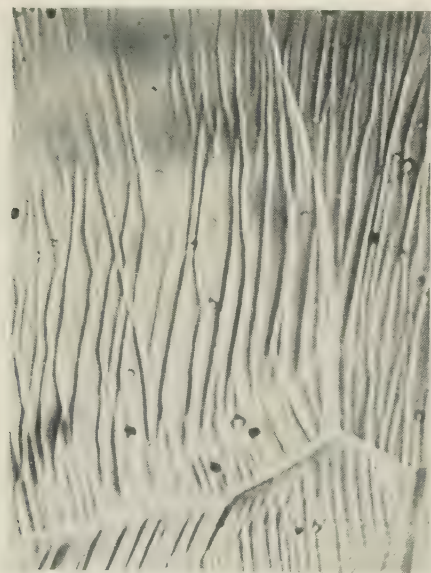
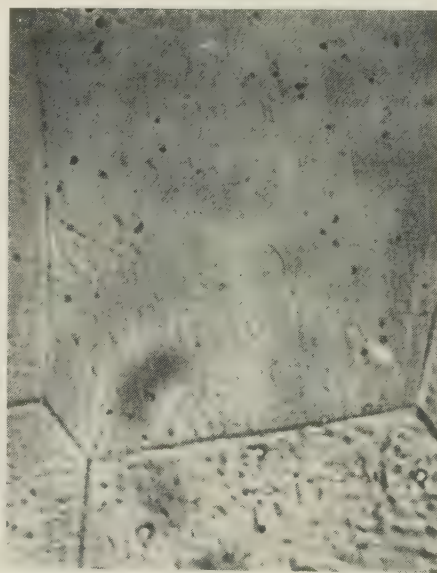


FIG. 10.—Grain-Boundary in Alloy Quenched from  $430^{\circ}\text{C}$ . Etched in Lacombe's Reagent.  $\times 1000$ .



(a)



(b)

FIG. 11.—Illustrating Difference in Appearance of Slip Bands in (a) Quenched and (b) Aged Alloy (2 Days at  $200^{\circ}\text{C}$ .), After Stressing to 80% of U.T.S.  $\times 1000$ .

walls (which are presumably becoming filmed over with oxide), and is the result of mechanical failure. If the stress was relaxed during the stage of rapid

TABLE II.—*Effect of Stress during the First Stages of Stress-Corrosion.*

Corrosive solution used: 3% NaCl solution in Cambridge tap-water.

Time of Corrosion without Stress	Time of Corrosion under Stress	Total Time to Failure
<i>Batch 1</i>		
	min.	min.
0	40	40
0	50	50
0	55	55
min.	min.	min.
50	5	55
50	10	60
50	10	60
50	10	60
50	10	60
50	10	60
50	10	60
50	10	60
<i>Batch 2</i>		
	hr.	hr.
0	1-2	<2
0	1-2	<2
0	1-2	<2
hr.	min.	hr.
4	<1	~4
4	<1	~4
4	<1	~4

hydrogen evolution, the evolution continued for an appreciable time, thus showing that at least part of the increase in corrosion rate is not directly due to the stress.

An attempt was made to follow cinematographically the progress of a crack and the evolution of hydrogen from it. Figs. 2 (a)–(c) (Plate XXXIV) show the rate of growth of hydrogen bubbles at a late stage (10–20 sec. before failure) in the life of a specimen. The film was taken at about 18 frames/sec. and there is about 1 sec. difference between each picture.

## V.—EFFECT OF CORROSION ON CRACKING

During the microscopic studies just described, with specimens having a life of about 1 hr., cracks became visible only a few minutes before actual failure. Those cracks which started at the edge of the specimen generally required 3–5 min. to advance a distance of one to two grains, but after that they progressed very rapidly and produced failure within a few seconds. It was also found that the presence of a crack could generally be detected by means of an extensometer, such as a Mercer dial instrument. Doubt was felt as to whether corrosion was still playing an essential part during this rapid final stage, and it was decided to investigate whether cracking could be halted by electrochemical means.

Specimens (solution-treated and aged for  $2\frac{1}{2}$  days at  $175^{\circ}$  C.) were loaded through levers to 37% of their ultimate tensile strength. The movement of a second lever, arranged to give a total mechanical advantage of 140, was recorded on a rotating drum. A glass cylinder containing 3% sodium chloride solution in tap-water was held in position round the specimen by means of a rubber cork. A steel spring was used to make electrical contact with one of the levers when the specimen had extended a given amount, thus completing a circuit which made the specimen cathodic with respect to a second electrode placed in the solution. Time/extension curves obtained with and without cathodic protection are shown in Fig. 3. Curve B was obtained when a current of about 0.3 amp. was applied to the specimen after it had extended  $2 \times 10^{-3}$  in., halting the crack despite the fact that it had already penetrated almost half-way into the specimen.

The mechanism of this cathodic protection is interesting, since it is impossible to obtain a potential low enough to produce equilibrium between aluminium and its ions in aqueous solution. The application of the external current presumably causes an increase in the pH of the solution inside the crack, which favours precipitation and filming of the surface. The formation of such films seems to be sufficient to halt the progress of the cracks. As a rule, cracking did not readily start again, even when the protective current was subsequently interrupted, and in one case at

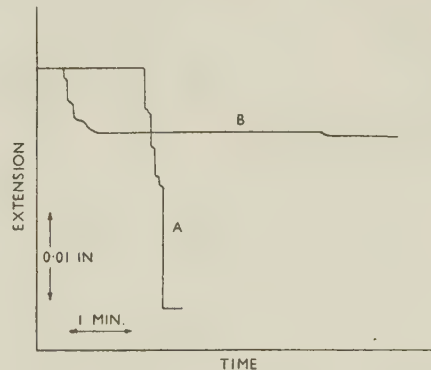


Fig. 3.—Time/Extension Curves for Specimen of Aluminium-7% Magnesium Alloy Failing by Stress-Corrosion.

Curve A: Normal.  
Curve B: Specimen protected cathodically after cracking had started.

least an entirely new crack is believed to have developed and caused failure, while the old crack remained inactive.

## VI.—EFFECT OF AGEING ON SUSCEPTIBILITY

The susceptibility to stress-corrosion of many aluminium alloys is known to increase to a maximum with time of ageing, and then to decrease. This maximum has been shown to correspond with the



beginning of an increase in hardness, in the case of aluminium-copper alloys, by Robertson,<sup>4</sup> who has also shown that the susceptibility practically vanishes by the time the maximum hardness has been attained.

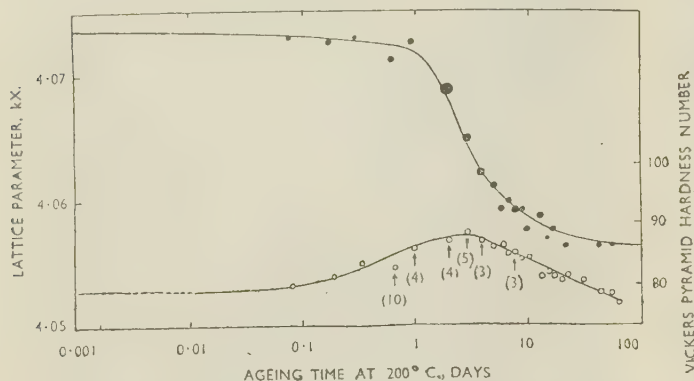


FIG. 4.—Variation of Lattice Parameter (upper curve) and Vickers Diamond Pyramid Hardness Number (lower curve) with Ageing Time at 200° C. for Aluminium-7% Magnesium Alloy. (Perryman and Hadden,<sup>8</sup>)

The arrows indicate ageing treatments used for stress-corrosion tests at an initial stress of 6.2 tons/in.<sup>2</sup> and the figures beside the arrows give the corrosion-stress lives in days.

Perryman and Hadden<sup>8</sup> studied the ageing of a commercial aluminium-7% magnesium alloy, and some of their results are reproduced in Fig. 4. Fig. 5 illustrates the stress-corrosion life of specimens cut from the sheet used by Perryman and aged together with his specimens, and subsequently tested by the present author. Comparison with Fig. 4 shows that, as with the aluminium-copper alloys, susceptibility is serious at a very early stage in the ageing process and probably before actual precipitation has occurred in the bulk of the alloy.

Precipitation of a second phase may take place most rapidly at the grain boundaries, and the possibility that the susceptible material at the grain boundary is the equilibrium second phase cannot be excluded, though there is at present no way of confirming this assumption. The microscopic evidence, based on etching, put forward by certain authors is not convincing, since the interpretation assumes, in the first place, a knowledge of the causes of preferential etching.

Microscopic examination of the aged aluminium-magnesium alloy has shown that the size of the so-called "particle" tends to increase with time of etching (see Figs. 6 and 7, Plate XXXIV). An electron-micrograph obtained by Dr. J. Nutting (Fig. 9, Plate XXXV) indicates that the grain-boundary etching marks are sometimes pits and that the shape of these is mainly determined by the orientation of the grains. This can also be demonstrated by means of Lacombe's reagent<sup>9</sup> ( $\text{HNO}_3\text{-HCl-HF}$ ), and Fig. 8 (Plate XXXIV) illustrates the appearance of an aged alloy etched with this reagent. It will be seen that the appearance of the boundaries is governed by the relative orientation of the boundary and the grains, and that one boundary which is favourably orientated

has become continuously etched. Under a low magnification, such a specimen gives the impression of having an uninterrupted layer of second phase at one boundary and particles at the remainder. The as-quenched alloy is not preferentially etched at the grain boundary, as shown by Fig. 10 (Plate XXXV), in which the presence of the various grains can only be inferred from the shape of the pits. It is therefore clear that ageing does render the boundary more susceptible to attack, but neither the shape nor the size of the pits or trenches seems to be connected with the original structural defect of chemical or physical origin, which caused the susceptibility. Preferential grain-boundary etching may not, therefore, be due to the presence of a second phase, as claimed by certain workers, but may be attributable for instance, to segregation of one of the components at the boundary. According to Whitwham and Evans,<sup>10</sup> physical strain may be responsible for such an attack, though it seems more likely that in the present case the presence of a higher proportion of relatively soluble magnesium compounds makes the boundary more reactive.

The increase, with ageing, in susceptibility to stress-corrosion (as opposed to intercrystalline attack) may not be entirely due to the increase in chemical reactivity of the boundary material, since the mechanical properties of the alloy also alter with ageing. The changes are not very noticeable when using conventional testing methods (U.T.S., hardness, &c.), but Figs. 11 (a) and (b) (Plate XXXV) show the appearance of slip bands on a quenched and an aged alloy strained to the same extent. The difference in the

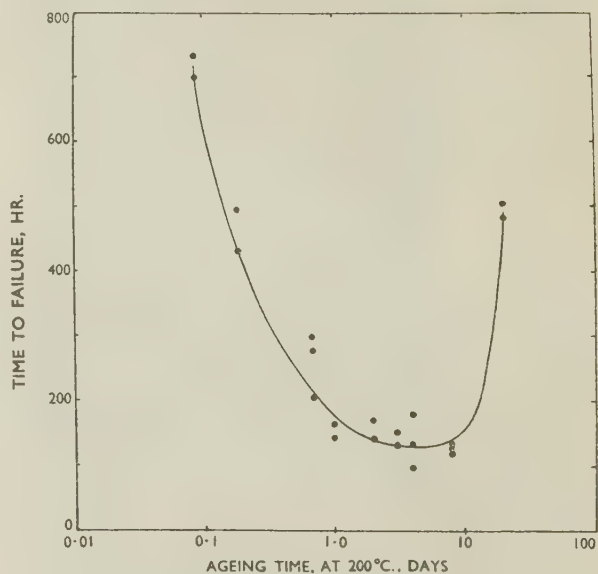


FIG. 5.—Showing Time to Failure of Specimens of Aluminium-7% Magnesium Alloy Aged at 200° C., Made Anodic in 10N-NaCl Solution Under an Applied E.M.F. of 2 V. and Stressed by Levers to 6.2 tons/in.<sup>2</sup>.

slip mechanism is clear. This observation has been confirmed by an electron-microscope study carried out by Dr. A. F. Brown.

## VII.—DISCUSSION

On ageing an aluminium-magnesium alloy a layer of easily corrodible material is formed at the grain boundaries. Analytical work tends to indicate that the width of this layer is submicroscopic, and metallurgical evidence shows that susceptibility to stress-corrosion is at a maximum at an early stage in the ageing process. It is therefore possible that the easily corrodible material is not the equilibrium second phase,  $\beta$ , but that the susceptibility is attributable to the segregation (adsorption) of solute atoms at the grain boundary as a first stage in the ageing process. It seems practically inevitable that such segregation must take place before the separation of the second phase, which, in the case of aluminium-magnesium alloys, has a large and complex unit cell. The retention of a layer at a grain boundary when real precipitation starts is unlikely, if the interfacial energy between the new phase and the parent metal is more than half that between two grains. The decline in susceptibility after longer periods of ageing may therefore be due to the separation of a second phase and the destruction of the original segregate grain-boundary layer.

It is believed that preferential attack will take place where the magnesium content is highest, but that the rate of attack per unit area at such points is not likely to be much greater than on pure aluminium. However, the presence of the paths of easy corrosion results in the active anodes remaining at the tips of the trenches, so that the very rapid penetration during intercrystalline corrosion is due more to the continuous attack at the boundary than to an actual increase in rate of attack.

With highly susceptible material, stress does not appear to play any essential role during the greater part of the life of a specimen. When visible cracking starts, there seems to be a slight increase in the rate of attack, although it is not known how much of this extra corrosion takes place at the tip of the crack.

Active anodes carry only very thin oxide films, and it may be that the absence of the normally thicker

films facilitates in some manner the propagation of cracks. This view is supported by work on single crystals of zinc and cadmium,<sup>11-13</sup> which has shown that the presence of oxide films can reduce greatly the rate of creep and presumably of other types of deformation. Menter and Hall<sup>13</sup> have suggested that the film hinders the movement of dislocations. It is interesting to note that, in the present case, cathodic treatment, which is believed to cause filming, halts the cracking.

A second way of explaining the rapid advance of cracks, in spite of the relatively slow rate of corrosion, is to assume that the removal of atoms from the lattice provides a continuous source of mechanical weakness.

## ACKNOWLEDGEMENTS

The author is indebted to Dr. U. R. Evans, F.R.S., in whose laboratory the work has been carried out, and to Dr. H. Sutton for much helpful advice. Thanks are due to many friends, and, in particular, to Mr. C. Taylor and other members of the laboratory staff at Cambridge.

## REFERENCES

1. R. B. Mears, R. H. Brown, and E. H. Dix, Jr., *Symposium on Stress-Corrosion Cracking of Metals (A.S.T.M.-A.I.M.E.)*, 1944, 323.
2. G. J. Metcalfe, *J. Inst. Metals*, 1946, **72**, 487.
3. P. Brenner and W. Roth, *J. Inst. Metals*, 1947-48, **74**, 159.
4. W. D. Robertson, *Trans. Amer. Inst. Min. Met. Eng.*, 1946, **166**, 216.
5. C. Edeleanu and U. R. Evans, *Trans. Faraday Soc.* (in the press).
6. A. Thiel and J. Eckell, *Z. Elektrochem.*, 1927, **33**, 370.
7. E. B. Sandell, "Colorimetric Determination of Traces of Metals", p. 117. New York: 1944 (Interscience Publishers, Inc.).
8. E. C. W. Perryman and S. E. Hadden, *J. Inst. Metals*, 1950, **77**, 207.
9. P. Lacombe and L. Beaujard, *J. Inst. Metals*, 1947-48, **74**, 1.
10. D. Whitwham and U. R. Evans, *J. Iron Steel Inst.*, 1950, **165**, 72.
11. E. N. da C. Andrade and R. F. Y. Randall, *Nature*, 1948, **162**, 890.
12. S. Harper and A. H. Cottrell, *Proc. Phys. Soc.*, 1950, [B], **63**, 331.
13. J. W. Menter and E. O. Hall, *Nature*, 1950, **165**, 611.





# THE PRODUCTION AND PROPERTIES OF OXIDE-REDUCED COPPER POWDER \*

1342

By E. C. ELLWOOD,† Ph.D., A.I.M., MEMBER, and W. A. WEDDLE,‡ B.Sc., STUDENT MEMBER

## SYNOPSIS

Conditions have been established under which scrap copper wire can be oxidized, mainly to cuprous oxide, comminuted, and subsequently reduced to a copper powder which is suitable for use in powder metallurgy. The effects of time and temperature of reduction by different gases and of other variables, such as stirring of the oxide and the rate of gas flow, have also been investigated, and the change in particle-size distribution during reduction observed.

The properties of powders of different size distribution, prepared by the reduction of the oxide by hydrogen and, to a limited extent, by carbon monoxide, are compared with those of commercially available powders produced by electrolysis and steam atomization. A comparison is also made of the properties of pressed compacts made from such powders before and after sintering. With the oxide-reduced powders, the best strength properties (12–13 tons/in.<sup>2</sup>) were obtained with high compacting pressures (60 tons/in.<sup>2</sup>) and relatively low sintering temperatures (600° C.); whereas with electrolytic and atomized powders the best results (10–11 tons/in.<sup>2</sup>) were obtained with compacting pressures of 40 tons/in.<sup>2</sup> and sintering temperatures of 1000° C. Oxide-reduced powders gave superior results, except at 1000° C. and compacting pressures of 40 and 60 tons/in.<sup>2</sup>, where large expansions occurred, particularly when hydrogen was the reducing gas. However, under the conditions for maximum tensile strength with oxide-reduced powders, the dimensional changes on sintering were remarkably small.

The high tensile-strength figures for oxide-reduced powders were reached without any appreciable decrease in hardness during sintering, indicating that it is possible for pronounced sintering to take place at temperatures below the recrystallization temperature.

## I.—INTRODUCTION

THE production of metal powders by reduction of the corresponding oxide is a well-established method, but little work seems to have been published on its application to copper, other than that of Drapeau.<sup>1</sup>

The work now described is a study of some of the principal variables in the oxidation of copper wire, the comminution of the oxide so produced, and its subsequent reduction to metallic copper powder. The properties of the powder and the effect on the final sintered product of variables in the production of the oxide and in subsequent pressing and sintering were also investigated.

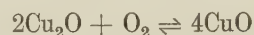
The work was carried out in collaboration with Durham Chemicals, Ltd., of Birtley, County Durham, and was not intended as a wholly academic study of the subject, but rather to serve as a guide in the event of the commercial development of the process and to explore the suitability of oxide-reduced copper powder for applications in powder metallurgy.

## II.—OXIDATION OF COPPER

### 1. OXIDATION OF SINGLE WIRES

The raw material was scrap copper wire of electrical purity, 0.007 in. in dia., and coated with approximately 1.0 wt.-% of tin.

It has been established by several investigators<sup>2-5</sup> that the oxidation curve for copper at temperatures above 600° C. is parabolic in form. The equilibrium temperature of the reaction :



is about 1025° C. at atmospheric pressure; below that temperature black cupric oxide is stable, while above it red cuprous oxide should be formed.

The aim in the oxidation process is to convert the copper completely to cuprous oxide. The formation of cupric oxide is economically undesirable, as the extra oxygen has to be removed in the reduction process, and any unconverted copper may prove troublesome in the milling operation. The two operative factors are, therefore, the rate of oxidation of the copper and the rate of conversion of cuprous oxide to cupric oxide.

In preliminary experiments on single strands of detinned wire, 0.007 in. in dia., the oxidation curve at 630° C. was parabolic in form, but complete oxidation was not obtained after 18 hr. At 720° C., the curve was almost parabolic, but oxidation was still not complete within a reasonable time. At 820° C. oxidation was complete in 3 hr., and up to that time the rate followed a parabolic law; a low and diminishing rate of weight increase was, however, recorded with

\* Manuscript received 26 February 1951.

† Lecturer in Metallurgy, King's College, University of Durham.

‡ Thomas Hedley and Co., Ltd., Newcastle-on-Tyne; formerly Post-Graduate Student, King's College, University of Durham.



longer times, presumably corresponding to conversion of cuprous to cupric oxide. After 3 hr. (when oxidation was complete), the increase in weight was 16%, corresponding to a mixture of oxides containing 72% cuprous oxide, and after holding at 820° C. for a further 13 hr., the increase had reached 22.8% (17.6% cuprous oxide). At 900° C. oxidation was complete in 90 min., the increase being 14.4% (84.8% cuprous oxide). Conversion of cuprous to cupric oxide took place at this temperature, though more slowly than at 820° C. These experiments confirmed that, under the conditions employed, the rate of oxidation followed an inverse-square law and that cupric oxide was more stable than cuprous oxide; but they also showed that it is possible for a very high proportion of cuprous oxide to be formed at temperatures below that at which cuprous oxide is the stable form.

The wire available for the main experiments was tinned, and it was therefore necessary to investigate the effect of the tin coating. Experiments at 820° C. showed that this was insignificant, and it was concluded that the tin diffused into the copper, forming a dilute bronze, which oxidized in a similar way to pure copper. It was therefore not removed.

## 2. OXIDATION OF WIRE IN BULK

The scrap copper wire was in the form of fairly compact semi-tangled masses. A gas-fired reheating furnace of internal dimensions 3 ft. × 1 ft. 6 in. × 1 ft. 2 in. was used for roasting. Table I gives the composition of the furnace atmosphere just above the charge at different operating temperatures.

TABLE I.—*Analysis of Furnace Atmosphere During Roasting.*

Temp., °C.	Time, hr.	Carbon Dioxide, %	Oxygen, %
800	1	4.0	6.0
	2	3.0	9.0
	3	3.5	8.0
900	1	5.0	3.0
	1.5	5.0	3.0
	2	5.5	4.0
	3	5.0	3.5
1000	2	6.0	1.0
	3	5.5	0.5

Three kg. of wire were treated as a charge, held in a box 12 × 12 × 4 in. made of iron-wire mesh ( $\frac{1}{4}$ -in. mesh, 16 S.W.G.). The box was supported at the corners and centre 2 in. from the furnace floor, so that air had free access. By analysis the iron content of the final oxide was found to be about 0.1%. This is higher than desirable, but it is thought that contamination would be much less using a heat-resisting steel box and insignificant with a Nichrome container.

Oxidation was carried out at 800°, 900°, and

1000° C. for periods up to 3 hr. at each temperature. The temperatures of furnace and charge were measured separately, and it was quickly observed that these were not even approximately the same during the early stages of roasting. If the temperature of the furnace was held steady, the temperature of the charge rapidly attained this value and went on increasing, owing, undoubtedly, to the exothermic nature of the reaction. In one such experiment at 900° C. the charge had reached 900° C. in 8 min. and in a further 7 min. had reached 1040° C. without any marked decrease in the rate of rise in temperature. To avoid fusion of the

TABLE II.—*Oxidation of Batches of Copper Wire.*

Copper determined electrolytically, and oxygen by difference, assuming the tin content to be constant at 1%.

Temp., °C.	Time, hr.	Copper, %	Oxygen, %
800	1	92.3	6.7
	2	90.3	8.9
	3	89.2	9.8
900	1	88.0	11.0
	1.5	86.3	12.7
	2	85.6	13.4
	3	85.0	14.0

charge, the furnace temperature was quickly lowered to 800° C. and then gradually raised again. In a further 55 min. the charge was down to 900° C., and after a further 10 min. the charge and furnace were both at 885° C. and were gradually brought to 900° C. At 800° C. the increase was much less, 870° C. being the maximum charge temperature recorded with a constant furnace temperature of 800° C. Roasting at 1000° C. was rendered very difficult by the heat of reaction, and even with careful supervision, temperature control was found to be uncertain and parts of the charge showed signs of fusion. Some experimental results were obtained, but it is considered that this temperature is too high for a production plant. The results obtained at 800° and 900° C. are shown in Table II.

At 800° C. the charge was uniformly oxidized throughout the iron-mesh box, but the wire had a residual copper core even after 3 hr. At 900° C. it was completely oxidized after 2 hr., and after 1.5 hr. there were only small areas where oxidation was not complete.

A charge of wire was then roasted at 850° C. for 2 hr., but this did not result in complete oxidation. A longer time would have done so, but economic considerations do not merit the longer time for a reduction in temperature of only 50° C. Furthermore, the lower temperature appeared, in the single-wire experiments, to yield more cupric oxide.

It was concluded that roasting for 2 hr. at 900° C. was the optimum condition of oxidation and 2 cwt. of oxide for the later experiments were made under these conditions.

## III.—COMMUNUTION OF COPPER OXIDE

## 1. EXPERIMENTAL

The overriding consideration in the comminution of the oxide is suitable size grading. Sieve analysis of samples of commercially available copper powders gave an average size distribution of about 5% of material of +120 mesh, 20% of -120/+200 mesh, 20% of -200/+300 mesh, and the balance -300 mesh. While it was thought probable that the size distribution would change during reduction, no estimate could be made, so that the initial aim was to produce oxide having a similar size grading. A wide range of conditions was examined, but some of the possible variables had to be eliminated. Thus, only dry milling in batches was carried out and the time factor dealt with by removing samples from the mill at 5- or 10-min. intervals. This is not wholly desirable, since the mill load is progressively reduced during milling. Continuous operations using air separation for dry milling or water separation for wet milling were not seriously considered, and, in any case, do not lend themselves readily to small-scale experiments.

The cylindrical mill (9 × 13 in.) was filled with 1.2-cm. polished steel balls nearly to the axis, the load being 20 kg. The critical speed was calculated as 88 r.p.m., but, since the balls were polished and the mill lining smooth, considerable slip occurred and the actual speed was found to be rather more than 120 r.p.m.

Because of the difference between the actual and theoretical critical speeds, observations of the ball action were made by fitting a wire screen over the end of the mill. The speeds finally decided upon were 60, 100, 106, and 116 r.p.m. At 60 r.p.m. the principal cause of comminution was attrition at the centre of the mass, changing to cascading of free balls down the surface heap as the speed was increased. At 100 r.p.m. the balls struck the breast of the mill at what might be called the four o'clock position. Coghill and DeVaney<sup>6</sup> have shown that the maximum rate of grinding occurs under this condition. The higher speeds were chosen to reduce attrition to a minimum, to see whether the amount of fines could be reduced in this way.

Details of the experimental conditions and the results obtained are shown in Figs. 1-3. Six particle-size groups were selected but, to simplify the figures, these have been grouped into four.

## 2. DISCUSSION OF MILLING EXPERIMENTS

## (a) General

Figs. 1-3 show that the particle-size distribution of the milled oxide is greatly affected by the conditions of grinding, but the general form of all the graphs is the same and is represented by Fig. 1 (5:1). The main variation is in the slope of curve *D*, the maximum values for *B* and *C*, and the slope of the initial part of

curve *A*. The ideal condition is a rapid decrease with time for curve *A* and a large value for the maximum of *B* and *C*, occurring at a time when *A* is very small. In other words, it is desired to produce a large amount of the intermediate -120/+300-mesh fraction, at a time when the coarse +120-mesh material has virtually disappeared and before the -300-mesh material has reached 50 wt.-%.

## (b) Variation of Ball-to-Charge Ratio and Time of Milling (Fig. 1)

The results plotted in Fig. 1 show that, as the ball-to-charge ratio is increased, the rate of grinding (measured by the slope of curve *A*) decreases, but the maximum value of *B* increases. The times required

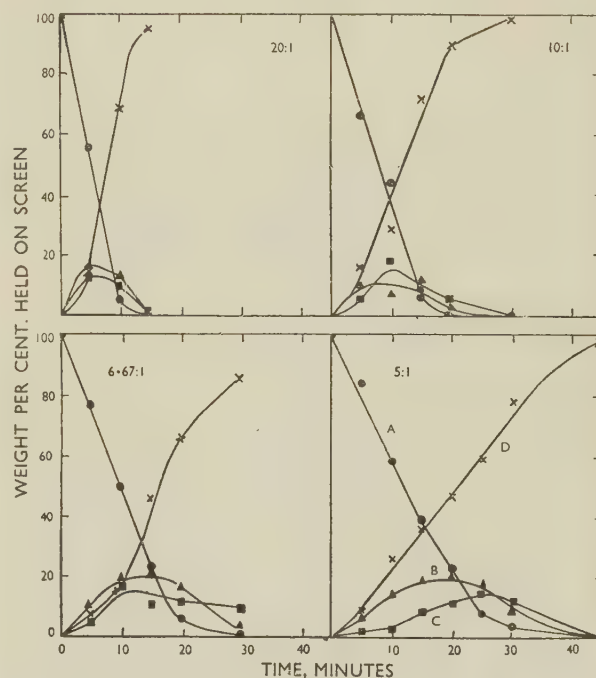


Fig. 1.—The Effect of Ball-to-Charge Ratio on Grinding. Speed 60 r.p.m.; ball load 20 kg.; ball dia. 1.2 cm.

KEY.

● +120 mesh.      ■ -200 to +300 mesh.  
▲ -120 to +200 mesh.      × -300 mesh.

to reach the optimum size distribution are 10, 15, 20, and 25 min. with ball-to-charge ratios of 20:1, 10:1, 6.67:1, and 5:1, respectively, and the percentage weights of the intermediate size (-120/+300 mesh) after these times are 25, 21.5, 27.5, and 33 with increasing ball-to-charge ratio. The rates of production of useful powder at the times required to reach optimum size distribution in the four experiments are 95, 125, 140, and 146 g./min. with the increasing ball-to-charge ratios given above. Thus, even if the time of unloading and recharging the mill is ignored, it will be seen that the 5:1 ratio requires less time to produce a given quantity of powder.



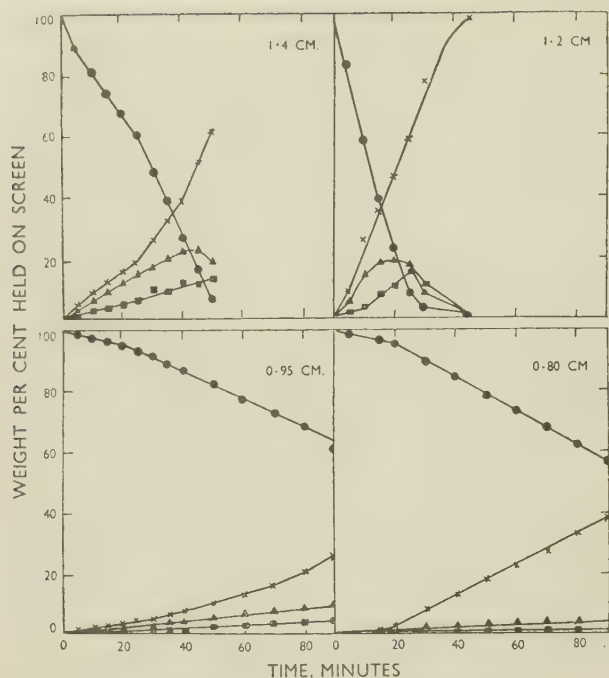


Fig. 2.—The Effect of Ball Diameter on Grinding. Speed 60 r.p.m.; ball-to-charge ratio 5:1; ball load 20 kg.

KEY.  
 ● +120 mesh.  
 ▲ -120 to +200 mesh.  
 ■ -200 to +300 mesh.  
 × -300 mesh.

(c) *Variation of Ball Size and Time of Milling (Fig. 2)*

With 0.8-cm.- and 0.95-cm.-dia. balls the rate of comminution of the +120-mesh fraction is very low, but any of this material which is broken down is converted almost immediately to -300 mesh size. While great in both cases, this tendency is highest with the smaller balls. It appears that while the small balls have a very large number of points of contact, the crushing impulse at any given point is too small to fracture much of the coarse material, although great enough to break such fines as are formed. With 1.2-cm. balls the initial slope of the curve for the +120-mesh material is high, indicating rapid grinding of the coarser fractions, while the build-up of the intermediate sizes is satisfactory after about 25 minutes' milling. The 1.4-cm. balls, with their extra weight, might have been expected to break down the coarse fraction even more quickly than the 1.2-cm.-dia. balls, but the slope of the curve for the +120-mesh material is not as great, indicating that the decrease in the number of points of contact has placed a restriction on the rate of grinding, not compensated by the greater crushing impulse. Of the ball sizes investigated, 1.2-cm.-dia. gives the best results.

(d) *Variation of Speed of Mill and Time of Milling (Fig. 3)*

A speed of 100 r.p.m. gives the most rapid breakdown of the coarse fraction, if the initial part of the

curve for 116 r.p.m. is ignored. At 116 r.p.m. the mill charge began to centrifuge after 7 minutes' operation and, while the size distribution of the -120-mesh material was satisfactory, a considerable amount of coarser material would have to be removed by sieving, and it was desired to avoid this if possible. Similar considerations apply to the tests at 106 r.p.m. At 60 r.p.m. the results obtained after 25 min. were satisfactory, but slightly better results were obtained from 15 min. milling at 100 r.p.m., coupled with the advantage of the slightly shorter milling time required.

This speed, with a ball-to-charge ratio of 5:1, a ball load of 20 kg., and a ball dia. of 1.2 cm., was used to produce 12 kg. of oxide for the experiments on the reduction of the oxide and the properties of the powder so produced. The size distribution of the milled oxide after sieving out the +120 mesh was 17.2% +200 mesh, 12.8% -200/+300 mesh, and 70% -300 mesh. The total percentage in the intermediate size range was less than expected.

The work on the milling of the oxide is by no means comprehensive, and it is not possible to say to what extent the results are affected by the size factor. They do appear to indicate, however, that the comminution of the coarse material without the production of excessive fines is likely to be difficult unless removal of the -120-mesh material can be carried out during milling by air separation or screening.

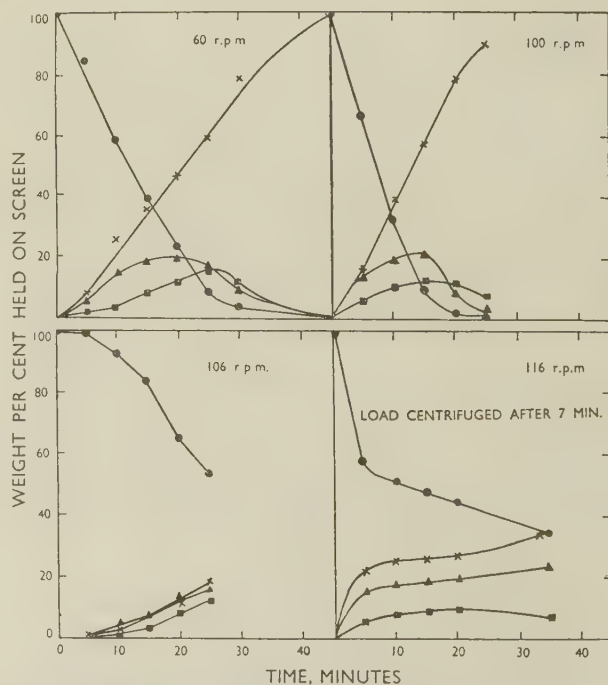


Fig. 3.—The Effect of Mill Speed on Grinding. Ball-to-charge ratio 5:1; ball load 20 kg.; ball dia. 1.2 cm.

KEY.  
 ● +120 mesh.  
 ▲ -120 to +200 mesh.  
 ■ -200 to +300 mesh.  
 × -300 mesh.

## IV.—REDUCTION OF COPPER OXIDE

## 1. GENERAL

Drapeau<sup>1</sup> recommends a temperature range of 175°–375° C. for reduction by hydrogen, but preferably one between 175° and 260° C. He gives 375° C. as the temperature at which sintering becomes pronounced.

Baëza<sup>7</sup> attaches considerable importance to the mode of occurrence of any residual oxide, stating that oxide on the surface of the particles does not interfere very markedly with the moulding operation or the subsequent strength of the compact. On the other hand, he regards occluded oxide as being very detrimental and resulting in a product of low tensile and impact strength. This indicates that complete removal of oxygen during reduction is important.

The variables considered were temperature, time, composition of reducing medium, particle size of the oxide, quantity of reducing medium, and degree of agitation of the oxide during reduction. With so many variables it was not possible to attach equal importance to all. The reducing media investigated were hydrogen, carbon monoxide, cracked ammonia, coal gas, and propane, and it was decided to study the effect of time and temperature for hydrogen and coal gas. With the other three gases the investigation was confined to one temperature, 400° C. Other variables were investigated using hydrogen as a reducing agent at 400° C.

The reason for investigating the suitability of cracked ammonia, coal gas, and propane, was that from an economic point of view they appeared to offer greater advantages than hydrogen or carbon monoxide. The latter gases were used because they are good reducing agents and also because of their different mechanism of reduction. Ransley<sup>8</sup> observed this fundamental difference in the case of massive copper containing oxide inclusions. In hydrogen reduction the process is essentially one of diffusion of the gas into the particles, so that internal reduction occurs, with the possibility of steam being trapped in the particles. With carbon monoxide, diffusion of the gas into the metal does not take place, so that reduction is a surface reaction controlled by the diffusion of the oxide to the surface. It was expected that cracked ammonia, which contains a high proportion of hydrogen, and nitrogen, which is presumed to be inert, would react in the same way as hydrogen; that propane would resemble carbon monoxide; and that coal gas which is mainly hydrogen, methane, and carbon monoxide, would react like hydrogen, since hydrogen would tend to diffuse into the particles and reduce the oxide before it reached the surface where carbon monoxide or methane could react.

## 2. EXPERIMENTAL

Reduction was carried out in a hard glass tube, 4.5 cm. in dia. and 60 cm. in length. This was drawn out to a fine jet at one end; and closed at the other

by a rubber bung incorporating a gas inlet and the thermocouple. The reducing gas was passed in through the rubber bung and burnt at the jet end. The copper oxide was confined to a 15-cm. length at the outlet end of the tube by tilting it slightly. The glass tube could be placed inside an electrically heated tube furnace 40 cm. long  $\times$  6.4 cm. internal dia. The length of the glass tube actually heated was about 30 cm., so that the outlet where the gas was burnt was approaching furnace temperature. This was necessary to avoid condensation of steam in the tube. The furnace was controlled by the temperature of the winding at its centre point; another thermocouple dipping in the powder enabled the temperature of the latter to be measured.

In some of the experiments the tube was rotated to agitate the contents, and for this purpose a slack-fitting rubber sleeve over the glass gas-inlet was found to provide a satisfactory joint. The couple was attached to two brass discs which dipped into pools of mercury to enable the temperature to be measured during rotation. To rotate the glass tube, it was clamped into a steel tube mounted in suitable bearings and driven by an electric motor through a belt. A glass rod was placed in the tube to improve agitation during rotation.

To carry out an experiment, the glass tube was removed from the apparatus, the gas supply connected up, and the gas flow regulated by a gas meter. When all the air had been swept from the tube, the gas was ignited and the tube placed in the furnace, which had previously been brought to the required temperature. After treatment for the required time the tube was removed from the furnace and allowed to cool with the reducing gas still flowing.

In all cases except those involving investigation of particle size, the copper oxide had a sieve analysis of 17.2% — 120/+200 mesh, 12.8% — 200/+300 mesh, and 70% — 300 mesh. (This is subsequently referred to as 17.2/12.8/70 oxide.)

The progress of reduction was followed by the chemical analysis of the powder at the end of each experiment. The oxygen content was determined by passing hydrogen over a sample of the powder at 1000° C. and weighing the water vapour produced, and determining the loss in weight of the sample.

Frequently the copper powder tended to sinter during reduction. The agglomerates so formed were easily broken down in a small Raymond swinging hammer mill, and it was usual to treat all powder in this mill before determining sieve analysis.

## 3. REDUCTION BY HYDROGEN

Results are shown in Table III.

A marked increase in the rate of reduction occurs as the temperature is increased from 175° to 250° C. Raising the temperature above this has very little effect on the reaction rate. Initially the rate of reduction is rather slow, while the oxide is being heated up, then increases rapidly, and finally slows



down. The oxygen content does not reach zero and appears to be dependent on temperature, being lowest at the highest temperature.

TABLE III.—*Variation of Oxygen Content with Time and Temperature of Reduction by Hydrogen.*

Gas flow 0.02 ft.<sup>3</sup>/min.; rotating tube; 17.2/12.8/70 oxide.

Temp., °C.	Time, min.						
	10	15	30	45	60	105	120
	Oxygen Content, wt.-%						
175	...	12.9	10.6	3.2	1.4	...	1.1
200	...	12	2.76	1.22	0.66	...	0.83
250	...	5.8	0.59	0.85	0.74	0.65	...
300	...	...	0.69	0.63	0.74	...	...
350	...	2.9	0.72	...	0.56	...	...
400	...	...	0.64	...	0.43	...	0.39
450	8.61	0.89	0.45	...	0.42	...	...

TABLE IV.—*Variation of Sieve Analysis of Copper Powder (after Breaking Down) with Time and Temperature of Reduction.*

Hydrogen flow 0.02 ft.<sup>3</sup>/min.; intermittent rotation; 17.2/12.8/70 oxide.

Reducing Conditions		Sieve Analysis, %	
Temp., °C.	Time, min.	+120 mesh	—120/+200 mesh
400	30	0.8	12.0
	45	1.5	11.8
	60	1.0	12.0
450	15	1.6	12.4
	30	4.5	12.5
	60	8.5	12.0

Fig. 4 shows the temperature of the powder during reduction at furnace temperatures of 200°–450° C. It will be seen by comparison with Table III that considerable heat is evolved when the maximum rate of reduction is obtained and that at elevated tempera-

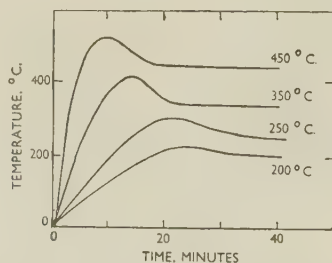


FIG. 4.—Temperature of Powder During Reduction by Hydrogen at Different Furnace Temperatures.

tures, at least, the temperature of the powder rises considerably above the temperature of the enclosure.

It is necessary to limit the temperature of reduction because of the sintering of the copper particles. At any temperature sintering takes place as soon as a

clean copper surface is formed, but below 250° C. the strength of the sintered agglomerates is small. At higher temperatures the strength increases, until at 450° C. quite hard lumps are formed. Table IV shows the sieve analysis of material broken down under identical conditions in the hammer mill. There is an appreciable increase in the proportion of +120 mesh material with increase in reduction temperature from 400° to 450° C.

When the minimum oxygen content, rate of reduction, and extent of sintering are considered, the optimum temperature of reduction would appear to be 400° C. However, it was thought that reduction temperature might exercise some unforeseen effect on the pressing and sintering properties of the copper powder. To test this, reduction temperatures of 400° and 250° C. were used to produce batches for experiments on the properties of the powder dealt with in Section V.

#### 4. REDUCTION BY COAL GAS

Comparison of the results obtained (Table V) with those for hydrogen (Table III) under comparable conditions shows that coal gas is less efficient, both as regards the degree and rate of reduction.

TABLE V.—*Variation of Oxygen Content with Time of Reduction by Coal Gas.*

Gas flow 0.02 ft.<sup>3</sup>/min.; continuous rotation; 17.2/12.8/70 oxide.

Temp., °C.	Time, min.						
	10	20	30	40	50	60	120
	Oxygen Content, wt.-%						
200	...	...	...	...	...	...	13.8
250	13.2	...	11.6	...	5.0	6.6	...
300	10.0	6.7	6.7	1.5	...	0.95	...
350	11.9	3.8	...	...	...	0.85	...
400	10.9	1.49	1.65	...	...	...	...
450	...	1.74	...	...	...	...	...

This result was rather unexpected, since, as shown in Table VI, the coal gas contained almost 50% of hydrogen by volume.

TABLE VI.—*Analysis of Coal Gas (vol.-%).*

Sulphur content 14–20 grains/100 ft.<sup>3</sup>.

H <sub>2</sub>	CO	N <sub>2</sub>	CH <sub>4</sub>	CO <sub>2</sub>	O <sub>2</sub>	Unsaturated Hydrocarbons
47.0	7.75	10.5	27.5	3.5	0.25	3.5

The powder reduced by coal gas was unstable, the colour changing from pink to dark brown or black in 10–30 days. Analysis showed that the sulphur content of partly or completely reduced copper oxide increased from zero to 0.004% during reduction by coal gas and remained constant at that figure after about 10 minutes' contact. It is thought that

the discoloration of the powder was connected with its sulphur content, since sulphur-free powders did not discolour in the same way, but this line of investigation was not followed up.

### 5. REDUCTION BY CARBON MONOXIDE

The results of experiments at 400° C. are given in Table VII. Comparison with Table III shows that the rate and extent of reduction by hydrogen and carbon monoxide are very similar. The reaction gives an increase in temperature of about 50° C. above the furnace temperature when proceeding at the maximum velocity.

TABLE VII.—*Variation of Oxygen Content with Time of Reduction by Carbon Monoxide at 400° C.*

Gas flow 0.02 ft.<sup>3</sup>/min.; intermittent rotation, 17.2/12.8/70 oxide.

Time, min.	15	30	60
Oxygen, wt.-% . .	0.69	0.58	0.33

The size distribution of the powders resulting from reduction by carbon monoxide and hydrogen are shown in Table VIII.

It would seem that the difference in the mechanism of reduction involves a change in the size distribution. With hydrogen the +200-mesh material has suffered a greater degree of decrepitation than with carbon monoxide, but this is offset by a greater tendency for sintering during hydrogen reduction, giving a decrease in the -300-mesh material.

Some indication of the difference is given by the appearance of the copper. There is a fairly marked similarity in surface between the oxide and the

TABLE VIII.—*Change in Size Distribution (wt.-%) on Reduction of Oxide by Hydrogen and Carbon Monoxide.*

1 hr. at 400° C.; gas flow 0.02 ft.<sup>3</sup>/min.; intermittent rotation.

Size Fraction	Oxide	Hydrogen-Reduced Copper Powder	Carbon-Monoxide-Reduced Copper Powder
-120/+200 mesh .	17.2	11.8	14.1
-200/+300 mesh .	12.8	28.8	20.6
-300 mesh . . .	70.0	59.4	65.2

carbon-monoxide-reduced powder, whereas the hydrogen-reduced copper has a spongy appearance.

### 6. REDUCTION BY CRACKED AMMONIA

A series of experiments was carried out at 400° C., using 0.02 ft.<sup>3</sup>/min. of gas with intermittent rotation. The results are shown in Fig. 5, together with results for similar experiments with hydrogen. It will be seen that cracked ammonia is a more efficient reducing agent than hydrogen, particularly in regard to the

residual oxygen content. The reason may be that part of the ammonia which remained in the gas after initial cracking was decomposed on the surface of the

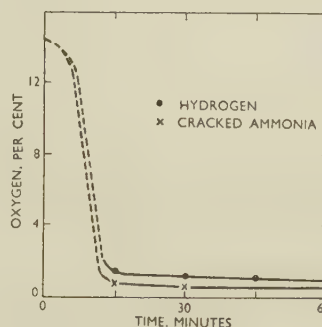


FIG. 5.—Reduction of Copper Oxide Using Hydrogen and Cracked Ammonia.

partly reduced oxide with the liberation of nascent hydrogen, which diffused rapidly into the particles, but this was not further explored.

### 7. REDUCTION BY PROPANE

The results of a series of experiments at 400° C. using 0.02 ft.<sup>3</sup> of propane/min. are shown in Table IX. The rate of reduction is very slow at this temperature.

TABLE IX.—*Variation of Oxygen Content with Time of Reduction by Propane at 400° C.*

Gas flow 0.02 ft.<sup>3</sup>/min.; 17.2/12.8/70 oxide; intermittent rotation.

Time, min.	15	30	60	120
Oxygen, wt.-% . .	5.80	3.68	1.53	2.41

At 500° C. reduction proved more rapid, but sintering of the powder was excessive. The propane tended to crack during treatment, with deposition of carbon. Analysis showed the amount of carbon present to be relatively small (0.02% after 15 min. and 0.05% after 2 hr.), but the effect on the appearance of the powder was very marked.

### 8. EFFECT OF AGITATION DURING REDUCTION

Experiments were carried out at 400° C. to study the effect of agitation during reduction. As described in Section IV, 2, reduction was carried out in a hard glass tube, which was capable of rotation. In one set of experiments the tube was held stationary, in the second the tube was rotated for 1 min. in every 5, and in the third rotated continuously. The results are shown in Table X. So far as the removal of oxygen is concerned there is little difference between continuous and intermittent rotation, but both procedures give more rapid removal of oxygen than no rotation.

There is another aspect that must be considered in connection with the use of a rotating tube. When continuous rotation was employed, the particles



tended to sinter together in the form of spheres, which, under the influence of the polishing effect of the glass tube, developed a hard surface. This glazed surface does not appear to have hindered reduction, but is detrimental, because it hinders the disintegration of the agglomerate after reduction and produces rejectable oversize material. This tendency is illustrated in Table XI, where the hard glazed material constitutes a high proportion of the +120-mesh fraction.

TABLE X.—*Variation of Oxygen Content with Degree of Agitation and Time of Reduction by Hydrogen at 400° C.*

Gas flow 0.02 ft.<sup>3</sup>/min.; 17.2/12.8/70 oxide.

Degree of Agitation	Time, min.			
	15	30	45	60
	Oxygen Content, wt.-%			
Continuous Rotation .	0.81	0.64	0.60	0.46
Intermittent Rotation	0.92	0.55	...	0.49
No Rotation . . . .	3.45	0.83	0.68	0.62

The appearance of a hard surface was noted even at 175° C. However, at this lower temperature, 2 hr. of rotation were required, whereas a very hard surface had developed after only 30 min. at 450° C.

With intermittent agitation the disadvantage of continuous motion was avoided without any serious

TABLE XI.—*Variation of Sieve Analysis of Copper Powder with Degree of Agitation and Time of Reduction (after Breaking Down in a Swinging-Hammer Mill).*

Degree of Agitation	Time of Reduction, min.	Sieve Analysis, %	
		+120 mesh	—120/+200 mesh
No rotation	30	1.5	11.0
	45	2.0	11.5
	60	1.0	11.0
Continuous rotation	15	2.0	11.0
	30	3.5	11.0
	45	7.0	11.8
	60	8.0	11.6

reduction in the rate of reaction, and this procedure was used when batches of material were produced for the work on the properties of oxide-reduced powders.

## 9. THE RATE OF GAS FLOW

The rate of flow of gas used in the previous experiments was 0.02 ft.<sup>3</sup>/min. This was not sufficiently rapid to blow the powdered oxide from the tube, yet was fast enough to carry out the steam formed before it condensed. The results of experiments using other rates of flow are given in Table XII. These suggest that there is an optimum rate of gas flow above which no appreciable increase in the rate

of reduction is obtained and below which the reaction is slowed down. The rate does not appear to affect the ultimate oxygen content of the copper.

TABLE XII.—*Variation of Oxygen Content with Rate of Gas Flow and Time of Reduction by Hydrogen at 400° C.*

17.2/12.8/70 oxide; intermittent rotation.

Rate of Gas Flow, ft. <sup>3</sup> /min.	Time, min.			
	15	30	45	60
	Oxygen Content, wt.-%			
0.01	8.44	4.89	...	0.44
0.02	0.81	0.69	0.60	0.46
0.03	0.71	0.38	...	0.39
0.04	...	0.59	...	0.49

## 10. EFFECT OF PARTICLE SIZE OF THE OXIDE

This aspect of reduction was investigated to find out if the very fine oxide could be completely de-oxidized, since none of the previous experiments had given any indication that complete removal of oxygen could be achieved in reasonable time. The results are given in Table XIII. It would appear

TABLE XIII.—*Variation of Oxygen Content with Particle Size of Oxide and Time of Reduction by Hydrogen at 400° C.*

Gas flow 0.02 ft.<sup>3</sup>/min.; intermittent rotation.

Time, min.	Particle Size (mesh)				
	—36/+72	—72/+120	—120/+200	—200/+300	—300
	Oxygen Content, wt.-%				
30	0.68	0.72	0.48	0.48	0.33
60	0.76	0.66	0.43	0.45	0.41

that with oxide of —120 mesh the particle size has little effect on the rate of reduction or ultimate oxygen content, but coarser metal has a higher residual oxygen content.

An interesting point which emerged is that sintering only becomes pronounced with the —300-mesh material. Reduction of the —200/+300-mesh fraction gave agglomerates which disintegrated readily, whereas the —300-mesh fraction produced much harder nodules.

## 11. EFFECT OF TEMPERATURE ON RELATION BETWEEN PARTICLE SIZE OF OXIDE AND REDUCED COPPER POWDER

Attention has already been drawn to the change in sieve analysis which occurs during reduction and a comparison made of the results with hydrogen and carbon monoxide as reducing agents. Table XIV compares reduction by hydrogen at 250° and 400° C., and appears to indicate that the decrepitation of the

larger oxide particles is independent of the temperature of reduction, but that at 400° C. the proportion of — 300-mesh material is reduced on account of sintering at that temperature.

TABLE XIV.—*Change in Size Distribution (wt.-%) on Reduction with Hydrogen for 1 Hr. at 250° and 400° C.*

Gas flow 0.02 ft.<sup>3</sup>/min.; intermittent rotation.

Size Fraction	Oxide	Reduced at 250° C.	Reduced at 400° C.
—120/+200 mesh .	17.2	11.3	11.8
—200/+300 mesh .	12.8	15.7	28.8
—300 mesh .	70.0	72.8	59.4

## V.—THE PROPERTIES OF OXIDE-REDUCED POWDERS

### 1. GENERAL

The purpose of this section of the work was to examine the properties of a number of selected grades of oxide-reduced copper powder and compare them with those of other types of commercially available copper powders. A study of nine powders has been made: six examples of oxide-reduced powder and three of commercial powders, two of the latter being produced by electrolysis and one by steam atomization.

Of the six oxide-reduced powders, four were used to investigate the effect of size distribution on the properties with hydrogen reduction at 400° C., one to determine the effect of reduction by carbon monoxide, and one to study the effect of hydrogen reduction at 250° C.

Since none of the powders produced by reduction had what was considered a satisfactory size distribution, the powders investigated were prepared by thoroughly blending mixtures of the appropriate size fractions.

The properties examined include the apparent density, flow behaviour, size distribution, and chemical composition of the unsintered powders. The effect of pressure during the pressing operation, and of temperature of sintering, on the mechanical properties and volume changes of compacts made from the various grades of powders after sintering, have also been studied.

### 2. EXPERIMENTAL

Of the various densities that could have been measured, only the apparent density of the powder and the density of compacts before and after sintering were investigated. The Powmet Flow-Factor Meter was used in determining the apparent density and comparing flow behaviour. This instrument consists of a smooth brass cone of 30° semi-vertical angle terminating in a  $\frac{5}{32}$ -in.-dia. orifice. In operation the orifice was closed by a metal disc and the cone filled

by pouring powder from 1 in. above its surface. The powder was levelled off with a scraper and the contents then allowed to pass through the orifice to a cup of 25 c.c. capacity. The powder in the cup was levelled off and weighed, permitting the apparent density to be calculated from the weight and volume of the powder.

The density of the compacts before and after sintering was calculated from their weight and their measured volume. Porosity was calculated employing a value of 8.91 g./c.c. for the density of copper.

Two types of compact were used; a cylindrical compact 0.5 in. in dia., somewhat variable in height, and weighing 10 g., for density and hardness measurements and micro-examination, where carried out; and a flat compact from the die illustrated in Fig. 6, for mechanical-property measurements.

The pressure was applied by 10- and 70-ton hand-operated hydraulic presses. For tensile specimens a constant volume of powder was pressed. A solution of stearic acid in benzene was used to lubricate the ram and die faces, but the lubricant was not mixed with the powder. The rate of loading was kept at 60 tons/in.<sup>2</sup>/min., as far as possible, and the pressure

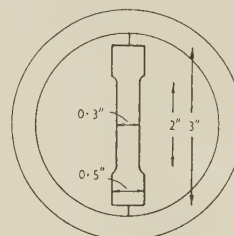


FIG. 6.—Diagram of Tensile Test-Piece Die.

maintained for 15 sec. on reaching the maximum value.

The compacts were sintered in a silica tube furnace through which a reducing gas could be passed or in which a vacuum could be maintained, as required. Since different temperatures were used for sintering, the rate of heating varied somewhat. The compacts were held at the sintering temperature for 30 min. and cooled either with the sintering gas passing through or *in vacuo*.

The tensile specimens were tested on a Hounsfield tensometer. The tensile strength, reduction in area, and elongation on a 1-in. gauge-length were the properties measured.

### 3. RESULTS AND DISCUSSION

#### (a) The Powders

Within the size range examined for hydrogen-reduced powders the variation of size distribution had no significant effect on the apparent density (2.75 g./c.c.).

Powders with the same size distribution but produced under different conditions of reduction showed a difference in apparent density. Thus, the



smoother carbon-monoxide-reduced particles gave a higher apparent density (3.20 g./c.c.) than the rougher hydrogen-reduced particles (2.74 g./c.c.). Reduction by hydrogen at 250° C. also appeared to give a higher apparent density than reduction at 400° C., presumably as a result of a less violent reaction and hence a smoother surface after reduction at 250° C.

The powder produced by steam atomization gave a much higher apparent density than any of the other powders. This is probably due to the smooth, rounded nature of the particles.

It was expected that the surface condition and shape of the powder particle would control the flow characteristic, but this was not found to be so. It appears that the proportion of —300-mesh material is of considerable importance with electrolytic and oxide-reduced powder, although not with atomized powder. Oxide-reduced powders with 60% —300-mesh material would sometimes flow, but it was found that the best results were obtained with less than 30% of this material, and that flow would not always begin when there was 45% —300-mesh material present.

#### (b) The Pressed Compacts

Owing to the failure of the cylindrical die in service and the difficulty of replacement, it was not possible

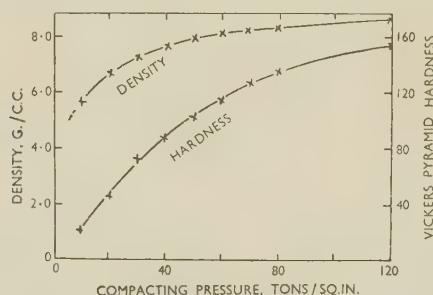


Fig. 7.—Density and Hardness of Pressed Compacts of Oxide-Reduced Powder No. 1 (100% —300 mesh).

to mould any cylindrical specimens of atomized or electrolytic powders. Four oxide-reduced powders containing 20–100% —300-mesh material were examined. The varying proportion of sub-sieve material had only a very slight effect on the density of a compact at any pressure. Since porosity and the compression ratio are a function of the density, these properties are also only slightly affected by the same factor. The variation of density and hardness with compacting pressure in a typical case is shown in Fig. 7. This is in good agreement with work by Goetzel<sup>9</sup> but conflicts with that of Kuzmick,<sup>10</sup> who concluded that a very close relation exists between hardness and density, the flattening out of both curves taking place at the same value of compacting pressure. The present work indicates that the hardness increases more rapidly than density at high compacting pressures. This may be because of work-hardening due to fairly severe deformation of individual grains as the final pores are filled up.

#### (c) The Sintered Compacts

A general survey of the effect of compacting pressure and sintering temperature on the properties of oxide-reduced powders was carried out before comparison with other powders was made. Compacting pressures of 10, 20, 40, and 60–70 tons/cm.<sup>2</sup>

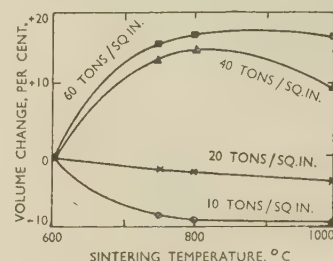


Fig. 8.—Volume Change on Sintering after Different Compacting Pressures.

were used, with sintering temperatures of 600°, 750°, 800°, and 1000° C. The specimens were heated as rapidly as possible to the sintering temperature, held for 30 min., and then allowed to cool. A hydrogen atmosphere was used throughout.

The combined effect of compacting pressure and sintering temperature on the volume of sintered compacts of oxide-reduced powder No. 2, containing 60% —300 mesh, is shown in Fig. 8. It will be seen that a very small shrinkage occurs at all compacting pressures at 600° C., but that above that temperature compacts made at 10 and 20 tons/in.<sup>2</sup> shrink, whereas those pressed at 40 and 60 tons/in.<sup>2</sup> expand very appreciably. This has also been observed by other investigators.

The effect of the particle size of powder on the density of sintered compacts is very slight. At any temperature the greatest values of density were found with powder No. 1 (100% —300 mesh) when the compacting pressure was 10 tons/in.<sup>2</sup>. At higher pressures, however, powder No. 2 gave slightly higher values. At low compacting pressures the fine powders showed a greater shrinkage than coarse ones, but again this effect was comparatively slight.

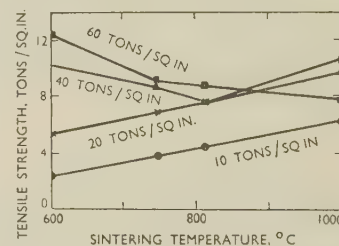


Fig. 9.—Strength of Compacts of Oxide-Reduced Powder at Different Compacting Pressures and Sintering Temperatures.

The tensile strength of compacts of powder No. 2 is plotted against sintering temperatures for different compacting pressures in Fig. 9. The strength of compacts produced at pressures of 10 and 20 tons/in.<sup>2</sup>

increases as the sintering temperature is raised, but with pressures of 60 tons/in.<sup>2</sup> the tensile strength decreases steadily as the sintering temperature is increased, while at 40 tons/in.<sup>2</sup> there is an initial decrease in strength followed by a slight increase at 1000° C. Comparison of Figs. 8 and 9 shows that the fall in tensile properties is accompanied by an expansion during sintering, indicating that any increase in the inter-particle bond strength is more than off-set by the development of gas-containing pores in the test-pieces. Hoar and Butler<sup>11</sup> have recently carried out a detailed examination of the volume changes accompanying the pressing and sintering of copper powder containing oxygen. The relations between pressure, temperature, and oxygen content are complex and will not be discussed here in detail.

These general observations refer to powder No. 2, but the shape of the tensile-strength/sintering-temperature curves is similar for the other oxide-reduced powders. The actual values of tensile strength, however, are slightly different for the four powders produced by this method. This is illustrated in Fig. 10 for a sintering temperature of 750° C., at which the maximum deviation for the four powders was observed. The general conclusion to be drawn is that at low compacting pressures the strength increases with the proportion of — 300-mesh material present, but that with high compacting pressures a very high proportion of — 300-mesh material gives inferior results.

Previous workers do not appear to have investigated the strength of compacts sintered at temperatures below 750° C. It will be seen from Fig. 9 that tensile figures of more than 12 tons/in.<sup>2</sup> were given by powder No. 2 sintered at 600° C. after compacting at 60 tons/in.<sup>2</sup>. This figure was confirmed by the results for powders 3 and 4 containing, respectively,

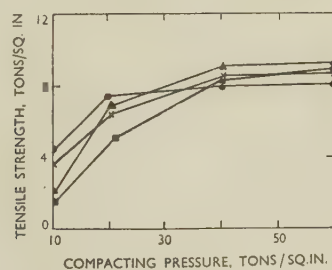


FIG. 10.—Strength of Sintered Compacts of Powders with Different Size Distribution. Sintering temperature, 750° C.

KEY.

- Powder No. 1 (100% — 300 mesh).
- × " No. 2 (60% " " " " ).
- ▲ " No. 3 (40% " " " " ).
- " No. 4 (20% " " " " ).

40 and 20% — 300-mesh material. A search of the literature did not reveal figures of much above 9 tons/in.<sup>2</sup> for oxide-reduced powder, but in all cases higher sintering temperatures were used.

The ductility, as measured by the reduction of area, was shown to follow the tensile strength of the

compacts very closely. This agrees with the observations of Cook and Pugh.<sup>12</sup>

From Fig. 11 it will be seen that the hardness of compacts does not change as they are heated, until the temperature exceeds 600° C. This applies to all compacting pressures, although it is to be expected

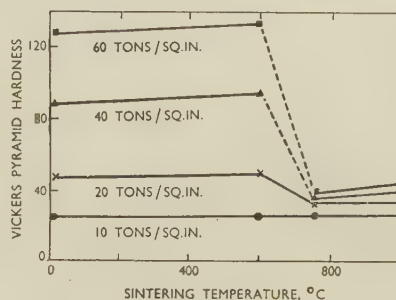


FIG. 11.—Variation with Compacting Pressure of the Hardness of Sintered Compacts of Oxide-Reduced Powder No. 2.

that the exact softening temperature will vary with the amount of deformation during pressing, that is, with the compacting pressure. In the present work the different sintering temperatures are too widely separated to show the exact softening temperature.

The observations on hardness lead to the conclusion, important from the fundamental aspects of sintering, that sintering may occur at temperatures below the recrystallization temperature, but this point has not been followed up.

The microstructure of the compacts will not be dealt with in detail. As is to be expected, the changes in porosity as measured by the density are reflected in the microstructure. The high hardness values of compacts sintered at 600° C. are accompanied by grain distortion in the microsections and the lower hardness values for higher sintering temperatures are accompanied by a recrystallized structure with several grains in a single particle. Sintering at 1000° C. tends to promote grain growth, but, even so, the original powder particles are far from being single crystals after sintering.

#### (d) Comparison of Sintered Compacts of Electrolytic, Atomized, and Reduced Powders

The strength and ductility of compacts of an electrolytic, a steam-atomized, and an oxide-reduced powder (No. 2) after sintering at 600°, 750°, and 1000° C., are shown in Fig. 12. Except for compacts pressed at 60 tons/in.<sup>2</sup> the strength of compacts of both electrolytic and atomized powders increases with sintering temperature. For compacts pressed at 10 and 20 tons/in.<sup>2</sup>, higher strength is obtained with oxide-reduced powder at any sintering temperature. Under the same condition the difference between electrolytic and atomized powders is very slight.

The pronounced expansion in volume that takes place on sintering reduced-powder compacts, pressed at 40 and 60 tons/in.<sup>2</sup> at 750° C. or above, is detrimental to their strength properties. Even so, at



750° C. the strength is greater than that of compacts from either electrolytic or atomized powders and at 1000° C. the reduced material is only slightly inferior.

The ductility of compacts prepared from electrolytic and atomized powders is similar after sintering at temperatures of 750° C. or higher and superior to that of compacts made from reduced powders. It is unfortunate that cylindrical compacts could not be prepared, so that the porosity and volume changes of compacts from the standard materials could be compared with compacts of oxide-reduced powder. The dimensions of the tensile test-pieces allow approximate assessments of the volume changes on sintering the standard materials to be made and suggest that under the optimum conditions for tensile properties (40 tons/in.<sup>2</sup> compacting pressure and sintering at 1000° C.) a shrinkage of about 3% occurs. Under the optimum conditions for oxide-reduced powder (60 tons/in.<sup>2</sup> and 600° C.) the corresponding figure is 0.6%.

The results obtained appear to conflict with those of Cook and Pugh,<sup>12</sup> who concluded that higher tensile values were possible using electrolytic powder than the oxide-reduced type. It is difficult to offer any wholly satisfactory explanation as to why the results should differ, except that in the earlier work sintering temperatures as low as 600° C. were not examined and it was at this temperature that the highest values for tensile strength were obtained. There may also have been some slight difference in

played any part in the higher strength obtained, since according to Alkins and Hallows<sup>13</sup> stannic oxide probably would not be reduced by hydrogen at 400° C.

#### (e) The Effect of the Reducing Gas

Reference has been made earlier to the fundamental differences in the mechanism of reduction by hydrogen and carbon monoxide. Table XV compares compacts

TABLE XV.—*Properties of Compacts of Hydrogen- and Carbon-Monoxide-Reduced Powders Sintered at 750° C.*

Powder Number	Reducing Medium	Compacting Pressure, tons/in. <sup>2</sup>	Elongation, %	Maximum Tensile Strength, tons/in. <sup>2</sup>	Change of Volume, %
2	Hydrogen	10	0	3.57	— 8.8
		20	1.6	6.41	— 1.7
		40	3.1	8.51	+ 13.4
		60	3.1	9.01	+ 15 *
5	Carbon monoxide	10	0	2.01	— 6 *
		20	1.6	3.74	0 *
		40	1.6	7.19	+ 5 *
		60	3.1	8.55	+ 8 *

\* Approximate values

of powders produced by hydrogen and carbon-monoxide reduction after sintering at 750° C. in hydrogen. It will be seen that the carbon-monoxide-reduced powder gives lower results for tensile strength than that reduced by hydrogen. This is probably connected with the difference in surface condition of the two types of powder. On the other hand, the volume changes on sintering are less with carbon-monoxide reduction.

#### (f) The Re-Oxidation of Hydrogen-Reduced Powder

It has been shown that completely oxygen-free powders were not obtained under the reducing conditions employed, and it was desired to assess the reason for this. As stated in Section II, 1, the copper contained about 1% of tin present as a coating on the original wire. Alkins and Hallows<sup>13</sup> have shown that reduction of stannic oxide in high-conductivity copper by hydrogen at atmospheric pressure begins at about 550° C. Under the conditions employed in this research, there is little chance of any appreciable reduction. If the whole of the tin were present as stannic oxide, the oxygen content of the powder from this source alone would be 0.27%. However, this figure would not account for all the residual oxygen in the powder and, to try and account for the remainder, experiments were made on the re-oxidation of hydrogen-reduced powder. For this purpose copper oxide was reduced in a hard-glass tube at 400° C. When reduction was as complete as possible, the glass tube was sealed off at two existing constrictions without allowing air into contact with the powder. When the tube was cold, it was weighed. Air was then admitted by breaking one of the seals at

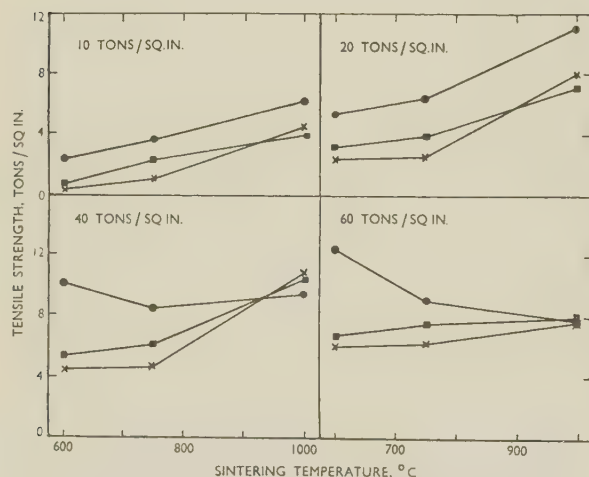


FIG. 12.—Variation with Compacting Pressure and Sintering Temperature of the Tensile Strength of Sintered Compacts.

KEY.

- Oxide-reduced powder.
- Electrolytic powder.
- × Atomized powder.

the powders used, since in the previous research reduction was carried out at 300° C. as compared with 400° C. in the present work. The powder used by Cook and Pugh may have had a higher residual oxygen content and a less irregular surface. It is doubtful whether the tin on the powder would have

the end of the tube, and weighing carried out as quickly as possible. It was found that a steady increase of weight of 0.2% had occurred in 30 hr. and that half this increase occurred in the first 5 min. of exposure. This indicates that re-oxidation takes place in air at room temperature, but that the re-oxidation process is probably confined to the surface layers of the metal. Since there was usually some delay in analysing for oxygen, it must be assumed that any oxygen figure quoted is from 0.1 to 0.2% higher than the actual oxygen content of the metal in the reducing chamber. This amount of oxygen, together with that which is almost certainly associated with the tin, accounts for the high residual oxygen contents of the powders. It would thus appear that, in the absence of tin, oxygen contents of the order of 0.2% might be obtained and that the powders would be stable towards oxygen after this initial re-oxidation had occurred. If sulphur was present in the metal or in the atmosphere, however, the experiments on reduction by coal gas suggest that some addition would have to be made to render the powder stable.

## VI.—SUMMARY

It is possible completely to oxidize tinned copper wire 0.007 in. thick in bulk by roasting at 900° C. for 2 hr. Some cupric oxide is found, but the greater part of the copper exists as cuprous oxide. The oxide is friable and easily broken down in a small ball-mill to powder suitable for reduction. However, there is a tendency for excessive amounts of fines to be produced and in bulk production some form of dry classification might be required to remove the fines as they are formed. The size distribution of the comminuted oxide may be altered by changes in ball-milling practice, but it is not suggested that the results obtained could be applied to a larger mill without further experiment.

Reduction of the comminuted oxide by hydrogen for 1 hr. at 400° C. gives the best results, but some sintering occurs which makes it necessary to break the agglomerates of powder in a mechanical mill. Material of — 300 mesh was largely responsible for the sintering. Coal gas was not satisfactory, as traces of sulphur rendered the powder unstable and liable to discolour when exposed to the atmosphere for periods of up to a month. If it were possible to remove the sulphur completely, coal gas might prove a useful reducing agent. Propane was not capable of reducing the oxide at a temperature below that at which sintering was serious. Partially cracked ammonia gave quicker and more thorough removal of oxygen than any other agent, probably on account of further cracking of the gas on the surface of the oxide in the reducing chamber, with the formation of nascent hydrogen, which diffused into the oxide particles rapidly. Carbon monoxide is a satisfactory reducing agent. Reduction is by a surface reaction, and the surface of the powder is smoother than that of powder reduced by hydrogen. This difference

between the two gases is also responsible for disruption of some of the larger particles when hydrogen is used. Some disruption occurs with carbon monoxide but not to the same extent. The proportion of — 300-mesh material is reduced during reduction by the sintering together of some of the fine particles, and in this case the decrease is greater with hydrogen than with carbon monoxide, indicating that the rough surface of the hydrogen-reduced powder assists in sintering.

Slight agitation of the powder during reduction is beneficial. There is a critical rate of gas flow above which no increase in the rate of reduction is attained.

A comparison between oxide-reduced and commercially available electrolytic and atomized copper powders showed that the apparent density of hydrogen-reduced powder is slightly lower than electrolytically prepared powder and considerably lower than atomized powder. Powder made by carbon-monoxide reduction has an apparent density higher than electrolytic powder but still considerably below that of the atomized product. The flow properties of the oxide-reduced powders are inferior to those of electrolytic or atomized powders of similar size-grading, and this property is seriously affected as the proportion of — 300-mesh material approaches 60%, when flow virtually ceases in the standard Powmet Flow-Factor Meter.

A study of pressed compacts of oxide-reduced powders suggested that particle-size distribution has a very slight effect on density and hence on porosity and compression ratio at any pressure. At compacting pressures of 10 and 60 tons/in.<sup>2</sup> the percentage porosities were about 37 and 9.3%, respectively.

The best properties were obtained by using compacting pressures of 60 tons/in.<sup>2</sup> and sintering temperatures of 600° C. At higher temperatures, with compacting pressures of 40 and 60 tons/in.<sup>2</sup>, the tensile strength was less. Sintering under these conditions is accompanied by large expansions, and it is concluded that any increase in the inter-particle bond strength is more than offset by the development of gas-containing pores in the test-pieces. At compacting pressures of 10 and 20 tons/in.<sup>2</sup>, lower figures for tensile strength are obtained, but sintering at 750° and 1000° C. is accompanied by relatively high shrinkage. At 600° C. the volume changes are very small and the change in hardness is also slight, indicating that sintering has taken place below the recrystallization temperature. At low compacting pressures the strength increases with the proportion of — 300-mesh material present, but with high pressures a very considerable proportion gives inferior results.

The ductility of the sintered compacts as measured by the reduction of area appears to follow closely the tensile strength.

A comparison of the strength and ductility of compacts of electrolytic, atomized, and oxide-reduced powders shows that with compacting pressures of 10 and 20 tons/in.<sup>2</sup> the reduced powder is superior at the three sintering temperatures examined.



With compacting pressures of 40 and 60 tons/in.<sup>2</sup>, the reduced powder gives better tensile properties at sintering temperatures of 600° and 750° C., but at 1000° C. the order is reversed, although the difference between the three powders is not great.

In ductility there is little to choose between the three types of powder until sintering temperatures of 1000° C. are reached. At this temperature, with compacting pressures of 40 and 60 tons/in.<sup>2</sup>, the electrolytic powder gives results superior to those for the reduced powders; even so, the ductility of the electrolytic powder is adversely affected with compacting pressures of 60 tons/in.<sup>2</sup>.

Sintered compacts prepared from hydrogen-reduced powder give better tensile figures than those from carbon-monoxide-reduced powder, but the volume changes accompanying sintering are less with carbon monoxide than with hydrogen.

At high sintering temperatures, when high compacting pressures have been used, the volume changes which accompany the sintering of hydrogen-reduced powder are larger and variable, but under the optimum

condition for obtaining maximum tensile strength (60 tons/in.<sup>2</sup> and 600° C.) shrinkage is 0.6%, as compared with 3% for electrolytic powder under the optimum condition for maximum tensile properties (40 tons/in.<sup>2</sup> and 1000° C.).

Atmospheric oxygen re-oxidizes hydrogen-reduced powder, though when an increase in weight of about 0.2% has been reached, no further oxidation occurs.

#### ACKNOWLEDGEMENTS

The authors are indebted to Durham Chemicals, Ltd., who provided the raw materials for this research, facilities for the grinding of the oxide and for pressing the compacts, and to members of their staff for their co-operation, particularly to Mr. C. E. Pearson for many helpful suggestions in planning the work, and to Mr. C. T. Morley-Smith, who supervised the oxygen determinations. Thanks are also due to Professor A. Preece for his constant interest and advice and for the provision of facilities in the Metallurgy Department of King's College, University of Durham.

#### REFERENCES

1. J. E. Drapeau, Jr., U.S. Patent No. 2,170,814, 1939.
2. W. H. J. Vernon, *J. Chem. Soc.*, 1926, **130**, 2273.
3. J. S. Dunn, *Proc. Roy. Soc.*, 1926, [A], **111**, 210.
4. N. B. Pilling and R. E. Bedworth, *J. Inst. Metals*, 1923, **29**, 529.
5. R. F. Tylecote, *J. Inst. Metals*, 1950-51, **78**, 327.
6. W. H. Coghill and F. D. DeVane, *Missouri School Mines Met. Bull.*, 1938, **13**, 1.
7. W. J. Baëza, "A Course in Powder Metallurgy". New York: 1943 (Reinhold Publishing Corp.).
8. C. E. Ransley, *J. Inst. Metals*, 1939, **65**, 147.
9. C. G. Goetzel, *J. Inst. Metals*, 1940, **66**, 319.
10. J. F. Kuzmick, *Trans. Amer. Inst. Min. Met. Eng.*, 1945, **161**, 612.
11. T. P. Hoar and J. M. Butler, *J. Inst. Metals*, 1950-51, **78**, 351.
12. M. Cook and S. F. Pugh, *Iron Steel Inst. Symposium on Powder Metallurgy, Special Rep. No. 38*, 1947, 162.
13. W. E. Alkins and A. P. C. Hallows, *J. Inst. Metals*, 1935, **56**, 125.

# UNRELATED SIMULTANEOUS INTERDIFFUSION AND 1343 SINTERING IN COPPER-NICKEL COMPACTS\*

By J. M. BUTLER,† M.A., Ph.D., JUNIOR MEMBER, and T. P. HOAR,‡  
M.A., Ph.D., F.I.M., MEMBER

## SYNOPSIS

Metallic interdiffusion during the heat-treatment of 50 : 50 (by volume) copper-nickel powder compacts has been assessed metallographically, and length changes have been followed, dilatometrically. At temperatures (500°–700° C.) below those where sintering begins, there is a large expansion and production of fissures (not found in either pure copper or pure nickel compacts) caused by unequal metallic interdiffusion. At higher temperatures (700°–800° C.), sintering shrinkage, very similar to that found in pure copper compacts, begins; isothermal sintering at 775° C. is also similar to that found with pure copper. These results show that although interdiffusion and sintering can take place simultaneously they are not causally related. It is inferred that neither interdiffusion nor self-diffusion is important as a mechanism for metal transfer in the sintering of metal compacts, which takes place rather by plastic deformation, i.e. slip, creep, or both, of mechanically weak hot metal under the action of surface forces.

## I.—INTRODUCTION

THE sintering of metal powder compacts, when no liquid phase appears, involves the collapse, spheroidizing, and eventual disappearance of the voids present in green compacts. There is widespread agreement<sup>1-6</sup> that the driving force for the process is the available surface energy of the metal particles, which tends to make the total void surface diminish; residual stress in the compressed particles<sup>7</sup> is now generally thought to be an unimportant driving force, since sintering frequently begins only at temperatures well above those necessary for stress-relief or even recrystallization, and indeed readily takes place in unpressed powder agglomerates. There is, however, considerable disagreement as to the mechanism through which the surface driving force acts. Kuczynski<sup>4</sup> studied the sintering of single particles of copper and of silver to plates of the same metal, gauging its progress from the widening of the metal-to-metal bridges; Dedrick and Gerds<sup>8</sup> have similarly studied the sintering of layers of particles. Kuczynski's mathematical analysis of the observed rate of growth led him to believe that sintering occurs by self-diffusion of metal atoms by the vacancy mechanism through the volume of the metal; Cabrera<sup>9</sup> has since shown that a mechanism of surface self-diffusion could also lead to the same functional relationship between metal transport and time. On the other hand, Mackenzie and Shuttleworth<sup>6</sup> have pointed out that the observed rates of compact shrinkage during the early stages of sintering are often much too rapid to be explained by atom-by-atom diffusion, and believe that the mechanism is one of plastic deformation or of creep under the influence of the surface forces. That surface energy

can produce creep shrinkage in fine copper wires at temperatures well below the melting point has been demonstrated by Udin, Shaler, and Wulff<sup>10</sup> in their elegant determination of the surface energy of solid copper.

If self-diffusion is important as a mechanism of metal transfer leading to sintering shrinkage of single-metal compacts, the generally faster interdiffusion might *a fortiori* be expected to be important in the sintering of compacts of two or more metals that interdiffuse. Silver-iron compacts, in which the very small mutual solid solubility makes interdiffusion negligible, undergo sintering very similar to that of a single metal.<sup>11</sup> In copper-zinc, copper-tin, and other mixed compacts of metals forming a series of intermediate phases, it can be shown metallographically that all the expected phases are formed during sintering,<sup>12</sup> but these systems are too complicated for any relationship between the progress of interdiffusion and that of sintering to be readily apparent. Copper-nickel and similar compacts of two metals forming a single solid solution over the entire composition range provide the simplest example of considerable interdiffusion during sintering,<sup>13, 14</sup> but the progress of interdiffusion during the important early stages of heating and of initially rapid sintering does not appear to have hitherto been studied.

In the work now reported the authors have found it possible to follow the progress of interdiffusion in copper-nickel compacts by metallographic examination of these compacts stained at room temperature with the vapour from aqueous ammonium polysulphide. This reagent rapidly forms interference-tint films of cuprous sulphide on copper-nickel solid solutions; the rate of film formation and hence the colour after exposure is sharply dependent on the

\* Manuscript received 25 July 1951.

† British Non-Ferrous Metals Research Association,

London; formerly Research Student, Cambridge University.

‡ Lecturer in Metallurgy, Cambridge University.



copper content, and consequently a semi-quantitative estimate of the progress of interdiffusion is possible. The progress of sintering of the same compacts has been studied dilatometrically by the use of the apparatus we have previously described.<sup>15</sup> The results of the experiments show that, although metallic interdiffusion and sintering can and do occur simultaneously, the two phenomena are not causally related, and also that interdiffusion can, in the early stages of heat-treatment, produce porosity and cause expansions that are the reverse of sintering. We believe it may be inferred from this lack of a relation between interdiffusion and sintering that the slower self-diffusion in single-metal compacts is also of little importance as a mechanism of sintering shrinkage, at least in the rapid early stages, and that consequently a mechanism such as that suggested by Mackenzie and Shuttleworth<sup>6</sup> is in better accord with the facts.

## II.—EXPERIMENTAL PROCEDURE

### 1. MATERIALS

The electrolytic copper powder used was superficially oxidized to 0.11 wt.-% oxygen; we have previously described the preparation, reduction, and controlled oxidation of this powder, and its principal characteristics.<sup>15</sup> The oxygen content of the powder was that found to be the lowest that can be maintained without further appreciable oxidation when the powder is exposed to the atmosphere.

The nickel powder, prepared by the carbonyl process, was supplied by The Mond Nickel Co., Ltd., and had the following characteristics :

Apparent density . . .	2.23 g./c.c.
Tap density . . .	3.17 g./c.c.
Oxygen content (determined by weight of water produced by heating in hydrogen at 850° C.) . . .	0.39 wt.-%.
Flowability (from 60° cone through orifice $\frac{3}{16}$ in. dia. and $\frac{1}{8}$ in. long) . . .	Nil.
Particle-size distribution . . .	The powder was extremely regular in shape and uniform in size; the particles were spherical with an average dia. of 4.5 $\mu$ .

### 2. PREPARATION OF COMPACTS

Cylindrical compacts 5 mm. in dia. and about 3.5 mm. long were prepared in the absence of lubricants with a compacting pressure of 20 tons/in.<sup>2</sup> by the method previously described.<sup>15</sup> The following powders were used :

A. Nickel powder alone.

B. A 50 : 50 mixture by volume of the copper and nickel powders, thoroughly mixed by tumbling.

C. A 50 : 50 mixture by volume of the copper and nickel powders, thoroughly mixed by tumbling and then reduced in hydrogen at 310° C. for 24 hr.

with constant shaking. This powder is referred to as the "low oxide" powder; its oxygen content was 0.1 wt.-%, estimated by weight of water produced by heating in hydrogen at 850° C. Compacts made from it were pressed and sintered as soon after the reduction as possible.

### 3. SINTERING TECHNIQUE

The compacts were sintered in a Chevenard differential dilatometer adapted for use with small specimens with up to 12% length change and for atmospheres other than air.<sup>15</sup> All experiments were performed in duplicate.

### 4. METALLOGRAPHIC TECHNIQUE

Green and sintered compacts were ground on emery papers and finally on 600-mesh carborundum powder mounted in paraffin wax, polished with fine, levigated magnesia on a selvyt pad, and lightly etched in a mixture of ammonium hydroxide and hydrogen peroxide. Copper-rich areas were revealed by the preferential staining of these areas caused by exposing the specimens to ammonium polysulphide vapour. Exposures of a few seconds only stained the very copper-rich areas to first-order interference colours, leaving all else unstained; successively longer exposures were useful in revealing areas progressively poorer in copper. It is proposed to develop this technique in quantitative detail later.

## III.—RESULTS AND INTERPRETATION

### 1. DILATOMETRIC RESULTS

Compacts of the unreduced copper-nickel powder mixture B, pressed at 20 tons/in.<sup>2</sup>, were sintered in hydrogen in the dilatometer. The compacts were heated to 755° C. at the rate of 20° C./min., held at that temperature for various periods of time, and cooled in the furnace at about 30° C./min. The dilation/temperature and dilation/time curves of these compacts were very reproducible; the curves for compacts heated for short times agreed precisely with the early parts of the curves for compacts heated for long times. Typical results are shown in Fig. 1 (a) and (b); evidently, a regular expansion occurs on heating up to about 250° C., whereafter the compact length changes only slightly until a temperature of about 500° C.; this period of little or no expansion is to be associated with the reduction of oxide.<sup>15</sup> Above about 500° C., however, a very marked expansion occurs, continuing up to 755° C. and, indeed, into the isothermal period of the treatment (Fig. 1 (b)); the expansion is maximal after about 10 min. at 755° C. The compact thereafter shrinks, rapidly at first and then more slowly, at rates comparable with those previously found for copper compacts,<sup>15</sup> for which dilation/temperature and dilation/time curves are included in Fig. 1 for comparison.



FIG. 5.—Green State.

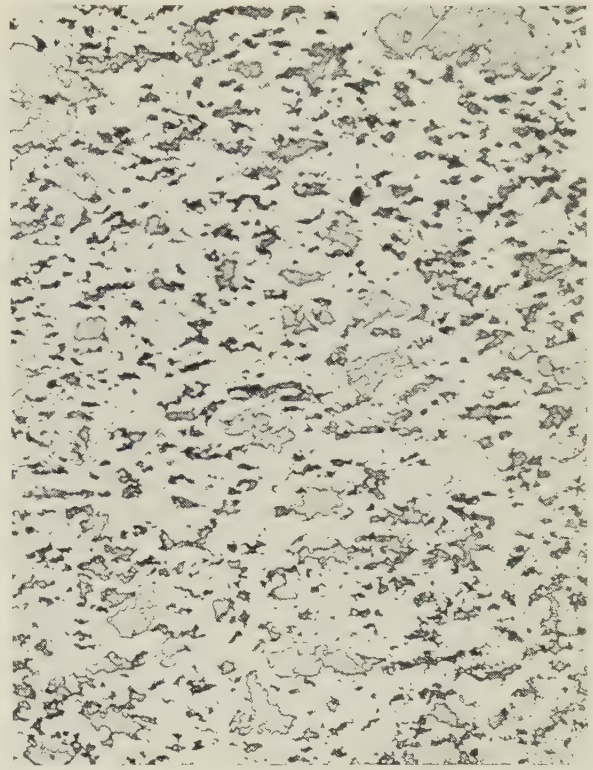


FIG. 6.—Heated to 755° C. in Hydrogen and Furnace Cooled.

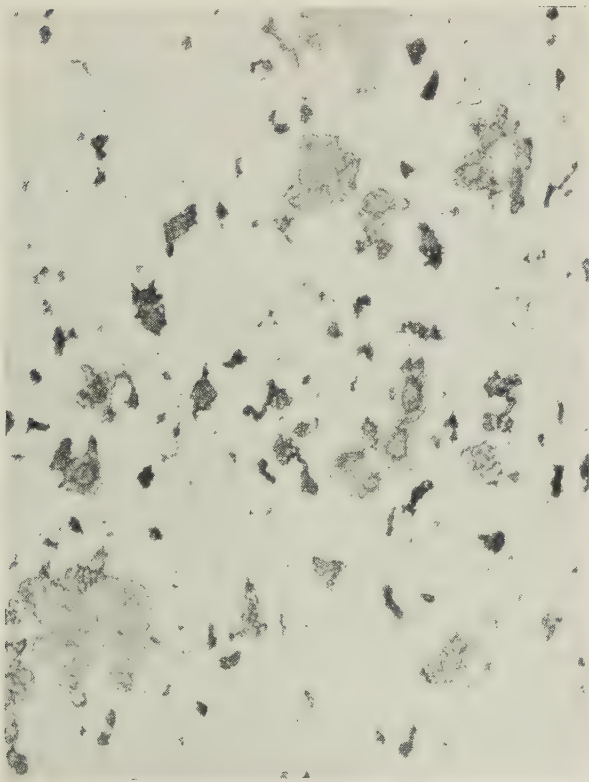


FIG. 7.—Heated at 755° C. in Hydrogen for 2 Hr.

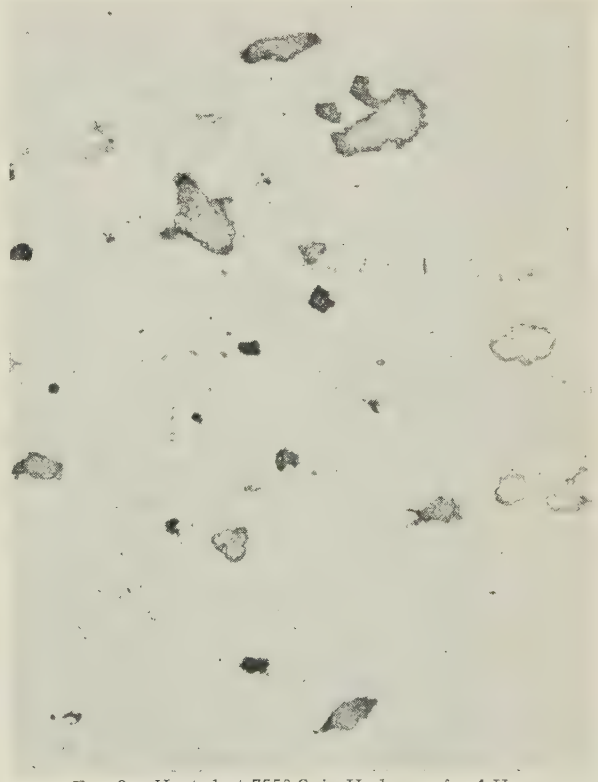


FIG. 8.—Heated at 755° C. in Hydrogen for 4 Hr.



PHOTOMICROGRAPHS OF COPPER-NICKEL COMPACTS.

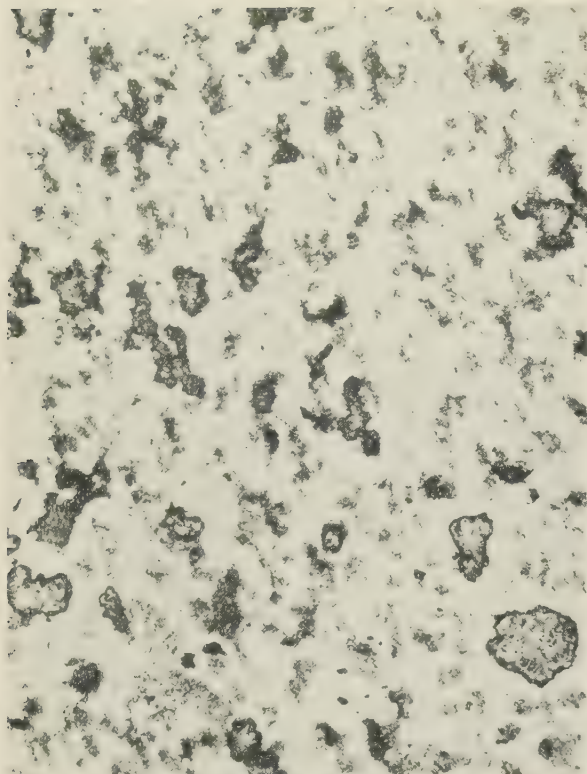


FIG. 9.—Heated at 755° C. in Hydrogen for 2 Hr. Heavily stained with polysulphide vapour.  $\times 100$ .

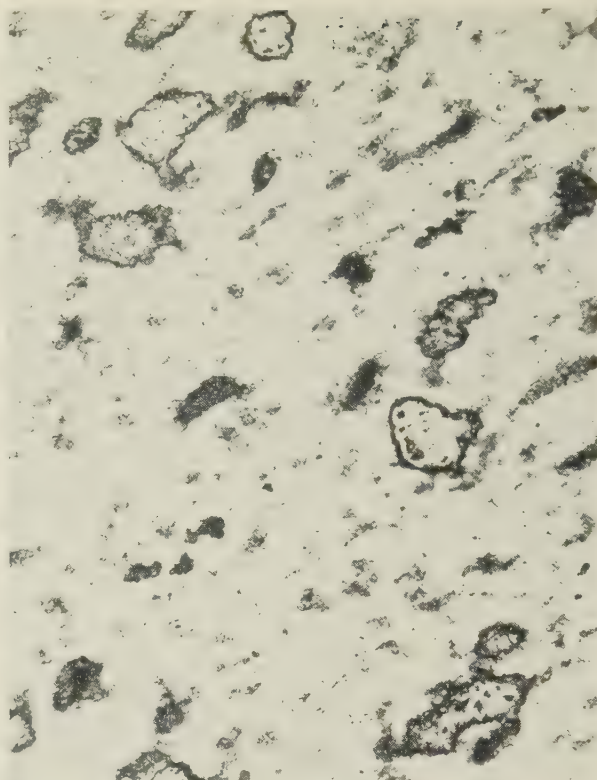


FIG. 10.—Heated at 755° C. in Hydrogen for 4 Hr. Heavily stained with polysulphide vapour.  $\times 100$ .



FIG. 11.—Heated at 755° C. in Hydrogen for 2 Hr. Showing porosity. Flowed layer removed, unstained.  $\times 1500$ .



FIG. 12.—As Fig. 11, but stained with polysulphide to approximately first-order interference colours.  $\times 1500$ .

Further dilatometric experiments were made to establish the cause of the expansion: (i) compacts of the nickel powder *A* were heated in hydrogen in the dilatometer to 755° C. at a rate of 20° C./min., (ii)

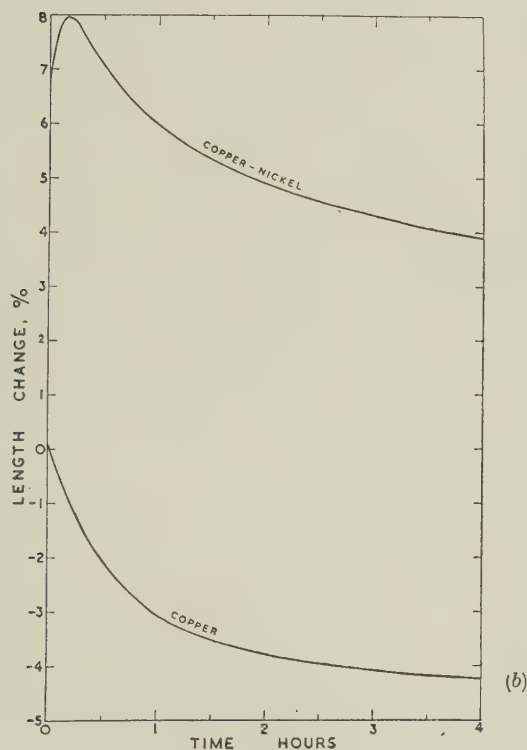
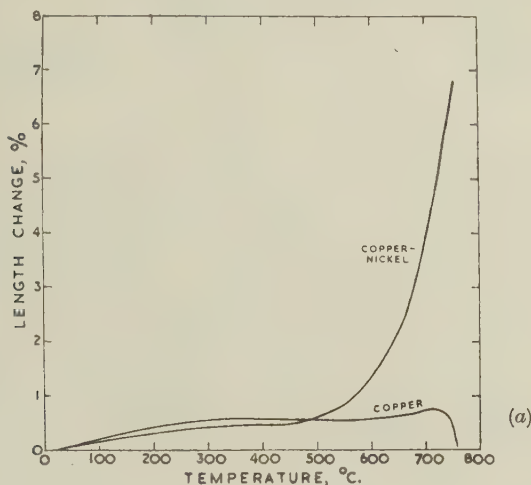


FIG. 1.—Length Changes During Heat-Treatment of Unreduced 50 : 50 (by volume) Copper-Nickel and Copper Compacts.

(a) Dilation/Temperature Curves. Heating rate: 20° C./min.  
(b) Dilation/Time Curves at 755° C.

compacts of the low-oxide copper-nickel powder *C* were heated in hydrogen and in argon in the dilatometer to 755° C. at a rate of 20° C./min.; and (iii) compacts of the unreduced mixture *B* were heated in hydrogen in the dilatometer to 900° C. at 20° C./

min. Typical dilation/temperature curves obtained in these experiments are shown in Figs. 2, 3, and 4,

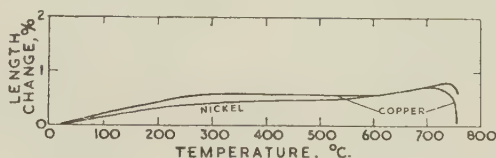


FIG. 2.—Dilation/Temperature Curves of Copper and Nickel Compacts Heated in Hydrogen to 755° C. Heating rate: 20° C./min.

together with the curve previously obtained<sup>15</sup> for compacts of the original copper powder pressed at 20 tons/in.<sup>2</sup> and heated in hydrogen to 755° C. at the rate of 20° C./min.

It may be seen that no abnormal expansion occurs during the heating of nickel compacts (Fig. 2). Clearly, therefore, the marked expansion of copper-nickel compacts is not a characteristic of the sintering of nickel.

The dilation/temperature curves of the low-oxide copper-nickel compacts heated to 755° C. in argon and in hydrogen (Fig. 3) are almost identical and very similar to those obtained by heating compacts of the unreduced powder in hydrogen (Fig. 1 (a)). Above about 250° C. the curves for the unreduced powder tend to lie slightly below those for the low-oxide powder; this is due to the small decrease of volume that occurs when the oxide in the former compacts is reduced to metal. However, it is clear that the expansion occurring above about 500° C. cannot be due to the production of gas by oxide reduction, since the expansion that occurs during the heating of compacts made from low-oxide powder is almost identical with that found during the heating of compacts made from the unreduced powder; furthermore, the expansion is still found when the compacts are heated in non-reducing argon.

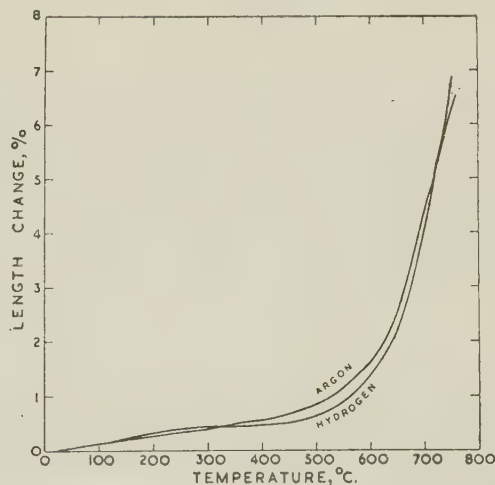


FIG. 3.—Dilation/Temperature Curves of Low-Oxide Copper-Nickel Compacts Heated to 755° C. in Hydrogen and in Argon. Heating rate: 20° C./min.



Compacts of the low-oxide powder heated at a rate of 20° C./min. to 900° C. (Fig. 4) give an expansion beginning at 550° C. and maximal at 800° C., followed by an extensive and rapid shrinkage. The maximum length increase is very nearly the same as that attained on heating compacts of unreduced powder to 755° C. and holding them at that temperature for about 10 min. (Fig. 1 (b)). This result, and the observed continuation of the expansion during isothermal treatment, indicate that the effect is not

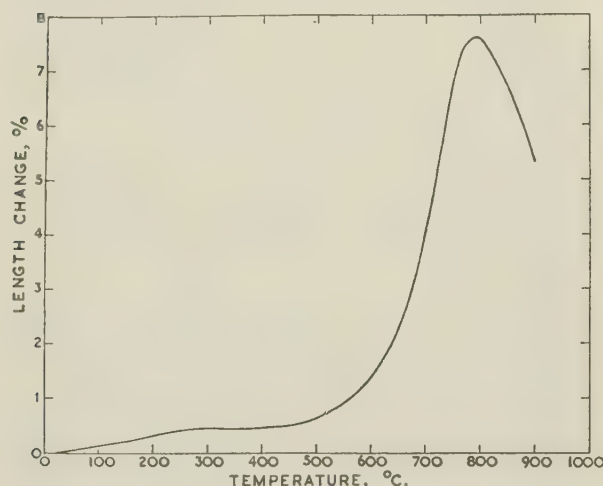


FIG. 4.—Dilation/Temperature Curve of Unreduced Copper-Nickel Compact Heated in Hydrogen to 900° C. Heating rate: 20° C./min.

due to differential thermal expansion of the two components of the compacts, a view supported by the known small difference in the coefficients of thermal linear expansion of solid copper and nickel,  $16.6 \times 10^{-6}$  and  $13.3 \times 10^{-6}$  cm./cm./°C. respectively.

It is highly probable, therefore, that the expansion is caused solely by metallic interdiffusion, as discussed in detail in the following section.

## 2. METALLOGRAPHIC RESULTS

Photomicrographs of a green copper-nickel compact, of a compact heated to 755° C. and immediately furnace-cooled, and of compacts held at 755° C. for 2 and 4 hr., are given in Figs. 5, 6, 7, and 8 (Plate XXXVI) respectively. The polysulphide staining was regulated to give films no thicker than those showing second-order interference colours, so that only areas rich in copper, where little nickel has penetrated, are stained. It will be seen that some reduction in the extent of the copper-rich areas occurs in compacts heated to 755° C. and at once cooled. Furthermore, the number of such copper-rich areas diminishes rapidly when the compacts are heated at 755° C.; after 2 hr. at this temperature the number of such areas is considerably reduced, and few remain after 4 hr.

However, heavy staining by polysulphide vapour of the 2- and 4-hr. sintered compacts reveals an

abundance of moderately copper-rich areas (Figs. 9 and 10, Plate XXXVII), doubtless located at the sites of the original copper particles in the green compacts. Thus homogenization even in the 4-hr. sintered compacts is by no means complete.

The results of these experiments show that interdiffusion in 50:50 copper-nickel compacts begins during the expansion phase of their heat-treatment, continues during the subsequent sintering shrinkage (of which the rate is substantially the same as that of pure copper compacts), but has not produced alloy homogeneity even after a 4-hr. treatment at 755° C., when sintering equivalent to that found in pure copper compacts has occurred. These facts jointly suggest that interdiffusion is not an important mechanism of sintering shrinkage, but rather that the two phenomena are largely independent.

Examination of sintered copper-nickel compacts under high magnification shows that many areas, appearing under lower magnifications as diffuse, unresolved patches, are regions of high porosity, containing elongated fissures (Fig. 11, Plate XXXVII). Staining to first-order interference colours with ammonium polysulphide vapour shows that these regions of high porosity are always closely associated with a copper-rich area, in which appears a network of metal less heavily stained than the surrounding material (Fig. 12, Plate XXXVII). This network is evidently relatively nickel-rich, presumably resulting from rapid diffusion of nickel along the grain boundaries within the polycrystalline (probably recrystallized) copper particles, and slower lattice diffusion from the grain boundaries into the grain margins. The diffusion rate of copper into nickel at 755° C. is less than that of nickel into copper,<sup>16-19</sup> and consequently there is a net transfer of material into the copper particles, causing them to expand. Owing to the rigidity of the cupro-nickel alloy thus formed, this expansion cannot all be accommodated by the space left by diffusion of nickel, but causes rupture of cold-welded areas, creates fissures in and near the original copper particles, and leads to the overall expansion described above. This view accords with recent work on the sintering of binary mixtures of gold and silver with other metal powders,<sup>11</sup> in which similar "diffusion porosity" was observed in systems known to form solid solutions.

It thus appears that interdiffusion in mixed metal powder compacts may create extensive porosity, in opposition to the surface forces tending to reduce porosity, and hence may somewhat delay sintering.

## IV.—DISCUSSION

The interdiffusion process is evidently able to produce expansion and porosity in opposition to sintering shrinkage at temperatures where the mechanical properties of cupro-nickel are suitable. It is of some interest to estimate the relative driving forces available for interdiffusion and for sintering caused by the decrease of surface.

The total available interdiffusion driving force (to produce complete composition homogeneity) is, in the system studied, simply the integral free energy of mixing for a 50:50 (by volume) copper-nickel mixture. Experimental data are lacking; but if ideal solution is assumed (a near approximation in this system) the free energy of mixing per gramme molecule is

$$\Delta G_M = RT(N_{\text{Cu}} \log_e N_{\text{Cu}} + N_{\text{Ni}} \log_e N_{\text{Ni}})$$

where  $R$  is the gas constant,  $T$  is the absolute temperature, and  $N_{\text{Cu}} = 0.48$  and  $N_{\text{Ni}} = 0.52$  are the mol fractions of copper and nickel respectively in their 50:50 by volume mixture. At  $755^\circ\text{C}$ .,  $\Delta G_M$  is about 1400 cal./g. mol.

The total available surface energy per gramme-molecule (to produce complete densification) can be only very approximately assessed. A liberal estimate may be made by assuming spherical particles of diameter  $2\ \mu$ —considerably smaller than the known sizes of the irregular powder particles. With usual values for the metal densities, this gives a total surface area per gramme molecule of 50:50 by volume copper-nickel mixture of some  $2 \times 10^5\text{ cm}^2$ , and if the surface energies of the metals are taken as about 1500 ergs/cm.<sup>2</sup>, the total available surface energy is about 7 cal./g.-mol. This is so very much smaller than the total energy available for interdiffusion that the predominance of the expansion caused by interdiffusion over the shrinkage caused by surface decrease—where the mechanical properties are suitable—is not at all surprising. Of course, a complete discussion of the matter would include consideration of the relative rates of the expansion and shrinkage processes, which depend upon activation-energy or resistance terms as well as upon the relative available driving forces. The application of quantitative rate theory to the present complex process involving interdiffusion and plastic flow is probably not yet profitable; but it may be pointed out that the resistance of the compact to plastic deformation is certainly much more highly temperature-dependent than is the resistance to interdiffusion, so that it is quite reasonable to find the expansion caused by interdiffusion overcome by the sintering shrinkage when the temperature is high enough.

The production of mechanical pressure by unequal diffusion of matter across an interface is a well-known effect in osmosis; indeed, the swelling pressure produced by the growing cupro-nickel particles may be regarded as an osmotic pressure. Just as in conventional liquid osmosis the continued maintenance of such a pressure depends on the mechanical ability of a semi-permeable membrane to sustain it, so in the present case the maintenance of the expansive condition can continue only while the cupro-nickel has sufficient mechanical strength. A rise of tempera-

ture into the region where creep or slip under the small surface forces becomes rapid leads to rapid sintering shrinkage, quite independent of the interdiffusion process. Also, under isothermal conditions, expansion will continue only while the interdiffusion process remains rapid enough to counter the sintering shrinkage-rate at the particular temperature.

The general conclusion that sintering is not assisted, and in the present case is hindered, by interdiffusional movement of metal is quite evident. The inference that the much slower self-diffusion is also unimportant as a sintering mechanism is almost as clear; to suppose that a rise of temperature from some  $700^\circ\text{C}$ ., where the expansion caused by interdiffusion is predominant, to  $800^\circ\text{C}$ ., where rapid sintering shrinkage sets in (Fig. 4), produces so great an increase of the rate of self-diffusion that this mechanism can account for the now predominant rapid shrinkage is scarcely reasonable. But this rise of temperature would be expected to produce just such a marked decrease in mechanical strength and increase of creep-rate as could account for plastic deformation (slip, creep or both), even under the small surface forces, sufficient to produce void collapse and sintering shrinkage independent of any kind of atom-by-atom diffusion.

Further evidence in favour of a non-diffusional sintering mechanism is provided by well-established phenomena in the hot-pressing of compacts:<sup>20-22</sup> by using quite low pressures, densification equivalent to that produced by unassisted sintering can be obtained in shorter times and at lower temperatures, a result inexplicable in terms of a diffusional mechanism but in harmony with one of plastic deformation. Again, Christensen and Calbick<sup>23</sup> have detected by electron microscopy the formation of terraces  $10^{-6}$  to  $2 \times 10^{-5}$  cm. high on the surface of metal particles during sintering; the conclusion that these terraces are slip bands formed during plastic deformation<sup>24</sup> can scarcely be escaped.

We do not suggest that diffusional movement of matter is *never* of any importance in sintering. We have previously pointed out<sup>15</sup> that the *very slow* final densification of compacts, with the removal of gas-filled closed voids, may well depend upon diffusion of gas molecules through metal lattices by a vacancy mechanism. We believe, however, that the evidence is now conclusive that the rapid early stages of sintering, which are of such great importance in practice, take place by plastic deformation independent of any atom-by-atom diffusion.

#### ACKNOWLEDGEMENT

The authors' thanks are due to the Department of Scientific and Industrial Research for a Maintenance allowance to one of them (J. M. B.), during the tenure of which the work was carried out.



## REFERENCES

1. J. Frenkel, *J. Physics (U.S.S.R.)*, 1945, **9**, 385.
2. F. N. Rhines, *Trans. Amer. Inst. Min. Met. Eng.*, 1946, **166**, 474.
3. A. J. Shaler, *Trans. Amer. Inst. Min. Met. Eng.*, 1949, **185**, 796.
4. G. C. Kuczynski, *Trans. Amer. Inst. Min. Met. Eng.*, 1949, **185**, 169.
5. F. N. Rhines, C. E. Birchenall, and L. A. Hughes, *Trans. Amer. Inst. Min. Met. Eng.*, 1950, **188**, 378.
6. J. K. Mackenzie and R. Shuttleworth, *Proc. Phys. Soc.*, 1949, [B], **62**, 833.
7. G. Grube and H. Schlecht, *Z. Elektrochem.*, 1938, **44**, 367.
8. J. H. Dedrick and A. Gerdts, *J. Appl. Physics*, 1949, **20**, 1042.
9. N. Cabrera, *Trans. Amer. Inst. Min. Met. Eng.*, 1950, **188**, 667.
10. H. Udin, A. J. Shaler, and J. Wulff, *Trans. Amer. Inst. Min. Met. Eng.*, 1949, **185**, 186.
11. E. Raub and W. Plate, *Z. Metallkunde*, 1949, **40**, 206.
12. P. Duwez, Internat. Symposium on Powder Metallurgy, Graz, 1948; for abridged report see *Metal Ind.*, 1948, **73**, 103, 129.
13. F. N. Rhines and R. A. Colton, *Trans. Amer. Soc. Metals*, 1942, **30**, 166; also *Powder Metallurgy (Amer. Soc. Metals)*, 1942, 67.
14. P. Duwez and C. B. Jordan, *Trans. Amer. Soc. Metals*, 1949, **41**, 194.
15. T. P. Hoar and J. M. Butler, *J. Inst. Metals*, 1950-51, **78**, 351.
16. G. Grube and A. Jedele, *Z. Elektrochem.*, 1932, **38**, 799.
17. P. P. Belyaev and A. A. Sladkov, *Vestn. Metalloprom.*, 1936, **16**, 95.
18. S. D. Gertzriken and M. A. Faingold, *Mem. Phys., Kiev*, 1940, **8**, 127.
19. L. C. C. da Silva and R. F. Mehl, *Trans. Amer. Inst. Min. Met. Eng.* (in *J. Metals*), 1951, **191**, 155.
20. F. Sauerwald, *Z. Metallkunde*, 1929, **21**, 22.
21. W. Trzebiatowski, *Z. physikal. Chem.*, 1934, [A], **169**, 91.
22. C. G. Goetzel, *Metals and Alloys*, 1940, **12**, 30.
23. H. Christensen and C. J. Calbick, *Phys. Rev.*, 1948, [ii], **74**, 1219.
24. A. F. Brown, *Metallurgical Applications of the Electron Microscope (Inst. Metals Monograph No. 8)*, 1950, 103.

# HEAT-TREATMENT OF TITANIUM-RICH TITANIUM-IRON ALLOYS\*

1344

By H. W. WORNER,† M.Sc., MEMBER

## SYNOPSIS

An exploratory investigation of the heat-treatment of titanium alloys containing 2-9.5 wt.-% iron is described. It has been shown that alloys with 2-6% iron can be hardened appreciably by water-quenching them from the  $\beta$ -titanium-iron solid-solution region. Some of the alloys which could be retained as  $\beta$ -solid solutions by water-quenching exhibited age-hardening effects when heated for a few hours in the range 220°-450° C.

## I.—INTRODUCTION

In an earlier investigation,<sup>1</sup> the author has established the general outlines of the titanium-iron constitutional diagram from titanium up to the intermetallic phase FeTi. It has been shown that the  $Ti_{\alpha} \rightleftharpoons Ti_{\beta}$  transformation-temperature range is depressed by the addition of iron to titanium. Whereas the maximum solid solubility of iron in  $\beta$ -titanium is 18-20 wt.-% from 600° to 900° C., the  $\alpha$ -solid-solution in the same temperature range is very restricted, being less than 1%. There is a eutectoid point lying approximately at 17% iron and 600° C., the products of the eutectoid change being the inter-

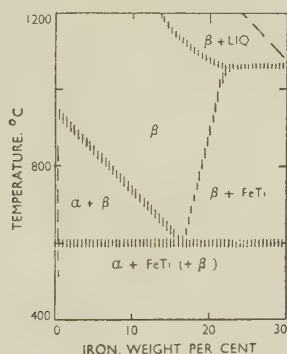


FIG. 1.—Titanium-Rich Portion of the Constitutional Diagram for Titanium-Iron Alloys Based on Commercially Pure Titanium.

metallic phase FeTi and  $\alpha$ -titanium with no more than 1% iron in solution.

The above features of the titanium-rich portion of the titanium-iron constitutional diagram are shown in Fig. 1. The  $\beta \rightarrow \alpha + FeTi$  eutectoid change has proved to be very sluggish. Even when heated for 3 weeks at temperatures of about 575° C., alloys close to the eutectoid composition still exhibited some residual  $\beta$ -solid solution. Thus the region below 600° C. in Fig. 1 is labelled  $\alpha + FeTi (+\beta)$ .

It is worthy of note that Fig. 1 pertains to alloys of commercial purity, i.e. alloys based on titanium made by the Kroll process.

Alloys containing less than 3.8% iron can not be retained as  $\beta$ -solid solutions by water-quenching from the  $\beta$  region in Fig. 1. This heat-treatment causes low-iron alloys to develop Widmanstätten structures like that shown in Fig. 2 (Plate XXXVIII). Such structures have also been found in titanium quenched from temperatures in the  $\beta$  range, and they have been taken as evidence of a rapid  $\beta \rightarrow \alpha$  transformation that occurs during the quench. X-ray-diffraction experiments have indicated that a more or less complete  $\beta \rightarrow \alpha$  change does actually occur when pure titanium is quenched from the  $\beta$  range. However, the X-ray-diffraction evidence of a 2% iron alloy water-quenched from 950° C. has not been very conclusive; there are some weak, broad reflections at low Bragg angles corresponding to  $\alpha$ -titanium, but no reflections which would indicate the retention of any  $\beta$  phase.

When water-quenched from the  $\beta$  field in Fig. 1, alloys containing 3.8% or more iron can be retained as  $\beta$ -solid solutions, the microstructures of which are illustrated by Fig. 3 (Plate XXXVIII). Little comment can be made on the existence of sub-boundaries in some grains of retained  $\beta$  solutions (cf. Fig. 3, Plate XXXVIII). It is perhaps worth noting that the existence of sub-boundaries does not appear to be related directly to the mechanical history of the alloys. The sub-boundaries have been observed in quenched specimens which have not received any previous mechanical working, just as they have also been found in specimens which have been hot and cold worked before the quenching treatment.

In view of the above general observations on the structure of quenched alloys, it was thought that it might prove possible to vary appreciably the mechanical properties of titanium-iron alloys by heat-treatments involving quenching from the  $\beta$  region and perhaps subsequent reheating to lower temperatures. It was considered that the development of Widman-

\* Manuscript received 16 April 1951.

† Senior Research Officer, Physical Metallurgy Section,

Commonwealth Scientific and Industrial Research Organization, Baillieu Laboratory, University of Melbourne, Australia.



stätten structures like that shown in Fig. 2 (Plate XXXVIII) might well be accompanied by hardening. It was also thought that  $\beta$ -solid solutions retained by quenching might be strengthened by reheating to comparatively low temperatures at which there might be a tendency for phases that were stable at low temperatures to form in a very finely dispersed form. These ideas formed the basis of the investigation to be outlined in the present paper.

Because of a marked tendency to intergranular cracking, alloys containing more than 9.5% iron could not be safely worked, even at temperatures as high as 900° C. Thus most of the investigation was limited to the composition range 1-9.5% iron.

## II.—EXPERIMENTAL

### 1. PREPARATION OF ALLOYS

All the alloys were made by melting iron and titanium powders together in an argon-arc furnace. The iron powder was made by the carbonyl process at the General Aniline Works, New Jersey, U.S.A. The titanium powder was made by the Kroll process in the laboratories of the U.S. Bureau of Mines. The chief impurities in the titanium were: oxygen 0.2, nitrogen 0.05, carbon 0.1, iron 0.2, and silicon 0.05 wt.-%.

Table I contains a list of the whole range of alloys employed in the work. The iron content of each alloy was determined by analysis.

TABLE I.—Alloys Used in the Investigation.

Alloy No.	Iron Content		Alloy No.	Iron Content	
	Wt.-%	At.-%		Wt.-%	At.-%
1	1.06	0.92	8	9.5	8.25
2	2.06	1.78	9	12.0	10.5
3	3.08	2.70	10	13.5	11.8
4	3.79	3.30	11	16.2	14.2
5	4.07	3.50	12	18.5	16.3
6	5.9	5.2	13	20.4	18.0
7	8.7	7.6	14	22.5	20.0

Alloys containing 1-9.5 wt.-% iron were homogenized by hot working at 700° C. and heating at 1000° C. for 30-40 hr. in argon. Since specimens with more than 9.5% iron could not be hot worked, they were homogenized by simply heating to 1000°-1030° C. in argon for about 50 hr. The author's earlier paper<sup>1</sup> may be consulted for a more detailed treatment of alloy preparation.

### 2. HEAT-TREATMENT TECHNIQUES

Heating in the  $\beta$  region before quenching was effected by immersing the specimens in a charcoal-covered bath of molten tin. As a general rule, heating for 10-20 min. at temperatures in the range 750°-950° C. was sufficient to produce wholly  $\beta$ -structures. The heating in molten tin caused slight superficial contamination of the specimens with

oxygen and tin. The contaminated layer was removed by pickling in a cool mixture of concentrated nitric acid (4-5 parts by volume) and 50% hydrofluoric acid (1 part by volume).

Either a molten salt bath or molten tin was used for reheating to produce age-hardening or tempering effects. The thin oxide coatings caused by these comparatively low-temperature treatments were removed by means of the nitric-hydrofluoric acid mixture.

### 3. HARDNESS OF QUENCHED ALLOYS

The hardness/composition relationship for alloys quenched from the  $\beta$  region is presented graphically in curve A of Fig. 5 (Plate XXXIX). The outstanding feature of the results is the fact that the hardness rises rapidly to a maximum at 4% iron, falls steeply to a minimum near 9.5 and 12% iron, and then the increase in hardness with increasing iron content follows a fairly smooth, progressive course in a manner which might have been expected over the whole composition range if unaltered  $\beta$ -solid solutions had been retained by the water-quench from 950° C. It has already been mentioned in the introduction that alloys containing up to 3% iron cannot be retained in the  $\beta$  form by quenching, and it might well be expected that the sudden change occurring in these alloys during a quench from 950° C. would cause some hardening. But it is very interesting to note that the quenched 4.07 and 5.9% iron alloys, both of which appear to consist of retained  $\beta$ , are also hard by comparison with quenched  $\beta$  alloys of higher iron content. It would seem that the 4.07 and 5.9% alloys may not actually be strictly unaltered  $\beta$ -solid solutions after the quench and the evidence obtained from observation under the microscope is inconclusive. X-ray-diffraction experiments on quenched powders yield patterns with broad lines, not only in the case of the 4.07 and 5.9% alloys, but also for retained  $\beta$ -solid solutions of higher iron content. At present it would be premature to attempt a detailed explanation for the comparative hardness of the 4.07 and 5.9% alloys after quenching from the  $\beta$  field.

Curve B in Fig. 5 indicates how the hardness increases with increasing iron content when the alloys have been brought close to equilibrium at 650° C. by heating at this temperature for at least 5 hr. after furnace cooling from 950° C. After this heat-treatment, alloys containing 1-13.5% iron consist of mixtures of  $\alpha$ -titanium and  $\beta$ -solid solution containing about 15% iron, the two phases being arranged in a Widmanstätten pattern similar to the well-known annealed ( $\alpha + \beta$ )-brass structures (cf. ref. 1). The 16.2% iron alloy quenched from 650° C. simply consists of retained  $\beta$ -solid solution and as would be expected, its hardness is practically identical with that of the same alloy quenched from 950° C. The 18.5, 20.4, and 22.5% iron alloys quenched from 650° C. consist of retained  $\beta$ -solid solution together with a small proportion of the intermetallic phase FeTi. These

latter structures are a little softer than the  $\beta$ -solid solutions of higher iron content retained by quenching from 950° C.

Comparison of curves *A* and *B* in Fig. 5 clearly reveals the extent to which the mechanical properties of alloys in the range 2-6% iron might be varied by quenching treatments. The points pertaining to curve *B* represent, for all practical purposes, the softest condition of the alloys. Heat-treatments at lower temperatures, even in the  $\alpha + \text{FeTi} (+\beta)$  field of Fig. 1, do not cause any reductions in hardness.

#### 4. EFFECTS OF HEATING QUENCHED ALLOYS IN THE RANGE 100°-750° C.

The results discussed in the previous section suggested that alloys quenched from the  $\beta$  region might exhibit age-hardening characteristics. This possibility was explored by means of some preliminary experiments in which the period of reheating or "ageing" after the quench was kept constant at 20 min. The effects which were obtained are shown graphically in Fig. 6 (Plate XXXIX). It was found that reheating the quenched  $\beta$ -solid solution alloys containing 4-9.5% iron caused hardening. The temperature range in which hardening occurred varied according to the iron content, as can be seen in Fig. 6. Reheating alloys with less than 4% iron content caused little effect until 350° C. was exceeded; then softening was observed.

There were no microstructural changes corresponding to the maxima in the curves shown in Fig. 6. However, 20 minutes' heating at 650° and 750° C. caused changes in microstructure, presumably due to precipitation of  $\alpha$ -titanium, and the final structures were of the type illustrated in Fig. 4 (Plate XXXVIII).

#### 5. AGE-HARDENING EFFECTS

Because the results recorded in Fig. 6 demonstrated the possibility of producing appreciable age-hardening effects in some of the alloys, an exploratory study of these effects was undertaken. Attention was concentrated chiefly on alloys containing 3.8, 5.9, 8.7, and

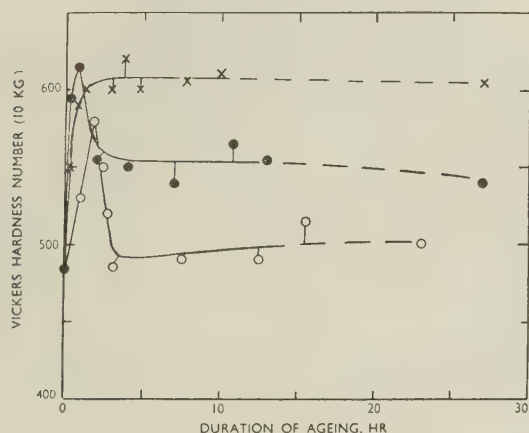


FIG. 7.—Age-Hardening of 5.9% Iron Alloy Water-Quenched from 950° C.

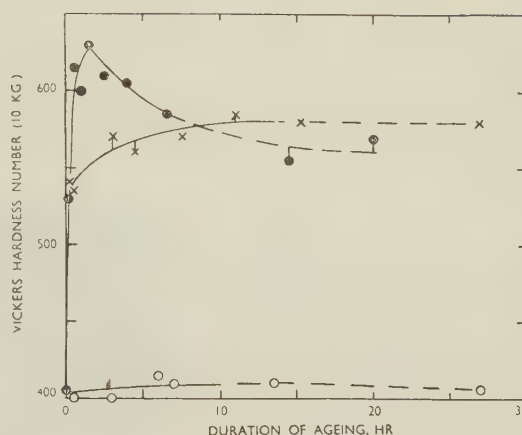


FIG. 8.—Age-Hardening of 8.7% Iron Alloy Water-Quenched from 950° C.

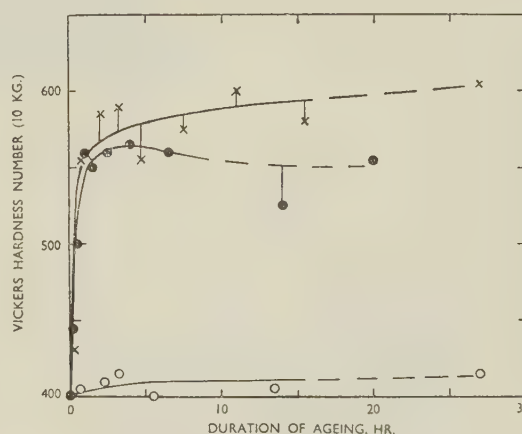


FIG. 9.—Age-Hardening of 9.5% Iron Alloy Water-Quenched from 950° C.

KEY.

○ Aged at 220° C.    × Aged at 360° C.    ● Aged at 440° C.

9.5% iron and the ageing treatments were conducted at three temperatures, namely 220°, 360°, and 440° C.

The 3.8% iron alloy exhibited no definite tendency to age-harden at 220° C., even after about 36 hr. heating, and only a slight tendency at 360° C. At this latter temperature, a maximum hardness of 515 V.P.N. was attained after 45 minutes' heating; thereafter slow softening occurred. Heating at 440° C. for only 15 min. caused a definite drop in hardness to occur and the softening proceeded as the duration of heating was increased. It would appear that the 3.8% alloy, like the 2.06 and 3.08% alloys, is practically in its hardest condition after quenching from the  $\beta$  region.

The 5.9, 8.7, and 9.5% iron alloys exhibited rather more interesting tendencies to age-harden as is shown in Figs. 7, 8, and 9. Striking increases in hardness were observed in the 8.7 and 9.5% alloys aged for a few hours at both 360° and 440° C. Softening tended to occur in all three alloys when ageing at 440° C. was extended beyond 2-4 hr.



The 5.9% alloy exhibited a rather peculiar age-hardening effect on heating at 220° C. Hardening developed if the duration of heating was  $\frac{3}{4}$ –2½ hr. However, further heating at 220° C. left the hardness at its original value for the "as-quenched"  $\beta$  alloy. No definite explanation of this phenomenon can yet be offered.

A very interesting feature of all the age-hardened alloys represented in Figs. 7, 8, and 9, including those in which over-ageing had occurred, was that their microstructures did not differ from those of the initial "as-quenched" alloys. Evidences of definite structural change were noted under the microscope only after the alloys had been very seriously over-aged. For example, after the 5.9% iron alloy had been kept at 440° C. for about 60 hr. and its hardness had dropped to 505 V.P.N., it possessed the structure illustrated in Fig. 4 (Plate XXXVIII). From this microphotograph, it is evident that the breakdown of the  $\beta$ -solid solution had occurred along crystallographic planes within the crystals, but beyond this, little can yet be stated concerning the nature of the age-hardening and over-ageing phenomena in these alloys.

The 16.2% iron alloy was subjected to a few ageing trials. Earlier work by the author<sup>1</sup> had indicated that the  $\beta$ -solid solutions close to the eutectoid composition decomposed only very slowly even at temperatures as high as 550°–600° C. It was therefore of some interest to ascertain whether age-hardening could be produced in such high-iron alloys. Actually, it was found that no age-hardening occurred in the 16.2% alloy when heated for periods up to 21 hr. at 220°, 360°, and 440° C. Likewise, these ageing treatments caused no change in microstructure.

### III.—POSSIBLE USEFULNESS OF ALLOYS

A survey of the results presented in this paper suggests that all alloys in the range 2–9.5% iron have interesting possibilities as heat-treatable materials. Practically, the alloys of greatest interest are probably those with 2.06, 3.08, and 3.8% iron. In this composition range, the alloys in their softened state are fairly easily shaped by working and machining. They can be hardened by simply water-quenching from about 950° C. After the quench-hardening, they can be tempered back to levels of hardness which might be suitable for a wide variety of practical applications.

Some results obtained in tensile tests on 2.06 and 3.8% iron alloys are recorded in Table II.

The results in Table II were obtained from specimens which were prepared under ideal conditions in the laboratory and it would be practically impossible to reproduce this quality of alloy on a commercial scale. However, while keeping this factor in mind, it can be stated that the properties of the heat-treated

alloys are very impressive. It would seem that this type of alloy is worthy of further study.

Although the 5.9, 8.7, and 9.5% iron alloys exhibit striking age-hardening effects, their appeal to the engineer is not likely to be very great, largely because they are difficult to cold-work and machine when in

TABLE II.—Some Mechanical Properties of Titanium Alloys Containing 2.06 and 3.8% Iron

Tensile test-bars:  $\frac{3}{16}$  in. dia., 1 in. gauge-length.

Fe, wt.-%	Heat-Treatment	Property		
		Vickers Hardness Number	Ultimate Tensile Stress, tons/in. <sup>2</sup>	Elonga- tion, % on 1 in.
2	Softened *	260	44	10
	W.Q. 950° C. Tempered for $\frac{1}{4}$ hr. at 440° C.	395	94	4
3.8	Softened *	305	61	7
	W.Q. 950° C. Tempered for $\frac{1}{4}$ hr. at 500° C.	445	106	3

\* Cooled at 20° C./min. from 950° to 650° C., held for 6 hr., and finally water-quenched.

their softest condition. Moreover, they tend to be brittle in the hardened condition, especially if the final hardness is above 450 V.P.N.

A problem encountered in the heat-treatment of all the alloys was the tendency for undesirably rapid grain growth to occur during heating in the  $\beta$  region. Unfortunately, it did not prove possible to refine the grain-size by heat-treatment alone. It was found that the only effective methods for grain refinement were:

(i) Hot working in the range 650°–800° C., followed by heating to about 20° C. above the  $\beta/(\alpha + \beta)$  boundary for  $\frac{1}{4}$ – $\frac{1}{2}$  hr.

(ii) Cold working followed by the same annealing treatment as outlined under (i).

### ACKNOWLEDGEMENTS

The investigation formed part of the programme of the Physical Metallurgy Section of the Commonwealth Scientific and Industrial Research Organization, Australia. This section is associated with the Baillieu Laboratory in the University of Melbourne.

The author wishes to record his appreciation of the assistance and facilities afforded by Professor J. Neill Greenwood. The analytical work was very ably performed by Mr. J. A. Corbett. Mr. J. D. Martin assisted very considerably in the heat-treatment experiments.

The titanium powder used in making the alloys was kindly provided by the United States Bureau of Mines.

### REFERENCE

1. H. W. Worner, *J. Inst. Metals*, 1951, **79**, (3), 173.

MICROSTRUCTURES OF TITANIUM-IRON ALLOYS.

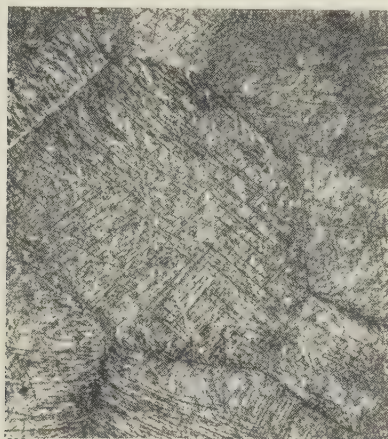


FIG. 2.—2.06% Iron Alloy, Water-Quenched from 950° C.  $\times 100$ .



FIG. 3.—9.5% Iron Alloy, Water-Quenched from 950° C.  $\times 100$ .

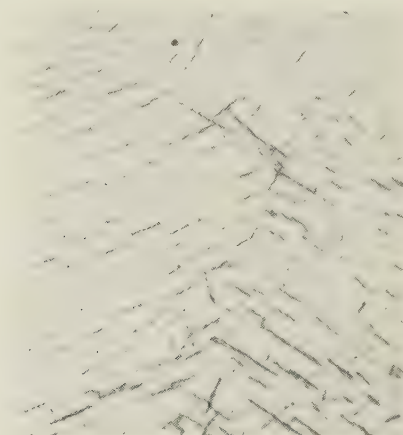


FIG. 4.—5.9% Iron Alloy, Water-Quenched from 950° C., and Aged at 440° C. for 60 Hr.  $\times 500$ .

Microspecimens etched in an aqueous solution containing 1 wt.-% HF and 0.5 wt.-%  $\text{H}_2\text{O}_2$ .



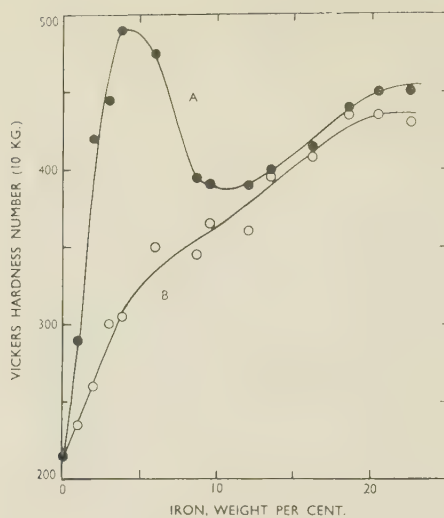


FIG. 5.—Variation of Hardness with Iron Content for Alloys Quenched from 950° C. (curve A) and 650° C. (curve B).

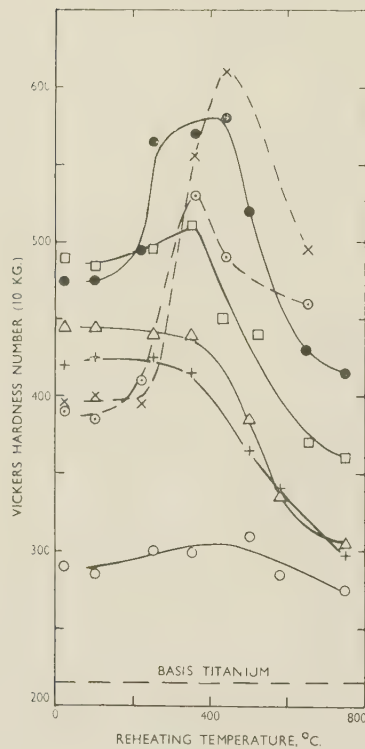


FIG. 6.—Effect of 20 Minutes' Reheating at Various Temperatures on the Hardness of Alloys Previously Water-Quenched from 950° C.

KEY.

○ 1.1 wt.-% Iron.	□ 3.8 wt.-% Iron.
+ 2.1 wt.-% Iron.	● 5.9 wt.-% Iron.
△ 3.1 wt.-% Iron.	× 8.7 wt.-% Iron.
○ 9.5 wt.-% Iron.	

By E. C. ELLWOOD,† Ph.D., A.I.M., MEMBER

## SYNOPSIS

The lattice spacings of the solid solutions of zinc in aluminium have been determined at room and elevated temperatures up to the solidus. The phase boundaries of the solid solutions, including the solidus, have been determined from the X-ray results and agree well with the published diagram.

At room temperature the lattice spacings show that the apparent atomic diameter of aluminium increases in two separate steps as zinc is added, and it is suggested that these increases are associated with the filling of Brillouin zones. At elevated temperatures the composition ranges over which the increase in apparent atomic diameter of aluminium occurs are extended. It is concluded that Brillouin-zone effects of the type found in this system are markedly sensitive to temperature.

Between 16.5 and 25 at.-% zinc the lattice spacing of the  $\alpha$  phase remains constant over a considerable range of temperature when in equilibrium with the  $\alpha'$  phase. This is apparently associated with the filling of a Brillouin zone. Density measurements show that vacant lattice sites form when Brillouin zones are being filled.

## I.—INTRODUCTION

THE work described in the present paper is part of an investigation into the factors affecting equilibrium in the alloys of aluminium which was begun in 1938, abandoned in 1939, and restarted in 1947.

Hume-Rothery and his collaborators have previously studied factors affecting equilibrium in the alloys of the monovalent solvents gold, silver, and copper and the divalent solvent magnesium. This work, together with the theories of Mott and Jones, has been summarized by Hume-Rothery.<sup>1</sup> In the present work it was desired to investigate the application of similar principles to the trivalent solvent aluminium.

The system aluminium-zinc was chosen for the initial experiments on account of the rather unusual form of the equilibrium diagram, which suggested that it might supply some clues as to the factors affecting equilibrium. The form of the diagram is now well established, the annotated diagram of Raynor<sup>2</sup> being generally accepted.

The experimental technique adopted involved the measurement of lattice spacings of the alloys at 25° C. and at elevated temperatures, and density at 25° C. A preliminary note on this work has been published.<sup>3</sup> Errors in detail revealed by further work are corrected in the present account.

## II.—EXPERIMENTAL PROCEDURE

## 1. SOURCE AND PREPARATION OF THE ALLOYS

Certain of the alloys were those used by Gayler and Sutherland<sup>4</sup> in their work on the aluminium-zinc system, and were kindly presented to the author by Dr. Gayler in 1938. These alloys were prepared from spectrographically pure zinc and high-purity aluminium containing as major impurities 0.001% iron,

0.005% silicon, and 0.001% copper, special precaution being taken to prevent contamination during melting and subsequent treatment. Alloys of lower zinc content were prepared for this research. The aluminium, kindly presented by The British Aluminium Co., Ltd., contained 0.0005% iron, 0.0005% silicon, and 0.0005% copper, giving 99.9985% aluminium (by difference). The zinc, which was presented by Imperial Smelting Corporation, Ltd., contained as impurities 0.002% iron, 0.002% lead, and 0.001% copper, with zinc 99.995% (by difference). The alloys were melted in a small alumina crucible in 50-g. lots and cast into an iron mould from temperatures just above their melting points after thorough mixing. The ingots were  $\frac{1}{4} \times 1$  in. in cross-section.

## 2. ANALYSIS OF THE SAMPLES

The alloys presented by Dr. Gayler were parts of micro-sections which had been heat-treated at temperatures close to the solidus and after micro-examination had been cut into two parts, one of

TABLE I.—Compositions of Alloys Used.

Zinc, Wt.-%	Zinc, At.-%	Zinc, Wt.-%	Zinc, At.-%
10.1	4.43	45.0	25.2
20.2	9.45	52.4 *	31.4
24.7	11.9	62.3 *	40.7
28.3	14.0	64.6 *	43.1
32.4	16.5	69.9 *	49.1
35.5	18.5	74.8 *	55.3
40.0	21.6	78.3	59.8

\* Alloys obtained from Dr. Gayler.

which was analysed. It is therefore to be expected that no error due to sampling was introduced. In the case of the alloys prepared by the author for this research, samples for X-ray examination were cut from the middle of the ingots and samples for chemical

\* Manuscript received 23 April 1951.

† Lecturer in Metallurgy, King's College, University of Durham.  
217



analysis taken from adjacent parts. The samples from all the alloys comprised the whole cross-section of the ingot. The analytical results are recorded in Table I. At a late stage in the work additional alloys containing less than 5 at.-% zinc were prepared. These were used for determining the lattice spacings of low-zinc alloys at 25° C. Since the results obtained by plotting nominal compositions were indistinguishable from those of Axon and Hume-Rothery,<sup>5</sup> the alloys were not analysed.

### 3. HEAT-TREATMENT AND PREPARATION OF X-RAY SAMPLES

The samples were heat-treated in lump form at 375° C. for three weeks to establish equilibrium. Filings for X-ray samples were taken immediately after quenching in water. Wherever possible it is customary to take filings from single-phase alloys, and the above procedure of lump annealing was undertaken with this end in view. Unfortunately the transformation at 275° C. cannot be suppressed by quenching, so that the high-temperature condition was not attained for alloys containing more than about 33% zinc.\*

Before X-ray examination of alloys in the duplex region below 275° C. the filings, sealed in silica tubes, were brought to equilibrium by prolonged annealing, quenched in water, and then placed in the high-temperature X-ray camera which had previously been adjusted to the annealing temperature. The specimens were heated for 1 hr. at the annealing temperature before exposure. A similar procedure was adopted in the ( $\alpha'$  +  $\beta$ ) phase field. It is inevitable that the equilibrium of the specimen will be disturbed during the initial heating up and that precipitation may be induced. Nothing in the results obtained indicated that the annealing time of 1 hr. in the X-ray camera was insufficient to restore equilibrium.

### 4. X-RAY TECHNIQUE

The high-temperature X-ray camera used has been described earlier,<sup>6</sup> but since that description was published supplementary knife edges have been inserted corresponding with Bragg angles of 45°, so that the diffraction lines with Bragg angles greater than 45° were recorded on a single strip of film. The camera was calibrated by direct measurement, the films corrected for shrinkage, and the true lattice spacing obtained by extrapolation. Measurement of the film was rendered difficult by lack of contrast between the lines and background, particularly at the higher temperatures. It was found by taking replicate measurements on a film exposed at about 400° C. that the average deviation from the mean for ten measurements was 0.00012 kX units, the standard deviation 0.00015 kX units, and the maximum

deviation from the mean 0.00028 kX units; so it cannot be claimed that any particular measurement is closer than  $\pm 0.0003$  kX units, although a series of points may be accurate to about  $\pm 0.0001$  kX unit.† This error is from measurement alone. The two other principal errors to be considered are that due to the composition of the alloy and that due to temperature measurement. The former is of the order of 0.0001 kX unit per 0.1% zinc, which is regarded as the probable maximum error in analysis, and the latter of the order of 0.0001 kX unit/°C. It is estimated that the temperatures recorded were too high by about 3° at 650° C. and 1° at 419.4° C. Larger temperature errors were reported in earlier work,<sup>7</sup> but these have now been reduced. This error is systematic and leads to a general displacement of the lattice-spacing/temperature curves.

Certain aspects of the attainment of equilibrium at elevated temperatures in the X-ray camera are mentioned in the previous section, and it remains to describe the general procedure adopted. Single-phase alloys were treated as pure metals, and little or no annealing time was allowed between exposures at the different temperatures. Alloys in the ( $\alpha$  +  $\alpha'$ ) loop were annealed for 1 hr. at constant temperature before exposure. This appeared to be adequate, good agreement being obtained on both rising and falling temperatures. Alloys in the ( $\alpha$  + liquid) field were allowed 1 hr. to reach equilibrium, and no X-ray photographs were taken at temperatures lower than the maximum reached in previous treatments in order to avoid any undesirable effects caused by coring. Measurable photographs were obtained at temperatures up to 35° C. above the solidus.

### 5. DENSITY MEASUREMENTS

The densities were measured at room temperature by the displacement method, using distilled water as the fluid. The specimens, which had previously been annealed for three weeks at 450° C., were degassed by annealing *in vacuo* for one week at 360° C., and then reduced in thickness by 50% by hammering at 450° C. They were placed on a small cradle of Nichrome wire, which was in turn suspended from the arm of the balance by very thin tungsten wire. The weight of the specimen in water was obtained by subtracting the weight of the cradle and suspension in water from the weight of the specimen plus cradle and suspension. In this way the effect of surface tension was allowed for. The surface-tension forces were small and consistent enough not to alter materially replicate weighings. The results were corrected for the density of water at the temperature of the measurement and for the buoyancy of air, and a final correction was made for the thermal expansion of the alloys between the temperature of measurement and 25° C. Thus the final density

\* All compositions quoted are in atomic per cent. zinc unless otherwise stated.

† The values given throughout the paper for the lattice

spacings are in kX units, and have not been corrected for refractive index.

figures were those for 25° C. The results in themselves are of no great value unless compared with some standard of reference. The standard used was the theoretical density calculated from the expression:  $\rho = mMN/a^3$ , where  $\rho$  is the density,  $m$  the mass of atom of unit atomic weight ( $1.66035 \times 10^{-24}$  g.),  $M$  is a composite atomic weight for the atoms in the alloy calculated from their international atomic weights (1947) and atomic percentages,  $N$  is the number of atoms/unit cell (four in this system), and  $a$  the lattice constant in absolute Ångströms ( $kX \times 1.00202 = \text{Å}$ ).

the lattice-spacing/temperature curves for different alloys are distinct, but that in the two-phase fields ( $\alpha + \beta$ ), ( $\alpha + \alpha'$ ), and ( $\alpha + \text{liquid}$ ) the lattice spacings obtained for one alloy are the same as those for any others at the same temperature. This is, of course, to be expected.

In Fig. 2 the same set of results is plotted in the form of isothermal lattice spacings for the alloys of different composition. Where there were insufficient points to establish a curve with certainty, it has been drawn parallel to lines that are well established. Fig. 2 does not contain any more information than

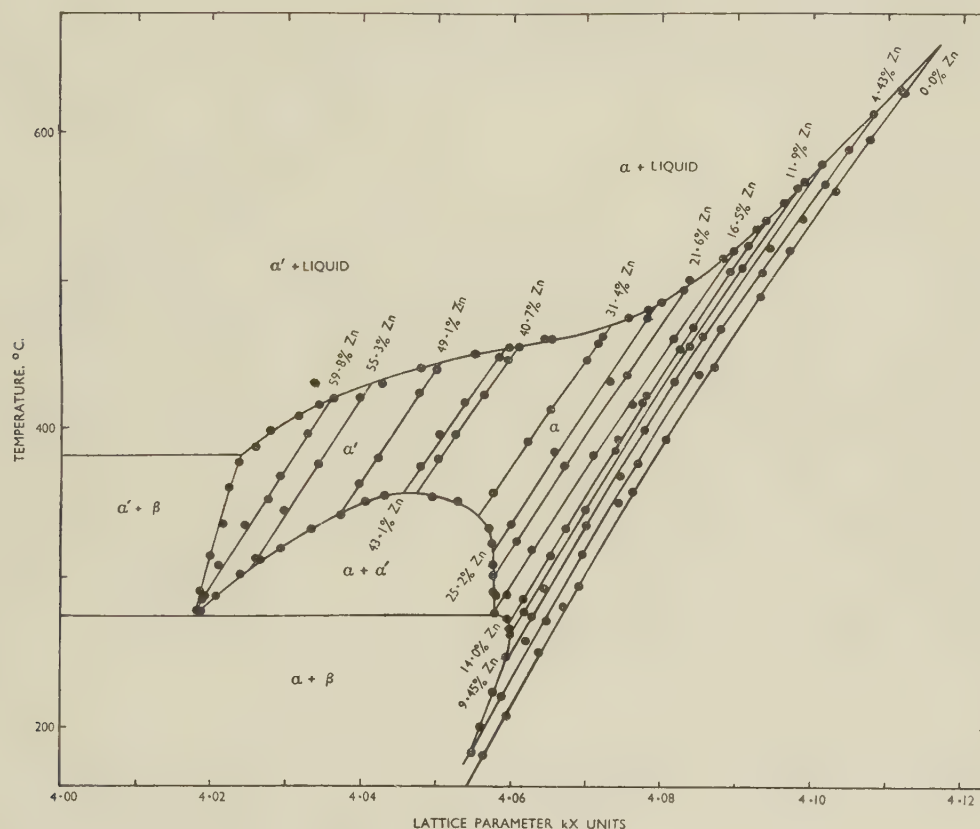


FIG. 1.—Lattice-Spacing/Temperature Curves of Aluminium-Zinc Solid Solutions.

The density experiments were repeated by Mr. N. Gibson, formerly a post-graduate student in the Metallurgy Department, who made and analysed a completely new set of samples in connection with another aspect of this investigation, using a very similar technique to that described. These results are included with those obtained by the author.

### III.—EXPERIMENTAL RESULTS

All the high-temperature X-ray results are shown on a composite diagram in Fig. 1, in which the lattice spacing in kX units is plotted against temperature. It will be seen that in the homogeneous phase field

Fig. 1, but it allows the  $\alpha'/(\alpha' + \beta)$  boundary to be determined by interpolation, and it is thought that this is quite a legitimate device to use.

Fig. 3 shows part of the equilibrium diagram as determined in the present work, and for comparison points taken from the diagram of Raynor<sup>2</sup> are included.

The room-temperature lattice spacings are shown in Fig. 4, with those at 360° C. for comparison, and the density results are shown in Fig. 5. The density results are interpreted in terms of percentage vacant lattice sites which are calculated from the expression:  $\%V.L.S. = 100(\rho_t - \rho)/\rho_t$ , where  $\rho_t$  and  $\rho$  are the theoretical and actual densities respectively.



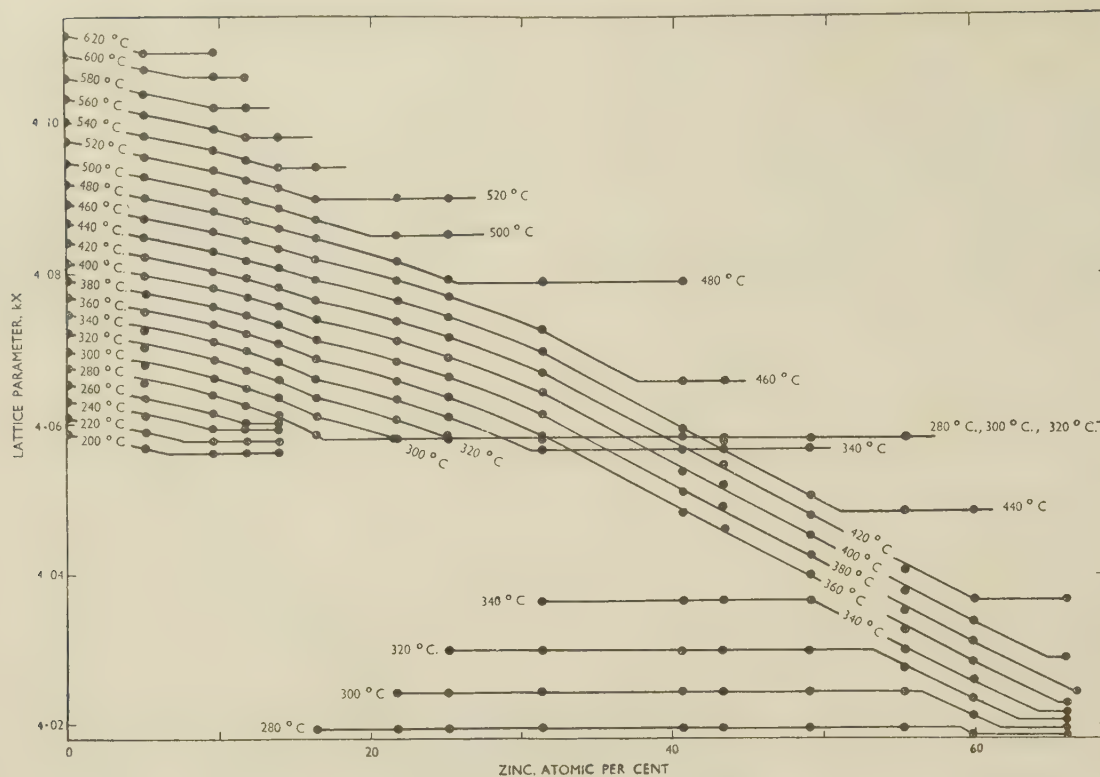


FIG. 2.—Isothermal Lattice Spacings of Aluminium-Zinc Solid Solutions. Drawn from Fig. 1.

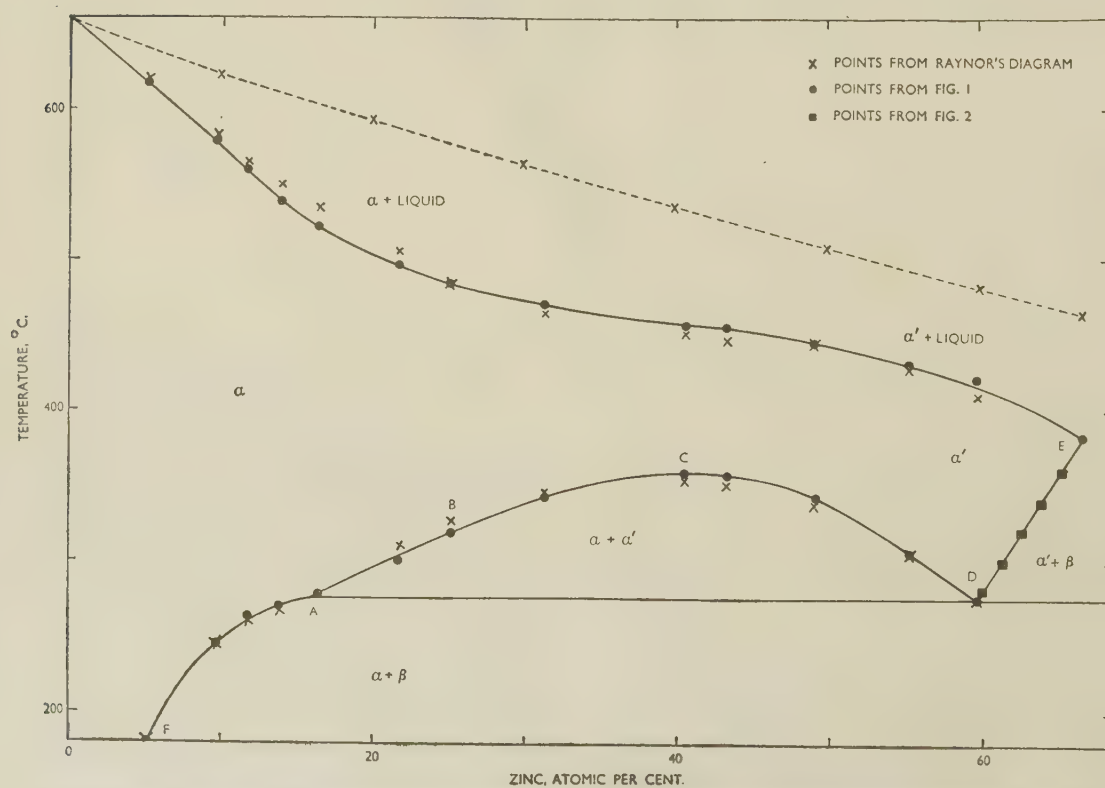


FIG. 3.—The Boundaries of the Solid-Solution Phases as Determined from the High-Temperature X-Ray Results.

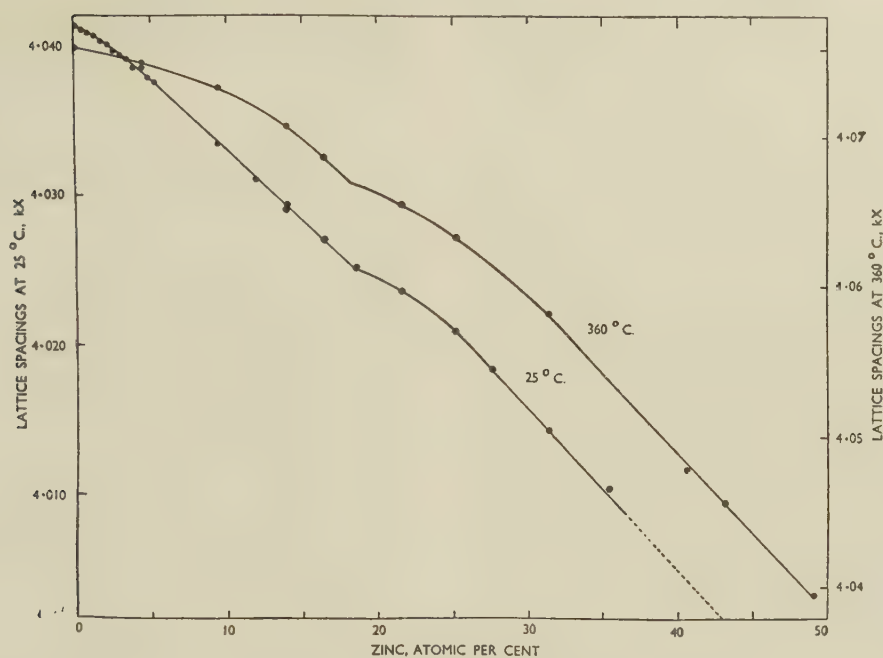


FIG. 4.—Lattice Spacings of Solid Solutions at 25° and 360° C.

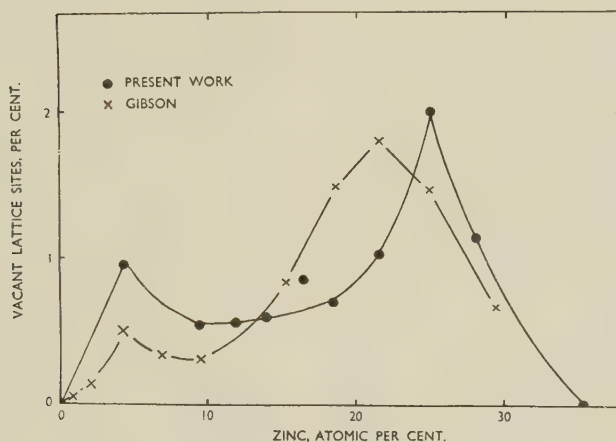


FIG. 5.—Percentage Vacant Lattice Sites in Aluminium-Zinc Alloys.

#### IV.—DISCUSSION OF RESULTS

Although this work is not concerned primarily with the accurate establishment of the aluminium-zinc equilibrium diagram, it is of general interest to compare the results of high-temperature X-ray work with those of classical metallography. This may be done by reference to Fig. 3. Agreement between the points from Raynor's diagram and the present work is not perfect, and in general Raynor's values are to be preferred, though the X-ray method has given a very fair degree of agreement over most of the range. The solidus curve calls for comment, since in the range 5-25% zinc considerable divergence from Raynor's diagram occurs. However, on checking Raynor's

sources<sup>2</sup> it was found that the curve drawn had not been determined experimentally but had been interpolated between the results of Butchers, Raynor, and Hume-Rothery<sup>8</sup> over the range 0-5% zinc and those of Gayler and Sutherland<sup>4</sup> over the range 23-50% zinc, as representing the most probable values. While it is not wished to put too much stress on the high-temperature X-ray results (so far as the author is aware this is the first determination of a solidus curve by such a method), it is thought that the solidus in this region may be worth exploring in detail, since, as will be shown later, the composition range is one in which vacant lattice sites are formed in the solid solutions.

Axon and Hume-Rothery<sup>5</sup> have determined the



lattice spacings of the alloys over the range 0–6% zinc, and the present results are in excellent agreement with theirs. Owen and Pickup<sup>9</sup> have published lattice spacings of the aluminium–zinc alloys at elevated temperatures, but the present work does not confirm their results. The alloys used by Owen and Pickup contained considerably more iron, silicon, and in some cases copper as impurities than those used for the present work, and this may have been responsible for the difference in results.

The lattice-spacing curve at 25° C. (Fig. 4) is unusual in that it can be divided into four parts. In the ranges 0–4.0 and 18.5–25.0% zinc a non-linear relationship between lattice spacing and composition is shown, whereas in the ranges 4.0–18.5 and 25.0–35.0% zinc a linear relationship exists. The lattice spacings at 360° C. show similar anomalies, except that the curved portions extend over a greater range of composition, the approximate limits being 0–14.0 and 17.0–30.0% zinc.

The significance of the curvature of the lattice-spacing/composition graphs becomes clearer if the effective diameters of the aluminium atoms are considered by extrapolating the linear parts of the curves obtained to zero zinc content. When this is done for the results at 25° C. atomic diameters of 2.8579, 2.8582, and 2.8672 kX units are obtained for aluminium with the zinc contents of 0, 4.0–18.5, and more than 25.0% respectively. Thus, when pure aluminium is alloyed with zinc the apparent atomic diameter increases in two steps and remains constant over a range of composition between the two increases and after the second. Jones,<sup>10</sup> in considering the change from the close-packed hexagonal  $\epsilon$  phase to the open hexagonal pure metal zinc, has shown that the change in axial ratio and the consequent change in structure is the effect of a Brillouin-zone overlap along the  $c$  axis of the hexagonal  $\epsilon$  phase, or that the effect of the Brillouin-zone overlap is to cause an expansion of the lattice in the direction of the overlap. Hume-Rothery and Raynor<sup>11</sup> have used this property to indicate Brillouin-zone effects in the primary solid solutions of multivalent metals in magnesium. It is thought, therefore, that the two increases in the effective atomic diameter of aluminium which occur when zinc is taken into solid solution correspond with the filling of Brillouin zones in the alloys. Such a conclusion is contrary, however, to what might be expected, since, in these alloys, the filling of the zones occurs on decreasing the electron/atom ratio rather than on increasing it, as is more usual.

It has recently been shown by Matyáš<sup>12</sup> that the symmetry of the  $s$ - and  $p$ -states in aluminium results in almost complete filling of the first Brillouin zone and that there is slightly more than one electron per atom in the states of the second zone but that no zone is filled. Such an  $N(E)$  curve is quite different from that which is indicated for a face-centred-cubic structure by the simple Brillouin-zone theory of Jones and Mott,<sup>13</sup> in which the condition for a trivalent metal is one following after the (200) overlap.

Although Matyáš's curve is unusual, it is confirmed to some extent by the shape of the soft X-ray emission bands for aluminium which have been obtained by Skinner.<sup>14</sup>

If the  $N(E)$  curve of Matyáš is not accepted, and it is assumed that aluminium behaves as a normal face-centred-cubic metal with an  $N(E)$  curve similar to that calculated by Jones and Mott,<sup>13</sup> a serious difficulty is encountered in that the electron/atom concentrations at which inflections in the curve occur are not even approximately those at which Brillouin-zone overlaps should occur. If, on the other hand, the  $N(E)$  curve of Matyáš is accepted, the difficulty mentioned earlier of explaining Brillouin-zone overlaps with decreasing electron concentrations has to be faced. This difficulty is perhaps not an insuperable one, for as Hume-Rothery<sup>1</sup> has pointed out aluminium, when dissolved in copper, behaves as a typical trivalent solute and has a solid-solubility curve very similar to that for the copper–gallium system. In other words the limit of solid solubility is controlled by a Brillouin-zone factor. Furthermore, the  $\beta$  phase in the aluminium–copper system falls symmetrically about the composition  $\text{Cu}_3\text{Al}$  with an electron/atom ratio of 3 : 2 and the  $\gamma$  phase embraces the composition  $\text{Cu}_9\text{Al}_4$  with an electron/atom ratio of 21 : 13. Thus, if we accept Matyáš's results, it must be postulated that in the aluminium–copper system the form of the diagram for the copper-rich alloys is dominated by the electronic structure of copper, whereas for the aluminium-rich alloys the electronic structure of aluminium affects the form of the equilibrium diagram, and that a transition from one form to the other must occur. As an explanation of the results obtained for the aluminium–zinc system, it is suggested that the factors which give rise to the unusual  $N(E)$  curve for aluminium become modified when zinc is added, and that the  $N(E)$  curves for the alloys in the  $\alpha$  and  $\alpha'$  solid-solubility fields take intermediate forms between that for aluminium calculated by Matyáš and that derived for the general case of face-centred-cubic metals by Jones and Mott.<sup>13</sup>

The effect of temperature on the lattice spacings is seen in Fig. 4. Over the ranges where a linear relation exists between lattice spacing and composition the slopes of the curves are approximately the same. (The linear portion of the curve below 18% zinc at 360° C. is not well marked, however.) This indicates that where the supposed Brillouin-zone effects are not operating additions of zinc affect the lattice spacing in a similar way both at room temperature (25° C.) and at 360° C. As indicated at the beginning of the present discussion the non-linear portions of the curves at 360° C. extend over a greater range than at room temperature. Although this does not affect the slope of the linear portions, it causes a displacement in them, so that when the curves are extrapolated to zero zinc content, the apparent atomic diameter of aluminium changes to a more marked extent at 360° C. than at 25° C. This effect is shown in Table II, where, for convenience, pure aluminium has been

designated  $Al_a$ , aluminium after the first expansion  $Al_b$ , and aluminium after the second expansion  $Al_c$ . The thermal expansions of the three forms of aluminium are also shown.

TABLE II.—*The Apparent Atomic Diameters of Aluminium before and after Brillouin-Zone Overlaps at 25° and 360° C.*

Aluminium Type	At. Dia. at 25° C., kX	At. Dia. at 360° C., kX	Coeff. of Expansion 25°–360° C.
$Al_a$ . .	2.8581	2.883(2)	$26.2 \times 10^{-6}$
$Al_b$ . .	2.8589	2.887(3)	$29.6 \times 10^{-6}$
$Al_c$ . .	2.8627	2.893(4)	$31.9 \times 10^{-6}$

The physical significance of these changes is not easy to assess, but there would appear to be two possible explanations if the assumption that they originate from Brillouin-zone effects is accepted.

(a) They may be the result of thermal excitation of the electrons of highest energy, giving rise to the Fermi tail on the  $N(E)$  curve. Skinner,<sup>14</sup> who used a soft X-ray spectroscopy technique, has shown that for pure aluminium the observed temperature broadening of the emission edges for aluminium agrees well with the calculated values obtained by using the Fermi formula for the effect of temperature on the electrons in a metal.

(b) A modification of the  $N(E)$  curve, quite apart from the Fermi tail, may occur with increase in temperature. Such a modification might arise from the redistribution of electrons in the  $s$ - and  $p$ -states. Skinner<sup>14</sup> has obtained some evidence which, though not conclusive, points to a change in the  $N(E)$  curve with temperature for aluminium.

Fig. 2 shows that the spread of the two expansions becomes more pronounced as the temperature is raised and that at 400° C. the inflection in the curves at about 16.5% zinc has almost disappeared. A point of general interest is that while the structure of the alloy may be preserved by water-quenching, the anomalies in lattice spacing cannot.

Another experimental finding of considerable interest is the constancy of lattice spacing of the  $\alpha$  phase when in equilibrium with the  $\alpha'$  phase in the range 275°–315° C. (Fig. 1). It would appear that the lattice constant of 4.0578 kX units is one that cannot be decreased any further by the addition of zinc over that particular temperature range. Since any further increases in zinc would normally decrease the lattice spacing below the critical value of 4.0578 kX unit, a new phase  $\alpha'$  of the same structure (face-centred cubic) is found, which has a much lower lattice constant. As the temperature increases more zinc is taken into solution, but the lattice spacing remains constant until a temperature of 315° C. is reached, when the lattice spacing, which appears to have been critical at lower temperatures, can be

decreased. The constancy of lattice spacing occurs over the range 16.5–25% zinc, which corresponds with the range over which aluminium of form  $Al_b$  changes to aluminium of the form  $Al_c$ .

It is again inferred that the constancy of lattice spacing is associated with a Brillouin-zone effect, but the author is not able to discuss this interesting point in any detail.

The work of the author on the densities has been confirmed in principle—if not in absolute detail—by that of Gibson. In general, there is some measure of correlation between the lattice-spacing/composition and the vacant-lattice-site/composition curves, in that where the lattice-spacing curves are non-linear, the number of vacant lattice sites is increasing; whereas the linear portion of the lattice-spacing/composition curves correspond with constant or decreasing numbers of vacant sites.

The interpretation placed upon these results is that the formation of vacant lattice sites is associated with the filling of Brillouin zones. In an alloy in which the electron/atom ratio is, say 2.75 electrons/atom, as calculated from the composition of the alloy, the appearance of vacant sites means that, on the average, there is an electron deficiency of 2.75 electrons/vacant site. The Brillouin zone will not be affected, however, since vacant sites will merely be equivalent to defects in the diffraction grating. Although they may affect the efficiency of the array of ions in diffracting electrons, the overall effect of the array will not be changed materially. The result may be compared with that obtained from an optical grating in which a proportion of the lines are missing in a random manner. Thus, while the vacant sites will not affect the Brillouin zone, they will reduce the electron concentration and hence the energy of the electrons on the Fermi surface. Where the electron movement is beginning to be restricted by the filling of a Brillouin zone, vacant sites may bring some measure of relief in just the same way as the change from face- to body-centred-cubic structure in the copper-zinc alloys.

Vacant lattice sites or defect lattices were first reported by Bradley and Taylor<sup>15</sup> in the nickel-aluminium system. Later investigations have shown that defect lattices occur also in the iron-nickel-aluminium,<sup>16</sup> copper-nickel-aluminium,<sup>17</sup> iron-copper-aluminium,<sup>18</sup> and cobalt-aluminium<sup>19</sup> systems, although in these cases the defect lattices are of a very special kind in that they occur in ordered structures and are connected with the systematic occupation of lattice sites by one or more kinds of atoms in the ordered structure. In a later paper, however, Lipson and Taylor<sup>20</sup> have discussed the effect of vacant lattice sites on the electron/atom ratios and have reached conclusions similar to those drawn from the present work, since the vacant sites appear in alloys having a body-centred-cubic structure when the valency-electron concentration is 1.5 electrons/atom. This concentration is just in excess of that required to fill the Brillouin zone which is bounded by the planes (110), so that restriction is placed on the



accommodation of any further electrons of higher energy.

In the aluminium-zinc system vacant sites occur at atomic compositions which do not correspond with any known ordered structure, and no ordering has been observed by the experimental technique used. Borelius and Larsson<sup>21</sup> however, have obtained indirect evidence which suggests that ordering may occur.

### V.—CONCLUSIONS

The most important conclusions which may be drawn from the work described are:

1. The equilibrium relations in aluminium-zinc alloys containing less than 40% zinc are determined by Brillouin-zone effects.

2. The  $N(E)$  curve for aluminium is of an unusual type and is probably similar to the form calculated by Matyáš.

3. The  $N(E)$  curve for aluminium may be profoundly modified by temperature changes.

4. On alloying there is a transition from the abnormal  $N(E)$  curve of Matyáš to the normal curve for the face-centred-cubic structure of Jones and Mott.

5. The appearance of vacant lattice sites may be a natural consequence of the filling of Brillouin zones.

### ACKNOWLEDGEMENTS

The author has pleasure in thanking The British Aluminium Co., Ltd., for presenting the high-purity aluminium and for carrying out the analysis of the alloys; Imperial Smelting Corporation, Ltd., for the gift of high-purity zinc; Dr. M. L. V. Gayler for the gift of certain of the alloys; and Professors C. E. Pearson and A. Preece for much encouragement while the work was in progress. The author also wishes to thank his colleagues in the University for helpful discussions.

### REFERENCES

1. W. Hume-Rothery, "The Structure of Metals and Alloys" (*Inst. Metals Monograph* No. 1), 1945.
2. G. V. Raynor, *Inst. Metals: Annotated Equilib. Diagr. Series* No. 1, 1944.
3. E. C. Ellwood, *Nature*, 1949, **163**, 722.
4. M. L. V. Gayler and E. G. Sutherland, *J. Inst. Metals*, 1938, **63**, 123.
5. H. J. Axon and W. Hume-Rothery, *Proc. Roy. Soc.*, 1948, [A], **193**, 1.
6. E. C. Ellwood, *J. Inst. Metals*, 1940, **66**, 87.
7. E. C. Ellwood and J. M. Silcock, *J. Inst. Metals*, 1947-48, **74**, 457.
8. E. Butchers, G. V. Raynor, and W. Hume-Rothery, *J. Inst. Metals*, 1943, **69**, 209.
9. E. A. Owen and L. Pickup, *Phil. Mag.*, 1935, [vii], **20**, 761.
10. H. Jones, *Proc. Roy. Soc.*, 1934, [A], **147**, 396.
11. W. Hume-Rothery and G. V. Raynor, *Proc. Roy. Soc.*, 1940, [A], **177**, 27.
12. R. Matyáš, *Phil. Mag.*, 1948, [vii], **39**, 429.
13. H. Jones and N. F. Mott, *Proc. Roy. Soc.*, 1937, [A], **162**, 49.
14. H. W. B. Skinner, *Phil. Trans. Roy. Soc.*, 1940, [A], **239**, 95.
15. A. J. Bradley and A. Taylor, *Proc. Roy. Soc.*, 1937, [A], **159**, 56.
16. A. J. Bradley and A. Taylor, *Proc. Roy. Soc.*, 1938, [A], **166**, 353.
17. A. J. Bradley and H. Lipson, *Proc. Roy. Soc.*, 1938, [A], **167**, 421.
18. A. J. Bradley and H. J. Goldschmidt, *J. Inst. Metals*, 1939, **65**, 389.
19. A. J. Bradley and G. C. Seager, *J. Inst. Metals*, 1939, **64**, 81.
20. H. Lipson and A. Taylor, *Proc. Roy. Soc.*, 1939, [A], **173**, 232.
21. G. Borelius and L. E. Larsson, *Arkiv. Mat., Astron. Fysik*, 1948, [A], **35**, (13).

## I.—Primary Resources of Ferrous and Non-Ferrous Metals

## Introduction

By PROFESSOR A. J. MURPHY,† M.Sc.

MY real Introductory Address to this discussion was delivered last March as the main topic of my Presidential Address.‡

In the discussion today, we shall doubtless find that more than one speaker will refer to the short-term and the long-term problems of supply and demand, and it would be difficult to deny the justice of this distinction. In the short-term, say during the next three years, the problem of ensuring a balance between supply and demand is easier in some respects, and more difficult in others, than when the long-term prospect is being considered. It is easier in the sense that emergency measures can be taken, for instance by raiding stocks intended to cater for forward requirements, by using highly uneconomic methods of mining and refining metals, or by denying supplies for applications which can be deferred for a time though not indefinitely—all of these are means which would have no relevance to a long-term policy. On the other hand, time, money, and men are the great obstacles when a quick, though temporary, alleviation has to be found. The limitation of time is especially intractable when the expansion of supply depends upon the construction of new plant and buildings, for instance, for electrical generating plant for the production of aluminium or magnesium from minerals which are plentiful. Money in the form of investment capital is not readily attracted to mines and factories which are to be developed rapidly for a current demand without a firm prospect of commercial success in the more distant future. Finally, the operative labour and skilled technicians must be drawn from an industry already claiming to be inadequately staffed.

In war all these difficulties are swept aside by the sheer necessity for survival. In the phase of peacetime rearmament in which we are now it is not possible to concentrate all effort on the simple objectives of providing the military machine with its needs and keeping the civilian population alive: a triple balance has to be maintained between immediate service requirements, building up reserves for security if war comes, and the supplies needed for civilian trade, especially for export.

In my Presidential Address I referred to the three

significant elements in the balance between supply and demand as: (1) the increasing population of the world, (2) the non-renewable character of mineral resources, and (3) the world-wide demand for higher standards of living. Statistics in plenty are available to show that, while the world population is rising by about 1% annually, the consumption of metals is swinging upwards at a much higher rate.

It is self-evident that if these rapidly accelerating inroads into a fixed amount of resources were to continue indefinitely the final exhaustion of metal supplies would be inevitable. The two vital questions are: what quantity of workable resources remains untapped and what are the prospects of the rate of winning metals from the earth (and the sea) keeping pace with the soaring demands? Here we find a cleavage of opinion among those who have studied these questions, and no doubt we shall be made aware of these differences as the meeting proceeds.

Those who find grounds for believing that critical and enduring shortages will be experienced within a generation consider that, among our present common metals, lead, zinc, and copper are destined to move into the category of relatively scarce commodities. At the other end of the scale, iron, aluminium, magnesium, and perhaps titanium are expected to remain plentiful for a much longer period.

Opponents of the view that we are within sight of the exhaustion of some of our staple metals point to the fact that in the past under the stimulus of growing demand the requisite increase in supplies of metals has always been forthcoming. They express the faith that in a free economy and given normal peace-time conditions the ordinary price mechanism will provide the incentive for mineral exploration and the exploitation of new sources and improved processes. The point has been well made in this connection that a more powerful stimulus than a high price for the mined product is an assured continuing demand.

I am sure that many other metallurgists will share my feeling of pleasure that in giving consideration to these matters today we have the benefit of the opinions of economists and of geologists. They will not need to be reminded how vitally important it is to metallurgical industry to arrive at a sound appraisal of the forces influencing the future trend of supply and demand of the basic metals. To take only three examples, we may mention galvanizing, copper for

\* Abridged report of a discussion held at a General Meeting of the Institute in London on 17 October 1951, with the President (Professor A. J. Murphy, M.Sc.) in the Chair.

† Professor of Industrial Metallurgy, University of Birmingham.

‡ *J. Inst. Metals*, 1951, 79, 117.



high-tension transmission lines, and lead in electrical accumulator batteries. Is the stringency in supplies of zinc likely to remain so severe, even when the needs of rearmament have been met, that alternative means of protecting steel will replace galvanizing permanently in many applications? Will a continuing critical shortage of copper lead to a large extension of the use of aluminium for overhead conductors? Will the depletion of lead resources cause the lead accumulator to be replaced by other types embodying other, more plentiful, metals?

An affirmative answer to any of these questions will imply as a consequence a change in production methods which may range from a simple adaptation of existing plant in one case to a complete upheaval in another, demanding the learning of new techniques of manufacture, control, and even of selling. For the metallurgist in industry the need for versatility and adaptability to cope with the new situation is obvious, but there is another phase of metallurgical activity in which it is important to have, as early as possible, guidance on the future trend of supplies. I refer to the work of the research metallurgist. In this country, with our limited resources of technical man-power and equipment, it is especially important that a substantial part of these resources should be engaged in the most useful and effective way, in relation to national needs. If we can know now that supplies of metal *B* will be plentiful while those of metal *A* will inevitably diminish, we can direct an intensified programme of metallurgical research to a study of metal *B*, and especially of its alloys.

This is not a matter which calls for help only from the technical metallurgist: the theoretical metallurgist must also be ready to commit himself to forecast technically useful compositions and treatments of unfamiliar alloys which are likely to be available when the better-known materials have become unobtainable.

Economic considerations and technical metallurgical factors are closely linked in almost every aspect of this subject. Others, more expert, will develop this theme, and I shall only refer briefly to two points. The first is the changed situation in the metal industry when scarcity pushes the price of a basic metal much higher relatively to the other main components in the cost structure of the product. Many visitors to America have described how the metal-working industry there has been built up on the acceptance of labour as a relatively scarce and costly commodity, expensive plant being installed to make the most economical use of human labour, and production schedules then being planned to keep the plant working at full output with the least possible interruption. If now a section of the industry has to reconcile itself permanently to a greatly enhanced cost of its raw material, it may be compelled to change this philosophy. In such new circumstances the most important requirement would be to eliminate every

cause of wastage of metal, and expenditure on plant and labour would diminish in significance. It would mean that the attitude of industry towards its metals would shift away from that of the mass-production iron foundry and steel mill towards that of the gold-mine and the silversmith.

As I have remarked previously, the problem can be expressed in the form of three questions:

- (1) What can we do to improve our supplies?
- (2) How can we make better use of what we have?
- (3) What substitutes can we use in place of the metals which have become difficult in supply?

The first question will fall for consideration in Part I of this discussion; the other two questions in Part II.

## The World Supply of Non-Ferrous Metals, Including the Light Metals

By R. LEWIS STUBBS \*

I am going to talk about copper, zinc, lead, tin, aluminium, and magnesium, and I shall try to assemble the facts on which any forecast of supply and consumption must be made.

TABLE I.—*World Production and Consumption of Copper, Zinc, Lead, Aluminium, and Tin, 1948–50.*

(Thousands of metric tons)

		1948	1949	1950
Copper	Refinery production	2291	2237	2537
	Consumption	2326	2075	2539
	U.S. Special Account purchases	13	163	208
Zinc	Smelter production	1564	1680	1819
	Consumption	1543	1478	1847
	U.S. Special Account purchases	54	103	115
Lead	Smelter production	1365	1510	1674
	Consumption	1327	1185	1560
	U.S. Special Account purchases	7	192	155
Aluminium	Smelter production	1117	1127	1285
	Consumption	1111	1024	1312
	U.S. Special Account purchases	...	11	20
Tin	Smelter production	160	171	175
	Consumption	136	117	149
	U.S. Special Account purchases	24	53	30 *

\* Estimated.

### Current Shortages

Let us analyse the extent and causes of present shortages. The figures of production and consumption in the free world issued by the Economic Co-operation Administration in Washington are given in

\* The British Non-Ferrous Smelters' Association.

Table I for the years 1948, 1949, and 1950. The United States "Special Account purchases", which are generally taken to represent the purchases for stockpiling, are shown separately. Table II sum-

TABLE II.—*Summary of Production and Consumption for 3-Year Period 1948-50.*

(Thousands of metric tons)

	Total Production	Total Consumption	Excess or Deficit	Total U.S. Special Account purchases for 3 Years	Total Excess or Deficit
Copper . . .	7065	6940	+125	384	-259
Zinc . . .	5063	4868	+195	273	-78
Lead . . .	4549	4072	+477	354	+123
Aluminium . .	3529	3447	+82	31	+51
Tin . . .	507	402	+104	107	-3

marizes the position for the period 1948-50. During those three years, the United States Government stockpiled some 5% of the world's total production of copper and zinc, 8% of that of lead, and no less than 21% of the total production of tin, and that is the

TABLE III.—*World Mine and Smelter Production of Copper, Zinc, and Lead 1948-1950.*

(Thousands of metric tons)

		1948	1949	1950
Copper	Mine production	2120	2051	2280
	Metal content of scrap	155	199	239
	Combined total	2275	2250	2519
	Refinery production	2291	2237	2537
Zinc	Mine production	1542	1593	1764
	Metal content of scrap	64	83	130
	Combined total	1606	1676	1894
	Smelter production	1564	1680	1819
Lead	Mine production	1282	1347	1466
	Metal content of scrap	68	137	143
	Combined total	1350	1484	1609
	Smelter production	1365	1510	1674

TABLE IV.—*Summary of Mine and Smelter Production for 3-Year Period 1948-50.*

(Thousands of metric tons)

	Mine Production + Scrap for Smelting	Smelter Production	Excess or Deficit
Copper . . .	7044	7065	-21
Zinc . . .	5176	5063	+113
Lead . . .	4443	4549	-106

cause of our present shortage. The mine production for the same three years (1948-50) is summarized in Tables III and IV.

Since 1950 the position has changed a little, and now I think that it is our defence requirements which

are throwing production and consumption out of balance. Stockpiling has been at a very much lower rate this year, and will probably be smaller still next year.

### *The Long-Term Demand*

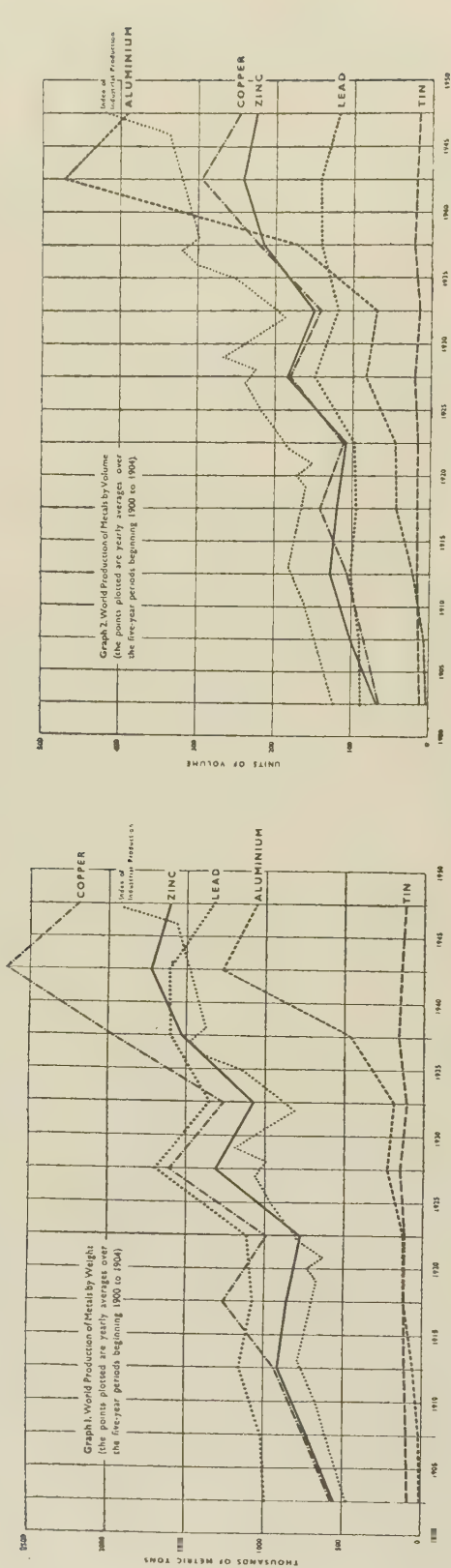
In a general way it is easy to determine roughly the requirements for the next few years, but it is very much more difficult to determine the consumption trends farther ahead. Recently we have been going through a period of accelerated industrial activity, and over the last fifty years there has been a steady upward trend in production, despite fluctuations. The most spectacular rise has been that of aluminium, particularly in terms of volume (Figs. 1 and 2).

Price also has a very important influence on the consumption of metals, though it is overshadowed just now by shortages. Between the wars there does not seem to have been any significant relationship between price and output, the slow downward trend in prices corresponding with the slow increase in the value of money as measured by the wholesale price indices (Fig. 3). Prices began to move upwards at the outbreak of war, and continued to do so until the middle of 1948, when there were some minor fluctuations. Prices have again started to mount, the falls being arrested by the new demands which occurred after the start of the Korean war. Between the wars the relationship between the prices of the different metals never changed significantly, but aluminium is now very much cheaper than the other non-ferrous metals by volume, and I think that this is of great importance, because the price gap between the old and new metals may become even wider in future (Fig. 4). The average costs of copper, zinc, and lead may be expected to rise when new production is brought in, since this will mean the use of lower-grade ores; but with aluminium and magnesium there are abundant supplies of ores, and new production will depend on increasing the supply of electric power. The prospects are good in many parts of the world, so that aluminium looks like competing favourably in the future on a cost basis.

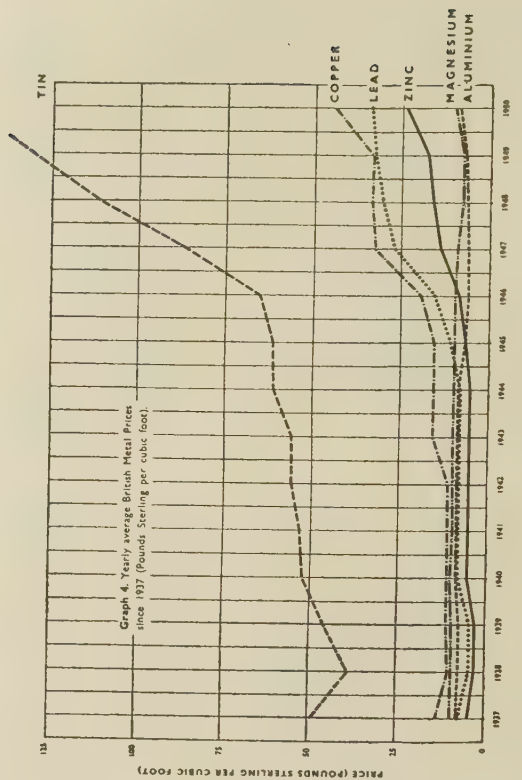
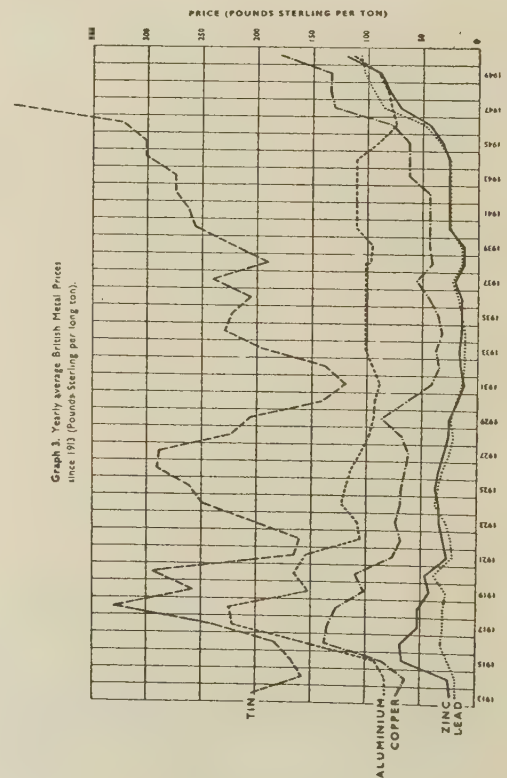
Magnesium is another metal which is likely to be very important in the future, on account both of its properties and of its comparatively low price. At present its price per pound in the United Kingdom is about twice that of aluminium, but its specific gravity is only 1.7, compared with 2.7, so that the price per cubic foot is not much greater. The price of magnesium is now much higher here than it was a year ago, probably because of the sudden increase in the demand as a result of rearmament. In the U.S.A., however, the price is still only 35% above that of aluminium. At the end of the war huge stocks of magnesium were left over, so that production virtually ceased, and it has only just started again.

The low prices of aluminium and magnesium when compared with the older metals on a volume basis mean that we are now faced with an entirely different pattern of consumption from that which prevailed





Figs. 1 and 2.—World Production of Metals (1) by Weight and (2) by Volume, 1900-50.



Figs. 3 and 4.—Average Annual Price of Metals in Britain (3) by Weight (1913-50) and (4) by Volume (1937-50).

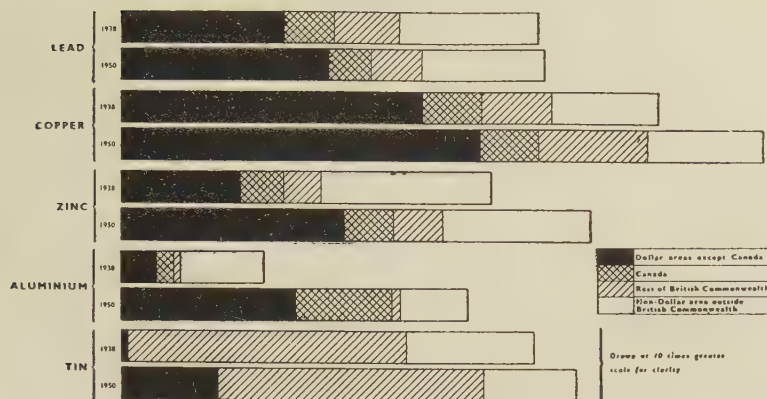


FIG. 5.—World Distribution of Metal Production Before and After the War.

between the wars, and that more and more non-ferrous metals are becoming available for general use. The indications are that, as consumption grows, aluminium and magnesium will take an increasing share of it, and thus the rise in the consumption of copper, zinc, lead, and tin is likely to be less steep than the rise in industrial production throughout the world. This has already occurred in the United Kingdom, where industrial production from 1946 to 1950 rose some 40%, though the consumption of various metals rose by very different percentages, e.g. aluminium 56, zinc 13, copper 6, and lead 3; while tin consumption actually fell. Hitherto, a certain conservatism has caused the older metals to be chosen for many purposes because they have always been so used. Now, however, aluminium is establishing a tradition of its own which will tend to increase its use at the expense of the older metals, and the same applies in a lesser degree to magnesium.

Titanium is another metal for which a great future is predicted, though it seems likely to compete more with steel than with the non-ferrous metals. Plastics may make big inroads into the non-ferrous metals field in the future.

#### *Circulation of Scrap*

In any survey of the pattern of future consumption, allowance must be made for the important role played by scrap, the amount of which will continue to rise in increasing proportion with the rise in consumption of virgin metal. Only when consumption rises quickly, as is now the case, does the available scrap tend to lag behind and to aggravate present shortages.

H. J. Miller estimates the total production of lead from 1847 to 1947 at 85 million tons, of which 65% may be ultimately recovered as scrap. In the same period 80 million tons of copper were produced, 60% of which may ultimately be recovered. This recoverable scrap constitutes a vast pool of metal which will continually be re-used and recirculated, virgin metal being constantly added to it as is necessary to meet demands.

Lead is the classic example of the importance of scrap, which nowadays amounts to some 40% of the

metal consumed. The greater part of this is recovered by salvage, the remainder being process scrap. The lead-scrap pool dates back a very long time, and its growing size may in fact account for the slight decline in the consumption of virgin metal. Until recently the main dissipating use of lead was in pigments, but now, of course, we have the very important use in the U.S.A. for high-octane petrol, and that may change the situation in a few years.

Copper is another almost indestructible metal, but its cycle of return to the pool is much longer. At present about 35% of the copper used comes from scrap, of which between one-half and two-thirds is the result of salvage, the remainder being process scrap. Copper has been used on a large scale only for a generation or two, and in twenty or thirty years from now the pool may have grown to be just as important as that of lead, or perhaps even more important. The only dissipating use is for copper sulphate.

With zinc, the scrap now represents only some 25% of the metal consumed, but the prospects of the pool growing are not so good, since some of the main uses of zinc require the complete loss of the metal, as in protective coatings and in pigments.

Tin is used mainly in an indestructible metallic form. Its chief use is in very thin coatings on steel, and most of this metal is not recovered, although, because of the high price, 20-30% of the tin used in this country and in America is secondary metal from various sources.

I feel that the best form of conservation lies in reclaiming metals rather than in prohibiting their use.

#### *The World Resources*

Before considering the resources of ores which are available to meet future requirements, some general observations on world resources may be worth making. First, up to the present certainly not more than two-thirds of the land surface of the earth can be said to have been explored for minerals. While it is probable that the remaining third will be found to contain less mineral wealth in proportion, there must



nevertheless be huge unknown resources still awaiting location. Most of the great discoveries in the past twenty years have been made in the so-called explored regions, and these will no doubt continue. It must not be forgotten also that the period between the two world wars was one of over-production, when there was no urge to seek new ores.

Another factor which has an important bearing on the estimation of world resources is that in the last twenty years important new methods of locating ore bodies have been introduced, although science has not yet succeeded in evolving any method of locating really deep deposits.

The present high prices have led to much more active prospecting, the results of which can be seen in the large number of new mines and workings now being opened up; and here it is to be noted that these ventures have been based on work begun when prices were much lower than they now are. Another result of the price stimulus will be the exploitation of poorer ores than those previously worked, and, as extraction techniques improve, the amount of such ores increases. The mining of ores at lower level will also prove economic. Many mining companies know quite well what additional reserves can be reckoned on as prices advance.

I now propose to deal with each metal separately and to examine the estimates of resources made by different experts.

*Aluminium.*—Aluminium constitutes 8% of the earth's crust, though only bauxite is being mined on a large scale. Bauxite is, however, found in large quantities in many parts of the world, and there is no immediate prospect of other sources having to be used. The only factor likely to limit aluminium production is the availability of electrical power, the cost of which constitutes about 60% of the present cost of the metal. The future of aluminium is very closely linked with the development of hydro-electric power or other large-scale plants for producing electricity cheaply. It is estimated that the total world output in 1951 will be 15% higher than in 1950, and by the end of 1953 as much as 50% higher than it is today. A dozen new smelters are in course of erection in different parts of the world, the largest being in North America.

*Magnesium.*—Magnesium is in a similar position to aluminium, in that it is very plentiful and is believed to constitute 2% of the earth's crust. It is obtained from deposits of magnesite and dolomite and from brines and sea-water, and so is virtually unlimited. Its production generally requires electric power, though thermal processes are also used. The U.S.A. consumed about 20,000 tons of magnesium in 1950, and expect to use some six times this amount annually by 1960. Production is being increased accordingly.

*Copper.*—Authoritative figures for the reserves of copper are difficult to obtain. The total "officially reported" in the Year-Book of the American Bureau of Metal Statistics for 1951 is approximately 60

million metric tons, but this does not include a number of the largest mines both in America and elsewhere. From recent company reports, it is evident that approximately 7.9 million tons should be added to the above figure, but even this fails to include many important mines for which no reserves have been published, though they may be estimated at about 16 million tons. It is therefore safe to assume that there is a reserve of at least 100 million tons of copper at present, or sufficient for at least 44 years at the current rate of consumption.

Prospecting for fresh deposits is continually going on, and valuable "finds" are not infrequently made; it should be remembered, for instance, that the enormous ore-bodies of the Northern Rhodesian copper belt were unknown until about a quarter of a century ago, and other deposits of comparable magnitude may well be discovered in years to come. It is apparent, too, that as methods of extraction improve, grades of ore previously regarded as uneconomical will become workable; and the development and continual improvement of the froth-flotation method of concentration is a dominating factor in this direction.

For these and other reasons there seem to be no grounds for supposing that supplies of copper will be insufficient to meet the essential requirements of an expanding economy for many years to come.

*Zinc.*—With zinc, we have more estimates of the resources than with most of the other metals. The latest and most authoritative survey was given in 1948 by K. C. Dunham, who observes that a high proportion of the estimated reserves mentioned falls within the possible and speculative (inferred) categories; nevertheless, the estimates are made by experienced mining engineers and are not flights of fancy. Other reliable estimates have been made by W. R. Ingalls, in 1931, and by W. P. Shea, in 1940 and 1947. The figures, given in Table V, are very

TABLE V.—*Zinc Consumption and Reserves.*  
(In millions of metric tons)

Year	Annual Rate of Consumption	Estimated Reserves
1931	1.1	24.5
1940	1.8	39
1947	1.6	57
1948	1.8	65

interesting, because these reserves appear to grow with each new estimate.

Discoveries of new zinc deposits are being made in many parts of the world, and are far too numerous for detailed mention. The most important are perhaps those in Canada and French North Africa. In Canada the new Barvue mine alone expects to produce 4000 tons of ore per day in 1950, and surface drilling has already outlined 17 million tons of ore.

The exploitation of poorer ores, as well as of the vast heaps of slag from lead blast furnaces which lie

all over the world, will be a further source of metal, assuming that present prices continue. Thus at Bergamo, in Italy, a new smelter is being built especially to deal with the abundant local supplies of poor-grade ore.

*Lead.*—In the case of lead there has so far not been any overall world shortage, though there have been local shortages in some countries which in future may become more serious, particularly if the shortages of zinc and copper continue. Since zinc and lead are generally found together, the new mines referred to under zinc will provide an important addition to the reserves of lead. Shea and Dunham have both made estimates of the world reserves of lead, shown in Table VI.

TABLE VI.—*Lead Consumption and Reserves.*  
(In millions of metric tons)

Year	Annual Rate of Consumption	Estimated Reserves
1947	1.8	32.5
1948	1.6	31

*Tin.*—Since the end of the war the production of tin has been in excess of consumption, the shortages experienced during and immediately after the war having allowed substitutes to become well established. It has been said that the resources in Malaya, from which about 35% of the world's tin is obtained, are rapidly being depleted, but the real trouble is that prospecting has been prevented by the local disturbances. Good reserves are known to exist in Indonesia, the Belgian Congo, and Bolivia.

In general, the reserves of the principal non-ferrous metals seem to vary according to likely future demands, with aluminium at the top of the list and lead at the bottom. It is fashionable nowadays to quote the known reserves of metals in terms of their life at the present rate of production. I have therefore reproduced in Table VII figures prepared in 1949 by

TABLE VII.—*Estimated World Reserves of Non-Ferrous Metals (1949).*

Metal	World Reserves	
	Thousands of Metric Tons	Years' Supply at Current Rate of Production
Bauxite (crude ore)	1,400,000	200
Copper (recoverable content)	100,000	45
Zinc (gross content)	70,000	39
Tin (recoverable content)	6,000	38
Lead (gross content)	40,000	33

Elmer W. Pehrson, of the U.S. Bureau of Mines. Since those estimates were made, there have been some substantial new discoveries, so that I do not think that they represent by any means the last word.

### *Overcoming the Present Shortages*

Having shown that the long-term supplies should cause little anxiety, I must now turn to the problems of the present shortages, where the position is much less clear. I think it is evident that they were brought on by stockpiling and are now being aggravated by the demands for defence. Furthermore, as always, every shortage seems to create an extra demand. The present situation appears likely to continue for some time, and to be followed by a fairly heavy demand for civilian consumption for an indefinite period. All this uncertainty affects the flow of investment towards the development of mining and smelting, and the time-lag between the decision to open a new mine or build a new smelter and actual production must always be allowed for. Moreover, it must be realized that this is almost the first time, apart from war conditions, when metal consumption has exceeded production, and producers naturally fear a sudden return to the former state of affairs. Nevertheless, many new mines are being opened up, and the *Engineering and Mining Journal* mentions no less than fifty new copper, zinc, or lead mines as having been opened during the first six months of this year. I believe that the real shortage is only a matter of a few per cent., and is likely to be over fairly soon; but we are always faced with the difficulty that we cannot determine the extent of the demand so long as consumption is limited by the shortage of metal.

Before considering our own prospects, it is interesting to see what has been happening to consumption in the leading countries since the shortage began. The figures in Table VIII show that consumption has risen in almost every country, with the exception of the United Kingdom and the U.S.A. In other words, the countries with the biggest purchasing power have felt the shortage more acutely than the others.

The causes of this situation seem to be fairly clear. First, there is the rapid growth of the fabricating industries in exporting countries such as Canada and Australia. In Australia the home consumption of zinc has been encouraged by the fixing of an exceptionally low internal price. More recently, the Canadian fabricators have been able to buy metals more cheaply than the users of Canadian metals in this country, and the same price differences can be seen in other exporting countries. This, of course, is not a new trend, but it is being given further encouragement now that the exporting countries find that money is losing its value and often does not command the equipment and machinery which they need.

Secondly, planning and control have become features of economic policy both here and in the U.S.A. In both countries efforts have been directed towards keeping the price of metals down, and recently even the U.S.A., with its colossal dollar purchasing power, has found itself outbid for foreign ores simply because it could not turn the ores into metal which it could sell at the home price.



The whole-hearted determination of America and ourselves to solve our difficulties and those of the free world generally by international planning and control is shown by the setting up of the International Materials Conference, which has the object of ensuring the fair distribution of the raw-material resources of the world. Here it may be remembered that previous schemes for the international distribution of metal have seldom proved successful, and it remains to be seen whether the threat of aggression may make the chances of success better now. If the International Materials Conference allocation scheme should fail, the U.S.A. may well resort to buying for its armament needs at higher prices in the open market. This in turn may lead to a general resumption of free trading in metals, and possibly to

E.C.A. funds, the loans being made to mines and smelters in Europe. Incentives to increase production and to bring new mines into operation have been adopted in other countries and, since the development of mining in the Commonwealth is still largely based on London, we might also take steps to ensure that incentives at least as effective are available to firms with mines in Britain itself and in the Commonwealth.

In the U.S.A. approved new mining and smelting projects can secure accelerated tax amortization. Eighteen of the new projects so favoured are expected to yield by 1955 96,000 metric tons of copper, 106,000 metric tons of lead, and 230,000 metric tons of zinc. Aluminium production is being increased by the same means, and a total of 1,175,000 tons is expected to be produced by 1955, and 178,000 tons of magnesium.

TABLE VIII.—*Consumption of Copper and Zinc (1938, 1949, 1950, and 1951).*

Copper		U.K.	U.S.A.	Belgium	France	Australia	Italy	Canada
1938	Quarterly average . . .	66,400	96,112	7,500	28,025	4,350	23,000	9,247
1949	Quarterly average . . .	80,975	234,750	11,750	30,050	8,325	15,800	23,000
1950	Quarterly average . . .	84,775	326,250	14,250	29,250	8,900	22,525	24,275
1951	First Quarter . . .	83,100	313,000	17,800	37,200	8,505	29,000	29,200
	Second Quarter . . .	87,700	316,000	19,200	31,300	8,900	29,000	...
	Fourth Quarter allocation .	87,450	317,460	16,480	35,030	8,500	23,080	27,580
Zinc								
1938	Quarterly average . . .	54,850	102,822	25,875	22,250	8,060	8,775	9,017
1949	Quarterly average . . .	50,475	171,500	15,000	26,750	11,250	7,025	10,350
1950	Quarterly average . . .	60,150	249,200	16,250	25,250	13,000	8,750	12,750
1951	First Quarter . . .	46,400	195,200	19,000	27,100	12,100	11,000	14,100
	Second Quarter . . .	46,600	...	29,000	27,900	13,100	11,000	15,400
	Fourth Quarter allocation .	58,450	221,461	22,160	26,910	13,010	9,390	12,780

the weakening of the present arrangements whereby we and the U.S.A. are able to get good supplies of metal more cheaply than most other countries.

The loss of the free market means that the planners have now to decide for what purposes metals or their substitutes are to be used. In any case, the pattern of control and planning seems likely to last for some time, and the prospects of an early return to free markets are rather remote. In this connection it is interesting to examine Fig. 5 (p. 229), which shows the changes in production that took place between 1938 and 1950. It will be seen that during that period nearly all the new production was in the dollar area. It seems to me that there are three ways in which we might consider improving our present position: (i) by placing long-term contracts, (ii) by encouraging production in non-dollar areas where we may expect to enjoy a first call on new output, and (iii) by maintaining and fostering ventures with headquarters in London.

We and the U.S.A. have already placed long-term contracts, often accompanied by loans, a condition of the loan being the repayment of the money in metal arising from the new production. An outstanding example is our arrangement with the Canadian aluminium producers. The U.S.A. has made rather similar arrangements with the use of

The United States authorities have also undertaken, in the event of a fall in prices, to purchase metal or concentrates at an agreed floor price in the case of other new ventures for a period sufficient to ensure the return of capital. In addition they have made advances for approved prospecting ventures repayable in terms of metal or ores. In Canada a new mine is allowed exemption from tax for three years, and the high rate of mining development there is good evidence of the effectiveness of that method of encouragement.

Before applying such incentives here, however, our taxation laws would appear to need overhauling, since at present they represent a serious drawback to London-based mining companies, which have tended to remove their headquarters elsewhere in recent years. We cannot overlook the fact that these London-based companies have been our best and most certain sources of supply in the past, and may be even more important to us in the future. It seems unfair that these companies, the operations of which are carried on overseas, should be liable to United Kingdom tax on all their profits, whether or not they are remitted to this country. Moreover, British-controlled mining companies do not enjoy depletion allowances comparable with those in other countries, and particularly in North America, where

large depletion funds can be built up out of tax-exempt current revenue, these funds being available for further exploitation when existing ore-bodies are worked out.

These are but a few of the changes which our taxation laws would seem to need, if British companies are to continue to play a part in opening up world resources. However equitable our mining taxation may be compared to that imposed on other United Kingdom industries, it falls far short of the practice in other countries, and that is the real criterion. Not a single mining company of any size has been floated in the United Kingdom since the war, and it seems certain that none will be under present conditions.

## Metals as Natural Resources

By PROFESSOR S. ZUCKERMAN,\* C.B., F.R.S.

The shortages with which we are concerned signify far more than transitory dislocations of the market. They mean that all over the world manufacturing industries are turning over much faster than production industries. The increase in population, the facts that standards of living are rising everywhere, that the backward races are becoming industrialized and that their consumption is going up, that rearmament is taking place, and that stockpiling is occurring all add pressure to the demand on resources. But not one of these factors, taken separately, is new. There are two things, however, that do seem to me to be new. The first is the fact that the rate of demand appears to have gone up enormously in the last ten years. The second is that, much to the surprise of a number of prophets, there has been no slump.

The central problem to which we have to direct ourselves is the disparity between demand and supply. This disparity was the theme of a series of articles which recently appeared in the *Economist* entitled "Agenda for the Age of Inflation". These expressed the view that as far as one can see ahead there is going to be too much money chasing too few goods. That is another way of saying that the rate of demand is going to rise at a greater rate than the rate of supply, and that the value of money will decrease.

In a recent paper, † Professor Lewis, the head of the Department of Economics at Manchester University, has assembled figures for countries on this side of the Iron Curtain to show that the fundamental reason for the overall problem which faces us today is not excessive demand but shortage of supply. He does not accept the conclusion that in the commodities field there will be a balance if one or two extraneous factors are removed.

He points out that if the rate of growth of world

industry over the past 70 years is plotted, it is found—surprisingly—that the rate of increase of growth of manufacturing industry has been falling off recently in the world and not rising. The rate of increase for the 40 years before 1914 was 3·7% per annum, and since then the rate of increase has fallen to 2·5%. The same trend is demonstrated in the figures for the U.S.A., where between 1873 and 1913 manufacturing industry increased at the rate of 4·8% per annum, whereas from 1913 to 1929 the rate of increase was 3·8%, and from 1929 to 1950 it was 3·1%. In other words, and relatively speaking, the rate of growth of demand has been declining.

Professor Lewis also provides figures which show that whereas before 1913 the raw-materials industries of the world were growing roughly at the same rate as manufacturing industry, since then there has been an increasing disparity (Table IX).

The growth of manufacturing industry is paralleled by the growth of the metals and fuel industries, and there is very little disparity there. The main disparities are in food production, population increase, and agricultural raw materials, which include, of course, all fibre production. Within each of these classes there are enormous differences between various commodities, and the separation of these classes is naturally very broad, but in general let us agree with Professor Lewis that there has been this divergence, and let us also accept the very important fact which emerges, namely that in the world today the primary reason for the disparity between supply and demand is

TABLE IX.—Increase in Productivity 1913–50.

	1913	1929	1937	1950
Manufacturing production	100	152	172	247
Food	100	116	125	131
Agricultural raw materials	100	149	194	178
Metals and fuel	100	150	170	239
All primary production	100	127	140	155
World population	100	113	124	138

shortage of production of primary materials and not excessive demand.

Turning to changes in the pattern of consumption—a factor which Mr. Stubbs has illuminated extremely well—we see these changes occurring partly because of the development of relative scarcities in the amounts of lead, tin, zinc, and so on, which are available, and also because of the intervention of new materials. As Mr. Stubbs has shown, these changes in availability have to be looked at not only in terms of volume, but also in terms of price. It is important to note here that, while the increase in scientific knowledge and in improved methods of dealing with minerals and metals has apparently reduced the cost of handling these commodities, nevertheless these economic benefits have become swamped, as far as

\* University of Birmingham; Chairman of the Natural Resources Technical Committee.

† Arthur W. Lewis, *District Bank Rev.*, 1951, (99), 1.



the old, conventional minerals are concerned, by increasing labour costs, transport costs, and so on.

This does not necessarily apply, as Mr. Stubbs has also shown, to some of the newer metals, as aluminium, for example, the price of which is fairly constant. You therefore have a change in the pattern of relative values and a change in the pattern of relative availability, and these two things determine the changes in the pattern of consumption and also what we call "substitution", which will occur and which has always occurred whenever there has been an economic advantage to be gained by it.

On the other hand, as far as I can make out, substitution does not mean, or has never yet meant, any reduction in the use of a material for which a substitute is being found. Even though the production of lead has been falling over the years, nobody has suggested that the amount of lead which is available is not being used.

So far as the world as a whole is concerned, obviously the only way to overcome these difficulties in the long term is to see that capital is attracted to the raw-materials industries. The position is difficult for private investment. Private investors rarely go into food production abroad in a big way, and today it is plain that many people are nervous about investment abroad, not only because of political uncertainties but also because at present the private investor has to reconcile the advice of pessimists talking about long-term shortages and difficulties with the fact that at any given moment there may be a glut of some particular commodity.

If the world problem of stimulating the primary-materials industry is not solved by private industry, clearly Government investment has to come in, but I do not want to go into that aspect of the problem.

Having talked so far about the world problem, I should like in conclusion to refer to our own particular problem. In this country we are importers: we live by the added value that we give to raw materials which we get from abroad and which we then export. We get 50% or more of our food and 80% of our raw materials of industry from abroad. Our capacity to secure these depends on our competitive position in the world markets. Our competitive position is not as strong as one would like. In fact, if there is one point on which I disagree with the analysis of Mr. Stubbs, it is his suggestion that this country and the U.S.A. have been the two most powerful countries since the end of the war as far as world trade is concerned. I would say that we have been extremely limited in our competitive power in obtaining materials at various times. Because we are in a weak position, we must remember not only that the International Materials Conference is very important, but also that development plans in other countries can affect us enormously.

I think, as Mr. Stubbs does, that every encouragement should be given to the mining industries. I

also feel that, in addition to overseas investment, we should not forget to survey our own country. It is unfortunate that the Mineral Development Commission was not set up. Circumstances prevented it, but it would have done a great deal towards a rational survey of the resources of this country. Furthermore, it might have done much to stimulate deep exploration, and at the same time it might have helped to bridge the gap between the gaining of new knowledge about our resources and the exploitation of those resources.

We have to take a rational view of the future. I myself am not convinced that the price mechanism alone is a sufficient guarantee that materials will be there when they are required. We have to reconcile private and public interests in some way and find a means whereby private initiative and skill and enterprise can be so unleashed that it will be to the public good, not only in this country but over the whole world.

## World Demand and Resources of Iron Ore

By T. P. COLCLOUGH,\* C.B.E., D.Sc.

The steel industry has been well described as one of the basic industries of the modern world, and the production of crude steel in the world has risen from about half a million tons in 1870 to over 160 million tons in 1950. The fundamental raw materials of steel are iron ore and scrap to furnish the metallic iron, and coal to supply the necessary heat required in the operations.

### Scrap Supplies

While the proportion of scrap used in steel-making may vary from country to country according to the process employed, the percentage of scrap arising over the world as a whole bears a fairly constant relationship to the gross tonnage of steel made. Taking a broad view, the rolling of steel, its processing into finished form, and the return of obsolete or used plant give in total a volume of scrap equal to roughly 50% of the ingot weight made.

### Pig-Iron Requirements

Again taking a broad view and averaging the yields for the various steel-making processes, the weight of metallics—scrap and pig iron—required for steel-making is approximately 110% of the ingot weight. It therefore follows that the pig iron required for steel-making is approximately 60% of the crude steel produced. To this must be added about 4% for the ferro-alloys consumed and pig iron used for the making of ingot moulds, giving a total blast-furnace product requirement of about 64% of the ingot weight made.

\* Technical Adviser, British Iron and Steel Federation.

The world production of 160 million ingot tons in 1950 required approximately 100 million tons of pig iron and ferro-alloys, as compared with a total pig-iron production of 113 million tons, the remaining tonnage being required for foundry and other types of pig iron.

### Iron Ore

The total world production of iron ore in 1949 is estimated at practically 220 million tons. Distribution of the production of iron ore, pig iron, and steel among the principal countries is given in Table X. For convenience, the steel-producing countries

TABLE X.—World Production of Iron Ore, Pig Iron, and Steel (1949).

(Million tons)

	Iron Ore	Pig Iron	Crude Steel
	%	%	%
U.S.A. . . . .	85.0—38.7	49.0—43.2	69.6—44.1
U.S.S.R. . . . .	35.0—16.0	16.4—14.5	23.2—14.7
France and Saar	31.4—14.3	9.9—8.7	10.9—6.9
Scandinavia . .	14.1—6.4	0.9—0.8	1.4—0.9
U.K. . . . .	12.5—5.7	9.5—8.4	15.6—10.0
W. Germany . .	9.4—4.3	7.1—6.3	9.2—5.8
North and West Africa . . . . .	5.4—2.5	...	...
S. America . . .	4.6—2.1	...	...
Belgium and Luxembourg . .	4.1—1.9	6.1—5.4	6.1—3.9
Canada . . . . .	3.3—1.5	2.1—1.8	2.8—1.8
India . . . . .	2.8—1.3	1.6—1.4	1.3—0.8
Australia . . . .	1.5—0.7	1.0—0.9	1.2—0.7
Others . . . . .	10.3—4.7	9.8—8.6	16.4—10.4
Total production	219.4 million tons	113.4 million tons	157.7 million tons

of the world may be divided into four groups: (a) the United States and Canada, (b) Western Europe and the United Kingdom, (c) the U.S.S.R. and its associated countries, and (d) the rest of the world—South America, South Africa, India, and Australia. The production figures for these four groups are given in Table XI. The data for the U.S.S.R. are all estimated, and no useful purpose would be served by a detailed examination. It may be assumed that the

TABLE XI.—1949 Production of Iron Ore, Pig Iron, and Steel.

(Million tons)

Group	Iron Ore	Pig Iron	Crude Steel
	%	%	%
(a) U.S.A. and Canada . . . . .	88.3—40.2	51.1—45.1	72.5—46.0
(b) Western Europe and U.K. (inc. N. and N.W. Africa) . . . . .	80.9—36.9	35.8—31.6	47.2—29.9
(c) U.S.S.R. and associated countries . .	38.0—17.3	20.2—17.8	29.6—18.8
(d) Others . . . . .	12.2—5.6	6.3—5.5	8.4—5.3
Total production .	219.4 million tons	113.4 million tons	157.7 million tons

ore and coal requirements for this group will prove adequate.

So far as group (d) is concerned, these industries exist principally to meet local demands and have adequate indigenous resources. It is not anticipated that, except in the case of South America, these resources can make a positive contribution to the requirements of the large consuming groups (a) and (b).

(a) *U.S.A. and Canada.*—The U.S.A. and Canada have a combined capacity for over 100 million tons of steel per year and require approximately 100 million tons of ore. The ore reserves are extremely large and, while enormous tonnages have already been extracted, further resources are being revealed. Experimental work on the beneficiation of the low-grade taconites, which are estimated at over 1 billion tons, has reached the stage of pilot-plant development, and large-scale production is expected within a very few years. Meanwhile, developments on a large scale are in hand for the exploitation of the vast reserves of high-grade ore in Venezuela and on the Quebec/Labrador border. Each will provide 10 million tons of ore per year. New developments are taking place in the American interests in West Africa, and there is a tendency to increase the import of ore from Sweden. These increased imports of ore must be used mainly at sea-board locations, and a second large steel-producing plant with a capacity of 2 million tons per year is planned for the Atlantic coast. The known resources of iron ore are estimated as adequate to assure the life of the industry in the U.S.A. for over 100 years.

Canada, with its limited steel production of about 3 million tons per year, has ample reserves of iron ore, and will undoubtedly act as an exporter of ore to both U.S.A. and Europe, the chief limiting factor being the severe winter conditions which restrict exports to about six months of the year.

(b) *Western Europe.*—For reasons of geographical proximity, it is convenient to regard the ore-producing countries of North Africa and Sierra Leone as an integral part of this group. In 1949 this area produced roughly 47 million tons of steel, 36 million tons of pig iron, and 81 million tons of ore. It is well known that the native ore resources of France, Germany, and Britain are of comparatively low grade as compared with the ores available in America and Sweden. As a result, the weight of material to be mined, carried, and processed per ton of product is higher in this group than in any other producing area in the world. The details of ore production, by country, are given in Table XII.

This table shows that approximately 95% of the ore produced in the area was consumed within its borders. Three countries show apparent deficiencies: the deficit of the largest importer, Belgium/Luxembourg, importing 9 million tons, is only apparent, since practically the whole of this ore is imported across the border from France. The two real importing countries are the United Kingdom and Western Germany, and to these countries supplies of ore from external sources are vital.



TABLE XII.—*Iron Ore Available to Western Europe in 1949.*

(Thousands of tons)

Country	Production *	Imports				Total
		Other W. European Countries	N. Africa and Sierra Leone	America	Others	
Sweden . . .	13,729	...	...	...	...	Nil
France/Saar . .	31,410	148	222	...	26	396
U.K. . . . .	12,457	4,391	3,569	713	22	8,695
W. Germany . .	9,362	4,100	289	67 †	62	4,518
Belgium/Luxembourg . .	4,137	8,920	110	38 †	23	9,091
Spain . . . . .	1,852	...	...	...	...	Nil
Austria . . . .	1,488	415	81	...	87	583
Italy . . . . .	521	...	99	...	66	165
Norway . . . . .	413	39	...	...	...	39
Switzerland . .	120	38	...	...	...	38
Netherlands . .	Nil	412	262	43 †	...	717
Totals . . . .	75,489	18,463	4,632	861	286	24,242
Algeria . . . .	2,500	...	...	...	...	...
Morocco . . . .	1,250	...	...	...	...	...
Tunis . . . . .	670	...	...	...	...	...
Sierra Leone . .	970	...	...	...	...	...
	5,390	...	...	...	...	...
<i>Summary of Western European Area</i>						
Total ore production . . . . .	...	...	...	...	80,879	...
Imports from America . . . . .	...	...	...	...	861	...
" " others . . . . .	...	...	...	...	286	...
Less : . . . . .	...	...	...	...	...	82,026
Exports to America . . . . .	...	...	...	...	2,191	...
" " others . . . . .	...	...	...	...	1,643	...
	...	...	...	...	3,834	...
Net ore available . . . . .	...	...	...	...	78,192	...

\* Includes some pyrites and manganese ores.

† Brazil.

*Future Requirements*

Each of the Western European countries is engaged upon the task of modernizing and expanding its steel production. The provision of the estimated increase in demand of raw materials presents one of the outstanding problems. The production of iron and crude steel of the different countries for the year 1949 and the target estimates for the middle 1950s are given in Table XIII. It will be noted that, while both pig-iron and steel targets show substantial increases, the proportion of pig iron to steel rises from 75% in 1949 to 82.5% in 1955. It is self-evident that the manufacture of over 50 million tons of pig iron per year will result in a substantial increase in the demand for iron ore. The first step to meet this, already in hand, is to increase production at the existing sources of supply, or to utilize more fully the present tonnage of materials mined.

In pre-war days considerable difficulty was experienced in disposing of fine ores which were inevitably produced in the mining operations. Mechanized and larger-scale operations will increase the proportion of these fine ores. This fine material must be utilized, and for this purpose all ore users have been urged to instal further sintering capacity in order to deal with iron-ore fines, pyritic residues, flue dust, and other iron-bearing materials. Considerable progress has been made in this direction in the United Kingdom,

TABLE XIII.—*Western European Production and Targets of Iron and Steel.*

(Thousands of metric tons)

Country	Pig Iron			Steel		
	1949	1955	Increase, %	1949	1955	Increase, %
Austria . . . .	838	1,200	42	835	1,300	55
Belgium . . . .	3,749	4,870	30	3,849	4,850	26
France and Saar . .	9,927	14,000	41	10,909	14,800	35
W. Germany . . .	7,140	11,500	61	9,156	13,500	47
Italy . . . . .	393	1,450	269	2,055	3,100	51
Luxembourg . . .	2,372	3,300	39	2,272	3,100	36
Netherlands . . .	434	540	24	437	770	76
Norway . . . . .	61	75	22	61	150	149
Spain . . . . .	615	800	30	710	1,000	41
Sweden . . . . .	811	1,250	54	1,370	2,050	50
United Kingdom . .	9,499	12,185	28	15,553	17,500	12
Totals . . . . .	35,839	51,170	42	47,207	62,120	31

and it is anticipated that by 1953 the production of sinter in this country will be of the order of 5.25 million tons, as compared with slightly over 3 million tons in 1949.

Each of the ore-producing countries in this group has submitted plans for the further development of its resources, and Table XIV gives an indication of the quantities of ore and their iron content which it is estimated will be available for the years 1953 and 1960 from these sources. It will be seen that the anticipated production of 48 million tons of iron would be approximately equal to the amount needed for the manufacture of 51 million tons of pig iron. It is, however, undesirable, if not impracticable, to continue imports and discontinue the export of ore to other groups. If the export of ore is to increase proportionally, say from 4 to 6 million tons per annum, then new additional sources of ore supply must be established.

It is well known that large reserves of iron ore in

TABLE XIV.—*Estimates of Iron Ore Production in Western European Area.*

(Millions of tons)

Country	Iron Content, %	1949		1953		1960	
		Ore	Iron	Ore	Iron	Ore	Iron
Sweden . . . .	63	13.73	8.65	16.7	10.52	19.5	12.28
Norway . . . .	66	0.41	0.27	1.33	0.88	2.5	1.65
France . . . .	32.5	31.41	10.21	39.0	12.67	40.0	13.00
Luxembourg . .	30	4.14	1.24	7.0	2.10	7.0	2.10
W. Germany . .	30	9.36	2.81	9.65	2.89	16.5	4.95
United Kingdom	30	12.46	3.74	15.5	4.65	18.3	5.49
Austria . . . .	36	1.49	0.54	2.55	0.92	3.0	1.08
Italy . . . . .	45	0.52	0.23	1.03	0.46	1.10	0.49
Spain . . . . .	48	1.85	0.89	2.3	1.10	2.35	1.12
Others . . . .		0.12	0.03	2.0	0.94	2.75	1.36
Algeria . . . .	52	75.49	28.61	97.06	37.13	113.00	43.52
Morocco : . . .		2.50	1.30	...	...	3.25	1.69
French . . . .	45	0.37	0.17	...	...	0.75	0.34
Spanish . . . .	58	0.88	0.51	...	...	1.20	0.70
Tunisia . . . .	52	0.67	0.35	...	...	1.00	0.52
Wabana . . . .	52	0.71	0.37	...	...	1.75	0.91
Brazil . . . .	60	0.15	0.09	...	...	0.30	0.18
Totals . . . .	...	5.28	2.79	...	...	8.25	4.34
Less exports . .	...	80.77	31.40	...	...	121.25	47.86
	...	3.83	2.37	...	...	6.00	3.70
Net available . .	...	76.94	29.03	...	...	115.25	44.16

North-West Africa which are as yet unsurveyed or undeveloped can, under certain conditions, be made available. The Sierra Leone deposits can be mined on a larger scale and exported through the present port of Pepel. Work is already in progress to develop mining operations and a port at Conakry in French Guinea, and survey work is proceeding on known deposits in Mauretania. These, if developed, should be capable of producing together a total of 8-10 million tons of ore.

### *Economic Considerations*

Britain, in particular, and Western Germany depend to a very marked extent on the import of ore. The new sources of supply in general present increasing costs of equipment and greater distances of transport. It is essential that these new enterprises should be based on a scale of production sufficiently large to carry the capital charges involved and at the same time reduce freight charges by the handling of the material in larger units of volume. This raises a further outstanding problem, namely the provision of new shipping to carry the increased tonnage and the building of ships of such a size and design as to give the maximum efficiency and economy in transport.

It further demands the installation of modern equipment and port facilities for the rapid unloading of the ore ships and avoidance of delays in port in order to secure the maximum economic use of the ships available. It is hoped by these means to offset in a large measure the increase in costs arising from present conditions. Steps to meet these demands are already in hand in this country.

Despite the magnitude of the problem, the difficulty arising from increased capital costs, and the necessity for more adequate shipping and unloading facilities, there would appear to be no doubt that the proposed iron and steel programmes can be met, provided that the plans already formulated are attacked with vigour and fully implemented.

## Discussion

**Professor W. R. Jones \*** : There is a great deal of difference between the connotation of the term "mineral reserves" to the geologist and the mining engineer on the one hand and to almost anybody else who is not closely associated with the mining industry on the other. Let me give an example. Five years ago, Mr. G. F. Laycock, in his Presidential Address to the Institution of Mining and Metallurgy, made this statement: "There would appear to be only sufficient known reserves of the ores of lead in the world at the present time to last about 14 years at the pre-war rate of production, and in the case of zinc probably about 21 years." That statement was quoted very widely, and as widely misinterpreted.

It was assumed that at the end of two decades the world would be faced with a very acute shortage of lead and zinc. The statement meant nothing of the kind. Mr. Laycock's object was to encourage the search for minerals; he knew—no one knew better—that in any mineral field the known reserves are often only a small fraction of the mineral resources of that field. There are many mines which fifty years ago had known reserves of four or five years, which have been in constant production ever since, and which today still have known reserves for four or five years. Many of them in twenty years' time will again have known reserves for four or five years.

It is true that in the decades preceding the first world war there was a spate of discoveries of enormous ore-bodies which have supplied, and continue to supply, the world's main production of metals. It is true that between the two world wars there were some notable discoveries, but they could not compare in magnitude or in diversity with the discoveries that preceded the first world war. It is also true that the demand for and the diversity of minerals have been increasing greatly. What is not true, however, is the conception that it has been established for any particular mineral that in twenty years or in forty years or even in a hundred years there will be a very acute shortage because of the exhaustion not of the proved reserves of today but of the mineral resources of the world.

I have time to deal only, and that very briefly, with the mineral reserves of zinc. Thirty years ago, W. R. Ingalls, who was a man of international reputation, took a great deal of trouble to estimate the reserves of zinc, and he came to the conclusion that on the consumption of that day there were enough proved reserves to supply the world with 27 million tons of metal. Twenty years later, in 1940, W. L. Shea estimated that the reserves would provide 43 million tons of the metal, and seven years later, as a result of further information, he changed the figure, and instead of 43 million tons for the whole world he said 43 million tons for foreign countries and 20 million for the U.S.A., bringing the total to 63 million, that is, two and a half times Ingalls's figure. Yet in the thirty years between Ingalls's estimates and Shea's over 30 million tons of the metal were produced, i.e. 3 million tons more than the total estimate of Ingalls for the world.

The spectacular increases in these estimates may strike one as being very extraordinary, but they are not at all extraordinary to the mining engineer or to the geologist, who know that a few bores put down in a few months may add hundreds of thousands of tons of ore reserves on a mining property.

There is also the fact that the increase in price of the metal at once increases the mineral reserves, because all the marginal reserves—those that were not previously considered because they were too low in grade—with the increase in price become potentially

---

\* Professor Emeritus of Mining Geology, Imperial College of Science and Technology, London.



useful. In addition, of course, the high prices create an added incentive for the discovery of new deposits. There is a lag, it is true, which may be of one or two years, but there is intense activity going on now.

In the U.S.A. certain mineral reserves are being depleted quicker than they are being added to, but that is not true in other parts of the world. For instance, Quebec, which in 1935 had not produced a pound of zinc, is producing thousands of tons at the present time, and mines are opening all over the place.

Whatever the factors are which have caused this shortage of zinc, they do not lie with Nature, and the blame does not fall on geologists and mining engineers. Take production: for the five years ended 1939, the average annual zinc production was 1,750,000 tons; for the four years ended 1949 it was 1,736,000 tons, a difference of 14,000 tons. That is just three months' production of the Baldwin mines in Burma, which have not been producing zinc in late years, not because of the depletion of the reserves but because of the political situation.

**Mr. L. Tarring\* :** In the short term, at any rate, bulk buying and wider governmental control over metal distribution (international as well as national) seem likely, and there is one particular aspect of this to which attention might be drawn. Until recently the centuries-old metal industry had progressed under the economic influences of supply and demand and the price factor. When demand was large in relation to supply, prices rose and new risk capital was attracted to the exploration and exploitation of metal deposits and more efficient collection of scrap. When demand was small in relation to supply, prices fell and marginal production declined.

With the more obvious, richer, and most easily exploitable deposits developed, attention has now been directed to the lower-grade, less accessible, and more complex deposits. Their development frequently involves lengthy exploration and development work and a large capital investment. The new and technologically improved methods of prospecting are also mostly much more expensive than the older methods. In view of the huge sums of money required, big inducements are needed to attract them from the private investor.

The present policy of attempting to stabilize prices at what may be adequately remunerative levels to existing mines may nevertheless have a deterrent effect on the search for, and development of, new mines to meet the requirements of the next generation. Coupled with the movement towards price stabilization has been the more or less world-wide establishment of high rates of mining taxation—few more penal than in this country, where there is also now the additional threat of dividend limitation—with the

result that the glittering rewards sometimes achieved by the mining industry in the past are practically impossible today.

It is true that in the United States the Government has recently encouraged the development of new mines by offering to buy the output from them over a period of years at a predetermined price, if above the market rate then ruling. This, however, does not take the risk out of mining, but merely transfers it from the mining company to the tax-payer. That is to say Governments are now gambling on the future price of metals instead of individuals.

Another aspect of metal price stabilization which deserves attention is that by regimentation of prices the normal competitive influences as between one metal and another, or between a metal and a non-metal, are emasculated or temporarily suspended, and in their place are put arbitrary restrictions banning certain uses by governmental decree. If the excess of demand over supply is to be very prolonged, as Professor Zuckerman envisages, and not confined to a temporary rearmament phase, it means that the pattern of metal consumption will be decided by a small group, irrespective of personal predilection or normal economic pressure.

Admittedly unrestricted commodity markets at times result in extremes of prices. But the more rapidly the extremes are reached the more rapidly the cures are brought into effect. If the world will pay £450 a ton for copper (as it is doing in places), such a price would more quickly bring new production into being than a price of £250, and would more quickly sort out the uses of copper which had become uneconomic.

War conditions and near-war conditions are economically unnatural, and admittedly may call for economically unnatural practices. But it is desirable to guard against measures necessitated by a nation's emergency becoming the plaything of theorists. No consumer likes to pay extravagantly high prices for the material he fabricates or manufactures, but he likes much less a condition of semi-permanent organized scarcity, which stultification of the normal economic influences seems to engender.

There can be no ultimate stability if the aim of mankind is towards an ever-higher standard of living. What is more, evidence is still completely lacking that there is any man or body of men sufficiently omniscient to plan and produce a system of continuing plenty and sweet stability in a world inhabited by men cast in their present imperfect mould, and by nations with sharply different ideologies and autarchic possibilities.

**Mr. C. F. Carter † :** The kind of thing which is in the minds of some of us when we get a little frightened about the future possibilities for raw-material production is this. First, the growth in world popula-

\* Joint Editor, *Metal Bulletin*, London.

† Lecturer in Economic Statistics, University of Cambridge; Joint Editor of the London and Cambridge Economic Service.

tion is considerable, and although we thought some years ago that it might be coming to an end in Western countries, that is now by no means certain. Secondly, the total amount of goods and services produced per head is rising fairly fast. In the last 45 years it has risen by 40% in this country, and by nearly 60% in the U.S.A., in terms of real income produced per head. Thirdly, industrial production grows faster than real income as a whole. In the United Kingdom it has risen in the past 45 years by 85%, and in the U.S.A. by 185%. Fourthly, engineering production has in this period been rising very much faster than industrial production as a whole. In the United Kingdom it has risen in the past 45 years by 260%. The U.S.A. figures are not easy to interpret, but in the latter half of the period engineering production has risen there by 140%.

It does not, of course, follow that the demand for metals will increase as fast as engineering production, and these facts do not justify any assumption by the economist that the rates, which tend to proceed, as far as one can see, on a geometrical progression rather than on a declining curve, will exhaust reserves. That is one matter about which we do not know very much. What I think the economist is justified in saying is that this enormous rate of growth will soak up reserves at so great a rate as to lead to much more rapid shifts in producing areas than have taken place in the past, and that those shifts may very well be extremely adverse for the established producing countries. What will happen is that iron ore will be fetched over greater and greater distances, or that more and more remote areas may have to be opened up for the mining of non-ferrous metals, and they may be remote not only geographic-

ally but also politically. A very large part of the unexplored area of the world is no longer open to British or United States capital.

I think, therefore, that what we may find is that the costs—the real costs, not merely money costs—of providing the raw materials of British industry will tend to rise. But what I should like to know, and what I find it quite impossible to decide from the figures or from the other evidence put before us today, is whether this means that prices have to go even higher than they are now, or whether we can hope that the growth of production will for a short period proceed a little faster, and that we can restore raw-material prices to some normal relationship with prices in general. In particular, I am thinking of those raw materials whose prices are running at four or five times the pre-war level.

Finally, I should like to refer to one problem which has not been mentioned specifically, though several speakers have touched on it, and that is the difficulty created for the world by the very high rates of production in the U.S.A. relative to the world as a whole—that enormous industrial predominance of the U.S.A. which tends to mean that the rest of us, whether we like it or not, are at the mercy of comparatively slight changes in American policy; things which perhaps to American eyes seem entirely their domestic concern and perhaps of no great importance, such as a temporary decision to stop stockpiling, or something of that kind. Such a decision can have devastating results in other parts of the world, and, in looking forward to a future of greater international co-operation in these problems, we have to realize that the contribution to be made by the U.S.A. in the wise use of its sovereignty is very great indeed.



## II.—Scrap Reclamation, Secondary Metals, and Substitute Metals

### The Scope for Conservation of Metals, Ferrous and Non-Ferrous

By C. A. BRISTOW,\* B.Sc., A.R.S.M., A. J. SIDERY,\* Assoc.Met., and H. SUTTON,\* D.Sc.

METAL economy can usefully start in the design stage. It is specially important that each particular product be considered critically in such ways as the following :

(a) Can the required performance be secured with the use of materials that are less difficult to obtain ?

(b) Does the design include anywhere material which could be economically excluded as being in excess of what is really required ?

(c) Can a less wasteful method of production be employed, without or with practicable modifications of design ?

(d) If good protection against corrosion or better resistance to creep were reasonably practicable, could less metal be used to produce a satisfactory or superior article ?

#### *Ferrous Materials*

The shortage of alloy additions to steel emphasizes the importance of the use, wherever possible, of low-alloy steels. The situation regarding alloy additions in steel differs somewhat from that prevailing during the last world war, but the experience gained then should assist greatly. The compositions of these steels in the light of information on current and prospective availability of the different ferro-alloys and additions, and the properties attainable by suitable and special techniques of steel-making, working, and heat-treatments in relation to sections of different mass will undoubtedly receive much study by manufacturers and users. Redesign and intensive testing are involved for many applications.

Low-tungsten high-speed steels or cutting materials free from tungsten, if capable of extensive use, would greatly relieve the difficult tungsten position.

In connection with stainless and heat-resistant steels, recent important developments will contribute substantially towards economy in the use of niobium, except in cases where welding or exposure to high temperature, or both, are concerned. The practicability and efficacy of low carbon content, and the value of titanium as a stabilizer, are well recognized by metallurgists, but possibly not yet sufficiently appreciated by engineers. In view of the special properties of niobium and of the very limited amount available, it is important that it should be used only

in essential applications, such as in heat-resisting steels and alloys and welding materials.

In the gas-turbine field substantial economies have already been achieved in alloying metals by the use of ferritic materials for discs—a development made possible by engineering design. Further economies may be realizable, but for special applications, such as gas turbines and steam plant, strong claims for the special elements used in heat-resistant materials will undoubtedly call for renunciation in other fields.

#### *Non-Ferrous Materials*

Copper, zinc, aluminium, and lead are the non-ferrous materials produced in greatest quantity, and for each of them, with the exception possibly of aluminium, demand at present exceeds supply. Aluminium has already found applications which, if it were not available, would require larger amounts of other materials for duties which, in many cases, are performed more effectively by aluminium.

Large amounts of copper are used in condensers for power plants. If aluminium or aluminium alloys can be used here, without corrosion problems for the user, much copper can be applied to other uses. The use of aluminium instead of copper for bus-bars would seem to be obvious.

In the cable and conductor field the increasing use of synthetic materials, such as polyethylene, protected by a light sheathing of aluminium instead of lead, is a matter of necessity. Battery plates made in lead alloys having improved mechanical properties appear likely to save lead, though performance in service is an important part of these developments.

An interesting development is the introduction of organic adhesives for joining metals to replace riveting and welding. Reinforced plastics, impregnated timber, &c., as structural materials are undergoing intensive study. Further economies in the use of valuable metals can be effected by the wider application of reinforced plastics as bearing and gear materials. The successful application of plastics to replace metals calls, however, for very careful consideration by the designer.

#### *Scrap Segregation and Recovery*

Increasing efficiency in the use of scrap and used material must be achieved. Miller forecasts that, unless an expansion of the production of low-grade alloys from scrap is achieved, it will be necessary to consider the adoption of processes for the treatment of scrap to recover the constituent metals in a high state of purity.

During the last world war, and to some extent since,

\* Ministry of Supply.

scrap segregation, making possible efficient re-use of the material, proved of great advantage. Colour markings for scrap from particular groups of light alloys or steels permitted the recovery of large amounts of valuable material. There is scope for much more action on these lines, thereby saving labour as well as material. In connection with the identification of alloys for secondary handling, a great deal of information and experience is available, ranging from rapid tests made in simple ways to the more elaborate analytical methods, including spectrography. Fewer different alloy specifications would help in this direction.

#### *Corrosion Losses*

Uhlig has estimated the value of the direct annual loss by corrosion and in combating corrosion in U.S.A. to be of the order of 5500 million dollars, and J. C. Hudson puts the loss in connection with corrosion and protection of iron and steel in the United Kingdom at £200 million annually. In many cases the engineer has to face risks of great consequential expenditure that may arise from a failure by corrosion and tends to over-design his pipes or other equipment to reduce that risk. Renewals made necessary by corrosion are not the only serious aspect of the subject, but these alone account for substantial demands for the metals involved. Great economies have been achieved in particular fields by the development and use of corrosion-resistant materials and of improved methods of protection of industrial metals. These aspects of protective coatings for metals have recently been presented by U. R. Evans.

#### *The Forward View*

Few indeed are the industrial metals for which there is encouragement to hope for greatly or rapidly increased rates of world production. Of the elements present in substantial amount in the earth's crust, silicon has hitherto defied the attempts which have been made to render it ductile. Ductile, workable silicon or silicon-rich alloys might do much to relieve present and prospective demands for industrial metals and alloys.

Aluminium is nearly a thousand times as abundant as copper in the earth's crust, and is one of the metals likely in future years to be called upon to serve mankind to a much greater extent than at present.

Magnesium is nearly 250 times as abundant as copper, and the raw material which is the main source of the metal in the U.S.A. and the United Kingdom is sea-water. Sea-water contains about 1272 mg. of magnesium per kilogramme, and Teed mentions that a cubic mile of ocean water contains about 5,400,000 tons of magnesium. Present world production is on a much smaller scale than for aluminium, but magnesium could be manufactured in much greater amounts than at present. Modern magnesium alloys have working properties, mechani-

cal properties, and durability such as to make them capable of much more extensive use in general engineering and many other applications. Alloys of high resistance to corrosion are now available in cast and wrought forms.

Titanium is about 65 times as abundant as copper in the earth's crust. Its oxide is an article of commerce, the amount now produced per day in the pigment industry in America being equivalent to 300 tons of metallic titanium content. The metal itself possesses very good corrosion-resistance and general mechanical properties. Titanium alloys of various types are known which offer good corrosion-resistance and general mechanical properties comparable with those of high-tensile steels. The low density (4.5-4.6 g./c.c.) of these materials, coupled with their general properties, claims for them a considerable future as materials of construction. Production of titanium is at present on a small scale, but is being advanced rapidly in the U.S.A. Important research and development work is in progress in the U.S.A., the United Kingdom, and other countries.

The authors thank the Chief Scientist, Ministry of Supply, for permission to present this paper.

## **Economy by Standardization of Alloys and of the Method of Reclamation of Scrap Metals**

By C. DINSDALE,\* M.Sc.

British Railways are substantial users of many kinds of ferrous and non-ferrous metals and alloys. Up to 1948 the four main-line railway companies were each using metals—especially non-ferrous ones—with widely differing compositions for the same component. Non-ferrous metal reclamation policy also varied. For many reasons it is most desirable, and indeed essential, that in future all Regions shall use, if at all possible, the same metal for the same purpose.

British Railways are at present using between 20,000 and 30,000 tons of non-ferrous metals and alloys each year on their rolling stock alone. The most recent ex-L.N.E. Class A.1 locomotive, for example, contains nearly  $5\frac{1}{2}$  tons of non-ferrous metals and alloys:  $3\frac{1}{4}$  tons of copper firebox plates and stays, 38 cwt. of bronze axle-boxes, 3 cwt. of bronze boiler mountings, 2 cwt. of bronze bushes and bearings, and 100 lb. of white metal being the main items. In addition, non-ferrous metals are used by the civil engineer in buildings, by the signal and telegraph engineer for cables and telephones, and by the electrical engineer for transmission purposes and for overhead wiring and bonds on electrified systems.

---

\* Railway Executive, Eastern and North Eastern Regions.



TABLE XV.—*Bronzes and Brasses for Future Use.*

Type of Alloy	Nominal Chemical Composition, %					Main Uses	Notes
	Cu	Sn	Pb	Zn	Others		
Phosphor-bronze	87.5	12	...	...	P 0.15 (min.)	Slide valves (superheated engines); unlined bushes; machinery bushes and details.	B.S. 1400-PB2
Leaded bronze	67.5	5	26	...	Ni 1.5	Slide valves (saturated engines); regulating valves (grid type).	...
Leaded gun-metal	86	7	2	5	...	Steam and boiler mountings; axle-boxes, lined bushes and brasses; carriage and wagon bearings, &c.	B.S. 1400-LG3
Yellow brass	66	...	2	32	...	Name and number plates; carriage fittings, &c.	B.S. 1400-B3
Brazing metal	90	...	...	10	...	Fittings which are to be brazed on to copper or steel pipe.	...

Nationalization of the British main-line railway companies as a result of the Transport Act, 1947, made it essential that standard non-ferrous metals and practices should exist in all regions, and in 1948 the member of the Railway Executive for Mechanical and Electrical Engineering set up a Committee to investigate the matter. A brief account of this Committee's main findings and recommendations is as follows:

(a) *Cast Bronze and Brasses.*—The large majority of the bronze and brass castings required for British Railways' rolling stock and machinery are made in the Railway Executive's 17 "brass" foundries, a total of some 11,000 tons of non-ferrous castings being produced annually. In 1948 these foundries between them were casting 37 copper-base alloys, each of which had a different composition. Fourteen mixtures were being used in small quantities only (less than 10 tons of each per year), whilst the two most important were 85:5:5:5 leaded gun-metal (over 4000 tons, or about 40% of the total) and 13½% tin bronze (3500 tons, about 35%). In addition, a further alloy was specified for certain purchased wagon bearing shells.

The five alloys listed in Table XV were recommended by the Committee, and have already been introduced in all Railway Executive foundries for the bronze and brass castings which are made for use on rolling stock and machinery.

It will be noticed that the 85:5:5:5 leaded gun-metal has not been included in this new list. Although large quantities of that alloy have been used for many years in locomotive construction, it was considered that a somewhat harder and better-wearing bronze was required, especially for components such as boiler mountings and axle-boxes. It is hoped that the 7% tin leaded gun-metal will give this increased life and so justify its extra cost. Certain axle-box trials are being made in the Eastern and North Eastern Regions using 7% tin leaded gun-metal instead of the 13½% tin alloy which has been the standard for many years, and also with the high-leaded bronze for slide valves. If the new alloys can be used successfully for the purposes suggested,

complete standardization will have been achieved and a list of 38 bronze and brass casting alloys reduced to five.

(b) *White Metals.*—The Railway Executive probably owns between 6000 and 7000 tons of various white-metal alloys. In 1948 some 18 white-metal alloys with 13 different compositions were being used for lining such components as locomotive and tender axle-boxes, bushes and brasses, eccentric straps, crossheads, and carriage and wagon bearing shells. The white metals being used, however, fell into four well-defined groups, viz.: (1) high-tin, lead-free, (2) high-tin, low-lead, (3) intermediate or tin-lead-base, and (4) lead-base alloys.

It was considered that, as a first step towards standardization, the number of compositions used should be reduced to four, one metal being specified to cover each of the four groups. The compositions of the four alloys now standard are those in Table XVI.

A practice which uses only one metal for all bearings is obviously attractive, owing to the simplicity of lining practice, scrap segregation, and store-keeping of ingot metal. The present high price of tin, however, immediately rules out the introduction of the 80% tin metal for all locomotive, carriage, and wagon bearings; and even the universal use of 60% tin white metal would involve the Railway Executive in additional expenditure. At present, therefore, extensive trials are being carried out on all Regions

TABLE XVI.—*Chemical Composition of White Metals.*

Type of Alloy	High-Tin, Lead-Free	High-Tin, Low-Lead	Lead-Tin Base	Lead Base
Tin, % . . . . .	84-86	80-85	58-60	11-13
Antimony, % . . . . .	9-11	9-11	9-11	12-14
Lead, % . . . . .	0.2 max.	0-5	27-29	73.5-75.5
Copper, % . . . . .	4-6	4-6	2-4	0-1
Max. total impurities, % (excluding lead)	0.30	0.30	0.35	0.40
Aluminium shall not exceed . . . . .	0.05	0.05	0.05	0.05
Arsenic shall not exceed . . . . .	0.10	0.10	0.15	0.20
Bismuth shall not exceed . . . . .	0.08	0.08	0.08	0.08
Iron shall not exceed . . . . .	0.08	0.08	0.08	0.08
Zinc shall not exceed . . . . .	0.05	0.05	0.05	0.05

with the use of these lower-tin-content white metals on locomotive, tender, carriage, and wagon bearings.

(c) *Packing Metals*.—Although much cast iron and non-metallic material is used for such purposes as piston-rod and piston-valve-rod packing, seven non-ferrous alloys were also in use.

The three alloys listed in Table XVII have now been introduced for the purposes indicated. The financial savings are, however, not large, as the quantities involved are small.

TABLE XVII.—*Metallic Packing.*

Type of Alloy	Nominal Chemical Composition, %		Typical Use
Antimonial lead	Antimony	20	Piston-rod and piston-valve-rod packing; saturated engines.
	Lead	80	
Copper lead	Copper	37	Piston-rod and piston-valve-rod packing; superheated engines.
	Lead	61	
	Nickel	1.25	
	Sulphur	0.75	
Leaded-bronze	Copper	67.5	Piston-rod, piston-valve-rod and McNamee packing; superheated engines.
	Lead	26	
	Tin	5	
	Nickel	1.5	

(d) *Wrought Metals*.—There was already considerable agreement among the Regions both as to the composition of the wrought non-ferrous metals being used in the construction of rolling stock and the purposes for which they are used. This was undoubtedly due to the fact that well-known and long-established British Standards existed for these materials, viz. B.S. 24, Part 5, B.S. 218, B.S. 249, &c.

(e) *Solders and Brazing Metals*.—In the main, the composition and uses of the soft solders and brazing metals used were based on the appropriate British Standard, e.g. 219 (soft solders), 263 (brazing spelter), and 206 (silver solder), but in a few instances solders with other compositions were being made and used. Small amounts of proprietary brazing materials were being used. Some 70 tons of soft solders are made each year in Railway Executive shops and 20 tons purchased. About 15 tons of brazing solder and  $\frac{1}{2}$  cwt. of silver solder are also bought.

As British Standards exist, or will shortly be issued, for most grades of soft and silver solders and brazing metals, the Railway Executive have not found it necessary to issue many of their own specifications for this class of material.

(f) *Aluminium and Magnesium Alloys*.—Although for many years certain Continental and American systems have made considerable use of light alloys in rolling-stock construction, in this country comparatively little use is being made of such alloys. "Alpax" vacuum and steam-heater pipes and connections, aluminium alloy castings for the road-motor department, foundry patterns and aluminium alloy carriage fittings appear to be the main uses. Where aluminium alloy was used in the wrought form for rolling-stock construction, it was only in an experimental stage.

When light alloys are required, the material will be ordered to a British Standard specification.

(g) *Schedule of Non-Ferrous Metals and Alloys*.—For the use of Railway Executive designers, metallurgists, &c., the Committee compiled a "Schedule of Non-Ferrous Metals and Alloys". This was along the lines of the B.S./S.T.A.7 Schedule, and contained details of the chemical composition, mechanical properties, and uses of all the standard alloys.

### *Iron and Steel*

A further Policy Committee has been formed to recommend specifications for steels for rolling stock, &c., but, as most of the steels used previously were in accordance with British Standards, the resulting standardization will not be so spectacular as in the case of some non-ferrous metals. Most grey cast-iron mixtures already include a high percentage of returned scrap, sometimes up to 95%, and further economies are not expected to be great.

### *Reclamation and Renovation of Non-Ferrous Scrap*

British Railways differ from most other engineering concerns in that their non-ferrous metals are in constant circulation throughout their own system, returning periodically to the workshops either for re-use or for scrapping. It is estimated that 27,000 tons of non-ferrous metal scrap are produced each year by British Railways as the result of machining operations and breaking-up and repairing programmes.

It is clear that under such conditions the reclamation and renovation for re-use of as much of this non-ferrous scrap as possible is an economic proposition, as the quantities of expensive virgin metals and alloys which would have otherwise to be purchased are thereby much reduced. It is therefore not surprising that all the former main-line companies carried out in their own workshops a certain amount of reclamation and renovation of those types of scrap which do not have to undergo complicated refining processes or require expensive plant. The L.M.S.R. had developed scrap reclamation to a high degree, and had in being a systematic scheme of scrap collection and segregation, together with a Central Reclamation Depot at Derby, which dealt with non-ferrous scrap from all departments. Established in 1933, this depot is treating annually nearly 4000 tons of non-ferrous scrap; white metal, packing metal, brass and bronze turnings and castings, zinc sheet, lead sheet and pipe, copper wire and cable, white-metal dross, shop sweepings, &c., are all being dealt with. Over 1500 tons of renovated white-metal ingots and 1500 tons of brass and bronze ingots are produced each year. The other Regions all carried out a certain amount of reclamation, but had not developed the process to such an extent as had the London Midland.

Inquiries by the Committee showed that some 80 different varieties of non-ferrous scrap are encountered in Railway Executive workshops and stores. As



different terms were being used in the various Regions for what appeared to be the same type of scrap, the Committee recommended that standard terms be used and drew up a schedule listing the type of scrap, how and where it arose, its present description, and the term recommended for future use. These standard terms have now been introduced and are in regular use.

Of the 27,000 tons of non-ferrous scrap produced in Railway Executive shops annually, some 12,000 are sold and the remainder used again by them. Surplus non-ferrous metal scrap and residues are accumulated in the stores at each main works, being segregated according to a standard classification.

The author wishes to thank Mr. R. A. Riddles, the member of the Railway Executive for Mechanical and Electrical Engineering, for permission to present this paper.

## The Influence of Specifications on Productivity and the Economic Utilization of Ferrous and Non-Ferrous Metals

By F. HUDSON \*

I shall try to correlate some of the more important aspects associated with the influence of specifications on productivity and the supply position, and to indicate one or two factors of major importance common to the subject as a whole.

Before maximum productivity can be obtained, in conjunction with the most efficient use of available raw materials, consideration must be given to the greater use of simplification, standardization, and specialization methods, so that manufacturing operations can be properly planned. According to the British Productivity Report "Simplification in Industry" these terms can be defined as follows:

*Simplification* is the process of reducing the number of types and varieties of products made.

*Standardization* is the process of organizing agreement on (i) a standard for a particular product, range of products, or procedure, and (ii) the application of that standard. A standard is a definition with reference to performance, quality, composition, dimensions, or method of manufacture or testing.

*Specialization* is the application of particular productive resources exclusively to the manufacture of a narrow range of products.

Simplification and standardization must go hand in hand, since too many specifications may be just as bad as none at all so far as efficient production methods are concerned. An endeavour should therefore be made to plan production so that the minimum number of standard metals and alloys is required. The ideal

would be the use of one metal or alloy, a condition which may be difficult to obtain in many factories.

In British Standard 970 (1947), covering wrought steels for use up to 6-in. rolling section for automobile and general engineering purposes, some 137 steels are listed. Are all of these really necessary? British Standard Schedule 1400 (1948), covering copper alloy ingots and castings, outlines 23 different alloys for castings. The bulk of industrial requirements for castings can probably be met by 10 copper-base alloys, and these can be readily grouped into 7 main types for production purposes. Agreement regarding tolerances on certain elements, normally considered as impurities, would reduce the number of alloys required still further. The simplification of alloys in this way assists productivity in both melting shop and foundry and aids the subsequent reclamation of scrap. Those responsible for the drafting of future standard specifications should keep this point particularly in mind. It is interesting to note in this connection that the full use of simplification methods has led to a reduction in the number of alloys employed in America. In the plants visited last year by the British Brassfoundry Productivity Team, approximately 75% of the total output of castings was in 85 : 5 : 5 : 5 gun-metal.

Manufacturers should take every opportunity of educating users of metal products to appreciate factors which promote high productivity, namely the use of a limited number of standard alloys and the importance of ordering components of the same design in sufficient quantity, so that mass-production methods may be employed. Users of metal articles should try to apply simplification methods to their products to the utmost possible extent. Whilst it is not always possible to reduce the variety of finished products, many components making up the whole can often be made identical, enabling sub-assemblies of one particular part of the final assembly to be produced in greater quantities.

The next most important factors in obtaining increased productivity in conjunction with the best use of available materials are undoubtedly design and quality control. Specifications in most cases cover only the quality of the metal in a test-bar, and this is of limited value to the engineer in designing a structure composed of rolled, forged, stamped, or cast components. There is particular need for greater attention to be given to the quality of castings, and for research on the relation between test-bar and casting. Designers and engineers today appreciate that neither integral nor separately cast test-bars normally exhibit mechanical properties representative of the casting. When designing castings the engineer therefore increases his section to ensure an adequate factor of safety. This obviously increases the weight of the casting and the amount of metal required. In discussing this matter with a firm of marine engineers of international repute, I was told that the design of

\* The Mond Nickel Co., Ltd.

bronze and gun-metal castings was based on 50% of the specified test-bar properties. In other words, the castings were twice as thick and twice as heavy as they need have been had the founder been able to produce castings having similar properties to those obtainable from separately cast test-bars. The production of castings of better quality, enabling designers to reduce the section and weight, will obviously lead to substantial economy in the use of metal.

The problem is, however, a long-term one. It is hoped that every brassfounder will give this matter serious attention, as indicated in a paper on "The Mechanical Properties of Some Copper-Base Alloy Castings", presented to the Institute of British Foundrymen by the Technical Committee of the Association of Bronze and Brass Founders in 1949. In that report it is suggested that improvements in the quality of cast products may be sought along several lines. First, by co-operation between designer and manufacturer with a view to evolving designs which will meet the designer's requirements and at the same time be conducive to the production of a sound casting. Secondly, by improvement in manufacturing technique derived from the results of fundamental research, allied with manufacturing experience. Thirdly, by research which promotes a better understanding of the casting characteristics of the materials, and to provide materials with improved casting characteristics.

Incidentally, the results given in the paper to which I refer support the belief that alloys with long freezing ranges, such as bronze and gun-metal, are liable to contain dispersed porosity which lowers their mechanical properties, whilst castings in alloys with a short freezing range, such as high-tensile brass and aluminium bronze, can be made completely sound and with properties equal to those of separately cast test-bars, provided the metal is not gassy and that the castings are properly fed. It might be suggested, therefore, that, to make the best use of available supplies of metal, wherever design and service conditions permit centrifugal and chill-casting methods should be used for the production of bronze and gun-metal castings, and greater consideration given to the use of high-strength alloys. This will enable the founder to produce castings with superior mechanical properties, which the designer can utilize for reducing section and weight.

In order to obtain increased productivity from available supplies of metal, it is essential that foundries should use metal more economically. This can be brought about by the production of castings of higher quality, enabling engineers and designers to reduce section and weight. Furthermore, this increase in quality must be obtained wherever possible by a reduction in the number of defective castings produced. In order to attain this ideal, brassfounders must give greater attention to the technical control of casting quality. To cover this subject fully would

require a separate paper, and at the moment it is possible only to make brief mention of one or two of the more important production factors which merit careful consideration.

These factors include: (i) more general use of degassing methods in conjunction with the development of a rapid control test to assess melt quality; (ii) more effective control of pouring temperatures; (iii) more effective control of the properties of moulding and core sands; (iv) improvements in running and feeding methods; and (v) the adoption of a standard inspection procedure, such as that covered by B.S. 1367 (1947) based on the assessment of actual casting quality, as distinct from the use of separately or integrally cast test-bars. Incidentally, some action on this last point is badly needed, as at the moment manufacturers have to deal with many inspecting bodies, each having its own particular inspection requirements, and this does not assist either productivity or the economic utilization of metals. It would be a great help if we could have one standard inspection system which would be acceptable to all inspecting bodies.

## Secondary Heavy Metals

By E. H. JONES \*

Cost of work versus value of metal determines the limits of both primary and secondary recovery, but no minimum concentration of general application can be calculated. Variation in the scale of operations possible and the chemical and physical state of the raw material are very important factors; for instance, the average discard slag of the tin smelter is often higher than the ores before initial concentration. Although it is likely that prices will continue to rise relative to the cost of work, and that the latter will also be lowered by technical advance, it is possible to make a rough division into recoverable and irrecoverable fractions. Only after a metal has been put to some use can it really be considered secondary, but since the cycling load of residues from smelting and fabricating operations is very large, and as secondary smelters treat considerable quantities of by-products from primary sources, the usual figures given are often misleading.

It is, however, possible to divide consumption into categories for most heavy metals in the U.S.A. and United Kingdom, usually for many years. An estimate of the average life of equipment containing the metals in one form or another can be made from standard depreciation tables and from trade inquiries. Where "old" scrap figures are given in statistics, these can then be related to the period of consumption and a fraction obtained representing what has been recovered (Table XVIII). It is possible to check the results to some extent by comparing those for different metals in the same alloy. The fraction

\* Copper Pass and Son, Ltd., Bristol.



recovered, multiplied by the consumption during the period calculated for the average time in use, will give the total recoverable stock under present economic conditions (Table XIX). Wegner\* has esti-

TABLE XVIII.—*Consumption and Recovery of Heavy Metals.*

		Element, %	Alloys, %	Coatings, %	Compounds, %	Total Recovered, %
Tin	Used	4	46	48	2	...
	Recovered	2	24	6	0	32
Copper	Used	57	39	...	4	...
	Recovered	38	20	...	0	58
Zinc	Used	7	45	35	13	...
	Recovered	4	25	0	0	29
Lead	Used	40	40	...	20	...
	Recovered	32	28	...	0	60
Antimony	Used	...	60	...	40	...
	Recovered	...	45	...	0	45

TABLE XIX.—*Recoverable Stock of Heavy Metals in Use.*

(Million tons)

	Tin	Copper	Zinc	Lead	Antimony
Author's estimate .	1.5	40	11	32	0.5
Wegner's estimate	...	70	49	70	...

mated the amount left after deducting loss by corrosion and wear from the total amount mined. His figures are given for copper, lead, and zinc; they appear high, especially that for zinc, but both sets of figures in Table XIX can be taken only as giving some idea of the amounts involved. The differences represent the secondary marginal reserves; an increase in price not only cuts consumption but increases collection from these reserves almost immediately.

The concentration of these stocks is not uniform; the U.S.A. must be increasing its holding as the other countries press manufactured articles on it in return for its highly desirable currency. All figures relate only to the free world.

Consumption, other than stockpiling, including secondaries is :

Tin . . . . .	180,000 tons
Copper . . . . .	2,800,000 "
Zinc . . . . .	2,100,000 "
Lead . . . . .	2,400,000 "
Antimony . . . . .	50,000 "

The use of secondary tin in alloys is around 60% of the total, but some of this is derived from the detinning of tinplate. Adjusting for this, it would seem that some 50% of the tin used in alloys is lost. This appears very high, but tin alloys, especially solders, are used in small portions at a time and are, therefore, well dispersed.

For zinc the figures given for coatings will appear low if referred to published statistics; this is because the tonnage delivered to galvanizers is some 20% higher than that sold on their products, owing to the redistillation of about this fraction from residues, mainly hard spelter, produced during galvanizing. The figure for recovery from zinc alloys is not too sound; it is too early to estimate the fraction for die-casting metal. Brass is the traditional metal for small articles such as screws, fittings, cheap jewellery, &c. This will tend to lower the fraction of alloys recoverable.

### Compounds

It will be seen that salts are considerable fractions and these are almost wholly lost. There are exceptions: for example, zinc used as blue powder as a reducing agent is mostly returned, although it then usually ends as pigment and is finally lost; litharge, if used as paste in storage battery manufacture, is recovered as metal. These uses have not been included in the compound fractions. Normally, a very large proportion is made from metal that has already been used as element or alloy; much low-grade brass is converted into copper sulphate and lithopone. As the price rises, substitution is almost automatic in most cases, but so far no fungicide with all the desirable properties of copper-containing mixtures has been found, and it seems that lead tetra-ethyl will continue to be used, even with lead at many times today's price, until the Diesel or the internal-combustion turbine replaces the high-compression petrol engine. This use of lead has increased in the last quarter of a century to about 10% of the total consumption and, since the metal is very effectively dispersed, no recovery is possible. If the use continues and increases with greater use of motor transport, it could in the end become the only large-scale use of lead until the adoption of alternative forms of prime-mover became general.

### Coatings

Although plating with nickel and silver is done for the sake of appearance, most coatings are applied to protect a metal with desired structural properties from corrosion. An exception is gilding metal on steel, used in small-arms ammunition, where the backing metal is used mainly to economize in the use of the other. In the case of alloys, the extent of secondary recovery depends very much on the size of the article, since this determines the difficulty of collection after use; but in the case of coatings the general use of steel as the backing metal adds the magnet as a collecting tool, and the proportion recovered is decided by other factors. These are so varied that it will be clearer to deal with the main coated products individually.

Collection of scrap tinplate, including old cans, is well organized, and the return of tin and steel is a significant fraction of the total consumption. As

\* *Metall*, 1950, 4, (7/8), 156.

there is no method of removing small amounts of tin from steel, it must be stripped from the plate before melting in the open-hearth furnace. Two processes are used, one depending on the volatilization of tin chloride and the other on the solution of tin in caustic soda. While metallic tin could be recovered by the chloride process, this process is normally used only to the extent that there is a demand for tin chlorides as mordants or reducing agents, and the metal is ultimately lost. The caustic-soda method yields metallic tin, and is the process used for most detinning.

It will be seen that the operation will be economic only if the value of the coating for unit area exceeds a certain minimum, this in turn being decided by the price of tin and the thickness. Should the value fall too low the scrap would remain untreated and, as the coating may still be too high to be tolerated by the mild-steel maker, both tin and iron would be lost. Assuming that 20% of the tinplate used is recovered when the average coating makes detinning just economical, a cut in the thickness by less than 20% would actually increase the net loss of tin. It is also apparent that a fall in the price of tin would necessitate an increase of coating thickness to avoid the same result; in normal circumstances this would, of course, occur, although there would be a rather long time-lag.

The value of the coating on galvanized iron has never been high enough to warrant dezincing on the lines of detinning operations, but there are also two other significant differences; the coating is to some extent sacrificed during use, and its removal at the steelworks is relatively easy. Zinc used in galvanizing is likely to continue to be lost; if the price rose very high it might pay to treat the material in open-hearth furnaces to make steel and a zincy fume, but the volume of gas to be treated per unit of zinc would be very large. Cadmium plating is mainly electrolytic and, although the price of the metal is very high, the coating is thin; nevertheless, if cadmium-plated articles were in more general use or not so widely dispersed, a leaching method of recovery would be economically possible.

The replacement of cupro-nickel by steel-backed gilding metal (copper 90%, zinc 10%), as with the bullet envelope in small-arms ammunition, brought recovery problems. Since only bullets collected at practice butts are recovered, the saving of copper and nickel must have been considerable, but the scrap strip from which the blanks had been punched, and the wasters, could no longer be re-melted and re-rolled. Although during the war at least two processes were recommended specifically to separate and recover the copper and iron, most of the scrap was used as flux in lead smelting with the formation of a leady copper matte, the copper ending as copper sulphate and the iron as silicate in the slag. There is no doubt that, with an assured supply warranting the investment in plant, either of the two processes mentioned above would have been much more efficient, but war is still considered a temporary state of affairs.

### *Alloys and Elements*

Except in the case of elemental zinc, corrosion and wear are probably not the cause of serious loss. Indeed, not all the products of corrosion are lost; they may adhere to the surface, or be collected, as in the case of lead sulphate from chemical plants, the metal content being recovered by the secondary smelter.

The proportion ultimately recovered of the metal used as the element, or as an alloy of which it is a major constituent, depends mainly on the size of the article manufactured. A very easy method of conserving, say, copper would be for the United Nations to insist that no end-use product of copper, brass or bronze should weigh less than a pound. The effect would be chaotic, but there is no doubt that the method would appeal to modern Governments much more than the traditional one of allowing the price to increase. Copper and zinc in screws, nuts and bolts, locks, keys, furniture fittings, and such small items must be written off as almost wholly lost.

The collected scrap can be divided into two main categories: (i) clean pieces that can be re-melted and, after adjustment of composition, cast into ingots for return to the fabricator; and (ii) material that by design or accident has become attached to other metals or inorganic materials so firmly that physical separation is difficult or impossible. The latter are smelted, and during the operation some of the metal is lost. Sometimes in the case of alloys the whole of one constituent may be wasted; for example, the presence of steel inserts, screws, &c., in brass articles has in the past caused considerable dispersion of zinc into the atmosphere. Even today, when most copper smelters' fume is collected, a process for the removal of iron from brasses and bronzes would save much metal and an even greater value in metallurgical work.

Smelting removes non-metallics, aluminium, magnesium, and some zinc in the slag, and volatilizes zinc and cadmium which are caught as an impure fume. The metallic product will normally be an impure mixture and, if this can be refined and adjusted to a marketable alloy, the loss and work will naturally be less than if the elements have to be produced to ensure sale. The alloy must normally meet some specification or other and, if the maximum metal is to be regained from scrap, it is essential that such specifications should be realistic. A very low limit put on, say, iron or nickel in brass, bronze, or solder, or on bismuth in lead alloys, because it is safer in the absence of information about the amount that could be tolerated without deleterious effects, wastes both work and metal.

The introduction of new alloys containing elements that were not previously used in the same range can increase the problems of the secondary smelter very considerably. Even if the greatest care is taken in segregation during collection, some mixing of scrap and residues is inevitable, and the abnormal elements must be removed by metallurgical means before an alloy of use as a basis for a saleable range can be



obtained. Examples are the use of nickel in bearing metals, tellurium in lead, and arsenic and silver in solders.

The effect of relative prices not only of the metals but of fuel, power, labour, &c., on the adjustment of the smelters' flowsheet, is considerable. When the price of zinc is low, the lead smelter will use it to remove impurities and ultimately lose it in slag; aluminium will be used to remove antimony from solder, instead of the more laborious process of liquation or fluoborate electrolysis. The optimum economic metal content of discarded residues, whether the slag of copper, tin, and lead smelting, or the retort residue in the case of zinc, is a varying equilibrium between value of recovery and cost of work done, and is the subject of constant calculation. It has been truly said that a smelter should never finally throw away anything, since the concentrations in Nature are being steadily exhausted and the relative value of the metal increasing. Dumps of slag and residues then become valuable reserves.

The secondary smelter very rarely treats only materials that have been used by the community; much of its raw material consists of complex concentrations of by-products from primary plants, and quite often complex minerals as well. The plant must be as flexible as possible and, therefore, the tonnages produced relative to the size of the enterprise seem very small compared to those of the primary smelter. The great variation in feed makes the production of a range of elements and alloys necessary, although usually these are kept to a minimum by selling by-products to other refiners. A convenient and competitive outlet for materials not suitable for treatment at the producer's plant is of great value. A comprehensive extractive metallurgical industry, comprising many plants each specializing in some field, was an important factor in the success of German pre-war secondary smelting.

There is scope for very considerable technical improvement; the treatment of complex arsenides is alone worth study, but it is doubtful whether the difference between present technique and perfection would materially alter the rate at which Man is scattering the metals under review beyond practical recovery. This need not worry us unduly; for most uses there are economically possible substitutes for each of these metals: reserves, primary and secondary, are sufficient to supply the remaining uses for a time stretching well beyond that within our power to foresee.

## Secondary Aluminium and Magnesium

By COLONEL W. C. DEVEREUX,\* C.B.E.

The production of secondary light metals and alloys from scrap and waste materials, as an integrated and scientifically controlled industrial process, was some-

what delayed in this country. In the U.S.A. and Germany, the basis of such an industry had been laid during the 1914-18 war, and by 1926 secondary aluminium in the U.S.A. had reached an estimated annual production of 44,000 tons.

The United Kingdom secondary aluminium industry as we know it today did not really get under way until the early thirties. In those days the consumption of aluminium in the United Kingdom was relatively small—about 20,000 tons of primary metal a year, out of a world total of 180,000 tons. Moreover, consumption in earlier years had been even smaller, so that the arisings of old scrap had not then been large enough to sustain a separate secondary industry. Once started, however, the secondary smelting industry advanced rapidly. At first the smelters had to content themselves with supplying second-grade foundry alloys and deoxidizing material and with exports; but by 1935 they had reached a production of about 10,000-12,000 tons a year.

By a vigilant policy of laboratory control of quality, they patiently set about overcoming the prejudices against their products, and by the outbreak of the

TABLE XX.—*Production and Consumption of Secondary Aluminium in United Kingdom.*

Year	Secondary Production, tons			Aluminium Consumption, tons			Percentage of Secondary Used
	Smelters	MPRD's *	Total	Virgin	Secondary	Total	
1940	37,000 †	900 †	37,900	102,300	32,200	134,500	24
1941	50,300	2,900	53,200	116,800	49,000	165,800	30
1942	75,300	3,500	78,800	195,300	63,800	259,100	25
1943	87,700	5,800	93,500	208,200	85,500	293,700	29
1944	95,900	8,600	104,500	150,100	71,700	221,800	32
1945	61,900	19,100	81,000	94,900	51,200	146,100	35
1946	48,600	26,300	74,900	114,600	82,600	197,200	42
1947	63,700	33,900	97,600	159,200	107,500	266,700	40
1948	63,300	16,800	80,100	173,700	69,400	243,100	29
1949	68,600	6,600	75,200	178,600	68,400	247,000	28
1950	86,400	...	86,400	181,400	93,800	275,200	34
1951 ‡	89,300	...	89,300	185,300	131,800	317,100	42

\* Ministry of Supply Recovery Plants.

† Estimated.

‡ Estimated as twice the figure for January-June 1951.

recent war it was generally accepted that secondary alloys were metallurgically equivalent to those made from primary material. The advent of the war brought about a complete change in the status of the industry, which now assumed a role of great importance and, although the discriminatory clauses were not removed from official specifications until after the war, they were tacitly ignored. Table XX shows production and consumption since 1940, when 32,000 tons of secondary metal were used. Since the war its use has continued to increase, reaching a record yearly rate of about 130,000 tons in the first half of 1951—over a third of the total raw material used by the aluminium fabricating industry. In terms of money this represents about £14 million.

The recovery of magnesium alloys from scrap had meanwhile also made progress. No statistical data

\* Managing Director, Almin, Ltd.; Chairman, International Alloys, Ltd.

are available, but it is estimated that of the total consumption, which at present is at the rate of 5500 tons per year, something between a quarter and a third is met by recovery from scrap.

### *Sorting of Scrap*

Hand sorting of large pieces of scrap is still done mainly by experienced but not technically trained workers, with the support of a few very simple tests. The so-called spot tests for identification of alloys have not found use as routine tests in sorting single pieces, as they are still too slow for this purpose. Recently, instruments have been developed which seem to offer possibilities of comparing in a few seconds the electrical and magnetic properties of alloys. Perhaps these instruments will in future become useful in routine sorting in special cases. A very striking improvement in sorting efficiency has been effected by one company by putting a skilled chemist on the job to guide and support the sorters with various tests and better general technical knowledge.

Sorting of small pieces can be economical only if it is mechanized, and so far is limited to magnetic separation of ferrous metals. Obviously there is great scope for further inventions in this field. Large-scale experiments with mechanized sorting on the sink-and-float principle were technically successful, but the present market situation does not permit exploitation of the process.

For composite structures containing light metal parts and other metals, sorting before the melting operation is often impracticable, and separation is effected by the use of liquation furnaces, a method which has been used on a large scale for aircraft scrap. As the use of the liquation furnace seems now firmly established, it will be interesting to compare views on the most suitable designs.

### *Melting and Metallurgical Treatment*

On the question of furnace equipment there is at present a division of opinion about the merits and limitations of the rotary furnace, which is built with capacities between 1 and 8 tons, and reverberatory furnace, which generally covers the range between 10 and 25 tons capacity. The Americans, with their generally larger output and their strong interest in mechanizing charging and pouring operations, have set themselves to adapting the reverberatory furnace to intensive flux treatment as necessary for the melting of scrap, and have produced very useful furnace designs. On the other hand, in Europe the rotary furnace, with its short melting cycle and great flexibility, is firmly established. The two methods have been compared recently by a mission of European specialists sent to America by O.E.E.C., and it is hoped that a useful clarification of opinions on this point will arise from their reports.

A recent development in the melting equipment is the use of the low-frequency induction furnace for melting many kinds of scrap, including turnings, as long as they are fairly clean. This equipment has

been operated mainly in Germany and America, and apparently has given good results in production.

Refining of aluminium and magnesium in the classic sense, i.e. for production of pure aluminium or magnesium, is at the present time technically possible but not economically justified, since, as a rule, all the metallic material available can be incorporated into useful alloys. The scope of the present refining technique is, therefore, confined to the elimination of metallic inclusions, oxide, &c., and of gases, the treatment consisting essentially of melting under a flux the action of which is to lift the oxide from the liquid melt by surface-tension forces and to keep it enveloped in slag. It has been shown that solution of oxide in the slag does not play any appreciable part in the slag treatment either of aluminium or of magnesium.

The only industrial refining operation in the more classic sense is the elimination of magnesium from aluminium alloys. The removal of other alloying elements is not at the moment economical.

High-class technical, and especially analytical, laboratory control is essential in all stages of scrap recovery, sorting, blending, furnace control, and release. Requirements in precision of analysis in secondary-metal production are often higher than in producing alloy from virgin material. As a consequence, the art of analysis, especially of aluminium, has received valuable contributions from the work of the laboratories of the remelting industry.

The production of secondary magnesium alloys proceeds technically on similar lines to the production of secondary aluminium alloys, with the well-known differences in fluxing and melting treatment. This applies to the more compact forms of scrap. Turnings and sawings can be re-melted with due precautions, but, apart from the flux consumption, the economy of this recovery is reduced by the precautions to be taken in storing and transporting this material, which is more sensitive to the influence of air and moisture than the corresponding aluminium scrap. The recovery of magnesium from skimmings and grindings is not practicable at the moment.

### *Scrap Arisings*

By no means all the scrap metal recovered is handled by the secondary smelters. There is always in the works of the fabricators a large amount of scrap runners and risers, discards, sheet clippings, &c., which nowadays never comes on to the market at all, but which goes straight back into the furnaces with the primary material. Material of this kind is termed *process scrap*.

*New scrap* is scrap arising at the second stage of manufacture, i.e. in the works of the users of semi-manufactures. The quality of this scrap ranges from fairly massive and therefore readily identifiable forms, such as off-cuts from sheet and extruded sections, and scrapped castings, to machine-shop swarf and turnings. Not all this is available to the secondary industry, owing to special arrangements sometimes



made by fabricators with their larger customers for the return of the more solid types of scrap. Since the turnover of this scrap is fairly rapid, the quantity available bears a fairly constant relationship to the scale of activity of the fabricating industry. This is true also of dross, skimmings, grindings, &c., which, although strictly coming under the heading of new scrap, require such specialized treatment that they constitute a separate class of their own, and are almost all handled by the remelting industry.

The third main group of scrap is *old scrap*, i.e. arisings from obsolete, damaged, or worn-out machinery, structures, utensils, &c. It also includes the special class of aircraft scrap.

The question of what proportions of our secondary metals derive from new and old scrap respectively is interesting and important to the study of future trends. New scrap arisings are directly related to the scale of use of aluminium at any given time and bear a fairly constant relationship to it, although this proportion is not fixed absolutely. If anything, it

TABLE XXI.—*Production of Secondary Aluminium in U.S.A.*

(Short tons)

Year	From New Scrap	From Old Scrap
1935-1939 (average)	16,000	35,000
1939	16,200	37,800
1940	34,600	45,800
1941	63,700	43,100
1942	154,800	41,600
1943	280,900	33,100
1944	302,700	22,900
1945	271,100	27,300
1946	187,500	90,500
1947	181,000	163,800
1948	191,100	95,000
1949	136,200	44,600

tends to fall as efficiency of utilization increases, a point well illustrated by the reduction in the proportion of turnings arising as the use of die-castings increases at the expense of sand castings. Unfortunately, we have no accurate statistics on this point, though we may learn something from the U.S. figures shown in Tables XXI and XXII.

It will be seen that in the pre-war years about 70% of secondary metal in the U.S.A. derived from old scrap, but that since then the proportion of new scrap has exceeded old scrap by a considerable margin. This is to be expected, since in 1935-39 the fabrication of aluminium was increasing only slowly, while expansion since then has been very great indeed. The really interesting thing about these figures is the trend of the old scrap figures. There is the effect of the scrap drive in 1940-42, and the shortage in 1943-45 as a result thereof. Note also the great increase in 1945-48, when aircraft scrap was used in large quantities, and the apparent return to normality in 1949.

### Supply and Demand

Generally speaking, the relation of supply to demand for scrap and secondary metal follows the same lines as for other basic commodities, being perhaps among the items most sensitive to economic conditions. While production of fabricated products

TABLE XXII.—*Consumption of Scrap by Remelters, Smelters, and Refiners in U.S.A. in 1949.*

(Short tons)

Source	New Scrap	Old Scrap
Pure clippings, wire foil, &c.	9,618	273
Castings, forgings	14,310	12,027
Alloy sheet	21,027	2,511
Scrap sheet, sheet utensils	...	5,900
Borings and turnings	27,532	...
Wrecked aircraft	...	10,188
Miscellaneous and dross	12,798	12,288
Total	85,285	43,187

risers, scrap arisings tend to fall behind demand because of their relation to the smaller scale of earlier production. Conversely, it would appear that a surplus of scrap should arise when production decreases, because the process scrap from previous larger output flows back to be combined with the present smaller production as shown in Table XXIII. It must be admitted that this is not borne out by the events of the past six years, but then special measures were adopted to utilize the accumulated aircraft scrap, for instance, by inclusion in the aluminium houses of which vast quantities were sold, much to our regret at the moment.

In an interesting article written in 1944, Korn calculated that there may come a time in the distant future when, under stable conditions of aluminium consumption, 75% of the total demand for alu-

TABLE XXIII.—*Aluminium Scrap Arisings and Consumption in the United Kingdom.*

Year	Arisings, tons	Consumption, tons	Total Consumption of Virgin and Secondary,* tons	Arisings as Proportion of Virgin and Secondary Consumption, %
1941	66,700	59,400	165,800	40
1942	97,300	91,700	259,100	38
1943	121,800	110,900	293,700	41
1944	125,400	123,500	221,800	57
1945	71,000	83,200	146,100	49
1946	73,700	70,200	197,200	37
1947	118,300	92,300	266,700	44
1948	131,100	102,100	243,100	54
1949	99,900	104,500	247,000	40
1950	92,800	118,500	275,200	34
1951 †	93,200	110,300	317,100	29

\* This total is somewhat in excess of actual consumption, since secondary output contains some virgin metal which is therefore included twice. However, although in the present circumstances this is higher than usual, the proportion of virgin metal is normally well below 10%.

† Estimated as twice the figure for January-June 1951.

minium could be supplied from secondary metal. We are not concerned here to look so very far ahead, but it is a suggestion of how the importance of secondary metal will tend to increase. At present in most industrial countries the proportion of secondary metal, excluding process scrap, incorporated into the total aluminium consumption tends to be around 30%, as shown in Table XXIV.

Overall United Kingdom production of secondary ingot since 1940 has been in excess of consumption, so that substantial stocks were built up, amounting to 118,000 tons at the end of 1949. In the last year, however, consumption has increased sharply and currently stocks are being consumed at the rate of about 40,000 tons a year, at which rate stocks will be exhausted by the end of 1952, if not before.

A similar situation exists in the case of scrap arisings. Excluding arisings of aircraft scrap consumed at Government scrap-recovery plant, the excess of arisings over consumption from 1941 to July 1951, was about 30,000 tons. At the current rate of excess of consumption over arisings of about 20,000 tons a

in which aluminium was chosen partly because of the very long life-span it offers. In particular, I would mention building applications, which have consumed about 250,000 tons since 1945. It will be many years before material so used will come on the market as scrap. Such uses are, however, balanced to some extent from the secondary point of view by a rapid rise of some very short-life uses, particularly in the packaging industry, but to exploit this potential source of scrap presents very considerable difficulties.

Since 1948 the use of aluminium for packaging has more than doubled. It is currently running at about 30,000 tons a year. Assuming 70% of this actually goes into food cans, bottle lids and caps, foil wrappings, &c., there is some 20,000 tons of potential scrap which should arise within a year or two of manufacture. This scrap is the most difficult to collect, relying mainly on collection by local authorities, charitable and voluntary organizations, hospitals, &c. However, this is potentially worth something like £1½ million a year, and seems likely to increase, so that it might be worth while considering expenditure of a few thousand pounds a year in propaganda to make the public aware of the importance of this and other forms of household scrap as dollar savers and to encourage their segregation and collection.

TABLE XXIV.—*Proportion of Secondary Metal in Aluminium Consumption of Various Countries.*

(In 1000 metric tons)

	Total Primary and Secondary Consumption			Secondary Consumption			Per cent. Secondary		
	1948	1949	1950	1948	1949	1950	1948	1949	1950
U.S.A. . . . .	883	742	1082	261	164	265	30	22	24
Total O.E.E.C. countries . . .	538	490	566*	163	140	170*	30	29	31
United Kingdom .	245	250	278	69	69	94	28	28	34
France . . . .	104	68	74*	25	20	20*	24	29	27
Germany . . .	75	59	75*	42	23	30*	56	39	40

Sources: For European countries, O.E.E.C. reports. For United States, Bureau of Mines. For United Kingdom, Ministry of Supply Light Metal Statistics.

\* Estimated.

year, this source will soon be exhausted. If the rate of scrap arisings were to remain as at present, i.e. about 95,000 tons, then the production of secondary aluminium would be limited to about 82,000 tons, i.e. about 8,000 tons below the rate in the first half of 1951 and nearly 50,000 tons below the current rate of consumption. These figures must not be taken too literally, as experience has shown that more scrap can usually be found when the time comes to "scrape the barrel"; but it is certain that even if the smelters can somehow maintain the present rate of output, the amount available for consumption must fall considerably.

What makes attempts at accurate forecasts very unreliable is the dynamic nature of such a young industry as ours, particularly in regard to the constantly changing pattern of the uses of aluminium. Before the war a very high proportion of the aluminium used went into machines of moderate life-span, e.g. motor vehicles, aircraft, &c., whereas some important post-war applications have been developed

#### *Influence of Export Drive*

The high rate of export of manufactured goods has a very profound influence on the arisings of scrap, since many of the commodities for which there are the largest export markets use large quantities of aluminium, e.g. motor vehicles, vacuum cleaners, washing machines, &c. Road vehicles, for example, are among the largest users of aluminium alloys, and before the war scrapped motor cars and components provided substantial quantities of material for secondary smelters.

Road vehicles consume nearly 50,000 tons of aluminium semi-manufactures a year. If we assume that 80% goes into the finished vehicle, then almost 40,000 tons is sent out of the country every year, leaving only 10,000 tons as potential arisings when the vehicles are scrapped, although, of course, with the present shortage of vehicles at home, we shall have to wait a long time for this. The actual arisings now are but a fraction of this figure, being about a quarter of the arisings from this source before the war, in spite of a 100% increase in vehicle production.

From these considerations it appears that we must anticipate a shortage of scrap during the next few years. The abnormally high rate of consumption of old scrap made possible by the channelling of all aluminium into short-lived structures during the war, the necessity to limit dollar imports, the high rate of indirect export of aluminium, the development of long-life uses of the past few years, the difficulty of collecting short-life scrap, and the current rearmament programme all tend to reduce the scrap arisings or increase demand.

In the long run, the more virgin aluminium that is



used the greater the potential scrap arisings, but in the immediate future it is difficult to see how a falling off in supplies can be avoided unless drastic steps are taken to improve the efficiency of scrap collection and utilization. This is not a matter which concerns the scrap merchants and secondary smelters alone. As previous speakers have emphasized, the utilization of scrap is an important factor in the national economy. Improved utilization requires the wholehearted co-operation of the fabricating industry and all users of light metals in scrap segregation and collection and the elimination of wasteful methods of remelting.

### Discussion

**Mr. G. L. Bailey \*** : I should like to suggest that the question of substitute metals must be divided into two parts. In the normal course of events, in say the next five to ten years, we can imagine that there will be available in the world more aluminium, more magnesium, and possibly more titanium. As those materials become available, the price factor and the availability will both conspire to cause people to use those materials, perhaps for purposes for which hitherto other and heavier metals have been used. Substitution of that sort is, I submit, not substitution, but permanent replacement. Such replacement must depend on the efficiency and the economy of the change; if it does not stand on those grounds, then it can be only temporary and will not come into effect on the ordinary basis of a peace-time economy. There will be such changes, and they will be gradual, and a great deal of work will be done to establish the suitability of this or that material, or the action that is necessary to make a particular material suitable for a particular application. Most substitution suggestions for a short-range basis have to face the fact that that substitution may well be uneconomic in money or in man-power or in some other respect. It may be desirable, but we have to face the fact that it is not something done for permanent, good reasons, but only because there is a temporary shortage.

On the question of secondary metals and scrap reclamation, we are all very impressed by what the aluminium industry has done, and I should very much like to see the scale of operations of the secondary copper industry similarly increased—not to the same scale, because the material is not available, but increased very largely.

There are some aspects of reclamation which I do not think have been touched on, for example, reclamation from liquid residues—from pickling solutions, plating solutions, and so on. There is no doubt that a great deal of copper sulphate is still thrown down the drain in this country, whereas its electrolysis would not only permit the recovery of the copper but make possible the regeneration of the sulphuric acid. Another thing which is also being gone into is

the recovery of plating solutions which find their way into the drains in one way or another. One firm has recently installed plant for running its wash water through synthetic resins to recover an extremely valuable metal which is present in very small amounts. Apart from that, drag-out losses from plating tanks can be very considerable, particularly in the nickel-plating industry. The recovery of drag-out from plating solutions is quite an important matter.

On the question of specifications, Mr. Hudson introduced into the title of his paper the influence of specifications on productivity, but I wonder whether he did not forget something about productivity when he talked of using high-strength alloys instead of ordinary gun-metals. No doubt it is possible to make valves of aluminium bronze instead of gun-metal with an economy in the weight of metal used, but I should have thought that that economy is probably offset by the loss of productivity, and, after all, man-power is still one of our most urgent questions, however short we may be of metals.

The possibility, however, that working to a limited number of specifications can greatly increase the economic use of metals is undoubted, and I should only like to be sure that, when people do so, they choose the right alloys from the productivity point of view as well as from the point of view of the availability of the metal.

**Mr. D. A. Oliver †** : In the paper by Bristow, Sidery, and Sutton reference is made to the fact that the designer has great scope for influencing the metal-economy side of the project. I should like to emphasize that point, because there is an idea abroad that metal shortages are a figment of someone's imagination in some Ministry, and that if only we hang on to our existing designs long enough things will right themselves and business will be as usual.

If we are going to make appreciable economies over the national industrial field, it will involve a very large amount of redesign, hard work, fresh development, and testing. In this connection I would draw attention to something that happened in the U.S.A. about a year ago. The radio and television manufacturers there were told that their industry was a luxury one, and that they could have only approximately two-thirds of the metal they had had before to meet a market that was soaring rapidly. They faced the situation, and sets which weighed 28 lb. were redesigned to weigh only 17½ lb. It was a brilliant piece of research from beginning to end.

Possibly it would be useful to mention a few figures for the consumption of scrap taken over this country as a whole. I am contrasting the year 1947 with the first half of 1951 and assuming that the other half of 1951 runs similarly to the first half. In the case of copper, the scrap consumption in 1947 was 35% and this year 40%, showing that either the price structure

\* Director, British Non-Ferrous Metals Research Association.

† Director of Research, B.S.A. Group Research Centre, Sheffield; Metals Economy Adviser, Ministry of Supply.

or the shortage has resulted in an increase of a considerable amount. In the case of lead, the two figures are 43% and 49%, and in the case of zinc 30% and 36%.

**Dr. U. R. Evans \*** : Bristow, Sidery, and Sutton state that corrosion control can contribute substantially to metal conservation. I fully agree. Conversely, prohibition of adequate corrosion control can contribute substantially to metal shortages; this, I think, is a very real danger at present, and is not fully realized at a time when, with a view to economy, the use of non-ferrous metals for the protective coating of steel is being cut down, and relatively large and valuable masses of manufactured steel are in consequence jeopardized.

In this situation, it is logical to consider the principles which govern the way in which protection varies with the thickness of a protective coating. It should be noted that the principles are different according to whether we are considering a metal which is anodic to the steel basis, such as zinc, or a metal like nickel, which is cathodic to the basis. In the case of zinc, it is frequently stated that the useful life of a coating is proportional to its thickness. That, I fear, is an over-simplification, but in certain situations it may serve, and, where it does, it should be relatively easy to decide what thickness of zinc should at the present time be used, having regard to the shortage of zinc and the value of the steel article to be protected.

It is very important to notice, however, that this rule fails completely if the zinc coating is not uniform. I have been told by an authority on galvanizing that below a certain mean thickness of zinc coat it is impossible to attain uniformity, and I think that it will generally be uneconomic to go below that limiting thickness.

The case of nickel is mathematically quite different, as was shown to some extent in recent work in our laboratory by Dr. Shome (work which will be published in the *Journal of the Electrodepositors' Technical Society*) but the outcome of it is the same. A very small reduction in thickness of nickel plating compared with what is customary may seriously cut down the effective protection. I am not a manufacturer, but I confess that one of the things which worry me at the present time is the possibility that our reputation for high quality in export goods will disappear because someone will be tempted to send abroad plated articles which look in the showroom very like those that have been sent in the past, but which will look very different after a short time in service.

That does not apply to metal plating alone, and I am well aware that it does not always result from a desire for economy; sometimes it is due to carelessness.

Speaking quite generally, I would say that there is little doubt that greater care in the choice and application of protective coatings, whether metallic or non-

metallic, would contribute to metal conservation quite as much as the organization of the return of the uncorroded residues to the metallurgical industry in the form of scrap.

**Mr. H. J. Miller †** : Secondary copper and copper-base materials arise from three different sources :

(1) Process scrap, recovered in engineering and other works from the fabrication of various products (sometimes termed "new scrap").

(2) Salvage or demolition scrap, obtained from operations consequent upon the obsolescence of equipment, apparatus, vehicles, buildings, &c. (often described as "old scrap").

(3) Residues comprising the slags, skimmings, and other by-products that arise from the metallurgical industry, which cannot be utilized directly.

The available statistical data reveal the predominant importance of the first two groups: the residue type of material, which needs special processing, arises in much lower quantities. Another point which might be deduced from the available data is that while over extended periods there is a fairly constant flow of scrap, there may be enormous variations in the supplies within short periods, depending entirely on the relative rates of activity of different branches of the industry and on the market sentiment.

Process scrap or new scrap becomes available after an interval of a few weeks or months from the time the semi-fabricated strip, sheet, rod, or other product has been manufactured. The amount of such scrap varies widely, say from 10% to 50% for individual products, though it is probable that it averages about 20% of the total quantity of semi-fabricated material. Clearly, in conditions of expanding trade, the time-lag which occurs before such scrap is returned to the metallurgical works results in a temporary scrap shortage; on the other hand, in conditions of contracting trade, it results in a glut.

The amount of scrap from demolition or salvage operations is subject to an altogether different series of variations. While it is generally recognized that the non-ferrous metals are largely indestructible, and therefore that they may ultimately be recovered, there is nevertheless a fairly large loss due to inevitable waste and the imperfections of salvaging and recovery. It is not possible to state accurately any average recovery factor, but I would place it at 65%—a figure, incidentally, which has previously been established for iron and steel products. This recovery factor may be expected to apply to copper and copper alloy products after they have reached an average life of 25 years. Thus the quantity of old scrap which comes forward at any given time bears a relation to the metal put into service in the previous generation.

\* Reader in the Science of Metallic Corrosion, University of Cambridge.

† British Insulated Callender's Cables, Ltd.



It follows that with conditions of stable industry over a period of 25 years—which conditions have never existed and indeed are unlikely ever to exist—new scrap would amount to 20% of the metallurgical industries' turnover for copper and copper alloys, and the raw material feed would be 65% old scrap. As in general there has been a gradual expansion in the consumption of copper, old scrap has never reached this absolute importance. It is of interest to note that in the years immediately before 1939 in the U.S.A., old scrap amounted to 28% and new scrap to 14%, thus giving a total of 42% of the copper consumption, the remaining 58% being virgin metal. This was an unusual state of affairs, to a large extent brought about by the more or less static industrial activity experienced in the decade 1930-39, and the performance has not been repeated since. In any event I think the figure of 14% for new scrap is on the low side, because of the incompleteness of the statistics.

As regards the uses to which copper and copper alloy scrap may be applied in the metallurgical industry, it is my view that the combined efforts of scrap-metal merchants and consumers have resulted in a satisfactory utilization of material.

I would estimate that on the average all branches of the copper industry can utilize up to 40% of total scrap, so that the virgin copper requirement is 60%. The figures published by the British Bureau of Non-Ferrous Metals Statistics for recent months confirm these percentages. Actually in pre-war years in England the proportions were probably nearer 30% scrap and 70% virgin metal. It is not reasonable to expect that the proportions of scrap can be increased to any considerable extent over the present values; indeed, if, as seems inevitable, there is an extended demand for semi-fabricated materials to have more uniform and superior properties, whether in respect of grain-size, cold-working characteristics, conductivity, or other properties, then the amount of scrap used may actually have to be reduced.

The overall conclusion is that it will not always be possible to absorb all the arising of new and old scrap directly; the excess amounts will of necessity have to be treated for recovery of the constituent metals. Indeed, in U.S.A., such recovery has been undertaken for a very long time now, and large quantities of electrolytic copper have been produced from secondary materials. Owing to the cost of the methods of extraction and purification, the prices which the scrap commands are lower than if it were used for direct production. Hence this recovery has only been made on marginal amounts, and, from the arguments which have been advanced, these marginal amounts will tend to become greater.

Efforts must always be made to ensure a greater direct use of scrap, as this is more economic. To facilitate this, it is most important that process or new scrap should be kept clean and well segregated, and that in the case of old scrap there should be the

most judicious classification. In all instances there should be a maximum up-grading.

**Mr. E. H. Bucknall \*** : The agenda covered earlier this year by the Joint Sub-Committee on the Utilization of Manganese, Nickel, Cobalt, Tungsten, and Molybdenum of the International Materials Conference in Washington included a review of existing specifications, the important problems of substitution and limitation (with special reference to end-uses), and the salvage and use of scrap in certain of the main fields of utilization of the five metals mentioned. In its deliberations, the Sub-Committee tried to adopt a practical outlook and to concern itself with measures which could be applied on the basis of existing technological knowledge.

In conformity with this essentially practical outlook, the discussion of the substitution of the five elements was limited to cases where it seemed likely to ameliorate the present shortages. It was found that great efforts were being made to increase the production of the metals; for example, the production of nickel is expected to be increased by over 30% by 1954. Those steps, however, are unlikely to be sufficient to remedy the present shortages.

It emerged from the Sub-Committee's discussions that one of the most effective means of increasing the availability of these metals was improved scrap salvage, and that measures which procured the return of scrap, so far as possible, to the original producers of the material are the most efficient means, since they put off the time at which the metal becomes so dispersed as to be irrecoverable. One may speculate whether there ought not to be special consideration given to limiting the employment of these metals in circumstances where they become completely unsalvageable, as I presume is the case with the use of cobalt in vitreous enamelling, and of lead in petroleum.

The Sub-Committee came to the conclusion that there were few fields of present application which could be regarded as non-essential, and none of the civilian fields of application which could be called frivolous. On the contrary, it was felt that even in the most favourable cases any substitution of one metal by another involves some sacrifice, and that there are many instances where a reduction in the content of one of the elements in a steel alloy or other product would lower its efficiency in service to an extent which would be intolerable. The Sub-Committee drew special attention to certain specific applications where it felt that there could be no diminution in efficiency and service still be obtained. One instance of that sort is the moving parts of jet aircraft engines. Incidentally, although that case comes from the military field, or from near to the military field, I do not think that anyone on the Sub-Committee held the opinion that all military uses are the most efficient, and that substitution in that field would not provide very great opportunities for conservation.

\* The Mond Nickel Co., Ltd.

# ELECTRIC FURNACES FOR THE THERMAL TREATMENT OF NON-FERROUS METALS AND ALLOYS \*

1347

By C. J. EVANS,† A.M.I.E.E., P. F. HANCOCK,‡ B.A., F.I.M.,  
MEMBER, F. W. HAYWOOD,§ Ph.D., B.Sc., F.R.I.C., F.I.M.,  
MEMBER, and J. McMULLEN,|| A.I.M., MEMBER

## SYNOPSIS

A review is given of the types of furnaces available for the thermal treatment of (a) light alloys and (b) copper, nickel, and their alloys. Reference is made to the use of suitable controlled atmospheres in each case.

Emphasis has been laid on furnaces of highly specialized design, which work in conjunction with conveying or handling gear to fit them into production lines.

## INTRODUCTION

ELECTRIC furnaces find uses, actual or potential, in practically every phase of manufacture of copper, nickel, and their alloys, and of light alloys, from the ingot, slab, or billet, right down to the finished product, wherever the proved advantages of electric heating can be shown to offset the generally higher installation costs as compared with fuel-fired equipment.

The temperatures employed for the various operations in this field extend from about 200° to 1250° C., within which range electric heating by means of metallic resistor elements of various kinds can provide satisfactory service. Nickel-chromium alloys are limited to a maximum temperature of 1200° C. The highest temperatures, however, are called for only in connection with the hot working of some of the higher-nickel alloys. The great majority of treatments on copper, brasses, bronzes, cupro-nickels, &c., produced in tonnage quantities, demand temperatures no higher than 1100° C. In the case of light alloys temperatures rarely exceed 550° C.

In the lower part of this range, up to about 750° C., much use is made in electric furnaces of forced convection, by means of circulating fans, to increase the speed of heat transfer from elements to the charge and so to shorten heating times. In operations where

cooling under a controlled atmosphere forms part of the procedure, similar methods may be employed for speeding up the rate of cooling.

For temperatures above 750° C., convection plays a rapidly diminishing part in heat transfer, and furnaces designed for operation in this range rely primarily on direct radiation from the elements to the charge. In suitable applications, and where the form of the charge permits, resort may be had to the "flash-heating" technique, i.e. the deliberate use of a high temperature gradient between furnace elements and charge to promote rapid transfer.

General furnace construction follows established practice for electric-resistor furnaces. The casings are of sheet steel, made gas-tight when necessary, and mounted on a structural steel framework to give a convenient working height. The heating-chamber lining is usually of light-weight refractory backed by insulation, hard refractory brick being employed only at points where the possibility of wear or damage by the charge renders this necessary. The resistor elements, of heat-resisting alloy in the form of sinuous strip or rod, coiled rod or wire, or occasionally tube, may be mounted in slots in the brickwork of the roof or walls, or suspended by means of hooks or pins. Elements may also be placed in the hearth, if the type of furnace and the operation to be performed make this desirable.

\* Manuscript received 29 September 1951. A contribution on behalf of the Electric Resistance Furnace Section of B.E.A.M.A., to a Symposium on "Equipment for the Thermal Treatment of Non-Ferrous Metals and Alloys", to be held in London on 26 March 1952.

† The General Electric Co., Ltd., England.

‡ Chief Metallurgist, Birlec, Ltd., Birmingham.

§ Technical Director, Wild-Barfield Electric Furnaces, Ltd., Watford; and Chief Metallurgist, G.W.B. Electric Furnaces, Ltd., Dudley and Watford.

|| Chief Metallurgist, Electric Resistance Furnace Co., Ltd., Weybridge.



When designing the furnace elements, care is taken to ensure that the rate of heat dissipation per unit area is selected in relation to their situation in the furnace and the furnace operating temperature regulated in such a way that they do not overheat. In addition, if a controlled atmosphere is being used, appropriate element material must be employed to guarantee long life.

It must be remembered that lubricant carried into the furnace volatilizes and cracks. It will be deposited in the form of soot on the brickwork and can cause short-circuiting between the elements. It may also carburize, or sulphur in it may attack the elements. A minimum of oil on the charge is therefore desirable.

Fully automatic temperature control, together with over-temperature protective devices, is regarded as standard practice, and is generally achieved by means of thermocouples suitably placed in the heating chamber, together with indicating or recording control instruments operating in conjunction with contactors on the power supply. Transformers are often employed to reduce the line voltage to a lower level suitable for connection to the heating elements, particularly when the latter are of heavy section, as is often desirable in order to ensure long element life.

Larger furnaces, particularly those of the continuous type, may be subdivided into several zones, in each of which the heating elements are independently controlled by separate thermocouples and control equipment, an arrangement which gives flexibility in matching the heat input to the demand in different parts of the furnaces, or in enabling any required temperature distribution to be obtained.

Zoning facilitates the maintenance of close temperature uniformity within a large furnace. By careful positioning of the control thermocouples, and by restriction of the lengths of the door zones, rapid establishment of a consistent temperature throughout the furnace is achieved after each operation of the door or doors.

The rapidly increasing use of special atmospheres to eliminate or minimize the incidence of scaling during heating and heat-treatment operations is particularly marked in the non-ferrous field, although it has not been necessary to devote as much attention to protection of the surface of light alloys as to the copper- and nickel-base alloys. In the section dealing with copper and nickel detailed reference is made to suitable atmospheres and generators.

Electric-furnace makers were the pioneers of bright annealing and similar processes, and electric-furnace equipment is specially well adapted for use with a

controlled atmosphere. Particular emphasis may be laid on this important feature and on the varieties of controlled atmosphere that are commercially available.

Many modern electric furnaces are of highly specialized design, built for maximum efficiency in the performance of one particular operation, the trend in this direction, as with machine tools and other industrial equipment, becoming more marked as time goes on.

Probably the choice of batch as against continuous treatment is made primarily on the score of output, size, and nature of the charge. However, when either process is feasible, a continuous process has many attractions, as generally speaking, it ensures the maximum heating and cooling speeds, uniformity of treatment, and should permit the attainment of the best uniform surface finish.

The various types of continuous furnace are designated by the method adopted—invariably automatic—for conveying the work through the furnace. Thus there are the mesh-belt or chain-belt conveyor, the driven-roller hearth, the walking-beam, the pusher, and the chain-conveyor types.

The loading, unloading, and conveying mechanisms are most important pieces of equipment. For slabs the mechanisms fall into three main types: the pusher with shoes on rollers or on skids; the chain conveyor; and the walking beam. For round billets, three further methods are available: the inclined hearth, so designed that the billets roll through the furnace; the diabolo-roller rail used in conjunction with a pusher; and the rotary-hearth furnaces.

Chain conveyors are reliable and satisfactory, when the load is in no way top-heavy, though possibly dearer in first cost. To employ a chain conveyor when there is any danger of the slab falling over, involves the use of "spikes" in the chain links, to maintain spacing. These are not only cumbersome, particularly when making arrangements for the chain return under the furnace, but are costly and not very reliable. Conveyor mechanisms are further discussed in Section A III, 2(c) of the paper.

It has been found convenient to deal with the furnaces for light alloys separately from those used for copper- and nickel-base alloys. The range and scope of the equipment described covers a wide field and, whilst the two sections are complementary to one another, there is some overlapping. This is inevitable, since the problems to be overcome when heating light alloys are frequently similar to those encountered when dealing with copper and nickel alloys.

## A.—Aluminium and Magnesium Alloys

The heat-treatment processes for the light alloys are such as to call for special furnaces, owing to the limited temperature range.

### I.—MAGNESIUM ALLOYS

The mechanical properties of most magnesium alloy castings are improved by suitable heat-treatment. For instance, solution heat-treatment produces maximum shock-resistance and toughness; precipitation-treatment subsequent to solution-treatment gives maximum hardness and yield strength with a loss of ductility. Solution heat-treatment is carried out within the temperature range 420°–425° C., and precipitation heat-treatment within the range 160°–220° C. Stabilization is a fairly recent process, which is really a higher-temperature ageing treatment, a typical example being carried out at 260° C. for a period of 4 hr.

The magnesium alloys are generally heat-treated in dry furnaces of the forced-circulation type, the higher-temperature treatments employing an atmosphere containing 1–2% of sulphur dioxide. This atmosphere is obtained either by the use of sulphur dioxide from bottles or, more generally, by preparing the sulphur dioxide *in situ* in the furnace from sulphur. Completely combusted gases are sometimes used. Salt baths using nitrate salt are not recommended.

### II.—ALUMINIUM ALLOYS

The heat-treatment of aluminium alloys covers the operations known as solution heat-treatment or solution-treatment; precipitation heat-treatment or precipitation-treatment; and annealing. The two former processes result in a change in the properties of the alloys, conferring enhanced strength, whilst annealing produces softening.

#### 1. SOLUTION-TREATMENT

Solution-treatment involves heating and maintaining the alloy at a specified temperature for a specified time under controlled conditions, followed by quenching. The usual temperature range is 470°–540° C., and whatever type of furnace is involved the control must be within at least  $\pm 5^\circ$  C. of the specified temperature. Only when the temperature is as high as practicable is the maximum hardening effect obtained, but the upper temperature limit is set by the risk of burning the alloy. The consistent development of satisfactory and reproducible mechanical properties is the criterion of sound heat-treatment. The required time at temperature cannot be given with the same accuracy as for precipitation-treatment. The soaking times in Table I, quoted for use with salt baths, give a very rough guide only.

TABLE I.—Solution-Treatment Times for Aluminium Alloys in Salt Baths.

	Dimensions	Soaking Time, min.
Sheet and strip	0.018–0.080 in. thick	10–25
	0.128–0.252 „	28–40
Bars or extrusions	Up to 0.5 in. dia.	30
	0.5–1.0 „	45
	For each additional 1 in.	45

After the alloy has been heated, it is removed and quenched, the time interval between removal of the work and complete immersion in the quenching medium being as short as possible. For wrought alloys it should not be more than a few seconds. For example, on sheet material up to 0.10 in. thick, in order to ensure maximum mechanical properties and resistance to corrosion, this time should not exceed 10 sec. However, for castings, a time lag of up to 1 min. can be tolerated.

The usual quenching media employed are water (either cold as a spray, or hot), oil, or air cooling, but the best corrosion-resistance is obtained by using cold water. The choice of medium is governed largely by the need to minimize distortion. Spray-quenching is being increasingly used for sheet material.

#### 2. PRECIPITATION-TREATMENT

In all age-hardening alloys, the strength begins to increase shortly after quenching. Some harden to a greater extent and more rapidly than others. When maintained for some days at normal shop temperature these so-called “natural-ageing” alloys develop their full mechanical properties.

The “artificial-ageing” alloys, whilst hardening slightly at normal temperatures after solution-treatment, do not give optimum mechanical properties unless subjected to precipitation-treatment. This involves heating the quenched alloy at a prescribed temperature between 100° and 200° C. for a definite time, depending upon the composition of the alloy and the required mechanical properties.

The precipitation-treatment temperatures for sheet and strip are between 155° and 185° C.; for tubes the range is 155°–200° C., and for forgings and sections 100°–200° C. The time at temperature varies between 2 and 24 hr. After precipitation-treatment, the method of cooling is not of great importance, although occasionally quenching is employed.

#### 3. ANNEALING

Annealing treatment varies with the composition and condition of the alloy. The strain-hardening resulting from working soft wrought alloys may be removed by annealing in the temperature range



320°–360° C. Heating above 360°–370° C. may cause partial solution-treatment and so prevent full softening, whilst annealing below 320° C. may not give complete recrystallization. Casting alloys are usually annealed in the as-cast condition at approximately 345° C. for about 2 hr. The annealing of heat-treated alloys is normally carried out at  $340^{\circ} \pm 10^{\circ}$  C., and the soaking time is usually 1 hr. Sometimes temperatures of 375° C. are used, but greater care is then necessary to avoid age-hardening.

When annealing, it is necessary to cool the alloy slowly, and in general the slower the rate of cooling the softer the material. However, when a completely heat-treated alloy has to be fully annealed, it is necessary to heat it for 2 hr. at 400°–425° C., followed by slow cooling at about 15° C./hr. until a temperature of 320° C. has been reached. The rate of cooling thereafter is not important.

Aluminium and its alloys are commonly heat-treated in two types of furnaces; salt baths—using nitrate salts—and forced-air-circulation furnaces. There is no need to use a protective atmosphere in the latter type of furnace.

### III.—FURNACES FOR HEAT-TREATMENT

For the sake of convenience heat-treatment furnaces may be split up into two main classes, batch and continuous furnaces. Two types of batch furnace are used, viz. salt baths and forced-air-circulation furnaces. The continuous furnaces are of the forced-air-circulation type. Details of a number of recent installations are given in the following sections.

#### 1. BATCH FURNACES

##### (a) *Salt Baths*

Whatever construction or mode of heating is employed; the salt used is either a nitrate, a mixture of nitrates, or a mixture of nitrates and nitrites, all of the alkali-metal type. Such baths have been in operation for many years, but it is well to stress, at the risk of over-emphasis, what may seem common knowledge. Nitrate and similar baths are very satisfactory if simple precautions are employed in their operation. These are as follows: avoid grease, oil, and organic matter in contact either with the alloys being heat-treated or the salt itself; work must be degreased and perfectly dry; do not overheat the salt bath; do not let other salts (which may be used in a normal heat-treatment shop where both aluminium alloys and steels are heat-treated), such as those containing cyanides, come into contact with the bath; magnesium alloys must not be treated in salt baths; avoid splashing hot salt around the shop.

Despite the many improvements in the design of air furnaces for light alloy heat-treatment and their undoubted superiority for many purposes, the salt bath still retains a field of application and for many purposes is favoured. Because of this it is of interest to draw a brief comparison between the two.

When the charge is immersed in the salt the drop in bath temperature is small and the time to recover temperature is short. Also the rate of heat input to the metal is rapid—an important factor in the prevention of grain growth. For the same reason the salt bath is at a disadvantage where alloys requiring different temperatures of treatment are to be treated in the one unit.

It is usually considered that uniformity of temperature is more easily assured in the salt bath than in the air furnace. This factor minimizes the possibilities of distortion due to uneven heating and, in the case of solution-treated work, allows of the bath being operated at a temperature near to the safe maximum for the alloy concerned. A further advantage is that since part of a load may be withdrawn from the bath as required without interfering with the rate of heat input to the remainder, the treatment of mixed loads of varying section is permissible. The rapid heating obtained in a salt bath is very useful for the treatment of clad alloys; interdiffusion between the cladding and the parent metal is minimized.

On the other hand, there are definite operational disadvantages. First, it is important that all traces of the salt be removed immediately after treatment; adequate washing facilities are therefore required. Second, de-sludging of the bath should be carried out at regular intervals; and finally, the usual precautions in storing and handling nitrate salts must be taken.

The salt bath therefore finds its widest use in the solution-treatment of aluminium alloys; has a limited, but less popular, application to artificial ageing; is not recommended for billet or slab heating; and is unsuitable for annealing.

(i) *Method of Heating*.—Internal heating by means of immersion heaters is now standard practice. External heating by means of elements located outside the pot has never been found satisfactory, as, apart from its well-known disadvantages, there is the difficulty of preventing creep of the salt into the heating chamber, with resulting attack on the elements.

Internal heaters are of the wire-wound resistance type. In some cases they are supported on refractory "spacers" or carriers and shrouded in metallic tubes, the heaters then being arranged along the bottom of the bath with the terminals at one end. In an alternative type of heater the spiral is embedded in insulating material which, in its compact form, has a high thermal conductivity. The elements housed in metallic sheaths are arranged round the sides of the bath and, in the case of the larger baths, they are placed in independently controlled zones graded to compensate for end losses.

(ii) *General Construction*.—The pot, usually rectangular, is built up from heavy-section Armco iron, or alternatively, from high-grade boiler plate, hammer welded externally, electrically welded internally, and stress-relieved after welding.

The tank is surrounded by an adequate thickness of

insulating brickwork and built into a steel outer casing which also serves as the supporting structure for the lid and operating mechanism.

As the maximum heat losses during working occur by radiation from the salt surface, all baths are provided with heavily insulated lids. In the smaller baths, the lids are hand-operated, either of the swing or roll-off type; whereas on the larger baths, the lids are power-operated and of the swing or lift- and roll-off type. The latter are usually push-button controlled.

Fig. 1 shows a cross-section of this type of bath. Such baths have been built in sizes up to 40 ft. long, suitable for extruded sections, sheets, &c. A typical bath for the treatment of extruded sections was 34 ft. long  $\times$  4 ft. deep and 3 ft. wide, and each of the ninety heaters, which were arranged in four independently controlled zones, was rated at  $3\frac{1}{2}$  kW. It

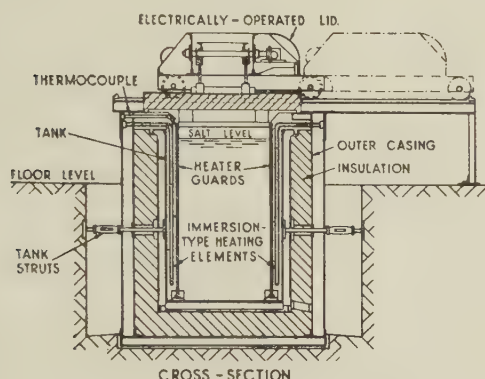


FIG. 1.—Cross-Section of a Salt Bath with Immersion-Type Heating Elements.

is usual to provide each heater with its separate fuse, so that the reduction in power input should an element fail is only fractional and the element can be quickly replaced during the next idling period. For both sheet and coiled strip, units have been built having pot dimensions 22 ft. long  $\times$  7 ft. 6 in. deep  $\times$  4 ft. wide, the rating in this case being 450 kW., controlled in five zones.

For installations such as that illustrated, a circuit-breaker forms the main isolating unit, and this is followed by a switch panel housing the relays and contactors by which the individual zones are controlled, in addition to the pilot lights and master switches. It is usual to instal a stepdown transformer to provide a reduced load to the heaters during soaking and idling periods, controlled by a hand-operated change-over switch. The temperature controllers and recorders are usually of the potentiometric type, and normally a master relay is incorporated which will shut down the whole plant in the event of the bath reaching a dangerous temperature limit. This, in addition, is usually signalled by an audible or visible warning device.

For solution-treatment, the complete plant also includes the quenching tank, together with—and depending upon the type of parts being treated—

some oscillating gear, which assists in the removal of salt from the work. A second tank, of similar dimensions, is used as a cold-water rinse.

#### (b) Forced-Air-Circulation Furnaces

The heating of light alloys presents problems peculiar to these materials. Heat-treatment temperatures are comparatively low, so that the rate of radiant heat transmission is small, while the reflectivity of the surface is high. These two factors, combined with a high heat content, mean that the material is slow to attain temperature. To assist the radiant heat by a measure of convected heat, fans are fitted in the roof of box furnaces, and these rotate in free air without any form of directive ducting. These fans produce a disturbance of the atmosphere, as distinct from a directed forced-air flow. To obtain greater outputs from a given furnace, it is necessary to pack the charge more densely, by such means as standing ingots on their thin edge, and in these circumstances radiation and free convection are comparatively ineffective.

Forced-air circulation, however, with the air made to follow well-defined paths, gives economical outputs. The method in which the fans and elements are applied to the furnace chamber varies considerably, the simplest form being, in effect, a shield fitted between the charge and the elements of the box furnace, so that the fan draws the air in at the top of the baffle and returns it via the heating-element space to the chamber at hearth level. Two large ingot-soaking furnaces have recently been put into commission employing this form of construction. In these particular furnaces the inner baffle is formed from brick side walls and arches, with metal-plate inserts at the fan and element positions. The elements, which are divided into six zones, one to a fan, are not evenly distributed over the side walls but placed in a bank between the two furnace arches. The total rating per furnace is 3720 kW. To cover holding requirements, each zone is further divided, so that the rating may be reduced to a fraction of the maximum. Each fan has a cubic capacity of 22,000 ft.<sup>3</sup>/min. and is capable of dealing with air at temperatures up to 700° C.

This form of air circulation has been effectively applied to coil-annealing furnaces dealing with tightly wound coils of aluminium strip.

The difference between this design and the billet heater lies in the baffle wall being of metal and not brick construction. Coils standing on end, are, of course, particularly suitable for vertical air flow, as the maximum area is exposed to the heating effect of the air stream.

A further development of forced-convection heating is to remove both the fan and the elements from inside the furnace chamber and mount them externally. This has the decided advantage of making the fan runner and the elements accessible for maintenance purposes, without the necessity of cooling off the whole of the furnace chamber; in fact, it may be possible to



run at a reduced output with one zone out of commission. This form can, however, prove inconvenient in construction in certain circumstances and involves a difficulty in effectively lagging the fan casing and element chamber. It is extremely cheap when applied to double-cased ovens which are used for precipitation-treatment.

A typical example of an installation of dry furnaces of the batch type is shown in Fig. 2 (Plate XL). The installation embraces two furnaces with their associated control and electrical equipment, an electrically heated water-quench tank, and a relatively high-speed hoist. Each furnace is designed to cater for the annealing and solution- and precipitation-treatments of light alloys and will accommodate a load of up to 3 tons of components. The effective dimensions of the charge carriers are 7 ft. dia.  $\times$  8 ft. deep. Each furnace has a rating of 150 kW., with means provided of reducing the input for the lower-temperature precipitation-treatment.

Furnaces of this class are generally provided with positive directional air circulation, the air being confined to a closed circuit and circulated continuously in a definite path. To achieve this, the fan is mounted either in the base or in the door behind a throat which engages with a cylindrical drum. An annular space is formed between the drum and the insulated walls of the chamber in which the heating elements are mounted. The air in circulation passes through the annular space, absorbing heat from the elements during its passage, and then passes through the charge. With the larger pit furnaces of the type illustrated, it is common practice to mount the fan and throat in the door, as this facilitates maintenance and at the same time avoids any complicated supporting structure which would otherwise be necessary for carrying a relatively heavy charge above the fan. The resultant door assembly is quite heavy, but is comparatively simple to operate. Both lifting and traversing movements are electrically operated, the lifting being accomplished by screw jacks, chain-driven, through a reduction gear unit, and the traversing through gear trains to the wheels of the door bogie. The two movements are remote-controlled and are interlocked and provided with limit switches to ensure foolproof operation.

Each furnace is of the single-zone pattern and the temperature is controlled by a non-indicating potentiometer with a separate two-point recorder connected to thermocouples at the bottom and top of the furnace, where they indicate, respectively, the controlling temperature of the furnace and the temperature of the charge. In addition to providing a permanent record of each batch of work treated, the recorder is also used to determine when the charge, as distinct from the furnace, has reached the required temperature, a fact which is indicated by the coincidence of the two records obtained. In addition, a further instrument is provided to act as a safety controller in the event of failure of the automatic temperature controller. This instrument is set to operate a few

degrees above the furnace-controlling temperature and if brought into operation will set in motion alarm devices.

The most recent trend, particularly in large air-circulation furnaces, has been to separate the work chamber from the heating chamber in order to ensure that radiant heating is eliminated completely and 100% forced convection assured. An example of this can be seen in Fig. 3 (a) (Plate XL), which shows a diagram of the vertical cylindrical type. Fig. 3 (b) is a photograph of a section of a model of the furnace. The principle, which is clear from the figure, was first used in furnaces designed for the tempering of steel parts and later adopted for the various types of furnace designed for the heat-treatment of aluminium and magnesium alloys. The important features of its design are: the work chamber is remote from the heating chamber, thereby eliminating radiant heating and minimizing the risk of physical damage to the heating elements. The heater unit is so designed that the entire bank can be removed bodily from the heater assembly for inspection or replacement purposes without interfering seriously with the progress of the charge. A small auxiliary fan fitted on the main shaft actuates an air switch connected to the elements so that they are disconnected when the fan is off. The larger-type muffle furnaces can be zoned, the working chamber being divided into two or more independently controlled zones, each with its own heater, fan, and temperature control, thus compensating for any variation in load density and heat losses at the various sections of the furnace.

## 2. CONTINUOUS FURNACES

### (a) Chain-Conveyor Furnace

The choice of method adopted to carry the charge through the furnace is decided by the economics involved and the shape and size of the parts, having in mind the high coefficient of friction and the extreme softness of aluminium alloys at the temperatures concerned.

An example of a chain-conveyor furnace used for the annealing of aluminium foil on spools is illustrated in Fig. 4 (Plate XLI), which shows the discharge end of a 300-kW. furnace built fairly recently for handling approximately 1 ton/hr. of foil ranging in thickness from 0.017 to 0.025 mm.

The furnace comprises a heating chamber 29 ft. long and a cooling chamber 77 ft. long, with door openings 6 ft. 6 in. wide  $\times$  2 ft. 9 in. high. The doors, which are of heavily lagged cast iron, are of the inclined sliding type, electrically operated, with their movements controlled by limit switches and synchronized with the high-speed chain conveyors. The inner metalwork of this furnace is aluminized mild steel. Between this lining and the outer casing is an adequate thickness of insulation.

The whole of the hearth is provided with recessed idle rollers carried on racks, the hearth itself being

constructed of brick piers running the full width and designed to support the transverse members which in turn support and locate the racks and conveyor chains. Inlet and outlet roller tables are provided.

There are four chain conveyors, two of which are high-speed units and two low-speed. One high-speed unit is for transferring the charge from the inlet roller table to a position inside the heating chamber; the other is for discharging from the end of the heating chamber to the cooling chamber. The two low-speed units convey the charge through the heating and cooling chambers, respectively. The chains are provided with pawls to engage on the tubular-type charge carriers, the pitch of the pawls being so arranged that the carriers are conveyed through the heating and cooling chambers independently.

This furnace incorporates a patented forced-air-circulation system, as illustrated in Fig. 3, but in this case the heat is dissipated in four independently controlled air zones. For this purpose four heaters are positioned along the side of the furnace, each comprising an easily removable heater bank, a centrifugal-type fan, a thermostat, and an air switch operated by a small fan carried on the main shaft to ensure that the heating elements and the fan are not independent. The heated air is blown via ducts provided at the furnace roof in each zone, through deflector plates initially adjusted to ensure uniform air flow through the zone, and returns through the charge via similar ducts provided at the side of the furnace below the rollers.

Four cooling fans, shown in Fig. 4, provide cold air to the cooling chamber, shutters being provided in the side walls and roof of the ducting to regulate the air as required. In this particular instance the air exhausted from the cooling chamber is used for other purposes in the factory.

Additional features are the provision of a system of dampers in the first two zones of the furnace to ventilate the vaporized lubricant from the work, which then passes through special ducting provided for the purpose.

Temperature control of the furnace, as distinct from the heaters, is effected by two thermocouples—one recording and one indicating—in each zone.

Operation of the furnace is automatic, since the movements of the inlet and outlet doors of the furnace chamber are synchronized with the high-speed chain conveyor. Also, the timing device is set to give the desired time sequence. The only manual work required is to load the charged carriers on to the inlet rollers from a roller-topped table.

#### (b) Flash-Annealing Furnaces

The air-circulation system used with flash-annealing furnaces is similar to that described for the billet-heating furnaces, except that the fans are placed on alternate sides of the roof. These fans draw air from the top of the side wall, discharging it through the elements, which are contained in the space between baffles and roof brickwork across the width of the

chamber, to enter the chamber on the opposite side. From here the air travels above and below the charge on the conveyor, coming into contact with both surfaces of the charge. The alternation of the direction of air flow (for example, in a 30 ft. furnace there are six fans, so that each covers a length of 5 ft.) removes the possibility of uneven heating of the charge.

Trouble was experienced initially in that heavy sheets required the maximum air speed and volume to effect the necessary heat transfer in the time available. When dealing with small, thin-gauge circles the air blast was so strong that they were either blown off the conveyor or made to flutter, which enhanced the marking troubles already experienced. This trouble was finally overcome by fitting D.C. motors to drive the fans, giving an impeller speed variation of the order of 6-1. This has proved satisfactory, because with the smaller circles less air is required to carry the heat taken up by the charge, so that the various factors are self-compensating.

Fig. 5 (Plate XLI) shows a flash-annealing furnace capable of handling 6-ft.-wide sheets and treating them at the rate of 1.75 tons/hr. The rating of 525 kW. is divided between three zones, each having two contra-flow fans.

#### (c) Conveying Mechanism

When treating slabs which may fall over while passing through the furnace, shoes, run either on their own rollers or on rail tracks of the type shown in Fig. 6 (Plate XLII), are the most suitable means of carrying the charge. The shoes for the large furnaces each take three slabs, the maximum size of which is  $126 \times 60 \times 9$  in. The chamber charge weight is 216,000 lb., made up of sixty slabs. Shoes, of course, introduce a complication in that provision has to be made for returning them to the charge end of the furnace on each occasion and, as with the chain in the conveyor furnace, they have to be heated up each time to no useful purpose. Some economy in shoes can be effected by making them suitable for carrying more than one billet. This is particularly useful when a range of billet sizes has to be handled; then the shoe can be made of such a length that it is in effect a common denominator of the various thicknesses.

When large slabs are to be treated, the loading up of pusher-type furnaces can be simplified by the use of transfer cars. The shoes and slabs are charged on to these cars before they are moved into position between the front of the furnace and the pusher head. An alternative is to load by hand, as shown on the left of Fig. 6.

Various methods have been devised for discharging slabs from a furnace, as it is not normally satisfactory to allow the charge-pusher to perform this function. It is necessary to close the discharge door between operations to conserve heat in the furnace, and also in the emerging billets. Otherwise they would lose temperature by being exposed to the atmosphere for a period before being picked up. Some form of "go-



getter" is therefore normally employed in the case of very large furnaces. The slabs are loaded three to a shoe, and at the discharge end an overhead crane of special design lifts out the slabs one at a time and places them on the live roller table; the shoes as they become empty are dealt with in a similar manner, being returned to the charge end by the special conveyor mounted between the two units.

Another form of discharge mechanism is illustrated in Fig. 7 (Plate XLII). Here, the shoes are withdrawn from the furnace by the hooks shown in the base and the billets are swung off the shoes and delivered to the roller discharge table by the arms.

Chain-conveyor furnaces also require some form of unloading device, as here again the speed of the chain is much too slow to discharge the billet at full temperature. It is also advisable to enclose the driving-shaft in the discharge end of the furnace and to return the chains through tunnels in the hearth insulation, to conserve, as far as possible, their heat content.

For cylindrical billets, the cheapest form of furnace is the gravity-hearth type. No mechanical device is required, other than a star wheel at the discharge end, to retain the furnace full of billets while one is taken out. These furnaces, however, are not very satisfactory where a range of billet lengths has to be catered for, and it is necessary to separate completely parallel tracks of billets passing through the furnace.

To reduce stoppages, it is also an advantage to machine the ends of the billets to prevent them from catching in the sides of the hearth metalwork. Furnace efficiency is slightly reduced by the necessity of providing poking doors at intervals along the sides of very long furnaces. With this form of conveyor, the furnace loading is reduced in proportion to the variation in billet length below the maximum; this point also applies to chain-conveyor furnaces.

With the diabolo-roller rail furnace, the billets pass through the furnace in the "end-on" position in parallel rows. This form of furnace has several advantages; for one thing the capacity of the furnace does not vary with the length of billet employed; and again there is no lost heat, as with chains or shoes. Quite a wide range of diameters and lengths of billet can be accommodated, if due regard is paid to this point at the design stage, so that the pusher and discharge mechanism can be pre-set to deal with various lengths.

A minor disadvantage, which it shares with all pusher-type furnaces, is that it cannot be emptied easily. Mechanical loading is satisfactorily provided by continuing the diabolo-rollers on to the shop floor and arranging a section of these in the form of a hoist to bring a row of billets into position in front of the pusher head. It is not necessary to provide a door at the charge end, as the billets can be pushed through circular holes and form their own heat seal, if the last row is allowed to fill the holes. It is probably advisable to fit doors at the ends, so that ready access can be had to the interior of the furnace, as occasion

demands. The charging holes may be cut in the door itself.

Automatic discharge is rendered possible by arranging the ends of the roller track on a drop mechanism, so that small tables incline at the discharge end and the billet rolls out by gravity. Here, again, it is possible to provide circular openings in the end door—normally sealed by flaps—so that it is not necessary to raise the door each time a billet is discharged.

The comparatively recent development of flash-annealing technique calls for particular care in the conveyor mechanism. The aluminium sheets, even when cold, are so soft that the slightest abrasion causes marking. Flash annealers installed to date have been fitted with interlaced rope conveyors, the loading section consisting of round leather ropes running in grooved pulleys, which at the furnace entrance are interlaced with similar grooved pulleys, carrying the stainless-steel ropes which convey the sheet material through the furnace and the cooling chamber. At the discharge table the conveyor reverts to the leather ropes in a manner similar to that employed at the charge end. This method has not proved completely satisfactory, as with large circles further marking troubles are experienced by reason of the fact that the discs expand as they pass through the furnace, even though the conveyor mechanism may be perfectly smooth and satisfactory from other points of view.

Prolonged experiments have been carried out to produce a completely mark-proof conveyor system, and development work has now been completed.

A further complication with flash-annealing conveyors is that the speed is necessarily high, of the order of 20 ft./min., so that unless care is taken to keep its mass low, excessive heat loss will result from the constant reheating of the conveyor. A new design in which the cooling-chamber and furnace conveyors are separate, enables the hot furnace conveyor to be returned along a heat-insulated duct and has the effect of considerably reducing the kWh. required to anneal a ton of sheets.

With the original wire-rope conveyors, considerable difficulty was experienced because of the uneven stretching of the various ropes, and this was finally overcome by introducing a separate spring and jockey-pulley tensioning device to each rope. It was also discovered that even minute differences in diameter of the driven drums, caused considerable relative creep of one rope with respect to another. These faults in themselves were sufficient to cause severe marking.

Solution-treatment furnaces dealing with castings are often of the pusher type, and the crates containing the castings travel through the furnace on to a loading deck which drops into the quench tank. By employing automatic power-operated motions, the time lag between leaving the furnace and entering the quench tank can be reduced below the 30 sec. normally required.

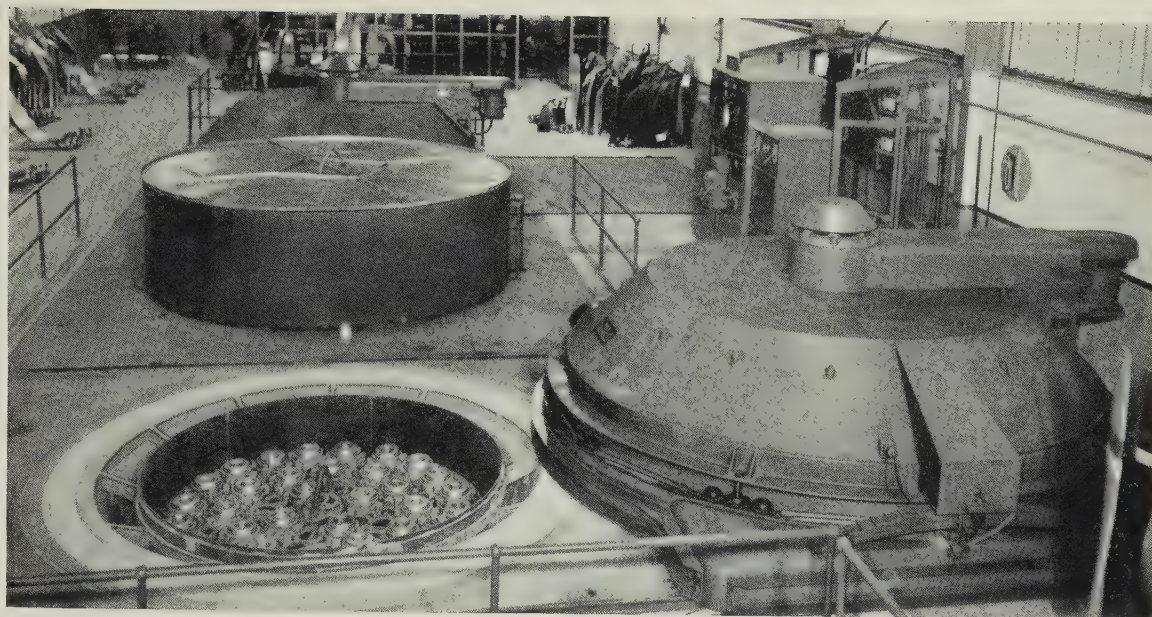


FIG. 2.—Battery of Batch-Type, Forced-Air-Circulation Furnaces, with Centrifugal Fans.

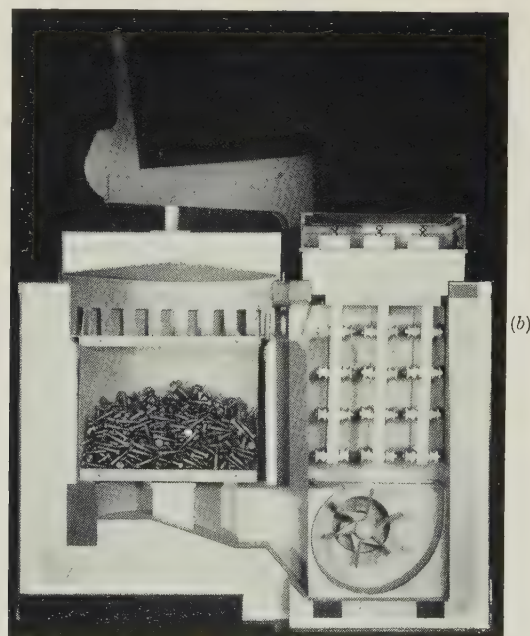
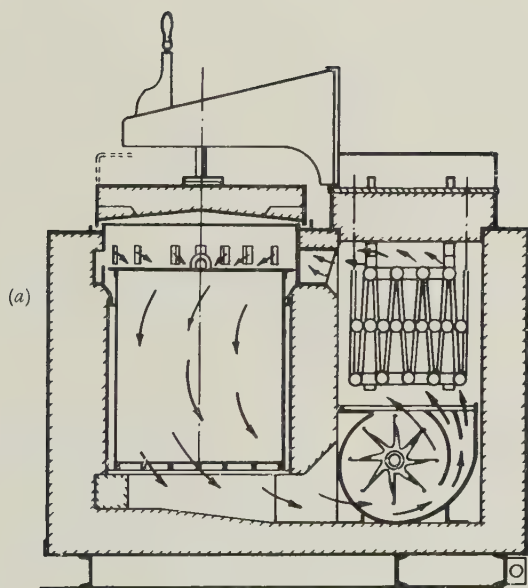


FIG. 3.—(a) Line Diagram and (b) Photograph of Patented Cyclone Furnace.



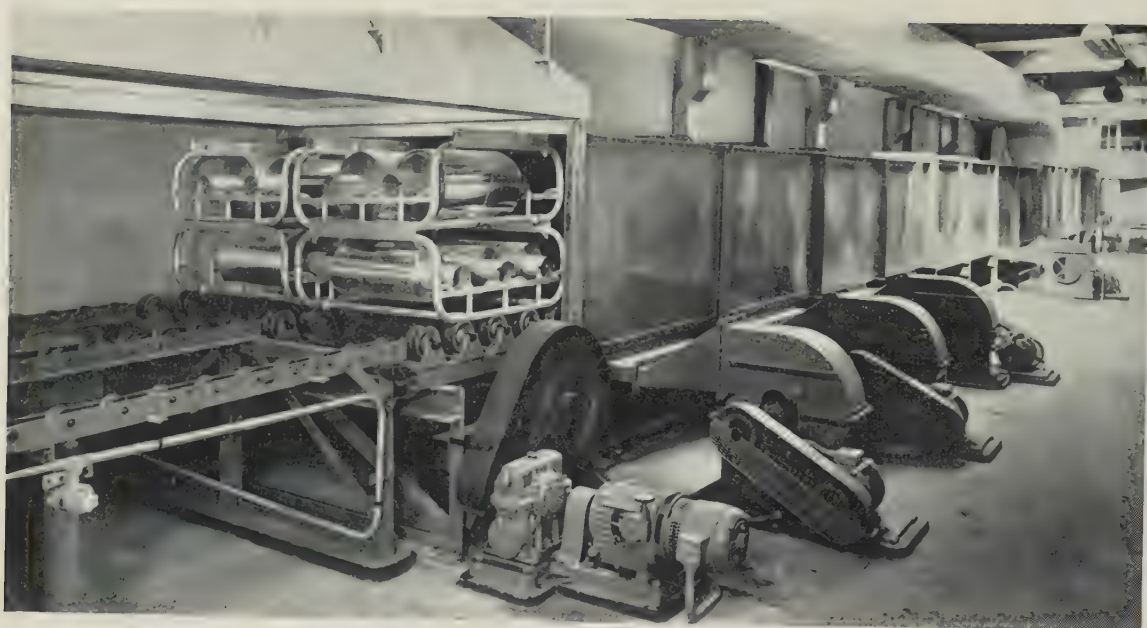


FIG. 4.—Discharge End of Chain-Conveyor Furnace for the Annealing of Aluminium Foil on Spools.



FIG. 5.—Flash-Annealing Furnace for Sheet Material up to 6 ft. wide.

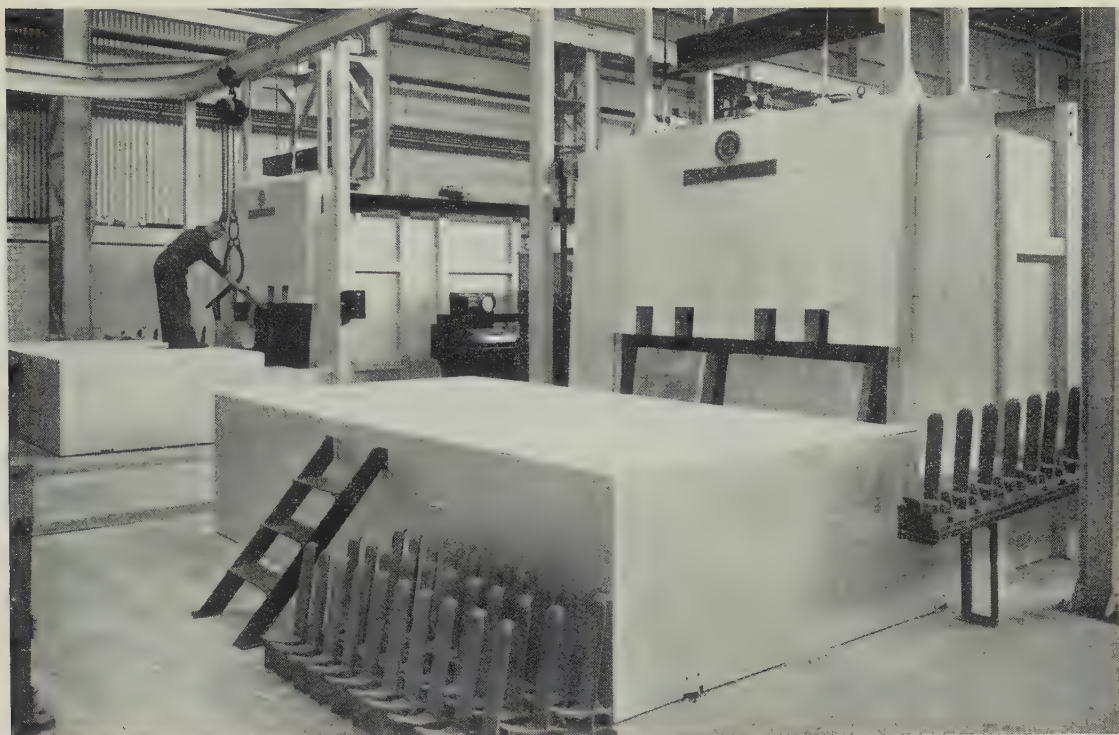


FIG. 6.—Two Billet-Heating Furnaces, Showing Method of Conveying Billets Through the Furnace.

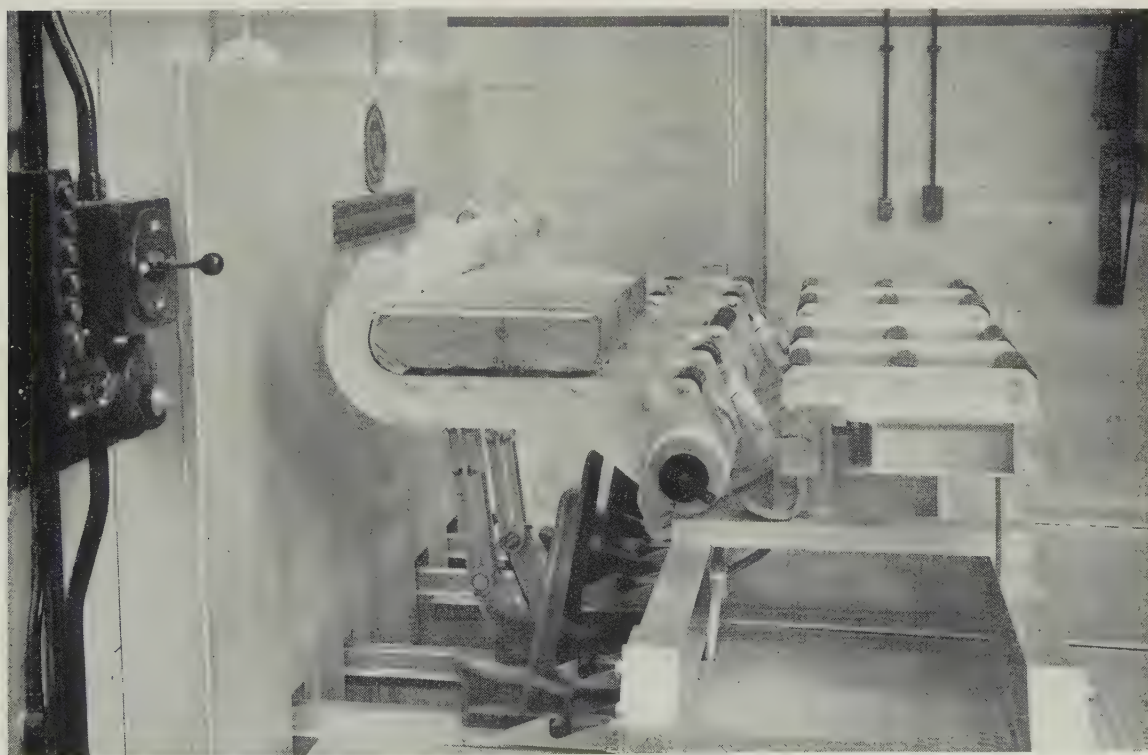


FIG. 7.—Discharge End of Billet-Heating Furnace, Showing Discharge Mechanism.



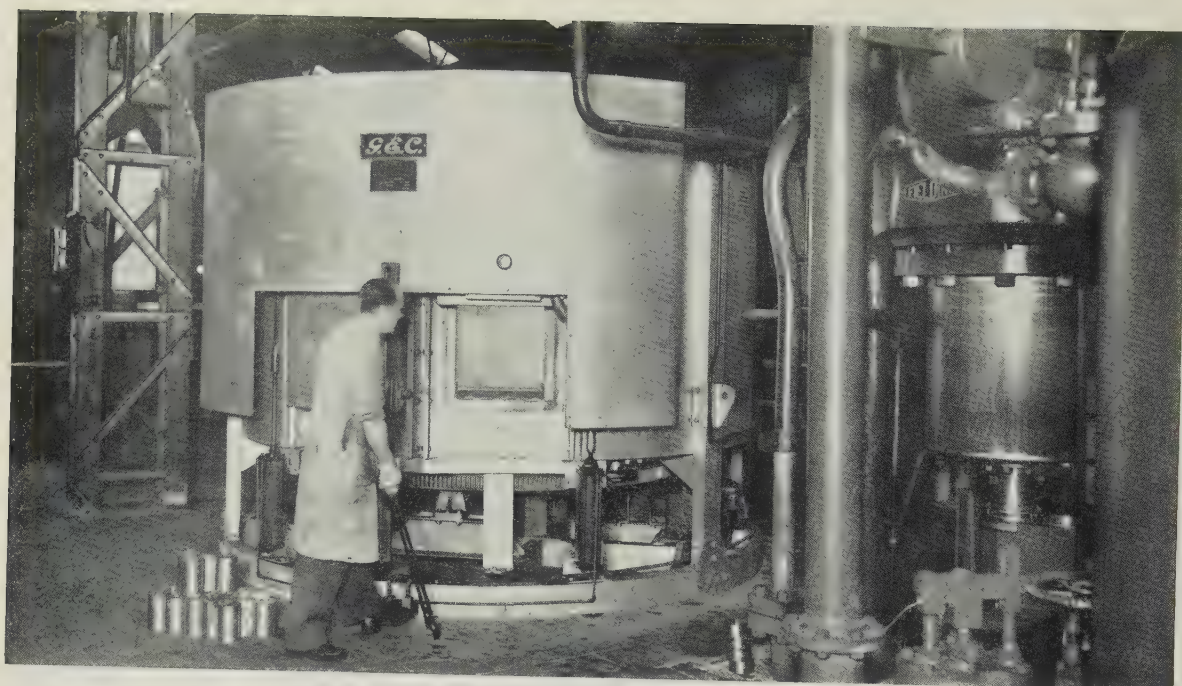


FIG. 8.—Front View of Rotary-Hearth, Billet-Heating Furnace.

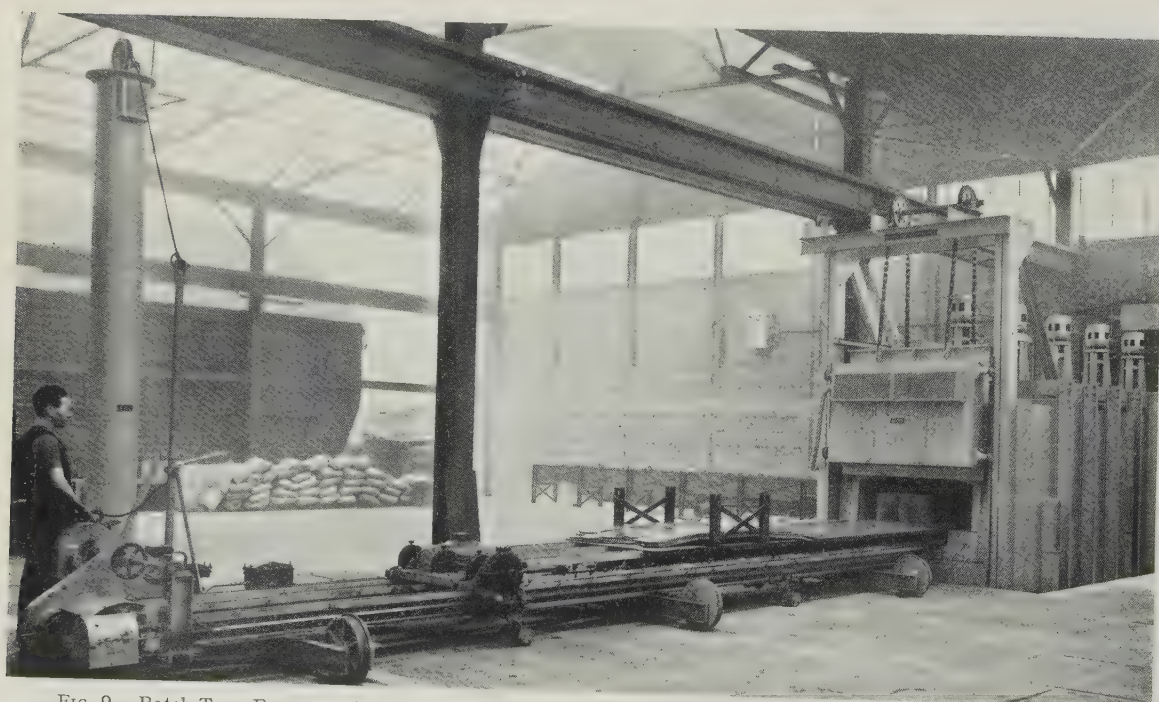


FIG. 9.—Batch-Type Furnace, with Charging Machine, for Annealing Copper and Copper Alloy Sheets, Tubes, &c.

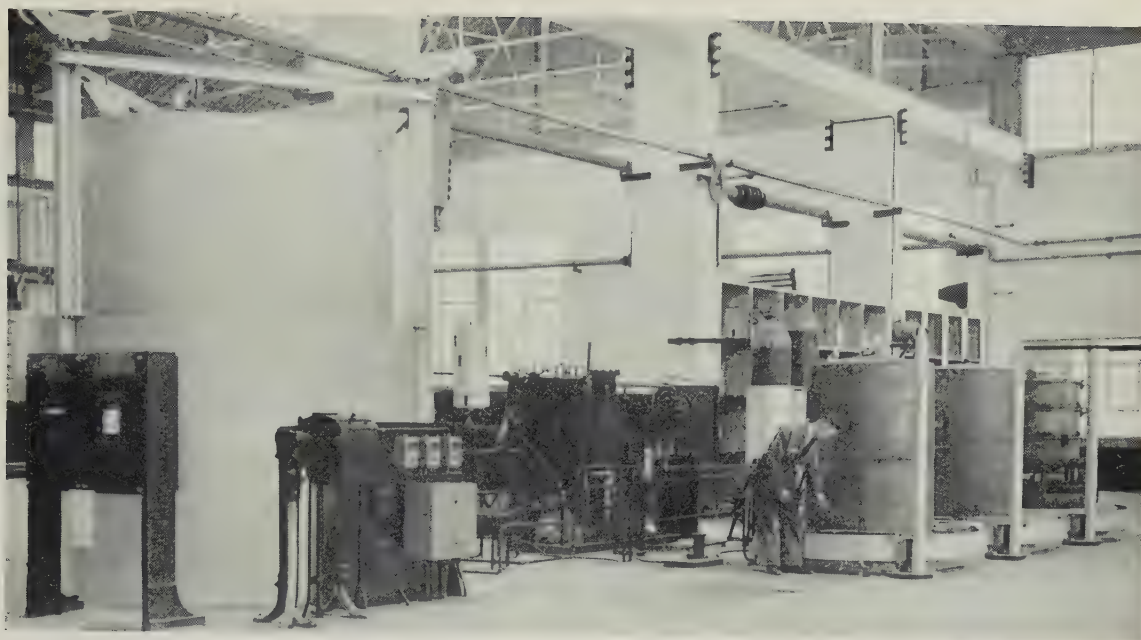


FIG. 10.—Bell Furnace with Regenerative Ammonia Burner for Bright Annealing Copper Wire.

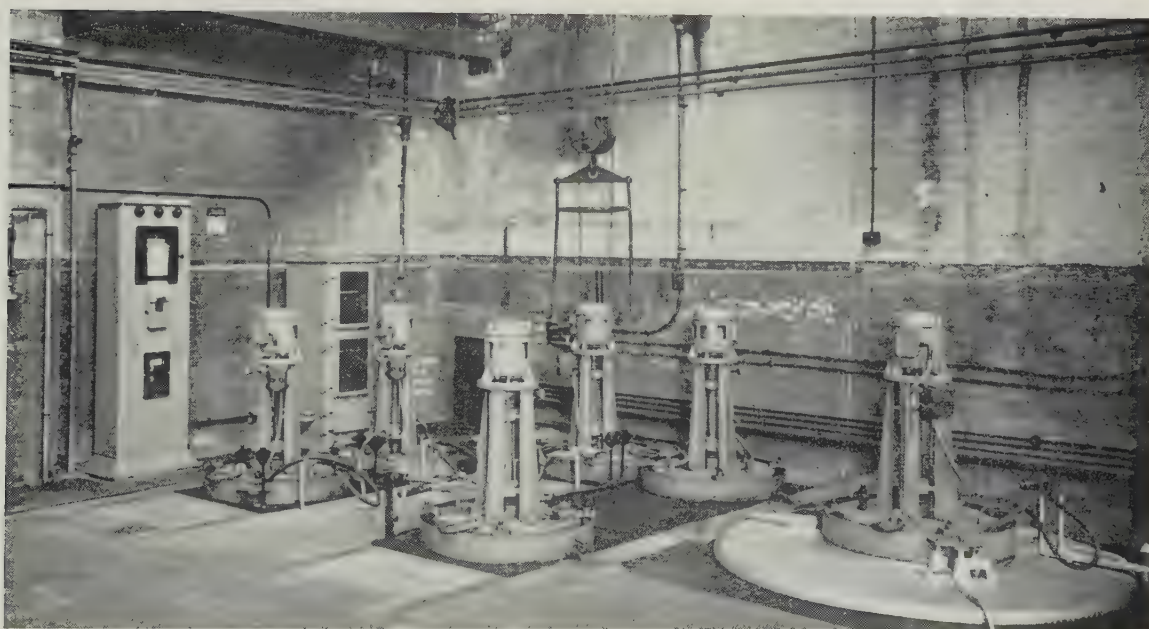


FIG. 11.—Pit Furnace for Bright Annealing Silver-Clad Copper Sheet in Coil Form.



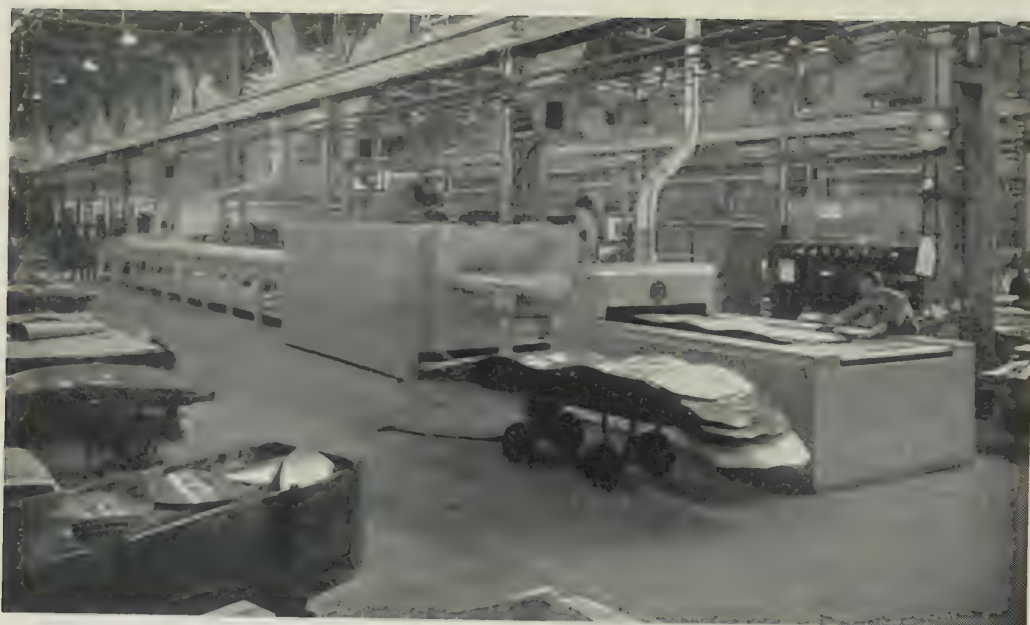


FIG. 12.—Belt Conveyor Type Continuous Furnace for Copper Sheets.

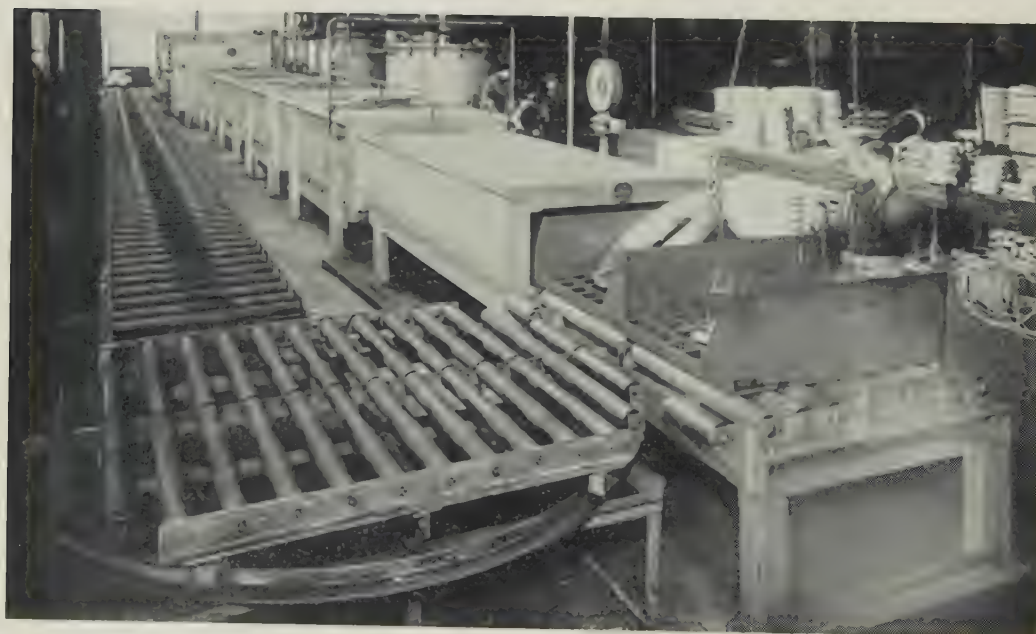


FIG. 13.—Continuous Bright-Annealing Pusher-Type Furnace.

## B.—Copper, Nickel, and Their Alloys

### I.—EQUIPMENT FOR HEATING BEFORE HOT WORKING

Electric furnaces, while potentially suitable for heating billets, slabs, &c., of most copper- and nickel-base alloys, for hot working, have not up to the present found a wide application in this field, fuel-fired equipment being almost universally employed.

Certain types of electric furnace have, however, been adopted for such uses. For example, general-purpose, horizontal batch-type furnaces are suitable for small-scale heating of brass billets for hot pressing. Such furnaces, of rectangular shape, have heating elements mounted on the side walls, roof, and door, and also beneath the hearth, the latter being in the form of a cast or fabricated heat-resisting alloy plate. The door may be hand- or foot-operated, for manual charging and unloading of the billets.

Of larger, continuous-type furnaces, a number of electrically heated rotary-hearth units have been built for heating copper, brass, and cupro-nickel tube billets before extrusion.

The furnace shown in Fig. 8 (Plate XLIII), feeding a press, has a mean hearth dia. of 5 ft. 9 in. and a hearth width of 16 in. The billets range in size from 4 in. dia.  $\times$  12 in. deep to 6 in. dia.  $\times$  15 in. deep and the output is from 15 to 20 cwt./hr. The electrical rating of the furnace is 175 kW.

This type of furnace is built gas-tight, the rotating hearth being sealed by means of downward-projecting flanges, which engage in fixed sand seals welded to the furnace casing. An atmosphere of partially burnt and desulphurized town gas is supplied through inlets in the back of the furnace and near the doors. Use of a controlled atmosphere is not necessary for brass, but for copper and certain copper alloys, where the required temperatures range up to 1100° C., it is found invaluable in ensuring the delivery of scale-free billets to the press. In the case of a multi-furnace installation, the hearths are arranged to rotate so that the discharge door of each is close to the press. Another feature deserving of mention is the provision of a separately controlled zone of elements near each discharge door, by means of which the discharge temperature of the billets is maintained within close limits of the pressing temperature, irrespective of the number of times the outlet door is opened.

### II.—EQUIPMENT FOR ANNEALING AND HEAT-TREATMENT

Electric furnaces for the annealing and heat-treatment of copper, nickel, and their alloys may be broadly subdivided into the following three categories :

#### 1. OPEN BATCH-TYPE FURNACES

Batch furnaces, of horizontal rectangular type, are built in a wide range of sizes for the open annealing

of coiled strip, sheets, plates, tubes, sections, &c., in brass and other copper alloys. They may be classified as general-purpose furnaces, and in all but the smallest sizes (4-ft. hearth or under) are arranged for operation in conjunction with a charging machine. They can be made suitable for operation at temperatures up to 1000° C., and in special cases up to 1100° C. Electric furnaces incorporating high-speed fans have been built for operation at temperatures up to 1050° C. For the treatment of non-ferrous materials, the use of fans is restricted to temperatures below 750° C., where their primary function is that of promoting heating by convection.

A typical example is shown in Fig. 9 (Plate XLIII). The hearth dimensions are 24 ft. long by 4 ft. 6 in. wide. The rating is 330 kW., elements being provided on the side walls, roof, and hearth, and on the inner face of the door. Five disturber-type fans are mounted in the roof along the centre line of the furnace. Loads of 6-7 tons are accommodated and the average output is 2 tons/hr. Discharging and recharging, by means of the charging machine provided, can be effected in about 3 min.

Similar furnaces are suitable for the solution heat-treatment of age-hardening alloys, such as chromium and other special bronzes, K Monel, Nimonic alloys, &c. For these purposes, a controlled atmosphere may sometimes be desirable to reduce the amount of scaling, particularly if a long soaking time at a high temperature is necessary, e.g. for chromium bronze. In this case, the furnace will be built gas-tight, i.e. with a seam-welded casing, and extra attention is paid to sealing the door, to contain the special atmosphere. An example of this type is provided by a furnace of hearth dimensions 10 ft. 6 in.  $\times$  3 ft. 6 in. and rating of 190 kW., employed with an atmosphere of partially burnt town gas for solution-treatment of chromium bronze bars and sections at 1050° C. The associated charging machine is of the electrically operated, cantilever type, working in conjunction with a mechanized quench tank, the latter being located between the charging machine and the furnace. The charge is withdrawn from the furnace on to the quenching platform, which then descends into the tank, the permitted time between opening of the furnace door and complete immersion of the charge being about 1 min.

Small vertical forced-air-circulation furnaces, of the type well known in their application to light alloy treatment and to tempering, also find a number of applications in the copper- and nickel-base alloy field. They are suitable for annealing brass and nickel silver pressings and other products at temperatures of 650°–750° C.; for stress-relief annealing (seasoning) of brass products; and finally for ageing treatments on heat-treatable bronzes and other age-hardening alloys. Sizes in common use are 10 in. dia.  $\times$  10 in. deep,



16 × 12 in., 20 × 18 in., 26 × 24 in., and 32 × 32 in., rated respectively at 4, 10, 20, 40, and 60 kW. Larger sizes and different ratios of diameter to depth have been built.

## 2. CONTROLLED-ATMOSPHERE BATCH-TYPE FURNACES

While the batch furnaces described above may sometimes be used with a controlled atmosphere to reduce the extent of scaling, a completely oxide-free finish cannot be produced, since there is no provision for cooling of the charge under atmosphere. Where true bright annealing is required on a batch basis, the pit or bell furnace is now regarded as standard equipment, with a separate atmosphere generator, operating from ammonia or town gas. These furnaces are mostly of cylindrical shape, for treatment of coiled rod, wire, strip, and tubing, though rectangular

cooling times, depending in turn on the material being treated.

A typical bell-furnace installation is illustrated in Fig. 10 (Plate XLIV). It is used for bright annealing copper wire and consists of a furnace rated at 75 kW. with four hearths, the charge space dimensions being 3 ft. dia. × 3 ft. deep. Atmosphere is supplied by a regenerative ammonia burner, and performance figures are: output 12–14 cwt./hr., power consumption 90–100 kW./ton, and ammonia consumption 1 lb./ton.

In the pit furnace, the heating chamber is fixed, and is partly sunk below floor level, the charge, in a sealed container previously purged with the atmosphere gas, being lowered into it. Thus, while differing from the bell furnace in physical construction, the operating procedure is similar, the sequence of charging, purging,

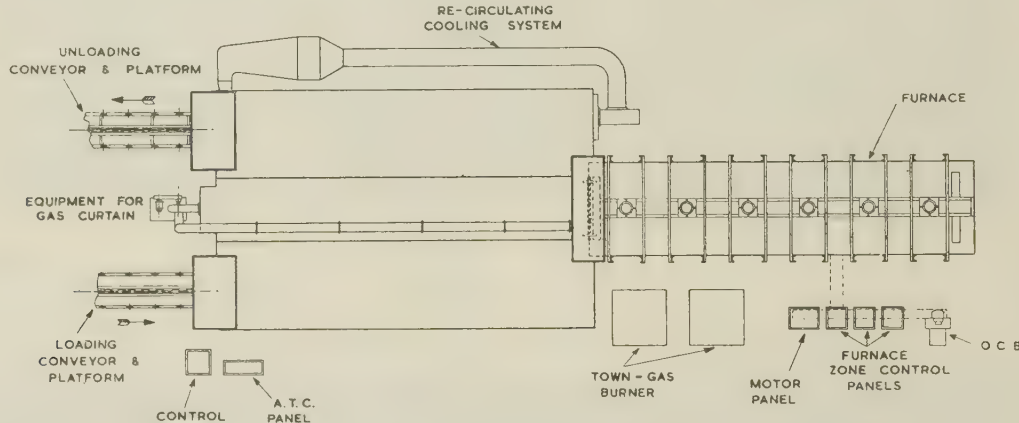


FIG. 14.—Layout of Intermittent-Type Furnace for Bright Annealing Copper Tube.

furnaces can also be built for sheets and straight lengths.

In the bell-type furnace, the charge rests on a stool on the hearth of the furnace, and is enclosed by a light sheet-metal cover which engages with a powder or liquid seal around the hearth to form a completely gas-tight enclosure. The furnace proper is in the form of a bell which is lowered over the covered charge. Three or more hearths are provided with each furnace.

The operating procedure is as follows. After loading a hearth, the cover is put in position, and a supply of protective atmosphere fed to it until all the air has been purged out. The furnace, already at the annealing temperature, is then lowered over it, and kept in position until the charge is fully heated and soaked. At the conclusion of this period, the furnace is lifted off, the atmosphere outlet from the hearth closed while the inlet remains open, and the charge allowed to cool under a slight pressure of atmosphere gas, until cool enough to be discharged into the air without oxidation. The furnace meanwhile has been transferred to a second hearth, and the same sequence of operations repeated. The number of hearths required per furnace is a function of the ratio of heating and

heating, soaking, cooling, and discharging being carried out in exactly the same manner.

The small installation shown in Fig. 11 (Plate XLIV), is used for bright annealing coils of copper clad with standard silver, and consists of a 45-kW. furnace with six containers, the atmosphere being partially combusted, desulphurized town gas.

Most annealing operations on non-ferrous metals and alloys, for which bell- or pit-type furnaces are used, require temperatures in the range 450°–700° C., in which forced circulation is of advantage. With a suitable design of fan, properly located in relation to the charge, considerable reductions in both heating and cooling times can be obtained, resulting in a significantly higher output from an installation of a given size.

There is technically little difference between bell- and pit-type furnaces, and the choice is generally governed by such factors as floor space, head room, and lifting facilities available on the site, rather than by any intrinsic difference in performance.

A third type of batch furnace is sometimes employed for bright annealing of bulky charges, for example, straight lengths of tube. This consists of a heating chamber essentially similar to the horizontal batch

furnace described in Section II, 1, with a purging and cooling chamber built on to the front of the heating chamber, charges being inserted first into the front chamber for purging, thence moved into the heating chamber, and finally returned to the front chamber for cooling before discharge. An installation of this type is illustrated in Fig. 14.

It has a charge space 32 ft. long by 5 ft. wide by 2 ft. high, is rated at 300 kW., and bright anneals 4–5-ton charges of copper tubes, employing an atmosphere of almost completely burnt propane, which is desulphurized. The charge of copper tubes is loaded from slings on to a mild-steel cradle in front of the right-hand door of the three-station cooling chamber. The door is opened and the cradle pushed into the right-hand compartment of a two-compartment carrier. The door is closed and in approximately  $\frac{1}{2}$  hr. the controlled atmosphere flowing through the cooling chamber removes completely any air taken in with the charge. The internal furnace door is then opened and an annealed charge is withdrawn from the furnace into the left-hand compartment of the carrier, whereupon the furnace door is closed and the carrier is traversed one station to the left, thus bringing the hot charge into the forced-cooling position and the purged charge in front of the furnace door. The purged charge is then fed into the furnace and recirculation of atmosphere over the hot charge and through a cooler is begun. In approximately 2 hr. the annealed charge is cold enough to be withdrawn through the left-hand door of the cooling chamber and the bright tubes unloaded. The carrier then moves one station to the right to receive a fresh load. Thus each charge is purged for  $\frac{1}{2}$  hr., heated for  $2\frac{1}{2}$  hr., and cooled for 2 hr., resulting in an output of one cradle-load of copper every  $2\frac{1}{2}$  hr. Handling consists of loading and unloading the tubes once every  $2\frac{1}{2}$  hr. and the intermediate push-button operation of traversing and charging. The loading and unloading position are side by side, thus enabling the tubes to be carried in a single line from the presses to the draw-benches, furnace, and stacking positions.

### 3. CONTINUOUS FURNACES

Continuous furnaces used for the treatment of copper and nickel alloys are of many types, which may be conveniently classified according to the type of conveying mechanism employed. Many are adaptable for use with or without an atmosphere, a cooling chamber (or in some instances means for rapid cooling of the charge by liquid quenching) following the heating chamber, if bright treatment is required. The following types are of importance.

#### (a) Pull-Through Furnaces

In these furnaces, employed for single-strand annealing of wire or strip, the material forms its own conveyor, being uncoiled at the charged end and recoiled after emerging from the furnace or cooling chamber. In the case of wire, the furnace is usually arranged to take a number of strands in parallel, each

strand passing through its own separate tube or compartment in the heating chamber and also in the cooling chamber, if one is fitted. When bright annealing is being carried out, each tube is fed with a supply of atmosphere gas.

These furnaces are usually horizontal, since, mechanically, this is the more convenient arrangement. Vertical construction, however, is also possible, and has the advantage of permitting the strip or wire to pass through the treatment chambers without appreciable contact with the hearth of the muffle. There is also some saving in floor space, but at the expense of considerable complication in construction, particularly if the furnace is of the bright-annealing type, with a cooling chamber following the heating chamber.

#### (b) Belt-Conveyor Furnaces

The continuous furnace employing an endless belt has a variety of uses in the non-ferrous industries, including the annealing of sheet, strip, straight lengths of tube, rod, and sections, and also light coils, pressings, and similar products. The belts are generally of woven heat-resisting wire mesh, but occasionally for special purposes they may be of the chain or slat type. This type of furnace is suitable for brazing and also finds a number of applications in the powder-metallurgy field, including annealing of metal powders, and sintering of pressed powder compacts.

Employing a wire-mesh belt, they have been built in sizes from 4 to 54 in. belt width and are generally adapted for use with a controlled atmosphere, a cooling chamber following the heating chamber. For some purposes, e.g. inter-annealing of copper sheets, spray-quench cooling may be substituted for the conventional water-jacketed cooling chamber, with a considerable saving of floor space.

A 54-in.-wide belt furnace (Fig. 12, Plate XLV), rated at 175 kW., is installed for the dry bright annealing of copper sheet, the output varying between 10 and 15 cwt./hr., according to the loading conditions. The overall length of the furnace is 89 ft.

#### (c) Roller-Hearth Furnaces

This type of furnace, in which the hearth consists of a series of suitably spaced transverse-driven rollers, and which is generally adapted for controlled-atmosphere treatment, is employed for annealing straight-length tubes, rod, strip, sheet, and sections at large outputs, the material being laid directly on the roller track. It is also used for the treatment of coiled products loaded on suitable alloy trays. It has been built with hearth widths from 12 in. upwards.

To keep down the length of the installation, spray-quench cooling may be employed where suitable, or, if a dry-type cooling chamber is essential, forced convection will probably be incorporated to assist in rapid cooling.

As an example, a furnace of this type, fitted with spray cooling, is used for the annealing of copper tubing in straight lengths. It has a rating of 270 kW.,



and an output of 2 tons/hr., the overall length being 87 ft. 6 in. The atmosphere is desulphurized partially burnt town gas.

#### (d) *Pusher-Tray Furnaces*

In these furnaces, which are employed for large-scale annealing of coiled products, large pressings, &c., the work is loaded in alloy trays and passes through the furnace on skids or roller rails by means of an intermittently operating pusher gear. They may be of open type, in which case advantage is sometimes taken of the possibilities of recuperation, either by having two tracks with the trays travelling in opposite directions, or by having a single track, which doubles back on itself so that trays emerge near the charging point. Alternatively, this furnace may be adapted for bright annealing, with a dry-type cooling chamber, usually incorporating forced convection. For bright annealing, a single straight-through track is preferred.

In view of the size of the end openings of such furnaces, special means are generally required to economize in atmosphere gas consumption; these may take the form of double-door lock-chambers, or of "bulkhead"-type trays, i.e. trays with a transverse vertical wall nearly equal in dimensions to the tunnel cross-section.

The controlled-atmosphere pusher furnace illustrated by the example (Fig. 13, Plate XLV) is used for bright annealing coils of copper wire, strip, and tube. The output is 15-20 cwt./hr. Bulkhead trays are used, and the consumption of atmosphere gas (desulphurized, partially burnt town gas) is about 3000 ft.<sup>3</sup>/hr.

#### (e) *Special Types*

Various special forms of continuous furnace have been built for treatment of particular products. An interesting example in this category is the rotary-drum furnace, for annealing cartridge cases and other small pressings, which has been built both as a simple straight-through unit, and in recuperative form. In the latter, the work travels forward in an inner drum, and transfers at the end of the hot zone to an outer annular drum, which surrounds the inner drum, and along which the work travels to the discharge opening, near to the charging point. These units are of a completely automatic type, being hopper-fed and the work passing through the furnace and its associated pickling, washing, and drying machines, without manual operations.

### III.—CONTROLLED ATMOSPHERES

Frequent reference has been made, in the preceding sections, to bright-annealing operations. Some further description is desirable of equipment for producing protective atmospheres, and the requirements of furnaces in which atmospheres are employed. Also, various special problems which arise in bright annealing deserve consideration.

For treatment of copper- and nickel-base alloys,

atmospheres are commonly derived from one of two sources: (a) anhydrous ammonia, and (b) town gas, or other fuel gases.

Atmospheres may be produced from ammonia either by cracking it into its constituent elements, in which case the product contains 75% hydrogen and 25% nitrogen; or, alternatively, by cracking followed by partial combustion and dehydration, the product then being mainly nitrogen, with between 2% and 15% of hydrogen, according to the combustion ratio employed. These atmospheres are of a high degree of purity, being quite free from sulphur, and in the case of the cracked gas exceptionally dry. This latter feature makes cracked ammonia especially suitable for the bright treatment of alloys containing readily oxidizable constituents such as chromium, silicon, or manganese. The cost of ammonia, however, is relatively high, and the use of the straight cracked or burnt gas is seldom justified, except for small-scale operation, or for treatment of materials of high intrinsic value.

In the case of the burnt gas considerable economy can be effected by the use of a regenerative system, the gas after use being collected, reconditioned, and reinserted in the furnace. By these means, the atmosphere costs can be held to a level competitive with alternative sources, but, on the other hand, the plant required is somewhat complicated, and not entirely satisfactory except when operated in conjunction with completely sealed furnaces, such as the pit- or bell-type.

The regenerative ammonia-burner plant comprises a cracker unit, mixing equipment, burner, condenser, and driers, if required, together with the necessary flowmeters, control valves, and other auxiliary equipment, e.g. gas holders or capacity vessels.

Undoubtedly the most widely used protective atmospheres for non-ferrous materials are those derived from town gas, by partial combustion followed by removal of excess water vapour. These atmospheres are cheap, and in view of the ready availability of town gas in industrial areas, convenient in use; moreover, the composition may be controlled over quite a wide range by simple adjustment of the combustion ratio. The limits, for a normal town gas of 450 B.Th.U./ft.<sup>3</sup> calorific value are about 2-15% hydrogen, 2-12% carbon monoxide, 4-10% carbon monoxide, balance nitrogen. If desirable, water vapour may be removed down to low limits by means of activated alumina or silica gel dryers; by the use of organic solvents such as the ethanalamines, which can be regenerated, carbon dioxide can be removed completely. In this way, an atmosphere consisting almost solely of nitrogen, can be produced from town gas. Similar mixtures are obtained by partial combustion of hydrocarbons, such as propane or butane, or of liquid hydrocarbon mixtures such as paraffin, and these alternatives may be used where there is no town-gas supply.

By means of a slightly different type of generator, atmospheres with up to 50% hydrogen may be

obtained from fuel gases, but highly reducing atmospheres of this kind are seldom required for non-ferrous metals, except for some operations in the powder-metallurgy field.

The following is a brief summary of the requirements of various classes of non-ferrous material. For pure copper, pure nickel, cupro-nickel alloys, and standard silver, a very slightly reducing atmosphere is all that is needed to prevent oxidation, and burnt ammonia with about 2% hydrogen, or partially burnt fuel gases with 2-5% of hydrogen plus carbon monoxide, are suitable. Such atmospheres are non-explosive. For non-deoxidized grades of copper, the hydrogen content must be kept to a low level, not higher than about 3%, if hydrogen embrittlement is to be avoided. High percentages of water vapour are not objectionable, and indeed "wet" atmospheres sometimes produce a better finish on copper, particularly when lubricant staining is a problem. In such cases, spray-quench cooling may be substituted for atmosphere cooling, where the form of the charge is suitable. In general, coiled or stacked materials are not suitable for spray quenching, owing to retention of water between the turns, which causes subsequent staining. It is generally applicable to single layers of tubes, rods, &c., where drying of the material can take place readily. Dry treatment, however, is generally preferred in all cases for finish annealing.

The above materials are sensitive to sulphur, suffering a staining of the surface, and in the case of nickel and its alloys intergranular attack as well. The exact amount of sulphur permissible in the atmosphere gas will depend on the time and temperature of treatment, but is generally in the range 0.05-1.00 grain/100 ft.<sup>3</sup>. Although attack is caused mainly by hydrogen sulphide, it is not sufficient to remove this compound alone from the atmosphere, since at treatment temperatures other sulphur compounds in the presence of hydrogen will react to form hydrogen sulphide. Consequently, all forms of sulphur must be rigorously excluded from the atmosphere. It must be remembered further, that many lubricants contain appreciable percentages of sulphur, and if degreasing before treatment is not possible, care must be taken in selecting a lubricant low in this element. It is plainly useless to provide for an atmosphere carefully purified from sulphur, if considerable quantities are permitted to enter the furnace from other sources. In this connection, the rate at which the oil vapours are purged from the annealing furnace is obviously of major importance.

Brasses and nickel silvers containing more than about 15% of zinc present a special problem in bright annealing, and no really satisfactory solution has yet

been found for production-scale operations. Much has been written about the bright annealing of brass, particularly in regard to brass strip in coils, since brass wire is an easier proposition. Brass strip in coils can be bright annealed fairly readily on a small scale, and it appears that each of the following factors will contribute to success or failure :

- (1) Degree of surface contamination before annealing.
- (2) The amount of oxygen, free or combined, in the controlled atmosphere.
- (3) The efficiency of purging.
- (4) The "dirtiness" of the internal surfaces of the annealing container.

In order to avoid oxidation, somewhat more reducing conditions are necessary than for pure copper; this in itself would present no great difficulty were it not for the fact that if the atmosphere is made fully reducing, the absence of a surface oxide film permits serious loss of zinc by volatilization, so that marked roughening and deterioration of the surface results. This effect is negligible if the heating time is very short, and thin wire and strip in single strands can be satisfactorily treated by the flash-annealing technique. It can be minimized also if the annealing temperature is kept low. If, however, full softening is required, and the material is of such a form that an appreciable heating time is necessary, zinc loss is inevitably a serious factor in the presence of a fully reducing atmosphere. For many purposes, however, "clean" annealing, i.e. confinement of oxidation to a thin film of zinc oxide, such as is obtained in a mildly reducing atmosphere, followed by flash pickling, provides a satisfactory compromise.

For bronzes and other copper alloys containing tin, lead, and low percentages of zinc, moderately reducing atmospheres are required, and no special problems arise, provided due attention is paid to sulphur purification. Special bronzes, containing aluminium, chromium, silicon, or beryllium, cannot be truly bright annealed except in highly reducing atmospheres, such as pure hydrogen or cracked ammonia; on the other hand "clean" treatment in which oxidation is confined to a thin layer of the oxide of the alloying element is simple, and for most purposes acceptable.

Nickel-chromium and nickel-chromium-iron alloys also require a highly reducing atmosphere for true bright annealing, and cracked ammonia is commonly used, in conjunction with a metallic muffle, the latter being necessary to maintain the required degree of atmosphere dryness and purity in the treatment chamber.





# GAS EQUIPMENT FOR THE THERMAL TREATMENT OF NON-FERROUS METALS AND ALLOYS\*

1348

By J. F. WAIGHT,† B.Sc.(Eng.), M.Inst.Gas E.

## SYNOPSIS

Constant chemical characteristics, together with the ease with which it can be burned and controlled, have combined to make town gas an accepted fuel in the non-ferrous metal industry. Town gas can be burned completely with its theoretical air requirements, and the mixture of gases produced by combustion acts as a working medium within a furnace enclosure. Convection and gas radiation are the primary methods by which heat is transferred from the hot gases to the furnace and the charge.

The burner systems in common use in the non-ferrous metal industry are discussed, and stress is laid on the importance of automatic mixture-control devices, a number of which are described in detail.

A brief review of furnace atmospheres is incorporated, and attention is called to the importance of sulphur for some applications. An account is given of a catalytic sulphur-removal plant of the type fitted to bright-annealing furnaces.

A number of furnace installations are described, illustrating the application of the various burner systems, and also the use of mechanical-handling equipment. These installations include a copper-billet-heating furnace, tube-annealing furnaces, and a cover furnace. In the field of light metals, billet-heating furnaces, salt baths, and forced-circulation hot-air furnaces are discussed.

## I.—INTRODUCTION

THE heat-treatment of non-ferrous metals and alloys is undertaken to produce physical properties which render the metals suitable for rolling, drawing, extrusion, or pressing. In all these processes temperature requirements are critical, and in most of them the heating must be carried out in an atmosphere that protects the surface of the work during treatment.

The use of town gas as a fuel and as a means of providing such protective atmospheres is extensive. It is natural that this should be so, since gas is a fuel easy to control and possessing chemical characteristics that allow it to be used as a basis for the preparation of furnace atmospheres. Town gas is a mixture of inert and combustible gases, and is supplied to the consumer at calorific values which must be maintained within 5% of the value declared by the gas-supply undertaking. In Great Britain 80% of the town gas produced is manufactured at calorific values lying within the range 450–500 B.Th.U./ft.<sup>3</sup>. Town gas may be burned to completion with its theoretical air requirements, and the resulting products of combustion from 1 ft.<sup>3</sup> of gas will contain, approximately, carbon dioxide 0.45, water vapour 0.95, and nitrogen 3 ft.<sup>3</sup>, and when the air is supplied at normal temperature all products of combustion will have an initial temperature of approximately 1950° C. If air is supplied in excess of the theoretical requirements, the initial temperature

of the products of combustion will be below this figure, and this will degrade the heating potential of the gas.

## II.—HEAT TRANSFER

In a gas-fired furnace, the products of combustion act as a working medium, since they carry sensible heat from the burners to the working space of the furnace, and by virtue of their temperature, velocity, carbon-dioxide and water-vapour content, they also provide the means of transferring their heat to the furnace enclosure and the charge. As far as town gas is concerned, two methods of heat transfer operate—convection and radiation.

### 1. CONVECTION

When a temperature gradient exists between a gas and a surface with which it is in contact, and when the gas has a velocity relative to the surface, a transfer of heat takes place by convection. When velocity is given to the gas by natural means, i.e. by density difference, the heat transfer is described as being by “natural convection”, and when the velocity is produced by mechanical means, the transfer is said to be by “forced convection”.

The study of aerodynamics shows that when a gas flows over a solid surface a thin layer of stationary gas exists adjacent to the surface; the thickness of

\* Manuscript received 31 October 1951. Contribution to a Symposium on “Equipment for the Thermal Treatment of

Non-Ferrous Metals and Alloys”, to be held in London on 26 March 1952.

† West Midlands Gas Board.



this layer may be reduced by increasing the velocity of the gas relative to the surface. Heat transferred by convection must pass across this layer by conduction and, since gases have low thermal conductivities, the thin stationary layer presents a formidable barrier to heat transfer by convection.

Other factors also influence the rate of transfer by convection. Namely, the temperature difference, the Reynolds number, and the size, shape, and position of the receiving surface. Unfortunately, because the shape factor is dimensionless, it is not possible to cover all the variations met with in practice with a general solution, and it is necessary in order to obtain the appropriate value for the convection coefficient, to treat each problem separately, using the heat-transfer data most appropriate to the conditions of the problem.

Convection formulæ which have proved to be of considerable value in furnace design are given below.

#### (a) Natural Convection

The heat loss by convection in still air from freely exposed surfaces, is given by the formula:

$$H = C \times 0.3 \times \theta^{5/4} \text{ B.Th.U./ft.}^2/\text{hr.}$$

where  $\theta$  is the temperature difference in °F. and  $C$  is a constant. The value of  $C$  for various surfaces is given in Table I.

TABLE I.—Values of  $C$  for Various Types of Surface.

Type of Surface		$C$
Plane vertical surface . . . . .		1.0
Plane horizontal surface	facing up and hotter than gas	1.3
	„ „ „ colder „ „	−0.65
	„ down „ hotter „ „	0.65
	„ „ „ colder „ „	−1.3

#### (b) Forced Convection

For forced convection to plane surfaces, data obtained by Jürges<sup>1</sup> and given in Table II, may be employed.

TABLE II.—Surface Coefficients for Various Types of Surface and Different Velocities (Jürges).

$H$  in B.Th.U./ft.<sup>2</sup>/hr./°F.  $V$  in normal ft./sec.

Type of Surface	Velocities Less than 16.5 ft./sec.	Velocities Higher than 16.5 ft./sec.
Smooth . . .	$H = 0.98 + 0.2V$	$H = 0.5V^{0.78}$
Rolled . . .	$H = 1.02 + 0.2V$	$H = 0.5V^{0.78}$
Rough . . .	$H = 1.09 + 0.22V$	$H = 0.52V^{0.78}$

For the calculation of the surface coefficients in ducts, Shack<sup>2</sup> recommends the formula:

$$H = 0.31V^{0.8}/D^{0.25},$$

where  $V$  is the velocity of gas in normal ft./sec. and  $D$  is the hydraulic diameter.

Etherington<sup>3</sup> suggests that where these formulæ give coefficients less than 1.5, the following formula should be used in order to obtain reasonable values for  $H$ :

$$H = 1 + \sqrt{V}/8.$$

## 2. RADIATION FROM PRODUCTS OF COMBUSTION

In most gas-fired furnaces combustion is completed rapidly at the burner, and the resulting products of combustion are non-luminous and free from solid particles. The radiant heat transfer from the combustion products for these conditions and for all practical purposes is due to the carbon-dioxide and water-vapour content of the hot gases. It has been shown by Shack<sup>2</sup> that heat transfer by gas radiation depends upon the partial pressure of water vapour and carbon dioxide, the thickness of the gas layer, and the temperatures of the hot gas and the receiving surface. The total radiation from a gas layer containing carbon dioxide and water vapour is approximately equal to the sum of the radiations from each of the gases at their respective partial pressures. The net radiation from a parallel layer of gas at a temperature  $T_1$  to a surface of emissivity  $E$  and temperature  $T_2$  is approximately  $E(R_1 - R_2)$ , where  $R_1$  is the gross radiation from the hot gas at temperature  $T_1$  for the given conditions of water and carbon-dioxide concentration and layer thickness, and  $R_2$  is the radiation which, under the same conditions, would be emitted by the gas at temperature  $T_2$ . The net radiation received by the surface in contact with the gas is additional to the heat transfer from the gas by convection.

In open-flame furnaces of the type employed for copper-billet heating and for annealing copper and nickel alloys, the coefficient of radiant transfer is likely to be greater than the coefficient of convective transfer. The effectiveness of gas radiation is increased by arranging that the layer of gas in the working chamber is as thick as possible. A limit must, however, be set to the area of furnace cross-section, since the walls of the furnace lose heat by conduction and it is important that the heat-losing area of the walls should be as low as possible. In order to minimize this loss, the designer must produce the optimum value for the furnace cross-section.

## 3. HEAT TRANSFER TO CHARGE

When the charge is contained within an open-fired furnace, the walls of which are standing at a temperature in excess of the charge, heat transfer to the charge will take place by the methods described above and also by surface radiation from the furnace walls. The heat radiated by the walls will, of course, be supplied initially by gas radiation and convection. The exchange of heat by surface radiation will take place approximately in accordance with the Stefan-Boltzmann law:

$$Q = 0.173 EA \left[ \left( \frac{T_1}{100} \right)^4 - \left( \frac{T_2}{100} \right)^4 \right] \text{ B.Th.U./hr.}$$

where  $A$  is the receptive area in ft.<sup>2</sup> and  $T_1$  and  $T_2$  are the absolute temperatures in °F. of the emitting and receiving surfaces, respectively.

If the charge is contained within a muffle, surface radiation will be the only method of heat transfer to the charge. This heat will be transmitted by conduction through the muffle walls and will be supplied to the outer surface of the muffle by gas radiation, by convection, and by surface radiation from the walls of the structure that contains the muffle.

In the case of forced-circulation furnaces employed for the heat-treatment of light metals, the design is so arranged that heat is supplied to the charge as far as possible by forced convection, and a high rate of air circulation is used in order to minimize temperature gradients.

The calculation of heat exchange in furnaces is complex, and owing to the divergence that often exists between the conditions of the practical problem and the conditions under which laboratory determinations of heat-transfer coefficients are made, the solution must sometimes rest on an approximation between the two. There is available, in the literature, a considerable amount of heat-transfer data, and the application of this information as far as possible to practical design enables the most economic furnace structure to be predicted with assurance.

### III.—BURNER SYSTEMS

It is the burner which produces the combustion products that form the working medium. A large number of town-gas burner systems are in use, but for the purpose of the present paper five systems will be considered which represent those mainly employed in non-ferrous-metal heat-treatment furnaces. They may conveniently be classified on the basis of the method of aeration as shown in Table III.

An important characteristic of any gas burner is its range of stability. It is well known that certain types of Bunsen burner are prone to light-back at low gas rates, a failing which also affects the industrial air-blast burner. The point at which light-back occurs is the lower limit of stability of the burner, and in planning burner equipment for industrial purposes, the designer must arrange that at the lowest rate of heat input required, the burners are operating above the lower stability limit. The turn-down range may be expressed in various ways. A common method, used in the last column of Table III, is to express the range as a ratio :

$$\frac{\text{maximum gas rate}}{\text{gas rate at lower limit of stability}}$$

The choice of any one of these systems depends on the design of the furnace and on what is required of the burner. In some cases ease of control is the only important consideration; in others a wide range of turn-down with no variation in the analysis of the products of combustion may be required. In the first case, natural draught with neat-gas burners

could be employed, and in the latter, a premix system would probably be necessary. No clearly defined criterion of burner performance exists, but generally

TABLE III.—*Classification of Furnace Burner Systems.*

	Burner System	Method of Aeration	Gas Pressure	Turn-Down Range
1	Neat-gas or post-aerated	All secondary	2.5 in. water gauge	5/1
2	Low-pressure Bunsen	Primary and secondary	2.5 in. water gauge	2.5/1
3	Air-blast injector-mixing	All primary	Atmospheric	3.5/1
4	Air-blast nozzle-mixing	All secondary	2.5 in. water gauge	5/1
5	Premixed gas and air	All or part primary	...	12/1

speaking it may be said that a burner system must be able to manufacture products of combustion of constant analysis at the highest possible temperature and over the widest range of turn-down.

#### 1. NEAT-GAS OR POST-AERATED BURNERS

This class of burner is extremely simple and is completely stable over the whole range of turn-down. Neat-gas burners are extensively employed where the temperature-control requirements demand a high

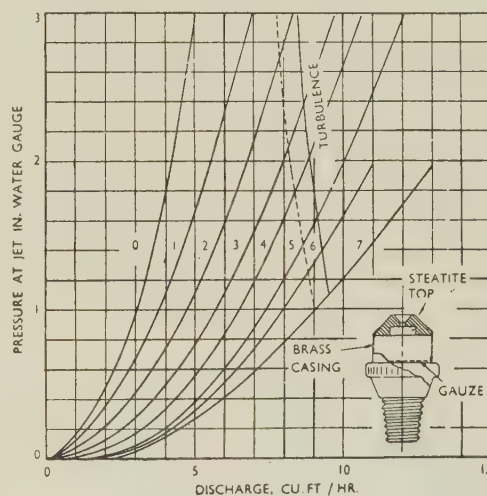


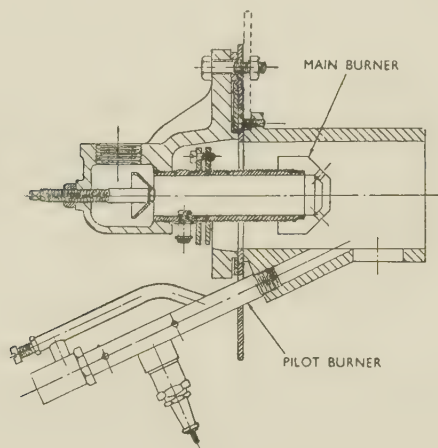
FIG. 1.—Diagram of Neat-Gas Burner, with Typical Pressure/Discharge Curves.

turn-down ratio and where a constant atmosphere is of relatively minor importance. They are widely used for salt baths and for forced-circulation ovens.

The neat-gas burner consists essentially of a jet from which gas is ejected without previous admixture of air, the air for combustion being supplied at and beyond the point of ignition as secondary air. The size of the jet, the gas pressure, and the gas density



determine the rate of heat liberation. Generally, the gas pressure employed does not exceed 2.5 in. water gauge. A common type is illustrated in Fig. 1, where typical pressure/discharge-rate curves are also shown. The curves relate to a 560-B.Th.U./ft.<sup>3</sup> gas, and the line marked "turbulence" indicates the



[Courtesy Keith Blackman, Ltd.]

FIG. 2.—Neat-Gas Burner Designed to Handle Large Gas Rates.

upper limit of stability for the burners. At the pressures given by this line the flames lose their stable shape and become turbulent.

The burner consists of a steatite jet supported in a stout brass casing and is made in ten sizes covering the ranges shown in Fig. 1. A similar jet is also made in heat-resisting metal. These jets are used mounted on manifolds, at a pitch small enough to ensure ignition of all the jets from one flame. The manifolds may be curved or straight, according to the requirements of the combustion chamber, and they must be arranged in such a way that the incoming air assists in cooling the jets. This type of burner is used in apparatus operating with natural draught. It is important that the flames from these jets should not impinge on any cold surface or on each other, for otherwise incomplete combustion and sooting will occur.

Large neat-gas burners are also employed, and Fig. 2 shows a burner designed to handle large gas rates and to operate with high suction in the combustion chamber. These burners may be fitted to induced-draught air heaters of the type required for some designs of forced-circulation furnaces.

## 2. ATMOSPHERIC BUNSEN BURNERS

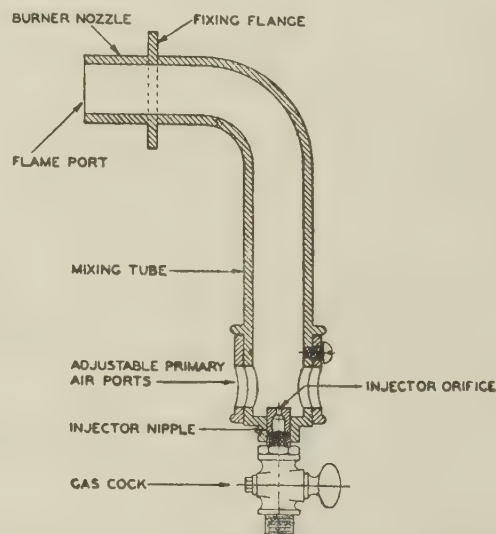
This type of burner operates with partial primary aeration and is designed for use with natural draught and with gas at normal supply pressures. A typical arrangement is shown in Fig. 3. Part of the air required for combustion passes into the gas stream before the point of ignition, through adjustable ports.

This admixture of primary air completely alters the character of the flame as compared with that produced

by the neat-gas burner, and enables it to come into contact with cold surfaces without producing soot. The remainder of the air required for combustion is supplied as secondary air.

With the primary-air shutter closed, the flame is luminous and has no definite shape. As the shutter is opened and air enters the gas stream, the flame assumes a definite shape and its colour changes to a reddish blue. With increased primary aeration, a green cone appears. This cone becomes blue in colour and smaller with increased aeration until the limit of stability is reached, when the cone becomes very short and the point of ignition will pass through the burner ports, causing combustion to take place within the mixture tube. This, as has already been indicated, is to be avoided, since the burner structure will become overheated and—what is more serious—combustion will be incomplete.

It is often the practice to operate Bunsen burners with enough primary aeration to take out all traces of the luminous flame and to supply the secondary air through a recuperator. When using these burners with sufficient primary aeration to form an inner cone, it is important that the latter should not impinge on a solid surface; otherwise combustion will be incomplete. Atmospheric Bunsen burners are used where natural draught is suitable. They are frequently employed with some types of cover furnaces, and are



[Courtesy H.M. Stationery Office.]

FIG. 3.—Atmospheric Bunsen Burner.

often fitted to the batch-type furnaces used for annealing small brass pressings and for preheating dies for extrusion presses.

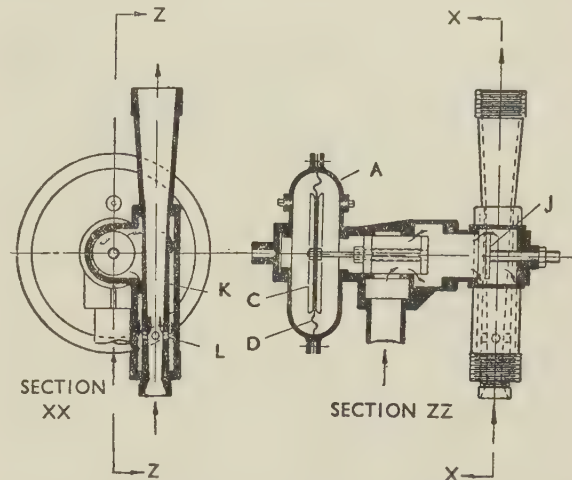
## 3. AIR-BLAST BURNERS, INJECTOR-MIXING

This type of burner is extensively employed in billet-heating and annealing furnaces and also in atmosphere-generating plants. It is capable of producing a short and intense flame against furnace

pressure. Air is supplied under pressure, usually at about 1 lb./in.<sup>2</sup>, and gas is at normal supply pressures. When intended for furnace heating, fully aerated mixtures are employed, and mixture pressures behind the burner ports of up to 10 in. water gauge may be produced when air is supplied at 1 lb./in.<sup>2</sup>. Mixture pressures of this magnitude would blow the flame from the burner port, and to prevent this happening the burners normally discharge into refractory tunnels built into the walls of the furnace enclosure. For this reason the burners are sometimes described as "tunnel burners".

A diagram of such a burner system is shown in Fig. 4, from which it will be seen that an air jet entrains gas through an adjustable restrictor, the resulting air/gas mixture then passing to the burner nozzle via a mixture tube. Provided that gas is supplied to the inlet of the restrictor at atmospheric pressure, the percentage of gas in the gas/air mixture passing to the nozzle will remain constant for all rates of air flow. For this reason, atmospheric gas governors are frequently fitted to air-blast burner systems, and turn-down for temperature-control purposes is effected by a controlling valve in the air line. This arrangement permits a considerable simplification of temperature-control systems and fuel economy is obtained, since the optimum air : gas ratio is maintained over the

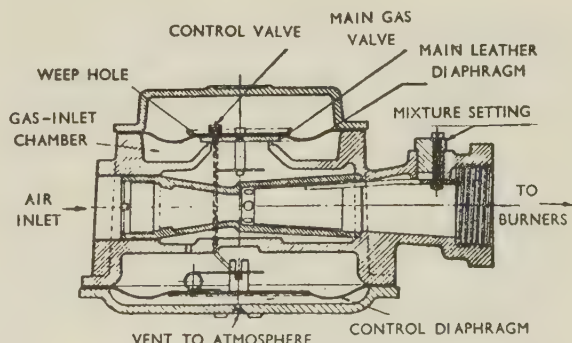
fitted as an integral part of the governor. The operation of the governor is as follows: two diaphragms are used, one carrying a gas valve and the



[Courtesy Walter King, Ltd.

Fig. 5.—Air-Blast Injector System Incorporating Atmospheric Gas Governor.

other a control diaphragm which is balanced against atmospheric pressure and is linked to a small valve which can open a small orifice in the main gas valve. This orifice allows the pressure on the outlet side of the main gas valve to communicate with the space above the gas-valve diaphragm. Gas also enters this space from the inlet side of the valve through another small orifice. If the pressure at the governor outlet exceeds atmospheric, the control diaphragm becomes distended and the small valve to which it is linked will close. The small supply of gas from the inlet side of the valve will then cause pressure to build up above the gas diaphragm and the gas valve will move towards the closed position; the reverse occurs when the pressure at the outlet of the governor falls below atmospheric.



[Courtesy Walter King, Ltd.

Fig. 6.—Air-Blast Injector System Incorporating Atmospheric Gas Governor.

turn-down range. The value of the air : gas ratio is fixed by setting the restrictor.

The diagrams in Figs. 5 and 6 illustrate two air-blast injector systems incorporating atmospheric governors. In the type shown in Fig. 5 the diaphragm of the atmospheric governor is mounted in a vertical plane and controls a piston gas valve. The diaphragm is open to atmosphere on the side remote from the valve, and the pressure of gas in the outlet side of the piston valve is communicated to the side adjacent to the valve. When this latter pressure exceeds atmospheric, the valve moves to close and vice versa.

The flow of gas past the restrictor, which is fitted on the downstream side of the governor, is therefore due solely to the suction caused by the air jet. It has been found that this suction is directly proportional to the air pressure, and the flow of gas into the system is, accordingly, dependent on the setting of the restrictor and is proportional to the rate of air flow.<sup>4</sup>

The controller depicted in Fig. 6 is similar in operation to that described above, but the atmospheric governor is of a sensitive type and the injector is

The first governor can be used to supply a number of separate air/gas injectors, but the latter is designed to supply one large burner nozzle or a number of

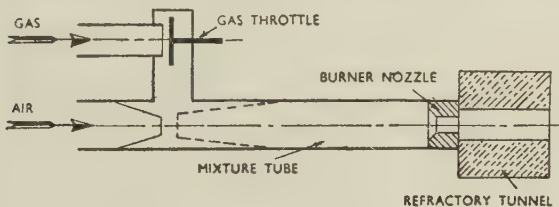
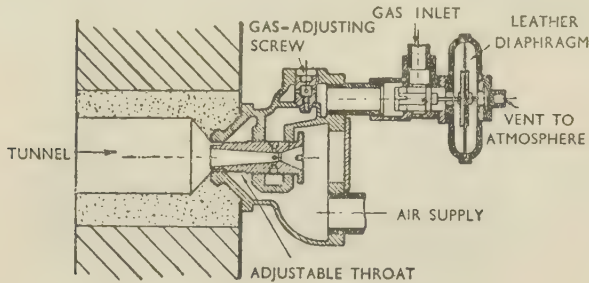


Fig. 4.—Air-Blast Burner System Employing Injector Mixing.



smaller ones. In the latter case it is most important to ensure that a minimum loss of mechanical energy occurs between the outlet of the injector and the entrance to the burner nozzle. For this reason the



[Courtesy Walter King, Ltd.]

FIG. 7.—Two-Stage Inspirator Type of Air-Blast Burner.

mixture manifold should be as short as possible and should have the minimum number of bends and changes of section. The range of turn-down obtainable with air-blast burners of this type is generally in the region of 3.5/1, when air is supplied at 1 lb./in.<sup>2</sup>. Higher air pressures enable the turn-down range to be increased.

Another type of air-blast burner, covered by the term "injector-mixing", is shown in Fig. 7. This is known as a two-stage inspirator burner, and differs from those previously described in that some of the air is supplied as secondary air through an annulus surrounding the burner port. Automatic mixture control can be applied to this burner in a manner similar to that described above. The arrangement increases the stability of the burner at low pressures and enables a certain amount of air preheat to be employed. Air preheat, when all the air is supplied as primary air, is not recommended, as fully aerated mixtures have a greater tendency to backfire.

#### 4. NOZZLE-MIXING BURNERS

In addition to the burners described above, air-blast burners are used in which the air and gas streams meet just before the point of ignition. Burners of this type are chosen when it is desired to preheat the whole of the air. They will not light-back and therefore have the widest possible turn-down range. Their chief disadvantages are that they tend to be noisy in operation and that, because the mixture is not intimately mixed before ignition, there is in certain circumstances a tendency to delayed combustion.

#### 5. PREMIXED GAS AND AIR

For this method of combustion, gas and air are mixed and compressed before distribution to the burners. The mixing plant consists essentially of a governing and mixing device and a rotary compressor compressing to about 81 in. water gauge. These machines can deliver a fully aerated mixture at high

pressure, and the advantage of this system lies in the fact that extremely high turn-down ranges can be obtained with a constant air:gas ratio over the whole range. Turn-down ranges of 12/1 may be obtained,<sup>5</sup> and this means that heavily insulated general-purpose furnaces may be built to operate satisfactorily at temperatures from 400° to 900° C., or over an even wider range.

The disadvantage of the fully aerated premix system is that the mixture is highly explosive and precautions have to be taken to prevent backfiring. Flame traps must be fitted to the outlet of the compressor and subsidiary flame traps to the individual burners. Flame traps which incorporate a fusible link or an electrical device that will shut off the main gas valve in the event of a flame reaching the trap, are often used.

Fig. 8 illustrates a typical burner. The burner nozzle is manufactured from heat-resisting steel, and the ports are of small diameter and have a length sufficient to provide a high resistance to flash-back. The burner nozzle discharges into a refractory tunnel which prevents blow off at maximum velocity.

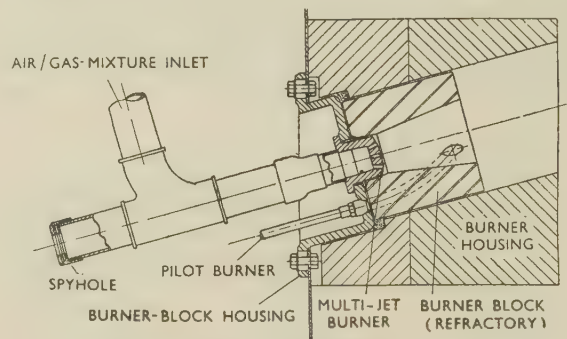


FIG. 8.—Burner System Employing Premixed Gas and Air.

#### 6. CONTROL OF AIR:GAS RATIO IN BURNER SYSTEMS

When air and gas are supplied by separate blowers, the control of the mixture may be effected manually with the aid of inferential flow meters. Automatic control is frequently applied, however, and the relay-type regulator is often employed, for this purpose. One form of this regulator depends for its action on the fact that if a jet of fluid issuing from a nozzle impinges normally on a flat surface its momentum is destroyed, with the result that a pressure is set up on the surface over an area equal to the cross-section of the jet. If an orifice were drilled in the flat surface, of the same diameter as the jet, and connected to a pressure gauge, the gauge would show a pressure slightly less than that existing behind the nozzle, when the jet of fluid completely covered the orifice. If the jet partially covered the orifice, the pressure shown by the gauge would be correspondingly reduced.

Fig. 9 shows how the principle is applied to the automatic control of air:gas ratio. The two gases to

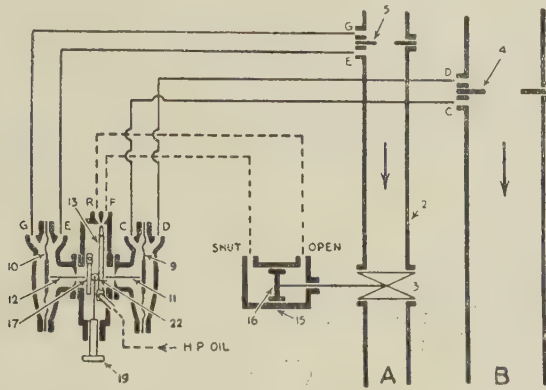
be mixed are flowing in mains *A* and *B*, the primary gas flowing in main *B* and the controlled gas in main *A*. Orifice plates are fitted in both mains, and the pressure loss across the orifice in main *A* is set up

that with the roller in this position the regulator is in equilibrium only when the forces in the push-rods are equal; if the diaphragms are of the same size, it follows that the differential pressures across the orifice plates are also equal.

Should the flow in main *B* increase, therefore, the differential pressure across the right-hand diaphragm will also increase, causing the jet to be deflected towards orifice *R*. This causes a build-up of pressure in the right-hand end of the double-acting control piston, and the main valve is opened. Thus, the flow of fluid in main *B* increases, the pressure drop across its orifice plate increases, and the left-hand diaphragm produces an opposing force which tends to deflect the jet to the right. When the jet has moved back to its mid position, the pressure drops across each orifice plate are again equal and the air : gas ratio is restored to the set value. Adjustment of the air : gas ratio is obtained by moving the contact roller to either side of its mid position. Screw (19) is fitted to enable this adjustment to be made.

An interesting development which incorporates a premix burner is that of the recuperative radiant tube illustrated in Fig. 10. This resulted from the need to produce a gas-furnace enclosure similar in characteristics to that of an electrical furnace. Its application is primarily to bright-annealing furnaces. The important feature of the design is that combustion is delayed to produce a uniform temperature along the working length of the tube. The burner is supplied with an air/gas mixture which carries 50% of the total air requirements. The remaining air for combustion is supplied as secondary air through a perforated inner tube, the perforations being so disposed that combustion is even along the length of the tube and is complete before the hot products leave the working section of the radiant tube. The inner tube is enlarged at the point where the gases of combustion leave the heating section, and this enlarged surface abstracts heat from the outgoing gases and transfers it to the incoming secondary air. A high efficiency is thereby obtained.

This design is in use in continuous and other types of furnace, and tubes located above and below a conveyor belt can be arranged to give any desired gradient through the furnace chamber. They are manufactured from spun-cast high-chrome alloys.



[Courtesy Reavell and Co., Ltd.]

FIG. 9.—Diagram Illustrating Automatic Control of Air : Gas Ratio.

across the left-hand diaphragm (10) and that across the orifice plate in main *B* is set up across the right-hand diaphragm (9). These diaphragms operate in the vertical plane. Diaphragm (9) is linked by a push-rod to a jet pipe, pivoted to swing in the horizontal plane. The arc of swing is restrained, so that at one extremity the jet covers orifice *R* and at the other orifice *F*.

The nozzle discharges oil at a high pressure, and when covering orifice *R* will cause a pressure approximating to the supply pressure to be applied over the whole area of the piston (16), which therefore provides a large force to open the main gas valve. The reverse happens when the jet covers orifice *F*, and the main valve closes. Intermediate positions of jet will cause finer correction, and floating control will be obtained. As a very small force is needed to deflect the jet, the ratio of correcting force to controlling force is extremely high. The left-hand diaphragm (10) is linked by a push-rod to a dummy jet pipe, and between this and the jet pipe proper there is a contact roller secured to a flexible steel blade. When the contact roller is in the mid position, it coincides with the centre lines of the two push-rods, and it follows

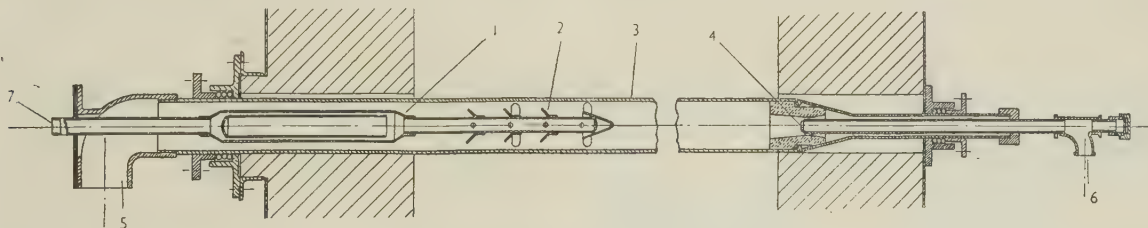


FIG. 10.—Recuperative Radiant Tube System.

KEY.

1. Recuperator (secondary air).
2. Defectors to encourage secondary air to mix with partly burned air/gas mixture.
3. Heat-resisting radiant tube.
4. Burner nozzle.
5. Exhaust outlet.
6. Air/gas mixture inlet.
7. Secondary air inlet.



#### IV.—FURNACE STRUCTURE AND HEAT LOSSES

The temperatures required for the heat-treatment of non-ferrous metals are not unduly high, and the task of selecting suitable refractory materials is, in consequence, fairly simple. Apart from the obvious need to produce a furnace structure that will be stable at the operating temperature, the selection is governed by the need to keep to a minimum the heat lost by conduction through the furnace walls and the heat loss due to the thermal capacity of the furnace structure.

For reasons of stability the furnace walls are usually laid up in widths that are multiples of  $4\frac{1}{2}$  in. The composition of the wall may consist of an inner  $4\frac{1}{2}$ -in. lining of refractory material, backed by suitable thicknesses of insulating material.

For copper-billet-heating furnaces and for the higher-temperature annealing furnaces, this type of wall structure is often used. It is necessary to employ an

TABLE IV.—*Thermal Characteristics of Furnace Wall Constructions.*

Furnace operating at approximately 1000° C. over 120 hr. continuous cycle, with a week-end shut down of 48 hr.  $K$  = thermal conductivity (B.Th.U./ft.<sup>2</sup>/hr./°F./in.).

Construction	9-in. Fire-brick ( $K = 7.8$ )	9-in. Hot-Face Insulation ( $K = 1.88$ )	9-in. Hot-Face Insulation ( $K = 1.88$ ) Backed by 2 in. Insulation ( $K = 0.74$ )
Loss by transmission via brickwork, B.Th.U./ft. <sup>2</sup> /week . . . . .	146,400	39,300	25,200
Heat-capacity loss, B.Th.U./ft. <sup>2</sup> /week-end . . . . .	20,090	6,540	6,810

inner lining of low permeability for furnace chambers in which protective atmospheres have to be retained. This implies an inner lining of refractory brick with close jointing. Such a lining, backed by the insulation, would be contained within a braced steel or cast-iron casing, rendered as gas-tight as possible, and provided that the temperature of the interface between refractory and insulation does not exceed 900° C., insulating bricks made from naturally-occurring diatomaceous earths can be employed. Above this temperature, it becomes necessary to use refractory insulating bricks, sometimes described as hot-face or high-temperature insulating bricks. These bricks are made from refractory clays and have a highly porous structure, the air-filled pores acting as insulating cells and giving the brick a low thermal conductivity and a low bulk density.

Refractory insulating bricks possess a fair strength, but they are permeable and have no resistance to abrasion. They are suitable generally for hot-face temperatures up to about 1100° C., although certain special types are now available for hot-face temperatures up to 1500° C. They can be used in place of

refractory material, where other conditions are suitable.

An interesting development is the bonding of a thin but dense refractory layer to one face of the brick during manufacture. This process is being applied to brick made from exfoliated mica or vermiculite, and the use of these bricks should enable improved thermal efficiencies to be obtained from intermittently operated furnaces. In Table IV, which gives the thermal characteristics of various furnace-wall constructions, the heat economy resulting from the use of hot-face insulating material is clearly indicated.<sup>6</sup>

##### 1. CONDUCTION BY STRUCTURE WALLS

The heat lost in unit time across a conducting diaphragm of area  $A$  ft.<sup>2</sup> and thickness  $L$  in., is given by the expressions :

$$H = \frac{(T_i - T_o)L}{KA}$$

where  $T_i$  = temperature of the inner hot face,  $T_o$  = temperature at the outer cool face, and  $K$  = coefficient of thermal conductivity.

For a number of conducting diaphragms in contact, the heat lost in unit time becomes :

$$H = \frac{(T_i - T_o)L}{\sum KA} = \frac{T_i - T_o}{\left(\frac{L_1}{K_1A_1} + \frac{L_2}{K_2A_2} + \frac{L_3}{K_3A_3} + \text{&c.}\right)}$$

This formula may be used to determine the heat lost through a composite furnace wall, provided that  $T_o$  is known. The determination of  $T_o$  is obtained from a graphical solution of the equation :

$$\frac{T_i - T_o}{\sum KA} = CA_3(T_i - T_o)^{5/4} +$$

$$0.173A_3E\left\{\frac{(T_o + 460)^4}{100} - \frac{(T_A + 460)^4}{100}\right\}$$

where  $A_3$  is the area of the outer surface and  $T_A$  is the ambient temperature in °F.

Having obtained the heat loss by conduction, the interface temperatures may be readily calculated, and

TABLE V.—*Thermal Conductivities of Furnace Constructional Materials.*

$K$  = thermal conductivity, B.Th.U./ft.<sup>2</sup>/hr./°F./in.

Type of Refractory	$K$
Aluminous firebrick (38/45% $\text{Al}_2\text{O}_3$ ) . . . . .	4.5-8.5
Firebrick (25/38% $\text{Al}_2\text{O}_3$ ) . . . . .	4.5-8.5
Sillimanite . . . . .	8-12
Silicon carbide . . . . .	60-100
Insulating fireclay refractory . . . . .	2-3.5
Diatomite insulating brick . . . . .	0.7-1.0

if these exceed the safe value for the insulating material, another choice of material must be made.

Table V gives the thermal conductivities of materials in common use for furnace construction.

## 2. THERMAL STORAGE

The heat stored by the structure when temperature equilibrium is reached may be determined from the interface temperatures and the density of the material of construction. The heat absorption takes place while the furnace is being heated, and continues for some considerable time after the working temperature is reached. In furnaces operated continuously over long periods, the proportion of heat lost due to storage is small, but for intermittently operated furnaces the loss may reach high proportions, particularly if dense refractory is used extensively in the wall structure.

There is, therefore, with intermittently used furnaces, a powerful case for the utmost use of insulating refractory material. In addition to the materials already mentioned, the following may be employed for certain special purposes :

Silicon carbide, a high-conductivity material, used for muffles, hearths in under-fired furnaces, burner tunnels, and in any situation where high thermal conductivity, refractoriness, abrasion-resistance, and strength are called for.

Sillimanite, often used for air-blast burner tunnels.

Aluminous firebrick, used for roof arches, combustion chambers, and in all situations where strength and fairly high refractoriness are required.

There is also available a wide variety of castable and plastic refractory materials for the production of special shapes and for the manufacture of jointless linings in some special types of furnace.

## 3. FLUE LOSSES

As has been indicated, the products of combustion in passing through the working chamber give up heat to the walls of the chamber and the charge, thereby suffering a loss in temperature. The heat carried by the products at the temperature at which they leave the heat-exchange surface is lost, if no heat-recovery device is used. The actual quantity of heat lost is a function of the exit temperature and of the composition of the products of combustion. Assuming that no unburned combustible is present, the heat quantity is composed of two factors :

- (1) The latent heat of the water vapour in the products of combustion.
- (2) The sensible heat of the products of combustion.

If no condensation takes place, the first factor will be constant and the percentage loss may be written as :

$$100 \left( 1 - \frac{CV \text{ net}}{CV \text{ gross}} \right)$$

The second factor is a function of temperature and waste-gas composition, and the percentage loss by sensible heat is expressed by :

$$\frac{100}{CV \text{ gross}} \cdot (T - 60)(aN_2 + bCO_2 + cH_2O + dO_2)$$

where  $N_2$ ,  $CO_2$ ,  $H_2O$ , and  $O_2$  are the volumes of these individual gases per unit of gas burned;  $a$ ,  $b$ ,  $c$ , and  $d$  are the mean specific heats at constant pressure between  $60^\circ \text{ F.}$  and  $T$ , the temperature of the products of combustion at the point at which they leave the heat-exchange surfaces.

It is convenient to rearrange this expression in terms of the products of combustion from the stoichiometric mixture and the excess air supplied to the burners. The equation may then be written :

$$\% \text{ loss by sensible heat} = \frac{100}{CV \text{ gross}} (fV_p + gV_a)$$

where  $V_p$  = volume of theoretical products per unit volume of gas burned;  $V_a$  = volume of excess air supplied per unit volume of gas burned;  $f$  = mean specific heat at constant pressure of the theoretical products between  $60^\circ \text{ F.}$  and  $T$ ; and  $g$  = the mean specific heat of air between  $60^\circ \text{ F.}$  and  $T$ .

The total percentage flue loss may be written thus :

$$100 \left( 1 - \frac{CV \text{ net}}{CV \text{ gross}} \right) + \frac{100}{CV \text{ gross}} (T - 60)(fV_p + gV_a)$$

It is clear from this expression that the two factors influencing the loss to the flue are the temperature of

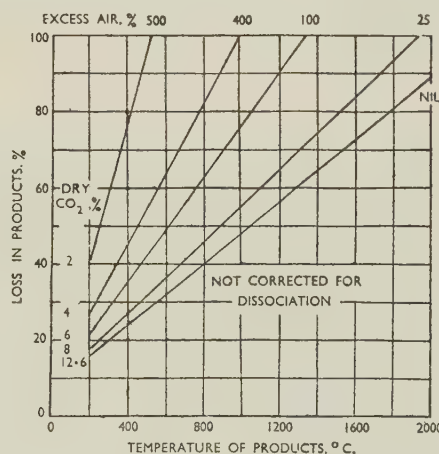


FIG. 11.—Chart Showing Percentage Flue Loss for Various Temperatures and Carbon Dioxide Concentrations.

the outgoing gases and the volume of the excess air supplied. This, in conjunction with the fact that excess air also reduces the temperature at which the products of combustion are manufactured at the burners, illustrates the vital importance of reducing the quantity of excess air admitted to the combustion chamber. Gaseous fuels are the only fuels which can, in practice, be burned completely with their theoretical air requirements.

The chart in Fig. 11 shows the percentage flue loss for various temperatures and  $CO_2$  concentrations in the flue gases. This chart has been constructed for complete combustion conditions.



## 4. CONDITIONS FOR EFFICIENT HEATING

From the sections on flue losses and on heat transfer, it will be clear that high working temperatures tend to reduce the efficiency of the heating process. This tendency may be offset by increasing the amount of insulation and by using outgoing hot gases to preheat the air for combustion. With some burner systems it is impossible to use preheated air, and in such cases the outgoing hot gases may be used to preheat the charge before this enters the working chamber proper.

In high-temperature furnaces radiation from the hot gases and the walls of the working chamber are the most effective methods of heat transfer, and the production of the most efficient furnace section is an important feature of design.

With low-temperature processes attention centres more and more on convection, which can be stimulated by employing mechanical means to increase the velocity of the hot gases and by exposing as much of the surface of the charge as possible to the moving gases.

Apart from considerations that affect heat transfer and thermal efficiency, there is the necessity in the case of copper and nickel alloys to ensure that the atmosphere surrounding the charge during its dwell in the furnace is such that the surface of the metal suffers as little damage as possible. The production and retention of protective atmospheres is, to some extent, a matter of furnace design, and examples will be described in the section on installations. It is appropriate, however, at this point, to review briefly the subject of furnace atmospheres.

## V.—FURNACE ATMOSPHERES

It has been shown that when town gas is burned with its theoretical air requirements, an atmosphere is produced which contains carbon dioxide, water vapour, and nitrogen. In addition, owing to the presence of sulphur compounds in the town gas, there will be small but significant quantities of these compounds in the furnace atmosphere. If the atmosphere is reducing, the sulphur will be present principally as hydrogen sulphide, but when the air supplied is the theoretical quantity it exists mainly as sulphur dioxide. If air is supplied in excess of the theoretical quantity, the sulphur will be present as sulphur dioxide and there will be, in addition, free oxygen in the furnace atmosphere.

In considering, therefore, the action of products of combustion of town gas on the non-ferrous metals, it is necessary to take into account the reactions of the metals with the following gases: oxygen, carbon dioxide, water vapour, hydrogen, carbon monoxide, sulphur dioxide, and hydrogen sulphide.

## 1. GAS REACTIONS

(a) *Oxygen*

This will readily oxidize copper at temperatures used for annealing, giving rise to a layer of oxides in

which cuprous oxide predominates next to the metal and cupric oxide on the outer skin. The attack increases with temperature and is aggravated by the presence of sulphur compounds. In bright annealing very small percentages of oxygen are sufficient to spoil the product.

Alloys of copper with silver and zinc will be subject to oxidation, which increases with rise in temperature. For some of these alloys annealing may be accomplished in oxidizing atmospheres, provided that the temperature of anneal is not high. Brasses may be clean annealed in forced-circulation hot-air ovens at 550° C.

(b) *Carbon Dioxide*

This gas is generally regarded as being inert to copper and very largely to copper alloys. High-zinc alloys are most susceptible to attack by carbon dioxide, but this may be minimized by adopting a reducing atmosphere.

(c) *Water Vapour*

This is regarded as being inert or slightly reducing to copper, so that steam atmospheres may be used for the bright annealing of copper. High-zinc alloys are susceptible to attack by water vapour, with the production of zinc oxide.

(d) *Hydrogen*

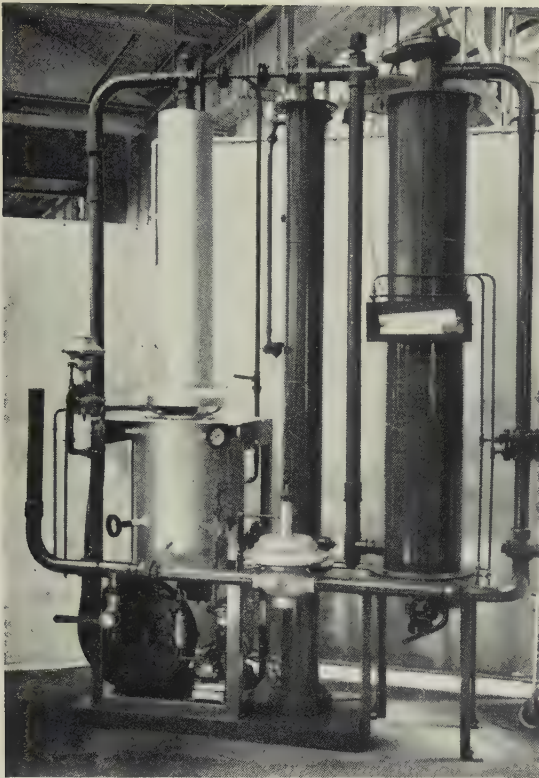
The effect of hydrogen on copper at temperature has been the subject of much investigation. With oxygen-free coppers it assists in bright annealing. On the other hand, with oxygen-bearing coppers percentages of hydrogen may give rise to embrittlement owing to the formation of water vapour in the body of the metal. Whether or not this will occur depends upon the temperature and the associated rates of diffusion of hydrogen and cuprous oxide; hence, for furnace atmospheres which come into contact with oxygen-bearing coppers the conditions should approximate to neutral, with hydrogen not exceeding 1%. In the case of brasses and other alloys, embrittlement does not take place.

(e) *Carbon Monoxide*

This gas may have an influence on the annealing of oxygen-bearing coppers, although its action is stated to be a surface one in contradistinction to the penetrative diffusion of hydrogen. Therefore, when its action is combined with that of hydrogen the total effect is greater than that of hydrogen alone, owing to an acceleration of the deoxidation of the copper surface. With copper alloys its action is not harmful, and it assists in bright annealing.

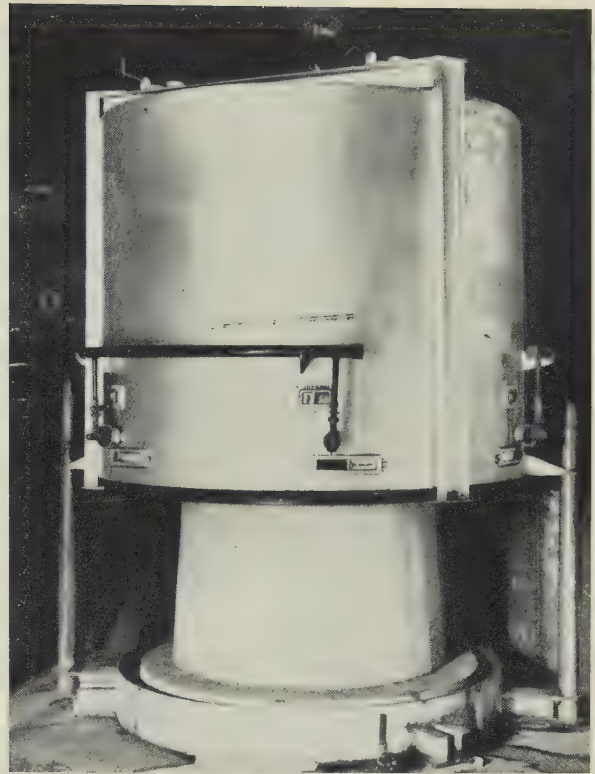
(f) *Sulphur Dioxide*

Copper and its alloys are practically immune from attack by sulphur dioxide. Accordingly, copper may be bright annealed in products of combustion that are slightly on the reducing side, provided that the town gas used has a low sulphur content. If the conditions



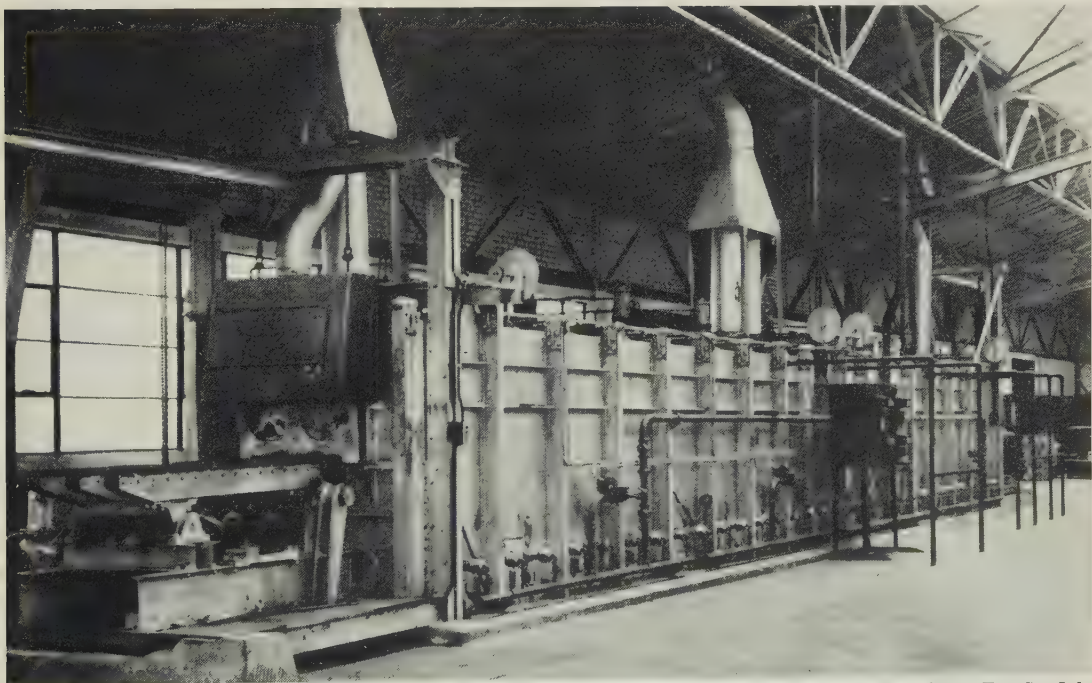
[Courtesy North Thames Gas Board.]

FIG. 18.—Sulphur-Removal Plant.



[Courtesy Incandescent Heat Co., Ltd.]

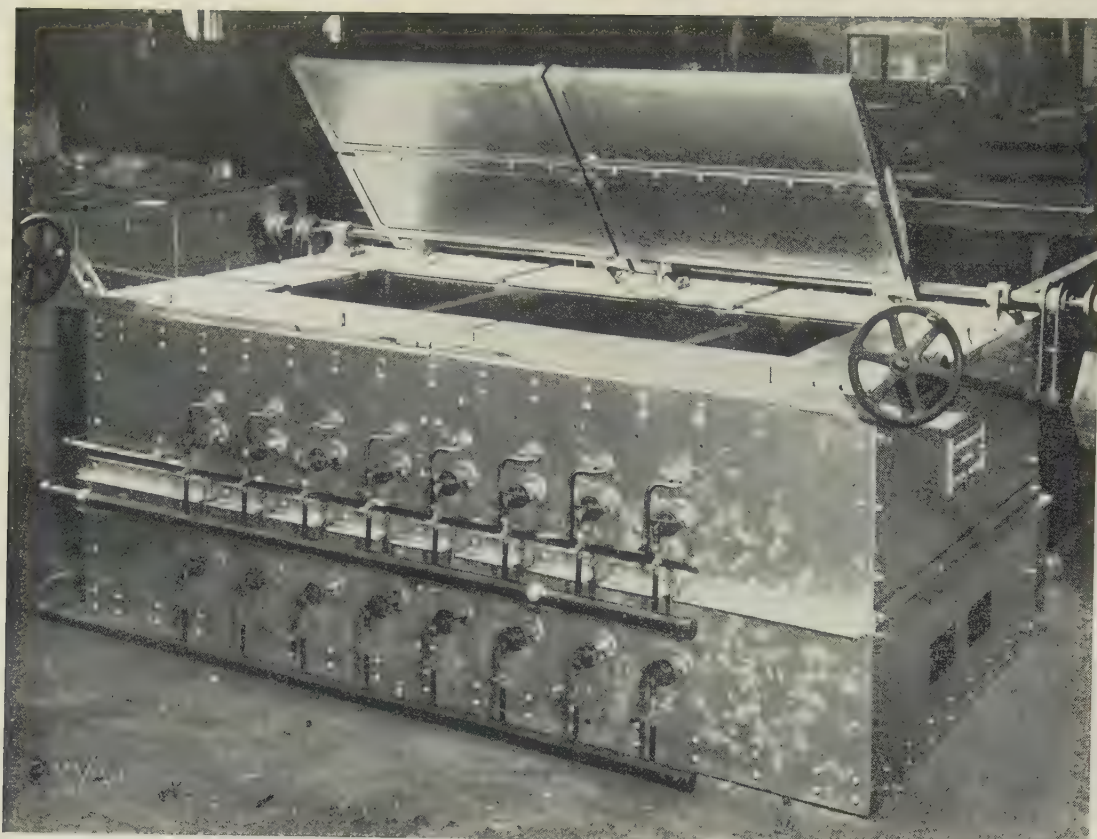
FIG. 19.—Cover Furnace.



[Courtesy Incandescent Heat Co., Ltd.]

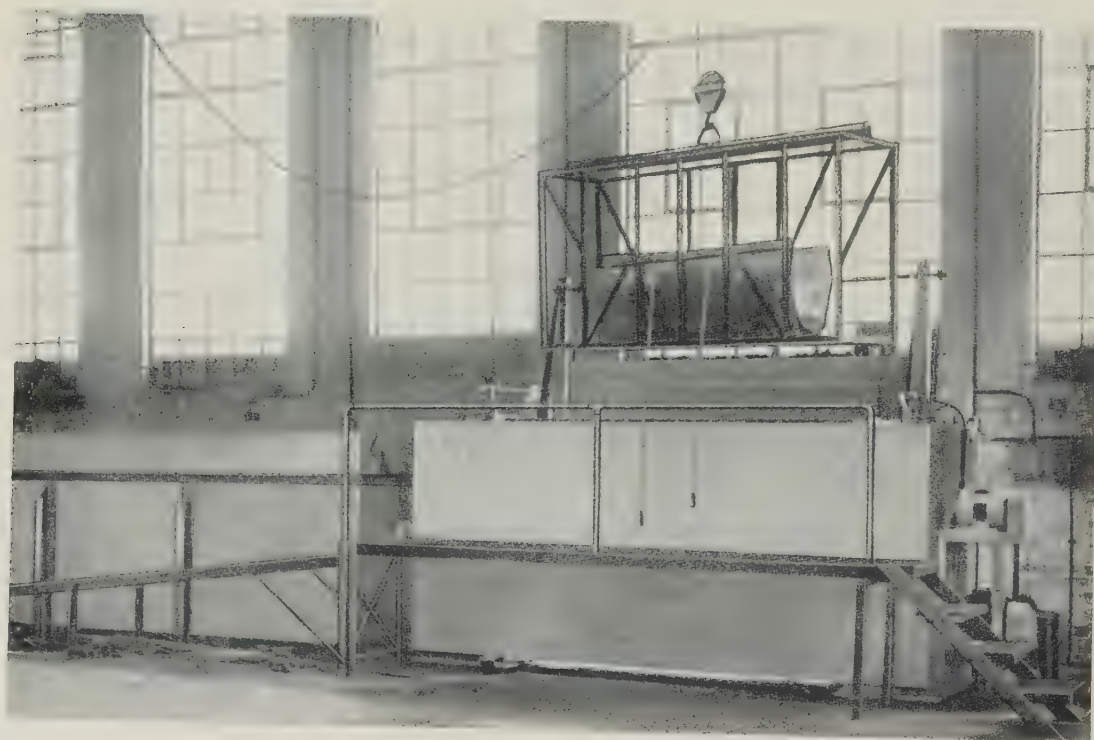
FIG. 20.—Continuous Light-Alloy Billet-Heating Furnace, Equipped with Chain Conveyors.





[Courtesy Incandescent Heat Co., Ltd.]

FIG. 21.—Gas-Fired Salt Bath, Showing Two-Stage Burner System.



[Courtesy J. L. S. Engineering Co., Ltd.]

FIG. 22.—Forced-Convection Oven for Heat-Treatment of Sheet.

are not too reducing, the sulphur compounds will be present in the oxidized state.

#### (g) Hydrogen Sulphide

The action of this gas, particularly on copper, is very pronounced, causing staining which can be removed only by cyanide solutions. Accordingly, for reducing atmospheres where hydrogen sulphide is likely to occur, its complete removal is advocated. Copper-silver alloys are much more prone to staining by this gas than is pure copper. For such alloys, steam atmospheres are advocated.<sup>7</sup>

### 2. SULPHUR REMOVAL

The neutral atmosphere produced by town-gas burners operating on the theoretical air:gas ratio can be used for the clean annealing of brass and nickel silver and for bright annealing copper, provided that the sulphur content of the town gas is below 6 grains/100 ft.<sup>3</sup>.

As most town gases contain sulphur in excess of this amount, it is necessary to desulphurize the gas before it is burned in the furnace.

The three important sulphur compounds present in town gas are :

	Sulphur-Content, grains/100 ft. <sup>3</sup> .
Carbon disulphide, CS <sub>2</sub> . . .	2-15
Carbon oxysulphide, COS . . .	3-10
Thiophen, C <sub>4</sub> H <sub>4</sub> S . . .	1-10

The carbon disulphide and carbon oxysulphide may be converted to sulphur dioxide and hydrogen sulphide in a catalytic sulphur-removal plant. These sulphur compounds may then be removed by washing and purification.

Thiophen cannot be removed by this process. A plant in common use is that developed by the North Thames Gas Board,<sup>8</sup> which will reduce the sulphur content from 20-25 to 3-4 grains/100 ft.<sup>3</sup>. A photograph of the equipment is shown in Fig. 18 (Plate XLVI).

The operation of the plant is as follows: The gas, together with a small proportion of added air, is heated to a temperature above 180° C., preferably 280°-320° C. The preheated gas then passes through the catalyst bed at about 1000 standard ft.<sup>3</sup>/ft.<sup>3</sup> of the bed. The active material is nickel subsulphide (Ni<sub>3</sub>S<sub>2</sub>) on small cylindrical pieces of porous, fired china clay. The carbon disulphide and carbon oxysulphide in the gas are converted to sulphur dioxide. Most of the oxygen in the gas, e.g. 0.5% by volume originally present and 0.5% added as air, reacts with some of the hydrogen to form water vapour. The catalytic combustion of hydrogen produces enough heat to give the required temperature of 380° C. near the outlet of the catalyst bed, this temperature being controlled by thermostatic adjustment of the air added at the plant inlet. Some of the sulphur dioxide formed near the inlet to the catalyst bed is reduced to hydrogen sulphide at the hot, oxygen-free end.

The treated gas, containing hydrogen sulphide, sulphur dioxide, and additional water vapour, then flows upwards through a washer-cooler. The counter-current wash of soda-ash solution or hard water removes the sulphur dioxide, the temperature and dew point of the gas being reduced almost to the temperature of the wash liquid.

Finally, the gas is freed from hydrogen sulphide in a purifier containing iron oxide, preferably a compact tower charged with specially active spherical oxide nodules. Gas flow in the tower is upward at the rate of about 200 ft.<sup>3</sup>/hr./ft.<sup>3</sup> of oxide nodules. Spent oxide is removed periodically in small quantities from the base of the tower and fresh nodules added at the top.

### 3. ATMOSPHERE REQUIREMENTS FOR INDIVIDUAL METALS

The products of combustion from desulphurized town gas burned with its theoretical air requirements can be used for bright annealing copper and high-copper brasses, cupro-nickels, &c., and also for the clean annealing of brasses, nickel silver, &c. No special-atmosphere plant is therefore required for gas furnaces dealing with these materials, and direct firing and the optimum conditions for thermal efficiency may be employed.

#### (a) Partially Burned Town Gas

For some metals, however, such as silver, high-silver alloys, and Monel metal, somewhat more reducing conditions are necessary and partially burned town-gas atmospheres are employed. This type of atmosphere has many points in its favour: it is cheap to produce, easy to control, and is generated from a readily available gas. It is generated separately from the furnace in a plant which would consist of the following: (1) a catalytic sulphur-removal plant; (2) a mixing device in which the gas and air are taken into the system and mixed in the required proportions; (3) a burner and combustion chamber in which the gas/air mixture is burned in contact with refractory material; (4) cooling, condensing, or washing apparatus for the removal of the water of combustion and some sulphur compounds; (5) iron oxide purifier for the removal of hydrogen sulphide; (6) a drying unit.

A plant of this kind<sup>9</sup> will provide atmosphere gas with a sulphur content of 0.2 grains or less/100 ft.<sup>3</sup>. The mixing of gas and air may be effected by hand control of gas and air with reference to suitable flow gauges, or may be done automatically in a compressor mixing machine to which gas and air are fed at atmospheric pressure through a ported sleeve valve, the vertical motion of which is actuated by a diaphragm which reflects the demand in the compressor. This valve may be rotated to control the air: gas ratio. The vertical motion controls the rate of mixture flow.

Other atmospheres which may be employed in muffled town-gas furnaces are those produced from ammonia by cracking and by partial combustion.



(b) *Cracked Ammonia*

Compressed liquid ammonia can be obtained commercially in a state of high purity, and forms, on cracking, a mixture of nitrogen and hydrogen which can be used as a protective atmosphere for the bright annealing of non-ferrous metals. The mixture is highly reducing in nature, with 75% hydrogen. The cracking is effected at about 520° C. in the presence of a catalyst, the reaction going almost to completion, so that the residual ammonia should not exceed 0.1%. This atmosphere, on account of its highly reducing nature and its high cost, has rather limited applications in the field of non-ferrous heat-treatment, but it is used on small plants where purity is essential.

and the application of various types of burner equipment.

## 1. COPPER-BILLET-HEATING FURNACE

This furnace is designed for an output of 8.5 tons/hr. of copper billets, heated to 850° C. The billets are 6 ft. long and vary from 3 to 6 in. in dia. The handling arrangements are fully automatic, the billets being mechanically fed from the magazine into the furnace through which they are carried by a walking beam. The mechanical system is such that charging and delivery are completely under the control of the press operator, who has only to push a button when a billet is required. Heat is provided by 24 burners of the

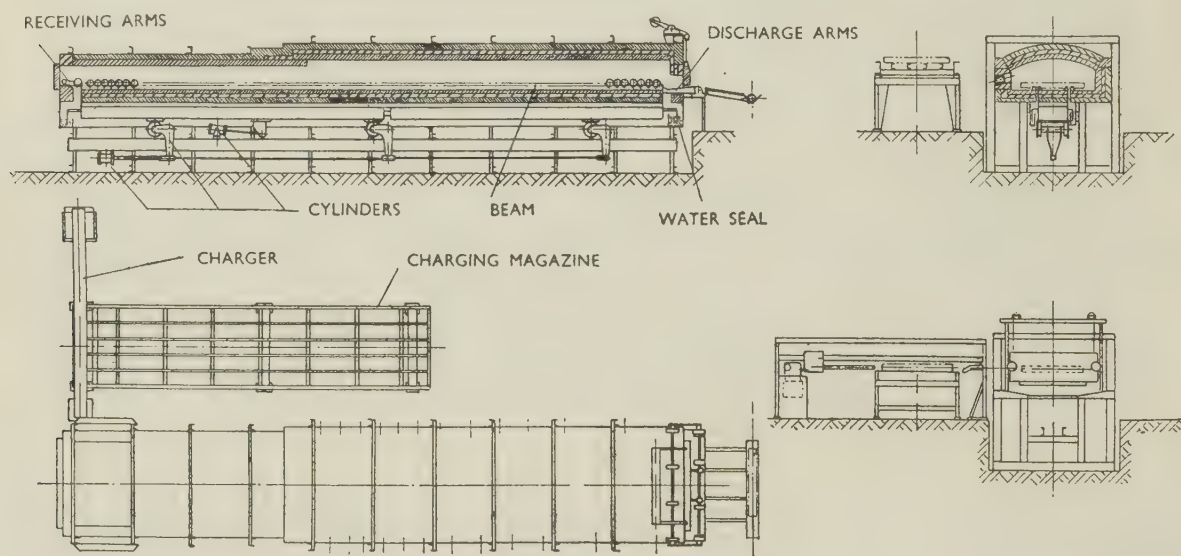


FIG. 12.—Copper-Billet-Heating Furnace.

[Courtesy Birlec, Ltd.]

(c) *Burned Ammonia*

The regulated combustion of cracked ammonia with various quantities of air leads to another range of prepared atmospheres of the same type, viz. hydrogen/nitrogen mixtures with lower proportions of hydrogen. For the completion of the combustion and the elimination of the presence of oxygen, catalytic means are adopted and hydrogen contents of approximately 10% are generally aimed at. On account of the high cost of this atmosphere, regeneration of the gases is desirable. This calls for careful attention to the design of the furnace plant in which the atmosphere is to be used. Burned-ammonia atmospheres may be used for the bright annealing of copper and the non-ferrous alloys where a particularly clean finish justifies the cost.

## VI.—GAS-FIRED FURNACE INSTALLATIONS

This section of the paper includes some brief descriptions of up-to-date furnace installations, chosen to illustrate methods of mechanical handling

type illustrated in Fig. 8 and these operate on pre-mixed gas and air. A fully aerated mixture is supplied, and each burner is fitted with a flame trap. The burner system is zoned into separately controlled groups of 4, 8, and 12 burners. The gas is not desulphurized, and the air : gas ratio is held constant by apparatus of the type shown in Fig. 9.

The furnace consists of a direct-fired heating chamber and a preheating section into which the billets are charged (Fig. 12). Along the length of the hearth run four parallel toothed bars, the inside pair being carried on the walking beam. The two outside bars are fixed to the hearth and form the rests that carry the billets when the beam disengages. The beam is operated by hydraulic cylinders and is completely water-sealed.

The charging magazine consists of a sloping table upon which the billets roll to the charger. The billets are held back on the charging table by a step which is adjustable for various billet diameters and which will also lift one billet at a time into a charging trough. A pusher operating in the charging trough transfers the billet from the trough into the furnace, where it is

received on cradle arms, which in turn place it on the toothed racks on the hearth.

The discharge gear works in conjunction with the furnace door. When the door is raised, arms which are permanently in the furnace lift the billet from the last position on the static toothed bars and form a sloping ramp down which it rolls to the piercing press. The action is completed by the discharged billet itself operating mechanism to shut the door. Loading and discharging operations are co-ordinated and the whole movement is performed by hydraulic cylinders controlled electrically by sequence and limit switching. The water-sealed beam prevents leakage of the furnace atmosphere, and the combustion gases leave the furnace enclosure through flues located at the end of the preheat section.

row fires above the roller hearth and the other below, the burner rows being fitted on opposite sides of the furnace chamber. The gas is desulphurized before combustion and a fully aerated mixture supplied to the burners, the mixture ratio being held constant by apparatus of the type shown in Fig. 9.

The cooling arrangements consist of a slow-cool and a spray chamber, the slow-cool chamber being located immediately after the heating section. The spray chamber is constructed from non-corrosive material, and the water temperature is thermostatically controlled to ensure maximum dryness and to prevent water staining. The cooling equipment consists of an array of high-pressure spray nozzles above and below the work, and a special weir which also provides an unbroken curtain of water to retain

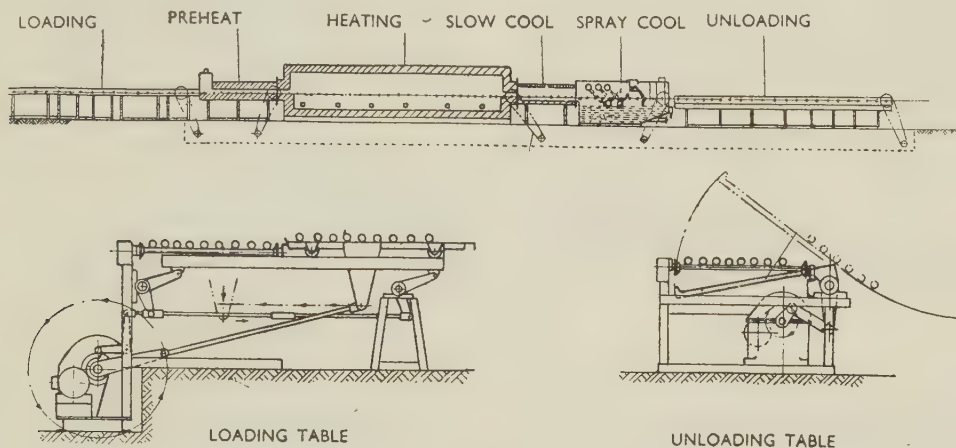


FIG. 13.—Bright-Annealing Furnace for Copper Tubes.

[Courtesy Birlec, Ltd.]

## 2. COPPER-TUBE ANNEALING FURNACE

This furnace is designed to bright anneal copper tube in straight lengths, and will raise 3 tons/hr. of tube to  $650^{\circ}\text{C}$ . It is a direct-fired, roller-hearth furnace fitted with cooling chambers and with mechanical arrangements for charging and discharging the copper tubes.

The rollers are of heat-resisting material in the heating chamber and mild steel elsewhere, except in the spray-cooling chamber, where they are made of a non-corrosive material. All the rollers are provided with collars to guide the tubes through the furnace; and to ensure gas-tightness all the rollers are fitted with specially sealed bearings. The roller drive, which is under push-button control, operates through a reduction gear and a variable-speed gear-box to chains and sprockets on the rollers.

The work enters the furnace through an adjustable door and through a system of baffles which restricts the egress of the products of combustion. The first part of the furnace acts as a preheater, and after passing through this zone the tubes enter the heating section, where heat is provided by two rows of multi-jet burners of the type illustrated in Fig. 8. One

the furnace atmosphere. Beyond the weir a series of baffles is fitted, together with a steam vent.

The loading and discharge arrangements are illustrated in Fig. 13. The loading table is 25 ft. long, with driven steel rollers. The mechanical loading device consists of a series of steel arms which carry the tubes to be charged and which move forward between the rollers where they are lowered to deposit the charge on to the rollers. The arms are then withdrawn to accept a fresh charge.

The horizontal and vertical movements of the arms are actuated by levers driven through a motor and gear-box. The unloading table is of the same length as the loading table, but in this case the unloading device consists of a series of arms which, operating between the rollers, lift and roll the tubes down to a suitable receptacle.

## 3. RADIANT-TUBE, ROLLER-HEARTH CONVEYOR FURNACE

This furnace is designed to bright anneal copper refrigerator coils and tubes at a temperature of  $650^{\circ}\text{C}$ . The coils are fed through the furnace on trays at the



rate of 600 lb./hr., and the total weight heated, including the trays, is equivalent to 1500 lb./hr. of copper. The furnace is illustrated diagrammatically in Fig. 14. It is an indirect-fired, roller-hearth furnace, fitted with forced-convection fans in the heating zone and in the water-jacketed cooling chamber.

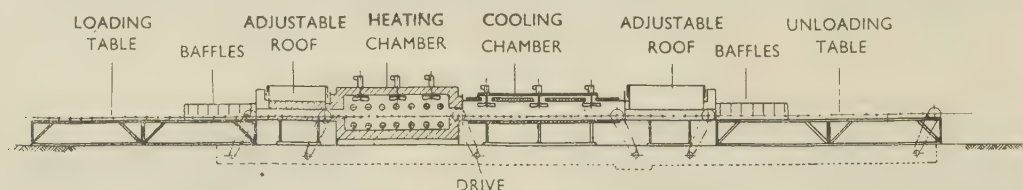
The furnace atmosphere is partially burned town gas, supplied by a separate generator equipped with sulphur-removal plant. The furnace chamber is heated by 14 recuperative radiant tubes, similar to that illustrated in Fig. 10. The radiant-tube array is split into two separately controlled zones, and three fans in the roof of the furnace circulate the protective atmosphere and ensure temperature uniformity.

The cooling chamber is of the water-jacketed type, and here again three circulating fans are fitted to assist cooling. The atmosphere provided by the generator is retained by baffles, and the roofs of the

cooling pipes in the sides and roof of the chamber. In the second stage a series of spray nozzles are fitted above and below the work. The spray system is of the thermostatically controlled, recirculating type, and produces cool work at maximum dryness. It is claimed that very clean annealing of nickel silver and other non-ferrous metals and alloys can be obtained from this type of furnace without desulphurizing the gas, provided that the normal sulphur content does not exceed about 25 grains/100 ft.<sup>3</sup>.

## 5. COVER FURNACES

These furnaces are used for dry bright annealing coiled non-ferrous wire and strip. A typical installation, part of which is shown in Fig. 19 (Plate XLVI), consists of one heating cover and four bases. The charge is supported on a perforated plate and is covered by a light sheet-steel cover, which fits into a sand seal around the base. This cover, which is aluminized



[Courtesy Birlec, Ltd.]

FIG. 14.—Radiant-Tube, Roller-Hearth Furnace for Bright Annealing.

inlet and outlet tunnels are adjustable to vary the height of the furnace opening to suit varying heights of work. These adjustable roofs are fitted with deep water seals.

## 4. NICKEL SILVER ANNEALING FURNACE

The furnace illustrated in Fig. 15 is a gas-fired furnace designed for the clean annealing of nickel silver. The work is carried through the furnace on a series of driven rollers made of materials suitable for the conditions encountered in the heating and cooling zones. Heat is provided by rows of air-cooled tunnel burners supplied with a correctly proportioned air : gas mixture which is maintained constant by the system shown in Fig. 5. Air is supplied at 1 lb./in.<sup>2</sup> by a blowing fan, and the burners are arranged to fire above and below the rollers.

The work enters the charge vestibule through canvas curtains. After obtaining a certain amount of preheat, it enters the heating chamber. This is fitted with heat-resisting drop doors at entry and exit which may be adjusted to give a minimum clearance over the work. The inner doors assist in retaining the atmosphere, but their main function is to prevent heat being radiated into the charge vestibule and cooling chamber.

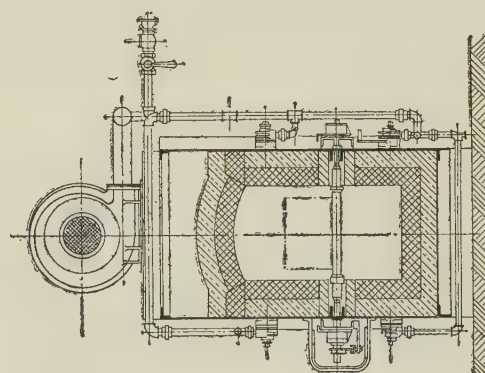
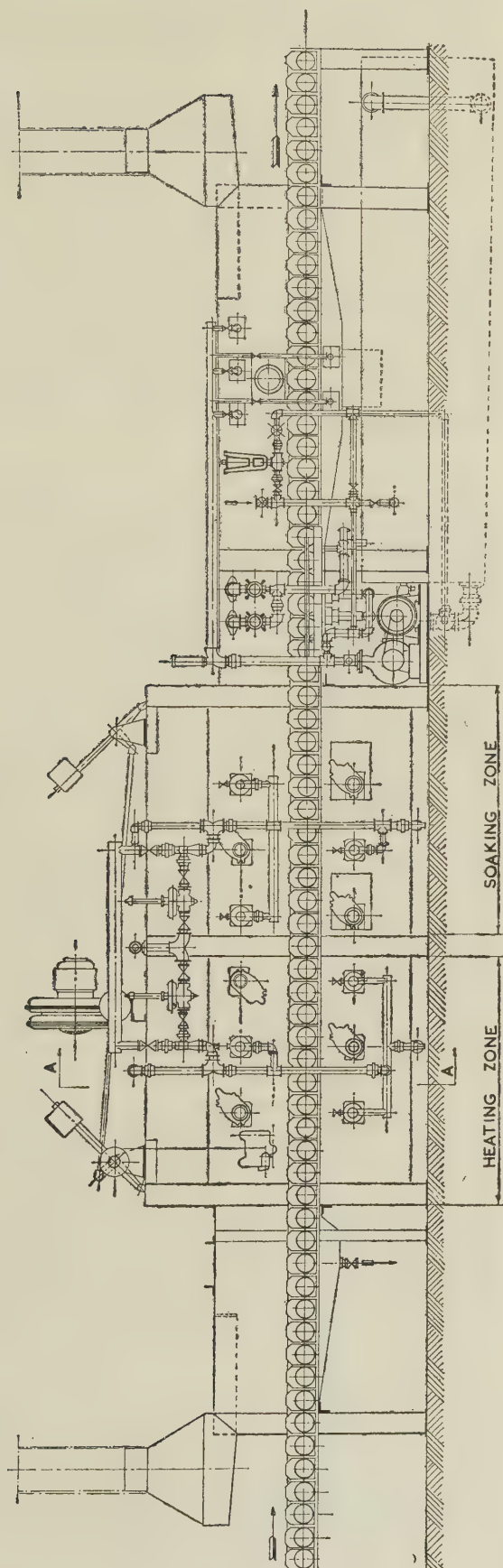
Cooling is carried out in two stages. In the first, heat is extracted by water-cooled rollers and by

on the outside, is also provided with a skirt which dips into a water trough, so providing an additional seal. The outer or heating cover is lined with a suitable refractory material and fitted with a system of low-pressure Bunsen burners. At each base there is provision for connecting the burners to the main gas supply.

Each base is fitted with a fan, which circulates a protective atmosphere within the light inner cover and materially assists in accelerating the heating and cooling cycles and in achieving temperature uniformity. Complete automatic controlling and recording equipment is provided, which operates with each base as it comes into use. Two thermocouples are employed with each base, one being placed in the outer edge at the top of the charge and the other inside the charge at the bottom. By this means the temperature is controlled within close limits.

In the furnace illustrated, the inside dia. of each inner cover is 2 ft. 10½ in. and the stacking height is 3 ft. The full capacity of each base is 1 ton of wire/load, the output varying from 7 to 10 cwt./hr., depending upon the gauge being treated. The working temperature ranges from 350° to 550° C. Of the four bases, one is used for the heating cycle and the others for cooling, loading, and unloading.

The design of the cover furnace enables any of the available furnace atmospheres to be employed with the minimum amount of loss.



SECTIONAL ELEVATION  
ON LINE A.A.

FIG. 15.—Arrangement of Roller-Hearth Furnace for Annealing  
Nickel Silver, &c.  
(Courtesy British Furnaces, Ltd.)



## 6. FURNACES FOR LIGHT ALLOYS

The furnaces used in the various thermal processes involved in the manipulation of the light alloys may be classified as follows:

(1) Furnaces in which the products of combustion form the furnace atmosphere and which employ fans to promote circulation.

(2) Molten salt baths.

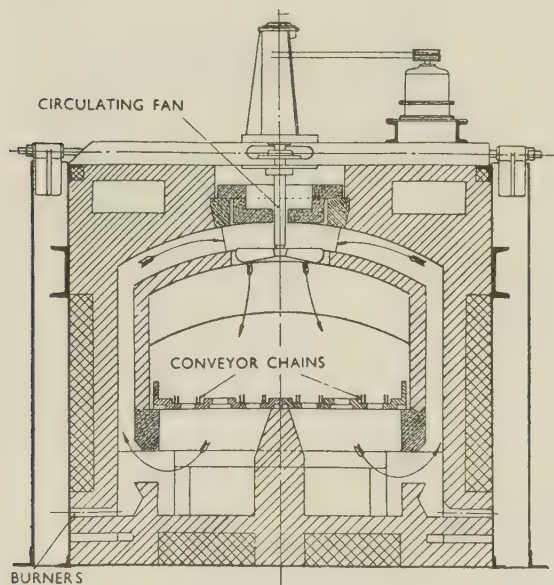
(3) Forced-circulation furnaces, in which an air atmosphere is circulated by means of fans.

Furnaces in the first category are usually employed for billet heating and for annealing and precipitation-treatments. Those in the third may be used for annealing, and for solution- and precipitation-heat-treatments. Salt baths are generally employed for the solution-treatment of light alloys, although it is possible, with the low-temperature salts now available, to use salt baths for precipitation-treatment. Salt baths must not be used for the heat-treatment of magnesium-rich light alloys.

The temperatures employed in the thermal treatment of the light alloys are low, but the requirements are precise and critical. It is for these reasons that accurately controlled forced-convection furnaces have found such favour in this field. Some examples of typical heat-treatment plant are described below.

## (a) Billet-Heating Furnace

Aluminium alloys at 400°–500° C. are soft and have a high coefficient of friction; for these reasons it is



[Courtesy Incandescent Heat Co., Ltd.]

FIG. 16.—Atmosphere-Circulation System in Billet-Heating Furnace for Light Alloys.

necessary in the design of continuous billet-heating furnaces, to avoid stressing or sliding the billet. Chain conveyors, slat conveyors, or roller hearths, are therefore, often employed. The furnace illustrated

in Fig. 20 (Plate XLVI) is an example of a continuous light-alloy billet-heating furnace equipped with chain conveyors.

The furnace is 55 ft. long  $\times$  3 ft. wide  $\times$  1 ft. 4 in. to the crown of the arch, and is designed to operate continuously up to temperatures of 520° C. The furnace deals with 16 billets/hr., each measuring 25  $\times$  12  $\times$  5 in., representing an output of 2550 lb./hr. The billets are carried through the furnace by two conveyor chains fitted 18 in. apart. Heat is supplied by two rows of low-pressure Bunsen burners evenly disposed along each side of the furnace. The products of combustion are circulated by 8 fans spaced along the roof of the furnace. The circulation path is indicated in Fig. 16. Heating is uniform and the billets are thoroughly soaked when they are discharged to the rolling mill.

## (b) Salt Baths

The molten salt bath was used by Wilm in the experiments that resulted in the discovery of age-hardening and the invention of Duralumin. Since that time the salt bath has remained popular for the solution-treatment of aluminium alloys. It is an extremely flexible piece of equipment, in that it can handle work in any form up to the limit of its capacity and can deal effectively with almost any type of section. Heat transfer to the work is rapid, the temperature distribution is uniform, and the molten salt gives some measure of uniform support to thin sections which would otherwise be likely to sag at the softening temperature.

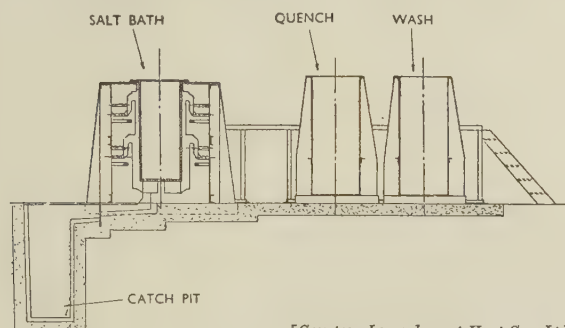
On the other hand, salt baths are not as clean as the forced-circulation furnace, and one consequence of this is that the quenching apparatus must be somewhat elaborate. To prevent subsequent corrosion, the work must be completely freed from salt after quenching, and a second quenching tank is often used in which the salt is removed by water circulating at high velocity or by high-pressure water sprays.

An example of a gas-fired salt bath is shown in Fig. 21 (Plate XLVII). It is heated by low-pressure Bunsen burners arranged in 4 rows, 2 rows being placed on each side. This two-stage arrangement is employed to ensure temperature uniformity over the depth of the bath. The burners fire behind vertical panel walls which prevent flame impingement on the metal wall of the bath, and the gases of combustion pass down over the sides of the bath to flues in the base of the setting. In some installations these flues are graded to a catch pit which will accommodate the molten salt should the bath fail. Fig. 17 shows a section of a typical arrangement of salt bath, quench tanks, and catch pit.

The molten-salt containers are manufactured from low-carbon steel, and may be of welded or riveted construction, with rounded corners to eliminate focal points of stress when the bath is heated and cooled.

The furnace setting surrounding the container is usually constructed from refractory insulating material contained within a braced steel casing. In order to

reduce heat loss from the surface of the molten salt, insulated covers are used. These may be hinged, rolling, or lift-off types. Power operation is employed for the larger lids.



[Courtesy Incandescent Heat Co., Ltd.]

FIG. 17.—Gas-Fired Salt-Bath Installation.

### (c) Forced-Convection Ovens with Air Atmosphere

This type of furnace employs forced convection as the means of transferring heat to the charge, and an air atmosphere is circulated at a high velocity in order to achieve a large coefficient of convective transfer. The rate of air displacement is also great, so as to reduce temperature gradients within the working space to a minimum. Sealed heat-exchangers are used to ensure that the gases of combustion do not mix with the air atmosphere in the working chamber. This is important in so far as it has been shown by Stroup<sup>10</sup> that products of combustion are likely to cause blistering of aluminium-base alloys containing magnesium. It would appear that the effect of products of combustion is not serious at temperatures below 400° C., and ovens in which such products are circulated can therefore be used for annealing and precipitation-treatment. Direct firing has the advantage of higher thermal efficiency, as compared with the indirect method. A forced-convection oven designed for the heat-treatment of sheet and parts fabricated from sheet, is shown in Fig. 22 (Plate XLVII).

The oven is designed for top loading, and the working space measures 8 ft. 9 in. long × 3 ft. 9 in. wide × 4 ft. 10 in. deep. The plant will deal with the whole range of light alloy heat-treatment, and the manufacturers guarantee a degree of uniformity within the working chamber of  $\pm 1^\circ$  at 530° C. The working space is heated by high-velocity air, which passes over the surface of two heat-exchangers built one into each side of the working space. The burner equipment consists of two rows of industrial-type neat-gas jets similar to that illustrated in Fig. 1, operating at a maximum gas pressure of  $2\frac{1}{2}$  in. water gauge. This burner equipment is controlled by temperature-indicating and -recording equipment.

## VII.—CONCLUSION

An outline has been given of present-day practice as it relates to the design of gas-fired furnaces employed by the non-ferrous metal industry. Unfortunately, the scope of the subject is so extensive that it has only been possible to deal with the various main branches in the briefest possible fashion.

It is hoped, however, that the omission of a more detailed treatment has not obscured the fact that the art of designing gas-fired furnace equipment is a branch of technology which is no longer dependent upon empiricism, but one which employs scientific knowledge and method in order to produce efficient plant eminently suitable for the work required of it.

## ACKNOWLEDGEMENTS

The author offers his grateful thanks to the following firms who have given assistance by providing photographs and information concerning their products: Birlec, Ltd., British Furnaces, Ltd., Incandescent Heat Co., Ltd., J.L.S. Engineering Co., Ltd., Keith Blackman, Ltd., and Reavell and Co., Ltd.

His thanks are also due to the Chairman and members of the West Midlands Gas Board for permission to publish this paper.

## REFERENCES

1. W. Jürges, *Beihefte Gesundheits-Ing.*, 1924, **1**, (19).
2. A. Schack, "Industrial Heat Transfer". New York: 1933 (John Wiley and Sons, Inc.); London (Chapman and Hall, Ltd.).
3. H. Etherington, "Modern Furnace Technology". London: 1938 (Charles Griffin and Co., Ltd.).
4. J. F. Waight, *Inst. Gas Eng., Commun.* No. **384**, 1951.
5. A. G. Robiette, *Metal Ind. (Lond.)*, 1939, **55**, 365.
6. "The Efficient Use of Fuel." London: 1944 (H.M. Stationery Office).
7. I. Jenkins, "Controlled Atmospheres for the Heat-Treatment of Metals", p. 477. London: 1946 (Chapman and Hall, Ltd.).
8. — *Gas Times*, 1951, **68**, (745), 174.
9. P. F. Hancock, *Metal Ind.*, 1949, **74**, 103.
10. P. T. Stroup, *Controlled Atmospheres (Amer. Soc. Metals)*, 1942, 207.





# BATCH AND CONTINUOUS ANNEALING OF COPPER AND COPPER ALLOYS\*

1349

By EDWIN DAVIS,† M.Sc., F.I.M., MEMBER, and S. G. TEMPLE,‡  
M.Sc., A.I.M., MEMBER

## SYNOPSIS

The more exacting quality requirements in respect, for example, of uniformity of crystal structure and properties and surface finish, and the need for improving operating efficiency and output, have resulted in recent years in considerable changes in annealing equipment and practices in the production of wrought copper and copper alloys. Some of these are outlined, and since they involve a knowledge and application of fundamental considerations, the annealing characteristics of representative copper-base alloys are discussed and reference made to the effect of impurities on the softening of copper alloys and to heat-treatment other than annealing to produce soft material, such as stress-relief annealing, solution heat-treatment, and tempering.

Various types of batch and continuous furnaces are described, and the factors influencing uniformity of annealing and the relative merits, limitations, and applications of both types of annealing are briefly considered. Since copper and copper alloys readily oxidize when annealed in air, the development of protective atmospheres has progressed rapidly and the conditions to be fulfilled in bright annealing are detailed. Particular reference is made to copper-zinc alloys which not only oxidize readily but from which zinc may volatilize, to the detriment of the surface appearance.

## I.—INTRODUCTION

ANNEALING as applied to copper and copper alloys may be defined as a heating and cooling operation designed to induce softness and effect recrystallization to produce a desired microstructure. It is an essential process in the production of these materials in such semi-fabricated forms as strip, sheet, wire, rod, and tubes. Until comparatively recently annealing practices were largely based on knowledge accumulated from past experience, supplemented by experiments conducted in an empirical manner in the plant. During the last 20 years or so more exacting requirements in respect of uniformity of hardness, grain-size, freedom from directional properties, improved surface finish, &c., of products have necessitated the development of annealing practices founded on more fundamental knowledge. Furthermore, the necessity for obtaining increased productivity has become more and more important, and when cold-working operations are involved high outputs can be obtained only when the annealing schedules, and of course the concomitant rolling schedules, are designed in the light of the most modern knowledge of annealing characteristics of the materials being processed. It is not within the scope of this paper to discuss the mechanism of recovery and recrystallization which takes place in annealing, and about which there is still considerable controversy, but much of the work done in this field is used to supplement the simpler basic know-

ledge of the effect of time and temperature on the hardness and grain-size.

The improvements in annealing technique brought about by increased knowledge of the fundamentals of the process have been paralleled by improvements in plant and equipment. Thus, the solid-fuel-fired furnaces of the early 20th century, in which the temperature could not be closely controlled, have been replaced by gas- or electrically-heated furnaces with provision for accurate temperature control, and with protective atmospheres where necessary. Indeed, without these improvements advantage could not be taken of the knowledge now available, the application of which demands precise control of the annealing conditions.

So wide is the range of copper and copper alloys produced in wrought forms that the annealing equipment required is very varied in type. The requirements for annealing brass strip, for example, differ to some extent throughout the processing schedule, and the carefully controlled operation for the final anneal may not be justifiable either metallurgically or economically for that following the initial cold rolling of cast ingots or hot-rolled stock, and the plant suited to either of these operations may be unsuitable for wire, rod, or tube. The purpose of this paper is to present a picture of present-day practices for annealing copper and copper alloys, to detail the influence of the requirements of annealed stock of various forms on plant design, and to indicate trends of future de-

\* Manuscript received 22 October 1951. Contribution to a Symposium on "Equipment for the Thermal Treatment of Non-Ferrous Metals and Alloys", to be held in London on 26 March 1952.

† Technical Officer, Imperial Chemical Industries, Ltd., Metals Division, Birmingham.

‡ Manager, Strip Rolling Mill, Imperial Chemical Industries, Ltd., Metals Division, Birmingham.



velopment. Since in the last two decades the annealing of strip and sheet has received most attention, as a result of more stringent demands by consumers—particularly in respect of surface finish and uniformity of properties—more frequent reference is made to the treatment of these products than to the annealing of wire, rod, or tube. The basic principles defined, however, apply to all types of products, and it is significant that the most recent improvements in tube-annealing plant, for example, follow closely earlier developments in strip and sheet annealing.

## II.—ANNEALING CHARACTERISTICS

The annealing characteristics of 90:10 gilding metal, 70:30 brass, and 18% nickel silver are shown in the form of isochronal annealing curves in Fig. 1 and relate to  $\frac{1}{2}$ -hr. annealing periods for material cold rolled 50% in thickness. Annealing curves of these three alloys are similar in general character, an initial increase of hardness occurring at low temperatures, the magnitude of which varies with the alloy and for any one alloy generally increases with the amount of cold work (see Fig. 2). As the temperature is increased, rapid softening takes place associated with the onset of recrystallization, the temperature at which softening begins depending not only on the composition of the alloy but also on the previous rolling treatment (see Fig. 2). When recrystallization is complete, further increase in annealing temperature affects the hardness to a lesser extent, but the gradient

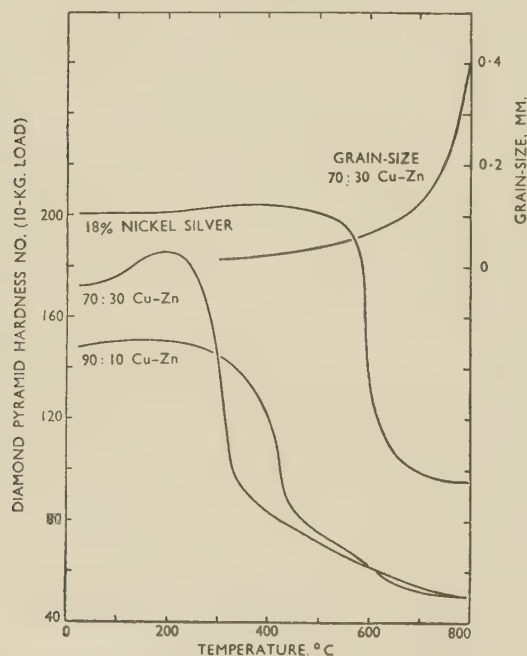


FIG. 1.—Isochronal Annealing Curves. Annealing period after 50% reduction in thickness:  $\frac{1}{2}$  hr.

of the curve varies considerably from alloy to alloy. Treatment of alloys in the temperature range over which a slight increase of hardness occurs is of prac-

tical interest only in stress-relief annealing, to which reference will be made later (Section VIII). For industrial annealing operations it is the lower portion

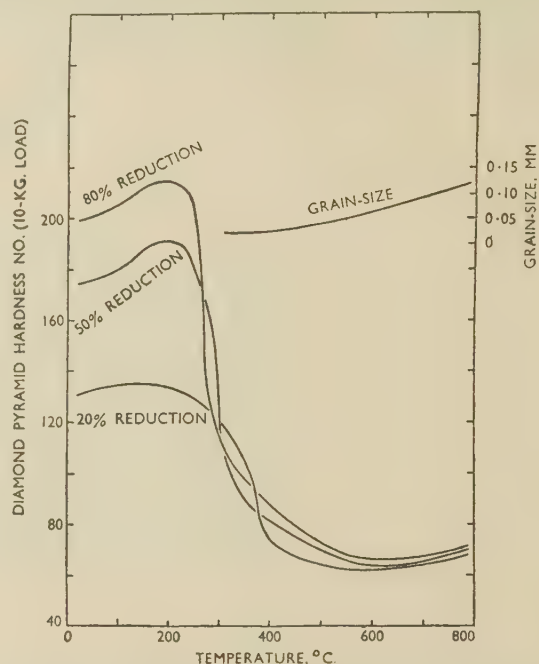


FIG. 2.—Isochronal Annealing Curves for 64:36 Brass. Annealing period after reduction in thickness:  $\frac{1}{2}$  hr.

of the curve, after complete recrystallization, which is of greatest importance, defining as it does, the conditions for full annealing, i.e. to a hardness value of about 60 D.P.N. in the case of 70:30 brass. For certain applications stock may be required not fully softened, and this may be produced by annealing at a temperature lower than is required for complete softening. Thus, for example, 64:36 brass strip or sheet with a hardness of some 80 D.P.N. is frequently produced by annealing at  $340^{\circ}$ – $400^{\circ}$  C., a process which is cheaper than cold rolling fully annealed stock, particularly in thin gauges. On the other hand it is not practicable to obtain hardness values lying on the vertical portion of the annealing curve, e.g. 100 D.P.N. for 64:36 brass, by annealing cold-rolled material, since the essential conditions are too critical to be realized in practice and strip of this order of hardness is produced by cold rolling.

Beyond the temperature at which recrystallization is complete, the hardness of any one copper-base alloy does not vary significantly with the previous rolling reduction, and thus in industrial annealing practice the operating temperature is not usually related to the degree of cold work, except when considerations of directional properties are paramount. Although hardness is not greatly affected by increase of annealing temperature after recrystallization, the grain-size increases with higher annealing temperatures (see Figs. 1 and 2).

The effect of annealing time is shown by isothermal annealing curves, a typical example for 70:30 brass

being given in Fig. 3. From this, it is apparent that after the initial recrystallization, which takes place in a very short space of time, grain growth is initially

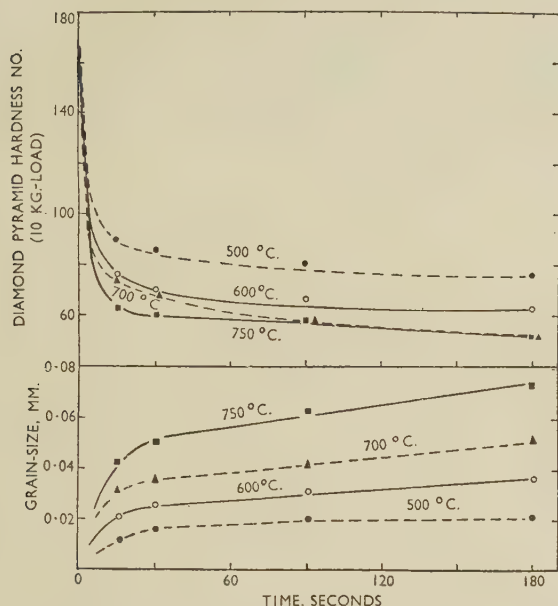


FIG. 3.—Effect of Annealing Time on Isothermal Annealing Curves for 70 : 30 Brass.

fairly rapid and then becomes much slower, whereas hardness is but little affected after the completion of recrystallization. From this isothermal curve, which is typical of those for most copper-base alloys of the single solid-solution type, and the extensive work on this aspect of annealing carried out by French,<sup>1</sup> it is clear that the relatively slow rate of grain growth and hardness change with time at temperatures below about 550° C. ensures that with reasonable control of temperature, batch-annealing time is not inherently a very critical factor. On the other hand, in certain types of continuous-annealing plants, particularly continuous strand-annealing furnaces, metal temperatures are high and heating times are short. If therefore the speed of the stock through the furnace and thus the time at temperature varies, significant variations in grain-size may well result. It is common practice, in order to increase the furnace output, to operate strand-annealing furnaces with a temperature lead, i.e. the furnace temperature is in excess of the maximum strip temperature; conditions which accentuate the ill-effects on grain-size that result from variations in speed.

Fig. 4 shows the relationship between the hardness and grain-size of annealed 70 : 30 brass compiled from results of a large number of determinations on stock previously cold rolled 50% or more in thickness before annealing. Although this relationship provides a useful guide, it does not hold if the previous rolling reduction is small, for under these circumstances the influence of the grain-size before the final rolling reduction may be marked, as shown by French.<sup>1</sup>

It is from data of the type illustrated in Figs. 1–3 that the industrial annealing conditions for the batch process have been laid down, and a number of these are quoted for a range of common alloys in Table I. The annealing temperatures quoted in this table are typical of those commonly adopted for final annealing. In process annealing it is not unusual for higher temperatures to be employed, since maximum soft-

TABLE I.—*Typical Industrial Annealing Ranges for Copper-Base Alloys.*

Alloy	Annealing Temperature, °C.	Diamond Pyramid Hardness No.
H.C. Copper	300–350	45–55
Deoxidized copper	400–450	45–55
90 : 10 Cu–Zn	550–600	55–65
80 : 20 Cu–Zn	500–600	60–70
70 : 30 Cu–Zn	500–600	60–70
60 : 40 Cu–Zn	525–575	80–90
95 : 5 Cu–Sn	600–650	75–85
93 : 7 Cu–Sn	650–700	80–90
95 : 5 Cu–Al	700–750	65–75
80 : 20 Cu–Ni	700–750	70–80
10% Nickel Silver	700–750	80–90
18% Nickel Silver	700–750	85–95

ness is often desirable in order that subsequent cold-working operations can be more easily effected. Increase of annealing temperature, however, may not always result in lower hardness values, and in this connection the brasses containing between 62 and 64% copper are of particular interest. Reference to Fig. 2 shows that as the annealing temperature increases above about 550° C. the hardness no longer decreases but begins to increase owing to the formation of the  $\beta$  phase, which under the prevailing cooling conditions is retained. Similarly, minimum hardness

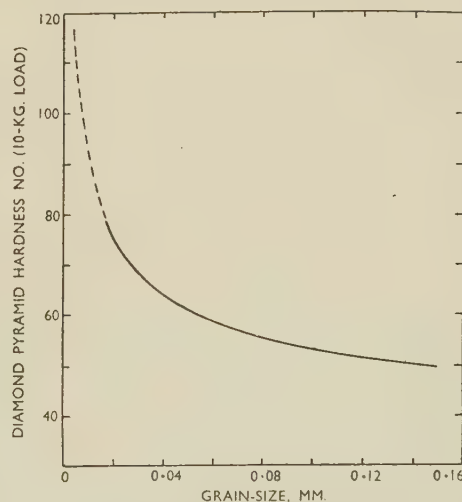


FIG. 4.—Relationship Between Hardness and Grain-Size of Annealed 70 : 30 Brass.

values on 60 : 40-type brasses are obtained by annealing at temperatures of about 550° C., at which the proportion of  $\beta$  phase is a minimum.



The data quoted in Table I and the annealing curves in Figs. 1-4 relate to commercially pure alloys, and significant changes in annealing characteristics may result from the presence of certain impurities. It is well known, for example, that the addition of about 0.05% silver to high-conductivity copper increases the softening temperature by about 100° C., and Cook and Miller<sup>2</sup> have described the effect of various elements on the annealing characteristics of 70:30-type brass. A marked change is brought about by the presence of as little as 0.04% phosphorus and 0.07% iron. On the other hand, up to 0.045% arsenic, 0.2% antimony, 0.068% aluminium, or 0.08% tin has no effect upon the annealing characteristics, and small quantities of lead, though refining the grain-size slightly, do not affect the hardness after

TABLE II.—Heat-Treatment Temperatures for Copper-Base Temper-Hardening Alloys.

Alloy System	Temperature, °C.	
	Solution Treatment	Tempering Treatment
Cu-Be . . . . .	775	315
Cu-Cr . . . . .	1000-1050	450
Cu-Ni-Al . . . . .	900	525-550
Cu-Zn-Ni-Al . . . . .	825	525
Cu-Ni-Si . . . . .	700-750	450

annealing. When lead is present in either  $\alpha/\beta$  or  $\alpha$  brasses, the annealing conditions must be chosen so as not to give rise to deleterious increase in the lead particle-size with corresponding reduction in machinability, for which purpose lead additions are made; in general, annealing temperatures must be restricted to about 550° C. to prevent significant agglomeration of the lead particles.

The foregoing relates only to the intermediate or final annealing of simple alloys for the purpose of obtaining material in the soft state for further cold working, but annealing or heat-treatment is also carried out on copper alloys for other purposes.

Of these other treatments, low-temperature annealing to prevent stress-corrosion cracking is probably the next most common, particularly as some copper alloys are very susceptible to this form of failure. The subject of the relationship of composition of these alloys to stress-corrosion cracking has recently been comprehensively surveyed by Cook.<sup>3</sup> For all practical purposes copper can be regarded as free from liability to stress-corrosion cracking, but copper-zinc alloys with more than 15% zinc are prone to this type of failure, although the addition of certain elements, particularly silicon, has a beneficial effect. Many other copper-base alloys are susceptible to stress-corrosion cracking, though with the exception of the nickel silvers, the tendency to failure is less marked than with the brasses.

In the production of temper-hardening copper-base alloys provision is necessary for solution heat-treat-

ment at high temperature, followed by quenching and subsequent re-heating to a lower temperature. Solution-heat-treatment temperatures for copper-base temper-hardening alloys are usually higher (see Table II) than the annealing temperatures for simple copper alloys, and tempering operations are usually carried out at temperatures between 400° and 600° C., according to the alloy. Specific plant requirements for heat-treating temper-hardening alloys will be referred to in Section VIII.

### III.—BATCH-ANNEALING FURNACES

The majority of annealing operations are carried out in batch-type furnaces which vary considerably in size from the small type capable of holding a few pounds of metal only, to those of several tons capacity with outputs of one or more tons per hour. The conventional rectangular box structure finds general application when a variety of forms of product are required to be annealed, as for example in sheet or strip mills, where initial cold-rolled stock in long lengths as well as coil or sheet has to be treated (Fig. 6, Plate XLVIII). For more specialized applications cylindrical furnaces may be used, these being horizontal for treatment of tubes or long rods (Fig. 9, Plate XLIX) or vertical for wire and strip coils (Fig. 10, Plate XLIX), particularly when floor space is restricted. The actual dimensions of the furnaces vary widely, often being dependent on other than metallurgical factors. With horizontal furnaces, for example, the usual practice is to charge by means of a fork-type machine with the product loaded on trays or cradles, as illustrated in Fig. 6 (Plate XLVIII).

TABLE III.—Details of Typical Batch-Annealing Furnaces for Copper-Base Alloys.

Product	Internal Dimensions	Average Charge, tons	Approx. Output, tons/hr.	Rating, kW.	Max. Gas Capacity, ft. <sup>3</sup> /hr.
Brass coils	Rectangular, 18 ft. 0 in. long, 6 ft. 0 in. wide, 16 in. high.	3.0	1.0	250	...
Copper wire	Vertical cylindrical, 2 ft. 6 in. dia., 8 ft. 6 in. high.	2.5	0.5	70	...
Brass tubes	Rectangular, 30 ft. 0 in. long, 8 ft. 0 in. wide, 2 ft. 0 in. high.	2.5	2.0	...	5000

These forks, carrying the load, move forward into the furnace along grooves; subsequent slight lowering of the forks enables them to be withdrawn without disturbing the charge. Thus the large overhang of the fork charger and weight of product to be annealed per batch restrict furnace length, and horizontal batch furnaces are rarely more than 30 ft. long. Vertical

furnaces are usually charged with overhead cranes, the work being suitably loaded on frames or stands, and the limits to size are the effective working height available and the rigidity of the frame or stands at operating temperatures. Where head room is restricted, vertical furnaces are often sunk below floor level. Details of typical examples of the larger types of furnace in the industry are given in Table III.

In batch-annealing furnaces the rates of heating of the charge may vary considerably in different parts of the furnace if, as is common, the charge is heated by either gas burners, radiant tubes, or electric-resistance elements, when inevitably the portion of the

reduce temperature differentials throughout the furnace. Heating elements may also be incorporated in the doors of horizontal furnaces. Moreover, to improve uniformity of heating, fans of various types may be introduced to circulate the atmosphere. Since annealing of copper-base alloys is generally carried out at temperatures at which radiation is of more importance in conveying heat to the product than is convection, the fans employed in furnaces for annealing copper alloys merely disturb the air, and do not effect a definite pattern of air flow as is common in furnaces for heat-treating aluminium or tempering steels. Furnaces with true forced-air cir-

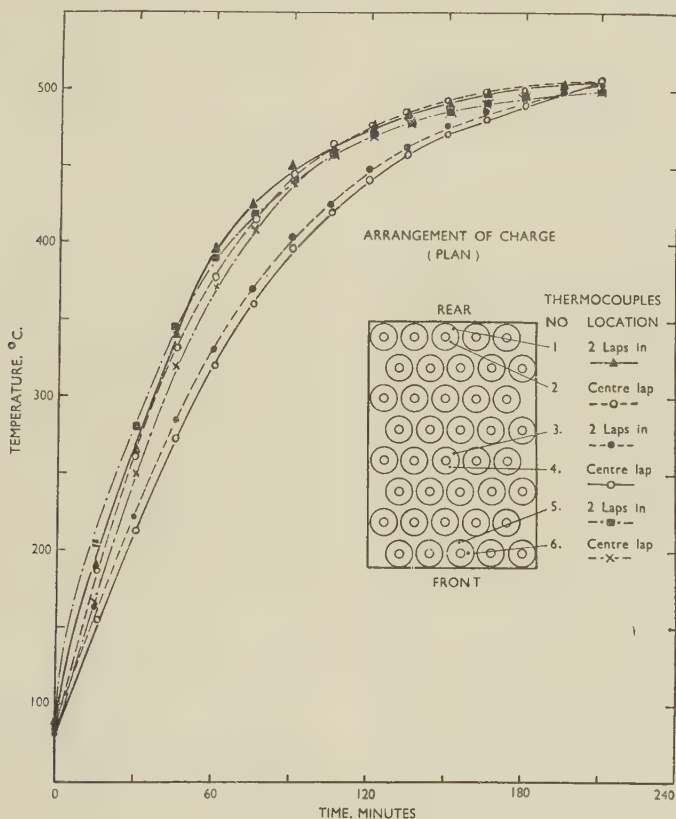


FIG. 5.—Time/Temperature Relationship During Batch Annealing of 40 Coils of 70:30 Brass Strip (Size:  $8\frac{1}{2} \times 0.035$  in. Total weight: 3 tons).

charges adjacent to these heating elements is heated more rapidly. In the case of tightly wound coils or wire the inner laps or strands are heated mainly by conduction from adjacent turns, whereas the edges of all the coils and the outer laps near the heating elements are subject to direct radiation. It has been suggested<sup>4</sup> that increased uniformity of heating of coiled strip can be obtained by loosening the laps or spacing them with distance pieces, but the cost of such methods generally renders them impractical.

The furnace itself is often divided into a number of zones, individually controlled by pyrometers suitably located in the furnace, so that the heat input in any one zone can be restricted or increased as required to

culcation should show economies in annealing costs and time, particularly for operating at the lower temperatures employed in stress-relieving of tubes or annealing of copper, but few such installations appear to be in operation, probably because of their high initial cost.

Different rates of heat absorption may arise from differences in the surface condition of the metal being annealed, for although after cold working copper and copper alloys are usually bright, lubricant may be present on the surface and if the conditions of heating are such as to promote cracking with subsequent deposition of carbon, then the bright areas reflect and the dull rapidly absorb the heat. Similarly, different



degrees of oxidation in the early stages of annealing may result in differential rates of heat absorption, for copper and most copper alloys form oxide films in air at temperatures in excess of about 150° C.

Even with the most modern batch furnaces tests are usually necessary to determine the characteristics of the unit with particular reference either to the annealing of the predominant types of charges handled or to the annealing of special batches for which the equipment was perhaps not specifically designed, to determine the most suitable locations for temperature-control thermocouples, or to establish the optimum distribution of the load in the furnace to secure uniform heating. Tests of this type usually consist of introducing thermocouples into various parts of the charge and establishing the time/temperature relationship. A typical series of curves from a batch furnace annealing some 40 coils of brass strip is shown in Fig. 5.

Factors other than uniformity of heating, however, have to be considered. For example, distribution of the charge affects the output of the furnace and possibly the labour costs of handling. Excessive handling as well as increasing costs may result in damage to the edges of coils or the surfaces of sheet, and thus in view of these conflicting requirements some compromise relating to distribution of the charge must be made. Such a compromise can usually be made satisfactorily for brass, as in view of its annealing characteristics mentioned in Section II, soaking can be extended to 3 or 4 hr., provided the temperature is not too high, without detriment to the properties of the final product.

#### IV.—CONTINUOUS-ANNEALING FURNACES

It has already been pointed out that in batch annealing the whole charge cannot be annealed under exactly the same conditions, and it was to overcome this disadvantage that continuous methods of annealing were developed. Ideally, in continuous annealing the product moves at a uniform speed through a heated zone or zones maintained at definite controlled temperatures so that in its passage through the furnace it all undergoes the same heating and cooling cycle. In practice, such ideal conditions are rarely achieved, although in strand annealing of wire they are very closely approached. The earliest type of continuous furnace was that with the moveable hearth, batches of the product to be annealed being placed on the hearth, which was then pushed or pulled through the furnace at a predetermined rate. Several installations of this type have been used for the annealing of hot-rolled brass and copper sheet, but the process is inherently inefficient, since the massive refractory hearths have to be heated and cooled during each cycle.

The continuous furnaces in use today are of three main types: the chain or roller conveyor, the mesh belt, and the continuous-strand furnace. In the first of these, trays are generally used to carry the charge

through the heated zone and out into the atmosphere, and to maintain high thermal efficiency these trays are made as light as practicable, within the limits imposed by the necessity for retention of shape at the annealing temperature. Long rods or tubes are annealed in roller-hearth furnaces without the use of tray conveyors, provided the work is sufficiently straight not to foul the rollers during passage through the furnace. A modern furnace for annealing copper tubes is illustrated in Fig. 7 (Plate XLVIII), the output of which is of the order of 2 tons/hr.

Mesh-belt or chain conveyors are also among the earliest examples of continuous furnaces, and hot-rolled copper sheets were frequently annealed in furnaces of this type, each individual sheet passing through the furnace, the oxide film formed being removed by quenching to give the desired iridescent matt finish. In modern practice the mesh-belt conveyor is used extensively for annealing sheets and small pressings, and plant has been installed for annealing brass and copper sheets up to 54 in. wide with outputs of one ton or more per hour (Fig. 8, Plate XLVIII).

Strand annealing of thin strip material was developed about 1925, and where the output is large and uniform in physical form plant of this type is economically justified. The usual practice is to employ a horizontal furnace, the strip (not exceeding about 0.040 in. thick) being decoiled at one end and recoiled at the other, each subsequent coil being either welded or stitched to its predecessor. During its passage through the furnace the strip may be supported on rollers or, alternatively, supported at the entrance and exit of the furnace only and allowed to assume the natural catenary in the heated zone.

Horizontal furnaces of this type require a considerable amount of floor space, for their length must be such that at the rate of travel of strip through the furnace the time in the heated zone is adequate for the metal to attain the defined annealing temperature. As in batch annealing, the surface condition of the strip markedly affects the rate at which it absorbs heat, and some installations incorporate gas jets or burners at the entrance of the furnace to act not only as an additional source of heat, but also to dull the strip surface and so increase the rate of heat absorption. It is quite common practice to equip continuous furnaces of this type with pickling, cleaning, and drying arrangements so that the whole process is carried out without the necessity for intermediate recoiling. The advantages of this are obvious, but complications in design are inevitably introduced, since the rate of travel through the plant must be adequate not only for annealing but also for pickling, and, of course, the floor space required is considerably increased.

To avoid the use of supporting rollers, inclined furnaces have been employed for the annealing of copper alloys; the most recent development, however, has been to instal vertical furnaces such as have been used in the steel industry for the last decade or

so. In the U.S.A. a furnace of this type has been quoted<sup>5</sup> as having an output of 90 tons of annealed brass in 24 hr., and it is certain that vertical continuous furnaces, if operated on strip of standard dimensions, are capable of giving high outputs, while at the same time conserving floor space and giving adequate support to the strip throughout the annealing process.

Strand annealing of wire is essentially similar to that of strip, and several designs of furnace for this process have been developed. Probably because of the need for higher operating speeds for comparable outputs, they have never attained the same popularity, but several furnaces embodying interesting features have been put on the market. The Snead furnace, for example, utilizes the resistance of the wire as the heating medium, and the temperature is controlled by the expansion of the wire, but it does not seem to have been used to any extent.

No attempt appears to have been made to develop strand-annealing furnaces for tubes, but the trend in this section of the industry has in the last few years been very marked indeed towards the employment of continuous furnaces, with the tubes either in straight lengths or in coils being carried on trays or fed through on a roller-hearth.

Furnaces of this type have the further advantage that tubes of any length can be annealed, a feature of considerable importance in view of the use of larger billets and correspondingly longer tube-lengths. A recent installation is illustrated in Fig. 7 (Plate XLVIII).

Although continuous furnaces would appear at first sight to be capable of providing uniform conditions, this result is in fact not so readily realized. Many of the factors influencing the uniformity of products in batch annealing apply equally to continuous annealing. Thus, for example, in continuous annealing of coiled strip or wire the outer laps are heated more rapidly than the inner laps, and similar conditions apply in continuous annealing of tubes or sheets unless one layer only is laid on the rollers or mesh belt. In continuous strand annealing of strip, the rate of heat absorption is not uniform across the width, the edges heating up more quickly, but on the other hand uniformity of heating can be readily obtained in strand annealing of wire. Differences in the reflectivity of strip surface, arising from variations in rate of oxidation, or the extent to which lubricant present on the surface cracks and deposits carbon, can result in marked variations in the strip temperature during continuous strand annealing, and consequent irregular annealing. The influence of all these factors is increased if the furnace is worked on a temperature lead, as is quite common. Continuous annealing is in fact more critical in its requirements than batch annealing, but once the correct conditions have been established for a particular type of product a high degree of reproducibility is obtainable, and continuous annealing plants of all types are becoming increasingly used where outputs are sufficiently large to warrant the high initial cost.

## V.—COMPARISON OF BATCH- AND CONTINUOUS-ANNEALING FURNACES

Throughout the preceding sections reference has been made as occasion arose to the relative merits of batch- and continuous-annealing furnaces under particular circumstances, but it is not possible to make a general comparison between the two types of plant. It is obvious that installation of continuous-annealing plant can be considered only when large-scale production of similar lines of products is required, but even when this basic requirement is fulfilled it does not necessarily follow that continuous-annealing plant is justified. The initial cost of continuous furnaces, with all their ancillary equipment, is usually greater than that of batch furnaces and associated charging equipment for similar work, and continuous furnaces are less versatile. On the other hand, the shorter annealing cycle of continuous furnaces facilitates a constant flow of material through the plant, and often the quality of the product is considerably superior to that of similar stock batch-annealed. Labour costs, output per man hour, and output per unit of energy vary so much according to the type of plant and product being handled that it is not possible to make a general comparison between the two classes of furnaces on these grounds.

In general, it would appear that in small plants the batch furnace will continue to be the standard equipment because of its flexibility. During the past few years there has been a tendency in large-scale manufacturing for continuous furnaces to replace batch-annealing equipment, as evidenced by the increasing number of mesh-belt or roller conveyors for annealing sheet or tube, and the time may come when, in big plants, batch annealing will be for the most part obsolete.

## VI.—PROTECTIVE ATMOSPHERES FOR COPPER AND COPPER ALLOYS

### 1. EFFECT OF VARIOUS GASES

When copper and its alloys are heated in air at temperatures at which annealing operations are conducted, oxidation occurs, resulting in the formation of a layer of surface scale, the nature and amount of which depends upon the alloy and the annealing time and temperature. For subsequent fabrication this scale requires to be removed by mechanical or chemical means, which not only involves an appreciable metal loss but also the installation of suitable plant.

Although copper and many copper-zinc alloys can be easily cleaned in sulphuric acid solutions, the scale on copper alloys containing aluminium, nickel, or silicon cannot be so readily removed by pickling in such media. It is not surprising, therefore, that techniques have been developed for carrying out annealing operations under conditions which prevent the formation of scale.

In considering the application of protective atmo-



spheres for annealing, reference must be made to the reaction of the metals or alloys with the various constituents of the atmospheres, which include nitrogen, carbon monoxide, carbon dioxide, hydrogen, water vapour, and sulphur compounds in proportions depending on the source of the atmosphere. The dissociation pressure of copper oxide is relatively high; hence, a reasonably high concentration of oxidizing gases can be tolerated in the normal controlled atmospheres without oxidation of copper occurring, e.g. in water vapour at a temperature of 725° C., oxidation of copper will not proceed if there is a trace of free hydrogen present. Copper is inert to nitrogen, and the rates of reactions with oxides of carbon below 600° C. are so slow as to be negligible; the rate of reaction with steam is of a similar order. Hydrogen does not attack pure copper, but the reaction with tough-pitch copper, as the hydrogen diffuses into the body of the metal and reacts with the cuprous oxide present, forms steam, which causes disruption of the metal. This is well known and has been described in detail by Ransley,<sup>6</sup> who has investigated also the reaction with carbon monoxide and a mixture of carbon monoxide and hydrogen. It is well established that provided the annealing temperature does not exceed 400° C., up to 2% hydrogen can be tolerated. Hydrogen sulphide rapidly attacks copper at elevated temperatures, producing a film of black copper sulphide which is not readily removed by the conventional pickling agents and requires treatment by alkaline cyanide solutions. Although sulphur dioxide and organic sulphur compounds are generally inert to copper, they are readily converted to hydrogen sulphide in the presence of hydrogen, a reaction assisted by the catalytic action of any steel present in the furnace or container. Copper alloys, other than those containing more than 15% zinc, to which reference will be made in Section VII, are affected by the gases referred to above in a manner similar to copper. Thus protective atmospheres for annealing copper and copper alloys, except brasses, should be free from sulphur-bearing gases, while for tough-pitch copper some restriction must be placed on the hydrogen content and/or the temperature. Protective atmospheres for bright annealing these materials are therefore basically of three types: steam, ammonia derivatives, and fuel-gas derivatives. Precautions to prevent the ingress of free oxygen and the presence of sulphur compounds must be taken, and the methods of accomplishing this in industrial annealing are dealt with below.

## 2. STEAM ATMOSPHERES

The earliest method adopted for annealing in steam atmospheres was the use of sealed containers with charcoal and water placed in the pot. From close annealing operations of this type, products superior in appearance to those annealed in open furnaces were obtained, but the thermal efficiency of the process was low and a prolonged annealing cycle was essen-

tial. The Bates and Peard continuous furnace, which had water seals and a steam atmosphere, was extensively employed during the early years of this century, and is still quite widely used today. A batch-type furnace having a protective steam atmosphere was developed in the U.S.A., and a number of these—Kenworthy—furnaces are still in use. Quenching the charge in water is an essential feature of both these types of furnace, and thus the annealed material is discharged below the temperature at which oxidation normally takes place, but unless operating conditions are carefully controlled the product frequently water stains. These furnaces were mainly developed for annealing copper wire, and it is for this purpose that they still find considerable application. It is interesting to note that bright annealing of wire was developed earlier than bright annealing of other forms of copper alloys because of the difficulty of chemically treating and cleaning coils of wire.

Apart from steam annealing just described, there was little development in the application of protective atmospheres for bright annealing copper until after the first world war, when the increasing use of electric-resistance furnaces enabled protective atmospheres to be introduced into the furnace body without admixtures of the gaseous products of the combustion of a fuel. Furthermore, it began to be appreciated about that time that secondary reactions could occur between the metal and oxygen-bearing and sulphur-bearing gases as well as primary oxidation of the metal by free oxygen.

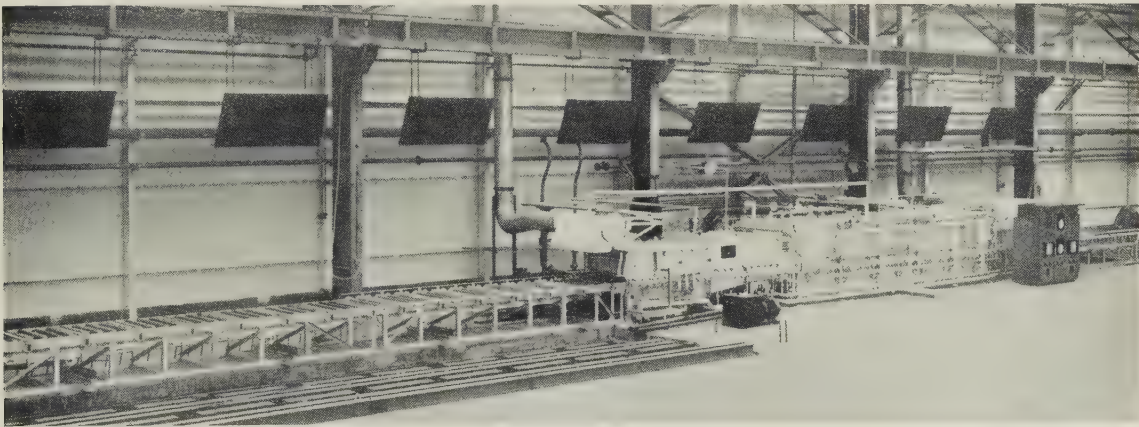
## 3. ATMOSPHERES OF AMMONIA DERIVATIVES

The protective atmospheres usually employed in this country in the annealing of copper and copper alloys are produced from two sources—ammonia and fuel gases. In the use of the former, anhydrous liquid ammonia in cylinders is fed in gaseous form to a cracking unit, where it passes over a catalyst maintained at about 520° C. The equipment used is both compact and well designed so as to be suitable for use under quite severe conditions. The cracker unit delivers a gas containing 75% hydrogen, which calls for care in furnace design, especially in continuous furnaces, to reduce the risk of explosion. The gas is extremely pure and free from moisture, but it is highly reducing in character, and for these reasons its application is limited. Reductions in cost of atmospheres of this type may be obtained by partially burning the cracker gas with air under controlled conditions, so that the hydrogen content is lowered to about 5%, when the risk of explosion in use is eliminated, and an increased volume is produced from the ammonia. Water vapour produced by combustion of hydrogen and oxygen is removed by condensation, and gas-drying plants in cases where oxidation of the metal can be caused by moderately high water-vapour contents of the atmosphere. These gas-drying plants incorporate alumina gel as a drying agent and are used to reduce the water-vapour





FIG. 6.—Batch Furnaces for Annealing Brass Coils.



*[Courtesy Stein and Atkinson, Ltd.]*

FIG. 7.—Gas-Fired Roller-Hearth Furnace for Annealing of Tubes.

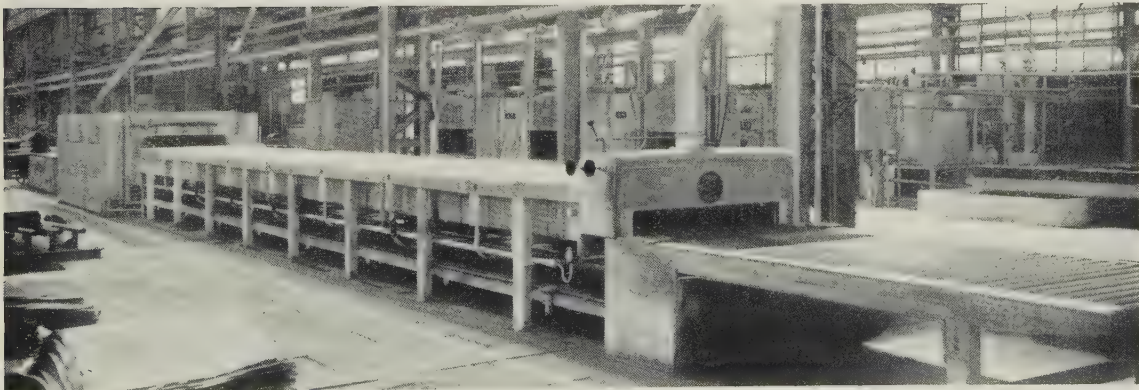


FIG. 8.—Mesh-Belt Conveyor Furnace for Annealing of Sheets.



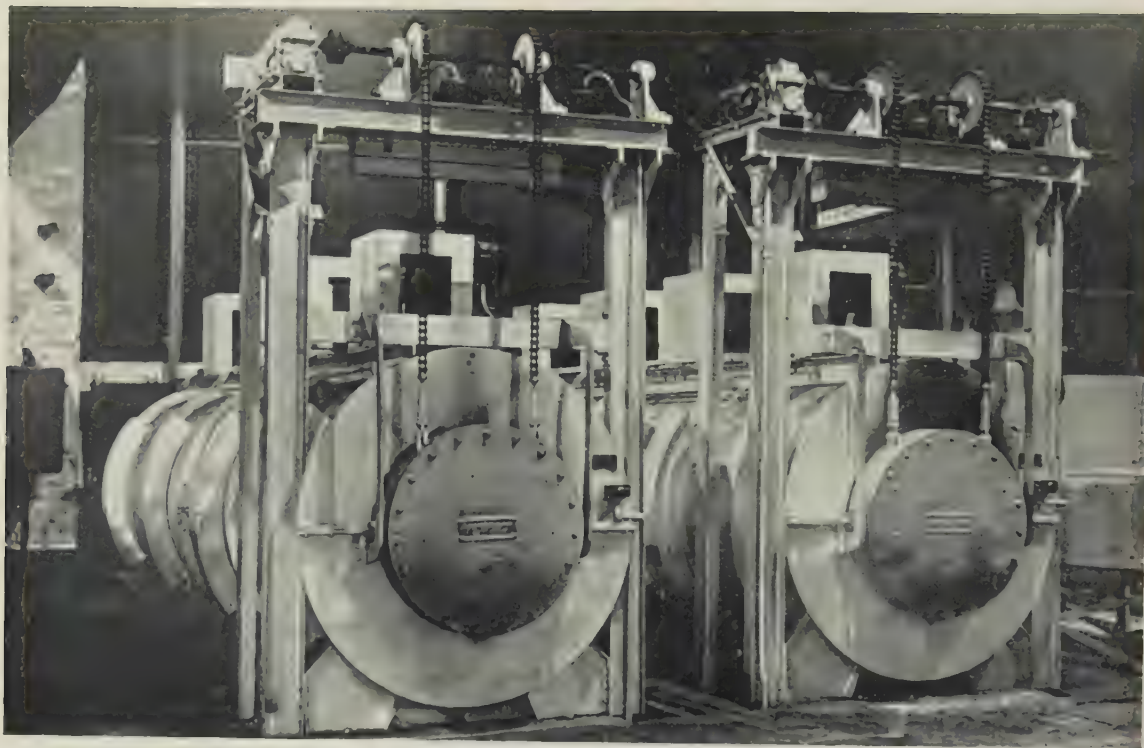


FIG. 9.—Cylindrical Furnaces for Annealing of Tubes.

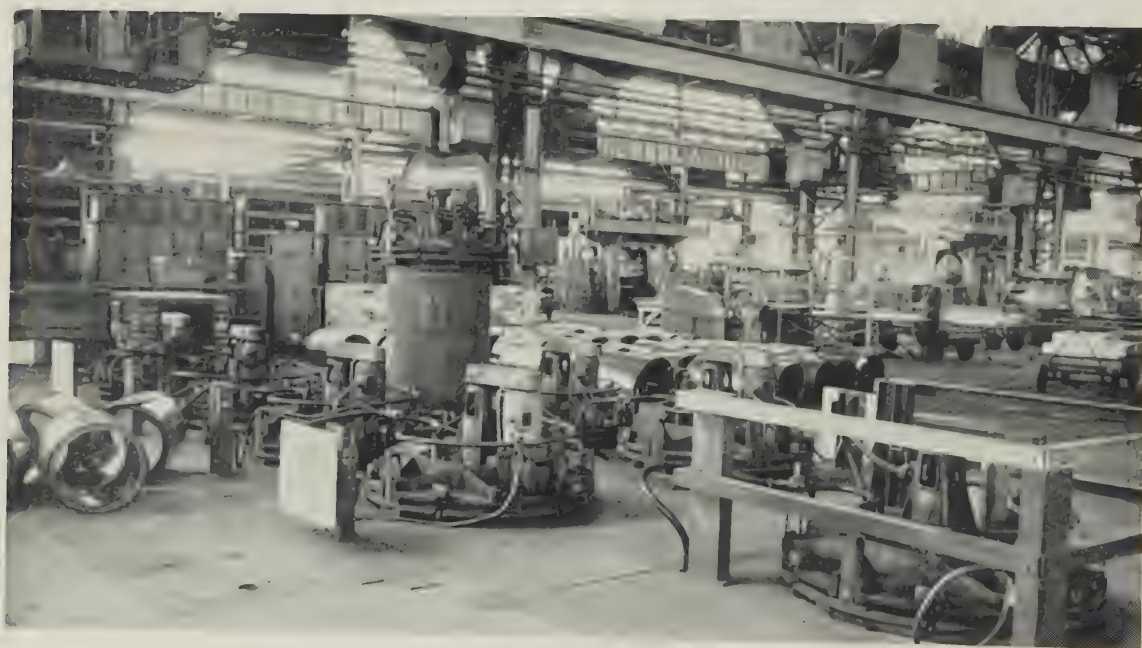


FIG. 10.—Pit Furnace for Annealing of Copper Wire and Strip.

content of the atmosphere to a small figure, and to lower the dew point to  $-40^{\circ}\text{C}$ . Protective atmospheres of this type are frequently recirculated to reduce the cost. Recirculation sometimes involves the installation of plant to clean the atmosphere after it has passed through the annealing furnace, where it may pick up oil vapour from rolling lubricants on the metal or contaminating gases arising from the charge itself or formed by reactions between the atmosphere and the container or charge. When recirculated ammonia burner gas becomes contaminated from lubricants on the charge, filters are sometimes incorporated in the return gas system to assist in oil-mist removal. Regenerated ammonia burner gas is widely used for protective atmospheres in the annealing of non-ferrous metals, but the initial capital outlay is high, and the furnace, especially the continuous type, requires to be carefully designed to avoid air contamination of the recirculated atmosphere.

#### 4. ATMOSPHERES OF FUEL-GAS DERIVATIVES

Partial burning of fuel gases produces atmospheres which are basically suitable for annealing non-ferrous metals, and although town gas is most widely used in this country, propane, butane, and acetylene are suitable; in the U.S.A. natural gas is widely employed. Town gas is readily available in quantity and the atmosphere produced from it is relatively cheap, but, because of its complex composition, purification is essential for many applications as well as a careful control of the degree of combustion, which may increase the final cost considerably. The products of combustion consist of the oxides of carbon, hydrogen, nitrogen, water vapour, and sulphur compounds in various proportions, depending upon the composition of the gas and the air : gas ratio employed in combustion. For the annealing of copper and its alloys it is essential that sulphur, particularly when present in the form of sulphuretted hydrogen, and organic sulphur compounds be eliminated, and scrubbers, iron oxide towers, and catalytic sulphur-removing towers are usually provided. Since burnt town-gas atmospheres are cheaper than burnt and cracked ammonia atmospheres, though not necessarily cheaper than regenerated ammonia burner gas, they are not recirculated, and thus build-up of contamination of the atmosphere by lubricant from the metal is avoided.

Recent developments have been in the direction of carrying out annealing in a direct-fired gas furnace in which the gas : air ratio is carefully controlled so that the products of combustion are such as to afford considerable, if not complete, protection to the material being annealed. Operating conditions, however, are critical, since the requirements of combustion to provide the suitable atmosphere may be opposed to those necessary to obtain and maintain the correct annealing temperature. The thermal efficiency of such furnaces may be considerably higher than that

of conventional electric-resistance or radiant-type gas-fired furnaces, and they are becoming of increasing importance in the non-ferrous metals industry.

#### VII.—PROTECTIVE ATMOSPHERES FOR BRASSES

Prevention of oxidation of zinc-containing alloys in which the zinc content is in excess of about 15% is much more difficult than with copper. Zinc oxide has a low dissociation pressure, and hence is readily formed in atmospheres containing only low concentrations of oxidizing gases. For example, at  $725^{\circ}\text{C}$ . in hydrogen, zinc oxide will be formed in the presence of small traces of water vapour. Furthermore, volatilization of zinc begins at temperatures in excess of  $450^{\circ}\text{C}$ ., increasing with time, temperature, and the zinc content of the alloy, and theoretically proceeding until equilibrium is established between the zinc vapour and solid states at the temperature of treatment. However, this static equilibrium is never attained in practice, since the passage of the controlled atmosphere through the furnace continually reduces the vapour pressure of zinc above the charge, so leading to further volatilization. Similarly, oxidizing gases in the controlled atmosphere, or those evolved from the alloy itself, combine with the volatilized zinc, which further reduces the zinc vapour pressure, and again promotes volatilization.

Thus, the conditions to be fulfilled in order to bright anneal brass include annealing temperatures sufficiently low to prevent zinc volatilization, the provision of a pure static atmosphere with a very low content of oxidizing gases, and a high degree of cleanliness of both product and muffle. In view of these stringent requirements it is not surprising that bright annealing of brass to the fully softened condition has not yet been completely realized on an industrial scale, except in isolated instances where special conditions apply. Many ingenious processes have been suggested, and under experimental conditions a number of them have shown some success. Experimentally, the best results have been obtained by degreasing the metal and annealing in cracked ammonia in a metallic chamber, but the cost of the whole process, including the degreasing, militates against its widespread adoption even when gas costs are reduced by purging with regenerated ammonia burner gas before the introduction of cracked ammonia. Vacuum treatment in the earlier stages of the annealing cycle, followed by the introduction of a protective atmosphere in the heating and cooling stages, is an alternative method which has been advocated<sup>7</sup> and tried with varying degrees of success.

The clean annealing of brass is carried out in a protective atmosphere either at a temperature sufficiently low to prevent significant zinc loss by volatilization, which yields a product not fully soft but satisfactory for many purposes, or at a temperature sufficiently high to produce soft material, and subsequently to



remove the thin layer of zinc oxide and sulphide stains which normally occurs by a flash-pickling treatment.

### VIII.—EQUIPMENT FOR SPECIAL PROCESSES

Reference has already been made to heat-treatment other than annealing, such as stress-relieving, solution-treatment, and tempering operations which may have to be carried out in non-ferrous metal production units. Batch furnaces are usually employed for these operations. The temperatures at which stress-relief anneals are effected are lower than normal annealing temperatures, and in fact are in the range in which forced-circulation air furnaces should be used to obtain the most satisfactory results. Treatment in furnaces designed for annealing at 600° C. is not to be recommended, because the charge is likely to be

irregularly heated, which results in the softening of some products and inadequate treatment of others.

For the solution heat-treatment of temper-hardening alloys, batch furnaces are generally used, and some provision for rapidly withdrawing the charge from the furnace and lowering it into water is essential. Protective atmospheres may be introduced to minimize oxidation at the high temperatures involved. The subsequent tempering treatment may well be carried out in conventional batch furnaces, for the temperatures required are of the same order as those for annealing the more usual copper-base alloys.

### ACKNOWLEDGEMENTS

The authors gratefully acknowledge the help and encouragement they have received from Dr. Maurice Cook, and the assistance of various colleagues in the preparation of this paper.

---

### REFERENCES

1. R. S. French, *Trans. Amer. Inst. Min. Met. Eng.*, 1944, **156**, 195.
2. M. Cook and H. J. Miller, *J. Inst. Metals*, 1932, **49**, 250.
3. M. Cook, *Symposium on Internal Stresses in Metals and Alloys (Inst. Metals Monograph and Rep. Series No. 5)*, 1948, 73.
4. I. Jenkins, "Controlled Atmospheres for the Heat-Treatment of Metals", p. 489. London: 1946 (Chapman and Hall, Ltd.).
5. "Productivity Report on Non-Ferrous Metals (Wrought)", p. 36. London: 1951 (Anglo-American Council on Productivity).
6. C. E. Ransley, *J. Inst. Metals*, 1939, **65**, 147.
7. British Patent No. 518,132, 1938.

# BRIGHT ANNEALING OF NICKEL AND ITS ALLOYS\*

1350

By H. J. HARTLEY,† M.Sc., F.I.M., MEMBER, and E. J. BRADBURY,‡ M.Eng., A.M.I.Mech.E., A.I.M., MEMBER

## SYNOPSIS

The historical development of bright-annealing plant and technique is briefly related, and the process defined as a special case of clean annealing in which lustre is retained. The conditions which must be fulfilled in each case are reviewed from a theoretical standpoint, and the variations in requirements of different alloys and the effects of sulphur and carbon in the annealing atmospheres are noted. The manner in which theoretical requirements were translated into practice in commercial furnaces for bright annealing wire and strip is described; the latter raised a special control problem necessitating the development of a photoelectric pyrometer controller. Clean annealing in belt-conveyor furnaces is briefly considered, and special attention is paid to the production of sulphur-free atmospheres from town gas, and to methods of testing the suitability of purging-gas atmospheres for use in annealing these alloys, including a method which avoids dew-point measurements.

## I.—INTRODUCTION

THE past twenty-five years have seen very considerable advances in the art of working metals, most of which derive almost entirely from the introduction of new tools. Before the development of tungsten carbide wire-drawing dies, high-pressure rolling mills, and modern methods of lubrication, the frequency of annealing required during the cold processing of many metals was inevitably much greater than it is today, and since all base metals and alloys oxidize in air to a greater or lesser extent at the usual annealing temperatures, equally frequent pickling treatments were necessary. Nickel and the majority of its alloys differ markedly from copper and iron in that "scaling" is virtually unknown, the oxides formed being usually comparatively thin continuous films, which are relatively resistant to chemical attack. The same features of the oxides that protect nickel alloys from excessive oxidation lead also to difficulties in pickling, and those acids which will break through the oxide layers frequently pit the underlying metal and produce extremely rough surfaces. Pickling solutions which do not result in such faults are slow working and often objectionable in use, and these facts gave considerable impetus to the search for a really satisfactory means of avoiding oxidation during the annealing operation.

The present paper gives a brief history of the development of bright annealing as applied to nickel and nickel alloys; provides an outline of the most important theoretical aspects of the process, and describes equipment for bright annealing wire and strip in these metals.

## II.—HISTORICAL DEVELOPMENT

Twenty-five years ago electric furnaces were in their infancy, and the fuels available for fuel-fired furnaces were too rich in sulphur to permit direct-fired furnaces to be operated under reducing conditions when annealing nickel and high nickel alloys. Thus, if clean annealing of such materials, implying the use of a reducing atmosphere, was to be achieved, the metal had first to be protected from the products of combustion, and secondly a specially prepared reducing atmosphere had to be provided in contact with the metal. Inevitably, therefore, pot annealing, where the metal is sealed in an externally heated vessel containing the required atmosphere, became the starting point.

The reducing or neutral atmospheres required were originally obtained by the use of wrought-iron pots, the lids of which were sealed with damp clay. In addition, charcoal was often used to fix the oxygen. These vessels were usually lined with scrap nickel sheet in order to avoid contamination by direct contact with the iron pot. External scaling of the pots was objectionable, and led to heavy replacement costs. When heat-resisting pots were used, it became essential to make provision for fixing the oxygen in the pot (previously removed by oxidation of the iron). With the advent of electric furnaces, designers recognized the opportunity to build a virtually gas-tight furnace, and further development followed two parallel lines: batch pot-annealing devices were rationalized, and electric furnaces of the conveyor type were designed. The latter were fed with reducing atmospheres prepared in an auxiliary plant.

\* Manuscript received 15 September 1951. Contribution to a Symposium on "Equipment for the Thermal Treatment of Non-Ferrous Metals and Alloys", to be held in London on 26 March 1952.

† Manager, Process Development Laboratory, Henry Wiggin and Co., Ltd., Birmingham.

‡ Development and Research Department, The Mond Nickel Co., Ltd., London.



The major difficulty designers experienced in modifying pot-annealing furnaces was to attain a practical work : container weight ratio. Electric furnaces were costly to build and power supplies expensive, but the overriding consideration that the furnace must be economical in service had to be met. Unfortunately the temperature of a large mass of metal, such as the charge and the container comprised, can be raised and lowered only slowly, and there was opportunity for nickel and nickel alloys to weld together during the process. Other drawbacks were that the product was frequently unevenly annealed and of poor surface quality and colour, and the long time cycles required the use of several units and a large area of floor space.

In an endeavour to avoid the use of an envelope between the charge and the heating elements, water seals, underwater rams for quenching, and other devices were developed, but they provided as many difficulties for the designer as for the user, and though the use of alcohol-water solutions enabled clean annealing to be achieved, water-quench annealing furnaces have never been widely used.

The modern large continuous clean-annealing furnaces developed slowly, mainly as a result of the difficulties of designing an economical gas-seal which would keep the volume of special atmosphere required for the furnace within reasonable limits. The preparation of the atmosphere also required considerable attention. As a result of the necessity to avoid the presence of sulphur in furnace atmospheres, mixtures of nitrogen and hydrogen were first tried, but the quantity of gas required to maintain a reducing atmosphere in the early roller-hearth furnaces proved quite uneconomical as a consequence of the very high gas leakage that occurred. The nitrogen used in this early attempt was prepared in a liquid-air plant, and the hydrogen from silicon and caustic soda.

This early experience proved of value, however, and designers turned their attention to conveyor-belt furnaces. These offered considerable advantages as compared with the roller-hearth type, so far as the design of gas-sealing devices was concerned. They also showed that traces of oxygen present in the cooling chamber must be avoided, since nickel and copper oxidize at temperatures down to 100° C., whereas reduction of their oxides by hydrogen ceases at about 180° C.

The next development was a conveyor furnace equipped with a means of water quenching. Quenching caused stains on the metal and distortion, and was abandoned in favour of extended cooling-chambers in which an oxygen-free reducing atmosphere, similar to that in the annealing section of the furnace, was maintained. This arrangement is similar to that used today.

In the first of this type of furnace the atmosphere was prepared by incomplete combustion of butane, and was manufactured in a special plant separate from the furnace. Liquid butane was comparatively cheap and contained little sulphur, but nevertheless the partially burnt butane was cooled and passed

through "bog iron ore" to remove any trace of sulphur that might be present as  $H_2S$  after the burning.

The change from a roller to a conveyor-belt design resulted in very substantial economies in the quantity of gas required to maintain the reducing atmosphere, for the use of a belt facilitated the fitting of smaller and more efficient gas-seals to prevent loss of the prepared gas and entry of air. A great deal of effort has been spent in perfecting designs for such seals, but apart from improvements in detail the general principles of conveyor-belt furnaces have not changed since 1935.

Metal annealed by any of the above-mentioned methods loses its lustre or brightness, and is properly referred to as "clean" annealed. When the lustre of the cold-worked metal is retained during annealing, the process is termed "bright" annealing. As commercial furnaces which gave satisfactory clean annealing of many nickel alloys became available, attention was turned to the problem of extending the process to the nickel-chromium alloys. Laboratory investigations showed that the conditions requisite for clean annealing these alloys were stringent. A laboratory pilot-plant furnace was constructed, in which nickel-chromium alloys in wire form were successfully bright annealed as early as 1930, and the standard commercial furnace was developed by 1932. No serious attention was given by Henry Wiggin and Co., Ltd., to bright annealing of strip until about 1937, by which time the design of furnaces for wire had become stabilized. Both these developments are dealt with more completely in Section V.

### III.—THEORETICAL CONSIDERATIONS

#### 1. GENERAL

By virtue of the wide range of annealing temperatures and corresponding times which may be used without significant differences in the physical properties of the annealed material, the design of clean-annealing plant for pure nickel and many of its alloys involves only the provision of a furnace in which a non-oxidizing atmosphere can be maintained and visible stains avoided. In the case of many of the alloys, the physical properties of flash-, conveyor-, and batch-annealed products are indistinguishable, except for the important property of electrical resistance. The use of rapid cooling frequently results in the metal having an electrical resistivity and temperature coefficient of resistivity different from the normal values for slowly cooled metal. The value of each of these properties is restored to normal on heating to 400°–500° C., followed by fairly slow cooling.

Flash annealing has a considerable advantage over other methods when a fine grain-size is required, since under these conditions recrystallization starts from many nuclei and leads to a considerable refinement of the grain, whereas the slower process of con-

veyor annealing may lead occasionally to exaggerated grain-growth. Flash annealing may also be advantageously employed for bright annealing. Fuller consideration of the differences in clean- and bright-annealing techniques will be dealt with in Section V.

The materials coming within the scope of the present paper are pure nickel, alloys of nickel with copper, and alloys of nickel with any one or more of the elements iron, chromium, and cobalt. In addition, minor additions of other elements, e.g. titanium, aluminium, and manganese, may be present and because of their tendency to selective oxidation, may complicate the design of a bright-annealing furnace.

When considering what conditions it will be essential to meet in order to bright anneal a particular alloy, it is necessary to take into account:

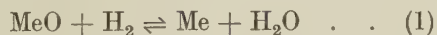
- (a) the composition of the alloy;
- (b) the affinity of each major element for oxygen;
- (c) the possible effect of minor elements;
- (d) the effect of sulphur;
- (e) the effect of carbon.

## 2. THE EFFECT OF MAJOR ELEMENTS

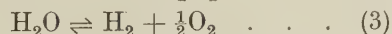
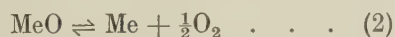
Nickel, copper, and nickel-copper alloys may be kept clean in steam with the addition of a very small percentage of hydrogen. Nickel-iron alloys, however, will oxidize at 900° C. if the  $H_2O : H_2$  ratio is in excess of approximately 1:3 and, if cooling from the annealing temperature is slow, the steam content of the atmosphere must be drastically reduced. Nickel-manganese alloys containing up to 5% manganese can tolerate the presence of steam if flash annealing can be used, but oxidize in slightly damp hydrogen if the annealing or cooling time is prolonged.

The alloys containing 13–20% chromium differ considerably from the others, and oxidize at room temperature in air to form an invisible oxide film which protects the metal from further oxidation. This oxide does not increase in thickness at temperatures below about 400°–500° C., depending on the alloy. The alloys oxidize visibly and quite rapidly at temperatures of 700° C. and upwards, in either air or damp hydrogen.

The reaction:



is balanced and may be considered in two stages:



Reaction (3) is a second-order gaseous reaction at all temperatures above 650° C., and the extent of the dissociation of water vapour increases with rising temperature, but is suppressed by dilution with hydrogen, as is shown by:

$$K_p = \frac{(p_{H_2})^2 \cdot (p_{O_2})}{(p_{H_2O})^2} \quad . \quad . \quad . \quad (4)$$

The affinity of chromium for oxygen decreases with rising temperature, and alloys containing chromium do not oxidize, or if they become oxidized the oxide can be reduced by hydrogen containing traces of water vapour, the permissible moisture content rising with the temperature. Approximate figures are shown in Table I.

TABLE I.—Permissible Moisture Content in Hydrogen Atmospheres Used with Cr-Bearing Alloys.

Temp., °C.	Partial Pressure of $H_2O$ in $H_2$ , mm. Hg	Dew-Point, °C.
1200	7.0	+ 6
1020	0.7	–21
700	0.008	–60

It follows that slow cooling of nickel-chromium alloys from the annealing temperature makes clean annealing virtually impossible, except on a laboratory scale. On the other hand, rapid cooling avoids the build-up of a visible oxide film even in hydrogen containing water vapour. This consideration leads to the choice of flash-annealing processes for alloys containing chromium.

Another factor which is of importance in selecting the annealing temperature for alloys containing chromium is the oxidation which occurs as the metal is being heated in the normal commercial design of furnace. This oxidation is probably the result of occlusion of oxygen and water on the surface of the metal. The oxide formed can not be reduced rapidly, even in exceptionally dry hydrogen below 1000° C., and it is therefore usual to endeavour to raise the metal to at least that temperature. In fact, these chromium-containing alloys do not flash anneal at an economical rate below that temperature.

## 3. THE EFFECT OF MINOR ELEMENTS

The effect of relatively small additions of elements with a high affinity for oxygen must also be considered. Additions of less than 1% of such elements have a negligible effect on bright- or clean-annealing procedures, though, if the equilibrium conditions permit, some of the trace elements will certainly be lost by oxidation at the surface.

If present in larger proportions, say 2–3%, these elements, if the conditions are such that oxidation of them occurs, may lead to the formation of an unwanted oxide coating on the metal, and in some cases to intergranular oxidation. The intergranular attack is slight, and may occur with the presence of such elements as aluminium or titanium.

## 4. THE EFFECT OF SULPHUR

The behaviour of sulphur towards nickel is also governed by balanced reactions. In a reducing atmosphere the sulphur is present in the form of hydrogen sulphide or carbon oxysulphide. (It may be mentioned that nickel alloys are comparatively immune from sulphur attack under oxidizing con-



ditions.) The proportion of carbon oxysulphide present is small and governed by the reaction:



so that only the direct action between nickel and hydrogen sulphide need be considered.

It has been shown that pure hydrogen reduces nickel sulphide, and that the equilibrium concentration of hydrogen sulphide varies rapidly with temperature. Other experiments have shown that nickel and nickel-copper alloys are immune from attack by sulphur when exposed to a normal purging gas containing approximately  $\text{N}_2$  80,  $\text{CO}_2$  8,  $\text{CO}$  6, and  $\text{H}_2$  6%, with  $\text{H}_2\text{S}$  not exceeding 0.08 grain/100 ft.<sup>3</sup>; whereas in the same gas with 0.40 grain/100 ft.<sup>3</sup> embrittlement by sulphur attack takes place quite rapidly at 700°–750° C.

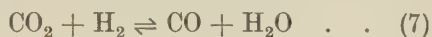
The presence of minor additions in the nickel or nickel alloy can affect the rate of attack by hydrogen sulphide. Sulphur attack on nickel and some high-nickel alloys proceeds catastrophically in reducing atmospheres at temperatures above approximately 700° C., with the formation of a low-melting-point nickel-nickel sulphide phase. The attack proceeds with the progressive formation of the phase along the grain boundaries, and leads eventually to disintegration of the metal. Magnesium as a minor addition may diffuse to the grain boundaries, and, by fixing the sulphur as magnesium sulphide, arrest or considerably slow down the rate of attack.

#### 5. THE EFFECT OF CARBON

Though it is at present not of practical importance, the fact may be noted that nickel alloys can be carbonized or decarbonized by suitable adjustment of the atmosphere composition. Of greater importance is the deposition of carbon (or soot) on nickel alloys annealed in a diluted water-gas atmosphere from which a large proportion of moisture has been removed without rebalancing the gaseous equilibrium. Many nickel alloys appear to catalyse the reaction:



at 700° C., at which temperature the reaction



is sluggish.

### IV.—COMPARISON OF CLEAN AND BRIGHT ANNEALING

The difference between clean and bright annealing was defined earlier with respect to the relative brilliance of the product, before and after annealing (Section II). The difference is mainly the result of the selection of the atmosphere used, clean annealing being obtained by the use of a composite atmosphere the constituents of which are liable to react, e.g. water gas diluted with nitrogen, and bright annealing by the use of virtually neutral gas, e.g. hydrogen diluted either by nitrogen or steam. In the former atmo-

sphere re-establishment of equilibrium between the constituents of the gas is catalysed by the metal, especially as the metal is only momentarily at the same temperature as the gaseous atmosphere, and consequently the metal becomes etched and loses lustre in the process. In the latter, the annealed product loses lustre only if the annealing time is relatively prolonged, and it may even appear to gain in brilliance when rapid strand-annealing is used. This effect may well be caused by such practical factors as the rapidity with which the contaminating vapours derived from residual lubricants are swept away from the work in the strand-type furnaces.

### V.—BRIGHT-ANNEALING EQUIPMENT AND PRACTICE

The brief description given above of the primary factors controlling the successful bright-annealing process leads naturally to a description of the technique and equipment developed for the bright annealing of nickel and nickel alloys in the forms of wire and strip. Bright annealing has not been applied to these materials in sheet form; it is therefore proper to make a brief reference to the conveyor-belt furnaces and practice used for the clean annealing of all normal forms of metal.

#### 1. THE BRIGHT ANNEALING OF WIRE

The bright annealing of wire was developed commercially several years before a similar process was available for strip. The process was intended originally as a means of clean annealing nickel-chromium alloy wire. The wire form lends itself to continuous processing, and as a result of laboratory experiments the basic scheme adopted from the beginning has been to employ a strand-annealing technique in which the wire is uncoiled and passed in a single strand through a heated tube which serves to raise the temperature of the wire, to support it at temperature, to maintain the controlled atmosphere around it, and finally to cool and recoil or spool it.

The original furnace used external heating of long horizontal lengths of silica tubing, but in view of the relatively high temperature initially employed, conventional laboratory tube-furnace windings on silica had a short life, and breakage of the silica tubing was frequent. It was therefore decided to use metallic tubing, though at that time solid-drawn tubes in heat-resisting alloys were not available, nor had a satisfactory technique for the welding of the 80:20 nickel-chromium alloy which it was proposed to use been perfected. Leakage of the atmosphere through pinholes occurred, and eventually a design was adopted in which two concentric tubes were used. The outer tube served two purposes; it acted as an atmosphere guard wall, and it also served as the heating element, for, by extending it beyond the furnace case, large water-cooled clamps could be attached, and a high-amperage current from a low-

voltage transformer could be passed through the tube to heat it. The inner tube was held more or less concentric with the outer tube by means of refractory rings spaced a few inches apart, and at the outgoing end of the furnace a metal plug was used to close the annular gap. At the ingoing end the corresponding gap was closed by means of a bonded asbestos plug. A slight positive pressure of hydrogen was maintained in the space between the two tubes.

The inner tube at the outgoing end was connected to another horizontal tube, which was externally water cooled, and a supply of hydrogen was fed into the inner tube at the junction. With open-ended horizontal tubes, roughly 95% of the hydrogen passed through the cold tube, and it was therefore necessary to devise a seal through which wire could pass, but which retained the gas in order to economize in hydrogen. Rubber bungs pierced with a needle, capillary glass tubes, felt in a compression joint, and old tungsten carbide dies all proved satisfactory, and the final choice became a matter for the individual, the decision being based on wear-resistance, ease of replacement, and in particular the ease of threading the furnace.

The dual-tube design, with twin supplies of hydrogen, proved successful, since leakage of the outer tube did not directly affect the annealing atmosphere and leakage of the inner tube at its worst could only admit somewhat impure hydrogen to the true annealing atmosphere. The scheme was in fact, so successful that endeavours to purify hydrogen beyond the dew-point attainable by using calcium chloride drying became worthwhile, and the furnace-tube life could correspondingly be increased by a slight reduction in annealing temperature and speed of passage of the wire.

Under such conditions it was found possible to maintain a satisfactory atmosphere in a single inner tube for the expenditure of 1 ft.<sup>3</sup>/hr. of hydrogen to each of the inner and outer tubes. The annealing rate for a hot zone 8 ft. long and with a probable peak wire-temperature of 1000° C. was approximately 6 lb. of wire/hr.

The problem of controlling such a furnace was novel, and here the laboratory prototype played a very useful part, for in this furnace it was possible to thread one or more exploratory thermocouples into the annular space and so gain information as to the speed with which the static temperature-distribution curve changed to the equilibrium dynamic distribution curve, and as to the point along the length of the furnace at which the peak temperature was reached under the latter conditions. As the furnace case was essentially a long rectangular box of square cross-section, and the insulation material a diatomaceous-earth powder, the two curves proved to be as shown in Fig. 1, the broken line being symmetrical and the peak of the full line lying at a point which was almost inside the constant-temperature zone, and the speed of change over from the one to the other was found to be rapid.

This was useful information, since experience showed that thermocouple maintenance in the annulus between the tubes was impossible, owing to the necessity to provide electrical insulation involving the use of very long, fragile refractory sleeves. The procedure adopted was, therefore, to insert a thermocouple in a light-weight metal-sheath into a pocket made from a short piece of tubing welded into a curved strip of metal. The latter was pressed against the external tube wall and the thermocouple spring loaded so as to maintain contact with the bottom of the pocket. Obviously the indications of such a thermocouple are only relative to the true furnace temperature, and form a very poor guide to the actual work temperature, but such limitations have to be accepted in any continuous furnace. Experience shows the system to be satisfactory.

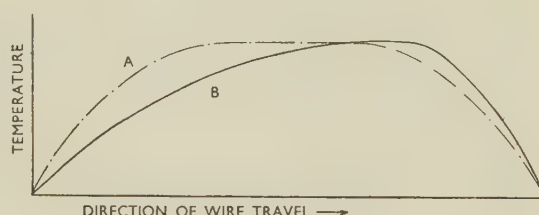


Fig. 1.—Temperature-Distribution Curves in Wire-Annealing Furnace.

A Static curve.

B Dynamic curve.

The typical modern industrial furnace developed from this prototype is shown in Fig. 2. It has several tubes enveloped by one large tube, the latter as before acting as the furnace resistor. The furnace casing is usually 12–15 ft. long, the cooling tubes 6 ft. long, and the work-rate 9 lb./hr./strand in 18–25 S.W.G. wire.

The complete layout of a multi-tube strand-annealing furnace comprises a swift rack for holding the wire to be annealed, a furnace, and a cooling extension, together with electrical equipment and the winding devices.

To avoid waste of time, several spare swifts and pegs are required. With rotating swifts, free running is essential, though it is permissible to use stationary swifts, since the twists introduced are killed during the annealing process. In either case a lot of floor space is required. In practice the stationary swift is inconvenient for use with a multi-tube furnace, since the corkscrew form of the wires leading to the latter is certain to cause entanglement. On the other hand, swifts must be kept in good condition and their free running checked if loss of gauge, or even breakage in the furnace, is to be avoided. For this reason it is preferable to use short furnaces, and a multitude of tubes, swifts, and coilers, so that the linear speeds used shall not be excessively high. Otherwise snatch effects may cause serious trouble.

A variety of winding devices may be used, depending on the space available and the layout required. For wires of heavy gauge, horizontal coilers (see



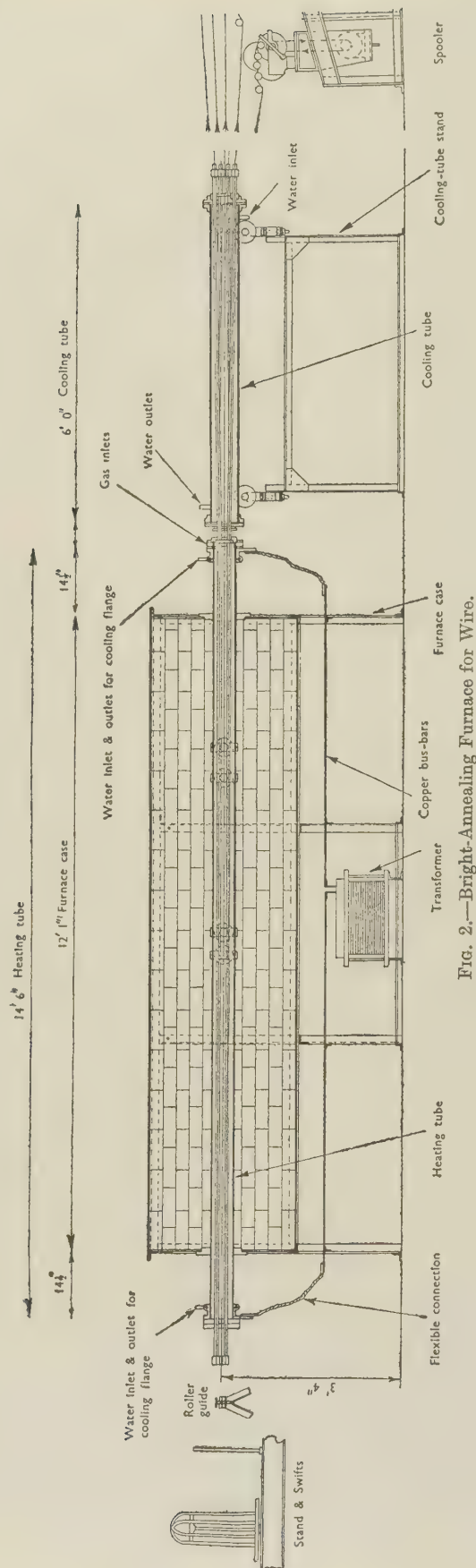


Fig. 2.—Bright-Annealing Furnace for Wire.

Fig. 3) are most convenient. Vertical drums share with them the advantage of constant speed, but special devices are required to force the wire to climb the block. Automatic spoolers are largely used for finished wire, thus avoiding rehandling. They must, however, be provided with devices to adjust the speed of rotation so as to maintain a reasonably constant rate of annealing from start to finish of a spool.

Bright annealing of nickel-chromium alloys in wire form is used both for finished wire and for inter-stage annealing. A low-melting-point metallic lubricant is normally used in drawing these alloys, and it has been shown that such a lubricant may be very satisfactorily applied as a coating directly to bright-annealed wire on which an invisible oxide layer has not been allowed to form. The operations of annealing and coating may therefore be combined by using less drastic cooling in tubes which are surrounded by air instead of water, and which are bent down into a bath of molten metal. These tubes are thereby completely sealed and the atmosphere in them is stagnant; consequently, the wire surface is chemically clean as it enters the molten metal, and good wetting is obtained without the aid of a flux. The wire leaving the bath is directly air-cooled before coiling. A typical arrangement is shown in Fig. 3.

Furnaces used for strand bright-annealing of nickel-chromium alloys make use of 80 : 20 nickel-chromium tubes for the resistors and "muffle" walls. This alloy has the disadvantage that in the event of the "muffle" walls being exposed to impure gas for any length of time, the oxide formed will be difficult to reduce, and until it is reduced bright annealing cannot be achieved. Alternative materials free from chromium, such as nickel and mild steel, are too weak, and although they have been used they had a short life, and frequent replacements were necessary. It is also important to choose materials which are not susceptible to intergranular attack when subjected to "differential oxidation", for it is inevitable that the atmosphere in the furnace tubes will at times be oxidizing to chromium or other constituents of the alloy and is probably nearly always oxidizing to chromium near the inlet end of the tube.

Recent work has shown that when the resistor and muffle are formed by the same tube, heat transfer to the work is much faster than when an inner muffle is used. The annealing speed which can be attained is illustrated by the fact that a nickel-alloy wire has been annealed by indirect heating, using a speed of traverse such that the heating and cooling cycle is completed in one-fifth of a second.

## 2. THE BRIGHT ANNEALING OF STRIP

The development of furnaces for bright annealing strip was stimulated by the need to increase deliveries of nickel-copper-zinc alloy strip 0.002 in. thick. The alloy was of a grade showing rapid work-hardening, and consequently for normal processing it required frequent annealing and pickling treatments. Difficulties were experienced also with staining of the metal after the final pickling treatment.

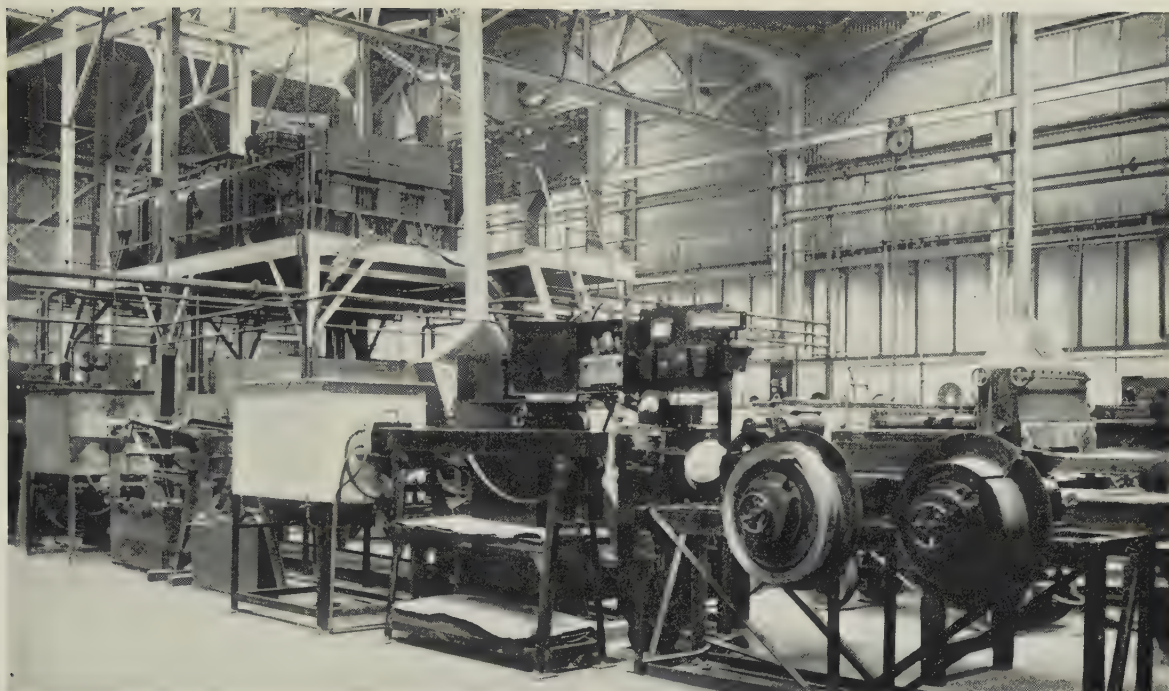


FIG. 6.—Bright-Annealing Furnace for Strip.

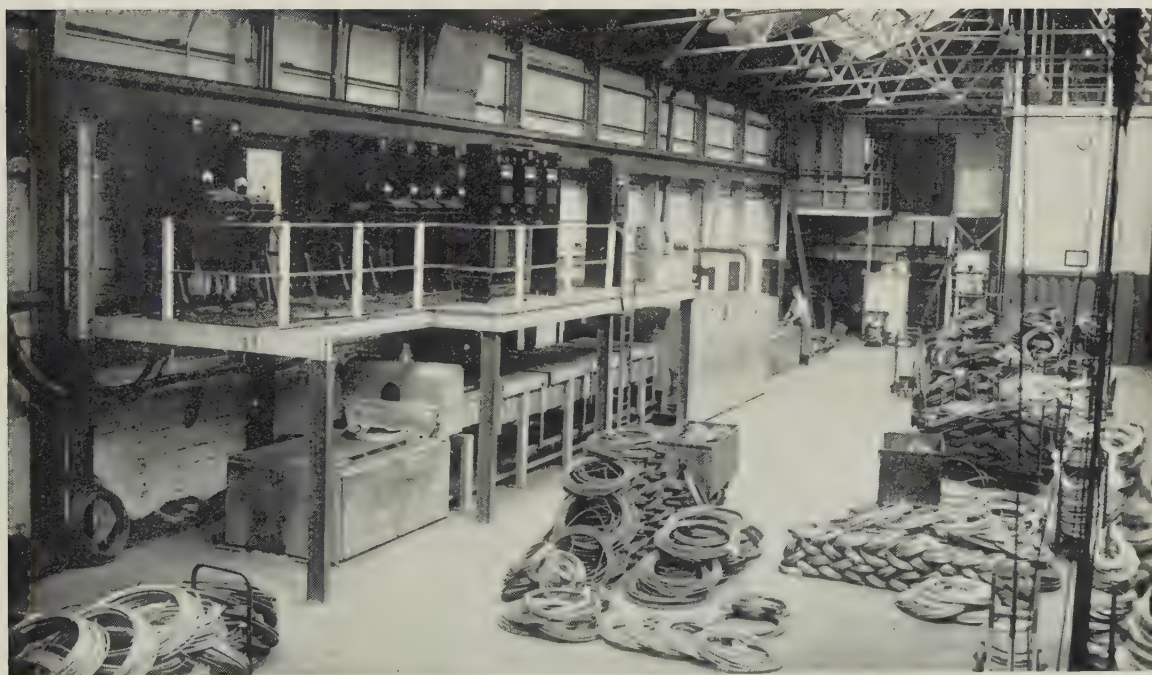


FIG. 7.—Belt-Conveyor Furnace for Clean Annealing.





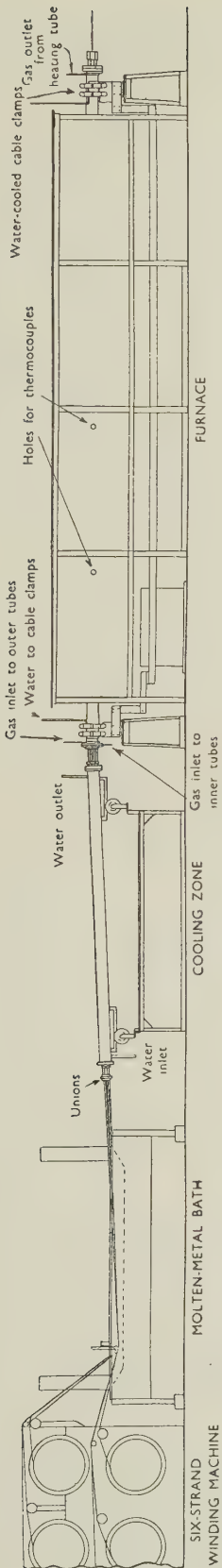


Fig. 3.—Annealing and Coating Furnace for Wire.

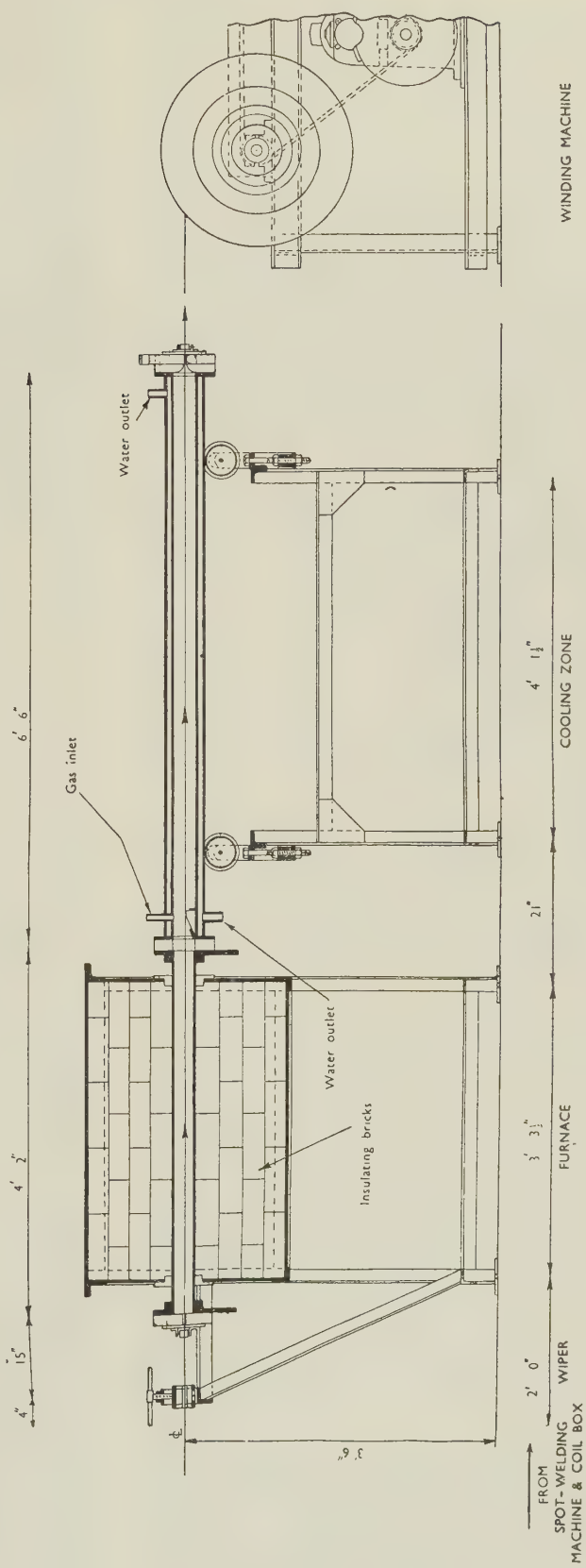


Fig. 4.—Bright-Annealing Furnace for Strip.



Preliminary laboratory tests were conducted, using a bell-jar in which an atmosphere of dry cracked ammonia was maintained and the strip was heated by passing a heavy current through it for a short period. Relatively thin strip was used, and after being degreased it was dried, weighed, annealed, re-weighed, and the final hardness determined. Heavy fuming of zinc occurred, but the actual weight loss was low, and it was also found that the rate of heating could be increased with consequent reduction in zinc loss without any increase in the final hardness. As a result of the high thermal conductivity of hydrogen, the rate of cooling was rapid, and eventually it was found possible to give the strip a true bright-annealing treatment. It should be noted here that the high thermal conductivity of hydrogen favours the rapid indirect heating as well as cooling of a metal in a hydrogen atmosphere.

These experiments suggested the design of a furnace having a short, oval, horizontal tubular heating zone with a comparatively short water-cooled extension for a cooling chamber. The dual tube as adopted for wire was unsuitable, both because it would be difficult to construct and because it was desired to use a higher temperature than could safely be used if the muffle were indirectly heated. The original furnaces were approximately 40 in. long, and the oval chosen permitted the annealing of strips up to 4 in. wide with a very slight tension provided by a felt-lined clamp, which also served to remove most of the rolling lubricant. A graphite block was fitted at the junction of the hot and cold zones of the furnace, and this and the cold zone itself were electrically insulated from the resistor tube. It was necessary to work with a very shallow catenary in the strip in order to avoid direct contact with the resistor tube, for if such contact occurred, fusion of the edges of the strip resulted.

With such a furnace it was considered essential to reduce the atmosphere requirements to a minimum. This required a careful design of the seal at the outgoing end, and it was found that with this seal in good condition, together with a slot  $4 \times \frac{3}{16}$  in. at the inlet, the furnace atmosphere could be maintained on an input of 2 ft.<sup>3</sup>/hr. A strip-annealing furnace of this type is shown in Fig. 4 and Fig. 6 (Plate L).

When used for annealing nickel silver, the atmosphere of the hot zone soon became laden with zinc vapour. This probably served two useful purposes: it reduced zinc loss by increasing the partial pressure of the zinc in the atmosphere, and it acted as a scavenger for any air or contaminant drawn in by the strip. Zinc dust and zinc oxide gradually accumulated in the cooling chamber and had to be removed occasionally.

The furnace was worked with a peak resistor temperature of about 1050° C., which is above the melting point of the alloy concerned. Careful attention had to be given to threading, which was effected by passing a nickel-chromium alloy strip through the furnace and fixing it to the coil winding-drum, spot-

welding the nickel silver strip to the leading strip, and starting the winding gear. The cutting clear of the leading strip and the reclamping of the nickel silver to a second drum was achieved without interruption in the flow of the strip.

This type of furnace brought a new problem in temperature control, for, as a result of the light weight of the resistor tube, backed up by diatomaceous-earth insulation, resistor temperature changes could be very rapid. A loading of 25 W./in.<sup>2</sup> was commonly employed, and the furnace could be brought to 1000° C. from cold in approximately 7-8 min. The use of a thermocouple and an ordinary temperature controller resulted in a very serious lag in response and in wide hunting of the resistor temperature, and consequent inequality of annealing. The final solution to the problem was worked out in conjunction with the electronic engineers of the British Thomson-Houston Co., Ltd., Rugby. The circuit of the photoelectric pyrometer controller developed for the purpose is illustrated in Fig. 5. A photoelectric pyrometer was coupled to a very simple current amplifier, and the output current, after conversion to a voltage, was compared with stable reference voltages by means of a pair of thyatrons. These were used to energize relays which gave bucking or boosting action to a motorized, on-load, stepless, variable-output-voltage transformer. Thus, the input to the furnace was kept closely matched to the demand at all times. The pyrometer was sighted upon a disc of the furnace resistor approximately  $\frac{3}{8}$  in. in dia., situated at the centre of a disc 1 in. in dia., which was exposed to view by means of a tube inserted through the insulation.

This type of pyrometer can be made to give a very open scale over any selected temperature range, and is therefore very useful for purposes of close temperature control; moreover, its overall response lag as a controller is very short. It is, however, necessary to use a thermocouple as a means of checking and calibrating the photoelectric pyrometer from time to time.

These strip furnaces were found to give excellent control of annealing characteristics.

The complete installation consisted of a coil box with space for two coils, an electric spot-welder, a screw clamp-wiper, the furnace, and cooling chamber, together with transformers and electrical control gear, and a twin- or triple-drum coil-winder. The latter was driven by a D.C. motor using Ward-Leonard speed control. The use of 18-in.-dia. drums made it easy for operators to maintain a reasonably constant speed throughout the length of coils of normal weight, by an occasional manual adjustment of the speed of rotation of the drums.

The use of a pure cracked-ammonia atmosphere leads to an enhancement of the surface appearance during annealing, and thin strip which has been annealed several times during preparation, can, with due attention to roll surface, be produced in the soft condition with an almost perfect mirror surface

without any other treatment. The use of purging gas of the nitrogen-diluted water-gas type causes deterioration of the surface, even when the strip passes through the hot zone in as short a period as 10 sec.

The above remarks apply equally to pure nickel, nickel coppers, and nickel silvers, but obviously this type of furnace cannot clean anneal nickel-chromium alloys when using the water-gas type of atmosphere. They do, however, give very satisfactory bright annealing of nickel-chromium alloys when purged by dry cracked ammonia, provided that sufficient attention is given to the maintenance of the furnace tube and to the joints between the heating and cooling chamber and the outlet seal.

Furnaces of this type are in general use today for annealing all classes of nickel alloys in widths up to

except that because of handling difficulties it is usual to drop the working temperature when annealing very thin strip and to accept a lower output.

### 3. CONVEYOR-FURNACE ANNEALING

Belt-conveyor furnaces fed with a partially burnt town-gas atmosphere are in general used both for sheet and wire annealing; a modern furnace is illustrated in Fig. 7 (Plate L). This type of furnace is especially economical in manpower when applied to wire, since there is no swifting to be done. Precise control of physical properties is not readily achieved, since the time/temperature cycle varies not only with belt speed and furnace temperature, but also with the weight and special distribution of work on the belt. The majority of nickel alloys (other than nickel chromes) may be clean annealed in this type of furnace,

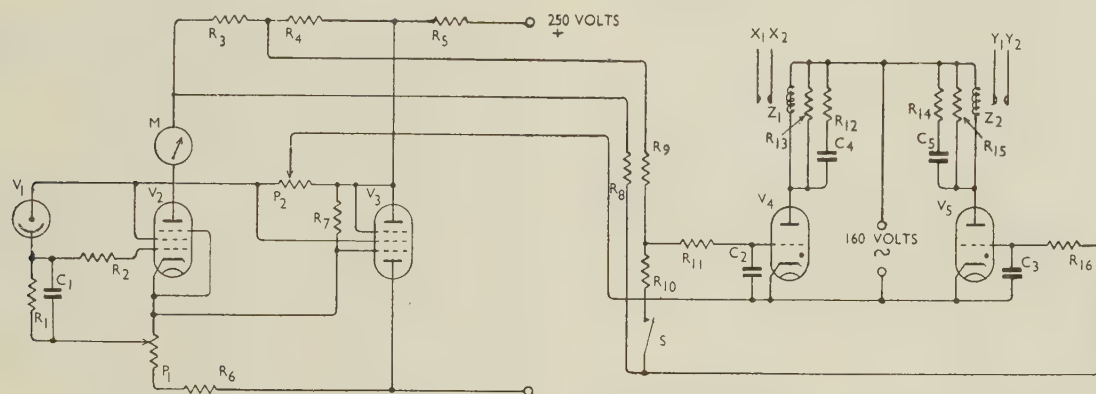


FIG. 5.—Circuit Diagram of Photoelectric Pyrometer Controller.

$C_1$ 0.01 $\mu$ F (mica).	$P_1$ 1200 $\omega$ .	$R_8$ 1000 $\omega$ .	$R_{11}$ 250,000 $\omega$ .	$S$ Switch, periodically closed by synchronous motor.	$V_4$ T41.
$C_2$ 0.01 $\mu$ F.	$P_2$ 5000 $\omega$ .	$R_9$ 10,000 $\omega$ .	$R_{12}$ 1000 $\omega$ .		$V_5$ T41.
$C_3$ 0.01 $\mu$ F.	$R_1$ 5,000,000 $\omega$ .	$R_7$ 100,000 $\omega$ .	$R_{13}$ 1000 $\omega$ .	$V_1$ P.E.S.	$X_1, X_2$ (Contacts energizing follower relays.
$C_4$ 0.1 $\mu$ F.	$R_2$ 100,000 $\omega$ .	$R_6$ 50,000 $\omega$ .	$R_{14}$ 1000 $\omega$ .	$V_2$ Pen 45DD	$Y_1, Y_2$
$C_5$ 0.1 $\mu$ F.	$R_3$ 2000 $\omega$ .	$R_5$ 50,000 $\omega$ .	$R_{15}$ 7000 $\omega$ .	$V_3$ STV 280-80.	$Z_1, Z_2$ Relays 30,000 $\omega$ .
$M$ Milliammeter.	$R_4$ 6000 $\omega$ .	$R_{10}$ 25,000 $\omega$ .	$R_{16}$ 250,000 $\omega$ .		

9 in. It is current practice to provide an electrical input of 20 W./in.<sup>2</sup> of resistor-tube surface, and this can be reduced to approximately 4 W./in.<sup>2</sup> by means of the variable-voltage transformer. A contactor is also fitted, but this is rarely called upon to operate so long as work is passing through the furnace.

The perimeter of the resistor is usually approximately  $3\frac{1}{2}$  times the width of the widest strip which the furnace is designed to anneal, and the resistor length is now generally about 50 in. Thus a furnace for  $4\frac{1}{2}$ -in.-wide strip will be loaded at about 14 kW. Since the current leads to the resistor have to be brazed and water cooled, this causes a loss of about  $1\frac{1}{2}$ –2 kW., and the loss via insulation will also be of the order of 2 kW. The remaining 10 kW. can be transferred to the work providing full-width strip is being annealed, and in consequence at this width an output of 130 lb./hr. can be obtained from such a furnace. The permissible output varies slightly from one alloy to another, and is directly proportional to the width of the strip, and independent of thickness,

though with the normal atmosphere the product is never bright.

This type of furnace should be designed for a particular type of work, since the requisite flow of purging gas is related directly to the width and roughly to the cube of the height of the apertures. Various designs of curtains and hinged flaps have been tried out with varying degrees of success, but the effective sealing of a furnace designed to admit tall coils of wire or strip is very difficult. Clearly the sealing is most effective in the case of a furnace designed for annealing fairly light-gauge sheet, since the product lies flat after annealing and the discharge aperture need not be more than 2–3 in. high. Inevitably these furnaces are subject to operating difficulties if located in draughty shops.

The belts used in such furnaces should also be designed with due reference to the work they have to perform. It has been found that a nickel-chromium-iron alloy containing approximately Ni 37, Cr 18, and Si 2%, gives reasonably satisfactory service for medium- to high-temperature annealing furnaces,



and is very much less susceptible to failure by green rot (a species of intergranular attack) than the majority of commercial nickel-chromium alloys.

It may be of interest to note that it is common practice to anneal nickel-chromium sheets in belt-conveyor furnaces. The atmosphere is oxidizing to chromium, but not to nickel. As a result, a rather spongy oxide may be formed, and if such annealing is repeated after further rolling, it is possible to obtain an apparently clean sheet, owing to the presence of a nickel-rich film at the surface, although on careful examination it may be found that there is an oxide layer below this film. Such an effect is disastrous if the metal is to be used as an electrical-resistance element.

## VI.—THE PRODUCTION OF ATMOSPHERES OF CONTROLLED COMPOSITION

### 1. ATMOSPHERES FOR BRIGHT ANNEALING

For the purpose of bright annealing, the most important atmosphere is cracked ammonia with pure hydrogen as an alternative. Theoretically, pure nitrogen or even an inert gas might be considered more desirable, but in practice the work invariably carries some contaminants into the furnace and these prevent bright or clean annealing in nitrogen, and, as mentioned earlier, occluded oxygen may also enter the furnace on the surface of the metal and result in oxidation.

Relatively few users would contemplate the installation of an electrolytic-hydrogen plant, on the score of both capital expense and running costs. Bottled hydrogen is expensive, and the gas as received is always contaminated with free oxygen; in consequence the gas has to be passed over a catalyst and, for some alloys, it requires drying before introduction into the furnace.

The use of cracked ammonia simplifies the problem, for anhydrous ammonia may be obtained in very large cylinders in the liquid form, which at once eases the handling problem and reduces costs. Catalytic crackers of standard design are available and give very reliable results, providing the temperature control for the catalyst is good and the throughput rating is not exceeded. Furthermore, the ammonia synthesis demands virtually complete freedom from both oxygen and moisture, and except in so far as a new charge of catalyst may introduce a little moisture by incomplete reduction of the oxides, the cracked ammonia may be relied upon to have a dew-point of  $-40^{\circ}\text{C}$ . or even lower. The gas obtained after cracking is not entirely free from ammonia, for the reaction  $2\text{NH}_3 \rightleftharpoons \text{N}_2 + 3\text{H}_2$  is a balanced one, and whilst the operating temperature is chosen so that the reaction shall be as complete as possible consistent with working the catalyst at a reasonably high space velocity, the equilibrium concentration of ammonia at atmospheric pressure is approximately 0.1%. For many purposes this residue of ammonia in the gas is

unimportant, and from the practical standpoint of locating leaks, its presence can be helpful.

When cracked ammonia is used for annealing nickel-chromium alloys, it is desirable, though not essential, to install an activated alumina (or silica gel) drier. Such a unit must be well designed, for otherwise the drier will be virtually useless, and it is important to ensure that all the alumina can be readily raised to  $250^{\circ}\text{C}$ . for revivification, that a current of dry gas can be passed through the charge in reverse direction to normal, and that the "dead pipework" at what is now the outlet can easily be raised to  $100^{\circ}\text{C}$ . to avoid the collection of water. With a really satisfactory design, a dew-point of  $-60^{\circ}\text{C}$ . is readily maintained.

### 2. ATMOSPHERE OF A WATER-GAS TYPE FOR CLEAN ANNEALING

In Section III, 4 it was stated that under certain conditions nickel and nickel alloys are attacked by sulphur. Town gas usually carries some 20 or more grains of sulphur per 100 ft.<sup>3</sup>, and when burnt to give about 10% of residual combustibles, the volume of purging gas available after rough drying is increased approximately threefold, so that the sulphur content of the final gas is of the order of 7 grains/100 ft.<sup>3</sup>. Most of this sulphur is present as hydrogen sulphide, which is readily absorbed by bog iron ore, providing the ore is maintained in an active condition. This condition is achieved if the plant is so arranged that several ore boxes are employed with interlinked valves, in order that they can be used in rotation. In such an installation (see Fig. 8 (a)), town gas is led through one purifier box, then through a catalytic unit in which the organic sulphur compounds, other than thiophene, are converted to hydrogen sulphide or to sulphur dioxide and hydrogen sulphide, according to whether a hydrogenation or an oxidation catalyst is used. After the catalyst, sulphur dioxide, if present, is removed by a sodium carbonate wash, and hydrogen sulphide by a second bog-iron-ore purifier. The gas now carries several grains (possibly up to 10) of sulphur per 100 ft.<sup>3</sup> in the form of thiophene. This high value results from the discontinuance of oil washing and the high sulphur content of coals used for carbonization at the present time. The gas is now burnt with a fixed proportion of air and after cooling and passing through a demister the gas is again purified by bog iron ore.

The active purifiers in the above train are handling gas which does not contain any free oxygen. Under these conditions the activity of the oxide rapidly decreases, and adsorption of hydrogen sulphide is incomplete. If, however, a fourth box is provided, cyclical interchange becomes practicable, since the spare box can be purged to atmosphere with town gas or with furnace purging gas, according to the position it is next to fill, and each active box can in turn be worked as a precatalyst box, and so be partially regenerated by the oxygen present in the town gas.

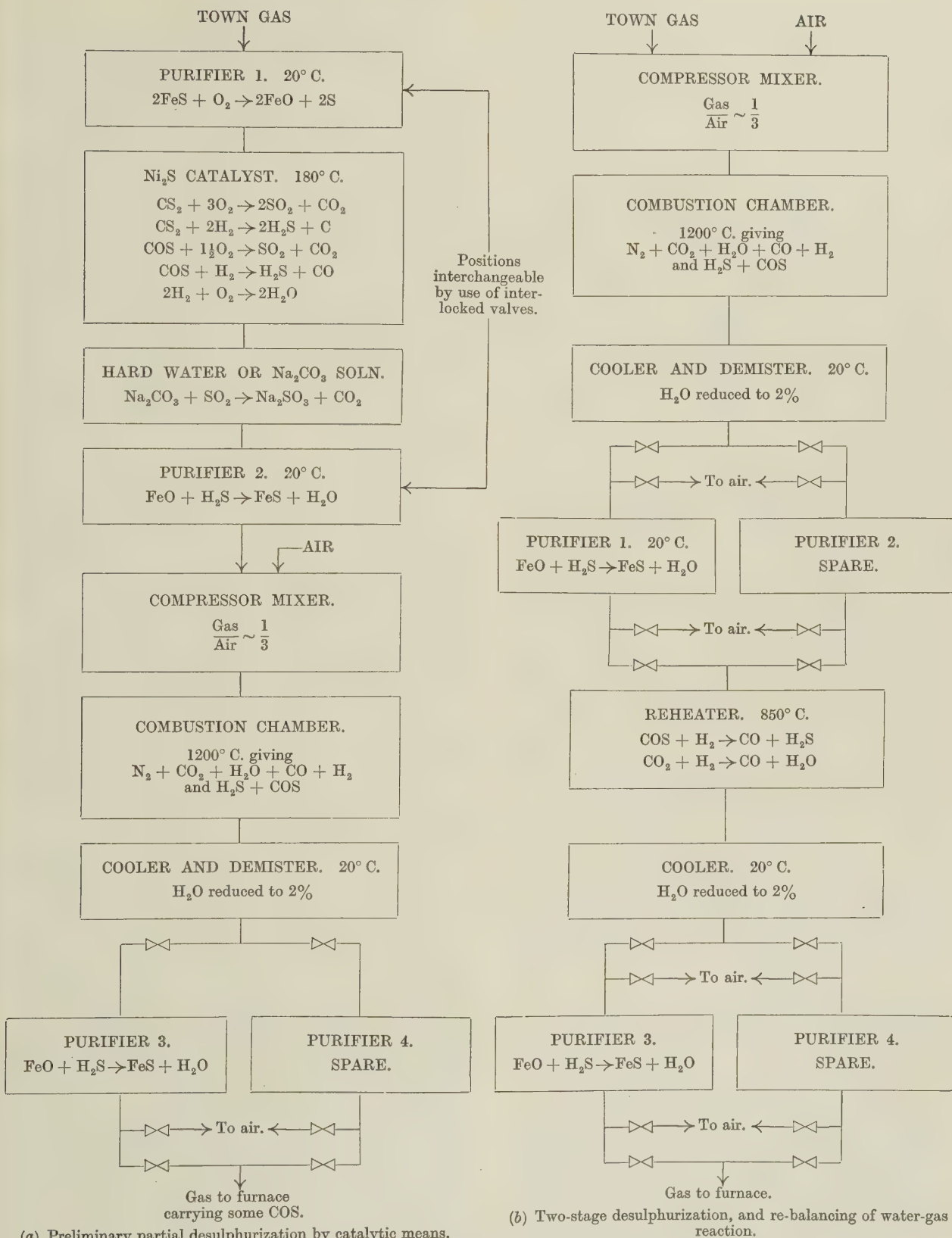


FIG. 8.—Operational Sequences for Production of Purging Gas from Town Gas.



These boxes are usually metal and surrounded by air, so that they should not be situated out of doors; otherwise in cold weather they will become sluggish. It is difficult to prevent boxes of this sort from becoming too damp, and downward flow through the oxide bed is therefore recommended. On the other hand, during a long spell of hot weather they may easily become too dry.

The scheme outlined above suffers from the disadvantage that thiophene is very difficult to convert to an easily removable sulphur compound. Atmosphere gas prepared from partially desulphurized town gas has a very low residual sulphur content if thiophene is not present in the town gas. If the sulphur present as thiophene is of the order of 5 grains/100 ft.<sup>3</sup>, the atmosphere gas will be unsuitable for nickel alloys. The scheme described below (see Fig. 8 (b)) is safer, since it can be relied upon to give atmosphere gas in which the sulphur content does not exceed 0.2 grains/100 ft.<sup>3</sup> even when the town gas carries 30 grains/100 ft.<sup>3</sup>. No catalytic unit is used, and instead the purging gas after the first-stage purification is reheated to about 850° C. Experience has shown that the final purifier in this system remains active for several months, and consequently the only problem is the first purifier. This difficulty, however, may be dealt with as follows. A small amount of oxygen may be added to the gas at any convenient point in the cooling train, for this oxygen will be burnt out at the reheater. The small amount of oxygen required may be most conveniently provided by leading a little of the pre-mixed gas and air from the blower via a by-pass to a point beyond the combustion chamber. The volume of oxygen required is of the order of 0.2% of the town gas that is being burnt in the plant; hence a little over 1% by volume of air is required. For example for a plant burning 1000 ft.<sup>3</sup>/hr. of town gas, about 10 ft.<sup>3</sup>/hr. air should be supplied to the purifier. If the temperature of the oxide and its moisture content are reasonable, a purifier may generally be kept in circuit for several months at a time. It is, however, desirable to have spare purifiers which may normally be open to the air, the air being replaced occasionally, so that if hydrogen sulphide slip is detected, the spare box may be purged with atmosphere gas and put in circuit as a purifier, while the fouled box is rested and revived by air; or, if need be, the oxide may be replaced without serious interruption of the supply of atmosphere gas to the furnace.

## VII.—TESTING OF ATMOSPHERE GAS

### 1. CRACKED AMMONIA

Two tests are required, for residual ammonia and for water vapour. The former is simple, being carried out by means of a Bunte burette, utilizing the extremely high solubility of ammonia in water. Since the only purpose of the test is to determine whether the ammonia content exceeds  $\frac{1}{4}\%$ , no refinements are necessary.

When dew-points of the order of  $-40^{\circ}$  to  $-60^{\circ}$  C. are involved, the simplest procedure is to carry out a qualitative test which is of real significance, rather than to attempt dew-point determinations, which by themselves are meaningless. A resistance-wire spiral may be mounted around a portion of a narrow-bore silica tube. Such a primitive furnace resembles the commonly used pencil element of an electric fire, and for any given voltage attains a steady temperature in a few minutes. The voltage/temperature relationship is readily determined, after which a voltmeter may be used instead of a thermocouple and a millivoltmeter for estimation of the temperature. To test the purity of the gas, the hydrogen or cracked ammonia is led through the tube, and a piece of nickel-chromium alloy tape is treated in the gas at any desired temperature for about a minute and withdrawn slowly through the open cold-end of the tube. Examination of the surface after treatment at one or more temperatures will directly establish the minimum temperature at which clean annealing can be achieved in the gas.

### 2. WATER-GAS-TYPE ATMOSPHERE

It is usually only necessary to know what proportions of combustibles are present in water-gas-type atmospheres, and whether sulphur elimination is satisfactory. An Orsat apparatus is satisfactory for the estimation of the former, but special tests are necessary to determine the latter.

The maintenance of an atmosphere plant depends on keeping the purifiers active, and tests for hydrogen sulphide should be made periodically. For this purpose it is most convenient to pass the gas through a known area of a rather coarse filter-paper, which has been impregnated with lead acetate solution and dried. If a constant-head device and constriction are used, and the gas is passed for, say, one minute, the severity of the slip may be estimated by the depth of sulphide stain formed.

Tests for actual sulphur content of gas are rarely required, and need a careful technique. The gas must be enriched with hydrogen or cracked ammonia and then burnt with a supply of pure air that has been scrubbed with soda lime. The products of combustion may be washed by hydrogen peroxide, which fixes sulphur dioxide and sulphur trioxide as sulphuric acid. If a sufficient quantity of gas is burnt, a volumetric method of estimation is possible.

In some instances it may be desirable to determine the sulphur content of the atmosphere gas, and also to determine the sulphur content of gas samples withdrawn from various points within the furnace, in order to decide what degree of contamination is occurring as a result of residual lubricants carried into the furnace by the work. Providing the investigator has mastered the technique of such tests, deliberate contamination of the atmosphere in this manner may be used to investigate whether the inlet positions for atmosphere gas, and the baffles provided are ensuring the correct flow of gas through the

urnace. More frequently it is desirable to establish whether staining of the work is caused by sulphur or by oxygen. This question may require the use of a very long sampling probe, which should be water cooled and made from either a nickel-chromium or an aluminium tube. Samples of gas may be withdrawn from well within either the heating or the cooling chamber and examined for hydrogen sulphide and free oxygen. Cases have occurred when air has been driven into a furnace via the extractors which are usually fitted to industrial conveyor furnaces utilizing atmospheres containing carbon monoxide.

It rarely happens that precise information is necessary, since for most purposes it is sufficient to know that the difficulty results from air infiltration rather than from the presence of sulphur, or vice versa, and it is sufficient, therefore, to prove that oxygen is or is not present at a point, say 8 ft. from the discharge vestibule of a long cooling chamber. If it is necessary to establish whether or not discoloration is due to sulphur, it will generally be necessary to decide whether the sulphur is present in the atmosphere gas as supplied, or whether it is being carried into the furnace by the work. In the case of clean-annealing furnaces, it is not the usual practice to degrease the work for annealing, even though this is the obvious way to prevent any contamination being carried into the furnace. Apart from the additional cost of the degreasing operation, another objection generally raised is that materials which have been degreased before annealing are much more liable to pressure welding. This may result from one of two causes. In the event of oxygen infiltration to the heating chamber, the presence of lubricants on the work may provide a vapour envelope which protects the work from oxidation; reduction of the oxide would inevitably follow and provide a porous surface which would weld more readily than the normal solid surface; or it may be that solid residues, possibly carbon, are left as the lubricant vaporizes, and these provide a separating medium which decreases the tendency to weld under pressure.

#### VIII.—DEFICIENCIES IN EXISTING EQUIPMENT

It will be apparent from what has been described earlier in this paper that the bright or clean annealing of nickel alloys requires careful control of the conditions of annealing and also of the general condition of the plant. Such control necessitates the availability of a continuous picture of the running conditions in the furnace and the ancillary equipment, and it is in the presentation of that picture that most deficiencies of the present equipment appear.

It is usual to find in belt-type furnaces that addi-

tional alternative positions for thermocouples are desirable so that the best position for control can be determined. Similarly, there is generally no provision for gas sampling which would enable control of the condition to be maintained.

In the atmosphere-generating-plant the provision of an adequate number of test cocks would enable pressure losses in the equipment to be measured and the location of blockages, such as soot deposits in a cooler, to be readily made. The provision of drains and the use of corrosion-resisting materials where moisture collects would be an advantage, and provision of means for cleaning blockages where these are most likely to occur would greatly assist in keeping the plant running.

One of the principal charges relating to belt furnaces is the cost of replacement belts, and any economical improvement in the life of belts would be of great assistance, both in reducing costs and improving availability of the furnace.

Other points which require attention are the design of sealing devices for economy in the use of the controlled atmosphere, and some arrangement to prevent the formation, in entry vestibules, of deposits of impurities, derived possibly from lubricants, which can fall on to the charge and cause trouble. In furnaces in which the controlled atmosphere is exhausted to air, the design of the exhaust chimney requires careful attention to prevent the occurrence of down draughts which can seriously affect the efficiency of the furnace.

The correct location of the furnace in the shop in relation to doors and windows rarely receives the careful consideration to which it is entitled, probably owing to the fact that it is seldom appreciated that the air velocities of draughts are probably at least as high as "light air" or "light breezes", which range from 2 to 3 and from 4 to 7 m.p.h. respectively, i.e. 3 to 4½ or 6 to 10 ft./sec. Neglecting temperature effects, and, assuming uniform horizontal motion of the gases in conveyor furnaces, velocities would rarely exceed 2½–3 ft./min., calculated on maximum economic inputs of purging gas and average vertical cross-section of typical furnaces. There is, therefore, real danger that a draught from a door or window will lead to contamination of the controlled atmosphere by air and a consequent failure to bright or clean anneal.

#### ACKNOWLEDGEMENTS

The authors wish to thank the British Thomson-Houston Co., Ltd., for permission to give details of the temperature-control circuit, and acknowledge their indebtedness to The Mond Nickel Co., Ltd., and to Henry Wiggin and Co., Ltd., for permission to publish this paper. Acknowledgements are also due to Mr. H. T. Kempson for his enthusiastic co-operation in the development of strip-annealing furnaces.





# BATCH THERMAL TREATMENT OF LIGHT ALLOYS\*

1351

By C. P. PATON,† B.Eng., MEMBER

## SYNOPSIS

After a brief description of the processes of annealing, solution-treatment, precipitation-treatment, and stabilizing, and the principal differences in thermal conditions which they entail, the factors affecting the choice of a furnace are listed. Technical considerations affecting this choice are then dealt with in greater detail under the headings: fuels, heating media, circulation of heating media, furnace atmospheres, temperature measurement and control, quenching and drying, general handling, and constructional materials. Descriptions of some different types of furnaces on which operational experience has been obtained are given, covering their construction, control, and operation, together with some critical comments.

Finally, criticism is made of current batch-furnace design, and attention is drawn to those points most in need of consideration. These include the present low thermal inputs and rates of air circulation in air furnaces and, in general, the need for improved construction if higher temperatures are to be used, of greatly facilitating loading and unloading, and of rendering maintenance and inspection as easy as possible without hindering the use of furnaces.

## I.—INTRODUCTION

It is not proposed in this contribution to deal in any detail with the theoretical aspects of the thermal treatment of light alloys, but to assume that the fundamental principles are known. Only brief descriptions of the various treatments will therefore be given in Section II.

In regard to the descriptions of equipment that follow, it must be appreciated that the decision to instal a particular type of furnace has often been influenced by the conditions obtaining at the time, and that in consequence ideal requirements could not always be met. For instance in the case of equipment installed during the last war, the primary consideration was the speed at which it could be obtained and put into operation; while the choice of method of heating was governed by local conditions such as the availability of coke-oven or producer gas, and the comparative cost at that time of operation with gas or electricity.

## II.—DESCRIPTION OF THERMAL-TREATMENT PROCESSES

Thermal treatments, broadly speaking, are treatments carried out below the melting point of a material to enhance one or more of its properties, such as strength or ductility. The following treatments are usually applied to light alloys: (i) annealing, (ii) solution-treatment, (iii) precipitation-treatment, and (iv) stabilizing.

### 1. ANNEALING

#### (a) *Partial or Temper Annealing of Strain-Hardened Material*

Partial annealing is a low-temperature treatment to effect partial strain-relief and is usually carried

out between 150° and 300° C. The result is a reduction in strength of the material and a considerable increase in elongation. It is also possible to decrease the difference between the longitudinal and transverse tensile properties which is associated with material that has been subjected to heavy directional cold work, such as occurs in strip rolling.

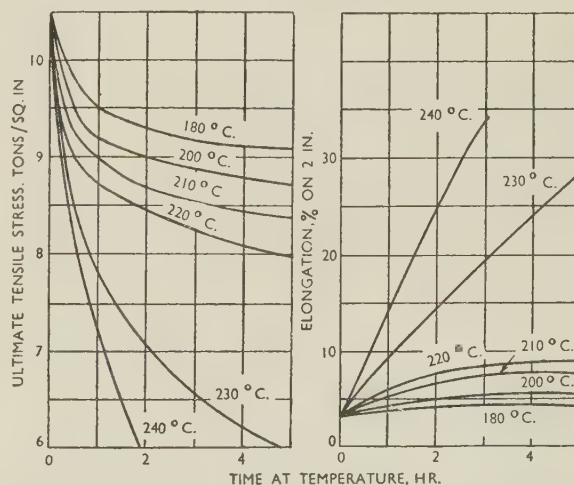


FIG. 1.—Effect of Time at Temperature on Transverse Properties of Cold-Rolled Commercial-Purity Aluminium.

Partial annealing takes place over a wide range of temperatures and is dependent upon the time at temperature, as shown in Figs. 1 and 2.

The history of the material has quite a considerable effect on the rate and extent of recovery in partial annealing. This includes the metal composition, method of casting, temperature and time of pre-heating the cast ingot, and whether or not the material

\* Manuscript received 22 November 1951. Contribution to a Symposium on "Equipment for the Thermal Treatment of Non-

Ferrous Metals and Alloys", to be held in London on 26 March 1952.

† Northern Aluminium Company, Ltd., London.



has been subjected to an intermediate anneal. The advantages of partial annealing are that, by a suitable choice of temperature and time, it is possible to

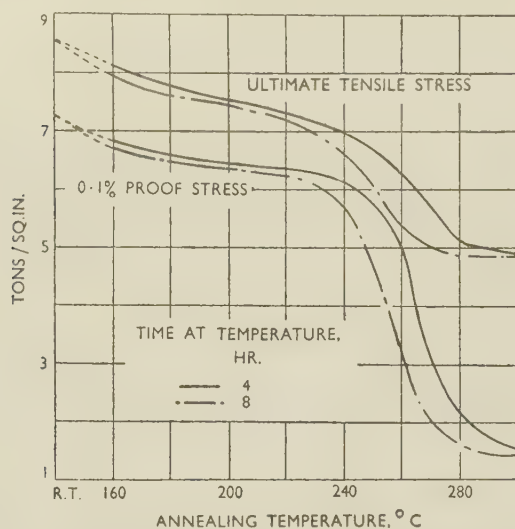


FIG. 2.—Effect of Annealing Time and Temperature on the Tensile Properties of Cold-Rolled 99.6% Aluminium.

obtain the intermediate tempers of half hard and three-quarters hard from hard-rolled material produced by modern rolling mills designed to give heavy reductions. In addition, the better ductility and reduced directionality of properties so obtained make the material more suitable for certain pressing operations than that produced by rolling to temper. This is illustrated by Table I.

TABLE I.—Mechanical Properties of 0.048-in. Sheet of Commercial-Purity Aluminium.

Condition	Longitudinal		Transverse	
	U.T.S., tons/in. <sup>2</sup>	Elongation on 2 in., %	U.T.S., tons/in. <sup>2</sup>	Elongation on 2 in., %
60% reduction	9.6	7	10.6	3
60% reduction and partial anneal of 8 hr. at 200° C.	8.3	10	8.5	8
30% reduction	8.2	8	8.6	4

One of the disadvantages of this low-temperature treatment which should be taken into consideration is the hazard of oil staining, particularly with material that has been rolled in modern flood-cooled mills. It also has to be borne in mind that material treated in this way does not possess the protective oil film present on temper-rolled material and is therefore more susceptible to damage in handling.

#### (b) Full Annealing of Strain-Hardened Material

Full annealing is a treatment applied for complete softening, and it leaves the material in an entirely strain-free condition. With most commercial alu-

minium alloys, the process of softening takes place within the range 340°–400° C. Normally, a temperature head well in excess of that required to give complete softening can be safely used to augment the rate of heating—a factor of major importance in controlling the grain-size of the material.

#### (c) Full Annealing of Heat-Treatable Material

This process provides full softening without age-hardening. While one object of the process is to remove the effect of cold working, it is also necessary to ensure that precipitation of the soluble constituents from the solid solution is as complete as possible. The process involves a soak within the range of 340°–400° C., followed by a slow, controlled rate of cooling of approximately 15° C./hr. to a temperature of not more than 260° C. After such a treatment the material is in a stable condition, and cold working can be carried out after protracted periods.

#### (d) Interstage Annealing of Heat-Treatable Material

This process is carried out on material on which it is intended to undertake cold working fairly soon after annealing. Under these conditions the slow, controlled rate of cooling necessary for full annealing is dispensed with. Treatment temperatures usually lie within the range 340°–400° C. Higher temperatures may result in solution rather than precipitation, with the hardening that would be expected from such a condition. After this treatment some age-hardening may take place, but the use of the process is fully justified when the flow of material from the annealing treatment to the next cold-working operation can be controlled to take advantage of the saving that occurs from this shortened annealing treatment.

## 2. SOLUTION-TREATMENT

Solution is the first stage of any thermal hardening treatment. It consists essentially of heating the metal and then quenching it rapidly in a suitable medium, such as water or oil, to retain in solution the hardening constituents. Temperatures employed vary from 460° to 530° C. for wrought products, and from 425° to 545° C. for cast products. The permissible variation from the accepted nominal temperature is usually stipulated as  $\pm 5^\circ$  C., but, in good works' practice, limits of  $\pm 3^\circ$  C. are generally maintained. The lower limit of the heat-treatment temperature range is governed by the fact that solution must be sufficiently complete and consequently the material have adequate strength, while the upper limit is controlled by the danger of partial melting with resultant cracking and deterioration of the mechanical properties.

The rate of heating and the time at temperature of most wrought products is of great importance. In the case of sheet, a large proportion of material produced in heat-treatable alloys is clad—that is, it consists of a core of heat-treatable strong alloy with a coating of approximately 5% of the total thickness on each side of a higher-purity metal anodic to the

core as a protection against corrosion. If the time at solution heat-treatment temperature is excessive, alloying elements will diffuse to an undesirable extent from the core into the cladding and thereby decrease the degree of protection. It can generally be accepted that some diffusion will take place at all temperatures above approximately 300° C.

With material that has been cold worked before solution heat-treatment, it is obvious that the thermal process must be accompanied by some degree of recrystallization. The resultant grain-size largely depends on the amount of cold work and the thermal conditions existing. The rate of heating, which is one of the thermal conditions, is of great importance in controlling the grain-size. In the case of castings, with their relative freedom from internal stresses at this stage, a slow rate of heating can be tolerated.

In all products the rate of cooling after the high-temperature solution-treatment is very important, since any delay allows the material to cool, with the corresponding reduction in the degree of supersaturation, lowering the strength and the corrosion resistance of the material. Such delays may arise either as a result of the time elapsing between removal from the solution-treatment furnace and quenching, or as a result of varying the type of quenching medium.

### 3. PRECIPITATION-TREATMENT

Precipitation-treatment is applied to certain of the heat-treatable alloys after solution heat-treatment to improve their strength further, at the expense of

shorten the time necessary to obtain the maximum properties. The combination of temperature and time has to be carefully chosen, however, to obtain the optimum properties from any particular alloy, as will be seen from the characteristic ageing curves shown in Fig. 3.

### 4. STABILIZING

Stabilizing of cast products may be required for two purposes: (a) to prevent progressive changes in mechanical properties at elevated operating temperatures, and (b) to prevent dimensional changes (distortion) at normal temperatures.

The former is accomplished by carrying out precipitation-treatment at a temperature equal to, or greater than, the known operating temperature. The latter result is attained by carrying out the heat-treatment in such a manner as to reduce the residual stresses to a minimum. Slow quenching, as in hot oil, is one way of obtaining this effect.

Stabilization of the aluminium-magnesium solid-solution alloys of the NS4 type when produced in the form of temper-rolled sheet, may be necessary, as, in this condition, the mechanical properties of these products change slightly over a period of time at normal temperatures. Their strength and hardness decrease and their elongation increases. Therefore, to bring the alloys into a stable condition before use, they may be subjected to a stabilization treatment of approximately 4 hr. at 150° C.

Works' practices must take account of the fact that all these treatments are progressive, i.e. metallurgical changes begin to take place at very much lower temperatures than those chosen for operating. For example, with large furnace loads the process of solution in heat-treatment in air furnaces may begin two or three hours before the nominal temperature is reached. The result is then that the soaking time given at a nominal temperature is usually somewhat less than the time calculated in the laboratory for a specific temperature.

In establishing procedures, account must be taken of the fact that uniform temperature conditions seldom exist throughout the whole of the load during the heating cycle. In some cases it may be found that one part of the load is at nominal temperature several hours before another part of the same load. This is particularly important in ageing and temper annealing, and temperatures and times must be chosen which will permit of this latitude of several hours.

### III.—FACTORS GOVERNING THE CHOICE OF FURNACE

In installing new equipment for batch thermal treatment, the main factors which have to be considered are as follows: (i) thermal treatment required (annealing, solution-treatment, artificial ageing, &c.); (ii) type of material (e.g. sheet, coil, extrusions, tube,

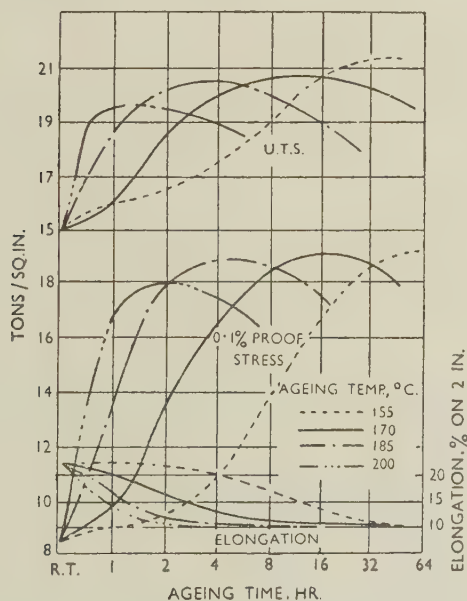


FIG. 3.—Artificial Ageing Curves for an Aluminium-1% Silicon-0.6% Magnesium Alloy 1-in.-Dia. Extruded Bar, After Solution-Treatment at 520° C.

ductility. The temperatures employed range from 100° to 200° C. Artificial ageing takes place within the whole of this range; the higher temperatures



wire, forgings, and castings); (iii) types of alloy to be treated; (iv) size of material to be treated; (v) tonnage to be treated; (vi) degree of flexibility required with regard to flow of material (the number of different alloys requiring different treatment); (vii) the types of fuel available; (viii) heating media to be employed; (ix) degree of uniformity of temperature required; (x) rate of heating and cooling required; (xi) the method of control to be employed (manual or automatic); (xii) special requirements (such as controlled atmosphere or freedom from the products of combustion); (xiii) method of handling to be employed; (xiv) space available for installation; (xv) total capital cost of furnace, buildings, and ancillary handling equipment; (xvi) estimated maintenance requirements; (xvii) the estimated total cost per ton of material treated; and (xviii) the availability of labour and the number of men required to operate the furnace.

#### IV.—TECHNICAL CONSIDERATIONS AFFECTING DESIGN OF FURNACES

In this section it is intended to describe some general characteristics which affect the design of heat-treatment furnaces. These factors include: (1) fuels, (2) heating media, (3) circulation of heating media, (4) furnace atmosphere, (5) temperature measurement and control, (6) quenching and drying, (7) general handling, and (8) constructional materials. These factors are interdependent, and there may therefore be some unavoidable duplication of the comments made under the different headings.

##### 1. FUELS

Most fuels can be used in suitably designed furnaces for the thermal treatment of aluminium and its alloys. The majority of furnaces, however, are designed to utilize electricity, coke-oven gas, or producer gas. The major factors governing the choice of fuel are availability and relative cost. The latter cannot be confined to the cost of fuel alone, but should take account of the capital cost of installing a furnace suitably designed to use the available fuel and to meet the specific metallurgical requirements of the thermal treatment it is intended to carry out.

Under present conditions the possibility of restriction in the supply of electricity has to be taken into consideration, and power which is produced on site may offer an advantage. Apart from these considerations electricity is usually preferred because of the following advantages:

- (i) The degree of cleanliness offered by its use.
- (ii) It lends itself to simplicity of furnace design without the restriction which is necessary under certain conditions with gas and oil of preventing the products of combustion coming into contact with the metal being treated.
- (iii) The ease and accuracy of control—usually gas- and oil-fired furnaces require a greater

amount of pyrometric equipment. Automatic control of gas-fired furnaces demands a source of clean gas and, in the case of producer gas, this becomes an expensive requirement.

The case of salt baths can be considered separately. Electric heating is to be preferred for these, especially in the case of large baths, because it can be easily applied internally, so providing greater ease of control and a longer tank life compared with external heating, whether electric, gas, or oil. In internally heated baths, resistance elements encased in nickel sheaths are suspended round the sides of the tank or, alternatively, large tubular elements may be laid along the bottom of the bath from end to end.

##### 2. HEATING MEDIA

The types of heating media in general use are heated air, the products of combustion from gas or oil fuel, and molten salt. The furnaces therefore fall into two main classes: (i) air furnaces, in which either heated air or the products of combustion from gas or oil fuel are circulated around the material to be treated, and (ii) salt baths containing molten salt in which the material is immersed.

The outstanding differences between salt baths and air furnaces may be summarized as follows:

(1) Salt-bath furnaces usually have a lower installed cost, especially in the larger sizes.

(2) Salt baths have a higher rate of heat transfer to the load, thus reducing the necessary total time in the furnace. In the solution heat-treatment of clad sheet this is an advantage in limiting diffusion from the core material into the high-purity cladding.

(3) The operating costs of air furnaces are lower than those of salt baths. The disadvantages of salt-bath furnaces in this respect are the drag-out of salt with each load and the necessity of washing the load.

(4) Air furnaces are much more flexible, as they may be shut down and re-started with comparative ease, and a single furnace may be used for a variety of thermal treatments such as solution-treatment, annealing, artificial ageing, &c.

(5) Salt baths, especially large units, require housing in a separate room to prevent the salt-laden atmosphere from contaminating other areas.

(6) Air furnaces generally produce a more even colour on sheet.

On account of the last four factors air furnaces have been generally adopted for all thermal treatments other than the solution-treatment of sheet.

It is probable that the reason why salt-bath furnaces are generally used in this country for the solution-treatment of sheet is that by far the larger proportion so treated is of the clad type. Air furnaces are very widely used for heat-treating flat sheets in North America, however.

Suitable salts for solution heat-treatment purposes are pure sodium nitrate, a eutectic mixture of sodium nitrate and potassium nitrate and/or nitrites. Such mixtures are more expensive than pure sodium nitrate, but have lower melting points, and are thus more fluid at heat-treating temperatures, consequently reducing the drag-out loss.

In the air furnace with gas or oil heating, one problem which has to be faced is that at high temperatures the products of combustion may cause blisters if they come into contact with aluminium alloys. Consequently there are two types of gas- or oil-fired air furnaces: (i) those in which the products of combustion from the gas pass over the load, and which are usually operated at low temperatures (such as annealing temperatures), and (ii) those which operate on a heat-exchange principle and in which the load chamber is entirely muffled from the products of combustion. In this latter group may be included the electrically heated furnaces.

### 3. CIRCULATION OF HEATING MEDIA

In any type of heat-treatment the aim is to bring the whole load to the desired temperature as quickly as possible. In air furnaces the natural convection currents are neither suitable nor strong enough to maintain an efficient circulation. Consequently all furnaces of this type are designed with some form of forced-air circulation. In general, it is not necessary to use assisted circulation in the case of salt baths, as the convection currents combined with the high value of the heat content of the salt have been found ample for the purpose.

Circulation in air furnaces should take place so that as many surfaces as possible to be heated come into direct contact with the air or the products of combustion. This is a difficult problem with stacks of flat sheet and coiled sheet, since, while the outer layers or edges may be exposed to the heating medium, the inner surfaces cannot be. The slight air space between the laminations acts as an insulator. With very large coils and stacks it is suggested that most of the heating of the middle of the mass is by way of conduction from the edges of the laminations. Extrusions, forgings, and castings, on account of their size and form, permit of more adequate spacing.

Generally speaking, it can be stated that the more rapid the air circulation the greater is the rate of rise of temperature of the load, but this is limited by the ability of the charge, because of its form and thermal characteristics, to absorb the available heat.

There are two main types of rapid circulation:

(a) End flow, in which the air or products of combustion pass down the length of the furnace and over the whole of the load. This type of furnace usually has one point of pyrometric control for the whole of the heat input, located at the point where the air enters the load chamber.

(b) Transverse flow, in which the air passes through the load along one of the minor dimen-

sions of the load chamber. This type of furnace lends itself to multi-point control, that is, the heat source can be divided into sections or zones, each zone having its own pyrometric control, thus improving the uniformity of temperature over the load as a whole.

Where the material to be treated allows adequate spacing, a simpler type of air circulation can be adopted, using the "paddle fan". With this type of furnace a fan is suspended by its shaft through the roof to draw the heated air up through the load to the top of the furnace, and to spread it out to pass down each side of the chamber over the heating elements before passing through the load again. This type of furnace is usually zoned.

In the muffle-type furnace, electrically or gas heated, the desired circulation is generally obtained by inserting a second lining inside the muffle. Fans are used to pass the air over the load and through the outer chamber and then to return it to the load. In the case of electric furnaces the heating elements are usually placed between the inner and outer shells.

With loads of larger dimensions, particularly as regards length, it is essential to make sure that all parts are brought to temperature as uniformly as possible. Periodic reversal of the direction of air flow is advantageous in effecting this, and also helps in the efficient use of the available heat.

### 4. FURNACE ATMOSPHERES

Exposure of some aluminium alloys at solution heat-treatment temperatures, i.e. in the region of 500° C., to an atmosphere containing the products of combustion of coke-oven and producer gas, give rise to the formation of blisters. Gas furnaces designed for use at these temperatures, therefore, are of the muffle type. But even with the muffle-type furnace, including those electrically heated, there is a blister hazard due to water vapour which may be introduced on the surface of the load carrier or from the shop atmosphere. The hazard is increased in the case of vertical furnaces, since a water tank is situated below the furnace for quenching purposes. In order to prevent the formation of these blisters, creosote, tallow, or similar hydrocarbons are painted on the surface of the metal or, alternatively, a small quantity is introduced into the furnace atmosphere when the cold load is charged. In North America sodium fluoroborate is sometimes used for the same purpose.

At annealing temperatures the products of combustion from gas do not present the same blister problem, particularly in clad strong alloys or commercial-purity sheet. Consequently, gas-fired furnaces with the products of combustion passing over the metal can be used for annealing purposes. Precautions have to be taken, however, against the risk of condensation staining. The danger of condensation does not exist if the sheets or coils are hot from the rolling operation, but if the material is cold arrangements should be made for it to be heated to



approximately 100° C. in a clean atmosphere before being loaded into the products of combustion at the higher temperature. This can be carried out by means of preheating chambers either electrically heated or gas fired on the heat-exchange principle.

Alloys containing magnesium are always liable to discolour when annealed in furnaces in which the products of combustion are recirculated through the working chamber. Apart from spoiling the appearance, the oxidation of such material may be a source of difficulty in subsequent welding, and the discoloration can be minimized by enveloping the alloy in a thin case of aluminium sheet.

#### 5. TEMPERATURE MEASUREMENT AND CONTROL

All furnaces used for the heat-treatment of aluminium should be equipped with automatic temperature controllers and recorders to maintain and record accurate temperatures within the specified heat-treatment limits.

It is generally accepted today that controllers and recorders of the potentiometric type afford the greatest accuracy of measurement and are the most reliable. It is advisable that the control and recording of the temperature be carried out by separate instruments, especially when the process being controlled is solution heat-treatment. With two installations operating independently, each acts as a continuous check upon the other.

For recording purposes, as wide a chart as possible is to be preferred, and the instrument should be so calibrated that the full width of the chart is used with the working range of temperatures. In air furnaces it is general practice that the thermocouples used for temperature-recording purposes shall be placed within the load.

After the installation of a new bath or furnace, or the starting up of a bath or furnace after a shut down for modification or maintenance, a complete pyrometric survey should be carried out in order to ensure that the temperatures obtained are within the accepted tolerances for the process. This is usually carried out both with the furnace empty and later charged with loads, by means of a number of wandering thermocouples attached to a suitable instrument.

#### 6. QUENCHING AND DRYING AFTER SOLUTION-TREATMENT

The usual method of quenching aluminium alloys after soaking at temperature is by total immersion in a tank of cold water. It is common practice to have a continuous flow of fresh clean water entering the quench tank, in order to spill the layer of hot water from the top of the tank and hold the temperature below approximately 30° C. In the case of quenching from salt baths a continuous change of water also keeps the salt content of the water under control.

The transfer from the furnace to the quench tank should be as rapid as possible as long delays in transfer impair the strength and corrosion-resistance of the

alloy. Transfer times of considerably under one minute are commercially feasible, and quench tanks should be located close to the furnace and at the same or a lower level to assist in obtaining the rapid quench.

Where it is necessary to reduce distortion and residual stresses which may manifest themselves later, such as is the case with forgings and castings in certain alloys, it is common practice to quench in hot water or oil, usually at about 60°–100° C.

Heating quenching oil by immersion heaters in the quenching tanks themselves is not to be recommended. Usually such tanks acquire a layer of sludge at the bottom, due to cracking of the oil and the collection of solid particles of sands, oxides, &c., washed off castings and the cage. In time this forms an effective insulating layer at the bottom of the tank, which results in overheating and failure of the heaters. The life of heaters under such conditions is very limited, and their replacement is usually an extremely troublesome business.

A better system is to heat the oil in a separate tank through which it may circulate and pass continuously to and from the quench tank. Such a tank may be of comparatively small dimensions, and the oil can be circulated through it at an extremely rapid rate, so that great rapidity of heating is obtainable.

After solution-treatment in a salt bath, sheet has to be thoroughly washed in order to remove the salt, and after this a drying operation is necessary in order to prevent the occurrence of corrosion and to present the material for flattening as soon as possible. The water used for washing purposes must have a low content of dissolved solids to prevent the formation of stains on drying.

Drying is usually carried out by subjecting sheet to a warm air blast. With some alloys the temperature of the sheet obtained in drying must not exceed approximately 60° C., for otherwise the natural ageing characteristics of the sheet may be inhibited.

If the quenching of forgings or castings has been carried out in oil, the oil is usually removed either by means of sawdust or, alternatively, by washing with water and detergents.

#### 7. GENERAL HANDLING

Any system of handling must take into consideration the susceptibility of aluminium and aluminium alloys to surface damage, particularly in view of the high standard of surface finish that present-day requirements demand. Methods of handling should be so designed as to minimize the effects of vibration or movement of the load during heat-treatment.

Because of the hazard of surface damage during loading and unloading, any system which permits load carriers that can be used both in the furnace and for general transport during operational process, is advantageous. The low strength of the metal at annealing and solution-treatment temperatures requires that it be adequately supported to minimize distortion, with a type of support that will not itself cause damage.

The spacing of loads should be arranged to permit of as large a proportion of the load as possible being in intimate contact with the heating media, and also, in the case of air furnaces, to take full advantage of the system of air circulation being employed.

Flat sheets for annealing are usually loaded on carriers in stacks supported on a firm base, such as perforated thick steel sheet. A furnace load, may, for instance, consist of many trays capable of being interlocked to facilitate handling the charge in and out of the furnace. Another method is to stand sheets on edge during annealing. This permits better spacing and simplifies loading.

Coiled strip is usually loaded vertically on steel trays, and charged in and out of the furnace by means of hydraulic rams, or stacked on several levels horizontally, in which case, to prevent collapse during treatment, they are previously wound on to aluminium-sprayed steel spools.

For solution-treatment flat sheet is either suspended on hangers attached to a lifting head, or held in vertical cradles. If cradles are used, they should be so designed that they provide a good support to the bottom edge of the sheet, and that there is reasonable allowance for free movement to accommodate distortion arising from either the heating or the quenching cycle. If coiled strip is solution-treated, it is advisable, on account of the compact mass making surface heating and quenching difficult, to use salt-bath furnaces, and to space the laps of the coils either by wire or by dimpling the edges. To prevent intermeshing the dimples are spaced at irregular intervals. Wire spacing is used only for heavier gauges of material which are not readily dimpled, as there is a danger with wire of scratching the sheet, and the greater risk of entrapment of nitrate or contaminated quench water.

Low-temperature treatment such as that for precipitation, where the need for support is not so necessary, allows stacks to be spaced at  $\frac{1}{2}$ –1 in. intervals with asbestos rope or extruded sections.

Extrusions, forgings, and castings are more easily handled and lend themselves to better load spacing. Loading may be in skips, cages, or suspension from spiders. The loading calls for careful thought and ingenuity to ensure that the best use is made of the maximum capacity of the furnace, consistent with maintaining the necessary metallurgical control. Time can be saved if duplicate sets of load carriers are available for each furnace, so that their loading can be proceeded with during the time that a previous load is being treated in the furnace.

## 8. CONSTRUCTIONAL MATERIALS

The requirements of constructional materials for furnaces for the thermal treatment of aluminium and its alloys are not exacting, because of the comparatively low level of temperatures employed. Mild steel is by far the most common metal used, both for furnace and load-carrier construction. The exceptions to this general rule are the general use of Armco

plate for salt baths and the use of alloy steels or irons for the heat-exchanger units in gas-fired muffle-type furnaces. In this latter case alloy steels are necessary, not only to prevent scaling but also in order that they shall stand up to an atmosphere containing sulphur compounds.

The practice is increasing of offering protection to load carriers and internal linings of furnaces made in mild steel by spraying with aluminium metal. A cheaper form of protection, although naturally with a much shorter life, can be obtained by the use of certain proprietary paints.

The bricks most commonly used are good-quality firebricks of approximately 40% alumina content, with fireclay of similar composition for jointing. Bricks of a high porosity are employed for insulation purposes. Insulating bricks are preferred to loose packing material such as slag wool, asbestos flock, or diatomaceous powders, owing to the tendency for the latter to consolidate with vibration, giving uneven insulation.

## V.—DESCRIPTION OF VARIOUS TYPES OF FURNACES

In selecting furnaces for inclusion in this section no attempt has been made to cover the whole range available, and it has been confined to a small number of representative types on which operational experience has been obtained. The description of each type covers the salient points of its construction, control, and operation, and is followed by comments on its shortcomings in the light of experience gained during operation.

### 1. GAS-FIRED FURNACE WITH RECIRCULATED PRODUCTS OF COMBUSTION FOR ANNEALING SLAB AND SHEET

In this furnace the products of combustion are passed through the load. They are then exhausted at the rate of 20,000 ft.<sup>3</sup>/min., to be reheated to the correct temperature, for recirculation, by a number of low-pressure gas burners disposed along each side of the furnace. The direction of flow of the hot products of combustion is reversed automatically every 20 min.

The outer casing consists of  $\frac{3}{8}$ -in. mild-steel sheet with suitable supports, and within this case the necessary flues, ducts, and load chamber are built with firebrick.

The furnace has 24 burners divided into six zones. Pyrometric control couples are inserted in the recirculation flues at the point where the recirculated gases are heated by individual burners. The four couples in each zone are connected to potentiometric controllers which average the four temperatures and operate the gas and air valves. It is possible also to determine the temperature recorded by each individual couple and, by manual adjustment of the burners, to ensure uniformity. Six iron/Constantan thermo-



couples located at intervals along the roof of the load chamber are used for recording the temperature of the recirculated gases. The temperature of the load is recorded on a separate potentiometric recorder by means of couples inserted in the load.

The load carrier comprises 24 interlocking trays. These trays, 6 × 6 ft., are used to transport the material to and from the furnace. Some 15 min. before the charging of any load, the supply of gas to the burners is turned off and the furnace atmosphere "purged" of the products of combustion. Two hours after charging the load, or when the load couples register 100° C., the gas burners are relit. The load is brought to, and held at, temperature for the requisite period, the time and temperature depending on the alloy and the form of the material being treated.

Aluminium-1½% manganese alloy sheet, which requires a rapid rate of heating to control the grain-size, can be annealed only in very small loads, for example in piles not more than 3 in. high, taking an overall time of about 6 hr.

*Comments.*—(1) The need for "purging" the furnace to avoid staining by condensation results in a loss in thermal efficiency and gives a slow rate of heating, making the furnaces unsuitable for annealing full loads of alloys susceptible to grain growth. (2) The instrumentation of control equipment presents a big maintenance problem. (3) The method of charging the load gives rise to indentations and pressure welds unless additional precautions such as loading on soft asbestos sheets is used. (4) The time taken to complete the annealing and cooling cycle necessitates the carrying of a heavy mill load.

## 2. GAS-FIRED HEAT-EXCHANGER AIR FURNACE FOR ANNEALING COILED SHEET

In this furnace clean air is recirculated over the load and obtains its heat from a gas-fired heat-exchanger placed externally to the furnace. The direction of the air flow within the furnace is downwards.

The furnace itself consists of a double tunnel, each tunnel being 4 ft. 6 in. wide × 6 ft. high × 80 ft. long. The tunnels are closed at each end by brick insulated doors and are divided into preheating and soaking zones by internal doors. The air circulation system is separate for each of these zones and provides respectively 25,000 and 28,000 ft.<sup>3</sup>/min. The main furnace has a casing of ¾-in. mild steel suitably strengthened. Within this casing the ducts and heating chambers are built with 9 in. of firebrick, backed by a minimum of 9 in. of insulating brick.

The heat-exchanger is divided into three sections, two of which provide heated air for the preheating and soaking zones of the furnace, while the third section utilizes the waste heat from these two in order to heat the air supply for the burners. Both gas supply and air supply to the burners are automatically controlled by means of thermocouples placed in the clean air stream.

Coils, of maximum size 39 in. dia. and 30 in. wide, are wound on 16-in.-dia. spools for loading on to special trays in which one coil is carried above another (Fig. 4, Plate LI).

Control of the overall temperatures of the two zones of the furnace is automatic, as already mentioned, but control within the zones is carried out by adjustment of dampers which control the flow of recirculated air. Some of the air is spilled from the preheating zone in order to get rid of the oil vapour picked up from the load.

The normal operating temperatures of this furnace for commercially pure aluminium and the 1½% manganese alloy are 550° C. in the preheat zone and 500° C. in the soaking zone. At these temperatures one tray is charged in each tunnel every 40 min., and the output of the furnace is 10,000 lb./hr.

*Comments.*—(1) This type of furnace has been expressly designed for long runs of material requiring the same annealing cycle, and light and heavy coils cannot be annealed together without risk of overheating the light coils. (2) The rate of heating of the load, which is dependent partly upon the furnace design and partly upon the form and weight of the load, is slower than necessary for the best control of grain-size. (3) The rate of heat input to the recirculated air is limited by the maximum permissible temperature of operation of the heat-exchanger unit.

## 3. ELECTRICALLY HEATED AIR FURNACE FOR ANNEALING SLAB AND SHEET

The main case of this furnace is of 4½-in. firebrick backed by 9 in. of insulating brick, the whole encased in ⅝-in. mild steel. An aluminium-sprayed mild-steel baffle is fixed 9 in. away from the side wall and the roof of the furnace. Nichrome tape elements are uniformly arranged in the space between the baffle and the roof, and are divided electrically to provide six independent control zones along the length of the furnace. The side walls of the baffle are perforated and have perforated dampers attached, by which the air flow can be adjusted. A fan is provided in each zone to give a high rate of air circulation from the heaters, through the side wall, across the load, and back to the heaters via the opposite side wall. The electrical input is 420 kW.

Temperature control is by means of six deflection-type indicating controllers connected to thermocouples situated one in each zone at the point where the air stream leaves the heating elements. Two 6-point potentiometric recorders are provided, each recording the temperature of the air stream before and after it passes over the load.

The load carrier consists of four trays arranged in tiers, each 30 ft. long × 5 ft. wide × 1 ft. high, and is mechanically charged on a roller track. Slab or flat sheet is loaded manually on to the trays and the carrier assembled on the shop floor and then lifted by crane on to the charging table. With a load of approximately 10 tons, the temperature of the air on the ingoing side reaches nominal temperature in

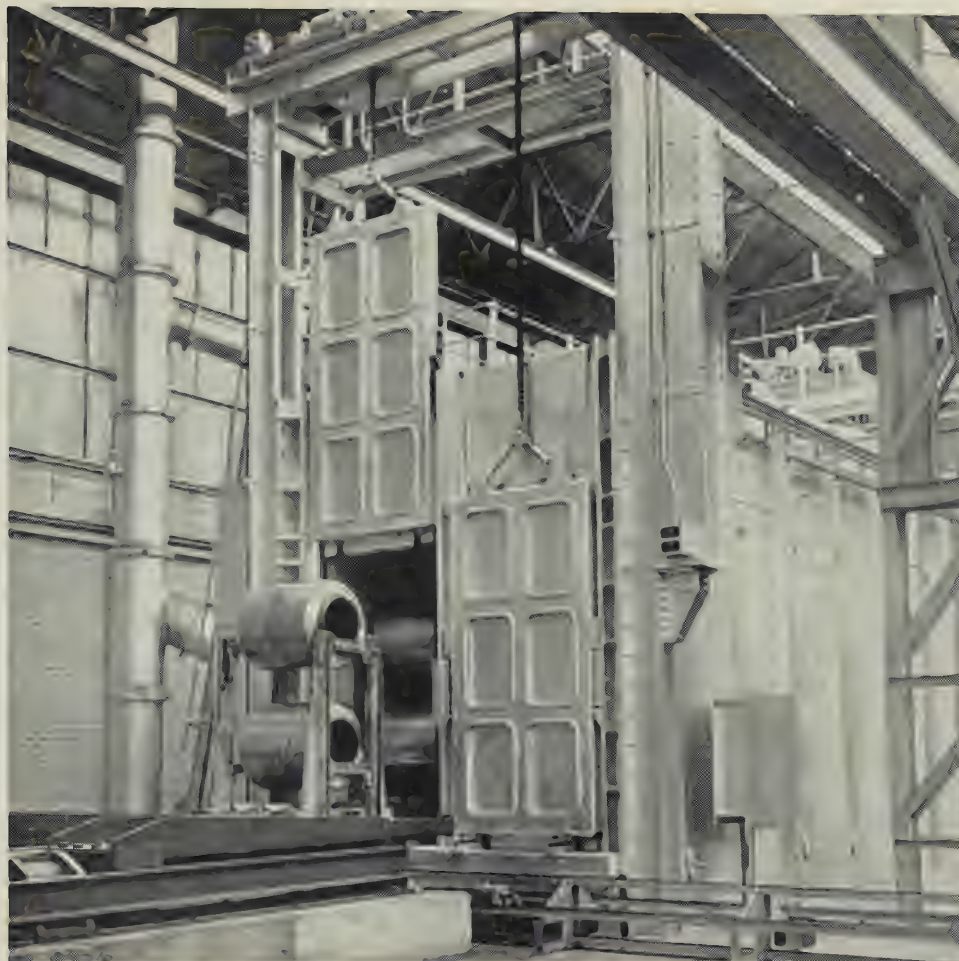


FIG. 4.—Coils Entering Gas Fired, Heat-Exchanger Air Furnace.

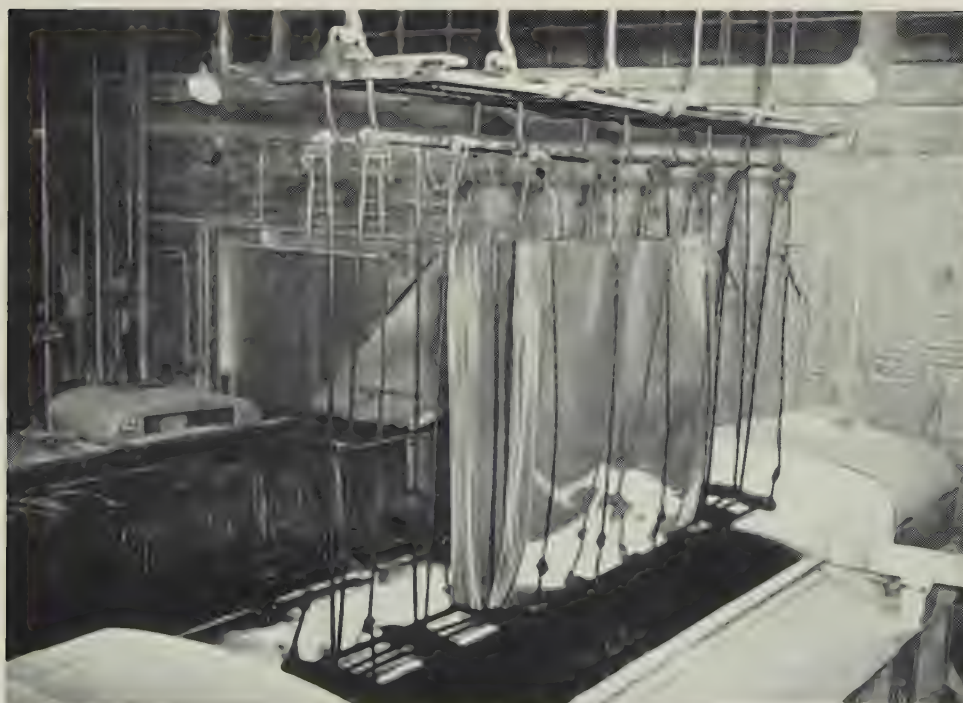


FIG. 5.—Solution-Treated Sheet Leaving a Salt Bath.



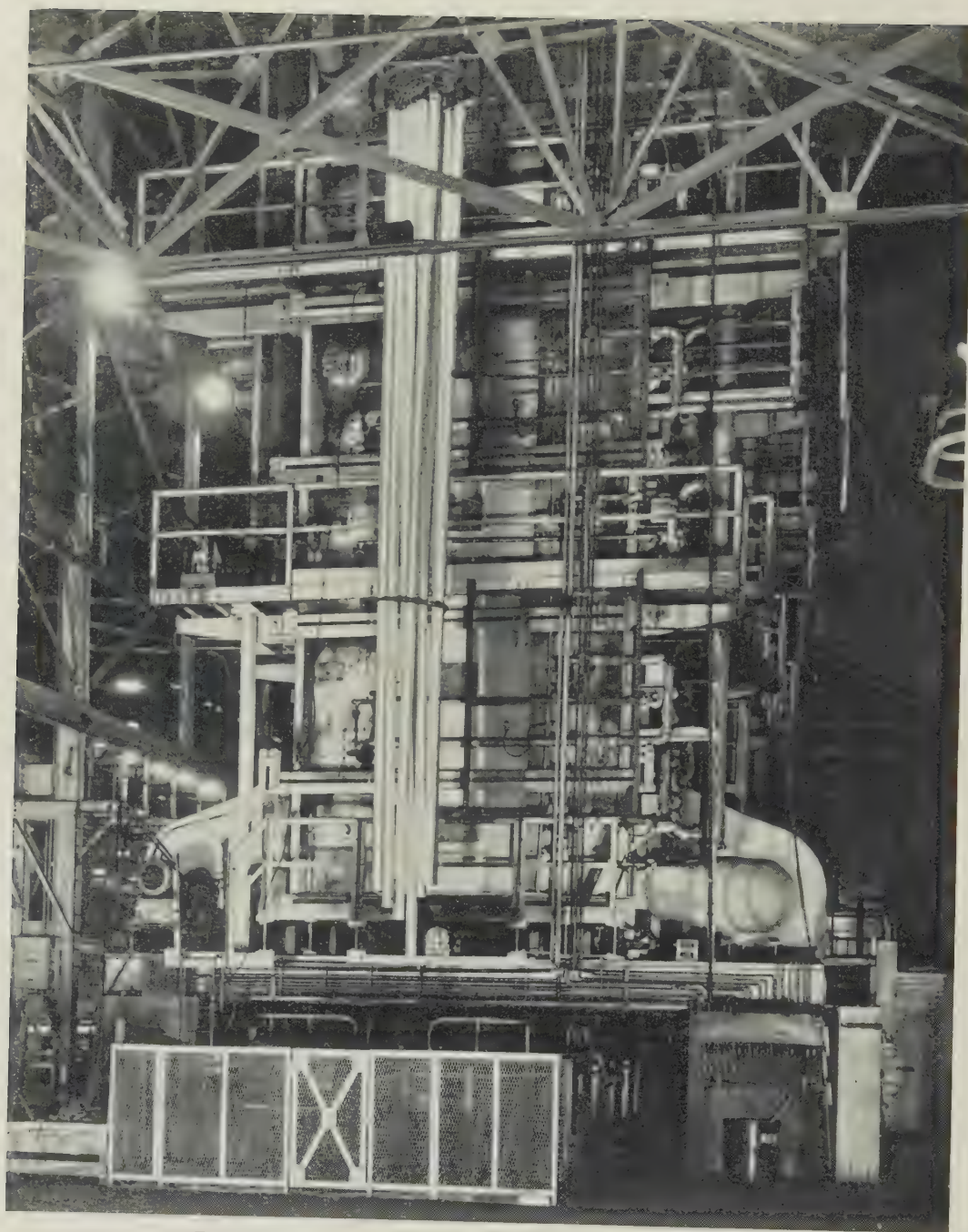


FIG. 6.—Gas-Fired Vertical Furnace with Load of Tubing on Spider.

approximately 3 hr. and the outgoing air in 6 hr., while the load itself, as ascertained by survey couples, requires 9 hr.

*Comments.*—(1) The design of this furnace prevents the easy use of load couples to follow load temperatures. (2) The rate of rise of temperature of the load is less than is desirable for satisfactory control of grain-size. (3) Furnaces of this type require a large amount of floor space. The furnace and its attendant mechanical-charging equipment must be accommodated, together with space for the cooling of treated material, and the formation of the new load.

#### 4. ELECTRICALLY HEATED SALT BATH FOR SOLUTION-TREATMENT OF SHEET

The bath holding the salt is made up of welded 1-in. Armco iron plate, having as usable dimensions a length of 21 ft., a width of 3 ft., and a depth of 6 ft. 6 in. It rests on 2-in. mild-steel I sections, which in turn are supported on 12 in. of insulating brick with a space between filled with slag wool. The sides are insulated by 7 in. of slag wool, supported in a 9-in. wall of firebrick, and the whole is encased by  $\frac{1}{8}$ -in. mild-steel sheet. Hinged along one side is a power-operated lid lagged with slag wool.

A bank of 15 immersion heaters enter from each end of the bath. Each heater is a  $3\frac{1}{4}$ -in. outside dia.,  $\frac{1}{8}$ -in. wall nickel tube encasing flexible resistors spaced with refractory discs. The heaters are supported about 6 in. from the bottom of the bath by nickel "spectacled" plate and protected from above by  $\frac{3}{16}$ -in. perforated Armco iron plate. The electrical input is 420 kW.

Temperature control is automatic, by means of sheathed Chromel/Alumel thermocouples at each end of the bath connecting to a deflection-type galvanometer. The temperature is recorded, using sheathed iron/Constantan thermocouples, again at each end of the bath, and a potentiometric instrument calibrated between 350° and 550° C. and giving approximately 10° C. per  $\frac{5}{8}$ -in. width of chart.

The bath holds 32 tons of synthetic sodium nitrate, and when in full use must be replenished with about 15 cwt. daily. The quench and wash tanks each hold 6000 gallons of water, which is continuously changed by an input of 50 gallons of water a minute to each tank. The cold-water quench and wash tanks may, in fact, be used for two salt baths, by suitably placing them between the salt baths.

Flat sheet is loaded vertically between protective cover sheets on a mild-steel cradle. Coil is loaded with its axis vertical on a flat perforated table. The load carrier is handled by an overhead traversing two-point hoist with a lift of 75 ft./min. and a traverse of 90 ft./min. Before each load is slowly lowered into the molten salt, the bath temperature is adjusted to within 3° C. higher than the nominal temperature required. Wide coils must be reciprocated to assist salt penetration between the laps. The reciprocating mechanism gently moves the load carrier through a vertical distance of  $4\frac{1}{2}$  in.

Upon the immersion of an average load of 800 lb., there is an immediate drop of between 5° and 8° C., which takes 10–15 min. to recover. The operation of the plant is centralized, the push-button controls and temperature control and recording instruments being in a raised pulpit from which a clear view of all operations can be obtained.

Generally, it is the gauge of the sheet being treated that determines the time of immersion. When this time has elapsed the load is lifted, held for 20 sec. above the bath to allow the molten salt to drain back, rapidly traversed, and quenched in the cold water. The entire operation takes about 35 sec. It is gently agitated in the quench water for about 1 min. and transferred to the wash tank for primary washing. The cradle is next unloaded and the sheets washed separately with water having a low content of dissolved solid and finally dried in a warm air blast.

A view of the furnace in operation is given in Fig. 5 (Plate LI).

*Comments.*—As mentioned elsewhere, the salt bath is open to objection on the score of cost, handling difficulties, the hazards associated with the medium of the bath, and so on. Against this must be set the advantages gained from the rapid heating possible on immersion in the nitrate medium. It would be useful if these times of treatments could be still further reduced by more rapid transfer of heat.

#### 5. ELECTRICALLY HEATED, PADDLE-FAN-CIRCULATION, ZONED FURNACE FOR SOLUTION- AND PRECIPITATION-TREATMENT OF EXTRUDED SECTIONS UP TO 70 FT. LONG

The working chamber of this furnace is a cylinder 4 ft. in dia. and 72 ft. long. The cylinder walls are of  $4\frac{1}{2}$ -in. firebrick backed by 9 in. of insulating brick and the whole supported by a  $\frac{1}{8}$ -in. mild-steel case, suitably stiffened. A mild-steel and brick door is provided at one end. The mechanically operated door lifts to open, and when closed is clamped against the furnace end.

Heating is by evenly spaced tape elements set on the firebricks in the furnace wall and divided electrically to give eight independently controlled zones along the length of the furnace. A paddle fan in the roof at the centre of each zone provides the circulation. A Chromel/Alumel couple placed in the centre of each zone automatically controls the temperature of the air before it meets the load. A load couple is provided in each zone in order that a record of the load temperature may be kept. Along the bottom of the furnace chamber is a track which extends to the quench tank. A skip of mild steel is moved mechanically on the track. The furnace operations are press-button controlled, the whole operation of quenching being completed in 20 sec.

For solution-treatment, the furnace is stabilized at the required temperature with all controllers on the same setting. The load is lifted mechanically on to the skip by means of padded slings and tied roughly in position by means of aluminium wire. The load is



then run into the furnace and the couples are lowered through the roof until they touch the load.

After the material has received its requisite soaking at temperature, the couples are lifted and the load brought out and quenched. It is necessary that the section remains in the quench water sufficiently long to be cooled down to 30°–40° C. For precipitation-treatment the load is so arranged as to assist vertical and transverse air flow. The maximum loads for the furnace are 1200 lb. for the solution-treatment of sections up to  $\frac{1}{2}$  in. thick, rising to 3500 lb. The maximum load for precipitation-treatment is 7000 lb.

*Comments.*—(1) Temperature is easily controlled in a furnace of this type, but, as may be expected with an air furnace used for treatment of aluminium alloy sections, the rate of heat transfer is slow. With a load of 3000 lb. solution-treatment may take about  $2\frac{1}{2}$  hr., which represents 60% of the working time of the furnace. (2) With this particular type of furnace, the skip, when resting on the quenching mechanism is approximately at shoulder height, which is inconvenient for handling purposes. (3) As is usual with horizontal furnaces, material which is solution-treated may be kinked by inadequate support.

#### 6. PRODUCER-GAS-FIRED, MUFFLE-TYPE, END-FLOW, VERTICAL FURNACE FOR SOLUTION-TREATMENT OF TUBING AND EXTRUSIONS

This furnace is heated by the circulation of the products of combustion of producer gas round the outside of an alloy-steel corrugated muffle. These are then exhausted before being passed back to the burner flues to be mixed with hot burner gases.

All the ducts and passages for the products of combustion are built in firebrick, and the whole is braced and supported by mild-steel casings and girder work. The furnace has 24 burners divided into six zones. Thermocouples are inserted in the recirculation flues at the point where the hot gas from each burner mixes with the recirculating gases. By this means the heating may be adjusted so to be as uniform as possible over the four burners within any zone. By suitable connections the temperatures of the four burners within the zone are averaged for automatic control of the gas and air supply to each zone.

The muffle is roughly a vertical tube closed at the top and with a door at the bottom. Inside the muffle, and running almost end to end, is a tubular baffle. This load chamber is approximately 30 ft. long  $\times$  3 ft. 6 in. in dia. A screw-type fan at the top of the furnace provides the end-flow circulation within the working chamber, and the direction of circulation is reversed automatically every 6 min. The quench tank is supported on a movable carriage in a pit below the furnace. The tank, of 4000 gallons capacity, has a water inlet at the bottom and overflows at the top.

To load the furnace, sections suitably drilled are shackled to the load carrier, which is supported on the movable carriage. Light sections can be handed down the pit and fixed to the load carrier by hand,

but heavy sections must be handled by mechanical appliances. To minimize heat-treatment blistering, large sections are painted with creosote before loading; with thin section a small pan of creosote is placed on top of the load carrier. The size of load varies with the shape and size of the section being treated from approximately 300 to 3000 lb.

After loading is completed, the carriage is moved to bring the load directly under the furnace chamber, where it is lifted into the furnace by means of three wrought-iron chains which pass through the top of the furnace. The door is mechanically closed against a sand seal. Thermocouples are inserted at the top and bottom of the furnace and from the side to register the temperature of the load on a potentiometric recorder.

When the solution-treatment cycle is finished, the quench tank is moved under the furnace opening and the furnace charge lowered quickly into it. An adequate flow of water must be maintained throughout the quenching cycle in order that the hot water at the top shall rapidly overflow. This is helped to some extent by displacement due to the load. After quenching, the quench tank is moved to the side of the furnace to facilitate the removal of the load by mechanical means. The load is usually held suspended for some little time in order that the water may drain away.

A view of the furnace is given in Fig. 6 (Plate LII).

*Comments.*—(1) The product from this type of furnace is free from the kinks imparted by supports in the horizontal furnace, but nevertheless there is a certain amount of distortion when quenching sections of unequal dimensions. The loading and unloading of this furnace are more laborious than for a horizontal furnace, though the method of suspension ensures adequate spacing. (2) The producer gas supplied to this furnace is water washed, but careful attention to valves and pipes is necessary. Even with the greatest care, conditions may lead to temporary manual control. (3) The control of the furnace necessitates considerable skill on the part of the operator, since the recirculated products of combustion are controlled at temperatures of the order of 700° C. to produce muffle temperatures of the order of 500° C. (4) This furnace takes about 24 hr. to heat up from cold to working temperatures and approximately 3 hr. to cool from 510° to 465° C., and 4 hr. for the reverse heating cycle.

#### 7. ELECTRICALLY HEATED, END-FLOW AIR FURNACE FOR PRECIPITATION-TREATMENT OF EXTRUSIONS, SHEET, AND TUBING

The main structure of this furnace consists of two concentric mild-steel tubes, 8 ft. 6 in. and 10 ft. in dia., and 25 ft. long, the whole of the space between the two cylinders being packed with insulating brick. Inside this structure is a mild-steel baffle, 7 ft. in dia., and reaching almost the complete length of the furnace. A large centrifugal fan at the back end of the furnace draws the air from the working chamber

and forces it over the electrically heated elements, which are hung in the 9-in. annular space. The air re-enters the load chamber at the front end of the furnace. The maximum electrical input is 300 kW., but this is reduced to 100 kW. as the nominal temperature is approached.

The heating is controlled automatically by a thermocouple placed at the point where the air stream leaves the electrical-heating elements. Load couples are provided to be inserted into the load at both ends of the furnace.

For extrusions, a "Christmas-tree" type of load carrier is provided, and for flat sheet a double tier of flat trays is used. Flat sheet loads are spaced in layers approximately  $\frac{3}{4}$  in. thick, by means of asbestos rope or extruded sections, to leave longitudinal air passages. The maximum load of sheet is 8000 lb. With such a load the furnace regains nominal temperature in approximately 2 hr., while the time the load requires to reach nominal temperature is approximately 7 hr. With extrusions, the load reaches temperature quicker than with sheet, owing to the greater surface area exposed.

The furnace is also suitable for the annealing of extruded sections and tubes, it being easy to arrange controlled slow cooling by switching off the heating, keeping the air circulating, and slightly lifting the door.

*Comments.*—This furnace gives extremely good temperature control. There is, however, a big difference between the time at which the material at the front end and that at the back end of the furnace reaches the nominal treatment temperature. In the case of thin extrusions this may be of the order of 1 or  $1\frac{1}{2}$  hr., while in the case of sheet it is of the order of 2–3 hr.

## VI.—CRITICISM OF CURRENT BATCH-FURNACE DESIGNS

In setting forth criticism of present batch furnaces, comments have been limited to those installed over the past ten years. Admittedly war-time exigencies resulted in the acceptance of much equipment that would not have been used under normal conditions. Furthermore, criticism must be tempered with the observation that in the last decade or two many changes have taken place in production techniques (particularly the advent of large strip mills), which have made much more exacting demands upon existing furnace designs.

(1) One of the most common complaints against the present air furnaces has been that their thermal input and rate of air circulation are too low. Of course, these two factors go hand in hand, high thermal input necessitating rapid air circulation to effect rapid heat transfer and to avoid deterioration of the heating elements. However, when high temperatures have been used, such as for the preheating of aluminium alloys, particularly those containing manganese, they have often resulted in rapid deterioration of the

constructional steelwork of the furnace. This emphasizes the complaint that present furnaces are not, in general, built for high enough temperatures.

(2) Another point which seems often to have been overlooked, both by designers and operators, is that one of the principal factors in the cost of thermal treatments is loading and unloading. Many installations require expensive manual loading, which also introduces the possibility of scratching and surface abrasion. For this reason, the aim should be to design furnaces to accommodate the racks or trays which can be used for conveying the material through the mill.

(3) Although the time lost in maintenance of furnaces is not usually very great, insufficient attention has been paid to minimizing it. For example, with the notable exception of those furnaces with modern panel-type heating units, it is necessary in most cases to shut down a furnace to replace a damaged heating element, while repairs to insulation usually necessitate a major shut-down. In addition, air and gas passages are not usually accessible for inspection.

(4) Many furnaces have also been installed without adequate provision for purging to remove the fumes from the combustion and vaporizing of the rolling or drawing lubricant, and this has contributed to the explosion hazard.

(5) A lesser complaint is that many furnaces suffer excessive heat loss through the doors, which leads to lack of temperature uniformity throughout the load. It would appear that additional elements or improved insulation should be provided for in this part of the furnace.

(6) A very small point is that the direction of rotation of fans is often not clearly indicated.

(7) A general criticism of gas-fired furnaces is that if heat-exchangers are not used the products of combustion cause serious staining of the material. In addition, heat-exchangers generally make for lower thermal efficiency, and many furnaces show considerable temperature variation owing to radiation effect. Maintenance of automatic controls on such furnaces usually proves to be expensive.

(8) In spite of the relatively high cost of electricity, experience with this medium has generally been the most favourable. However, the common practice of locating elements within the heating chamber means that to effect repairs the furnace must be shut down. In other designs, the adjustment of the ports to regulate heat distribution also frequently necessitates shutting down and cooling the furnace.

(9) Solution-treatment furnaces, in particular, provide considerable scope for improvement. In North America some excellent vertical types for sheet and extrusions were developed some years ago, the former permitting quenching times of as little as 4 sec. Loads of several tons are accommodated. However, the furnaces are generally unsuitable for coiled material in the clad form, since it is not possible to bring up the temperature quickly enough to prevent diffusion of the alloying constituents into the liner



plates. Vertical furnaces for extrusions, while causing a minimum of distortion and allowing very rapid quenching, are usually difficult to load efficiently. In most air furnaces, clamping and racking devices are clumsy. On the other hand, air furnaces of the horizontal type are usually less satisfactory for sheet or extruded or drawn products. Not only do they distort complex sections, but also the quenching periods are apt to be excessive.

(10) The shortcomings of salt baths have already been discussed at length, though it may be repeated that they are generally expensive to operate at part capacity, as is often the case in peace-time. Furthermore, while the initial cost of such furnaces is low, the need for setting them up in a separate building to minimize the danger of explosions, and to keep the nitrate powder out of the works (to avoid corrosion of steelwork and damage to work in process), usually means the total cost is high. Costs of transport into a separate department should also not be ignored. Further complaints include the low capacity of salt baths and the slow quenching period that is necessary if nitrate consumption is to be reasonable, and the tendency of the nitrate to stain the sheet.

## VII.—FUTURE TRENDS

It is likely that the trend in the immediate future will be towards large annealing furnaces (to match large rolling mills), accommodating large loads of heavy coiled material.

It is difficult to predict whether the "box type" or the semi-continuous "tunnel" type will ultimately prove the more desirable, but in either case the trend will be to pass the material through the furnace on the same racks as are used for conveying it throughout the works.

The vertical type of heat-treating furnace will probably gain favour, and for extruded or drawn products lengths of 50–60 ft. will be required, since it is desirable to heat-treat and stretch sections in the maximum length which can be extruded.

Thermal input will be considerably greater than at present, and the rate of air circulation will be increased. Obviously, with rising costs of fuel, high thermal efficiency will be of paramount importance.

Probably many furnaces will have to be fitted with means for controlling the atmosphere in view of the increasing use of alloys containing magnesium.

There is no doubt that in the future greater use will be made of furnaces incorporating separate heating units and working areas. This will permit the use of gas, electricity, or solid fuel as the heating

medium, and, by the use of efficient heat-exchangers, render possible a controlled atmosphere in the working chamber. A further development may be the use of one heating unit with two or more working chambers for example, so that one chamber can be used for heating while the second chamber is being slowly cooled and a third is being charged ready for heating. Possibly some form of recuperation can be incorporated in such a design.

Many of the shortcomings listed previously will probably be overcome, and some furnaces will be designed for working temperatures of up to 650° C. (which involves the use of alloy steels). Presumably provision will be made for repairing the heating elements without cooling down the entire furnace, while methods for quickly replacing sections of defective insulation will be evolved.

It is conceivable that for certain operations, such as heating up hubs for propellor blades for upsetting, small high-powered induction furnaces will play an increasingly important part.

Finally, some comment may not be out of place on the effect of development of other methods of thermal treatment upon the batch treatments dealt with in this paper.

Most fabricators are studying with considerable interest proposals for the thermal treatment of large coils of strip and wire by induction or internal-resistance methods. The obvious advantages of these methods of heating, for example, for the annealing of strip, lie in the increased efficiency in the use of electricity and some aspects of handling and simplification of equipment. The use of coils instead of the present practice of cutting up into sheets is attractive. It is also conceivable that by annealing in this way it would be possible to eliminate the need for long pre-heats on continuously cast ingots.

The adoption of such processes would inevitably modify the demand for thermal treatments by the older methods and consequently eliminate the need for some of the improvements outlined in this paper. It is certain, however, that such new processes are not likely to be immediately available, and there is still plenty of scope for improvement of the batch furnace.

## ACKNOWLEDGEMENTS

The author wishes to thank the Northern Aluminium Co., Ltd., for permission to publish this paper, and acknowledges the help afforded by his associates in Aluminium Laboratories Limited, and Northern Aluminium Co., Ltd., in obtaining material for its preparation.

By R. T. STAPLES,† MEMBER

## SYNOPSIS

Results obtained from treatments carried out on light alloys in a flash-annealing furnace show that a wide range of thermal treatments can be successfully accomplished, and the view is expressed that such furnaces represent an advance in technique over the batch-treatment type.

The theoretical case in favour of employing high rates of heating to secure a fine grain-size on recrystallization is briefly presented and supported by evidence obtained in industrial practice. The practical desirability of fine grain-size is related to the needs of sheet producers and users.

From technological and metallurgical considerations unit cross-section thermal treatment is to be recommended. The factors governing the design of a single-sheet, conveyor-type furnace are reviewed and performance data reported.

## I.—INTRODUCTION

NEITHER in principle nor in practice is flash annealing new. Its application to light alloys as a fully developed process has, however, taken place only in the last few years. Only two specially designed flash-annealing furnaces have been described in the British technical literature.<sup>1, 2</sup> A schematic drawing of one of them is shown in Fig. 1, and a photograph in Fig. 6

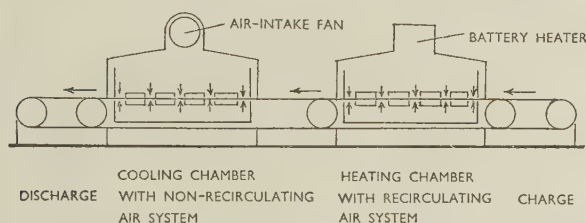


Fig. 1.—Schematic Drawing of Single-Sheet, Conveyor-Type Flash-Anneal Furnace (cf. Fig. 6, Plate LIII).

(Plate LIII). Such a recent development probably indicates that the need for flash-annealing furnaces is not a primary one, but arises from the technical requirements of large-scale production, and to meet specialized demands now being dealt with in sufficient volume to justify separate equipment.

The case for flash annealing has been well set out in the paper by Thomas and Fowler.<sup>3</sup> The general problem which it is designed to meet arises out of the imperfect success attending the recrystallization annealing of large coils and large masses of cut sheet in the sizes now typical of production. The essential limitations of the older design of equipment are :

- (i) Imperfect grain-size control.
- (ii) Occurrence of annealing stains.
- (iii) Unsuitability for the exploitation of the recovery effect.

- (iv) Non-availability of continuous-heat-treatment equipment to make possible the treatment of coils of unit weight of about 1 ton.

The particular case dealt with in the present paper is that of single-sheet treatment by means of a conveyor-type furnace. In some degree, the single-sheet furnace may be regarded as a pilot plant for the continuous strip furnace, but in addition it meets a separate production requirement, as the shearing of sheet or the blanking of circles in the soft condition is not normally regarded as a satisfactory production technique. In consequence, continuous-strip annealing cannot be employed when the final product has to be supplied annealed.

The widespread use of aluminium and its alloys has brought with it not only an appreciation of the versatile performance of the metal, but also a clear understanding of its limitations. In sheet form, the outstanding demand has been for uniform fine-grained material, consistent in all batches. The practical requirements have been reproducible performance when work in press or drawing tools has to be undertaken, and maximum economy in the final finishing operations. While the attainment of a good surface is a more subtle matter than the simple avoidance of the "orange-peel effect" associated with coarse grain, a minimum grain-size is essential. Producer and consumer needs have thus led to a common demand for furnaces capable of producing in bulk uniformly fine-grained material.

## II.—BASIC METALLURGICAL CONCEPTS

## 1. PRODUCTION OF FINE GRAIN-SIZE

The general relationship<sup>4</sup> between degree of plastic strain and grain-size after recrystallization of a wrought material, is well known. Though capable of simple application to sheet-rolling practice, this is

\* Manuscript received 29 October 1951. Contribution to a Symposium on "Equipment for the Thermal Treatment of Non-Ferrous Metals and Alloys", to be held in London on

26 March 1952.

† Production Metallurgist, T.I. Aluminium, Ltd., Birmingham.



inadequate in itself to permit of the consistent production of a fine grain or to explain the multiplicity of effects encountered in bulk production.

Petersen <sup>5</sup> lays down the following conditions as favourable to the formation of a fine grain-size on recrystallization :

- (1) An annealing temperature as high as possible, with correspondingly reduced annealing time.
- (2) Highest possible rate of heating.
- (3) A method of deformation as inhomogeneous as possible, but not too non-uniform throughout the section (drawing in dies is better than unrestricted elongation).
- (4) Lowest possible cold-working temperature.
- (5) Highest possible working temperature for the preceding hot working.
- (6) Highest possible rate of deformation.
- (7) Choice of suitable alloying elements (generally very small additions are adequate).
- (8) An initial structure with a medium grain-size.
- (9) Previous strengthening by cold working is permissible, if the final deformation is thereby further removed from the critical degree of deformation.
- (10) Recrystallization as soon as possible after cold working.

In this list small importance is attached to the influence of cold work. In sheet practice this low rating does not apply, but it should be noted that the attention which cold working has received is due to the fact that, together with factors (1) and (2), it is readily controlled, as opposed to the other items, the individual effects of which are less readily apparent in industrial practice.

One factor omitted from the above list is of considerable industrial importance and, in certain cases, can be a dominant one, namely, the necessity for obtaining a homogeneous state if any uniform response on recrystallization is to be expected. In recent years this has assumed greater importance owing to the widespread use of the direct-cooling casting method. While this provides material of generally uniform composition without gross segregation effects, the high rate of cooling leads to the phase states being more remote from equilibrium than was the case with older methods.

The significance of the phase state has been clearly set out by Beck, Holzworth, and Sperry <sup>6</sup> and is discussed in Section IV.

In the annealing process itself, the only permissible variables are the rate of heating, the annealing temperature, and the time at temperature, all other factors being predetermined. Economic considerations dictate that the rate of heating should be as high, the annealing temperature as low, and the soaking time as short as possible. In practice the conditions adopted will be a compromise between technological possibility and metallurgical necessity.

The latter, as the controlling factor, will be discussed first.

## 2. PRINCIPLES OF RECRYSTALLIZATION

The individual stages encountered in full recrystallization may be distinguished as induction, nucleation, grain growth, coalescence, and secondary recrystallization. These are seldom dealt with independently in commercial practice, and the less specific terms recovery, recrystallization, and grain growth are more appropriate to large-scale annealing. It is valuable, however, in examining a new process to study the implications of the separate stages shown to exist by detailed study. In this connection no paper is more helpful than that of Anderson and Mehl,<sup>7</sup> from which the following data have been extracted.

### (a) Induction

For pure aluminium (Si 0.01, Fe 0.03, Cu 0.01%, Ti nil) sheet 0.125 in. thick, the induction times quoted in Table I and grain-sizes given in Table II were found. The onset of recrystallization was determined by microscopical examination.

TABLE I.—*Variation of Induction Period of Recrystallization of 0.125-in. Aluminium Sheet with Deformation and Temperature (Anderson and Mehl<sup>7</sup>).*

Elongation, %	Induction Period, min.			
	310° C.	325° C.	350° C.	370° C.
5	1750	550	41.6	1.6
10	416	130	16.6	4.5
15	...	...	...	1.0

TABLE II.—*Effects of Temperature and Deformation on Final Grain-Size in 0.125-in. Recrystallized Aluminium Sheet (Anderson and Mehl<sup>7</sup>).*

Temp., °C.	No. of Grains/cm. <sup>2</sup>		
	5% Elongation	10% Elongation	15% Elongation
310	145	345	...
325	305	575	1330
350	400	530	1090
370	550	755	815

Table I indicates that the induction period is critically sensitive to temperature and degree of plastic strain, and if the required minimum period is to be assured, then heavy plastic strain and a high temperature must be employed. The presence of a high degree of plastic strain may be taken for granted in most sheet-rolling practice; hence choice is limited to temperature. The influence of temperature on the other aspects of recrystallization is considered below.

### (b) Nucleation and Grain Growth

It has been demonstrated<sup>7</sup> that, for normal industrial conditions, both nucleation and grain growth increase exponentially with temperature, but

nucleation increases the more rapidly with increasing cold work, and whereas grain growth reaches a limiting value at about 15% deformation, nucleation continues to increase with degree of deformation. In relation to time, nucleation initially increases, reaches a maximum, and then declines; whereas grain growth is invariable. To achieve the minimum grain-size it is clear that the highest possible temperature must be employed. This ensures maximum nuclei formation and so avoids the necessity of allowing significant time for grain growth.

### (c) Coalescence

The relationships described above do not by definition include coalescence, which is the growth of grains after recrystallization. As the movement is towards a state of minimum stress, it is a much more complex phenomenon than simple grain growth, and on external evidence requires protracted times to reach completion, even at high temperature.

Whilst it is known that the recrystallized and final grain-sizes in aluminium do not differ markedly, the importance of the difference in the two states is not clearly defined. From practical experience there is no evidence to indicate that the recrystallized structure differs in performance from the final structure, if no size-factor is present. Nor is there evidence to suggest that the more fully coalesced structures obtained after a low-temperature batch anneal are in any way superior to similar structures obtained after high-temperature flash annealing, which gives recrystallization with little coalescence. Were this not the case, and had time to be allowed for a fully stress-free structure to be developed, the design of any flash-annealing furnace would need to be modified. The compromise in practice is to use the maximum temperature feasible. The total time to be allowed for grain growth and coalescence is discussed in Section III.

### (d) Discussion of Theoretical Concepts

On all counts a high annealing temperature is to be preferred, and if grain growth is not to be allowed to occur on an extensive scale, minimum time at temperature is essential. The highest possible rate of heating is also desirable. Sufficient time must, however, be allowed for grain growth to take place, and as

TABLE III.—Grain-Sizes for Flash-Annealed Aluminium (99.4%) Sheet.

Gauge, in.	Cold Work, %	No. of Grains/in. <sup>2</sup> *	Ratio of Grain Radii	Ratio of Sheet Thickness
0.032	30.5	320,000	1.0	1.0
0.064	30.75	160,000	1.42	2.0
0.092	27.5	110,000	1.72	2.88
0.128	30.5	80,000	2.0	4.0

\* Approx.

this is a fixed rate with time it may be related to grain-size and, hence, in some degree to sheet thickness (see Table III). Practical experience shows that an

unspecified lapse of time at temperature may also be required, sufficient to permit some measure of coalescence to occur.

## III.—TEMPERATURE OF ANNEALING IN PRACTICE

### 1. EFFECT ON GRAIN-SIZE

From the theory discussed above it would appear that, considered by itself, the temperature at which recrystallization occurs is not important in relation to final grain-size. In works' procedure, however, this is apparently not the case. A temperature in excess of the critical temperature is adopted so as to give the optimum result for the conditions employed, having regard to the final purpose for which the material is destined. The occurrence of an apparent optimum is to be explained by the combined effects of grain growth and nucleation in relation to a time interval fixed by such factors as thermal-exchange efficiency and load: furnace-rating ratio. As any increase in temperature, if the physical conditions are fixed, of necessity leads to a protracted time interval, no desirable alteration in nucleation: grain-growth ratio occurs, and a greater opportunity is afforded for growth to occur. Hence, in works' practice it is common to find that higher temperatures of working tend to be associated with larger grain-sizes. In fact,

TABLE IV.—Effect of Temperature of Annealing on Grain-Size of Cold-Worked Aluminium Sheet (Chevigny<sup>8</sup>).

Material	Grain-Size, $\mu$					
	250° C.	300° C.	350° C.	550° C.	600° C.	630° C.
Super-pure aluminium	B.R.	45	55	1000	1700	2000 *
99.5% aluminium	N.R.	45	60	70	69 *	80 *
99.0% aluminium	N.R.	32	48	70	62	105 *

B.R. = Beginning of recrystallization.

N.R. = Not recrystallized.

\* Occasional very large crystals.

many reported data exhibit this effect, but as in most cases works-scale thermal cycles have been deliberately reproduced in the paper, the results must be regarded as empirical only and not as a clear guide to the temperature to be employed in such a different process as flash annealing.

A recent study<sup>8</sup> shows the relationship between annealing temperature and grain-size for sheet treated in batches (Table IV). The values quoted are selected on account of the wide range of temperatures explored and the fact that the influence of impurities is apparent.

A response of this type may be expected for any non-heat-treatable alloy. For heat-treatable materials there is not the same freedom of choice of temperature, owing to the onset of solution effects before the completion of softening due to recrystallization. If complete softening is to be accomplished, then protracted slow cooling must be given to reprecipitate all the alloying constituents taken into



solution at the recrystallization temperature adopted. The slow rate of cooling necessary to achieve full precipitation may be regarded as an index of the rate of solution of the soluble elements. It follows that, if recrystallization, which is completed in a short space of time at the working temperature, can be accomplished without previous prolonged treatment at lower temperatures, then solution effects will be reduced proportionately. The necessity for slow cooling will thus be reduced, and rapid air cooling, such as is adopted in flash annealing, becomes a possibility.

## 2. INFLUENCE OF TEMPERATURE ON CRYSTAL FORM

While specific evidence is lacking of the practical significance of crystal form, it is reported that in the recrystallization of heavily cold-worked material the grains formed at low temperatures have an oblate spheroidal form with a high major to minor axis ratio; but that as the temperature is increased, a nearer approach to a sphere is obtained. This effect is stated to be independent of coalescence. In the absence of confirmatory evidence, the spherical type of grain would appear to be the more desirable.

## 3. EFFECT OF RATE OF HEATING

It has been seen that of the variables at the annealing-treatment stage, rate of heating is that to which grain-size is most directly related. This has been long appreciated, and such devices as reduction of load weights, use of superheat, high power rating of electrically heated furnaces, and load spacing have all been employed, wherever considerations of quality over-ruled the economy of heating in large loads.

These trends towards perfect batch treatment have culminated in the equipment for the solution-treatment of the alloys of the aluminium-copper-magnesium type in sheet and coiled-strip form, but despite intensive efforts economic advantages have only been achieved at some loss in quality as compared with material treated in nitrate salt baths. It seems clear that no form of batch treatment will ever yield material of optimum quality, and the need is apparent for equipment based on unit cross-section treatment on a continuous basis. In Table V a comparison is made of the influence of heating rate on grain-size as

TABLE V.—Effect of Rate of Heating on Grain-Size Produced in Salt Baths and Air Furnaces.

Material	Cold Work, %	Salt Bath Grain-Size, mm.	Air Furnace Grain-Size, mm.	Ref. No.
99.5% Aluminium	...	0.03	0.04	9
Aluminium + 1% Mg <sub>2</sub> Si	5 75	0.20 0.062	0.45 0.12	10
Aluminium + Mg + Si	...	0.2	2-5	11

produced in air furnaces and salt baths. No actual heating rates are quoted, but it may be assumed that whereas the salt-bath treatment gives a rate of the order of 60° C./sec., a typical air-furnace treatment will give 1-6° C./min., a mean ratio of 1 : 1000. The results vary.

When treating aluminium-copper-magnesium alloys<sup>12</sup> in the heavily cold-worked state (50-70% reduction) (see Fig. 2), it has been found that the rate

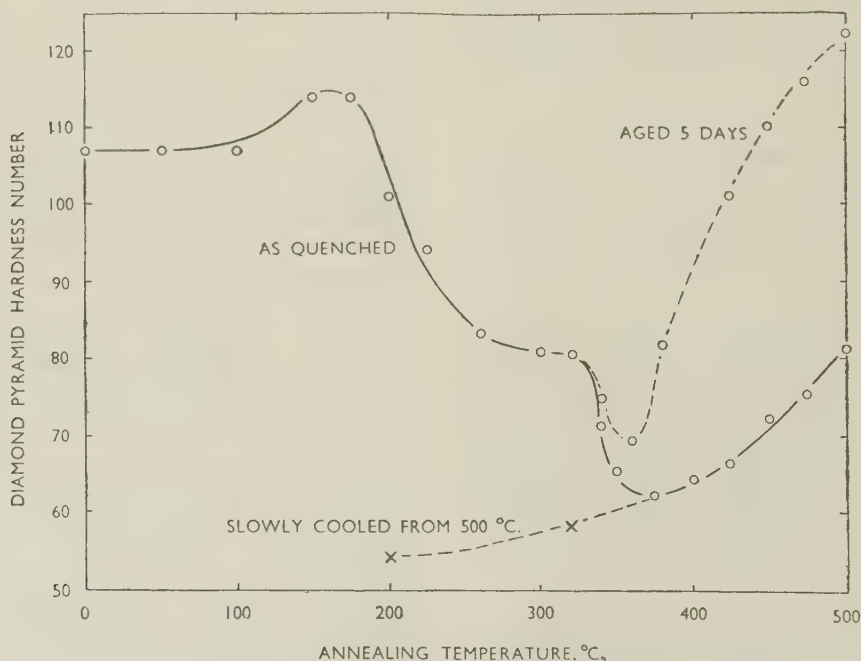


FIG. 2.—Annealing Curve of Al-Cu-Mg Alloy Strip After 50% Cold Rolling. (Chadwick, Richards, and Summer.<sup>12</sup>)

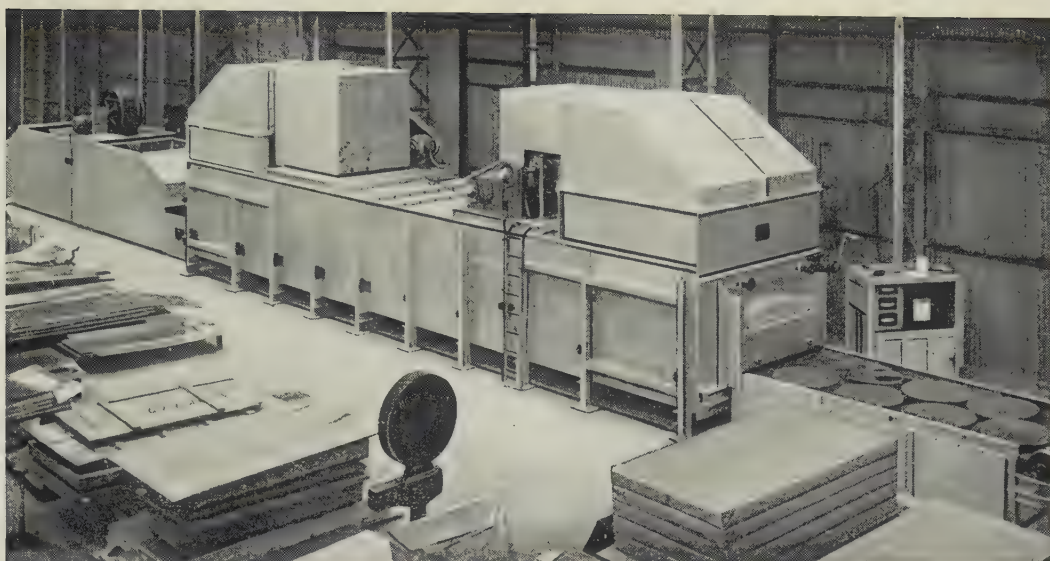


FIG. 6.—Single-Sheet, Conveyor-Type, Flash-Annealing Furnace.

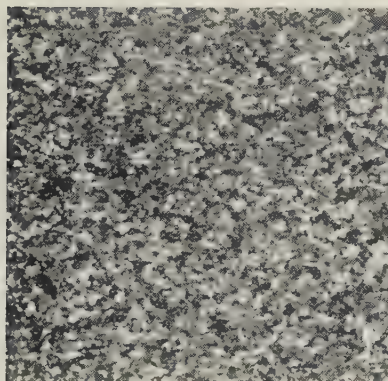


FIG. 7.—Batch Annealed.

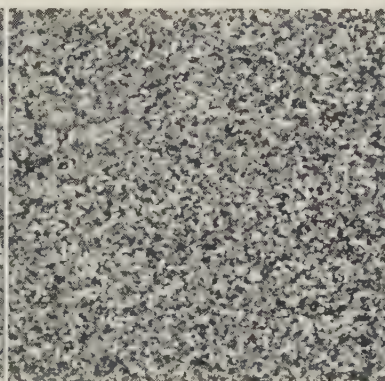


FIG. 8.—Flash Annealed.



FIG. 9.—Salt-Bath Annealed.

FIGS. 7-9.—Photomicrographs of Al-Mg-Si-Mn Sheet Illustrating Effect on Structure of Differences in Rate of Heating. All treatments were carried out at  $450^{\circ}\text{C}$ ., i.e. in the heterogeneous region.  $\times 2$ .

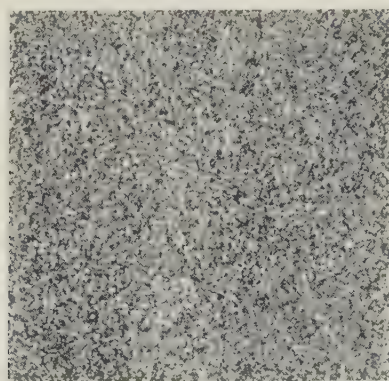
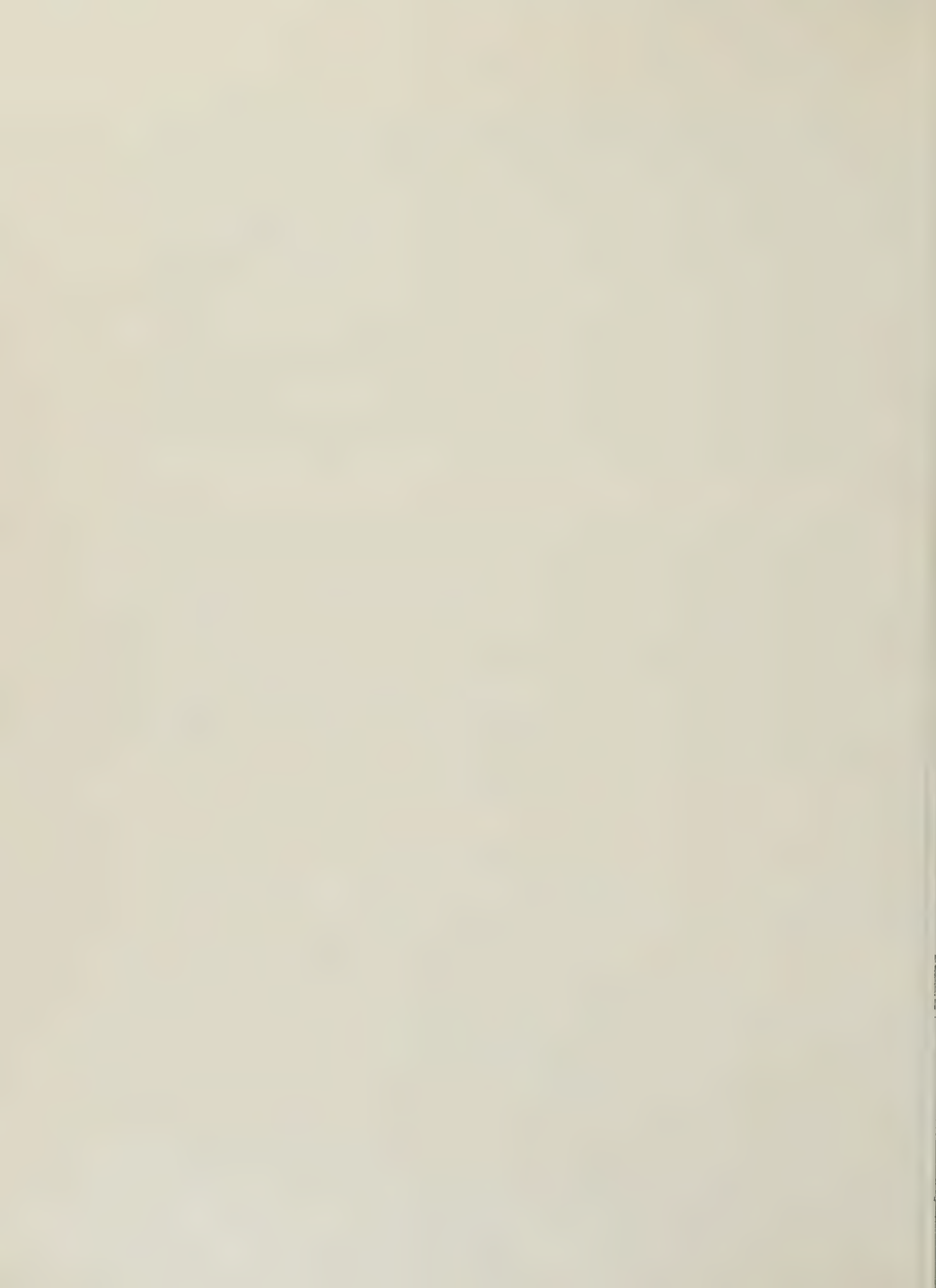


FIG. 10.—Structure of Sheet after Salt-Bath Treatment at  $530^{\circ}\text{C}$ ., i.e. in single-phase field.  $\times 2$ .





of heating was the only significant factor, but that the ratio of grain-sizes typical of the two treatments employed never exceeded 2:1. This confirms the consistent effect of the heating rate, but consideration of the degree of grain refinement achieved leads to the conclusion that attention to this factor is not always justified. The results quoted are from laboratory-scale experiments, or trials in which processes have been adopted of much greater complexity than would normally be feasible in production, and are not thought to represent the conditions obtaining in works' practice. This point is of considerable importance, since, if it were possible to reproduce the quality of slowly heated laboratory specimens, it is doubtful whether any economic justification would exist for the provision of the complex flash-annealing type of furnace. The main reason for variation between laboratory and production tests is considered to be the different degrees of equilibrium existing in the phase states. The choice, then, is between prolonged homogenization of the cast blank and flash annealing of the wrought form. The latter is the cheaper process.

#### IV.—INFLUENCE OF COMPOSITION

##### 1. EFFECT OF PHASE STATE

The most helpful general guide to the effect of composition on the recrystallization process is that covering the response of single-, double-, and heterogeneous-phase systems (Table VI).<sup>10</sup> It has been

TABLE VI.—*The Effect of Composition on the Recrystallized Grain-Size of Aluminium Alloys (Eastwood, Jones, and Bell<sup>10</sup>).*

Composition	Initial Grain Dia., mm.	Rolling Reduction, %	Grain Dia. after 30 min. at 400° C., mm.	
			Slow Heating	Rapid Heating
Single-Phase Alloy				
99.95% Al	0.09	5	0.25	0.25
		75	0.20	0.20
Two-Phase Alloy at Annealing Temp., Single-Phase near Solution Temp.				
Al + 4% Cu	0.016	5	1.0	0.08
		75	0.030	0.02
Heterogeneous Alloys.				
Al + 3% Mn	Not recrystallized	30	A *	C
		75	D	F

\* Very large grain-size, decreasing from A to F.

shown that the heating rate is not critical for single-phase alloys, but is critical for two-phase and heterogeneous alloys. In those cases where the annealing temperature is high enough to take the other phases into solution, the effect of heating rate decreases, although it remains very marked if an insoluble phase persists.

These general effects are common industrial experience, the outstanding case being that of the aluminium-manganese alloy, which invariably yields erratic, coarse-grained structures unless both homogenized by prolonged treatment at 570° C. in the cast state and salt-bath- or flash-annealed at the intermediate and final treatments.

The advantages of recrystallizing as a single phase are frequently attainable, as most of the two-phase and heterogeneous systems belong to the heat-treatable group. Hence, final recrystallization is carried out at the optimum temperature to ensure the maximum degree of solution and fine recrystallization.

In those cases where the soft state of a heat-treatable alloy is required, a real advantage will be gained if the general coarsening associated with multiple phases can be minimized by using a high heating rate right up to the recrystallization temperature from which undesirable heat-treatment effects would result.

#### 2. EFFECTS OF ALLOYING ELEMENTS

Manganese and silicon are outstanding amongst the insoluble and slightly soluble alloying elements of commercial importance; 1% manganese<sup>9, 13</sup> is reported to raise the recrystallization temperature of commercially pure aluminium by 60° C., and silicon<sup>9, 13</sup> depresses the recrystallization temperature by 30° C. These powerful effects offer a partial explanation for the recrystallization of families of crystals much ahead of the remaining portions of the material, when sheet produced from non-homogenized 1% manganese alloy is annealed in the critical range. These families are considered to be the product of the cored cast crystals, the centre of which has a lower alloy content and a lower recrystallization temperature.

#### V.—TECHNOLOGICAL CONSIDERATIONS

##### 1. PAST PRACTICE

The preceding sections have indicated the extent of present knowledge regarding the influence of rate of heating on recrystallization. Its beneficial effect was reported by Röhrig as far back as 1924.<sup>13</sup>

When using convection batch-type furnaces, reduction of load size, spacing of loads, and increasing the air-temperature head have all been tried, but in no case has the near ideal of the salt-bath treatment been approached. The introduction of the nitrate salt-bath made available a method of treatment desirable in all but its economic aspects, and in the absence of bulk demands this method has been commonly used.

For non-heat-treatable alloys a system employing a salt bath as the heating medium might well be adopted, if a suitable method of loading and unloading were to be devised and provision made for salt recovery, washing, and drying facilities. There is, however, no record of the existence of such equipment.

Comparison of the products of the salt-bath and of various batch-anneal processes demonstrates clearly



that unit cross-section treatment must be adopted when using convected air, if the ideal of the salt-treated material is to be approached. The single-sheet, conveyor-type furnace is, then, the logical outcome of a demand for a high-output flash-anneal furnace. The factors governing the selection of the design are discussed below.

## 2. FURNACE-DESIGN FACTORS

### (a) Heating Rates

Data recently published by Mohr<sup>14</sup> include heating rates of unclad aluminium-copper-magnesium alloys immersed in a large air furnace. Table VII shows values read off the published curves. The significance of a degree of superheat is obvious.

TABLE VII.—Time of Heating to 350° C. of 1.2-mm. Sheet Specimens of Unclad Al-Cu-Mg Alloys (Mohr<sup>14</sup>).

Furnace Air Temp., °C.	Superheat, °C.	Approx. Time to Reach 350° C., min.	Heating Rate, °C./sec.
450	100	3.2	1.8
520	170	1.7	3.4
600	250	1.1	5.3
700	350	0.6	9.7

Table VII may be compared with Table VIII, which gives observed heating rates for pure aluminium sheet in a flash-anneal furnace.

TABLE VIII.—Heating Rates of Pure Aluminium Sheet in Flash-Anneal Furnace.

Furnace air temperature 550° C. Sheet 8 ft. × 4 ft. × 0.048 in.

Conveyor Speed, ft./min.	Rate of Heating to 350° C., °C./sec.	Observed Temperature, °C.			Computed Temperature, °C.		
		Middle	Left Edge	Right Edge	Left-Half Mean	Right-Half Mean	Mean Sheet
5.2	3.34	350	430	400	390	375	382½
9.55	4.28	350	390	365	370	357½	363½
14.0	4.02	350	405	380	377½	365	371½
18.3	3.96	350	395	380	372½	365	368½
23.2	4.07	350	390	375	370	362½	366½
27.9	4.42	350	380	380	365	365	365
33.0	4.45	350	390	380	370	365	367½
35.0	4.58	350	390	375	370	362½	366½

The irregularities in the results in Table VIII are due to the fact that the values are for sheet heated on one side only but with air spill at the edges. A value for 550° C. air temperature interpolated from Fig. 3 gives 4° C./sec. for the heating rate which may be compared with the average value of 3.94° C./sec. for the heating rates shown in Table VIII. This is in better agreement than the nominal relative heat-exchange areas suggest.

As the heating rate governs the furnace length, heating on both sides is to be desired on the grounds of minimizing length and achieving uniformity of temperature.

### (b) Use of Superheat

The values in Table VII leave no doubt as to the advantageous increase in rate to be gained by the use of superheat, and as few limitations arise the full range observed may be employed where appropriate in unit cross-section treatment. The permissible extended use of superheat is in direct contrast to batch treatment, where variations in load temperature increase in proportion to the degree of superheat employed, and in consequence a figure higher than 100° C. is seldom adopted, even for non-critical treatments. For critical batch treatment no superheat is possible.

The successful employment of the maximum degree of superheat will depend largely on the heated air being introduced uniformly to all faces where heat transfer may take place. If this is not done, a temperature gradient will exist. In practice, using

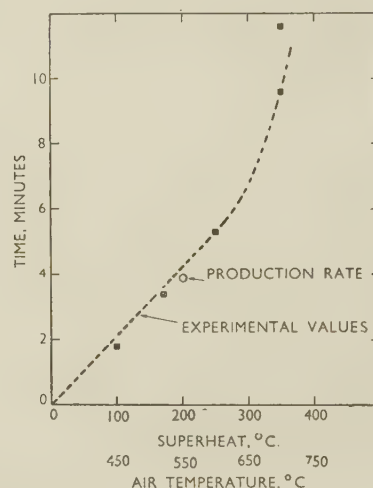


FIG. 3.—Influence of Air Temperature on Heating Rate of Pure Aluminium Sheet.

primarily single-side heating, the grain-size has been found to differ as between the side of the sheet heated directly and the side receiving its heat by conduction. Turbulence at the edges, causing air spill to the lower face, has also led to the edge areas being maintained in a heat balance with a temperature much above that of the centre. It will be seen later that the heat transfer at the surface is nearly constant for all gauges of sheet between 0.028 and 0.128 in.; hence, the edge/centre difference should be relatable to gauge, the values being highest for the thin sheet which has the lowest heat content. In practice, this has not been found to be the case. At speeds below 15 ft./min. conduction appears to be greater than the localized heat intake, and a smaller difference occurs with decreasing speed. Above 15 ft./min. a temperature difference, constant within the limits of experimental error, is recorded for all thicknesses.

Those observations are of significance only in emphasizing the necessity for correct heat introduction

to all faces, if a furnace capable of precision treatment is to be developed.

Fig. 3 shows that with air temperatures above 550° C. a radiation effect is imposed upon the convection effect. To some extent this limits the amount of superheat, because, if the temperature is taken too high, an accidental stoppage might easily lead to the sheet being overheated or even melted, owing to the residual radiant heat in the structure. A temperature of 650° C. appears to be sufficiently high for all requirements, but not so high as to be difficult to handle in design or practice.

### (c) Air Flow

The two furnaces mentioned in Section I are continuous furnaces having a longitudinal air flow. Whilst this simplifies the construction, successful transfer of heat to the load becomes increasingly dependent on the satisfactory development of tur-

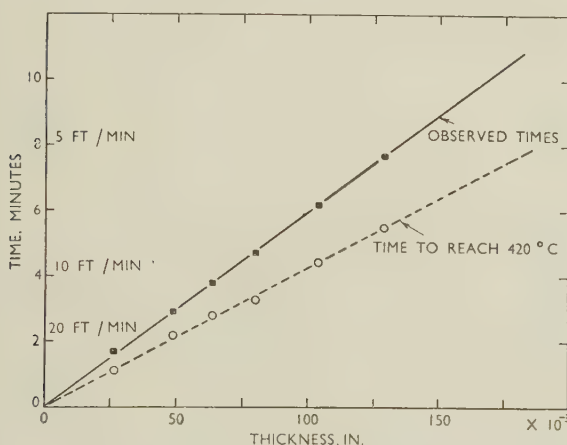


FIG. 4.—Conditions for Annealing Aluminium-14% Manganese Alloy Sheet. Furnace air temperature 550° C.

bulent flow. A strict limit is imposed on the degree of turbulence, as one of the main functions of flash annealing is the treatment of circles, which are lifted if too vigorous or too turbulent a flow is developed; hence, a serious bar to efficient exchange is imposed.

Flow or counter-flow of the air does not appear to be of major significance, considering normal air-flow speeds and conveyor working speed. Transverse flow would achieve the slight advantage of a uniform temperature head along the length of the furnace, but still produces the generally unsatisfactory effect of flow parallel to the sheet face. Multiple-point introduction of the air at 90° to the load, with adjacent off-takes, would appear to give the optimum conditions, the full requirement being a set of inlet points above and below the load. These inlets should be opposed, to counter any lifting affects which the lower jets might exercise.

The need to obtain optimum air-flow conditions is well illustrated in Fig. 4, from which it will be seen that the total time in the furnace for any selected

treatment is closely related to gauge and to no other factor. The values used are determined empirically, guided by metallographic and tensile tests, and confirmed by subsequent pressing trials. If the total time in the furnace is broken down into the two significant stages—time to recrystallization temperature and time above recrystallization temperature—the linear relation is preserved for both stages. The time above recrystallization temperature may be considered in relation to Table III. The linear response further indicates a constant total heat requirement for recrystallization of a unit mass, and also a constant rate of heat transfer, independent of conveyor speed and gauge, which in turn demonstrates clearly that the air/metal-surface relationship is the factor to which design attention must be given. Heating rates double the reported values are obtained if small samples, fully exposed on both sides, are passed through the furnace.

### (d) Conveyor Design and Operation

It has been deduced that conveyor speed is not a critical factor, so that little loss of efficiency or effect on the critical heating rate need be expected if choice of speed is governed by other factors. Two main considerations are output and handling problems. As the first is directly determined by the width and length of the furnace, attention is given here only to the latter.

Circles in sizes ranging from 5 to 15 in. dia. and with thicknesses between 0.022 and 0.040 in. are one of the main products treated in a flash-anneal furnace. As individual handling is involved, the high conveyor speed which the thickness would indicate is impracticable, unless mechanical handling is adopted. This is expensive, and a simpler solution appears to be to use a wide furnace and a low conveyor speed. Such a furnace would still be suitable for sheet annealing.

In all forms of material, damage is to be avoided. With the highly polished finish normal to sheet and circles this is particularly difficult, owing to the rapid loss of strength and hardness with temperature that takes place in aluminium and its alloys. At temperature, even when subjected only to its own weight, polished sheet abrades if any movement relative to the conveyor occurs. Abrasions of this type are important, as not only is the surface appearance impaired but the damage can lead to failure in circles on deep drawing.

For sheet, the furnace width is limited to multiples of the maximum sheet width, and if no other factor intervenes, the conveyor speed should be such that the labour engaged in loading and unloading is steadily employed, while maintaining the furnace working at capacity. The labour factor is the major economic disadvantage of flash annealing, as a charging and discharging team must be employed for each furnace, in contrast to batch-type furnaces where a small team can operate a battery.

If operating conditions are a critical factor in



specifying a furnace, it may be necessary to consider the economics of three-shift as opposed to two- or one-shift working. The structure is large compared with the load, and hence starting costs are high. It might well prove better to work continuously at a low conveyor speed than intermittently at a high speed. The importance of these points must be weighed against the fact that flash-annealing costs are twice as high as those of batch annealing.

If the rate of loading, either mechanically or manually, determines the conveyor speed, it would appear to be a logical development to make this speed the standard for the average thickness to be treated and maintain it as far as possible by utilizing the great flexibility in changing the heating rate obtainable by varying the degree of superheat.

So far, no consideration has been given to cooling. Two factors may operate which will in turn affect the conveyor speed. If air is used, the temperature difference becomes a fixed interval, and so the cooling rate of the thickest material to be treated will decide the length of the cooling chamber. This length has to be considered in relation to the conveyor speed. For the reverse case, where a high rate of cooling is

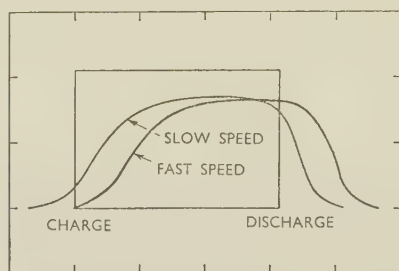


Fig. 5.—Schematic Representation of Influence of Speed on the Relative Position of the Heating Curve.

required, as in quenching from solution-treatment temperature, and where, moreover, the temperature at which quenching effectively takes place is critical, it may be necessary to adopt a conveyor speed to give the effect shown in Fig. 5.

Above a critical minimum speed it appears that the rate of heat loss of the sheet to still, cool air is equal to or less than the heat pick-up from superheated fast-moving air in the furnace, and so the sheet remains at a near-constant temperature for half the length of the sheet (4 ft.). Table IX shows minimum speeds at which this effect operates, the sheet being still-air-quenched only.

In assessing these speeds relative to normal heat-treatment operations, it is usual to attempt to quench a load in less than 15 sec. after removal from the furnace, and the quenching operation is done by a crane having a typical speed of drop of 50 ft./min. These values show that, if desired, quite a good heat-treatment effect can be achieved with existing arrangements, and with further modifications considerable improvements should be possible.

In discussing the conveyor design for this type of furnace it is to be noted that the problem common to

all continuous furnaces, namely that of minimizing heat loss through the conveyor, is exaggerated by the very low density of aluminium, although this is offset to some extent by its high specific heat. The ideal would be a conveyor fully contained in the hot chamber, but this is not entirely practicable, since if a

TABLE IX.—Relation of Conveyor Speed to Sheet Thickness in Controlling Cooling Rate.

Sheet Thickness, in.	Conveyor Speed, ft./min.
0.028	30
0.048	20
0.064	15
0.080	5
0.104	5
0.128	5

transfer of load from a charging conveyor to the main conveyor and then to the discharge conveyor is carried out at temperature, the probability of damage to the heat-softened metal surface is too high to risk. The problem is further complicated by the fact that the size of units for treatment varies from 5-in.-dia. circles to 4-ft.-wide sheets, and the conveyor must be designed for the smaller unit. As complete efficiency is clearly not to be attained with this wide range, the provision of separate furnaces designed for the individual requirements of circles and sheet is desirable wherever production quantities permit.

A more serious question is that of damage. While leather-thong conveyors at each end of the furnace solve the charging and discharging problems, the movement of the metal from the hot-zone conveyors to the cooling-zone conveyors has yet to be perfected. The maximum permissible metal temperature is limited by the success of the conveyor system, and in this respect much study needs to be undertaken by the furnace manufacturers.

#### (e) Heating Source and Method

So far, electricity has been assumed to be the source of heat. This is in accordance with what is almost standard practice in the industry for the annealing of sheet forms. The use of other heat sources is not precluded, but simplicity and accuracy of control make electricity the obvious choice for a furnace where a wide range of load variations can be met with in a short time. Clean air is unchallenged as the transfer medium, since it is non-reactive and readily available.

In view of the very small heat requirement for unit area of the load, it is essential that the heat be uniformly dispersed. To some degree the method of air distribution will ensure this, but uniform heating of the air is a first essential. To achieve this the battery-type heater is preferable to the strip-resistor type. The latter depends on turbulence, an effect which is seldom complete and results in some stratification of the air, with consequent temperature variations. The battery-type heater has, moreover, the advantage

that it relies on convection only, and incidental radiation is avoided. A very high degree of control can thus be maintained, as even with the large air masses essential to provide a constant degree of superheat, the total specific heat in the air is small, and as air temperature is used as the control index the heat input can be regulated to a very fine degree.

#### (f) Temperature Control

Uniformity of load temperature will result from single-sheet loading and the successful design of the furnace to produce even heat distribution. The temperature attained is related to the air temperature and the time of immersion in the heated air, i.e. the conveyor speed. Both are capable of precise control, which in turn permits a similar degree of control of the load temperature, if the other factors are constant. Unfortunately, surface condition plays a large part in determining the heat-transfer rates (see Table X).

TABLE X.—Heat Emissivity of Solid Surfaces of Aluminium. (Black Body = 1.)

Surface Condition	100° F. (38° C.)	500° F. (260° C.)	1000° F. (538° C.)	Ref. No.
Polished . . .	0.04	0.05	0.08	15
Rough . . .	0.072	...	...	...
Oxidized . . .	0.85	...	0.50	16

For this reason the development of the lead-sulphide-cell, low-temperature radiation pyrometer is of particular interest, though its performance is again dependent on surface condition. Despite this limitation, an advance is offered over the existing procedure, where no direct indication is given of any temperature change.

The use of contact pyrometers might be envisaged, but as the main problem is avoidance of damage in the hot state, their employment does not appear to be justified.

In practice there has not been much difficulty in achieving very good consistency, employing indirect control. This applies, however, only when handling stock directly from the rolls, when the sheet surfaces are in prime condition. Stock (oxidized) sheet has been found to give a different response, but this effect has not been fully studied.

From trials, it would appear that no better accuracy than  $\pm 30^\circ$  C. can be assumed. Most of this variation is attributable to surface condition of the sheet, rather than to the equipment. Of the equipment variables it should be emphasized that the conveyor-speed settings must be reproducible to a very high order, if accuracy of temperature is to be maintained.

#### (g) Atmosphere Control

In practice the free escape of oil fumes from the surfaces, rendered possible by single-sheet loading, prevents staining, and the use of a normal atmosphere allows a fully acceptable quality of finish to be achieved. The need for further control is not envisaged.

### 3. APPLICATION

#### (a) General

As stated in the Introduction, the scope of the present paper is limited to single-sheet treatment by means of a conveyor furnace. It should be emphasized that the observations made are valid only for unit cross-section treatment; if even two-deep treatment is attempted, there is wide divergence of temperature in the individual sheets and no economy is effected. Thermally the limits are not close and a great variety of treatments can be carried out, limited only by the time intervals permitted by the conveyor system. In practice, even this has been extended by intermittent working of the conveyor.

#### (b) Recovery

The exploitation of the recovery effect, which involves heating at a temperature below the critical recrystallization temperature, has not yet found wide application, despite the attractive balance of mechanical properties resulting from this type of treatment. In batch annealing it is a prolonged process, as no temperature head is possible owing to the fact that a near approach to the recrystallization temperature must be made and that the consequent probability of locally exceeding the recrystallization temperature has to be avoided.

Only meagre details of practical results have been published, typical values for pure aluminium are reproduced in Table XI.

TABLE XI.—Comparative Elongation Values Produced by Temper Rolling and Letting Down in Aluminium Half-Hard Sheet (Thomas and Fowler<sup>3</sup>).

Temper Rolling		Letting Down	
Mean U.T.S., tons/in. <sup>2</sup>	Elongation, % on 2 in.	Mean U.T.S., tons/in. <sup>2</sup>	Elongation, % on 2 in.
7.3	2.5-7	7.4	17-18
8.2	2-5	8.1	9

In the case of pure aluminium the relative economy of full annealing and temper rolling, as opposed to hard rolling and letting down, is in doubt; although in the case of very thin sheet, the letting-down process permits the development of tempers not readily achieved by rolling. The delicate heat balance of the flash-annealing furnace makes it ideal for the accomplishment of such treatments at an economic rate.

Particular attention has been devoted to the recovery effect as a means of overcoming the difficulties found in flattening sheets of the aluminium-magnesium-manganese alloy type. This group of alloys responds very rapidly to cold working and develops low proof-stress: U.T.S. ratios, so that there is a very small plastic range available for the flattening operation to be made effective. With air temperatures between  $300^\circ$  and  $500^\circ$  C. and conveyor speeds between 10 and 40 ft./min., the recovery effect



has been fully utilized to increase the plastic range to a controlled degree.

Results of laboratory tests designed to explore the feasibility of employing short-time treatments to accomplish this effect are given in Table XII. Blanked and prepared sheet specimens were immersed

TABLE XII.—Results of Short-Time Heat-Treatments on Aluminium and Aluminium Alloys.

Treatment Temperature, °C.	0.1% Proof Stress, tons/in. <sup>2</sup>	U.T.S., tons/in. <sup>2</sup>	Elongation, % on 2 in.	Vickers Pyramid Hardness Number
<i>Commercially Pure Aluminium (99.5%)</i>				
As rolled	6.65	8.0	5.0	37.1
180	6.35	7.55	6.0	36.1
200	6.25	7.65	8.0	37.1
240	5.87	7.25	9.0	34.7
280	5.6	7.1	10.0	34.4
320	4.73	6.5	16.0	31.9
<i>Aluminium-1.25% Manganese Alloy</i>				
As rolled	9.5	11.2	11.0	52.2
200	8.65	11.1	9.0	51.3
240	8.55	10.9	10.0	50.9
280	8.45	10.7	13.0	49.9
320	8.1	10.2	14.0	49.9
<i>Aluminium-2.5% Magnesium Alloy</i>				
As rolled	15.4	16.8	4.0	83.2
180	12.9	16.2	6.0	76.1
200	12.15	15.6	8.0	74.9
240	12.3	15.5	8.0	76.1
280	12.4	15.1	7.0	76.6
320	11.65	14.8	8.0	74.0

TABLE XIII.—Results Obtained from Production Treatments on Aluminium-2.5% Magnesium Alloy Sheet, 0.064 in. Thick.

Furnace air temperature 500° C.

Conveyor Speed, ft./min.	0.1% Proof Stress, tons/in. <sup>2</sup>	U.T.S., tons/in. <sup>2</sup>	Elongation, % on 2 in.	Bend Value, $r = t$
Series A				
As rolled	14.0	16.7	6.0	$\frac{1}{2}t$
35	10.0	14.0	11.0	
30	9.8	13.8	13.6	Flat
25	9.0	13.6	17.0	
20	6.0	12.0	22.0	
15	4.8	11.9	25.3	
Series B				
As rolled	18.0	19.4	3.5	$1t$
25	13.0	15.9	11.0	
24	12.9	16.0	11.0	Flat
23	12.9	16.0	11.0	
22	13.1	14.5	14.0	
21	10.9	14.8	11.0	
20	7.3	13.0	22.0	
15	6.2	12.3	23.0	
10	5.6	12.0	25.0	

in a bath of fused salt previously brought to the test temperature in a small muffle furnace. The total time of immersion was 1 min. for each specimen treated individually.

The tensile-test values of Series B, Table XIII clearly illustrate the two states of recovery and recrystallization. The demarcation between the two

is shown to be only 1 ft./min. of conveyor speed, but as the recovery values extend over a wide range of speeds, it is possible to handle the production variables without entering the critical range. In addition, the range can be extended if necessary by reduction of the superheat temperature. A further illustration of the influence of degree of superheat on the consistency of mechanical properties is shown in Table XV.

In practice no difficulty has been experienced in determining and applying treatments to produce sheet showing consistent properties.

### (c) Annealing

Annealing beyond the recrystallization point is the specific function for which the flash-annealing furnace was designed. If recrystallization is the only requirement, then alloys of all types can be treated successfully and freely, as an adequate temperature range is available. Notable success has been attained in treating the 1¼% manganese alloy which, because of its heterogeneous state at the minimum recrystallization temperature, is particularly prone to erratic and large grain-size when heated slowly through the recrystallization range. Treatment in the new type of furnace overcomes this difficulty.

Considering the examples given above to illustrate the effect of heating rate, it is plain that for bulk-produced sheet, where the amount of cold work will be high or constant, the main factor of significance, other than the phase state at the temperature at which recrystallization takes place, is the rate of heating. The rates available in a furnace of the type illustrated in Fig. 1 appear to be adequate to permit a general realization of the benefit of a high rate of heating.

A study of the alloy structures shown in the photomicrographs (Fig. 7-9, Plate LIII) clearly shows that the difference in the rate plays a significant part. Fig. 7 is from a batch treatment, Fig. 8 from flash-annealing treatment, and Fig. 9 from salt-bath treatment. All treatments were carried out at 450° C.

The dominance of phase state over the effect of heating rate is well illustrated by a comparison of Figs. 7-9 with Fig. 10 (Plate LIII). All samples were cut from a sheet of aluminium-magnesium-silicon-manganese alloy, which at 450° C. is heterogeneous but at 530° C. will be essentially single-phase. Fig. 10 shows the result of salt-bath treatment at 530° C.

The limitation imposed by the phase state is not so severe as might at first appear, for most of the heterogeneous alloys of commercial interest belong to the heat-treatable group and are finally treated at the highest permissible temperature in the single-phase region.

If recrystallization and softening are required, then the adverse influence of phase state must be accepted in those alloys subject to a solution-hardening effect. This does not include the 1¼% manganese alloy, but does apply to the aluminium-magnesium-silicon-manganese and aluminium-copper-magnesium-silicon-manganese groups. Even so, the beneficial effect

of a high rate of heating will be achieved, and if several cycles of annealing and cold work are necessary, then the resultant grain-size will be significantly finer.

Experimental values for short-time annealing treatments of an aluminium-copper-magnesium alloy are given by Mohr<sup>14</sup> (Tables XIV and XV). A comparison of these tables illustrates the degree to which undesirable solution effects can be avoided by the rapid attainment of the recrystallization temperature.

A further aspect of some importance is the limited time available for diffusion to take place. When clad aluminium-copper-magnesium-silicon-manganese alloys are processed, the diffusion of the alloying elements into the cladding is undesirable. As diffusion at a given temperature is related to time, it is essentially suppressed by the use of a flash-anneal treatment of 2-3 minutes' duration only, as opposed to the normal batch treatment of 4-5 hr.

TABLE XIV.—*Effect of Batch-Annealing Treatment on Tensile Properties of Aluminium-Copper-Magnesium Alloy (Mohr<sup>14</sup>).*

Condition	Yield Stress, tons/in. <sup>2</sup>	U.T.S., tons/in. <sup>2</sup>	Elongation, %
Hard rolled	16.7	17.2	4.7
After 1½ hr. at 365° C.	6.42	13.45	15.7
After 1½ hr. at 345° C.	9.32	13.8	11.6

TABLE XV.—*Effect of Flash Annealing on Tensile Properties of Aluminium-Copper-Magnesium Alloy (Mohr<sup>14</sup>).*

Furnace temperature 600° C.

Time of Immersion, min.	Test Temp., °C.	Yield Stress, tons/in. <sup>2</sup>	U.T.S., tons/in. <sup>2</sup>	Elongation, %
1	350	4.98	13.2	16.4
1½	370	5.68	15.25	17.2
1½	400	9.52	20.1	15.0
2	420	11.42	23.5	18.0

The values given in Table XV are worthy of particular note, in that 600° C. represents the limit of the range of superheat likely to be employed. The reason for the values found after the flash anneal being lower than those after the batch anneal is that solution effects were almost entirely avoided owing to the short duration of the treatment and were not present from any previous treatment. This is in accordance with the practical evidence regarding super-annealing; very slow rates of cooling have to be employed in order to achieve full precipitation, which is possibly some index of the solution rates.

The annealing of the aluminium-copper-magnesium-manganese alloy, D.T.D. 390, on a production basis, is illustrated by the results in Table XVI.

It will be seen that a close approximation to the normal batch-annealed properties can be obtained by flash-annealing. The ultimate stress value of 1.8 tons/in.<sup>2</sup> higher for the flash anneal than the batch anneal is not considered unsatisfactory and can be

TABLE XVI.—*Effect of Annealing on Properties of D.T.D. 390.*

(a) Furnace Air Temperature 500° C.

Conveyor Speed, ft./min.	Seven Days after Anneal *		
	0.1% Proof Stress, tons/in. <sup>2</sup>	U.T.S., tons/in. <sup>2</sup>	Elongation, % on 2 in.
15.0	11.0	21.3	17.0
17.5	9.72	19.45	15.0
19.0	6.45	14.95	15.0
20.0	6.5	14.5	14.5
21.0	7.8	15.35	11.0
22.5	14.35	17.9	9.0
25.0	11.6	16.4	9.0

(b) Furnace Air Temperature 450° C.

Conveyor Speed, ft./min.	Immediately after Anneal		
	0.1% Proof Stress, tons/in. <sup>2</sup>	U.T.S., tons/in. <sup>2</sup>	Elongation, % on 2 in.
10.0	6.36	15.4	17.0
12.5	5.83	14.25	15.5
15.0	6.24	14.25	14.0
17.5	13.9	17.7	10.0

Conveyor Speed, ft./min.	Seven Days after Anneal *		
	0.1% Proof Stress, tons/in. <sup>2</sup>	U.T.S., tons/in. <sup>2</sup>	Elongation, % on 2 in.
10.0	10.3	20.1	16.5
12.5	6.5	14.65	16.0
15.0	6.45	14.7	15.5
17.5	13.1	17.25	10.0

(c) Comparative Properties.

0.1% Proof Stress, tons/in. <sup>2</sup>	U.T.S., tons/in. <sup>2</sup>	Elongation, % on 2 in.
<i>As Rolled</i>		
15.4	19.1	6.0
<i>As Batch-Annealed</i>		
6.0	12.9	14.0

\* All values are obtained after standing for 7 days at room temperature.

explained partly by the smaller grain-size. No difficulty has been experienced in rolling material treated in this way.

Typical production conditions for recrystallization annealing are shown in Fig. 4 (p. 329). The main feature of interest is the fact that the recrystallization temperature has to be exceeded by an amount which is related to gauge, apparently by reason of the grain-size/gauge relationship. No detailed study has been made of this point, but the view is expressed in the knowledge that the production variables have been adjusted with considerable precision, and hence the suggested analysis of the total time is considered to be legitimate.

(d) Solution Heat-Treatment

In the recrystallization annealing of the heat-treatable alloys some difficulty arises owing to the



necessity of avoiding solution-hardening effects. The close relation to temperature of the degree of these effects experienced is shown by Mohr's figures in Table XV and by those quoted in Table XVI. In each case it is clear that the properties are closely associated with the temperature attained, despite the short time intervals. This being so, it may be anticipated that if solution-treatment temperatures are reached, then a full heat-treatment effect can be obtained if provision is made for quenching.

Working with alloy systems having a solution-response range greater than the temperature variation of the furnace, this effect has been utilized and properties only a few per cent less than the optimum have been recorded. Since this has been done with equipment not designed for the purpose, a study of the relevant factors should enable continuous single-sheet solution-heat-treatment to be put on a practical footing.

## VI.—FUTURE PROSPECTS

### 1. EQUIPMENT

The justification of the flash-anneal furnace lies in the heating rate which it offers. It has been seen that the rates at present achieved fall far short of the standard set by the salt-bath treatment. A rate of heating twice that at present possible will be made available if successful double-side heating can be developed. A further increase will be achieved if designs are introduced utilizing the full superheat which experience suggests is fully practicable, i.e. 650° C. air temperature. Even with these modifications the rate will still be much below that given by the salt bath, and an interesting development in this connection is the proposal contained in French Patent No. 959,650 to use induction heating. Comparative rates of heating for 1-mm.-thick material are: induction heating 50° C./sec., and salt-bath treatment 60° C./sec., as against 10° C./sec. as the apparent optimum for an air-transfer treatment, and 5° C./sec. for existing flash-anneal furnaces. This tenfold increase is worth achieving, in view both of the finer grain-size to be expected and of the reduction in furnace length. A soaking chamber of a length governed by the time needed for grain growth and the required degree of coalescence would appear to be an essential, and is probably also necessary to achieve

uniformity of temperature. In the patent mentioned the claim is for solution heat-treatment, and provision is made for a long holding chamber. This is presumably to provide the requisite time for the desired degree of solution to be attained.

The outstanding problem at present is that of improving conveyor design so that damage to the surface of the sheet is avoided. It seems likely that no equipment to suit all cases is available and that furnaces must have conveyors specially adapted to the load.

Greater uniformity of temperature is needed, if consistency of results is to be obtained. It has been found, for instance, that blanks for subsequent deep drawing proved unsatisfactory if annealed in sheet subsequently cut to make several blanks. This was undoubtedly due to the edge temperature being higher than the temperature at the centre of the sheet, with a corresponding effect on the degree of recrystallization. Metallographically, no difference could be detected.

### 2. CONCLUSION

The examples quoted show that the application of theoretical considerations to the heating rate is a matter of practical significance, and further prototype flash-annealing furnaces to exploit the effect have been successfully produced. The operation of these furnaces has proved that continuous treatment offers a most versatile and economic method of preparing sheet forms in the physical state required, an optimum result being obtained in many cases.

The effects of recovery, recrystallization, coalescence, and solution-treatment, can also be exploited in any selected degree.

Secondary recrystallization effects are not eliminated by continuous annealing.

### ACKNOWLEDGEMENTS

The author wishes to thank the Directors of T.I. Aluminium, Ltd., for permission to publish this paper.

Acknowledgement must also be made to the Staff of Reynolds Rolling Mills, Ltd., for assistance in preparing the paper. In particular thanks are extended to Mr. L. Walker, B.Sc., and to Mr. S. Beard, who were responsible for carrying out at various times the experimental work recorded.

### REFERENCES

1. — *Sheet Metal Ind.*, 1949, **26**, 2605.
2. — *Sheet Metal Ind.*, 1950, **27**, 19.
3. W. J. Thomas and W. A. Fowler, *J. Inst. Metals*, 1948–49, **75**, 921.
4. H. C. H. Carpenter and C. F. Elam, *J. Inst. Metals*, 1920, **24**, 83.
5. C. Petersen, *Metallforsch.*, 1947, **2**, 289.
6. P. A. Beck, M. L. Holzworth, and P. R. Sperry, *Trans. Amer. Inst. Min. Met. Eng.*, 1949, **180**, 163.
7. W. A. Anderson and R. F. Mehl, *Trans. Amer. Inst. Min. Met. Eng.*, 1945, **161**, 140.
8. R. Chevigny, *Rev. Aluminium*, 1946, (122), 153.
9. H. W. L. Phillips, *J. Inst. Metals*, 1942, **68**, 47.
10. L. W. Eastwood, R. W. Jones, and R. F. Bell, *Trans. Amer. Inst. Min. Met. Eng.*, 1939, **133**, 124.
11. J. Hérenghuel and F. Santini, *Rev. Mét.*, 1948, **54**, 468.
12. R. Chadwick, T. Ll. Richards, and K. G. Sumner, *J. Inst. Metals*, 1948–49, **75**, 627.
13. H. Röhrig, *Z. Metallkunde*, 1924, **16**, 265.
14. E. Mohr, *Metall*, 1951, **5**, (15/16), 328.
15. M. Jakob and G. A. Hawkins, "Heat Transfer and Insulation", Chapter XI, p. 175. London: 1942 (Chapman and Hall, Ltd.).
16. "The Efficient Use of Fuel", p. 130. London: 1944 (H.M. Stationery Office).

# CONTINUOUS HEAT-TREATMENT OF ALUMINIUM ALLOYS OF THE DURALUMIN TYPE \*

1353

By MARCEL LAMOURDEDIEU,† MEMBER

## SYNOPSIS

A description is given of a plant designed for the continuous heat-treatment of Duralumin-type alloys, and the results of some tests on 24S Alclad are reported.

## I.—INTRODUCTION

In 1945 the Société Centrale des Alliages Légers and the United Engineering and Foundry Company of Pittsburgh, Pa., decided to collaborate in designing and building an experimental furnace for the continuous heat-treatment of aluminium alloys.

As a result of experiments over a period of several years, the conditions have been determined under which continuous heat-treatment can be applied to aluminium alloy strip of the Duralumin type.

The plant was first erected at the New Castle, Pa., works of the United Engineering and Foundry Corporation, and it was there that all the early experiments were made. It is now being re-erected in the works of the Société Centrale des Alliages Légers at Issoire (Puy-de-Dôme).

## II.—DESCRIPTION OF THE PLANT

The general arrangement of the plant is shown in Fig. 1. It is suitable for the heat-treatment of alloy strip having a maximum width of 56 in. and a thickness varying from 0.10 to 0.080 in. The speed of the strip can be varied from 0 to 50 ft./min.

The plant includes :

- (1) Decoiler.
- (2) Felt-lined wiper for braking the strip as it is unwound.
- (3) Pneumatic guillotine shears for squaring the ends of the strip.
- (4) Stapling or welding machine for joining the ends of different pieces of strip.
- (5) A pair of tension rolls on each side of the loop pit, which is provided to facilitate the joining of the strips without interfering with the continuous heat-treatment.
- (6) Guide roll.
- (7) Induction coil for rapid heating of the strip.
- (8) Electric forced-air stabilizing furnace.
- (9) Quenching bath. This is situated immediately below the furnace, and consists of a series of cooling sprays between which the strip passes.

To ensure furnace tightness and to avoid premature air cooling of the strip, the furnace outlet is placed below water level.

(10) Hot-air drier. This consists of two longitudinal pipes between which the strip passes as it comes out of the quench tank. The air jet instantly dries the strip and prevents any water being carried into the tension rolls and re-coiling machine. The fan for this drier is driven by a 20-h.p. motor.

(11) A pair of tension rolls on each side of the loop pit, making it possible to shear the strip without impeding the continuous operation of the plant.

(12) Roller leveller driven by a 10-h.p., D.C. motor.

(13) Coiler with automatic stripping device, driven by a 10-h.p., D.C. motor.

## III.—METHOD OF HEATING

The strip is heated by means of :

(1) A single-phase induction coil of 1875 kVA., operating at 60 c./s. and 440 V., for rapid pre-heating to the approximate temperature for solution-treatment. The strip reaches a suitable temperature in a few seconds.

(2) A stabilizing furnace. This is an electric forced-air circulation furnace, designed to bring the strip to the exact temperature required for solution-treatment, to provide even heating throughout its full width, and to maintain it at the correct temperature for the minimum time required.

The strip is then quenched in water or sprayed by means of water jets as it emerges from the furnace.

## IV.—ELECTRICAL EQUIPMENT

This includes the necessary switchgear for bringing in the supply and regulating the heat of the inductor; and also special equipment operated by voltage control, to give a variable speed by means of D.C. motors driving various rolls.

\* Manuscript received 12 November 1951. Contribution to a Symposium on "Equipment for the Thermal Treatment of Non-

Ferrous Metals and Alloys", to be held in London on 26 March 1952. † Director, Société Centrale des Alliages Légers, Paris.



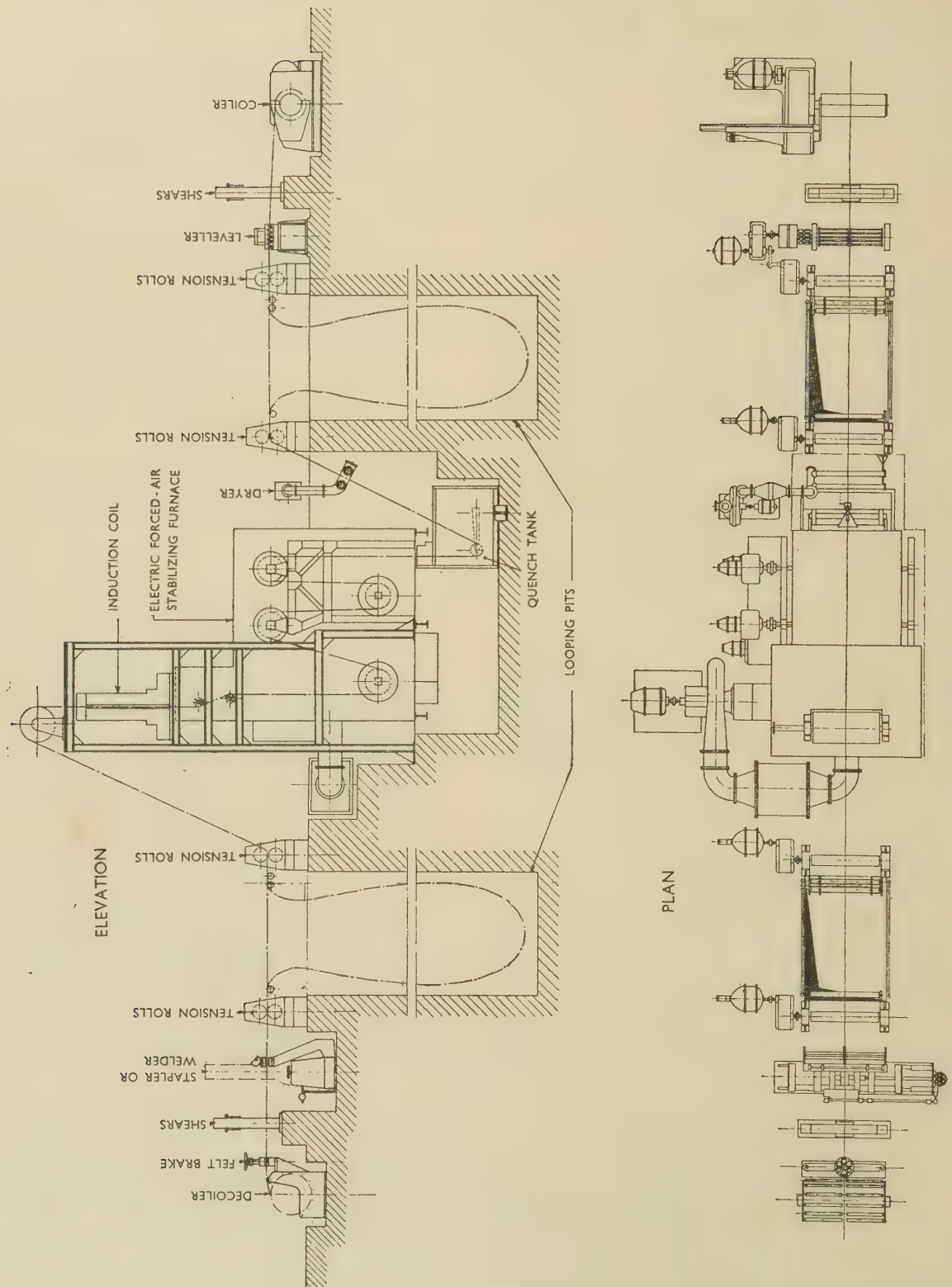


Fig. 1.—Continuous Heat-Treatment Plant for Aluminum Alloys.

### 1. CONTROL OF THE INDUCTOR

The schematic diagram of this equipment is shown in Fig. 2. The coil is fed by a single-phase, 440-V., 60-c./s. supply through a two-pole, remote-control, air-break switch. The voltage of the supply can be varied between 440 and 110 by means of a transformer. There is an air-cooled, single-phase, auto-transformer suitable for 60 c./s., 440 V. primary, and 353 V. secondary, and an induction voltage regulator.

The power for induction heating is 1875 kVA., 444.3 kW., 490 V., 60 c./s. The induction coil is water-cooled. The gap between the poles for the passage of the strip is 3 in., with a possible adjustment of  $\pm \frac{1}{2}$  in.

On each half of the coil there are fixed water-cooled edge protectors to avoid overheating the

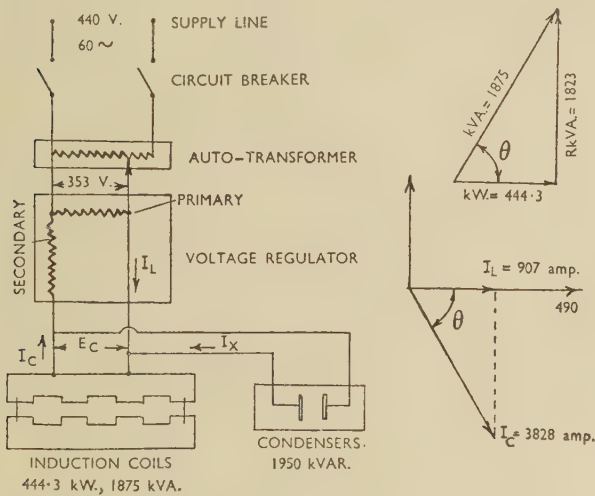


FIG. 2.—Diagram of Inductor.

$$\text{RkVA.} = \text{kVA.} \sin \theta = 1875 \times 0.915 = 1823.$$

$$I_L = \frac{1823 \times 1000}{490} = 3720 \text{ A.}$$

$$E_C = 490 \text{ V.}$$

$$P = 444.3 \text{ kW.}$$

$$I_L = \frac{444.3 \times 1000}{490} = 907 \text{ A.}$$

$$I_C = 3828 \text{ A.}$$

edges of the strip. An arrangement of photoelectric cells makes it possible to adjust the edge protectors for any width of strip between 30 and 56 in., and the lateral movement of the strip can be automatically followed to  $\pm 2$  in.

A single-phase battery of condensers of 1950 kVAR., 575 V., 60 c./s. is arranged in parallel with the induction coil, and corrects its power factor.

### 2. VARIATION OF SPEED BY VOLTAGE CONTROL

The power for this equipment is obtained from a 40-kW. Ward-Leonard set, operated by a 3-phase, 75-h.p. induction motor. By this method it is possible to regulate individually the speed of each

motor, so that the speed of the strip on each pair of rolls is the same throughout the installation, and there is no slipping of the strip on the rolls. It is also possible to synchronize the speed of all the motors.

### 3. PURPOSE OF EDGE PROTECTORS

These protectors are shown in section in Fig. 3. They are made of water-cooled copper and have a

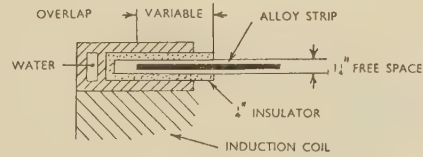


FIG. 3.—Edge Protector.

lining of fibro-cement insulating material. The width of overlap on the strip can be varied from 0 to 4 in.

In the first experiments the protectors were fitted with guide rolls touching the edge of the strip, so as to keep the protectors in the correct position. This method was quickly abandoned, however, as various difficulties, including damage to the edge of the strip, resulted.

With the strip passing at a speed of 12 ft./min., and a variable current in the induction coils, it is possible to maintain an even temperature at the centre and the edges of the strip by varying the position of the edge protectors. Without them there would be a considerable difference of temperature between the centre and the edge.

The temperature is measured on the travelling strip, at the point where it emerges from the induction coil, by means of a thermocouple fixed on the end of a long bar and clamped on to the strip while the temperature reading is taken. Many different experiments have all given results similar to those shown in Fig. 4.

If no edge protectors are used, or if they are spaced wide apart, there is a considerable difference of

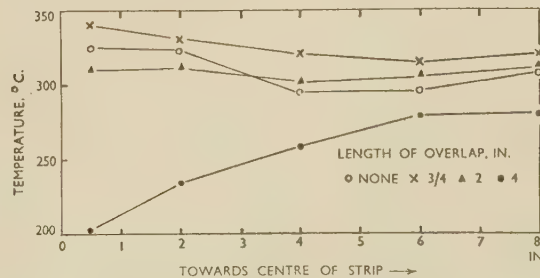


FIG. 4.—Variation of Temperature Between Sides and Centre of Strip for Four Different Positions of the Edge Protectors.

temperature between the edge and centre of the strip, e.g. 610°–615° F. (321°–324° C.) at the edge,



and 560°–565° F. (293°–296° C.) 6 in. from the edge. With the protectors overlapping by  $3\frac{1}{8}$ –4 in., the temperature may be as much as 80° C. lower than the centre, e.g. 390°–400° F. (199°–205° C.) at the edges; 530°–540° F. (277°–282° C.) at the centre. If the edge protectors overlap by  $1\frac{1}{8}$ –2 in., the difference between the hot and cold extremes varies from 6° to 10° C.

TABLE I.—*Effect of Position of Edge Protectors on Properties of Strip.*

Mechanical Properties	At Edge	8 in. from Edge	At Centre
Before heat-treatment :			
Yield strength, kg./mm. <sup>2</sup> .	27.1	27.2	27.4
Tensile strength, kg./mm. <sup>2</sup> .	28.1	28.3	28.3
Elongation, % . . . .	3.4	3.4	3.4
After continuous heat-treatment :			
Yield strength, kg./mm. <sup>2</sup> .	12.7	11.2	11.8
Tensile strength, kg./mm. <sup>2</sup> .	23.7	21.6	22.5
Elongation, % . . . .	19.9	20.7	21.7

The curves in Fig. 4 show quite clearly the importance of control by means of edge protectors. In a continuous heat-treatment test carried out at a speed of 18 ft./min., protectors overlapping by  $1\frac{3}{4}$ – $1\frac{7}{8}$  in. the properties shown in Table I were obtained. The stabilizing furnace operated at 635°–650° F. (335°–343° C.) and the induction coil was regulated so as to give a temperature of 650° F., where the strip came out of the coil.

## V.—TEMPERATURE MEASUREMENT ON THE MOVING STRIP

One of the most important problems, which was not finally solved during the experiments in America, was the measurement of the temperature of the moving strip.

At first a sensitive pyrometer couple was placed inside a loop made by two sections of the strip passing close to one another. The objection to this method was that the pyrometer was situated at a considerable distance from the induction coil, and, consequently, was too slow in indicating the temperature of the strip as it left the coil.

A contact pyrometer was also considered; this was clamped on to the moving strip and travelled with it for the time necessary to read the temperature. It was proposed that this pyrometer clamp should then return and take a new hold on the strip coming out of the induction coil. This method has been used for all the experiments so far, but has been operated by hand.

The final method to be employed was developed by the Leeds-Northrup Company. It consists of a very sensitive total-radiation pyrometer which embodies an aluminium plate resistance-heated to a predetermined temperature equal to that required in the strip. The heat rays are reflected several times between the aluminium plate and the strip, and finally give the average temperature of the plate and the strip. The results are theoretically very accurate when the plate and the strip are at approxi-

TABLE II.—*Mechanical Properties of 24S Alclad Aged after Continuous Heat-Treatment.*

Space between coils 3 in. Overlap of edge protectors 2 in. Temp. in air stabilizing furnace 940° F. (505° C.) at point of entry of hot air.

Position	Speed : 19 ft./min. 2400 Amp.			Speed : 19 ft./min. 2450 Amp.			Speed : 30 ft./min. 3000 Amp.		
	Yield Strength, kg./mm. <sup>2</sup>	Tensile Strength, kg./mm. <sup>2</sup>	Elongation, %	Yield Strength, kg./mm. <sup>2</sup>	Tensile Strength, kg./mm. <sup>2</sup>	Elongation, %	Yield Strength, kg./mm. <sup>2</sup>	Tensile Strength, kg./mm. <sup>2</sup>	Elongation, %
Right edge *	26.6	41.3	...	28.7	41.5	16.7	25.0	38.3	13.6
	25.8	42.5	15.1	27.1	41.3	19.0	23.3	38.3	15.6
	27.5	42.1	16.0	27.9	40.7	16.1	23.3	37.3	18.8
Centre *	26.6	43.0	19.2	26.2	41.3	17.9	23.9	38.8	12.6
	27.9	42.8	16.0	29.2	42.5	17.5	22.5	37.3	18.4
	28.3	42.5	16.0	28.3	42.1	17.3	23.3	38.0	14.4
Left edge *	27.1	41.4	16.0	27.5	40.3	15.0	22.1	36.3	16.4
	26.3	41.6	14.5	27.0	40.1	17.6	...	37.5	15.0
	25.8	41.2	18.5	27.1	41.3	18.4	22.1	36.1	14.0
Right edge †	27.1	40.4	15.1	27.9	42.1	15.3	24.2	38.0	15.5
	25.8	40.4	12.9	27.9	42.0	18.7	23.3	37.6	17.3
	24.6	40.4	15.4	25.0	41.3	15.0	25.4	38.6	17.0
Centre †	25.4	41.1	17.0	27.5	42.2	16.2	25.8	39.2	16.7
	26.3	40.9	15.4	28.3	42.1	18.6	24.2	39.8	15.1
	26.3	41.5	16.5	28.3	42.0	15.6	25.4	38.9	15.5
Left edge †	26.3	40.3	16.7	26.7	40.7	16.5	...	37.5	16.7
	25.8	40.8	17.8	28.3	41.3	15.4	24.2	37.2	15.3
	27.9	40.5	16.2	...	41.7	15.0	...	37.1	13.7

\* Specimens taken from first half of a coil of strip.

† Specimens taken from the second half.

mately the same temperature. Laboratory experiments have proved very encouraging, but in practical operation results have been very irregular—sometimes very good, sometimes bad.

This pyrometer equipment has been modified by the Leeds-Northrup Company and will be installed in the plant at Issoire. When further experience has been gained, it should be possible to give a more definite verdict on the value of this method of pyrometry, which is one of the most important matters connected with the development of the new plant.

#### VI.—HEAT-TREATMENT RESULTS

The tests at New Castle were made on strips, 40 in. wide and 0.040 in. thick, of 24S Alclad having the following average composition: Cu 4.31, Mg 1.48, Mn 0.56, Fe 0.50, Si 0.14%. Results are given in Table II.

#### VII.—CONCLUSIONS

It will be noted that in the last series of tests, carried out at 30 ft./min., the properties of the metal are not up to standard, although the tests at 19 ft./min. gave satisfactory results. This does not prove, however, that 19 ft./min. is the maximum speed possible with the present installation. The plant was in operation for a long period at 19 ft./min., whereas only one test was made at 30 ft./min., owing to lack of 24S strip.

In the course of the trials in America, several important problems were solved; for example: (1) feeding the strip into the furnace, (2) control of the speed and tension of the strip in the furnace, and (3) measurement of the temperature of the moving strip. A number of modifications will be made when the plant is re-erected in France.



### Metal Economics : a Correction

In the contribution by Mr. R. Lewis Stubbs, which appeared in the January 1952 issue of the *Journal*, Table V (p. 230) should have read :

TABLE V.—*Zinc Consumption and Reserves.*  
(In millions of metric tons)

Year	Annual Rate of Consumption	Estimated Reserves
1931	1·2	27
1940	2·0	43
1947	1·75	63
1948	1·8	70

# REPORT OF COUNCIL

## FOR THE YEAR ENDED 31 DECEMBER 1951

THE Council feels that it can look back on the year 1951 with considerable satisfaction. For the next seven years its anxieties regarding the Institute's finances have been largely removed by the generous response by industry to its appeal for support of the Institute's work.

The Council cannot express too strongly its sincere appreciation of the quick and generous response made by so many firms in the metallurgical and engineering industries, and would particularly mention the support received from metallurgical firms in the United States and Switzerland. This recognition by industry of the value of the Institute's work is a matter of gratification to the members as a whole. As the costs of the Institute's services, and especially of its publications, are continually increasing, further subscriptions in response to this appeal will be welcomed.

The most notable event of the year was the Autumn Meeting in Italy, which was held by invitation of the Associazione Italiana di Metallurgia and was attended by about 250 members and ladies, in addition to those resident in Italy. The Council desires to place on record its sense of gratitude to the Associazione Italiana di Metallurgia, and all those who so warmly received and generously entertained members and ladies during this memorable meeting, which it is hoped has done much to bring together more closely those, in Europe in particular, who are concerned with the science and practice of metallurgy.

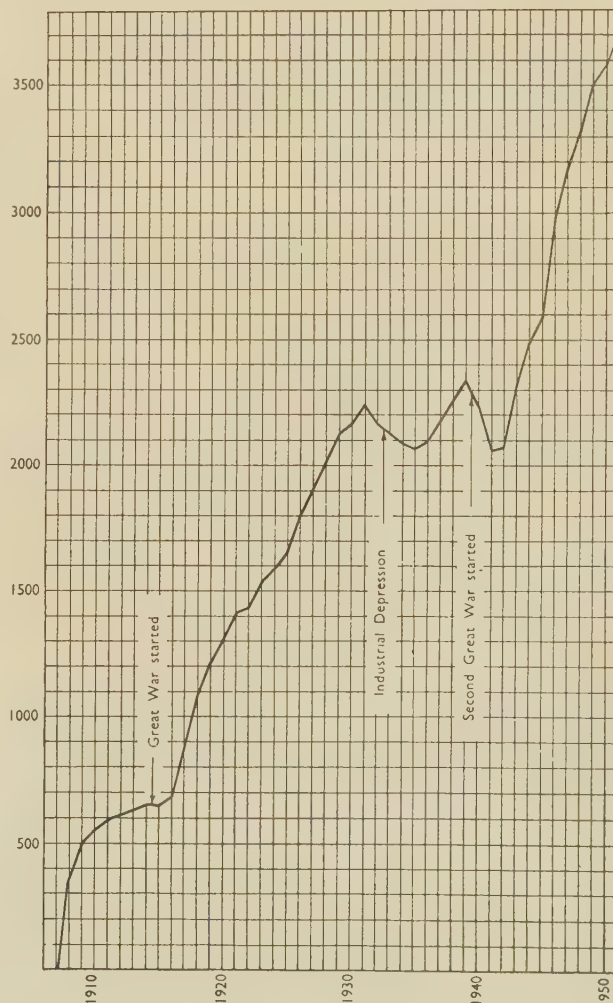
During the year a Meetings Sub-Committee was appointed, under the chairmanship of the Senior Vice-President, to consider, in the light of changes of circumstances since the formation of the Institute, and having in mind the financial aspects of these matters, all questions relating to the organization of General Meetings. The Committee of eight members was representative of the different interests within the Institute and its report, as accepted by the Council, is printed, in abridged form, in the *Bulletin* for October 1951, pp. 9 and 10.

### MEMBERSHIP

As the following table shows, the membership of the Institute has continued to show a steady increase. During the forthcoming year a special effort is to be made to develop the membership—both in the British Isles and overseas—and it is hoped that members will co-operate by bringing the value of the Institute's services to the notice of their friends and by inviting suitable persons to join. The Institute aims to serve science and industry without regard to nationality. Copies of a quarto pamphlet entitled

“The Institute of Metals: Particulars of its Objects, Work, and Membership” are available to all who can make use of them for development purposes.

At 31 December	1944	1945	1946	1947	1948	1949	1950	1951
Honorary Members . . .	6	6	6	9	9	11	11	11
Fellows . . .	7	6	6	7	6	9	10	8
Ordinary Members . . .	2153	2213	2414	2491	2546	2685	2815	2941
Junior Members . . .	...	...	...	...	...	...	291	305
Associate Members . . .	15	12	25	17	19	18	...	...
Student Members . . .	305	361	529	655	746	783	452	462
Active List . . .	2486	2598	2980	3179	3326	3506	3579	3727
Suspense List . . .	200	179	58	36	55	67	97	124
Total . . .	2686	2777	3038	3215	3381	3573	3676	3851



Active Membership at 31 December 1908–1951.



## OBITUARY

The Council deeply regrets to record the deaths of Professor Emeritus Thomas Turner, Past-President, Fellow, and Original Member; Mr. Harry Davies, a Member of Council; Mr. A. H. Munday, a former Member of Council; and Mr. R. C. Stanley, an Institute of Metals (Platinum) Medallist.

It also much regrets to record the deaths of the following members, which were notified during the year: Mr. J. M. Allan (an Original Member), Mr. A. Allcock, Mr. F. L. Baer, Mr. R. L. Brunton, Mr. R. Burn, Mr. P. D. Caldicott, Mr. H. Carr-Walker, Mr. K. W. Caulfield, Mr. G. Chelioti, Mr. G. C. Clayton, Mr. A. Crowther, Mr. A. Delruelle, Mr. F. W. Dingwall (an Original Member), Mr. J. D. Ellis, Mr. D. M. Fairlie, Mr. K. V. Haig, Mr. F. W. R. Harris, Mr. E. H. Hill, Mr. A. W. Hothersall, Mr. J. Howeson, Mr. A. F. Hutt, Mr. G. A. Inglis, Ing. J. Lagerquist, Dr. P. J. M. Leemans, Mr. A. B. Lisle, Mr. J. R. McKellar, Mr. G. H. Rogers, Mr. E. C. Roglin, Mr. R. de H. St. Stephens, Mr. A. Vigne, Mr. F. Walker, and Mr. L. W. T. Webb.

## OFFICERS OF THE INSTITUTE

The following members were declared elected to fill vacancies as honorary officers of the Institute with effect from the 1951 Annual General Meeting:

*President:*

Professor A. J. MURPHY, M.Sc.

*Vice-Presidents:*

A. B. GRAHAM

P. V. HUNTER, C.B.E.

*Ordinary Members of Council:*

K. W. CLARKE

CHRISTOPHER SMITH

Subsequently, Mr. Alfred BAER, B.A., and Mr. N. I. BOND-WILLIAMS, B.Sc., were elected Ordinary Members of Council, to fill vacancies.

In accordance with Article 42, the Council elected Dr. C. J. SMITHELLS, M.C., as Senior Vice-President for the year 1951-52.

## HONORARY CORRESPONDING MEMBERS TO THE COUNCIL

The Council desires to express to all Honorary Corresponding Members its appreciation for their help and advice during the past year. The list of Honorary Corresponding Members to the Council is as follows: *Australia*: Professor H. K. Worner, D.Sc.; *Belgium*: H. P. A. Féron; *Canada*: Professor B. Chalmers, Ph.D., D.Sc., and Professor G. Letendre, B.A., Ph.D.; *France*: Professor P. A. J. Chevenard and Jean Matter; *India*: N. P. Gandhi, M.A., B.Sc., A.R.S.M., D.I.C.; *Italy*: Leno Matteoli, Dott.Chim.; *Netherlands*: M. Hamburger; *South Africa*: G. H. Stanley, D.Sc., A.R.S.M., and Professor L. Taverner, A.R.S.M., D.I.C.; *Spain*: Professor J. Orland,

M.Sc., M.A., Ph.D., D.D.; *Sweden*: Professor Carl A. F. Benedicks, Fil.Dr., Dr.Ing.e.h., Dr.Techn.h.c., and Professor Axel Hultgren; *Switzerland*: Professor A. von Zeerleder, Dr.Ing.; *United States of America*: Professor R. F. Mehl, Ph.D., Hon.Eng.D., Hon.Sc.D., Professor C. S. Smith, Sc.D., and Dr. R. A. Wilkins.

On leaving the country, Mr. H. N. Bassett resigned as Honorary Corresponding Member for Argentina, and the Council expresses its thanks for his long services to the Institute.

## INSTITUTE OF METALS MEDAL

The Institute of Metals (Platinum) Medal for 1951 was awarded to Dr. R. W. DIAMOND, Vice-President and General Manager of the Consolidated Mining and Smelting Company of Canada, Ltd., Trail, B.C., in recognition of his outstanding services to the non-ferrous metal industries in connection with researches on differential flotation as applied to the complex Sullivan ore and as manager of the largest combined lead and zinc producer in the world.

## W. H. A. ROBERTSON MEDAL

The W. H. A. Robertson Medal was awarded to Mr. CHRISTOPHER SMITH for his paper on "The Extrusion of Aluminium Alloys", published in the *Journal*, 1949-50, vol. 76, pp. 429-451.

## ROSENHAIN MEDAL

The first award of the Rosenhain Medal was made to Professor G. V. RAYNOR, M.A., D.Phil., D.Sc., Professor of Metal Physics at the University of Birmingham, for his outstanding contributions in the field of physical metallurgy in connection with our knowledge of the constitution and formation of alloys.

## CAPPER PASS AWARDS

During the year Capper Pass Awards of £50 each were made (a) jointly to Mr. R. G. WILKINSON, B.Sc., and Dr. F. A. Fox for their paper on "The Hot-Working of Magnesium and Its Alloys" (*Journal*, 1949-50, vol. 76, pp. 473-500); and (b) jointly to Mr. J. J. HOBEN and Mr. J. F. MULVEY for their paper on "The New Continuous Brass Mill of the Scovill Manufacturing Company, Waterbury, Conn., U.S.A." (*Journal*, 1950, vol. 77, pp. 357-388).

## STUDENTS' ESSAY PRIZES

The Council has approved the annual award of two prizes of 20 guineas each (£10. 10. 0. in cash and £10. 10. 0. in the form of books) for essays by Student Members of the Institute or Associate Members of Local Sections eligible for Student Membership. Each year essays of 2500-3500 words will be invited under two subject headings, and it is hoped that prize-winners will be offered opportunities to read their papers before their Local Sections. Full particulars will be published in the *Bulletin*, and it is intended that the first competition shall be held in 1952.

## PUBLICATIONS

For reasons that have already been announced, the format of the *Journal* was changed from octavo to quarto with effect from the issue for September 1951, and at the same time a new feature—the *Bulletin*—was introduced. No doubt many members will have regretted the disappearance of the *Journal* in its old, familiar form, and it is appreciated that the new size may present problems where there is fixed shelving. The Council feels confident, however, that the change has been in the interests of the Institute, and that members will appreciate the advantages of the new format. It is intended that, in addition to news, the *Bulletin* (which may be separately bound) shall contain a selection of papers read before the Local Sections and that it shall become a medium for the discussion, by correspondence, of all non-ferrous topics which come within the field of the Institute.

During the year 1951 a total of 56 papers and addresses was published in the *Journal*.

*Metallurgical Abstracts* has been brought further up to date, and 855 periodicals are now regularly searched, in addition to many others which are searched at irregular intervals. The publication of the index for 1950 took place later than had been hoped, but the printing of the index for 1951 is well advanced, and it is confidently believed that the issue of the annual indexes will in future be made much more promptly than has been the case for some years.

In the *Monograph and Report Series* there were published during the year: No. 9: "The Hot-Working of Non-Ferrous Metals" and No. 10: "Non-Destructive Testing of Metals", by Dr. R. F. Hanstock. In addition, No. 11: "Thermodynamics of Alloys", by Mr. J. Lumsden has been printed and copies are about to be delivered, and No. 12: "The Cold-Working of Metals and Alloys", is in the press. A completely revised edition of Monograph No. 3: "Atomic Theory for Students of Metallurgy", by Dr. W. Hume-Rothery, F.R.S., is also in the press, and should be published early in 1952.

Two new *Annotated Equilibrium Diagrams* were published during the year: No. 8—Iron–Zinc and No. 9—Antimony–Lead, both prepared by Professor G. V. Raynor.

## GENERAL MEETINGS

The Forty-Third Annual General Meeting was held in London on 13, 14, and 15 March 1951, when Professor A. J. MURPHY, M.Sc., was inducted into the Chair. One day of the meeting was devoted to an all-day Symposium on "Metallurgical Aspects of the Cold-Working of Non-Ferrous Metals and Alloys".

On 23 May 1951, at the Royal Institution, Albemarle Street, London, W.1, The Right Hon. Sir JOHN ANDERSON, P.C., G.C.B., G.C.S.I., G.C.I.E., F.R.S., delivered the Forty-First May Lecture on "Science in the Service of the Community".

The Autumn Meeting was held in Italy from 15 to

25 September 1951, by invitation of the Associazione Italiana di Metallurgia. Exclusive of those resident in Italy, about 250 members and ladies took part. After four days in Venice, at which the scientific discussions were held and a series of works was visited, members proceeded to visit metallurgical works at Bolzano, Milan, Turin, and—from Florence—Fornaci di Barga. The meeting was one of the most successful of its kind that the Institute has held, and the Council has expressed to the President of the Associazione Italiana di Metallurgia, on behalf of the members, the Institute's warm sense of gratitude to its hosts for the most friendly and generous way in which members and their ladies were received and entertained.

At a General Meeting in London on 17 October 1951, an all-day discussion was held on "Metal Economics", a report of which has appeared in the *Journal*.

## STUDENTS' EDUCATIONAL TOUR

An Easter vacation educational tour for Junior and Student Members was held in South Wales from 13 to 19 April 1951, inclusive. It was attended by 23 Junior and Student Members, and 7 works were visited. The Council records its gratitude to the Directors of the works visited, and to the Committee of the South Wales Local Section, which acted as an advisory committee, for their co-operation in making this tour a success.

Before making arrangements for an educational tour in 1952, it was considered advisable to ascertain whether it is felt that such tours do provide valuable educational facilities for young men in industry. The managements of 24 well-known firms in the non-ferrous industry were accordingly asked for their opinion, and their replies have been almost unanimously in favour of the continuance of the tours, which the majority have undertaken to support both by encouraging suitable young men to take part in them and by assisting in the payment of the very moderate expenses involved.

An Easter vacation educational tour for Junior and Student Members has therefore been arranged in 1952 to be held in South Lancashire, and full particulars will be published in the *Bulletin* and sent to all who are eligible to take part in it.

## LOCAL SECTIONS AND ASSOCIATED SOCIETIES

During the year an additional Local Section was formed at Oxford. It opened its session with about 100 members and associates drawn mainly from the University, the Atomic Energy Research Establishment at Harwell, and the metallurgical and engineering industries within a radius of about 25 miles round the city of Oxford.

The other five Local Sections (Birmingham, London, Scottish, Sheffield, and South Wales) had good programmes of meetings in the winter session.



Members also continued to enjoy the privilege of free membership of the Leeds Metallurgical Society, Liverpool Metallurgical Society, and Manchester Metallurgical Society.

The President and Secretary again paid official visits to some of the Local Sections and Associated Societies, and appreciated these opportunities to obtain the views of local members on the work of the Institute.

#### SPECIAL COMMITTEES

The Metal Physics Committee had 3 meetings during the year, and is arranging a Symposium on the Properties of Metallic Surfaces, to be held in London in the late Autumn of 1952. The Council has agreed to a request that one half-day session shall be allocated at the Annual General Meeting and Autumn Meeting in 1952 for the discussion of papers on metal physics. In addition, it has approved a proposal to hold informal discussions for those interested in metal physics.

The Metallurgical Engineering Committee met 3 times. It has arranged an informal discussion to be held in Birmingham, on 3 January 1952, on "Tool and Die Materials for the Extrusion of Non-Ferrous Metals and Alloys", and also a whole-day Symposium on "Equipment for the Thermal Treatment of Non-Ferrous Metals and Alloys", to be held in connection with the 1952 Annual General Meeting.

*Ad hoc* Committees have again discussed problems relating to the abstracting of metallurgical literature and the publication of reviews of progress in metallurgy, and, by invitation of the Council, representatives of the Iron and Steel Institute, the Institution of Mining and Metallurgy, and the Institute of British Foundrymen have met representatives of the Institute of Metals to consider whether any co-operation on these matters is desirable and practicable.

#### STAFF

In April 1951 the Secretary completed 40 years' connection with the Institute's staff, on which he has served successively as Assistant Secretary, Editor of Publications, Assistant Secretary and Editor, Secretary and Editor, and as Secretary.

During the year Mr. S. R. Williams, B.Sc., joined the staff as Editorial Assistant.

#### JOINT ACTIVITIES

##### JOINT LIBRARY AND INFORMATION DEPARTMENT

As in previous years, the services of the Joint Library have been in great demand, not only by members but also by Government Departments, Research Associations, Universities, and other teaching establishments. The number of publications

borrowed during 1951 was 11,617, the corresponding figure for 1950 being 11,060. A further 279 textbooks were added to the Library's book-shelves, many by presentation, and the Council offers its best thanks to the many donors for their valuable contributions.

Members are reminded that the use of the Lending Library is a valuable privilege of membership. Books and periodicals are sent post free to members resident in Great Britain. In addition to the books filed in the Joint Library, members may borrow—through the Librarian—publications from the Science Library and the National Central Library. Assistance is also given to all members, in Great Britain and overseas, to obtain photostat copies of articles, which can be supplied under certain conditions. A total of 46 photostat copies and 19 microfilms was supplied to members during the past year.

The work of the Information Department is an important part of the service. The Department is prepared to answer scientific and technical enquiries from members, but it is not its function to give the type of advice which comes within the field of the metallurgical consultant.

On 31 December 1951, Mr. R. Elsdon, the Joint Librarian, retired from the staff of The Iron and Steel Institute; he had been with that Institute for over forty-seven years. The Council of the Institute takes this opportunity to thank Mr. Elsdon for his valuable services to the Joint Library since it was set up in 1938 and to offer him its best wishes for much happiness in his retirement.

##### JOINT COMMITTEE ON METALLURGICAL EDUCATION

The Committee held four meetings during 1951. It received and considered comments on its "Recommendations on University Full-time Degree Courses in Metallurgy", published in 1950, and discussed the subject of its current enquiry and report.

Of the 1000 copies of the Committee's "Recommendations on University Full-time Degree Courses in Metallurgy" which were printed in 1950, 200 were distributed to Universities, Government Departments, and other bodies concerned with higher teaching and Research Associations, and approximately 700 have been issued in response to requests.

Mr. D. R. O. Thomas (United Steel Companies, Ltd.) agreed to become Chairman of the Committee in May 1951, in succession to Mr. E. G. Lawford (Rio Tinto Company, Ltd.), who was obliged to resign owing to pressure of other business.

Dr. Leslie Aitchison was appointed Assessor to the Committee in May 1951, when it was decided to conduct an enquiry into metallurgical education with particular reference to metallurgical education other than at universities. Dr. Aitchison has since held discussions with the Committee on the scope of the enquiry and various aspects of the subject. The Committee will shortly consider a draft Report.

JOINT COMMITTEE FOR NATIONAL CERTIFICATES  
IN METALLURGY

At its four meetings held in 1951, the Committee has considered and approved four schemes for Ordinary National Certificate Courses, two schemes for first year Courses at contributory centres, and six schemes for Higher National Certificate Courses (including one new "sandwich" type scheme for the Higher Certificate with additional endorsement subjects).

The number of Courses in operation during 1951 has been :

Ordinary Certificate Courses . . .	28
Contributory Centre „ . . .	6
Higher Certificate „ . . .	17

The comparative figures of entries to final examinations in the years 1950 and 1951 are :

	1950	1951
Ordinary Certificate . . .	281	314
Higher Certificate . . .	62	110

and the number of Technical Colleges holding final examinations :

	1950	1951
Ordinary Certificate . . .	20	25
Higher Certificate . . .	11	16

## SIR GEORGE BEILBY MEMORIAL FUND

During the year, the assessors made awards (for 1950), each of one hundred guineas, to Mr. William

Albert Baker, B.Sc., F.I.M., in recognition of his experimental contributions to knowledge of the factors determining the production of sound castings of non-ferrous metals and alloys, and to Dr. Gordon Whittingham, M.A., in recognition of his experimental contributions to knowledge of the combustion products of fuels containing sulphur and their effects on corrosion.

## MOND NICKEL FELLOWSHIPS COMMITTEE

During 1951, Mr. W. A. C. Newman replaced the late Lieut.-Colonel Sir John Greenly as representative of the Institute on the Committee.

The following awards were made for 1951 :

Mr. P. J. HILL (Public Works Department of Western Australia) to study, in the United Kingdom, the application of research to the development of corrosion-resistant metals for use in the mechanical engineering industry.

Mr. J. PRESTON (British Non-Ferrous Metals Research Association) to study, in Great Britain, the United States of America, and Canada, specialized methods of production and fabrication of metals, with particular reference to powder-metallurgical techniques.

Mr. P. E. WHITE (J. B. and S. Lees, Ltd.) to study the metallurgy and detailed production technique of high-quality strip steels in the United Kingdom, Scandinavia, United States of America, and Canada, with particular reference to hardened and tempered steel strip, stainless steels, and silicon steels.



## APPENDIX I

## CONTRIBUTORS TO THE INDUSTRIAL DONATIONS FUND UP TO 31 DECEMBER 1951

## A.—ANNUAL DONATIONS, UNDER COVENANT, FOR NOT LESS THAN 7 YEARS.

Donor	Net Donation	Gross, after Recovery of Tax by the Institute	Donor	Net Donation	Gross, After Recovery of Tax by the Institute.
	£ s. d.	£ s. d.		£ s. d.	£ s. d.
Enfield Rolling Mills, Ltd. (incl. Enfield Copper Refining Co., Ltd.; Enfield Rolling Mills (Aluminium), Ltd.; Holloway Metal Roofs, Ltd.; and London Zinc Mills, Ltd.)	275 0 0	500 0 0	Birmingham Aluminium Casting (1903) Co., Ltd.	25 0 0	45 5 0
Mond Nickel Co., Ltd., The (incl. Birlec, Ltd.; Henry Wiggin and Co., Ltd.; and associated companies in the United States and Canada)	275 0 0	500 0 0	Bristol Aeroplane Co., Ltd., The	25 0 0	45 5 0
Consolidated Zinc Corporation, Ltd., The (incl. The Broken Hill Corporation, Ltd.; Imperial Smelting Corporation, Ltd.; The National Smelting Co., Ltd.; New Broken Hill Consolidated, Ltd.; Northern Smelting and Chemical Co., Ltd.; Sulphide Corporation Pty., Ltd.; and The Zinc Corporation, Ltd.)	250 0 0	454 10 0	British Metal Corporation, Ltd., The	25 0 0	45 5 0
Goodlass Wall and Lead Industries, Ltd.: Associated Lead Industries, Ltd.	£100		Chloride Electrical Storage Co., Ltd., The	25 0 0	45 5 0
Fry's Metal Foundries, Ltd. (incl. Antifriction Bearing Co., Ltd., The; Atlas Metal and Alloys Co., Ltd.; and The Eyre Smelting Co., Ltd.)	50		London and Scandinavian Metallurgical Co., Ltd.	25 0 0	45 5 0
Mufulira Copper Mines, Ltd.	150 0 0	272 14 0	Rotol, Ltd.	25 0 0	45 5 0
Roan Antelope Copper Mines, Ltd.	150 0 0	272 14 0	Star Aluminium Co., Ltd. (incl. Anglo-Swiss Aluminium Co., Ltd.)	25 0 0	45 5 0
Imperial Chemical Industries, Ltd. and its subsidiary companies	137 10 0	250 0 0	Sterling Metals, Ltd.	25 0 0	45 5 0
British Aluminium Co., Ltd., The (incl. Aluminium Corporation, Ltd.; William Mills, Ltd.; and North British Aluminium Co., Ltd.)	100 0 0	181 18 0	Telegraph Construction and Maintenance Co., Ltd., The (incl. Submarine Cables, Ltd.)	25 0 0	45 5 0
McKechnie Brothers, Ltd.	100 0 0	181 18 0	Wolverhampton Metal Co., Ltd., The (incl. James Bridge Copper Works, Ltd.)	25 0 0	45 5 0
Magnesium Elektron, Ltd. (incl. F. A. Hughes and Co., Ltd.)	100 0 0	181 18 0	Hughes-Johnson Stampings, Ltd., The	21 0 0	38 3 8
Metallo-Chemical Refining Co., Ltd.	100 0 0	181 18 0	Light Metal Forgings, Ltd.	21 0 0	38 3 8
Consolidated Tin Smelters, Ltd. (incl. The Cornish Tin Smelting Co., Ltd.; Eastern Smelting Co., Ltd.; The Penpoll Tin Smelting Co., Ltd.; and Williams, Harvey and Co., Ltd.)	50 0 0	90 19 0	Ferranti, Ltd.	20 0 0	36 8 0
Enthoven (H. J.) and Sons, Ltd.	50 0 0	90 19 0	Gibbons Brothers, Ltd. (incl. The Thermic Equipment and Engineering Co., Ltd.)	20 0 0	36 8 0
High Duty Alloys, Ltd.	50 0 0	90 19 0	Parkinson Stove Co., Ltd., The	20 0 0	36 8 0
Venesta, Ltd.	50 0 0	90 19 0	British Tin Investment Corporation, Ltd.	15 15 0	28 8 0
Whiley (Geo. M.), Ltd.	50 0 0	90 19 0	Derby and Co., Ltd.	15 15 0	28 8 0
Associated Electrical Industries, Ltd., on behalf of the A.E.I. Group of Companies	27 10 0	50 0 0	London Electric Wire Company and Smiths Ltd., The (incl. Liverpool Electric Cable Co., Ltd.)	15 15 0	28 8 0
Dale (John), Ltd.	27 10 0	50 0 0	Bolton (Thomas) and Sons, Ltd.	15 0 0	27 5 5
Murex, Ltd. (incl. Murex Welding Processes, Ltd.)	27 10 0	50 0 0	British Lead Mills, Ltd.	15 0 0	27 5 5
Morgan Crucible Co., Ltd., The	26 5 0	47 14 0	Holroyd (John) and Co., Ltd.	13 15 0	25 0 0
Essex Aero, Ltd.	25 0 0	47 12 4	Phosphor Bronze Co., Ltd., The	10 10 0	22 12 4
A.P.V. Company, Ltd., The	25 0 0	45 5 0	International Alloys, Ltd.	11 0 0	20 0 0
Birmetals, Ltd.	25 0 0	45 5 0	Allen (Edgar) and Co., Ltd.	10 10 0	18 8 6
			British Tin Smelting Co., Ltd., The	10 10 0	18 8 6
			General Electric Co., Ltd., The	10 10 0	18 8 6
			Saunders-Roe, Ltd.	10 10 0	18 8 6
			Curran (Edward) Engineering, Ltd.	10 0 0	18 4 0
			Rollet (H.) and Co., Ltd.	10 0 0	18 4 0
			Wolverhampton Die-Casting Co., Ltd., The	10 0 0	18 4 0
			Scottish Non-Ferrous Tube Industries, Ltd.	8 5 0	15 0 0
			Loewy Engineering Co., Ltd., The	7 10 0	13 12 8
			Central Marine Engine Works (William Gray and Co., Ltd.)	5 5 0	9 14 0
			Harland Engineering Co., Ltd., The	5 5 0	9 14 0
			Wild-Barfield Electric Furnaces, Ltd.	5 5 0	9 14 0
			Bound Brook Bearings (G. B.), Ltd.	5 0 0	9 1 10
			Hunt and Mitton, Ltd.	5 0 0	9 1 10
			Jenkinson (W. G.), Ltd.	5 0 0	9 1 10
			Shaw, Son and Greenhalgh, Ltd.	5 0 0	9 1 10
			Stein (John G.) and Co., Ltd.	5 0 0	9 1 10
			Betts and Co., Ltd.	4 4 0	7 12 6
			Glenfield and Kennedy, Ltd.	4 4 0	7 12 6
			Platt Metals, Ltd.	2 0 0	3 12 9

## B.—ANNUAL DONATIONS TO BE RENEWED (WITHOUT OBLIGATION), BUT NOT UNDER COVENANT.

	£	s.	d.		£	s.	d.
United States Copper and Brass Industry : individual subscriptions, totalling \$2400, by the following :				Wednesbury Tube Co., Ltd., The	42	0	0 *
American Brass Co., The	854	12	0	English Electric Co., Ltd., The (incl. D. Napier and Son, Ltd.)	26	5	0 *
Bridgeport Brass Co.				Head, Wrightson and Co., Ltd.	26	5	0
Bristol Brass Corporation, The				Braby (Fredk.) and Co., Ltd.	25	0	0 (5)
Chase Brass and Copper Co., Inc.				British Timken, Ltd. (incl. Fischer Bearings Co., Ltd.)	25	0	0
Lewin-Mathes Co.				British United Shoe Machinery Co., Ltd., The	25	0	0 *
Revere Copper and Brass, Inc.				Gardner (Henry) and Co., Ltd.	25	0	0 *
Scovill Manufacturing Co.				Telegraph Construction and Maintenance Co., Ltd., The	25	0	0 †
Wolverine Tube Division, Calumet and Hecla Consolidated Copper Co., Inc.				Metal Box Co., Ltd., The	22	1	0 *
Aluminium Laboratories, Ltd. (incl. Alumi- nium Union, Ltd.; Northern Alumi- nium Co., Ltd.; and Stand, Ltd.)				Almin, Ltd.	21	0	0
Tube Investments, Ltd. (incl. The Chester- field Tube Co., Ltd.; Mersey Cable Works, Ltd.; Reynolds Light Alloys, Ltd.; Rey- nolds Rolling Mills, Ltd., South Wales Aluminium Co., Ltd., and T. I. Aluminium, Ltd.)	200	0	0 *	Fulmer Research Institute, Ltd.	21	0	0
Aluminum Company of America (\$500)	178	0	6	Philips Electrical, Ltd.	21	0	0 *
N'changa Consolidated Copper Mines, Ltd.	150	0	0 (7)	Deloro Stellite, Ltd.	20	0	0
Rhodesia Broken Hill Development Co., Ltd., The	150	0	0 *	Park Gate Iron and Steel Co., Ltd., The	20	0	0 *
Rhokana Corporation, Ltd.	150	0	0 (7)	Renfrew Foundries, Ltd.	20	0	0 *
British Insulated Callender's Cables, Ltd. (incl. British Copper Refiners, Ltd.)	100	0	0	Sheffield Smelting Co., Ltd., The	20	0	0 *
Capper Pass and Son, Ltd. (incl. George Pizey and Co., Ltd.; The Tyne Solder Co.; and Victor G. Stevens, Ltd.)	100	0	0 *	Fry's Diecastings, Ltd.	10	10	0 (7)
Johnson, Matthey and Co., Ltd.	100	0	0	Glynn Brothers, Ltd.	10	10	0 *
General Electric Co. (U.S.A.) \$250	88	19	5	Hoover, Ltd.	10	10	0
Manganese Bronze and Brass Co., Ltd., The	52	10	0	Incandescent Heat Co., Ltd., The	10	10	0
Fairey Aviation Co., Ltd., The	50	0	0	Lawley (Thomas), Ltd., and Jones and Rooke (1948), Ltd.	10	10	0 *
G. K. N. Group	50	0	0 *	Crittall Manufacturing Co., Ltd., The	10	0	0
Lucas (Joseph), Ltd. (incl. Rotax, Ltd.)	50	0	0 *	Electric Furnace Co., Ltd.	10	0	0 (3)
				Electric Resistance Furnace Co., Ltd.	10	0	0 (3)
				Rothschild (N. M.) and Sons	10	0	0 *
				Pascall Engineering Co., Ltd., The	6	6	0 *
				United Wire Works (Birmingham), Ltd.	6	6	0 *
				Ratcliffs (Great Bridge), Ltd.	5	5	0 *
				Linread, Ltd.	5	5	0 *
				Langley Alloys, Ltd.	5	0	0 (7)
				Follisain-Wycliffe Foundries, Ltd.	2	2	0
				Jenks (E. P.), Ltd.	1	1	0 *

\* = received as an "annual donation". Where a fixed number of donations is promised, the total number is shown in parentheses.

† see also donations under covenant.

## C.—OTHER DONATIONS, SOME OF WHICH MAY BE RENEWED FOR UNSPECIFIED AMOUNTS.

	£	s.	d.		£	s.	d.
Babcock and Wilcox, Ltd. (incl. The Caloriz- ing Corporation of Great Britain, Ltd.)	250	0	0	Belliss and Morcom, Ltd. (incl. W. Sisson and Co., Ltd.)	10	10	0
General Motors, Ltd. (incl. A. C. Sphinx Spark Plug Co., Ltd., Delco-Remy-Hyatt, Ltd., and Frigidaire, Ltd.)	200	0	0	Carborundum Co., Ltd., The	10	10	0
Allen (W. H.), Sons and Co., Ltd.	105	0	0	Clifford (Charles) and Son, Ltd.	10	10	0
Vickers-Armstrongs, Ltd.	105	0	0	Dennison Watch Case Co., Ltd., and Birming- ham Associated Chain Co., Ltd.	10	10	0
Booth (James) and Co., Ltd. (incl. John Wilkes, Sons and Mapplebeck, Ltd.)	100	0	0	Highton and Son, Ltd.	10	10	0
Davy and United Engineering Co., Ltd.	100	0	0	Hills (West Bromwich), Ltd.	10	10	0
Johnson (Richard) and Nephew, Ltd.	100	0	0	Newey and Tayler, Ltd. (incl. Newey Brothers, Ltd.; and D. F. Tayler and Co., Ltd.)	10	10	0
Rylands Brothers, Ltd., and The Whitecross Co., Ltd.	100	0	0	North Thames Gas Board	10	10	0
Stone (J.) and Co. (Charlton), Ltd.	100	0	0	Vauxhall Motors, Ltd.	10	10	0
Beral Tin and Wolfram, Ltd.	52	10	0	Elliot Brothers (London), Ltd.	10	0	0
Mallory Metallurgical Products, Ltd.	52	10	0	Metro-Cutanit, Ltd.	10	0	0
Austin Motor Co., Ltd., The	50	0	0	Strebor Diecasting Co., Ltd., The	10	0	0
Rolls-Royce, Ltd.	50	0	0	West Yorkshire Foundries, Ltd. (Subsidiary of Leyland Motors, Ltd.)	10	0	0
Weir (G. and J.), Ltd. (incl. Argus Foundry, Ltd.)	50	0	0	Acton Bolt, Ltd.	5	5	0
Copper and Alloys, Ltd.	25	0	0	Barnard (H. B.) and Sons, Ltd.	5	5	0
Messina (Transvaal) Development Co., Ltd., The	25	0	0	Blackwells Metallurgical Works, Ltd.	5	5	0
Plessey Co., Ltd., The	25	0	0	Cohen (Leonard), Ltd.	5	5	0
Roe (A. V.) and Co., Ltd.	25	0	0	Corfield-Sigg, Ltd.	5	5	0
Rover Co., Ltd., The	25	0	0	Easdale (R. M.) and Co.	5	5	0
Thompson (John) (Wolverhampton), Ltd.	25	0	0	Emery Brothers, Ltd.	5	5	0
Bull's Metal and Melloid Co., Ltd.	21	0	0	Headley, Birch and Co., Ltd.	5	5	0
Delta Metal Co., Ltd., The (incl. Heaton and Dugard, Ltd.)	21	0	0	Jacks (William) and Co., Ltd.	5	5	0
Harrison (Birmingham), Ltd.	21	0	0	Lead Wool Co., Ltd., The	5	5	0
Monotype Corporation, Ltd., The	21	0	0	New Metals and Chemicals, Ltd.	5	5	0
Brightside Foundry and Engineering Co., Ltd., The	20	0	0	Preece, Cardew and Rider	5	5	0
Hall and Pickles, Ltd.	20	0	0	Rigby (John) and Sons, Ltd.	5	5	0
Hard Metal Tools, Ltd.	20	0	0	Vincent Engineering Co., Ltd.	5	5	0
Société Anonyme pour l'Industrie de l'Alu- minium (Lausanne, Switzerland)	20	0	0	Wilkinson (John) and Sons (Saltley), Ltd.	5	5	0
Marconi's Wireless Telegraph Co., Ltd.	15	15	0	Cambridge Instrument Co., Ltd.	5	0	0
Perry Barr Metal Co., Ltd.	15	0	0	Hoyt Metal Company of Great Britain, Ltd., The	5	0	0
Brotherhood (Peter), Ltd.	12	12	0	Blakeborough (J.) and Sons, Ltd.	4	4	0
				Kincaid (John G.) and Co., Ltd.	4	4	0
				Mining and Chemical Products, Ltd.	3	3	0
				Walterisation Co., Ltd., The	3	3	0
				Beryllium and Copper Alloys, Ltd.	2	2	0
				Carobronze, Ltd.	2	2	0
				Tungum Sales Co., Ltd.	2	2	0



## APPENDIX II

## COMMITTEES

The main committees of the Institute which have served during the year were constituted as follows at 31 December 1951 :

## FINANCE AND GENERAL PURPOSES COMMITTEE

BALL, Major C. J. P. ( <i>Chairman</i> ).	TASKER, Mr. H. S.
BAILEY, Mr. G. L.	<i>Ex-officio :</i>
BOLTON, Mr. E. A.	President.
GRAHAM, Mr. A. B.	Senior Vice-President.
GUETERBOCK, Colonel Sir Paul.	Honorary Treasurer.
HIGNETT, Mr. H. W. G.	Chairman, Publication Committee.
SMOUT, Sir Arthur.	

## LOCAL SECTIONS COMMITTEE

HIGNETT, Mr. H. W. G. ( <i>Chairman</i> ).	ARNOTT, Mr. John ( <i>Chairman, Scottish Local Section</i> ).
CLARKE, Mr. K. W.	HAY, Mr. Matthew ( <i>Hon. Secretary, Scottish Local Section</i> ).
GARSDIE, Dr. J. E.	HALLETT, Mr. M. M. ( <i>Chairman, Sheffield Local Section</i> ).
GRAHAM, Mr. A. B.	MACDOUGALL, Mr. A. J. ( <i>Hon. Secretary, Sheffield Local Section</i> ).
JONES, Mr. E. H.	HONTOIR, Mr. E. A. ( <i>Chairman, South Wales Local Section</i> ).
KENNETT, Dr. S. J.	SPRING, Mr. K. M. ( <i>Hon. Secretary, South Wales Local Section</i> ).
WALTON, Mr. J. S.	
THOMAS, Mr. Bernard ( <i>Chairman, Birmingham Local Section</i> ).	
BUCKNALL, Mr. E. H. ( <i>Hon. Secretary, Birmingham Local Section</i> ).	
LIDDIARD, Mr. E. A. G. ( <i>Chairman, London Local Section</i> ).	
RHODES, Dr. E. C. ( <i>Hon. Secretary, London Local Section</i> ).	
FINNISTON, Dr. H. M. ( <i>Chairman, Oxford Local Section</i> ).	
FROST, Dr. B. R. T. ( <i>Hon. Secretary, Oxford Local Section</i> ).	
	<i>Ex-officio :</i>
	President.
	Senior Vice-President.
	Honorary Treasurer.

## MEDAL COMMITTEE

PRESIDENT ( <i>Chairman</i> ).	Not more than four medallists who are, or have been, Members of Council (to be selected by the President).
SENIOR VICE-PRESIDENT.	
and	

## METAL PHYSICS COMMITTEE

QUARRELL, Prof. A. G. ( <i>Chairman</i> ).	NUTTING, Dr. J.
BARRETT, Professor C. S.	OLIVER, Mr. D. A. (representing the Iron and Steel Institute and B.I.S.R.A.).
BOWDEN, Dr. F. P.	RICHARDS, Dr. T. Ll.
COTTRELL, Professor A. H.	ROTHERHAM, Mr. L.
FRANK, Dr. F. C.	
HIGNETT, Mr. H. W. G.	<i>Ex-officio :</i>
HUME-ROTHERY, Dr. W.	President.
KING, Mr. R.	Chairman, Publication Committee.
LOMER, Mr. W. M.	
MCLEAN, Mr. D.	
NABARRO, Mr. F. R. N.	

## METALLURGICAL ENGINEERING COMMITTEE

SMITH, Mr. Christopher ( <i>Chairman</i> ).	SWINDELLS, Dr. N.
BAKER, Mr. W. A.	THOMAS, Mr. W. J.
BOLTON, Mr. E. A.	WALTON, Mr. J. S.
BOWMAN, Mr. W. H.	WILKINSON, Mr. R. G.
CAMPBELL, Mr. D. F.	
DAVIES, Mr. C. E.	<i>Ex-officio :</i>
MILLER, Mr. H. J.	President.
PATON, Mr. Charles.	Chairman, Publication Committee.
SINGER, Dr. A. R. E.	

## NOMINATIONS COMMITTEE

PRESIDENT ( <i>Chairman</i> ).	TASKER, Mr. H. S.
SMOUT, Sir Arthur.	SENIOR VICE-PRESIDENT.

## PUBLICATION COMMITTEE

O'NEILL, Professor H. ( <i>Chairman</i> ).	POWELL, Mr. A. R.
BAILEY, Mr. G. L.	SULLY, Mr. W. J.
COTTRELL, Professor A. H.	THOMPSON, Professor F. C.
FOX, Dr. F. A.	TURNER, Mr. T. Henry.
GADD, Mr. E. R.	
HIGNETT, Mr. H. W. G. ( <i>representing the Local Sections Committee</i> ).	<i>Ex-officio :</i>
INGLIS, Dr. N. P.	President.
JENKINS, Dr. Ivor.	Chairman, Finance and General Purposes Committee.
JONES, Mr. E. H.	Honorary Treasurer.
LIDDIARD, Mr. E. A. G.	Chairman, Metal Physics Committee.
PHILLIPS, Mr. H. W. L.	Chairman, Metallurgical Engineering Committee.

# REPORT OF THE HONORARY TREASURER

## FOR THE YEAR ENDED 30 JUNE 1951

THE year has been one of continued expansion of the Institute's activities which has been accompanied by more than a proportionate increase in the running costs due, mainly, to rises in printing and paper charges. It has also been marked by the accession of funds under the schemes originated by a former President, Mr. H. S. Tasker, and by the need to draw upon those funds for the first time in order to meet over-expenditure.

The income and expenditure account discloses that there has been a net increase of income of £936, of which £357 was due to expansion of membership and £572 to enlarged *Journal* sales and advertisement revenue. The net increase in expenditure amounted, however, to £1845. Thus the annual deficiency has increased by £909 (from £1497 to £2406), and would have been some £1760 greater but for a direct net income from the sale of Special Publications.

The items of expenditure showing the largest rises are salaries, printing and publication of the *Journal*, and grants to Local Sections (40%).

For the first time the Institute has been assessed for rates on the accommodation which it occupies. It also bears a part of the assessment on rooms which it shares with the Iron and Steel Institute.

The considerable advances in the price of paper and the cost of printing react most unfavourably on all bodies whose principal activity is publication. In the case of the Institute it is estimated, for instance, that had the increases notified only since June 1951 been operative in the financial year now under consideration the adverse balance of expenditure would have risen by £2185 to a total of £4600 for the identical matter issued in the octavo volume for 1950-51.

The balance sheet shows that the current assets have risen by £2114 and the current liabilities have diminished by £1425. The reserves and current surplus are up by £4466. There has been little change in the investments.

Up to 30 June 1951 the Industrial Donations Fund appeal resulted as follows, inclusive of income tax recoverable :

*Gross Annual Income with  
Income Tax at Present Rate*

A. Annual donations under covenant for not less than seven years . . . . .	£5028
B. Annual donations to be renewed (without obligation), but not under covenant . . . . .	2686
C. Other donations . . . . .	1612

This is the culmination of very strenuous efforts to strengthen the financial structure of the Institute. It must be emphasized again, however, that this extra income is only secure during seven years, and that this period of seven years is but a breathing space. Before its end it is hoped that, by increases in membership and by other means, the gap between income and expenditure will have been filled on a more permanent basis.

The excess of expenditure of £2406 has been met by :

(1) Transferring the balance of £1890 from the War-Time Emergency Fund to the General Account. In this way a resource provided by generous donors during war time to meet post-war difficulties is wound up. It has served an extremely useful purpose and during the last six years has been a stabilizing influence when financial anxiety might have arisen.

(2) Transferring £516 from the new Tasker or Industrial Donations Fund. Since the War-Time Emergency Fund balance included £950 invested in 3% Funding Stock, this has been taken over by the Industrial Donations Fund in exchange for cash.

The problem of the continued existence of learned societies is one which is not only exercising our own Council but also many others. The *Manchester Guardian*, dealing with this question in May 1951, said "The learned society is an institution that has nowhere been more successfully developed than in this country. . . . Its function has become indispensable and if hard times threaten its existence or continued efficiency something must be done about it which few of the individual societies may be able to do for themselves."

With the continued expansion of research in Universities, research organizations, and private firms, and the necessity for making the results of such research widely known and readily applicable, the cost of publication may very soon become more than any Society can bear without heavy endowments or without raising its terms to individual members to such an extent that they become prohibitive, more particularly to the younger member who should be encouraged.

The change in format of the *Journal* from octavo to demy quarto appears generally to have been well received, but the financial advantages to be gained from this change will not be fully felt until the year 1952-53.

The accumulation of papers ready for publication, resulting in much delay, has troubled the Publication Committee and the Council very considerably. For some time there have not been sufficient liquid funds, without encroaching on capital, for this situation to be met adequately. With funds now in hand, however, it is hoped to work off arrears by the end of 1952 and thereafter to have a pre-publication period of only about four months, which is the minimum necessary for efficient publication.

Following the alterations to the Institute's Articles of Association, deemed to be necessary in view of the general statement by the Chancellor of the Exchequer in 1950 on the validity of certain charitable institutions, the Inland Revenue authorities have recognized the claim by the Institute for the repayment of £477 income tax on investment revenue and of £3150 on the Mond Nickel Fellowships Fund. These items were referred to in last year's report.



THE INSTITUTE OF METALS  
BALANCE SHEET AS AT 30 JUNE 1951

[illegible]

REPORT TO THE MEMBERS OF THE INSTITUTE OF METALS

We have audited the above Balance Sheet dated 30 June 1951, and the annexed Income and Expenditure Account for the year ended 30 June 1951, and report that we have obtained all the information and explanations which to the best of our knowledge and belief were necessary for the purposes of our audit.

In our opinion, proper books of account have been kept by the Institute, so far as appears from our examination of those books.

The above mentioned Balance Sheet and annexed Income and Expenditure Account are in agreement with the books of Account.

The said Accounts give the information required by the Companies Act 1948, in the manner so required, and give a true and fair view, in the case of the Balance Sheet, of the state of the Institute's affairs as at 30 June 1951, and in the case of the Income and Expenditure Account of the excess of expenditure over income for the year ended 30 June 1951.

THE INSTITUTE OF METALS  
INCOME AND EXPENDITURE ACCOUNT FOR THE YEAR ENDED 30 JUNE 1951

£	30.6.50 £	£	30.6.50 £
876	12,180	MEMBERS' SUBSCRIPTIONS AND DONATIONS	12,537
151		INTEREST ON INVESTMENTS	
114		General Fund	489
1,141		Endowment Fund	769
			1,265
7,948			
545			
559			
646			
89			
21			
52			
226			
240			
151			
10,457			
694			
802			
298			
1,100			
76			
500			
725			
60			
95			
58			
834			
154			
91			
14,471			
5,342			
5,772			
11,114			
3,357			
11,899			
4,334			
4,736			
—			
20,969			
1,422			
1,008			
1,036			
3,466			
21,435			
227,792			
1,422			
1,008			
1,036			
3,466			
21,435			
227,792			
1,422			
1,008			
1,036			
3,466			
21,435			
227,792			
1,422			
1,008			
1,036			
3,466			
21,435			
227,792			
1,422			
1,008			
1,036			
3,466			
21,435			
227,792			
1,422			
1,008			
1,036			
3,466			
21,435			
227,792			
1,422			
1,008			
1,036			
3,466			
21,435			
227,792			
1,422			
1,008			
1,036			
3,466			
21,435			
227,792			
1,422			
1,008			
1,036			
3,466			
21,435			
227,792			
1,422			
1,008			
1,036			
3,466			
21,435			
227,792			
1,422			
1,008			
1,036			
3,466			
21,435			
227,792			
1,422			
1,008			
1,036			
3,466			
21,435			
227,792			
1,422			
1,008			
1,036			
3,466			
21,435			
227,792			
1,422			
1,008			
1,036			
3,466			
21,435			
227,792			
1,422			
1,008			
1,036			
3,466			
21,435			
227,792			
1,422			
1,008			
1,036			
3,466			
21,435			
227,792			
1,422			
1,008			
1,036			
3,466			
21,435			
227,792			
1,422			
1,008			
1,036			
3,466			
21,435			
227,792			
1,422			
1,008			
1,036			
3,466			
21,435			
227,792			
1,422			
1,008			
1,036			
3,466			
21,435			
227,792			
1,422			
1,008			
1,036			
3,466			
21,435			
227,792			
1,422			
1,008			
1,036			
3,466			
21,435			
227,792			
1,422			
1,008			
1,036			
3,466			
21,435			
227,792			
1,422			
1,008			
1,036			
3,466			
21,435			
227,792			
1,422			
1,008			
1,036			
3,466			
21,435			
227,792			
1,422			
1,008			
1,036			
3,466			
21,435			
227,792			
1,422			
1,008			
1,036			
3,466			
21,435			
227,792			
1,422			
1,008			
1,036			
3,466			
21,435			
227,792			
1,422			
1,008			
1,036			
3,466			
21,435			
227,792			
1,422			
1,008			
1,036			
3,466			
21,435			
227,792			
1,422			
1,008			
1,036			
3,466			
21,435			
227,792			
1,422			
1,008			
1,036			
3,466			
21,435			
227,792			
1,422			
1,008			
1,036			
3,466			
21,435			
227,792			
1,422			
1,008			
1,036			
3,466			
21,435			
227,792			
1,422			
1,008			
1,036			
3,466			
21,435			
227,792			
1,422			
1,008			
1,036			
3,466			
21,435			
227,792			
1,422			
1,008			
1,036			
3,466			
21,435			
227,792			
1,422			
1,008			
1,036			
3,466			
21,435			
227,792			
1,422			
1,008			
1,036			
3,466			
21,435			
227,792			
1,422			
1,008			
1,036			
3,466			
21,435			
227,792			
1,422			
1,008			
1,036			
3,466			
21,435			
227,792			
1,422			
1,008			
1,036			
3,466			
21,435			
227,792			
1,422			
1,008			
1,036			
3,466			
21,435			
227,792			
1,422			
1,008			
1,036			
3,466			
21,435			
227,792			
1,422			
1,008			
1,036			
3,466			
21,435			
227,792			
1,422			
1,008			
1,036			
3,466			
21,435			
227,792			
1,422			
1,008			
1,036			
3,466			
21,435			
227,792			
1,422			
1,008			
1,036			
3,466			
21,435			
227,792			
1,422			
1,008			
1,036			
3,466			
21,435			
227,792			
1,422			
1,008			
1,036			
3,466			
21,435			
227,792			
1,422			
1,008			
1,036			
3,466			
21,435			
227,792			
1,422			
1,008			
1,036			
3,466			
21,435			
227,792			
1,422			
1,008			
1,036			
3,466			
21,435			
227,792			
1,422			
1,008			
1,036			
3,466			
21,435			
227,792			
1,422			
1,008			
1,036			
3,466			
21,435			
227,792			
1,422			
1,008			
1,036			
3,466			
21,435			
227,792			
1,422			
1,008			
1,036			
3,466			
21,435			
227,792			
1,422			
1,008			
1,036			
3,466			
21,435			
227,792			
1,422			
1,008			
1,036			
3,466			
21,435			
227,792			
1,422			
1,008			
1,036			
3,466			
21,435			
227,792			
1,422			
1,008			
1,036			
3,466			
21,435			
227,792			
1,422			
1,008			
1,036			
3,466			
21,435			
227,792			
1,422			
1,008			
1,036			
3,466			
21,435			
227,792			
1,422			
1,008			
1,036			
3,466			
21,435			
227,792			
1,422			
1,008			
1,036			
3,466			
21,435			
227,792			
1,422			
1,00			



THE INSTITUTE OF METALS

## ENDOWMENT FUND

ENDOWMENT FUND					
				£	£
30.6.50	To Transfer to General Fund—Investment Interest	.	.	769	
	" Balance at 30 June 1951	.	.	21,294	21,294
				<u>769</u>	
					769
				<u>£22,063</u>	<u>£22,063</u>
					£22,063

## WAR-TIME EMERGENCY FUND

[illegible]

## INDUSTRIAL DONATIONS FUND

INDUSTRIAL DONATIONS FUND		
	£	£
To Cost of Appeals		
" Amount payable to General Fund, being part Excess of Expenditure over	290	
" Income for the Year ended 30 June 1951	516	
" Balance at 30 June 1951	6,366	
	<u>£7,092</u>	
		By Donations received
		7,092
		<u>£7,092</u>

MOND NICKEL FELLOWSHIPS FUND

MOND NICKEL FELLOWSHIPS FUND	
£	£
To Grants to Fellows, including travelling	£
3,361	3,793
20	—
87	34
4	4
—	27
20,557	23,837
£24,035	£27,875
	£24,035
	£27,875
	£
By Balance at 30 June 1950	20,557
" Donations received	7,000
" Interest on investments and Bank Interest	318
	£

## CAPPER PASS FUND

CAPPER PASS FUND	
£	£
To Grants	By Balance at 30 June 1950
150	258
316	200
" Balance at 30 June 1951	Donations received
	200
	8
	" Bank Interest
	"
£466	£466
	£525
	£525

## W. H. A. ROBERTSON FUND

W. H. A. ROBERTSON FUND			
£	£	£	£
To Cost of Medal	100	By Donation received	100
Balance at 30 June 1950 due to The Institute of Metals	30	Balance at 30 June 1951 due to The Institute of Metals	32
Expenditure during year	2		
	<u>£32</u>		<u>£130</u>
£130			£32

SCHEDULE OF SECURITIES. 30 JUNE 1951

[illegible]

# THE SINTERING OF COPPER-ZINC POWDER COMPACTS\*

1354

By D. D. HOWAT,† B.Sc., Ph.D., F.R.I.C., R. L. CRAIK,† B.Sc., A.R.T.C., and J. P. CRANSTON,‡ B.Sc., Ph.D., A.R.T.C.

## SYNOPSIS

It is shown that data obtained by differential thermal analysis, together with changes in volume and in electrical resistivity, may be taken as criteria of the sintering and alloying processes occurring when compacts of copper and zinc powders are heated. The effects of particle size and compacting pressure on the mechanism have also been investigated.

The first stage in sintering of the compacts is the transfer of zinc atoms to the surfaces of copper particles and the formation of the body-centred cubic  $\beta$  phase of the copper-zinc system. X-ray-diffraction evidence indicates that substantially all the zinc in the compact is transferred to the copper particles, forming  $\beta$  phase. Phase changes on further heating are shown to be due to diffusion of the metals in the solid state and to the volatilization of zinc from the  $\beta$  phase.

## I.—INTRODUCTION

ALTHOUGH the mechanism of the sintering of single-metal powder compacts has been intensively studied during the past few years, no completely satisfactory theory has been formulated to explain all the experimental facts.

The present paper deals with compacts of copper and zinc powders, into the study of which two new factors enter, viz. the relatively high vapour pressure of zinc and the possible formation of new solid phases by interaction of the two metals. Transfer of the zinc to the copper through the vapour phase may be expected to occur, with subsequent alloy formation on the surface of the copper particles.

Differential thermal analysis has been employed, and changes in volume and in electrical resistance of the compacts measured, to assess the value of the data thus obtained as criteria of sintering and in throwing light on the mechanism of the changes taking place. The alloy phases produced have been identified by X-ray methods.

Duwez<sup>1</sup> carried out some work on the volume changes occurring during the sintering of copper-zinc compacts. His results agree closely with those described in the present investigation, as was pointed out in the discussion of his paper.<sup>2</sup>

## II.—EXPERIMENTAL TECHNIQUE

Three different batches of copper powder were used during the experiments. All sizes given refer to B.S. sieves.

### Atomized Copper Powder

(A) A fine powder, all — 300 mesh.

(B) A rather coarser powder with the following sieve analysis:

+ 100 mesh	.	.	.	0.09
100/150 mesh	.	.	.	9.93
150/200 mesh	.	.	.	21.15
200/300 mesh	.	.	.	17.02
— 300 mesh	.	.	.	51.80

(C) — 100 mesh, separated into various grades for specific tests.

### Schori Zinc Powder

Grade "A" All — 300 mesh.

Grade "B" Separated into various grades for specific tests.

Coarser zinc powders, used in some of the experiments, were prepared by filing samples of "Tadanac" "A" grade zinc from Trail, B.C. The filings were sieved into closely graded fractions.

The compacts for test were pressed cold into the form of thin flat discs. Discs weighing 10 g. were used for all tests except for differential thermal analysis, for which 25-g. discs were required. The mould used was a hollow steel cylinder, 3.25 in. in external dia. and 2.4 in. long, with a 1.15-in.-dia. bore. The base plug was 1 in. long, the plunger being chromium plated. With this mould it proved possible to prepare compacts at pressures from 5 to 80 tons/in.<sup>2</sup>. Even with the chromium-plated plunger, considerable trouble was experienced with particles of metal which found their way between the plunger and the wall of the cylinder. Both copper and zinc formed flat slivers which adhered closely to the cylinder wall.

All the experimental work reported was carried out in a vacuum of under 1 mm., produced by an Edwards Hyvac pump. The furnace was wound with Nichrome wire and contained a 2-in.-dia.

\* Manuscript received 6 December 1950.

† Metallurgy Department, The Royal Technical College,

Glasgow.

‡ Metallurgy Department, University of Manchester.



working tube of fused silica. The rate of heating was between  $2.5^{\circ}$  and  $3^{\circ}$  C./min., unless otherwise stated.

### III.—EXPERIMENTAL RESULTS

#### 1. VOLUME CHANGES ON HEATING COMPACTS

To study volume changes on heating, the furnace arrangement shown in Fig. 1 was adopted, the cold-

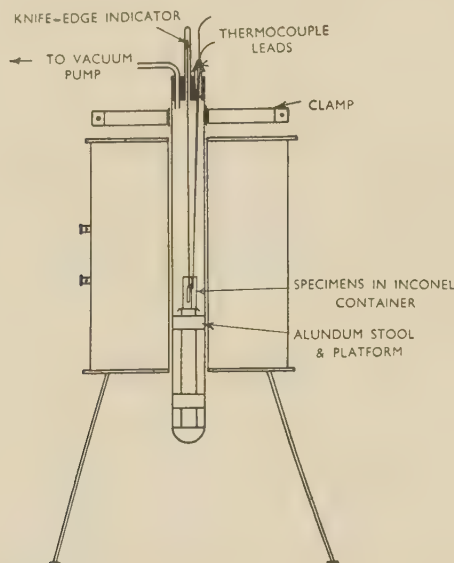


FIG. 1.—Apparatus for Studying Dilatometric Changes.

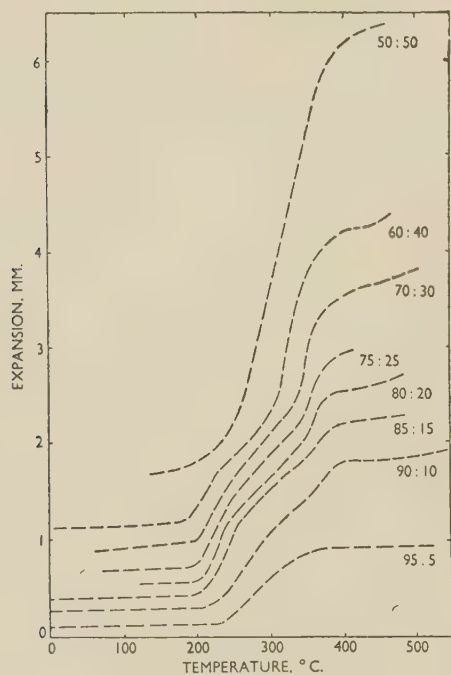


FIG. 2.—Thermal-Expansion Curves for Copper-Zinc Compacts. Pressed at 20 tons/in.<sup>2</sup> and heated *in vacuo*.

pressed disc being arranged vertically in a split Inconel container. Changes in volume were indicated by a thin fused-silica sheath, the lower end of which

passed through a drilled hole in the container and rested on the edge of the disc. The upper end of the sheath was contained within a glass tube in the rubber bung, the movements of a knife-edge resting on the top of the sheath being observed by means of a cathetometer. The thermocouple junction was inserted through another hole drilled in the Inconel container. Cathetometer readings were taken at each 0.1-mV. temperature interval.

The results of some of the expansion tests are shown in Figs. 2 and 3, the expansion across the 1.15-in.-dia. discs being plotted against temperature.

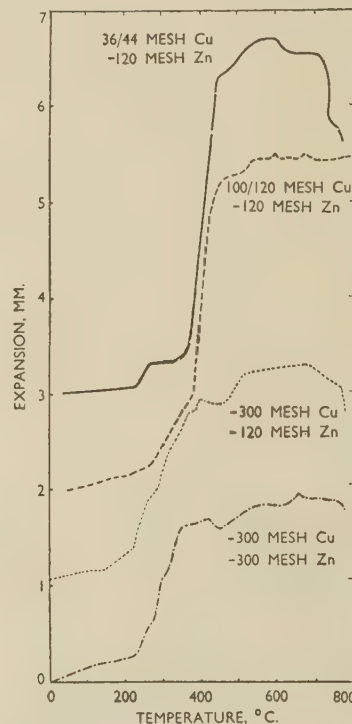


FIG. 3.—Thermal-Expansion Curves for 50:50 Copper-Zinc Compacts, with Varying Mesh Grades of Powders. Pressed at 50 tons/in.<sup>2</sup> and heated *in vacuo*.

All tests gave a pronounced and usually fairly rapid expansion in the region  $200^{\circ}$ – $380^{\circ}$  C. Fig. 2 shows that the magnitude of this expansion is roughly proportional to the zinc content, at least up to 50%.

TABLE I.—Effect of Particle Size on Expansion of 50:50 Copper-Zinc Specimens.

Copper Particle Size	Zinc Particle Size	Observed Expansion	
		mm.	%
36/44 mesh	— 120 mesh	3.66	12.52
100/120 mesh	„ mesh	3.38	11.57
— 300 mesh	„ mesh	2.52	8.63
„ mesh	— 300 mesh	1.96	6.71

The effect of particle size on expansion is illustrated in Fig. 3 and in Table I, for 50:50 copper-zinc compacts. In the range  $200^{\circ}$ – $300^{\circ}$  C. expansion declines with decrease in particle size.

The effect of compacting pressure is shown in Table II for discs containing 70% copper and 30% zinc, the powders used being — 300 mesh. With powders of this size minimum expansion occurs at a compacting pressure of 30–50 tons/in.<sup>2</sup>.

TABLE II.—Effect of Compacting Pressure on Expansion of 70 : 30 Copper-Zinc Specimens.

Compacting Pressure, tons/in. <sup>2</sup>	Expansion in Range 180°–380° C.		Temp. of Start of Expansion, °C.	Temp. of End of Expansion, °C.	Rate of Expansion, mm./°C.	Temp. Range of Expansion, °C.
	mm.	%				
10	2.31	7.91	216	324	0.021	108
20	2.27	7.78	215	332	0.019	117
30	1.69	5.78	226	346	0.014	120
50	1.32	4.52	200	385	0.007	185
50	1.50	5.13	200	385	0.008	185
70	1.72	5.88	179	385	0.0085	206

## 2. CHANGES IN ELECTRICAL RESISTANCE OF DISCS

Fig. 4 shows the horizontal-furnace arrangement adopted for the study of changes in electrical resistance. Two holes of about  $\frac{3}{32}$ -in. dia. were bored through the disc sample at  $\frac{3}{4}$ -in. centres. The disc was then bolted with Inconel screws to the ends of two lengths of  $\frac{1}{4}$ -in. copper rod, the ends of which were drilled and tapped. Two heavy asbestos clamps inside the furnace tube kept the copper rods rigid, the rods passing through holes in the rubber bung. The thermocouple wires passed through a glass tube inserted

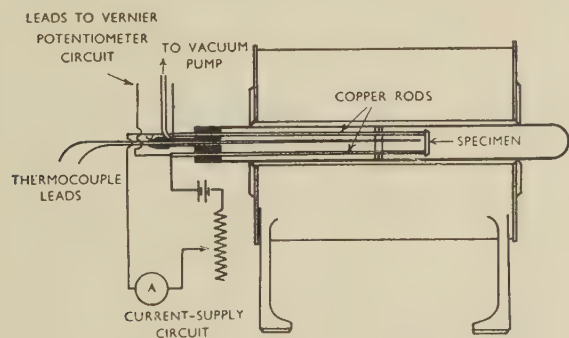


FIG. 4.—Apparatus for Measuring Relative Resistance.

in the rubber bung, another glass tube being connected to the Hyvac pump. The junction of the thermocouple was arranged just to touch the disc. A current of about 5 amp. was passed through the disc by means of the heavy copper rods, the potential drop across it being measured by a Tinsley vernier potentiometer at intervals of 2.5° C.

No attempt was made to calculate resistance figures in ohms/cm.<sup>3</sup>, because of the large volume changes in the discs, and the results are expressed in terms of potential drop across the specimen against temperature. Figs. 5, 6, and 7 show the changes in resistance with temperature of copper-zinc discs under specified conditions of composition, particle size, and compacting pressure.

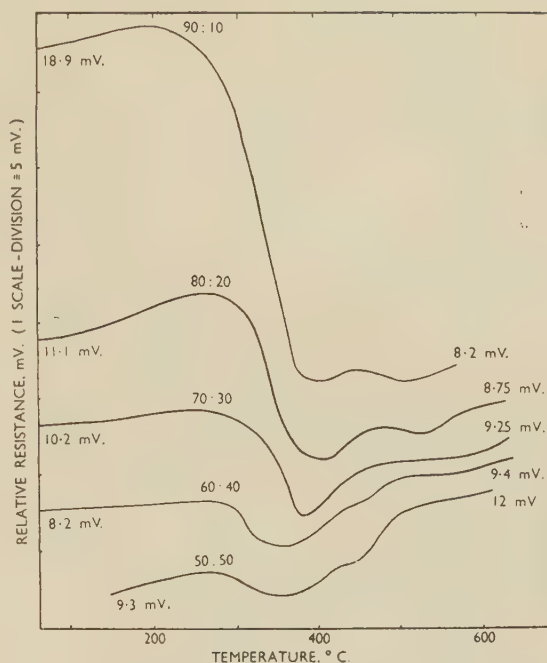


FIG. 5.—Relative-Resistance Curves for Compacts Composed of Coarse (B) Copper Powder with — 300-Mesh Zinc Powder. Pressed at 50 tons/in.<sup>2</sup> and heated *in vacuo*. Initial and final resistance values are given for each curve.

A few tests were carried out to determine the resistance changes in discs made from pure copper powder, two typical results being given in Fig. 8. The first drop in resistance occurred at 120° C., i.e. at a lower temperature than any of the copper-zinc discs. For the disc pressed at 80 tons/in.<sup>2</sup> the

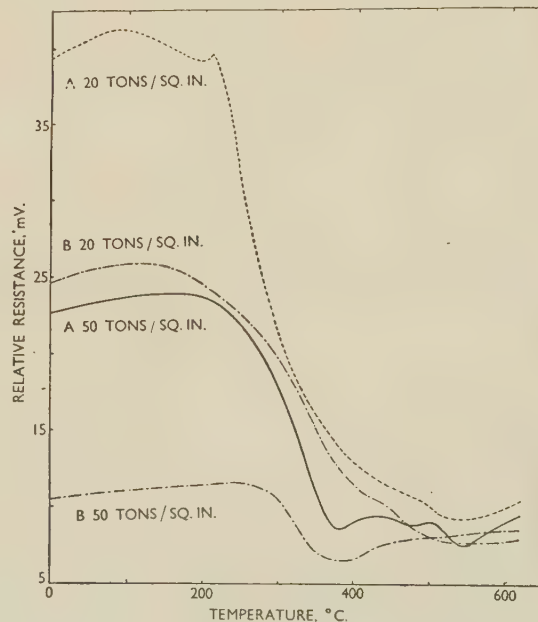


FIG. 6.—Relative-Resistance Curves for 80 : 20 Compacts Composed of Fine (A) and Coarse (B) Copper Powders with — 300-Mesh Zinc Powder. Pressed at 20 and 50 tons/in.<sup>2</sup> and heated *in vacuo*.



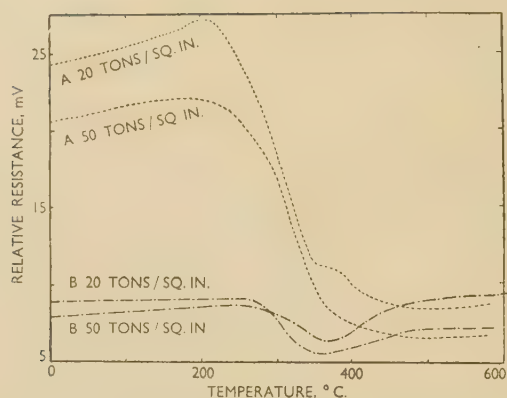


FIG. 7.—Relative-Resistance Curves for 60:40 Compacts Composed of Fine (A) and Coarse (B) Copper Powders with — 300-Mesh Zinc Powder. Pressed at 20 and 50 tons/in.<sup>2</sup> and heated *in vacuo*.

resistance curve gives a positive coefficient with temperature after heating to 525° C., while the disc pressed at 50 tons/in.<sup>2</sup> did not show a positive coefficient until it had been heated to 800° C.

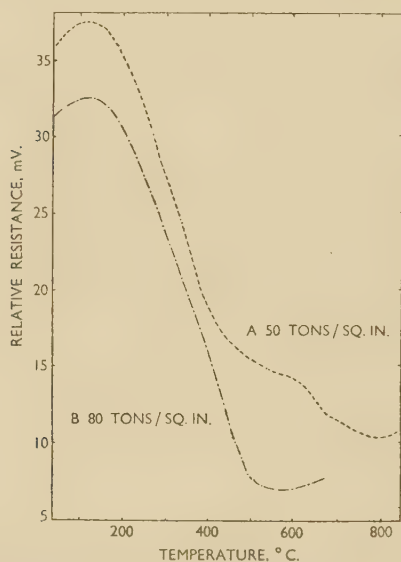


FIG. 8.—Relative-Resistance Curves for Pure Copper Compacts Composed of Fine (A) and Coarse (B) Powders. Pressed at (A) 50 and (B) 80 tons/in.<sup>2</sup> and heated *in vacuo*.

### 3. DIFFERENTIAL THERMAL ANALYSIS

Differential thermal curves were obtained, using copper as the standard and a half disc (weighing 12½ g.) as the test specimen. The standard and test specimens, of the same shape, size, and weight, were placed inside an Alundum container, made with two appropriate recesses. The junction of the temperature-measuring thermocouple was inserted into a small hole in the centre of the Alundum container (see Fig. 9).

Fig. 10 gives the differential thermal curves for a series of discs made from — 300-mesh copper

powder and — 120-mesh zinc powder. The percentage of zinc varied from 10 to 50, the compacting pressure being 50 tons/in.<sup>2</sup>. The most notable feature of these curves is the sudden and pronounced exothermic change, with a maximum occurring at 250° C. The magnitude of this thermal change is

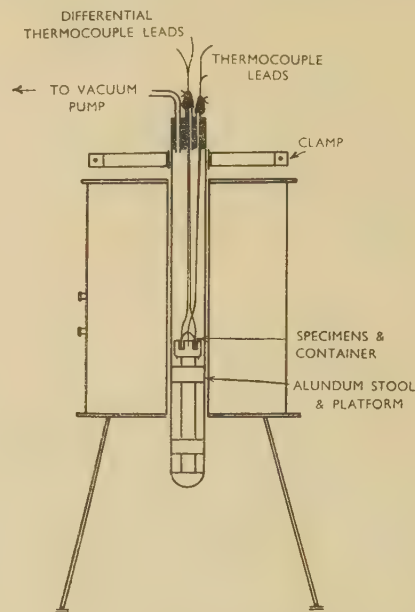


FIG. 9.—Apparatus for Studying Thermal Changes.

greatest at between 40 and 50% zinc. Secondary changes following the main change are much smaller and extend over a much wider range.

Figs. 11 and 12 illustrate the effect of variation in the particle size of the copper and the zinc, respectively, on the differential thermal curves for

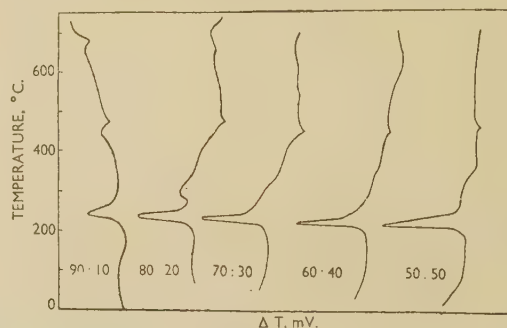


FIG. 10.—Differential Thermal Curves for Compacts of Varying Composition Made from — 300-Mesh Copper and — 120-Mesh Zinc Powders. Pressed at 50 tons/in.<sup>2</sup> and heated *in vacuo*.

50:50 copper-zinc discs pressed at 50 tons/in.<sup>2</sup>. The thermal change at 250° C. does not occur with copper particles larger than 120 mesh, but there is a definite change at about 420° C. corresponding to the melting point of zinc or a zinc-rich phase. A similar effect is obtained by varying the sizes of the zinc particles, as shown in Fig. 12. The effects

are less marked than those produced by variation in the copper-particle sizes, e.g. the thermal change

#### 4. X-RAY STUDY OF PHASES PRODUCED DURING SINTERING

The discs were studied by means of a Philips X-ray machine equipped with a Geiger-counter spectrometer. Table III shows the main X-ray

TABLE III.—X-Ray Lines Used in Phase Identification.

2 $\theta$ Values, degrees	Miller Indices
<i>Copper Lines</i>	
43.2	222
50.2	211
73.4	111
<i><math>\beta</math>-Phase Lines</i>	
43.4	110
62.76	200
79.8	211
<i>Zinc Lines</i>	
36.3	204
38.95	222
42.25	300
54.20	402
69.90	... *
70.40	501
81.80	510

\* Line probably due to Cu  $K_{\alpha}$  radiation.

lines used in the identification of the phases present in the discs.

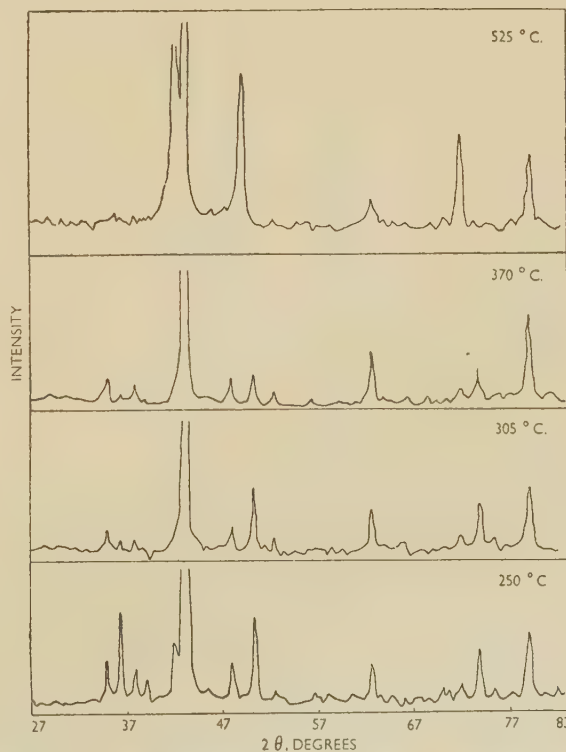


FIG. 14.—X-Ray-Diffraction Curves for 50 : 50 Compacts Made from — 300-Mesh Copper Powder and — 120-Mesh Zinc Powder. Heated for 2 hr. at the temperatures indicated.

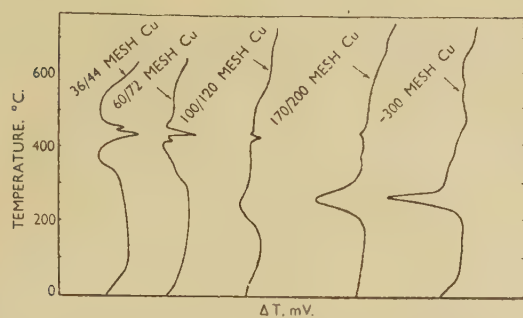


FIG. 11.—Differential Thermal Curves for 50 : 50 Compacts Composed of — 120-Mesh Zinc Powder with Various Grades of Copper Powder. Pressed at 50 tons/in.<sup>2</sup> and heated *in vacuo*.

at 420° C. occurs only when the zinc particles are larger than 36 mesh.

Fig. 13 shows that with copper and zinc particles



FIG. 12.—Differential Thermal Curves for 50 : 50 Compacts Composed of — 300-Mesh Copper Powder with Various Grades of Zinc Powder. Pressed at 50 tons/in.<sup>2</sup> and heated *in vacuo*.

finer than 300 mesh, variation in the compacting pressure from 10 to 75 tons/in.<sup>2</sup> has very little effect on the thermal changes. Only in the case of discs

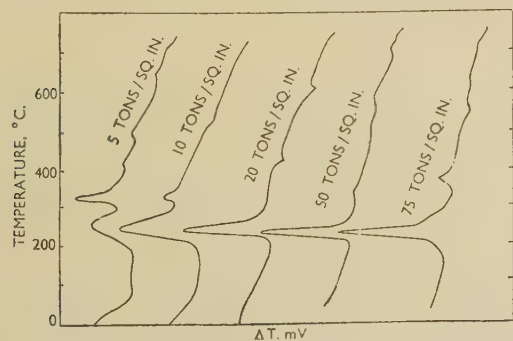


FIG. 13.—Differential Thermal Curves for 50 : 50 Compacts Made from — 300-Mesh Copper and — 300-Mesh Zinc Powders with Varying Pressures and Heated *in vacuo*.

pressed at 5 tons/in.<sup>2</sup> is there any significant difference in the change, which becomes less well defined, showing two maxima at 265° and 320° C., respectively.



The X-ray data for a series of copper-zinc powder compacts, heated to 750° C. and allowed to cool slowly, are presented in Table IV. This shows that discs containing up to 50% zinc, pressed at 50 tons/in.<sup>2</sup> and heated to 750° C., are composed of the same solid phases that would be expected in the corresponding series of alloys made by melting and casting mixtures containing the appropriate amounts of the two metals. Some loss of zinc occurs by volatilization, so that, for example, the disc made up to 60 : 40 composition contains less  $\beta$  than would be

TABLE IV.—X-Ray Data for Copper-Zinc Powder Compacts.

Series made from atomized copper powder (A) and Schori Grade "A" zinc powder.

All compacts were made under pressure of 50 tons/in.<sup>2</sup>, heated gradually to 750° C. and allowed to cool slowly.

Composition of Compact, %	Major Lines in X-Ray Spectra		
	Angle, degrees	Plane of Reflection	Phases Present
Cu 100 {	43.3	222	...
	50.3	211	...
	73.9	111	...
Zn 100 {	43.3	...	...
	36.3	...	...
	39.0	...	...
	54.2	...	...
	69.9	...	...
	81.9	...	...
Cu 90 Zn 10 {	42.9	222	} $\alpha$
	50.0	211	
	73.3	111	
Cu 80 Zn 20 {	42.7	222	} $\alpha$
	49.7	211	
	72.9	111	
Cu 70 Zn 30 {	42.5	222	} $\alpha$
	49.4	211	
	72.4	111	
Cu 60 Zn 40 {	42.2	222	} $\alpha$ $\beta$ $\alpha$ $\alpha$
	43.3	110	
	49.2	211	
	71.9	111	
Cu 50 Zn 50 {	43.3	110	} $\beta$
	62.5	200	
	79.1	211	

expected, while the disc made up to 50 : 50 composition contains no  $\gamma$ , and may contain a small quantity of  $\alpha$ .

A series of compacts were prepared in order to study the new solid phases formed on heating to various temperatures. The important variables in this connection were composition, particle size, temperature, compacting pressure, and time of heating at the given temperature. The differential thermal curves had shown that a highly significant exothermic change occurred at 250° C. on heating the compacts. This was accordingly one of the selected temperatures for the series of tests, the other

temperatures being 305°, 370°, and 525° C. Table V gives particulars of the compacts prepared for this series of tests.

The results of the X-ray investigation were all plotted on large-scale graph paper. The appropriate data from each plot were abstracted and are correlated in Table VI. Fig. 14 is a typical X-ray

TABLE V.—Data on Copper-Zinc Powder Compacts Prepared for X-Ray Examination.

Compact No.	Composition, %	Particle Size (B.S. Mesh Sieves)	Compacting Pressure, tons/in. <sup>2</sup>	Time of Annealing at Temperature, hr.
1	Cu 90 Zn 10	— 300 — 300	50	2
2	Cu 70 Zn 30	— 300 — 300	50	2
3	Cu 50 Zn 50	60/72 — 120	50	2
4	Cu 50 Zn 50	170/200 — 120	50	2
5	Cu 50 Zn 50	— 300 — 120	50	2
6	Cu 50 Zn 50	170/200 — 120	100	2
7	Cu 50 Zn 50	170/200 — 120	50	4
8	Cu 50 Zn 50	— 300 — 120	50	4
9	Cu 50 Zn 50	100/120 — 120	50	12
10	Cu 50 Zn 50	36/44 — 120	50	2

plot for compacts prepared from — 300-mesh copper and — 120-mesh zinc powders and heated to the temperatures indicated for 2 hr.

The data obtained from the X-ray examination of test specimens treated as shown in Table V indicate that :

(1) The initial stage in sintering is the formation of  $\beta$  phase. Even in discs where  $\alpha$  is the equilibrium phase,  $\beta$  forms first and no appreciable quantities of  $\alpha$  appear until practically all the zinc has been transformed into  $\beta$ . Thereafter  $\alpha$  is formed by diffusion.

(2) The rate of  $\beta$  formation is speeded by increase in compacting pressure and decrease in particle size of copper and, to a lesser extent, of zinc. A higher temperature is required for the conversion of all the zinc to  $\beta$  as the particle size of the copper is increased.

(3) The lowest temperature at which  $\beta$  begins to form is 170° C., the maximum rate of formation occurring at about 250° C. in the discs made with the finest powders.

TABLE VI.—X-Ray Data for Copper-Zinc Powder Compacts.

Compact No.	Possible Phases Present	Temperature to Which Compact was Heated			
		250° C.	305° C.	370° C.	525° C.
1	Cu Zn $\beta$ $\alpha$	Strong Absent Very slight Absent	Strong Absent Slight Absent	Strong * Absent Very slight Absent	Absent " " Strong
2	Cu Zn $\beta$ $\alpha$	Strong Weak Slight Absent	Strong * Absent Moderate Absent	Absent " Weak Strong	Absent " " Strong
3	Cu Zn $\beta$ $\alpha$	Strong " Very slight Absent	Strong Weak Moderate Absent	Moderate * Absent Moderate Absent	Absent " Strong Slight
4	Cu Zn $\beta$ $\alpha$	Strong Moderate Slight Absent	Strong Absent Strong Absent	Moderate * Absent Strong Absent	Absent " Strong Slight
5	Cu Zn $\beta$ $\alpha$	Strong Weak Moderate Absent	Strong * Absent Strong Absent	Absent " Strong Slight	Absent " Moderate Strong
6	Cu Zn $\beta$ $\alpha$	Strong Moderate † Strong Absent	Moderate Absent Strong Absent	... ... ... ...	... ... ... ...
7	Cu Zn $\beta$ $\alpha$	Moderate Absent Strong Absent	Moderate Absent Strong Absent	... ... ... ...	... ... ... ...
8	Cu Zn $\beta$ $\alpha$	Moderate Absent Strong Absent	... ... ... ...	... ... ... ...	... ... ... ...
9	Cu Zn $\beta$ $\alpha$	Strong Weak Moderate Absent	... ... ... ...	... ... ... ...	... ... ... ...
10	Cu Zn $\beta$ $\alpha$	Strong Moderate Very faint Absent	Strong Moderate " Absent	... ... ... ...	... ... ... ...

\* Indicates that the copper lines showed very slight displacement owing to the beginning of the formation of  $\alpha$ . When this displacement becomes more pronounced with rise in temperature,  $\alpha$  is recorded as present and copper as absent.

† Absent after 4 hr. at 250° C.

## IV.—DISCUSSION OF RESULTS

### 1. GENERAL

Discs of powdered metals may be considered as composed of particles touching one another at certain points. With discs made from metals of low vapour pressure, sintering may occur by diffusion at the points of contact between the particles. With spherical particles this contact area is limited and, for the same weight of disc, decreases as the particle size increases. In copper-zinc discs the relatively high vapour pressure of the zinc removes this limiting factor, so that, in effect, the total surface area of the copper particles may be regarded as the diffusion interface. Further, Smigelskas and Kirkendall<sup>3</sup> have shown that the diffusion of zinc into copper occurs much more rapidly than that of copper into zinc, so that the sintering of the discs of copper and zinc powders may be pictured almost entirely in terms of

the transfer of the zinc to the copper surface and the subsequent diffusion of the zinc into the copper.

Although the disc is at a uniform temperature, the zinc can be deposited on the copper surfaces, because the  $\beta$  which forms has a lower zinc vapour pressure than that of the pure metal. This may be shown by extrapolating Hargreaves's<sup>4</sup> figures for the vapour pressures of copper-zinc alloys to the temperature range used in the present experiments. Theoretically, therefore, complete transfer of the zinc to the copper may occur. The limiting factors are the surface area of the copper particles and the speed of diffusion of zinc. If the quantity of zinc volatilized in any given time is greater than can be absorbed by the copper owing to either of these limiting factors, then zinc vapour is lost from the disc.

This conception of the mechanism of sintering in copper-zinc compacts has been confirmed by the dilatation, electrical-resistance, and thermal-analysis investigations. The beginning of the formation of  $\beta$  was marked in each of these tests by physical changes within the range 130°–380° C., the actual temperature depending on various secondary factors such as composition, particle size, and compacting pressure.

### 2. DILATATION TESTS

A sudden expansion occurred in all the discs in the range 175°–380° C., the magnitude being proportional to the zinc content. This expansion is due to the growth of the individual copper particles, caused by the absorption and diffusion of the zinc and by the atomic re-arrangement involved in the change from the face-centred cubic lattice of the copper to the body-centred cubic lattice of  $\beta$ .

#### (a) Effect of Particle Size

It would be expected from geometrical considerations that the increase in voids due to the growth of the copper particles would be greater the larger the particles. This is confirmed by Fig. 3, which shows that, for a constant composition, the total disc expansion becomes greater as the size of the copper particles increases.

#### (b) Effect of Compacting Pressure

The effect of compacting pressure on expansion, as indicated in Table II, may also largely be explained in terms of growth of copper particles and voids. Increase in compacting pressure leads to a decrease in the initial voids and a greater mechanical strength of the disc. It appears that up to a compacting pressure of 25–35 tons/in.<sup>2</sup>, the combination of these two factors prevents expansion of the disc from occurring to the same extent. With packing pressures above this range, the voids have been reduced to such an extent that the growth of the individual copper particles results in an increased expansion of the disc.



### 3. ELECTRICAL-RESISTANCE TESTS

As shown in Figs. 5-8, the electrical resistance of all discs increases slightly on heating to 130°-250° C. and then decreases suddenly throughout the temperature range in which  $\beta$  is forming most rapidly. Since the electrical resistance of  $\beta$  is greater than that of either copper or zinc, the observed decrease might at first sight appear anomalous. Such a conclusion takes no account, however, of the physical structure of the disc, which is an agglomerate of separate particles bonding only at isolated points and separated to a large extent by air films and pockets. During the initial heating to 130°-250° C., before any changes take place, the electrical resistance shows the slight positive coefficient associated with any normal conductor. When  $\beta$  begins to form, there is an immediate increase in the contact area between the particles. There are thus two opposing influences at work: the  $\beta$  phase formed has a higher resistance than the parent metals, whereas the growth of the contact areas tends to increase the conductivity. The observed drop in the resistance of the discs proves that the extension of the contact areas is the dominant factor.

It is axiomatic that the electrical conductivity of a disc depends upon the number and the area of the contacts between the constituent particles. The number of contacts may be increased by combining various sizes of particles in suitable proportions to give a mixture with a high packing density. This is illustrated by the results shown in Fig. 5. The value of the initial resistance of the disc decreases as the proportion of fine zinc powder to coarse copper powder is increased. As the initial area of contact becomes greater, there is a correspondingly smaller drop in resistance when the disc is heated within the range 130°-250° C. In addition, as the proportion of zinc increases, greater quantities of  $\beta$  are formed, the change in conductivity becoming increasingly dominated by this factor. In the case of the 60:40 and 50:50 copper-zinc discs, the final resistance is higher than the initial resistance.

In the discs made from — 300-mesh powders the initial resistance is higher than that of the previous series. While particle-size distribution may play a part, it is probable that the effects of surface condition, oxide film, air film, and moisture film, exercise the predominant influence, and the higher internal resistance of discs made from these fine powders is easily explained.

### 4. SINTERING OF PURE COPPER DISCS

As is evident from Fig. 8, the resistance curves obtained on heating discs made from pure copper powder show the same general features as those of the copper-zinc discs. These tests were completed before publication of the work of Shaler and Wulff,<sup>5</sup> Kuczynski,<sup>6</sup> and Rhines, Birchenall, and Hughes.<sup>7</sup> In the light of their much more exhaustive work, it

is difficult to offer any very definite views on the resistance curves.

According to Hüttig<sup>8</sup> and to Shaler<sup>9</sup> the alterations that occur as a powder-metal disc is heated may be subdivided into "transient" and "steady-state" phenomena. Hüttig<sup>8</sup> holds that the following changes occur in the order given as the disc is heated slowly: (1) the desorption of physically adsorbed gases; (2) atomic re-arrangement of the surface; (3) breakdown of chemically adsorbed surface compounds; and (4) recrystallization. The characteristics of the steady-state phenomena are: (i) spheroidization of voids; and (ii) densification of the compact.

On these definitions the changes in resistance in the discs made from pure copper may be described as transient phenomena, but it may be pointed out that they cover a temperature range extending from the transient up to the steady-state phenomena of densification. The magnitude of the changes in resistance is significant, the resistance of the disc after heating being only about one-fifth of the initial value. Considerable re-arrangement of the atoms in the surface layers is obviously involved before a change of this magnitude can occur.

### 5. DIFFERENTIAL THERMAL ANALYSIS

As already noted, in the differential thermal curves for discs made with fine copper and zinc powders the formation of  $\beta$  is marked by a large heat evolution which reaches a maximum at 250° C. Fig. 10 shows that this heat evolution increases with the zinc content up to 40-50%.

#### (a) Effect of Particle Size

The effect of particle size on the heat changes is shown in Figs. 11 and 12. Increase in the size of the copper particles reduces the area on which the zinc may be absorbed, and therefore reduces the heat evolved at any given moment. If the area of the copper becomes too small for equilibrium to be attained with the heating rate employed, the free zinc left in the disc melts when the temperature reaches 419° C. These changes are clear from Fig. 11. With copper particles of 100/120 mesh the heat evolution is indistinct and diffuse, and there is a faint indication of the melting of a zinc-rich material. Very decided evidence of fusion of zinc-rich material occurs with larger-sized copper particles, as shown in Fig. 11.

Increase in the size of the zinc particles reduces the number of solid contacts between the particles of copper and zinc, and diminishes the total surface area from which zinc may volatilize. The rate of  $\beta$ -phase formation is thereby reduced and the heat evolution is less well defined, as shown in Fig. 12. An important difference between Figs. 11 and 12 is that no indication of fusion of the zinc phase occurs until very large zinc particles (+ 36 mesh) are used. With zinc particles of 44/60 mesh,

there is a distinct heat evolution at 370° C. Quite pronounced formation of  $\beta$  is, therefore, occurring with these comparatively coarse zinc particles at temperatures well below the melting point of zinc, confirming that transport of zinc to the copper surfaces takes place to a large extent through the vapour phase.

(b) *Effect of Compacting Pressure*

It can be seen from Fig. 13 that in discs made with very fine copper and zinc powders, variation in compacting pressure has very little effect on the temperature of formation of  $\beta$  or on the rate at which it occurs. With all pressures between 10 and 75 tons/in.<sup>2</sup>, formation of  $\beta$  begins at 150°–180° C. and reaches a maximum at about 250° C. Only when compacting at 5 tons/in.<sup>2</sup> is the heat evolution

slightly diffuse, with the maximum occurring at higher temperatures. This also is in agreement with the postulate that transport of zinc to copper occurs through the vapour phase. If solid/solid contact between the particles were the predominant factor, an increase in packing pressure would be expected to exert a profound influence on  $\beta$  formation.

ACKNOWLEDGEMENTS

The authors wish to thank colleagues in the Metallurgy Department, The Royal Technical College, for helpful discussion and criticism of this paper.

They are much indebted to Professor R. Hay, Head of the Metallurgy Department, who first suggested research work on this problem and whose encouragement and constructive criticism have been of great value at all times.

---

REFERENCES

1. P. Duwez and H. Martens, *Trans. Amer. Inst. Min. Met. Eng.*, 1949, **185**, 571.
2. D. D. Howat, R. L. Craik, and J. P. Cranston, *ibid.*, 1950, **188**, 1046 (discussion).
3. A. D. Smigelskas and E. O. Kirkendall, *ibid.*, 1947, **171**, 130.
4. R. Hargreaves, *J. Inst. Metals*, 1939, **64**, 115.
5. A. J. Shaler and J. Wulff, *Indust. and Eng. Chem.*, 1948, **40**, 838.
6. G. C. Kuczynski, *Trans. Amer. Inst. Min. Met. Eng.*, 1949, **185**, 169.
7. F. N. Rhines, C. E. Birchenall, and L. A. Hughes, *ibid.*, 1950, **188**, 378.
8. G. F. Hüttig, *Kolloid-Z.*, 1941, **97**, 227, 281; 1942, **98**, 6, 263.
9. A. J. Shaler, *Trans. Amer. Inst. Min. Met. Eng.*, 1949, **185**, 796.





# THE EFFECT OF THE ELEMENTS OF THE FIRST LONG PERIOD ON THE $\alpha \rightleftharpoons \beta$ TRANSFORMATION IN TITANIUM \*

1355

By A. D. McQUILLAN,† Ph.D., B.Sc.

## SYNOPSIS

The method in which the hydrogen pressure in equilibrium with an extremely dilute solution of hydrogen in a titanium-rich alloy is measured as a function of temperature in order to follow the phase transformations occurring in the alloy, described in a previous paper (*J. Inst. Metals*, 1951, 79, 73), has been used for a systematic investigation of the effects of vanadium, chromium, manganese, nickel, and cobalt on the  $\alpha \rightleftharpoons \beta$  transformation in titanium. The maximum amount of each addition element used was approximately 5 at.-%.

It is found that all these elements, when added to titanium, depress the allotropic transformation, and that, with the exception of vanadium, they are not appreciably soluble in the low-temperature ( $\alpha$ ) form of titanium. The extent of the depression of the  $\beta/(\alpha + \beta)$  boundary is substantially the same for equal atomic fractions of all the addition elements, except in the case of vanadium, which is slightly less effective in this respect than the others. The experimentally determined  $\beta/(\alpha + \beta)$  boundaries have been compared with an idealized theoretical boundary obtained from the known latent heat of transformation of pure titanium.

The experimental data have been used to determine the effect of addition elements on the hydrogen solubility in  $\beta$ -titanium. Vanadium caused the greatest change in this property, the other elements having but little effect.

## I.—INTRODUCTION

THE application of the measurement of the change with temperature of the hydrogen pressure in equilibrium with very dilute solutions of hydrogen in titanium metal and titanium-rich alloys to the study of phase transformations in these materials has previously been described by the author.<sup>1, 2</sup> The results have shown that the method is accurate and extremely convenient for the examination of titanium-rich alloys. It has therefore been employed for a systematic investigation of the effect of addition elements of the first long period of the Periodic Table on the  $\alpha \rightleftharpoons \beta$  transformation in titanium. From the experimental results obtained, it has been possible to investigate the effect of the addition elements on the hydrogen solubility in the  $\beta$  solid solution of the various systems.

## II.—PREPARATION AND ANALYSIS OF SPECIMENS

The titanium metal used in this investigation was prepared at Philips's Gloeilampenfabrieken by the van Arkel method. The metal was 99.93% pure, the impurities being iron, oxygen, and faint traces of a number of other metallic elements. The addition elements used in the preparation of the alloys were of the highest available purity, and were all, with the

exception of vanadium, at least 99.9% pure. The manganese, chromium, and cobalt were prepared electrolytically by the U.S. Bureau of Mines, the high-purity carbonyl nickel was manufactured by The Mond Nickel Co., Ltd., and the vanadium of greater than 99% purity was prepared by Johnson, Matthey and Co., Ltd. As was to be expected, the major impurity in the vanadium was oxygen, which was present to an extent sufficient to make the metal somewhat brittle.

The alloys were prepared by melting together the component metals in an arc furnace containing an atmosphere of carefully purified argon at a reduced pressure. The details of the melting and subsequent homogenizing processes applied to the specimens are fully described in a previous paper.<sup>2</sup> Since the subsequent experiments on the alloy samples showed that all began to transform very sharply at the boundaries in the constitutional diagrams, it would appear that the method of preparation, and the homogenizing and cleaning treatments of the alloys, were satisfactory.

After each series of hydrogen-pressure/temperature measurements the alloy specimen was analysed. A semi-microchemical colorimetric method<sup>3</sup> was used for all elements except vanadium. The results were shown by control experiments to be accurate to between 1 and 2%. The analysis of vanadium, for which no colorimetric method has at present been

\* Manuscript received 11 May 1951.

† Formerly Senior Research Officer, Commonwealth Scientific and Industrial Research Organization, University

of Melbourne, Australia; now Senior Research Fellow, Department of Metallurgy, University of Birmingham.



devised, was carried out by ordinary chemical methods. For this purpose a quantity of alloy in excess of the specimen used for the hydrogen-pressure measurements was necessary, and the analysis was, therefore, carried out on the alloy remaining from the melt after a specimen had been prepared. This may have had the effect of diminishing the accuracy of the analytical results for the titanium-vanadium alloys.

### III.—EXPERIMENTAL PROCEDURE

In the hydrogen-pressure method of investigating phase transformations occurring in alloys which exhibit a marked affinity for hydrogen, a very small quantity of pure hydrogen, prepared by the thermal decomposition of titanium hydride, is dissolved in the alloy specimen. On heating the specimen in a closed system of small internal volume, hydrogen is liberated until the hydrogen pressure in the system has reached a value at which it is in equilibrium with the hydrogen still dissolved in the specimen. The equilibrium hydrogen pressure depends on the temperature of the specimen, the concentration of dissolved hydrogen, and the solubility of hydrogen in the phase or phases present in the alloy. The details of the apparatus, the method of procedure in carrying out these investigations, and the precautions to be observed when using the hydrogen method have been described in an earlier paper.<sup>2</sup>

The change in equilibrium hydrogen pressure  $p$  of a dilute solution of hydrogen in a single homogeneous phase at a temperature  $T$  is given by the equation:

$$p = kc^2e^{Q/RT} \quad \dots \quad (1)$$

where  $c$  is the concentration of the dissolved hydrogen,  $R$  is the gas constant,  $Q$  is the heat of solution of molecular hydrogen in the alloy phase, and  $k$  is a proportionality constant. In general, the values of  $Q$  and  $k$  change with the composition of a phase and are different for different alloy phases. Over the temperature range covered by the present investigation, both quantities are independent of temperature. The equation shows that, for a specimen in a single-phase condition,  $\log p$  should be proportional to  $1/T$ , ( $T$  being in  $^{\circ}\text{K}.$ ). Any departure from linearity in the curves of  $\log p$  against  $1/T$  for an alloy indicates that the alloy is no longer in the single-phase condition.

The standard procedure could not be used for the manganese alloys, because at the higher temperatures these alloys lost manganese rapidly by volatilization. It was not possible in this system, therefore, to cover the temperature range by starting at the highest temperature and taking readings at successively lower temperatures, since the rate of evaporation of manganese from the surface of the specimen was sufficiently great to cause serious concentration gradients. This had the effect of rounding off the discontinuities at the beginning of the  $\alpha \rightleftharpoons \beta$  transformation, and rendering the results valueless. Therefore, results were obtained for the series of

manganese alloys by annealing the specimens, in which the required amount of hydrogen had previously been dissolved, for a prolonged period at  $700^{\circ}\text{C}.$ , until the hydrogen pressure remained stationary, indicating that the alloys were in metallurgical equilibrium. Pressure readings were then taken at progressively increasing temperatures until a point was reached at which the evaporation of manganese became appreciable and it was no longer possible to obtain a constant hydrogen pressure at any fixed temperature. The experiment was then abandoned. The temperature at which evaporation of the manganese became appreciable was above the  $\beta/(\alpha + \beta)$  boundary for all titanium-manganese alloys containing less than 4 at.-% manganese. In the case of the 5 at.-% alloy, it was impossible to obtain a sharp discontinuity in the pressure/temperature curve at the  $\beta/(\alpha + \beta)$  boundary.

### IV.—EXPERIMENTAL RESULTS

The experimentally determined families of curves of  $\log p$  against  $1/T$  for the series of alloys in the various systems examined were all of the same general form. The curves for the titanium-chromium alloys (Fig. 1) are typical of the results obtained. The temperature at which a sharp discontinuity occurs

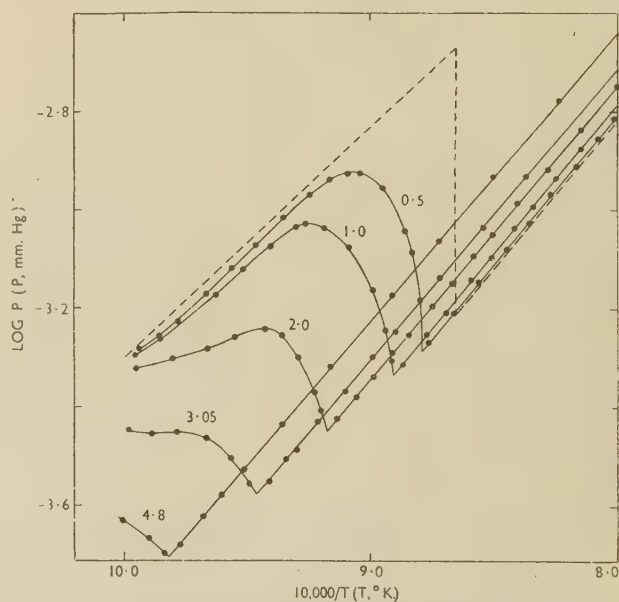


FIG. 1.— $\log p$  against  $1/T$  Curves for a Series of Titanium-Chromium Alloys Containing 0.05 at.-% Dissolved Hydrogen. The figures on the curves are the chromium content in at.-%. The broken line represents the curve for pure titanium containing the same amount of hydrogen.

between the high-temperature linear relationship between  $\log p$  and  $1/T$  and the curved relationship found at lower temperatures marks the beginning of the  $\beta \rightleftharpoons (\alpha + \beta)$  transformation. Over the whole range of temperature in which the  $\log p$  against  $1/T$  curves are non-linear, the alloys are in the two-phase  $(\alpha + \beta)$  region.

MICROSTRUCTURES OF TITANIUM-VANADIUM ALLOYS.  $\times 200$ .



FIG. 3.—0.5 At.-% Vanadium Alloy, Slowly Cooled from 900° to 700° C., Held for 18 hr. at 700° C., and Quenched.



FIG. 4.—1.0 At.-% Vanadium Alloy, Slowly Cooled from 900° to 700° C., Held for 18 hr. at 700° C., and Quenched.



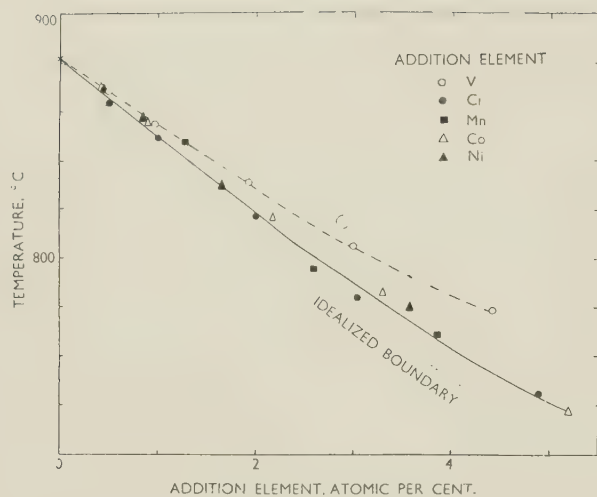


FIG. 5.—The  $\beta/(a + \beta)$  Boundary of a Number of Titanium Alloy Systems Compared with an Idealized Theoretical Boundary.

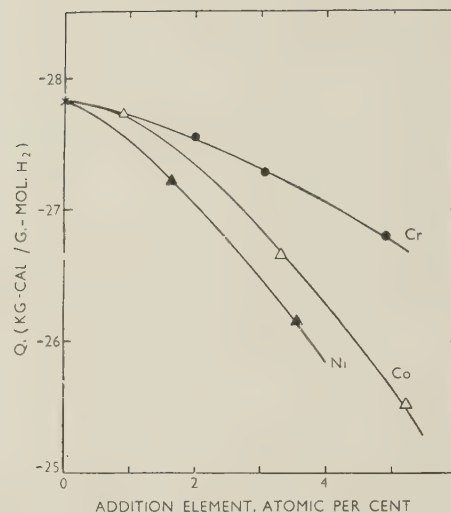


FIG. 6.—Heat of Solution of Hydrogen  $Q$  in the  $\beta$  Phase of Titanium-Chromium, Titanium-Cobalt, and Titanium-Nickel Alloys as a Function of the Addition Element Content.

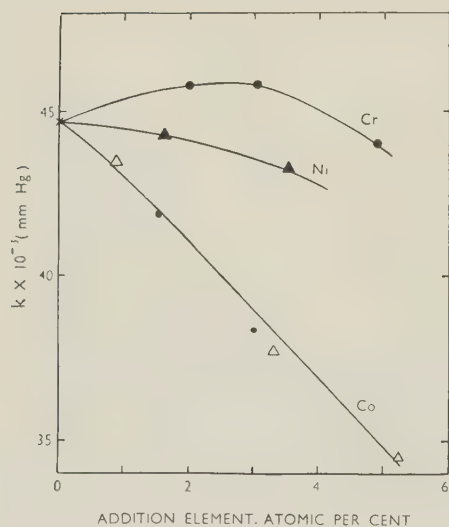


FIG. 7.—Values of  $k$  for Dilute Solutions of Hydrogen in the  $\beta$  Phase of Titanium-Chromium, Titanium-Cobalt, and Titanium-Nickel Alloys as a Function of the Addition Element Content.

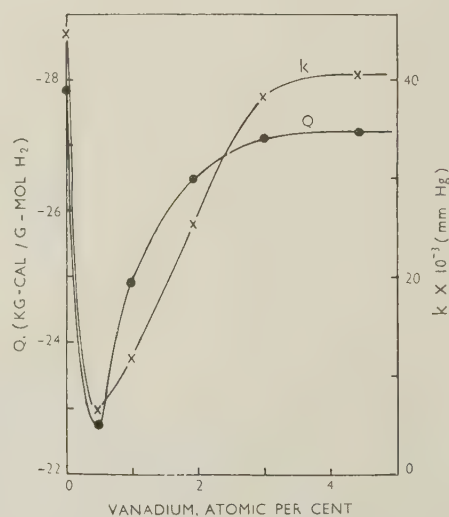


FIG. 8.—Heat of Solution of Molecular Hydrogen  $Q$  and Values of  $k$  for Dilute Solutions of Hydrogen in a Series of  $\beta$ -Phase Titanium-Vanadium Alloys as a Function of the Vanadium Content.

The results obtained show that the effects of chromium, manganese, nickel, and cobalt on the  $\alpha \rightleftharpoons \beta$  transformation of titanium are almost identical. From the shape of the  $\log p$  against  $1/T$  curves in the  $(\alpha + \beta)$  region it can be deduced<sup>2</sup> that these addition metals are almost completely insoluble in the hexagonal close-packed, low-temperature  $\alpha$ -titanium. They have, however, an extensive solubility in the body-centred cubic, high-temperature,  $\beta$  form of the metal. The extent of the depression of the  $\beta/(\alpha + \beta)$  boundary caused by all the addition elements is the same, within the limits of experimental error, when the concentration of the element is expressed as an atomic percentage. Vanadium differs from the other elements in the first long period in having a greater solubility in  $\alpha$ -titanium, and is consequently less effective in depressing the  $\beta/(\alpha + \beta)$  boundary. This greater solubility of vanadium can almost certainly be attributed to the smaller difference in atomic size between titanium and vanadium compared with the size-factors of titanium and the other elements of the present series.

There is, on the experimentally determined  $\log p$

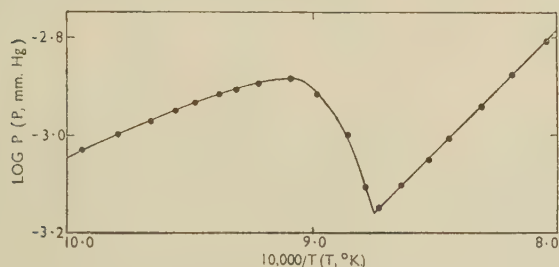


FIG. 2.— $\log p$  against  $1/T$  Curve for a 0.5 at.-% Vanadium Alloy Containing 0.05 at.-% Dissolved Hydrogen.

against  $1/T$  curves, no indication of a eutectoid horizontal in any of the systems examined, although in all systems, since the  $\beta/(\alpha + \beta)$  boundary is depressed by the addition element, such a transformation must occur. When an alloy specimen undergoes an eutectoidal transformation at which the remaining  $\beta$  solid solution breaks down isothermally, the  $\log p$  against  $1/T$  curve shows a vertical discontinuity. This type of behaviour has been observed in titanium-copper alloys at 776° C.<sup>2</sup>

The  $\log p$  against  $1/T$  curves for the series of vanadium alloys differ from those of the other systems in one respect. The curve for a 0.5 at.-% vanadium alloy (Fig. 2) appears to become linear again at a temperature below that of the  $\beta/(\alpha + \beta)$  boundary. It would seem, therefore, that this alloy becomes single-phase at low temperatures. No sharp transition from the non-linear  $(\alpha + \beta)$  portion of the pressure/temperature curve to the linear  $\alpha$ -solution part of the curve can, however, be observed. The microstructure of the specimen after cooling slowly from 900° to 700° C. and annealing for 18 hr. at 700° C. (Fig. 3, Plate LIV) shows only the single-phase  $\alpha$  solid solution. This structure may be compared with that of a 1 at.-% vanadium alloy, annealed under

identical conditions and quenched from the same temperature, shown in Fig. 4 (Plate LIV). The 1 at.-% alloy has the typical  $(\alpha + \beta)$  structure obtained by slow cooling from the  $\beta$  solid solution to the  $(\alpha + \beta)$  range. In the titanium-vanadium system the  $\alpha/(\alpha + \beta)$  boundary must lie, therefore, between 0.5 and 1 at.-% vanadium at 700° C. Since the discontinuity on the  $\log p$  against  $1/T$  curve of the 0.5 at.-% vanadium alloy corresponding to the  $\beta/(\alpha + \beta)$  boundary is sharp, the lack of a marked discontinuity representing the  $\alpha/(\alpha + \beta)$  boundary cannot be attributed to contamination of the specimen. Therefore, the reason for the lack of a sharp transition at the lower boundary must be that at a vanadium concentration of 0.5 at.-% the boundary is almost parallel to the temperature axis of the constitutional diagram. On cooling the alloy through the  $(\alpha + \beta)$  region of such a system, the last traces of the  $\beta$  solid solution would disappear only very gradually, and no marked discontinuity at the  $\alpha/(\alpha + \beta)$  boundary would be expected.

The experimentally determined positions of the  $\beta/(\alpha + \beta)$  boundaries obtained from an examination of the  $\log p$  against  $1/T$  curves for a series of alloys in each of the systems investigated have been collected together in Fig. 5 (Plate LV). The results for the systems of titanium with chromium, manganese, cobalt, and nickel are so grouped that the  $\beta/(\alpha + \beta)$  boundaries for all these systems may be represented by a single curve (within the limits of experimental error). The points representing the  $\beta/(\alpha + \beta)$  boundary for the titanium-vanadium system lie above the general boundary for the above-mentioned systems by an amount which increases with increasing concentration of the addition element. Microsections of some of the alloys used were examined, and their structures were found to be in accordance with the position of the boundaries as shown in Fig. 5.

Besides giving information on the  $\beta/(\alpha + \beta)$  boundaries of the various systems, the families of  $\log p$  against  $1/T$  curves also indicate the effect of addition elements on the solubility of hydrogen in  $\beta$ -titanium. In view of the rather interesting results that have been obtained on the effect of copper on the solubility of hydrogen in titanium-rich  $\beta$  solid solutions,<sup>2</sup> an investigation of the effect of the present series of addition elements on the quantities  $Q$  and  $k$  in equation (1), as applied to the  $\beta$  solid solutions, was carried out. In order to increase the accuracy of the determination of these values for the various alloys, that part of the  $\log p$  against  $1/T$  curve representing the  $\beta$  solid solution was repeated for a number of different hydrogen concentrations up to a maximum of 5 at.-%. In all cases it was found that the hydrogen solution still behaved as an ideal solution up to this hydrogen concentration, and that the additional hydrogen had no measurable effect on the values of  $Q$  and  $k$ . The results for the effect of the addition elements on  $Q$  and  $k$  are, therefore, more accurate than could be obtained from the single pressure/temperature curves.



The effect of chromium, nickel, and cobalt on the solution of hydrogen in  $\beta$ -titanium is illustrated in Figs. 6 and 7 (Plate LV), in which  $Q$  and  $k$  are plotted as functions of the concentration of the addition element. These elements have relatively little effect on the numerical values of  $Q$  and  $k$ , and behave much like iron in this respect. There is, however, a general tendency in the three systems for  $Q$  and  $k$  to decrease slightly with increasing amounts of addition element, the rate of decrease becoming greater at higher concentrations. Vanadium has a very marked effect on the values, and the curves of  $Q$  and  $k$  as functions of vanadium concentration are quite unlike any of the other curves. Both curves, given in Fig. 8 (Plate LV), show that the numerical values of  $Q$  and  $k$  decrease rapidly with the first addition of vanadium, and then, at concentrations between 4 and 5 at.-% vanadium, tend towards a steady value which is approximately the same as that for pure  $\beta$ -titanium. No results on the effect of manganese on these quantities have been obtained, owing to the high rate of evaporation of manganese over most of the temperature range in which the  $\beta$  solid solution exists.

## V.—DISCUSSION OF RESULTS

### 1. THE $\beta/(\alpha + \beta)$ BOUNDARIES

On the assumption that an addition element forms an ideal solution when dissolved in small quantities in  $\beta$ -titanium and that it is completely insoluble in  $\alpha$ -titanium, it is possible, knowing the latent heat of transformation of pure titanium, to calculate the form of the  $\beta/(\alpha + \beta)$  boundary which would occur in this ideal case. The free energy,  $F$ , of an ideal solid solution, expressed as a function of the atomic fraction of the addition element,  $x$ , is given by the equation:

$$F = RT [x \ln x + (1 - x) \ln (1 - x)] \quad (2)$$

in which the free energy of pure  $\beta$ -titanium at any temperature is taken to be zero. The composition of the  $\beta$  solid solution in equilibrium with  $\alpha$ -titanium at any temperature at which such an equilibrium is possible can be determined by finding the point of contact of the tangent to the free-energy/composition curve of the solid solution, which passes through the free-energy axis at a point at which the free energy is equal to the difference between the free energies of  $\alpha$ - and  $\beta$ -titanium at that temperature. Although some information on the difference between the free energies of the two forms of titanium as a function of temperature has been obtained,<sup>4</sup> the data are not sufficiently accurate for the solution of this particular problem. Such information as is available indicates, however, that the relationship is almost linear at temperatures close to the transformation temperature, and this will be assumed to be the case in the subsequent calculations. The tangent of the angle between the tangents to the free-energy/temperature curves for  $\alpha$ - and  $\beta$ -titanium at the transformation temperature will be  $L/T_0$ , where  $L$  is the latent heat of trans-

formation. The free-energy difference between the two forms of titanium,  $F_{\alpha\beta}$ , as a function of temperature will, therefore, be taken to be represented by the equation:

$$F_{\alpha\beta} = \frac{L}{T_0} (T_0 - T) \quad (3)$$

At any temperature,  $T$ , the equation of the tangent to the free-energy/composition curve for the solid solution which passes through the point the distance from zero of which represents the free-energy difference between  $\alpha$ - and  $\beta$ -titanium will be:

$$F = RT x \ln \frac{x'}{1 - x'} + \frac{L}{T_0} (T_0 - T) \quad (4)$$

where  $x'$  is the concentration at the point of contact of the tangent to the free-energy curve. Substituting  $x'$  for  $x$  in equations (2) and (4), the free-energy values given by these two equations must be equal, and the expressions can be equated thus:

$$\begin{aligned} RT[x' \ln x' + (1 - x') \ln (1 - x')] \\ = RTx' \ln \frac{x'}{1 - x'} + \frac{L}{T_0} (T_0 - T). \end{aligned}$$

Hence

$$\ln (1 - x') = \frac{L}{R} \left( \frac{1}{T} - \frac{1}{T_0} \right) \quad (5)$$

which is the equation for the idealized  $\beta/(\alpha + \beta)$  boundary. Using the values  $L = 678$  cal./g.-atom and  $T_0 = 882.5^\circ \text{C}$ ,<sup>4</sup> the idealized boundary, shown as a dotted line in Fig. 5 (Plate LV), may be obtained. The calculated boundary will be accurate only at temperatures close to the transformation temperature of pure titanium. It is expected, however, that at  $700^\circ \text{C}$ . the calculated values of the points on the idealized boundary will lie within the limits of the experimental error in the results for real systems if the assumptions made regarding the nature of the solution apply in these cases.

In a real system of this type there are a number of reasons for deviation of the  $\beta/(\alpha + \beta)$  boundary from the idealized boundary: (1) the possibility of some solubility of the addition element in  $\alpha$ -titanium, (2) a departure from the conditions of ideal solution when the addition element is dissolved in  $\beta$ -titanium, and (3) a large difference in size between the atoms of the addition element and those of titanium. The effect of solubility in the  $\alpha$  form of titanium can best be seen by consideration of the relation:

$$\left[ \left( \frac{dx'}{dT} \right)_\beta - \left( \frac{dx'}{dT} \right)_\alpha \right]_{T=T_0} = \frac{L}{RT_0^2} \quad (6)$$

where  $\left( \frac{dx'}{dT} \right)_\beta$  and  $\left( \frac{dx'}{dT} \right)_\alpha$  are, respectively, the limiting slopes of the  $\beta/(\alpha + \beta)$  and  $\alpha/(\alpha + \beta)$  boundaries at zero concentration of addition element. Since the angle between the limiting slopes of these two boundaries is fixed by the values of  $L$  and  $T_0$ , any increase in  $\left( \frac{dx'}{dT} \right)_\alpha$  due to increased solubility in

$\alpha$ -titanium must cause an increase in  $\left(\frac{dx'}{dT}\right)_\beta$ . The existence of a range of solution in  $\alpha$ -titanium thus has the effect of elevating the  $\beta/(\alpha + \beta)$  boundary above that for the idealized case in which it is assumed that there is no such solubility. If the solution of the addition element in  $\beta$ -titanium does not obey the conditions for ideal solution, equation (2) must be replaced by the equation:

$$F = RT[x \ln x + (1 - x) \ln (1 - x) + \frac{2T_c}{T} x(1 - x)] \quad (7)$$

which is the free-energy curve for a regular solution having a critical temperature  $T_c$ . In such a system, assuming that no intermetallic compounds exist, there would be a miscibility gap, symmetrically placed in the centre of the system, the width and height of which would depend only on the value of  $T_c$ . An ideal solution is a special case of a regular solution for which  $T_c$  is zero. The effect of the extra term in the free-energy equation of the  $\beta$  phase serves to modify equation (5), which now becomes:

$$\ln(1 - x') + \frac{2T_c}{T} (x')^2 = \frac{L}{R} \left( \frac{1}{T} - \frac{1}{T_0} \right) \quad (8)$$

It can readily be shown that the  $\beta/(\alpha + \beta)$  boundary obtained in the case of the formation of a regular solution, given by equation (8), will lie above the boundary obtained in the case of an ideal solution (equation (6)) for all positive values of  $T_c$ . Thus any departure from the conditions of ideal solution in the  $\beta$  solid solution will raise the  $\beta/(\alpha + \beta)$  boundary to a position above that of the ideal boundary. Similarly, the effect of the difference in the atomic sizes of the alloying elements and titanium can be shown<sup>5</sup> qualitatively to have the effect of increasing the free energy of the solid solution and hence elevating the  $\beta/(\alpha + \beta)$  boundary. Thus all three factors likely to influence the position of the  $\beta/(\alpha + \beta)$  boundary in real systems act in the same direction, i.e. towards a decrease in the depression of the boundary, and hence the idealized boundary is the limit below which the boundaries in real systems cannot lie.

The experimental points for the  $\beta/(\alpha + \beta)$  boundaries in the systems of titanium with chromium, manganese, nickel, and cobalt lie close to the idealized boundary and slightly above it. In these systems, therefore, the idealized conditions must be a close approximation to the actual conditions governing the form of their constitutional diagrams. The distance between the actual boundaries and the ideal boundary tends to increase with increasing concentration of addition element. It would seem reasonable to attempt to explain this deviation by the assumption that the  $\beta$  solid solutions behave not as ideal solutions but as regular solutions with a low critical temperature. It is found, however, that equation (8) cannot be made to represent the form of the boundaries for the real systems if a single value of  $T_c$ ,

independent of the concentration of addition element, is used. The departure from ideal behaviour shown by the real systems may, therefore, be due, either partially or totally, to the existence of some solubility of the addition elements in  $\alpha$ -titanium. The solution in  $\alpha$ -titanium would be expected, however, to be very limited, and to be less than 0.1 at.-% at 700°C., which is the upper limit of the  $\alpha$  solid solution range estimated from the form of the experimentally determined  $\log p$  against  $1/T$  curves.

The  $\beta/(\alpha + \beta)$  boundary in the titanium-vanadium system lies well above the equivalent boundaries for the other systems. In this system it has been shown experimentally that the addition element is soluble in  $\alpha$ -titanium to the extent of at least 0.5 at.-% at 700°C. The greater deviation from the ideal form of the  $\beta/(\alpha + \beta)$  boundary in this system may, therefore, be attributed for the most part to the relatively extensive solubility of vanadium in  $\alpha$ -titanium. The same argument applies to the boundaries in the titanium-copper<sup>2</sup> and titanium-hydrogen<sup>4</sup> systems, in which there are fairly extensive  $\alpha$  solid solutions and hence large deviations from the ideal boundary. In the titanium-iron system,<sup>2</sup> however, although the  $\beta/(\alpha + \beta)$  boundary has only about half the depression per unit concentration that the ideal boundary has, there is no evidence of any appreciable  $\alpha$  solid solution range. The behaviour of the titanium-iron system appears, therefore, to be anomalous, though the reason for this is not at present clear.

## 2. HYDROGEN SOLUBILITY IN THE $\beta$ SOLID SOLUTIONS

At the outset of this investigation it was hoped that information which would be obtained on the effect of various addition elements on the hydrogen solubility in  $\beta$  solid solutions in titanium systems would throw some light on the factors governing the relationships between  $Q$  and  $k$ , which control these solutions, and the concentration of the addition element. It was found, however, that in the case of the  $\beta$  solid solutions of chromium, nickel, and cobalt in titanium the addition element had only a very small effect on  $Q$  and  $k$ . The effect of vanadium on  $Q$  and  $k$  is very marked, but it is quite unlike that of any other element investigated, and does not allow of any general conclusions.

At present it would seem that the only conclusion which can be drawn from the curves of  $Q$  and  $k$  as functions of the concentration of the alloying element is that numerically  $Q$  and  $k$  almost always change in the same direction; small additions of chromium, however, cause a slight increase in  $k$  at first, whereas  $Q$  decreases continuously. The fact that  $Q$  and  $k$  often change together is very apparent in the case of vanadium alloys, in which both quantities show minima at 0.5 at.-% vanadium and both tend to a constant value not greatly different from the respective values for pure  $\beta$ -titanium. Although there is, therefore, a tendency for the changes in  $Q$  to be mirrored in the form of the  $k$ -curve, there appears to be little



correlation between the effects of the various elements on the two quantities. In Figs. 6 and 7 (Plate LV) nickel is seen to be the most effective metal in depressing the numerical value of  $Q$ , whereas cobalt causes the greatest depression in  $k$ .

It had been thought that a solid solution could be treated thermodynamically as an assembly of different types of interstices, each type being characterized by different proportions of addition-element atoms occupying the surrounding lattice sites. Hägg<sup>6</sup> has

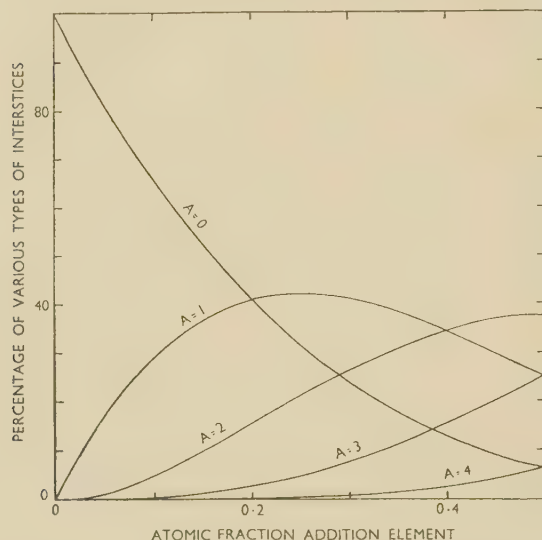


Fig. 9.—The Percentage of the Total Number of Tetrahedral Interstices in a Body-Centred Cubic Lattice of a Binary Solid Solution of Two Components, X and Y, having 0, 1, 2, 3, and 4 Atoms of One Component Surrounding the Interstitial Holes.

$A = 0$	0 atoms of X, 4 atoms of Y.
$A = 1$	1 atom of X, 3 atoms of Y.
$A = 2$	2 atoms of X, 2 atoms of Y.
$A = 3$	3 atoms of X, 1 atom of Y.
$A = 4$	4 atoms of X, 0 atoms of Y.

(Curves for only half the composition range have been drawn. At concentrations greater than 50 at.-%, the curve for  $A = 0$  is continued as the mirror image of the  $A = 4$  curve about a plane perpendicular to the composition axis at a composition of 50 at.-%. Similarly,  $A = 1$  is continued as the mirror image of  $A = 3$  and so on for the curves  $A = 2, 3$ , and 4. The  $A = 2$  curve is, therefore, symmetrical about the composition 50 at.-%.)

assembled evidence which seems to show that dissolved hydrogen atoms in  $\beta$ -titanium are situated in the tetrahedral interstices of a body-centred cubic lattice. If this is assumed to be correct, it is possible to calculate the percentage of the total number of interstices in the metal lattice which have 0, 1, 2, 3, and 4 addition-element atoms surrounding the interstitial holes. Fig. 9 shows the way in which the fraction of the various types of interstices present in the solid solution vary with the concentration of the addition

element. It is assumed, in computing these curves, that the distribution of the metal atoms among the lattice sites is completely random.

At concentrations of addition element less than about 3 at.-%, the only interstices in the alloy which need be considered are those having 0 and 1 addition-element atoms among their four surrounding atoms. If such a solid solution could be treated as an assembly of two types of interstices, each with a different affinity for hydrogen, dissolved hydrogen would partition itself between the two types in a manner similar to the way in which it partitions itself in a specimen containing two alloy phases, the values of  $Q$  and  $k$  being different in the two phases. Such a partition of hydrogen in a solid solution would mean that the effective values for  $Q$  and  $k$  for that alloy would themselves be functions of temperature. This has not been observed in any of the experimental results for real systems. It would seem, therefore, that a dissolved hydrogen atom situated in an interstitial site is influenced by more than its closest-neighbour metallic atoms and that the bonding energy and partition function of a hydrogen atom dissolved in a dilute solid solution are more or less independent of the particular interstice in which, at any instant, it may find itself.

#### ACKNOWLEDGEMENTS

The work presented in this paper forms part of the research programme being carried out by the Physical Metallurgy Section of the Australian Commonwealth Scientific and Industrial Research Organization. The author would like to express his gratitude to Professor J. N. Greenwood of the Baillieu Laboratory, University of Melbourne, for his encouragement and for the laboratory facilities which have enabled this work to be undertaken.

The author's thanks are also due to Miss Y. Tobin for her very able assistance in obtaining the experimental results contained in this and previous papers published while the author was at the Baillieu Laboratory.

#### REFERENCES

1. A. D. McQuillan, *J. Inst. Metals*, 1950–51, **78**, 249.
2. A. D. McQuillan, *J. Inst. Metals*, 1951, **79**, 73.
3. J. A. Corbett, *Analyst*, 1950, **75**, 475.
4. A. D. McQuillan, *Proc. Roy. Soc.*, 1950, [A], **204**, 309.
5. R. H. Fowler and E. A. Guggenheim, "Statistical Thermodynamics", p. 366. London: 1939 (Cambridge University Press).
6. G. Hägg, *Z. physikal. Chem.*, 1931, [B], **11**, 433.

# DETERMINATION OF ELASTIC CONSTANTS AND STRESS/STRAIN RELATIONSHIP TO FRACTURE OF SINTERED TUNGSTEN CARBIDE-COBALT ALLOYS \*

1356

By E. LARDNER,† B.Sc., A.I.M., MEMBER, and N. B. MCGREGOR ‡

## SYNOPSIS

Since an accurate knowledge of Young's modulus and Poisson's ratio is important in engineering design, an investigation has been carried out to determine these constants, as well as the stress/strain relationship to fracture, for sintered tungsten carbide-cobalt alloys containing 5–25% cobalt. Three alloys having in addition 5–15% titanium were also included. The data have been obtained by three different methods, none of which was capable of supplying completely the information required. The results show that at room temperature Young's modulus decreases considerably, and Poisson's ratio increases slightly, with rise in the cobalt content. Determinations of Young's modulus between room temperature and 600° C. indicate a total decrease of the order of 5–6% at 600° C., the rate of decrease being almost uniform and independent of the amount of cobalt. There is evidence from the stress/strain relationship that when cobalt exceeds about 11%, some plastic deformation occurs at stresses well below the room-temperature fracture strength.

The effect of replacing some of the tungsten carbide by titanium carbide is further to lower Young's modulus. Variations in grain-size between the limits investigated do not appear to cause any systematic change in Young's modulus or Poisson's ratio.

The energy to fracture in slow bending has also been determined and appears to be a more useful criterion of the service performance of sintered tungsten carbide-cobalt alloys than the bend strength or the impact-resistance as measured by the usual methods.

## I.—INTRODUCTION

SINTERED hard metals have been well established as cutting materials for many years, but recently their field of application has been considerably increased. The early applications for cutting-tool tips and drawing dies depended mainly on the great hardness and wear-resistance of these alloys. It was well known that their compressive strength was high, but otherwise they were regarded as being rather brittle, and care was taken in the design of tools to eliminate or to minimize as far as possible any impact or tensile stresses.

Recent successful applications for such purposes as blanking dies and punches, large rings for deep-drawing dies, and cold-heading dies and punches have meant that the hard metals are now being subjected to more severe conditions than were formerly considered possible. In addition, for applications such as drawing rings, which are made in sizes up to 20 in. in dia., the elastic deformation during use reaches values which warrant consideration.

The entry of hard metals into such fields of application demands a more thorough knowledge of the mechanical properties of the various alloys now available. So far, information has been rather scanty. The most comprehensive data are those given by Engle,<sup>1</sup> who reported the Rockwell hardness, transverse rupture strength, and compressive strength

of most of the hard-metal alloys commonly used in America in 1941. In addition, values of the Young's modulus, proportional limit in compression, impact strength, and endurance limit are given for a few of the alloys. In many cases the value of these data is limited by lack of detailed information regarding the actual composition. In the 1948 edition of the A.S.M. Handbook the above results are reproduced in the form of a table<sup>2</sup> with the addition of a few more values for Young's modulus and several values for Poisson's ratio.

Both Young's modulus and Poisson's ratio are of importance in a study of the elastic behaviour of hard metals in the field of engineering design. In the paper by Engle,<sup>1</sup> the values of Young's modulus are stated to have been obtained by W. H. Davenport of the Norton Co., by what is described as "the musical-pitch method".

It has generally been assumed that for hard metals the stress is proportional to strain right up to the point of fracture. However, there is evidence to suggest that some plastic deformation can occur. For instance, hardness impressions show clearly that permanent deformation without fracture can take place at normal temperatures. It was, therefore, considered possible, especially with the high cobalt content used in applications involving impact stresses, that some significant amount of plastic deformation might occur before fracture.

\* Manuscript received 14 June 1951.

† Research Metallurgist, Hard Metal Tools, Ltd., Coventry.

‡ The Brown-Firth Research Laboratories, Sheffield.



Accordingly, in the present investigations it seemed desirable to study the stress/strain relationship up to the point of fracture. As will be explained, this was made possible by a refinement of the transverse rupture test now generally used to determine the bending strength (Method I). The test was not suitable for the determination of Poisson's ratio, however, and so the latter was obtained from compression tests on hard-metal cylinders of suitable dimensions (Method II).

In view of the fact that hard-metal parts, as a result of the arduous duties imposed upon them, frequently work well above room temperature, it was considered necessary to determine Young's modulus at elevated temperatures. This part of the investigation was carried out by means of a vibration method developed by Roberts and Nortcliffe<sup>3</sup> (Method III).

The work described was carried out in two laboratories; the research laboratories of Hard Metal Tools, Ltd., and The Brown-Firth Research Laboratories. Method I was used by the former, and Methods II and III by the latter. The specimens tested by Methods I and III were produced by Hard Metal Tools, Ltd., and those tested by Method II were produced by Firth-Brown Tools, Ltd.

## II.—EXPERIMENTAL TECHNIQUE

### 1. RANGE OF COMPOSITION INVESTIGATED

The useful cobalt range of tungsten carbide-cobalt alloys extends from about 4 to about 25%. The specimens produced lay in this range, and included

TABLE I.—Composition and Properties of Alloys Tested by Method I.

Nominal Composition			Vickers Pyramid Hardness No.	Density, g./c.c.	Grain-Size, microns
WC, %	TiC, %	Co, %			
94	...	6	1650	14.84	0.7
94	...	6	1470	14.92	1.2
89	...	11	1300	14.21	1.2
80	...	20	1100	13.43	1.2
86	5	9	1390	12.91	1.2
79	15	6	1550	11.22	1.2
77	15	8	1460	11.31	1.2

TABLE II.—Composition and Properties of Alloys Tested by Method II.

Composition			Vickers Pyramid Hardness No.	Density, g./c.c.	Grain-Size, microns
Total C, %	Co, %	Fe, %			
5.8	4.72	0.20	1700	14.95	0.7
5.75	6.38	0.27	1475	14.8	1.5
5.53	9.16	0.18	1420	14.6	2.4
5.45	11.04	0.20	1320	14.4	1.7
5.33	12.96	0.14	1250	14.15	1.0
5.33	12.96	0.24	1200	14.2	1.7
5.33	12.95	0.55	1020	14.0	2.4
4.93	20.2	0.23	1015	13.5	1.2
4.90	20.12	0.13	980	13.5	2.0
5.00	20.12	0.52	850	13.4	2.6
4.55	25.5	0.25	930	12.8	1.2

specimens similar in composition but with considerable variations in grain-size. In addition, three alloys containing titanium carbide were prepared.

Tables I, II, and III give details of the composition, hardness, density, and grain-size of the various alloys tested.

TABLE III.—Composition of Alloys Tested by Method III.

Nominal Composition		
WC, %	TiC, %	Co, %
95	...	5
94	...	6
94	...	6
91	...	9
90	...	10
89	...	11
85	...	15
80	...	20
86	5	9
79	15	6
77	15	8

### 2. METHOD I

#### Determination of Young's Modulus, Fracture Strength, and Stress/Strain Relationship to Fracture by the Transverse-Rupture-Test Method

In this test a plain rectangular test-piece, supported at both ends and loaded at the middle, was used, but in order to make possible the accurate determination of the stress/strain relationship up to fracture, a refined form of the test was devised, whereby the load and the deflection of the test-piece could be measured simultaneously. The sensitivity of such a method depends mainly on the magnitude of the deflection and the accuracy with which it can be measured.

The deflection ( $\delta$ ) at the centre of a rectangular beam is given by the expression :

$$\delta = \frac{WL^3}{4bd^3 \cdot E} \quad \dots \quad (1)$$

where  $W$  = load applied at centre of span,  $L$  = distance between supports,  $b$  = width of beam,  $d$  = thickness of beam, and  $E$  = Young's modulus. Hence the greatest accuracy can be attained by making the test-piece as long and thin as possible. A specimen 6 in. long (which could be loaded between rollers spaced 5 in. apart), 0.25 in. wide, and 0.1 in. in thickness was finally decided upon. This specimen was expected to give deflections of the order of 0.1 in. with loads of 50 kg. It was also possible for the load to be applied to the specimen by dead-weight loading, and the deflections to be measured accurately with a conventional dial-gauge indicator.

The apparatus used, with the test-piece in position, is illustrated in Fig. 1 (Plate LVI). The dial-gauge was taken from a Rockwell hardness testing machine. Each dial division was found to be equal to 0.0004 in. and estimates better than 0.0001 in. could readily be made.

From equation (1) the value for Young's modulus may be rewritten :

$$E = \frac{3WL}{2bd^2} \cdot \frac{d\delta}{2L^2} \quad . \quad . \quad . \quad (2)$$

where  $\frac{3WL}{2bd^2} = \text{skin stress} \quad . \quad . \quad . \quad (3)$

and  $\frac{d\delta}{2L^2} = \text{strain} \quad . \quad . \quad . \quad (4)$

Test-pieces were accurately ground to the required dimensions on a surface grinder. No trouble was experienced in observations of the deflection readings caused by bedding down of the various load-transmitting members, and perfectly linear results were obtained down to the minimum load applied. In some cases this was 2·380 kg., which was the weight of the scale pan, roller, &c., but this was generally deliberately increased to 4 kg., at which load the dial-gauge was set at zero.

In the calculation of the bending strength at fracture, the initial load was included in the breaking load, but Young's modulus was calculated on the deflection between the second and penultimate increments of load in order to eliminate inaccuracies due to bedding down in the supports, and any uncertainty as to the actual value of the load at the time of fracture.

### 3. METHOD II

#### *Determination of Young's Modulus and Poisson's Ratio by a Compression Method*

The object of this method was primarily to determine Young's modulus and Poisson's ratio from direct measurement of the longitudinal and lateral strain by loading in compression specially prepared cylinders of carbide. The cylinders used were accurately ground to the following dimensions: length 3 in., dia. 0·798 in. (area =  $\frac{1}{2}$  in.<sup>2</sup>).

Longitudinal strain measurements were made by means of a 2-in.-gauge Lamb's roller extensometer which embodied two mirrors mounted on separate rollers and a sensitive optical lever. This instrument was capable of measuring accurately a strain of 0·00001. Lateral strain measurements were obtained by a Lamb's lateral extensometer, which is designed on the same principle and is capable of measuring a strain of 0·0000025, on a cylinder of 0·798 in. dia.

It was not possible, however, to mount both these extensometers in the same 2 in. of the cylinder. As a practical length of cylinder was 3 in., it was decided where possible to use two identical cylinders, mounted carefully one on the other, end to end, and to measure the longitudinal strain on the top cylinder and the lateral strain on the bottom cylinder. Compression loading of the cylinders in this manner was carried out in an Avery universal testing machine, which satisfied A1 Board of Trade requirements. The cylinders were mounted between two specially pre-

pared compression plates of hardened steel. Fig. 2 (Plate LVI) shows the testing arrangement with two cylinders on test and the extensometers in position.

The maximum compressive stress was 42 tons/in.<sup>2</sup>, the first reading of strain being observed at 2 tons/in.<sup>2</sup>, and then at each 2 tons/in.<sup>2</sup> increment up to 42 tons/in.<sup>2</sup>.

By the above arrangement one set of longitudinal and lateral strains were observed from which Young's modulus and Poisson's ratio could be calculated. In cases where a straight-line plot was obtained on the first application of stress, the cylinders were interchanged and a second set of readings obtained. By this means it was possible to ensure that no undue error was introduced by any dissimilarity between the two cylinders under test, and Poisson's ratio could be calculated from longitudinal and lateral strain observed for the same cylinder or for two identical cylinders.

In some tests only one cylinder was available for a particular grade of carbide, and in these cases the longitudinal strain was determined during the first and the lateral strain during the second application of stress to the same cylinder. This was permissible practice where no plastic deformation was observed during the first stressing of a cylinder, but for some of the grades of carbide containing more than 13% cobalt, evidence of a non-linear stress/strain relationship was observed, and this meant that the lateral-strain readings were taken on a cylinder which had undergone some plastic deformation during a previous application of stress.

The following results illustrate the consistency of results obtained under the above conditions :

(a) In the test on the 4·72% cobalt alloy sample linear plots were obtained right up to 42 tons/in.<sup>2</sup> for several loadings on two cylinders, interchanging one for the other between loadings.

Young's Modulus, $\times 10^4$ tons/in. <sup>2</sup>	Poisson's Ratio
39,200-39,600 (8 loadings)	0·209-0·213
Average : 39,360	Average : 0·211

(b) In the test on the 20·12% cobalt alloy sample (coarse grain-size) during the first application of stress to determine Young's modulus and Poisson's ratio using two cylinders, the stress/strain relationship was non-linear for both longitudinal and lateral strain. A subsequent application of stress gave a linear stress/strain relationship up to 42 tons/in.<sup>2</sup>.

Test	Young's Modulus, $\times 10^4$ tons/in. <sup>2</sup>	Poisson's Ratio	Type of Plot
1	33,000	0·216	non-linear
2	32,700	0·217	linear

From these results it would appear that no great errors in Young's modulus or Poisson's ratio are introduced when :

(1) Identical cylinders are tested, one for longitudinal strain and the other for lateral strain on the first loading, or when the cylinders are interchanged and reloaded.



(2) Identical cylinders are tested and do not give a linear stress/strain relationship on the first loading, and are subsequently reloaded when the stress/strain relationship has become linear.

#### 4. METHOD III

##### *Determination of Young's Modulus by a Vibration Method*

This method,<sup>3</sup> used to determine Young's modulus at room temperature and elevated temperatures, is based upon that of Förster and Köster,<sup>4</sup> and consists essentially of setting up transverse vibrations in a cylindrical rod and measuring the resonant frequency.

The characteristic frequency depends upon the dimensions of the rod and upon the density and Young's modulus of the material under test. The modulus is then given by the formula:

$$E = 1.041 \left( \frac{L}{d} \right)^4 \cdot \frac{m}{L} \cdot f^2 \times 10^{-8} \text{ tons/in.}^2$$

where  $L$  = length of rod (cm.),  $d$  = dia. of rod (cm.),  $f$  = natural frequency of rod (c./s.), and  $m$  = weight of the rod (g.). The dimensions of the test-bar were 6 in. long  $\times \frac{3}{16}$  in. dia. and the maximum temperature used was 600° C.

#### 5. PRESENTATION OF RESULTS

Values for Young's modulus at room temperature determined by all three methods are plotted against cobalt content in Fig. 3, and those for Poisson's ratio, obtained by Method II, are plotted in the same way in Fig. 5. Young's modulus values at room temperature and at 200°, 400°, and 600° C. for the range of cobalt content investigated, are plotted in Fig. 4. Young's modulus for the samples of titanium-bearing hard metals are given in Table IV and in Fig. 4 for elevated temperatures. The breaking strength and energy to fracture determined by Method I are given in Table V.

### III.—DISCUSSION OF RESULTS

#### 1. EFFECT OF COMPOSITION ON YOUNG'S MODULUS

Agreement between the three methods of determining Young's modulus is extremely good at 5–6% cobalt, and even up to 11% cobalt the differences are not great, but some scatter, probably connected with sintering temperature and grain-size, is apparent at higher cobalt contents. No conclusive evidence of the effect of grain-size is clear, however, from the results obtained.

As will be seen from Fig. 3, the effect of increasing the amount of cobalt is to cause a rapid drop in the modulus, which, over the range of cobalt content investigated, is closely proportional to the cobalt content. Such a large variation of the modulus in any alloy system as a result of the increase in the

proportion of one element is not usual, and it is probably caused by the changes in structure of the alloys. The modulus for any one composition appears to be the mean of the moduli of the carbide and of the cobalt bonding phase in terms of their relative volumes.

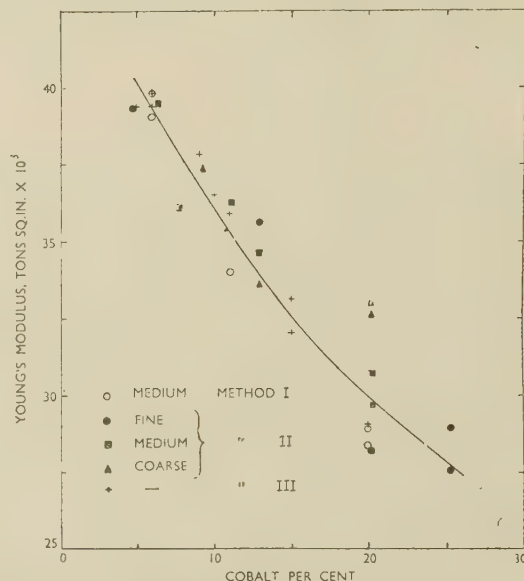


FIG. 3.—Effect of Cobalt Content on Young's Modulus for Sintered Tungsten Carbide-Cobalt Alloys.

"Fine" grain-size = 0.7–1.2 microns.  
 "Medium" grain-size = 1.5–2.0 microns.  
 "Coarse" grain-size = 2.4–2.6 microns.

Substitution of titanium carbide for tungsten carbide results in a further reduction of Young's modulus, as can be seen from Table IV. The alloy with 15% titanium carbide and 8% cobalt has almost the same volume of cobalt phase as the alloy with 94% tungsten carbide, 6% cobalt (modulus 39,300 tons/in.<sup>2</sup>), yet the modulus is more than 20% lower.

TABLE IV.—Effect of Titanium Carbide on Young's Modulus.

Nominal Composition		Young's Modulus, $\times 10^6$ tons/in. <sup>2</sup>
TiC, %	Co, %	
5	9	33,300
15	6	33,300
15	8	31,800

The amount of titanium carbide by volume is, of course, much greater than 15%, because of its very low density compared with that of tungsten carbide, and it also takes into solution a large amount of tungsten carbide. Consequently in such an alloy more than half the volume consists of the TiC-WC solid solution.

#### 2. EFFECT OF TEMPERATURE ON YOUNG'S MODULUS

The results obtained by the vibration method for Young's modulus are of especial interest (Fig. 4). The decrease in the values with increasing temperature

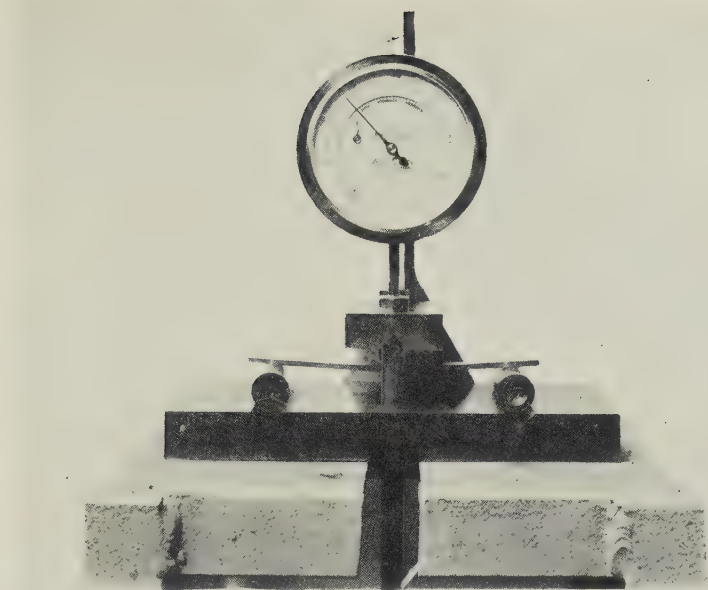


FIG. 1.—Apparatus Used for Bend Testing.

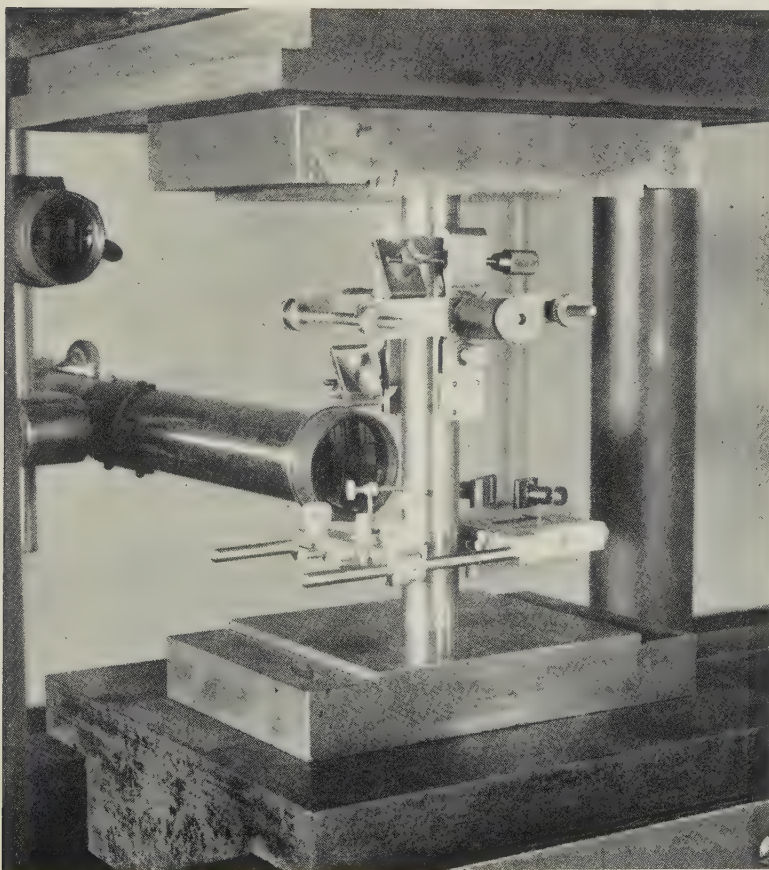


FIG. 2.—Apparatus Used for Compression Testing.





is small, being of the order of only 5–6% between room temperature and 600°C. Over this range the decrease is independent of the cobalt content. For steels, values of the modulus decrease by about 20% over the same temperature range<sup>3</sup> and by about 25–30% for cobalt-base alloys.<sup>5</sup>

The small decrease in the value of the modulus for

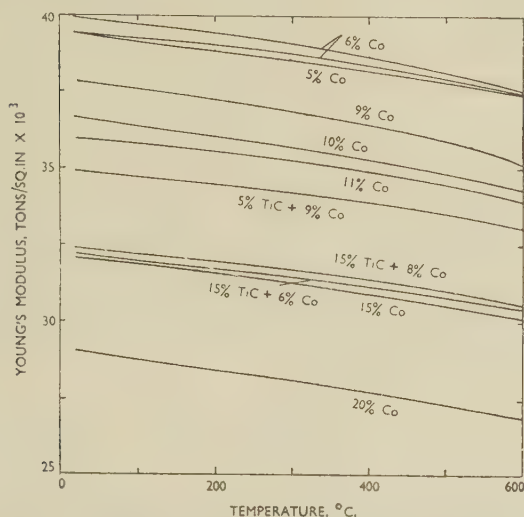


FIG. 4.—Effect of Temperature on Young's Modulus for Sintered Tungsten Carbide-Cobalt Alloys.

the tungsten carbide-cobalt alloys can hardly be due to the properties of the cobalt, and so must indicate that the temperature has only a slight influence on the modulus of the carbide. This fact is rather unexpected, but it is probably due to the fact that in sintered carbides, the carbide-to-carbide bond accounts for an appreciable amount of the strength of the alloys.

### 3. EFFECT OF COMPOSITION ON POISSON'S RATIO

The effect of increasing the amount of cobalt in a tungsten carbide alloy is to increase slightly the value of Poisson's ratio in proportion to the amount of

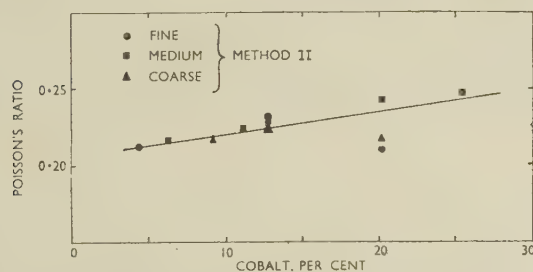


FIG. 5.—Effect of Cobalt Content on Poisson's Ratio for Sintered Tungsten Carbide-Cobalt Alloys.

"Fine" grain-size = 0.7–1.2 microns.  
 "Medium" grain-size = 1.5–2.0 microns.  
 "Coarse" grain-size = 2.4–2.6 microns.

cobalt over the range investigated (Fig. 5); the increase between 5 and 25% cobalt, however, is not great.

### 4. FORM OF THE STRESS/STRAIN CURVE

A most interesting feature of the work carried out at the two laboratories is to be found in the form of the stress/strain curve. In the case of the 6 and 11% cobalt alloys tested by the transverse rupture test (Method I), the stress is directly proportional to the strain, within the limits of sensitivity of the apparatus, right up to the point of fracture. The 20% cobalt alloy, however, when tested under the same conditions, showed a slight but distinct deviation from the straight-line relationship.

In order to verify this effect, a further test was carried out on a second test-piece of the 20% cobalt alloy. In this test the load was increased until the stress approached the maximum obtained in bending in the first test, and it was then removed. This loading cycle was repeated twice, but on the third cycle the loading was continued to fracture. The non-linear form of the stress/strain relation was again evident during the first cycle of loading, but subsequent loading and unloading gave straight lines parallel to the linear portion of the initial loading curve.

This disappearance of the non-linear relationship on repetition of the initial loading cycle was also observed in a compression test (Method II) on the 20-12% cobalt alloy sample and has been described in Section II, 3. In the series of compression tests carried out by Method II, some evidence was obtained of the presence of the non-linear form of the stress/strain curve in the 13% cobalt alloy and at a stress in the neighbourhood of 40 tons/in.<sup>2</sup>. In the curves for the alloys of higher cobalt content tested by the same method, the departure from proportionality took place at lower stresses than this, e.g. the 25.5% cobalt alloy appeared to have a proportional limit at about 20 tons/in.<sup>2</sup>. It would, therefore, seem probable that any permanent deformation that occurs in these alloys under load is confined entirely to the cobalt-rich phase and that this phase work-hardens in the usual way.

### 5. ENERGY TO FRACTURE

Tests to indicate the degree of resistance of carbide alloys to impact, are not generally carried out as a means of control, owing to the difficulty of obtaining a suitable test. Engle<sup>1</sup> has given values for unnotched test-pieces,  $\frac{1}{4}$  in. square, tested in a Charpy impact-testing machine. Values between 0.73 and 1.75 ft.-lb. were obtained for alloys of tungsten carbide and 6–20% cobalt, but this form of test does not lend itself to the determination of the impact strength of hard and brittle materials. The energy to fracture in bending is a good indication of toughness, but it cannot readily be obtained in the usual form of transverse rupture test used in the control of cemented carbides, as the deflection is very small. However, the energy may be obtained from the test data of Method I.

The values for bending strength given in Table V



are fairly typical, if somewhat low, owing to the large span of the test-piece, but they show an increase of about 25% with rise in cobalt content from 6 to 20%. This increase in the bending strength does not account for the increase in impact-resistance encountered in practice in some applications. For example, such properties as resistance to cracking during brazing

TABLE V.—*Results of Tests by Method I.*

Nominal Composition	Bending Strength, tons/in. <sup>2</sup>	Young's Modulus, $\times 10^4$ tons/in. <sup>2</sup>	Thickness of Test-Piece, in.	Deflection at Fracture,* in.	Energy to Fracture,† ft.-lb.
6% cobalt (fine grain-size)	82.8	38,900	0.1038	0.0780	0.23
6% cobalt	92.9	39,800	0.1154	0.0829	0.28
6% cobalt	87.5	39,000	0.1015	0.0830	0.25
6% cobalt	82.6	39,100	0.1045	0.0728	0.22
11% cobalt	82.8	34,000	0.1050	0.0714	0.26
11% cobalt	112.0	34,000	0.0942	0.126	0.48
20% cobalt	114.1	28,300	0.0745	0.203	0.60
20% cobalt	107.0	28,850	0.1232	0.1225	0.52
5% TiC, 9% cobalt	97.8	33,300	0.1177	0.0974	0.37
5% TiC, 6% cobalt	78.7	33,300	0.0840	0.0964	0.24
5% TiC, 8% cobalt	85.2	31,850	0.095	0.0776	0.30

\* The deflection due to the weight of scale pan is not included.

† Calculated for a test-piece  $0.25 \times 0.1$  in. over a span of 5 in.

or grinding suggests that the 20% cobalt alloy has a much greater toughness than the 6% cobalt alloy. This is certainly not indicated by the 25% increase in transverse strength. On the other hand, the values of the energy to fracture given in Table V show an increase of 125% over the same cobalt range. This property does take into account the deformation before fracture, and it may give a much better indication of the toughness of hard metals.

#### IV.—CONCLUSIONS

(1) It has been shown that sintered alloys of tungsten carbide and cobalt do not suffer any significant plastic deformation when the cobalt content is 13% or less. This includes all those grades which are suitable for cutting tools. Alloys of higher cobalt content undergo a small amount of plastic deformation, which increases as the cobalt content is increased to 25%.

(2) The values of Young's modulus determined by the three methods employed are considered on the whole to be in good agreement and to have been determined with sufficient accuracy to be a reliable guide in design formula.

(3) The values for Poisson's ratio determined by the compression method agree closely with those quoted by Engle<sup>1</sup> for cobalt contents between 4.5 and 13%.

(4) Doubt remains as to the effect of grain-size on the data presented, and further work is required.

(5) The modulus of elasticity is well maintained at elevated temperatures, the decrease being only about 5–6% between room temperature and 600° C.

(6) The modulus of elasticity of tungsten carbide-cobalt alloys is outstandingly high, and it is possible that the usefulness of these alloys may be extended in fields where fairly small components of great stiffness are required. At present, the only common application which takes advantage of the high modulus is for solid carbide boring bars.

(7) Determinations have been made of the energy to fracture on slow bending of the various grades, which give figures more indicative of the known performance of the alloys than does the bend strength or the impact-resistance as determined by the usual methods.

#### ACKNOWLEDGEMENTS

The authors are indebted to the Directors of Hard Metal Tools, Ltd., and to Dr. C. Sykes, F.R.S., Director of Research, The Brown-Firth Research Laboratories, for permission to publish this paper. They also wish to thank Mr. A. E. Oliver, F.I.M., Chief Metallurgist to Hard Metal Tools, Ltd., for his helpful interest in the work, Dr. E. J. Sandford, also of Hard Metal Tools, Ltd., who suggested the bending method for determining Young's modulus, and Mr. H. Burden, B.Sc., of Firth-Brown Tools, Ltd., who suggested the compression method and supervised the production of the necessary carbide cylinders.

#### REFERENCES

1. E. W. Engle, "Powder Metallurgy", edited by J. Wulff, p. 436. Cleveland, O.: 1942 (American Society for Metals).
2. "Metals Handbook", p. 62. Cleveland, O.: 1948 (American Society for Metals).
3. M. H. Roberts and J. Nortcliffe, *J. Iron Steel Inst.*, 1947, 157, 345.
4. F. Förster and W. Köster, *J. Inst. Elect. Eng.*, 1939, 84, 558; also *Engineer*, 1938, 166, 626.
5. "Metals Handbook", p. 579. Cleveland, O.: 1948 (American Society for Metals).

# THE CONSTITUTION OF THE COPPER-RICH COPPER-ZINC-GERMANIUM ALLOYS \*

1357

By P. GREENFIELD,† Ph.D., B.Sc., STUDENT MEMBER, and  
PROFESSOR G. V. RAYNOR,‡ M.A., D.Sc., MEMBER OF COUNCIL

## SYNOPSIS

As part of a systematic examination of the factors affecting the formation of ternary alloys, the constitution of the system copper-zinc-germanium has been examined by micrographic methods, with confirmatory X-ray experiments. Isothermals have been established at 550° and at 400° C.; at the latter temperature the body-centred cubic copper-zinc electron compound ( $\beta'$ ) has an ordered structure. The general forms of the two isothermal diagrams are similar. Simple two-phase equilibrium exists between the  $\zeta$  phase of the copper-germanium system and the  $\beta$  and  $\beta'$  phases of the copper-zinc system. Both phases, however, have considerable ranges of homogeneity in the ternary system. The hexagonal  $\zeta$  phase is able to dissolve 21 at.-% zinc, and at this limit the germanium content is 10 at.-%. The cubic  $\beta$  phase is able to accommodate 7.5% germanium. The extent to which the binary electron compounds penetrate the ternary system is effectively independent of temperature.

The results are discussed in relation to atomic-size effects and electron:atom ratios. It is shown that the form of the primary solid-solubility isothermals, which are convex towards the copper-rich corners of the diagrams, is consistent with the fact that both zinc and germanium expand the copper lattice, bearing in mind that the local distortion introduced by 1 at.-% germanium is greater than that introduced by 1 at.-% zinc, and that the limiting solid solution of zinc in copper must be considered as a concentrated solution. The ranges of homogeneity of the 3/2 electron compounds are discussed in terms of the effective size-factor in ternary systems, and confirm the general principle that these ranges of homogeneity tend to correspond with zones of effective size-factor similar to those in which the same structures occur in the relevant binary alloys.

The experiments revealed that the  $\zeta$  phase tends to precipitate in thin plates parallel to the (111) planes of the copper-rich solid-solution matrix. This phenomenon is discussed.

## I.—INTRODUCTION

THE constitutions of a number of ternary silver-rich and copper-rich alloy systems have been discussed in recent publications, with particular reference to the factors affecting ternary equilibrium. Special attention has been paid to the extent to which third metals are soluble in binary electron compounds of electron:atom ratio 3/2 (the  $\beta$ ,  $\mu$ , and  $\zeta$  phases), and it has been suggested that these ranges of homogeneity may be interpreted in terms of the effective size-factors in the ternary systems. If, in the system  $ABC$ , the size-factors of the solutes  $B$  and  $C$  with respect to the solvent  $A$  are respectively  $F_B$  and  $F_C$ , then to a first approximation the effective size-factor for a ternary alloy containing  $X$  at.-% of  $B$  and  $Y$  at.-% of  $C$  may be written as  $\frac{XF_B + YF_C}{X + Y}$ .<sup>1</sup> According to the data of Hume-Rothery, Reynolds, and Raynor,<sup>2</sup> the crystal structures assumed by the 3/2 electron compounds in binary alloys of copper and silver with metals of the  $B$  sub-groups of the periodic table depend upon the value of the size-factor. In general, close-packed hexagonal  $\zeta$  structures appear at low size-factors (approximately  $-6$  to  $+3$ ), while outside these limits body-centred cubic  $\beta$  phases

are favoured. The cubic structure is unlikely to occur within the size-factor range from  $-4.5$  to  $+3$ . Increasing valency of the solute tends to favour the hexagonal structures, whereas increasing temperature favours the cubic structures. Using the conception of the effective size-factor in ternary systems, very similar considerations appear to apply in the ternary alloys previously investigated. From studies of the systems silver-antimony-zinc,<sup>3</sup> copper-aluminium-silicon,<sup>4</sup> and silver-magnesium-tin,<sup>5</sup> it may be concluded that, in general, the 3/2 electron compounds occupy ranges of effective size-factor which are closely similar to the ranges of size-factor over which the same structures exist in the binary alloys. This conclusion must be modified, however, if the size-factors of the two solutes with respect to the solvent are of opposite sign and differ considerably, or if there is a very strong electrochemical interaction between the two solutes.

The effect of greatly differing size-factors is illustrated by reference to the silver-magnesium-zinc system.<sup>6</sup> The size-factors of magnesium and zinc with respect to silver are respectively  $+10.65$  and  $-7.77$ ; it would be expected, therefore, that the close-packed hexagonal  $\zeta$  phase of the silver-zinc system would persist in the ternary alloys until a low

\* Manuscript received 31 May 1951.

† Research Student, University of Birmingham.

‡ Professor of Metal Physics, University of Birmingham.



effective size-factor in the range 0 to +3 had been reached. Experiment shows, however, that the range of homogeneity of this phase in the ternary system is limited; it is necessary, when the two binary size-factors differ appreciably, to consider specifically the effect of introducing large atoms into a lattice which is contracted relatively to that of the solvent.

A strong electrochemical interaction between the

packed hexagonal  $\zeta$  phase of the silver-antimony system.

In an extension of the work on the theory of ternary alloys of this class, the system copper-zinc-germanium has been examined. This was selected for the following reasons:

(i) The size-factors of zinc and germanium with respect to copper are respectively +4.23 and -4.15,

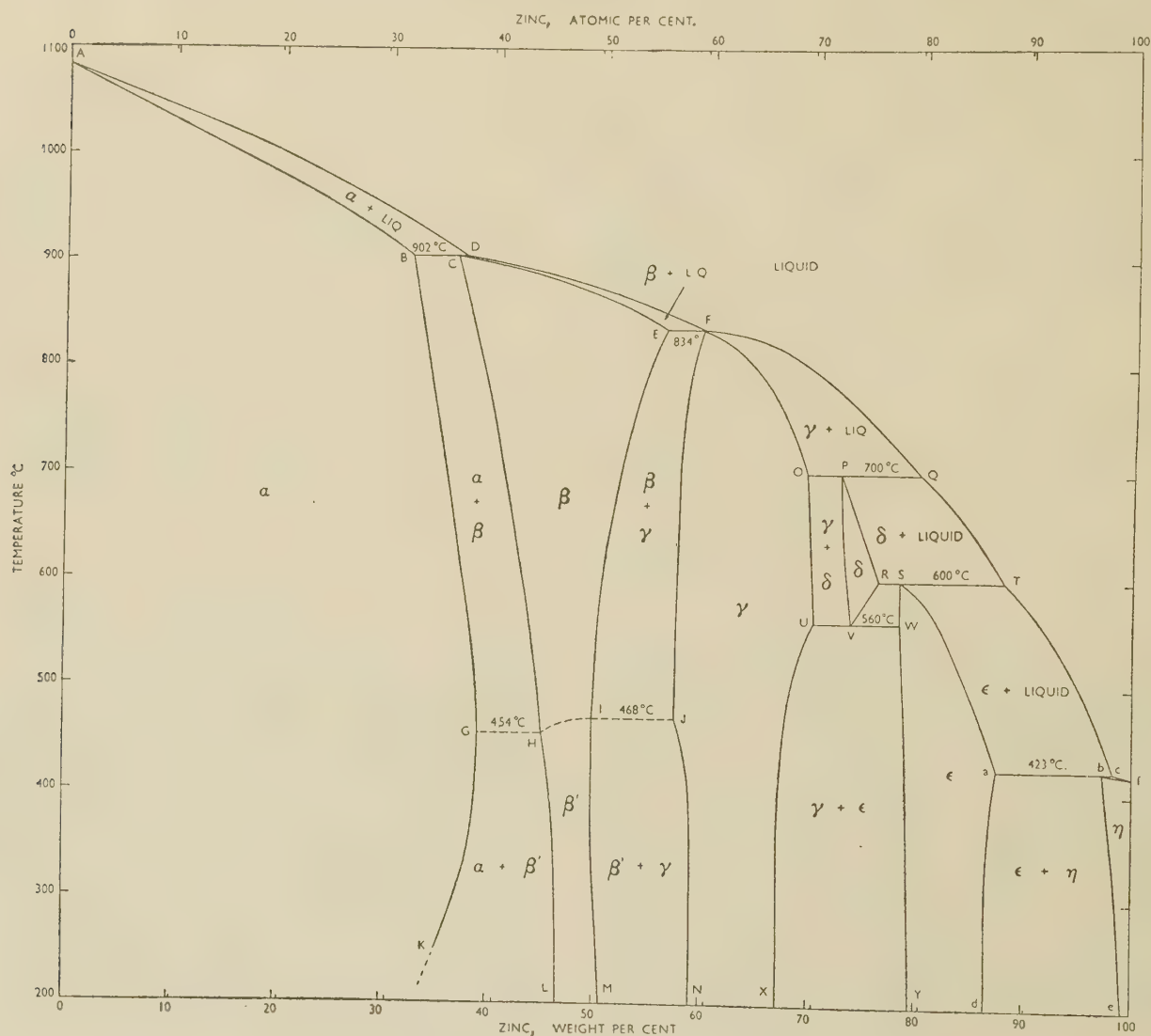


FIG. 1.—The Equilibrium Diagram of the Copper-Zinc Alloys.

solute metals, which leads to the formation of a stable binary intermetallic compound, may greatly restrict the ranges of homogeneity of the  $3/2$  electron compounds in ternary systems. This is well illustrated by the constitution of the silver-magnesium-antimony alloys<sup>7</sup>; in this system the stable intermetallic compound  $Mg_3Sb_2$  enters into equilibrium with the primary silver-rich solid solution, thereby effectively preventing equilibrium between the body-centred cubic  $\beta'$  phase of the silver-magnesium system and the close-

and thus lie symmetrically on either side of zero. The difference between these size factors is much less than in the case of the silver-magnesium-zinc alloys.

(ii) The copper-zinc system contains a body-centred cubic  $3/2$  electron compound  $\beta$  which orders to a caesium chloride structure  $\beta'$  at approximately  $450^\circ\text{C}$ ., while the copper-germanium system contains a close-packed hexagonal  $\zeta$  phase at the electron : atom ratio  $3/2$ . The equilibria involved are thus similar to those in the silver-magnesium-zinc system, but

are not complicated by an abnormally large size-factor difference. A considerable range of homogeneity of the  $\zeta$  phase and a zinc-rich limit corresponding to an effective size-factor at least of approximately zero would thus be expected.

(iii) By comparing the results of experiments carried out below 450° C. with those obtained at higher temperatures, equilibria involving the ordered  $\beta'$ -phase of the copper-zinc system may be compared with those involving the disordered  $\beta$ -phase.

(iv) No stable intermetallic compounds exist in the binary zinc-germanium system; the equilibrium relationships in the copper-rich ternary alloys should therefore be uncomplicated by the electrochemical factor, and simple two-phase ( $\beta + \zeta$ ) or ( $\beta' + \zeta$ ) alloys should be observed in the appropriate composition ranges.

crystal structure of the caesium chloride type. The  $\gamma$  phase, based on the composition  $\text{Cu}_5\text{Zn}_8$ , is a typical 21/31 electron compound with a characteristic complex cubic structure containing 52 atoms in the unit cell. The crystal structure of the  $\epsilon$  phase, which is a 7/4 electron compound, is close-packed hexagonal. Only the  $\alpha$ ,  $\beta$ ,  $\beta'$ , and  $\gamma$  phases are of importance to the present investigation.

## 2. THE COPPER-GERMANIUM SYSTEM

No satisfactory complete diagram for this system has been reported. The entire range of compositions has been investigated by Schwarz and Elstner,<sup>9</sup> but the equilibrium relationships are incompletely defined. Further work by Maucher<sup>10</sup> and by Weibke<sup>11</sup> has shown that copper dissolves approximately 10 at.-% germanium, and that the primary solid solution

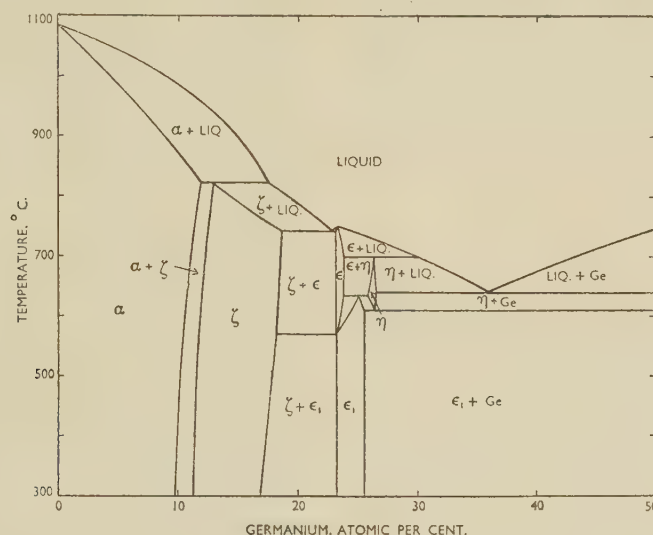


FIG. 2.—The Most Probable Equilibrium Diagram of the Copper-Germanium Alloys.

Isothermal diagrams at 550° and 400° C. have been established by micrographic and X-ray examination of a large number of ternary alloys, in order to examine the equilibria involved.

## II.—THE BINARY SYSTEMS

### 1. THE COPPER-ZINC SYSTEM

The equilibrium diagram for this system has been discussed by Raynor<sup>8</sup> and is reproduced as Fig. 1. The details have been accurately established by means of X-ray, micrographic, and thermal analysis. The limits of the face-centred cubic primary  $\alpha$  solid-solution are satisfactorily determined, and the fall in the solubility below 454° C. has been confirmed by several independent investigations. The  $\beta$  phase, based on the composition  $\text{CuZn}$ , is a random body-centred cubic 3/2 electron compound, which undergoes an order-disorder transformation at the temperatures indicated by the broken line in Fig. 1. Below these temperatures, the  $\beta'$  phase is stable, with a

enters into equilibrium in the solid state with an intermediate phase ( $\zeta$ ) containing approximately 13–16 at.-% germanium. According to Weibke,<sup>11</sup> the  $\zeta$  phase is succeeded, on increasing the germanium content, by a  $\gamma$  phase, which decomposes eutectoidally into the  $\zeta$  and  $\epsilon$  phases at approximately 560° C. The primary solid-solubility curve has been accurately established by Hume-Rothery, Raynor, Reynolds, and Packer,<sup>12</sup> who have obtained results in excellent agreement with the earlier work of Hume-Rothery, Mabbott, and Channel-Evans.<sup>13</sup> At the same time, the form of the  $\zeta$  phase area has been more accurately defined<sup>12</sup> and has been shown to extend over a considerably wider range of compositions than was previously supposed. Corrections to the region of the diagram involving Weibke's  $\gamma$  phase have recently been made by Hume-Rothery and Betterton,<sup>14</sup> who have shown that a high-temperature phase, denoted  $\epsilon$ , decomposes eutectoidally into the  $\zeta$  and  $\epsilon_1$  phases at 570° C.\*

\* The authors are grateful to Dr. Hume-Rothery and Dr. Betterton for permission to use these data.



Fig. 2 represents the most probable equilibrium diagram for these alloys, in the relevant composition range, and is based upon the most reliable of the researches outlined above; the X-ray researches of Owen and Rowlands<sup>15</sup> and Owen and Roberts<sup>16</sup> have also been taken into account. The  $\alpha$  solid-solubility limit is 11.9–12.0 at.-% germanium at the peritectic temperature of 822.5° C., and the  $\zeta$  phase has a maximum composition range of 11.5–18.7 at.-% germanium. The crystal structure of the  $\zeta$  phase, which is a 3/2 electron compound, is close-packed hexagonal; the structures of the  $\epsilon$  and  $\epsilon_1$  phases are not completely determined, but neither phase is isomorphous with  $\gamma$  brass.

### 3. THE ZINC-GERMANIUM SYSTEM

This system has been examined by Gebhardt,<sup>17</sup> who reported a simple eutectiferous series of alloys, with the eutectic at 6 at.-% germanium and 398° C. The mutual solid solubilities of zinc and germanium are extremely small. No stable intermetallic compounds are formed, and the system is not of great importance to the present work.

### III.—MATERIALS USED

Because of the relative scarcity of germanium metal, only a proportion of the alloys used were prepared from the constituent metals. Many specimens had to be prepared by remelting previously cast alloys with appropriate additions of copper, zinc, or germanium, or by melting together two existing alloys. The remelting technique employed was unavoidable; analytical tests were, however, made to ensure that no contamination was introduced by the procedure adopted.

Over 100 ternary alloys were prepared, and of these approximately one-quarter were made directly from the component metals. The following materials were used:

1. Oxygen-free, high-conductivity copper, 99.99% pure.
2. "Crown Special" zinc, 99.99% pure, which was kindly presented by the Imperial Smelting Corporation, Ltd., Avonmouth.
3. Spectrographically standardized germanium, which was supplied by Johnson, Matthey and Co., Ltd., and which was of a very high degree of purity.

### IV.—EXPERIMENTAL METHODS

In general, alloys rich in the two solute metals were prepared from the pure components, and in subsequent work their compositions were changed towards the copper-rich corner of the ternary composition diagram by remelting weighed amounts with the appropriate quantity of pure copper. In all cases, melting methods were closely similar. Carefully weighed

amounts of the components were melted in graphite crucibles, using a small spark-gap H.F. furnace. Only small melts were prepared, in order to conserve germanium; initially the alloys were made in 5-g. quantities, but this was later reduced to 3 g. The crucibles used were specially made from high-conductivity graphite containing less than 0.01% impurity, and were of  $\frac{3}{4}$  in. external dia. and  $\frac{1}{4}$  in. bore. Owing to the narrow bore, only a very small area of the melt was exposed to the air; this circumstance, combined with the very rapid heating obtained with the induction furnace and the reducing atmosphere produced by the slow burning of the crucibles, made it unnecessary to use flux protection or controlled atmospheres. Subsequent analyses showed that only slight zinc losses occurred, while analysis of an alloy melted or remelted four times (with various additions of copper and zinc) indicated that no appreciable amount of impurity was introduced in the preparation.

When molten, alloys were vigorously stirred with a preheated recrystallized alumina rod, and then quickly cast into a cylindrical mould bored in a heavy copper block, to give ingots  $\frac{1}{4}$  in. in dia. and approximately  $\frac{1}{2}$  in. long. The fine chill-cast structures obtained hastened the attainment of equilibrium on subsequent annealing.

Specimens of the alloys were annealed, *in vacuo*, in horizontal electric-resistance furnaces, controlled to within  $\pm 1^\circ$  C. of the required temperature by automatic regulators. In general, the chill-cast alloys were slowly heated to 650° C. and given a homogenizing treatment for 3 days at this temperature. The specimens were then cooled to the required annealing temperature (either 550° or 400° C.), and annealed for periods of at least 5 days at the higher temperature, or 8 days at the lower. Tests showed that the annealing periods used were sufficient for the establishment of equilibrium. After the annealing treatments, all alloys were rapidly quenched in cold water.

Temperatures were measured throughout with a platinum/platinum-rhodium thermocouple, used in conjunction with a sensitive potentiometer, and standardized frequently against the freezing points of pure metals.

For the micrographic examination, fresh surfaces of the quenched alloys were exposed with a fine saw; the specimens were mounted in Diakon cement, and prepared in the usual manner. Etching techniques are referred to in the next section. As a check on the micrographic interpretations, or where these were doubtful, X-ray experiments were carried out. For this purpose fine filings were prepared from the quenched alloys, and were reheated to the quenching temperature for the relief of mechanical strain. The annealing was carried out in evacuated hard-glass tubes, which shattered when the specimens were quenched in cold water, giving a rapid chill. Air cooling was found by experiment to be insufficiently drastic, and incapable of retaining the high-temperature structure of the ternary alloys. The washed

and dried quenched filings were made into cylindrical specimens, without sieving, using either Canada balsam or gum tragacanth as adhesive, and diffraction patterns were obtained by exposure to copper  $K_\alpha$  radiation in a 9- or 19-cm. Debye-Scherrer X-ray camera.

In view of the volatility of zinc, all critical alloys were chemically analysed. The actual specimens examined in the micrographic work were submitted for analysis, after removal of the outer surfaces to avoid errors resulting from possible volatilization losses during annealing. Analyses were carried out by Johnson, Matthey and Co., Ltd., by Mr. L. James and Miss Archer of the Metallurgy Department, University of Birmingham, or by one of the authors (P. G.). Results from the three sources were concordant. In general, all three of the component elements were determined, and the analytical totals confirmed the absence of accidental impurities. As an example, the analysis figures for an alloy which had been remelted three times after the initial preparation totalled 99.94%; the analytical deficit is within the limits of experimental accuracy, when it is considered that the total weight of sample available did not exceed 0.2 g.

In the following sections, when it is necessary to refer to individual alloys, this will be done in terms of their alloy content; thus, alloy 6.27/12.38 contains 6.27 at.-% zinc and 12.38 at.-% germanium.

## V.—METALLOGRAPHY

Throughout the work, only phases based upon those present in the binary systems were observed. These five phases  $\alpha$ ,  $\beta$  (or  $\beta'$ ),  $\zeta$ ,  $\gamma$ , and  $\epsilon_1$ , were distinguishable micrographically in the combinations in which they occurred. Two reagents were found generally useful: (1) a fresh solution of ammonium hydroxide (0.88 sp. gr.) with the addition of approximately 5% of 20-vol. hydrogen peroxide; and (2) a solution of ferric chloride made up from 10 g.  $\text{FeCl}_3$ , 25 c.c. hydrochloric acid, and 200 c.c. water.

Solution 1 was used as an immersion etch; the etching time was not critical, and varied with the constitution of the alloy examined. Solution 2 was most useful when applied with a swab of cotton-wool.

The copper-rich  $\alpha$  solid solution was readily recognizable on account of prolific twinning. When present with the  $\zeta$  phase, the primary solid solution was coloured light yellow, but when the  $\beta$  (or  $\beta'$ ) phase was present, the yellow colour tended towards light brown. Both etching treatments left the  $\zeta$  phase white, and in  $(\alpha + \zeta)$  alloys increased colour contrast was obtained by immersion in alcoholic ferric chloride after initial treatment with ammoniacal hydrogen peroxide. In  $(\zeta + \epsilon_1)$  alloys, the  $\epsilon_1$  phase etched a steel-blue colour, while in  $(\beta + \zeta)$  and  $(\beta + \alpha)$  alloys, the  $\beta$  phase was coloured a very light blue, and frequently contained a number of fine cracks. In  $(\beta + \gamma)$  alloys, the  $\gamma$  phase was coloured mauve, and the  $\beta$  phase yellow, as in homogeneous alloys. The

colours quoted refer to direct observation without the use of colour filters.

In a number of alloys, the  $\zeta$  phase tended to precipitate preferentially along certain crystallographic planes of the  $\alpha$  solid solution in the form of long thin plates. This effect gave rise to unusual microstructures, some of which are illustrated later in the paper; the phenomenon is discussed in Section VII.

## VI.—EXPERIMENTAL RESULTS

The results obtained may be conveniently summarized in the form of isothermal diagrams at 550° and 400° C.

### 1. THE 550° C. ISOTHERMAL DIAGRAM

The results of experiments on annealed chill-cast specimens (Section IV, p. 378) are summarized in Fig. 3, in which unanalysed alloys have been distinguished by black vertical bars. The isothermal contains seven well-defined areas, within the range of compositions examined.

The primary solid-solubility isothermal does not

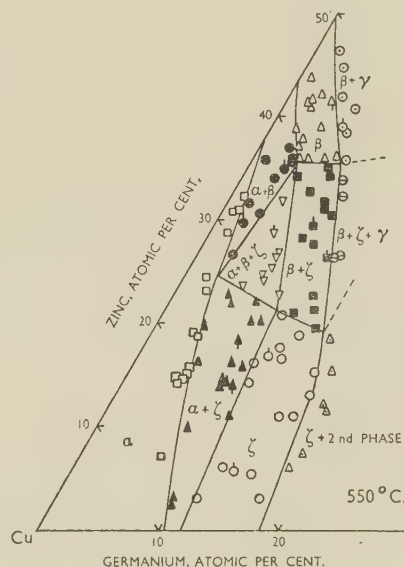


FIG. 3.—The 550° C. Isothermal.

KEY.					
□ $\alpha$	△ $\beta$	▲ $\alpha + \zeta$	○ $\beta + \gamma$	△ $\zeta + 2\text{nd phase}$	
○ $\zeta$	● $\alpha + \beta$	■ $\beta + \zeta$	⊖ $\beta + \zeta + \gamma$	▽ $\alpha + \beta + \zeta$	

appear to be a straight line joining the binary solid-solubility limits, which are accurately established by previous work. The ternary solubility is slightly less than in the ideal case. The  $\alpha/(\alpha + \zeta)$  boundary is accurately fixed by alloys 15.95/4.66, 16.28/5.05, 18.68/3.98, and 19.81/3.82, which determine its course over the range 15–20 at.-% zinc. At lower zinc contents, the bracket is given by alloys 2.6/10.0, 3.42/9.76, and 7.51/6.58.

The  $\alpha/(\alpha + \beta)$  boundary is also satisfactorily located, and appears to join smoothly on to the



$\alpha/(\alpha + \zeta)$  boundary, within the limits of accuracy obtained. It is considered that the boundaries of the homogeneous  $\beta$  and  $\zeta$  phases are also well established. In particular, it is to be noted that the straight-line boundaries of the three-phase ( $\alpha + \beta + \zeta$ ) field cannot be moved appreciably from the positions shown in Fig. 3 without violating the micrographic results obtained in adjacent phase fields.

It was not intended, during this work, to investigate the equilibrium relationships at higher solute concentrations than those corresponding to the solute-rich boundaries of the 3/2 electron compounds. From several X-ray experiments, however, it may be proved that the  $\beta$  phase, along the whole of its solute-rich boundary, enters into equilibrium with the  $\gamma$  structure based on the  $\gamma$  phase in the copper-zinc alloys. The alloy 35.69/7.69, for instance, which is very close to the corner of the three-phase triangle involving the solute-rich limits of the  $\beta$  and  $\zeta$  phases, contains the  $\beta$  and  $\gamma$  structures only. The adjacent three-phase triangle must thus involve the  $\beta$ ,  $\zeta$ , and  $\gamma$  phases, and is appropriately labelled in Fig. 3. Since it is unlikely that the copper-zinc  $\gamma$  phase and the copper-germanium  $\epsilon_1$  phase, having different crystal structures, form a continuous series of solid solutions, the  $\zeta$  phase, along its solute-rich boundary must enter into equilibrium with both the  $\gamma$  and  $\epsilon_1$  phases over the appropriate composition ranges. Micrographically, however, there was no indication of these separate phase fields, and accordingly the alloys lying beyond the solute-rich boundary of the  $\zeta$  phase have been designated merely as ( $\zeta + 2nd$  phase). It is hoped to investigate the  $\gamma$ - $\epsilon_1$  equilibria in the near future. All the other areas in the diagram were confirmed by the diffraction patterns of filings made from quenched alloys. Preliminary experiments with an alloy having the  $\beta$  structure at 550° C., but consisting of ( $\alpha + \beta'$ ) at 400° C. showed that the high-temperature state could be retained only by quenching; after air cooling, diffraction lines due to precipitated  $\alpha$  were observed.

Photomicrographs of typical microstructures produced by quenching from 550° C. are reproduced in Figs. 7 and 8 (Plate LVII). The former shows needles of second phase which have precipitated at 550° C. from the  $\zeta$  matrix in alloy 6.32/17.77; the latter shows the ( $\alpha + \zeta$ ) structure of alloy 9.97/7.53.

The main feature of the isothermal diagram shown in Fig. 3 is the pronounced extension of the  $\zeta$  field (close-packed hexagonal crystal structure) into the body of the diagram, and the simple two-phase equilibrium between the two 3/2 electron compounds, which necessitates the presence of the ( $\alpha + \beta + \zeta$ ) three-phase triangle. The  $\zeta$  phase dissolves a maximum of 21 at.-% zinc, at which limit the germanium content is only 10 at.-%; the phase thus contains twice as many zinc atoms as germanium atoms, while still retaining the close-packed hexagonal crystal structure. The  $\beta$  phase can dissolve a maximum of 7.5 at.-% germanium without losing its body-centred cubic structure.

## 2. THE 400° C. ISOTHERMAL DIAGRAM

In determining this isothermal, the alloys already annealed at 550° C. were re-annealed at the lower temperature for a period of not less than 8 days, and tests for the complete attainment of equilibrium were again applied. The results of the experiments are summarized in Fig. 4, in which the various phase boundaries are adequately defined by the points plotted. Although the general form of the equilibrium diagram remains unaltered, some differences in detail may be noted. Thus, several alloys which consisted of the homogeneous  $\alpha$  phase at 550° C. contain small amounts of the  $\beta'$  or  $\zeta$  phases at 400° C. The deviation of the ternary solid-solubility isothermal from linearity is therefore even more pronounced at the lower temperature, in spite of the fact that comparatively little change in the binary solid solubilities has taken place. The major part of the ( $\alpha + \zeta$ )/ $\zeta$

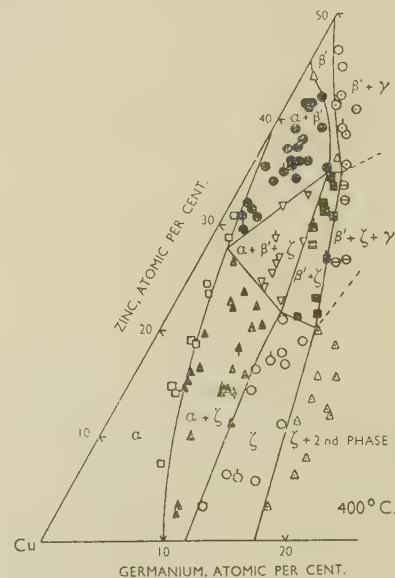


Fig. 4.—The 400° C. Isothermal. Key as for Fig. 3.

boundary appears to be unchanged in position, although, from a consideration of the binary limits in the copper-germanium system, it would be expected to lie slightly nearer the copper-rich region by an amount of approximately 0.2 at.-%. The solute-rich boundary of the  $\zeta$  phase, however, lies much nearer the copper-rich region at 400° C. than at 550° C., in agreement with the change in the binary  $\zeta/(\zeta + \epsilon_1)$  boundary between these temperatures. The  $\zeta$  field is clearly less wide than at 550° C., but its projection into the ternary diagram appears to be unchanged, as shown by the compositions of the alloys which locate the  $\zeta/(\beta' + \zeta)$  boundary.

The  $\beta'$  field at 400° C. is considerably narrower than the  $\beta$  field at 550° C.; this is a consequence of the order-disorder transformation in the binary copper-zinc alloys. Eleven of the thirteen alloys which consisted of homogeneous  $\beta$  at the higher temperature became two-phase during annealing at 400° C. The two which remained homogeneous were confirmed as

$\beta'$  by X-ray diffraction methods. It will be noted that the germanium-rich limit of the homogeneity range of the  $\beta'$  phase is not reached by the homogeneous alloy 36.44/7.45, since alloys 35.40/6.43 and 35.69/7.69 contain respectively the  $(\alpha + \beta')$  and  $(\beta' + \gamma)$  phases. In spite of the marked narrowing of the  $\beta'$  field, the maximum extent to which germanium may dissolve in the body-centred cubic phase appears to be quite unaffected by the fall in temperature.

The restricted width of the  $\beta'$  field gives rise to a narrowing of the  $(\beta' + \zeta)$  area, and an enlargement of the three-phase  $(\alpha + \beta' + \zeta)$  triangle, as compared with the constitution at 550° C. It is also to be noted that the copper-rich apex of this three-phase triangle is displaced towards higher zinc contents. This feature is particularly well illustrated by the fact that alloy 26.49/3.0, which contained the  $\alpha$  and  $\beta$  phases at 550° C., possessed an  $(\alpha + \zeta)$  microstructure at 400° C.; the corresponding changes in other alloys confirm the displacement. As at 550° C., the boundaries of the three-phase triangle cannot be moved appreciably from the positions plotted in Fig. 4 without causing conflict with the results in adjacent phase fields.

All the phase fields occurring between the copper-rich corner of the diagram and the solute-rich boundaries of the 3/2 electron compounds were confirmed by X-ray-diffraction experiments. Alloy 35.69/7.69 was again shown to consist of the  $\beta'$  and  $\gamma$  phases by these means, and confirmatory experiments were carried out on three other alloys nearer to the copper-zinc axis of the diagram. The two-phase alloys lying beyond the solute-rich boundary of the  $\zeta$  phase again showed no evidence of the expected  $(\zeta + \gamma)$  and  $(\zeta + \gamma + \epsilon_1)$  fields, and, to avoid confusion, have again been plotted as  $(\zeta + 2\text{nd phase})$ .

Figs. 9-12 (Plate LVII) show typical microstructures obtained in the alloys quenched from 400° C. Fig. 9 illustrates clearly the form in which the  $\zeta$  phase is precipitated in the  $\alpha$  matrix, and it is to be noted particularly how the twin boundaries in the  $\alpha$  phase are heavily outlined by the  $\zeta$  plates, and that, in general, the precipitation tends to occur so that the traces of the  $\zeta$  plates are parallel to the twin boundaries. Fig. 10 shows a portion of the same alloy at higher magnification. A typical two-phase alloy lying to the solute-rich side of the  $\zeta$  phase is shown in Fig. 11. Fig. 12 is another example of plate-like  $\zeta$  crystals precipitated in twinned  $\alpha$  crystals in an alloy which consisted, at the higher temperature, of the  $\alpha$  and  $\zeta$  phases in a relatively coarse admixture.

## VII.—DISCUSSION OF THE RESULTS

Certain features of the constitution of the copper-zinc-germanium system are of interest in relation to the theory of ternary-alloy formation, and may be considered separately.

### 1. THE PRIMARY SOLID-SOLUBILITY ISOTHERMALS

The forms of ternary primary solid-solubility isothermals have been discussed previously,<sup>18</sup> and in

the absence of compound formation, three cases have been distinguished. In particular, where both solutes are of favourable size-factor with respect to the solvent, the isothermals approximate to straight lines joining the binary solubility limits. If, however, the solution is relatively dilute, and one solute markedly increases the distortion of the lattice produced by the other, the ternary solubility tends to be more restricted than in the ideal case. Relief of the distortion produced by one solute on addition of the other conversely tends to cause the solubility to exceed the ideal value. In cases where the solid solution is insufficiently dilute for the system to be considered as a solvent framework containing centres of relatively intense local distortion, these tendencies are modified; the more appropriate picture is that of a framework of both solvent and solute atoms, with a lattice spacing markedly different from that of the solvent. The atoms of the second solute may then be of unfavourable size-factor with respect to the alloy framework, leading to a more restricted ternary solid solution than in the ideal case. The present alloy system may be discussed in the light of these conceptions.

The solid solubilities of zinc and germanium in copper are widely different, when expressed in terms of atomic percentages, so that the ternary solid solution may be regarded, from one point of view, as dilute near the copper-germanium axis and concentrated near the copper-zinc axis. The solubility relationships may thus be expected to be complex. The interatomic distances in the crystals of the elements concerned in the present work are: copper, 2.551 Å.; zinc, 2.659 Å.; germanium, 2.445 Å. The solvent, therefore has an atomic diameter midway between those of the solutes, but, as shown in Figs. 3 and 4, the ternary solubility isothermals are not consistent with the relief of a positive distortion due to the zinc atoms by a distortion in the opposite sense caused by the smaller germanium atoms. The observed boundary shows a lower solubility than in the ideal case, the deviation being more pronounced at the lower temperature. Consideration of the relative atomic diameters of the component metals is insufficient to give a reliable guide to the relative distortion effects, and the relative valencies must also be considered. In a solid solution in copper or silver, the observed lattice distortion may be regarded as the resultant of two factors.<sup>18</sup> The atomic factor, which depends upon the relative atomic sizes, may be positive or negative, according to whether the solute atoms are larger or smaller than those of the solvent; whereas the valency factor, whose magnitude depends upon the difference in valency between the component metals, is positive where the solute valency exceeds that of the solvent. The dependence of the valency factor on the valency of the solute has been discussed previously.<sup>19</sup> Thus, in spite of its smaller atomic diameter, germanium expands the lattice of copper,<sup>20</sup> the positive distortion due to the high valency of germanium over-



compensating the effect of its small atomic diameter. Both zinc and germanium, therefore, expand the copper lattice, and mutual relief of lattice distortion in the sense considered above does not occur.

The general tendency is for ternary solid-solubility isothermals in equilibrium diagrams of the type considered here to correspond to the maintenance of an approximately constant electron : atom ratio. When, therefore, zinc replaces germanium in the saturated solid solution of the latter in copper, approximately three zinc atoms replace one of germanium. Since the distortion of the copper lattice produced by one atom of zinc is approximately 0.6 of that produced by one atom of germanium,<sup>20</sup> the inclusion of zinc will lead to an increase in the total distortion to be accommodated by the lattice, and in addition there will be more centres of distortion. Thus the decrease in solubility as compared with the ideal case may be understood. Conditions are somewhat different when germanium is introduced into the saturated solid solution of zinc in copper, which cannot be considered dilute. Here the lattice contains a large number of centres of distortion and is greatly expanded relative to pure copper; \* although only one germanium atom enters the lattice in place of three zinc atoms, thereby reducing the total distortion to be accommodated, it is unlikely that the already highly distorted lattice will easily accommodate the introduced centres of intense local distortion, considering that the lattice expansion produced in copper by one germanium atom is approximately 1.6 times that produced by one zinc atom. The relative restriction in solubility at the zinc-rich end of the solubility isothermals may therefore also be interpreted. It is of interest to note that the more marked deviation from a straight line joining the binary limits occurs on substituting zinc for germanium, and suggests that increasing total distortion, and increasing numbers of centres of distortion, are more effective in restricting the solubility than the introduction of a few intense centres of distortion into an already strained lattice, if these are partially compensated for by a decrease in the total distortion to be accommodated. The interpretation of the form of the isothermals in terms of distortion effects is consistent with the more pronounced deviations from linearity observed at the lower temperatures, since the effects of thermal agitation would be expected to facilitate the accommodation of local lattice distortions.

## 2. THE 3/2 ELECTRON COMPOUNDS

As shown by Figs. 3 and 4, the equilibrium between the  $\beta$  and  $\zeta$  phases, and between the  $\beta'$  and  $\zeta$  phases, is simple, and the projection of the area corresponding to each into the body of the ternary diagram is considerable. The  $\zeta$  phase, as noted above, is able to maintain its hexagonal structure even when the number of zinc atoms contained in it is twice the

number of germanium atoms. The  $\beta$  and  $\beta'$  phases will dissolve a maximum of approximately 7 at.-% germanium. In Section I it was noted that, in general, ternary electron compounds were stable at effective size-factors closely similar to the size-factors at which they occurred in binary systems based on copper and silver. The work of Hume-Rothery, Reynolds, and Raynor<sup>2</sup> shows that, for the silver alloys, the  $\zeta$  structure occurs in the systems silver-tin (size-factor,  $-3.0$ ) and silver-antimony (size-factor,  $+0.5$ ), but gives way to the  $\beta$  structure at high temperatures in the system silver-cadmium (size-factor,  $+3.1$ ). For copper alloys the  $\zeta$  and  $\beta$  structures are stable in the systems copper-germanium (size-factor,  $-4.15$ ) and copper-zinc (size-factor,  $+4.23$ ); no systems with 3/2 electron compounds fall between these size-factor limits. By comparison with the silver series, it would be expected that, in the ternary copper-zinc-germanium system, the  $\zeta$  structure would persist to an effective size-factor of more than  $+0.5$ , but would become unstable with regard to the cubic  $\beta$  phase before the effective size-factor of  $+3$  was reached. On general grounds, persistence of the  $\zeta$  phase, at the temperatures considered in the present paper, to an effective size-factor of approximately  $+2$  would be expected. Since, in the silver series of alloys, the cubic phase is not observed below a size-factor of  $+3$  until a negative size-factor of  $-5.65$  is reached (silver-aluminium system), the copper-zinc-germanium  $\beta$  and  $\beta'$  phases would not be expected to persist below an effective size-factor of approximately  $+3$ .

The experiments summarized in Figs. 3 and 4 show that at  $550^\circ\text{C}$ . the  $\zeta$  phase actually persists from a size-factor of  $-4.15$  at the copper-germanium axis to an effective size-factor of  $+1.6$  at the copper-rich end, and  $+0.6$  at the solute-rich end, of the  $\zeta/(\zeta + \beta)$  boundary. At  $400^\circ\text{C}$ . the corresponding limits are at effective size-factors of  $+1.6$  and  $+0.9$ . The ternary hexagonal phase thus becomes unstable at a maximum effective size-factor of  $+1.6$ , in good qualitative agreement with the values at which the same change occurs in the binary systems.

The body-centred cubic phase based upon CuZn extends from the copper-zinc axis (size-factor,  $+4.23$ ) to an effective size-factor of  $+3.38$  at the copper-rich end, and  $+2.8$  at the solute-rich end, of the  $\beta/(\beta + \zeta)$  boundary. At  $400^\circ\text{C}$ ., the limits of the  $\beta'$  phase occur at corresponding effective size-factors of  $+2.9$  and  $+2.8$  respectively. These figures are in excellent agreement with the values expected from a study of the relevant binary systems. It will be noted that the dilution of the copper-germanium  $\zeta$  phase with zinc reinforces the effective size-factor, since solutes of low valency in general tend to stabilize the body-centred cubic structure.

The above discussion of the homogeneity ranges of the 3/2 electron compounds confirms the general

\* The percentage distortion of the copper lattice at the maximum solid-solubility of zinc  $\left(\frac{\delta a}{a} \times 100\right)$ , where  $a$  is the

lattice spacing of copper) is approximately 2.47, whereas the corresponding value for germanium in copper is approximately 1.08.<sup>15</sup>

principle that a qualitative guide to the extent of the projection of a 3/2 electron compound into the body of a ternary isothermal diagram may be obtained by a consideration of the effective size-factor in the ternary system, in conjunction with a study of the

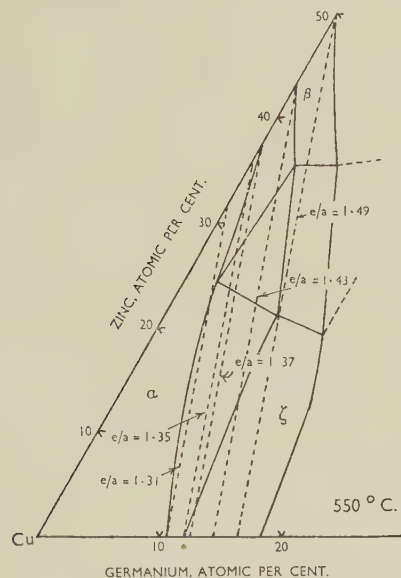


FIG. 5.—The  $\beta$ - and  $\zeta$ -Phase Boundaries Compared With Lines of Constant Electron : Atom Ratio at 550° C.

relationship between structure and size factor in the relevant binary alloys. The system under consideration bears a striking resemblance to the copper-aluminium-silicon system,<sup>4</sup> in which, at temperatures above that at which the copper-aluminium  $\beta$  phase decomposes eutectoidally, the hexagonal  $\zeta$  structure exists between effective size-factors of  $-8$  (copper-silicon system) and  $+2$ , and the cubic structure exists between effective size-factors of  $+6.6$  (copper-aluminium system) and  $+3.2$ . The effective size-factors at which the hexagonal and cubic phases become unstable relative to each other are very similar in the two systems.

It has been noted that the ternary  $\beta'$  phase at 400° C. is very much narrower than the ternary  $\beta$  phase at temperatures above that of the order-disorder transformation (Section VI, 2). This is not unexpected, since the replacement of zinc by germanium, if the characteristic electron : atom ratio of approximately 1.5 is not to be greatly exceeded, involves a composition change towards the copper-rich side of the line representing the maintenance of an ideal caesium chloride arrangement. Under these conditions it is unlikely that the ternary  $\beta'$ -structure, which owes its stability mainly to the operation of electronic factors, will be able to tolerate an excess of either copper or zinc, since the difficulty of maintaining the ordered arrangement would be increased.

Since the most important factor affecting the formation of the  $\beta$  and  $\zeta$  phases is electronic in origin, it is of interest to examine the electron : atom ratios corresponding to their phase boundaries. In Fig. 5,

the various boundaries at 550° C. have been plotted as full lines, and lines of constant electron : atom ratio, corresponding to the limits in the binary systems, have been inserted as broken lines. Fig. 6 shows a corresponding diagram for the 400° C. isothermal. It is clear that there is neither a tendency for the ternary isothermal boundaries to follow a line of constant electron : atom ratio, nor to approximate to the electron : atom ratios characteristic of the limits of homogeneity in the binary systems. Instead, as zinc is added to the copper-germanium  $\zeta$  phase, both the copper-rich and solute-rich boundaries move towards higher electron : atom ratios; the same is true of the ternary  $(\alpha + \beta)/\beta$  and  $\beta/(\beta + \gamma)$  boundaries. This is consistent with the behaviour of 3/2 electron compounds in the corresponding binary alloys,<sup>2</sup> in which an increase in the numerical magnitude of the size-factor tends to shift the composition of the electron compound as a whole to lower electron : atom ratios, and conversely. In the ternary alloys considered, the numerical value of the effective size-factor decreases towards zero both on the addition of zinc to the copper-germanium  $\zeta$  phase and on the addition of germanium to the copper-zinc  $\beta$  or  $\beta'$  phases. It is of great interest to note that the junction of the  $(\alpha + \zeta)/\zeta$  and  $(\beta + \zeta)/\zeta$  boundaries, at both the temperatures investigated, occurs almost exactly at the ideal electron : atom ratio of 1.5 (Figs. 5 and 6). Another point of interest is that, although the homogeneity range of the ternary  $\beta$  phase at 550° C. includes the electron : atom ratio 1.5, the range of

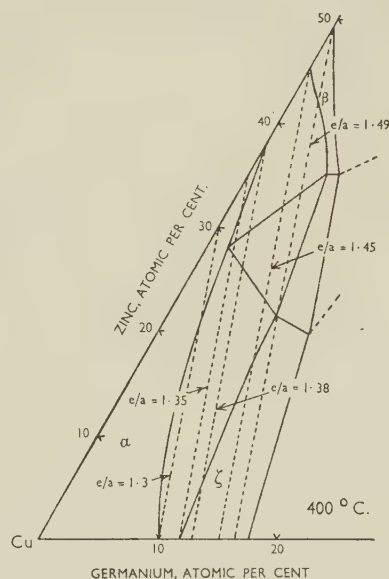


FIG. 6.—The  $\beta$ - and  $\zeta$ -Phase Boundaries Compared With Lines of Constant Electron : Atom Ratio at 400° C.

homogeneity of the  $\beta'$  phase at 400° C. does not include this ratio at germanium contents greater than about 1.7 at.-% (Fig. 6). The junction of the  $\beta/(\beta + \gamma)$  and  $\beta/(\beta + \zeta)$  boundaries occurs at both temperatures investigated, at the composition 7.5 at.-% ger-



manium and 35.2 at.-% zinc, corresponding to an electron : atom ratio of 1.58.

### 3. THE PRECIPITATION OF THE $\zeta$ PHASE FROM THE $\alpha$ PHASE

In Section V, and in Figs. 9, 10, and 12 (Plate LVII), attention has been drawn to the precipitation of the  $\zeta$  phase preferentially along certain crystallographic directions in the solid-solution matrix, in the form of thin plates. The form of a precipitate is, in general, greatly affected by surface-energy considerations, and there is a marked tendency for precipitation to occur in such a way that the atomic planes in the respective phases which are parallel to each other on either side of the bounding surface are similar both as regards atomic positions and atomic spacings. In the present case, the plates of precipitated  $\zeta$  phase were, in general, parallel to the twin boundaries, and in many cases twins in the  $\alpha$ -solid-solution matrix were outlined by plates of precipitate. Since it is known that twinning in the face-centred cubic structure of copper occurs along the (111) planes, it would appear that the  $\zeta$  phase precipitates along the (111) planes of the matrix. This would be expected from structural considerations. The lattice spacing of the copper-germanium alloys at the maximum solid-solubility limit is 3.646 Å.,<sup>15</sup> whereas that of the copper-zinc alloys at 34.25 at.-% zinc (close to the solubility limit) is 3.685 Å.<sup>16</sup> Along the  $\alpha/(\alpha + \zeta)$  boundary, therefore, we may consider the average lattice spacing to be approximately 3.666 Å. The average distance between atoms in the (111) planes, in which the atomic arrangement is hexagonal, is thus  $3.666/\sqrt{2}$  or 2.592 Å. The lattice spacings of the binary  $\zeta$  phase have been measured by Maucher,<sup>10</sup> who quotes values for the  $a$  spacing of 2.606 and 2.616 Å., respectively, at 14.06 and 18.07 at.-% germanium. Assuming a linear variation of the  $a$  spacing with composition, the appropriate value at the copper-rich phase boundary of the  $\zeta$  phase is 2.598 Å. Thus the atomic spacing in the (00,1) planes of the hexagonal  $\zeta$  phase, in which there is a hexagonal atomic arrangement, is closely similar to that in the (111) planes of the copper-rich solid solution, and the form of precipitation observed may be understood. The  $\zeta$  phase precipitates in such a

way that the two planes with similar atomic spacing and arrangement in the  $\zeta$  and  $\alpha$  phases lie parallel to each other.

### ACKNOWLEDGEMENTS

This research was carried out in the Metallurgy Department of the University of Birmingham, under the general supervision of Professor D. Hanson, D.Sc., to whom the authors' thanks are due for his interest and support. The authors also express their gratitude to the Department of Scientific and Industrial Research, the Royal Society, the Chemical Society, and Imperial Chemical Industries, Ltd., for generous financial assistance.

### REFERENCES

1. G. V. Raynor, *Phil. Mag.*, 1948, [vii], **39**, 212.
2. W. Hume-Rothery, P. W. Reynolds, and G. V. Raynor, *J. Inst. Metals*, 1940, **66**, 191.
3. G. V. Raynor, *Phil. Mag.*, 1948, [vii], **39**, 218.
4. F. H. Wilson, *Trans. Amer. Inst. Min. Met. Eng.*, 1948, **175**, 262.
5. G. V. Raynor and B. R. T. Frost, *J. Inst. Metals*, 1948-49, **75**, 777.
6. G. V. Raynor and R. A. Smith, *J. Inst. Metals*, 1949-50, **76**, 389.
7. B. R. T. Frost and G. V. Raynor, *Proc. Roy. Soc.*, 1950, [A], **203**, 132.
8. G. V. Raynor, *Inst. Metals: Annotated Equilib. Diagr. Series No. 3*, 1947.
9. R. Schwarz and G. Elstner, *Z. anorg. Chem.*, 1934, **217**, 289.
10. H. Maucher, *Forschungsarb. Metallkunde u. Röntgen-metallographie*, 1936, (20).
11. F. Weibke, *Metallwirtschaft*, 1936, **15**, 299.
12. W. Hume-Rothery, G. V. Raynor, P. W. Reynolds, and H. K. Packer, *J. Inst. Metals*, 1940, **66**, 209.
13. W. Hume-Rothery, G. W. Mabbott, and K. M. Channel-Evans, *Phil. Trans. Roy. Soc.*, 1934, [A], **233**, 1.
14. W. Hume-Rothery and J. O. Betterton, Jr., unpublished work.
15. E. A. Owen and V. W. Rowlands, *J. Inst. Metals*, 1940, **66**, 361.
16. E. A. Owen and E. W. Roberts, *Phil. Mag.*, 1939, [vii], **27**, 294.
17. E. Gebhardt, *Z. Metallkunde*, 1942, **34**, 255.
18. W. Hume-Rothery, *Phil. Mag.*, 1936, [vii], **22**, 1013.
19. G. V. Raynor, *Trans. Faraday Soc.*, 1949, **45**, 698.
20. W. Hume-Rothery, G. F. Lewin, and P. W. Reynolds, *Proc. Roy. Soc.*, 1936, [A], **157**, 167.



## MICROSTRUCTURES OF COPPER ZINC-GERMANIUM ALLOYS.

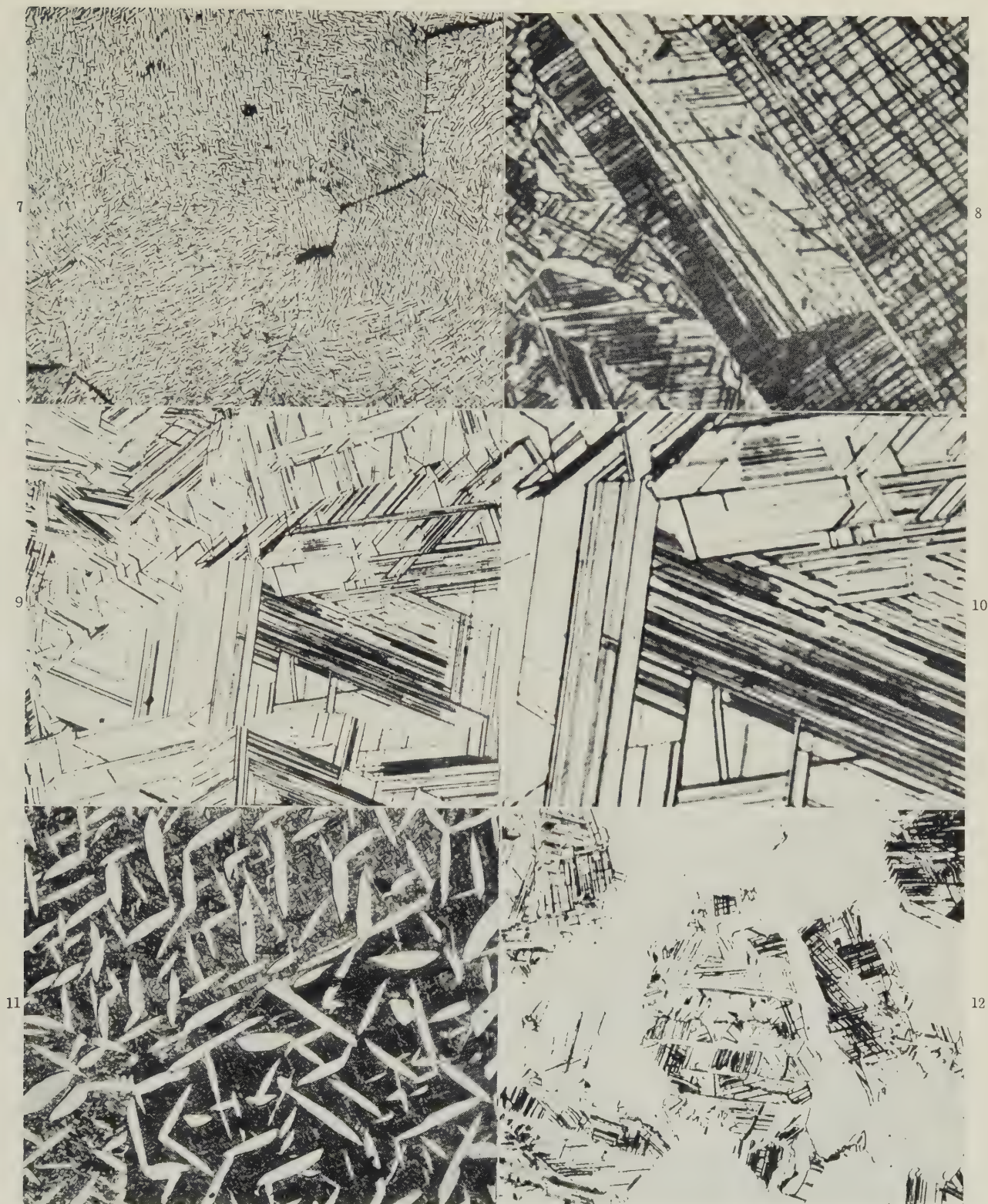

 FIG. 7.—6.32 At.-% Zn, 17.77 At.-% Ge Alloy, Quenched From 550° C. Needles of second phase in light matrix.  $\times 200$ .

 FIG. 8.—9.97 At.-% Zn, 7.53 At.-% Ge Alloy, Quenched From 550° C. Dark  $\zeta$  in twinned  $\alpha$ .  $\times 450$ .

 FIG. 9.—16.28 At.-% Zn, 5.05 At.-% Ge Alloy, Quenched From 400° C. Precipitated plate-like  $\zeta$  in twinned  $\alpha$ .  $\times 200$ .

 FIG. 10.—As Fig. 9.  $\times 450$ .

 FIG. 11.—6.32 At.-% Zn, 17.77 At.-% Ge Alloy, Quenched From 400° C. Second phase precipitated from  $\zeta$ .  $\times 200$ .

 FIG. 12.—20.17 At.-% Zn, 7.76 At.-% Ge Alloy, Quenched From 400° C. Plate-like  $\zeta$  crystals in twinned  $\alpha$  crystals in an alloy consisting of ( $\alpha + \zeta$ ) at 500° C.  $\times 200$ .

All specimens etched in ammoniacal hydrogen peroxide.

[To face p. 384.





# MICROGRAPHIC ASPECTS OF THE DIFFUSION OF ZINC AND ALUMINIUM IN COPPER \*

1358

By H. BÜCKLE,† Dr.-Ing., MEMBER, and J. BLIN †

## SYNOPSIS

Diffusion experiments carried out on brasses containing 10, 20, and 30% zinc and on a copper-7% aluminium alloy, in contact with pure copper, have confirmed the observations made by Smigelskas and Kirkendall (*Trans. Amer. Inst. Min. Met. Eng.*, 1947, **171**, 130), viz. (1) that the interface between the copper and the alloy is displaced during diffusion in such a way that the copper expands and the alloy contracts; and (2) that holes appear in the diffusion zone, though on the alloy side only. In certain cases, particularly in the copper-aluminium alloy, the holes have the shape of regular octahedra with their faces parallel to the (111) planes of the crystal.

Various possible explanations of the phenomenon are considered. The authors favour that which assumes the existence of two different mechanisms of diffusion of the atoms of the alloying element which proceed concurrently.

## I.—INTRODUCTION

AN anomaly in intermetallic diffusion has been observed by Smigelskas and Kirkendall,<sup>1</sup> who, using molybdenum wires as markers in a study of the inter-diffusion of copper and zinc in a specimen of 70 : 30 brass electroplated with copper, found that the original interface between the two specimens was displaced in the course of diffusion treatment towards the brass side. From this they concluded that zinc diffused more rapidly than copper, contrary to the classical conception of diffusion in a phase having a substitution structure.

Bückle<sup>2</sup> had earlier reported a similar anomaly in the formation by diffusion of a phase in the silver-zinc system, and Herman<sup>3</sup> also found a displacement of the interface in the case of a copper-aluminium alloy. These phenomena have been the subject of several investigations of a more or less theoretical character, seeking to explain the mechanism responsible for them.<sup>4-6</sup>

The object of the present investigation was to obtain additional experimental data on various doubtful points. In particular, it was desired: (1) to confirm the phenomenon of contraction using specimens of various zinc contents; (2) to repeat the experiment with a copper-aluminium alloy, in order to exclude the possible effects of the high vapour pressure of zinc; (3) to carry out experiments in the opposite direction, that is to say, with the copper specimen at the centre and brass on the outside, by which means it should be possible to eliminate certain hypotheses of the mechanism of contraction; and (4) to study more closely the pitting observed in the

structure of the diffusion zone by Smigelskas and Kirkendall.<sup>1</sup>

## II.—EXPERIMENTAL PROCEDURE

The alloys used were brasses containing 10, 20, and 30% zinc and a copper-aluminium alloy containing 7 wt.-% (16 at.-%) aluminium. Specimens  $12 \times 4 \times 4$  mm. were prepared, having two polished parallel surfaces. A little very fine molybdenum powder (average grain dia.  $2\mu$ ) was spread on these two faces and fixed in position by lightly pressing between two polished plates.

The various couples were made in two ways: (a) the alloy specimens were plated with a layer of copper 2 mm. thick (a very thin layer was first deposited from a cyanide bath, and the remainder built up in a sulphate bath); (b) sandwiches were formed, with copper at the centre and brass outside, or the reverse. In order to ensure good adherence between the interfaces ( $4 \times 12$  mm.), the sandwiches were placed in a special small press for 24 hr. at  $800^\circ\text{C}$ . in an atmosphere of purified nitrogen. They were then coated with copper to a thickness of 0.5 mm. in order to preserve them from oxidation during the prolonged diffusion treatment. All the specimens were treated for 25 days at  $800^\circ\text{C}$ . in sealed silica tubes.

Micrographic examination of the brass and copper revealed traces of impurities uniformly distributed. In order to determine the effect of these impurities on diffusion, purer specimens were prepared in the following way. Copper powder (containing  $99.923 \pm 0.003\%$  copper,  $<0.007\%$  iron), after being reduced in a current of purified hydrogen, was sintered into

\* Manuscript received 9 May 1951.

† Ingénieurs de Recherches, Office National d'Etudes et de Recherches Aéronautiques, Paris.



cylinders, 15 mm. in dia.  $\times$  150 mm. long, at 800° C. in the same atmosphere. These were melted *in vacuo* to produce dense cylinders 15 mm. in dia. To obtain pure brass some of the sintered copper cylinders were cut into discs 5 mm. thick, and arranged in piles with alternate discs of 99.99% zinc, 1 mm. thick. When these piles were heated *in vacuo* to a temperature below the melting point of the brass to which they corresponded, liquid zinc passed into the spongy, sintered-copper discs. The brass was then made by melting *in vacuo* for a very short time, followed by cooling *in vacuo*. The bars thus obtained (15 mm. in dia.) were lightly cold worked by hammering and annealed to ensure perfect homogenization. A layer 1.5 mm. thick was then turned off the bars so as to remove any impurities introduced into the surface by the various treatments. Sandwiches of copper/brass/copper and brass/copper/brass were then made from these bars and bars of pure copper, all of which were analysed.\*

After the diffusion treatment, the specimens were cut perpendicularly to the interface and the cross-section carefully polished. By means of the traces of molybdenum powder, it was possible to measure, with a microscope having a calibrated micrometer ocular, the distance between the opposite interfaces. Their initial positions being known from the thickness of the brass, it was thus possible to determine the displacement of the interfaces during diffusion.

Several causes of error arose in these measurements: (i) it was difficult to obtain two planes which were strictly parallel; (ii) it was essential to cut the specimen exactly perpendicularly to the interface—an error of 3° involved an error of about 6  $\mu$  in the displacement; and (iii) a certain amount of irregularity in the lateral faces of the specimens, due to diffusion, was observed.

### III.—EXPERIMENTAL RESULTS

#### 1. MEASUREMENT OF DISPLACEMENT

The results of the measurements of the displacement of the interface are summarized in Table I. It will be seen from these that there is a marked shift of the interface in all cases, the extent of it increasing with the zinc content. The direction of the displacement is always such as to be equivalent to a contraction of the alloy (whether brass or copper-aluminium) and an expansion of the copper. For a given brass (e.g. 30% zinc) the expansion of the copper is greater and more uniform than the contraction of the brass (cf. specimens 5 and 6 with 1 and 2). This latter phenomenon led to an investigation of the micrographic aspect that revealed the presence of holes in the diffusion zone, always occurring on the alloy side. These holes are to be seen only as a result of very careful mechanical polishing. Polishing on emery paper causes them to be filled up, and it is only by taking special precautions in polishing on felt and

velvet that they can be rendered visible. Thus, it is possible to distinguish the true holes from the oxide and other inclusions which sometimes occur to a limited extent, particularly near the surface, and which might be confused with the holes in a badly polished section.

TABLE I.—Displacement of Interface After Heating for 25 Days at 800° C.

Specimen No.	Constitution of Specimen	Displacement of Interface, $\mu$	Probable Error, $\mu$	Remarks
1	Cu/70 : 30 brass/Cu (electrolytic coating)	— 96	$\pm 7$	Average of 2 measurements. ...
2	Cu/70 : 30 brass/Cu (sandwich)	— 121	$\pm 10$	
3	Cu/80 : 20 brass/Cu (electrolytic coating)	— 57	$\pm 10$	...
4	Cu/90 : 10 brass/Cu (electrolytic coating)	— 34	$\pm 10$	...
5	70 : 30 brass/Cu/70 : 30 brass (sandwich)	+170	$\pm 5$	Average of 4 measurements.
6	70 : 30 brass/Cu/70 : 30 brass (sandwich)	+172	$\pm 5$	
7	Cu/Cu-7% Al/Cu (electrolytic coating)	— 35	$\pm 5$	Average of 4 measurements.

Fig. 3 (Plate LVIII) shows the distribution of the holes in the diffusion zone of a copper/brass specimen. It will be seen that they are strictly confined to the alloy side of the interface; on the copper side any natural defects (such as microporosity) have been closed up by the expansion. The presence of these holes easily explains why smaller values are obtained for the contraction of the brass than for the expansion of the copper. Measurements of the size of the holes have been made with a planimeter on photographs at a magnification of 200, and the additional contraction corresponding to their volume calculated. With this correction, values were obtained corresponding to those for the expansion of copper, within the limits of experimental error. The displacement of the interface, corrected in this way, has been plotted against the atomic percentage of zinc in the brass in Fig. 1. The value of 85  $\mu$  for the 30% brass (after 25 days at 800° C.) agrees well with the value of 80  $\mu$  (after 25 days at 785° C.) given by Smigelskas and Kirkendall.<sup>1</sup> The figure obtained for the copper-aluminium specimen lies a little below the curve for brass.

#### 2. APPEARANCE OF THE HOLES

The holes are empty and are of approximately polygonal cross-section, especially in the case of the copper-aluminium alloy. The sides of the polygons are parallel to the twin boundaries in the brass, that is to say, to the (111) planes. The cross-sections are rectangles, triangles, and hexagons. From this it is concluded that the holes are octahedra with faces parallel to the (111) planes. Figs. 5 and 6 (Plate LVIII) illustrate the typical appearance of the holes and their orientation in relation to the twins. Holes having

\* Copper prepared in this way analysed 99.967  $\pm$  0.003%, with traces of iron.

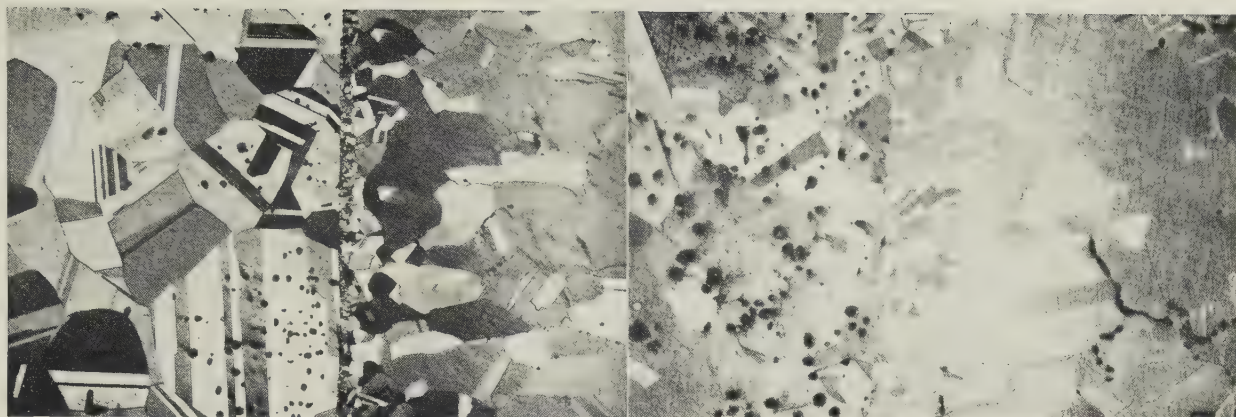


FIG. 3.—Distribution of holes in the diffusion zone on the alloy side.

FIG. 4.—Taken near the edge of the specimen and showing the micro-cracks at the copper boundaries (*right*).

FIGS. 3 and 4.—Copper/70 : 30 Brass Specimen after Diffusion for 25 Days at 800° C. Etched in ammoniacal copper chloride solution.  $\times 50$ .

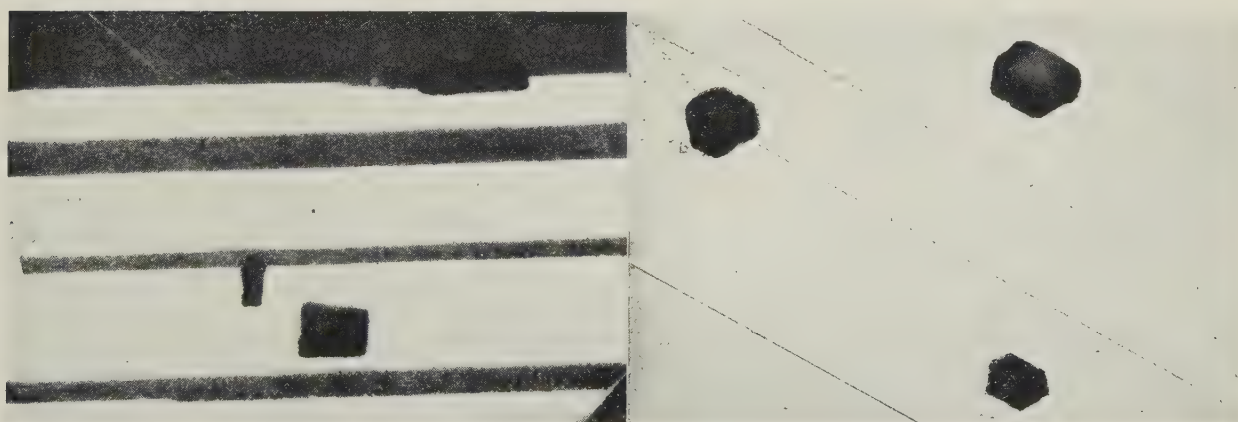


FIG. 5.—  $\times 350$ .

FIG. 6.—  $\times 400$ .

FIGS. 5 and 6.—Copper/Copper-7% Aluminium Alloy Specimen after Diffusion for 25 Days at 800° C., showing the Shape of the Holes formed in the Diffusion Zone on the Alloy Side and their Orientation with Respect to the Twins. Etched in ammonium persulphate solution.





less regular cross-sections have also been found, particularly in brass. This may be due in part to lack of care in polishing, but the reproducibility of the shape of the holes leads to the conclusion that it is mainly due to rounding of the holes in sintering. This point is considered further in the discussion.

In certain specimens holes were also found on the copper side, though not in the diffusion zone. These holes were never polygonal, but took the form of small cracks around the grain boundaries (Fig. 4, Plate LVIII). It can be shown that these represent micro-fissures caused by irregular blisters due to the special shape of certain of the specimens (sandwiches covered by a protective layer of electrolytic copper).

### 3. DIFFUSION COEFFICIENTS

Although the determination of the coefficients of diffusion was not the object of the present work, the polished specimens have been used in an attempt to

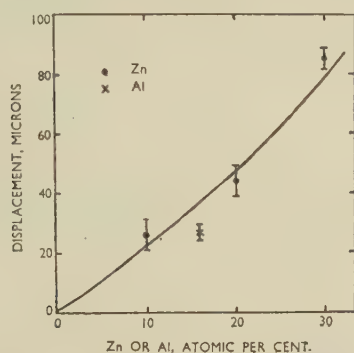


FIG. 1.—Displacement of Original Boundary after Diffusion for 25 Days at 800° C.

establish a diffusion curve by means of microhardness measurements.<sup>7</sup> No great accuracy can be claimed for the results, as the effect of grain-size, twins, and particularly the presence of holes, led to a rather large scatter in the microhardness values. In addition, reliable calibration curves relating microhardness to composition were not available. Fig. 2 shows the variation in microhardness with distance from the original interface as revealed by the grains of molybdenum powder. It relates to the copper/copper-16 at.-% aluminium alloy specimen. By taking account of the effect of the holes, and by assuming a linear relationship between microhardness and composition, it was possible to obtain values of the coefficients of diffusion between  $3 \times 10^{-10}$  and  $6.7 \times 10^{-10}$  cm.<sup>2</sup>/sec. over the range 1–15 at.-% aluminium. At low concentrations, the value agrees well with that obtained by the classical methods,<sup>8,9</sup> although the effect of concentration is much less pronounced in the present determinations.

### IV.—DISCUSSION OF RESULTS

First, it should be emphasized that the results now obtained show without doubt that the formation of

holes is connected with diffusion. It is equally certain that there is a displacement of the original interface in such a way as to cause a contraction on the alloy side and an expansion on the copper side. In this connection it should be mentioned that the existence of holes has also been found by Rhines and Nelson,<sup>10</sup> in the oxidation at high temperatures of brasses containing 10–30% zinc. These workers noted that the holes extended well beyond the maximum penetration of oxidation, and they emphasized the fact that it was a question in this zone of true holes, quite distinct from oxide inclusions such as occur near the surface. They attributed the phenomenon to insufficiently rapid contraction of the brass in comparison with the rate of diffusion of zinc. Although this explanation does not pretend to be fundamental in character, the importance of Rhines and Nelson's work is clear.

It may be pointed out that the variation in lattice parameter with composition cannot be responsible for the contraction of the brass, as that would account for only a very small fraction of the observed effect.

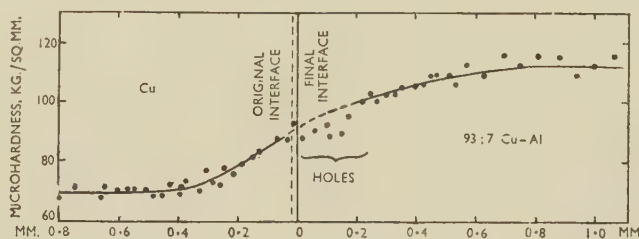


FIG. 2.—Microhardness Curve for a Copper/Copper-7% Aluminium Specimen after Diffusion for 25 Days at 800° C.

The conclusion that zinc or aluminium leaves the alloy more rapidly than copper enters it therefore seems inevitable. At this stage we may conveniently consider an explanation commonly advanced, namely, the effect of the zinc vapour. Assuming the existence of micro-fissures, zinc vapour could find its way through them into the copper. The variation in the lattice might assist in this by enlarging slightly the cracks in the brass and reducing those in the copper. Mehl has described a case of this kind.<sup>11</sup> A serious objection to this explanation lies in the contraction of, and formation of holes in, the copper-aluminium alloy. The vapour pressures of copper and aluminium are approximately equal and are  $10^6$  times smaller than that of zinc. In addition, no trace has been found of the supposed cracks, even after electrolytic polishing, which generally enlarges such defects. Finally, the presence of isolated holes in the interior of the brass crystals (Fig. 3, Plate LVIII), cannot be explained by this theory alone.

On the other hand, there is no doubt that the vapour phase plays a certain part, even if not a decisive one. The plated layer of copper on the specimens is subject to blisters which can give rise to cavities, particularly at the corners of the alloy core. Zinc vapour finds its way through these cavities into the zone adjacent to the copper, thereby locally in-



creasing the diffusion and the contraction of the brass. As a result, the plane of separation will be curved. This curvature has been taken into account as far as possible in the present measurements. Moreover, zinc vapour present in the holes formed in the course of diffusion will accelerate diffusion in that region. But in these cases the action of the zinc vapour is a consequence of the contraction of the brass (or the expansion of the copper) and not its cause.

Nor is it believed that impurities are responsible for the anomaly, as no appreciable difference has been observed between specimens of different purities. In theory, thermal dissociation of the inclusions might produce bubbles of gas. But the formation of holes is restricted to the diffusion zone and is accompanied by a contraction. The polyhedral shape of certain of the holes is also contrary to such a theory. Finally, preferential diffusion along the grain boundaries will explain neither the contraction nor the presence of holes in the interior of the grains, and such a hypothesis runs counter to the observed facts.

## V.—THEORETICAL DISCUSSION

The fact that all the evidence shows that zinc or aluminium leaves the alloy more rapidly than copper enters it, cannot be explained by the classical conception of the mechanism of diffusion in a solid solution of the substitutional type, unless additional assumptions are made. Explanations commonly advanced (influence of the vapour phase, &c.) do not accord with the results of the present experimental work, and we are led to the same conclusion as Smigelskas and Kirkendall,<sup>1</sup> namely, that zinc diffuses more rapidly than copper in the brass solid solution.

In accepting the validity of the Gibbs–Duhem equation, which is normally applicable to a binary system, it must also be assumed that the mobilities of zinc and copper atoms are different. This is possible only on the basis of a vacancy mechanism of diffusion, the direct exchange of atoms being excluded. The mobilities can be a function of the concentration, or more precisely, of the chemical activity, but they certainly do not depend only on the latter, at least if the validity of the Gibbs–Duhem equation is to be maintained.

Several hypotheses may be advanced to explain the observed facts:

(i) It can be assumed that the Gibbs–Duhem equation ceases to be valid in the diffusion zone. The effect of impurities could be seen there. In fact, this relation is valid only in a binary system, and by assuming the presence of impurities the system becomes a ternary or higher one, with the following expression<sup>4</sup> for the coefficient of diffusion of atoms of type  $i$  in the case of a vacancy mechanism:

$$D_i = M_i kT \left( 1 + \frac{\partial \log \gamma_i}{\partial \log N_i} \right)$$

where  $M_i$  is the mobility,  $\gamma_i$  the chemical activity, and  $N_i$  the molecular concentration of atoms of type  $i$ .

Even assuming equal mobility for the zinc and copper atoms, the coefficients  $D$  would be different, because the expression in parentheses is no longer identical for the different kinds of atoms, as is the case in a binary system.

The experimental data are not sufficient either to confirm or disprove this hypothesis, but we do not regard it as a likely one, for it does not in itself explain the presence of holes in the diffusion zone.

(ii) A mass flow, homogeneous or otherwise, can be assumed to be superimposed on the movement by diffusion. This hypothesis has been advanced by several workers,<sup>4, 5</sup> and the flow can be explained by the movement of vacant sites. Seitz<sup>5</sup> has developed a theory in which such a movement, starting at the exterior surface of the copper, traverses the specimen towards the brass side, where the vacant sites amalgamate, being no longer in equilibrium. The mathematical treatment of such a hypothesis leads to an expression which more or less explains formally the observed phenomena. According to Darken,<sup>4</sup> the expression for the coefficient of diffusion is:

$$D = kT(N_A M_B + N_B M_A) \left( 1 + \frac{\partial \log \gamma_A}{\partial \log N_A} \right)$$

where  $N_A$  and  $N_B$  are the molecular concentrations,  $M_A$  and  $M_B$  the mobilities, and  $\gamma_A$  the activity of the atoms  $A$ . There are thus different coefficients of diffusion for each kind of atom,  $i$ :

$$D_i = M_i kT \left( 1 + \frac{\partial \log \gamma_A}{\partial \log N_A} \right)$$

But the fact that in the present work the specimens in which the copper was on the inside and the brass on the outside, showed the same phenomena as those in which the metals were reversed, appears to contradict this hypothesis. It is not easy to see the cause of such a movement of vacant sites, or to reconcile the theory with the present observations.

(iii) We believe that two concurrent mechanisms of diffusion of zinc atoms may operate, the first corresponding to the classical vacancy mechanism and involving an equivalent movement of copper atoms in the opposite direction; the second an interstitial movement of zinc atoms independent of the copper atoms. For this to be possible, it must be assumed that imperfections in the crystals exhibit disorder of the Frenkel type<sup>12</sup>; that is to say, that part of the zinc atoms leave their normal positions on the lattice, causing vacancies, and are to be found in the interstices. The degree of disorder is a function of temperature and concentration. By assuming a greater mobility on the part of the interstitial atoms, it is possible to explain the observed contraction and the occurrence of holes in the following way.

The interstitial atoms of zinc which have rapidly diffused towards the copper side, will be replaced by atoms of zinc moving from their ordinary lattice sites in order to re-establish thermodynamic equilibrium. In consequence, there will be an excess of vacant sites which can amalgamate to form holes.

The octahedral shape of the latter is a point in favour of this hypothesis. On the copper side there will be an excess of interstitial atoms of zinc which will insert themselves in the lattice, thus giving rise to expansion. The contraction of the brass is a logical consequence of the hole formation. It is the result of sintering, which tends to make the holes round and to reduce their volume. It is quite natural for sintering to be the least rapid process, being governed as it is by self-diffusion, which is always slower than the diffusion of dissolved atoms. Thus, the coefficient of self-diffusion of copper<sup>13, 14</sup> at 800° C. is about  $4 \times 10^{-11}$  cm.<sup>2</sup>/sec., while that of zinc in copper<sup>8</sup> is  $8 \times 10^{-9}$  cm.<sup>2</sup>/sec.

We are aware that this hypothesis is open to objection on thermodynamic grounds. Frenkel disorder, while well known in certain heteropolar compounds (oxides, sulphates, &c.), has not been observed in metallic solid solutions, and it is difficult to imagine its occurring there. At the same time the possibility cannot be entirely rejected, for it may be realized under certain conditions (for example, a special or ordered distribution of the vacant sites and of the interstitial atoms). In this connection reference may be made to the work of Seith and Keil,<sup>15</sup> who showed by means of radioactive tracers that the diffusion of gold atoms in a lead-gold solid solution is  $8 \times 10^6$  times more rapid than that of atoms of lead in the same alloy. Johnson<sup>16</sup> has also found by the use of radioactive tracers that there is a difference in the rates of diffusion of silver and of gold in a 50:50 gold-silver alloy. It is true that this latter case can be interpreted as a ternary diagram,<sup>17, 18</sup> but the differences here are much less important (1-2.5).

(iv) Finally, mention must be made of the possibility of surface diffusion along internal surfaces, such as mosaic boundaries<sup>19</sup> or sub-microscopic cracks set up by stress.<sup>6</sup> This hypothesis cannot be completely refuted, though it is very doubtful whether such faults, enlarged by diffusion, would remain invisible on well-polished sections.

## VI.—CONCLUSIONS

(1) The vapour phase, although it assists in the phenomenon, does not play a decisive part and cannot be the cause of the displacement of the interface.

(2) The theory of a movement of vacant sites which originate at the surface and proceed towards the interior of the specimen must be discarded.

(3) It must be assumed that in the alloys the mobilities of the atoms of copper, aluminium, and zinc are different.

(4) If a partial interstitial diffusion of zinc is assumed, it is possible formally to explain the

phenomena observed by making a special assumption as to the nature of the crystalline faults (Frenkel disorder). The verification of this last hypothesis, however, needs further experiments outside the scope of the present work.

### Note Added in Proof

After completion of the present work, which was carried out in the Metallurgical Laboratory of O.N.E.R.A. in 1949, a paper on the same subject was published by da Silva and Mehl,<sup>20</sup> who confirmed the Smigelskas and Kirkendall phenomenon in the systems copper-zinc, copper-aluminium, copper-nickel, copper-tin, copper-gold, and silver-gold. They also have assumed a vacant-site mechanism in which the sites arise in the diffusion zone itself, but they observed porosity only in the diffusion zone in copper-zinc alloys. We believe, however, that the apparent absence of holes is not contrary to our hypothesis, as the number of holes depends not only on the mechanism of diffusion proper, but also on the subsequent sintering, which tends to close them up.

### ACKNOWLEDGEMENTS

The authors wish to thank the Director of O.N.E.R.A. for permission to publish this paper. They also wish to thank Mme. C. Bückle for carrying out the delicate preparation of the specimens, as well as for taking the photomicrographs.

### REFERENCES

1. A. D. Smigelskas and E. O. Kirkendall, *Trans. Amer. Inst. Min. Met. Eng.*, 1947, **171**, 130.
2. H. Bückle, *Metallforschung*, 1946, **1**, 175.
3. M. R. Herman, *Trans. Amer. Inst. Min. Met. Eng.*, 1947, **171**, 140 (discussion).
4. L. S. Darken, *ibid.*, 1948, **175**, 184.
5. F. Seitz, *Phys. Rev.*, 1948, [ii], **74**, 1513.
6. C. S. Smith, *Trans. Amer. Inst. Min. Met. Eng.*, 1947, **171**, 136 (discussion).
7. H. Bückle, *Z. Metallkunde*, 1942, **34**, 130.
8. F. N. Rhines and R. F. Mehl, *Trans. Amer. Inst. Min. Met. Eng.*, 1938, **128**, 185.
9. E. O. Kirkendall, L. Thomassen, and C. Upthegrove, *ibid.*, 1939, **133**, 186.
10. F. N. Rhines and B. J. Nelson, *ibid.*, 1944, **156**, 171.
11. R. F. Mehl, *ibid.*, 1936, **122**, 11.
12. J. Frenkel, *Z. Physik*, 1926, **35**, 652.
13. W. A. Johnson, *Trans. Amer. Inst. Min. Met. Eng.*, 1941, **143**, 107.
14. G. C. Kuczynski, *ibid.*, 1949, **185**, 169.
15. W. Seith and A. Keil, *Z. physikal. Chem.*, 1933, [B], **22**, 350.
16. W. A. Johnson, *Trans. Amer. Inst. Min. Met. Eng.*, 1942, **147**, 331.
17. L. S. Darken, *ibid.*, 1948, **175**, 194-201 (discussion).
18. A. D. Le Claire, *ibid.*, 1948, **175**, 194-201 (discussion).
19. A. Smekal, "Handbuch der Physik", 1933, **24**, (II), 880.
20. L. C. C. da Silva and R. F. Mehl, *ibid.*, 1951, **191**, 155.



By A. E. L. TATE,† A.I.M., and D. McLEAN,† B.Sc., MEMBER  
(Communication from the National Physical Laboratory.)

## SYNOPSIS

A sub-crystal structure has been detected microscopically in cold-rolled aluminium. The sub-crystals are about twenty times larger linearly than those detected by X-rays.

Hot-rolled aluminium rod, when rolled under conditions which do not produce complete recrystallization by self-annealing and examined using the anodic film and polarized-light technique, has been found to contain a sub-crystal structure within each deformed grain.<sup>1</sup> It is fairly certain that this sub-crystal structure is similar to that observed by Wilms and Wood<sup>2</sup> to form in aluminium during creep and thought by the present authors to be due to polygonization.

Cold-rolled rod rolled from room temperature and given a reduction of 33% in cross-sectional area also showed indications of an undeveloped sub-crystal structure. It appeared likely that if the degree of cold deformation was progressively increased, thus increasing the lattice strain and the temperature rise due to deformation, a more distinct sub-crystal structure might be developed. It also appeared likely that lowering the temperature of rolling would reduce the distinctness of the sub-crystal structure.

Some qualitative experiments were therefore made to determine the effect of the rolling temperature and degree of deformation on the microstructure of rolled rod. Annealed super-pure aluminium rod, 0.9 in. in dia., was rolled under the following conditions:

- (a) Rolled from an initial temperature of about 20° C. and given 50, 74, and 84% reductions.
- (b) Rolled from 0° C. giving the same reductions and quenching into iced water after each pass through the rolls.
- (c) Rolled from -73° C., again giving the same reductions, but quenching into a CO<sub>2</sub>-acetone mixture (-73° C.) after each pass through the rolls.

The materials were examined microscopically and the hardness determined after each reduction under each set of conditions. The temperature increased to about 60°, 70°, and 75° C. in material rolled under condition (a) and given 50, 74, and 84% reduction, respectively. It may be assumed that there was a substantially smaller temperature rise for conditions (b) and (c).

The initial grain structure of the material before cold rolling is shown in Fig. 1 (Plate LIX). The structure after hot rolling to 50% reduction is illustrated in Fig. 2 (Plate LIX), and shows a fully developed sub-crystal structure. Material rolled under condition (a) and given 30% reduction showed only slight evidence of a sub-structure, but the sub-structure was developed more distinctly by increasing the deformation, as may

be seen by comparing Fig. 3 (Plate LIX), showing the microstructure after 30% reduction, with Fig. 4 (Plate LIX), showing the microstructure after 50% reduction. The latter is clear evidence that a sub-crystal structure can be produced by cold working aluminium.

The set of micrographs Figs. 2, 4, 5, and 6 (Plate LIX), form a regular sequence showing the structures produced by 50% reduction at different temperatures, namely (400°-180° C.), (20°-60° C.), 0° C., and -73° C., respectively. There is less evidence of a sub-crystal structure, the lower the temperature of rolling.

The X-ray-diffraction patterns from cold-worked metals have been interpreted by Wood and Rachinger<sup>3</sup> to mean that the original crystals are broken into small crystallites by cold rolling. Whereas Wood<sup>4</sup> and Kellar, Hirsch, and Thorpe<sup>5</sup> deduced a minimum crystallite size for cold-worked aluminium of 10<sup>-4</sup> cm. dia., the sub-crystals in Figs. 2 and 4 were about 20 × 10<sup>-4</sup> cm. in dia. The sub-crystals were therefore 20 times larger than the crystallites and cannot have been the same as the latter. The sub-crystal size did not appear to be greatly dependent on temperature of deformation.

An X-ray-diffraction pattern from hot-rolled material showed many quite sharp spots, so that some of the sub-crystals must have been relatively strain-free. It is tempting to suggest, as Beck<sup>6</sup> and Cahn<sup>7</sup> have done, that these sub-crystals are the germ crystals for recrystallization, i.e. that certain of them eventually grow and absorb their neighbours.

Hardness tests on the various materials rolled as indicated above showed that the hardness increased less rapidly with deformation the higher the rolling temperature. It appeared that for a given degree of reduction the hardness was lower, the more distinct the sub-crystal structure. This is likewise consistent with the formation of a sub-crystal structure being associated with crystal recovery and also with the softening attributed to the latter process.

## REFERENCES

1. D. McLean and A. E. L. Tate, *Rev. Mét.*, 1951, **48**, (10), 765.
2. G. R. Wilms and W. A. Wood, *J. Inst. Metals*, 1949, **75**, 693.
3. W. A. Wood and W. A. Rachinger, *ibid.*, 1949, **75**, 571.
4. W. A. Wood, *Proc. Phys. Soc.*, 1940, **52**, 110.
5. J. H. Kellar, P. B. Hirsch, and J. S. Thorpe, *Nature*, 1950, **165**, 556.
6. P. A. Beck, *J. Appl. Physics*, 1949, **20**, 633.
7. R. W. Cahn, *Proc. Phys. Soc.*, [A], 1950, **63**, 323.

\* Manuscript received 14 December 1951.

† Metallurgy Division, National Physical Laboratory, Teddington.

MICROSTRUCTURES OF SUPER-PURE ALUMINIUM ROD.  $\times 150$ .

FIG. 1.—Annealed at 350° C.

FIG. 3.—Cold-rolled 30% Reduction from 20° C. (condition (a)).

FIG. 5.—Cold-rolled 50% Reduction from 0° C. after Each Pass (condition (b)).

FIG. 2.—Hot-rolled 50% Reduction at 400°–180° C.

FIG. 4.—Cold-rolled 50% Reduction from 20°–60° C. (condition (a)).

FIG. 6.—Cold-rolled 50% Reduction from –73° C. after Each Pass (condition (c)).





# FUNDAMENTAL REACTIONS IN THE VACUUM-FUSION METHOD AND ITS APPLICATION TO THE DETERMINATION OF O<sub>2</sub>, N<sub>2</sub>, AND H<sub>2</sub> IN Mo, Th, Ti, U, V, AND Zr\*

1360

By H. A. SLOMAN,† M.A., F.R.I.C., F.I.M., MEMBER, and C. A. HARVEY.† With an Appendix by O. KUBASCHEWSKI,†  
Dr. phil. nat. habil., MEMBER

(Communication from the National Physical Laboratory.)

## SYNOPSIS

In a previous publication (*J. Inst. Metals*, 1945, **71**, 391), the application of the vacuum-fusion method to the determination of oxygen, nitrogen, and hydrogen in certain non-ferrous metals and alloys was described. The present paper deals with the application of the method to six further metals. The optimum conditions for each are discussed, and a mechanism for the reactions forming the basis of the method, derived from practical results and thermodynamical calculations, is postulated.

Results showing the relation between the gas contents and the methods of preparation or subsequent treatments of the various metals are included, together with some observations on the effects of the gaseous elements on their properties.

The detailed derivations of the thermodynamical data used in the paper are given in an Appendix.

## I.—INTRODUCTION

INTEREST in the production and properties of the rarer metals has been increasing rapidly over the past few years. This is particularly true of such metals as molybdenum, titanium, vanadium, and zirconium, which by reason of their high melting points offer possibilities as heat-resistant materials, and of other metals such as thorium and uranium, because of their use in the application of nuclear energy. In its turn this interest has stimulated the development of methods of analysis applicable to the determination of impurities in these metals. Such impurities include the gaseous elements oxygen, nitrogen, and hydrogen, and as part of the research programme carried out at the National Physical Laboratory during the past five or six years, attention has been devoted to developing a method for the determination of these elements in molybdenum, thorium, titanium, uranium, vanadium, and zirconium.

As a result of the success which one of the authors (H. A. S.) obtained in extending the use of the vacuum-fusion method, originally developed for the determination of the gaseous elements in steel, to a large number of non-ferrous metals and alloys,<sup>1</sup> investigations were undertaken to find conditions under which the method might be applied to the six metals mentioned above.

The apparatus and operation of the method have been comprehensively described.<sup>1</sup> The method depends upon the decomposition in a liquid-metal bath at high temperatures of metallic oxides and, possibly, nitrides by carbon, yielding carbon monoxide and nitrogen. By carrying out the decomposition in a high vacuum and thus removing the gaseous products very rapidly, the reactions can be made quantitative. As regards hydrogen, carbon probably plays no part in its evolution, which is controlled only by the temperature and degree of vacuum. At the same time as the reaction with carbon is taking place any oxygen or nitrogen present in solution in the metal is evolved (the oxygen as carbon monoxide). The method thus permits a simultaneous and quantitative determination of the total oxygen, nitrogen, and hydrogen in a metal sample, no matter in what form or forms these elements may be present. The essentials are that the carbon shall be brought into intimate contact with the oxides and nitrides, and that the temperature and vacuum shall be high enough to ensure rapid reaction.

The problem in the cases of the six metals now under consideration was approached in the same way as for the other non-ferrous metals discussed in the earlier paper,<sup>1</sup> and will be conveniently illustrated, first by some general thermodynamic considerations and then by describing in detail the experiments

\* Manuscript received 9 August 1951.

† Metallurgy Division, National Physical Laboratory, Teddington.  
391



carried out to establish the correct conditions for one of them.

## II.—THERMODYNAMIC CONSIDERATIONS

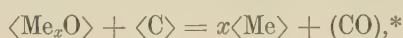
Where available, thermodynamic data have proved very valuable for determining the basic mechanism of the method and for giving a close indication of the temperature required for the reduction of a particular compound, thus limiting the number of exploratory experiments yielding negative results.

Since there are so few non-ferrous metals or alloys with which it is possible to operate the method without a large iron bath, it will be assumed in what follows that iron is always present in excess.

### 1. APPLICATION TO OXIDES

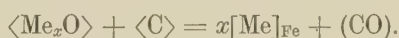
Several mechanisms may be postulated to explain the quantitative determination of oxygen by the vacuum-fusion method :

(1) The oxide of the metal reacts with carbon to form carbon monoxide, any reaction of the metal so formed being too slow to contribute to the free energy of the gas evolution. This mechanism may be represented by the equation :

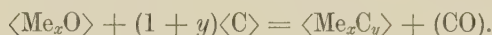


or  $x\{\text{Me}\} + (\text{CO}).$

(2) The oxide of the metal reacts with carbon and with molten iron to form carbon monoxide and a solution of the metal in the iron :



(3) The oxide of the metal reacts with carbon to form carbon monoxide and the metal carbide :

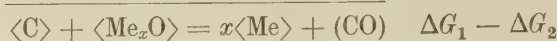
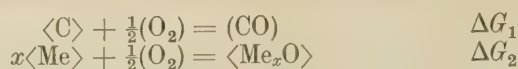


(4) The reaction in any particular case is controlled by mechanism (2) or (3), depending on whether the affinity of the particular metal for iron or for carbon is the higher.

Other more complex mechanisms may be possible, such, for example, as a simultaneous occurrence of mechanisms (2) and (3), but these have not been considered. The relevant free-energy equations for the formation of the oxides and carbides of the six metals under consideration, together with those for the solution of these metals in iron are given in the Appendix (p. 405). The corresponding equations for silicon and aluminium are also given for comparison.

Let us now consider what information may be derived from these free-energy equations, and use the simplest mechanism, i.e. the first, for illustrative purposes.

By combining the free energy of formation of a particular oxide with that of carbon monoxide as follows :



a value for the pressure of CO in equilibrium with the oxide at any temperature may be calculated from the following equation :

$$\log p_{\text{CO}} = -\frac{\Delta G_1 - \Delta G_2}{4.57 T} \quad (1)$$

using the data given in the Appendix. It will be noted that where more than one oxide exists, it is only the free energy of formation of the most stable, that is, the lowest, oxide which is given in the Appendix and which needs to be considered.

In Table I these equilibrium pressures have been calculated for two temperatures : 1700° and 2000° K.

TABLE I.—Pressure of Carbon Monoxide (in mm. Hg) in Equilibrium with Various Oxides at Two Temperatures.

Temperature		MoO	SiO <sub>2</sub>	VO	Al <sub>2</sub> O <sub>3</sub>
°K.	°C.				
1700	1427	1 × 10 <sup>7</sup>	2.3 × 10 <sup>2</sup>	3.7 × 10	1.5 × 10 <sup>-1</sup>
2000	1727	...	6.6 × 10 <sup>3</sup>	1.1 × 10 <sup>3</sup>	1.4 × 10

Temperature		ZrO <sub>2</sub>	UO <sub>2</sub>	TiO	ThO <sub>2</sub>
°K.	°C.				
1700	1427	1.1 × 10 <sup>-1</sup>	4.2 × 10 <sup>-2</sup>	2.0 × 10 <sup>-2</sup>	1.2 × 10 <sup>-3</sup>
2000	1727	8.8	4.3	2.2	1.9 × 10 <sup>-1</sup>

An alternative method of calculation is to find from equation (1) the temperature at which the equilibrium pressure of carbon monoxide over any oxide has a certain value. It is apparent that the various oxides may be placed in a series of descending values for the equilibrium pressure of carbon monoxide at a given temperature (as in Table I), or in one of ascending temperatures for a given pressure of carbon monoxide (as in Table II), and that the order in which the oxides appear will be the same whichever method of compiling the series is employed. This series may be extended to incorporate any metallic oxide for which the necessary thermodynamic data are available.

Now it had been established<sup>1, 2</sup> that the temperature required for the rapid and quantitative reduction of Al<sub>2</sub>O<sub>3</sub> under the conditions pertaining in the apparatus at the National Physical Laboratory is 1600° C. or slightly lower. From equation (1) it can be calculated that the pressure of CO in equilibrium with Al<sub>2</sub>O<sub>3</sub> at 1600° C. is 2.4 mm. Hg. Using the same equation, the temperature at which the pressure of carbon monoxide over any other oxide has the same value can be found. This has been done

\* Different brackets are used to indicate different phases : <solid>; {liquid}; (gaseous); and [dilute solution]<sub>solvent</sub>.

(Table II) for those oxides which are more stable than alumina. Similar calculations have not been made for oxides less stable than alumina (i.e. those in the upper half of Table I), since these are all readily reduced below  $1600^\circ C.$  and present no difficulties.

TABLE II.—*Temperatures at Which the Equilibrium Pressure of CO over Various Oxides is 2.4 mm. Hg.*

Oxide	Temp., $^\circ C.$
$MoO_2$ . . . .	<1550
$SiO_2$ . . . .	<1550
$VO$ . . . .	<1550
$Al_2O_3$ . . . .	1600
$ZrO_2$ . . . .	1640
$UO_2$ . . . .	1710
$TiO$ . . . .	1770
$ThO_2$ . . . .	1950

Turning now to the other postulated mechanisms, equation (1) requires modification by the inclusion of another free-energy term appropriate to the particular additional reaction assumed to occur. Apart from this, the calculations are similar in every respect to those described above. Taking as a basis in each case the known fact that the reduction of  $Al_2O_3$  necessitates a temperature of  $1600^\circ C.$ , a series of temperatures may be calculated for each mechanism similar to those given in Table II for mechanism (1). These, together with the experimentally determined temperatures, are collected in Table III.

TABLE III.—*Temperatures at Which Various Oxides Should Behave Like  $Al_2O_3$  at  $1600^\circ C.$ , According to Different Mechanisms of Reaction.*

Oxide	Exptl. Temp., $^\circ C.$	Temperature ( $^\circ C.$ ) According to Mechanism			
		1	2	3	4
$MoO_2$ . . . .	<1550	<1550	<1550	<1550	<1550
$SiO_2$ . . . .	<1550	<1550	<1550	<1550	<1550
$VO$ . . . .	<1550	<1550	<1550	<1550	<1550
$Al_2O_3$ . . . .	1600	1600	1600	1600	1600
$ZrO_2$ . . . .	1625	1640	1670	700	945
$UO_2$ . . . .	1700	1710	1710	1120	1440
$TiO$ . . . .	1750	1770	1785	720	1030
$ThO_2$ . . . .	1900	1950	1950	1330	1640

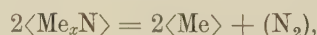
From Table III it is obvious that mechanisms (3) and (4) lead to temperatures and sequences of the metals so far removed from those determined experimentally that neither can be true. On the other hand, the temperatures for both mechanisms (1) and (2) are close to those observed, and the sequence in each case is correct. It seems unlikely that the very simple postulate of mechanism (1) can be true; it must therefore be concluded that the conditions required for the determination of oxygen by the vacuum-fusion method are controlled by mechanism (2), i.e. by reaction of the oxide with carbon and solution of the metal in liquid iron. It may be pointed out that complete agreement between the observed temperatures and those calculated for

mechanism (2) is not to be expected, since the free energy of solution of a metal in iron is certainly somewhat changed by the presence of carbon, and the data used in the calculations apply strictly only to the solution of a pure metal in pure iron. The reason why mechanism (1), although not the true one, leads to results not very different from those given by the more complex equation for mechanism (2), is that the free energies of solution of the metals in iron do not differ greatly from one another. This term in the equation is thus nearly a constant, and its introduction into equation (1) has little effect. Empirically, therefore, one may for simplicity assume that mechanism (1) holds and equation (1) may be used in its simplest form when predicting the behaviour of a new metal which dissolves in iron. Experience has shown that this procedure indicates at once the relative ease or difficulty of quantitatively reducing a particular oxide by carbon in the vacuum-fusion apparatus and that, having found by experiment the correct temperature for one oxide ( $Al_2O_3$  in the present case), a close estimate may be made of that necessary for any other. It may be pointed out that the preliminary exploratory experiments with the oxides of each of the six metals under consideration were conducted at temperatures deduced from calculations based on mechanism (1) and, as will be seen from Table III, no temperature was more than  $50^\circ C.$  in error, so that much wasted effort was avoided in determining the correct conditions of operation.

## 2. APPLICATION TO NITRIDES

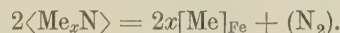
The possible mechanisms to explain the quantitative determination of nitrogen by the vacuum-fusion method are somewhat different from those postulated for the oxides. They are:

(5) Thermal dissociation of the nitride:

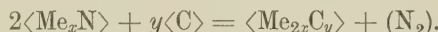


or  $2\{Me\} + (N_2).$

(6) Thermal dissociation of the nitride and solution of the metal in liquid iron:



(7) Reaction of the nitride with carbon to form nitrogen and the metal carbide:



(8) The reaction in any particular case is controlled by mechanism (6) or (7), depending on whether the affinity of the metal for iron or for carbon is the higher.

It will be noted that carbon is not involved, except perhaps catalytically, in mechanisms (5) and (6), and once again more complex postulates, which have not been considered, are possible. As before, the calculations are based on the experimentally determined temperature needed for the rapid and quantitative decomposition of one compound, in this case a



nitride. This temperature was determined most accurately for titanium nitride, TiN, as 1800° C., and in Table IV are given the temperatures for the various nitrides calculated according to the mechanisms postulated above, together with the experimentally determined values. The relevant free-energy equations are given in the Appendix (p. 405).

Table IV shows that mechanisms (5) and (6) lead to results which are close to each other and nearest to the temperatures determined experimentally. Once again, the reason for the agreement between these two mechanisms is that the free energies of solution of the various metals in iron do not differ greatly from one another. Of the two postulates it seems probable that mechanism (6) is the operative one. The agreement with the observed temperatures is not good, but the sequence is correct with the exception of zirconium. This exception may be due to an error in the experimental results from which the free-energy formula for ZrN was derived.

TABLE IV.—*Temperatures at Which Various Nitrides Should Behave Like TiN at 1800° C. According to Different Mechanisms of Reaction.*

Nitride	Exptl. Temp., °C.	Temperature (°C.) According to Mechanism			
		5	6	7	8
Mo <sub>3</sub> N . . .	<1550	<500	<500	1160	1030
Si <sub>3</sub> N <sub>4</sub> . . .	<1550	<500	<500	1200	1100
VN . . .	<1550	<500	910	1235	1235
AlN . . .	<1550	840	855	2300	1830
UN . . .	<1550	1380	1420	2330	2330
ZrN . . .	1750	1970	1930	1670	1670
TiN . . .	1800	1800	1800	1800	1800
Th <sub>3</sub> N <sub>4</sub> . . .	1750 *	1720	1685	2400	2400

\* See p. 399 (application to thorium).

Unfortunately the free energies of nitride formation are but inaccurately known, so that the calculated results can be no more than a rather rough guide. Nevertheless, they indicate at once whether the nitride of a particular metal is likely to cause greater difficulty than the oxide and so necessitate an even higher operating temperature.

It will be noted that the most probable mechanism for the behaviour of the nitrides (No. 6), is analogous to that for the oxides (No. 2); both involve solution of the metal in liquid iron and not carbide formation. This analogy considerably strengthens the view that this reaction is in fact that which takes place during a vacuum-fusion analysis and determines the temperature needed.

### 3. APPLICATION TO HYDROGEN

With every metal except uranium, so far examined, the vacuum conditions and the operating temperature of 1600° C. or over required for the oxides and/or the nitrides ensure the complete removal of the hydrogen. In the light of this fact and in view of the incomplete and somewhat uncertain nature of the available

thermodynamical data for hydrogen, very little would be gained by any attempt to formulate mechanisms for this element. The exceptional case of uranium is referred to later.

## III.—PRACTICAL CONSIDERATIONS

### 1. COMPOSITION OF BATH

As already mentioned, the essential practical conditions of operation of the vacuum-fusion method are that carbon be brought, in sufficient excess, into intimate contact with the oxide and, possibly, nitride in the metal specimen. This condition is only satisfied if the reactions are allowed to proceed in a mobile liquid-metal bath in which an adequate amount of carbon is dissolved. Iron and steel are ideally suited to this purpose. A sample of either melted in a graphite crucible yields a mobile liquid containing several wt.-% of carbon at any temperature above, say, 1500° C. Moreover, the presence of the carbon so reduces the vapour pressure of the iron that volatilization in the high operating vacuum (10<sup>-5</sup>–10<sup>-6</sup> mm. Hg) is very slow. There are, however, very few non-ferrous metals or alloys for which the method may be operated in the direct manner applicable to steels, i.e. with a liquid bath consisting of the particular metal itself. The main reasons for this are:

- (i) The melting point of the metal may be too high.
- (ii) The metal may be largely converted to a high-melting-point carbide, so producing a pasty or solid mass.
- (iii) Solution of carbon in the metal may be so slow that an adequate excess of this element is not available in the short time desired.
- (iv) The temperature required for the rapid reduction of the oxide and/or nitride may be too far above the melting point of the metal, thus leading to excessive volatilization of the metal.

The problem of excessive volatility is of considerable importance. If a molten metal is volatile in a high vacuum at high temperatures, the cold walls of the furnace tube above the reaction crucible quickly become coated with a highly reactive condensed metal film. This film, if it attains appreciable thickness during the course of an experiment, will adsorb any gas subsequently evolved from the specimen, so leading to low results. Once such a film has formed, the determinations must be stopped and the apparatus dismantled for cleaning. With many metals even the results from the first specimen introduced into the crucible would be suspect, were not some means of avoiding rapid film formation employed.

In general, therefore, recourse is had to the technique described earlier,<sup>1</sup> of diluting the non-ferrous metal with iron. Reaction then takes place in a

ternary liquid bath consisting of iron, second metal, and carbon, in which the concentration of the second metal may be controlled. The use of iron serves several purposes:

(a) It may lower the melting point of the second metal, so that the method may be applied to, say, molybdenum or tungsten.

(b) In every case so far examined, it ensures that at the required operating temperature a mobile liquid bath containing an adequate amount of carbon is obtained.

(c) The partial vapour pressure of the second metal is lowered, so reducing volatilization and the rate of film formation at a given temperature.

Three limitations to the universal application of this dilution technique may be encountered. First, high-melting-point binary or ternary compounds may be formed, converting the bath into a solid or semi-solid mass. This may usually be avoided by careful control of the relative amounts of iron and second metal employed. Secondly, the addition of the second metal to the liquid iron-carbon alloy may reduce the solubility of the carbon. If this occurs to a considerable extent sufficient "kish" may be thrown out of solution to give a pasty mass through which the gaseous products of reaction find it difficult to diffuse. In doing so they may produce a froth which can overflow the crucible. No remedy for this has been found, and in the one case so far experienced (namely, with silicon) the use of iron had to be abandoned.<sup>1</sup> None of the present series of metals gave rise to this particular difficulty in the smallest degree. Thirdly, complex phenomena, such for example as immiscibility ranges, may occasionally be encountered.

## 2. OPERATING TEMPERATURE

The phrase "operating temperature" has already been used in the text, and it will be useful at this point to define it. There are several reasons why it is undesirable that an analysis should take longer than 20 min. During that time all the oxygen, nitrogen, and hydrogen originally present in the specimen must have been extracted and collected. The "operating temperature" for a given material has therefore been quite arbitrarily defined as the lowest temperature, 1550° C. or over,\* at which oxygen, nitrogen, and hydrogen are completely removed from a specimen of the material within 15–20 min. of its introduction into the crucible.

The practical tests employed to check whether any particular temperature is the correct one for the material are:

(a) The vacuum in the apparatus at the end of the 20-min. period has returned to its original value of  $5 \times 10^{-6}$  mm. Hg.

(b) No further gas is evolved from the specimen if the experiment is continued beyond the 20-min. period.

(c) A similar experiment conducted at a temperature, say, 100° C. higher, does not alter the amount or composition of the evolved gas in any way.

## 3. EXPLORATORY TESTS

Assuming now that the dilution technique is to be used, the following steps are necessary to ascertain the correct conditions for a particular material.

### Step 1.

The operating temperatures for the oxide, nitride, and, where possible, hydride of the metal are separately determined as follows using synthetically prepared materials.

A small amount of, say, the oxide, contained in an extremely light pure iron capsule of very low, known, gas content is introduced into a previously degassed iron bath held at a pre-selected temperature. The weight of oxide taken should be such as to yield 5–10 ml. of carbon monoxide. (For the nitride or hydride, the weights should yield the same volume of nitrogen or hydrogen, respectively). A series of experiments is conducted at temperature intervals of 50° C. beginning, say, 50° C. below that deduced thermochemically as the temperature necessary for the particular compound. In this way very few experiments serve to determine the operating temperatures† for oxygen, nitrogen, and hydrogen, respectively. It is usually found that the individual temperatures for the three gases differ from one another and, accordingly, the highest is taken as the operating temperature for the subsequent steps in the investigation.

### Step 2.

A sample of the metal of the highest purity available is selected. A series of experiments, each lasting 20 min., is carried out in which different (increasing) amounts of this material are added to an iron bath of constant weight held at the operating temperature as determined in Step 1. If the sample is of a form from which cylindrical specimens can be prepared, it is introduced direct. If not, the metal specimens are placed inside pure iron capsules. During these experiments the relation between rate of film formation and concentration of metal is observed. The maximum permissible rate is a matter of experience with the particular apparatus; it must be less than that which would lead to absorption of gas evolved at any time during a 15–20 min. period.

The liquid-metal surface in the crucible is constantly

\* Temperatures below 1550° C. are not considered, since experience has shown that it is not desirable to operate an iron bath below that temperature.

† No attempt is normally made to "bracket" the operating

temperature within the 50° C. intervals. If, for example, it is found that a temperature  $T^\circ$  C. is too low, while  $(T + 50)^\circ$  C. is satisfactory, a trial at a temperature of  $(T + 25)^\circ$  C. may be carried out, if desired.



watched to ascertain whether at any concentration of the second metal it changes in appearance, indicating the formation of high-melting-point compounds or the ejection of carbon. The maximum permissible concentration of the second metal is thus assessed.

#### *Step 3.*

Having determined the maximum permissible concentration of the metal in the iron, the next step is to determine accurately the gas content of the selected sample of metal. Keeping its concentration well below the maximum determined in Step 2, an analysis is conducted at the temperature indicated by the experiments in Step 1. If this temperature is in fact correct, the conditions (a), (b), and (c) listed on p. 395 will be satisfied, and analysis of the gas collected will give acceptable values for the oxygen, nitrogen, and hydrogen contents of the sample.

Several repeat experiments are carried out to check the homogeneity of the sample and the experimental procedure. A further series is then conducted in which the concentration of the metal is increased until it reaches the previously determined maximum, in order to ascertain how closely this may be approached before low results due to absorption of gas by metallic films begin to be obtained.

#### *Step 4.*

The last phase of the investigation is to combine Steps 1 and 3. In the experiments in Step 1 the concentration of oxygen, nitrogen, or hydrogen, respectively, is relatively high, while that of the metal is very low (only a few hundredths of a gramme). Since the metal used in Step 3 is normally reasonably pure, the reverse is the case in these experiments. It remains therefore to examine the effect of a relatively high concentration of the metal on the extraction of large amounts of the three gaseous constituents. Step 1 is accordingly repeated, but the capsules are made from the sample of metal used in Step 3. Moreover, instead of being very light they are arranged to weigh about 20 g. (i.e. the weight of an average metal specimen). Since the gas content of this material has been established, due allowance can be made in the calculations for its presence, and the completeness of recovery from the oxide, nitride, or hydride determined. So far no case has been found in which the results of these experiments have necessitated modifications of the conclusions from earlier steps. Nevertheless, it is a test which should not be omitted with a new metal. It is even more effective as a check on procedure if it is possible to increase the oxygen, nitrogen, or hydrogen content of the metal sample chemically, rather than physically, as in the case when the metal is used as a capsule.

#### 4. PRACTICAL APPLICATION OF METHOD

We are now in a position to apply the method to the analysis of different samples of the particular metal. Determinations are conducted as follows:

After degassing the empty graphite crucible for

2–3 hr. at 2400°–2500° C., the temperature is lowered to the operating temperature and the “blank” of the apparatus determined. The requisite number of ferrous specimens (cylinders each weighing 18–20 g.) to give the desired weight of bath are now introduced into the crucible. They may be prepared from any ferrous material (iron, steel, pig or cast iron) which does not have an unduly high gas content and does not contain appreciable amounts of film-forming constituent, particularly manganese. In order to save time the material should degas quickly, that is, it should not contain stable oxides or nitrides such as aluminium oxide, titanium nitride, &c. After the ferrous bath has been degassed, the first specimen of metal is introduced and the extraction of gas from it completed in less than 20 min. This is followed by the second specimen, and so on.

The weights of the metal specimens are arranged to be such as to yield at least 2 ml., and not more than 10 ml., of gas. The maximum weight of an individual specimen is limited, for practical reasons, to 20 g. If a particular sample is so pure that a specimen weighing 20 g. will not yield even 2 ml. of gas, two or more specimens, each of this weight, may be introduced into the crucible and treated as one. If the sample is of a form such that solid cylinders can be prepared from it, these are used as specimens. If, however, it is in the form of powder, nodules, or other irregular shapes, each specimen is enclosed in a very light iron capsule.<sup>1</sup>

It should be noted that when several specimens are analysed consecutively, it will not usually be possible to permit the concentration of the second metal to rise to the maximum determined in the exploratory tests. The conclusions derived from these tests are based on the film produced by a certain concentration of the metal during the time (20 min.) required for a single determination. When several specimens are involved, the experiment may last up to about 2 hr., and it is readily seen that film formation will be considerably increased. For example, suppose that during an exploratory test lasting 20 min. it was found that with an iron bath weighing 60 g., 40 g. (i.e. a concentration of 40%) of the second metal could be tolerated. Assume now that this 40 g. is in the form of 2 specimens each weighing 20 g., which are to be analysed consecutively, and that the rate of film formation is proportional to the concentration of metal in the bath. Then at the end of the first 20-min. period, during which the concentration would have been 25%, just over half the permissible growth of film would have occurred, and within 10 min. of the introduction of the second specimen, which would have raised the concentration to 40%, the other half would have formed. During the remaining 10 min. of the analysis of the second specimen the maximum growth would have been exceeded and the result for this specimen might easily be low.

It is a simple matter to work out whether any particular number of specimens of given weight can

be safely analysed consecutively. A few combinations in further illustration of the above example are given below:

(a) 40-g. specimen (i.e. 2 of 20 g. each, treated as one); or (b) 20-g. specimen; or (c) 15-g. specimen; or (d) 10-g. specimen, followed by one of 10 g. or less; or (e) 5-g. specimen, followed by one of 20 g. or less; or (f) 5-g. specimen, followed by two of 5 g. (the last may be somewhat doubtful); &c.

From (b) and (e) it will be apparent that, while in the particular circumstances postulated above it would be safe to follow a 5-g. specimen with one of 20 g., it is not safe to reverse the order. The specimen of smallest weight should therefore always be analysed first and the heaviest last.

The "blank" of the apparatus, i.e. the gas evolved from the graphite parts at the operating temperature after the normal preliminary degassing period of 2-3 hr. at a temperature considerably higher than the operating one, is very important when analysing non-ferrous metals or alloys. Its size depends on the design of the apparatus, the purity of the graphite, the duration and temperature of the degassing period, and finally on the operating temperature itself. Since for many metals and alloys this last is considerably higher than that required for steels, a blank which might perhaps be acceptable in the routine analysis of steel would become unacceptably large at the higher temperatures. For example, the temperature necessary for thorium has been found to be 1900° C., as compared with 1560°-1600° C. for steels. In the apparatus at the National Physical Laboratory a degassing temperature of 2400°-2500° C., maintained for 3 hr., is standard. After this, the blank of the apparatus is 0.005-0.007 ml. at N.T.P./hr. at 1600° C. and 0.04-0.05 ml./hr. at 1900° C., i.e. about 10 times greater. Ratios of this order are likely to be true for any apparatus, irrespective of the actual magnitude of the blank at 1600° C., provided that a similar degassing temperature and time are employed. If this temperature is lowered, the ratio between the volumes of the blank at 1600° and 1900° C. will be correspondingly increased. For example, with a degassing temperature of 2200° C. the blank at 1600° C. in a particular apparatus might be 0.01 ml./hr. At 1900° C. it would not, however, be about 1 ml. but probably about 3 ml./hr., or even more. Now a blank of 0.1 ml./hr. might be tolerated for a specimen needing 20 min. and yielding 4-5 ml. of gas; but one of 1 ml./hr. for another also requiring the same time and yielding the same volume of gas, would render the analytical results open to considerable doubt. A blank of 3 ml./hr. would render them quite useless.

The extremely low blank of the apparatus at the National Physical Laboratory is entirely negligible even at the highest operating temperatures so far found necessary, and renders practicable analyses of very small or very pure specimens from which con-

siderably less gas is evolved than the 2 ml. recommended earlier as the desirable minimum evolution from each specimen.

It may be pointed out that if the equipment is used continuously for the analysis of non-ferrous metals the value of the blank, at say 1600° C., gradually increases on successive occasions from the normal volume of about 0.005 to 0.03-0.04 ml./hr., after which it remains constant. If now, ferrous samples only are employed, the blank will fairly rapidly return to its normal value. This effect is due to contamination of the graphite powder which surrounds the crucible, by small amounts of the condensed metal films. When the apparatus is opened to air after a run these films oxidize rapidly and, during the dismantling operation, small quantities become detached from the walls of the furnace tube and mix with the graphite powder. During the next degassing period these oxide particles react with the graphite at a rate depending on their stability and on the temperature. Since, however, the temperature of most of the powder is relatively low, the rate of reaction is slow, so that at the end of the degassing period oxide particles may still be present and may be reduced. The resulting carbon monoxide added to the normal gas evolution leads to the higher blank. It is obvious that the increase in the blank will be most rapid when the apparatus is being used for metals which may have very stable oxides and are themselves appreciably volatile at the operating temperature. The value of the blank may be brought back to normal at any time, either, as indicated above, by interposing a short series of runs using only ferrous materials, or by treating the powder for 2-3 hr. at, say, 2400° C., in a high vacuum. This may be done by placing it inside the reaction crucible of the apparatus itself or alternatively by setting up another suitable apparatus for the purpose. Nothing is gained by discarding the powder when it shows signs of contamination and using fresh material. This material is itself to some degree contaminated and will therefore give rise to a high blank on the first few occasions of use. It can only be brought into a satisfactory condition by avoiding additional contamination, that is, by using ferrous samples only.

TABLE V.—Operating Temperatures and Maximum Concentrations for Mo, Th, Ti, U, V, and Zr.

Metal	Operating Temperature (°C.)			Final Operating Temperature, °C.	Maximum Concentration in the Bath,* wt.-%
	Oxygen	Nitrogen	Hydrogen		
Mo .	<1550	<1550	<1550	1560	40
V .	<1550	<1550	<1550	1560	20
Zr .	1625	1750	<1625 †	1750	30
U .	1700	<1550	1750-1800	1750-1800	20
Ti .	1750	1800	<1650 †	1800	20
Th .	1900	1750 ‡	<1750 †	1900	20

\* On the basis of an experiment lasting 20 min. only.

† Lower temperatures than those given have not been explored.

‡ See p. 399 (application to thorium).



In Table V are given the complete experimentally determined conditions for the six metals under consideration.

#### IV.—EXAMINATION OF INDIVIDUAL METALS

##### 1. MOLYBDENUM

During the development, several years ago, of the vacuum-fusion method for steel<sup>3</sup> and its application to ferro-alloys<sup>4</sup> used in steelmaking, some work had been done on the determination of oxygen, nitrogen, and hydrogen in molybdenum. A complete re-examination was, however, considered desirable since interest now centred in the gas content of relatively pure samples of the metal and its alloys in connection with the development of new high-temperature materials. The determinations present no difficulties; a working temperature of 1560° C. only is required, and at this temperature the metal itself is not appreciably volatile at concentrations up to about 40 wt.-%. Beyond this concentration the liquidus temperatures of the binary iron-molybdenum alloys begin to rise steeply to the melting point of molybdenum. With this metal, therefore, a rise in the liquidus temperature rather than film formation limits the maximum permissible concentration. As a result, the length of an experiment, i.e. the number and weights of specimens analysed consecutively, is not very important, provided a total concentration of about 40 wt.-% is not exceeded.

Owing to the well-known volatility of molybdenum oxide at high temperatures, the chief point which had to be investigated in determining the optimum conditions for the analysis of the metal was whether some or all of the oxide would be lost before reaction with carbon could occur. This should be more likely to occur in the exploratory tests, in which oxide is introduced into the crucible in a capsule, than in the analysis of a metal sample in which the oxygen is uniformly dispersed. Experience showed, however, that even in the exploratory tests recovery of oxygen was quantitative. Pure MoO<sub>3</sub> was used in the tests and evolution of CO at 1560° C. was extremely rapid, being complete within 2–3 min. of the introduction of the capsule. Some examples of the results obtained are given in Table VI.

TABLE VI.—*Recovery of Oxygen from MoO<sub>3</sub> at 1560° C.*

Wt. of MoO <sub>3</sub> Used, g.	Oxygen Content of MoO <sub>3</sub> , g.	Oxygen Recovered, g.
0.045	0.015	0.014 <sub>8</sub>
0.045	0.015	0.015 <sub>1</sub>
0.015	0.005	0.004 <sub>9</sub>
0.003	0.001	0.001 <sub>1</sub>

Molybdenum containing nitrogen was prepared by heating metal powder in ammonia gas at 700° C. for 24 hr., which yielded a material containing 94.7%

molybdenum and 5.3% nitrogen as determined by increase in weight. X-ray analysis showed this to consist of a mixture of the metal and the nitride, Mo<sub>2</sub>N. The recovery of nitrogen from this material was quantitative, evolution at 1560° C. being very rapid and complete within 2–3 min. of the introduction of the sample into the apparatus. Some examples of the results are given in Table VII.

TABLE VII.—*Recovery of Nitrogen from Molybdenum Containing 5.3% Nitrogen at 1560° C.*

Wt. of Sample, g.	Nitrogen Content of Sample, g.	Nitrogen Recovered, g.
0.20	0.010 <sub>8</sub>	0.010 <sub>3</sub>
0.20	0.010 <sub>8</sub>	0.011 <sub>0</sub>
0.10	0.005 <sub>3</sub>	0.005 <sub>7</sub>
0.025	0.001 <sub>3</sub>	0.001 <sub>4</sub>

The tests for oxygen and nitrogen recovery were repeated using capsules of molybdenum metal weighing about 20 g., and gave equally satisfactory results. No attempt was made to prepare molybdenum hydride, since samples of the metal containing substantial amounts of hydrogen were shown to evolve it very readily at 1560° C., and increasing the temperature of operation did not lead to further evolution.

The method has been successfully applied to a study of the relation between the gas content of molybdenum and its method of preparation and subsequent treatment, with particular reference to operations involved in powder-metallurgy techniques. Molybdenum alloys, especially those with such metals as chromium, have also been examined. In dealing with such alloys the requirements characteristic of the second metal have to be borne in mind when deciding on the concentration in the bath, temperature of operation, &c.

##### 2. THORIUM

Thorium is the most troublesome of the metals so far examined, because its oxide requires a very high temperature for decomposition by carbon. The nitride, although not so refractory as the oxide, also needs a high temperature. The conclusions reached from thermochemical calculations for both compounds (see Tables III and IV) are fully borne out by experiment, from which it has been established that an operating temperature of 1900° C. is necessary. At this temperature volatilization of the metal is serious and 20 wt.-% in the bath should not be exceeded. The condensed metallic film is not easy to remove from the walls of the silica furnace tube. In part this may be due to its passivity to both acids and alkalies, but also there seems to be some attack on the glazed surface of the silica itself, which may arise because, with the crucible at 1900° C., the external water cooling, adequate with lower crucible temperatures, does not in fact keep the walls of the tube quite cold.

In the exploratory tests on the oxide, pure ThO<sub>2</sub> was employed and extraction was found to be complete within 15–20 min. at 1900° C. Recovery of the added oxide was quantitative. Difficulties were encountered in attempts to prepare pure thorium nitride; the product always contained appreciable amounts of thorium oxide, probably derived from the starting material. It was soon found that, as predicted thermochemically, the nitride needed a considerably lower temperature than did the oxide, but it was impossible to determine this temperature accurately owing to the contaminated nature of the sample. For example, at 1750° C., gas evolution, which began shortly after the introduction into the crucible of a sample of the nitride, continued rapidly for several minutes. The rate then slowed down to a trickle which continued steadily for over  $\frac{1}{2}$  hr. By collecting the gas in several portions it was found that up to the stage when the evolution rate became slow and steady, the gas was essentially nitrogen with some carbon monoxide. After this stage the gas was carbon monoxide with a little nitrogen. It was known that 1750° C. was too low for decomposition of the oxide, so that the slow evolution of CO was explained, but the reason for the slow removal of the residual nitrogen is not clear, and no means was available of ascertaining whether the pure nitride would behave similarly. As the temperature of the experiment was increased the amount of nitrogen in the last fractions of gas became smaller, until at 1900° C. complete evolution of both nitrogen and carbon monoxide was rapid. It seems probable that 1700°–1750° C. or even lower, would prove adequate for the nitride alone, but since 1900° C. has to be employed for the oxide, no attempt has been made to prepare pure nitride and examine its behaviour.

The extraction of hydrogen from thorium does not present any difficulty. The lowest temperature at which it can be quantitatively removed has not been ascertained; there is some indication that it is below 1750° C. At 1900° C. it is evolved completely during the first few minutes of the experiment.

A considerable number of samples of thorium metal, consisting mostly of powders produced by reducing a halide with magnesium or calcium, have been analysed. The following figures illustrate the range of gas contents encountered:

	Wt.-%
Oxygen . . . . .	0.2 –1.3
Nitrogen . . . . .	0.1 –0.2
Hydrogen . . . . .	0.05–0.15 (560–1700 ml./100 g.)

The extremely high proportion of hydrogen in these powders probably results from the method of leaching out excess magnesium or calcium in dilute acid.

Melting compacted thorium powder in a thorium crucible in a high vacuum has given material containing:

	Wt.-%
Oxygen . . . . .	0.07 –0.08
Nitrogen . . . . .	0.02 –0.03
Hydrogen . . . . .	0.001–0.0015 (10–15 ml./100 g.)

As might be expected, the principal purification is in the hydrogen, but at the same time both oxygen and nitrogen are reduced in quantity. In the former case this is probably due to flotation of oxide to the top of the melt. In the latter, while some nitride may float to the top, it is most likely that the reduction arises chiefly from decomposition at the high temperature and under the high vacuum employed.

### 3. TITANIUM

Titanium is one of the metals whose nitride is more stable than the oxide under the conditions of a vacuum-fusion determination. Inability to prepare the nitride free from oxide did not, therefore, interfere with its behaviour during the exploratory tests, as did similar contamination in the case of thorium nitride. These tests established the temperature needed for the oxide as 1725°–1750° C., while that for the nitride was 1800° C. Titanium hydride, again rather impure, yielded its hydrogen very readily at 1650° C. or below, and the temperature for hydrogen was not explored further.

The final operating temperature for titanium was thus fixed at 1800° C. At this temperature the metal is appreciably volatile, and its maximum concentration in the bath should not be allowed to exceed 20 wt.-%.

TABLE VIII.—Gas Contents of Titanium Produced by Various Methods.

Sample	Method of Preparation	Form	O <sub>2</sub> , wt.-%	N <sub>2</sub> , wt.-%	H <sub>2</sub> , wt.-%
A	Reduction of TiCl <sub>4</sub> by Mg	Powder	0.06 0.07	0.01 0.02	0.08 0.10
B	As for A	Powder	0.05	0.02	0.15
C	As for A	Powder	0.13	0.02	0.18
D	Reduction of TiCl <sub>4</sub> by Mg	Sponge	0.12	<0.01	0.005
E	As for D	Sponge	0.24	<0.01	0.02
F	Reduction of TiCl <sub>4</sub> by Na	Powder	0.38	0.02	0.1
G	Reduction of TiO <sub>2</sub> by Ca	Powder	0.37 0.42	0.12 0.09	0.5 0.5
H	Van Arkel iodide process	Rod	0.021 0.023	<0.01 0.01	0.001 0.001

Much of the early interest in the gas contents of titanium samples was in relation to the method of preparation. Apart from the van Arkel iodide process, the other methods depend essentially on the reduction of a compound of titanium by an alkali metal or alkaline-earth metal. These reactions lead to the production of titanium in powder form contaminated by the reactants. The latter are normally removed either by acid leaching or by vacuum distillation. The former process leaves the titanium as a powder, while the latter produces a spongy product.

The gas contents of some typical samples are given in Table VIII.

In three cases duplicate results are given in Table VIII to illustrate the repeatability of the



vacuum-fusion method. Apart from sample *H*, prepared by the iodide process and containing considerably less impurities than any of the others, the chief point of interest lies in the hydrogen results. The effect of hydrogen pick-up during leaching is very marked (samples *A*, *B*, *C*, *F*, and *G*) when compared with those samples (*D* and *E*) in which vacuum distillation was employed to separate the metal from the reactants. On a small scale, the hydrogen content of titanium may be very largely reduced by treating it in a vacuum at about 600° C. for 2–3 hr., e.g. from 0.2 to 0.001%. Sintering in a vacuum also reduces the hydrogen content to a similar extent but tends to increase the oxygen, probably as a result of residual air in the pores of the compact. For example, the following results were obtained on a sintered compact which had been made from sample *A* (Table VIII):

	Wt.-%
Oxygen . . . .	0.2
Nitrogen . . . .	0.02
Hydrogen . . . .	0.002 (22 ml./100 g.)

Because of its high melting point and strong affinity for carbon, hydrogen, nitrogen, and oxygen, the melting of titanium presents special difficulties. The molten metal reduces the refractory oxides  $\text{Al}_2\text{O}_3$ ,  $\text{BeO}$ ,  $\text{CaO}$ ,  $\text{MgO}$ , and  $\text{ThO}_2$ , and reacts with carbon forming a carbide; consequently these materials cannot be used for crucibles without some contamination of the melt. Preliminary experiments revealed that titanium melted in a crucible of any of the oxide refractories mentioned above was extremely hard and brittle and might contain 1% or more of oxygen. From work carried out in the United States it appeared that contamination with carbon, provided the amount introduced was not excessive, had less effect in rendering the metal brittle than contamination with oxygen. Small-scale exploratory tests were therefore carried out in which titanium was melted in graphite crucibles, and the vacuum-fusion method was employed to investigate the effects of different conditions of melting on the gas content. The titanium used in these experiments was the powder referred to as sample *A* in Table VIII containing oxygen 0.06, nitrogen 0.01, and hydrogen 0.08%. The powder was compacted into suitable cylinders. The earliest experiments were carried out in a vacuum in a high-frequency induction furnace, but the graphite and thermal insulating material were not pre-treated in any way. Oxygen contents as high as 1.0% and nitrogen values of 0.1% were obtained. Subsequently the crucible and surrounding insulation were pre-treated by heating them to about 1900° C. in a vacuum for about 2 hr. before introducing the titanium compact. A marked improvement in gas content was found, as follows:

	Wt.-%
Oxygen . . . .	0.20–0.28
Nitrogen . . . .	0.01–0.03
Hydrogen . . . .	0.005–0.01 (55–110 ml./100 g.)

These values are very similar to those obtained on vacuum sintering the same powder. While the length of time the metal was held molten had a very pronounced effect on the pick-up of carbon, the duration of the experiment had no significant influence on the gas content.

The most suitable method so far developed for melting reactive metals such as titanium without contamination is to use an electric arc. Melting is carried out very rapidly in a water-cooled copper chamber. To this, after evacuation, is admitted a small pressure of pure argon to stabilize the arc, and, if normal care is taken, samples may be melted entirely without contamination. In this way it is possible to study the effects on the properties of the metal of added elements without interference from unwanted impurities. This method is being used at the National Physical Laboratory to study the titanium–oxygen and titanium–nitrogen systems, the vacuum-fusion method being utilized to determine how closely the true compositions of the alloys lie to the nominal ones. A few examples are given in Table IX.

TABLE IX.—*Comparison of Nominal and True Gas Contents of Titanium–Oxygen and Titanium–Nitrogen Alloys Prepared by Arc Melting.*

Initial Oxygen Content, wt.-%	Oxygen Added, wt.-%	Oxygen Determined, wt.-%
0.2	0.2	0.42
	0.3	0.50
	12.0	11.7
0.02	0.1	0.11
	0.5	0.51
Initial Nitrogen Content, wt.-%	Nitrogen Added, wt.-%	Nitrogen Determined, wt.-%
0.03	0.2	0.18
	0.3	0.26

#### 4. URANIUM

Uranium is one of the more difficult metals to which the method has been applied. This difficulty arises from two causes, first, the anomalous behaviour of hydrogen, to which reference will be made below, and secondly, the necessity for an operating temperature (1750°–1800° C.) so much above the melting points of the metal and its alloys with iron.<sup>5</sup> Quantitative and reasonably rapid reduction of uranium oxide ( $\text{UO}_2$  was employed) is effected at 1700° C., while uranium containing nitrogen (made by heating metal turnings in pure nitrogen) is easily decomposed at the lowest temperature examined, namely, 1550° C. From the results of these tests it would seem that a working temperature of about 1700° C. would be satisfactory, since normally the third element being determined, namely, hydrogen, does not present any difficulties at temperatures suitable for the decomposition of oxides and/or nitrides. The fact

that hydrogen in uranium behaves anomalously was, however, noted during the earliest experiments with samples of the metal. These analyses were carried out at  $1700^\circ C$ . It was found that while most of the gas was extracted in 12–15 min., the vacuum did not return to its normal "base" value of about  $5 \times 10^{-6}$  mm. Hg, and a small amount of gas continued to be evolved for a further 15–20 min. This phenomenon is typical of the effect of too low an operating temperature, and it was at first thought the residual gas was carbon monoxide. By collecting the gas in fractions it was shown, however, to be hydrogen. No explanation of the difficulty of extracting this gas quantitatively was available at that time, but by working at different temperatures it was found that the trouble could be overcome at  $1800^\circ C$ ., at which temperature a determination could be completed in 15 min. As a result of subsequent work, to be discussed below, it was shown that the solubility of hydrogen in liquid uranium is high and there is some thermodynamical evidence that it increases with temperature. It is thus only under a very high vacuum that the metal will part with the last traces of the gas and, if the thermodynamical evidence is correct, the temperature should be as low as possible (just above the melting point,  $1125^\circ C$ .). Since, however, operation at this temperature is impracticable if an iron bath is being employed and the oxygen and nitrogen contents of the sample are to be determined at the same time, the only alternative, if the analysis is to be completed within the desired time, is to operate at a temperature at which both oxygen and nitrogen are extracted very rapidly in, say, 5–6 min. This leaves the major portion of the extraction period available for the removal of the residual hydrogen. The use of a working temperature of about  $1800^\circ C$ . has become standard practice for the analysis of uranium samples.

Most of the uranium analysed for the gaseous elements by the vacuum-fusion method has given results within the following ranges :

	Wt.-%
Oxygen . . .	0.0003–0.003
Nitrogen . . .	0.0005–0.005
Hydrogen . . .	0.0004–0.002 (5–25 ml./100 g.)

The solid solubility of oxygen in the metal is extremely small. Microscopical evidence of the presence of oxide particles having characteristic shapes and etching properties was seen in samples containing as little as 0.0003% oxygen.

No constituent that could be associated with the presence of nitrogen has been identified microscopically, and no data have been obtained on the solid solubility of this element in uranium. Samples of the metal heat-treated at about  $600^\circ C$ . in pure nitrogen acquire a heavy surface scale of uranium nitride, but the rate of diffusion must be extremely slow, since the nitrogen content of the metal below the scale is unaffected. As a result of this very slow diffusion rate, the scale appears to attain a certain thickness, after which it acts as a protective coating.

It is, however, very easily detached. When this happens attack begins again, and under these conditions it is possible to convert the metal almost completely to the nitride.

The solubility of hydrogen in uranium has been studied in some detail. If, after the metal reduction has been completed, the surface of the molten uranium under its fluoride flux is watched while the metal is cooling and solidifying, bubbles of gas may sometimes be seen breaking through the flux and burning on contact with the air. This gas is undoubtedly hydrogen, evolved as the metal cools owing to decreasing solubility. The source of the hydrogen may be moisture in the material from which the reaction mould is made, or slight hydration of one or both of the reactants. Reference to the range of hydrogen contents in typically reduced metal given above shows that, even after solidification, as much as 25 ml. of hydrogen per 100 g. of metal may be retained. With this concentration of hydrogen the metal may show gas porosity, so that the solid solubility of the gas at or just below the melting point must be less than this amount. (Evidence discussed below suggests that the solid solubility at temperatures just below the melting point is 18–20 ml./100 g.). On the other hand, the fact that such amounts may be present in the solid metal means that just above the melting point the liquid solubility of hydrogen is equal to or greater than 25 ml./100 g. There must therefore be a sharp drop in solubility as the metal solidifies.

The solid solubility of hydrogen in uranium has been measured at various temperatures, but before proceeding with these determinations it appeared desirable to obtain some information on the formation and stability of uranium hydride. Experiments were therefore carried out using discs of uranium 1–2 mm. thick and about 10 mm. in dia., held in a silica boat in a transparent silica tube in which a pressure of 1 atm. of hydrogen was maintained. Exploration was carried out starting at  $600^\circ C$ . The cold tube containing the specimens and already full of hydrogen was introduced into a furnace running at  $600^\circ C$ . and held for 1 hr. At the end of this period the tube was withdrawn, the specimens examined by inspection through the tube, and the whole replaced in the furnace. The temperature was then lowered to  $550^\circ C$ . and the experiment repeated. No change apart from slight superficial oxidation was observed in the specimens after 1 hr. at  $600^\circ$ ,  $550^\circ$ ,  $500^\circ$ ,  $450^\circ$ , or  $400^\circ C$ ., but after a similar period at  $350^\circ C$ . they were found to have completely disintegrated into a dark-brown powder which was very bulky.

A similar series of experiments was conducted starting at  $100^\circ C$ . and increasing the temperature in steps of  $50^\circ C$ . At  $100^\circ$  and  $150^\circ C$ . an exposure of 1 hr. produced no change in the specimens. At  $200^\circ C$ . there was a small amount of the dark-brown powder on the surface, while at  $250^\circ C$ . the disintegration of the metal was complete.



The effect of longer times at particular temperatures was next examined. It was found that even 24 hr. at 400° C. left the specimens quite unaffected, so that the upper limit of formation of uranium hydride could reasonably be assumed to be below 400° C. (but well above 350° C.). The lower limit of formation was not definitely established. Twenty-four hours at 200° C. produced complete conversion, while a similar period at 150° C. led to partial disintegration. It seemed probable therefore that, given sufficient time, the hydride might be formed even at room temperature.

Experiments were then conducted to determine the stability of the hydride. Once formed, it is stable down to room temperature in hydrogen, in an inert gas, or in a vacuum, but decomposes with explosive violence on contact with air even in the cold. On heating to 400° C. or over in hydrogen,

passed through the tube continuously at 1 atm. pressure.

At the end of the 24-hr. period the specimen was quenched into mercury by fusing the suspension wire. Preliminary experiments had shown that uranium could be quenched from any temperature up to 1050° C. (the highest examined) in this manner without suffering amalgamation or any other deleterious effect. The mercury was contained in a steel crucible inside the bottom of the silica tube. Immediately after the quenching operation the hydrogen was pumped from the system, replaced by air, and the specimen extracted from the mercury within about 2 min. An immediate determination of hydrogen in the specimen was made by the vacuum-fusion method.

On being quenched, the uranium cylinder sank to the bottom of the crucible containing the mercury,

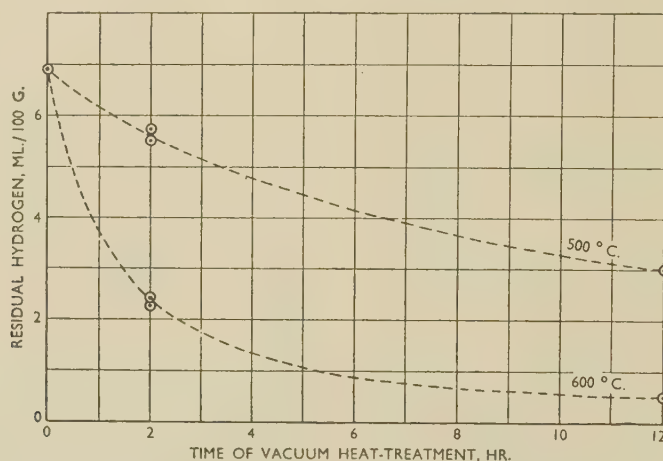


FIG. 1.—Removal of Hydrogen from  $\alpha$ -Uranium by Vacuum Heat-Treatment.

the hydride is completely decomposed. The powder shrinks on itself and changes colour to that of uranium. On cooling this powder in hydrogen below 400° C., the hydride is again formed very rapidly and the cycle may be repeated at will. If the metal powder is allowed to cool, not in hydrogen but in a vacuum or in an inert gas, no change takes place down to room temperature. It oxidizes pyrophorically, however, on exposure to air.

Having established the conditions for the formation of hydride and the upper limit of its stability, attention was directed to determinations of the solid solubility of hydrogen in uranium. Five temperatures were employed: two in the  $\alpha$ -range, one in the  $\beta$ -range, and two in the  $\gamma$ -range. The method was as follows:

A cylinder of uranium about 5 mm. in dia. and 10 mm. long was suspended by means of a fine tungsten wire in a heated, vertical silica tube which formed part of a vacuum-tight system. The specimen was heated to 400° C. *in vacuo* and hydrogen was then admitted. The temperature was adjusted to 450°, 600°, 720°, 800°, or 1000° C. and held steady for 24 hr., a very slow stream of hydrogen being

and no signs of gas evolution were seen during the short period after quenching and before removal from the mercury. It may reasonably be assumed that no significant loss of hydrogen occurred before the analysis was carried out. The uranium used in these experiments contained initially 10 ml./100 g.

TABLE X.—Solid Solubility of Hydrogen in Uranium at Various Temperatures under 1 atm. Pressure.

Temperature, °C.	Solid Solubility of Hydrogen, ml./100 g.
$\alpha$ -range } 450	5
600	3
$\beta$ -range } 720	8
$\gamma$ -range } 800	15
1000	16

of hydrogen. The respective amounts found after the treatments at the temperatures specified above, and which represent the solid solubilities relating to those temperatures, are given in Table X.

The results in Table X show that above the upper limit of stability of uranium hydride (i.e. above  $400^\circ\text{C}$ .) there is only a small solubility of hydrogen in  $\alpha$ -uranium and that this solubility decreases with increasing temperature. The solubility increases again at the  $\alpha$ - $\beta$  transition and rises sharply at the  $\beta$ - $\gamma$  change point. The values obtained at  $800^\circ$  and  $1000^\circ\text{C}$ . suggest, as stated above, that the solubility increases to 18–20 ml./100 g. at the melting point.

The effect of vacuum heat-treatment on the hydrogen content of  $\alpha$ -uranium has been investigated by holding portions of the same sample in a vacuum for different times at different temperatures, and then determining the residual hydrogen by the vacuum-fusion method.

The results are illustrated in Fig. 1. The number of points on each curve (one curve showing the results of the treatment at  $500^\circ\text{C}$ . and the other those at  $600^\circ\text{C}$ .) is insufficient to determine its exact shape. The general form may nevertheless be taken as established and enables the following conclusions to be drawn: (1) the rate of evolution per hour decreases with time, i.e. with the actual hydrogen content remaining in the metal; and (2) the temperature of the treatment is very important, exerting a marked influence on the rate of removal. This effect is in line with the solid-solubility values given in Table X over this temperature range.

## 5. VANADIUM

Vanadium, like molybdenum, offers no serious difficulties to the application of the vacuum-fusion method. A low working temperature,  $1560^\circ\text{C}$ ., only is required, and most samples so far examined have yielded their gas very readily indeed; sometimes in as short a period as 5 min. Unlike molybdenum, however, vanadium is appreciably volatile, and it has been found necessary to limit its concentration in the bath to 20 wt.-%. An additional trouble has also been noted, namely, that the volatilized film, even when quite thin, is very difficult to remove from the walls of the furnace tube and also from the sighting window at the top of the furnace head. Oxalic acid appears to be the most satisfactory solvent, if the use of abrasive scouring agents is to be avoided. It would probably be desirable in any equipment set up primarily to analyse vanadium samples to incorporate an internal shield below the window, so that the latter need be exposed to the gaseous metal only for limited periods when observations are being made.

Chief interest in the gas contents of vanadium samples has lain in comparisons between different methods of producing the metal. The reduction of vanadium pentoxide by calcium, which has been studied at the National Physical Laboratory, yields metal of reasonably high purity (99.7–99.9%) in the form of beads of various sizes, together with a substantial amount of powder (or very small beads). As would be expected, the beads are of higher purity

than the powder. Typical results of gas analysis on beads are:

	Wt.-%
Oxygen . . .	0.05–0.6
Nitrogen . . .	0.02–0.09
Hydrogen . . .	0.004–0.008 (45–90 ml./100 g.)

Powder samples may contain as much as 8% oxygen and 0.5% hydrogen. These high values are probably associated, at least in part, with the necessity for leaching the material with dilute acid to remove calcium compounds.

Individual beads from the same experiment may vary considerably in oxygen content, e.g. 0.03–0.08%. The hardness increases with increased oxygen. The nitrogen content is very sensitive to nitrogen present during the reaction. On different occasions abnormally high nitrogen values have been traced to residual nitrogen in the vanadium pentoxide (prepared from ammonium vanadate) or to nitrogen in a particular batch of calcium. Values as high as 0.4% nitrogen have been obtained from one or other of the above causes.

Vanadium prepared in the form of sponge or powder, by the reduction of vanadium tetrachloride with magnesium, contains about the same level of gaseous impurities as does that made by the reduction of the oxide. The main problem in handling the sponge or powder is the separation from magnesium and magnesium chloride. If this is done by leaching with dilute acid the hydrogen content of the metal may rise to an extraordinary degree owing to the small particle size of the vanadium. Values of 1.0–1.5% are not uncommon. On the other hand, by removing the magnesium by vacuum distillation, metal with a hydrogen content of 0.01% or less may be obtained.

An interesting series of experiments made possible by the application to vanadium of the vacuum-fusion method, has been in connection with the free energies in the vanadium–oxygen system. The free-energy diagram had been reasonably well established by earlier workers from the composition  $V_2O_5$  down to beyond the composition  $VO$ . Uncertainty still existed, however, in the range of lower oxygen concentrations. The slope of the free-energy curve in this range was determined at the National Physical Laboratory for one temperature ( $1000^\circ\text{C}$ .) by establishing equilibria between a vanadium–oxygen solid solution (containing about 4.5% oxygen) and molten barium, magnesium, or calcium at this temperature.<sup>6</sup> Under these conditions the oxygen content of the vanadium should be reduced until its pressure is equal to the dissociation pressure of the oxide of the alkaline-earth metal. The excess reducing metal and its oxide were removed, and the oxygen content of the vanadium determined by the vacuum-fusion method. From these results and the known free energies of formation of  $BaO$ ,  $MgO$ , and  $CaO$ , three points on the curve of the free energy of solution of oxygen in vanadium at  $1000^\circ\text{C}$ . were obtained, thus enabling the diagram to be completed.



## 6. ZIRCONIUM

Zirconium, like titanium, has a nitride which, under the conditions of a vacuum-fusion determination, is more stable than the oxide. In this case, however, the difference in stabilities is even more marked, so that whereas the oxide is readily reduced by carbon at 1600°–1650° C., the nitride is only decomposed easily at about 1750° C. The hydride presents no difficulties; hydrogen being quickly and quantitatively extracted at 1625° C., the lowest temperature examined. Owing to the stability of the nitride, a working temperature of 1750° C. is necessary, and at this temperature volatilization of the metal is rather serious, so that a concentration of 30 wt.-% in the bath should not be exceeded.

Attention may be drawn to one other consequence of the high operating temperature required. If a sample containing an appreciable amount of oxygen (0.1% or more) is dropped into the crucible at 1750° C., the reaction of the oxide with carbon is so violent that large quantities of the molten metal may be thrown up to the crucible lid causing the ball stopper to stick to it. To avoid this possibility, samples known or suspected to contain much oxygen are introduced into the crucible at a temperature of about 1625° C. About 3–5 min. are allowed for the oxide/carbon reaction to take place, and the temperature is then raised rapidly to 1750° C., taking about 3 min. In spite of the fact that this procedure causes some 6–8 min. to elapse before a temperature of 1750° C. is attained, an analysis can always be completed within the desired period of 15–20 min.

The application of the vacuum-fusion method to zirconium is perhaps best illustrated by a consideration of the results obtained on a series of samples received through the courtesy of the United States Bureau of Mines, Oregon. These samples consisted of parts of ingots obtained by melting in graphite crucibles *in vacuo*. Eight samples in all were provided, and details of the original materials and additions, if any, are given in Table XI.

TABLE XI.—*Preparation Details of Zirconium Samples.*All samples melted in graphite crucibles *in vacuo*.

Sample	Initial Material	Additions of O <sub>2</sub> During Melting, wt.-%
A	Foote Mineral Co. metal (Van Arkel iodide process)	Nil
B C D E F	Bureau of Mines metal (Kroll process)	Nil 0.1 0.2 0.3 0.5
G H	Similar to B	Nil

Analysis figures for iron and carbon in the samples were supplied by the Bureau of Mines, and the gas contents and hardness values were determined at the National Physical Laboratory. The results are collected in Table XII. Duplicate results for oxygen, nitrogen, and hydrogen are given in three cases (samples C, D, and F) as an indication of the homogeneity of the materials and the reproducibility of the vacuum-fusion results.

TABLE XII.—*Analyses of Zirconium Samples.*

Sample	Fe, wt.-%	C, wt.-%	O <sub>2</sub> , wt.-%	N <sub>2</sub> , wt.-%	H <sub>2</sub> , wt.-%	Vickers Pyramid Hardness No., 10-kg. load (mean of 4 impressions)
A	0.077	0.14	0.01 <sub>s</sub>	0.01	0.001	130 (128–134)
B	0.086	0.15	0.05 <sub>s</sub>	0.01	0.001 <sub>s</sub>	170 (167–173)
C	0.065	0.14 {	0.28 0.26	0.02 <sub>s</sub> 0.03	0.002 <sub>s</sub> 0.002	236 (233–242)
D	0.059	0.09 {	0.16 0.17	0.01 0.01	0.002 0.001 <sub>s</sub>	198 (198–206)
E	0.076	0.16	0.29	0.02	0.001 <sub>s</sub>	241 (236–247)
F	0.067	0.29 {	0.61 0.58	0.02 <sub>s</sub> 0.02	0.001 0.002	376 (363–397)
G	0.03	0.18	0.07 <sub>s</sub>	0.01	0.001	157 (150–161)
H	0.37	0.15	0.08 <sub>s</sub>	0.01	0.001	184 (182–185)

The results obtained on one other sample of zirconium are of interest. The material was produced by the van Arkel iodide process, and vacuum-fusion analysis gave the following results:

	Wt.-%
Oxygen . . . . .	0.006
Nitrogen . . . . .	0.01
Hydrogen . . . . .	0.008 (90 ml./100 g.)

While both oxygen and nitrogen are very low, the hydrogen is high, some eight times higher for instance than in the samples discussed above. It seems probable that this hydrogen was derived from the starting material. This would be very likely if the original metal were powder or sponge produced by the Kroll process and had been leached in dilute acid. However this may be, it is a significant observation that such a large amount of hydrogen (90 ml./100 g.) may be present in zirconium produced by the van Arkel method.

## ACKNOWLEDGEMENTS

The work described above has been carried out as part of the research programme of the National Physical Laboratory and is published by permission of the Director.

The authors desire to acknowledge the assistance of Dr. O. Kubaschewski, who compiled the free-energy equations in Table XIII and discusses their derivations in the Appendix.

## APPENDIX

By O. KUBASCHEWSKI, Dr. phil. nat. habil.

The vacuum-fusion method involves the reaction of metal oxides and nitrides with molten iron saturated with carbon to form carbon monoxide and nitrogen. Mechanisms which would conform to the experimental observations have been postulated and discussed on pp. 392 and 393. Generally, the oxides, nitrides, and carbides of the metals under

(2) What temperatures are required for the evolution of carbon monoxide and nitrogen for a certain metal? Such "characteristic" temperatures have been observed for several metals, and these results may be used for comparison with the calculated values.

For this purpose the free energies of formation of the oxides, nitrides, and carbides of the metals

TABLE XIII.—Free-Energy Equations.

Reaction	$\Delta G$ , cal.	Accuracy, $\pm$ kg.-cal.	Temp. Range, $^{\circ}K$ .	Ref.
<b>A. Oxides with Carbon</b>				
1. $\frac{1}{2}\langle O_2 \rangle + \langle C \rangle = \langle CO \rangle$	$-26,700 - 20.95T$	1	1500–2500	7
2. $\frac{1}{2}\langle MoO_2 \rangle + \langle C \rangle = \frac{1}{2}\langle Mo \rangle + \langle CO \rangle$	$40,100 - 42.5T$	6	1500–1800	7
3. $\frac{1}{2}\langle SiO_2 \rangle + \langle C \rangle = \frac{1}{2}\langle Si \rangle + \langle CO \rangle$	$81,100 - 45.35T$	4	1700–1973	7 *
4. $\langle VO \rangle + \langle C \rangle = \langle V \rangle + \langle CO \rangle$	$76,300 - 38.9T$	5	1500–2000	6
5. $\frac{1}{3}\langle Al_2O_3 \rangle + \langle C \rangle = \frac{2}{3}\langle Al \rangle + \langle CO \rangle$	$102,100 - 43.1T$	3	1500–2200	7
6. $\frac{1}{2}\langle ZrO_2 \rangle + \langle C \rangle = \frac{1}{2}\langle Zr \rangle + \langle CO \rangle$	$99,400 - 40.85T$	2	1800–2100	9
7. $\frac{1}{2}\langle UO_2 \rangle + \langle C \rangle = \frac{1}{2}\langle U \rangle + \langle CO \rangle$	$105,000 - 42.2T$	7	1800–2200	8, 9
8. $\langle TiO \rangle + \langle C \rangle = \langle Ti \rangle + \langle CO \rangle$	$103,000 - 40.0T$	8	1800–2000	9
9. $\langle TiO \rangle + \langle C \rangle = \langle Ti \rangle + \langle CO \rangle$	$107,500 - 42.2T$	8	2000–2200	9
10. $\frac{1}{2}\langle ThO_2 \rangle + \langle C \rangle = \frac{1}{2}\langle Th \rangle + \langle CO \rangle$	$114,000 - 40.5T$	12	1800–2100	9
<b>B. Nitrides</b>				
1. $2\langle MoN \rangle = 4\langle Mo \rangle + \langle N_2 \rangle$	$33,200 - 43.0T$	6	1500–2000	Estimated
2. $\frac{1}{2}\langle Si_3N_4 \rangle = \frac{3}{2}\langle Si \rangle + \langle N_2 \rangle$	$94,400 - 49.25T$	9	1800–2000	9
3. $2\langle VN \rangle = 2\langle V \rangle + \langle N_2 \rangle$	$79,600 - 39.4T$	20	1800–2000	8
4. $2\langle AlN \rangle = 2\langle Al \rangle + \langle N_2 \rangle$	$127,000 - 55.0T$	8	1800–2200	8 *
5. $2\langle ZrN \rangle = 2\langle Zr \rangle + \langle N_2 \rangle$	$164,400 - 44.0T$	23	1800–2100	9
6. $2\langle UN \rangle = 2\langle U \rangle + \langle N_2 \rangle$	$142,500 - 46.4T$	9	1800–2200	9
7. $2\langle TiN \rangle = 2\langle Ti \rangle + \langle N_2 \rangle$	$160,500 - 45.7T$	12	1800–2100	9
8. $\frac{1}{2}\langle Th_3N_4 \rangle = \frac{3}{2}\langle Th \rangle + \langle N_2 \rangle$	$155,200 - 44.85T$	10	1800–2100	8
<b>C. Solutions in Iron</b>				
1. $\langle Mo \rangle = [Mo]_{Fe}$	$6,300 - 8.0T$	4	1800–2100	10 *
2. $\langle Si \rangle = [Si]_{Fe}$	$-29,000 - 0T$	3	1800–2100	10 *
3. $\langle V \rangle = [V]_{Fe}$	$4,200 - 6.8T$	4	1800–2000	10 *
4. $\langle Al \rangle = [Al]_{Fe}$	$-18,500 - 1.3T$	4	1800–2100	9, 10, mean
5. $\langle Zr \rangle = [Zr]_{Fe}$	$-9,500 - 5.3T$	5	1800–2100	Estimated
6. $\langle U \rangle = [U]_{Fe}$	$-10,000 - 5.6T$	5	1800–2100	See p. 406
7. $\langle Ti \rangle = [Ti]_{Fe}$	$-14,500 - 2.8T$	4	1800–2000	Estimated
8. $\langle Th \rangle = [Th]_{Fe}$	$-6,000 - 7.8T$	5	1800–2100	„
<b>D. Carbides</b>				
1. $2\langle Mo \rangle + \langle C \rangle = \langle Mo_2C \rangle$	$4,200 - 4.8T$	6	–1800	8
2. $\langle Si \rangle + \langle C \rangle = \langle SiC \rangle$	$-37,200 + 7.4T$	6	1800–2000	9
3. $\langle V \rangle + \langle C \rangle = \langle VC \rangle$	$-28,000 + 1.6T$	9	1800–2000	6 (estimated)
4. $4\langle Al \rangle + 3\langle C \rangle = \langle Al_4C_3 \rangle$	$-51,600 + 7.1T$	5	1500–2200	See p. 406
5. $\langle Zr \rangle + \langle C \rangle = \langle ZrC \rangle$	$-40,000 - 7.7T$	5	1500–2000	8, 9
6. $\langle U \rangle + 2\langle C \rangle = \langle UC_2 \rangle$	$-43,800 + 6.7T$	9	1500–2000	From E, A
7. $\langle Ti \rangle + \langle C \rangle = \langle TiC \rangle$	$-54,000 + 2.7T$	12	1500–2000	See p. 406
8. $\langle Th \rangle + 2\langle C \rangle = \langle ThC_2 \rangle$	$-43,800 + 4.0T$	10	1500–2100	From E, A
<b>E. Oxides and Carbides</b>				
1. $\frac{1}{3}\langle Al_2O_3 \rangle + \frac{2}{3}\langle C \rangle = \frac{1}{3}\langle Al_4C_3 \rangle + \langle CO \rangle$	$97,600 - 44.1T$	5	1500–2200	See p. 406
2. $\frac{1}{3}\langle ZrO_2 \rangle + \frac{2}{3}\langle C \rangle = \frac{1}{3}\langle ZrC \rangle + \langle CO \rangle$	$79,400 - 44.7T$	5	1800–2200	„
3. $\frac{1}{2}\langle UO_2 \rangle + 2\langle C \rangle = \frac{1}{2}\langle UC_2 \rangle + \langle CO \rangle$	$83,100 - 38.85T$	12	1800–2000	„
4. $\frac{1}{2}\langle ThO_2 \rangle + 2\langle C \rangle = \frac{1}{2}\langle ThC_2 \rangle + \langle CO \rangle$	$92,100 - 38.5T$	8	1800–2200	8

\* Original formulæ slightly amended (see p. 406).

investigation are solid below 2000° C. The metals may be either solid or liquid, but no reaction will be considered which involves more than one gaseous constituent, either carbon monoxide or nitrogen.

Two questions can be answered by the application of thermochemical calculations: (1) What is the chemical mechanism of the vacuum-fusion method?

and their free energies of solution in liquid iron are required. These data should be known for the temperature range 1500°–2000° C. The free energies of formation of many metal oxides have been established with some accuracy; those of the nitrides and carbides and the free energies of solution, however, are not accurately known for most of the metals under



consideration. Approximate figures can be obtained by checking the available information carefully and introducing estimates based upon general experience in metallurgical thermochemistry. Since the liquid iron is in direct contact with an excess of graphite throughout the experiments, the activity of carbon must be taken as unity, and formation of iron carbide need not be considered in the free-energy calculations.

Table XIII gives the free-energy equations finally obtained, their probable accuracy, and the sources from which they have been derived. For simplicity, the data are expressed in two-term formulæ:

$$\Delta G = A + BT$$

Some of the free-energy equations in Table XIII could be taken directly from published critical compilations, such as that by Richardson and Jeffes.<sup>7</sup> Some of the formulæ required small corrections; these are denoted by an asterisk. The published free-energy equation for silica,<sup>7</sup> for instance, applies to quartz, whereas tridymite is generally formed when silica is precipitated from molten iron. Hence the heat of transformation (2800 cal.) must be taken into account. Kelley's  $\Delta G$  equations,<sup>8</sup> which have also been used, generally contain more than two terms. These formulæ have been simplified to two-term expressions. Kelley has also evaluated some oxide/carbide equilibria quoted under Section E of Table XIII. These have been completely re-evaluated. Kelley's estimated  $\Delta C_p$  terms appear to be unreasonably high. Smaller values have been introduced and the standard entropies estimated. The present equations agree with Kelley's at the temperatures of the basic measurements, and since they involve more probable entropies at room temperature they are to be preferred to Kelley's earlier evaluations. For the reaction of alumina with carbon (E1, Table XIII) a new heat of formation of aluminium carbide<sup>9</sup> was introduced and again a numerically lower  $\Delta C_p$  was assumed. With these alterations a new free-energy equation is obtained, which yields a standard entropy of 31.3 cal./deg./mole for  $\text{Al}_4\text{C}_3$ ; this is more probable than Kelley's estimate<sup>8</sup> of 25 cal./deg./mole.

The free energies of formation of the carbides have been obtained from the new equations E if no information from direct measurements was available. The formula for vanadium carbide is an estimate.<sup>6</sup>

The free energies of formation of the nitrides are much less accurate than the other values quoted in Table XIII. Calculations based upon the nitride equations cannot therefore be really conclusive. They are, however, included in order to give an approximate idea of the order of magnitude.

Most of the free energies of solution of the metals in liquid iron are estimated. The principles on which these estimates are based have been discussed.<sup>9, 10</sup> They are relatively simple where regular solution can be assumed (vanadium, molybdenum). They are more difficult for non-regular solutions, indicated by an appreciable heat of solution. Some measurements are available for silicon and aluminium.<sup>9, 10</sup>

For uranium the observation by Grogan<sup>5</sup> has been taken into account, that there is a heat effect when the metal is dissolved in molten iron. Similar behaviour may be expected in thorium. Some of Chipman's free-energy formulæ have been employed, but they are altered in order to apply to a concentration of 10% by weight of the metal in iron. This is an average figure for the concentrations used in practice. Actually, the concentrations vary within wide limits. It is considered, however, that the entropy, which mainly accounts for the change in concentration, though considerably altered at very low concentrations, becomes less sensitive to such changes if a concentration of, say, 5 at.-% is exceeded. Thus, the error introduced in the evaluations by the free-energy equations C is probably not larger than that in the equations for the oxides and nitrides.

Table XIII contains all the information required for the calculation of the carbon-monoxide and nitrogen pressures in reactions (1)–(8) (pp. 392 and 393) for the metals under consideration. These pressures are obtained in atmospheres from the equation:

$$\log p_{\text{CO}} \text{ or } \log p_{\text{N}_2} = \Delta G_x / 4.575 T$$

$\Delta G_x$  is obtained from the free energies in Table XIII in the following way:

Mechanism	$\Delta G_x =$
(1)	$\Delta G_A$
(2)	$\Delta G_A + x\Delta G_{\text{CO}}$
(3)	$\Delta G_A + x\Delta G_{\text{D}}$
(5)	$\Delta G_B$
(6)	$\Delta G_B + 2x\Delta G_{\text{CO}}$
(7)	$\Delta G_B + 2x\Delta G_{\text{D}}$

For the simplest mechanism of CO evolution, i.e. mechanism (1), the pressures obtained in this manner have been given (in mm. Hg) in Table I (p. 392). As already stated (p. 393), the sequence of calculated pressures follows the same order as that observed experimentally for evolution of carbon monoxide.

Instead of calculating CO and  $\text{N}_2$  pressures first, information can be obtained directly from the free-energy equations by a relative method. The temperature of carbon-monoxide evolution in the presence of alumina has been determined as 1600° C. This corresponds to a free energy of 21,300 cal. in equation (A5). If this quantity is subtracted in all the other equations for  $\Delta G_A$ , a temperature  $T_{\text{CO}}$  is obtained from:

$$\Delta G_A = A - 21,300 + BT$$

for  $\Delta G_A = 0$ . If the mechanism represented by one of the formulæ (1)–(3) is correct, these temperatures  $T_{\text{CO}}$  should be equal to those observed for the gas evolution within the limits of error of the basic  $\Delta G$  equations. This method has been adopted in order to derive the temperatures in Tables III and IV. The value of the numerical term in the equation given above is, of course, different for each mechanism. The corresponding calculations in the case of the nitrides are not based on observations with aluminium, but on the more reliable results with titanium, which showed a nitrogen evolution at 1800° C. (p. 399).

There is some uncertainty in the selection of the value of  $x$  in formulæ (2), (3), (6), and (7). The oxides and nitrides selected in Table XIII (A) and (B) are the lowest for which data could be derived having regard to the fact that the free energy of the lowest compound determines the total reduction to the metal. This arbitrary method is accurate so far as the free energy is concerned. The chemical equations, however, do not necessarily represent the actual mechanism. The equation for titanium, for instance (48, Table XIII), could as well be written for  $TiO_2$  or any other composition in place of  $TiO$ , retaining the free-energy relationship, i.e. equations A (Table

XIII) can be considered as representing partial molar free energies. To eliminate as far as possible the error introduced by this uncertainty, the calculations have been carried out for equal amounts of metal Me, i.e.  $x$  in formulæ (2) and (3) is taken to be unity throughout. If, for instance,  $x$  is taken to be equal to the mole fractions indicated by equations A, the temperatures obtained are close to those obtained for  $x = 1$ ; only for titanium is an appreciably lower value ( $160^\circ C.$ ) found. For the nitrides the difference in the two methods is still smaller.

The results of the calculations have been discussed at some length on pp. 392–394.

#### REFERENCES

1. H. A. Sloman, *J. Inst. Metals*, 1945, **71**, 391.
2. H. A. Sloman, *Iron Steel Inst. Special Rep.*, 1937, (**16**), 96.
3. H. A. Sloman, *ibid.*, 1939, (**25**), 46.
4. W. H. Hatfield and W. C. Newell, *J. Iron Steel Inst.*, 1943, **148**, 351p.
5. J. D. Grogan, *J. Inst. Metals*, 1950, **77**, 571.
6. N. P. Allen, O. Kubaschewski, and O. von Goldbeck, *J. Electrochem. Soc.*, 1951, **98**, 417.
7. F. D. Richardson and J. H. E. Jeffes, *J. Iron Steel Inst.*, 1948, **160**, 261.
8. K. K. Kelley, *U.S. Bur. Mines Bull.*, 1937, (**407**).
9. O. Kubaschewski and E. Ll. Evans, "Metallurgical Thermochemistry". London: **1951** (Butterworth-Springer, Ltd.).
10. J. Chipman, *Basic Open-Hearth Steelmaking by (A.I.M.M.E.) Cttee. on Phys. Chem. of Steelmaking*, 1944, **17**, 466.





# THE OPAQUE-STOP MICROSCOPE AS A MEANS OF STUDYING SURFACE RELIEF\*

1361

By W. M. LOMER,† M.Sc., B.A., and P. L. PRATT,‡ B.Sc.

## SYNOPSIS

Small undulations and slopes of a specimen surface are difficult to detect under the conventional microscope, especially at high powers. The insertion of suitable opaque stops in the optical train enables much smaller changes of slope to be detected and estimated. The improvement in sensitivity to angle is by a factor of about thirty. Some results obtained by this method are illustrated.

## I.—OUTLINE OF THE METHOD

THE conventional microscope reveals the structure of an object only if there is a true difference in the brightness of the light leaving different parts of the object. Oblique illumination may, however, show up slopes and tilts of the surface invisible in normal illumination, while Zernicke's phase-contrast microscope uses the information contained in the *phase* of the light to show the details of a slightly distorted surface. The "opaque-stop microscope" to be described is similar in arrangement to the phase-contrast microscope, and makes the advantages of oblique illumination available at high magnification.

The principle of the method is shown in Fig. 1,

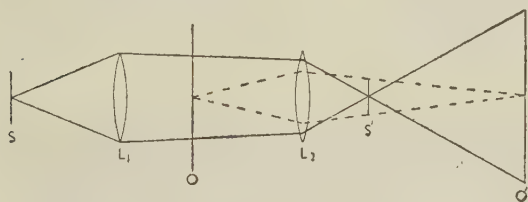


FIG. 1.—Principle of Method.

drawn for transmitted light for clarity. An image of the object  $O$  is formed by the lens  $L_2$  at  $O'$ , as shown by the dotted lines. The illumination is provided by the source  $S$ , whose image would be formed by  $L_1$  and  $L_2$  at  $S'$  were the object not present; to ensure a uniformly bright field of view,  $S'$  must not be too far from the back focal plane of  $L_2$ . An opaque stop is placed in the plane  $S'$  of such a shape and size as to intercept the light not deviated by the object, while allowing that which is to pass on to form the image in  $O'S$ .

It is convenient to speak of two ways in which light

may be deviated by an object; i.e. either by geometrical reflection or refraction of the beam as a whole, or by diffraction, which becomes important when studying structures of a size comparable with the resolving power of the objective. The geometrical deviations of the beam produce contrast in the image, since light from one area of the object may be intercepted by the opaque stop, while that from an inclined area is allowed to pass. The linear separation of the images of  $S$ , formed in the plane of the opaque stop after reflection by such areas, is the product (angle between areas)  $\times$  (distance  $L_2S'$ ); by measuring the displacement of the opaque stop necessary to cut out light from different areas in turn, the angle between them can be found. For appreciable contrast with the best setting of the stop, the separation of the images of  $S$  must be, say, one-fifth of the diameter of each image. As  $L_2S'$  is roughly equal to the focal length of  $L_2$  in practice, the sensitivity to angle is about (diameter of image of  $S$ )/(5  $\times$  focal length). Without an opaque stop, appreciable contrast is obtained only when rays from some areas fail to enter the objective at all, and the partial interception of the broad circular beam by the objective mount gives a very poor initial sensitivity. The effective angular sensitivity is then of the order of (diameter of objective)/(focal length); that is, about  $\sin^{-1}$  (numerical aperture). In practice, to obtain sufficient brightness of the final image, the image of  $S$  must be at least one-tenth as large as the objective aperture at high magnifications, but may be smaller for low magnifications without an eyepiece. Thus a gain of sensitivity by a factor of about thirty is quite feasible, and is in fact usually attained even in high-magnification systems.

The interpretation of the images produced in the diffraction region is more difficult. As diffraction

\* Manuscript received 17 May 1951.

† Cavendish Laboratory, Cambridge.

‡ Research Fellow, Atomic Energy Research Establishment, Harwell; formerly Cavendish Laboratory, Cambridge.

§ An opaque-stop microscope has already been described by Hallimond,<sup>1</sup> in which the stop was made similar to the source, so that only the *undeviated* light was allowed to pass.

In order to avoid a drastic loss in resolution, some of the most widely deviated rays were also admitted. It seems more desirable to preserve all the deviated image-forming rays and obtain the contrast desired by removal of the intense direct beam, especially since this arrangement can give both dark-field and oblique-illumination effects.



effects are more noticeable at high magnification, where we are concerned not to lose resolution, it will be assumed that the stop at  $S'$  is complementary to  $S$ ; in this case it can be arranged that only the direct, and none of the diffracted, light is cut out. With the opaque stop in such a position, dark-field illumination of a particularly sensitive kind results; not only are scratches, sharp steps, and similar structures shown up, but also comparatively gently sloping regions. It is, however, usually more instructive to move the stop slightly to one side, so that some of the undeviated light is allowed to pass, and the diffracted light on one side removed. The images given by this Schlieren arrangement look rather like those resulting from oblique illumination, and give a very useful general view of the topography of a surface.

A theoretical treatment of a similar arrangement has been given by Zernicke,<sup>2</sup> which is valid for slightly imperfect surfaces. He shows that the brightness of the image is linearly dependent on a function which is effectively the slope of the surface, though sharp corners appear rounded. This general effect is not unlike that produced by geometrical deviation of the beam, the interpretation of which is independent of the degree of deformation of the surface; it thus seems reasonable to assume Zernicke's calculation to be approximately valid for highly distorted surfaces.

## II.—EXPERIMENTAL TECHNIQUES

Fig. 2 shows the arrangements of the apparatus used for examining opaque objects. For low magnifications, up to  $\times 10$ , the apparatus is set up on an optical bench, the lens  $L_2$  being a high-quality camera or process lens of about 5 in. focal length, adjusted to give the desired magnification of the primary image  $O'$ . A long bellows camera, with its lens removed,

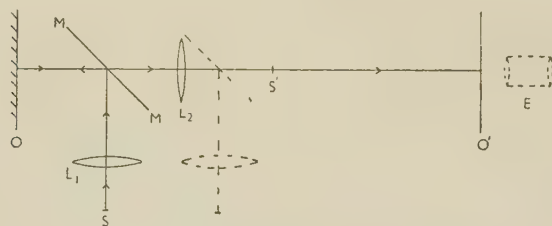


Fig. 2.—Arrangement of Apparatus for Examining Opaque Objects.

Full lines—low-power arrangement.  
Broken lines—high-power arrangement.

forms a very convenient plate-holder to record this image and screens the plate from stray light. The illumination is produced by a Pointolite lamp, or for more critical work, a Western Electric 10-W. "concentrated arc" lamp, and it is brought to a parallel beam by  $L_1$ , a lens of fairly good quality. This beam is introduced from one side using the glass slip  $MM$  in front of the lens  $L_2$ . The stop  $S'$ , carried on a separate slide on the optical bench, is brought into the focal plane by placing a piece of plane mirror at  $O$  and sliding the stop  $S'$  until the best image of the

source is formed on it. The mirror is then replaced by the object, and  $S'$  is traversed until the desired structure is displayed to the best advantage. For quantitative work a straight-edge stop is used, and the distance it must be traversed to cut out light from the inclined areas in turn is measured.

Rather higher magnifications can be obtained by using a low-power microscope objective for  $L_2$  and adding a projection eyepiece  $E$  further to magnify  $O'$ . In practice, it is convenient to slot the tube of a microscope about 1 in. behind the objective mount and insert  $S'$  at this position. The convergence of the illuminating beam must then be adjusted to a value which will allow an image of the source to be formed in the plane of the slot, and will be different for different objectives. Since most of the direct light from the object is intercepted by  $S'$ , any glare produced by reflection of light from the objective lens can very much reduce the available contrast, and, if the working distance of the objective is large enough, it is desirable to use  $MM$  in front of the objective.

At high magnification, it is impossible to introduce the slip  $MM$  between the objective and the specimen, and it must be replaced by a more conventional type of metallurgical vertical illuminator, shown dotted in Fig. 2. It is desirable that this slip should be as close as possible to the objective  $L_2$ , since it is essential that  $S'$  shall be behind the illuminator slip and as near the back focal plane of the objective as is feasible. To suppress glare in this arrangement, it is necessary to prevent light passing axially down through the objective  $L_2$ , and the most satisfactory arrangement is to use as source a narrow annular stop, like that used in a phase-contrast microscope. The stop  $S'$  is a thin metal ring which just covers the image of the source. This arrangement introduces one further complication, for the image of the source must not only be in the plane of  $S'$  but also be of the correct size. The necessary extra degree of freedom is conveniently provided by making both  $L_1$  and  $S$  adjustable on an optical bench. It is not difficult to find the correct placing of the two by trial and error, focusing  $S$  into the plane of  $S'$  by removing the microscope eyepiece and using parallax to fix the position accurately. The positions can then be marked on the bench for each objective, and changes made fairly readily. It is necessary to provide one of the annular stops with suitable traversing arrangements to position the image of  $S$  correctly on to  $S'$ . Any good phase-contrast metallurgical system can be adapted to this opaque-stop use by simply replacing the phase ring by an opaque ring. An interchangeable pair would be very useful in practice, since some of the effects seen in phase-contrast work depend more on the fact that the phase-ring absorbs light than on its phase-shifting properties. A comparison with the opaque-stop images might often enable more confident interpretation of phase-contrast pictures to be made.

The sensitivity to angle of slope of the surface depends on the magnification of the system. The minimum angle which can be measured is about



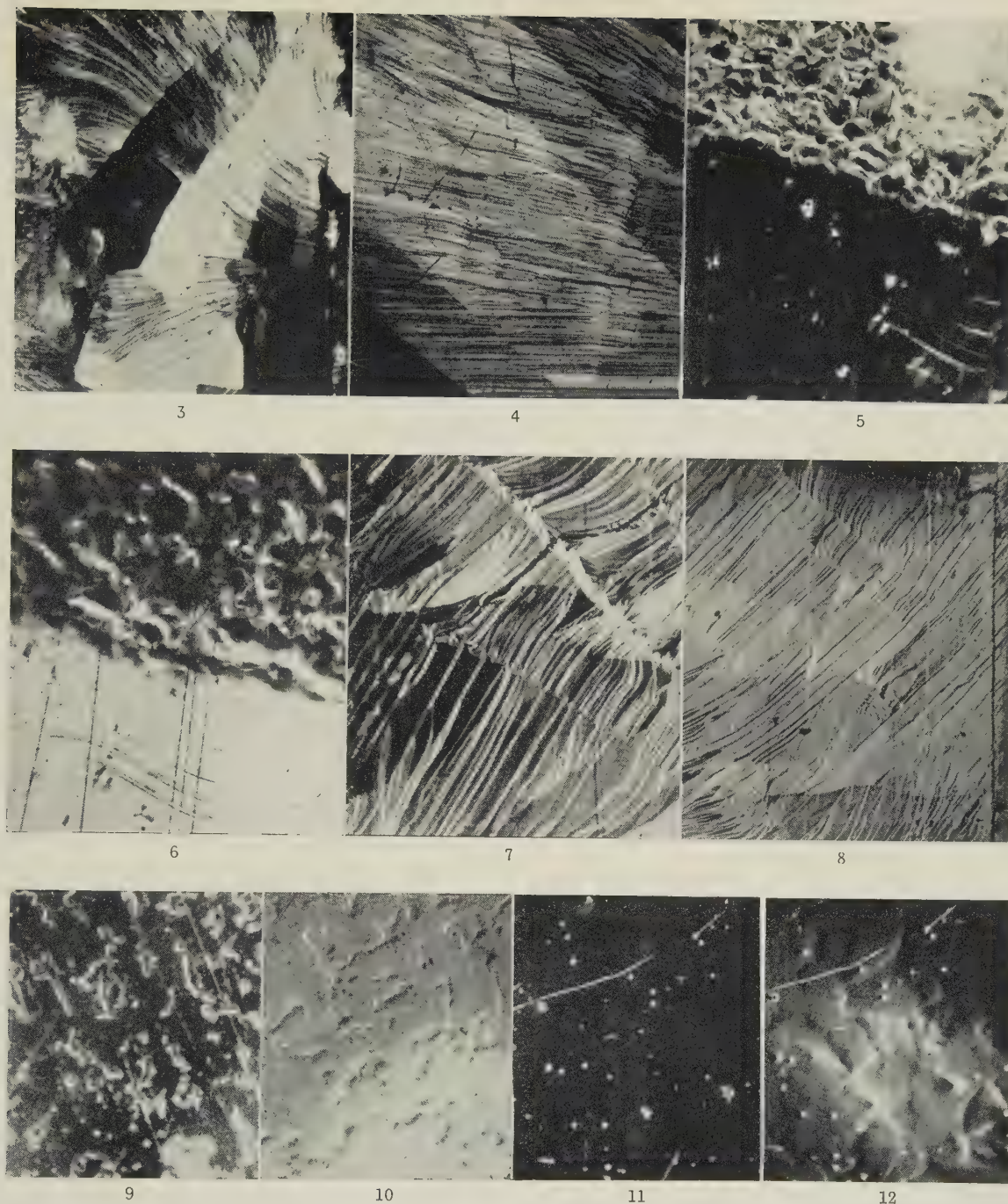


FIG. 3.—Macromosaic Structure in Crystal of NaCl.  $\times 12$ . Point source, edge stop.  
 FIG. 4.—Macromosaic Structure in LiF; Good Specimen.  $\times 6$ . Point source, edge stop.  
 FIG. 5.—Lüders Band in Mild Steel.  $\times 80$ . Annular stops.  
 FIG. 6.—Same as Fig. 5, with Stop Moved to Reverse Contrast.  
 FIG. 7.—Cleavage Steps on Surface of NaCl Crystal Seen in Sensitive Dark Field.  $\times 24$ . Point source, edge stop.  
 FIG. 8.—Deformation Lines in NaCl, Produced by Cleavage; Schlieren Arrangement.  $\times 24$ . Point source, edge stop.

FIGS. 9-12.—Polished Mild Steel with Raised Particles of Pearlite on Surface. Unetched.  
 Reduced by one-quarter linear in reproduction.

FIG. 9.—Sensitive Dark Field.  $\times 50$ . Annular stops.  
 FIG. 10.—Same as Fig. 9, Schlieren Arrangement.  $\times 50$ . Annular stops.  
 FIG. 11.—Same as Fig. 9.  $\times 150$ .  
 FIG. 12.—Same as Fig. 10.  $\times 150$ .





(diameter of  $S'$ )/(focal length of  $L_2$ ), and the diameter of  $S'$  is determined, since it controls the brightness of the final image, which cannot be allowed to decrease without unduly prolonging the exposure times. For a given exposure time, the diameter of  $S'$  is fixed, and the sensitivity is therefore approximately proportional to the focal length of  $L_2$ , or inversely proportional to the magnification. The following figures indicate the order of sensitivity obtained; with a single lens of 5 in. focal length giving a magnification of  $\times 6$ , angles of  $1'$  could be seen, while at a magnification of  $\times 200$ , using a lens of NA 0.45, the sensitivity dropped to  $1^\circ$ .

### III.—DESCRIPTION OF PHOTOGRAPHS

Photographs showing the contrast which results mainly from geometrical deviations of the beam, are shown in Figs. 3, 4, and 5 (Plate LX). A typical macromosaic structure on the cleaved surface of a nearly perfect single crystal of sodium chloride is shown in Fig. 3. The difference in orientation which produced the contrast between adjacent areas is of the order of  $1^\circ$ . A crystal of lithium fluoride having a less-marked mosaic structure, used for an X-ray monochromator, appears in Fig. 4; the disorientation here is only a few minutes of arc. Fig. 5 shows a Lüders band in mild steel; the deformed area at the top is inclined at about  $3^\circ$  to the undeformed area at the bottom, and the marked rumpling of the deformed surface is easily visible. Fig. 6 (Plate LX) shows the same specimen with the opaque stop traversed a distance corresponding to the angle between the two areas.

Effects produced by diffraction are shown in Figs. 7–12 (Plate LX). The bright lines in Fig. 7 are low cleavage steps on the surface of a sodium chloride single crystal shown up by the sensitive dark-field type of illumination mentioned above. On this same crystal, plastic deformation has caused the black and white vertical lines in Fig. 8; these are visible only where some direct light has passed the opaque stop. This corresponds to the Schlieren arrangement discussed above, and the black and white lines are interpreted as narrow regions of opposite slope. Figs. 9 and 10 show a specimen of mild steel polished so that areas of pearlite stand above the general level of the surface, which is unetched. Fig. 9 illustrates the effect of a central stop, corresponding to the dark-field arrangement; the particles are outlined in light, and scratches and inclusions are seen. (The haze in

the upper left corner is the result of glare from the objective.) A similar field is shown in Fig. 10 with the Schlieren arrangement; the relief effect is quite clear, and the spurious rounding of the corners is visible, for the particles are in fact very nearly flat-topped. The same specimen under a higher magnification is seen in Figs. 11 and 12; the central stop shows only a trace of evidence for the particles (which would be invisible under the conventional microscope), while the Schlieren pictures show the relief quite clearly.

### IV.—SUMMARY

The study of slopes and surface irregularities under the conventional microscope is difficult because the high numerical aperture means that the objective collects light reflected over a wide range of angles (up to  $\sin^{-1}$  NA); and only if the slopes of the surface are comparable with this angle will the structure be visible. The opaque-stop microscope enables the sensitivity to angle to be increased by a factor of about thirty, so that at a magnification of  $\times 6$  with a single lens of 5 in. focal length a sensitivity of  $1'$ , and with NA 0.45 (total magnification  $\times 200$ ) a sensitivity of about  $1^\circ$  can be obtained.

In addition, the opaque-stop arrangement can give the effect of either sensitive dark-field, or of oblique, illumination, and is available even at high magnification where the objective-mount design prevents the use of true oblique illumination. These effects must play some part in the formation of phase-contrast images, especially where heavily absorbing phase rings are used. It would perhaps be useful to be able quickly to replace the phase ring by an opaque stop in order to compare the images and eliminate some of the possible errors of interpretation.

### ACKNOWLEDGEMENTS

This work was done at the suggestion of Dr. E. Orowan, while both the authors were in receipt of maintenance grants from the Department of Scientific and Industrial Research, to whom grateful acknowledgement is made.

### REFERENCES

1. A. F. Hallimond, *Nature*, 1947, **159**, 851.
2. F. Zernicke, "Achievements in Optics", edited by A. Bouwers, p. 116. Amsterdam: 1946 (Elsevier Publishing Co.).





# A MODIFIED DEW-POINT METHOD FOR VAPOUR-PRESSURE MEASUREMENTS OF LEAD-MERCURY ALLOYS \*

1362

By B. R. BURGAN,† R. C. HALL,† and R. F. HEHEMANN ‡

## SYNOPSIS

A modification of the dew-point method for determining the vapour pressure of a volatile component over an alloy system is described. The vapour pressure of mercury over several lead-mercury alloys has been determined for a range of temperatures. The activities of mercury and of lead were calculated for 324° C. and agreed well with the results of Hildebrand, Foster, and Beebe (*J. Amer. Chem. Soc.*, 1920, **42**, 545).

THE dew-point method for determining the vapour pressures of alloy systems in which one of the components has a negligible vapour pressure in comparison to the other, has recently been applied to a number of systems.<sup>1-3</sup> In these investigations, the alloy was sealed in an evacuated tube and heated in a furnace which produced a temperature gradient along the length of the tube. Equilibrium of the vapour of the more volatile component with the alloy and with the pure component was established by keeping the temperature constant at the alloy end of the tube and reducing the temperature of the condensate end until condensation of the vapour was observed. A small auxiliary coil surrounding the condensate end of the tube was used to narrow the temperature range between condensation and evaporation so that an accurate temperature measurement of the condensation point could be obtained.

The method used by the previous investigators employed manual adjustment of the current through the auxiliary coil and visual observation of condensation. At higher temperatures, this observation becomes more difficult because of the incandescence of the tube. In order to make the temperature at the condensate end of the tube self-adjusting instead of manually controlled and to eliminate the necessity for visual observation, the sample tube in the present work was modified by sealing two tungsten wires in the condensate end of the tube, as shown in Fig. 1. The suitability of this modification was studied by determining the vapour pressures of several lead-mercury alloys over a range of temperatures.

The furnace employed in this investigation was similar to that of Hargreaves.<sup>1</sup> The space between the tungsten wires in the condensate end of the tube was approximately 0.01 in. The tungsten wires were connected in series with a relay which controlled the power to the auxiliary coil at the condensate end of the tube. Condensation of mercury on the contact

points activated the relay and heated the auxiliary coil until evaporation of the mercury occurred. Preliminary experiments showed that when the wires merely projected into the tube, contact was made upon condensation of the mercury; but, probably because of the surface-tension relationships between tungsten and mercury, the droplet would fall from the tungsten wires, thereby opening the power circuit to the auxiliary heating coil. These wires were therefore located at the bottom of the tube to maintain contact with the mercury until evaporation had occurred.

Five-g. samples of various compositions (Table I) were prepared from high-purity lead and mercury.

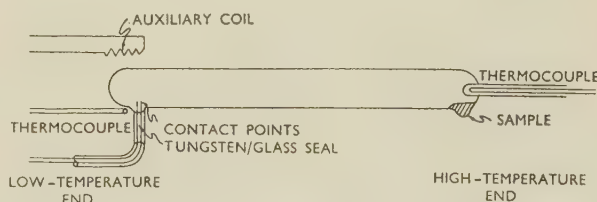


FIG. 1.—Apparatus for Determination of Vapour Pressure.

Each sample was sealed in an evacuated tube and heated to a uniform temperature for several hours—usually overnight. The temperature of the condensate end was lowered, and the auxiliary coil operated until the condensation and evaporation temperatures were within 2° C. of each other. The temperature at the alloy end of the tube was then changed and the process repeated. After readings had been obtained at several temperatures, the tube was quickly cooled and the mercury content of the alloy determined by standard chemical techniques.

From the vapour-pressure/temperature data for pure mercury,<sup>4</sup> the vapour pressure of mercury over the alloy at each temperature was determined from the corresponding condensation temperature of

\* Manuscript received 5 March 1951.

† Student, Department of Metallurgical Engineering, Case Institute of Technology, Cleveland, O., U.S.A.

‡ Instructor, Department of Metallurgical Engineering, Case Institute of Technology, Cleveland, O., U.S.A.



mercury at the condensate end of the tube. Table I and Fig. 2 give the vapour pressures of several lead-mercury alloys over the range 215°–575° C.

TABLE I.—*Vapour Pressure of Lead-Mercury Alloys at Various Temperatures.*

Hg, at.-%	Temp., °C.	V.P., mm. Hg	Hg, at.-%	Temp., °C.	V.P., mm. Hg
85.2	329	375	29.4	338	219
	306	254		307	145
	303	240		255	44.0
	272	118		241	30.5
	220	29.3	17.1	288	44.2
	216	25.5		279	38.0
44.9	338	365		267	28.5
	302	155		245 *	20.6
	285	118	5.0	573	520
29.4	410	720		480	210
	395	560		375	57

\* This temperature is below, all others above the liquidus.<sup>5</sup>

Hansen<sup>5</sup> has summarized the data on the equilibrium diagram of the lead-mercury system. The diagram is well known for temperatures above 0° C. and apparently exhibits a modified eutectic behaviour, with the eutectic temperature at  $-37.6^{\circ}$  C; however, Hansen expresses some doubt concerning whether or not a peritectic reaction exists at low temperatures and small lead contents. Lead is essentially insoluble

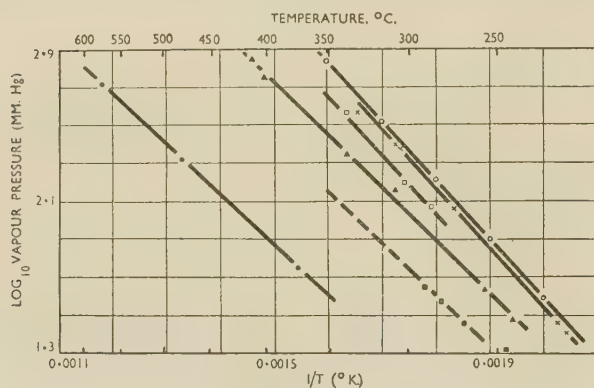
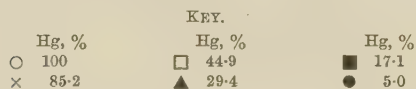


FIG. 2.—Vapour Pressures of Lead-Mercury Alloys.



in solid mercury, but a large field of solid solubility exists at the lead-rich end of the diagram, extending from approximately 66 to 100 at.-% lead at the eutectic temperature. The thermodynamic properties of lead-mercury alloys at ambient temperature have been studied by Tammann and Ohler<sup>6</sup> by calorimetric measurements and by Hoyt and Stegemann<sup>7</sup> using e.m.f. measurements. Hildebrand, Foster, and Beebe<sup>8</sup> determined the activity of mercury over

lead-mercury alloys at 324° C. from vapour-pressure measurements by using a manometric method.

In order to compare the results of the present investigation with those of Hildebrand, Foster, and Beebe, the activities of lead and mercury were evaluated at 324° C. The activity of mercury was calculated from the vapour-pressure temperature data and that of lead by a graphical integration of the Gibbs-Duhem equation. The activities of lead and

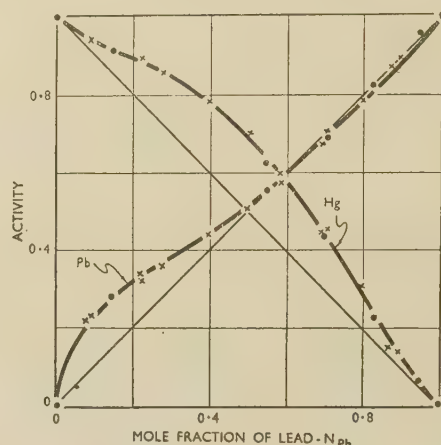


FIG. 3.—Activities of Lead and Mercury at 324° C. as a Function of Composition.

● Present author.      × Hildebrand, Foster, and Beebe.

mercury at 324° C., as now determined and as determined by Hildebrand, Foster, and Beebe, are presented in Fig. 3 as a function of composition. The data are seen to agree well.

The activity of mercury shows positive deviations from Raoult's law over the entire composition range; however, an inflection point may be noted at approximately 30% mercury. The activity of lead also exhibits positive deviations from Raoult's law for low lead contents, but, as a result of the inflection mentioned above, the activity of lead shows slightly negative deviations for high lead contents. This behaviour suggests that the Hg-Pb bond is stronger than the Hg-Hg or Pb-Pb bond at high lead contents and may reflect a change in the effective co-ordination number as the lead content decreases.

## REFERENCES

1. R. Hargreaves, *J. Inst. Metals*, 1939, **64**, 115.
2. C. E. Birchenall and C. H. Cheng, *Trans. Amer. Inst. Min. Met. Eng.*, 1949, **185**, 428.
3. A. Schneider and E. K. Stoll, *Z. Elektrochem.*, 1941, **47**, 527.
4. "Handbook of Chemistry and Physics", 23rd edn. Cleveland, O.: 1939 (Chemical Rubber Publishing Co.).
5. M. Hansen, "Der Aufbau der Zweistofflegierungen". Berlin: 1936 (Julius Springer).
6. G. Tammann and E. Ohler, *Z. anorg. Chem.*, 1924, **135**, 118.
7. C. S. Hoyt and G. Stegemann, *J. Phys. Chem.*, 1934, **38**, 753.
8. J. H. Hildebrand, A. H. Foster, and C. W. Beebe, *J. Amer. Chem. Soc.*, 1920, **42**, 545.

# THE EFFECT OF GRAIN-SIZE ON THE STRUCTURAL CHANGES PRODUCED IN ALUMINIUM BY SLOW DEFORMATION \*

1363

By W. A. RACHINGER,† M.Sc., JUNIOR MEMBER

## SYNOPSIS

X-ray-diffraction and metallographic methods have been used to study the internal derangement of aluminium polycrystals of various grain-sizes after slow deformation at elevated temperatures. Previous work had shown that, for a given grain-size, the deformation markings were influenced by both the temperature and the rate of deformation. The present work indicates that for a given temperature and rate of straining the effect of an increase in grain-size is roughly equivalent to a decrease in temperature or an increase in strain rate. Further evidence is produced to confirm the existence of a deformation-induced sub-structure within the grains.

## I.—INTRODUCTION

PREVIOUS work<sup>1,2</sup> on the mechanism of creep deformation in aluminium has been directed towards elucidating the effect of temperature and rate of straining. X-ray-diffraction methods have shown that plastic deformation causes a sub-structure to form within the grains, the size of the units of the sub-structure increasing with increasing temperature or decreasing strain rate. Parallel microscopic observations showed a considerable change in the deformation markings. With increasing temperature or decreasing strain rate, it was found that slip lines became coarser and more widely spaced and finally disappeared, giving way to surface markings which were suggestive of a cellular structure within the grains.<sup>1,2</sup> Greenough and Smith<sup>3</sup> have verified the X-ray observations and have proposed a mechanism of formation of the sub-structure.

It was considered worthwhile to extend the earlier work to include investigations of coarse-grained material with a view to obtaining more detailed information about the sub-structure and also to determining, if possible, the effect of grain-size on the mechanism of deformation.

## II.—EXPERIMENTAL METHOD

The material used was aluminium of 99.98% purity in the form of sheet tensile specimens of gauge-length 1.6 in. and cross-section  $0.3 \times 0.060$  in. Specimens having three different grain-sizes were produced, namely 0.2 and 1 mm. dia. and very large-grained aggregates having only 2 or 3 crystals within the gauge-length. The specimens were deformed in a tensile-testing machine, which imposed a constant overall rate of elongation of 0.15%/hr. Tests on specimens of the three grain-sizes were carried out at

250°, 350°, and 400° C. The temperature variation along the gauge-length was never greater than 3° C. and the temperature at the centre of the specimen was controlled to  $\pm 1^\circ$  C.

The investigation was carried out by X-ray-diffraction and metallographic methods. Two types of X-ray back-reflection methods were used. One was the standard technique in which both the film and the specimen were stationary, and in the other the film and specimen were oscillated in synchronism through  $\pm 5^\circ$ . This latter method is useful for the determination of the orientation range of the deformed crystals, the area of spread of the X-ray reflections being essentially a measure of the disorientation of the reflecting planes. Furthermore, the orientation range in any particular direction can be determined, and this technique may therefore be used as an alternative to the Laue method suggested by Calnan and Burns.<sup>4</sup> The specimen holder in the X-ray camera was designed so that the same point of the specimen could be irradiated even after the specimen had suffered a large deformation. Cobalt radiation was used exclusively for the X-ray investigations.

Each specimen was electrolytically polished and etched before deformation, and the surface was examined microscopically after deformation. It was found that by repolishing and re-etching after deformation it was possible to produce metallographic evidence for a sub-structure within the grains.

## III.—EXPERIMENTAL OBSERVATIONS

The main findings of the investigation were:

(a) The earlier results obtained with fine-grained aluminium were verified, and it was further shown that the same tendencies (increase in the size of the sub-structure units with increasing temperature) were also evident in the case of coarser-grained material.

\* Manuscript received 2 August 1951.

† Aeronautical Research Laboratories, Melbourne, Australia.



(b) It was possible to develop a sub-structure within the grains by etching, thus allowing the configuration of the cells to be studied. In some cases it was observed that the sub-units tended to lie in bands transverse to the slip lines. There was evidence that the cells are not merely units of the original mosaic structure which have become disoriented by the deformation.

(c) Although the coarse grains broke down into cells at temperatures where the fine grains exhibited no cellular structure, there was no indication of a clear-cut variation of absolute cell size with grain-size for a given temperature.

(d) For a given temperature, the slip mechanism of deformation tended to become more prevalent the larger the grain-size. Thus, in as far as the deformation markings are concerned, an increase in grain-size is roughly equivalent to a decrease in temperature.

Since the results consist mainly of X-ray-diffraction photographs and photomicrographs, the description of the work will take the form of a commentary on the illustrations.

### 1. FINE-GRAINED MATERIAL

Fig. 1 (Plate LXI) is a stationary back-reflection photograph from an annealed fine-grained specimen. After 13% slow (0.15%/hr.) elongation at 250° C., the diffraction pattern assumes the appearance shown in Fig. 2 (Plate LXI). There has been a considerable increase in the density of spots on the Debye circles. It was suggested in earlier work that the multiplication of spots was due to the breaking down of the grains into smaller units which become disoriented, each sub-unit then giving rise to a reflection spot. This hypothesis is substantiated by microscopic evidence. Fig. 3 (Plate LXI) shows a typical area of the deformed structure, and Fig. 4 (Plate LXI) shows the same area after repolishing and heavy etching. The fine sub-boundaries are visible in the interior of the grains, indicating that the grains consist of small blocks tilted with respect to each other. Since the same grain boundaries appear in each photograph, it is evident that recrystallization has not occurred.

At 350° C. it is found that the grains suffer little or no internal breakdown. Fig. 5 (Plate LXI) shows the diffraction pattern from the annealed specimen and Fig. 6 (Plate LXI) the pattern from the same area after 13% slow strain at 350° C. There has been no appreciable increase in the number of diffraction spots and hence no internal breakdown of the grains. At 400° C. similar behaviour was observed. This verifies the earlier hypothesis<sup>2</sup> of the increase in cell size with increasing temperature.

### 2. COARSE-GRAINED (1-MM.) MATERIAL

The work on coarse-grained aluminium was undertaken in the hope that a more detailed examination of the sub-structure of the deformed grains could be

made. It was also considered that a knowledge of the effect of grain-size on the surface markings would be of interest, since the results of Hanson and Wheeler<sup>5</sup> suggested that with increasing grain-size the occurrence of slip becomes more prevalent.

Fig. 7 (Plate LXI) shows an oscillation back-reflection X-ray photograph from an annealed specimen. The size of the beam is such that only 2 or 3 grains are irradiated. After 20% slow elongation at 250° C., the photograph shown in Fig. 8 (Plate LXI) was taken from the same area. The original spots have now been smeared out into areas which contain a large number of fine spots. The area of diffusion of the reflections indicates that the range of orientation of the crystals has been increased, while the spottiness of the areas implies the existence of a block-like structure within the grains. Fig. 9 (Plate LXII), a stationary back-reflection photograph from the same area, illustrates the same features, the peripheral spread of the reflection being indicative of a range of orientation within the grains and the discreteness of the reflections indicating the existence of a sub-structure.

Fig. 10 (Plate LXII), a typical photomicrograph of the deformed surface, exhibits surface markings suggestive of a cellular sub-structure, and this is verified by repolishing and etching. Fig. 11 (Plate LXII) shows a grain which was traversed by coarse slip lines, traces of which remain after repolishing. Heavy etching develops a network of sub-boundaries, the most prominent of which lie transverse to the slip lines. This banded appearance is quite typical and occurs in most cases where the grains contain a large number of cells. Another interesting feature of Fig. 11 is the wavy appearance of the grain boundary. Similar effects have been observed in zinc<sup>6</sup> and have been attributed to the preferential absorption of some cells by the migrating boundary.

As in the case of the fine-grained material, the cell size is increased by increasing the temperature of deformation. A slow elongation of 15% at 350° C. causes the diffraction pattern of Fig. 12 (Plate LXII) to change to that shown in Fig. 13 (Plate LXII). These photographs show the usual increase in orientation range and break up into discrete units. The X-ray spots in Fig. 13 are larger and more discrete than those of Fig. 8, thus indicating an increase of cell size with increasing temperature.

Fig. 14 (Plate LXII) is a typical area of the deformed surface, and Fig. 15 (Plate LXII) shows the same area after repolishing and etching. The cells are much larger than those obtained by deformation at 250° C. (Fig. 11), thus verifying the temperature effect. It may be observed also that the cells are not arranged in an orderly fashion as in Fig. 11, though an orderly array could hardly be expected since there are so few cells within each grain.

The results obtained by slow deformation of a coarse-grained aggregate at 400° C. are very similar to those obtained at 350° C., no significant increase in the cell size being observed.

### 3. VERY LARGE-GRAINED AGGREGATES

The specimens which consisted of only two or three crystals were produced by slow solidification from the melt, and consequently had a dendritic structure. Slow deformation at 250° C. produced the usual X-ray evidence of disorientation and formation of a sub-structure; the surface markings are predominantly slip, as shown in Fig. 16 (Plate LXII). The effect of grain-size on the surface markings can be seen by a comparison of Figs. 3 and 16, both being taken from specimens deformed at 250° C., the former from a fine-grained aggregate, the latter from a bicrystal. With increasing grain-size the cellular structure of Fig. 3 becomes replaced by the more familiar slip lines of Fig. 16.

The tensile specimen used for the test at 350° C. was a tricrystal with transverse boundaries. After 20% overall extension the centre grain of the specimen was found to exhibit heavy surface rumpling, while the two end grains showed the normal widely spaced slip bands.

Figs. 17 and 18 (Plate LXII) are oscillation photographs from the central grain before and after deformation. The large disorientation within the grain is obvious from the spread of the reflections over quite a considerable area. The two lightly deformed end grains suffered much less disorientation than the heavily deformed central grain, the area of spread of reflections on the oscillation photograph being much less in the case of the end grains (Fig. 19, Plate LXII) than with the heavily distorted central grain (Fig. 18).

The microstructure revealed after repolishing and etching this specimen proved to be quite interesting. Fig. 20 (Plate LXII), a typical area of the heavily deformed central grain, shows two networks of boundaries, the heavy discontinuously dotted ones being dendrite boundaries, the continuous ones being cell boundaries. The fact that no obvious relationship exists between the positions of the two boundaries indicates that the cells are not the units of any fault structure which was initially present in the material, since the boundaries of these units would not be expected to be continuous across the dendrite boundaries, as are the cell boundaries. The dependence of cell size on the temperature and rate of deformation would also indicate that the cells could not be identified as any unit of structure present in the original undeformed material.

### IV.—DISCUSSION

One of the foremost aims of this work was to determine the effect of grain-size on the mechanism of slow deformation in aluminium at elevated temperatures. Both X-ray and microscopic evidence failed to indicate any marked variation of *absolute* cell dimensions with grain-size, although of course the number of cells per grain increased with increasing grain-size. The most striking feature of the observations was the change in deformation markings as illustrated by Figs. 3, 10, and 16. It is clear from

these that, for a given temperature, the occurrence of slip becomes more marked as the grain-size increases. If the intensity of visible slip is assumed to be a measure of the deformation of the grains themselves, then one may conclude that, under the conditions considered, the grains of a coarse aggregate suffer more internal deformation than those of a fine-grained aggregate.

Such a conclusion can be shown to be in agreement with current ideas on the mechanism of creep. Under conditions of slow deformation it is considered that there are two factors contributing to plastic flow, namely, the change in shape of the grains and the relative movements of the grains. At higher temperatures the latter mechanism is preferred, but its actual contribution to the overall deformation will depend on the amount of grain-boundary material present, i.e. it will be dependent on the grain-size. If the grain-size is small, relative grain movements may account for nearly all the plastic flow, but if the grain-size is large, this process may be insufficient to cope with the required flow, and the grains themselves will be compelled to alter their shape by drastic internal changes and so contribute to the deformation. Of course, in the limiting case of a single crystal, the change in shape of the grain is the sole contributor to the deformation. Thus, on the basis of present-day ideas, one would expect the deformation of the grains—and hence the intensity of the slip markings—to increase with increasing grain-size, i.e. the effect of an increase in grain-size would be expected to be roughly equivalent to that of a decrease in temperature or an increase in rate of straining. This in fact was the result obtained from these experiments, and the observations may therefore be considered to give indirect support to the hypothesis of relative grain movements.

One topic which will probably remain in doubt for some time is the nature of the transition region between neighbouring cells. Photomicrographs such as Fig. 15 indicate that apart from the fact that the cell boundaries do not etch as deeply as the grain boundaries—presumably because of the smaller orientation difference—the two are essentially similar. Thus the etching characteristics of cell boundaries at least gives a rough indication that they are of the same nature as grain boundaries.

It now remains to discuss the rather controversial question of the configuration and the mode of formation of the sub-structure. Although it is not known whether the sub-units make an important contribution, by virtue of their relative rotations or translations, to the actual deformation, it is likely that their presence has some influence on the deformational properties, e.g. strain-hardening. From this aspect alone it is of vital importance to investigate not only the effect of the cell structure on mechanical properties, but also—from the more fundamental viewpoint—the mode of formation of the sub-structure and the way in which it is modified as deformation proceeds.

The dependence of the size of the sub-units on the



rate and temperature of deformation has been satisfactorily explained by the dislocation hypothesis as described by Crussard<sup>8</sup> and by Greenough and Smith.<sup>3</sup> This theory can also account, in a general manner, for the mode of formation of the sub-structure and its subsequent disorientation. Essentially the theory suggests that local lattice curvatures are formed during the deformation and that, under the influence of stress and temperature, the dislocations move into stable positions in an array which is in fact the cell-boundary network. Such a process might be termed "polygonization under stress", the atomic mechanism of cell formation being similar to that of ordinary polygonization, except that the temperature and time required for the process are reduced drastically because of the applied stress field. If, in the limiting case, the process takes place almost instantaneously, then this theory reduces, for all practical purposes, to a hypothesis of direct dissociation of the grains into sub-units, as was suggested by Wilms and Wood.<sup>1</sup> The formation of a dislocation array, whether instantaneously or not, would account for both the initial dissociation of the grain into a sub-structure and its progressive disorientation.

One feature requires further explanation, however, namely the banded appearance of the sub-structure (Fig. 11), which is typical of cases in which the cell size is much smaller than the grain-size. Several explanations of this phenomenon are possible, although at present it is difficult to determine which is

the most suitable. One obvious explanation is that, as was suggested in the case of recovery of bent aluminium crystals,<sup>7</sup> the dislocations assemble on planes perpendicular to the slip planes, thus giving rise to boundaries of the type shown in Fig. 11. Here again the process may be considered to be either instantaneous or to require the passage of time.

Honeycombe<sup>9</sup> has observed a similar banded structure in aluminium single crystals under conditions where he considers a polygonization process unlikely to occur, namely deformation at room temperature, and consequently suggests that kinking is the operative mechanism. Another process likely to give rise to an ordered array of cells would be the Taylor crystallite "roller" effect or a similar mechanism involving the rotation of the sub-units about one or more axes, as suggested by Calnan and Burns.<sup>4</sup>

Of all these possible mechanisms it is at the moment very difficult to make a definite choice, but it is hoped that future work will allow such a choice to be made.

#### ACKNOWLEDGEMENTS

This work forms part of a joint research programme on plastic deformation of metals under the general direction of Mr. H. A. Wills of the Aeronautical Research Laboratories, Department of Supply, and Professor J. N. Greenwood and Dr. W. A. Wood of the Baillieu Laboratory, University of Melbourne, to whom the author expresses his thanks.

#### REFERENCES

1. G. R. Wilms and W. A. Wood, *J. Inst. Metals*, 1948-49, **75**, 693.
2. W. A. Wood and W. A. Rachinger, *J. Inst. Metals*, 1949-50, **76**, 237.
3. G. B. Greenough and Edna M. Smith, *J. Inst. Metals*, 1950, **77**, 435.
4. E. A. Calnan and B. D. Burns, *J. Inst. Metals*, 1950, **77**, 445.
5. D. Hanson and M. A. Wheeler, *J. Inst. Metals*, 1931, **45**, 229.
6. J. A. Ramsey, private communication.
7. R. W. Cahn, *J. Inst. Metals*, 1949-50, **76**, 121.
8. C. Crussard, *J. Inst. Metals*, 1948-49, **75**, 1125 (discussion).
9. R. W. K. Honeycombe, *Proc. Phys. Soc.*, 1950, [A], **63**, 672.

# OBSERVATIONS ON THE STRUCTURE AND PROPERTIES OF WROUGHT COPPER- ALUMINIUM-NICKEL-IRON ALLOYS\*

1364

By MAURICE COOK,† D.Sc., Ph.D., F.I.M., MEMBER, W. P.  
FENTIMAN,‡ B.Sc., A.I.M., and EDWIN DAVIS,‡ M.Sc.,  
F.I.M., MEMBER

## SYNOPSIS

A study has been made of the structure and properties of complex aluminium bronzes containing 8–12% aluminium and 4–6% each of nickel and iron.

Four phases,  $\alpha$ ,  $\beta$ ,  $\delta$ , and  $\kappa$ , have been identified, with random face-centred cubic, random body-centred cubic,  $\gamma$ -brass type, and ordered body-centred cubic structures respectively, and the phase fields for equilibrium conditions have been approximately determined. Structurally, the alloys can be divided into three classes: (1) alloys containing 8–9% aluminium, which, consisting of  $\alpha$  and  $\beta$  at 1000° C., change to  $\alpha$  and  $\kappa$  at lower temperatures; (2) alloys containing 10% aluminium, consisting of  $\beta$  at 1000° C.,  $\alpha$ ,  $\beta$ , and  $\kappa$  between 800° and 900° C., and  $\alpha$  and  $\kappa$  at lower temperatures; and (3) alloys containing 11–12% aluminium, consisting of  $\beta$  at 1000° C., changing from  $\beta + \kappa$  to  $\alpha + \beta + \kappa$  over the range 800°–600° C., and finally changing to  $\alpha + \kappa + \delta$ .

The mechanical properties of alloys containing 8, 10, and 12% aluminium with 5% each of nickel and iron, representative of the three main structural classes, have been determined in the quenched, quenched and tempered, hot-rolled, and hot-rolled and annealed conditions, and these properties have been related to the structures. In general, optimum properties were obtained with the 10/5 alloy. The effect of cold rolling on the mechanical properties of this alloy has been determined, and the structure and properties of extruded and annealed rod have also been studied.

## I.—INTRODUCTION

As a contribution to the study of complex aluminium bronzes in wrought forms containing appreciable amounts of both nickel and iron, in which increasing interest is being shown, the results are briefly described of some preliminary investigations into the structure, hardness, and tensile properties of alloys within the ranges 8–12% aluminium and 4–6% each of nickel and iron.

For the preliminary investigations on structure and properties, ingots weighing 10 lb. each were cast and hot rolled into 0.30 and 0.10-in.-thick strip. This part of the work is described in Sections II, 1, 2, and 3, the first of which is concerned with structure of the alloys under equilibrium conditions between 1000° and 500° C. Section II, 2 deals with the structural changes that take place when the alloys are brought into equilibrium at 1000° C. and subsequently tempered between 300° and 900° C. for periods up to 256 hr. The mechanical properties of representative alloys, both as quenched after bringing into equilibrium at various temperatures and after various tempering procedures following quenching at 1000° C., are detailed in Section II, 3

and related to the structural changes described in Section II, 1 and 2.

As a result of the studies described in Section II, six alloys were selected for processing on a larger scale, and observations on the effects of hot and cold rolling and subsequent thermal treatments on structure and properties are included in Section III. Information obtained in the course of a study of selected alloys in the form of extruded rod is given in Section IV.

To facilitate speedy identification of the various alloys referred to throughout the paper, a simple numerical code has been adopted, three figures being used to indicate the percentage of aluminium, nickel, and iron, respectively. Thus, for example, the material referred to as the 10/4/6 alloy contains 10% aluminium, 4% nickel, and 6% iron.

## II.—GENERAL INVESTIGATION OF STRUCTURE AND PROPERTIES

### 1. STRUCTURES OF QUENCHED ALLOYS

The purpose of the first part of this work was to define the approximate positions of the phase boundaries under equilibrium conditions and to

\* Manuscript received 28 November 1951.

† Joint Managing Director, Metals Division, Imperial Chemical Industries, Ltd., Birmingham.

‡ Technical Officer, Metals Division, Imperial Chemical Industries, Ltd. Birmingham.



relate the structure with the mechanical properties. To ensure that the alloys were in structural equilibrium at the various temperatures, the following procedure of annealing, soaking, slow cooling, and final quenching was adopted.

Specimens cut from strip of each of the twenty-five alloys listed in Table I were heated to 1000° C.

TABLE I.—Composition of Alloys Used in Structural Investigation.

Cast No.	Nominal			By Chemical Analysis *			
	Al, %	Ni, %	Fe, %	Al, %	Ni, %	Fe, %	Cu, %
1	8	4	4	8.16	4.00	4.09	83.7
2	8	4	6	8.02	4.15	5.74	81.9
3	8	5	5	7.87	4.99	4.90	82.1
4	8	6	4	7.83	6.03	4.15	81.9
5	8	6	6	8.06	5.97	5.70	80.2
6	9	4	4	9.25	3.81	3.85	82.8
7	9	4	6	8.96	4.06	5.76	81.1
8	9	5	5	8.97	4.85	5.30	80.8
9	9	6	4	8.97	6.30	3.91	80.8
10	9	6	6	8.99	5.91	6.08	78.9
11	10	4	4	9.86	4.40	3.98	81.7
12	10	4	6	10.24	4.33	5.68	79.7
13	10	5	5	10.13	4.86	5.04	79.9
14	10	6	4	10.38	5.79	4.07	79.8
15	10	6	6	10.00	6.00	5.88	78.1
16	11	4	4	11.01	4.14	4.05	80.8
17	11	4	6	11.09	4.17	5.61	79.1
18	11	5	5	11.04	4.72	5.01	79.1
19	11	6	4	11.00	5.65	3.75	79.5
20	11	6	6	11.11	5.87	5.96	77.05
21	12	4	4	11.63	4.07	4.06	80.2
22	12	4	6	11.98	3.86	5.84	78.3
23	12	5	5	11.99	4.73	4.99	78.2
24	12	6	4	11.97	5.85	5.86	76.3
25	12	6	6	11.97	6.10	5.80	76.1

\* Spectrographic analysis showed :

Zn . . .	Nil	Ag . . .	0.003%
Sn . . .	<0.01%	Bi . . .	<0.001%
Pb . . .	<0.01%	As . . .	0.005%
Mn . . .	0.01-0.02%	Si . . .	0.01-0.02%

and after 24 hr. at that temperature one specimen of each alloy was withdrawn and quenched in water. The temperature was then slowly reduced to 900° C. and after soaking for one day at that temperature further specimens were quenched. Successive batches of samples were quenched at temperature intervals of 100° C. and in some cases at closer intervals, the rate of cooling being decreased and the time of soaking increased so that samples quenched from 800°, 700° . . . 100° C. were heat-treated for 3, 5, 8, 12, 17, 23, 30, and 38 days, respectively.

The phases existing in the copper-aluminium-nickel-iron system have been variously named by different investigators, but in the present paper the following nomenclature has been adopted. The random face-centred cubic, random body-centred cubic, and  $\gamma$ -brass type structures similar to those in the copper-rich binary copper-aluminium alloys are referred to as  $\alpha$ ,  $\beta$ , and  $\delta$ , respectively. The

fourth phase, believed to be a nickel-iron-aluminium complex with an ordered body-centred cubic structure similar to that of NiAl and FeAl, is referred to as  $\kappa$ .

To facilitate identification of the various phases, an etching procedure, established after many experiments, was used throughout the work. Samples were etched first in aqueous 10% ammonium persulphate solution, which coloured  $\alpha$  pale yellow,  $\kappa$  grey-blue, and acicular  $\beta$  brown. To develop the structure of the acicular  $\beta$  and examine its decomposition products, the samples etched in persulphate were lightly repolished with magnesia and water and immersed in a solution of  $\frac{1}{2}$ % nitric acid in 20 vol. hydrogen peroxide. Positive identification of  $\delta$  was realized by staining it blue with aqueous 20% sodium hydroxide solution, used immediately after etching in persulphate, and washing. Re-etching in persulphate removed the blue stain from  $\delta$ , leaving it distinctly whiter than any  $\kappa$  present.

The results of the structural survey are presented in two series of schematic diagrams (Figs. 1 and 2), in which the phase boundaries have been approximately interpolated. Fig. 1 represents the structural constitution of all alloys considered at temperatures ranging from 500° to 1000° C., and Fig. 2 gives sections at various nickel and iron contents.

In general, the microstructural forms of  $\alpha$  and  $\beta$  resemble those of the binary aluminium bronzes (Figs. 3, 8, 10, 16, Plates LXIII and LXIV), and, in fact, apart from the presence of  $\kappa$  in the complex system,

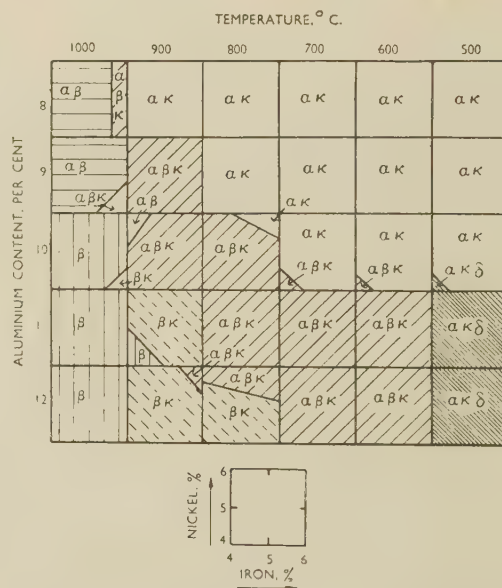


FIG. 1.—The Approximate Relationship between Composition, Temperature, and Phase Fields in Cu-Al-Ni-Fe Alloys. Isothermal sections. Each square represents a section at constant temperature and constant aluminium content.

the diagrams at constant nickel and iron contents bear a general resemblance to the copper-aluminium diagram in the region 7½-11% aluminium. When a substantial proportion of  $\beta$  is retained undecomposed, acicular marks are produced by etching (Fig. 13,

Plate LXIII), similar to those observed in quenched  $\beta$  in binary copper-aluminium alloys. The  $\beta$  phase cannot be retained unchanged by quenching, for a martensitic-type transformation occurs, accompanied sometimes by decomposition to an extent dependent on the aluminium, nickel, and iron contents.

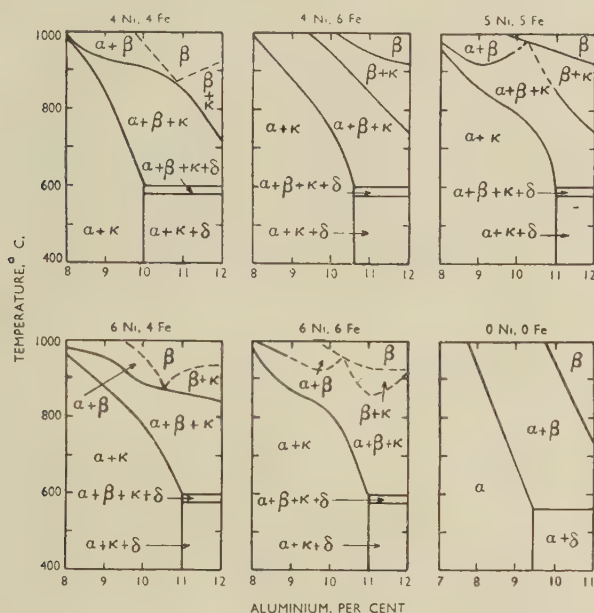


FIG. 2.—The Approximate Relationship between Composition, Temperature, and Phase Fields in Cu-Al-Ni-Fe Alloys. Sections at constant nickel and iron contents.

The 8 and 9% aluminium alloys consist of polygonal  $\alpha$  in  $\beta$  at 1000° C. until the iron content reaches about 5½%, when a small amount of  $\kappa$  is also present. On quenching from 1000° C., however, the  $\beta$  largely decomposes and secondary  $\alpha$  is precipitated both as a grain-boundary film and within the grains in the typical needle-like forms of the Widmannstätten pattern illustrated in Figs. 4, 6, and 8 (Plate LXIII). Below 900° C., 8% aluminium alloys consist exclusively of  $\alpha$  and  $\kappa$  (Fig. 5, Plate LXIII), irrespective of the nickel content. Similarly, the 9% alloys consist of  $\alpha$  and  $\kappa$  below 800° C., but a region of  $\alpha$ ,  $\beta$ , and  $\kappa$  (Fig. 7, Plate LXIII) exists between 1000° and 800° C., the extent of the three-phase region varying with the nickel and iron contents. The  $\kappa$  phase is precipitated from  $\beta$  in a characteristic form of rosettes or small spheres.

Over the range 8–10% aluminium also, the  $\beta$  content increases progressively, the 10% alloy consisting mainly of  $\beta$  at 1000° C. (Fig. 9, Plate LXIII), and on quenching a higher proportion of the  $\beta$  is retained undecomposed than in alloys containing less aluminium,  $\alpha$  being precipitated at the grain boundaries only. At 900° and 800° C., the 10% alloys consist of  $\kappa$  and Widmannstätten  $\alpha$  in  $\beta$  (Fig. 11, Plate LXIII) and at 700° C. and below of  $\alpha$  and  $\kappa$  (Fig. 12, Plate LXIII). At constant aluminium content, the proportion of  $\beta$  at 900° and 800° C. decreases, and the proportion of  $\kappa$  at 500° C. increases, with increasing nickel

content. At low concentrations of iron and nickel,  $\delta$  is formed below 600° C. by a three-phase-four-phase three-phase reaction, leaving  $\alpha$ ,  $\kappa$ , and  $\delta$ .

Alloys containing 11–12% aluminium, quenched from 1000° C., consist entirely of  $\beta$ , and there is no evidence of decomposition into  $\alpha$ , although the martensitic transformation occurs (Fig. 13, Plate LXIII). Except those of highest nickel and iron content, alloys quenched between 900° and 800° C. consist of  $\kappa$  in a matrix of acicular  $\beta$  (Fig. 14, Plate LXIII); at still lower temperatures  $\alpha$  also precipitates in Widmannstätten form, the structures consisting of  $\beta$ ,  $\alpha$ , and  $\kappa$  (Fig. 15, Plate LXIV). When the 12% aluminium alloys are quenched from between 700° and 600° C.,  $\alpha$  and  $\kappa$  are precipitated together in eutectoid form (Fig. 16, Plate LXIV). Finally, the residual  $\beta$  changes into  $\delta$ , and the structure after quenching from 500° C. is as shown in Fig. 18 (Plate LXIV). Fig. 17 (Plate LXIV) illustrates the structure in the four-phase zone ( $\alpha$ ,  $\beta$ ,  $\kappa$ , and  $\delta$ ) obtained in this instance by quenching from 590° C. The proportion of  $\delta$  present increases with decrease of nickel and increase of aluminium. At constant aluminium content, the proportion of  $\beta$  present at 700° C. increases, and the proportion of  $\kappa$  at 500° C. decreases, as the nickel content decreases.

Reverting to the behaviour of the alloys on quenching from 1000° C., the critical cooling rate for suppression of the  $\beta$  decomposition decreases with increasing aluminium content, that for 11 and 12% alloys being exceeded under the standard quenching conditions employed, whereas that for alloys of lower aluminium content was not attained. Thus the 8 and 9% aluminium alloys precipitate  $\alpha$  at grain boundaries and in a Widmannstätten pattern, whilst the 10% alloy precipitates  $\alpha$  at grain boundaries only. Increasing the severity of the quench reduces the amount of  $\beta$  decomposition in 8, 9, and 10% aluminium alloys. The martensitic transformation, however, is not influenced by the quenching rate, and in no circumstances was it found possible to suppress this change.

On the basis of the structural observations described above and illustrated in Figs. 1 and 2, the alloys can be grouped into three classes: (1) alloys containing 8 and 9% aluminium, consisting of  $\alpha + \beta$  at 1000° C. and changing to  $\alpha + \kappa$  at lower temperatures; (2) alloys containing 10% aluminium, consisting of  $\beta$  at 1000° C.,  $\alpha + \beta + \kappa$  at 800°–900° C., and  $\alpha + \kappa$  at lower temperatures; (3) alloys with 11 and 12% aluminium consisting of  $\beta$  at 1000° C. and changing through  $\beta + \kappa$  to  $\alpha + \beta + \kappa$  over the range 800°–600° C. and at lower temperatures to  $\alpha + \kappa + \delta$ .

## 2. STRUCTURES AFTER QUENCHING AND TEMPERING

To determine the structural changes occurring on tempering, the alloys listed in Table I were quenched from 1000° C. and tempered for  $\frac{1}{16}$ ,  $\frac{1}{8}$ ,  $\frac{1}{4}$ , . . . 256 hr. at 300°, 400°, 500°, 550°, 600°, 700°, 800°, and 900° C. All microstructures produced by quenching and tempering were examined and can



be exemplified by reference to the structural changes in three alloys only, namely, the 8/5/5, 10/5/5, and 12/5/5 alloys, which are representative of the three main groups noted in Section II, 1.

The 8/5/5 alloy consists of  $\alpha$  and partially decomposed  $\beta$  as quenched, and on tempering at all temperatures the  $\beta$  completely decomposes to small particles of  $\kappa$  in  $\alpha$ , whilst further precipitation of  $\kappa$  as fine plates takes place in the  $\alpha$  areas (Figs. 19 and 20, Plate LXIV).

As quenched, the 10/5/5 alloy consists of acicular  $\beta$  from which, on tempering at 900° C., plates of  $\alpha$  and fine, rounded particles of  $\kappa$  precipitate (Fig. 21, Plate LXIV). At 800° C. fine plates of  $\kappa$  in  $\alpha$  occur, with some small areas of residual  $\beta$  (Fig. 22, Plate LXIV).

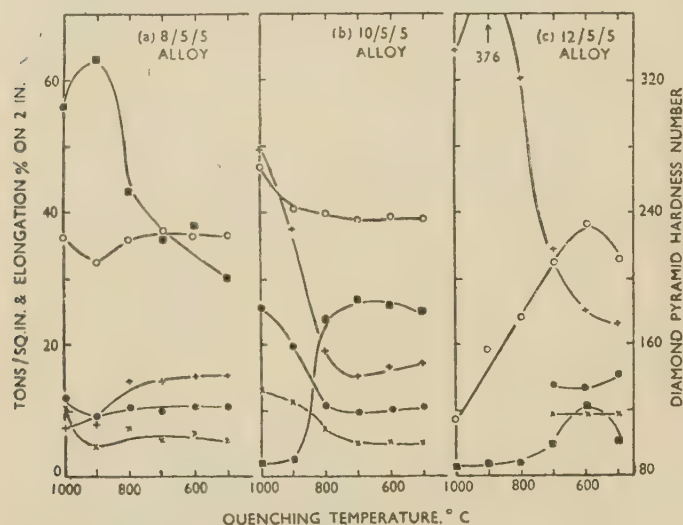


FIG. 51.—Mechanical Properties of Cu-Al-Ni-Fe Alloys after Slow Cooling from 1000° C. to Various Temperatures and Quenching.

KEY TO FIGS. 51-54.

×---× Limit of proportionality.  
●—● 0.1% Proof stress.  
○—○ Ultimate tensile strength.  
□—□ Elongation % on 1 in.

decomposes to  $\alpha + \kappa$  or  $\alpha + \kappa + \delta$ , although decomposition is not always complete. At low tempering temperatures,  $\kappa$  is more readily precipitated from  $\beta$  than from  $\alpha$  and tends to be spheroidal in character, in contrast with the plate-like formation it assumes on precipitation from  $\alpha$ .

### 3. MECHANICAL PROPERTIES OF QUENCHED AND TEMPERED ALLOYS

#### (a) Quenched Alloys

The mechanical properties of all the alloys detailed in Table I were determined on 0.1-in.-thick hot-rolled strip after various heat-treatments, and were related to the microstructures. In general, differences

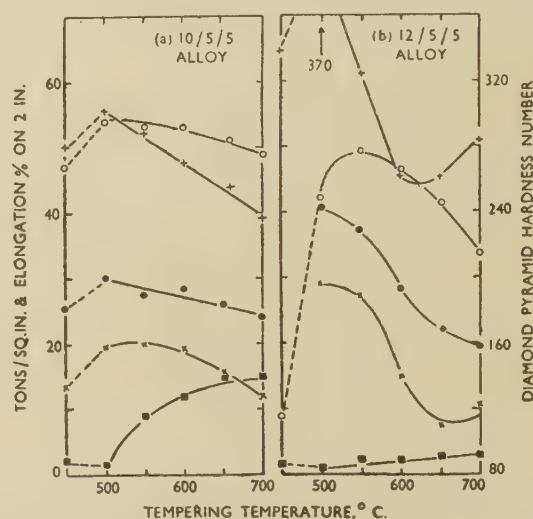


FIG. 52.—Mechanical Properties of Cu-Al-Ni-Fe Alloys Tempered for 2 Hr. at Various Temperatures.

When the alloys are tempered at 700° C. or below, the structures are very fine and difficult to interpret, but it appears that  $\kappa$  is readily precipitated from  $\beta$  in fine spheroidal form whereas formation of  $\alpha$  is slower, proceeding mainly by growth from the grain boundaries. When precipitation is complete, the structure consists of fine, rounded particles of  $\kappa$  in an  $\alpha$  matrix (Fig. 23, Plate LXIV).

On tempering the 12/5/5 alloy at 900° or 800° C., rosettes of  $\kappa$  are formed in the acicular  $\beta$  present in the quenched condition. Tempering at 700° or 600° C. causes  $\beta$  to break down to fine  $\kappa$  in an  $\alpha$  matrix (Figs. 24 and 25, Plate LXIV), and at still lower temperatures  $\alpha$ ,  $\kappa$ , and  $\delta$  are formed. As in the 10/5/5 alloy, decomposition of  $\beta$  below 600° C. proceeds mainly by growth of  $\alpha$  from the grain boundaries (Fig. 26, Plate LXIV),  $\delta$  being precipitated in fine irregular particles.

On tempering,  $\kappa$  is generally precipitated from the  $\alpha$  areas in the form of fine plates, and acicular  $\beta$

in properties which resulted from varying the nickel and iron contents were not marked, and the effect of heat-treatment on the properties of these complex alloys is illustrated by reference to the 8/5/5, 10/5/5, and 12/5/5 alloys numbered 3, 13, and 23, respectively, in Table I, which are typical of the three structural groups. These alloys, after re-heating to 1000° C., were slowly cooled to lower temperatures and quenched as indicated in Section II, 1. The mechanical properties of the alloys after the various heat-treatments are illustrated in Fig. 51, and since no significant changes took place when the final quenching temperature was below 500° C., data for these low temperatures are not included.

As quenched from 1000° C., the 8/5/5 alloy consists of  $\alpha$  and partially decomposed  $\beta$ . No  $\beta$  is present on quenching from 900° C., and so the ductility is slightly increased and the limit of proportionality and proof stress decreased. As the quenching temperature is further reduced, there is little change in the properties,

except for a decrease in elongation and an increase in hardness due to increasing precipitation of  $\kappa$ . The proof stress and ultimate tensile strength remain approximately constant at 10 and 35 tons/in.<sup>2</sup>, respectively (Fig. 51 (a)).

The 10/5/5 alloy, like all those containing 10% aluminium, is very sensitive to minor variations in the rate of quenching from 1000° C., but under the

The 12/5/5 alloy is brittle after quenching from temperatures between 1000° and 900° C., but the ductility is improved by quenching from lower temperatures, and the elongation reaches a maximum value of 12% after quenching from 600° C. Further lowering of the quenching temperature again decreases the ductility, as a result of the formation of the brittle  $\delta$  phase. The tensile strength of the alloy

TABLE II.—Diamond Pyramid Hardness Numbers after Quenching from 1000° C. and Tempering.

Heat-Treat- ment Temp., °C.	Hardness as Quenched from 1000°C.	Tempering Time, hr.												
		$\frac{1}{16}$	$\frac{1}{8}$	$\frac{1}{4}$	$\frac{1}{2}$	1	2	4	8	16	32	64	128	256
8/5/5 Alloy (No. 3, Table I)														
300	112	112	110	110	112	115	120	119	113	112	111	116	...	...
400	112	112	114	110	114	116	112	113	121	131	118	120	126	...
500	112	114	116	118	123	123	124	128	144	152	176	238	233	236
550	112	120	120	124	124	130	136	146	161	198	207	202	...	...
600	112	125	128	130	128	135	147	164	184	191	187	...	...	...
700	112	128	155	157	167	173	186	177	...	...	...	...	...	...
800	112	167	169	180	174	174	...	...	...	...	...	...	...	...
900	112	139	135	132	130	123	...	...	...	...	...	...	...	...
10/5/5 Alloy (No. 13, Table I)														
300	283	400	418	418	422	411	413	412	412	413	415	...	...	...
400	283	425	425	425	422	421	420	420	418	418	409	400	379	323
500	283	411	420	415	393	329	308	300	...	...	...	...	...	...
550	283	337	320	308	308	...	...	...	...	...	...	...	...	...
600	283	301	295	289	287	...	...	...	...	...	...	...	...	...
700	283	272	265	247	242	...	...	...	...	...	...	...	...	...
800	283	242	238	221	209	...	...	...	...	...	...	...	...	...
900	283	262	262	264	268	...	...	...	...	...	...	...	...	...
12/5/5 Alloy (No. 23, Table I)														
300	334	374	370	377	393	388	384	391	404	400	402	398	...	...
400	334	398	394	394	402	404	406	402	398	397	404	400	320	...
500	334	383	400	401	406	329	317	312	308	302	298	295	290	281
550	334	375	377	301	275	278	272	266	257	260	257	253	...	...
600	334	285	276	270	260	258	262	256	255	245	243	...	...	...
700	334	277	269	269	258	258	258	255	...	...	...	...	...	...
800	334	314	312	309	307	305	...	...	...	...	...	...	...	...
900	334	326	308	315	311	309	...	...	...	...	...	...	...	...

TABLE III.—Effect of Heat-Treatment on Mechanical Properties of 8/5/5 Alloy (No. 3, Table I).

Quenching Treatment		Reheating Treatment		Limit of Proportionality, tons/in. <sup>2</sup>	0.1% Proof Stress, tons/in. <sup>2</sup>	Ultimate Tensile Strength, tons/in. <sup>2</sup>	Elongation % on 2 in.	D.P. Hardness (30 kg.)
Temp., °C.	Time, hr.	Temp., °C.	Time, hr.					
1000	$\frac{1}{2}$	—	—	10.1	12.0	35.9	56	112
1000	$\frac{1}{2}$	500	64	8.5	22.4	46.7	13	238
1000	$\frac{1}{2}$	700	2	11.9	16.6	39.1	23.5	186

standard quenching conditions it consists mainly of  $\beta$  and the diamond pyramid hardness value is some 280 (Fig. 51 (b)). By slow cooling before quenching,  $\alpha$  and  $\kappa$  precipitate from  $\beta$ , resulting in a sharp drop in the hardness value with initial progressive lowering of the ultimate tensile strength to about 38 tons/in.<sup>2</sup> after quenching from 700° C., a value which is maintained with lower quenching temperatures and is associated with limits of proportionality and proof stresses of approximately 5 and 10 tons/in.<sup>2</sup>, respectively. The elongation value increases from 2% as quenched from 1000° C. to 25% as quenched from 700° C.

was at a maximum of some 38 tons/in.<sup>2</sup> after quenching from 600° C. (Fig. 51 (c)).

#### (b) Tempered Alloys

Tempering experiments were carried out on the same series of twenty-five alloys after quenching from 1000° C., so that all consisted as far as possible of  $\beta$  or  $\alpha + \beta$ . Details of the mechanical properties are given in graph form in Fig. 52 for two of the more interesting alloys.

The 8/5/5 alloy, on tempering at 300°–400° C. after quenching from 1000° C., does not show any marked hardening, since  $\beta$  has already decomposed



during quenching. The slight hardening taking place at these low temperatures is due to precipitation of  $\kappa$ , and thus as the temperature is increased and more  $\kappa$  is precipitated, the hardness increment becomes greater. The optimum tempering temperature is 500° C., and after 64 hours' tempering the diamond pyramid hardness value is 238 (Table II), associated with increases in both tensile strength and proof stress, but a decrease in the ductility (Table III). As the tempering temperature is raised above 500° C., the maximum hardness attained becomes progressively lower, and the optimum time of tempering also decreases, so that on tempering at 700° C. a maximum hardness value of 186 is reached in 2 hr. (Tables II and III).

The hardness of the 10/5/5 alloy after quenching from 1000° C. increases with tempering temperatures between 300° and 500° C., maximum hardness rapidly being attained and thereafter tending to decrease with increased tempering time. Hardness changes on tempering at 400° C., for example, are accompanied by rapid increases in the limit of propor-

existing after quenching the 10/5/5 alloy or the 12/5/5 alloy from 1000° C. is similar (see Fig. 52).

Comparison of the 10/5/5 alloy, quenched from 900° C., with the 8/5/5 alloy, quenched from 1000° C., is of special interest. After these treatments both are structurally similar, consisting mainly of  $\alpha + \beta$ . As already noted, however, the  $\beta$  phase in the 8/5/5 alloy quenched from 1000° C. has already partially decomposed and therefore on tempering at 400° C. does not show the marked improvement in mechanical properties which occurs in the 10/5/5 alloy without any visual changes in microstructure (Tables II and IV).

The results so far discussed indicate that, in general, alloys containing  $\beta$  or  $\delta$  are lower in strength and ductility than those which consist solely of  $\alpha$  or  $\kappa$ . The distribution of  $\alpha$  and  $\kappa$  has a marked influence on the mechanical properties, and with alloys containing 10% aluminium, where fine spheroidal  $\kappa$  is formed in  $\alpha$  by decomposition of  $\beta$ , the proof stress and tensile strength are higher than those of 8 and 9% aluminium alloys, where acicular  $\kappa$  in  $\alpha$  is formed

TABLE IV.—Effect of Heat-Treatment on Mechanical Properties of 10/5/5 Alloy (No. 13, Table I).

Quenching Treatment		Reheating Treatment		Limit of Proportionality, tons/in. <sup>2</sup>	0.1% Proof Stress, tons/in. <sup>2</sup>	Ultimate Tensile Strength, tons/in. <sup>2</sup>	Elongation % on 2 in.	D.P. Hardness (30 kg.)
Temp., °C.	Time, hr.	Temp., °C.	Time, hr.					
1000	1	...	...	12.9	25.6	51.5	2	287
1000	1	400	1	32.6	50.1	55.3	1	421
1000	1	600	1	23.2	33.8	53.3	7	287
1000	1	800	1	11.4	19.65	50.0	9	221
1000	1	900	1	14.4	22.7	43.2	3	268
900	1	...	...	14.0	23.0	43.8	3	268
900	1	400	1	12.7	30.5	52.2	1	317
900	1	550	16	18.6	28.9	51.6	7	253

tionality and proof stress (Table IV), but there are no visible changes in the microstructure. As the tempering temperature is increased, the limit of proportionality, proof stress, tensile strength, and hardness decrease and reach a minimum after treatment at 800° C. (Table IV), the subsequent increase on tempering at 900° C. being due to the formation of  $\beta$ . The mechanical properties of the 10/5/5 alloy quenched from 1000° C. and subsequently tempered for 2 hr. at 500°–700° C. are shown in Fig. 52 (a).

Hardness changes on tempering the 12/5/5 alloy (Table II) are generally similar to those in the 10/5/5 alloy, the greatest hardness increments resulting from low tempering temperatures. Details of the effect of reheating the quenched alloy for 2 hr. at 500°–700° C. are illustrated in Fig. 52 (b). The tensile strength is a maximum at 49 tons/in.<sup>2</sup> after tempering at 550° C., and an increase in the tempering temperature causes the strength to fall progressively owing to the re-formation of  $\beta$ , the proof stress and limit of proportionality falling in a similar manner. The elongation of the 12/5/5 alloy as quenched is only some 2%, and on tempering it increases slightly with the temperature. In general, therefore, the effect of tempering the  $\beta$ -phase complex

from supersaturated  $\alpha$ . Alloys containing 11% aluminium or more are lacking in ductility (cf. Figs. 51 (c) and 52 (b)), as a result of the presence of either  $\beta$  or  $\delta$ , depending on the heat-treatment.

### III.—STRUCTURE AND PROPERTIES OF ROLLED PLATE

In the light of results obtained in the work described in Section II, some alloys in the most promising range of composition, namely, 5–6% each of nickel and iron with 8.5–10.5% aluminium, were prepared on a larger scale for further observation. This study was confined to a consideration of the structural features and mechanical properties of material in the conditions obtained in normal industrial operations of hot and cold rolling, &c., and no attempt was made to establish equilibrium conditions.

#### 1. STRUCTURES AND PROPERTIES IN THE HOT-ROLLED CONDITION

The compositions of the alloys studied are given in Table V. Five of them were cast in the form of 100-lb. ingots of 1½ in. thickness and the sixth as

an 18-cwt. cake of  $6\frac{3}{4}$  in. thickness. The 100-lb. ingots were preheated to 975° C. and hot rolled in five passes to  $1\frac{9}{16}$  in. thick. The hot rolling of the

TABLE V.—Chemical Analyses of Ingots for Hot Rolling.\*

Al, %	Ni, %	Fe, %	Cu, %
8.61	5.21	5.71	80.43
9.22	5.79	5.43	79.51
9.61	5.56	5.57	79.22
10.09	5.47	5.20	79.19
10.00	5.11	4.84	79.85 †
10.71	5.30	6.10	77.84

\* Spectrographic analysis showed:

Zn . . .	Nil	Ag . . .	0.003%
Sn . . .	<0.01%	Bi . . .	<0.001%
Pb . . .	<0.01%	As . . .	0.005%
Mn . . .	0.01-0.02%	Si . . .	0.02%

† 18-cwt. casting, hot rolled as detailed in Table VI.

TABLE VI.—Hot-Rolling Programme for 10/5/5 Alloy († in Table V).

Material
Machined flat-cast 18-cwt. cake approx. 3 ft. × 2 ft. 3 in. × $6\frac{3}{4}$ in.
Hot Rolling
Heated to 975° C. and rolled from $6\frac{3}{4}$ to 6 in.
Turned through 90°, reheated to 975° C., and rolled to $4\frac{1}{2}$ in.
Reheated to 975° C. and rolled to $1\frac{3}{4}$ in.; turned through 90° at $2\frac{1}{2}$ in.
Reheated to 975° C. and rolled to 1 in.
(a) Reheated to 975° C. and rolled from 1 to $\frac{9}{16}$ in.
(i) Reheated to 925° C. and rolled from $\frac{9}{16}$ to $\frac{5}{16}$ in.
(ii) Reheated to 925° C. and rolled from $\frac{5}{16}$ to $\frac{3}{16}$ in.
(iii) Reheated to 925° C. and rolled from $\frac{3}{16}$ to $\frac{1}{8}$ in.
(iv) Reheated to 800° C. and rolled from $\frac{3}{16}$ to $\frac{1}{16}$ in.
(b) Reheated to 800° C. and rolled from 1 to $\frac{13}{16}$ in.
(i) Reheated to 900° C. and rolled from $\frac{13}{16}$ to $\frac{1}{2}$ in.

18-cwt. cake was begun at the same temperature and continued with reheatings as necessary, the complete sequence of operations being shown in Table VI. All the ingots cooled appreciably during the hot

rolling, the extent of cooling varying with the pre-heating temperature and the plate thickness. The effect of these two factors has been investigated by preparing plate from the 18-cwt. cake reheated to either 800° or 925° C. and rolling to different thicknesses as indicated in Table VI.

As hot rolled, the alloy containing 8.61% aluminium consists mainly of  $\alpha$  with a few bands of fine  $\kappa$  and large rosettes of  $\kappa$  which are probably formed either in the cooling of the original casting or in an early stage of the rolling process. In the three alloys containing 9.22, 9.61, and 10.09% aluminium, the matrix consists of fine  $\kappa$  and  $\alpha$  with areas of distorted  $\alpha$  and the  $\kappa$  rosettes already referred to (Fig. 27, Plate LXV), while in the 10.71% aluminium alloy the structure is similar, though the areas of  $\alpha$  are absent. The finely distributed  $\kappa$  in these alloys results from decomposition of  $\beta$  during cooling from 975° C. to room temperature, and considerable precipitation of  $\alpha$  from  $\beta$  takes place in the alloys containing 10.0% aluminium or less during the earlier stages of rolling.

The mechanical properties of alloys with 8.5–10.5% aluminium are detailed in Table VII for plate (a) as rolled, (b) rolled and annealed 2 hr. at 650° C., and (c) rolled, quenched from 1000° C., and tempered 2 hr. at 650° C. In all three conditions the limit of proportionality, proof stress, tensile strength, and hardness increase with the aluminium content, and the elongation values generally decrease. The effect on the mechanical properties of annealing or annealing and quenching under the defined conditions varies from alloy to alloy, but in no instance is there any very marked change. These observations on the structure and properties of hot-rolled plate indicate that alloys containing 9.2–10.7% aluminium and about 5% each of nickel and iron possess substantially similar properties and have the most attractive combination of properties. A more detailed study of the effect of rolling temperature and subsequent annealing on hot-rolled 10/5/5 plate was therefore, made.

Reheating the 10/5/5 alloy to above 950° C., at

TABLE VII.—Mechanical Properties of Hot-Rolled Plate.

Condition	Al, %	Limit of Proportionality, tons/in. <sup>2</sup>	0.1% Proof Stress, tons/in. <sup>2</sup>	Ultimate Tensile Strength, tons/in. <sup>2</sup>	Elongation % on $4\sqrt{A}$	D.P. Hardness (30 kg.)	Izod Value, ft.-lb.
(a) Hot rolled from $1\frac{3}{8}$ to $\frac{9}{16}$ in. thick, beginning at 975° C.	8.61	17.4	23.9	44.1	18	210	8
	9.22	19.7	27.6	50.6	20	222	9
	9.61	18.3	26.4	48.4	13	230	8½
	10.09	20.6	29.5	49.3	12	240	7
	10.71	23.8	30.9	53.5	10	254	5½
(b) Hot rolled and annealed 2 hr. at 650° C.	8.61	18.5	28.6	46.0	20	231	9
	9.22	18.6	30.4	51.2	18	256	5
	9.61	16.8	28.2	49.8	17	257	6
	10.09	18.9	31.2	51.9	17	250	5½
	10.71	17.0	29.7	51.2	18	263	7
(c) Quenched from 1000° C. and tempered 2 hr. at 650° C.	8.61	11.2	22.7	46.4	20	191	12
	9.22	16.1	23.1	48.5	21	223	13
	9.61	17.9	26.5	49.2	16	249	11
	10.09	16.3	28.1	51.2	16	254	8
	10.71	19.8	34.3	54.4	14	265	4



which temperature  $\beta$  only is present, and re-rolling does not alter the structure significantly, both small and large particles of  $\kappa$  being present in the  $\alpha$ . The mechanical properties are also substantially unchanged as evidenced by the values quoted for the 1-in.- and  $\frac{9}{16}$ -in.-thick re-rolled plates in Table VIII. On the other hand, when the reheating temperature is below 950° C., the effect of subsequent rolling reductions tends to be cumulative, producing fine striations of  $\alpha$  in decomposed  $\beta$ . These structural differences produced by rolling can be seen by comparing the structure of plate hot-rolled from a casting (Fig. 27, Plate LXV) with that of plate at thicknesses of  $\frac{1}{8}$ ,  $\frac{3}{16}$ ,  $\frac{9}{16}$ , and 1 in. (Figs. 28–31, Plate LXV), fabricated as detailed in Table VI and in the captions. With thinner plate, in addition to the effect of increased total reduction, the greater chill and also the higher aluminium content of the  $\beta$  present at the lower reheating temperature reduces the tendency to precipitation of  $\alpha$  in the earlier stages of rolling and

re-rolling at 800° C. are similar to those of plate hot rolled at 975° or 900° C., as indicated by comparison of the values quoted in the upper portion of Table VIII.

## 2. ANNEALING OF HOT-ROLLED PLATE

The foregoing examples show the very considerable dependence of properties in the hot-rolled condition on differences in structure which are associated not only with composition but also with the thermal changes taking place during the sequence of rolling operations. The major factors that influence structure in the hot-rolled condition are the thickness of the plate, which affects the rate of cooling, and the original hot-rolling temperature. Further, thermal treatment of hot-rolled material results both in structural changes and in softening or annealing after recrystallization, but these cannot be fully illustrated by a single example. They are shown in Fig. 53, in which annealing curves are plotted for

TABLE VIII.—*Mechanical Properties of Hot-Rolled Plate of 10/5/5 Alloy († in Table V).*

Final Hot-Rolling Details			Limit of Proportionality, tons/in. <sup>2</sup>	0.1% Proof Stress, tons/in. <sup>2</sup>	Ultimate Tensile Strength, tons/in. <sup>2</sup>	Elongation % on		D.P. Hardness (30 kg.)	Izod Value, ft.-lb.
Initial Thickness, in.	Reheating Temp., °C.	Final Thickness, in.				1 in.	2 in.		
$1\frac{3}{4}$	975	1	22.7	31.0	51.4	...	20 *	226	12
1	975	$\frac{9}{16}$	24.9	32.0	52.7	18 *	...	247	8
$\frac{19}{32}$	900	$\frac{1}{2}$	22.1	32.2	52.5	18 *	...	234	...
1	800	$\frac{19}{32}$	24.2	31.0	51.1	17 *	...	239	$9\frac{1}{2}$
$\frac{5}{16}$	925	$\frac{3}{16}$	30.5	43.0	58.0	7	6	287	...
$\frac{3}{16}$	925	$\frac{1}{8}$	34.2	44.8	57.9	11	8	266	...
$\frac{9}{16}$	800	$\frac{13}{64}$	33.4	49.9	60.5	2	1	325	...

\* Round test-piece with  $4\sqrt{A}$  gauge-length.

also the extent to which  $\beta$  decomposes on cooling to room temperature. Thus, whereas  $\beta$  in the 1-in.- and  $\frac{9}{16}$ -in.-thick plate has almost completely decomposed to  $\alpha$  and  $\kappa$  on cooling, that in the  $\frac{3}{16}$ -in.- and  $\frac{1}{8}$ -in.-thick plate has precipitated some  $\kappa$  but is still essentially  $\beta$ , the differences being illustrated in Figs. 32 and 33 (Plate LXV). Partial retention of  $\beta$  results in higher strength in thin plate than in thick plate, as indicated by the properties quoted in Table VIII.

When reheated to temperatures at which small proportions only of  $\beta$  are present, this phase is heavily distorted during rolling (Fig. 34, Plate LXV), and the matrix of the material is structurally similar to that of material reheated to temperatures within the  $\alpha + \kappa$  field and then rolled, consisting of fine particles of  $\kappa$ , formed during reheating, in an  $\alpha$  matrix. Strain-hardening of the  $\alpha$  which occurs under these rolling conditions causes a considerable increase in strength, as illustrated by the properties given in Table VIII for  $\frac{13}{64}$ -in.-thick plate rolled from  $\frac{9}{16}$  in. thick, reheated to 800° C. for rolling.

On the other hand, provided the plate thickness is  $\frac{1}{2}$  in. or more, the mechanical properties after

two thicknesses of plate rolled from high and low preheating temperatures. All these data were obtained on material from a single plate of 10/5/5 alloy at different stages in the rolling sequence, as indicated in Table VI, and therefore the differences in properties are associated entirely with structural differences and not with variations in composition.

In  $\frac{3}{16}$ -in.-thick plate, hot rolled from the higher preheating temperature of 925° C., annealing at 400° or 450° C. does not affect the structure of  $\alpha$ , but  $\beta$  breaks down into fine particles of  $\kappa$  in  $\alpha$ , resulting in a marked fall in the limit of proportionality and proof stress (Fig. 53 (a)). Annealing at 500° C. precipitates  $\kappa$  from  $\alpha$ , and the amount increases as the annealing temperature is raised, resolvable particles of  $\kappa$  being identifiable when the annealing temperature is 600° C. (Figs. 35 and 36, Plate LXV). As the annealing temperature is further increased, the  $\kappa$  particles increase in size (Fig. 37, Plate LXV), and at 750° C. the microstructure consists of fine particles of  $\kappa$  evenly disseminated in the  $\alpha$  matrix (Fig. 38, Plate LXV). Small proportions of  $\beta$  are formed on annealing at 800° C. and the  $\kappa$  is spheroidized (Fig. 39, Plate LXVI). The proportion of  $\beta$  and the size of the polygonal

$\alpha$  and  $\beta$  grains increase with temperature (Figs. 40 and 41, Plate LXVI) until at 1000° C. the structure consists wholly of coarse grains of  $\beta$ . The effect of these various annealing treatments on the mechanical properties of the alloy is indicated in Fig. 53 (a).

When the reheating temperature between rolling operations is sufficiently high to absorb all the  $\alpha$ , the size of the  $\kappa$  particles formed on subsequent annealing at any given temperature is determined by the magnitude of the rolling reduction, being greatest for the heaviest reductions (Fig. 43, Plate LXVI). On the other hand, when the reheating temperature is low and therefore the amount of  $\beta$  present is small, there is a tendency for local concentrations of  $\kappa$  to form from  $\beta$  on annealing after rolling, and a heavy final hot-rolling reduction is necessary.

annealing at temperatures in excess of 500° C., owing to recrystallization of  $\alpha$ . The amount of  $\kappa$  precipitated from  $\alpha$  on annealing both thick and thin plates rolled at 800° C. is less than that in material rolled at a higher temperature, a slight irresolvable precipitate forming only in material annealed at 550° C. (Fig. 44, Plate LXVI). Annealing at higher temperatures results in a dissemination of fine  $\kappa$  similar to that present in material rolled at higher temperatures (Figs. 45 and 46, Plate LXVI).

Annealing the hot-rolled 10/5/5 alloy above 750° C. brings about the formation of  $\beta$ , and this is accompanied by a substantial falling off in ductility. Maximum ductility is obtained by annealing within the range 700°–750° C., in which strain-hardening is removed, and the structure consists mainly of  $\alpha$

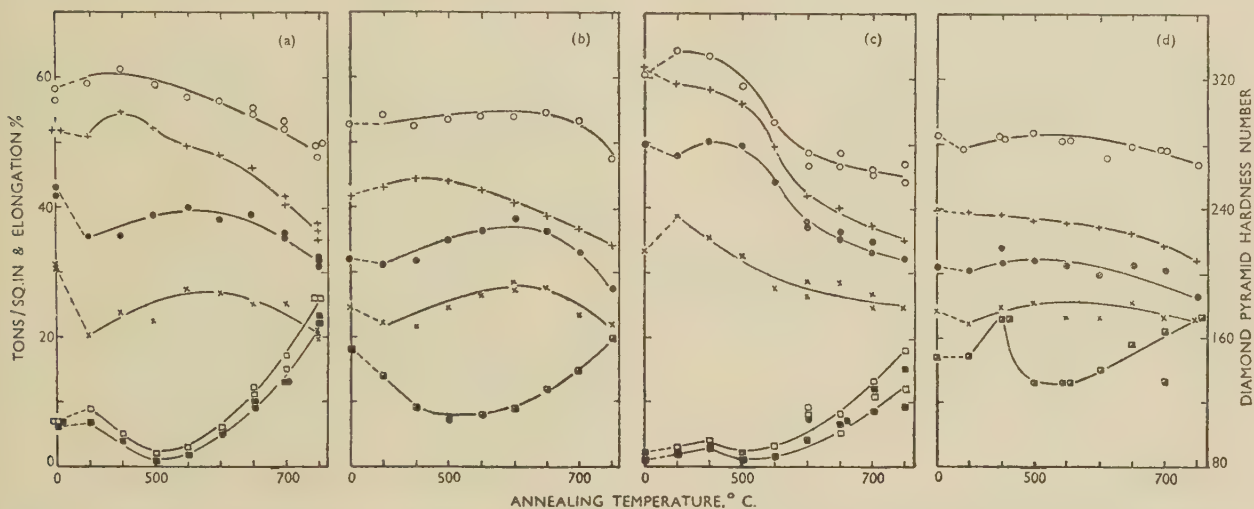


FIG. 53.—Effect of Annealing for 2 Hr. at Various Temperatures on the Mechanical Properties of 10/5/5 Alloy. For key see Fig. 51.

(a)  $\frac{3}{16}$  in. plate hot rolled from  $\frac{1}{8}$  in. thick at 925° C.  
(b)  $\frac{3}{16}$  in. „ „ „ 1 in. „ „ 975° C.

(c)  $\frac{13}{32}$  in. plate hot rolled from  $\frac{9}{16}$  in. thick at 800° C.  
(d)  $\frac{13}{32}$  in. „ „ „ 1 in. „ „ „

Annealing of thicker plate, e.g.  $\frac{9}{16}$  in. hot rolled from 1 in., from the higher preheating temperature of 975° C. (Fig. 53 (b)) results in much smaller changes in mechanical properties, and, in particular, there is a much smaller reduction in limit of proportionality, proof stress, and elongation.

Thick and thin plates rolled from the lower reheating temperature of 800° C. consist structurally of  $\kappa$  in  $\alpha$  with a small amount of partially decomposed  $\beta$ , and on annealing at 450° C. further decomposition of the  $\beta$  occurs with a corresponding increase in elongation (Figs. 53 (c) and (d)). At high annealing temperatures, the changes in properties of  $\frac{13}{32}$ -in.-thick plate rolled from 800° C. (Fig. 53 (d)) are similar to those occurring in the alloy rolled at 925° and 975° C. (Figs. 53 (a) and (b)). In the thinner,  $\frac{13}{64}$ -in.-plate there is, however, some evidence that the relief of strain-hardening is greater than in the other three plates, in which structural changes have the major influence. Thus, tensile strength, proof stress, limit of proportionality, and hardness all fall rapidly after

with relatively small particles of  $\kappa$ . Values for the tensile properties obtainable on material in this condition are: tensile strength 46–50 tons/in.<sup>2</sup>, limit of proportionality 20–25 tons/in.<sup>2</sup>, and elongation 13–20%, with a diamond pyramid hardness of 210–230.

Structures resulting from annealing followed by slow cooling have been investigated, and those which occur in the 10/5/5 alloy are of special interest. As already indicated, heating above 750° C. results in the formation of  $\beta$ , but on cooling to a lower temperature  $\beta$  again breaks down into  $\alpha$  and  $\kappa$ . On annealing at 800° C. and slowly cooling to 750° C.,  $\kappa$  particles are produced larger in size but less numerous than those formed by direct annealing at 750° C. (Fig. 42, Plate LXVI). As the annealing temperature is raised, the size of the  $\kappa$  particles is further increased, until annealing at 900° C., followed by slow cooling to 750° C., produces plates of  $\kappa$ , and treatment at 1000° C. results in the formation of structures similar to that illustrated in Fig. 12 (Plate LXIII).



The mechanical properties corresponding to these structures are indicated in Table IX. It will be noted that alloys quenched from 800° to 1000° C., in which  $\beta$  is present, have a high strength but low ductility and that by furnace-cooling the elongation

and reduces the number of  $\kappa$  particles. Plate so treated can be cold rolled with successive reductions of about 25% with intermediate annealing at 750° C., and the effect of cold rolling on the mechanical properties is illustrated in Fig. 54. The reason for

TABLE IX.—Effect of Quenching and Furnace Cooling on Mechanical Properties of Plate of 10/5/5 Alloy ( $\dagger$  in Table V) after Annealing at 800°–1000° C.

Heat-Treatment		Mode of Cooling	Limit of Proportionality, tons/in. <sup>2</sup>	0.1% Proof Stress, tons/in. <sup>2</sup>	Ultimate Tensile Strength, tons/in. <sup>2</sup>	Elongation % on 2 in.	D.P. Hardness (30 kg.)
Temp., °C.	Time, hr.						
800	1	Quenched in water	11.0	23.0	48.5	15	206
800	1	Furnace cooled	8.3	22.3	45.0	24	176
900	1	Quenched in water	9.1	16.2	43.1	3½	256
900	1	Furnace cooled	8.8	14.6	41.3	28	158
1000	1	Quenched in water	15.8	25.2	53.1	2	362
1000	1	Furnace cooled	7.5	11.9	38.1	26	153

values are substantially increased, although changes in the limit of proportionality, proof stress, and tensile strength are, in some instances, slight.

### 3. EFFECT OF COLD ROLLING ON MECHANICAL PROPERTIES

The effect of cold working on the mechanical properties of the alloys is exemplified by results obtained with the 10/5/5 alloy. Plate hot rolled to  $\frac{19}{32}$  in., as indicated in Table VI, and annealed at

the observed initial drop in the limit of proportionality produced by cold rolling is not yet known, but the shape of the stress/strain curve for annealed material shows a marked break at the limit, whereas that for the cold-worked material is in the form of a smooth curve, making precise location of the point of deviation from a straight line difficult.

### IV.—STRUCTURE AND PROPERTIES OF EXTRUDED ROD

For the investigation of the structure and properties of extruded rod, charges of 1500 lb. were melted in an oil-fired furnace, cast into 7-in.-dia. cast-iron moulds, and subsequently sawn into slugs 18 in. long. Extrusion was carried out on a 7-in.-dia. press to produce rod 1.5, 0.75, 0.5, and 0.29 in. in dia., using single-, two-, three-, and six-hole dies, respectively. The temperature was varied from 925° C. for the largest-diameter rod to 1025° C. for the smallest. After the usual discards had been made from the leading and rear ends of each extruded rod, samples 6 ft. in length were taken from the front and back ends and from the middle portions, and it was on these samples (designated front, back, and middle) that the structure and mechanical properties were determined. The compositions of the alloys are given in Table X.

In general, the structural characteristics of extruded alloys containing nominally 10–10.5% aluminium and 5.0–5.5% each of nickel and iron are similar to those observed in hot-rolled plate. The front end of a 10/5/5 alloy extruded rod, 0.29 in. in dia., for example, consists mainly of  $\beta$  at the extrusion temperature (1025° C.), and then as the material cools plates of  $\alpha$  are precipitated (Fig. 47, Plate LXVI). On the other hand, when the composition (10.5/5.5/5.5) and extrusion temperature (0.75 in. dia. extruded at 950° C.) are such that  $\alpha$  is present during extrusion, elongated particles of  $\alpha$  are formed at the front end (Fig. 48, Plate LXVI). When, at the extrusion temperature, alloys consist of striations of  $\alpha$  and  $\beta$ , the

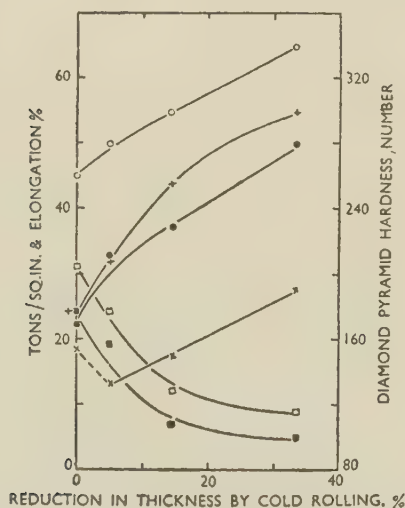


FIG. 54.—Mechanical Properties of 10/5/5 Alloy Plate Cold Rolled to Various Reductions, after Annealing at 825° C. and Slow Cooling to 750° C. For key see Fig. 51.

750° C. can be initially reduced in thickness by cold rolling to the extent of about 30% before edge cracking begins, but cracks develop on subsequent cold working after annealing at 750° C., since  $\alpha$  only partially recrystallizes. To obviate this difficulty, it is essential, before cold rolling, to anneal the hot-rolled stock at 825° C. and slowly cool it to 750° C.; as indicated earlier, this treatment increases the size

latter break down on cooling to  $\alpha$  and  $\kappa$ , as illustrated in Fig. 49 (Plate LXVI), which is typical of the structure existing in the middle portion. Back-end structures are always of fine  $\kappa$  in  $\alpha$ , as indicated in Fig. 50 (Plate LXVI).

The mechanical properties of the 10/5/5 alloy rod were found not to vary appreciably with the

TABLE X.—Composition of Extruded Rod.

Content, %	0.29 in. dia.	0.75 in. dia.
Copper . . . . .	79.56	78.15
Aluminium . . . . .	9.91	10.44
Nickel . . . . .	4.90	5.49
Iron . . . . .	5.33	5.69
Manganese . . . . .	0.17	0.19
Tin . . . . .	0.01	Trace
Lead . . . . .	0.01	0.01
Arsenic . . . . .	0.01	Nil

diameter, apart from an increase in the elongation value from 10 to 15% as the diameter increases from 0.29 to 0.75 in. (Fig. 55). The limit of proportionality and 0.1% proof stress of the back ends of extruded rods are 28 and 33 tons/in.<sup>2</sup>, respectively, as compared with values of 18 and 24 tons/in.<sup>2</sup>, respectively, for the front end and middle of the rods, except in the case of the 0.33-in.-dia. rod.

Annealing extruded rod at 750° C. and cooling in air causes complete decomposition of any  $\beta$  remaining, the middle and back-end portions then consisting

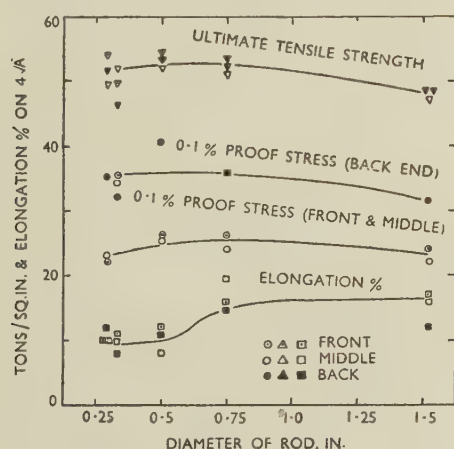


FIG. 55.—Effect of Size of Extruded Rod on Mechanical Properties of 10/5/5 Alloy.

of fine rounded  $\kappa$  particles in  $\alpha$ , and the front end containing finer  $\kappa$  particles, some plates of  $\kappa$ , and occasional  $\alpha$ -rich areas. Annealing between 800° and 850° C., followed by slow cooling to 750° C., and finally air cooling produces a structure of finely

rounded  $\kappa$  in an  $\alpha$  matrix, whilst annealing above 850° C. results in the formation of plates of  $\kappa$ .

The mechanical properties of extruded rod of the 10/5/5 alloy after annealing are illustrated in Fig. 56. Both tensile strength and proof stress generally diminish as the annealing temperature is increased. Differences in proof stress and limit of proportionality along the length (Figs. 55 and 56) are not eliminated by annealing below 1000° C., although the microstructures of the front, middle, and back end of the rod produced by heating below 1000° C. are identical. By annealing at 1000° C., however, when all the  $\alpha$  is taken into solution, uniformity of properties is

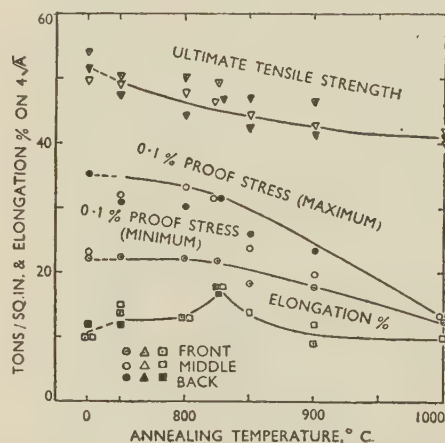


FIG. 56.—Effect of Annealing on Mechanical Properties of 0.29-in.-dia. 10/5/5 Alloy Rod, Subsequently Slowly Cooled from Annealing Temperature to 750° C.

obtained along the entire length. Maximum elongation values are obtained by annealing at 825° C., followed by slow cooling to 750° C., but even under these conditions the ductility is lower than that of hot-rolled plate. The lower elongation values of the extruded rod as compared with hot-rolled plate would appear to be due to marked preferred orientation of  $\alpha$  along the whole length of the rod, (111) and (100) fibre textures occurring approximately in equal proportions, as is not uncommon in extruded rods of other materials. These textures persist even after annealing at 1000° C. and slow cooling to 750° C., when the  $\alpha$  and  $\kappa$  are taken into solution and reprecipitated. Thus, although the microstructure of rod treated in this manner is identical with that of hot-rolled plate similarly treated, the ductility of the rod is less than that of the plate.

#### ACKNOWLEDGEMENT

The authors wish to record their thanks to several colleagues for much valuable help in connection with various aspects of the work described in this paper.





99.98% ALUMINIUM.



FIG. 1.—Stationary Back-Reflection Photograph of Fine-Grained Specimen Before Extension.



FIG. 2.—Fine-Grained Specimen After 13% Elongation at 250° C.



FIG. 3.—Microstructure After 13% Elongation at 250° C.  $\times 1000$ .

FIG. 4.—Same Area as Fig. 3, After Re-polishing and Etching.  $\times 100$ .



FIG. 5.—Stationary Back-Reflection Photograph of Fine-Grained Specimen Before Extension.

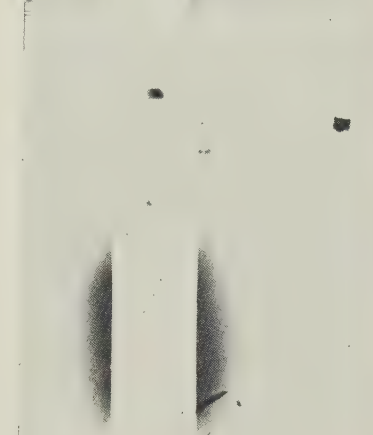


FIG. 6.—Same Area as Fig. 5, After 13% Elongation at 350° C.

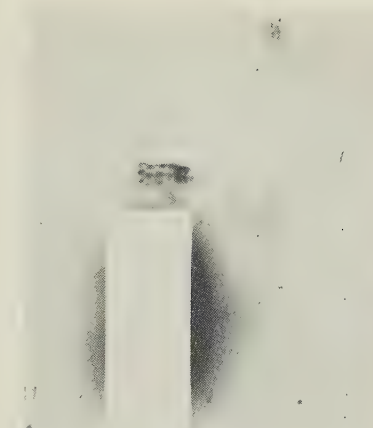


FIG. 7.—Oscillation Back-Reflection Photograph of Annealed Coarse-Grained (1-mm.) Specimen.

FIG. 8.—Oscillation Photograph of Same Area After 20% Elongation at 250° C.



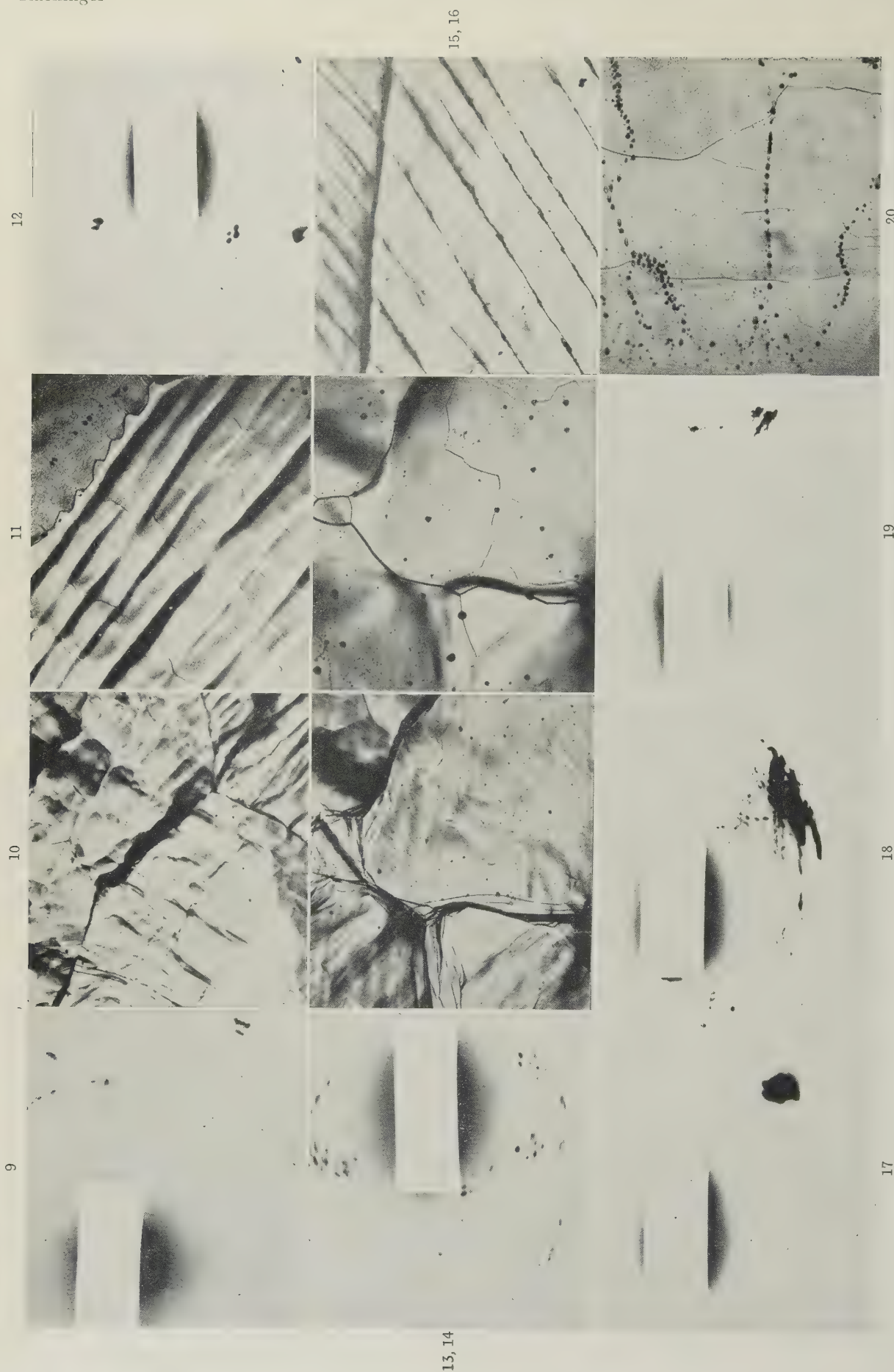


FIG. 9.—Stationary Photograph from Same Area as Fig. 8.

FIG. 10.—Typical Microstructure of Coarse-Grained Material After 20% Elongation at 250° C.  $\times 100$ .

FIG. 11.—Coarse-Grained Specimen After 20% Elongation at 250° C. and Repolishing and Etching.  $\times 100$ .

FIG. 12.—Initial Oscillation Photograph of Coarse-Grained (1-mm.) Specimen.

FIG. 13.—Oscillation Photograph of Same Area After 15% Elongation at 350° C.

FIG. 14.—Typical Microstructure After 15% Elongation at 350° C.  $\times 100$ .

FIG. 15.—Same Area as Fig. 14 After Repolishing and Etching.  $\times 100$ .

FIG. 16.—Typical Microstructure of a Bicrystal After 8% Elongation at 250° C.  $\times 100$ .

FIG. 17.—Oscillation Photograph from Central Grain of a Tricrystal. (See text.)

FIG. 18.—Oscillation Photograph from This Grain After 20% Overall Elongation at 350° C.

FIG. 19.—Oscillation Photograph from a Lightly Deformed End Grain of this Specimen After 20% Overall Extension at 350° C.

FIG. 20.—Typical Microstructure from the Heavily Deformed Central Grain After Repolishing and Etching.  $\times 100$ .



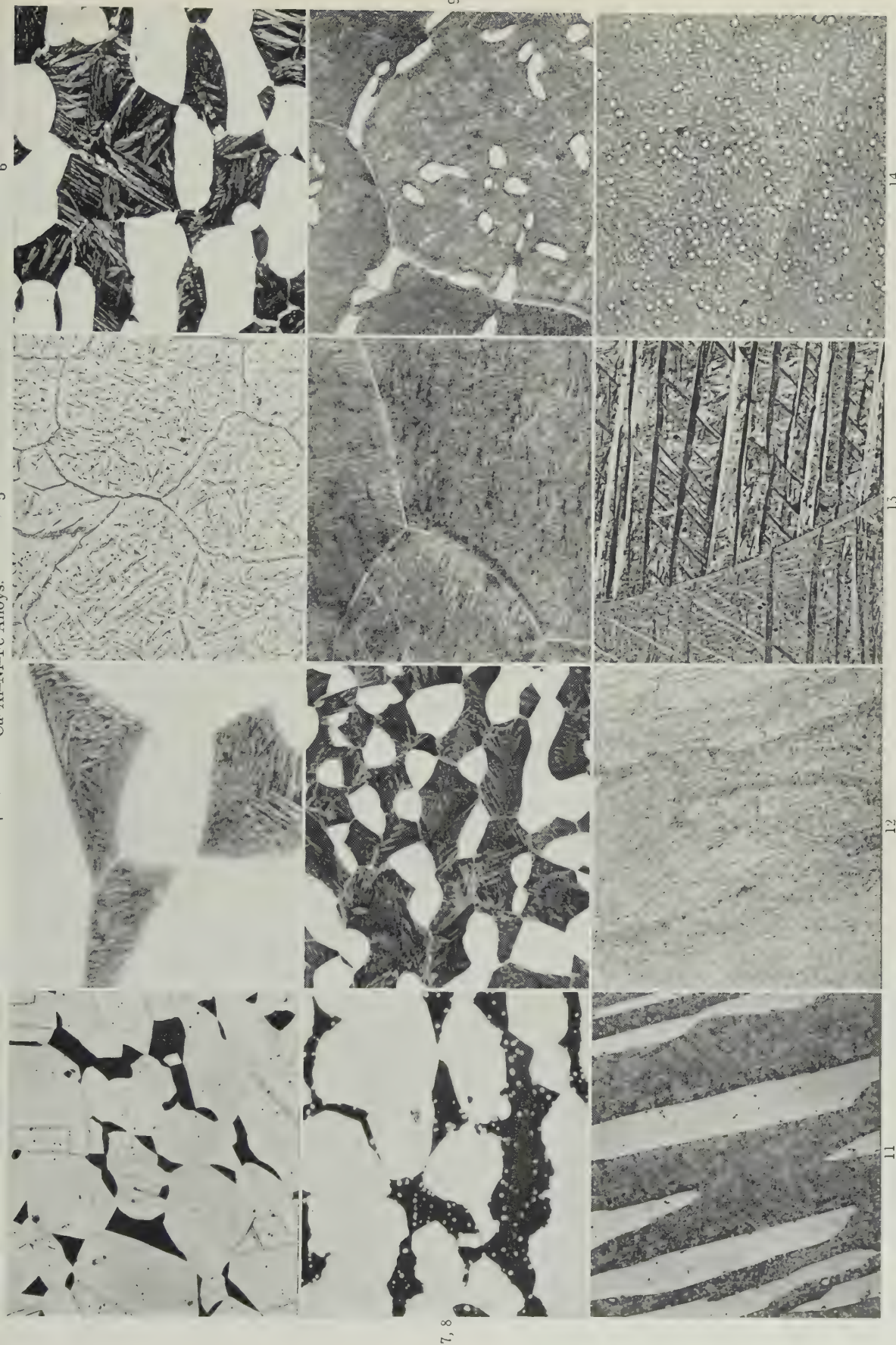


FIG. 3.—8/5/5 Alloy. Quenched from 1000° C.  $\alpha$  + decomposed  $\beta$ .  $\times 100$ .

FIG. 4.—Detail of Fig. 3.  $\times 500$ .

FIG. 5.—8/5/5 Alloy. Slowly cooled from 1000° to 600° C. and quenched.  $\alpha$  +  $\kappa$ .  $\times 100$ .

FIG. 6.—9/5/5 Alloy. Quenched from 1000° C.  $\alpha$  + decomposed  $\beta$ .  $\times 100$ .

FIG. 7.—9/5/5 Alloy. Slowly cooled from 1000° to 900° C. and quenched.  $\alpha$  +  $\beta$  +  $\kappa$ .  $\times 100$ .

FIG. 8.—9/6/6 Alloy. Quenched from 1000° C.  $\alpha$  + decomposed  $\beta$ .  $\times 100$ .

FIG. 9.—10/5/5 Alloy. Quenched from 1000° C. Martensitic  $\beta$  +  $\alpha$  (at boundaries).  $\times 100$ .

FIG. 10.—10/5/5 Alloy. Slowly cooled from 1000° to 975° C. and quenched.  $\alpha$  + martensitic  $\beta$ .  $\times 100$ .

FIG. 11.—10/5/5 Alloy.  $\beta$  +  $\kappa$ .  $\times 100$ .

FIG. 12.—10/5/5 Alloy.  $\beta$  +  $\kappa$ .  $\times 100$ .

FIG. 13.—12/5/5 Alloy. Quenched from 1000° C. Martensitic  $\beta$ .  $\times 100$ .

FIG. 14.—12/5/5 Alloy.  $\beta$  +  $\kappa$ .  $\times 100$ .

FIG. 10.—10/5/5 Alloy. Slowly cooled from 1000° to 975° C. and quenched.  $\alpha$  + martensitic  $\beta$ .  $\times 100$ .

FIG. 11.—10/5/5 Alloy.  $\beta$  +  $\kappa$ .  $\times 100$ .

FIG. 12.—10/5/5 Alloy.  $\beta$  +  $\kappa$ .  $\times 100$ .

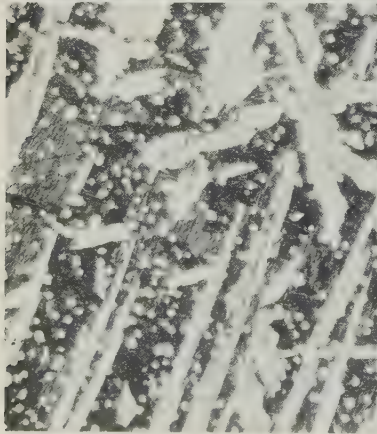
FIG. 13.—12/5/5 Alloy. Quenched from 1000° C. Martensitic  $\beta$ .  $\times 100$ .

FIG. 14.—12/5/5 Alloy.  $\beta$  +  $\kappa$ .  $\times 100$ .

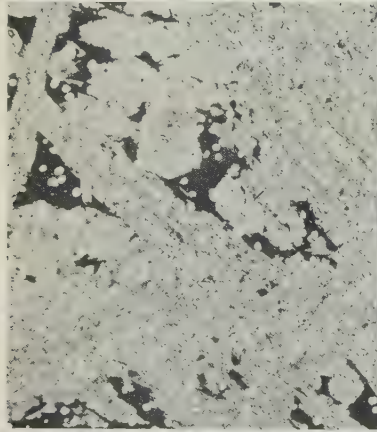


## Cu-Al-Ni-Fe Alloys.

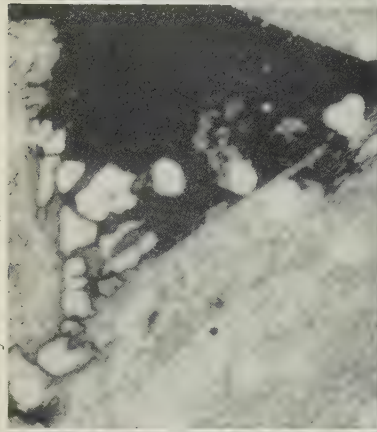
15



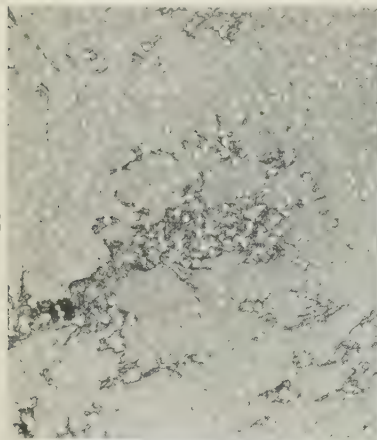
16



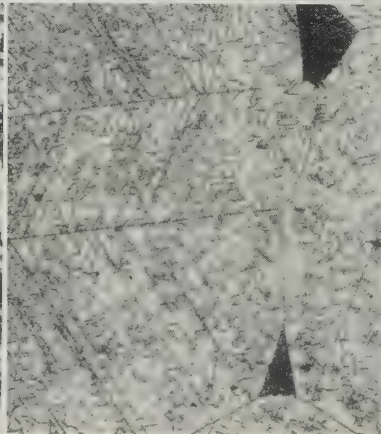
17



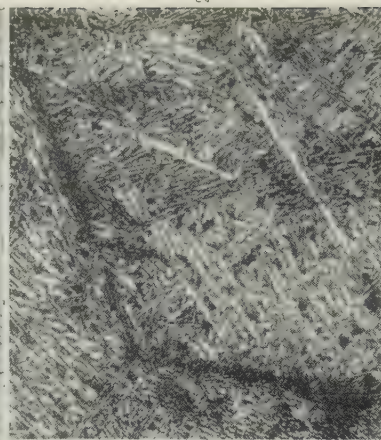
18



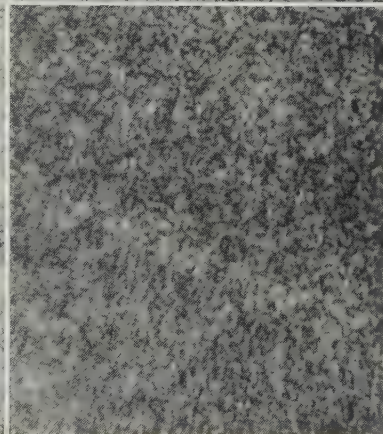
19, 20



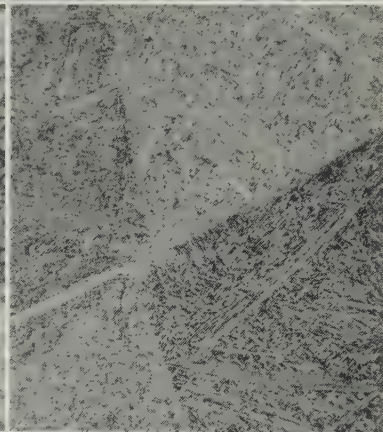
21, 22



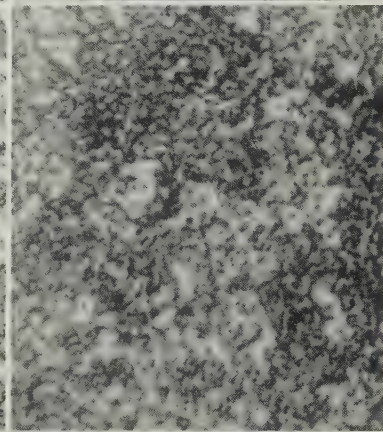
23



24



25



26

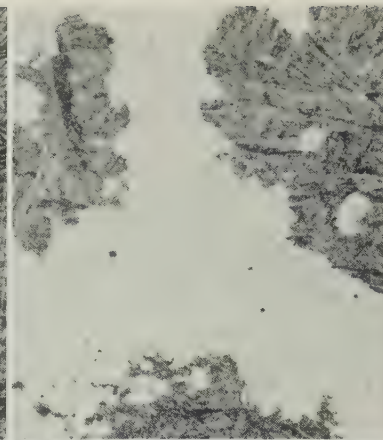
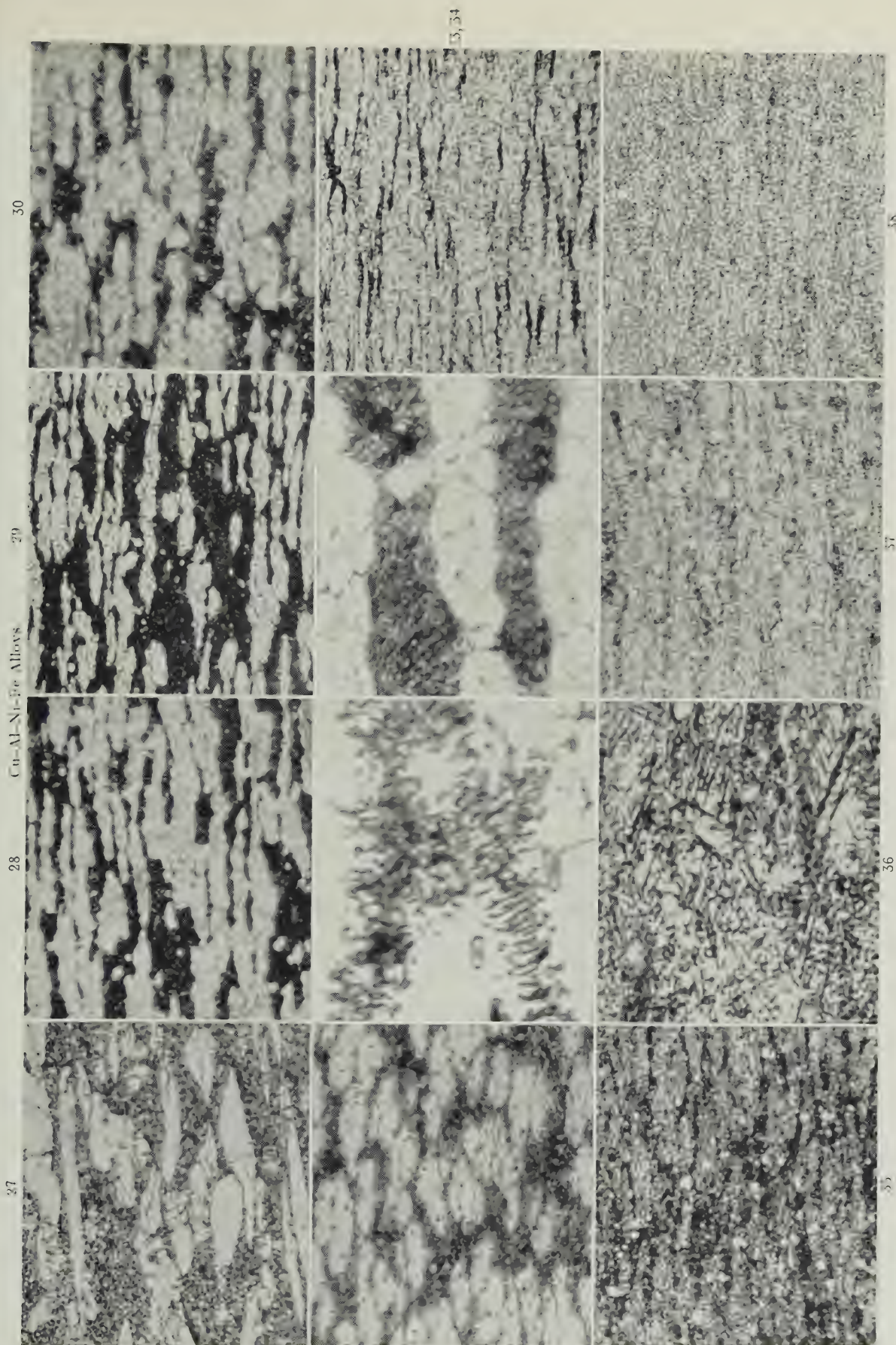


FIG. 15.—12/5/5 Alloy. Slowly cooled from 1000° to 700° C. and quenched.  $a + \beta + \kappa$ .  $\times 100$ .  
 FIG. 16.—12/5/5 Alloy. Slowly cooled from 1000° to 600° C. and quenched.  $a + \beta + \kappa$ .  $\times 100$ .  
 FIG. 17.—12/5/5 Alloy. Slowly cooled from 1000° to 590° C. and quenched.  $a + \beta + \kappa + \delta$ .  $\times 500$ .  
 FIG. 18.—12/5/5 Alloy. Slowly cooled from 1000° to 500° C. and quenched.  $a + \kappa + \delta$ .  $\times 100$ .  
 FIG. 19.—8/5/5 Alloy. Quenched from 1000° C. and tempered 4 hr. at 700° C.  $a + \kappa$ .  $\times 500$ .  
 FIG. 20.—8/5/5 Alloy. Quenched from 1000° C. and tempered 256 hr. at 500° C.  $a + \kappa$ .  $\times 100$ .  
 FIG. 21.—10/5/5 Alloy. Quenched from 1000° C. and tempered 1/3 hr. at 900° C.  $a + \beta + \kappa$ .  $\times 500$ .  
 FIG. 22.—10/5/5 Alloy. Quenched from 1000° C. and tempered 1/3 hr. at 800° C.  $a + \beta$  (small dark patches) +  $\kappa$ .  $\times 500$ .  
 FIG. 23.—10/5/5 Alloy. Quenched from 1000° C. and tempered 1/3 hr. at 600° C.  $a + \kappa$ .  $\times 2500$ .  
 FIG. 24.—12/5/5 Alloy. Quenched from 1000° C. and tempered 1 hr. at 600° C.  $a + \beta + \kappa$ .  $\times 100$ .  
 FIG. 25.—Detail of Fig. 24.  $\kappa$  particles in  $a$ .  $\times 2500$ .  
 FIG. 26.—12/5/5 Alloy. Quenched from 1000° C. and tempered 1 hr. at 500° C.  $a + \kappa + \delta$ .  $\times 100$ .  
 Penetration at grain boundary.  $\times 100$ .



FIG. 27.—Plate as Rolled from  $1\frac{3}{8}$  to  $\frac{1}{16}$  in., beginning at  $975^{\circ}\text{C}$ .  $a + \kappa$ .  $\times 500$ .FIG. 28.—Plate as Rolled from  $\frac{1}{16}$  to  $\frac{1}{8}$  in., beginning at  $925^{\circ}\text{C}$ .  $a + \kappa$  + partially decomposed  $\beta + \kappa$ .  $\times 500$ .FIG. 29.—Plate as Rolled from  $\frac{5}{16}$  to  $\frac{3}{16}$  in., beginning at  $925^{\circ}\text{C}$ .  $a + \kappa$  + partially decomposed  $\beta + \kappa$ .  $\times 500$ .FIG. 30.—Plate as Rolled from  $1\frac{3}{8}$  in. to  $\frac{1}{16}$  in., beginning at  $975^{\circ}\text{C}$ .  $a + \kappa$ .  $\times 500$ .FIG. 31.—Plate as Rolled from  $1\frac{3}{8}$  to  $1$  in., beginning at  $975^{\circ}\text{C}$ .  $a + \kappa$ .  $\times 500$ .FIG. 32.—Detail of Fig. 31.  $a + \kappa$ .  $\times 2500$ .FIG. 33.—Detail of Fig. 28.  $a + \kappa$  + partially decomposed  $\beta + \kappa$ .  $\times 500$ .FIG. 34.—Plate as Rolled from  $\frac{1}{16}$  to  $0.2$  in., beginning at  $800^{\circ}\text{C}$ .  $a + \kappa$  + partially decomposed  $\beta + \kappa$ .  $\times 500$ .FIG. 35.— $\frac{1}{16}$  in. Plate Rolled at  $925^{\circ}\text{C}$ . Annealed 2 hr. at  $600^{\circ}\text{C}$ .  $a + \kappa$ .  $\times 500$ .FIG. 36.—Detail of Fig. 35.  $a + \kappa$ .  $\times 500$ .FIG. 37.— $\frac{1}{16}$  in. Plate Rolled at  $925^{\circ}\text{C}$ . Annealed 2 hr. at  $700^{\circ}\text{C}$ .  $a + \kappa$ .  $\times 500$ .FIG. 38.— $\frac{1}{16}$  in. Plate Rolled at  $925^{\circ}\text{C}$ . Annealed 2 hr. at  $750^{\circ}\text{C}$ .  $a + \kappa$ .  $\times 500$ .



Cu-Al-Ni-Fe Alloys.

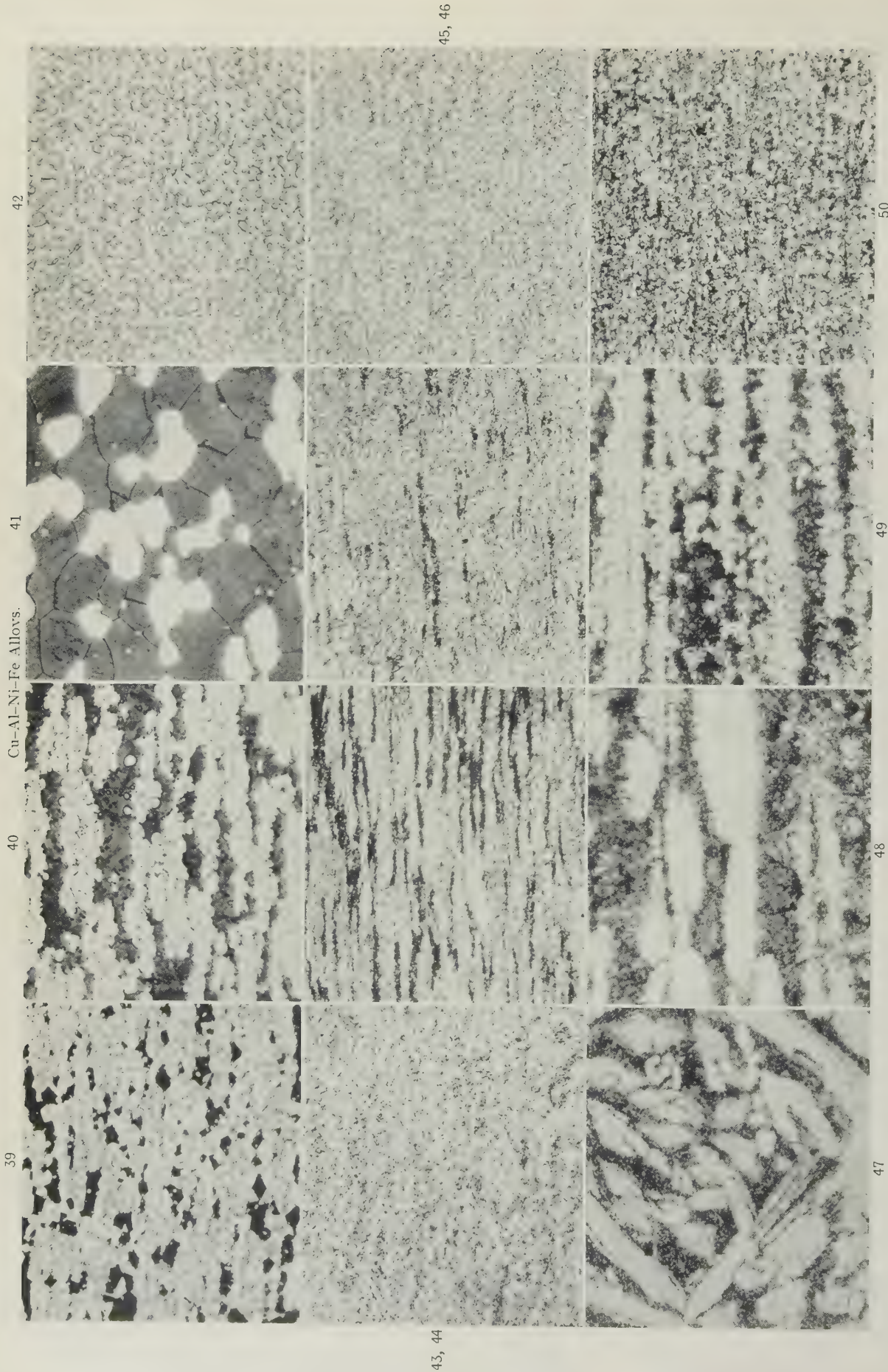


FIG. 39.— $\frac{1}{8}$ -in. Plate Rolled, beginning at 925° C., Annealed 2 hr. at 800° C., and Quenched.  $\alpha + \beta + \kappa$ .  $\times 500$ .  
 FIG. 40.— $\frac{1}{8}$ -in. Plate Rolled, beginning at 925° C., Annealed 2 hr. at 850° C., and Quenched.  $\alpha + \beta + \kappa$ .  $\times 500$ .  
 FIG. 41.— $\frac{1}{8}$ -in. Plate Rolled, beginning at 925° C., Annealed 2 hr. at 900° C., and Quenched.  $\alpha + \beta + \kappa$ .  $\times 500$ .  
 FIG. 42.— $\frac{1}{8}$ -in. Plate Rolled, beginning at 925° C., Annealed at 800° C., and Slowly Cooled to 750° C.  $\alpha + \kappa$ .  $\times 500$ .  
 FIG. 39.— $\frac{1}{8}$ -in. Plate Rolled, beginning at 925° C., Annealed 2 hr. at 800° C., and Quenched.  $\alpha + \beta + \kappa$ .  $\times 500$ .  
 FIG. 40.— $\frac{1}{8}$ -in. Plate Rolled, beginning at 925° C., Annealed 2 hr. at 850° C., and Quenched.  $\alpha + \beta + \kappa$ .  $\times 500$ .  
 FIG. 41.— $\frac{1}{8}$ -in. Plate Rolled, beginning at 925° C., Annealed 2 hr. at 900° C., and Quenched.  $\alpha + \beta + \kappa$ .  $\times 500$ .  
 FIG. 42.— $\frac{1}{8}$ -in. Plate Rolled, beginning at 925° C., Annealed at 800° C., and Slowly Cooled to 750° C.  $\alpha + \kappa$ .  $\times 500$ .

FIG. 43.— $\frac{1}{8}$ -in. Plate Rolled, beginning at 975° C., Annealed 2 hr. at 750° C.  $\alpha + \kappa$ .  $\times 500$ .  
 FIG. 44.— $\frac{1}{8}$ -in. Plate Rolled, beginning at 800° C., Annealed 2 hr. at 550° C.  $\alpha + \kappa$ .  $\times 500$ .  
 FIG. 45.— $\frac{1}{8}$ -in. Plate Rolled, beginning at 800° C., Annealed 2 hr. at 600° C.  $\alpha + \kappa$ .  $\times 500$ .  
 FIG. 46.— $\frac{1}{8}$ -in. Plate Rolled, beginning at 800° C., Annealed 2 hr. at 750° C.  $\alpha + \kappa$ .  $\times 500$ .  
 FIG. 47.—Front End of 0.29-in.-dia. Rod, as Extruded.  $\alpha + \text{concentrations of fine } \kappa$ .  $\times 500$ .  
 FIG. 48.—Front End of 0.75-in.-dia. Rod, as Extruded.  $\alpha + \text{concentrations of fine } \kappa$ .  $\times 500$ .  
 FIG. 49.—Middle of 0.75-in.-dia. Rod, as Extruded.  $\alpha + \text{concentrations of fine } \kappa$ .  $\times 500$ .  
 FIG. 50.—Back End of 0.75-in.-dia. Rod, as Extruded. Fine  $\kappa$  in  $\alpha$ .  $\times 500$ .



## ALUMINIUM ALLOYS CONTAINING TIN, INDIUM, OR CADMIUM.

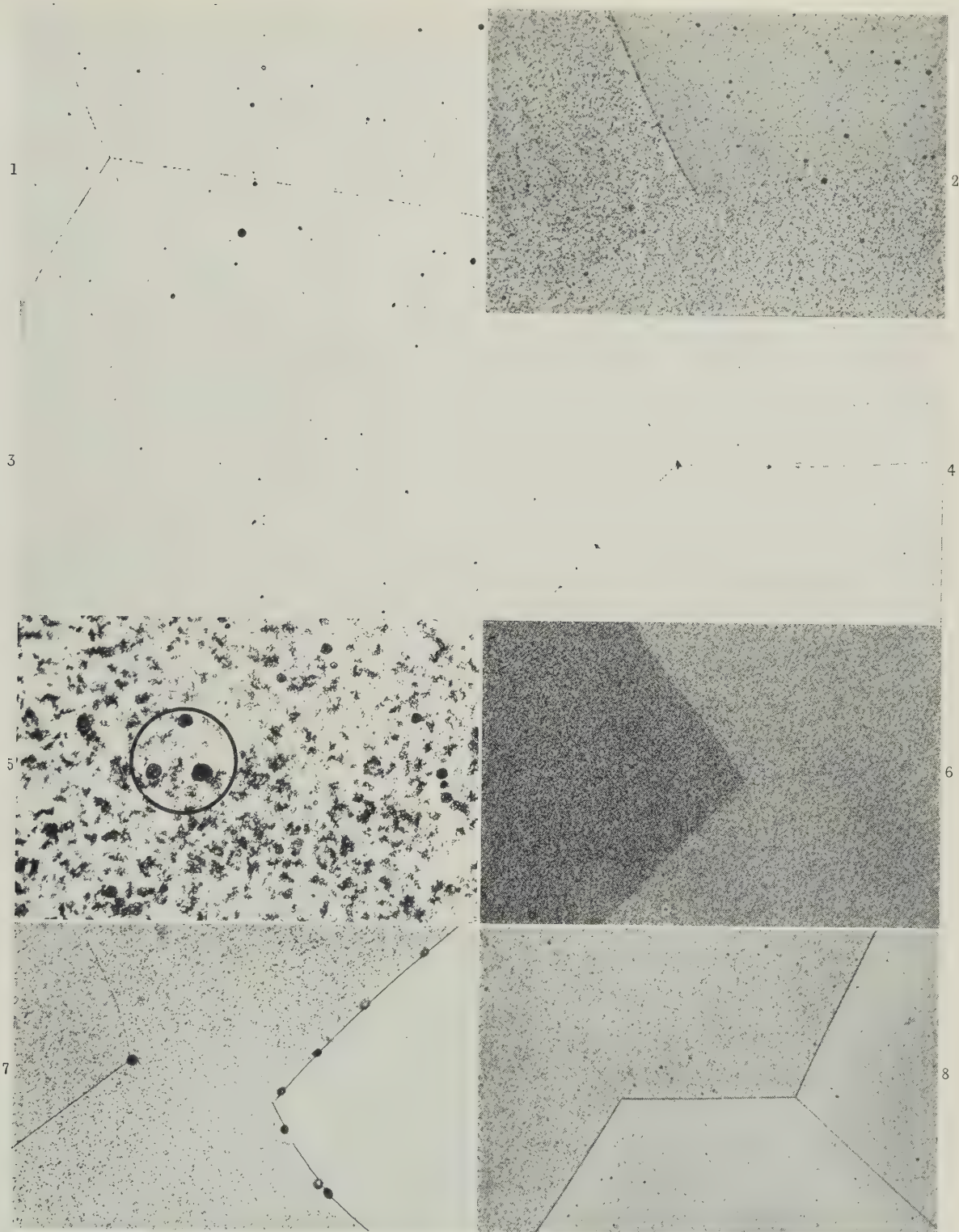


FIG. 1.—0.055% Sn, as Quenched from 530° C.  
 FIG. 3.—0.028% Sn, as Quenched from 530° C.  
 FIG. 5.—0.1% In, as Quenched from 530° C.  
 FIG. 7.—0.24% Cd, as Quenched from 530° C.

FIG. 2.—0.055% Sn, Aged at 165° C. after Quenching from 530° C.  
 FIG. 4.—0.045% Sn, as Quenched from 615° C.  
 FIG. 6.—0.045% In, Aged at 165° C. after Quenching from 530° C.  
 FIG. 8.—0.1% Cd, Aged at 165° C. after Quenching from 530° C.

All etched in 1% HF solution. × 250.



## ALUMINIUM ALLOYS CONTAINING TIN OR CADMIUM.



FIG. 9.—0.05% Sn, Aged at 165° C. after Quenching from 560° C.  $\times 500$ . FIG. 10.—0.08% Sn, as Quenched from 650° C.  $\times 500$ . FIG. 11.—0.39% Cd, as Quenched from 590° C.  $\times 250$ .

All electrolytically polished in Jacquet's solution; unetched.

## ALUMINIUM-CHROMIUM-IRON ALLOYS.



FIG. 6.—Typical Slowly Cooled Alloy. Primary crystal of  $\text{CrAl}_7$  in Al-rich matrix containing secondary  $\text{FeAl}_3$ . Etched in 20%  $\text{H}_2\text{SO}_4$  at  $70^\circ\text{C}$ . for 20 sec.  $\times 70$ .



FIG. 7. Irregular Prisms of  $\text{CrAl}_7$ .  $\times 70$ .

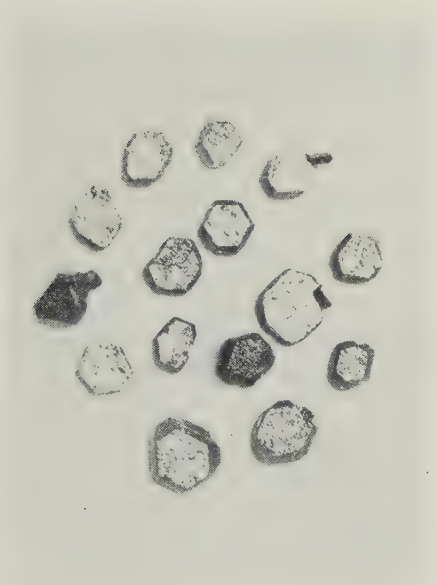


FIG. 8.—Equi-axed Crystals of Type Different from  $\text{CrAl}_7$ .  $\times 70$ .



FIG. 9.—Flat Needles of  $\text{FeAl}_3$ .  $\times 70$ .



COPPER-GALLIUM ALLOYS

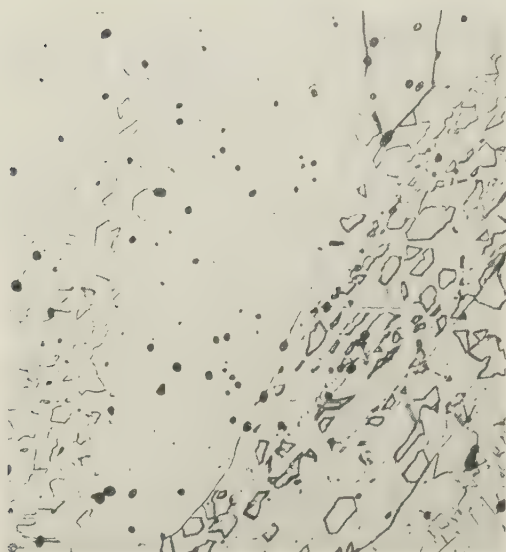


FIG. 9.—37.65 at.-% Gallium. Annealed 37 days at 353.5° C. Etched 30 sec. in aq.  $\text{FeCl}_3$  solution.  $\times 125$ .

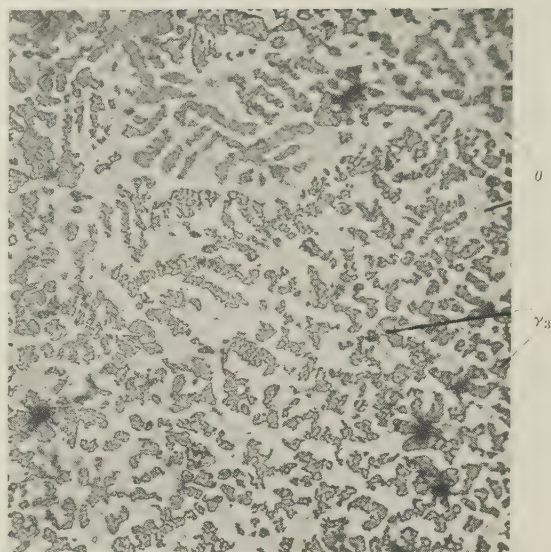


FIG. 10.—56.59 at.-% Gallium. Annealed 17 hr. at 250° C. after 30 days at 195° C. Etched 10 sec. in alcoholic  $\text{FeCl}_3$  solution.  $\gamma_3 + \theta$ .  $\times 120$ .

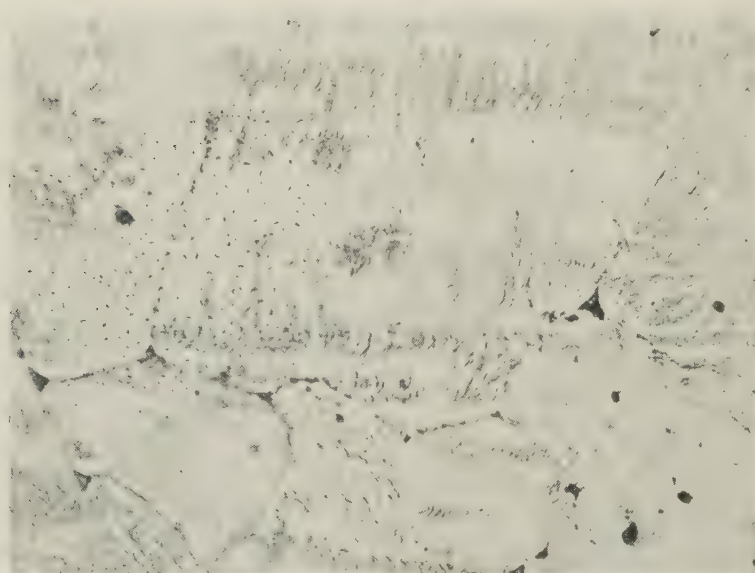


FIG. 11.—66.52 at.-% Gallium. Annealed 30 days at 195° C. Etched 10 sec. in alcoholic  $\text{FeCl}_3$ .  $\theta$  + trace of chilled liquid.  $\times 300$ .

# THE SOLID SOLUBILITIES OF CADMIUM, INDIUM, AND TIN IN ALUMINIUM\*

1365

By H. K. HARDY,† Ph.D., M.Sc., A.R.S.M., A.I.M., MEMBER

## SYNOPSIS

The solid solubilities of cadmium, indium, and tin in aluminium at temperatures of 530° C. and above have been estimated metallographically on electrolytically polished specimens. The solubilities of cadmium and indium increased to maximum values of 0.45 and 0.11%, respectively, at their monotectic temperatures. Aluminium-tin alloys showed a retrograde curve, with a maximum solubility of 0.1% at about 610° C.

## I.—INTRODUCTION

It has been shown recently that a small quantity of cadmium, indium, or tin exerts a pronounced influence on the ageing processes of aluminium-copper alloys.<sup>1,2</sup> The binary alloys of aluminium with cadmium, indium, or tin underwent age-hardening at 165° C., when quenched from 530° C. The results indicated that the solubility of these metals at the latter temperature was of the order of 0.05 wt.-%. A previous estimate of the solid solubility of tin in aluminium at 530° C., based on microscopic examination and lattice-parameter measurements, had indicated the same value.<sup>3</sup>

The solid solubilities of cadmium, indium, and tin in aluminium have now been determined at 530° C. and above. The very small solubility range introduced considerable experimental difficulties, but it was believed that a suitable metallographic method could be developed.

## II.—SPECIMEN PREPARATION AND HEAT-TREATMENT

A series of binary aluminium alloys was prepared from materials of the highest available purity, using an alumina-lined crucible and H.F.-furnace melting. Tests showed that this technique caused no more than a negligible reduction in purity. Billets of 1½ in. dia. were cast by water chilling and machined to 0.6 in. dia.; ½-in. lengths were flattened along a diameter to 0.2 in. thick and stamped for identification.

The specimens were loosely surrounded by aluminium foil and heat-treated in a circulating-air furnace, at a temperature within  $\pm 2^\circ$  C. of the nominal value, followed by quenching in cold water. The samples were heat-treated for 16 hr. at 650°, 16 hr. at 640°, 24 hr. at 615°, 32 hr. at 590°, 48 hr. at 560°, or 72 hr. at 530° C. No microstructural differences were observed between specimens heat-treated for

48 hr. instead of 72 hr. at 530° C., indicating that equilibrium had been reached. A duplicate set of specimens was aged for 16 hr. at 165° C.

## III.—PREPARATION OF MICROSPECIMENS

Microspecimens were cut in such a way that the surface for examination lay approximately  $\frac{1}{8}$  in. beneath the end of the heat-treated sample. The specimens were rubbed down with 000 emery, using a mixture of paraffin and liquid paraffin (BP) as a lubricant.

A modification of de Sy and Haemers's method of electrolytic polishing<sup>4</sup> was employed, in which the solution consisted of four parts of absolute alcohol to one part of perchloric acid. The potential across the cell was controlled at 10–15 V., giving a polishing time of 3–5 min. Initially, the same technique was followed as had been used on aluminium-tin alloys,<sup>4</sup> and the microspecimens were examined after etching in 1% HF. But, as shown below, it was found that alloys containing more than about 0.04% indium or tin possessed a markedly enhanced tendency to pit on etching, which masked any effects due to small undissolved particles. A further experimental technique was therefore sought.

The microspecimens polished in de Sy and Haemers's solution were repolished by the process due to Jacquet.<sup>5-7</sup> The solution consisted of 65% acetic anhydride and 35% of 60% perchloric acid. The potential drop across the cell was controlled at 25–30 V., the polishing time being about 10 min. The current density was too low to allow this method to be used directly on ground specimens, and a preliminary polish in the alcohol-perchloric solution was always necessary.

Examination of alloys with increasing concentration indicated that the presence of insoluble particles led to pitting during electropolishing. Fink, Willey, and Stumpf<sup>8</sup> had previously taken small pits in electrolytically polished specimens of aluminium-

\* Manuscript received 23 July 1951.

† Head of Physical Metallurgy Section, Fulmer Research Institute, Stoke Poges, Bucks.



sodium alloys as an indication of the presence of undissolved particles. The method is extremely sensitive in comparison with normal metallographic techniques, but a difficulty lies in distinguishing between very small pits due to insoluble particles and minor polishing defects. The merit of the Jacquet process was that it produced a minimum of polishing blemishes. Etch pits were occasionally formed during polishing, but were easily distinguished by their straight sides. Gas bubbles on the anode could also lead to pitting, but these pits were normally many times larger than the structural ones. After polishing, the specimens were rinsed rapidly in distilled water and dried in absolute alcohol in order to reduce drying stains to a minimum.

#### IV.—ANALYSES AND EXPERIMENTAL ACCURACY

Analyses were made on at least one of the micro-specimens solution-heat-treated at each temperature; the whole specimen was dissolved for this purpose. The duplicate specimens were also analysed in any doubtful or critical cases. The chemical analysis was thought to be accurate to  $\pm 0.01\%$  of the alloy content. The difficulty of preparing perfectly polished specimens also limited the accuracy, but the solubility curves are believed to be correct to between  $\pm 0.02$  and  $\pm 0.05$  wt.-%, depending on the number of experimental points and the alloy content. Any spurious effects due to grain-boundary segregation, as discussed below, would lead to low results.

A closely allied metallographic technique has given the maximum solid solubility of sodium in aluminium as less than  $0.003\%$ .<sup>8</sup> It is therefore encouraging to note that a completely different experimental method, based on diffusion experiments, enabled Ransley and Neufeld<sup>9</sup> to place the maximum solubility at  $0.002\%$  sodium.

#### V.—METALLOGRAPHIC BEHAVIOUR

##### 1. SPECIMENS ETCHED IN 1% HF

The technique followed was that used previously for aluminium-tin alloys.<sup>4</sup> The specimens were polished in de Sy and Haemers's bath, and the time required to etch fully a specimen aged at  $165^\circ\text{C}$ . was noted. The same length of time was then allowed for etching the corresponding quenched specimens.

The microstructure of the alloy with  $0.055\%$  tin, quenched from  $530^\circ\text{C}$ . and aged at  $165^\circ\text{C}$ ., is illustrated in Fig. 2 (Plate LXVII). In the quenched condition, the alloy showed pits at the grain boundaries (see Fig. 1, Plate LXVII). An aluminium- $0.028\%$  tin alloy (Fig. 3, Plate LXVII) gave no pits at the grain boundaries when solution-treated at  $530^\circ\text{C}$ . Closely similar results were obtained after heat-treatment at all temperatures, in that grain-boundary pitting was always present when the alloy contained more than about  $0.04\%$  tin. A further example is shown

in Fig. 4 (Plate LXVII), for an alloy with  $0.045\%$  tin quenched from  $615^\circ\text{C}$ .

The results obtained on etching the aluminium-indium alloys were very similar. An alloy with  $0.1\%$  indium, quenched from  $530^\circ\text{C}$ ., showed a number of black circular patches, and three of these may be seen within the circle in Fig. 5 (Plate LXVII). They did not occur in the alloy with  $0.045\%$  indium (Fig. 6, Plate LXVII), but further etching tests revealed that alloys with more than about  $0.05\%$  indium also possessed a seriously enhanced tendency to pit on etching, sufficient to mask effects due to genuine undissolved particles.

An alloy with  $0.24\%$  cadmium, solution-treated at  $530^\circ\text{C}$ . (Fig. 7, Plate LXVII) showed pits at the grain boundaries that were absent from the  $0.1\%$  cadmium alloy (Fig. 8, Plate LXVII). Little general pitting occurred in any of the alloys with cadmium, so that small pits at the grain boundaries were not masked.

Comparison of the microstructure in Figs. 1 and 2, 5 and 6, 7 and 8, shows how the etching characteristics were affected by the ageing treatment.

##### 2. SPECIMENS POLISHED IN THE JACQUET BATH

The microspecimens were examined without etching, and the occurrence of pitting was taken as evidence of undissolved particles. The pits in the aluminium-tin or aluminium-indium alloys were often composed of a number of smaller ones and were usually outlined by stains (see Fig. 9 (Plate LXVIII)). An example of grain-boundary fusion in an aluminium- $0.08\%$  tin alloy, quenched from  $650^\circ\text{C}$ ., is shown in Fig. 10 (Plate LXVIII). Only individual pits normally occurred in aluminium-cadmium alloys containing insoluble particles (Fig. 11, Plate LXVIII) and these were usually free from stains.

#### 3. DISCUSSION OF THE METALLOGRAPHIC OBSERVATIONS

The multiple pitting and staining in the Jacquet bath, associated with the insoluble particles, were probably related to the etching behaviour of the tin and indium alloys. Atoms of these elements may have been re-deposited on the surface of the specimen from the polishing bath or etching solution, and have caused preferential attack of the aluminium in their immediate neighbourhood. Apparently cadmium atoms did not lead to this effect under the conditions employed.

Work on copper-antimony alloys by McLean,<sup>10</sup> and on copper-bismuth alloys by Samuels,<sup>11</sup> has shown that special grain-boundary etching effects can be produced by segregation of solute atoms to the grain boundaries in the absence of a second phase. The microstructural features of the alloys examined in the present work were quite different in appearance from those shown by Samuels, although the tendency of the grain boundary to pit on etching may indicate that grain-boundary segregation was present.

## VI.—SOLUBILITY CURVES

The experimental results are given in Figs. 12 and 13. The straight-line relationship between the logarithm of the solute concentration and the reciprocal of the absolute temperature, which holds for many aluminium alloys,<sup>12</sup> has been used in selecting the exact form of the solubility curve. As illustrated by Fig. 14, the straight-line relationship holds within the limits of the experimental error probably because the composition of the liquid in equilibrium with the solid solution is nearly independent of temperature over the range investigated.

The solubility in aluminium of cadmium (Fig. 12) and of indium (Fig. 13) increases continuously as the

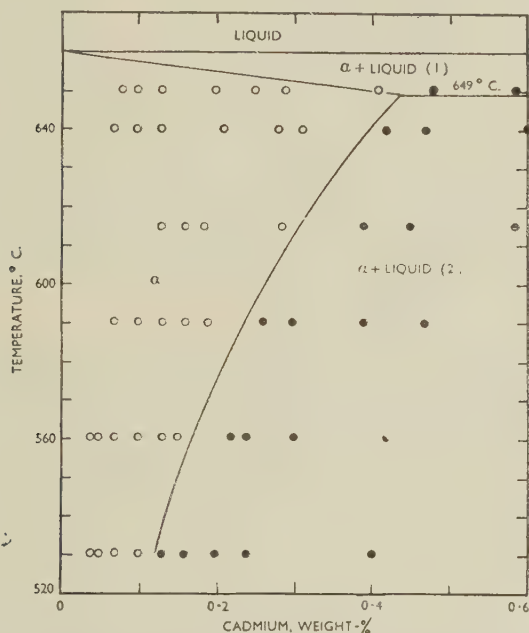


FIG. 12.—Solid-Solubility Relationships for Aluminium-Cadmium Alloys.

temperature is raised. However, the solubility of tin in aluminium passes through a maximum and thus gives a retrograde curve. Extrapolation of the straight line in Fig. 14 indicates a cadmium solubility of 0.0002 wt.-% at 165° C. The solubility of indium and tin at this temperature is of the same negligibly small order.

## VII.—THE FORM OF THE EQUILIBRIUM DIAGRAMS

## 1. ALUMINIUM-CADMIUM ALLOYS

The equilibrium diagram gives a monotectic at 649° C. and 7.5% cadmium, whilst the miscibility gap extends nearly to pure cadmium.<sup>13</sup> The maximum solid solubility of 0.45% (Fig. 12) is approximately half that deduced by Hansen and Blumenthal<sup>14, 15</sup>

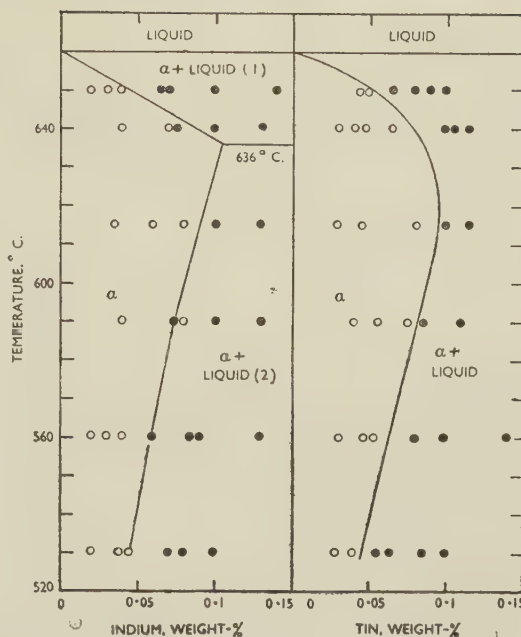


FIG. 13.—Solid-Solubility Relationships for Aluminium-Indium and Aluminium-Tin Alloys.

from the absence of a secondary arrest point on their cooling curves. The equation:

$$\log_{10} \frac{a_1}{a_2} = \frac{H}{4.575} \left( \frac{1}{T} - \frac{1}{T_M} \right) \quad (1)$$

relates the activity of the solvent in the solid  $a_1$  with the activity of the solvent in the liquid  $a_2$ , where  $H$  is the latent heat of solidification of the solvent (2520 cal./g.-atom for aluminium),  $T_M$  is the melting point of the pure solvent (933.3° K.), and  $T$  is the temperature. The relation can be applied to aluminium-cadmium alloys at the monotectic temperature by assuming that the activities can be replaced by the atomic fractions. Taking the solubility as 0.45 wt.-% and the monotectic temperature as 649° C., the calculated value of the monotectic cadmium content

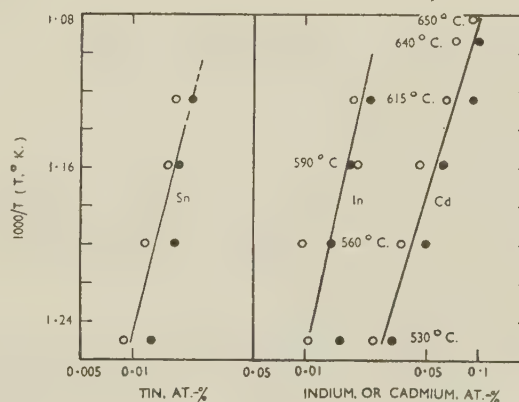


FIG. 14.—Relationships Between Log (Solute Concentration) and the Reciprocal of the Absolute Temperature.



is 6.7 wt.-%, which is in reasonable agreement with the experimental value of 7.5 wt.-%.

A value of less than 0.2 wt.-% cadmium at 150° C. has been based on age-hardening investigations of alloys of different cadmium content.<sup>15, 16</sup> A value of 0.12 wt.-% at 245° C., suggested recently by Dorn, Pietrokowsky, and Tietz<sup>17</sup> and based on lattice-parameter measurements, is greater than would be expected from the present work.

## 2. ALUMINIUM-INDIUM ALLOYS

The equilibrium diagram shows a monotectic at approximately 636° C., extending from 15 to 95% indium.<sup>18</sup> The solid-solubility curve increases up to the monotectic temperature (see Fig. 13). Taking the solubility at the monotectic temperature as 0.11 wt.-% and inserting the appropriate values in equation (1) gives the calculated monotectic indium content of 13.5 wt.-%, which is in reasonable agreement with the experimental value.

No values have previously been reported for the solubility of indium. The reason for the low solubility and for the miscibility gap in the liquid state is obscure, since the relative size-factor and valencies are not dissimilar.<sup>19</sup>

## 3. ALUMINIUM-TIN ALLOYS

A smoothly continuous liquidus curve falling to a eutectic at about 99.5% tin and 228.3° C. was found when the equilibrium diagram was studied previously.<sup>3</sup> Lattice-parameter measurements and ageing tests were used in the earlier work and gave a solubility of approximately 0.05 wt.-% tin at 530° C.<sup>3</sup> Hunsicker<sup>20</sup> has quoted unpublished work indicating a tin solubility of 0.025% at 300°, 0.045% at 400°, and 0.06% at 510° C., but no details were given of the experimental methods employed. The solid-solubility curve (Fig. 13) has a maximum, and is thus a retrograde curve.<sup>21-23</sup> The thermodynamics of retrograde solubility curves, which are frequently solidus

curves, has been studied by Meijering.<sup>24</sup> He gave a diagram, reproduced in Fig. 15, by which an alloy system may be tested for the existence of a retrograde curve, provided that the solubility and the composition of the liquid phase at a temperature well below that of maximum solubility are both known.

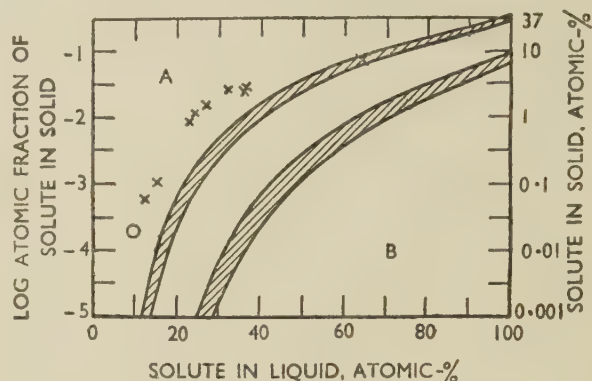


FIG. 15.—Graphs Used to Determine Whether or Not a Solidus is Retrograde. The two shaded bands represent the limiting conditions when the entropy of melting is made equal to 1.1 and 2.5  $R$ , respectively. The crosses refer to maximum solubilities found when surveying the literature. (Meijering.<sup>24</sup>)

A. Region of negative  $dt/dx$  (normal solidus).  
B. Region of positive  $dt/dx$  (retrograde solidus).  
O Al-Sn alloys.

Application to the aluminium-tin system shows that a retrograde curve is to be expected, since the solubility at the eutectic temperature is appreciably less than the critical value of 37 at.-% (72 wt.-%) tin. The decrease of solubility close to the melting point of pure aluminium is due to the increasing influence of the liquidus.<sup>24</sup>

## ACKNOWLEDGEMENT

The author's thanks are due to his colleagues at the Fulmer Research Institute who contributed to the experimental work.

## REFERENCES

1. H. K. Hardy, *J. Inst. Metals*, 1950-51, **78**, 169.
2. H. K. Hardy, *ibid.*, 1951-52, **80** (in the press).
3. A. H. Sully, H. K. Hardy, and T. J. Heal, *ibid.*, 1949-50, **76**, 269.
4. A. de Sy and H. Haemers, *Aluminium*, 1942, **24**, 96.
5. P. Jacquet, *Métaux et Corrosion*, 1943, **18**, 198.
6. P. Jacquet, *Metal Finishing*, 1949, **47**, (11), 62.
7. P. Lacombe and L. Beaujard, *J. Inst. Metals*, 1948, **74**, 1.
8. W. L. Fink, L. A. Willey, and H. C. Stumpf, *Trans. Amer. Inst. Min. Met. Eng.*, 1948, **175**, 364.
9. C. E. Ransley and H. Neufeld, *J. Inst. Metals*, 1950-51, **78**, 25.
10. D. McLean, *ibid.*, 1947, **73**, 791 (discussion).
11. L. E. Samuels, *ibid.*, 1949-50, **76**, 91.
12. W. L. Fink and H. R. Freche, *Trans. Amer. Inst. Min. Met. Eng.*, 1934, **111**, 304.
13. W. L. Fink and L. A. Willey, *Metals Handbook (Amer. Soc. Metals)*, 1948, 1157.
14. M. Hansen and B. Blumenthal, *Metallwirtschaft*, 1931, **10**, 925.
15. B. Blumenthal and M. Hansen, *ibid.*, 1932, **11**, 671.
16. M. Hansen, "Der Aufbau der Zweistofflegierungen", p. 90. Berlin: 1936 (Julius Springer).
17. J. E. Dorn, P. Pietrokowsky, and T. E. Tietz, *Trans. Amer. Inst. Min. Met. Eng.*, 1950, **188**, 933.
18. H. M. Davis, *Metals Handbook (Amer. Soc. Metals)*, 1948, 1162.
19. H. J. Axon and W. Hume-Rothery, *Proc. Roy. Soc.*, 1948, [A], **193**, 1.
20. H. Y. Hunsicker, "Sleeve Bearing Materials", p. 82. Cleveland, O.: 1949 (American Society for Metals).
21. E. Scheil, *Z. Metallkunde*, 1942, **34**, 96.
22. E. Raub and A. von Polaczek-Witteck, *ibid.*, 1942, **34**, 93.
23. E. Raub and A. Engel, *Metallforschung*, 1946, **1**, 76.
24. J. L. Meijering, *Philips Research Rep.*, 1948, **3**, 281.

# THE CONSTITUTION OF THE ALUMINIUM-CHROMIUM-ZINC ALLOYS AT LOW CHROMIUM CONTENTS\*

1366

By A. R. HARDING,† B.Sc., Ph.D., STUDENT MEMBER, and  
PROFESSOR G. V. RAYNOR,‡ M.A., D.Sc., MEMBER OF COUNCIL

## SYNOPSIS

In continuation of work on aluminium-rich systems containing transition-metal solutes, and to gain information as to the behaviour of such solutes in zinc-rich alloys, the system aluminium-chromium-zinc has been examined, by metallographic and X-ray methods, at low chromium contents. No ternary compounds were found to occur in the range investigated. The surfaces of primary separation involve the crystallization of the aluminium-rich solid solution ( $\alpha$ ), the zinc-rich solid solution ( $\beta$ ),  $\text{CrAl}_7$ ,  $\text{Cr}_2\text{Al}_{11}$ ,  $\text{CrAl}_4$ , chromium, and the  $\theta$  (Zn-Cr) binary intermediate compound. The primary  $\text{CrAl}_4$  field is extensive, and this phase crystallizes from the melt at zinc contents exceeding 99%. The primary  $\alpha$  and primary  $\text{CrAl}_7$  fields are restricted, and are extremely narrow above 50% zinc. Both persist to zinc contents of 95-95.5%, and the  $\alpha$  and  $\text{CrAl}_7$  phases crystallize, together with  $\beta$ , at a ternary eutectic containing 95% zinc and not more than 0.01% chromium.

Equilibrium relations above 95% zinc are complex, and the primary Cr,  $\theta$  (Zn-Cr), and  $\beta$  fields occur in this region. Annealing experiments have established an isothermal at 371°C., in which the chief feature is a large ( $\alpha + \text{CrAl}_7 + \beta$ ) three-phase triangle. The  $\beta$  phase thus enters into equilibrium with  $\text{CrAl}_7$ ; the other equilibria involving  $\beta$  in the zinc-rich region could not be established owing to the impossibility of attaining equilibrium by annealing chill-cast alloys. The constitution of solid alloys above 95% zinc is dictated by the crystallization process; complex composite crystals of intermetallic compound are formed as a result of successive peritectic reactions, and annealing for long periods makes little difference to the as-cast structure. By the analysis of crystals extracted from slowly cooled alloys, it has been shown that  $\text{CrAl}_7$  dissolves zinc, most probably by replacement of aluminium, up to at least 14.7 wt.-% (7.6 at.-%).

The results of the investigation are briefly discussed.

## I.—INTRODUCTION

IN the course of a series of investigations on ternary aluminium-rich alloys containing, as solutes, two transition metals or one transition and one non-transition metal, the systems formed by alloying aluminium and manganese with chromium, iron, cobalt, nickel, copper, silver, zinc, cadmium, and silicon, respectively, have been examined in detail. Particular attention has been paid to the formation of ternary compounds, to the solid solubility of third elements in the binary compounds formed by aluminium and a transition metal, and to the alloying characteristics of transition metals. Ternary compounds, which enter into equilibrium with the aluminium-rich solid solution, are observed when the second solute is chromium, nickel, copper, zinc, or silicon. The significance of these ternary compounds has been discussed in a recent paper.<sup>1</sup> The data for the alloys of aluminium, manganese, and a third metal are particularly complete, but comparatively little is known of the corresponding alloys containing chromium in place of manganese, which would provide an interesting comparison. Accordingly,

a study has now been made of the aluminium-chromium-zinc system. Zinc was chosen as the second solute because its atomic size, relative to those of aluminium and the transition metals, appears to be favourable for the formation of ternary compounds, provided that no factor peculiar to the individual alloy system interferes.

Work on aluminium-rich alloys has supported the suggestion that, in a polyvalent solvent which donates to the structure as a whole a sufficient number of free electrons per atom, transition-metal atoms may accept electrons; the probable number of free electrons accepted per atom decreases as the atomic number of the transition metal rises.<sup>1</sup> It is of considerable interest to define the conditions under which this acceptance of electrons takes place, so that information on the behaviour of transition metals in solvents other than aluminium is required. Zinc, with a valency of two, forms a suitable solvent for comparison with aluminium. The present work was therefore extended to include the zinc-rich alloys, and the whole composition range from aluminium to zinc has been studied, with chromium additions varying from 9.5% at the aluminium-

\* Manuscript received 14 July 1951.

† Research Fellow, University of Birmingham.

‡ Professor of Metal Physics, University of Birmingham.



rich end to 2.0% at the zinc-rich end. The methods employed included micrographic analysis, the examination of slowly cooled alloys, and the extraction, chemical analysis, and X-ray investigation of primary crystals where possible.

## II.—PREVIOUS WORK

### 1. THE BINARY SYSTEMS

#### (a) Aluminium-Chromium

The most probable equilibrium diagram for the aluminium-rich alloys is shown in Fig. 1, which is based on the work of Fink and Freche,<sup>2</sup> Bradley

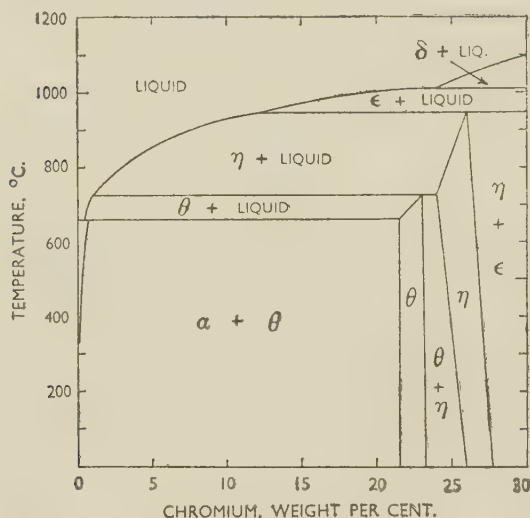


Fig. 1.—The Aluminium-Rich Portion of the System Aluminium-Chromium.

and Lu,<sup>3</sup> and Raynor and Little.<sup>4</sup> The essential features for the present work are as follows:

(1) There are three aluminium-rich intermediate phases.  $\text{CrAl}_4$  ( $\epsilon$ ) is formed peritectically at approximately  $1000^\circ\text{C}$ . At higher aluminium contents, this phase reacts peritectically with the melt to form  $\text{Cr}_2\text{Al}_{11}$  ( $\eta$ ), which in turn forms  $\text{CrAl}_7$  ( $\theta$ ) by peritectic reaction with the liquid. The transformation temperatures are given as  $930^\circ$  and  $725^\circ\text{C}$ ., respectively.\*  $\text{CrAl}_7$  reacts peritectically at  $661^\circ\text{C}$ . with the aluminium-rich melt to form the primary solid solution, which is denoted  $\alpha$ .

(2) The crystal structures of  $\epsilon$ ,  $\eta$ , and  $\theta$  are very similar, and give rise to closely similar diffraction patterns.

(3) Owing to supercooling, alloys in the range 1.0–3.0% chromium frequently fail to deposit

primary  $\eta$  on cooling and only the  $\theta$  phase is observed. In other cases,  $\eta$  may separate above the peritectic temperature and  $\theta$  below this temperature, without any micrographically detectable evidence of a peritectic relationship between the two phases.<sup>5</sup>

(4) The solid solubility of chromium in aluminium is limited, and is 0.72% at  $661^\circ\text{C}$ ., diminishing to 0.03% at  $350^\circ\text{C}$ .

A complete diagram, differing little from that given in Fig. 1, together with a brief review of the relevant experimental work, has been published by Falkenhagen and Hofmann.<sup>6</sup>

#### (b) Aluminium-Zinc

Fig. 2 shows the equilibrium diagram for the aluminium-zinc alloys.<sup>7</sup> No intermediate phases are formed, and the mutual solid solutions of the two metals form a eutectic at 95% zinc and  $382^\circ\text{C}$ . The solubility of zinc in aluminium is extensive, but that of aluminium in zinc does not exceed 1% at the eutectic temperature. In the range  $365^\circ$ – $275^\circ\text{C}$ ., and between 31.6 and 78% zinc, the face-centred cubic  $\alpha$  solid solution decomposes into a mixture of two face-centred cubic solid solutions of different compositions.

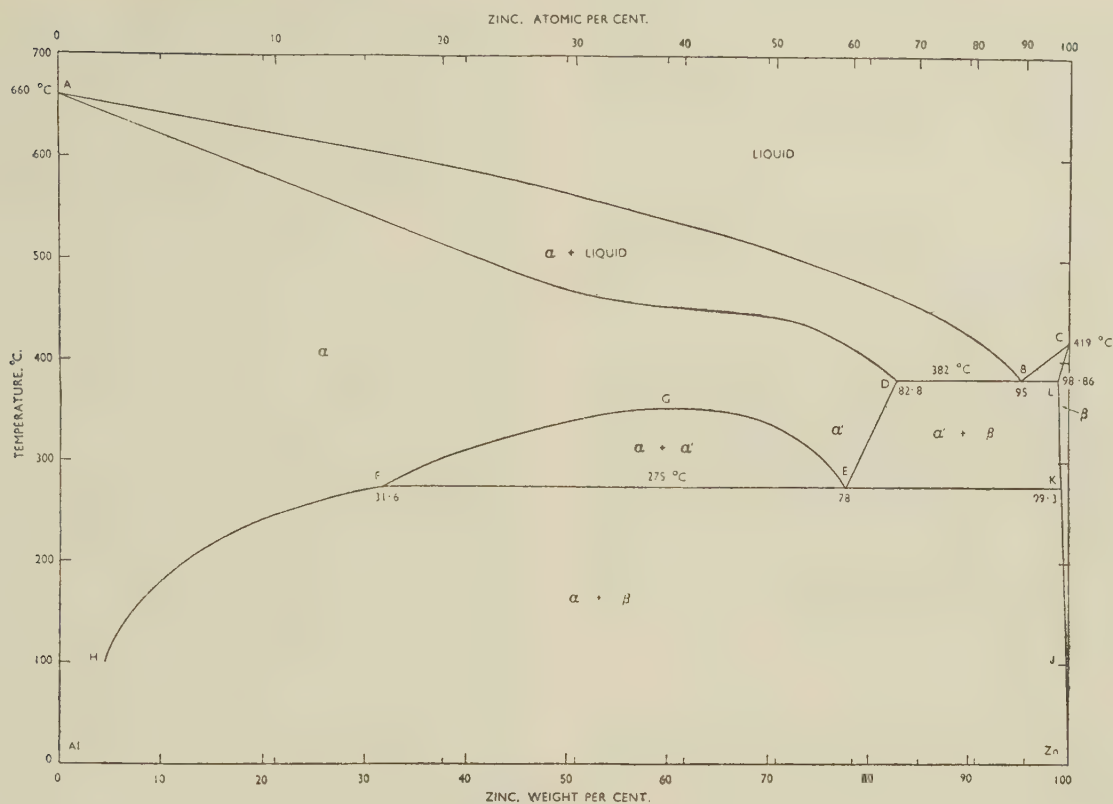
#### (c) Zinc-Chromium

Little work has been carried out on this system; the literature contains references only to the zinc-rich portion. Earlier work by Weisse, Blumenthal, and Hanemann<sup>8</sup> and by Hanemann<sup>9</sup> was checked by Heumann,<sup>10</sup> who gave the maximum solid solubility of chromium in zinc as 0.034% at the eutectic temperature ( $415^\circ\text{C}$ .). Three points were obtained by thermal analysis on the curve of primary separation of an intermediate phase,  $\theta$  (Zn-Cr), and the eutectic composition (0.22% chromium) was estimated from the point of intersection of this curve with the eutectic horizontal. The  $\theta$  (Zn-Cr) phase is the only intermediate phase present; its exact range of homogeneity is unknown. Heumann repeated previous attempts to define its composition by extraction and analysis, and obtained a value of 5.13% chromium. This figure, however, may be in error owing to contamination with free chromium. Attempts to characterize the phase from the relative amounts of  $\theta$  (Zn-Cr) and zinc-rich solid solution ( $\beta$ ) present in microsections suggested a figure of 4% chromium, which is probably low owing to errors involved in the method. The information available is summarized in Fig. 3, in which the  $\theta$  (Zn-Cr) phase is shown as invariant at 4% chromium.† The phase has a hexagonal crystal structure, and is formed peritectically at  $464^\circ\text{C}$ .

\* There is evidence<sup>5</sup> that the  $\text{Cr}_2\text{Al}_{11} + \text{liquid} \rightleftharpoons \text{CrAl}_7$  reaction takes place at a temperature higher than  $725^\circ\text{C}$ .

† In Fig. 3, and throughout the paper, the chromium-rich

solid solution has, for convenience, been denoted "chromium" or Cr.

FIG. 2.—The Equilibrium Diagram of the Aluminium-Zinc Alloys.<sup>7</sup>

## 2. THE TERNARY SYSTEM

The constitution of the ternary system in the region 0–10% of both zinc and chromium has been examined by Little, Axon, and Hume-Rothery,<sup>11</sup> using micrographic and X-ray techniques. In this composition range, CrAl<sub>7</sub> is the only phase to enter into equilibrium with the  $\alpha$  solid solution, which exists over a narrow range of chromium content close to the aluminium-zinc axis of the ternary diagram. The 460° C. isothermal is shown in Fig. 4. The surfaces of primary separation were not examined in detail, but the analysis of four samples of CrAl<sub>7</sub>, extracted

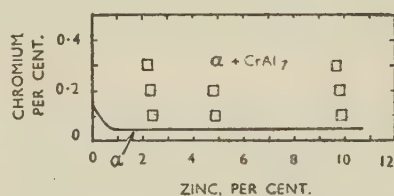


FIG. 4.—The System Aluminium-Chromium-Zinc : 460° C. Isothermal.

from slowly cooled alloys, showed that this phase is able to dissolve at least 2.81% zinc.

No information about the zinc-rich alloys is available, except for the composition of the ternary eutectic. This was found to lie at 5.19% aluminium, 0.007% chromium, and a temperature of 381.25° C.<sup>8</sup> This composition is very close to that of the binary aluminium-zinc eutectic. No indication was given as to the nature of the three phases that separate at the ternary eutectic.

## III.—EXPERIMENTAL

### 1. MATERIALS USED

All alloys were prepared from the constituent metals, or from binary master alloys made from pure materials.

#### (a) Zinc

Alloys required for slow-cooling experiments intended to define the surfaces of primary separation

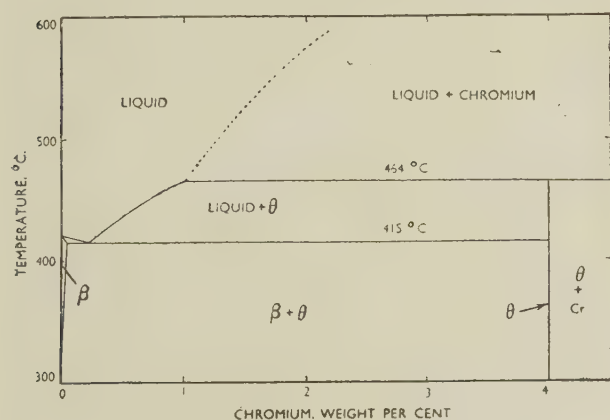


FIG. 3.—The Zinc-Rich Portion of the System Zinc-Chromium.



were made from Crown Special zinc of 99.99% purity. For the annealing experiments, and the preparation of zinc-chromium master alloys, a purer grade of zinc was used, in which the only impurities detected spectrographically were: lead 0.0001, cadmium 0.00005, and calcium 0.0001%.

#### (b) Aluminium

Super-pure aluminium, obtained from The British Aluminium Co., Ltd., was used throughout the work. The purity was 99.997%.

#### (c) Aluminium-Chromium Master Alloys

Two master alloys were used. One, containing 1.03% chromium, was made by reducing a mixture of chromium trioxide and chromium chloride (Analar) with super-pure aluminium; details are given below. The other alloy was prepared from super-pure aluminium and electrolytic chromium by The British Aluminium Co., Ltd., and had the following composition: silicon 0.009, iron 0.005, copper 0.0005, manganese 0.0005, chromium 10.4%.

#### (d) Zinc-Chromium Master Alloys

Two alloys were prepared by a method described below involving the reduction of chromium chloride with the purer grade of zinc; the purities of these materials were as given in (a) and (c) above. The chromium content of the alloys obtained was, respectively, 0.23 and 0.54%. At a later stage in the work, an alloy containing 1.94% chromium was made by direct solution, in molten zinc, of electrolytic chromium.

## 2. PREPARATION OF MASTER ALLOYS

#### (a) Aluminium-Chromium Alloys

Before the 10.4% chromium alloy became available, attempts were made to produce suitable material by the reduction of chromium compounds with molten aluminium. Initially, dehydrated chromic chloride was mixed with a standard flux containing magnesium, potassium, and sodium chlorides, and calcium fluoride. This was added in small quantities to molten aluminium, at 800° C., contained in an alumina-lined crucible. After thorough stirring, the resulting alloy was granulated by casting into cold water. It was found impossible by this method to introduce more than 0.5% chromium; oxidation losses were serious and uncontrolled. Experiments using the trioxide were somewhat more successful, but again oxidation losses were heavy. The method finally adopted was to add to molten aluminium, at 750°–800° C., a mixture of one part of chromium oxide and two parts of dehydrated chromic chloride, together with the standard flux. Reaction proceeded vigorously, and by this means it was possible to produce 90 g. of granulated master alloy, containing 1.03% chromium.

#### (b) Zinc-Chromium Alloys

The preparation of a zinc-chromium master alloy, by means of which alloys in the zinc-rich region could be made up, presented some difficulty. According to previous workers,<sup>9, 10, 12</sup> solid chromium dissolves in molten zinc only to a very small extent, so that attempts to prepare alloys in this way lead to the presence of considerable quantities of free chromium. Le Chatelier,<sup>13</sup> in attempting to prepare alloys by reducing chromium chloride with molten zinc, also obtained a large amount of free chromium; Hanemann,<sup>9</sup> however, found it possible to produce alloys without free chromium by adding solid zinc to the chloride dissolved in a molten flux. Since no success was obtained by the addition of dehydrated chromic chloride to molten zinc, Hanemann's method was employed in the present work. An alumina-lined fireclay crucible was half-filled with a flux containing 59.5 mol.-% potassium chloride and 40.5 mol.-% lithium chloride, and the temperature raised to 100° C. above the melting point of the flux. At this stage the dehydrated chromium chloride was added until the mixture became pasty, and the temperature was raised to 800° C. Preheated pieces of zinc, of approximately 10 g. in weight, were then added, with thorough stirring; time to re-attain the temperature of 800° C. was allowed between each addition. When the zinc had been added, the mixture was stirred for 2 hr. to achieve complete solution of the chromium, after which it was granulated in cold water. Two alloys made in this way, containing respectively 0.23 and 0.54% chromium, proved very convenient for examining the extreme zinc-rich region of the system. No free chromium was visible micrographically. The success of the method depends entirely on the operating temperature, which is that at which the speed of reduction of the chloride equals the rate of solution of the chromium produced. Below 800° C., the speed of reduction is the greater and results in the presence of free chromium. At temperatures above 800° C., the chloride, under the conditions of the experiment, tends to become converted to the sesquioxide, with consequent difficulty in reduction.

In addition to these materials, a master alloy richer in chromium was required. It was found possible to obtain this by direct solution of electrolytic chromium in molten zinc, in spite of previous statements to the contrary. After preliminary experiments, the following method was adopted. Sufficient zinc and electrolytic chromium to provide an alloy with approximately 2% chromium were sealed *in vacuo* in a hard-glass tube. The mixture was annealed for 3 weeks, with thorough shaking at regular and frequent intervals, at a temperature of 450° C. This temperature was chosen so that the alloy would correspond with the (liquid +  $\theta$  (Zn-Cr)) field of the equilibrium diagram, and would thus contain no free chromium if complete solution was achieved. After 3 weeks, the tube was shattered by plunging in cold water, and the resulting granulated alloy was

found to contain 1.94% chromium. Examination of the structures of alloys subsequently prepared from this master alloy confirmed the absence of free chromium. Subsidiary experiments showed that negligible contamination by silicon from the glass tubes occurred; for example, a similar alloy containing 0.75% chromium was found by analysis to contain less than 0.01% silicon.

### 3. GENERAL METHODS

Alloys were prepared by melting together carefully weighed quantities of the pure metals and master alloys, with thorough stirring. For the annealing work, quantities of 15–25 g. were made, and cast into cold copper moulds. Alloys intended for slow-cooling experiments were made in quantities of 50–150 g., except in the extreme zinc-rich region of the system, where up to 300 g. of alloy were prepared to enable very small proportions of chromium to be introduced in the form of accurately weighable amounts of master alloy. In general, the aluminium was first melted and heated to 800° C. before addition of the aluminium-chromium master alloy; where the amount of the latter was appreciable, this procedure was reversed. The zinc, or zinc-rich master alloy, was added and quickly stirred in immediately before casting or slow cooling. Slow-cooling experiments were carried out at  $\frac{3}{4}$ ° C./min., using a potentiometric programme controller to ensure a uniform rate.\* When cold, each slowly cooled ingot was sectioned vertically, and one half was examined micrographically. The other half, if suitable, was used for the extraction of the primary intermetallic compounds present.

From aluminium-rich alloys, primary crystals were extracted by anodic solution of the matrix in 7½% hydrochloric acid at a current density of 0.5 amp./in.<sup>2</sup> and a potential of 8 V. The crystals settled to the bottom of the cell, and were washed successively with 50% nitric acid, water, and alcohol, and finally dried. Clean, well-formed crystals were picked out under a binocular microscope for chemical and X-ray analysis. With increasing percentages of zinc, the primary crystals of the aluminium-chromium phases became much smaller and fewer in number, and it was necessary to modify the usual method of extraction to ensure as complete and uncontaminated a collection of crystals as possible. Also, a weaker electrolyte (1–4% hydrochloric acid) was employed, in view of the greater reactivity of the crystals from zinc-rich alloys. The apparatus is shown in Fig. 5 (a), and is self-explanatory. Extracted crystals collected on the glazed paper, from which they could easily be removed after washing and drying; these processes were carried out in the funnel. Such crystals were usually too small for accurate sorting and too few for chemical analysis; they were used for the X-ray work. In several cases it was necessary to

obtain X-ray-diffraction patterns from the very small crystals present in chill-cast alloys which had been annealed and quenched. Extraction of these crystals was carried out in the apparatus shown in Fig. 5 (b), which again is self-explanatory. A very low current density was employed, and the electrolyte was frequently changed. At the end of an experiment, the glass container was removed; the contents of the paper sack were washed with distilled water and alcohol and finally dried by gentle heating. Microscopic examination at a magnification of 500 dia. showed the extracted crystals to be slightly contaminated by matrix material, which was, however, insufficient to cause any interference on Debye-Scherrer diffraction films.

For annealing treatments, alloys were sealed in evacuated glass tubes; contact with the glass was avoided by the use of sheaths made from high-grade

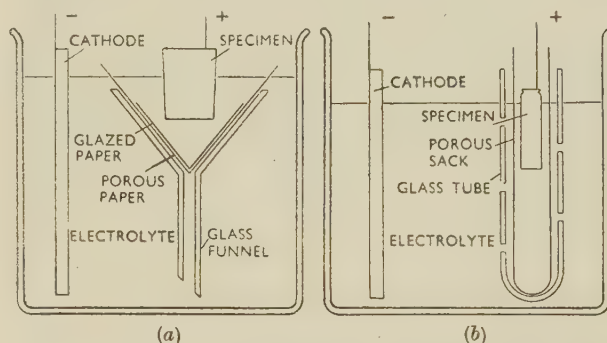


FIG. 5.—(a) Cell for Extraction of Small Crystals from Zinc-Rich Alloys. (b) Cell for Extraction of Very Small Crystals from Annealed Alloys.

alumina cement. Annealing was carried out in tubular electric resistance furnaces automatically controlled to within  $\pm 1$ ° C. of the required temperature. Temperature measurements throughout the work were made with a periodically calibrated platinum/platinum-13% rhodium thermocouple, used in conjunction with an accurate potentiometer.

Standard X-ray techniques were employed to obtain diffraction patterns of extracted crystals. The crystals were crushed in an agate mortar, and were initially mounted on hairs or glass fibres with Canada balsam. Later, improved results were obtained by mixing the powder with a minimum of gum tragacanth, moistening with water, and extruding thin rods of the resultant paste. Specimens were exposed to copper  $K_\alpha$  radiation in either a 9- or 19-cm. Debye-Scherrer camera of the van Arkel type.

Critical alloys and a number of samples of intermetallic compounds were analysed chemically, either in the authors' laboratory, or by Johnson, Matthey and Co., Ltd. Results from the two sources were consistent.

\* In the region of the ternary eutectic, the fields of primary separation become very narrow, and a cooling rate of  $\frac{1}{4}$ ° C./min. proved more satisfactory.



## 4. METALLOGRAPHY

No ternary compounds were observed during the course of the work, so that only phases based upon those present in the respective binary systems occurred. The preparation of microsections was carried out using relatively standard techniques, finishing by a light polish on a pad of blanket felt with fine-grade alumina as the polishing medium.

(a) *Aluminium-Rich Alloys*

Examination of unetched sections showed the presence of hard silver-grey crystals of an intermediate phase, sometimes containing cores of slightly harder, darker material, set in the aluminium-rich matrix. Because of their similarity to the crystals occurring in binary aluminium-chromium alloys, these were tentatively identified as  $\text{CrAl}_7$ , with cores of  $\text{Cr}_2\text{Al}_{11}$ . Etching methods described by Little, Axon, and Hume-Rothery<sup>11</sup> were therefore initially used in the examination of these alloys, but the results were found to be somewhat non-reproducible. Further etching treatments were therefore examined, and the more reliable are summarized in Table I. Several reagents revealed very fine duplex structures in the matrix, arising from the decomposition of the aluminium-zinc solid solution; larger-scale duplex structures were observed in alloys richer in zinc, owing to the presence of the zinc-rich solid solution.

TABLE I.—*Etching Treatments for Aluminium-Rich Alloys.*

	Reagent *	Time, sec.	Results
1	0.5% HF, 2.0% HCl, in water	10	Grain-boundary reagent; crystals unattacked.
2	15 g. ammonium molybdate, 100 c.c. 50% $\text{HNO}_3$ , 100 c.c. water	20	Crystals coloured green, blue, and brown; distinction between cores and rims of duplex crystals uncertain.
3	5% $\text{HNO}_3$ in water	5	$\beta$ light brown to dark blue; $\alpha$ , or ( $\alpha + \alpha'$ ) decomposition structure, blue grey; crystals unattacked.
4	0.5-1.0% HF, 1-3% $\text{HNO}_3$ , 1-2% HCl, in water.	15	Deep attack on matrix; crystals unattacked.
5	10 g. KOH, 10 g. $\text{K}_3\text{Fe}(\text{CN})_6$ , 100 c.c. water.	20	Grain boundaries revealed; $\beta$ white; $\alpha$ , or ( $\alpha + \alpha'$ ) decomposition structure, grey to black; crystals unattacked.
6	Thermal etching.	...	Accentuated grain boundaries; differentiated cores of duplex crystals.

\* Reagents 1-5 used cold.

No reagent was found to give a satisfactory and reproducible attack on the crystals of intermediate compounds or to differentiate with certainty between  $\text{CrAl}_7$  and  $\text{Cr}_2\text{Al}_{11}$ . The best results were obtained by a sequence of etches consisting of 10 sec. in reagent (5), 20 sec. in reagent (1), and finally a further 30-60 sec. in reagent (5). After this treatment the cores in duplex crystals were slightly attacked and showed a greenish tinge. The general unreactive nature of the particles of the intermediate

phases was consistent with their being derived from the aluminium-chromium compounds, but more reliable evidence than that given by etching was clearly necessary.

Several reagents adequately distinguished the two-phase and three-phase alloys present in the system, but the most reliable was found to be reagent (5).

(b) *Zinc-Rich Alloys*

Many of the zinc-rich alloys prepared contained the  $\theta$  (Zn-Cr) phase, which was, by contrast with the aluminium-chromium compounds, soft and not readily visible in relief in the unetched specimens of lowest aluminium content. Several etching reagents satisfactorily differentiated  $\theta$  (Zn-Cr) from the matrix; the most generally useful was reagent (5) in Table I. This coloured the matrix yellow, and on etching for 15 sec. the  $\theta$  (Zn-Cr) crystals in binary zinc-chromium alloys were yellowish brown. Longer etching times coloured the compound crystals varying shades of brown according to orientation, until, after 60 seconds' immersion, a relatively uniform dark-blue coloration was produced. With increasing aluminium content of the alloy under examination, the crystals became progressively harder and more resistant to attack; longer periods of etching (up to 2 min.) were necessary to produce any coloration. At aluminium contents greater than 0.5%, the crystals were scarcely attacked even by prolonged etching.

The experimental results obtained are described in Section IV. Where it is desirable to refer to individual alloys, these are denoted by their chromium and zinc contents; thus, alloy 1/30 refers to an alloy containing 1 wt.-% chromium and 30 wt.-% zinc.

## IV.—EXPERIMENTAL RESULTS

The equilibrium relationships in the ternary system were investigated by the metallographic examination of slowly cooled alloys, and of alloys annealed and quenched from various temperatures. The crystals of intermetallic compound present in many of the slowly cooled alloys were separated, and, where possible, analysed. The identification of the crystals was confirmed or established by X-ray methods.

## 1. THE SURFACES OF PRIMARY SEPARATION

In all, some 150 alloys, covering all compositions lying on the aluminium-zinc side of a line joining the compositions (90% Al, 10% Cr) and (98% Zn, 2% Cr) were slowly cooled and examined. The majority of these alloys lay in the zinc-rich region of the constitutional diagram, as the equilibria were found to be complex between 95 and 100% zinc. Microsections revealed the presence in all alloys of crystals of primary intermetallic compound, which were unusually small and tended to become even smaller with increase in the chromium or zinc content. Numerous attempts were made to increase the crystal

size by modifications in cooling rate and programme, but without success. Consequently, it was found impracticable to obtain samples of uncontaminated crystals for chemical analysis by sorting residues from electrolytic extractions, except in the case of alloys containing less than 1% chromium and 40% zinc.

The results of the experiments are summarized in Figs. 6, 7, and 8, which are plotted on a progressively larger scale to show the complexity of the zinc-rich alloys. These diagrams are most conveniently considered in terms of the general types of microstructure observed.

#### (a) Alloys Depositing Primary $\text{CrAl}_7$ Crystals

The alloys denoted in Fig. 6 by open circles, after slow cooling, gave microstructures in which the primary crystals visible were very similar to those obtained by slowly cooling binary aluminium-chromium alloys. The primary crystals were homogeneous, and no peritectic cores were visible in the etched sections. Crystals were extracted from several alloys, and consisted of a mixture of flat plates and hexagonal prisms exactly similar to the mixture of crystal forms obtained by extraction from binary aluminium-chromium alloys of such compositions that  $\text{CrAl}_7$  separates as primary crystals. Debye-Scherrer photographs of both types of crystal separated from ternary alloys were identical with that of  $\text{CrAl}_7$ . In addition, X-ray work showed the crystals extracted from alloys 1/10, 1/30, 3/10, and 1/40 to be  $\text{CrAl}_7$ , while the analysis of good-quality crystals from alloys 1/30 and 1/40 gave the following results, which are consistent with solid solution of zinc in  $\text{CrAl}_7$ :

Alloy	Cr, wt.-%	Zn, wt.-%
1/30	20.90	10.05
1/40A	20.36	11.98
1/40B	19.86	11.72

The expected field of primary separation of  $\text{Cr}_2\text{Al}_{11}$  therefore does not appear; all the alloys under consideration deposit primary  $\text{CrAl}_7$ . This difficulty has also been met with in other ternary systems involving the addition of a third metal to the aluminium-chromium system (e.g. the aluminium-chromium-iron system<sup>5</sup>) and is very probably due to the marked tendency towards supercooling of  $\text{Cr}_2\text{Al}_{11}$ . From experience in this and other systems, it appears likely that marked supercooling takes place until the temperature of the melt is in the region of the  $\text{Cr}_2\text{Al}_{11} + \text{liq.} \rightleftharpoons \text{CrAl}_7$  peritectic, when  $\text{CrAl}_7$  is deposited from supersaturated solution. The unusually small size of the crystals extracted from these alloys is consistent with this interpretation. Since the slow cooling rates employed may have accentuated this difficulty, certain alloys were cooled more rapidly; cooling rates of 1°–2° C./min. made no difference to the type of microsection observed, but at rates of 5°–10° C./min. cores were observed in the crystals of intermetallic compound deposited from melts that would be expected to lie in the primary

$\text{Cr}_2\text{Al}_{11}$  field. There is little doubt, therefore, that under equilibrium conditions a primary  $\text{Cr}_2\text{Al}_{11}$  field would appear in the ternary diagram, and the  $\text{liq.} + \text{Cr}_2\text{Al}_{11} \rightleftharpoons \text{CrAl}_7$  peritectic line has been inserted in Fig. 6 in such a position as to be consistent with the peritectic point in the binary aluminium-chromium diagram.

It will be observed that, in Fig. 6, the primary  $\text{CrAl}_7$  field has been continued to a composition close to 95% zinc. This has been done on the basis of the structures of the alloys to be described below, and because metallographic experiments show (Section V) that the three phases in equilibrium at the ternary eutectic are  $\alpha$ ,  $\beta$ , and  $\text{CrAl}_7$ .

#### (b) Alloys Depositing Primary $\text{CrAl}_4$ Crystals

Many of the alloys examined fell into this group. The more aluminium-rich among these showed crystals of intermediate compound containing hard, dark cores set in what appeared, from their metallographic characteristics, to be  $\text{CrAl}_7$  crystals. As the zinc content became higher the dark cores increased in size, at the expense of the material forming the outer rims of the crystals, and eventually the rims disappeared entirely. At still higher zinc contents, rims of phase identified as the  $\theta$  (Zn-Cr) compound appeared.

The first-mentioned group is distinguished in Fig. 6 by full circles bearing a small vertical bar. Electrolytic extractions were made from several alloys, but only in the cases of alloys 1/50 and 1/70 were the residues sufficient in quantity for suitable crystals to be hand picked for analysis. Analyses were made of these extracts with the following results:

Alloy	Cr, wt.-%	Zn, wt.-%
1/50	20.99	13.31
1/70	24.15	14.73

The chromium content is greater than in the case of extracts from alloys 1/30 and 1/40, showing that the material of the cores represents a phase richer in chromium than  $\text{CrAl}_7$ . X-ray exposures were made of the extracts from alloys 1/60, 9.36/10, and 1/70. In the micro-sections of the first two, only small, hard cores were visible, and the X-ray pattern was typical of that of  $\text{CrAl}_7$ . This justifies the extension of the  $\text{CrAl}_7$  primary field to high zinc contents, as shown in Fig. 6. Alloy 1/70, however, showed cores of appreciable size in the  $\text{CrAl}_7$  crystals, and the diffraction pattern contained well-defined lines in addition to those of  $\text{CrAl}_7$ . The extra lines agreed exactly with those obtained in diffraction patterns of the core material free from  $\text{CrAl}_7$ , obtained from alloys richer in zinc.

The microsections of the alloys of this class contained, in addition to the cored crystals, a matrix of aluminium-rich solid solution together with ternary eutectic material.

Alloys in which the rims of  $\text{CrAl}_7$  had disappeared are indicated in Figs. 6 and 7 by full circles. The micrographic characteristics of the primary crystals were almost identical with those of  $\text{CrAl}_7$ , and



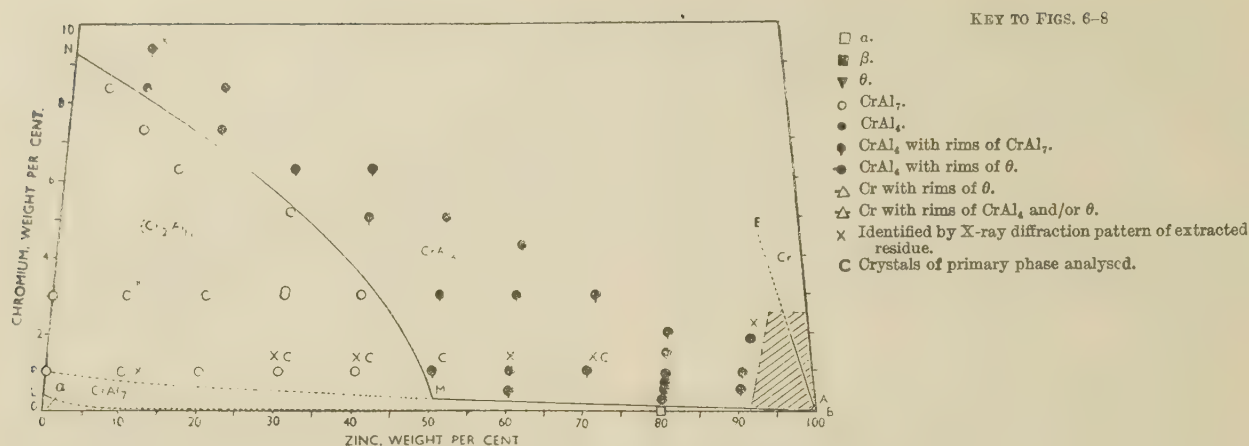


FIG. 6.—The System Aluminium-Chromium-Zinc: Surfaces of Primary Separation.

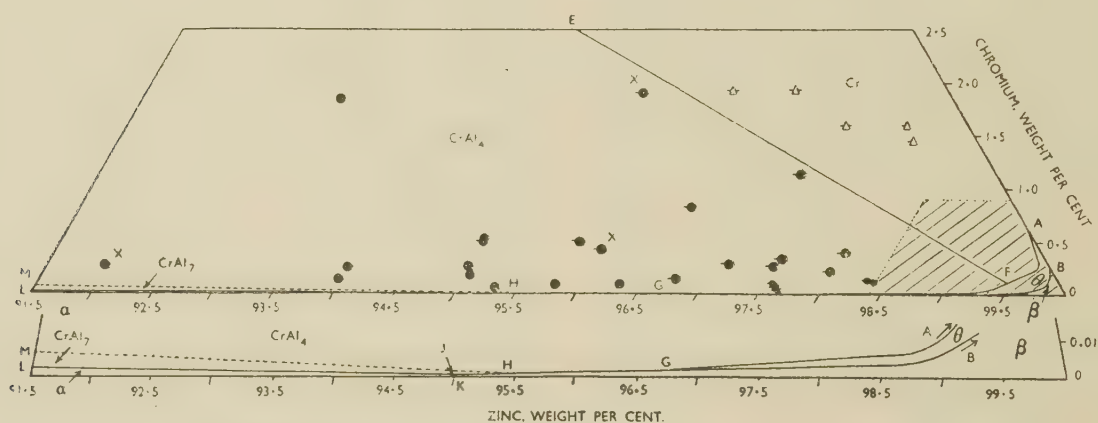


FIG. 7.—The System Aluminium-Chromium-Zinc: Surfaces of Primary Separation in the Region 0-2.5% Chromium and 0-8.5% Aluminium.

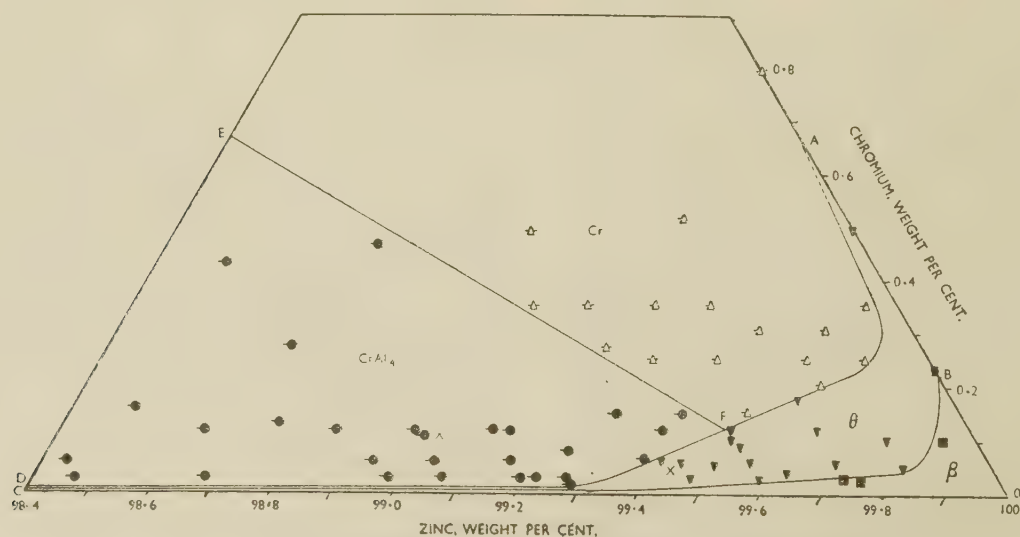


FIG. 8.—The System Aluminium-Chromium-Zinc: Surfaces of Primary Separation in the Region 0-0.9% Chromium and 0-1.6% Aluminium.

although the phase could be distinguished from rims of the  $\text{CrAl}_7$  phase, when both were present together, no reliance could be placed on etching experiments to distinguish the new phase from  $\text{CrAl}_7$  in separate specimens. Accordingly, the crystals were extracted from several alloys and the more successful residues submitted to X-ray examination. Residues from alloys 1.79/90.71 and 0.25/92 gave identical diffraction patterns, which did not agree with those of  $\text{CrAl}_7$ ,  $\text{Cr}_2\text{Al}_{11}$ , or with the  $\gamma$ -brass or tetragonal phases of the aluminium-chromium system. They were, however, closely similar to the diffraction pattern of  $\text{CrAl}_4$  published by Bradley and Lu<sup>3</sup> and the crystals were identified as consisting of this phase. The reason for the disappearance of rims of  $\text{CrAl}_7$  in these alloys is connected with the fact that the primary  $\text{CrAl}_7$  field, at corresponding zinc contents, has shrunk to a very narrow strip parallel to the aluminium-zinc axis of the diagram. The temperature of the cooling alloy thus very quickly traverses the range within which crystallization of  $\text{CrAl}_7$  is possible.

With still further increase in zinc, the  $\text{CrAl}_4$  crystals become rimmed by  $\theta$  (Zn-Cr). The alloys in this class are distinguished in Figs. 7 and 8 by full circles bearing a horizontal bar. During cooling, the composition of the liquid remaining after primary crystallization of  $\text{CrAl}_4$  traverses the line separating the primary  $\text{CrAl}_4$  and primary  $\theta$  (Zn-Cr) fields, and the alloys deposit some primary  $\theta$  (Zn-Cr) and secondary crystals of this material.

Extracts were obtained from several alloys, and those from alloys 0.42/96, 0.25/92, and 1.79/90.71 gave unmistakable diffraction patterns of  $\text{CrAl}_4$ . In alloys 1.89/95.61 and 0.10/99 appreciable quantities of  $\theta$  (Zn-Cr) were present, and the correct identification of this phase was confirmed by the X-ray-diffraction pattern obtained from extracts from these alloys. It may be noted that alloy 0.06/99.38 lies very close to the boundary of  $\text{CrAl}_4$  separation; the primary crystals were almost entirely  $\theta$  (Zn-Cr), with small  $\text{CrAl}_4$  cores.

#### (c) Alloys Depositing Primary Chromium

Twenty-four alloys in the zinc-rich region showed primary crystals of chromium, which were rimmed, in most cases heavily, by either  $\text{CrAl}_4$ ,  $\theta$  (Zn-Cr), or both. The possibility that the free chromium was not a true primary deposit, but had been present in the master alloys used, was carefully considered. It was concluded that the material represented true primary particles, because the alloys, apart from 1.91/96.34, 1.92/96.84, 1.58/97.42, and 1.59/97.91, were prepared from master alloys obtained by the reduction of chromium chloride; as shown by examination, these master alloys contained no free chromium, and no free chromium was observed in alloys prepared from them and lying in fields of primary separation other than that of primary chromium.

In Figs. 7 and 8, open triangles represent alloys in which primary chromium was observed. A

horizontal bar denotes rimming by  $\theta$  (Zn-Cr), and two such bars denote rimming by  $\text{CrAl}_4$  and  $\theta$  (Zn-Cr). Alloys in the latter class usually showed, because of the mode of crystallization, inner cores of chromium surrounded successively by rims of  $\text{CrAl}_4$  and  $\theta$  (Zn-Cr). This is consistent with the fields of primary separation shown. Alloys in which rimming of primary chromium by  $\theta$  (Zn-Cr) only was observed clearly lie at such compositions that the composition of the liquid alters, on primary precipitation of chromium, in such a way as to strike the boundary  $FA$  without crossing the boundary  $FE$ .

It may be noted that the binary alloys 0.79/99.21 and 0.5/99.5 were prepared by direct synthesis and annealed at 600° C. Both these alloys should, according to the diagram due to Heumann,<sup>10</sup> deposit primary  $\theta$  (Zn-Cr) on cooling. Alloy 0.79/99.21, however, deposited primary chromium on slow cooling after annealing for 28 days, while alloy 0.5/99.5 deposited only  $\theta$  (Zn-Cr) on slow cooling after annealing for 21 days. The point representing the composition of the liquid at the temperature of the liq. + Cr  $\rightleftharpoons$   $\theta$  (Zn-Cr) peritectic must thus occur at a smaller chromium content (approx. 0.7%) than that given by Heumann.

#### (d) Alloys Depositing Primary $\theta$ (Zn-Cr)

The alloys which deposited primary  $\theta$  (Zn-Cr) crystals are indicated in Fig. 8 as full inverted triangles, and it will be seen that they adequately define the field of primary  $\theta$  (Zn-Cr) separation down to approximately 99.4% zinc. X-ray examination of the extract from alloy 0.06/99.41 confirmed the identification of the primary phase. Below 99.4% zinc no alloys containing primary  $\theta$  (Zn-Cr) alone were observed experimentally. The corresponding field of primary separation must, however, continue to much lower zinc contents, since rims of  $\theta$  (Zn-Cr) were observed surrounding primary  $\text{CrAl}_4$  particles down to approximately 96.7% zinc.

#### (e) Alloys Depositing Primary $\beta$ and Primary $\alpha$

Fig. 8 shows three alloys which were obtained in the primary  $\beta$  field, and serve to confirm the general shape of the boundary between the primary  $\theta$  (Zn-Cr) and primary  $\beta$  fields. Only two primary  $\alpha$  alloys were observed, and no attempt was made to examine the primary  $\alpha$  field in detail.

#### (f) The General Form of the Surfaces of Primary Separation

As noted above, no alloys were obtained, except at rates of cooling too high for the use of the results in any diagram approximating to equilibrium conditions, in which the phase  $\text{Cr}_2\text{Al}_{11}$  occurred either as primary particles or as spines in other crystals. The line dividing the primary  $\text{Cr}_2\text{Al}_{11}$  field in the ternary diagram from the  $\text{CrAl}_7$  field has therefore been inserted, as a dotted line (Fig. 6), in its most probable position. The primary  $\text{CrAl}_7$  and primary



$\alpha$  fields must both extend to the ternary eutectic close to 95% zinc, since rims of  $\text{CrAl}_7$  are observed round primary  $\text{CrAl}_4$  particles, and since  $\alpha$ ,  $\text{CrAl}_7$ , and  $\beta$  crystallize together from the ternary eutectic (see Section IV, 2). At  $M$  (Fig. 6) the boundary separating the primary  $\text{CrAl}_4$  field from that of primary  $\text{Cr}_2\text{Al}_{11}$  makes contact with the primary  $\text{CrAl}_7$  field. This point occurs at approximately 50% zinc, and 0.4% chromium. At 50% zinc, therefore, the  $\text{CrAl}_7$  and  $\alpha$  primary fields are already very narrow.

Evidence for the position of the ternary eutectic point  $J$  (Fig. 7) is obtained from alloys 0.125/94 and 0.25/94. In the former, in addition to primary  $\text{CrAl}_4$  crystals, secondary  $\alpha$  crystals are visible in a ternary eutectic matrix; in the second alloy, there are primary  $\text{CrAl}_4$  crystals, and secondary  $\beta$  crystals set in the eutectic matrix. Taking into consideration the composition of the primary phase, the eutectic point  $J$  must lie very close to the composition of the binary aluminium-zinc eutectic, in agreement with the work of Weisse, Blumenthal, and Hanemann.<sup>8</sup> Since alloy 0.03/95.32 contains primary  $\text{CrAl}_4$  crystals, it is clear that the chromium content of the eutectic must be less than 0.01% and is probably nearer 0.01%.

The point  $H$  (Fig. 7) at which the line separating the  $\text{CrAl}_4$  and  $\text{CrAl}_7$  fields meets that separating the  $\text{CrAl}_4$  and  $\beta$  fields is difficult to locate owing to the extreme narrowness of the  $\text{CrAl}_7$  and  $\beta$  fields in the region of the ternary eutectic. Point  $H$  must lie at a higher zinc content than that of the eutectic, but, since the  $\text{CrAl}_7$  field is very narrow, cannot differ greatly from the eutectic composition. It has therefore been placed at 95.5% zinc and 0.001% chromium.

The lines separating the  $\theta$  (Zn-Cr) and  $\beta$  fields, the chromium and  $\theta$  (Zn-Cr) fields, and the  $\text{CrAl}_4$  and  $\theta$  (Zn-Cr) fields are well established by the alloys examined above 99.3% zinc. The line  $FE$  (Fig. 7) separating the primary chromium and primary  $\text{CrAl}_4$  fields is also well defined; the point  $F$  falls at 0.12% chromium and 99.48% zinc. The primary  $\beta$  field must extend back to the ternary eutectic, but must be extremely narrow at zinc contents less than 99.3%, since alloy 0.01/99.29 contains primary  $\text{CrAl}_4$ .

It will have been noted that primary  $\text{CrAl}_4$  crystals may be rimmed by  $\text{CrAl}_7$ , by  $\theta$  (Zn-Cr), or not rimmed at all. The alloy richest in aluminium that showed rims of  $\theta$  (Zn-Cr) was alloy 0.5/95. Alloys 0.48/95.81, 0.42/96, and 0.14/96.77 showed appreciable amounts of this phase. Assuming the composition of  $\text{CrAl}_4$ , the point  $G$  (Fig. 7) may be estimated to lie approximately at the composition 96.75% zinc and 0.001% chromium; at this point  $\text{liq.} + \theta \text{ (Zn-Cr)} \rightleftharpoons \beta + \text{CrAl}_4$ .

The outstanding feature of the projection of the surfaces of primary separation is the crowding of the  $\theta$  (Zn-Cr) and  $\beta$  primary fields into the extreme zinc-rich corner of the diagram, and the persistence of the field of primary separation of  $\text{CrAl}_4$  up to 99.5% zinc. A further feature of interest is the extension of

the primary fields of the aluminium-chromium and zinc-chromium compounds almost to the aluminium-zinc axis of the diagram. The addition of very small quantities of chromium to aluminium-zinc alloys therefore results in the presence of  $\text{CrAl}_7$  at zinc contents below 50%, and of  $\text{CrAl}_4$  between 50 and 99.5% zinc.

## 2. THE CONSTITUTION IN THE SOLID STATE

In order to make a preliminary exploration of the equilibrium relations in the solid state, four groups of alloys were prepared, and annealed at the highest safe temperature, which was established by preliminary solidus experiments. These four groups of alloys possessed compositions as illustrated in Fig. 9, and received annealing treatments as follows:

- Group 1. 21 days at 448° C.
- Group 2. 21 days at 519° C. + 14 days at 519° C.
- Group 3. 21 days at 431° C.
- Group 4. 21 days at 371° C.

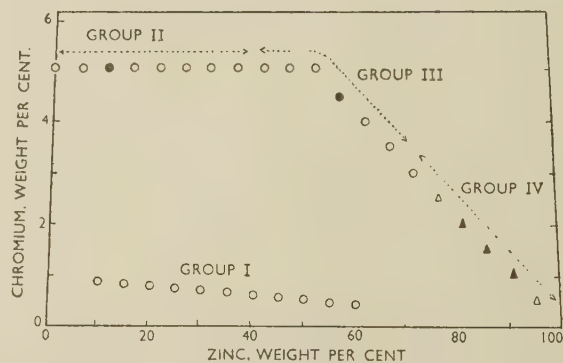


FIG. 9.—Exploratory Experiments in the Solid State.

KEY.  
 ○ ●  $\alpha + \text{CrAl}_7$ .       $\Delta \blacktriangle \alpha + \beta + \text{CrAl}_7$ .  
 Solid symbols indicate identification from X-ray diffraction pattern of extracted residues.

On micro-examination, all alloys in groups 1, 2, and 3 showed hard particles set in an aluminium-zinc alloy matrix, which, at zinc contents from approximately 25–60%, showed evidence of the decomposition of the  $\alpha$  phase into two phases on quenching, in the form of scarcely resolvable grey patches frequently associated with grain boundaries. The hard particles were micrographically similar to  $\text{CrAl}_7$ , and their identification as this phase was confirmed by the X-ray-diffraction patterns of the crystals extracted from alloys 5/10 and 4.5/55. In the case of the most zinc-rich alloys of group 3, some of the larger  $\text{CrAl}_7$  crystals contained very small cores of a second intermediate phase, which, from the evidence obtained with slowly cooled alloys, was probably  $\text{CrAl}_4$ . These, however, were neglected, since their complete absorption could not affect the general interpretation of the microstructures.

In group 4, only alloy 3.0/70 showed the  $(\alpha + \text{CrAl}_7)$  structure. The remainder were three-phase, showing the presence of the  $\beta$  phase (solid solution of aluminium in zinc). The amount of  $\beta$  increased with increasing

zinc content. Again, some  $\text{CrAl}_7$  crystals contained cores, which could not be completely removed even by 8 weeks' annealing. Crystals were extracted from alloys 2/80, 1.5/85, and 1.0/90, and subjected to X-ray experiments. The diffraction pattern of

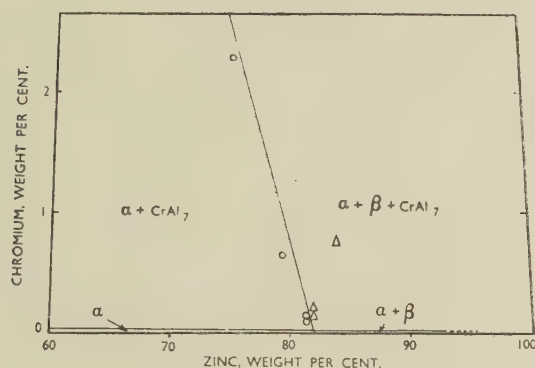


FIG. 10.—Zinc-Rich Alloys: Constitution in the Solid State.

KEY.  
 $\circ$   $\alpha + \text{CrAl}_7$ ,  $\Delta$   $\alpha + \beta + \text{CrAl}_7$ .  
 All analysed compositions.

the residue from 2/80 was clearly that of  $\text{CrAl}_7$ , but the patterns from the other two alloys showed  $\text{CrAl}_4$  to be present in recognizable amount. These experiments confirmed that complete equilibrium had not been attained at  $371^\circ\text{C}$ . The  $\text{CrAl}_4$  cores, however, were insufficient in amount to modify the structure appreciably on complete absorption.

All the alloys of groups 1-4 were re-annealed for 21 days at  $371^\circ\text{C}$ ., to provide a complete isothermal at this temperature. No metallographic changes were observed. These preliminary experiments thus established that a three-phase triangle involving the  $\alpha$ ,  $\beta$ , and  $\text{CrAl}_7$  phases exists in the ternary system; since  $\alpha$  and  $\beta$  are associated in the binary eutectic, the ternary eutectic must involve  $\alpha$ ,  $\beta$ , and  $\text{CrAl}_7$ .

The preliminary work also established that alloys 3.0/70 and 2.5/75 bracket the  $(\alpha + \text{CrAl}_7)/(\alpha + \beta + \text{CrAl}_7)$  boundary. Further alloys were prepared to define this boundary more closely; after annealing for 21 days at  $371^\circ\text{C}$ . microsections were examined and the critical alloys analysed. The results are shown in Fig. 10. Since the ternary eutectic contains certainly not more than 0.01% chromium, the width of the  $(\alpha + \beta)$  field in the ternary diagram cannot exceed this in terms of chromium content. The point of contact of the  $(\alpha + \text{CrAl}_7)/(\alpha + \beta + \text{CrAl}_7)$  boundary with the  $(\alpha + \text{CrAl}_7)/\alpha$  boundary must therefore be practically coincident with the limit of solubility of zinc in aluminium at  $371^\circ\text{C}$ . ( $82.0 \pm 0.3\%$ ). This fact has been utilized in drawing Fig. 10.

Some difficulty was experienced in attempts to locate the  $(\alpha + \beta + \text{CrAl}_7)/(\beta + \text{CrAl}_7)$  boundary, which must intersect the  $(\beta + \text{CrAl}_7)/\beta$  boundary at a point very close to the solid-solubility limit of aluminium in zinc at  $371^\circ\text{C}$ . ( $98.9 \pm 0.1\%$ ). A series of alloys containing 0.1% chromium and, respectively, 0.1, 0.2, 0.4, 0.6, 0.7, 0.9, and 1.0% aluminium was annealed at  $371^\circ\text{C}$ . for 24 weeks. All showed crystals of intermetallic compound in a  $\beta$  matrix, but the crystals were too small in size for identification. Two further alloys, 0.05/98.75 and 0.02/98.68, were similarly treated; the microstructure of alloy 0.05/98.75 was similar to those described above, while the matrix of alloy 0.02/98.68 contained, in addition to the  $\beta$  phase, small amounts of the aluminium-zinc  $\alpha$  phase.

A further series of 9 alloys was prepared, with compositions lying approximately on the line joining 94.7% zinc on the aluminium-zinc axis to 2.0% chromium on the zinc-chromium axis.\* These alloys were annealed for 46 days at  $371^\circ\text{C}$ ., after which treatment they were clearly not in equilibrium; little change from the as-cast structure had occurred. Subsequent re-annealing for a total of 17 weeks failed to remove the complex coring from the crystals of intermetallic compound, and no certain identification was possible except for alloy 1.73/97.71, which was

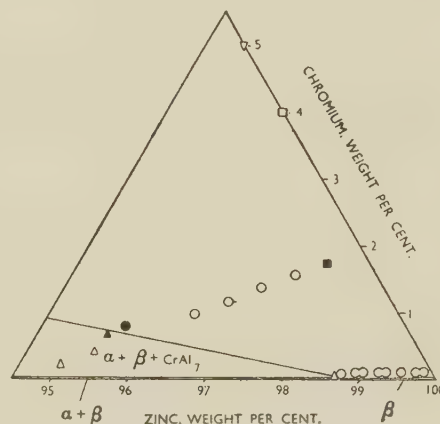


FIG. 11.—Experiments in the Solid State at Zinc Contents Greater than 95%.

KEY.  
 $\Delta$   $\alpha + \beta + \text{CrAl}_7$ ,  $\circ$   $\beta$ ,  $\square$   $\beta + \theta$ ,  $\nabla$   $\theta + \text{Cr}$ .  
 $\circ$ —X-ray diffraction pattern of extracted residues shows presence of  $\theta$ .  
 Solid symbols indicate analysed alloys.

$(\beta + \theta)$  in structure. A change in the matrix from  $\beta$  to  $(\alpha + \beta)$  was, however, observed between the compositions 0.78/95.59 and 0.62/95.41. These results are summarized in Fig. 11. It is of interest to note that the crystals extracted from alloy

\* During the preparation of these alloys the temperature was carefully controlled to avoid overheating the 1.94% chromium master alloy, and the consequent formation of free chromium. As a result of this precaution, the crystals of

intermediate phase in the alloys prepared were somewhat large, and this factor added to the difficulty of obtaining equilibrium on annealing.



1.36/97.05 gave a pattern in which only the diffraction lines due to  $\theta$  (Zn-Cr) could be recognized.

Although complete equilibrium was not attained in these alloys, it is probable that the boundary shown in Fig. 11 approximates closely to the  $(\alpha + \beta + \text{CrAl}_7)/(\beta + \text{CrAl}_7)$  boundary. The general directions of this boundary and the  $(\alpha + \text{CrAl}_7)/(\alpha + \beta + \text{CrAl}_7)$  boundary are consistent with intersection to form the third corner of the three-phase triangle, at the maximum solid solubility of zinc in  $\text{CrAl}_7$ , as determined by analysis of extracted crystals.

### 3. THE $\theta$ (Zn-Cr) COMPOUND

The preparation of alloys containing this phase has already been described. Attempts to separate sufficient for analysis were unsuccessful, owing to the relative reactivity of the crystals. To obtain an approximate confirmation of the composition of  $\theta$  (Zn-Cr), two alloys, of composition 5/95 and 4.02/95.98, were prepared by the method developed

zinc content. The ternary eutectic ( $\text{liq.} \rightleftharpoons \alpha + \beta + \text{CrAl}_7$ ) is very close in composition to the binary aluminium-zinc eutectic, and contains much less than 0.01% chromium. By contrast to the  $\text{CrAl}_7$  field, the field in which  $\text{CrAl}_4$  separates as primary crystals is remarkably extensive, pointing to a very high stability for this phase.

As noted previously, the primary  $\text{Cr}_2\text{Al}_{11}$  field does not appear to be present under conditions of slow cooling ( $\frac{3}{4}^\circ \text{C./min.}$ ), owing to super-cooling difficulties. The boundary  $MN$  (Fig. 6) between structures containing compound crystals in which  $\text{CrAl}_4$  occurs as pronounced cores, and structures containing primary  $\text{CrAl}_7$  crystals without cores, is, however, well established. In view of the fact that experiments using rapid cooling rates produced cored  $\text{CrAl}_7$  crystals in alloys having compositions within the area  $PMN$ , it is very probable that the ternary system, under equilibrium conditions, contains a region in which  $\text{Cr}_2\text{Al}_{11}$  separates as primary crystals, as shown in Fig. 6.

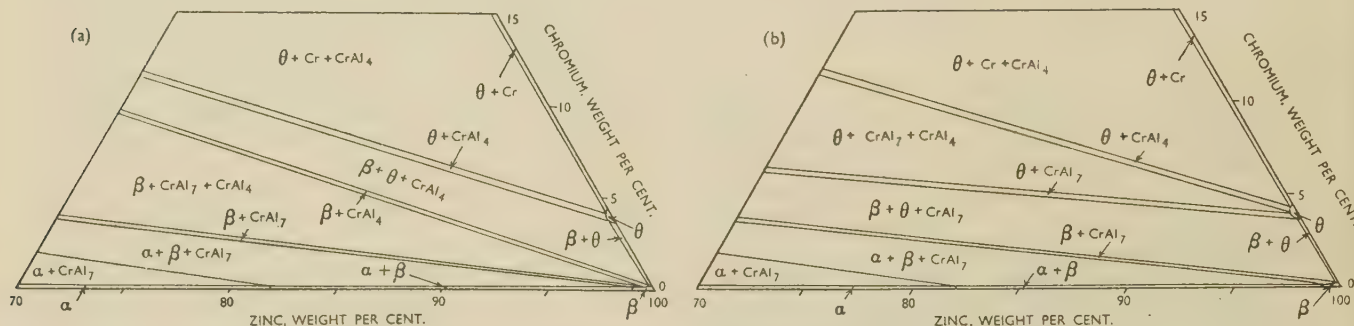


FIG. 12.—Possible Forms of Equilibria Involving the  $\beta$  Phase, in the Solid State.

for the binary zinc-chromium alloys used in the slow-cooling experiments. These were quenched from the liquid state, and annealed for 17 weeks at  $371^\circ \text{C.}$  After this treatment the 4% chromium alloy was  $(\beta + \theta \text{ (Zn-Cr)})$  in structure, while the 5% chromium alloy contained the  $\theta$  (Zn-Cr) phase in association with chromium. Those limits agree with the estimate made by Heumann,<sup>10</sup> and the structures confirm that no other intermediate phase occurs in the binary system.

### V.—DISCUSSION

The nature of the surfaces of primary separation in the system aluminium-chromium-zinc is peculiar, in so far as phases characteristic of the binary aluminium-chromium system are deposited as primary crystals at high zinc contents, while the introduction of a few tenths of a per cent. of chromium to aluminium-zinc alloys over most of the composition range causes the appearance of hard intermetallic-compound crystals or crystals of free chromium. The primary  $\alpha$  and primary  $\beta$  fields are very limited, while the primary  $\text{CrAl}_7$  field shrinks rapidly with increasing

The primary field in which  $\theta$  (Zn-Cr) separates is confined to a very small range of compositions in the zinc-rich corner of the diagram, which has, however, been accurately established.

From the slow-cooling experiments, it is difficult to decide whether the boundary dividing the  $\text{CrAl}_7$  and  $\text{CrAl}_4$  fields meets the line separating the  $\text{CrAl}_7$  and  $\alpha$  fields or that separating the  $\text{CrAl}_7$  and  $\beta$  fields. The existence of a three-phase  $(\alpha + \beta + \text{CrAl}_7)$  field in the solid state, however, makes it clear that the former alternative cannot be correct. Somewhat similar uncertainty exists with regard to the exact composition of the point  $G$ , terminating the primary  $\theta$  (Zn-Cr) field (Figs. 6 and 7). The relatively sharp onset of rimming of the primary  $\text{CrAl}_4$  particles by the  $\theta$  (Zn-Cr) phase (Fig. 7) suggests strongly that the boundary between the  $\text{CrAl}_4$  and  $\theta$  (Zn-Cr) fields meets the boundary between the  $\text{CrAl}_4$  and  $\beta$  fields, as plotted. In this case the equilibrium relations in the solid state for zinc-rich alloys are complex, since the following three-phase equilibria are implied: (i)  $\alpha$ ,  $\text{CrAl}_7$ , and  $\beta$ ; (ii)  $\text{CrAl}_7$ ,  $\text{CrAl}_4$ , and  $\beta$ ; (iii)  $\text{CrAl}_4$ ,  $\theta$  (Zn-Cr) and  $\beta$ ; (iv)  $\text{CrAl}_4$ ,  $\text{Cr}$ , and  $\theta$  (Zn-Cr). The equilibria involving the  $\beta$

phase, according to this scheme, are sketched schematically in Fig. 12 (a). If, however, the point *G* (Fig. 7) falls to the aluminium-rich side of point *H*, thus meeting the  $\text{CrAl}_7/\text{CrAl}_4$  boundary, the implied equilibria are: (i)  $\alpha$ ,  $\text{CrAl}_7$ , and  $\beta$ ; (ii)  $\text{CrAl}_7$ ,  $\text{CrAl}_4$ , and  $\theta$  (Zn-Cr); (iii)  $\text{CrAl}_7$ ,  $\theta$  (Zn-Cr), and  $\beta$ ; (iv)  $\text{CrAl}_4$ , Cr, and  $\theta$  (Zn-Cr). The corresponding constitution in the zinc-rich region is given schematically in Figure 12 (b). Owing to the difficulty of obtaining equilibrium by annealing chill-cast alloys in this region, it is not possible to decide between these alternatives, but, from the results of the slow-cooling experiments, Fig. 12 (a) is regarded as the more probable.

The solid solubility of zinc in  $\text{CrAl}_7$  is of interest, for comparison with those of manganese and iron in this phase. The analysed compositions of  $\text{CrAl}_7$  crystals extracted from alloys 1/30, 1/40, 1/50, and

behaviour of zinc therefore contrasts strongly with that of manganese and iron, which dissolve in  $\text{CrAl}_7$  partly by replacement of chromium and partly by filling vacant lattice sites in the  $\text{CrAl}_7$  structure.<sup>5, 14</sup> Manganese and iron each dissolve until a total solute concentration of 14.5 at.-% is reached; it will be noted that this solute concentration is exceeded by the zinc solid solution even before the limiting solubility is reached. Further, at the solubility limits of manganese and iron in  $\text{CrAl}_7$ , the number of 3*d* and 4*s* electrons supplied by the transition metals per solute atom is constant at 6.4; it is clearly impossible for this value to be attained by the solution of zinc. The mode of solution of a non-transition metal in  $\text{CrAl}_7$ , therefore, appears to be different from that of a transition metal, and it would be of interest to examine the solubility limits of other metals in the structure.

The detailed study of the ternary aluminium-chromium-zinc system reported in this paper shows that no ternary compounds, of the type observed in the aluminium-manganese-zinc system, occur. As has been previously demonstrated, there is considerable evidence that ternary compounds in aluminium-rich ternary alloys containing the transition metals manganese, iron, cobalt, and nickel are similar in many respects to electron compounds, and that the transition-metal atoms accept electrons from the structure as a whole. In some cases, chromium behaves in a similar manner; thus, ternary compounds of similar electron:atom ratio, calculated on the assumption that chromium and manganese may accept, respectively, 4.66 and 3.66 electrons per atom,<sup>1</sup> occur in the systems aluminium-chromium-magnesium<sup>11</sup> and aluminium-manganese-magnesium.<sup>15</sup> From the present work, however, it may be inferred that the alloying behaviour of chromium is not necessarily similar to that of manganese or the other transition metals of the first long period, and further systematic work is needed to define the conditions under which the different types of behaviour may be expected.

#### ACKNOWLEDGEMENTS

The work described was carried out in the Metallurgy Department of the University of Birmingham, under the general supervision of Professor D. Hanson, D.Sc., to whom the authors' thanks are due for his interest and encouragement.

Grateful acknowledgement is also made to the Department of Scientific and Industrial Research, the Royal Society, the Chemical Society, and Imperial Chemical Industries, Ltd., for financial assistance and the loan of apparatus.

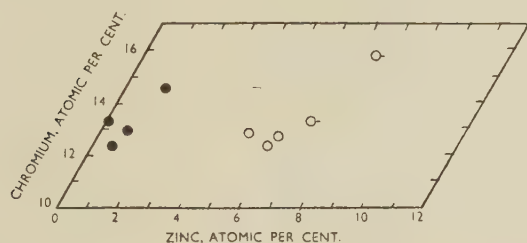


FIG. 13.—Compositions of Extracted Crystals. Solid symbols indicate results of other workers; primed symbols indicate crystals contained cores of  $\text{CrAl}_4$ .

1/70 are plotted in Fig. 13. It will be recalled that the samples from alloys 1/50 and 1/70 contained cores of  $\text{CrAl}_4$ , and the analyses are thus unreliable, except in so far as they show a marked solid solubility of zinc in  $\text{CrAl}_7$ . The compositions of the uncontaminated samples from alloys 1/30 and 1/40 are consistent with those obtained by analysis of samples from alloys richer in aluminium in the work of Little, Axon, and Hume-Rothery,<sup>11</sup> which have been included in Fig. 13 as full symbols. Above 70% zinc, no crystals suitable for analysis could be obtained; it is probable therefore that the maximum solid solubility of zinc in  $\text{CrAl}_7$  has not been reached in these experiments, but this maximum can hardly lie above 8.5 at.-% zinc.\* If the two contaminated samples are ignored, the results in Fig. 13 indicate that, on solution of zinc, the chromium content remains approximately constant. There is no tendency for a constant aluminium content to be maintained, and the evidence suggests that zinc replaces aluminium in the  $\text{CrAl}_7$  structure. The

\* This figure may be estimated by extrapolation, to the ternary eutectic composition, of the curve of zinc content of

extracted crystals against zinc content of the parent, slowly cooled alloy.



## REFERENCES

1. J. N. Pratt and G. V. Raynor, *Proc. Roy. Soc.*, 1951, [A], **205**, 103.
2. W. L. Fink and H. R. Freche, *Trans. Amer. Inst. Min. Met. Eng.*, 1933, **104**, 325.
3. A. J. Bradley and S. S. Lu, *J. Inst. Metals*, 1937, **60**, 319.
4. G. V. Raynor and K. Little, *ibid.*, 1945, **71**, 481.
5. J. N. Pratt and G. V. Raynor, *ibid.*, 1952, **80**, 449.
6. G. Falkenhagen and W. Hofmann, *Z. Metallkunde*, 1950, **41**, 191.
7. G. V. Raynor, *Inst. Metals: Annotated Equilib. Diagr. Series No. 1*, **1943**.
8. E. Weisse, A. Blumenthal, and H. Hanemann, *Z. Metallkunde*, 1942, **34**, 221.
9. W. Hanemann, *ibid.*, 1940, **32**, 91.
10. T. Heumann, *ibid.*, 1948, **39**, 45.
11. K. Little, H. J. Axon, and W. Hume-Rothery, *J. Inst. Metals*, 1948-49, **75**, 39.
12. G. Hindrichs, *Z. anorg. Chem.*, 1908, **59**, 427.
13. H. Le Chatelier, *Compt. rend.*, 1895, **120**, 835.
14. K. Little, unpublished work.
15. D. W. Wakeman and G. V. Raynor, *J. Inst. Metals*, 1948-49, **75**, 131.

# THE ALUMINIUM-RICH ALLOYS OF THE SYSTEM ALUMINIUM-CHROMIUM-IRON\*

1367

By J. N. PRATT,† B.Sc., Ph.D., MEMBER, and PROFESSOR G. V.  
RAYNOR,‡ M.A., D.Sc., MEMBER OF COUNCIL

## SYNOPSIS

The system aluminium-chromium-iron has been examined, in the aluminium-rich region, by metallographic and X-ray methods and by the chemical analysis of primary crystals extracted from slowly cooled alloys. In the solid state only  $\text{CrAl}_7$ , with iron in solution, and  $\text{FeAl}_3$ , with chromium in solution, enter into equilibrium with the primary solid solution. No ternary compound is encountered in the aluminium-rich alloys. In the slowly cooled alloys, however, the  $\text{Cr}_2\text{Al}_{11}$  phase occurs; although its presence is frequently unrecognizable micrographically, the crystal form of this constituent in the extracted residues is sufficiently different from that of  $\text{CrAl}_7$  to permit separation, chemical analysis, and X-ray study.

Examination of the results shows that a strong analogy exists between the aluminium-rich alloys of this system and those of the system aluminium-chromium-manganese. The total solute concentrations at the solubility limits of manganese and iron in  $\text{CrAl}_7$  are equal. The structure, however, accommodates approximately twice as many manganese atoms as iron atoms, and it is shown that the numbers of  $3d$  and  $4s$  electrons per solute atom are closely similar at the two limits. The electron:atom ratios are also closely similar whatever effective valency  $V$  is assumed for chromium, provided that the effective valencies of manganese and iron are taken respectively as  $(V+1)$  and  $(V+2)$ . Somewhat similar relationships are observed for  $\text{Cr}_2\text{Al}_{11}$ . In this case, the solubility limits of iron and manganese do not agree so well with a constant total solute content, so that the electron:atom ratios do not correspond closely. The number of  $3d$  and  $4s$  electrons per solute atom, however, is still important. The close analogies between the two structures are discussed in terms of the nature of the binary compounds.

## I.—INTRODUCTION

As part of a research programme on aluminium-rich ternary alloys containing, as solutes, two transitional metals of the first long period of the Periodic Table, the system aluminium-chromium-manganese has already been examined.<sup>1</sup> In this system, the form of the equilibrium varies with temperature. Above  $590^\circ\text{C}$ . the aluminium-rich solid solution enters into equilibrium, at the appropriate compositions, with either  $\text{MnAl}_6$  or with a solid solution of manganese in  $\text{CrAl}_7$ . No ternary compound exists in equilibrium with the aluminium-rich solution or with the aluminium-rich liquid in this temperature range. Below  $590^\circ\text{C}$ ., however, the ternary compound  $G$  comes into equilibrium with the aluminium-rich solid solution. The most outstanding feature of the constitutional diagram is the extent of the solid solubility of manganese in the binary phases  $\text{CrAl}_7$  and  $\text{Cr}_2\text{Al}_{11}$ . The  $\text{CrAl}_7$  phase may dissolve a maximum of 11.5 wt.-% manganese. The solution does not correspond with direct replacement of one chromium atom by one manganese atom, but with replacement of chromium atoms by manganese atoms in the ratio 2:3. In this respect, the solid solution in  $\text{CrAl}_7$  is different from the solid solutions of iron in  $\text{MnAl}_6$ , and of iron, nickel, and silicon in  $\text{Co}_2\text{Al}_9$ , where the replacement

proceeds atom for atom, the aluminium content remaining constant. The  $\text{Cr}_2\text{Al}_{11}$  phase may dissolve a maximum of 28 wt.-% manganese; in this case the replacement of chromium by manganese follows no simple scheme. The composition tends towards  $\text{Mn}_3\text{Al}_{14}$ , and, although the solid solution ends before it reaches the binary aluminium-manganese wall of the ternary model, almost all the chromium may be replaced by manganese without alteration in crystal structure. In view of the peculiar behaviour of the phases  $\text{CrAl}_7$  and  $\text{Cr}_2\text{Al}_{11}$ , as compared with that of other aluminium-rich intermetallic compounds containing transitional metals, it was decided to examine the equilibrium relationships in the system aluminium-chromium-iron for comparison. The present paper reports the results of this investigation.

## II.—PREVIOUS WORK

### 1. THE BINARY ALUMINIUM-IRON SYSTEM

The equilibrium diagram of the aluminium-rich aluminium-iron alloys is shown in Fig. 1. This diagram is based on the work of Gwyer and Phillips,<sup>2</sup> Phillips,<sup>3</sup> and Bradley and Taylor.<sup>4</sup> As was shown by Edgar,<sup>5</sup> the solubility of iron in aluminium is extremely small, decreasing smoothly from 0.052 wt.-% at  $655^\circ\text{C}$ . to 0.006 wt.-% at  $590^\circ\text{C}$ . At 1.7 wt.-%

\* Manuscript received 31 May 1951.

† Research Fellow, Department of Metallurgical Engineering, University of Toronto, Canada; formerly Research

Fellow, University of Birmingham.

‡ Professor of Metal Physics, University of Birmingham.



iron and a temperature of  $655^{\circ}\text{C.}$ , this solid solution and the phase  $\text{FeAl}_3$  are deposited as a eutectic from the melt.  $\text{FeAl}_3$  is of limited homogeneity, and,

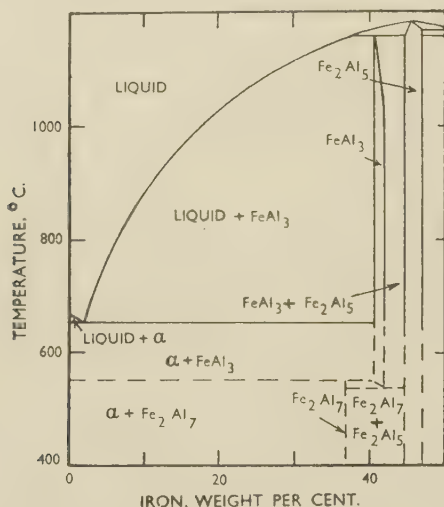


FIG. 1.—Equilibrium Diagram for the Aluminium-Iron Alloys.

according to the X-ray investigations of Bradley and Taylor, decomposes at some temperature below  $600^{\circ}\text{C.}$  to give a mixture of  $\text{Fe}_2\text{Al}_5$  and  $\text{Fe}_2\text{Al}_7$ . Since the transformation temperature has not been accurately determined, equilibrium relationships in the neighbourhood of this transformation have been indicated by broken lines. For uniformity with previous publications, the phase in equilibrium with the aluminium-rich solid solution is referred to as  $\text{FeAl}_3$  throughout this paper.

## 2. THE BINARY ALUMINIUM-CHROMIUM SYSTEM

The aluminium-rich portion of the equilibrium diagram for the aluminium-chromium system is reproduced as Fig. 2, which is based upon investiga-

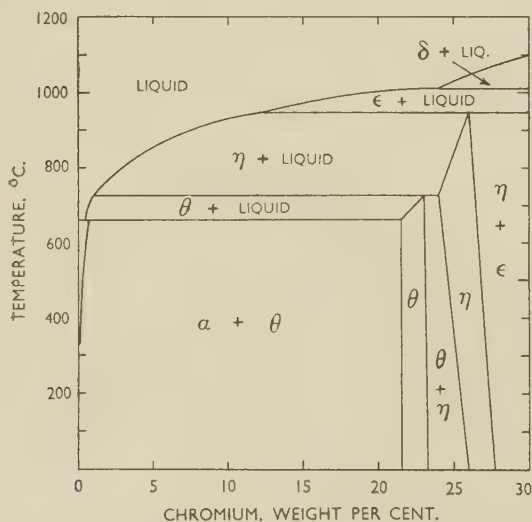


FIG. 2.—Equilibrium Diagram for the Aluminium-Chromium Alloys.

tions by Bradley and Lu,<sup>6</sup> Gotō and Dogane,<sup>7</sup> Fink and Freche,<sup>8</sup> and Raynor and Little.<sup>9</sup> The solid solubility of chromium in aluminium is limited, and falls from a maximum of 0.72 wt.-% at  $661^{\circ}\text{C.}$  to approximately 0.03 wt.-% at  $350^{\circ}\text{C.}$  At low temperatures, therefore, practically the whole of the chromium present exists in the form of the  $\theta$  phase, which corresponds with the "formula"  $\text{CrAl}_7$ . As shown in Fig. 2, two intermediate phases occur within a very narrow range of composition. The higher-melting of these phases ( $\eta$ ) is based upon the composition  $\text{Cr}_2\text{Al}_{11}$ , and exists over the maximum range of 24–27.5 wt.-% chromium; the precise limits of homogeneity are somewhat temperature-dependent. At a temperature of approximately  $725^{\circ}\text{C.}$  the  $\eta$  phase reacts peritectically with the melt to form the  $\theta$  phase ( $\text{CrAl}_7$ ), which exists from 21.6 to 23.25 wt.-% chromium, the limits being in this case practically independent of temperature. The  $\theta$  phase in turn reacts peritectically with the liquid at  $661^{\circ}\text{C.}$  to form the primary aluminium-rich solid solution.

According to the X-ray investigation of Bradley and Lu, the crystal structures of the  $\theta$  and  $\eta$  phases

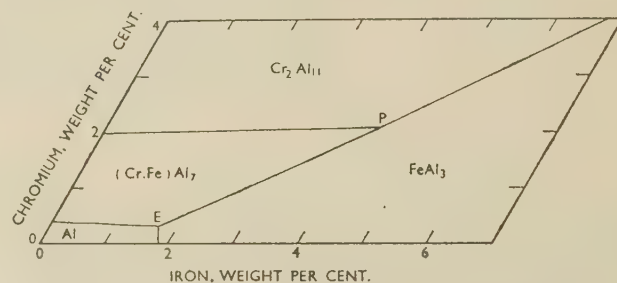


FIG. 3.—Surfaces of Primary Separation: Aluminium-Chromium-Iron System (Mondolfo).

are closely related, and give rise to very similar diffraction patterns.

## 3. THE TERNARY ALUMINIUM-CHROMIUM-IRON SYSTEM

Previous investigations of this system have been concerned primarily with the properties of the alloys, and little information on the constitutional features appears in the literature. According to the early work of Taillandier,<sup>10</sup> only the binary compounds  $\text{FeAl}_3$  and " $\text{CrAl}_3$ " exist in equilibrium with the aluminium-rich solid solution; a ternary eutectic involving these three phases is reported at approximately 2 wt.-% chromium and 1 wt.-% iron, the temperature of the reaction being given as  $635^{\circ}\text{C.}$  Mondolfo,<sup>11</sup> on the basis of this work and limited further investigation, proposed the diagram given in Fig. 3 for the surfaces of primary separation in the aluminium-rich region. No ternary compound was reported, and only the  $\text{Cr}_2\text{Al}_{11}$ ,  $\text{CrAl}_7$ ,  $\text{FeAl}_3$ , and  $\text{Fe}_2\text{Al}_7$  phases were observed. Iron was said to be soluble to a certain extent in  $\text{CrAl}_7$ , forming a phase with characteristics slightly different from those of

$\text{CrAl}_7$ , and denoted  $(\text{CrFe})\text{Al}_7$ . It will be noted that, as written, this "formula" suggests direct atomic replacement of chromium by iron. The diagram contains two invariant points: (i) a peritectic point  $P$ , at which the  $\text{CrAl}_7$ ,  $\text{Cr}_2\text{Al}_{11}$ ,  $\text{FeAl}_3$ , and liquid phases are in equilibrium (approximately 4.2 wt.-% iron and 2.1 wt.-% chromium); and (ii) a eutectic point  $E$ , involving the liquid phase, aluminium,  $\text{FeAl}_3$ , and  $(\text{CrFe})\text{Al}_7$  (approximately 1.7 wt.-% iron and 0.3 wt.-% chromium;  $640^\circ\text{C}$ ).

In the course of work on the properties and methods of production of the ternary alloys, Kornilov<sup>12</sup> carried out limited constitutional studies, and confirmed the non-existence of a true ternary compound.

### III.—EXPERIMENTAL METHODS

In view of the limited data already available, the ternary system has been studied by metallographic and X-ray methods, and by the examination of slowly cooled alloys, from which the intermetallic compounds were separated for X-ray investigation and chemical analysis.

#### 1. MATERIALS USED

Throughout the work alloys were prepared from super-pure aluminium, as supplied by The British Aluminium Co., Ltd., and from binary master alloys made up from pure materials. The master alloys used were kindly presented by The British Aluminium Co., Ltd., and were of the following compositions:

(i) *Aluminium-Iron Master Alloys*.—Two alloys were employed. One contained 5.7 wt.-% iron, with 0.0035% silicon and 0.0035% copper as impurities. The second contained 5.85 wt.-% iron, and had an impurity content of 0.0015% silicon, copper, and manganese.

(ii) *Aluminium-Chromium Master Alloys*.—The bulk of the work was carried out using an alloy containing 10.4 wt.-% chromium, and impurity contents as follows: silicon 0.009, iron 0.005, manganese 0.0005, copper <0.0005%.

Certain experiments were carried out with an alloy containing 8.66 wt.-% chromium, and of a somewhat higher purity than the first alloy.

#### 2. PREPARATION AND TREATMENT OF ALLOYS

Alloys for metallographic or slow-cooling experiments were prepared by melting together weighed quantities of the materials in alumina-lined crucibles. After thorough stirring, the melts were either cooled slowly (approximately  $\frac{3}{4}^\circ\text{C}/\text{min.}$ ) or cast into heavy copper moulds. Slow cooling was controlled by a potentiometric programme controller of standard design, and a heavy cylindrical furnace liner of copper was employed to minimize temperature fluctuations in the melt. For alloys of composition such that no peritectic reaction was expected, cooling was continued to room temperature. Where a peritectic reaction was

known or suspected to occur, the cooling process was halted above the peritectic temperature, and the alloy was held in the semi-liquid region for approximately 1 hr., before being finally quenched into cold water. When cold, each slowly cooled ingot was sectioned vertically; one-half was examined metallographically and the other reserved for the extraction of primary crystals of intermetallic compounds, if suitable.

For metallographic work, small sections of chill-cast alloys were sealed in evacuated glass capsules; contact with the glass was avoided by the use of alumina sheaths, and throughout the work no evidence of contamination with silicon was obtained. Annealing was carried out in tubular resistance furnaces controlled by temperature regulators to within  $\pm 1\frac{1}{2}^\circ\text{C}$ . of the required temperature, and all annealing treatments were ended by quenching the alloys in cold water. In order to ensure equilibrium, alloys were annealed until no further change could be detected micrographically.

Crystals of the intermetallic compounds present after slow cooling were separated from several alloys by anodic solution of the aluminium-rich matrix. The specimen was made the anode in a simple electrolytic cell, the cathode of which was a pure nickel strip. Using as electrolyte a 7½% aqueous hydrochloric acid solution, and a current density of approximately 0.1 amp./in.<sup>2</sup> at a potential difference of 8 V., clean separations of the compound phases were obtained. The crystals were washed with nitric acid (50%) and well rinsed with distilled water. The water was removed by rinsing with alcohol, and the residue was allowed to dry and then examined with a binocular microscope. In many cases the residues were homogeneous, and the most perfectly formed crystals were removed with forceps for analysis or X-ray examination. In some cases, however, crystals of more than one type occurred. The types present were readily distinguishable by their crystalline forms, and were separated from each other by careful hand-sorting. Examples of the crystals obtained are given later.

X-ray diffraction patterns were obtained from many of the samples of intermetallic compound separated. The brittle crystals were crushed to a fine powder in an agate mortar. Owing to the brittle nature of the compounds, no stress-relieving annealing treatment was necessary. Powder specimens were exposed in van Arkel-type Debye-Scherrer cameras (9 or 19 cm. in dia.) to cobalt or copper  $K_\alpha$  radiation from a demountable Metropolitan-Vickers X-ray machine.

Chemical analysis of the compounds obtained was carried out either in the analytical laboratory of the Department of Metallurgy, Birmingham University, or by Johnson, Matthey and Co., Ltd. Results from the two sources were consistent. Test analyses of specimens used in the annealing work were also made. The results agreed closely with the intended compositions, and in view of the relative simplicity of the equilibrium relations in the solid state, synthetic compositions have been employed throughout this paper.



Alloys are referred to in terms of the concentrations of solute metals present. Thus an alloy containing 2 wt.-% chromium and 4 wt.-% iron is referred to as "alloy 2/4".

Throughout the work temperatures were measured with a carefully calibrated platinum/platinum-rhodium thermocouple, used in conjunction with a deflection potentiometer. At all times the cold junction of the thermocouple was immersed in melting ice.

#### IV.—METALLOGRAPHY

Alloys for metallographic examination were sectioned to expose an entirely new surface, which was prepared for microscopic observation by standard techniques. Relief effects shown by the hard inter-metallic compound crystals were initially troublesome, but were subsequently avoided by the following method. After grinding on paraffin-soaked emery paper, the worst scratches were removed by a very brief polish with "Brasso" on Selvyt cloth. This treatment was followed by light hand polishing, first on blanket-felt, using a medium-grade proprietary magnesia powder, and then with a fine-grade magnesia or alumina powder on chamois leather. It was found essential to restrict the final stages to as brief a polish as possible. Some fragmentation of the large primary crystals present in the slowly cooled alloys appeared to be unavoidable.

Throughout the work, only the phases  $\text{CrAl}_7$  and  $\text{FeAl}_3$  were observed, in addition to the primary solid solution, in annealed alloys.  $\text{CrAl}_7$ , which was silver-grey in colour, was easily distinguished in the unetched condition from  $\text{FeAl}_3$ , which was blue-grey in colour. In the slowly cooled alloys, these phases could again be distinguished in the unetched state, both by reason of their colour difference and because primary  $\text{CrAl}_7$  crystals were large and irregular, whereas primary  $\text{FeAl}_3$  crystals occurred as long, thin needles. Many of the slowly cooled alloys contained, in addition, the  $\text{Cr}_2\text{Al}_{11}$  phase. This usually occurred as peritectic spines in  $\text{CrAl}_7$  crystals, and in this condition could be differentiated from  $\text{CrAl}_7$  by the presence of a pinkish tinge and an apparently slightly greater hardness. When present as discrete primary crystals, however, the  $\text{Cr}_2\text{Al}_{11}$  phase was almost impossible to distinguish from  $\text{CrAl}_7$ .

All alloys were examined in the etched condition. The most generally useful reagents were:

(i) 0.5% aqueous hydrofluoric acid. On etching for 15 sec. by swabbing,  $\text{CrAl}_7$  remained unattacked, while  $\text{Cr}_2\text{Al}_{11}$  and  $\text{FeAl}_3$  were both coloured light brown.

(ii) Mixed acid reagent (0.5% hydrofluoric acid, 1.5% hydrochloric acid, 2.5% nitric acid, remainder water). After immersion of the specimen for 5 sec.,  $\text{CrAl}_7$  was unaffected,  $\text{FeAl}_3$  slightly darkened, and  $\text{Cr}_2\text{Al}_{11}$  coloured light brown.

(iii) 20% aqueous sulphuric acid, used at 70°C. Alloys were immersed for 20 sec.;  $\text{FeAl}_3$  was heavily darkened, whereas  $\text{CrAl}_7$  and  $\text{Cr}_2\text{Al}_{11}$  remained unattacked.

The results of etching experiments on the annealed alloys were in all cases clear and easy to interpret, in spite of a tendency to etch unevenly on the part of  $\text{FeAl}_3$ . Owing to the large size of the primary crystals, however, and the consequent non-uniformity of etching characteristics, difficulty was experienced in interpreting the microstructures of slowly cooled alloys. Although  $\text{CrAl}_7$  could be distinguished from  $\text{FeAl}_3$ , and peritectic spines of  $\text{Cr}_2\text{Al}_{11}$  in  $\text{CrAl}_7$  could be detected, distinction between discrete crystals of the latter two phases was frequently uncertain. For these alloys, examination of unetched specimens, together with the separation and X-ray examination of typical crystals, provided the most satisfactory method of identification of the various constituents.

The microstructures of the annealed alloys were typical and showed no unusual features; it has therefore not been considered necessary to reproduce photomicrographs. A photomicrograph typical of most of the slowly cooled alloys examined is given in Fig. 6 (Plate LXIX); this shows a large primary crystal of  $\text{CrAl}_7$ , in an aluminium-rich matrix containing secondary  $\text{FeAl}_3$  crystals.

#### V.—EXPERIMENTAL RESULTS

##### 1. PRELIMINARY INVESTIGATIONS

In view of the limited data available, a preliminary exploration of the aluminium-rich region was carried out by means of a series of ten alloys, prepared in 10-g. quantities, and slowly cooled from the liquid state to room temperature. The series included the binary alloys 4/0 and 0/4, in order to facilitate identification of phases in the ternary alloys by direct comparison with typical binary structures. The results of these experiments are summarized in Table I. It will be noted that, although alloy 4/0 lies in the reported field of separation of primary  $\text{Cr}_2\text{Al}_{11}$ , no signs were detected of the expected peritectic reaction:  $\text{liq.} + \text{Cr}_2\text{Al}_{11} \rightleftharpoons \text{CrAl}_7$ . Only large irregular prisms of silver-grey primary  $\text{CrAl}_7$  were visible in the aluminium-rich matrix. This phenomenon appears to be due to severe undercooling, and is paralleled in the structures of alloys 3/1 and 3/4. These alloys lie in the field denoted as primary  $\text{Cr}_2\text{Al}_{11}$  by Mondolfo (Fig. 3). Since, by comparison with Fig. 2, Mondolfo's  $(\text{CrFe})\text{Al}_7$  field appears to be much too extensive in terms of chromium content, peritectic cores of  $\text{Cr}_2\text{Al}_{11}$  would also be expected in alloy 2/2. The supercooling clearly causes suppression of the primary  $\text{Cr}_2\text{Al}_{11}$  deposition.

Table I indicates that the aluminium-rich liquid enters into equilibrium only with  $\text{Cr}_2\text{Al}_{11}$ ,  $\text{CrAl}_7$ , and  $\text{FeAl}_3$ . No evidence for the formation of a ternary compound was observed during the experiments.  $\text{CrAl}_7$  was recognized as the primary constituent in

the majority of the alloys, and thus has a large effective field of primary separation under the normal conditions of slow cooling. The primary  $\text{FeAl}_3$  field is limited to compositions lying close to the aluminium-iron binary axis. Except in alloys containing the highest proportions of chromium, the primary separation of  $\text{Cr}_2\text{Al}_{11}$ , which would be expected under equilibrium conditions, tends not to take place.

TABLE I.—Microstructures of Aluminium-Chromium-Iron Alloys.

Alloy	Microstructure	Remarks
4/0	Primary $\text{CrAl}_7$ in Al-rich matrix.	$\text{Liq.} + \text{Cr}_2\text{Al}_{11} \rightleftharpoons \text{CrAl}_7$ , peritectic suppressed.
3/1 } 2/2 }	Primary $\text{CrAl}_7$ , secondary $\text{FeAl}_3$ , in Al-rich matrix. }	No $\text{Cr}_2\text{Al}_{11}$ cores observed.
1/3	Primary and secondary $\text{CrAl}_7$ ; secondary $\text{FeAl}_3$ and some abnormally large $\text{FeAl}_3$ crystals.	...
0/4	Primary $\text{FeAl}_3$ in Al-rich matrix.	...
1/1 } 1/2 }	Primary $\text{CrAl}_7$ , secondary $\text{FeAl}_3$ in Al-rich matrix. }	...
6/2	Large $\text{CrAl}_7$ crystals containing $\text{Cr}_2\text{Al}_{11}$ cores; secondary $\text{FeAl}_3$ in Al-rich matrix.	Showed unmistakable evidence of peritectic reaction.
3/4	Primary and secondary $\text{CrAl}_7$ ; secondary $\text{FeAl}_3$ and some large $\text{FeAl}_3$ crystals.	Only small amount of large $\text{FeAl}_3$ crystals.
1/5	Primary $\text{FeAl}_3$ , secondary $\text{CrAl}_7$ , in Al-rich matrix.	...

In order to confirm the absence of any ternary compound, fourteen chill-cast alloys, containing 2 or 4 wt.-% of total solute, were annealed for 21 days at  $560^\circ\text{C}$ . After quenching, metallographic examination revealed only  $\text{CrAl}_7$  and  $\text{FeAl}_3$  in equilibrium with the aluminium-rich solid solution. Nine of the alloys contained the three phases  $\alpha$  (aluminium-rich solid solution),  $\text{CrAl}_7$ , and  $\text{FeAl}_3$ ; no evidence of a ternary compound or of  $\text{Cr}_2\text{Al}_{11}$  was observed in these alloys.

## 2. THE CONSTITUTION IN THE SOLID STATE

Investigation showed that the aluminium-rich alloys did not enter the semi-liquid region at  $600^\circ\text{C}$ . A series of twenty-six chill-cast alloys was therefore annealed at  $600^\circ\text{C}$ . until no further structural change was observed (60 days). The compositions and observed structures are summarized in Fig. 4, in which the binary solid-solubility limit of chromium in aluminium is taken from the previous work of Raynor and Little.<sup>9</sup> As indicated by the preliminary work, no ternary compound exists at this temperature in equilibrium with the aluminium-rich solution, while only one three-phase triangle ( $\alpha + \text{CrAl}_7 + \text{FeAl}_3$ ) exists; there is no indication that  $\text{Cr}_2\text{Al}_{11}$  enters into equilibrium with the  $\alpha$  phase. Fig. 4 shows that  $\text{CrAl}_7$  must be able to dissolve appreciable quantities of iron, and that  $\text{FeAl}_3$  is able to dissolve small amounts of chromium.

In the aluminium-chromium-manganese alloys, the ternary compound  $G$  is formed at  $590^\circ\text{C}$ .; in order to confirm that no similar phenomenon occurred in the present system, fourteen alloys were annealed to equilibrium at  $425^\circ\text{C}$ . (45 days). The results, which are summarized in Fig. 5, again show that only the phases present at  $600^\circ\text{C}$ . take part in the equi-

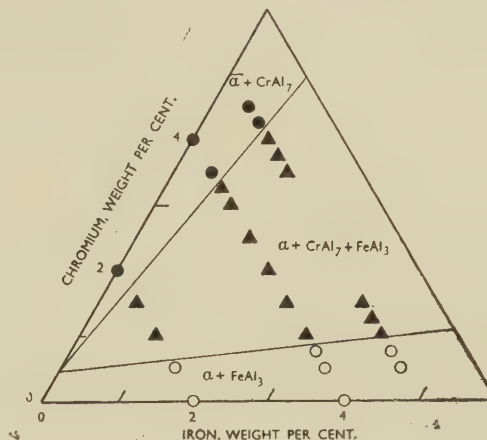


FIG. 4.—The Aluminium-Chromium-Iron System :  $600^\circ\text{C}$ . Isothermal.

●  $\alpha + \text{CrAl}_7$ . ○  $\alpha + \text{FeAl}_3$ . ▲  $\alpha + \text{CrAl}_7 + \text{FeAl}_3$ .

librium relationships at this temperature. No attempt was made to define the boundaries of the three-phase triangle any more closely than is indicated in Fig. 5, since the two-phase alloys 3.5/0.5 and 0.5/1.5 suggest that the boundaries do not deviate appreciably from those examined in detail at  $600^\circ\text{C}$ . The general tendency is for solid solutions to become

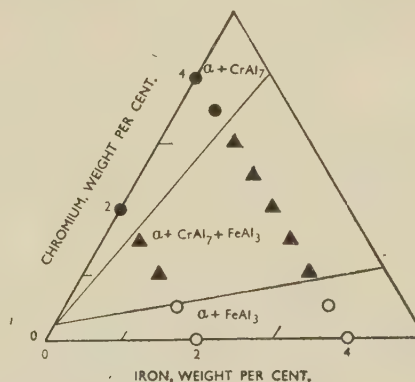


FIG. 5.—The Aluminium-Chromium-Iron System :  $425^\circ\text{C}$ . Isothermal.

●  $\alpha + \text{CrAl}_7$ . ○  $\alpha + \text{FeAl}_3$ . ▲  $\alpha + \text{CrAl}_7 + \text{FeAl}_3$ .

more restricted with decreasing temperature, so that any change in the solubilities of iron in  $\text{CrAl}_7$  or chromium in  $\text{FeAl}_3$  would be expected to cause the alloys 3.5/0.5 and 0.5/1.5 to precipitate a third phase. It should be noted that the microstructures of the preliminary alloys annealed at  $560^\circ\text{C}$ . were the same as those indicated in Fig. 5; the form of the



equilibrium relationships between 600° and 425° C. is therefore virtually independent of temperature.

### 3. EXPERIMENTS ON SLOWLY COOLED ALLOYS

In order to isolate samples of the intermetallic compounds present in the aluminium-rich alloys, melts were prepared in quantities of 50 g. and slowly cooled to room temperature. The compositions and microstructures of these alloys are given in Table II;

TABLE II.—Summary of Microstructures and Extracted Crystals.

Alloy No.	Composition, wt.-%		Apparent Microstructure	Extracted Crystals
	Cr	Fe		
1*	3.5	0.5	$\alpha$ + CrAl <sub>7</sub> (primary) + FeAl <sub>3</sub> (secondary). No evidence of liq. + Cr <sub>2</sub> Al <sub>11</sub> $\rightleftharpoons$ CrAl <sub>7</sub> peritectic.	Long irregular prisms, often of hexagonal cross-section; CrAl <sub>7</sub> type.
2*	3.0	1.0		
3*	2.5	1.5		
4	2.25	1.75	$\alpha$ + Cr <sub>2</sub> Al <sub>11</sub> + CrAl <sub>7</sub> + FeAl <sub>3</sub> . The peritectic reaction was observable.	Long irregular prisms; CrAl <sub>7</sub> type.
5†	2.0	2.0	$\alpha$ + CrAl <sub>7</sub> (primary) + FeAl <sub>3</sub> (secondary). No evidence of peritectic.	Long irregular prisms of CrAl <sub>7</sub> type, mixed with small equi-axed or flat-tish prisms.
6†	2.0	2.0		
7†	1.75	2.25	$\alpha$ + CrAl <sub>7</sub> (primary) + FeAl <sub>3</sub> (secondary). No evidence of peritectic.	Long irregular prisms of CrAl <sub>7</sub> type, mixed with equi-axed prisms.
8†	1.5	2.5	$\alpha$ + CrAl <sub>7</sub> (primary) + FeAl <sub>3</sub> (primary or very coarse secondary). No evidence of peritectic.	Flat needles.
9†	1.25	2.75	As for Alloy No. 8.	Residue of unsatisfactorily small crystals.
10†	1.0	3.0	As for alloy No. 8.	Equi-axed or flat prisms, mixed with flat needles.
11	0.75	3.25	$\alpha$ + FeAl <sub>3</sub> (primary) + CrAl <sub>7</sub> (secondary).	Flat needles.
12†	0.5	3.5	As for alloy No. 8.	Equi-axed or flat prisms, mixed with flat needles.

\* Analysis of extracted crystals indicates that in addition to CrAl<sub>7</sub>, these initial alloys probably contained Cr<sub>2</sub>Al<sub>11</sub>, which passed unnoticed in both the microstructure and the extracted residues.

† Examination of extracted crystals shows that in general these alloys also contained Cr<sub>2</sub>Al<sub>11</sub>, which the metallographic examination of the slowly cooled ingots failed to distinguish from CrAl<sub>7</sub>.

it will be noted that the microstructures are consistent with those of the preliminary series. Again Cr<sub>2</sub>Al<sub>11</sub> apparently fails to crystallize from the melt at the expected compositions, and only CrAl<sub>7</sub> can be recognized micrographically. Table II also contains a description of the residues extracted from these alloys by anodic solution of the matrix. The first four alloys gave residues apparently consisting entirely of long irregular prisms, frequently of hexagonal cross-section. This crystal form is characteristic of CrAl<sub>7</sub>, and is similar to that of the manganese-bearing CrAl<sub>7</sub> crystals separated in the earlier work of Raynor and Little.<sup>1</sup> The alloy 2/2, however, gave a residue containing, in addition to the long irregular prisms of CrAl<sub>7</sub>, small flat or approximately equi-axed crystals. These two types of crystal are illustrated

in Figs. 7 and 8 (Plate LXIX); the difference in form made it possible to separate the two types by hand-sorting under the binocular microscope, and separate samples were reserved for analysis. A similar residue was obtained from alloy 1.75/2.25. Alloys 1.0/3.0 and 0.5/3.5 gave residues consisting of

TABLE III.—Composition of Extracted Crystals and their Structures.

Alloy No.	Composition of Extracted Crystals, at.-%		Type of Structure by X-Ray Examination	Remarks
	Cr	Fe		
1	13.47	0.48	CrAl <sub>7</sub>	...
2	13.15	0.92	CrAl <sub>7</sub>	...
3	13.00	1.44	CrAl <sub>7</sub>	...
4	...	...	...	Not analysed because of peritectic inclusions.
5	11.79	2.21	CrAl <sub>7</sub>	Long irregular prisms.
	13.25	4.25	Cr <sub>2</sub> Al <sub>11</sub>	Equi-axed prisms.
6	12.06	2.21	CrAl <sub>7</sub>	Long irregular prisms.
	...	...	...	Flat prisms, insufficient for analysis.
7	11.5	3.02	...	Long irregular prisms.
	11.78	5.71	...	Flat prisms.
8	1.28	23.53	FeAl <sub>3</sub>	...
9	...	...	...	No crystals suitable for analysis.
10	11.46	7.74	Cr <sub>2</sub> Al <sub>11</sub>	Flat prisms.
	2.1	23.01	FeAl <sub>3</sub>	...
11	0.90	22.31	FeAl <sub>3</sub>	...
12	11.81	6.75	Cr <sub>2</sub> Al <sub>11</sub>	Small flat prisms.
	2.64	24.87	FeAl <sub>3</sub>	...

relatively equi-axed prisms together with flat needles (Fig. 9, Plate LXIX) characteristic of FeAl<sub>3</sub>. The remaining residues were almost entirely FeAl<sub>3</sub>. Carefully selected samples of the crystal types obtained were submitted for chemical analysis, and the results are given in Table III. Fig. 10 shows these results

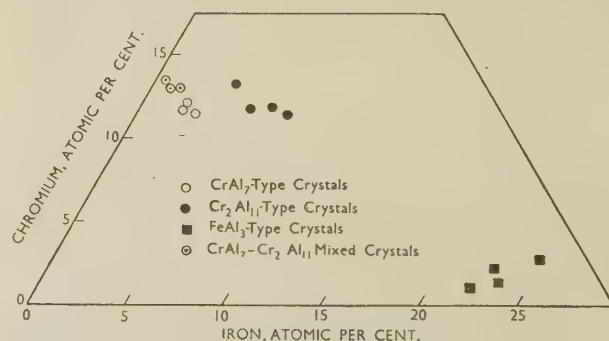


Fig. 10.—Compositions of Extracted Crystals: ○ long irregular prisms; ● equi-axed prisms; ■ flat needles; ○ mixed crystals.

plotted in atomic percentages. The results make it clear that not all the primary crystals interpreted micrographically as CrAl<sub>7</sub> do in fact consist of that phase. The relatively equi-axed crystals are significantly richer in both chromium and iron, and are consistent with the solution of iron in the Cr<sub>2</sub>Al<sub>11</sub>

phase. This interpretation is confirmed by means of the X-ray results also recorded in Table III. The long irregular prisms gave diffraction patterns identical with that of  $\text{CrAl}_7$ , and with those of the samples of the solid solution of manganese in  $\text{CrAl}_7$  obtained in previous work. The equi-axed prisms gave diffraction patterns of a distinctly different type; although not identical in all respects with that of  $\text{Cr}_2\text{Al}_{11}$ , they were very similar, and the slight differences observed could easily arise from a distortion of the structure by the iron present. The analysis and X-ray work indicate that, in the microstructures, absence of evidence of the  $\text{liq.} + \text{Cr}_2\text{Al}_{11} \rightleftharpoons \text{CrAl}_7$  reaction does not necessarily indicate the absence of the  $\text{Cr}_2\text{Al}_{11}$  phase. It is apparently possible for  $\text{Cr}_2\text{Al}_{11}$  to separate as primary crystals above the peritectic temperature and for  $\text{CrAl}_7$  to separate at temperatures lower than that of the peritectic, without the peritectic reaction taking place to any metallographically recognizable extent. In other cases, the primary crystallization of  $\text{Cr}_2\text{Al}_{11}$  may itself be missing. Assessment of the amounts of the two types of crystal present in the residues obtained indicated that the amount of  $\text{Cr}_2\text{Al}_{11}$  relative to that of  $\text{CrAl}_7$  increased as the iron content of the parent alloy increased, in spite of the fact that, micrographically, the  $\text{Cr}_2\text{Al}_{11}$  could not be adequately distinguished from the  $\text{CrAl}_7$ . It is probable that the presence of iron in solid solution causes the etching characteristics of these phases to become even more similar than in the binary alloys.

The compositions of the samples of  $\text{CrAl}_7$  extracted from alloys 3.5/0.5, 3.0/1.0, and 2.5/1.5 require explanation, since the specimens are richer in chromium than the other samples obtained, although giving rise to the  $\text{CrAl}_7$  diffraction pattern. These residues were analysed before the confirmation of the fact that two types of crystal occurred; as explained above, the equi-axed crystals ( $\text{Cr}_2\text{Al}_{11}$  containing iron) increase in amount as the iron content of the parent alloy increases. The most probable explanation of the abnormal compositions of the residues in question is, therefore, that the residues, though assumed to be entirely  $\text{CrAl}_7$ , did in fact contain a certain amount of the more equi-axed crystals, and consequently gave a higher chromium figure on analysis than would correspond to crystals of the  $\text{CrAl}_7$  type.

#### 4. EXPERIMENTS WITH QUENCHED SEMI-LIQUID ALLOYS

From Fig. 10 it will be noted that no samples of the solid solution of iron in  $\text{Cr}_2\text{Al}_{11}$  containing less than 4.25 at.-% iron were obtained. In an effort to obtain specimens with compositions closer to that of the binary compound, a number of alloys were slowly cooled to a temperature below that of the liquidus but above that of the peritectic reaction  $\text{liq.} + \text{Cr}_2\text{Al}_{11} \rightleftharpoons \text{CrAl}_7$  (reported as occurring at 725° C.), and quenched in cold water. Alternatively, the alloys were cooled to room temperature, reheated to above the peritectic temperature, annealed for 1–2 hr., and

quenched. Six ternary alloys were examined together with two binary aluminium–chromium alloys; in general the physical state of the quenched alloys prevented adequate micro-examination, but where this was possible the primary crystals appeared to be free from peritectic contamination. The primary crystals were successfully extracted from these alloys, and, though somewhat mixed, consisted mainly of the long irregular prisms characteristic of  $\text{CrAl}_7$ . Selected portions of these crystalline residues were examined by X-rays, and all gave rise to diffraction patterns of the  $\text{CrAl}_7$  type. Since the quenching temperatures ranged from 730° to 765° C., it appears possible that the peritectic temperature in the binary alloys is considerably higher than previously supposed. In view of the difficulty of obtaining samples of  $\text{Cr}_2\text{Al}_{11}$  for analysis from these alloys, the experiments were discontinued.

#### 5. THE SURFACES OF PRIMARY SEPARATION

As will be appreciated from the description of the slowly cooled alloys, it is extremely difficult to decide the compositions at which the boundary between the primary  $\text{Cr}_2\text{Al}_{11}$  and primary  $\text{CrAl}_7$  field falls. The expected criterion, i.e. the presence of visible signs of a peritectic reaction, is untrustworthy in these alloys; only the evidence obtained from extracted residues is admissible, and this is not sufficiently detailed to define the boundary accurately. The results suggest, since alloy 1.0/3.0 gave a residue consisting of  $\text{FeAl}_3$  and the iron-bearing  $\text{Cr}_2\text{Al}_{11}$  phase, that along the line representing 96 wt.-% aluminium the primary  $\text{Cr}_2\text{Al}_{11}$  and primary  $\text{FeAl}_3$  fields touch. The primary  $\text{CrAl}_7$  field must therefore be much more restricted than in the diagram suggested by Mondolfo,<sup>11</sup> but is not accurately fixed by the present work.

#### VI.—DISCUSSION

The results obtained in the work reported in Section V show clearly that no ternary compound exists in equilibrium with the primary aluminium-rich solid solution. In the solid state, only  $\text{FeAl}_3$  and  $\text{CrAl}_7$  are found in addition to the primary solid solution, and the boundaries of the three-phase ( $\alpha + \text{CrAl}_7 + \text{FeAl}_3$ ) triangle suggest strongly that both the  $\text{CrAl}_7$  phase and the  $\text{FeAl}_3$  can dissolve the appropriate third element. In slowly cooled alloys, however, the  $\text{Cr}_2\text{Al}_{11}$  phase makes its appearance. By the analysis of extracted samples of the intermetallic compounds, it has been shown that  $\text{CrAl}_7$  can dissolve iron up to a maximum of 3.02% by atoms; at this composition, the chromium content is 11.5 at.-%. The solubility of iron in  $\text{Cr}_2\text{Al}_{11}$  is more extensive, and reaches 7.74 at.-% iron at a chromium content of 11.45 at.-%. In neither case does the replacement of chromium by iron appear to follow any simple atomic scheme.

The equilibrium relations in the system aluminium–chromium–iron thus appear to bear a superficial resemblance to those reported for the aluminium–



chromium-manganese alloys above 590° C. In neither case is a ternary compound formed, while in both cases the compounds  $\text{CrAl}_7$  and  $\text{Cr}_2\text{Al}_{11}$  dissolve the third element. The solubilities of manganese in the two compounds are, however, much greater than the solubilities of iron. In spite of this, the analogy between the two systems is very much closer than a superficial comparison would indicate.

The compositions of the limiting solid solution of iron and manganese in the binary compounds are:

$\text{CrAl}_7$ : Fe 3.02 and Cr 11.5 at.-%.  
 Mn 6.44 and Cr 7.99 at.-%.  
 $\text{Cr}_2\text{Al}_{11}$ : Fe 7.74 and Cr 11.45 at.-%.  
 Mn 15.37 and Cr 1.83 at.-%.

Thus, in each case the amount of iron which can be taken up is approximately one-half of the maximum possible amount of manganese. The solubility figures are compared in Fig 11; it will be seen that the lines

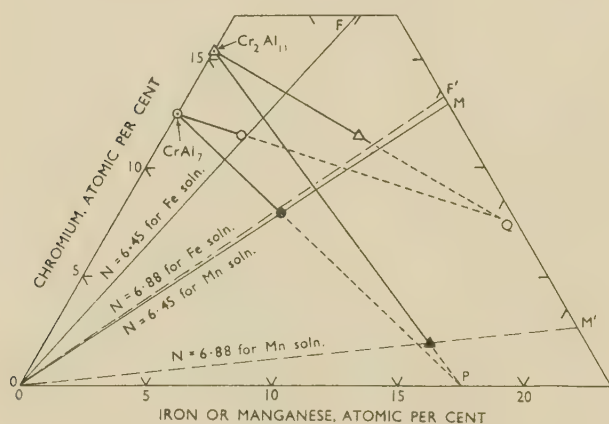


FIG. 11.—Solubilities of Iron and Manganese in  $\text{CrAl}_7$  and  $\text{Cr}_2\text{Al}_{11}$ .

- Solution of iron in  $\text{CrAl}_7$ .
- Solution of manganese in  $\text{CrAl}_7$ .
- △ Solution of iron in  $\text{Cr}_2\text{Al}_{11}$ .
- ▲ Solution of manganese in  $\text{Cr}_2\text{Al}_{11}$ .

representing the solution of manganese in the two compounds, if extrapolated, would meet on the aluminium-manganese axis at approximately 17.6 at.-% manganese (point P), so that, if it were possible to replace the whole of the chromium by manganese in both compounds the composition  $\text{Mn}_3\text{Al}_{14}$  would be obtained. In the case of solution of iron, the corresponding lines intersect at point Q; this point lies at a chromium percentage which is exactly half of the chromium content of  $\text{Cr}_2\text{Al}_{11}$ , and corresponds to the hypothetical formula  $\text{CrFe}_2\text{Al}_{10}$ . The solubility limit of iron in  $\text{Cr}_2\text{Al}_{11}$  falls almost at the composition  $\text{Cr}_{1.5}\text{FeAl}_{10.5}$ .

These curious relationships are difficult to understand without a detailed knowledge of the crystal structures of  $\text{CrAl}_7$  and  $\text{Cr}_2\text{Al}_{11}$ , or of the effective valency of chromium in these alloys.

The crystal structure of  $\text{CrAl}_7$  has been examined by Hofmann and Wiehr<sup>13</sup> and by Bradley and Lu<sup>14</sup>;

the cell dimensions reported are, however, not in agreement, as shown by the following comparison:

Hofmann and Wiehr: monoclinic cell with  $a = 20.43$ ,  $b = 7.62$ ,  $c = 25.31$  Å;  $\beta = 155^\circ 10'$ .

Bradley and Lu: orthorhombic cell with  $a = 19.99$ ,  $b = 12.47$ ,  $c = 34.51$  Å.

More recently, the cell dimensions of single crystals of  $\text{CrAl}_7$ , extracted from a binary aluminium-chromium alloy by methods similar to those described in this paper, have been determined by Little,<sup>15</sup> who has reported the unit cell to be orthorhombic, with the dimensions  $a = 24.8$ ,  $b = 24.7$ ,  $c = 30.2$  Å. The density of  $\text{CrAl}_7$  crystals was found to be less than that estimated from the densities of the constituent metals, and, when combined with the lattice-spacing measurements, enabled the number of units of  $\text{Cr}_2\text{Al}_{14}$  per unit cell to be estimated as 72 or 73. The compound  $\text{Cr}_2\text{Al}_{11}$  was also examined by Little, and the cell dimensions were found to be, within the limits of experimental error, identical with those of  $\text{CrAl}_7$ . The density was again less than that calculated additively, giving rise to an estimate of 93 units of  $\text{Cr}_2\text{Al}_{11}$  per cell. According to this work, therefore, the unit cells of the two compounds are not only very similar, but also contain similar numbers of aluminium atoms (1008 or 1022 for  $\text{CrAl}_7$ ; 1023 for  $\text{Cr}_2\text{Al}_{11}$ ). Since the unit cell of  $\text{Cr}_2\text{Al}_{11}$  can accommodate approximately 40 more chromium atoms than that of  $\text{CrAl}_7$  without significant change in dimensions, it is difficult to escape the conclusion that the structure of  $\text{CrAl}_7$  contains vacant lattice sites, which may, under the appropriate conditions, be filled by extra transition-metal atoms. In this connection, it is significant that, at the limits of solubility of iron and of manganese in  $\text{CrAl}_7$ , the total solute concentrations are closely similar. As shown in Fig. 12, these concentrations are respectively 14.52 and 14.43 at.-%. It is probable, therefore, that in both cases solution of the third metal in  $\text{CrAl}_7$  proceeds by the filling of vacant lattice sites up to a total solute concentration of approximately 14.5 at.-%. This is not the only factor involved, however, since the solubility of manganese is twice that of iron.

The numbers of outer electrons (3d and 4s) for chromium, manganese, and iron are respectively 6, 7, and 8. The solubility limit of manganese thus corresponds to a contribution from the transition-metal atoms of 93.02 3d and 4s electrons per 85.57 aluminium atoms. If it is assumed that this contribution is critical and also that it governs the solubility of iron in  $\text{CrAl}_7$ , it may be calculated that the composition of the iron-rich limit would be 3.2 at.-% iron, 11.2 at.-% chromium, and 85.57 at.-% aluminium. These values are in excellent agreement with the experimentally observed limit. The analogy between the two ternary systems thus suggests strongly that solid solution of manganese and iron in  $\text{CrAl}_7$  is dependent partially on replacement of chromium atoms, and partially on the filling up of vacant lattice sites to a maximum of 14.5 at.-% total

solute, subject to the attainment of a specific electron concentration. Although, in the above discussion, the total numbers of  $3d$  and  $4s$  electrons contributed by the transition-metal atoms were considered, it is clear that an analogous result is obtained by assuming any effective valency  $V$  (positive or negative) for chromium, provided that the effective valencies of manganese and iron are taken as  $(V + 1)$  and  $(V + 2)$ , respectively. It is therefore not possible to gain evidence from this work with regard to the effective valencies of the transition metals, but the importance of the electronic factor is clear.

It is probable that the same general factors apply to the phase  $\text{Cr}_2\text{Al}_{11}$ , though here the experimental correlation is less good. Here again the numbers of extra  $3d$  and  $4s$  electrons introduced with the second transition metal are approximately equal in the two cases (15.4 for manganese, 15.5 for iron), but the chromium content at the iron solubility limit is greater

of iron in  $\text{CrAl}_7$  falls close to this line. The broken lines  $OM'$  and  $OF'$  represent  $N = 6.88$  for the two systems; the correlation for the solubilities of manganese and iron in  $\text{Cr}_2\text{Al}_{11}$  is less close than for the case of  $\text{CrAl}_7$ , but similar principles are involved.

Fig. 10 shows that the analytical results for the extracted crystals of  $\text{FeAl}_3$  are too scattered to define the mode of replacement of iron by chromium. It is certain, however, that the solubility of chromium does not exceed 3.0 at.-%, from the position of the  $(\alpha + \text{CrAl}_7 + \text{FeAl}_3)/(\alpha + \text{FeAl}_3)$  boundary (see Fig. 4). The small solubility of chromium, and similarly of manganese, in  $\text{FeAl}_3$  is in marked contrast to the relatively extensive solubility of cobalt in this structure. This is in agreement with the general principle that intermetallic compounds formed by aluminium and transition metals form extensive solid solutions only with other transition elements which increase the number of electrons per atom. Transition metals which reduce the electron concentration do not, in general, dissolve appreciably in this type of compound.

## VII.—SUMMARY

In the system aluminium–chromium–iron, only  $\text{CrAl}_7$ , with iron in solution, and  $\text{FeAl}_3$ , with chromium in solution, enter into equilibrium with the aluminium-rich solid solution. In semi-liquid alloys, however,  $\text{Cr}_2\text{Al}_{11}$  is also found, and the solubilities of iron in  $\text{CrAl}_7$  and  $\text{Cr}_2\text{Al}_{11}$  may be determined by the analysis of crystals extracted from slowly cooled alloys. It is found that  $\text{CrAl}_7$  will dissolve 3.02 at.-% iron, while  $\text{Cr}_2\text{Al}_{11}$  will dissolve 7.74 at.-% iron. In this respect the system is analogous to the aluminium–chromium–manganese system, where  $\text{CrAl}_7$  and  $\text{Cr}_2\text{Al}_{11}$  respectively dissolve 6.44 and 15.37 at.-% manganese. Detailed examination of the two systems has shown the following analogies:

(i) The total solute concentrations at the solubility limits of iron and manganese in  $\text{CrAl}_7$  are almost identical.

(ii) The electron:atom ratios at the solubility limits of iron and manganese in  $\text{CrAl}_7$  are very similar whatever effective valency  $V$  is assumed for chromium, provided that the effective valencies of manganese and iron are taken as  $(V + 1)$  and  $(V + 2)$  respectively.

(iii) The numbers of  $3d$  and  $4s$  electrons per transitional solute atom at the iron and manganese limits in  $\text{CrAl}_7$  are closely similar, and the same is true to a lesser degree of accuracy at the solubility limits of iron and manganese in  $\text{Cr}_2\text{Al}_{11}$ .

(iv) The number of  $3d$  and  $4s$  electrons per solute atom is increased from 6 to approximately 6.45 by the solution of iron or manganese in  $\text{CrAl}_7$ , and to approximately 6.9 by the solution of these two elements in  $\text{Cr}_2\text{Al}_{11}$ . The increase permitted in the case of  $\text{Cr}_2\text{Al}_{11}$  is therefore twice that permitted for  $\text{CrAl}_7$ .

The full interpretation of these striking correspondences is not possible until the crystal structures

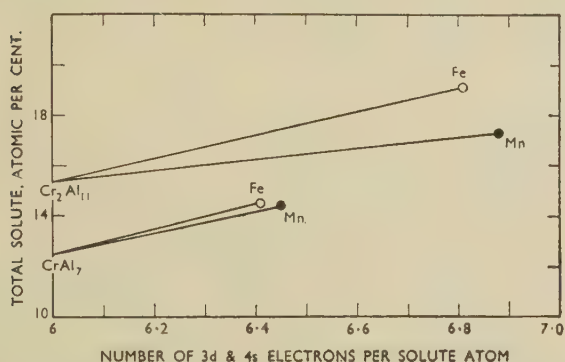


FIG. 12.—Correlation of Total Solute Concentration with Number of  $3d$  and  $4s$  Electrons per Solute Atom for the Solid Solutions of Iron and Manganese in  $\text{CrAl}_7$  and  $\text{Cr}_2\text{Al}_{11}$ .

than would be expected if exactly the same conditions applied as for  $\text{CrAl}_7$ . The  $\text{Cr}_2\text{Al}_{11}$  structure is apparently able to support a larger total solute concentration than is actually reached on solution of manganese.

The importance of the electronic factor may be appreciated from Fig. 12, in which the total solute concentration is plotted against the number of  $3d$  and  $4s$  electrons per atom of transition metal ( $N$ ). This diagram shows that the values of  $N$  at the solubility limits of iron and manganese in  $\text{CrAl}_7$  are closely similar. The numbers of transition-metal atoms are also almost identical. Although the total solute concentration at the solubility limit of iron in  $\text{Cr}_2\text{Al}_{11}$  is greater than that at the solubility limit of manganese, the values of  $N$  are similar. It may be noted that the increase in  $N$  permitted for  $\text{Cr}_2\text{Al}_{11}$  is approximately twice that permitted for  $\text{CrAl}_7$ .

Fig. 11 summarizes the electronic features discussed above. The full line  $OM$  in Fig. 11 represents  $N = 6.45$   $3d$  and  $4s$  electrons per solute atom for the system aluminium–chromium–manganese, while the full line  $OF$  represents the same value of  $N$  for the aluminium–chromium–iron system. The solubility



of the two binary compounds have been determined. Preliminary work has shown, however, that the crystal structures of both must be very similar; the constancy of the unit cell dimensions in spite of a variation in the relative numbers of aluminium and chromium atoms has led to the suggestion that both structures contain the same numbers of aluminium atoms per cell, and a number of vacant lattice sites which are available to accommodate extra transition-metal atoms. In the case of  $\text{CrAl}_7$ , this suggestion is strengthened by the observation now made that the total numbers of solute atoms present at the solubility limits of iron and manganese in  $\text{CrAl}_7$  are equal. Both manganese and iron dissolve in  $\text{CrAl}_7$  partly by substitution of chromium atoms and partly by the filling of vacant lattice sites until the same total solute concentration is reached; at the same time there is an electronic restriction which prevents the number of  $3d$  and  $4s$  electrons from increasing beyond approximately 6.45 per solute atom. It appears probable that similar considerations apply in principle to  $\text{Cr}_2\text{Al}_{11}$ , since solution of iron and manganese again

proceeds to a comparable number of  $3d$  and  $4s$  electrons per solute atom; the increase above 6 is approximately twice that permitted for  $\text{CrAl}_7$ . The total solute content, however, is not equal at the two solubility limits.

The analogy between the systems aluminium-chromium-iron and aluminium-chromium-manganese is therefore much closer than a superficial comparison would suggest.

#### ACKNOWLEDGEMENTS

This research forms part of a programme in progress in the Department of Metallurgy, Birmingham University, under the general supervision of Professor D. Hanson, D.Sc., to whom the authors' thanks are due for his interest and support. The authors also express their gratitude to the Department of Scientific and Industrial Research, the Royal Society, the Chemical Society, and Imperial Chemical Industries, Ltd., for generous financial assistance and for the loan of apparatus.

#### REFERENCES

1. G. V. Raynor and K. Little, *J. Inst. Metals*, 1945, **71**, 493.
2. A. G. C. Gwyer and H. W. L. Phillips, *J. Inst. Metals*, 1927, **38**, 29.
3. H. W. L. Phillips, *J. Inst. Metals*, 1941, **67**, 275.
4. A. J. Bradley and A. Taylor, *Proc. Roy. Soc.*, 1938, [A], **166**, 353; and *J. Inst. Metals*, 1940, **66**, 53.
5. J. K. Edgar, *Trans. Amer. Inst. Min. Met. Eng.*, 1949, **180**, 225.
6. A. J. Bradley and S. S. Lu, *J. Inst. Metals*, 1937, **60**, 319.
7. M. Gotō and G. Dogane, *Nippon Kōgyō Kwai Shi*, 1927, **43**, 931.
8. W. L. Fink and H. R. Freche, *Trans. Amer. Inst. Min. Met. Eng.*, 1933, **104**, 325.
9. G. V. Raynor and K. Little, *J. Inst. Metals*, 1945, **71**, 481.
10. G. Taillandier, *Rev. Mét.*, 1932, **29**, 315, 348.
11. L. F. Mondolfo, "Metallography of Aluminium Alloys". New York: 1943 (John Wiley and Sons, Inc.).
12. I. I. Kornilov, "Iron Alloys. I.—Iron-Chromium-Aluminium Alloys". Moscow: 1945 (Academy of Sciences).
13. W. Hofmann and H. Wiehr, *Z. Metallkunde*, 1941, **33**, 369.
14. A. J. Bradley and S. S. Lu, *Z. Krist.*, 1937, **96**, 20.
15. K. Little, private communication.

# THE EQUILIBRIUM DIAGRAM OF THE SYSTEM COPPER-GALLIUM IN THE REGION 30-100 AT.-% GALLIUM\*

1368

By J. O. BETTERTON,<sup>†</sup> JR., D.Phil., B.S., and WILLIAM  
HUME-ROTHERY,<sup>‡</sup> O.B.E., F.R.S., MEMBER

## SYNOPSIS

The equilibrium diagram of the system copper-gallium has been investigated in the region 30-40 at.-% gallium, and some information has been gained as to the constitution of the gallium-rich alloys. According to the previous work of Weibke (*Z. anorg. Chem.*, 1934, **220**, 293), a phase denoted  $\delta$ , with a  $\gamma$ -brass structure, existed at low temperatures in the range 30-40 at.-% gallium, and at high temperatures underwent a transformation into a phase denoted  $\gamma$ , whose structure was not determined. The present work shows that this transformation is an order-disorder change, and that the high-temperature  $\gamma$  phase has a typical  $\gamma$ -brass structure. At low temperatures the  $\delta$  phase of Weibke is shown to consist of three different modifications of the  $\gamma$ -brass structure, denoted  $\gamma_1$ ,  $\gamma_2$ , and  $\gamma_3$ , which are characterized by slight differences in the intensities of some of the weaker X-ray-diffraction lines. Measurements of densities and lattice spacings show that the  $\gamma_1$  phase contains the full number of 52 atoms per unit cell at its copper-rich boundary, but that increasing gallium content results in a slight decrease in the number of atoms per unit cell. On passing to the  $\gamma_2$  and  $\gamma_3$  fields, there is a marked diminution in the number of atoms per unit cell, and this dropping out of atoms occurs in such a way as to maintain a constant electron concentration. No evidence is found for the existence of the  $\epsilon$  or  $\epsilon'$  phases postulated by Weibke, and the  $\theta$  phase which he placed at 56 at.-% gallium is shown to correspond almost exactly with the formula  $\text{CuGa}_2$ .

## I.—INTRODUCTION

THE equilibrium diagram of the system copper-gallium in the region 0-30 at.-% gallium has been determined by Hume-Rothery, Mabbott, and Channel-Evans<sup>1</sup> and by Hume-Rothery and Raynor,<sup>2</sup> whose work showed that the diagram of Weibke<sup>3</sup> was incorrect in some respects. Later work by Owen and Rowlands<sup>4</sup> has substantially confirmed the  $\alpha$ -solid-solubility curve of Hume-Rothery and his co-workers, and the copper-rich end of the diagram, which may be regarded as well established, is shown on the left-hand side of Fig. 1.

The remainder of the diagram, shown on the right-hand side of Fig. 1, was investigated by Weibke,<sup>3</sup> according to whom there is a  $\delta$  phase with a typical  $\gamma$ -brass structure in the region 30-40 at.-% gallium, and this undergoes a transformation into a high-temperature phase, denoted  $\gamma$ , whose structure was not determined. On the gallium-rich side of the  $\gamma$  phase, the diagram of Weibke showed two horizontals at 478° and 467° C., respectively, which were regarded as connected with the formation of phases denoted  $\epsilon$  and  $\epsilon'$ , but the diagram was unconvincing in this region, and as drawn in Fig. 1 is in contradiction to the Phase Rule. At higher concentrations of gallium, Weibke claimed to have established the existence of a phase denoted  $\theta$  at about 56 at.-% gallium, but the evidence for the composition of this phase was not conclusive.

The present paper describes a detailed determination of the diagram in the region of the  $\gamma$  and  $\delta$  phases of Fig. 1, and some information has also been gained as to the constitution of the gallium-rich alloys.

## II.—EXPERIMENTAL

### 1. MATERIALS

The copper used in the present work was electrolytic metal of 99.998% purity kindly presented by the British Non-Ferrous Metals Research Association. The gallium was supplied by Johnson, Matthey and Co., Ltd., and was specially refined metal of 99.94% purity.

### 2 MELTING TECHNIQUE

The alloys for microscopical and X-ray work were melted in crucibles machined from pure graphite, and were poured into heavy copper moulds to give ingots of  $\frac{1}{4}$  in. or  $\frac{3}{8}$  in. dia. Numerous alloys were analysed for both copper and gallium, and no evidence of contamination was obtained. These and all other analyses were carried out by Johnson, Matthey and Co., Ltd., and we must express our thanks to Mr. A. R. Powell for his help and attention.

### 3. LIQUIDUS DETERMINATION

The first cooling-curve experiments in the range 31-37 at.-% gallium were with ingots of 16-20 g. melted in graphite crucibles fitted with graphite lids,

\* Manuscript received 13 August 1951.

<sup>†</sup> Metallurgist, Oak Ridge National Laboratory, Tenn., U.S.A.

<sup>‡</sup> Royal Society Warren Research Fellow and University Lecturer in Metallurgical Chemistry, Oxford.



and contained in a closed silica tube filled with argon. The rates of cooling were  $1^{\circ}$ – $2^{\circ}$  C./min., and the platinum/platinum-13% rhodium thermocouples used were of specially thin wire contained in thin silica sheaths. The stirring rods were also of silica. The experimental methods resembled those of Hume-Rothery and Reynolds<sup>5</sup> and Andrews, Davies, Hume-Rothery, and Oswin,<sup>6</sup> and gave satisfactory primary arrests, though later arrests were very weak, and with increasing gallium content the primary arrests became smaller. This was partly due to the high thermal conductivity of the graphite, and some stronger arrests were obtained by using silica crucibles; the

ingots have been deduced by subtracting 0.2% from the nominal compositions based on the weights of metals used. The liquidus below  $500^{\circ}$  C. was determined by a differential method, with one junction of the differential thermocouple in a block of solid copper, and the other in the molten alloy, both being contained in thin silica sheaths coated with alundum cement. Under these conditions well-marked arrests were obtained. In order to reduce the consumption of gallium, the first cooling curve was made on a 97.5 at.-% alloy which was then remelted with the addition of an accurately weighed amount of a 32 at.-% alloy. This process was repeated a number

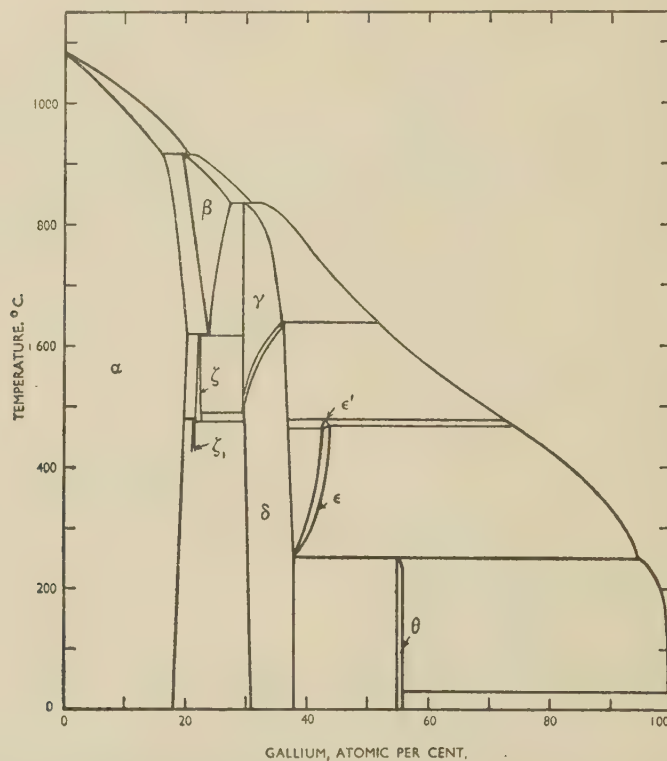


FIG. 1.—The Equilibrium Diagram of the System Copper-Gallium in 1947. The diagram in the  $\alpha$ ,  $\beta$ ,  $\zeta$ , and  $\zeta_1$  regions is due to Hume-Rothery, Mabbott, and Channel-Evans<sup>1</sup> and to Hume-Rothery and Raynor.<sup>2</sup> The remainder of the diagram is due to Weibke.<sup>3</sup>

resulting ingots were, however, slightly contaminated by silicon, which was present to the extent of 0.03, 0.025, and 0.09% in alloys 37.92, 49.12, and 64.22,\* respectively. Later experiments were carried out in alumina crucibles using silica stirrers and thermocouple sheaths coated with alundum cement, and contamination was prevented; the weight of the ingots was increased to 36 g. in these experiments. For all but two of the points on the liquidus above  $500^{\circ}$  C., the complete cooling-curve ingot was dissolved for analysis and the total percentages of the gallium and copper lay between 99.94 and 100.04. There was usually a slight loss of gallium during the experiment, and the compositions of the two un-analysed

of times, until the composition calculated to be 72.4 at.-% gallium was reached, after which the ingot was analysed and found to contain 72.48 at.-% gallium. The good agreement between the calculated and analysed compositions justifies using the former for the intermediate alloys.

#### 4. SOLIDUS DETERMINATION

The solidus was first determined by the standard microscopical method, using specimens previously homogenized at suitable temperatures. The specimens were usually heated for 30 min. at the desired temperature, which was controlled to within  $\pm \frac{1}{2}^{\circ}$  C. by the hand adjustment of resistances. After quench-

\* For convenience, alloys are referred to by their atomic percentages of gallium; thus alloy 32.0 means an alloy containing 32.0 at.-% gallium.

ing in water, the specimens were examined microscopically by the methods referred to below. This method was satisfactory, but proved difficult owing to the brittle nature of the alloys, and a second determination of the solidus was therefore made by taking heating curves. The alloys were too brittle to be drilled, and were therefore cast in a graphite mould with a central graphite core which produced

the analysis of the same batch of filings (after heat-treatment) from which the X-ray specimen was made.

### 5. MICROSCOPICAL EXAMINATION OF SOLID ALLOYS

The microscopical examination of the alloys was difficult owing to their brittleness and the presence of free gallium in many specimens. The alloys were usually split by cleavage, and then ground directly for prolonged periods on 000 emery paper; an automatic machine using very light pressure was designed for this purpose. Alloys that contained free gallium were ground on a glass plate surrounded by solid carbon dioxide, the alloy itself being mounted in an insulating substance, and pressed at intervals against another piece of solid carbon dioxide. Numerous etching reagents were used, and the effects of these are summarized in Appendix I.

### 6. X-RAY TECHNIQUE AND DENSITY DETERMINATIONS

Room-temperature Debye-Scherrer photographs were taken in a 19-cm. Unicam camera, and the lattice spacings determined by standard extrapolation methods. In this work the alloys were annealed to equilibrium in lump form and quenched. Powders prepared by grinding in a mortar were treated with alcohol and ether (cf. Hume-Rothery and Reynolds)<sup>5</sup>, and re-annealed in sealed evacuated silica tubes. By using filtered copper  $K_\alpha$  radiation, very satisfactory diffraction films were obtained. Some high-temperature photographs were also taken in the Debye-Scherrer camera of Hume-Rothery and Reynolds,<sup>7</sup> and these are referred to later. Preliminary density determinations were made on homogenized lumps of alloy, which were weighed in air and when immersed in liquid ethylene dibromide. Owing to the difficulty of obtaining perfectly sound ingots, the work was repeated using coarsely powdered alloys in a silica container; about 10 g. of alloy were used in each determination. The method was a modification of that of Egerton and Lee,<sup>8</sup> and prolonged evacuation was necessary to remove adhering gas bubbles. The probable error of the method was estimated as being of the order of 1 part in 5000, and the observed differences between duplicate measurements lay between 1 part in 4000 and 1 part in 80,000. In the X-ray work, the chemical analysis was usually carried out on the same batch of filings (after heat-treatment) as that from which the specimen was prepared, and in 12 determinations the percentages of gallium and copper determined analytically lay between 99.94 and 100.07. In a few cases it was possible only to use the analysis of the specimens in lump form; these results are distinguished in both tables and diagrams.

### III—THE LIQUIDUS

The primary liquidus arrests obtained on cooling curves are shown in Table I, and are plotted in Fig. 3. The good agreement between the result for alloy 64.22, which contained 0.09% silicon, and that for alloy 64.35, free from silicon, shows that the three ingots

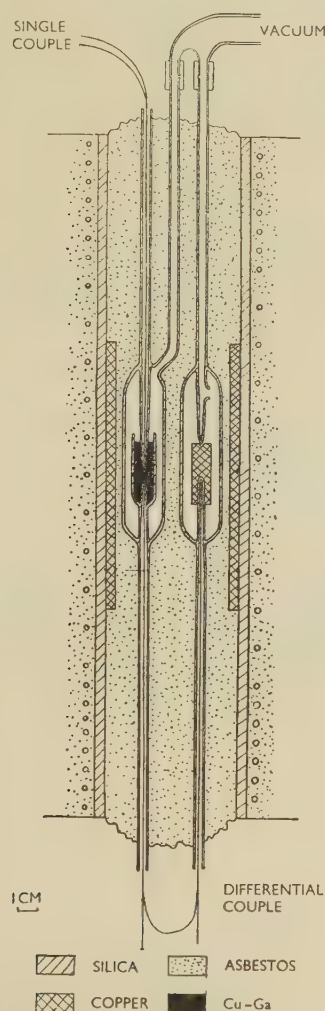


Fig. 2.—Differential-Heating-Curve Apparatus Used for Solidus Determinations.

a cylindrical specimen with a hole down the centre. After homogenization at a suitable temperature, heating curves were taken in the apparatus shown in Fig. 2, which is self-explanatory. Two further points on the solidus curve of the 21/13 electron compound were also obtained by standard X-ray lattice-spacing methods, using the lattice-spacing/composition curves of Section IV in conjunction with the lattice spacings of specimens from just within the semi-liquid region. In work on the solidus, the composition was determined by the analysis of the actual specimen used for the microscopical or thermal work, and by



TABLE I.—Liquidus Points.

Gallium, at.-%	Liquidus Arrest, °C.	Notes *	Gallium, at.-%	Liquidus Arrest, °C.	Notes *
30.85	833.9	A	64.22	548	S3
32.77	829.2	A	64.35	545	A
34.34	821.0	A	72.48	494	AX7
35.08	815.7	A	77.6	458.5	EX6
37.92	794	S1	83.3	415	EX5
43.8	729	ES	87.0	383	EX4
49.12	671	S2	91.74	328	EX3
51.57	649	A	96.0	256	EX2
54.54	619	A	97.5	225	EX1
60.77	571	E			

\* In all cases the complete cooling-curve ingot was dissolved for analysis. In general, a small insoluble residue of graphite, alumina, &c., was found owing to flaking or powdering of the refractories. After allowing for this, the totals of gallium + copper determined analytically lay between the limits 99.94 and 100.03 for the alloys marked A or AX. The alloys marked S1, S2, and S3 contained 0.03, 0.025, and 0.095% silicon, but the good agreement between the results for alloys 64.22 and 64.35 suggests that this exerted a negligible effect on the liquidus point. In the alloys marked E the composition was estimated by subtracting 0.2 at.-% from the value calculated from the weights of metals used, and the alloy marked ES is thought to possess a silicon content lying between those for the alloys marked S1 and S2. As explained in the text (p. 460), the alloys EX1 to AX7 were prepared by using first a 97.5 at.-% gallium alloy, to which additions of a 32 at.-% alloy were made until an intended composition of 72.4 at.-% gallium was reached. The resulting ingot was analysed and gave the value 72.48 recorded for the alloy marked AX7; the compositions of the alloys EX1 to EX6 were then estimated from the weights of metals used.

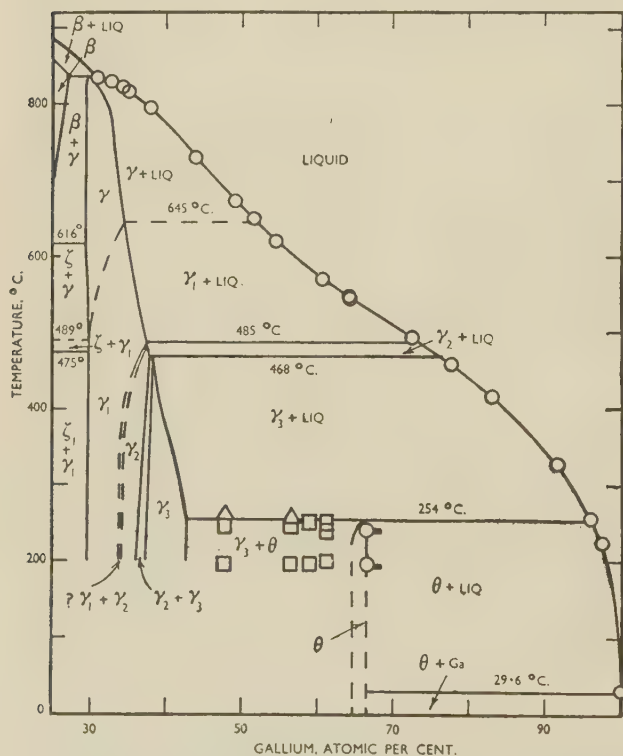


FIG. 3.—The Equilibrium Diagram of the System Copper-Gallium in the Region 25-100 at.-% Gallium. The liquidus points of the present work, and the results of annealing experiments in the region 50-70 at.-% gallium are included. For the  $\gamma$  regions the details are given in Fig. 5.

referred to on p. 460 may legitimately be included in the diagram. The results are in general agreement with those of Weibke, but the present curve is slightly higher, probably as a result of the slower rates of cooling. The liquidus curve shows a change in direction at 51.8 at.-% gallium and 645° C., and secondary arrests were observed for this transformation, which is discussed in detail later. The cooling curves also confirmed the existence of two arrests in the region of 460°-480° C., and of the low-temperature horizontal at 254° C. (Weibke, 249° C.). The interpretation of the transformations giving rise to these arrests proved very difficult, and is described in the following sections.

#### IV.—THE $\gamma$ AND $\gamma_1$ PHASES

According to Weibke, the  $\delta$  or low-temperature modification of the 21/13 electron compound undergoes a transformation into a high-temperature modification denoted  $\gamma$ . The temperatures of this transformation were determined by Weibke from arrests

TABLE II.—Lattice Spacings of Alloy 32.13 at High Temperature.

The same specimen was taken through the following sequence of temperatures with the results shown.

Experiment No.	Temperature, °C.	Lattice Spacing, kX units	Experiment No.	Temperature, °C.	Lattice Spacing, kX units
1	20.7	8.7179	6	404.6	8.7958
2	521.8	8.8237	7	603.8	8.8465
3	536.2	8.8275	8	22.0	8.7173
4	507.1	8.8188	9	701.0	8.8677
5	23.4	8.7174	10	22.2	8.7172

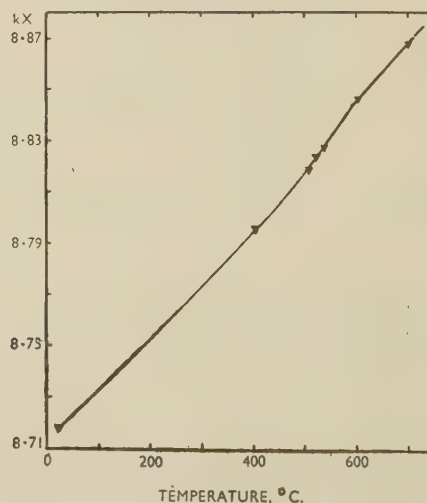


FIG. 4.—The Lattice-Spacing/Temperature Curve for the Alloy Containing 32.13 at.-% Gallium.

on cooling curves and rose from 489° C. on the copper-rich side to 639° C. on the ( $\gamma/\gamma + \text{liq.}$ ) boundary. The present experiments have shown that this transformation is an order-disorder change, the evidence for which is summarized below. The X-ray work described in Sections V and VI has shown that at the

lower temperatures there are three distinct modifications of the 21/13 electron compound, and these have therefore been denoted by  $\gamma_1$ ,  $\gamma_2$ , and  $\gamma_3$ , whilst retaining Weibke's symbol of  $\gamma$  for the high-temperature modification. The evidence for the order-disorder change is as follows:

(1) Alloys quenched from the  $\gamma$  and  $\gamma_1$  regions were indistinguishable microscopically and gave similar

X-ray-diffraction patterns, typical of the  $\gamma$ -brass structure.

(2) High-temperature X-ray-diffraction photographs showed no difference between the structures above and below the transformation temperature. The lattice spacings of alloy 32.13 at high temperatures are shown in Table II, and the lattice-spacing/temperature curve is shown in Fig. 4 and indicates a slight

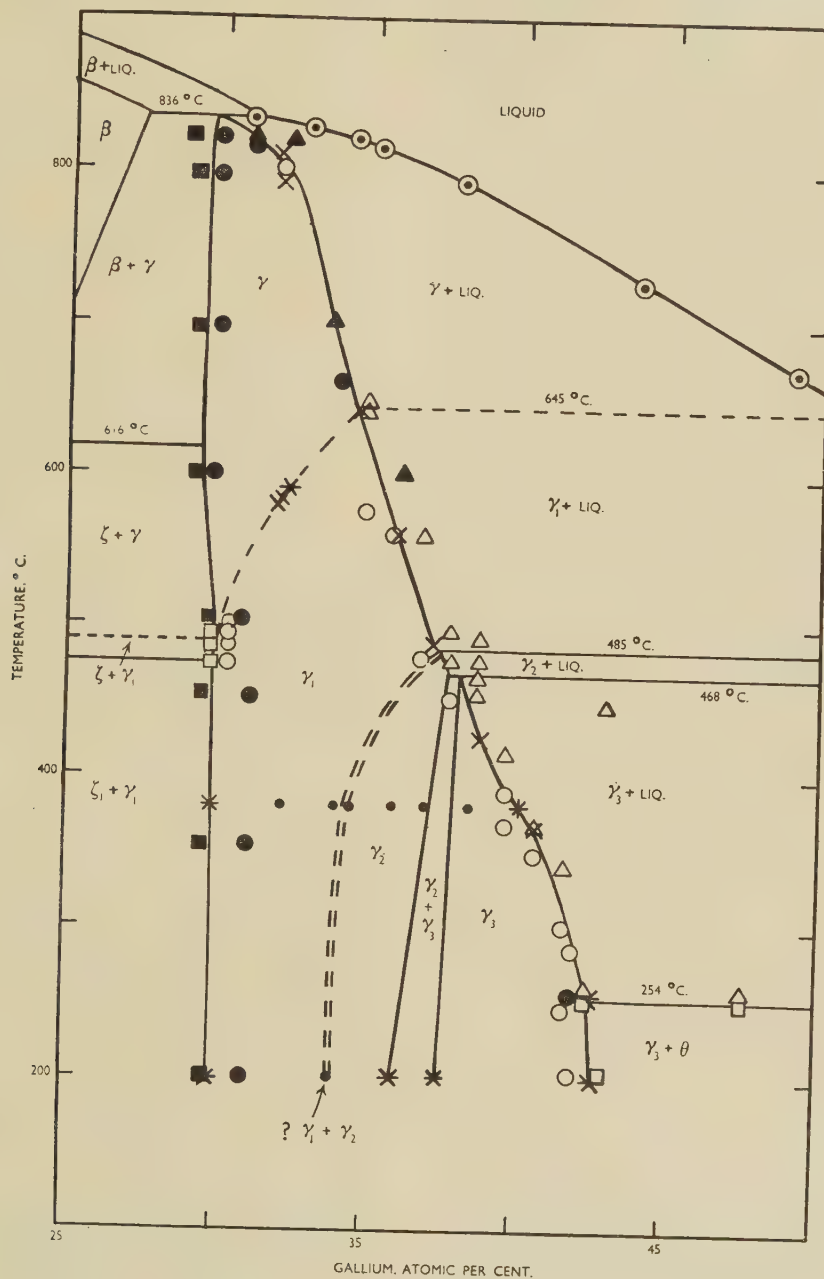


FIG. 5.—The Equilibrium Diagram of the System Copper-Gallium in the Region 25-50 at.-% Gallium.

- KEY.
- |  |                           |
|--|---------------------------|
| ○ Liquidus points by thermal analysis.                           | ○ ● Single-phase alloys.  |
| × Solidus points from heating curves.                            | □ ■ Two-phase alloys.     |
| * Points determined by lattice-spacing methods.                  | △ ▲ Partly liquid alloys. |
| ● Alloys examined by X-ray methods for identification of phases. |                           |

The full circles, squares, and triangles refer to alloys specimens of which were analysed after quenching from the temperatures concerned. The open symbols refer to alloys whose compositions were obtained by analysis of specimens quenched from other temperatures, or were estimated from the weights of metals used.



change in direction in the region of 590° C. This temperature is in good agreement with those of the thermal arrests for two alloys of slightly lower gallium content (see Fig. 5).

(3) The thermal arrests of three alloys were studied in detail, and in all cases the arrest on a cooling curve was fairly sharp and died away gradually. Heating curves revealed no sudden arrests, but instead there was a gradual deflection of the curve, ended by a sharp swing back in the direction opposite to that expected for an arrest. This clearly suggested an order-disorder transformation, and approximate determinations of the changes in specific heat were therefore made.

For this purpose the heating-curve apparatus was provided with a heavy copper tube in order to obtain a uniform temperature inside the furnace. A third thermocouple was placed in the space between the specimen and the standard body (of copper), and by moving this thermocouple up and down it was shown that the temperature was satisfactorily constant. In this way readings were made of the furnace temperature, the temperature of the alloy under investigation, and the difference in temperature between the alloy and the standard body. This apparatus does not embody the full refinements of that devised by Sykes<sup>9</sup> for tubular specimens, but the equations of Sykes may legitimately be used to obtain the approximate variation of the ratio of the specific heats of the alloy and the standard body. Fig. 6 shows the approximate variation of the specific heat of alloy 31.72 in the middle of the  $\gamma$ ,  $\gamma_1$  region, and the form of the curve is typical of an order-disorder change. Alloy 34.6,

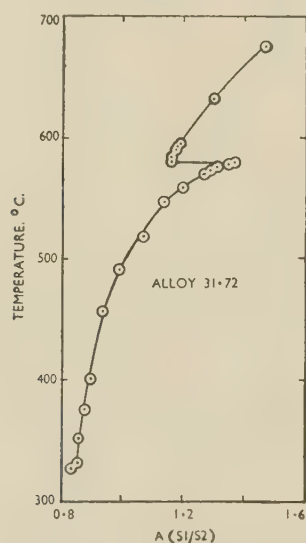


Fig. 6.—The Variation with Temperature of the Ratio of the Specific Heat of Alloy 31.72 ( $S_1$ ) to That of Copper ( $S_2$ ).

whose transformation temperature is on the edge of the semi-liquid region, gave an analogous curve slightly complicated by the latent heat of fusion at the solidus point. It may therefore be concluded that

the  $\gamma \rightleftharpoons \gamma_1$  transformation is an order-disorder change whose temperature runs across the phase field until it reaches the solidus at the temperature of the 645° C. horizontal (Weibke, 639° C.). For the three alloys

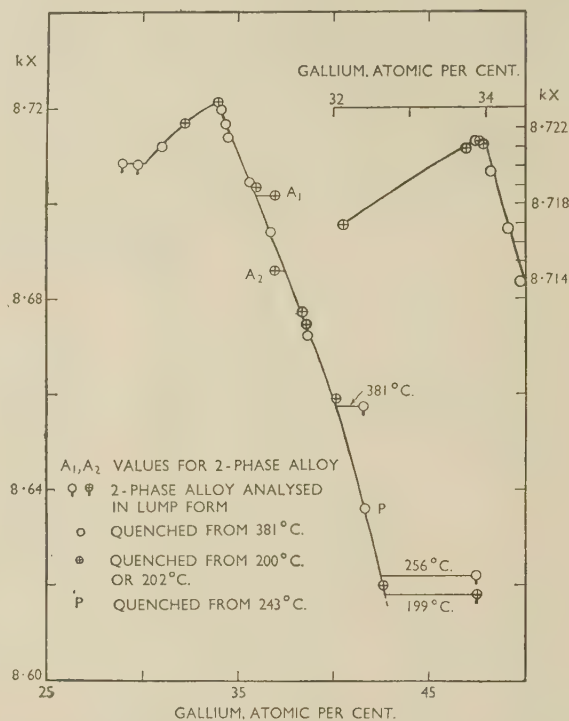


Fig. 7.—The Lattice Spacing/Composition Relationship for Copper-Gallium Alloys in the  $\gamma_1$ ,  $\gamma_2$ , and  $\gamma_3$  Regions. All specimens were analysed in powder form except those indicated as having been analysed in lump form. The small inset figure shows the results at the peak of the curve for alloys whose compositions lie too close together to be shown in the main figure.

studied in detail, the peak on the specific-heat/temperature curve was 5°–6° C. higher than the uppermost temperature given by Weibke, who regarded the change as a normal phase change involving a two-phase region. In view of the above results, the transformation has been represented by a single broken line to indicate an order-disorder change.

The phase boundaries of the  $\gamma$  and  $\gamma_1$  phases on the copper-rich side were determined by microscopical methods with the results shown in Fig. 5; a summary of the annealing times is given in Appendix II. Alloys were examined after annealing at five temperatures between 475° and 503° C., but no evidence could be found for an abrupt change in composition of the  $\gamma$  phase such as would be expected if the transformation at 489° C. were of a eutectoid or peritectoid type. At the lower temperatures two points on the  $\gamma_1$  solubility curve were determined by the lattice-spacing method, and, as will be seen from Fig. 5, these results confirm those of the microscopical work.

The lattice-spacing/composition curve of the  $\gamma_1$  phase is shown in Fig. 7. With increasing gallium content the lattice spacing of the  $\gamma_1$  phase increases

steadily until slightly below 34 at.-% gallium, after which the  $\gamma_2$  phase is present and the lattice spacing diminishes. The exact values are given in Table III.

TABLE III.—Lattice Spacings at 18° C. of Copper-Gallium Alloys in the  $\gamma$  Regions.

Gallium, at.-%	$a$ , kX units	Annealing Temp., °C.	Notes
29.68 *	8.7083	381	$\gamma_1$ + trace of $\alpha$
29.68 *	8.7084	381	
31.01	8.7120	381	
32.13B	8.7169	200	...
33.73B	8.7209	200	...
33.84B	8.7213	381	...
33.90B	8.7201	202	...
33.90B	8.7213	200	...
33.96B	8.7211	200	...
34.06B	8.7197	381	...
34.29	8.7167	381	...
34.44B	8.7139	381	...
35.57B	8.7048	380	...
35.89	8.7035	200	...
36.69B	8.6940	380	...
36.93	{ 8.6860 8.7017 }	202	{ Two-phase film $\gamma_2 + \gamma_3$
38.40	8.6774	202	
38.60B	8.6722	381	...
38.59	8.6747	202	...
40.14	8.6593	200	...
41.65	8.6362	243	...
42.64 *	8.618	200	...

For the alloys marked \* the composition was determined by the analysis of the alloy in lump form after homogenization. For the remaining alloys the analyses were carried out on the powder after its final annealing treatment, except that for alloy 41.65 the analysis was made on a sample of the powder annealed at 200° C. For the analyses of the alloys marked B, both metals were determined, and the sums of the analytical percentages lay between the limits 99.94 and 100.07. For the remaining analyses, copper alone was determined.

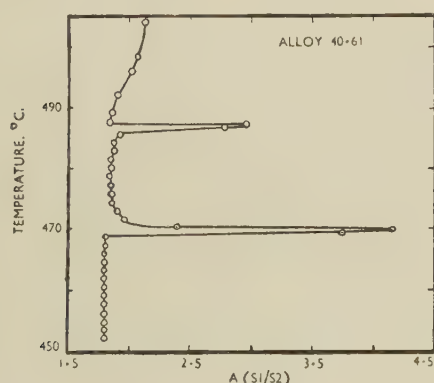


FIG. 8.—The Variation with Temperature of the Ratio of the Specific Heat of Alloy 40-61 ( $S_1$ ) to that of Copper ( $S_2$ ). The curve indicates two phase changes and should be contrasted with that of Fig. 6.

The solidus curves of the  $\gamma$  and  $\gamma_1$  regions were determined by microscopical and thermal methods, and, as will be seen from Fig. 5, the results are in good agreement, except that the thermal arrest for alloy 31.8 appears slightly too low. The heating curves of several alloys were carried up to the temperature of

the 645° C. horizontal, and the resulting arrests were characteristic of an order-disorder transformation, rather than of a true phase change. In agreement with the work of Weibke, these experiments showed the existence of two horizontals at 485° and 468° C. (Weibke, 478° and 467° C.). In contrast to the arrests for the  $\gamma \rightleftharpoons \gamma_1$  transformation, the thermal arrests at 485° and 468° C. were those of true phase changes; Fig. 8 shows the specific-heat curve for alloy 40-61, and the contrast with the curve of Fig. 6 is apparent. It appears, therefore, that the arrests at 485° C. correspond to the peritectic reaction  $\text{liq.} + \gamma_1 \rightleftharpoons \gamma_2$ , and that this is a genuine phase change. No microscopical distinction could be made between the  $\gamma_1$  and  $\gamma_2$  phases, and the boundary between these is discussed below.

## V.—THE $\gamma_2$ AND $\gamma_3$ PHASES

Fig. 7 shows that beyond 34 at.-% gallium, the lattice spacing of the  $\gamma$  phase decreases rapidly. In this region changes occur in the intensities of some of the weakest lines of the Debye-Scherrer films. In all these alloys the general  $\gamma$  structure is retained, and all the lines can be indexed as belonging to the cubic cell of side 8.6-8.7 kX. The films divide themselves into three main types, and Table IV shows the variation of intensity of the characteristic weak diffraction lines. These variations of intensity do not necessarily imply phase changes, since they may result from variations of structural parameters or from a dropping out of atoms from some of the structural sites, but they are sufficiently pronounced to be regarded as indicating the existence of three modifications of the  $\gamma$  phase, which will be referred to as  $\gamma_1$ ,  $\gamma_2$ , and  $\gamma_3$ . On passing from  $\gamma_1$  to  $\gamma_2$ , there is a strengthening of the reflections for which  $\Sigma h^2 = 6, 9, 10, 11, 27$ , and 40, and a weakening of those for which  $\Sigma h^2 = 20, 21, 74$ , and 100. On passing to the  $\gamma_3$  modification, there is a further weakening of the lines for which  $\Sigma h^2 = 20$  and 100, and a strengthening of the lines for which  $\Sigma h^2 = 9, 10, 11, 17$ , and 19.

The lattice-spacing/composition curve for homogeneous alloys shows no appreciable change in direction on passing from the  $\gamma_2$  to the  $\gamma_3$  region. Alloy 36.93 after annealing at 202° C. gave a diffraction film with two sets of lines, showing that a real phase change is involved on passing from the  $\gamma_2$  to the  $\gamma_3$  modification. The lines at high angles were sufficiently separated for the lattice spacings of the  $\gamma_2$  and  $\gamma_3$  phases to be measured, and the resulting lattice parameters gave the compositions of the phases in equilibrium as  $\gamma_2 = 35.9$  and  $\gamma_3 = 37.5$  at.-% gallium, whilst at 380° C. only the  $\gamma_2$  phase was present. The existence of a two-phase ( $\gamma_2 + \gamma_3$ ) region suggested that the 468° C. horizontal determined by thermal analysis was that of the peritectic reaction  $\text{liq.} + \gamma_2 \rightleftharpoons \gamma_3$ , and careful examination was therefore made to see whether the  $\epsilon$  phase of Weibke's diagram could be observed. An alloy quenched from the middle of the supposed  $\epsilon$  phase field was found to contain large



amounts of chilled liquid, and chilled liquid was also found in several alloys quenched from the region in which, according to Weibke, the structures should have been solid ( $\delta + \epsilon$ ), or ( $\gamma_2$  or  $\gamma_3 + \epsilon$ ) in the present notation. No evidence could be found for the existence of the  $\epsilon$  phase claimed by Weibke, and, as

TABLE IV.—Intensities of Characteristic Weak Diffraction Lines Distinguishing  $\gamma_1$ ,  $\gamma_2$ , and  $\gamma_3$  Phases.

Modification of $\gamma$ Phase	$2\theta^\circ =$												
	6	9	10	11	17	19	20	21	27	40	41	74	100
$\gamma_1$	C	C	A	A	C	B	W	C	B	C	C	W	W
$\gamma_2$	W	W	B	B	C	B	C	B	C	W	B	C	C
$\gamma_3$	W	M	C	C	W	C	B	B	C	W	B	C	A

KEY.

A = Absent.  
B = Barely visible.  
C = Clear but very faint.

W = Weak.  
M = Medium to weak.

shown in Fig. 5, the results for the solidus curve of the  $\gamma_1$ ,  $\gamma_2$ , and  $\gamma_3$  phases determined by microscopical, X-ray, and thermal methods are in good agreement, and the solidus curve of the  $\gamma_3$  phase ends at  $254^\circ \text{C.}$ , the temperature of the  $\text{liq.} + \gamma_3 \rightleftharpoons \theta$  peritectic horizontal.

The change from  $\gamma_1$  to  $\gamma_2$  is less pronounced than that from  $\gamma_2$  to  $\gamma_3$ . Fig. 7 shows that several alloys were examined in the region of the peak on the lattice-spacing/composition curve. Apart from these, other films were taken whose results are not included in Table IV, but no films were obtained with two sets of diffraction lines. With specimens quenched from  $381^\circ \text{C.}$ , alloys 32.13 and 33.84 gave typical  $\gamma_1$  diffraction patterns, whilst alloys 34.44 and 35.57 gave the patterns characteristic of  $\gamma_2$ . In alloy 34.29 the intensities of the faint lines of Table IV were intermediate between those of the  $\gamma_1$  and  $\gamma_2$  types. At  $202^\circ \text{C.}$  alloy 35.89 consisted of  $\gamma_2$ , whilst alloy 33.85 showed lines whose intensities were intermediate between those of the  $\gamma_1$  and  $\gamma_2$  types; this indicates that the  $\gamma_1/\gamma_2$  boundaries move in the direction of lower gallium content as the temperature falls. If these changes in intensity indicate a phase change, this may reasonably be identified with the change occurring at the  $485^\circ \text{C.}$  horizontal determined by thermal analysis, but the sharpness of the lines on the diffraction films suggests that the difference between the compositions of the two phases must be very small. This region has therefore been shown by closely spaced broken lines passing through the points 33.84 at  $200^\circ \text{C.}$ , 34.29 at  $381^\circ \text{C.}$ , and then to the intersection of the solidus curve with the  $485^\circ \text{C.}$  horizontal. No etching reagent was found which would distinguish clearly between the different modifications of the  $\gamma$  phase, although on etching with dilute aqueous ferric chloride, many of the alloys in the  $\gamma_3$  and  $\gamma_2$  regions developed a polygonized structure within the individual crystals (see Fig. 9, Plate LXX), whereas those in the  $\gamma_1$  region did not. Unfortunately this effect became weak at

the copper-rich side of the  $\gamma_2$  region, and as it depended on the orientation of the crystal it could not be used to determine the  $\gamma_1/\gamma_2$  boundaries. It is perhaps significant that a similar etching effect is produced on the analogous copper-aluminium alloys.

Below the  $254^\circ$  peritectic horizontal, the  $\gamma_3/(\gamma_3 + \theta)$  solubility curve was determined by both microscopical and X-ray methods, as shown in Fig. 5, and the results were in agreement.

## VI.—DENSITIES AND NUMBERS OF ATOMS PER UNIT CELL FOR $\gamma$ -PHASE ALLOYS

The densities of the  $\gamma$ -phase alloys are given in Table V, which shows that the density begins to decrease more rapidly after the peak on the lattice-spacing/composition curve of Fig. 7. The third column of Table V shows the number of atoms per unit cell. In the  $\gamma_1$  region there is a slight fall in the number of atoms per unit cell as the gallium content increases. A completely filled cell contains 52 atoms, and graphical extrapolation of the data in Table V shows that alloys on the extreme copper-rich side of the  $\gamma$ -phase field of Fig. 5 will contain the full number of 52 atoms per unit cell. On passing into

TABLE V.—Densities and Atomic Structure of  $\gamma$ -Phase Alloys.

Gallium, at.-%	Density, g./c.c.	No. of Atoms per Unit Cell	No. of Electrons per Unit Cell
30.85	8.471(6)	51.85	83.8
32.79	8.411(9)	51.43	85.2
33.75 *	8.40	51.4(4)	86.2
34.51	8.360(9)	51.06	86.3
34.60 †	8.356	51.01	86.3
35.81	8.317(0)	50.52	86.7
36.69	8.248(0)	49.90	86.5
38.60	8.1704	49.11	87.0
42.03	7.987(3)	46.98	86.5

\* Owing to the smallness of the sample, the results for this alloy are less certain than the others in the Table.

† This composition was estimated from the weights of metals used in making the alloy. The remaining compositions were obtained by analysis of the density powders.

the  $\gamma_2$  and  $\gamma_3$  regions, increasing gallium content results in a much more rapid dropping out of atoms from the structure, and column 4 of Table V shows that this process occurs so as to maintain an approximately constant number of valency electrons per unit cell if copper and gallium are given their normal valencies of 1 and 3. The significance of this is discussed in a separate paper by Betterton, Hume-Rothery, and Reynolds.<sup>10</sup>

## VII.—THE GALLIUM-RICH SECTION OF THE DIAGRAM

The present paper is concerned mainly with the copper-gallium  $\gamma$  phases, but some information has also been gained regarding the gallium-rich alloys. According to Weibke (Fig. 1) the next phase in the system, denoted  $\theta$ , contains approximately 56 at.-% gallium. Several alloys were examined in this region,

but all contained two phases in comparable amounts; Fig. 10 (Plate LXX) shows the structure of alloy 56.59 after annealing for 17 hr. at 250° C. after 30 days at 195° C. No evidence could be obtained for the existence of Weibke's  $\theta$  phase, which has therefore been omitted from Fig. 3. Examination showed that homogeneous alloys existed near to the composition required by the formula  $\text{CuGa}_2$ , and this phase has been called  $\theta$ , in view of the analogous phase  $\text{CuAl}_2$  which is usually denoted  $\theta$  in the system copper-aluminium. Fig. 11 (Plate LXX) illustrates the structure of alloy 66.52 after annealing for 30 days at 195° C., and this shows nearly homogeneous  $\theta$  with traces of chilled liquid. The markings on the surface of the grain are typical, and the phase is relatively soft and of an entirely different character from the  $\gamma$  phases. Small deformations of the  $\theta$  phase result in noises which suggest a twinning process. Annealing treatments were carried out at temperatures between 195° and 248° C., and as far as could be estimated by the lever rule, the  $(\theta + \gamma_3)/\theta$  boundary remained nearly vertical at approximately 64.5 at.-% gallium from 200° to 240° C., and then moved slightly in the gallium-rich direction as the 254° C. peritectic horizontal was approached. The amount of chilled liquid increased only slightly when alloy 66.52 was annealed at 240° C., as compared with 195° C., and taking into account the curvature of the liquidus, the  $\theta/(\theta + \text{liquid})$  boundary is nearly vertical, but it was not possible to examine this region in detail. According to Zintl and Treusch,<sup>11</sup> the  $\theta$  phase of the system copper-gallium has a tetragonal structure with  $a = 2.83$ ,  $c = 5.835$  kX, and 3 atoms per unit cell. These investigators found that a powder photograph of an alloy containing 58 at.-% gallium showed diffraction lines from the above structure, together with some lines of the  $\gamma$ -brass structure ( $\delta$  in the notation of Weibke and of Zintl and Treusch). This would agree with the present diagram, which shows the  $\theta$  phase as lying at approximately 66.5 at.-% gallium. Zintl and Treusch regarded the  $\theta$  phase as containing less than 60 at.-% gallium, but it is not clear whether this was the result of their own work or was based on an acceptance of the diagram of Weibke.

## VIII.—DISCUSSION AND CONCLUSIONS

The preceding results suggest that the diagram of Weibke requires considerable modification in the region 35-100 at.-% gallium. The theoretical significance of the present results is to be discussed in a separate paper, but we may here emphasize the resemblance between the general form of the equilibrium diagrams of the systems copper-aluminium and copper-gallium. Each system has a typical  $\alpha$ ,  $\beta$ ,  $\gamma$  sequence of phases, and when the electron concentration exceeds 1.68-1.70, atoms drop out of the normal  $\gamma$  structure so as to maintain a constant number of electrons per unit cell. In the region 40-50 at.-% of the trivalent element, the copper-aluminium diagram is more complicated than that of copper-gallium,

but with still higher percentages of the trivalent elements analogous compounds  $\text{CuAl}_2$  and  $\text{CuGa}_2$  occur. If the present interpretation is correct, the copper-gallium diagram is of interest as an example of a system where an order-disorder change extends across a phase field until it involves equilibrium with the liquid phase.

## ACKNOWLEDGEMENTS

The authors must express their thanks to Professor Sir Cyril Hinshelwood, F.R.S., for laboratory accommodation, and to Dr. F. M. Brewer for many other facilities which have greatly encouraged the present research. Grateful acknowledgement is also made to the Council of the Royal Society and to the British Non-Ferrous Metals Research Association for financial assistance towards the general research programme of which this work forms a part.

## APPENDIX I

### Etching Reagents

Reagent *A*.—12.5 g. ferric chloride, 5 c.c. conc. HCl, 240 c.c. alcohol.

Reagent *B*.—10 g. ferric chloride, 3 c.c. conc. HCl, 100 c.c. water.

These were the most satisfactory reagents for revealing the grain boundaries of the different  $\gamma$  phases, but did not distinguish between the different modifications, or between grains of different orientation. With most alloys, swabbing with cotton wool was used to prevent uneven staining. After swabbing, the colour of the alloy was light orange tan, and the reagents revealed the polygonized structure in the  $\gamma_2$  and  $\gamma_3$  alloys referred to on p. 466.

Reagent *C*.—2.5 g. copper chloride, 5 g. magnesium chloride, 5 c.c. conc. HCl, 250 c.c. alcohol.

This reagent was similar in effects to Reagent *A*, but with a greater tendency to reveal microporosity, and a lesser tendency to stain the surface.

Reagent *J*.—60 g. copper sulphate, 120 c.c. ammonia ( $d$  0.880), 400 c.c. water.

This reagent reveals differences between crystal orientations by colour variations from brown to white, but leads to difficulties owing to indiscriminate staining.

Reagent *N*.—10 c.c. conc. HCl, 10 g. ferric chloride, 2 g. ferric sulphate, 10 g. alum, 10 g. tartaric acid, 50 c.c. alcohol, 100 c.c. water.

This reagent is due to Schramm and reveals the grain boundaries well, whilst leaving the grains a light tan colour.

The above notes refer to the effects of the reagents on alloys in the  $\gamma$ ,  $\gamma_1$ ,  $\gamma_2$ , and  $\gamma_3$  regions. In general, no difficulty was encountered in revealing the structures of alloys in the  $(\gamma + \text{decomposed } \beta)$ ,  $(\gamma_1 + \zeta)$  or  $(\gamma_3 + \theta)$  fields.



## APPENDIX II

*Summary of Heat-Treatments of Alloys Used for Determining the Phase Boundaries of the  $\gamma$ ,  $\gamma_1$ ,  $\gamma_2$ , and  $\gamma_3$  Fields*

For the phase boundaries on the copper-rich side of the  $\gamma$  fields, the chill-cast alloys were given preliminary homogenization treatments varying from 4-6 to 10 days at approximately 600° C. The critical alloys on which the diagram depends were then re-annealed for the times and temperatures (in °C.) given below :

17 hr. at 822°.  
 1 day at 797°.  
 2 days at 697°.  
 3 days at 495° + 7 days at 503°.  
 17 days at 500°.  
 3 days at 492° + 10 days at 495°.  
 29 days at 475°-503° + 9 days at 486°.  
 20 days at 473°.  
 36-37 days at 353°.  
 30 days at 200°.

Chill-cast alloys on the gallium-rich side of the  $\gamma_3$  region contained low-melting constituents, and the first annealing treatments consisted of slowly heating up from room temperature, in order to absorb the

low-melting phases. For the points at 200°-205° C., the alloys then received a preliminary anneal of 21 or 31 days at 230°-255° C. followed by final anneals of 31 or 44 days at 203° C. and 205° C., respectively.

## REFERENCES

1. W. Hume-Rothery, G. W. Mabbott, and K. M. Channel-Evans, *Phil. Trans. Roy. Soc.*, 1934, [A], **233**, 1.
2. W. Hume-Rothery and G. V. Raynor, *J. Inst. Metals*, 1937, **61**, 205.
3. F. Weibke, *Z. anorg. Chem.*, 1934, **220**, 293.
4. E. A. Owen and V. W. Rowlands, *J. Inst. Metals*, 1940 **66**, 361.
5. W. Hume-Rothery and P. W. Reynolds, *Proc. Roy. Soc.*, 1937, [A], **160**, 282.
6. K. W. Andrews, H. E. Davies, W. Hume-Rothery, and C. R. Oswin, *ibid.*, 1941, [A], **177**, 149.
7. W. Hume-Rothery and P. W. Reynolds, *ibid.*, 1937, [A], **167**, 25.
8. A. C. Egerton and W. B. Lee, *ibid.*, 1923, [A], **103**, 487.
9. C. Sykes, *ibid.*, 1935, [A], **148**, 422.
10. J. O. Betterton, Jr., W. Hume-Rothery, and J. Reynolds, *J. Inst. Metals*, 1951-2, **80** (in the press).
11. E. Zintl and O. Treusch, *Z. physikal. Chem.*, 1936, [B], **34**, 225.

# PRESIDENTIAL ADDRESS \*

1369

By C. J. SMITHELLS,† M.C., D.Sc., F.I.M.

I WANT first to thank you for the great honour you have conferred on me in making me your President for the coming year. When I think of Rosenhain, Carpenter, and other distinguished men who have occupied this Chair, I realize that there is no higher honour that can be bestowed on a metallurgist. Though I feel that I may not hope to contribute in the same measure as my predecessors, I assure you that I will do everything in my power to further the interests of the Institute. I count it as a special privilege that you should have chosen me as your President this year, while I am still holding a similar office in the Institution of Metallurgists. This dual role will be of short duration, but it may give me a unique opportunity to draw the Institute and the Institution still more closely together. There has, of course, always been the closest co-operation between the two societies, and it is important that their future development should cement these bonds more firmly.

The Institute is now 44 years of age, and we have had 24 Presidents and 22 Presidential Addresses. While some Presidents in their addresses have reviewed the progress of the Institute and made valuable suggestions for future policy, others have dealt with technical or scientific matters. I do not propose to do either, but I have followed the example of many of my predecessors and have re-read all the addresses that have been given. I felt that it would be interesting to see how far the hopes and ideals of those who set the Institute on its feet had in fact been realized, and whether some proposals that had not materialized were worthy of new consideration.

I had listened to 15 of these addresses, and found on reading them again that they were even more interesting and instructive than I had remembered, and I have been filled with admiration for the foresight of the founders of the Institute. The addresses present an extraordinarily clear picture not only of the progress of the Institute, but also of the development of the science of metals and of the non-ferrous metals industry during the past 40 or 50 years, and leave one with no doubt as to the important part that the Institute of Metals has played in these developments.

Many of you will not have time to read or to re-read these addresses, so I thought that it might interest you if I tried to give you a picture of the changes that have taken place during the short life of the Institute. I shall not attempt anything in the nature of a history; my remarks will be more like a Noel

Coward revue—unfortunately without music—presenting different facets of the Institute's activities.

## MEMBERSHIP

The Institute was formed in 1908 and held its first meeting in Birmingham. On 31 December 1908, there were 355 members, and four years later the number had risen to 606. It was not, however, until the Institute was 10 years old (1918) that the membership reached 1000. It is interesting to note that in his Presidential Address that year, Sir Harold Carpenter said: "My own view, taking everything into consideration, is that we ought to be able in due time to raise the membership of the Institute to at least 1500, and to maintain it there. I am not going to prophesy, but I think it can and will be done." Carpenter's forecast was, I am sure, based on the number of metallurgists then engaged in the non-ferrous metal industry, and the fact that our membership greatly exceeded this figure in less than 10 years is an indication of the rapid growth of the industry and the increasing number of people engaged in it. Carpenter's 1500 was reached within 5 years, the 2000 mark in 1928, 3000 in 1947, and to-day the membership is 3832.

The comparatively slow growth of the Institute during the early years is of some interest, and was due to two main causes. The first was the very much smaller size of the non-ferrous metals industry in those days, the aluminium industry, for instance, being virtually non-existent, and the much smaller number of metallurgists engaged in the industry. This is reflected by the number of students being trained in metallurgy at the Universities and Technical Colleges. I have tried to obtain reliable figures, and it appears that in 1910 about 50 students graduated with metallurgy as their principal subject, while in 1951 the figure was 1009, of whom 236 took University degrees and 773 obtained the Licenciateship of the Institution of Metallurgists, the Higher National Certificate, or the certificate of the City and Guilds of London Institute. The second cause was the character of the industry itself, when the production of non-ferrous alloys was mainly an art, and where science played little part. Coupled with this was a degree of secrecy on the part of manufacturers which to-day seems almost incredible.

Sir William White, in his first Presidential Address in 1909, threw an interesting light on this matter

\* Delivered at the Annual General Meeting, London, 25 March 1952.

† Director of Research, The British Aluminium Co., Ltd., Gerrards Cross, Bucks.



when he remarked that many firms in the industry attached great importance to the preservation of secrecy in respect of processes of manufacture and were not prepared to disclose these processes or to permit inspection of their works. He added that he confidently anticipated, however, that, as time passed and experience was gained, members of the Institute who had control of works and the direction of processes of manufacture would voluntarily assume a more generous attitude.

The same kind of secrecy had originally existed in the iron and steel industry, but had largely disappeared by this time, as a result, to a great extent, of the existence of the Iron and Steel Institute. The founders of the Institute of Metals evidently expected a similar result in the non-ferrous industry, for Sir William White remarked that in the Iron and Steel Institute broader and more liberal methods found favour as the society grew older, and the traditions of secrecy, which played an important part in the earlier days of steel manufacture, had to a great extent been abandoned.

In his address in 1913 Professor Huntington said : " The progress in the iron and steel industries in the last twenty-five years has been extraordinary, and I have no hesitation in saying that a large share of it is due to the existence of the Iron and Steel Institute. The members of those industries are no longer working against one another in a very narrow spirit, being afraid to confide their ideas one to another lest they should give a competitor an advantage. All this narrowness has disappeared, and now members visit one another's works and discuss everything concerning them at every opportunity." It was many years, however, before the non-ferrous metals industry followed the same course, and many Presidents had occasion to refer to this matter in their addresses. However, in 1938, Dr. C. H. Desch was at last able to say that the desire for secrecy concerning technical improvements, although legitimate and comprehensible in some instances, played, he believed, a diminishing part in governing the supply of communications, and that members could congratulate themselves that the existence of the Institute had itself done much to break down old prejudices in this respect.

There is no doubt that scientific societies like ours, as well as the Research Associations and Development Associations, have had a major share in bringing about the more broad-minded attitude now adopted by most of the larger industrial organizations. I think that there is still room for improvement in this respect in some sections of the industry, but co-operation is now much more fashionable than secrecy. Curiously enough, in my experience it is the smaller firms, with the most to gain by co-operation, which tend to remain secretive.

This earlier insistence on secrecy on the part of the manufacturers, and their refusal to take an active part in the meetings of the Institute, led to a vicious circle and provided them with the excuse that there was not a sufficient number of practical papers to

interest them. No less than ten Presidents appealed in their addresses for more practical papers. I do not propose to quote them all, but it is interesting to note that, in his first Presidential Address, Sir William White said : " If we are to succeed in this endeavour, the proceedings of the Institute of Metals must embrace contributions from users as well as makers of non-ferrous metals and their alloys; and there must be free and friendly discussion between the two classes when difficulties have to be faced or doubts removed ". Succeeding Presidents in 1910, 1911, and 1914 appealed for more encouragement and support from the manufacturers and referred to complaints that the Institute was too much a body of scientists and not sufficiently a practical association. I rather like Mr. Leonard Sumner's understatement, in 1922 : " I think there is a feeling, which at first sight would seem justifiable, that manufacturers do not contribute their quantum to this Institute ". The position was little better in 1928, when Dr. Rosenhain was President, and even he appealed for more practical papers. He tempered this appeal, however, with the very wise comment that it must be remembered that the world-wide reputation of the Institute rested largely on its essentially scientific work. Dr. Seligman, two years later, made the same point, and it seems that at last the Institute was getting at least a fair share of practical papers.

There is no doubt that the reputation of the Institute has been made by the quality of the original research work that has been published in its *Journal*. It is important that papers of this kind should be read and discussed, but such discussion tends to be more and more restricted to experts in particular fields, and research papers are becoming less suitable as bases of discussion at large General Meetings of the Institute.

## MEETINGS

The problem of satisfying all classes of our membership has been considered by the Council on many occasions, but we hope that it has now to a large extent been solved by changes in the character of the General Meetings of the Institute.

From its inception, it was the custom of the Institute to hold two General Meetings each year, in the spring and autumn. The Annual General Meeting, in the spring, was devoted almost entirely to the business of the Institute and the presentation and discussion of papers, whereas the Autumn Meeting also included visits to works, greater opportunities for social contacts, and was often held abroad. For the first 15 or 20 years this arrangement appears to have been satisfactory, and most of those who attended were genuinely interested in a good proportion of the papers presented. You may have heard members who attended meetings in the early 1920's refer to the excellent and lively discussions that took place, and regret that that is no longer the case. The chief reason is that the fundamental principles of scientific



metallurgy were being established then, and that these were of general interest both to the manufacturer and to the research worker, no matter in what particular metal their main interest was centred. Papers were concerned with such fundamental things as grain growth and recrystallization, the effect of cold work on structure as revealed by X-ray diffraction, the formation of single crystals by various methods, the interpretation of equilibrium diagrams, the mechanism of age-hardening, and whether Rosenhain's amorphous theory was right or wrong. Many of these things were being argued about for almost the first time, since it was not until the Institute of Metals provided the arena that such conflicts could be staged.

These were all matters of the greatest interest to all metallurgists and naturally there were some lively—and at times very heated—arguments. Many of you will remember how well Hatfield and Rosenhain disagreed and entertained us.

I feel sure that some of us forget how very recent is the science of metals, and how the facts and theories which every student now learns first appeared as original papers in our *Journal* and had to stand the criticism of discussion at our meetings. To emphasize this I should like to quote from some earlier Presidential Addresses: Sir Gerard Muntz, in 1910, said: "General knowledge of the non-ferrous metals is simply appalling by its absence; it leaves the greater scope for the work of the Institute of Metals". Professor A. K. Huntington, in 1913, remarked: "It must be remembered that metallography for practical purposes has only come into existence within the last fifteen years or so. The difference it has made in understanding what happens to metals and alloys in course of manufacture and in use is incalculable." And Vice-Admiral Sir Henry Oram in 1914 said: "Methods in brass foundries are often still of the haphazard and rule-of-thumb variety, and close supervision by the chemist or other scientist, which is essential to continuous success, is often wanting. Pyrometers, although more largely used than formerly, are still often unknown, temperature being frequently judged by the eye. One finds generally a lack of scientific precision and knowledge in the melting, mixing, and pouring, which, if it existed and were combined with practical experience, would greatly add to the value of an establishment."

Sir George Beilby referred to the almost complete absence in the *Journal* of papers on light alloys, and commented that though the early enthusiasm with which aluminium was welcomed as an industrial metal was largely based on the belief that its combined lightness and strength would enable it to take a place in serious structural and machine work, its mechanical properties were found to have been greatly over-rated, while its resistance to wind and water left much to be desired. I also found, in the first volume of the *Journal*, a statement that no doubt railway companies using steam traction will in due time grasp the advantage to be obtained by using aluminium, thus

lightening their train loads and economizing generally in their running expenses. Perhaps, in due time, they will!

Even as late as 1928, Dr. Rosenhain thought it necessary to devote one half of his Presidential Address to giving "something in the nature of an explanation—even a defence—of the equilibrium diagram . . . addressed essentially to the practical man who may perhaps care to know why these things are determined, what they are, and how they can be applied to practical purposes", and the other half to explaining the age-hardening of aluminium alloys.

These examples will, I think, make it clear why the papers presented to the Institute more readily gave rise to good general discussions. In course of time, however, the papers became more specialized and of less general interest, and there was a good deal of criticism and poor attendance when such papers were presented. Chairmen were often worried lest there might be no speakers in the discussion, and thus there arose the habit of canvassing speakers in advance. This practice robbed many discussions of spontaneity, and also tended to produce such lengthy contributions that a time limit had to be set for each speaker. That, by the way, was no novelty, for at the very first meeting of the Institute, in 1908, the President in opening the discussion limited the speakers to five minutes. I am glad to say that we seem to have got over those difficulties and a great improvement has been noticeable in our recent discussions.

Although Dr. Harold Moore, in his address in 1934, suggested that discussions or symposia on subjects appealing to selected groups of members should be organized, it was not until 1947 that this suggestion was really put into effect. In October of that year the first symposium, "Internal Stresses in Metals and Alloys", was held, and was a real success. This was followed by a series of symposia on subjects of interest to the industrial metallurgist: "Metallurgical Aspects of Non-Ferrous Metal Melting and Casting of Ingots for Working", in March 1949; "Metallurgical Aspects of the Hot Working of Non-Ferrous Metals and Alloys" in 1950; and "Metallurgical Aspects of the Cold Working of Non-Ferrous Metals and Alloys", in 1951. An important, and well-attended, symposium on "Metallurgical Applications of the Electron Microscope" was also held in November 1949.

Professor Murphy said last year that he believed that the practical man, whose loyal wailings of neglect used to fill the air periodically, no longer felt that he received less than a fair share of attention at our meetings; and that the successive symposia on different aspects of metallurgical production had been enthusiastically received and well attended.

In the past, the Council has been reluctant to agree to the formation of separate Groups or Divisions within the Institute. In 1944, however, a Metal Physics Committee was appointed to provide a closer



link between physicists who are studying metals and academic and industrial metallurgists. Several attempts have been made to define "metal physics", and I do not propose to enter the competition seriously. Metal physics is not restricted to any particular field of metallurgical science, but implies an attitude of mind in approaching the subject which is natural to the physicist and may be different from that of the professional metallurgist.

The Metal Physics Committee has been responsible for organizing, with the co-operation of other societies, the symposia on "Internal Stresses in Metals and Alloys", and "Metallurgical Applications of the Electron Microscope", to which I have referred above. Both led to most successful discussions between those interested in these subjects from widely different points of view, and the Committee is arranging a further symposium on "The Properties of Metallic Surfaces" in the autumn of this year.

In 1949 another special committee—the Metallurgical Engineering Committee—was formed to promote the study of equipment and instrumentation. It was concerned with the arrangement of the symposia on hot working and cold working, held in 1950 and 1951, and in January this year it organized a very successful informal discussion in Birmingham on "Tool and Die Materials for the Extrusion of Non-Ferrous Metals and Alloys". The symposium on "Equipment for the Thermal Treatment of Non-Ferrous Metals and Alloys", to be held to-morrow, also owes its origin to the Metallurgical Engineering Committee. Hitherto the *Journal* has contained very few papers dealing with the plant and equipment used in the industry, and we hope this important field will now receive the consideration that it deserves.

A Sub-Committee has recently considered the organization of future meetings of the Institute with the object of meeting the needs of the widest possible range of members. Its recommendations, which have been approved by the Council, ensure that in the future at Annual General Meetings one whole day will be devoted to a symposium on a subject of interest to production metallurgists and metallurgical engineers, while three half-days will be set aside for the discussion of other papers which have been published in the *Journal*. The suggestion of concurrent sessions on widely differing subjects is being tried again in connection with the present meeting, and both the Metal Physics Committee and the Metallurgical Engineering Committee have been authorized to arrange informal discussions. While, therefore, the presentation and discussion of original papers will still be the main feature of Institute meetings, the needs of the practical man and the specialist should be met by these arrangements.

## PUBLICATIONS

The presentation of papers and the holding of General Discussions are closely linked with problems of publication. From the appearance of the first

volume, in 1909, the *Journal* was an immediate success, and sales of the *Journal* became an important source of income to the Institute. These sales, which amounted to only £12 in 1909, had increased to £1100 in 1919–20 and to the very considerable figure of £4531 in 1950–51.

The second volume of the *Journal*, published in 1909, contained 40 pages of abstracts, and this section soon became one of the most important of the Institute's contributions to metallurgy. Our abstracts of non-ferrous metallurgical literature have been, and I believe still are, the most accurate and complete of any that are published in the world, and have played a large part in establishing the reputation of the Institute.

Until 1931 our *Journal* appeared every six months, in bound form only, with the abstracts in a section at the end of the volume. This practice had certain disadvantages, to which Dr. Richard Seligman drew attention in his Presidential Address of 1930, as follows: "In one respect it seems that our abstracts, complete as they are and carefully as they are prepared, fall short of what is required; they appear much too infrequently and, indeed, at such intervals that some of their value is lost. Moreover, when they do appear they come in such numbers as to make it very difficult for busy men to assimilate the mass of information they contain. It would be far better from every point of view if a suggestion made by Professor Hanson some time ago could be revived, and if this section of our *Journal* could be issued monthly."

The Institute owes a great debt of gratitude to Dr. Seligman for his guidance on many matters relating to our publications—he was Chairman of the Publication Committee for many years—and it must have been a great satisfaction to him to see the monthly appearance of the *Journal* and abstracts in 1931, during his Presidency. As you will know, since that year the Abstracts have been bound separately from the *Journal*, which its increasing size would have rendered necessary in any case, and in 1934, under the title *Metallurgical Abstracts*, they formed a separate periodical, with their own volume numbers. The number of abstracts published continues to increase each year. In the first volume in which they appeared in 1909 there were 93, in 1930 there were 3274, and in 1950 there were about 6000 occupying 1024 pages of *Metallurgical Abstracts*. In 1932 Sir Henry Fowler said that, in the case of abstracts from all important sources, they would be published within four to six weeks of their appearing in the original publication. Unfortunately it is no longer possible to maintain that ideal, but with difficulties in printing and publishing (it takes two months for the abstracts to pass through all stages of the Press), I think that the staff are to be congratulated that from the date of issue of the originals to the date of publication of the abstracts the average time has now been reduced to about four months for the more important periodicals.

Another innovation recorded by Dr. Moore in his Address was the advance publication of all our papers in the monthly *Journal*, which began in 1933. The advantages which he said most appealed to him were earlier publication of papers, their receipt by members continuously throughout the year instead of in two large batches, and the convenience of being able to consult them until they appeared, reimposed, in the half-yearly volumes of the *Journal*.

While on this subject, I feel that I should refer to another proposal for which Dr. Moore made a strong appeal in 1934. He said: "It was a dream of mine in those earlier years that if the Iron and Steel Institute and the Institute of Metals could have collaborated in the publication of a monthly periodical, it might have been the best metallurgical journal issued in the English language, and probably in the world. According to my vision it would have contained all the papers presented to the two Institutes, complete abstracts, ferrous and non-ferrous, authoritative reviews of progress in particular branches of our work, with other articles and matter of permanent value. The financial and other difficulties of such a scheme were great even twenty years ago, and have probably increased considerably with passage of time, but even now is it too late to consider co-operation in some form in the publication of abstracts?"

There has not unnaturally been some criticism from time to time of the duplication in abstracting which results from the publication of their own separate abstracts by each of the three British metallurgical Institutes: the Iron and Steel Institute, the Institute of Metals, and the Institution of Mining and Metallurgy. There is not, perhaps, so much duplication as some people suppose, but the suggestion of issuing one common abstract journal has been made several times on the grounds of economy and convenience.

Quite recently, a meeting of representatives of the three Institutes was held, at our instigation, to consider whether agreement could be reached to publish one comprehensive British abstracts periodical in place of the present three series. Your Council was prepared to go a long way to see this objective reached, but I am sorry to say that the representatives of the other two Societies were not prepared to recommend to their Councils the discontinuance of their own separate abstracts, and the Council of one of the Societies has definitely decided to maintain its own separate series. Although with the present high costs of printing, paper, and postage no financial saving would have been effected, the prestige which would result from such a British publication is something that we should keep in mind, in the hope that eventually a solution may be found.

Another service to metallurgical science was started by the Institute in 1936 with the publication of the first volume of the Monograph Series, on "The Structure of Metals and Alloys", by Dr. W. Hume-Rothery, of which about 8000 copies have now been sold, and about 1300 distributed free to members. The success

of this venture led to the adoption of the monograph as a recognized feature of our activities. There have now been eleven in this series, and another is in the press.

The Institute's publications, while producing about half of our normal revenue, also account directly for 48.4% of our total expenditure, excluding overheads, or 89.7% including all direct and indirect overheads. The increases in costs of everything connected with publication have forced the Council to consider the financial position very carefully. For many years it has been the Council's policy that the Institute should publish all original papers submitted to it which reach the required high standard. With the growth of the industry and the number of metallurgists engaged in research, the volume of matter acceptable for publication is constantly growing. This not only increases the labour and cost of publication, but presents the reader with a mass of material that he no longer has time to read and of which only a proportion can be of direct interest to him. The Council has been seriously concerned that the costs of publication might increase at a greater rate than our income, about half of which, as you know, is derived from membership subscriptions, and that drastic measures might have to be taken to balance our budget in future years. The Publication Committee has appointed a Sub-Committee to consider and report what economies in production are possible without seriously affecting the value or readability of the *Journal*, and it may be that we shall have to make some rather revolutionary changes in our procedure.

Many of our Presidents have in the past appealed to authors to express themselves in fewer words. Professor Thomas Turner devoted part of his address in 1924 to this subject, and he said that one method of meeting the difficulty was by a more rigid censorship of papers, and by the adoption of a less diffuse style in writing. He reminded members that the ability to express important facts in simple language was an indication of experience and of clearness of thought, and that in many cases the permanent value of a communication varied inversely as the square of its length.

In 1934 Dr. Moore made a similar appeal, and our immediate Past-President, Professor Murphy, felt impelled to comment again last year that there were few papers which would not actually be improved in clarity by an hour or two of the author's time being devoted to the removal of superfluous words and phrases.

There is still room for some improvement in this respect, although I think this alone will not meet the case. I feel that there should be some method of presenting the results of scientific research in a more condensed form than is now customary, yet without losing anything of value. This in itself is a subject for research, and if the Publication Committee can devise something of this nature it will perform a real service not only to the Institute but to other publishing societies.



## LOCAL SECTIONS

I should now like to refer briefly to some of the Institute's other activities. The formation of Local Sections was first suggested by Sir Gerard Muntz in 1910 in these words: "A much more frequent intercourse is needed. Such could be obtained by the establishment of local centres in all the larger provincial cities, where there is a sufficiency of members to make it worth while, as well as in the Metropolis, where meetings could be more frequently held, and where matters of interest—which occur almost daily—might be brought forward and discussed." But there was to be no nonsense about them, and he added: "If local centres are established, they must be prepared to support themselves, and must not look to the parent society to bear their expenses: neither must they expect to have their proceedings published in the *Journal* of the Institute".

The first Local Section was formed in Birmingham in 1910, and to-day we have Local Sections in six centres, and, in addition, members of the Institute enjoy free membership of local metallurgical societies in Leeds, Liverpool, and Manchester. The restrictions proposed by Sir Gerard Muntz no longer apply. Local Sections are now encouraged to submit suitable papers for publication in the *Bulletin*, and practically all their expenses are defrayed by the Institute. I was a member of the London Local Section from the time when I started my metallurgical career, and for nearly twenty years I seldom missed a meeting. I am sure that I learnt more metallurgy and made friends with more metallurgists in that way than in any other, and I do urge all our younger members to take an active part in the work of their own Local Section. There is no better way of learning to take part in discussion—or to make an impression on your seniors!

## INTERNATIONAL CO-OPERATION

I need hardly stress the cosmopolitan character of the Institute; our membership is international. The value of the closest co-operation with metallurgists in other countries has been stressed by many Presidents in the past. Many of our Autumn Meetings have been held in Europe at the invitation of other metallurgical societies. The Council has now decided that, in future, in every three Autumn Meetings, one shall be held outside the British Isles, one shall be held in the provinces, and one in London, when a foreign metallurgical society will be invited to hold its meeting side-by-side with that of the Institute. We hope that in this way we shall have an opportunity of returning some of the hospitality which we have received so often from kindred societies abroad. We have Honorary Corresponding Members to the Council in 12 different countries, and very friendly ties with the leading metallurgical societies in Europe and America.

## RESEARCH

An activity which occupied the attention of the Institute in its early years was the prosecution of metallurgical research. Many of you may have forgotten this, but you must remember that practically all the industrial research laboratories with which we are now familiar were founded 5, 10, or 15 years after the formation of the Institute. It therefore seemed right to our founders that the Institute should be prepared to carry out co-operative research for the industry. Sir Gerard Muntz in 1910 suggested that "A system might be initiated by which any member meeting with some obscure problem, upon which he desired light, might communicate it to the Secretary of the Institute". I don't know what Colonel Guilan's reaction to such a request would be, but I have no doubt that he would be equal to the occasion. And Muntz continued: "Until the Institute is in a position to establish a laboratory and research staff of its own, it must look to its members individually for the necessary help and research in any work which it desires to undertake. It must be some time yet before we are rich enough to think of such an establishment, but there is no harm in dreaming of the days which may be."

The Institute did in fact sponsor research into the corrosion of condenser tubes by sea-water, which was at that time a matter of grave concern to the Admiralty. A Corrosion Research Committee was set up in May 1910, with Dr. Bengough as the Institute's first (and honorary) investigator. Experimental work was carried out initially at Liverpool University, and was transferred in 1916 to the Royal School of Mines. At its inception the cost was borne by contributions from the Admiralty, the industry, and shipowners. Subsequently both the Department of Scientific and Industrial Research and the British Electrical and Allied Manufacturers' Association became contributors, and the work was extended to cover light alloys at the request of the Air Ministry. Work of great value, which led eventually to the development of the aluminium-brass condenser tube, was continued by the Institute until 1930, when the research was taken over by the British Non-Ferrous Metals Research Association.

Another matter in which the Institute has played its part is in the practical application of scientific knowledge to industrial processes. Sir George Goodwin in 1920 commented that while he had read and heard a great deal about the advantages that must result from the application of science to industry, a large portion of it had remained for a long time, and still remained, in the abstract and was not really applied. And Dr. Rosenhain, in 1928, said "It is not a bad thing, even for the most scientific worker, to pause at times and consider the nature and possible practical utility of the work on which he is engaged". Sir Henry Fowler in 1932 again laid great stress on this matter and said that one of the great problems of the day was the

"marrying up" of research with the practical application of the results obtained. He felt, therefore, that one of the objects which should always be borne in mind was to get the improvements they thought they were able to make put to a practical test as early as possible.

It was not until about 1948, however, that someone in official circles invented the term "operational research" to cover this activity, which had been constantly in our minds and had long been one of the normal tasks of industrial research teams. The various symposia which we have held in recent years have been a very direct contribution in this field.

There is another metallurgical field, however, which the Institute has deliberately refrained from entering until very recently, namely that of metal reserves and metal conservation. In 1924 Professor Turner quoted the opinion of Sir Thomas Holland that the whole of the known base-metal supplies of the world would not last for many years at the current rate of consumption, and that a shortage of supply could be expected within the lifetime of persons then living. He added that it was clear that the supply of base metals in future was likely to be restricted to an extent which had not hitherto been contemplated. Of aluminium alone, he said, there appeared to be an unlimited supply. Dr. Desch returned to the subject in 1938, but added that: "To discuss these questions, tempting as they are, would be to travel far beyond the scope of this Institute".

However, last year, Professor Murphy, realizing the increasing importance of this subject, said that it appeared to him that there was a clear opportunity for the Institute to perform a public service by devoting some attention to those aspects of metallurgical science and industry concerned with the resources of metals on which the non-ferrous metallurgical industry is based and with the most efficient utilization of those resources. Following this suggestion, the Institute organized a General Discussion on this subject in October last year, to which contributions were made not only by metallurgists, but also by leading geologists, economists, and representatives of Government Departments. While the world situation is creating a serious shortage at the present time, the pessimistic forecasts which have appeared at intervals for the last 50 years would hardly seem justified, at least while so much of the North American Continent remains unexplored.

## EDUCATION

I cannot omit some reference to another subject in which the Institute has had a continued interest, namely metallurgical education. The importance of metallurgical training has been stressed on many occasions by our Presidents, and eventually we had an opportunity to express our views in a most effective manner. Mr. H. S. Tasker, who devoted much time and thought to this subject on our behalf, dealt with this subject in his address in 1950.

In 1943 the Department of Scientific and Industrial Research appointed a Committee to consider the steps necessary to secure an adequate supply of trained metallurgists in the post-war period. At the same time the Board of Education, as it was then, approached the various institutions interested in metallurgy, pressing for the establishment of National Certificates in Metallurgy, and there was also among working metallurgists a demand that a qualifying organization concerned specifically with the science and practice of metallurgy should come into being. Discussions on these matters took place with the Iron and Steel Institute, the Institution of Mining and Metallurgy, and the Institute of British Foundrymen, as a result of which the Joint Committee on National Certificates in Metallurgy was formed; a draft of a constitution for an Institution of Metallurgists was produced; and the four institutes set up their Joint Committee on Metallurgical Education, on which the Institution of Metallurgists is now also represented.

National Certificates are now firmly established, the Institution's qualifications are becoming widely recognized, and valuable work has been done by the Joint Committee on Metallurgical Education in making recommendations for full-time University degree courses in metallurgy.

I hope that these scenes from the life of the Institute will have been of some interest to you. It is difficult in a short time to give an adequate picture of all that the Institute has done, or to show you to what a great extent the progress of our industry has been made possible by the existence of the Institute of Metals. Nearly all the ideals of our founders have been realized, and in many directions we have progressed further than they could have hoped. The Institute is still young and vigorous and I am sure there are many directions in which we can still develop and so increase our service to the science of non-ferrous metallurgy.





# A STUDY OF SOME FACTORS INFLUENCING THE YOUNG'S MODULUS OF SOLID SOLUTIONS\*

1370

By A. D. N. SMITH,† B.A.

## SYNOPSIS

The values of Young's modulus for a series of binary solid solutions of copper with zinc, gallium, germanium, silicon, and arsenic, and of silver with cadmium, indium, and tin, have been measured dynamically at room temperature. In agreement with earlier work, it was found that, in any one system, the modulus decreases approximately linearly with the atomic percentage of the solute, although the rate of decrease differs for each system. This rate of decrease depends not only on the difference in atomic radii of the solute and solvent, as suggested by Zener (*Acta Cryst.*, 1949, 2, 163), but also on the difference in valency between the two constituents. It appears that this latter effect may be proportional either to the square of the valency of the solute or to the electron concentration of the solution, the experimental evidence slightly favouring the former. A close relation is found to exist between the rates of decrease of the modulus and of the solidus temperature for any given solution of copper or of silver, both for the author's results and for those given by Köster and Rauscher (*Z. Metallkunde*, 1948, 39, 110). The results obtained by the latter investigators for solid solutions of gold do not follow the laws outlined above, probably owing to the relative ease with which the gold ion can be polarized.

## I.—INTRODUCTION

It is usually desirable that Young's modulus ( $E$ ) of a structural material should be as high as possible, since the buckling strength in compression is directly proportional to it, and hence an understanding of the factors which govern it is very desirable. Formulæ correlating the elastic moduli with the absolute melting temperature, specific volume, specific heat, coefficient of thermal expansion, &c., have been derived in the past, both empirically and, in a very few cases, theoretically.

Mack,<sup>1</sup> reviewing the literature published up to 1945, found that the most successful empirical formulæ were those due to Portevin<sup>2</sup> and to Andrews.<sup>3</sup> The first of these is the simpler

$$E = kT_m^a/V^b \quad (1)$$

where  $k$  is a constant,  $T_m$  the absolute melting temperature,  $V$  the specific volume, and  $a$  and  $b$  are constants having values of approximately 1 and 2 respectively. Andrews' formula is:

$$E = V^{-\alpha} \cdot A \exp(-\beta T/T_m) \quad (2)$$

where  $T$  is the absolute temperature of measurement and  $A$ ,  $\alpha$ , and  $\beta$  are constants which have two sets of values according as  $T/T_m$  is greater or less than 0.5. The two sets of constants are necessary to take account of the sudden drop in the modulus/temperature curve in the region of  $T \simeq 0.5 T_m$ . This reduction in  $E$  was recognized by Andrews as being probably due to viscous flow during the static tests which were used to measure the constant, an explanation that was confirmed 20 years later by Ké's

experiments on grain-boundary slip.<sup>4</sup> Neither of these formulæ, however, do much more than show the rough trend of the modulus.

The theoretical calculation of the elastic constants of single crystals has been carried out by Fuchs for the alkali metals and for copper,<sup>5</sup> from quantum-mechanical considerations, the agreement between the observed and the predicted values being good. More recently Leigh<sup>6</sup> has calculated the elastic constants of aluminium corresponding to a pure shear without change of volume, and has shown why aluminium crystals are approximately isotropic. Nevertheless, such calculations are very difficult and have not yet been extended to other metals.

The effect on Young's modulus when one metal is alloyed with another has been studied extensively by Köster and Rauscher,<sup>7</sup> who found that: (1) when one metal is completely soluble in another, the curves of modulus plotted against atomic percentage of solute are usually linear, e.g. Cu-Au, Cu-Ni, Cu-Pt, exceptions being the systems Ag-Au, Ag-Pd, and Au-Pd, in which the curves are concave downwards at room temperature; and (2) when the solubility is limited, there is a linear relation between the modulus and atomic percentage of solute in the region of solid solubility. In copper- and silver-rich alloys, the modulus decreases, and the rate of decrease increases as the limit of solid solubility decreases. However, this is not always the rule for alloys of other elements, as is shown by the results for gold, for which some alloys (Au-Mg, Au-Fe, Au-Cd) show a rise in modulus.

A theoretical explanation of the behaviour typified by the copper and silver alloys has been put forward

\* Manuscript received 25 August 1951.

† Royal Aircraft Establishment, Farnborough, Hants.



by Zener,<sup>8</sup> who, by starting from a thermodynamic equation, shows that any difference in the size of the solvent and solute atoms lowers the modulus, and that the magnitude of the decrease observed by Köster and Rauscher is in rough agreement with his predictions for most alloys of copper and of silver. It is plain that this argument must be an oversimplification, since it ignores all other differences between solvent and solute, some of which may be expected to influence the modulus considerably.

It seemed probable from the work of Hume-Rothery<sup>9</sup> and his collaborators that the valency difference is likely to be important, particularly in alloys in which the difference in atomic size is fairly small. It was therefore decided to measure Young's modulus for a series of binary alloys of copper with each of the succeeding four elements in the Periodic Table (zinc, gallium, germanium, and arsenic) and also for the corresponding series of alloys of silver (cadmium, indium, tin, and antimony), together with pure copper and pure silver. The advantage of these two series is that the differences in atomic size and weight are kept fairly small, so that any effects due to valency should be dominant; furthermore, these series of alloys have been the subject of extensive research by Hume-Rothery and his collaborators into the factors that control the equilibrium diagrams. When the work on these two series of alloys was completed, the results indicated that useful information might be gained from a study of copper-silicon alloys, so this series has also been investigated.

## II.—EXPERIMENTAL PROCEDURE

### 1. APPARATUS

Young's modulus was measured dynamically, using apparatus similar in design to Förster's.<sup>10</sup> The specimen, in the form of a uniform round bar 6 mm. in dia. and 10–15 cm. long, was suspended by two fine threads attached to the bar close to the nodes of the "free-free" mode of vibration. The other ends of the threads were attached to the coil of a moving-coil loudspeaker and to a gramophone pick-up, respectively. The loudspeaker was driven by a variable-frequency oscillator of high accuracy, and the gramophone pick-up was connected, via an amplifier, to a cathode-ray oscilloscope. When the frequency of the oscillator approached the fundamental resonant frequency of the bar, vibrations started to build up in the latter which were detected by the pick-up and made visible on the cathode-ray tube. Thus the specimen could easily be tuned to resonance and the frequency ( $f$ ) was then read directly from the decade dials of the oscillator. Knowing the length ( $l$ ), the diameter ( $d$ ), and the density ( $\rho$ ) of the bar, Young's modulus was determined from the equation:

$$E = 1.262\rho f^2 l^4 / d^2$$

The accuracy with which each of the quantities could be measured was estimated to be  $\pm 0.1\%$ , and

hence it may be shown that the average error in  $E$  due to errors of observation is  $\pm 0.5\%$ , with a maximum of  $\pm 1\%$ .

### 2. MATERIALS

The alloys were supplied in the form of 6-mm. rod by Johnson, Matthey and Co., Ltd. All the material was spectroscopically pure, the maker's analysis for each bar being given in Table I.

TABLE I.—*Analysis of Specimens.*

Copper Alloys					Silver Alloys		
Zn, at.-%	Ga, at.-%	Ge, at.-%	As, at.-%	Si, at.-%	Cd, at.-%	In, at.-%	Sn, at.-%
1.17	0.97	1.02	2.16	0.90	0.88	1.05	0.93
3.62	3.13	3.03	3.94	3.04	3.50	3.10	3.13
5.23	8.18	4.94	6.29 *	5.30	5.53	8.06	4.90
8.01	16.20	8.10	...	8.05	7.45	16.19	7.90
16.31	...	...	...	...	15.78	...	...
32.15	...	...	...	...	32.42	...	...

\* This alloy could not be drawn and no reliable values for its modulus were obtained.

The method of manufacture of each alloy was to melt the solvent under charcoal and to introduce the solute beneath the surface of the molten metal. After solidification, the ingots were cold rolled to  $\frac{1}{4}$ -in. square bar and finally drawn down to 6 mm. dia. Each bar was radiographed for porosity, but none was found. All the silver-antimony alloys proved to be too brittle to be drawn, and no specimens on which modulus determinations could be made were obtained.

Each bar listed in Table I (except that marked \*) was annealed at a temperature sufficiently high to ensure that it had recrystallized; this was confirmed by taking X-ray back-reflection photographs of sample bars. X-ray transmission photographs were also taken of samples to estimate the amount of preferred crystallographic orientation present. It was most important that this should be small, as the anisotropy of the crystal combined with a fibre structure may cause large changes in the elastic moduli, e.g. Kuczynski<sup>11</sup> has shown that the Young's modulus of copper wire may be increased by 36% when most of the grains have their [111] axes lying along the wire axis. It was gratifying, therefore, that there appeared to be little preferred orientation present in most of the bars examined after annealing. However, in two bars (Cu-Zn 32% and Ag-Cd 32%) it did appear to be appreciable, and the results from these have therefore been discarded.

### III.—EXPERIMENTAL RESULTS

Fig. 1 shows Young's modulus ( $E$ ) plotted against atomic percentage of solute present ( $C$ ) for the five series of copper-rich alloys. There are only two points plotted for the copper-arsenic series since, as

mentioned in Table I, one alloy was too brittle to be drawn. Fig. 1 also shows the results for the series of silver-rich alloys, although, since there were no

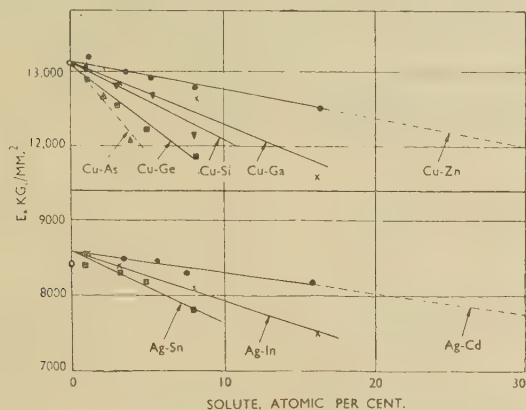


FIG. 1.—Variation of Young's Modulus ( $E$ ) with Atomic Per Cent. of Solute ( $C$ ) for Copper and Silver Alloys.

satisfactory silver-antimony alloys only results for cadmium-, indium-, and tin-containing alloys are plotted.

#### IV.—DISCUSSION

##### 1. GENERAL

It can be seen in Fig. 1 that for any one series of alloys the points lie roughly on a straight line whose slope differs for each system, and an attempt was made to determine the factors that control the magnitudes of these slopes.

The empirical formulæ of Portevin and of Andrews (equations (1) and (2), Section I) both relate Young's modulus to the absolute melting temperature. This seems plausible from general considerations, since the modulus is a measure of the differential coefficient of the cohesive force between adjacent atoms in a lattice, and thus is related to the binding energy and hence to the melting temperature. It therefore seems possible that the factors which affect the modulus of an alloy also affect its melting tem-

perature of an alloy in the range of solid solubility is usually a straight line, a convenient comparison of the modulus and the solidus temperature for any one series of alloys may be made by plotting the slopes of the two straight-line graphs  $dE/dC$  and  $dT/dC$  against one another, as in Fig. 2 for the copper alloys and in Fig. 3 for the silver alloys, in both of which the results of Köster and Rauscher<sup>7</sup> have been included. It should be noted that in Fig. 3 the results for silver-gold and silver-palladium alloys are plotted in the wrong quadrant, since both  $dE/dC$  and  $dT/dC$  were positive for these alloys. When the modulus or solidus curves were not straight lines, as sometimes occurs when a continuous series of solid solutions are formed, the slopes of these curves at zero atomic per cent. of solute have been plotted.

It can be seen that the results are grouped quite well round a straight line in each case, bearing in mind that when  $dE/dC$  is large the accuracy is poor, since Köster and Rauscher's results have been taken from published figures drawn to quite small scales. Hence it can be concluded that the modulus and the solidus temperature of an alloy are closely related,

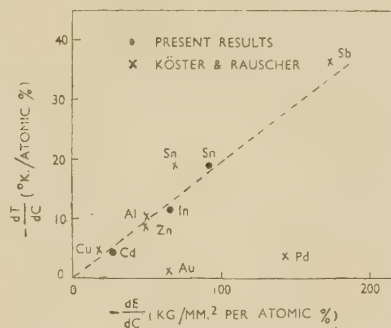


FIG. 3.—Relation Between the Slopes of the Solidus Line ( $dT/dC$ ) and the Corresponding Modulus Line ( $dE/dC$ ) for Silver Alloys.

and that factors which affect the former also affect the latter and vice versa.

Jones<sup>12</sup> has advanced a theory to account for the form of the solidus curve. He shows that the internal energy is governed primarily by two factors: (1) the Fermi energy, which is sensitive to changes in electron concentration even when there is no change in atomic volume, and (2) the energy of the lowest level of the valency electrons, which is mainly influenced by change in atomic size. Thus the steepness of the solidus line should increase as either the valency of the solute element increases or as the difference in atomic radii between solvent and solute increases, or both, and this does in fact happen. It was the atomic-size effect alone which was considered by Zener<sup>8</sup> in his explanation of Köster and Rauscher's results, but since the modulus and the solidus temperature are so closely linked, it seems likely that the valency difference between solvent and solute also plays an important part. Of the other factors likely to affect  $E$ , the difference in behaviour of the

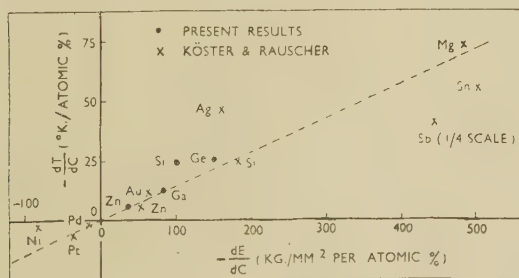


FIG. 2.—Relation Between the Slopes of the Solidus Line ( $dT/dC$ ) and the Corresponding Modulus Line ( $dE/dC$ ) for Copper Alloys.

perature (which may be taken to be the solidus temperature rather than the liquidus, since it is the former which marks the boundary between solid and liquid phases). Since, to a first approximation,



underlying *d*-band of electrons is probably the most influential. Each of these three effects will now be considered in turn.

## 2. THE EFFECT OF ATOMIC SIZE

Zener<sup>8</sup> concluded from his theory that, if a solute atom of radius  $R + \delta R$  is dissolved in a solvent of radius  $R$  (the radius being defined as half the closest distance of approach of the atoms), the slope of the modulus/at.-% solute curve ( $dE/dC$ ) will be given by:

$$\frac{1}{E} \cdot \frac{dE}{dC} = \frac{4(\delta R)^2}{(R)^2} \cdot (Nk)^{-1} \frac{d\mu}{dT} \quad (3)$$

where  $d\mu/dT$  is the slope of the curve of shear coefficient of the pure metal plotted against temperature,  $N$  the number of atoms per unit volume, and  $k$  Boltzmann's constant. It should be noted that all the quantities on the right-hand side of this equation are known, i.e. it contains no arbitrary constants. If this formula is correct, then the difference between the value of  $dE/dC$  given by it and that observed experimentally should be due to a valency or ionic effect. This difference is examined below, but no very accurate result should be expected, except where the contribution from equation (3) is very small compared with the experimental value, since Zener's equation is an approximation. Moreover, it is frequently difficult to assign a precise value to the atomic radius of an element when in solution with another. The best figure to use seems to be the "apparent atomic radius" proposed by Axon and Hume-Rothery.<sup>13</sup> This is the radius that it is necessary to assign to the solute element to account for the lattice constant of the particular solid solution considered. Thus the apparent radius is not a characteristic of the solute element alone, but also depends on the solvent.

Table II shows the observed values of  $-\frac{dE}{dC}$  ( $X$ ), Zener's values of  $-\frac{dE}{dC}$  ( $Z$ ), and the differences between them. In addition to the present results, Köster and Rauscher's values for alloys of copper, silver, and gold are given for comparison. The list includes all their results with the exception of alloys of the transition elements, in which the partly filled lower *d*-bands probably play an important part in the binding forces, and of the silver-gold system, in which  $dE/dC$  varies continuously from +67 to -40 kg./mm.<sup>2</sup>/at.-%.

This table shows that, as expected, Zener's atomic-size effect does not, in general, account for the whole of the observed decrease in the modulus. However, where the valency difference between solvent and solute is small, while the difference in atomic radii is appreciable (e.g. Cu-Ag, Cu-Au, Cu-Mg), Zener's value is quite a good approximation to the observed value.

Another point brought out by Table II is that the agreement between Köster and Rauscher's results

and those of the present work is not very close. There are several possible causes for this, and it is difficult to say which is the most likely. Firstly, there was a marked difference in purity in the materials used, Köster and Rauscher using commercially pure

TABLE II.—The Observed Value of  $dE/dC$  Compared With Zener's Estimate, for Alloys of Copper, Silver, and Gold.

Source of Result	Solvent	Solute	$-\frac{dE}{dC}$ kg./mm. <sup>2</sup> /at.-%		$X - Z$ kg./mm. <sup>2</sup> /at.-%
			$X$ (Observed)	$Z$ (Zener)	
Present work	Cu	Zn	37	20	17
		Ga	82	36	46
		Ge	150	47	103
		Si	102	1	101
		As	240	95	145
Köster and Rauscher <sup>7</sup>	Cu	Ag	164	144	20
		Au	63	95 *	-32
		Mg	480	380 *	100
		Zn	51	20	31
		Si	182	1	181
		Sn	500	450	50
		Sb	1780	410	1370
Present work	Ag	Cd	27	17	10
		In	65	36	29
		Sn	92	68	24
Köster and Rauscher <sup>7</sup>	Ag	Cu	18	47	-29
		Mg	17	3	14
		Zn	49	17	32
		Al	50	6	44
		Sn	69	68	1
		Sb	172	133	39
Köster and Rauscher <sup>7</sup>	Au	Cu	-46	19	-65
		Mg	-80	39 *	-119
		Zn	0	8	-8
		Cd	-43	6	-49
		Sn	181	29	+152

\* The "apparent atomic radius" was not known for these alloys, so Goldschmidt's atomic radius for a co-ordination number of 12 has been used instead.

copper in their alloys, whereas spectroscopically pure material was used in the present work. Secondly, it is most important, for the results to be comparable, that the specimens should be completely annealed, since, as shown by Kuntze<sup>14</sup> and by Kawai,<sup>15</sup> even small amounts of cold work may have a considerable effect on  $E$ . Köster and Rauscher certainly used annealed bars, but it is not clear whether the degree of crystal perfection (i.e. sharp spots on an X-ray-diffraction photograph) was the same as that obtaining in the author's material. Finally, there is the possibility that some preferred orientation existed in Köster's bars.

## 3. THE RELATIVE VALENCY EFFECT

The results obtained in the present work show that, after allowance has been made for the size effect, the value of  $(X - Z)$  increases with the valency ( $v$ ) of the solute element (the valencies used here are the

conventional ones, viz. Cu and Ag, 1; Zn and Cd, 2; Ga and In, 3; Ge, Si, and Sn, 4; As, 5). In trying to determine the precise effect that the valency has on the modulus, it should be borne in mind that the values of  $(X - Z)$  are liable to appreciable error, since not only is  $Z$  an approximation, but the value of  $X$  cannot be closely determined from the experimental curves. It was to obtain a series of alloys

it is permissible to say on the present evidence is that the valency of the solute has an appreciable effect on the Young's modulus of an alloy, and that either the effect increases linearly with  $v^2$ , or linearly with the electron concentration, although the former is slightly to be favoured.

Further experimental work is necessary to decide which law is correct, but unless the accuracy of the

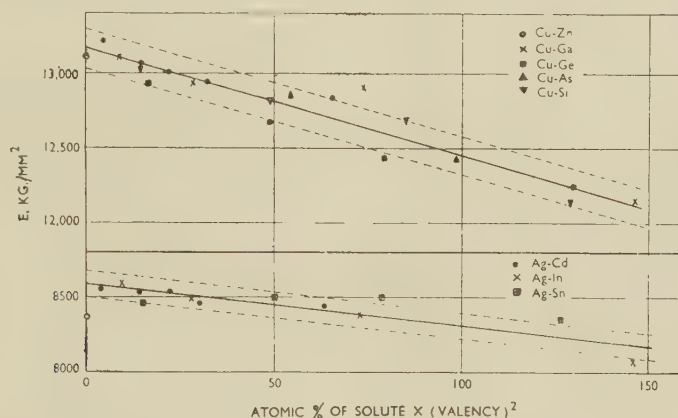


FIG. 4.—Young's Modulus as a Function of (Valency)<sup>2</sup> for Copper and Silver Alloys. Allowance has been made for size effect.

in which  $Z$  was reduced to a minimum that the copper-silicon alloys were investigated, the "apparent atomic radius" of silicon being almost the same as that of copper when the two are in solution. It is encouraging to note that, after allowing for the size effect, the value of  $(X - Z)$  for the copper-germanium alloys is almost identical with that for copper-silicon alloys and again shows that Zener's equation is probably quite a good approximation to the truth.

From the results for the copper alloys, it seems possible that  $(X - Z)$  increases as the square of the valency of the solute. If this is the case, then for any one alloy containing  $C$  at.-% solute of valency  $v$ , the decrease in  $E$  due to the valency effect alone should vary as  $Cv^2$ . Thus, if we assume that only the atomic size and valency effects are important, by plotting  $(E + C \cdot Z)$  against  $Cv^2$  for all the copper alloys investigated, we should obtain a straight line. This plot is made in Fig. 4 for both the copper and the silver series, from which it will be seen that the points are grouped around a straight line in each case. Furthermore, if two lines are drawn to represent the limits of experimental error (shown dotted in Fig. 4), most of the points lie within this zone.

However, from the work of Hume-Rothery<sup>9</sup> and his collaborators, it would seem possible that the valency effect varies with the electron concentration rather than with  $v^2$ . If this is the case, then  $(E + C \cdot Z)$  should vary with  $1 + \frac{C(v-1)}{100}$ , and this

plot is given in Fig. 5, which shows that although more points lie outside the zone of experimental error, the fit is sufficiently good for there to be a distinct possibility that this law is correct. All that

method is improved, it is doubtful whether the fresh evidence would be conclusive. However, if the experimental error of the determination of  $E$  on a given specimen is reduced, then the possibility of error due to the small amount of preferred orientation remaining in the bar after recrystallization cannot be ignored. Since it is very difficult to obtain a fine-grained specimen with a truly random crystallo-

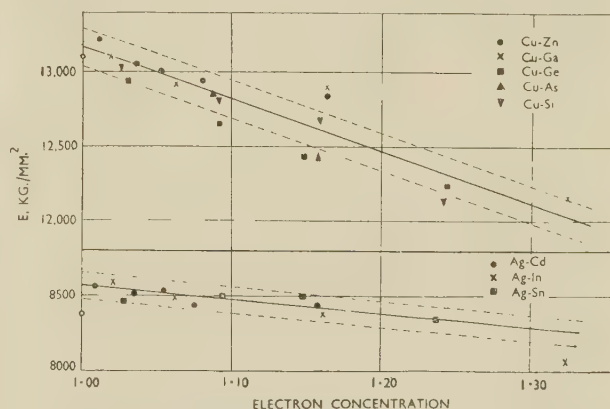


FIG. 5.—Young's Modulus as a Function of the Electron Concentration for Copper and Silver Alloys. Allowance has been made for size effect.

graphic orientation, the most profitable line of attack for work of high accuracy would seem to be to use single crystals.

#### 4. THE IONIC EFFECT

It can be seen from Table II that Köster and Rauscher's results for alloys of gold with magnesium, cadmium, or zinc do not conform to the pattern of



the copper or silver alloys, since the modulus actually increases as the amount of solute increases. Gold has the same valency as copper and silver, and furthermore the atomic radius of pure gold is practically the same as that of silver, so that some effect must be present in the case of gold which is powerful enough to overcome the effects of valency and atomic size. It seems most likely that the explanation lies in the behaviour of the electrons in the completely filled *d*-bands, as may be seen from the following simplified picture of the forces giving rise to cohesion.

The valency electrons may be regarded as drawing the atoms together, thereby giving rise to a strong attractive force, which is supplemented to a small extent by a force of the van der Waals type between the outermost electrons of the *d*-bands moving in harmony with one another. In the noble metals (copper, silver, and gold) with which we are concerned, the balancing repulsive forces arise almost entirely from the overlap of the electron clouds of the *d*-bands. Thus, these metals may be regarded as being made up of hard spheres (the ions) held in contact by the valency electrons.

There is, however, a modification to be made to this picture in the case of gold, since, as pointed out by Hume-Rothery,<sup>16</sup> the gold ion may be more easily polarized than either the silver or the copper ion, with the result that it may be more easily deformed. That this is so is shown by the facts that: (a) gold and copper form a continuous series of solid solutions at room temperature, while silver and copper do not, in spite of the atomic radii of silver and gold being almost identical, and (b) Young's modulus for gold is much lower than that for copper (8000 compared with 13,000 kg./mm.<sup>2</sup>), whereas the bulk modulus is greater (17,000 compared with

13,500 kg./mm.<sup>2</sup>), which shows that the resistance of gold to hydrostatic pressure is far greater than to a unidirectional force. This may be put another way by saying that Poisson's ratio is higher for gold than for either silver or copper<sup>17</sup> (0.42 against 0.38 and 0.34).

Now if some of the gold atoms are replaced by atoms of another element whose ions are not so readily polarized, the new ions may be expected to stiffen the lattice with respect to shearing forces, with a resultant increase in Young's modulus. It follows from this theory that if the bulk moduli of the alloys were measured, they would be found to decrease with increasing alloy content, since this modulus should be unaffected by the change in ions, but would be subject to the decrease arising from the valency change.

It is possible that this ionic effect begins to make itself felt in the silver alloys, since the valency effect is apparently much less in these alloys than in the copper alloys. The fact that Poisson's ratio for silver lies midway between the values for copper and gold may be significant, but this idea of the part played by the ions is purely qualitative and no prediction of the magnitude of the effect can be made.

#### ACKNOWLEDGEMENTS

The author is deeply indebted to Mr. L. Rotherham, formerly Head of the Metallurgy Department, Royal Aircraft Establishment, who instigated this work, and also to Dr. G. B. Greenough, formerly at the Royal Aircraft Establishment, for many useful discussions and much helpful advice. Acknowledgement is also made to the Chief Scientist, Ministry of Supply, and to the Controller, H.M. Stationery Office, for permission to publish this paper.

#### REFERENCES

1. D. J. Mack, *Trans. Amer. Inst. Min. Met. Eng.*, 1946, **166**, 68.
2. A. Portevin, *Compt. rend.*, 1923, **177**, 634.
3. J. P. Andrews, *Phil. Mag.*, 1925, [vi], **50**, 665.
4. T. S. Kê, *Phys. Rev.*, 1947, [ii], **71**, 533.
5. K. Fuchs, *Proc. Roy. Soc.*, 1936, [A], **153**, 622; **157**, 444.
6. R. S. Leigh, *Phil. Mag.*, 1951, [vii], **42**, 139.
7. W. Köster and W. Rauscher, *Z. Metallkunde*, 1948, **39**, 110.
8. C. Zener, *Acta Cryst.*, 1949, **2**, 163.
9. W. Hume-Rothery, "The Structure of Metals and Alloys" (*Inst. Metals Monograph and Rep. Series No. 1*), 1949.
10. F. Förster, *Z. Metallkunde*, 1937, **29**, 109.
11. G. Kuczynski, *Nature*, 1950, **165**, 562.
12. H. Jones, *Proc. Phys. Soc.*, 1937, **49**, 243.
13. H. J. Axon and W. Hume-Rothery, *Proc. Roy. Soc.*, 1948, [A], **193**, 1.
14. W. Kuntze, *Z. Metallkunde*, 1928, **20**, 145.
15. T. Kawai, *Sci. Rep. Tôhoku Imp. Univ.*, 1930, [i], **19**, 209.
16. W. Hume-Rothery, "Atomic Theory for Students of Metallurgy" (*Inst. Metals Monograph and Rep. Series No. 3*), 1948.
17. G. W. C. Kaye and T. H. Laby, "Tables of Physical and Chemical Constants." London: 1948 (Longmans, Green and Co., Ltd.).

# THE AGEING CHARACTERISTICS OF TERNARY ALUMINIUM-COPPER ALLOYS WITH CADMIUM, INDIUM, OR TIN\*

1371

By H. K. HARDY,† Ph.D., M.Sc., A.R.S.M., A.I.M., MEMBER

## SYNOPSIS

Hardness/ageing-time curves have been obtained between 30° and 240° C. for aluminium-copper alloys containing 2, 3, or 4% copper with 0.01 or 0.05% indium or tin. Work on similar alloys containing small amounts of cadmium was limited by the loss of that element from the surface during salt-bath heat-treatment. The loss is completely negligible, however, in alloys of commercial purity.

The presence of indium or tin favoured single-stage ageing curves which passed smoothly through peak-hardness values. Only slight evidence was found of the two-stage ageing curves met with in the binary aluminium-4% copper alloy at 130° C.

The ageing process was accelerated and the peak-hardness values considerably raised at certain temperatures, compared with the corresponding binary aluminium-copper alloys. Analysis of the results suggested that the presence of cadmium, indium, or tin facilitated the nucleation of the Guinier-Preston zones [2]. The mechanism of the process may be based on heterogeneous nucleation associated either with prior precipitation of the cadmium (indium or tin) atoms or with short-range grouping of copper atoms around the cadmium (indium or tin) atoms during solution-treatment.

A thermodynamic analysis of short-range ordering in ternary solid solutions has shown that some grouping of the solute elements is to be expected under appropriate conditions. A semi-quantitative application to an aluminium-copper-tin alloy gave indecisive results for the significance of short-range grouping in relation to the ageing behaviour of the alloys.<sup>1</sup>

## I.—INTRODUCTION

RECENT work has shown that small quantities—of the order of 0.05–0.1 wt.-%—of cadmium, indium, or tin exert a pronounced influence on the response of aluminium-copper alloys to artificial ageing. The rate of artificial ageing is greatly enhanced and the tensile properties, notably the proof stress, are considerably increased.<sup>1-3</sup> Small quantities of magnesium militate against the effects of indium or tin, but do not influence additions of cadmium.<sup>2</sup> The latter element is also unaffected by the simultaneous presence of iron, silicon, manganese, nickel, or zinc.<sup>4</sup>

The effects of cadmium, indium, and tin result from their slight solubility in aluminium at temperatures in the region of 500° C.,<sup>2, 5</sup> and two hypotheses have been discussed to account for the acceleration in the rate of artificial ageing.<sup>2</sup> In one of these it is supposed that a precipitate of cadmium (indium or tin) atoms, coherent with the matrix, is capable of acting as a nucleus for the aluminium-copper decomposition product formed on artificial ageing. This hypothesis received some support because the binary alloys of these three elements with aluminium show age-hardening at elevated temperatures.<sup>2</sup> The second hypothesis postulated that short-range grouping of “small” copper atoms occurred around the “large”

cadmium (indium or tin) atoms during solution-treatment. Such groups act as nuclei during artificial ageing. The high-purity cast alloys showed a diminished capacity for natural ageing when they contained cadmium (indium or tin). This was taken to support the second hypothesis, since the short-range groups might be sufficiently stable to take no part in the ageing at room temperature.

A clarification of the mechanism by means of which the cadmium (indium or tin) atoms exert such a large effect would be of considerable interest. This is greatly to be desired in view of the possibility—particularly if the hypothesis of short-range grouping were confirmed—of using very small additions of suitable elements to enhance the age-hardening of other systems.

A detailed examination has therefore been undertaken of the ageing characteristics of alloys of various copper contents with additions of cadmium, indium, or tin. Hardness/ageing curves have been determined in this initial study, using experimental methods similar to those for binary aluminium-copper alloys.<sup>6</sup> It is intended that metallographic and single-crystal X-ray examinations shall subsequently be allied to this approach. The work described in the present paper forms part of a more general investigation into the ageing processes of aluminium-copper alloys and the effects caused by the presence of third constituents.

\* Manuscript received 23 July 1951.

† Head of Physical Metallurgy Section, Fulmer Research Institute, Stoke Poges, Bucks.



## II.—EXPERIMENTAL PROCEDURE

Full details of the methods adopted have been given previously<sup>6</sup> and will only be summarized here. Materials of the highest available purity were carefully melted and water-chill-cast to  $1\frac{1}{4}$ -in.-dia. billets. These were scalped, annealed, and cold forged to 0.52 in. square, homogenized, annealed, and flattened to 0.22 in. thick and  $1-1\frac{1}{4}$  in. wide. The specimens were prepared as fully as possible before heat-treatment, in order to minimize their subsequent handling, and only required final grinding on 00 emery paper before hardness testing.

The initial solution-treatment was for not less than 48 hr. at 520° C. in a salt bath, followed by quenching in water at  $20^\circ \pm 1^\circ$  C. The specimens were dried by rinsing in acetone and aged at 30°, 130°, 165°, 190°, and 220° C. The aluminium-4% copper-0.05% tin alloy only was aged at 240° C. The time between quenching and placing in the ageing furnace did not exceed 5 min. The 30° and 165° C. treatments were carried out in oil baths. Circulating-air-furnaces were used at 130°, 190°, and 220° C., and a salt bath at 240° C. The temperature fluctuations were not greater than  $\pm 1\frac{1}{2}^\circ$  C. The time for the specimens to reach a temperature 2° C. lower than that of the furnace was approximately 5 min., except for the salt bath, in which the specimens required 1.5 min. These times have been allowed in plotting the ageing curves.

Five Vickers diamond pyramid hardness tests were made on each specimen after ageing. Duplicate specimens were used for the early portions of the ageing curves. Specimens were not re-aged unless their initial ageing treatment had been fairly lengthy in relation to the peak on their ageing curve.

The melt analyses of the alloys all fell within  $\pm 0.1\%$  of the desired copper contents (e.g.  $4.0 \pm 0.1\%$ ), whilst the quantities of the third elements did not vary from their nominal figures by more than 10% (e.g.  $0.05 \pm 0.005\%$ ). Spectrographic analysis showed no changes in composition of the aluminium-copper-indium or aluminium-copper-tin alloys during heat-treatment. As will be shown later, a loss of cadmium occurred and prevented full ageing curves being obtained for this element.

As in the previous work on the binary aluminium-copper alloys,<sup>6</sup> an incubation value has been adopted to indicate the time to the beginning of ageing. This is obtained by extrapolating the rising ageing curve back to the hardness value during the incubation period. This incubation value falls between the incubation period and the time to the maximum rate of hardening.

## III.—EXPERIMENTAL RESULTS

## 1. ALUMINIUM-COPPER-CADMIUM ALLOYS

Spectrographic analysis of the surfaces of specimens prepared before solution-treatment revealed that a serious loss of cadmium had occurred, as shown in

Table I. This was reflected by the hardness/ageing curves, which reproduced the results obtained on the

TABLE I.—*Variation of Cadmium Content with Depth Below the Surface for Aluminium-4% Copper-Cadmium Alloys Solution-Treated 48 hr. in a Salt Bath at 520° C.*

Nominal: 0.1% Cd		Nominal: 0.25% Cd	
Depth, cm.	Cd, %	Depth, cm.	Cd, %
Nil	0.03	Nil	0.005
0.047	0.06	0.012	0.03
0.073	0.075	0.047	0.12
0.091	0.085	0.085	0.22
0.137	0.09	0.102	0.22
...	...	0.130	0.21

binary aluminium-copper alloys.<sup>6</sup> Some improvement was obtained if the specimens were prepared after their initial solution-treatment and subsequently re-heat-treated for 5 min. only. Even so, the acceleration of the ageing was less than expected, and some loss of cadmium occurred. Preparation of the specimens after full heat-treatment was not entirely satisfactory, as the hardness measurements were then carried out on a surface which had been somewhat cold worked. Only a few hardness/ageing curves were therefore plotted on the aluminium-copper-cadmium alloys and they have not been reproduced here.

Cadmium additions are known to be effective in very high-purity cast aluminium-4% copper-0.15% titan-

TABLE II.—*Averaged Tensile-Test Results on Wrought Al-4.5% Cu-0.15% Ti Alloys of Very High Purity.*

$2\frac{1}{4}$ -in.-dia. water-chill-cast billets, annealed at 425° C., furnace cooled and cold forged to  $\frac{3}{4}$  in. square, solution-treated 16 hr. at 530° C. in a salt bath, cold-water quenched, and aged as indicated.

Cd, %	Aged 14 Days at Room Temp.			Aged 16 Hr. at 165° C.		
	0.1% Proof Stress, tons/in. <sup>2</sup>	Max. Stress, tons/in. <sup>2</sup>	Elongation, %	0.1% Proof Stress, tons/in. <sup>2</sup>	Max. Stress, tons/in. <sup>2</sup>	Elongation, %
Nil	6.1	16.1	38 $\frac{1}{2}$	13.5	20.7	12 $\frac{1}{2}$
0.08	5.7	15.5	41 $\frac{1}{2}$	21.5	25.2	5
0.1	5.6	15.8	42 $\frac{1}{2}$	22.0	25.4	5

ium alloys,<sup>2</sup> and in cast or wrought aluminium-copper alloys of commercial purity.<sup>4</sup> The results in Table II show that the same effect occurs in wrought alloys of very high purity. Therefore, it will be assumed in the subsequent discussion that the behaviour of aluminium-copper-cadmium alloys is essentially similar to that of the alloys with indium or tin. Only a negligible loss of cadmium occurs during solution-treatment of commercial-purity alloys, in either a salt bath or an air furnace.<sup>3</sup>

## 2. ALUMINIUM-COPPER ALLOYS WITH 0.05% INDIUM OR TIN \*

### (a) Quenched Hardness Values

It will be seen from Table III that the ternary alloys with indium or tin were always softer than the

TABLE III.—Vickers Pyramid Hardness Values on Quenched Specimens.

Each figure is the average of five impressions on 10–12 specimens, except for the alloys with 0.01% indium or tin, where 7–8 specimens were used. The hardness tests were carried out between 5 and 15 min. after quenching.

Addition, %	Copper Content, %				
	2.0	3.0	3.5	4.0	4.5
Nil *	39.65	51.2	57.1	63.2	69.0
0.01 In	...	...	...	60.2	...
0.05 In	36.7	46.3	...	57.35	...
0.01 Sn	...	...	...	58.7	...
0.05 Sn	36.7	45.7	...	56.2	...

\* Values previously determined.<sup>6</sup>

corresponding binary alloy immediately after quenching. The presence of 0.05% indium or tin diminished the hardness of the alloys with 3.0 and 4.0% copper by an amount equivalent to a reduction in copper content of approximately 0.5%. This effect was slightly less marked in the alloys containing 2.0% copper, since the reduction in hardness was roughly proportional to the copper content.

### (b) Ageing at 30° C. (Fig. 1)

The ternary alloys with 3.0 or 4.0% copper showed a slower rate of ageing than the corresponding binary

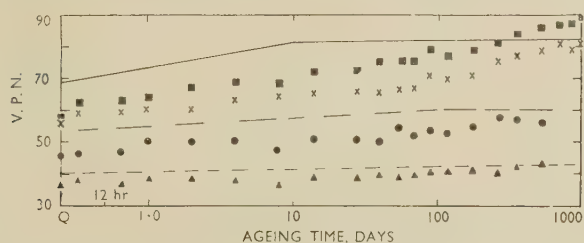


FIG. 1.—Hardness Curves for Alloys Aged at 30° C. Each point represents the average of 5 impressions on each of 2 specimens.

KEY TO FIGS. 1-5, 10, 11

■	Al-4% Cu-0.01% Sn.	—	Al-4% Cu.
+	Al-4% Cu-0.05% Sn (In).	- - -	Al-3% Cu.
○	Al-3% Cu-0.05% Sn (In).	- - - -	Al-2% Cu.
△	Al-2% Cu-0.05% Sn (In).		

aluminium-copper alloys. However, the effect was much less marked in the ternary alloys with 2.0% copper, as the binary alloy aged only very slowly. The aluminium-4.0% copper-0.05% tin alloy took

about 1000 days to reach the same hardness as the binary aluminium-4% copper alloy. The aluminium-4.0% copper-0.01% tin alloy also aged more slowly than the corresponding binary alloy, but reached a greater hardness.

At first sight these results appear to confirm the conclusion reached earlier on cast alloys of very high purity,<sup>2</sup> that additions of cadmium, indium, or tin greatly diminished the natural ageing capacity of aluminium-copper alloys. Typical tensile-test results are given in Table IV, from which it will be seen that the proof-stress values of the high-purity alloys were greatly reduced in the presence of cadmium, indium, or tin. A check on the cast aluminium-

TABLE IV.—Averaged Tensile-Test Results on Cast Aluminium-Copper Alloys.

Sand-cast D.T.D. bars, solution-treated 16 hr. in a circulating-air furnace at 530° C., cold-water quenched, and aged 14 days at room temperature.

Addition, %	0.1% Proof Stress, tons/in. <sup>2</sup>	Max. Stress, tons/in. <sup>2</sup>	Elongation, %
<i>Al-4.0% Cu-0.15% Ti Alloy (high-purity) <sup>2</sup></i>			
Nil	10.0	18.1	18
0.05 Cd	7.6	16.1	22
0.05 In	4.8	13.9	22½
0.05 Sn	4.35	12.8	20
<i>Al-4.0% Cu-0.15% Ti Alloy (high-purity), present work</i>			
Nil	8.9	17.7	17
<i>Al-4.5% Cu-0.22% Fe-0.1% Si-0.15% Ti Alloy <sup>4</sup></i>			
Nil	7.6	17.7	17
0.05 Cd	7.5	16.6	14
0.25 Cd	6.1	15.8	15

4.0% copper alloy gave a proof stress slightly lower than the original value—8.9 against 10.0 tons/in.<sup>2</sup>—but still considerably above the results on the other alloys.

Only a much smaller reduction in properties after natural ageing was observed in the commercial-purity cast alloys as a result of additions of cadmium<sup>4</sup> (see Table IV). This also applied to the wrought alloys of commercial purity, and of high purity (Table II). Natural-ageing tests on sheet alloys revealed only a very slight reduction in properties due to the presence of cadmium.<sup>3</sup>

The reduction in natural-ageing capacity is clearly much smaller than was deduced previously from the behaviour of the high-purity cast alloys.<sup>2</sup> It is particularly to be noted that the proof-stress value of the high-purity cast aluminium-4.0% copper-0.15% titanium alloy (Table IV) is greater than that of the wrought aluminium-4.5% copper-0.15% titanium alloy (Table II). This may indicate a difference between very high-purity cast and wrought materials which is lost when the purity is reduced.<sup>4</sup> Dehlinger

\* Only the ageing curves for the aluminium-copper-tin alloys have been reproduced. Those for the aluminium-copper-indium alloys were very similar and have been deposited in the Joint Library of the Institute of Metals and the

Iron and Steel Institute, together with full-scale drawings of the curves for the aluminium-copper-tin alloys. Points taken from the experimental results on the aluminium-copper-indium alloys are included in Figs. 8–11.



*et al.*<sup>7-10</sup> have postulated that cast single crystals of aluminium possess a more strongly marked mosaic structure than crystals formed by recrystallization.

It seems safe to conclude that additions of cadmium, indium, or tin diminish the natural-ageing capacity to a slight extent, since the properties of alloys containing these elements are always somewhat lower than those in which they are absent. The ternary additions may diminish the natural ageing by: (a) slowing down the rate of diffusion by blocking movement along dislocations or by retarding the move-

that the first half of the hardness rise took place more rapidly than the second half.

The incubation values were much closer together than in the binary alloys. The peak on the curves occurred at much shorter times and at higher hardness values, particularly in the 2% copper alloys.

(d) Ageing at 165° C. (Fig. 3)

The ageing curves passed smoothly through their peak-hardness values. The alloys with 2% copper showed a very wide hardness peak.

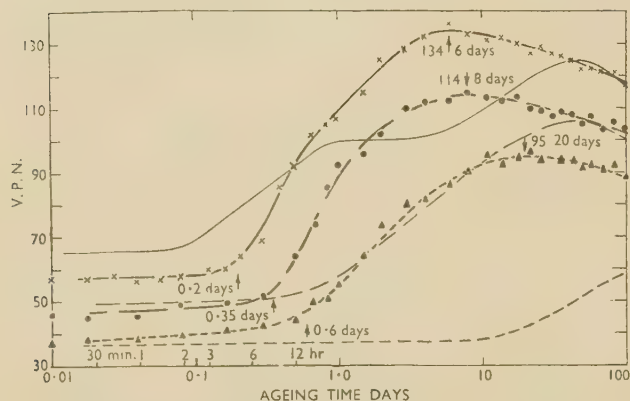


FIG. 2.—Hardness Curves for Alloys Aged at 130° C. Each point represents the average of 5 impressions on each of 2 specimens. (For key see Fig. 1.)

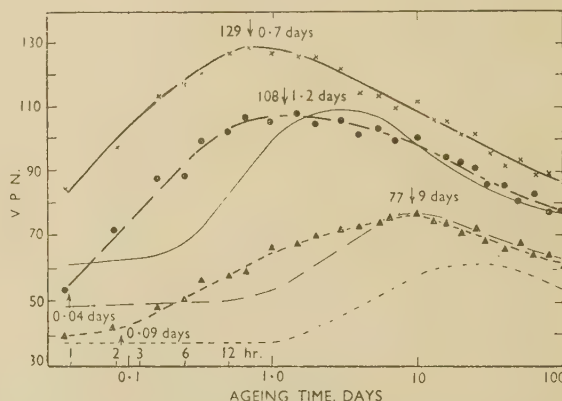


FIG. 3.—Hardness Curves for Alloys Aged at 165° C. Up to 7 days each point represents the average of 5 impressions on each of 2 specimens; single specimens were used at longer ageing times. (For key see Fig. 1.)

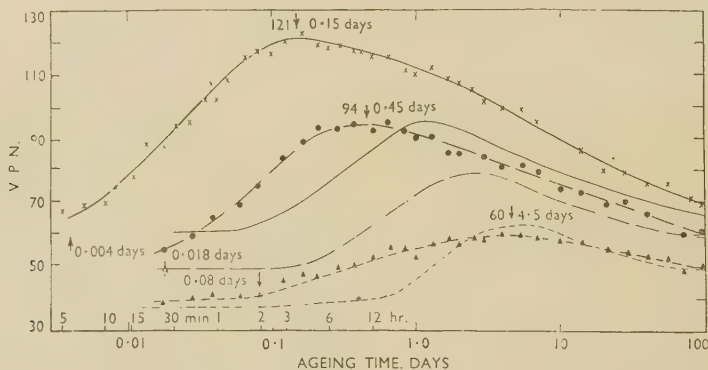


FIG. 4.—Hardness Curves for Alloys Aged at 190° C. Up to 28 days each point represents the average of 5 impressions on each of 2 specimens; single specimens were used at longer ageing times. (For key see Fig. 1.)

ment of vacant lattice sites, (b) reducing the quenching strains, (c) decreasing the effective copper content owing to an accumulation of copper atoms around the cadmium (indium or tin) atoms, or (d) a reduction in the quenching strains.

(c) Ageing at 130° C. (Fig. 2)

The binary alloy of aluminium with 4.0% copper had given a very strong indication of a two-stage ageing process at this temperature,<sup>6</sup> as evidenced by the flat on the ageing curve. This was absent from the ageing curves of the 4.0% copper alloy containing 0.05% indium or tin, although there were indications

(e) Ageing at 190° C. (Fig. 4)

The general appearance of the ageing curves was very similar to that at 165° C., except that the peak hardness of the ternary alloys with 2% copper did not exceed that of the corresponding binary alloy. The curves for the ternary alloys with 2% copper were also much flatter than those of the binary alloy.

(f) Ageing at 220° C. (Fig. 5)

The relationship between the ageing curves of the ternary and binary alloys was similar to that at 190° C.

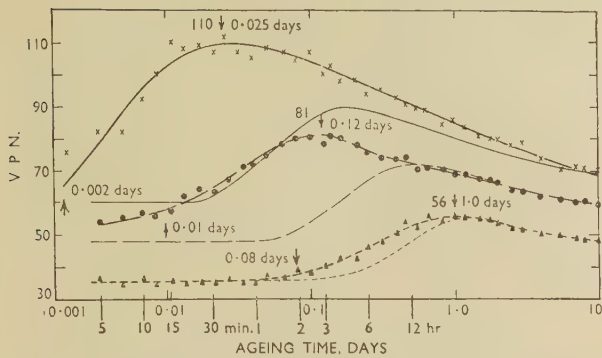


FIG. 5.—Hardness Curves for Alloys Aged at 220° C. Each point represents the average of 5 impressions on each of 2 specimens. (For key see Fig. 1.)

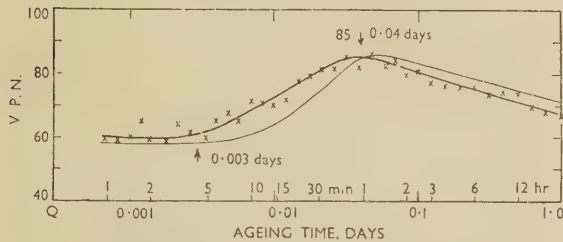


FIG. 6.—Hardness Curve (x—x) for Aluminium-4% Copper-0.05% Tin Alloy Aged at 240° C. Each point represents the average of 5 impressions on each of 2 specimens. — Al-4% Cu.

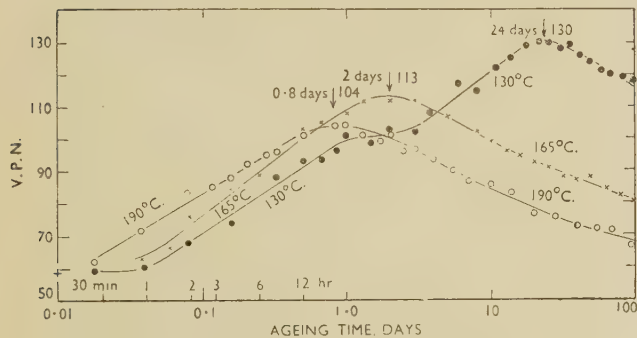


FIG. 7.—Hardness/Ageing Curves for Aluminium-4% Copper-0.01% Tin Alloy.

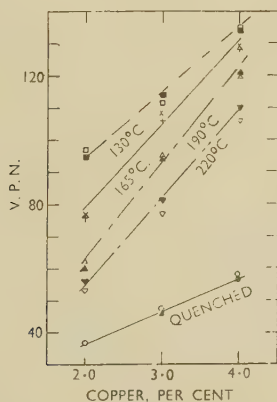


FIG. 8.—Relation Between Peak Hardness and Copper Concentration for Alloys with 0.05% Indium ( $\square$ ,  $+$ ,  $\Delta$ ,  $\nabla$ ,  $\circ$ ) or Tin ( $\blacksquare$ ,  $\times$ ,  $\blacktriangle$ ,  $\blacktriangledown$ ,  $\bullet$ ).

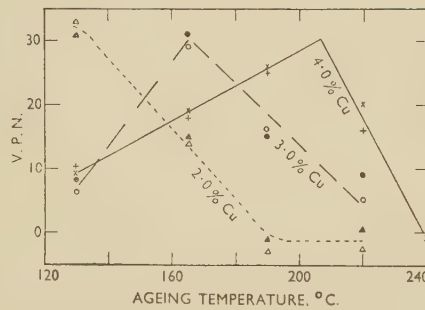


FIG. 9.—Relation Between Peak-Hardness Difference (Ternary minus Binary Alloys) and Ageing Temperature for Alloys with 0.05% Indium ( $\Delta$ ,  $+$ ,  $\circ$ ) or Tin ( $\blacktriangle$ ,  $\times$ ,  $\bullet$ ).

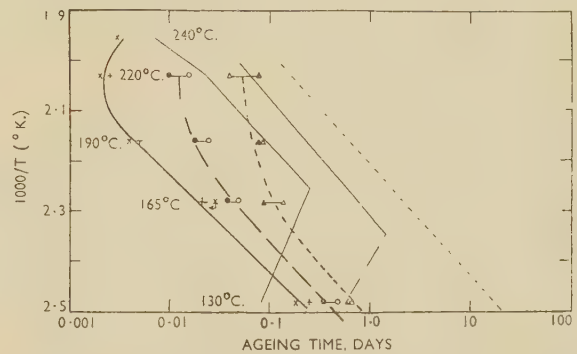


FIG. 10.—Relation Between Incubation Value and Ageing Temperature for Alloys with 0.05% Indium or Tin. (For key see Fig. 1.)

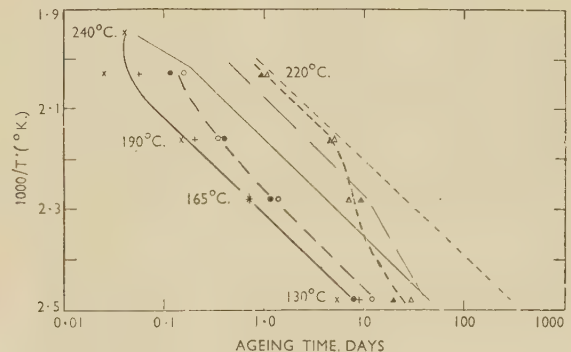


FIG. 11.—Relation Between Time-to-Peak Hardness and Ageing Temperature for Alloys with 0.05% Indium or Tin. (For key see Fig. 1.)

### (g) Ageing at 240° C. (Fig. 6)

The incubation value and peak hardness occurred after times only slightly shorter than in the case of the binary alloy. In this respect the relationship was the same as that of the aluminium-2% copper-0.05% tin and aluminium-2% copper alloys at 220° C.

### 3. ALUMINIUM-4% COPPER ALLOYS WITH 0.01% INDIUM OR TIN

The ageing curve at 30° C. has been given in Fig. 1, and the curves in Fig. 7 are for ageing at 130°, 165°, and 190° C. The alloys with 0.01% tin or indium



were normally intermediate in behaviour between the binary aluminium-copper alloys and the ternary alloys with additions of 0.05% tin or indium. Inflected curves were obtained at 130° C., giving evidence of a two-stage ageing process.

#### 4. ANALYSIS OF RESULTS

##### (a) *Peak-Hardness/Concentration Relationships (Fig. 8)*

The quenched-hardness values showed a linear relationship with concentration of copper in the alloys with 0.05% indium or tin. The dependence of peak hardness on concentration could best be represented by straight lines at all the temperatures investigated. This indicates a marked difference from the behaviour of the binary alloys, in which the peak-hardness values fell into an upper and a lower group connected by an inflected curve (see Fig. 11 of ref. 6).

##### (b) *Peak-Hardness/Ageing-Temperature Relationships*

The peak-hardness values tended to fall as the ageing temperature increased, and comparison of the ageing curves shows that this applied equally to the binary and ternary alloys. The binary aluminium-2% copper alloy possessed peak-hardness values almost independent of the ageing temperature, but the ternary alloys with 2% copper showed greater hardness at 110° and at 130° C. than at the higher ageing temperatures.

##### (c) *Peak-Hardness Difference (Ternary minus Binary)/Ageing-Temperature Relationships (Fig. 9)*

The maximum difference in hardness was approximately 30 V.P.N. and was substantially independent of copper content. Small differences in the peak-hardness values occur at low ageing temperatures (high degrees of supersaturation) when the binary alloys possess enhanced hardness associated with the two-stage ageing process.<sup>6</sup> The difference in peak hardness is again small at high temperatures, when the degree of supersaturation is considerably lower.

##### (d) *Incubation Value/Temperature Relationships (Fig. 10)*

The binary aluminium-copper alloys had been examined previously<sup>6</sup> and had given two branches for the curve relating the logarithm of the incubation value and the reciprocal of the absolute temperature. This had been interpreted as evidence that there were different initial decomposition products, associated with each branch of the curve, at very high and at high degrees of supersaturation.

The ternary aluminium-copper-0.05% indium and aluminium-copper-0.05% tin alloys examined in the present paper possessed relatively simple C curves. The ternary alloys normally showed smaller incubation values than those of the corresponding binary alloys. The ternary 2% copper alloys aged at 165° and 130° C. showed the effect very markedly, but the reverse applied to ternary alloys with 4% copper aged at 130° C.

##### (e) *Time-to-Peak-Hardness/Temperature Relationships (Fig. 11)*

The acceleration of the ageing process is illustrated by comparing the peak-hardness times of the binary and ternary alloys. The curve for the ternary alloy with 2% copper is particularly noteworthy, as it shows at 190° and 220° C. peak-hardness times similar to those of the binary alloy, but much shorter times than the binary alloy at lower ageing temperatures.

#### IV.—DISCUSSION OF RESULTS

The initial decomposition product of binary aluminium-copper alloys passes with decreasing supersaturation through the series Guinier-Preston zone [1] → G.P. zone [2] →  $\theta'$  →  $\theta$ . The lower branch of the curve relating the incubation value of the binary alloys with temperature (Fig. 10) was associated with the formation of G.P. zones [1]. The upper branch of this curve was associated with the formation of G.P. zones [2] as the initial decomposition product.<sup>6</sup>

The additions of indium or tin exercised their greatest influence in transposing the upper branch of the curve for the incubation values of the binary alloys to shorter ageing times (Fig. 10). The conclusion can therefore be drawn that the acceleration in the rate of ageing is due to an enhanced rate of formation of the G.P. zones [2]. Since the two-stage ageing curve is well developed in the binary aluminium-4% copper alloy aged at 130° C., but only indicated to a smaller extent in the ternary 4% copper alloy with 0.01% indium or tin, it appears that the addition of indium or tin favours the formation of the G.P. zones [2] at the expense of the G.P. zones [1]. It is not certain how far the G.P. zones [2] are favoured at the expense of  $\theta'$ . The latter may become the initial precipitate at low degrees of supersaturation. The flatter maximum on the curve for the ternary 2% copper alloys aged at 190° C. might be associated with the rapid formation of the initial decomposition product, which is unable to grow quickly owing to the small quantity of copper present.

The increased hardening brought about by the additions of cadmium, indium, or tin can readily be explained, since the number of particles of precipitate is increased.<sup>2</sup> The maximum difference in the peak-hardness values (ternary minus binary) (Fig. 11) probably occurs when the degree of supersaturation is most favourable to the G.P. zones [2] in the ternary alloy and unfavourable to the G.P. zones [1] in the binary alloy, so that it does not result in the two-stage ageing process. The reduction in the difference between ternary and binary peak-hardness values at higher ageing temperatures can be associated with the formation of  $\theta'$  or  $\theta$  as the initial decomposition product in the ternary as well as in the binary alloys.

A complete description of the cause of the results arising from the presence of cadmium, indium, and tin must await X-ray-diffraction studies. It is not

yet known how far the third elements modify the structures of the decomposition products and affect any polymorphic transformations. However, the acceleration of the ageing process is most probably due to some factor facilitating the nucleation of the G.P. zones [2]. Alternative views, such as the precipitation of a completely new phase, or ageing effects due to the simultaneous precipitation of cadmium (indium or tin), have been dismissed earlier.<sup>2</sup> The ternary aluminium-copper-tin phase diagram shows that only  $\text{CuAl}_2$  and tin are in equilibrium with the aluminium solid solution.<sup>11</sup> Similar conditions would probably apply in the aluminium-copper-cadmium and aluminium-copper-indium systems. Furthermore, the quantity of cadmium (indium or tin) precipitate would be insufficient to account for the very considerable effects described, on the basis that the age-hardening was due to the sum of the independent precipitates of cadmium and copper.

It is not possible to decide from the present work the exact mechanism by which the cadmium, indium, and tin atoms facilitate the nucleation of the G.P. zones [2]. These third elements could promote homogeneous nucleation if they lowered the interfacial tension between the initial decomposition product and the matrix, with a consequent reduction in the height of the energy barrier to nucleation.<sup>12</sup> The reduction in the coherency strains associated with the G.P. zones [2] would also lower the hardening effect, although this would be compensated by an increased number of particles. An alternative explanation—that the energy barrier is reduced because the addition elements increase the free-energy drop per atom of precipitate<sup>12</sup>—seems unlikely in view of the very small amounts of cadmium, indium, or tin required. As described previously,<sup>2</sup> prior precipitation of the ternary elements or short-range grouping of the copper atoms around the cadmium (indium or tin) atoms during solution-treatment could provide nuclei for the rapid formation of the G.P. zones [2]. Heterogeneous nucleation<sup>13, 14</sup> is well known in the crystallization of solids from gases (e.g. ice crystals from water vapour<sup>15, 16</sup>) and of solids from liquids (e.g. solid aluminium from the melt by titanium carbide<sup>17</sup>). Though rarely described for reactions within solids, it seems the most likely explanation in the present case.

Lattice-strain-energy considerations were suggested previously as a possible origin of local ordering,<sup>2</sup> but an alternative cause resides in the thermodynamic relationships between the component metals. It may be noted that aluminium-copper and copper-cadmium (indium or tin) alloys have a negative heat of solution, whereas aluminium-cadmium (indium or tin) alloys have a positive one. A reduction of the statistical disorder of the solid solution is to be expected in the ternary alloys, since cadmium (indium or tin) atoms will prefer copper rather than

aluminium atoms as their nearest neighbours. A thermodynamic analysis has been made in the Appendix (below), but a semi-quantitative treatment did not lead to a clear decision as to the importance of this process in relation to the ageing behaviour.

It is worth mentioning again<sup>2</sup> that a marked acceleration occurs at ageing temperatures in excess of the melting point of indium ( $156.4^\circ\text{C}$ .), when a liquid phase is the stable precipitate in binary aluminium-indium alloys. However, the initial decomposition product may be coherent with the matrix, since the binary alloys show age-hardening at  $165^\circ\text{C}$ .<sup>2</sup> A further factor which may allow the ageing characteristics of the ternary alloys to return to those of the binary aluminium-copper alloys as the temperature is raised, is that the precipitate of cadmium, indium, or tin will tend to favour a non-coherent form.

#### ACKNOWLEDGEMENTS

The author's thanks are due to his colleagues at the Fulmer Research Institute who assisted with the experimental work, and to Dr. A. H. Sully for helpful discussions.

#### APPENDIX

##### SHORT-RANGE ORDERING IN TERNARY SOLID SOLUTIONS

Small additions of cadmium, indium, or tin are known greatly to accelerate the ageing process in aluminium-copper alloys at elevated temperatures. One of the hypotheses put forward to account for the results postulates short-range grouping of the copper atoms around the ternary atoms during solution-treatment.

It was thought that thermodynamic calculations could be used to assess the short-range ordering hypothesis. A certain degree of short-range order is to be expected from qualitative considerations, since binary aluminium-copper alloys<sup>18, 19</sup> and copper-tin alloys<sup>20</sup> have a negative heat of solution, whereas aluminium-tin alloys<sup>21</sup> have a positive one.\* For simplicity it will be assumed that the behaviour of tin atoms is also typical of cadmium and indium.

##### 1. PREVIOUS WORK

Adoption of the nearest-neighbour assumptions<sup>22, 23</sup> allows the free energy of a binary solid solution to be written as:

$$F = n_{AA} V_{AA} + n_{BB} V_{BB} + n_{AB} V_{AB} - TS,$$

where  $n_{AA}$ ,  $n_{BB}$ , and  $n_{AB}$  are the numbers of AA, BB, and AB bonds, respectively.  $V_{AA}$ ,  $V_{BB}$ , and  $V_{AB}$  are the corresponding interaction bond energies for appropriate pairs of atoms.

It is easily shown that the configurational free

\* A thermodynamically negative heat of solution, usually taken as positive in thermochemistry, is associated with a

negative deviation from Raoult's law and an exothermic reaction.



energy of a statistical disordered solid solution may be put, in similar terms, as :

$$F_c = \frac{ZN}{2}[\alpha^2 V_{AA} + \beta^2 V_{BB} + 2\alpha\beta V_{AB}] + RT(\alpha \ln \alpha + \beta \ln \beta),$$

where  $Z$  is the co-ordination number,  $N$  is Avogadro's number, and  $\alpha$  and  $\beta$  the atomic fractions of A or B atoms.

By defining a term  $V_1 = 2V_{AB} - (V_{AA} + V_{BB})$  this equation can be transformed to :<sup>24</sup>

$$F_c = \frac{ZN}{2}[\alpha V_{AA} + \beta V_{BB} + \alpha\beta V_1] + RT(\alpha \ln \alpha + \beta \ln \beta) \quad (1)$$

Equation (1) conforms to the hypothesis of a "regular" solution.<sup>25, 26</sup>

The excess free energy of solution  $\Delta F_c$  is obtained from equation (1) by dropping the terms which are linear functions of  $\alpha$  and  $\beta$ , and will be used in the following treatment. This is formally equivalent to placing  $V_{AA} = V_{BB} = 0$ .  $V_1$  is zero for an ideal solution.

Takagi<sup>27</sup> examined the statistical mechanics of several binary lattices with order-disorder reactions. In the absence of long-range order all the expressions reduced to the same equation, which is readily written in a form similar to that of equation (1) :

$$\Delta F_c = \frac{ZN}{2}(\alpha - a)V_1 + \frac{ZRT}{2}[a \ln a + 2(\alpha - a) \ln (\alpha - a) + (1 - 2\alpha + a) \ln (1 - 2\alpha + a)] - RT(Z - 1)(\alpha \ln \alpha + \beta \ln \beta) \quad (2)$$

where  $a$  is the fraction of AA bonds out of all the bonds. For statistical disorder  $a = \alpha^2$ . Equation (2) is formally identical with equation (2.17) of Guggenheim and McGlashan,<sup>28</sup> except that the equilibrium value of  $a$  ( $= \bar{a}$ ) is presumed in the latter. With this assumption, equation (2) can readily be reduced to :

$$\Delta F_c = RT(\alpha \ln \alpha + \beta \ln \beta) + \frac{1}{2}ZRT\left(\alpha \ln \frac{\bar{a}}{\alpha^2} + \beta \ln \frac{\bar{b}}{\beta^2}\right)$$

where  $\bar{b}$  is the fraction of BB bonds out of all the bonds. This equation is formally identical with equation (2.29) of Guggenheim and McGlashan.<sup>28</sup>

The equation resulting from minimizing  $\Delta F_c$  with respect to  $a$ ,<sup>27</sup> fulfils the requirements of quasi-chemical equilibrium, and has been used by Guttman<sup>29</sup> and Oriani<sup>30</sup> to calculate the short-range ordering in  $\alpha$ -brass and  $\text{Cu}_3\text{Au}$  alloy.

The equation for the excess configurational free energy of a statistically disordered ternary solid solution is :

$$\Delta F_c = \frac{ZN}{2}[\alpha\beta V_1 + \beta\gamma V_2 + \gamma\alpha V_3] + RT(\alpha \ln \alpha + \beta \ln \beta + \gamma \ln \gamma) \quad (3)$$

$$\text{where } \left. \begin{aligned} V_1 &= 2V_{AB} - (V_{AA} + V_{BB}) \\ V_2 &= 2V_{BC} - (V_{BB} + V_{CC}) \\ V_3 &= 2V_{CA} - (V_{CC} + V_{AA}) \end{aligned} \right\} \quad (4)$$

and  $\alpha$ ,  $\beta$ , and  $\gamma$  are the atomic fractions of the A, B, and C atoms, respectively. Hirone and Katayama<sup>31</sup> calculated the tie-lines for certain ratios of  $V_1 : V_2 : V_3$ , and showed how these lead to typical equilibrium diagrams. A thorough examination of the effect of all positive and negative values of  $V_1$ ,  $V_2$ , and  $V_3$  on the form of the equilibrium diagrams has been given by Meijering.<sup>32, 33</sup>

No work appears to have been carried out on short-range order in ternary solid solutions. Guggenheim<sup>34</sup> has given a generalized partition function, but remarks that the explicit solution of short-range order is intractable.

## 2. PRESENT WORK

### (a) Theoretical

The following identities hold in a ternary solid solution :

$$\left. \begin{aligned} 2n_{AA} + n_{AB} + n_{AC} &= ZN_A \\ n_{AB} + 2n_{BB} + n_{BC} &= ZN_B \\ n_{AC} + n_{BC} + 2n_{CC} &= ZN_C \\ N_A = N\alpha, N_B = N\beta, N_C = N\gamma \end{aligned} \right\} \quad (5)$$

where  $n_{AA}$ ,  $n_{BB}$ , &c., are the numbers of AA bonds, BB bonds, &c.;  $N_B$  and  $N_C$  are the numbers of A, B, or C atoms, respectively;  $\alpha$ ,  $\beta$ , and  $\gamma$  are the atomic fractions; and  $Z$  is the co-ordination number.

Let  $a$  be the fraction of AA bonds,  $b$  of BB bonds,  $c$  of CC bonds,  $2p$  of AB bonds,  $2q$  of BC bonds,  $2r$  of CA bonds, and since the total number of bonds is  $ZN/2$  :

$$\left. \begin{aligned} n_{AA} &= \frac{ZN}{2}a & n_{BB} &= \frac{ZN}{2}b & n_{CC} &= \frac{ZN}{2}c \\ n_{AB} &= ZNp & n_{BC} &= ZNq & n_{CA} &= ZNr \end{aligned} \right\} \quad (6)$$

so that equation (5) gives rise to the following identities :

$$\left. \begin{aligned} a + p + r &= \alpha \\ p + b + q &= \beta \\ r + q + c &= \gamma \end{aligned} \right\} \quad (7)$$

$$a + b + c + 2p + 2q + 2r = \alpha + \beta + \gamma = 1$$

By adopting the combinatory method of Fowler and Guggenheim,<sup>35</sup> also used by Guggenheim and McGlashan,<sup>28</sup> the total number of distinct configurations in a ternary solid solution with short-range order can be written as :

$$g(N\alpha\beta\gamma a b c p q r) = \frac{N!}{N\alpha! N\beta! N\gamma!} \times \frac{(\frac{1}{2}ZN\alpha^2)! (\frac{1}{2}ZN\beta^2)! (\frac{1}{2}ZN\gamma^2)!}{(\frac{1}{2}ZN\alpha)! (\frac{1}{2}ZN\beta)! (\frac{1}{2}ZN\gamma)!} \times \frac{[(\frac{1}{2}ZN\alpha\beta)!]^2 [(\frac{1}{2}ZN\beta\gamma)!]^2 [(\frac{1}{2}ZN\gamma\alpha)!]^2}{[(\frac{1}{2}ZNp)!]^2 [(\frac{1}{2}ZNq)!]^2 [(\frac{1}{2}ZNr)!]^2} \quad (8)$$

The bond fractions for statistical disorder, namely :

$$\left. \begin{aligned} a &= \alpha^2 & b &= \beta^2 & c &= \gamma^2 \\ 2p &= 2\alpha\beta & 2q &= 2\beta\gamma & 2r &= 2\gamma\alpha \end{aligned} \right\} \quad (9)$$

have been used in setting up equation (8).

Using Stirling's formula to simplify the logarithm of equation (8) leads to :

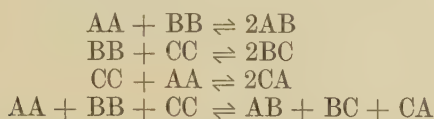
$$\Delta F_c = \frac{ZN}{2}(pV_1 + qV_2 + rV_3) - RT(Z-1) \\ (\alpha \ln \alpha + \beta \ln \beta + \gamma \ln \gamma) + \frac{ZRT}{2}(a \ln a + b \ln b + \\ c \ln c + 2p \ln p + 2q \ln q + 2r \ln r) \quad (10)$$

for the excess configurational free energy of solution, and is the logical extension of equation (2).

Suitably minimizing equation (10) yields :

$$\left. \begin{aligned} \frac{p^2}{ab} &= e^{-V_1/kT}, \quad \frac{q^2}{bc} = e^{-V_2/kT}, \\ \frac{r^2}{ca} &= e^{-V_3/kT}, \quad \frac{pqr}{abc} = e^{-(V_1+V_2+V_3)/2kT} \end{aligned} \right\} \quad (11)$$

which are exactly the equations which would be derived from the quasi-chemical equilibrium<sup>36, 37</sup> of the following bond reactions :



This identity of results follows because the combinatory method contains the hypothesis of the non-interference of pairs.<sup>34</sup>

Expressions (7) and (11) contain six independent equations which, in theory, allow the bond fractions to be solved in terms of the atomic fractions and energy constants  $V_1$ ,  $V_2$ , and  $V_3$  (equation (4)). In practice, the final equations containing only one of the variables  $a$ ,  $b$ ,  $c$ ,  $p$ ,  $q$ , or  $r$  are so complicated that they are useless, confirming Guggenheim's statement of their intractable nature.<sup>34</sup>

However, the bond fractions in the case of statistical disorder are readily found from equation (9) for any chosen alloy. Instead of attempting to solve between equations (7) and (11) for selected values of  $V_1$ ,  $V_2$ , and  $V_3$ , it is easier to alter the bond fractions from the values for complete disorder and to solve for the corresponding energy constants in equation (11). A series of trials readily leads to the desired values of  $V_1$ ,  $V_2$ , and  $V_3$ .

#### (b) Application to Alloys

Very approximate values of the energy constants can be derived from the equilibrium diagrams. The value of  $V_1$  and the critical temperature corresponding to complete solubility are obtained from equation (1) :

$$V_1 = \frac{4kT_c}{Z} = \frac{kT_c}{3}$$

and can be regarded as independent of temperature. Tin has only a very slight solubility in aluminium at 500° C.<sup>5</sup> The straight line resulting from plotting the logarithm of the tin content against the reciprocal of the absolute temperature gives  $T_c$  (0.5 tin soluble)  $\approx 10,000^\circ$  K. Mutual solubility would indicate a

lower value of  $T_c$ , but this figure will be used to show the maximum possible effect. Hence

$$V(\text{Al-Sn}) = \left( \frac{kT}{3} \cdot \frac{T_c}{T} \right)_{T=770^\circ \text{K.}} \approx (+5kT)_{T=770^\circ \text{K.}}$$

The value of  $V_1$  at the critical temperature corresponding to an  $A_2B$  order-disorder reaction in a body-centred cubic lattice is given by :<sup>38</sup>

$$V_1 = -2.92 kT_c$$

although the value is very dependent on the particular model chosen.

$V(\text{Al-Cu})$  and  $V(\text{Cu-Sn})$  have been taken as  $-2kT$  at 500° C. and  $V(\text{Al-Ni})$  as  $-4kT$ , since NiAl has one of the highest heats of formation.  $V(\text{Ni-Cu})$  is zero for an uninterrupted series of solid solutions with no ordering reactions.

The  $\beta$  phase of the copper-aluminium system was investigated first, as the atomic fractions involved were more suitable for numerical handling without practice than that of tin in the ternary aluminium-copper-tin alloys. The binary equilibrium diagram suggests that the  $\beta$  phase at 25 at.-% aluminium shows short-range ordering.<sup>40</sup> The ideal and chosen bond fractions of two copper-aluminium-nickel alloys are given in Tables V and VI. It will be seen that the "real" solutions show appreciable divergences from statistical disorder.

The ideal and chosen bond fractions for the aluminium-4 wt.-% copper-0.05 wt.-% tin alloy are set

TABLE V.—Ideal and Chosen Bond Fractions for Alloy Containing Cu 69, Al 23, Ni 8 at.-%.

	Ideal Solution	Chosen Solution
Bonds	Bond Fraction	Bond Fraction
Cu-Cu . . .	0.4761	0.4725
Al-Al . . .	0.0529	0.0100
Ni-Ni . . .	0.0064	0.0025
Cu-Al . . .	0.3174	0.3600
Al-Ni . . .	0.0368	0.0800
Ni-Cu . . .	0.1104	0.0750
	1.0000	1.0000
Numbers of nearest neighbours surrounding each . . .	Cu, Ni, or Al Atom	Ni Atom
	5.52 Cu	3.75 Cu
	1.84 Al	4.00 Al
	0.64 Ni	0.25 Ni
Corresponding energy constants : *		
$V(\text{Cu-Al})$ . . .	0	-1.92 $kT$
$V(\text{Al-Ni})$ . . .	0	-4.16 $kT$
$V(\text{Ni-Cu})$ . . .	0	-0.17 $kT$

\*  $V(\text{Cu-Al}) = 2V_{\text{Cu-Al}} - (V_{\text{Cu-Cu}} + V_{\text{Al-Al}})$ , &c.

out in Table VII. In order to give the required energy constants, each tin atom would have approximately  $2\frac{1}{2}$  copper atoms amongst its nearest neighbours which is ten times greater than the number in the statistically disordered solid solution.

Short-range ordering, giving rise to less than one or more than five copper atoms as nearest neighbours of tin atoms, could be regarded as significantly opposing or favouring the hypothesis of short-range order as a



TABLE VI.—Ideal and Chosen Bond Fractions for Alloy Containing Cu 73.5, Al 24.5, Ni 2.0 at.-%.

Bonds	Ideal Solution	Chosen Solution
	Bond Fraction	Bond Fraction
Cu-Cu . . .	0.54020	0.50432
Al-Al . . .	0.06000	0.01380
Ni-Ni . . .	0.00040	0.00012
Cu-Al . . .	0.36020	0.44200
Al-Ni . . .	0.00980	0.02040
Ni-Cu . . .	0.02940	0.01936
	1.00000	1.00000
Numbers of nearest neighbours surrounding each . . .	Cu, Ni, or Al Atom	Ni Atom
	5.88 Cu	3.872 Cu
	1.96 Al	4.080 Al
	0.16 Ni	0.048 Ni
		Al Atom
Corresponding energy constants: *		7.22 Cu
		0.45 Al
		0.33 Ni
$V$ (Cu-Al) . . .	0	-1.95 $kT$
$V$ (Al-Ni) . . .	0	-4.18 $kT$
$V$ (Ni-Cu) . . .	0	-0.38 $kT$

\*  $V$  (Cu-Al) =  $2V_{\text{Cu-Al}} - (V_{\text{Cu-Cu}} + V_{\text{Al-Al}})$ , &c.

TABLE VII.—Ideal and Chosen Bond Fractions for Alloy Containing Al 98.25, Cu 1.74, and Sn 0.01 at.-%.

Bonds	Ideal Solution	Chosen Solution
	Bond Fractions	Bond Fractions
Al-Al . . .	0.96530625	0.96508000
Cu-Cu . . .	0.00030276	0.00004100
Sn-Sn . . .	0.00000001	0.00000100
Al-Cu . . .	0.03419100	0.03468000
Cu-Sn . . .	0.00000348	0.00003800
Sn-Al . . .	0.00019650	0.00016000
	1.00000000	1.00000000
Numbers of nearest neighbours surrounding each . . .	Al, Cu, or Sn Atom	Sn Atom
	11.7900 Al	9.6000 Al
	0.2088 Cu	2.2800 Cu
	0.0012 Sn	0.1200 Sn
		Cu Atom
Corresponding energy constants: *		11.958 Al
		0.028 Cu
		0.013 Sn
$V$ (Al-Cu) . . .	0	-2.02815 $kT$
$V$ (Cu-Sn) . . .	0	-2.17520 $kT$
$V$ (Sn-Al) . . .	0	+5.01580 $kT$

\*  $V$  (Al-Cu) =  $2V_{\text{Al-Cu}} - (V_{\text{Al-Al}} + V_{\text{Cu-Cu}})$ , &c.

cause of easy nucleation. The figure of  $2\frac{1}{4}$  copper atoms around each tin atom must be regarded as indecisive. This number of tin atoms does not seem sufficient to lead to easy nucleation, but additional factors may operate. The grouping may involve sheets of tin atoms and, in any case, the calculations apply to mean values and do not indicate fluctuations

that would increase the number of copper atoms around some of the tin atoms.

### (c) Conclusions

The thermodynamic approach indicates that a certain degree of simple short-range grouping is to be expected. Ignorance of the exact values of the interaction energy parameters militates against a firm conclusion regarding its importance in the ageing processes of aluminium-copper-tin alloys.

### REFERENCES

1. A. H. Sully, H. K. Hardy, and T. J. Heal, *J. Inst. Metals*, 1949-50, **76**, 269.
2. H. K. Hardy, *ibid.*, 1950-51, **78**, 169.
3. H. K. Hardy, unpublished work.
4. H. K. Hardy, *J. Inst. Metals*, 1950-51, **78**, 657.
5. H. K. Hardy, *ibid.*, 1951-52, **80**, 431.
6. H. K. Hardy, *ibid.*, 1951, **79**, 321.
7. U. Dehlinger, *Physikal. Z.*, 1933, **34**, 836.
8. U. Dehlinger and F. Gisen, *ibid.*, 1934, **35**, 862.
9. F. Gisen, *Z. Metallkunde*, 1935, **27**, 256.
10. H. Bumm and U. Dehlinger, *Metallwirtschaft*, 1936, **15**, 89.
11. C. A. Edwards and J. H. Andrew, *J. Inst. Metals*, 1909, **2**, 29.
12. H. K. Hardy, *ibid.*, 1950, **77**, 457.
13. J. H. Hollomon, *Thermodynamics in Physical Metallurgy* (Amer. Soc. Metals), **1950**, 161.
14. D. Turnbull, *J. Chem. Physics*, 1950, **18**, 198.
15. V. J. Schaefer, *Science*, 1946, **104**, 457.
16. B. Vonnegut, *J. Appl. Physics*, 1947, **18**, 593.
17. A. Cibula, *J. Inst. Metals*, 1949-50, **76**, 321.
18. F. Weibke and O. Kubaschewski, "Thermochemie der Legierungen", p. 139. Berlin: **1943** (Springer Verlag).
19. G. Grube and P. Hantelmann, *Z. Elektrochem.*, 1942, **48**, 399.
20. F. Weibke and O. Kubaschewski, *loc. cit.*, p. 228.
21. F. Weibke and O. Kubaschewski, *loc. cit.*, p. 149.
22. E. A. Guggenheim, *Proc. Roy. Soc.*, 1935, [A], **148**, 304.
23. H. A. Bethe, *ibid.*, 1935, [A], **150**, 552.
24. R. Becker, *Z. Metallkunde*, 1937, **29**, 245.
25. J. H. Hildebrand, *Proc. Nat. Acad. Sci.*, 1927, **13**, 267.
26. J. H. Hildebrand and R. L. Scott, "The Solubility of Non-Electrolytes", 3rd edn. New York: **1950** (Reinhold Publishing Corp.).
27. Y. Takagi, *Proc. Phys.-Math. Soc. Japan*, 1941, [iii], **23**, 44.
28. E. A. Guggenheim and M. L. McGlashan, *Proc. Roy. Soc.*, 1951, [A], **206**, 335.
29. L. Guttman, *Trans. Amer. Inst. Min. Met. Eng.*, 1948, **175**, 178.
30. R. A. Oriani, *J. Appl. Physics*, 1950, **21**, 1068.
31. T. Hirone and T. Katayama, *Sci. Rep. Tohoku Imp. Univ.*, 1942, [i], **30**, 109.
32. J. L. Meijering, *Philips Research Rep.*, 1950, **5**, 333.
33. J. L. Meijering, *ibid.*, 1951, **6**, 183.
34. E. A. Guggenheim, *Proc. Roy. Soc.*, 1944, [A], **183**, 203, 213.
35. R. H. Fowler and E. A. Guggenheim, *ibid.*, 1940, [A], **174**, 189.
36. R. H. Fowler and E. A. Guggenheim, "Statistical Thermodynamics", pp. 350-366. Cambridge: **1949** (University Press).
37. G. S. Rushbrooke, *Proc. Roy. Soc.*, 1938, [A], **166**, 286.
38. "Introduction to Statistical Mechanics", p. 301. Oxford: **1949** (Clarendon Press).
39. R. H. Fowler and E. A. Guggenheim, "Statistical Thermodynamics," p. 602. Cambridge: **1949** (University Press).
40. F. C. Nix and W. Shockley, *Rev. Modern Physics*, 1938, **10**, 1.
41. W. Hume-Rothery, P. W. Reynolds, and G. V. Raynor, *J. Inst. Metals*, 1940, **66**, 191.

# RESIDUAL STRESSES IN CHILL-CAST AND CONTINUOUSLY CAST ALUMINIUM ALLOY BILLETS\*

1372

By R. A. DODD,† M.Sc., Ph.D., A.I.M., A.R.I.C., MEMBER

## SYNOPSIS

The effect of the following variables on the magnitude of the internal stresses in chill-cast (water-cooled mild-steel moulds) B.S.S. 2L42 (R.R.59) aluminium-alloy billets has been studied: (a) length of billet, (b) diameter of billet, (c) pouring temperature, and (d) rate of flow of cooling water.

The stresses were determined mechanically by Sachs's boring method, electric-resistance strain-gauges being used to measure the dimensional changes. The stresses are shown to be independent of the billet dimensions and of the rate of flow of the cooling water, but to increase approximately linearly with increase in pouring temperature.

Although the results are not directly comparable because of differences in alloy composition, the stresses were generally found to be considerably lower than those quoted by previous workers for billets directly sprayed with water, i.e. continuously cast, and only slightly higher than those found in chill-cast (air-cooled mould) billets. This is explained on the basis of the formation of an insulating air-gap between the water-cooled mould and the billet surface, and it appears that the relative coefficients of thermal expansion of the mould and casting are the most important factors determining the stress magnitude in castings of this type.

The effect of pouring temperature and rate of pouring on residual stresses in semi-continuously cast 17S (Superduralumin) billets has also been studied. Over the range investigated, temperature is shown to have little influence, but an increase in the pouring rate results in an increase in the stress, particularly in the longitudinal component. Certain of these observations that are at variance with those of previous workers are examined in detail.

## I.—INTRODUCTION

RESIDUAL stresses in cast cylindrical billets occur as a result of non-uniform cooling in the mould. The mechanism of stress formation, involving initial plastic deformation of the outer skin of the casting and subsequent inability of the core to contract fully, is well known, the final result, as thermal equilibrium is established throughout the metal mass, being that the outer layers of the casting are subjected to compressive stresses, balanced by tensile stresses in the core. The maximum compressive stress is at the billet surface, and the maximum tensile stress at the centre.

The magnitude of the internal stresses is determined by the temperature gradient from the centre to the surface of the casting during cooling; the steeper the gradient, the greater is the magnitude of the stresses. The stresses become of appreciable magnitude only as a result of a steep gradient such as is obtained by water-cooling. In industrial practice, therefore, interest centres largely in the high stresses formed during the continuous or semi-continuous casting of extrusion billets and rolling slabs. In the continuous process, after the metal has solidified in a short mould, it is directly sprayed with cold water, and this drastic quenching treatment frequently

results in the formation of internal stresses of such a magnitude as to cause internal or external cracking before or during subsequent fabrication.

## II.—PREVIOUS WORK

Many papers have been published on internal stresses in solution-treated and quenched cylindrical metal specimens and on stresses in cold-rolled rods, &c., but no attempt was made until 1942 to investigate stresses in cylindrical cast billets. In that year, Roth, Welsch, and Röhrig<sup>1</sup> investigated the variation in stress in continuously cast billets of eutectic aluminium-silicon alloy with certain factors, the stresses being measured on 35-cm. lengths of the billets by the boring method due to Sachs.<sup>2</sup> The results are illustrated in Fig. 1, and can be summarized as follows:

(a) *Effect of Pouring Speed.* (164-mm.-dia. billet).—Two speeds were investigated: 12 and 23 kg./min. Only negligible differences in stress were found (Fig. 1 (a)).

(b) *Effect of Irregularities in Pouring Speed.* (145-mm.-dia. billet).—An even rate of 9 kg./min. was compared with an irregular rate varying between 10 and 17 kg./min. over the experimental length of the billet. Irregularities in the pouring rate resulted in an appreciable increase in the magnitude of the

\* Manuscript received 28 April 1951.

† Department of Metallurgy, University of the Wit-

watersrand, Johannesburg, South Africa; formerly Research Fellow in Industrial Metallurgy, University of Birmingham.



longitudinal stress component (Fig. 1 (b)), of the order of 40% at the billet axis. The radial-stress component also increased perceptibly, while the tangential stress remained unchanged. The effect of cross-section of the billets with even pouring was not appreciable (cf. Figs. 1 (a) and (b)).

(c) *Effect of Length of Mould.* (164-mm.-dia. billet).—The use of a mould four times the normal length resulted in a considerable reduction in the stresses (Fig. 1 (c)).

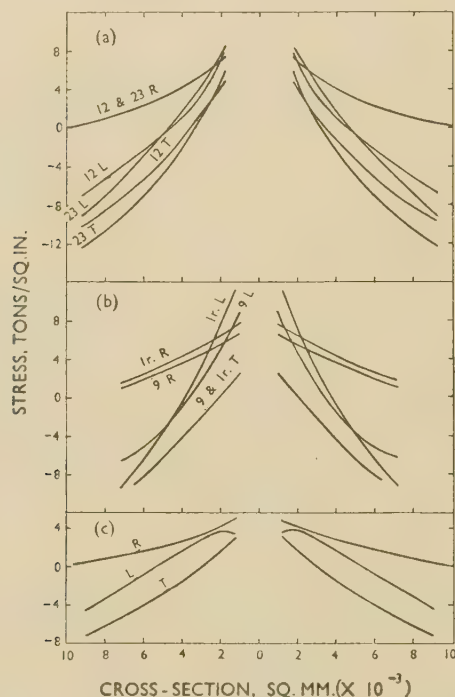


FIG. 1.—Effect on Stress in Continuously Cast Al-Si Billets of (a) Pouring Speed (164-mm.-dia. billet); (b) Irregularities in Pouring Speed (145-mm.-dia. billet); (c) Length of Mould ( $4 \times$  normal length; 164-mm.-dia. billet). (Roth, Welsch, and Röhrig.<sup>1</sup>)

L = Longitudinal stress. T = Tangential stress. R = Radial stress. Ir. = Irregularly poured. Figures refer to pouring speed in kg./min.

The paper by Roth *et al.* is the only published work of importance, although the presence of high internal stresses in continuously cast billets has been confirmed by Doyle,<sup>3</sup> who, using the X-ray-diffraction technique for stress measurement, found the tangential stress component at the surface of a  $4\frac{1}{2}$ -in.-dia. R.R.56 aluminium-alloy billet to be 11.9 tons/in.<sup>2</sup> (compressive), and the principal stress sum at the billet axis to be 10.5 tons/in.<sup>2</sup> (tensile).

This paucity of experimental data is probably mainly due to the fact that reliable methods for determining the stresses are tedious and experimentally complex, e.g. Sachs's boring method, but it is also likely that a certain amount of secrecy still attaches to the continuous method of casting.

### III.—SCOPE OF PRESENT INVESTIGATION

Particular importance attaches to the problem of internal stresses in continuously cast billets and slabs, but it was considered of interest to investigate first internal stresses in chill batch castings. In such billets, longitudinal temperature gradients are sensibly absent, and the radial temperature gradient is the sole factor determining the stresses, whereas in continuous casting the temperature gradients are much more complex.

The four variables chosen as likely to affect the temperature gradients, and hence the internal stresses, in water-cooled batch-cast billets were: billet length, billet diameter, pouring temperature, rate of flow of cooling water.

Research into continuous casting was restricted to a preliminary investigation into (i) pouring temperature and (ii) pouring speed. The billets were supplied by James Booth and Co., Ltd., and the variables were so chosen that no interference with normal production casting machines was necessary. It is not therefore implied that they have any major theoretical or practical significance, but simply that they represent the most convenient experimental cases and were thought likely to lead to measurable variations in stress. Moreover, these particular variables had, in part, been investigated by Roth and his co-workers and the results obtained would decide whether their conclusions were of universal application, or whether the nature of the stresses was a function of a combination of variables.

### IV.—EXPERIMENTAL PROCEDURE

#### 1. MATERIALS

The purpose of the research required that high stresses be developed in the castings, in order that the variables investigated should give rise to easily measurable changes in their magnitude. As the residual stresses in a metal body can never exceed the yield stress for that metal, it was necessary to use an alloy having a reasonably high yield stress in the chill-cast (water-cooled) condition. This requirement was met by the aluminium alloy to British Standard Specification 2L42\* (R.R.59), which when quenched from 525° C. into water at 20° C. has a yield stress of approximately 9.5 tons/in.<sup>2</sup>. This treatment approximates to chill casting, and the figure represents the upper limit of internal stress to be expected. The semi-continuously cast billets were of Super-duralumin (17S).†

#### 2. CASTING APPARATUS

A schematic representation of the casting apparatus is shown in Fig. 2 (a). The mould (A) consists of a welded 16-gauge mild-steel cylinder, the diameter of

\* Specification limits: Cu 1.5–3.0, Ni 0.5–1.5, Mg 1.2–1.8, Fe 1.0–1.5, Ti  $\geq$  0.2, Si  $\geq$  1.3%, Al remainder.

† Nominally Cu 4, Mg 0.5, Mn 0.5%, Al remainder.

which was varied between 3 and 6 in., and the length between 4 and 12 in. A base (*B*), also of 16-gauge mild steel, is welded on to the cylinder. The mould is supported on an angle-iron framework (*C*) by means of a steel plate (*D*),  $\frac{1}{4}$  in. in thickness, in which the mould is located by means of a recessed hole of the appropriate diameter. The mould is held rigidly in position by the screws (*E*) (Fig. 2 (*b*)). During the casting operation the mould is supported on refractory bricks, it being assumed that the thermal conductivity of these is too low to affect to any extent the

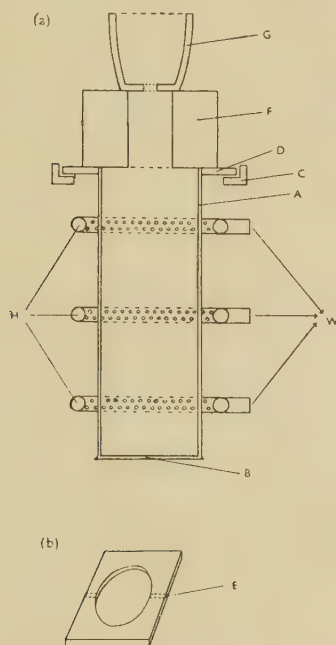


FIG. 2.—Billet-Casting Apparatus (for key see text).

temperature gradients in the cooling casting. Pipe formation in the casting is avoided by the use of a refractory "hot-top" (*F*) of  $6\frac{1}{2}$  in. dia. and 4 in. high, with a centrally situated, slightly tapered hole of 2 in. dia. which serves as a feeding head. The refractory top is separated from the metal plate (*D*) by a single thickness of asbestos paper, which is adequate to prevent leakage of liquid metal at this junction. Pouring is effected by the use as a liquid-metal reservoir of a small plumbago crucible (*G*), in the bottom of which is drilled a  $\frac{3}{8}$ -in.-dia. hole.

The charge required to produce a sound billet free from piping and yet insufficient to leave more than approximately 1 in. of solid metal in the refractory top was calculated from the known density and liquid-metal-contraction data of the alloy, and subsequently verified experimentally.

The cooling water is applied by means of annular sprays (*H*) made by bending and welding aluminium tubing. The spray holes are  $\frac{1}{32}$  in. in dia., the smallest size compatible with an uninterrupted water flow, and are so arranged that one spray is sufficient to cool uniformly a 4-in. length of mould. As the

diameter of the cast billets varied from 3 to 6 in., sprays of two different diameters, 6 and 8 in., were necessary. The sprays are connected to the main water supply (*W*) via a four-way junction and pressure gauge, the gauge being recalibrated in terms of rate of water flow through the sprays.

### 3. MELTING AND CASTING TECHNIQUE

The charge, which varied in weight between 7 and 35 lb. according to the billet dimensions, was melted in a gas-fired pit furnace and was suitably degassed and fluxed before casting. Pouring temperatures were measured potentiometrically, using a Chromel/Alumel thermocouple. The mould was coated with a water suspension of colloidal graphite and dried at  $150^{\circ}\text{C}$ ., while the refractory top and crucible were preheated to a temperature of the order of that of pouring and placed in position on the mould immediately before the operation. On completion of pouring, the water spraying was at once begun at the predetermined rate of flow and was continued for approximately  $\frac{1}{4}$  hr., at the end of which time the mould was quite cold.

### 4. STRESS MEASUREMENT

The stresses were determined by the method developed by Sachs,<sup>2</sup> which allows of the solution of a three-dimensional stress system in a cylindrical metal body. A hole is drilled up the centre of the cylinder, which is then bored out in steps, each of the order of 10% of the cross-section. The dimensional changes of the cylinder, i.e. changes in external diameter and length, are measured accurately after each successive step in the machining operation, and the residual stresses originally present in the cylinder are given by the following equations, deduced by Sachs on the basis of elasticity theory:

$$S_L = \frac{E}{1 - \nu^2} \left\{ (F_b - F) \frac{d\Lambda}{dF} - \Lambda \right\}$$

$$S_T = \frac{E}{1 - \nu^2} \left\{ (F_b - F) \frac{d\theta}{dF} - \frac{(F_b + F)}{2F} \cdot \theta \right\}$$

$$S_R = \frac{E}{1 - \nu^2} \left\{ \frac{(F_b - F)}{2F} \cdot \theta \right\}$$

where  $E$  = modulus of elasticity,  $\nu$  = Poisson's ratio,  $F_b$  = total cross-sectional area,  $F$  = area of bored-out cross-section,  $\Lambda = (\lambda + \nu\delta)$ , and  $\theta = (\delta + \nu\lambda)$ ,  $\lambda$  and  $\delta$  being the longitudinal and circumferential strains, respectively.  $S_L$ ,  $S_T$ , and  $S_R$  are the longitudinal, tangential, and radial stress components respectively at a point  $r_1$ , on the cross-section where  $F = \pi r_1^2$ . The differentials  $d\Lambda/dF$  and  $d\theta/dF$  are determined by drawing tangents to the curves obtained by plotting  $\Lambda$  and  $\theta$  against  $F$ .

An improved experimental technique utilizing electric-resistance strain-gauges, which obviates certain errors to which Sachs's method is liable and which has been described elsewhere,<sup>4</sup> was used throughout the research.



V.—EXPERIMENTAL RESULTS

1. BATCH-CAST BILLETS

Table I gives a set of results typical of those for batch-cast billets. The curve relating the strain functions  $\Lambda$  and  $\theta$  to the bored-out cross-section,  $F$ , from which  $d\Lambda/dF$  and  $d\theta/dF$  are derived, is shown in Fig. 3. This again is a typical curve, all curves relating to batch-cast billets being of the same form. The longitudinal, tangential, and radial stress components are shown plotted against percentage cross-section in Fig. 4.

Since the stress distribution was found to differ markedly from billet to billet, the effect of the variables investigated was assessed by plotting the areas under the curves of the longitudinal stress components (i.e. integrated stress) against the appropriate variable (Fig. 5). The choice of the longitudinal component was quite arbitrary, but the tangential and radial components were found to give similar results, i.e. the relationship between the three principal stress components appeared to be constant throughout the series of billets. This is in fact apparent from the stress curves.

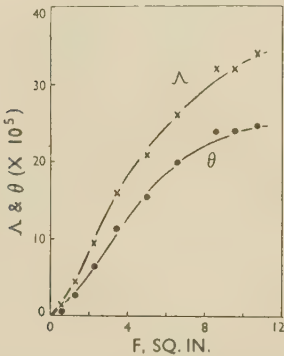


FIG. 3.—Typical Plot of Strain Functions  $\Lambda$  and  $\theta$  Against Bored-Out Cross-Section  $F$ . Values of  $\Lambda$ ,  $\theta$ , and  $F$  taken from Table I.

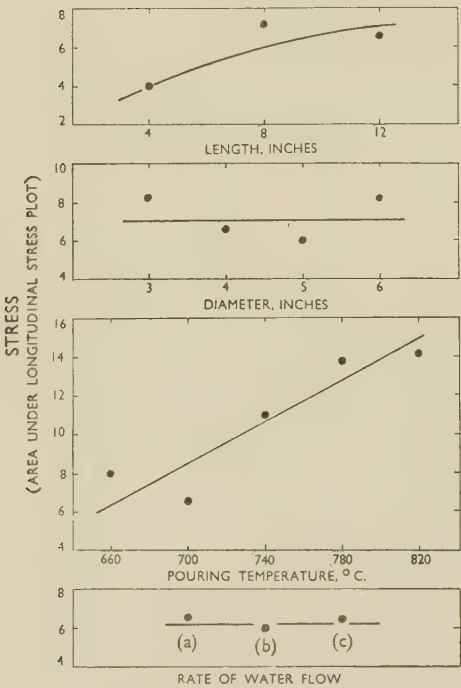


FIG. 5.—Effect of Variables on Magnitude of Residual Stresses in Water-Cooled Batch-Cast Cylindrical Billets. (a) 0.0023; (b) 0.0017; (c) 0.0011 ft.<sup>3</sup>/min./in.<sup>2</sup>.

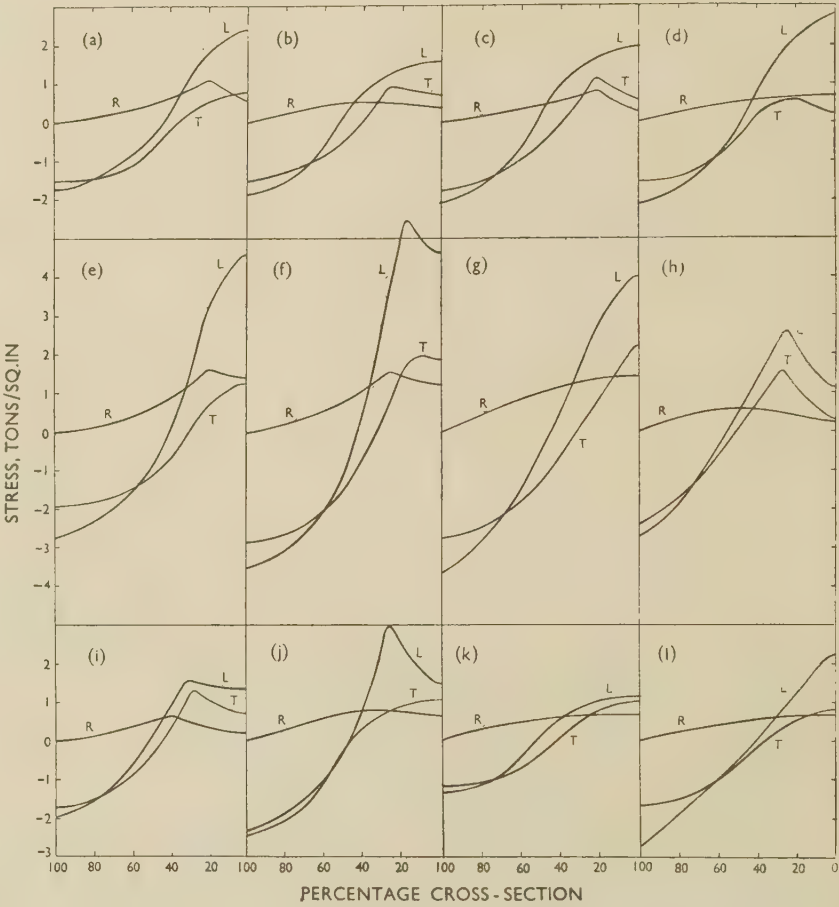


FIG. 4.—Residual Stresses in Water-Cooled Batch-Cast Cylindrical Billets.

KEY.

	Length, in.	Dia., in.	Pouring Temp., °C.	Water Flow, ft. <sup>3</sup> /min./in. <sup>2</sup>
a	12	4	700	0.00232
b			700	0.00172
c			700	0.00106
d			660	0.00232
e		740		
f		780		
g		820		
h		3	700	
i	5			
j	6			
k	4			
l	4			

TABLE I.—Typical Results Obtained by Applying Sachs's Method of Residual-Stress Analysis to Water-Cooled Batch-Cast Billets.

Length of billet, 12 in.; dia., 4 in.; pouring temperature, 700° C.; rate of water flow, 0.0023 ft.<sup>3</sup>/min./in.<sup>2</sup>.

$F$	$\lambda \times 10^5$	$\delta \times 10^5$	$\Lambda \times 10^5$	$\theta \times 10^5$	Stress, tons/in. <sup>2</sup>		
					Longi- tudinal	Tan- gential	Radial
0.64	1.4	...	1.4	0.5	2.52	0.96	0.58
1.33	4.1	1.4	4.6	2.8	2.43	0.90	0.70
2.27	8.3	3.8	9.6	6.6	2.20	0.76	0.95
3.46	13.9	6.8	16.2	11.4	1.12	0.35	0.81
4.91	18.0	9.7	21.2	15.7	0.10	-0.28	0.64
6.61	22.1	12.7	26.3	20.1	-0.60	-0.86	0.48
8.55	27.2	14.9	32.2	24.0	-1.22	-1.29	0.29
9.62	27.3	14.9	32.3	24.0	-1.45	-1.38	0.20
10.75	29.4	15.1	34.4	24.9	-1.63	-1.44	0.13

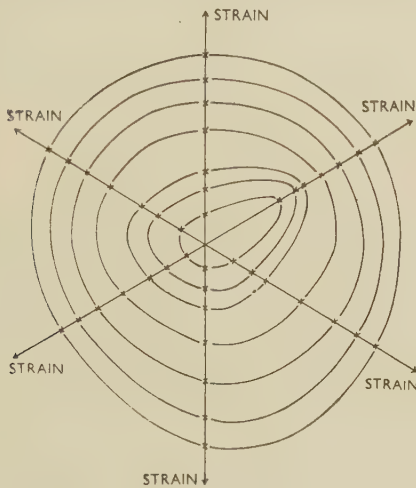


FIG. 6.—Degree of Symmetry of Stresses in Semi-Continuously Cast Billet.

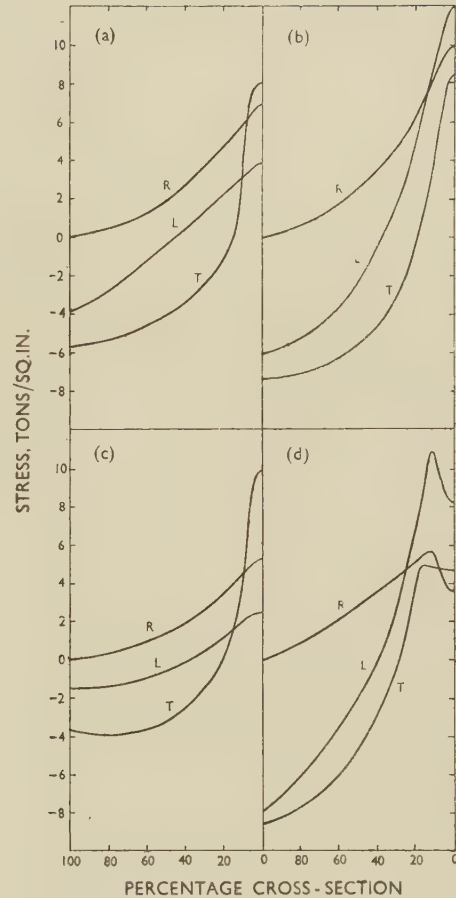


FIG. 8.—Residual Stresses in Semi-Continuously Cast Cylindrical Billets.

Key as Fig. 7.

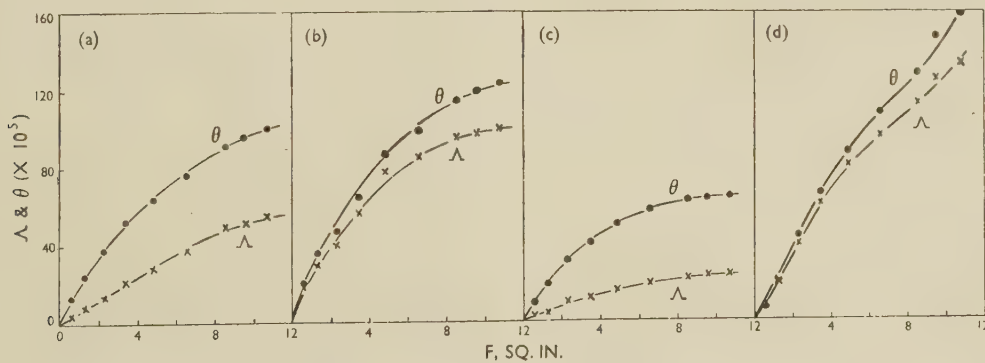


FIG. 7.—Plot of Strain Functions  $\Lambda$  and  $\theta$  Against Bored-Out Cross-Section  $F$  in Semi-Continuously Cast Billets.

KEY.

	Pouring Temp., °C.	Rate of Withdrawal, in./min.
(a)	650	4
(b)		8
(c)	700	4
(d)		8



TABLE II.—Results Obtained by Applying Sachs's Method of Residual Stress Analysis to Semi-Continuously Cast Billets, 12 in.  $\times$  4.1 in. dia.

(a) Pouring Temperature 650° C.; rate of withdrawal 4 in./min.

$F$	$\lambda \times 10^5$	$\delta \times 10^5$	$\Lambda \times 10^5$	$\theta \times 10^5$	Stress, tons/in. <sup>2</sup>		
					Longi- tudinal	Tan- gential	Radial
0.64	0.0	14.2	4.7	14.2	3.42	6.35	6.19
1.33	0.3	25.3	8.7	25.4	3.01	2.52	6.10
2.27	1.0	37.7	13.6	38.0	2.40	-1.10	5.44
3.46	5.0	51.3	22.1	53.0	1.74	-2.36	3.93
4.91	7.7	61.8	28.3	64.4	0.93	-2.99	2.88
6.61	13.5	72.3	37.6	76.8	-0.09	-3.62	2.02
8.55	22.5	83.0	50.2	90.5	-1.60	-4.62	1.27
9.62	23.2	87.6	52.4	95.3	-2.19	-4.99	0.95
10.75	23.5	93.0	54.5	100.8	-2.77	-5.30	0.58

(b) Pouring Temperature 650° C.; rate of withdrawal 8 in./min.

$F$	$\lambda \times 10^5$	$\delta \times 10^5$	$\Lambda \times 10^5$	$\theta \times 10^5$	Stress, tons/in. <sup>2</sup>		
					Longi- tudinal	Tan- gential	Radial
0.64	13.5	15.9	18.8	20.4	11.76	6.93	9.28
1.33	20.8	28.0	30.1	34.9	7.88	2.73	7.98
2.27	27.7	37.7	40.3	46.9	5.67	-1.42	7.09
3.46	39.8	52.1	57.2	65.4	2.84	-2.31	5.26
4.91	54.7	68.4	77.5	86.6	0.11	-3.89	3.88
6.61	59.2	79.0	85.5	98.7	-2.42	-5.46	2.70
8.55	65.2	92.8	96.1	114.5	-4.20	-6.51	1.65
9.62	65.2	99.3	98.3	121.0	-4.78	-6.83	1.21
10.75	65.2	102.0	99.2	123.7	-5.20	-6.98	0.72

(c) Pouring Temperature 700° C.; rate of withdrawal 4 in./min.

$F$	$\lambda \times 10^5$	$\delta \times 10^5$	$\Lambda \times 10^5$	$\theta \times 10^5$	Stress, tons/in. <sup>2</sup>		
					Longi- tudinal	Tan- gential	Radial
0.64	-0.4	9.8	2.9	9.7	2.21	8.40	4.90
1.33	-2.2	19.3	4.2	18.7	1.94	2.21	4.34
2.27	-1.1	32.4	9.7	32.0	1.52	0.42	3.73
3.46	-1.4	41.5	12.4	41.1	0.84	-1.10	3.04
4.91	-1.8	50.5	15.0	49.9	0.11	-2.47	2.23
6.61	0.0	57.7	19.2	57.7	-0.50	-3.31	1.51
8.55	1.8	61.3	22.2	61.9	-0.89	-3.78	0.88
9.62	2.1	62.3	22.9	63.0	-1.09	-3.73	0.63
10.75	2.0	63.3	23.1	64.0	-1.21	-3.62	0.37

(d) Pouring Temperature 700° C.; rate of withdrawal 8 in./min.

$F$	$\lambda \times 10^5$	$\delta \times 10^5$	$\Lambda \times 10^5$	$\theta \times 10^5$	Stress, tons/in. <sup>2</sup>		
					Longi- tudinal	Tan- gential	Radial
0.64	8.1	6.0	10.1	8.7	8.82	4.67	4.12
1.33	15.5	16.9	21.1	22.1	10.09	4.94	5.16
2.27	27.9	33.8	39.2	43.1	9.24	4.94	5.44
3.46	43.9	51.1	60.9	65.7	4.99	1.63	4.74
4.91	58.6	67.4	81.1	86.9	1.00	-2.57	3.88
6.61	67.9	86.4	96.7	109.0	-1.68	-4.46	2.86
8.55	79.0	101.9	113.0	128.2	-3.94	-5.88	1.87
9.62	85.7	118.1	125.1	146.7	-4.88	-6.72	1.44
10.75	91.0	129.0	134.0	159.3	-5.99	-7.72	0.92

## 2. SEMI-CONTINUOUSLY CAST BILLETS

The semi-continuously cast billets were 4.1 in. in dia. and 12 in. long, the required length being sawn from stock approximately 6 ft. in length. As it was thought that the sawing operation might lead to a reduction and redistribution of the residual stresses which would be manifest by an asymmetrical stress distribution round the billet axis, a billet was examined on which were glued longitudinally six resistance strain-gauges, at intervals of 60° round the circumference and half-way along the length, the strains recorded by these gauges on boring out the billet indicating the degree of symmetry of the stresses (see Fig. 6).

The results for the semi-continuously cast billets are given in Table II (a-d), and the plots of  $\Lambda$  and  $\theta$  against  $F$  in Fig. 7. The calculated stresses are shown in Fig. 8.

## VI.—DISCUSSION OF RESULTS

## 1. BATCH-CAST BILLETS

## (a) General Observations

The stresses in the billets were calculated using an average of three strain readings in both the longitudinal and circumferential directions. As these average strains resulted from individual readings differing in certain cases by as much as 50%, it is clear that the stresses were not, in general, symmetrical about the billet axes. Furthermore, the stress distribution was frequently such that the maximum tensile stress did not occur at the centre of the billet. It is probable that both the above observations are accounted for by the axis of maximum temperature being displaced from the longitudinal axis of the billet by uneven cooling, which was probably mainly due to the water sprays employed for cooling purposes. As already explained, these differences in stress distribution necessitated an assessment of the effects of the variables by plotting the areas under the longitudinal-stress curves against the appropriate variable.

Although not directly comparable because of differences in alloy composition, the results in general are intermediate in magnitude between those quoted by Roth and his co-workers<sup>1</sup> for continuously cast billets (maximum stress approx. 10 tons/in.<sup>2</sup>) and for chill-cast billets (maximum stress approx. 2 tons/in.<sup>2</sup>), which might be anticipated on the basis of the temperature gradients present during cooling. It appeared that the rate of cooling of the billets was retarded by the formation of an air-gap between the water-cooled mould and the billet surface, owing to the considerable difference in the coefficients of thermal expansion of the steel mould and the aluminium-alloy billet. The magnitude of the stresses is therefore largely determined by the temperature of the billet when the insulating effect of the air-gap becomes appreciable, this in turn depending on the

relative coefficients of thermal expansion of the mould and the casting.

### (b) Effect of Billet Dimensions

(i) *Length*.—As indicated in Fig. 5, the stresses are independent of billet length except when the latter is of the same order as, or less than, the diameter. Since cooling proceeds radially and no longitudinal temperature gradients are present, this result would be anticipated. The reduction in stress when the length : diameter ratio is reduced to, or below, 1 : 1 is due to the fact that although under these conditions chilling still occurs mainly in the radial direction, longitudinal temperature gradients are probably also present. In other words, "end-effects" become of appreciable magnitude.

(ii) *Diameter*.—Although the results plotted in Fig. 5 exhibit considerable scatter, the stresses appear to be independent of billet diameter. It must, then, be concluded that although the rate of cooling of the billet decreases with an increase in diameter (at constant length), the temperature gradients remain substantially unchanged. As previously stated, a similar conclusion was reached by Roth.<sup>1</sup>

### (c) Effect of Casting Variables

(i) *Pouring Temperature*.—It is evident (Fig. 5) that the stresses tend to increase with rise in pouring temperature. However, the limits of the temperature range investigated are well outside those normal in industrial practice, so that stress variations of the present order would not occur. To account for the increase in stress there must be an increase in the temperature gradient. This can be explained on the assumption that an increase in pouring temperature does not materially affect the time that elapses between pouring and the beginning of solidification, as observed by Paschkis<sup>5</sup> in the case of 4-in.-thick sand-cast steel plates. It must further be assumed that differences in the temperature gradient persist down to the temperature range at which residual stresses are set up, though temperature measurements would be required to verify this postulated mechanism.

(ii) *Rate of Flow of Cooling Water*.—Over the range investigated the stresses are independent of the rate of flow. It appears, then, that in each case the volume of cooling water was sufficient to extract heat from the casting at the maximum possible rate, a fact probably associated with the formation of the air-gap round the casting. Tests showed that a reduction in the rate of water flow below that used in the research resulted in uneven spraying, which rendered the test impracticable.

## 2. SEMI-CONTINUOUSLY CAST BILLETS

### (a) General Observations

Fig. 6 indicates the very high degree of symmetry of the stresses round the billet axis. No stress reduction or redistribution occurs as a result of the

sawing of the billet from the cast stock, and the stresses quoted are therefore true stresses, i.e. those actually present in the as-cast billets. The sawing operation may modify the stresses in the vicinity of the saw-cut but the effect does not extend to the region of the strain-gauges, which, being situated at the half-length position, are 6 in. away. It is possible that methods of strain measurement in which the total change in length is measured are liable to appreciable end-effect errors.

It will be noted from Table II (c) that throughout the whole series of boring operations very small longitudinal strains were measured, although the circumferential strains were considerable. If, therefore, an approximate method of stress measurement such as that of Heyn,<sup>6</sup> which assumes only longitudinal stresses to be present, had been used, the billet would have been reported as being free from residual stresses. In fact, as shown in Fig. 8, considerable stresses are present, the tangential stress at the centre of the billet attaining a value of 10 tons/in.<sup>2</sup>, although the longitudinal stress at the billet axis is, naturally enough, only of the order of 2 tons/in.<sup>2</sup>. In view of the fact that Heyn's and other approximate methods of stress measurement are still used to a considerable extent, it is important that their very serious shortcomings be fully realized.

### (b) Effect of Casting Variables

(i) *Pouring Temperature*.—It is evident (Fig. 8) that for pouring speeds of both 4 and 8 in./min. the effect of pouring temperature is, over the range investigated, very small, a slight decrease in stress being obtained at the higher temperature. The decrease does not, however, appear to be of any significance, and as the chosen temperatures represent the practical limits, it may be concluded that pouring temperature is of no importance as a stress-controlling variable in the range of experimental conditions studied. The observed decrease in stress may be due to the fact that at higher pouring temperatures the billet is at a higher temperature on final emergence from the cooling system, and a certain amount of stress relief is therefore able to take place before it finally cools down to room temperature.

(ii) *Pouring Speed*.—The effect of the speed of pouring is much more pronounced, a 50% reduction resulting in a very substantial decrease in stress. It is difficult to assess its effect on the overall rate of cooling because, although the billet cast at the lower speed emerges from the cooling system at a lower temperature, it has been in contact with the cooling system for a longer time, and the two factors of speed and time are not easily separated. It is clear, however, that a reduction in pouring speed leads to a reduction in the longitudinal temperature gradient, and an alteration in pouring speed would therefore be expected to affect mainly the longitudinal stress component. This is in fact observed. At a pouring temperature of 650° C. the longitudinal stress component at the billet axis is reduced from



13 to 4 tons/in.<sup>2</sup> for a reduction in pouring speed from 8 to 4 in./min., while the radial stress component is reduced only from 10 to 6 tons/in.<sup>2</sup> and the tangential stress component at the billet axis remains constant at 8 tons/in.<sup>2</sup>. A similar effect is observed with a pouring temperature of 700° C. It has already been remarked that the measured longitudinal strains in the case of billets cast at low speeds are very small, from which it follows that the longitudinal stress is entirely due to the Poisson effect.

These results are in contradiction to those of Roth, Welsch, and Röhrig,<sup>1</sup> who, for pouring speeds of 12 and 23 kg./min. (8.4 and 16.1 in./min.) found only negligible differences in stress. This may be due to the higher pouring speeds used in their work, and rendered possible by the relatively low-melting aluminium-silicon eutectic alloy which freezes at a fixed temperature instead of over a range. The fact that the two investigations employed billets of different diameters (6.46 and 4.1 in.) is perhaps not so important, in view of Roth's conclusion that stress is independent of diameter. The effects of volume of cooling water, &c., which may have differed in the two cases cannot, however, be disregarded, and further work is needed to investigate individually the effects of all the variables associated with the continuous-casting process.

## VII.—CONCLUSIONS

The main conclusions drawn from the work described are as follows:

(1) The residual stresses in batch-cast water-cooled aluminium-alloy billets seldom attain such a magnitude that their presence is likely to be of importance during subsequent fabrication of the billets.

(2) The stresses in these batch castings are mainly determined by the insulating air-gap which forms between the cooling casting and the steel mould, and are independent of billet dimensions and rate of flow of cooling water. They tend to increase with increase in pouring temperature, though this appears to be of no practical significance.

(3) The residual stresses in continuously cast aluminium-alloy billets vary markedly with casting conditions. Within the range of experimental conditions studied, the rate of pouring exerts an appreciable effect, a 50% reduction resulting in a considerable decrease in stress, particularly in the longitudinal component. The effect of pouring temperature is negligible, but in view of the differences between the results described in this paper and those quoted previously by Roth,<sup>1</sup> it is apparent that the stresses are a function of a combination of variables and the results are not, therefore, of universal application.

## ACKNOWLEDGEMENTS

The author wishes to thank Professor L. Aitchison and Professor A. J. Murphy for their interest and encouragement and Dr. V. Kondic for much valuable help and advice. Thanks are also due to James Booth and Co., Ltd., who supplied the continuously cast billets.

## REFERENCES

1. A. Roth, M. Welsch, and H. Röhrig, *Aluminium*, 1942, **24**, 206.
2. G. Sachs, *Z. Metallkunde*, 1927, **19**, 352.
3. W. M. Doyle, *Metal Ind.*, 1945, **66**, 370, 390.
4. R. A. Dodd, *Metallurgia*, 1952, **45**, (269), 109.
5. V. Paschkis, *Trans. Amer. Found. Assoc.*, 1948, **56**, 373.
6. E. Heyn, *J. Inst. Metals*, 1914, **12**, 3.

By W. A. WOOD,† D.Sc., MEMBER, and J. W. SUITER,† B.Sc.,  
STUDENT MEMBER

## SYNOPSIS

Previous work has shown that when annealed aluminium is slowly deformed at elevated temperatures the grains break down into a substructure, the size of which tends to an equilibrium value typical of the temperature and rate of deformation. In the present work the changes in strength and structure were observed during the deformation of aluminium in which the grains had already been broken down to a fine substructure by previous straining. It was found that growth of the fine substructure could be initiated within the grains, and that this could be controlled by suitably altering the temperature and the rate of strain. Further, the growth produced by such simultaneous heating and straining was of an order of magnitude greater than that obtainable by heating alone and sometimes termed "recovery". The new effects are therefore termed "stress-recovery". Finally, the strength of the metal under particular conditions of deformation was proved to be inversely proportional to the size of the substructure.

A general interpretation of the phenomenon is given on the view that the conditions of deformation determine the nature of the substructure, which in turn governs the strength of a metal.

## I.—INTRODUCTION

ATTENTION has recently been directed to the structural changes occurring during the slow deformation of aluminium at elevated temperatures, and the way in which the changes differ from those produced by ordinary deformation at room temperature.<sup>1-5</sup> The main finding has been that at the higher temperatures the grains do not deform by the ordinary slip mechanism but by one associated with the development of a coarse substructure, which has two outstanding features: (1) The size of the elements is determined by the conditions of deformation; in particular, if deformation proceeds at a fixed rate, then the elements tend to an equilibrium size characteristic of the temperature and strain rate, and this size becomes progressively larger with increase of temperature or decrease of strain rate. (2) The size of the elements appears to be closely related to the strength of the metal, which increases as the size of the element decreases. A point of special interest was that the strength did not change appreciably with continued deformation once the equilibrium size had been reached; that is, strain-hardening ceased.

In most of the earlier work, the metal before testing was in the annealed condition. The initial structure of each grain was therefore as nearly perfect as possible, and the process studied was essentially a breaking down of this perfect structure. In the present work, the reverse process has been investigated; the grains have been broken down by preliminary deformation, and the changes occurring during subsequent deformation of this broken-down condition have been studied.

A notable feature was a "building up" of the preliminary broken-down condition. By deformation at a particular temperature and strain rate the broken-

down structure could be made to grow within the grains to a coarse substructure of relatively perfect elements. Growth set in when the preliminary structure was smaller than the characteristic equilibrium size for the temperature and strain rate applied, and continued until that equilibrium size was attained. This growth was activated by straining rather than by heating. Thus, if two specimens with a similar initial substructure were held at the same temperature, one being unstrained and the other subjected to continuous straining, growth in the former was negligible in comparison with that in the latter.

A close connection was also observed between the size of the substructure and the strength of the metal, which provides direct support for the block or crystal-lite theory of strength.

## II.—EXPERIMENTAL PROCEDURE

(a) *Straining Apparatus*

The apparatus constructed was one which subjected a test specimen to a constant rate of strain at a constant temperature and was similar to that described by Polanyi.<sup>6</sup> The strength of the specimen became the stress required at each instant to maintain the particular rate of strain applied. It thus measured literally the resistance of the metal to deformation.

(b) *Specimens*

The test material, as in the earlier work, was aluminium of 99.98% purity. Flat tensile specimens were prepared with a parallel gauge-length of 1.7 in., 0.3 in. wide, and 0.06 in. thick. These were annealed to give a standard grain-size of about 0.02 cm., though a few specimens were prepared with a coarser

\* Manuscript received 8 August 1951.

† Baillieu Laboratory, University of Melbourne, Australia.



grain-size. The desired types of initial substructure were then produced by pre-straining; fuller details are given in describing the results on particular examples. The specimens were next electropolished to remove all slip lines or markings produced by the preliminary straining. Except for the main grain boundaries, the specimens therefore appeared structureless before testing.

### (c) Test Procedure

The pre-strained specimens were mounted in the machine and observations made of the variations in strength as they were extended at a chosen temperature and strain rate. A similar but unstressed specimen, placed in the furnace beside the main specimen, served to indicate to what extent, if any, the changes in the latter were due to heating alone. At intervals the extension was interrupted, and the specimens allowed to cool, to permit X-ray and metallographic examination to be carried out. Back-reflection diffraction patterns were obtained using cobalt  $K\alpha_1$ ,  $\alpha_2$  radiation.

## III.—STRESS-RECOVERY EFFECT

As already stated, simultaneous heating and straining produce large changes in the substructure, whereas heating alone causes minor changes only. The latter have already been extensively studied, being commonly referred to as "recovery" effects.<sup>7, 8</sup> It is proposed to designate the much more marked changes caused by simultaneous heating and straining by the term "stress-recovery". Previous isolated observations of the effect have been made independently by Wood and Scrutton,<sup>3</sup> and by Greenough and Smith.<sup>5</sup>

The specimen used in the experiments described below had a grain-size of 0.1 cm.; this was coarser than the standard size, but the changes in individual grains can be more easily seen. The initial deformed condition was produced by stretching 5.7% at 20° C. As might be expected, this extension resulted in great numbers of slip lines, which were removed by electropolishing to give the structureless appearance shown by Fig. 1 (Plate LXXI).

That the grains were considerably broken down internally is, however, clear from the X-ray-diffraction pattern of the initial state, which shows the usual transition from the sharp reflection spots typical of annealed grains (Fig. 2, Plate LXXI) to the apparently continuous arcs typical of deformed grains (Fig. 3, Plate LXXI). This transition is considered to indicate that the initially homogeneous grains have broken down to form a virtual mosaic of elements about  $10^{-4}$  cm. or less in size, an interpretation which has recently been supported by an interesting application of micro X-ray beams.<sup>9</sup> By their aid the apparently continuous arcs obtained from deformed aluminium can be resolved into fine but discrete spots, so proving that the reflecting units in the grains are themselves discrete elements. This fine structure of

the arcs can indeed usually be discerned by the ordinary X-ray technique, especially if the arcs are lightly exposed; under such conditions it is known that the separate reflection spots appear to coalesce as soon as the reflecting elements approach a size of about  $10^{-4}$  cm.

The onset of stress-recovery, induced in the present instance by straining at the rate of 0.15%/hr. at 250° C., first shows itself by the development of a coarse substructure (see Fig. 4, Plate LXXI, obtained after an additional 8% extension). The previously continuous arcs have broken up into well-marked separate reflection spots, showing that the corresponding reflecting elements in the grains are distinctly coarser than before the test. By comparison of the number of the spots on the ring, with those from materials of known grain-size, it was estimated that the size of the elements at this stage was about  $5 \times 10^{-3}$  cm. Examination of the X-ray pattern at earlier stages showed that growth began almost immediately on deformation, and continued with increasing strain, but at a slower and slower rate. At the additional 8% extension illustrated in Fig. 4, the substructure appeared to approach an equilibrium size. During this growth the grains did not deform by visible slip (Fig. 5, Plate LXXI), a rule which held for all specimens examined. This is significant because it confirms that slip is a process which breaks down the grains, and it would thus be impossible to have both the slip and the growth processes proceeding simultaneously. Instead of slipping, the grains developed a cellular appearance, as also illustrated by Fig. 5. This cellular structure was noted in earlier work,<sup>1</sup> and was then attributed to relative movements of the coarse elements to which initially annealed grains broke down during deformation. It would now appear that, even if the grains before straining are already broken down, the process of deformation inside the grains must produce a superposed set of sub-boundaries on a coarser scale. The growth of the preliminary substructure then proceeds within these coarse sub-boundaries.

## IV.—CELL GROWTH

When the cells are of a size that produces X-ray-diffraction arcs consisting of separate reflection spots, as in the experiment just described, there can be no doubt that they represent discrete elements within a grain. Having been brought to that size, they can be made to grow further, if desired, by raising the temperature of deformation or by reducing the rate of strain. The straining of the specimen at 250° C. was discontinued after 8% extension and the same specimen then formed the starting point for the following tests.

Fig. 6 (Plate LXXI) shows the change in the substructure produced by a further 4% deformation at 350° C., the rate of strain being 0.15%/hr. as before. If Fig. 6 is compared with Fig. 4, it is clear that the further deformation has greatly reduced the number of

reflecting elements in the grain, i.e. the elements are larger; the cell-size at this stage was estimated to have increased to  $10^{-2}$  cm. It has also caused the reflection spots to become scattered more uniformly around the diffraction ring, indicating that the orientation of the coarse cells departs progressively from the orientation of the parent grains, presumably as a result of continued movements associated with the process of deformation of the grains and of the specimen as a whole.

Increase in the temperature of straining to  $450^{\circ}\text{C}$ . produced still further growth of the substructure, confirming that the growth process is controllable and is related to the conditions of deformation. Straining of the same specimen was continued at  $450^{\circ}\text{C}$ . and at  $0.15\%$ /hr. and the resulting growth of the substructure is clear from Fig. 7 (Plate LXXI) obtained after  $4.7\%$  extension, which shows a still further reduction in the number of X-ray-reflection spots. Again, the grains did not deform by the ordinary slip mechanism, the absence of slip lines being evident from Fig. 8 (Plate LXXI), which shows the condition of the surface after deformation at  $350^{\circ}\text{C}$ .

The results of these two tests are typical of all those undertaken. The general principle, as already indicated, was that there appeared to be an equilibrium size of substructure for a given temperature and strain rate. If the preliminary substructure in a specimen subjected to deformation was less than the equilibrium value for the temperature and strain rate applied, then it would increase until that equilibrium was approached; if larger, then it would break down to that value. It is unnecessary to illustrate this latter case, since it corresponds, in effect, to beginning with specimens in the annealed state, which was the subject of the earlier work.

## V.—METALLOGRAPHIC OBSERVATIONS

The changes in the internal structure of the grains revealed by X-rays were not the product of recrystallization as normally defined. The usual test for recrystallization was made, the test specimen being electrolytically repolished to remove surface markings, and etched to bring up the grain boundaries. It was found in all cases that the grains present were the same as at the beginning of the tests and that no new boundaries had been produced at any point. Fig. 9 (Plate LXXII), a photomicrograph of the specimen after slow straining at  $350^{\circ}\text{C}$ ., shows essentially the same field of grains as in the initial state (Fig. 1). Only minor modifications have occurred in the shape of the grains, and these are due to ordinary boundary migrations. Elementary tests showed that if recrystallization were deliberately produced, the polishing and etching techniques employed invariably showed up a new set of grain boundaries.

\* To avoid accidental straining of the specimen, it was so mounted in the machine that a certain amount of slack had to be taken up before the tension was transmitted to the specimen. The time occupied by this stage, being small in

This persistence of the original grains provides full evidence that the substructures indicated by the X-ray photographs do in fact grow and change within the original grain boundaries. A further indirect confirmation is suggested by the characteristic wavy nature of the final grain boundaries (cf. Figs. 1 and 9). This feature is in keeping with the idea that the grains after deformation are virtually aggregates of irregularly shaped cells, so that the main grain boundary is built up out of the irregular sub-boundaries. The sub-boundaries can in fact be discerned in the grain indicated by arrows in Fig. 9, and they appear to set the shape of the main boundary.

It was found that the substructure could often be brought out visually by the following device. The specimen after straining was electropolished to remove strain markings and to provide a flat surface. It was then etched to bring up the main grain boundaries and such sub-boundaries as would respond to normal etching. Theoretically, all the sub-boundaries should become visible, because the X-ray observations show that neighbouring cells must differ in orientation. In practice, the difference was so small—estimated at about  $0.5^{\circ}$ —that the sub-boundaries did not always show up, and when they did so they were usually faint (Fig. 9). But if the specimen was then subjected to a small further deformation under the same or equivalent conditions, some relative movement of the cells occurred which was usually sufficient to disturb its surface contour at the sub-boundaries, so that the cells stood out prominently under the microscope. The condition of the surface of the test specimen after polishing and etching is shown in Fig. 9; the further extension of  $4.7\%$  applied slowly at  $450^{\circ}\text{C}$ . sufficed to emphasize the sub-boundaries in the manner described (Fig. 10, Plate LXXII).

One object of rendering the sub-boundaries visible was to examine their shape, shown by Fig. 10 and other photographs to be quite irregular. It was difficult to believe that such irregular shapes could result from the slip process; indeed it appeared that the cells bore no direct relation to the crystallography of the metal.

## VI.—CELL-SIZE AND MECHANICAL STRENGTH

The variations in strength during extension of the specimen previously described are plotted in Fig. 13, curve I.\* The extension at  $250^{\circ}\text{C}$ . is indicated by curve IA, the extension at  $350^{\circ}\text{C}$ . by curve IB, and that at  $450^{\circ}\text{C}$ . by curve IC.

### (a) Variation in Strength at One Temperature

The strength rises rapidly to a maximum when deformation begins and then falls away. The rise is caused by the specimen taking up the applied

comparison with the period of the test, is included in the time scale of the graph. During this initial interval, however, the specimen registers no stress.



stress. The maximum represents, in effect, the strength of the preliminary fine substructure, which has not had time to grow appreciably in the relatively short period required to reach the maximum. This was confirmed by X-ray examination. The subsequent fall in strength coincides with growth of the substructure within the grains, as already illustrated. This also was confirmed by X-ray examination. These observations were repeated on many other

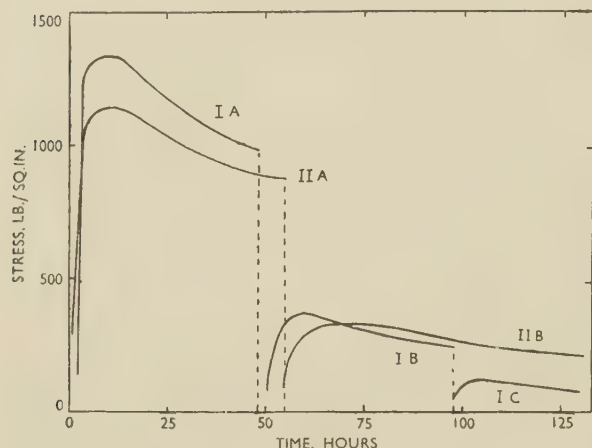


FIG. 13.—Strength/Extension Curves During Stress-Recovery.

Curve IA, extension at 250° C.; Curve IB, 350° C.; Curve IC, 450° C. (Specimen pre-strained 5.7%, grain-size 0.1 cm.)

Curve IIA, 250° C.; Curve IIB, 350° C. (Specimen pre-strained 3.3%, grain-size 0.02 cm.)

specimens, and the general conclusion reached that, to a first approximation, the strength of resistance to deformation exhibited by the metal is inversely proportional to the size of the substructure produced by that deformation.

#### (b) Variation in Strength with Temperature

As might be expected, the strength decreases with increasing temperature, but Fig. 13 brings out the point in an interesting manner, since it gives the strength of virtually the same substructure at two different temperatures. Thus, the end point on curve IA is the strength of a particular substructure at 250° C. The maximum to which curve IB rises when straining is continued at 350° C, is the strength of essentially the same substructure at that temperature, since, as already stated, no considerable growth could occur in the short interval taken in reaching that maximum. Therefore the difference in strength is due primarily to the difference in temperature. Thus, the resistance of the substructure to the applied strain rate falls from approximately 900 to 400 lb./in.<sup>2</sup> when the temperature is raised from 250° to 350° C. The corresponding fall between 350° and 450° C. is much less, from some 250 to 100 lb./in.<sup>2</sup>.

It is interesting to consider what the decrease in strength measures, for, as indicated, there is reason to believe that the major part of the deformation of specimens under the above conditions is associated

with relative movements of the grains at the main grain boundaries, and possibly to a lesser extent at the sub-boundaries. If this is so, then the measurements of strength give the "viscous" resistance of the disordered material at the grain boundaries. By extended measurements it would be possible to measure directly the dependence of this resistance on temperature and strain rate.

#### (c) Variation with Pre-Strain

The curves marked IIA and IIB in Fig. 13 show the variation in strength for a second specimen which had been subjected to a smaller extension at room temperature, namely, 3.3 as against 5.7%. The initial grain-size was also smaller, 0.02 as compared with 0.1 cm. They illustrate the behaviour of grains which initially were in a less broken-down condition. As might be expected, when this specimen was strained at 250° C. the strength of the initial substructure, shown by the early rise to a maximum, was less than for the first specimen. But after sufficient straining, as shown by curve IIB at 350° C., the specimens tended to the same order of strength; and X-ray examination showed that the substructure had reached the same order of size. This suggested that specimens which initially exhibited very different degrees of structural breakdown would always show the same size of substructure and same order of strength after sufficiently prolonged straining at the same temperature and strain rate. The results of other experiments which were carried out specifically on this aspect confirmed the point. Moreover, the same order of size and strength was reached when the test specimen was initially in the annealed condition. Thus, temperature and strain rate appear to be the overriding factors in determining the mechanical and structural behaviour.

### VII.—STRESS-RECOVERY VERSUS ORDINARY RECOVERY

By ordinary recovery is meant the changes that may be brought about, previous to recrystallization, merely by heating a pre-strained metal. It is known that in aluminium these changes often include some removal of strain-hardening,<sup>10</sup> and it has been shown recently that they may also involve detectable modifications of the deformed structure.<sup>8, 11</sup> It is not proposed to discuss these effects in detail here, since they have been treated extensively by many authors,<sup>7</sup> it is desired rather to show by direct experiment how they differ in important respects from those described in the present paper and referred to as "stress-recovery".

#### (a) Degree

A significant difference in magnitude between stress-recovery and ordinary recovery effects may be illustrated by a typical test. Two similar specimens were pre-strained by the same amount at room temperature, each being extended 17%. One specimen was then subjected to straining at 0.15%/hr.

at 250° C; the other was suspended alongside it in the furnace, free from any stress. When both specimens were examined by X-ray diffraction after similar periods of time, it was found that the strained specimen rapidly developed a substructure of relatively coarse but perfect elements in the manner already described, whereas the free specimen showed no signs of such a substructure. The contrast is evident on comparing Figs. 11 and 12 (Plate LXXII), obtained after some 70 hr. during which the strained specimen extended by 10%. The diffraction ring from the strained specimen is composed of clearly resolved reflection spots, whereas that from the free specimen is still continuous, as it was before heating. This result was obtained with all specimens sufficiently deformed to give a continuous diffraction ring, and it may be concluded that the growth produced by heating alone is negligible compared with that produced by simultaneous heating and straining, and also that straining plays an essential part in initiating the growth.

#### (b) Relation to Recrystallization

The use of a heavily pre-strained specimen for the test described above proved particularly valuable, because it was further found that no systematic substructure could be produced in the unstrained specimen by prolonging the heating at 250° C., or by heating at higher temperatures; instead, the specimen entered directly into the recrystallization stage. On the other hand, an equivalent specimen subjected to combined heating and straining showed no tendency to recrystallize, however prolonged the deformation. It appeared that the coarse substructure, once formed, resisted recrystallization. The only way to produce recrystallization in these tests was by using a heavily pre-strained specimen and subjecting it to such a high temperature of deformation that sufficient inducement was given for recrystallization to set in rapidly before the substructure associated with stress-recovery had an opportunity to form. This, however, was a very special case. Under other conditions, where recrystallization would normally involve heating for at least a few hours, it could occur in a pre-strained specimen which was heated only, but not in an equivalent specimen which was simultaneously heated and slowly strained. Evidently ordinary recrystallization, and what by analogy might be termed "stress-recrystallization", obey different laws because the preliminary ordinary recovery and "stress-recovery" are quite different in degree, if not in kind.

#### (c) Relation to Degree of Pre-Strain

It has been pointed out that during the stress-recovery of a pre-strained specimen the substructure appeared ultimately to reach the same order of size whatever the extent of the pre-straining, but it would be surprising if any substructure produced by heating alone, as in ordinary recovery, were independent of the pre-strained condition. Such evidence as is available shows that ordinary effects do in fact depend considerably on the pre-strained condition, as has been

discussed fully by Burgers.<sup>7</sup> This was confirmed by the present observations. Thus, signs of a substructure could be produced by heating alone much more easily in lightly worked and coarse-grained aggregates than in heavily worked specimens; the substructures, however, never had the clarity obtained with stress-recovery.

### VIII.—INTERPRETATION OF THE OBSERVATIONS

The final position may be summarized by reference to Fig. 14, which also serves to illustrate the interpretation placed by the authors on their present and related observations, and to provide a basis for discussing their possible contribution to current views on the processes of deformation.

Row (i) illustrates the essential effects as observed in a grain subjected to slow deformation at an elevated temperature, the grain being initially in the annealed state so that before straining (a) it is perfect and homogeneously oriented. After straining at a fixed slow rate and constant temperature, a coarse cell structure is developed, composed of equally perfect elements differing slightly in orientation (b). The size of the cells is characteristic of the temperature and strain rate; if the temperature is raised or the strain rate lowered, the size becomes larger (c). As far as can be ascertained by experiment, if this second temperature and strain rate had been applied in the first place, the annealed grain would have broken down directly to the size corresponding to (c) without going through a smaller intermediate size. Moreover, during the

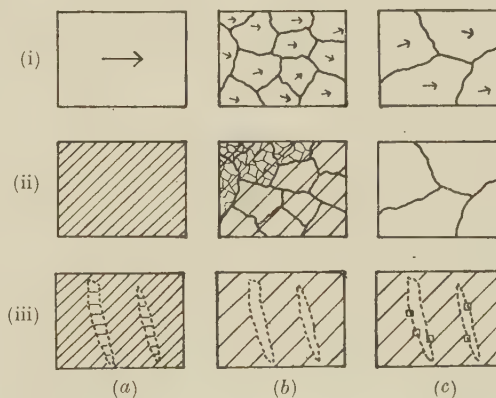


FIG. 14.—Row (i). Formation of Cell Structure by Slow Straining of Annealed Grain. Row (ii). Stress-Recovery by Slow Straining of Pre-Strained Grain. Row (iii). Ordinary Recovery by Heating Only of Pre-Strained Grain.

whole process, if the temperature was high enough and the strain rate low enough to produce cell formation, the deforming surface would show no signs of ordinary slip lines.<sup>4</sup>

Row (ii) illustrates the process of stress-recovery. It is supposed that pre-straining has occurred by the slip mechanism, as suggested by (a), producing a very fine substructure of disoriented elements. (It is



believed that this substructure is to be identified physically with the small blocks between the main slip lines and the still finer lamellæ which, as shown by the electron-microscope studies of Brown,<sup>12</sup> and of Heidenreich and Shockley,<sup>13</sup> compose the macroscopic slip lines themselves.)

It is then considered that the slow deformation at the elevated temperatures causes the grains to develop a coarse set of sub-boundaries independently of what fine substructure may be already present, as indicated by (b); and, moreover, that this superposed substructure is of the same order of size as that which would have been formed had the grains been in the annealed state at the beginning of the test. Otherwise it is difficult to explain why the ultimate size is practically independent of the degree of pre-straining, and why it is decided essentially by the temperature and strain-rate.

Next, it is supposed that the preliminary fine substructure within each of the coarse sub-boundaries progressively disappears, so that the ultimate condition of the grain, as indicated by (c), resembles the condition reached by grains that were initially in the annealed state. During the disappearance, intermediate sizes of substructure are observed. Therefore the disappearance presumably occurs by the preferential growth of some of the fine elements at the expense of others in the originally deformed substructure. The growth is possible because the sub-boundaries between the very fine elements are redundant in the new conditions of deformation, the coarse sub-boundaries alone being sufficient for the high-temperature deformation, as in the case of the annealed grain. Energy to activate the growth would be available from the removal of the redundant sub-boundaries; but it must also come from the strains introduced by the applied stress, since, as already shown, heating alone is insufficient to produce much growth.

Row (iii) contrasts stress-recovery with the process of ordinary recovery. One essential difference follows from the fact that heating alone, in comparison with simultaneous straining and heating, is relatively ineffective in activating growth inside a grain. This

suggests that heating is likely to affect only those regions in a grain that are excessively deformed. It is known from the work of Barrett and Levenson<sup>14</sup> and others that such areas, or deformation bands, invariably accompany deformation by slip. They are usually characterized by a different orientation from the parent grain, and this is indicated by the fuller representation of the pre-strained condition shown in (a). It is considered, then, that ordinary recovery in the first place consists largely of the removal of internal distortion in such deformation bands, with the resulting production of islands of relatively perfect structure in an otherwise deformed grain, as depicted by (b). Prolonged heating does not appear to produce appreciable further growth in aluminium but leads to formation of recrystallization nuclei as indicated by (c). These views have been confirmed by other experiments in the Baillieu Laboratory.<sup>15</sup> They are in keeping also with observations on recovery by Crussard<sup>16</sup> and by Cahn.<sup>11</sup>

In the second place, there is the possibility that recovery simplifies the heavily deformed regions associated with a single slip line by causing absorption of the multiple lamellæ composing the slip line into the main blocks between the slip lines. Reasons why a very thin lamella should become unstable in this way have been given by Bragg.<sup>17</sup> Their disappearance would also contribute to the partial removal of radial diffusion from the X-ray lines of cold-worked metals which has often been noted in specimens that have been heated.

The feature of ordinary recovery on this view, therefore, and its essential difference from stress-recovery, is that it results in a slight modification of the initial cold-worked condition and not in the creation of a new independent condition within the grains.

#### ACKNOWLEDGEMENT

The authors are deeply indebted to Professor J. N. Greenwood, University of Melbourne, for his invaluable advice and encouragement during the course of these experiments.

#### REFERENCES

1. G. R. Wilms and W. A. Wood, *J. Inst. Metals*, 1948-49, **75**, 693.
2. W. A. Wood and W. A. Rachinger, *ibid.*, 1949-50, **76**, 237.
3. W. A. Wood and R. F. Scrutton, *ibid.*, 1950, **77**, 423.
4. W. A. Wood, G. R. Wilms, and W. A. Rachinger, *ibid.*, 1951, **79**, 159.
5. G. B. Greenough and E. M. Smith, *ibid.*, 1950, **77**, 435.
6. M. Polanyi, *Z. techn. Physik*, 1925, **6**, 121.
7. W. G. Burgers, *Proc. K. Ned. Akad. Wetensch.*, 1947, **50**, 601.
8. R. W. Cahn, *J. Inst. Metals*, 1949-50, **76**, 121.
9. J. N. Kellar, P. B. Hirsch, and J. S. Thorp, *Nature*, 1950, **165**, 554.
10. P. C. Varley, *J. Inst. Metals*, 1948-49, **75**, 185.
11. R. W. Cahn, *ibid.*, 1951, **79**, 129.
12. A. F. Brown, *Metallurgical Applications of the Electron Microscope* (*Inst. Metals Monograph No. 8*), **1950**, 103.
13. R. D. Heidenreich and W. Shockley, *Phys. Soc.: Rep. Conf. on Strength of Solids*, **1948**, 57.
14. C. S. Barrett and L. H. Levenson, *Trans. Amer. Inst. Min. Met. Eng.*, 1940, **137**, 112.
15. J. A. Ramsey, private communication.
16. C. Crussard, *Rev. Mét.*, 1944, **41**, 111, 133.
17. W. L. Bragg, *Proc. Phys. Soc.*, 1940, **52**, 105.

# CREEP PROCESSES IN COARSE-GRAINED ALUMINIUM\*

1374

By D. McLEAN,† B.Sc., MEMBER

(Communication from the National Physical Laboratory.)

## SYNOPSIS

A specimen of super-pure aluminium was extended under a constant load of  $\frac{1}{2}$  ton/in.<sup>2</sup> at 200° C. to fracture, which occurred at 65% extension in 850 hr. Observations were made of slip-band and grain-boundary movements, on a previously polished surface. The movements were measured, mainly by means of an interference microscope, and their respective contributions to the creep extension calculated. They accounted for only about one-half of the total extension, and it was necessary therefore to seek the cause of the "missing" creep.

It was believed that fine slip, difficult to detect, or viscous flow might be responsible. Evidence was found that fine slip occurred throughout the extension, and polygonization in the second stage, the latter involving viscous flow by the diffusion of dislocations; there was also some evidence that the known breakdown of the original crystals into sub-crystals operated in this case by the specific mechanism of polygonization. It was possible to measure the orientation tilts between adjacent sub-crystals, and the creep extension attributable to fine slip was thus calculated to be of the same order of magnitude as the missing creep.

It is concluded that, under the conditions of the experiment, creep occurred by coarse slip, fine slip, and grain-boundary displacement.

## I.—INTRODUCTION AND RESULTS

EXPERIMENTAL evidence or theoretical arguments have been advanced in support of a number of creep-deformation mechanisms, and it is often supposed that the various stages of a typical creep curve are due to different processes. For example, the initial, transient, stage of relatively rapid, but decelerating, extension has been associated with normal work-hardening<sup>1</sup> and with grain interior slip.<sup>2</sup> The second stage of approximately constant rate of extension has been thought to represent a running balance between work-hardening and thermal softening,<sup>3,4</sup> or to be due partly to grain-boundary flow.<sup>2,5</sup> That such flow actually occurs has been demonstrated by Rosenhain and Humfrey.<sup>6</sup> Rotherham<sup>7</sup> has summarized the various points of view.

It was the aim of the present work to detect the various deformation processes operating in a particular case and to measure the creep extension due to each. The conditions applied produced a creep rate of about 3%/100 hr., a rate which, though well outside the domain of engineering practice, facilitated study. The grain-boundary and visible slip displacements were measured, and from the average displacements and the number of grain boundaries and visible slip bands, their individual contributions to the creep extension were calculated. It was found that at all stages the slip and grain-boundary contributions formed only about one-half of the total extension, so that, assuming the calculations to be correct, some other quite important process was involved. The work of Hanson and Wheeler<sup>8</sup> had indicated that this

was the case, but it was uncertain how much "missing" creep was to be expected.

Direct proof of deformation additional to that due to the grain boundaries and visible slip bands was obtained from some micrographs of the deformed specimen surface, which showed shear of considerable magnitude in the spaces between the visible slip bands. It was thought that fine slip, not easily detectable, and viscous flow due to stress-directed diffusion, might be responsible for the missing creep, and examination was accordingly made with the phase-contrast and the electron microscopes. Fine slip took place in the early stages, and both processes occurred in the later stages as part of the polygonization by which the original crystals broke down into sub-crystals, and which can be regarded as a combination of fine slip and a type of viscous flow. This flow consists of the diffusion of dislocations which necessarily occurs during polygonization and which probably contributes somewhat to the extension. Other evidence indicated that no viscous flow unrelated to the crystal structure occurred. A crucial point was reached when the extension attributable to fine slip was calculated from the tilts between neighbouring sub-crystals and was found to be of the same magnitude as the missing creep. The final conclusion was, therefore, that deformation occurred by easily visible slip, by grain-boundary displacement, and by fine slip, the sum of the individual contributions being of the same magnitude as the measured extension; there was no evidence of any other important process.

Because of the large grain-size of the specimen examined, grain-boundary displacement contributed

\* Manuscript received 27 October 1951.

† Metallurgy Division, National Physical Laboratory, Teddington.  
507



only a small part of the total creep extension. This process has, nevertheless, throughout been regarded as an important one, since, in the more general case of specimens of medium or small grain-size, a simple calculation shows its contribution to be large.

## II.—EXPERIMENTAL DETAILS

The specimen, of gauge-length  $2\frac{1}{2} \times \frac{3}{8} \times \frac{1}{4}$  in., was machined from strip produced from recast super-pure aluminium. The strip analysed 0.002–0.003% iron, 0.003% silicon, and 0.003% copper. After machining, the specimen was polished, annealed for 24 hr. at 325° C., furnace-cooled to 200° C., and finally electropolished to produce an unworked surface suitable for metallographic examination. The grain-size at this stage was such that 104 grain boundaries/cm. were intercepted by a straight line.

The specimen was then extended in creep by 2% at 200° C. under a load of  $\frac{1}{2}$  ton/in.<sup>2</sup>. Sufficient movement occurred at all grain boundaries for these to become easily visible. Recrystallization to a large grain-size, such that 21.7 boundaries/cm. were intercepted, was effected by heating to 270° C. The original boundaries were not obliterated, and acted as fine marker lines for measuring displacements parallel to the surface at slip bands and grain boundaries during subsequent creep.

During the subsequent straining evidence gradually accumulated that the recrystallized structure was not randomly orientated. This was advantageous in that only one set of slip bands occurred over most of the area of each crystal, and the interpretation of the deformation was thus simplified; but it was disadvantageous in that the rates of deformation might differ from those for a specimen of random orientation.

The specimen was then extended at 200° C. under a load of  $\frac{1}{2}$  ton/in.<sup>2</sup>, being periodically removed from the creep machine for examination and measurement. The curve of extension against time is given as "total creep" in Fig. 1. The extension excluding the necked region is also shown.

Measurements were made of the slip-band and grain-boundary displacements, the component normal to the specimen surface,  $v$ , and the component parallel to both the specimen surface and the direction of displacement as projected on to the surface,  $l$ , being measured separately; the latter is the displacement seen directly under the microscope. The measurements of  $v$  were made at first with a Linnik Zeiss \* interference microscope, giving a sensitivity of about 500 Å., but towards the end of the test, when the displacements became large, they were measured with a normal microscope, by determining with the fine-focus adjustment the shift in focus from top to bottom of the slip band or grain-boundary; the sensitivity was

then about 5000 Å. The measurements of the component parallel to the surface were made with a scale eye-piece and were sensitive to 5000–10,000 Å. To obtain a mean value for each measurement, 100 separate slip bands or grain boundaries, or on one occasion 200, were measured and averaged, except for the first few measurements of grain-boundary displacement, for which between 10 and 50 measurements were averaged. The slip bands and grain boundaries were chosen in a random way; the microscope stage was traversed a short distance without watching the field and the five slip bands measured nearest the centre of the arbitrary field thus brought into position; the stage was then

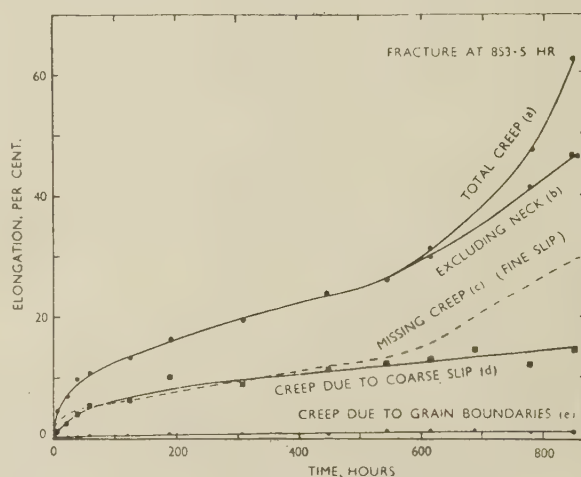


FIG. 1.—Curves Showing Total Creep and Contributions of Various Processes.

Curves (a) and (b) were measured directly; (d) and (e) were computed from measurements of slip-band and grain-boundary displacements; (c) was obtained by subtracting (d) + (e) from (b).

traversed a further short distance, and so on. A similar procedure was adopted for grain boundaries, ten successive boundaries being measured in each randomly chosen field.

A measure of the number of slip bands was obtained by counting the number intercepting a line parallel to the specimen length and 1 cm. long before creep began. So that the measurement should be an average over the specimen surface, the line was actually composed of five well-separated segments, each 0.2 cm. long.

## III.—STRUCTURAL FEATURES AND CHANGES OBSERVED

### 1. COARSE OR VISIBLE SLIP BANDS

The slip bands now discussed are those easily seen. As observed at high power with the optical microscope, they fell into three categories: (i) single slip

can be removed by placing a shutter in the path of the beam going to the reference surface, or their spacing and direction can be controlled by movement of an optical wedge in the path of the same beam. These facilities were particularly useful in the present work.

\* This is a two-beam interference microscope. The illuminating beam is split, one part going via the objective to the specimen, the other going via a similar objective to a reference reflecting surface. The two reflected beams are recombined and produce interference fringes. The fringes

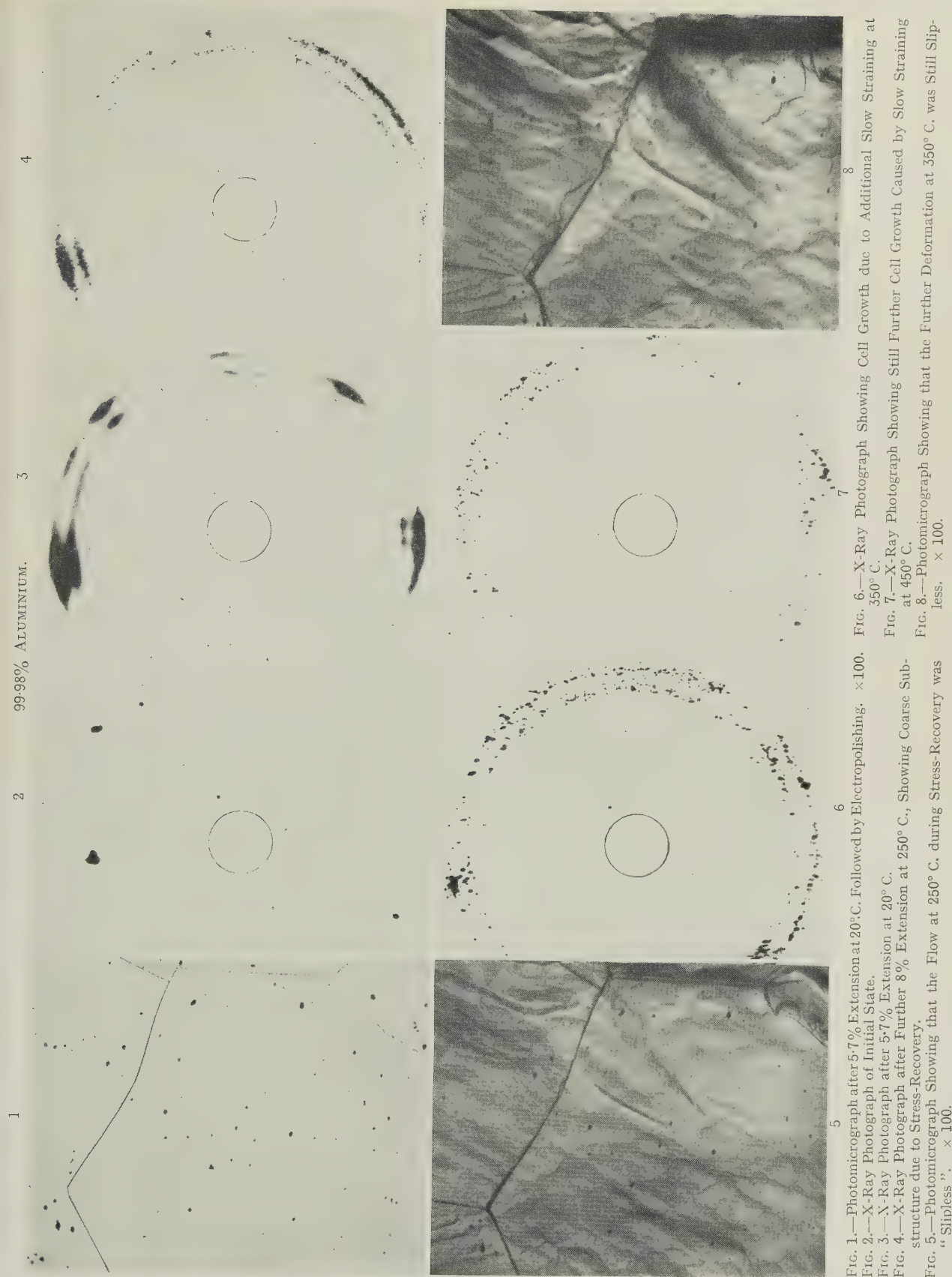


FIG. 1.—Photomicrograph after 5.7% Extension at 20°C. Followed by Electropolishing.  $\times 100$ .  
 FIG. 2.—X-Ray Photograph of Initial State.  
 FIG. 3.—X-Ray Photograph after 5.7% Extension at 20°C.  
 FIG. 4.—X-Ray Photograph after Further 8% Extension at 250°C., Showing Coarse Sub-structure due to Stress-Recovery.  
 FIG. 5.—Photomicrograph Showing that the Flow at 250°C. during Stress-Recovery was "Slipless".  $\times 100$ .

FIG. 6.—X-Ray Photograph Showing Cell Growth due to Additional Slow Straining at 350°C.  
 FIG. 7.—X-Ray Photograph Showing Still Further Cell Growth Caused by Slow Straining at 450°C.  
 FIG. 8.—Photomicrograph Showing that the Further Deformation at 350°C. was Still Slipless.  $\times 100$ .



## 99.98% ALUMINIUM.

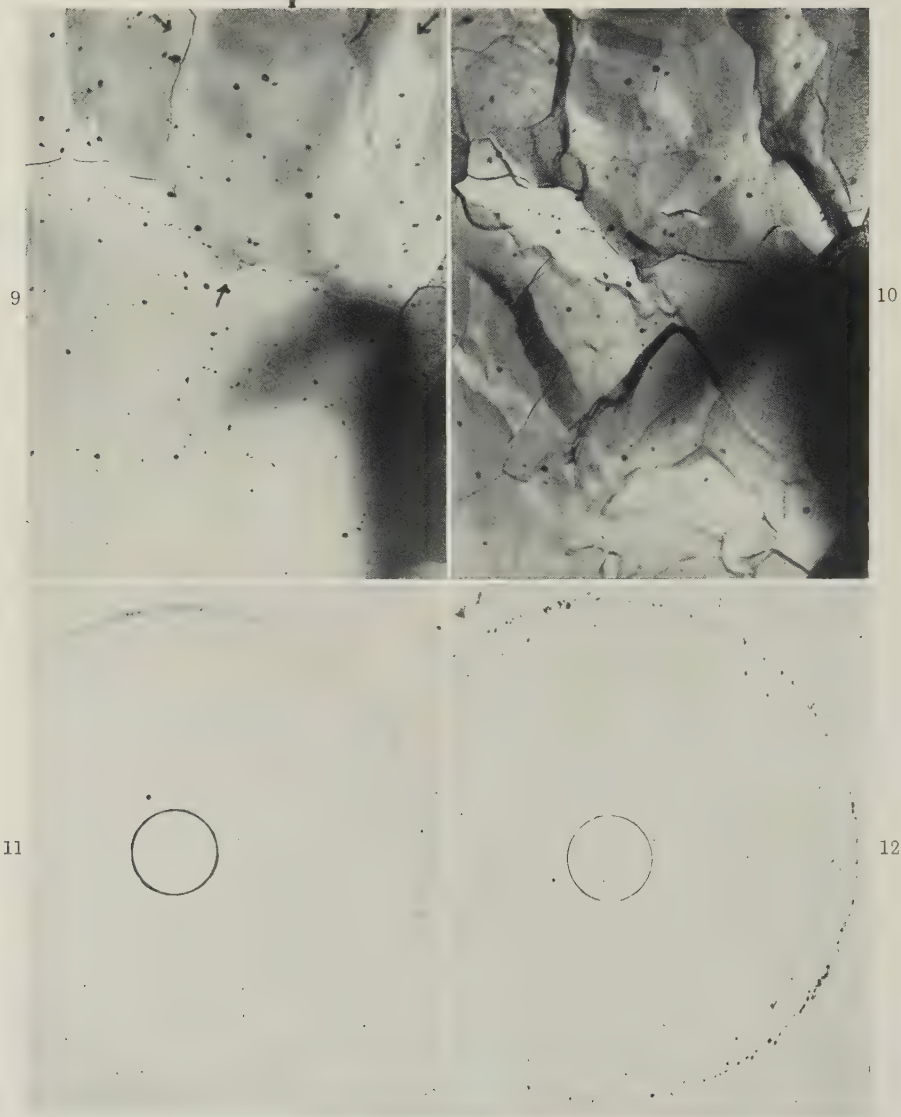


FIG. 9.—Photomicrograph of Specimen Repolished after Straining at 350° C., Showing Traces of Cell Structure but No Recrystallization.  $\times 100$ .

FIG. 10.—Photomicrograph of Specimen Strained at 450° C., Showing Emphasized Cell Structure.  $\times 100$ .

FIG. 11.—X-Ray Photograph of Specimen Pre-Strained 17% at 20° C., then Heated for 70 hr. at 250° C., Showing Negligible Effect of Ordinary Recovery.

FIG. 12.—X-Ray Photograph of Specimen Pre-Strained 17% at 20° C., then Slow-Strained for 70 hr. at 250° C., Showing Marked Effect of Stress-Recovery.

## VISIBLE SLIP BANDS IN COARSE-GRAINED ALUMINIUM.

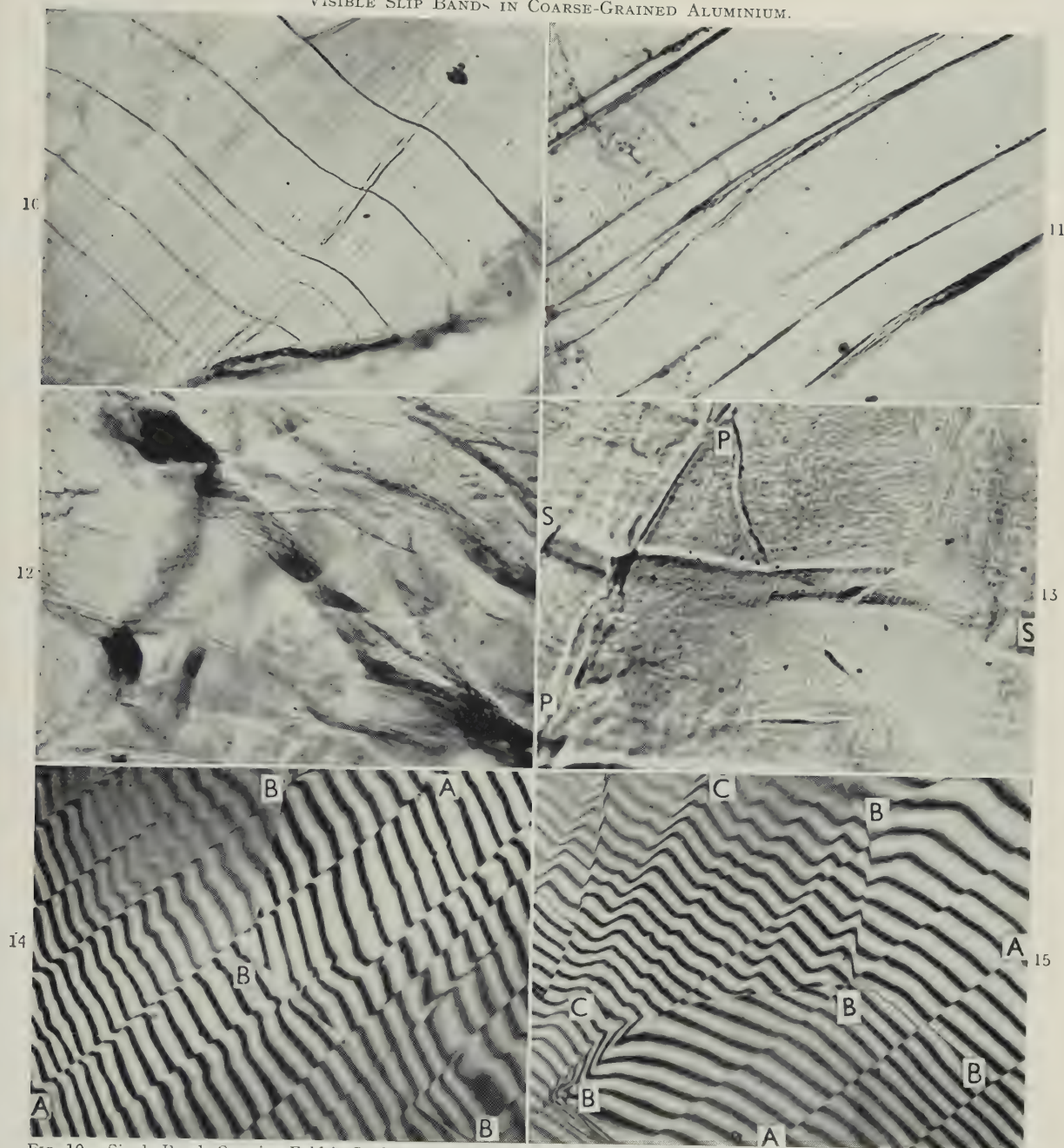


FIG. 10.—Single Bands Crossing Fold in Surface Caused by Polygonization. 31.2% Elongation.  $\times 1000$ .

FIG. 11.—Multiple Bands. 31.2% Elongation.  $\times 1000$ .

FIG. 12.—Very Complex Deformation Involving Multiple Bands. Necked region;  $>100\%$  elongation (after 848 hours' creep).  $\times 750$ .

FIG. 13.—Wide Band. 47% Elongation.  $\times 1000$ .

FIG. 14.—Interference Micrograph Showing Slip Bands (AA) and Old Grain Boundaries (BB). 7.1% Elongation.  $\times 500$ .

FIG. 15.—Interference Micrograph Showing New Slip Bands (AA), Old Slip Bands (CC), and Old Grain Boundaries (BB). 7.1% Elongation.  $\times 500$ .



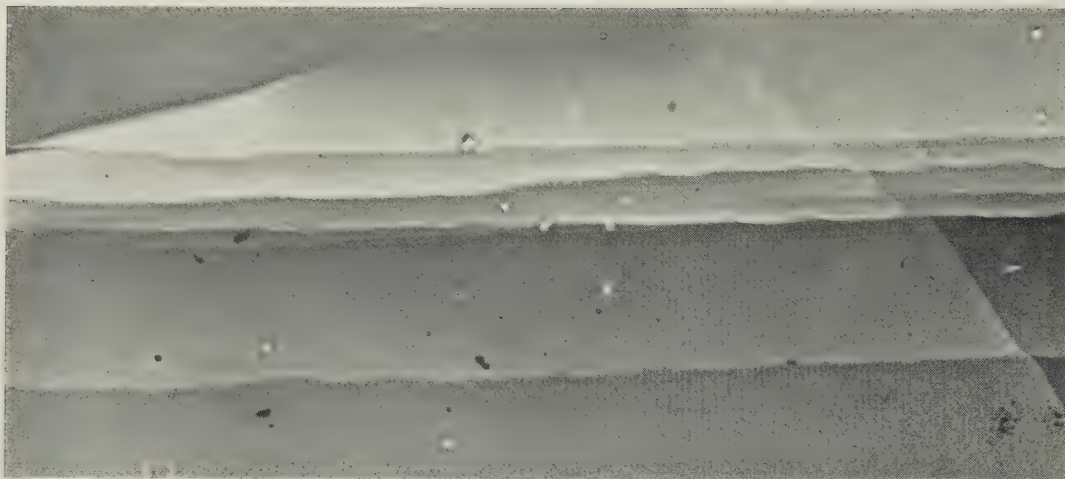


FIG. 16.—Electron Micrograph Showing Serrated Structure of Slip Bands. 4.6% Extension. Unshadowed plastic replica.  $\times 5000$ . (Trotter.)



FIG. 17.—Optical Micrograph Showing Serrated Structure of Slip Band. 47% Elongation.  $\times 1500$ .

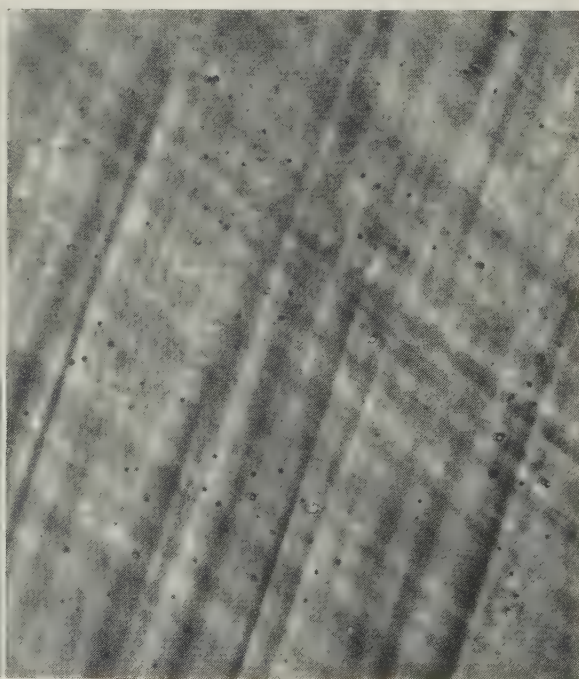
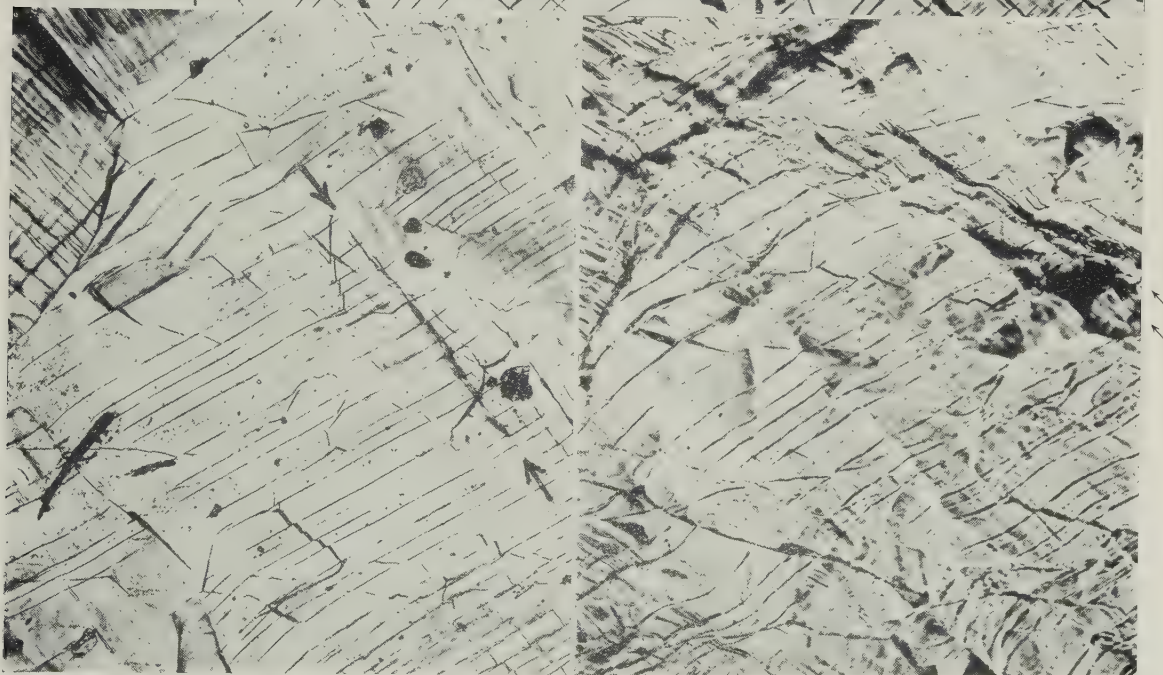
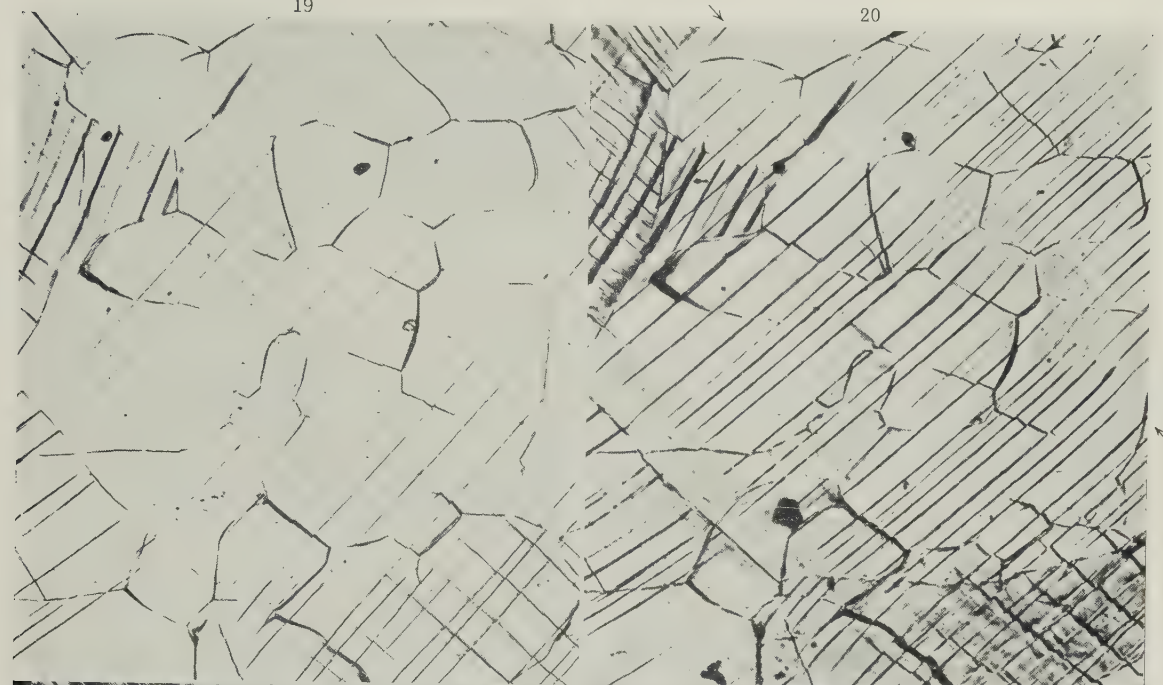


FIG. 18.—Phase-Contrast Micrograph Showing Fine Slip at 0.9% Extension.  $\times 1500$ .

## SLIP PROCESSES IN SAME FIELD AT INCREASING EXTENSION.

19

20



21

22

FIG. 19.—4.6%.  
FIG. 21.—16.4%.

FIG. 20.—9.5%.  
FIG. 22.—46.6%.

All  $\times 150$ .Arrows point to a prominent bend in the slip bands (polygonization fold). Specimen length axis  $\longleftrightarrow$



## SLIP PROCESSES IN SAME FIELD AT INCREASING EXTENSION.

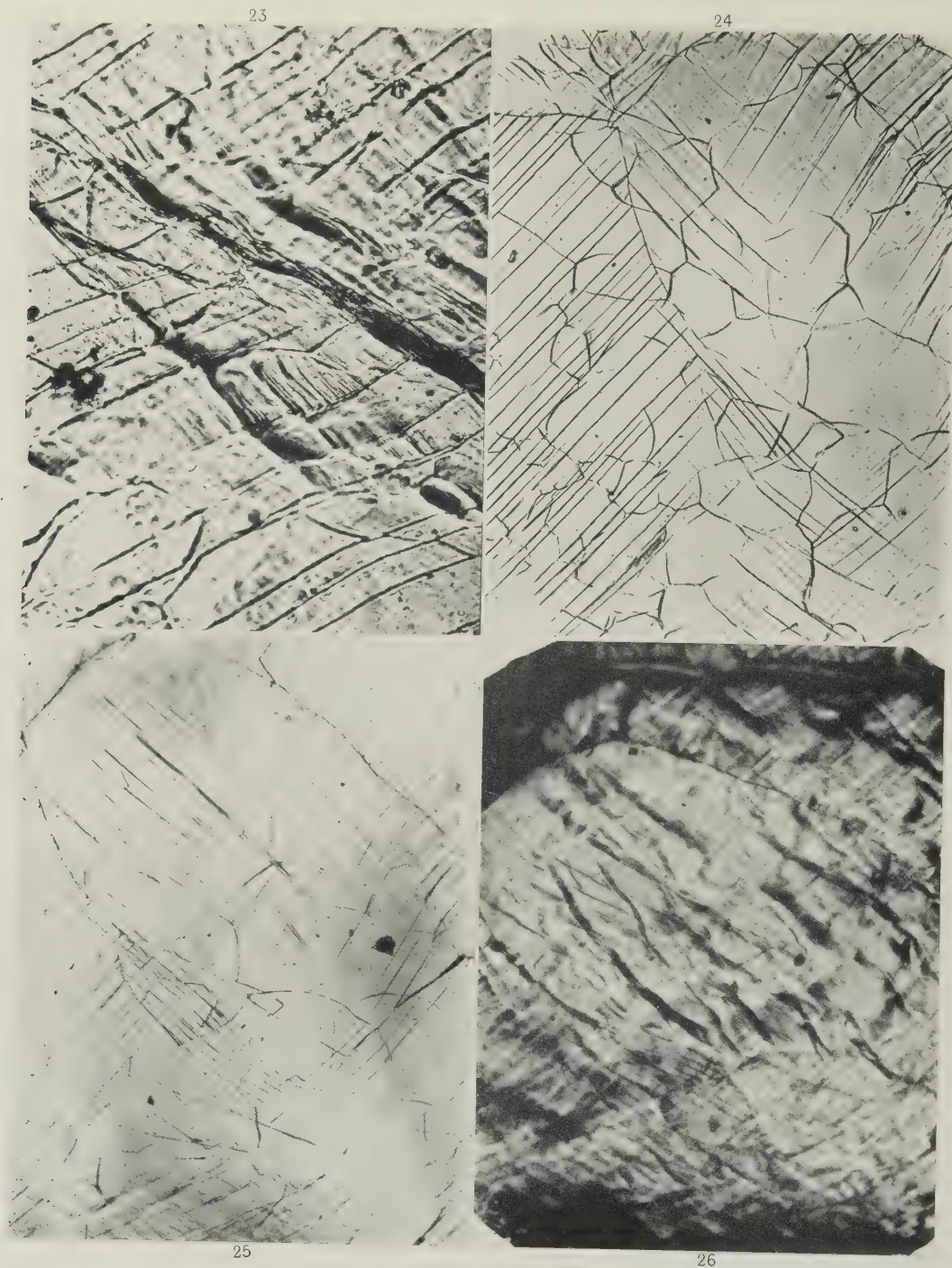


FIG. 23.—Part of Field of Figs. 19–22 at Higher Power Showing Stepped Structure in Polygonized Band. 41% extension.  $\times 500$ .

FIGS. 24–26.—Crystal Containing Two Sets of Slip Bands, Showing Development of Multiple Bands, Polygonization Folds, and Grain Rotation.

FIG. 24.—4.6%.

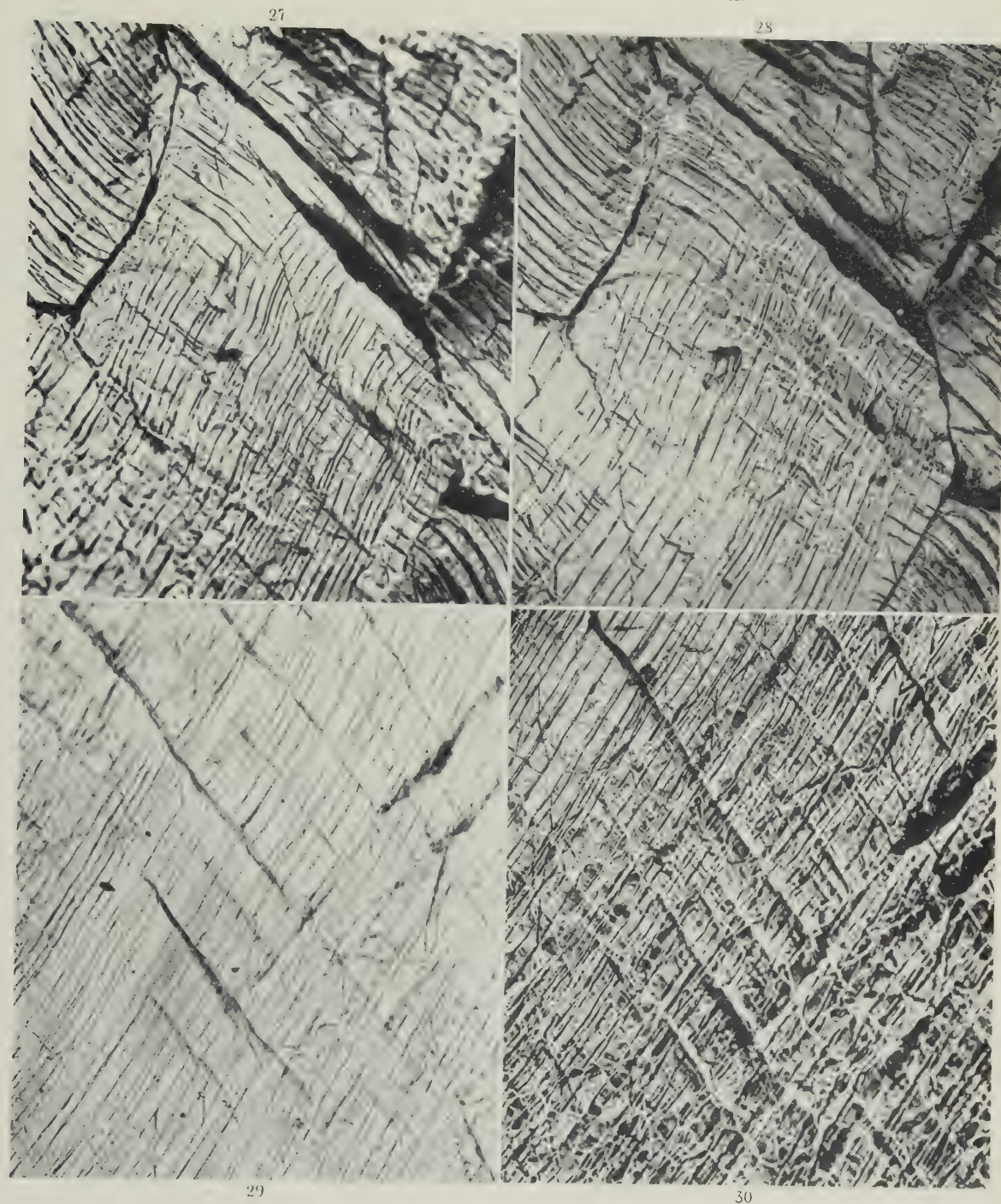
FIG. 25.—13.5%.

FIG. 26.—45%.

All  $\times 100$ . Specimen length axis  $\longleftrightarrow$ .



## POLYGONIZATION IN COARSE-GRAINED ALUMINIUM.

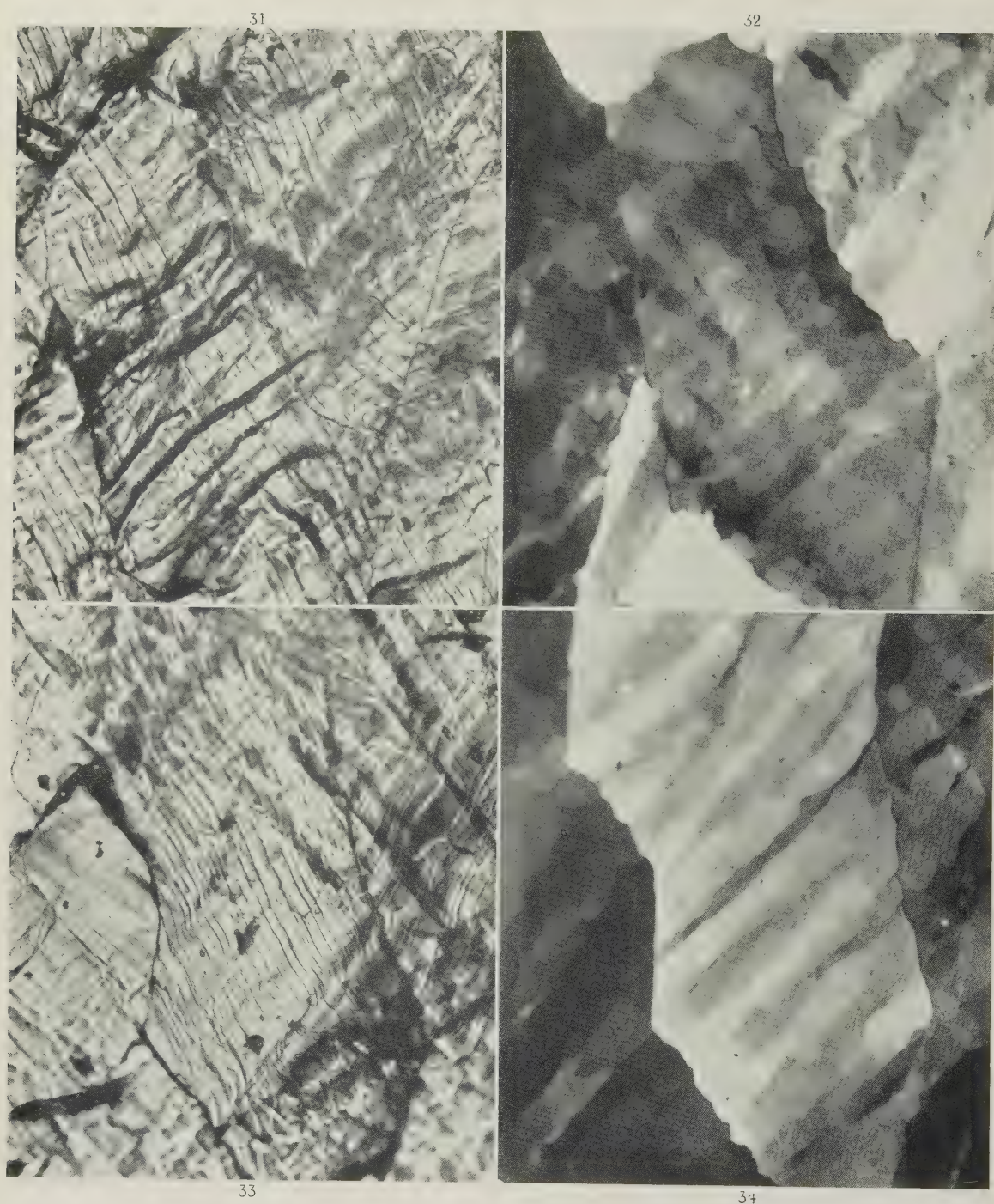
FIGS. 27-30.—Al 31.2% Extension.  $\times 150$ .

FIGS. 27 and 29 in focus, nearly full aperture.

FIGS. 28 and 30 racked about  $35\mu$  inside focus, small aperture. The white lines are an optical effect and indicate convex bends in the surface.



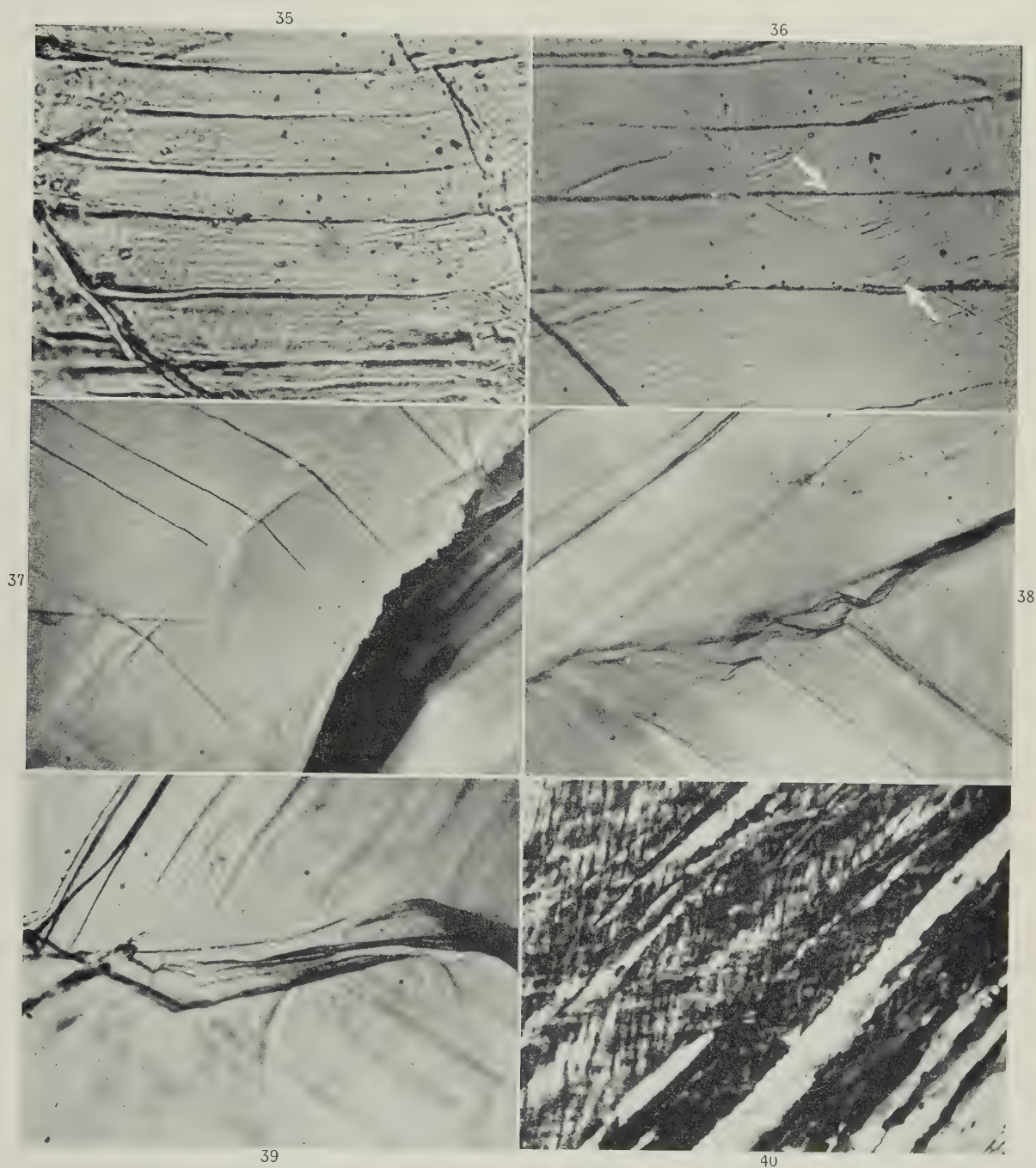
## POLYGONIZATION IN COARSE-GRAINED ALUMINIUM.



FIGS. 31 and 33.—Surface Appearance After 47% Elongation (853 hours' creep), Showing Slip Bands and Polygonization Folds. FIGS. 32 and 34.—Same Field as Figs. 31 and 33 respectively After Polishing Flat and Anodic Oxidation. Banding parallel to polygonization folds and slip bands. Photographed under crossed polaroids.

All  $\times 150$ .

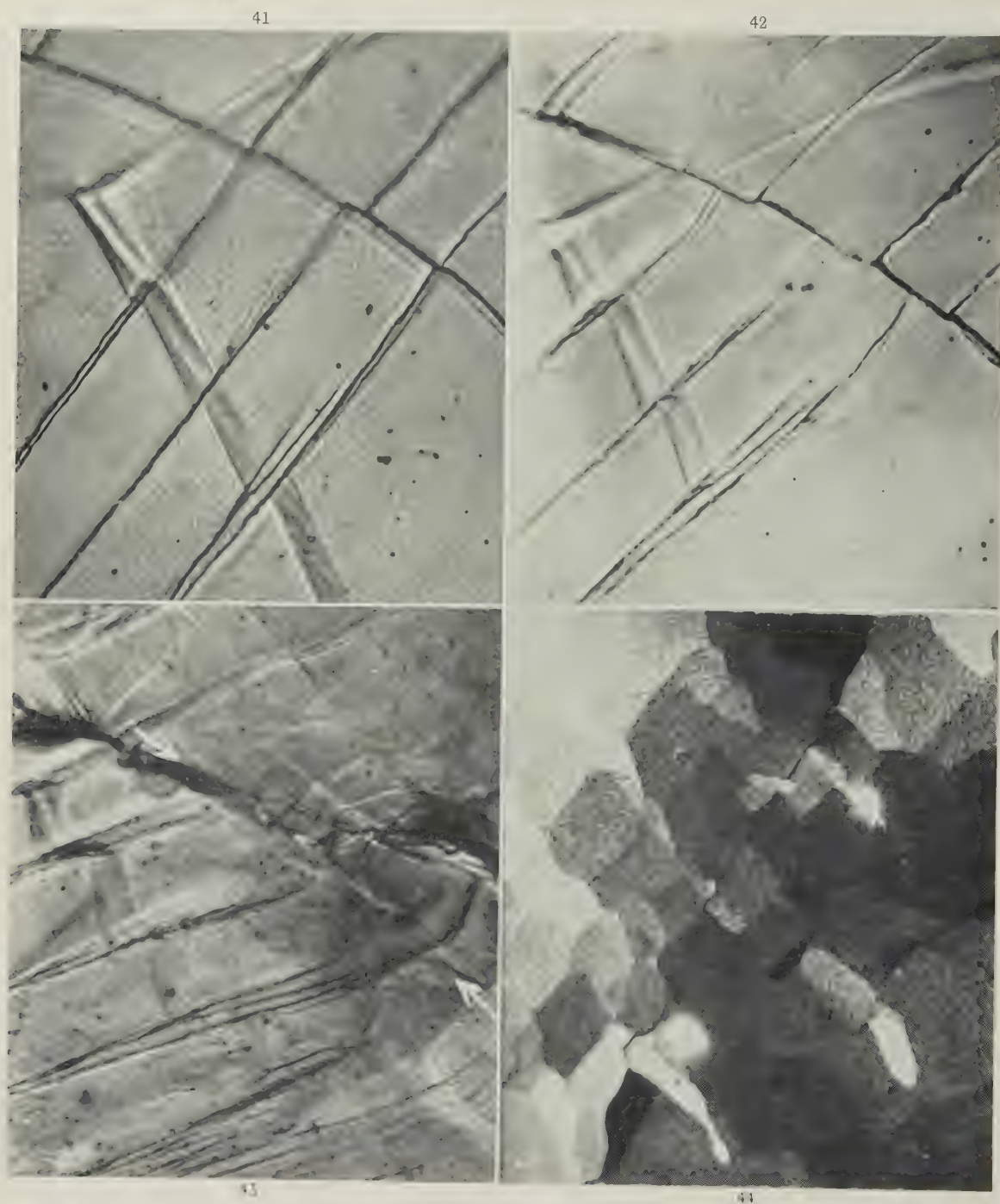




FIGS. 35 and 36.—Fine and Coarse Slip Bands. 47% Extension (853 hours' creep).  $\times 1000$ .  
 FIG. 37.—Polygonization Tilts Around Two Axes. 31.2% Extension.  $\times 1000$ .  
 FIGS. 38 and 39.—Grain Boundary After Movement. 31.2% Extension.  $\times 1000$ .  
 FIG. 40.—Section Near Fracture.  $\times 200$ .



## INTERACTION BETWEEN GRAIN-BOUNDARIES AND SLIP BANDS IN SAME FIELD AT INCREASING EXTENSION.

FIG. 41.—7.1% Extension.  $\times 1500$ .FIG. 42.—13.5% Extension.  $\times 1500$ .FIG. 43.—41% Extension.  $\times 1500$ .FIG. 44.—47% Extension, Showing Grain Boundary Conforming to the Sub-Crystal Structure Developed During Creep.  $\times 400$ .

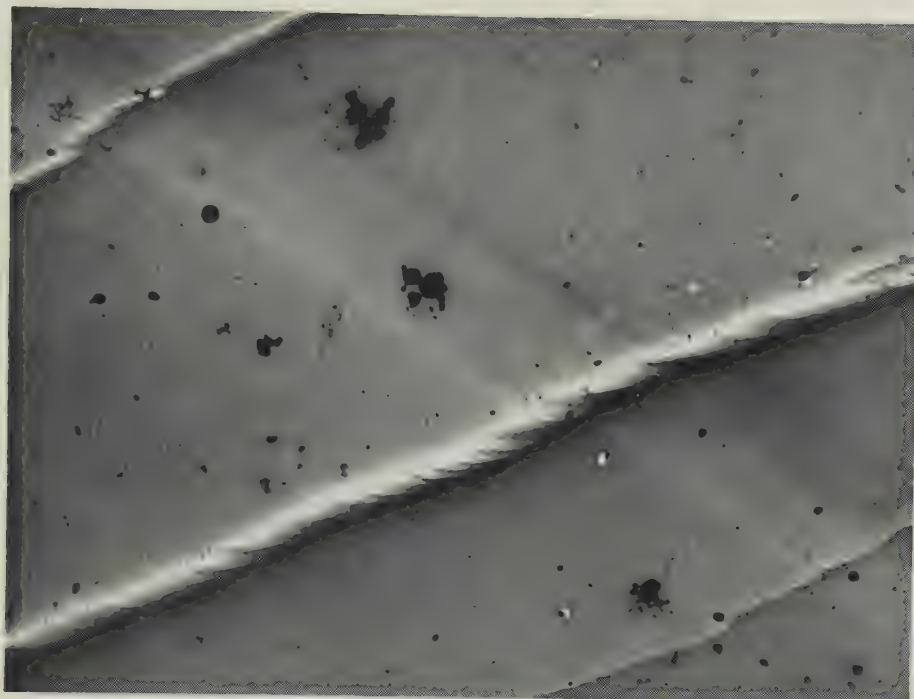


FIG. 3.

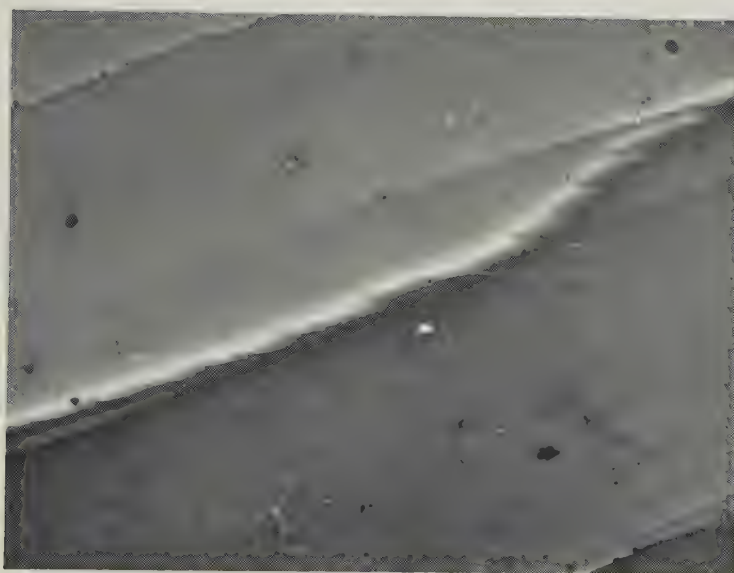


FIG. 4.

FIGS. 3 and 4.—99.98% Aluminium After 9.5% Extension at 200° C.  $\times 5000$ .  
Unshadowed plastic replica.



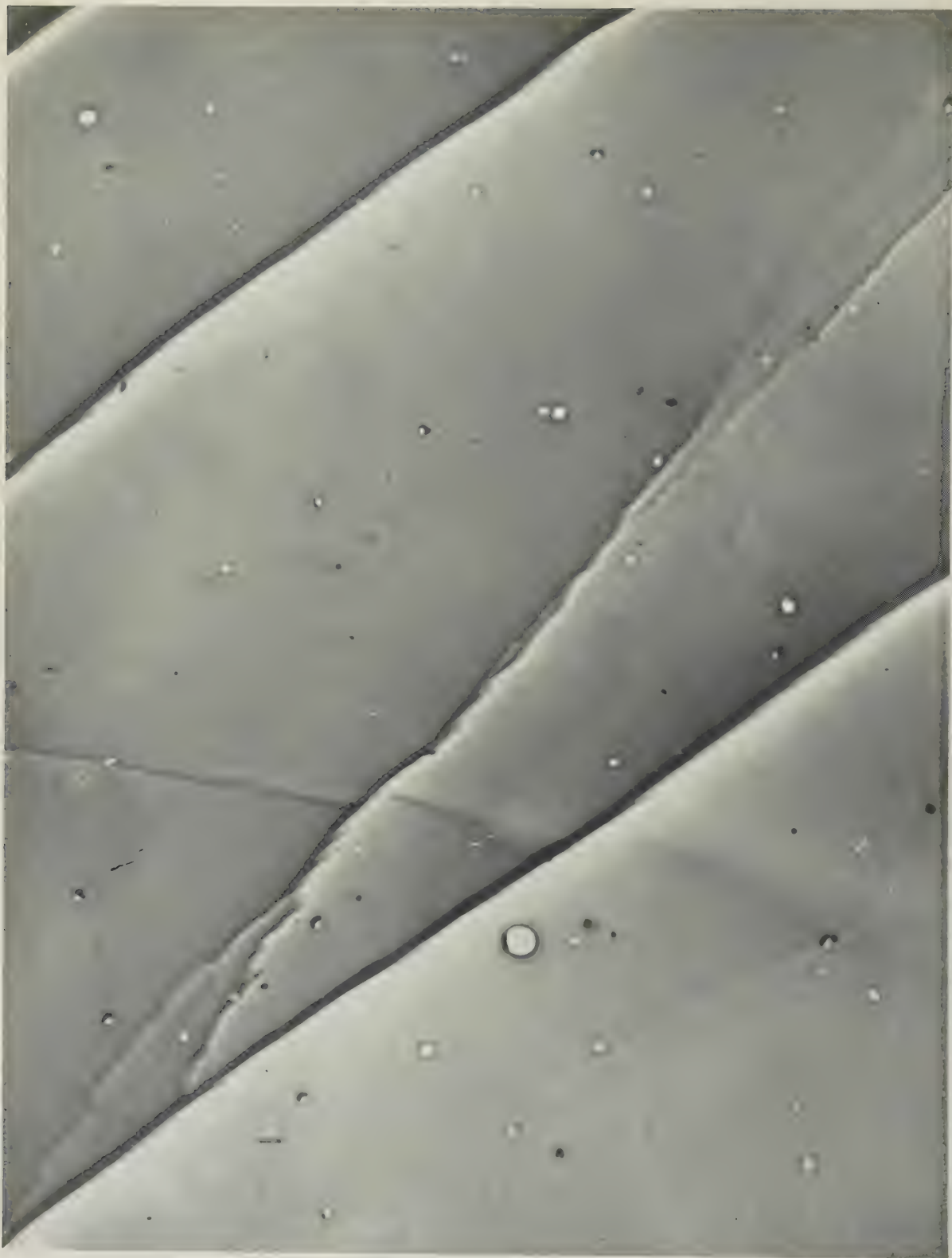


FIG. 5.—99.98% Aluminium After 62.5% Extension at 200° C.  $\times 5000$ . Unshadowed plastic replica.



FIG. 6.—99.98% Aluminium After 13.5% Extension at 200° C.  $\times 5000$ . Unshadowed plastic replica.

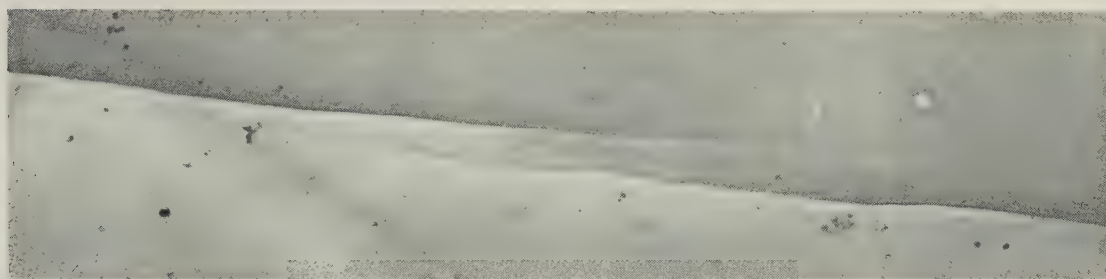


FIG. 7.—99.98% Aluminium After 9.5% Extension at 200° C.  $\times 5000$ . Rotation-shadowed with chromium.

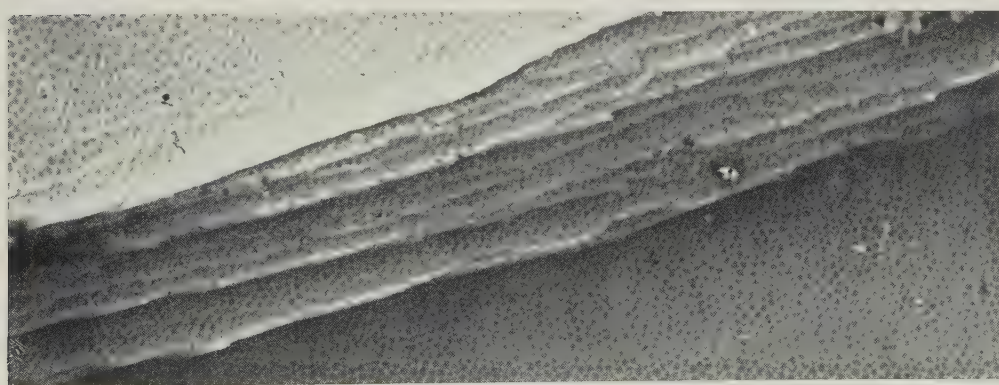


FIG. 8.—99.98% Aluminium After 23.6% Extension at 200° C.  $\times 11\,000$ . Unshadowed plastic replica.



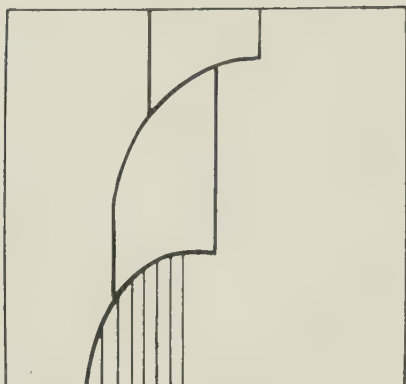


FIG. 9 (a).—Plan of Lamellar Slip and Cross-Slip in Fig. 2.

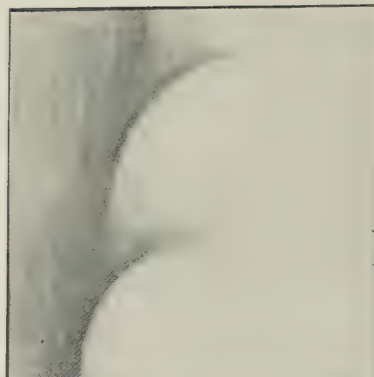


FIG. 9 (b).—Contrast to be Expected in an Electron Micrograph Due to Feature in Fig. 9 (a).



FIG. 10.—99.98% Aluminium After 17.7% Extension at 200° C.  $\times 5000$ . Unshadowed plastic replica.

bands (Figs. 10, Plate LXXIII; 19,\* Plate LXXV; and 37, Plate LXXIX), (ii) multiple bands made up of closely spaced irregular lines, each perhaps comprising a single slip band (Figs. 11 and 12, Plate LXXIII); and (iii) wide, relatively structureless bands (SS Fig. 13, Plate LXXIII). At low power these various types usually appeared as black lines of different widths.

Single slip bands were most frequent, but as deformation progressed, a few of the single slip bands developed into multiple bands (see Figs. 24 and 25, Plate LXXVI, showing the same field at 4.6 and 13.5% extension, respectively\*). Some bands which appeared to be single at 4.6% extension had clearly become multiple at 13.5%. The majority, however, remained single.

An examination of the slip bands with the electron microscope is described more fully elsewhere,<sup>9</sup> and only the main feature is referred to here. With this instrument the single and multiple bands were detected, but apparently not the wide ones. The extra resolution of the electron microscope revealed a serrated structure of practically all slip bands detected, an example being shown in Fig. 16 (Plate LXXIV). A suggestion of this structure was frequently visible with the optical microscope (e.g. in Fig. 11), and occasionally it was on a coarse enough scale to be resolved distinctly. Fig. 17 (Plate LXXIV) shows that it is a genuine structure on the metal surface and not an electron-microscope artefact. The most likely interpretation of the serrated structure is that slip occurs on one plane for a short length only, and then transfers to a neighbouring plane. Thus, the appearance of a slip band on the specimen surface resembles that of a pack of cards which has been sheared, as viewed from the side, each card corresponding to the active length of a slip plane and the thickness of the pack corresponding to the direction of the slip band as a whole. This direction had no specific connection with the orientation of the slip plane, although as a rule the two were quite close together. Consequently, the slip bands might well be curved, as, in fact, most of these appeared to be.

Typical behaviour of the slip bands as a whole, as deformation progressed, is illustrated in Figs. 19–22 (Plate LXXV), showing the same field at 4.6, 9.5, 16.4, and 46.6% extension, respectively. The number of slip bands increased in the early stages and they became bent (Fig. 20, 9.5% extension); the bend intensified into a fairly sharp fold, seen as a rather broad black line oriented at about 90° to the slip bands (Fig. 21; 16.4% extension); which developed a stepped structure and extended lengthwise. This feature was apparently similar to that observed by Wyon and Crussard.<sup>10</sup> Other bends and folds developed, and a network formed which could be revealed as white lines by suitable adjustment of the

microscope (Fig. 22, 47% extension). The significance of this is discussed later. The stepped structure is seen more clearly at higher power in Fig. 23 (Plate LXXVI) showing a portion of the same field after 41% extension.

Most slip bands lay initially within about 35°–55° of the specimen length axis; these shown in the centre of Figs. 19–22 are typical in this respect. This indicated a preferred orientation such that the slip planes lay approximately normal to the specimen surface and at about 45° to the specimen axis. In agreement with this, measurement of the displacement of the slip bands of Figs. 19–22 normal to the specimen surface and parallel to the slip band showed that the slip direction lay at about  $\frac{1}{2}$ ° to the specimen surface. The fact that the fold intersects the slip bands approximately at right angles means then that the plane of the fold, assuming that the lattice disturbance of which it is the indication extends below the surface, is approximately at right angles to the slip planes themselves. In most crystals having only one set of coarse slip bands the folds formed fairly closely to 90° from the slip bands, suggesting, in view of the preferred slip-band orientation, that such an angle was usual. With increasing deformation the angle moved away from 90° as was to be expected; this development can be seen in Fig. 22.

The behaviour, as deformation progressed, of one of the comparatively rare crystals containing two sets of slip bands is illustrated in Figs. 24–26 (Plate LXXVI), showing the same field at extensions of 4.6, 13.5, and 45%, respectively. The difference from the previous series is that the folds in Fig. 16 are not at an angle of 90° from either set of slip bands, but have taken up a compromise position, a matter referred to later. Besides the numerous “marker-line” grain boundaries of the first recrystallization, the boundaries of a large lenticular-shaped grain of the second recrystallization can be seen. The longitudinal axis of the specimen was placed horizontal for these micrographs, and the lenticular-shaped grain has rotated very considerably and has elongated somewhat at the stage shown in Fig. 26. This field lay in the region that eventually necked, thus undergoing a very large elongation. Necking had just begun at the stage shown in Fig. 26; later, the elongation became very pronounced, the grain rotation increased, and the surface distortion became very complex (see Fig. 12, showing at higher power another field in the necked zone, the extension being over 100%).

The displacement was not uniform along the length of a slip band even though no visible obstruction could be observed, as may be seen along the slip band AA in the interference micrograph Fig. 14 (Plate LXXIII). The fringe displacements show the movements at different points along the slip band.† Such non-uniformity is to be expected from the current dislocation theory of slip. Moreover, if slip

\* The network of boundaries (“marker lines”) corresponding to the first recrystallization to a small grain-size is to be

seen in these and many of the later micrographs.

† A displacement of one fringe amounted to 2730 Å.



was prevented at one part of a slip band by some obvious agency, it continued elsewhere. An example is shown in Figs. 41–43 (Plate LXXX), illustrating the same field at 7.1, 13.5, and 41.2% extension, respectively. A grain boundary runs in an arc from left to right of the field, slip bands occur in both grains, and marker lines indicate the directions and amounts of displacement. In this field no slip displacement occurred at the grain boundary itself, but there was a displacement of about  $1\mu$  in each slip band, 10–15  $\mu$  from the boundary, as can be seen by the displacements of the marker line.

The displacements  $v$  and  $l$ , respectively normal and parallel to the specimen surface, were measured for each slip band as a whole without regard to detailed structure. Figs. 14 and 15 (Plate LXXIII) show the type of interference image from which the measurements of  $v$  were made, and Figs. 41–43 the marker-line displacements from which the measurements of  $l$  were made. The mean values  $\bar{v}$  and  $\bar{l}$  are plotted against time in Fig. 2 (a).

The increase in displacement was very rapid in the first 50 hr. and for  $\bar{v}$  is shown on a more open time-scale in Fig. 2 (b). The initial rate of vertical displacement ( $d\bar{v}/dt$ ) was 0.4 Å./sec. (~10 atomic dia./min.) but suffered a sharp decrease until a fairly

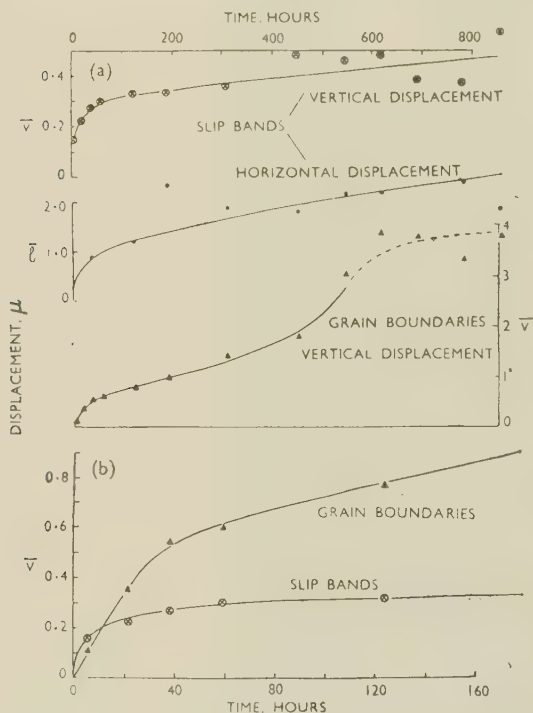


FIG. 2 (a) and (b).—Slip-Band and Grain Boundary Displacements Plotted Against Time. (b) On enlarged time scale.

steady rate of 0.0007 Å./sec. (~1 atomic dia./hr.) was reached after about 100 hr. The measurements became less reproducible as extension progressed, as can be seen from the scatter of the later points in Fig. 2. This was due partly to the growing difficulty of

making accurate measurements as the complexity and roughness of the specimen surface increased and partly to the fact that the slowing down of the displacement of most slip bands was greater than indicated in Fig. 2, the gradual increase in  $\bar{v}$  and  $\bar{l}$

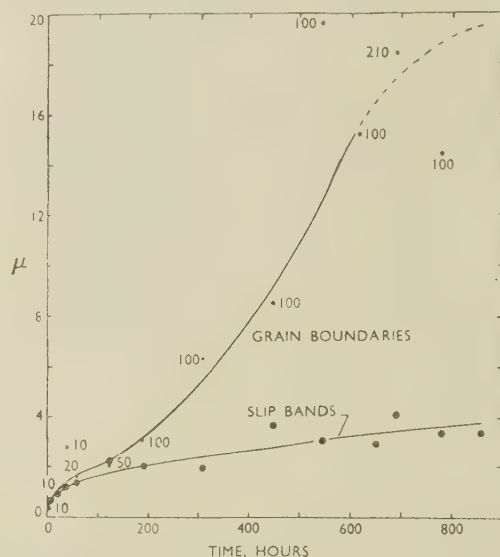


FIG. 3.—Maximum Height of Slip Bands and Grain Boundaries Plotted Against Time.

Slip bands: mean of 3 largest in count of 100.

Grain Boundaries: 1 largest in count of 10 or 20; 2 largest in 50; 3 largest in 100; 6 largest in 210 (see figures against points).

being mainly due to a few bands of large displacement; thus, the 100 slip bands measured included fewer and fewer effective slip bands and so gave a poorer and poorer average. This point is clear on comparing Fig. 2 with Fig. 3, which shows, plotted against time, the mean of the three slip bands having the largest vertical displacement. After 25 hours' extension the ratio  $v_{\text{max.}}/\bar{v}$  was 4, but after 800 hours' extension it was 9.

Rather surprisingly, wide slip bands of the type shown in Fig. 13 (Plate LXXIII), as well as multiple slip bands (e.g. Fig. 11), gave larger vertical displacements in general than single slip bands (e.g. Fig. 10).

The number of slip bands is plotted against time in Fig. 4. There was a rapid initial generation of slip bands but no fresh ones appeared after about 50 hr. A plot (not given) of  $\log(N_0 - N)$  against time, where  $N_0$  is the final number of slip bands, and  $N$  the number at time  $t$ , deviated from the straight-line behaviour that would be obtained if there were  $N_0$  sources of the same unchanging probability in the direction that indicates a decrease in probability as  $N$  grows.

## 2. POLYGONIZATION AND FINE SLIP

The network of white lines referred to in Section III, 1 (e.g. Fig. 22, Plate LXXV and Fig. 28, Plate LXXVII) is similar to the "cell structure" observed by Wilms and Wood<sup>11</sup> and by Wyon and Crussard<sup>10</sup>, which in

turn is probably a surface manifestation of a sub-crystal structure resembling that noted many years earlier by Jenkins and Mellor<sup>12</sup> in creep specimens of iron.

To bring up the white lines prominently, the microscope stage had to be racked inside focus by several  $\mu$  and the aperture stopped down. The lines were symmetrical. According to a suggestion by Mr. W. M. Lomer, they therefore represent bends in the surface, as shown diagrammatically in Fig. 5, the effect of racking the stage upwards being to bring into focus the bright virtual image of the cylindrical contour.

It was known from work by Calnan and Burns<sup>13</sup> and by Greenough and Smith,<sup>14</sup> as well as from other work not yet published, that polygonization should be far advanced at a stage where the white-line pattern could be made prominent (beyond about 20% extension). Polygonization consists of the development of a sub-crystal structure, with, in the ideal case, a set of sub-crystal boundaries lying on planes at right angles to the slip planes.<sup>15</sup> It has been

30–40  $\mu$  inside focus and with reduced aperture to bring up the lines. The folds seem to be a development of the white lines which occurred as deformation proceeded. The appearance of the surface during deformation was therefore consistent with the idea that polygonization had caused prominent sub-boundaries, of comparatively large lattice tilt, to form at right angles to the slip bands, and had also caused a network of sub-boundaries of smaller lattice tilts, indicated by the network of white lines, to form in more or less accidental positions.

After the creep test was completed, it was possible to make a check on this conclusion, as follows. Five fields were photographed, repolished until flat, and examined under the microscope in polarized light after anodic filming; with this technique the crystal structure is revealed in intensity contrast by virtue of orientation differences<sup>18,19</sup>. Two comparisons are made in Figs. 31 and 32 and 33 and 34 (Plate LXXVIII). Figs. 32 and 34 show that the original crystals had broken down into sub-crystals of size similar to that

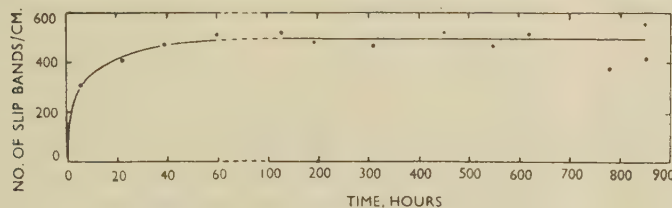


FIG. 4.—Increase of Number of Slip Bands with Time.

Based on number intercepting a line parallel to the specimen length and 1 cm. long before creep began.

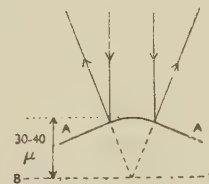


FIG. 5.—Diagram Indicating How a Sub-Boundary Can Appear as a White Line under the Microscope.

AA Section through surface.  
BB Plane of focus.

explained qualitatively in terms of dislocations,<sup>16</sup> on the basis that edge dislocations originally in the slip bands collect into rows lying in planes at right angles to the slip planes, for the reason that such an arrangement is a stable one.<sup>17</sup> They must do this by diffusing outwards from, and moving parallel to, the slip bands. This arrangement of dislocations constitutes a sub-boundary, in the sense that the parts of the originally straight lattice on either side of a row of dislocations are tilted with respect to each other by the presence of the extra planes of atoms associated with the dislocations. At the specimen surface, such a lattice tilt should produce a bend in the surface similar to that shown in Fig. 5, the bend being sharper the more completely the dislocations have gathered into rows. Thus, the white-line appearance is the optical evidence of polygonization to be expected. As the folds referred to in Section III, 1 almost invariably formed nearly at right angles to the slip bands where only one set of bands occurred, they were situated in the position where rows of dislocations would theoretically be expected. The folds, which did not end abruptly, were often continued as white lines, examples being shown in Figs. 27 and 28 and Figs. 29 and 30 (Plate LXXVII), the second of each pair being taken

of the cell structure (cf. Figs. 28 and 30). The sub-crystals lie in bands, indicating that approximate planes exist across which a tilt in the lattice occurs, and comparison with Figs. 31 and 33 shows that the bands are parallel to the folds on the unpolished deformed surface. This parallelism was found in four out of the five fields examined (in the fifth field no obvious banding occurred). It was therefore concluded that the folds and white-line or cell structure were both indications of polygonization.

In Fig. 32 banding is evident also in the direction parallel to the slip planes in Fig. 31. This was observed in the other photographs, although in all cases the more pronounced banding was parallel to the folds. The parallel banding could be caused by polygonization due to screw dislocations, which would produce a lattice rotation about the normal to the slip planes.

The dislocation argument as set out applies to, and predicts the behaviour observed in, only those crystals containing a single direction of slip bands. In crystals where two sets of slip bands occurred, the folds took up a compromise position, as has been noted. The presence of dislocations with Burgers vectors in additional directions due to a second set of



slip bands, should affect the interaction in such a way that the arrangement of lowest energy becomes one in which the dislocations are arranged in planes that are a compromise between those at right angles to each set of slip bands.

Faint slip lines could be seen between the coarse slip bands after about 20% extension, as in Fig. 35 (Plate LXXIX). Since polygonization was developing markedly at this stage, the presence of the fine slip bands was consistent with the idea that during polygonization dislocations move parallel to the slip direction of the coarse slip bands.

It may be remarked, in connection with the serrated structure of the coarse slip bands referred to earlier, that occasionally the fine slip bands were inclined at an appreciable angle to the coarse bands, as in Fig. 36 (Plate LXXIX). However, at points along the coarse bands in this figure a serrated structure can be detected with the serrations approximately parallel to the fine slip. It thus seems that the fine slip indicates the actual slip direction.

In Fig. 36 some of the fine slip bands end on a line (indicated by arrows) which, at lower power, could be seen to be part of a white line of the "cell structure". This is consistent with the idea that dislocations have moved up to a sub-boundary and come to rest therein.

What appeared to be polygonization-tilts around two axes were sometimes observed, e.g. Fig. 37 (Plate LXXIX), where one occurs at the sub-crystal boundary visible in this field and one at the sharp edge; the sharp edge was merely an unusually sharp tilt as could be seen by changing the focus. (This field is contained at lower power in Fig. 28, Plate LXXVII.) The behaviour shown here seems to demand the operation of a set of edge dislocations, to produce one tilt, and two sets of screw dislocations, to produce a tilt at the sharp edge about an axis normal to the slip plane.

It was expected that sub-boundaries of the opposite tilt to that shown in Fig. 5, i.e. making the surface concave, would show as white lines under the microscope when racked outside focus, but this was rarely so. It was the general rule that concave bends were considerably less sharp than convex. It could also be seen from the bends in the slip bands that those of one type were distinctly sharper than those of the other type, e.g. Fig. 29 (Plate LXXVII). The reason for this difference is not known. However, as no corresponding appearance was observed with the polarized light-anodic-film technique in sections below the surface, it is perhaps a surface effect.

Sometimes a slight displacement was noted at a sub-boundary; for example, at part of the sub-boundary in Fig. 37 and at the long sub-boundary *PP* in Fig. 13. In general, however, the displacements, if any, at sub-boundaries, were far smaller than at

ordinary grain boundaries in spite of the fact that, as shown later, tilts of tens of degrees occurred. This suggests that sub-boundaries due to polygonization differ somewhat from ordinary grain boundaries and, conversely, that grain boundaries should not be regarded simply as composed of dislocations. This is consistent with the observation that a polygonized structure can confer strength in creep.<sup>20</sup>

### 3. DEFORMATION AT AND NEAR GRAIN BOUNDARIES

The grain boundaries exposed by vertical movement were terraced, partly owing to the slip-band outcrop, as in Fig. 38 (Plate LXXIX), and partly, it appears, independently of slip, as in Fig. 39 (Plate LXXIX).

Interaction between grain boundaries and slip bands took place and is illustrated in the series Figs. 41-43 (Plate LXXX), showing the same field at 7.1, 13.5, and 41.2% extension, respectively. The marker lines indicate that the rim of the lower grain has rotated anti-clockwise with respect to the upper grain. The slip bands in the lower grain are also bent in an anti-clockwise direction near the grain boundary, thus proving that the grain rotation has not been caused by a couple exerted elsewhere, for then the bands would tend to bend in the opposite direction owing to the restraining drag of the upper grain. The rotation seems, in fact, to have been enforced by the slip itself. At the stage shown in Fig. 42, 5000-10,000 dislocations have travelled past the marker lines,\* but have not reached the grain boundary. They must, therefore, be concentrated in the space between the marker line and boundary. They cannot be concentrated along the slip band itself, for that would demand a prohibitive strain far beyond the elastic limit. They must have diffused outward from the slip band, and in Fig. 43 there is evident the plane (marked by arrows) along which they have collected, (initially approximately at right angles to the slip band), to form a polygonized boundary and to produce the sharp change in lattice orientation manifested by the bend in the slip bands. It is this bend in the lattice which has necessarily produced at least part of the observed grain-boundary displacement.

If the dislocation model of plastic deformation be accepted, this set of micrographs affords direct proof that diffusion of dislocations outwards from slip bands does occur. Such diffusion has the result that grain boundaries or similar obstructions do not prevent slip continuing at other points along the slip band, as noted previously.

The relation just described between direction of slip, direction of bending of slip bands, and direction of grain-boundary rotation was nearly always found. If the excess (or deficit) of metal near the grain

\* Measurements of vertical and horizontal displacement showed that the slip direction in Fig. 42 was within a degree or two of the specimen surface. The slip displacement at the marker lines is about  $2\mu$ , and this is therefore practically

the displacement in the slip direction. The passage of one dislocation causes slip displacement of 1 atomic dia. ( $2.8\text{ \AA}$ . for aluminium), so to produce  $2\mu$  displacement the passage of about 7000 dislocations is necessary.

boundary were accommodated by a viscous flow unrelated to the crystal structure, which is an alternative explanation to the dislocation theory, it is not clear why the observed relation of slip and grain-boundary movement should be so consistently found. As might be expected, rotation also occurred where, over long lengths of a grain boundary, no slip bands ended.

From general examination it appeared that polygonization proceeded most rapidly near grain boundaries. On microstructures prepared after the test was finished, the originally smooth crystal boundaries

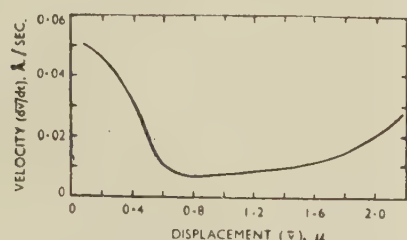


FIG. 6.—Grain-Boundary Velocity Plotted Against Grain-Boundary Displacement.

Both ordinate and abscissa refer to vertical component only.

had become irregular. As Fig. 44 (Plate LXXX) shows, the irregularities coincided with the sub-crystal structure.

The curve of mean vertical displacement against time is given in Fig. 2 (a), the initial part being plotted on a larger scale in Fig. 2 (b). Up to 600 hr. the mean curve (Fig. 2 (a)) is similar to the total creep curve (Fig. 1), exhibiting transient, secondary, and tertiary portions at about the same times. The exact shape of the grain-boundary curve beyond 600 hr. is considered uncertain and is shown dashed.

The curve for the few largest displacements is shown in Fig. 3. The ratio of maximum displacement to mean displacement was not as great as for slip bands. All the grain boundaries continued to move regularly as creep progressed. The increasing mean displacement was not due to a few large displacements to the same extent as for the slip bands.

Fig. 6 contains the curve, derived from Fig. 2 (a), of the velocity component of grain-boundary displacement in the direction normal to the specimen surface, plotted against that displacement. The velocity was 0.5 Å./sec. ( $\sim 1$  atomic dia./min.) at the first measured point and decreased steadily to a minimum value of 0.005 Å./sec. ( $\sim 7$  atomic dia./hr.) at about 0.7  $\mu$  displacement. This decrease is due to some obstruction force which increases with displacement and is presumably set up at grain corners and protuberances. The velocity subsequently increased, presumably because of the increasing stress per unit area caused by the decreasing cross-section of the specimen.

#### IV.—CONTRIBUTIONS OF THE DIFFERENT DEFORMATION PROCESSES TO EXTENSION

##### 1. VISIBLE SLIP BANDS

From the mean displacement and number of slip bands the extension associated with them was calculated in the manner described in the Appendix. The procedure is clear from Fig. 7 (p. 517), where  $S$ ,  $S$  are slip bands,  $a_0$  lies in the original direction of the specimen surface,  $a$  in the final direction, and  $p$  is the slip displacement. The problem is simply to calculate the average increase of  $a$  over  $a_0$ . The extensions so obtained ( $E\%$  slip) are given in Table I and plotted in Fig. 1. It is clear from the latter that in

TABLE I.—Measurements of Extension, &c.

No. of grains/cm. = 21.7 by linear-intercept method. Initial Vickers hardness number = 13.5.

Time, hr.	Creep Extension, %	Vickers Diamond Hardness Number	Slip Bands							Grain Boundaries					
			No. of Slip Bands *	Vertical † Displacement, $\bar{v}$ , $\mu$	Max. ‡ $v$ , $\mu$	$\bar{v}$ max. $\bar{v}$	Horizontal § Displacement, $\bar{l}$ , $\mu$	$\bar{l}$ $\bar{v}$	Creep Due to Slip Bands, %	Vertical † Displacement, $\bar{v}$ , $\mu$	Max. $v$ , $\mu$	$\bar{v}$ max. $\bar{v}$	Horizontal § Displacement, $\bar{l}$ , $\mu$	$\bar{l}$ $\bar{v}$	Creep Due to Grain Boundaries, %
5½	4.5	14.3	310	0.153	0.63	4.1	...	...	1.3	0.11	0.3	2.85	...	...	0.1
22	7.1	13.8	410	0.222	0.90	4.05	...	...	2.5	0.35	1.1	3.15	...	...	0.31
38½	9.5	14.6	472	0.27	1.22	4.5	...	...	4.1	0.54	2.75	5.10	...	...	0.50
59½	10.6	...	510	0.302	1.38	4.55	0.85	2.8	5.4	0.60	1.65	2.75	...	...	0.55
124	13.5	15.1	518	0.329	2.22	6.75	1.20	3.7	6.2	0.77	2.05	2.7	3.74	4.9	0.65
190	16.4	...	478	0.326	2.03	6.25	2.3	7.1	10.0	0.96	3.1	3.25	5.9	6.4	0.80
308	19.8	...	362	0.355	1.93	5.45	1.85	5.2	8.9	1.42	6.3	4.45	...	...	0.95
378	21.3	...	...	...	...	...	...	...	...	...	...	...	...	...	...
449	23.6	...	514	0.48	3.65	7.6	1.78	3.7	11.3	1.81	8.5	4.7	6.0	3.3	0.85
545	26.2	...	462	0.46	3.03	6.55	2.12	4.6	12.1	3.05	19.6	6.4	4.4	1.4	1.15
616	31.2	...	509	0.48	2.91	6.1	2.15	4.5	12.9	3.88	15.2	3.95	9.3	2.4	1.45
690	41.2	...	...	0.38	4.1	10.8	2.96	7.8	14.7	3.77	18.4	4.53	8.5	2.1	1.3
779	47.8	...	375	0.37	3.4	11.1	2.36	6.3	12.2	2.82	14.4	5.1	8.0	2.8	1.05
848	46.6	...	548	...	...	...	...	...	...	...	...	...	...	...	...
853½ (fracture)	46.6	15.4	413	0.57	3.35	5.9	1.82	3.2	14.7	3.77	23.0	6.1	...	...	1.3

\* The number of slip bands/original cm. along a line parallel to the length axis of the specimen.

† Measured normal to the surface.

‡ The mean of the three largest readings in a count of one hundred.

§ Measured in the direction of displacement as projected on to the specimen surface.

|| Including necked region which began to develop between 545 and 616 hr. All other measurements refer to the parallel portion of the test-piece.



so far as the calculations are accurate, the slip bands contributed one-third to one-half of the total extension, excluding the necked region.

## 2. GRAIN-BOUNDARY DISPLACEMENTS

The extension due to the displacements at grain boundaries was calculated similarly, details also being given in the Appendix. The results ( $E\%$  g.b.) are included in Table I and plotted in Fig. 1 and show that the grain boundaries contributed one-twentieth to one-fortieth of the total creep.

## 3. FINE SLIP ("MISSING" CREEP)

The curves of ( $E\%$  slip) and ( $E\%$  g.b.) in Fig. 1 were added together and then subtracted from the curve for the measured extension, excluding the necked region, to give the curve labelled "missing" creep (fine slip) in Fig. 1. This amounts to roughly half the total extension.

The situation at this stage was thus that three main deformation processes had been observed, clearly visible slip, grain-boundary displacement, and fine slip, and that assuming that the calculations could be relied upon, the deformation corresponding to the first two accounted for not more than half the measured creep.

The fine slip would cause shear between the coarse slip bands. As far as the later stages of the creep test were concerned, direct proof that such a shear did occur is provided by a comparison of the micrographs Figs. 41 and 43 (Plate LXXX), showing the same field at 7.1 and 41% extension, respectively. The angle between the marker lines and slip bands has quite clearly changed during the intervening exten-

TABLE II.—Comparison of Shear In and Between Slip Bands.

Values refer to the increase in shear, extension, or missing creep between the early and the later micrograph of each pair.

	(a) Shear/ Slip Band, cm.	(b) Shear/ Inter- space, cm.	(b) ÷ (a)	(c) Slip * Exten- sion, %	(d) Missing * Creep, %	(d) ÷ (c)
Field of Figs. 41 and 43 (Plate LXXX)	0.8	0.4	0.5	12	17	1.4
Another field	0.27	0.4	1.5	13.7	22.5	1.6

\* Average value for the whole specimen.

sion, and this can only be due to shear in the spaces between the bands. The same effect was found in another pair of micrographs (not shown) where a fortunate choice of field had been made in the early part of the test. The relative magnitudes of the shear at the coarse slip bands and between the bands is given in Table II for these two fields. The values of slip extension, proportional to the mean shear at coarse slip bands, and of missing creep, expected to be

proportional to the mean shear between slip bands, are also given for comparison.

The shear in the interspaces in these two arbitrary fields is thus of the same order of magnitude as that in the slip bands themselves, which is consistent with the missing creep being due to fine slip between the coarse bands.

### (a) Second-Stage Creep, Involving Polygonization

The qualitative observations already described showed that polygonization occurred prominently during the second stage of creep. An estimate is made below on the basis of the dislocation theory of the extension associated with polygonization, to see if it is of the right magnitude to be identified with the missing creep occurring during the second stage. The estimate is approximate, depending on an assumption about the distance dislocations move during polygonization, but with this proviso it gives an average value over the whole uniform part of the specimen.

During polygonization the dislocations move under the influence of the applied stress in that direction which increases the extension, positive dislocations moving in one direction and negative dislocations in the other.\* The extension during polygonization is due partly, and in all probability mainly, to the movement parallel to the slip planes, although the diffusion movement normal to these planes doubtless causes some extension.

The number of dislocations that have moved into sub-boundaries can be estimated from the orientation tilts between neighbouring sub-crystals. If the average tilt is  $\theta$  radians,

$$\theta = n\lambda$$

where  $n$  is the number of dislocations in the sub-boundary (i.e. row of dislocations) per unit length of sub-boundary normal to the dislocation axis, and  $\lambda$  is the unit slip distance caused by the passage of a single dislocation. If  $d$  is the spacing between sub-boundaries,

no. of dislocations/cm.<sup>2</sup> due to one set of

$$\text{sub-boundaries} = \rho = \frac{\theta}{d\lambda} \quad (1)$$

If each dislocation moves a distance  $x$  parallel to the slip bands, the shear per dislocation is  $x\lambda$ , so the total

$$\text{shear} = \frac{\theta}{d\lambda} x\lambda = \frac{\theta x}{d}$$

Since the slip bands lie approximately at 45° to the length axis,

$$\text{extension } E = 100 \frac{\theta x}{2d} \% \quad (2)$$

The extension calculated therefore depends linearly on the value taken for  $x$ . The distance  $x$  will be of order  $d$ , since a dislocation will continue moving until it reaches a row of dislocations, and will probably be captured by the first row of correct sign it comes to,

\* The applied stress thus helps to sort out the dislocations, and this constitutes a difference between polygonization under stress and in the absence of stress.

except in the early stages when the rows are very incomplete. Alternate rows contain positive and negative dislocations, so the average distance a dislocation moves should be closely equal to  $d$  in the later stages of polygonization but probably greater than  $d$  in the early stages. Putting  $x = d$  in equation (2) gives the value, probably therefore on the low side:

$$E = \frac{100\theta}{2} \% \quad . \quad . \quad . \quad (3)$$

It should be emphasized that equation (3) refers to the elongation corresponding to the formation of one set of sub-boundaries, i.e. the sub-crystals are lamellae extending right across the main crystal. It has been

TABLE III (a).—*Extension Associated with Polygonization Calculated from Measurements of Angle of Bend  $\alpha$  of Slip Bands at Sub-Boundaries.*

Each value is the mean of 50 readings.

Time, hr.	Missing Creep, %	Angle of Bend ( $\alpha$ ), degrees		$\theta$ , degrees	Extension, %, Calculated from Equation (4)
		Values	Mean		
779	20	8.2	8.2	11.6	20
848	24	13.7, 8.1	10.9	15.4	27
853	25	11.7, 9.6	10.7	15.1	26

shown that another set of about equal spacing occurred approximately at right angles to the first (Figs. 32 and 34, Plate LXXVIII) with a similar but smaller value of  $\theta$  (see also Table III (b)); the elongation associated with the formation of both sets will therefore be nearly twice that given by equation (3). Hence:

$$E \sim 100\theta \% \quad . \quad . \quad . \quad (4)$$

The value of  $\theta$  was obtained in two ways. In the first, the angle of bend  $\alpha$  of the slip bands at sub-boundaries was measured under a microscope. This angle corresponds to the component of  $\theta$  projected on to the specimen surface; on the average, there is an equal component at right angles, so:

$$\cos \theta = \cos^2 \alpha$$

For each mean value, 50 measurements were

made, 5 consecutive measurements in each of 10 crystals. The results, together with the extension calculated from equation (4), are given in Table III (a). The missing creep values refer to that occurring during the second stage, taken for this purpose to begin at 50 hours' creep.

The scatter is considerable, but it is clear that there is agreement in magnitude between the missing creep and that calculated from the disorientation. In view of the approximations made, the good degree of numerical agreement must be regarded as fortuitous.

The second method of obtaining  $\theta$  could only be employed after the creep test was finished. A section of the test-piece was polished and anodically filmed. It appears that the film bears a certain orientation relationship to the underlying aluminium, for general observation in other work has shown that the more extensive the creep deformation, the greater the contrast under polarized light between neighbouring sub-crystals. Unless some epitaxial relation is obeyed there seems no reason why this should be so. Accordingly, the difference between extinction angles of adjacent sub-crystals was measured with a rotating stage to give an angle corresponding to  $\alpha$  for slip bands. Measurements were made separately for sub-boundaries forming the more prominent bands, assumed from the previous evidence to be those parallel to the polygonized bands, and for the sub-crystal boundaries forming the less prominent bands, assumed to be parallel to the slip bands. These measurements were made on a section parallel to, and just underneath, the specimen surface, on a mid-section parallel to the surface, and on a longitudinal mid-section normal to the surface (parallel to the specimen thickness). The purpose of measuring in these positions was to see if surface and interior behaved similarly. The results are given in Table III (b).

Again, there is agreement of magnitude between missing creep and extension associated with polygonization. In view of the scatter in the measurements, the difference between the orientation tilts as determined from slip bands and under polarized light, or between the measurements made in different positions, are not large enough to be significant.

TABLE III (b).—*Extension Associated with Polygonization Calculated from Measurements of Difference in Extinction Angle under Polarized Light.*

Each value is the mean of 50 readings. Measurements made after 853 hours' creep. Missing creep in second stage 25%.

Position of Measurement	(A) Across Polygonized Boundaries				(B) Across Slip Bands				Total $E\%$ (A) + (B)
	Extinction Angle, degrees		$\theta$ , degrees	$E\%$ from Equation (3)	Extinction Angle, degrees		$\theta$ , degrees	$E\%$ from Equation (3)	
	Values	Mean			Values	Mean			
Just under surface	7.3, 10.0	8.6	12.1	10½	5.0, 7.1	6.0	8.5	7½	18
Mid-section parallel to surface	11.1	11.1	15.6	13½	9.0	9.0	12.7	11	24½
Longitudinal mid-section normal to surface	8.1	8.1	11.4	10	5.1	5.1	7.2	6½	16½



Although it is clear that during polygonization dislocations move parallel to the slip planes, the extension in Tables III (a) and (b) can only be additional to the extension due to the visible slip bands in so far as the movement of dislocations to which it relates does not occur in these; in so far as it occurs in these bands it will have been included in the measurements of slip-band displacement. However, Table II shows that a large proportion of the deformation during polygonization takes place outside the visible slip bands.

It is therefore permissible to count a large proportion of the calculated polygonization extension as additional to the calculated slip-band extension. Consequently this proportion can be identified with the missing creep, supporting the conclusion that the missing creep during the second stage is due to the movement of dislocations along slip planes in the interspaces between the coarse slip bands, i.e. to fine slip on these planes.

The measurements of disorientation due to polygonization given here differ from those made by X-rays,<sup>11,21</sup> since they refer to the average tilt between adjacent sub-crystals, whereas the X-ray measurements record either the total spread or the average angular separation between adjacent spots on the X-ray film which come from unidentifiable sub-crystals. The largest single tilt recorded among the slip-band measurements was  $48\frac{1}{2}^\circ$ , and among the measurements under polarized light  $42^\circ$ .

Table III (b) shows that although the tilts across the slip bands are smaller than those across the polygonized bands, they are still of the same magnitude. If the tilts across the slip bands were due to non-uniform polygonization along the main polygonization bands at right angles to the slip bands, they would almost certainly be much smaller than those across polygonized bands. Since it was rare for more than one set of slip bands to form, the former tilts must generally be due to dislocations in these bands, and appear to be explicable only if polygonization due to screw dislocations occurs to produce rotation about the normal to the slip plane, as suggested earlier.

#### (b) *Transient Part of Missing-Creep Curve*

Despite this general agreement as regards the later stages of the creep test, the position was still unsettled for the early stages, since the missing-creep curve (Fig. 1) is of the wrong shape at the origin to be due to a process such as polygonization which involves diffusion. It seemed very likely, however, that the steep initial rise in the curve was due to undetected fine slip, for interference micrographs such as Figs. 14 and 15 (Plate LXXIII) gave direct proof at a fairly early stage that appreciable shear had occurred in the spaces between the slip bands, since the fringes did not always quite preserve the same direction on crossing a band.

To check this point a further specimen was prepared, which was recrystallized in a normal way to a large grain-size (10 grains/cm.) by heating at  $500^\circ\text{C.}$ , and

was examined after short periods of extension under the same conditions ( $\frac{1}{2}$  ton/in.<sup>2</sup> at  $200^\circ\text{C.}$ ). After  $\frac{1}{2}$  min. (0.9% extension) numerous fine slip bands could be seen in most fields with the phase-contrast microscope; an example is shown in Fig. 18, (Plate LXXIV). The spacing appears to be about  $1\mu$ , but there may be many other bands beyond the resolving power of the microscope. Judging from experience, the height of the faint bands is of the order of  $100\text{ \AA.}$ , so from equation (6) (see Appendix) they should cause an extension of the order of 1%. Hence at this stage the bulk of the extension appeared to be due to fine slip. After 30 min. (1.9% extension) very little fine slip was visible. The only explanation seems to be that the fine slip bands had become so close together as to be unresolvable. After 8 hr. (4.1% extension) virtually no fine slip was seen. This corresponds approximately with the first observation made on the original specimen. It thus seems reasonable to conclude that the failure to observe early fine slip in that specimen was because, when the first observation was made, the fine slip bands were too close together to be resolved, and that the steep initial rise in the missing creep curve is due to very fine slip.

#### 4. EXTENSION IN NECKED REGION

After 848 hours' creep the extension in the necked region was 230% and in the parallel part 47%. The number of slip lines was counted and found to be the same in the necked zone (544/cm. original length) and the parallel part (552). The surface was too cockled to measure the slip displacements in the necked zone, but it was thought that, if coarse slip bands were responsible for much of the extra rather rapid extension, many new bands would have been formed.

On the other hand, polygonization had obviously progressed, the apparent sub-crystal size being about one-quarter of that in the parallel part, i.e. three new polygonized boundaries had formed for every one existing before. The mean angle of bend of slip bands at all the boundaries was  $14.1^\circ$ . In calculating the extension, due to polygonization in the necked region, it is a good enough approximation to assume a structure of original size and tilt  $14.1^\circ$  to form first and a finer structure of tilt  $14.1^\circ$  to form subsequently, giving the extension (see equation (4))  $35 + 35 = 70\%$ , compared with 20% (see Table III (a)) for the parallel part. It thus seems that a considerable part, if not all, of the neck extension is due to fine slip.

After fracture, examination of a micro-specimen under polarized light confirmed that in the necked region the sub-crystal size was much smaller than elsewhere; Fig. 40 (Plate LXXIX) shows the structure. The rather indistinct polygonized structures suggest that the sub-crystals are in a state of strain, i.e. that a large proportion of dislocations have not reached the sub-crystal boundaries. This is an aspect in which the necked part probably differs from the parallel part (see below). It appears that during the rapid

extension involved in necking, fresh dislocations are generated faster than they can diffuse to the sub-boundaries.

### V.—CALCULATION OF DISLOCATION DENSITY

The dislocation density, counting only dislocations in sub-crystal boundaries, can be calculated from equation (1) if the sub-crystal size is found. Equation (1) gives the density for one set of boundaries only; as two occur of similar spacing, (1) has to be multiplied by a factor of 2. The number of sub-boundaries/cm. parallel to the longitudinal direction was found to be 304 on a micro-section just under the surface, 350 on a mid-section parallel to the surface, and 386 on a mid-section parallel to the side. The differences are probably not significant. Because of the irregularity of the sub-crystal structure it is a good enough approximation to take the mean value for  $d = \frac{1}{336}$  unaltered. For  $\theta$ , the mean of all the values given in Tables III (a) and (b) for 848 and 853 hr. was taken ( $\alpha = 9.30^\circ$ ,  $\theta = 13.1^\circ = 0.23$  radian).

Inserting in equation (1) and multiplying by 2:

$$\rho = \frac{2 \times 0.23 \times 336}{2.8 \times 10^{-8}} \\ = 5.5 \times 10^9 \text{ dislocations/cm.}^2$$

If it is assumed, on account of the apparent perfection under the microscope and on a back-reflection X-ray pattern of the sub-crystals (excluding the necked region), that few dislocations lay within the sub-crystals at any instant, this figure is close to the total density. The hardness of the specimen rose from 13.5 before the test began to 15.4 at the end; on this assumption the small increase is due to this density of dislocations arranged in a more or less regular way.

### VI.—DISCUSSION

The interference measurements of displacement are self-consistent up to about 20% elongation; beyond this there is increasing scatter. The horizontal measurements from marker lines are less satisfactory. The measurements of different processes add together in a reasonably satisfactory way; the greatest improvement would come from a knowledge of the distance that dislocations move during polygonization.

However, practically all these measurements were made on the specimen surface, and this raises an obvious objection. Part of the anisotropy of the displacements might be attributable to some surface effect, though, as there was evidently a preferred orientation, it is unlikely that all of it was due to this. It would be very useful to make equivalent measurements of displacement in the specimen interior, but there seems no way of doing so at present. One reassuring feature in this connection is that for the tilt between sub-crystals, which it was possible to measure on the surface, just under the surface, and in

the specimen interior, rough agreement was found in all positions. Moreover, no difference was observed between microstructures from different regions.

In the specimen studied polygonization proved to be the deformation process in each individual crystal characteristic of the second stage of creep. Since polygonization involves diffusion of dislocations, and since creep rates as a function of temperature are often governed by an activation energy, it is tempting to regard this process as that controlling the creep rate. However, in a polycrystal the situation may well be complicated by the fact that each crystal must accommodate itself to the movement of its neighbours.

The polygonization process involves fine slip that may be extremely difficult to detect, e.g. it may involve no more than one dislocation travelling along a given slip plane. It is rather striking that so much of the extension (about one-half) in the present work was due to fine slip. This was foreshadowed by Hanson and Wheeler<sup>8</sup> and makes it necessary to regard with caution the interpretation of Wood and his co-workers<sup>22</sup> that creep can occur without slip.

Since the demonstration by Ewing and Rosenhain<sup>23</sup> that visible slip bands were produced as steps in the surface during plastic deformation of metals, it has been tacitly assumed that slip is confined to isolated planes or groups of planes, separated by perhaps  $1\mu$ , the lamellae between remaining undeformed. As, in the present work, a multitude of slip bands of very small displacement were formed down to, and presumably beyond, the limit of sensitivity of the phase-contrast microscope (the most powerful instrument yet available for this kind of examination), it seems that this assumption may not be correct. Numerous small displacements, perhaps down to unit slip distance, may be general but may have escaped detection.

### ACKNOWLEDGEMENTS

The author desires to acknowledge the assistance given by Mr. M. H. Farmer, who prepared the specimens and took many of the measurements and photographs. Mr. R. W. Ridley was responsible for the creep straining, and the electron micrograph was taken by Mr. J. Trotter.

The work was carried out in the Metallurgy Division of the National Physical Laboratory as part of the general research programme, and is published by permission of the Director.

### APPENDIX

#### CALCULATION OF EXTENSION FROM DISPLACEMENT AND ORIENTATION MEASUREMENTS

##### 1. Slip Bands

The formulæ on p. 518 are worked out for a single crystal. Aluminium has twelve slip systems, one of which must always lie near the direction of maximum shear even with random orientation. Because of this, it is considered that the formulæ also apply



closely for a polycrystalline specimen. The direction of maximum shear is  $45^\circ$  from the stress axis.

The situation is therefore as shown in Fig. 7, in which  $a_0$  lies in the initial direction of the

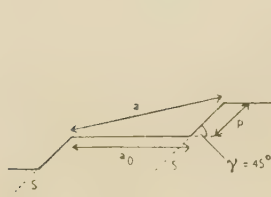


FIG. 7.  
 $S =$  Slip bands.

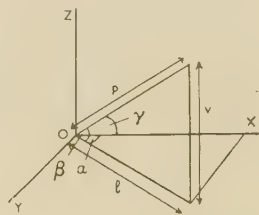


FIG. 8.  
 $OXY$  is the plane of the specimen surface.  
 $p$  is the total slip displacement.

specimen axis, and  $p$  is the slip on one slip band and lies in the slip direction. The new direction of the specimen axis due to crystal rotation caused by slip is that in which  $a$  lies. The elongation:

$$E \text{ slip} = (a - a_0)/a_0 \\ = \frac{\sqrt{(a_0^2 + p^2 + 2a_0p \cos 45^\circ)} - a_0}{a_0} \quad (5)$$

If there are  $n$  slip bands/cm. of the original length of the specimen,  $a_0 = 1/n$  on average.

$$E \text{ slip} = 100[\sqrt{1 + \sqrt{2}np + n^2p^2} - 1]\% \quad (6)$$

Putting  $\gamma = 45^\circ$  in equations (5) and (6) is equivalent to assuming that all the crystal rotation arises from this slip. This was not so, since considerable fine slip also occurred, but the error at 50% total extension was only about (-2%) in  $E$  slip (calculated from the amount of fine slip deduced to occur). Corrections at intermediate values were rather arbitrary, since the necessary data were not available; this correction has therefore been omitted.

In Fig. 8,  $OXY$  is the plane of the specimen surface,  $p$  is the actual displacement in the slip direction, as in Fig. 7,  $v$  is the component normal to the surface, and  $l$  the component parallel to the surface in the direction of movement as projected on to the surface. Clearly  $p = \sqrt{v^2 + l^2}$ . In equations (5) and (6) a mean value of  $p$  is required. To allow for the variation of  $v/l$  with the angle  $\beta$ , the value required is strictly the mean of  $(v^2 + l^2)$ . The measurements did not give this, as  $v$  and  $l$  were not usually recorded for the same individual movements, so the value  $\sqrt{\bar{v}^2 + \bar{l}^2}$ , which should not differ greatly, is used instead.

Apart from assuming that slip occurs in a direction at  $45^\circ$  to the axis, no assumption has so far been made about randomness of displacement direction (i.e. ratio of the angles  $\alpha$  and  $\beta$  in Fig. 8). Such an assumption was not permissible for this particular specimen, for, as noted, the slip bands initially nearly all lay close to  $45^\circ$  from the specimen axis, indicating preferred orientation such that  $\beta$  was small and  $\alpha$

approached  $45^\circ$  in most grains. It was possible to check this by comparing the measured value of  $\bar{l}/\bar{v}$  with that computed for random direction of displacement, as follows:

Ratio of  $\bar{l}/\bar{v}$

(a) With  $\gamma = 45^\circ$  as for slip bands:

$$\bar{l} = \frac{4}{\pi} \bar{p} \int_0^{\pi/4} \cos \beta d\beta \\ = \frac{2\sqrt{2}\bar{p}}{\pi}$$

$$v = \frac{2}{\pi} \frac{\bar{p}}{\sqrt{2}} \int_0^{\pi/2} \sin \theta d\theta$$

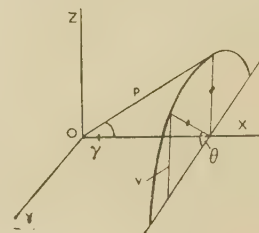


FIG. 9.—Variation of  $v$  (Vertical Displacement) with Direction of  $p$  (Total Slip Displacement).  
 $OX$  is the specimen axis.

since for a given value of  $\gamma$   $v$  varies as  $\sin \theta \times p \sin \gamma$  (Fig. 9).

$$\therefore \bar{v} = \frac{\sqrt{2}\bar{p}}{\pi}$$

$$\therefore \bar{l}/\bar{v} = 2 \quad (7)$$

(b) It is interesting to note that, making one assumption, essentially the same result is obtained if  $\gamma$  takes any direction between  $0$  and  $90^\circ$ , as, for example, it must do for grain boundaries. The applied force  $F$  acts along  $OX$  (Fig. 8). It is necessary to make some assumption about the relation between  $\gamma$  and  $p$ . Assume the displacement in any direction to be proportional to the shear stress in that direction, then:

$$F \sin 2\gamma = ap, \text{ where } a \text{ is some constant.}$$

$$\text{Now } l = p \cos \beta = \frac{F}{a} \sin 2\gamma \cos \beta$$

$$\therefore l = \frac{2F}{\pi a} \int_0^{\pi/2} \int_0^{\pi/2} \frac{\sin 2\gamma}{\gamma} \cos \beta d\gamma d\beta$$

$$= \frac{2F}{\pi a} \int_0^{\pi/2} \frac{\sin 2\gamma \sin \gamma d\gamma}{\gamma}$$

$$= \frac{2F}{\pi a} \times 0.8845 \text{ by numerical integration}$$

$$\therefore \bar{l} = \frac{F}{a} \times 0.563$$

Similarly :

$$\begin{aligned} \bar{v} &= \frac{2}{\pi} \frac{F}{\pi a} \int_0^{\pi/2} \int_0^\pi \sin 2\gamma \sin \gamma \sin \theta d\gamma d\theta \\ &= \frac{4F}{\pi^2 a} \int_0^{\pi/2} 2 \sin^2 \gamma \cos \gamma d\gamma \\ &= \frac{8F}{3\pi^2 a} \\ &= \frac{F}{a} \times 0.270 \quad . \quad . \quad . \quad . \quad . \quad . \quad . \end{aligned} \tag{8}$$

[illegible]

which is very close to equation (7). The difference is within the experimental error. It is therefore taken that for both slip bands and grain boundaries  $l/\bar{v} = 2$  when there is no preferred orientation. For slip bands the actual measured ratio was about 3 at the earliest measurement and increased to about  $5\frac{1}{2}$  at large extension. This increase is close to the calculated increase due to crystal rotation, but the high initial value points to preferred orientation, in the sense that the slip direction lay near to the plane of the specimen surface, and so supports the previous observation.

Since  $l$  is considerably larger than  $v$ , a direct calculation of  $\bar{p}$  from  $\sqrt{\bar{l}^2 + \bar{v}^2}$  gives a set of values for which  $l$  predominates. To obtain another set in which  $v$  predominated, the ratio  $\bar{l}/\bar{v}$  at different extensions was determined from smoothed curves;  $\bar{l}$  was then obtained by multiplying  $\bar{v}$  by  $\bar{l}/\bar{v}$ , and  $\bar{p}$  from  $\bar{v}$  and this  $\bar{l}$ . The mean  $\bar{p}$  of these two determinations was used to compute  $E\%$  slip from equation (6). The values are given in Table I and the curve in Fig. 1.

By this procedure each point on the curve is made the mean of the 200 measurements of  $l$  and  $v$  instead of only the 100 measurements of  $l$ .

## 2. Grain Boundaries

The extension due to grain-boundary displacement was also computed from equation (6). A little consideration of the value to be taken for the angle  $\gamma$  is necessary: in this case  $\gamma$  actually takes all values and, strictly, there should be an integration over these according to some law. However, as the extension due to grain boundaries is quite small, from the point of view of synthesizing the total creep a simplifying approximation here is permissible. Consequently  $\gamma$  was taken to be  $45^\circ$  at all stages of creep, giving the term  $\sqrt{2np}$  in equation (6).

A further consideration was that the ratio  $\bar{l}/\bar{v}$  was initially nearly six and decreased with extension to about two. This indicates that the movements changed direction as extension proceeded, the initially faster horizontal movement slowing down relatively to the vertical movement until the average behaviour was isotropic. It appears that the unusual mode of recrystallization caused some preferred orientation of crystal interfaces as well as crystal lattices. It was thus not possible to compute extensions from  $\bar{v}$  alone, making the assumption that the average behaviour was isotropic. This would have been desirable, since the  $\bar{l}$  measurements showed much scatter, probably because it was difficult in practice to distinguish corresponding reference marks on the two sides of a boundary. However, in order to weight the computation with  $\bar{v}$ , they were made by the second method used for slip bands. The results are given in Table I, and plotted in Fig. 1.

## REFERENCES

1. D. Hanson, *Trans. Amer. Inst. Min. Met. Eng.*, 1939, **133**, 15.
2. A. H. Sully, "Metallic Creep and Creep-Resistant Alloys". 1949: London (Butterworths Scientific Publications).
3. R. W. Bailey, *J. Inst. Metals*, 1926, **35**, 27.
4. H. C. H. Carpenter and J. M. Robertson, "Metals". 1939: London (Oxford University Press).
5. E. N. da C. Andrade, *Phys. Soc.: Rep. Conf. on Strength of Solids*, 1948, 20.
6. W. Rosenhain and J. C. W. Humphrey, *J. Iron Steel Inst.*, 1913, **87**, 219p.
7. L. Rotherham, "Creep of Metals". 1951: London (Institute of Physics).
8. D. Hanson and M. A. Wheeler, *J. Inst. Metals*, 1931, **45**, 229.
9. J. Trotter, *J. Inst. Metals*, 1951-52, **80**, 521.
10. G. Wyon and Ch. Crussard, *Rev. Mét.*, 1951, **48**, 121.
11. G. R. Wilms and W. A. Wood, *J. Inst. Metals*, 1948-49, **75**, 693.
12. C. H. M. Jenkins and G. A. Mellor, *J. Iron Steel Inst.*, 1935, **132**, 179p.
13. E. A. Calnan and B. D. Burns, *J. Inst. Metals*, 1950, **77**, 445.
14. G. B. Greenough and E. M. Smith, *J. Inst. Metals*, 1950, **77**, 435.
15. R. W. Cahn, *J. Inst. Metals*, 1949-50, **76**, 121.
16. A. H. Cottrell, "Progress in Metals Physics" (edited by B. Chalmers), Vol. I., p. 77. 1949: London (Butterworths Scientific Publications).
17. J. M. Burgers, *Proc. K. Ned. Akad. Wetensch.*, 1939, **42**, 293.
18. P. Lacombe, *Chim. et Ind.*, 1945, **53**, 222.
19. A. Hone and E. C. Pearson, *Metal Progress*, 1948, **53**, 363.
20. D. McLean and A. E. L. Tate, *Rev. Mét.*, 1951, **48**, 765.
21. A. Guinier and P. Lacombe, *Métaux et Corrosion*, 1948, **23**, 212.
22. W. A. Wood, G. R. Wilms, and W. A. Rachinger, *J. Inst. Metals*, 1951, **79**, 159.
23. J. A. Ewing and W. Rosenhain, *Phil. Trans. Roy. Soc.*, 1900, [A], **195**, 279.





# ELECTRON-MICROSCOPIC STUDIES OF SLIP IN ALUMINIUM DURING CREEP \*

1375

By J. TROTTER †

(Communication from the National Physical Laboratory.)

## SYNOPSIS

The slow deformation of a specimen of 99.98% aluminium at 200° C. has been studied by means of the electron microscope, using the plastic-replica process. It is shown that the slip zones do not consist of bundles of long parallel slip lamellæ of the type found by Heidenreich and Shockley (*J. Appl. Physics*, 1947, **18**, 1029) in room-temperature deformation, but of intimate segments of primary and cross-slip. A direct consequence of this is that the direction of a slip zone does not, under the conditions of the present experiment, coincide with the trace of the slip plane and, indeed, it may be far removed from it.

## I.—INTRODUCTION

THE present work forms part of an investigation of creep deformation, of which the results obtained using optical and interference microscopy are described by McLean.<sup>1</sup> It is convenient to describe the electron microscopy separately, since some of the features it has revealed merit more detailed discussion than would be appropriate in a general account of the complete investigation.

The electron microscope has recently been used to study the slip zones in aluminium by Heidenreich and Shockley<sup>2</sup> and Brown,<sup>3</sup> who employed the aluminium-oxide-replica technique with considerable success. Since, however, this method involves the destruction of the specimen, it was not suitable for the present work, in which successive optical and electron-optical observations were to be made on a particular specimen during creep deformation. A plastic-replica method, which had proved very satisfactory for the examination of steels,<sup>4,5</sup> was therefore used.

## II.—EXPERIMENTAL

A tensile test specimen of rectangular cross-section, 0.375 in. by 0.25 in., and with a test length of 2 in. was prepared from aluminium of purity 99.98%. The specimen was extended under a constant load of 0.5 ton/in.<sup>2</sup> at 200° C. and removed from the creep machine for examination at each of the following points on the extension/time curve:

Time, hr.:	5.5	22.0	38.5	59.5	124.0	449.0	779.0	848.0
Extension, %:	4.5	7.1	9.5	10.6	13.5	23.6	47.8	62.5

The replicas were prepared by first pipetting on to the specimen surface a 0.5% solution of Formvar (polyvinyl formal) in chloroform. The specimen was then placed in a vertical position and allowed to drain. The resulting plastic coating was backed

with a film of nitrocellulose applied in a similar manner. The composite film was removed under water and picked up on a 200-mesh specimen grid with the nitrocellulose uppermost. Finally, the nitrocellulose was dissolved away with amyl acetate. Both the primary and the backing films obtained in this way were thicker than those usually employed, but this was necessary to enable the Formvar film to withstand the stresses of stripping from a heavily disturbed surface. In spite of these precautions, the replicas frequently broke down at places where there were large and abrupt changes in the surface contour, that is, where there had been a large amount of slip.

Some attempts were made to improve the contrast by "shadowing" the replica with chromium metal. Both low-angle shadowing—the more usual method—and rotation shadowing were employed. The former method enables fine slip lines to be observed only if they are approximately perpendicular to the shadowing direction, and if they are not screened from the source of metal atoms by large surface features. These limitations are largely overcome if the replica is rotated during shadowing about an axis making a suitable angle with the shadowing direction. This process gives a fairly uniform layer of metal over the surface and produces a metal replica similar in character to the aluminium-oxide replica. There was some improvement in resolution with these replicas, but they showed no detail that could not be seen on the unshadowed replicas.

In all some 200 electron micrographs were obtained, most of them showing the "orange peel" background effect which appears to be characteristic of aluminium.<sup>3</sup>

## III.—RESULTS AND DISCUSSION

There is a general similarity of the slip zones over the whole range of extension, the zones are well defined, slightly wavy, and widely spaced. The

\* Manuscript received 14 June 1951.

† Metallurgy Division, National Physical Laboratory, Teddington, Middlesex.



same features appear throughout the whole series of electron micrographs, which, in addition, by virtue of the superior resolution of the electron microscope, show interesting fine detail. Striking examples of this detail are the slip zones illustrated in Figs. 3 and 4 (Plate LXXXI), which have the appearance of cords lying on the surface. It is believed that these result from regular and intimate segments of primary and cross-slip. The detailed analysis by which this conclusion is reached is as follows:

Primary and primary cross-slip are defined as slip in a common direction on two planes which may or may not be of the same crystallographic form. This relationship may be seen in Fig. 1. Slip of this kind clearly cannot account for either the apparent semi-

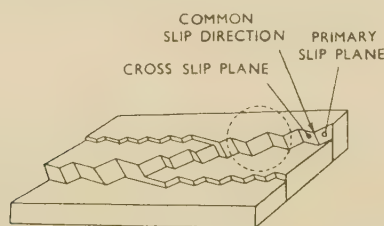


FIG. 1.—Segments of Primary and Cross-Slip Producing the Corded Structure Seen in Fig. 4 (Plate LXXXI).

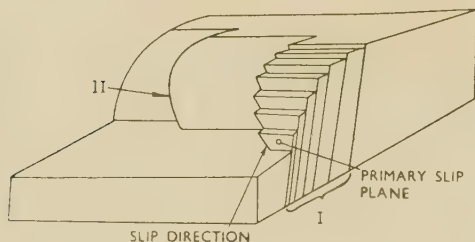


FIG. 2.—Detail Within Circle of Fig. 1. Lamellar slip (I) on a primary slip plane gives a curved trace (II) of the cross-slip plane on the slip zone.

circular section of the slip zone or the curvature of the markings across the zone. The former could be entirely an artefact due to the flow of the plastic replica material over the abrupt changes in surface contour as shown in Fig. 1, an effect that was discussed extensively in the Institute of Metals Symposium on "Metallurgical Applications of the Electron Microscope."<sup>6,7</sup> The curvature of the markings, however, can be due only to the intersection of one or both of the slip planes with a curved surface, and thus the true shape of the slip zone must be as indicated in Fig. 2. Although there is no direct evidence in the electron micrographs, it is reasonable to suppose that the curved surface results from fine lamellar slip, as shown in Fig. 2. It has been suggested that the curvature of the markings might arise from flexing of the replica after stripping, but this is unlikely, since the observed curvatures would demand flexing through 45°–90°. The interpretation

of the cording in Fig. 3 in the light of these considerations is illustrated in Fig. 9 (Plate LXXXIV). The cord-like markings across the slip zone thus appear to be the traces of one of the operative slip planes. Without a knowledge of the crystal orientation, the crystallographic indices of the operative planes cannot be determined and, in general, distinction cannot be made between primary and cross-slip planes. For convenience these markings will be considered here as corresponding to the cross-slip plane.

Other examples of the corded structure are to be found in Figs. 5, 6, and 10 (Plates LXXXII–LXXXIV). The spacing of the markings varies from the close cording in Figs. 3 and 4 to the wide spacing in Fig. 5. There is no correlation between the spacing and the extension undergone by the specimen.

It is evident from the diagrams that the direction of a slip zone is not generally the same as the trace of the primary slip plane, but is determined by the relative lengths of the primary and cross-slip traces. Furthermore, a change in the direction of the slip zone may be brought about by a change in these relative lengths. On this basis the main feature in Fig. 4 is readily explained. It will be noted, however, that there is in addition some continuation beyond the cross-over of both parts of the slip zone. The interpretation of this observation has already been shown diagrammatically in Fig. 1. With suitable modification of the amounts and lengths of primary and cross-slip, the same diagram will serve to explain the frequently observed branching of slip zones, as for example in Figs. 5 and 6. The last example is a particularly interesting case of multiple branching, where the general direction of the branch zones is very different from that of the parent zone. The amount of slip appears to be divided between the parent and branch zones, and thus, with further subdivision of the branch zones, the amount of slip on each becomes correspondingly less. This may continue until the bundle of fine slip zones vanishes. Since there is no reason to believe that the limiting amount of slip coincides with the limit of resolution in these particular micrographs, it is possible that a slip zone continues to branch and the amount of slip diminishes until it corresponds to a shear of a few atomic distances. There is evidence from comparison of successive optical micrographs of the same area that considerable shear, due presumably to slip, has occurred in the regions between the main slip bands. Fine slip lines which could account for this have been observed by phase-contrast methods after about 1% extension, but with increasing deformation they became too closely spaced to be resolved. There are no electron micrographs relating to this early stage, and indeed it is doubtful whether, with the present technique, the lines could have been observed. In some of the micrographs grain boundaries and slip bands relating to a previous stage in the specimen's history are visible. These were produced by a short creep extension after the specimen had been recrystallized

to a small grain-size before recrystallization to the large grain-size used in these experiments.

Cahn<sup>8</sup> has reported somewhat similar features in deformed aluminium from optical-microscopic examinations, but he has not resolved any of the fine detail described here and thus attributes the cross-over to slip on a single cross-slip plane. Rosi and Mathewson<sup>9</sup> have, however, mentioned one case in which they were able to resolve the cross-over into segments of the primary and the usual cross-slip planes. Cahn also illustrates a case where the cross-over occurs in several stages over a distance of about 20  $\mu$ , each stage causing one slip zone to become narrow while the other is correspondingly broadened. The feature in Fig. 7 (Plate LXXXIII) is probably an extreme case of this effect, with the individual stages so numerous and small as to be unresolved.

Among the micrographs of the present investigation there are many examples of bundles of approximately parallel slip zones. They display a wide variation of appearance, ranging from the complex type shown in Fig. 8 to simple bundles, well defined as in Fig. 16 (Plate LXXIV) of McLean's paper.<sup>1</sup> There is little doubt that they are the result of the branching phenomenon discussed above, differing in the frequency of the occurrence of the branching but maintaining, between branching, a fairly constant ratio of lengths of primary and cross-slip, i.e. maintaining the same general direction of the slip zone.

There are comparatively few examples of two intersecting sets of slip zones of markedly different general directions which could be attributed to the classical primary and conjugate slip systems. One example of this is shown in Fig. 10 (Plate LXXXIV), in which the cording on both sets of slip zones implies that there is cross-slip associated with both the primary and conjugate systems.

Under the conditions of the present investigation—slow deformation of aluminium at 200° C.—it would appear that an essential feature of the deformation process is the incidence of intimate cross-slip. This occurs throughout the deformation range and provides an explanation of the cording, branching, cross-over, &c., of the slip zones described in the preceding paragraphs. The changes of direction of the slip zones formed at high temperatures have been mentioned by Brown,<sup>3</sup> who also ascribed them to cross-slip. This has been confirmed, but in addition, it

is now clear that even the apparently straight portions of a slip zone are frequently the result of regular and intimate slip on the primary and cross-slip planes, and indeed most of the slip zones are of this type. That the ratio of the lengths of primary and cross-slip should remain virtually constant over many alternations of the two systems, as shown in Fig. 3, seems more than fortuitous. It cannot be due to a stress system homogeneous over the whole area, for if this were such as to initiate the two slip systems, then two intersecting sets of slip zones would result. Thus it appears necessary to conclude that the stress system must vary on the scale of the elements of the corded structure in such a way as to produce the alternate segments of slip.

The question then arises as to whether this variation is a fundamental feature of slow deformation at elevated temperatures or whether it is the result of some form of external constraint. In this latter category the corded structure may be ascribed to the presence of a surface oxide coating which at the beginning of testing was somewhat thicker than usual owing to the preliminary recrystallization treatments. If the oxide film sheared along its direction of maximum resolved shear stress, namely at 45° to the stress axis, the underlying metal in adopting this deformation would do so by slipping on elements of the two systems. This type of constrained slip may well be an example of the complex deformation occurring at grain boundaries within the bulk of the metal. It must be pointed out, however, that the regularity of the fine structure of the slip lines makes the possibility that this is an entirely spurious effect due to cracking of the oxide film most unlikely. It is hoped that work in progress will throw further light on this problem.

#### ACKNOWLEDGEMENTS

The author wishes to acknowledge the co-operation of Mr. D. McLean in making available the specimen and the results of his own observations, and the advice and assistance of Dr. C. J. Birkett Clews and Mr. E. A. Calnan in the interpretation of the electron micrographs.

The work has been carried out as part of the research programme of the National Physical Laboratory, and this paper is published by permission of the Director of the Laboratory.

#### REFERENCES

1. D. McLean, *J. Inst. Metals*, 1951-52, **80**, 507.
2. R. D. Heidenreich and W. Shockley, *J. Appl. Physics*, 1947, **18**, 1029; *Phys. Soc.: Rep. Conf. on Strength of Solids*, 1948, 57.
3. A. F. Brown, "Metallurgical Applications of the Electron Microscope" (*Inst. Metals Monograph and Rep. Series No. 8*), 1950, 103.
4. J. Trotter and D. McLean, *J. Iron Steel Inst.*, 1949, **163**, 9.
5. J. Trotter, D. McLean, and C. J. B. Clews, "Metallurgical Applications of the Electron Microscope" (*Inst. Metals Monograph and Rep. Series No. 8*), 1950, 75.
6. G. L. J. Bailey and S. Vernon-Smith, *ibid.*, 48.
7. J. Nutting and V. E. Cosslett, *ibid.*, 70.
8. R. W. Cahn, *J. Inst. Metals*, 1951, **79**, 129.
9. F. D. Rosi and C. H. Mathewson, *Trans. Amer. Inst. Min. Met. Eng.*, 1950, **188**, 1159.





# ALLOTROPIC TRANSFORMATION IN TITANIUM-ZIRCONIUM ALLOYS\*

1376

By PROFESSOR POL DUWEZ,† D.Sc., MEMBER

## SYNOPSIS

In titanium-zirconium alloys, the transformation from the high-temperature body-centred cubic  $\beta$  solid solution to the low-temperature hexagonal close-packed  $\alpha$  solid solution is shown to take place, at least partially, at all compositions and at rates of cooling as high as 8000° C./sec. This transformation is not complete, however, and the amount of the  $\beta$  solid solution that is retained is a maximum in alloys containing 50 at.-% of each metal.

## I.—INTRODUCTION

THE early work of Fast<sup>1</sup> on the titanium-zirconium system revealed the existence of an uninterrupted series of solid solutions. Since both metals have an allotropic transformation from a hexagonal close-packed structure ( $\alpha$ ) to a body-centred cubic structure

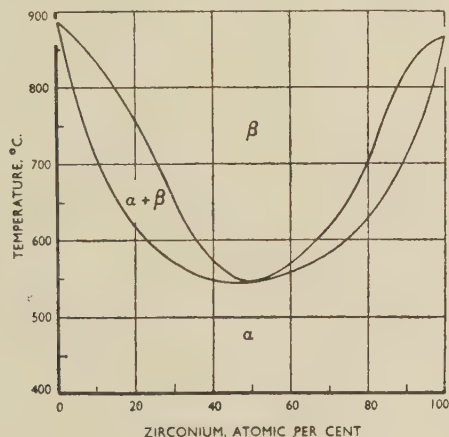


Fig. 1.—Boundaries between  $\beta$  and  $\alpha$  Solid Solutions, According to Fast.<sup>1</sup>

( $\beta$ ) stable at high temperatures, the solid solutions are also hexagonal close-packed at low temperatures and body-centred cubic at high temperatures.

In the phase diagram established by Fast, the  $\alpha$  and  $\beta$  solid-solution fields are separated by a narrow two-phase region, in which both cubic and hexagonal solid solutions are in equilibrium (Fig. 1). The purpose of the present study was to determine whether or not the  $\beta \rightarrow \alpha$  transformation of the solid solutions could be suppressed by rapid cooling, and, if it were not suppressed, to what extent the transformation temperature could be depressed.

## II.—MATERIALS AND PROCEDURE

Pure titanium and zirconium metals, prepared by the iodide process, were received from the New

Jersey Zinc Company and the Foote Mineral Company, respectively. The alloys were melted in a helium arc furnace on a water-cooled copper block.<sup>2</sup> After melting, the specimens, weighing approximately 10 g. each, were slightly cold worked by rolling, then sealed in evacuated fused silica capsules, and given a homogenization treatment for 10 days at 980° C.

The technique used for the determination of the transformation temperature during rapid cooling was essentially that described by Greninger<sup>3</sup> in his study of the martensite arrest in carbon steels. This same technique had been used more recently for the study of titanium-molybdenum and titanium-vanadium alloys.<sup>2,4</sup> The specimens consisted of two pieces of metal about 0.020 in. thick and  $\frac{1}{16}$  in. square; 0.005-in. Chromel/Alumel thermocouple wires were placed between the two pieces and the assembly spot-welded. The specimens were heated in vacuum or in helium and rapidly cooled by a helium jet. The temperature was recorded on a rotating-drum-type oscillograph.<sup>2</sup> With the exception of a few tests, the break in the cooling curve was quite easy to locate and the accuracy of measurement of the transformation temperature was approximately  $\pm 5^\circ$  C.

## III.—RESULTS OF RAPID-COOLING EXPERIMENTS

Alloys containing 2.5, 5, 7.5, 10, 15, 20, and up to 90 by steps of 10 at.-% zirconium in titanium were studied with cooling rates in the range 100°–8000° C./sec. For each alloy composition, from 5 to 10 cooling curves were recorded at various speeds. Results obtained on alloys containing up to 50% zirconium are presented in Fig. 2, from which it will be seen that, within the range of cooling rates used for these experiments, the temperature at which a thermal arrest was observed appeared to be independent of the cooling rate, except in the case of the alloy containing 2.5% zirconium, for which a slight decrease in temperature (about 20° C.) was observed. No effect of rate of cooling was observed

\* Manuscript received 1 November 1951.

† Associate Professor of Mechanical Engineering, California Institute of Technology, Pasadena, Calif., U.S.A.



in alloys containing 60, 70, 80, and 90 at.-% zirconium.

The temperature at which the thermal arrest was observed is plotted against zirconium content in Fig. 3. In this graph, a vertical bar is used for pure

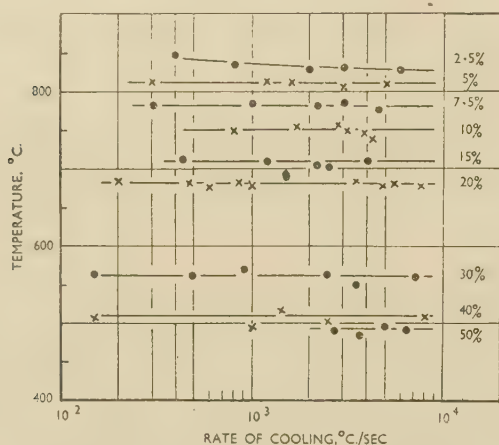


Fig. 2.—Effect of Rate of Cooling on the Transformation Temperature of  $\beta$  Solid Solution for Various Atomic Percentages of Zirconium.

titanium, pure zirconium, and for the 2.5 at.-% zirconium alloy. This vertical bar indicates that in these cases the transformation temperature was depressed by rapid cooling by an amount corresponding to the length of the bar. By comparing Fig. 3 with Fig. 1, it is apparent that under conditions of

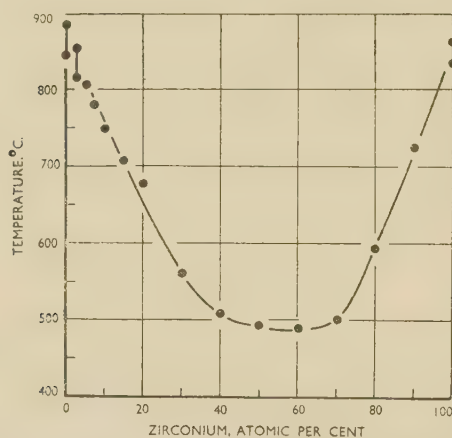


Fig. 3.—Transformation Temperature of Rapidly Cooled Titanium-Zirconium Alloys.

rapid cooling, the  $\beta \rightarrow \alpha$  transformation takes place at temperatures somewhat lower than those corresponding to equilibrium conditions. However, since the transformation temperatures are not appreciably affected by the rate of cooling in the range 100°–8000° C./sec., it is logical to assume that the transformation is diffusionless and that the atomic mechanism involved is similar to that of a martensitic

reaction. The slight decrease in transformation temperature with increasing rate of cooling observed for the 2.5 at.-% zirconium alloy is compatible with the fact that a similar effect exists in pure titanium. If experiments had been made with alloys rich in zirconium (above 95%), a similar situation would probably have been found. The curve in Fig. 3 may therefore be considered as independent of the rate of cooling, except for concentrations approaching 0 and 100% zirconium. In any case, the effect of cooling rate on the transformation temperature of titanium-rich or zirconium-rich alloys would be smaller than that observed for pure titanium and pure zirconium (cf. vertical bars on Fig. 3).

#### IV.—STRUCTURE OF QUENCHED ALLOYS

Although the results of the thermal analysis discussed in the previous section showed the existence of a thermal arrest for titanium-zirconium alloys over the entire range of composition, the possibility that the  $\beta \rightarrow \alpha$  transformation takes place only partially must not be ignored. In fact, it was observed that the thermal arrest was much less pronounced for the alloys containing about equal amounts of titanium and zirconium than for the alloys rich in either titanium or zirconium. This observation led to the conclusion that some of the  $\beta$  phase might be retained after rapid cooling, in alloys whose compositions lay in the centre of the phase diagram. This fact had already been mentioned by previous investigators in a metallographic study of titanium-zirconium alloys prepared by melting together the two metals obtained in sponge form by the Kroll process.<sup>5</sup> In the present study, an X-ray-diffraction investigation was made in order to identify the phases present in the alloys quenched from 980° C. The X-ray-diffraction patterns were obtained with a 143.2-mm.-dia. powder camera, in which the Straumanis film arrangement was used. The radiation was  $\text{Cu } K_\alpha$  filtered through nickel foil. In an attempt to reduce to a minimum the line-broadening effect due to thermal stresses and cold working, the powder was first filed from the quenched specimens, sealed in an evacuated fused silica tube, reheated for 5 min. by introducing the tube into a furnace at 980° C., and then quenched in liquid argon.\*

Analysis of the X-ray-diffraction patterns revealed that the patterns of the alloys containing 10 and 90% zirconium were those of the hexagonal close-packed  $\alpha$  phase, and all the others from 20 to 80% zirconium, by steps of 10%, contained both the hexagonal  $\alpha$  and the body-centred cubic  $\beta$  reflections. In addition, the relative intensities of the  $\beta$  and  $\alpha$  patterns varied with composition in such a manner that the intensity of the  $\beta$  pattern increased between 20 and 50 at.-% and then decreased between 50 and 80 at.-% zirconium; the change in the intensity of the  $\alpha$

\* As explained elsewhere,<sup>6</sup> titanium and titanium alloy powders react with water during quenching and a change in

lattice parameter, probably due to oxygen absorption, has been observed.

pattern was in the opposite direction. It is therefore quite clear that the  $\beta \rightarrow \alpha$  transformation during rapid cooling is not complete. The extent of this transformation decreases with the addition of zirconium to titanium as well as with the addition of titanium to zirconium and reaches a minimum in the alloy containing equal atomic proportions of the two metals (65.6 wt.-% zirconium).

The X-ray-diffraction measurements lead to some interesting observations concerning the variation of lattice parameter of the predominant phase in the quenched alloys. The parameters of the  $\alpha$  phase were measured for the alloys containing 10, 20, 30,

transformation is accompanied by a change in volume. Since the change in volume occurs over limited portions of the powder particles, internal stresses are set up.

Considering the degree of accuracy in lattice-parameter measurements just discussed, the plot of the variation of lattice parameter with concentration shown in Fig. 4 may be regarded as very nearly linear. The straight line drawn through the parameters of the cubic  $\beta$  phase extrapolates to 3.27 kX for titanium and 3.58 kX for zirconium. These values could be compared quantitatively with those measured around 900° C., namely 3.32 kX for titanium<sup>7</sup> and 3.61 kX for zirconium,<sup>8</sup> if sufficiently accurate thermal-expansion curves were available for both metals up to at least 900° C.

## V.—CONCLUSIONS

1. In titanium-zirconium alloys, the high-temperature  $\beta$  solid solution transforms, at least partially, into  $\alpha$  solid solution at rates of cooling as high as 8000° C./sec. Since the temperature at which the transformation takes place is not appreciably affected by the rate of cooling, the reaction is most probably of the martensitic type.

2. Retained  $\beta$  solid solution is noticeable in alloys containing 10 at.-% of either titanium or zirconium, and the amount increases progressively with addition of one metal to the other, so as to reach a maximum in the alloy containing approximately 50 at.-% of each metal.

3. Within the limits of accuracy imposed by the lack of sharpness of diffraction patterns of quenched alloys, the lattice parameters of the retained  $\beta$  phase and of the  $\alpha$  phase resulting from the rapid transformation of  $\beta$  during quenching vary approximately linearly with composition.

## ACKNOWLEDGEMENTS

This work was sponsored by the Office of Naval Research, United States Navy, under contract number N6onr-24430. The author wishes to thank Mr. Paul Pietrokowsky, for preparing the alloys and conducting the X-ray-diffraction experiments, and Mr. W. V. Wright, Jr., for carrying out the rapid-cooling experiments.

## REFERENCES

1. J. D. Fast, *Rec. Trav. Chim.*, 1939, **58**, 973.
2. P. Duwez, *Trans. Amer. Inst. Min. Met. Eng.*, 1951, **191**, 765.
3. A. B. Greninger, *Trans. Amer. Soc. Metals*, 1942, **30**, 1.
4. P. Pietrokowsky and P. Duwez, unpublished work.
5. E. T. Hayes and A. H. Roberson, *U.S. Bur. Mines Norwest Electrodevelopment Lab. Progress Rep.*, No. **3**, 1950.
6. P. Duwez and J. L. Taylor, *Amer. Soc. Metals Preprint* No. **3**, 1951.
7. J. D. Fast, *Z. anorg. Chem.*, 1939, **241**, 42.
8. R. Vogel and W. Tonn, *ibid.*, 1931, **202**, 292.

\* This statement is confirmed by the fact that if pure titanium or zirconium powder is quenched in liquid argon,

very sharp X-ray-diffraction patterns with resolved doublets can be obtained.

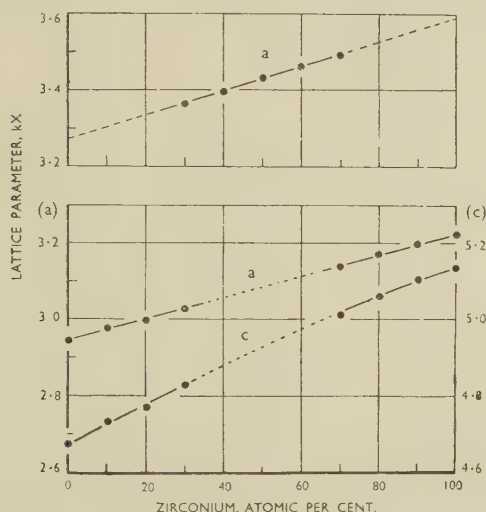


FIG. 4.—Lattice Parameters of Retained  $\beta$  (above) and  $\alpha$  (below) in Titanium-Zirconium Alloys Quenched from 980° C.

70, 80, and 90% zirconium and those of the  $\beta$  phase for alloys containing 30, 40, 50, 60, and 70% zirconium. A plot of lattice parameter against concentration is shown in Fig. 4. The accuracy of the parameter values is approximately  $\pm 0.005$  kX for the values of  $a$  and  $\pm 0.01$  kX for the values of  $c$ . The main limitation in obtaining a greater accuracy was the lack of sharpness of the high-angle reflections, for which the  $K_\alpha$  doublets were not resolved. As explained before, cold working of the powder or quenching stresses were eliminated as causes of line broadening.\* A possible explanation for the lack of sharpness of the patterns of the quenched titanium-zirconium alloys is that, during quenching, the partial transformation from  $\beta$  to  $\alpha$  takes place without the changes in composition which would occur if the alloys were cooled extremely slowly through the two-phase region of Fast's equilibrium diagram (Fig. 1). The coexisting  $\alpha$  and  $\beta$  phases after quenching are therefore under strain because they are supersaturated with one or other element. Another possible reason for the presence of internal stresses in the quenched alloys is that the  $\beta \rightarrow \alpha$



## Discussion

# The Alloys of Molybdenum and Tantalum

By G. A. GEACH and D. SUMMERS-SMITH

(*Journal*, this vol., p. 143.)

Dr. S. F. RADTKE,\* Professor W. C. SCHUMB,\* and Professor M. B. BEVER † (Member): The heavy metals in groups VA and VIA of the Periodic System melt at high temperatures and react readily with common gases and refractories. The resultant experimental difficulties are considerable and have tended to retard the investigation of these metals and especially of their alloys. The results reported in this paper are therefore a welcome contribution to a largely undeveloped field.

The authors state that no loss of molybdenum by evaporation occurred and that the greatest deviation from the nominal composition was less than 1.5 wt.-%. Obviously, the differences between intended compositions and analysed compositions in their Table I cannot be caused by evaporation of molybdenum, since in all but one instance the molybdenum content increased. The authors may wish to explain the loss of tantalum which must have occurred.

Composition changes in the preparation of the alloys are of no consequence in evaluating subsequent measurements, but they hold some interest for the experimenter. Table A gives pertinent data for some specimens of our own. These samples were prepared by arc fusion of sintered compacts followed by annealing.† The recoveries were probably affected by slight differences in the execution of the arc fusion, but a tendency towards higher molybdenum losses with higher molybdenum contents is evident. In five of the samples the loss was less than 1.5%.

Table A also presents hitherto unpublished densities of the alloys. The values are the averages of measurements by the pycnometer method and by the method of Archimedes, which agreed closely without any systematic difference. A plot of the densities shows a slight positive deviation from linearity, which is in agreement with the negative deviation from Vegard's law found by the authors. The average values

of the densities we determined are only slightly lower than those reported by the present authors and some of our individual measurements agree exactly with theirs.

TABLE A

Composition of Pressed Ta-Mo Compacts, Ta at.-%	Composition of Annealed Ta-Mo Ingots, Ta at.-%	Density, g./c.c. at 26.3 ± 1.3° C.
0	0	10.16
9	10.10	10.83
19	20.08	11.65
29	30.02	12.25
39	39.96	12.91
49	49.47	13.43
59	61.21	14.47
69	71.47	14.92
79	82.77	15.44
89	91.42	15.96
100	100	16.55

Macrohardness and microhardness measurements on our specimens showed the behaviour typical of solid solutions. The macrohardness and microhardness curves exhibited a flat maximum which was displaced to the high-tantalum side of the equi-atomic composition. These findings confirm the authors' observations.

The AUTHORS (*in reply*): We are very pleased to see these further data and to have this support for our observations. The loss of tantalum, which almost always occurred on making up the alloys, baffled us, and we have as yet no satisfactory explanation of it.

\* Department of Chemistry; † Department of Metallurgy, Massachusetts Institute of Technology, Cambridge, Mass., U.S.A.

‡ For details, see W. C. Schumb, S. F. Radtke, and M. B. Bever, *Indust. and Eng. Chem.*, 1950, **42**, 826.

# THE PLACE OF PLASTICS IN THE ORDER OF MATTER \*

1377

By J. J. P. STAUDINGER,† Dr.-Ing.

## SYNOPSIS

After a brief description of the nature of plastics and of their properties, an account is given of various fields of application in which plastics are replacing metals. Some composite metal-plastic articles are also mentioned.

## I.—INTRODUCTION

It is perhaps most fitting that I should introduce this year's May Lecture with a remark from last year's lecture when Sir John Anderson stated: "The production of plastics has become an industry of the first importance, providing materials now regarded as essential for a great variety of purposes". This succinct phrase it is, on which I have based the theme of to-day's lecture, in the course of which I shall outline to what extent and for what reasons the development of plastics may affect the utilization of metals.

The life of man from ages past to the present day has been closely linked with the use of materials by which he could provide himself with food and comfort, with shelter and defence, and the advent of a new material has influenced—if not his moral attitude—at least the mode of his secular occupations. Whereas, in the past, man has had to rely upon naturally occurring materials of mineral, vegetable, or animal origin, which, with the growth of his knowledge, he could improve and diversify, the last few decades has seen the introduction of synthetic materials with designed performance characteristics. These new synthetic materials—and I refer here to those generally known as plastics—are no longer to be considered substitutes for one or the other material, but by their unique combination of properties must now be recognized as a new species of matter. Otherwise, it would be difficult to explain the rapid growth of this industry which has become an important feature of our economic life. The spread of usage of plastics in all branches of industry and for all aspects of our life has been remarkable in extent and variety, and life without plastics would mean a life without electronics, without radar, without wireless and television, and without a good many other things. Thus it came about that these synthetic materials, by virtue of

their properties or economics or availability, penetrated into the fields of rubber, fibres, wood, leather, glass, clay, and metal. This sure and swift progress has caught the imagination of a wide public which has come to look upon plastics as the cure-all for many material deficiencies and raw-material shortages. This over-enthusiasm has led the public Press to describe our days as the beginning of the "Plastics Age". As I cannot entirely disagree with this view, I face the audience of the Institute of Metals with the trepidation which the early metallurgists must have experienced when, at the onset of the Iron and Bronze Age, they extolled the virtues of metals to the experts and artisans of the then highly developed flint and stone industry.

When, in the course of this lecture, I betray my enthusiasm for polymers and plastics, I pray you will consider it pardonable on the grounds of the fascinating spell which this new branch of science, i.e. polymer chemistry, casts over its disciples. Through the growing knowledge of the fundamental reactions, which lead to these polymer molecules and through the better understanding of their configuration and their behaviour, it has become possible to design and produce synthetically new materials of construction having predetermined characteristics, which range from products with rubber-like elasticity to hard plastics and to fibre-forming materials, and which can be transparent or opaque, crystalline or amorphous, soft or hard, elastic or brittle.

## II.—THE NATURE OF PLASTICS

Unfortunately, the term "plastics" is used indiscriminately to describe any of these materials, without distinction of their chemical origin or their properties. The number of chemicals that can be converted into plastics is so great and their nature so diverse that for a clearer understanding of their

\* Delivered at the Annual General Meeting, London, 24 March 1952.

† Director of Research, British Resin Products Ltd., Sully, Penarth, Glam.



properties, a very brief glimpse into the chemistry of a few of these materials may not be amiss.

I should mention here that every student of organic chemistry has at one time or other, synthesized, unwillingly and unwittingly, some polymers in the form of a sticky or pitchy residue in his reaction flask, which, in his quest for the distillate, he has neglected and relegated to the sink. To-day, however, science recognizes and industry acknowledges the importance of such substances, which are merely the large molecules from which plastics can be produced.

These large molecules we call "polymers", and evidence shows that they are not always infinitely complex and ramified in their structure, but are built up by successive repetition of small units, which we call the "monomers". Nature herself produces a variety of polymers such as starch, cellulose, rubber, and proteins, which by means of some chemical modification we can turn into plastics; but the greater proportion of our polymers we produce *ab initio*, using identical or different unit molecules, for their construction. When speaking of these large molecules, we must think in terms of molecular weights of several tens of thousands up to hundreds of thousands; even molecules with weights of up to one million or more have been identified and measured in some species of polymers. To get some idea of these giant molecules, I should like you to compare them with a molecule which, also in the limelight, is considered already large by the standards of organic chemistry, namely streptomycin with a molecular weight of 581. According to present knowledge it consists of three individual fragments—or three different monomer units—covalently linked by single oxygen atoms, as in Formula 1.

Against this I quote a few prototypes of polymers, which demonstrate their comparative simplicity of structure:

(1) The reaction of phenol and formaldehyde, one of the earliest discovered reactions, may lead to a polymer of the type shown in Formula 2.

In the case of this phenolic resin the properties of the final product will depend not only on the mode and degree of condensation, but also on the nature of the initial materials. For example, ring substitution can lead to products of greatly varying properties. To this class belong also the reaction products of formaldehyde with urea or melamine.

(2) The condensation of alkylene diamines with dicarboxylic acids leads to a polymer of the type shown in Formula 3.

Should the number of carbon atoms in the diamine as well as in the dicarboxylic acid happen to be six, then the polymer is known as Nylon fibre. It is, however, possible by changing the nature of the dibasic acid or the diamine, to produce polymers without any fibre-forming tendencies, and these are very useful for plastics moulding. Furthermore, by alkyl substitution on the nitrogen, one can impart rubber-like elasticity to the polymer.

(3) The polymerization of a vinyl- or vinylidene-

type monomer leads to polymers of the type shown in Formula 4.

Here again most profound variations of characteristics can be achieved by changing the nature of the lateral substituents *X* and *Y*, and without any structural changes in the polymer molecule, the resultant polymer may be a rubber or a hard plastic or may even have fibre-forming properties:

<i>X</i>	<i>Y</i>	Nature of Polymer	Type of Polymer
H	H	Crystalline	Polyethylene
CH <sub>3</sub>	CH <sub>3</sub>	Rubbery	Polyisobutene
H	O.OC.CH <sub>3</sub>	Plastic	Polyvinyl acetate
H	CO.O.CH <sub>3</sub>	Rubbery	Polymethyl acrylate
CH <sub>3</sub>	CO.O.CH <sub>3</sub>	Plastic	Polymethyl methacrylate
Cl	Cl	Fibre-forming	Polyvinylidene chloride
H	Cl	Plastic	Polyvinyl chloride
H	Phenyl	Plastic	Polystyrene
H	CN	Fibre-forming	Polyacrylonitrile

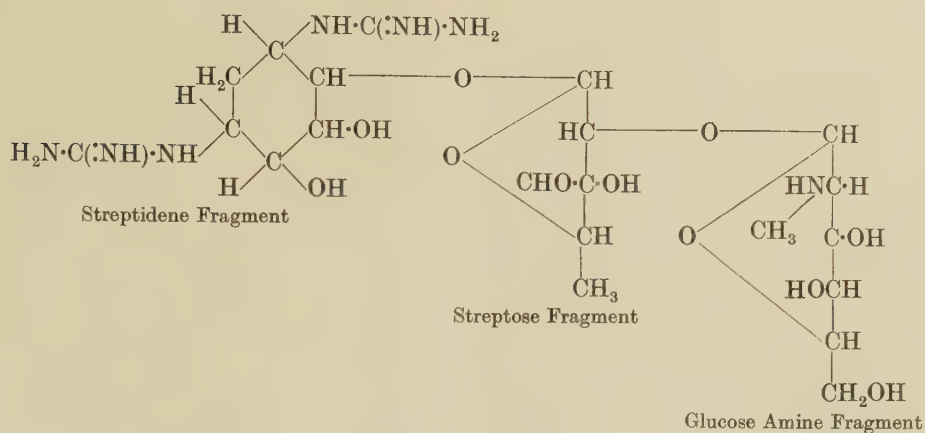
I referred here to the effect of the chemical constitution upon polymer properties merely to stress the fact that the simple tools, the standard reactions, and the established techniques of organic chemistry are required to achieve these far-reaching changes in the performance of a plastic. As might be expected, an infinite variety of properties can result from starting with a mixture of different monomers, and, provided that they co-react, the permutations, combinations, and complexities of effects are almost limitless. Such operations are now common practice, and many plastics are based on copolymers obtained from binary or ternary systems. In its results copolymerization between two, three, or more monomers is not dissimilar from the process of alloying of metals.

The two principal types of reactions, polycondensation and polymerization, can lead to macromolecules only if the reactants are polyfunctional, and, according as to whether these reactions occur between bifunctional monomers or between monomers with a functionality higher than two, we distinguish their end-products as thermoplastic or as thermosetting. The thermoplastics—for example, polystyrene, polymethyl methacrylate, or polyvinyl chloride—remain throughout their existence in a state in which heat and pressure suffice to render them plastic again; whereas the thermosetting plastics—such as the phenolic or urea resins—lose this faculty on the last lap of their course to the end-use type of article.

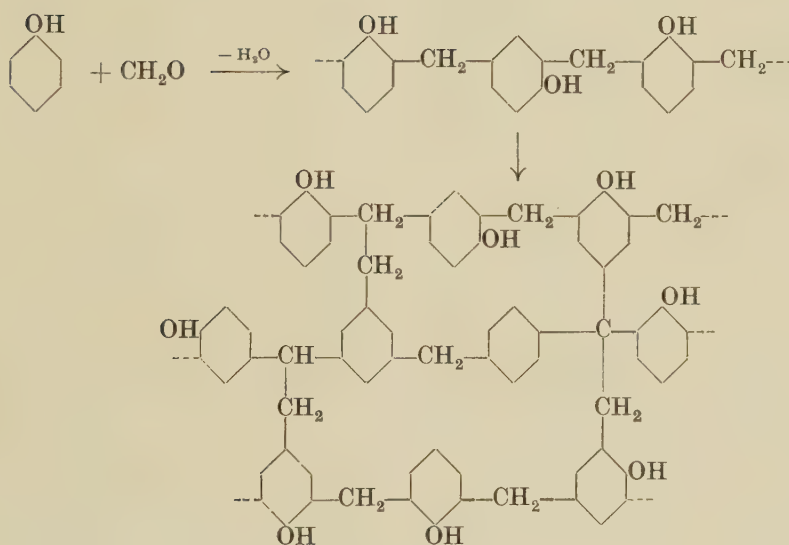
### III.—PROPERTIES OF PLASTICS

When evaluating these plastic materials in relation to metals, it is tempting to look for the basic differences in the nature of matter. It is fortunate that the polymers have one common denominator, namely the fact that their structure is based on the covalent bond between carbon-carbon, carbon-oxygen, carbon-nitrogen, and in a few cases carbon-sulphur and carbon-silicon; in other words the characteristics of the chemical bond must be set against those of the metallic bond.

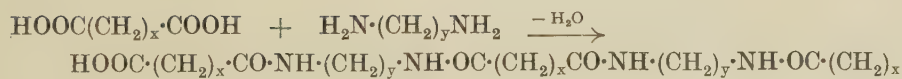
Our present knowledge enables us to accept as correct certain features of the covalent bond, such as



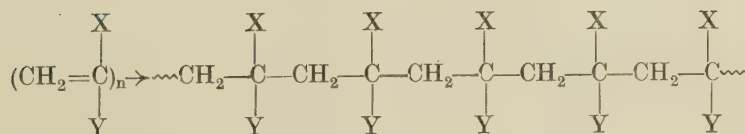
FORMULA 1.



FORMULA 2.



FORMULA 3.



FORMULA 4.



the constancy of primary bond lengths, the constancy of valence angles, and the existence of secondary valence forces. Information on inter-atomic distances as well as on the magnitude of valence angles is available with remarkable accuracy, and this has made it possible to reconstruct, with the aid of models, the structure of polymer molecules and to study their internal mobility. The combination of this morphological approach with the study of the chemical and physical behaviour of polymer molecules in solution, has given us considerable insight into the structural peculiarities of these giant molecules.

We know that a covalent single bond requires energies of between 50 and 100 kg.cal./mol. for its disruption; yet we cannot arrive by sheer mathematical deduction at the practical strength of a plastic, as the ratio of rupture of primary bonds to secondary valence bonds cannot be assessed quantitatively. However, if I may theorize on the supposition that the work necessary to rupture an aggregate of parallel polymer molecules of equal lengths is equal to the chemical work required to sever the primary valence bonds, then a cellulose fibre of 1 mm.<sup>2</sup> would require a force corresponding to 1100 tons/in.<sup>2</sup> to rupture all polymer chains at one C-O linkage. This information about the limiting value for the tensile strength of an ideal chain polymer aggregate is useful, as it indicates the upper limit to what might be accomplished by scientific development. Such strikingly high values are, however, not found in practice. Firstly, the degree of randomness of polymer molecules is very high, so that any applied stress is not taken up by all molecules; secondly, the dimensions of the single polymer molecules are small, from a practical point of view; and thirdly, the forces of cohesion between polymer chains are of a comparatively small order, even if we assume that the macromolecules attract one another in the same way as do small molecules in a gas, a liquid, or a crystal. All this points to the possibility of slippage between adjacent polymer molecules under conditions of high stress. This is one of the peculiarities of polymers.

Whereas organic compounds of low molecular weights possess sharp melting points—as is also the case with metals—this no longer holds for polymers of high molecular weight. Although comparatively little energy in the form of heat is required to dissociate the forces of cohesion and permit thermal agitation of the molecular groups or relaxation of chain segments, the only effect is one of softening.

The temperature at which polymer molecules would exist in the molten state is often near or above the temperature at which they start to decompose or depolymerize. Between the softening point and the decomposition temperature there exists a range of plasticity, and it is this plasticity which is one of the most valuable characteristics of polymers, for it makes possible the convenient conversion of the shapeless tangle of polymer molecules into the desired shape by the moulding process.

These then are some of the factors which are respon-

sible for such properties of plastics, as strength, extensibility, resilience, creep, second-order transition, and flow.

I now venture to set against these characteristics of the metallic bond which are not possessed by products based on the covalent bond, namely the high thermal and electrical conductivity, malleability, ductility, and cold workability of metals. By emphasizing these metallic virtues, a comparison between metals and plastics might be seen more easily in the right perspective.

That the metallic bond is different from the chemical bond is obvious from the fact that it cannot be defined in terms of the covalent-bond laws (atomic distance, bond strength, valence angle, electron sharing, and charge cloud distribution), and also from the fact that the metallic bond forces are often greater than could be attributed to covalent bonds. This is evident from the high melting points and the high heats of evaporation of some metals. Consequently, there must exist a characteristic new form of linkage, concerning which I can say with certainty only that I know very little about it. However, certain considerations point to the fact that in a metal, positively charged ions are embedded in an electron atmosphere distributed throughout the whole crystal. This type of linkage may arise from the fact that the bond electrons leave their sharply defined circuit and begin to permeate into and to move within the three-dimensional field of the atomic lattice. As these electrons are distributed over the whole lattice region, the good electrical conductivity, which is one of the peculiarities of the metallic state, could thereby find a plausible explanation. Such a concept would also entail a lack of direction in the bonding forces which in turn would account for the fact that atoms in the metal lattice may be moved past one another without any essential change in environment. This would explain why metals can suffer large deformation without their properties changing materially, ductility, malleability, and cold workability, which are characteristic of the metallic state, being a consequence.

From this short description it would appear that metals and plastics have very little in common and would not find a field in which both could compete, were it not for such factors as specific strength, resilience, elasticity, and toughness which are common to both types of materials.

When considering these criteria, i.e. strength (tensile value at break), stiffness (modulus of elasticity), elasticity (yield point), resilience (resilient energy), and toughness (energy absorption without break), in relation to plastics, I must emphasize again that temperature and time factors are of greater importance than they are with most metals. It is by the nature of the covalent bond that elevated temperature will bring about thermal unrest within the polymer molecules, so that plastics cannot compete at all with metals as structural components at elevated temperatures. It is essential therefore to know the softening point of plastics because it gives the temperature up

to which they can safely be used. The phenomena of cold flow and creep, which in plastics are greater by many orders of magnitude, particularly in cases where stresses are applied for prolonged periods and/or at temperatures above the ambient region, are also handicaps to the use of plastics. This summary of negatives might appear to weigh heavily against plastics, but once these limitations are recognized and taken into account, the merits and virtues of plastics more than outweigh these deficiencies. In comparing certain properties of plastics and metals it is only fair that we should include the tensile strength on the basis of specific gravity (see Table I).

TABLE I.—Some Properties of Plastics and Metals.

	Specific Gravity	Specific Tensile Strength, lb./in. <sup>2</sup>	Elastic Modulus lb./in. <sup>2</sup> × 10 <sup>6</sup>	Impact Strength, ft. lb./in.	Heat Distortion Temp., °F.
Phenol formaldehyde: Wood-flour filled . . .	1.25	6,400	7.5	0.3	260
String filled . . .	1.32	7,000	12.0	3.0	280
Paper laminate . . .	1.35	20,700	26.0	6.0	270-300
Melamine formaldehyde, cellulose filled . . .	1.47	6,700	13	0.35	400
Silicon resin, glass-fibre filled . . .	1.70	2,000	...	4.5	600
Nylon (moulded) . . .	1.14	8,700	4.0	1.0	360
Polyvinyl chloride/vinyl acetate (rigid) . . .	1.33	6,700	4.0	0.6	150
Polyvinyl chloride (rigid) . . .	1.39	6,470	5.0	0.5	185
Polyvinylidene chloride (moulded) . . .	1.65	3,030	0.8	1.0	150
Polyester/glass fibre laminate . . .	1.80	22,000	2.7	16	...
Polyester resins . . .	1.10	9,900	4.0	0.4	240
Polystyrene . . .	1.05	6,600	5.0	0.4	195
Methylmethacrylate . . .	1.18	6,800	4.5	0.5	165
Polychlorotrifluoroethylene . . .	2.10	2,710	1.9	3.6	>360
Polyethylene . . .	0.92	1,520	0.2	>16	110
Brass (rolled hard) . . .	8.52	7,740	...	...	...
Bronze (cast annealed) . . .	8.78	4,950	...	...	...
Copper (rolled) . . .	8.85	3,620	...	...	...
Iron (cast) . . .	7.13	2,250	...	...	...
Steel (0.71% C, annealed) . . .	7.70	14,000	...	...	...
Steel (casting) . . .	7.55	10,000	...	...	...
Structural steel . . .	7.85	5,200	290	...	...
Aluminium alloy 24ST . . .	2.75	25,000	103	...	...
Magnesium alloy AM585 . . .	1.80	25,500	65	...	...
Elektron alloy Z6Z . . .	1.81	21,000	65	2.1	...
Elektron alloy AZ91 . . .	1.83	17,500	65	2.5	...

#### IV.—REPLACEMENT OF METALS BY PLASTICS

One thing stands out in the table, and that is the fact that some of the alloys of aluminium and magnesium are superior in specific tensile properties to plastics and also to many of the heavy metals, with the exception perhaps of the highly specialized steels. On that score alone there would appear to be little inducement to replace them by plastics, but as one more example of the melancholy truth that nothing in this world is perfect, even the light metals have their failings, and must concede to plastics some of their domain. Whereas the impact resistance of plastics is generally better, the elastic modulus is lower than that of metals. Nevertheless, the very satisfactory strength of plastics, particularly of the laminated and reinforced varieties, in which the plastic com-

ponent represents about 50% by weight, is the reason why these materials are being increasingly used in the construction of fuselage and other structural aircraft components, small naval craft (see Fig. 7, Plate LXXXVI), dinghies and other pleasure boats, housings for portable and transportable mechanical tools and agricultural machinery, bobbins and other textile machinery components, mining helmets, and even bullet-proof body protection. You will notice that in many of these instances aluminium or its alloys is the metal that can be, and has been, replaced.

An application in which such reinforced plastics have not as yet been able to establish themselves, although some progress has been made in that direction, is in car-body construction. The strength/weight ratio is satisfactory and manufacturing processes are adaptable to mass-production requirements; but another aspect had to be taken into account, namely that resulting from the lack of skill in the motoring performance of the other fellow on the road, who on occasion is held responsible for some indentation, penetration, or distortion of the car-body. Now, with a conventional body such defects are comparatively easy to mend owing to the ductility and malleability of the metal; not so, however, with a plastics body. Nevertheless the reduced steel allocation may tempt car manufacturers to make in plastics at least those parts of the car body which could easily be exchanged as a whole, such as doors, bonnet, or boot covers. Sometimes the attributes of ductility and malleability are undesirable, as, for example, in the case of housings for domestic gadgets such as vacuum cleaners and carpet sweepers, and also in textile appliances such as bobbins, pirns, spools, and weaver's beam flanges and slip rollers, where a high shock-resisting and dent-proof plastic ensures a long life of the component (Fig. 1, Plate LXXXV).

The laminated or reinforced plastics can also be used for bearings and bushings, particularly where lubrication with oil presents difficulties. But even with oil as lubricant or with no lubricant at all, plastics provide satisfactory materials for load-bearing, low-friction surfaces. For such purposes the metal-powder- or fabric-filled phenolic plastics have been developed, and one of the outstanding successes is the use of a fabric-filled phenolic plastic for bearings of all sorts of steel rolling mills (Fig. 3, Plate LXXXV).

Recently some new plastics have entered this field, namely the fluorinated ethylene polymers, which without lubrication have extremely low friction coefficients (of the order of 0.05), and although still in the early development stage, they are potentially capable of much wider use. In addition, all these materials are chemically inert and resistant to the action of moisture and various acids and salt solution.

In all these applications there is one more respect in which plastics are superior to metals, and that is their sound-dissipating, vibration-absorbing, and resonance-dampening effects. This is of significant value in view of the compelling urge of modern man for ever higher speeds, which brings with it a series of problems



in accentuated form, such as noise, vibration, resonance, and even new problems such as rain erosion. In addition, the reduction of the noise-level in factories, in transport machinery, and even in the home is a psychological necessity of our times, and here, too, some of the plastics, by virtue of their ability to absorb mechanical energy, have helped in overcoming difficulties in the design of structural parts, as for example in gears (Fig. 4, Plate LXXXV), couplings, slipper-pads and other metal-to-metal motion elements, railway tie-plates, rail connecting rods, and even in such machinery as typewriters, adding and computing machines, printing and engraving machines, and gyroscopes.

It is difficult to decide what to mention and what to omit in demonstrating the versatility of plastics in the realm of metals, but I shall pay little attention to applications where shortage of metals is the sole compelling motive for the engineer to turn to plastics, nor shall I stress the applications of purely military significance, such as plastic grenades, plastic bombs, plastic shell noses, plastic proximity fuse heads, plastic mine-detectors, or plastic gun-flash simulators (Fig. 2, Plate LXXXV). That such applications are of a transient nature in more senses than one, I am only too aware. In quoting only the few examples where plastic materials can compete successfully with metals on a strength/weight basis, I hope to have conveyed at least some idea of the scope of their application.

But mechanical strength is not the sole consideration where the employment of metals is concerned. For lack of a more suitable material, metals were often selected because of their adaptability to mass production. For example, the great variety of encapsulations used in the low-power electricity distribution system, such as fuse boxes, switch cases, joint and distribution boxes, conduits, terminals, relay cases, are now increasingly made from plastic materials, mainly of the phenolic, urea, or melamine type. Previously many of these articles were made from metal or wood, or even ceramic materials, but none of these possessed the combination of properties which are so desirable in these applications, namely excellent insulating properties, satisfactory strength, light weight, durability, corrosion-resistance, and in addition economy in production; and here the use of plastics is spreading.

Electricity distribution consumes also considerable quantities of lead, and its replacement by plastics such as polyvinyl chloride or polyethylene has now become an established practice. These multitudinous electrical components and the protection of cables with lead cut heavily into the country's stock of metals, and in addition to making an even better job, plastics have enabled these stocks to be conserved.

I have not yet stressed one aspect in favour of plastics which in nearly all applications is of considerable importance, that is the ease of production by the modern moulding processes, which permit most complicated designs, even with multiple undercuts, to be made in one piece, with the greatest accuracy of

dimensions, to very close tolerances, with all the necessary inserts fixed into their right positions, at high production rates, and at low reject rates. In addition, surface finish and colour are built-in features with plastics, resulting in less assembly time and fewer finishing operations. These manufacturing assets will prove plastics to be more economical for mass production than metals in a great number of cases.

In this connection I may perhaps mention one of the most interesting examples of plastics as successors to a variety of metals, namely in the construction of refrigerators, deep freezers, and ice-cream machinery. The low thermal conductivity, the inertness to moisture and to the chemicals contained in food, the hygienic appearance of plastics, and the saving in cost have made this change-over quite universal. Ice-cube trays, drip trays, food boxes, and freezer-compartment doors are only a few instances where polystyrene or polyethylene have taken the place of aluminium. This is a typical case where plastics on account of performance, economy, and appearance satisfy the requirements better than any other material.

There are still other fields, where the resistance of certain plastics (polyethylene, polystyrene, polyvinyl chloride, polyvinylidene chloride, polyfluoro-ethylene, and some of the phenol/formaldehyde plastics) to the action of corrosive liquids, vapours, and fumes has broadened their industrial application considerably. With the progress in the techniques of fabrication, plastics will oust metals from a variety of applications, such as tanks, containers, pipes, tubes, ducts, valves, pump housings, impellers, and fans, where resistance to hydrochloric and hydrofluoric acid, to dilute sulphuric and sulphurous acids, to organic acids, to oxidizing chemicals, and other corrosive media is required. It is possible to-day to manufacture and assemble large and fairly complicated structures from plastics by the use of hot-air torch welding or plastic riveting or synthetic-resin gluing, using metal in some cases merely as external supports (see Fig. 8, Plate LXXXVI). All-plastic frosting tanks for glass treatment, all-plastic ventilation systems and fume ducting, and all-plastic pickling tanks are no longer curiosities in the chemical industry, and no doubt such applications will multiply to the exclusion of metals. Even in the domestic sphere such prosaic utilities as plumbing and sanitation, down to the nursery necessities, have offered plastics many opportunities to outdo metals, and no doubt the increasing tendency towards prefabrication will favour plastics.

Although from this short description it may appear that the philosophy of usefulness is the sole motive for the expanding applications of plastics, this is far from being the case, as many applications are based on their aesthetic appeal; the unlimited colour possibilities of plastics and their low thermal conductivity make these materials pleasing to the eye, comforting to feel, and friendly to touch, so that a countless host of plastic articles for personal, domestic, and industrial use are now accepted. Tool handles, brush handles, buttons and buckles, hair curlers, cosmetic



and other containers, kitchen equipment, furniture trimmings, trays, and screw-cap closures are only a few examples where plastics are increasingly chosen on grounds of visual and sensuous appeal. This field will expand not merely at the rate at which metals will become scarcer for such usage, but even more as a result of their attributes of appearance and low cost.

As well as replacing metals, plastics can join forces with them to give improved combinations. The application of a plastic in the form of a surface coating or in the form of a layer moulded on to a metallic core combines the advantages of both materials, and indeed in such examples as door handles, furniture fittings (Fig. 5, Plate LXXXV), steering-wheels (Fig. 6, Plate LXXXV), car fittings, deck rails, bathroom equipment, the strength and dimensional stability come mainly from the metal core, generally die-cast, and the outward appearance, such as colour and surface finish, feel, and the protection against corrosion, derive from the plastic. In articles of this type the amount of metal replaced by plastics is not very great, as only about one-third of the article is plastic; but no doubt this field of plastics utilization is going to expand, as the desire to have the best of both worlds is such a natural human trait.

Lest I be accused of partiality, I must mention also the reverse process in which metals give the desired surface to a light-weight core of plastics. The hankering after the glitter of shining metal has led to the development of processes for metallizing plastics either by spraying or by electrolytic or vacuum deposition. Apart from the low cost of production of the plastic article, the saving in metal, such as nickel, chromium, silver, or gold, is very great indeed, when one considers that an ounce of metal can cover an area equal to a football pitch. I can visualize that in a very severe metal shortage, practical use could be made of this process by chromium or nickel plating plastics in the form of such simple components as tubes, pipes, containers, agitator blades, and the like. This may save a lot of metal, and an innovation of this type may have great possibilities for plastics.

A point which may be somewhat outside the scope of the present discourse, but which should not be left unmentioned as it demonstrates the versatility of synthetic polymers and as it is closely linked to some metallurgical operations, is the use of synthetic resins as binders in foundry work, in the shell moulding process (Fig. 9, Plate LXXXVI), in sand cores, and also as template material instead of wax composition for precision casting. I would say that among the plastics now picked for greatest future development are those used for foundry work.

## V.—THE FUTURE OF PLASTICS

On the score of the strength/weight ratio, the plastic materials have ample opportunities to replace the heavier metals in a very great variety of applications, although the light metals, aluminium, magnesium and their alloys, appear to be the most serious

competitors of plastics, since they combine the lightness of plastics with the metallic virtues. However, to the pro-plastic factors of appearance, durability, corrosion-resistance, low thermal and electrical conductivity, and low production cost must be added one other important factor, namely that of availability of raw materials.

In our present economy, with the dual priorities for rearmament and export, the raw-material aspect may induce the engineer to consider plastics as an alternative to aluminium or magnesium and their alloys. It may be argued that some of the precursors of the chemicals from which we manufacture the plastics raw materials have to be imported in the same way as, for example, bauxite; and for this reason a short account of the sources from which plastics are derived may not be out of place. Firstly, there is imported oil, which, with the expanding development of the petroleum chemicals industry, is becoming an increasingly important—perhaps the most important—source of supply; secondly, we have indigenous coal, which either via coal tar, via carbide, or via other chemical operations is already a raw-material source of considerable importance; and, thirdly, there are the products and by-products of vegetation such as starch, molasses, cotton-waste, wood-pulp, and seaweed.

You will recognize that these are potentially abundant, easily accessible, and reasonably cheap source materials. You will also be aware that the trend in procurement of raw materials is to use the cheapest and most abundant of these materials, to pass them through an industrial—usually chemical—operation, and to turn them into valuable raw materials. On the other hand, some materials based on geographically ill-located mineral resources are likely to become progressively scarcer or dearer, so that a change from metals to plastics, wherever possible on grounds of technical merit, emphasizes what, plastically speaking, is a healthy, natural, and logical trend.

Now, what does all this replacement of light metals by plastics amount to, in terms of quantities? Assuming a yearly production of aluminium of 1.4 million tons and making a very rough, but optimistic, estimate of 8000–10,000 tons of plastics used instead of aluminium, that would correspond to about 1%. Whereas a doubling of this would mean a very great progress to the plastics industry, it would still constitute only a minor inroad into the volume of metal, which may be more than compensated by the natural growth of the light-metal industry itself.

The place of plastics in the order of matter is now firmly established as the essential link between the natural organic materials, such as pitch, shellac, rosin, rubber, wax, horn, and wood on the one hand, and the minerals (glass, clay, stone) and metals on the other. The organic materials, with the exception of horn and wood, have thermal and mechanical characteristics too low to be useful for structural purposes, while horn and wood, though still light in weight and



possessing already good mechanical properties, do not lend themselves to such a wide variety of applications as plastics do. It is here that plastics fill the gap and ensure the continuity of characteristics between the natural organic materials and the minerals and metals.

By virtue of their position in the order of matter, plastics frequently combine some of the good features of both groups, and for this reason the application of plastics will not only cover those fields where previously other materials have been misapplied for lack of anything better, but will also greatly expand on their own account, as, for example, in the increasingly important fields of electronics, television, and radar. Here, the developments on an industrial scale would not be possible without the aid of plastics. I firmly believe that plastics, which have only begun to show their mettle, will become one of the major materials of construction in our age which becomes more and more dependent on manufactured materials and fabricated goods.

The multitudinous aspects of plastics may not all have become apparent here, as in this discourse I could cover only the narrow area of rivalry between plastics and metals, thus leaving the fascinating story of the all-plastic shoe, the all-plastic ship, and the all-plastic sealing-wax an unrevealed romance.

The plastics age is not yet upon us, but the mind of

modern man is not unaware of the importance of plastics in our life, although acceptance, approbation, and admiration are on occasions still mingled with an undertone of disparagement and doubt. This I found nicely and neatly expressed in a little poem published in *Punch* with which I should like to conclude this short story of plastics in the realm of metals.

"It serves as adjective or noun, just as you wish,  
Like a verbal blancmange, that's flopped from any old dish;  
It has all colours, every one of them shiny,  
It may be tremendous, it may be tiny.  
The stuff takes any shape,  
With the senseless imitation of the ape.  
We may wear it, or eat upon it,  
Play with it, or take a seat upon it.  
With hot things it is hot,  
With cold things it is not.  
It can flap upon occasion like cloth,  
But it denies food to the moth;  
It can even look like lace,  
Boiled hard, devoid of grace.  
It cuts like inferior steel,  
Or turns when shaped like a wheel.  
You can make it whistle as a recorder,  
It will even twang to order.  
It may be sawn or moulded,  
Snipped, nailed, glued, sand-papered or folded,  
It is gymnastic, elastic,  
It is PLASTIC."\*

\* Excerpt from "Deliver Us", reproduced by permission of the Proprietors of *Punch*.

By K. E. PUTTICK,† B.Sc., and RONALD KING,‡ B.Sc.,  
MEMBER

## SYNOPSIS

Specimens of tin consisting of two crystals meeting in a straight boundary were stressed in shear to cause relative movement of the crystals at the boundary. The relation between relative movement and time under steady stress was examined at a number of stresses and temperatures, for a standard type of specimen in which the *c* axes of the crystals were at right angles to one another and at 45° to the boundary.

Over the range of stresses (500–2100 g./cm.<sup>2</sup>) and temperatures (180°–225° C.) employed, the initial rate of relative movement obeyed the relation:

$$\text{rate of movement} = A\sigma \exp(-19,200/RT),$$

where  $\sigma$  is the shear stress across the boundary. The behaviour of the crystal boundary was therefore analogous to that of a viscous liquid.

The physical character of the boundary was found to depend on the nature of the impurities present in the tin. Boundaries in cast specimens of two samples of tin of similar total impurity content, but differing in the relative amounts of impurities, were of different appearance. Straining and annealing produced similar boundaries in the two types of tin.

## I.—INTRODUCTION

It has been known for some time that relative motion of the crystals plays a part in the deformation of polycrystalline metals under low stresses at elevated temperatures,<sup>1,2</sup> but quantitative information on the behaviour of the grain boundary has been lacking until fairly recently, when Kê,<sup>3</sup> by the comparison of certain anelastic phenomena in aluminium, demonstrated that for small relative displacements ( $\sim 10^{-5}$  cm.) of the grains, the material at the grain boundary behaves like a viscous fluid. He found that the rate of relative movement of the grains could be expressed:

$$v = A\sigma \exp(-H/RT)$$

where  $v$  is the rate of relative movement in cm./sec.,  $\sigma$  the shear stress,  $R$  the gas constant,  $T$  the absolute temperature,  $A$ , a constant = 18(cm./sec.)/(dyne/cm.<sup>2</sup>), and  $H$ , the energy of activation = 34,000 cal./g.-atom.

Making the assumption that the boundary layer, was about one atom thick, Kê obtained an expression for the viscosity which when extrapolated to the melting point gave fair agreement with the experimentally determined viscosity of the liquid metal. Although such behaviour would be consistent with the earlier conception of the grain boundary as an amorphous layer similar to an undercooled liquid cementing the grains together, it is not necessary to postulate such a layer to explain the results. Kê has proposed<sup>4</sup> a mechanism for the behaviour in terms of localized readjustments of small disordered regions, which he suggests is also responsible for steady-state creep

within the crystals and for self-diffusion. In the case of aluminium, the activation energy for all these processes is about 34,000 cal./g.-atom.

An alternative mechanism was suggested by Mott,<sup>5</sup> who pictured the boundary as comprising islands of good fit and regions of bad fit. On the assumption that localized melting of the islands due to thermal fluctuations enabled relative movement to occur, he derived an expression for the rate of flow in good agreement with Kê's experimental results.

Kê's results represent an average for a large number of grain boundaries varying in disposition relative to the stress, and possibly of different properties, since they lay between crystals of different relative orientation. The displacements were small. Experiments have therefore been performed by the present authors to provide information concerning the behaviour of a single grain boundary undergoing larger displacements.

## II.—EXPERIMENTAL PROCEDURE

Specimens consisting of two crystals separated by a single straight boundary were tested in shear at different temperatures. In all cases the orientations of the crystals were the same and the boundary was disposed in the same way in the specimen. As far as practicable, the specimens were therefore identical. Tin was chosen because a certain amount of experience had already been gained in the preparation of both single-crystal and bicrystal specimens, and preliminary experiments<sup>6</sup> had shown that measurable displacements occurred under convenient experi-

\* Manuscript received 18 June 1951.

† Physics Laboratory, British Iron and Steel Research Association, London; formerly at the Royal Aircraft Establishment, Farnborough.

‡ Assistant Director, Davy-Faraday Research Laboratory of the Royal Institution of Great Britain, London; formerly at the Royal Aircraft Establishment, Farnborough.



mental conditions. Chempur tin was used in all cases except those referred to in Appendix II.

### 1. PRODUCTION OF SPECIMENS

The specimens were prepared by the moving-furnace method already described in its application to tin by Chalmers.<sup>7</sup> Single crystals were grown in cylindrical moulds with a small constriction at one end. The metal was melted, and the furnace then slowly moved away so that solidification proceeded from the constriction. The single crystals so formed were used as "seeds" from which the bicrystals were grown.

Bicrystals were grown in boats as indicated in Fig. 1. The mould was filled as far as the two end grooves and the two single-crystal seeds were inserted in the grooves at the required orientations. The furnace was moved over the mould from the closed end until the ends of the seeds melted and joined on to the charge in the boat. The furnace was then moved steadily away from the seeded end, solidification proceeding from the seeds along the mould. In general, this treatment produced a specimen consisting of two crystals having the orientations of the original seeds and separated by a reasonably straight boundary. The specimen was 2 cm. wide, about 0.5 cm. thick, and 10 cm. long. The speed of movement of the furnace could be varied over quite a wide range without affecting the result; a speed of 10 cm./hr. was normally used.

From these specimens were cut lengths of 2 cm. upon which boundary-slip determinations were made. Originally, the specimens were grown in plain boats and the required lengths cut off by means of a small

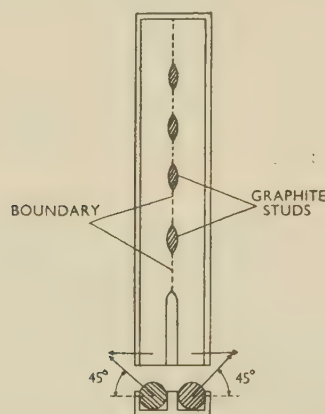


Fig. 1.—Diagram of Mould for Bicrystals, Showing Relative Orientations of Seed Crystals. Arrows indicate  $c$  axes.

blow-pipe flame to avoid the deformation and consequent recrystallization caused by mechanical separation, but this method resulted in uneven edges which presented difficulties both in the determination of the boundary area and in fixing the specimen in the stressing apparatus. Specimens were therefore grown in the type of boat shown in Fig. 1. Graphite studs were pegged to the bottom of the boat and the

crystals grew around them. The boundaries were in general produced as indicated and specimens could then be separated off by sawing, without deformation in the neighbourhood of the boundary itself. Recrystallization following this treatment did not usually extend to the boundary.

To ensure that the specimens were as nearly identical as possible, they were all grown from crystals

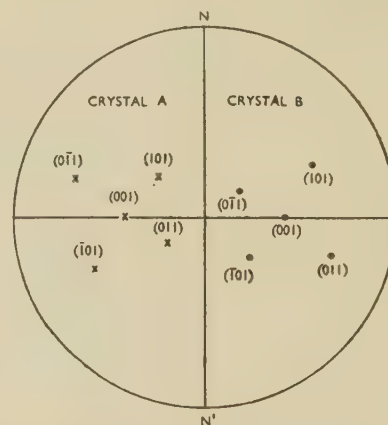


Fig. 2.—Stereographic Projections of the Two Crystals of the Bicrystal Specimens.  $NN'$  = specimen axis.

produced from one original seed crystal grown in a glass mould. The  $c$  axes of the crystals were normal to the specimen axis and in the bicrystals, normal to one another and at  $45^\circ$  to the boundary plane. The orientation of the bicrystal specimens is shown in Fig. 2.

Some information on the conditions necessary for the production of satisfactory specimens is included in Appendix I (p. 543).

### 2. THE OBSERVATION OF GRAIN-BOUNDARY SLIP

The relative movement of the two halves of the bicrystal specimens under a shear stress was observed microscopically. For this purpose the specimens were first electrolytically polished, using perchloric acid.<sup>8</sup> A series of reference lines were then made, perpendicular to the grain boundary, by touching the surface lightly with a razor blade. This treatment produced a fine clear line.

The apparatus for stressing the specimens is illustrated in Fig. 11 (Plate LXXXVII). A simple heater  $H$ , of Nichrome wire wound on a Sindanyo former, is contained in a box made of Sindanyo, in the lid of which is set a small glass window. Two stainless-steel rollers  $Q$  rest on supports fixed to the walls of the box and carry the two clamps  $C_1$  and  $C_2$  in which the specimen is gripped. The  $C_1$  clamp is stationary and is held in position by the threaded rod  $R_1$ , which is fixed to the box by lock-nuts.  $C_2$  is a movable clamp and can be pulled to the right by means of the rod  $R_2$ , which passes out through a hole in the box to a spring assembly by means of which the load is applied. Each clamp consists of a main block to which the rod  $R$  is attached and a stirrup which fits over one crystal of the

specimen and pulls it up against a stop in the main block by the action of the screw  $S_1$  or  $S_2$ . The specimen is so set in the clamps that  $R_1$ ,  $R_2$ , and the boundary are in line. In this way the boundary is subjected to a pure shearing force. While it has been shown<sup>9</sup> that in an elastic solid such a system of loading would lead to a non-uniform distribution of shear stress across the median plane, it is clear that in the case of a grain boundary capable of stress relaxation in a manner similar to a viscous liquid, the shear stress must be uniform.

To investigate the temperature distribution, preliminary tests were carried out with a specimen in which were set a number of fine thermocouples. It was found that the specimen temperature did not vary significantly from point to point in the neighbourhood of the boundary and could be controlled to within  $\pm 2^\circ\text{C}$ . by means of a standard commercial temperature controller.

The tests were carried out in air. While oxidation during the course of the test tended to obscure the fiducial marks, measurements of the displacement with the accuracy desired never proved impracticable.

The polished and marked specimen was adjusted in the clamps and the temperature allowed to settle to the required value before the stress was applied. Observation of displacement of the reference marks was made at regular intervals through the window. A 16-mm. objective was used in the microscope. This had a working distance of about 6 mm., and it was found that no cooling of the objective was necessary, as a complete set of measurements on all the reference lines took only a few minutes. Displacements were measured to within  $2.5 \times 10^{-4}$  cm. by means of an eyepiece micrometer.

Tests were carried out at temperatures from  $180^\circ$  to  $225^\circ\text{C}$ . and at stresses between 500 and 2100 g./cm.<sup>2</sup>.

### III.—RESULTS

Within the range of temperature and stress examined, observable relative movement of the two crystals took place in a reasonable time, and in general the deformation was limited to a very narrow region at the boundary. The two portions of the reference line separated cleanly, and in the absence of boundary migration showed no sign of distortion. Fig. 12 (Plate LXXXVII) illustrates a typical displacement. (The mottled appearance of the surface and the thickening of the reference lines in Figs. 12 and 13 are due to oxidation.)

In many cases the boundaries changed their shapes in the course of the test. Lateral movements of as much as 0.5 mm. took place in parts of the boundary, and large irregularities were thus produced. Fig. 13 (Plate LXXXVII) shows a typical case. It is of interest to observe that in places the reference line is curved, proving that displacement at the boundary was taking place continuously as the boundary advanced, whereas in other sections the line remains straight and shows a step at a well-marked boundary position.

In the main, tests were carried out on specimens having reasonably straight boundaries. Whereas displacements were generally the same at all points along the boundary, in a number of cases they were found to differ markedly from point to point; deformations of the crystals themselves, in addition to their sliding past one another, must therefore have occurred between these points. This phenomenon occurred at stresses as low as 500 g./cm.<sup>2</sup> at  $225^\circ\text{C}$ . To examine whether such behaviour could be related to irregularities in the boundary, specimens were separated along the boundary by immersion in mercury. The mercury diffuses along the boundary, and after a few minutes the crystals can be pulled apart to expose the boundary surface. The difference between specimens showing non-uniform slip and those showing uniform slip was not sufficiently well defined to provide a clear reason for the varying behaviour in the two cases, but the treatment led to an interesting observation on the appearance of the boundary surface. (See Appendix II, p. 544.)

Curves relating displacement and time were drawn for those specimens in which the displacement was uniform along the boundary. Typical curves are reproduced in Figs. 3 and 4. These are representative

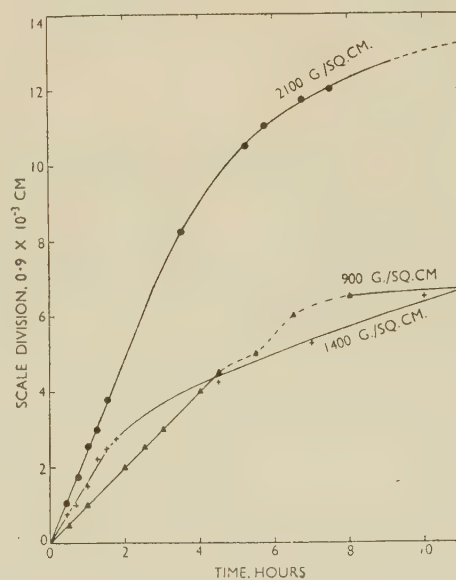


Fig. 3.—Displacement/Time Curves of Type A for Different Stresses at  $200^\circ\text{C}$ .

of the curves most usually obtained (type A). They show that the displacement occurred relatively rapidly at first and then slowed down continuously to become very small after 30–40 hr. This low rate was, however, found to persist for some days. The initial rate of displacement is of the order of  $10^{-3}$  cm./hr. and the total displacement in the time of the test roughly  $10^{-2}$  cm. It is characteristic of these curves that the initial portion is sensibly linear. At lower temperatures this initial steady rate may persist



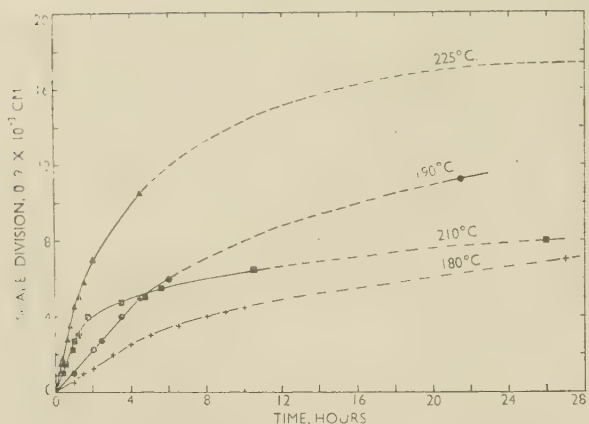


FIG. 4.—Displacement/Time Curves of Type A for Different Temperatures under a Stress of 1500 g./cm.<sup>2</sup>.

for some hours; at higher temperatures the linear portion is not so clearly defined.

Fig. 5 shows another type of curve (B), obtained on

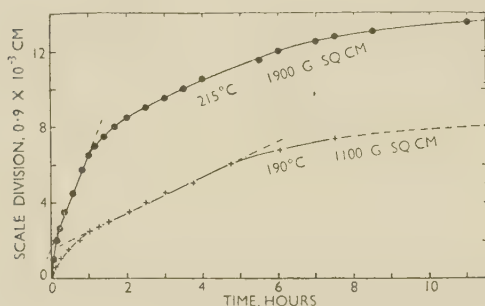


FIG. 5.—Displacement/Time Curves of Type B.

a few occasions. The rate of displacement does not decrease continuously, but there is a short period during which the initial very rapid rate decreases to a

value which remains constant for a time, then decreases, as in the first set of curves.

Fig. 6 shows a curve (type C), two examples of which were recorded. This starts off like a type-A curve and then, after the initial rate has decreased for a certain time, the rate increases again, only to decrease and then increase once more before finally attaining a low value.

It is clear that the behaviour of the boundary is not fully reproducible. Even type-A curves differ con-

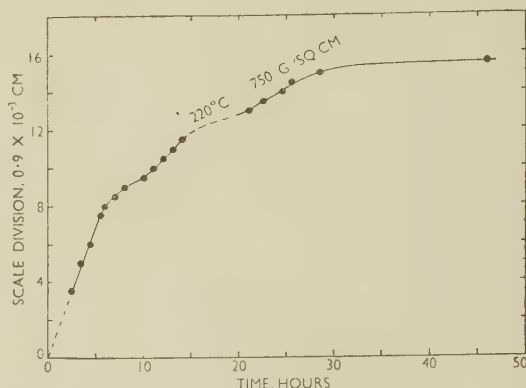


FIG. 6.—Displacement/Time Curves of Type C.

siderably under the same experimental conditions in total displacement, persistence of initial rate, and rate of decrease of slip velocity. Type-A curves are, however, reproducible in one important respect. Fig. 7 shows the relation between initial rate of displacement  $v$  and stress  $\sigma$  for a number of temperatures. The rate is seen to be proportional to stress at any given temperature.

The points marked A are derived from type-A curves; those marked B are derived from type-B curves and correspond to the linear portion of the

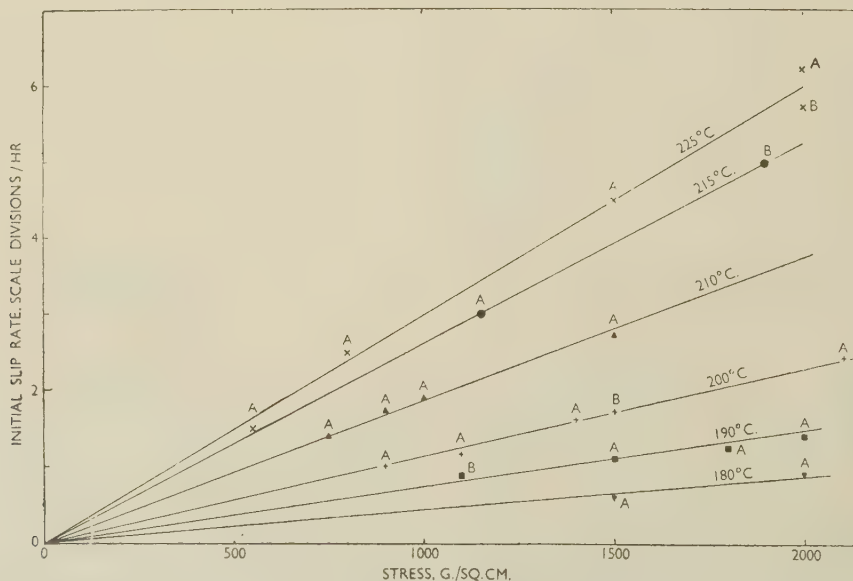


FIG. 7.—Relation Between Initial Rate of Displacement and Stress for Different Temperatures. Points marked A and B are derived from type-A and type-B curves, respectively.

curve following the initial stage of decreasing rate of displacement. There is clearly a close correspondence between this rate and the initial rate of type-*A* curves.

Since at any temperature  $v$  appeared to be proportional to  $\sigma$ , a relation was sought between the ratio and the temperature. In Fig. 8,  $\log_{10} (v/\sigma)$  is

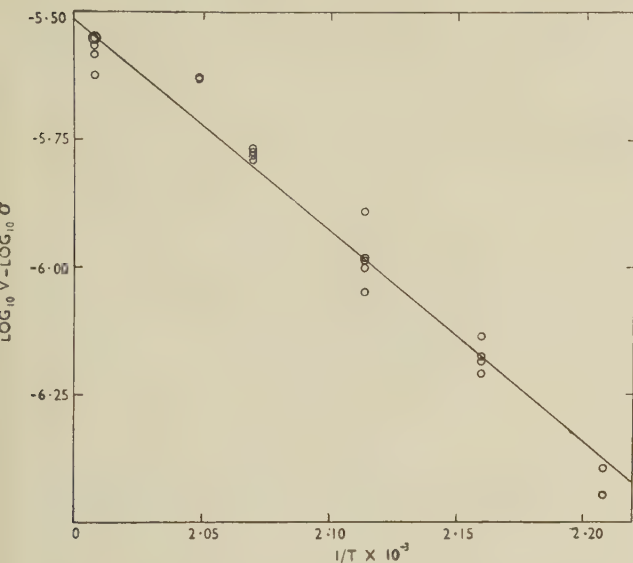


FIG. 8.—Plot of  $\log_{10} (v/\sigma)$  Against  $1/T$  for Points of Fig. 7.

$v$  = initial slip rate in cm./hr.

$\sigma$  = stress in g./cm.<sup>2</sup>.

$T$  = absolute temperature.

plotted against  $1/T$  ( $T$  = absolute temperature) for all the points of Fig. 7. Analysis of the results showed that these points could be fitted by the straight line shown with a correlation coefficient of 0.98. The relationship is therefore of the form :

$$\log (v/\sigma) = a - b/T,$$

or

$$v = A\sigma \exp(-H/RT) \quad (1)$$

Within 95% confidence limits, the value of the activation energy  $H$  is  $19,200 \pm 1500$  cal./mole and the constant  $A$  has a probable value of  $2.29 \times 10^{-4}$  (cm./sec.)/(dyne/cm.<sup>2</sup>). The uncertainty in  $A$  is quite large, the value within the 95% confidence limits ranging from  $4.3 \times 10^{-5}$  to  $1.2 \times 10^{-3}$  (cm./sec.)/(dyne/cm.<sup>2</sup>).

#### IV.—DISCUSSION OF RESULTS

The general nature of the results is in keeping with Kê's observations, but the relative displacement of the grains becomes more difficult as the displacement proceeds. Since this work was completed, Rotherham, Smith, and Greenough<sup>10</sup> have carried out experiments on tin similar to those of Kê on aluminium. Analysis of their results leads to the expression :

$$v = 54 \sigma \exp(-19,000/RT)$$

for the rate of relative displacement (cm./sec.) at the grain boundary in polycrystalline tin. Their results

are in general accord with those of Kê, and extrapolation to the melting point gives values of the viscosity in reasonable agreement with the measured viscosity of liquid tin.

Comparison of this expression with equation (1), shows that while there is excellent agreement in the values of the activation energies for the processes, the value of the coefficient  $A$  is very much larger for the internal-friction measurements than for the macroscopic deformation of the bicrystals. The initial rates of deformation observed in the type-*A* curves for bicrystals are thus some hundred thousand times smaller than those occurring by the Kê mechanism for small displacements. It is clear then that the values recorded in the present paper for the initial rate of displacement correspond to a later stage in the process, when some "hardening" of the boundary has occurred. The existence of type-*B* curves, and the agreement of their constant-rate portions with those of type-*A* curves, are in accord with this conclusion. The two types of curve are therefore probably the same, the initial decelerating portion taking place so rapidly in type-*A* curves that it is not observed on the gross scale of the experiments. The striking feature of the results, then, is that there exists an *intermediate* period in the deformation, which at low temperatures may persist for some hours, during which the deformation proceeds at a constant rate, the deformation being characterized by the same activation energy as for very small displacements. The "hardening" of the boundary may be explained by the fact that it is not originally perfectly straight, although the deviations are small. When the stress is applied, the crystals move relative to one another, as in Kê's experiments, but such movement is soon hindered by the interlocking of the projections in the intercrystalline surfaces. Further movement may then occur by one or both of the following mechanisms :

(i) The stress concentrations at the irregularities may be sufficient to cause deformation in the crystals themselves, either by crystalline slip or by local readjustments in small groups of atoms, as suggested by Orowan<sup>11</sup> as a mechanism operative in steady-state creep.

(ii) Local migration of the boundary may occur in such a manner as to allow further slip, the actual deformation being limited to a small boundary layer and proceeding by the Kê mechanism.

That local deformation of the crystals may occur in the neighbourhood of the boundary, at these low stresses, is clearly shown by those specimens in which the displacements of the reference lines was not the same at all points on the boundary. This could only be brought about by the deformation of the crystals. Evidence for non-uniform deformation of the crystals in the region of an irregularity is given by Fig. 14 (Plate LXXXVIII), in which a sub-structure is clearly indicated. This is taken to be the polygonized structure now recognized as arising on recovery after inhomogeneous deformation. However, in the specimens for which displacement curves are recorded, the



displacement was uniform along the boundary and for the greater part of the displacement the movement was limited to a very narrow region at the boundary, giving separation of the reference lines similar to that shown in Fig. 12. No cases of sub-structure formation were observed. In view of these facts and the magnitude of the displacement attained, it is felt that deformation of interlocking regions did not play a major part in allowing further motion to take place after interlocking had occurred. There was no evidence of large interlocking regions in the specimens until well towards the end of the deformations recorded. Smaller interlocking regions which may have been present but were not detectable, would need to have been completely sheared before displacements of the magnitude observed could have taken place. It is true that there may have been larger interlocking regions within the specimen capable of deforming by amounts sufficient to allow displacements of the required magnitude, but since the mechanical behaviour would depend completely on the magnitude of such regions, the reproducibility of the behaviour would require that such deviations from straightness were the same in all specimens, an occurrence which is not considered likely.

It is suggested, therefore, that the major part of the displacement is made possible by local migrations of the boundary. Under the action of thermal fluctuations the boundary is constantly experiencing small changes of position. In the highly stressed regions such changes will take place preferentially in such a direction as to reduce the strain energy, i.e. the boundary will tend to straighten out so that further slip may occur and transfer the stress to other regions of interlocking.

In the regions between interlocking points, which are free from stress, fluctuations will take place in random fashion and new irregularities are produced which take up the stress as it is relieved at other points by the straightening of the boundary. Such spontaneous straightening of the boundary can occur only where the irregularities are small. When a large irregularity has been built up, as will happen by chance, the probability of its removal is small and further displacement is limited to that consequent upon deformation of the crystals in this region: the fact that the formation of a large irregularity is purely a matter of chance would account for the differences in the value of the total deformation observed for different specimens, and the duration of the period of uniform rate of displacement. It would be expected that such irregularities would occur more readily at higher temperatures, and this would explain the observation that the duration of the period of uniform rate of displacement was generally less at such temperatures. The occasional removal of a relatively large irregularity would account for the behaviour indicated by type-C curves.

This mechanism does not of necessity lead to a period of constant rate of displacement, but such a period would not be inconsistent with it, owing to the

likelihood that the irregularities produced by thermal fluctuations would remain reasonably constant in size and number, until the formation of a large one upset the general distribution of stress.

The close agreement of the observed value of the activation energy  $H$  with the value obtained by Rotherham, Smith, and Greenough<sup>10</sup> is significant. It would suggest that the same elementary process is responsible for the local migration of the grain boundary at an irregularity, as for slip in a straight boundary. Mott<sup>5</sup> has in fact suggested that the localized melting of regions of the boundary due to thermal fluctuations is responsible for both processes.

While the results of the comparatively gross experiments now recorded throw very little light directly upon the mechanism of relative movement at a straight grain boundary, they do serve to show that certain mechanisms which have been suggested cannot be entirely responsible for the process. Read and Shockley,<sup>12</sup> developing the dynamics of a boundary composed of arrays of dislocations, suggested that relative movement of the grains may proceed by the movement of dislocations along the slip planes. For boundaries consisting of dislocations of one type only, the process is relatively simple, but for boundaries of mixed dislocations it involves diffusion of the dislocations perpendicular to the slip planes, as well as movement along them. Such movement of dislocations could play an important part in the internal-friction measurements of Kê and others, and might be expected to occur readily in the simple boundaries formed on polygonization after inhomogeneous deformation, but it is clear that this is not the only mechanism by which the grains may move past each other. For each of the boundary types considered by Read and Shockley, a given relative movement of the grains should be accompanied by a comparable lateral movement of the boundary. Fig. 12 (Plate LXXXVII) shows clearly that large relative movement may occur without noticeable lateral migration.

Considerable lateral movement was observed in many cases, and it is probable that such movement plays an important part in prolonged intergranular creep in polycrystalline specimens, the readjustments at the grain corners enabling movement to proceed when it would otherwise cease, but the primary process of slip on straight boundaries clearly does not demand such lateral migration.

There is nothing in the present results to conflict with the suggestion by Kê that boundary slip occurs by the re-arrangement of disordered groups of atoms. Kê, however, arguing from the cases of aluminium,  $\alpha$ -brass, and  $\alpha$ -iron, in which the activation energy was found to be the same for boundary slip, self-diffusion, and creep in single crystals, suggested that the same mechanism was responsible for all three processes. Such a theory would suggest that information on diffusion could be obtained from the experimentally simpler observation of internal friction. In the case of tin, however, the published figures<sup>13</sup> for the activation energy of self-diffusion (5900 cal./mole. along the

$c$  axis and 10,500 cal./mole along the  $a$  axis) differ considerably from the value for boundary slip. The elementary process would appear to be different for the two phenomena, and observations upon grain-boundary slip cannot in general be expected to provide information on diffusion.

The local melting of islands of good fit suggested by Mott as a mechanism for boundary slip is very similar to that of Kê, and there appears to be no means of distinguishing experimentally between them. It is probable that some such mechanism produces both boundary slip and lateral migration. Further experiments now proceeding may throw further light on the problem.

#### ACKNOWLEDGEMENTS

The work described was carried out in the Royal Aircraft Establishment, Farnborough, and acknowledgement is made to the Chief Scientist, Ministry of Supply, and to the Controller, H.M. Stationery Office, for permission to publish this paper.

#### APPENDIX I

##### *The Effect of Mould Material on the Growth of Crystals and the Conditions for Straight Boundaries*

Single crystals were grown in glass tubes, and single-crystal and bicrystal specimens in moulds both of graphite and of Sindanyo. The material of the mould was found to exercise a marked influence on the condition of the resultant specimen.

There was a strong tendency for specimens grown in glass to have similar orientations; in the majority of

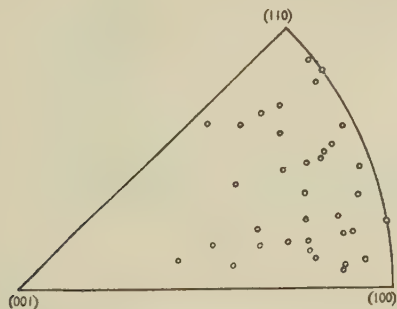


FIG. 9.—Diagram Showing the Orientation of Single-Crystal Specimens Grown in Graphite Moulds. The circles are projections of the specimen axes on the stereographic triangle.

cases the  $c$  axis of the crystal was normal to the axis of the specimen. In graphite moulds, where the conditions of growth were otherwise identical, there was not the same strong tendency for this type of orientation. Fig. 9 shows the relation of the specimen axis to the crystal axes in 38 specimens grown in graphite. While there is a tendency for the specimen axis to make a large angle with the  $c$  axis, there is not the marked tendency for an angle of  $90^\circ$  so typical of specimens grown in glass. Relatively few specimens were grown in Sindanyo moulds without seeding from

another crystal, but it appeared that the dispersion of the angle between the  $c$  axis and the rod axis was intermediate between that for graphite moulds and that for glass.

Comment has been made by a number of workers (see, for example, Chalmers<sup>14</sup>) on the "macromosaic" structure in large crystals grown from the melt. In tin crystals the structure is revealed by etching in ferric chloride solution, showing as a series of bands running generally in the direction of growth of the crystals. The bands are about 1–2 mm. wide and



FIG. 10.—Diagram Indicating the Effect of Crystal Orientation on the Direction of the Boundary.  $c$  axes symmetrical to the vertical plane in each case.

- (a)  $c$  axes not normal to specimen axis.
- (b)  $c$  axes normal to specimen axis.

X-ray and optical examination of a few specimens showed that each specimen in fact consisted of a number of long crystals corresponding to these bands and differing in orientation by angles of a few degrees. There was a strong tendency for this macromosaic structure to be present in single crystals grown in glass, but in crystals grown in Sindanyo and graphite the individual crystals were larger, and the range of angles between them smaller, than for glass-grown specimens.

In the growth of bicrystals for experiments on grain-boundary slip, efforts were naturally directed to producing specimens in which the boundary was sensibly straight and preferably running parallel to the axis of the specimen. Such a boundary is formed when the two component crystals are so orientated that a rotation about the specimen axis will bring the crystal axes into coincidence. If the crystals are not so disposed, the boundary grows at an angle to the specimen axis. The explanation offered by Chalmers<sup>14</sup> is that the temperature of equilibrium between a crystal and the liquid metal varies with the crystallographic orientation of the interface; when both crystals present the same plane at the solid/liquid interface the boundary grows parallel to the axis of the specimen. It was found, however, that even when this condition was satisfied, in cases where the  $c$  axes of the two crystals were not normal to the specimen axis, the boundary, while forming generally along the axis of the specimen, did not remain in a vertical plane and tended to twist, as illustrated in Fig. 10. Only in the case where the  $c$  axes were normal to the direction of growth and symmetrically oriented on each side of the boundary were straight boundaries produced with reasonable consistency in Sindanyo moulds. Even this condition did not produce satisfactory boundaries in graphite moulds. In these moulds, the boundaries, while running generally parallel to the specimen axis, were irregular.

These limited observations indicate the importance of mould material in the preparation of single-crystal



and large-grained specimens. The thermal properties of the mould will clearly affect the temperature gradient and rate of growth for given furnace conditions. Teghtsoonian and Chalmers<sup>15</sup> have shown that the rate of growth has a marked effect on the size of the macromosaic units. It is worthy of note that the spread of orientations in the macromosaic structure within a single specimen is greatest under those conditions which lead to the smallest spread in the mean orientation from specimen to specimen.

## APPENDIX II

### *Some Observations on Grain-Boundary Surfaces*

In an attempt to find an explanation of irregular grain-boundary slip in certain bicrystal specimens, some specimens were immersed in mercury for a few minutes to allow diffusion of the mercury to occur along the boundary, after which the crystals could be pulled apart to expose the boundary surfaces.

It was found that specimens of Pass No. 1 tin had fine corrugations running along the boundary. Polycrystalline specimens also showed these corrugations, so that they are not due to the special conditions of growth of bicrystals. Further, in specimens grown in flat, open moulds the corrugations were roughly perpendicular to the bottom of the mould, while in cylindrical specimens they were approximately radial; specimens cast under these different conditions are shown in Figs. 16 and 15 (Plate LXXXVIII). The corrugations therefore follow the direction of cooling.

Prolonged annealing did not alter this appearance; but if a specimen was strained before annealing, the boundaries when exposed were smooth. It is interesting to note how in a polycrystalline specimen, slightly strained and annealed, the process of boundary ad-

justments during grain growth could be followed. In Fig. 17 (Plate LXXXVIII) parts of the grain surfaces show a corrugated appearance, while others are smooth. The smoothing out of the surfaces always started at the grain vertices and spread gradually over the faces, suggesting, as might be expected, that the concentration of strain energy following slight deformation was greatest at the grain vertices. Fig. 18 (Plate LXXXVIII) shows the complete removal of corrugations by further annealing.

It was anticipated that the corrugations were in some way due to the presence of impurities, which might be expected to collect at the boundary during solidification. To test this, similar tests were carried out on Chempur tin. In this case the grain boundaries were smooth (Fig. 19, Plate LXXXVIII). The compositions of the two samples of tin were:

	Cu, %	Bi, %	Fe, %	Sb, %	As, %	S, %	Pb, %
Chempur	0.0006	0.0008	0.0004	0.0032	0.0005	0.0004	0.0021
Pass No. 1	...	Less than 0.00005	0.0033	0.007	0.0004	0.0001	0.0017

The total impurity content varies only slightly, but there are significant differences in antimony and iron content. It is to be expected that small differences of impurity content might have a profound effect on the nature of the grain boundary, but these experiments bring out in addition a significant difference between cast and recrystallized boundaries in tin of a certain purity. It is often found that metals in the as-cast condition show better creep-resistance properties than wrought material. If, as is thought, grain-boundary slip plays an important part in creep, especially at elevated temperatures, a possible explanation of this fact might be found in a difference in the boundary configuration. This point is being examined in tin, as is also the possibility of following the progress of boundary readjustments after straining.

## REFERENCES

1. D. Hanson and M. A. Wheeler, *J. Inst. Metals*, 1931, **45**, 229.
2. H. F. Moore, B. B. Betty, and C. W. Dollins, *Univ. Illinois Bull.*, 1935, (272).
3. T. S. Kê, *Phys. Rev.*, 1947, [ii], **71**, 533; **72**, 41.
4. T. S. Kê, *J. Appl. Physics*, 1949, **20**, 274.
5. N. F. Mott, *Proc. Phys. Soc.*, 1948, **60**, 391.
6. R. King, R. W. Cahn, and B. Chalmers, *Nature*, 1948, **161**, 682.
7. B. Chalmers, *Proc. Roy. Soc.*, 1940, [A], **175**, 100.
8. K. E. Puttick, *Metallurgia*, 1949, **41**, 120.
9. E. N. da C. Andrade, *Proc. Roy. Soc.*, 1911, [A], **85**, 448.
10. C. E. Inglis, *ibid.*, 1923, [A], **103**, 598.
11. L. Rotherham, A. D. N. Smith, and G. B. Greenough, *J. Inst. Metals*, 1951, **79**, 439.
12. E. Orowan, *J. West Scotland Iron Steel Inst.*, 1946-47, **54**, 45.
13. W. T. Read and W. Shockley, *Phys. Rev.*, 1950, [ii], **78**, 275.
14. W. Boas and P. J. Fensham, *Nature*, 1949, **164**, 1127; 1950, **165**, 178.
15. B. Chalmers, *Proc. Roy. Soc.*, 1949, [A], **196**, 64.
16. E. Teghtsoonian and B. Chalmers, *Canad. J. Physics*, 1951, **29**, 370.



FIG. 1.—Beam Flanges (String-Filled Phenolic), Spools (Cellulose Acetate), and Pin (Filled Cellulose Acetate).

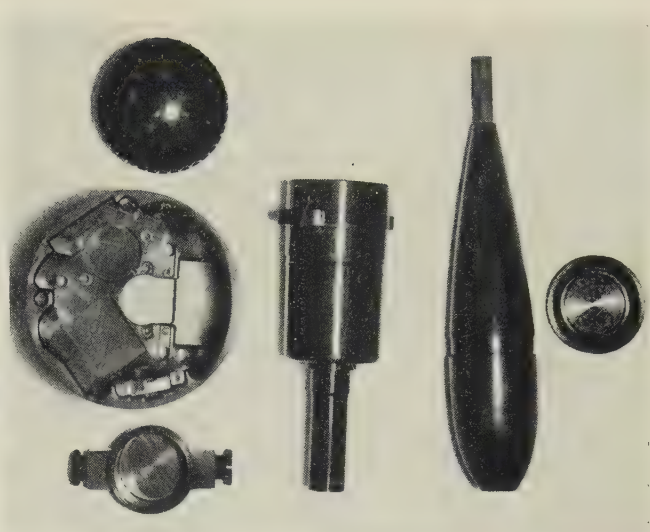


FIG. 2.—Grenade, Practice Bomb, Mine-Detector Parts, and Cartridge Lid (Phenolic Plastics). By courtesy of the Advisory Service on Plastics and Rubber, Ministry of Supply.

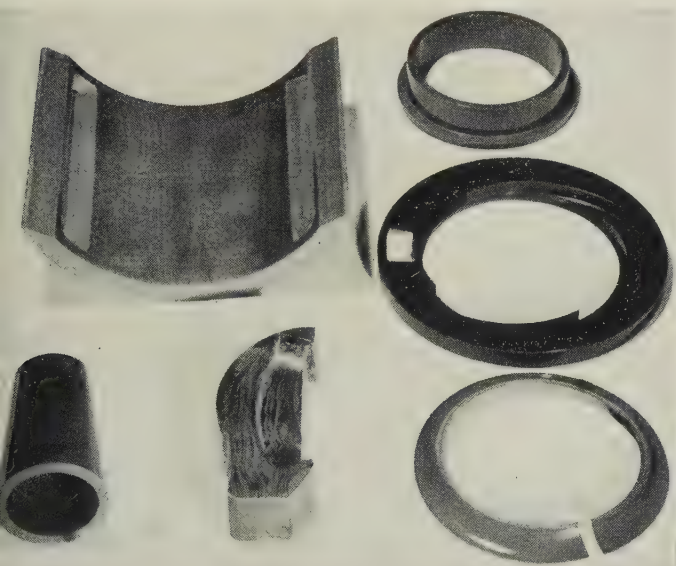


FIG. 3.—Rolling-Mill Bearing, Piston Ring, Thrust Bearing Race Collar, Blade Centre Bush (Fabric-Filled Phenolic Plastics). By courtesy of The Bushing Co., Ltd.

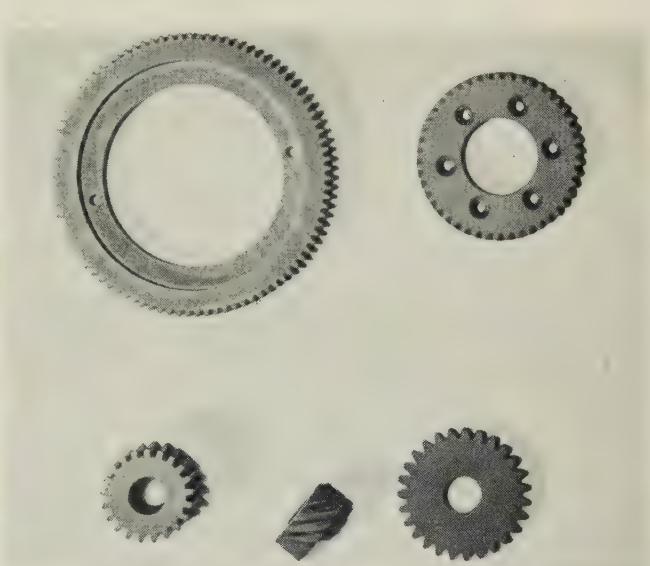


FIG. 4.—Shock-Resistant, Silent Gear Wheels (Fabric-Laminated Phenolic Plastic). By courtesy of Tufnol, Ltd.

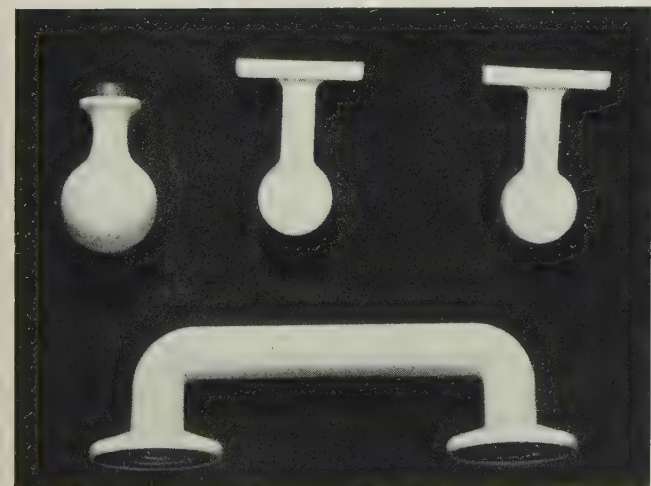


FIG. 5.—Door-Knob, Rail Supports, and Bathroom Handgrips (Die-Cast Metal Core with Moulded-On Polyvinyl Chloride Layer).

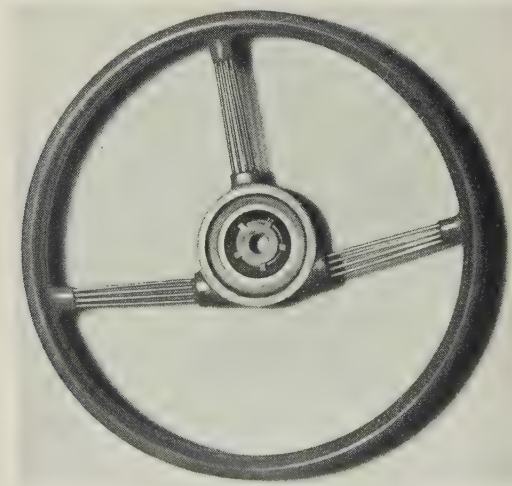


FIG. 6.—Steering Wheel (Metal Skeleton with Moulded-On Cellulose Acetate).





FIG. 7.—U.S. Naval Landing Craft (Polyester/Glass Fibre Laminate). By courtesy of *Modern Plastics*.

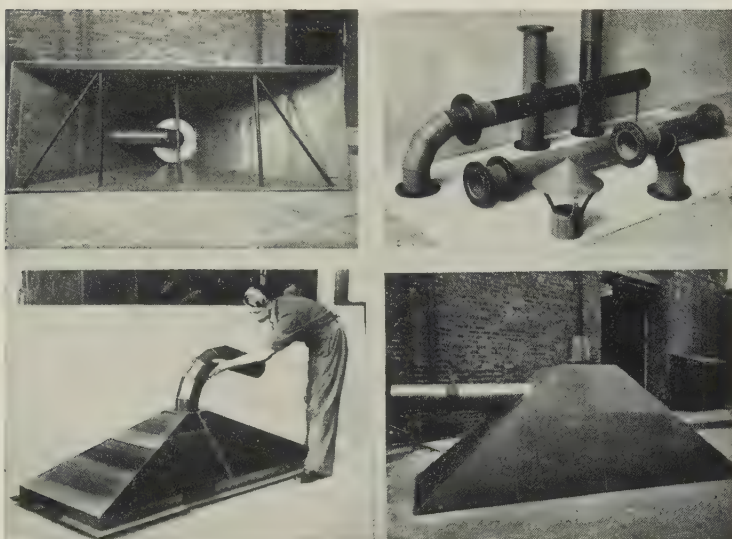


FIG. 8.—Acid-Resisting Fume Hoods and Ducts (Polyvinyl Chloride). By courtesy of Tanks and Linings, Ltd., and Prodorite, Ltd.

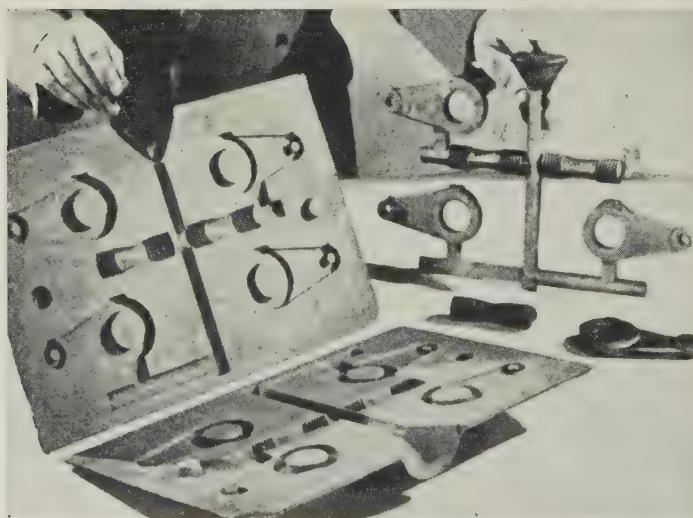


FIG. 9.—Resin-Bonded Sand Moulds for Shell-Moulding Process (Phenolic Resin).

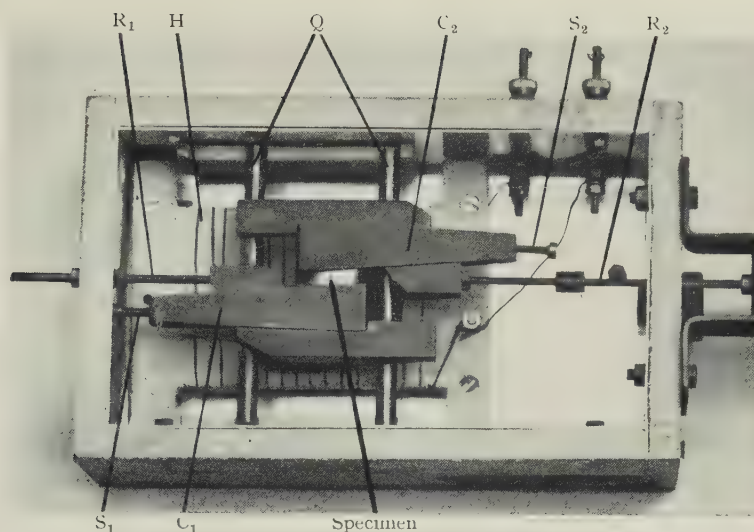


FIG. 11.—Apparatus for Stressing Specimen. Lid removed.  $\times \frac{2}{3}$ .

BOUNDARY SLIP IN BICRYSTALS OF TIN.

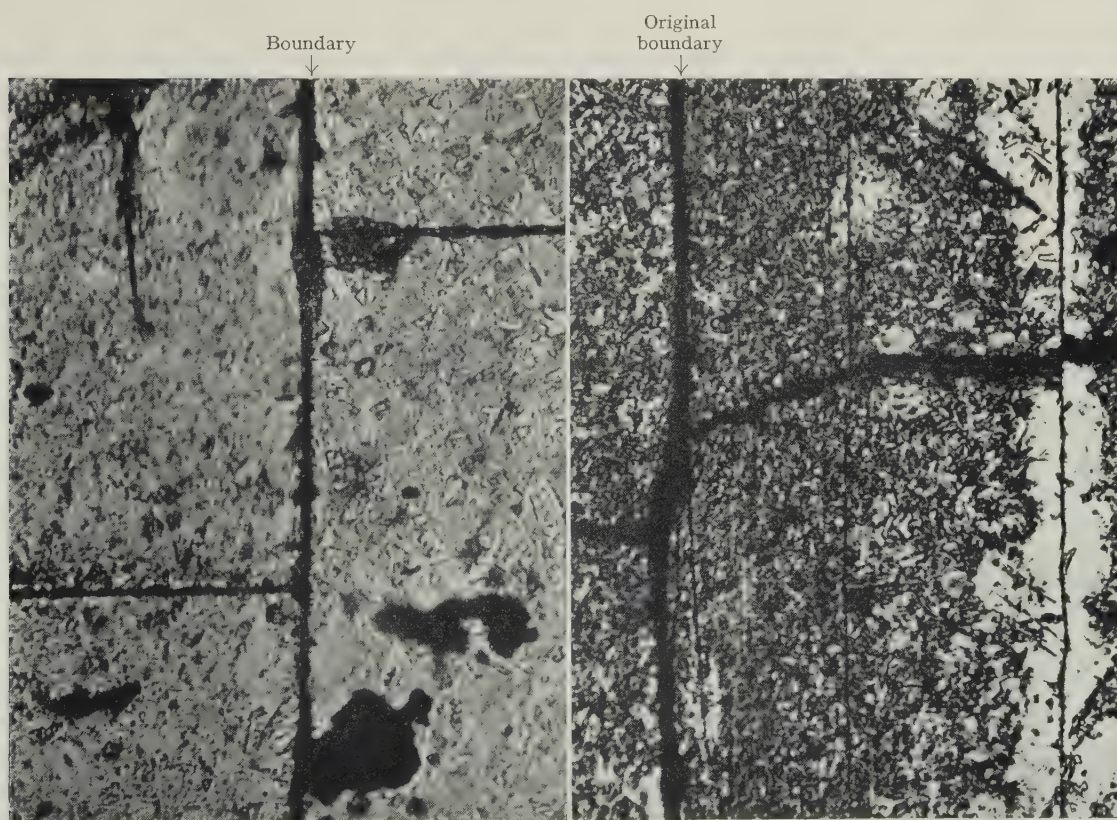


FIG. 12.—Showing Typical Displacement of Reference Line at Grain Boundary.  $\times 550$ .

FIG. 13.—Showing Boundary Slip Accompanied by Boundary Migration.  $\times 400$ .



## GRAIN-BOUNDARY STRUCTURES IN TIN CRYSTALS.



FIG. 14.—Showing Sub-Structure Around an Irregularity in the Boundary.  $\times 400$ .

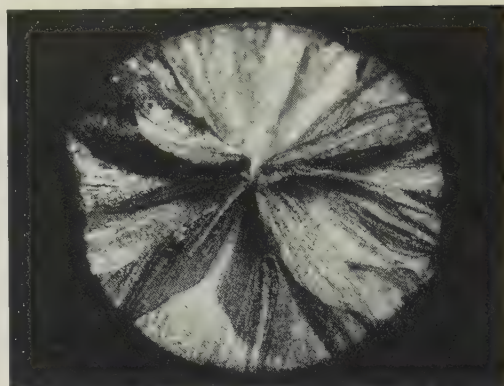
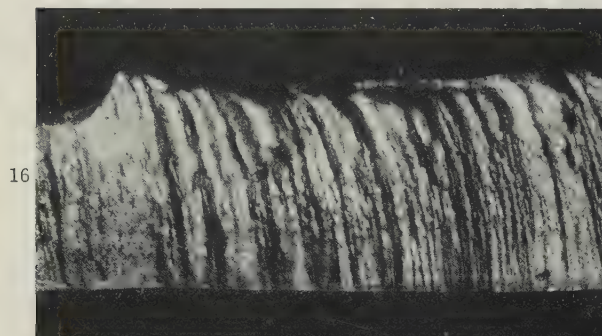


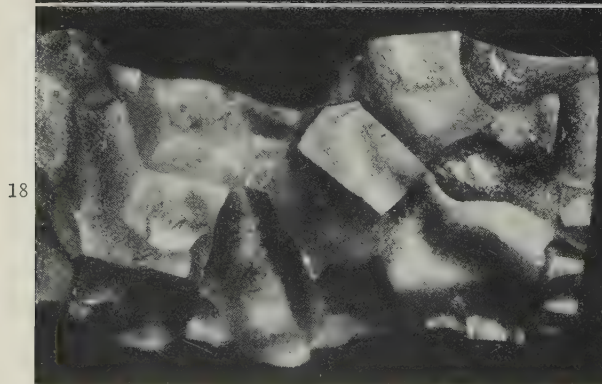
FIG. 15.—Specimen Cast in Cylindrical Mould and Separated Along Grain Boundaries. Pass No. 1 tin.  $\times 6$ .



16



17



18



19

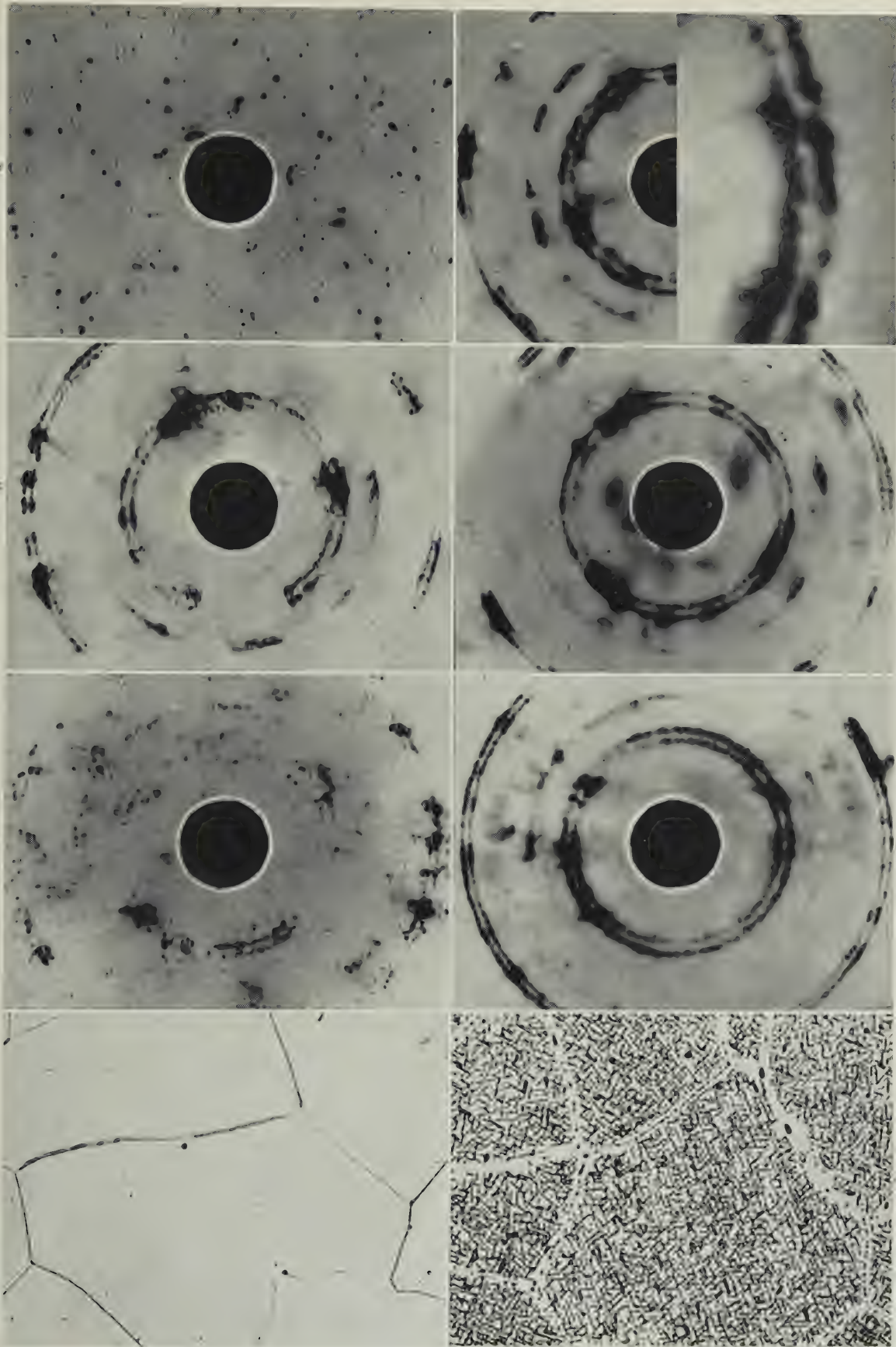
FIG. 16.—Specimen Cast in Flat Mould and Quickly Cooled, then Separated Along Grain Boundaries. Pass No. 1 tin.  $\times 6$ .

FIG. 17.—Specimen Cast in Flat Mould, Slightly Strained, and Annealed for  $\frac{1}{2}$  hr. at  $220^{\circ}\text{C}$ .; then Separated Along Grain Boundaries. Pass No. 1 tin.  $\times 6$ .

FIG. 18.—Specimen Similar to that of Fig. 17, Annealed for  $2\frac{1}{2}$  hr. at  $220^{\circ}\text{C}$ .  $\times 6$ .

FIG. 19.—Specimen of Chempur Tin Cast in Flat Mould and Quickly Cooled, then Separated Along Grain Boundaries.  $\times 6$ .

Figs. 16-19 reduced by  $\frac{1}{4}$  linear in reproduction.



Figs. 1-3.—Al-0.5% Ag Alloy.

FIG. 2.—Creep of 8.3% in 66 hr. at 300° C. (390 lb./in.<sup>2</sup>), then annealed 68 hr.

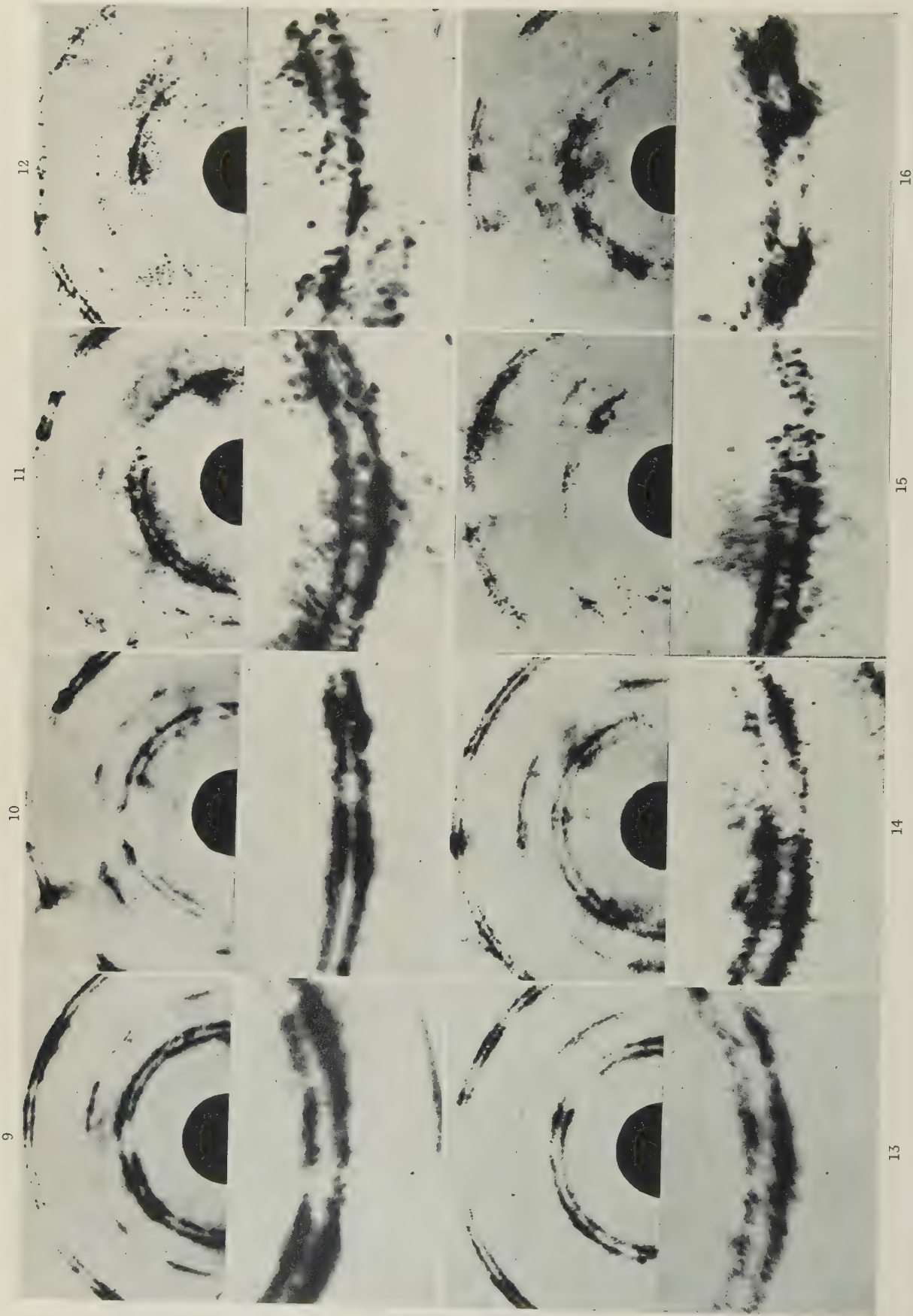
Figs. 4-7.—Al-2% Ag Alloy.

FIG. 5.—Photomicrograph of initial state.  $\times 200$ .  
FIG. 7.—Extension of 8.1% in 1 min. at 300° C. (5000 lb./in.<sup>2</sup>), then annealed 69 hr.

FIG. 8.—Pure Aluminium. Specimen 10B. Extended 6.1% at 20° C.

FIG. 1.—X-ray photograph of initial state.





FIGS. 9-14.—Recovery of Pure Aluminium at 300° C., Initially Extended at 20° C.

FIG. 9.—Specimen 10A; annealed 69 hr.

FIG. 12.—Specimen 17A; creep of 4.8% in 319 hr.

FIG. 10.—Specimen 20A; creep of 0.3% in 67 hr.

FIG. 13.—Specimen 9B; extension of 3.1% in 1 min.

FIGS. 15 and 16.—Recovery of Pure Aluminium, Initially Extended at 300° C.

FIG. 15.—Specimen 2F; creep of 1.0% in 87 hr. at 300° C.

FIG. 16.—Specimen 4F; annealed 36 hr. at 400° C.

FIG. 11.—Specimen 17A; creep of 1.9% in 202 hr.

FIG. 14.—As Fig. 13, then annealed 66 hr.



## NICKEL-ALUMINIUM ALLOYS.

FIG. 2.—No. 200. 21.1 at.-% Al.

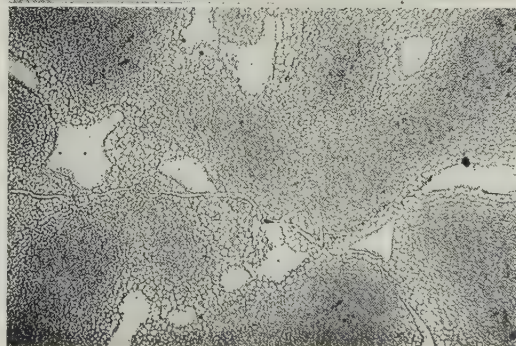


FIG. 4.—No. 203. 26.4 at.-% Al.

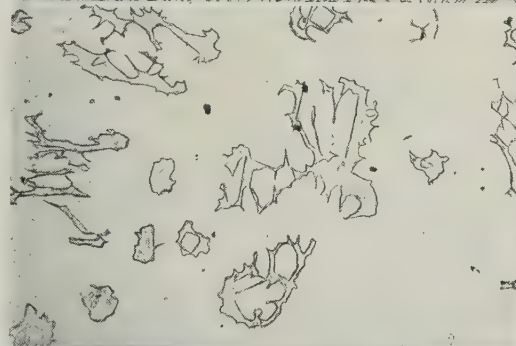
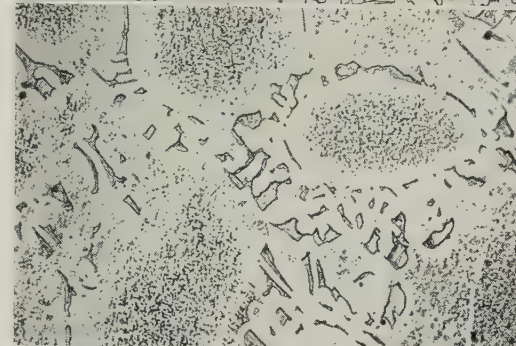


FIG. 6.—No. 205. 31.0 at.-% Al.



FIG. 8.—No. 218. 22.8 at.-% Al, 2.7 at.-% Cr.



## NICKEL-ALUMINIUM-CHROMIUM ALLOYS.

FIG. 10.—No. 216. 26.6 at.-% Al, 2.5 at.-% Cr.



FIG. 3.—No. 201. 23.2 at.-% Al.

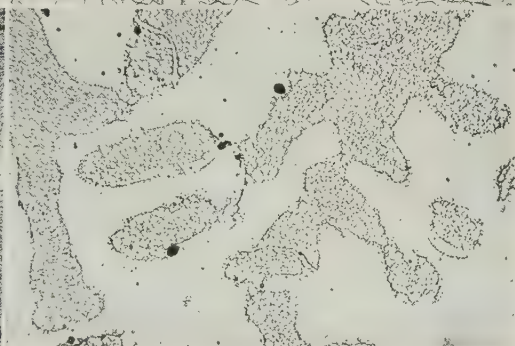


FIG. 5.—No. 204. 27.8 at.-% Al.

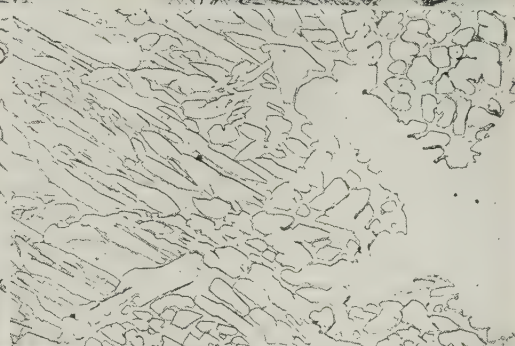


FIG. 7.—No. 204. 15 min. at 1365° C., Water Quenched.



FIG. 9.—No. 217. 25.5 at.-% Al, 2.4 at.-% Cr.

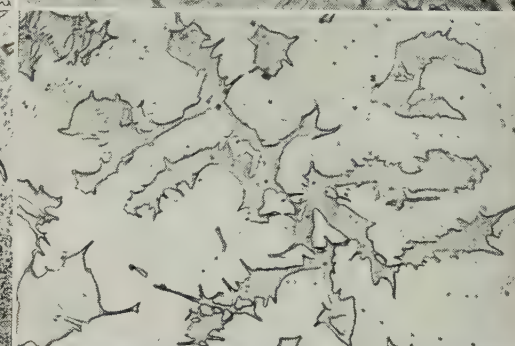
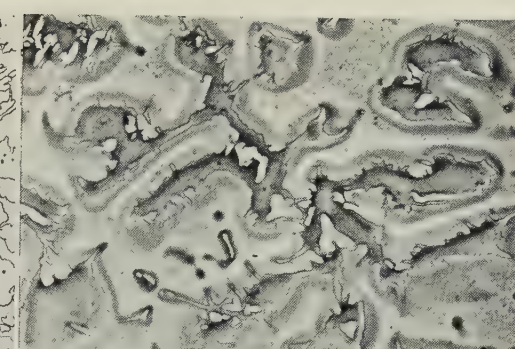


FIG. 11.—As Fig. 9, but with Phase-Contrast Illumination.



All etched electrolytically in 5% HF + 10% glycerine solution.  $\times 200$ . Reduced by  $\frac{1}{10}$  linear in reproduction.



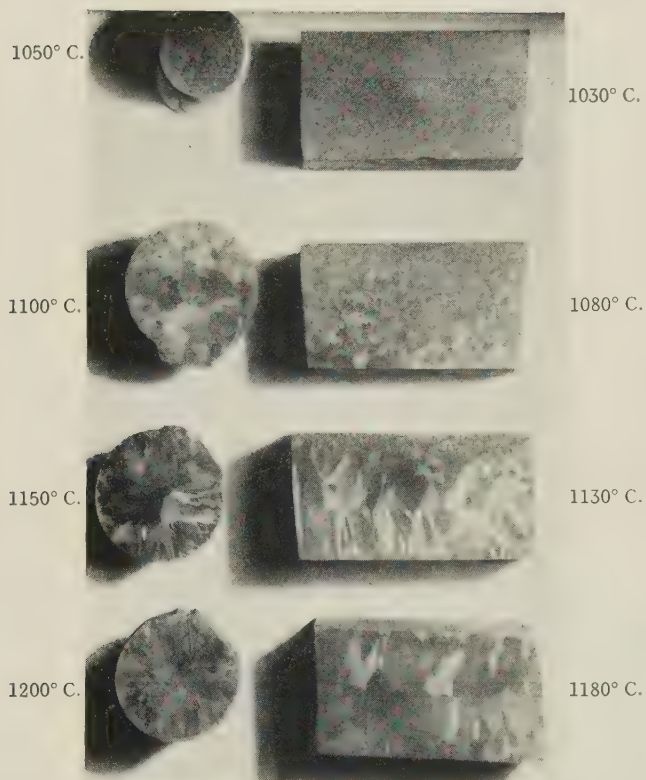


FIG. 16.—Effect of Pouring Temperature on Grain-Size of 85 : 5 : 5 : 5 Gun-Metal Castings (1-in.-dia. bars and 1-in. thick plates) Containing less than 0.01% Phosphorus. Drag face of plate specimens uppermost.

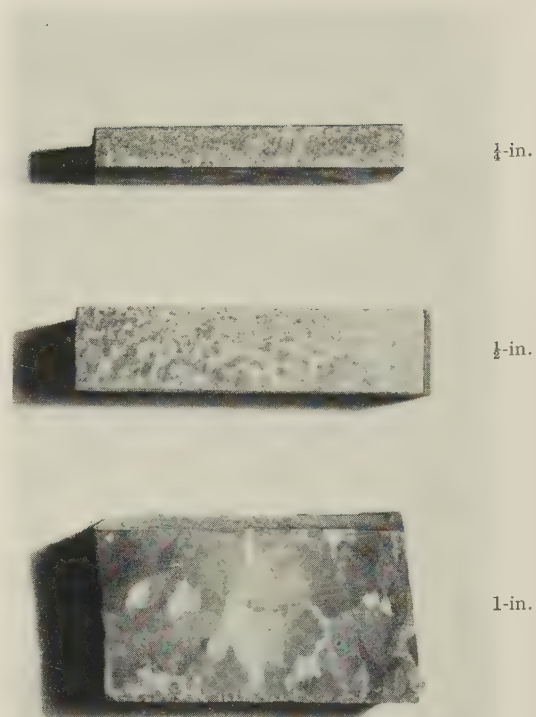


FIG. 17.—Effect of Section Thickness on Grain-Size of 85 : 5 : 5 : 5 Gun-Metal Castings (ribbed plates) Poured from 1180° C. and Containing 0.008% Phosphorus. Cope face uppermost.

# X-RAY DIFFRACTION STUDIES IN RELATION TO CREEP \*

1379

By G. B. GREENOUGH,† Ph.D., MEMBER, (MRS.) CATHERINE  
M. BATEMAN,‡ B.Sc., JUNIOR MEMBER, and (MRS.) EDNA M.  
SMITH,§ B.A.

## SYNOPSIS

To investigate a hypothesis regarding the mechanism of creep put forward by Greenough and Smith (*J. Inst. Metals*, 1950, **77**, 435), two aluminium-silver alloys, one a solid solution and the other containing a precipitate, were examined. While the former behaved in the same manner as pure aluminium and showed marked cell development during creep, the latter exhibited no traces of such cells. Experiments were also carried out on the recovery of specimens quickly pulled at either 20° or 300° C. It was confirmed that whereas annealing at 300° C. in the absence of stress caused little recovery, cell development occurred if the specimens were allowed to creep at this temperature. The cell development did not become apparent until the creep strain was appreciable; the influence of the strain rate appeared to be small.

It is considered that the ideas based on dislocation theory and polygonization provide a simple explanation of the experimental results and are more satisfactory than an explanation in terms of boundary micro-movements.

## I.—INTRODUCTION

THE application of X-ray diffraction methods to the study of the creep deformation of polycrystalline metals was much encouraged by the observation of Wood and Tapsell<sup>1</sup> that, while the rapid deformation of aluminium at 300° C. gave blurred diffraction spots which did not recover sharpness during soaking at that temperature, creep deformation caused each initial diffraction spot to dissociate into several, equally sharp, spots. The interpretation of this observation is that the creep deformation causes the original grains to dissociate into "cells", the lattices of which are almost perfect and differ slightly in orientation from one cell to the next. The conditions governing the development of these cells have been carefully examined by Wood and his collaborators.<sup>2-5</sup> That the effect is not confined to aluminium has been demonstrated by Gifkins,<sup>6</sup> who noted similar effects in a polycrystalline lead-thallium alloy, and by Cottrell and Aytekin,<sup>7</sup> who showed microscopically that cells of slightly different orientation formed within the grains of polycrystalline zinc during creep. On the other hand, Greenough and Smith<sup>8</sup> found that if an aluminium of commercial purity was used for the experiments, the cell development was suppressed.

The several authors do not agree on the explanation of the observations. Wood and his collaborators view the breakdown of the grains into fragments, more or less perfect according to the experimental deformation conditions, as fundamental in itself. They have correlated the size of the cells formed during

experiments at various constant strain rates with the stresses necessary to produce the strain,<sup>3</sup> and they suggest that after the development of the cells, deformation proceeds by the relative displacement of the cells at their boundaries, steady-state creep appearing when sufficient boundary has been developed for the total of the "micro-movements" at all boundaries to account for the external strain.<sup>5</sup> That movement of one grain relative to another occurs at the boundary during high-temperature creep is beyond doubt; but whereas Wood, Wilms, and Rachinger<sup>5</sup> claim that cells can be seen microscopically to be displaced relative to one another after creep, Wyon and Crussard<sup>9</sup> consider that there is no such displacement. In point of fact it is very difficult to imagine how an assembly of rigid blocks could extend solely by sliding over one another at their surface unless the blocks were extremely regular in shape, which is not the case. It seems inevitable that any viscous boundary sliding would have to be accompanied by some deformation within the cells or grains.

An alternative explanation, supported by most of the other workers,<sup>7-9</sup> is that the formation of the cells is due to a type of polygonization.<sup>10</sup> Greenough and Smith,<sup>8</sup> in particular, have examined the details of this explanation closely and brought forward experimental evidence to support the views expressed.

The discussion<sup>11</sup> on the papers by Wood and Scrutton, by Greenough and Smith, and by Calnan and Burns<sup>12</sup> is extremely instructive, since it contains many views on the points of interest involved.

One of the comments made by Honeycombe during

\* Manuscript received 13 August 1951.

† Metallurgy Department, Sheffield University; formerly at the Royal Aircraft Establishment.

‡ Royal Aircraft Establishment, Farnborough, Hants.

§ Fulmer Research Institute, Stoke Poges, Bucks.; formerly at the Royal Aircraft Establishment.



that discussion was that none of the solutions advanced mentioned the phenomenon of deformation, or kink, bands which usually appear during the plastic deformation of aluminium. Cahn<sup>13</sup> has since described a detailed investigation of this phenomenon in aluminium, but was unable to explain the origin of the bands, although it was clear why they became more marked as the deformation increased. These bands are regions in the lattice where the orientation differs from that of the remainder of the lattice and are associated with lattice curvature, i.e. with concentrations of dislocations of one sign.

Cahn showed that such regions could be polygonized in single crystals by heating the specimens to about 430° C. in the absence of an applied stress, but that if a stress were applied polygonization occurred much more rapidly, thus directly supporting the polygonization theory of the creep phenomena. In addition to providing regions where polygonization is possible, deformation bands may be of fundamental importance.

It was also suggested to the present authors privately that the effects might be confined entirely to the surface layer of crystals. To test this, photographs were taken of specimens after layers of metal had been removed electrolytically, but no significant changes in appearance were noted. The effects appear to extend throughout the bulk of the aluminium.

The present paper describes experimental work carried out in an attempt to test the truth of the dislocation interpretation of cell formation during creep. In the main, the work has been designed to investigate in much greater detail the points established earlier by Greenough and Smith.<sup>8</sup>

In the earlier paper, the commercial-purity aluminium was given as an example of an alloy containing foreign atoms. Its composition was such that there was present some precipitate of the ternary aluminium-iron-silicon compound, in addition to foreign atoms in solution. It was not possible to decide which was the more important in preventing the formation of cells. It was therefore decided to carry out further experiments on two aluminium-silver alloys, in one of which all the silver was in solution and in the second of which there was a precipitate of  $\text{AlAg}_2$  in addition to silver in solution. Silver was chosen as the alloying element because it is known to have the same effective atomic radius as aluminium in solution and was therefore thought unlikely to exercise much effect on the deformation characteristics of the solid-solution alloy.

The effect of an applied stress on the recovery of pure aluminium after extension at room temperature had already been briefly described. Further research was undertaken to determine more precisely the conditions under which cell formation occurred in worked specimens. This is also described below.

## II.—EXPERIMENTAL

Flat specimens of 1 in. gauge-length,  $\frac{1}{4}$  in. wide, and  $\frac{1}{8}$  in. thick, were employed throughout; stresses were

applied by axial loading shackles of conventional design. Except in the case of room-temperature deformation, tests were made at 300° C., maintained along the gauge-length within  $\pm 5^\circ$  C.

All diffraction photographs were taken by the back-reflection method, using unfiltered radiation from a cobalt target operating at 48 kV. and a film-specimen distance of 7 cm. All X-ray photographs from any one specimen were of approximately the same area in the middle of the gauge-length.

### 1. ALUMINIUM-SILVER ALLOYS

The limits of solid solubility of silver in aluminium at temperatures down to 100° C. have been carefully determined by Larke and Rotherham,<sup>14</sup> who found that at 300° C. approximately 0.8 at.-% silver is soluble. In the present work, two alloys were used, containing nominally 0.5 and 2% silver, respectively. The former should contain no precipitate, while the latter should contain 1.2% of silver in the form of a precipitate of  $\text{AlAg}_2$  when in equilibrium at 300° C. The exact analyses of the alloys were as follows:

(i) Ag 0.52, Fe 0.01, Si 0.01, Cu 0.005 at.-%, Mn, Ni, Ti nil, Al (by difference) 99.46 at.-%; (ii) Ag 2.17, (nominal 2.0), Fe 0.01, Si 0.01, Ni, 0.005, Cu 0.002 at.-%, Mn, Ti nil, Al (by difference) 97.80 at.-%.

The material was in the form of  $\frac{7}{8}$ -in.-dia. bar. This was rolled to a strip of  $\frac{1}{8}$  in. thickness from which specimens were machined. All specimens were annealed at 450° C. for  $\frac{1}{2}$  hr. *in vacuo*; in the case of the 2% alloy the specimens were then heated at 300° C. for 24 hr. to enable the material to reach metallurgical equilibrium at that temperature (the work of Larke and Rotherham had shown this time to be sufficient). The specimens were always cooled rapidly to room temperature, and then stored at  $-2^\circ$  C. to ensure that slow precipitation did not take place.

Micrographs of the two alloys after their respective heat-treatments are shown in Figs. 1 and 5 (Plate LXXXIX). Whereas no precipitate was apparent in the 0.5% alloy, the 2% alloy showed a well-defined Widmanstätten structure. X-ray photographs of the two alloys both resembled Fig. 4 (Plate LXXXIX), which contains quite sharp spots, thus indicating that all specimens were initially strain-free.

Specimens of both alloys were deformed at 300° C. at various rates and quickly cooled again to room temperature; further X-ray photographs were then taken. The rates of deformation were chosen so as to fall roughly into two groups: (i) of the order of 0.1%/hr., referred to as deformation by creep, (ii) of the order of 10%/min., referred to as fast deformation. All the specimens strained quickly were subsequently heated again to 300° C. and left for periods similar to the duration of the corresponding creep tests.

X-ray diffraction photographs taken after test from specimens of the 0.5% alloy are shown in Figs. 2 and 3 (Plate LXXXIX). These may be compared with photographs taken from high-purity aluminium after comparable fast and slow deformations shown in the

earlier paper by Greenough and Smith<sup>8</sup> (Plate XLIX). The effects are similar for the two materials.

The photographs taken after creep show that the original grains have broken down into smaller strain-free units, whereas the diffuse diffraction effects found after rapid deformation indicate that the units are either distorted or are extremely small. This structure is but little affected by a long recovery period at test temperature, and since the photographs taken immediately after deformation were so similar to those after recovery, they have not been reproduced. A careful comparison of the photographs of specimens after creep and after rapid deformation indicates that the difference is due mainly to the amounts of lattice distortion in the units, rather than to a difference in their size (see Section III).

X-ray-diffraction photographs from specimens of the 2% alloy after test are reproduced in Figs. 6 and 7 (Plate LXXXIX). Both show diffuse diffraction rings, and there is very little difference between those obtained from the creep specimen and those from the quickly extended specimen. However, a comparison of many photographs, particularly from specimens after higher deformations, shows that on the whole the creep specimens give slightly sharper photographs with more discontinuous rings.

## 2. RECOVERY OF PURE ALUMINIUM SHOWING DIFFUSE REFLECTIONS

The aluminium used was from the same batch as before and was of 99.95 at.-% purity. The cast ingots were first roughly machined to a thickness of  $\frac{1}{2}$  in., and then rolled to strip  $\frac{1}{8}$  in. thick from which specimens were machined. These were heated *in vacuo* for  $\frac{1}{2}$  hr. at 450° C., to produce perfectly annealed grains of suitable size.

Two series of experiments were performed. In the first, annealed specimens were extended quickly at room temperature by amounts between 2 and 9%. These were then either soaked at 300° C. or higher temperature without an applied stress, or deformed further at 300° C. by various amounts and using various strain rates. In the second series, annealed specimens were extended rapidly by 5–7% at 300° C. and then treated in the same way as the first series.

### (a) Specimens Extended at Room Temperature

The preliminary results of this work were shown in Figs. 13–15 (Plate LII) of the paper by Greenough and Smith.<sup>8</sup> Details of some of the additional tests are given in Table I, and the photographs are shown in Figs. 8–14 (Plates LXXXIX and XC). In these figures the upper half is taken from the original X-ray negative with a magnification of  $\times 0.9$ , and the lower half shows a portion of the negative at  $\times 2.7$ .

The photographs published in the previous paper had demonstrated that the initial cold extension caused considerable diffuseness of the X-ray reflections, and that a creep deformation gave a marked sharpening of the diffraction spots, although soaking

the specimen at 300° C. without an applied stress had little effect. This, in general, was confirmed by the present work, but several additional details became apparent.

It was clear from all the tests that a creep deformation does not cause the blurred diffraction rings to split up into sharp spots until the extension reaches

TABLE I.—*Recovery Experiments after Deformation at 20° C.*

Specimen No.	Rapid Deformation at 20° C.		Recovery Conditions			
	Stress, lb./in. <sup>2</sup>	Strain, %	Stress, lb./in. <sup>2</sup>	Temp., °C.	Time	Strain, %
10B	5300	6.1	...	...	...	...
10A	5400	6.8	...	300	69 hr.	...
20A	4500	5.6	64	300	67 hr.	0.3
17A	5400	8.3	350	300	202 hr.	1.9
17A	5400	8.3	350	300	319 hr.	4.8
9B	4800	5.8	2200	300	1 min.	3.1
		followed by	...	300	66 hr.	...

about 2%. In Fig. 10 (Plate XC), for instance, the slight extension of 0.3% produced by the small applied stress has had little effect on the structure. If the extension exceeds 2%, the diffraction spots become more clearly separated, cf. Fig. 12 with Fig. 11 (Plate XC), paying particular attention to the upper part of each print. Experiments were carried out under different stresses to determine whether the figure of 2% necessary to develop the sharp spots was influenced by the strain rate used. Although a small variation was found from specimen to specimen in the minimum strain necessary to produce the cell structure, there was no correlation with strain rate.

The effect of a rapid extension at 300° C. is interesting. In Fig. 13 (Plate XC) the rapid extension of 3.1% has had a noticeable effect on the diffraction photograph. A comparison with Fig. 9 (Plate XC), for instance, shows that by deformation a more marked development of diffuse spots has been produced than by annealing the cold-extended specimen at 300° C. for many hours. The rapid extension at 300° C., then, brings about considerable recovery in the cold-worked specimen, and Fig. 14 (Plate XC) shows that annealing at 300° C. after this extension causes further recovery. Other experiments indicated that rapid extensions at 300° C. of greater amounts did not cause a progressive recovery such as occurred during increasing creep extensions.

Lastly, attempts were made to produce "true" polygonization by heating the cold-extended specimens in the range 400°–500° C. It proved impossible to obtain a structure showing diffraction spots as well separated as those of creep specimens. While heating at 400° C. did cause some small development of diffuse reflection spots in about 30 hr., attempts to increase the distinctness of the effect by prolonging the time of anneal, or by raising the



temperature, failed because true recrystallization always intervened.

(b) *Specimens Extended at 300° C.*

In these recovery tests annealed specimens were extended rapidly by about 5–7% at 300° C., and then either allowed to creep at that temperature under various stresses or heated to a higher temperature with no applied stress. Details of two typical tests are given in Table II.

TABLE II.—*Recovery Experiments After Deformation at 300° C.*

Specimen No.	Rapid Deformation at 300° C.		Recovery Conditions			
	Stress, lb./in. <sup>2</sup>	Strain, %	Stress, lb./in. <sup>2</sup>	Temp., °C.	Time, hr.	Strain, %
2F	1820	6.6	480	300	87	1.0
4F	1820	6.7	...	400	36	...

The specimens deforming by creep were examined at frequent stages during the deformation. When the applied stress was so small that little, i.e. <0.1%, creep occurred, there was little change in the diffraction photograph. But when the creep strain had increased to about 0.3%, several small sharp spots became visible. These spots became more numerous, and the diffuse regions less extensive, as creep proceeded. Fig. 15 (Plate XC) is taken after a strain of 1% and the original negative showed almost all the pattern to be composed of sharp spots; these are, however, in many places very close together and are not resolved in the reproduction, which has not the same range of contrast. Larger creep strains increased the separation of the spots and also appeared to cause some increase in their size.

Within the range of creep rates employed, it was clear that the development of the cell structure was largely independent of the creep rate, and was controlled rather by the magnitude of the strain. The behaviour was thus analogous to that of specimens deforming at 300° C. after an initial cold extension, though in the latter case a larger creep strain was required before the cell structure became apparent.

Experiments were also made with specimens rapidly extended at 300° C., to determine whether, in the absence of an applied stress, polygonization would occur on heating to higher temperatures. Fig. 16 (Plate XC) shows the effect of annealing for 36 hr. at 400° C., and it is seen that some sub-structure has developed; this is rather more marked than that exhibited by the cold-worked specimens. However, attempts to increase the extent of the polygonization again failed because recrystallization set in.

It is interesting to note that recrystallization was never observed in specimens in which the polygonized structure was developing during creep. It thus appears that the application of a stress has a greater effect on polygonization than on recrystallization.

### III.—DISCUSSION

It must be remembered that it depends to a great extent on the geometry of the apparatus employed, as well as on the lattice-orientation difference between neighbouring units, whether or not small units of a crystal in which the lattice is perfect will give rise to separate spots in a Laue photograph. The experiments described have all been carried out with the same X-ray apparatus, and the results are thus comparable; the results may also be directly compared with those of other workers who have employed similar techniques, e.g. Wood and his collaborators. However, care must be taken when comparison is made with the results of Guinier and Tennevin,<sup>15</sup> who employed accurate focusing conditions; with those of Kellar, Hirsch, and Thorp,<sup>16</sup> who used a micro-beam technique; and with the deductions which Hall<sup>11</sup> makes from his intensity observations. In all the latter experiments, conditions were such that individual units could be detected when smaller or less disorientated than the units necessary to give separate spots in the present work.

In this work very well-defined cell formation on a relatively coarse scale is necessary before the resulting spots can easily be separated. It was estimated that in the most favourable circumstances, viz. cells of about  $10^{-3}$  cm. and free from strain, clearly separated spots would be visible when the angular difference of orientation of the cells was about  $10^\circ$ . In a specimen giving a photograph in which the diffraction spots are not well separated, it is not necessarily true to say that there is no cell formation; all that is certain is that the cells, if present, are smaller or less perfect than in a specimen showing well-defined spots. This difference in techniques probably accounts for the fact that Guinier and Tennevin<sup>15</sup> could observe well-defined polygonization in cold-worked aluminium specimens after annealing at 400° C., while in these similar experiments the polygonization was not well marked (although the lower purity of the aluminium used will also have contributed to this difference).

#### 1. ALLOYS

Since the silver atoms are effectively of the same size as the aluminium atoms, they should cause little, if any, distortion of the lattice when in solution and thus would not be expected to act as dislocation traps. It follows that the aluminium alloy containing 0.5% silver should behave in the same way as the pure aluminium during deformation at 300° C. A comparison of Figs. 2 and 3 with those given earlier for pure aluminium, both by Greenough and Smith and by Wood, shows this to be completely verified.

It is interesting to compare the results for the aluminium-silver solid-solution alloy with those of Gifkins<sup>6</sup> for a lead-thallium alloy. In the latter case, the solute atom has an atomic radius somewhat different from that of lead, and the alloy does not show cell formation with anything like the clarity of either aluminium or the 0.5% silver alloy. This

may arise from some difference between lead and aluminium,\* but it may also be because the foreign atoms of different size in the lead alloy affect the dislocation movements.

In the earlier paper by Greenough and Smith,<sup>8</sup> it was concluded that precipitated particles in the crystals would probably act as effective dislocation traps. The mutual attraction of the dislocations in such a case is relatively less important than the interaction of the dislocations with the stress fields of the precipitates, and it is unlikely that a polygonized structure would form in such an alloy. It is clear from Fig. 6 of the present paper, that there is no sign of a cell structure developing during the creep of the aluminium-silver alloy containing the precipitate; in fact, the photographs of the creep specimens are very similar to those of the rapidly extended specimens. The experimental results thus substantiate the earlier theoretical ideas.

Since the alloy in which the silver was in solid solution showed development of the cell structure, the silver in solution in the 2% alloy cannot be held responsible for the prevention of cell formation. It is clear that the precipitate must be responsible. It thus appears likely that the presence of the precipitate in the commercial-purity aluminium examined earlier might be responsible for the suppression of the cell formation. It is still not clear, however, whether cell formation would be prevented in solid solutions when the dissolved atoms and those of the parent lattice were dissimilar in size.

## 2. RECOVERY EFFECTS

The results showing the effect of various treatments at 300° C. on specimens previously extended at 20° C. are a direct continuation of the work reported earlier.<sup>8</sup> Specimens in which the grains were initially distorted show far less evidence of strain after creep and eventually become almost strain-free. The initial grains are divided up into smaller parts in the same way as the grains of specimens allowed to creep from the annealed state. The present work, however, indicates that the important criterion in the production of cells is the creep strain of the specimen. The presence of a small stress is in itself ineffective, unless it is large enough to cause a certain strain, and neither the strain rate nor the time for which the stress is applied seems important. Presumably this is because the movement of the dislocations from their initial random arrangement to positions in a polygonized array must be accompanied by some plastic deformation, and consequently some creep strain is to be expected during the process.

During his work on polygonization in the absence of stress, Cahn<sup>10</sup> noted that zinc polygonized more readily if the initial deformation was carried out at room temperature rather than at -180° C. The corresponding temperatures for aluminium are prob-

ably higher, and it was thought that a comparison of the behaviour of aluminium specimens after initial extensions at 300° and 20° C. might give results analogous to those of Cahn. The results did, in fact, show that, when subsequently heated at about 400° C., specimens which had been extended at 300° C. tended to polygonize more markedly than those extended at 20° C., although the difference was small. A comparison of the two groups of specimens after creep at 300° C. showed that the cell structure developed at lower creep strains in the specimens initially extended at 300° C., and in this case the difference was more marked. The experimental results are thus generally similar to those of Cahn.

These recovery results, then, are in accord with the explanations advanced earlier and are readily interpreted in terms of dislocation theory. It is less easy to understand the effect of subjecting a cold-extended specimen to a rapid deformation at 300° C. The X-ray photographs show that although the diffraction rings remain diffuse in parts, in general they sharpen considerably and a definite fine structure develops. In the earlier paper it was suggested that the stress necessary to cause the deformation would be so large that no dislocation array could form; it now seems more likely that the process of polygonization takes place to some extent in both cases and that the difference is only in the size and degree of perfection of the sub-crystals formed. This idea is supported by recent work of McLean and Tate,<sup>18</sup> who examined super-pure aluminium after various deformations, using both X-ray and microscopic methods to detect small orientation differences in the grains. They confirmed that a very clearly marked sub-structure appeared during creep at 300° C., but they also found evidence of a smaller and less well-defined structure after hot rolling. It is just possible that this sub-structure forms after the deformation, in the short interval during which the specimen is at the deformation temperature before cooling, but this does not seem probable.

If it is accepted that the polygonized structure does form during rapid deformation at 300° C., even though it is less well developed than that formed during creep, then the earlier explanation, which did not envisage any degree of polygonization during fast deformation, must be an over-simplification.

## 3. EXTENSION OF POLYGONIZATION THEORY

In a criticism of the polygonization theory of cell formation during creep, Wood, Wilms, and Rachinger<sup>5</sup> advance the argument that true polygonization is a two-stage process. First, the grain is disordered, and then the disordered lattice dissociates into units with perfect lattices, the range in orientation of which is usually similar to that in the disordered lattice. This, they state, does not occur during creep, where the initial spots of the annealed material divide into several

\* The earlier experiments by Greenough and Smith on lead were probably vitiated by the presence of the peculiar

layer on the surface of the drawn wires described by Gifkins and Coe.<sup>17</sup>



spots with little initial disordering, their angular separation increasing during further creep. These points were well brought out by Wood and Scrutton<sup>4</sup> (although, as pointed out during the discussion of the paper,<sup>11</sup> the technique used is too crude to permit the statement that *no* initial disordering occurs), but are illustrated generally throughout the work by Wood and his co-workers.

In their own explanation, this observation is interpreted as showing that the cells form early in the creep deformation and then rotate slowly with respect to one another. In the dislocation interpretation, such an increase of angle between the two lattices would be caused by a gradual increase of dislocation density in the wall between two cells during creep. In other words, during the creep subsequent to the production of the cells, dislocations are continually created within the lattice and move to the polygon walls, where they remain. This process, since it involves the continuous plastic shearing of the units of perfect lattice, explains how two neighbouring lattices can rotate relative to one another and yet remain in geometrical contact.

Wood and his collaborators<sup>2,3</sup> showed that the stage during which the cells were constant in size but gradually increasing in orientation difference, corresponded to secondary (steady-state) creep of the specimen. If the alternative explanation of the continuous increase of the density of dislocations in the boundary between two cells is accepted, then steady-state creep must be associated with motion of dislocations. Most earlier theories viewed primary creep as being associated with the motion of dislocations, and secondary creep as due to some other process, such as viscous flow (the ideas accepted earlier by Greenough and Smith). But, in the case of zinc single crystals, Cottrell and Aytakin<sup>7</sup> have shown that steady-state creep is due to a running balance between strain-hardening and a recovery process, and that the deformation mechanism remains the same throughout the primary and secondary stages. While these authors did not suggest that this was true in general, and for polycrystalline aluminium in particular, they have cast doubt on the widely held view that secondary creep differs fundamentally from primary creep. At the moment, then, the polygonization ideas cannot be ruled out because they indicate that secondary creep involves the motion of dislocations.

#### 4. ALTERNATIVE EXPLANATION

It is of interest to examine the experimental results described in the present paper in the light of the general explanation put forward by Wood, Wilms, and Rachinger.<sup>5</sup> Essentially, this explanation is that the elemental motion responsible for the plastic deformation is a micro-movement at a boundary. If a stress is applied to a specimen, the initial grains divide up until there is sufficient boundary area (either between grains or between cells) to enable enough micro-movements to take place to give the observed

steady strain rate. If conditions are altered, e.g. temperature increased or rate of deformation reduced, then presumably there would be a transition period while the cells increased in size until the reduced boundary area was sufficient to produce the requisite number of micro-movements.

It is difficult to see, on this picture, how alloys would be expected to behave. It is not clear whether the presence of a precipitate at a boundary would increase or decrease the probability of micro-movements there. Thus, this explanation could fit the experimental facts if it were supposed that the precipitate reduced the number of micro-movements taking place per unit area of boundary.

On the other hand, the application to the recovery results is, in general, quite clear. Creep deformation at 300° C. requires far less boundary area to cause the necessary micro-movements and consequently the very small units produced by the cold extension grow until they reach the equilibrium state. That a certain interval must elapse before the new state is reached is to be expected, although it might be anticipated that a time interval would be important, whereas experimentally it is observed to be a strain interval. In particular, it is very difficult to imagine how the growth could be so rapid as to explain the change when a cold-worked specimen is pulled a further 3% in 1 min. at 300° C.

Essentially, however, the difficulty of deforming an aggregate of rigid units solely by means of movements at their boundaries remains, and, while this theory is not completely contrary to the experimental facts, it is felt to be less satisfactory than that based on dislocation theory.

#### ACKNOWLEDGEMENTS

Acknowledgement is made to the Chief Scientist, Ministry of Supply, and to the Controller of H.M. Stationery Office for permission to publish this paper.

#### REFERENCES

1. W. A. Wood and H. J. Tapsell, *Nature*, 1946, **158**, 415.
2. G. R. Wilms and W. A. Wood, *J. Inst. Metals*, 1948-49, **75**, 693.
3. W. A. Wood and W. A. Rachinger, *ibid.*, 1949-50, **76**, 237.
4. W. A. Wood and R. F. Scrutton, *ibid.*, 1950, **77**, 423.
5. W. A. Wood, G. R. Wilms, and W. A. Rachinger, *ibid.*, 1951, **79**, 159.
6. R. C. Giffkins, *ibid.*, 1951, **79**, 233.
7. A. H. Cottrell and V. Aytakin, *ibid.*, 1950, **77**, 389.
8. G. B. Greenough and E. M. Smith, *ibid.*, 1950, **77**, 435.
9. G. Wyon and C. Crussard, *Rev. Mét.*, 1951, **48**, 121.
10. R. W. Cahn, *J. Inst. Metals*, 1949-50, **76**, 121.
11. —, *ibid.*, 1950, **77**, 597 (discussion).
12. E. A. Calnan and B. D. Burns, *ibid.*, 1950, **77**, 445.
13. R. W. Cahn, *ibid.*, 1951, **79**, 129.
14. L. W. Larke and L. Rotherham, unpublished work.
15. A. Guinier and J. Tennevin, *Acta Cryst.*, 1949, **2**, 133.
16. J. N. Kellar, P. B. Hirsch, and J. S. Thorp, *Nature*, 1950, **165**, 554.
17. R. C. Giffkins and H. C. Coe, *Metallurgia*, 1951, **43**, 47.
18. D. McLean and A. E. L. Tate, *Rev. Mét.*, 1951, **48**, 765.

# THE FORMATION OF THE $\text{Ni}_3\text{Al}$ PHASE IN NICKEL-ALUMINIUM ALLOYS\*

1380

By R. W. FLOYD,† B.Sc., A.I.M., MEMBER

## SYNOPSIS

The  $\text{Ni}_3\text{Al}$  phase forms so rapidly during the solidification of alloys of nickel and aluminium containing about 25 at.-% aluminium, that the difficulties in interpreting the results of investigations of this part of the phase diagram have led to two different reactions being proposed. The present work demonstrates that the  $\text{Ni}_3\text{Al}$  phase is the product of a peritectic reaction between the melt and the  $\beta(\text{NiAl})$  phase. This has been established by a comparison of the microstructures of small ingots of a series of binary nickel-aluminium alloys containing 20–30 at.-% aluminium, with those of a corresponding series in which  $2\frac{1}{2}$  at.-% of the nickel had been replaced by chromium.

## I.—INTRODUCTION

ALTHOUGH a phase of composition  $\text{Ni}_3\text{Al}$  is shown in a nickel-aluminium phase diagram published by Iitaka<sup>1</sup> in 1924, the existence of such a phase was first established with any certainty by Bradley and Taylor<sup>2</sup> in the course of their studies of the system by X-ray analysis. While the  $\text{Ni}_3\text{Al}$  phase, referred to below as  $\gamma'$ , was separated at room temperature from the nickel solid solution ( $\gamma$ ) by a miscibility gap extending from 11–23 at.-% aluminium, Bradley and Taylor's X-ray photographs indicated that the two phases merged at temperatures above about 1100°C.

Alexander and Vaughan,<sup>3</sup> using thermal and micrographic analysis, established that the  $\gamma'$  phase exists up to the solidus and is formed as a result of a peritectic reaction which occurs at 1395°C. between the  $\text{NiAl}$  solid solution ( $\beta$ ) and the melt, and that it yields a

aluminium-molybdenum,<sup>4</sup> and iron-nickel-aluminium<sup>5</sup> systems, and it may be presumed that they have been confirmed by the authors of those papers.

The findings of Alexander and Vaughan were challenged, however, by Schramm,<sup>6</sup> who concluded that  $\gamma'$  results from a peritectic reaction occurring at 1362°C. between the  $\gamma$ -phase and the melt, and that it forms a eutectic with the  $\beta$  phase at 1360°C. (Fig. 1 (b)). This conclusion was based primarily on cooling-curve studies, and Schramm found it necessary to introduce a very involved argument to account for the microstructures which he used as supplementary evidence. Nevertheless, a paper by Köster, Zwicker, and Moeller<sup>7</sup> on the copper-nickel-aluminium system incorporates Schramm's results on the binary nickel-aluminium alloys and places the peritectic on the nickel side of the eutectic.

Examination of the published evidence provides no direct clue to indicate which, if either, of the two diagrams is correct, although the complexity of Schramm's argument suggests that the more straightforward case advanced by Alexander and Vaughan is more probable. The present work was undertaken to determine qualitatively the nature of the reaction by which  $\text{Ni}_3\text{Al}$  is formed, without attempting to establish the temperature of its formation or the precise position of any phase boundaries.

## II.—EXPERIMENTAL METHOD

It was clear from the previous work that, whatever the mechanism of formation of  $\text{Ni}_3\text{Al}$ , it took place too rapidly in the binary nickel-aluminium alloys for its progress to be observed directly by micro-examination of quenched alloys. Likewise, the eutectic was very difficult to detect on account of the broadening of the  $\gamma'$  phase field immediately below the solidus. In contrast to the rapid rate of reaction in nickel-aluminium alloys, the response to heat-treatment of alloys of nickel with chromium was known to be sluggish, and it seemed reasonable to suppose that the

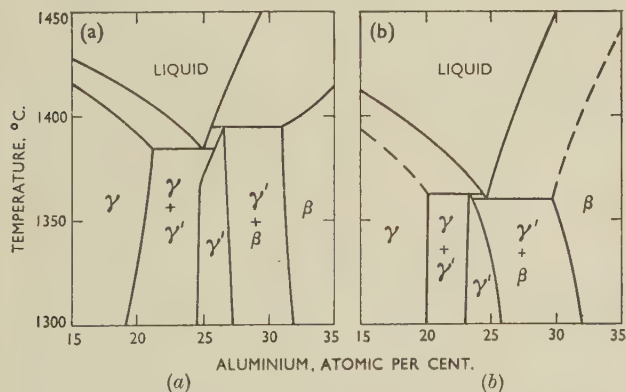


Fig. 1.—The Nickel-Aluminium Phase Diagram in the Region of  $\text{Ni}_3\text{Al}$  According to (a) Alexander and Vaughan,<sup>3</sup> and (b) Schramm.<sup>6</sup>

eutectic with the  $\gamma$  phase at 1385°C. (Fig. 1 (a)). Between 1395° and 1385°C.  $\gamma'$  is also deposited directly from the melt. These results have been incorporated in papers dealing with the nickel-

\* Manuscript received 7 November 1951.

† The Mond Nickel Co., Ltd., Birmingham.



replacement in nickel-aluminium alloys of a small part of the nickel by chromium would slow down the rate of any reaction taking place during solidification. Evidence obtained by the author from other work<sup>8</sup> showed that the addition of chromium in small amounts did not introduce any new phase. Accordingly, a microscopical examination has been made of a series of binary nickel-aluminium alloys containing 20–30 at.-% aluminium and of a corresponding series of nickel-chromium-aluminium alloys containing 2½ at.-% chromium at the same aluminium levels.

The alloys were prepared by melting together selected Mond nickel pellet, high-purity aluminium from The British Aluminium Co., Ltd., and Murex chromium with a purity of about 99.6%. Charges of 100 g. were melted in alumina-lined crucibles in a small high-frequency induction furnace under an atmosphere of hydrogen at a low pressure, the pressure being reduced to about  $10^{-3}$  mm. during the solidification of the alloys in the crucible. As soon as the ingots appeared to be solid, they were removed from the furnace and quenched in water to eliminate changes in structure due to solubility changes with decreasing temperature. It is probable that the quenching temperature in all cases was over 1200° C.

The chemical analyses of the alloys are given below in atomic percentages:

Alloy No.	Composition, at.-%		
	Ni *	Al	Cr
200	78.9	21.1	...
201	76.8	23.2	...
202	74.9	25.1	...
203	73.6	26.4	...
204	72.2	27.8	...
205	69.0	31.0	...
218	74.5	22.8	2.7
217	72.1	25.5	2.4
216	70.9	26.6	2.5

\* Nickel figures obtained by difference.

Microspecimens were cut from the as-cast ingot, the remainder of which was annealed at 1200° C. for 3 days to promote homogeneity. Additional microspecimens from some of the annealed ingots were heat-treated to provide further evidence. The specimens were etched electrolytically in a solution of hydrofluoric acid and glycerine in water.

### III.—EXPERIMENTAL RESULTS

The microstructures of the binary nickel-aluminium alloys in the as-cast state, shown in Figs. 2–7 (Plate XCI), are essentially the same as those published by Alexander and Vaughan in their account of the system. They are presented as a series in order of increasing aluminium content so that the relationships between the  $\gamma'$  phase and the  $\gamma$  and  $\beta$  phases may be compared. Alloy 200 (Fig. 2) consists of cored primary  $\gamma$  solid solution in which extensive precipitation of  $\gamma'$  has occurred and an aluminium-rich infilling which has become entirely  $\gamma'$ . As would be expected, the structure exhibited by alloy 201 (Fig. 3) is very similar, except that there is a much larger proportion

of  $\gamma'$  phase. The unusual cellular structure appears to be characteristic of  $\gamma + \gamma'$  alloys in which the two phases have separated at a high temperature. Alloy 202 consisted entirely of regular polyhedral grains of  $\gamma'$ . With further increase in aluminium content the  $NiAl$  phase ( $\beta$ ) appears (Figs. 4–6). Although the published phase diagrams indicate that the  $\beta$  phase should be the first to separate from the melt, it is not obvious from the microstructures that this is so, unless they are viewed at low magnifications, when the dendritic pattern is clearly seen. The conspicuous feature of these structures, particularly as seen in alloys 203 and 204 (Figs. 4 and 5), is the outline of the  $\beta$  phase, which suggests that the  $\gamma'$  phase has been formed by a very rapid reaction involving the  $\beta$  phase. It is maintained by Schramm<sup>6</sup> that this structure is produced by the rapid rejection of  $\gamma'$  from supersaturated  $\beta$  as the solubility decreases with fall in temperature. This explanation seems to be open to doubt, particularly if reference is made to the structure of the centre of the  $\beta$  dendrites in alloy 205 (Fig. 6). At the solidus, this alloy consists almost entirely of  $\beta$  phase, and since there is no opportunity for the metal at the centres of the dendrites to react with any possible traces of residual liquid, all the  $\gamma'$  present must have been formed by precipitation from the solid  $\beta$  phase. To confirm that this type of structure was due to solid-solubility changes, a small specimen of alloy 204 was annealed at 1365° C. for 15 min. and quenched in water. Such a treatment was thought adequate to permit any reaction at the solidus to become complete, while restraining any change occurring during cooling. The structure obtained is shown in Fig. 7, from which it can be seen that within the areas which consisted entirely of  $\beta$  at the annealing temperature, much precipitation of  $\gamma'$  has taken place, giving a pattern similar to that in Fig. 6, although finer, as would be expected from the more effective quenching. Thus it would appear that the form of the  $\beta$  phase in alloys 203 and 204, as cast, is due to a reaction occurring during solidification, but it has not been found possible to demonstrate this conclusively by experiments on the binary alloys alone.

The structures of the 2½% chromium alloys, as cast, are shown in Figs. 8–10 (Plate XCI), again in order of increasing aluminium content. The extent to which the rate of formation of the  $\gamma'$  phase is retarded is well demonstrated by the structure of alloy 218 (Fig. 8). In this can be seen cored primary dendrites of  $\gamma$ , in which  $\gamma'$  is precipitated in a finely dispersed form, together with an infilling which has the appearance of a coarse ( $\gamma + \beta$ ) eutectic. Alloy 217 (Fig. 9), on the other hand, consists of primary  $\beta$  dendrites, whose edges have an appearance similar to that of corresponding binary nickel-aluminium alloys, with a lightly etched infilling. Close examination of both these structures reveals that there are clear envelopes around the  $\beta$  phase separating it from the  $\gamma$  phase. These envelopes must consist of a phase intermediate in composition between  $\gamma$  and  $\beta$ , which can only be  $\gamma'$ . Under particularly favourable conditions these envelopes can be etched fairly clearly,

as in Fig. 10, alloy 216, while it has been found that in all cases they are readily visible under phase-contrast illumination (Fig. 11, Plate XCI).

From Figs. 10 and 11 it is evident that the envelopes of  $\gamma'$  phase are formed by a reaction between the solid  $\beta$  dendrites and the infilling, which consists of the  $\gamma$  and  $\gamma'$  phases intermixed either as a eutectic or by precipitation of  $\gamma'$  from the original  $\gamma$ . The fact that the  $\beta$  phase solidified first from the melt is sufficient to indicate that the reaction is:  $\text{liq.} + \beta \rightleftharpoons \gamma'$ .

Additional evidence is provided by the shape of the envelopes, which have an irregular outline at the  $\beta$  interface, while the interface with the  $\gamma$  phase is smooth, showing that during the formation of the  $\gamma'$  phase the  $(\gamma + \gamma')$  infilling was liquid.

There remains the possibility that the addition of chromium to nickel-aluminium alloys results in a change-over from a reaction involving solid  $\gamma$  phase to one involving solid  $\beta$  phase. Such a case has not been disproved experimentally, but it is known that in the nickel-chromium-aluminium system the eutectic and peritectic of the nickel-aluminium binary system merge,<sup>8</sup> as in the iron-nickel-aluminium system.<sup>5</sup> This being so, it would be quite impossible to construct a ternary phase diagram for the nickel-chromium-aluminium system in which any transposition of the eutectic and peritectic occurred between the nickel-aluminium side of the system and the point at which the peritectic merges into the eutectic.

#### IV.—DISCUSSION

In the determination of phase diagrams, it is usual to establish in the first place the nature of phase relationships in the component systems. In the case of binary diagrams a knowledge of the melting points and transformations of the pure metals is an obvious starting point. Again, the relationships between phases in ternary systems can rarely be explored until the contiguous binary phase systems have been established, and the resultant phase diagram must

be consistent in all respects with the binary phase diagrams by which it is contained.

It is because of the essential consistency of a more complex phase system with the simpler component systems that it has been possible in the present work to apply the observations made on nickel-chromium-aluminium alloys to the interpretation of the structures of binary nickel-aluminium alloys. While this is the reverse of the usual procedure, the method is inherently sound, and it may be that in other cases where a reaction is either too rapid or too slow for observation by direct methods, the introduction of another, suitably chosen, element will so affect the rate of the reaction that its progress can be easily followed and its mechanism understood. It is essential to the satisfactory application of results on a complex system to those of a less complex one, that sufficient be known about the effects of the additional element; otherwise serious difficulties in interpretation can occur, as has been shown in studies of systems where the presence of impurities has been unavoidable owing to limitations in the raw materials available or in the techniques by which the alloys had been prepared.

#### ACKNOWLEDGEMENT

The author wishes to thank The Mond Nickel Co., Ltd., for permission to publish this paper.

#### REFERENCES

1. I. Iitaka, *Tetsu to Hagane*, 1924, **10**, 1.
2. A. J. Bradley and A. Taylor, *Proc. Roy. Soc.*, 1937, [A], **159**, 56.
3. W. O. Alexander and N. B. Vaughan, *J. Inst. Metals*, 1937, **61**, 247.
4. H. V. Kinsey and M. T. Stewart, *Canad. J. Research*, 1949, [F], **27**, 80.
5. A. J. Bradley, *J. Iron Steel Inst.*, 1949, **163**, 19.
6. J. Schramm, *Z. Metallkunde*, 1941, **33**, 347.
7. W. Köster, U. Zwicker, and K. Moeller, *Z. Metallkunde*, 1948, **39**, 225.
8. A. Taylor and R. W. Floyd, to be published shortly.



# NOTICE TO AUTHORS OF PAPERS FOR THE "JOURNAL" AND CONTRIBUTORS TO DISCUSSIONS

1. **Papers will be considered for publication from non-members as well as members of the Institute.** They are accepted for publication in the *Journal* and not necessarily for presentation at any meeting of the Institute. MSS. should be addressed to The Editor of Publications, The Institute of Metals, 4 Grosvenor Gardens, London, S.W.1.

2. **Papers suitable for publication** may be classified as:

(a) Papers recording the results of original research.  
(b) First-class reviews of, or accounts of progress in, a particular field.

(c) Papers descriptive of works methods, or recent developments in metallurgical plant and practice.

(d) Papers in classes (a), (b), and (c) above, previously published in languages other than English, French, German, or Italian, if of sufficient merit.

3. **Manuscripts and illustrations** should be submitted in duplicate. MSS. must be typewritten (*double-line spacing*) on one side of the paper only, and authors are requested to sign a declaration that neither the paper nor a substantial part thereof has been published elsewhere. Exceptions may be made in certain cases where a paper has been published in a language other than English, French, German, or Italian (see 2(d) above). MSS. not accepted are normally returned within 6 months of receipt.

In the interests of economy, all papers must be written as concisely as possible; in general, internal research reports are not in suitable form for publication as papers in the *Journal*. All but the simplest mathematical expressions should be written by hand, with capital and small letters clearly distinguished. Superscript and subscript letters should also be plainly indicated. Greek letters and special signs should be identified in the margin. For style, spelling, and abbreviations used, any recent issue of the *Journal* may be consulted.

4. **Synopsis.** Every paper must have a synopsis (not exceeding 250 words in length) which, in the case of a paper reporting original research, should state its objects, the ground covered, and the nature of the results. The synopsis will appear at the beginning of the paper, and should be in a form suitable for use by abstracting organizations. Extracts from a "Guide for the Preparation of Synopses" drawn up by the Abstracting Services Consultative Committee are reproduced below.

5. **References** must be collected at the end of the paper and must be numbered in the order in which they occur in the MS. Initials of authors must be given, and the Institute's official abbreviations for periodical titles (as used in *Metallurgical Abstracts*) should be employed, where known. References to papers should be set out in the style:

A. L. Dighton and H. A. Miley, *Trans. Electrochem. Soc.*, 1942, 81, 321 (i.e. year, volume, page).

References to books should be in the following style:

C. Zener, "Elasticity and Anelasticity of Metals". Chicago: 1948 (University of Chicago Press).

6. **Illustrations.** Each illustration must have a number and description; only one set of numbers must be used in one paper, and it is desirable to number the half-tone illustrations consecutively, rather than to intersperse them with the line figures. The captions should be typed on a separate sheet.

The set of **line figures** sent for reproduction must be drawn (about twice the size to appear in the *Journal*) in Indian ink on smooth white Bristol board, good-quality drawing paper, co-ordinate paper, or tracing cloth, which are preferred in the order given. Co-ordinate paper, if used, must be blue-lined, with the co-ordinates to be reproduced finely drawn in Indian ink. Curves should be drawn boldly (i.e. at least twice the thickness of the frame). Experimental points should be indicated by open or closed circles, triangles, squares, &c. (preferably not crosses). Curves should be broken on each side of such symbols and plenty of allowance should be made for closing up in blockmaking. All lettering and numerals, &c., should preferably be in *pencil*, so that the Institute's standard lettering may be affixed, and ample margins must be left outside the framework of the figures to enable this to be done. The second set of line illustrations may be photostat copies.

**Photographs** must be restricted in number, owing to the expense of reproduction, and photomicrographs should be trimmed to the smallest possible of the following sizes consistent with adequate representation of the subject: 4 in. deep by 3 in. wide: 2 in. deep by 3 in. wide: 2 in. square. Magnifications of photomicrographs must be given in each case. Photographs for reproduction should be loose, not pasted down (and not fastened together with a clip, which damages them), and the figure number and author's name should be written on the back of each. Captions should be given to the photomicrographs, but these should be kept as brief as possible.

Because of the present high cost of printing and paper it is imperative that authors restrict illustrations (particularly photographs) to the absolute minimum deemed necessary to support their argument. Only in exceptional cases will illustrations be reproduced if already printed and readily available elsewhere.

7. **Tables or Diagrams.** Results of experiments, &c., may be given in the form of tables or figures, *but* (unless there are exceptional reasons) *not both*. Tables should bear Roman numbers, and each should have a heading that will make the data intelligible without reference to the text.

8. **Corrections.** A certain number of corrections in proof are inevitable, but any modification of the original text is to be avoided. Since corrections are very expensive, the Institute reserves the right to require authors to contribute towards their cost if the Editor deems them to be excessive. The Institute also reserves the right to require a contribution to the cost of remaking any block where this is necessitated by an error on the author's part.

9. **Reprints.** Individual authors are presented with a maximum of 25, and two or more authors with a maximum of 50 reprints from the *Journal*, without covers. Limited numbers of additional reprints can be supplied at the author's expense, if ordered before proofs are passed for press. (Orders should preferably be placed when submitting MSS.)

10. **Discussion.** Except in the case of special symposia, shorthand records of discussions are not taken at meetings. Written discussion may be submitted on any paper, preferably typewritten (*double-line spacing*). References should be given in the form of footnotes. Paragraphs 6 and 7 above are also applicable to such contributions. Reprints of discussion cannot be supplied to contributors.

## GUIDE FOR THE PREPARATION OF SYNOPSES

(As recommended by the Abstracting Services Consultative Committee)

1. **Purpose.** The synopsis is not part of the paper; it is intended to convey briefly the content of the paper, to draw attention to all new information, and to the main conclusions. It should be factual.

2. **Style of writing.** The synopsis should be written concisely and in normal rather than abbreviated English. It is preferable to use the third person. Where possible use standard rather than proprietary terms, and avoid unnecessary contracting.

It should be presumed that the reader has some knowledge of the subject, but has not read the paper. The synopsis should therefore be intelligible in itself without reference to the paper; for example, it should not cite sections or illustrations by their numerical references in the text.

3. **Content.** The title of the paper is usually read as part of the synopsis. The opening sentence should be framed accordingly and repetition of the title avoided. If the title is insufficiently comprehensive, the opening should indicate the subjects covered. Usually the beginning of a synopsis should state the objective of the investigation.

It is sometimes valuable to indicate the treatment of the subject by such words as: brief, exhaustive, theoretical, &c.

The synopsis should indicate newly observed facts, conclusions of an

experiment or argument and, if possible, the essential parts of any new theory, treatment, apparatus, technique, &c.

It should contain the names of any new compound, mineral species, &c., and any new numerical data, such as physical constants; if this is not possible, it should draw attention to them. It is important to refer to new items and observations, even though some are incidental to the main purpose of the paper; such information may otherwise be hidden, though it is often very useful.

When giving experimental results the synopsis should indicate the methods used; for new methods the basic principle, range of operation, and degree of accuracy should be given.

4. **References.** If it is necessary to refer to earlier work in the summary, the reference should always be given in full and not by number. Otherwise references should be left out.

When a synopsis is completed, the author is urged to revise it carefully, removing redundant words, clarifying obscurities, and rectifying errors in copying from the paper. Particular attention should be paid by him to scientific and proper names, numerical data, and chemical and mathematical formulæ.

# THE EFFECT OF METAL/MOULD REACTION ON 85 : 5 : 5 : 5 LEADED GUN-METAL SAND CASTINGS\*

1381

By N. B. RUTHERFORD,† B.Sc., A.I.M., MEMBER

(Communication from the British Non-Ferrous Metals Research Association.)

## SYNOPSIS

Earlier work had shown that the controlled absorption of gas arising from metal/mould reaction improved the strength and pressure-tightness of phosphor bronze or gun-metal sand castings having marked heat centres. The present work was designed to examine further the effect with leaded gun-metals, in view of their increasing popularity as casting materials.

Varying degrees of metal/mould reaction were induced in 85 : 5 : 5 : 5 leaded gun-metal by casting it into green-sand moulds from four pouring temperatures between 1050° and 1200° C., and by varying the residual phosphorus content from 0.002 to 0.15%. The castings were in the form of ribbed plates,  $\frac{1}{4}$ ,  $\frac{1}{2}$ , and 1 in. thick, and 1- and 2-in.-dia. bars. The plates were intended to simulate poorly fed industrial castings.

The amount of gas arising from metal/mould reaction that was absorbed was calculated from the densities of the castings. Its effect on the properties was determined from tensile test-pieces. The work was designed as a factorial experiment, and the results were examined by statistical methods, details of which are given in an Appendix. Concurrently with the laboratory work, trials were run in two foundries making valve castings in 85 : 5 : 5 : 5 gun-metal.

It was concluded that the value of metal/mould reaction as a means of increasing the proportion of pressure-tight castings is less with leaded gun-metal than with phosphor bronze or lead-free gun-metal. With 85 : 5 : 5 : 5 leaded gun-metal it may be used with advantage where the rate of solidification is rapid, as in castings with section thicknesses of the order of  $\frac{1}{4}$  in., or in thicker-section castings poured from temperatures lower than 1100° C.

## I.—INTRODUCTION

It is generally recognized that tin bronzes and gun-metals are superior to many other casting alloys in that simple and inexpensive methods of gating and feeding suffice to produce pressure-tight castings of complex shape. Nevertheless, a proportion of the castings leak under pressure, usually at bosses, junctions of sections, or other similar heat centres. Such centres function as local feeders for the adjacent parts of the casting and, being themselves unfed, may be highly porous when solid.<sup>1</sup>

It was shown in earlier work<sup>1-4</sup> that the pressure-tightness and strength of the poorly fed parts of special test castings made in phosphor bronze or lead-free gun-metal were substantially improved if the metal was slightly gassy (equivalent to 1.5–2.5% voids in a sand-cast, D.T.D.-type test-bar) instead of being thoroughly degassed, and that even better results were obtained by using degassed metal and causing some gas to be absorbed by the casting while it froze in the mould. This absorption, termed metal/mould reaction, was achieved by the introduction of a suitable residual phosphorus content into the metal; the mechanism of the reaction and the effect of variations

in composition and moulding conditions have been discussed elsewhere.<sup>1, 5</sup>

The improvement in pressure-tightness is believed to arise in the following way. Because of the much lower solubility of the gas (hydrogen<sup>1</sup>) in the solid metal than in the liquid, much of it is rejected during solidification of those parts of the casting adjoining the heat centre, leaving small amounts of well-distributed interdendritic porosity. Consequently, less feeding of these parts is needed, and more metal remains to solidify in the heat centre, so increasing its soundness. Provided that the amount of gas in the liquid metal is not excessive, the net effect is a redistribution of the porosity that would have been present had the castings been made from hydrogen-free metal. Unfortunately, hydrogen diffuses rapidly through molten metal, and during solidification tends to segregate in the residual liquid in the heat centres. If there is sufficient time for this segregation to become marked, the porosity distribution may be worse, and the heat centre finally less sound, than with gas-free metal. It is for this reason that gas absorbed from the mould during solidification is more effective in dispersing shrinkage porosity than gas present in the metal before casting, since in the former case the gas

\* Manuscript received 30 May 1951. The work described in this paper was made available to members of the B.N.F.M.R.A. in a confidential report issued in 1949.

† Research Investigator, British Non-Ferrous Metals Research Association, London.



has less time to diffuse towards the heat centres. For the same reason, the beneficial effect of absorbed gas should be most marked when solidification is rapid, i.e. when the average section thickness of the casting is small and/or when the pouring temperature is low.

The previous work had thrown no light on the practical significance of the last two factors, because pouring temperature and section thickness were arbitrarily standardized in order to study the effect of other variables. In that work<sup>1-3</sup> the test casting was a  $\frac{3}{8}$ -in.-thick disc fed via a restricted ingate attached to a central boss, and the casting temperatures used were fairly high.\* Under those conditions, it was found that, although, as noted above, suitable amounts of gas absorption during solidification greatly improved the pressure-tightness of phosphor bronze and lead-free gun-metal castings, with the leaded gun-metals now in common use gas absorption had an adverse effect. Beneficial effects of mould reaction could be demonstrated with this alloy only when the ingate was further restricted,<sup>3</sup> so that, in the absence of mould reaction, the proportion of leaky castings rose towards that found with the other alloys.

Since that work was done, the good casting characteristics of the leaded gun-metals have led to their increasing use for pressure-tight parts, and there is little doubt that less trouble is experienced from leakage than with the lead-free gun-metals. However, a small proportion of leaded gun-metal castings do leak under pressure, and the purpose of the present work was to see whether mould reaction might be used to increase the yield of sound castings. To this end, works' trials were made in the foundries of two member firms of the B.N.F.M.R.A. and, concurrently, laboratory tests were carried out under carefully controlled conditions to determine the conditions of pouring temperature and residual phosphorus content most beneficial in castings of various section thicknesses. The laboratory tests are described in detail below. The results of the works' trials, some of which are more fully described elsewhere,<sup>6</sup> are briefly reported and their relation to the laboratory tests is discussed.

## II.—EXPERIMENTAL TECHNIQUE

### 1. METHOD

The earlier work<sup>1-3</sup> had established that the results of tensile tests on inadequately fed parts of castings, though not quite so sensitive, corresponded with the results of pressure tests. The latter were "go or no-go" tests, and large numbers of castings had to be tested to obtain significant results. In the present work, therefore, a test casting was selected in the form of a  $9 \times 6$  in. plate, which provided a number of tensile specimens whose mean strength was taken as a measure of pressure-tightness.<sup>4</sup> The casting had double ribs which produced a less severe heat centre

than the boss of the disc casting. It was made in three section thicknesses ( $\frac{1}{4}$ ,  $\frac{1}{2}$ , and 1 in.) and the amount of metal/mould reaction was varied by using different residual phosphorus contents (0.002–0.15%) and pouring temperatures (1050°–1200° C.). The volume ratios between the ribs and the plate and between the test casting and the feeder were kept the same for each section thickness. Castings without heat centres, and castings made in moulds sprayed with aluminium–magnesium paint to inhibit metal/mould reaction,<sup>5</sup> were also cast from each melt. The investigation was planned as a factorial experiment † and melts were made in random order.

### 2. MATERIALS, MELTING, AND CASTING

Two tons of commercial ingots (B.S. 1400/LG2) from a single cast of 85:5:5:5 leaded gun-metal were obtained. Chemical analysis of samples from three ingots, taken at random, gave the following composition: Sn 5.25–5.38, Zn 4.68–4.86, Pb 5.28–5.52, P 0.0008–0.0063, Fe 0.22–0.25%, Al trace, Mn nil (Ni 0.3, Bi 0.02%, Si nil, by spectrographic analysis of a single sample), remainder Cu.

Previous work<sup>5</sup> had shown that 0.5% iron in phosphor bronze increased the gas absorption from the sand mould. As the material now being used contained over 0.2% iron, a few supplementary tests were made with high-purity melts of 85:5:5:5 alloy. The addition of 0.3% iron to the metal caused small variations in the amount of porosity in the castings, but it was concluded that they were not significant.<sup>4(a)</sup>

The commercial ingots were remelted in some forty 120-lb. heats, using clay–graphite crucibles and a gas-fired furnace. All except the first few melts included about 15% of heads, &c., from previous casts. The melts were heated to about 100° C. above the pouring temperature before turning off the flame. Phosphor copper was added and the melts degassed by blowing a vigorous stream of nitrogen through the metal for 10 min.<sup>7</sup> Impurities in the phosphor copper were determined spectrographically as follows: As 0.04; Ni 0.004; Ag 0.004%; Fe, Sn, Sb, each 0.001%; Bi 0.0006%; Pb, Si, trace; Co, Mn, Te, Zn, not detected.

Besides the ribbed plate castings described above, simple cylinders without a heat centre and with large superimposed feeding heads, were poured from each melt. These bars were of 1- and 2-in. dia., the 1-in. bar being to the pattern recommended by the D.T.D. specification for tensile tests (Figs. 1 and 2). The plates and one bar of each diameter were made in moulds of green Mansfield sand (5–5.5% moisture) and one bar of each diameter was also made in a mould sprayed with 100-mesh aluminium–magnesium alloy powder suspended in a commercial volatile resinous base. This paint virtually prevents gas

\* A  $\frac{1}{2}$ -in.-thick plate casting with a heat centre formed by a single or double rib, similar to the test castings described later in the present paper, was used in some of the experi-

ments with lead-free gun-metal.<sup>4</sup>

† This and other statistical terms are explained in the Appendix (p. 564).

absorption from the mould, so that these castings show whether the melts were thoroughly degassed<sup>5</sup> and, also, if the porosity found in the bars from the unsprayed moulds exceeds that in the bars from the

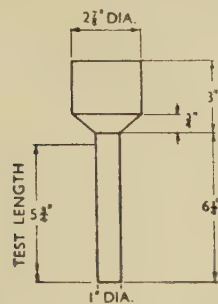


FIG. 1.—1-in.-dia. Test-Bar (D.T.D.-type), as cast; yield approx. 20%.

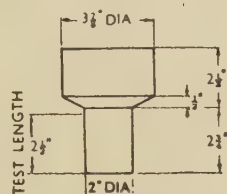


FIG. 2.—2-in.-dia. Test-Bar, as cast; yield approx. 20%.

sprayed moulds, gas absorption from metal/mould reaction has occurred with the former moulds. The order of pouring and average time/mould are given in Table I.

TABLE I.—Pouring Conditions for Bars and Plates.

Order of Pouring	Type of Casting	Pouring Time/Mould, sec.	Fall in Pouring Temp. from Start, °C.
1	1-in.-dia. bar (sprayed mould)	6.5	0
2	„ „ (unsprayed mould)	6.5	5
3	1/4-in. ribbed plate	8	10
4	1/2-in. „ „	10	20
5	1-in. „ „	17	30
6	2-in.-dia. bar (sprayed mould)	6	40
7	„ „ (unsprayed mould)	6	45

Temperatures were measured to better than  $\pm 5^\circ \text{C}$ . Four initial pouring temperatures were used;  $1050^\circ$ ,  $1100^\circ$ ,  $1150^\circ$ , and  $1200^\circ \text{C}$ . However, the average of a number of observations showed the metal temperature in the crucible before pouring each casting to be below that for the first casting by approximately the amount shown in Table I. Two-in.-dia. bars from a cast in which pouring began at  $1100^\circ \text{C}$ . have therefore been compared with 1-in.-dia. bars from a cast in which pouring began at  $1050^\circ \text{C}$ ., and so on. The observed temperatures were spread up to  $10^\circ \text{C}$ . on either side of the appropriate figures quoted in Table I, and, as an aid to appreciation of the results of the experiment, it is therefore justifiable to group the castings according to type and pouring temperature in the following way (cf. Table I):

	Pouring Temp., °C.
Group 1: 1-in.-dia. bars . . .	1100
Group 2: plates . . .	$1100 - 20 = 1080$
Group 3: 2-in.-dia. bars . . .	$1100 - 50 = 1050$

This grouping is used in the rest of the paper.

\* Formula (ii) is based on previous B.N.F.M.R.A. work<sup>8</sup> and information from other sources,<sup>9,10</sup> and its validity for all practical purposes has been shown.<sup>1-3,5</sup> The addition of

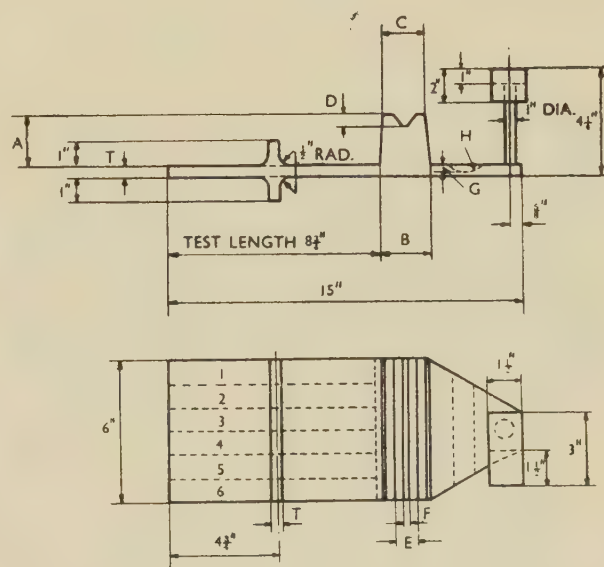
### 3. EXAMINATION OF CASTINGS

After removal of the feeders and thorough cleaning, the overall densities of the castings were determined correct to better than 1 part in 1000. From these the overall porosity was calculated using the following formulæ:

$$(i) \text{ Porosity (vol.-%)} = \left( \frac{\text{max. density} - \text{observed density}}{\text{max. density}} \right) \times 100$$

$$(ii) \text{ Max. density} = 8.93 - (0.013 \times \% \text{ Zn}) + (0.025 \times \% \text{ Pb}) - (0.1 \times \% \text{ P}) = 8.990 - (0.1 \times \% \text{ P}).^*$$

The ribs were removed from the plate castings and the outer 1-in. strips (see Fig. 3) discarded to avoid the edge effects shown to exist by other work.<sup>4,12</sup> Strips 2-5 (Fig. 3) were machined into tensile test-pieces,



Casting	Dimensions, in.									Volume Ratio	
	T	A	B	C	D	E	F	G	H	Casting Feeder	Plate Rib
1/4" plate	1/4	1 1/2	1 1/2	1 1/2	1 1/2	1 1/2	1 1/2	1 1/2	1 1/2	1.0	4.5
1/2" " "	1/2	2 1/2	2 1/2	2 1/2	2 1/2	2 1/2	2 1/2	2 1/2	2 1/2	1.0	4.5
1" " "	1	3 1/2	3 1/2	3 1/2	3 1/2	3 1/2	3 1/2	3 1/2	3 1/2	0.9	4.5

FIG. 3.—Double-Ribbed Plates, as Cast. The strips (2-5), used for tensile tests after removing the rib, are indicated by dotted lines.

the cast surfaces being removed in amounts proportional to the thickness. The nominal dimensions of the test-pieces were: 1/4-in. plate,  $8 \frac{3}{4} \times \frac{7}{8} \times \frac{3}{16}$  in.; 1/2-in. plate,  $8 \frac{3}{4} \times \frac{7}{8} \times \frac{3}{8}$  in.; 1-in. plate  $8 \frac{3}{4} \times \frac{7}{8} \times \frac{3}{4}$  in. The 1-in. test-bars were machined and tested as 0.564-in.-dia. test-bars (B.S.18). Gauge-lengths of

tin to copper has little effect on the density.<sup>11</sup> The nominal composition 85:5:5:5 was assumed in obtaining the constant figure of 8.990.



2 in. were used on all test-bars. The nature of the fractures was noted.

It was assumed that the removal of the cast surface would not affect the interpretation of the results, which involves a comparison between porosity due to metal/mould reaction and the corresponding tensile strengths, for the following reason. A brief examination<sup>13</sup> of the distribution of porosity in 2-in.-dia., well-fed castings of 10% tin phosphor bronze (which freeze at about the same rate as a 1-in.-thick plate<sup>14</sup>) had shown that metal/mould reaction causes no concentration of porosity towards the cast surface, as it does in aluminium-magnesium alloy castings.<sup>15</sup>

All heats were analysed for residual phosphorus content, samples being taken from the base of the head of the  $\frac{1}{2}$ -in. ribbed plate. Samples taken from other places and other castings showed no significant variation within a given heat.

### III.—RESULTS AND DISCUSSION

#### 1. GAS POROSITY CAUSED BY MOULD REACTION

The porosity found in the test castings is shown in Table II, and the more pertinent observations are summarized in Figs. 4, 5, and 6.

The results were treated statistically by methods for the analysis of variance,\* and in this way the effects were determined of residual phosphorus content, pouring temperature, and section thickness on the amount of porosity in the castings, and a measure of their significance\* was obtained. The independent variables\* in the statistical analysis were:

(i) Residual phosphorus content at four levels: \* 0.002–0.010%, average 0.007%; 0.028–0.037%, average 0.032%; 0.043–0.063%, average 0.055%; and 0.081–0.15%, average 0.11%.

(ii) Pouring temperature at three or four levels †: 1050°, 1100°, 1150°, and 1200° C. for the 1-in.-dia. bars; 1080°, 1130°, 1180° C. for the plates; and 1000°, 1050°, 1100°, 1150° C. for the 2-in.-dia. bars.

(iii) Section thickness at two or three levels: 1 and 2 in. dia. for the cylinders; and  $\frac{1}{4}$ ,  $\frac{1}{2}$ , and 1 in. thickness for the plates.

Variations in porosity have been neglected if the statistical analysis showed there to be a chance greater than 5 times in 100 that they were accidental. Where figures such as  $1.00 \pm 0.48\%$  porosity are given, they represent the mean porosity in the castings, for the conditions specified in the text, and the corresponding 95% fiducial limits.\*

#### (a) 1-in. and 2-in.-Dia. Bars

When pouring began from 1050° C. air bubbles were trapped in the last bar cast (2-in.-dia., unsprayed mould), the temperature in the crucible having then fallen to 1000° C. The results from these bars were

TABLE II.—Porosity in 85:5:5:5 Gun-Metal Sand Castings.

Melt No.	Residual P, %	Porosity, vol.-%						
		1-in.-dia. Bars		Ribbed Plates			2-in.-dia. Bars	
NTY		S *	U *	$\frac{1}{4}$ -in.	$\frac{1}{2}$ -in.	1-in.	S *	U *
Pouring Temp.: 1050° C.		1030° C.					1000° C.	
13	0.002	1.8	1.7	...	1.8	1.6	3.0	...
27	0.028	1.9	2.0	...	1.8	1.6	2.5	3.9 †
45	0.031	1.7	1.9	...	1.9	1.7	2.5	3.9 †
38	0.033	1.8	2.1	...	1.8	1.8	1.9	3.8 †
39	0.058	1.8	1.9	...	1.9	1.8	2.0	4.1 †
41	0.063	1.9	2.0	...	1.9	1.8	2.3	2.9 †
21	0.094	2.0	2.1	...	1.9	1.3	2.5	3.8 †
37	0.15	1.7	2.4	...	2.1	2.4	2.7	5.1 †
Pouring Temp.: 1100° C.		1080° C.					1050° C.	
12	0.004	1.3	1.7	...	1.9	4.0	1.8	2.2
40	0.010	1.3	1.6	...	1.4	1.3	1.4	1.7
44	0.033	1.4	1.8	2.0	3.1	1.8	1.8	2.3
22	0.037	1.3	1.5	2.2	2.5	2.2	1.8	2.1
23	0.055	1.4	1.9	2.4	2.0	2.5	1.8	3.8
36	0.055	1.4	1.9	2.3	2.1	2.1	2.3	2.0
24	0.11	1.5	2.6	3.0	3.3	4.1	2.2	3.1
42	0.15	1.6	1.9	...	3.8	3.4	2.3	3.3
Pouring Temp.: 1150° C.		1130° C.					1100° C.	
10	0.002	1.3	1.4	1.5	1.4	1.6	2.0	...
48	0.007	1.2	1.5	2.0	1.6	1.6	1.7	2.7
25	0.008	1.2	1.3	1.8	1.5	1.2	2.2	2.0
8	0.011	1.4	1.6	...	2.6	3.4	1.5	3.3
47	0.022	1.3	1.5	1.9	1.9	2.2	2.3	2.3
14	0.030	1.3	1.9	2.4	2.1	2.5	2.0	2.2
34	0.032	1.4	2.1	1.9	2.5	2.5	2.2	2.7
32	0.062	1.3	4.0	2.6	2.9	4.3	2.6	3.3
15	0.11	1.5	2.4	2.9	4.0	4.0	2.2	3.2
33	0.12	2.4	4.2	3.7	5.3	4.7	1.8	2.7
37	0.15	...	...	...	4.4	...	...	...
Pouring Temp.: 1200° C.		1180° C.					1150° C.	
26	0.008	1.1	1.4	2.0	2.3	2.1	1.9	2.0
43	0.008	1.2	1.3	1.9	1.9	2.1	1.7	3.4
9	0.010	1.8	1.8	2.5	2.9	2.8	2.0	2.2
28	0.028	1.3	1.7	2.8	2.9	3.1	2.5	2.9
46	0.034	1.5	2.5	2.8	3.6	3.6	2.7	2.6
11	0.043	1.5	3.8	2.4	5.3	5.7	2.5	3.7
29	0.050	1.3	2.3	2.7	3.2	3.7	2.7	3.2
20	0.081	1.9	5.6	4.8	5.9	6.0	2.0	3.7
35	0.12	2.7	6.2	5.3	6.0	7.3	3.6	5.1

\* S = mould sprayed with aluminium-magnesium paint.  
U = unsprayed mould.

† This high porosity was caused by gas trapped during pouring and not by metal/mould reaction.

therefore ignored in the statistical analysis; nor are they included in Fig. 5.

The statistical analysis showed the outstanding effect on the amount of (shrinkage) porosity in the 1- and 2-in. castings made in sprayed moulds to be

\* This, and other statistical terms used in the paper are explained briefly in the Appendix, where also a summary of the results of the statistical analysis is given.

† The  $\frac{1}{4}$ -in. plates would not run with the lowest pouring temperature used; the analysis of variance was therefore confined to the three highest temperatures.

that due to section size, and there was a significant interaction\* between section size and pouring temperature. As the difference between the two sizes of bars were clearly a consequence of their differing geometry, the results for the two sizes of bar made in unsprayed moulds were treated independently.

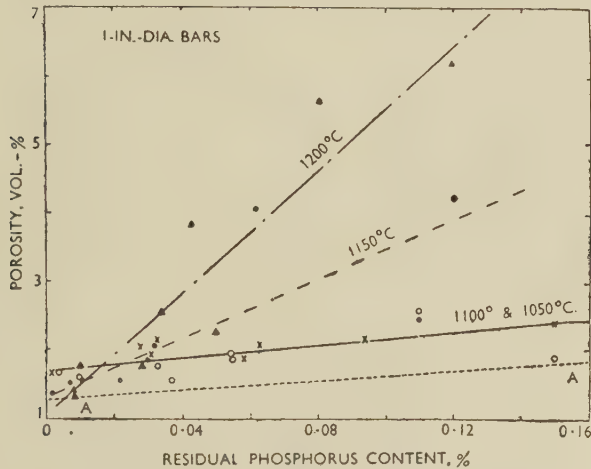


FIG. 4.—Porosity Due to Metal/Mould Reaction in 1-in.-dia. Bars Cast from Degassed 85 : 5 : 5 : 5 Leaded Gun-Metal, Compared with Shrinkage Porosity in Bars Cast in Sprayed Moulds.

KEY: Pouring Temp., °C.: ▲ 1200; ● 1150; ○ 1100; × 1050. A ---- A, bars cast in moulds sprayed with Al-Mg paint.

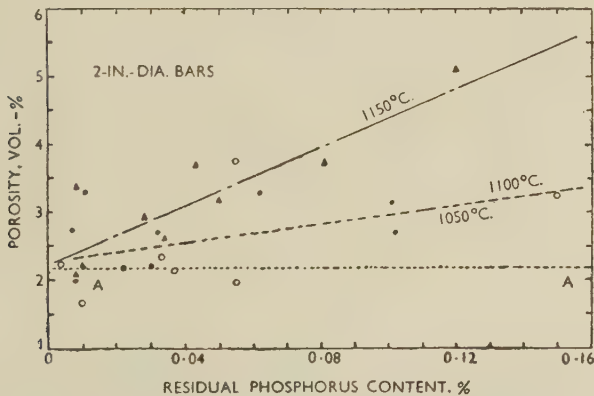


FIG. 5.—Porosity Due to Metal/Mould Reaction in 2-in.-dia. Bars Cast from Degassed 85 : 5 : 5 : 5 Leaded Gun-Metal, Compared with Shrinkage Porosity in Bars Cast in Sprayed Moulds.

KEY: Pouring Temp., °C.: ▲ 1150; ● 1100; ○ 1050. A ---- A, bars cast in moulds sprayed with Al-Mg paint.

For the bar castings made in unsprayed moulds an increase in either phosphorus content or pouring temperature caused an increase in porosity due to metal/mould reaction (see Figs. 4 and 5). The effect of phosphorus was of the greater statistical significance.†

For the 1-in.-dia. bars, the effect of phosphorus became greater with higher pouring temperatures and, similarly, the effect of temperature was greater with higher phosphorus contents;‡ for instance, the difference between the amount of porosity in 1-in.-dia.

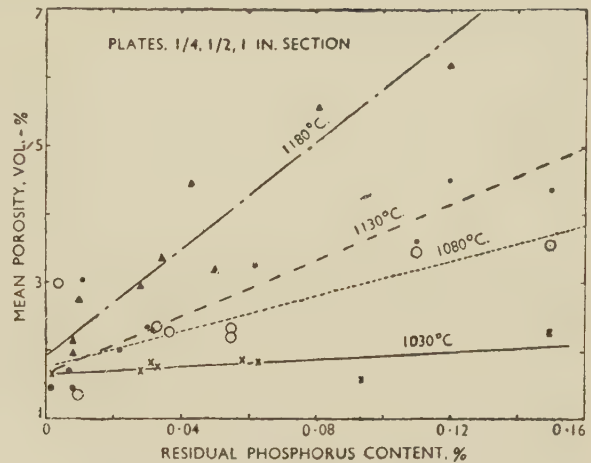


FIG. 6.—Porosity Due to Metal/Mould Reaction in Double-Ribbed Plate Castings Made from Degassed 85 : 5 : 5 : 5 Leaded Gun-Metal.

KEY: Pouring Temp., °C.: ▲ 1180; ● 1130; ○ 1080; × 1030.

castings with average phosphorus contents of 0.007 and 0.055% was  $0.26 \pm 0.18\%$  when poured from 1100°C., and  $2.61 \pm 1.87\%$  when poured from 1150°C.

Although the effects of residual phosphorus content and pouring temperature are probably also interdependent for the 2-in.-dia. bars (cf. Fig. 5), this interdependence was not significant in the present observations. The independent effects of phosphorus content and pouring temperature on these bars, as indicated by the statistical analysis, are illustrated diagrammatically in Figs. 7 and 8, where, for simplicity, the

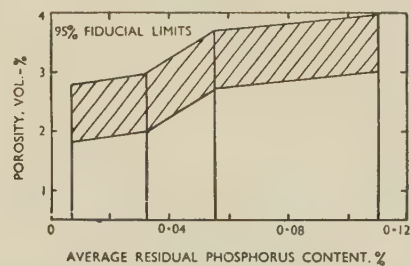


FIG. 7.—Effect of Residual Phosphorus Content on Porosity Due to Metal/Mould Reaction in 2-in.-Dia. Test Castings Poured from 1050° to 1150° C., as Indicated by Statistical Analysis.

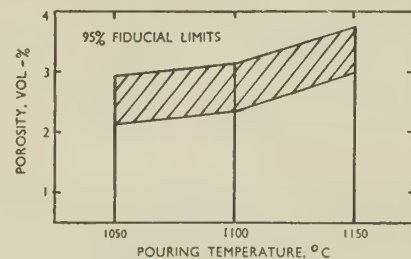


FIG. 8.—Effect of Pouring Temperature on Porosity Due to Metal/Mould Reaction in 2-in.-Dia. Test Castings with Residual Phosphorus Contents up to 0.15%, as Indicated by Statistical Analysis.

\* See Appendix for the meaning of this term.

† See Appendix for the meaning of this term and for the figures on which the statement is based.

‡ Statistical significance did not obtain over the full ranges examined.



average phosphorus contents and not the corresponding ranges have been plotted.

### (b) Ribbed Plates

In the plates the amount of porosity due to metal/mould reaction increased slightly with thickness, independently of pouring temperature or phosphorus content, being  $2.61 \pm 0.27\%$  for the  $\frac{1}{4}$ -in. plates,  $3.07 \pm 0.27\%$  for the  $\frac{1}{2}$ -in. plates, and  $3.34 \pm 0.27\%$  for the 1-in. plates.

The effects of residual phosphorus content and pouring temperature were much more significant. As with the 1-in.-dia. bars, an increase in either caused an increase in the effect of the other. This is shown in Fig. 6, where the actual observations are plotted and where plates of different section thicknesses all cast

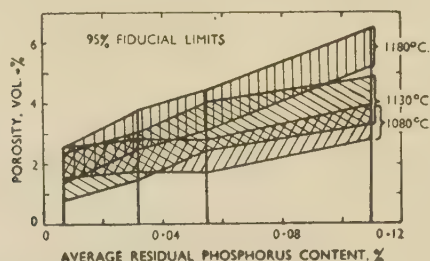


Fig. 9.—Effect of Residual Phosphorus Content on Porosity Due to Metal/Mould Reaction in Plate Castings of  $\frac{1}{4}$ ,  $\frac{1}{2}$ , or 1 in. Section, Poured from Different Temperatures, as Indicated by Statistical Analysis.

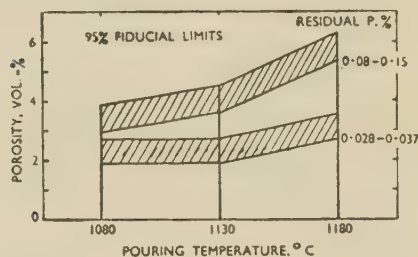


Fig. 10.—Effect of Pouring Temperature on Porosity Due to Metal/Mould Reaction in Plate Castings of  $\frac{1}{4}$ ,  $\frac{1}{2}$ , or 1 in. Section, with Varying Residual Phosphorus Contents, as Indicated by Statistical Analysis.

from one heat are averaged. The statistically significant variations in porosity arising from metal/mould reaction are indicated in Figs. 9 and 10. The effects were more significant at the higher levels, and the effect of phosphorus was more significant than that of temperature.

## 2. TENSILE PROPERTIES

The tensile strengths of the castings are given in Table III and the variations with pouring temperature and phosphorus content are summarized in Fig. 11. The figures were analysed statistically in a similar manner to those for porosity. Values obtained for the elongation of the test-pieces are not given, and were not analysed, because they almost completely reflected changes in strength; they ranged from 2 to 25% on the 1-in.-dia. bars and from 2 to 15.5% on the plates.

TABLE III.—Ultimate Tensile Strength of 85 : 5 : 5 : 5 Gun-Metal Sand Castings.

Melt No.	Residual P, %	Ultimate Tensile Strength, tons/in. <sup>2</sup>				
		1-in.-dia. Bars		Ribbed Plates †		
		S *	U *	$\frac{1}{4}$ -in.	$\frac{1}{2}$ -in.	1-in.
NTY						
Pouring Temp. :		1050° C.		1030° C.		
13	0-002	8.7	12.6	...	8.3	10.4
27	0-028	12.6	14.8	...	10.7	10.9
45	0-031	11.6	14.8	...	11.0	13.0
38	0-033	12.0	15.1	...	12.2	12.7
39	0-058	11.5	13.1	...	13.2	13.0
41	0-063	11.7	14.5	...	13.2	13.2
21	0-094	10.8	16.5	...	13.0	12.4
37	0-150	14.1	16.8	...	11.9	11.5
Pouring Temp. :		1100° C.		1080° C.		
12	0-004	11.2	13.0	...	8.4	12.2
40	0-010	12.0	12.9	...	12.7	13.0
44	0-033	9.2	14.5	9.2	11.3	12.0
22	0-037	12.3	13.3	10.1	10.4	10.7
23	0-055	12.6	15.2	11.2	12.8	10.7
36	0-055	11.4	15.3	9.0	11.3	11.4
24	0-11	12.0	11.3	10.5	10.4	8.9
42	0-15	12.5	...	...	9.2	9.1
Pouring Temp. :		1150° C.		1130° C.		
10	0-002	10.4	12.4	13.2	10.4	11.0
48	0-007	10.0	11.6	9.9	11.0	10.3
25	0-008	10.5	11.7	9.8	12.2	11.7
8	0-011	10.1	13.5	...	9.7	9.5
47	0-022	10.4	12.9	11.5	11.7	9.6
14	0-03	11.3	11.4	10.1	10.2	9.0
34	0-032	12.4	10.9	10.3	9.5	9.1
32	0-062	15.2	9.8	10.2	9.8	9.6
15	0-11	10.9	12.9	10.6	9.1	8.6
33	0-12	7.9	11.2	10.7	8.2	9.0
37	0-15	...	...	...	8.7	...
Pouring Temp. :		1200° C.		1180° C.		
26	0-008	11.8	14.8	10.6	10.6	10.5
43	0-008	12.0	15.0	10.3	9.8	9.7
9	0-010	6.9	12.2	9.5	9.7	10.8
28	0-028	10.8	13.1	10.3	11.6	10.5
46	0-034	10.7	14.2	11.7	9.0	9.7
11	0-043	12.6	7.3	10.6	7.6	8.1
29	0-050	13.6	14.3	11.0	9.4	10.6
20	0-081	11.0	7.6	8.2	7.37	8.1
35	0-12	10.1	7.2	8.6	7.9	7.8

\* S = mould sprayed with aluminium-magnesium paint.

U = unsprayed mould.

† Mean value of four strips cut from each plate.

### (a) 1-in.-Dia. Bars

Despite less porosity, the tensile strengths of the bars cast from 1150° C. or less in sprayed moulds were generally lower (3 out of 25 were higher) than for those cast in unsprayed moulds. Similarly, with up to 0.034% residual phosphorus, bars poured from 1200° C. were weaker when cast in sprayed moulds than when cast in unsprayed moulds. This suggests that, in these well-fed castings, gas absorption from the mould

produced porosity that was more uniformly dispersed and hence less harmful than that due to shrinkage alone.<sup>1, 4</sup>

However, when phosphorus content and pouring temperature were both high, the gas absorption was excessive and, for 3 of the 4 observations made, the strengths of the bars cast into unsprayed moulds were only of the order of two-thirds those of the bars cast into sprayed moulds.

Variations in phosphorus content and pouring temperature produced irregular effects on the strength of the bars cast both in the sprayed and the unsprayed moulds: for both types of mould interdependence between the effect of the residual phosphorus content and of the pouring temperature was significant, but the dispersion of the observations was such that the changes of strength for given changes in pouring temperature or phosphorus content were not always significant.

### (b) Ribbed Plates

Section thickness exercised no significant effect on the strength of the plates, but residual phosphorus content and pouring temperature did so, the effect of phosphorus being the more highly significant.

The strength of castings poured from 1080° C. or higher fell as either phosphorus content or pouring temperature increased, showing that gas absorption from the mould was having a harmful effect. The observations are plotted in Fig. 11, where each point shows the mean strength of all test-pieces from plates cast from each heat. Figs. 12 and 13 summarize the results of the analysis of variance. Although the increase in the volume of gas absorption was continuous throughout the range of phosphorus contents examined (Fig. 9), raising the average phosphorus

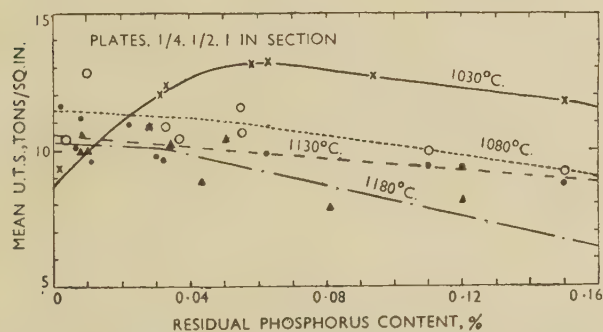


FIG. 11.—Effect of Metal/Mould Reaction on Tensile Strength of Inadequately Fed Parts of Double-Ribbed Plate Castings made from Degassed 85:5:5:5 Leaded Gun-Metal. (Cf. Fig. 6.)

Each point represents the mean of twelve tests, four from each plate of  $\frac{1}{4}$ ,  $\frac{1}{2}$ , and 1 in. section.

content from 0.032 to 0.055% caused no fall in strength parallel to the corresponding increase in porosity (Fig. 12). Evidently metal/mould reaction in this region had the expected effect of redistributing the porosity, so that the strength remained unaffected in spite of the increasing unsoundness.<sup>1, 4</sup>

P P

On the other hand, the strength of the  $\frac{1}{2}$ -in. and 1-in. plates poured from 1030° C. (the  $\frac{1}{4}$ -in. plates would not run at this temperature) improved from a mean of 11.2 tons/in.<sup>2</sup> with phosphorus contents of 0.002–0.033%, to a mean of 13.0 tons/in.<sup>2</sup> with contents of 0.058–0.094% (Fig. 11), the probability

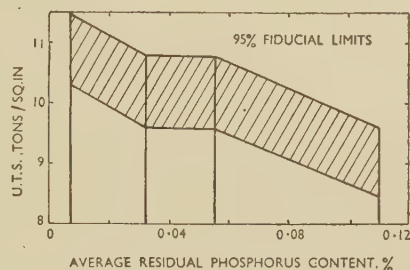


FIG. 12.—Effect of Residual Phosphorus Content on Mean Tensile Strength of Inadequately Fed Parts of Plate Castings of  $\frac{1}{4}$ ,  $\frac{1}{2}$ , or 1 in. Section, Poured from 1080° to 1180° C., as Indicated by Statistical Analysis.

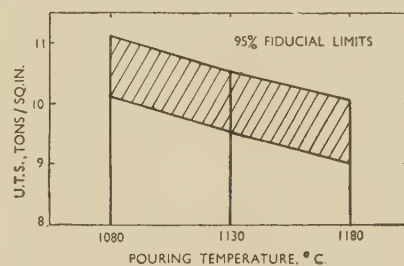


FIG. 13.—Effect of Pouring Temperature on Mean Tensile Strength of Inadequately Fed Parts of Plate Castings of  $\frac{1}{4}$ ,  $\frac{1}{2}$ , or 1 in. Section, with Residual Phosphorus Contents up to 0.15%, as Indicated by Statistical Analysis.

of the difference having occurred by chance being only 1 in 1000. This effect is similar to that found with lead-free bronzes in the earlier work.<sup>1, 2</sup>

While phosphorus itself had no effect on grain-size (see Section III, 4), so that the improvement in strength can be attributed to metal/mould reaction, it may be that the small grain-size produced by pouring from 1030° C. was a contributory factor, since the chance of spreading the porosity is greater the smaller the grains.<sup>16</sup> There was no significant change in the amount of porosity in these castings as their phosphorus content rose (Fig. 6).

The value of 13 tons/in.<sup>2</sup> obtained under the above conditions was the highest strength realized in the plate castings (Fig. 11), and is of the same order as the strengths attained by the 1-in.-dia. test-bars.

### 3. RELATION BETWEEN OVERALL POROSITY AND STRENGTH

The earlier work<sup>1-3</sup> showed that, with phosphor bronze poured from 1130° C. and with 88:8:4 lead-free gun-metal and 85:5:5:5 leaded gun-metal poured from 1180° C., the tensile strength of 1-in.-dia. bars (D.T.D.-type) fell off proportionally to the increase in porosity caused by metal/mould reaction. A linear relationship was also found between porosity



due to inherent gas and the tensile strength of 1-in.-dia. bars for phosphor bronze, 88 : 8 : 4 lead-free gun-metal, and 85 : 5 : 5 : 5 leaded gun-metal, but for 86 : 7 : 5 : 2 leaded gun-metal the relationship was not quite linear. However, for the disc castings made in phosphor bronze or 88 : 8 : 4 gun-metal, the strength of the inadequately fed part and the pressure-tightness of the castings *increased* with the first increase in porosity caused by gas arising from metal/mould reaction and then stayed at a high level. With inherent gas the initial rise in strength or pressure-tightness was followed by a fall. In the two leaded gun-metals the strength fell continuously as porosity from inherent gas increased. No information on the effect of porosity arising from metal/mould reaction was obtained for 86 : 7 : 5 : 2 alloy; the meagre data for 85 : 5 : 5 : 5 alloy showed a rise in strength for increased porosity due to metal/mould reaction.<sup>3</sup>

In agreement with the earlier work,<sup>3</sup> the present results show a fall in the strength of 85 : 5 : 5 : 5 gun-metal cast into 1-in.-dia. bars, as the overall porosity increases from the effects of metal/mould reaction, but, in contrast to the results from the disc castings,<sup>3</sup> the strength of the ribbed plates fell as metal/mould reaction increased. The respective correlation coefficients for the relations shown in the present work were  $-0.685$  and  $-0.682$ , being well above the corresponding  $0.1\%$  significance levels.\* When the results are plotted graphically (Figs. 14 and 15) the wide spread of 5–6 tons/in.<sup>2</sup> in the tensile strengths with the lower amounts of porosity is evident. Thus, there is no significant correlation for the bars containing  $2.6\%$  porosity or less, nor for the plates containing  $2.1\%$  porosity or less, which includes all but two of the

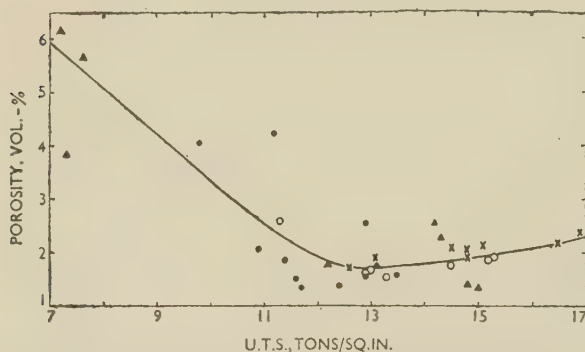


FIG. 14.—Relation Between Porosity and Tensile Strength for 1-in.-Dia. Bars, Poured into Unsprayed Moulds.

KEY: Pouring Temp., °C.: × 1050; ○ 1100; ● 1150; ▲ 1200.

plates poured from 1030° C. However, in spite of the spread of the results, the negative correlation for plates is still above the  $0.1\%$  significance level, even when only those containing up to  $2.6\%$  porosity are considered.

\* The increase in strength with increasing phosphorus content of the plates cast from 1030° C., noted above (p. 561), occurred without any change in the overall porosity,

The lack of correlation between porosity and strength at the lower porosities—less than  $2.6\%$  for the bars or  $2.1\%$  for the plates—is no doubt attributable to variations in the form and distribution; the porosity figures are for the whole castings, while the strengths are determined by local weaknesses.\* Micro-examination of sections prepared through the

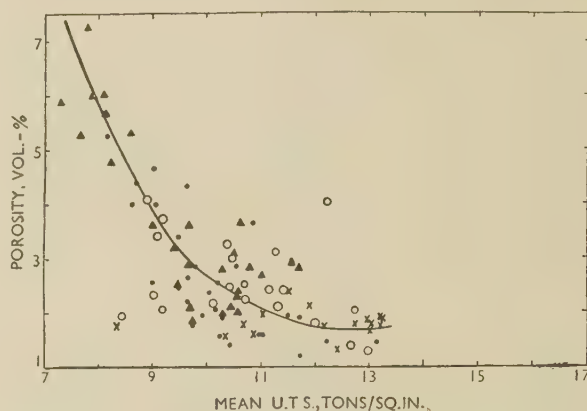


FIG. 15.—Relation Between Overall Porosity and Mean Tensile Strength for Inadequately Fed Parts of  $\frac{1}{4}$ ,  $\frac{1}{2}$ , and 1 in. Section Plate Castings.

KEY: Pouring Temp., °C.: × 1030; ○ 1080; ● 1130; ▲ 1180.

fractures of fourteen of the test bars machined from the 1-in. bars, failed to show any correlation between the amounts of microporosity visible near the fractures and the strengths of the bars.

There was also a wide spread in the strengths of the bars containing only shrinkage porosity. Of the 35 1-in. bars protected from gas absorption by pouring into sprayed moulds, 33 contained between 1 and  $2\%$  porosity, and for these the strengths ranged from 6.9 to 15.2 tons/in.<sup>2</sup>. This range is half as much again as that for the bars cast in unsprayed moulds, where metal/mould reaction occurred. In conjunction with the decreasing spread of strengths with increasing metal/mould reaction already discussed (Fig. 14), this suggests once again that the gas absorbed from the reaction assisted in distributing porosity uniformly.<sup>1,4</sup>

#### 4. FRACTURE AND GRAIN-SIZE

During the breaking of the tensile test-pieces, note was made of the position and appearance of the fracture, and also of the grain-size of the material as indicated by the "orange-peel" effect.

The first pieces machined from the bar castings broke at various places along the gauge-length. Except in one or two test-pieces from the plates cast from 1180° C., fracture of all the  $\frac{1}{4}$ -in. samples occurred just to the head side of the rib position. A similar tendency was noted in the thicker plates, though at the higher temperatures many broke just on the

and is attributable to the effect of the metal/mould reaction on the distribution of the porosity<sup>1,4</sup> (cf. Figs. 6 and 11).

opposite side of the rib and a number failed under the rib. At first sight one might expect the weakest part of the castings to be always under the rib, but the tendency for failure to occur on the head side can be attributed to the asymmetrical temperature distribution during cooling, caused by the absence of a similar head of hot metal at the far end of the plate. With the higher pouring temperatures and greater section thicknesses, the sand around the casting gets hotter, and the thermal gradients in the casting are consequently flatter when the solidification range is reached; <sup>14</sup> this explains why the tendency for failure to occur on the head side of the rib is less marked.

Micro- and macro-shrinkage were more obvious on the fractured faces of the test-pieces from the plates as the pouring temperature rose and the section thickness increased. Test-pieces from both the 1-in. and  $\frac{1}{2}$ -in. plates had coarse columnar fractures when cast from 1180° C., and the fractures of the test-pieces from the 1-in. plates cast from 1130° C. were also coarse. These fractures corresponded, as would be expected, with a coarse "orange-peel" (grain-size) appearance on the surface of the test-piece after pulling; a similar correspondence occurred with the test-piece from the bars. The relation between grain-size and fracture was confirmed by micro-examination, and the most important observation was that the castings poured from the lowest temperature, whether plates or bars, had grain-sizes of the order of  $\frac{1}{10}$ th of those of castings poured from the highest temperature (Fig. 16, Plate XCII). The grain-size increased with section thickness, the effect being marked at the highest pouring temperature (Fig. 17, Plate XCII). Phosphorus content had no effect on the grain-size.

#### IV.—RESULTS OF PRODUCTION TRIALS

Concurrently with the laboratory work, production trials, some of which are described more fully elsewhere,<sup>6</sup> were carried out in two foundries making small 85 : 5 : 5 : 5 sand castings. In both foundries small valve bodies, with section thicknesses in the range  $\frac{1}{8}$ – $\frac{3}{8}$  in., had been prone to leak under pressure at the junctions between the valve bodies and valve seats. Normal pouring temperatures were 1160°–1130° C., and the metal had variable initial gas contents equivalent to 2.0–3.8% porosity in a D.T.D. bar.

In the trials, 400-lb. heats were halved and poured from 200-lb. ladles; to one ladle the normal addition of copper-phosphorus for deoxidation was made and to the other a greater addition to promote metal/mould reaction. Each ladleful of metal produced 50–80 castings; the drop in temperature of the metal in the ladle while these were being cast was of the order of 50° C. The extra phosphor copper increased the residual phosphorous content from the normal 0.01–0.02% to 0.06–0.09%, and the effect was greatly to reduce the proportion of leaky castings—in one foundry from 28% to 15% (one melt) and in the other from 16% to nil (two melts).

These results are not directly comparable with those obtained in the laboratory, because of the higher initial gas content of the metal used in the industrial trials. However, there was some indication with the laboratory castings most nearly comparable, i.e. the  $\frac{1}{4}$ -in. plates cast from 1130° C., that here too the properties improved (the improvement was non-significant) as the residual phosphorus content rose above 0.01%; as noted earlier (p. 556), the tensile tests used in the laboratory are a rather less sensitive measure than pressure tests.

With a heavier valve-head casting ( $\frac{1}{4}$ – $\frac{3}{4}$ -in. section) made in one of the foundries, increasing the phosphorus content of the metal caused undue gas unsoundness and the proportion of the castings that leaked under pressure rose from 20 to 57% (two melts). Practice was similar to that outlined above, except that only 12–14 castings were made from each ladle. While it was found that the yield of sound castings could be increased to 100% (2 melts) by using the lowest practicable pouring temperature, 1050°–1080° C., this was inconvenient for production purposes.

Although this marked improvement in yield appears to parallel the laboratory experiments, where metal/mould reaction was found greatly to improve the properties of the  $\frac{1}{2}$ - and 1-in. plate castings only when they were poured from below 1100° C., the metal used for the industrial trials was initially more gassy. The true comparison was found in later trials.

These showed that, by degassing the metal before casting, so that a 1-in.-dia. test-bar contained less than 2% porosity, yields of 96–100% could be obtained with both the higher and the lower residual phosphorus contents (2 melts).<sup>6</sup> It is evident from these latest trials that the feeding characteristics of the casting were such as to produce pressure-tight castings provided good-quality (low-gas-content) metal was used.

The following conclusions may therefore be drawn for this heavier casting. If poor-quality metal is used, enough time elapses during freezing for the dissolved hydrogen to diffuse and concentrate sufficiently at the heat centre to cause leakage under test, unless pouring temperatures are some 80° C. lower than those normally employed. On the other hand, with good-quality metal, the subsequent absorption of gas from the mould during freezing is not deleterious, because there is then not enough time for diffusion to occur.

A similar effect is apparent in the laboratory tests, where, in the 1-in. bars poured from all temperatures, the introduction of gas due to metal/mould reaction, up to the equivalent of about 3% porosity in the bars, did not affect their strength; only with the highest residual phosphorus contents (roughly 0.08%), combined with the highest pouring temperature (1200° C.), was the strength reduced.

The practical value of metal/mould reaction is well demonstrated by the subsequent experience of the foundry making the heavier casting. After the trials, the phosphorus additions to the metal were increased



sufficiently to maintain residual phosphorus contents of around 0.06% throughout the general production of both light and heavy valves and similar castings, amounting to about 3000 pieces per week. There was a consequent increase of 2% in the already high overall yield of sound castings. This improvement was obtained without the introduction of degassing.\*

## V.—CONCLUSIONS

In drawing the following conclusions, both the laboratory experiments and the industrial trials have been taken into consideration.

(1) Metal/mould reaction may be used as a possible means of improving the yield of pressure-tight sand castings containing heat centres. When compared with earlier work, the results now reported indicate that the advantage to be gained with leaded gun-metal is less than with phosphor bronze and lead-free gun-metal. (The earlier work showed that leaded gun-metals are less prone to develop localized and harmful porosity than are the phosphor bronzes and lead-free gun-metals.)

(2) Laboratory experiments and industrial trials have shown that metal/mould reaction can improve the strength and pressure-tightness of 85:5:5:5 leaded gun-metal castings containing heat centres, when the rate of solidification is rapid, either because of the thinness of the section or the use of a low pouring temperature.

(3) Additions of phosphorus to the leaded gun-metals to promote metal/mould reaction should not, therefore, be made indiscriminately. In castings with section thicknesses of  $\frac{1}{2}$  in. or more metal/mould reaction may be harmful unless the pouring temperature is kept as low as possible consistent with running the casting. For the conditions described in this paper the pouring temperature must be below 1100°C. In foundry practice it is usual to pour a number of castings from one crucible or ladle, and some latitude in pouring temperature is necessary. In some circumstances, therefore, a restriction on pouring temperature may prove impracticable.

(4) The presence in the metal before pouring of moderate amounts of gas (equivalent to about 3% porosity in a D.T.D.-type test-bar) may cause leakage in what would otherwise be sound castings, but the absorption of similar amounts of gas from the mould during freezing does not have this deleterious effect.

(5) The application of aluminium-magnesium alloy paint to the surface of sand moulds prevents the absorption by 85:5:5:5 leaded gun-metal of gas arising from metal/mould reaction.

(6) When 85:5:5:5 leaded gun-metal with a high residual phosphorus content (greater than

0.04%) is cast into unpainted sand moulds from a high pouring temperature (1200°C.) marked gas absorption occurs; this may reduce the tensile strength of 1-in.-dia. D.T.D.-type test-bars by over one-third. The application of the inhibiting paint under these conditions gives improved tensile properties.

(7) Bars with smaller amounts of absorbed gas due to metal/mould reaction (equivalent to about 3% or less porosity in the test bar) have strengths some 25% higher than those in which gas absorption is prevented by painting the mould with aluminium-magnesium alloy paint.

(8) The grain-size of sand-cast 85:5:5:5 leaded gun-metal is markedly dependent on pouring temperature; with section thicknesses of  $\frac{1}{4}$  in.-1 in. castings poured from 1050°C. have grain-sizes of the order of one-tenth of those in similar castings poured from 1200°C.

## ACKNOWLEDGEMENTS

The author wishes to thank the Director and Council of the British Non-Ferrous Metals Research Association for permission to publish this paper, and Mr. W. A. Baker for much helpful discussion. Mr. E. C. Mantle of the Association's Liaison Department supervised the production trials.

## APPENDIX

### I.—STATISTICAL EXAMINATION

The laboratory work described in the paper was designed as a factorial experiment, and the results have been analysed by statistical methods. Consequently, in describing the work it was necessary to use various terms which may be unfamiliar to some readers. Brief explanations of these are given below. Brownlee,<sup>17</sup> while avoiding the theoretical background, has given fuller explanations and illustrative examples of the terms and treatment used in experimentation based on statistical methods. The underlying theory is dealt with by Fisher<sup>18</sup> and by Yule and Kendall.<sup>19</sup>

#### (a) Purpose and Method of Analysis of Variance

Suppose in an experiment a deliberate variation is made in some controllable factor, such as pouring temperature, with the object of assessing the effect of this change on some property. The factor deliberately altered is known as the *independent variable* and the property observed as the *dependent variable*. In the present paper, phosphorus content, pouring temperature, and section thickness are the independent variables, and porosity or tensile strength is the dependent variable. The purpose of analysing the results statistically is to determine quantitatively whether the observed change in the dependent variable is significantly greater than the experimental error involved. *Significance* is assessed in terms of the probability that the observed change could have occurred purely by chance. Thus, it may be calculated by statistical methods that, on the average, the observed difference in the values of the dependent variable for two values of an independent variable could have occurred by chance once in every ten observations made, i.e. there is a 10% probability that the observed difference happened purely by chance. This may be regarded as too great a probability to justify the drawing of a conclusion from the observations.

\* As a result of recent and more extensive trials with the heavier casting described above, degassing is now to be intro-

duced and there is no evident reason why a further improvement in overall yield should not follow.

In fact, a 5% chance probability is commonly taken to represent a level of significance at which it is reasonable to draw conclusions about the effect of the independent variable, though more strict requirements, the 2% or 1% levels of significance, are frequently adopted. The attainment of the 5% level of significance has been considered to permit the drawing of conclusions in the present work.

#### (b) *Advantages of the Factorial Experiment*

By using statistics in conjunction with a properly planned experiment, it is possible to obtain more information with less experimental work than when the classical method of experimentation is adopted.

In the *classical experiment* all factors are held constant except one, and the value of the property being measured (the dependent variable) is determined at two or more values of this variable factor (the independent variable). To obtain an estimate of the experimental error involved in the determination, it is necessary at least to duplicate the measurements at each value of the variable factor. Thus, the effect of residual phosphorus content on the porosity due to metal/mould reaction in a casting might be measured as  $V_1$ ,  $V_2$ ,  $V_3$ , and  $V_4$  at four phosphorus contents  $P_1$ ,  $P_2$ ,  $P_3$ , and  $P_4$ , while pouring temperature was held constant at  $T_1$  and section thickness at  $S_1$ . In duplicate this would require eight observations. Similar experiments to determine the effect of pouring temperature, using say four different temperatures (*levels*), while residual phosphorus content and section thickness were constant, and the effect of section thickness at three levels, while residual phosphorus content and pouring temperature were held constant, would require a further fourteen observations.

But, after completion of the classical experiment, it would still not be known whether phosphorus would have the same effect when the pouring temperature was  $T_2$  (or  $T_3$ , or  $T_4$ ) as when it was  $T_1$ , the temperature at which the observations were made. In fact, the results noted in the paper (p. 559) show that, for this particular example, a given increase in the residual phosphorus content causes a bigger change in the amount of porosity in the casting when the pouring temperature is raised. A similar effect for tensile strength is referred to on p. 561. In statistics such interdependence, i.e. the effect of one factor being dependent upon the value of another factor, is called an *interaction*. The effect of the residual phosphorus content may also be different for castings of different section thickness.

Similar remarks to those for phosphorus might apply equally to the effect of temperature and section thickness. Consequently to cover in duplicate all possible variations in this example by classical experiment it would be necessary to make 96 observations.

In a *factorial experiment* observations of the dependent variable are made at all combinations of the values of the independent variables; from these observations more accurate determinations of the sizes of the effects of the independent variables are obtained than from the equivalent classical experiment and, in addition, a measure of the significance of these effects and measures of the size and significance of the interactions involved. Thus, for the above example, a single observation of the porosity would be made at all combinations of  $P$ ,  $T$ , and  $S$ , making only 48 observations in all. From these 48 observations and with the help of statistics the following information would be forthcoming: a measure of the experimental error, not an estimate as in the classical experiment; consequently, a quantitative measure of the significance of any interactions that may exist; if interactions do exist, a measure of the significance of the effects of the independent variables on the property observed, and a measure of the size of the effect as the differences between the means of three ( $P$  and  $T$ ) or four ( $S$ ) observations instead of two as in the classical experiment; if interactions do not exist, a measure of the significance of the effects of the independent variables on the property observed, and a measure of the size of the effects as the differences between the means of twelve ( $P$  and  $T$ ) or sixteen ( $S$ ) observations.

#### (c) *The Analysis of Variance*

The above information would be obtained by a method of statistical analysis known as the *analysis of variance*.

The *variance* of a number of experimental observations is a measure of their scatter about their mean value. The variance has the valuable attribute that the total variance of a number of observations can be split into components due to changes in the known and controlled factors and to a residual due to uncontrolled factors (i.e. to experimental errors). For example, suppose the ultimate tensile strengths of test-bars poured from different batches of metal and from different pouring temperatures are being measured. The total variance of all the results may then be divided into a component due to metal batch, a component due to pouring temperature, a component due to interaction between these two factors, and a residual due to the experimental error.

The *variance ratio* for a particular factor is the ratio of the variance due to that factor to that due to the residual. It is obvious that the larger this ratio (i.e. the bigger the effect of the factor in comparison with that of the error) the more significant is the effect of the factor. Hence the value of the variance ratio is a measure of the significance of the effect of the factor. The variance ratio is also used to test the significance of interactions. To determine the level of significance the calculated ratios are compared with those given for equivalent conditions in published statistical tables.

The *analysis of variance* consists in calculating these different components of the total variance and determining the significance of the effects they represent.

From the residual component of variance it is possible to make further calculations that determine the limits between which, on the average, a certain proportion of a series of observations of a property will fall. These limits are termed the *fiducial limits*. Thus if, as in the present paper, the 95% fiducial limits are calculated as  $x$  and  $y$ , on the average 95 out of every 100 observations will fall between  $x$  and  $y$ .

#### (d) *The Comparison Between Two Means*

On p. 561 of the paper statistics are used to determine simply the significance of the difference between the means of two sets of observations. For this purpose a test for significance devised by *Student* and known as the "*t*" test is used. This is different from the variance-ratio test described above, but the method of testing is similar, i.e. the value of  $t$  is calculated for the experimental observations and compared with the figures for equivalent conditions at various levels of significance that are available in published statistical tables.

#### (e) *The Relation Between Two Variables*

Another example of the use of statistical methods occurs in Section III, 3 of the paper, where the relation between the porosity and strength of the castings is discussed. From the experimental data a statistical function known as the *correlation coefficient* was calculated. The characteristic of this function is that, when the observed values fall exactly on a straight-line plot, it has the value +1 for a line of positive slope and -1 for a line of negative slope, and when a plot of the data shows points entirely at random it has the value 0. Thus, as the calculated numerical value of the correlation coefficient rises, it indicates that the observations fall more nearly on a straight line. As with the variance ratio and Student's  $t$ , it is possible to test whether the value of the correlation coefficient calculated from the experimental data is greater than the value which might have been obtained accidentally with the same number of observations, and thus a level of significance can be assigned to the apparent relation between the variables.

## II.—SUMMARIZED RESULTS OF STATISTICAL CALCULATIONS

The results of the calculations to determine the significance of various effects are summarized below. In addition, a few tables of mean values and fiducial limits not quoted in the text of the paper or given in the figures, are included.



The following abbreviations are used:

- $P$  = mean residual phosphorus content (%)  
 $T$  = pouring temperature (°C.)  
 $S$  = section thickness (in.)  
 U.T.S. = ultimate tensile strength (tons/in.<sup>2</sup>)  
 $D.F.$  = degrees of freedom  
 $M.S.$  = mean squares  
 $S(V.R.)$  = significance level from variance-ratio test (%)  
 $N.S.$  = non-significant  
 $F.L.$  = fiducial limits  
 $r$  = correlation coefficient

(a) Variance of Porosity

(i) 1-in. and 2-in.-Dia. Bars Made in Sprayed Moulds

$P$  = 0.007, 0.032, 0.055, 0.11.

$T$  = 1050, 1100, 1150.

$S$  = 1, 2.

Values for porosity under each condition were generally means of two observations. Second-order interaction was neglected.

Zero moved to 2% porosity and figures  $\times 100$ .

Source of Variance	D.F.	M.S.	S(V.R.)
Between $P$ . . . .	3	2,058	5
" $T$ . . . .	2	492	N.S.
" $S$ . . . .	1	22,632	...
$P \times T$ interaction . .	6	566	N.S.
$T \times S$ " . . . .	2	4,416	1
$S \times P$ " . . . .	3	657	N.S.
Residual . . . .	6	381	...

$T \times S$  interaction significant (see p. 559); therefore split into two-factor experiments:

$P \times T$

Source of Variance	D.F.	$S = 1$		$S = 2$	
		M.S.	S(V.R.)	M.S.	S(V.R.)
Between $P$ . . . .	3	561	N.S.	2154	N.S.
" $T$ . . . .	2	2199	2	2709	N.S.
Residual . . . .	6	294	...	653	...

$S$	$T$	Mean Porosity, %	95% F.L.
1	1050	1.83	} $\pm 0.22$
	1100	1.41	
	1150	1.44	

$S \times P$

Source of Variance	D.F.	$T = 1050$		$T = 1100$		$T = 1150$	
		M.S.	S(V.R.)	M.S.	S(V.R.)	M.S.	S(V.R.)
Between $S$ . . . .	1	162	N.S.	11,400	3	19,900	1
" $P$ . . . .	3	378	N.S.	445	N.S.	2,367	N.S.
Residual . . . .	3	407	...	521	...	490	...

$T$	$S$	Mean Porosity, %	95% F.L.
1100	1	1.41	} $\pm 0.35$
	2	2.17	
1150	1	1.44	} $\pm 0.35$
	2	2.44	

(ii) 1-in.-Dia. Bars Made in Unsprayed Moulds

$P$  = 0.007, 0.032, 0.055, 0.11.

$T$  = 1050, 1100, 1150, 1200.

Generally two results for each condition.

Zero moved to 2% porosity and figures  $\times 100$ .

Source of Variance	D.F.	M.S.	S(V.R.)
Between $P$ . . . .	3	56,781	...
" $T$ . . . .	3	27,958	...
$P \times T$ interaction . .	9	17,773	0.1
Residual . . . .	16	2,269	...

$P \times T$  interaction significant; experiment has therefore to be broken down into single-factor experiments:

Porosity, % (means of two observations)

$P \backslash T$	1050	1100	1150	1200
0.007	1.67 *	1.63	1.43	1.37
0.032	2.09	1.65	1.96	2.14
0.055	1.99	1.89	4.04 *	3.04
0.11	2.27	2.32	3.33	5.90

\* Single observations.

Student's  $t$  test was used to determine the significance of the difference between these means; as might be expected from the spread of the observations and their limited number, significance was only attained in certain cases (cf. p. 559).

(iii) 2-in.-Dia. Bars Made in Unsprayed Moulds

$P$  = 0.007, 0.032, 0.055, 0.11.

$T$  = 1050, 1100, 1150.

Generally two results for each condition.

Zero moved to 2% porosity and figures  $\times 100$ .

Source of Variance	D.F.	M.S.	S(V.R.)
Between $P$ . . . .	3	19,626	0.7
" $T$ . . . .	2	13,310	4
$P \times T$ interaction . .	6	1,983	N.S.
Residual . . . .	12	3,531	...

(See Figs. 7 and 8, p. 559.)

(iv) Plate Castings

$P$  = 0.007, 0.032, 0.055, 0.11.

$T$  = 1080, 1130, 1180.

$S = \frac{1}{4}, \frac{1}{2}, 1$  in.

Values for porosity under each condition generally mean of two observations. Second-order interaction neglected.

Zero moved to 2% porosity and figures  $\times 100$ .

Source of Variance	D.F.	M.S.	S(V.R.)
Between $P$ . . . .	3	106,358	...
" $T$ . . . .	2	48,944	...
" $S$ . . . .	2	16,014	0.5
$P \times T$ interaction . .	6	9,267	1
$T \times S$ " . . . .	4	1,496	N.S.
$S \times P$ " . . . .	6	3,092	N.S.
Residual . . . .	12	2,209	...

$S$  main effect independent of  $P$  and  $T$  (see p. 560).

$P \times T$  interaction significant; experiment therefore broken down into two-factor experiments:

$T \times S$ 

Source of Variance	D.F.	P = 0.007		P = 0.032		P = 0.055		P = 0.11	
		M.S.	S(V.R.)	M.S.	S(V.R.)	M.S.	S(V.R.)	M.S.	S(V.R.)
Between $T$ . .	2	2,047	N.S.	7,029	5	18,836	N.S.	48,817	0.3
Between $S$ . .	2	655	N.S.	1,419	N.S.	12,358	N.S.	10,859	3
Residual . .	4	1,565	...	845	...	4,695	...	1,024	...

(See Fig. 10, p. 560.)

 $S \times P$ 

Source of Variance	D.F.	T = 1080		T <sub>2</sub> = 1130		T <sub>3</sub> = 1180	
		M.S.	S(V.R.)	M.S.	S(V.R.)	M.S.	S(V.R.)
Between $S$ . .	2	1,483	N.S.	4,765	N.S.	12,758	5
Between $P$ . .	3	11,686	1	35,379	0.8	77,826	<0.1
Residual . .	6	1,721	...	3,437	...	2,350	...

(See Fig. 9, p. 560.)

(b) *Variance of U.T.S.*(i) *1-in.-Dia. Bars* $P = 0.007, 0.032, 0.055, 0.11.$  $T = 1050, 1100, 1150, 1200.$ 

Generally two results for each condition.

Zero moved to 10.0 tons/in.<sup>2</sup> and figures  $\times 100.$ 

Source of Variance	D.F.	Sprayed Moulds		Unsprayed Moulds	
		M.S.	S(V.R.)	M.S.	S(V.R.)
Between $P$ . .	3	821	...	372	...
Between $T$ . .	3	29	N.S.	1892	...
$P \times T$ interaction	9	488	0.3	1068	0.1
Residual . .	16	111	...	179	...

 $P \times T$  interaction significant; experiments therefore broken down into two single-factor experiments:*U.T.S. tons/in.<sup>2</sup>* (means of 2 observations)

$P \backslash T$	Sprayed Moulds				Unsprayed Moulds			
	1050	1100	1150	1200	1050	1100	1150	1200
0.007	8.7 *	11.6	10.3	11.9	12.6 *	13.0	11.7	14.9
0.032	12.3	10.8	11.9	10.8	15.0	13.9	11.2	13.7
0.055	11.6	12.0	15.2 *	13.1	13.8	15.3	9.8 *	10.8
0.11	12.5	12.3	9.4	10.6	16.7	11.3 *	12.1	7.4

\* Single observations.

Student's  $t$  test was used to determine the significance of the difference between these means; as might be expected from the spread of the observations and their limited number, significance was not attained in all cases (cf. p. 561).(ii) *Plates* $P = 0.007, 0.032, 0.055, 0.11.$  $T = 1080, 1130, 1180.$  $S = \frac{1}{4}, \frac{1}{2}, 1$  in.

Values for U.T.S. under each condition generally means of two observations. Second-order interaction neglected.

Zero moved to 10 tons/in.<sup>2</sup> and figures  $\times 100.$ 

Source of Variance	D.F.	M.S.	S(V.R.)
Between $P$ . . . .	3	52,346	0.2
Between $T$ . . . .	2	35,053	2
Between $S$ . . . .	2	1,707	N.S.
$P \times T$ interaction	6	8,608	N.S.
$T \times S$ . . . .	4	10,036	N.S.
$S \times P$ . . . .	6	11,673	N.S.
Residual . . . .	12	5,298	...

(See Figs. 12 and 13, p. 561.)

(c) *Comparison of Mean Strengths*(i) *1-in.-Dia. Bars Poured from 1150° C. or Less*

Sprayed moulds : mean U.T.S. = 11.4 (26 observations).

Unsprayed moulds : mean U.T.S. = 13.3 (25 observations).

Student's  $t = 4.07$ ;  $\therefore$  significance level for difference between means = 0.1% (cf. p. 560).(ii) *1-in.-Dia. Bars Poured from 1200° C. and Containing 0.034% Phosphorus or Less*

Sprayed moulds : mean U.T.S. = 10.4 (5 observations).

Unsprayed moulds : mean U.T.S. = 13.9 (5 observations).

Student's  $t = 3.21$ ;  $\therefore$  significance level for difference between means = 2% (cf. p. 560).(iii) *Plates Poured from 1030° C.* $P = 0.002-0.003$  : mean U.T.S. = 11.2 (8 observations). $P = 0.058-0.094$  : mean U.T.S. = 13.0 (6 observations).Student's  $t = 4.65$ ;  $\therefore$  significance level for difference between means = 0.1% (cf. p. 561).(d) *Correlation Coefficients for Porosity vs. U.T.S.*(i) *1-in.-Dia. Bars Made in Unsprayed Moulds*

All observations (34 pairs of observations):

$$r = -0.685,$$

significance level =  $>0.1\%$  (cf. p. 562).

Bars containing up to 2.6% porosity only (29 pairs of observations):

$$r = +0.223,$$

significance level =  $>10\%$ , i.e. non-significant (cf. p. 562).(ii) *Plates*

All observations (94 pairs of observations):

$$r = -0.682$$

significance level =  $\ll 0.1\%$  (cf. p. 562).

Plates containing up to 4.0% porosity only (81 pairs of observations):

$$r = -0.396$$

significance level = 0.1% (cf. p. 562).

Plates containing up to 2.6% porosity only (57 pairs of observations):

$$r = -0.465$$

significance level = 0.1% (cf. p. 562).

Plates containing up to 2.1% porosity only (41 pairs of observations):

$$r = -0.125,$$

significance level =  $>10\%$ , i.e. non-significant (cf. p. 562).



## REFERENCES

1. W. A. Baker, F. C. Child, and W. H. Glaisher, *J. Inst. Metals*, 1944, **70**, 373.
2. W. H. Glaisher, *ibid.*, 1949-50, **76**, 377.
3. W. H. Glaisher, *B.N.F.M.R.A. Research Rep.* No. **A.718**, 1946.
4. N. B. Rutherford, *ibid.*, No. **A.804**, 1948.
- 4<sup>(a)</sup>. N. B. Rutherford, *ibid.*, No. **A.831**, 1949.
5. N. B. Rutherford, *J. Inst. Metals*, 1951, **79**, 189.
6. L. Buckley and E. C. Mantle, *Foundry Trade J.*, 1951, **91**, 727.
7. W. A. Baker and F. C. Child, *J. Inst. Metals*, 1944, **70**, 349.
8. R. Genders and G. L. Bailey, "The Casting of Brass Ingots" (B.N.F.M.R.A. Research Monograph No. 3), pp. 159 ff. **1934**: London.
9. D. Hanson, S. L. Archbutt, and Grace W. Ford, *J. Inst. Metals*, 1930, **43**, 41.
10. E. A. Owen and Ll. Pickup, *ibid.*, 1934, **55**, 215.
11. N. P. Allen and S. M. Puddephat, *ibid.*, 1935, **57**, 79.
12. R. W. Ruddle, *ibid.*, 1950, **77**, 1.
13. N. B. Rutherford, B.N.F.M.R.A. unpublished work, 1948.
14. R. W. Ruddle, "The Solidification of Castings" (Inst. Metals Monograph and Rep. Series No. 7), p. 49. **1950**: London.
15. B. W. Peck, *B.N.F.M.R.A. Research Rep.*, No. **A.806**, 1948.
16. A. Cibula and R. W. Ruddle, *J. Inst. Metals*, 1949-50, **76**, 361.
17. K. A. Brownlee, "Industrial Experimentation". **1948**: London (H.M. Stationery Office).
18. R. A. Fisher, "Statistical Methods for Research Workers". **1946**: London (Oliver and Boyd).
19. G. U. Yule and M. G. Kendall, "An Introduction to the Theory of Statistics". **1940**: London (Charles Griffin).

# SEGREGATION OF IRON AND PHOSPHORUS AT THE GRAIN BOUNDARIES IN 70 : 30 BRASS DURING GRAIN GROWTH\*

1382

By H. M. MIEKK-OJA,† Sc.D.

## SYNOPSIS

During an investigation into the influence of impurities on grain growth in 70 : 30 brass, it was found that if the iron content is 0.007% or more, small amounts of phosphorus (0.002–0.019%) strongly inhibit grain growth at temperatures up to 670° C. Consequently grain-sizes of 0.020–0.050 mm. are readily obtainable by annealing over a wide temperature range. However, the larger grain-sizes, such as the American 0.070, 0.100, and 0.120 mm., are not easily obtained, and a non-uniform structure is often formed on annealing in the range 575°–670° C. When the iron content is 0.005% or less, small amounts of phosphorus accelerate grain growth at high temperatures, and therefore any desired grain-size can be secured only with great difficulty. In the absence of phosphorus, the grain-size/temperature curve rises slowly and steadily, making it possible to produce 70 : 30 brass in several annealed tempers, as is customary in the United States.

To explain the anomalies found in the grain-size/temperature curves with small amounts of various impurities, it is suggested that during grain growth iron and phosphorus segregate, without forming any separate phase, at the grain boundaries, where they hinder the migration of parent atoms through the transition zone. This segregation is assumed to occur because the decreases in both binding and strain energy which accompany it outweigh the effect on the free energy of the simultaneous decrease of entropy. However, when the temperature is high enough, the influence of entropy predominates, resulting in the dispersion of the impurity atoms throughout the lattice. Thicknesses of the layers of iron atoms at the transition zone are calculated.

## I.—INTRODUCTION

As the most important structure variable of homogeneous metals, the mean grain-size has been the subject of numerous investigations, which have thrown light upon the internal mechanism of the grain-growth process. Normal grain growth during annealing, i.e. the development of practically perfect crystals at the expense of others, is now known to be a manifestation of a tendency towards a diminution of free energy, which requires a reduction of the total area of the crystal boundaries. While the grains are growing, the driving force for grain-boundary migration decreases, until the grains stabilize in sizes depending mainly on the annealing temperature. The normal course of grain-boundary migration may, however, be disturbed by various factors which alter the activation energy of the grain-growth process, with a resulting change in the final grain-size. Among such factors, the effect of impurities, particularly in the form of inclusions of a second phase, is generally known.

The results of studies on the effect of impurities do not, however, agree in detail, which is quite understandable in view of the numerous factors involved in grain growth. With quite small amounts of impurities for instance, a region is entered where the influences of different impurities conflict with each

other. Thus, the quantitative results published in the literature cannot always be directly applied in works' practice. This difficulty was encountered at the Outokumpu Metal Works in connection with the annealing of 70 : 30 brass, and led to the closer investigations which form the subject of the present paper.

Preliminary experiments showed that phosphorus and iron, if present simultaneously, play a major role in the grain growth of 70 : 30 brass, a fact referred to by Burghoff<sup>1</sup> among others. For this reason, the investigations were concentrated first upon the influence of these particular impurities. The iron content of the 70 : 30 brass produced at the Outokumpu Works is on an average 0.005% and only exceptionally exceeds 0.01%. Phosphorus was added deliberately with a view to obtaining the 0.005% customarily introduced in Europe to prevent season-cracking and excessive grain growth.<sup>2</sup>

## II.—EXPERIMENTAL

The research scheme was quite simple: samples of 70 : 30 brass containing phosphorus and iron in varying small quantities were, after cold rolling, annealed at different temperatures, each for the same period of time, and the mean grain-size and Brinell hardness determined.

\* Manuscript received 6 November 1951.

† Technical Adviser to the Outokumpu Metal Works, Pori,

Finland; Acting Professor of Physical Metallurgy at the Finland Institute of Technology.



Three lines were followed in the investigations, viz.: the influence on final grain-size of (a) phosphorus, (b) iron, (c) phosphorus + iron. Samples selected by means of spectrographic analysis showed the variations in content given in Table I.

TABLE I.—Results of Spectrographic Analysis of Samples.

	(a)	(b)	(c)
P, %	0.000–0.027	0.000	0.000–0.019
Fe, %	0.004–0.005	0.004–0.100	0.007–0.029
Ni, %	0.005–0.006	0.005–0.006	0.005–0.025
Pb, %	0.001–0.002	0.001–0.017	0.002–0.012
Sn, %	0.000	0.000	0.000–0.050
Cu, %	70.2–70.8	70.1–71.5	69.1–72.1
Zn, %	remainder	remainder	remainder

The samples were taken partly from sheets selected from the current works' production, partly—when large amounts of impurities were needed—from sheets specially prepared for the purpose. Those from production were cold rolled after hot rolling and annealing, while the separately prepared sheets went through three cold-rolling and annealing operations. To eliminate the influence of varying thickness on grain growth, all sheets were rolled to 3.0 mm. The reduction in final rolling was 50%, and annealing before final rolling was carried out for 3 hr. at 630° C.

In order to diminish the effect of annealing time on

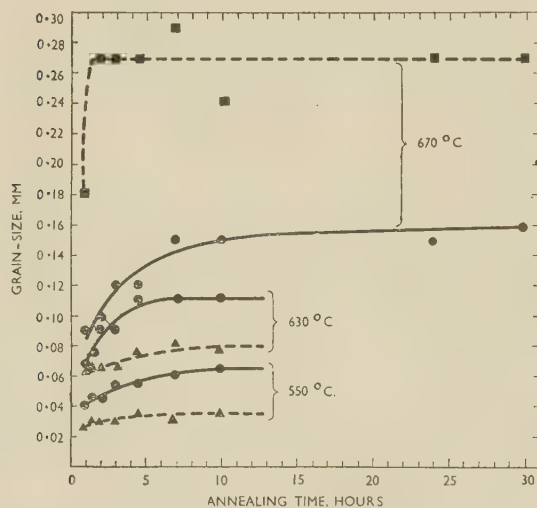


FIG. 1.—Isothermal Grain-Growth Curves Showing Variation of Grain-Size with Time in 70 : 30 Brass.

KEY.

Cu, %	70.5	70.2	70.4
P, %	0.000	0.012	0.002
Fe, %	0.004	0.004	0.004
Pb, %	0.001	0.002	0.002
Ni, %	0.006	0.006	0.006
Zn, %	remainder	remainder	remainder

final grain-size, a 3-hr. period was adopted for all treatments. As the investigations were intended to serve practical ends, a longer time was not chosen,

in spite of the fact that preliminary experiments showed a slight increase in grain-size during prolonged annealing (Fig. 1). Annealing was carried out in a

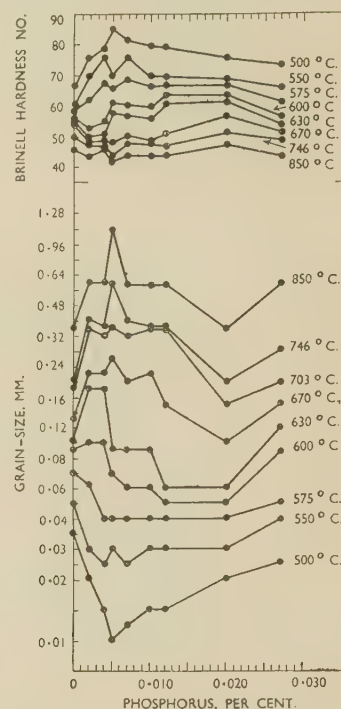


FIG. 2.—Effect of Phosphorus on Grain Growth and Brinell Hardness of 70 : 30 Brass.

small laboratory furnace with the temperature controlled to  $\pm 5^\circ \text{C}$ . The final temperature was attained, as a rule, within 30 min. of charging. Grain-size measurements were made on the edge of the sample, which was polished and etched electrolytically, by means of A.S.T.M. grain-size charts using a magnification of 75; for grain-sizes of 0.200 mm. and upwards, a magnification of 25 was used. The Brinell hardness was measured on the rolled surface of the sample in the usual way.

The results obtained are given in Figs. 2–4. These show the effect of phosphorus and iron content on hardness and final grain-size for different annealing temperatures. As can be seen from Table I, during the experiments on the influence of phosphorus (Fig. 2), the iron content was practically constant at 0.004%. In experiments on the influence of iron (Fig. 3), only traces of phosphorus were present. The combined effects of phosphorus and iron are shown graphically (Fig. 4) as a function of phosphorus content; the iron contents (0.007–0.029%) appear below the graph. In addition to the phosphorus and iron, all samples contained minor amounts of other impurities, especially nickel and lead (see Table I). These impurities exercise their own influence, which, however, seems to be obscured by that of iron and phosphorus.

The grain structure in the samples, including those of large grain-size, was fairly uniform, and mean

grain-size could therefore easily be estimated. Certain samples, however, which contained both phosphorus and iron, showed a mixed grain structure, a

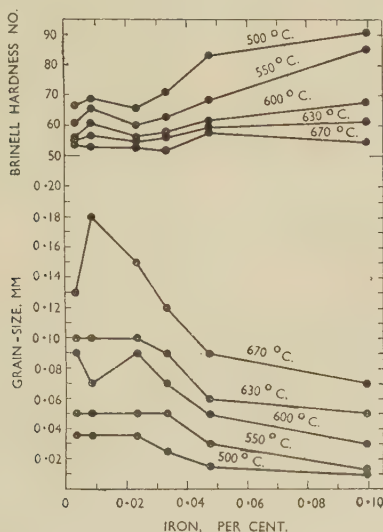


FIG. 3.—Effect of Iron on Grain Growth and Brinell Hardness of 70 : 30 Brass.

phenomenon referred to by Burghoff<sup>3</sup> amongst others. The results in question are indicated by a query-mark on the graph (Fig. 4).

### III.—DISCUSSION OF EXPERIMENTAL RESULTS

Figs. 2-4 show that, depending on the annealing temperature and the presence of impurities, grain-size and Brinell hardness vary considerably; the former from 0.010 to 1.12 mm., the latter from 42 to 91. To estimate the interdependence of grain-size and hardness, the results, up to a size of 0.440 mm., are collected in Fig. 5, where hardness is plotted as a function of grain-size. Bearing in mind the statistical character of grain growth and the resulting inaccuracy in the conception of "mean" grain-size, it can be seen that there is a definite correlation between hardness and grain-size. This correlation, it is true, is not in full agreement with Gensamer's law,<sup>4</sup> as can be seen when taking the logarithm of grain-size as the abscissa. On the other hand, the A.S.T.M. charts do not count twins as separate grains, although free paths are cut off at the twinning planes.

It should be emphasized that the interdependence of grain-size and hardness values is not systematically influenced by variations in impurities and annealing temperature, e.g. a certain small grain-size is connected with the same hardness value, whether it is the result of impurities or of a low annealing temperature. This means that the effect of foreign atoms on the resistance to deformation, represented by indentation hardness, is due to their influence on the grain boundaries. The small amounts of impurities

involved do not increase the deformation resistance of the lattice itself to an extent that could be revealed by the measurements made in this work.

If the curves in Figs. 2, 3, and 4 are compared with the results of other authors,<sup>1</sup> a certain measure of agreement is apparent. This is especially the case as regards the effect of iron, in respect of which differences are mainly quantitative. An obvious dissimilarity, however, is found in the combined influence of small amounts of phosphorus and iron on the final grain-size. In contradiction to previous results, it appears from Fig. 2 that above a certain temperature small amounts (0.002-0.012%) of phosphorus increase the final grain-size when the iron content is as low as 0.004%.

Fig. 6 was drawn to illustrate the results of the work as a whole, and shows final grain-size as a function of annealing temperature for different critical amounts of impurities. These curves clearly indicate that the dependence of grain-size on annealing temperature is controlled by extremely small variations in phosphorus and iron content.

Significant, moreover, is the fact that the final grain-size, with few exceptions, is not determined by incidental factors, as, for example, in discontinuous and exaggerated grain growth. On the contrary, a practically identical grain-size is always obtained when 70 : 30 brass with the same phosphorus and

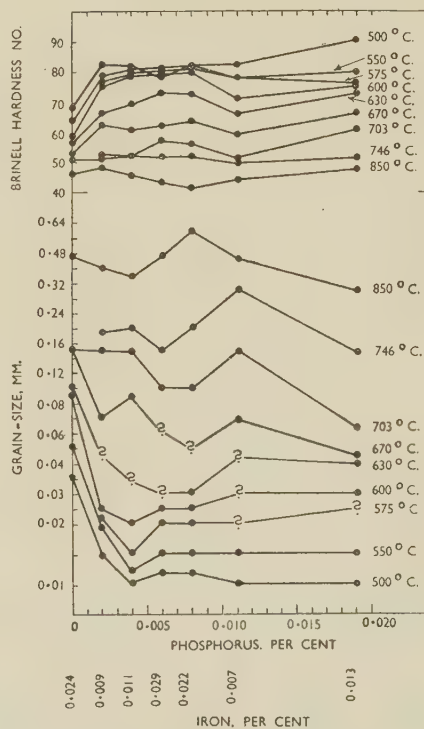


FIG. 4.—Effect of Phosphorus + Iron on Grain Growth and Brinell Hardness of 70 : 30 Brass.

iron content is annealed at the same temperature, at least up to a grain-size of 0.200 mm. and when other impurities are of the order given ( $\text{Ni} < 0.006\%$ ,



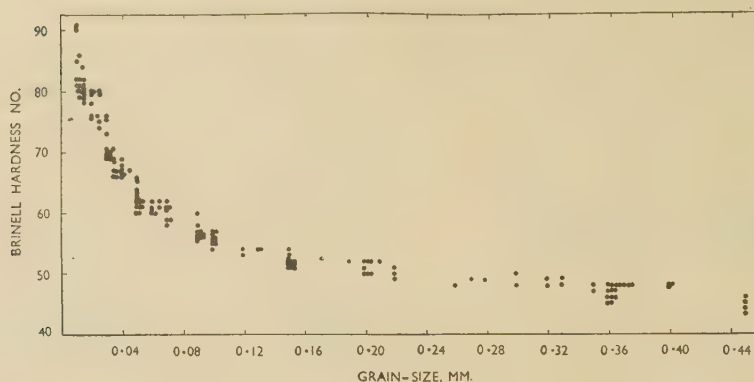


Fig. 5.—Correlation between Brinell Hardness and Grain-Size in Annealed 70 : 30 Brass.

Impurities : P 0.000–0.027, Fe 0.004–0.100, Ni 0.005–0.025, Pb 0.001–0.017, Sn 0.000–0.050%. Annealing temperature 500°–850° C.

Pb < 0.002%), as in the case of the 70 : 30 brass made at Outokumpu. This was established by control experiments and in connection with other investigations into grain-size, carried out both in the laboratory and on a production scale.

In Fig. 6 the curve 0.000 P may be regarded as corresponding to "pure" 70 : 30 brass, in spite of the impurities (Fe 0.004, Ni 0.006, Pb 0.001%), because in the absence of phosphorus such small amounts of these impurities are not known to affect the grain-size;<sup>1</sup> while an increase in iron content to 0.024%

did not produce any change in the 0.000 P curve. Moreover, curve 0.000 P is in fair agreement with the results of other authors for "pure" 70 : 30 brass.<sup>1</sup>

With the iron content still as low as 0.004%, the influence of increasing amounts of phosphorus on the final grain-size is shown by curves 0.002 P, 0.007 P, 0.012 P, and 0.020 P; other impurities (nickel and lead) being present in the same amounts as in sample 0.000 P. The difference between curve 0.000 P and curves 0.002 P–0.020 P may not, however, be due to phosphorus alone, for there is reason to believe that phosphorus acts in conjunction with the iron. At 550° C. and below, phosphorus exercises a marked stabilizing effect on grain growth. Final grain-size is independent of phosphorus content, at any rate from 0.002 to 0.020%, at the temperatures mentioned, as is evident from Fig. 6.

With an increase in phosphorus content alone from 0.002% upwards, this stabilizing effect is maintained at higher temperatures. On the other hand, small increases in the iron content, even from 0.004 to 0.009%, result in a further considerable decline in grain-size when phosphorus is present (curve 0.002 P/0.009 Fe). An increase in iron content beyond 0.009%, at any rate up to 0.022%, does not noticeably strengthen this effect at low temperatures (curve 0.008 P/0.022 Fe). With higher iron contents the stabilizing effect is extended to higher temperatures.

In the presence of relatively large amounts of iron (0.007–0.029%) a non-uniform grain structure may be found in the annealing range 575°–670° C. (Fig. 4). This phenomenon, to which reference was made in Section II, does not occur in the absence of phosphorus.

When phosphorus is not present, the obstructing influence of iron on grain growth sets in when the iron content is about 0.034% and grows stronger with increasing amounts (Fig. 3). With 0.050% iron the same grain-sizes are obtained at various temperatures as with 0.004% iron combined with small amounts of phosphorus; 0.100% iron is needed to produce the same effect as 0.009% iron + 0.002% phosphorus (cf. Fig. 6, curves 0.100 Fe and 0.002 P/0.009 Fe).

The marked rise in curves 0.002 P–0.012 P at high

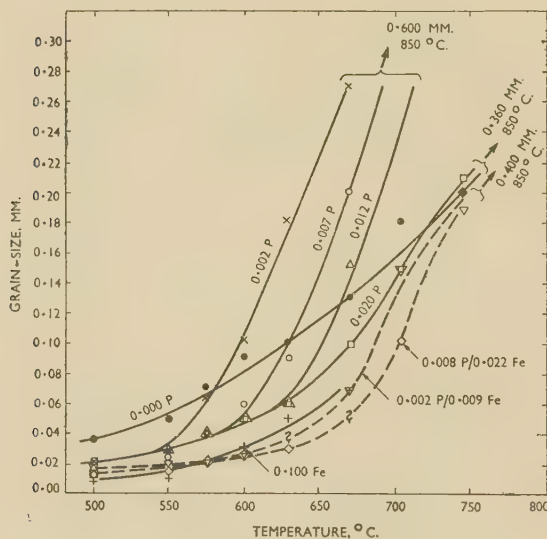


Fig. 6.—Grain-Size/Temperature Curves for 70 : 30 Brass, Containing Different Critical Amounts of Phosphorus and Iron.

Thickness of sample 3.0 mm., cold rolled 50%, annealing time 3 hr.

KEY.

	●	×	○	△	□	▽	◇	+
	0.00 P	0.002 P	0.007 P	0.012 P	0.020 P	0.002 P/ 0.009 Fe	0.008 P/ 0.022 Fe	0.100 Fe
Cu, %	70.5	70.4	70.5	70.2	70.7	70.9	69.1	70.1
P, %	0.000	0.002	0.007	0.012	0.020	0.002	0.008	0.000
Fe, %	0.004	0.004	0.005	0.004	0.005	0.009	0.022	0.100
Ni, %	0.006	0.006	0.006	0.006	0.005	0.025	0.007	0.005
Pb, %	0.001	0.002	0.002	0.002	0.001	0.002	0.002	0.002
Sn, %	...	...	...	...	...	0.001	0.050	...

temperatures (Fig. 6) deserves particular attention. Although a certain caution is always necessary in dealing with large grain-sizes, it is evident that small amounts of phosphorus considerably increase the final grain-size at high temperatures. True, it may be argued that phosphorus does not actually accelerate grain growth, but merely eliminates the stabilizing influence of other impurities; to resolve this question definitely would require iron-free brass. However, if curve 0.000 P represents the grain-size/temperature dependence of "pure" 70 : 30 brass, as is assumed by the author, the amounts of phosphorus mentioned really accelerate the grain growth at high temperatures; this may be looked upon as a catalytic effect.

#### IV.—PRACTICAL SIGNIFICANCE

The results of the present work, as summarized in Fig. 6, clearly indicate that variations in phosphorus and iron content as small as from 0.000 to 0.010% cause considerable differences in the final grain-size in annealed 70 : 30 brass. Under practical annealing conditions the effect of such variations in these two impurities obscures that of other factors involved in grain growth, provided, of course, that additional effective impurities are not present.

Considering, first, an iron content of 0.007% and above, customary in commercial products, it is seen that an addition of 0.002% phosphorus or more produces a strong stabilizing effect on grain growth. This effect is essentially independent of variations in phosphorus content, at least from 0.002 to 0.020%, and in iron content from 0.007 to 0.029%. Consequently, by adding phosphorus, a relatively small grain-size of 0.020–0.050 mm., suitable for most purposes, is readily obtained over a wide temperature range of 550°–650° C. This is plainly the main reason for the European custom of adding phosphorus to 70 : 30 brass.

On the other hand, the presence of phosphorus causes difficulties when larger grain-sizes are required, such as the American 0.050, 0.070, 0.100, and 0.120 mm.<sup>5</sup> These are obtained at high temperatures, 650° C. and above, where the dependence of final grain-size on temperature and iron content is so sensitive that the necessary constant temperature cannot be readily attained in practice. Furthermore, there is the danger of a non-uniform grain structure when annealing is carried out at 575°–670° C. (Fig. 4).

The situation alters appreciably as soon as the iron content falls to 0.005% or below. Addition of phosphorus then either obstructs or accelerates the grain growth, depending on the amount of phosphorus and on the temperature. It is, in consequence, extremely difficult to obtain a desired grain-size, especially as the exact amount of phosphorus cannot be fixed and because there may, on a production scale, be variations in the iron content from 0.005 to 0.007% or more.

In the absence of phosphorus, the dependence of grain-size on temperature conforms with curve

0.000 P (Fig. 6) and also with variations in iron content, at least up to 0.024%. The increase in final grain-size is then fairly uniform and slow, making it possible to produce 70 : 30 brass in several annealed tempers, corresponding, for example, to grain-sizes of 0.015, 0.025, 0.035, 0.050, 0.070, 0.100, and 0.120 mm. This is apparently why phosphorus is avoided as far as possible in the United States; an additional advantage is that no danger of non-uniform grain structure then arises.

#### V.—THEORETICAL DISCUSSION

When considering the results of this work, due weight should be given to the fact that they are reproducible and appear to conform to definite laws, particularly as regards the influence of impurities. This proves that the latter obey thermodynamic laws of equilibrium in the control they exercise over grain-boundary migration, and that grain growth is not determined by incidental factors, even in the presence of only small amounts of impurities.

It should be emphasized that even small quantities of impurities have a decisive influence on the final grain-size. To take an example, an alteration in phosphorus and iron contents from 0.002/0.004 to 0.002/0.009%, brings about a decrease in grain-size from 0.100 to 0.025 mm. when annealing at 600° C. (Fig. 6). This can hardly be explained without assuming that the influence of the atoms in question is concentrated at the grain boundaries; within the lattice they would scarcely be able to produce such a strong effect. Furthermore, it suggests that the grain boundary is narrow, a few atoms thick only, as required by the transition theory.

These considerations give rise to the assumption that the impurity atoms collect at the grain boundaries, without forming any separate phase. Similar segregation of solute atoms at grain boundaries has actually been observed, e.g. as a result of investigations into intercrystalline corrosion in various metals.<sup>6</sup> It may be assumed that the partition of impurities between the lattice and the transition zone is determined by the minimum free energy  $F = E - TS$ . The accumulation of impurity atoms in the transition zone would result in a decrease of the internal energy  $E$ , whereas their dispersion throughout the lattice would lead to an increase of the entropy  $S$ ; an increase in temperature  $T$  would shift the equilibrium towards the higher entropy state, and vice versa. This being the case, we have to deal with a special kind of "segregation within a single phase" (*Einphasenentmischung*). This conception and its great metallurgical significance have been elucidated by Houdremont.<sup>7</sup> In substitutional solid solutions the segregation of solute atoms into certain local zones in the matrix is known to occur, e.g. in connection with precipitation-hardening, where the decrease in internal energy is attained mainly through the liberation of binding energy, great enough to cause segregation in spite of the fact that it results, not only



in a decrease of entropy, but also in an increase of strain energy. However, the accumulation of solute atoms into coherent zones does not lead to an equilibrium state in the parent matrix, since there is a possibility of a further decrease of the internal energy through precipitation, when the coherent zones have grown large enough.<sup>8</sup> As shown by Cottrell<sup>9</sup> and by Nabarro,<sup>10</sup> segregation within a single phase may also occur in interstitial solid solutions; these authors speak of a carbon and nitrogen "atmosphere" around dislocations in steel. Here the internal energy decreases mainly as a result of strain-energy relief when interstitial atoms segregate around dislocations. The resulting inhomogeneous solid solution may be considered to be in an equilibrium state,<sup>11</sup> which is determined by the minimum free energy. At such high temperatures as just below the  $A_{c1}$  point, the interstitial atoms disperse from the neighbourhood of the dislocation into the lattice, a fact which is apparent from the absence of a yield point (break in the stress/strain curve) in freshly quenched material. During slight annealing (ageing), as well as during slow cooling, e.g. in connection with soft annealing and normalizing, the interstitial atoms accumulate again around the dislocations and a yield point reappears.<sup>11</sup>

Reverting to the experimental results, curve 0.000 P in Fig. 6 is considered to represent approximately the interdependence of final grain-size and temperature for "pure" 70 : 30 brass, in spite of amounts of impurities as great as 0.004% iron, 0.006% nickel, and 0.001% lead. It should be borne in mind that iron and nickel atoms in particular are, as regards both atomic diameter and chemical character, so similar to copper and zinc atoms that no marked diminution in internal energy can be expected as a result of segregation within a single phase. It is evident, therefore, that enrichment of these atoms at the grain boundaries does not take place to any noticeable extent. This view is supported by the fact that an increase in iron content from 0.004 to 0.024% does not perceptibly change the course of curve 0.000 P. According to Burghoff,<sup>1</sup> nickel, at any rate up to 0.13%, also has no effect upon grain growth.

The picture becomes quite different, however, as soon as phosphorus is introduced, its presence even seeming to be a necessary condition for grain-growth anomalies. The diameter of the phosphorus atom, whether in the atomic or the ionic state, and its chemical character, differ considerably from the corresponding properties of other atoms present. Consequently, the enrichment of phosphorus atoms at the grain boundaries may result in a marked decrease in the internal energy. Taking into account the great energy of the bond between phosphorus and iron atoms, the maximum reduction of internal energy will obviously be obtained if phosphorus and iron atoms accumulate at the grain boundary simultaneously.

The following hypothesis is advanced to explain the

powerful effect of small amounts of phosphorus and iron on the final grain-size in 70 : 30 brass. At such low temperatures, where the influence of entropy on free energy is not decisive, phosphorus and iron atoms segregate simultaneously at the transition zone between the grains, without the formation of a second phase. The decrease of binding energy and of strain energy which this occasions outweighs the decrease in the entropy of mixing, thus enabling segregation to occur. But the decrease of binding energy is not sufficient to cause the formation of coherent zones in the matrix, and still less the formation of separate precipitates. It is suggested that the phosphorus atoms take up positions in the interstices at the transition zone, while the iron atoms replace the parent atoms; no detailed assumptions as to the bonds between the different atoms or as to possible molecule formation are made, however. The iron atoms, bound by phosphorus atoms at the transition zone, hinder the migration of copper and zinc atoms across the zone, thus counteracting grain growth. The higher the temperature, the greater the number of iron atoms needed to check growth. With rising temperature, when the entropy term  $TS$  increases, the iron atoms gradually pass over into the lattice, and their obstructive influence on grain-boundary migration decreases correspondingly.

Let us examine first samples 0.002 P, 0.007 P, 0.012 P, and 0.020 P (Fig. 6), where the phosphorus content varies from 0.002 to 0.020%, while the iron content remains practically constant at 0.004%. If, as a rough approximation, it is assumed that all iron atoms are located at the transition zone—as if they were swept forward during primary grain growth—they would form layers there, the thickness of which depended on mean grain-size, so that 0.010 mm. grain-size corresponded approximately to 1.3 Å., 0.020 mm. to 2.7 Å., 0.040 mm. to 5.3 Å., 0.100 mm. to 13.3 Å., and so on. The diameter of the iron atom is 2.52 Å., and as it belongs to the "hard" atoms it will not contract appreciably, even if the bond is heteropolar. There would in consequence exist in the transition zone, of, say, a 0.020-mm. grain, a layer that is one iron atom thick. At the temperature involved, 500°C., this layer may be supposed to prevent the migration of copper and zinc atoms across the transition zone. With increase in temperature, a thicker layer is needed, which allows the growth of larger grains; e.g. at 575°C., when grains grow to 0.040 mm., the layer is about two atoms thick, if all the iron atoms are retained in the transition zone.

At 550°C. and below, the grain-size remains practically unchanged while the phosphorus content varies from 0.002 to 0.020% (iron constant at 0.004%), as can be seen from Fig. 6. To explain this it must be remembered that the atomic weight of phosphorus is approximately half that of iron, and consequently when the phosphorus content is 0.002% and the iron content 0.004%, the number of atoms of each is about the same. Further, the possibility of phosphorus

binding the iron atoms corresponds at least to the relation  $\text{Fe}_2\text{P}$ ; 0.004% of iron may, therefore, well be bound at the transition zone by as little as 0.002% phosphorus, and an increase in phosphorus content will not lead to any change. The fact that an increase up to 0.020% does not strengthen the stabilizing effect produced by 0.002% phosphorus, lends support to the assumption that phosphorus atoms, at any rate at the transition zone, are situated in interstices.

If this hypothesis is correct, an increase in the iron content above 0.004% would increase the number of iron atoms at the transition zone. This would produce a stronger stabilizing effect on grain growth and, consequently, a diminution of final grain-size. That this is actually the case can be seen from Fig. 6, curve 0.002 P/0.009 Fe. For quantitative treatment of the effect envisaged let us take a temperature of 600°C., when the grain-size is 0.050 mm. with 0.004% iron, and 0.025 mm. with 0.009% iron. With some simplifying approximations, the layer of iron atoms corresponds in the former case to 6.7 Å., and in the latter to 7.5 Å., thicknesses which are practically the same. This means that at a given temperature a certain thickness of the layer of iron atoms is needed to stabilize the grains. At 600°C., the layer corresponds to about three iron atoms, i.e. to the assumed thickness of the transition zone. The zone would thus be fully occupied by iron atoms, and an increase in the iron content above 0.009% would have no additional effect in preventing grain growth. Experiments with iron contents up to 0.029% showed this to be the case.

In contradiction to the results of previous research, it appears from Fig. 6 that small amounts of phosphorus have an accelerating influence on grain growth at high temperatures when the iron content is small (0.004%). A similar but still stronger effect was found by the author in O.F.H.C. copper, in agreement with the results of Yen.<sup>12</sup> To explain this effect in brass, it may be assumed that after the dispersion of the iron atoms into the lattice at a given temperature, at least part of the phosphorus atoms still remain in the transition zone and possibly in its neighbourhood, in the "zone of accommodation".<sup>13</sup> This being the case, phosphorus atoms alter the strain energy of the parent atoms at the transition zone, and also around it, with the result that the energy barrier which prevents them from passing over from the transition zone into the lattice and vice versa, is lowered. Phosphorus would thus act in a way analogous to that of catalysts in chemical reactions. Actually, the influence of phosphorus is not restricted to its effect on final grain-size, but affects also the rate of isothermal grain growth. At 670°C., for instance, the grains attain their final size very rapidly in the presence of 0.002% phosphorus (Fig. 1), whereas grain growth in phosphorus-free brass takes place more or less in accordance with the relationship  $D = k \cdot t^n$ , where  $D$  = grain-size,  $t$  = time, and  $k$  and  $n$  are constants.<sup>14</sup> This effect of phosphorus clearly shows that the presence of very small amounts of impurities—as little as

0.002% phosphorus—may completely obscure the results of investigations into isothermal grain growth.

As is evident from the experimental results (Figs. 4 and 6), some annealing treatments carried out between 575° and 670°C. led to a mixed grain structure. This is the temperature range in which the dependence of grain-size on impurities is most sensitive. The phenomenon was already well known, and is explained as being due to non-uniform dispersion of impurities in the metal,<sup>3</sup> which agrees well with the above argument. Below 550°C. the final grain-size is so little dependent on differences in the amount of impurities that no one grain can grow large in comparison with the others, although great local differences in concentration may exist. Above 700°C. all grains grow relatively large, regardless of the amounts of impurities. In the critical range, 575°–670°C., however, the final grain-size is greatly dependent on impurities, e.g. annealing at 630°C. gives grain-sizes of 0.180 and 0.030 mm. when the impurities are 0.002% phosphorus and 0.004% iron, or 0.002% phosphorus and 0.009% iron, respectively. Under these conditions, in areas low in iron, the grain may easily grow to such a size, in comparison with others, that its surfaces are all convex in relation to those of its neighbours, which promotes its further growth.

In connection with the influence of impurities on grain growth, normal or discontinuous, the presence of a second phase is generally assumed.<sup>15</sup> In the present work, however, no second phase could be detected, at least on a microscopic scale, in spite of careful examination. Furthermore, the above considerations show that the inhibiting effect of impurities on grain growth can be explained without assuming the presence of a second phase. Where quite small amounts of impurities are concerned, the presence of a second phase is improbable. As the crystal, in order to be stable, must reach a certain minimum size, the small amounts of impurities in question are not likely to be sufficient to form such a network of crystals at the grain boundaries as could explain their marked and consistent influence. In addition, it must be remembered that the boundaries are moving during grain growth. To obstruct this movement and finally to stabilize the grains in sizes appreciably smaller than those in a pure metal, the small amounts of impurities in question are expected to keep pace with the grain boundaries and segregate there during grain growth. It is not easy to understand how crystals of a second phase or even coherent zones in the matrix would be able to do so.

On examining the effect of iron alone in 70 : 30 brass, without phosphorus, it was found that here too the inhibiting influence on grain growth sets in without the presence of a second phase. While Bauer and Hansen<sup>16</sup> give for the solid solubility of iron the values of 0.05% at 500°C., 0.15% at 600°C., and 0.3% at 700°C., the present results show a marked effect on grain growth with iron contents of 0.035% at 500°C., and 0.045% at 600° and 670°C. This



effect cannot be explained on the basis of the hypothesis given above, since the presence of phosphorus was postulated as a condition for the accumulation of iron atoms in the transition zone. However, it must be remembered that the change from a one- to a two-phase field is not very abrupt. In solid solutions, especially near the limit of solubility, perceptible fluctuations in concentration occur. In the two-phase field again, the small nuclei of a new phase tend to redissolve if the concentration lies so near to the equilibrium concentration that  $\partial^2 F / \partial \alpha^2$  is still positive ( $F$  = free energy,  $\alpha$  = concentration), which results in "downhill" diffusion.<sup>17, 18</sup> Consequently, when the iron content is 0.035–0.045%, fine-scale fluctuations in concentration probably reach a high figure, especially close to the grain boundaries, where the number of iron atoms may be considered to be statistically greater than elsewhere. Near the grain boundary the iron atoms may be thought to obstruct the migration of parent atoms through the boundary. Comparing the curves of 0.100 Fe and 0.002 P/0.009 Fe (Fig. 6), it can be seen that with iron alone, ten times the amount is required to produce the same effect in final grain-size as when phosphorus and iron are present together. This means that when bound at the transition zone by phosphorus, iron atoms hinder grain growth more effectively than if they are merely present by themselves in the lattice near the grain boundary.

## VI.—CONCLUSIONS

The conception that solute atoms segregate at grain boundaries, used by the author in explaining the marked influence of small amounts of phosphorus and iron on grain growth in 70 : 30 brass, is by no means new. To explain such a segregation, it is suggested that it is due to the requirements of minimum free energy, which call for a compromise between the maximum of the entropy of mixing on the one hand and the minimum of internal energy on the other, internal energy being represented mainly by the binding and strain energies. The anomalies in the grain-size/temperature curves and also the occurrence of discontinuous grain growth are believed to be better accounted for by alterations in the partition of impurity atoms between grain boundary and lattice, than on the basis of submicroscopical precipitations. This applies particularly to small amounts of impurities which, in order to be effective, must keep pace with the grain boundaries during grain growth.

It is held that the part played by inclusions of a second phase in preventing grain growth is trivial, even where general precipitation is concerned. However, even in the presence of such inclusions, if these are not finely dispersed, segregation of solute atoms may influence grain-boundary migration, in conjunction with the precipitates. That segregation is possible in the presence of precipitates is proved by the fact that it can also occur from a solution which is not even saturated, as is the solution which is in

equilibrium with precipitates. The case is analogous to the formation of carbon atmospheres around dislocations in steel, i.e. in ferrite, which may be in equilibrium with iron carbide; as shown by Gruhl,<sup>19</sup> this equilibrium is attained by ageing for 1 hr. at 200° C. Here, too, the segregation of solute atoms into distorted regions around dislocations occurs, with a resulting depletion of the solution and subsequent dissolution of carbon atoms from the carbide precipitates.

The work described was intended to serve purely practical ends. Consequently, the theoretical results need support by other, specially planned investigations. These should naturally not be confined to segregation of atoms of certain pairs of metals at grain boundaries, but should also be directed to distorted zones in the lattice.

## ACKNOWLEDGEMENTS

The author would like to express his thanks to Dr. Eero Mäkinen, General Manager of the Outokumpu Company, for his encouragement during the investigations and for permission to publish this paper. He also wishes to acknowledge his indebtedness to his colleagues at the Metal Works in Pori, especially to Mr. J. Kinnunen, M.A., who made the spectrographic analyses, and to Mr. J. Neva, who carried out all the experimental work.

## REFERENCES

1. H. Burghoff, *Grain Control in Industrial Metallurgy* (Amer. Soc. Metals), 1949, 185.
2. J. D. Jevons, "The Metallurgy of Deep Drawing and Pressing", p. 139. 1945: London (Chapman and Hall, Ltd.).
3. H. Burghoff, *Grain Control in Industrial Metallurgy* (Amer. Soc. Metals), 1949, 198.
4. M. Gensamer, E. B. Pearsall, W. S. Pellini, and J. R. Low, Jr., *Trans. Amer. Soc. Metals*, 1942, 30, 983.
5. —, *A.S.T.M. Standards* E79–49T.
6. R. King and B. Chalmers, "Progress in Metal Physics", Vol. I, p. 157. 1949: London (Butterworths Scientific Publications).
7. E. Houdremont, *Arch. Eisenhüttenwesen*, 1951, 22, 63.
8. F. R. N. Nabarro, *Inst. Metals: Symposium on Internal Stresses in Metals and Alloys*, 1948, 245. (Monograph and Report Series No. 5.)
9. A. H. Cottrell, *Phys. Soc.: Rep. Conf. on Strength of Solids*, 1948, 30.
10. F. R. N. Nabarro, *ibid.*, 38.
11. G. Masing, *Arch. Eisenhüttenwesen*, 1950, 21, 322.
12. M.-K. Yen, *Trans. Amer. Inst. Min. Met. Eng.*, 1949, 185, 61.
13. A. H. Geisler, "Symposium on Phase Transformations in Solids", p. 430. 1951: New York (John Wiley and Sons, Inc.); London (Chapman and Hall, Ltd.).
14. P. A. Beck, J. C. Kremer, and L. Demer, *Phys. Rev.*, 1947, [ii], 71, 555.
15. J. E. Burke, *Grain Control in Industrial Metallurgy* (Amer. Soc. Metals), 1949, 47.
16. O. Bauer and M. Hansen, *Z. Metallkunde*, 1934, 26, 121.
17. A. H. Cottrell, "Theoretical Structural Metallurgy", p. 234. 1948: London (Edward Arnold and Co.).
18. R. Smoluchowski, "Symposium on Phase Transformations in Solids", pp. 149, 166. 1951: New York (John Wiley and Sons, Inc.); London (Chapman and Hall, Ltd.).
19. W. Gruhl, *Z. Metallkunde*, 1950, 41, 173.

# THE CONSTITUTION OF NICKEL-RICH ALLOYS OF THE NICKEL-CHROMIUM-TITANIUM SYSTEM \*

1383

By A. TAYLOR,† Ph.D., F.I.M., F.Inst.P., MEMBER, and R. W. FLOYD,‡ B.Sc., A.I.M., MEMBER

## SYNOPSIS

The binary nickel-chromium and nickel-titanium systems have been re-examined by X-ray diffraction and micrographic techniques, and new equilibrium diagrams for them are presented. A detailed investigation has also been carried out on nickel-rich nickel-chromium-titanium alloys, from which partial equilibrium diagrams corresponding to the 750°, 1000°, and 1150° C. isothermals have been constructed. Isoparametric contours have been drawn for the nickel-rich primary solid solution, or  $\gamma$  phase, and it is shown that the hexagonal phase,  $\text{Ni}_3\text{Ti}$ , grows epitaxially on the octahedral planes of  $\gamma$  on account of the close similarity in their interatomic distances. The boundary separating magnetic from non-magnetic ternary  $\gamma$ -phase alloys at 20° C. is indicated in the nickel-chromium-titanium equilibrium diagram.

## I.—INTRODUCTION

THE constitution of the nickel-chromium system has been known for many years, and commercial alloys of nickel and chromium have been used for many applications where their high electrical resistivity and high strength at elevated temperatures make them an obvious choice. However, except in the case of iron, comparatively little is known about the effect of other elements on the properties and structures of nickel-chromium alloys. The work described in the present paper was designed to establish the effect of additions

## II.—EXPERIMENTAL PROCEDURE

In general, the same methods of treatment and examination were applied to all the alloys, irrespective of composition, although there were some deviations from the main scheme. The alloys were all synthesized by melting together the component metals, either in a small 4-kW. valve-operated H.F. induction furnace or in a Kroll-type argon-arc furnace. The latter was employed only for the chromium-rich alloys and for a very few alloys with high titanium contents. The raw materials used in the preparation of the alloys

TABLE I.—*Analysis of Raw Materials (Wt.-%).*

	Ni	Cr	Ti	Cu	Fe	Al	Mn	S	Si	O	V	Mg	O <sub>2</sub>
Nickel . . . . .	bal.	...	...	0.002	0.018	...	...	0.001	0.002	0.034	...	...	...
Chromium (Murex) . . . .	0.01	bal.	0.01	0.015	0.08	0.1	0.15	...	0.03	...	0.01	...	...
Chromium (Johnson, Matthey) . . . . .	0.02	bal.	0.008	0.015	0.02	0.008	0.005	...	...	...	...	0.002	0.5
Titanium . . . . .	...	...	bal.	...	0.015	0.15	0.04	...	0.08	...	...	0.03	...

of titanium to nickel-chromium alloys, and consists of an investigation by X-ray and micrographic analysis of the structure of nickel-rich alloys containing up to about 30 at.-% titanium. Before studying the ternary alloys, it was found necessary to examine both the binary nickel-chromium and nickel-titanium systems, because of inconsistencies in the published diagrams, or because of the low purity of the alloys previously studied.

For convenience the paper is divided into sections dealing, respectively, with the experimental methods adopted, each of the component binary phase systems individually, and the ternary nickel-chromium-titanium system.

were selected Mond nickel pellet, electrothermally reduced chromium (Murex, Ltd.), high-purity electrolytic chromium (Johnson, Matthey and Co., Ltd.), and magnesium-reduced titanium (Metal Hydrides, Ltd.). The compositions of these metals, mainly estimated visually from their spectra, are given in Table I. The Murex chromium was used for all the nickel-rich alloys, the Johnson-Matthey chromium being used only for the chromium-rich alloys. Alloys prepared in the induction furnace were melted from 50-g. charges in alumina- or magnesia-lined crucibles under an atmosphere of hydrogen at about 10 cm. pressure. The melts were superheated until the thin oxide skin on the surface was broken up, leaving a

\* Manuscript received 17 November 1951.

† Horizons Inc., Cleveland, O., U.S.A.; formerly with

The Mond Nickel Co., Ltd., Birmingham.

‡ The Mond Nickel Co., Ltd., Birmingham.



clean metal surface. At this stage the pressure was reduced to remove as much gas as possible from the alloys, which were then allowed to solidify in the crucible *in vacuo*.

Towards the end of the investigation the arc furnace became available, and this was used for melting the alloys containing more than 80% chromium, which had proved difficult to make in the induction furnace. Melting was carried out under argon at a pressure of about one-fifth of an atmosphere, using charges weighing 30 g. Although it was known that the electrolytic chromium contained some oxygen, no attempt was made to remove this by previous treatment. The effective composition of these alloys was obtained from chemical determination of the metallic chromium and nickel contents, assuming the insoluble non-metallic matter to be inert.

All the alloys were homogenized *in vacuo* for up to 4 days at temperatures between 1150° and 1300° C., depending on their composition, and then quenched to retain the high-temperature condition. Samples for chemical analysis were machined from the ingots, and filings for X-ray examination were taken from the machined surface. Alloys containing a high proportion of titanium or chromium were too hard for machining, and both analytical and X-ray samples were prepared by crushing in a tungsten carbide percussion mortar. Specimens for micro-examination were obtained from the remaining metal.

The nickel-chromium system was explored almost entirely by X-ray analysis, while both X-rays and micro-specimens were used in the case of the nickel-titanium and nickel-chromium-titanium systems. Both types of specimen were quenched after being heat-treated according to the same scheme of times and temperatures, whereby the time of treatment is approximately doubled for each fall in temperature of 50° C., as follows:

Temperature, °C.	Annealing Time
1200	1 hr.
1150	2 hr.
1100	4 hr.
1000	1 day
900	5 days
850	10 days
750	3 weeks

X-ray samples were heat-treated in alumina tubes sealed in evacuated silica capsules, and photographed in a 9-cm. Debye-Scherrer camera, using copper, manganese, or chromium  $K_{\alpha}$  radiation. Phase boundaries were located by visual inspection of the diffraction patterns and by lattice-parameter measurements, which were obtained to a high degree of accuracy using the  $\frac{1}{2}(\cos^2 \theta / \sin \theta + \cos^2 \theta / \theta)$  extrapolation of Taylor and Sinclair<sup>1</sup> and corrected for refractivity. Micro-specimens were annealed in continuously evacuated Inconel tubes and polished on  $\gamma$ -alumina. The structures were revealed by electrolytic etching in an aqueous solution containing 5% hydrofluoric acid and 10% glycerine, or in a saturated solution of oxalic acid.

### III.—THE BINARY SYSTEMS

#### 1. NICKEL-CHROMIUM

A comprehensive review of investigations of the nickel-chromium system carried out before 1937 is given by Jenkins, Bucknall, Austin, and Mellor,<sup>2</sup> who reproduce the phase diagram of Hansen,<sup>3</sup> based on the work of Matsunaga<sup>4</sup> and of Nishigori and Hamasumi.<sup>5</sup> Their own diagram, derived from the results of a thorough exploration of the system up to 91 at.-% chromium by thermal analysis and micro-examination of specimens quenched above 800° C., substantially confirms the earlier Japanese work, except as regards the position of the boundary of the solid solution of chromium in nickel,  $\gamma$ , which Jenkins *et al.* place higher by about 6 at.-%. The diagram is that of a eutectiferous series with a wide nickel primary solid solution,  $\gamma$ , the solubility of chromium in which decreases linearly from 50 at.-% at the eutectic temperature of 1345° to 43 at.-% at 800° C. The solubility of nickel in chromium at the eutectic temperature is 29 at.-%, falling rapidly to 17.5 at 1200° and then more slowly to 8 at.-% at 800° C. Since no alloys containing more than 91 at.-% chromium were examined by Jenkins and his co-workers, there is little evidence in their paper from which to estimate the solubility of nickel in chromium at temperatures below 1000° C. The only published work on the extent of the chromium solid solution below 1100° C. is that of Jette, Nordstrom, Queneau, and Foote,<sup>6</sup> who carried out X-ray studies on the solid solubilities of the system at temperatures between 524° and 1113° C. The limit of the chromium solid solution was shown to be about 9 at.-% nickel at 1100° C., falling to 1.6 at.-% at 500° C. This curve could be extrapolated to meet the corresponding one on Jenkins's diagram at about 1200° C. An outstanding feature of Jette's work is the placing of the  $\gamma$ -phase boundary so that at 1100° C. it lies at the same composition as the eutectic established by the thermal and microscopic examinations, and shows a steady fall in the solubility of chromium down to 35 at.-% at 500° C. To bring this boundary into agreement with that of Jenkins necessitates a considerable degree of retrograde solubility above 1100° C. It is clear that the factors contributing to this peculiar result are the inadequacy of the heat-treatment given to the lump alloys before the X-ray powder samples were obtained, and the lack of a single-phase alloy sufficiently near the  $\gamma$ -phase boundary, aggravated further by inaccuracies in parameter determination due to the use of a focusing camera.

For these reasons it was deemed essential to re-examine the binary nickel-chromium system by X-rays and to determine whether agreement could be obtained between X-ray and micrographic methods. Additional interest lay in the possibility of superlattice formation in the region of  $\text{Ni}_3\text{Cr}$ . No superlattice lines had been reported in the early X-ray work of Jette, although anomalies in the resistivity of  $\text{Ni}_3\text{Cr}$

were shown by Yano<sup>7</sup> to occur in the region of 530° C. and tentatively attributed, among other causes, to an order-disorder transformation. More recently<sup>8</sup> it had been found that certain complex alloys based on Ni<sub>3</sub>Cr gave quite clearly defined superlattice lines in their diffraction patterns, from which it could be inferred that Ni<sub>3</sub>Cr itself underwent an order-disorder transformation.\*

(a) *Face-Centred Cubic Alloys of the  $\gamma$  Phase*

A series of binary alloys containing 10–70 at.-% chromium, mostly at 5 at.-% intervals, were lump-annealed at 1200° C. for 4 days, and filings for X-

aries derived are shown in the revised equilibrium diagram of the nickel-chromium system given in Fig. 2.

The lattice parameter for the  $\gamma$  phase of boundary composition tends to increase slightly above the true value when excessively large amounts of  $\alpha$  phase are present, probably on account of differential stresses set up during contraction in quenching. The boundary composition of the  $\gamma$  phase has accordingly been obtained by drawing horizontals through the points for duplex alloys lying nearest the lattice parameter/composition curve for the single-phase alloys. Above 950° C. the boundary of the  $\gamma$  phase, as determined by

TABLE II.—Compositions, Lattice Parameters, and Structures of Nickel-Chromium Binary Alloys.

Alloy No.	Composition, at.-%		Lattice Parameter, kX, at 20° C.						Phases Present
			Quenching Temperature					Slowly Cooled	
	Ni	Cr	1200° C.	1100° C.	1000° C.	900° C.	750° C.		
1	90.2	9.8	3.5271	...	3.5274	3.5274	3.5270	3.5273	$\gamma$ (face-centred cubic)
2	84.8	15.2	...	3.5327	...	...	3.5317	3.5315	
3	80.2	19.8	3.5387	...	3.5388	3.5386	3.5380	3.5374	
4	75.1	24.9	3.5448	3.5457	3.5455	3.5446	3.5437	3.5441	
5	70.2	29.8	3.5532	...	3.5521	3.5522	3.5518	3.5509	
6	65.2	34.8	3.5604	3.5602	3.5589	3.5594	3.5591	3.5582	
7	60.7	39.3	3.5689	3.5674	3.5660	3.5670	3.5646	3.5657	$\gamma + \alpha$
8	55.5	44.5	3.5758	3.5752	3.5732	3.5701	3.5646	3.5656	
59	52.9	47.1	...	...	3.5766	...	...	...	
9	50.2	49.8	3.5830	3.5810	...	3.5707	3.5649	3.5666	
30	40.7	59.3	3.5862	{	3.5823	3.5773	3.5721	3.5649	
					2.8688	2.8749	2.8759	2.8769	
31	29.9	70.1	3.5871	{	3.5850	3.5780	3.5742	3.5649	
					2.8694	2.8760	2.8762	2.8769	
293	26.1	73.9	...	...	...	...	...	...	
292	23.2	76.8	...	...	...	...	...	...	
291	22.7	77.4	...	...	...	...	...	...	
277	20.6	79.4	...	2.8719	2.8743	...	2.8771	...	
276	13.8	86.2	...	2.8724	2.8729	2.8767	2.8767	...	
274	11.0	89.0	...	2.8735	2.8747	2.8768	2.8771	...	
275	10.7	89.3	...	...	...	2.8768	2.8767	...	
273	5.3	94.7	...	2.8757	2.8766	2.8772	2.8776	...	
272	2.8	97.2	...	2.8772	...	2.8772	2.8774	...	
271	0	100	...	...	2.8784	2.8785	...	...	$\alpha$ (body-centred cubic)

ray examination were heat-treated at various temperatures for standard times and quenched. Lattice parameters were determined from X-ray Debye-Scherrer patterns taken with manganese  $K_{\alpha}$  radiation, which gives a clearly resolved (311)  $\alpha$ -doublet at a Bragg angle of approximately 78°. Alloy compositions, heat-treatment conditions, and lattice-parameter data are presented in Table II. The compositions are based on the chemical determination of the chromium content, and the nickel figures, obtained by difference, include the very small amount of impurity present.

Lattice parameter is plotted against composition for the  $\alpha$  and  $\gamma$  phases in Fig. 1, and the phase bound-

X-rays in the present investigation, approximates very closely to that of Jenkins *et al.*,<sup>2</sup> but at lower temperatures the solubility of chromium in nickel decreases rather more rapidly than they had estimated. This difference in boundary position is probably inherent in the methods of investigation. At low temperatures, the formation of small amounts of a second phase of dimensions large enough to be visible under the microscope frequently takes a considerable time, whereas the rate of precipitation, and hence the approach to equilibrium, is considerably accelerated in filings owing to the large degree of cold work absorbed in preparation. Furthermore, the lattice parameter of

\* Since the preparation of this paper, Bloom and Grant<sup>9</sup> have published a phase diagram of the nickel-chromium system showing a high-temperature form of chromium which

breaks down eutectoidally at 1180° C., but no supporting evidence for this has been found by the present authors.



the  $\gamma$  boundary is obtained by calculation and is not dependent on observing the presence of  $\alpha$  phase, which may exist in too small an amount or in too high a state of dispersion to be detected by its diffraction pattern or by means of the microscope. The consistency of the parameter values obtained from specimens quenched at 750° C. suggests that this point on the boundary has been established by the X-ray method with a high degree of precision.

One of the remarkable features of the lattice parameters of the  $\gamma$  phase is the closeness with which they approach the parameters of face-centred cubic nickel-iron binary alloys, almost as though iron and chromium had identical atomic radii when in solution in nickel. It will be noted that in the nickel-iron system, in the region of  $\text{Ni}_3\text{Fe}$ , which has a high initial magnetic permeability on account of its zero magnetostriction, there is a well-marked inflection in the lattice-parameter/composition curve, as if a small contraction of the lattice had occurred.<sup>10</sup> An almost identical inflection is found near  $\text{Ni}_3\text{Cr}$ , although in this case the alloys are non-magnetic even at the temperature of liquid nitrogen.

It is probable that the inflection is in some way connected with the tendency to form an ordered lattice. In the case of  $\text{Ni}_3\text{Fe}$ , Leech and Sykes<sup>11</sup> have shown the presence of superlattice lines in the X-ray-diffraction patterns of carefully annealed specimens, but even after very closely controlled heat-treatments it has not been possible to obtain powder patterns of  $\text{Ni}_3\text{Cr}$  in which the superlattice lines could be detected with certainty, although the ratio of main lattice lines to superlattice lines using manganese  $K_\alpha$  radiation should be 40:1. This may be due to the fact that fully-ordered anti-phase nuclei have not grown to a size sufficient for the correspondingly

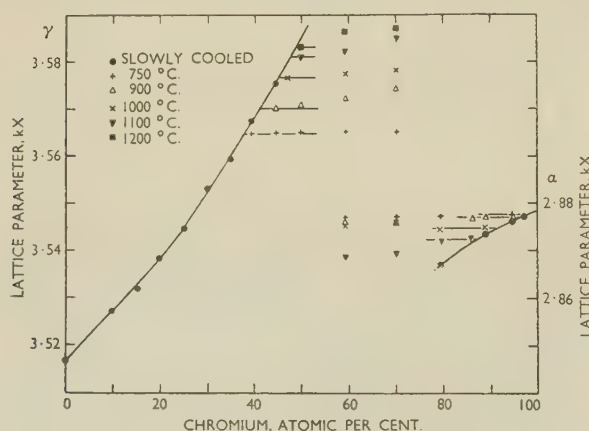


FIG. 1.—Lattice Parameter/Composition Curves for the  $\alpha$  and  $\gamma$  Phases in Nickel-Chromium Alloys.

sharpened superlattice reflections to be brought above the visibility level on the background of the diffraction pattern. In any event, powder patterns are much less sensitive than single-crystal photographs for indicating the presence of superlattice reflections and a diffraction pattern from a coarse-grained solid specimen

used in specific-heat determinations gave faint reflections which could be identified as superlattice lines. When a superlattice forms there is a marked tendency for the ordered alloy to have a somewhat lower lattice parameter than when disordered,<sup>12, 13</sup> and the same tendency in this direction is found in the

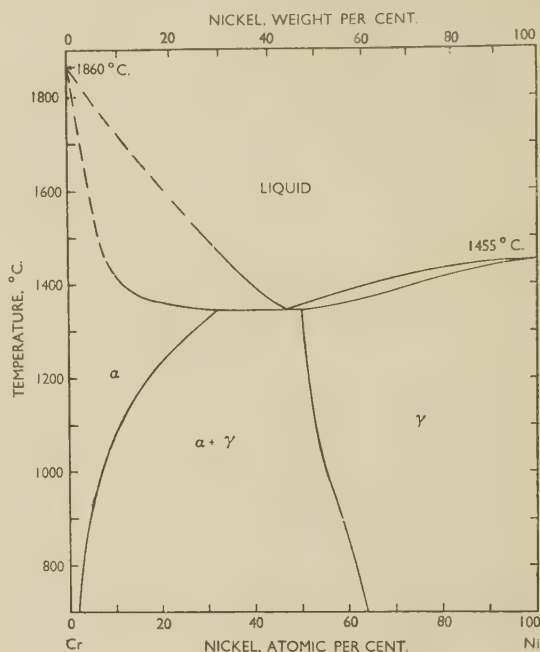


FIG. 2.—The Nickel-Chromium Phase Diagram.

case of  $\text{Ni}_3\text{Cr}$ , where the lattice parameter for the slowly cooled alloy is slightly lower than for the alloy quenched from a high temperature. Final X-ray proof of the tendency of  $\text{Ni}_3\text{Cr}$  to become ordered is given by the strong superlattice lines observed when as little as one-fifth of the chromium is replaced by aluminium.

**Magnetic Properties.**—The Curie temperature of nickel is rapidly lowered by the addition of chromium in solid solution. As shown by Marian,<sup>14</sup> 8.0 at.-% of chromium lowers the Curie point of nickel linearly from 358° C. to room temperature.

#### (b) Body-Centred Cubic Alloys of the $\alpha$ Phase

When the nickel content of binary nickel-chromium alloys falls below 20%, the melting point rises rapidly to that of chromium. The melting of these alloys in the induction furnace proved difficult, owing to the volatility of the chromium near its melting point and to its tendency to form a thin refractory oxide skin, which prevents the nickel from going into solution. Because of this, it was found more convenient to prepare all the chromium-rich alloys in the Kroll-type argon-arc furnace. To reduce inhomogeneity to a minimum, the alloys after melting were turned over on the water-cooled copper hearth and remelted, the process being repeated a number of times.

X-ray-diffraction patterns of the body-centred cubic chromium-rich alloys were taken with chromium

$K_\alpha$  radiation, which gives a useful high-order (211) reflection at  $77^\circ$ . Lattice parameters and compositions of the alloys are given in Table II. It will be noted that the replacement of chromium by nickel produces only a very small change in lattice parameter, which is again analogous to the small parameter changes observed in the body-centred cubic iron-rich alloys of the iron-nickel system,<sup>10, 15, 16</sup> except that in the latter case the addition of nickel leads to an increase in the iron parameter. The slight change in parameter of the  $\alpha$ -phase alloys, coupled with errors in measurement occasioned by the low ratio of line intensity to background in the diffraction patterns, together lead to appreciable errors in the derived values of the solubility limit for different temperatures. The position of the  $\alpha$ -phase boundary below  $1100^\circ\text{C}$ . is probably correct to within  $\pm 1.0$  at.-%, and is in good agreement with the boundary originally established by Jette *et al.*<sup>6</sup> by X-ray methods, but differs quite markedly from the later work of Jenkins.<sup>2</sup> It will be observed, however, that the present boundary fits smoothly on to the boundary established by Jenkins for temperatures above  $1200^\circ\text{C}$ . and accordingly, as the best compromise, Fig. 2 shows the boundary of the  $\alpha$  phase as determined by X-rays below  $1100^\circ\text{C}$ . and by micrographic methods above  $1200^\circ\text{C}$ .

### (c) The Tendency to $\sigma$ -Phase Formation

It has now been established that the  $\sigma$  phase found in the iron-chromium system at FeCr has its counterpart in many systems containing transition elements.<sup>17-21</sup> It is of interest to note, however, that to date there has been no report of a  $\sigma$ -phase structure occurring in the nickel-chromium system, although a theory of  $\sigma$ -phase formation put forward by Sully<sup>22</sup> predicts the occurrence of such a phase at about 70 at.-% chromium. An investigation of the chromium-cobalt-nickel system by Beck and Manly<sup>21</sup> has shown that at  $1200^\circ\text{C}$ . the  $\sigma$  phase occurring at CoCr extends deep into the ternary system as a long narrow tongue, until well over half the cobalt atoms are replaced by atoms of nickel with very little change in chromium content. This clearly indicates that nickel itself has a certain tendency to form a  $\sigma$  phase with chromium, which becomes strongly operative in the presence of a sufficient amount of cobalt.

A study of the shape of the  $\gamma$ -phase boundary at temperatures near the eutectic also reveals the tendency to form an intermediate phase. According to Le Chatelier's equation  $\log S = -L/RT + C$ , where  $S$  is the molecular fraction of alloying element,  $L$  the molal heat of solution,  $R$  the gas constant,  $T$  the absolute temperature, and  $C$  a constant of integration. Consequently, the composition of the phase boundary expressed as  $\log S$  should vary linearly with  $1/T$ . Any inflection in the curve in the region of the eutectic temperature indicates, according to Raynor and Wakeman,<sup>23</sup> a tendency towards compound formation due to a factor which appears to be electronic in character.

Plotting  $\log S$  against  $1/T$  for the newly determined  $\gamma$ -phase boundary, as in Fig. 3, does in fact give a well-defined kink in the region of the eutectic temperature, and closely resembles the results obtained by Raynor and Wakeman for the aluminium-silver system. Thus the tendency to form a  $\sigma$  phase is confirmed. It should be noted that the original boundary of Jenkins *et al.* has a rather different shape, which, on conversion to a  $\log S$  versus  $1/T$  plot, does not indicate a tendency to compound formation.

In accord with Sully's prediction that  $\sigma$  phase should form in the region of 70 at.-% chromium, three alloys containing 60, 70, and 80 at.-% chromium were lump-annealed at  $1250^\circ\text{C}$ ., the temperature increasing to  $1320^\circ\text{C}$ . over 24 hr., and quenched. Microspecimens and X-ray samples were then annealed for several

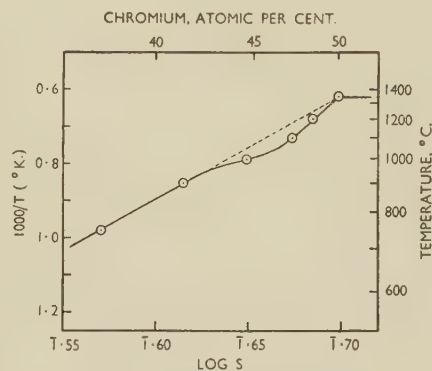


Fig. 3.—Plot of  $\log S$  Against  $1000/T$  for the  $\gamma$ -Phase Boundary of the Nickel-Chromium System.

hundred hours at temperatures between  $600^\circ$  and  $750^\circ\text{C}$ ., but the results were entirely negative, no phases other than  $\alpha$  and  $\gamma$ , as predicted by the equilibrium diagram, being found.

## 2. NICKEL-TITANIUM

The first diagram of the nickel-titanium system to be published was that of Vogel and Wallbaum,<sup>24</sup> who established the existence of an intermediate phase  $\text{Ni}_3\text{Ti}$  and determined the liquidus and solidus as far as 34 at.-% titanium. They found that the solubility of titanium in nickel was about 8 at.-% at  $1150^\circ\text{C}$ ., falling to 3.5 at.-% at  $750^\circ\text{C}$ . The compound  $\text{Ni}_3\text{Ti}$  was shown to exist only at the stoichiometric ratio, its structure being, according to Laves and Wallbaum,<sup>25</sup> close-packed hexagonal. An accurate determination has been made by the authors,<sup>26</sup> of the unit cell of  $\text{Ni}_3\text{Ti}$ , whose parameters were shown to be  $a = 2.5454$ ,  $c = 8.2900$  kX,  $c/a = 3.2569$ .

Wallbaum<sup>27</sup> has shown that, in addition to  $\text{Ni}_3\text{Ti}$ , a body-centred cubic phase with the CsCl-type of structure exists at  $\text{NiTi}$ , and a face-centred cubic phase at  $\text{NiTi}_2$ . The existence of these phases has been confirmed by Duwez and Taylor,<sup>28</sup> but the speculative extension of the phase diagram by Wallbaum to the titanium-rich end has not been substantiated by Long



and his co-workers,<sup>29, 30</sup> working on high-grade titanium-rich alloys containing up to 40% nickel. These latter investigators have shown that the melting point of titanium is considerably depressed by the addition of quite small amounts of nickel to a eutectic with 28.5 at.-% nickel at 960° C., rising again to

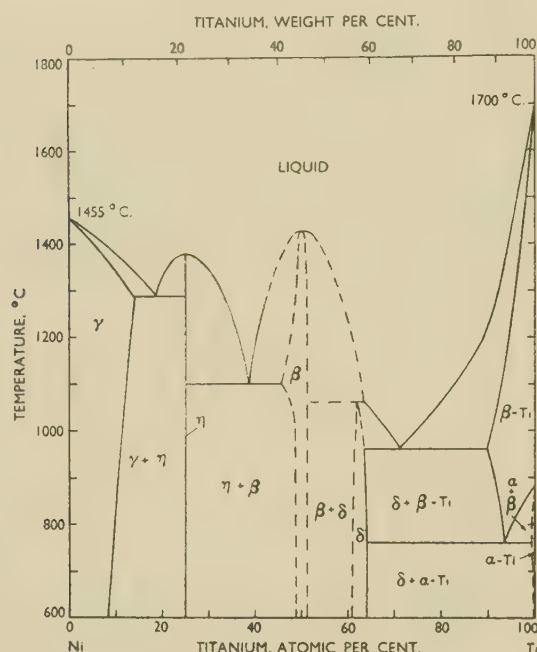


FIG. 4.—The Nickel-Titanium Phase Diagram.

1060° C. at a composition approximating to  $\text{NiTi}_2$ , where they found an intermediate phase,  $\delta$ , with a body-centred cubic structure. The high-temperature  $\beta$  form of titanium is shown to decompose eutectoidally at 760° C. into  $\alpha$ -titanium and the  $\delta$  phase.

The diagram is not in conformity with the experimental data, since many of the alloys did not obey the phase rule owing to the presence of minor impurities. A. D. McQuillan<sup>31</sup> has since shown that impurities of the type found in Kroll titanium, as used by Long, could modify the range over which the transformation from  $\alpha$ - to  $\beta$ -titanium takes place. Thus, extremely pure van Arkel titanium, made by thermal decomposition of titanium iodide, transforms quite sharply at 882° C., whereas Kroll titanium changes over the range 860°–960° C. This would cause titanium alloys likewise to transform over a temperature range and lead to difficulties in the interpretation of the experimental observations. It is of interest to note that the breakdown of  $\beta$ -titanium by a eutectoid reaction to  $\alpha$ -titanium and an intermediate phase, as tentatively proposed by Long for the nickel-titanium system, has since been shown to occur in the iron-titanium system explored by Werner<sup>32</sup> and in the chromium-titanium system described by M. K. McQuillan.<sup>33</sup> Hence it would appear that the tentative diagram derived by Long must be accepted for the time being, although the experimental results

presented indicate a need for a re-investigation using alloys made with van Arkel titanium.

A probable form of the complete phase diagram of the nickel-titanium system is shown in Fig. 4, in which the titanium-rich end proposed by Long is linked to the nickel-rich part of the diagram as determined by Vogel and Wallbaum, but with the position of the  $\gamma$  boundary suitably revised to accord with the results of X-ray and micrographic investigation described below.

#### (a) The Face-Centred Cubic $\gamma$ Phase

The work on nickel-rich alloys of the nickel-chromium-titanium system was originally based on the position of the  $\gamma$ -phase boundary given by Vogel and Wallbaum for the nickel-titanium system, but at an early stage it was discovered that their solubility limit for nickel was far too low. Accordingly, a series of nickel-titanium binary alloys was prepared, and the boundary of the  $\gamma$  phase determined from lattice-parameter measurements and confirmed by micro-examination. The composition, structure, and lattice parameters of these alloys are given in Table III and the lattice-parameter/composition relationship of the  $\gamma$ -phase alloys is plotted in Fig. 5. From these data, the boundary of the  $\gamma$  phase can be placed at 13.0 at.-% titanium at 1150° C., falling to 9.4 at.-% at 750° C., as indicated in the complete equilibrium diagram (Fig. 4).

The low solubility of nickel in titanium observed by Vogel and Wallbaum<sup>24</sup> is almost certainly due to their titanium, which was only 95% pure, as compared with the titanium used in the present investigation, which had a purity of 99.6%. The new position of the  $\gamma$ -phase boundary of the binary system conforms

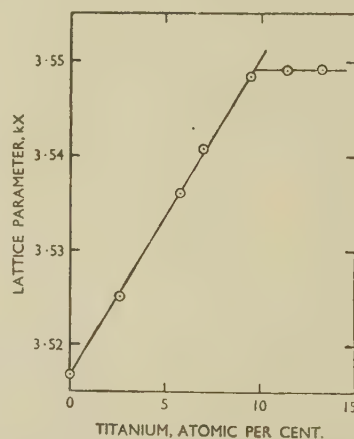


FIG. 5.—Lattice Parameter/Composition Curve for the  $\gamma$  Phase in Nickel-Titanium Alloys.

well with the results obtained on the more complex ternary nickel-chromium-titanium alloys. Metallographic examination of duplex alloys containing small amounts of  $\text{Ni}_3\text{Ti}$  showed that this phase occurs in the form of very thin plates lying in the octahedral planes of the  $\gamma$  matrix. This form of epitaxial growth is to be

expected, since the (001) planes of hexagonal  $\text{Ni}_3\text{Ti}$  correspond to the (111) planes of the face-centred cubic lattice of the nickel-rich solid solution and the interatomic distances on these planes are approximately equal.

**Magnetic Properties.**—A series of rough determinations carried out on  $\gamma$ -phase alloys quenched from  $1200^\circ\text{C}$ . indicate that the Curie point falls linearly with additions of titanium, from  $358^\circ\text{C}$ . at 0% to  $0^\circ\text{C}$ . at 9.2 at.-% titanium. This is in agreement with the observations of Marian<sup>14</sup> and confirms the

of the system has had to be based solely on the phase diagrams of the contiguous binary systems. The primary objects of the present investigation were to determine the extent of the nickel solid solution,  $\gamma$ , and the range over which this is in equilibrium with the intermetallic compound  $\text{Ni}_3\text{Ti}$ ,  $\eta$ . A further point of interest was the effect on the  $\text{Ni}_3\text{Cr}$  superlattice of replacing part of the chromium by titanium.

The compositions, lattice parameters, and structures of the ternary alloys are given in Table IV. In the first instance the general lay-out of the phase diagram was

TABLE III.—Compositions, Lattice Parameters, and Structures of Nickel-Titanium Alloys.

Alloy No.	Composition, at.-%		Phases Present			Structure	Lattice Parameter, kX, at 20° C.	Magnetic Curie Point, °C.	Reference
			Quenching Temperature						
	Ni	Ti	1150° C.	1000° C.	750° C.				
...	100	...	γ	γ	γ	} f.c.c. {	3.5168	358	...
152	97.4	2.6	γ	γ	γ		3.5252	...	...
153	94.2	5.8	γ	γ	γ		3.5363	...	...
154	93.0	7.0	γ	γ	γ		3.5409	85	...
155	90.5	9.5	γ	γ	γ		3.5485	— 12	...
156	88.6	11.4	γ	γ	γ + η		3.5492	— 86	...
157	86.8	13.2	γ + η	γ + η	γ + η	...	3.5493	...	...
28	75	25	Ni <sub>3</sub> Ti (η)			h.c.p.	a = 2.5454 c = 8.2900	...	Taylor and Floyd <sup>26</sup>
191	50	50	NiTi (β)			CsCl	3.005	...	...
...	37	63	δ			b.c.c.	?	...	Long <sup>30</sup>
...	...	...	NiTi <sub>2</sub>			f.c.c.	11.310	...	Duwez and Taylor <sup>23</sup>
...	...	...	α-Ti (below 882° C.)			h.c.p.	a = 2.9504 c = 4.6833	...	Halla <sup>37</sup>
...	...	...	β-Ti (above 882° C.)			b.c.c.	3.32 (at 900° C.)	...	...

position of the  $\gamma$  boundary established in the present investigation.

### 3. CHROMIUM-TITANIUM

Since the  $\gamma$  and  $\eta$  phases of the nickel-chromium-titanium system are in equilibrium with the chromium-rich  $\alpha$  solid solution of the binary chromium-titanium system, it is necessary to include a brief description of this latter system. M. K. McQuillan<sup>33</sup> has shown that chromium and titanium are completely soluble in each other at temperatures between  $1360^\circ$  and  $1400^\circ\text{C}$ ., and that below  $1360^\circ\text{C}$ . the solid solution breaks down into a mixture of  $\text{Cr}_3\text{Ti}_2$  and a body-centred cubic solid solution based on either chromium or  $\beta$ -titanium. The  $\beta$ -titanium undergoes a eutectoid transformation at about  $700^\circ\text{C}$ . to form  $\text{Cr}_3\text{Ti}_2$  and  $\alpha$ -titanium.

## IV.—THE NICKEL-CHROMIUM-TITANIUM SYSTEM

No reference to previous investigations of the nickel-chromium-titanium system has been found in the literature, so that the work on the nickel corner

established from the X-ray-diffraction patterns given by powder samples slowly cooled from  $900^\circ\text{C}$ . to room temperature over a period of about 14 days. Comparison of the results obtained on X-ray samples and micro-specimens annealed at  $750^\circ$  and  $850^\circ\text{C}$ ., respectively, showed that the slow-cooling heat-treatment gave equilibrium conditions corresponding to about  $800^\circ\text{C}$ . Subsequently, the movement of phase boundaries as the temperature was raised to  $1000^\circ$  and  $1150^\circ\text{C}$ . was determined by micro-examination of selected alloys. The ternary diagram corresponding to equilibrium at  $750^\circ\text{C}$ . is given in Fig. 6, and superimposed isothermal sections of the phase diagram corresponding to  $750^\circ$ ,  $1000^\circ$ , and  $1150^\circ\text{C}$ . in Fig. 7. A typical series of X-ray-diffraction patterns covering the portion of the ternary system under investigation is shown in Fig. 8 (Plate XCIII).

At  $1150^\circ\text{C}$ . the face-centred cubic  $\gamma$  solid solution based on nickel extends to 47.8 at.-% chromium along the nickel-chromium edge of the diagram. It will take titanium into solution in amounts increasing from 5.5 at.-% at 37 at.-% chromium to 13 at.-% in the chromium-free nickel-titanium alloys. The extent of the phase field decreases with temperature in accordance



with the boundary movements of the binary systems. The change with temperature in the solubility of titanium in the  $\gamma$  phase is approximately the same at all chromium contents. For example, at 25 at.-% chromium the  $\gamma$  phase will dissolve 6.5 at.-% titanium at 1150°, 4.7 at.-% at 1000°, and 2.7 at.-% at 750° C.

the lattice parameter of the  $\gamma$  phase at the boundary remains almost constant, and is such that there is a close match of atomic spacing with the  $\text{Ni}_3\text{Ti}$  structure. The lattice parameter of the  $\gamma$  phase at the boundary lies within the range 3.548–3.56 kX, depending on the temperature, giving an interatomic distance in the

TABLE IV.—Compositions, Lattice Parameters, and Structures of Nickel–Chromium–Titanium Ternary Alloys.

Alloy No.	Composition, at.-%			Phases Present			Lattice Parameter of $\gamma$ -phase, kX, at 20° C.		Alloy No.
				Quenching Temperature			Slowly Cooled	Quenched from 750° C.	
	Ni	Cr	Ti	1150° C.	1000° C.	750° C.			
120	90.3	7.2	2.5	...	...	$\gamma$	3.5277	...	120
51	87.4	10.1	2.5	...	...	$\gamma$	...	...	51
123	85.6	11.7	2.7	...	...	$\gamma$	3.5305	...	123
127	80.2	17.1	2.7	...	...	$\gamma$	3.5404	...	127
52	75.6	22.1	2.3	...	...	$\gamma$	...	...	52
121	90.7	4.7	4.6	...	...	$\gamma$	3.5325	...	121
124	85.5	10.3	4.2	...	...	$\gamma$	3.5373	...	124
128	80.8	14.4	4.8	...	...	$\gamma$	3.5404	...	128
122	90.2	3.9	5.9	...	...	$\gamma$	3.5366	...	122
125	86.1	7.6	6.3	...	...	$\gamma$	...	...	125
160	90.4	1.9	7.7	...	...	$\gamma$	...	...	160
131	75.5	20.0	4.5	$\gamma$	$\gamma$	$\gamma + \eta$	3.5507	3.5501	131
136	73.0	22.9	4.1	$\gamma$	$\gamma$	$\gamma + \eta$	...	...	136
138	71.3	24.5	4.2	$\gamma$	$\gamma$	$\gamma + \eta$	3.5545	...	138
137	70.4	26.5	3.1	...	...	$\gamma + \eta$	...	...	137
142	69.1	27.4	3.5	$\gamma$	$\gamma$	$\gamma + \eta$	3.5574	...	142
143	66.4	31.1	2.5	$\gamma$	$\gamma$	$\gamma + \eta$	3.5586	3.5598	143
129	80.4	12.5	7.1	$\gamma$	$\gamma$	$\gamma + \eta$	3.5449	...	129
132	75.4	17.6	7.0	$\gamma$	$\gamma + \eta$	$\gamma + \eta$	3.5513	...	132
139	71.9	21.9	6.2	$\gamma$	$\gamma + \eta$	$\gamma + \eta$	3.5539	...	139
161	85.8	5.1	9.1	$\gamma$	$\gamma$	$\gamma + \eta$	...	...	161
93	83.5	6.7	9.8	$\gamma$	$\gamma$	$\gamma + \eta$	...	...	93
130	81.1	9.8	9.1	$\gamma$	$\gamma + \eta$	$\gamma + \eta$	...	...	130
133	76.0	14.8	9.2	$\gamma + \eta$	$\gamma + \eta$	$\gamma + \eta$	3.5495	3.5503	133
140	71.2	19.8	9.0	$\gamma + \eta$	$\gamma + \eta$	$\gamma + \eta$	3.5570	...	140
126	84.8	2.5	12.7	$\gamma$	$\gamma + \eta$	$\gamma + \eta$	3.5468	...	126
53	81.2	5.4	13.4	$\gamma + \eta$	$\gamma + \eta$	$\gamma + \eta$	...	...	53
134	76.2	12.5	11.3	$\gamma + \eta$	$\gamma + \eta$	$\gamma + \eta$	3.5488	3.5504	134
141	72.6	14.7	12.7	$\gamma + \eta$	$\gamma + \eta$	$\gamma + \eta$	3.5547	...	141
135	76.4	5.0	18.6	$\gamma + \eta$	$\gamma + \eta$	$\gamma + \eta$	3.5480	3.5480	135
166	63.0	35.5	1.5	$\gamma$	$\gamma$	$\gamma + a$	...	...	166
144	63.8	34.1	2.1	$\gamma$	$\gamma$	$\gamma + \eta + a$	...	3.5598	144
167	60.6	37.0	2.4	$\gamma$	$\gamma$	$\gamma + \eta + a$	3.5642	...	167
55	65.5	29.8	4.7	$\gamma$	$\gamma + \eta$	$\gamma + \eta + a$	3.5617	...	55
168	61.5	34.5	4.0	$\gamma$	$\gamma + \eta$	$\gamma + \eta + a$	...	...	168
172	56.1	39.4	4.5	$\gamma + a$	$\gamma + \eta + a$	$\gamma + \eta + a$	...	...	172
163	63.0	29.9	7.1	$\gamma + \eta$	$\gamma + \eta + a$	$\gamma + \eta + a$	...	...	163
169	60.9	32.3	6.8	$\gamma + \eta$	$\gamma + \eta + a$	$\gamma + \eta + a$	...	...	169
164	66.1	25.0	8.9	$\gamma + \eta$	$\gamma + \eta$	$\gamma + \eta + a$	3.5628	...	164
170	61.2	30.0	8.8	$\gamma + \eta$	$\gamma + \eta + a$	$\gamma + \eta + a$	...	...	170
173	56.0	35.3	8.7	$\gamma + \eta + a$	$\gamma + \eta + a$	$\gamma + \eta + a$	3.5674	...	173
165	66.4	19.9	13.7	$\gamma + \eta$	$\gamma + \eta + a$	$\gamma + \eta + a$	...	...	165
171	61.6	24.9	13.5	$\gamma + \eta + a$	$\gamma + \eta + a$	$\gamma + \eta + a$	...	...	171
94	71.3	5.7	23.0	...	...	$\gamma + \eta + a$	3.5645	...	94

Beyond this boundary lies a two-phase region in which  $\gamma$  coexists with the hexagonal  $\eta$  phase based on  $\text{Ni}_3\text{Ti}$ .

Lattice parameters of the nickel solid solution were measured from X-ray photographs of many of the alloys given the slow-cooling heat-treatment or annealed at 750° C. From these the isoparametric contours shown in Fig. 6 were obtained. It is of interest to observe that up to about 25 at.-% chromium

octahedral planes of 2.51–2.52 kX, while the interatomic distance in the basal planes of  $\text{Ni}_3\text{Ti}$  is 2.545 kX. It appears likely that the equilibrium between the two phases is conditioned by the tendency of the two structures to grow epitaxially on a common plane in which the interatomic distances are equal, so that there is a minimum of strain at the interface and therefore a state of lowest potential energy. It may well be that at high temperatures the interatomic

distances are still more nearly equal, diverging on cooling owing to changes in the composition of the  $\gamma$  phase as  $\text{Ni}_3\text{Ti}$  precipitates, and to differences in the coefficients of thermal expansion of the coexisting structures. The difference in interatomic distance at room temperature is very small and corresponds to lattice faults occurring at intervals of about 100 atoms.

Similar matching of interatomic distances of phases in equilibrium with each other is to be found in other alloy systems. For instance, in the iron-nickel-

$\text{CuAl}_2$ , from the solid solution is preceded by the formation of the intermediate  $\theta'$  phase with a structure fitting closely that of the matrix.<sup>36</sup>

The two-phase ( $\gamma + \eta$ ) region is almost triangular in shape, since, as far as can be ascertained,  $\text{Ni}_3\text{Ti}$  takes into solution practically no nickel, chromium, or titanium. The variations in microstructure of the alloys in this phase field are shown in Figs. 9-13 (Plate XCIV). Near the  $\gamma/(\gamma + \eta)$  boundary, the  $\eta$  phase appears in the form of very thin plates lying on the octahedral planes of the  $\gamma$  phase (Fig. 9), while at

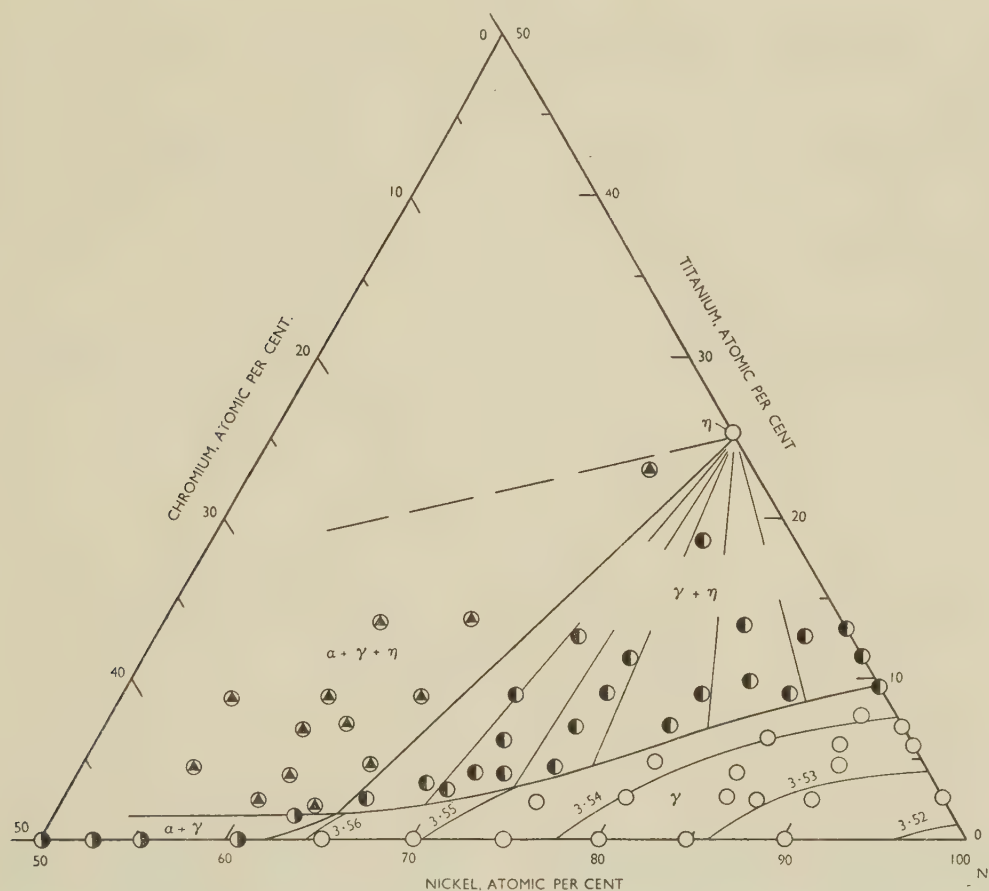


FIG. 6.—The Nickel-Chromium-Titanium Phase Diagram: Isothermal Section for 750° C.

aluminium system there is a miscibility gap in the body-centred cubic  $\beta$ -phase region, alloys in which break down into two  $\beta$  phases, one ordered, the other disordered, with equal lattice parameters.<sup>34</sup> Again, in the copper-nickel-aluminium system, there is coincidence of the lattice parameters of the conjugate solid solutions of alloys in the face-centred cubic ( $\alpha + \alpha'$ ) phase field, the two phases being differentiated by the existence of the  $\alpha'$  superlattice.<sup>35</sup> The tendency for matrix and precipitating phases in age-hardening systems to have the same interatomic distance on a common plane has also been observed; for example, in the aluminium-4% copper alloy the precipitation of  $\theta$ ,

rather higher titanium contents the plates are thicker and more regular in form (Fig. 10). In alloys consisting of approximately equal proportions of the  $\gamma$  and  $\eta$  phases, the plates of  $\eta$ , while still forming a Widmanstätten pattern, assume a still more massive form, as illustrated in Fig. 11. Where there is a preponderance of  $\eta$  in the structure, it occurs as large primary columnar crystals with an infilling of  $\gamma$ , from which fine needles of  $\eta$  have precipitated. This structure is represented in Fig. 12, and again in Fig. 13 at a lower magnification to show the presence of the  $\gamma + \eta$  eutectic remaining from the as-cast condition. It seems likely from the microstructures that



the  $(\gamma + \eta)$  eutectic of the nickel-titanium system links up with the  $(\gamma + \alpha)$  eutectic of the nickel-chromium system.

At the chromium-rich end of the  $\gamma$ -phase field, the boundary moves towards the nickel corner as the temperature falls, the change being about the same as in the binary nickel-chromium system. Beyond this boundary a side of the  $(\alpha + \gamma + \eta)$  three-phase triangle lies close to the nickel-chromium edge of the composition triangle, in accordance with M. K.

detected, even when present in quite small amounts, in the diffraction patterns of the three-phase alloys provided there is not too much  $\eta$  phase present.

Only the side of the  $(\alpha + \gamma + \eta)$  ternary triangle adjacent to the  $(\gamma + \eta)$  two-phase field has been accurately located, although the approximate positions of the other two sides are indicated in Figs. 6 and 7. A few alloys on the titanium-rich side of the  $(\alpha + \gamma + \eta)$  field have been examined, but it has not been possible to identify all the phases satisfactorily,

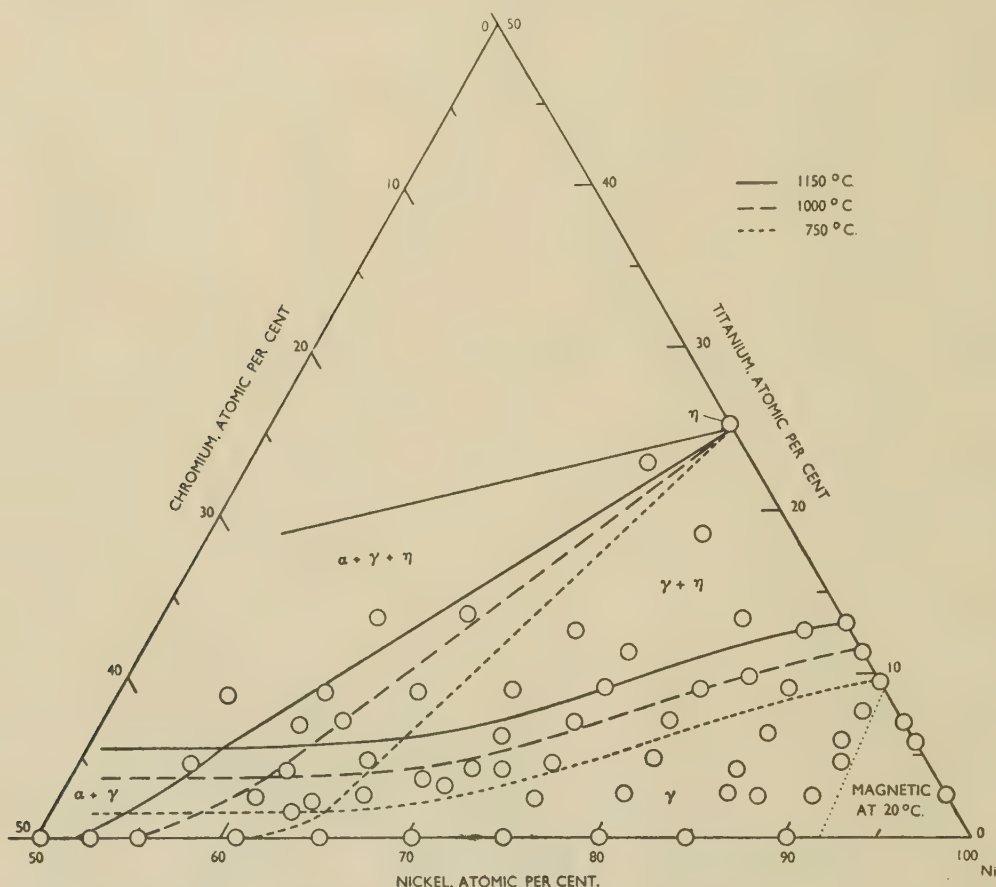


FIG. 7.—The Nickel-Chromium-Titanium Phase Diagram: Isothermal Sections for 750°, 1000°, and 1150° C.

McQuillan's<sup>33</sup> findings on the low solubility limit of titanium in the  $\alpha$ -chromium phase of the chromium-titanium system.

Over a wide range of temperature, the boundary between the  $(\gamma + \eta)$  and  $(\alpha + \gamma + \eta)$  regions is a straight line pivoting round  $\text{Ni}_3\text{Ti}$ , and its position can easily be located by the incidence of  $\alpha$  phase in the alloys. The actual detection of  $\alpha$  phase in the microstructures of alloys containing  $\eta$  is not easy, since both the  $\alpha$  and  $\eta$  phases are very resistant to attack by etching reagents as compared with the  $\gamma$  phase. However, the  $\alpha$  phase is slightly different in colour from the  $\eta$  phase, and the use of a monochromatic bluefilter enables it to be identified with certainty as the lighter areas in Fig. 14 (Plate XCIV). It can also be

and this portion of the diagram awaits further investigation.

**Magnetic Properties.**—The behaviour of the Curie point of nickel with chromium and with titanium in solution has already been mentioned. The boundary separating magnetic from non-magnetic nickel-chromium-titanium alloys at room temperature is shown in Fig. 7, and extends across the composition triangle as a straight line joining 8 at.-% chromium, 92 at.-% nickel to 9 at.-% titanium, 91 at.-% nickel, approximately.

#### ACKNOWLEDGEMENT

The authors wish to thank The Mond Nickel Company, Ltd., for permission to publish this paper.

## REFERENCES

1. A. Taylor and H. Sinclair, *Proc. Phys. Soc.*, 1945, **57**, 108.
2. C. H. M. Jenkins, E. H. Bucknall, C. R. Austin, and G. A. Mellor, *J. Iron Steel Inst.*, 1937, **136**, 193p.
3. M. Hansen, "Der Aufbau der Zweistofflegierungen". 1936: Berlin (Julius Springer).
4. Y. Matsunaga, *Kinzoku no Kenkyu*, 1929, **6**, 207; *Japan Nickel Rev.*, 1933, **1**, 347.
5. S. Nishigori and M. Hamasumi, *Kinzoku no Kenkyu*, 1929, **6**, 219; *Sci. Rep. Tōhoku Imp. Univ.*, 1929, [i], **18**, 491.
6. E. R. Jette, V. H. Nordstrom, B. Queneau, and F. Foote, *Trans. Amer. Inst. Min. Met. Eng.*, 1934, **111**, 361.
7. Z. Yano, *Rikwagaku Kenkyū-jo Ihō*, 1940, **19**, 110; *Japan Nickel Rev.*, 1941, **9**, 17.
8. A. Taylor and R. W. Floyd, to be published.
9. D. S. Bloom and N. J. Grant, *J. Metals*, 1951, **3**, 1009.
10. A. J. Bradley, A. H. Jay, and A. Taylor, *Phil. Mag.*, 1937, [vii], **23**, 545.
11. P. Leech and C. Sykes, *Phil. Mag.*, 1939, [vii], **27**, 742.
12. A. J. Bradley and A. H. Jay, *J. Iron Steel Inst.*, 1932, **125**, 339p.
13. W. Betteridge, *J. Inst. Metals*, 1948-49, **75**, 559.
14. V. Marian, *Ann. Physique*, 1937, [xi], **7**, 502.
15. E. A. Owen and A. H. Sully, *Phil. Mag.*, 1941, [vii], **31**, 314.
16. E. A. Owen and E. L. Yates, *Proc. Phys. Soc.*, 1937, **49**, 307.
17. H. J. Goldschmidt, *Research*, 1951, **4**, 343.
18. G. J. Dickinson, A. M. B. Douglas, and W. H. Taylor, *J. Iron Steel Inst.*, 1951, **167**, 27; *Nature*, 1951, **167**, 192.
19. C. W. Tucker, Jr., *Acta Cryst.*, 1951, **4**, 425.
20. P. Duwez and S. R. Baen, *A.S.T.M. Symposium on the Nature, Occurrence, and Effects of Sigma Phase*, 1950, 48.
21. P. A. Beck and W. Manly, *Trans. Amer. Inst. Min. Met. Eng.*, 1949, **185**, 354.
22. A. H. Sully, *Nature*, 1951, **167**, 365.
23. G. V. Raynor and D. W. Wakeman, *Phil. Mag.*, 1949, [vii], **40**, 404.
24. R. Vogel and H. J. Wallbaum, *Arch. Eisenhüttenwesen*, 1938, **12**, 299.
25. F. Laves and H. J. Wallbaum, *Z. Krist.*, 1939, **101**, 78.
26. A. Taylor and R. W. Floyd, *Acta Cryst.*, 1950, **3**, 285.
27. H. J. Wallbaum, *Arch. Eisenhüttenwesen*, 1941, **14**, 521.
28. P. Duwez and J. L. Taylor, *Trans. Amer. Inst. Min. Met. Eng.*, 1950, **188**, 1173.
29. J. R. Long, E. T. Hayes, D. C. Root, and C. E. Armantrout, *U.S. Bur. Mines Rep. Invest.*, No. **4463**, 1949.
30. J. R. Long, *Metal Progress*, 1949, **55**, 364.
31. A. D. McQuillan, *J. Inst. Metals*, 1950-51, **78**, 249.
32. H. W. Worner, *ibid.*, 1951, **79**, 173.
33. M. K. McQuillan, *ibid.*, 1951, **79**, 379.
34. A. J. Bradley and A. Taylor, *Proc. Roy. Soc.*, 1938, [A], **166**, 353; *J. Inst. Metals*, 1940, **66**, 53.
35. A. J. Bradley and H. Lipson, *Proc. Roy. Soc.*, 1938, [A], **167**, 421.
36. G. D. Preston, *Phil. Mag.*, 1938, [vii], **26**, 855.
37. F. Halla, "Kristallchemie und Kristallphysik metallischer Werkstoffe", 2nd edn. 1951: Leipzig (J. A. Barth).

## Discussion

## Structural Changes Accompanying Creep in a Tin-Antimony Alloy

By W. BETTERIDGE and A. W. FRANKLIN

(*Journal*, this vol., p. 147.)

Mr. R. C. GIFFKINS,\* B.Sc., A.I.M. (Member): There are one or two points concerning the interpretation of micrographs upon which I should like to comment. The boundary broadening illustrated in Figs. 7, 8, and 9 (Plate XXVII), has been noted here in several metals, and on the basis of my own observations with aluminium and lead alloys, I question the interpretation of the dark-ground illumination photograph. The fact that the boundary shows bright with this illumination does not necessarily indicate a steep slope. This is because the dark-ground image is formed from the diffracted light only, the direct beam being stopped-out, so that bright parts of the image correspond to features having microscopic detail capable of causing diffraction. Similarly, the rumpling within grains could still be steep and yet not be revealed by dark-ground illumination, provided the local changes in curvature were nowhere great enough to cause diffraction effects. The arguments put forward by the authors on the evidence of Fig. 9 would be correct for oblique illumination, although even then diffraction effects could give misleading results.

There is a suggestion of a fine structure in the boundary in Fig. 8, running more or less lengthwise along the boundary,

and I have observed such structures in many similarly broadened boundaries of aluminium, zinc, and lead alloys, and confirmed their presence with phase-contrast and multiple-beam interferometry. The latter technique shows that a boundary such as *C* in Fig. 7, which appears dark with ordinary illumination and bright with dark-ground illumination, may be inclined with respect to the level grain at an angle of only 6°.

The second point concerns the displacement of scratches at boundaries, &c., which it is stated must be due to movements in the plane of the surface of the specimen. Whilst this is so for large displacements, small ones can be produced by a combination of movements consisting of (a) the production of a step, and (b) the tilting of the whole group of grains concerned, so that the specimen is viewed obliquely. Thus, although the interpretation of the displacements shown is probably justified, the possibility of this other effect should be noted, particularly when the examination is made at a high magnification.

The explanation given for the strain marks from grain-boundary triple-points (Fig. 15 (c) (p. 149) and Fig. 7) is very interesting; I have noticed such marks on many specimens,

\* Baillieu Laboratory, University of Melbourne, Australia.



but have not appreciated their significance; Wyon and Crussard\* also refer to them in a recent paper. I find on re-examining multiple-beam interferograms of such features that a small step is often present at the strain mark.

Mr. E. C. W. PERRYMAN, † M.A., A.I.M. (Member): The paper is extremely interesting in that the authors show clearly that viscous movement between two grains can lead to localized strain within the grain that lies ahead of the grain-boundary plane upon which movement has taken place. I have observed a similar phenomenon in an aluminium-10% zinc alloy. This alloy after solution-treatment decomposes at room temperature, with the formation at the grain boundaries of zinc-rich zones and a new solid solution in equilibrium at the temperature of ageing.‡ In this condition the material is subject to intercrystalline fracture, if stressed in air. If, however, the rate of straining is increased, the fracture becomes transcrystalline. It was considered, therefore, that the soft new solid-solution zones at the grain boundary allowed grain-boundary slip to take place, this process ultimately leading to intercrystalline fracture. A piece of this alloy which had been aged at room temperature was electrolytically polished and bent, after which it was observed that one edge of the new solid solution had become black (see Fig. A, Plate XCV), probably because of grain-boundary slip perpendicular to the plane shown in the figure. In addition to this, localized strain marks can be seen running from the point of intersection of the grain boundaries. Another example of this phenomenon is shown in Fig. B (Plate XCV). These strain marks were never seen to run completely across the grain, always stopping at a short distance from the point of intersection of the boundaries.

A rather similar effect has been found by Schulz and Wassermann,§ who show a photograph of an aluminium-6.3% zinc-1.2% magnesium alloy solution-treated and aged at 200° C. Strain, as evidenced by precipitation on slip planes, was produced during quenching from the solution-treatment temperature. In addition, the photograph shows precipitation at the grain boundaries, and a continuation of these boundaries into adjacent grains. It is not impossible that the stresses set up during quenching were sufficient to cause some grain-boundary slip which in turn gave rise to localized strain in the adjacent grains, forming a localized area at which precipitation could take place. Can Dr. Betteridge and Mr. Franklin say whether the localized strain marks were in general parallel to slip lines and also whether they increased in length as the magnitude of grain-boundary slip increased? It must be remembered that, when viewing the surface, two dimensions only, are explored, and it is possible that the grains in which these localized strain marks are seen are in fact wedge-like, being very thin at the point of intersection of the grain boundaries. Do the authors think that such grains are responsible for this localized strain becoming visible?

Another example showing the presence of stress concentrations produced during grain-boundary movements occurred in some experiments I carried out on a  $\beta$ -brass. At elevated temperatures such brasses break with an intercrystalline fracture and it is thought that viscous flow at the grain boundaries takes place. Fig. C (Plate XCV) shows cracks formed away from the fracture in a specimen tested at 400° C. At the base of the crack, which lies at about 45° to the direction of the applied stress, there is a region containing new recrystallized grains. Evidently the plastic deformation at the base of this crack was sufficient to cause the material to recrystallize at the temperature of testing.

The AUTHORS (*in reply*): It is satisfactory to find that the strain marks we noted are to be observed in suitably strained samples of a number of different alloys.

With regard to the interpretation of the dark-ground illumination photograph, features revealed by this technique could be due either to diffracted light or to reflected light, and in the latter case the reflecting surface must be within a suitable range of angles of tilt. Since all the grain boundaries are not shown up, as they should be if they were diffracting centres, we decided that those visible must be attributed to reflection. On the other hand, since no cell boundaries are revealed these cannot be diffracting, nor can they be tilted sufficiently to fall within the reflecting range. It is surely not likely that all cell boundaries are tilted beyond the reflecting range. We consider, therefore, that the interpretation of Fig. 9 which we put forward is correct.

Mr. Giffkins's proposed alternative explanation of the observed displacement of scratches is certainly possible for very small displacements.

Nevertheless, a consideration of the depth of focus of the objective used and the observed length of the grain boundary which is in focus, enables a maximum possible angle of tilt of the whole group of grains to be established, from which the maximum scratch displacement explicable by Mr. Giffkins's mechanism can be derived. It is found that the observed displacements are about 100 times as great as the maximum possible by the mechanism proposed by Mr. Giffkins.

It is unfortunately not possible to answer with any certainty Mr. Perryman's question as to whether the localized strain marks were parallel to slip directions, since under the conditions of testing employed for the tin-antimony alloys, the slip lines were usually very irregular in direction. Neither can we say whether the length of the strain marks increased with progressive grain-boundary flow, since repeated observations during the course of a test were not made. It is not thought likely that the localized strain markings are to be associated with wedge-shaped grain sections which are very thin at the point of intersection of the boundaries, since too many examples were observed. It may well be, however, that the effect only occurs at the surface, where there is less restraint than in the body of the metal.

\* G. Wyon and C. Crussard, *Rev. Mét.*, 1951, **48**, 121.

† Research Investigator Aluminium Laboratories, Ltd., Kingston, Ont., Canada; formerly at British Non-Ferrous Metals Research Association, London.

‡ E. C. W. Perryman and J. C. Blade, *J. Inst. Metals*, 1950, **77**, 263.

§ E. Schulz and G. Wassermann, *B.I.O.S. Rep. Gp2/HEC* 3758.

# THE CONSTITUTIONAL DIAGRAM OF THE CHROMIUM-TUNGSTEN SYSTEM \*

1384

By H. T. GREENAWAY,† B.Met.E.

## SYNOPSIS

The chromium-tungsten phase diagram has been investigated by metallographic, X-ray, and thermal analysis. The liquidus rises, slowly at first and then more rapidly, from the freezing point of chromium towards that of tungsten. Above 1500° C. the solid alloys consist of a continuous series of solid solutions; below 1500° C. the single phase breaks down into two limited solid solutions, which thus form a solubility gap in the diagram.

## I.—INTRODUCTION

THE chromium-tungsten diagram was first studied by Isida, Asada, and Higashimura,<sup>1</sup> who used metallographic, X-ray, and thermal analysis. They found the system to contain a eutectic at approximately 35 wt.-% tungsten; their alloys, however, were prepared by aluminothermic methods and contained considerable amounts of aluminium, thus making their results doubtful. Kubaschewski and Schneider,<sup>2</sup> using electrolytic chromium and reduced tungsten, found, by means of X-rays, complete miscibility of the two metals in the solid state. The liquidus curve was stated to pass through a minimum at 30 wt.-% tungsten,  $1720^{\circ} \pm 50^{\circ}$  C.

The most accurate work published to date is that of Trzebiatowski, Ploszek, and Lobzowski,<sup>3</sup> who, by using X-rays, found a two-phase region in the diagram below 1430° C. They did not investigate the system at higher temperatures, however.

The present paper gives the constitutional diagram as determined by metallographic and X-ray examination of the whole range of alloys, and by thermal analysis of alloys containing up to 44 wt.-% tungsten.

## II.—EXPERIMENTAL PROCEDURE AND RESULTS

### 1. METALS USED

The chromium used was a special electrolytic grade prepared in the Aeronautical Research Laboratories, using a high bath temperature and a high current density. Spectrographic analysis showed it to contain no metallic impurities. The total oxygen content averaged 0.06 wt.-% and the nitrogen content less than 0.001%. The preparation of this material has been described earlier.<sup>4</sup> Chromium powder was made from the lump material by grinding in a chromium-plated steel ball-mill containing chromium-plated steel balls.

The tungsten powder used was prepared by reducing very pure tungstic acid with hydrogen, and its purity was approximately 99.99%. Spectrographic

examination showed slight traces of copper, calcium, silicon, chromium, and zinc.

### 2. DETERMINATION OF THE LIQUIDUS CURVE

Thermal analysis of alloys containing up to 44 wt.-% tungsten was carried out using the apparatus and technique previously described.<sup>4</sup> A beryllia crucible and an alumina thermocouple sheath were used for alloys containing up to 15 wt.-% tungsten. The melting points of alloys containing more than 15% tungsten were found to be too high for alumina ware to be used. Beryllia is unsuitable for the sheath material<sup>4</sup> (owing to contamination of the couple), and hence magnesia ware was used. A new technique for its preparation was developed. This consisted of slip casting magnesia into double-weight paper extraction thimbles, as is done in normal slip casting into plaster moulds. The paper thimble was then burnt off the magnesia shape during the firing operation. Magnesia was found to be very suitable both for sheaths and crucible.

At least two cooling curves were obtained for each alloy. Heating curves were also taken in some cases. The liquidus values obtained for each alloy were within the accuracy of the calibration of the molybdenum/tungsten thermocouple, namely  $\pm 10^{\circ}$  C. Alloys were analysed chemically at the end of each determination. The results obtained were:

Tungsten, wt.-%	Liquidus Temp., °C.
0	1845
6.0	1845
10.0	1849
16.8	1853
25.7	1872
34.3	1922
44.0	1987

These values have been used in the constitutional diagram given in Fig. 7. Solidus values could not be definitely determined from the cooling curves. The small slope of the liquidus indicates that the differences between liquidus and solidus temperatures for the above alloys are small; hence the solidus arrest could not be differentiated from the normally larger liquidus arrest.

\* Manuscript received 19 November 1951.

† Aeronautical Research Laboratories, Department of Supply, Melbourne, Australia.



### 3. PREPARATION OF ALLOYS FOR DETERMINATION OF SOLID PHASE BOUNDARIES

Alloys containing up to 60 wt.-% tungsten were prepared from lump chromium and tungsten powder by melting in a tungsten-arc furnace made to the design of H. W. Worner of the Baillieu Laboratory, Melbourne University. A similar type of furnace was recently described by Geach and Summers-Smith.<sup>5</sup> The argon atmosphere used was purified immediately before the melting operation by melting an additional piece of chromium-tungsten alloy placed on the hearth at some distance from the metals to be alloyed. In order to ensure uniform distribution of the two metals, the alloy button was inverted and quickly remelted several times. Above 60 wt.-% tungsten the loss of chromium by volatilization (due to the very high melting points of such alloys) was too great to produce a reasonably uniform non-porous melt. However, it was noted that the furnace was capable of melting pure tungsten quite satisfactorily. Alloys containing nominally 5, 10, 15, 20, 30, 40, 50, and 60 wt.-% tungsten and weighing 15 g. were melted in this way. Alloys containing 70, 80, 90, 95, 98, and 99 wt.-% tungsten were prepared by powder methods. Compacts  $1\frac{1}{2} \times \frac{3}{8} \times \frac{3}{8}$  in. were pressed at 12 tons/in.<sup>2</sup>, then sintered for 3 hr. at 1600° C. in an induction furnace, using a purified hydrogen atmosphere.

### 4. METALLOGRAPHIC AND HARDNESS INVESTIGATIONS

Metallographic examination of the melted alloys showed them to be dendritic single-phase materials, with very marked coring. They were homogenized by induction heating in a hydrogen atmosphere at 1600° C. for 6 hr. This produced homogeneous single-phase alloys in all cases. The sintered alloys were found to be homogeneous single-phase solid solutions, and hence did not require further annealing. Chemical analyses were carried out on all alloys at this stage.

The phase diagram below 1600° C. was then investigated by metallographic examination of small portions of each of these alloys annealed in argon at various temperatures and water-quenched. New samples were used for each temperature investigated. The times of heating, at each temperature, which were found necessary to attain equilibrium were:

Temp. of Anneal, °C.	Time of Anneal, hr.
1375	50
1250	260
1150	400
1000	460

Annealing was done in a controlled-temperature platinum-wound furnace, fitted with a gas-tight alumina tube. A static atmosphere of purified argon was used, and as an extra safeguard against contamination of the alloys, they were covered with a layer of chromium powder. A thin interlayer of alumina prevented sintering of the chromium powder on to the specimens. After these treatments, the alloys had a thin contaminated skin, but otherwise were unaffected by oxygen and nitrogen attack.

Metallographic examination, carried out on the centre portions of these alloys, showed that a two-phase region existed in the phase diagram and established its approximate position. Figs. 1 and 2 (Plate XCVI) show typical microstructures of alloys in the single- and two-phase regions. It will be seen that the tungsten-rich phase precipitates in the chromium-rich solid solution in a form resembling a eutectic. The specimens were etched electrolytically in a 10% potassium ferricyanide, 10% potassium hydroxide aqueous solution, with 2 V. across the electrodes.

The position of the phase boundary around the maximum of the solubility gap (in the region of 1500° C.) was obtained by metallographic examination of small samples of alloys vacuum-annealed at various temperatures and water-quenched in the furnace described earlier.<sup>6</sup> In this apparatus the alloy was supported by a platinum/platinum-rhodium thermocouple and heated by radiation from two electrically

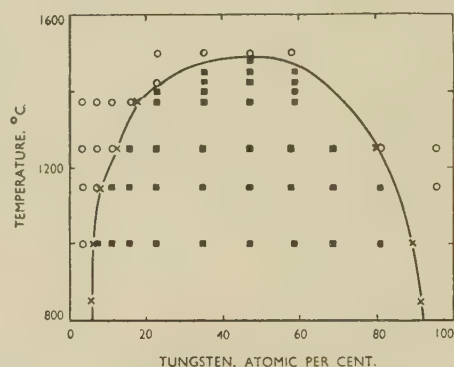


FIG. 3.—The Two-Phase Region of the Cr-W System.

KEY.  
 ○ Single-phase alloys } as determined by X-ray and metallo-  
 ■ Two-phase alloys } graphic methods.  
 × Phase boundaries as determined by X-ray methods.

heated molybdenum strips. The whole was contained in an evacuated, water-cooled jacket. Quenching was carried out by a stream of water which was allowed to impinge directly on the alloy at the end of the annealing treatment; hence it was more drastic than that given to the alloys annealed as previously described. A rapid quench is essential in the determination of flat or almost flat phase boundaries, since any temperature drop before water-quenching makes a larger difference in the determined position of this type of boundary than it does in steep boundaries. Moreover, the high temperature at the top of the solubility gap would be expected to result in relatively rapid rates of reaction.

The metallographic results are given in Fig. 3, together with the X-ray results described later. Hardness tests were carried out on the centre portions of the metallographic specimens which had been prepared by melting. The results are given in Table I.

### 5. X-RAY INVESTIGATIONS

X-ray investigations were carried out to establish the exact position of the two-phase region. Debye-

Scherrer photographs were first taken on powder samples of the range of alloys homogenized at 1600° C. The results given in Fig. 4 show that a complete

TABLE I.—Hardness Determinations.

Tungsten, wt.-%	Vickers Diamond Pyramid Hardness No.			
	6 hr. at 1600° C.	260 hr. at 1250° C.	400 hr. at 1150° C.	460 hr. at 1000° C.
19.9	370	414	418	450
30.1	447	507	505	552
40.2	508	562	575	577
51.4	557	602	573	575

series of solid solutions exists at this temperature. The system was then investigated at lower temperatures in a similar manner to that described for the metallographic examination. The alloys were annealed in the powder form where possible, because of

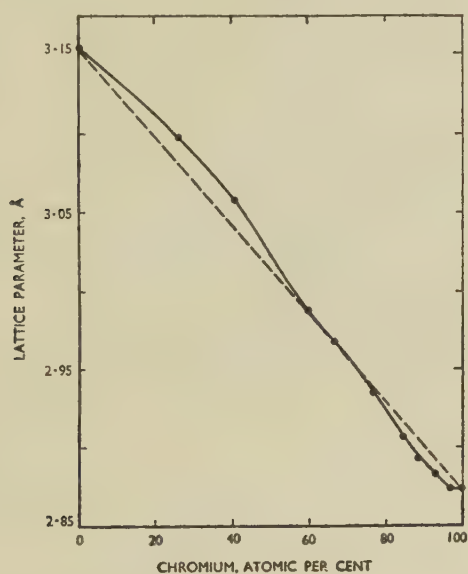


FIG. 4.—Lattice Parameters of Chromium-Tungsten Alloys.

the possibility of lattice straining when alloys are powdered after annealing and of the claim that annealing is more rapid in the powder form.<sup>7</sup>

Below 1000° C. clear silica can be used for annealing and is suitably gas-tight; hence two series of alloys were ground in a percussion mortar, sealed under vacuum in clear silica tubes, and annealed at 1000° and 850° C. for 500 and 3000 hr., respectively. These long annealing times were found to be necessary to obtain a satisfactory X-ray photograph. Their lattice parameters were then measured, using a Bradley-type 19-cm. camera and Cr  $K_{\alpha}$  radiation.

The lack of a suitably gas-tight refractory and the extremely rapid rate of attack of nitrogen and oxygen on the alloys made annealing of powders undesirable above 1000° C. Portions of the lump samples annealed above 1000° C. for metallographic work were therefore used for X-ray lattice-parameter determina-

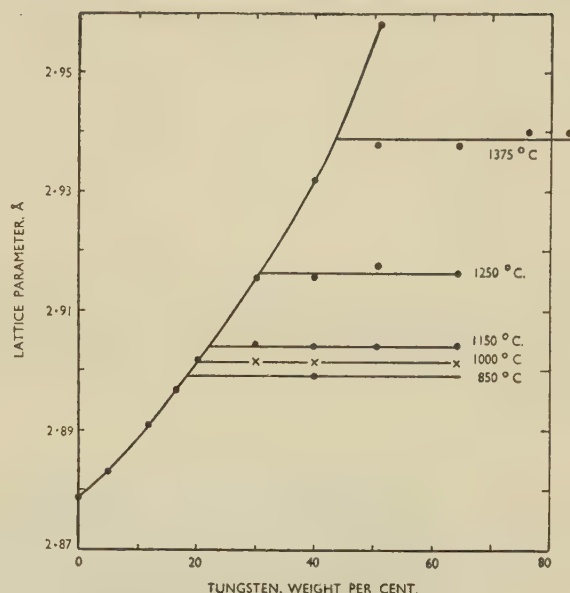


FIG. 5.—Lattice-Parameter Determinations on Chromium-Rich Chromium-Tungsten Alloys.

tions. The grain-size of the sintered alloys (tungsten-rich) was sufficiently small to give satisfactory X-ray photographs of solid alloys in a back-reflection flat-plate camera, using copper  $K_{\alpha}$  radiation. The melted alloys (up to 60% tungsten) were coarse grained and would not give a suitable X-ray photograph in the solid form; they were therefore lightly ground in a percussion mortar, and the powders photographed satisfactorily in a back-reflection flat-plate camera using chromium  $K_{\alpha}$  radiation. Stress-relieving of these ground powders was found to have no effect on the lattice-parameter measurements, and hence was not normally carried out.

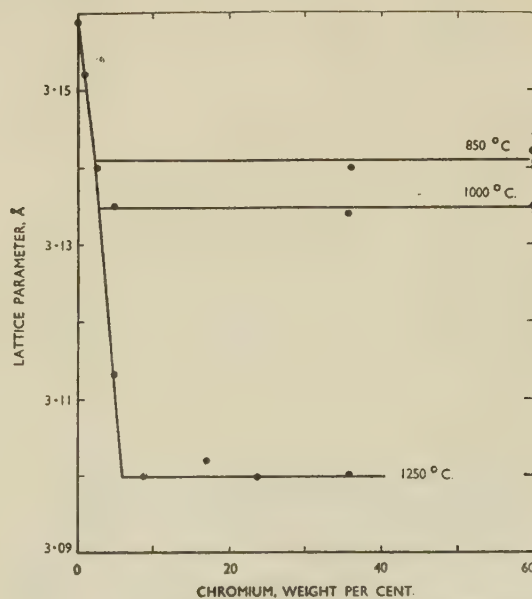


FIG. 6.—Lattice-Parameter Determinations on Tungsten-Rich Chromium-Tungsten Alloys.



The lattice parameters obtained have been plotted in Figs. 5 and 6. The following phase-boundary positions were obtained from these results:

Temp., °C.	Chromium-Rich Tungsten, at.-%	Tungsten-Rich Tungsten, at.-%
1375	17.8	...
1250	11.5	81.0
1150	7.8	...
1000	6.6	90.0
850	5.8	91.8

The metallographic determination of the top of the two-phase region was checked by X-ray photographs taken on the metallographic specimens. The results agreed with those previously obtained. Fig. 3 shows the two-phase region as determined by X-rays.

#### IV.—CONSTITUTIONAL DIAGRAM AND DISCUSSION

The chromium-tungsten constitutional diagram, as determined in this work, is given in Fig. 7. It is of the

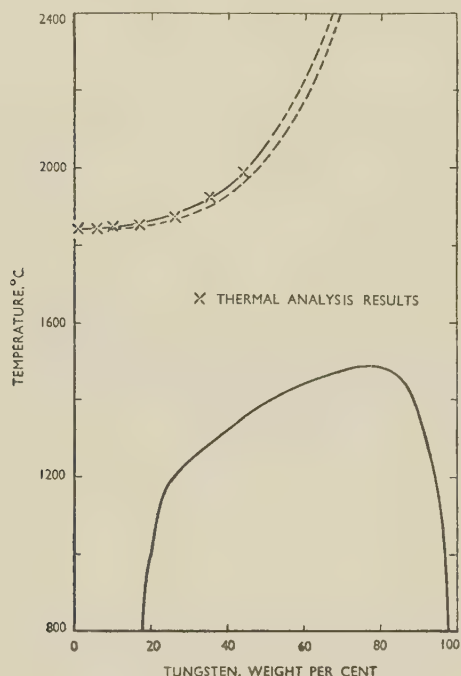


Fig. 7.—The Constitutional Diagram of the Cr-W System.

type to be expected from the lattice structure and dimensions of the parent metals. Hume-Rothery<sup>8</sup> has put forward the hypothesis that metals of the

same crystal structure having atomic diameters differing by less than 14% should form considerable, or a complete series of, solid solutions. Chromium and tungsten fall just within this limit, and a complete series of solid solutions has been found at higher temperatures. The fact that the "size-factor" is close to the limit of 14% in this case is consistent with the observed breakdown into two solid solutions.

The thermal-analysis results do not agree with those of the earlier workers,<sup>1,2</sup> who found a minimum in the liquidus at about 35 wt.-% tungsten. No such minimum was found in the present work, the liquidus rising, slowly at first, from the melting point of chromium towards that of tungsten. During metallographic examination it was noticed that alloys containing 20–40% tungsten appeared to be more prone to attack by nitrogen than were pure chromium and the alloys outside this range. Hence it is likely that the minimum observed by earlier workers at about 35% tungsten is attributable to a lowering of the freezing point of such alloys by nitrogen contamination. It is also possible that the "eutectic" appearance of the two-phase microstructures led Isida, Asada, and Higashimura<sup>1</sup> to believe that a eutectic existed in the system.

The position of the two-phase region agrees reasonably well with that obtained by Trzebiatowski *et al.*<sup>3</sup> Fig. 4 shows that the lattice parameters of alloys homogenized at 1600° C. deviate slightly from Vegard's linear law, to an extent normally found in solid-solution alloy systems.

The hardness values show that a portion of the system is of the age-hardening type, in that alloys containing more than 19.9 wt.-% tungsten show increased hardness when annealed at 1250° C. and below, after being quenched from 1600° C., while the 19.9% alloy shows hardening at 1000° C. only. It is probable that the duplex alloys investigated are in the over-aged condition, and that they could be further hardened by suitable heat-treatment.

#### ACKNOWLEDGEMENTS

This work was carried out as part of the high-temperature metals programme of the Aeronautical Research Laboratories, Department of Supply. The author's thanks are due to the Chief Scientist of the Department for permission to publish this paper. The X-ray work was carried out by N. F. Dewsnap of these laboratories, to whom acknowledgement is gratefully made.

#### REFERENCES

1. S. Isida, H. Asada, and S. Higashimura, *Rep. Aeronaut. Research Inst., Tokyo Imp. Univ.*, 1938, **13**, 195.
2. O. Kubaschewski and A. Schneider, *Z. Elektrochem.*, 1942, **48**, 671.
3. W. Trzebiatowski, H. Ploszek, and H. Lobzowski, *Analyt. Chem.*, 1947, **19**, 93.
4. H. T. Greenaway, S. T. M. Johnstone, and M. K. McQuillan, *J. Inst. Metals*, 1951–52, **80**, 109.
5. G. A. Geach and D. Summers-Smith, *Metallurgia*, 1950, **42**, 153.
6. M. K. McQuillan, *J. Inst. Metals*, 1951, **79**, 379.
7. E. A. Owen and D. P. Morris, *ibid.*, 1949–50, **76**, 145.
8. W. Hume-Rothery, "The Structure of Metals and Alloys" (*Inst. Metals Monograph and Rep. Series No. 1*), p. 60. London: 1950.

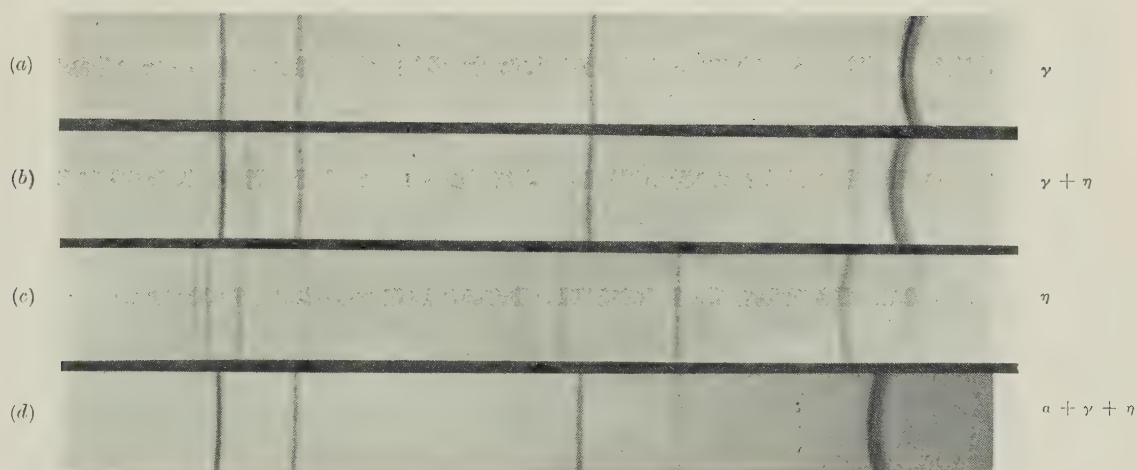


FIG. 8.—X-Ray-Diffraction Patterns of Alloys, Slowly Cooled from 900° C. Mn  $K_{\alpha}$  radiation.

(a) No. 128. 80.8/14.4/4.8 Ni-Cr-Ti.

(b) No. 133. 76.0/14.8/9.2 Ni-Cr-Ti.

(c) No. 28. 74.7/25.3 Ni-Ti.

(d) No. 172. 56.1/39.4/4.5 Ni-Cr-Ti.



## MICROSTRUCTURES OF NICKEL-CHROMIUM-TITANIUM ALLOYS.

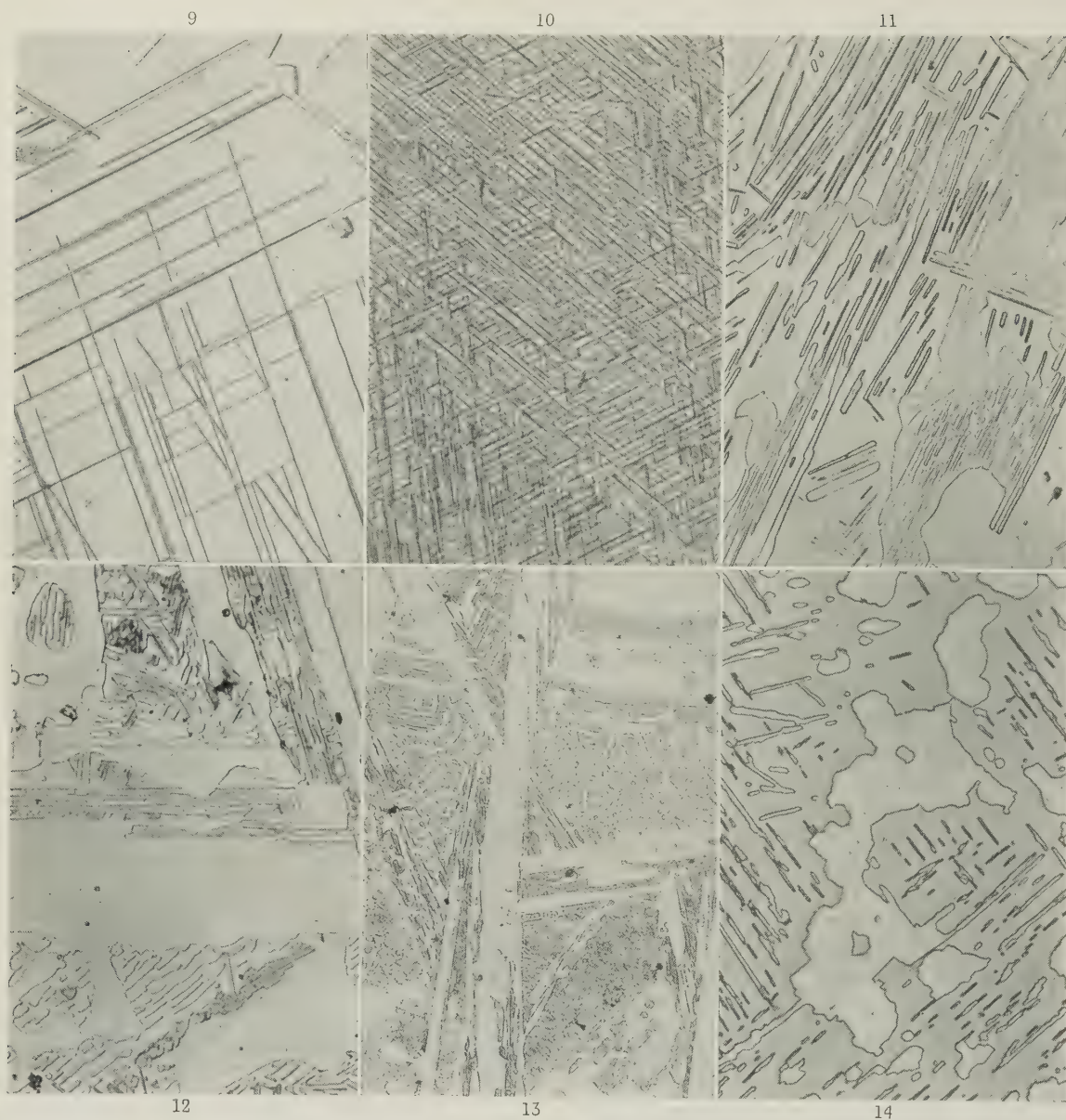


FIG. 9.—No. 126. 84.8/2.5/12.7 Ni-Cr-Ti. 1000° C.  $\gamma + \eta$ .  $\times 500$ .  
 FIG. 10.—No. 139. 71.9/21.9/6.2 Ni-Cr-Ti. 1000° C.  $\gamma + \eta$ .  $\times 500$ .  
 FIG. 11.—No. 141. 72.6/14.7/12.7 Ni-Cr-Ti. 1150° C.  $\gamma + \eta$ .  $\times 500$ .  
 FIG. 12.—No. 135. 76.4/5.0/18.6 Ni-Cr-Ti. 850° C.  $\gamma + \eta$ .  $\times 500$ .  
 FIG. 13.—As Fig. 12. Primary  $\eta$  in  $\gamma + \eta$  eutectic.  $\times 100$ .  
 FIG. 14.—No. 173. 56.0/35.3/8.7 Ni-Cr-Ti. 1150° C.  $\alpha + \gamma + \eta$ .  $\times 500$ .

FIGS. 9-13.—Etched electrolytically in 5% HF, 10% glycerine.  
 FIG. 14.—Etched electrolytically in saturated oxalic acid.



FIG. A.—Al-10% Zn Alloy Aged at Room Temperature, Electropolished, and Bent.  $\times 1500$ .

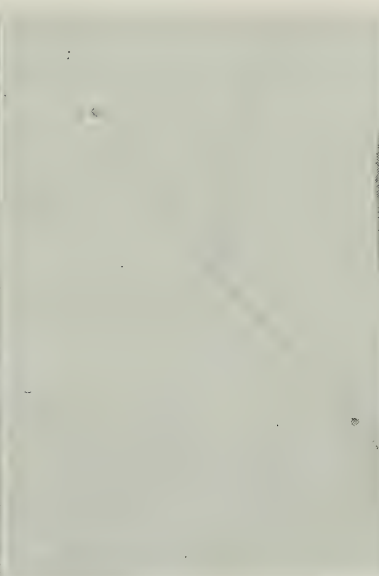


FIG. B.—As Fig. A.  $\times 500$ .

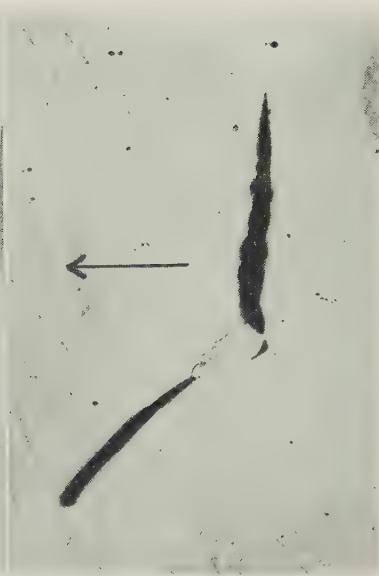


FIG. C.— $\beta$ -Brass Fractured at  $400^{\circ}\text{C}$ .  $\times 200$ . Arrow shows direction of applied stress.





FIG. 1.—51.4% Tungsten Alloy Annealed at 1600° C. for 6 hr. Single solid solution.  $\times 250$ .

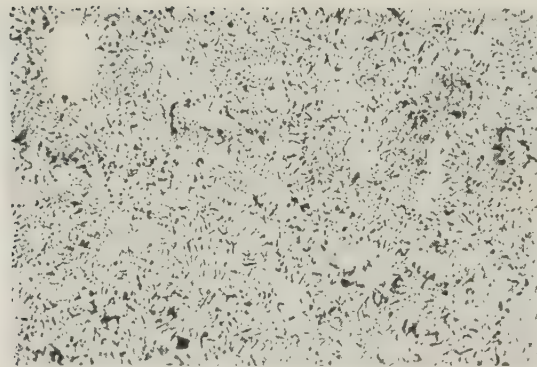


FIG. 2.—51.4% Tungsten Alloy Annealed at 1250° C. for 260 hr. Two solid solutions.  $\times 250$ .

Both etched electrolytically in alkaline potassium ferri cyanide.

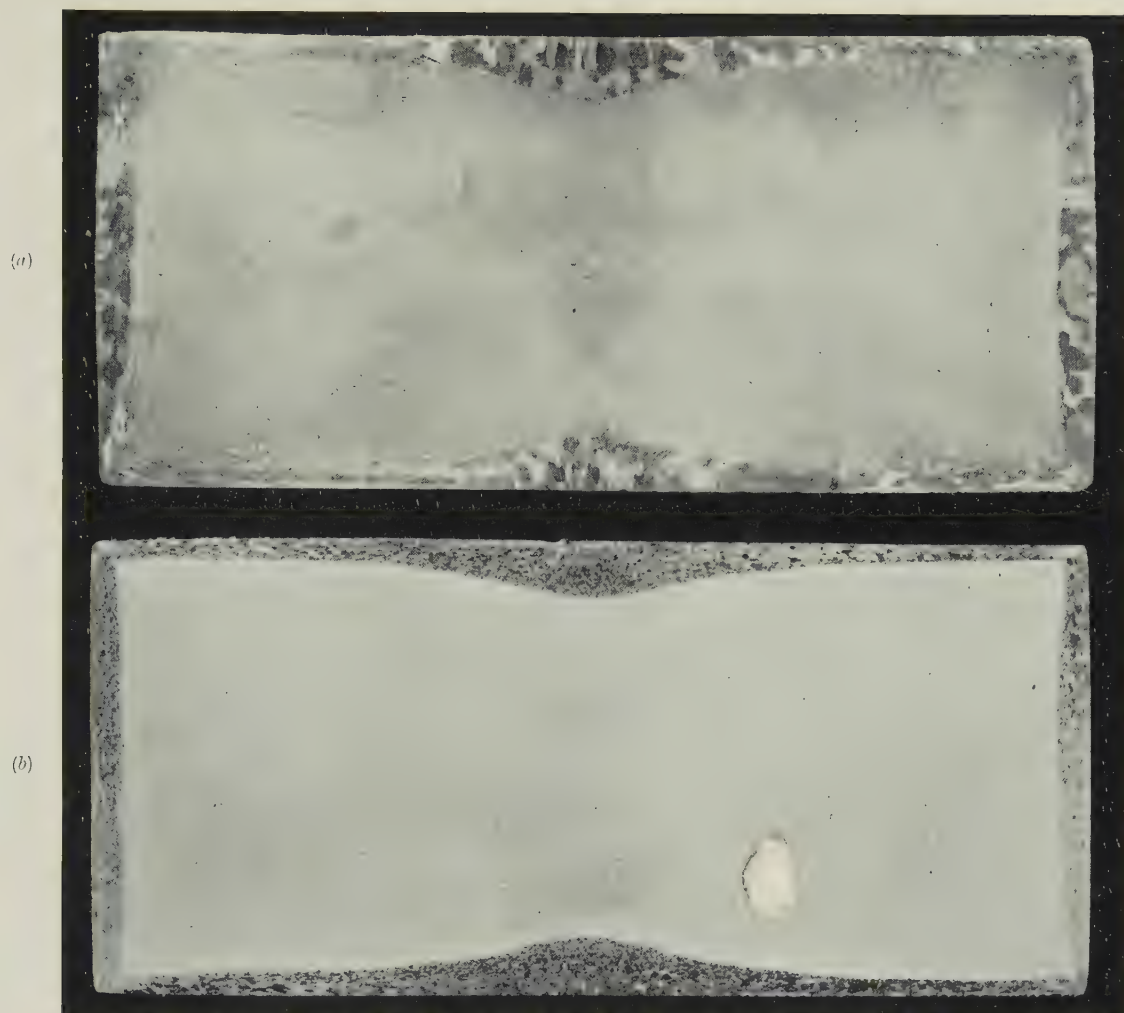


FIG. 6.—Macrostructure of FR Alloy (a) Without and (b) With 0.27% Zirconium. Solution-treated 29 min. in a salt bath at 505° C., followed after an interval of 52 sec. by quenching into water at 41° C. Approx.  $\times 1$ .

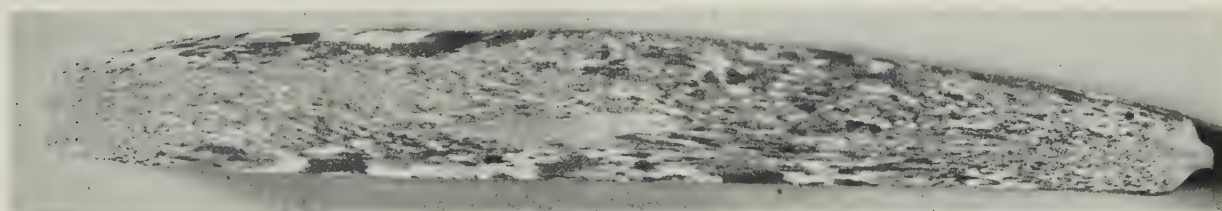


FIG. 7.—Macrostructure of Typical Airscrew Blade in Ordinary FR Alloy. Approx.  $\times 0.8$ .





FIG. 8.—Macrostructure of Double-Flanged Bar in FR Alloy Containing 0.22% Zirconium + 0.24% Manganese, Showing Fine Uniform Grain-Size. Approx.  $\times 0.6$ .

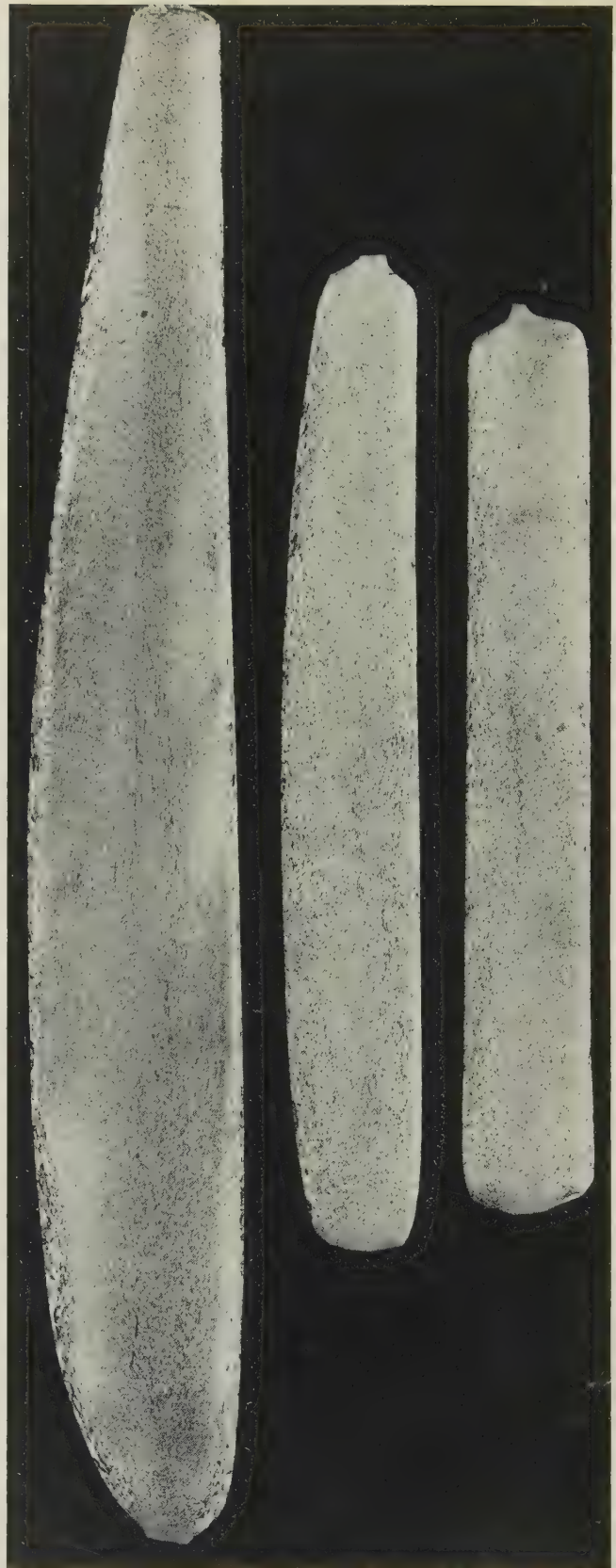


FIG. 9.—Macrostructure of Finished Airscrew Blades in FR Alloy Containing 0.22% Zirconium + 0.24% Manganese, Showing Fine Uniform Grain-Size, with Border of Slightly Larger Grains. Approx.  $\times 1$ .

# THE EFFECT OF ZIRCONIUM ON THE PROPERTIES AND STRUCTURE OF SUPERDURALUMIN, WITH PARTICULAR REFERENCE TO FORGINGS\*

1385

By M. TOURNAIRE,† MEMBER, and M. RENOARD,‡ MEMBER

## SYNOPSIS

Superduralumin A-U4 GI (Duralumin FR) is frequently used in France for high-strength forgings. However, these forgings, particularly those of large size, are susceptible to quenching cracks and in addition, like forgings in ordinary Duralumin, they show considerable variations in grain-size in different parts of the same section.

In the course of researches aimed at rendering forged Superduralumin less liable to quenching cracks, it has been found that if the manganese content of the alloy is replaced, wholly or partly, by 0.25% zirconium (it is impossible to add more than 0.25%), forgings are obtained whose mechanical properties are in no way inferior but which have a remarkably fine and uniform grain-size. This advantage, valuable in itself, is not the only one resulting from the addition of zirconium, for the new alloy can be cast, by the semi-continuous method, into very large billets with less risk of fissures than with ordinary Superduralumin, and it can be forged with greater ease.

## I.—INTRODUCTION

IN France the high-strength alloy Superduralumin (Duralumin FR) usually has the composition: copper  $4.40 \pm 0.20$ , magnesium  $1.60 \pm 0.20$ , manganese  $0.65 \pm 0.10$ , silicon  $< 0.30$ , iron  $< 0.50\%$ , remainder aluminium. As quenched and aged, this alloy, which is practically identical with the American alloy 24S, gives excellent properties in the form of bars, extrusions, sheet, and strip, namely, 0.2% proof stress 28–45, tensile strength 45–62 kg./mm.<sup>2</sup>, and elongation 25–10%.

The alloy is also used for forgings, especially for airscrew blades, though it had disadvantages for this purpose, as the forging operation is somewhat difficult and quenching is apt to cause intercrystalline surface cracks, especially in regions of relatively large grain-size. Their formation is promoted by surface defects and by a solution-treatment temperature of 500° C. or over. Normally these cracks are averted by quenching from below 500° C. (at 490°–495° C.) and by allowing a short interval to elapse before the quench (20–60 sec., according to the size of the forging). Nevertheless, quenching alloy FR is a delicate operation, and inadequate control may lead to heavy rejects.

One of the factors that render the quenching temperature critical is the presence in the alloy of the ternary eutectic  $\text{Al} + \text{CuAl}_2 + \text{Cu}_2\text{Mg}_2\text{Al}_5$ , which

melts at about 500° C., but it is clearly impossible to remove this without completely altering the composition of the alloy. Another factor that promotes quenching cracks in forgings is the formation of large grains at the surface, and sometimes also in the interior. It is not easy to avoid these large grains by controlling the working conditions, and it was decided therefore to introduce a grain-refining element in the alloy.

To a certain extent manganese has the desired effect, raising the recrystallization temperature and increasing the critical degree of cold working, but its influence is inadequate, at any rate in forgings. The elements known to refine the as-cast structure of aluminium and its alloys almost all belong to the transition group, namely, titanium, zirconium, vanadium, molybdenum, and tungsten, of which the first two appear to be the most efficacious.

Although refinement of the cast structure does not, *a priori*, necessarily lead to a refined structure on recrystallization, this has proved to be the case when using zirconium. This metal was preferred to titanium because, according to previous work, it reduces the tendency to intercrystalline cracking in certain alloys, and it was thought that, if this were so with alloy FR, it would diminish the number of quench cracks.

Tests on extruded bars had shown that zirconium could entirely replace manganese in alloy FR without

\* Manuscript received 2 August 1951.

† Director of Research, Compagnie Générale du Duralumine et du Cuivre, Paris.

‡ Head of Research Laboratory, Compagnie Générale du Duralumin et du Cuivre, Rive-de-Gier (Loire).

§ These figures relate to the longitudinal direction, the lowest strength corresponding to quasi-isotropic, recrystallized products, and the highest to markedly anisotropic, unrecrystallized ones.



any loss in properties. In this connection reference may be made to the well-known effect of manganese on the mechanical properties of Duralumin and Superduralumin extrusions. In unpublished work by one

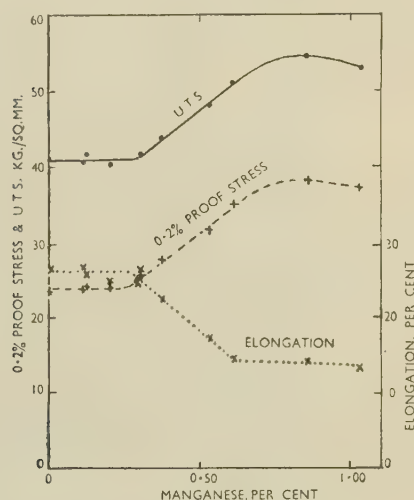


Fig. 1.—Variation with Manganese Content of the Mechanical Properties of Extruded 20-mm.-dia. Bars of Normal FR Alloy in the Quenched and Aged Condition.

Composition: Cu 4.25, Fe 0.15, Mg 1.50, Si 0.15, Mn 0.1–1%, Al remainder.

of the authors (M. T.), the mechanical properties of 20-mm.-dia. bars, quenched from 495° to 500° C., have been determined as a function of manganese content (Fig. 1). It will be seen that the effect of manganese begins to be appreciable only at a content approaching 0.30%; this probably represents the point at which recrystallization ceases to be complete in about 20 min. at 495°–500° C.

## II.—ALLOYS CONTAINING ZIRCONIUM

It was at first assumed that the effect of zirconium would also not be apparent below a certain content, and it was proposed to make up two melts, one containing 0.30 and the other 0.60% zirconium. But in the event it proved impossible to add more than 0.25–0.30% and the two casts had the following closely similar compositions:

Ref. No.	Cu, %	Mg, %	Mn, %	Si, %	Fe, %	Zr, %
751P	4.14	1.52	0.02	0.12	0.14	0.27
752P	4.29	1.51	0.01	0.08	0.14	0.26 *

\* In this cast, which was intended to contain 0.60% zirconium, the excess was deposited at the bottom of the furnace, and was found in the ingots cast last.

The zirconium was introduced by means of an aluminium–5% zirconium hardener, added to the melt before the magnesium. In industrial practice, where up to 50% of the charge might consist of scrap, it would probably be desirable to utilize instead potassium fluozirconate, in slight excess, to counteract the retarding effect on the reaction of the magnesium

present in the scrap. This has the additional advantage of purifying the bath. For comparison a cast of ordinary FR alloy was made, which analysed: copper 4.32, magnesium 1.57, manganese 0.54, silicon 0.12, iron 0.24%.

From these three melts, forged bars were produced by the following procedure:

- Semi-continuous casting of 400-mm.-dia. billets;
- extrusion of 160-mm.-dia. bars;
- forging to bars 130 mm. square;
- forging the squares to rectangular bars, either (i) of approximately constant cross-section (140 × 120, 140 × 110, 170 × 100, 200 × 80, and 200 × 60 mm.), or (ii) of constant width (130 mm.) and various depths viz. 120, 100, 80, 60, 45, and 28 mm.

The initial forging temperature was 450°–470° C., and the final temperature 370°–450° C. In the course of working it was noted that the zirconium-containing alloys forged more easily than the ordinary alloy, since they cracked less. Bars of the three alloys were quenched simultaneously after solution-treatment for 29 min. in a salt bath at 505° C.; an interval of 52 sec. was allowed before quenching into water at 41° C. Except for the temperature, these conditions were not severe, and no quenching cracks were observed in any of the alloys.

Macrographs revealed in all cases a marked superiority of the zirconium-containing alloys in regard to

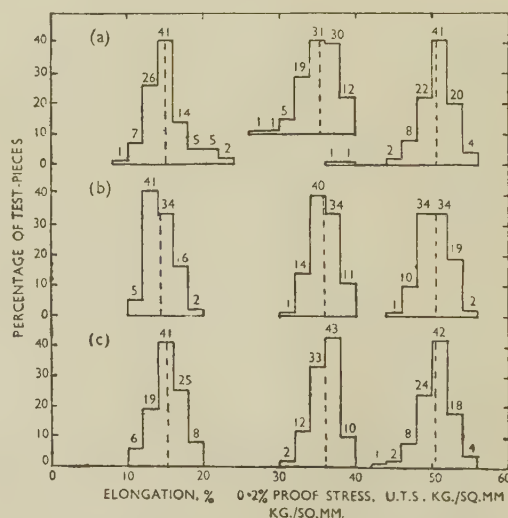


Fig. 2.—Mechanical Properties in the Longitudinal Direction of Rectangular Forged Bars of FR Alloy, with and without Zirconium, in the Quenched and Aged Condition.

(a) Normal FR; (b) Melt No. 752P, Zr 0.26%; (c) Melt No. 751P, Zr 0.27%.

fineness of grain in the surface regions (Fig. 6, Plate XCVII). X-ray diffraction diagrams also showed a clear difference. This very appreciable improvement occurred in all the sections examined, but was chiefly

apparent in the most heavily worked sections, where the coarse-grained zones tend to increase in depth. Comparison with specimens from ordinary FR alloy, previously forged under similar conditions, confirmed the improvements produced by zirconium.

The mechanical properties in the longitudinal direction, generally speaking, exhibit no very apparent correlation with the position of the test-piece in the section or with the degree of hot working. The mechanical properties of the two alloys are sensibly

properties. It did not, however, show whether zirconium reduced the tendency to quench cracking, since none was found, even in the normal alloy.

### III.—ALLOYS CONTAINING MANGANESE AND ZIRCONIUM

While the work described was in progress, a more general investigation, carried out in the Research Department of the Compagnie P  chiney, showed that an alloy containing both manganese and zirconium possessed the same good qualities as those conferred by zirconium alone in respect of grain-size, with perhaps a very slight gain in strength. A new series of tests was therefore begun with an alloy containing manganese + zirconium, with the following objectives:

(a) To confirm the superior forgeability of the zirconium-containing alloy.

(b) To study the grain-size and static mechanical properties of industrial products (forged angles, forged and die-forged airscrew blades),

(c) To determine the possible effect of zirconium on the dynamic mechanical properties (impact and fatigue).

(d) To examine more closely the effect of zirconium on quenching cracks.

The last factor was investigated first. In work on quenching cracks in FR alloy forgings, it had been found that bars  $40 \times 20$  mm., forged from extrusions 80 mm. in dia., reduced to 60-mm. squares, lent themselves particularly well to experiments of this kind, because of the invariable presence of surface defects which served as sites for cracks. Bars,  $40 \times 20$  mm., containing zirconium and manganese were therefore compared with similar bars of ordinary FR alloy.

In this particular case, the introduction of zirconium brought about no improvement in the susceptibility to cracking. With or without zirconium, cracks were generally observed on quenching without any interval from  $495^\circ \text{C.}$ , or from  $500^\circ \text{C.}$  after an interval of 20 sec., though admittedly these are severe tests.

These tests were not pursued further, for at this stage the value of the zirconium addition appeared to be principally in the refining and homogenization of the grain-size in forgings and in the improvement of forgeability. This improvement was clearly brought out in some new experiments on FR alloy containing zirconium + manganese. It is estimated that FR alloy containing zirconium (or zirconium + manganese) is at least as easy to forge as ordinary Duralumin, i.e. it is much easier to forge than FR alloy.

Various forgings are described in the following sections, made from a casting of the following com-

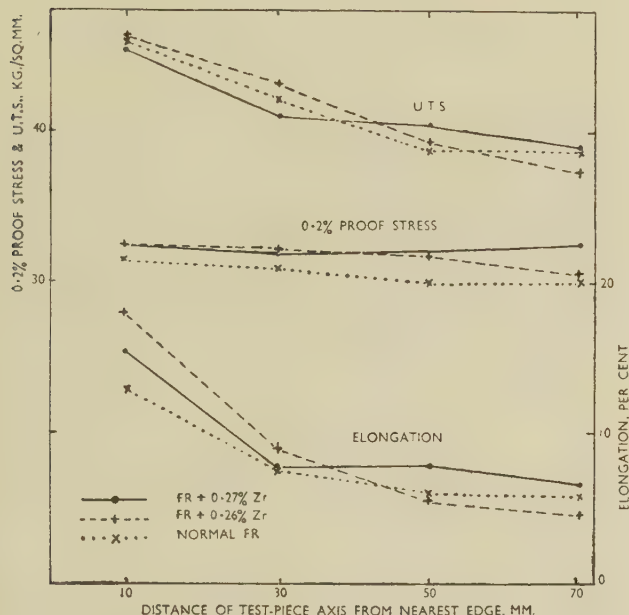


FIG. 3.—Mechanical Properties in the Transverse Direction of Rectangular Forged Bars of FR Alloy, with and without Zirconium, in the Quenched and Aged Condition.

the same, as shown by the histograms in Fig. 2. The mean values are:

Alloy	0.2% P.S., kg./mm. <sup>2</sup>	U.T.S., kg./mm. <sup>2</sup>	Elongation, %	No. of Test-Pieces
751P	36.0	50.5	15.2	300
752P	35.8	50.3	14.4	292
FR	35.3	50.5	15.0	305

The transverse properties, on the other hand, with the exception of the proof stress, are markedly affected by the position of the test-piece, being higher the nearer the specimen is to the surface (Fig. 3). Overall, the transverse properties are about the same for the three alloys, though in the surface regions elongation of the zirconium-containing alloys appeared slightly better, probably because the grain-size was finer.\*

This experiment proved that the replacement of manganese by zirconium in alloy FR effected considerable grain refinement, particularly in the surface regions, without any alteration of the static mechanical

\* There was in all cases a marked positive correlation between the elongation and tensile strength, particularly in the unrecrystallized or incompletely recrystallized interior of the bar. The test-pieces then broke on the ascending part

of the stress/strain curve and, as the latter appeared to be almost the same for all the test-pieces, the highest tensile strengths are associated with the greatest deformations.



TABLE I.—Mechanical Properties of Forged Double-Flanged Bars.

	Longitudinal						Transverse			
	Flanges (16 test-pieces)		Centre (16 test-pieces)		Overall		Flanges (8 test-pieces)		Centre (10 test-pieces)†	
	Mean	Deviation *	Mean	Deviation *	Mean	Deviation *	Mean	Deviation *	Mean	Deviation *
0.2% Proof Stress, kg./mm. <sup>2</sup>	30.1	0.9	29.4	0.9	29.8	...	28.1	0.8	30.0	0.8
U.T.S., kg./mm. <sup>2</sup>	45.1	0.6	44.8	0.6	44.9	0.6	44.4	0.4	43.4	1.1
Elongation, %	20.9	1.4	23.1	1.7	22.0	...	21.6	1.2	13.6	2.3

\* Deviation  $\sigma$  is given by the formula  $\sigma = \sqrt{\frac{\sum(x - \bar{x})^2}{N - 1}}$ , where  $\sum(x - \bar{x})^2$  represents the sum of the squares of the deviations and  $N$  the number of tests.

† Horizontal, vertical, and diagonal test-pieces.

position: copper 4.18, magnesium 1.61, manganese 0.24, zirconium 0.22, silicon 0.14, iron 0.15%, aluminium remainder.

### 1. DOUBLE-FLANGED BAR

Two continuously-cast billets of 30 mm. dia. were forged into two double-flanged bars (see Fig. 8, Plate XCVIII) in three operations: (i) rough hammer-forging

one another revealed no preferred orientation; recrystallization appeared to be complete. The mechanical properties in the longitudinal direction were sensibly the same throughout the section, with an appreciable increase in elongation at the centre. The transverse properties differed little from the longitudinal in the flanges, but in the centre section there was a marked difference, particularly in elongation, the test-pieces breaking on the ascending part of the stress/strain curve (Table I).

### 2. ROUGH BLADES

Three rough blades (Fig. 4) were forged at 440°–450° C., in one operation, from extruded bar 180 mm. in dia. One of the blades was solution-treated for

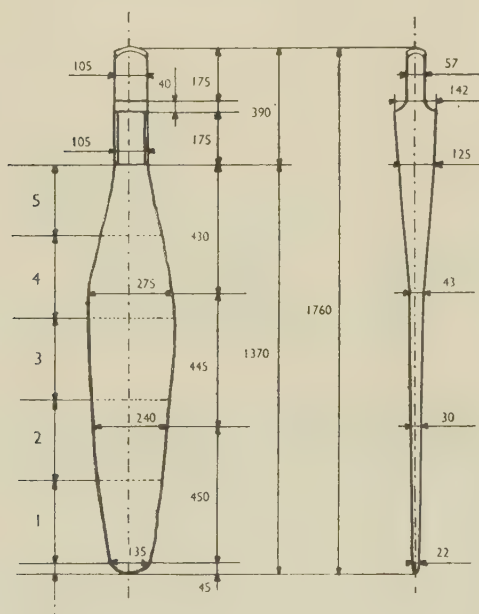


FIG. 4.—Diagram of Forged and Quenched Blade in FR Alloy Containing Zirconium + Manganese, Showing Position of Test-Pieces. Approx.  $\frac{1}{2}$  actual size.

to a rectangular section 160 × 80 mm. (temperature 460° and 455° C.); (ii) rough die-forging (temperature: 445° and 435° C.); and (iii) finish die-forging (temperature: 390° and 385° C.) One of the forgings was then solution-treated for 30 min. in a salt bath at 500° C., and quenched into water at 32° C. after an interval of 30 sec. When aged, its structure was examined and its mechanical properties determined. The grain proved to be uniformly fine (Fig. 8) and X-ray diagrams taken in three planes at right angles to

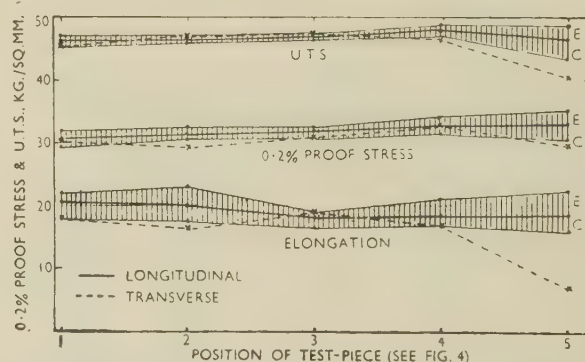


FIG. 5.—Mechanical Properties of Forged and Quenched Blade in FR Alloy Containing 0.22% Zirconium + 0.24% Manganese.

30 min. in a salt bath at 500° C. and quenched into water at 32° C. after an interval of 30 sec. After ageing, it was examined macro- and micrographically and subjected to the usual mechanical tests, as well as to fatigue tests. The structure was fine and uniform, with a border of slightly larger grains round the edge which were not found in the flanged beams.

The mechanical properties are shown in Fig. 5. Except at the centre, they differ little in the longitudinal and transverse directions and correspond to those of recrystallized metal. That the metal had recrystallized was confirmed by X-ray-diffraction photographs. The fatigue limit was 14 kg./mm.<sup>2</sup>,

the normal value for quenched and aged recrystallized Superalumin.

### 3. FINISHED BLADES

Four airscrew blades were produced from extruded bars, 100 mm. in dia., by the following procedure: (i) rough hammer-forging; (ii) die-forging under the hammer, and (iii) die-forging under the press. The blades were numbered 6-9. Nos. 6, 7, and 9 were quenched under the following conditions:

	No. 6	No. 7	No. 9
Solution Temp., °C. . . . .	504	495	499
Time at Temp., min. . . . .	30	30	20
Interval before Quench, sec. . . . .	30	35	30
Temp. of Quench Water, °C. . . . .	19	18	warm

The macrostructure was everywhere fine and uniform, with a border of slightly larger grains (Fig. 9, Plate XCVIII). The improvement due to the introduction of zirconium is clear on comparing Fig. 9 with Fig. 7 (Plate XCVII), which shows a typical blade in ordinary FR alloy. The average mechanical properties of the blade proper (excluding the root) are shown in Table II.

The fatigue limit determined on blade No. 9 was 13.8 kg./mm.<sup>2</sup>. The other mechanical properties of this blade were similar to those given in Table II.

TABLE II.—*Mechanical Properties of Airscrew Blade.*

	Blade No. 7 (quenched from 495° C.)		Blade No. 6 (quenched from 504° C.)	
	Long.	Trans.	Long.	Trans.
0.2% Proof Stress, kg./mm. <sup>2</sup>	35.8	34.6	35.8	34.2
U.T.S., kg./mm. <sup>2</sup> . . . . .	49.7	46.4	50.0	47.5
Elongation, % . . . . .	16.8	14.8	17.1	15.7
Impact Strength, kg./cm. <sup>2</sup> . . . . .	3.9	2.5	3.7	2.1

### IV.—CONCLUSIONS

The second series of tests confirmed the first in regard to the improvement in forgeability and grain

refinement brought about by the use of zirconium. In addition it showed that in commercial forgings, the mechanical properties, both static and dynamic, of FR alloy containing zirconium are comparable with those of the ordinary alloy, and are quite satisfactory.

Interest in zirconium addition is not necessarily limited to forgings or to alloys of the Duralumin type. Reference has already been made to the extensive investigations of the Research Department of the Compagnie Pechiney, which have included a wide range of alloys, while in the laboratories of the Compagnie Générale du Duralumin et du Cuivre the effect of zirconium on extruded bars of FR alloy, ordinary Duralumin, and Almasilium has been studied. Generally speaking, zirconium, like manganese, tends to raise the recrystallization temperature and the critical degree of cold working, though usually it is more effective in this respect than manganese.

An important application of the addition of zirconium to FR alloy is for the semi-continuous casting of large-diameter billets, which are often very difficult to produce in ordinary FR alloy when the diameter exceeds 300 mm. Although experience is at present limited, it is estimated that the improvement is very appreciable and in certain tests rejects due to cracking have been negligible. Care, must, however always be taken in casting billets over 400 mm. in dia., to avoid the formation of aluminium-zirconium crystals, which are hard and brittle. No effect has been found, by micrographic or X-ray examination, of zirconium on the as-cast structure of Superalumin, though only semi-continuous casting on an industrial scale has so far been investigated.

The addition of zirconium to light alloys is of interest in a wide variety of cases, but it is probably for forging that the zirconium-containing alloys will primarily be developed, since the small increase in price due to the partial replacement of manganese by zirconium will be offset by the increased ease of casting and forging, and in addition, the uniformity and fineness of structure should ensure safety in service.



# The Reaction of Aluminium-Magnesium Alloys with Steam

By A. J. SWAIN

(*Journal*, this vol., p. 125.)

Mr. R. W. RUDDLE,\* M.A. (Member): One of the most generally accepted theories of the oxidation of metals is that of Hoar, Price, and Thomas.† These authors, basing their conclusions on work carried out previously by Wagner,‡ suggest that the system may be treated as an electrolytic cell of the type metal|metal oxide|oxygen and that progressive oxidation occurs as the result of the diffusion of metal ions, oxygen ions, and electrons through the oxide film. This theory indicates that the increase in the thickness,  $y$ , of the oxide film should follow a parabolic law:

$$y^2 = \frac{2Jkn_e(n_e + n_a) \Delta G^0 t}{\rho Z F^2}$$

where  $J$  = equivalent weight of oxide.

$k$  = electrical conductivity of oxide.

$n_e, n_o, n_a$  are the transport numbers, respectively, of electrons, cations, and anions.

$\Delta G^0$  = standard free energy of formation of oxide.

$t$  = time.

$\rho$  = density of oxide.

$Z$  = valency of metal.

$F$  = Faraday's number.

Of the constants in this equation, the term  $n_e(n_e + n_a)$  cannot be greater than 0.25 and, with the exception of the conductivity, the others do not vary by more than about an order of magnitude from one oxide to another. However, the conductivity of metal oxides varies over an enormous range (about 10 orders) and, if the theory is right, is the principal factor governing rate of growth of oxide films.

The oxidation of many metals follows this parabolic law, but with some, e.g. aluminium and beryllium, oxidation suddenly stops when the film is still very thin. Mott§ has proposed another theory (to some extent complementary to that of Hoar *et al.*) to account for this. Like Hoar, Mott assumes that oxidation takes place by diffusion of metal ions and electrons (he discounts the possibility that oxygen ions can pass through the film), but suggests that in some instances the ability of the electrons to pass into the oxide layer may be the controlling factor. In the case of oxides of stoichiometric composition (these are the "insulators"), electrons must pass over a high potential barrier in going from the metal to the oxide. Hardly any of the electrons in a metal have enough energy for this, and on the basis of the old quantum theory oxidation of the metal surface should be impossible. However,

according to the newer wave-mechanical theory, a certain number of electrons of low energy can pass through the potential barrier; this number depends upon the thickness of the film and decreases sharply almost to zero when a certain critical film thickness is reached. Mott's picture of the oxidation of these metals is, then, that oxidation at first proceeds according to the parabolic law (much as described by Hoar *et al.*), the electrons passing through the oxide by the "tunnel" effect described above. However, once the critical thickness is reached, passage of electrons virtually ceases and oxidation stops. Mott has applied his theory to the oxidation of aluminium and has predicted that oxidation should cease when the film thickness reaches about 50 Å. at room temperature, in good agreement with the observed limiting thickness of 40 Å.

Work done at The British Non-Ferrous Metals Research Association by Mr. A. R. Heath has shown that the oxide films on aluminium-magnesium alloys at elevated temperatures consist mainly of magnesia, although a layer of alumina may be present as well in some cases.|| Both these oxides are of very low electrical conductivity and are stoichiometric; the films on these alloys should therefore be protective if they are *continuous*. I suggest, therefore, that the fact that the films formed on these alloys are not protective may be due to the film being *discontinuous*, and that oxidation proceeds as the result of fissuring of the film and not, as is sometimes suggested, because the rate of diffusion of magnesium ions through the oxide is high.

The AUTHOR (*in reply*): Mr. Ruddle's contribution is valuable in suggesting that the non-protective nature of the oxide films obtained on aluminium-magnesium alloys may be ascribed to discontinuity of the films and that oxidation proceeds as the result of fissuring.

Although it is indicated on p. 128 of the paper that continued disruption of the surface may have occurred owing to the violent nature of the reaction, it is more difficult to conceive a mechanism whereby fissuring could occur when the thickness of the film is of the order of the limiting thickness of the normal protective film on aluminium.

There is obviously much work remaining to be done on the formation of oxide films on these alloys, and it is from an investigation of the nature and structure of the film that a satisfactory explanation of the various phenomena encountered may be expected.

\* Head of Casting Section, British Non-Ferrous Metals Research Association, London.

† T. P. Hoar and L. E. Price, *Trans. Faraday Soc.*, 1938, **34**, 867; L. E. Price and G. J. Thomas, *J. Inst. Metals*, 1938, **63**, 21.

‡ C. Wagner, *Z. physikal. Chem.*, 1933, [B], **21**, 25.

§ N. F. Mott, *Trans. Faraday Soc.*, 1939, **35**, 1175; 1940, **36**, 472.

|| L. de Brouckère, *J. Inst. Metals*, 1945, **71**, 131.

# LATTICE-SPACING RELATIONSHIPS IN ALUMINIUM-RICH SOLID SOLUTIONS OF THE ALUMINIUM-MAGNESIUM AND ALUMINIUM-MAGNESIUM-COPPER SYSTEMS\*

1386

By D. M. POOLE,† B.Sc., STUDENT MEMBER, and H. J. AXON,‡ D.Phil., JUNIOR MEMBER

## SYNOPSIS

The lattice-spacing/composition relationship for the aluminium-rich aluminium-magnesium solid solution has been re-investigated, using two samples of magnesium of different purities. Increasing the purity of the magnesium reduces the curvature of the relationship at low concentrations of magnesium and causes the linear portion of the curve to become more steep.

The aluminium-rich ternary aluminium-magnesium-copper solid solution has also been investigated, using magnesium of high purity; in this solid solution there is a slight negative deviation from the additive effect which might be expected from copper and magnesium separately. Accurate control of alloy composition is of great importance and is likely to hold up research in this field.

## I.—INTRODUCTION

THE lattice spacings of the primary solid solutions formed when copper, silver, zinc, magnesium, silicon, germanium, and lithium are dissolved in aluminium have already been reported for the binary alloy systems.<sup>1</sup> The purpose of the present work was to extend the measurements to aluminium-rich ternary solid solutions. The system first investigated was that of the aluminium-magnesium-copper alloys, but before the ternary system was studied it was necessary to re-determine the relationship for the binary aluminium-magnesium alloys, in view of a discrepancy between the result of the two most recent investigations.<sup>1,2</sup> The present work has shown that the lattice-spacing/composition relationship in the aluminium-magnesium system is extremely sensitive to the purity of the metals used.

## II.—EXPERIMENTAL METHODS

### 1. METALS USED

The aluminium was super-purity metal, supplied by The British Aluminium Co., Ltd., and analysed 99.991% aluminium, with silicon 0.0030, iron 0.0030, copper 0.0030, manganese <0.0005, and zinc 0.001%. The authors must thank Mr. H. W. L. Phillips, of The British Aluminium Co., Ltd., for his kindness in arranging this analysis.

The copper was similar to that used in the previous work,<sup>1</sup> and was of 99.995% purity.

Two samples of magnesium were used in order to investigate the influence of impurities on the lattice-

spacing relationship. The less-pure magnesium was supplied by Magnesium Elektron, Ltd., and had the following analysis: sodium 0.01, zinc 0.02–0.03, iron 0.005, copper 0.002, silicon 0.002, and magnesium 99.95%. This magnesium was used to produce the "impure" series of binary alloys.

The magnesium of higher purity was supplied in the form of spectrographic electrodes by Johnson, Matthey and Co., Ltd., who gave the following chemical analysis: iron 0.013, manganese 0.0023, and lead 0.0013%; magnesium was estimated as 99.98%. Spectrographic examination revealed traces of silicon, copper, aluminium, calcium, and sodium. This magnesium was used to produce the "specpure" series of binary alloys and also all the ternary alloys.

### 2. PREPARATION AND HEAT-TREATMENT OF INGOTS

The aluminium was melted in crucibles lined with pure alumina. The copper was added to the melt in the form of a 55% copper-aluminium master alloy. The magnesium was added immediately before casting and was stirred into the melt with a rod of sintered alumina. No flux was used. The alloy was cast into a heavy iron mould to give an ingot 2 in. long and  $\frac{3}{8}$  in. in dia. The chill casting resulted in a small grain-size, which facilitated the attainment of equilibrium on annealing. Portions of the ingots were wrapped in several layers of aluminium foil to prevent contact with the evacuated glass capsules in which they were annealed. All annealing treatments were carried out at 450°C., the eutectic temperature in the aluminium-

\* Manuscript received 28 November 1951.

† Inorganic Chemistry Laboratory, Oxford; formerly

University of Manchester.

‡ Lecturer in Electrometallurgy, University of Manchester.



magnesium system. The binary alloys were annealed for 7 days, and the ternary alloys for 10 days. At the end of the anneal, the ingots were quenched into cold water. The surface layer of each ingot was removed to a depth of about 1 mm., and the remainder of the ingot was then used in the preparation of filings.

### 3. PREPARATION AND HEAT-TREATMENT OF FILINGS

About 1 g. of filings was prepared from each ingot, care being taken to avoid contamination during the process. The filings were washed in ether to remove organic contamination and then annealed for 6 hr. at 450° C. During this anneal the filings were contained in alumina collars inside evacuated hard-glass capsules. At the end of the anneal, the capsules were quenched into cold water. The capsules broke on quenching, and the water came into immediate contact with the filings. The filings were then washed, dried, and sieved through copper gauze of 60 meshes to the linear inch. This removed coarse particles of metal, but enabled the chemical analysis to be done on material which was identical with that used for the X-ray specimen.<sup>1</sup>

### 4. X-RAY TECHNIQUE AND LATTICE-SPACING MEASUREMENTS

In the present work the same methods of specimen preparation and chemical analysis were used as have already been reported.<sup>1</sup> The chemical analyses were again carried out by Johnson, Matthey and Co., Ltd., and the authors wish to express their thanks to Mr. A. R. Powell for his careful attention to this matter.

Unfiltered CuK radiation was obtained from a Metropolitan-Vickers "Raymax" unit. The camera was a 19-cm.-dia. Debye-Scherrer model made by Unicam Instruments, Ltd. It was found that the resolution of the camera could be improved by reducing the height of the collimator slit from 4 to 3 mm. The camera as supplied had a built-in motor unit which rotated the specimen at 1 revolution every 7½ min. Detailed work on the measurement of exposure temperature in this camera<sup>3</sup> showed that the motor warmed the camera when in operation. The built-in motor was therefore removed, and the specimen was rotated at 1 revolution every 2 min. by means of an external pulley and motor arrangement. It was also necessary to enclose the camera completely in a cardboard box to prevent temperature fluctuations caused by air currents and radiation from the lamps which illuminated the X-ray room. In the final experimental arrangement, the exposure temperature was measured by a mercury-in-glass thermometer graduated in 1/16° C. The thermometer was placed, with its bulb freely suspended in the air, inside the X-ray camera, as near to the specimen as possible without obstructing the X-rays. The X-ray specimen was thermally insulated from the metal work of the camera, and it is considered that the air inside the camera, the X-ray specimen, and the thermometer bulb should all

be at the same temperature. During an exposure, the temperature of the air inside the camera was maintained constant to within 0.4° C. by altering the ventilation of the X-ray room.

Those films which were straight and of good quality were measured on a Cambridge Universal Measuring Machine, the micrometer head of which allowed readings to 0.01 mm. and interpolation to 0.002 mm.

The lattice spacings were calculated by standard methods, using the tables of Edwards, Lipson, and Wilson,<sup>4</sup> and the extrapolation function of Nelson and Riley.<sup>5</sup> All lattice spacings were corrected to a temperature of 25° C., using a value of  $23.1 \times 10^{-6}$  as the coefficient of linear expansion of aluminium and its solid-solution alloys.

The final values for the lattice spacings at 25° C. are given in kX units, and no correction has been made for refraction.

## III.—EXPERIMENTAL RESULTS

### 1. PURE ALUMINIUM

The mean value of five experimental determinations of the lattice spacing of the pure aluminium used in the present work was 4.0412(1) kX at 25° C., the extreme values being 4.0411(9) and 4.0412(4) kX. The mean value of 4.0412(1) kX is used in all the graphs and calculations which follow.

It was considered important to determine whether the alloys picked up any impurity in the processes of melting, casting, and lump-annealing. This was investigated by preparing X-ray specimens of super-purity aluminium by alternative methods. In the first method, filings were prepared direct from the large ingot supplied by The British Aluminium Co., Ltd. These filings were given a stress-relieving heat-treatment of 6 hr. at 450° C. and quenched. In the second method, the super-purity aluminium was remelted under conditions as similar as possible to those under which the "impure" and "specpure" series of binary alloys were made. The molten super-purity aluminium was cast and lump-annealed for 7 days at 450° C. Filings were taken from the annealed lumps and given the usual stress-relieving heat-treatment. The two methods gave values which agreed within the limits of the extreme values quoted above, indicating that there was no contamination of the aluminium during melting, casting, and lump-annealing.

Table I contains a selection of recent values for the lattice spacing of aluminium at 25° C. Lu and Chang<sup>8</sup> reported a value of 4.0411 kX, with an estimated probable error of 0.0001 kX at 20° C., and in Table I their result is calculated as 4.041(5) at 25° C. Dorn, Pietrokowsky, and Tietz<sup>2</sup> investigated two samples of aluminium of slightly different purity, but all their aluminium-magnesium alloys were made from the sample of 99.987% purity. It will be seen from Table I that the value obtained in the present work is slightly low in comparison with those reported

by most recent investigators, and this is probably to be explained by slight variations in the purity of the materials used and in the accuracy with which the specimen temperature was controlled and measured. The effect of temperature errors probably plays the

TABLE I.—*Lattice Spacings of Aluminium at 25° C.*

Date	Authors	Purity of Al, %	Lattice Spacing, kX
1935	Jette and Foote <sup>6</sup>	99.97	4.0413(6)
1936	Levins and Straumanis <sup>7</sup>	99.992	4.0414(3)
1941	Lu and Chang <sup>8</sup>	99.992	4.041(5)
1941	Wilson <sup>9</sup>	99.992	4.0413(1)
1948	Axon and Hume-Rothery <sup>1</sup>	99.994	4.0413(4)
1949	Hume-Rothery and Boulton <sup>10</sup>	99.994	4.0414(2)
1950	Dorn, Pietrokowsky, and Tietz <sup>2</sup>	99.987	4.0413(0)
		99.984	4.0412(6)
		99.991	4.0412(1)
	Present Work		

greater part,\* and a study of the published information suggests that the best temperature control so far was obtained in the present work.

## 2. ALUMINIUM-MAGNESIUM ALLOYS

In order to investigate the effect of impurities on the form of the lattice-spacing relationship, this system has been investigated twice, using two batches of magnesium of different purities. The results at 25° C. for the "impure" series of alloys, in which magnesium of 99.95% purity was used, are collected below and plotted as curve *I* in Fig. 1.

Analysed Composition, Magnesium, at.-%	Lattice Spacing, kX
0.35	4.0418(7)
0.69	4.0431(6)
1.01	4.0444(9)
1.99	4.0490(9)
2.38	4.0505(8)
2.75	4.0520(6)
2.99	4.0533(5)
3.37	4.0548(6)
4.01	4.0576(0)
6.71	4.0700(3)
7.63	4.0737(5)

In addition, a further alloy with a synthetic composition 0.166 at.-% magnesium was prepared. This gave a lattice spacing of 4.0414(6) kX. The specimen was not analysed, but the corresponding point is plotted in Fig. 1 (lowest square).

The results at 25° C. for the "specpure" series of alloys, in which magnesium of >99.98% purity was used, are given below and plotted as curve *S* in Fig. 1.

Analysed Composition, Magnesium, at.-%	Lattice Spacing, kX.
0.18	4.0415(7)
0.32	4.0422(4)
0.62	4.0434(4)
1.28	4.0460(3)
1.93	4.0489(2)
7.15	4.0723(5)

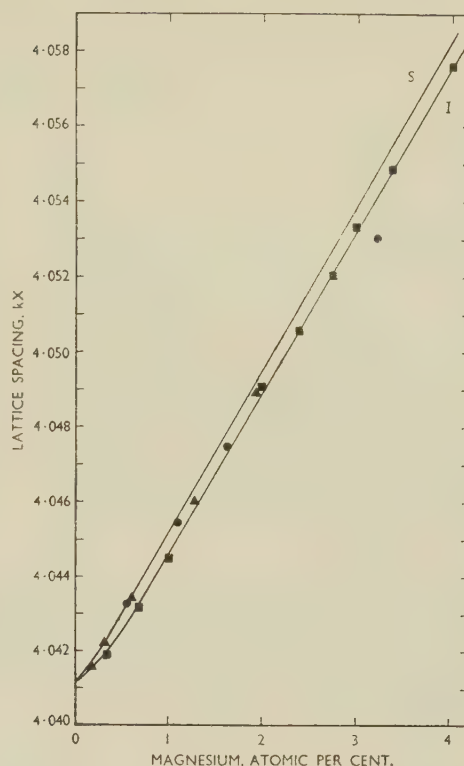


FIG. 1.—The Variation of Lattice Spacing with Atomic Composition for the Aluminium-Rich Solid Solution of Aluminium and Magnesium.

Curve *I* for "impure" magnesium (■).  
Curve *S* for "specpure" magnesium (▲).

The circular points are due to Dorn, Pietrokowsky, and Tietz. All experimental points are not shown on this figure, but they have all been taken into consideration in drawing the curves.

## 3. ALUMINIUM-MAGNESIUM-COPPER ALLOYS

The synthetic compositions of all the ternary alloys investigated are shown in Fig. 2. All these alloys fall within the ternary solid-solution region at

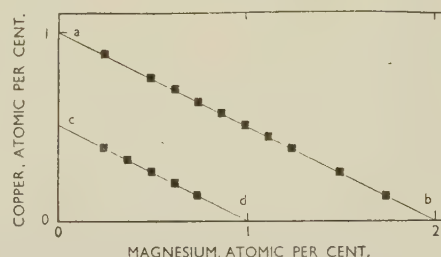


FIG. 2.—The Synthetic Composition of Alloys Investigated in the Ternary Aluminium-Magnesium-Copper Solid Solution.

460° C.,<sup>11</sup> and micro-examination of the alloys after annealing at 450° C. for 10 days confirmed that all the alloys were homogeneous. The lattice spacings of these alloys are collected in Table II, which also con-

\* An error of 1° C. corresponds to approximately 0.0001 kX.



TABLE II.—The Correction of Observed Lattice Spacings to Values Appropriate to the Synthetic Compositions of the Alloys in the Ternary Aluminium–Magnesium–Copper System.

Magnesium of "specpure" quality. Data corrected to 25° C.

Synthetic Composition		Analysed Composition		Composition Corrections		Lattice-Spacing Corrections			Observed Lattice Spacing, kX	Corrected Lattice Spacing, kX
Mg, at.-%	Cu, at.-%	Mg, at.-%	Cu, at.-%	$\Delta M$	$\Delta C$	$\Delta aM$	$\Delta aC$	$\Delta aM + \Delta aC$		
0.25	0.375	0.189	0.367	0.061	0.008	0.0002(1)	—0.0000(4)	0.0001(7)	4.0397(9)	4.0399(6)
0.50	0.25	0.456	0.247	0.044	0.003	0.0001(9)	—0.0000(2)	0.0001(7)	4.0415(7)	4.0417(4)
0.75	0.125	0.655	0.119	0.095	0.006	0.0004(2)	—0.0000(3)	0.0003(9)	4.0428(4)	4.0432(3)
0.25	0.875	0.202	0.880	0.048	—0.005	0.0001(6)	0.0000(2)	0.0001(8)	4.0376(6)	4.0378(4)
0.50	0.75	0.414	0.750	0.086	0.000	0.0003(8)	0.00000	0.0003(8)	4.0390(9)	4.0394(7)
0.75	0.625	0.637	0.628	0.113	—0.003	0.0005(0)	0.0000(2)	0.0005(2)	4.0407(9)	4.0413(1)
1.00	0.50	0.927	0.500	0.073	0.000	0.0003(2)	0.00000	0.0003(2)	4.0425(3)	4.0428(5)
1.25	0.375	1.247	0.362	0.003	0.013	0.0000(1)	—0.0000(6)	—0.0000(5)	4.0442(6)	4.0442(1)
1.50	0.25	1.311	0.246	0.189	0.004	0.0008(3)	—0.0000(2)	0.0008(1)	4.0450(4)	4.0458(5)
1.75	0.125	1.608	0.127	0.142	—0.002	0.0006(2)	0.0000(1)	0.0006(3)	4.0468(2)	4.0474(5)
0.375	0.313	0.356	0.302	0.019	0.011	0.0000(8)	—0.0000(5)	0.0000(3)	4.0409(0)	4.0409(3)
0.625	0.188	0.578	0.179	0.047	0.009	0.0002(1)	—0.0000(4)	0.0001(7)	4.0423(7)	4.0425(4)
1.125	0.438	1.058	0.422	0.067	0.016	0.0002(9)	—0.0000(8)	0.0002(1)	4.0430(7)	4.0432(8)
0.625	0.688	0.570	0.659	0.055	0.029	0.0002(4)	—0.0001(4)	0.0001(0)	4.0395(6)	4.0396(6)
0.875	0.563	0.804	0.521	0.071	0.042	0.0003(0)	—0.0002(0)	0.0001(0)	4.0408(3)	4.0409(3)

tains the values of the synthetic compositions, the analysed compositions, and details of the correction which has been applied in order to evaluate the lattice-spacing values appropriate to the *synthetic* composition for each alloy.

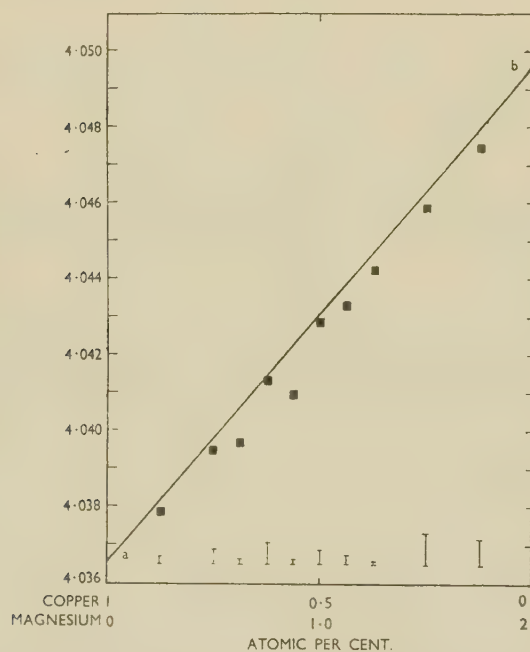


FIG. 3.—The Variation of Lattice Spacing with Composition in the Ternary Aluminium–Magnesium–Copper Alloys with Synthetic Compositions along Line *ab* of Fig. 2. The vertical lines indicate the correction which has been made to the lattice spacing (see Table II).

The lattice-spacing measurements were carried out within 24 hr. of quenching the filings; duplicate measurements were also made on certain alloys 3, 11, and 23 days after quenching the filings. All duplicate values agreed with the initially determined values to within the normal experimental scatter, thus indicat-

ing that room-temperature ageing effects do not influence the results.

The analyses of the alloys showed a departure from the synthetic compositions, and since it was desired to examine the variation of lattice spacing along the lines *ab* and *cd* of Fig. 2, a correction was applied to the observed lattice spacing in the following way:

$\Delta M$  and  $\Delta C$  are respectively the differences between synthetic and analysed magnesium and copper contents in atoms per cent.

$\Delta aM$  and  $\Delta aC$  are respectively the corresponding corrections which have to be applied to the observed lattice spacing in order to give the lattice spacing appropriate to the synthetic composition. The corrections  $\Delta aM$  and  $\Delta aC$  are taken from the binary lattice-spacing/composition curves for aluminium–magnesium alloys (Fig. 1, curve *S* for the "specpure" magnesium), and aluminium–copper alloys.<sup>1</sup>

The lattice-spacing/composition relationship is linear for aluminium–copper alloys, but for aluminium–magnesium the relationship shows a slight curvature at low percentages of magnesium; this curvature was taken into consideration in applying the correction. The method of correction and final corrected values appropriate to the synthetic compositions are set out in Table II.

These synthetic compositions and corrected values of lattice spacing are plotted in Figs. 3 and 4. Fig. 3 is drawn for the series of alloys whose synthetic compositions lie on line *ab* of Fig. 2. The straight line in Fig. 3 is drawn between two points from the binary systems aluminium–magnesium and aluminium–copper. The point *a* of Fig. 3 corresponds to point *a* of Fig. 2 and represents an alloy containing 1 at.-% copper with a lattice spacing of 4.0365 kX at 25° C.<sup>1</sup> Similarly, point *b* in Figs. 2 and 3 represents an aluminium–magnesium alloy of the "specpure" series, with 2 at.-% magnesium and a lattice spacing of 4.0495(5) at 25° C. The vertical lines below each experimental point show the amount of correction

which has been applied to the measured lattice spacing in order to produce the corrected lattice spacing.

Fig. 4 represents the variation of lattice spacing with composition along the line *cd* of Fig. 2. Point *c* represents an aluminium-copper alloy with 0.5 at.-% copper and a lattice spacing of 4.0389 kX.<sup>1</sup> Point

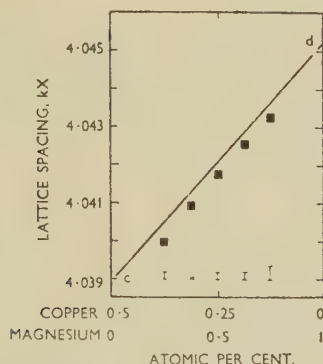


Fig. 4.—The Variation of Lattice Spacing with Composition in the Ternary Aluminium-Magnesium-Copper Alloys with Synthetic Compositions along Line *cd* of Fig. 2. The vertical lines indicate the correction which has been made to the lattice spacing (see Table II).

*d* represents an aluminium-magnesium alloy of the "specpure" series with 1 at.-% magnesium and a lattice spacing of 4.0451(6) kX at 25° C. It will be seen that the experimentally determined values for lattice spacing in the ternary solid solution tend to lie slightly below the linear relationship represented by lines *ab* and *cd* of Figs. 3 and 4.

#### IV.—DISCUSSION

The value of the lattice spacing of pure aluminium obtained in the present investigation is slightly lower than recently published values obtained by other investigators. This is partly due to slight differences in the purity of the different samples of aluminium, but, in the absence of detailed and accurate chemical analyses of the various materials, little more can be said. The discrepancy is about 0.0001 kX. It is unlikely that the discrepancy is due to faulty calibration of the camera, since the calibration was done by direct measurement of the knife edges and camera diameter; and a discrepancy of 0.0001 kX in the lattice spacing of aluminium would correspond to errors of 0.002 in. in the measurement of the knife edges or 0.01 in. in the diameter. Errors of this magnitude are unlikely.

The two curves *S* and *I* of Fig. 1 show that small amounts of impurity in the magnesium have a pronounced effect on the lattice-spacing relationship. Both these curves lie above the curve of Axon and Hume-Rothery.<sup>1</sup> The curvature reported by these authors at low concentrations of magnesium is

apparent in both curves in the present work, but decreases as the purity of the magnesium increases. Increasing purity of the magnesium is also associated with a steeper linear portion to the relationship. It must be concluded that the effective purity of the magnesium was least in the experiments of Axon and Hume-Rothery<sup>1</sup> and greatest in the "specpure" series of the present work. The amount of impurity is exceedingly small in all three cases, and it is difficult to be certain what the effective impurity is. Preliminary calculations have shown, however, that the form and magnitude of the effect may be explained on the supposition that the effective impurity is silicon, if the additional assumption is made that the electrochemical effect between magnesium and silicon, in a ternary solid solution of aluminium, causes a decrease of lattice spacing over and above that calculated from the effect due to the two elements separately. This suggestion is supported by the fact that the closest distance of approach of atoms in  $\text{Mg}_2\text{Si}$  is 2.75 kX, whereas the closest distance of approach calculated for a hypothetical mixture of magnesium and silicon atoms, in the ratio of 2:1 is 2.9 kX. This point can be settled only by further work on the lattice spacings of the ternary aluminium-magnesium-silicon solid solution, but accurate chemical analysis is likely to be difficult in such experiments.

The four experimental points due to Dorn, Pietrowsky, and Tietz<sup>2</sup> plotted as circles in Fig. 1 show that their three points of lowest magnesium content agree well with the results of the present work, and are not inconsistent with a curved relationship at low magnesium contents. The fourth point, which is placed \* at 3.228 at.-% magnesium lies below the best straight line drawn through the three lower points; this straight line is not shown in Fig. 2, but if it is extrapolated backwards to 100% aluminium, a value of 4.0410(9) kX is obtained. If this value is compared with the published value of 4.0413(0) obtained by the American workers for pure aluminium, it suggests the presence of a "low-concentration curvature" in their relationship.

The previous results of Axon and Hume-Rothery<sup>1</sup> were used to evaluate an apparent atomic diameter of magnesium when dissolved in aluminium. The new results presented above give rise to a modified value of the apparent atomic diameter of magnesium, but do not in any way alter the arguments of Axon and Hume-Rothery, as is shown below, since the apparent atomic diameter is still appreciably less than the atomic diameter in the pure metal.

	Apparent Atomic Dia., kX
Specpure series . . . .	3.172
Impure series . . . .	3.167
Axon and Hume-Rothery <sup>1</sup> . . . .	3.15
Dorn, <i>et al.</i> <sup>2</sup> . . . .	3.12
Atomic dia. for metallic Mg . . . .	3.19

\* It is unfortunate that Dorn and his colleagues did not analyse the X-ray specimens. Their chemical analyses refer to samples taken from the molten alloy before the metal was

cast. It is well known that the tendency to lose magnesium increases as the total magnesium content of the alloy increases.



The results for the ternary solid solution of magnesium and copper in aluminium are plotted in Figs. 3 and 4. In these figures the linear relationships *ab* and *cd* are drawn between the previously determined lattice-spacing values for the binary solid solutions. Figs. 3 and 4 suggest that in the ternary solid solution there is a small negative deviation from the postulated linear relationship. A highly unsatisfactory aspect of these diagrams is the correction which has to be made because the analysed composition does not agree with the synthetic composition; and in general the magnitude of the negative deviation is of the same

order as the applied correction. It is highly suggestive that the deviation is always negative, but, in the absence of more careful control of composition or more accurate chemical analysis, it is impossible to say more. It is in these respects, rather than in the measurements on the X-ray side, that work on ternary solid solutions is likely to be difficult.

#### ACKNOWLEDGEMENTS

The authors thank Professor F. C. Thompson for research facilities and encouragement, and the Royal Society for a grant in aid of the research.

---

#### REFERENCES

1. H. J. Axon and W. Hume-Rothery, *Proc. Roy. Soc.*, 1948, [A], **193**, 1.
2. J. E. Dorn, P. Pietrokowsky, and T. E. Tietz, *Trans. Amer. Inst. Min. Met. Eng.*, 1950, **188**, 933.
3. D. M. Poole, unpublished work.
4. O. S. Edwards, H. Lipson, and A. J. C. Wilson, "Tables for Facilitating the Calculation of Lattice Spacings for Cubic Crystals." Cambridge: 1940 (Crystallographic Laboratory).
5. J. B. Nelson and D. P. Riley, *Proc. Phys. Soc.*, 1945, **57**, 160.
6. E. R. Jette and F. Foote, *J. Chem. Physics*, 1935, **3**, 605.
7. A. Ievinš and M. Straumanis, *Z. physikal. Chem.*, 1936, [B], **33**, 265.
8. S. S. Lu and Y. L. Chang, *Proc. Phys. Soc.*, 1941, **53**, 517.
9. A. J. C. Wilson, *ibid.*, 1941, **53**, 235.
10. W. Hume-Rothery and T. H. Boulton, *Phil. Mag.*, 1949, [vii], **40**, 71.
11. D. J. Strawbridge, W. Hume-Rothery, and A. T. Little, *J. Inst. Metals*, 1947, **74**, 191.

# FACTORS AFFECTING EQUILIBRIUM IN CERTAIN ALUMINIUM ALLOYS \*

1387

By E. C. ELLWOOD,† Ph.D., F.I.M., MEMBER

## SYNOPSIS

The lattice spacings and densities of solid solutions of copper, magnesium, and silver in aluminium have been measured at 25° C. No anomalies were found in the aluminium-copper solution. In the aluminium-magnesium solution the slight curvature in the lattice-spacing/composition curve reported by Axon and Hume-Rothery (*Proc. Roy. Soc.*, 1948, [A], **193**, 1) is confirmed, and vacant sites are formed in the solid solution. An expansion in the lattice occurs between 10 and 14 at.-% silver in the aluminium-silver system, but no vacant sites are found. It is deduced that the anomalies are the result of Brillouin-zone overlaps and that the two latter solid solutions resemble that of zinc in aluminium in some respects. The solid solutions are not identical in their behaviour, and it is concluded that the effects produced are characteristic of the alloying element. It is shown that where Brillouin-zone effects are found the solid solutions are not ideal.

## I.—INTRODUCTION

IN a recent study <sup>1</sup> of the aluminium-zinc system by the author, it has been found that anomalous lattice spacings and densities occur. These have been attributed to Brillouin-zone effects, and it was desired to investigate other aluminium-rich primary solid solutions to find whether similar effects occurred in them. Only the solutions of magnesium and silver cover the electron concentrations at which the anomalous effects are found in the aluminium-zinc alloys, and the lattice spacings and densities of these alloys, together with those of the aluminium-copper alloys used by Ellwood and Silcock,<sup>2</sup> have been measured at 25° C.

## II.—EXPERIMENTAL PROCEDURE

### 1. MATERIALS AND PREPARATION OF THE ALLOYS

Details of the purity, preparation, and analysis of the aluminium-copper alloys were given in an earlier publication.<sup>2</sup> The remaining alloys were made from aluminium, containing iron 0.0005, silicon 0.0005, and copper 0.0005%, giving 99.9985% aluminium (by difference). The silver was "spectrographically pure", and the magnesium contained as impurities silicon 0.002, iron 0.002, copper 0.001, nickel 0.0003, manganese 0.003, sodium 0.003%, and traces of aluminium and zinc.

The alloys were prepared in 50-g. lots by melting the aluminium in an alumina crucible, adding the alloying element and stirring with a carbon rod before casting into a warm iron mould. The ingots were  $\frac{1}{4} \times 1$  in. in cross-section.

### 2. SAMPLING AND ANALYSIS

With the silver alloys it was possible to take filings for lattice-spacing measurements, measure the density,

and carry out the analysis on a  $\frac{3}{8}$ -in. section cut from the centre of the ingot. A considerable quantity of filings was prepared from the aluminium-magnesium alloys and samples for analysis and X-ray diffraction taken from them after the final stress-relieving anneal. Samples for density and analysis measurements were taken separately from adjacent parts of the ingot. In all cases the samples comprised the whole cross-section of the ingot. The analytical results for the aluminium-magnesium system are discussed in an Appendix.

The analysis for magnesium was carried out in the Research Laboratories of The British Aluminium Co., Ltd. Analysis for silver was made by the author, the silver being estimated as chloride.

### 3. HEAT-TREATMENT

The silver and copper alloys were homogenized by annealing sections of the ingots for 2 weeks *in vacuo* at 536° and 546° C., respectively. Sections from the magnesium alloys were sealed in a hard-glass container in argon and annealed for 12 days at 448° C. After homogenization, filings for X-ray examination were taken from each alloy. Those from the silver and copper ingots were sealed in silica tubes and heated for 1 hr. at the homogenizing temperature and quenched before diffraction patterns were taken.

As indicated in the previous section, a considerable quantity of filings was prepared from the aluminium-magnesium alloys, so that sufficient should be available for analysis. The whole of the filings were stress-relieved by annealing at 448° C. for 1 hr. in an alumina tube sealed in Pyrex in an atmosphere of argon. The filings were water-quenched, washed in alcohol, and dried before sealing into a thin silica tube for use as X-ray specimens.

\* Manuscript received 19 January 1952.

† Lecturer in Metallurgy, King's College, University of Durham, Newcastle-upon-Tyne 1.



## 4. X-RAY TECHNIQUE

The diffraction patterns were obtained on a 9-cm.-dia. camera, using copper radiation. The lattice spacings were calculated by standard methods, making a correction for film shrinkage and using the extrapolation function of Nelson and Riley.<sup>3</sup> The lattice spacings were corrected to 25° C. on the assumption that their coefficients of expansion were the same as that of pure aluminium. The values for the lattice spacing are in kX units and have been calculated, using 1.537395 kX as the wave-length of Cu  $K_{\alpha}$  radiation. No correction for refractive index has been applied.

## 5. DENSITY MEASUREMENTS

After homogenizing, the specimens were heated to 430° C. and hammered to reduce the thickness by 50% where possible. The alloys containing more than 7% \* magnesium and that containing 2.17% copper were hard and tended to crack during hammering, so that the reduction was less than 50% for these alloys. The worked specimens were heat-treated for 1 hr. at the homogenizing temperature to restore equilibrium, and any cracks were filed out before the densities were determined. The experimental methods, corrections applied, and constants used in the density determinations were similar to those described for the aluminium-zinc alloys.<sup>1</sup> The density results for the aluminium-magnesium alloys are expressed as percentages of vacant lattice sites. It is not claimed that these figures are more than an approximation to the number of vacant sites actually present.

## III.—RESULTS AND DISCUSSION

## 1. THE ALUMINIUM-COPPER SOLID SOLUTION

Previous work<sup>2,5</sup> has shown that the lattice-spacing/composition relation is linear. The following density results show that there are probably no vacant sites formed in alloys containing less than 2% copper.

Copper, at.-%	Theoretical Density, g./c.c.	Measured Density, g./c.c.
0.41	2.715	2.712
0.84	2.736	2.732
1.28	2.753	2.754
1.73	2.777	2.774
2.17	2.798	2.788

There is a slight discrepancy in the alloy containing 2.17% copper, but this was hard and not reduced as much as the other alloys by hammering, so that the difference may be due to unclosed pores. The linear lattice-spacing/composition relationship and the probable absence of vacant sites suggest that there are no Brillouin-zone effects in these alloys.

## 2. THE ALUMINIUM-SILVER SOLID SOLUTION

The lattice-spacing/composition relation is shown in Fig. 1. The density results are as follows:

Silver, at.-%	Theoretical Density, g./c.c.	Measure Density, g./c.c.
0.50	2.737	2.737
1.59	2.826	2.824
2.06	2.864	2.863
5.85	3.170	3.170
9.64	3.477	3.471
14.0	3.828	3.835
20.0	4.320	4.319
23.3	4.579	4.590

The lattice spacing of aluminium is practically unchanged by addition of up to 6% silver; between 6 and 14% silver there is a small but definite increase

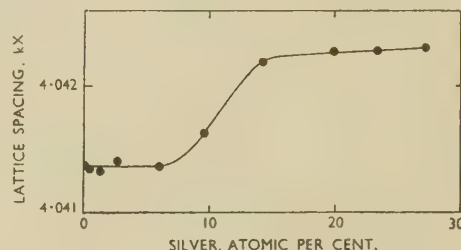


Fig. 1.—Lattice Spacings of the Aluminium-Silver Solid Solution.

in spacing, while silver additions between 14 and 27% probably cause no further increase in spacing, the small change shown in Fig. 1 being within the normal experimental error. The increase in lattice spacing between 6 and 14% silver is interpreted as being associated with the filling of a Brillouin zone. As in the aluminium-zinc system, the zone is filled as the electron/atom ratio is decreased, but no vacant sites are formed. The zone appears to be filled when 14% silver is present, corresponding with an electron/atom ratio of 2.72 : 1.

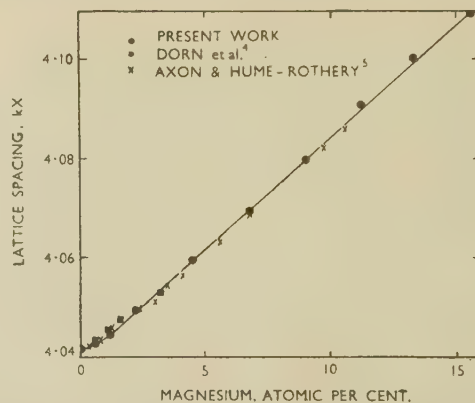


Fig. 2.—Lattice Spacings of the Aluminium-Magnesium Solid Solution.

## 3. THE ALUMINIUM-MAGNESIUM SOLID SOLUTION

The lattice-spacing/composition relation is shown in Fig. 2. The percentages of vacant lattice sites, as calculated from the theoretical and actual densities, are shown in Fig. 3. Lattice-spacing results by Dorn, Pietrowsky, and Tietz<sup>4</sup> and by Axon and Hume-

\* This and all subsequent compositions are expressed in atomic per cent.

Rothery<sup>5</sup> are also shown in Fig. 2. The former authors claim that the lattice-spacing/composition relation is linear, whereas Axon and Hume-Rothery's results show that there is some curvature at low magnesium contents. The present results clearly support Axon and Hume-Rothery, but there is a tendency for the results to be slightly higher than theirs at higher magnesium contents. Other than the slight curvature, there is no evidence of any Brillouin-zone effects in the lattice-spacing/composition relationship. Vacant lattice sites are found, however, and there appears to be a peak in the vacant-lattice-site/composition curve at 1% magnesium and a gradual increase in the number of vacant sites from 5% magnesium to the limit of solid solubility. Some inaccuracy may have been introduced by the difficulty of working alloys containing more than 8% magnesium, but the results at lower alloy contents are probably fairly reliable. The vacant lattice sites suggest that two Brillouin zones are filled as magnesium is added to aluminium, although no

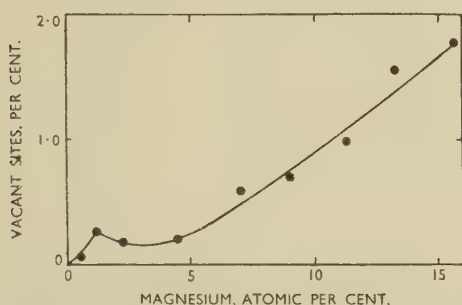


Fig. 3.—Vacant Lattice Sites in the Aluminium-Magnesium Solid Solution.

evidence to support this is shown by the lattice spacings. In fact, the lattice spacings show a decrease in the effective atomic diameter of aluminium, whereas in other systems the effective atomic diameter increases.

If a vacant lattice site is regarded as an atom of zero diameter and Vegard's law is applied, it is apparent that vacant lattice sites would decrease the lattice spacing. In this case the number of vacant sites is sufficient to cause a much greater decrease in spacing than is actually observed. It is tentatively suggested that at low magnesium contents, where the rate of increase of vacant sites with composition is highest, the effect of the vacant sites in contracting the lattice is greater than that of the Brillouin-zone effect in expanding it, so that the net result is a less-rapid expansion of the lattice.

#### 4. GENERAL DISCUSSION

The three systems described and the aluminium-zinc system discussed earlier<sup>1</sup> may now be considered together.

Raynor and Wakeman<sup>6</sup> have discussed the solubility of silver and zinc in aluminium and shown that the inflection in the solubility curve of the aluminium-

silver system corresponds with the maximum of the  $(\alpha + \alpha')$  loop in the aluminium-zinc system when the composition is expressed in terms of electron/atom ratios. The concentration of vacant lattice sites and the lattice spacings suggest that the filling of the Brillouin zone occurs at somewhat lower alloy contents than the phenomena discussed by Raynor and Wakeman, but the change taking place at 14% silver appears to correspond with that occurring at 25% zinc rather than that at about 4% zinc.

It seems likely that in the aluminium-magnesium system two zones are filled, one at about 1% magnesium and the other at a higher magnesium content. There is no definite evidence to show the exact composition at which this other zone is filled, and it may not be filled even at the limit of solid solubility. A figure for the electron concentration will be calculated on the assumption that the zone is filled at the limit of solid solubility at 450° C., although there is little justification for doing so.

The results given earlier<sup>1</sup> for the aluminium-zinc system indicate that zones are filled at about 4.3 and 25% zinc in that system. Taking into account vacant lattice sites, the following list, showing the electron/atom ratios at which Brillouin zones are filled, may be drawn up:

	Zone a	Zone b
Al-Cu	...	...
Al-Ag	...	2.72
Al-Mg	2.97	2.77
Al-Zn	2.93	2.70

No Brillouin zones appear to be filled in the aluminium-copper system. The limit of solid solubility is little more than 2% copper, so it is unlikely that zone b would be approached; but the electron/atom ratio of 2.97 at which zone a is filled in the aluminium-magnesium system is included in the solid solution. However, there is no sign of zone a in the aluminium-silver alloys, so it is perhaps not surprising that it does not appear in the aluminium-copper alloys. Zone b occurs in the aluminium-silver alloys, although zone a does not. The electron/atom ratio at which it appears corresponds closely with that for zone b in the aluminium-zinc alloys. Agreement with the aluminium-magnesium alloys is not so good; but there is some uncertainty about the exact composition at which zone b occurs in this system. Zone a is filled in both the latter alloy systems. Agreement is reasonable, but not by any means perfect.

In the aluminium-zinc system zone effects are accompanied by expansion of the lattice and formation of vacant sites; in the aluminium-silver system lattice expansion occurs but no vacant sites; while in the aluminium-magnesium system vacant sites are formed without an expansion of the lattice. It is concluded that the addition of silver and magnesium to aluminium modifies the  $N(E)$  curve of the pure metal, just as zinc does, but that the electron/atom ratios, and the exact phenomena associated with the modifications are different for the various alloying elements.



For ideal solutions in equilibrium with a phase of invariant composition, it can be shown that the plot of  $\log S$  against  $1/T$  gives a straight line, where  $S$  is the saturation concentration of the solute and  $T$  the absolute temperature. In the systems under consideration this plot gives a straight line for the solution of copper, the solution of silver at low concentrations, and the solution of magnesium at high concentrations. The solution of zinc does not give a straight line. In the cases of silver and magnesium the departures from linearity do not coincide exactly with the supposed zone effects, although there is fair correlation. The departure from linearity indicates that the solutions are not ideal, and it is suggested that where Brillouin-zone effects occur solid solutions may become non-ideal.

#### IV.—CONCLUSIONS

The conclusions which may be drawn from the work described are:

1. Silver and magnesium when alloyed with aluminium modify the  $N(E)$  curve for aluminium and cause the filling of Brillouin zones as the electron/atom ratio is decreased, in the same way as does zinc.

2. Copper has no similar effect up to the limit of solubility.

3. The effect of each alloying element is characteristic of the element itself. Different elements act in different ways.

4. Brillouin-zone effects cause solid solutions to behave in a non-ideal way.

It is tentatively suggested that the initial curvature of the aluminium-magnesium lattice-spacing/composition curve is associated with the formation of vacant lattice sites which act in the same way as small atoms in tending to reduce lattice spacing.

#### ACKNOWLEDGEMENTS

The author has pleasure in thanking The British Aluminium Co., Ltd., for the gift of the high-purity aluminium and for carrying out the analysis of the aluminium-magnesium alloys; F. A. Hughes and Co., Ltd., for the gift of the high-purity magnesium; Mr. D. Hardie, B.Sc., of the Metallurgy Department, King's College, for preparing the filings and measuring the lattice spacings of the aluminium-magnesium alloys; and Professor A. Preece for his encouragement while the work was in progress.

#### APPENDIX

##### *Changes in Composition During the Annealing of Aluminium-Magnesium Alloy Filings*

Hume-Rothery and Raynor<sup>7</sup> are very insistent on the need for analysing samples of the filings from which the final X-ray specimen is prepared. The author believes this may introduce errors (for instance, Ellwood and Weddle<sup>8</sup> have shown that copper powder may pick up 0.2% oxygen when exposed to the atmosphere), and has not found it necessary until working on the aluminium-magnesium system. Lattice-spacing measurements were erratic, suggesting an irregular loss of magnesium during the final stress-relieving anneal. To determine the lattice spacing a little more than 1 g. of filings of each alloy was prepared and the final stress-relieving treatment carried out on all the filings by the procedure adopted by Axon and Hume-Rothery.<sup>5</sup> Samples for X-ray examination were prepared and the remainder of the filings sent for analysis. The results are as follows:

Magnesium, at.-%		Lattice Spacing, kX at 25° C.
Ingot	Filings	
0.59	0.59	4.0427 <sub>3</sub>
1.19	1.19	4.0444 <sub>4</sub>
2.37	2.21	4.0494 <sub>3</sub>
4.56	4.48	4.0595 <sub>3</sub>
6.85	6.72	4.0695 <sub>3</sub>
9.15	9.01	4.0797 <sub>8</sub>
11.3	11.2	4.0908 <sub>1</sub>
13.5	13.3	4.1002 <sub>1</sub>
16.2	15.6	4.1092 <sub>5</sub>

There is a small irregular loss of magnesium when filings of these alloys are stress-relieved. This phenomenon has not been observed in the other systems investigated, and the results are included to give an indication of the changes in composition involved.

#### REFERENCES

1. E. C. Ellwood, *J. Inst. Metals*, 1951-52, **80**, 217.
2. E. C. Ellwood and J. M. Silcock, *ibid.*, 1948, **74**, 457.
3. J. B. Nelson and D. P. Riley, *Proc. Phys. Soc.*, 1945, **57**, 160.
4. J. E. Dorn, P. Pietrowsky, and T. E. Tietz, *Trans. Amer. Inst. Min. Met. Eng.*, 1950, **188**, 933.
5. H. J. Axon and W. Hume-Rothery, *Proc. Roy. Soc.*, 1948, [A], **193**, 1.
6. G. V. Raynor and D. W. Wakeman, *Phil. Mag.*, 1949, [vii], **40**, 404.
7. W. Hume-Rothery and G. V. Raynor, *J. Sci. Instruments*, 1941, **18**, 74.
8. E. C. Ellwood and W. A. Weddle, *J. Inst. Metals*, 1951-52, **80**, 193.

# THE FACTORS AFFECTING THE FORMATION OF 21/13 ELECTRON COMPOUNDS IN ALLOYS OF COPPER AND OF SILVER \*

1388

By W. HUME-ROTHERY,† O.B.E., F.R.S., MEMBER, J. O. BETTERTON, Jr.,‡ D.Phil., B.S., MEMBER, and J. REYNOLDS,§ B.A.

## SYNOPSIS

An attempt is made to discover the factors that control the composition limits of phases with the  $\gamma$ -brass structure in different alloy systems. The Brillouin zone of the structure is described; this gives rise to a double peak on the  $N(E)$  curve, and then to two relatively steep falls in the curve before the final descent to zero as the zone is filled. Data for copper-aluminium and copper-gallium alloys show that, when the electron concentration reaches about 1.70, atoms begin to drop out of the structure in such a way that the number of electrons per unit cell remains constant. Considered empirically, the data for all the systems point to the fact that this is a critical electron concentration beyond which a normal  $\gamma$  structure with its full complement of atoms cannot exist, and it is suggested that this corresponds to one of the steep falls in the  $N(E)$  curve. Increasing size-factor displaces the compositions of  $\gamma$  phases in the direction of lower electron concentration; this tendency resembles that previously found for  $\beta$  phases. Increasing electrochemical factor displaces the compositions of  $\gamma$  phases in the direction of higher electron concentration. The Pauling valencies do not give such a good generalization of the  $\gamma$ -phase compositions as that given by the conventional valencies. With the exception of the  $\text{Ag}_3\text{Li}_{10}$  phase, the wide range of data agrees with accepted theory.

## I.—INTRODUCTION

In alloys of copper and silver with metals of the B Sub-Groups and of the first two Short Periods, the first additions of the solute metal usually result in the formation of a primary substitutional solid solution. In systems where the size-factors are favourable, the limit of the primary substitutional solid solution is reached when the electron concentration has increased to a value of about 1.36–1.40, and this has been explained by the electron theory of H. Jones.<sup>1</sup> Further additions of the solute element result in the appearance of a new phase whose composition in many systems lies at an electron concentration of about 3/2. Such phases may be called the 3/2 electron compounds, and are of three main types: the  $\beta$  and  $\beta'$  phases with random and ordered body-centred cubic structures, respectively, the  $\zeta$  and  $\zeta'$  phases with close-packed hexagonal structures, and the  $\mu$  phases with the structure of  $\beta$ -manganese. The factors which affect the relative stabilities of these phases have been discussed by Hume-Rothery, (P. W.) Reynolds, and Raynor,<sup>2</sup> and there is general agreement that where the size-factors are favourable the  $\alpha \rightleftharpoons \beta$  equilibrium is determined mainly by the electron concentration. To a higher degree of accuracy the  $\alpha \rightleftharpoons \beta$  equilibrium is affected by the lattice distortion produced by the solute element,<sup>3</sup> and in systems where the size-factor is on the edge of the favourable zone (e.g. copper-

indium, copper-tin) the  $\alpha$ -phase boundaries are displaced in the direction of lower electron concentration.

With still higher percentages of the solute element, phases with a characteristic  $\gamma$ -brass type of structure are formed in many systems at an electron concentration of  $21/13 = 1.615$ .<sup>4,5</sup> The normal  $\gamma$ -brass structure is cubic, with a lattice spacing of the order of 8.5–9 kX, and the unit cell contains 52 atoms. Modifications of the structure are found, some of which (e.g.  $\text{Cu}_{31}\text{Sn}_9$ ) are based on a cell of double this size (and hence eight times the volume) containing 416 atoms per cell; whilst in some systems (e.g. copper-gallium, copper-aluminium) defect structures are formed with the same general structure but fewer than 52 atoms per unit cell. Apart from these cubic structures, distorted modifications (e.g.  $\text{Cu}_9\text{In}_4$ ) of the general  $\gamma$ -type of structure are found,<sup>6</sup> in which the symmetry is lower. The object of the present paper is to survey the systems in which  $\gamma$  phases are formed, in the hope of establishing the factors that affect the stabilities and composition limits.

## II.—THE BRILLOUIN ZONE OF THE $\gamma$ -BRASS STRUCTURE

The first Brillouin zone of the  $\gamma$ -brass structure was calculated by H. Jones<sup>7</sup> and is shown in Fig. 1. The zone is bounded by two sets of faces corresponding to the satisfying of the Bragg equation for reflection from

\* Manuscript received 31 October 1951.

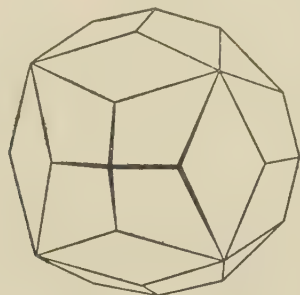
† Royal Society Warren Research Fellow and University Lecturer in Metallurgical Chemistry, Oxford.

‡ Metallurgist, Oak Ridge National Laboratory, Tenn., U.S.A.

§ Inorganic Chemistry Laboratory, Oxford.



the (330) and (411) planes of the crystal; it is these planes which give rise to the very strong  $\Sigma h^2 = 18$  diffraction line in X-ray powder films. The completely filled zone contains 90 electrons per unit cell, and so corresponds to an electron concentration of 1.73, if the cell contains the full number of 52 atoms. If the energy contours within the zone are assumed to be



[Courtesy Clarendon Press.]

FIG. 1.—The Brillouin Zone of the  $\gamma$ -Brass Structure.

spherical, the Fermi sphere which touches the zone surfaces corresponds to an electron concentration of 1.54, if all the lattice points are occupied. The corresponding compositions of alloys of copper and silver with solutes of higher valency are shown in Table I, and these are fundamental for the understanding of the alloys.

TABLE I.—Copper and Silver Alloys.

Valency of Solute	Atomic-% Solute Corresponding to :	
	Inscribed Fermi Sphere (Electron Concentration 1.54)	Completely Filled Zone (Electron Concentration 1.73)
2	54	73
3	27	36.5
4	18	24.3

It was first shown by Ekman<sup>8</sup> that phases with a  $\gamma$ -brass structure are formed by some of the transition elements, and that these appear at the same electron concentration, 21/13, if the transition element is given a zero valency. These phases are of widely varying composition, and probably no great significance attaches to an exact zero valency, because the facts would be covered equally well by a small positive or

TABLE II.—Alloys of Transition Elements.

Valency of Solute	Atomic-% Solute Corresponding to :	
	Inscribed Fermi Sphere (Electron Concentration 1.54)	Completely Filled Zone (Electron Concentration 1.73)
2	77	86.5
3	51.3	64.3
4	38.5	43.3

negative valency of the transition element. If a zero valency is assumed, Table II shows the percentages of solute elements of valencies 2, 3, and 4 which correspond to the tangency of the Fermi sphere and to the completely filled zone in alloys of the transition

elements, assuming that the unit cell contains its full complement of 52 atoms.

The conventional description of the  $\gamma$ -brass phases as founded on an electron:atom ratio of  $21/13 = 1.615$  originated with the X-ray crystal-structure work which showed that the phases in the systems copper-zinc and copper-aluminium were based on the compositions  $\text{Cu}_5\text{Zn}_8$  and  $\text{Cu}_5\text{Al}_4$ . The electron concentration of 1.615 therefore lies slightly beyond the peak on the  $N(E)$  curve, if a spherical Fermi surface is assumed (Fig. 2 (a)). In the zone of the actual crystal structure the Fermi surfaces are not spherical, and although the centres of the (330) and (411) faces lie at the same distance from the origin of  $k$ -space, the Fermi surface will not in general touch the two kinds of face at exactly the same energy,  $E$ . This means that the true  $N(E)$  curve usually has a double peak, as in Fig. 2 (b), or a flattened top, as in Fig. 2 (c).

The Brillouin zone for the  $\gamma$ -brass structure has three kinds of corner at different distances from the origin of  $k$ -space. With increasing electron concentration the occupied states spread outward in  $k$ -space, and a marked fall in the  $N(E)$  curve occurs as a particular set of corners is filled, because at this stage electron states in a number of directions are no longer available. The high-energy end of the  $N(E)$  curve

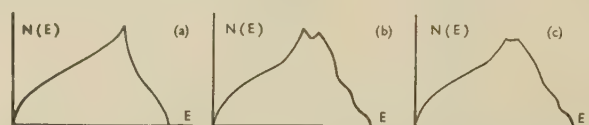


FIG. 2.— $N(E)$  Curves for  $\gamma$ -Brass Phases.

for the  $\gamma$ -brass zone is therefore of the general form shown in Figs. 2 (b) and (c), in which there are two relatively steep falls before the final descent to zero.

### III.—DEFECT STRUCTURES AND THE CRITICAL ELECTRON CONCENTRATION

The above description refers to the electron:atom ratios and the Brillouin zones of the normal  $\gamma$  structure when the unit cell contains the full complement of 52 atoms. In the system copper-aluminium,<sup>9</sup> the X-ray and density data show that the number of

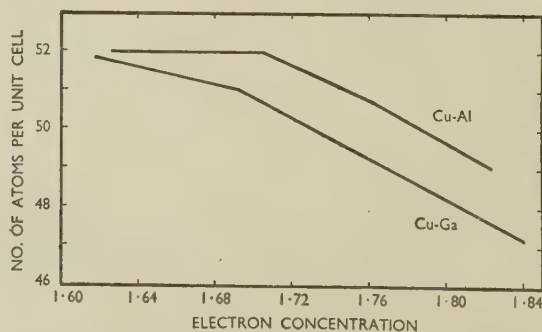


FIG. 3.—The Number of Atoms per Unit Cell in the  $\gamma$  Phases of the Systems Copper-Gallium and Copper-Aluminium as a Function of Composition.

atoms per unit cell is approximately constant at about 52 from the composition  $\text{Cu}_5\text{Al}_4$  to about 35.3 at.-% aluminium, after which atoms begin to drop out more rapidly in such a way as to maintain an approximately constant number of 89 electrons per unit cell. This was first pointed out by Konobeevsky,<sup>10</sup> although he made some mistakes in Brillouin-zone theory. In

In a recent note Bradley<sup>12</sup> has suggested that the atoms drop out of the copper-aluminium  $\gamma$  structure in such a way that a valency electron replaces an atom, and the total sum of (atoms + valency electrons) per unit cell remains constant. A detailed examination has been made by the present authors of the data of Bradley, Goldschmidt, and Lipson,<sup>9</sup> and the scatter of

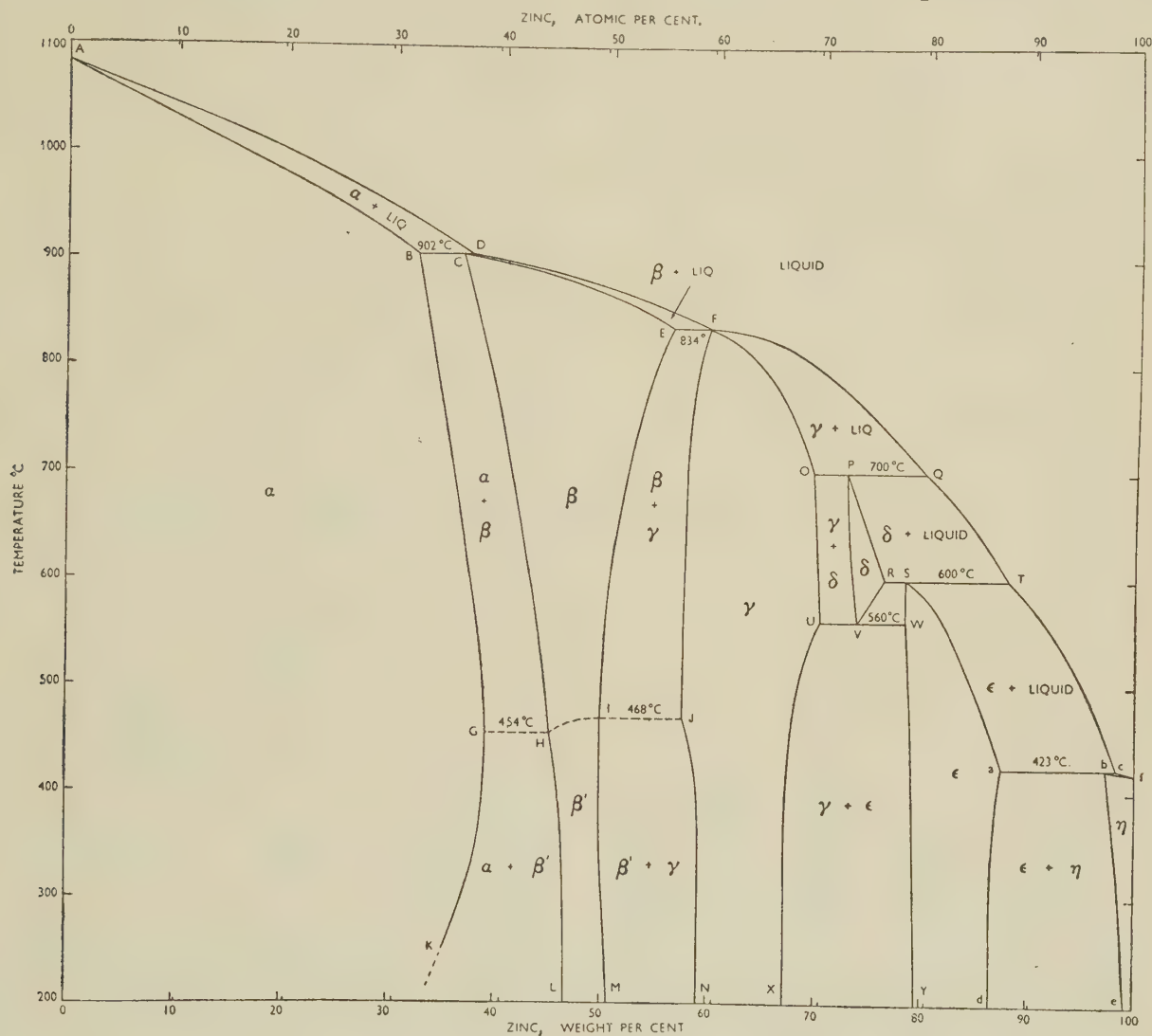


FIG. 4.—The Equilibrium Diagram of the System Copper-Zinc.

the system copper-gallium<sup>11</sup> the number of atoms per unit cell is 52 at the copper-rich boundary of the  $\gamma$ -phase area, and then diminishes very slightly with increasing gallium content up to 34.5 at.-% gallium, after which the atoms drop out more rapidly so that a constant number of 86.5 electrons per unit cell is maintained. Fig. 3 shows the number of atoms per unit cell as a function of the composition, and the consistently higher values for the copper-aluminium alloys may be due to the higher electrochemical factor producing increased cohesion; this is reflected in the markedly higher melting points of these alloys.

the points is found to be too great to permit a conclusive decision to be made between the two hypotheses of a constant number of electrons, or of (electrons + atoms) per unit cell, although the former hypothesis is slightly favoured. For the system copper-gallium<sup>11</sup> the data are conclusively in favour of a constant number of electrons per unit cell, and it is suggested that the structures of the  $\gamma$  phases do not offer any real support for Bradley's hypothesis of electrons replacing atoms on lattice points.

Fig. 3 suggests that the composition 34-35 at.-% aluminium or gallium marks a critical stage in the



filling of the Brillouin zone, and that beyond an electron concentration of about 1.70 the increase in electronic energy becomes so marked that atoms drop out of the structure to prevent the number of electrons per unit cell from increasing. Alternatively, the effect might be due to the difference in size of the two kinds of atom making it impossible to replace more than a certain percentage of the copper atoms by the larger atoms of gallium or aluminium. Examination of the structure of  $\text{Cu}_9\text{Al}_4$  determined by Bradley<sup>13</sup> has failed to show a correlation between the composition 34–35 at.-% of aluminium and the stage at which any one of the structurally equivalent groups of copper might be completely replaced by atoms of aluminium. This suggests that the effect is electronic.

Support for this view is found by a study of the  $\gamma$ -phase boundaries in the system copper–zinc. In this

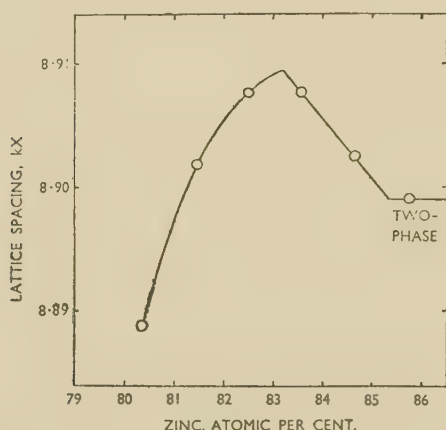


FIG. 5.—The Lattice Spacing/Composition Curve in the System Nickel–Zinc.

system no density/composition data are available, but the accurate work of Owen and Pickup<sup>14</sup> shows the lattice spacing/composition curve to be smooth. Fig. 4 gives the equilibrium diagram of the system, from which it will be seen that the limit of the  $\gamma$  phase occurs at about 70 at.-% zinc, and hence at an electron concentration (1.70) almost the same as that at which the atoms begin to drop rapidly out of the  $\gamma$  structure in the systems copper–aluminium and copper–gallium.

The next phase, denoted  $\delta$ , has been shown<sup>15</sup> to possess a body-centred cubic structure containing numerous defects or unoccupied lattice points. When it is remembered that the  $\gamma$ -brass structure is itself a distorted b.c.c. structure from which 2 atoms out of 54 have been removed, the resemblance between the two systems is apparent. In each case the normal  $\gamma$  structure continues up to an electron concentration of the order 1.70. Beyond this electron concentration atoms drop out of the copper–gallium \*  $\gamma$  struc-

ture in such a way that the general type of structure is retained, whilst in the system copper–zinc, the dropping out of atoms is more drastic and the alloy reverts to a defective form of the body-centred cubic structure from which the  $\gamma$  phase may be regarded as originally derived.

In the system nickel–zinc the lattice spacing/composition curve for the  $\gamma$  phase (Fig. 5) rises to a sharp peak at about 83 at.-% zinc. This atomic ratio is quite different from those in the systems copper–aluminium and copper–gallium, but if nickel is regarded as zero valent the electron concentration corresponding to 83 at.-% zinc is 1.66 and is thus nearly the same as that in the alloys of copper with trivalent metals.

The above facts suggest that normal  $\gamma$  structures containing nearly the full complement of 52 atoms per unit cell become unstable when the number of electrons per unit cell exceeds about 87–88 (electron concentration 1.68–1.70). It must be emphasized that the number of electrons per unit cell is the real characteristic of Brillouin-zone theory, and that the simple electron-concentration rules are the result of the fact that in most structures all the lattice points are occupied. Since the  $\gamma$  phases may involve defect structures, strictly speaking the phase boundaries of the different  $\gamma$  phases should be compared in terms of electrons per unit cell, but in the absence of density measurements in most systems Fig. 6 has been drawn so as to show the phase boundaries with electron concentration as abscissæ and temperature as ordinates. The scales are the same in each case, and the different systems are arranged in the order of size-factors,† and are spaced out to avoid overlapping. In each system the vertical line represents an electron concentration of 21/13. Fig. 7 is a similar diagram for the  $\gamma$  phases of transition elements. In this figure the abscissæ are atomic percentages, because the exact valency of the transition element is unknown; the vertical dotted lines represent an electron concentration of 21/13, if a zero valency for the transition element is assumed.

In Fig. 6 the wide extent of the  $\gamma$  phases in the systems copper–aluminium and copper–gallium is correct as expressing the range of composition, but is misleading in that the figure does not indicate the point (electron concentration = 1.68–1.70) beyond which defect structures are formed. Of the other copper, silver, and gold alloys, the system gold–zinc is the only one in which the electron concentration exceeds 1.70. The gold–zinc  $\gamma$ -phase region is very wide, and almost certainly involves a defect structure, because if all the lattice points were occupied the phase boundary would extend beyond the point corresponding to a completely filled zone, and this is improbable. In no other system does the electron concentration of

\* The above description is based on the lattice spacings of copper–gallium alloys after quenching from 381° and 200° C. If the diagram of Betterton and Hume-Rothery<sup>11</sup> is correct, the  $\gamma_1$  modification extends as far as 37 at.-% gallium at high temperatures, but the number of atoms per unit cell is not

known in this region.

† The systems are arranged in order of the size-factors and not on a regular scale, because the latter would involve overlapping.

the  $\gamma$  phase exceed 1.70, and considered empirically this appears to be a critical value beyond which a normal  $\gamma$  structure cannot exist. It may be suggested that this critical electron concentration corresponds with one of the steep falls in the  $N(E)$  curve, since a fall in the  $N(E)$  curve means an increase in the energy required to introduce further electrons.

If the transition elements are assumed to exert a zero valency, an electron concentration of 1.68–1.70 corresponds to 84–85 at.-% of a divalent element, and from Fig. 7 it will be seen that in the systems manganese-zinc, cobalt-zinc, and nickel-zinc the  $\gamma$ -phase

near to these values, the exact figures being shown below:

System	At.-% Solute
Cu-Zn	57
Ag-Zn	58
Ag-Cd	58
Ag-Hg	57
Cu-Al	30
Cu-Ga	29
Ag-In	32
Cu-Si	18

It may be concluded, therefore, that in systems where the structure of the alloy is controlled mainly by the electron concentration, the normal  $\gamma$  phases are

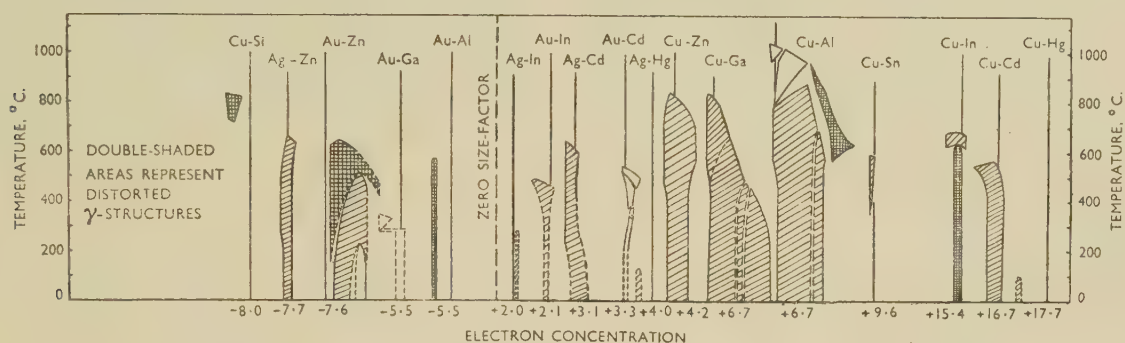


FIG. 6.—The Phase Fields of the Known  $\gamma$  Phases. The systems are spaced out in the order of the size-factors so as to avoid overlapping. The vertical lines indicate the composition corresponding to the electron : atom ratio of 21/13.

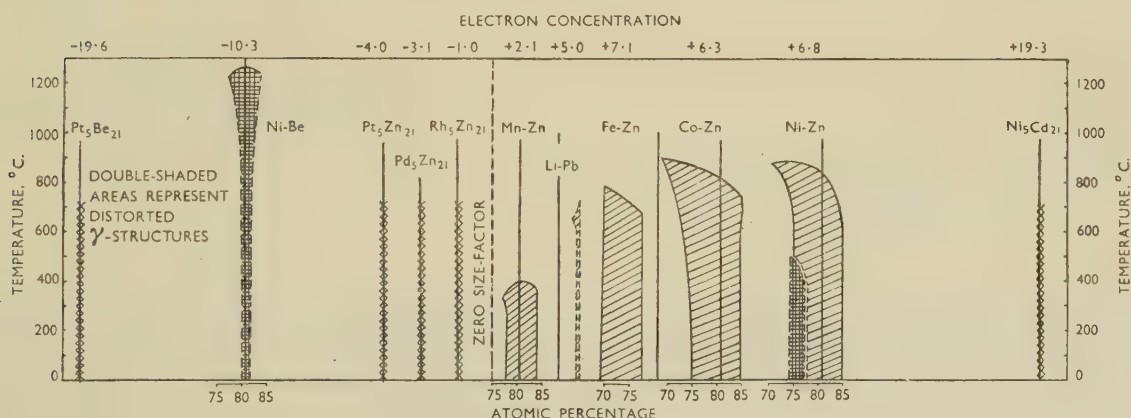


FIG. 7.—The Phase Fields of  $\gamma$  Phases in Alloys of Transition Metals. The vertical lines represent the electron : atom ratio of 21/13 on the assumption that the transition element has a zero valency.

region extends up to this percentage of zinc, and in no case is this value exceeded for the divalent elements.

#### IV.—THE EFFECTS OF SIZE-FACTOR AND ELECTROCHEMICAL FACTOR

As shown in Table I, the assumption of a spherical Fermi surface leads to a peak on the  $N(E)$  curve at an electron concentration of 1.54, which corresponds with 54, 27, and 18 at.-% of di-, tri-, and tetravalent solutes, respectively. Fig. 6 shows that in the systems where the size-factors are favourable and the electrochemical factors are not very large, the boundaries of the  $\gamma$  phase on the copper-, silver-, or gold-rich side lie very

stable from an electron concentration near to that of the peak on the  $N(E)$  curve of the simple theory to a critical value of about 1.70.

Fig. 6 shows that with a given valency the effect of increasing size-factor is to displace the composition of the  $\gamma$  phases in the direction of lower electron concentration. This is shown clearly by comparing the diagrams for copper-zinc and copper-cadmium, and for copper-aluminium, copper-gallium and copper-indium, all of which are established accurately. This principle is the same as that found for the  $\beta$  phases,<sup>2</sup> but an exception is shown by the system silver-mercury, where the  $\gamma$  phase has a lower electron concentration than would be expected.



From Fig. 6 it is clear that for the alloys of copper, silver, and gold the  $\gamma$  phases reach their maximum stability when the atomic diameters of solvent and solute are neither too nearly equal nor differ too greatly, whereas close-packed hexagonal phases are favoured by almost equal atomic diameters. In the system silver-aluminium there is no  $\gamma$  phase, but the two close-packed hexagonal phases based on electron concentrations of  $3/2$  and  $7/4$  join together to form a single phase, as shown in Fig. 8. It is perhaps significant that although in this system the conventional size-factor is  $-5.5\%$ , the two kinds of atom are so nearly similar that no appreciable lattice distortion occurs when silver dissolves in aluminium. In the system gold-aluminium the conventional size-factor is the same as for silver-aluminium, but a greater lattice distortion is found, and a phase with a distorted  $\gamma$  structure occurs. Fig. 6 makes it plain that

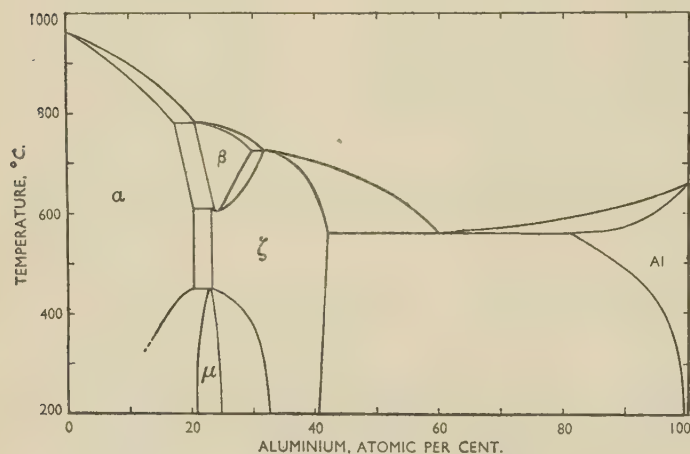


Fig. 8.—The Equilibrium Diagram of the System Silver-Aluminium.

$\gamma$  phases are stabilized by a moderate size-factor, and this may be because the  $\gamma$  structure is essentially a body-centred cubic structure from which atoms have dropped out. In a naïve way one may imagine that, if the atoms are all of the same size, there is no reason why one kind should fall out, whilst if they are of different sizes one kind may be squeezed out with a re-arrangement of the remainder to form the more stable groupings of the  $\gamma$  structure.

As pointed out previously,<sup>16</sup>  $\gamma$  phases are formed in systems (e.g. copper-cadmium) where the size-factor is too great to permit the formation of an appreciable primary solid solution. Figs. 6 and 7 suggest that the critical value of the size-factor is slightly greater than 20%, as compared with 15% for primary solid solutions. No  $\gamma$  phases are formed in the few systems where the size-factor exceeds 20%. From the point of view of size-factor, there is no reason why  $\gamma$  phases should not be formed in alloys of silver or gold with fully ionized lead or thallium, and the non-existence of such phases suggests that the latter elements are incompletely ionized in these alloys.

Fig. 6 shows that, so far as the normal and defect  $\gamma$  structures are concerned, the effect of increasing electrochemical factor is to displace the composition of the  $\gamma$  phase in the direction of higher electron concentration. This is seen clearly by comparing the position of the 21/13 line relative to the phase boundaries for the systems copper-gallium and copper-aluminium, where the electrochemical factor is greater in the latter case, and for copper-zinc, silver-zinc, and gold-zinc, where the size-factors are all favourable and the electrochemical factor increases in the order  $\text{Cu} < \text{Ag} < \text{Au}$ . In the system gold-zinc there is a very stable  $\beta'$  phase with a CsCl structure, rising to a maximum freezing point, and the displacement of the boundary of the  $\gamma$  phase in the direction of higher electron concentration can be interpreted in terms of the free-energy curves (see Fig. 9), since it has already been shown<sup>2</sup> that, considered empirically,

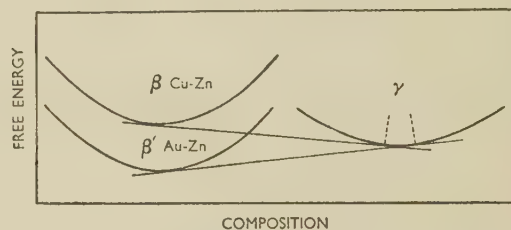


Fig. 9.—Hypothetical Free-Energy Curves Showing How the Displacement of the  $\gamma$ -Phase Boundary May Occur in the System Gold-Zinc.

the stability of the  $\beta'$  phases is increased by increasing electrochemical factor. It is perhaps for this reason that  $\gamma$  phases are not found in the systems silver-magnesium and gold-magnesium, where the electrochemical factor is even larger and very stable  $\beta'$  phases are formed. As shown in Table I, with a divalent solute the differences between the composition of the 21/13 ratio (61.5 at.-% zinc) and the full zone (73 at.-% zinc) is only 11.5 at.-%; whilst the difference between the 21/13 ratio and the empirically established critical electron:atom ratio of 1.70 (= 70 at.-% Zn) is only 8.5 at.-%. If, therefore, in the system gold-zinc the gold-rich boundary of the  $\gamma$  phase has been displaced to 63 at.-% zinc, it can be understood how the much higher electrochemical factor in the alloys with magnesium may displace the boundary so far from the characteristic electron:atom ratio that a  $\gamma$  phase is not formed. These considerations are quite general, and if, when considering the phase boundaries of a structure X in a series of alloys, a system is found where X is adjacent to a phase Y which is of great stability, we may expect the com-

position of the  $X/(X + Y)$  boundary to be displaced in the direction \* away from  $Y$ .

Fig. 6 shows that in the systems copper-zinc, copper-gallium, and copper-aluminium the composition ranges of the  $\gamma$  phases lie almost entirely on the high electron-concentration side of the ratio 21/13. Bernal,<sup>18</sup> who regarded the ratio 21/13 as fundamental, suggested that this was an illustration of the principle that where a structure involved a definite number of covalent bonds, it was more serious to have too few electrons than to have too many. It seems improbable that the  $\gamma$  phases really illustrate this principle, because the electron theory suggests that no particular significance attaches to the exact electron : atom ratio

$\gamma$  phases have been found in the systems lithium-lead and silver-lithium. In view of the interest aroused by the Pauling scheme of valencies,<sup>19</sup> an examination has been made of the degree to which these permit a generalization of the compositions of the  $\gamma$ -brass phases in the different alloys. Fig. 10 (a) shows the electron-concentration ranges of the  $\gamma$  phases in all the systems where they have been conclusively established. The generalization is clearly satisfactory, except for the system silver-lithium, the electron concentration for which must be 1.0 (this system is referred to below). Fig. 10 (b) gives the corresponding diagram for the Pauling valencies. Here, not only is the system silver-lithium an exception, but considerable diver-

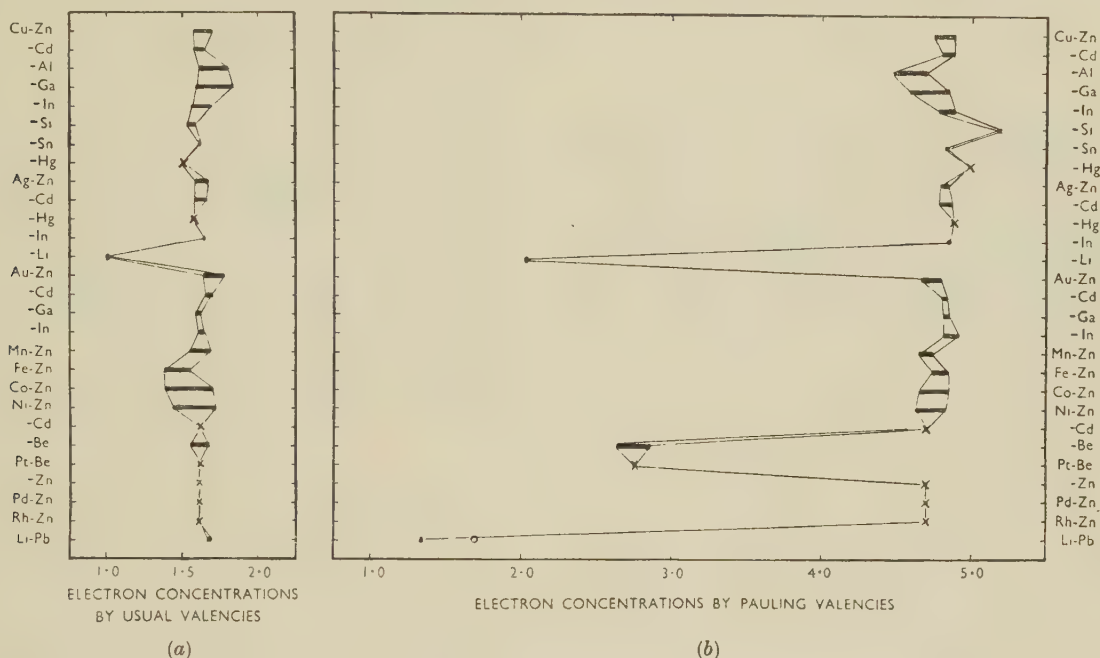


FIG. 10.—The Extent of the  $\gamma$ -Phase Region in Terms of Electron Concentration in the Different Systems, Using (a) the Normal Valencies and (b) the Pauling Valencies.

of 21/13, and also provides an alternative explanation of the diamagnetism of  $\gamma$ -brass which Bernal regarded as evidence for the existence of covalent bonds. Further, Fig. 6 shows not only that increasing size-factor moves the compositions of the  $\gamma$  phases to lower electron concentrations (copper-cadmium, copper-indium, copper-tin), but that even when the size-factor is favourable, the  $\gamma$  phase may (e.g. silver-cadmium) lie more to the low- than to the high-electron side of the 21/13 ratio.

## V.—DISCUSSION

In the preceding discussion and in the diagrams, use has been made of the conventional valencies, namely, 0 for transition metals; 1 for Cu, Ag, Au; 2 for Be, Zn, Cd, Hg; 3 for Al, Ga, In; and 4 for Si, Ge, Sn. Apart from the alloys of copper, silver, and gold,

gencies are shown by several other systems which fall into line when the normal valencies are used. Some workers regard the compound  $\text{Na}_{31}\text{Pb}_8$  as possessing a structure identical with, or closely similar to, that of the  $\gamma$  phases, although the details are not yet certain. If this compound is properly regarded as a  $\gamma$  phase, it falls into place when the normal valencies are used, but cannot be reconciled with the Pauling valencies, unless sodium is given a valency of 5.44. It may be concluded, therefore, that considered from the point of view of the empirical generalization of the facts relating to  $\gamma$  phases, the Pauling valencies are less successful than the normal valencies.

The composition of the  $\text{Ag}_3\text{Li}_{10}$  phase which occurs in the system silver-lithium is in contradiction to any of the previous theories, since both metals are univalent and it is improbable that higher valencies are

\* This principle is similar to that advanced by Raynor<sup>17</sup> for the effect of increasing stability of an intermediate phase on the limits of a primary solid solution.



exerted in their alloys. The atomic scattering powers of the two metals are here very different, and a detailed examination of the positions of the atoms in the unit cell of the  $\text{Ag}_3\text{Li}_{10}$  phase would thus be of great interest.

The present paper shows that, apart from this one example, the wide range of  $\gamma$  phases is in good agreement with the accepted theory, and some of the effects of size-factor and electrochemical factor can now be seen. The conclusion that the critical electron : atom ratio is 1.70, instead of the previously accepted value for the full zone (1.73), is also of interest, and suggests that more detailed calculations for the band structure of  $\gamma$  phases are desirable.

#### ACKNOWLEDGEMENTS

The authors must express their thanks to Professor Sir Cyril Hinshelwood for laboratory accommodation, and to Dr. F. M. Brewer for many other facilities which have greatly encouraged the present research. Thanks are also due to the Council of the Royal Society and to the British Non-Ferrous Metals Research Association for financial assistance towards the research programme of which this work forms a part.

#### REFERENCES

1. H. Jones, *Proc. Phys. Soc.*, 1937, **49**, 250.
2. W. Hume-Rothery, P. W. Reynolds, and G. V. Raynor, *J. Inst. Metals*, 1940, **66**, 191.
3. K. W. Andrews and W. Hume-Rothery, *Proc. Roy. Soc.*, 1941, [A], **178**, 464.
4. A. Westgren and G. Phragmén, *Phil. Mag.*, 1925, [vi], **50**, 311.
5. A. J. Bradley and J. Thewlis, *Proc. Roy. Soc.*, 1926, [A], **112**, 678.
6. W. Hume-Rothery and J. Reynolds, unpublished work.
7. H. Jones, *Proc. Roy. Soc.*, 1934, [A], **144**, 225.
8. W. Ekman, *Z. physikal. Chem.*, 1931, [B], **12**, 57.
9. A. J. Bradley, H. J. Goldschmidt, and H. Lipson, *J. Inst. Metals*, 1938, **63**, 149.
10. S. Konobeevsky, *J. Inst. Metals*, 1938, **63**, 161 (discussion).
11. J. O. Betterton, Jr., and W. Hume-Rothery, *J. Inst. Metals*, 1951-52, **80**, 459.
12. A. J. Bradley, *Nature*, 1951, **168**, 661.
13. A. J. Bradley, *Phil. Mag.*, 1928, [vii], **6**, 878.
14. E. A. Owen and L. Pickup, *Proc. Roy. Soc.*, 1933, [A], **140**, 179.
15. K. Schubert and E. Wall, *Z. Metallkunde*, 1949, **40**, 383.
16. W. Hume-Rothery, "The Structure of Metals and Alloys". (*Inst. Metals Monograph and Rep. Series*, No. 1), 1950: London.
17. G. V. Raynor, "Progress in Metal Physics." Vol. I, p. 4. London: 1949 (Butterworths Scientific Publications).
18. J. D. Bernal, *Trans. Faraday Soc.*, 1929, **25**, 367.
19. L. Pauling, *Phys. Rev.*, 1938, [ii], **54**, 899; *J. Amer. Chem. Soc.*, 1947, **69**, 542.

# THE LATTICE SPACINGS AND DENSITIES OF GOLD-NICKEL ALLOYS AT 25° C.\*

1389

By E. C. ELLWOOD,† Ph.D., F.I.M., MEMBER and K. Q. BAGLEY,‡ Ph.D.

## SYNOPSIS

Anomalies in lattice spacing and density have been found in the solid solution of gold and nickel. It is concluded that Brillouin-zone overlaps occur in the solid solution, accompanied by the formation of vacant lattice sites. By analogy with other gold-rich solid solutions and from the calculation by Jones and Mott (*Proc. Roy. Soc.*, 1937, [A], 162, 49) of the  $N(E)$  curve for the face-centred cubic metal copper, it is concluded that nickel has a valency of 3.2 when dissolved in gold up to 60 at.-%.

## I.—INTRODUCTION

It has recently been shown by one of the authors<sup>1</sup> that certain anomalies in the lattice spacing and density of the aluminium-zinc solid solutions in the range of the  $(\alpha + \alpha')$  immiscibility loop are probably associated with Brillouin-zone effects. It was desired to examine another system containing a similar loop to see whether such effects were common or were confined to the aluminium-zinc system. The gold-nickel system was chosen because the maximum temperature of immiscibility appeared to be lower than that found in other systems.

## II.—EXPERIMENTAL METHODS

The gold was more than 99.99% pure. The nickel, kindly presented by The Mond Nickel Co., Ltd., contained copper 0.003, iron 0.013, carbon 0.040, and sulphur 0.001%. The carbon was removed, or considerably reduced, by treatment with moist hydrogen for 48 hr. at 720° C. It is likely that some of the sulphur was removed at the same time.

The alloys were prepared in 5-g. lots by the general method of Owen,<sup>2</sup> modified to suit our conditions as required. In particular, vacuum-melting in a H.F. furnace in alumina thimbles was used for the high-melting-point nickel-rich alloys. The maximum loss in weight was 2 mg. or four parts in ten thousand, and the average loss was nearer two parts in ten thousand. The International Atomic Weight of gold (1947) is given to five parts per ten thousand, so that the accuracy obtained by synthesis appears to be greater than can be used in calculating the atomic percentage of gold.

After preparation, the alloys were annealed *in vacuo* at 900° C. for a month and tested for homogeneity by measuring the lattice constants of filings taken from different parts of the ingot. When it had been shown

that any particular ingot was homogeneous, the lattice spacing obtained was assigned to the intended composition.

To determine the lattice spacing, the filings were sealed in evacuated silica tubes, annealed for 1 hr. at 900° C., and quenched in water. The diffraction patterns were obtained using a 9-cm.-dia. camera and copper radiation, and the spacings calculated in kX units, taking 1.537395 kX as the wave-length of  $\text{CuK}_{\alpha}$  radiation. The films were corrected for shrinkage, but no correction for refraction was applied. The values of the lattice spacing were obtained by extrapolation and adjusted to 25° C., on the assumption that the coefficient of expansion varied linearly with atomic composition from  $14.4 \times 10^{-6}$  for gold to  $13.0 \times 10^{-6}$  for nickel.

The theoretical densities of the alloys were calculated from the atomic weights and lattice spacings in the usual way, using  $1.66035 \times 10^{-24}$  g. as the mass of an atom of unit atomic weight and a factor of 1.00202 to convert kX units to Ångströms.

Attempts were made to work the alloys before the densities were measured. Up to 25 and above 85 at.-% nickel, the alloys could be cold worked without cracking. At intermediate compositions the alloys were too hard to cold work appreciably. The ingots were so small that they lost heat very rapidly when transferred to a cold anvil for hammering, and thus could not be hot worked satisfactorily by that method. An attempt was made to heat the ingots in a heat-resisting steel die and to hammer them *in situ*, but the die appeared to be much softer than the ingots at 850° C., and little useful deformation was obtained. Most of the ingots of intermediate composition were deformed to some extent by a combination of hot and cold working, but the actual amount was variable and small. The fact that four of the eight alloys in this composition range attained the theoretical density, together with the absence of visible micro-porosity,

\* Manuscript received 16 January 1952.

† Lecturer in Metallurgy, King's College, University of Durham.

‡ Ministry of Supply, Atomic Energy Production Division; formerly of Metallurgy Department, King's College, University of Durham.



may perhaps be taken as evidence that the alloys were sound.

The densities were determined in the way described earlier.<sup>1</sup> Extreme accuracy was not considered essential, and by weighing to 0.1 mg. the maximum accuracy in determining the density of gold and nickel is 0.01 and 0.0015 g./c.c. respectively. This allows an accuracy of about 0.05 and 0.02 in the calculation of the percentage vacant sites in the gold- and nickel-rich alloys, respectively. There may be errors in weighing, and in general the calculation of percentage vacant sites is probably accurate to within 0.1%. No claim is made that the figure obtained represents the actual percentage of vacant sites, although it probably gives an approximate value when suitable precautions are taken.

### III.—RESULTS AND DISCUSSION

The lattice spacings are given in Table I, and the lattice-spacing/composition and percentage-vacant-

abnormal expansion of the lattice and the appearance of vacant lattice sites coincides with the filling of Brillouin zones in the alloy. If gold is regarded as a normal monovalent solvent and nickel as a solute of

TABLE I.—Lattice Spacings of Gold-Nickel Alloys.

Ni, at.-%	Lattice Spacing, kX	Ni, at.-%	Lattice Spacing, kX
0.0	4.0703	65.0	3.7472
10.0	4.0398	70.0	3.7170
20.0	3.9907	75.0	3.6840
25.0	3.9625	80.0	3.6545
30.0	3.9354	85.0	3.6258
40.0	3.8902	90.0	3.5904
50.0	3.8410	95.0	3.5561
60.0	3.7771	100.0	3.5169

unknown valency  $x$  and the points  $B$  and  $D$  (Fig. 1) as corresponding with the first two peaks at 1.40 and 2.10 electrons/atom on the  $N(E)$  curve for the face-centred cubic structure, as deduced by Jones and

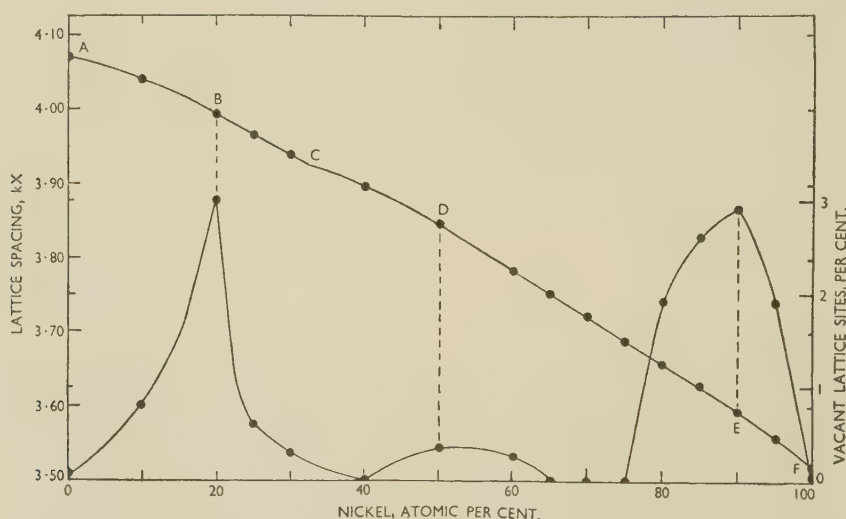


FIG. 1.—Lattice-Spacing/Composition and Vacant-Lattice-Site/Composition Curves for Gold-Nickel Alloys.

lattice-sites/composition curves are shown in Fig. 1. There is good correlation between the two curves. In the regions  $AB$  and  $CD$ , where the normal lattice contraction with increasing nickel is retarded, the number of vacant sites is increasing. In the ranges  $BC$  and  $DE$ , where the lattice spacing varies linearly with composition, the lattice vacancies are either decreasing or constant until  $E$  is approached. The change occurring between  $F$  and  $E$  is regarded as being a mirror image of the changes between  $AB$  and  $CD$ . In passing from  $F$  to  $E$  an abnormal expansion of the lattice occurs, which corresponds with an increase in the number of vacant lattice sites. As soon as this abnormal expansion is passed, the lattice-spacing/composition relationship becomes linear and the number of lattice defects decreases.

These results are interpreted in the same way as the results on aluminium-zinc alloys,<sup>1</sup> namely that the

Mott,<sup>3</sup> we have (allowing for the vacant lattice sites):

$$19.4x + 77.6 = 140, \text{ from which } x = 3.21$$

$$\text{and } 49.8x + 49.8 = 210, \text{ from which } x = 3.22$$

It would thus appear that the effective valency of nickel when in solution in gold up to about 60 at.-% is approximately 3.2. In considering the above figures due allowance must be made for the lack of precision in determining exactly where the points  $B$  and  $D$  occur in Fig. 1. For the purpose of the calculations  $B$  and  $D$  have been taken at 20 and 50 at.-% nickel, respectively.

The point  $E$  in Fig. 1 cannot be treated in the same simple way, because it appears to be an instance of the filling of a Brillouin zone on decreasing the electron concentration. It is suggested that the phenomena may involve the modification of the  $N(E)$  curve for

nickel in a manner similar to that postulated by Ellwood<sup>1</sup> for aluminium when zinc is added, although the supporting evidence of the  $N(E)$  curve is not available.

The experimental results are interpreted as showing that Brillouin zones are filled as nickel is added to gold. In many of the alloy systems in which gold is a solvent, the filling of such zones is accompanied by a change in structure from face-centred to body-centred cubic. It would appear that both structures are equally stable for monovalent metals and their dilute alloys in which the electron concentration is close to unity. Fuchs<sup>4</sup> has suggested that the face-centred cubic structure is most commonly found because the greater interatomic distances in the face-centred structure cause less overlap of the electron clouds of the ions. In the present case, nickel causes considerable lattice contraction, and it is possible that the alloys could not accommodate the further contraction in interatomic distance induced by a change in co-ordination number from 12 to 8. As an alternative to a change in phase, vacant sites are formed.

#### IV.—CONCLUSIONS

The conclusions drawn from this work are as follows:

1. That Brillouin-zone overlaps take place in the solid solutions of gold and nickel and are accompanied by the formation of vacant lattice sites, and therefore, that this phenomenon is not confined to the solid solutions of zinc in aluminium.

2. That nickel contributes about 3.2 electrons per atom when dissolved in gold up to 60 at.-%.

3. That a Brillouin-zone overlap occurs when gold is added to nickel, that is on a decreasing electron concentration, suggesting that the  $N(E)$  curve of nickel is complex and that it suffers modification on alloying.

#### ACKNOWLEDGEMENTS

The authors have pleasure in thanking Professor A. Preece and their colleagues for helpful discussions.

#### REFERENCES

1. E. C. Ellwood, *J. Inst. Metals*, 1951-52, **80**, 217.
2. E. A. Owen, *ibid.*, 1943, **69**, 2.
3. H. Jones and N. F. Mott, *Proc. Roy. Soc.*, 1937, [A], **162**, 49.
4. K. Fuchs, *ibid.*, 1935, [A], **151**, 585; 1936, [A], **153**, 622.



# NOTICE TO AUTHORS OF PAPERS FOR THE "JOURNAL" AND CONTRIBUTORS TO DISCUSSIONS

1. Papers will be considered for publication from non-members as well as members of the Institute. They are accepted for publication in the *Journal* and not necessarily for presentation at any meeting of the Institute. MSS. should be addressed to The Editor of Publications, The Institute of Metals, 4 Grosvenor Gardens, London, S.W.1.

2. Papers suitable for publication may be classified as:

(a) Papers recording the results of original research.  
(b) First-class reviews of, or accounts of progress in, a particular field.

(c) Papers descriptive of works methods, or recent developments in metallurgical plant and practice.

(d) Papers in classes (a), (b), and (c) above, previously published in languages other than English, French, German, or Italian, if of sufficient merit.

3. Manuscripts and illustrations should be submitted in duplicate. MSS. must be typewritten (double-line spacing) on one side of the paper only, and authors are requested to sign a declaration that neither the paper nor a substantial part thereof has been published elsewhere. Exceptions may be made in certain cases where a paper has been published in a language other than English, French, German, or Italian (see 2(d) above). MSS. not accepted are normally returned within 6 months of receipt.

In the interests of economy, all papers must be written as concisely as possible; in general, internal research reports are not in suitable form for publication as papers in the *Journal*. All but the simplest mathematical expressions should be written by hand, with capital and small letters clearly distinguished. Superscript and subscript letters should also be plainly indicated. Greek letters and special signs should be identified in the margin. For style, spelling, and abbreviations used, any recent issue of the *Journal* may be consulted.

4. Synopsis. Every paper must have a synopsis (not exceeding 250 words in length) which, in the case of a paper reporting original research, should state its objects, the ground covered, and the nature of the results. The synopsis will appear at the beginning of the paper, and should be in a form suitable for use by abstracting organizations. Extracts from a "Guide for the Preparation of Synopses" drawn up by the Abstracting Services Consultative Committee are reproduced below.

5. References must be collected at the end of the paper and must be numbered in the order in which they occur in the MS. Initials of authors must be given, and the Institute's official abbreviations for periodical titles (as used in *Metallurgical Abstracts*) should be employed, where known. References to papers should be set out in the style:

A. L. Dighton and H. A. Miley, *Trans. Electrochem. Soc.*, 1942, 81, 321 (i.e. year, volume, page).

References to books should be in the following style:

C. Zener, "Elasticity and Anelasticity of Metals". Chicago: 1948 (University of Chicago Press).

6. Illustrations. Each illustration must have a number and description; only one set of numbers must be used in one paper, and it is desirable to number the half-tone illustrations consecutively, rather than to intersperse them with the line figures. The captions should be typed on a separate sheet.

The set of line figures sent for reproduction must be drawn (about twice the size to appear in the *Journal*) in Indian ink on smooth white Bristol board, good-quality drawing paper, co-ordinate paper, or tracing cloth, which are preferred in the order given. Co-ordinate paper, if used, must be blue-lined, with the co-ordinates to be reproduced finely drawn in Indian ink. Curves should be drawn boldly (i.e. at least twice the thickness of the frame). Experimental points should be indicated by open or closed circles, triangles, squares, &c. (preferably not crosses). Curves should be broken on each side of such symbols and plenty of allowance should be made for closing up in blockmaking. All lettering and numerals, &c., should preferably be in pencil, so that the Institute's standard lettering may be affixed, and ample margins must be left outside the framework of the figures to enable this to be done. The second set of line illustrations may be photostat copies.

Photographs must be restricted in number, owing to the expense of reproduction, and photomicrographs should be trimmed to the smallest possible of the following sizes consistent with adequate representation of the subject: 4 in. deep by 3 in. wide: 2 in. deep by 3 in. wide: 2 in. square. Magnifications of photomicrographs must be given in each case. Photographs for reproduction should be loose, not pasted down (and not fastened together with a clip, which damages them), and the figure number and author's name should be written on the back of each. Captions should be given to the photomicrographs, but these should be kept as brief as possible.

Because of the present high cost of printing and paper it is imperative that authors restrict illustrations (particularly photographs) to the absolute minimum deemed necessary to support their argument. Only in exceptional cases will illustrations be reproduced if already printed and readily available elsewhere.

7. Tables or Diagrams. Results of experiments, &c., may be given in the form of tables or figures, but (unless there are exceptional reasons) not both. Tables should bear Roman numbers, and each should have a heading that will make the data intelligible without reference to the text.

8. Corrections. A certain number of corrections in proof are inevitable, but any modification of the original text is to be avoided. Since corrections are very expensive, the Institute reserves the right to require authors to contribute towards their cost if the Editor deems them to be excessive. The Institute also reserves the right to require a contribution to the cost of remaking any block where this is necessitated by an error on the author's part.

9. Reprints. Individual authors are presented with a maximum of 25, and two or more authors with a maximum of 50 reprints from the *Journal*, without covers. Limited numbers of additional reprints can be supplied at the author's expense, if ordered before proofs are passed for press. (Orders should preferably be placed when submitting MSS.)

10. Discussion. Except in the case of special symposia, shorthand records of discussions are not taken at meetings. Written discussion may be submitted on any paper, preferably typewritten (double-line spacing). References should be given in the form of footnotes. Paragraphs 6 and 7 above are also applicable to such contributions. Reprints of discussion cannot be supplied to contributors.

## GUIDE FOR THE PREPARATION OF SYNOPSES

(As recommended by the Abstracting Services Consultative Committee)

1. Purpose. The synopsis is not part of the paper; it is intended to convey briefly the content of the paper, to draw attention to all new information, and to the main conclusions. It should be factual.

2. Style of writing. The synopsis should be written concisely and in normal rather than abbreviated English. It is preferable to use the third person. Where possible use standard rather than proprietary terms, and avoid unnecessary contracting.

It should be presumed that the reader has some knowledge of the subject, but has not read the paper. The synopsis should therefore be intelligible in itself without reference to the paper; for example, it should not cite sections or illustrations by their numerical references in the text.

3. Content. The title of the paper is usually read as part of the synopsis. The opening sentence should be framed accordingly and repetition of the title avoided. If the title is insufficiently comprehensive, the opening should indicate the subjects covered. Usually the beginning of a synopsis should state the objective of the investigation.

It is sometimes valuable to indicate the treatment of the subject by such words as: brief, exhaustive, theoretical, &c.

The synopsis should indicate newly observed facts, conclusions of an

experiment or argument and, if possible, the essential parts of any new theory, treatment, apparatus, technique, &c.

It should contain the names of any new compound, mineral species, &c., and any new numerical data, such as physical constants; if this is not possible, it should draw attention to them. It is important to refer to new items and observations, even though some are incidental to the main purpose of the paper; such information may otherwise be hidden, though it is often very useful.

When giving experimental results the synopsis should indicate the methods used; for new methods the basic principle, range of operation, and degree of accuracy should be given.

4. References. If it is necessary to refer to earlier work in the summary, the reference should always be given in full and not by number. Otherwise references should be left out.

When a synopsis is completed, the author is urged to revise it carefully, removing redundant words, clarifying obscurities, and rectifying errors in copying from the paper. Particular attention should be paid by him to scientific and proper names, numerical data, and chemical and mathematical formulae.

By B. W. MOTT,† M.A., MEMBER, and H. R. HAINES †

## SYNOPSIS

Methods of preparing uranium for examination under polarized light are discussed, and the relative merits of various solutions for electrolytic polishing are given. Details of the structures observed on uranium sections taken from material in the cast, swaged, and hot-worked conditions are described, together with the effects of heat-treatment and recrystallization. It is considered that the anisotropic reflection from electrolytically polished sections of uranium is due to the properties of the uranium/uranium oxide film interface; by heating specimens polished in perchloric acid solutions up to about 250° C. in air, a birefringent film is formed which leads to marked ellipticity of the reflected beam. Thermal etching occurs when electrolytically polished specimens are heated in the upper  $\alpha$  range. Future developments are discussed.

## I.—INTRODUCTION

IN a recent paper,<sup>1</sup> an apparatus which can be used for the examination of surfaces under polarized light has been described, together with recommendations based on experience obtained by the authors. In addition, the results obtained by other workers in the field have been reviewed. A general summary of the effect of crystal structure, surface films, and etching on the reflection of normally incident, plane polarized light has also been included. More recently, a mathematical analysis has been made<sup>2</sup> of the intensity of the light reflected from anisotropic metals, and the conclusions have been confirmed by experimental observation; the effect of rotation of the analyser from the crossed position and of strain in the objective lens has also been discussed in some detail.

In the present paper, it is proposed to discuss the metallography of uranium as elucidated in the Metallurgy Division of the Atomic Energy Research Establishment, with particular reference to the application of polarized-light techniques. The work has been carried out either on a Beck Universal microscope No. 50 or a Cooke, Troughton, and Simms Vickers microscope of standard design. Certain minor modifications have been made to both types of instrument to comply with the needs of the present work, and reference to these changes has been made in the earlier paper.<sup>1</sup> It cannot be over-emphasized that, in view of the low intensities normally transmitted by the analyser and the dependence of the effects on a critical setting of all parts of the optical train, the results obtained will be related to the accuracy with which the adjustments are made. Suitable objectives, good polarizing units, and accurate alignment are essential for a critical, full-field examination of metals under polarized light, especially at high powers.

## II.—EXAMINATION OF URANIUM SECTIONS

## 1. GENERAL

Uranium is one of the more important elements in the field of atomic energy, and an understanding of its metallurgy demands a metallographic study of its microstructure. The pure metal<sup>‡</sup> has a Brinell hardness of about 200 in the annealed condition and can be polished mechanically for microscopical examination by conventional methods, using an aqueous suspension of alumina or chromic oxide for final polishing. Surfaces prepared in this way can be used satisfactorily for the examination of inclusions, second phases, and porosity in the metal.

All attempts to etch the material in the conventional reagents used for revealing the grain-size of other metals and alloys have failed to yield a reliable etching treatment for the examination of the grain structure, &c. Several electrolytes<sup>3</sup> can be used for the anodic etching of uranium, but the results depend to a large extent on the metallurgical condition of the material. The macrostructure is only clearly defined on material that has been fully annealed after cold working; other conditions result in effects that are not easily interpreted. On cast material, for example, the character of an etched surface varies with the form of illumination, and no exact grain-size can be attributed to the metal. The effect is best described in terms of small facets which form various groups of grains, the members of a given group varying with the direction of the incident light.

The failure of standard procedures to provide a satisfactory means of examining the structure of uranium led to the use of polarized-light techniques. Since uranium has an orthorhombic structure at room temperature and shows marked anisotropy of properties, it may be expected to show grain contrast

\* Manuscript received 1 March 1952.

† Metallurgy Division, Atomic Energy Research Establishment, Harwell, Berks.

‡ Some of the more important physical data on uranium are given in an Appendix (p. 627).



when suitably prepared sections are examined under crossed polarizers.

## 2. METHODS OF PREPARATION

When uranium specimens which have been polished by normal mechanical methods are examined under polarized light, no grain structure is observed, and the only light transmitted by the analyser is that caused by scattering from surface imperfections, e.g. pits and scratches. Chipman<sup>4</sup> has confirmed this observation and states that it is necessary to polish the surface electrolytically to produce a reaction to polarized light. The electrolyte he recommends contains 5 parts orthophosphoric acid, 5 parts ethylene glycol, and 8 parts ethyl alcohol, but no details of the polishing conditions are given. More recently, Metz and Woods<sup>5</sup> have described an attack method of mechanical polishing which gives a suitable surface for examination under polarized light. A dilute solution containing hydrofluoric and nitric acids is used as a suspension medium for the polishing powder, and the metal surface is finally swabbed in concentrated nitric acid. Specimens prepared in this way give good grain contrast, but are not as suitable for the examination of fine detail as those prepared by electrolytic polishing. (The authors prefer hydrofluoric acid only in the suspension medium, since the presence of nitric acid causes marked tarnishing of the surface.)

The electrolyte described by Chipman was used for the early work at the A.E.R.E., but investigation showed that replacement of the ethylene glycol by glycerol (which was more readily available) gave equally satisfactory results. The solution for routine preparation contains equal proportions of phosphoric acid, glycerol, and ethyl alcohol. The best current density is 0.1–0.2 amp./cm.<sup>2</sup>. The solution is cooled by passing a stream of water through a glass coil which is immersed in the bath and surrounds both electrodes. Stirring is not necessary, but the bath has to be kept free from water; otherwise marked staining of the surface occurs during both polishing and subsequent drying. The usual procedure is to immerse the specimen in ethyl alcohol immediately after switching off the current and to wipe the surface gently with a camel-hair brush. Finally, the specimen is washed in absolute alcohol and dried in a stream of hot air.

With the above solution and a cathode of uranium, platinum, or steel, (in this order of preference), specimens can be polished after preparation on 000 emery paper to give a surface suitable for examination under polarized light. It takes 30–40 min. to remove scratches completely, and during this time the flatness of the surface deteriorates and some pitting may occur at oxide particles and other inclusions. If a flat, undisturbed surface is required for critical examination, it is preferable first to polish the specimen mechanically, for the time required for electrolytic polishing can then be reduced to 5–10 min.

Numerous other solutions have been investigated as

possible electrolytes, and from nearly a hundred, four have been chosen as having useful application to uranium.

The most successful solution<sup>3</sup> to date contains 1 vol. orthophosphoric acid, 2 vol. concentrated sulphuric acid, and 2 vol. water. Polishing is carried out at a current density of 0.5–0.75 amp./cm.<sup>2</sup>, and the technique which gives the best results is to remove the anodic layer continuously during polishing by wiping with a camel-hair brush. Polishing is more rapid than with the glycerol solution, and gives a very flat uniform surface even after relatively prolonged electrolysis, so that there is less chance of staining on drying off the specimen after this treatment. Most of the inclusions, and especially the oxide particles which are always present in uranium, are not attacked significantly. The quality of the surface after several minutes' polishing in this solution can be judged from Fig. 1 (Plate XCIX), in which the oxide particles are clearly revealed. The reaction to polarized light is generally more satisfactory than with the glycerol solution owing to increased flatness and less interference from imperfections in the surface.

Of the three other electrolytes, two are based on perchloric acid. Very rapid polishing occurs with 60% perchloric acid (sp. gr. 1.54) at current densities approaching 1 amp./cm.<sup>2</sup>, and this treatment is especially useful for removing the effects of cold work before X-ray examination. Surfaces polished by this method do not give good grain contrast under polarized light, however: the oxide particles and other inclusions are deeply etched; some grain and twin boundaries are delineated; any iron impurity present as U<sub>6</sub>Fe particles is usually attacked; and the whole surface becomes irregular and assumes an appearance of relief owing to different rates of polishing in different grains. A similar effect has been observed by Roth<sup>6, 7</sup> in the electropolishing of zirconium, using a mixture of perchloric and acetic acids as an electrolyte. A section of cast uranium polished in this mixture is shown in Fig. 2 (Plate XCIX), in which most of the effects mentioned can be observed. It might be expected that this treatment could be used as the basis of an etch to reveal grain structure, &c., but so far, no modifications have led to a reliable interpretation of the structure. Only the boundaries between grains of markedly different orientation are delineated, and small differences are not revealed.

Greater control over the polishing process is obtained by adding acetic acid, and an electrolyte containing 1 vol. perchloric acid and 4 vol. acetic acid is a type most commonly used. The general effects, however, are similar to those produced by perchloric acid alone. Jacquet<sup>8</sup> has described an electrolyte containing 20 vol. acetic acid and 1 vol. perchloric, and claims that surfaces so prepared are suitable for examination under polarized light, but in the authors' experience the contrast obtainable is not as good as with other solutions.

A more recent development is an electrolyte based on pyrophosphoric acid, the most satisfactory com-

position being 10 g. pyrophosphoric acid, 10 g. chromium trioxide, 40 ml. orthophosphoric acid, 100 ml. concentrated sulphuric acid, and 200 ml. distilled water. After the specimen has been prepared on 000 emery, a good polish can be obtained at a current density of about 0.5 amp./cm.<sup>2</sup> in about 5 min. The polished surface has a high reflectivity, and the oxide or other inclusions are relatively unattacked. The electrolyte appears suitable for polishing many uranium alloys.

### 3. CAST URANIUM UNDER POLARIZED LIGHT

A possible reason for the failure of the etching reagents to distinguish clearly the grains in cast uranium is the close orientation of adjacent grains. In general,<sup>2</sup> if the polarizer and analyser are exactly crossed and stray polarization effects due to the objective are negligible, each grain will give four maxima and minima of intensity per rotation of the stage. Thus, for any two grains of different orientation, there are eight positions of the stage for which the intensities of their reflected rays are exactly equal. The smaller the angle between the principal directions of two given grains and the more nearly equal their maximum reflecting powers, the larger will be the range of azimuth angle over which the grains will reflect at nearly the same intensity. Frequently, in cast uranium, the presence of two grains in a given area is revealed only by a marked difference in intensity over a narrow range of azimuth angle.

Contrast between grains can be considerably improved by slight rotation of the analyser from the crossed position, and this is accompanied by a change in the number of maxima and minima per complete rotation of the stage from four to two.<sup>2</sup> Usually, for uranium, the rotation of the analyser from the crossed position for which maximum contrast is obtained is between 1° and 2°, and for examination and photography this is the normal operating condition.

The bands which appear light in dark grains and vice versa were originally described by Chipman<sup>4</sup> and termed "deformation bands". They occur in approximately parallel families in a given grain, but vary in direction with the orientation of the grain surface examined. The majority of these markings have been established as deformation twins. Cahn<sup>9</sup> has shown that uranium commonly deforms by twinning, although slip also occurs as in other metals.<sup>10</sup> In unworked uranium, the twins result from the anisotropic expansion, and the form and extent of twinning depend on the rate of cooling in the  $\alpha$  range.

Examples of the variation in appearance of the twinning in cast uranium are given in Figs. 3-10 (Plate XCIX). Fig. 3 shows the normal structure of chill-cast material of up to about 1 in. section, in which the twins are fairly straight and are most prominent in two directions. Fine twins in several directions in the same grain are often observed, and up to nine families are quite frequent. Since there are four

planes of the general form (*hkl*) in the orthorhombic system, at least three types of twin plane must operate in uranium. Actually, Cahn<sup>9</sup> has identified four types by a combination of X-rays and microscopical examination. The existence of four sets of twins can be observed in the left-hand grain of Fig. 4. Some twins interpenetrate, whereas others stop at the interface between the twin and the untwinned portion.

In the study of deformation twins, care must be taken to ensure that the material affected by mechanical deformation of the surface during preparation has been completely removed. To take an extreme case of erroneous interpretation where such care has not been taken, the structures shown in Figs. 5 and 6 should be compared. Fig. 5 illustrates the structure revealed in a section of cast material in which a milled surface was electrolytically polished for 15 min. in the phosphoric acid-glycerol-alcohol electrolyte and etched for 5 min. in the same bath at a low current density. Fig. 6 shows the structure in the same specimen under polarized light after preparation on 000 emery paper and polishing for 5 min. in the phosphoric acid-sulphuric acid bath. The broad bands in Fig. 5 are deformation twins produced by the milling operation, whereas the twins produced by thermal stresses in the casting are much finer.

For the determination of the grain-size of uranium from back-reflection X-ray photographs, patterns were obtained from specimens at various stages of polishing a milled surface. Diffuse patterns were obtained from all mechanically polished surfaces, and in one series of experiments the effect of milling was detected after more than 0.25 mm. had been removed by electrolytic polishing. The X-ray patterns showed no change in appearance beyond about 0.4 mm. from the surface; this depth of cold working is the same as that reported by Bulian and Fahrenhorst<sup>11</sup> for magnesium, but is considerably higher than the figure of 0.03 mm. found by Schmid and Boas<sup>12</sup> for aluminium. No significant change in the appearance of the structure under polarized light, however, can be detected after about 0.05-0.08 mm. of material has been removed. Early work indicated that the average grain-size deduced from the X-ray photographs was usually smaller than the value obtained metallographically by a factor of 20-40. This has been attributed by Chipman<sup>4</sup> to the close relationship of the orientation of the  $\alpha$  grains and the inability of polarized light to differentiate between them. He refers to a "litter" of closely oriented  $\alpha$  grains from a given mother  $\beta$  grain. An alternative partial explanation is that each family of twins behaves as a separate crystallite and contributes to the number of spots on the X-ray film; if this is so, it would account for some of the discrepancy. In some cast specimens, on careful rotation of the stage, positions extending over a few degrees only can be found in which small areas of an "apparent" grain do appear with a slight difference in intensity. In addition, slight kinks may be observed where the twins cross the boundaries of



subgrains of this type, and examination has shown the presence of "sub-facets" on fractures through coarse-grained material. Further support for the Chipman theory is afforded by the fact that in fully annealed cold-worked material which has been cooled slowly from the annealing temperature, the X-ray grain-size, although smaller than that revealed by polarized light, is of the same order. However, in such material the average number of twins/grain is less than unity, so that the second possibility may be a contributory factor. More detailed study has shown that the X-ray crystallite size corresponds more closely to that of the "litter" units, and it is feasible that the latter may be a "macro-polygonization" effect associated with the transformation from  $\beta$ - to  $\alpha$ -uranium.

The majority of the twins in Figs. 4 and 6 are slightly curved. This could arise from a process similar to that described by Kaufmann, Gordon, and Lillie<sup>13, 14</sup> for beryllium, viz. twisting or bending due to further deformation after twinning. Alternatively, it may be a result of non-uniform growth from the twins. Fig. 7 shows a further stage in this process in a larger casting and at the same time illustrates the complicated forms taken by the twinning in cast material. The fine, bright lines crossing the half-tone twins in Fig. 7 are due to secondary twinning, and this appearance is a common feature of chill-cast material of large cross-section and relatively large grain-size. An extreme form of this is shown in Fig. 8, in which the broad bands are the primary twins, and the other twins crossing at various angles represent further stages of deformation. (The bright spots in Fig. 8 are oxide particles.)

A study of the patterns produced by multiple twinning in a given grain is of interest. Examination of Figs. 2-9 shows that some twins intersect without any apparent interference, whereas others appear to suffer some displacement. In addition, cross-twinning can occur in what is primarily an untwinned portion of a grain bounded by two twins which formed at an early stage. The effect observed in any given case will obviously depend on the crystallographic parameter of the twins. This has been examined in detail by Cahn.<sup>9</sup> The change in intensity at the junctions of interpenetrating twins in Fig. 9 is worth noting, since it indicates that the orientation at the intersection of two twins is different from that of either twin, but is related by a shear direction common to both twins.

#### 4. RECRYSTALLIZATION OF CAST MATERIAL

On annealing cast material for periods up to 3 hr., no marked change in microstructure occurs until the temperature reaches 500° C., when some grains grow at the expense of others. Slight changes in structure have been observed after 3 days' anneal at 420° C., but these are mainly confined to straightening of the grain boundaries. Long periods of annealing in the  $\alpha$  range above 500° C. result in a more marked straightening of the grain boundaries and an increase

in grain-size. In specimens annealed for over 100 hr. at 650° C., broad bands that suggest a peculiar form of grain growth were observed in some grains (Fig. 10, Plate XCIX). The very fine twins in Fig. 10 were probably formed on air cooling from 650° C. or possibly during the preparation of the surfaces. The origin of the bands is not fully understood, but a possible mode of formation is that recrystallization started at the interface between the twins and the parent metal as observed by Zolotov<sup>15</sup>, and that the bands are formed by coalescence of the growing crystals with identical orientation.

The most remarkable recrystallization effects have been observed on samples which have undergone a number of thermal cycles in the  $\alpha$  range. Recrystallization appears to be initiated at certain positions on the deformation twins, especially in grains having a marked difference in orientation from their neighbours. Subsequent growth can produce local broadening of the twins, as shown in Fig. 11 (Plate XCIX), where irregular growth has occurred, or the new crystallites can grow from the junction of interpenetrating twins. Fig. 12 (Plate XCIX) shows a structure in which recrystallization has been initiated at numerous positions along the twins, and it is easy to visualize that growth of some crystallites at the expense of others would eventually result in a coarse grain structure of the type illustrated in Fig. 13 (Plate C).

#### 5. THE EFFECT OF MECHANICAL WORKING ON THE MICROSTRUCTURE

In uranium which has been severely deformed by rolling, extrusion, or swaging at temperatures below 400° C., the structure is very confused and difficult to interpret, and the existence of highly deformed areas often leads to difficulties in obtaining a satisfactory electrolytic polish. As might be expected, the deformed metal shows preferred orientation, the degree of orientation depending on the percentage reduction achieved and the temperature of deformation. A qualitative estimate of the preferred orientation was made metallographically by observing the percentage area of a given section which shows the same variation in intensity as the stage is rotated under crossed polarizers. Other optical methods which have been used for estimating preferred orientation are similar to those described previously.<sup>1</sup> The appearance of the structure in a longitudinal section through hot-worked material shows a marked variation, and Fig. 14 (Plate C) illustrates the highly deformed structure in which no recrystallization occurred during working.

Deformation in the higher  $\alpha$  range is sometimes accompanied by recrystallization in the more highly deformed regions and at the twin boundaries, as shown in Fig. 15 (Plate C). The small recrystallized grains subsequently grow (Fig. 16, Plate C), and usually result in a preferred orientation. Recrystallization and growth occurs more rapidly on heating into the  $\beta$  range, i.e. between 660° and 775° C.

and yields a random, rather than a preferred texture. On subsequent cooling through the  $\alpha$ - $\beta$  change point, further recrystallization is possible, so that the material will have an appearance similar to that of a cast structure.

## 6. RECRYSTALLIZATION OF COLD-WORKED MATERIAL

The results of annealing swaged material after various percentage reductions may be summarized as follows:

The onset of recrystallization in swaged material is governed by the percentage reduction. Little change in the structure was observed in samples which had received up to 46% reduction in area on annealing at 300° C. for up to 18 hr. After 5 hr. at 400° C., some nucleus grains were visible in material reduced by 46–35%, but not in material reduced by 22%. A remarkable phenomenon of multiple twinning was observed in the most heavily worked specimen. An example of this is given in Fig. 17 (Plate C), which shows several primary twins in a grain, each twin containing one or two sets of secondary twins. At higher magnifications, it is possible to resolve a finer set of twins within the secondaries. The primary twinning had presumably occurred during swaging, whereas the finer twins had most probably formed on air-cooling from 400° C. after annealing.

At 420° C., recrystallization was more rapid, and after 3 days all specimens which had been reduced by 35% and over consisted of entirely new, very fine grains. In a sample swaged by 22%, recrystallization had only occurred at the more highly deformed regions. Similar results were obtained after 3 hr. at 450° C., but prolonging the time at this temperature or increasing the temperature resulted in some recrystallization throughout all the materials swaged by more than 20%, although the grain-size showed considerable variation. During 5 hours' anneal at 500° C., some grain growth occurred in material reduced by 45% and over, the grain boundaries being more polygonal than after shorter anneals. In samples swaged by 35%, the grain-size was relatively fine and uniform. At 600° C. and above, recrystallization in specimens swaged by more than about 10% was incomplete after  $\frac{1}{2}$  hr. but almost complete after 1 hr., the resulting grain-size depending on the reduction and, to some extent, on the rate of heating to temperature. The structure in a bar swaged by 35% and heated at 650° C. for 1 hr. is shown in Fig. 18 (Plate C).

An effect of the degree of cold work on the grain-size of recrystallized metal was observed in a small tensile test-piece which was machined from recrystallized swaged uranium and annealed for 63 hr. at 625° C. after an extension of about 2%. The structure along the gauge-length was fine and uniform, but in the shoulder, where the deformation was less, the grain-size was very variable, as shown in Fig. 19 (Plate C). This indicated that the strain of 2% and recrystallization temperature of 625° C. were close to the critical values required for marked grain growth.

There are some interesting features in material that is annealed after cold working. The grain boundaries are much straighter than in cast material, and very often the grains are polygonal in outline. The twins in cast material are usually curved or kinked and are often present in three or more directions in one grain; in recrystallized worked material, the twins formed on cooling are straight and usually confined to one direction per grain. (This also applies to the twins produced by cold working during preparation for polishing.) Very often, the true size of discrete grains can be ascertained only by careful positioning of the stage to give maximum contrast between adjacent grains. This feature is shown by Fig. 20 (Plate C) in which many areas that appear to consist of one grain are actually composed of two or three, as indicated by the re-entrant angles of the boundaries. Normally an overall preferred orientation exists after recrystallization to a degree depending on the amount of cold work and the temperature and time of annealing.

The results of annealing uranium in the  $\beta$  range are relatively unaffected by its previous thermal history, a coarse-grained structure being produced similar to that of as-cast material but with an irregular outline to the grain boundaries. Some coarsening may occur on prolonged treatment in this range, and the structure may also depend on the rate of cooling and other factors.

## 7. OTHER EFFECTS OBSERVED ON URANIUM UNDER POLARIZED LIGHT

The so-called "optical cross"<sup>16, 17, 18</sup> formed under crossed polarizers as a result of the nature of the light produced by multiple reflections at oblique incidence from the sides of a spherical cavity or a transparent inclusion, has been observed in uranium sections. The most perfect crosses are formed by reflection from gas cavities in cast material, an example of which is shown in Fig. 21 (Plate C). The cross in the cavity is reasonably perfect and shows the fringes produced by successive multiple reflections.

The most common non-metallic inclusion in uranium is a relatively opaque oxide (either UO or UO<sub>2</sub>), so that light is transmitted only through very thin sections. Normally, the particles are very prismatic and thicker than the critical thickness for transmission, so that under crossed polarizers and especially at low magnifications, they appear bright owing to a scattering effect from the exposed surface. However, under oil-immersion objectives, the transmission colour and the optical cross are occasionally observed in the smaller particles, especially those which have globularized during annealing. The transmission colour when a white source is used is normally a reddish-brown, and the reflected colour is light grey, which is consistent with the data given by Dana<sup>19</sup> for uranite. The most interesting effects were obtained in a section taken through a reduction cross. The oxide in this case was in the form of an



intimate mixture of thin plates and fine globules which had a greyish lustre under ordinary illumination. Under polarized light, the smaller globules transmitted the reddish-brown colour and showed the optical cross effects, as in Fig. 22 (Plate C). The plates and larger globules were generally opaque but some light was transmitted through the thinner sections of the plates, as may be observed in Fig. 22.

Polarized light has also been used in an investigation of the "cores" in the oxide particles shown in Fig. 1 (Plate XCIX). As mechanically polished, these were sharply delineated and under ordinary illumination are an appreciably darker grey than the rest of the particle. No difference can be observed under polarized light. After etching in 50% nitric acid for about 15 sec. or after polishing electrolytically, the core is darkened considerably, suggesting complete solution. This is confirmed by the formation of the optical cross under crossed polarizers. Gray, at Harwell, has separated the prismatic inclusions and, since he found only  $\text{UO}_2$  lines in X-ray powder photographs, he concluded that the coring effect was due to changes in oxygen content within the phase composition limits of the  $\text{UO}_2$  structure. In view of the above evidence, however, it would appear that this explanation is incorrect, and it is possible that the X-rays did not penetrate the  $\text{UO}_2$  sufficiently to yield lines from the cores.

### III.—THE NATURE OF POLARIZED LIGHT REFLECTED FROM URANIUM

Theoretical considerations show that a plane polarized beam of light is reflected from the polished surface of an anisotropic metal as an elliptically polarized wave. The degree of ellipticity for a given metal depends on the crystal symmetry, the orientation of the reflecting surface, the wave-length of the radiation, and the azimuth angle which the direction of the plane of polarization of the incident ray makes with the principal direction in the section. No quantitative measurements have been made in this work of the ellipticity values which are associated with various metals, but it is to be expected that uranium and other metals of biaxial symmetry will reflect with a more marked ellipticity than those belonging to a uniaxial system. As far as can be ascertained with a sensitive tint-plate inserted between the vertical reflector and the analyser, the ellipticity from an electrolytically polished surface of uranium is low and of the same order as in the case of uniaxial metals, e.g. tin, (tetragonal) and zinc, cadmium, zirconium, and titanium (hexagonal).

It has been reported<sup>20</sup> that electrolytically polished specimens of uranium are covered with a film of uranium oxide, up to 200 Å. thickness, corresponding to about 60 atoms, and electron-diffraction patterns obtained at the A.E.R.E. from similar surfaces are consistent with this view. There is, however, some doubt as to which oxide is present, and from the results of electron-diffraction work it would appear

that it is either the cubic  $\text{UO}_2$  or the orthorhombic  $\text{U}_3\text{O}_8$ , depending on the electrolyte and polishing conditions used. Although the presence of a  $\text{UO}_2$  film results in a change in the values of the effective refractive indices by a factor of  $1/n_f$  (where  $n_f$  is the refractive index of the film), the relative orientation of the oxide and metal does not affect the nature of the reflected wave from a given grain. If the film were of the orthorhombic oxide, it is doubtful whether a thickness of 200 Å. would be sufficient to result in marked variations of ellipticity from grain to grain. It has been found, however, that if an electrolytically polished specimen is heated to about 100° C. (a convenient way of doing this is by directing a stream of hot air from a hair dryer on to the surface), the nature of the reflected wave is affected, and marked colour effects are obtained when a sensitive tint-plate is inserted between the vertical reflector and the analyser.

These changes on heating have so far been observed only on specimens that have been polished in the perchloric acid-acetic acid bath and to a lesser degree in the phosphoric acid-sulphuric acid bath. In view of the marked increase in the ellipticity of the reflected wave, it would appear that, on heating, an anisotropic film is built up of such a thickness as to identify each grain with a given degree of ellipticity of the reflected wave. As the grains are truly revealed by the elliptically polarized reflected light, it is essential that either the thickness or the orientation of the film be related to the orientation of the underlying uranium grains. (This would necessitate that the original oxide film produced by electrolytic polishing shows these characteristics also.) The anisotropic film is also formed during annealing for periods up to 30 min. in a moderate vacuum or in a closed silica tube at temperatures up to about 270° C. In such specimens, a faint delineation of the grain boundaries, but no grain contrast, is observed under ordinary illumination.

When specimens which have been polished in the perchloric acid-acetic acid bath are heated for long periods at low temperatures, a heat-tinting etch is produced which may or may not show interference-colour effects when examined under the microscope in ordinary illumination. An example of the etch obtained by heating a section from a recrystallized rolled bar for 1 hr. at about 100° C. is shown in Fig. 23 (Plate C). On increasing the time of heating, the film on such specimens becomes too thick for examination under polarized light. Annealing at temperatures higher than 270° C. destroys the ability of all surfaces to react to polarized light, and specimens then behave as if they were isotropic. No satisfactory explanation of this phenomenon has so far been advanced, but it is obviously related to a change in either the composition or the structure of the oxide film.

As the annealing temperature is raised, thermal etching occurs which delineates both the grain boundaries and some twin boundaries. Fig. 24 (Plate

C) shows the structure of a specimen (similar to that of Fig. 23) which was heated *in vacuo* for a total of about 1 hr. to a maximum temperature of 720° C. at which it was held for about 10 min. The boundaries observed in Fig. 24 are therefore the grain boundaries of both the initial and final structures and also of the twins formed on cooling from 720° C. Chalmers, King, and Shuttleworth<sup>21</sup> have reported that in general, during the thermal etching of silver, the grooves move forward with the boundaries, so that no scars are left at the previous position. By comparison, the above results can be explained on the basis that the initial grain boundaries are "recorded" by thermal etching at temperatures below that at which grain growth occurs, but once the latter is initiated the grooves progress with the boundaries, and the second set mark the position of the final boundaries resulting from grain growth. This obviously affords a method of investigating the mechanism of recrystallization and grain growth in uranium, especially if a suitable high-temperature microscope can be constructed.

#### IV.—DISCUSSION

The observations recorded in this paper illustrate the usefulness of polarized light in the metallographic study of uranium. The techniques involved in routine structural examination of this metal have been satisfactorily evolved, but further developments in the application of polarized light in the study of uranium are possible. For example, Woodard,<sup>22</sup> using a photomultiplier unit in conjunction with a polarizing microscope, has been able to make a qualitative estimate of the degree of preferred orientation in worked Monel metal. This required the formation of a surface film which produced anisotropic reflection of polarized light. This technique has been applied to uranium sections, but it is apparent that, owing to the difference in the nature of the reflected light in the two cases (that from the surface of treated Monel metal has

an appreciably greater ellipticity), the results on uranium are affected to a far greater extent by stray polarization effects in the apparatus. These effects are due to various causes, but originate mainly from reflection at oblique incidence on the glass-slip illuminator and internal strain in the objective lens. Methods of compensating for these effects are under consideration, and it is felt that if they can be eliminated, it may be possible not only to investigate preferred orientation in uranium qualitatively, but also to provide some quantitative check on the nature of the orientation by accurate analysis of the effect of reflection of plane polarized light by the specimen.

#### APPENDIX

##### SOME PHYSICAL DATA ON URANIUM

The  $\alpha$  phase is stable from room temperature to 660° C. and has an orthorhombic structure with  $a = 2.85$ ,  $b = 5.87$ , and  $c = 4.95$  Å.

The  $\beta$  phase, which is stable from 660° to 775° C., has a tetragonal structure similar to that of the  $\sigma$  phase which is formed in various alloys of the transition elements. The parameters are  $a = 10.52$  and  $c = 5.57$  Å.

The  $\gamma$  phase is body-centred cubic with  $a = 3.43$  Å., as extrapolated to room temperature, and is stable from 775° C., to the melting point at 1128° C.

The coefficients of expansion along the three crystallographic axes of the  $\alpha$ -phase between 25° and 650° C. are  $28 \pm 2$ ,  $-1.4 \pm 1$ , and  $22 \pm 1 \times 10^{-6}/^{\circ}\text{C.}$ , respectively.

##### ACKNOWLEDGEMENTS

The authors wish to express their thanks to Sir John Cockcroft, Director of the Atomic Energy Research Establishment, Harwell, for his kind permission to publish this paper. They also wish to acknowledge the interest shown in the work by Dr. J. Woodrow of the Engineering Division, and many helpful discussions with Dr. R. W. Cahn.

#### REFERENCES

1. B. W. Mott and H. R. Haines, *Research*, 1951, **4**, 24, 63.
2. J. Woodrow, B. W. Mott, and H. R. Haines, *Proc. Phys. Soc.*, 1952, [B], **65**, in the press.
3. B. W. Mott and H. R. Haines, *Metallurgia*, 1951, **43**, 255.
4. J. Chipman, *U.S. Atomic Energy Commission Publ.*, 1946, (MDDC-539).
5. D. Boyd Metz and H. W. Woods, *U.S. Atomic Energy Commission Publ.*, 1950, (SEP-42).
6. H. P. Roth, *U.S. Atomic Energy Commission Publ.*, 1950, (AECD-2882).
7. H. P. Roth, *Metal Progress*, 1950, **58**, 709.
8. P. A. Jacquet and R. Caillat, *Compt. rend.*, 1949, **228**, 1224.
9. R. W. Cahn, *Acta Cryst.*, 1951, **4**, 470.
10. C. S. Barrett, "The Structure of Metals", p. 316. 1943: New York (McGraw-Hill Book Company).
11. W. Bulian and E. Fahrenhorst, "Metallography of Magnesium and Its Alloys", p. 6. 1944: London (F. A. Hughes and Co. Ltd.).
12. E. Schmid and W. Boas, *Naturwiss.*, 1932, **20**, 416.
13. A. R. Kaufmann, P. Gordon, and D. W. Lillie, *Metal Progress*, 1949, **56**, 664.
14. A. R. Kaufmann, P. Gordon, and D. W. Lillie, *Trans. Amer. Soc. Metals*, 1950, **42**, 785.
15. V. A. Zolotov, *Compt. rend. (Doklady) Acad. Sci. U.R.S.S.*, 1943, **39**, 180.
16. R. W. Drayton, *Trans. Amer. Inst. Min. Met. Eng.*, 1935, **117**, 119.
17. S. L. Hoyt and M. A. Scheil, *ibid.*, 1935, **116**, 405.
18. P. Schafmeister and G. Moll, *Arch. Eisenhüttenwesen*, 1936, **10**, 155.
19. E. S. Dana, "A Text-Book of Mineralogy", 7th Edition, Vol. 1, p. 611. 1944: New York (John Wiley and Sons).
20. R. M. Treco, *Trans. Amer. Inst. Min. Met. Eng.*, 1950, **188**, 1042 (discussion).
21. B. Chalmers, R. King, and R. Shuttleworth, *Proc. Roy. Soc.*, 1948, [A], **193**, 465.
22. D. H. Woodard, *Trans. Amer. Inst. Min. Met. Eng.*, 1949, **185**, 722.





# THE APPLICATION OF POLARIZED LIGHT TO THE EXAMINATION OF VARIOUS ANISOTROPIC METALS AND INTERMETALLIC PHASES\*

1391

By B. W. MOTT,† M.A., MEMBER, and H. R. HAINES †

## SYNOPSIS

The application of polarized light to a study of various anisotropic metals and of some anisotropic constituents of alloys is discussed. Details are included of the methods of preparation of each metal, both as described in the literature and as developed by the authors, and photographs illustrate the results obtained. A tentative explanation of the observations made on mechanically polished specimens under polarized light is given in terms of the various possible surface layers produced during preparation.

## I.—INTRODUCTION

ALTHOUGH the techniques for the microscopical examination of metals under polarized light have been known and used since the beginning of the century, their application to metallurgical problems has considerably increased during the last few years, especially in the United States. The authors have recently reviewed<sup>1</sup> the literature on the use of polarized light in metallography and have described the apparatus required. The present paper deals with the application of polarized light to the examination of anisotropic metals, including uranium, which is also discussed elsewhere.<sup>2</sup> It is felt that for many of the less-common metals, the electrolytes which may be used for polishing are not generally known and that a review of the available techniques will be of value. Only a selection of the references is included, but others may be found in the reviews given by Perryman,<sup>3</sup> Jacquet,<sup>4</sup> and Kemsley and Tegart.<sup>5</sup>

The use of reflected polarized light at normal incidence in the study of the structure of metals and alloys may be divided under the following two headings: (a) examination of the structural characteristics of a homogeneous phase; and (b) identification of inclusions and differentiation between various phases of a complex structure.

Both anisotropic and isotropic phases can be investigated for grain-size, incidence of twinning and general deformation, and degree of preferred orientation. For a study of anisotropic materials, sections may be polished either by suitable mechanical or electrolytic methods, but for isotropic materials it is necessary to prepare the surface in such a way that the reflection of polarized light is made dependent on the orientation of the metal.

The preparation of anisotropic metals to give a suitable polish for examination under polarized light often presents difficulty. Ideally, the surfaces should be free from scratches, pits, and relief effects which give spurious reflections. In addition, most of the

anisotropic metals twin easily on mechanical deformation, and quite often the twins formed on mechanical polishing give a completely false impression of the condition of the material. As stated by Walker<sup>6</sup> for various anisotropic metals, in general, the better the mechanical polish and freedom from surface defects, the better the results under polarized light. Walker considers that the formation of a surface film by mechanical polishing does not extinguish the anisotropic reflection, which usually becomes stronger with time of polishing. This may be true, but undoubtedly the flowed layer can reduce the reaction to polarized light, since the results on beryllium, uranium, and zirconium are considerably improved by using the attack-polish method suggested by Metz and Woods<sup>7</sup> which continuously removes the flowed layer during polishing. The contrast is also invariably better on surfaces prepared by a suitable electrolytic polish which will remove not only the flowed surface but also the metal deformed by mechanical treatment. The advantages of electrolytic polishing over mechanical methods have been stressed by Capdecombe and his co-workers,<sup>8</sup> who found that the former gives more consistent values for the reflecting powers.

It is often difficult to decide whether the anisotropic reflection of etched specimens is due to metal anisotropy, surface contour, or the presence of a birefringent film. For example, Hone and Pearson,<sup>9</sup> who developed an anodic treatment for aluminium, and Woodard,<sup>10</sup> who worked with Monel metal, claim that an anisotropic film results from etching. On the other hand, Perryman and Lack,<sup>11</sup> after forming a silver film 800 Å. thick by vacuum deposition on the etched surfaces of aluminium and Monel metal, obtained similar results under polarized light to those before silvering. This is a strong indication that the surface contour is at least an important factor in the method of examination. No attempt is made in this paper to distinguish effects due to a surface film and those due to surface contour, except in the more obvious cases.

\* Manuscript received 13 March 1952.

† Metallurgy Division, Atomic Energy Research Establishment, Harwell, Berks.



## II.—EXAMINATION OF ANISOTROPIC METALS

### 1. ANTIMONY (RHOMBOHEDRAL)

This metal is difficult to polish mechanically owing to its brittleness and the ease with which it forms mechanical twins. As far as is known, no method of electrolytic polishing has been reported in the literature and no suitable electrolyte has been found by the authors. However, a specimen mechanically polished on soft alumina showed some effects under polarized light, but the grain contrast was not as high as might have been expected from Walker's observations or from those of Capdecombe,<sup>12</sup> who examined natural cleavage faces on antimony crystals and estimated the maximum angle of rotation as  $3.5^\circ$ .

### 2. BERYLLIUM (HEXAGONAL)

In the mechanically polished condition, the grain contrast\* under polarized light is very poor (Fig. 1, Plate CI), mainly owing to surface flow during preparation. As reported by Kaufmann and his co-workers<sup>13, 14</sup> and by Gordon,<sup>15</sup> the contrast is improved by etching in 2% hydrofluoric acid solution, the main effect of which appears to be the removal of the flowed layer, since a greater number of scratches are usually revealed after this treatment. The structure in an etched specimen is shown in Fig. 2 (Plate CI), some of the twins in which were probably produced by mechanical polishing. Further improvement is obtained by the attack-polish method of preparation of Metz and Woods,<sup>7</sup> which involves the use of a weak solution of oxalic acid as a suspension medium for the polishing powder. With this technique, the chance of deformation twins being formed is not as great, but care is needed to avoid staining, especially if the surface contains voids, as, for example, in cast metal or powder compacts; the contrast under polarized light, however, is generally superior to that for polished and etched specimens.

It was found that the metal may be polished in 98% phosphoric acid to which about 50 ml. concentrated sulphuric acid are added per litre. Some grain contrast is obtained under ordinary illumination by etching at a current density of 1 amp./cm.<sup>2</sup>. The reaction to polarized light is good, and strong colour effects are obtained when a sensitive tint-plate is used in the optical system. The best results are produced by polishing in the following solution at a current density of 2–4 amp./cm.<sup>2</sup>:

Orthophosphoric acid . . . . .	100 ml.
Conc. sulphuric acid . . . . .	30 ml.
Glycerol . . . . .	30 ml.
Absolute ethyl alcohol . . . . .	30 ml.

Treatment in this electrolyte gives a good metallographic polish without any delineation of the grains under ordinary illumination, but with a marked reaction to polarized light. Fig. 3 (Plate CI) represents a sample of hot-pressed beryllium powder

containing voids and Fig. 4 (Plate CI) the same area under polarized light. Surfaces prepared in this way apparently reflect a plane polarized beam without producing any marked ellipticity and do not give marked colour effects when the sensitive tint-plate is used.

### 3. BISMUTH (RHOMBOHEDRAL)

From an examination of natural cleavage surfaces, Capdecombe<sup>12</sup> estimated the maximum angle of rotation as  $3.5^\circ$ . Good grain contrast under polarized light has been obtained by the authors after hand polishing, although care has to be exercised to prevent undue flowing of the surface, which partially masks the effects. Fig. 5 (Plate CI) shows the appearance after a light mechanical polish. Little change in contrast under crossed polarizers is obtained by etching in dilute fluoboric acid, but the reflected ray then shows marked ellipticity, so that beautiful colour contrast between the grains is observed with the use of the sensitive tint-plate. The colour effects are quite marked, even with a mercury-vapour lamp as source, but are most brilliant with a carbon-arc source. Changes in intensity with maxima at  $90^\circ$  intervals can also be observed on etched specimens on stage rotation with the polarizer unit in position and the analyser removed, suggesting that the polarization effects are associated with surface contour.

If bismuth sections are lightly etched in dilute nitric acid, some increase in grain contrast is obtained between crossed polarizers, but the colour differences are only slight when the sensitive tint-plate is used. This indicates that the reflected beam is effectively plane polarized and that the action of this etching treatment is to remove the flowed layer only, thus supporting the observations of Jones,<sup>16</sup> who found that if bismuth is lightly etched in nitric acid, alternate pairs of maxima differ markedly in intensity unless the analyser is exactly crossed with the polarizer.

Tegart and Vines<sup>17</sup> have described a method of electrolytically polishing bismuth in a saturated solution of potassium iodide acidified with hydrochloric acid and claim that the polish gives grain contrast under polarized light. Satisfactory surfaces for polarized-light work have been prepared by the authors by polishing in a solution containing 1 vol. orthophosphoric acid, 2 vol. sulphuric acid, and 2 vol. distilled water at about 1 amp./cm.<sup>2</sup>. This solution yields a fairly flat surface which is freer from pits than after the treatment recommended by Tegart and Vines.

### 4. CADMIUM (HEXAGONAL)

Only slight polarization effects were observed on a mechanically polished cadmium specimen, probably owing to the surface flowing on polishing in addition to an inherently weak rotation of the plane of polarization. Several authors<sup>3, 18–20</sup> have recommended solutions based mainly on perchloric acid for polishing

\* The authors have attempted to make the contrast in the photographs representative of that observed on visual examination.

the metal electrolytically. The present authors have polished cadmium electrolytically in concentrated perchloric acid, but the surface produced gives only a weak grain contrast under polarized light.

Both Perryman<sup>3</sup> and Capdecombe and Schwob<sup>19</sup> have recommended the use of an aqueous solution of phosphoric acid at a relatively low current density for polishing cadmium. Perryman and Lack<sup>11</sup> concluded that the grain contrast under polarized light in specimens prepared in this way was due to true anisotropic reflection, since no effects were observed after a thin silver film had been deposited on the surface. Capdecombe and Schwob<sup>19</sup> showed that a cubic oxide film was present and that the maximum rotation angle was about  $0.5^\circ$ , but by anodic oxidation in potassium hydroxide solution a surface film of anisotropic cadmium hydroxide could be deposited that was strongly birefringent and resulted in rotations of the plane of polarization of up to  $7^\circ$ .

The best results were obtained in the present work by polishing in an electrolyte containing 2 parts phosphoric acid, 2 parts glycerol, and 1 part distilled water at a current density of about  $0.4 \text{ amp./cm.}^2$ . Good grain contrast with a fairly marked reaction with the sensitive tint-plate was shown. This would suggest that some etching accompanies electrolytic polishing and gives increased reaction to polarized light. An example of the fine structure produced by cold deformation followed by annealing at  $150^\circ \text{C.}$  is illustrated in Fig. 6 (Plate CI).

#### 5. COBALT (HEXAGONAL)

Few workers have used polarized light in the metallographic examination of cobalt, although the metal has been polished electrolytically for a study of ferromagnetic domain structures. The anisotropic optical properties are apparently very weak, and poor grain contrast is obtained on mechanically polished specimens under polarized light. Cobalt can be polished electrolytically in phosphoric acid (density 1.35), as recommended by Elmore,<sup>21</sup> but this treatment produces etch pits or a macro-etch, especially at lower current densities. Grain-boundary delineation is obtained by polishing at about  $2.5 \text{ amp./cm.}^2$  in a solution containing equal volumes of hydrochloric acid and ethyl alcohol. Such specimens give fairly marked grain contrast and delineation of twins when viewed under crossed polarizers, but only slight colour contrast is obtained when the sensitive tint-plate is used. Fig. 7 (Plate CI) shows the grain-structure and twinning in a cobalt ingot which has been melted in an argon-arc furnace.

#### 6. MAGNESIUM (HEXAGONAL)

Some grain contrast can be obtained on mechanically polished magnesium under polarized light, but since the metal is liable to twin during this treatment, spurious deformation structures are often found. There is no great improvement by electrolytic polishing in phosphoric acid-ethyl alcohol mixtures, as

suggested for normal microscopical examination by Larke and Wicks,<sup>22</sup> Perryman,<sup>3</sup> and Jacquet,<sup>23, 24</sup> but the perchloric-acetic anhydride solution recommended by the Magnesium Metal Corporation<sup>25</sup> is more effective, although the polished surface usually contains pits which interfere with examination under polarized light (Fig. 8, Plate CI).

Capdecombe<sup>12</sup> obtained maximum rotation angles of up to  $4^\circ$  on specimens polished in a solution of chromic oxide in alcohol, indicating quite marked anisotropy, although it is not clear whether an anisotropic film was contributing to the reflection. Ernst and Laves<sup>26</sup> failed to obtain sufficient grain contrast on surfaces prepared either mechanically or electrolytically, and they describe a complex treatment for depositing uniaxial birefringent films to improve the results. They observed that the birefringence of the film on a plane with the normal approximately parallel to the symmetry axis was nil or very weak and suggested that an estimate of the orientation of a given grain could be made from the degree of birefringence in the surface film. George<sup>27</sup> has suggested a different technique for increasing grain contrast and estimating the orientation. He etched mechanically polished surfaces in an aqueous solution of picral and glacial acetic acid which produces facets of the basal plane in each grain, so that the ellipticity produced by reflection of a plane polarized beam depends on the orientation of the facet and hence of the grain.

The best results have been obtained by electrolytic polishing for about 60 sec. in a solution containing 10 ml. concentrated hydrochloric acid in 135 ml. carbitol at a current density of  $0.1\text{--}0.15 \text{ amp./cm.}^2$ . A thick passive film is formed on the specimen, which is partly removed by washing in a stream of water and dissolved completely by immersion in a weak solution of potassium hydroxide. The specimen is then dried and re-treated in the above electrolyte for about 20 sec. and washed in water. Any residual film remaining from the initial polishing treatment is completely removed by the second polish, so that the immersion in caustic potash may be omitted. The grain boundaries are only faintly delineated by this treatment and the surface is fairly flat, as shown in Fig. 9 (Plate CI), which represents a section from an extruded magnesium rod after annealing. Fig. 10 (Plate CI) shows the same area under polarized light and reveals the presence of small groups of grains of similar orientation (cf. the results reported for recrystallized uranium<sup>2</sup>). Surfaces prepared in this way give fairly distinct colour effects when the sensitive tint-plate is inserted in the microscope, and it is considered likely that the elliptical polarization arises from reflection within minute facets on the surface.

#### 7. TIN (TETRAGONAL)

Contrary to the suggestion of Walker<sup>6</sup> and to the fact that Capdecombe<sup>12</sup> gives maximum angles of rotation of  $1.5^\circ$ , tin is one of the few metals which give marked anisotropic effects on mechanically polished specimens. The typical appearance of a specimen



prepared in this way and viewed under polarized light is shown in Fig. 11 (Plate CI). The metal may be polished electrolytically in 60% perchloric acid, as recommended by Puttick,<sup>28</sup> and although not reported by him, surfaces so prepared give good reaction to polarized light. Others<sup>3, 8, 29</sup> have described various solutions based on perchloric acid for electrolytically polishing tin, but the concentrated solution above has given the most satisfactory results.

Fig. 12 (Plate CI) shows the same specimen as that in Fig. 11, after polishing in 60% perchloric acid. The material now appears to be twin-free, indicating that the markings in Fig. 11 are mechanical twins formed during hand polishing. The veining in Fig. 12 is probably due to segregation of impurities in the grain boundaries on solidification, which suggests that considerable grain-boundary migration has occurred on cooling to room temperature. (A similar effect has been reported by Jacquet<sup>38</sup> on zirconium.) Fig. 13 (Plate CII) shows a sample of tin that was deformed at room temperature and partly recrystallized at about 100° C. The material appears to be recrystallizing from nuclei associated with the deformation twins, especially at the junction of interpenetrating twins. A similar phenomenon has been reported for uranium<sup>2</sup> and also for zinc by Zolotov.<sup>30</sup>

#### 8. TITANIUM (HEXAGONAL)

Mechanically polished titanium appears to have a flowed surface layer which masks the true structure of the metal, so that the grain structure is rarely observed under polarized light when prepared in this way. Craver<sup>31</sup> removed the distortion and surface flow which occurs on mechanical polishing by adding a few drops of 5% oxalic acid to the suspension medium. Specimens which have been electrolytically polished in weak solutions of perchloric acid in acetic acid, as recommended by Perryman,<sup>3</sup> Roth,<sup>32</sup> and Sutcliffe, Forsyth, and Reynolds,<sup>33</sup> give a marked grain contrast under polarized light, comparable with that obtained under ordinary illumination after etching in a mixture of nitric and hydrofluoric acids. Jacquet<sup>34, 35</sup> recommends an electrolytic etch at a low current density in a solution similar to that described above for polishing to improve the grain contrast under polarized light. A section from an argon-arc-melted ingot after polishing in the perchloric acid-acetic acid mixture is shown in Fig. 14. (Plate CII).

#### 9. URANIUM (ORTHORHOMBIC)

A full account of the use of polarized light in the examination of uranium is given elsewhere,<sup>2</sup> and it is necessary to give only a brief summary of the results in so far as they affect the discussion at the end of this paper. No grain contrast has been observed on specimens mechanically polished by conventional methods, but good results have been obtained by the attack-polish procedure and by electrolytic polishing. Surfaces prepared by electrolytic polishing show only slight colour contrast between the grains when viewed with the sensitive tint-plate, but the contrast is fairly

marked after an attack-polish as a result of an unidentified film which is apparently birefringent.

In cast uranium, groups of grains with closely related orientations are often observed and, since the individual units are resolved only for a narrow range of azimuth angle, the use of a rotating stage is essential for a true interpretation of the structure. To illustrate this, Fig. 25 (Plate CIII) shows photographs of a vacuum-cast bar after six successive rotations of 30° with the analyser rotated slightly from the crossed position. Areas which appear single-grained for one stage setting are identifiable as composed of more than one grain on stage rotation, so that a false impression of the true grain structure would have resulted from the use of a non-rotating stage.

#### 10. ZINC (HEXAGONAL)

Some grain contrast is obtained on zinc after mechanical polishing, but, as pointed out by Capdecombe, Dargent, and Orliac,<sup>8</sup> there is a marked tendency for deformation of the surface layers which may be accompanied by twinning or recrystallization. Despite these difficulties, Capdecombe<sup>12</sup> used mechanically polished specimens for measurements of the maximum angle of rotation and obtained a value of about 4°.

Etching in concentrated nitric acid will remove the flowed layer, but deformation twins due to polishing may persist even after deep etching. For this reason, it is preferable to polish zinc electrolytically to obtain the true structure, and various solutions have been recommended. Capdecombe and his co-workers<sup>8, 36</sup> found that specimens polished in a solution of potassium or sodium hydroxides gave good contrast under polarized light and that a birefringent film of hexagonal zinc oxide was formed. In an investigation of the recrystallization of zinc at 110° C. under polarized light, Brinson and Moore<sup>37</sup> used the orthophosphoric acid electrolyte originally recommended by Jacquet.<sup>24</sup> Perryman and Lack<sup>11</sup> found that a zinc specimen polished in a phosphoric acid-ethyl alcohol bath gave a suitable surface for polarized-light examination and showed that no results were obtained after silvering by vapour deposition, indicating that the original anisotropic effects were probably due to the structure of the metal rather than to surface contour.

Orthophosphoric acid solution (98%) gives an excellent polish, and is usually employed by the authors for zinc. To obtain good colour contrast with the sensitive tint-plate, specimens may be polished in an electrolyte containing 1 vol. nitric acid to 2 vol. methyl alcohol, followed by etching in the same solution at low current density. Fig. 15 (Plate CII) shows a zinc specimen which was recrystallized at 100° C. after deformation and polished in the methyl alcohol-nitric acid solution. The apparent double grain boundaries in some areas of Fig. 15 are due to a relief effect produced by polishing, which results in a marked grain-boundary delineation under normal illumination.

### 11. ZIRCONIUM (HEXAGONAL)

As with uranium, no results have been obtained on zirconium after conventional mechanical polishing, but good grain contrast is shown when specimens are polished with a few drops of hydrofluoric acid on the pad. Jacquet and Caillat<sup>38</sup> and Roth<sup>39,40</sup> recommend weak solutions of perchloric acid in acetic acid for electrolytic polishing. The grain contrast in cast zirconium treated in this way is illustrated in Fig. 16 (Plate CII). Since the surface produced has an appearance of relief owing to preferential rates of attack depending on the orientation, the solution has been further developed by the authors to eliminate this effect, with some success when a higher ratio of perchloric acid to acetic acid and additions of carbitol or ethylene glycol have been used. The best results have been obtained with a mixture of 50 ml. perchloric acid, 175 ml. acetic acid, and 100 ml. ethylene glycol at a current density greater than 1 amp./cm.<sup>2</sup>. An alternative modification described by Jacquet<sup>41</sup> consists of perchloric acid in a mixture of ethyl alcohol and 2-butoxy-ethanol, but, with this solution, there is a tendency for the formation of an adherent film which tends to mask the structure.

The A.E.R.E. modified solution appears to be more suitable for cast zirconium than for recrystallized wrought material. Typical lenticular twins in zirconium are illustrated in Fig. 17 (Plate CII), in which the primary twin in the centre of the field is crossed by fine parallel secondary twins, as reported for other metals.

## III.—EXAMINATION OF ANISOTROPIC CONSTITUENTS OF ALLOYS

### 1. MANGANESE-URANIUM ALLOYS

In an investigation of the etching characteristics of a manganese-uranium alloy containing 2.5 at.-% uranium, it was found that a twinning structure was revealed by etching mechanically polished specimens in 2% nital (Fig. 18, Plate CII). Examination of this specimen between crossed polarizers gave marked intensity contrast between the twins and different grains as in Fig. 19 (Plate CII), and beautiful colour contrast when a sensitive tint-plate was used in conjunction with a white light source. After electrolytic polishing in a solution containing 1 vol. orthophosphoric acid, 2 vol. sulphuric acid, and 2 vol. distilled water, the contrast under polarized light was poor. This would indicate that the etching treatment in nital had produced a birefringent film similar to that obtained by Worrell<sup>42</sup> on a tetragonal manganese-copper alloy with 12% copper. (Worrell found that both etching in 5% citric acid and polishing in alcoholic perchloric acid gave marked anisotropic reflection.)

### 2. MARTENSITIC STEELS

In the normal way, it is difficult to assess the grain-size of martensitic steels after etching and under bright-field illumination. If, however, an etched

specimen is examined between crossed polarisers, the grain contrast is markedly improved (Figs. 20 and 21, Plate CII), and can be further enhanced by using a sensitive tint-plate which gives useful colour effects. The etching treatment may be carried out either in nital or a solution containing 10 ml. hydrochloric acid, 3 ml. nitric acid, and 100 ml. methyl alcohol after mechanical polishing. Alternatively, the specimens may be electrolytically polished in a solution containing 4 parts acetic acid to 1 part perchloric acid. Heindlhofer and Bain<sup>43</sup> suggest that the grain contrast under polarized light is the result of anisotropy in the crystal structure of the tetragonal martensite and that failure to obtain any effect as polished is due to a flowed layer which may be removed by etching. Since the martensitic structure is only a light distortion of a body-centred cubic lattice, the birefringence expected would be small, and it is more probable that the effects are caused by the surface contour of the etched specimen. This is confirmed by the fact that the contrast is a maximum for an optimum etching treatment when the martensitic needles (which are approximately parallel in a given grain) are only just resolved, as in Fig. 21, and that the contrast under polarized light decreases with deeper etching.

### 3. THORIUM-ALUMINIUM ALLOYS

The complete constitution of the thorium-aluminium system has not been reported, but it is apparent that there are at least two compounds. In an examination of thorium-aluminium alloys at the A.E.R.E., Murray<sup>44</sup> found that one compound in the region of ThAl was markedly anisotropic and under polarized light was easily distinguishable from the phases with which it was in equilibrium. The optical anisotropy of the compound was apparent after mechanical polishing and also after electrolytic polishing in a phosphoric acid-acetic acid mixture, as illustrated in Fig. 22 (Plate CII).

### 4. THORIUM-SELENIUM ALLOYS

Several intermediate phases have been shown by Murray and D'Eye<sup>45</sup> to exist in thorium-selenium alloys, some cubic and others of lower symmetry. The microstructure of the alloys is complicated, but the use of polarized light was found to be of considerable help in separating the cubic phases from the non-cubic and also in distinguishing between the various anisotropic constituents. As an example, one alloy consisted of a eutectic that was not revealed under ordinary illumination, but was clearly resolved under polarized light as a result of the different anisotropic properties of the constituent phases (Fig. 23, Plate CII).

### 5. TUNGSTEN CARBIDE COMPACTS

In an investigation of the hot-pressing characteristics of tungsten carbide powder (WC), Williams<sup>46</sup> was able to use polarized light to identify the grain-size in compacted specimens. The normal procedure is to



etch the carbide in a boiling solution of alkaline potassium ferricyanide as described by Bleecker.<sup>47</sup> This reveals the grain boundaries, but gives no grain contrast. Since tungsten carbide is hexagonal, a section mechanically polished with four suspensions of successively finer diamond dust gave good grain contrast between crossed polarizers, and the definition was superior to that given by the somewhat drastic etch described above. A typical section is illustrated in Fig. 24 (Plate CII).

#### 6. URANIUM-ALUMINIUM ALLOYS

The constitution of uranium-aluminium alloys has been reported by Gordon and Kaufmann.<sup>48</sup> The system contains three compounds,  $UAl_2$  and  $UAl_3$ , which are cubic, and one in the region  $UAl_4$ - $UAl_5$ . It has recently been shown<sup>49</sup> that the third compound is  $UAl_4$  and that it is orthorhombic. The three compounds are differentiated only by a slight difference in colour when they occur together, and no etching reagent has been found to colour any of them. Alloys have been examined under polarized light at the A.E.R.E., and a marked contrast between  $UAl_3$  and  $UAl_4$  has been obtained, such that the distribution and mode of occurrence of either compound could be studied with ease.

#### IV.—FACTORS AFFECTING THE PRODUCTION BY MECHANICAL POLISHING OF A SATISFACTORY SURFACE FOR EXAMINATION BY POLARIZED LIGHT

On the basis of the results from seven mechanically polished metals, Walker<sup>6</sup> concluded that the anisotropic properties were not extinguished by the formation of a polish film and that "the metals having the least percentage of reflection of the incident beam gave the strongest anisotropic properties" (see Table I). No indication was given of how the anisotropy was assessed, but presumably it was based on the grain contrast shown between crossed polarizers by a multi-grained specimen with random orientation. Walker's results do not agree with the authors' observations (also summarized in Table I), and it is worth while considering possible explanations of these differences.

For a perfectly polished section, it would be expected that the maximum possible contrast between two grains would be related to the ratio of the principal reflectivities, which governs the maximum angle of rotation of the plane of polarization on reflection. Capdecombe's\* values for this angle have been included in Table I, and the order in which magnitudes of the rotation occur is not the order of the strongest anisotropy observed on mechanically polished specimens as given by Walker or the present authors. In

addition, for the hexagonal metals, there is no obvious correlation between the apparent or measured anisotropic properties and the departure of the axial ratio from that of the ideal close-packed structure.

Bowden and his collaborators<sup>50</sup> postulate that metallic polishing occurs by a progressive melting of the ridges followed by a flowing of the liquid into the valleys; this transfer of atoms finally results in a

TABLE I.—Summary of Crystallographic Observations and Some Physical Properties of Various Anisotropic Metals and Alloys.

Metal	Crystal Structure	Axial Ratio	Reflectivity, %	Grain Contrast Normally Obtained on Mechanically Polished Specimens	Maximum Rotation Angle, °†	Melting Point, °C.
Tin	Tetragonal	0.546	82	Very good	1.5 +	232
Bismuth	Rhombohedral	...	55	Good	3.5	271
Cadmium	Hexagonal	1.885	98	Moderate	0.5	321
Zinc	Hexagonal	1.856	74	Moderate	4.0	420
Antimony	Rhombohedral	...	53	Weak	3.5	631
Magnesium	Hexagonal	1.624	73	Weak	4.0	650
Uranium	Orthorhombic	...	...	None	...	1128
Beryllium	Hexagonal	1.585	...	Weak	...	1350
Cobalt	Hexagonal	1.624	...	None	...	1450
Titanium	Hexagonal	1.601	...	None	...	1800
Zirconium	Hexagonal	1.589	...	None	...	1900
$UAl_4$	Orthorhombic	...	...	Very good	...	~1500
WC	Hexagonal	0.973	...	Very good	...	~2800
Martensite	Tetragonal	...	...	None	...	...

\* Given by Walker<sup>6</sup> for mechanically polished condition. Tellurium was also included by Walker, but not investigated at A.E.R.E.

† Given by Capdecombe.<sup>12</sup>

levelling of the whole surface. If only a few atoms are involved during melting, then when the liquid solidifies, it is most likely to assume the orientation of the solid with which it is in contact, although a thick liquid layer might solidify with a structure independent of the underlying metal. The amount of liquid present at any one instant will depend on the melting point and thermal conductivity of the metal and the pressure applied during polishing, and is likely to be greatest for low-melting-point metals polished with heavy pressures. The fact that spurious grain structures are often observed on tin and zinc after heavy mechanical polishing is easily understood on this basis.

Since the metal may be cold worked to an appreciable depth during preliminary preparation of the section, such as sawing, filing, or grinding, the structure observed on mechanically polished sections will be determined by the deformation characteristics of the metal. If deformation occurs mainly by slip, the structure will be that of the parent metal, but if deformation twins are possible, these will be observed as for magnesium and beryllium.

For very brittle materials which fracture easily, the mechanism of polishing must be considered as a grinding process in which there is a mechanical breakdown of the ridges. Compounds such as  $UAl_4$  and WC therefore give good results on mechanically polished specimens, and although martensitic steels might be

\* Some of Capdecombe's results were obtained on cleavage surfaces and electropolished sections; where mechanically

polished sections were examined, the results were in the same order for all three conditions.

expected to behave similarly, the observed lack of grain contrast is easily explained. The rotation of the plane of polarization that could be expected from the anisotropy of the crystal structure, which is only a slight distortion of a body-centred cube, is inherently small. Thus only slight grain contrast is possible on polished specimens, and it is necessary to etch to give a suitable contour effect to produce different degrees of ellipticity of the reflected rays from different grains.

Although many of the observations described in this paper may be explained, it is difficult to understand why mechanically polished sections of uranium, cobalt, titanium, and zirconium usually behave as if they reflect light isotropically. One factor which has been ignored so far is surface oxidation. The oxide film present on the ground specimen is probably broken up and trapped in the surface during polishing, forming an intimate metal-oxide mixture which may account for the general conclusion from electron-diffraction investigations that the surface layer is either amorphous or consists of very small crystals. If the thickness and absorption characteristics of the metal-oxide mixture results in the surface film being opaque, then no change in azimuth of the plane polarized beam will occur on reflection and the metal will appear to be isotropic. This may explain the behaviour of metals such as uranium and the fact that good grain contrast is obtained on uranium, beryllium, and zirconium if an acid solution is used as the suspension liquid during mechanical polishing. The acid would serve to loosen the oxide and keep the surface relatively clean.

It is possible that the characteristics of the metal-oxide layer may change with the polishing conditions, such as the pressure on the specimen, and this could account for the difference between the authors' observations and those of Walker. The complete polishing treatment used by Walker occupied several hours with very low pressures which were automatically controlled to fine limits, whereas in the present work the metals were polished with pressures similar to those normally used in metallographic preparation. Evidence to support this was obtained by polishing a magnesium specimen on an automatic machine for 2 hr., taking care to use only a light pressure at all stages of preparation. Subsequent examination under polarized light gave improved grain contrast over that obtained on the same specimen prepared by the more normal procedure, although it was inferior to that after electrolytic polishing.

## V.—CONCLUSIONS

It is evident that polarized light is a useful aid in the metallographic examination of anisotropic metals and alloys. In some cases, it is doubtful whether any marked advantages are obtained in the use of polarized light to obtain grain contrast over the results of the more conventional etching techniques, but this is by no means always true. For example, no reliable etching treatment has been found for revealing the

grain structure in uranium, and all the data obtained so far at the A.E.R.E. on the effect of thermal and mechanical treatments on the structure of this metal have been from examination under polarized light. In general, however, since the technique can be used on sections in the as-polished condition, lack of definition due to the possible deterioration of the surface on etching is avoided. A good example is that of tungsten carbide, where the ferricyanide etch normally employed is not only messy but has a tendency to pit and stain the surface.

In theory, it is possible to observe grain contrast on a mechanically polished surface of any material which has a crystal structure other than that of cubic symmetry, but owing to various factors which are not properly understood, the results vary greatly with the metal under examination. In some cases, material affected by polishing may be removed by a simple etching treatment, but usually superior results are obtained by suitable electrolytic polishing. In addition to those solutions already described in the literature, possible alternatives are suggested in the light of developments at the A.E.R.E., in particular for beryllium, bismuth, magnesium, uranium, and zirconium. It should be appreciated that in electrolytic polishing the results may be greatly affected by small variations in the polishing conditions, such as the temperature, composition, and impurity content of the electrolyte, and in the method of handling, shape, and the composition of the specimen.

It is often difficult to decide whether the presence of a birefringent surface film or of a regular surface contour contributes to the inherent anisotropic reflection of a non-cubic metal, but on the assumption that perfect metallic reflection introduces only slight ellipticity, some indication of the magnitude of the interfering effect can be obtained from the degree of colour contrast between the grains when a sensitive tint-plate is inserted below the analyser. In those cases in which the contrast due to the anisotropic reflection of the metal is poor, it may often be advantageous to form a regular pattern of facets or a birefringent surface film by a modification of the electrolytic treatment.

Polarized light may sometimes be used to distinguish between intermediate phases in an alloy system whose similar etching characteristics make difficult a distinction by examination under ordinary illumination. Such a technique is not restricted to alloys in which one constituent is cubic and the other of lower symmetry, since often there is sufficient difference in the birefractivity of two anisotropic phases to enable a distinction to be made between them.

## ACKNOWLEDGEMENTS

This paper is published by kind permission of Sir John Cockcroft, F.R.S., Director of the Atomic Energy Research Establishment, Harwell. The authors are grateful to Mr. L. Kent for his assistance with the illustrations.



## REFERENCES

1. B. W. Mott and H. R. Haines, *Research*, 1951, **4**, 24, 63.
2. B. W. Mott and H. R. Haines, *J. Inst. Metals*, 1951-52, **80**, (12), 621.
3. E. C. W. Perryman, *Metal Ind.*, 1951, **79**, 23.
4. P. A. Jacquet, *Proc. Third Internat. Electrodeposition Conf.*, 1947, **3**.
5. D. S. Kemsley and W. J. McG. Tegart, *Council Sci. Indust. Research (Australia), Div. Tribophysics, Phys. Met. Rep. No. 7*, 1948.
6. H. L. Walker, *Metal Progress*, 1939, **35**, 562.
7. D. Boyd Metz and H. W. Woods, *U.S. Atomic Energy Commission Publ.*, 1950, (SEP-42).
8. L. Capdecombe, R. Dargent, and M. Orliac, *Métaux, Corrosion-Usure*, 1942, **17**, 53.
9. H. Hone and E. C. Pearson, *Metal Progress*, 1948, **53**, 363.
10. D. H. Woodard, *Trans. Amer. Inst. Min. Met. Eng.*, 1949, **185**, 722.
11. E. C. W. Perryman and J. M. Lack, *Nature*, 1951, **167**, 479.
12. L. Capdecombe, *Bull. Soc. franç. Minéral.*, 1941, **64**, 160.
13. A. R. Kaufmann, P. Gordon, and D. W. Lillie, *Trans. Amer. Soc. Metals*, 1950, **42**, 785.
14. A. R. Kaufmann, P. Gordon, and D. W. Lillie, *Metal Progress*, 1949, **56**, 664.
15. P. Gordon, *U.S. Atomic Energy Commission Publ.*, 1949, (AECD-2869).
16. O. Jones, *Phil. Mag.*, 1924, [vi], **48**, 207.
17. W. J. McG. Tegart and R. G. Vines, *Rev. Mét.*, 1951, **48**, 245.
18. J. Liger, *Bull. Soc. Chim. France*, 1944, **11**, 568.
19. L. Capdecombe and Y. Schwob, *Métaux, Corrosion-Usure*, 1943, **18**, 173.
20. R. W. K. Honeycombe, *Symposium on the Recent Advances in Physical Metallurgy, Part I* (Australian Inst. Metals), 1944.
21. W. C. Elmore, *Phys. Rev.*, 1938, [ii], **53**, 757.
22. L. W. Larke and E. B. Wicks, *Metallurgia*, 1950, **41**, 172.
23. P. A. Jacquet, *Métaux, Corrosion-Usure*, 1943, **18**, 1.
24. P. A. Jacquet, *Métaux, Corrosion-Usure*, 1944, **19**, 71.
25. — Brit. Patent No. 550,175 and 550,176, 1942.
26. T. Ernst and F. Laves, *Z. Metallkunde*, 1949, **40**, 1.
27. P. F. George, *Trans. Amer. Soc. Metals*, 1947, **38**, 687.
28. K. E. Puttick, *Metallurgia*, 1949, **41**, 120.
29. P. A. Jacquet, *Internat. Tin Research Development Council, Publ.*, No. 90, 1939.
30. V. A. Zolotov, *Compt. rend.*, (Doklady) Acad. Sci. U.R.S.S., 1943, **39**, 180.
31. C. B. Craver, *Metal Progress*, 1951, **59**, 371.
32. H. P. Roth, *ibid.*, 1951, **59**, 816b.
33. D. A. Sutcliffe, P. J. E. Forsyth, and J. A. Reynolds, *Metallurgia*, 1950, **41**, 283.
34. P. A. Jacquet, *Compt. rend.*, 1951, **232**, 71.
35. P. A. Jacquet, *Metal Treatment*, 1951, **18**, 176.
36. L. Capdecombe and M. Orliac, *Compt. rend.*, 1941, **213**, 383.
37. G. Brinson and A. J. W. Moore, *J. Inst. Metals*, 1951, **79**, 429.
38. P. A. Jacquet and R. Caillat, *Compt. rend.*, 1949, **228**, 1224.
39. H. P. Roth, *U.S. Atomic Energy Commission Publ.*, 1950, (AECD-2882).
40. H. P. Roth, *Metal Progress*, 1950, **58**, 709.
41. P. A. Jacquet, *Metallurgia*, 1950, **42**, 268.
42. F. T. Worrell, *J. Appl. Physics*, 1948, **19**, 929.
43. K. Heindlhofer and E. C. Bain, *Trans. Amer. Soc. Steel Treat.*, 1930, **18**, 673.
44. J. R. Murray, Unpublished work.
45. J. R. Murray and R. W. M. D'Eye, Unpublished work.
46. A. E. Williams, *Metal Treatment*, 1951, **18**, 445.
47. W. H. Bleecker, *Iron Age*, 1950, **165**, (21), 71.
48. P. Gordon and A. R. Kaufmann, *Trans. Amer. Inst. Min. Met. Eng.*, 1950, **188**, 182.
49. B. S. Borie, *U.S. Atomic Energy Commission Publ.*, 1950, (ORNL-810).
50. F. P. Bowden and D. Tabor, "The Friction and Lubrication of Solids", Chapter III. 1950: Oxford (University Press).

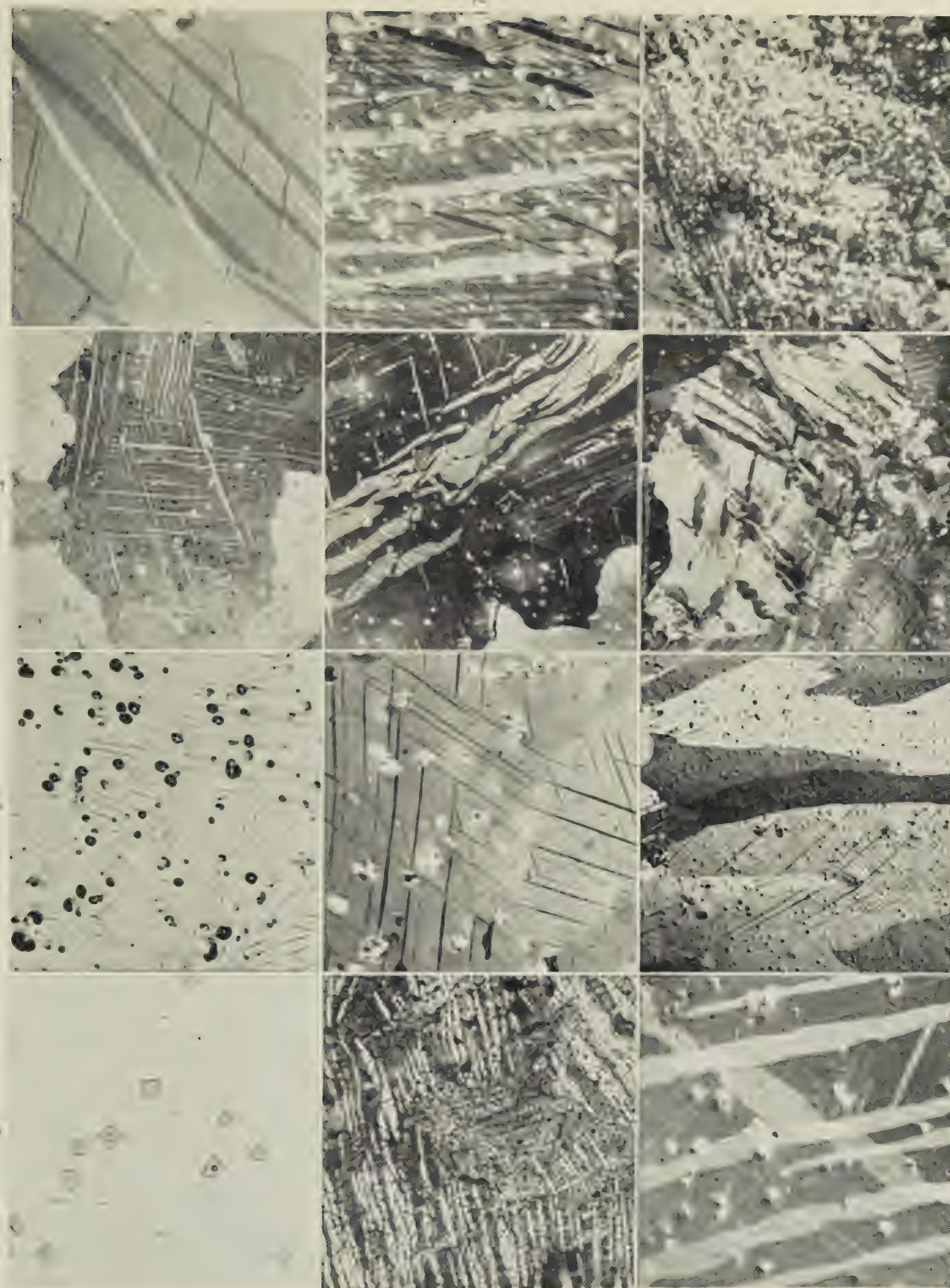


FIG. 1.—Oxide Particles.  $\times 500$ .

FIG. 2.—Electropolished in Perchloric Acid, Acetic Acid Bath.  $\times 100$ .

FIG. 3.—Structure of 1-in. dia. Chill-Cast Bar.  $\times 150$ .

FIG. 4.—Twining in 2-in. dia. Bar.  $\times 750$ .

FIG. 5.—Twining Revealed by Electropolishing a Milled Surface.  $\times 100$ .

FIG. 6.—Same as Fig. 5 After Repolishing on 000 Emery Paper and Electro-polishing.  $\times 300$ .

Figs. 1, 2, 5, 23, and 24 taken with ordinary illumination. All others under polarized light.

FIG. 7.—Dislocation and Multiple Twinning.

FIG. 8.—Primary and Secondary Twinning in 2-in.-dia. Bar.  $\times 200$ .

FIG. 9.—Intersection of Twins.  $\times 200$ .

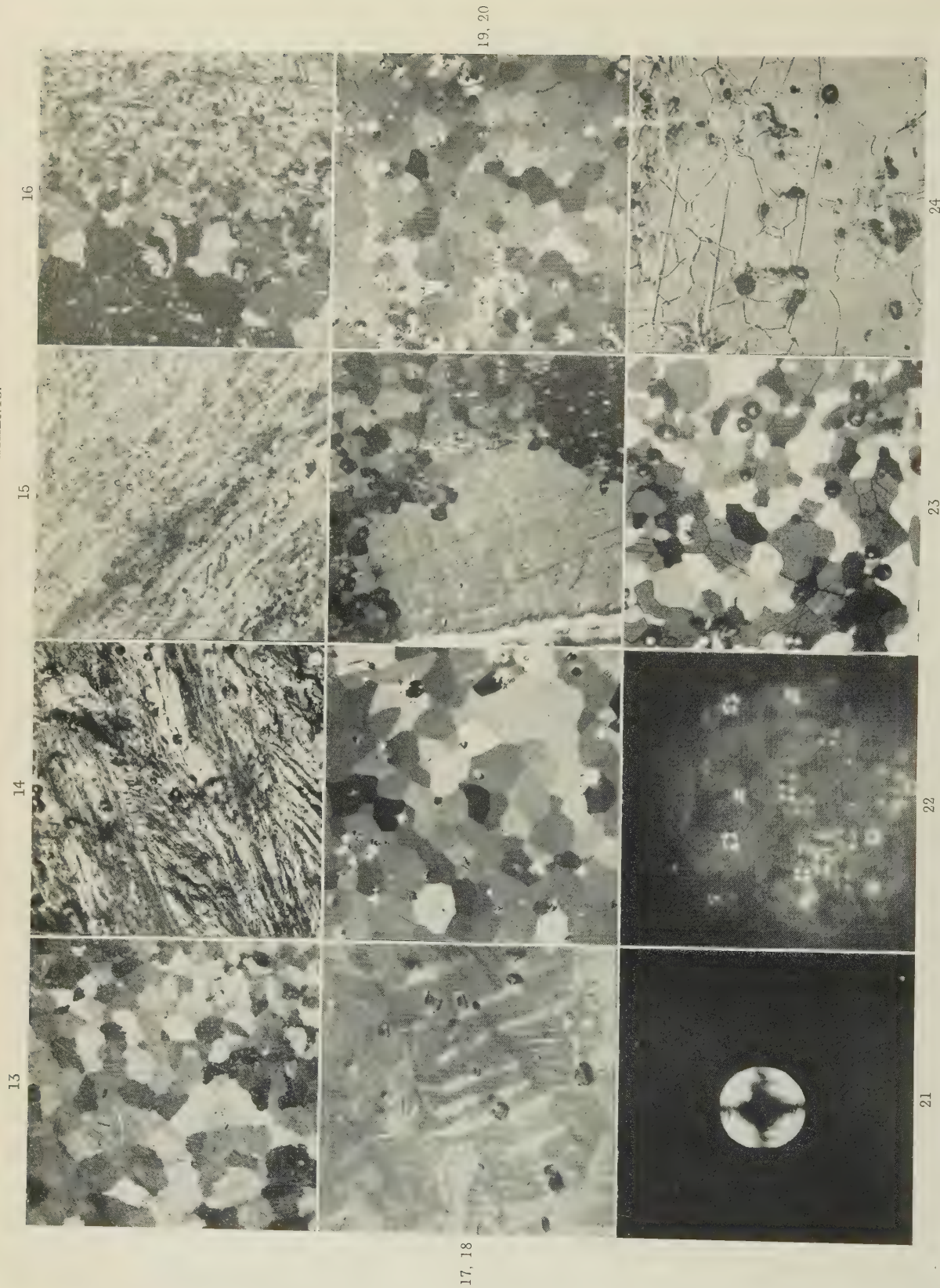
FIG. 10.—Annealed for 250 Hr. at  $650^{\circ}\text{C}$ .  $\times 100$ .

FIG. 11.—Thermally Cycled in  $\alpha$  Range.  $\times 200$ .

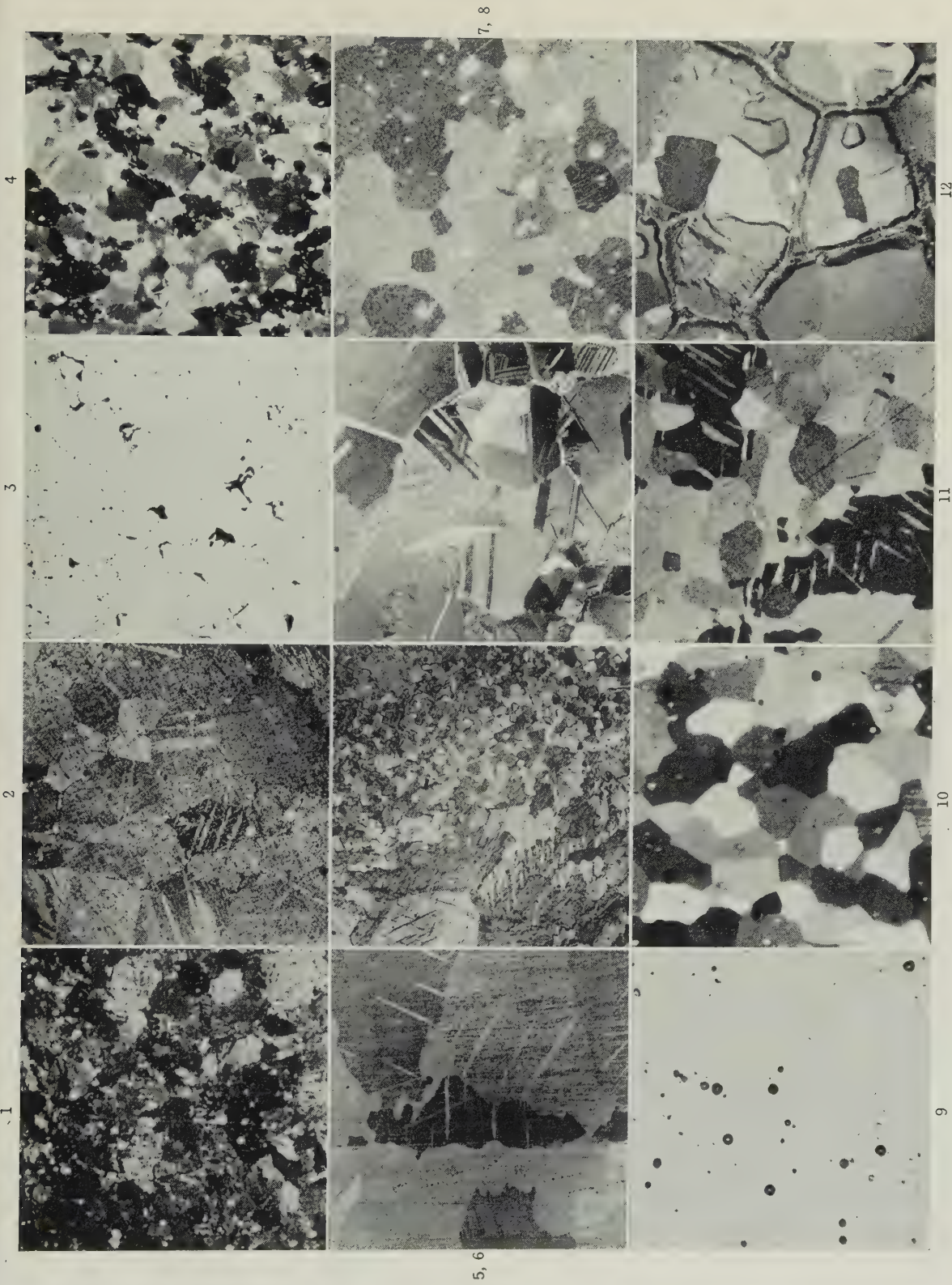
FIG. 12.—As Fig. 11, Showing Recrystallization Along Twins.  $\times 75$ .



## MICROSTRUCTURES OF URANIUM AFTER VARIOUS TREATMENTS.

FIG. 13.—As Fig. 11, Showing Coarse Grain Structure.  $\times 75$ .FIG. 14.—Longitudinal Section of Bar Hot Worked in  $\alpha$  Range. Highly deformed structure showing no recrystallization.  $\times 100$ .FIG. 15.—Recrystallization in Material Hot Worked in Higher  $\alpha$  Range.  $\times 200$ .FIG. 16.—Growth of Small Recrystallized Grains Resulting in Preferred Orientation.  $\times 100$ .FIG. 17.—Swaged Bar Annealed at  $400^{\circ}\text{C}$ . Showing Primary and Secondary Twins.  $\times 150$ .FIG. 18.—Bar Swaged by 35% and Heated at  $650^{\circ}\text{C}$ . for 1 Hr. ShowingFIG. 19.—Structure at the Shoulder of Tensile Test-Piece Machined from Recrystallized Swaged Uranium and Annealed for 63 Hr. at  $625^{\circ}\text{C}$ . after 2% Extension.  $\times 175$ .FIG. 20.—Recrystallized Cold-Rolled Bar.  $\times 200$ .FIG. 21.—“Optical Cross” Formed by Gas Cavities in Cast Material Under Crossed Polarizers.  $\times 100$ .FIG. 22.—“Optical-Cross” Effects Obtained from Oxide Globules in Reduction Dross.  $\times 1000$ .FIG. 23.—Section of Recrystallized Rolled Bar Heat-Tinted at  $108^{\circ}\text{C}$ . for 1 Hr.







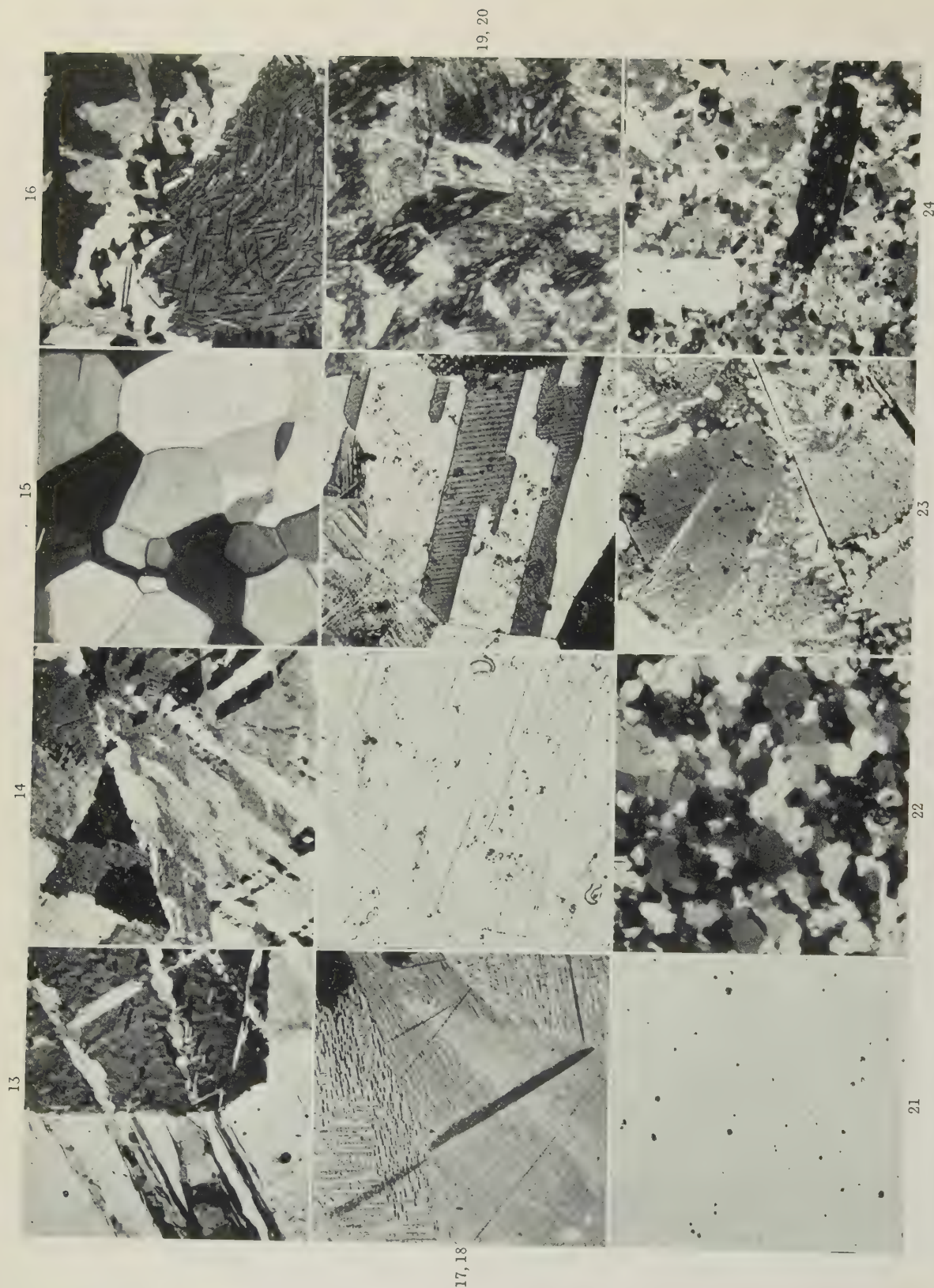


FIG. 13.—Sn Deformed at Room Temp. and Partly Recrystallized at 100° C., under Polarized Light. Electropolished in perchloric acid.  $\times 75$ .  
 FIG. 14.—Ti under Polarized Light. Electropolished in perchloric acid.  $\times 100$ .  
 FIG. 15.—Zn under Polarized Light. Electropolished in methyl alcohol-nitric acid soln.  $\times 75$ .  
 FIG. 16.—Zr under Polarized Light. Electropolished in perchloric acid.  $\times 75$ .  
 FIG. 17.—Zr under Polarized Light. Electropolished in A.E.R.E. soln.  $\times 75$ .  
 FIG. 18.—Mn-U Alloy. Mech. polished and etched in Nital.  $\times 400$ .

FIG. 19.—As Fig. 18, under Polarized Light.  $\times 400$ .  
 FIG. 20.—Martensitic Steel under Polarized Light. Etched.  $\times 200$ .  
 FIG. 21.—As Fig. 20, under Normal Illumination.  $\times 200$ .  
 FIG. 22.—Th-Al Alloy under Polarized Light. Electropolished in phosphoric acid-acetic acid soln.  $\times 200$ .  
 FIG. 23.—Th-Se Alloy under Polarized Light. Mech. polished.  $\times 300$ .  
 FIG. 24.—WC under Polarized Light. Polished with diamond dust.  $\times 300$ .

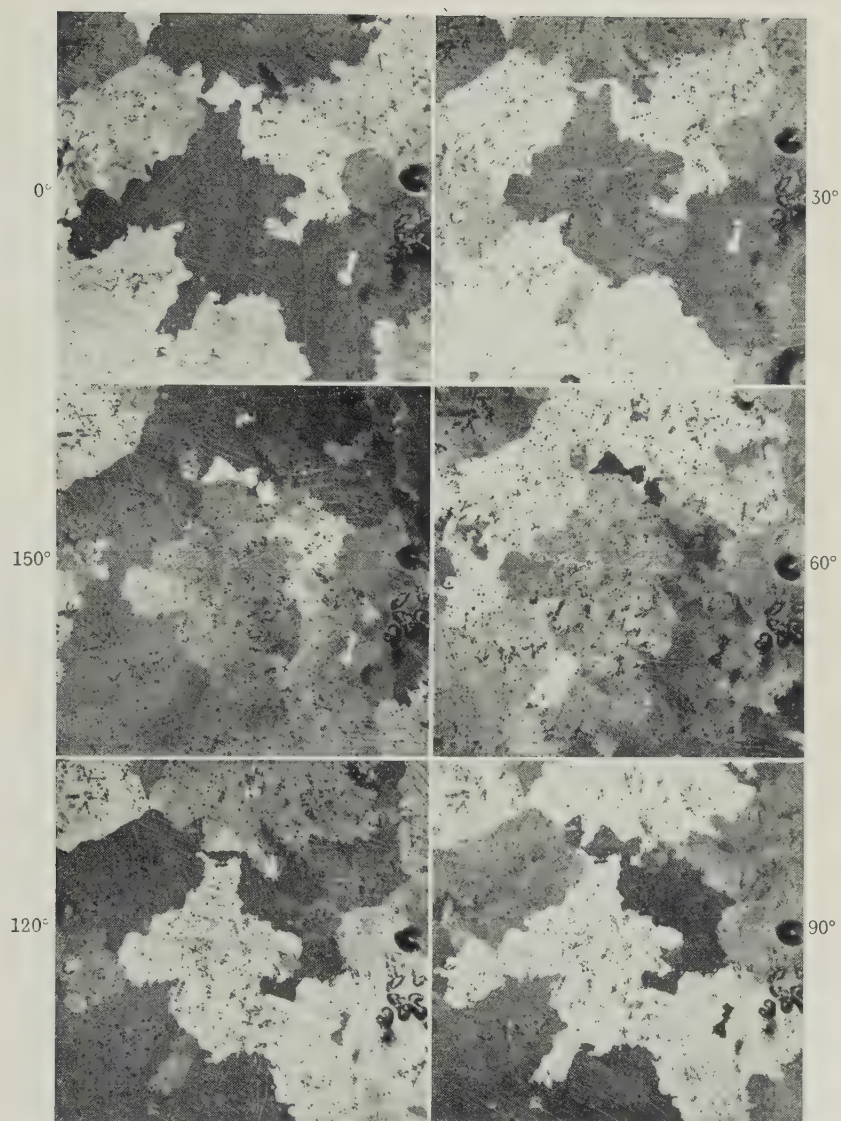


FIG. 25.—Vacuum-Cast Uranium after Six Rotations of  $30^\circ$ . Analyser rotated slightly from the crossed position.  $\times 100$ .



## COPPER-INDIUM ALLOYS.

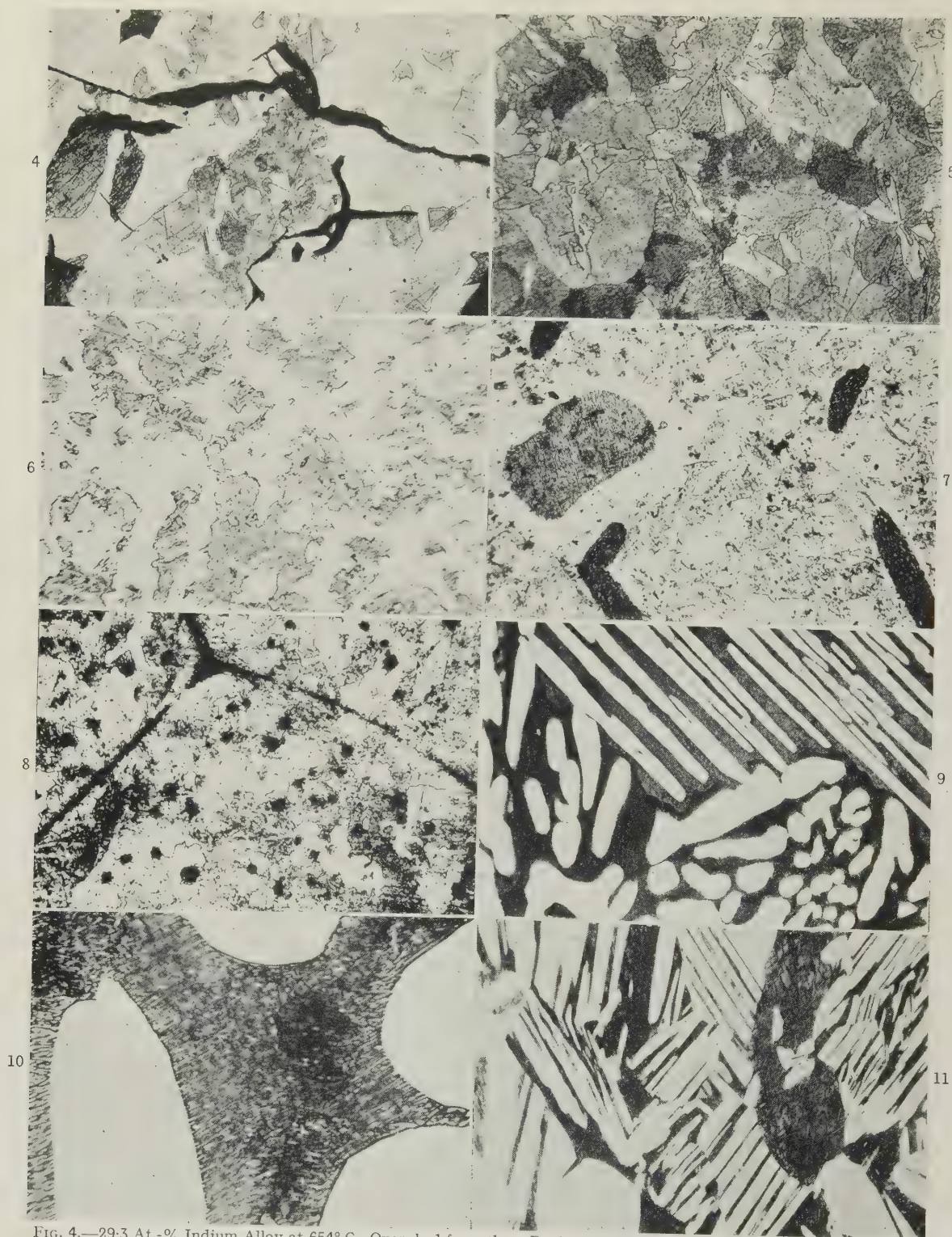


FIG. 4.—29.3 At.-% Indium Alloy at 654° C., Quenched from the  $\gamma$ -Region.  $\times 175$ .

FIG. 5.—30.3 At.-% Indium Alloy at 654° C., Quenched from the  $\gamma$ -Region.  $\times 90$ .

FIG. 6.—30.8 At.-% Indium Alloy at 630° C., Quenched from the  $\gamma$ -Region.  $\times 150$ .

FIG. 7.—31.45 At.-% Indium Alloy Quenched from 661° C. Two-phase appearance.  $\times 150$ .

FIG. 8.—30.75 At.-% Indium Alloy Quenched from 675° C. Decomposed  $\eta$  precipitated in decomposed  $\gamma$ .  $\times 175$ .

FIG. 9.—28.5 At.-% Indium Alloy Quenched from 619° C.  $\delta$  and eutectoidally-decomposed  $\gamma$ .  $\times 120$ .

FIG. 10.—As Fig. 9.  $\times 600$ .

FIG. 11.—32.0 At.-% Indium Alloy Furnace-Cooled from 660° to 611° C. and Quenched.  $\delta$  and decomposed  $\eta$ .  $\times 150$ .



NICKEL-VANADIUM ALLOYS.



FIG. 12.—Alloy C50 after Thermal Analysis.  $a + \text{eutectic}$ .  $\times 200$ .

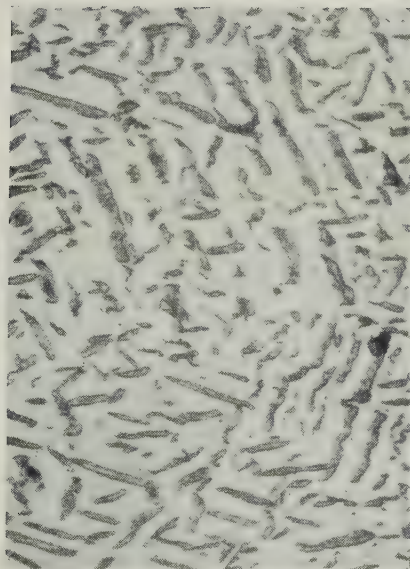


FIG. 13.—Alloy E20.3, Quenched from  $932^{\circ}\text{C}$ .  $\times 750$ .

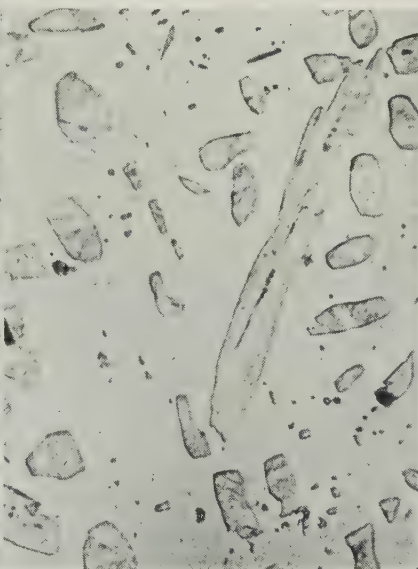


FIG. 14.—Alloy H23.7, Quenched from  $1034^{\circ}\text{C}$ .  $\times 750$ .

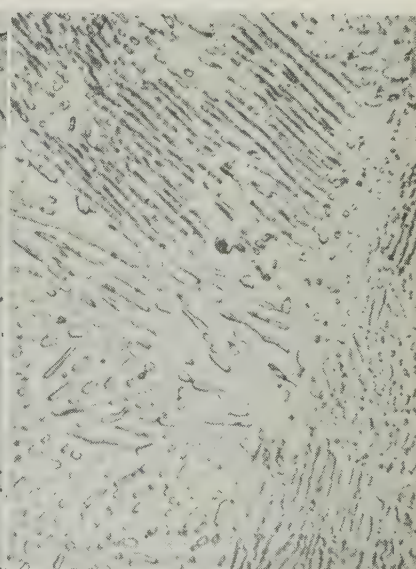


FIG. 15.—Alloy H37.3, Quenched from  $877^{\circ}\text{C}$ .  $\times 750$ .



## NICKEL-VANADIUM ALLOYS.

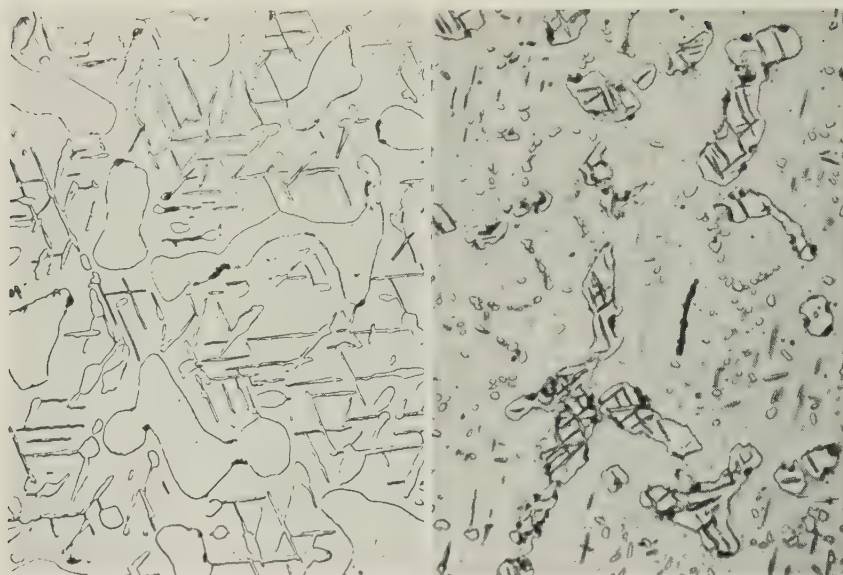


FIG. 16.—Alloy H45, Quenched from 1044° C.  $\times 300$ . FIG. 17.—Alloy S53, Quenched from 851° C.  $\times 500$ .

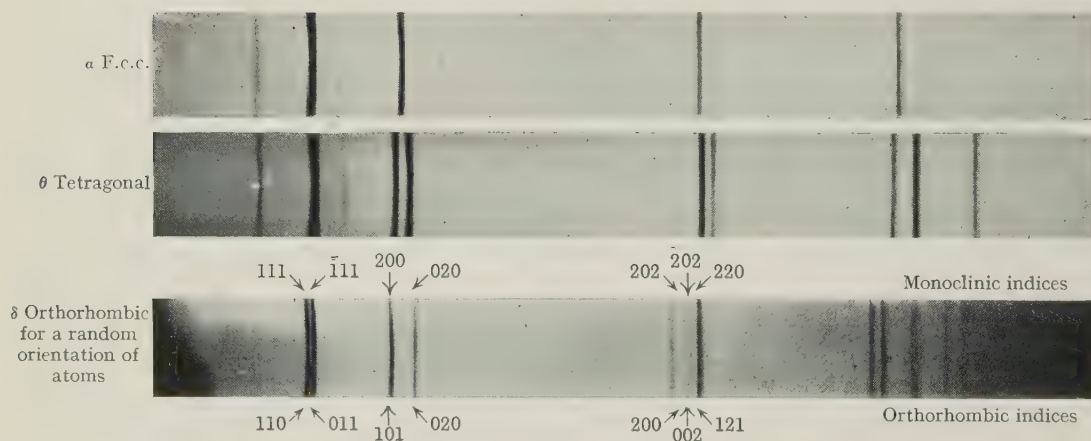
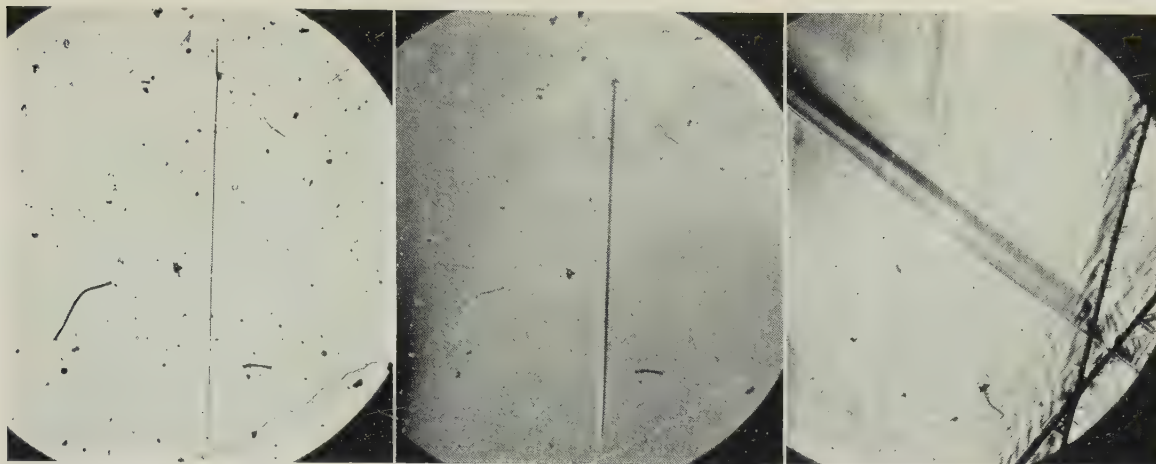
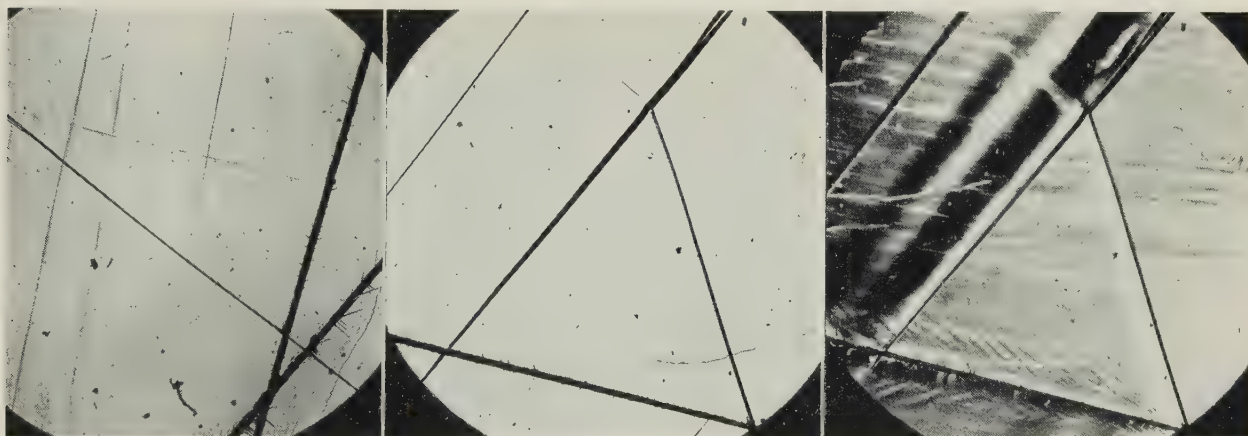
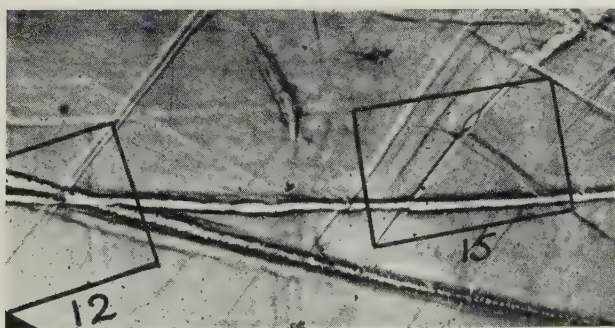
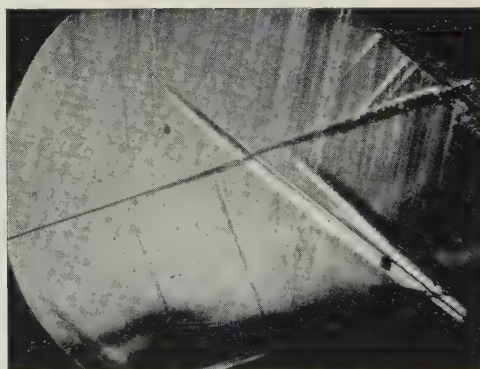


FIG. 18.—Showing the Relationship between the Face-Centred Cubic  $\alpha$  Structure and the  $\theta$  and  $\delta$  Structures. Unfiltered Cu radiation. The photograph of the  $\delta$  phase was taken in a high-temperature camera at about 850° C.

FIG. 10.—Twin Trace on Cleavage Face in Zinc.  $\times 15$ .FIG. 11.—As Fig. 10, with Opaque Stop.  $\times 15$ .FIG. 12.—Twin Marked by Intersecting Scratches. Opaque stop.  $\times 30$ .FIG. 13.—As Fig. 12. Normal illumination.  $\times 30$ .FIG. 14.—Multiple Twins near Scratch on Crystal Shown in Fig. 13.  $\times 30$ .FIG. 15.—As Fig. 14, with Opaque Stop.  $\times 30$ .FIG. 16.—X-Ray Micrograph of Crystal in Figs. 12-15, Showing Areas of Lattice Rotation.  $\times 12$ .FIG. 17.—Crossing Twins and Kinks. Opaque stop.  $\times 30$ .



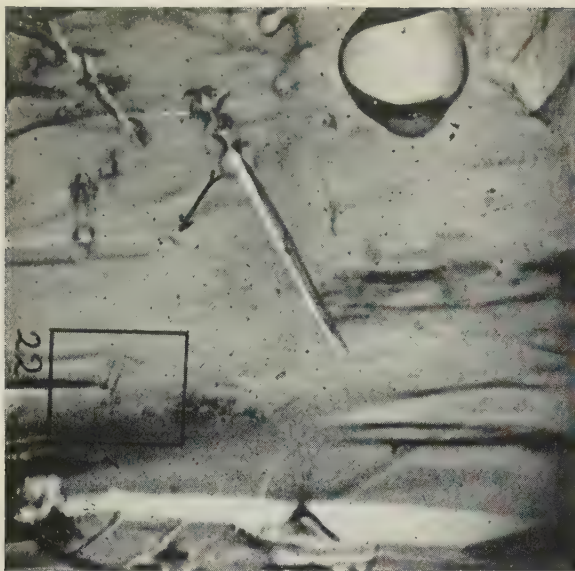


FIG. 18.—X-Ray Micrograph, Showing Twins and Kink Bands.  
× 12.

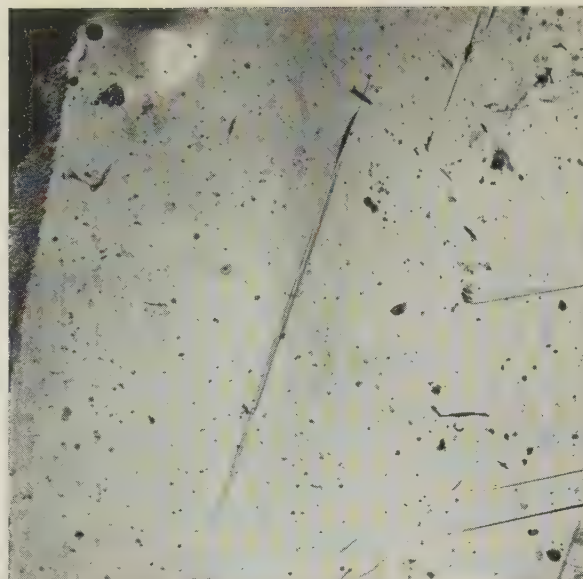


FIG. 19.—Optical Micrograph of Area Shown in Fig. 18.  
× 12.



FIG. 20.—Twins Shown in Figs. 18 and 19. Opaque stop. × 15.



FIG. 21.—Kink Band at End of Twin in Fig. 10. Opaque stop. × 30.

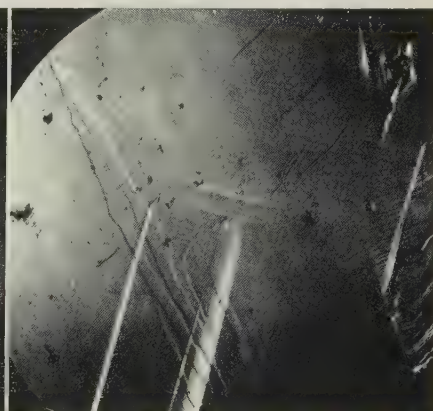


FIG. 22.—Area Marked by Square in Fig. 18, with Accommodation at Ends of Twins. Opaque stop. × 30.



FIG. 23.—Narrow Twins Ending Within the Crystal. Opaque stop. × 30.



FIG. 24.—As Fig. 23. Normal illumination. × 30.

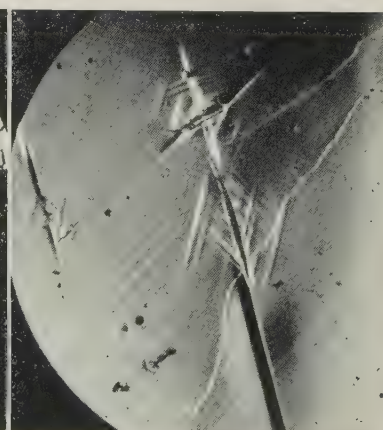


FIG. 25.—Distorted Area at End of Twin in Fig. 20. Opaque stop. × 30.

MANGANESE-COPPER ALLOYS.



FIG. 8.—94% Mn Alloy. Etched 5 sec. in citric acid. Normal illumination.  $\times 175$ .

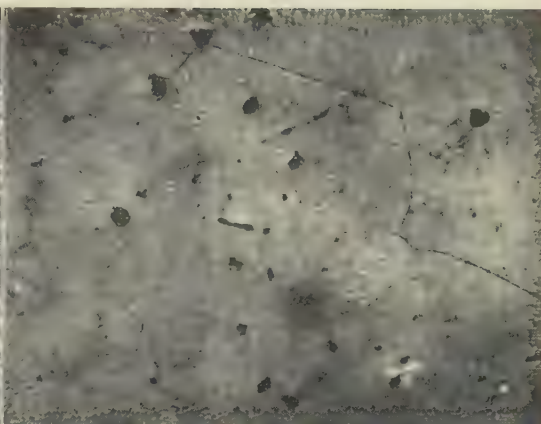


FIG. 9.—85% Mn Alloy. Etched 20 sec. in citric acid. Normal illumination.  $\times 250$ .

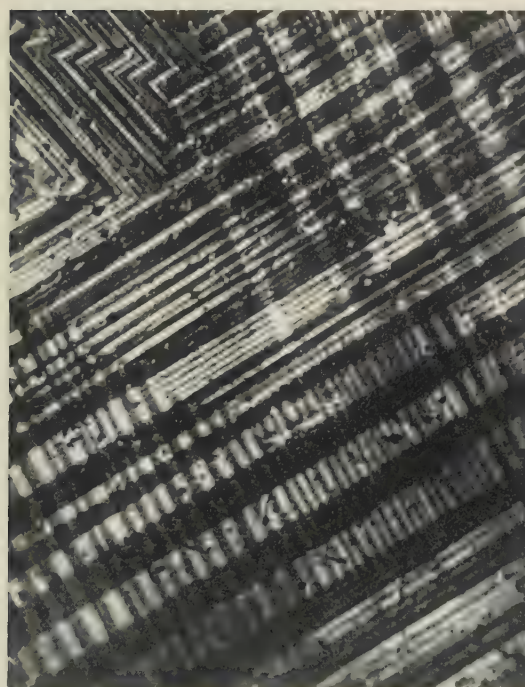


FIG. 10.—93.5% Mn Alloy. Unetched. Photographed at room temperature under oblique illumination.  $\times 150$ .

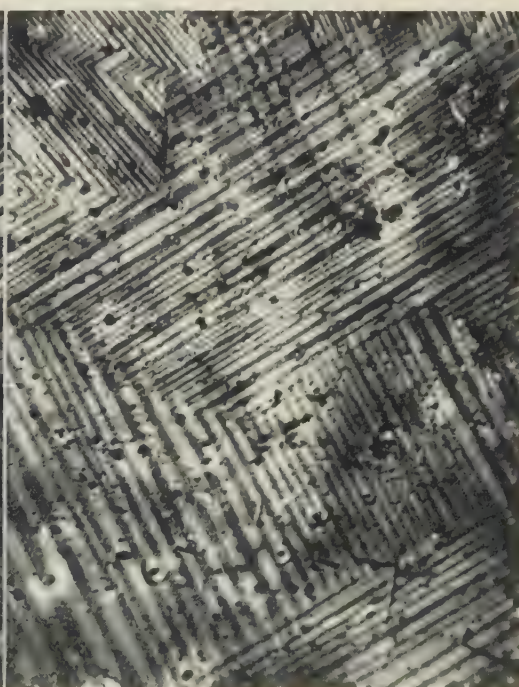


FIG. 11.—Same Area as Fig. 10. Photographed at 200° C. under oblique illumination.  $\times 150$ .





# THE EQUILIBRIUM DIAGRAM OF THE SYSTEM COPPER-INDIUM IN THE REGION 25-35 At.-% INDIUM \*

1392

By J. REYNOLDS,† B.A., W. A. WISEMAN,† and W. HUME-ROTHERY,‡ O.B.E., F.R.S., MEMBER

## SYNOPSIS

Thermal, microscopical, and X-ray methods have been used to determine the equilibrium diagram of the system copper-indium in the range 25-35 at.-% indium. In this region there is a phase with a  $\gamma$ -brass structure whose liquidus rises to a maximum at 29.6 at.-% indium and 682° C. On the copper-rich side, the liquidus falls to a eutectic with the  $\beta$  body-centred cubic phase, and on the indium-rich side there is a peritectic horizontal at which an  $\eta$  phase with a NiAs structure is formed by reaction between  $\gamma$  and liquid. No evidence has been obtained for the existence of the  $\epsilon$  phase postulated by Weibke and Eggers (*Z. anorg. Chem.*, 1934, 220, 273). The  $\gamma$  phase is stable only at high temperatures, and on cooling it undergoes a transformation at about 630° C. to a phase denoted  $\delta$ , whose X-ray powder diffraction pattern suggests a tetragonal cell with  $a = 8.97$ ,  $c = 9.14$  kX, and  $c/a = 1.020$ .

## I.—INTRODUCTION

THE first complete equilibrium diagram for the system copper-indium was determined by Weibke and Eggers,<sup>1</sup> and is reproduced in part in Fig. 1. Their

within the limits of experimental error. With increasing indium content there is, according to Weibke and Eggers, a phase denoted  $\gamma$  whose liquidus curve rises to a maximum at 29.1 at.-% indium. This phase could not be retained by quenching, and on cooling it transformed into a phase denoted  $\delta$ , which was described as possessing a  $\gamma$ -brass type of structure. At higher indium contents, Weibke and Eggers deduced the existence of the  $\epsilon$  phase shown in Fig. 1, and of a phase denoted  $\eta'$ , which, on the basis of weak thermal arrests, was regarded as probably undergoing a transformation at about 389° C. into a low-temperature form  $\eta$ . As this part of the diagram was not established conclusively, we have made a redetermination of the  $\gamma$ ,  $\delta$ , and  $\epsilon$  regions which are of interest in connection with the theory of  $\gamma$  phases. Conclusive evidence has not been obtained of a  $\eta \rightleftharpoons \eta'$  change, and the symbol  $\eta$  has been used for the whole region of this phase, whose copper-rich boundary has been determined. Since the present work was begun, a paper has appeared by Hellner and Laves,<sup>4</sup> according to whom the  $\gamma$  and  $\epsilon$  phases of Weibke and Eggers have identical structures of the  $\gamma$ -brass type, while the  $\delta$  phase has a superlattice based on the NiAs type of structure, and the  $\eta$  phase has the normal NiAs structure.

## II.—EXPERIMENTAL DETAILS

The copper used in the present work was specially pure electrolytic metal, kindly presented by The British Non-Ferrous Metals Research Association. Most of the indium used was supplied by Johnson, Matthey and Co., Ltd., and was of 99.99% purity; later in the work an ingot of Canadian origin was ob-

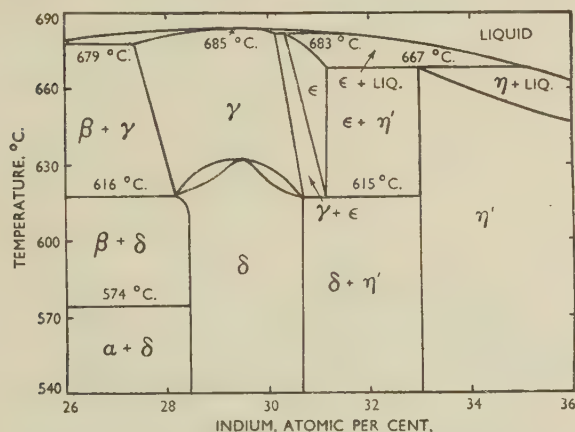


FIG. 1.—The Copper-Indium Diagram in the Range 26-36 At.-% In, According to Weibke and Eggers.<sup>1</sup>

diagram shows an  $\alpha$  solid solution followed by a  $\beta$  phase, which was later found to have a body-centred cubic structure. The solid-solubility curves of the  $\alpha$  and  $\beta$  phases were redetermined by Hume-Rothery, Raynor, (P. W.) Reynolds, and Packer,<sup>2</sup> and the  $\alpha$  solid-solubility curve of these investigators has been substantially confirmed by the X-ray work of Owen and Morris.<sup>3</sup> The  $\alpha$  solubility curve of these workers shows a slightly smaller solubility at high temperatures, but as no experimental details were published it is not possible to say whether the difference is

\* Manuscript received 17 January 1952.

† Inorganic Chemistry Laboratory, Oxford.

‡ Royal Society Warren Research Fellow, and University Lecturer in Metallurgical Chemistry, Oxford.



tained through the Pure Metals Committee of the D.S.I.R., which was of 99.99+ % purity.

For the cooling-curve experiments ingots of 50 g. were used. Melting was carried out in graphite crucibles having graphite lids provided with holes for the stirrer and thermocouple sheath, which were made of silica. The whole assembly was contained in a closed silica tube heated in a long tubular resistance

to the ( $\beta + \gamma \rightleftharpoons$  liquid) eutectic point at 25.5 at.-% indium and 677° C. (Weibke and Eggers gave 25.8 at.-%, 679° C.), while on the indium-rich side the liquidus falls to a peritectic horizontal at 667° C., the nature of which is considered later. The exact liquidus points are given in Table II.

TABLE II.—*Liquidus Points.*

Indium, at.-%	Primary Arrest, °C.	Second Arrest, °C.
26.32	678	677
27.84	681.0	...
29.56	682.3	...
30.52	682.0	...
32.21	679.0	...
32.94	676.8	667.6
33.80	672.7	667.1
34.75	671.3	667

TABLE I.—*Etching Reagents.*

Reagent	Method of Application	Time, sec.	Remarks
1. $\text{FeCl}_3 + \text{HCl} + \text{water}$	Swabbing	5-15	Used for alloys containing $\gamma$ , $\delta$ , or $\eta$ phases or chilled liquid.
2. $\text{FeCl}_3 + \text{HCl} + \text{ethyl alcohol}$	Swabbing	ca. 10	Used to produce a colour contrast in $\gamma$ , $\delta$ , and $\eta$ alloys, whose grain boundaries are revealed by reagent 1.
3. $(\text{NH}_4)_2\text{S}_2\text{O}_8$ soln.	Immersion	30-90	Used as 2.
4. $\text{CrO}_3 + \text{HCl} + \text{water}$	Swabbing	5-15	Used for ( $\gamma + \delta$ ) alloys ( $\gamma$ darkened).

furnace. An inert gas was not used, because the reducing atmosphere produced by the graphite was found adequate to prevent oxidation. The precautions taken to ensure accuracy were similar to those described by Hume-Rothery and (P. W.) Reynolds.<sup>5</sup> The whole of each cooling-curve ingot was dissolved for analysis, and the sums of the percentages of the two metals determined analytically lay between the limits 99.97 and 100.07.

For the microscopical and X-ray investigations, the first alloys were melted in graphite crucibles under charcoal, and were cast into heavy moulds to give ingots of  $\frac{1}{4}$ -in. dia. For some of the later alloys, melting was carried out using "Analar" potassium chloride as flux. The experimental methods for annealing, quenching, microscopical examination, and X-ray metallography resembled those described by Betterton and Hume-Rothery,<sup>6</sup> unless otherwise stated. The etching of some of the alloys was found to be difficult, and a list of reagents not previously used is given in Table I.

### III.—THE $\gamma$ -PHASE REGION

As shown in Fig. 2, the liquidus of the  $\gamma$  phase rises to a very flat maximum at 682.3° C., 29.6 at.-% indium (Weibke and Eggers reported 685° C., 29.1 at.-%). On the copper-rich side, the liquidus falls

The solidus from 33 to 35 at.-% indium was determined by the quenching method. In alloys containing 33.5 and 34.4 at.-% indium, the first traces of chilled liquid in the grain boundaries were detected at 658° and 644° C., respectively.

It was found impossible to retain the structure of the  $\gamma$  phase by quenching, and the various decomposition structures obtained are described below. A high-temperature X-ray powder photograph of alloy

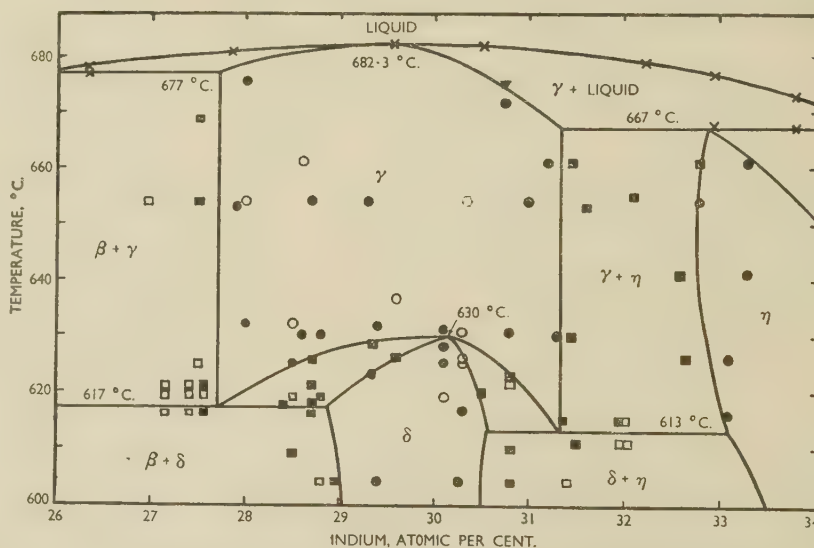


Fig. 2.—The Diagram in the Region 26-34 At.-% In and above 600° C. (Present Work).

KEY.  
 × Thermal arrests.      □ ■ Two-phase alloys.  
 ○ ● Single-phase alloys.      ▽ ▴ Alloys containing chilled liquid.  
 Solid symbols represent analysed alloys.

29.6\* was taken at 650° C., and, in agreement with Hellner and Laves,<sup>4</sup> the structure was found to be of the  $\gamma$ -brass type. Forty-two diffraction lines were sufficiently intense to be measured, and all agreed with a cubic cell whose side was determined as 9.2317 kX by standard extrapolation methods.

\* Alloys will be denoted by their indium content in atomic percentages.

The  $(\beta + \gamma)/\gamma$  boundary was determined microscopically, using specimens which were homogenized by annealing for 36 hr. at 665° C. The temperature of the furnace was then lowered, and alloys were removed

decomposition changes with increasing indium content. Figs. 4, 5, and 6 (Plate CIV) show the decomposed structures obtained on quenching alloys 29.3, 30.3, and 30.8 from the  $\gamma$  region. Although the last\* of them may at first appear to possess a two-phase structure, the irregular boundaries between the light and dark areas are not shaped like those for two phases in equilibrium at the quenching temperature, but are characteristic of those of partly decomposed alloys in many systems. Further, as shown in Fig. 7 (Plate CIV), the same structure was found in alloy 31.45, in which the  $\eta$  phase was present after prolonged annealing, and this clearly suggests that the structure of Fig. 6 is not that of an alloy which was two-phase before quenching.

The structure of an alloy of some interest in connection with the decomposition of  $\gamma$  on quenching is shown in Fig. 8 (Plate CIV). This is the result of annealing alloy 30.75 at 675° C. in the  $(\gamma + \text{liq.})$  region. The chilled liquid can be seen outlining the original  $\gamma$  grain boundaries, and is also to be observed inside the grains. The photograph also shows the typical decomposition of  $\gamma$  in this region, and indicates that it has taken place across  $\gamma$  grain boundaries as well as within individual grains of  $\gamma$ . This alloy was used to fix the solidus above the  $\gamma$  phase on the indium-rich side of the maximum. Weibke and Eggers' paper contained no thermal evidence for the supposed  $\epsilon$  phase, and the above results, with those of Hellner and Laves, suggest strongly that it is non-existent.

The  $(\gamma + \eta)/\eta$  boundary was also determined microscopically, with the results shown in Fig. 2. The times of annealing were similar to those used for the other high-temperature boundaries. Alloy 32.6, quenched from 626° C., showed a higher proportion of the  $\gamma$  phase than when quenched from 641° C., and as the  $\gamma/(\gamma + \eta)$  boundary is almost vertical, it may be concluded that the  $(\gamma + \eta)/\eta$  boundary slopes towards the indium-rich side at lower temperatures. The  $(\beta + \delta)/\delta$ ,  $(\alpha + \delta)/\delta$ ,  $\delta/(\delta + \eta)$ , and  $(\delta + \eta)/\eta$  boundaries, determined by microscopical methods, were found to be vertical below 500° C., within the limits of the experiments (Fig. 3). If the transformation in the  $\eta$  phase suggested by Weibke and Eggers is genuine, there will be a corresponding slight modification of the  $(\delta + \eta)/\eta$  boundary at about 390° C., but this has not been studied.

#### IV.—THE $\gamma \rightleftharpoons \delta$ TRANSFORMATION

The  $\gamma \rightleftharpoons \delta$  transformation is a real phase change accompanied by changes in the X-ray-diffraction pattern which are described below. The transformation temperature rises to a maximum at 630° C. and 30.15 at.-% indium, and on either side of this maximum two-phase  $(\gamma + \delta)$  alloys are found. On the

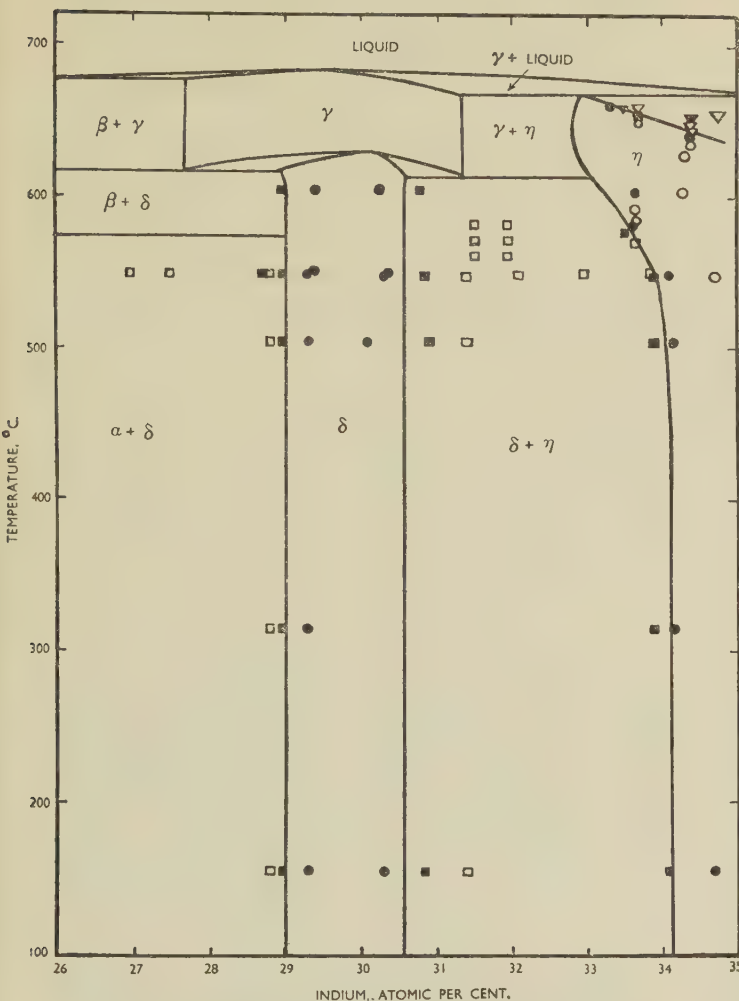


FIG. 3.—The Diagram in the Region 26-35 At.-% In and down to 100° C. (Present Work). Key as for Fig. 2.

and quenched after 3 days at the temperatures concerned. This boundary is very nearly vertical, in contrast with the diagram of Weibke and Eggers, which showed the boundary sloping in the direction of higher indium contents with falling temperature.

The  $\gamma/(\gamma + \eta)$  boundary, determined in the same way, is also nearly vertical, and corresponds roughly with the  $\epsilon/(\epsilon + \eta')$  boundary of Weibke and Eggers. Careful examination of the microstructures of the quenched alloys gave no evidence for the existence of the supposed  $\epsilon$  phase; this agrees with the high-temperature X-ray work of Hellner and Laves,<sup>4</sup> who showed that both the  $\gamma$  and  $\epsilon$  phases possessed the  $\gamma$ -brass structure. All alloys in the  $\gamma$  region undergo decomposition on quenching, but the nature of the

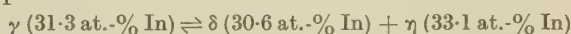
\* This composition does not lie within the  $(\gamma + \epsilon)$  region of Weibke and Eggers' diagram.



copper-rich side, the phase boundaries were determined by microscopical methods using specimens homogenized at 660° C. and then annealed for one week at the temperatures shown in Fig. 2. There is a eutectoid point corresponding to the reaction :



and the quenching experiments showed this to lie at  $617^\circ \pm 1.5^\circ$  C. Figs. 9 and 10 (Plate CIV) show the structure of alloy 28.5 after quenching from the ( $\gamma + \delta$ ) area at 619° C., the photograph at high magnification showing the fine eutectoidal structure produced during quenching. On the copper-rich side of the maximum, the phase boundaries determined microscopically were in good agreement with the thermal arrests obtained by Weibke and Eggers, but on the indium-rich side their arrests were distinctly lower than the transformation temperatures indicated by the microstructures after prolonged annealing. On the indium-rich side, the  $\gamma$  phase undergoes a eutectoid transformation at 613° C. which may be represented :



Quenched alloys do not show a characteristic eutectoidal structure, although the  $\gamma$  phase always decomposes during quenching. If alloys are homogenized above the eutectoid horizontal and are then re-annealed below it, the eutectoid coarsens to form a characteristic plate-like structure. Thus Fig. 11 (Plate CIV) shows the structure of alloy 32.0 after being homogenized and furnace-cooled from 660° C., and then re-annealed at 611° C. The dark areas represent  $\eta$  phase which has decomposed on quenching, whilst the bulk of the alloy consists of a coarse plate-like structure of  $\delta$  and decomposed  $\gamma$ .

The crystal structure of the  $\delta$  phase was examined by X-ray powder methods, and was found to be closely related to that of the  $\gamma$  phase. The transformation  $\gamma \rightarrow \delta$  could not be suppressed by quenching, and slowly cooled alloys in the homogeneous  $\delta$  region gave powder-diffraction films which were indistinguishable from those of the same alloys when quenched from above the transformation temperature. Comparison of films for  $\delta$  alloys with those for the  $\gamma$  phase taken in the high-temperature camera showed that the first strong diffraction line ( $\Sigma h^2 = 18$ ) had apparently split into two lines of roughly equal strength, whilst many other lines of the  $\gamma$  structure had become multiplets.

The film was difficult to interpret because of the frequent overlapping of lines, but it could be seen that the  $\Sigma h^2 = 66$  line of the  $\gamma$  structure at a Bragg angle =  $43^\circ$  had split into several lines for which the  $\alpha_1\alpha_2$  doublets were resolved and were usually free from overlapping. By a modification of the method described by Bradley and Lu<sup>7</sup> for rhombohedral splitting, it was shown that the multiplets agreed with a tetragonal cell for which  $a = 8.97$ ,  $c = 9.14$  kX, and  $c/a = 1.020$ . The cubic line  $\Sigma h^2 = 66$  corresponds with the (811), (741), and (554) reflections, and the combination of high and low indices makes it suitable

for the accurate determination of the axial ratio. The first 33 lines of the film were measured, and of these 30 gave  $d$  values which agreed within 1% with possible reflections from a cell of the above dimensions. The remaining three lines agreed with possible reflections to within 4.7%, 3.6%, and 1.6% of the  $d$  values. The two greatest discrepancies were for the first line ( $\theta = 9.9^\circ$ ) and for a very faint line at  $\theta = 17.5^\circ$ , for which measurement was very difficult. In view of the faintness of many of the lines, it was felt that the above agreement is as good as could be expected. The tetragonal axial ratio  $c/a = 1.020$  has the effect of making the (330) and (411) reflections overlap, so that the strong  $\Sigma h^2 = 18$  line of the  $\gamma$  structure appears at first sight to have split into two lines of comparable strength, although more careful examination reveals the remaining component resulting from the splitting of the (330) and (411) lines of the cubic structure.

Examination was also made to see whether the splitting of the  $\Sigma h^2 = 66$  line could be reconciled with a rhombohedral distortion of the cubic cell, but although a fairly good agreement could be obtained, it led to the difficulty that one line had to be indexed as an  $\alpha_2$  reflection without the expected stronger  $\alpha_1$  component. For this and other reasons, the above tetragonal deformation of the cubic  $\gamma$  structure appears the most probable. Further progress requires the examination of single crystals, which have now been prepared. It is hoped that an examination of these will lead to a determination of the structure, and will show how this is related to the NiAs superlattice proposed by Hellner and Laves. The present paper is concerned only with the equilibrium diagram of the system copper-indium in the region of the  $\gamma$  and  $\delta$  phases, and the bearing of the results on the general theory of  $\gamma$  phases has been discussed in a separate paper by Hume-Rothery, Betterton, and Reynolds.<sup>8</sup>

#### ACKNOWLEDGEMENTS

The authors must express their thanks to Professor Sir Cyril Hinshelwood, F.R.S., for laboratory accommodation, and to Dr. F. M. Brewer for many other facilities which have greatly encouraged the present research. Grateful acknowledgement is also made to the Council of the Royal Society and to The British Non-Ferrous Metals Research Association for financial support to the general research programme of which this work is one part.

#### REFERENCES

1. F. Weibke and H. Eggers, *Z. anorg. Chem.*, 1934, **220**, 273.
2. W. Hume-Rothery, G. V. Raynor, P. W. Reynolds, and H. K. Packer, *J. Inst. Metals*, 1940, **66**, 209.
3. E. A. Owen and D. P. Morris, *ibid.*, 1949, **76**, 145.
4. E. Hellner and F. Laves, *Z. Naturforsch.*, 1947, [A], **2**, 177.
5. W. Hume-Rothery and P. W. Reynolds, *Proc. Roy. Soc.*, 1937, [A], **160**, 282.
6. J. O. Betterton, Jr., and W. Hume-Rothery, *J. Inst. Metals*, 1951-52, **80**, 459.
7. A. J. Bradley and S. S. Lu, *Z. Krist.*, 1937, **96**, 20.
8. W. Hume-Rothery, J. O. Betterton, Jr., and J. Reynolds, *J. Inst. Metals*, 1951-52, **80**, 609.

# THE CONSTITUTION AND STRUCTURE OF NICKEL-VANADIUM ALLOYS IN THE REGION 0-60 At.-% VANADIUM \*

1393

By W. B. PEARSON,† D.F.C., M.A., MEMBER, and W. HUME-ROTHERY,‡ O.B.E., F.R.S., MEMBER

## SYNOPSIS

The equilibrium diagram of the system nickel-vanadium has been investigated by thermal, microscopical, and X-ray methods in the range 0-60 at.-% vanadium. There is a wide solid solution of vanadium in nickel, and with increasing vanadium content the liquidus falls to a eutectic point at 51 at.-% vanadium and 1202° C., at which temperature the liquid is in equilibrium with the  $\alpha$  (nickel-base) solid solution of composition 42.7 at.-% vanadium, and with a phase denoted  $\sigma$ , which has the same general type of crystal structure as the  $\sigma$  phase in iron-chromium alloys. At 1045° C. the  $\alpha$  solid solution gives rise to a phase denoted  $\theta$ , which is a tetragonal superlattice based on the composition  $\text{Ni}_3\text{V}$ . The  $\theta$  phase is of variable composition, and its crystal structure has been determined. In the region of 33.5 at.-% vanadium, a second intermediate phase, denoted  $\delta$ , separates from the  $\alpha$  solid solution. This is of almost fixed composition and has a body-centred orthorhombic structure which may be regarded as the result of a monoclinic distortion of the face-centred cubic structure. The effects of composition on the lattice spacings of the  $\alpha$ ,  $\theta$ , and  $\sigma$  phases have been studied, and the bearing of the results on the general theory of alloys is discussed briefly.

## I.—INTRODUCTION

THE only previous work on the nickel-vanadium system is that of Giebelhausen,<sup>1</sup> who obtained twelve liquidus and solidus points for nickel-rich alloys, and stated that alloys containing more than about 20% vanadium contained two phases. In this work the alloys were melted in air, and the ensuing oxidation is probably responsible for the fact that the results obtained bear little resemblance to those of the present investigation.

When the present work was started, it was expected that vanadium metal of 99.8% purity would be available, but unfortunately the metal obtainable was of variable purity, which was often considerably lower than that stated. In the work described below, no serious discrepancies have arisen between the results obtained with pure and impure metal, whilst closely agreeing results were obtained for alloys contaminated by iron with little or no oxygen or nitrogen, and by other alloys contaminated by oxygen or nitrogen, but almost free from iron. We think that the general form of the diagram is established conclusively, and that the phase boundaries are likely to be accurate to within 1 at.-% on the composition axis.

## II.—MATERIALS USED

The nickel used consisted of two batches of Mond nickel shot, both supplied by the kindness of Mr. H. W. G. Hignett. The first of these contained

99.94% nickel, with carbon 0.04, iron 0.013, and copper 0.003% as the chief impurities. The second batch contained 0.02% carbon, and 0.02% iron. Before being used, the shot was washed with ether and pickled in *aqua regia*.

The first vanadium used was nominal 99.6% metal of American origin. Analysis showed that the globules were of variable composition, the vanadium content lying between 99.0 and 99.5%, with nitrogen and carbon as the chief contaminating elements, together with about 0.1% of iron and calcium; the last element was probably removed on melting in a vacuum. This metal was used for the determination of the liquidus and solidus by thermal analysis, and for preparing some of the first nickel-rich alloys.

By the kindness of Mr. A. R. Powell, one of the present authors (W. B. P.) was enabled to work at the laboratories of Johnson, Matthey and Co., Ltd., and prepared calcium-reduced vanadium of 99.3-99.5% purity. Vacuum-fusion revealed 0.4% nitrogen and 0.05% oxygen; only a trace of iron could be detected. This metal was thus of the same type as the purer globules of the American metal, and alloys prepared from both these grades of vanadium are denoted by the same letters *E* or *C* (according to the date of the work), followed by the atomic percentage of vanadium. Thus alloy *E*25.4 indicates an alloy containing 25.4 at.-% vanadium prepared from one of the above two grades of metal.

Alloys denoted by the symbol *J* were prepared from

\* Manuscript received 11 February 1952.

† Low-Temperature Solid-State Physics Department, National Research Council, Ottawa, Canada formerly Inorganic Chemistry Laboratory, Oxford.

‡ Royal Society Warren Research Fellow, and University Lecturer in Metallurgical Chemistry, Oxford.



English calcium-reduced vanadium of purity 99.5–99.9%, the impurity being almost entirely oxygen, with comparatively small amounts of carbon, nitrogen, and iron. Another series of alloys, denoted *H*, was prepared from similar vanadium containing only 0.05% nitrogen and less than 0.05% carbon, but variable amounts of iron; this contaminated the alloys by amounts of the order of 0.2–1.0% iron, the exact details being referred to later.

Alloys denoted by *S* were made from magnesium-reduced vanadium from Magnesium Elektron, Ltd. This metal was stated to be 99.6% pure, and to contain little impurity except oxygen.

In the course of the work a large amount of chemical analysis has been carried out by Johnson, Matthey and Co., Ltd., and we must thank Mr. A. R. Powell and Dr. J. C. Chaston for their interest. The analyses have shown that little or no contamination of the alloys occurred during their preparation by the methods described below. Because of this and of the use of a small quantity of high-purity 99.9+ % vanadium, sufficient really pure alloys have been obtained to show that the main form of the equilibrium diagram is conclusively established, and that the details are not seriously wrong.

### III.—PRODUCTION OF ALLOYS

The alloys for the present investigation were prepared in an H.-F. induction furnace in a vacuum or under a low pressure of purified argon which was admitted after thorough degassing of the refractories at 900°–1200° C. Preliminary experiments showed that vanadium could not be melted in magnesia crucibles without a reaction between the metal and the magnesia, although the latter has been used by several investigators for melting vanadium. Satisfactory melts were obtained in crucibles of thoria and zirconia, and also in  $\frac{3}{4}$ -in.-dia. crucibles of lime prepared by calcining blocks of marble in which holes had been drilled. Molten vanadium reacted slowly with Morgan  $\Delta$  RR alumina crucibles, and 0.88% aluminium was found in a 15-g. ingot which had been kept molten for 11 min. Vacuum-melting of the *H* metal in a thoria crucible gave a product which was so malleable that it could be cold rolled to a sheet 0.0002 in. thick. For the nickel-rich alloys, alumina crucibles were suitable for vanadium contents up to 25%, and alumina crucibles lined with thoria for the range 25–60% vanadium.

After cooling in the induction furnace, the alloys were cleaned by grinding away the outside layers. Some alloys were homogenized by heating in the induction furnace for 2–2½ hr. at temperatures about 20° C. below the solidus. Others were homogenized by heating for 60–170 hr. at temperatures from 70° to 170° C. below the solidus in alumina collars in sealed evacuated silica tubes heated in a platinum resistance furnace. The latter method was used for the first annealing treatments at the higher temperatures, but below about 1000° C. no contamination

resulted if the alumina collars were omitted and the specimens were annealed in sealed evacuated silica tubes and quenched in iced water. The general annealing methods were those standard in this laboratory, and have been described by Carlile, Christian, and Hume-Rothery,<sup>2</sup> and by Coles and Hume-Rothery.<sup>3</sup>

### IV.—PREPARATION OF ALLOYS FOR MICROSCOPICAL EXAMINATION

The nickel-rich alloys with less than 15 at.-% vanadium could be cut with a saw, but many of the remaining alloys were hard and were sectioned with alumina cutting wheels, after which they were polished and etched by conventional methods.

As described later, the nickel–vanadium diagram is characterized by the existence of: (1) a wide solid solution of vanadium in nickel, denoted  $\alpha$ ; (2) a tetragonal superlattice phase in the region of 25 at.-% vanadium ( $\text{Ni}_3\text{V}$ ), denoted  $\theta$ ; (3) an orthorhombic phase based on the composition  $\text{Ni}_2\text{V}$ , denoted  $\delta$ ; and (4) a phase with a typical “ $\sigma$ ” structure in the region 55–74 at.-% vanadium (see Fig. 1). Apart from these genuine constituents of the system, some alloys contained impurity particles due to the carbon, oxygen, and nitrogen in the original vanadium.

The most useful etching reagent was found to be 50% aqueous nitric acid, which was used for the whole range of alloys examined. This reagent revealed the structure in homogeneous  $\theta$  and  $\delta$  alloys, and outlined the two phases in alloys of the  $(\alpha + \theta)$ ,  $(\alpha + \delta)$ ,  $(\alpha + \sigma)$ ,  $(\theta + \delta)$ , and  $(\delta + \sigma)$  types; it also revealed the presence of chilled liquid. The etching characteristics of the phases were not, however, always the same, and although the nitric acid reagent distinguished clearly between homogeneous and two-phase alloys, it could not always be used for the identification of a phase.

A 50% aqueous solution of hydrofluoric acid with the addition of a little nitric acid was sometimes used when increased definition of the grain boundaries was required.

In the region 35–45 at.-% vanadium, it was difficult to distinguish between traces of chilled liquid and particles of the  $\sigma$  phase or of the *X* impurity phase referred to below. It was found that if, after etching in nitric acid, the alloy were repolished and treated with a saturated solution of manganous chloride in dilute hydrochloric acid, only the areas of chilled liquid were attacked and stained, and in this way identification was possible, but the etching of these alloys was difficult and required considerable experience.

### V.—IMPURITY PARTICLES IN THE ALLOYS

In drawing the equilibrium diagram, the uniform policy has been adopted of ignoring the impurities, scaling up the analysed percentages of nickel and

vanadium to a total of 100, and then converting to atomic percentages. Thus an alloy which on analysis gave vanadium 20.0, nickel 79.5, nitrogen 0.1, and iron 0.4% was taken to contain 20.1% vanadium and 79.9% nickel. In so far as the formation of carbides and nitrides removes vanadium rather than nickel from the alloys, this procedure tends to overestimate the vanadium content, but the difference is small. The method was found to lead to results which were consistent among themselves, whereas attempts made to correct compositions by assuming that the iron replaced either nickel or vanadium led to inconsistencies.

The small amounts of iron present in the alloys entered into solid solution in the phases of the nickel-vanadium system and did not produce new constituents. The *H* alloys were thus almost free from impurity particles, and the *S* alloys were also relatively

## VI.—DETERMINATION OF THE LIQUIDUS

Thermal analyses were carried out in the H.F. induction furnace, using the apparatus of Carlile, Christian, and Hume-Rothery,<sup>2</sup> modified so as to be used with a thermocouple instead of an optical pyrometer. Alumina or thoria thermocouple sheaths 7-in. long were sealed into the brass tube by a water-cooled Apiezon wax seal, as shown by Hume-Rothery, Christian, and Pearson.<sup>4</sup> The thermocouple tube was thus isolated from the furnace tube, and the thermocouple could be used in air or in an atmosphere of argon. Crucibles and thermocouple sheaths of alumina were used for alloys containing up to 20 at.-% vanadium, and crucibles of alumina lined with thoria, or of pure thoria for the alloys of higher vanadium content, for which thoria thermocouple sheaths were used. With ingots of 50-55 g. and

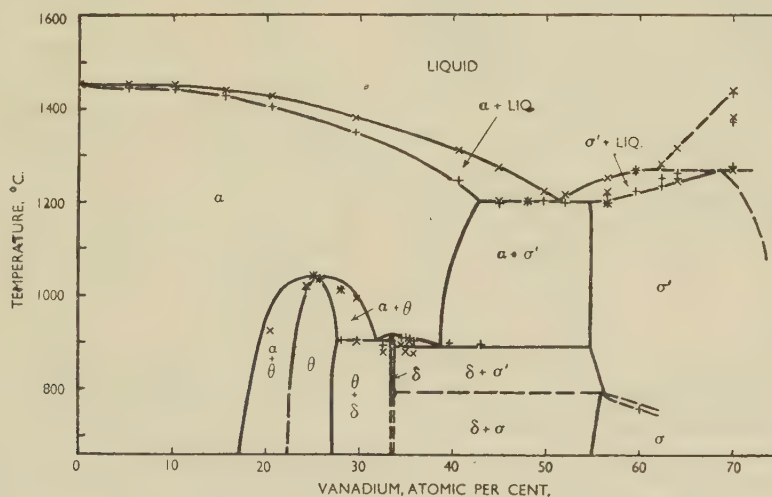


FIG. 1.—Investigation of Nickel-Vanadium Alloys by Thermal Analysis. (See also Appendix, p. 652.)

x Cooling-curve arrests. + Heating-curve arrests.

clean. The *C* and *E* alloys contained impurity particles whose number increased with the vanadium content, and these alloys were therefore not used for microscopical work beyond 30 at.-% vanadium. Up to this limit the contamination of these alloys was not serious. Thus alloy *C*29.56, which was used for thermal analysis (see below), was held molten for about 1 hr., and the analysis of the ingot showed the presence of aluminium 0.02, nitrogen 0.09, nickel 70.27, and vanadium 29.67%, making a total of 100.05%, and the contamination by aluminium will be less for alloys which were solidified immediately after melting.

The *J* series of alloys sometimes showed small particles of nickel oxide, but the main impurity phase occurred in white or very pale blue particles which were denoted *X*. Some alloys were prepared from oxidized vanadium powder, and on annealing it appeared that nickel oxide was gradually converted into *X*, which is thus probably a metallic phase containing oxygen.

rates of cooling of the order of 2° C./min., satisfactory thermal arrests were obtained. Table I shows the

TABLE I.—*Liquidus and Solidus Points for the C Series of Alloys.*

Vanadium, at.-%	Liquidus Arrest from Cooling Curve, °C.	Solidus Point from Heating Curve, °C.	Remarks.
0	1453	...	Standard Ni point
10.18	1451	1441	
15.59	1439	1428	
20.51	1427	1403	
29.56	1379	1348	
40.59	1311	1246	

results for alloys containing up to 40.59 at.-% vanadium, and the remaining points are included in Fig. 1. For the alloys in Table I, the analysed percentages of nickel and vanadium never totalled less than 99.90, and the purity was satisfactory, diminishing gradually with increasing vanadium content. Be-



yond this point the contamination increased rapidly and erratically. Thus alloy C59-57 gave a (nickel + vanadium) total of only 99.07, whilst for alloy C61-06 the total was 99.78. In four alloys the ingots contained a few particles of free vanadium. The particles appeared not to dissolve because they were surrounded by a sheath of insoluble substance, and as they had clearly not melted, and were not dissolved during the analysis, they were removed and weighed and not included in the vanadium content.

Fig. 12 (Plate CV) shows the structure of the cooling-curve ingot of alloy C50 containing primary  $\alpha$  and eutectic.

Fig. 1 shows that the liquidus of the  $\alpha$  solid solution in nickel falls gradually with increasing vanadium content until a eutectic point is reached at 51 at.-% vanadium and 1202° C. The eutectic temperatures for alloys C48 (not analysed) and C49-73 were 1201° and 1202° C., respectively, and with higher vanadium contents the temperature fell to as low as 1196° C. We have, therefore, taken the highest observed value, and the temperature for a perfectly pure nickel-vanadium alloy is probably about 1203°–1204° C. The solid constituents of the eutectic are the  $\alpha$  and  $\sigma'$  phases, containing 43 and 55 at.-% vanadium, respectively. (For detailed results, see Appendix.)

With increasing vanadium content the liquidus of the  $\sigma'$  phase rises, but this part of the diagram was not studied in detail.

## VII.—DETERMINATION OF THE SOLIDUS

The solidus points determined from heating curves were confirmed by microscopical methods. The standard technique was used, in which previously homogenized lumps were annealed for 30 min. at increasing temperatures and then quenched. Chemical analysis showed that no contamination occurred during the annealing treatments, which were carried out in the double-walled furnace described by Hume-Rothery, Christian, and Pearson.<sup>4</sup>

For the solidus of the  $\alpha$  phase the microscopical method gave the results shown in Fig. 5 (p. 647), which are in good agreement with those obtained by thermal analysis. The microscopical method placed the eutectic horizontal as lying between 1201° and 1204° C., in good agreement with the value (1202° C.) obtained from the cooling curves. The solidus curve of the  $\sigma$  phase is thought to have been determined to within 10° C., but the increasing amounts of impurity make this part of the diagram less certain.

## VIII.—THE $\theta$ -PHASE REGION

As will be seen from Fig. 1, the  $\alpha$  solid solution is of considerable extent at high temperatures, and at lower temperatures the  $\theta$  phase is formed in the region of 25 at.-% vanadium. The form of the diagram is such that at high temperatures the  $\theta$ -phase area is surrounded by the  $\alpha$  phase on both sides, whereas at

lower temperatures the  $\theta$  phase is in equilibrium with the  $\delta$  phase on the vanadium-rich side. At the higher temperatures the equilibrium diagram was established by microscopical methods, using specimens which, after preliminary homogenization, were annealed for periods ranging from 10–15 days at 1040° C. to 77 days at 672° C. At the lower temperatures, the limits of the  $\alpha$  and  $\theta$  phases were determined by X-ray lattice-spacing methods, using the lattice spacing/composition curves described on pp. 648 and 649, whilst some microscopical work was also done.

The results in this region of the diagram are shown in Figs. 2 and 3, the X-ray and microscopical data

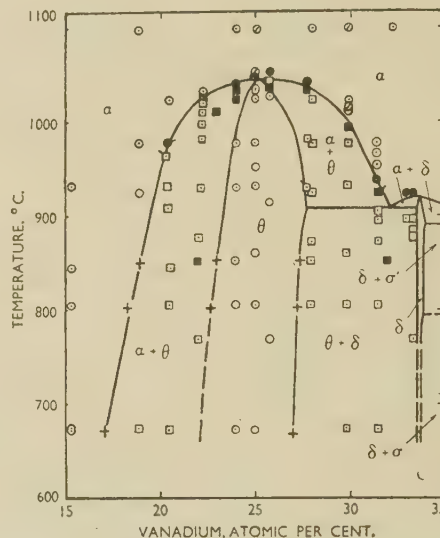


Fig. 2.—The Constitution of Nickel-Vanadium Alloys in the Range 15–33 At.-% Vanadium, as Determined by Microscopical Observation of Quenched Alloys.

KEY.  
 ○ One-phase alloys.  
 □ Two-phase alloys.  
 ● and ■ indicate analysed alloys.  
 + Phase boundaries determined by lattice-parameter measurements.

being in good agreement, except that at 980° C. there was a discrepancy of 1% in the nickel-rich  $\alpha/(\alpha + \theta)$  boundary. The limits of the  $\theta$  phase rise to a maximum temperature of 1045° C. at the composition corresponding to the formula  $\text{Ni}_3\text{V}$ . On the nickel-rich side the  $(\alpha + \theta)/\theta$  boundary is smooth and moves to lower vanadium contents as the temperature falls. On the vanadium-rich side the boundary of the  $\theta$  phase shows a change in direction at 908° C., the temperature of the  $(\alpha \rightleftharpoons \theta + \delta)$  eutectoid transformation. The solubility curve of the  $\theta$  phase rises to a maximum at 25 at.-% vanadium, but is not symmetrical about this point.

When quenched supersaturated  $\alpha$ -phase alloys are re-annealed in the  $(\alpha + \theta)$  region, the  $\theta$  phase is precipitated in a Widmanstätten type of structure. Fig. 13 (Plate CV) shows the structure of alloy E20-3 after quenching from 932° C., and Fig. 14 (Plate CV) shows alloy H23-7 after quenching

from 1034° C.; in the latter many of the  $\theta$  crystals are twinned. In the ( $\alpha + \theta$ ) region alloy *E22-3* and in the homogeneous  $\theta$  region alloys *E25-0* and *J25-8* were free from iron, whilst on the vanadium-rich side alloys *S27-7* and *E29-8* were also satisfactory. In all these alloys the analysed percentages of (nickel + vanadium) were never lower than 99.93, and we think that this part of the diagram is established satisfactorily because there was good agreement between the results for *E*, *H*, *J*, and *S* alloys.

### IX.—THE $\delta$ -PHASE REGION

As shown in Section XIII the  $\delta$  phase may be regarded as a distorted superlattice of the  $\alpha$  phase at the

closed in thin-walled silica capillaries. Under these conditions the heating-up of the specimen and the first exposure resulted in a change of composition of the order of 2-3% in the nickel-rich direction, and this was followed by a much more gradual change when the specimen was maintained at the high temperature for periods up to 35 hr.

This change of composition was confirmed by chemical analyses of the specimens, and by the proportion of the phases present, as indicated by the relative intensities of the diffraction lines. The lines were sharp and extra lines were usually absent or extremely weak, and the fact that the capillaries withstood repeated or prolonged heating suggested that the loss of vanadium was not due to any extensive reaction with

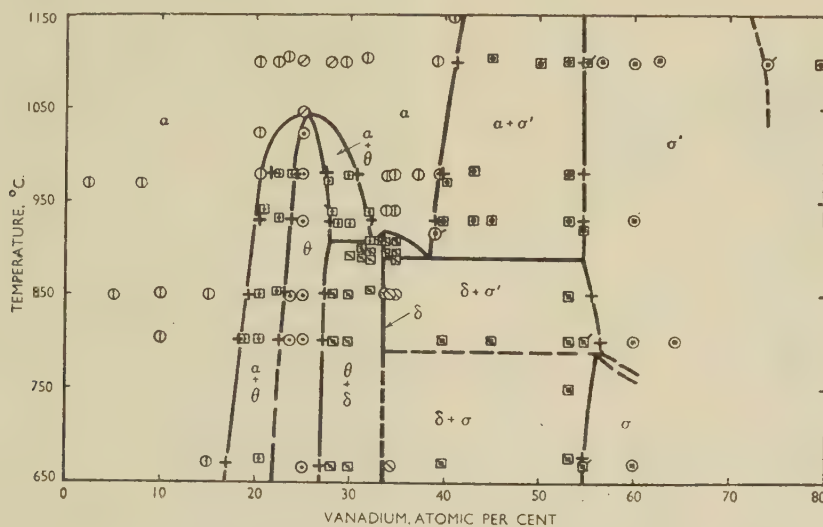


FIG. 3.—X-Ray Investigation of Quenched Nickel-Vanadium Alloy Powders.

#### KEY.

- |                              |                                    |
|------------------------------|------------------------------------|
| ⊙ $\alpha$ phase.            | ⊞ $\alpha + \theta$ .              |
| ⊖ " decomposed on quenching. | ⊞ $\theta + \delta$ .              |
| ⊙ $\theta$ .                 | ⊞ $\alpha + \sigma$ .              |
| ⊙ $\delta$ .                 | ⊞ $\delta + \sigma$ .              |
| ⊙ $\sigma$ .                 | ⊞ $\sigma + \text{vanadium (?)}$ . |
|                              | ⊞ $\alpha + \delta$ .              |

+ Phase boundaries determined by lattice-parameter measurements.

composition  $\text{Ni}_2\text{V}$ . As with the  $\theta$  phase, the  $\delta$ -phase region projects into the  $\alpha$  field; the  $\alpha/(\alpha + \delta)$  boundary passes through a maximum, and on the vanadium-rich side sinks to a eutectoid point at 890° C. and 38.5 at.-% vanadium, at which temperature the  $\alpha$  phase decomposes into ( $\delta + \sigma$ ). The equilibrium diagram in this region, determined mainly by microscopical methods, is shown in Fig. 4; the annealing times were usually 10-15 days in the range 920°-880° C., but some anneals were extended to 25 days, and specimens from some of the shorter anneals were checked by cold working and re-annealing. X-ray investigation of re-annealed and quenched powders made from alloys microscopically examined confirmed the phases present (Fig. 3).

The results were also confirmed by experiments in the high-temperature X-ray camera, using filings en-

silica that would affect the results. The results were further checked, using a rod specimen, which was photographed while the camera was highly evacuated. The same crystal structure was observed, but photographs showed a larger change of composition due to loss of vanadium than when the specimens were enclosed in silica capillaries.

The X-ray films formed a quite consistent series in which the different phases appeared in the same order as that indicated by the microscopical work, but the change in composition of the specimens during the high-temperature experiments prevented these X-ray results from being used for the exact determination of phase boundaries, other than the temperature horizontals. Attempts to analyse the actual X-ray specimens led to many difficulties not only in determining the very small quantities of vanadium, but



also because the vanadium lost by the filings could not be removed mechanically from the silica. There was thus an uncertainty as to how much of the vanadium on the silica had dissolved before the latter was removed by filtration, and with the very small quantities available, no further progress was possible.

The results showed conclusively that alloys in the  $\delta$  region transformed to the face-centred cubic  $\alpha$  phase at

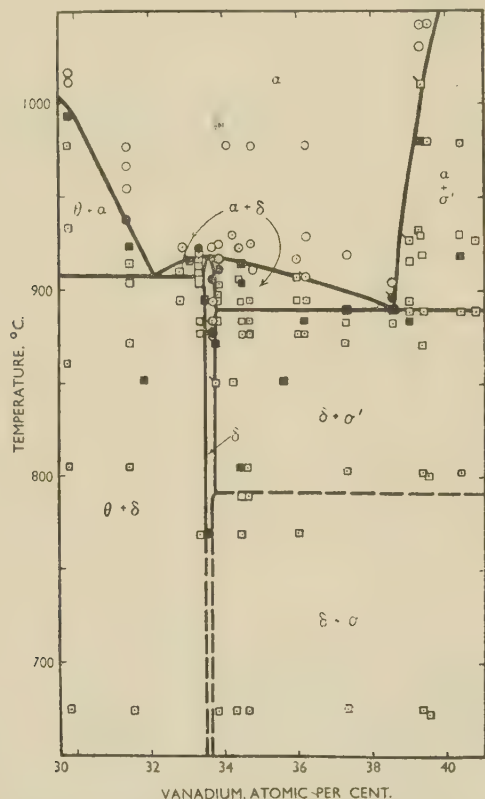


FIG. 4.—The Constitution of Nickel-Vanadium Alloys in the Range 30–40% Vanadium, as Determined by Microscopical Observation of Quenched Alloys.

KEY.  
○ One-phase alloys.      □ Two-phase alloys.  
● and ■ indicate analysed alloys.

high temperatures, and that alloys which at low temperatures were in the  $(\delta + \sigma)$  field changed to alloys of the  $(\delta + \alpha)$  type at about 885° C. On the nickel-rich side of the  $\delta$  phase, the  $\alpha$  solubility curve sinks to a second eutectoid point at 908° C. and 32.1 at.-% vanadium, and here the  $\alpha$  phase decomposes eutectoidally into  $(\theta + \delta)$ . The high-temperature X-ray photographs confirmed that alloys which at low temperatures were in the  $(\theta + \delta)$  field became of the  $(\theta + \alpha)$  type above 908° C. Alloys in the small

$(\alpha + \delta)$  field on the nickel-rich side of the  $\delta$  phase were identified by microscopical examination and in a powder photograph of quenched filings.

The composition range of the  $\delta$  phase does not exceed about 0.5 at.-%. Homogeneous  $\delta$  structures were observed for alloys J33.6, J33.69, and J33.73 after annealing at 769°, 877°, and 906° C., respectively. Alloy 33.4 was in the  $(\theta + \delta)$  region below the 908° C. eutectoid horizontal, and above this temperature it was in the  $(\alpha + \delta)$  region on the nickel-rich side of the  $\delta$  field. Alloy 34.48 at 915° C. was in the  $(\alpha + \delta)$  region lying on the vanadium-rich side of the  $\delta$  phase. Two analytical results were slightly anomalous, in that alloys J33.64 and J33.80 at 895° and 769° C., respectively, were of the  $(\theta + \delta)$  and not of the  $(\delta + \sigma)$  type. We think the discrepancies are due to a slightly uneven composition of the ingots,\* and the evidence as a whole indicates a narrow  $\delta$ -phase region in the range 33.6–34.1 at.-% vanadium. These alloys were all made from the pure vanadium and were almost free from iron, whilst the analysed totals of (nickel + vanadium) were always better than 99.9. The structures of the *H* series of alloys, which were contaminated by iron, were in agreement with those for the purer alloys. Fig. 15 (Plate CV) shows  $\sigma'$  and  $\delta$  in alloy H37.3 quenched from 877° C.

The boundaries of the  $\delta$  phase have been established by microscopical methods down to 770° C. At lower temperatures the nature of this phase is not completely certain, owing to the difficulty of interpreting microstructures and to the fact that the X-ray diffraction lines on quenched powder specimens were always diffuse. Diffraction photographs taken in the high-temperature camera at 650° and 670° C.† gave sharp reflections which showed that the  $\delta$  phase persisted at these temperatures, although the degree of orthorhombic distortion was markedly decreased. It is possible that this change in the axial ratios may account for the diffuse lines obtained from quenched powders.

Alloys of series *H*, containing iron, placed the vanadium-rich  $\alpha/(\alpha + \delta)$  boundary and the  $(\alpha \rightleftharpoons \delta + \sigma)$  and  $(\alpha \rightleftharpoons \theta + \delta)$  eutectoid horizontals about 7° C. lower than those of the iron-free *J* series. The higher temperatures have been preferred, and this discrepancy explains why a few single-phase alloys are shown in the two-phase  $(\alpha + \delta)$  region of Fig. 4, and alloys containing  $\alpha$  in the  $(\theta + \delta)$  region of Fig. 3.

The transitions between the  $\alpha$  and the  $\theta$  and  $\delta$  phases were also investigated by thermal analysis conducted on homogenized alloys in a platinum resistance furnace. The arrests obtained (shown in Fig. 1) were very strong in the regions 25.0 and 33.5–35.0 at.-% vanadium.

\* Only the result J33.80 is in serious contradiction to the remaining analyses, and this specimen came from an ingot of which different portions gave slightly different analytical results. Although several sections were examined microscopically before the specimen was sent for analysis, it is

possible that local segregation may have been present and not observed microscopically.

† The powders were prepared from lumps annealed at 670° C., and the specimen was then annealed in the camera at 650° or 670° C. before exposure.

## X.—THE EQUIATOMIC REGION

Fig. 5 shows that the eutectic point lies slightly to the vanadium-rich side of the equiatomic composition. If the impurities depress the true liquidus and solidus curves, this effect is likely to be greater for the  $\sigma$  than for the  $\alpha$  phase, and it is possible that with really pure metals the diagram would confirm Stockdale's principle of simple atomic ratios for eutectics.<sup>5</sup> In any case the deviation from this principle is slight.

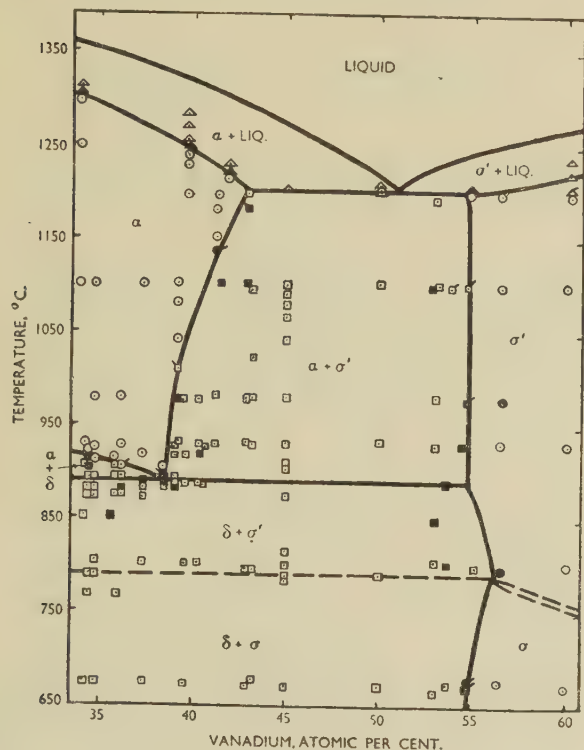


FIG. 5.—The Constitution of Nickel–Vanadium Alloys in the Range 35–60 At.-% Vanadium, as Determined by Microscopical Observation of Quenched Alloys.

## KEY.

- One-phase alloys.    □ Two-phase alloys.    △ Partly liquid alloys.  
●, ■, and ▲ indicate analysed alloys.

Where a point is marked with a tick, only a trace of the second phase was present.

The heating curves showed arrests which suggested that the  $\sigma$  phase underwent a transformation at about 760° C., and for convenience we call the high-temperature modification  $\sigma'$  and the low-temperature form  $\sigma$ . The genuineness of this transformation is confirmed by a change in direction of the solubility curve of the  $\sigma$  phase on the nickel-rich side. The nature of this transformation is at present unknown, but high-temperature X-ray powder photographs showed the same principal low-angle diffraction lines above and below the transition temperature. Fig. 6 shows the  $a$  and  $c$  parameters of the  $\sigma$  phase in both homogeneous and two-phase alloys. Increase in vanadium content produces an increase in both  $a$  and  $c$ , and a decrease in axial ratio  $c/a$ , these effects being

in the same direction as those found by Martens and Duwez<sup>6</sup> when vanadium is added to replace chromium in a 50 : 50 iron–chromium alloy.

Fig. 5 shows the  $\alpha/(\alpha + \sigma')$  boundary to slope in the direction of lower vanadium content with decreasing temperature. In agreement with this, precipitation of the Widmanstätten type occurs in the  $\alpha$  phase when  $(\alpha + \sigma')$  alloys are homogenized and then re-annealed at a lower temperature (see Fig. 16, Plate CVI). The  $(\alpha + \sigma')/\sigma'$  boundary is almost vertical, and no

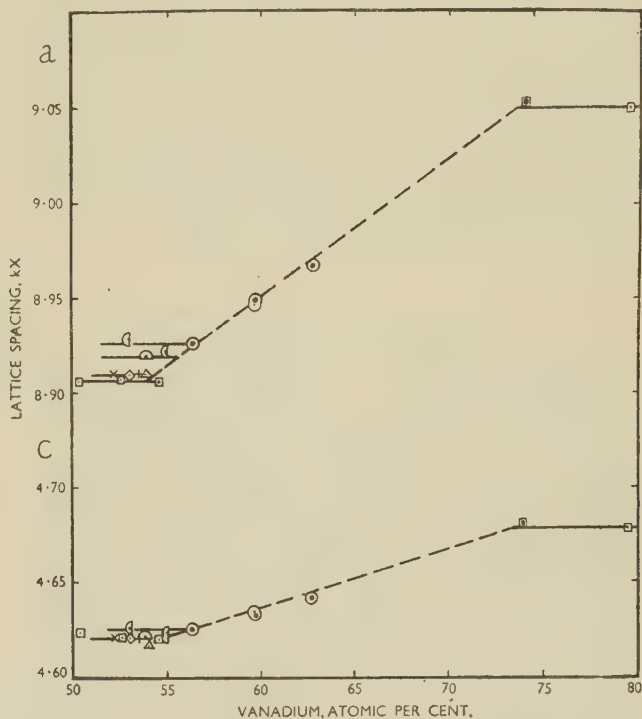


FIG. 6.—Lattice Parameters of the  $\sigma$  Phase, Corrected to 18° C.

## KEY.

- Homogeneous alloys (chemically analysed).  
◇ 2-phase alloys quenched from ca. 1190° C.  
□ " " " " 1100° C.  
× " " " " 980° C.  
+ " " " " 930° C.  
△ " " " " 850° C.  
◐ " " " " 800° C.  
▲ " " " " 672° C.

Widmanstätten precipitation was found in the  $\sigma'$  phase on annealing at lower temperatures in the  $(\alpha + \sigma')$  field, although the slope of the  $\alpha$  boundary means that the proportion of the  $\sigma'$  phase increases in accordance with the lever rule. Since the X-ray films do not distinguish clearly between the  $\sigma$  and  $\sigma'$  phases, results from alloys quenched from the  $\sigma'$  region must be accepted with caution, but it is interesting to note that with quenched specimens the  $\sigma'$  diffraction lines were sharp, and their lattice spacings gave an  $(\alpha + \sigma')/\sigma'$  boundary agreeing exactly with that obtained by microscopical methods.

At 890° C. the  $(\alpha \rightleftharpoons \delta + \sigma')$  eutectoid transformation occurs, and below this temperature the  $(\delta + \sigma')/\sigma'$  boundary bends in the direction of higher vanadium



content with falling temperature. This results in an additional fine precipitation of  $\delta$  from  $\sigma'$  when alloys are slowly cooled, or are re-annealed at a lower temperature in the two-phase field (see Fig. 17, Plate CVI). This change in direction of the  $\sigma'$  boundary was confirmed by lattice-spacing measurements. Below the temperature of the transformation in the  $\sigma$  phase, the  $\sigma$ -phase boundary bends back in the direction of lower vanadium content with falling temperature; this was confirmed by both microscopical and lattice-spacing methods. It was not possible to study the  $\sigma$  transformation in detail, but the evidence obtained suggests that this is of the peritectoid type, and the dotted horizontal line is drawn at  $790^\circ\text{C}$ .

The existence of a phase with the characteristic  $\sigma$  structure in the system nickel-vanadium was reported by Pearson, Christian, and Hume-Rothery,<sup>7</sup> and the structure was further investigated by single-crystal methods by Pearson and Christian.<sup>8</sup>

### XI.—THE LATTICE SPACINGS OF THE $\alpha$ SOLID SOLUTION

For the determination of the lattice spacings of the  $\alpha$  phase, the lump ingots were first homogenized and quenched, after which filings were prepared and re-annealed. For all but the lowest vanadium contents, the filings had to be quenched in order to suppress the transformations associated with the formation of the  $\theta$  and  $\delta$  phases. In the region 15–24 at.-% vanadium, the  $\alpha$  phase could be retained without difficulty, but alloys containing 25 and 28% vanadium could not be retained in the  $\alpha$  state even with very rapid silica-capillary quenches, and the 30% alloy was retained only with difficulty when quenched rapidly after annealing in thin-walled, evacuated silica capillaries. Ordinary quenching methods were sufficient in the 33–40% vanadium region, and excellent X-ray films were obtained. The rate of transition of  $\alpha$  to  $\delta$ , which occurred at lower temperatures, was much less than the transition of  $\alpha$  to  $\theta$ . Alloys containing less than 15 at.-% vanadium were sufficiently soft for filings to be prepared by several methods, but with higher vanadium contents difficulties were encountered owing to the hardness of the quenched ingots. Filings could be prepared with a tungsten carbide wheel in an atmosphere of argon, but were contaminated by tungsten, and it was not possible to determine to what extent alloying took place on subsequent annealing. The best results were obtained by the use of steel files, followed by careful cleaning of the product by magnet, and then washing with carbon tetrachloride, alcohol, and ether. The powder photographs were taken with copper radiation in a 19-cm. Unicam camera, and the lattice spacings determined by standard extrapolation methods.

The lattice spacing/composition curve obtained is shown in Fig. 7. Phase boundaries obtained by the use of this curve agreed well with microscopical

investigations up to 20% vanadium, but at higher vanadium contents the presence of iron in the  $H$  series of alloys, which were used mainly to establish this curve, probably results in the parameters being too low. The iron content of the powder was in most cases included in the vanadium analytical totals. If this is allowed for so that all alloys throughout the diagram are plotted on the same basis, then reasonable agreement is generally found between phase boundaries determined by microscopical and by

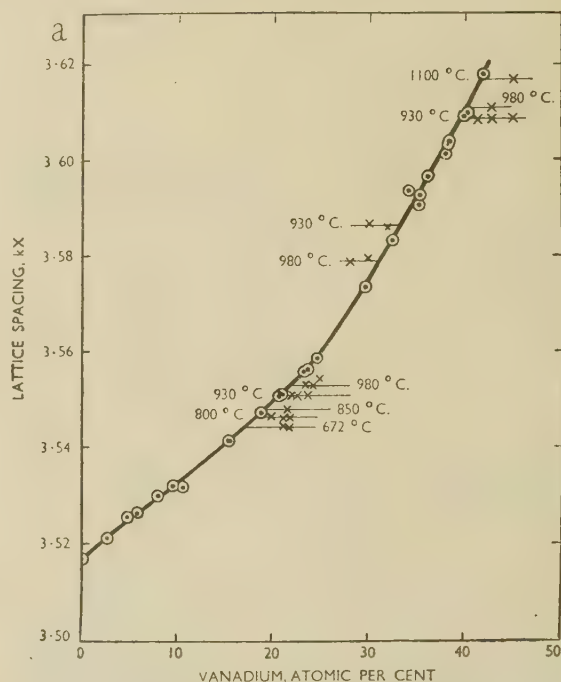


FIG. 7.—Lattice Parameters of the  $\alpha$  Solid Solution for Nickel-Vanadium Alloys, Showing the Parameters for  $\alpha$ ,  $(\alpha + \theta)$ , and  $(\alpha + \sigma)$  Alloys.

○ Homogeneous alloys (chemically analysed).  
× Two-phase alloys.

X-ray investigation. If it is not allowed for, the X-ray boundaries lie at about 1% higher vanadium content.

### XII.—CRYSTAL STRUCTURE AND LATTICE SPACINGS OF THE $\theta$ ( $\text{Ni}_3\text{V}$ ) PHASE

The structure of the  $\theta$  phase was determined from Debye-Scherrer photographs of quenched filings. Using  $\text{CuK}_\alpha$  radiation, films were obtained whose lines could be indexed as belonging to a simple face-centred tetragonal cell with  $a = 3.53 \text{ kX}$  and  $c/a = 1.02$  approximately. With this radiation the scattering powers of nickel and vanadium atoms are too similar for a superlattice structure to be revealed, and photographs were therefore taken with  $\text{CrK}_\alpha$  radiation. The resulting films showed a number of additional faint lines, of which all but three could be indexed as belonging to a tetragonal cell with the same value of  $a$  but with double the axial ratio suggested by the preliminary photographs with Cu radiation. When

referred to this cell (see Fig. 8 (a)), all the indexed lines corresponded to reflections for which  $(h + k + l)$  was even, and the structure was thus identified as that of the  $\text{Al}_3\text{Ti}$  type. The cell contains 2 vanadium

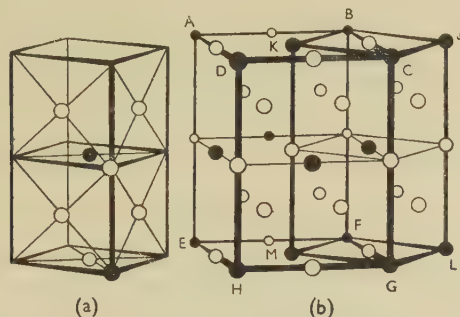


FIG. 8.—The  $\theta$  Phase. (a) The unit cell. (b) The relationship of the 8-atom unit cell to the cell containing 16 atoms in terms of which  $\text{Al}_3\text{Ti}$  types of structure are generally described.

atoms in the positions  $(000, \frac{1}{2}, \frac{1}{2}, \frac{1}{2})$  and 6 nickel atoms at  $(00\frac{1}{2}, \frac{1}{2}, 0, 0\frac{1}{2}, 0\frac{1}{2}, \frac{1}{2}, 0\frac{1}{2}, \frac{1}{2}, 10\frac{1}{2}, \frac{1}{2}, 10\frac{1}{2}, \frac{1}{2})$ . The figure shows clearly that if the difference between the atoms is ignored the structure is face-centred tetragonal with a cell one-half the height of that in Fig. 8 (a). The three lines which could not be indexed on this basis were all very weak, and we think they must be due

TABLE II.—X-Ray Results for Alloy Containing 26.12 At.-% Vanadium.

Photographed with  $\text{CrK}\alpha$  radiation.

Bragg Angle	$hkl$	$a$ Calculated for $c/a = 2.0362$	Intensity *	$ F ^2 P \times \frac{1 + \cos^2 2\theta}{\sin^2 \theta \cos \theta}$
18.49	002	3.540(5)	vvw	8
21.13	101	3.533(5)	w	25
22.02	...	...	vw	...
25.82	...	...	vvw	...
27.21	110	3.535(8)	vvw	6.3
33.851	112	3.533(6)	vs	522
35.11	103	3.539(2)	vvw	7
39.452	004	3.534(1)	m	85
40.303	200	3.534(7)	ms	156
46.078	202	3.536(3)	vvw	3.5
47.734	211	3.536(5)	vw	7.0
51.49	114	3.536(2)	vvw	3.3
58.976	105	3.536(8)	vvw	4.2
59.950	213	3.536(5)	vw	9
64.958	$204a_1$	3.5352	s	176
65.182	$204a_2$	3.5358	...	...
66.076	$220a_1$	3.5353	ms	92
66.315	$220a_2$	3.5348	...	...
69.91	...	...	vvw	...
75.35	$222a_1$	3.535(8)	vvw	6.7
79.19	$301a_1$	3.535(9)	vvw	8.0
...	006	...	Not observed	1.2

\* vs = very strong, s = strong, ms = moderately strong, m = medium, w = weak, vw = very weak, vvw = extremely weak.

to impurity, but it has not been possible to identify them.

Table II shows the results obtained for an alloy containing 26.12 at.-% vanadium. In this, the first

column shows the measured Bragg angle of the reflection, and the second column the index of the plane referred to the unit cell of Fig. 8 (a) containing 8 atoms. The third column shows the values of  $a$  calculated for an axial ratio  $c/a = 2.0362$ ; by standard extrapolation methods the true value of  $a = 3.5353 \text{ kX}$ . The fourth column shows the visually estimated intensities, and the fifth column the relative intensities calculated from the expression

$$|F|^2 P \times \frac{1 + \cos^2 2\theta}{\sin^2 \theta \cos \theta}.$$

The atomic scattering factors were corrected for the anomalous effects in the region of the absorption edge, but as the intensities were estimated visually, it was thought reasonable to omit the absorption and temperature factors because these act in opposite directions, and although the absorption factor is predominant, its effect at high angles is, from the point of view of visual observation, counterbalanced by the broadening of the lines.\*

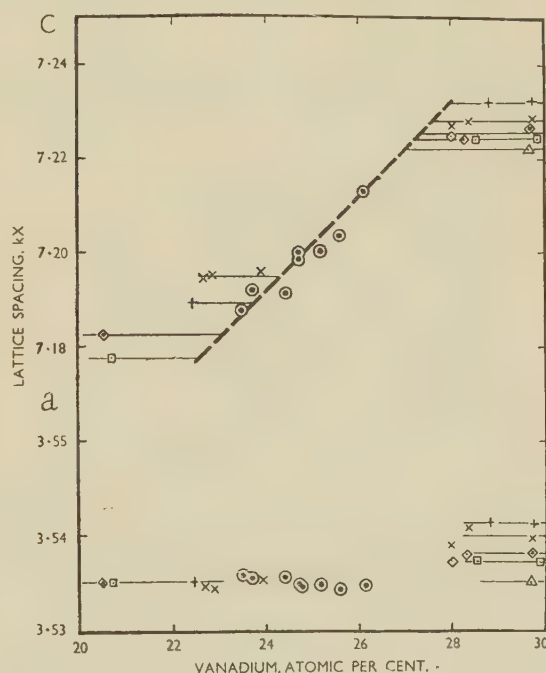


FIG. 9.—Lattice Parameters of the  $\theta$  Phase, Corrected to  $18^\circ \text{C}$ .

KEY.  
 ○ Homogeneous alloys (chemically analysed).  
 × 2-phase alloys quenched from ca.  $980^\circ \text{C}$ .  
 + " " " "  $930^\circ \text{C}$ .  
 ◇ " " " "  $850^\circ \text{C}$ .  
 □ " " " "  $800^\circ \text{C}$ .  
 △ " " " "  $672^\circ \text{C}$ .

For the high-angle lines where the  $K\alpha$  doublet was resolved, the calculated value for the  $\alpha_1$  line was reduced by one-third to compare with the values for unresolved lines. The calculated and observed values are in good agreement, and the failure to observe the (006) reflection is in agreement with the relative calculated values for the neighbouring (301) and (222)

\* This, of course, does not apply if integrated intensities are measured photometrically.



superlattice lines. The  $\text{Al}_3\text{Ti}$  type of structure is generally referred to a larger cell, which is denoted  $ABCDEFGH$  in Fig. 8 (b), where  $BJCKFLGM$  is the unit cell of the present paper; and the most symmetrical space group is  $I4/mmm$ .

The lattice-spacing/composition relations for the phase are shown in Fig. 9, and are of interest because the equilibrium-diagram work shows that the phase extends on both sides of the exact composition corresponding to  $\text{Ni}_3\text{V}$ . The lattice-spacing data show that the  $a$  parameter of the unit cell is little affected by the composition, although the  $c$  parameter increases rapidly with increasing vanadium content, as would be expected from the atomic diameters of nickel and vanadium. The structure of Fig. 8 is such that horizontal layers of nickel atoms are interleaved by layers consisting of equal numbers of atoms of nickel and vanadium.

### XIII.—CRYSTAL STRUCTURE AND LATTICE SPACINGS OF THE $\delta$ PHASE

Powder specimens quenched from the  $\delta$  region gave diffraction films with diffuse lines, but satisfactory photographs were obtained with a high-temperature

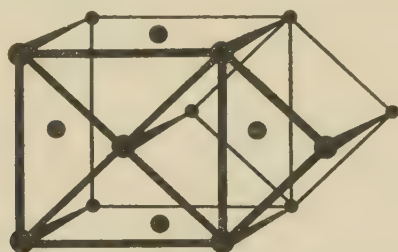


FIG. 10.—The  $\delta$  Phase, Showing the Relationship of the Monoclinic and Orthorhombic Unit Cells.

Unicam camera modified so as to use the hemispherical furnaces described by Basinski, Pearson, and Christian.<sup>9</sup> The structure can be understood by considering the results obtained for alloy  $H34.5$  at  $850^\circ\text{C}$ .

The lines on this photograph were clearly related to the lines of the face-centred cubic  $\alpha$  solid solution, and also to those of the face-centred tetragonal  $\theta$  structure (Fig. 18, Plate CVI). The lines of the face-centred cubic structure had split, but the number of lines formed was not that expected from tetragonal or orthorhombic distortion of the original cube. Examination showed that the number of lines formed would be accounted for if the original face-centred cube had undergone a monoclinic distortion such that  $a = c = 3.6680 \pm 0.0002 \text{ kX}$ ,  $b/a = 0.9646$ , and  $\beta = 89.0747^\circ$ . The condition  $a = c$  means that the non-rectangular side of the unit cell is a rhomb, and, since the two diagonals of a rhomb are perpendicular, the structure is body-centred orthorhombic with  $a = 2.6145$ ,  $b = 3.5382$ ,  $c = 2.5726 \text{ kX}$ . The relations between the two unit cells are shown in Fig. 10, and although the structure is properly described as having the higher symmetry of the body-centred ortho-

rhombic arrangement, the relation between the structures of the  $\delta$  and face-centred cubic phases is shown most clearly by considering the face-centred monoclinic cell. Table III shows the angles of the observed lines with the indices and the calculated values of  $a$  for both monoclinic and orthorhombic cells. The body-centred orthorhombic cell containing two atoms, shown in Fig. 10, is the simplest cell that can be chosen for a *random* orientation of atoms. As the composition of the phase is  $\text{Ni}_2\text{V}$ , the *true* unit cell must be larger and contain multiples of three atoms.

### XIV.—DISCUSSION

The bearing of the present work upon the general theory of the transition metals and their alloys is being discussed elsewhere, but the following points of general interest may be noted here. The crystal

TABLE III.—X-Ray Results on  $\delta$  Phase.

Photographed with  $\text{CuK}$  radiation in high-temperature camera at *ca.*  $850^\circ\text{C}$ .

Angle of Diffraction Line.	Intensity *	Monoclinic Index	$a$ Monoclinic	Orthorhombic Index	$a$ Orthorhombic
21.686	vs	111	3.632	110	...
21.926	vs	$\bar{1}11$	3.632	011	...
25.033	s	200	3.637	101	...
26.004	m	020	3.638	020	...
36.227	m	$202a_1$	3.650	$200a_1$	...
36.906	mw	$\bar{2}02a_1$	3.650	$002a_1$	...
37.339	s	$220a_1$	3.651	$121a_1$	...
37.458		$a_2$	3.650	$a_2$	...
44.173	s	$311a_2$	3.655	$211a_1$	...
44.332		$a_2$	3.654	$a_2$	...
44.659	s	$\bar{3}11a_1$	3.656	$112a_1$	...
44.804		$a_2$	3.656	$a_2$	...
45.823	m	$131a_1$	3.657	$130a_1$	...
46.000	ms {	$a_2$	3.655	$a_2$	...
46.177		$\bar{1}31a_1$	3.656	$031a_1$	...
47.159	m	$a_2$	3.654	$a_2$	...
47.342		$222a_1$	3.658	$220a_1$	...
47.827	m	$a_2$	3.656	$a_2$	...
47.998		$\bar{2}22a_1$	3.657	$022a_1$	...
57.1336	m	$a_2$	3.656	$a_2$	...
57.3393		$400a_1$	3.661	$202a_1$	2.610
		$a_2$	3.662	$a_2$	2.610
65.4240	m	040		040	...
65.7204		$313a_1$	3.6639	$310a_1$	2.6116
67.3861	ms	$a_2$	3.6644	$a_2$	2.6120
67.7276		$\bar{3}13a_1$	3.6649	$013a_1$	2.6123
68.1110	s	$a_2$	3.6650	$a_2$	2.6124
68.4677		$331a_1$	3.6656	$231a_1$	2.6128
68.8096	s	$a_2$	3.6656	$a_2$	2.6128
		$\bar{3}31a_1$	3.6660	$132a_1$	2.6131
These two lines overlap		$\bar{3}31a_2$		$132a_2$	...
		$402a_1$		$301a_1$	...
70.707	w	$402a_1$	3.6662	$103a_1$	2.6133
These two lines overlap		$402a_2$	...	$103a_2$	...
		$420a_1$	...	$222a_1$	...
71.2880	...	$420a_2$	3.6661	$222a_2$	2.6132
74.8371	vs	$240a_1$	3.6668	$141a_1$	2.6136
75.3800	...	$a_2$	3.6667	$a_2$	2.6135

\* For key, see Table II.

Extrapolated Values:

Referred to Monoclinic cell,  $a = c = 3.6680$ ,  $b/a = 0.9646$ ,  
 $\beta = 89.0747^\circ$ .  
 " " Orthorhombic cell,  $a = 2.6145$ ,  $b = 3.5382$ ,  
 $c = 2.5726$ .

structure and atomic diameters (taken as the closest distance of approach of the atoms in the crystal) of the elements from titanium to copper are given in Table IV. It is now almost certain that the crystal structure of  $\gamma$ -manganese is face-centred cubic, and that the previously reported tetragonal structure with axial ratio 0.934 is the result of strains produced during quenching. In the absence of other data, the value (2.62 kX) given for manganese is the mean of the two

vanadium crystallize in the body-centred cubic structure, it is probably more correct to increase their atomic diameter by 3% (the Goldschmidt correction) in order to make them comparable with those from the structures with co-ordination number 12. The resulting size-factor differences are shown in the last row of the table, and will be used for discussion.

The figures in the last row of Table IV show that from the point of view of size-factor, vanadium

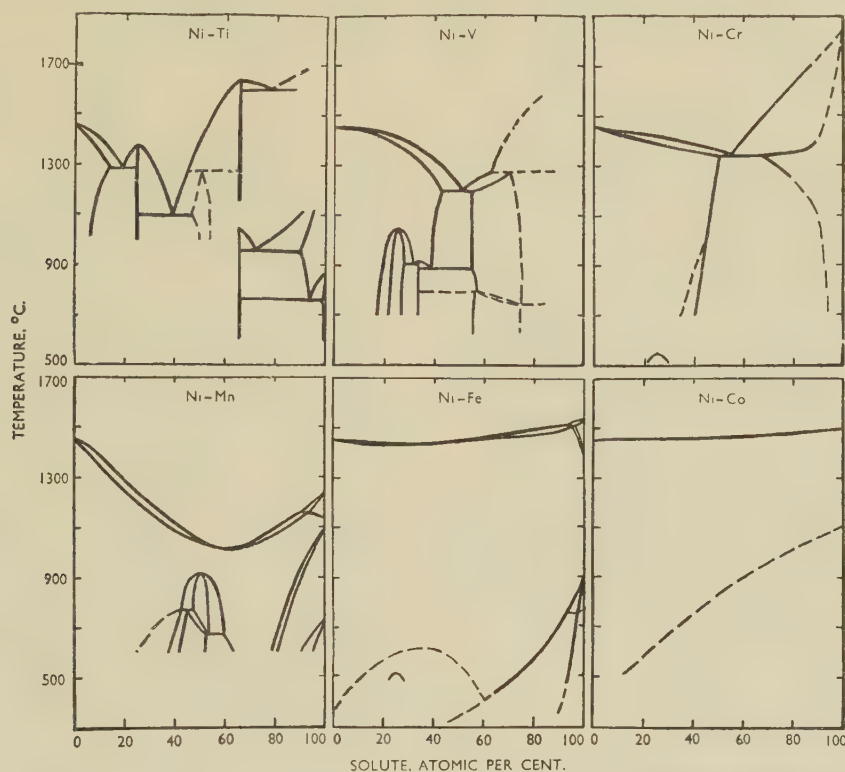


FIG. 11.—The Ni-Ti, Ni-V, Ni-Cr, Ni-Mn, Ni-Fe, and Ni-Co Equilibrium Diagrams.

close distances of approach in the tetragonal structure (2.58 kX and 2.67 kX). The third row in Table IV shows the percentage difference between the atomic diameters and that of nickel. Since chromium and

TABLE IV.—Crystal Structures and Atomic Diameters of Transition Metals.

Element	Ti	V	Cr	Mn	Fe	Co	Ni	Cu
Crystal structure	c.p.h.	b.c.c.	b.c.c.	f.c.c.	f.c.c.	c.p.h.	f.c.c.	f.c.c.
Atomic diameter, kX	2.91	2.63	2.49	2.62	2.52	2.50	2.49	2.55
Difference (%) from that of Ni	+16.8	+5.6	...	+5.0	+1.2	...	...	+2.4
Difference (%) from that of Ni adjusted to refer to co-ordination No. 12	+16.8	+8.8	+3	+5	+1.2	...	...	+2.4

\* The limits of the vanadium-rich solid solution have not been determined in the present paper, but the existence of the Ni-V  $\sigma$  phase makes it clear that the two primary solid

(+8.8) occupies a critical position between titanium, whose size-factor (+16.8) is slightly outside the usually accepted favourable zone ( $\pm 15\%$ ), and the series of elements Cr, Mn, Fe, Co, and Cu, for which the size-factors are very favourable. The equilibrium diagram in the range considered reflects this in several ways. The size-factor is still sufficiently favourable for the formation of a wide solid solution of vanadium in nickel, but as will be seen from Fig. 11, the range of the two primary solid solutions in the system Ni-V is distinctly less than those\* in the systems Ni-Cr, Ni-Mn, Ni-Fe, Ni-Co, and Ni-Cu, where the size-factors are more favourable. The moderately large size-factor (+8.8%) in the system Ni-V is clearly related to the formation of the  $\theta$  and  $\delta$  phases, which, as the previous work shows, are both slightly distorted forms of the face-centred cubic arrangement, and are

solutions in this system occupy at high temperatures a smaller proportion of the diagram than in the system Ni-Cr.



undoubtedly formed in order to relieve the strain caused by the relatively large vanadium atoms.

The equilibrium diagrams reproduced in Fig. 11 show the remarkable effect of the size-factor upon the stabilities of the phases of the type  $Ni_3X$ . In the Ni-Ti system, where the size-factor is unfavourable, a compound  $Ni_3Ti$ , with the DO 24-type of hexagonal structure, gives rise to a maximum in the liquidus at 1378° C. In the system Ni-V,  $\theta$  ( $Ni_3V$ ) is stable up to a maximum temperature of 1045° C., and then breaks down to the face-centred cubic solid solution. In the systems Ni-Cr, Ni-Mn, and Ni-Fe, the corresponding  $Ni_3X$  phases are stable up to 544°, about 520°, and 506° C., respectively. It is of interest to note that there is an approximately linear relation between these temperatures and the size-factors, in spite of the fact that  $Ni_3Ti$  separates from the liquid and not from the face-centred cubic solid phase.

One interesting point noted in the course of the work was the formation of the compound  $V_3Si$  by reaction between vanadium vapour and silica containers. After a lump of an alloy containing approximately 70% vanadium had been annealed at 1100° C. in an alumina collar sealed inside an evacuated silica tube, a crystalline deposit was found inside the tube and on the alumina collar. X-ray examination of this deposit, using chromium radiation, identified the substance as  $V_3Si$ , having a  $\beta$ -tungsten type of structure with  $a = 4.7145$  kX at 18° C. Chemical analysis of the very small quantity of the crystals showed 61.0% vanadium, 17.3% silicon, with the remainder unaccounted for. The X-ray reflections due to  $V_3Si$  were very sharp and strong, whilst the film showed other much weaker reflections.

## APPENDIX

The small scale of Fig. 1 prevents the liquidus and solidus curves from being read to the degree of accuracy justified by the work. As explained on p. 643, the ingots containing up to 40.59 at.-% vanadium were satisfactorily pure, and it is hoped that the data given in Table I are accurate. With higher vanadium contents, the degree of contamination increased, but was erratic (see p. 644). Tables

V and VI give the results obtained by thermal analysis and by the microscopical method. The temperatures will tend to be too low by amounts which in general increase with the vanadium content, but the erratic contamination makes it impossible to estimate the errors.

TABLE V.—*Thermal-Analysis Results.*

Vanadium, at.-%	Liquidus Arrest on Cooling Curve, ° C.	Solidus Arrest on Heating Curve, ° C.	Notes
44.9	1274	1195	Eutectic alloy; not analysed.
48	1201	1202	
49.7	1223	1202	
52.1	1215	1198	
56.6	1252	1197	
59.6	1267	1224	{ Synthetic compositions; not analysed.
61.1	1282	1234	
64	1316	1250	
70	1441	1277	

TABLE VI.—*Temperature Brackets for Solidus by Microscopical Method.*

Vanadium, at.-%	Temp. Bracket, ° C.	Notes
33.97	1297-1305	$\alpha$ + trace $\sigma$ . $\alpha$ + liquid. $\alpha$ + (?) trace liquid.
39.66	1238-1249	
41.87	1215-1220	
42.90	1201	
45 *	1204	
50 *	1204	Analytical total 99.97% (0.04% N). $\sigma$ + trace liquid.
55 *	1201-1206	
59.9	1200-1207	
65 *	1235	

\* These alloys were not analysed and the values given are the synthetic compositions.

## ACKNOWLEDGEMENTS

The authors must express their gratitude to Professor Sir Cyril Hinshelwood, F.R.S., for laboratory accommodation, and to Dr. F. M. Brewer for many facilities which have greatly encouraged the present work. They must also acknowledge the help received from Mr. D. J. H. Hawes in connection with the preparation of alloys for microscopical examination.

## REFERENCES

1. H. Giebelhausen, *Z. anorg. Chem.*, 1915, **91**, 254.
2. S. J. Carlile, J. W. Christian, and W. Hume-Rothery, *J. Inst. Metals*, 1949-50, **76**, 169.
3. B. R. Coles and W. Hume-Rothery, *J. Inst. Metals*, 1951-52, **80**, 85.
4. W. Hume-Rothery, J. W. Christian, and W. B. Pearson, "Metallurgical Equilibrium Diagrams". London: 1952 (Institute of Physics).
5. D. Stockdale, *Proc. Roy. Soc.*, 1935, [A], **152**, 81.
6. H. Martens and P. Duwez, *Trans. Amer. Soc. Metals*, 1952, **44**, 484.
7. W. B. Pearson, J. W. Christian, and W. Hume-Rothery, *Nature*, 1951, **167**, 110.
8. W. B. Pearson and J. W. Christian, *Nature*, 1952, **169**, 70.
9. Z. S. Basinski, W. B. Pearson, and J. W. Christian, *J. Sci. Instruments*, 1952, **29**, 154.

By P. L. PRATT,† B.Sc., Ph.D., and S. F. PUGH,‡ M.A.,  
A.I.M., MEMBER

## SYNOPSIS

A study of the plastic deformation of single crystals of zinc has been made, using the opaque-stop and X-ray microscopic techniques to examine cleavage faces. By these complementary methods, the stresses arising from the twinning shear are shown to be relieved by accommodation kinking.

## I.—INTRODUCTION

IN view of the development of new metals of hexagonal structure and the problems connected with their plasticity, it was considered that a more detailed study of the deformation mechanism in zinc, using more sensitive methods of examination, would be valuable. The behaviour of zinc single crystals under simple tension is well known,<sup>1</sup> and, depending on the orientation of the crystal relative to the stress axis, deformation occurs by slip on the basal plane along one of the three close-packed rows of atoms, or by twinning on one of the  $\{10\bar{1}2\}$  pyramidal planes with shear in the corresponding  $\langle 10\bar{1}1 \rangle$  direction.

Following the work of Zapffe,<sup>2</sup> Jillson<sup>3</sup> studied markings on cleavage faces of zinc crystals deformed by large amounts in an arbitrary manner, and concluded that, in addition to the first-order twin markings, two sets of bands essentially perpendicular, and one set parallel, to the twin traces could be seen. The perpendicular sets were considered to be primary kinks at right angles to the slip system, and the parallel sets probably a first-order lattice bending. Although this work represents a valuable contribution to the problem of the plasticity of zinc, Jillson's method of deformation, by bending, straightening, and rumpling, makes the results difficult to interpret; the heavy deformation was necessary, however, to make the markings visible under the microscope.

The opaque-stop microscope,<sup>4</sup> developed to study surface slopes and tilts, is well fitted for the examination of deformation markings on cleavage faces, although no direct information is given about the crystal lattice beneath the deformed surface. A complementary use of the Berg-Barrett<sup>5</sup> technique of X-ray microscopy reveals changes in lattice orientation and enables a more complete picture of the deformation to be obtained.

## II.—PREPARATION OF SINGLE CRYSTALS

Single crystals of high-purity zinc were grown from the melt in a vertical gradient furnace, by a

method similar in principle to that described by Jillson.<sup>6</sup>

A vertical tube furnace with a tapped winding was set up, with a heavy-gauge aluminium tube projecting from the lower end. This furnace provided a suitable temperature gradient, when the currents in the end and main furnace windings were adjusted to the correct values with the shunt resistor  $R_1$  (Fig. 1). The average temperature in the furnace was controlled by the Variac setting, while the temperature

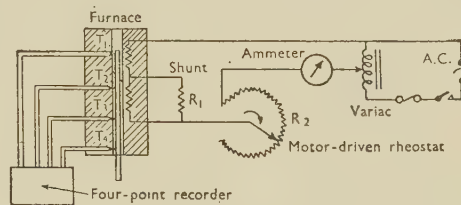


FIG. 1.—Gradient-Furnace Circuit Diagram.

gradient was monitored by four thermocouples between the aluminium tube and the furnace winding in the positions  $T_1$ – $T_4$  indicated in the figure. The whole furnace assembly was surrounded by insulating brick to eliminate rapid fluctuations in temperature due to draughts or changes in room temperature. Directional freezing from the bottom was obtained by slowly reducing the furnace current, and hence the temperature, with a motor-driven rheostat  $R_2$ .

Single crystals were grown from 99.999% purity zinc, melted, skimmed, and poured into a 0.5-in.-bore Pyrex tube, coated inside with graphite. Dissolved gas was removed from the molten metal by an oil-diffusion pump. The evacuated tube was sealed off and transferred to the gradient furnace, and the temperature allowed to settle down with the top of the Pyrex tube at 560° C. and the bottom at 455° C. The motor driving the rheostat  $R_2$  was then started, reducing the furnace current gradually so that freezing began at the lower, pointed end of the Pyrex tube. The full resistance was in after 8 hours' running, by which time the temperature at the top of the tube had

\* Manuscript received 10 May 1952.

† Research Fellow, Atomic Energy Research Establishment, Harwell, Berks.

‡ Senior Scientific Officer, Atomic Energy Research Establishment, Harwell, Berks.



fallen to 400° C. After cooling, the sealed Pyrex tube was broken at one end and the zinc crystal withdrawn. The method has so far invariably yielded single crystals. To prepare cleavage discs, the rods were placed in a bath of liquid air, and cleaved by sharp taps with a chisel placed parallel to the determined basal plane.

### III.—CRYSTALLOGRAPHY OF CLEAVAGE FACES

The six known twin planes  $\{10\bar{1}2\}$  (Table I), constituting a first-order pyramid (Fig. 2), intersect the basal plane in three parallel pairs of lines lying along the three directions  $\langle\bar{1}2\bar{1}0\rangle$ , inclined at 60° to each other. These twin traces in the basal plane are parallel to the close-packed rows of atoms in the basal plane (Fig. 3), and hence parallel to the slip directions. Since the composition plane of the twin lies approximately along the twin plane, the twin traces on the cleavage face will lie along these three directions inclined at 60°, and they will incidentally reveal the slip directions. As the axis of kinking lies in the slip plane normal to the slip direction, it follows that kink bands of the conventional type in zinc are normal to the twin traces in the basal plane and parallel to

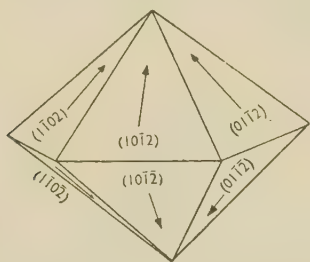


FIG. 2.—Twin Planes and Shear Directions in Zinc.

$\langle\bar{1}100\rangle$  directions; these are the traces of the second-order pyramid in the basal plane (Fig. 4). When examining a cleavage face after deformation, the types of marking to be expected are therefore those

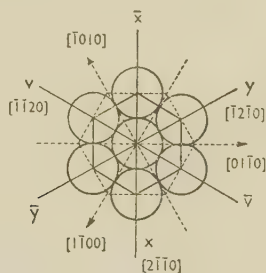


FIG. 3.—Atom Configurations in the Basal Plane.

illustrated in Fig. 5. Hess and Barrett<sup>7</sup> have also observed kinking about  $\langle\bar{1}2\bar{1}0\rangle$  axes, when the axis of the applied bending stress was parallel to this direction. This they consider to occur when the shear

stress along two of the possible slip directions is equal, so that slip occurs equally on both systems; and it results in slip in a direction along a line bisecting the angle between the two active slip systems. The

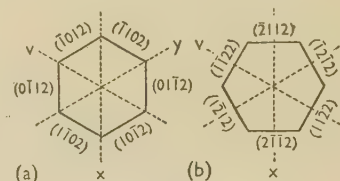


FIG. 4.—Trace of (a) First-Order, (b) Second-Order Hexagonal Pyramid in the Basal Plane.

traces of these first-order  $\langle\bar{1}2\bar{1}0\rangle$  kinks in the basal plane will be parallel to the twin traces.

A section perpendicular to the basal planes and to the direction of the twin trace in the basal plane, is

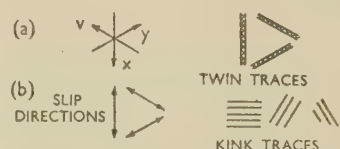


FIG. 5.—Directions of (a) Twin, and (b) Kink Traces in the Basal Plane.

illustrated in Fig. 6 (a). The section contains twins on  $(10\bar{1}2)$  and  $(\bar{1}012)$  planes which have parallel traces on the basal plane. By atomic rearrangement during twinning,<sup>8</sup> the  $c$ -axis in the parent becomes a basal plane direction in the twin, thus producing the same result as a lattice rotation of 90°; but the angle between the basal plane and the twin plane  $(0001)$

TABLE I.—Twin Planes in Zinc and Directions of Twin Traces and Kink Traces in the Basal Plane.

Twin Planes	Twin Traces	Kink Traces
$(10\bar{1}2), (\bar{1}012)$	$[\bar{1}2\bar{1}0] \parallel [\bar{1}2\bar{1}0]$	$[10\bar{1}0] \parallel [10\bar{1}0]$
$(1\bar{1}02), (\bar{1}102)$	$[\bar{1}120] \parallel [\bar{1}120]$	$[1100] \parallel [1100]$
$(01\bar{1}2), (0\bar{1}12)$	$[2\bar{1}10] \parallel [2\bar{1}10]$	$[0110] \parallel [0110]$

$(10\bar{1}2)$  is 46° 59', and therefore the mechanical shear during twinning is  $(2 \times 46^\circ 59') - 90^\circ = 3^\circ 58'$ . This shear is important in the present investigation, since it results in a displacement of the basal plane by an amount  $w \tan 3^\circ 58'$  in the  $c$  direction, where  $w$  is the width of the twin trace shown in Fig. 6 (b). If under pure shear a twin of uniform thickness completely crosses a single crystal, the net result is a displacement of the parent crystal on either side of the twin (see Fig. 8 (a), p. 656). This rarely occurs in practice, and it is more common to find twins which begin and end inside the crystal, causing inhomogeneous displacement of the crystal. The resulting distortion of the basal plane must be accommodated either elastically, or by local slip or kinking.

Since the shear directions for twins on different twin planes are neither parallel to each other nor to the lines of intersection of the twin planes (Fig. 2), it follows that twins in zinc cannot intersect. Consequently in

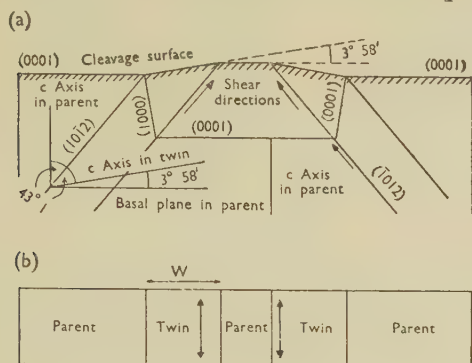


FIG. 6.—(a) Section Perpendicular to Cleavage Plane Twinned on (1012) and (1012) After Cleaving. (b) Appearance of Cleavage Surface of Section.

regions where one twin meets another high stresses must occur and the lattice must distort in some way to accommodate this strain.

#### IV.—EXPERIMENTAL TECHNIQUES

##### 1. X-RAY MICROSCOPE

The X-ray microscope was first used by Berg<sup>9</sup> to examine deformed crystals of rock salt with a monochromatic parallel beam of X-rays reflecting on to a photographic plate close to the crystal. Later Barrett<sup>5</sup> studied lightly deformed metal surfaces, magnifying the images optically up to  $\times 250$ , and also oscillating the specimen and film through a small angle to produce effectively a non-parallel incident beam. The technique has recently been used by Honeycombe<sup>10</sup> to study deformed single crystals of aluminium and other cubic metals.

Owing to the slight distortion introduced during cleaving, the lattice orientation varies from point to point over the surface of the crystal. As a result, with

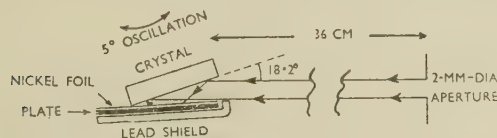


FIG. 7.—Arrangement for X-Ray Microscopy.

a parallel beam of X-rays, a stationary cleavage face gives a reflection from only a small area of its surface even under the most favourable conditions. By oscillating the specimen through 5° about a vertical axis, the whole surface can be brought into the correct position for a strong  $K_\alpha$  reflection, and in this way uniform images of large, slightly distorted crystals can be obtained. The sensitivity to lattice bending is but little reduced, especially about an axis at right angles

to the oscillation, although a displaced image due to the  $K_\beta$  reflection is introduced. This image, together with some of the fluorescent radiation, is conveniently removed by a  $\beta$ -filter placed next to the photographic plate.

A plan of the experimental arrangement used in this work is illustrated in Fig. 7. The specimen was mounted on the spindle of a Unicam Universal camera and set with the cleavage face at 18.2° to the incident beam, to give a basal plane reflection with  $\text{CuK}_\alpha$  radiation. The beam emerged through a 2-mm.-dia. aperture on the X-ray set, and, after reflection from the specimen, passed through a nickel filter on to a Kodak B 10 plate. This plate was set almost parallel to the crystal surface, and as close to it as possible without blocking the incident beam. The plate-to-crystal distance was about 2 mm., and the crystal-to-pinhole distance 36 cm. The specimen was oscillated through 5° about the vertical axis, with an exposure time of about 1 hr. Images were also obtained using the pyramidal plane reflections, but these appeared at higher angles and overlapped each other.

##### 2. THE OPAQUE-STOP MICROSCOPE

The opaque-stop microscope has been developed recently<sup>4</sup> to detect slopes and surface tilts with a higher sensitivity than can be obtained using a normal microscope. It is particularly suitable for the study of slightly distorted cleavage surfaces, where most of the specimen is nearly flat. By inserting suitable opaque stops in the optical train of a normal microscope, it is possible to obtain a sensitivity to angle of better than 1' at  $\times 6$ , and about 1° at  $\times 200$ , the sensitivity being inversely proportional to the magnification. In this work a point source of illumination was used, with a straight-edge stop close to the back focal plane of the objective. The stop was adjusted until a suitable contrast was obtained, and the images were recorded with a Beck eyepiece camera. For the interpretation of the images, it should be noted that difference of intensity corresponds to difference of surface inclination.

#### V.—EXPERIMENTAL RESULTS

The basal planes of crystals, cleaved under liquid air, were examined by the sensitive techniques outlined above, without further deformation in most cases. The deformation introduced by the cleavage process was sufficient to make clear the mechanism of deformation, although in some crystals heavier deformation was produced by lightly scratching the surface with a razor blade.

##### 1. ACCOMMODATION PARALLEL TO THE TWIN

Fig. 10 (Plate CVII) shows the cleavage face of a crystal under the ordinary microscope. A twin running through the body of the crystal intersects the cleavage face as the black vertical straight line, with a



dark irregular cleavage step at one end, and a fragmentary twin at  $60^\circ$  at the other. Inserting the opaque stop (Fig. 11, Plate CVII) accentuates the irregular cleavage step and shows a pattern of very low bright and dark steps covering the surface. In addition, the lattice accommodation around the twin is revealed as a first-order surface tilt, appearing as a dark band parallel to the twin and to the right. Further small markings near the ends of the twin can be seen, and they will be examined more closely in a later Section. The single surface tilt on one side of the twin is the simplest type of parallel accommodation observed in this work.

Wider accommodation tilts, made up of folds of alternate slope, appear in Fig. 12 (Plate CVII), and their detailed structure changes along the length of the

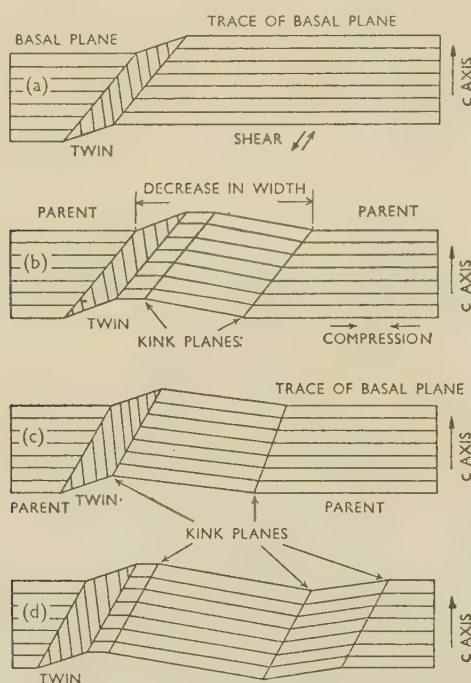


Fig. 8.—Appearance of Twin Lamellae and Kink Planes in Sections Normal to the Basal Plane and Twin Plane.

twin. With the opaque stop removed (Fig. 13 Plate CVII), the corresponding curvature of the twin can be seen by sighting at a glancing angle to the print. The position of this twin was marked by light intersecting scratches on the surface of the crystal, thus enabling this area to be recognized on the X-ray micrographs. Under normal illumination, short twins can be seen along the course of the scratch, arising from the deformation, while the opaque stop shows a much wider area of lattice distortion made up of tilts nearly perpendicular to the twin traces.

An interesting area of the same specimen, a little farther along one of the scratches, is shown in Fig. 14 (Plate CVII). Two parallel twins of the same system can be seen, together with a twin of another system making up a triangle with the scratch as base. At

the point where the twins meet, faint markings perpendicular to the first set of twins appear, and the broader of the parallel twins splits into two just above this point. The accommodation tilts parallel to the broad twin (Fig. 15, Plate CVII) revealed by the opaque stop, are complex, and extend a long way from it, while those of the fine twins are narrower and more simple. The perpendicular markings at the meeting point of the twins are seen to be surface tilts superimposed on the normal accommodation, and parallel to those produced by the deformation near the scratch.

The X-ray micrograph of this crystal (Fig. 16, Plate CVII) shows that the surface tilts, revealed by the opaque stop in the areas marked 12 and 15, are the result of lattice rotation beneath the surface; and the tilted regions are, in fact, kink bands, involving local slip, with the kink planes separating the tilted lattice from the parent lattice and the twin. Possible configurations of twin and kink plane have been drawn in Fig. 8 with the shear angle exaggerated for ease of illustration. In Fig. 8(a) the twin is shown in an undistorted lattice without accommodation; in Figs. 8(b) and (c), owing to lattice restraints, the kink plane appears away from the twin and at the composition plane, respectively; while in Fig. 8(d) buckling of the lattice occurs with the formation of kink bands of opposite sense. The resolution of the X-ray technique is not as high as that of the optical technique, but the twins, being unable to reflect, appear white, while the kink plane itself gives a strong reflection due to focusing effects. The cleavage steps, visible under the microscope, do not appear.

Twins in zinc do not have a common shear direction, and therefore true intersections cannot be formed. However, twins of different systems can be found apparently passing through each other, as in Fig. 17 (Plate CVII). Close examination, with the opaque stop removed, shows that one of the twins passes straight through the point of meeting, while the other is displaced by about 0.01 mm. More frequently, as in Fig. 14, the twins fail to penetrate, and the accommodation kinks merge together as the twins approach. In this specimen (Fig. 17) strong kinks perpendicular to the two twin systems can be seen, together with the usual cleavage steppings.

At this stage a further development of the use of the X-ray microscope was attempted. An image was obtained of an area of crystal containing a short twin visible to the naked eye, and after enlargement (Fig. 18, Plate CVIII) areas showing marked distortion were noted. The crystal was then examined optically, and the normal microscope showed little more than the twins, and larger cleavage steps. It should be noted, however, that the boundaries of kinked areas can nearly always be detected by defocusing the normal microscope, and this effect is shown in Fig. 19 (Plate CVIII). The photograph was taken on a Vickers microscope, using a single cine-camera projection lens without an eyepiece, and for this reason the image is inverted laterally with re-

spect to the X-ray image. A similar view of the twin with the opaque-stop microscope (Fig. 20, Plate CVIII) shows that the parallel accommodation kink is on the left side, in agreement with the X-ray image, while the upper end of the twin shows considerable distortion and rotation. In addition, a short kink, marked with an arrow, at the tip of the inclined twin to the left, can just be seen by both techniques. Owing to the relative positions of specimen and film, the X-ray image is foreshortened in the vertical direction, and a white band appears to the left of the parallel kink boundary.

## 2. ACCOMMODATION AT THE ENDS OF TWINS

An area marked in the lower left-hand corner of Fig. 18 shows parallel markings close to the end of

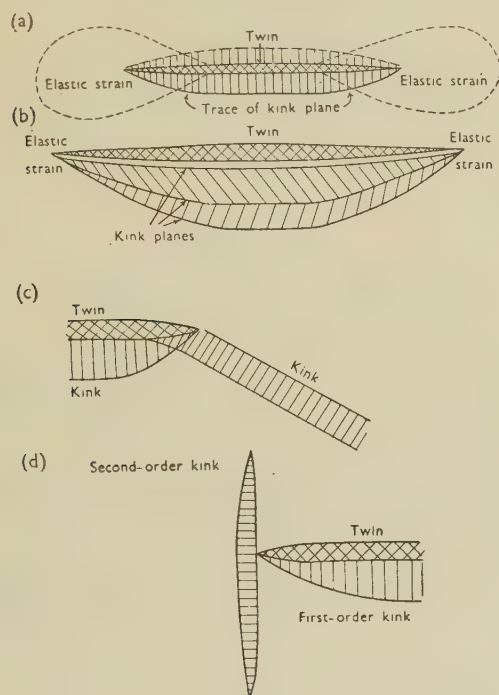


FIG. 9.—Appearance of Cleavage Facets Illustrating Accommodation Kinking Parallel to, and at the Ends of, Twin Lamellae.

two parallel twins. Optically in this area (Fig. 22, Plate CVIII), two intersecting sets of second-order kink bands can be seen, one perpendicular and one at  $30^\circ$  to the ends of the twins. Two interrupted cleavage markings can be seen on this specimen on the arc of a circle in the low cleavage steps, together with further perpendicular kinks at the end of the short twin in the top right-hand corner.

End accommodation, with a single lattice kink about an axis perpendicular to the length of the twin, is the type most frequently found (Fig. 9(b)), but kinks of the other second-order systems have also been observed. These usually appear on the same side of the twin as the parallel accommodation band, as in Figs. 21 and 22 (Plate CVIII) and 9(c), although the lower twin in Fig. 20 shows a kink across the tip in the

other direction. Twins with no end accommodation can be seen in Fig. 23 (Plate CVIII), but these have parallel accommodation kinks on both sides of the twins, and the twins themselves taper slowly to a very fine point (Fig. 24, Plate CVIII). At the left of the figures, two large cleavage steps originate from a point.

## 3. CHANGING WIDTH OF TWIN

In a previous Section (Fig. 15), it was found that the width of the twin appeared to determine the width of the parallel accommodation kink band. Where a lenticular twin ends within the crystal, the width of the first-order kink band decreases with the width of the twin, vanishing at the end of the twin. This behaviour can be seen in Fig. 21, for example, and has been sketched in Figs. 9(a) and (b).

Where the width of the twin changes sharply, second-order kink bands are found, as in Fig. 25 (Plate CVIII), showing the distorted end of the twin in Fig. 20. The two intersecting second-order kinks on each side of the wider part of the twin continue the lattice rotation of the single first-order kink seen below the twin on the left. The twin ends in a complex arrangement of all three second-order kinks, together with twins of another system.

## VI.—DISCUSSION OF RESULTS

The general appearance of the basal plane of deformed crystals is in good agreement with the predictions made in Section III, and with the results of earlier workers, in particular Zapffe<sup>2</sup> and Jillson.<sup>3</sup> Traces of the three first-order twin systems were found, inclined at  $60^\circ$  to each other, together with the second-order kink traces at right angles to the slip directions (cf. Fig. 5). By the use of the more sensitive methods of examination, it was possible to study crystals very lightly deformed during cleavage, and so to detect features masked at the higher deformations previously used.

Twins ending within the crystal are found to be invariably associated with wide first-order accommodation kink bands, parallel to the twin traces, where the kink angle rarely exceeds about  $45'$ . Because of this maximum angle, the width of the parallel accommodation kink band is proportional to the width of the twin, and the kink band curves towards, and ends at, the tip of lenticular twins.

These first-order kink traces, being parallel to twin traces, are perpendicular not to a possible slip direction, but to the line bisecting the angle between two slip directions. The formation of such a kink band involves slip in equal amounts in two slip directions in the basal plane, and this provides a possible reason for the observed limited angle of kinking, since it must involve dislocations moving in different directions on the same slip plane.

Hess and Barrett<sup>7</sup> have observed first-order macro-kinking about  $\langle 1\bar{2}10 \rangle$  axes when the stress system was favourable, but the angle of kinking was not stated.



An externally applied bending moment about other axes in the basal plane can be relieved by conventional kinking about  $\langle 10\bar{1}0 \rangle$  axes on one or more independent systems, although Jillson and the earlier workers have observed kinking on only two of the three possible systems at high deformations. At low deformations, kinking on all three systems has occasionally been observed in this work, at the centre of spherical indentations. It seems reasonable to suppose that the orientation of the accommodation kink bands parallel to the twin is due to the particular stress system set up during inhomogeneous twinning, since the shear direction in twinning necessitates a bending of the parent lattice accurately about a  $\langle \bar{1}2\bar{1}0 \rangle$  axis, and not about one of the usual  $\langle 10\bar{1}0 \rangle$  second-order kinking axes.

If the  $\langle \bar{1}2\bar{1}0 \rangle$  accommodation kinking angle is limited in value, certain features of the deformation of zinc can be explained. At high deformations, the accommodation kinks will be masked by the conventional  $\langle 10\bar{1}0 \rangle$  kinks, since the angle of kinking for the latter is not limited by the single slip system involved. However, when the twins grow to such a thickness that their associated displacement cannot be accommodated fully by the limited  $\langle \bar{1}2\bar{1}0 \rangle$  kinks, parting between the twin and parent will occur along the composition plane.

The distortion at the ends of finely tapering twins can be accommodated elastically in the lattice, but, more usually, kinking about a  $\langle 10\bar{1}0 \rangle$  axis is necessary where the angle of tapering is large. The accommodation can be conveniently illustrated by considering the behaviour of a pile of sheets of paper. If a wedge-shaped ridge, tapering to a point in the centre, is formed at one end of the pile, then the far side of the pile is raised. The sheets of paper are considered to represent the basal planes, while the ridge represents the twin and its accommodation kink. When the provision is made that sheets can slip over one another

only in one of three directions, so that the pile folds about one of three axes normal to or at  $30^\circ$  to the ridge, all the observed combinations of twin and kink can be demonstrated.

The opaque-stop microscope, in combination with X-ray microscopy, has proved a powerful tool in studying low-angle kinking. In the above investigation kink bands always appeared as areas of constant tilt, bounded by sharp kink planes. By modifying the apparatus it is proposed, in a further investigation, to watch the growth of twins with their accommodation kinks, and to discover the way in which the kink bands form. In addition, an investigation of the nature of twins and kink bands formed in other crystals will be undertaken.

#### ACKNOWLEDGEMENTS

The authors are indebted to Dr. H. M. Finnieston for his continual encouragement throughout this work, to Mr. L. Kent for producing the photographs, and to the Director, Atomic Energy Research Establishment, Harwell for permission to publish this paper.

#### REFERENCES

1. E. Schmid and W. Boas, "Plasticity of Crystals". London: 1950 (F. A. Hughes and Co., Ltd.).
2. C. A. Zapffe, *Metal Progress*, 1947, **51**, 428.
3. D. C. Jillson, *Trans. Amer. Inst. Min. Met. Eng.*, 1950, **188**, 1009.
4. W. M. Lomer and P. L. Pratt, *J. Inst. Metals*, 1951-52, **80**, 409.
5. C. S. Barrett, *Trans. Amer. Inst. Min. Met. Eng.*, 1945, **161**, 15.
6. D. C. Jillson, *ibid.*, 1950, **188**, 1005.
7. J. B. Hess and C. S. Barrett, *ibid.*, 1949, **185**, 599.
8. N. Thompson and D. J. Millard, *Phil. Mag.*, 1952, [vii], **43**, 422.
9. W. F. Berg, *Z. Krist.*, 1934, **89**, 286.
10. R. W. K. Honeycombe, *J. Inst. Metals*, 1951-52, **80**, 39.

# THE CUBIC-TETRAGONAL TRANSFORMATION IN MANGANESE-COPPER ALLOYS \*

1395

By Z. S. BASINSKI,† B.A., STUDENT MEMBER, and J. W. CHRISTIAN,‡ M.A., D.Phil., JUNIOR MEMBER

## SYNOPSIS

Manganese-rich manganese-copper alloys, quenched from the  $\gamma$ -phase field, have been studied by X-ray and microscopical methods. High-temperature Debye-Scherrer photographs taken in the equilibrium  $\gamma$  field show that the structure is face-centred cubic. Quenched alloys with more than 82% manganese are tetragonal at room temperature and are reconverted to a cubic structure by heating to moderate temperatures (180° C. for 93.5% manganese). Alloys in the cubic region at room temperature (containing <82% manganese) become tetragonal when cooled to lower temperatures. The transformation temperatures for powder specimens containing 70–95% manganese have been determined as occurring between –183° and +200° C., depending on the composition. The transformation is of the diffusionless (martensitic) kind, and takes place over a temperature range which is about 30° C. for powder and much smaller for lump specimens.

Etched microspecimens of tetragonal alloys show a banded structure, the bands lying on {110} planes, as in the analogous indium-thallium alloys. The banded structure is also produced by heating and cooling electropolished specimens through the transformation range. The transformation has been studied in detail in this way. The nature of the surface changes occurring during the transition and the orientations of the banded surfaces have been determined by an optical method. The results are in agreement with the double-shear mechanism of transformation proposed for indium-thallium alloys. Some difficulties in connection with possible dislocation theories of the actual atom movements are indicated.

## I.—INTRODUCTION

THE most recent investigation of the equilibrium diagram of copper-manganese alloys<sup>1</sup> shows a continuous solid solution at high temperatures between copper and the  $\gamma$  form of manganese.  $\gamma$ -Manganese is usually assumed to have a face-centred tetragonal structure, and X-ray photographs show that quenched alloys with more than 82 wt.-% manganese are tetragonal, the axial ratio increasing continuously with copper content until the structure becomes cubic. Worrell<sup>2</sup> has discovered that alloys containing about 88% manganese appear to be highly twinned on {110} planes after quenching from the  $\gamma$ -phase field. Zener<sup>3</sup> has suggested that the high-temperature phase field is cubic and that in manganese-rich alloys a diffusionless transformation to a face-centred tetragonal structure occurs on quenching. According to this theory, the microstructure observed by Worrell is due to heavy twinning to avoid high residual stresses. The suggestion that  $\gamma$ -manganese may have a face-centred cubic structure had been made previously by Walters and Wells.<sup>4</sup> Structures similar to those observed by Worrell have been found in chromium-manganese alloys,<sup>5</sup> and they probably exist also in many other manganese systems.

Microstructures of almost identical appearance have been found recently in indium-thallium alloys by Guttman,<sup>6</sup> who showed that these were a result of a transformation on cooling from a disordered face-

centred cubic phase to a disordered face-centred tetragonal phase. Bowles, Barrett, and Guttman<sup>7</sup> studied this transformation in detail and suggested that it occurs by means of two shears on {110} planes at 60° to each other. According to these authors, neighbouring bands observed on the microstructure are regions in which the first shear has occurred in opposite directions and the bands are not twin orientations.

The present work had the initial aim of proving that the high-temperature  $\gamma$ -manganese phase is really cubic, and that transformation to a tetragonal structure takes place by a shear process on quenching. X-ray and microscopical methods have been used in a detailed study of the transformation.

## II.—EXPERIMENTAL METHODS

### 1. PREPARATION OF THE ALLOYS

All alloys were prepared by melting in an induction furnace under a small pressure of purified hydrogen. The materials used were electrolytic manganese of 99.98% purity, supplied by Johnson, Matthey and Co., Ltd., and electrolytic copper (99.99%) presented by The British Non-Ferrous Metals Research Association. The ingots were sectioned with a slitting wheel, and after severe cold working the pieces were sealed in evacuated silica capsules and annealed at temperatures near to the solidus for 3–7 days and then quenched into ice-cold water. At temperatures above 940° C.

\* Manuscript received 26 February 1952.

† Inorganic Chemistry Laboratory, Oxford.

‡ Pressed Steel Co., Ltd., Research Fellow, Inorganic Chemistry Laboratory, Oxford.



alumina collars were used to prevent contact between the alloy and the silica tube. This treatment was effective in removing segregation present in the furnace-cooled alloys.

## 2. HIGH-TEMPERATURE DEBYE-SCHERRER PHOTOGRAPHS

X-ray photographs at temperatures up to 845° C. were taken in a 19-cm. Unicam camera, modified by installing hemispherical furnaces and new-type ring thermocouples; details of the alterations and of the performance of the camera have been published.<sup>8</sup> Solid-rod specimens of 1 mm. dia. were filed to shape on a lathe and then sealed in thin-walled silica capillaries. Photographs were also taken at temperatures between 20° and 250° C., and for these comparatively low temperatures powder specimens were used, the powder having been annealed previously in the  $\gamma$  region to remove the effects of cold work.

All Debye-Scherrer X-ray photographs were taken with either iron or manganese radiation. The latter gave more accurate results, but it was not available in the early stages of the work. A room-temperature exposure was taken as a check after each high-temperature photograph.

## 3. LOW-TEMPERATURE DEBYE-SCHERRER PHOTOGRAPHS

Powder photographs were taken in the range 20° to -120° C., using the cooling device described by Hume-Rothery and Strawbridge,<sup>9</sup> in conjunction with the film cassette from the Unicam high-temperature camera. A number of exposures were also made at the temperature of liquid oxygen (-183° C.), using the apparatus described by Lonsdale and Smith.<sup>10</sup> Specimens for low-temperature photographs were made by mixing powder with a dilute solution of Canada balsam in xylol and gently rolling thin cylinders on glass fibres.

## 4. PREPARATION OF MICROSPECIMENS

Alloys quenched from the  $\gamma$ -phase field were sectioned, ground on successive grades of emery paper, and mechanically polished with coarse alumina and water followed by magnesia and water. The alloys were then electrolytically polished, using as electrolyte one part of phosphoric acid, one part of glycerol, and two parts of absolute alcohol by volume. A potential of 18 V. was used across the cell, corresponding to a current density of about 0.28 amp./cm.<sup>2</sup>. These conditions differ slightly from those recommended by Worrell.<sup>2</sup> Specimens were etched in a 5% citric acid solution, washed in distilled water and alcohol, and dried in a stream of hot air.

## 5. MICROSTRUCTURAL CHANGES DURING HEATING AND COOLING

Microscopical observations on alloys heated and cooled through the transformation range were made, using the simple apparatus shown in Fig. 1. The

alloy was held by ordinary soft solder in a copper rod, which was heated by a Nichrome coil. Temperatures were observed by means of a thin-wire platinum/platinum-13% rhodium thermocouple inserted as near to the specimen as possible. The specimen was polished after mounting, and the apparatus was used up to 200° C., the surface being observed with a microscope, using oblique illumination.

## 6. X-RAY EXAMINATION OF LUMP SPECIMENS

The apparatus shown in Fig. 1 was also used to follow the transformation in lump specimens by X-ray methods. The specimen was mounted in a

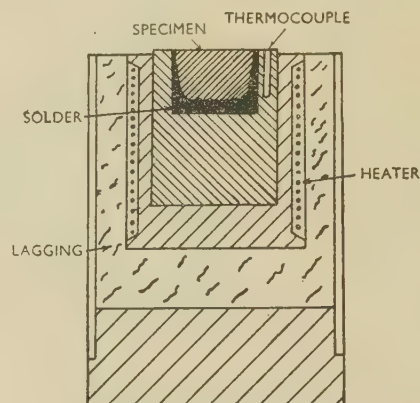


FIG. 1.—Apparatus for Observation of Microstructural Changes during Heating and Cooling.

Unicam single-crystal camera, and glancing-angle photographs were taken with iron radiation, the film being arranged to record the (220) and (202) reflections which were used to indicate the structure of the alloy. The grain-size of the specimens was sufficiently small to give smooth Debye rings.

## 7. OPTICAL EXAMINATION OF THE SURFACE

As described later, a banded relief structure was developed on the surface of electropolished specimens heated through the transformation range. An optical method was used to investigate the nature of the surface in more detail. The specimen was mounted on a small goniometer head and observed under a microscope, using vertical illumination. By using a very narrow pencil of light and removing the eyepiece of the microscope, it was possible to see two images of the pinhole source from each set of bands, which reflected the light in two different directions. These images were observed in the eyepiece of the microscope by inserting an auxiliary lens to act as a Bertram lens. The images were not sharp spots, as each set of bands acted as a reflection diffraction grating producing subsidiary maxima, and in the case of white light a coloured diffraction pattern. For reasonably broad bands, however, this effect was not important.

The angle between the surfaces in neighbouring light and dark bands was measured by means of an eyepiece with a crosswire. The specimen was tilted

on a goniometer in a direction perpendicular to a set of broad bands until the two main reflections were brought in turn on to the crosswire. The field was stopped down to include only two or three bands, and the accuracy of the method is believed to be quite high.

Direction images from a specimen mounted in the apparatus shown in Fig. 1 were also observed with the Bertram lens arrangement during heating and cooling through the transformation.

#### 8. CHEMICAL ANALYSIS OF THE ALLOYS

Analyses of the alloys were carried out by Johnson, Matthey and Co., Ltd. In the case of high-temperature X-ray photographs, the actual specimens were analysed for both copper and manganese; the analytical totals all exceeded 99.98%.

### III.—THE MICROSTRUCTURES OF QUENCHED $\gamma$ -PHASE ALLOYS

Attempts to obtain the banded structure described by Worrell<sup>2</sup> by etching mechanically polished speci-

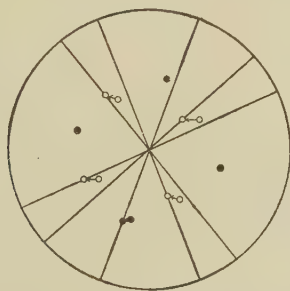


FIG. 2.—Stereographic Analysis of Traces in a Transformed Grain. Solid symbols are {111} poles, open symbols {110} poles of a standard (001) projection. In this grain there were 4 sets of {110} traces and 1 {111} twin.

mens were unsuccessful, but after electrolytic polishing it proved comparatively easy to develop this structure in alloys containing more than 85% manganese. The bands become more pronounced and slightly less regular as the manganese content increases. The appearance of the main bands is shown in Fig. 8 (Plate CIX). Each grain is crossed by one or more sets of bands, which in some cases meet at an angle, while in others they interweave. Some of the bands in the centre of Fig. 8 appear to contain fine sub-bands as observed in indium-thallium alloys.<sup>6</sup> Several attempts were made to confirm this observation, but despite careful etching and examination under polarized light it proved impossible to develop the sub-band structure again. Siefert and Worrell<sup>11</sup> have also recently published a photomicrograph of a manganese-copper alloy in which the sub-bands are just visible.

Several grains in the microstructures of alloys containing 88%, 92%, and 94% manganese were analysed by stereographic projection, and it was

established that interwoven sets of bands always arose from {110} planes at 60° to one another and that bands on planes at 90° to each other always met in a sharp line. These observations are in agreement with those of Bowles *et al.*<sup>7</sup> on indium-thallium alloys. Fig. 2 illustrates a typical stereographic analysis.

When etched after mechanical polishing, alloys having a tetragonal structure showed a curious mottled structure which was not present in alloys with a cubic structure. It was also found that electropolished alloys developed this structure when heavily etched. Fig. 9 (Plate CIX) shows a specimen after etching for 20 sec. in the citric acid solution; the banded structure is partially obscured by mottling.

### IV.—STRUCTURE OF THE HIGH-TEMPERATURE $\gamma$ PHASE

The similarity of the structures of the quenched  $\gamma$ -phase alloys to those found in indium-thallium alloys clearly indicates that a cubic-tetragonal transformation has occurred on cooling. In order to prove this directly, a number of exposures were made in the high-temperature  $\gamma$ -phase field at 845° C. These all showed a face-centred cubic structure. The films had rather heavy backgrounds, and the accuracy of the parameter measurements is thought only to be of the order of  $\pm 0.001$  Å.

The lattice parameters plotted against analysed compositions lie on a smooth curve, as shown in Fig. 3, the spacing decreasing with increasing manganese content. Satisfactory photographs could not be obtained with alloys containing more than 87.5% manganese, owing to the higher temperatures of the  $\beta \rightleftharpoons \gamma$  transformation and the increasing reactivity of the manganese with the silica. The results show, however, that the  $\gamma$ -phase alloys are cubic to at least 87.5% manganese, and it seems almost certain that the whole of the  $\gamma$  phase is cubic. In fact, this has been directly proved for alloys up to 95% manganese (see below).

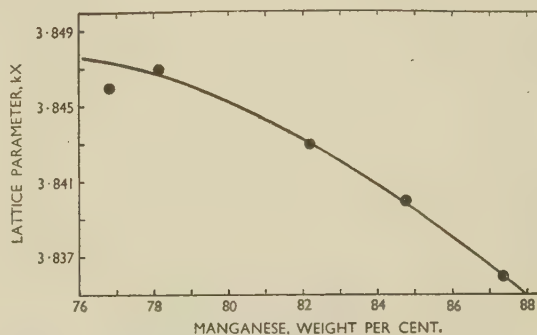


FIG. 3.—Lattice-Parameter/Composition Curve for the Equilibrium  $\gamma$ -Phase Field at 845° C.

The room-temperature photographs taken after each high-temperature exposure all showed the usual quenched structure, but some of the lines, in particular {200}, were slightly broadened.



### V.—DETAILED X-RAY STUDY OF THE TRANSFORMATION IN POWDERS

Alloys with less than 82% manganese are cubic after quenching to room temperature, but by cooling to lower temperatures these alloys could be made to transform to a tetragonal structure. Similarly, alloys with more than 82% manganese reverted to a face-centred cubic structure when heated to temperatures between 20° and 250° C. A series of alloys ranging in composition from 70 to 95% manganese were studied from -183° to +250° C., after first quenching from the  $\gamma$ -phase field. In each case the structure was tetragonal at lower temperatures and cubic at higher temperatures, the transformation temperatures varying with the composition. It should be emphasized that all these alloys were in metastable states, the equilibrium structure being a mixture of  $\alpha$ -manganese and a copper-rich face-centred cubic solid solution.

In contrast to the results of Dean *et al.*,<sup>1</sup> the transformation between the two structures appeared to be non-homogeneous, and a two-phase region in

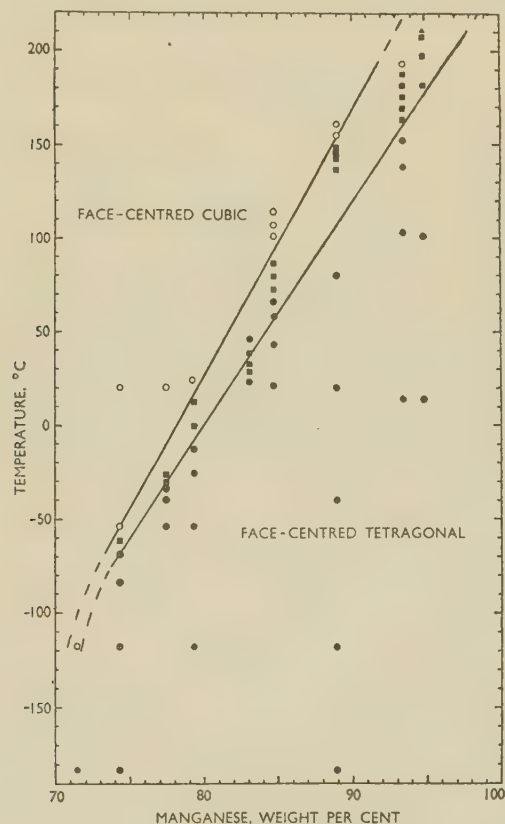


FIG. 4.—Results of Debye-Scherrer Powder Photographs.

KEY.  
 ● Tetragonal alloys.  
 ○ Cubic alloys.  
 ■ Cubic and tetragonal alloys.  
 ▲ Decomposed alloy.

which both structures co-existed was always found. Similar behaviour was observed by Bumm and Dehlinger<sup>12</sup> in manganese-gold alloys, and has recently

been reported by Zwicker<sup>13</sup> for many other manganese systems. In our powder photographs this gap is of the order of only 2%, and may thus have escaped detection

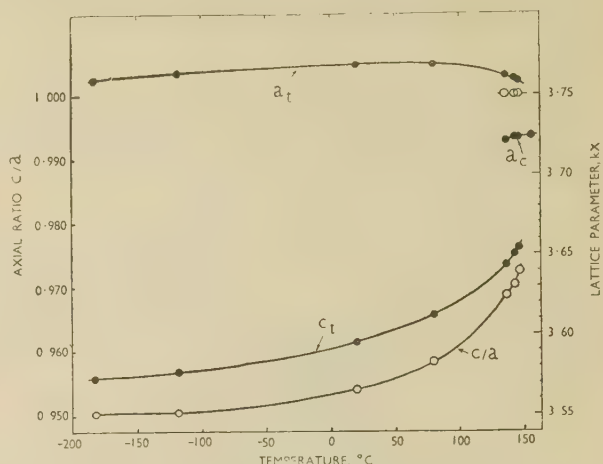


FIG. 5.—Lattice Parameter/Temperature Curves for an Alloy Containing 88.9% Mn.

KEY.  
 ● Lattice parameters.  
 ○ Axial ratios.

in previous work, especially as the tetragonal lines are usually rather diffuse. The two-phase photographs are not, however (as Zwicker suggests), to be interpreted as a region in which cubic and tetragonal phases are in equilibrium; they are rather to be regarded as indicating a temperature interval over which transformation takes place.

The axial ratio of the first tetragonal phase which appeared on cooling was definite, but varied with the composition of the alloy, approaching unity as the manganese content decreased. In cases where the separation of the tetragonal lines was large enough to avoid overlap with cubic lines, the transformation could be studied closely. The mean transformation temperature increased with increasing manganese content from -183° C. for ~70% manganese to between 160° and 200° C., for 93.5% manganese. The cubic phase in an alloy containing 95% manganese began to appear at 180° C., but the whole transformation could not be investigated, as this alloy began to decompose into the equilibrium phases above 200° C.

The results of all X-ray investigations on the transformation range are given in Fig. 4, the alloys, having been analysed in each case. The width of the transformation range cannot be correlated exactly with temperature (or composition), and probably depends on the grain-size. The range seems to become wider at higher temperatures.

Detailed lattice spacing/temperature curves were plotted for several alloys, and one of these for an alloy containing 88.9% manganese is shown in Fig. 5. The axial ratio of the tetragonal alloy decreases with temperature, at first abruptly and then more and more slowly, until it reaches an almost constant value about 200°–300° C. below the transformation range. The  $a$  parameter first increases with decreasing

temperature and then begins to decrease again about 50° C. below the transformation temperature. In the region where the two phases coexist, the parameters are not constant, but lie on the extrapolated expansion curves of the cubic and tetragonal regions. The parameters are such that the tetragonal phase which appears on cooling has the same volume as the cubic phase from which it is formed, within the limits of experimental error.

The results proved conclusively that the transformation is dependent only on temperature and not on the time for which a specimen is held at a given temperature. X-ray exposures on a specimen were not made consecutively as the temperature was raised or lowered, but were selected at random; the order of exposure had no noticeable effect on the amount of transformation. The transformation was almost instantaneous even at liquid-air temperature.

It is clear from these results that the transformation is diffusionless. The temperatures of the beginning and end of the transformation are, on this view,  $M_s$  and  $M_f$  temperatures, and as in the case of other martensitic transformations, e.g. cobalt, the transformation range may be very dependent on grain-size. Some confirmation of this has been obtained from the results described in the next section.

## VI.—THE TRANSFORMATION IN LUMP SPECIMENS

Bowles, *et al.*<sup>7</sup>, obtained the banded structure in indium-thallium alloys as a surface relief effect by allowing flat cubic specimens to transform to the tetragonal structure. The reverse procedure was used for manganese-copper alloys; electropolished tetragonal alloys were heated through the transformation range, using the apparatus shown in Fig. 1. An alloy containing 93.5% manganese was examined in detail, and the changes occurring are illustrated in Fig. 6. One or more sets of light and dark bands appeared in each grain and became gradually plainer as the temperature was raised. At a critical temperature, however, each dark band suddenly became much blacker. This change occurred at different times (or temperatures) in different bands, but was complete in a very small temperature interval. The order in which individual bands suddenly transformed was random, in general, but occasionally propagation along a series of bands (1, 2, 3 in Fig. 6 (d)) was observed.

The sudden change in the appearance of a band is believed to correspond to a region of the crystal, having the band as its surface, transforming from tetragonal to cubic. The description above, and Fig. 6, imply that this change was confined to the dark bands, but this was an optical illusion, as the eye sees only contrast. By varying the oblique illumination, it could be seen that both light and dark bands changed suddenly in the transformation range (see also Section VII). Rotation of the strongly banded structure resulted in a continuous variation of

contrast, with a reversal of black and white bands after 180° rotation. The banded structure was, therefore, probably caused by distortion of the flat surface into a surface with a saw-toothed cross-section, as shown in Fig. 6 (e).

On cooling, the reverse changes occurred. The strong bands changed abruptly to faint bands at a temperature about 6° C. below the heating transformation, and as the temperature was lowered further the bands gradually disappeared. A number of heating and cooling cycles were observed, and the band structure which appeared on each heating half-cycle appeared to be identical, as judged visually or from photomicrographs. The structure disappeared almost completely at room temperature, but the thermal cycling in the tetragonal region caused

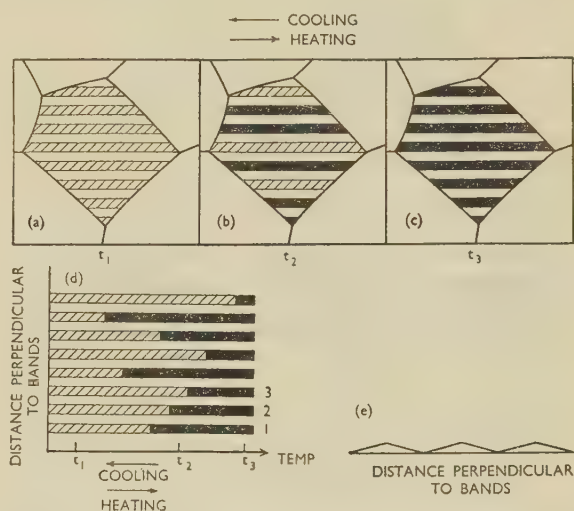


FIG. 6.—Microscopical Observation of the Transformation (Diagrammatic only).

- (a) Faint bands (tetragonal).
- (b) Partly transformed (tetragonal + cubic).
- (c) Strong bands (cubic).

some plastic deformation. Residual markings, similar to slip bands, appeared and increased in number with the number of cycles, as in the experiments of Boas and Honeycombe.<sup>14, 15</sup> The transformation temperatures on heating (181° C.) and cooling (175° C.) were reproducible.

Glancing-angle X-ray photographs confirmed that there was a very small transformation range on heating and cooling. Both the X-ray and the microscopical evidence indicated that this range increased slightly as the number of cycles increased. The much larger range for the powdered specimens described in Section V is presumably a grain- or particle-size effect.

Another specimen of the same alloy, which had been very slightly cold-worked by holding in a vice, produced bands when heated into the cubic region. These bands, however, did not disappear on cooling, but instead were crossed by a second set of bands, which were parallel to the first bands in some places and at an angle to them in others. In subsequent



cycles the transformation occurred reversibly by the appearance (in the tetragonal region) and disappearance (in the cubic region) of this second set of bands, the first set remaining equally prominent throughout; this is illustrated in Fig. 7 (a). The second set of bands were wider than the first set in all grains. It seems that cold working induced the transformation on a new set of planes.

Figs. 10 and 11 (Plate CIX) show an area in which two sets of bands were formed in this way. The broad bands on the lower half of Fig. 10 are on the same set of  $\{110\}$  planes as the narrower primary bands on the centre and bottom right of the figure, and on a different

cooling, but on heating they could be seen to disappear by migration of the boundaries perpendicular to their length. This difference is shown in Fig. 7 (b) and (c), and was very striking visually. After about 20 cycles, the cooling transformation gradually changed. A band appeared first as a thin line which grew by a series of discontinuous and apparently instantaneous jumps into the final band (Fig. 7 (d)). It was concluded that the cooling transformation was being retarded by plastic deformation.

A specimen, given a 10% reduction by squeezing, also produced bands on first heating, although much of the surface was too distorted to show them. On cooling, broad secondary bands appeared in the way shown in Fig. 7 (d). The effect of plastic deformation is evidently to inhibit the transformation, and ultimately to promote transformation on a new set of planes.

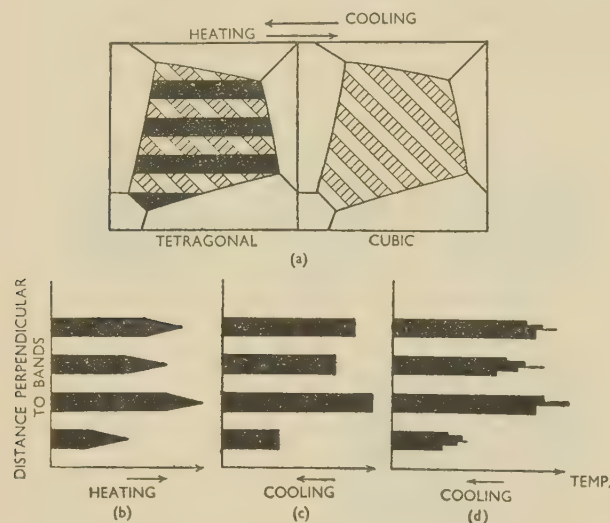


FIG. 7.—Transformation in Slightly Cold-Worked Alloy (Diagrammatic only).

set of planes from the primary bands on the bottom left of the photograph. These two sets of primary bands meet at an angle with slight interpenetration. There is another set of secondary bands on the top right of the photograph. The directions of the bands suggest that in this grain a  $\{001\}$  plane lies almost in the surface and the shearing movements have taken place in  $\{110\}$  planes at  $45^\circ$  to the surface. This was confirmed by stereographic analysis, using the traces mentioned above and the traces of the  $\{111\}$  twin and the  $\{110\}$  planes reflected across it in the top left of the photograph. The result showed that the surface was only a few degrees from a  $(001)$  plane and that the broad bands were then traces of the  $(101)$  planes. The polar co-ordinates  $\rho$  and  $\phi$  (Greninger and Troiano<sup>16</sup>) were  $\rho = 44^\circ$  and  $\phi = 6^\circ, 174^\circ$  for shears in the  $[\bar{1}01]$ ,  $[10\bar{1}]$  directions respectively.  $\rho$  is the angle between the normal to the plane of the surface and the shear plane, and  $\phi$  the angle between the trace normal of the surface in the shear plane and the shear direction.

Fig. 11 shows the same area as Fig. 10 photographed in the cubic region where the broad dark bands have disappeared. This area was observed for many cycles. The broad bands appeared abruptly on

## VII.—ORIENTATIONS OF THE SURFACE

From the above microscopical observations it was impossible to determine with certainty the nature of the banded surface, and in particular whether the surfaces of neighbouring bands were tilted in opposite directions, or whether only alternate bands were tilted in one direction with respect to the original surface. In some cases the appearance of the surface suggested that the bands were some form of rumpling into hills and valleys, but this was an optical illusion, and alteration of the inclination of the specimen in direction perpendicular to a given set of bands confirmed that the banded structure was in fact produced by tilting of the surface.

The method described in Section II, 7 was used to measure the angle between the surfaces of the broad bands at the bottom of Fig. 10 (Plate CIX). The zero-order reflection from the two sets of bands on the bottom left of Fig. 10 should give a pattern of 4 spots arranged in a rectangle, but the spots were drawn out in the direction of the broad bands into two line-diffraction patterns, resulting from the set of fine bands. It was, however, possible to distinguish the two zero-order maxima of the broad bands clearly. These bands were tilted  $2^\circ 5'$  with respect to each other.

A fourth specimen of the 93.5% manganese alloy was used to observe surface-orientation changes during heating and cooling. During heating the single strong reflection from the original surface lengthened out into a line-diffraction pattern (actually two overlapping diffraction patterns). When the transformation to the tetragonal structure occurred, the pattern separated into two diffraction patterns. On cooling, the separation of the central maxima of the two patterns suddenly jumped to a much smaller value when transformation took place. It was readily observable that each spot moved towards the other by approximately equal amounts, so that the bands were each tilted with respect to the flat surface, and represented regions sheared in opposite directions.

## VIII.—DISCUSSION

## 1. THE TWO-SHEAR TRANSFORMATION MECHANISM

The results detailed above may be summarized as follows:

(1) The often-suspected face-centred cubic structure of the high temperature  $\gamma$ -manganese phase has been established.

(2) The structure transforms to face-centred tetragonal by a shear process. The temperatures at which the transformation begins and ends depend on the composition of the alloy and are also influenced by grain-size and by cold work.

(3) The transformation occurs by shears on  $\{110\}$  planes of the cubic structure. The surface of the specimen is divided into bands, neighbouring bands representing regions sheared in opposite directions.

(4) Single bands form very rapidly on cooling, in a manner analogous to the formation of plates of martensite or mechanical twins. The transformation on heating is slower and occurs by migration of the band interface in a direction perpendicular to its length.

(5) The shear process is reversible, and in successive cycles the band-structure is identical after transformation.

Bowles, *et al.*<sup>7</sup>, in proposing a detailed mechanism for the corresponding transformation in indium-thallium alloys, have suggested that the process takes place by two shears on  $\{110\}$  planes at  $60^\circ$  to each other. The main bands represent traces of planes in which the first shear has occurred in opposite directions, and the sub-bands planes on which the second shear has been reversed. In the case of manganese alloys the axial ratio is less than one, whereas for indium-thallium alloys it is greater than one. The proposed double-shear mechanism is, however, applicable to both cases. A given  $\{110\}$  plane has four sets of  $\{110\}$  planes intersecting it at  $60^\circ$ . Oppositely directed shears on each of two of these planes give rise to two sets of sub-bands within a main band. If the first shear is of magnitude  $2\epsilon$ , the axial ratio of the tetragonal structure produced by this process is  $1 + 3\epsilon$ . Oppositely directed shears on the other two sets of planes give a tetragonal structure with an axial ratio of  $1 - 3\epsilon$ . The proof of this is identical with that given in the appendix to the paper by Bowles *et al.*<sup>7</sup> For pure  $\gamma$ -manganese the angles between the axes differ from  $90^\circ$  by  $5'$  and  $3''$  respectively, and the difference in length of the two  $a$  axes is about 4 parts in  $10^4$ . The alloys, having larger axial ratios, show even smaller divergencies from an exact tetragonal structure after the proposed two shears. This mechanism permits only two sets of sub-bands to be formed within a given main band, in agreement with observations for indium-thallium alloys.

The sub-bands were not observed sufficiently clearly in the present work, but other results in agreement with the two-shear mechanism, e.g. the interpenetration of main bands on  $\{110\}$  planes at  $60^\circ$  to each other and the

equal volumes of the cubic phase and the tetragonal phase formed from it, have been confirmed for manganese-copper alloys. The main evidence in support of this mechanism for manganese-copper alloys, however, comes from the results obtained for surface orientation. It was proved conclusively that during transformation shearing movements in opposite senses occur in one set of main bands. In the area of Fig. 10 the surface angle between the broad bands was  $2^\circ 5'$ . Greninger and Troiano<sup>16</sup> have shown that for a shear  $\gamma$  the angle  $\gamma'$  between the original and final positions of any plane is given by:

$$\tan(\rho + \gamma') = \tan \rho + \tan \gamma \cos \phi$$

where  $\rho$  and  $\phi$  have the meanings defined in Section VI. The axial ratio of the alloy shown in Fig. 10 was 0.948 at room temperature, so that for the double shear mechanism  $\epsilon = 0.017_3$  radians and  $\gamma = 2\epsilon = 1^\circ 59'$ . Substituting the experimental values for  $\rho$  and  $\phi$ , the angle  $\gamma'$  between the surface and one band is  $1^\circ$  and between the surface and the other band  $-1^\circ 2'$ . The angle between the two bands should thus be  $2^\circ 2'$ , which agrees very well with the experimental value. If the main bands had been the traces of twins, the angle between one main band and the surface would have been  $3^\circ$ .

This calculation is based on the room-temperature axial ratio, as were the pole figures used in the case of indium-thallium alloys. Bowles, *et al.*<sup>7</sup>, concluded from the observed agreement that the change in axial ratio with temperature takes place by further shears during cooling. In fact, it is not necessary to assume this, and such a mechanism seems most improbable, as it either involves an infinite number of infinitesimal shears or a discontinuous variation of axial ratio with temperature, which is contrary to the observed results. An infinite number of shears is either meaningless, or is merely another way of stating that the thermal expansion is anisotropic. Once the tetragonal orientations have been determined by the first shear, it is easy to see that anisotropic thermal expansion is able to produce further tilting of the surface in such a way that the tilt for any axial ratio is identical with that produced by a direct shear to that structure. We suggest, therefore, that the gradual tilt in the surfaces of the specimens produced during heating and cooling can be completely accounted for in this way.

## 2. ATOMIC MECHANISM OF THE TRANSFORMATION

The double-shear mechanism is in full agreement with the observations of this paper, but its validity is not finally established. If it is true, it describes the path taken by each atom during the transformation. It does not, however, give any further information about the way in which these movements occur.

Observations agree that the bands grow in a direction perpendicular to their length. The difference in behaviour on heating (where the interface could be



seen to move) and cooling (where bands formed apparently in an instantaneous click or a series of such clicks) may be one merely of velocity, though it is difficult to account even for this. The process seems to be one in which the shearing movement passes through successive atomic planes, as would be expected. The growth and disappearance of the bands occurred in a manner very similar to that recently described by Jillson<sup>17</sup> for the formation of mechanical twins in zinc.

With the small shears involved in this process, each atomic plane has only to move a very small distance over its neighbouring plane. Nevertheless, it seems scarcely possible that all the atoms in a plane move simultaneously, and the shears must therefore involve the motion of dislocation lines. A description of one process permitting the motion of an imperfect dislocation (i.e. a dislocation with a Burgers vector not equal to a lattice vector) from plane to plane has been given by Cottrell and Bilby,<sup>18</sup> and has been applied by them to the production of mechanical twins in body-centred cubic materials. A similar mechanism is expected for a martensitic transformation.

Serious difficulties are encountered, however, on attempting to apply dislocation theory to the shears involved in this transition. A lattice dislocation in the face-centred cubic lattice is of the type  $\frac{a}{2}[10\bar{1}]$  and, as shown by Heidenreich and Shockley,<sup>19</sup> this is dissociated into imperfect dislocations  $\frac{a}{6}[11\bar{2}]$  and  $\frac{a}{6}[2\bar{1}\bar{1}]$ . The first shear required for the indium-thallium alloy, however, would be produced by the

passage of a dislocation line  $\frac{a}{84}[101]$  down a series of  $(10\bar{1})$  planes, and this seems scarcely possible. The same difficulty applies to manganese-copper alloys.

Even if such an improbable dissociation occurred, there is the further difficulty of the change of axial ratio with composition, which means that each alloy would have to form a different imperfect dislocation. It thus appears probable that the whole process, if it occurs by dislocation movements, is much more complicated than the simple motion of one dislocation down a series of atomic planes. The geometry of dislocations in actual crystal lattices is at present very imperfectly developed. The difficulties summarized above apply equally, of course, to all shear transformations or twinning processes in which the amount of shear is very small; that is for most of the transformations known to occur by a shear mechanism.

The theory of Cottrell and Bilby<sup>18</sup> suggests that the shearing process may start at a stacking fault caused by the presence of an imperfect dislocation which is sessile. The reversibility of the process may indicate the presence of relatively stable nuclei, from which the transformation is initiated and which do not disappear when the reverse transformation occurs.

#### ACKNOWLEDGEMENTS

The authors would like to thank Sir Cyril Hinshelwood, F.R.S., for laboratory accommodation, Dr. W. Hume-Rothery, O.B.E., F.R.S., for his interest, and Mr. G. B. Harris for suggesting the optical method used for the surface-orientation determination. One of us (Z. S. B.) would also like to acknowledge financial assistance from the Committee for the Education of Poles in Great Britain.

#### REFERENCES

1. R. S. Dean, J. R. Long, T. R. Graham, E. V. Potter, and E. T. Hayes, *Trans. Amer. Soc. Metals*, 1945, **34**, 443.
2. F. T. Worrell, *J. Appl. Physics*, 1948, **19**, 929.
3. C. Zener, "Elasticity and Anelasticity of Metals", p. 162. Chicago: 1948 (University of Chicago Press).
4. F. M. Walters, Jr., and C. Wells, *Trans. Amer. Soc. Metals*, 1935, **23**, 727.
5. S. J. Carlile, J. W. Christian, and W. Hume-Rothery, *J. Inst. Metals*, 1949-50, **76**, 169.
6. L. Guttman, *Trans. Amer. Inst. Min. Met. Eng.*, 1950, **188**, 1472.
7. J. S. Bowles, C. S. Barrett, and L. Guttman, *ibid.*, 1478.
8. Z. S. Basinski, W. B. Pearson, and J. W. Christian, *J. Sci. Instruments*, 1952, **29**, 154.
9. W. Hume-Rothery and D. J. Strawbridge, *ibid.*, 1947, **24**, 89.
10. K. Lonsdale and H. Smith, *ibid.*, 1941, **18**, 133.
11. A. V. Siefert and F. T. Worrell, *J. Appl. Physics*, 1951, **22**, 1257.
12. H. Bumm and U. Dehlinger, *Metallwirtschaft*, 1934, **13**, 23.
13. U. Zwicker, *Z. Metallkunde*, 1951, **42**, 246.
14. W. Boas and R. W. K. Honeycombe, *Proc. Roy. Soc.*, 1946, [A], **186**, 57; 1947, [A], **188**, 427.
15. W. Boas and R. W. K. Honeycombe, *J. Inst. Metals*, 1947, **73**, 433.
16. A. B. Greninger and A. R. Troiano, *Trans. Amer. Inst. Min. Met. Eng.*, 1949, **185**, 590.
17. D. C. Jillson, *ibid.*, 1950, **188**, 1005.
18. A. H. Cottrell and B. A. Bilby, *Phil. Mag.*, 1951, [vii], **42**, 573.
19. R. D. Heidenreich and W. Shockley, *Phys. Soc.: Rep. Conf. on Strength of Solids*, 1948, 46.

## Equipment for the Thermal Treatment of Non-Ferrous Metals and Alloys\*

Mr. W. A. BAKER,† B.Sc., F.I.M. (Member), who acted as rapporteur, introduced the seven papers contributed to the Symposium and summarized their contents. In doing so he raised the following individual points of discussion:

In the paper on electric furnaces, an interesting type for annealing copper tubes in a controlled atmosphere is described (p. 264). It is a batch furnace, in which the tube charges are withdrawn from the hot furnace into a cooling chamber through which the controlled atmosphere is circulated as a cooling medium. From the description, it is not clear whether any attempt is made to effect heat transfer from the cooling work to the work awaiting heat-treatment in the adjoining chamber, but I have calculated that if this could be done without detriment to the quality of the controlled atmosphere or incurring other difficulties, at least 40% and probably a good deal more of the energy supplied to the furnace could be conserved. The actual saving in cost per ton of metal annealed is quite small, but considering the amount of energy used in the non-ferrous metal industry, any attempt to economize might be profitable from the point of view of overall consumption. It might, for example, be a comparatively easy matter in some types of continuous plant to arrange for counter-current flow of the work through the furnaces.

A further point of interest arising from the paper by Davis and Temple, is the problem of purging long copper alloy tubes when attempts are made to clean or bright anneal them.

Mr. W. A. FOWLER,‡ F.I.M. (Member): I propose to deal mainly with light alloys and to quote a few examples where there seems to be doubt as to what type of furnace should be used for a given treatment to yield the best all-round results.

Taking as a first instance the heat-treatment of extruded sections, there seem to be two distinct schools of thought, one which proclaims the virtues of the vertical furnace and another which advocates the horizontal furnace. The vertical furnace is largely standard practice in America and is becoming increasingly popular in this country. In many instances it has superseded the horizontal batch type. The horizontal furnace of a continuous type has such protagonists as the Société Centrale des Alliages Légers, and I would refer particularly to the paper by MM. Matter and Lamourdedieu published two years ago.§ Mr. Paton claims that the vertical furnace gives a product free from the kinks imparted by the supports in the horizontal furnace, but there is a certain amount of distortion when quenching sections of unequal dimensions. He states that the loading and unloading of the furnace are more laborious than for a horizontal furnace, and from knowledge acquired from other sources there is also a doubt as to the temperature control. It seems that the vertical furnace is not all that could be desired in this respect. On the other hand, it has been argued that the quenching associated with the horizontal furnace, whether by sprays or by tank immersion, results in such distortion as to make it extremely difficult, if not impossible, to straighten the section by any subsequent treatment.

The capital costs involved in the installation of a vertical furnace are very formidable, and the method of loading and unloading is both cumbersome and costly, whereas with a horizontal furnace of the continuous type it is possible to charge direct from the extrusion press, as well as to have a direct discharge of the section either into a spray box or into a quenching tank.

It may be that each system is superior in its own field of application. If so, we should know where the dividing line comes and what factors should influence our choice. The degree of distortion imparted to the material on quenching should only become important if the distortion is such that it cannot readily be rectified by any subsequent de-twisting or stretching operation. Presumably the kinks imparted to the material by the supports in the horizontal furnace are not easily removed by stretching. If concentrated attention could be given to the design of the horizontal furnace and this problem solved, its advantages in respect of ease of handling and lower capital and operating costs should place it well ahead of its vertical competitor.

My second example concerns the flash-annealing of light-alloy sheet. There are now a number of continuous flash-annealing furnaces for single sheets in operation in this country. The economic disadvantages compared with batch annealing are well recognized and, were it not for the fact that a rapid rate of heating in certain materials is essential for metallurgical reasons, it is doubtful whether these furnaces, for the light-metal industry at least, would ever have been developed. For the same metallurgical reasons as obtain for sheet, it is desirable to apply a flash-anneal to strip, and no doubt a continuous furnace for this purpose will be available before long. There is some difference of view, however, as to whether, if electricity is used, the heating should be carried out by radiation from electric-resistance elements, perhaps assisted by convection, or by induction heating.

The furnace builders do not seem to be in agreement on this point. Theoretically, induction heating should possess the important advantage of requiring less space. On the other hand, it is clear from the paper by Davis and Temple that a continuous furnace of the electric-resistance type has given satisfactory results in the annealing of copper strip, and one might expect that a furnace of a similar type would be equally satisfactory for light metals. However, I consider induction heating to be an attractive proposition, not only on the score of economy of space, but also because of the rapidity with which the strip can be brought to the required temperature.

The paper by M. Lamourdedieu describes a furnace of this type for the solution-treatment of light alloy strip, but it incorporates a resistance-heated holding zone necessary to maintain the heat-treatment temperature with the required degree of precision. Would such a holding furnace be required for a flash-annealing process, which does not call for the same tolerance in final temperature? Subject to satisfactory temperature control being assured, and to there being no offsetting disadvantages, induction heating for the continuous

\* Joint discussion at a Symposium held in London on 26 March 1952, on Papers Nos. 1347-1353 (*Journal*, this vol., pp. 255-339).

† Senior Metallurgist, British Non-Ferrous Metals Research Association, London.

‡ Production Manager (Manufactured Materials), The British Aluminium Co., Ltd., London.

§ J. Matter and M. Lamourdedieu, *J. Inst. Metals*, 1948-49, 75, 899.



annealing of strip should warrant further investigation. It would be interesting to have the views of the furnace builders, particularly on such matters as comparative energy consumption and installation and operating costs. The furnace builders and the electrical engineers should try to reconcile their differences of opinion on the pros and cons of induction and other types of heating, and speak to the users with one voice.

My final example concerns furnaces for the solution-treatment of strong alloy sheets. Salt baths, both electrically and gas-heated, are discussed in the papers, and so are vertical-quenching, forced-air-circulation furnaces, designed for the same purpose. The upper temperature limits to which a salt bath can be worked with safety are accurately known, but, as the heat-treatment temperatures for most of the strong alloys fall well within the safe range, the two types of furnace can in some respects at least be regarded as competitive.

There are certain metallurgical advantages in the rapid heating achieved in the salt bath, and for this reason its retention is more or less assured, but I am particularly struck by the fact that the vertical, forced-air furnace has been installed in recent years at large and important centres, among them the Isoire works of the Société Centrale des Alliages Légers. The British Aluminium Company has had experience of both types of furnace and gained a good idea of their limitations. The salt bath has fairly high operating costs, but the forced-air-circulation furnace is by no means a cheap unit. Whilst it would be of interest to learn the experience of other users in this matter, I hold that this is another important instance of different types of plant being used for the same purpose, and that it is the furnace builders who, with their wide knowledge of diverse conditions, should be able to say which is the more economic type of equipment to select.

Sufficient has been said to suggest that, in view of the large capital costs involved in the installation of modern furnaces, what is required is a comparative study of the various types designed to do precisely the same job. This would be of great service to the industry as a whole. If I may throw out a hint to our President, perhaps the Institute of Metals might be prepared to sponsor the formation of a panel composed of furnace builders and users to look into the matter further.

Turning to the question of costs, a recent survey of one of our mills showed that, of the total electricity used for all purposes, thermal treatment of the metal (excluding melting) was responsible for about 60%. For purposes of comparison, the gas-fired units were converted to an all-electric basis. The capital cost of the furnaces amounted to 15% of the total cost of all the plant and equipment installed, and they occupied approximately 25% of the total factory floor area, again excluding melting. We all know what these figures mean in terms of capital outlay and operating costs, and can appreciate the necessity of reducing them to the minimum.

The advent of large unit weights and special metallurgical requirements has created a demand for much-improved handling equipment, which now represents an imposing proportion of the total cost of the complete furnace installation. For instance, the handling gear for a slab pre-heating furnace represented about 30% of the total cost, and in an estimate for a continuous flash-annealing furnace for strip, handling equipment accounted for some 70%. It is unfortunate that these expensive handling devices are not always accompanied by a reduction in operating costs. Even where such economies have been effected, they are not so good as they might be owing to a relatively low pay-load ratio, that is, the ratio of the weight of the metal to be heated to the total weight of the charge. In a slab pre-heating furnace, although this ratio has progressively improved, with the modern pusher-type of furnace the iron carriers or trays still represent about 12½% of the furnace charge. Apart from the heat wasted, the disposal of the trays involves special gear and extra costs, and represents a quite unwelcome additional operation.

Fortunately, the heating space utilizable in these furnaces can be high; otherwise the pay-load ratio would suffer still more.

To mention one more example, in the annealing of coiled strip on spools, each spool requires a separate carrier, and this not only reduces the pay-load ratio but also the space-utilization factor. In a batch-type box furnace we found that whereas an output of, say, 2 tons/hr. could be achieved with plain coils, when spools and their carriers were used the output was reduced to about half. The spools and carriers formed over 20% of the weight of the charge, and the space utilization was only 65% of that with the plain coils. It seems obvious that many of the present popular forms of heating are thermally very unsatisfactory. Heating the furnace structure and the various carriers and conveyors employed at many stages from the initial slab to the final product, is a grossly inefficient practice. All the available heat should be directed into the metal itself and furnace builders and users should not be satisfied until this is achieved.

Dr. C. J. SMITHELLS, M.C., F.I.M. (President): Whether a small panel such as Mr. Fowler has suggested can be formed is, I am sure, a matter which the Council will be glad to consider. The British Non-Ferrous Metals Research Association are contemplating the setting-up of a rather similar panel representing the steelmakers and the users, following the discussion held in Birmingham last January on "Tool and Die Materials for the Extrusion of Non-Ferrous Metals and Alloys".

Mr. C. P. PATON,\* B.Eng. (Member): Mr. Fowler has raised some interesting questions with regard to the relative merits of the vertical and horizontal types of extrusion heat-treating furnace. Unfortunately, I have no figures available giving relative capital costs, but since the vertical arrangement requires a deep quenching pit and a high building, it will probably prove more expensive. However, the higher mill recoveries due to lower rejections for dents and distortion, should more than offset the higher depreciation charges of the vertical furnace.

Although loading a vertical furnace is somewhat more difficult, I doubt whether this will be reflected in the costs. In either case, the load is made up horizontally. With the vertical arrangement, each piece must be wired or otherwise attached at one end to a supporting rack; while with horizontal furnaces, the entire load must be wired down to the quenching rack to minimize distortion.

With regard to air circulation, I think that this matter can be handled as easily in vertical furnaces as in horizontal ones, and I am not aware that we have encountered any great difficulty.

I should say that the great advantages of the vertical arrangement are:

- (i) There is less distortion due to quenching. If an irregular section is quenched horizontally, it tends to bow sharply and to suffer damage where it is restrained by the wires holding the load together.
- (ii) Handling large sections vertically results in considerably less danger of their abrading each other when in a near-liquid condition, particularly during quenching.
- (iii) The vertical arrangement permits a much more uniform circulation of air around the sections and a more uniform and rapid quench.

For these reasons, vertical furnaces are particularly desirable for the heat-treatment of tubing. Perhaps the best proof of their overall merits is the fact that while we and our associates in North America have used both vertical and horizontal furnaces for sheet and extrusions in the various works, I believe that when production is at less than full capacity, the horizontal furnaces are usually the ones shut down.

It has been stated by one of the authors of the paper on electric furnaces, that the problem of abrasion of sheet and circles by the supporting wires in continuous annealing

\* Northern Aluminium Co., Ltd., London.



furnaces, has now been overcome. This is a development of which we are unaware, and we should be interested in further details on how this problem has been solved.

I should like to ask M. Lamourdedieu some questions about his new continuous induction heat-treating furnace at Issoire. I believe everyone in the non-ferrous metals industry is following this brave experiment with great interest. We have always feared that difficulties with breakage would be encountered in heat-treating the thinner gauges of sheet, which must be very close to its melting point and yet must, it is presumed, be subjected to considerable tension. Has there not also been difficulty due to adhesion of this semi-molten aluminium to the rolls over which it must pass during the heating and holding period? Does it appear likely that by heat-treating and quenching under tension, strip will emerge sufficiently flat for subsequent stretching and levelling operations to be reduced or eliminated?

M. Lamourdedieu states that at present he is obtaining speeds of about 20 ft./min. Does he feel that at this speed the continuous machine will be able to compete in economy with the more conventional types of batch heat-treating furnace. Recently our company prepared some theoretical figures upon the cost of annealing strip continuously, and concluded that to be comparable in cost with conventional furnaces the continuous machine would have to operate at closer to 100 ft./min.

Professor Dr.-Ing. A. VON ZEERLEDER\* (Honorary Corresponding Member to the Council for Switzerland): On the question of the relative advantages of continuous and batch-type furnaces for the solution-treatment of alloy sections and sheets, whether vertical or horizontal, there is another point which is important from the production aspect, and that is that Duralumin-type alloys need to be stretched very quickly after quenching, before age-hardening starts. With batches that is a disadvantage, because a large number of sheets or sections have to be dealt with at the same time, and a corresponding number of stretching or flattening machines are needed. With continuous heat-treatment, there is a regular flow of the products coming out of the furnace and going through the stretching installation.

I should like to direct attention to what I think is a not very well-known system of temperature measurement, using not thermo-electric couples but resistance thermo-elements. This has the great advantage of eliminating control of the cold end of the thermocouple, as the resistance element has no cold end, but records temperature only by the difference in the resistance of a very small coil of platinum wire of 100 ohms which is placed in the furnace.

Mr. A. H. HOLDEN,† B.Sc., A.I.M. (Member): As a furnace builder I am greatly interested in the opinions of users in these papers. Furnace building is still very much of an art. Mr. Waight gives us a great deal of mathematics, which we try to apply to the best of our ability, but I am afraid that anyone who attempts to build a furnace on mathematical grounds alone will be in serious trouble. This is particularly the case as regards convection heating, as will be known to those who have asked various builders for a quotation for a furnace employing heating of this type. Of four furnace builders, one will arrange the recirculation from side to side, another from top to bottom, another from bottom to top, and the fourth from end to end; and it is left to the engineer who is going to install the furnace to decide which of these methods is the right one. I wish we knew!

In the opening paragraph of the paper by Evans, *et al.*, it is implied that a gas- or fuel-fired furnace must cost less than an electric furnace. That is not the case. It handicaps us to some extent if it is assumed in the first place that we have to produce a cheaper furnace than the electric-furnace makers, to do the same work. We use radiant tubes, possibly, where

they use heating elements. If a controlled atmosphere is employed, there is very little difference. The handling gear, as has already been stated, accounts for a large proportion of the cost, and must be supplied. I cannot see any basis, therefore, for the assumption that a gas- or fuel-fired furnace should cost less than a comparable electric one.

Regarding the effects of sulphur in annealing, a point which is constantly being raised, we installed in 1934 a furnace for treating silver, without any arrangements for sulphur removal, and with no special atmosphere other than that derived from the heating burners, and this has been producing bright work steadily and consistently. A similar furnace was later installed in the same works and has been doing bright work on gilding metal and copper, as a finish anneal without any treatment and with no special atmosphere other than that from the burners. This effects considerable economy. The main difficulty, I suggest, is not sulphur in particular but variations in gravity of the gas, and this will apply even with a controlled atmosphere from a separate unit. It is not easy to hold the atmosphere within the required limits when the gravity of the town gas varies quite considerably from day to day or even hour to hour. A change from carburetted water gas to town gas produces an alteration in the relative density of the gas, which will upset any proportioning device. This point is of increasing importance at the present time, with the increased use of atmosphere control.

The employment of the electric furnace with radiant heating for clean rolled work with a high reflecting surface, involves a considerably longer time in the furnace heating chamber than is necessary with a fuel-fired furnace, which has a fair amount of direct convection other than forced convection by fans. This shorter time in the furnace helps to produce work which is to all intents and purposes bright, even with up to 30 grains/100 ft.<sup>3</sup> of sulphur present, but the carbon monoxide in the furnace atmosphere must be kept below 1.6%. The removal of sulphur does seriously increase the capital cost on a comparatively small installation.

For some time we have been building furnaces with direct-fired convection heating from heaters external to the furnace and recirculating. Although the heat-transfer rate is considerably higher and the temperature uniformity better, the application of the method is not quite straightforward. Hot-gas radiation can produce differences in temperature on thin sections, as can unequal distribution of the hot gases. A convection-heated furnace may be as economical on fuel as a direct-fired type, but generally speaking I do not think that convection heating makes for economy of operation. Recirculation demands heavy-H.P. fans, which are a considerable expense to install and run. Convection heating is not particularly new, but even so, many improvements can still be effected. No furnace builder cares to build two furnaces alike, because he usually finds that some improvements on the first can be incorporated in the second.

Speaking unofficially for the furnace builders, we would welcome, I think, any panel on which builders and users could get together, as we have done to-day, for free and frank discussion.

M. MARCEL LAMOURDEDIEU‡ (Member): I should like first to answer some of the questions put by Mr. Fowler on heat-treatment. I agree with Mr. Paton that the vertical type of batch furnace is certainly better, or at any rate easier to use in some cases, than the horizontal batch type, and certainly produces less distortion. At Issoire, however, we have a horizontal continuous furnace, and that, in my opinion, is far better than either type of batch furnace. The handling of extrusions is very easy, because they emerge directly from the press on to a roller table and so into the furnace, and out of the furnace into the quenching equipment. They come out very straight, and light stretching only is needed on the big sections. On small sections we have not yet had much

\* Director, Research Laboratories, S.A. pour l'Industrie de l'Aluminium Chippis, Neuhausen-am-Rheinfall, Switzerland.

Y Y

† British Furnaces, Ltd., Chesterfield.

‡ Director, Société Centrale des Alliages Légers, Paris.



experience. Small sections, about  $3 \times 3$  in. and  $\frac{1}{4}$  in. thick, have been extruded and showed more distortion than the larger sections, but they were very easy to stretch, and not much work was needed to get a perfectly straight extrusion.

Mr. Fowler also asked about flash annealing by induction heating. When we started to use the continuous heat-treatment furnace, the first operation undertaken was annealing, which is very easy with this type of furnace. No holding zone is required, but at the moment I cannot say whether it is more economical to use an induction furnace rather than one of the convection type. The induction furnace is certainly more expensive to install, and I do not think that it is necessary to use this type of equipment for flash annealing, although the results are most satisfactory. We were anxious to proceed to heat-treatment and did not make enough flash-annealing tests to establish the costs and consumption of electric power, &c. We did get a very good surface.

With regard to the continuous heat-treatment of aluminium alloys, Mr. Paton enquired about the problem of annealing thin strip. The thinnest strip run on this furnace was 0.5 mm. (about 0.02 in.), and this came out very well. A difficulty encountered from the beginning, and one still unsolved, is how to measure the temperature in the induction coil, but from the tests made it has been found that strip at  $500^{\circ}\text{C}$ . can support a tension of about 100 g./mm.<sup>2</sup>. That is not much, but a certain amount of tension can be applied to thin strip. The strip comes out of the furnace very flat. There is a roller leveller at the end of the furnace, as can be seen in Fig. 1 (p. 336), and a coiler with some tension between it and the roller leveller. The strip does not need any further flattening or stretching.

The other question is that of marking, which is certainly a major problem. No marking is encountered at the start, when there is a very good surface on the roll, but after some tests have been made, particularly if some of the strip has been burnt in the furnace, as occurred in our experiments, the rolls have to be cleaned again. I have not yet decided what is the material to use for these rolls. In earlier tests on a furnace for continuous heat-treatment the main difficulty lay in the rolls and the handling of the strip through the furnace. We did not succeed in using a convection furnace to heat the coil for heat-treatment, because there was too long a portion of strip in the furnace to obtain the right temperature and synchronization was not easy. It has meant considerable progress to be able to get the correct heat-treatment temperature very quickly, and to have only a short section of strip in the furnace during the holding period of 2–3 min.

Dr. SMITHELLS: With induction heating, is the temperature very sensitive to variation in thickness, much more so than it would be with the normal form of radiation heating or hot-air heating? I refer to variations in thickness of the strip, particularly when dealing with thin strip, because the temperature is a function of the induction and of the thickness of the material.

M. LAMOURDEDIEU: We can use fewer ampères to heat the thin sheet, or we can use the same current and heat it more quickly.

Dr. SMITHELLS: But if the sheet varies at all in thickness from its nominal gauge, does that mean that the temperature is not going to be what you expected?

M. LAMOURDEDIEU: Yes, certainly, but the variation in thickness is quite small in the continuous rolling of strip. That is why we have to try to keep the temperature in the induction coil at a minimum, so that if there is some variation the strip is not burnt. That, however, does not require continuous control by an operator.

Mr. CHRISTOPHER SMITH,\* F.I.M. (Member): I should like to raise two points regarding the present design of furnaces.

The space that continuous-annealing furnaces occupy is quite disproportionate to the amount of work done. I wonder whether the provision of tiers in furnaces would effect an economy in space, and whether it would be possible instead of progressing the work longitudinally through a continuous furnace to progress it laterally, in order to save shop space.

Those who use furnaces heated by air convection are appalled by the inefficiency of the heat transfer. Mr. Paton referred to this and asked for faster air speeds inside such furnaces. I should like to have some opinions from the furnace manufacturers with regard to the centrifugal-type fan and what is called the end-type fan, which I have always felt should be more economical.

Some years ago it was suggested that sheets should be heated by conduction. By pressing the sheets together and heating from the edges only, a very high rate of conduction would be obtained and the effect of the air pockets between the various kinds of sheets would be completely nullified. Have furnace builders given any thought to this type of furnace, or is it impracticable?

Mr. J. C. HARRIS:† In answer to Mr. Christopher Smith's question, edge-heating of coils or stacks of sheets has been seriously considered by furnace designers. A longer time is required to obtain approximately equal temperature at the centre and surface or edge when edge-heating, than when surface-heating across the air gaps, if the coil or stack of sheets is of considerable width, say 3 ft. or greater, and the total thickness is comparatively small, say 9 in. or under. Heating times are drastically reduced on the rare occasion that operating conditions permit spacing the sheets apart from one another, so that heated air passes between them.

With regard to Mr. Holden's reference to the power taken by fans in the convection-heated furnace, it is important to remember that that power is not lost, since almost the whole of the thermal energy of the fan goes into the heated air stream; even with a fan of very low efficiency the heat is not dissipated, but reduces that which has to be supplied by the main source of heat for the air, e.g. the radiant tubes, heating elements, &c.

Mr. Christopher Smith referred to the centrifugal fan versus the "end" fan. The centrifugal fan is used as an "end" fan as well as the axial-flow fan, and it is a question of the design of the furnace as to which is preferable. In a furnace with very high inherent resistance a centrifugal fan will often prove superior, since higher pressures can be developed at lower speeds.

Mr. Waight, in Fig. 10 (p. 275) of his paper, illustrates a recuperative type of radiant tube using premixed gas and air. Present-day practice is to limit premixing to those furnaces where it is desired closely to control the air: gas ratio, so that the products of combustion can be collected from the tubes, cooled, and returned to the furnace as protective atmosphere. An interesting example of a furnace employing this principle is one similar to that illustrated in Fig. 13 (Plate XLV) of the paper on electric furnaces, in which the atmosphere is derived from radiant tubes in the first zone of the furnace, since this zone has the most stable demand, and therefore the quantity of atmosphere will not vary appreciably with the demand of the furnace. In other cases, where it is not required to use the atmosphere from the radiant tubes—and these constitute the majority—nozzle mix is now employed, thus avoiding the necessity to make provision against lighting-back. Similar means of introducing secondary air for uniform temperature distribution and of obtaining recuperation are incorporated in both the premix and the nozzle-mix types of radiant tubes.

Mr. Paton, on p. 315 of his paper, refers to periodic reversal of the direction of air flow as being advantageous in promoting temperature uniformity. I think that this needs qualification. In general, the highest practicable air velocity over the charge should be the aim. In order to achieve this velocity, it may be necessary to use centrifugal-type fans to overcome un-

\* Works Superintendent, James Booth and Co., Ltd., Birmingham.

† Birlec, Ltd., Birmingham.



avoidable high circuit resistances. With this type of fan, flow reversal necessitates not reversal of fan rotation but redirection of the air stream after it leaves the fan, and this involves the use of ducts and change-over dampers which may increase the air resistance, so that the air velocity is greatly reduced. The net effect is that, while eliminating temperature differences at the extreme ends of the charge, a greater drop from end to centre may result.

On p. 320, Mr. Paton briefly describes an end-flow type of furnace in which air is drawn from the work chamber into the fan and then blown over the heating elements, re-entering the work chamber at the door end. This has the disadvantage that any contact of the recirculated air with a cold door lowers the air temperature before it enters the work chamber, and since the pressure of the air stream is highest outside the work chamber, any leakage causes short-circuiting of the air stream by air which has not passed the temperature-control point. A better arrangement is one in which the work chamber forms an inner tunnel, through which the air is blown directly as it leaves the fan. If the temperature-control point is situated at the fan outlet, no uncontrolled air enters the work chamber, and should any leakage occur in the walls of the tunnel, only outward leakage of controlled air results. Another important point is that, since the work chamber is surrounded by the returning air stream, heat-conduction losses from the external walls can be prevented from affecting its temperature.

With a correct size of fan and cross-section of work chamber, even with a high velocity over the charge maintaining high surface conductance, the rapid rate of circulation ensures a low temperature drop in the air stream from one end to the other and the limiting factor is then often the temperature, not from end to end of a long charge, but from outside to centre of its cross-section.

On p. 319, Mr. Paton says that it would be useful if times of treatment in salt baths could be still further reduced by more rapid transfer of heat. Is it suggested that, when heating sheets vertically suspended in the bath, the transfer of heat from the salt to the charge lowers the salt temperature, and that it takes too long to displace the cooled salt between the sheets by hotter salt from the main body of the bath, or that the rate of heat input from elements in the body of the salt is too slow? In the latter case, all that seems necessary is to provide more heating units, but in the former, some type of forced convection in the salt seems desirable, and the problem is not easily solved if uniform circulation over a large salt bath is to be achieved.

Mr. Paton suggests (p. 321) that furnaces should be designed to accommodate the racks or trays which can be used for conveying the material through the mill. This is a point on which furnace designers and users should collaborate, but it is doubtful whether it is practicable, since the trays necessary to convey material through the mill are rather heavy, while those for the furnaces need to be (a) light in weight to keep down the thermal capacity, thus saving power and minimizing heating-up time, and (b) designed to offer the minimum resistance to air circulation.

MR. A. J. FIELD,\* M.C., B.Sc., F.I.M. (Member): Although the tonnage of coal used annually for heating in the non-ferrous metal trade is only perhaps 1 million out of a total of about 220 millions, any saving possible must be made, particularly in future, and I suggest that we should evaluate our equipment on the basis of the coal-equivalent (per ton of material) for all the different types of furnace.

In connection with the annealing of non-ferrous metals, the practice in the steel trade may be studied with advantage. Steel-makers have arrived at a standardized form of annealing in bell-type furnaces, nearly always heated by gas; radiant tubes are customarily used, but direct heating has promise. Inside the outer bell, each stack of coils is housed in a canister which has inside it an inert atmosphere, the circulation of which helps to distribute the temperature.

In the annealing of aluminium, much use is made of box-type annealing furnaces, and these have many virtues. The efforts of the pioneers in the conveyor- and band-type furnace will be watched with interest, but in the meantime the box furnace, for the most part electrically heated and working on the batch system, remains the standard type.

Mr. Paton expresses a desire to force the annealing furnaces, but this must be a matter of compromise, because, if forced excessively, detriment to the material and undesirable variations in its properties will result. The first cost and efficiency of box-type furnaces can be somewhat improved by building them in batteries, as has already been done. With this arrangement it is important to ensure that the chambers are fairly well insulated from one another, so that each one can work independently as a unit. Another point is door loss, as stated by Mr. Paton. He also brought out the importance of heat conservation and suggested that the hot coils be taken into other chambers and blown, so that the heat from them is transferred to another set of coils which are initially cold. That is attractive, but it would seem that the maximum heat that could be recovered would be half the sensible heat in the coils, using two chambers.

As regards the unprofitable weight to be heated when steel trays are used for carrying the charge, mention should be made of the advantages of the roller-arm type of charging machine invented by van Marle,† by means of which it is possible to charge a load into a box furnace without any steel whatever.

In the case of heat-treatment, another standard item of equipment is the salt bath, the high uniformity of temperature of which is impressive. Our aircraft specifications call for a difference of  $\pm 5^\circ\text{C}$ .—a range of  $10^\circ\text{C}$ .—but even the biggest modern salt bath can do very much better than that. The rapidity of heating of the charge is also very high, and this gives good results in the heat-treatment of strong alloy sheets.

I was interested in Mr. Paton's reference on p. 315 to the heating medium in salt baths, where he advises that an addition of potassium nitrate to the sodium nitrate will give less drag-out loss. My own impression is that the fluidity of the molten sodium nitrate when used alone is very high. It would be interesting if he could give a figure of how much drag-out would be saved, and whether the cost would come out on the right side, as the nitrate of potash is more expensive.

With regard to the paper by Mr. Staples, the type of flash annealing described is likely to be commercially necessary only for one of the aluminium alloys, namely the aluminium-14% manganese alloy. I do not think it would be quite so satisfactory for the "letting-down" process, as he terms it, or the "partial-anneal" process, as Mr. Paton calls it, since with short times and more elevated temperatures there is danger of overrunning and of the material becoming too soft, in which case it would be entirely wasted.

I was most interested in Mr. Paton's statement (p. 312) that in sheet aluminium treated by this partial-annealing process the directional properties are more uniform than in that produced by an ordinary furnace anneal. My experience has been rather the reverse. Could he advise us of the nature of the preceding process which would bring about this desired result?

We all wish M. Lamourdedieu success in his pioneer venture with his interesting furnace. At a rough estimate, there is about 30 ft. of strip in the heating and soaking chambers combined, and at the speeds named the heating time is about  $1\frac{1}{2}$ –2 min. That is a rather shorter time than we find satisfactory for the salt-bath heat-treatment of strong aluminium alloys.

Finally, I would make an appeal that we should be orthodox in our terminology. I suggest that we adopt the terminology of the Institute for the generic title and call it "thermal treatment", and do not include annealing as a branch of heat-treatment, also that we should refer to "solution heat-treatment" and "precipitation heat-treatment". Furthermore, for the assistance of our members overseas, and others

\* Works Manager, The British Aluminium Co., Ltd., Falkirk.

† British Patents Nos. 116,949 and 169,042.



interested, we should be specific in our designations of material compositions.

Mr. W. N. ISMAY \*: After reading these papers I formed the impression, rightly or wrongly, that there is a distinct preference in the non-ferrous industry for electrically heated furnaces. I would like to question whether we are justified in installing as many electric furnaces as we do. They are certainly easier to operate, and in general require less maintenance, but, although we have progressed a long way from the time when coal and coke were used, coal is still our primary fuel.

Gas-fired furnaces possess several major advantages, which in many cases cannot be offset by easier operation or maintenance. In the first place, efficient gas-fired furnaces use less coal, and that is important not only in the national interest but from the standpoint of manufacturing costs. Secondly, more and more applications nowadays require controlled atmospheres. With electrically heated furnaces, the cost of providing those atmospheres is a significant item in terms both of heat energy wasted and of money. As Mr. Waight points out, means are now available to control the products of combustion of direct gas-fired furnaces so that a protective atmosphere can be obtained without additional expense.

Last year, I inspected most of the furnaces at one of the largest copper and brass manufacturing plants in America. Apart from melting furnaces, over 90% of the annealing and re-heating furnaces were gas-fired. The cost of power and fuel in New England is about the same as it is in England at the present rate of exchange, but relative to wages, is only about one-third of the price paid here. One might therefore assume that American manufacturers need be less concerned with effecting economies than we are. However, the price differential in America between electricity and gas is significant, and is of the same order, about 3 : 1, as in this country.

After making these visits, I wondered whether our preference for electric furnaces was due to our attitude of mind towards them or to the design of gas-fired furnaces. To my mind, it is a little of both. British gas-furnace designers have been slow to exploit the advantages of heating by forced convection and the application of automatic controls. Past experience in many cases has proved the electric furnace to be superior from the standpoint both of quality of product and process costs. A comparison of modern designs of gas and electric furnaces, however, shows that very careful consideration of all sides of the problem is necessary and justified.

Coming now to specific points raised by Mr. Waight, I hope that the gas industry may soon be able to do more than meet its statutory obligation to provide a fuel of constant calorific value, and will provide fuels of more constant composition and lower sulphur content. In some areas, variations in composition upset flow-ratio control devices and thereby affect the composition of the furnace atmosphere. The classification of burner systems given in the paper shows the limited range of turn-down possible with gas-fired furnaces. This emphasizes the need for users to specify their exact requirements for output, and for designers not to be too liberal with the gas supply to furnaces. If margins of safety are allowed by all concerned with the furnace from conception to installation, the result may well be a most inefficient piece of equipment. In cases where very varied duty or intermittent operation is demanded, the case for electrically heated furnaces is often stronger.

Of the burners and combustion systems described, that which offers closest control of atmosphere for clean and bright annealing is the total pre-mix system. Other systems should be satisfactory for constant output, but they often have too limited a range of turn-down for widely fluctuating throughputs. The explosion hazard with total pre-mix systems must be regarded seriously, but with a reasonable standard of operation and maintenance, the danger is less than that associated with many other industrial hazards. With a properly designed

system, and with reasonable standards of maintenance and operation, users need not have much fear. Of the furnaces that I inspected in America, the majority employed such systems of combustion, and most users were of the opinion that the close control possible more than outweighed the occasional hold-up due to ruptured explosion discs.

A feature which impressed me in America was the use of controlled atmospheres when annealing brass. Much work has been done in this country to develop a means of bright annealing brass, but no satisfactory method has yet been evolved. Most United States firms consider it worth while to have a controlled atmosphere derived from town gas, natural gas, or propane, because it facilitates the subsequent pickling operations.

Mr. Waight mentions the use of gas/air mixing machines. Although these are convenient and efficient, particularly where a large range of turn-down is required, they represent a potential danger which can, however, be reduced if separate air and gas blowers are employed in conjunction with a mixing chamber of light construction. An explosion in an air/gas mixing compressor will be more dangerous and involve more costly repairs than one in a thin-sheet mixing chamber.

The control of gas : air flow ratio by instruments depending on orifice-plate measurements is accurate only for a limited range of turn-down—about 7 : 1, I believe—and therefore does not make it possible to take advantage of the range of turn-down of total pre-mix burners, which Mr. Waight quotes as 12 : 1. It is therefore necessary with well-insulated furnaces to ensure that the maximum gas flow is limited to that required to give the maximum output from the furnace.

Mr. Waight mentions the possibility of recovering waste heat from the flue gases. In my experience load recuperation is generally the most efficient method in the non-ferrous industry, but if carried too far, it may well result in condensation at the entry of a continuous furnace, with subsequent damage by corrosion to the structural steelwork.

In the batch furnace versus continuous furnace controversy I would stress that careful consideration should be given to each requirement. We tend to say that it is all very well for the Americans, but they have long runs of the same gauge of material and the same alloy, &c. My impression, however, was that the Americans handle just as many alloys and just as many small orders as we do, but the proportion of continuous or semi-continuous furnaces in American is significantly higher, with consequent improvement in quality in many cases and certainly greater economy in man-power.

Dr. I. JENKINS,† F.I.M. (Member of Council) : Only in the light-alloy field have real problems been put forward, and those seem to be more concerned with handling equipment than with furnace design. One of the difficulties, from the furnace manufacturers' point of view, is that of having clearly presented to them the requirements of the user. I think that perhaps, before a panel is established to consider these matters, liaison between individual furnace makers and the user industry needs considerable improvement.

A great deal has been said about economy of operation. I am not sure whether the user is being completely fair to the furnace manufacturer. Let me quote one point that I have in mind, with all deference to Mr. Paton. Mr. Paton says : "We want a furnace that is thermally efficient, much more efficient than anything we have had before." On the other hand, he says : "Why do electric-furnace manufacturers put their heating elements inside the heating chamber?" The electric-furnace manufacturer replies : "I do that to give you the best thermal efficiency and the best heat transfer." Difficulties of that kind need resolving, and can only be resolved if the furnace manufacturer and the user get together much more closely than in the past.

Mr. Holden mentioned a furnace that had been installed without desulphurization equipment and had worked very

\* Furnace Design Engineer, Imperial Chemical Industries, Ltd., Metals Division, Birmingham.

† Chief Metallurgist, Research Laboratories of The General Electric Co., Ltd., Wembley.



satisfactorily in the bright annealing of silver for the last twenty years. Do we know why? It is very important to establish not only the causes that lead to staining but also the reasons that prevent it. Information about why processes work is just as important for the development of thermal equipment and the solution of some of the problems presented to-day, as information about why they do not work.

Mr. J. F. WAIGHT,\* B.Sc.(Eng.), M.Inst.GasE.: We in the gas industry are interested in the design, construction, and use of gas-fired furnace equipment, particularly from the point of view of thermal efficiency, as we are anxious that our consumers should obtain the maximum amount of work for the minimum expenditure of fuel. To that end we investigate problems associated with furnace design, construction, and usage. I disagree with Mr. Holden, in that I am of the opinion that gas furnace design can be based on first principles, but I agree with him that the specific gravity of town gas does vary, within fairly narrow limits, and that this variation will upset the operation of any mixture-control device which depends upon pressure drop across a resistance, or the discharge of gas through an orifice.

I was interested in Mr. Holden's statement that in forced-convection furnaces it was likely that radiant heat transfer from the gases would cause temperature gradients to be produced in the charge. I think that this statement needs qualification to allow for those furnaces which operate with a small concentration of carbon dioxide and water vapour in the circulating furnace atmosphere, and for those in which air only is used as the convecting medium. When the concentration of water vapour and carbon dioxide is low, their heat-radiating power will be very small and will not be likely to cause undesirable temperature gradients.

Mr. Christopher Smith mentioned the possibility of reducing the size of furnace for a given output. Furnace size ultimately depends upon the rates of heat transfer that can be achieved in the working chamber. In the case of convection, the heat-transfer rate can be increased by raising the velocity of the gas in relation to the charge, or by increasing the temperature of the gas in relation to the charge. The first method is fairly easy, since it is only necessary to employ fans which will produce higher pressures and higher gas speeds and to arrange that the furnace is more effectively sealed. The latter method presents more difficulty. If the temperatures of the heat-transferring media are increased in relation to the final temperature of the charge, the control of the heating process must be achieved by limiting the period during which the charge is exposed in the furnace working chamber. If this is not done, over-heating or undesirable temperature gradients may be produced in the work.

Mr. Ismay mentioned the effect of variation in gas composition on furnace atmospheres. To some extent this variation is due to the variable coals which the Gas Industry is called upon to carbonize, but particularly to the use of water-gas plants for meeting peak loads.

In regard to Mr. Ismay's remarks concerning recuperation, load recuperation is very often preferable to air recuperation, since with the latter there is some difficulty in designing burners that will handle pre-heated air and at the same time deliver products of combustion with a composition sufficiently constant to meet the requirements of the non-ferrous metal industry.

Professor Dr.-Ing. A. VON ZEERLEDER: The question of how to cut down the amount of space needed for furnaces is a very important one, both in production and from the point of view of reducing costs. A possibility would be the use of the Paternoster type of vertical furnace, as developed twenty years ago for billet annealing. The weight of the billets eventually became too heavy, and introduced a mechanical difficulty in building these furnaces. A system comprising

an endless chain with platforms on it, going up one side and down the other, offers certain advantages in annealing sheets, for instance. The openings are at the base, so that heat loss is a minimum and the smallest possible amount of space is occupied for the maximum volume in the furnace. For soft annealing there is even a possibility of heat exchange, if the upper part only of the furnace is heated and in the lower part heat transfer takes place from the heated pieces to the pieces entering the furnace.

For solution-treatment in the muffle furnace, especially in America, it is standard practice for the sheets to be vertical. The furnace is closed at the top and there is an opening at the bottom, with the quenching tank immediately beneath it, so that the sheets are quenched instantaneously. In this way there is minimum heat loss, whereas when the furnace opens at the top there is a very substantial heat loss at the moment of opening.

I always wonder why in melting a ton of aluminium in the induction furnace the heat consumption is 450-500 kWh., while for annealing a ton of sheets at 500° C., or for solution-treating them at 500° C., between 600 and 2000 kWh. are required; i.e. much more heat is needed in the heat-treatment furnace than for melting. Of course, the volume of the furnace compared with the tonnage of metal is considerably greater, but much could be done structurally to improve the efficiency of heat-treatment furnaces.

How do the furnace builders determine the speed of air circulation? It must be borne in mind that at 500° C. the weight of the air is only a quarter of what it is at room temperature, and so the efficiency is also only a quarter. In the type of furnace to which I have referred, we found that the ventilation must be from top to bottom, and not exceed 5-7 m./sec., because with the direction reversed the sheets became damaged.

Mr. H. J. HARTLEY,† M.Sc., F.I.M. (Member): One thing we have learned when working with nickel silver may prove useful to other furnace users. We found it possible to use a considerable degree of superheat with tremendous advantage for continuous annealing of strip, and obtained a very uniform product. End welding demands a considerable degree of speed and accuracy on the part of the furnace operator. We were working at temperatures above the melting point of our product, and any carelessness resulted in torn strip and the need to re-thread the furnace.

In our experience, the variation in gravity of town gas is much more important with a fuel-fired furnace than with, say, an electric annealing furnace with separate atmosphere generators. In the latter case, one can work, and usually does work for most non-ferrous alloys, with something of the order of 5-10% of combustibles in the gas. Under these conditions the atmosphere gas never becomes so lean as to cause oxidation in the furnace, at least in the case of nickel alloys. On the other hand, a gas-fired furnace incorporating gravity-control methods will shift its characteristics quite substantially owing to gravity changes.

There are two questions that I should like to put to M. Lamourdedieu. One is to what extent supply voltage variations affect the temperature achieved in the induction heating of strip.

M. Lamourdedieu describes the annealing of very wide material. Is the process applicable to materials in the range from, say, 1 to 6 in. in width? It has, of course, the tremendous advantage from the bright-annealing point of view that, where no holding is required, the whole of the structure is cold, which means that the retention of a protective atmosphere is very simple and eases many maintenance problems.

Mr. E. A. BOLTON,‡ M.Sc., F.I.M. (Member of Council): If a panel of furnace manufacturers and users were set up, the whole problem should be considered. Heat-treatment is not com-

\* West Midlands Gas Board.

† Manager, Process Development Laboratories, Henry Wiggin and Co., Ltd., Birmingham.

‡ Factory Manager, Imperial Chemical Industries, Ltd., Metals Division, Birmingham.



pleted until the metal has regained atmospheric temperature; cooling is as important as heating. That need is partially met in heat transfer by contra-flow, but I am thinking not only of heat conservation but also of time conservation. Frequently, it takes longer to cool the metal than it does to heat it, with a delay in the whole process cycle.

Mr. P. F. HANCOCK,\* B.A., F.I.M. (Member): Direct gas-fired bright-annealing furnaces are referred to by several of the authors. In the paper by Davis and Temple, the suggestion is made on p. 295 that the requirements of combustion to provide a suitable atmosphere may be opposed to those necessary to reach and maintain the correct annealing temperature and to secure maximum thermal efficiency. As far as most non-ferrous materials are concerned, that conflict fortunately does not arise, because for, say, pure copper, pure nickel, cupro-nickels, and, I think, standard silver, the best atmosphere is one which is only very slightly on the reducing side of complete combustion—about 95–98% of complete combustion—and that is also the condition near to giving maximum thermal efficiency.

The way in which inefficiency may arise with such furnaces is rather different, and concerns not so much the quality of the combustion products as their quantity. Applied to a continuous furnace with open ends, say, for annealing straight lengths of tubing, the volume of products of combustion will generally be ample when the burners are at maximum; but on stand-by or light-load conditions, when the burners are on turn-down, there may be an insufficient volume of products to maintain the furnace fully purged.

There are various possible solutions of the problem. One is to seal the ends of the furnace as far as possible. This will generally be done, but will equally generally not prove adequate. It is then necessary either deliberately to render the furnace somewhat inefficient, so that the amount of gas required to be burned on turn-down is enough to supply the atmosphere requirements, or to install a separate atmosphere generator, perhaps embodying a gas holder, with an arrangement such that an extra supply of combustion products is fed to the furnace when the burners are on turn-down.

Another point in relation to these furnaces, which has been discussed by several speakers, is that of sulphur purification. Mr. Holden suggested that it was generally unnecessary, and instanced a furnace which had been operating for many years successfully without it. It is not possible to say whether or not sulphur purification is necessary without considering all the conditions of operation. In particular, of course, the time of contact is very important, but more important still is the hydrogen content of the atmosphere. If the degree of combustion can be controlled so that the hydrogen content remains very low (of the order of 1% or less), probably the amount of sulphur present in normal town gas will not prove deleterious; but it is extremely difficult to make sure of maintaining that condition of very nearly neutral atmosphere. Two factors are liable to upset it. First, the gas: air ratio may be set to give just the right conditions, and then, if a load of work is introduced with a considerable amount of lubricant adhering to it, considerably more reducing conditions arise and sulphur staining sets in at once. This trouble occurred with the first furnace which my Company installed, about 12 years ago, for bright annealing copper tubes. If the tubes were perfectly clean, there was no sulphur contamination, but with the normal amount of lubricant present things went wrong at once.

There is also the difficulty arising from the variations which, as Mr. Waight has pointed out, are inevitable under present conditions in the composition of the raw town gas. If the composition is liable to vary over a certain range, obviously the ratio has to be set to give slightly reducing conditions when the calorific value is at its lowest point; that means

that if the calorific value increases a little the atmosphere will automatically become slightly more reducing, and again sulphur troubles occur. Generally speaking, sulphur purification is desirable as an insurance against such variations.

Mr. G. W. WEEKS,† A.I.M. (Member): In the aircraft industry we are concerned with comparatively small quantities of material, and the accent is on quality and strength. As regards the vertical versus horizontal furnace, we employ vertical furnaces with two considerations in mind. One is that vertical furnaces give us a little more floor space. The second represents a confirmation of what Professor von Zeerleder said about quenching speeds. We employ a furnace somewhat similar to that to which he referred, of a depth from the base to the top of about 6 ft. This is about 10 ft. above floor level, and there is a pit beneath, also of about 10 ft. The interval between the time of beginning to open the furnace and complete coverage of the cage is about 8 sec. We consider that is good, and it gives us the results we want on very thin sheet material, where quenching speed is critical.

The furnace is a gas-fired one, and the products of combustion pass through the furnace chamber. There is a tendency to blister with some types of alloys, mainly the unclad materials, and more particularly the higher-magnesium-bearing alloys. We have tried creosote and fluorides, which are mentioned in one of the papers, but we doubt how beneficial they are. What work we have done indicates that the water content in the furnace is quite important, and percentages ‡ up to 15 or 17 begin to give trouble. There is always some water present, as a consequence of the products of combustion. The blistering problem, however, is not very serious for us.

A particular point that I want to bring forward, in the hope that it is receiving consideration and that I may obtain some useful information, refers to a recent innovation, at least as far as this country is concerned. It is referred to as the hot bending of high-strength aluminium alloys. The word "hot" is a little misleading; the reference is to temperatures of 130°–140° C. Recent experiments, which we have confirmed in our own laboratories, have proved that materials such as D.T.D. 363 and 364 are much more readily adjusted at slightly elevated temperatures. It is all very well to bend test-pieces in a laboratory, where they can be warmed and there is only a foot or two to deal with, but when production lengths of 12 or 16 ft. are involved, the problem of warming them while carrying out the bending operation is a more difficult matter. The advantages to be gained, however, are so great that I cannot help feeling that someone may have progressed further than we have in the problem of heating individual pieces to carry out this bending operation.

Mr. J. O. HITCHCOCK,|| B.Sc., F.I.M. (Member): Heating metals is a costly business. For hot working, the cost of heating is at present repaid by the greater amount of work that can be done hot as compared with cold, and the cost of annealing by the greater degree of cold work that can subsequently be applied to the annealed material as compared with hard. Final heat-treatment to develop specific properties is a different matter, and does not lend itself so evidently to critical examination on a cost basis.

Furnace builders must, I think, appreciate that many modern metal-working developments are directed towards applying increasing amounts of hot work for each heating and increasing amounts of cold working between successive anneals, thus reducing the required furnace capacity. High capital expenditure on equipment to this end can in most cases be justified by saving in fuel costs. Typical examples of improved working methods are the use of the Sendzimir type of cold-rolling mill, the use of viscous lubricants in extrusion to permit very high extrusion ratios, the use of

\* Chief Metallurgist, Birlec, Ltd., Birmingham.

† Chief Metallurgist, Aircraft Division, The de Havilland Aircraft Co., Ltd., Hatfield, Herts.

‡ By volume as steam at 500° C.

|| Assistant Managing Director, Henry Wiggin and Co., Ltd., Birmingham.



improved cold-drawing lubricants, the use of tube-reducing machines, and so on.

Much of this development springs from the high costs and inconvenience of heat-treatment processes. What therefore are the possibilities of reducing these costs? This probably represents the first major direction in which improvements are required. In general, present-day furnaces are ingenious in design and capable of producing products which are excellent in every way from the metallurgical point of view, but they are not economical in fuel and labour. Admittedly, much of the wastage arises from the fact that the furnaces are frequently not operated at their rated capacity or for the actual purposes for which they were designed; nevertheless, there is scope for the reduction of heat losses due to dead weight of furnace-charge carriers, and to losses due to door and other openings.

Improved methods of handling charges, and better location of furnaces in relation to the equipment they serve, can also reduce costs. It is suggested, for instance, that more consideration should be given to making the heating units integral with the mechanical-working equipment, so that the metal manufacturer could, as one example, buy a hot-rolling mill with a heating unit feeding the hot metal right into the rolls, or, as another example, a wire-drawing machine with an annealing furnace incorporated. Progress on these lines is being made, but there is scope for more.

Correct use of furnaces, once installed, is the responsibility of the metal manufacturer. The cost of operating electric batch furnaces, where the charge and time of heating can easily vary, can be doubled by incorrect operation; belt furnaces, provided they are regularly fed, are less prone to misuse, so that while it might be expected that a lower annealing cost could be achieved on a batch furnace because there is no belt to heat up and no belt-replacement cost, actual figures on one installation where both furnaces are used for similar work, showed that over a period of some months lower costs were achieved by the belt furnace. A pull-through strip-annealing furnace showed even lower relative annealing costs. Highest annealing costs on similar work were shown by a pusher-tray type of furnace, owing partly to the fact that smaller coils were being charged than those for which the furnace was designed. No doubt other furnace users could quote similar instances.

Other directions in which furnace design and operation might be improved lie in the use of some of the new heat-resisting alloys now available. In the case of the pusher-tray furnace already mentioned, the trays are at present in heavy cast heat-resisting alloy. The trays have been redesigned in a modern creep-resisting alloy, and the weight has been cut to about 30%. There are, no doubt, other structural and moving parts where advantage can be taken of the high load-carrying capacity at high temperatures offered by these new alloys.

I am a little disappointed that the symposium does not include a paper on the salt-bath pickling process. Admittedly this is of interest to only a section of the non-ferrous industry, but a description of what is now possible might be of interest to other sections. Here, one visualizes combined pickling and heat-treatment operations.

Operating costs and production are fundamentals in our consideration of these papers, and the time is more than ripe for them to be brought right out.

Mr. D. F. CAMPBELL,\* M.A., A.R.S.M., F.I.M. (Member): I should like to say a few words about the stages in the development of electric furnaces. At first they were boxes heated by resistance elements and insulated most carefully because the heat was very expensive. The gas-furnace designers learned a great deal from the electric-furnace makers in this matter. Fundamentally, a great many of the furnaces built to-day are very much larger than they need be. The system of resistors

involves a certain number of square feet to dissipate a certain amount of energy, and a time is coming when we may have to consider entirely new principles of design and fall back on induction more and more. By induction it is possible to dissipate a much greater amount of heat in a very small space, and the paper by M. Lamourdedieu is especially interesting from the point of view of the space factor. The induction heater in the furnace he describes is only a fraction of the size of any other heater that would do the same work.

The question of time enters into some heat-treatment operations, but there are a great many operations in which time is not essential. The softening of aluminium and the heat-treatment of Duralumin are entirely different operations. M. Lamourdedieu's paper is concerned rather with Duralumin, but, for the simple heating of aluminium, induction heating gives great economy in both space and time.

The space factor is very important in all furnace design, because factories now cost up to £4/ft.<sup>2</sup>, and, if a 40-60-ft. furnace can be replaced by a very much shorter one, it is obviously more economic in capital expenditure, and the problems of insulation and controlled atmosphere become very much easier and less costly. The induction heating of billets, as compared with heating in pusher furnaces, is an interesting example. Where heat-treatment of steel and such materials is effected by heating them for 3-4 sec., that is done for the specific reason that surface heating only is required; but there is no difficulty in obtaining absolutely even heating through a billet by induction methods, if the time of heating is extended to, say, 8, 10, or 15 min. The advantage is that a furnace can be started up at 7 a.m. and at 7.15 the first of the metal can be out, thus avoiding the necessity of a large pusher furnace, which means bringing men in on the night shift, so that other men can start in the morning.

Electric-furnace makers are very anxious for more information from the operators about how far metal working is going to become a continuous process. We now have continuous casting. We have strip rolling at astonishing speeds; steel wire rod is to-day being rolled in this country at 5300 ft./min. So much for casting and rolling. In the field of heat-treatment, how far are furnace makers going to be asked to produce continuous as compared with batch processes?

Finally, in considering electric furnaces and comparing them with other furnaces, the amenities for the workman must be taken into consideration. Great advances have been made by the introduction of electric furnaces in melting shops, where fume and heat are now controlled, resulting in better amenities and health. Much remains to be done, however, to improve the working conditions in many forges, rolling mills, and pickling plants in non-ferrous works.

Dr. R. T. PARKER,† B.Sc., A.R.S.M., F.R.I.C., F.I.M. (Member): In both the design and the operation of furnaces the metallurgist's point of view should be remembered. It should be kept in mind particularly at this juncture, when the engineer in the works is saying: "We must do this and that operation faster; we must get higher rates of heat transfer"; and the furnace designer is saying: "We can meet your wishes in some degree".

For example, Mr. Campbell mentioned the use of induction heating for pre-heating billets, and I think that is one case where the metallurgist's opinion should be taken before the process is put into operation. In the past, because of the limitations of the methods available, billets have been heated relatively slowly. If we now proceed to a very much faster rate of heating, we may finish up with a structure that is not quite so amenable to extrusion or forging. The same principle possibly applies to some other methods of heating metals, and I should like to ask M. Lamourdedieu whether in his process of heat-treatment, the times for which are relatively short, he is satisfied that there is complete solution of the alloying constituents.

\* Chairman, Electric Furnace Co., Ltd., Weybridge, Surrey.

† Director of Research, Aluminium Laboratories Limited, Banbury.



In the suggested panel of works engineers and furnace makers there should be at least one metallurgist who could say what is required of furnaces from the metallurgical viewpoint.

Dr. E. G. STANFORD \* M.Sc.: Some years ago I experimented with a method for heating aluminium alloy strip, by induction methods, in a manner similar to that described by M. Lamourdedieu, and I came to the conclusion that it would not prove satisfactory on an industrial scale because the speed at which the strip could be heat-treated would be too slow.

In equipment of the type being used at Issoire, the efficiency of energy transfer from the work coils to the work is very low, and the use of edge-cooling channels, such as M. Lamourdedieu describes, serves to decrease this efficiency still further. The method suffers the disadvantage that the heating over the plane of the strip is not uniform, and, in particular, there is a concentration of heat along the edges. This disadvantage can be overcome by having magnetic poles which do not extend across the full width of the strip, and by suitable adjustment of the distance between the poles in a line parallel to the plane and direction of forward movement of the strip. Thus, the heat that is concentrated at the edges can be spread over the plane of the strip and something approaching uniformity of heating attained without further decrease in efficiency.

When making his choice of equipment for the induction heating of strip, I wonder why M. Lamourdedieu did not select a method in which the direction of electric current flow in the strip is parallel to its length. Such a method suffers the disadvantage that damage to the surface of the strip is likely to occur at the electric contacts that have to be made with it, but this difficulty can be overcome and uniform heating can be achieved at strip speeds considerably greater than those envisaged by M. Lamourdedieu.

Mr. W. A. BAKER: Why cannot a salt-bath medium be used for continuous heat-treatment of light-alloy strip? Drag-out losses would be rather a formidable disadvantage, but molten salt is a very suitable medium from the point of view of speed of heating, and if the strip were run through rollers lubricated in the salt the conditions would probably be conducive to elimination of marking.

Professor Dr.-Ing. A. VON ZEERLEDER: Ten years ago I heard of a salt bath being used for aluminium strip with the strip going in and running through the salt bath and then entering the quenching tank. In practice, this should work, and the patent has been published,† but I do not know whether it has been used anywhere.

Mr. C. P. PATON: I can foresee a number of practical difficulties in adapting a salt bath for the continuous heat-treatment of aluminium strip. Not only is the metal practically molten as it emerges, but it is without any protective coating of oil. In passing over a number of rollers before quenching, this strip would be particularly susceptible to breakage, distortion, and surface abrasion. It must be realized that a very slight increase in inspection rejections due to the above causes would quickly offset any other economic advantages of the process.

Mr. Harris observed that in my paper I had mentioned the need for speeding up the heat transfer in salt baths, and asked whether I had in mind a different form of salt or more rapid circulation. Actually, I had in mind the possibility of increasing the agitation within the bath to ensure more rapid transfer of heat.

Mr. Harris also questioned the suggestion that the trays used for annealing coils should be used, wherever possible, for transferring the material to the next operation or series

of operations. I believe this to be important. We have been discussing the importance of cutting fuel costs—say, a matter of a fraction of a penny per pound—but it must be remembered that if part of a coil is rejected for internal damage sustained during subsequent handling operations when the surfaces lack oil protection, this will more than offset the saving on fuel. Those who have read of the handling arrangements in the large aluminium strip-rolling mills built in North America in recent years, will no doubt have observed that material passes through the annealing furnaces on trays and is carried, without off-loading, by crane through successive cooling and storage operations to the point where the coils are charged into the next rolling mill. This is one of the major reasons for the high quality now being obtained from these works.

Mr. Field asked what reduction in drag-out losses in salt baths might be expected from using a mixture of potassium and sodium nitrate. I believe that the reduction is of the order of 15%, but I understand that the present difference in price between the two nitrates is such that there is little, if any, advantage to be obtained from using the compound salt. He also questioned the statement that better directional properties are obtained when aluminium has been partially, rather than fully, annealed. What I had in mind was that sheet that has been partially annealed for temper shows more uniform directional properties than sheet rolled to temper.

I should like to support Dr. Parker's view that there is some need for caution in the wholesale adoption of induction heating for extrusion or sheet ingots. There has not yet been a great deal of experience on the more complex alloys, and there is evidence to indicate that in some cases poor surface and lower extrusion speeds result from a very rapid preheat. This is not in any way a condemnation of induction heating, which unquestionably offers many advantages over a large range of alloys, but I think that one should be careful before applying it wholesale.

Mr. CHRISTOPHER SMITH: This discussion has centred very largely on aluminium alloys. Could someone on the copper-base alloy side express an opinion about rapid heating? Are those alloys open to the same possible objections as some of the aluminium alloys, even though the latter need homogenization to a greater extent than the copper alloys?

Mr. H. E. BENNETT,‡ F.I.M. (Member): From the metallurgical aspect both the rates of heating and of cooling of the charge are most important factors. For example, I recently had an experience with beryllium copper where the charge was put into a furnace together with a large amount of steelwork in the form of jigs holding the parts to be annealed, and the temperature was of necessity raised very slowly. This resulted in precipitation-hardening taking place at too low a temperature. We are investigating the effect of this, but we believe that it results in discontinuous precipitation, which later gives rise to undesirable brittleness in the alloy. At the other end of the scale, the speed at which the metal cools down can be equally important. In annealing standard silver, for instance, if it is cooled too slowly, one tends to get precipitation, which results in undesirable hardening. These two factors, therefore, must be borne in mind when considering the particular materials being heat-treated.

Another important point is the maintenance of an even temperature, particularly in the lower temperature ranges. I am thinking of a bell-type furnace, where a large spider is lowered into the bell and the thermocouple, for convenience of loading and to prevent damage, is located at the top part of the furnace. In a job which needed a control within at least 20° C., tests showed that this degree of evenness was not being obtained over the furnace. By inserting specially long thermocouples, it was found that the temperature variations throughout the mass were very considerable. There are

\* Aluminium Laboratories Limited, Banbury.

† Swiss Patent No. 285,591.

‡ Deputy Chief Metallurgist, Johnson, Matthey and Co., Ltd., Wembley.



difficulties to be overcome, but furnace makers should bear in mind the importance of evenness of temperature and of satisfactory methods of recording the temperatures reached.

Dr. R. H. BARFIELD : \* There have been a good many arguments for and against the rapid heating obtained with induction furnaces. Some reluctance is shown to apply it in British industry, but it has been widely introduced in America. Surely none of the points argued can really be settled until the method has been tried out, and there is great need for experiment in this direction.

There are one or two points to which I should like to refer in connection with the design of the strip heater described by M. Lamourdedieu. The strip passes between a gap in the poles of the magnets about 3 in. wide. We have looked into the problem of the design of these furnaces, and that gap seems to be very large. Could it not be made smaller? The gap represents money, because it is the distance between the poles that decides the cost of the power-factor-correcting condensers. I estimate that the cost could be as much as £2000/in. If the strip, in running through, could have a smaller clearance, a considerable saving in capital cost would be effected.

Has M. Lamourdedieu any figures to show how much of the heating is going into the cooling water and how much into the aluminium strip?

Mr. J. C. HOWARD, † B.Met. (Member) : I feel that induction heating of strip will have very wide applications in the future for such purposes as bright annealing.

Bright annealing and bright heat-treatment have come to stay, and we are familiar with the problem of maintaining a suitable and correct atmosphere, particularly where a muffle is operated at furnace temperature. One of the advantages of induction heating is that the muffle can be kept outside the inductors, thus making the problem simpler than for any muffle that has to operate at temperature. It can have airtight gaskets and spy holes with easily removable covers. It is possible to thread the strip through the inductors and through the cooling chamber. Heating-up can be very rapid indeed, but of course this must be applied only to such metal as will not suffer any detriment from a metallurgical point of view. With many of the other non-ferrous alloys there is not the same limitation to the speed of heating-up as there is with certain aluminium alloys and with some steels.

In order to take full advantage of this speed of heating, it must also be possible to cool sufficiently rapidly, so that the whole equipment will take the minimum of space. Ideas and schemes now being developed give promise that the rapid cooling, where permissible, can also proceed.

I contest the view that induction heating is not very efficient. If it is a question of very thin strip with a poor coupling, the efficiency is not as high as that of other methods of heating; but even then induction heating can still compare favourably, especially when it is borne in mind that one can stop and start as desired and that it is not necessary to have a furnace running at temperature for long hours at meal times, or during the night. One must take into consideration the power consumption over the whole of the time and not just the power consumption while there is actually work going through.

With regard to the various types of inductors, the most efficient for narrow strip and thin material is the transverse-flux type described by M. Lamourdedieu. There has been reference to a patent for an inductor that would cause the induced currents in the strip to flow in the plane of the strip itself. There are some points in favour of that idea, but contact difficulty might develop between the strip and the two rollers. There may be circulating currents through the roller and the machine. It would be necessary to ensure that there was no arcing at that point, for otherwise problems would arise similar to those that occur in using the strip itself as a resistor and passing the current directly through it.

When it comes to thicker materials, such as tubes, bars, billets and other quite wide sections, then the induced currents, which are always a mirror image of the actual currents in the inductors, do flow through the workpiece without any tendency to overheat locally, as may be the case with strip.

Mr. J. C. BAILEY, ‡ B.Sc., A.I.M. (Member) : I wish to refer to the problem of heating large aluminium-alloy rivets (over ½ in. dia.) for hot driving, a problem which is encountered in constructional shops and in shipyards making use of aluminium in rather heavier and thicker pieces than have been supplied in the past. The problem is not proving as easy of solution as might be expected.

Aluminium-5% magnesium alloys are used for rivets that are driven hot, and also for fairly substantial extruded sections which require to be hot formed, and the operation is probably best carried out at 400°–500° C. Through tradition, the riveters want to heat light-alloy rivets in the same way as steel rivets—on a coke brazier—and in fact they have tried to do so. The results have been disastrous.

The first quick answer to the problem—a temperature-indicating paint on the rivet—has been tried without success. The use of such paints is too refined a procedure, and is also unsatisfactory in that the paints do not respond quickly enough to the temperature changes. Similarly, attempts have been made to heat the rivets in sand trays placed on the coke brazier. Temperature control again is quite inadequate.

When hot-forming extruded sections, heating with an oxy-acetylene torch actually playing on the section in the particular areas it is desired to form, proves a slow and unsatisfactory process. A temperature-indicating paint, or a pine stick used as a temperature indicator, is rather misleading because of temperature variations in different parts of the section and the occurrence of skin heat.

Another method tried for heating sections was to insert an inner chamber in the ordinary type of oil-fired or gas-fired furnace used for heating steel sections, and to put the section inside that in order to damp down the temperature. Again, this does not effect sufficiently good temperature control. Attempting to operate at 400° or 500° C., a furnace which is designed to give much higher temperatures for the hot working of steel, is bound to prove an unsatisfactory procedure.

All these devices have been resorted to because there has not been a case—in the first instance at least—for incurring the expense of building a special furnace operating in the temperature range required, 400°–500° C.

Greater success has been obtained in heating rivets by adapting the normal electric-resistance-heating machine long used for steel rivets. Calibration as regards power input and heating period has first to be done, but this is not difficult. Using this machine, aluminium-magnesium rivets can be uniformly heated to the correct temperature, in a matter of seconds. Unfortunately these rivet-heating machines are not usually portable.

A rivet-heating furnace very often requires to be portable, and this sets a limitation on design. The principal requirements are that it must not be too heavy; there must be pyrometric control; the furnace must have sufficient capacity so as not to take too long to heat the rivets; and at the same time there must be no danger of overheating. These requirements are not satisfactorily met by any existing design.

As regards either the local or general heating of a fairly heavy extrusion, one method found satisfactory which avoids the high cost of a large furnace, is to build an extremely light furnace perhaps 20 ft. long × 8 or 9 in. wide × 4 in. deep, lined with very light insulation and having long heating elements. The section is put into the furnace and heated for a period which experiment has shown to be the correct period to attain the desired working temperature. It would be interesting to have the views of the furnace manufacturers on such a technique, which provides the uniform heating required for these large extrusions, without great expense.

\* Wild-Barfield Electric Furnaces, Ltd., Watford, Herts.

† Director, Electric Furnace Co., Ltd., Weybridge.

‡ Chief Metallurgist, The Aluminium Development Association, London.



Mr. CHRISTOPHER SMITH: Another problem in this field involves the bending at 300° or 400° C. of the newer types of aluminium alloys, which may be supplied to constructors in the fully heat-treated condition. The condition of bending these spars hot is that they should be heated very rapidly—in a matter of minutes—to the temperature necessary, and that the bending should be performed on the site where the heating is carried out, thereby causing a marked reduction in internal stress while scarcely affecting the mechanical properties of the material. It would be interesting if a furnace manufacturer could advise us about such problems and the possibilities of meeting them.

Dr. E. VOCE,\* M.Sc., F.I.M. (Member): With regard to the extrusion of copper alloys, billet heating by induction methods seems attractive, but would certainly be too rapid in some cases to ensure homogeneity of structure. One of the copper alloys most frequently extruded is 60 : 40 brass, which has an ( $\alpha + \beta$ ) structure; it is important that it should be brought more or less into a condition of equilibrium before extrusion. Certain alloys of copper, such as the cupronickels, are difficult to homogenize; the cored structure seems to persist for a long time, and I do not think that rapid heating would be very satisfactory in such cases.

On the question of induction heating, some time ago I saw a notice of a Swiss patent for a type of induction heater, intended for billets or slabs, which embodied a magnet rotating on a spindle. The magnetic field was rotated in place of the H.F. current generally used. I wonder whether the experts on furnace equipment could say anything about this.

The auxiliary equipment of furnaces is also important. The last paragraph of the paper by Davis and Temple states: "For the solution heat-treatment of temper-hardening alloys, batch furnaces are generally used, and some provision for rapidly withdrawing the charge from the furnace and lowering it into water is essential." Could any furnace maker give a little more information about the type of equipment normally installed for quenching these heat-treatable materials? I have no doubt that in the aluminium industry they are very widely used, since fairly rapid quenching methods are essential. Relatively few of the copper-base alloys require such rapidity of quenching, but some of them do, and I am not sure what kind of equipment to recommend for the purpose.

Professor Dr.-Ing. A. VON ZEERLEDER: The method of induction heating to which Dr. Voce referred was developed by Brown-Boveri, and the installation was tried in the Selve works. Two D.C. magnets rotate at either side of the billet and induce a current in it. No H.F. is employed, and it is only the D.C. magnetic field that induces heat in the billet. The installation did not prove satisfactory, because it was not possible to obtain uniform heat distribution. The billet became much hotter at the centre than at the corners, and as it was necessary for the two magnets to be as near together as possible—a distance of only 5 or 10 mm.—it was not possible to put any heat insulation between them. The thermal efficiency was not very good, and the installation was dismantled and is no longer in use.

Mr. F. KING,† A.I.M. (Member): A question was asked by Mr. Weeks about the heating of large extrusions for hot forming. Is there any need to use a complicated furnace for this purpose? Would not an oil bath with a high-flash-point oil be quite suitable and give good temperature uniformity?

A second matter to which I should like to refer is that of edge-heating a pack of sheets under pressure, as suggested by Mr. Smith. This is a condition which one gets when annealing a large coil with a build-up of 6 in. or more, wound under tension; the heating is essentially from the edges, and it will

be found that the uniformity of properties is quite good throughout such a coil. By attempting to anneal sheets under pressure, there is a serious risk of some form of pressure-welding between them, causing surface damage.

In his paper, Mr. Staples refers to the 1% manganese alloys and says that the choice is between prolonged homogenizing treatment and flash annealing, and that the latter is the cheaper method. Is that statement made on the basis of the cost of heating per ton, and has the author taken into account the greater risk of damage by flash annealing, with consequent reduction in overall recovery?

Mr. C. J. EVANS,‡ A.M.I.E.E. (Member): Mr. Baker, when speaking about electric furnaces, suggested that it might be possible on the tube-annealing furnace shown in Fig. 14, (p. 264) of our paper, to utilize 40% of the heat content of a hot charge by preheating a following one. This is a feasible proposition, but there are two important points which the furnace maker must consider:

(1) The dimensions of the cooling chamber would have to be increased by 40–50%.

(2) There must be a heat interchanger to transfer efficiently the heat from the hot to the cold charge, as well as the existing cooling unit used to cool the charge to below oxidizing temperature.

Thus, in addition to increased installation costs and floor-space requirements, there would be certain complications both in regard to general design and the maintenance of the controlled atmosphere in the chamber.

Another matter that Mr. Baker raised is the purging of air from the centre of tubes. On short tubes this is a comparatively easy matter, but many of those to be dealt with are up to 30 ft. long. It would be desirable to have fans blowing down the length of the tubes and taking the air straight out, but those familiar with forced circulation know from experience that that is a very difficult thing to do. In the furnace described in our paper, the long semi-continuous type, we get excellent purging of 3 or 4 tons of tubes in a matter of 2–3 hr. With regard to output, 1 or 2 tons/hr. of copper tubes is a reasonable one, even on a semi-continuous basis, if we are to ensure that an absolutely bright finish is obtained inside the tubes.

In the paper by Mr. Hartley and Mr. Bradbury reference is made to sulphur removal from the controlled atmosphere. The method they describe is not peculiar to nickel for bright annealing; it has been used quite widely and successfully for copper.

Mr. Fowler raised a very important point in regard to the cost of the ancillary gear on a furnace. I agree with the modern tendency to utilize continuous furnaces as much as possible; but first we should consider what forced circulation does. It gives more rapid heating, and so makes it possible to maintain the furnace temperature at a safe figure. But forced circulation alone at a low temperature cannot impart heat to an object faster than that object—copper, brass, &c.—can transfer the heat to the core. Therefore, the obvious step is to employ temperature gradients, possibly of 200° or 300° C., to get the maximum output. If the furnace is fairly large, there must be a considerable amount of coiling gear to maintain these big outputs of 2, 3, or 10 tons/hr. Assuming that a furnace costs £60,000 or £70,000, of which the coiling gear represents £30,000 or £40,000, who is going to risk installing such equipment unless it can be guaranteed to work?

The suggestion has been made that a panel should be formed to discuss this and other matters between furnace makers and furnace users. In my opinion, the furnace makers and users should consult with the rolling-mill or coiling-gear experts and work the problem out between them, to a certain extent on a financial basis. Then we should have continuous furnaces in this country treating copper, brass, and such other metals as aluminium, as successfully as in some other countries.

\* Senior Metallurgist, Copper Development Association, Radlett, Herts.

† Works Metallurgist, Northern Aluminium Co., Ltd., Rogerstone, Mon.

‡ The General Electric Co., Ltd., London.



On the question of end-heating and heating through the laps of a coil of metal, a great deal of practical experience leads us to believe that the resistance to heat conduction is about four times as great through the successive laps as it is directly through the material, although this figure will vary with the tightness of coiling and the metal being heated. This may give us some lead on the maximum width of material in relation to thickness of coil on which to work when trying to apply heat either through the sides of the material or down through the edge of the material.

Reference has been made to cooling. Naturally, cooling of a charge is a very important matter. The only solution that we can offer is an efficient fan system, because at the lower temperatures there is not a very steep gradient between ambient and material temperature, with a consequent limit to the speed of cooling. Fans are the best way known for cooling the charges and at the same time keeping the number of bases per furnace, and thereby the floor space, down to a minimum. The use of external fans blowing cold air over the cooling pots or hoods also has an appreciable effect on cooling times.

Mr. A. B. ASHTON,\* M.Sc., F.I.M. (Member): I should like to make a few remarks about the annealing of high-conductivity copper in the smaller sizes of wire used for cable making.

If, on a laboratory scale, the annealing curves of these wires are determined for a period of say  $\frac{1}{2}$  hr., it is found that the wires can be completely softened at a temperature of 150°–170° C. But on a factory scale, when heating not a 12-in. length of wire but a furnace charge of 1–2 tons, it is necessary to adopt a furnace temperature of the order of 250°–300° C., and a time of perhaps 2–3 hr. Thus, one is doing more than the copper actually needs to soften it. The reason for this lies in the fact that heat must be forced into the charge at such a rate that the whole of its mass will reach at least 150°–170° C. in a reasonably short time.

This is a point to which furnace designers should pay attention. That higher temperature and that longer time represent money; they may also lead to sticking owing to the welding together at local spots of adjacent turns of wire. Another important aspect is that the higher the temperature at which a charge is heated, the longer it takes to cool and the longer it occupies a furnace unproductively. The matter is becoming increasingly important because of the tendency towards larger and larger pieces, and bigger and heavier coils of wire and strip. Obviously, the greater the mass, the more exaggerated will be these tendencies.

These considerations lead to the point that it is desirable to increase the rate of heat transfer into the charge during heating and out of it during cooling. This should be regarded as a primary objective by furnace makers.

I should like now to refer to a method of heating which I think has not been mentioned at all, namely, heating by passing a current through the metal to be annealed by ordinary circuit methods using contacts (that is, as distinct from induction methods). In any furnace operation there is heated up, besides the metal in which one is interested, a very high proportion of structural material. Looking at a bell-type bright-annealing furnace being charged, and seeing the mass of the steel stands upon which the coils of wire are placed, the mass of the steel hood, the mass of the refractories and heater elements lowered over the hood, one thinks of the ratio between the metal it is desired to heat and the metal and refractories that one is forced to heat, and realizes what a proportion of the energy being put into that assembly is quite useless. The attraction of generating heat within the metal itself is that those increments of power consumption are completely eliminated. The heat is generated where one wants it and nowhere else.

I have seen strip in H.C. copper (which, of course, is the worst possible material to tackle from this point of view)

heated up to annealing temperature in a matter of seconds by the use of quite heavy currents fed into it by contacts; and also fine copper wires annealed continuously by running over contact pulleys with a potential across them at speeds of thousands of feet a minute.

My own view is that the furnace methods of annealing, at any rate in connection with some copper products, are on the slippery slope of obsolescence.

Mr. H. J. HARTLEY: In connection with the annealing of copper at 150°–170° C., the obvious method of getting up to that temperature is probably to use high-pressure steam in an autoclave.

Mr. Ashton also referred to the annealing of fine copper wire at very high speeds. There is one impression which I think I ought to correct. The only equipment that I have seen and which, so far as I know at the moment, is put on the market commercially for the resistance-annealing of copper wire gets over the fundamental difficulty of marking the wire at the hot contact at the expense of a very considerable loss of electrical energy. Instead of having the wire at its maximum temperature at the moment when it reaches the second contact, it first passes through 12 or 18 in. of water, used to bring the temperature down and keep the second contact cold. I believe this does significantly improve the condition that would otherwise occur at that contact.

In the laboratories of Henry Wiggin and Co., we have experimented with this type of resistance heating for materials that cannot be quenched in water and will not tolerate the presence of any moisture at all, if one is to achieve bright annealing. Attempts to overcome the difficulties have had to be abandoned, as we could not avoid serious pitting due to arcing at the second contact.

Dr. E. VOCE: So much has been said about the cost of cooling, the space required for cooling, and the general inconvenience of cooling that it might almost be more economical in some cases to introduce refrigeration. Has that ever occurred to any furnace manufacturer, and is it possible?

Turning to a different subject, there is a tendency now, I believe, to produce half-hard or quarter-hard materials (I am thinking mainly in terms of copper-base alloys) by partial annealing; that is to say, instead of taking fully annealed material and cold working it to a definite level, to take a relatively heavily cold-worked material and give it a light anneal. I should think this would need very accurate control, and I should be glad to have any information on the equipment and method to be used.

Mr. EDWIN DAVIS,† M.Sc., F.I.M. (Member): In reply to Dr. Voce, I should like to take the opportunity of emphasizing the impracticability of partially annealing a material to a hardness such as is represented by a point on the almost vertical portion of the annealing curve for any copper or copper-base alloys.

At first sight it seems an attractive proposition to render material half-hard by an annealing process, thus saving a final cold-working reduction. Actually, if the costs of the annealing operation and the cold-working operation are examined, for strip, sheet, or tube (and a large proportion of copper tube is produced in the half-hard condition), the economics are only just in favour of the partial-annealing procedure.

When the practical aspects are considered, however, the difficulties become apparent, since the annealing characteristics are influenced by the previous cold-working reduction and by the presence of minor impurities, so much so indeed, that the vertical portion of the annealing curve must in practice be replaced by a zone of appreciable width. Without knowing, therefore, the precise annealing characteristic of each and every production batch, it is impossible to anneal stock consistently

\* Research Manager, Frederick Smith and Co., Ltd., Manchester.

† Technical Officer, Imperial Chemical Industries, Ltd., Metals Division, Birmingham.



to this required value, and attempts to do so by selecting annealing conditions from one ideal curve result in a large proportion of material either remaining fully hard or being almost fully softened. Thus, for example, in experimental work designed to produce deoxidized copper tubes to fulfil the requirements of B.S. 659:1944 by giving a final annealing operation, some 30% of the tubes annealed under the most stringent conditions were either too hard or too soft.

The above remarks apply only to attempts to anneal copper or copper-base alloys to hardness values lying on the vertical portion of the relevant annealing curves, for, as indicated in our paper (p. 288), it is practicable to anneal to hardness values slightly higher than that of fully softened material.

Mr. A. J. FIELD: The question has been asked whether partial annealing, or temper letting-down, is being used in practice. In the case of commercially pure aluminium and some of the non-heat-treated aluminium alloys, it is being so used. Curves of the rate of softening at various temperatures are produced by our research staff, and it is a matter of selecting the curve at which the rate of softening is slow. We have then to bring a large mass of metal up to that temperature as uniformly as possible, and allow it to stay there until its strength has decreased to the desired extent. There is danger in using too high a temperature, in which case one, as it were, falls over the precipice and is left with a coil of nearly annealed metal which is of no use whatever. The tendency, therefore, is to underdo the letting-down rather than to overdo it.

It is a characteristic of this partially annealed material that its ductility increases rather more than its tensile strength drops. The method is therefore a practical one, but I do not think that it has, for the general run of commercial aluminium, any advantage over the normal full annealing and subsequent temper-rolling. When a coil of metal is completely annealed, it is all in the same state, and after the same rolling treatment one finishes up with a very uniform product.

On the question of resistance-annealing, it is an attractive proposition to put into the material only as much energy as is required to raise it to its annealing temperature. In practice, however, on the commercial scale, there are complications. For one thing, the size of section to be dealt with in sheet rolling is very large; a common section to be annealed in 99% pure aluminium, half-hard temper, is 48 in.  $\times$  0.064 in., that is 3 in.<sup>2</sup> in cross-section. That would require a very heavy current. Moreover, that is not the only cross-section to be annealed. One might get 10 or 20 tons of that size, and then change to a completely different size and require a completely different current. I should think that there would be electrical complications in applying that current.

Furthermore, after energy has been put into the metal it has then to be rejected. That is one of the tragedies of many metallurgical operations, such as casting, annealing, and heat-treatment. It does not matter whether the energy is rejected by refrigeration or by cooling off slowly in air—the heat is dissipated and is lost to mankind. There appears to be only one way of recapturing it, and that is by the so-called counter-current method. A vertical furnace has been mentioned by Professor von Zeerleder, with the strip going up on one side, being heated at the top, and coming down on the other side in close proximity and exchanging its heat at the bottom. That type of furnace should be thermally as efficient as could be got, but it is a band furnace and subject to all the complications inherent in that type.

Mr. F. KING: Some considerable tonnages of pure aluminium and the 1% manganese alloy have been produced by the partial-annealing treatment, and Fig. 2 (p. 312) of Mr. Paton's paper shows the effect of time and temperature on the mechanical properties of 99.6% pure aluminium.

The factors of importance in producing intermediate tempers by partial annealing can be summarized briefly as

preheat temperature and time, and the purity of the material being treated. With the higher purities the temper-annealing temperatures are less critical than with low-purity aluminium. Increasing the rolling reductions reduces the temperature range over which the process can be carried out. With 99.6% pure aluminium (see Fig. 2), the half-hard temper can be obtained with soaking times of between 4 and 8 hr. This means that the batch-type annealing furnaces built for the full annealing of aluminium alloys can be utilized for this method of manufacture of half-hard sheet in widths up to 48 in.

Mr. D. F. CAMPBELL: When talking about rapid induction heating, it is advisable to define the word "rapid". In the case of a 6-in. billet of aluminium, during the heating operation, which has a normal duration of 8–10 min., the temperature at the centre lags slightly behind the temperature at the outside; but, when the current is cut off, the outside naturally begins to cool and there comes a time when the temperature throughout the section of the billet is absolutely uniform. It has been proved very accurately by experiment that there is a period of 8–10 min. during which the variation is less than  $\pm 5^\circ$ , which is ample time for transferring the billet to the press, and, furthermore, a centre hotter than the outside can be obtained, if required. With normal-frequency induction heating, 8–10 min. is the time necessary to get uniform heating of a 6-in. aluminium billet for extrusion or rolling. With very rapid high-frequency induction heating, of course, it is possible to melt a steel bar in a few seconds on the outside and have it stone cold at the centre.

Mr. C. P. PATON: Mr. Campbell has observed that it is possible to have the centre of an ingot preheated by the induction method either hotter or cooler than the outside surface. I think that we should prefer to have an extrusion ingot slightly cooler on the outside and at the back than in the centre. Since the flow within the ingot is not uniform, these points tend to heat up more rapidly than others, and if they were at a lower temperature just before extrusion, it should mean that all parts of the ingot are at substantially the same temperature when they reach the die surface. This is one of the advantages of induction furnaces, and its possibilities should not be overlooked.

Mr. G. A. OXBY,\* B.Met. (Member): Mr. Bennett mentioned trouble experienced during batch-annealing of beryllium copper due to too slow heating and premature age-hardening. I have had experience of the same kind of trouble during batch-heating of beryllium copper for softening, previous to the hardening process. We get a very uniform product by the continuous-annealing procedure.

In connection with continuous-annealing furnaces, one point not hitherto mentioned is the possibility of measuring continuously some physical property of the product as it passes out of the furnace or out of the heat-treatment equipment. For example, the continuous measurement of the resistivity or even, in some cases, of the magnetic properties, or something similar, might provide a very useful control of the quality of the material. That would be a much less expensive operation than the sampling of pieces from the coils.

In the continuous annealing of bright strip the rate of heat transfer to the strip is low, because of its very bright surface, and in some cases one has to resort to deliberate oxidation of the strip to accelerate this rate. One of the big advantages of the induction heater is its rapid rate of heating, irrespective of the reflectivity of the strip.

Mr. A. HOLDEN: With reference to the bright annealing of silver and silver alloys in sulphur atmospheres, which I mentioned earlier, the control is fairly close, but not beyond the capacity of a completely untrained and unscientific operator. The furnace is working continuously with only very occasional serious trouble, due to enormous variations

\* Assistant Senior Metallurgist, Telegraph Construction and Maintenance Co., Ltd., Greenwich.



in the quality of the gas supply. The operator has by experience come to know the type of flame that he gets at the burner, which is visible through an inspection hole, and can control the atmosphere by visual means alone.

Several speakers have referred to the economics of furnaces and said that fuel conservation is much to be desired. There is an aspect of this matter that deserves careful consideration, namely the relative cost of the economies to be made. Assume that a furnace is relatively inefficient and that one is going to effect an economy of, say, 25%—a very high figure. The furnace must be extremely inefficient for it to be possible to effect such an economy by a new installation. It might mean that, using 2000 ft.<sup>3</sup>/ton on some process, one would save 500 ft.<sup>3</sup>/ton. Reduced to shillings and pence, as against the finished cost of the material, this would be a small matter, and would not merit the expenditure of very much capital.

This is particularly noticeable with higher-alloy steels, where some of the annealing processes are most inefficient. I know of figures of 11,000 and 12,000 ft.<sup>3</sup>/ton which are considered to be quite satisfactory, although it is possible to carry out the same process on 4500 ft.<sup>3</sup>. But when the selling price of the material is over £600 a ton, the saving is a comparatively small one, and no arguments that either the fuel experts or the furnace makers can advance will get manufacturers to spend money on installing comparatively expensive plant.

Everyone seems to assume that high rates of convection are desirable, but even in a fully convection-heated furnace, with the source of heat outside and all the heat distributed by convection, the amount transferred to the stock is still very low, probably of the order of 15%. I have not had the courage to try it yet, because in practice we do quite well on the existing methods, but it might be possible by ensuring an even distribution, to use very low velocities, so that the radiation is more effective, and not incur the cost of fully convection-heated furnaces with high velocities. As an example, I know of one furnace with four 25-h.p. fans, each handling 25,000 ft.<sup>3</sup>/min., and the economics are not particularly good. That is understandable, because the high velocities are in the fan ducts and not in the furnace. If the flow is vertical in a comparatively large furnace, it is obvious that the cross-sectional area over which the total flow is spread is very large. Consequently, the mean velocity is very low, and 90 ft./sec. may drop to a mean velocity of 2 ft./sec. That is not very high for convection purposes. The local velocity of the gas in heating the work will be considerably higher. These high velocities demand a considerable pressure difference from one part of the furnace to another, which in a continuous furnace with open ends leads to trouble in loss of heating gases or by cold air being drawn in. This accounts for the low thermal efficiency of convection-heated furnaces.

With reference to the low-temperature process mentioned for annealing copper wire on spools at 200° and 250° C., we tried this in about 1938, and I am prepared to admit a failure. The furnace was a full-convection type, and we spent a lot of money on it. The whole process was supposed to be completed in 2½ hr., with a maximum of 3 hr. The work was dry and remained dry, which did away with the water quenching previously used. After some time we had to take the furnace out, because the rate of cooling was slow and the economics terrible. I do not think it is possible to cool wire on spools very quickly.

Mr. J. J. STORDY,\* B.Sc. (Member): As a furnace manufacturer, I think we have dealt with this question of convection

and speed in quite the wrong way. The speed at which air is put through will have nothing whatever to do with the temperature control of the furnace. If we take a tubular type of furnace, 3 ft. in dia. × 30 ft. long, and circulate a certain volume of air from end to end, then the speed of the air will be fixed by the cross-sectional area of the furnace. While the heat transfer may be raised by rubbing and disturbance of the difficult skin that clings to the metal, the control will be no more precise than in a furnace of the same dimensions with the air brought in all along the sides of the furnace for its full length, because the only thing that affects the temperature of the furnace is the weight of the air circulating.

From the point of view of furnace accuracy that is what matters. If we load a furnace to 1000 kW. and the metallurgist or engineer lays down a furnace-temperature limit, then the weight of air (I am assuming that air is the only vehicle of heat and that there is no radiation in the furnace) is fixed by natural laws, and has to be such that in dropping through that temperature head the 1000 kW. will be released to the system. So I think that we stress speed and directional flow unnecessarily, and that the important factor is the heat-carrying capacity of the air. Unfortunately, we work with a very poor vehicle of heat transfer, and extremely large weights of air have to be circulated.

The furnace manufacturer also works under certain limitations in the manufacture of fans. We always, as far as possible, put the fan after the heater battery. I am speaking now of a furnace in which the heater battery is entirely remote from the work chamber. Our idea is to bring the air through, say, an electrical heater battery or through a combustion chamber—which may be gas- or oil-fired, or fired in some other way—and then to take it through the fan and deliver it to the furnace, so preventing any stratification due to the heat coming through the heating medium and direct to the furnace. But 20,000–30,000 ft.<sup>3</sup>/min. at a temperature of 650° C., is about the maximum limit of satisfactory operation for a fan which has the duty of conveying the whole heat capacity of the furnace, and the maximum temperature that ordinary heat-resisting materials, apart from very special steels, will give. The air circulated through the furnace is fixed by that consideration. Of course, if the furnace temperature itself has to be 650° C., the fan can be put on the re-circulation side of the furnace and the heat can come from the heater battery or combustion chamber at a higher temperature.

With regard to the question of conveyors for flash-annealing furnaces, I have heard that there is a method by which the sheets can be put on sky hooks and taken through without any marking whatever. I personally do not know of any way that will prevent marking of the soft annealed sheet. However, we have at last moved away from wire ropes and effected a considerable improvement by introducing a type of multi-formed strips on which the sheet can lie. A successful method of joining these strips has been found, but there can still be a very slight marking of the sheets as they come off the flash-annealing furnace.

Mr. W. A. BAKER: One of the main features that has emerged from the discussion has been a very strong plea for closer liaison between the manufacturers of furnaces and the users. If there is anything that The British Non-Ferrous Metals Research Association can do to foster development by such closer liaison, it will be only too happy to do so.

\* Director, Stordy Engineering Ltd., Wolverhampton.



# The Creep and Softening Properties of Copper for Alternator Rotor Windings

By N. D. BENSON, J. McKEOWN, and D. N. MENDS

(*Journal*, this vol., p. 131.)

Mr. L. E. BENSON,\* M.Sc., F.I.M. (Member): The work reported in this paper was carried out under the direction of a Committee on which the suppliers of copper for rotor windings and the manufacturers of electricity generators were represented, and I know that the Research Association will take no exception to my comment that the guidance of such committees should be acknowledged in the publication of work carried out in these circumstances. Technically, the work done is very useful and helpful and my remarks will be mainly directed towards emphasizing the conclusions which the authors have set out.

It is only fair to the investigators to point out that when the work was started it was not possible to define the real problem clearly. After a generator has been run up to speed and put on load, heat is generated in the windings, which warm up in advance of the steel rotor. This time lag, and the difference in coefficient of expansion between copper and steel, provide one explanation of heavy stress in the windings. As the rotor warms up this stress is reduced, but, if everything behaves elastically, some stress will remain until the machine stops. The stress in any winding is also affected by temperature differences between the windings themselves. Now it was not known—and I think it is still not known—whether the most important factor in the copper shortening mechanism is a high stress operating for a comparatively brief period each time a machine is started, or a lesser stress operating substantially all the time the machine is running. In the former case, softening of the copper might be of prime importance, but in the latter case the creep strength of the material would very likely be important too. The magnitude of the stresses operating in service were also not known, so that the problem was reduced to comparing ordinary tough-pitch copper with silver-bearing copper in a general sort of way, both as regards softening characteristics and creep strength over long periods.

Long-time creep strength does not necessarily bear any relationship to hardness, but on both counts the investigation has shown the silver-bearing copper to possess a big advantage—in terms of temperature perhaps approaching 100° C. This is a most important conclusion, and one which experience is beginning to confirm.

Unfortunately—owing probably to limitations of space—the authors have not been able to set out their data in such a way that the advantage will be as clear to engineers as it might be, so I should like to supplement some of their observations a little.

With regard first of all to softening; the graphs in Figs. 1 and 2 (pp. 134–135) may not be very convincing to engineers. The points plotted, however, have been obtained from hardness and time experiments, and Fig. A shows some of the hardness/time curves obtained. The upper graph, which refers to 130° C.—substantially the temperature of rotor windings in service—shows immediately that ordinary tough-pitch copper will soften badly in a lifetime, i.e. 100,000–

200,000 hr. Silver-bearing copper looks fairly good up to 10,000 hr., but the engineer wants to know if it will remain good for a further 90,000 hr. or more. This is where Figs. 1 and 2 come in. The real point about these graphs is that the slope of the curves tells us something about a characteristic of the metal. Furthermore, they form a family of straight lines, and previous experience indicates that they can be extrapolated with fair confidence. Therefore, by doing a little simple plotting, we can find that 100,000 hr. at 130° C. is equivalent to about 3 hr. at 225° C. for silver-bearing copper and about 30 hr. for tough-pitch copper, although the degree of softening for the two alloys is different. Now, looking at the lower graph in Fig. A, we can see that

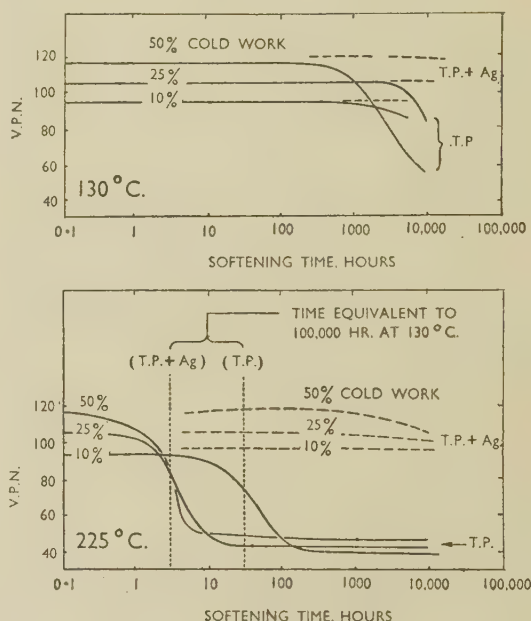


Fig. A.—Softening of Tough-Pitch and Silver-Bearing Copper at 130° and 225° C.

the silver-bearing copper has not started to soften in 3 hr. at 225° C. and therefore should not start to soften in 100,000 hr. at 130° C. The silver-free copper, however, has softened appreciably in 30 hr. at 225° C. and therefore would soften appreciably in 100,000 hr. at 130° C. Incidentally, the behaviour of tough-pitch copper in the upper and lower graphs supports the extrapolation made.

With regard to creep strength, the conclusion based on Fig. 5 (p. 137) is that silver-bearing copper at 225° C. behaves similarly to tough-pitch copper at 130° C. (cf. the two curves which intersect on the right-hand side). Whilst this com-

\* Research Laboratories, Metropolitan-Vickers Electrical Co., Ltd., Trafford Park, Manchester 17.

parison holds good for a degree of strain commensurate with that troubling the electrical engineers, it is based on tests lasting only 1000 hr. and does not afford as much comfort as designers would like.

Again, the authors have not had space to include all the available data, but, if I may take data from the original creep curves and resort to the expedient of plotting stress against log time for a given plastic strain, graphs can be produced for tough-pitch copper at 130° C. and silver-bearing copper at 225° C. which permit of some extrapolation, and which offer a fair hope that the advantage shown by the silver-bearing material will be largely maintained over longer periods (see Figs. B and C). Incidentally, these graphs make use of creep-test results lasting up to 10,000 hr., and the points have not been averaged as in Fig. 5 of the paper. Comparing Figs. B and C, it will be seen that the creep characteristics for, say, 0.2% strain are substantially the same, although the testing temperature for the silver-bearing copper was 95° C. higher than for silver-free copper.

I hope that the B.N.F.M.R.A. may be persuaded to undertake some hardness tests on creep-test specimens to see

have been a little more explicit. Thus 100,000 hr. at 130° C. is equivalent to about 30 hr. at 225° C. for tough-pitch copper, both treatments producing half softening of the copper. For the silver-bearing copper on the other hand, 3 hr. at 225° C. produces no measurable softening, and the equivalent treatment of 100,000 hr. at 130° C. should likewise produce no softening.

The softening tests are being continued on the silver-bearing tough-pitch coppers, and the following additional results help to make this point still clearer. In the samples with 10% and 25% cold work, no decrease in hardness has occurred after 35,000 hr. at 225° C. and lower temperatures. In the samples with 50% cold work no decrease in hardness has occurred after 35,000 hr. at 200° C. and lower temperatures. In these latter samples 50% softening occurred after 3000 hr. at 250° C. and after 20,000 hr. at 225° C. If these points are added to Fig. 2 (a) of the paper, they confirm the slope of the lines drawn through the earlier experimental points and give greater confidence in any extrapolation of the lines. On making such extrapolation it is found that the sample with 50% cold work would be expected to soften 50%

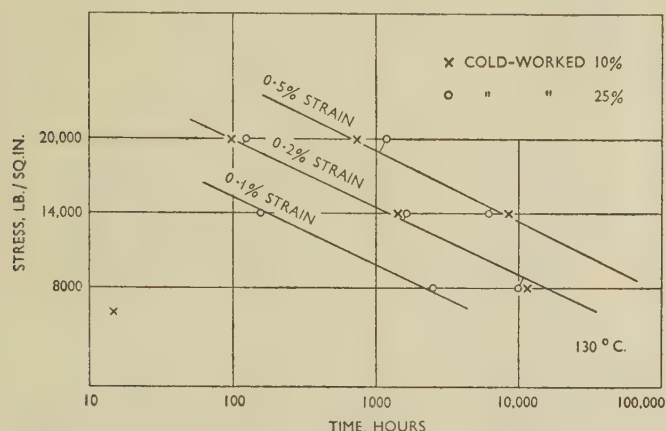


Fig. B.—Creep-Test Results on Tough-Pitch Copper at 130° C.

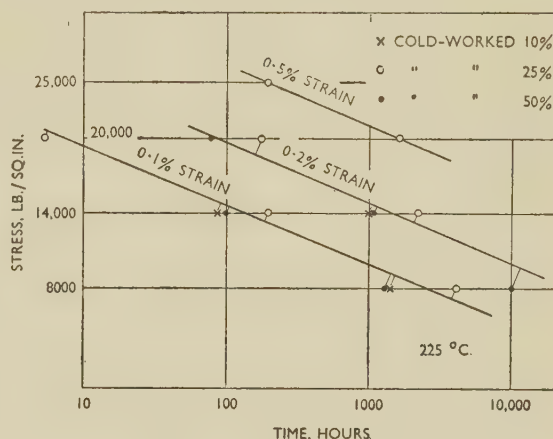


Fig. C.—Creep-Test Results on Silver-Bearing Copper at 225° C.

whether the rate of softening is appreciably affected by the specimen being loaded and subject to creep while hot. Other questions on which we are still incompletely informed concern the effect of cold work on creep, particularly at stresses where little initial strain occurs on loading and over long periods. Also, we know nothing at all about the accidental variations in creep strength between different batches of material. Judging by experience with other alloys, this may be quite important.

The AUTHORS (*in reply*): The work described in the paper was, as is usual in the Research Association, carried out under the general guidance of a Committee, and in this case the membership of the Committee included representatives of suppliers of copper for rotor windings and of manufacturers of electricity generators. Mr. L. E. Benson was a member of this Committee, representing a large manufacturer. The authors are very happy to place on record their thanks to the members of the Committee for helpful discussions during the progress of the work.

Mr. Benson's contribution to the discussion emphasizes the considerably higher resistance to softening of the silver-bearing compared with the silver-free copper, a point which we had felt was sufficiently covered by our statement on p. 135 that "the softening of cold-worked copper used for alternator windings at temperatures up to 225° C. can be completely avoided by the use of silver-bearing copper." We think that in his use of equivalent temperatures and times he might

in 10<sup>7</sup> hr. at 170° C. and those with lower degrees of work in still longer times. At 130° C. times to 50% softening would be expected to be of the order of at least 10<sup>10</sup> hr., and hence it is not difficult to visualize that in 100,000 hr. the silver-bearing coppers would not suffer any measurable reduction in hardness at this temperature.

The comparisons of the creep properties of silver-free and silver-bearing tough-pitch coppers made by Mr. Benson in Figs. B and C are certainly useful. We made a point on p. 135 that the longer-duration tests up to 10,000 hr. showed that the comparisons obtained at the longer times were the same as those obtained at 1000 hr. From this it would follow that the comparisons made in Fig. 5 would be equally true if the plastic strain were taken at 10,000 instead of at 1000 hr.

We regret that the creep specimens have been scrapped, and hence it is not possible to carry out any hardness tests with the object of comparing softening of the various coppers under stress as opposed to stress-free conditions. It is questionable, however, whether a worth-while comparison would have been obtained from such tests because of the confusing effect which might arise from the presence of creep strains. Special tests would have to be designed to make this comparison free from extraneous effects.

While, as Mr. Benson points out, much more work could be done in a research on creep properties, it has not been possible to spare the creep-testing units for further experiments to examine the effects of cold work at low stresses or the reproducibility of creep data using different batches of material.



# NOTICE TO AUTHORS OF PAPERS FOR THE "JOURNAL" AND CONTRIBUTORS TO DISCUSSIONS

1. Papers will be considered for publication from non-members as well as members of the Institute. They are accepted for publication in the *Journal* and not necessarily for presentation at any meeting of the Institute. MSS. should be addressed to The Editor of Publications, The Institute of Metals, 4 Grosvenor Gardens, London, S.W.1.

2. Papers suitable for publication may be classified as:

(a) Papers recording the results of original research.

(b) First-class reviews of, or accounts of progress in, a particular field.

(c) Papers descriptive of works methods, or recent developments in metallurgical plant and practice.

(d) Papers in classes (a), (b), and (c) above, previously published in languages other than English, French, German, or Italian, if of sufficient merit.

3. Manuscripts and illustrations should be submitted in duplicate. MSS. must be typewritten (*double-line spacing*) on one side of the paper only, and authors are requested to sign a declaration that neither the paper nor a substantial part thereof has been published elsewhere. Exceptions may be made in certain cases where a paper has been published in a language other than English, French, German, or Italian (see 2(d) above). MSS. not accepted are normally returned within 6 months of receipt.

In the interests of economy, all papers must be written as concisely as possible; in general, internal research reports are not in suitable form for publication as papers in the *Journal*. All but the simplest mathematical expressions should be written by hand, with capital and small letters clearly distinguished. Superscript and subscript letters should also be plainly indicated. Greek letters and special signs should be identified in the margin. For style, spelling, and abbreviations used, any recent issue of the *Journal* may be consulted.

4. **Synopsis.** Every paper must have a synopsis (not exceeding 250 words in length) which, in the case of a paper reporting original research, should state its objects, the ground covered, and the nature of the results. The synopsis will appear at the beginning of the paper, and should be in a form suitable for use by abstracting organizations. Extracts from a "Guide for the Preparation of Synopses" drawn up by the Abstracting Services Consultative Committee are reproduced below.

5. **References** must be collected at the end of the paper and must be numbered in the order in which they occur in the MS. Initials of authors must be given, and the Institute's official abbreviations for periodical titles (as used in *Metallurgical Abstracts*) should be employed, where known. References to papers should be set out in the style:

A. L. Dighton and H. A. Miley, *Trans. Electrochem. Soc.*, 1942, **81**, 321 (i.e. year, volume, page).

References to books should be in the following style:

C. Zener, "Elasticity and Anelasticity of Metals". Chicago: 1948 (University of Chicago Press).

6. **Illustrations.** Each illustration must have a number and description; only one set of numbers must be used in one paper, and it is desirable to number the half-tone illustrations consecutively, rather than to intersperse them with the line figures. The captions should be typed on a separate sheet.

The set of **line figures** sent for reproduction must be drawn (about twice the size to appear in the *Journal*) in Indian ink on smooth white Bristol board, good-quality drawing paper, co-ordinate paper, or tracing cloth, which are preferred in the order given. Co-ordinate paper, if used, must be blue-lined, with the co-ordinates to be reproduced finely drawn in Indian ink. Curves should be drawn boldly (i.e. at least twice the thickness of the frame). Experimental points should be indicated by open or closed circles, triangles, squares, &c. (preferably not crosses). Curves should be broken on each side of such symbols and plenty of allowance should be made for closing up in blockmaking. All lettering and numerals, &c., should preferably be in *pencil*, so that the Institute's standard lettering may be affixed, and ample margins must be left outside the framework of the figures to enable this to be done. The second set of line illustrations may be photostat copies.

**Photographs** must be restricted in number, owing to the expense of reproduction, and photomicrographs should be trimmed to the smallest possible of the following sizes consistent with adequate representation of the subject: 4 in. deep by 3 in. wide: 2 in. deep by 3 in. wide: 2 in. square. Magnifications of photomicrographs must be given in each case. Photographs for reproduction should be loose, not pasted down (and not fastened together with a clip, which damages them), and the figure number and author's name should be written on the back of each. Captions should be given to the photomicrographs, but these should be kept as brief as possible.

Because of the present high cost of printing and paper it is imperative that authors restrict illustrations (particularly photographs) to the absolute minimum deemed necessary to support their argument. Only in exceptional cases will illustrations be reproduced if already printed and readily available elsewhere.

7. **Tables or Diagrams.** Results of experiments, &c., may be given in the form of tables or figures, *but* (unless there are exceptional reasons) *not both*. Tables should bear Roman numbers, and each should have a heading that will make the data intelligible without reference to the text.

8. **Corrections.** A certain number of corrections in proof are inevitable, but any modification of the original text is to be avoided. Since corrections are very expensive, the Institute reserves the right to require authors to contribute towards their cost if the Editor deems them to be excessive. The Institute also reserves the right to require a contribution to the cost of remaking any block where this is necessitated by an error on the author's part.

9. **Reprints.** Individual authors are presented with a maximum of 25, and two or more authors with a maximum of 50 reprints from the *Journal*, without covers. Limited numbers of additional reprints can be supplied at the author's expense, if ordered before proofs are passed for press. (Orders should preferably be placed when submitting MSS.)

10. **Discussion.** Except in the case of special symposia, shorthand records of discussions are not taken at meetings. Written discussion may be submitted on any paper, preferably typewritten (*double-line spacing*). References should be given in the form of footnotes. Paragraphs 6 and 7 above are also applicable to such contributions. Reprints of discussion cannot be supplied to contributors.

## GUIDE FOR THE PREPARATION OF SYNOPSIS

(As recommended by the Abstracting Services Consultative Committee)

1. **Purpose.** The synopsis is not part of the paper; it is intended to convey briefly the content of the paper, to draw attention to all new information, and to the main conclusions. It should be factual.

2. **Style of writing.** The synopsis should be written concisely and in normal rather than abbreviated English. It is preferable to use the third person. Where possible use standard rather than proprietary terms, and avoid unnecessary contracting.

It should be presumed that the reader has some knowledge of the subject, but has not read the paper. The synopsis should therefore be intelligible in itself without reference to the paper; for example, it should not cite sections or illustrations by their numerical references in the text.

3. **Content.** The title of the paper is usually read as part of the synopsis. The opening sentence should be framed accordingly and repetition of the title avoided. If the title is insufficiently comprehensive, the opening should indicate the subjects covered. Usually the beginning of a synopsis should state the objective of the investigation.

It is sometimes valuable to indicate the treatment of the subject by such words as: brief, exhaustive, theoretical, &c.

The synopsis should indicate newly observed facts, conclusions of an

experiment or argument and, if possible, the essential parts of any new theory, treatment, apparatus, technique, &c.

It should contain the names of any new compound, mineral species, &c., and any new numerical data, such as physical constants; if this is not possible, it should draw attention to them. It is important to refer to new items and observations, even though some are incidental to the main purpose of the paper; such information may otherwise be hidden, though it is often very useful.

When giving experimental results the synopsis should indicate the methods used; for new methods the basic principle, range of operation, and degree of accuracy should be given.

4. **References.** If it is necessary to refer to earlier work in the summary, the reference should always be given in full and not by number. Otherwise references should be left out.

When a synopsis is completed, the author is urged to revise it carefully, removing redundant words, clarifying obscurities, and rectifying errors in copying from the paper. Particular attention should be paid by him to scientific and proper names, numerical data, and chemical and mathematical formulae.

## Discussion

# Grain Refinement of Castings\*

Mr. E. A. G. LIDDIARD,† M.A., F.I.M. (Member): Research on grain refinement is rendered extremely difficult, as indeed is all foundry work, by the large number of variables, which it is almost impossible to control satisfactorily.

Although these papers stress the influence of nuclei, it must be kept in mind that the grain-size of a casting is affected by a number of other factors, e.g. cooling rate, alloy composition (particularly those variations which affect the concentration gradient or which cause alterations in interfacial tension between the solid and liquid phases), and turbulence (whether arising in pouring or from gas evolution or reaction). This is why it is often necessary to make a large number of experiments and to treat the results statistically, before drawing any definite conclusions. The careful and exhaustive work of the B.N.F.M.R.A. investigators, and the ingenious use of the centrifuging technique, has, I think, given us convincing evidence of the vital part played by nuclei in grain refinement and has provided us with results of immediate practical application and importance.

At the Fulmer Research Institute we have done a certain very limited amount of work confirming the practical implications of Mr. Cibula's paper, but although we are in whole-hearted general agreement with him that titanium and boron, probably together as the boride, make excellent grain-refining agents, we find that the salts method of refining is more satisfactory in practice than the use of hardeners. We experienced considerable difficulty in obtaining the correct boron content by hardener additions in the few experiments carried out. Moreover, no tendency was found to mould reaction in alloys in which the boron was introduced via salts, but there was a marked mould reaction when similar quantities of boron were introduced by a hardener. I should like to have Mr. Cibula's comments.

Turning to the paper by Mr. Reynolds and Mr. Tottle, I feel that the work has suffered from a rather hasty enthusiasm, which has led to a lack of appreciation of other factors that influence grain refinement. It is a little disturbing to find no details in the section on experimental technique on the composition of the so-called "commercial purity" materials used, particularly in view of the tremendous influence that traces of impurities can exert on grain-size. Similarly, the melting and casting techniques are not described, and this seems regrettable in view of the importance of, for example, gravity segregation of grain-refining nuclei as a result of holding the metal molten in the furnace. There is also little information on reproducibility of results, which is always difficult to establish in foundry work. The authors would, I think, have been wise to keep to one mould material and to obtain more results without introducing this additional variable.

A result quoted in Table III (p. 96) shows that thorium as a mould coating caused no grain refinement of aluminium and this is attributed to the fact that it had an unsuitable lattice spacing, but in the experiments recorded in Table V (p. 97) thorium did produce a significant grain refinement because, according to the authors, it reduced alumina. This makes one wonder to what extent they have selected specific results to support their views on mechanism.

The evidence for the authors' deoxidation theory seems very

thin. I cannot understand by what mechanism solid nuclei are formed as a result of reaction between the oxide on the cast metal and the metal of the mould coating. The oxide film is presumably at the same temperature as the molten cast metal, and if the metal on the mould face is to reduce the oxide film on the cast metal the reaction must be exothermic, in which case I cannot see any likelihood of precipitation of solid nuclei as a result of the reaction.

One error of fact that needs correction is that the authors quote Vernon and his collaborators‡ as providing evidence for the composition of the oxide film on 18 : 8 chromium-nickel austenitic steel, but appear to have overlooked the fact that this relates to the oxide film on the polished surface. Vernon and his co-authors go on to show that heating steel at temperatures up to 500° C. increases the ratio of iron oxide to chromic oxide far beyond that found on the polished surface. Their paper does not, and is not supposed to, contain any evidence on the composition of the film on the *molten* 18 : 8 chromium-nickel steel.

The fact that one can in practice grain refine, at least on the surface, by nucleation from the mould face is, however, a most valuable practical observation.

Dr. D. V. ATTERTON,§ M.A. (Junior Member): I would like to support Mr. Liddiard's remarks on the advantages of grain refining by means of salt mixtures containing potassium titanofluoride and potassium borofluoride, rather than the hardeners used by Mr. Cibula. For large melts it is comparatively simple and cheaper to add a salt mixture, and a more uniform dispersion of titanium and boron will be achieved. In his experiments Mr. Cibula used 3-kg. melts. Can he give us any information on the relative ease of adding either hardeners or salt mixtures to larger melts?

Mr. Reynolds and Mr. Tottle mention (p. 96) that in the case of copper cast against iron powder no effect was observed with a casting temperature below 1200° C., and they attribute this to the fact that the  $\gamma$  state had not been reached by the iron coating under these conditions. It is difficult to accept this, as the metal/mould interface temperature for such a casting must be considerably in excess of 910° C.

Mr. W. A. BAKER,|| B.Sc., F.I.M. (Member): I am surprised that the technique adopted by Mr. Reynolds and Mr. Tottle should have yielded useful results, because I should have expected most, if not all, of the metallic powders used as mould coatings to oxidize rapidly before or immediately after the metal was poured into the mould. However, some very interesting results have been obtained, though I am by no means satisfied with the interpretation of some of the observations. In particular, I do not see why reduction of an oxide film on the metal being cast should produce solid particles of that metal, bearing in mind that the reaction involved is exothermic and that the heat evolution, however small, could hardly favour the formation of solid particles of the reduced metal. I wonder whether the difficulty could be resolved by assuming that the oxide-coated metal penetrates slightly into the pores of the metal-powder coating on the mould face; in such circumstances the small amount of heat evolved in a reaction occurring at the bottom of the pore might be rapidly

\* Joint discussion on the papers by A. Cibula (*J. Inst. Metals*, this vol., p. 1) and by J. A. Reynolds and C. R. Tottle (this vol., p. 93).

† Director, Fulmer Research Institute, Stoke Poges, Bucks.

‡ W. H. J. Vernon, F. Wormwell, and T. J. Nurse, *J. Iron*

*Steel Inst.*, 1944, 150, 81p.

§ Research and Development Manager, Foundry Services, Ltd., Birmingham.

|| Research Manager, British Non-Ferrous Metals Research Association, London.



dissipated and the metal reduced in the reaction might then appear as a solid particle.

Mr. A. CIBULA: Compounds having structures suitable for the nucleation of a liquid metal can, in practice, be used for grain refinement only if their solubility in the melt is small. In general, therefore, the difficulty of finding a suitable grain refiner increases with the melting point of the metal to be refined, as the solubility of several possible constituents of the nuclei (e.g. carbon, boron, sulphur, and silicon) is large in the high-melting-point liquids. In the novel method of refinement described by Mr. Reynolds and Mr. Tottle, the substances causing nucleation are in contact with the melt only for a short time before solidification, and their opportunity to become inactive by solution is correspondingly reduced; it is possible, therefore, that castings of some of the high-melting-point metals may be more easily refined by the use of mould coats than by the introduction of grain refiners into the melts; alternatively, the amount of refiner required may be much smaller if it is used as a mould coat rather than as an addition to the melt.

However, there still remains the danger of rendering the mould coat inactive by melting it, particularly when the nucleating particles are formed by exothermic reduction; the difficulty of nucleating solidification would then, of course, apply as much to the particles of metal in the molten coating as to the casting itself. It seems probable that several of the coatings used by the authors proved ineffective, not because the lattice dimensions were unsuitable, as they suggest, but simply because the coatings were melted before the casting began to solidify, e.g. lead coatings used with aluminium and copper, and so-called isomorphous aluminium coatings used with copper (see Table III, p. 96, of the paper). For a similar reason, the effect of several of the coatings should depend on the degree of superheat of the metal entering the mould; it would be interesting to know whether any such influence of casting temperature was detected with, say, copper or lead poured into, respectively, copper- or lead-coated moulds.

A possible disadvantage of the use of mould coats for refinement is that the reduction in grain-size is largely confined to the columnar grains growing from the surface of the casting, owing to the absence of nuclei from the interior. This degree of refinement may well be sufficient for some purposes, such as improving ductility, but it would probably have little influence on the general soundness or the distribution of porosity in a casting. The authors describe an interesting use of their technique in refining a stainless steel casting; it is unwise, however, to assume, as they do, that "the improvement in mechanical properties was no doubt considerable" or that a reduction in grain-size invariably improves these or other properties. Grant *et al.*\* have shown, for example, that the properties of cast turbine blades, made in a refractory nickel-chromium-cobalt-iron alloy, varied in a rather complex way with changes in macrostructure; coarse columnar grains produced better properties than the equiaxial grain structures obtained by using a graphite mould.

Dr. L. J. G. VAN EWIJK † (Member): Mr. Cibula shows in Table VI (p. 11) the value of additions of titanium and boron in preventing grain coarsening in aluminium-magnesium alloys when high casting temperatures are used; previous work by Cibula and Ruddle ‡ has indicated that such grain coarsening greatly reduces the tensile properties of the high-strength aluminium casting alloys. In my experience, the

general precaution of avoiding grain coarsening by employing low casting temperatures is not necessary with the aluminium-10% magnesium alloy (B.S.S. L53); chlorine-degassing melts at low temperature (700°–720° C.) has never given the optimum results, whereas degassing at 750°–760° C. has resulted in values of 26.5 tons/in.<sup>2</sup> tensile strength and 24% elongation in at least three out of ten bars cast-to-shape in sand, in spite of the fact that the grain-sizes could not be described as fine. A very rough test, carried out by hammering a test-bar over the sharp edge of a vice and bending it through 360°, shows the high quality of these coarse-grained bars.

Mr. Cibula has also discussed, in a previous paper § the influence of grain-size on the distribution of porosity in a casting; it is difficult to understand, however, why columnar crystal growth in aluminium-copper alloys should result in a shrinkage pipe, while equiaxial growth produces a shallow surface depression and dispersed porosity. One might expect that the liquid metal would feed through the tortuous interdendritic channels of a columnar structure only with great difficulty, and that this would result in dispersed shrinkage cavities and a small pipe; in an equiaxial structure, on the other hand, mass-feeding might proceed over a longer period, and consequently residual shrinkage cavities in the casting would be less dispersed, being concentrated in the feeder. I should appreciate Mr. Cibula's opinion on this point.

Mr. A. J. FIELD, || M.C., B.Sc., F.I.M. (Member): From the practical standpoint it would be of interest to know what advantage in the process or product is found from grain refinement of the casting in the case of wrought aluminium or aluminium alloys, having in mind that the grain-size of the wrought material after recrystallization by anneal is unrelated to the grain-size of the original cast ingot.

Mr. N. B. RUTHERFORD, ¶ B.Sc. A.I.M. (Member): Mr. Cibula has developed in this and earlier papers a well-substantiated theory for the mechanism of grain refinement, based on the presence of nucleating particles. On the other hand, Crossley and Mondolfo \*\* support the peritectic mechanism of grain refinement, although their grain refinement/equilibrium diagrams, with the exception possibly of that for aluminium-titanium, are quite unconvincing because of the paucity of points. However, the conditions used by the different investigators varied widely. In particular, Mr. Cibula based his work on the cooling rates pertaining to  $\frac{3}{8}$ -in. and 2-in.-dia. castings in sand moulds, while Crossley and Mondolfo used very much slower rates (6°–7° C./min.). Is it possible that grain refinement can occur by either mechanism, depending on the rate of cooling, and that nucleation is ineffective at very slow rates, so that, for example, sufficient titanium has to be added to allow the peritectic mechanism to operate?

Mr. P. C. VARLEY, †† M.B.E., M.A., T.D., F.I.M. (Member): Mr. Cibula shows that the grain-refining effect of titanium in aluminium alloys is much enhanced in the presence of quite small amounts of boron. Now, normal commercial aluminium contains about 1 part per million (0.0001%) of boron, a quantity which when used as an addition to an aluminium-titanium alloy provides some appreciable refinement (Table IV, p. 9). I wonder, therefore, whether the author has considered the possibility of this alternative explanation of the effect of titanium additions to aluminium alloys. In his earlier paper § he ascribed this to the formation

\* N. J. Grant, L. W. Kates, and N. E. Hamilton, *Foundry*, 1950, **78**, 86, 234.

† Metallurgist in Charge of Laboratories, N.V. "Industrie", Vaassen, Netherlands.

‡ A. Cibula and R. W. Ruddle, *J. Inst. Metals*, 1949–50, **76**, 361.

§ A. Cibula, *ibid.*, 321.

|| Works Manager, The British Aluminium Co., Ltd., Falkirk.

¶ Investigator, British Non-Ferrous Metals Research Association, London.

\*\* F. A. Crossley and L. F. Mondolfo, *Trans. Amer. Inst. Min. Met. Eng.*, 1951, **191**, 1143.

†† Metallurgist, The British Aluminium Co., Ltd., Gerrards Cross, Bucks.



of nuclei of titanium carbide, basing the identification on the X-ray examination of centrifuged particles. I do not suggest that this identification was in error, but if the observed grain refinement were really due to titanium boride, its presence might well be masked by a larger quantity of the carbide and so remain undetected and unsuspected.

To me it has always been one of the difficulties of the carbide theory that, while additions of boron exercise their expected effect, in whatever manner they are added, neither addition of carbon nor titanium carbide to the melt has any effect on grain refinement. This has been attributed by Mr. Cibula to the difficulty of getting such substances to dissolve in molten aluminium, but there is one easy way of introducing carbon into aluminium. Manganese carbide reacts quantitatively with molten aluminium, producing manganese and aluminium carbide, both of which go into solution. Such an alloy, rich in carbon, has been used as an addition to aluminium-titanium alloys, but has produced no further grain refinement, although titanium carbide must have been formed in large quantities.

Mr. CIBULA (*in reply*): I have had similar experience to that described by Mr. Liddiard with some commercial master alloys of high nominal boron contents, owing to the presence in them of large quantities of borate slag: the inclusions occur because of the difficulty of separating the molten slag and the aluminium-boron solution produced by aluminothermic reduction during the manufacture of the alloys. When the boron contents of the alloys were determined by analysis, the figures obtained included the boron present as borate slag as well as that in solution, but the oxidized boron did not, of course, produce refinement after addition to a melt, but only slag inclusions. We avoided this difficulty in our work by preparing an intermediate, dilute master alloy from the concentrated commercial product and absorbing the borate slag in a cryolite flux cover; however, quite satisfactory commercial alloys containing 1-2% boron have recently become available. The presence of borate slag in the master alloy may explain why boron proved more effective when added via a salt in the experiments described by Mr. Liddiard, but it does not explain why there was greater mould reaction when a hardener was used.

Mr. LIDDIARD: Mr. Cibula may well have provided the explanation. It is known that sand treated with boric acid can cause marked mould reaction in aluminium alloys containing silicon, although the mechanism is not understood. Reaction by the same mechanism might be anticipated in the case of borates arising from the hardener.

Mr. CIBULA: It is quite possible that inclusions of borate slag promote metal/mould reaction, as Mr. Liddiard suggests, presumably where they come into contact with the sand. However, it is unlikely that borate particles were responsible for the mould reaction and gas pick-up in the work described in the paper, as no slag particles were visible in microsections of the alloys and the mould-reaction porosities appeared to be related consistently to the boron and titanium contents. It seems more probable that dissolved boron affected the composition and properties of the oxide film on the alloys (e.g. by forming aluminium borate-alumina films) and thus allowed mould reaction to proceed unhindered; phosphorus behaves similarly in gun-metal, and small additions of beryllium are known to produce the opposite effect in aluminium-magnesium alloys.

In the few experiments described in the paper, boron and titanium introduced from salts were not as effective as master

alloys in producing refinement; however, the two methods have not been compared with large melts, and the salts process could doubtless be improved in a number of ways, if this were necessary. It is therefore not possible to recommend one particular method of adding the refining elements, except in the case of the magnesium-containing alloys, to which the transference of boron was poor from salts but virtually complete from master alloys; a similar influence of magnesium on the transference of boron and titanium from salts has been described in detail by Mrs. Eborall.\*

Master alloys have been used successfully for the refinement of foundry melts of up to 300 lb., in which the stream of nitrogen used for degassing ensured a uniform distribution of the added refining elements. Considerable difficulty has been experienced, however, in dispersing boron uniformly in larger melts of several tons when master alloys were used, owing to the difficulty of stirring such melts effectively; it is possible that the addition of salts would be more effective in these cases.

Very little has been published on the influence of the grain-size of the ingot on the working properties of cast aluminium and its alloys and on the properties of the wrought product. The following examples may illustrate the possible advantages of grain refinement.

(1) Although, as Mr. Field states, the grain-size of the final product after recrystallization is unrelated to the macrostructure of the original casting, there appears to be a marked relation between the orientation of patches of fine grains in the wrought material and the orientation of the crystals in the ingot from which these grains were derived. Work by Pearson (quoted by Kasz and Varley †) indicates that this correlation may result in pronounced directional properties in the rolled sheet prepared from coarse-grained ingots.

(2) Weak intergranular constituents formed by impurities are more uniformly distributed in fine-grained than in coarse-grained castings. Genders and Bailey ‡ have shown that in this way grain refinement counteracts the harmful effects of lead and other impurities on the working properties of brass and aluminium bronze, and it seems likely, therefore, that the influence of brittle iron- and silicon-rich impurities in aluminium alloys may be similarly reduced. Helling and Hahn § demonstrated that the rolled sheet produced from a fine-grained aluminium ingot had higher corrosion-resistance because the uniform distribution of impurities in the ingot persisted in the sheet.

(3) In some alloys the distribution of intermetallic compounds which have to be dissolved by heat-treatment is similarly improved by grain refinement, and homogenization times are thus reduced.¶ This does not occur in alloys in which most of the intermetallic compound lies within the grains, as the spacing of the dendrite arms, between which the eutectic constituents are situated, does not generally vary with the grain-size.¶

(4) Grain refinement also has a favourable influence on the amount and distribution of intergranular porosity in aluminium alloys,† and refinement should therefore improve the working properties of ingots which, when coarse-grained, contain appreciable shrinkage or gas porosity.

(5) Murphy \*\* has pointed out that grain refinement may be particularly valuable in maintaining ductility when the extent of working is limited by the size of the ingot, e.g. in making a large forging.

Although these several advantages appear to be considerable, the lack of quantitative data regarding them makes it difficult to assess their importance except in the case of a few specific alloys.

Mr. Rutherford suggests that the  $TiAl_3$  particles in hyperperitectic alloys of aluminium and titanium may nucleate

\* M. D. Eborall, *J. Inst. Metals*, 1949-50, **76**, 295.

† F. Kasz and P. C. Varley, *ibid.*, 407.

W. K. J. Pearson, *ibid.*, 754 (discussion).

‡ R. Genders and G. L. Bailey, "The Casting of Brass Ingots" (B.N.F.M.R.A. Research Monograph No. 3), pp. 63-65, 138. 1934: London.

§ W. Helling and E. Hahn, *Aluminium*, 1944, **26**, 32.

¶ F. A. Fox, *J. Inst. Metals*, 1948-49, **75**, 1094 (discussion).

¶ A. Cibula and R. W. Ruddle, *ibid.*, 1949-50, **76**, 361.

\*\* A. J. Murphy, *ibid.*, 762 (discussion).



solidification only at slow rates of cooling. I agree that this might occur if the more active nuclei were removed in some way during the early stages of freezing; for example, if cooling were sufficiently slow, the deposition of solid metal on to the most effective nuclei would cause them to sink to the bottom of the melt, owing to the difference in density between solid and liquid metals, and only small  $\text{TiAl}_3$  crystals (and other less effective particles) might remain suspended in the melt. However, the experimental evidence indicates that the  $\text{TiAl}_3$  crystals are not sufficiently good nuclei to produce very marked refinement. For example, in the earlier work\* we were able to remove active nuclei from an aluminium-0.29% titanium alloy by passing nitrogen through the melt under a flux cover, at a temperature at which the  $\text{TiAl}_3$  crystals were in solution; after solidification in sand at normal rates of cooling, the alloy had only a moderately fine grain-size, although particles of  $\text{TiAl}_3$  were present during freezing.

Mr. Varley's observations are very pertinent. We were unaware of the effect of traces of boron in our earlier work on the identification of nuclei in titanium-refined alloys, and we were, moreover, unable to determine boron contents of the order of 0.0001%; sufficient titanium boride may therefore have been present to cause part of the observed refinement, particularly as recent work indicates that the boride could have formed in addition to the carbide.† However, I think it unlikely that boride was the important constituent of the nucleating particles, for the following reasons. First, almost the maximum refinement was produced by the addition of super-purity aluminium to an equal quantity of an aluminium-titanium alloy from which the original nuclei had previously been removed; if it is assumed that the boron contents of the batches of super-purity aluminium were, at most, equal to that of the commercial-purity metal, the boron contents of the fine-grained castings were less than 0.00005%, which, according to our latest results, would have been insufficient to produce marked refinement. Secondly, it is not correct to say that carbon additions did not have any effect on grain refinement, for, in the presence of an active flux, such additions invariably produced the finest grain-sizes in the titanium alloys from which nuclei had previously been removed; flux composition has a very similar influence on the refinement of magnesium alloys by carbon additions and superheating. Titanium carbide additions or the use of carbon-containing crucibles also produced grain refinement with a suitable flux. Manganese was found to cause marked grain-coarsening in titanium-containing alloys, which was shown by the results of undercooling measurements to be due to decomposition of the nuclei; the fact that refinement did not occur when manganese was added together with the carbon to titanium-containing alloys is therefore not surprising, whatever the identity of the nuclei. Thirdly, titanium carbide and diboride have similar lattice structures and dimensions and chemical properties, and it therefore seems unlikely that the carbide would have nucleating properties much inferior to those of the boride in aluminium melts. Finally, it seems more than a coincidence that only those transition metals which can form simple interstitial carbides act as grain refiners in aluminium alloys; this correlation suggests that the carbides are the nuclei. Unfortunately, owing to lack of information on the composition and stability of the various borides formed by the transition metals in aluminium melts, it is not possible to attempt a similar correlation of grain refinement with boride formation. The evidence available is admittedly not conclusive, but it supports the conclusion that carbide particles can nucleate aluminium melts.

The results obtained by Dr. van Ewijk suggest that his cast-to-shape bars are fed so well, owing to their shape and the method of running, that the bars are virtually free from intergranular shrinkage porosity. We have found, however, that a fine grain-size is essential in D.T.D. test-bars and in

normal commercial castings, as these contain considerable intergranular porosity which is harmless only if uniformly and finely dispersed by grain refinement. The low casting temperatures found by Dr. van Ewijk to be unsuitable are, in fact, commonly used for test-bars in this country to obtain the tensile properties he quotes.

It is true, as Dr. van Ewijk points out, that in aluminium-copper castings with equiaxial structures, mass-feeding occurs at the beginning of solidification, causing a general depression in the top surface as the metal contracts. Eventually, however, the dendrites form a coherent network throughout the casting, and liquid metal then flows through the interstices of the network. Since both mass-feeding and interdendritic flow become increasingly difficult as the dendrite arms thicken, solidification contraction at the end of freezing creates voids which are dispersed throughout the network of grains. On the other hand, in alloys of low copper content (up to about 1%)—and hence short freezing range—mass-feeding hardly occurs to any important extent, as the skin formed by grains nucleated at the surface of the casting is fairly coherent, as shown by simple pour-out tests; feeding can then occur solely by the flow of liquid metal from the centre of the casting, and the continual depression of the surface of the liquid creates a pipe whose growth is stopped only by the bridging of the columnar dendrites near the end of solidification. In other words, the shrinkage which appears as a pipe in the columnar castings is partly replaced by the general depression of the top surface which accompanies mass-feeding in the equiaxial casting, and is partly dispersed throughout the network of grains. The dispersed porosity in the equiaxial casting can be reduced by decreasing the grain-size and thus prolonging mass-feeding during solidification.

Mr. REYNOLDS and Mr. TOTTLE (*in reply*): We are well aware of the numerous factors that can influence grain refinement in cast metals, and cannot accept Mr. Liddiard's suggestion that we suffered from hasty enthusiasm. Details of the metals used were not given for reasons of brevity, and the term "commercial-purity" was employed to indicate that super-purity or specially prepared metals were not involved. It is pointed out in the paper, under "Experimental Methods" (p. 94), that in initial experiments with double moulds, coatings were applied to one face only, leaving seven untreated faces for comparison. Variables introduced by metal composition and melting conditions were thus applicable to both untreated and treated faces. We believe that this fact, and the consistency with which results could be reproduced, dispose of Mr. Liddiard's criticism. The effects noted on treated faces, when these were successful in producing grain refinement, were so marked that they could not, in our opinion, be attributed to any other cause. Under "Examination of Ingots" (p. 95) such treatment is stated to have resulted in grain refinement from 10 to 25 times that due to all other variables.

We regret that Table III (p. 96) included unsuccessful results using thorium coatings with cast aluminium. These should not have been given without further explanation, as they are attributed to the thorium powder having an excessive coating of oxide. Later samples of thorium with very thin oxide films gave successful refinement, and the results are included in Table V (p. 97).

We do not agree with Mr. Liddiard and other contributors who suggest that solid particles are unlikely to be produced at the mould face by deoxidation of the cast metal. Experiments designed to measure mould-face temperatures are difficult to assess, but extreme care was taken in positioning the thermocouple junctions to obtain some idea of the rate of rise of temperature of the mould face. In discussing the investigation (p. 94) it is stated that the mould face frequently attained a temperature less than 70% of the freezing point of the cast metal, and this only some time after solidification had

\* A. Cibula, *J. Inst. Metals*, 1949-50, **76**, 321.

† F. W. Glaser, *Trans. Amer. Inst. Min. Met. Eng.*, 1952, **194**, 391.

begun. The mould faces were very carefully examined after cooling, and melting of the coating was found only where the melting point was far below that of the cast metal. We agree with Mr. Cibula that the degree of superheat must influence the nucleation where melting of the coating may occur, and would refer him to Table III, where the degree of refinement produced in copper cast against a copper coating is shown to vary with temperature.

Mr. Liddiard rightly points out that the oxide film on molten 18:8 chromium-nickel austenitic steel is not necessarily that found on a polished surface in the solid state at lower temperatures. We did not intend to imply that this was so, but that the oxide of chromium might influence the nucleation by our suggested mechanism of deoxidation.

We thank Mr. Baker for his suggestion that oxide-coated

metal may penetrate into the pores of the coating and so minimize the effect of the exothermic reaction which we suggest does occur. We believe that thin oxide films already present on the coating may assist in delaying the reaction until they are broken by differential expansion, exposing the metal beneath. The effect of this oxide film will then be completely to prevent the reaction, when the film reaches a certain thickness, dependent on the temperatures involved, the particle-size of the coating, and the physical properties of the oxide involved.

Finally, we have since found it possible to reproduce the results quoted in the paper many more times than is indicated in the relevant tables. One of us (C. R. T.) has been informed by private communication that a Continental foundry has used the method of mould coating successfully for some commercial castings.

## Discussion

# The Occurrence of Stretcher-Strain Markings in an Aluminium-Magnesium Alloy

By R. CHADWICK and W. H. L. HOOPER

(*Journal*, this vol., p. 17.)

Dr. E. W. FELL,\* M.Sc., F.I.M. (Member): I think it is possible, and desirable, to identify without any ambiguity the so-called "random" markings in aluminium alloy, and therefore I would go somewhat further than Mr. Chadwick and Mr. Hooper have done in Section III (p. 22) of their paper and state that the strain markings in the aluminium-3% magnesium alloy are undoubtedly the same phenomenon as the well-known Lüders lines in steel. Fig. 2 (Plate III) and Fig. 5 (Plate IV) of the paper afford conclusive evidence that the markings present the same visual appearance as in steel. Further, the remarkable similarity in the way in which the phenomenon occurs confirms that it is the same for both materials (see Table A, where the authors' results are

TABLE A.—*Random Markings in Aluminium-3% Magnesium Alloy Compared with Lüders Lines in Steel.*

Material	Angular Inclination of Strained to Unstrained Regions	Elongation Associated with the Spreading of Random Markings Over the Entire Gauge-Length, %	Elongation after Fracture, %	Approximate Upper Limit to the Size of the Crystals Composing the Aggregate, mm.
Al-3% Mg alloy	<1'	About 1	26	0.04
Soft steel †	About 2°	About 5	30	0.07

used). Chadwick and Hooper's view that random markings may be of relatively rare occurrence because few metals or alloys can readily be obtained with the fine grain-size that experiments indicate to be essential, is a conclusion I had reached in my own researches.

It is interesting to compare measurements of the actual surface distortion made by the authors on their aluminium

alloy, with similar measurements on steel I made by different methods.† In my own work, the movement of the metal in a direction normal to the surface of the test-piece was measured by means of a microscope, and the movement in a direction parallel to the surface by inscribing fine lines on the test-piece and then observing their new position caused by the formation of a Lüders line. The authors give the angle of inclination of the adjoining surfaces, at the boundary of a random marking, as generally less than 1' in the aluminium-magnesium alloy sheet, whereas observations showed the angle of inclination for steel bar to be as much as 1°, measured in a direction of shear.† Again, the permanent extension associated with the spreading of random markings over the whole of the gauge-length of the test-piece in the aluminium-magnesium alloy sheet is given by the authors as about 1%; for this to occur in soft steel bar the permanent extension necessary may easily be as much as 5%. The percentage elongation after fracture of the test-piece is included in Table A for purposes of comparison, and its value will be seen to be much larger than the permanent extension associated with the spreading of random markings over the gauge-length. Table A also shows the upper limit of crystal size, in the aggregate of crystals forming the test-piece, for random markings to occur, and it will be seen that these crystal sizes for the aluminium alloy and soft steel (Armco iron ‡) are not very different. There are, no doubt, other close similarities in properties to be found, but those I have indicated suffice to show that Lüders lines in steel are the same as the random markings in the aluminium-magnesium alloy and that they are quite distinct from other kinds of strain marking. Although the distortion and strain associated with Lüders lines in steel are considerably greater than for the aluminium alloy, to judge from the figures for the angular inclination of the strained regions and for the percentage elongation (Table A), yet scientifically we may now speak of Lüders lines in aluminium alloy.

\* Lecturer in Metallurgy, Technical College, Bradford.

† E. W. Fell, *J. Iron Steel Inst.*, 1935, **132**, 75 and Fig. 5 (Plate VIII).

‡ E. W. Fell, *Carnegie Schol. Mem., Iron Steel Inst.*, 1937, **26**, 157.



The AUTHORS (*in reply*): We agree that the term "Lüders lines" could well be applied to strain markings in aluminium alloy. However, before our investigation on aluminium alloys, the clear distinction between the two different types of marking, which we have called random markings and parallel bands, does not appear to have been realized, and terms such as "stretcher strains" and "Lüders lines" were used indiscriminately.

The comparison which Dr. Fell draws between our results, using a Talysurf instrument, and his own earlier work, employing rather less sensitive measuring devices, is, we feel, misleading, and the differences in behaviour between steel and aluminium-magnesium alloy are much smaller than he supposes. A paper comparing these two materials, in which one of the present authors (W. H. L. H.) participated, has recently been published in the *Bulletin* of the Institute of Metals.\* The markings obtained with light straining were measured mechanically on the Talysurf instrument and optically by Tolansky's interferometric method. This latter method provides a particularly accurate measure of the angular inclination of neighbouring regions in the strain-marked areas, and indicates that in steel this varies from 5' to 50' with most values in the range 20'-30'. The earlier measurement of less than 1' in aluminium alloy was confirmed. The maximum overall roughness associated with stretcher-strain markings is, however, about the same in both materials, viz. 0.0003 in.

The minimum permanent extension associated with the spreading of random markings over the entire gauge-length is not at all easy to determine. Straining is, of course, discontinuous, and when the whole length is affected by markings, some parts may have stretched more than others. However, our most careful measurements indicate that both

in aluminium-magnesium alloy and in mild steel, random markings are fully developed within about 0.5% extension. With continued stretching the markings in aluminium alloy are smoothed out at about 2% extension, but they may well persist up to 4% extension in steel.

We have already indicated that in aluminium-magnesium alloys a second form of strain marking, which we have termed "parallel bands" occurs with extensions greater than 2%. On the other hand, no corresponding form of strain marking appears to have been observed in steel once the first strain markings have been pulled out. Our more recent studies of strain markings or Lüders lines in steel indicate that, in fact, they are not of one kind but two, and that random markings and parallel bands can be present in the same specimen. In aluminium alloy random markings are characterized by being initially at right angles to the direction of stress (their random direction developing later owing to unequal stretching) and consist of kinking in the sheet. Parallel bands, on the other hand, are at a definite acute angle (57° in aluminium-magnesium) to the stress direction, the sheet being thinned or necked. Fig. A (Plate CX) shows strain markings on a mild-steel specimen stretched to a ½% elongation, along with the Talysurf traces of the surface. The broad lines at right angles to the stress are clearly accompanied by kinking, while the narrow lines subtending an angle of about 50° are accompanied by necking. Our interpretation of this picture is that the two types of marking, observed at different extensions in aluminium alloy, can occur simultaneously in steel. We do not know whether they always occur together at some stage of stretching mild steel, but certainly both develop with quite small extensions. We hope that Dr. Fell will be able to resume his studies of the straining of steel, in which there is obviously much of interest still to be learned.

## Discussion

# The Plastic Deformation of Metals†

Mr. F. R. N. NABARRO,‡ M.B.E., M.A., B.Sc. (Member): Dr. Cahn has concentrated his attention on the side surface of the crystal, where deformation bands are observed. This has led him to postulate two processes, neither of which seems to have been entirely plausible at the time the paper was written: first, the formation of small kink bands by the production of pairs of dislocations, and second, the migration of these kink bands as a whole along the crystal. Recently Frank and Stroh§ have shown theoretically that the first can occur if the angle of the kink is at least 2° (much smaller angles of kink are observed in practice), while Washburn and Parker|| have observed the second effect experimentally.

Dr. Brown, who concentrates on explaining the appearance of slip lines on the top surface, has also been led into an unverified hypothesis, namely that there exists a mechanism for softening a crystal in the immediate neighbourhood of a newly formed slip line. Such a mechanism has now been found in the release of vacant lattice sites during the slip process. Brown's interpretation of slip lines completely neglects the existence of deformation bands; Cahn's interpretation of deformation bands neglects, and is at first sight incompatible with, the observed fine structure of slip lines.

Progress must depend on a reconciliation of these two viewpoints.

Finally, Dr. Honeycombe seems anxious to attribute most of the work-hardening to the formation of deformation bands. His evidence for a connection is impressive, but three arguments can be brought against him. The "most convincing support" which he received from the experiments of Röhm and Köchendorfer is now not as firm as was originally thought; the reduction in the free path of dislocations produced by the presence of deformation bands is analogous to a grain-size effect, and would not by itself be expected to put up the critical stress greatly; it can hardly be a coincidence that crystals which slipped on two glide systems from the beginning of deformation formed no deformation bands, but hardened at roughly the same rate as crystals which formed kink bands.

Dr. B. JAOUŁ and Professor C. CRUSSARD¶: The stress/strain curves of all metals exhibit a singular point where the curvature changes suddenly. This transition point corresponds to a change in the rate of strain-hardening, i.e. a change in the mechanism of cold working. We have studied this phenomenon extensively, mainly on polycrystalline aluminium-base alloys.\*\* Although the exact mechanism is not clearly under-

\* W. H. L. Hooper and J. Holden, *Bull. Inst. Metals*, 1951-53, 1, (18), 161.

† Joint discussion on the papers by R. W. Cahn (*J. Inst. Metals*, 1951, 79, 129), R. W. K. Honeycombe (this vol., p. 45), and A. F. Brown (this vol., p. 115).

‡ Lecturer in Metallurgy, University of Birmingham.

§ Unpublished work.

|| J. Washburn and E. R. Parker, *Univ. California Inst. Eng. Research, Tech. Rep.*, 1951, (27/3).

¶ Centre de Recherches Métallurgiques, Ecole des Mines, Paris.

\*\* B. Jaoul and C. Crussard, *Rev. Mét.*, 1950, 47, 589.

stood, the change represents a stage in deformation where discrete spots become clearly visible on the asterism streaks of X-ray back-reflection photographs, thus indicating a kind of polygonization or kinking within the grains. Microscopic examination of samples electropolished before deformation, revealed a certain amount of intimate cross-slip at all stages of deformation, and was more extensive in the case of the less pure metals. Prominent cross-slip became apparent only after the transition point had been reached.

The transition point is also related to the spacing of the slip bands, which in turn depends on the content of alloying elements. If  $\epsilon_p$  is the elongation reached at the transition point, and  $x$  the atomic concentration of solute elements, then  $\epsilon_p$  is proportional to  $x^{1/3}$ , being 1.5% for 99.99% aluminium and 3% for 99.8% aluminium. For a given elongation, the average spacing of the slip bands varies inversely as  $\epsilon_p$ ; this means that the step, or unit glide per slip band varies inversely as the concentration, or rather some power of it near to  $x^{1/3}$ . Thus, the factor governing the shape of the stress/strain curve would seem to be the influence of alloying elements on the development of individual slip bands.

The transition point on the stress/strain curve is also observed in the case of single crystals. One of us (C. C.) has shown previously\* that two types of crystal should be distinguished:

Type I. Crystals in which only one slip system operates in the first stages of elongation.

Type II. Crystals in which two slip systems operate from the beginning (specimens whose axis lies in a direction near to [100] or [111]).

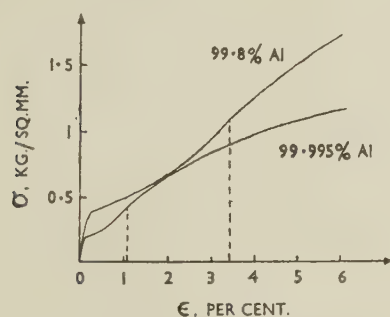


FIG. A.—Stress/Strain Curves of Aluminium Single Crystals (Type I).

Type-II crystals early exhibit strong asterism and extensive strain-hardening at first, which do not increase very much in the course of deformation; in agreement with Honeycombe's observations, they have no kink bands, but frequently display what he calls "bands of secondary slip". Type-I crystals do not strain-harden much at first, but after a small percentage elongation hardening and asterism occur and kink bands become visible. This proves that easy glide on a single slip system does not cold work the metal to any considerable degree, in agreement with the results of Röhm and Kochendörfer's experiments on the shear of aluminium crystals,† and Andrade and Henderson's experiments on silver and gold.‡ Strain-hardening and asterism are mainly due to the same cause—blocked dislocations. These may either group themselves to form kink bands (Type I) or remain dispersed on a smaller scale, like Burgers's "local curvatures" (Type II), according to the orientation of the crystals.

In crystals of Type I the transition point on the stress/strain curve is very well marked, corresponding to an inflection (Fig. A) where kink bands become distinct. Microscopic

examination shows cross-slip close to the kink bands (Fig. B, Plate CXI), while there is no trace of such slip in the intervals between the bands (Fig. C, Plate CXI). For such crystals, therefore, the transition point, kinking, and cross-slip are all closely related. With Type-II crystals the question is complicated by the fact that the rate of deformation seems to exert an important influence on the shape of the stress/strain curve.

There is thus a considerable resemblance between the phenomenon as it occurs in polycrystals and in single crystals. In both cases some factor (probably structural defects connected with pre-existing dislocations or variations in concentration) blocks the dislocations, which can then either pile up in a band (kink band) or change direction (cross-slip).

We have examined the possibility that kink bands originate in pre-existing sub-boundaries and have come to the conclusion that this is not the case. Fig. D (Plate CXI) shows the surface of a crystal electropolished, treated with a special reagent designed to produce fine etch pits, and pulled some 5% in tension. Sub-boundaries, some of which are almost straight, are clearly visible; their orientation has been determined to be about (112). Kink bands can also be easily distinguished. These lie, however, on a completely different plane, the (110) plane normal to the glide direction, as shown by Cahn. The sub-boundaries are, therefore, not the origin of the kink bands, although they may influence them, as shown in Fig. D, where two kink bands end on sub-boundaries.

In the course of our experiments we have observed that kink bands can be clearly revealed by electropolishing, as the metal dissolves more rapidly in their vicinity.

Dr. HONEYCOMBE (*in reply*): Mr. Nabarro states that crystals slipping on two sets of glide planes from the beginning of deformation do not develop deformation bands. This is not so, for while no kink bands are formed, bands of secondary slip are often particularly prominent, an observation which has been made both by Jaoul and Crussard and by the writer. In the circumstances it seems very desirable to avoid use of the general term "deformation band" when referring to a specific type of inhomogeneity. It is difficult to separate the contribution of the two types of inhomogeneity to the strain-hardening of aluminium crystals. However, it does seem that for cubic metals there is some degree of correlation between the occurrence of kink bands and the shape of the stress/strain curve. Furthermore, in hexagonal crystals deformed in tension, where the degree of strain-hardening is much less, both types of inhomogeneity are absent.

Mr. Nabarro's statement that crystals deforming on one or two glide systems harden at roughly the same rate is somewhat misleading, because in the early stages of deformation at least, there are significant variations in the rate of strain-hardening. M. Jaoul and Professor Crussard have shown in their contribution that the inflection in the stress/strain curve marking the end of easy glide is also associated with the distinct appearance of kink bands. More recently, Dalton and I§ have noted the same behaviour in copper crystals deforming on a single set of glide planes, which in most cases passed through a region of easy glide at an early stage of the deformation, before kink bands could be observed. If the inhomogeneities dominate the trend of the stress/strain curve, then it is not surprising that crystals deforming by duplex slip harden initially at a more rapid rate than those deforming by single slip, because in the former case large bands of secondary slip are present in the crystals from the earliest stages of deformation, whereas in the latter case, the kink bands are a later development.

M. Jaoul and Professor Crussard's stress/strain curves for two aluminium crystals of different purity are very revealing.

\* C. Crussard, *Rev. univ. Mines* (Congrès A.I.Lg., Section Métallurgie physique), 1947, 41.

† F. Röhm and A. Kochendörfer, *Z. Metallkunde*, 1950, 41, 265.

‡ E. N. da C. Andrade and C. Henderson, *Phil. Trans. Roy. Soc.*, 1951, [A], 244, 177.

§ A. L. Dalton and R. W. K. Honeycombe, unpublished work.



The less-pure crystal has hardened at a more rapid rate, and the region of easy glide is below 0.5% strain. My observations indicate that in crystals of similar purity (99.5%) kink bands are visible (in X-ray micrographs) after 0.5–1% strain; they are very closely spaced (0.05 mm.) and the spacing does not noticeably decrease with increasing deformation. How-

ever, with crystals of higher purity (99.99%) the kink bands appear to develop more gradually and at a rather later stage of the deformation; the minimum spacing is much greater (0.1–0.2 mm.), and as Jaoul and Crussard show, the rate of strain-hardening is less. Here perhaps is the grain-size effect which Mr. Nabarro seeks.

## Discussion

# The Flow of Liquid Metals on Solid Metal Surfaces

By G. L. J. BAILEY and H. C. WATKINS

(*Journal*, this vol., p. 57.)

Mr. R. CHADWICK,\* M.A., F.I.M. (Member): It is apparent from a study of this paper that considerable difficulty has been experienced in devising experiments to evaluate the factors which go to make up solderability. Indeed, the authors acknowledge this and do not claim the results to be anything but preliminary in character. Nevertheless the work has been extensive, and progress has been made, at least in the physical basis of interpretation of solder behaviour. It is, however, important to draw attention to the lack of metallographic observations, such conclusions as the authors draw with regard to phase relationships in joints being inadequately supported by evidence, and consequently misleading. There is little justification, for example, for the statement on p. 64, in which the absence of intermetallic compounds is deduced from the external appearance of drops which had spread over a large area; and on p. 71 it is somewhat surprising to note the authors' apprehension regarding the possible difficulty of detecting alloy layers by micrographic examination of sections.

Reference to earlier published investigations clearly indicates that molten tin and tin-lead alloys react rapidly with copper at soldering temperatures, with the formation of intermetallic compounds, principally  $\epsilon$  and  $\eta$ . I have shown † that the  $\epsilon$  compound film could readily be detected in microsections of joints in which the solder was molten for only about 1 sec. With longer times of reaction the amounts of intermetallic compounds were substantial, as several photomicrographs of joints indicate. Conditions comparable to those obtaining in some of the experiments under discussion are reproduced in the section illustrated in Fig. A (Plate CX), which shows needles of the  $\eta$  phase more than 0.1 mm. in length in a film of pure tin heated for 15 min. at 500° C. in contact with H.C. copper sheet. From data given on p. 62 of the paper by Bailey and Watkins, simple calculation shows that the standard drop of 0.05 ml. volume, after the normal initial spread to 10–12 mm. dia., would be about 0.5 mm. in thickness, while 30 min. later, when secondary spread had ceased, drop thickness would range between 0.1 and 0.5 mm., according to solder composition and temperature. It is evident, therefore, that some of the drops may have enclosed sufficient solid intermetallic-compound particles to affect flow significantly. The extent of interference would, moreover, depend on solder composition, since interlacing crystals of intermetallic compound grow out into the liquid metal only with pure tin or alloys of high tin content. As lead is progressively increased, so do compounds tend to form thinner and more sharply defined layers. Thus, the small amount of secondary spreading in the area B of Fig. 7 (p. 63) may be accounted for by the retention of liquid

in the sponge-like network of intermetallic compounds, while in area A the alloy layer would be more uniform and compact.

Another effect of the reaction between tin and copper would be to reduce substantially the tin content of the liquid solder. It seems not unlikely, therefore, that if data were available to permit replotting of the curves shown in Fig. 4 (p. 62), on the basis of residual rather than initial tin content, it would lead to a more rational result, with maximum spread at all four temperatures occurring at the same tin content.

Apart from these details of interpretation, it should be noted that the period over which the experiments extended was generally so long that the results have little practical significance. In the best soldering practice the solder is held in the molten condition for the briefest possible interval, and secondary spread is seldom involved. The development of techniques for studying flow over short periods should therefore be the authors' next concern.

Important and full of interest though soldering operations with tin-lead alloy may be, there is no doubt that the use of such a reactive metal as tin so complicates the issue that it is impossible to separate the many factors involved, and purely physical concepts must necessarily represent the summation of many variables. Simpler systems not involving compound formation should therefore be studied.

Finally, perhaps it would be as well to point out that the paper is concerned only with the first stage of the soldering operation, i.e. the flow of the solder into the joint. The second stage, involving the solidification of the liquid solder, is just as important. Eutectic solders, because of the absence of freezing range, are the most likely to succeed in difficult applications, and many soldering failures have occurred in the past by the use of mixtures with a freezing range in which stresses may develop before the solidus is reached. Compositions with a long freezing range and small eutectic content, such as the high-lead solders, are particularly unsuitable on that account, and may have little merit as solders even if the wetting difficulties can be overcome.

Dr. J. C. CHASTON, ‡ B.Sc., A.R.M.S., A.Inst.P., F.I.M. (Member): This will undoubtedly rank as an outstanding paper in the literature of the metallurgy of soldering. It represents the first really serious attempt to come to grips with the problem of "solderability", why one solder is easier to use than another; and all those privileged to follow the work of the B.N.F.M.R.A. investigators will know that it has been a difficult and often disappointing piece of work.

One important conclusion has now been quite definitely established—that the flow of a liquid metal over a surface

\* Assistant Research Manager, Imperial Chemical Industries, Ltd., Metals Division, Birmingham.

† *J. Inst. Metals*, 1938, 62, 277.

‡ Manager, Research Laboratories, Johnson, Matthey and Co., Ltd., Wembley, Middlesex.



may be affected by changes in the surface resulting from diffusion and also from reactions with the flux.

One of the underlying assumptions of the paper is that wetting and adhesion are two different properties. The authors write that "although lead failed to wet copper and iron, the adhesion was strong when it was allowed to solidify in contact with either". If this assumption is accepted, the whole problem of choice of solders becomes very much simplified; for the strength of a joint can be taken as equal to that of the solder, the work, or any interfacial layers, whichever is the weakest. There is, however, a limit beyond which this assumption does not apply; thus, molten metals will not, when solidified, adhere to glass, ceramics, or many oxidized surfaces. Can the authors give us any idea as to where the dividing line is to be drawn between materials which will or will not adhere to molten metals solidified on their surface? Will lead, for instance, adhere to any metal or alloy, whatever its lattice structure or parameters; and at what thickness does an unbroken oxide film become a barrier to adhesion?

In considering the factors which make one metal either flow over another, or dewet it, there is a possibility, I think, that Table II (p. 67) may be misleading. It is obvious that the flooding tests on which it is based are not very informative, and it is doubtful whether the results of preliminary work should be recorded at such length. Thus, the Table lists tin as a metal which wets copper at 400° C., but it is evident that this result needs qualification, since it appears that at 450° C., when the  $\epsilon$  phase  $\text{Cu}_3\text{Sn}$  is formed, the copper would dewet.

Although the conclusions of this work are undoubtedly important, it is not easy to apply them to practical experience. The authors, for instance, are particularly concerned with explaining the spread-of-drop tests, shown in Fig. 1 (p. 58), which suggest that 50:50 tin-lead alloys spread more readily on copper than any others in the system; and that with all alloys the spread is greater for 60° C. superheat than for 150° C. superheat. As I understand it, the suggestion is that the rate of diffusion of tin from the 50:50 tin-lead alloy into copper at 60° C. superheat is such as to favour the formation of  $\text{Cu}_5\text{Sn}_2$  rather than  $\text{Cu}_3\text{Sn}$  at the surface. If rate of diffusion is, in fact, the governing factor, it is difficult to understand why a 45% tin alloy should not spread just as much as a 50% tin alloy, if applied at a sufficiently high temperature so as to increase the diffusion rate to the optimum value. In other words, I should have thought that by suitable choice of temperature it should be possible to make any of the alloys poorer in tin than the 50% alloy spread as much as the 50% alloy, if diffusion rate were the only factor concerned.

I have long wondered why—in spite of such well-established spread-of-drop curves as those in Fig. 1—so many users find the eutectic tin-lead alloy easier to use than the 50:50 alloy. For making soldered joints in tinned-copper wiring in telephone and radio assemblies, for instance, it is quite certain that the eutectic alloy is easier to use, is more economical (far less is consumed), and is more certain in its results than any other alloy. The answer surely is that in this particular application the contact angle does not come into the question. The contact angle and the ease of wetting are probably here adequate with any tin-lead solder, but as the eutectic alloy has the lowest melting point, joints are made more quickly and surely with it (when using a given size of iron) than with any solder of higher melting point.

Finally, it should be emphasized that the results shown in Fig. 4 (p. 62) apply only to the spread of drops after the long period of 30 min.; and I would like to add a word about the general presentation of the results. To my mind, this paper rather too obviously is a compilation from a series of separate reports, and there seems a little too much anxiety to include reference to *all* the work done in the investigation. I hope that it will eventually be possible to give, perhaps in a monograph, a connected account of the conclusions without any

special reference to the order in which the work has been done.

Mr. R. G. HARPER,\* M.Sc. (Member): All who have followed the investigations of Dr. Bailey and his colleagues at the B.N.F.M.R.A. during the last few years have been impressed and delighted by the range of experimental techniques employed for the investigation of wetting phenomena. The present paper, a macedoine of physical, chemical, and metallurgical observation, typifies the kind of work carried out. It illustrates, too, in the sections dealing with nickel additions and with surface roughness, some practical and theoretical advances which have accrued.

Clearly, however, soldering is such a complex process that the greatest care must be taken when fitting the experimental findings into their practical context to avoid giving an unmerited prominence to any one factor. This applies particularly to the area-of-spread tests; despite the authors' careful phrasing, their final remarks may leave the reader with the impression that there can be a single criterion of solder performance.

It is perhaps an obvious point, but it bears re-emphasizing, that, within the standard range of lead-tin solders, the choice of composition is usually decided by considerations of soldering power. Near-eutectic solders are used for critical bit-soldering applications where the heat input must be restricted. Alloys of lower tin content are permissible where greater heat input and higher working temperatures are feasible. The choice, then, is based first on the melting characteristics of the alloy and their relation to the heating equipment available to the solderer.

Thus, industrial preference from the standard range of solders is more accurately represented by fluidity-spiral measurements than by the relevant section of Fig. 1 (p. 58). It must also be remembered that there is a big difference in spreading results of solders on copper and on steel, which is not reflected in industrial practice.

Where, then, lies the importance of spreading-test determinations as a measure of soldering power? Presumably, the standard solders all reach an acceptable level, beyond which the differences are largely masked by variations in the melting range. Certainly, with the solders outside this range which are more difficult to apply, such as the lead-base alloys of low tin content, the areas of spread (on copper) are much lower, and the results appear to coincide more closely with practical experience.

This criticism is directed at one point in what is necessarily an interim report—a report which shows solid progress. It can be hoped that the further work at the B.N.F.M.R.A. will yield a still clearer picture of this complicated but fascinating subject.

Mr. R. F. TYLECOTE,† M.A., M.Sc., A.I.M. (Member): I was particularly interested in the authors' findings with regard to the effect of the addition of nickel to lead on the wetting of copper and iron. Some years ago, I had occasion to investigate some of the properties of brazed joints. In joints between tungsten and mild steel, made by copper-brazing for about 15 min. at 1120° C. in hydrogen, I noticed the existence of a third phase between the copper and the tungsten. Since, as far as I am aware, copper and tungsten do not form an alloy, it was assumed that iron was dissolving in the copper and forming a copper-iron-tungsten phase on the copper-tungsten interface. A number of tests were made which supported this assumption. Efforts to copper-braze tungsten to tungsten resulted in a very weak joint, with no evidence of an interfacial alloy layer.

During this work, I needed to melt copper at 1120° C. in small mild-steel "cupels", in an atmosphere of hydrogen. With the normal turned surface I had difficulty in keeping the copper in place in the "cupel" owing to the fact that wetting of the steel by the copper caused the copper to run out over the

\* Technical Manager, Fry's Metal Foundries, Ltd., London.

† I.C.I. Research Fellow, Royal School of Mines, London.



top. However, this was obviated by metallographically polishing the top of the "cupel".

The AUTHORS (*in reply*): Both Mr. Chadwick and Dr. Chaston are concerned that the duration of many of our spreading experiments should have been as long as 30 min. Mr. Chadwick, in particular, suggests that the development of techniques for studying flow over short periods should be our next concern. While this has been done in later work, not yet reported, it must be pointed out that in the experiments described in the paper the liquid and solid metals were not brought into contact until the testing temperature had been reached. The short-term flow characteristics were thus, in fact, observable. In these experiments we were concerned, by the use of hydrogen as a flux, to simplify the study of spreading by eliminating effects due to the decomposition of liquid flux, thereby arriving at conclusions about the inherent ability of the liquid metal itself to spread on a clean solid surface. The occurrence of slow secondary spreading in these experiments provides evidence, not previously available, to indicate that one important function of zinc chloride flux is to promote rapid spreading through the occurrence, not possible with resin flux, of an electrolytic tinning reaction. The general correspondence of areas of spreading in rapid tests using zinc chloride flux and in our long-duration tests, is evidence that flow in the long-term tests was not significantly constricted by the growth of intermetallic compounds. Further evidence that the inherent spreading capacity (or contact angle) was in fact observed (subject to the qualifications occasioned by surface roughness referred to in the paper) is given by the statement (p. 63) that a drop of 40% tin alloy applied at a temperature above 300° C. began to spread rapidly on cooling. These remarks are relevant also in connection with Dr. Chaston's comments on diffusion rate. We agree that this is not the only factor concerned, the other important considerations being surface roughness and inherent contact angle.

Our belief that the spreading we observed was not unduly influenced by retention of the liquid in a sponge-like network of intermetallic compounds, led us to seek explanations for the variation of contact angle elsewhere. The results of micrographic examinations of alloy layers, the absence of which from the paper Mr. Chadwick deplores, were unhelpful,

and are not reported for this reason. The suggestion made by Mr. Chadwick to account for the variation of maximum area of spread with tin content may well be correct, however.

We would point out, in further reply to Mr. Chadwick, that we have reported elsewhere\* a study of a system in which no compounds are formed.

In reply to Dr. Chaston, what is regarded as "wetting" is a matter of definition. A surface is sometimes regarded as wetted by a liquid which rests upon it with a contact angle of less than 90°. We have taken the existence of a contact angle low enough to ensure the removal of a relatively stable liquid coating on a solid surface dipped into the melt, to constitute wetting. No close correlation is to be expected between wetting by the liquid and adhesion of the solidified liquid to the surface upon which it rests.

Table II, the wisdom of including which is questioned by Dr. Chaston, is considered useful, if read in context, in covering a wider field than was possible in later, more critical experiments.

Mr. Harper lays particular emphasis on the extent to which our work is capable of being fitted into a practical context. We have not attempted in this paper to draft our conclusions primarily in this sense, nor does the work claim to be concerned with the evaluation of all the relevant practical factors. In particular, we do not feel that area of spread provides directly even one of the criteria for solder performance. It is proposed in a later paper to discuss the practical bearing of this and later work.

In connection with Mr. Tylecote's interesting remarks we would refer him to work by Parker and Smoluchowski† in which silver was prevented from spreading on a steel surface by polishing, and add that we do not believe the existence of an interfacial alloy layer to be essential for good adhesion. Lead/steel and lead/copper provide examples in support of this contention. It seems likely that the contact angle between pure liquid and solid metals in general falls with increase in temperature. We were able to obtain coatings of lead on copper by dipping at temperatures above 500° C., followed by rapid cooling. In this connection it has been reported to us that at sufficiently elevated temperatures copper exhibits a low contact angle against tungsten, which facilitates brazing.

## Discussion

### Constitution of Transition-Metal Alloys‡

Dr. K. W. ANDREWS,§ B.Sc., F.I.M. (Member): The equilibrium diagram of the Ni-Mn system determined by Dr. Coles and Dr. Hume-Rothery contains some very interesting features. Thus, the authors have shown that there is complete solid solubility between  $\gamma$ -manganese and nickel, although there is an axial ratio change from the face-centred tetragonal structure of  $\gamma$ -manganese until a face-centred cubic structure is attained. Does this convergence of the  $a$  and  $c$  axial lengths occur at a simple ratio of atoms, or can any theoretical significance be attached to it? Alternatively, is it possible that a high-temperature X-ray camera would

reveal a continuous face-centred cubic solution, and that the tetragonal lattice of  $\gamma$ -manganese is formed only on quenching? It would also be of interest to know whether the authors have since carried out further work, or have developed an explanation of the sequence of phases at the equi-atomic composition. This is especially interesting in view of the change: face-centred cubic (close-packed)  $\rightarrow$  body-centred cubic  $\rightarrow$  face-centred tetragonal (close-packed, but ordered CuAu type). If the third of these phases is identical with the first, apart from the ordering, then the sequence is not dissimilar to that for the allotropy of pure iron, except that in

\* G. L. J. Bailey and H. C. Watkins, *Proc. Phys. Soc.*, 1950, [B], **63**, 350.

† E. R. Parker and R. Smoluchowski, *Trans. Amer. Soc. Metals*, 1945, **35**, 362.

‡ Joint discussion on papers from this volume of the *Journal* by B. R. Coles and W. Hume-Rothery (p. 85); G. A. Geach and D. Summers-Smith (p. 143); A. H. Sully

(p. 173); P. Duwez (p. 525); R. W. Floyd (p. 551); A. Taylor and R. W. Floyd (p. 577); H. T. Greenaway (p. 589); W. B. Pearson and W. Hume-Rothery (p. 641); and Z. S. Basinski and J. W. Christian (p. 659).

§ Head, X-Ray Section, United Steel Companies, Ltd., Research and Development Dept., Rotherham, Yorks.

the latter case the close-packed structure is that which occurs intermediate between two body-centred cubic forms. Can this phenomenon be associated with the fact that iron lies between manganese and nickel in the Periodic Table? Thus, in the neighbourhood of iron and cobalt, very little difference in free energy exists between the body-centred cubic and the face-centred cubic lattices. That the  $\alpha \rightleftharpoons \gamma$  transformation in the system Fe-Co is nearly horizontal, but gives a small maximum in the 50% region, may be connected with this fact (cf. also the apparently even smaller free-energy difference between the two forms of cobalt).

The  $\sigma$  phases provide an interesting link between non-ferrous and ferrous metallurgy, in view of their occurrence in a number of alloy systems involving iron as one component.\* Dr. Sully's theory was the first attempt to explain the occurrence of  $\sigma$  phases in terms of the electronic structure of the transition elements involved, and as such, will have stimulated further valuable research. It may be doubted, however, whether his interpretation is correct in detail. If it were so, a  $\sigma$  phase could not become ferromagnetic at any temperature, whereas it appears that the Fe-Cr  $\sigma$  phase does become ferromagnetic at about  $-113^\circ\text{C}$ .† It would also be expected that, since according to this theory the number of electrons taking part in interatomic bonding is considerably reduced, the structure would be weaker than say a body-centred cube of the same composition (as in Fe-Cr). The  $\sigma$  phases all appear to be hard and brittle. Furthermore, the  $\sigma$  phase in Fe-Cr is more dense than the body-centred cubic lattice, whereas it should be less dense. The following data illustrate this point:

	Density g./c.c.
Fe-Cr:	
$\sigma$ phase . . . . .	7.625 ‡
Body-centred cubic . . . . .	7.533 §
Fe 55.44-Cr 41.71-Ni 2.85 at.-%:	
$\sigma$ phase . . . . .	7.636 (at $20^\circ\text{C}$ )
Body-centred cubic . . . . .	7.569 ( „ „ )

It seems, therefore, that Dr. Sully's postulate that bonding electrons enter the vacant atomic orbitals until these are filled, is not justified. It does not necessarily follow that some other valid theoretical significance cannot be attached to the relationships suggested by his Figs. 4 and 5 (p. 176). Beck *et al.*¶ have, however, shown that  $\sigma$ -phase boundaries in a number of ternary alloy systems are approximately parallel to lines of constant electron vacancy. This discovery may point to a somewhat different interpretation from that of Dr. Sully, although both interpretations start from Pauling's theory of the transition metals.

Since  $\sigma$  phases in some binary systems occur at simple atomic ratios, with solid solution, it might have been supposed that superlattice formation was partly responsible for their occurrence. There is, for example, a pronounced maximum in the transformation  $\alpha \rightarrow \sigma$  in the systems Fe-V and Fe-Mo. In the systems Mn-Cr and Mn-V, however, the  $\sigma$  phases occur over a composition range that includes a 3:1 ratio (75% manganese). The position in regard to several of the other systems is not so simple. It is possible, however, that  $\sigma$  phases owe their origin to a combination of an electronic effect and a tendency to form a superlattice. The latter

tendency need not necessarily arise from differences in atomic radii, but could depend upon effects arising from the empty  $d$  shells, as suggested by Hume-Rothery and Christian.\*\* This possibility, viz. that  $\sigma$  phases arise from the operation of two factors, should not be ignored.

Dr. Sully refers, on p. 178, to the suggestion of Bradley and Goldschmidt that there are similarities between the X-ray pattern of the (Fe-Cr)  $\sigma$  phase and that of  $\alpha$ -manganese. I do not consider that the resemblance is actually very striking, but the suggestion was of value in view of the implication that the similarity was associated with the fact that iron and chromium lay one on either side of manganese in the Periodic Table.  $\sigma$  phases have now been reported in eleven binary alloy systems and, apart from the special cases of Mn-V and Mn-Cr, the alloying elements in each case invariably obey the rule that one of them lies to the right of the manganese group (VII) and one to the left in the Periodic Table. I have discovered †† that an intermetallic constituent which has an X-ray powder pattern practically identical with that of manganese and a lattice parameter of 8.860 kX units, does in fact exist. Furthermore, this constituent appears to be closely related to the  $\sigma$  phase, since it forms as an apparent alternative structure in closely similar alloys, in particular in steels containing chromium, nickel, and molybdenum (e.g. the so-called "18:8:3" types). The occurrence of this constituent known as the  $\chi$  phase has since been confirmed by workers in other laboratories. The existence of an intermediate phase similar in structure to manganese, may thus help in the understanding of  $\sigma$  phase and other intermediate constituents formed in alloys of the transition elements.

Dr. D. S. BLOOM ‡‡ and Dr. N. J. GRANT §§ B.Sc.: The paper by Dr. Taylor and Mr. Floyd presents some very welcome information on the Cr-Ni system. There are, however, several items that merit additional comment and question.

The authors mention in a footnote (p. 579) that they found no supporting evidence for the existence of the eutectoid reaction at  $1180^\circ\text{C}$ , that we reported. Unfortunately, no direct evidence is presented. There are two points on which we would like their opinion.

The first concerns the lack of lattice-parameter values in Table II (p. 579) for the chromium-rich phase in the alloys quenched from  $1200^\circ\text{C}$ . It was our experience that only with a most vigorous quench could the high-temperature chromium phase be retained, and the quenching rates obtained by the authors, therefore, may not have been adequate to retain the  $1200^\circ\text{C}$  equilibrium condition. As a result, an intermediate, non-equilibrium structure may exist, and this may explain the absence of the normal body-centred-cubic chromium lines.

The second point relates to the interesting form of the nickel solid-solution boundary as presented in the phase diagram of their Fig. 2 (p. 580). If the eutectoid reaction takes place at about  $1180^\circ\text{C}$ , then the shape of the boundary could be quite easily explained if the kink in the boundary is raised about  $100^\circ\text{C}$ .

Dr. B. R. COLES, |||| B.Sc. (Junior Member): I am particularly interested in the magnetic properties of these metals, and in this connection I would suggest that it is wrong to classify ruthenium, rhodium, osmium, and iridium with iron, cobalt, nickel, palladium, and platinum. The former group

\* Commercial ferro-vanadium supplied to the United Steel Companies' laboratory appears to consist entirely of  $\sigma$  phase (based on FeV).

† K. W. J. Bowen and T. P. Hoar, *Research*, 1950, **3**, 484.

‡ G. J. Dickens, A. M. B. Douglas, and W. H. Taylor, *J. Iron Steel Inst.*, 1951, **167**, 27.

§ Calculated from lattice parameter (cf. F. Adcock, G. D. Preston, and C. E. Webb, *ibid.*, 1931, **124**, 99).

|| Measured values from United Steel Companies' laboratory.

¶ S. Rideout, N. D. Manly, E. L. Kamen, B. S. Lement,

and P. A. Beck, *Trans. Amer. Inst. Min. Met. Eng.*, 1951, **191**, 872.

\*\* *Phil. Mag.*, 1945, [vii], **36**, 835.

†† K. W. Andrews, *Nature*, 1949, **164**, 1015.

K. W. Andrews and P. E. Brookes, *Metal Treatment*, 1951, **18**, 301.

‡‡ Michelson Laboratory, China Lake, Calif., U.S.A.

§§ Associate Professor, Massachusetts Institute of Technology, Cambridge, Mass., U.S.A.

|||| Lecturer in Metal Physics, Imperial College of Science and Technology, London.



exhibit temperature-independent paramagnetism like that of vanadium and chromium, while the paramagnetic susceptibilities of the latter group are strongly temperature-dependent in a roughly Curie-Weiss manner.

The magnetic properties of  $\sigma$  phases afford an important clue to their nature, and it may therefore be of interest to record that Dr. J. Crangle at Sheffield has examined the  $\sigma$  phases in the Fe-V and Ni-V systems. The former shows a strong Curie-Weiss type of paramagnetism, and the latter a temperature-independent paramagnetism of the order of that of vanadium. This seems to suggest that the occurrence of  $\sigma$  is independent of any particular electronic configuration in the  $d$ -band. Dr. Crangle and I hope to extend this work to the phases in other systems.

In all the  $\sigma$  phases so far reported, one metal has a Curie-Weiss paramagnetism and the other a temperature-independent paramagnetism. If this is a general condition, Mo-Rh and W-Os would differ from Fe-Cr by not showing  $\sigma$  phases.

Mr. H. J. GOLDSCHMIDT,\* M.Sc., F.Inst.P. (Member): These valuable papers, taken in conjunction, throw much more light on the systematics of alloy formation than the individual papers would suggest.

In Coles and Hume-Rothery's work on the Ni-Mn system, convincing proof is given that  $\gamma$ -manganese forms a continuous series of solid solutions with nickel, and the tetragonal structure of  $\gamma$ -manganese assumed earlier shows how misleading deductions from quenching experiments can be. That  $\gamma$ -manganese is face-centred cubic is in itself most important in bringing this metal, at least to some extent, "back into the fold" of simple metal structures.

As the face-centred tetragonal  $\theta$  phase at composition NiMn is isomorphous with the Ni-V  $\theta$  phase, I wonder whether Dr. Hume-Rothery would suggest that the two form a complete series of solid solutions. The comparison between these two systems focuses attention on the Ni-Cr system, which logically should be intermediate, though in fact it has the very simple eutectic form shown in Taylor and Floyd's paper. Is it not probable that this Ni-Cr diagram is really metastable only, and that true equilibrium is considerably more complex? For instance, a face-centred tetragonal  $\theta$  analogue suggests itself in the region of 40 at.-% chromium, where in fact the  $\gamma$ -phase boundary is known to lie. Taylor and Floyd do not find such a distortion, and in our own work a careful inspection of X-ray pictures also failed to detect it, though this is no disproof, since it may appear only at a low-temperature equilibrium extremely sluggish of attainment. Actually, Taylor and Floyd, in their Figs. 2 and 3 (pp. 580-581) show a break in the  $\gamma$ -boundary at about 1000°C., which is interpreted as being connected with  $\sigma$  formation, though it may equally well indicate an incipient  $\theta$ -phase distortion; significantly, the maximum temperatures for formation of  $\theta$  given by Dr. Hume-Rothery for Ni-Mn and Ni-V lie on either side of the Ni-Cr break, namely at about 950° and 1050°C., respectively.

The Ni-Cr system seems therefore to contain several inhibited phase transformations, and the tendency to nucleation of the  $\theta$  or  $\sigma$  phases will already exist within the matrix on a lattice scale and be likely to produce strains and ageing effects, which may in part explain the well-known special properties of Ni-Cr alloys.

It appears from Table III (p. 91) of Coles and Hume-Rothery's paper that the  $\beta$ -manganese lattice expands on addition of nickel, while  $\gamma$ -manganese contracts, to judge by the values given for the  $\gamma$ -manganese solid solution in the equi-atomic region. This is most interesting, and I wonder whether a more complete lattice-spacing curve for the  $\gamma$ -Mn-Ni solution is yet available. The indications are that it would show a maximum closely resembling the case of the Fe-Ni system. This would again confirm that the electron

valencies of the constituent metals vary with the nickel : manganese ratio, and supersede atomic size as the determining factor.

Are the lattice dimensions of the body-centred cubic  $\beta$  phase in the Ni-Mn system known, and are they similar to those of  $\alpha$ -iron, as might be expected in theory? If so, a continuous solid-solution link between  $\beta$ -NiMn and  $\alpha$  ( $\delta$ ) iron would suggest itself, a point which would have an important bearing on alloy-steel constitution. In this connection the equivalence (to a large extent) of nickel and manganese addition to steel should also be remembered.

Referring to the tetragonal  $\theta$  phases in the Ni-V and Ni-Mn systems, I wonder whether they should really be regarded as independent compounds, or whether they might better be looked upon as subsidiary transformations within the face-centred cubic primary ( $\alpha\gamma$ ) region. Is it not likely that the change is a diffusionless one? This perhaps raises a question of principle in phase-diagram work, namely when a "separate phase" becomes a "separate phase", and whether a lattice distortion like that under discussion actually represents a new compound. It may be said that one criterion is the existence of a two-phase region, but then the co-existence of a cubic phase and its tetragonal derivation may represent only a metastable equilibrium (as in the case of Basinski and Christian's banding effect in Mn-Cu alloys), and not a true two-phase condition.

The same question applies to the Ni-V  $\delta$  phase (face-centred with monoclinic distortion). Support for the continuity of this phase with the  $\alpha$  region comes in fact from the observed change of axial ratio with temperature, which suggests a gradual merging into the cubic field. Such continuity would further seem to be possible from the simple lattice relationships shown in Pearson and Hume-Rothery's Figs. 8 and 10 (pp. 649 and 650).

Regarding the structure of the  $\theta$  phase Ni<sub>3</sub>V, we have observed a very similar face-centred tetragonal distortion in the Ni-Mo system, in agreement with the work of Ellinger† and of Grube and Schlecht.‡ The lattice dimensions are also of the same order, but the atomic composition is somewhat nearer the nickel end. The Ni-Mo tetragonal phase is again a low-temperature product of the face-centred cube, but here there appears to be a continuous transition cubic  $\rightarrow$  tetragonal, without a duplex field.

I was most interested in the high-temperature X-ray investigation of the  $\delta$ -region. To what factor is the reported loss of vanadium from the sample attributed?

Regarding Dr. Hume-Rothery's  $\sigma$ -phase, as distinct from  $\sigma$ , is it yet known how this differs structurally from true  $\sigma$ , and are its interplanar spacings available? There may be a relation between  $\sigma'$  and a certain ternary compound we observed in the Fe-Cr-Mo and the Co-Cr-Mo systems.

I would like to corroborate the suggestion in Taylor and Floyd's paper that  $\sigma$  phase should occur in the Ni-Cr binary diagram, by another piece of evidence; namely, that in the ternary system Ni-Cr-Mo a large, but purely ternary  $\sigma$  field occurs, stopping short by about 6 at.-% of the binary Ni-Cr side, opposite the composition Ni<sub>2</sub>Cr<sub>3</sub>, indicating that if only lower-temperature equilibrium could be attained in a reasonable time,  $\sigma$  would indeed reach this side.

In the ternary system Ni-Cr-Ti is the  $\eta$  compound Ni<sub>3</sub>Ti the only intermetallic phase occurring, or is it still an open question whether a ternary compound may not also appear?

The fact that Ni<sub>3</sub>Ti has the hexagonal close-packed structure raises another interesting point. It means that by the addition to nickel of certain types of atoms, a cobalt-like structure can be produced. Ni<sub>3</sub>Ti is fully isomorphous with hexagonal cobalt (the X-ray photograph of  $\eta$  shown in Fig. 8 (Plate XCIII) of Taylor and Floyd's paper agrees well with one of pure cobalt), and is also of similar lattice dimensions. We have found the same type of effect in the Ni-Mo system, and quite probably other solutes of Group IV, V, or VI metals

\* Research Physicist and X-Ray Crystallographer, B.S.A. Group Research Centre, Sheffield.

† F. H. Ellinger, *Trans. Amer. Soc. Metals*, 1942, **30**, 607.

‡ G. Grube and H. Schlecht, *Z. Elektrochem.*, 1938, **44**, 413.

will act similarly. This relationship is emphasized by Taylor and Floyd's suggestion of epitaxial growth, and a close match of the nickel and  $\text{Ni}_3\text{Ti}$  lattices; it would further seem probable, though this has not yet been reported, that Lipson lattice-faults occur during this process, of the type described for cobalt transforming from hexagonal to cubic close-packing. Perhaps we may say in a simplified way that nickel can structurally be "rendered akin to cobalt" by the device of substituting for some of its atoms certain larger transition-metal ones.

Dr. A. D. McQUILLAN,\* B.Sc. (Member): There is, at present, an almost complete lack of knowledge of the form of the free-energy relationships in alloy systems of the transition elements. In the Cr-W system, Greenaway has shown that there exists an immiscibility gap in the solid state. The boundary of this gap is, of course, directly dependent on the form of the free energy of the Cr-W solid solution as a function of alloy composition and temperature. It is of interest, therefore, to compare the experimentally determined boundary of the immiscibility gap with a theoretical boundary based on the simplest possible set of assumptions and to survey critically the deviations between the two curves.

The simplest statistical thermodynamic treatment of this problem for a binary system having two components with the same crystal structure, is that given by Cottrell † for a regular solid solution. It is assumed, among other things, that the solid solution is completely disordered and that only closest-neighbour atom interactions need be considered. This leads to an equation relating the temperature  $T$  and atomic fraction of addition element  $c$  along the boundary of the immiscibility gap, of the form :

$$\ln \frac{c}{1-c} = \frac{2T_c}{T} c(2c-1) \quad (1)$$

where  $T_c$  is the critical temperature above which there exists complete miscibility between the two components in the solid state. It is not possible to derive an accurate value for  $T_c$  from purely theoretical grounds and, therefore, for the purpose of comparing the theoretical and experimental boundaries,  $T_c$  has been chosen equal to  $1490^\circ\text{C}$ ., which is the minimum temperature at which complete solid solubility

chromium-rich side of the diagram indicates, however, that the form of the actual free-energy/composition curves for the solid solution must depart considerably from that given by the simple theory of regular solutions, and that the good agreement on the other side of the diagram is almost certainly fortuitous. At temperatures below  $1000^\circ\text{C}$ . the theoretical boundary continuously approaches the temperature axes with

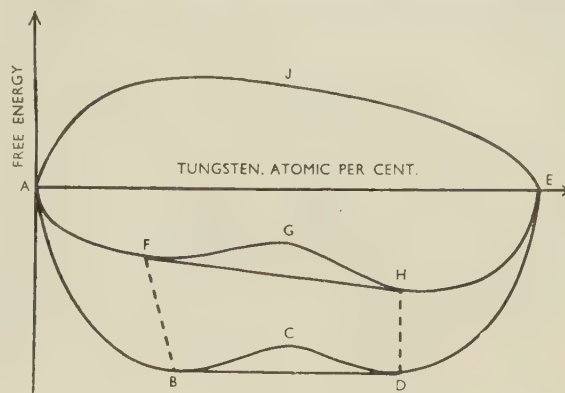


FIG. B.

decreasing temperature and would tend to the conditions for complete immiscibility as absolute zero is approached. Greenaway's boundary on both sides of the diagram becomes, however, almost vertical below  $1000^\circ\text{C}$ ., which strongly suggests that below this temperature his alloy specimens were no longer in equilibrium. Lacking decisive evidence on this last point, it would perhaps be best to limit the discussion of the experimental results to higher temperatures.

The interatomic distances of the pure elements of tungsten and chromium are 2.735 and 2.493 Å. respectively. A tungsten atom may, therefore, be considered as being 9.73% larger in diameter than a chromium atom and a chromium atom 8.87% smaller than a tungsten atom. Because of the asymmetrical nature of the attractive and repulsive components of the binding forces between metallic atoms, it is reasonable to expect in a binary solid solution, provided there is no great dissimilarity in elastic constants of the two types of atoms, that, when a large atom is introduced into the matrix of smaller atoms, there will be created a greater increase in the strain energy than would be the case when a small atom is introduced into a matrix of larger atoms. In the particular case of the Cr-W system considerations both of atomic size and elastic constants suggest that tungsten additions to the chromium would cause a proportionately larger effect on the free energy of the solid solution than would be the case for the addition of chromium to tungsten. It would be expected, therefore, that the strain energy as a function of alloy composition would be of the form shown in curve  $AJE$  in Fig. B. Curve  $ABCDE$  in this diagram represents the free-energy/composition curve for a regular solution of the type used to obtain the broken boundary curve in Fig. A. The points of contact of the tangent with curve  $ABCDE$  give the compositions of the two solid solutions that can co-exist at the particular temperature considered and are symmetrically placed about a composition of 50 at.-%. If the strain-energy curve given by curve  $AJE$  is added to the free energy of the regular solution a new free-energy/composition curve of the form  $AFGHE$  is obtained. The points of contact of the common tangent  $FH$  with this curve are now no longer symmetrical about the composition of 50 at.-%. In the case illustrated, the composition of the boundary of the immiscibility gap on the chromium-rich side has been decreased from  $B$  to  $F$ , while the boundary on the tungsten-rich side has, entirely fortuitously, remained unaltered.

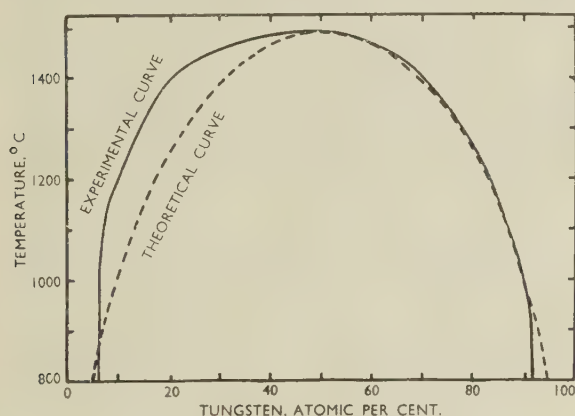


FIG. A.

exists in the Cr-W system as determined by Greenaway. Fig. A shows the resulting boundary computed from equation (1) compared with Greenaway's experimental boundary. The agreement between the experimental boundary and the idealized theoretical boundary on the tungsten-rich side of the diagram is surprisingly good. The displacement of the boundary towards lower tungsten compositions on the

\* Senior Research Fellow, Department of Metallurgy, Birmingham University.

† A. H. Cottrell, "Theoretical Structural Metallurgy". 1948: London (Edward Arnold and Co.).



It would be extremely interesting, therefore, if it were possible to obtain further experimental evidence that would lead to a more accurate delineation of the boundary of the immiscibility gap. This would make possible a better assessment of the contribution of the strain energy to the form of this system and would also help to decide whether the rapid change of slope of the boundary at a composition of 20 at.-% tungsten is a real effect.

side is surprisingly good and, I agree, probably fortuitous. It is much better than that found in other similar systems.

There is, however, one point which I wish to raise. The simple statistical thermodynamic treatment used by Dr. McQuillan assumes, among other things, that the bonding energy between atoms of chromium is of the same order as that between atoms of tungsten. In view of the wide disparities of the elastic constants and of the melting points of

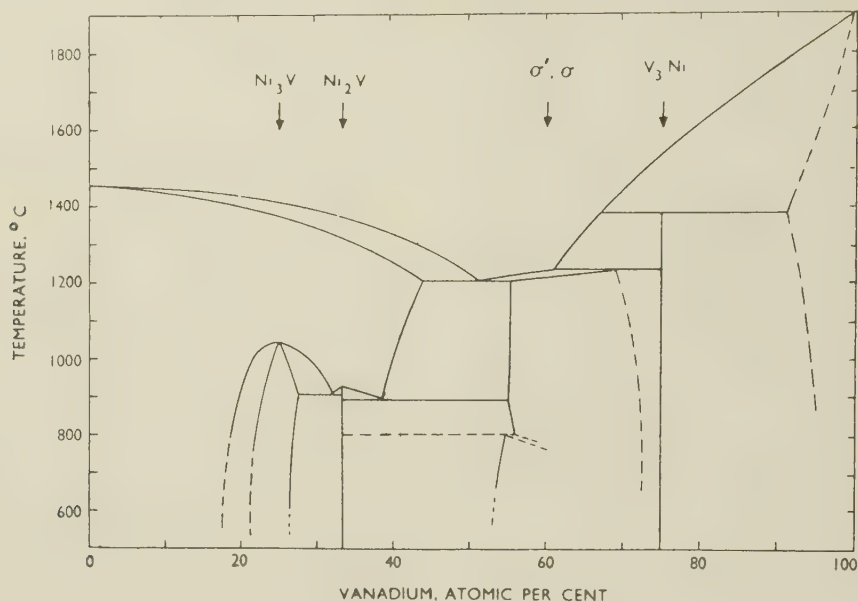


FIG. C.—The Nickel-Vanadium Diagram.

Dr. W. ROSTOKER,\* M.A.Sc.: Recent work at the Armour Research Foundation on the vanadium-rich end of this system may be added to complete the V-Ni diagram given by Mr. Pearson and Dr. Hume-Rothery. Alloys were prepared by argon-arc melting in a water-cooled copper crucible. The vanadium metal had a purity of about 99.76% as a typical value. Studies in the range 0-30 at.-% nickel, by both metallographic and X-ray-diffraction methods, yielded the following information:

(a) The solubility limit of nickel in vanadium is about 9 at.-%.

(b) An intermediate phase of the atomic proportions  $V_3Ni$  occurs between the terminal solid solution and the  $\sigma$  phase field.  $V_3Ni$  was found to be isomorphous with  $V_3Si$  and  $V_3Co$ , having a  $\beta$ -tungsten type of structure with  $a = 4.70$  kX. The  $V_3Ni$  phase appears metallographically to form as the product of a peritectic reaction.

(c) The melting point of vanadium of this purity may be fixed at  $1900^\circ \pm 25^\circ C$ .

In Fig. 1 (p. 643) of the paper an unrelated thermal arrest at  $1380^\circ C$  is recorded for the 70 at.-% vanadium alloy. This is likely to be the arrest for the peritectic reaction: liquid + vanadium solid solution  $\rightleftharpoons V_3Ni$ . The liberty has been taken in Fig. C of connecting these phase relationships with the partial diagram presented in the paper. The authors are to be complimented on their careful and detailed treatment of a difficult alloy system.

Mr. GREENAWAY (*in reply*): It is indeed interesting that the two-phase boundary as calculated by Dr. McQuillan from simplified theory agrees so well with the experimentally determined position. The agreement on the tungsten-rich

the two metals, it is not surprising that a discrepancy exists between the theoretical and experimental phase boundaries. Instead of advancing an additional *ad hoc* hypothesis for strain energy, as Dr. McQuillan has done, it seems more logical to alter the initial assumptions upon which the theoretical considerations rest. If the expression for the internal energy is modified to account for the difference of the bonding energies, the resultant free energy variation leads to a solubility-limit curve of the form shown in Fig. D. This curve, on the whole, agrees much better with the experimental curve, particularly at the lower temperatures.

With reference to the question of equilibrium below  $1000^\circ C$ .

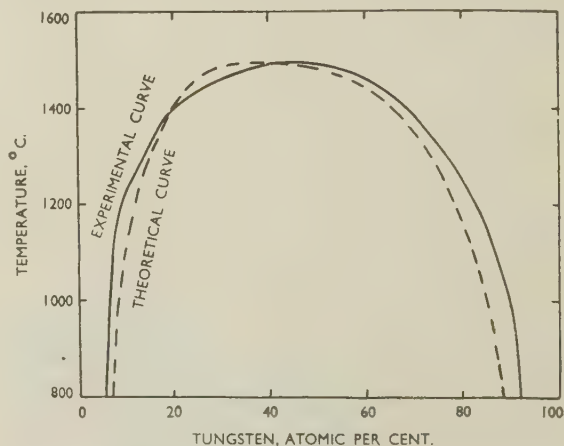


FIG. D.

\* Research Metallurgist, Metals Research Department, Armour Research Foundation of the Illinois Institute of Technology, Chicago, U.S.A.

raised by Dr. McQuillan, I believe that the times of heating employed were sufficient for complete, or very nearly complete, annealing at these temperatures. Recent metallographic work has agreed with this contention, in that it has shown that most of the transformation occurs in much shorter times than those employed in the phase-diagram work.

Dr. HUME-ROTHERY and his co-authors (*in reply*): We would point out to Dr. Andrews that since the work on Ni-Mn alloys was published, increasing evidence has accumulated that  $\gamma$ -manganese is face-centred cubic, and that the face-centred tetragonal modification is characteristic of quenched specimens.\* The results given in our paper are thus correct for quenched specimens, but the exact significance of the spacings for the tetragonal structure is uncertain.

Further work on the constitution of the alloys in the equi-atomic region is in progress. In view of the occurrence of face-centred tetragonal phases at equi-atomic compositions in the systems Ni-Zn, Pd-Zn, Pt-Zn, Pd-Cd, and Pt-Cd, the axial ratios often departing markedly from unity, and the general resemblance already noted between Ni-Mn and Ni-Zn, it is probable that the appearance of such phases is not controlled simply by superlattice effects.

To Dr. Goldschmidt's interesting communication we would reply as follows:

The tetragonal superlattice phases in the systems Ni-Mn and Ni-V have axial ratios less than, and greater than, unity, respectively, and the formation of a complete series of solid solutions is not, therefore, likely.

We do not think that the system Ni-Cr should "logically" be intermediate between the two systems Ni-V and Ni-Mn. In the system Ni-Cr, the size-factor is very favourable, the atomic diameters, as defined by the closest distances of approach of the atoms in the crystals of the element, being Ni 2.49 and Cr 2.49 kX; the latter value should perhaps be increased a little to allow for the difference between the co-ordination numbers (Ni 12, Cr 8). The corresponding value for vanadium (co-ordination number 8) is 2.63, and for  $\gamma$ -manganese (co-ordination number 12) *ca.* 2.6. The size-factor for Ni-Cr is, thus, not intermediate between those for Ni-V and Ni-Mn. In so far as one may argue from the physical properties of the element, it seems most probable that chromium has a slightly higher valency than manganese, and there is not a regular sequence on passing from V  $\rightarrow$  Cr  $\rightarrow$  Mn. This difference in electronic structure is reflected in the apparent atomic sizes. We suggest that it is the abnormal behaviour of manganese that is responsible for the lack of regular sequence noted by Mr. Goldschmidt.

The lattice spacing of the body-centred cubic  $\beta$  phase in the Ni-Mn system is given in the paper as 2.968(3) kX at 745° C., and this may be compared with the value of 2.861 kX for iron at 20° C.

The face-centred cubic and face-centred tetragonal structures are certainly different phases. Recent work† has shown that the 50 at.-% Co-Pt superlattice change is really a first-order phase change, and it is increasingly probable that many, if not all, superlattice changes are thermodynamically phase changes of the first order.

The loss of vanadium in the high-temperature X-ray work was not due to imperfect vacuum conditions, but to reaction with the silica capillaries. The quantities available were, unfortunately, too small for accurate analysis.

The  $\sigma$  and  $\sigma'$  phases both gave typical " $\sigma$ " structures on diffraction films, but detailed comparison of interplanar spacings would involve a knowledge of the coefficients of expansion which is not yet available.

Dr. SULLY (*in reply*): Dr. Andrews raises several interesting points, and I fully agree with him that recent work on the magnetic properties of the  $\sigma$  phase rules out the possibility that it is a full zone structure. The measurements to which

he and Dr. Coles refer are confirmed by some information privately communicated to me by Professor P. A. Beck, who has found that a number of  $\sigma$  phases become ferromagnetic at low temperatures. It seems, therefore, as Dr. Andrews states, that the model proposed in my paper is incorrect in detail and that the facts cannot be fully accounted for by the Pauling hypothesis. There can, however, be little doubt that the starting point of a relationship between 3d shell vacancies and  $\sigma$  occurrence is well founded, and the work of Beck *et al.* to which Dr. Andrews refers, on the accord between  $\sigma$ -phase boundaries in ternary systems and lines of constant electron vacancy, strongly supports this relationship.

I do not attach much importance to Dr. Andrews's argument based on the brittle nature of the  $\sigma$  phase, since the complex structure is probably more important than the bond strength in determining deformation behaviour.

Dr. Andrews suggests that superlattice formation is partly responsible for the occurrence of  $\sigma$  phase. An answer to this point must await a detailed analysis of atomic positions in the structure, but it must be noted that in some systems the  $\sigma$ -phase region does not include any simple stoichiometric ratio, and in others, e.g. Fe-Cr, although it lies near a simple ratio, it nevertheless lies entirely to one side of the ratio.

It is indeed possible that the origin of  $\sigma$  phases is not to be explained in terms of electronic effects alone. Size-factor considerations may also be involved. Further information is clearly required on several points, the most important in my view being a study of the magnetic properties of  $\sigma$  and its associated phases, detailed structure analyses of the phase to locate the positions of the different atoms, and a study of hitherto unexplored binary systems involving transitional elements of the other long periods, to determine whether  $\sigma$  phases occur in these systems and, if so, over what ranges of composition.

Dr. TAYLOR and Mr. FLOYD (*in reply*): Dr. Bloom and Dr. Grant comment on the absence of lattice-parameter data for the  $\alpha$ -chromium phase in alloys quenched from 1200° C. and suggest that the normal body-centred cubic chromium lines might have been absent. We would point out that we make no claim to have determined the boundary of the  $\alpha$ -phase at temperatures above 1100° C. As a matter of fact, we heat-treated most of the chromium-rich alloys at 1200° C., and all the diffraction patterns showed lines corresponding to a body-centred cubic structure. The reason we did not include lattice-parameter data for these samples in Table II is that the values were too inconsistent to give a satisfactory position for the phase boundary. In one or two cases we did observe lines additional to those of the  $\alpha$  and  $\gamma$  phases, but these were found to be due to unsatisfactory protection of the filings during heat-treatment, resulting in the formation of a chromium nitride. We obtained no evidence whatsoever of a structure corresponding to the high-temperature form of chromium proposed by Bloom and Grant, and we suggest that their own X-ray evidence is hardly convincing, if a study is made of the relative intensities of the diffraction lines attributed to this phase.

Whatever uncertainty there may be concerning the chromium-rich end of the diagram, we believe the boundary we obtained for the  $\gamma$  phase to be accurate to within  $\frac{1}{2}$  at.-% and that the change in slope occurs at about 1000° C. From this temperature upwards the boundary runs smoothly to the end of the eutectic horizontal, as determined by earlier investigators. There is no inflection in the neighbourhood of 1180° C. to support Bloom and Grant's diagram, and alloys on the chromium side of the boundary at 1200° C. showed clearly the characteristic diffraction lines of the body-centred cubic chromium phase. It may be that some of the anomalies in Bloom and Grant's diagram are due to the use of copper radiation, which is generally not suitable for diffraction

\* See Z. S. Basinski and J. W. Christian, *J. Inst. Metals*, this vol., p. 659.

† J. B. Newkirk, R. Smoluchowski, A. H. Geisler, and D. L. Martin, *J. Appl. Physics*, 1951, 22, 290.



studies on chromium-rich alloys owing to the proximity of the chromium absorption edge.

While we have associated the inflection in the  $\gamma$ -phase boundary with the suppressed formation of a  $\sigma$  phase, Mr. Goldschmidt suggests that it may equally well be taken to indicate an inhibited  $\theta$  phase similar to those found in the Ni-Mn and Ni-V systems. He also raises the question of whether a structural modification such as the  $\theta$  phase can be considered as a separate phase. It appears to us that the structure in the Ni-Cr system corresponding to the Ni-V  $\theta$  phase is the ordered modification of the  $\gamma$  phase in the region of Ni<sub>3</sub>Cr which occurs at temperatures below 540° C. On this point we find ourselves supported by Dr. Pearson and Dr. Hume-Rothery in the last section of their paper on the Ni-V system (p. 651).

Mr. Goldschmidt also raises two questions regarding the  $\eta$  compound Ni<sub>3</sub>Ti. This is certainly not the only intermetallic phase occurring in the Ni-Cr-Ti system: there are other binary compounds of the Ni-Ti and Cr-Ti systems, and there is the possibility of ternary phases in the unexplored part of the system beyond the ( $\alpha$  +  $\eta$ ) two-phase region. The suggestion that the addition of titanium atoms to nickel produces a cobalt-like structure is certainly interesting. The structure of Ni<sub>3</sub>Ti can be regarded as consisting of planes of atoms parallel to the basal hexagonal plane, occurring in the order *ABACABAC* . . . , and may be considered as being intermediate between the face-centred cubic and close-packed hexagonal structures. It therefore may be likened to cobalt with a regular "mistakes" lattice. However, the diffraction pattern bears only a superficial resemblance to that of cobalt.

## Discussion

# Constitution of Copper-Base Alloys\*

Dr. N. P. ALLEN,† M.Met., F.I.M. (Member): In the group of papers under discussion, that by Professor Guillet and his colleagues differs from the rest in that it puts forward a new technique for detecting phase changes in alloys by measurement of elastic constants, whereas the others present and discuss the results of phase-diagram studies.

Developments in electronic methods have given us many convenient ways of measuring elastic constants, but there are certain points that must be understood. The changes of the elastic constant are much more reliable indications of phase changes than changes of internal friction, for there are many processes within a given phase that can affect its internal friction. The elastic constants are more influenced by preferred orientations in the sample than would at first be imagined, and before drawing conclusions from the differences of the elastic constants of two different samples it is necessary to ensure that the samples are free from differences of texture.

This difficulty does not arise when the changes on heating and cooling a single sample are under observation, but another difficulty appears. When stress is applied to a substance there is in general an instantaneous deformation, followed by a deformation requiring time. The rate at which this second part of the deformation occurs increases as the temperature is raised. Consequently, at a sufficiently high temperature or sufficiently low frequency of vibration it will have time to occur, and the experiment will therefore yield the "relaxed" modulus. But at a sufficiently low temperature or high frequency it will not have time to occur, and the "unrelaxed" modulus will be measured. The change-over occurs moderately sharply, and is accompanied by a peak in the internal friction. Consequently, on obtaining curves such as Fig. 11 (p. 156 of Professor Guillet's paper), one cannot be certain that a phase change has occurred. Curves such as Fig. 7 (p. 154), however, showing a quite definite break in the temperature/modulus curve, are much more reliable. Cases in which the changes are due to a switch from the unrelaxed to the relaxed modulus can, however, be distinguished by altering the frequency, when the temperature at which the drop of modulus occurs will alter if it is due to a relaxation effect, but not if it is due to a true phase change. The systematic use of this test is much to be recommended.

Coming now to the equilibrium-diagram studies, we may consider how the general project for arriving at the factors

determining alloy formation from the systematic study of phase equilibria is getting on. A phase boundary occurs by definition at the composition at which two different phases come to equilibrium, and its position is determined by the properties of both phases. I think all our authors are fully aware of this, but there is a tendency to forget it. In the paper by Mr. Greenfield and Professor Raynor, for example, the discussion of the primary solid-solubility isothermals is written as if the explanation of the shape of these isothermals is to be found entirely in the structure of the  $\alpha$  solid solution, and is thus essentially wrong in outlook. The discussion of the 3/2 electron compounds which follows, on the other hand, keeps continually in mind that the position of the boundaries is determined by a balance between factors affecting the stability of the body-centred cubic phase and factors affecting the stability of the hexagonal phase, and thus is essentially right. It is interesting to note the prominence that these authors give to size-factor considerations and the relative lack of success of the electron-concentration consideration in explaining the positions of the boundaries. It is very evident from Figs. 5 and 6 (p. 383), for example, that electron:atom ratios are playing a relatively minor part. Attempts at predicting the alloying behaviour of metals such as titanium, uranium, or zirconium, have been more successful when based on size-factor than when based on other considerations. This is a point worth further study, for it suggests that intermediate-phase formation is very largely a matter of the packing of unlike atoms.

In this situation, the paper by Dr. Hume-Rothery, Dr. Betterton, and Mr. Reynolds has a special interest, for it tries to show that the boundaries of the " $\gamma$ -brass" phases are indeed decided principally by considerations of electron concentration. There is a slight change of emphasis, for whereas formerly the ratio of electrons to atoms was regarded as the primary factor, we now consider the number of electrons per unit cell to be dominant, and what in effect is argued is that when the number of electrons per unit cell rises above a certain figure, the free energy of the  $\gamma$  phases rises so steeply that no matter what the free energy of the adjacent phase the phase boundary cannot be far from that corresponding to an electron:atom ratio of 1.7. So far as the alloys of gold, silver, and copper are concerned, the case seems to be argued cogently enough, but doubt arises with the transition metals,

\* Joint discussion on papers from this volume of the *Journal* by R. Cabarat, P. Gence, L. Guillet, and R. LeRoux (p. 151); P. Greenfield and G. V. Raynor (p. 375); J. O. Betterton, Jr., and W. Hume-Rothery (p. 459); W. Hume-

Rothery, J. O. Betterton, Jr., and J. Reynolds (p. 609); and J. Reynolds, W. A. Wiseman, and W. Hume-Rothery (p. 637).

† Superintendent, Metallurgy Division, National Physical Laboratory, Teddington, Middlesex.

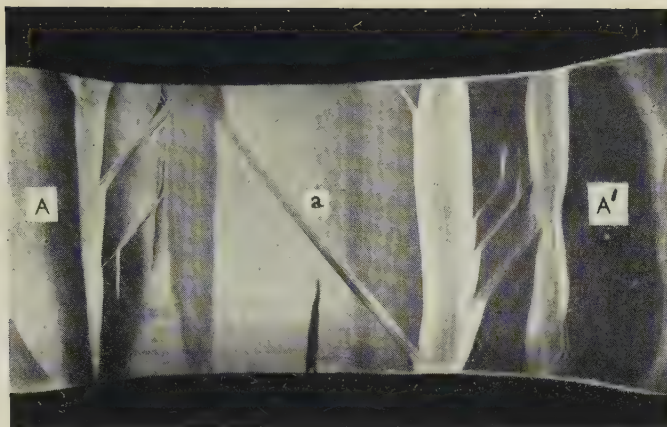


FIG. A.—Stretcher-Strain Markings in Steel Stretched  $\frac{1}{2}\%$  ( $\times 1$ ) and Corresponding Talysurf Traces ( $\times 1000$  vertical magnification). Wedge-shaped markings and kinks, present together. (*Chadwick and Hooper's reply.*)

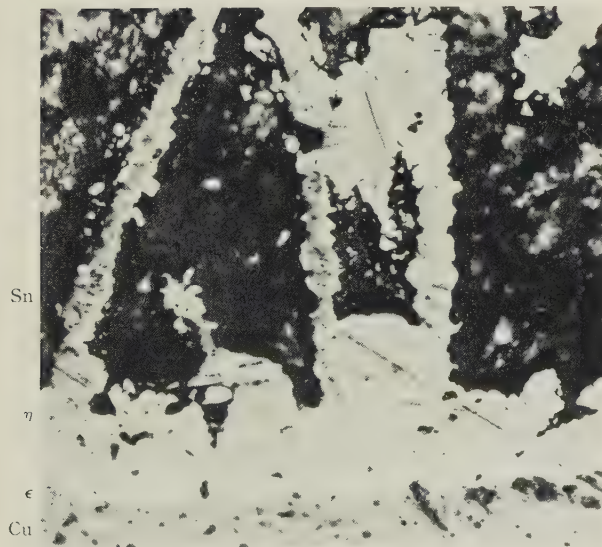
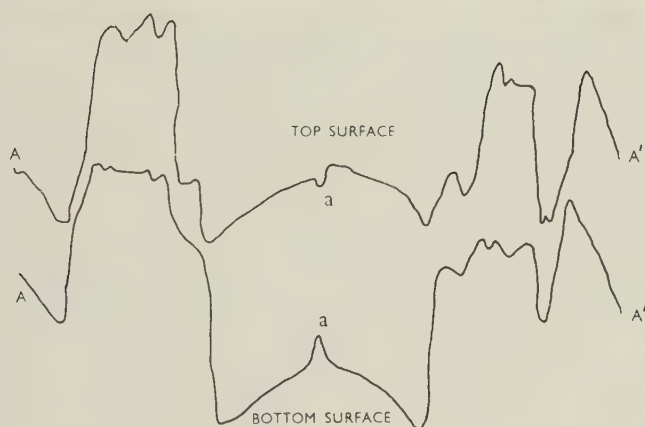


FIG. A.—Film of Pure Tin Heated for 15 Min. at  $500^{\circ}\text{C}$ . in Contact with H.C. Copper Sheet, Showing Needles of  $\eta$  Fringed with  $\epsilon$ .  $\times 500$ . (*Chadwick on Bailey and Watkins.*)

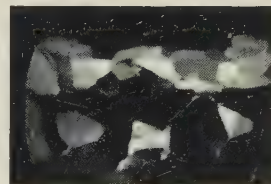


FIG. E.—Crystal Rod Formed by Sucking Molten Zinc into a Cool Glass Tube.  $\times 10$ . (*Puttick on Pratt and Pugh.*)

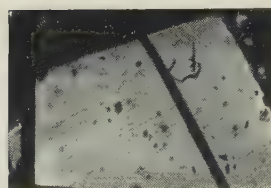


FIG. F.—Twin Formation in Zinc Crystal and Lines Attributable to Kink Bands.  $\times 75$ . (*Puttick on Pratt and Pugh.*)

[To face p. 700.]



PLASTIC DEFORMATION OF 99.99% ALUMINIUM.



FIG. B.—Region of a Kink Band, Showing Cross-Slip.  
400.



FIG. C.—Region Between Kink Bands.  $\times 400$ .

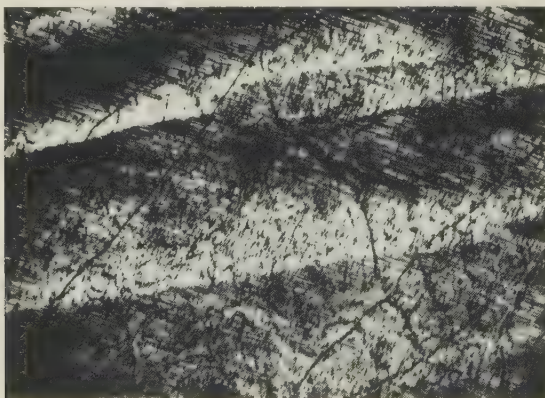


FIG. D.—Extended 5%. Etched.  $\times 50$ .  
(Jaoul and Crussard.)

STRESS-CORROSION IN ALUMINIUM-MAGNESIUM ALLOYS.



FIG. A.—High-Purity Aluminium-7% Magnesium Alloy, Solution Heat-Treated, Quenched, Electropolished, and Aged for 8 Days at 150° C. Etched for 10 min. in 10% phosphoric acid.  $\times 1000$ . (*H. K. Farmery, cited by Evans.*)

FIG. B.—Same specimen as Fig. A, but etched for a further 50 min., making 60 min. in all.  $\times 1000$ . (*H. K. Farmery, cited by Evans.*)

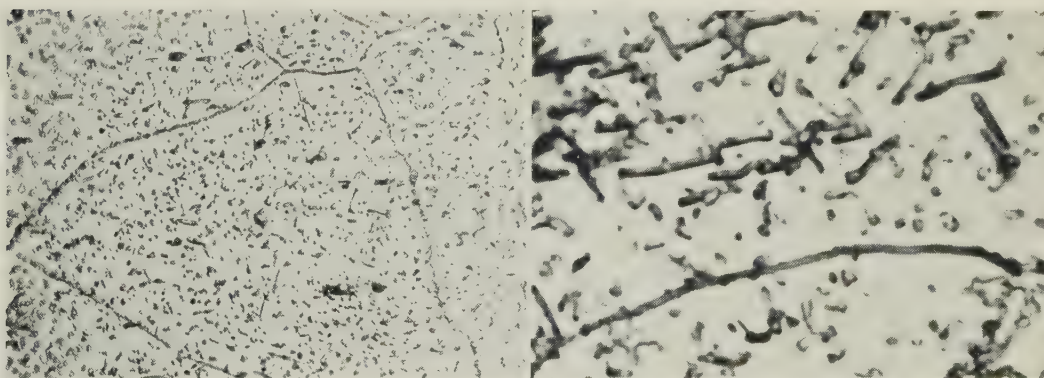


FIG. D.—Aluminium-7% Magnesium Alloy, Solution-Treated and Aged for 3 Days at 200° C.  $\times 1000$ . (*Perryman.*)

FIG. E.—Aluminium-7% Magnesium Alloy, Solution-Treated and Aged for 78 Days at 125° C.  $\times 3000$ . (*Perryman.*)



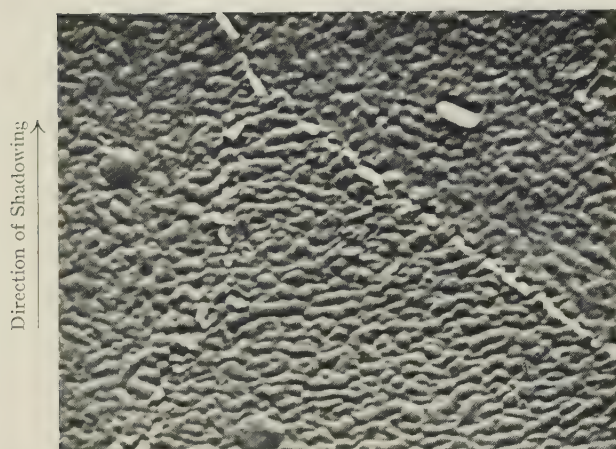


FIG. F.—Aluminium-7% Magnesium Alloy, Solution-Treated, 10% Overstrained, and Aged for 24 Hr. at 125° C. Electropolished and etched for 8 sec. in 10% NaOH at 55° C. Electron micrograph; collodion replica shadowed with gold.  $\times 13,500$ . (*Gilbert.*)

for we really do not know how many electrons these elements contribute to the structure. I find Fig. 10 (p. 615) particularly disturbing, for Fig. 10 (a) is based on the assumption that transition metals contribute no electrons, and Fig. 10 (b) on the basis that they contribute about 5, and yet both lead to the conclusion that  $\gamma$  phases are based on a constant electron : atom ratio. The authors do show that Fig. 10 (a) fits the facts better than Fig. 10 (b), but how long could an investigator making an erroneous assumption such as might be represented by Fig. 10 (b) continue to deceive himself that his assumptions were being confirmed by experiment, before deciding that the number of exceptions to the rule was really more than could be tolerated?

Our knowledge of the electron contributions of the various elements in the various phases is very uncertain. Dr. Sully\* would like to advance the idea that the  $\sigma$  phase is an electron compound, but to do so he must employ the Pauling valencies which Dr. Hume-Rothery rejects. Furthermore, he gets just as good constancy of electron : atom ratio when he assumes that the 4s electrons contribute to the bonding as when he assumes that they do not. Dr. Hume-Rothery assumes that manganese contributes no electrons to the  $\gamma$ -Mn-Zn compounds, but he would very much like it to have a valency of 2 in the  $\beta$ -Mn-Ni constituent, and nickel to have a valency of 1. Of course, there is no reason why an element should not have a certain effective valency in one structure and an entirely different one in another, but we do lack a clear and decisive method of discovering what these effective valencies actually are. Spectrographic methods may be helpful, but are likely to be slow and difficult. There is a further method which may perhaps be worth trying. We have a fairly good explanation of the elastic properties of copper based on the assumption that the effective valency is 1, and, through the work of Professor Jones, there is also an idea of the way in which additional atoms of varying valency should affect the behaviour. There is a continuous solid solution between copper and nickel, and if the elastic constants were measured carefully on single crystals, we might be able to calculate what contribution each addition of nickel is making to the factors affecting elasticity. Eventually, we should build up a reliable picture of the electronic state of solid nickel. Nickel forms continuous solid solutions with a great many of the transition metals—iron, cobalt, platinum, manganese—and by a similar procedure the factors affecting the elastic strength of these metals might be elucidated. The method might prove too difficult, but would in any case accumulate data on the elastic behaviour of these solid solutions, and such information is on its own account of value to the metallurgist and the engineer.

Mr. A. P. Miodownik,† B.Sc., L.I.M. (Student Member): Dr. Hume-Rothery puts forward two alternative methods whereby the increasing instability of the  $\beta$ -phase at electron concentrations greater than 1.5 can be relieved; namely, transformation to the complex  $\gamma$  phase, or the formation of defect lattices. It has also been suggested that the ion shape is possibly modified as the electron concentration increases. May I suggest, without any confirmatory investigation or calculation, that these two facts are related? If the ion shape, or volume, is not appreciably altered by increasing electron concentration, the  $\beta \rightarrow \gamma$  transition can be expected; while if the ionic shape is modified, the simple body-centred cubic configuration can be retained with the aid of a few vacancies.

Dr. K. Schubert‡: Dr. Hume-Rothery, Dr. Betterton, and Mr. Reynolds, following the present trend of metallurgical

chemistry, have endeavoured to supply simple solutions of the phenomena encountered in the investigation of the constitution of alloys. Their explanations can be amplified in certain respects. Westgren and Phragmén§ carried out density and lattice-constant measurements on the  $\gamma$ -Cu-Zn phase. The lattice constant increases with the zinc content, as does the number of valency electrons in the cell, whilst the number of atoms in the cell decreases.|| The  $\gamma$ -Cu-Zn phase is thus similar to the  $\gamma_1$ -Cu-Ga phase. The behaviour of the  $\gamma$ -Cu-Zn phase has been explained|| as due to an increasingly close fit of the Fermi surfaces and the Brillouin-plane polyhedron. This would be in agreement with the authors' suggestion that the rapid decrease in the atoms in the cell observed in the  $\gamma_2$ -Cu-Ga phase is connected with the steep fall of the  $N(E)$  curve. The slope, in relation to the concentration of valency electrons in the  $\gamma_2$  phase, is as steep as in NiAl, i.e. the number of electrons in the cell remains practically unaltered.

Before attempting to explain the behaviour of the  $\gamma_3$ -Cu-Ga phase, it is necessary to consider in which respects the  $\gamma$ -brass structure differs from the body-centred cubic (A2) structure. There are concentrations of the NiAl phase which have as many vacant sites as the  $\gamma$ -Cu-Zn phase, without, however, giving  $\gamma$  patterns in Debye photographs. Accordingly, a characteristic process must take place in the  $\gamma$ -brass structure, which differs from an A2 structure with statistically distributed vacant sites. In the absence of definite knowledge, this may be regarded as a displacement of the atoms towards the vacant site they surround. Assuming that the atoms of the first, second, and third zones round the vacant site are involved in this displacement, exactly 26 atoms would be ordered round each vacant site. This makes it clear that the  $\gamma$ -brass structure is, geometrically, typical of the vacant-site structures related to the A2 structure. In NiAl the Al portion of the lattice is so stable that the distortion mechanism described cannot take place. Results of earlier X-ray investigations¶ do not, however, rule out the possibility of such distortion in the  $\delta$ -Cu-Zn phase, as only the sub-structure was then studied. It is suggested that, like the  $\delta$ -Cu-Zn phase,\*\* the  $\gamma_3$ -Cu-Ga phase has a Fermi surface overlapping the Brillouin plane (330,411). It has been found†† that such overlapping takes place in a remarkably small range of concentration. This would have to be confirmed by electromagnetic measurements. Such measurements have been carried out on the A2 phases of the Cu-Sn system.‡‡ The process of vacant-site formation with increasing valency-electron concentration is governed by the crystallographic law that structures are the less closely bound, the higher the concentration of valency electrons. The reasons for this have been fully discussed.§§ It is therefore of interest to note that the structure of CuGa<sub>2</sub> may be considered as a tetragonally distorted A2 structure, in which every fourth atom is missing. On the other hand, the structure of this phase is closely related to that of gallium, in so far as the Ga structure is less closely bound than CuGa<sub>2</sub>, which resembles Cu<sub>2</sub>Sb in structure.||||

Dr. HUME-ROTHERY and Mr. REYNOLDS ¶¶ (in reply): We must thank Dr. Allen for his interesting communication. This covers a wide range, and perhaps the following comments may be made:

(1) We think Dr. Allen is incorrect in suggesting that Professor Raynor's discussion of phase boundaries is in terms of size-factor rather than of electron concentration. The position of the phase boundaries in the binary systems when

\* A. H. Sully, *J. Inst. Metals*, this vol., p. 173.

† Research Demonstrator, Metallurgy Department, Battersea Polytechnic, London.

‡ Max-Planck Institut für Metallforschung, Stuttgart.

§ A. Westgren and G. Phragmén, *Phil. Mag.*, 1925, [vi], 50, 311.

|| K. Schubert, *Z. Metallkunde*, 1948, 39, 88.

¶ K. Schubert and E. Wall, *ibid.*, 1949, 40, 383.

3 A

\*\* K. Schubert and G. Brandauer, *Naturwiss.*, 1952, 39, 208.

†† K. Schubert, *Z. Metallkunde*, 1952, 43, 1.

‡‡ Cf. K. Schubert and G. Brandauer, *ibid.*, 1952, 43, 262.

§§ K. Schubert, *ibid.*, 1948, 39, 88; 1950, 41, 417.

¶ K. Schubert and H. Pfisterer, *ibid.*, 1950, 41, 433.

|||| K. Schubert, *Z. Naturforsch.* (in the press).

¶¶ Owing to Dr. Betterton being in America, it has not been possible to include his views in this reply.



the size-factor is favourable is determined mainly by electron concentration, with the size-factor as a minor correction.\* Raynor's discussion starts from this point, and therefore involves electron concentration as well as size-factor.

(2) Theoretically, the important factor has always been the number of valency electrons per unit cell, and it is only because many structures have few defects that the principles can often be expressed in terms of valency electrons per atom. So far as constant ratios of electrons to atoms are concerned, it is a matter of algebra that alternative valency schemes will fit the facts. Thus, with the well-known  $\beta$ -phases CuZn, Cu<sub>3</sub>Ga, and Cu<sub>5</sub>Sn, the normal valencies give an electron : atom ratio of 3 : 2. But a series of valencies Cu =  $n$ , Zn =  $n \pm a$ , Ga =  $n \pm 2a$ , Sn =  $n \pm 3a$ , will give electron : atom ratios of:

$$\begin{aligned}\text{CuZn} \quad \frac{n + n \pm a}{2} &= n \pm \frac{a}{2} \\ \text{Cu}_3\text{Ga} \quad \frac{3n + n \pm 2a}{4} &= n \pm \frac{a}{2} \\ \text{Cu}_5\text{Sn} \quad \frac{5n + n \pm 3a}{6} &= n \pm \frac{a}{2}\end{aligned}$$

The normal valencies correspond to  $n = 1$ ,  $a = +1$ , whilst the Pauling valencies correspond to  $n = 5.4$ ,  $a = -1$ . The fact that a series of phases occur at a constant electron : atom

ratio with one set of valencies does not, therefore, imply that the valencies concerned have been chosen correctly, and a correct choice can be made only when something is known of the physics, chemistry, and electron theory of the metals concerned. The Pauling scheme of valencies may be criticized on the grounds that both physics and chemistry suggest that a valency of 4.4 for zinc is improbable. Pauling himself would not agree with this, and Fig. 10 (b) (p. 615) was thus included to show that, even if his valencies were accepted, they led to a less satisfactory generalization than the ordinary valencies.

(3) In alloys of the transition metals we regard it as quite certain that a given metal may exert different valencies, not only in different systems but in different composition ranges of one system. It is, thus, improbable that any simple scheme of valencies will explain these alloys.

In reply to Mr. Miodownik, we would point out that the  $\gamma$ -brass structure is itself a slightly distorted defect structure of the body-centred cube. The suggestion that the deformability of the ion is an important factor can be tested by comparing the alloys of silver (ion relatively undeformable) with those of copper and gold (ions more easily deformed).

We have been most interested in the series of papers which Dr. Schubert has published, and much appreciate his communication, to which we hope to reply fully in a later publication.

## Discussion

### Titanium and Its Alloys†

Dr. N. P. ALLEN,‡ M.Met., F.I.M. (Member): The authors of this group of papers are to be congratulated both on the excellence of their work and on their enterprise in taking up the study of titanium alloys at an early stage, when the future of the metal was still uncertain. The past year has been decisive in the history of the development of titanium, in that it has become clear that before long its alloys will be used, for example, in aircraft, and that a titanium industry of some magnitude will develop. The most important problem is still to find a cheap way of extracting the metal, and the size to which the industry will grow will depend upon the price ultimately attained. Nevertheless, the purposes to which titanium alloys can be applied at the present price are such that it is important to develop their best properties, and to this end a comprehensive study of the equilibrium diagrams of the alloys is needed.

The metallography of titanium alloys is governed by the transition from the hexagonal  $\alpha$  phase to the body-centred cubic  $\beta$  phase. This occurs at about the same temperature as the transition from  $\alpha$  to  $\gamma$  in iron, but there are certain important differences. With iron the small atoms, such as carbon and nitrogen, are more soluble in the high-temperature phase than in the low-temperature phase. In titanium the reverse is the case, and that is the main reason why hardening reactions analogous to those that occur in steel do not take place. In iron, the substitutionally dissolved elements, such as nickel, manganese, and chromium, are substantially soluble in both phases, but in titanium the solubilities of these elements in the  $\beta$  phase are generally high, and in the  $\alpha$  phase, low. (Aluminium is an exception.) As a result,

substitutionally dissolved elements generally lower the temperature of the  $\alpha$ - $\beta$  transition of titanium, and bring about the existence of a wide temperature range in which the  $\alpha$  and  $\beta$  phases coexist. In this condition the  $\beta$  phase contains a greater proportion of the alloying element, and is correspondingly hardened, whereas the  $\alpha$  phase is proportionately softened.

The hexagonal  $\alpha$  phase has only moderately good working properties, whereas the cubic  $\beta$  phase is more ductile. Consequently, a condition in which the hardening element is concentrated in the more ductile phase is favourable to the working properties of the alloys, and alloys of this kind seem to show their best properties when they consist of a suitable finely divided mixture of  $\alpha$  and  $\beta$ .

The position is rather different when interstitially dissolved elements, such as oxygen and nitrogen, are present. These elements are more soluble in the  $\alpha$  and, when dissolved in that phase, embrittle it severely. In duplex alloys, the oxygen or nitrogen is concentrated in the  $\alpha$ , giving a material consisting of a very hard and brittle phase intermingled with a more ductile phase. This condition is not favourable, and probably is to be avoided.

The metallography of titanium is likely to be concerned principally with adjusting the quantities of these two phases, their composition, distribution, and properties. It is therefore impossible to know too much about the equilibria between the phases and the modes of transformation from one to the other.

Dr. B. R. COLES,§ B.Sc. (Junior Member): My main interest in work on titanium and its alloys is to consider

\* See K. W. Andrews and W. Hume-Rothery, *Proc. Roy. Soc.*, 1941, [A], 178, 464.

† Joint discussion on the following papers published in the *Journal*: N. Karlsson (1951, 79, 391); A. D. McQuillan (1950-51, 78, 249; 1951, 79, 73, 371; this vol., p. 363); M. K. McQuillan (1951, 79, 379); H. W. Worner (1951, 79,

173; this vol., p. 213); A. E. Jenkins and H. W. Worner (this vol., p. 157).

‡ Superintendent, Metallurgy Division, National Physical Laboratory, Teddington.

§ Lecturer in Metal Physics, Imperial College of Science and Technology, London.

what conclusions can be drawn concerning the electronic structure of this extremely interesting metal. One of the first questions to be asked is whether or not it is to be regarded as a transition metal. This question is meaningful, however, only if the term "transition metal" is restricted to those metals in which the electrons can be regarded as distributed between two overlapping bands, one composed mainly of *d*-states and the other mainly of *s*-states. A "normal" metal will then be one, such as sodium, magnesium, or aluminium, in which all the outer or valency electrons are distributed in one broad band, the energy breadth of which (as shown by soft X-ray spectroscopy) is of the order of that which would be given by perfectly free electrons, although several Brillouin-zone overlaps may, in fact, have occurred. This latter picture is probably appropriate for potassium, calcium, and scandium, and if extended to titanium (the next element in the Periodic Table) would imply that the electrons are spread in energy over a range of about 13 eV.

As Dr. McQuillan suggests, the hydrogen-absorption results for titanium alloys are probably controlled largely by the electronic structures of the alloys, and it seems to me that the results are in support of the picture of a "broad electronic energy band" for titanium. Thus, initial additions of vanadium have an effect quite different from that of other first-transition-group elements, and it is to be noted that the magnetic properties of nickel-vanadium alloys suggest that all five of the outer electrons of vanadium can behave as effectively free in alloys. On the other hand, manganese, iron, cobalt, and nickel tend to enter into solid solution in many non-transition metals as ions of definite *3d* configuration. I suggest, therefore, that iron, cobalt, and nickel, even in very small amounts, enter titanium as ions with definite electronic configurations in their atomic *3d*-shells, whereas vanadium (in small concentrations) can contribute all five of its outer electrons to the broad electronic band of titanium. Since titanium and vanadium are neighbours in the Periodic Table, a common band structure at dilute concentrations is quite probable, and it is possible that chromium might behave similarly at very small concentrations. (In solid solution in nickel, chromium seems to behave more like vanadium than like the later group of elements.) I should be much interested to hear of any further results on very dilute alloys with chromium, and also of any results on alloys with scandium, the element preceding titanium.

If the ability of titanium to absorb hydrogen depends, like that of palladium, on a high density of states at the Fermi limit, the marked lowering effect of vanadium, while collective band formation occurs, resembles the effect of silver on palladium, and suggests that the density-of-states curve for titanium falls fairly steeply near the Fermi limit.

Dr. McQuillan's results on the electrical resistance of titanium are of great interest, although difficult to explain. The curve for the low-temperature form, extrapolated back to room temperature and absolute zero, shows a marked concavity downwards. Mott has given an explanation of this effect in the transition metals proper, palladium showing it very markedly, but an essential feature of this explanation is that the *d*-band is almost full. The effect for titanium is greater still, but even if this metal does possess a *d*-band (and this seems unlikely), it cannot be nearly full. It is probable, however, that any model of the electronic structure giving a falling density-of-states curve at the Fermi limit would account for such an effect, and its occurrence is thus in good agreement with the explanation given for the effect of vanadium on the hydrogen absorption. Such a fall in the curve would occur if the Fermi surface lay near a prominent Brillouin-zone boundary.

The temperature dependence of the resistance of body-centred cubic titanium is even smaller, and implies still greater curvature in the region below the transformation point. An approximate value for the room-temperature

resistance of pure body-centred titanium might be obtained by extrapolation from the values for a series of titanium-iron alloys in which the structure can be retained.

Mr. M. H. DAVIES,\* B.Sc. (Junior Member): Age-hardening phenomena, even in systems that have been extensively investigated, are difficult of interpretation. In those systems such as aluminium-copper where the phenomenon is associated merely with a change of solubility with temperature, no completely adequate explanation exists, and it is to be expected, therefore, that there will be major complications where a phase transformation is also involved and where the mode of transformation itself probably changes.

In the titanium-iron system, dealt with in Mr. Worner's paper, the pure metal and alloys of low iron concentration probably transform predominantly by a martensitic reaction, and the transformation is completed during the quench. At intermediate iron concentrations a partial martensitic reaction may obtain during the quench, and subsequent ageing may result in growth of the  $\alpha$  formed in the quench in addition to the nucleation and growth of  $\alpha$  from untransformed  $\beta$ . At higher iron concentrations, when  $\beta$  is fully retained during quenching, it is probable that nucleation and growth will play the major part in the transformation during ageing.

The peak hardness observed in alloys quenched from 950° C. is probably associated with an optimum intensity of the martensite-type reaction, coupled with maximum dispersion of discrete precipitated particles. Since age-hardening begins to become apparent only in alloys of composition approximating to that corresponding to the peak in the 950° C. quench/hardness curve, it is presumably at this composition that  $\beta$  begins to be retained on quenching.

Mr. Worner appears to interpret the age-hardening observed as being due to the breakdown of the  $\beta$  solid solution, but the results are offered only for alloys with 5.9-9.5% iron quenched from 950° C. These alloys are in the intermediate range of composition, where the reactions during quenching and subsequent ageing are most complicated. It appears extremely unlikely from Fig. 5 (Plate XXXIX) that the alloys in the quenched state do indeed consist of completely untransformed  $\beta$ .

The hardening of the 5.9% alloy exhibits, as the author himself remarks, most peculiar behaviour, in that sudden peaks are observed in the time/hardness curves of this alloy aged at 220° and 440° C., but the alloy aged at 360° C. attains a maximum hardness which is not reduced by prolonged ageing times.

It would be interesting to know whether ageing has been observed in alloys relating to the smooth part beyond the peak of the 950° C. curve in Fig. 5, i.e., above about 12% iron, and also in the alloys quenched from 650° C. Those alloys quenched from the two-phase field at 650° C. will contain varying amounts of  $\beta$  of constant composition and should presumably show varying degrees of hardening as the amount of  $\beta$  increases with iron content.

One other point remains. The increasing hardness with iron concentration of alloys as quenched from the two-phase field is apparently associated with the relative amounts of  $\alpha$  and  $\beta$  present, but it is difficult to understand why no softening should take place on annealing when there is a relatively large increase in the amount of  $\alpha$  present plus a small amount of compound formed. Hardness values for the individual phases could elucidate this point, and it would therefore be of value if Mr. Worner could give information on the hardness of  $\alpha$ - and  $\beta$ -titanium in the alloys quenched from 650° C. and also on the hardness of  $\alpha$ -titanium and the compound FeTi in the fully annealed material. Such figures might also indicate whether precipitation from a super-saturated  $\alpha$  solid solution is playing any part in the hardening process, which might well be the explanation of the anomalous behaviour of the 5.9% alloy aged at 220° C.

\* Physical Metallurgist, Fulmer Research Institute, Ltd., Stoke Poges, Bucks.



Dr. M. HANSEN\* (Member): Dr. McQuillan stressed the desirability of having available information on the phase boundaries in binary titanium-rich alloy systems based on van Arkel titanium, as compared with those of the same systems based on magnesium-reduced titanium. Some work along these lines has been done recently,<sup>†</sup> when studying the phase diagram of the titanium-molybdenum system by means of micrographic analysis. The results are given in Fig. A.

The full curve, as determined by the data points given, represents the  $\beta/(\alpha + \beta)$  boundary of the alloys based on magnesium-reduced titanium, and the dotted curve represents the boundaries of the  $(\alpha + \beta)$  field as determined by using van Arkel titanium-base alloys. No data points are given

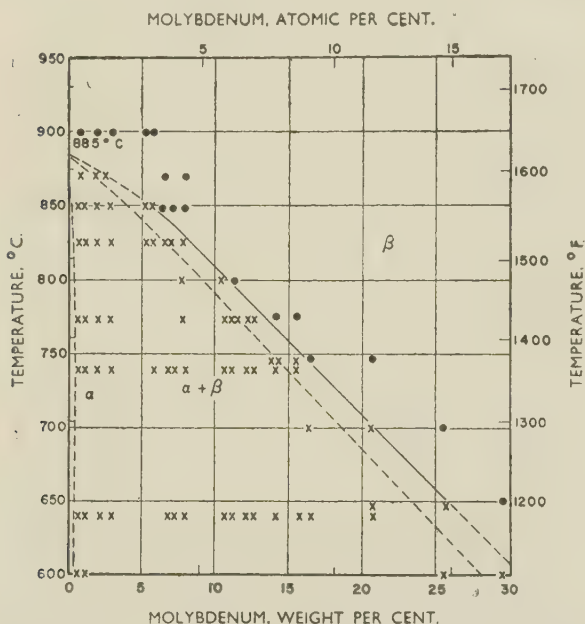


FIG. A.—The Extent of the  $(\alpha + \beta)$  Field in Titanium-Molybdenum Alloys Based on Magnesium-Reduced Titanium (full curve), Compared with the Field Determined by Means of Alloys Based on van Arkel Titanium (dotted curve).

for the latter. The magnesium-reduced titanium was 99.7% pure, and contained iron 0.10, oxygen 0.14, nitrogen 0.007, and carbon 0.02%. Similar results have been obtained with titanium-rich titanium-iron and titanium-chromium alloys. In all cases, the  $\beta/(\alpha + \beta)$  boundary for the systems based on magnesium-reduced titanium was shifted to higher contents of the alloying metal. It is to be expected that the degree of displacement of this boundary will increase in some way with the decrease in purity of the titanium used.

Dr. M. HANSEN\* (Member) and Dr. W. ROSTOKER<sup>‡</sup>: Mr. Karlsson believes he has found evidence that the phase  $\text{CuTi}_2$ , reported by Laves and Wallbaum to have a face-centred cubic lattice with 96 atoms per unit cell, does not exist, but that there exists a copper-titanium oxide, varying in composition between  $\text{Cu}_3\text{Ti}_2\text{O}$  and  $\text{Cu}_3\text{Ti}_4\text{O}$ . He further states that the phases  $\text{MnTi}_2$ ,  $\text{FeTi}_2$ ,  $\text{CoTi}_2$ , and  $\text{NiTi}_2$ , which,

according to Laves and Wallbaum, are isomorphous with  $\text{CuTi}_2$ , are probably identical with oxide phases analogous to  $\text{Cu}_3\text{Ti}_2\text{O}$ . In a recent paper on the intermediate phases of iron, cobalt, and nickel with titanium, Duwez and Taylor<sup>§</sup> have reported that the phases  $\text{FeTi}_2$ ,  $\text{CoTi}_2$ , and  $\text{NiTi}_2$  do exist, and that they have the crystal structure found by Laves and Wallbaum. Lattice parameters of these phases, as prepared by powder-metallurgy methods, were determined. On the other hand, Worner,<sup>||</sup> in his study of the constitutional diagram of the titanium-iron system, was unable to detect the compound  $\text{FeTi}_2$ . As far as the phase  $\text{NiTi}_2$  is concerned, metallographic data by Long *et al.*<sup>¶</sup> indicate that this phase does occur.

This brief summary of the data available shows that information on the existence of some of the  $\text{MeTi}_2$  phases mentioned above is highly inconsistent. It is to be hoped that more light will be shed on this problem by Mr. Karlsson's further work, as well as by studies of the phase diagrams of the systems titanium-copper, titanium-manganese, titanium-cobalt, and titanium-nickel, which are at present under way in various laboratories in the U.S.A.

The titanium-iron system has also been under study at this laboratory. Both melted and sintered binary alloys have been prepared and subjected to several types of heat-treatment cycles. In no case could the phase  $\text{FeTi}_2$  be identified. This is in agreement with Worner's<sup>||</sup> work. Following Mr. Karlsson's suggestion that the observed  $\text{MeTi}_2$  phases may in fact be ternary phases containing oxygen, a melt having the composition  $\text{Fe}_2\text{Ti}_4\text{O}$  was prepared and examined by the Debye-Scherrer diffraction method. The pattern so obtained agreed almost exactly with the structure for  $\text{FeTi}_2$  reported by Duwez and Taylor.<sup>§</sup> This would seem to lend substantial support to Mr. Karlsson's view on the origin of some of the  $\text{MeTi}_2$ -type phases. Further work is in progress and it is hoped that a fuller report will be published in the near future.

*Note added in proof.*—Since the above was written, work by one of us\*\* and by Mr. Karlsson<sup>††</sup> has demonstrated the existence of a family of ternary phases based on the formula  $\text{Ti}_4\text{X}_2\text{O}$ , where X may be Cu, Ni, Co, Fe, or Mn.

Mr. KARLSSON (*in reply*): A brief note concerning the oxides having the structure of the high-speed-steel carbide has been published, as Dr. Hansen and Dr. Rostoker say, and a detailed report will appear shortly.

I have found no evidence of the existence of the phases  $\text{MnTi}_2$ ,  $\text{FeTi}_2$ ,  $\text{CoTi}_2$ ,  $\text{NiTi}_2$ , or  $\text{CuTi}_2$ , in my work, in which the greatest care was taken to eliminate oxygen during preparation of the alloys. The manganese used was distilled in a high-frequency vacuum induction furnace and the iron, cobalt, and nickel were reduced with dry hydrogen immediately before the alloys were prepared. Without these precautions the melts in most cases contain oxygen, and X-ray powder photographs then show the presence of the corresponding oxides with the high-speed-steel carbide structure.

Dr. A. D. McQUILLAN (*in reply*): As pointed out by Dr. Coles, the form of the electrical resistivity/temperature curve of titanium is certainly interesting, and it would seem very probable that its shape is strongly dependent on the electronic structure of the metal and the change of this structure with temperature. If the resistivity/temperature curve for titanium is compared with the equivalent curves for zirconium and hafnium,<sup>‡‡</sup> it can be seen that there is a close similarity

\* Chairman, Metals Research Department, Armour Research Foundation, Illinois Institute of Technology, Chicago 16, Ill., U.S.A.

† M. Hansen, E. L. Kamen, H. D. Kessler, and D. J. McPherson, *Trans. Amer. Inst. Min. Met. Eng.*, 1951, **191**, 881.

‡ Research Metallurgist, Metals Research Department, Armour Research Foundation, Illinois Institute of Technology, Chicago 16, Ill., U.S.A.

§ P. Duwez and J. L. Taylor, *Trans. Amer. Inst. Min.*

*Met. Eng.*, 1950, **188**, 1173.

|| H. W. Worner, *J. Inst. Metals*, 1951, **79**, 173.

¶ J. R. Long, E. T. Hayes, D. C. Root, and C. E. Armantrout, *U.S. Bur. Mines Rep. Invest.*, No. **4463**, 1949.

\*\* W. Rostoker, *Trans. Amer. Inst. Min. Met. Eng.*, 1952, **194**, 209.

†† N. Karlsson, *Nature*, 1951, **168**, 558.

‡‡ H. K. Adenstedt, *Trans. Amer. Soc. Metals*, 1952, **44**, 949.

§§ J. D. Fast, *J. Appl. Physics*, 1952, **23**, 350.

in the form of the curves for the three Group IVA elements. Zirconium, which undergoes  $\alpha$ - $\beta$  transformation at 865° C., has a resistivity curve very closely resembling that for titanium, and shows a gradual decrease in the temperature coefficient of resistance in the  $\alpha$  form, beginning at about 450° C. below the transformation temperature and falling almost to zero immediately below the transformation temperature. Hafnium, on the other hand, shows no appreciable decrease in the temperature coefficient of resistance at 400° C., but has, very significantly, a similar decrease in temperature coefficient at about 450° C. below its  $\alpha$ - $\beta$  transformation, which according to Fast\* occurs at about 1950° C. It would seem, therefore, that the  $\alpha$ - $\beta$  transformation in these elements occurs only after the resistance/temperature curve departs markedly from the effectively linear temperature relationship found in metals obeying Grüneisen's law.

The resistivities of titanium, zirconium, and hafnium are all in the neighbourhood of  $40 \times 10^{-6}$  ohm-cm., at room temperature. These high values suggest that there is considerable restriction on the mobility of the electrons in the metal at room temperature, and this may be quoted as further evidence in support of Dr. Coles's very reasonable hypothesis that there is a steeply falling density of electron states at the top of the Fermi band in the hexagonal close-packed form of these metals. The departure of the resistivity/temperature curves from the almost linear increase with temperature which would be expected if thermal scattering of electrons were the only factor affecting the resistivity of the metal, suggests that the thermal scattering effect is being counterbalanced by a progressive increase in the number of electrons or electronic states able to contribute to the electrical conductivity as the metal approaches the  $\alpha$ - $\beta$  transformation temperature.

Dr. Coles's suggestion that a value of the room-temperature resistivity of  $\beta$ -titanium could be obtained by extrapolation to zero content of an addition element which depresses the  $\alpha$ - $\beta$  transformation, has been carried out by Adenstedt *et al.* for the vanadium system.† Vanadium forms a continuous series of solid solutions with  $\beta$ -titanium and the body-centred cubic structure can be retained in all alloys containing more than 30 at.-% vanadium. The relevant data are given in Fig. B. It would seem from these results that an extrapolation of the abnormally linear resistivity/composition curve of titanium-vanadium  $\beta$  solid solutions would yield the remarkable value of  $164 \times 10^{-6}$  ohm-cm. for pure  $\beta$ -titanium at room temperature. The temperature coefficient of resistivity/composition curve for the titanium-vanadium alloys cannot, because of its shape, be so readily extrapolated, but it would seem to suggest a value very close to zero for the temperature coefficient of resistance of  $\beta$ -titanium between 0° and 100° C. At a temperature immediately above the transformation temperature,  $\beta$ -titanium has a resistivity of  $94 \times 10^{-6}$  ohm-cm., and would therefore appear to increase its resistivity with decreasing temperature. In view of the anomalous effect of additions of only a few atomic per cent. of vanadium on the heat of solution of hydrogen in  $\beta$ -titanium, the validity of the extrapolation of resistivity values may be doubtful. It is possible that the effect of small additions of vanadium have a profound effect on the resistivity and temperature coefficient of resistance of the  $\beta$ -titanium and that, as in the case of the heat of solution of hydrogen, further additions have little effect and hence give rise to a linear resistivity/composition law. It would seem that further work on this and other similar systems is required before the value of  $164 \times 10^{-6}$  ohm-cm. for the resistivity, and of zero for the temperature coefficient of resistance of  $\beta$ -titanium at room temperature, are accepted. It is suggested that the experimental determination of the resistivity/temperature curves for a series of titanium-vanadium alloys containing less than 5 at.-% vanadium, at temperatures at which the  $\beta$  solution is stable, would indicate the probable validity of the extrapolation. Should this

linear law be found to be true for low vanadium concentrations, a series of results on high-vanadium alloys over a wide range of temperatures between 1000° C. and the lowest available temperature would be extremely interesting.

The amount by which the resistivity of  $\alpha$ -titanium deviates from the expected linear relationship with temperature as the temperature approaches 882° C. increases with temperature in a manner closely approximating to an exponential, and this strongly suggests that a thermally activated process is occurring as the temperature is increased. This effect would be expected to change the shape of the free energy/temperature curve of  $\alpha$ -titanium, and since its onset appears to determine the subsequent transformation at a higher temperature, it must be supposed that the free-energy curve of  $\alpha$ -titanium deviates from the normal curve, obtained by lattice-vibration considerations, in a direction that leads it to intersect the free energy/temperature curve of  $\beta$ -titanium and hence cause the metal to undergo an allotropic transformation. In such a case, it would be expected that the free-energy curves would intersect at a somewhat greater angle than normal, since one at least of the curves is abnormally dependent on the temperature. The difference of slopes of the two free energy/tempera-

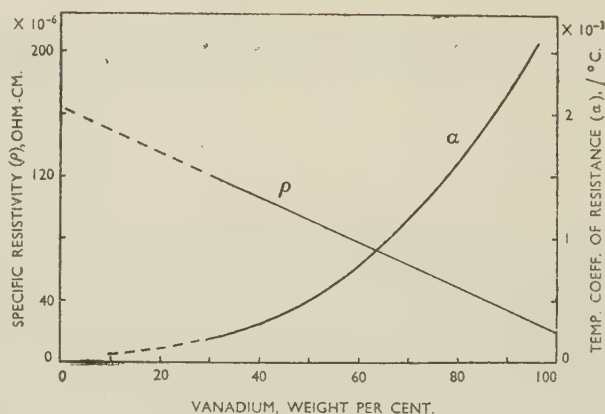


Fig. B.—Room-Temperature Specific Resistivity ( $\rho$ ) and Temperature Coefficient of Resistance ( $\alpha$ ) of  $\beta$ -Solid-Solution Titanium-Vanadium Alloys as a Function of Vanadium Content.†

ture curves at the transformation point is given by the entropy change on transformation and for titanium and zirconium (no data are available for hafnium) the entropy values are, respectively, 0.587 cal./°C.‡ and 0.624 cal./°C.§ These values are large compared with 0.287 and 0.227 cal./°C. for the iron transformations and 0.158 and 0.185 cal./°C. for the manganese transformations, and suggest that the change in thermal entropy of the atomic vibrations does not account for all the entropy change in the  $\alpha$ - $\beta$  transformation in titanium and zirconium. Electronic-structure configurations of the type considered by Dr. Coles would, therefore, seem to play a large part in the determination of the properties of titanium and its alloys.

In conclusion, I would like to thank Dr. Hansen for the information about the effect of impurities on the  $\beta$ /( $\alpha$  +  $\beta$ ) boundary in the titanium-molybdenum system. This would appear to agree very well with my results on the comparison of hydrogen-titanium system with magnesium-reduced and van Arkel titanium. I would, however, like to suggest that the dotted extrapolation of the  $\beta$ /( $\alpha$  +  $\beta$ ) boundary in the magnesium-reduced titanium system (Fig. A) is unlikely to meet the temperature axis at 885° C. (Dr. Hansen's figure for the transformation temperature of pure titanium). Since

\* J. D. Fast, *loc. cit.*

† H. K. Adenstedt, J. R. Pequignot, and J. M. Raymer, *Trans. Amer. Soc. Metals*, 1952, **44**, 990.

‡ A. D. McQuillan, *Proc. Roy. Soc.*, 1950, [A], **204**, 309.

§ C. J. Smithells (edited by), "Metals Reference Book", 1949: London (Butterworths).



the experimental points are in no way incompatible, it would perhaps be better to continue the  $\beta/(\alpha + \beta)$  boundary to meet the temperature axis at about 900° C. The impurities which would elevate the  $\beta/(\alpha + \beta)$  boundary by 20° C. would also cause the transformation in the unalloyed titanium to occur over a similar temperature range.

Mr. H. W. WORNER (*in reply*): Mr. Davies asks whether age-hardening was observed (a) in alloys containing more than 12% iron, and (b) in alloys quenched from 650° C. An alloy with 16.2% iron was aged at 220°, 360°, and 440° C. for periods up to about 24 hr. These treatments caused no detectable changes in hardness or microstructure. Alloys quenched from 650° C., that is, from the  $(\alpha + \beta)$  and  $(\beta + \text{FeTi})$  fields, were not submitted to ageing experiments, chiefly because these alloys all contained  $\beta$  solid solution with approximately 16% iron. As mentioned above, the 16.2% iron alloy

showed no signs of age-hardening when aged under the conditions covered in the investigation.

Mr. Davies refers to the more or less surprising fact that annealed alloys, that is, those slowly cooled down into the  $\alpha + \text{FeTi}$  ( $+\beta$ ) region, were no softer than those quenched from 650° C. Although the eutectoid transformation yields only a relatively small amount of the compound FeTi, it should be realized that the latter is very finely dispersed throughout the  $\alpha$  phase. This, together with the fact that there is always undecomposed  $\beta$  present, probably accounts for the comparative hardness of the annealed alloys. I have not determined the hardness values for the phases actually present in duplex and three-phase alloys. It would be practically impossible to carry out micro-hardness tests on the eutectoidal  $\alpha$  and FeTi phases in the annealed alloys. Hence it would be very difficult to throw any further light on the last point mentioned by Mr. Davies.

## Discussion

# The Deformation of Polycrystalline Zinc

By J. A. RAMSEY

(*Journal*, this vol., p. 167.)

Dr. G. B. GREENOUGH,\* M.A. (Member): Mr. Ramsey's paper interests me as a contribution to the controversy on the mechanism of cell formation during slow rates of straining at temperatures high relative to the melting point. As far as I can see, the experimental evidence put forward is in excellent agreement with the polygonization explanation, yet in the discussion this explanation is rejected.

If a cell boundary were a wall of dislocations, as postulated in the polygonization theory, then the wall would be expected to lie roughly perpendicular to the active slip direction. If, then, the active slip direction were nearly parallel to the surface of the crystal, one would expect most of the cell boundaries present in the crystal to appear on its surface. On the other hand, if the active slip direction were roughly perpendicular to the surface, few of the cell boundaries would intersect the visible surface. Since marked slip would be seen microscopically only in grains in which the slip direction was steeply inclined to the surface, grains showing most slip would be expected to exhibit cell boundaries but rarely, while grains showing little evidence of slip would be expected to exhibit many cell boundaries.

The experimental evidence presented by Mr. Ramsey would appear to support this argument very well. Two quotations from the second column on p. 168 may be cited:

"In some grains of zinc, no slip was observed; this was always the case in those grains manifesting the most clearly developed cell structure."

"It was found that grains containing a very well-developed cell structure . . . showed less tendency to slip than others" (during room-temperature straining after the development of the cells at a higher temperature).

Despite this latter statement, however, in the Discussion (first column on p. 171), it is stated that in grains showing a cell structure "slip appeared when the specimen was repolished and re-etched and then strained at room temperature", and this is the reason given for rejecting the polygonization theory of cell formation. The two statements need not be contradictory. Although slip cannot readily be seen on grains showing marked cell development, it may be

that Mr. Ramsey feels that if slip eventually becomes visible at larger extensions it is sufficient to disprove the polygonization theory. If so, then I would disagree.

Dr. P. L. PRATT,† B.Sc.: I think it probable, as Dr. Greenough has suggested, that those grains which showed cell structures but no visible slip had their basal plane nearly parallel to the surface of the specimen. The author states that slip occurred in the vast majority of grains at all temperatures, and this implies that the basal plane of most grains intercepted the surface at a high angle. This is consistent with the recrystallization texture to be expected in this material, where but few grains should have their basal plane close to the rolling plane.

This point is raised by the author in his Discussion, and he dismisses the possibility, since further strain at room temperature, after repolishing, produced parallel markings (Fig. 9, Plate XXX) which he attributed to slip. These markings are unlike basal-plane slip in appearance, and, without further evidence, it seems probable that they are kink markings similar to those observed on cleavage faces of zinc.

The AUTHOR (*in reply*): As regards Dr. Greenough's remarks, at the time the work was done I felt that there were two alternative reasons for the non-appearance of slip in grains such as Fig. 3 (Plate XXX). One was that the slip plane and, therefore, the slip direction were more or less parallel to the specimen surface, giving, as Dr. Greenough suggests, a marked sub-grain structure but no slip traces. The other reason, resting on Wood's hypothesis of cell formation and movement, was that some grains had deformed at the elevated temperature by the "cell mechanism" without slipping. To distinguish between these alternatives, specimens containing grains of the type referred to were deformed at room temperature, not simply for the sake of extra deformation as implied by Dr. Greenough, but because, according to the cell hypothesis, slipping would be more likely to occur at the lower temperature. The appearance of what was interpreted as traces of slip suggested that the basal plane was not

\* Metallurgy Department, Sheffield University.

† Research Fellow, Atomic Energy Research Establishment, Harwell, Berks.

parallel to the surface, and therefore slip had probably not occurred during the deformation at elevated temperature. This appeared to be an argument against interpreting the formation of the sub-structure in terms of the polygonization theory.

Dr. Pratt has questioned the interpretation of the markings in Fig. 9 (Plate XXX) as being slip traces. Whilst part of the oddness in appearance is no doubt due to using the microscope slightly out of focus, even when the instrument was correctly focused it must be admitted that the markings did appear peculiar, as Dr. Pratt remarks. However, they seemed more like slip traces than any kink markings in zinc with which I am familiar. I agree that more evidence than slight differences or similarities in appearance is needed on this point.

Dr. Greenough's more general remark that "the experimental evidence . . . is in excellent agreement with the poly-

gonization explanation" perhaps requires some comment. The mode of formation and site of the sub-grain boundary seems to be the main difficulty in applying ideas developed on the basis of annealing bent single crystals to specimens deformed at elevated temperature. During deformation at elevated temperature it seems improbable that the sub-grain boundaries are produced from a uniform lattice curvature by the meeting of two oppositely moving dislocation streams, as a result of heating alone. It seems more feasible that the deformation results in narrow regions of heavy curvature separating larger zones of slight curvature, and, with continued deformation, a migration and trapping of dislocations at the lines of greater curvature results in the substructure. Some recent experiments by Kelly and Gifkins\* on zinc deformed at elevated temperature and examined by multiple-beam interference fringes appear to confirm this view.

## Discussion

# A Mechanism of Stress-Corrosion in Aluminium-Magnesium Alloys

By C. EDELEANU

(*Journal*, this vol., p. 187.)

DR. U. R. EVANS,† M.A., Sc.D., F.I.M., F.R.S. (Member): One of the most important points brought out in the paper, which accords with results obtained by Dr. D. Whitwham (also at Cambridge), is that the total time needed for failure is much the same whether stress is applied in the early stages of corrosion or not. This conclusion was reached through work with materials in an unusually sensitive condition. If material in a less sensitive condition behaves in the same way, the practical importance is very great. Aircraft, for instance, are subjected to the highest stresses only for short periods. If their protective coatings are inadequate, slow corrosion may proceed day and night over long periods; when later a high stress is applied momentarily, cracking may occur almost as easily as though high stress and corrosion had been acting together throughout the entire life.

It would seem that when an alloy carrying an intergranular network more susceptible to corrosion than the grain interiors, is exposed to a corrosive environment, intergranular corrosion occurs along numerous grain boundaries. The damage, however, develops slowly, partly because the attack is distributed among a large proportion of the grain boundaries, and partly because, in practice, there will be some boundaries free from susceptible matter, so that even after very long periods of corrosion, the grains may be held together by resistant bridges. The fact that in unalloyed aluminium certain grain boundaries can remain immune from attack under conditions where others are attacked, was brought out by Lacombe‡; immunity can arise, it seems, if a certain relation exists between orientations within the two grains and that of the boundary. The immunity of certain grain boundaries appears to occur in aluminium-magnesium alloys, as brought out in microsections produced by Mr. Farmery.§ The effect seems to be a real one, since it is independent of the time of etching, as shown by comparing Fig. A (Plate CXII) which

represents 10 minutes' etching in 10% phosphoric acid, with Fig. B (Plate CXII), which represents 60 minutes' etching. If, when the intergranular corrosion has reached an advanced stage, stress is applied, there will be a tendency for the damage to be concentrated on a limited number of paths running roughly at right angles to the direction of applied stress. Consequently, the damage will now progress much more quickly. The fact that stress helps the advance of the intergranular attack may be due to the mechanical rupture of the resistant bridges, which would otherwise delay it. Obviously, a bridge which has been isolated by corrosion will be subjected to great stress intensification, and a load far too small to rupture uncorroded material would break such a bridge and allow the crack to advance once more. There is little doubt that even in the fairly advanced stages of corrosion cracking, corrosion as well as stress is needed for the crack to progress. It is even then not a question of pure mechanical breakdown. The experiment described on p. 189 of Dr. Edeleanu's paper shows how corrosion can be halted by application of a cathodic current, despite the fact that it has already penetrated almost halfway into the specimen. Other examples could be quoted from Mr. Farmery's work.

One possible objection to the idea of the simple mechanical rupture of the resistant bridges has been raised by Farmery. He points out that the corrosion almost invariably takes an intergranular course, whereas, if there was rupture, occasional transgranular sections of the path would be expected. It is possible that the effect of the stress is to increase the susceptibility of intergranular material which would otherwise be only slightly susceptible. Simnad's|| work on steel shows that strain can shift the potential in a direction such as to make metal more attackable. This has been denied by some investigators on the ground that the energy unaccounted for when metal is deformed would be sufficient to shift the

\* J. W. Kelly and R. C. Gifkins. To be published shortly.

† Reader in the Science of Metallic Corrosion, Cambridge University.

‡ P. Lacombe and N. Yannaquis, *Rev. Mét.*, 1948, 45, 68.

§ Unpublished work, Cambridge University.

|| M. Simnad and U. R. Evans, *Trans. Faraday Soc.*, 1950, 46, 175.



electrode potential by only a few millivolts. However, such calculations appear to have been based on the assumption that the energy stored up in deformed metal is equally distributed throughout the mass. If it were localized in certain small volumes, it would probably suffice to make a metal locally much more reactive than is normally the case—the potential being shifted towards that of potassium and away from that of platinum. Another objection sometimes raised is based on actual measurements of electrode potentials, which have been found to shift comparatively little when metal is deformed. However, the potential measured in a corrosive liquid is a compromise value, being the potential at which the anodic and cathodic currents become equal. If the effect of the strain is to facilitate both anodic and cathodic reaction, it might well be that the potential would remain almost unchanged by the strain, although the current flowing between the anode and cathode would be greatly increased. Simnad's measurements have, in fact, shown that this does occur on iron, and it is believed that these results remove the difficulty in accepting the view that cold work can shift potentials locally in the direction favourable to corrosive attack; such a shift may play a very serious part in corrosion-fatigue cracking.

Dr. T. P. HOAR,\* M.A., F.R.I.C., F.I.M. (Member): Dr. Edeleanu, by his elegant photomicrography, has shown that great care must be taken if etch figures formed preferentially at grain boundaries are not to be confused with a precipitate of a second phase. This part of his work will be of value to all workers in the intricate fields of intergranular and stress corrosion, and indeed to those more generally engaged on the effects of possible grain-boundary precipitation.

He has also clearly demonstrated the effects that can be produced by the application of cathodic protection to a stress-corroding alloy. I have always found it somewhat difficult to understand, not only how such cathodic protection can be effective, but also how a stress-corrosion cell, with a large cathode on the metal surface, and a small anode at the end of an advancing crack, can operate. At first sight one would think that the electrolytic resistance of the cell, between the surface cathode and the anode perhaps some millimetres inside the metal, would be very high relative to that of other cells, such as one between the metal surface and the sides of the crack near its mouth, or one between the sides of the crack near its end and its actual end. Can Dr. Edeleanu and Dr. Evans tell us in a little more detail how they envisage the operation of the stress-corrosion cell, and how cathodic protection operates in this case?

In work on the stress corrosion of 18:8-class steels, Mr. J. G. Hines and I have recently found that the measured electrode potential of a stress-corroding specimen in tension falls by several hundred millivolts over a period of some 2–10 min. immediately before the ultimate failure of the specimen. Whatever the process that is occurring, it is evidently fast compared with ordinary corrosion processes, but slow compared with ordinary tensile failure. Has Dr. Edeleanu any evidence of a similar phenomenon in the present case, or any views on what it is?

Dr. U. R. EVANS: In reply to Dr. Hoar, I would express my own view thus: When susceptible material is being removed from the tip of an intergranular crevice in an alloy, this tip (*A*) must be the anode, whilst there are two possible cathodes,  $C_1$  on the face outside the crevice (or perhaps on the walls of the crevice close to the mouth), and  $C_2$  at the inner part of the crevice close to *A*. At  $C_1$  the cathodic reaction can be the reduction of oxygen, whilst at  $C_2$  only the liberation of hydrogen can occur. It is clear that the e.m.f. of the cell  $A/C_2$  is lower than that of  $A/C_1$ , but its resistance is very much less, so that it will generate more current, provided that the

walls of the crevice at  $C_2$  are free from film. However, the reaction will produce aluminium ions and hydroxyl ions close together, and the walls will become coated with film, practically stopping the flow of current. The long-path current between *A* and  $C_1$  will produce (acidic) aluminium salts at the anode *A*, and alkali far away at the cathode  $C_1$  and the cathodes will remain relatively free from film. Thus, the only type of attack that will produce steady penetration inwards is the oxygen-reduction type, and the B.N.F.M.R.A. investigators have shown that if the oxygen supply is shut off, the advance of the crack ceases, starting again when oxygen is re-admitted. True, hydrogen is evolved in the cracks when fresh film-free metal is exposed. The action proceeds jerkily, as is shown by the sudden movements of the Mercer dials in the Cambridge work and the fluctuation of potential in the B.N.F.M.R.A. work; the jerks will be associated with the exposure of film-free metal in the cracks, and until this has been covered with film, hydrogen evolution is possible. But the destruction is bound up with the long-path cell for which oxygen is required.

There is, however, a manner—other than the shutting off of oxygen—in which stress-corrosion cracking can be halted. If, as illustrated in Fig. C, a block (*A'*) of some anodic metal such as magnesium is joined to the alloy, then the whole of the oxygen reaching the main cathodic surface  $C_1$  will be used up in corroding *A'*, and attack at *A* will practically cease. The

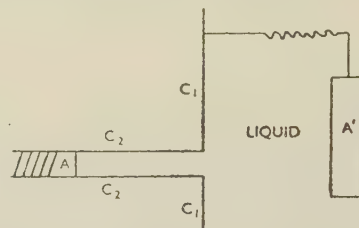


FIG. C.—Diagrammatic Representation of Method of Cathodic Protection to Prevent Stress-Corrosion Cracking.

same result will occur if *A'* is some other material (platinum or carbon), an external e.m.f. being applied so as to make *A'* anodic to the alloy. In both cases, the resistance of the cell  $C_1/A'$  will be much smaller than  $C_1/A$ , whilst its e.m.f. will, in most cases, be greater. The function of the external anode *A'* is *not* to send current along the high-resistance path to *A*, but to provide an alternative path of low resistance, and thus stop attack at *A*.

Mr. E. C. W. PERRYMAN,† M.A., A.I.M. (Member): While I do not want to discuss this paper from the corrosion standpoint, I should like to ask why on p. 188 Dr. Edeleanu states that it is *probable* that during corrosion without stress, corrosion is taking place at numerous grain boundaries. Surely it has often been shown that many grain boundaries are attacked and that it is only when stress is applied that the corrosion crack follows a single path. The author nowhere explains what effect applied stress has. That it does have a real effect is shown by the fact that in a neutral solution, without applied stress, the intercrystalline corrosion penetrates only to a depth of a few grains before stopping. It would be very interesting if Dr. Edeleanu could give us in rather more detail his views on why, when a stress is present, rapid cracking occurs.

Turning to the effect of ageing on stress-corrosion susceptibility, the author has reproduced some curves of mine in Fig. 4 (p. 190) and has reached the conclusion from this and his Fig. 5 that the stress-corrosion susceptibility is serious at a very early stage in the ageing process and probably before

\* Lecturer, Department of Metallurgy, Cambridge University.

† Research Investigator, Aluminium Laboratories, Ltd., Kingston, Ont., Canada; formerly British Non-Ferrous Metals Research Association, London.



actual precipitation has occurred in the bulk of the alloy. It is clear from my results and the author's that the stress-corrosion susceptibility increases with ageing time, reaching a maximum after 3-4 days. After this time the lattice parameter was reduced from about 4.074 kX to about 4.064 kX, corresponding to the precipitation of about 2% magnesium out of solid solution. Furthermore, after this ageing time copious resolvable precipitate was visible. The fact that with a much longer ageing time the stress-corrosion susceptibility was reduced (see Fig. 5) can be explained by the fact that after this time of ageing the precipitate at the grain boundaries had coalesced, resulting in much less continuous grain-boundary films. The above points are illustrated by Fig. D (Plate CXII) and by Fig. 6 of the paper by Perryman and Brook.\* These observations show that the stress-corrosion susceptibility is influenced strongly by the presence of a true second phase. Further evidence supporting the idea that a true second phase is produced on ageing at 200° C. is provided by the fact that after an ageing time of 3 days at 200° C. X-ray-diffraction lines were obtained from the precipitated phase.\* These lines did not correspond to those of the equilibrium  $\beta$  phase ( $Mg_2Al_3$ ). After 53 days at 200° C., however, X-ray-diffraction lines from the equilibrium  $\beta$  phase ( $Mg_2Al_3$ ) were predominant, and it was therefore supposed that the precipitate formed in the early stages of ageing is a transitional form of the equilibrium  $Mg_2Al_3$ . In view of the above, it seems fairly conclusive that with the ageing time and temperature used by the author (2 days at 200° C.), a true precipitate was present, although this may have been a transitional form of the equilibrium  $\beta$  phase ( $Mg_2Al_3$ ). I would like to know how the author reconciles his statement in the first paragraph on p. 190 and the last sentence in the first paragraph of the discussion on p. 191 with the above results.

Dr. Edeleanu criticizes microscopic evidence based on observations of how a second phase reacts to different etching reagents. While agreeing with him that much more needs to be known about the etching process, it must be remembered that this is one of the metallurgist's oldest tools and that the results obtained by its use have in general agreed with those obtained by the more recent X-ray techniques. With regard to the author's results on the aluminium-7% magnesium, it is perhaps unfortunate that he has made a bad choice of etching reagent. He has chosen a very aggressive etch to reveal a very chemically reactive phase; this is shown by the very short etching time he had to use (10 sec.). It is not surprising that the  $\beta$  precipitate was eaten away and that small pits formed after etching for 10 sec. became much larger after 2 min. By using a less vigorous etchant, such as 10% orthophosphoric acid, the precipitate formed on ageing at 200° C. can be clearly resolved under the normal metallurgical microscope, as can be seen in the figures referred to above. On ageing at lower temperatures, such as 125° C., the first sign of a structural change is the formation of small pits at the grain boundaries, and with longer times of ageing continuous troughs are formed at the grain boundaries which have been, I think wrongly, called continuous films of the  $\beta$  phase. With a lower ageing temperature the minimum stable nucleus size of precipitate is smaller than with the higher ageing temperature, and so the precipitated particles at 125° C. are likely to be smaller than at 200° C. On etching with 10% orthophosphoric acid, large particles of the  $\beta$  precipitate are always heavily outlined. This is probably due to a trough being formed around the particles by the etchant. With very small particles it will not be possible to distinguish between the troughs on each side of the particle, and so the particles appear as black spots. Also, if the etching process

is too drastic, a pit may well be produced. On this evidence alone, I agree with the author that it is impossible to ascribe the change in structure as being due to precipitation of a second phase. With very long ageing times at 125° C., however, the precipitated particles grow in size, and it becomes possible to resolve them (see Fig. E, Plate CXII). Without evidence to the contrary, this observation, together with the fact that according to the equilibrium diagram a second phase should be formed at low temperatures, implies that it is not unreasonable to make the assumption that the pits or grain-boundary grooves formed in the early stages of ageing are due to a true second phase. I agree with Dr. Edeleanu that in the aluminium-magnesium system there may well be "equilibrium segregation" of magnesium at the grain boundaries, because the magnesium atom, being much larger than that of aluminium, will be able to concentrate at the large holes in the distorted grain-boundary lattice, with a resultant decrease in free energy of the system. Although such a concentration of solute atoms has been observed by several investigators † in other systems, I do not think that this effect is responsible for the susceptibility to stress-corrosion cracking in the aluminium-magnesium alloys. Firstly, if "equilibrium segregation" is taking place, then it should be present in material which has been quenched from temperatures above the solid-solubility limit, i.e. with all the magnesium in solid solution. However, when the aluminium-7% magnesium alloy is given such a treatment it is known not to be susceptible to stress-corrosion. Secondly, with "equilibrium segregation" the grain-boundary concentration of solute at a given temperature will increase with increasing concentration of solute within the grains. Thus, when precipitation of the second phase is allowed to take place, the grain-boundary concentration would be expected to decrease. Therefore, if the stress-corrosion susceptibility is due to magnesium-rich grain boundaries, as the author suggests, the susceptibility should decrease as precipitate is formed and not increase, as is observed. To sum up, although I think it is probable that the grain boundaries in single-phase aluminium-magnesium alloys may have a higher concentration of magnesium than the grains, I am still of the opinion that it is the precipitated second phase which is responsible for the stress-corrosion cracking.

Dr. P. T. GILBERT, ‡ A.R.I.C., A.I.M. (Member): While the author has made a number of interesting and valuable experiments and observations on factors connected with the stress-corrosion of aluminium-7% magnesium, I feel that he has not put forward any complete mechanism of the process. There appears to be no attempt to give a connected account of the processes leading to rapid failure under the combined influence of stress and corrosion. In particular, the function of stress is not made at all clear.

The application to stress-corrosion of Dr. Edeleanu's views on the autocatalytic nature of the corrosion process on aluminium and its alloys in neutral solutions is very interesting. These views may help to explain the occurrence of local attack at the grain boundaries on aluminium-7% magnesium alloy in certain metallurgical conditions. But there is a vast difference between the slow intercrystalline corrosion on unstressed material and the rapid failure of stressed specimens of the same material in the same environment. The function of stress in bringing about this rapid failure needs careful explanation.

One would like to have the author's views on such matters as how stress localizes damage on to one or two of the many paths available; whether stress causes a series of mechanical fractures at the tip of the advancing crevice, as suggested by Hadden and myself §; or whether it functions merely by

\* E. C. W. Perryman and G. B. Brook, *J. Inst. Metals*, 1951, 79, 19.

† D. McLean and L. Northcott, *J. Iron Steel Inst.*, 1948, 158, 169.

D. McLean, *J. Inst. Metals*, 1947, 73, 791 (discussion).

D. McLean and L. Northcott, *ibid.*, 1946, 72, 538.

L. E. Samuels, *ibid.*, 1949-50, 76, 91.

M. T. Stewart, R. Thomas, K. Wauchope, W. C. Winegard, and B. Chalmers, *Phys. Rev.*, 1951, [ii], 83, 657.

E. C. W. Perryman, unpublished work.

‡ Head, Corrosion Section, British Non-Ferrous Metals Research Association, London.

§ P. T. Gilbert and S. E. Hadden, *J. Inst. Metals*, 1950, 77, 237.



breaking films of corrosion product, or because stressed metal is anodic to unstressed metal.

Mr. Perryman, has dealt at some length with the question of the nature of the anodic path in "susceptible" material. I agree with him that there seems little doubt about the presence of a second phase in material aged for a few days at 200° C. It is less easy to produce convincing evidence for the presence of a second phase in material aged at lower temperatures, because of the fineness of such precipitate, and the doubts about the precise mechanism of etching referred to by Dr. Edeleanu. Even in material aged for short times at 125° C., however, careful metallographic examination gives indications that there are particles present at the grain boundaries. My colleague, Mr. Hadden, has shown that these can be detected by light etching in dilute phosphoric acid or in sodium hydroxide solution (which should not preferentially attack the  $\beta$  phase). The results of such metallographic examination are supported by electron-microscope examination, as shown in Fig. F (Plate CXIII). This photograph shows that a series of particles are produced at the grain boundaries on ageing at 125° C., similar to, but on a much smaller scale than, the structure produced on ageing at 250° C. Perryman and Hadden\* have shown that material in both these conditions is susceptible to stress-corrosion. In general, the susceptibility to stress-corrosion appears to increase as the proportion of the grain boundary occupied by such particles increases, and material in which the particles are few or far apart is not susceptible to stress-corrosion.

It might be mentioned that Dr. Edeleanu's experiments, showing that only an extremely small amount of material is corroded away during stress-corrosion, is no evidence against the presence of particles of second phase and their function in constituting an anodic path. There is no reason to think that the particles are completely corroded away during stress-corrosion cracking, and we have photomicrographs showing a crack which has travelled along the boundaries between the particles and the matrix. I think, however, that there is some danger of over-emphasizing the importance of knowing the precise nature of the grain-boundary material. We are all agreed that when stress-corrosion occurs there is an anodic or "easily corroding" path at the grain boundaries, and we are agreed that this path is relatively rich in magnesium. Even if the path does not consist, in part at least, of  $\beta$  phase, one must attribute to it similar electrochemical properties, e.g. to explain the behaviour of stressed specimens in acid and alkaline solutions.† From some points of view, therefore, the precise metallurgical character of the anodic path is not a matter of major importance.

The AUTHOR (*in reply*): I would like first to correct two errors in Fig. 5 (p. 190). The solution used was N/10-NaCl and not 10 N and the time to failure should be read in minutes and not in hours.

Dr. Evans has made some very useful and interesting comments. The idea that some of the cracking is purely mechanical seems reasonable, but, as noted by Farmery, it is impossible to find the evidence microscopically in highly susceptible alloys. Dr. Evans rightly points out that strain energy can cause an increase in corrosion rate, but the effect in this case is comparatively small, as indicated by the evidence in the paper. The cracks in the later stages are advancing at rates certainly greater than 1 cm./min., and corrosion rates even approaching that order of magnitude are inconceivable to me. We are therefore forced to assume that a relatively low corrosion rate causes rapid cracking by assisting in some way the mechanism of cracking. This assumption, I feel, is not unreasonable, since numerous workers have already reported that surface effects can alter the mechanical properties of single crystals. The speed of stress-corrosion is brought out by Fig. G, in which load/extension curves are drawn for specimens strained at a constant rate. Curve A is for a normal specimen, while B and C

represent specimens wetted with a drop of 4% NaCl solution a few seconds before starting the experiment. Such curves were obtained for the high-purity and for the commercial alloy, but in both cases only a proportion of the specimens tested wet gave the lower U.T.S. values. Specimens giving low U.T.S. values had cracked, as far as could be judged, in an entirely intercrystalline manner. Perhaps Dr. Evans will agree that, although strain may accelerate corrosion, in the later stages of stress-corrosion the accelerating effect of the corrosion on the cracking mechanism may be the more important factor.

Dr. Hoar's opening remarks, when read in conjunction with the criticism by Dr. Gilbert and by Mr. Perryman, emphasize how unsatisfactory the micrographic method can be when one is forced to use it beyond its proper scope.

As regards cathodic protection, my own view is that it operates successfully in this case because the passage of a

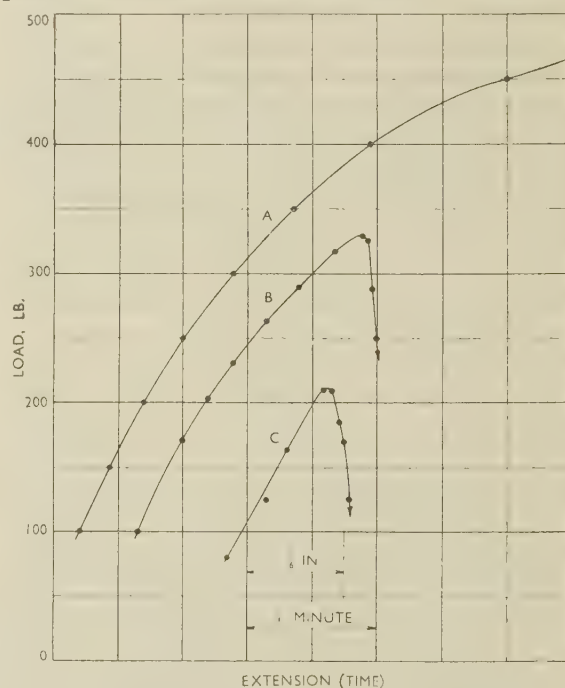


FIG. G.—Load/Extension Curves for Aluminium-Magnesium Alloys Showing Speed of Stress-Corrosion. Curve A: normal specimen. Curves B and C: specimens tested in presence of 4% NaCl solution.

minute current (a few micro-coulombs) would be sufficient to start the precipitation of aluminium hydroxide and thus reverse the whole process which allows localized corrosion to take place. Cathodic protection is, however, a misnomer in this case, since the cathodic polarization can lead to a very serious rise in the general corrosion rate owing to an increase in the pH round the specimen. Localized corrosion, which, I contend, depends on an autocatalytic mechanism, cannot occur in alkaline solutions in the case of aluminium, since the solubility of the aluminate ion, unlike that of the aluminium ion, decreases with a fall in pH. The faster the anodic reaction at any particular point, the lower would be the local pH and, in the case of alkaline solutions, the greater the chance of refilming. I feel that I cannot add anything to the very clear explanation of the corrosion-cell mechanism given by Dr. Evans, but the question raised a few fundamental points which I should like to take up elsewhere.

I have noticed potential drops similar to those mentioned by Dr. Hoar, and I feel that these are due to a slight increase in corrosion rate. Dr. Hoar will probably agree that large

\* E. C. W. Perryman and S. E. Hadden, *J. Inst. Metals*, 1950, 77, 207.

† P. T. Gilbert and S. E. Hadden, *ibid.*, 237.

drops in potential do not necessarily indicate considerable increases in corrosion rate, since, if the corrosion rate exceeds even slightly the rate of arrival of oxygen, a large drop in potential is to be expected.

As far as I can, I have already dealt with Mr. Perryman's first point. I have a high regard for his work on the precipitation mechanism in this type of alloy, and much of my own unpublished work supports his findings. I do not deny the existence of a second phase, for instance, after a few days' ageing at 200°C., but what I question is that this second phase is actually responsible for stress-corrosion and that it is present in all conditions which cause susceptibility to this type of failure. The observation that the  $\beta$  phase is surrounded by a trench during etching in itself affords proof that it may not be the most reactive part of these alloys. I feel that the weakness of metallography, in cases like the present, is the fact that choice of reagent and of time of etching can be arbitrarily made to prove a particular point. As it happens, the two very interesting photographs by Farmery (Figs. A and B, Plate CXII) show, besides the point raised by Dr. Evans, that the reagent recommended by Mr. Perryman can be used to support my contention. Two boundaries in Fig. A, after 10 minutes' etching, seem to exhibit only a few  $\beta$  particles, but the same boundaries are shown as continuously etched in Fig. B.

Perhaps the only reagent it is fair to use in this case is the sodium chloride solution which causes the stress-corrosion, and 4 hours' immersion in this solution gives no indication of visible etching, although it would appear from Table II (p. 189), that that amount of etching results in sufficient intercrystalline corrosion to cause failure in less than 1 min. in subsequent stressing. The fact that the width of the susceptible zone is sub-microscopic is supported by electron micrographs published by Bailey and Vernon-Smith,\* as

well as by the analytical work in the present paper. I cannot follow Dr. Gilbert's objection to this latter evidence, since as far as I can see he confirms that it is not the  $\beta$  phase that is being attacked.

The boundary layer I visualize is not the result of "equilibrium segregation". It arises from something more akin to adsorption, and its presence would naturally depend on temperature. It does not necessitate nucleation energy, and would be continuous at the boundaries. When sufficient magnesium gathers in the boundaries, a second phase may be formed at certain places in the same manner as at liquid interfaces when more than a monolayer has gathered. The disappearance of susceptibility after longer periods of ageing shows, I think, that (1) the interfacial energy between the new phase and the parent metal is more than half that between two grains, and (2) the amount of adsorption at boundaries between grains with low magnesium content is comparatively small. As Dr. Gilbert points out, the matter may not be of vital importance, unless, of course, it suggests a new method of approach to the problem. It would be interesting to know whether the addition of some metal that forms ions with a solubility product somewhat lower than  $10^{-33}$  and that is likely to precipitate on ageing, affects the stress-corrosion of this type of alloy.

I regret that the title of the paper led Dr. Gilbert to expect a more detailed theory, but I feel that further research is still necessary. I can, however, say that careful examination of the cine-films I have taken, leads me to think that the process at the tip of the crack is a continuous one, or, if it is not, that the cyclic mechanism postulated by Dr. Gilbert occurs on a very fine scale. For reasons given in the paper and in another publication,† I do not think that the anode becomes covered to any appreciable extent by films, and hence that the function of the stress is to rupture the oxide films.

## Discussion

# Powder Metallurgy of Copper and Copper Alloys‡

Mr. R. S. BARNES §: Verification of the conclusion reached by Butler and Hoar that the interdiffusion of copper and nickel is able to produce expansion and porosity has already been briefly reported|| and a full account has now been published.¶ The experiments described in these two publications demonstrate in a manner more direct than is possible in a necessarily complex sintering experiment that solid copper-nickel couples expand and become porous as a result of diffusion. However, porosity arises not because "there is a net transfer of material into the copper particles causing them to expand", but, on the contrary, because there is a net loss of atoms from the copper particles, causing contraction and making pore formation possible. This is in agreement with the results of previous experiments that the diffusion rate of copper into nickel is greater (and not less, as quoted) than that of nickel into copper.

Dr. H. H. HAUSNER \*\*: In regard to the X-ray data presented by Howat, Craik, and Cranston, it seems that the authors' remarks about the formation of  $\beta$  first should be

clarified. Whether alloying takes place because of direct zinc-to-copper particle contact or by deposition of zinc vapour on copper, a diffusion couple must occur at the interface, and until all the zinc is dissolved every phase in the copper-zinc system must be present, whether or not these phases are in sufficient quantity for X-ray identification, and this is seldom the case in any alloy system. Thus, as the zinc diffuses in,  $\beta$  must form before  $\alpha$ , and apparently it forms in sufficient quantity to be predominant in X-ray identification. Thus, if one makes a diffusion couple of copper/zinc, a rather large band of  $\beta$  would form relative to the size of the bands of other phases.

The effect of compacting pressure on the dilation tests needs further explanation, as I doubt whether it can be explained on the basis of voids. First, it must be remembered that the expansion was measured only linearly. Secondly, in compacting, the particles are generally plastically deformed and may be in a condition of strain. Since the pressure was applied normal to the direction of expansion measurement, one would expect less expansion in this direction for either

\* G. L. J. Bailey and S. Vernon-Smith, *Inst. Metals: Symposium on Metallurgical Applications of the Electron Microscope, 1949*, p. 43. (Monograph and Report Series No. 8).

† C. Edeleanu and U. R. Evans, *Trans. Faraday Soc.*, 1951, **47**, 1121.

‡ Joint discussion on the papers by E. C. Ellwood and W. A. Weddle (*J. Inst. Metals*, this vol., p. 193), J. M. Butler

and T. P. Hoar (this vol., p. 207), and D. D. Howat, R. L. Craik, and J. P. Cranston (this vol., p. 353).

§ Atomic Energy Research Establishment, Harwell, Berks. || A. D. Le Claire and R. S. Barnes, *Trans. Amer. Inst. Min. Met. Eng.*, 1951, **191**, 1060 (discussion).

¶ R. S. Barnes, *Proc. Phys. Soc.*, 1952, [B], **65**, (7), 512.

\*\* Manager, Atomic Energy Research and Development, Sylva Electric Products, Inc., Bayside, N.Y., U.S.A.



or both of two reasons: (1) Strain relief or recovery would tend to restore the particle to its original shape. Thus, it would tend to contract normal to the direction of pressing and expand in the direction of pressing. (2) Ordinary surface-tension phenomena indicate that the particle should assume the shape of a sphere upon heating and thus again tend to recover from its compressed condition.

At the higher pressures, then, the tendency for linear contraction normal to the compacting direction is greater, and thus the net amount of expansion is decreased. It is more difficult to explain the greater growth at very high pressures, and one must look to the alloying that occurs. Assuming no interference, the zinc should deposit itself from the vapour uniformly on the copper particle regardless of shape. The growth should be uniform in all directions. Interference does occur, however, and at higher pressure there may be more copper-to-copper particle contacts normal to the direction in which expansion was measured. This prevents some expansion owing to lack of deposition of the zinc in the direction not measured and precludes more relative growth in the measured direction. Further, the formation of relatively more  $\beta$  in the measured direction would increase the tendency to expand in this direction.

Even if it is assumed that the zinc did not become transferred primarily in the vapour phase, it can be postulated that more copper-to-zinc contacts occur in the direction normal to the pressing direction. Thus more  $\beta$  would tend to form at these contacts and lead to relatively more expansion in this direction.

The data presented on the effect of compacting pressure on the differential thermal analysis and the line of reasoning used by the authors to explain these data, seem to bear out the above ideas along the lines of vapour transport of the zinc.

To clarify this question data are needed for pure copper and for perhaps two compositions other than that reported in Table II (p. 355). I should like to ask the authors if they have such data and, if not, would suggest that they make these additional measurements. The information would render this paper an even more valuable contribution to the fundamental knowledge of powder metallurgy.

Dr. T. P. HOAR,\* M.A., F.R.I.C., F.I.M. (Member): Dr. Ellwood and Mr. Weddle emphasize that their work on the production of copper powder from scrap copper wire has a practical basis, and they disclaim credit for fundamental investigation. Nevertheless, I think that they have clearly demonstrated a number of fundamental points; the section on the milling of the oxide is of quite general importance in the comminution of powders, and indeed those who are mainly interested in principles rather than processes will find much to claim their attention throughout the research. The work is an excellent example of what can be achieved by the co-operation of industrial and university interests.

I agree with the authors that it is impossible to store copper powder in an absolutely oxygen-free condition, owing to the formation of surface oxide. Dr. Butler and I found that 0.1% oxygen was the lower limit for air-stability of a fairly coarse electrolytic powder. The comparatively poor stability of the coal-gas-reduced powder, found by Dr. Ellwood and Mr. Weddle, may well be due to the presence of sulphur; impure oxide films on copper, containing sulphide, thicken very readily, presumably because the sulphide impurity leads to a film of which the electronic and ionic conductivities are higher, and the cation vacancies more numerous, than in the case of a relatively pure oxide.

Dr. E. SCHEUER † (Member): With regard to the expansion observed in sintering compacts which form solid solutions, it may be of interest to recall similar observations reported some 15 to 25 years ago in connection with the solidification of certain alloys, e.g. bronzes and zinc-copper alloys. ‡§

During the final stages of solidification of these alloys, expansions have been observed which seem best explained on the assumption that the primary crystals which are unsaturated owing to the coring effect, pick up solute from the liquid eutectic surrounding them and incorporate it into their lattice by diffusion. By this process the crystals expand and push each other apart, thus producing intercrystalline cavities. The expansions observed in the case of zinc-copper alloys with about 85% zinc are of the order of 10%.

Dr. BUTLER and Dr. HOAR (*in reply*): We are grateful to Dr. Scheuer for pointing out the interesting cases of diffusion-produced expansions during the solidification of bronzes and zinc-copper alloys: as mentioned in our paper, Duwez and Jordan || have more recently noted the expansion effect in the zinc-copper system during the sintering of powder compacts. These experiments, together with our own and those of Mr. Barnes on the copper-nickel system, form a considerable body of evidence for expansion initiated by intermetallic diffusion.

Mr. Barnes is right in querying our suggestion that "there is a net transfer of material into the copper particles causing them to expand", but we think the situation is more complicated than his remarks imply. The diffusion rate of copper in nickel is less than that of nickel in copper for dilute solutions of the one metal in the other, as shown by the tail ends of composition/distance curves such as those of da Silva and Mehl; ¶ this is what might be expected, since nickel has a considerably higher melting point and presumably many fewer vacancies than copper at temperatures in the region 700°–1000° C. But the marker movements in da Silva and Mehl's work show clearly that there is a net transfer of material across the position of the original interface in the direction copper → nickel; copper moves more readily than nickel in concentrated solutions, that is, in alloys of composition in the range of, say, 25–75% of either metal. Thus, our suggestion in the paper is clearly wrong, although it does not affect either the experimental fact of the overall expansion or our general argument concerning the subsequent sintering contraction. It is, in fact, very likely that the net gain of material by the original nickel particles is responsible for the overall expansion, while the loss from the original copper particles produces local contractions and porosity.

The formation of porosity in the copper may be due to the condensation of vacancies (as suggested by Mr. Barnes in a private communication and in his paper), a mechanism similar to that advanced by Dunnington, Beck, and Fontana \*\* to explain porosity in iron undergoing oxidation at 1090° C., created in the metal just below the oxide film. While a diffusion mechanism may be partly responsible in the present case, we think that mechanical tearing—tensile or shear failure—of the weak hot metal is likely to occur by the movement of metal under stress by a mechanism similar to that causing sintering shrinkage.

Dr. E. C. ELLWOOD and Mr. W. A. WEDDLE (*in reply*): We thank Dr. Hoar for his remarks, and in particular for drawing attention to the fact that our paper was the result of co-operation between industrial and university interests. We fully agree that such work can often lead to practical results.

\* Lecturer, Department of Metallurgy, Cambridge University.

† Chief Metallurgist and Head of Laboratories, International Alloys, Ltd., Aylesbury, Bucks.

‡ G. Masing and E. Scheuer, *Z. Metallkunde*, 1933, **25**, 176.

§ K. Iokibe, *J. Inst. Metals*, 1924, **31**, 225.

|| P. Duwez and C. B. Jordan, *Trans. Amer. Soc. Metals*, 1949, **41**, 194.

¶ L. C. C. da Silva and R. F. Mehl, *Trans. Amer. Inst. Min. Met. Eng.*, 1951, **191**, 155.

\*\* B. W. Dunnington, F. H. Beck, and M. G. Fontana, *Corrosion*, 1952, **8**, 2.

Dr. HOWAT, Mr. CRAIK, and Dr. CRANSTON (*in reply*): We agree entirely with Dr. Hausner's remarks in his first paragraph, and regret that in the text of the paper we did not make it clear that all that was claimed was that the formation of  $\beta$  was the predominant reaction. In the recent work by da Silva and Mehl, the diffusion coefficient of zinc into copper is shown to increase very rapidly at about the limit of the  $\alpha$  phase. This also helps to confirm the rapid formation of  $\beta$  and the existence of only a thin band of  $\alpha$  solid solution.

The explanation put forward to correlate the effects of compacting pressure and dilatation tests was admittedly tentative, and we have read Dr. Hausner's suggestions with interest. The possibilities of strain relief and recovery are well worth considering. We feel, however, that the temperatures involved are too low to permit surface-tension phenomena to exert any appreciable effect. We agree that the more

difficult problem of greater growth of the compacts at high compacting pressures may possibly be associated with more rapid alloy formation.

It is difficult to assess what degree of plastic deformation of the individual particles occurs in compacting, but it does not appear to us very probable that more copper-to-copper particle contacts should be formed at high pressures. Possibly at the high compacting pressures some of the zinc particles are fractured, so creating a greater surface area and the possibilities of an increase in the number of copper/zinc contacts. The final explanation may be bound up with Dr. Hausner's suggestion about the degree of alloying which occurs and possibly with the kinetics of the alloy formation.

We regret that we have not the data referred to by Dr. Hausner in his last paragraph and have not as yet had a suitable opportunity to carry out the additional tests.

## Discussion

# The Solid Solutions of Zinc in Aluminium

By E. C. ELLWOOD

(*Journal*, this vol., p. 217.)

Dr. K. SCHUBERT\* and Dr. W. AUERHAMMER\*: Many references are to be found in the literature to the anomalies presented by aluminium-zinc solid solutions. As long ago as 1924, Tanabe† recognized that the two-phase field between the  $\alpha$  and  $\alpha'$  phases must be narrow. The question whether a two-phase field exists appears to be immaterial, however, from the point of view of the bond structure of the alloys. Von Schwarz and Summa‡ established the identity of lattice type of the two phases. From X-ray studies of quenched specimens,§ and subsequently from high-temperature X-ray photographs,|| Schmid and Wassermann reached conclusions which did not conflict with the constitutional diagram proposed by Tanabe, though, in contrast to him, they did regard a continuous series of solid solutions as possible. The existence of such a continuous series was recognized by Fink and Willey¶ and confirmed by Gayler and Sutherland\*\* by thermal analysis and micro-examination. Lattice-parameter measurements by Owen and Pickup†† revealed an anomaly in the region of 50 at.-% aluminium, which was confirmed by Auer's‡‡ magnetic measurements. Further X-ray investigations at high temperatures carried out by Petrov and Badaeva§§ also showed a marked anomaly in the lattice parameter in the region of homogeneous solid solutions. The same anomaly can be detected in the measurements reported by Ellwood in the present paper. In addition, Petrov and Badaeva measured the electrical resistance of the alloys, and this also clearly revealed an anomaly.

Hume-Rothery and Raynor||| were the first to attribute such anomalies to the overlapping of the (200) plane of the Brillouin zone by the Fermi surface. Raynor and Wakeman,¶¶ who discovered an analogous effect in the silver-aluminium system, abandoned the explanation, however, in view of Matyáš's\*\*\* calculation of the bond structure of aluminium, which gave no overlapping of the (200) plane. One of us (K. S.), without knowing of Hume-Rothery's proposal, suggested the overlapping of the (200) plane of the Brillouin zone by the Fermi surface, first as an alternative explanation,††† and subsequently as the sole explanation,‡‡‡ and later demonstrated §§§ in connection with the phase  $\text{TiAl}_3$  and by a new calculation, that the theory of the (200) plane overlap can be upheld. Calculations of the elastic constants of aluminium by Leigh|||| are based on this assumption.

Apart from the effect at a valency-electron concentration of about 2.1–2.5, which is due to the filling up of spaces beyond the (200) plane, similar "surface-overlap" effects are not to be expected up to a valency-electron concentration of 3.0, but only "edge-overlap" effects. However, the latter have not so far been correlated with physical anomalies. Auer's curves form an exception, for, though lacking confirmation, these showed a marked anomaly at about 80 at.-% aluminium—a region in which, it may be noted, Ellwood's lattice-constant curves show a slight inflection. It may be assumed that here the edge-overlap effect is operative.¶¶¶

\* Max-Planck Institut für Metallforschung, Stuttgart, Germany.

† T. Tanabe, *J. Inst. Metals*, 1924, **32**, 433.

‡ M. v. Schwarz and O. Summa, *Metallwirtschaft*, 1932, **11**, 369.

§ E. Schmid and G. Wassermann, *ibid.*, 373.

|| E. Schmid and G. Wassermann, *Z. Metallkunde*, 1934, **26**, 148.

¶ W. L. Fink and L. A. Willey, *Trans. Amer. Inst. Min. Met. Eng.*, 1936, **122**, 244.

\*\* M. L. V. Gayler and E. G. Sutherland, *J. Inst. Metals*, 1938, **63**, 123.

†† E. A. Owen and L. Pickup, *Phil. Mag.*, 1935, [vii], **20**, 774.

‡‡ H. Auer, *Vorträge der Hauptversammlung 1938 der*

*Deut. Ges. Metallkunde*, 1938, 48.

§§ D. A. Petrov and T. A. Badaeva, *Zhur. Fiz. Khim.*, 1947, **21**, 785.

||| W. Hume-Rothery and G. V. Raynor, *Proc. Roy. Soc.*, 1940, [A], **174**, 471.

¶¶ G. V. Raynor and D. W. Wakeman, *Phil. Mag.*, 1949, [vii], **40**, 404.

\*\*\* Z. Matyáš, *Phil. Mag.*, 1948, [vii], **39**, 429.

††† K. Schubert, *Metallforschung*, 1947, **2**, 349.

‡‡‡ K. Schubert, *Z. Metallkunde*, 1948, **39**, 88.

§§§ K. Schubert, *ibid.*, 1950, **41**, 417.

|||| R. S. Leigh, *Phil. Mag.*, 1951, [vii], **42**, 139, 876.

¶¶¶ K. Schubert, "Zur Kristallchemie dichter Kugelpackungen". 1951: Stuttgart.



The density effect found by the author need not necessarily be due to vacant lattice sites, but may be caused by structural defects. Fig. 5 (p. 221) of the paper might be interpreted as follows: From 100 to about 95 at.-% aluminium precipitation of zinc from the aluminium matrix takes place below 200° C. As the matrix cannot adapt itself sufficiently, a fall in density occurs, i.e. there is an apparent increase in the number of holes. Between 95 and 83 at.-% aluminium precipitation of zinc proceeds, but as the matrix adjusts itself more readily, the number of holes decreases. Between 83 and 75 at.-% aluminium a new process becomes operative, namely, precipitation of  $\alpha'$  from the matrix, which gives rise to a new source of structural defects so that the apparent number of holes increases again. Below 75 at.-% aluminium, however, this increase is masked by the contraction accompanying the decomposition of  $\alpha'$ .\*

Further investigations appear to be needed to determine whether the observed effects can be explained by the band model or not.

The AUTHOR (*in reply*): As Dr. Schubert and Dr. Auerhammer point out, there was doubt as to the form of the aluminium-zinc equilibrium diagram until the work of Fink and Willey, and of Gayler and Sutherland, was published. Its form is now generally accepted, and nothing in the present work conflicts materially with the Annotated Equilibrium Diagram of Raynor.† I regret that in my search of the literature, I missed Dr. Schubert's interesting work.

Leigh's papers on the elastic constants of aluminium and on the aluminium-zinc system had not been published when my work was written up, and consequently the discussion is based on the earlier work of Matyáš. Leigh's calculations account, in part, for the anomaly at about 20 at.-% zinc, but they do not predict that which occurs at about 5 at.-%,

nor do they explain the increase in apparent atomic diameter of aluminium which takes place in two steps as zinc is added, i.e. as the electron concentration is decreased. The calculations of Jones‡ and experimental work by Hume-Rothery and Raynor§ suggest that the reverse effect should be observed if the zones are being filled in the normal manner with increasing electron concentration. I have been careful not to suggest which zones are being filled, because this cannot be deduced from the experimental results.

The suggestion that the anomalies in density might be due to structural defects is interesting, but I am reluctant to accept it. The alloys certainly show precipitation effects, and those containing about 5 at.-% zinc over-age in comparatively short times at room temperature. It is possible that the density results might be affected, but the scale of the effect at 5 at.-% zinc, i.e. a density anomaly of 1%, is rather larger than that normally associated with structural defects. Repeated quenching from 360° C., with sufficient time at room temperature between each quench to over-age the specimens, does have a significant effect on the density. If the structural defects are not eliminated each time the specimens are solution-treated, some change in density should be observed. Further measurements at 360° C. in molten salt give anomalous densities.

The suggestion that structural defects associated with precipitation are responsible for the density results shown in Fig. 5 could be tested quite easily by carrying out dilatation measurements on quenched samples during ageing.

While I believe that my interpretation of the anomalous densities as being due to vacancies is correct, I am aware that it is most desirable to check this by some means that does not involve density measurements, and suggest that a possible line of approach might be to study carefully the background scatter on X-ray-diffraction films.

## Discussion

# Micrographic Aspects of the Diffusion of Zinc and Aluminium in Copper

By H. BÜCKLE and J. BLIN

(*Journal*, this vol., p. 385.)

Mr. E. LARDNER, || B.Sc., A.I.M. (Member): The cavities described in this paper appear to be very similar to cavities sometimes observed to be produced during the solution heat-treatment of magnesium-aluminium alloys of the Elektron AZ91 type. In such alloys the cavities are in the form of hexagonal prisms, with the hexagonal faces lying in the basal planes of the grains in which they occur. The dimensions vary considerably, but a typical cavity would measure about 15  $\mu$  across the flats of the hexagon and be about 8  $\mu$  wide.

The cavities are not universally present in solution-treated magnesium-aluminium alloys; in fact, they are the exception rather than the rule. It is evident that some condition as well as a suitable solution heat-treatment must be fulfilled, if they are to be formed, but unfortunately this has not yet been identified.

However, a considerable amount of work has been carried out on this subject, and it seems probable that in the case of the magnesium alloys the cavities are not produced during the progress of the heat-treatment, but during cooling from the heat-treatment temperature. It is hoped to publish further information regarding the phenomenon at a later date.

The AUTHORS (*in reply*): At first sight the similarities between the cavities described by Mr. Lardner and those which we observed are striking. It is not very likely, however, that the relatively short heat-treatment times used, taken in conjunction with the restricted segregation zones characteristic of the magnesium-aluminium alloys, would have favoured the formation, by the Kirkendall effect, of such large cavities. The structure and composition of commercial alloys of the Elektron AZ91 type are too com-

\* T. Tanabe, *loc. cit.*

E. Gebhardt, *Z. Metallkunde*, 1941, **33**, 329.

† G. V. Raynor, *Inst. Metals: Annotated Equilib. Diagr. Series*, No. 1, 1944.

‡ H. Jones, *Proc. Roy. Soc.*, 1934, [A], **147**, 396.

§ W. Hume-Rothery and G. V. Raynor, *ibid.*, 1940, [A], **177**, 27.

|| Research Metallurgist, Hard Metal Tools, Ltd., Coventry; formerly with Magnesium Elektron, Ltd.

plex, and the heat-treatment conditions too varied, to permit of one simple explanation of the phenomenon, which seems, moreover, to be produced only by chance. If it can be confirmed that the cavities are formed during cooling, the hypothesis that they are due to a diffusion mechanism must be abandoned. In that case, incomplete homogeniza-

tion, giving rise to internal stresses, might result in preferential attack during polishing and etching and the formation of cavities of regular shape. We observed such behaviour in the case of a specimen of zinc containing traces of copper; the cavities, which took the form of hexagonal prisms, were usually associated with twins.

## Discussion

# The Opaque-Stop Microscope as a Means of Studying Surface Relief

By W. M. LOMER and P. L. PRATT

(*Journal*, this vol., p. 409.)

Dr. J. W. CHRISTIAN,\* M.A. (Junior Member): The authors are to be congratulated on the way in which they have developed this simple and elegant method. In studying surface topography, now increasingly important, we must consider small differences in both height and orientation. Height differences are best observed qualitatively with the phase-contrast microscope, and interference techniques may be used for quantitative measurements. The authors' work shows that the opaque-stop microscope is probably the most sensitive method of revealing orientation differences. It would be interesting if they could state more definitely the advantages of the opaque stop, when used in the Schlieren arrangement, over the more usual method of slightly displacing the illumination system.

Dr. Lomer and Dr. Pratt have also shown that the opaque-stop microscope may be used for quantitative measurements of orientation differences. At low magnifications the sensitivity of this method is very high, but at high magnifications it seems inferior to the Bertrand-lens arrangement mentioned by Mr. Harris in the discussion on Mott and Haines's papers (p. 720). If the images of the source in the back focal plane of the objective, produced by two adjacent regions, are examined in this way, the angle between the surfaces can be measured by tilting the specimen on a small goniometer head until each image in turn is brought on to the eyepiece crosswire. Mr. Basinski and I found this method quite sensitive ( $\sim 5'$ ) at magnifications up to  $\times 400$ , whereas the figures given by the authors show that the sensitivity of the opaque-stop method is worse than  $1^\circ$  at this magnification. It is not necessary to tilt the surface to measure each angle required, and it is simpler to use a photographic method in which a plate is calibrated at a fixed magnification by tilting a flat polished surface by known amounts. The surface angles between four

or more neighbouring regions can then be measured accurately by photographing the direction images at the same magnification. The sensitivity of all optical methods of measuring orientation decreases at high magnifications, because diffraction effects are more pronounced and it is difficult to recognize the central diffraction maximum.

The AUTHORS (*in reply*): The main advantage of using a stop system, rather than displacing the illumination, is one of sensitivity, especially for nearly flat surfaces. With annular stops a small tilt of the surface allows a great deal of light to pass the stop to form the image, whereas if the effects are produced by the light beam overlapping the objective mount, the initial sensitivity is lower. In addition, it is convenient in practice to leave the illuminating train correctly aligned and to be able, simply by removing the stop from the illuminating train, to change quickly back to a normal set-up.

We agree with Dr. Christian that the sensitivity quoted in our paper seems to compare adversely with that of the method mentioned by Mr. Harris. The difference is, however, largely a question of the type of object studied. It was assumed by us that the object had detail of such size as to repay examination with the microscope at high magnification, and in this case diffraction sets a limit to the accuracy of about  $1^\circ$  for structures a few microns in diameter. The opaque-stop microscope allows one to reach substantially this sensitivity even when examining a field so complex that the back focal plane contains no clearly resolved images of the source stop. If it were used on an area of simple structure, the sensitivity would be much nearer that reached by Dr. Christian and Mr. Basinski, since both methods of measuring depend upon displacements of the image in the back focal plane.

\* Pressed Steel Co., Ltd., Research Fellow, Inorganic Chemistry Laboratory, Oxford University.



## Discussion

## The Structure and Properties of Wrought Copper-Aluminium-Nickel-Iron Alloys

By MAURICE COOK, W. P. FENTIMAN, and EDWIN DAVIS

(Journal, this vol., p. 419.)

Mr. W. A. BAKER,\* B.Sc., F.I.M. (Member): My colleagues and I have had advance information of a large part of the metallographic work described in this paper and have found it invaluable in investigations we are making into the mechanical properties of these alloys. In the course of our work we had occasion to compare the structures of materials heat-treated for relatively short times, of the order likely to be involved in commercial heat-treatment (e.g. 1 hr. in the range 700°–900° C. and 4–24 hr. in the range 400°–590° C.) with those to be expected from the phase diagram published in the paper. We found a close similarity, and the authors' diagrams are thus proved to be of immediate and practical value to those concerned with the commercial heat-treatment and use of these materials.

With reference to the marked dependence of the mechanical properties of some of the alloys on their earlier heat-treatment, can the authors enlarge on their observations on the effects resulting from breakdown of the  $\beta$  phase on cooling at various rates from temperatures in the  $\beta$ ,  $(\alpha + \beta)$ , and  $(\alpha + \beta + \kappa)$  fields? My colleagues have found that the hardnesses of alloys quenched from various temperatures in these fields are distinctly higher for materials whose compositions fall above and to the right of a line defined approximately by the points 900° C., 10% Al and 750° C., 11% Al in the authors' Fig. 2 (p. 421), for alloys containing 5% each of iron and nickel. The marked differences between the hardnesses of quenched alloys on either side of this line may be due to some odd shape of the phase space through which the diagram is a section. I confirm the authors' observation that rapid cooling of alloys of this type never preserves the  $\beta$  phase completely unchanged. I think that the characteristic acicular marks seen in the quenched  $\beta$  phase are a result of a martensitic transformation to a distorted face-centred cubic structure. It is clear that the presence of this constituent tends to embrittle the alloys, and I hope that the authors may be able to amplify the information given in their Table IX (p. 428) by giving data for the properties of alloys cooled from high temperatures at rates intermediate between the water-quenched and furnace-cooled rates cited.

Mr. A. P. MIODOWNIK,† B.Sc., L.I.M. (Student Member): I am engaged on some work involving the stability of certain copper-base  $\beta$  alloys, and consequently am familiar with the problem of distinguishing between the several types of reaction that occur and that seem to represent alternative methods of decomposition of the  $\beta$  phase. While appreciating the difficulties with which the authors were faced, I feel that the nomenclature used in the paper is liable to misinterpretation.

At the bottom of p. 420 the following statement appears: "When a substantial proportion of  $\beta$  is retained undecomposed, acicular marks are produced by etching (Fig. 13, Plate LXIII), similar to those observed in quenched  $\beta$  in binary copper-aluminium alloys. The  $\beta$  phase cannot be retained unchanged by quenching, for a martensitic-type transformation occurs,

accompanied sometimes by decomposition to an extent dependent on the aluminium, nickel, and iron contents." In the second column of p. 421 the authors write: "... the critical cooling rate for suppression of the  $\beta$  decomposition decreases with increasing aluminium content. ... Thus the 8 and 9% aluminium alloys precipitate  $\alpha$  at grain boundaries and in a Widmannstätten pattern, whilst the 10% alloy precipitates  $\alpha$  at grain boundaries only. Increasing the severity of the quench reduces the amount of  $\beta$  decomposition in the 8, 9, and 10% aluminium alloys. The martensitic transformation, however, is not influenced by the quenching rate, and in no circumstances was it found possible to suppress this change." From these quotations it appears that the authors have used the terms "transformation" and "change" to describe the martensitic reaction  $\beta \rightarrow \beta'$ , and the terms "decomposition" and "precipitation" for any reactions other than this, notably the formation of  $\alpha$ . This distinction has been rigidly adhered to throughout the paper, and represents a clear-cut division into reactions primarily based on shear and those based on diffusion processes. Work on binary systems such as copper-aluminium and copper-beryllium has shown that it is an over-simplification to separate the various types of reaction that can occur, since partial transformation to one product can affect subsequent transformation to other products.

With reference to the extract from p. 421, I disagree with the statement that the martensitic transformation is not influenced by the quenching rate. Incipient precipitation of  $\alpha$  will interfere with the nucleation and propagation of martensite needles, rendering these much shorter and resulting in different internal stresses. Furthermore, any appreciable precipitation of  $\alpha$  alters the composition of the remaining  $\beta$ , which therefore automatically has a different  $M_s$  temperature. Consequently, although there may be no direct effect on the  $\beta \rightarrow \beta'$  transformation from altering the cooling rate, there are very appreciable indirect effects.

The paper has the essentially practical purpose of correlating the mechanical properties of the alloys with the structures obtained by various heat-treatments. A proper understanding of the structures is therefore of paramount importance. The authors' division of the reactions into two clearly defined types, although probably adequate for the purposes of the present paper, will present serious difficulties when their work is extended. The transformation of steels was originally considered in this manner, with the result that the nomenclature of the various products became imprecise and confusing and had to be revised when  $TTT$  curves were subsequently established. The transformations taking place in non-ferrous alloys are, if anything, more complicated than those in the ferrous alloys.

Mr. CHRISTOPHER SMITH,‡ F.I.M. (Member): The information given in the paper is invaluable to workers using these interesting materials. I should like to ask a practical question. When these alloys are produced in large sizes, say,

\* Research Manager, British Non-Ferrous Metals Research Association, London.

† Research Demonstrator, Metallurgy Department, Batter-

sea Polytechnic, London.

‡ Works Superintendent, James Booth and Co., Ltd., Birmingham.

extruded bars of 6 in. dia., it is not practicable to obtain the highest mechanical properties by heat-treatment, as the bars crack in quenching from a high temperature. Owing to the slow rate at which such bars cool in air, properties are likely to be lower than on the smaller sizes. Can the authors suggest a treatment which will enable the high-strength properties of such large masses to be realized?

Mr. Z. STOKOWIEC,\* F.I.M., A.M.I.Mech.E.: At the David Brown Foundries Company we are dealing, not with wrought materials, but with sand or centrifugally spun castings. It may be of interest, however, to compare the results obtained by heat-treatment of sand castings in D.T.D. 412, which is very similar in composition to some of the alloys used by the authors. An increase of U.T.S. from 40 to 48 tons/in.<sup>2</sup>, and of 0.1% proof stress from 16 to 32 tons/in.<sup>2</sup>, together with a decrease in elongation from 12 to 5%, resulted from the following treatment of section up to 1 in. thick: (a) Soaking at 900°–965° C. for 40 min.; (b) quenching in water; (c) tempering at 600°–650° C. for 1–2 hr.; (d) quenching in water.

I should like to have the authors' comments on the addition of manganese to aluminium bronzes. We found that in order to obtain these remarkable results, as far as proof stress is concerned, it was necessary to have an addition of at least 1.2% manganese; without this addition the aluminium bronze would not respond to the heat-treatment.

Dr. H. SUTTON,† C.B.E., F.R.Ae.S., F.I.M. (Member): The paper represents a valuable contribution to the knowledge of the relation between the constitution and properties of a group of alloys whose importance as engineering materials has increased substantially in recent years. I should like to ask the authors whether they have found that alloys of lower aluminium content can be rather less easily hot worked than those containing higher percentages of aluminium, as has been the experience of some manufacturers? If so, can they offer any explanation?

The first sentence of the last paragraph in Section II of the paper (p. 424) might be read as indicating that the  $\kappa$  phase has a ductility comparable with that of the  $\alpha$  phase, but possibly a reference to  $\alpha + \kappa$  was intended.

It is unfortunate that the reproduction of some of the diagrams, e.g. Fig. 51 (a), (b), and (c), is not on a sufficiently large scale to permit of identification of certain curves.

The AUTHORS (*in reply*): We are glad to learn from Mr. Baker that his observations on the structures of these alloys are in agreement with what would be expected from the phase diagram given in the paper. The marked differences between the hardness of quenched alloys on either side of the line defined, from Fig. 2 of the paper, by the points 900° C., 10% Al and 750° C., 11% Al, for alloys containing 5% each of iron and nickel, may, we suggest, be due to the fact that this line corresponds to a proportion of some 20%  $\beta$  in the alloy. We have noted that as the  $\beta$  content increases above 20% the rate of increase of hardness becomes much more rapid than with lower  $\beta$  contents, but we have no evidence of a sudden discontinuous increase in hardness with change in quenching temperature.

We have made no systematic examination of the effects of different cooling rates on the breakdown of  $\beta$ , but air-cooling of sections  $\frac{1}{8}$  in. or more in thickness is usually

sufficiently slow to result in almost complete decomposition. On the other hand, the presence of  $\beta$  in hot-wrought material implies severe chilling during working, e.g. by the forming dies in forging, or, as we have shown, by the rolls during hot rolling of thin sheet.

In the absence of systematic data it is not possible to answer Mr. Smith's question with precision, but we would suggest that oil-quenching a 6-in.-dia. extruded bar of the 10:5:5 alloy might provide a sufficiently rapid rate of cooling over the important range 900°–600° C. to retain  $\beta$  without producing cracking. Optimum mechanical properties resulting from heat-treatment are only realized if this is so designed as to ensure that substantial proportions of martensitic  $\beta$  are retained by quenching and subsequently decomposed by tempering. The hardness of the quenched  $\beta$  phase and the further hardness increment taking place during the initial stages of tempering appear to be associated with the iron content, for the presence of nickel, or for that matter zinc and manganese, in binary aluminium bronzes in quantities up to those sufficient to depress  $M_s$  below room temperature, do not give rise to the marked increase in hardness noted when iron is present. The effect of manganese additions on the properties of castings referred to by Mr. Stokowiec would appear to be due mainly to a resultant increase in the amount of  $\beta$  present at the soaking temperature.

As Dr. Sutton has pointed out, the first sentence of the last paragraph in Section II (p. 424) should read " $\alpha$  and  $\kappa$ " not " $\alpha$  or  $\kappa$ ". Differences in the ease of hot working of alloys of different aluminium contents can be attributed partly to the influence of the  $\beta$  content, which is more readily deformed at high temperature than  $\alpha$ , and partly to the tendency of  $\alpha$ , when present in quantity, to strain-hardening at low hot-working temperatures. Thus, for ease of hot working, compositions and working temperatures should be so selected that there is a high proportion of  $\beta$  present.

We entirely agree with Dr. Sutton's comments about the difficulty in reading some of the diagrams. All were originally supplied as large clear drawings, but were, in our view, made far too small in reproduction.

We have, as Mr. Miodownik has noted, made a clear-cut distinction between reactions of the nucleation-and-growth type on the one hand and the diffusionless reaction of the martensitic type on the other, precisely because these reactions are different, and, therefore, quite contrary to what he suggests, the nomenclature we have used is not likely to be misinterpreted but to be explanatory and helpful. It is characteristic of the martensitic-type reaction that it is not affected by quenching rate. Although we are familiar with the work of Smith and Lindlie,‡ Mack,§ and Klier and Grymko,|| for example, to which Mr. Miodownik is presumably referring, in our experience and to our knowledge, no heat-treatment of the "austempering" type or of any kind which depends on controlled rate of cooling, yields mechanical properties in aluminium bronze superior to those obtainable by simpler methods. Although Mr. Miodownik has expressed his disagreement with the statement that the martensitic transformation is not affected by cooling rate, in so doing he is merely making an assertion which is contrary to existing evidence. Whilst it is true that the  $M_s$  temperature of  $\beta$  will vary with its composition, in these alloys it was above room temperature in all instances in which sufficient  $\beta$  was present to allow positive identification.

\* Bronze Foundry Superintendent, David Brown Foundries Co., Ltd., Penistone, nr. Sheffield.

† Director of Research and Development, Aircraft Materials, Ministry of Supply, London.

‡ C. S. Smith and W. E. Lindlie, *Trans. Amer. Inst. Min. Met. Eng.*, 1933, **104**, 69.

§ D. J. Mack, *ibid.*, 1948, **175**, 240.

|| E. P. Klier and S. M. Grymko, *ibid.*, 1949, **185**, 611.



## Discussion

## Metal/Mould Reaction in Copper-Base Alloys\*

Mr. N. B. RUTHERFORD,† B.Sc., A.I.M.: The aluminium-35% magnesium alloy was chosen for the tests with protective mould coatings purely because it is the eutectic mixture and was known to be brittle and easily ground to powder. The commercial paint subsequently produced contained more magnesium (50%), and was found to involve some fire risk in production. Furthermore, because the powder was granular, instead of flaked as with the grindings in aluminium paint, settling was rather rapid, and constant stirring in use was needed. Consequently, alternatives were looked for.

One might expect, from the vigorous nature of the metal/mould reaction experienced in the founding of the aluminium-10% magnesium alloy, that this mixture would serve satisfactorily in paint for inhibiting the metal/mould reaction in copper-base alloys. Some tests have been made with such a paint, in co-operation with one of the members of the B.N.F.M.R.A. who markets foundry materials. The tests were carried out using gun-metals with unusually high phosphorus additions in order to intensify the reaction. The results are given in Table A and show the paint to be com-

TABLE A.—Inhibition of Metal/Mould Reaction in Gun-Metals by Aluminium-Magnesium Alloy Paints.

Melts degassed with 6 l./min. of nitrogen for 8 min. Green Mansfield sand moulds. D.T.D.-type, 1-in.-dia. test-bars.

Alloy Composition	Pouring Temp., °C.	Order of Pouring	Mould Coat	Test-Bar	
				Density, g./c.c. at 17° C.	Porosity,* %
Cu 88, Sn 10, Zn 2, P 0.15%	1150	1	Al-10% Mg	8.802	1.0
		6	"	8.803	1.0
		2	None	8.533	4.0
		5	"	8.479	4.7
		3	Al-50% Mg	8.691	2.2
		4	"	8.681	2.3
Cu 85, Sn 5, Zn 5, Pb 5, P 0.15%	1170	1	Al-10% Mg	8.814	1.8
		6	"	8.837	1.6
		2	None	8.502	5.4
		5	"	8.557	4.9
		3	Al-50% Mg	8.697	3.1
		4	"	8.660	3.6

\* Based on maximum density calculated from nominal compositions and the formulæ given in the papers under discussion.

pletely satisfactory, and even better than the aluminium-50% magnesium paint, results for which were also obtained.

Comparison of the figures for 85:5:5:5 leaded gun-metal given in Table A with approximately corresponding ones given in Table II (p. 558) of my second paper, where the paint referred to contained 35% magnesium, indicates a

falling degree of inhibition as the magnesium content rises, though the data are limited. An explanation for this is hard to see, unless it be that the rate of reaction of the paint with the steam increases so much with increase in magnesium content, that the time over which the limited amount available can afford protection is shortened, and becomes less than the time during which metal/mould reaction can occur with the cast metal. The inference is, then, that there may be some optimum magnesium content for the alloy paint between 0 and 10% magnesium. This has not yet been explored, but it leaves open the possibility of further improving inhibition and of reducing the settling tendency of the alloy paints.

Dr. D. V. ATTERTON,‡ M.A. (Junior Member): I would like to ask Mr. Rutherford for further information on the exact mechanism of metal/mould reaction. Does he consider that the major part of the gaseous absorption by the metal takes place over an extended period of time and depends on the diffusion of the gaseous element through solid metal into liquid metal in the interior of the casting? I have asked this question, as in several parts of the papers the author has stressed, and given experimental results to support, the importance of the chilling or thermal-conducting properties of the mould face. For example, on p. 194 of the 1951 paper it is suggested that the lower porosity of the 2-in.-dia. as compared with the 1-in.-dia. test-bars may be due partly to the drop in temperature of 30°–50° C. that occurred during pouring. This suggests that the metal/mould reaction is a comparatively slow process, since the solidification of the metal at the metal/mould interface is most certainly rapid and is not substantially affected by relatively small differences in pouring temperature, as has been demonstrated experimentally by Dr. Paschakis in America.

There is one other point I would like to raise regarding the effect of the chilling properties of the mould face on metal/mould reaction. During an investigation at Foundry Services, Ltd., into various methods of inhibiting metal/mould reaction, lower porosity values were observed when a hard-rammed unpainted mould was used than with a lightly-rammed mould. This experiment was carried out intentionally to determine the effect of this variable. Presumably, Mr. Rutherford would explain this by the higher thermal conductivity of the hard-rammed sand. If so, can he suggest a suitable method of controlling this variable in experimental investigations?

Turning to the prevention of metal/mould reaction, I was impressed by the author's explanation of the mechanism of inhibition by aluminium paint, but there is one objection I would like to mention. The two possible processes for explaining the action of aluminium paint suggest that it should always give at least some degree of inhibition and never accelerate the metal/mould reaction, as the experimental results indicate (e.g. line ref. nos. 32, 28, and 27, Table II, p. 196, of the first paper). However, perhaps the aluminium is acting on some occasions in a similar manner to a getter in a vacuum system and is leaving a clean, unoxidized metal surface through which hydrogen can readily diffuse. I cannot see why, theoretically, an aluminium-magnesium paint should improve this state of affairs and reduce metal/mould reaction, although the experimental results both of the present author and others indicate this.

\* Joint discussion on papers by N. B. Rutherford (*J. Inst. Metals*, 1951, 79, 189 and this vol., p. 555).

† Remarks made in introducing his papers at the Autumn

Meeting of the Institute, held in Oxford, September 1952.

‡ Research and Development Manager, Foundry Services, Ltd., Birmingham.

On the influence of various addition elements to the melt on metal/mould reaction, it seems that very often an element which gives a retarding effect for one alloy has an accelerating effect on others. I came across an interesting example of this recently,\* where it was found that percentages of aluminium even as low as 0.01% had a very unfavourable effect on the pressure-tightness of copper alloys, and in particular on gun-metals, whereas aluminium exercised an inhibiting influence in the case of phosphor bronze melts.

Finally, I would appreciate the author's views as to why in his experiments there was a greater porosity in the 2-in.-dia. bars than in the 1-in.-dia. test-bars for 85 : 5 : 5 : 5 gun-metal, whereas the converse was true for phosphor bronze, although in each case the fall in temperature between pouring the two sets of bars was substantially the same.

Mr. R. W. RUDDLE,† M.A., A.I.M. (Member): The question of mould coatings, such as aluminium-magnesium paint, which inhibit mould reaction has been raised by Dr. Atterton, who points out that the degree of inhibition afforded by aluminium and aluminium-magnesium paints in Mr. Rutherford's experiments varied considerably. In one case painting the mould with aluminium paint resulted in more reaction than that generally obtained in unpainted moulds under the same conditions. It seems that we really know very little about the factors governing the effectiveness of the protection from mould reaction which these paints confer, and I wonder whether the thickness of the paint layer may not be an important variable; possibly this factor, which was uncontrolled in Mr. Rutherford's experiments, may account for the scatter in his results. It would be most interesting to have Mr. Rutherford's views on this point.

Mr. Z. STOKOWIEC,‡ F.I.M., A.M.I.Mech.E.: At Penistone we are using the metal/mould reaction for making large pressure-tight gun-metal castings. Mr. Rutherford's papers are practical and useful, but foundrymen feel that the metal/mould reaction does not provide the only remedy for all foundry troubles. Personally I think that one can get results from it, if at the same time one can wisely apply the use of chills, properly control the melting process, and adopt top-pouring methods to direct the solidification of the metal in the mould.

I should like to ask Mr. Rutherford whether he has had any experience of metal/mould reaction in cement sand? Would this be similar to the reaction in naturally bonded sand? What would be the best dressing to inhibit the metal/mould reaction in a permanent chill mould?

The AUTHOR (*in reply*): I am afraid I cannot satisfy Dr. Atterton's request for more information on the exact mechanism of metal/mould reaction beyond that suggested in my papers. Much further work of a more delicate nature than that described would probably be needed to elucidate this. It is suggested in the introduction to the 1951 paper that the reaction may accelerate towards the end of freezing because of concentration of phosphorus in the residual liquid. On the other hand, Swain§ has shown a maximum rate at a fixed temperature, independent of composition, for metal/mould reaction in aluminium-magnesium alloys. Though the period of reaction may be extended beyond this, I do not consider that any significant absorption of gas would occur after the formation of a solid skin of metal. However, it has been demonstrated|| by careful measurements of metal temperatures in various parts of a solidifying casting, that for alloys of the type under discussion, i.e. alloys with wide freezing ranges, solidification is not by skin formation, but by gradual freezing throughout the mass. That passages

to the mould face remain open even in the late stages of freezing is well illustrated by the phenomenon of tin sweat. This being so, reaction may continue for some time, particularly in large castings where the rate of solidification is slow.

Nevertheless, I was not suggesting on p. 194 of the earlier paper that the lower porosity in the 2-in.-dia. bars was a result of more rapid freezing, but that it followed from the lower rate at which the reaction proceeds as the temperature falls; evidence for this is provided by Glaisher¶ and in the later of the two papers under discussion. In paragraph (b) on p. 194 and on p. 199 it is suggested that chilling may account for some of the observed differences in the amount of porosity in the test-bars, implying that there is then less time for the reaction to proceed. That the rate of freezing does exert an effect is shown by the later work, where porosity in the plate castings increased with section thickness (p. 560).

Dr. Atterton's test with moulds rammed to different hardnesses appears to support this contention. To keep the degree of ramming constant is not easy, but some control can be exercised on the mould face by designing moulds so that a hardness tester can be used on the important faces.

Dr. Atterton is wrong in saying that line ref. no. 32 indicates that aluminium paint may stimulate metal/mould reaction, as a comparison with line ref. no. 33 shows. The high porosity is a result of the high phosphorus content of this melt. Line ref. no. 28 refers to a dried mould and shows 1% more porosity than for a green mould cast at the same time (line ref. no. 27). Comparable results for unsprayed moulds are given in line ref. nos. 2 and 4. It will be seen that only in the case of the dried mould does significant stimulation of the reaction appear to have occurred. As Dr. Atterton says, his explanation for this is difficult to accept, especially since aluminium-sprayed moulds have afforded other castings some degree of protection. It may be that an excessive coating was applied inadvertently to this mould, too soon before pouring to allow adequate evaporation of solvent. Slight blowing might then have occurred, though evidence of this was not noticed on the castings.

A possible explanation for the difference in behaviour of the aluminium and aluminium-magnesium paints is given on pp. 200-201 of the earlier paper.

Mr. Ruddle also comments on the irregular results from aluminium-sprayed moulds (only one of the ten castings made in aluminium-magnesium sprayed moulds had porosity outside the range  $0.85 \pm 0.25\%$ ) and suggests that the thickness of the paint layer may offer some explanation for this. This is not unreasonable, if the second mechanism suggested on p. 200 of the 1951 paper is accepted. One would, of course, expect such an effect to be marked if some areas were left uncoated. However, care was taken in spraying the moulds to obtain coats as similar to one another as possible. With the 2-in.-dia. bars, for which a number of results are available, there was no noticeable difficulty in doing this. Yet the porosity found in them ranged from 1.3 to 3.5%.

Dr. Atterton concludes from Larsson's tests that aluminium is ineffective in preventing metal/mould reaction in gun-metal. I believe that this conclusion is invalid. It is well known that small amounts of aluminium in these alloys, or in bronzes, when run and gated by the usual methods, will cause leakage under pressure test. The gating used in Larsson's tests would be expected to give this result. To test whether aluminium will prevent metal/mould reaction in gun-metals, as in bronze, the use of properly gated, well-fed test bars is essential.

On his last point, I can suggest only that the reversal,

\* A. V. Larsson, *Amer. Foundrymen's Soc.*, 1952, Preprint No. 52-70.

† Head of Melting and Casting Section, British Non-Ferrous Metals Research Association, London.

‡ Bronze Foundry Superintendent, David Brown Foundries Co., Ltd., Penistone, nr. Sheffield.

§ A. J. Swain, *J. Inst. Metals*, this vol., p. 125.

|| R. W. Ruddle, *ibid.*, 1950, 77, 1.

¶ W. H. Glaisher, *ibid.*, 1949-50, 76, 377.



for 85:5:5:5 gun-metal and phosphor bronze, of the difference between the amount of porosity in 1-in. and 2-in. dia. bars cast 50° C. apart arises from their widely differing compositions and consequent variations in constitution and freezing characteristics. The presence of lead in the former alloy may be an important factor, and some support for this suggestion is given by the figures for leaded and lead-free gun-metal in Table III (p. 203) of my earlier paper.

To Mr. Stokowiec I am grateful for lending further support to that given in the second paper, showing the value of metal/mould reaction as a practical tool for obtaining better castings in the foundry. However, I agree entirely that

metal/mould reaction is not the only remedy for all foundry troubles, and I would not suggest this intentionally for one moment. It is simply a useful and often powerful tool for improving the yield of good castings, and is additional to the use of chills, exothermic and insulating sleeves and pads, and proper running, gating, and feeding techniques.

Cement-bonded sand is uncommon in non-ferrous foundries, and no tests have been made with it. However, metal/mould reaction is quite likely to occur with this sand, since combined water, if not moisture, will be present. Reaction of the type under discussion does not normally occur with a permanent chill mould.

## Discussion

### Use of Polarized Light in the Examination of Metals\*

Dr. N. P. ALLEN,† M.Met., F.I.M. (Member): In the early days of the metallography of uranium, interest was largely centred on purity, and on tracing the origin of the many curious structures displayed by various samples of uranium. At that time ordinary metallographic methods sufficed, and the parts played by iron, oxygen, carbon, and other impurities were satisfactorily disentangled. On the removal of these impurities interest was focused on the grain structure of the metal. The grain structure of uranium proved most difficult to reveal, but Mr. Mott and Mr. Haines by using polarized light have found it possible to develop the very elegant structures presented in their first paper. No doubt the anisotropic character of the uranium crystal tends to give this result.

The authors mention that twins may result from the anisotropic expansion of the metal, but they have scarcely emphasized sufficiently how remarkable this expansion is. The data in the Appendix (p. 627) show that the coefficient of expansion of the  $\alpha$  form is large in two directions and actually negative in the third which, a fact which, as far as I am aware, was first demonstrated in this country by Mr. Wainwright during an investigation into certain curious differences of coefficient of expansion observed in bars. Very large stresses can thus be developed when random arrays of crystals are heated and cooled, and these stresses are no doubt responsible for the changes of structure that take place when cast uranium is annealed. The formation of twins is one of the effects produced.

Presumably, when uranium is annealed at some temperature at which it is reasonably soft, say, 600°–700° C., it gradually relieves itself of all stress, but when it cools, new stresses inevitably develop. It has been observed that when a temperature around 1000° C. is reached, a faint high-pitched "cry" like that of tin, is emitted. This sound is so high-pitched that not everybody can hear it, and so far as I know, it was first heard by Mr. G. B. Harris when he was working at the National Physical Laboratory.

The non-metallic inclusions in uranium are principally  $\text{UO}_2$ , but a certain amount of X-ray evidence has been produced, suggesting that the dark cores might be  $\text{UO}$ . This is somewhat unexpected. It might be thought that if a peritectic reaction is concerned, the reaction would be  $\text{UO}_2 + \text{U} = 2\text{UO}$ . The reason why  $\text{UO}_2$  surrounds  $\text{UO}$  is not clear.

Mr. G. B. HARRIS,‡ M.A. (Member): The metallographic methods described by Mr. Mott and Mr. Haines in these and other papers are analogous to the methods of examining

transparent mineral or rock sections between crossed polarizers. Comparison of the two techniques suggests that, as a means of identifying phases and studying crystal orientations, the metallographic technique might usefully be supplemented by examination of the conoscopic interference figures formed in the focal plane of the objective when a single crystal is examined between crossed polarizers. These figures are observed by first examining the specimen between crossed polarizers, as described by the authors, then stopping the field down to include only one crystal, removing the eyepiece of

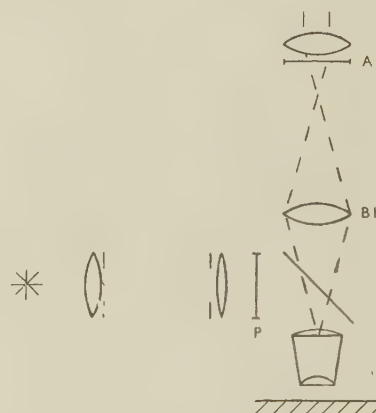


FIG. A.

the microscope and examining the image in the focal plane of the objective. Alternatively, by the use of a Bertrand lens, a standard fitting on petrological microscopes, the eyepiece can be used to magnify the image in the focal plane of the objective, as indicated in Fig. A. This shows the usual optical system of a metallurgical microscope with polarizing filters inserted at  $P$  and  $A$ ; the Bertrand lens  $BL$  has a focal length equal to one-quarter of the "tube-length" of the microscope.

The essential feature of an interference figure is that each point in the focal plane of the objective corresponds to one particular direction of the incident light beam, so that the observed figure is a chart of the amplitude and phase changes produced by the reflection of polarized light incident in

\* Joint Discussion on papers by B. W. Mott and H. R. Haines (*J. Inst. Metals*, this vol., pp. 621 and 629).

† Superintendent, Metallurgy Division, National Physical

Laboratory, Teddington, Middlesex.

‡ B.I.S.R.A. Research Bursar, Inorganic Chemistry Laboratory, Oxford.

different directions. Simple theory of reflection shows that isotropic materials, both metals and dielectrics, should give a figure consisting of a diffuse dark cross with its arms parallel to the vibration directions of the polarizing filters, with bright zones in the corners of the field at  $45^\circ$  to these directions. This figure is in fact observed when the optical system described is focused on a glass microscope slide or a polished metal mirror. The "optical cross" shown in Fig. 21 (Plate C) of Mott and Haines's paper on uranium is a distorted figure of this type, focused by the spherical surface of a gas cavity. The figures from metals and dielectrics can presumably be distinguished by inserting a sensitive tint plate in the optical train, with its principal vibration directions at  $45^\circ$  to those of the polarizer and analyser. In dielectrics, the bright zones arise from the splitting of the incident polarized beam into two components differing in amplitude, so that the figure is merely changed from black and white to light and dark purple. In metals, however, the two components differ both in amplitude and in phase, so that, with a sensitive tint plate, the dark cross becomes purple and pairs of opposite bright zones become red and blue, respectively.

The theory of the reflection of polarized light at oblique incidence from arbitrarily oriented anisotropic crystals is much more complex, but, as observations accumulate and the general laws of behaviour of interference figures become clear, this method may well prove a useful tool for the identification of phases and determination of orientations on areas of  $\sim 0.01$  of a square mm. in a micro-section. In general, both with anisotropic metals and with anisotropic surface films, such as the anodic film on aluminium produced by Hone and Pearson's method,\* one gets figures consisting of two dark hyperbolæ on a bright background; when the specimen is rotated, the vertices of the hyperbolæ rotate with it, but their asymptotes remain parallel to the vibration directions of the polarizer and analyser, so that in two positions of the specimen an "optical cross" figure is formed. The distance between the vertices varies from grain to grain. The figures described bear a superficial resemblance to those obtained with biaxial crystals in transmission, except for the varying distance between the vertices, which for the transmission case is an optical constant of the material. Probably this figure, when observed in reflection, is typical of a uniaxial crystal (trigonal, tetragonal, or hexagonal symmetry) with the optic axis inclined to the normal to the surface, and the vertices of the hyperbolæ correspond to the directions of rays incident and reflected along the optic axis. I should be interested to know if Mr. Mott and Mr. Haines have made any observations which would confirm or disprove this, and also whether they have observed these figures on uranium grains, in which the orthorhombic symmetry of  $\alpha$  uranium might produce more complex effects.

With reference to their observations on the behaviour of single grains of tin under polarized light, with the analyser rotated from the crossed position, the strong maxima and minima of brightness at  $180^\circ$  intervals seem to indicate that tin crystals have an enormous anisotropy in their reflection coefficients.

In connection with the anomalies produced by strain in the microscope objective, its effect on the interference figures is often to produce the hyperbola type of figure on reflection from isotropic materials, so that the polarizer and analyser cannot be properly crossed.

(Mrs.) PAMELA DUNSMUIR,† M.Sc., A.Inst.P.: These two papers provide a very good basis for an assessment of the general usefulness of polarized light as a tool for the metallurgist. They show, I think, that usually one may obtain all the information required concerning grain-size, orientation of

crystals, identification of phases, &c., without recourse to polarized light. Uranium seems to be rather an exception in defying examination by ordinary metallographic means involving etching. It is when we turn from the examination of static characteristics of a metal, such as I have mentioned above, to the study of dynamic processes, that the polarized-light method of examining anisotropic metals offers its fullest scope. For instance, recrystallization, grain-growth, and so on may be watched as they happen, without the need for etching. Ciné films showing recrystallization occurring in such anisotropic metals as tin, zinc, or cadmium have been quite widely circulated, and we can also envisage the application of polarized light to the study of recrystallization processes in anisotropic metals having much higher melting points. Such a technique would probably have to be carried out in conjunction with a microscope of long working distance specially designed for the examination of hot objects.

Similar possibilities offer when we think of the work on ferromagnetic materials which is at present being done using polarized light. In this case the magnetic Kerr effect is used to produce contrast between one magnetic domain and the next, and American workers have recently succeeded in observing the domains in cobalt‡ and (less strikingly) in silicon-iron.§ Such static observations of domains can, of course, be made very easily by using the Bitter-figure technique (i.e., covering the metal surface with a magnetic colloid), and the polarized-light method possesses no advantages. But dynamic processes occurring to the domains at high temperature and at high speed near the Curie point of the metal cannot at present be studied by means of Bitter figures. Here, possibly, polarized light may open up a new field of study.

Mr. Mott and Mr. Haines rightly stress the necessity of using suitable types of microscope components, correctly adjusted, in order to avoid misleading results. Perhaps in this country more attention should be directed to the Foster-type polarizing vertical illuminator, which appears to be a great asset to American workers in this field.

My last point concerns the difficulty which the authors mention of separating effects due to metal anisotropy, surface contour, and the presence of a birefringent film. Experiments of mine may be of some interest here. It was shown that changes in the state of polarization of light reflected from a polycrystalline silicon-iron sample were due to surface contour, by electrodepositing a film of copper on the surface, peeling it off, and examining the under-surface in polarized light. There was seen to be a pattern corresponding to the pattern of the grains of silicon-iron viewed directly in polarized light. Perhaps the use of a replica of the surface in this way may enable other workers to elucidate the cause of the effects which they observe in polarized light.

MR. D. McLEAN,|| B.Sc. (Member): These two papers come at a propitious moment. The two "new" metals, titanium and uranium, which seem destined to play a big part in future metallurgy, are both anisotropic and hence reactive to polarized light, and ways are being found of rendering isotropic metals reactive. It is therefore likely that polarized light will be used more in the future than in the past.

Some of the micrographs, especially those of the same field in normal and in polarized light in Figs. 3 and 4, 9 and 10, 20 and 21 (Plates CI and CII) of the second paper, are so striking that they may indeed lead to an over-estimation of the value of polarized light. Sometimes structures which are difficult to develop well in normal light and which are effectively revealed by polarized light are also well revealed in other ways, e.g. in phase-contrast illumination. This is so, for example, with the martensitic structure shown in Figs. 20

\* A. Hone and E. C. Pearson, *Metal Progress*, 1948, **53**, 363.

† Research Laboratories, British Thomson-Houston Co., Ltd., Rugby.

‡ H. J. Williams, F. G. Foster, and E. A. Wood, *Phys.*

*Rev.*, 1951, [ii], **82**, 119.

§ C. A. Fowler, Jr., and E. M. Fryer, *ibid.*, 1952, [ii], **86**, 426.

|| Metallurgy Division, National Physical Laboratory, Teddington, Middlesex.



and 21. It would, however, be wrong to endeavour to decide from such instances whether the polarized-light technique is more or less valuable in general than the phase-contrast or other techniques. The correct conclusion is that it is desirable to have all available and to use the one most suited to the particular problem.

In the first paper the authors mention that they tried about a hundred electrolytic polishing baths for uranium. In the second they give recommendations for a further fifteen metals. Clearly, much work has been involved, but it will be largely wasted if the warnings which the authors give in their other papers,\* are not heeded. These warnings have been abundantly confirmed by experience at the National Physical Laboratory. Objective lenses must be free from strain; an objective may be perfectly suitable for normal use and yet give poor results in polarized light, even with a contrasty subject, while being practically incapable of revealing some of the more delicate effects illustrated in micrographs accompanying these papers. The coated-and-bloomed type of glass reflector in the vertical illuminator gives better results than the plain glass type. It is necessary to orient the polarizer and analyser correctly with respect to the microscope as well as with respect to each other. Because polarized light will probably be more widely used in the future, it seems desirable that new equipment should comply with the more stringent requirements for successful use with polarized light, especially as the extra cost is small.

In the first paper it is suggested, following Chipman,† that each crystal seen with the microscope actually consists of a number of crystals too similarly oriented to be distinguished, the reason for the suggestion being that the number of crystals shown by X-ray patterns is several times larger than the number seen under the microscope. This situation is similar to that occurring in iron after cooling through the  $\alpha \rightarrow \gamma$  transformation, for there is fairly convincing X-ray evidence ‡ that each crystal is then composed of many slightly misoriented sub-crystals; under the microscope each  $\alpha$  crystal shows the pattern known as "veining", and it is reasonable to suppose that the veining lines are the sub-boundaries. When  $\alpha$ -iron is recrystallized below the transformation temperature, no veining lines occur, and X-ray evidence indicates that the new crystals are not fragmented. It would be interesting to know whether in  $\alpha$ -uranium, recrystallized below the transformation temperature, the new crystals are also unfragmented.

In their second paper, the authors mention that the effective anisotropy of a metal surface is sometimes due to an overlying anisotropic film produced, for example, during electrolytic polishing, and sometimes to facets developed in this film or in the metal surface. With the isotropic metal aluminium, which can be rendered effectively anisotropic by suitable anodic oxidation, there is evidence from work at the National Physical Laboratory that in some cases at least the effect is largely due to transmission through an anisotropic film. When the film was removed, the underlying metal surface showed little reactivity, so that the effect was not due to facets on this surface. Examined in transmission, the film, however, showed in quite good contrast the crystal structure of the metal. As the film was fairly transparent, an effect due to facets on its surface could produce only a weak effect in transmission. Moreover, filmed specimens give a conoscopic interference figure (i.e. the figure seen at the back of the objective on removing the eyepiece when polarizer and analyser are in position and are crossed) similar to that of a biaxial mineral in transmission, whereas I have not seen interference figures from deliberately produced etch pits that are clear or distinct enough to be sure of their character.

This evidence seems to run counter to that of Perryman and Lack, who concluded that the effect with aluminium was due to facets.§ However, Mott and Haines give evidence that in some cases the effect is due to facets, in others to transmission through a film. Possibly there is also variability with any one metal, depending on the method of preparation.

The AUTHORS (*in reply*): Dr. Allen has rightly drawn attention to the remarkable thermal expansion of uranium, the effects of which are revealed by the marked twinning that occurs on cooling. The extent of the twinning is little affected by the rate of cooling in a given specimen, so that the bulk of it would appear to be due to the stresses arising from the anisotropic contraction rather than to thermal stresses. The "cry" mentioned by Dr. Allen has been heard many times at Harwell when specimens of uranium and its alloys have been quenched and also on removal of small ingots from the argon-arc furnace. Dr. Cahn has amplified the sounds emitted on plastic deformation and has used the technique for determining the temperature range over which the metal deforms by twinning.

On the question of the cubic inclusions in uranium, we agree with Dr. Allen that the reason for a UO core occurring in a UO<sub>2</sub> particle is not clear. There is a possibility that the cubes may not consist simply of uranium and oxygen, but may also contain other elements, such as nitrogen and carbon. In spite of several attempts to make a complete identification of these inclusions, their precise nature remains a mystery.

We have not overlooked the possibilities of conoscopic observations, as suggested by Mr. Harris, but have not investigated these in great detail. Earlier tests showed that the nature of the optical figure could be appreciably altered by the presence of internal strain in the objective, and this has been confirmed by Neuerburg|| and by Green.¶ It is only in special cases, in which the strain is symmetrical, that the interference figure observed in conjunction with an isotropic specimen is a simple hyperbola: if the strain system is very complicated, the figure may be unrecognizable. We feel, however, that a wealth of information on the symmetry and orientation of the reflecting surface could be obtained from a detailed study of these figures.

We consider that Mr. Harris's deductions from the intensity curves for tin are misleading. The change in the intensity maxima on rotation of the analyser from the crossed position is dependent not only on the ratio of the reflection coefficients, but also on the offset of the analyser. On the other hand, the maximum angle through which the plane of polarization is rotated is directly related to the ratio of the reflectivities, and can be more conveniently used for a comparison of various materials.

While agreeing with Mrs. Dunsmuir that for most metals the use of polarized light does not yield any more information than can be obtained by suitable etching, we feel that the clarity of a particular structure may be better under polarized light, as deep etching often results in loss of definition. The direct observation of structural changes at elevated temperatures is a useful application of polarized light, but can be very complicated in the case of easily oxidized metals, even if the specimen is maintained in a vacuum of 10<sup>-6</sup> mm. Hg. Apart from the possibility of growth of the oxide film, surface changes may occur which make it impossible to examine the metal under polarized light. For example, in the case of uranium, above about 500°C., a UO film forms which appears to be opaque and eliminates the anisotropic reflection. No apparent change in structure was observed under polarized light when an electrolytically polished specimen

\* B. W. Mott and H. R. Haines, *Research*, 1951, 4, 24, 63.  
J. Woodrow, B. W. Mott, and H. R. Haines, *Proc. Phys. Soc.*, 1952, [B], 65, 603.

† J. Chipman, *U.S. Atomic Energy Commission Publ.*, 1946, (MDDC-539).

‡ A. Guinier, "Imperfections in Nearly Perfect Crystals"

(edited by W. Shockley, *et al.*), p. 402. 1952: New York (John Wiley and Sons); London (Chapman and Hall).

§ E. C. W. Perryman and J. M. Lack, *Nature*, 1951, 167, 479.

|| G. J. Neuerburg, *Amer. Mineralogist*, 1948, 33, 496.

¶ L. H. Green, *Econ. Geol.*, 1952, 47, 451.

of beryllium was heated *in vacuo* to about 800° C., but an examination of the specimen after repolishing showed that recrystallization had clearly taken place. Presumably in this case the reaction to polarized light is associated with the oxide film, which does not reproduce epitaxy as the structure of the metal changes.

The method suggested by Mrs. Dunsmuir for determining the origin of the anisotropic effects seems to be most useful, and could be advantageously applied in doubtful cases. The Foster-type of vertical illuminator is certainly a simple method of obtaining the crossed-polarizer condition, but it suffers from the disadvantage that the exact equivalent of rotating the analyser in other systems cannot be produced. A compromise can be made by inserting a fractional  $\lambda$ -wave plate, and this helps in obtaining improved contrast, but an analysis of the intensity of reflected light, as reported elsewhere,\* would not be possible with the Foster prism.

We agree with Mr. McLean that the use of polarized light in metallography should be considered as an additional tool

to the methods employing phase contrast, interference microscopy, &c. To obtain the maximum information on any one specimen it is desirable to make intelligent use of all the techniques available.

In our experience, recrystallization of uranium in the  $\alpha$  condition does not normally result in the sub-structure reported for material that has been cooled through one or both transformations; this suggests that the closely orientated grains, are, as in  $\alpha$ -iron, the result of crystallographic transformation. A similar type of structure may arise, however, if the material is strained during recrystallization, indicating that the effect may be due to a type of polygonization. It is of interest to note that more recent work by Mr. P. E. Madsen at Harwell has resulted in a much closer agreement between the grain-sizes as determined by polarized-light examination and by X-rays. This is due to improvements in the polarized-light technique which enable grains of closer orientation to be distinguished, and also to modifications in the formula used for calculating the X-ray grain-size.

## Discussion

# Twin Accommodation in Zinc

By P. L. PRATT and S. F. PUGH

(*Journal*, this vol., p. 653.)

Dr. R. W. CAHN,† B.A. (Junior Member): I would like to congratulate Dr. Pratt and Mr. Pugh on a paper as ingenious in execution as it is interesting in results, and I look forward very much to reading the results of their continued researches.

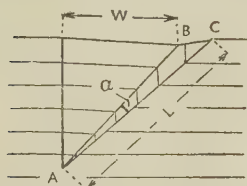


FIG. A.—Twin and Accommodation Bend. (After Jillson.)

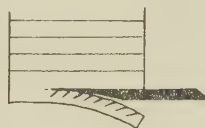


FIG. B.—Twinning Due to Cleavage.

There is one respect, however, in which I cannot help thinking they must have gone wrong. In their Fig. 8 (p. 656), the bend planes are shown as parallel to the composition plane of the twin. I imagine this state of affairs was inferred because each bend plane was normally so close to the twin to which it belonged. On the other hand, Jillson‡ has drawn a diagram (see Fig. A) which seems reasonable, since the bend planes, like polygonization boundaries, can be stable only if they are more or less perpendicular to the slip plane (i.e. the basal plane).

In that case, how is one to interpret the close proximity of twin lamellae and bend plane, as observed on the cleavage surface? I believe this to be due to the peculiar nature of the deformation associated with cleavage. If a comparatively thin slice is cleaved off, it is almost invariably somewhat bent (Fig. B). This is often associated with copious twinning on the stretched side only; compression in the basal plane of zinc cannot produce twins. So one gets twins which never go

right through the lamella, even a thin one. This is borne out by observations at Birmingham University. If the cleavage fragment is thicker, it will not bend bodily, but close to the surface only. This peculiar mode of deformation is made possible by the operation of bend planes which gradually fade out towards the interior of the fragment. The effect again is to produce twins which are short if measured along their shear direction ( $L$  in Fig. A).

The result of all this is that  $W$  (Fig. A) is always fairly small, as indeed the authors have observed. Another result is that the value of  $L$  is constant along most of the width of the twin (i.e.  $L' \simeq L''$ ), and therefore  $W$  is constant (see Fig. C). That is why cleavage is such a good mode of deformation for this kind of study, leading to neat bend-plane traces parallel to the twin traces on the cleavage surface. At the tips the bend-plane trace curves round (i.e.  $W$  decreases) because  $L$  gets progressively less (i.e.  $L''' < L'$ ).

In the general case of a twin lamella inside a large single

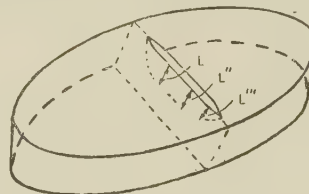


FIG. C.—Cleavage Fragment Containing a Twin (seen as if it were transparent).

crystal, the shape is rather different. As Yakutovich and Yakovleva§ have shown, the value of  $L$  alters from point to point. The associated bend plane should be quite complicated in shape in this case, since it has to intersect the

\* J. Woodrow, B. W. Mott, and H. R. Haines, *Proc. Phys. Soc.*, 1952, [B], 65, 603.

† Lecturer, Department of Metallurgy, Birmingham University.

‡ D. C. Jillson, *Trans. Amer. Inst. Min. Met. Eng.*, 1950, 188, 1005.

§ M. V. Yakutovich and E. S. Yakovleva, *Zhur. Eksper. Teoret. Fiziki*, 1939, 9, 882.



leading edge of the twin everywhere and yet remain normal to the slip plane. (A first-order bend plane consists of two kinds of dislocations with different slip directions and a plane cannot be perpendicular to two directions at once.)

The authors state that the distance  $W$  (Fig. A) depends on the thickness of the twin lamella. This follows also from the model I am putting forward, but only indirectly. It is to be presumed that the magnitude of the wedge angle  $\alpha$  (Fig. A) at the leading edge of the twin is limited because the shear gradient near the leading edge is proportional to  $\alpha$  and therefore most twins, except the very thinnest, will have the fixed maximum value of  $\alpha$ . The thickness of the twin as seen at the cleavage surface is roughly proportional to  $L$ . (This is exactly true only if  $AB$  and  $AC$  (Fig. A) are straight.)  $W$  is also proportional to  $L$ , and so we have the observed correlation between thickness and  $W$ .

As I have suggested elsewhere,\* when we compare different metals, generally speaking the thickness of typical twins is less the greater the crystallographic shear  $s$  (which is a characteristic of each metal). This is reasonable on this model, since, for a higher shear, a smaller wedge angle  $\alpha$  will suffice to produce a stress concentration as great as a bend plane can accommodate without localized fracture. The angle  $\beta_{lim}$  of the bend plane required for accommodation depends geometrically on this limiting value of  $\alpha$ . Presumably, then, for zinc a limiting bend-plane angle of  $45^\circ$ , as observed, is associated with a limiting wedge angle of the twins. From

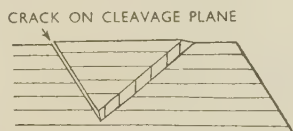


FIG. D.—Twinning and Accommodation Crack in Calcite.

data given in a recent paper by Holden,† it can be calculated that for zinc and magnesium,  $\beta_{lim} \propto s$  approximately.

According to the authors' observations, it looks as if accommodation bending is a necessary adjustment of lenticular twins. It is interesting to see whether other metals have potential bend planes which can act analogously to those in zinc. From the known plastic crystallography of bismuth, iron, and uranium, for instance, it looks as if bend planes that will serve can be found in each case. In one instance ( $\{130\}$  twins in uranium) the bend planes have an axis of rotation (i.e. normal to the slip direction and lying in the slip plane) which is just right for accommodating the twins. Here, only one kind of dislocation is needed.

The importance of accommodation bending is brought out by Rose's classical observation ‡ that if a twin lamella, even an extremely thin one, stops inside a crystal of calcite, the crystal tears apart at the leading edge of the lamella, as indicated in Fig. D. Calcite cannot slip and therefore cannot form bend planes.

A final comment relates to what happens to a twin lamella on annealing. The Russian school under Garber have shown that in several substances, including one metal, bismuth,§ thin twins are reabsorbed by the matrix on prolonged annealing. This has also been found in America for the case of zinc,|| though no detailed study has been made. It seems to me that a contributing factor, at least, may be the difficulty of moving a bend plane. For a bend plane of the first kind, composed of two kinds of dislocation, this difficulty must be

considerable (though not insuperable, as the authors have convincingly shown). It seems reasonable to assume that the difficulty will be the less, the smaller the bend-plane angle. For fresh absorption to begin, the bend plane must presumably move along with the edge of the lamella, and we can then see why only a thin twin can be absorbed, for only a thin twin has a small value of  $\alpha$ , and therefore has a small-angle bend plane associated with it.

Dr. A. J. W. MOORE ¶ (Member): At Cambridge we have also been interested in a study of the structure of cleaved zinc surfaces from the point of view of surface topography and have combined microscopical examination with results obtained with a stylus-type profile recorder (Talysurf). It has been found that the accommodation kinking can be easily observed by using the 33-mm. lens in the Vickers microscope, and profile records of the same areas enable the angles to be determined. For a simple accommodation kink the angle has been shown to be  $0^\circ 47' \pm 2.5'$ , which can be compared to an angle of approximately  $45'$  quoted by Dr. Pratt and Mr. Pugh. An example has also been found of a single twin showing two parallel accommodation bands, the angle of each changing along the length of the twin. Within the area that could be observed the kink nearest the twin changed from  $40'$  to  $20'$  angle, while the one furthest from the twin changed from  $10'$  to  $20'$  angle. These angle changes were in the opposite sense. It appears, therefore, that the observed area is a transition region and that a different kink predominates at each end of the twin. These measurements show that the accommodation angle may cover a range of values, and the maximum observed is about  $47'$ . This work has been more fully described elsewhere.\*\*

Mr. K. E. PUTTICK,†† B.Sc.: I have recently observed surface effects on zinc crystals prepared in rather a novel way. If liquid zinc is cooled under a low vacuum with a temperature gradient normal to the surface, the latter becomes clothed with crystals, a millimetre or so wide but extremely thin in the direction normal to the surface, the plane of which is (0001).

This phenomenon was first observed by Mr. A. J. Forty ‡‡ on small droplets of molten zinc slowly cooled; he suggested that the highly reflecting basal faces were formed by evaporation after solidification. However, I have recently seen the same formation on rods formed by sucking molten zinc into cool glass tubes, when the suction creates sufficient vacuum to prevent oxidation, and the crystals are seen to form in a very short time. It seems, therefore, that the crystals grow by deposition from the melt, but that the usual dendritic growth, due to the more rapid diffusion to corners of a growing crystal, is for some reason absent in this case. Fig. E (Plate CX) shows the appearance of such a rod.

Many of the crystals are not plane, but distorted by the presence of numerous kinks, formed presumably by bending due to the constraint of neighbouring crystals during cooling. After plastic deformation the crystals in such an aggregate show, as might be expected, twins and sets of lines which can be ascribed to kink bands (Fig. F, Plate CX), but I have not yet observed accommodation bands. Possibly they are absent in such thin crystals.

The AUTHORS (in reply): We agree with Dr. Cahn that a tapering twin such as he draws in Fig. A should be accompanied by a kink plane nearly normal to the basal plane; and we feel that it is reasonable to suggest that the kinking angle of  $45'$  arises from this fact, together with the limitations

\* R. W. Cahn, *Trans. Amer. Inst. Min. Met. Eng.*, 1951, 191, 542 (discussion).

† J. Holden, *Phil. Mag.*, 1952, [vii], 43, 976.

‡ G. Rose, *Physikal. Abhandl. Kgl. Akad. Wiss. Berlin*, 1868, 57.

§ I. A. Gindin and V. I. Startsev, *Zhur. Eksper. Teoret. Fiziki*, 1950, 20, (8), 738.

|| C. H. Mathewson and A. J. Phillips, *Trans. Amer. Inst.*

*Min. Met. Eng., Inst. Metals Div.*, 1927, 143.

¶ Research Group on the Physics and Chemistry of Surfaces, Laboratory of Physical Chemistry, Cambridge University.

\*\* A. J. W. Moore, *Proc. Phys. Soc.*, 1952, [B], 65, 956.

†† British Iron and Steel Research Association; at present at H. H. Wills Physical Laboratory, Bristol University.

‡‡ A. J. Forty, *Phil. Mag.*, 1952, [vii], 43, 949.

imposed by the elastic restraints of the lattice on the wedge angle  $\alpha$  in his figure. In this respect Fig. 8 of our paper may be somewhat misleading, since the twins are not drawn tapering to a wedge in the lattice. In practice it is more common to find a series of kink planes associated with each twin, rather than the single plane depicted by Jillson. Where the single plane does occur, we attempt to show, in Fig. 8 (c), that there is a kink plane coinciding with the twin composition plane, while in the more common case (Fig. 8 (b)) this kink plane is detached from the twin. In more complex cases (Fig. 8 (d)), it is not clear how the kink planes are situated beneath the surface, and it would be instructive to study sections normal to the twin trace in the basal plane.

We are interested in Dr. Cahn's comment on the re-absorption of thin twins during prolonged annealing. We agree that a contributing factor may be the difficulty of moving a kink plane, but it seems to us that the relaxation of the shear stresses around the twin by the kink plane itself, is more important from the point of view of stability of the twin during annealing. If these stresses were not relaxed by kinking of the lattice, the twin would be re-absorbed very rapidly. We have shown, in work not yet published, that the kink plane moves readily under the shear stress applied as the twin thickens, but this does not contradict

the fact that these boundaries should be stable at high temperature, since they adopt the position of lowest energy in the lattice. We do not believe that detwinning necessarily involves movement of the associated kink plane, since during mechanical detwinning a kink plane is driven out from the twin to absorb the original kink, leaving the surface of the specimen flat; it is possible that the same process occurs during thermal detwinning, and markings have been found which suggest that this may be so.

We are pleased to note that Dr. Moore's measurements of the kinking angle agree closely with our own. Both simple and complex kinks have been observed with the 33-mm. C.T.S. objective, but by using opaque stops it was possible to measure the angles directly.

We would not expect to find accommodation bands in the thin crystals mentioned by Mr. Puttick, since the twins should pass right through the crystal. We are interested in his observations, since we have found similar small crystals of magnesium showing faces of types (0001), (10 $\bar{1}$ 1), and (10 $\bar{1}$ 0). These appear to have condensed in the cooler parts of the tube as spherical droplets, and to have been etched thermally to show very perfect and uniform faces. Unfortunately, those found so far have been so small that they could only be handled under the microscope.



# NAME INDEX

To the *Journal*, Vol. 80, and *Monograph No. 13*

- Allen, N. P. Discussion on "Constitution of Copper-Base Alloys", 700; discussion on "Titanium and Its Alloys", 702; discussion on "Use of Polarized Light in the Examination of Metals", 720.
- Andrade, E. N. da C. Paper: "The Effect of Surface Conditions on the Mechanical Properties of Metals, Mainly Single Crystals", *Monograph No. 13*, page 133.
- Andrews, K. W. Discussion on "Constitution of Transition-Metal Alloys", 694.
- Ashton, A. B. Discussion on "Equipment for the Thermal Treatment of Non-Ferrous Metals and Alloys", 679.
- Atterton, D. V. Discussion on "Grain Refinement of Castings", 685; discussion on "Metal/Mould Reaction in Copper-Base Alloys", 718.
- Auerhammer, W. See Schubert, K.
- Axon, H. J. See Poole, D. M.
- Baer, Alfred. Elected Member of Council, xii.
- Bagley, K. Q. See Ellwood, E. C.
- Bailey, G. L. Discussion on "Scrap Reclamation, Secondary Metals, and Substitute Metals", 252; elected Vice-President for 1952-53, xii.
- Bailey, G. L. J., and H. C. Watkins. Paper: "The Flow of Liquid Metals on Solid Metal Surfaces and Its Relation to Soldering, Brazing, and Hot-Dip Coating", 57; reply to discussion, 694.
- Bailey, J. C. Discussion on "Equipment for the Thermal Treatment of Non-Ferrous Metals and Alloys", 677.
- Baker, W. A. Discussion on "Equipment for the Thermal Treatment of Non-Ferrous Metals and Alloys", 667, 676, 681; discussion on "Grain Refinement of Castings", 685; discussion on "The Structure and Properties of Wrought Copper-Aluminium-Nickel-Iron Alloys", 716.
- Barfield, R. H. Discussion on "Equipment for Thermal Treatment of Non-Ferrous Metals and Alloys", 677.
- Barnes, R. S. Discussion on "Powder Metallurgy of Copper and Copper Alloys", 711.
- Barwell, F. T. Paper: "The Effect of Lubrication and Nature of Superficial Layer after Prolonged Periods of Running", *Monograph No. 13*, page 101.
- Basinski, Z. S., and J. W. Christian. Paper: "The Cubic-Tetragonal Transformation in Manganese-Copper Alloys", 659.
- Bateman, (Mrs.) Catherine M. See Greenough, G. B.
- Bennett, H. E. Discussion on "Equipment for Thermal Treatment of Non-Ferrous Metals and Alloys", 676.
- Benson, L. E. Discussion on "The Creep and Softening Properties of Copper for Alternator Rotor Windings", 682.
- Benson, N. D., J. McKeown, and D. N. Mends. Paper: "The Creep and Softening Properties of Copper for Alternator Rotor Windings", 131; reply to discussion, 683.
- Betteridge, W., and A. W. Franklin. Paper: "An Investigation of the Structural Changes Accompanying Creep in a Tin-Antimony Alloy", 147; reply to discussion, 588.
- Betterton, J. O., Jr. See Hume-Rothery, W.
- and W. Hume-Rothery. Paper: "The Equilibrium Diagram of the System Copper-Gallium in the Region 30-100 At.-% Gallium", 459; reply to discussion, 701.
- Bever, M. B. See Radtke, S. F.
- Blin, J. See Bückle, H.
- Bloom, D. S., and N. J. Grant. Discussion on "Constitution of Transition-Metal Alloys", 695.
- Bolton, E. A. Discussion on "Equipment for Thermal Treatment of Non-Ferrous Metals and Alloys", 673.
- Bond-Williams, N. I. Elected Member of Council, xii.
- Bowden, F. P., and D. Tabor. Paper: "The Influence of Surface Films on the Friction and Deformation of Surfaces", *Monograph No. 13*, page 197.
- Bradbury, E. J. See Hartley, H. J.
- Bristow, C. A., A. J. Sidery, and H. Sutton. Paper: "The Scope for Conservation of Metals, Ferrous and Non-Ferrous", 240.
- Brown, A. F. Paper: "Slip Bands and Hardening Processes in Aluminium", 115.
- Bückle, H., and J. Blin. Paper: "Micrographic Aspects of the Diffusion of Zinc and Aluminium in Copper", 385; reply to discussion, 714.
- Bucknall, E. H. Discussion on "Scrap Reclamation, Secondary Metals, and Substitute Metals", 254.
- Burgann, B. R., R. C. Hall, and R. F. Hehemann. Paper: "A Modified Dew-Point Method for Vapour-Pressure Measurements of Lead-Mercury Alloys", 413.
- Butler, J. M., and T. P. Hoar. Paper: "Unrelated Simultaneous Interdiffusion and Sintering in Copper-Nickel Compacts", 207; reply to discussion, 712.
- Cabarat, R., P. Gence, L. Guillet, and R. Le Roux. Paper: "Thermoelastic Analysis of Transformations in Copper Alloys", 151.
- Cahn, R. W. Discussion on "Twin Accommodation in Zinc", 723.
- Campbell, D. F. Discussion on "Equipment for Thermal Treatment of Non-Ferrous Metals and Alloys", 675, 680.
- Carter, C. F. Discussion on "Primary Resources of Ferrous and Non-Ferrous Metals", 238.
- Chadwick, R. Discussion on "The Flow of Liquid Metals on Solid Metal Surfaces", 692.
- and W. H. L. Hooper. Paper: "Some Observations on the Occurrence of Stretcher-Strain Markings in an Aluminium-Magnesium Alloy", 17; reply to discussion, 690.
- Chambers, R. G., and A. B. Pippard. Paper: "The Effect of Method of Preparation on the High-Frequency Surface Resistance of Metals", *Monograph No. 13*, page 281.
- Chaston, J. G. Discussion on "The Flow of Liquid Metals on Solid Metal Surfaces", 692.
- Christian, J. W. Discussion on "The Opaque-Stop Microscope as a Means of Studying Surface Relief", 715; see also Basinski, Z. S.
- Cibula, A. Paper: "The Grain Refinement of Aluminium Alloy Castings by Additions of Titanium and Boron", 1; reply to discussion, 686, 687.
- Coleclough, T. P. Paper: "World Demand and Resources of Iron Ore", 234.
- Coles, B. R. Discussion on "Constitution of Transition-Metal Alloys", 695; discussion on "Titanium and Its Alloys", 702.
- and W. Hume-Rothery. Paper: "The Equilibrium Diagram of the System Nickel-Manganese", 85; reply to discussion, 699.
- Cook, Maurice, W. P. Fentiman, and Edwin Davis. Paper: "Observations on the Structure and Properties of Wrought Copper-Aluminium-Nickel-Iron Alloys", 419; reply to discussion, 717.
- Craik, R. L. See Howat, D. D.
- Cranston, J. P. See Howat, D. D.
- Crussard, C. See Jaoul, B.
- Davies, C. E. Awarded W. H. A. Robertson Medal, xii.
- Davies, M. H. Discussion on "Titanium and Its Alloys", 703.
- Davis, Edwin. Discussion on "Equipment for Thermal Treatment of Non-Ferrous Metals and Alloys", 679; see also Cook, Maurice.
- and S. G. Temple. Paper: "Batch and Continuous Annealing of Copper and Copper Alloys", 287.
- Devereux, W. C. Paper: "Secondary Aluminium and Magnesium", 248.
- Dinsdale, C. Paper: "Economy by Standardization of Alloys and of the Method of Reclamation of Scrap Metals", 241.
- Dodd, R. A. Paper: "Residual Stresses in Chill-Cast and Continuously Cast Aluminium Alloy Billets", 493.
- Dorey, S. F. Elected Vice-President for 1952-53, xii; elected Senior Vice-President for 1953-54, xiv.
- Dovey, D. M., I. Jenkins, and K. C. Randall. Paper: "Diffusion Coatings", *Monograph No. 13*, page 213.
- Dunsmuir, (Mrs.) Pamela. Discussion on "Use of Polarized Light in the Examination of Metals", 721.
- Duwez, Pol. Paper: "Allotropic Transformation in Titanium-Zirconium Alloys", 525.
- Edeleanu, C. Paper: "A Mechanism of Stress-Corrosion in Aluminium-Magnesium Alloys", 187; reply to discussion, 710.
- Ellwood, E. C. Papers: "Factors Affecting Equilibrium in Certain Aluminium Alloys", 605; "The Solid Solutions of Zinc in Aluminium", 217; reply to discussion, 714.
- and K. Q. Bagley. Paper: "The Lattice Spacings and Densities of Gold-Nickel Alloys at 25° C.", 617.
- and W. A. Weddle. Paper: "The Production and Properties of Oxide-Reduced Copper Powder", 193; reply to discussion, 712.
- Emley, E. F., A. C. Jessup, and W. F. Higgins. Paper: "The Effect of Phosphorus on the Corrosion-Resistance of Magnesium and Some of Its Alloys", 23.
- Evans, C. J. Discussion on "Equipment for Thermal Treatment of Non-Ferrous Metals and Alloys", 678.
- P. F. Hancock, F. W. Haywood, and J. McMullen. Paper: "Electric Furnaces for the Thermal Treatment of Non-Ferrous Metals and Alloys", 255.
- Evans, U. R. Paper: "Chemical Behaviour as Influenced by Surface Condition", *Monograph No. 13*, page 253; discussion on "A Mechanism of Stress-Corrosion in Aluminium-Magnesium Alloys", 707, 708; discussion on "Scrap Reclamation, Secondary Metals, and Substitute Metals", 253.
- van Ewijk, L. J. G. Discussion on "Grain Refinement of Castings", 686.
- Fell, E. W. Discussion on "The Occurrence of Stretcher-Strain Markings in an Aluminium-Magnesium Alloy", 689.
- Fentiman, W. P. See Cook, Maurice.
- Field, A. J. Discussion on "Equipment for Thermal Treatment of Non-Ferrous Metals and Alloys", 671, 680; discussion on "Grain Refinement of Castings", 686.
- Floyd, R. W. Paper: "The Formation of the Ni<sub>3</sub>Al Phase in Nickel-Aluminium Alloys", 551; see also Taylor, A.
- Forsyth, P. J. E. Paper: "Some Metallographic Observations on the Fatigue of Metals", 181.
- Fowler, W. A. Discussion on "Equipment for Thermal Treatment of Non-Ferrous Metals and Alloys", 667.
- Franklin, A. W. See Betteridge, W.
- Gay, P., and P. B. Hirsch. Paper: "The Crystalline Character of Abraded Surfaces", *Monograph No. 13*, page 123.
- Geach, G. A., and D. Summers-Smith. Paper: "The Alloys of Molybdenum and Tantalum", 143; reply to discussion, 528.
- Gence, P. See Cabarat, R.
- Gifkins, R. C. Discussion on "Structural Changes Accompanying Creep in a Tin-Antimony Alloy", 587.

- Gilbert, P. T. Discussion on "A Mechanism of Stress-Corrosion in Aluminium-Magnesium Alloys", 709.
- Goldschmidt, H. J. Discussion on "Constitution of Transition-Metal Alloys", 696.
- Grant, N. J. See Bloom, D. S.; Servi, Italo S.
- Greenaway, H. T. Paper: "The Constitutional Diagram of the Chromium-Tungsten System", 589; reply to discussion, 698.
- S. T. M. Johnstone, and Marion K. McQuillan. Paper: "High-Temperature Thermal Analysis Using the Tungsten/Molybdenum Thermocouple", 109.
- Greenfield, P., and G. V. Raynor. Paper: "The Constitution of the Copper-Rich Copper-Zinc-Germanium Alloys", 375.
- Greenough, G. B. Discussion on "The Deformation of Polycrystalline Zinc", 706.
- (Mrs.) Catherine M. Bateman, and (Mrs.) Edna M. Smith. Paper: "X-Ray Diffraction Studies in Relation to Creep", 545.
- Guillet, L. See Cabarat, R.
- Guinier, André. Awarded Rosenhain Medal 1952, xli.
- Gurney, C. Paper: "The Effect of Surface Condition on the Strength of Brittle Materials", *Monograph No. 13*, page 145.
- Haines, H. R. See Mott, B. W.
- Hall, R. C. See Burgan, B. R.
- Hancock, P. F. Discussion on "Equipment for Thermal Treatment of Non-Ferrous Metals and Alloys", 674; see also Evans, C. J.
- Hansen, M. Discussion on "Titanium and Its Alloys", 704.
- and W. Rostoker. Discussion on "Titanium and Its Alloys", 704.
- Harding, A. R., and G. V. Raynor. Paper: "The Constitution of the Aluminium-Chromium-Zinc Alloys at Low Chromium Contents", 435.
- Hardy, H. K. Papers: "The Ageing Characteristics of Ternary Aluminium-Copper Alloys with Cadmium, Indium, or Tin", 483; "The Solid Solubilities of Cadmium, Indium, and Tin in Aluminium", 431.
- Harper, R. G. Discussion on "The Flow of Liquid Metals on Solid Metal Surfaces", 693.
- Harris, G. B. Discussion on "Use of Polarized Light in the Examination of Metals", 720.
- Harris, J. C. Discussion on "Equipment for Thermal Treatment of Non-Ferrous Metals and Alloys", 670.
- Hartley, H. J. Discussion on "Equipment for Thermal Treatment of Non-Ferrous Metals and Alloys", 673, 679.
- and E. J. Bradbury. Paper: "Bright Annealing of Nickel and Its Alloys", 297.
- Harvey, C. A. See Sloman, H. A.
- Hausner, H. H. Discussion on "Powder Metallurgy of Copper and Copper Alloys", 711.
- Haywood, F. W. See Evans, C. J.
- Hehemann, R. F. See Burgan, B. R.
- Higgins, W. F. See Emley, E. F.
- Hirsch, P. B. See Gay, P.
- Hitchcock, J. O. Discussion on "Equipment for Thermal Treatment of Non-Ferrous Metals and Alloys", 674.
- Hoar, T. P. Discussion on "A Mechanism of Stress-Corrosion in Aluminium-Magnesium Alloys", 708; discussion on "Powder Metallurgy of Copper and Copper Alloys", 712; see also Butler, J. M.
- Holden, A. H. Discussion on "Equipment for Thermal Treatment of Non-Ferrous Metals and Alloys", 669, 680.
- Honeycombe, R. W. K. Papers: "A Simple Method of X-Ray Microscopy and Its Application to the Study of Deformed Metals", 39; "Inhomogeneities in the Plastic Deformation of Metal Crystals" (i. Occurrence of X-Ray Asterisms) 45, (ii. X-Ray and Optical Micrography of Aluminium) 49; reply to discussion, 691.
- Hooper, W. H. L. See Chadwick, R.
- Howard, J. C. Discussion on "Equipment for Thermal Treatment of Non-Ferrous Metals and Alloys", 677.
- Howat, D. D., R. L. Craik, and J. P. Cranston. Paper: "The Sintering of Copper-Zinc Powder Compacts", 353; reply to discussion, 713.
- Hudson, F. Paper: "The Influence of Specifications on Productivity and the Economic Utilization of Ferrous and Non-Ferrous Metals", 244.
- Hume-Rothery, W. See Betterton, J. O., Jr.; Coles, B. R.; Pearson, W. B.; Reynolds, J.
- J. O. Betterton, Jr., and J. Reynolds. Paper: "The Factors Affecting the Formation of 21/13 Electron Compounds in Alloys of Copper and of Silver", 609; reply to discussion, 701.
- Inglis, N. P. Elected Member of Council, xli.
- Ismay, W. N. Discussion on "Equipment for Thermal Treatment of Non-Ferrous Metals and Alloys", 672.
- Jaoul, B., and C. Crussard. Discussion on "The Plastic Deformation of Metals", 690.
- Jenkins, A. E., and H. W. Worner. Paper: "The Structure and Some Properties of Titanium-Oxygen Alloys Containing 0-5 At.-% Oxygen", 157.
- Jenkins, I. Discussion on "Equipment for Thermal Treatment of Non-Ferrous Metals and Alloys", 672; elected Member of Council, xli; see also Dovey, D. M.
- Jessup, A. C. See Emley, E. F.
- Johnstone, S. T. M. See Greenaway, H. T.
- Jones, E. H. Paper: "Secondary Heavy Metals", 245; elected Honorary Treasurer, xli.
- Jones, W. R. Discussion on "Primary Resources of Ferrous and Non-Ferrous Metals", 237.
- Karlsson, N. Reply to discussion on "X-Ray Study of the Phases in the Copper-Titanium System", 704.
- King, F. Discussion on "Equipment for Thermal Treatment of Non-Ferrous Metals and Alloys", 678, 680.
- King, Ronald. See Puttick, K. E.
- Kubaschewski, O. Appendix to paper: "Fundamental Reactions in the Vacuum-Fusion Method and its Application to the Determination of  $O_2$ ,  $N_2$ , and  $H_2$  in Mo, Th, Ti, U, V, and Zr", 405.
- Lamourededieu, Marcel. Paper: "Continuous Heat-Treatment of Aluminium Alloys of the Duralumin Type", 335; discussion on "Equipment for Thermal Treatment of Non-Ferrous Metals and Alloys", 669, 670.
- Lardner, E. Discussion on "Micrographic Aspects of the Diffusion of Zinc and Aluminium in Copper", 714.
- and N. B. McGregor. Paper: "Determination of Elastic Constants and Stress/Strain Relationship to Fracture of Sintered Tungsten Carbide-Cobalt Alloys", 369.
- Le Roux, R. See Cabarat, R.
- Liddiard, E. A. G. Discussion on "Grain Refinement of Castings", 685, 687.
- Lomer, W. M., and P. L. Pratt. Paper: "The Opaque-Stop Microscope as a Means of Studying Surface Relief", 409; reply to discussion, 715.
- Love, R. J. Paper: "The Influence of Surface Condition on the Fatigue Strength of Steel", *Monograph No. 13*, page 161.
- McGregor, N. B. See Lardner, E.
- McKeown, J. See Benson, N. D.
- McLean, D. Paper: "Creep Processes in Coarse-Grained Aluminium", 507; discussion on "Use of Polarized Light in the Examination of Metals", 721; see also Tate, A. E. L.
- McMullen, J. See Evans, C. J.
- McQuillan, A. D. Paper: "The Effect of the Elements of the First Long Period on the  $\alpha \rightleftharpoons \beta$  Transformation in Titanium", 363; reply to discussion, 704; discussion on "Constitution of Transition-Metal Alloys", 697.
- McQuillan, Marion K. See Greenaway, H. T.
- Mends, D. N. See Benson, N. D.
- Miekk-oja, H. M. Paper: "Segregation of Iron and Phosphorus at the Grain Boundaries in 70:30 Brass During Grain Growth", 569.
- Miller, H. J. Discussion on "Scrap Reclamation, Secondary Metals, and Substitute Metals", 253.
- Miodownik, A. P. Discussion on "Constitution of Copper-Base Alloys", 701; discussion on "The Structure and Properties of Wrought Copper-Aluminium-Nickel-Iron Alloys", 716.
- Moore, A. J. W. Discussion on "Twin Accommodation in Zinc", 724.
- Mott, B. W., and H. R. Haines. Papers: "The Application of Polarized Light to the Examination of Various Anisotropic Metals and Intermetallic Phases", 629; reply to discussion, 722; "The Metallography of Uranium", 621; reply to discussion, 722.
- Murphy, A. J. Introduction to discussion: "Metal Economics", 225.
- Nabarro, F. R. N. Discussion on "The Plastic Deformation of Metals", 690.
- Newman, W. A. C. Presents Honorary Treasurer's Report and Accounts, xi.
- Oliver, D. A. Discussion on "Scrap Reclamation, Secondary Metals, and Substitute Metals", 252.
- Oxby, G. A. Discussion on "Equipment for Thermal Treatment of Non-Ferrous Metals and Alloys", 680.
- Parker, R. T. Discussion on "Equipment for Thermal Treatment of Non-Ferrous Metals and Alloys", 675.
- Paton, C. P. Paper: "Batch Thermal Treatment of Light Alloys", 311; discussion on "Equipment for Thermal Treatment of Non-Ferrous Metals and Alloys", 668, 676, 680.
- Pearson, W. B., and W. Hume-Rothery. Paper: "The Constitution and Structure of Nickel-Vanadium Alloys in the Region 0-60 At.-% Vanadium", 641; reply to discussion, 699.
- Perryman, E. C. W. Discussion on "A Mechanism of Stress-Corrosion in Aluminium-Magnesium Alloys", 708; discussion on "Structural Changes Accompanying Creep in a Tin-Antimony Alloy", 588.
- Phillips, H. W. L. Paper: "The Nature and Properties of the Anodic Film on Aluminium and Its Alloys", *Monograph No. 13*, page 237.
- Piontelli, Roberto. Autumn Lecture: "Electrochemistry and the Science of Metals", 99.
- Pippard, A. B. See Chambers, R. G.
- Poole, D. M., and H. J. Axon. Paper: "Lattice-Spacing Relationships in Aluminium-Rich Solid Solutions of the Aluminium-Magnesium and Aluminium-Magnesium-Copper Systems", 599.
- Pratt, J. N., and G. V. Raynor. Paper: "The Aluminium-Rich Alloys of the System Aluminium-Chromium-Iron", 449.
- Pratt, P. L. Discussion on "The Deformation of Polycrystalline Zinc", 706; see also Lomer, W. M.
- and S. F. Pugh. Paper: "Twin Accommodation in Zinc", 653; reply to discussion, 724.
- Pugh, S. F. See Pratt, P. L.
- Puttick, K. E. Discussion on "Twin Accommodation in Zinc", 724.
- and Ronald King. Paper: "Boundary Slip in Bicrystals of Tin", 537.
- Rachinger, W. A. Paper: "The Effect of Grain-Size on the Structural Changes Produced in Aluminium by Slow Deformation", 415.
- Radtke, S. F., W. C. Schumb, and M. B. Bever. Discussion on "The Alloys of Molybdenum and Tantalum", 528.
- Ramsay, A. G. Elected Member of Council, xli.
- Ramsey, J. A. Paper: "Some Observations on the Deformation of Polycrystalline Zinc", 167; reply to discussion, 706.
- Randall, K. C. See Dovey, D. M.
- Raynor, G. V. See Greenfield, P.; Harding, A. R.; Pratt, J. N.
- Renouard, M. See Tournaire, M.
- Reynolds, J. See Hume-Rothery, W.
- W. A. Wiseman, and W. Hume-Rothery. Paper: "The Equilibrium Diagram of the System Copper-Indium in the Region 25-35 At.-% Indium", 637; reply to discussion, 701.



- Reynolds, J. A., and C. R. Tottle. Paper: "The Nucleation of Cast Metals at the Mould Face", 93; reply to discussion, 688.
- Robinson, Ian R. See Spear, Peter.
- Robinson, William Sydney. Awarded Institute of Metals (Platinum) Medal 1952, xii.
- Rostoker, W. Discussion on "Constitution of Transition-Metal Alloys", 698; see also Hansen, M.
- Ruddle, R. W. Discussion on "Metal/Mould Reaction in Copper-Base Alloys", 719; discussion on "The Reaction of Aluminium-Magnesium Alloys with Steam", 598.
- Rutherford, N. B. Paper: "The Effect of Metal/Mould Reaction on 85:5:5:5 Lead Gun-Metal Sand Castings", 555; reply to discussion, 719; discussion on "Grain Refinement of Castings", 686; discussion on "Metal/Mould Reaction in Copper-Base Alloys", 718.
- Schatz, Frederick V. Paper: "The Spectrochemical Determination of Zinc, Lead, and Iron in Copper and Copper Alloys", 77.
- Schubert, K. Discussion on "Constitution of Copper-Base Alloys", 701.
- and W. Auerhammer. Discussion on "The Solid Solutions of Zinc in Aluminium", 713.
- Schumb, W. C. See Radtke, S. F.
- Servi, Italo S., and N. J. Grant. Paper: "Creep and Stress Rupture as Rate Processes", 33.
- Sidery, A. J. See Bristow, C. A.
- Simnad, Massoud T. Paper: "Radioisotopes in the Study of Metal Surface Reactions in Solutions", *Monograph No. 13*, page 23.
- Sloman, H., and C. A. Harvey. Paper: "Fundamental Reactions in the Vacuum-Fusion Method and its Application to the Determination of  $O_2$ ,  $N_2$ , and  $H_2$  in Mo, Th, Ti, U, V, and Zr", 391.
- Smith, A. D. N. Paper: "A Study of Some Factors Influencing the Young's Modulus of Solid Solutions", 477.
- Smith, Christopher. Discussion on "Equipment for Thermal Treatment of Non-Ferrous Metals and Alloys", 670, 676; discussion on "The Structure and Properties of Wrought Copper-Aluminium-Nickel-Iron Alloys", 716.
- Smith, (Mrs.) Edna M. See Greenough, G. B.
- Smithells, C. J. Elected President for 1952-53, xii; Presidential Address, 469; discussion on "Equipment for Thermal Treatment of Non-Ferrous Metals and Alloys", 668, 670.
- Spear, Peter, Ian R. Robinson, and K. J. B. Wolfe. Paper: "The Influence of Machining and Grinding Methods on the Mechanical and Physical Condition of Metal Surfaces", *Monograph No. 13*, page 59.
- Stanford, E. G. Discussion on "Equipment for Thermal Treatment of Non-Ferrous Metals and Alloys", 676.
- Staples, R. T. Paper: "Flash Annealing of Light Alloys", 323.
- Staudinger, J. J. P. May Lecture: "The Place of Plastics in the Order of Matter", 529.
- Stokowiec, Z. Discussion on "Metal/Mould Reaction in Copper-Base Alloys", 719; discussion on "The Structure and Properties of Wrought Copper-Aluminium-Nickel-Iron Alloys", 717.
- Stordy, J. J. Discussion on "Equipment for Thermal Treatment of Non-Ferrous Metals and Alloys", 681.
- Stubbs, R. Lewis. Paper: "The World Supply of Non-Ferrous Metals, Including the Light Metals", 226.
- Suiter, J. W. See Wood, W. A.
- Sully, A. H. Paper: "The Sigma Phase in Binary Alloys of the Transition Elements", 173; reply to discussion, 699.
- Summers-Smith, D. See Geach, G. A.
- Sutton, H. Elected Member of Council, xii; discussion on "The Structure and Properties of Wrought Copper-Aluminium-Nickel-Iron Alloys", 717; see also Bristow, C. A.
- Swain, A. J. Paper: "Experiments on the Reaction of Aluminium-Magnesium Alloys with Steam", 125; reply to discussion, 598.
- Taber, D. See Bowden, F. P.
- Tarring, L. Discussion on "Primary Resources of Ferrous and Non-Ferrous Metals", 238.
- Tate, A. E. L., and D. McLean. Paper: "Note on Sub-Crystal Structure in Cold-Rolled Aluminium", 390.
- Taylor, A., and R. W. Floyd. Paper: "The Constitution of Nickel-Rich Alloys of the Nickel-Chromium-Titanium System", 577; reply to discussion, 699.
- Teed, P. Litherland, Elected Member of Council, xii.
- Temple, S. G. See Davis, Edwin.
- Thomas, W. J. Elected Member of Council, xii.
- Thompson, F. C. Elected Senior Vice-President for 1952-1953, xii.
- Tolansky, S. Paper: "Specialized Microscopical Techniques in Metallurgy", *Monograph No. 13*, page 1.
- Tottle, C. R. See Reynolds, J. A.
- Tournaire, M., and M. Renouard. Paper: "The Effect of Zirconium on the Properties and Structure of Superduralumin, with Particular Reference to Forgings", 593.
- Trotter, J. Paper: "Electron-Microscopic Studies of Slip in Aluminium During Creep", 521.
- Tylecote, R. F. Discussion on "The Flow of Liquid Metals on Solid Metal Surfaces", 693.
- Varley, P. C. Discussion on "Grain Refinement of Castings", 686.
- Voce, E. Discussion on "Equipment for Thermal Treatment of Non-Ferrous Metals and Alloys", 678, 679.
- Waight, J. F. Paper: "Gas Equipment for the Thermal Treatment of Non-Ferrous Metals and Alloys", 269; discussion on "Equipment for Thermal Treatment of Non-Ferrous Metals and Alloys", 673.
- Watkins, H. C. See Bailey, G. L. J.
- Weddle, W. A. See Ellwood, E. C.
- Weeks, G. W. Discussion on "Equipment for Thermal Treatment of Non-Ferrous Metals and Alloys", 674.
- Wiseman, W. A. See Reynolds, J.
- Wolfe, K. J. B. See Spear, Peter.
- Wood, W. A., and J. W. Suiter. Paper: "Stress-Recovery in Aluminium", 501.
- Worner, H. W. Paper: "Heat-Treatment of Titanium-Rich Titanium-Iron Alloys", 213; reply to discussion, 706; see also Jenkins, A. F.
- von Zeerleder, A. Discussion on "Equipment for Thermal Treatment of Non-Ferrous Metals and Alloys", 669, 673, 676, 678.
- Zuckerman, S. Paper: "Metals as Natural Resources", 233.







**DATE DUE**

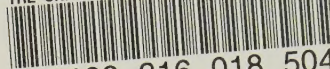
FEB 20 1983

RETD. FEB 1983

**PERIODICALS MUST BE RETURNED  
TO PERIODICALS DESK ONLY**



THE UNIVERSITY OF ILLINOIS AT CHICAGO



3 8198 316 018 504



